

ZOOLOGICAL SCIENCE

An International Journal

VOLUME 6
1989

published by
The Zoological Society of Japan

CONTENTS

VOLUME 6

REVIEWS

- Malacinski, G. M., A. W. Neff, G. Radice and H.-M. Chung: Amphibian somite development: contrasts of morphogenetic and molecular differentiation patterns between the laboratory archetype species *Xenopus* (anuran) and Axolotle (urodele) 1
- Engström, W., G. Möllermark, L. E. Kängström and O. Larson: Some molecular characteristics of canine mammary tumours and their relationship to biological malignancy and prognosis 15
- Oguro, C.: Evolution of the development and larval types in asteroids 199
- Selman, K. and R. A. Wallace: Cellular aspects of oocyte growth in teleosts 211
- Skadhauge, E.: Hormonal regulation of sodium absorption and chloride secretion across the lower intestines of birds 437
- Ozato, K., K. Inoue and Y. Wakamatsu: Transgenic fish: biological and technical problems 445
- Chieffi, G.: New trends in the regulation of the gonadal activity in vertebrates: paracrine and autocrine control 623
- Michibata, H.: New aspects of accumulation and reduction of vanadium ions in ascidians, based on concerted investigation from both a chemical and biological viewpoint 639
- Ueck, M., K. Wake and H. Kobayashi: Nervous organization of the pineal complex in lower vertebrates 817
- Oami, K. and Y. Naito: Bioelectric control of effector responses in the marine dinoflagellate, *Noctiluca miliaris* 833
- Murakami, T.: Scanning electron microscopy of vascular casts: A methodological review with some comments on the angioarchitecture of rat hypophysis 1047
- Hayashi, S. and M. Aihara: Neonatal estrogenization of the female rat: A useful model for analysis of hypothalamic involve-

ment of gonadotropin release 1059

ORIGINAL PAPERS

Physiology

- Kurahashi, T. and T. Shibuya: Membrane responses and permeability changes to odorants in the solitary olfactory receptor cells of newt 19
- Horiuchi, S., H. Kitani, Y. Koshida, F. Tokunaga, and T. Takeuchi: Immunofluorescent staining of visual cells from various species by monoclonal antibodies against bovine rhodopsin 31
- Minato, K.: Cell cycle in the epidermis during larval instars of the saturniid moth *Samia cynthia ricini* (Lep.) 35
- Tokunaga, F., T. Iwasa, M. Takao, S. Sato, and T. Takeuchi: Preparation and properties of anti-bovine rhodopsin monoclonal antibodies (COMMUNICATION) 167
- Tagawa, T., A. Ishikawa, W. C. Su and K. Okamoto: Autonomic innervation of intra and extra-cranial arteries in the amphibia 233
- Eguchi, E., K. Arikawa, S. Ishibashi, T. Suzuki and V. B. Meyer-Rochow: Growth-related biometrical and biochemical studies of the compound eye of the crab, *Hemigrapsus sanguineus* 241
- Okajima, A. and M. Watanabe: Electrophysiological identification of neuronal pathway to the prothoracic gland and the change in electrical activities of the prothoracic gland innervating neurones during larval development of a moth, *Mamestra brassicae* 459
- Ohtsu, K.: Flash-induced depression of the ERP under the Ca^{2+} -free condition in the octopus retina 469
- Fujii, R., H. Kasukawa, K. Miyaji and N. Oshima: Mechanisms of skin coloration and its changes in the blue-green damselfish, *Chromis viridis* 477

Sato, E. and S. Tagawa: Oscillations of membrane potential and membrane resistance during the cell cycle in the newt egg macromeres	649
Kimura, K., T. Tanimura and T. Shimozawa: Mosaic fate mapping of the behavioral and the muscular defects induced by a <i>Drosophila</i> mutation, <i>abnormal proboscis extension reflex C (aperC)</i>	659
Lorenzo, A., P. Santana, T. Gómez and P. Badia: Sodium and chloride transport in the lizard duodenum	667
Okajima, A. and K. Kumagai: The inhibitory control of prothoracic gland activity by the neurosecretory neurones in a moth, <i>Mamestra brassicae</i>	851
Okajima, A., K. Kumagai and M. Watanabe: The involvement of afferent chemoreceptive activity in the nervous regulation of the prothoracic gland in a moth, <i>Mamestra brassicae</i>	859
Tamamaki, N.: Visible light reception of accessory eye in the giant snail, <i>Achatina fulica</i> , as revealed by an electrophysiological study	867
Tamamaki, N.: The accessory photosensory organ of the terrestrial slug, <i>Limax flavus</i> L. (Gastropoda, Pulmonata): morphological and electrophysiological study	877
Shiga, T., Y. Oka, M. Satou, N. Okumoto and K. Ueda: Retinal projections in the himé salmon (landlocked red salmon, <i>Oncorhynchus nerka</i>)	885
cells of frog taste organ	487
Kuroda, Y., Y. Takada and T. Kasuya: Use of the laser microbeam for preserving frozen <i>Drosophila</i> embryos	499
Sugino, Y. M. and M. Ishikawa: The intercellular bridge of a blood cell in the ascidian, <i>Ciona savignyi</i> (COMMUNICATION)	599
Okai, Y.: A human embryo fibroblast-derived peptide suppresses the formyl-Met-Leu-Phe (FMLP)-induced activation in human polymorphonuclear leukocytes (COMMUNICATION)	603
Higashi, K., T. Gomi, M. Soeda, S. Sasa, A. Kimura and Y. Kikuchi: New morphological aspects of the brush cells in the main excretory ducts of the rat submandibular glands	675
Iwasaki, S., K. Miyata and K. Kobayashi: Fine structure of the lingual dorsal epithelium of the Japanese toad, <i>Bufo japonicus</i> (Anura: Bufonidae)	681
Wago, H. and T. Tanaka: Synergistic effects of calyx fluid and venom of <i>Apanteles kariyai</i> Watanabe (Hymenoptera: Braconidae) on the granular cells of <i>Pseudaletia separata</i> Walker (Lepidoptera: Noctuidae)	691
Asashima, M., T. Oinuma and S. Komazaki: Electron microscopical and histochemical studies of the spontaneous tumors of <i>Xenopus laevis</i>	899
Yashika, K. and P. H. Hashimoto: Annulate lamellae in prothoracic gland cells of brainless pupae of the swallowtail, <i>Papilio xuthus</i> (Lepidoptera)	907

Cell Biology

Shigenaka, Y., K. Yano and M. Imada: Axopodial contraction evoked by electrical stimulation and its ultrastructural analysis in a heliozoan <i>Echinospheerium</i>	45
Tachi, C. and U. Zor: Effect of calcium ionophore A23187 upon the rate of leukotriene C ₄ production and the cellular morphology in highly purified mouse peritoneal macrophages cultured <i>in vitro</i>	251
Iwasaki, S. and K. Kobayashi: Fine structure of the lingual dorsal epithelium in the bullfrog, <i>Rana catesbeiana</i>	259
Suzuki, Y. and M. Takeda: Filaments in the	

Genetics

Kamezaki, N.: Karyotype of the loggerhead turtle, <i>Caretta caretta</i> , from Japna (COMMUNICATION)	421
Hosono, R., T. Sassa and S. Kuno: Spontaneous mutations of trichlorfon resistance in the nematode, <i>Caenorhabditis elegans</i> ...	697

Immunology

Han, S. S. and A. P. Gupta: Arthropod immune system. II. Encapsulation of implanted nerve cord and "plain gut" surgical	
-------------------------------------------------------------------------------------------------------------------------	--

- suture by granulocytes of *Blattella germanica* (L.) (Dictyoptera: Blattellidae) 303
- Okai, Y. and S. Ishizaka: Spontaneous release of B lymphocyte-enhancing factors for growth and differentiation by YH-1 cells in serum-free culture media-Identification of interleukin 1 activities..... 523
- Shozawa, A., C. Suto and N. Kumada: Superoxide production by the haemocytes of the freshwater snail, *Biomphalaria glabrata*, stimulated by miracidia of *Schistosoma mansoni* (COMMUNICATION) 1019
- Biochemistry**
- Kenmochi, N. and K. Ogata: A comparative study of 40S ribosomal proteins in *Artemia salina* and rat liver: Peptide analysis by limited proteolysis and sodium dodecyl sulfate acrylamide gel electrophoresis 55
- Sakai, T., N. Tabata, and M. Suiko: Occurrence of biliverdin IX_α in the gallbladder bile of hagfish, *Eptatretus burgeri* (COMMUNICATION)..... 173
- Suzuki, T., M. Shiba, T. Furukohri and M. Kobayashi: Hemoglobins from the two closely related clams *Barbatia lima* and *Barbatia virescens*. Comparison of their subunit structures and N-terminal sequence of the unusual two-domain chain 269
- Yasugi, S., T. Matsunaga and T. Mizuno: Pepsinogen-like immunoreactivity in ascidian stomach and intestine: Immunohistochemical and biochemical study 283
- Michibata, H., Y. Zenko, K. Yamada, M. Hasegawa, T. Terada and T. Numakunai: Effects of vanadium ions in different oxidation states on myosin ATPase extracted from the solitary ascidian, *Halocythia roretzi* (Drasche) 289
- Kenmochi, N. and K. Ogata: The 5S RNA binding protein of *Artemia salina* ribosomes: Identification and immunological comparison with that of rat liver 295
- Yoshizaki, N.: Comparison of two lectins isolated from *Xenopus* cortical granules 507
- Sonobe, H.: Studies on embryonic diapause in the *pnd* mutant of the silkworm, *Bombyx mori*: characterization of protein synthesis during early development 515
- Hu, D. H., S. Kimura, S. Kawashima and K. Maruyama: Calcium-activated neutral protease quickly converts α -connectin to β -connectin in chicken breast muscle myofibrils (COMMUNICATION) 797
- Suzuki, T., T. Takagi, K. Okuda, T. Furukohri and S. Ohta: The deep-sea tube worm hemoglobin: subunit structure and phylogenetic relationship with annelid hemoglobin 915
- Developmental Biology**
- Tazawa, E., A. Fujiwara, and I. Yasumasu: Stimulating effect of dimethylsulfoxide on unfertilized eggs of the echinoid, *Urechis unicinctus* 63
- Uchiyama, H. and T. Mizuno: Sexual dimorphism in the genital tubercle of the duck: Analysis by sex-steroid administration and steroid autoradiography 71
- Shimizu, T. and E. Ohnishi: The stimulatory effect of 2-deoxyecdysone on spermiogenesis of the diapausing cabbage armyworm, *Mamestra brassicae* (Lepidoptera: Noctuidae), *in vitro* (COMMUNICATION) 177
- Wada, K.: Interbreeding experiments of the two forms of *Macrophthalmus japonicus* (Crustacea: Brachyura: Ocypodidae) (COMMUNICATION) 181
- Horiuchi, S. and Y. Koshida: Effects of foodstuffs on intestinal length in larvae of *Rhacophorus arboreus* (Anura: Rhacophoridae)..... 321
- Nakamura, S., C. Ohmi and M. K. Kojima: Effects of zinc ion on formation of the fertilization membrane in sea urchin eggs .. 329
- Myohara, M. and J. H. Willis: Control of cuticle formation in wing epidermal cells of the fleshfly, *Sarcophaga bullata* 533
- Sawa, M., A. Fukunaga, T. Naito and K. Oishi: Studies on the sawfly, *Athalia rosae* (Insecta, Hymenoptera, Tenthredinidae). I. General biology 541
- Sawa, M. and K. Oishi: Studies on the sawfly, *Athalia rosae* (Insecta, Hymenoptera, Tenthredinidae). II. Experimental

activation of mature unfertilized eggs	549
Sawa, M. and K. Oishi: Studies on the sawfly, <i>Athalia rosae</i> (Insecta, Hymenoptera, Tenthredinidae). III. Fertilization by sperm injection	557
Sawai, T. and K. Higuchi: Cytostatic effect of the cytoplasm of mature oocytes in the newt, <i>Cynops pyrrhogaster</i>	709
Asao, T.: The alkaline substances and other constituents of blastocoel fluid of the newt embryo	715
Sakairi, K., M. Yamamoto, K. Ohtsu and M. Yoshida: Environmental control of gonadal maturation in laboratory-reared sea urchins, <i>Anthocidaris crassispina</i> and <i>Hemicentrotus pulcherrimus</i>	721
Kawashima, T. and T. Nakazawa: Transient increase in mitochondrial protein synthesis of starfish embryo before gastrulation (COMMUNICATION)	801
Tanaka, A. and M. H. Ross: Tibia to femur ratios of unaltered and regenerated legs of the stumpy mutant of the German cockroach	927
Hamaguchi, Y.: Effect of ATP _γ s on fertilization envelope elevation of sand dollar eggs (COMMUNICATION)	1023

Reproductive Biology

Fujihara, N., H. Nishiyama and O. Koga: <i>In vitro</i> viability and fertilizing capacity of guinea fowl spermatozoa	731
Lattaud, C. and R. Marcel: Stimulating influence of cerebral ganglia on <i>in vitro</i> incorporation of tritiated leucine into ovaries of <i>Eisenia fetida</i> Sav. (Annelida: Oligochaeta)	741
Kobayashi, T. and H. Iwasawa: The role of Sertoli cells adjacent to efferent ductules in sperm transport in <i>Rana porosa porosa</i>	935
Awaji, M. and I. Hanyu: Seasonal changes in ovarian response to photoperiods in orange-red type medaka	943
Kobayashi, T., A. Oshimi and H. Iwasawa: Development of an <i>in vitro</i> spermiation system in the frog, <i>Rana nigromaculata</i> (COMMUNICATION)	1028

Endocrinology

Takagi, Y., T. Hirano, and J. Yamada: <i>In vitro</i> measurements of calcium influx into isolated goldfish scales in reference to the effects of putative fish calcemic hormones	83
Shimizu, A.: Role of internalization of follicle-stimulating hormone (FSH)-receptor complex on down-regulation of FSH receptor in mouse Sertoli cells	91
Mori, T. and H. Nagasawa: Causal analysis of the development of uterine adenomyosis in mice	103
Masaki, T., K. Endo, and K. Kumagai: Neuroendocrine regulation of the development of seasonal morphs in the Asian comma butterfly, <i>Polygonia c-aureum</i> L.: Stage-dependent changes in the activity of summer-morph-producing hormone of the brain-extracts	113
Kimura, M., S. Sakurai, T. Nakamachi, M. Nariki, S. Niimi, T. Ohtaki, Y. Fujimoto, F. Hata, and N. Ikekawa: Qualitative and quantitative analysis of juvenile hormone in the larvae of the silkworm, <i>Bombyx mori</i>	121
Dixit, A. S. and P. D. Tewary: Circadian periodicity in termination of photorefractoriness in the female yellow-throated sparrow, <i>Gymnorhis xanthocollis</i>	129
Peter, M. C. S. and O. V. Oommen: Effects of thyroid and gonadal hormones <i>in vitro</i> on hepatic succinate dehydrogenase activity of the teleost, <i>Anabas testudineus</i> (Bloch) (COMMUNICATION)	185
Hyodo, S., M. Sato and A. Urano: Molecular- and immuno-histochemical study on expressions of vasopressin and oxytocin genes following water deprivation	335
Iwamuro, S., N. Mamiya and S. Kikuyama: Pituitary hormone-dependent aldosterone secretion in <i>Xenopus laevis</i>	345
Koike, S. and T. Noumura: Effects of post-weaning differential housing on serum testosterone levels in male mice throughout aging	351
Kobayashi, Y. and C. Iga: Erythrocyte diapedesis in anterior pituitary hemorrhage	

- after intraperitoneal injection of hypertonic solution in mice359
- Sasayama, Y., K. Matsuda, C. Oguro and A. Kambegawa: Immunohistochemical demonstration of calcitonin gene-related peptide in the ultimobranchial gland of some lower vertebrates and in the nervous tissues of some invertebrates (COMMUNICATION)423
- Sasayama, Y., K. Matsuda, C. Oguro and A. Kambegawa: Immunohistochemical study of the ultimobranchial gland in chum salmon fry (COMMUNICATION)607
- Matsuda, K., Y. Sasayama, C. Oguro and A. Kambegawa: Calcitonin-immunoreactive cells found in the extra-ultimobranchial areas of the salamander, *Hynobius nigrescens*, during larval development (COMMUNICATION)611
- Akai, H. and H. Rembold: Juvenile hormone levels in *Bombyx* larvae and their impairment after treatment with an imidazole derivative KK-42 (COMMUNICATION) ..615
- Yamauchi, K., R. Horiuchi, S. Koya and H. Takikawa: Uptake of 3,5,3'-L-triiodothyronine into bullfrog red blood cells mediated by plasma membrane binding sites749
- Kobayashi, T., S. Kikuyama, A. Kume, J. Okuma and M. Ohkawa: [³⁵S]-sulphate uptake by *Xenopus laevis* cartilage: the influence of plasma from the growth hormone-treated animal757
- Uchibori, M. and S. Kawashima: Stimulation of nuclear volume enlargement and neuronal process growth by estrogen in the hypothalamic and limbic nuclei of the rat 763
- Maitra, G. and S. Bhattacharya: Seasonal changes of triiodothyronine binding to piscine ovarian nuclei771
- Tazawa, H., M. Mukai and M. Ogawa: Immunohistochemical studies of juxtaglomerular cells and the corpuscles of Stannius in the eel, *Anguilla japonica* (COMMUNICATION)805
- Shimizu, I., T. Matsui and K. Hasegawa: Possible involvement of GABAergic neurons in regulation of diapause hormone secretion in the silkworm, *Bombyx mori* (COMMUNICATION)809
- Fujii, K., N. Ohta, T. Sasaki, Y. Sekizawa, C. Yamada and H. Kobayashi: Immunoreactive FMRamide in the nervous system of the earthworm, *Eisenia foetida*951
- Takada, K., M. Itoh, H. Nishio and S. Ishii: Purification of toad (*Bufo japonicus*) gonadotropins and the development of their homologous radioimmunoassays963
- ### Morphology
- Yee, Win Win, S. Takahashi and S. Kawashima: Age-related changes and sex difference in the ultrastructure of renal glomerulus in Wistar/Tw rats777
- ### Behavior Biology
- Kabasawa, H. and S. Ooka-Souda: Circadian rhythms in locomotor activity of the hagfish, *Eptatretus burgeri* (IV). The effect of eye-ablation135
- Yamanouchi, K. and Y. Arai: Lordosis-inhibiting pathway in the lateral hypothalamus: Medial forebrain bundle (MFB) transection141
- Munro, A. D.: Lack of influence of photoperiod on the brood interval of the guppy (*Poecilia reticulata*) (COMMUNICATION)191
- Tabata, M., M. Minh-Nyo, H. Niwa and M. Oguri: Circadian rhythm of locomotor activity in a teleost, *Silurus asotus*367
- Tabata, M. and M. Minh-Nyo: Dual photo-behavioral response in catfish (COMMUNICATION)427
- Tomioka, K. and Y. Chiba: Photoperiod during post-embryonic development affects some parameters of adult circadian rhythm in the cricket, *Gryllus bimaculatus*565
- Watanabe, M. and H. Terami: Excessive transitory migration of guppy populations. II. Analysis of possible conspecific-following tendency573
- Spieler, R. E. and J. J. Clougherty: Free-running locomotor rhythms of feeding-entrained goldfish (COMMUNICATION) 813
- Terami, H. and M. Watanabe: Excessive transitory migration of guppy populations.

III. Analysis of perception of swimming space and a mirror effect.....	975
Yamashita, J., S. Hayashi and Y. Hirata: Reduced size of preputial glands and absence of aggressive behavior in the genetically obese (ob/ob) mouse (COMMUNICATION)	1033
Kusaka, S., H. Nagasawa, K. Yamanouch and Y. Arai: Induction of male behaviors by administration of testosterone using silastic tubes in castrated male and female rats (COMMUNICATION)	1037
Taxonomy and Systematics	
Kubota, S.: Systematic study of a paedomorphic derivative hydrozoan <i>Eugymnanthea</i> (Thecata-Leptomedusae)	147
Toda, M. J. and T. X. Peng: Eight species of the subgenus <i>Drosophila</i> (Diptera: Drosophilidae) from Guangdong Province, southern China	155
Sawada, I. and M. Harada: Cestode parasites of some Taiwanese shrews	377
Miura, T. and L. Laubier: <i>Nautilina calyptogenicola</i> , a new genus and species of parasitic polychaete on a vesicomid bivalve from the Japan Trench, representative of a new family Nautilinidae	387
Okada, T.: A proposal of establishing tribes for the family Drosophilidae with key to tribes and genera (Diptera)	391
Oda, S. and H. Mukai: Systematic position and biology of <i>Pectinatella gelatinosa</i> Oka (Bryozoa: Phylactolaemata) with the description of a new genus	401
Yoshida, I., Y. Obara and N. Matsuoka: Phylogenetic relationships among seven taxa of the Japanese microtine voles revealed by karyological and biochemical techniques	409
Shimazu, T.: Two new species of the genus <i>Diploproctodaeum</i> (Trematoda: Leporecreadiidae: Diploproctodaeinae), with some comments on species in the subfamily Diploproctodaeinae, from Japanese marine fishes	579
Matsuoka, N. and H. Suzuki: Electrophoretic study on the phylogenetic relationships among six species of sea-urchins of the family Echinometridae found in the Japanese waters	589
Brusle, S.: Cytological differences in early germ cells of three genera of grey mullets, <i>Mugil</i> , <i>Liza</i> and <i>Chelon</i> (Teleostei: Mugilidae)	789
Nagatomi, A., H. Imaizumi and H. Nagatomi: Revision of <i>Molobratia</i> from Japan and Taiwan (Insecta, Diptera, Asilidae)	983
Saitoh, M., N. Matsuoka and Y. Obara: Biochemical systematics of three species of the Japanese long-tailed field mice; <i>Apodemus speciosus</i> , <i>A. giliacus</i> and <i>A. argenteus</i>	1005
Others	
Proceedings of the 60th Annual Meeting of the Zoological Society of Japan	1069
Announcements	1228
Author index	1229
Instructions to Authors	195
Errata	198, 433, 1246

Vol. 6 No. 1

February 1989

ZOOLOGICAL SCIENCE

An International Journal

JUN 27 1989

LIBRARIES

PHYSIOLOGY
CELL and MOLECULAR BIOLOGY
GENETICS
IMMUNOLOGY
BIOCHEMISTRY
DEVELOPMENTAL BIOLOGY
REPRODUCTIVE BIOLOGY
ENDOCRINOLOGY
BEHAVIOR BIOLOGY
ENVIRONMENTAL BIOLOGY
ECOLOGY and TAXONOMY

published by Zoological Society of Japan

distributed by Business Center for Academic Societies Japan
VSP, Zeist, The Netherlands

ISSN 0289-0003

ZOOLOGICAL SCIENCE

The Official Journal of the Zoological Society of Japan

Editor-in-Chief:

Hideshi Kobayashi (Tokyo)

Managing Editor:

Chitaru Oguro (Toyama)

Assistant Editors:

Yuichi Sasayama (Toyama)

Hitoshi Michibata (Toyama)

Miëko Komatsu (Toyama)

The Zoological Society of Japan:

Toshin-building, Hongo 2-27-2, Bunkyo-ku,
Tokyo 113, Japan. Tel. (03) 814-5675

Officers:

President: Nobuo Egami (Tokyo)

Secretary: Hideo Namiki (Tokyo)

Treasurer: Tadakazu Ohoka (Tokyo)

Librarian: Masatsune Takeda (Tokyo)

Editorial Board:

Howard A. Bern (Berkeley)

Horst Grunz (Essen)

Susumu Ishii (Tokyo)

Koscak Maruyama (Chiba)

Kazuo Moriaki (Mishima)

Hideki Sato (Nagoya)

Ryozo Yanagimachi (Honolulu)

Walter Bock (New York)

Robert B. Hill (Kingston)

Seiichi Kawashima (Tokyo)

Roger Milkman (Okazaki)

Tokindo S. Okada (Okazaki)

Hiroshi Watanabe (Shimoda)

Aubrey Gorbman (Seattle)

Yukio Hiramoto (Chiba)

Yukiaki Kuroda (Mishima)

Hiromichi Morita (Fukuoka)

Andreas Oksche (Giessen)

Mayumi Yamada (Sapporo)

ZOOLOGICAL SCIENCE is devoted to publication of original articles, reviews and communications in the broad field of Zoology. The journal was founded in 1984 as a result of unification of Zoological Magazine (1888-1983) and *Annotationes Zoologicae Japonenses* (1897-1983), the former official journals of the Zoological Society of Japan. ZOOLOGICAL SCIENCE appears bimonthly. An annual volume consists of six numbers of more than 1100 pages including an issue containing abstracts of papers presented at the annual meeting of the Zoological Society of Japan.

MANUSCRIPTS OFFERED FOR CONSIDERATION AND CORRESPONDENCE CONCERNING EDITORIAL MATTERS should be sent to:

Dr. Chitaru Oguro, Managing Editor, Zoological Science, Department of Biology, Faculty of Science, Toyama University, Toyama 930, Japan, in accordance with the instructions to authors which appear in the first issue of each volume. Copies of instructions to authors will be sent upon request.

SUBSCRIPTIONS. ZOOLOGICAL SCIENCE is distributed free of charge to the members, both domestic and foreign, of the Zoological Society of Japan. To non-member subscribers within Japan, it is distributed by Business Center for Academic Societies Japan, 6-16-3 Hongo, Bunkyo-ku, Tokyo 113. Subscriptions outside Japan should be ordered from the sole agent, VSP, Utrechtseweg 62, 3704 HE Zeist (postal address: P. O. Box 346, 3700 AH Zeist), The Netherlands. Subscription rates will be provided on request to these agents. New subscriptions and renewals begin with the first issue of the current volume.

All rights reserved. No part of this publication may be reproduced or stored in a retrieval system in any form or by any means, without permission in writing from the copyright holder.

© Copyright 1989, The Zoological Society of Japan

[Publication of Zoological Science has been supported in part by a Grant-in-Aid for
Publication of Scientific Research Results from the Ministry of Education, Science
and Culture, Japan.]

REVIEW

Amphibian Somite Development: Contrasts of Morphogenetic and Molecular Differentiation Patterns between the Laboratory Archetype Species *Xenopus* (anuran) and Axolotl (urodele)

GEORGE M. MALACINSKI¹, ANTON W. NEFF², GARY RADICE¹,
and HAE-MOON CHUNG³

¹Department of Biology, and ²Medical Sciences Program (School of Medicine),
Indiana University, Bloomington, IN 47405, U.S.A. and

³Department of Biology, College of Education,
Seoul National University, Seoul 151, South Korea

ABSTRACT—Despite the overall similarity in superficial aspects of somitogenesis (e.g., segmentation of mesoderm into blocks, differentiation in the cranial to caudal direction, etc.), the actual details of pattern formation, morphogenesis, and differentiation are markedly different between the two laboratory prototype species, *Xenopus laevis* (anuran) and *Ambystoma mexicanum* (urodele—"axolotl"). The cells which comprise the mesoderm originate in different locations within the late blastula/early gastrula embryo. Differentiation (e.g., synthesis of actin and myosin) begins remarkably early in *Xenopus*, and surprisingly late in the axolotl embryo. The cellular mechanics (e.g., cell arrangement/shape/re-orientations) of segmentation are very different in those amphibia, and the structure of individual myotome cells (e.g., whether multinucleated) is also divergent.

Generalizations, sets of rules, or unifying principles which govern somitogenesis among various amphibian species are, therefore, difficult, if not impossible, to formulate. Legitimate discussion of the similarities and differences between somite development in *Xenopus* and axolotl embryos should focus on the sharp contrasts which characterize these laboratory species.

INTRODUCTION

Somite development has been a favorite subject of experimentation for several generations of embryologists. A variety of advantageous features characterize amphibian somitogenesis and largely account for the voluminous literature of the subject. Among the most notable properties are the following: (1) somites comprise the single largest tissue mass of the early embryo; (2) the metamerism displayed by somites is striking, and has therefore attracted the attention of biological model builders (e.g., [1]); (3) somite tissue is readily accessible for microsurgical manipulation; (4) the

cellular composition of a somite is relatively homogeneous; (5) somite functions (e.g., muscle contraction) are well understood; (6) biochemical markers for differentiation (e.g., monoclonal antibodies [MoAbs]; cDNAs) are available; (7) amphibian somite development patterns bear at least a superficial resemblance to somitogenesis in other vertebrates and hence serve as an experimentally convenient paradigm; and (8) somites in some organisms (e.g., *Xenopus*) differentiate relatively early, and therefore can be exploited as a model system for early embryonic organogenesis.

Since a large body of data is available an attempt should naturally be made to formulate generalization about the key features of somitogenesis, first, among various amphibians (e.g., anurans and

urodeles), and second, among other vertebrates (e.g., amphibian, avian and mammalian species). For amphibian model systems, *Xenopus* has emerged as the most commonly studied anuran, while the axolotl is certainly the most studied urodele embryo. Those species are among the easiest amphibians to maintain and breed in the laboratory, hence their substantial and worldwide popularity. As will be emphasized in this review the differences between almost all aspects of *Xenopus* and axolotl somitogenesis are more striking than the similarities. Those differences impede attempts to prepare generalizations. The strategy of this review is to discuss the key similarities and major differences between somitogenesis in *Xenopus* and *Ambystoma mexicanum*, and to consider several unresolved issues.

EVOLUTION OF ANURANS AND URODELES

Since the major differences in somitogenesis which will be described in this review can probably be traced to divergent evolutionary pathways, a brief discussion of amphibian phylogeny is called for.

Urodeles traditionally have been considered to be more primitive than anurans. It is generally agreed that the urodele body plan did indeed

evolve earlier (from lobe-finned fishes). However, some morphological features of some urodeles are shared with various primitive anurans. That could represent either (1) true close phylogenetic relationships; or (2) anatomical adaptations to specialized niches which have yielded superficial similarities. Some authors have even suggested that urodeles and anurans evolved from different fish groups (e.g., [2]): Urodeles from the more primitive porolepiforms, and anurans from the more advanced osteolepiforms. Although usually grouped together as the "Rhipidistia" those categories of fishes are considered by Jarvik [2] to be sufficiently different to warrant separation into two orders. Figure 1 summarizes Jarvik's view of amphibian phylogeny. That presumed polyphyletic origin of amphibia is, however, the subject of considerable discussion (e.g., see [3, 4]). The absence of a complete fossil record continues to impede resolution of the polyphyletic origin issue [5].

In addition to variant general morphogenetic features, major differences between *Xenopus* and axolotl embryogenesis exist. These include the origin of the mesoderm (internal in *Xenopus*, external in axolotl—see below), the mode of primordial germ cell development, and the method of fertilization (anurans=monospermic; urodeles=

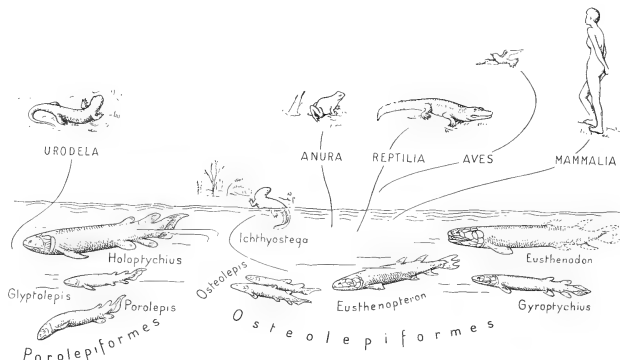


Fig. 1. Summary of evolutionary scheme for origin of anurans, urodeles and other vertebrates. Illustration kindly provided by Jarvik.

polyspermic).

Based upon the foregoing it is difficult to predict the extent to which somitogenesis should be either similar or different in *Xenopus* and the axolotl.

MAJOR CELLULAR COMPONENTS OF THE AMPHIBIAN SOMITE

Both *Xenopus* and axolotl somites consist of three main components: myotome, schlerotome, and dermatome. Those individual components are most readily observed in histological cross section (Fig. 2). As can be readily seen in those cross sections, axolotl and *Xenopus* somites exhibit similar relative amounts of the three components of the somite. The schlerotome consists of a small number of mesenchymous cells on the medial/ventral aspect of the somite. The dermatome consists of mesenchymous cells between the myotome and epithelium. This pattern is radically different from what is observed in the chick at a comparable stage in development. Here the mesenchymous schlerotome is the major component. The myotome is a relatively minor component which emerges from the anterior/medial edge

of the dermatome [6] which is epithelial. Clearly, both in the axolotl and in *Xenopus* the myotome is the primary component of the early somite. In contrast, in the chick embryo the myotome is a minor component of the early somite.

BRIEF REVIEW OF MAIN FEATURES OF AMPHIBIAN SOMITE MORPHOGENESIS

In *Xenopus*, at the late gastrula/early neurula stage, the paraxial (presomite) mesoderm is two cell layers thick and is underlain by a continuous layer of endoderm (i.e., the archenteron roof) (see Fig. 10). Somite segmentation begins as early as the neural fold stage. Superficially similar features are exhibited by axolotl embryos. The paraxial mesoderm is, however, often as much as three-cell layers thick.

By the neural fold stage *Xenopus* paraxial mesoderm becomes progressively organized along the cranial to caudal axis into somitomeres (pre-patterned arrays of loosely arranged prospective somite cells) (Fig. 3). A similar prepatterning has been discovered recently in axolotl somitomeres also. It generally resembles the *Xenopus* prepat-

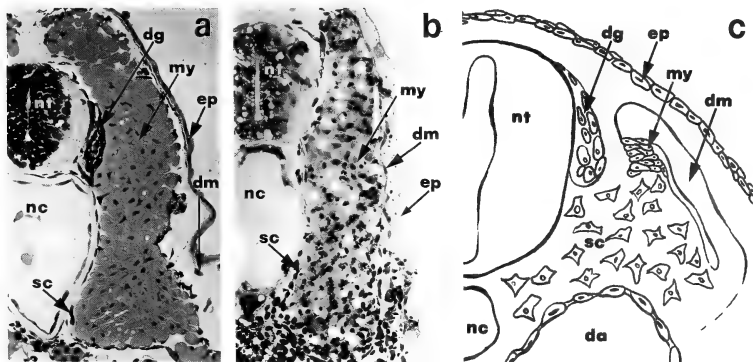


FIG. 2. Cross section of prehatching amphibian embryos and for comparison a diagram of the cross section to a comparable stage chick embryo. (a) Trunk region of a stage 36/37 *Xenopus laevis*. (b) Trunk region of a stage 40 *Ambystoma mexicanum*. (c) Chick embryo (33 somite stage). In (a) and (b) the schlerotome (sc) consists of individual cells between the myotome (my) and notochord (nc) and spinal cord (nt). The dermatome (dm) consists of mesenchymous cells between the myotome and the overlying epithelium (ep). In (c) the differences can be readily appreciated. The chick myotome is a minor component at this stage. Other abbreviations: dg = dorsal ganglion; da = dorsal aorta.

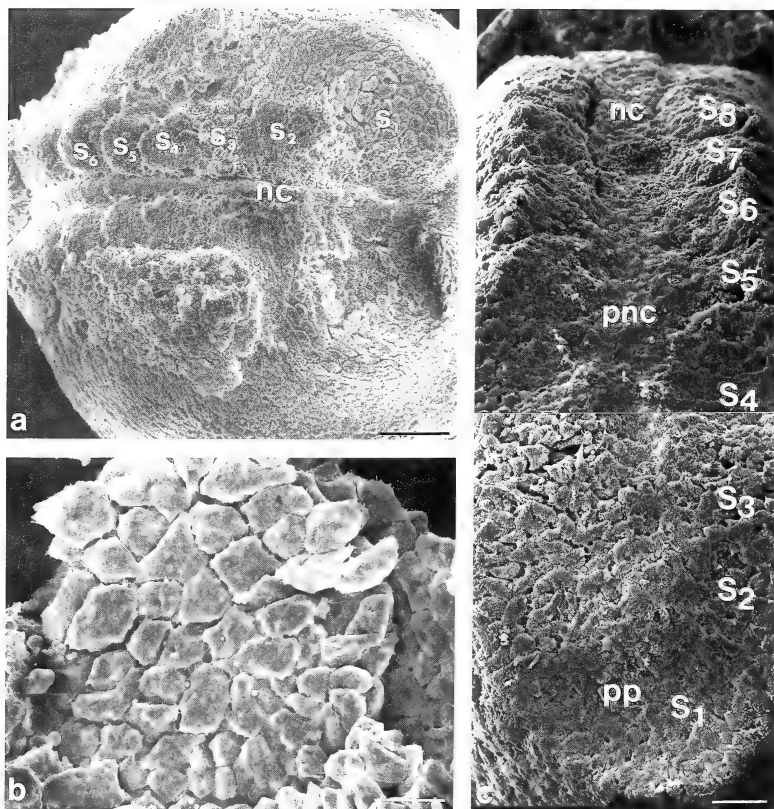


FIG. 3. Somitomeres (concentrically organized, patterned arrays of prospective somite cells) in *Xenopus* and axolotl embryos. Somitomeres have also been observed in many other vertebrate embryos (reviewed in [13]). (a) *Xenopus* embryo (dorsal view, cranial end on right) from which the epidermis and neural plate have been removed exhibits somitomeres (S_1 – S_4) and segmented somites (S_5 – S_6). (b) Single somitomere from *Xenopus* embryo displays concentric cell patterning. (c) Stage 14/15 axolotl somitomeres (S_1 – S_4). The beginning of segmentation of the somites is evident (S_5 – S_8). Abbreviations: nc = notochord; pnc = presumptive notochord; pp = prechordal plate. (a) and (b) generously provided by A. G. Jacobson. Bars in a = 0.2 mm; in b = 0.05 mm; c = 0.1 mm.

tern, as comparison of the scanning electron micrographs in Figure 3 reveals.

Careful examination has revealed that changes in shape occur among prospective somite cells

even before somitomeres can first be detected (Fig. 4). Those early (end of gastrulation/early neurulation) cell morphology changes offer the important clue that part of the program for somite

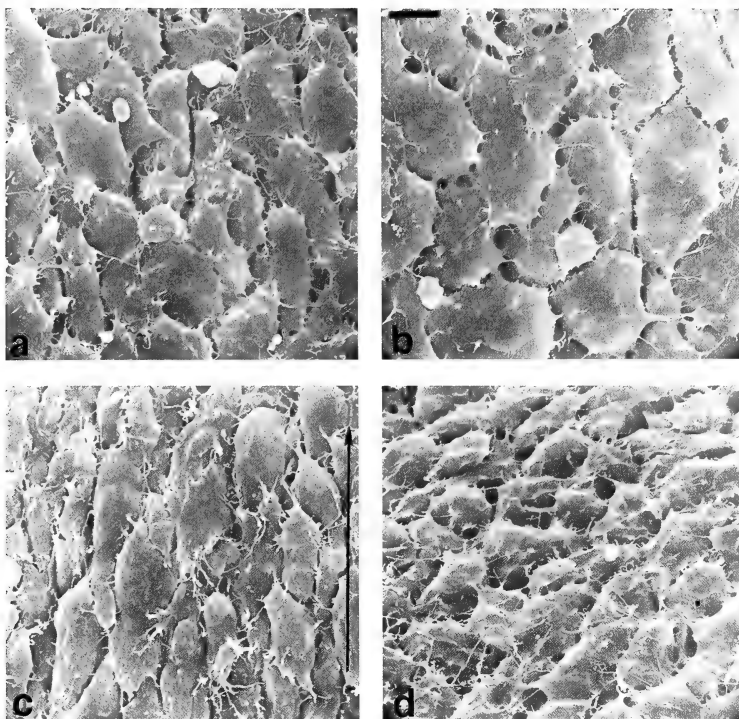


FIG. 4. Subtle differences in cell shape distinguish presomitic cells from lateral mesoderm cells as early as late gastrulation/early neurulation, before the somitomeres (Fig. 3) develop. The surfaces of presomite mesoderm cells (a) are smaller than nearby lateral mesoderm surfaces (b). By early neurulation, presomitic cells become elongated (c), in comparison to lateral mesoderm cells (d). Arrow in (c) shows dorsal/ventral direction. Bar in (b) = 10 μ m for each photo. Taken from Youn *et al.* [14].

morphogenesis is already established. The translocation experiments described later in this review (e.g., see Fig. 7) revealed no change in cell fate when somite cells were relocated, a fact which is not surprising in view of the information in Figure 4.

In *Xenopus* once a set of cells have segmented into a block, individual cells in a block change shape and often bend as they begin to rotate 90 degrees. Eventually all the myotome cells which

were initially perpendicular to the notochord come to lie parallel to it (Fig. 5). The result is that single, mononucleated cells extend the length of individual somites. In axolotl embryos cells become organized into rosettes about a myocoel immediately following segmentation (Fig. 5b). That prominent myocoel (Fig. 6), which is completely lacking from *Xenopus* somites, eventually disappears as relatively small individual myocytes fuse to form large multinucleated myocytes.

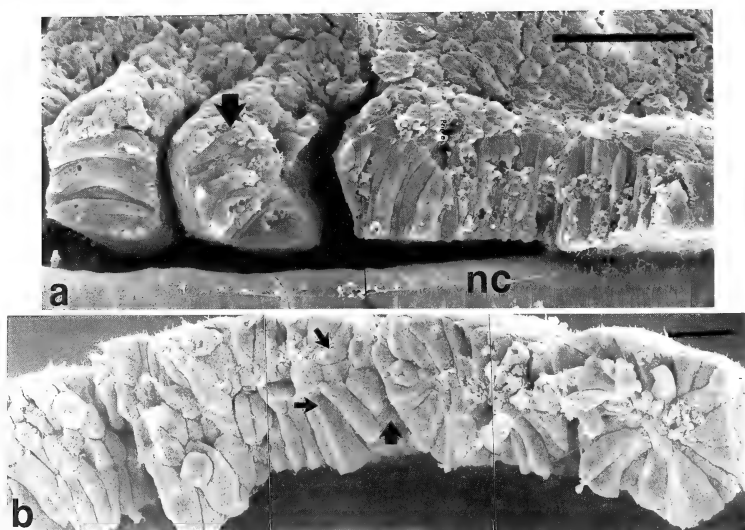
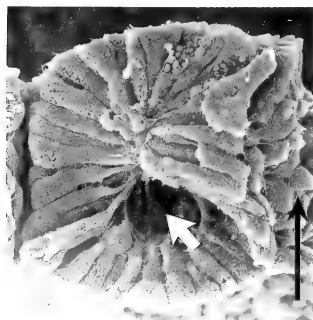


FIG. 5. Scanning electron micrographs of cell rearrangements which follow somite segmentation. (a) Dorsal view of longitudinally fractured *Xenopus* somite file. Arrow indicates the last segmented somite. Ninety degree rotation of individual cells within a block, rather than rotation of the block as a whole, generates myoblasts which lie parallel to the notocord (nc). (b) Mediolateral view of parasagittally fractured axolotl embryo. Rosette arrangement is displayed by two somites on the right. Large arrow indicates the caudal segmentation line. Short arrows point to cells which appear to be changing shape and rotating. Orientations: left in (a)=cranial; left in (b) = caudal. Bars: (a)=0.1 mm; (b)=50 μ m. (a) Taken from Youn and Malacinski [7]; (b) Taken from Youn and Malacinski [15].



Clearly both the cellular mechanics (blocks vs. rosettes) and final results (mononucleated vs. multinucleated cells) of somite morphogenesis are very different in those two species.

SIMILARITIES BETWEEN *XENOPUS* AND AXOLOTL SOMITOGENESIS

Morphogenesis

Several features of somite morphogenesis are

FIG. 6. Dorsal view of a longitudinally fractured axolotl somite which displays the myocoel (small arrow). The long arrow indicates the lateromedial direction of the somite. Taken from Youn and Malacinski [15].

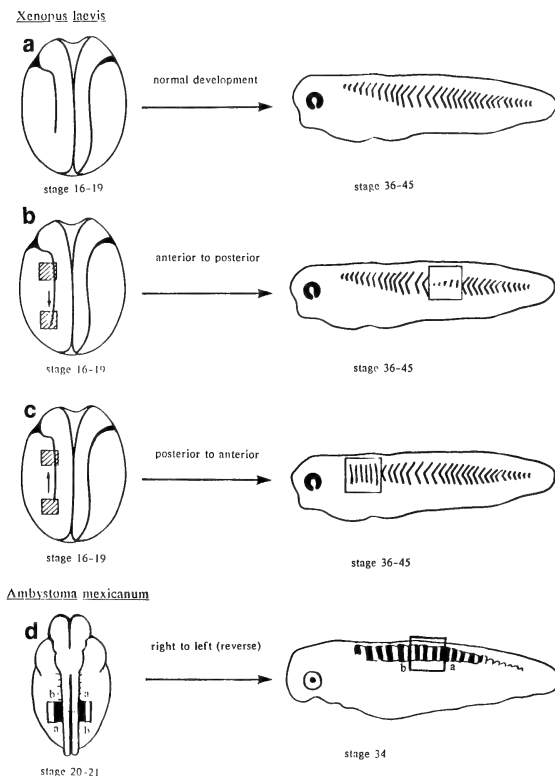


FIG. 7. Experimental analyses which reveal that many features of somite morphogenetic pattern formation are completed by neurulation. In *Xenopus* the cranial somites degenerate by stage 47 (Nieuwkoop and Faber [16]; Chung *et al.*, manuscript submitted). (b) Transplantation of this cranial presomitic somite into the trunk region results in degeneration in their new location. (c) Conversely, grafting trunk presomitic mesoderm into the head region results in myotomes that do not degenerate. (d) Myocytes differentiate within axolotl myotomes in a transient polar anterior to posterior and medial to lateral polarity (Neff *et al.*, manuscript submitted). Grafting experiments in which 180° inversion of the tissue is achieved has shown that the anterior-posterior pattern is already established before segmentation of the somites. The morphology of the myotomes in these experiments was monitored by indirect whole-mount immunocytochemistry using monoclonal antibodies against muscle non-cytoplasmic actin and myosin as probes (Neff *et al.*, manuscript submitted).

shared by both species. These include the following:

- (1) Both *Xenopus* and axolotl myotome pre-

cursor cells are arranged as "somitomeres" (Fig. 3).

- (2) In both species somite cell differentiation

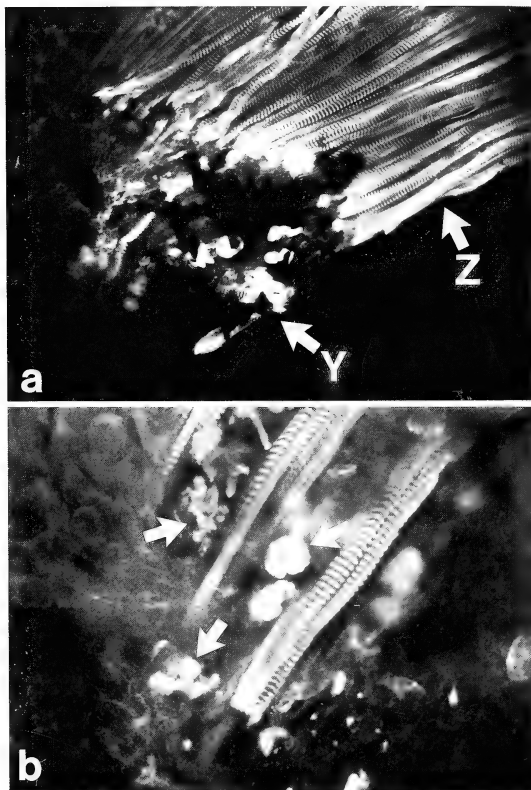


FIG. 8. Reduction of *Xenopus* cranial myotomes. Between stages 26 and 47 the 5 most cranial myotomes degenerate in a cranio-caudal sequence (Nieuwkoop and Faber [16]). (a) illustrates a confocal microscopic image of whole mount immunostained (muscle-specific actin) cranial myotomes Y and Z. Myotome Y to the left displays degeneration and myotome Z exhibits striated muscle cells. (b) illustrates an enlarged region of myotome Y showing degenerating cells (rounded and disordered sarcomeres—arrows) adjacent to intact striated muscle fibers.

patterns appear to be fixed before the somites segment from the paraxial mesoderm. In both axolotl and *Xenopus* neurula stage embryos, transplantation of unsegmented presomitic mesoderm into different locations along the somite file

indicates that many features of cranial and trunk myotome differentiation patterns are already established (Fig. 7).

- (3) The presence of the notochord is not required for somite morphogenesis in either *Xenopus* or axolotl embryos. Contrary to

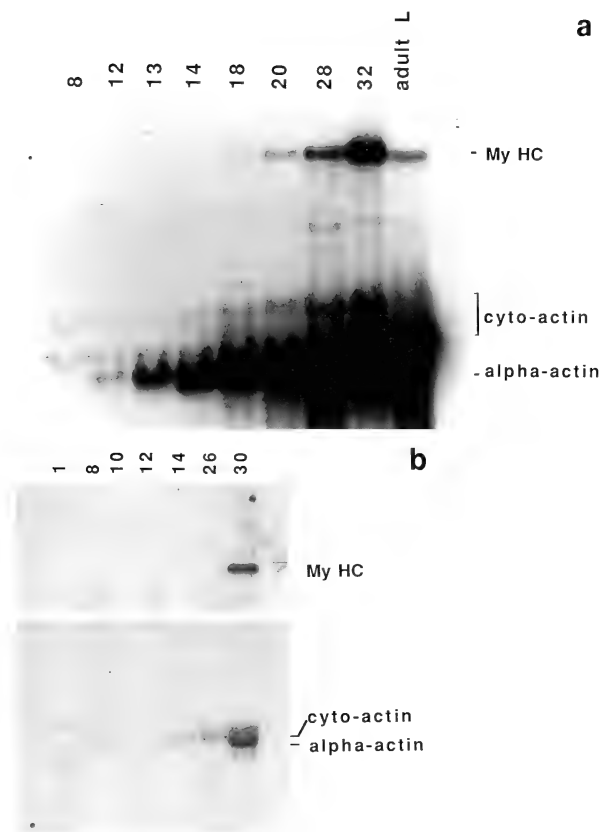


FIG. 9. Skeletal actin and myosin heavy chain mRNAs first appear during embryogenesis earlier in *Xenopus* than in *axolotl*. Northern blots of 10 μ g total RNA from various developmental stages were hybridized with a myosin heavy chain cDNA probe from *Xenopus* embryos (MyHC) and with spAC-9, a cardiac α -actin cDNA probe from *Xenopus* (kindly provided by Igor Dawid, NIH). The MyHC probe hybridizes to a single, 7.0 kb transcript, whereas spAC-9 hybridized to cytoplasmic as well as α -actin. In *Xenopus* (a), α -actin and muscle myosin heavy chain first appear at late gastrula-early neurula (st. 13-14), whereas in *axolotl* (b), these transcripts do not appear until after stage 26.

earlier reports, an interaction between the notochord and surrounding mesoderm is not a prerequisite for normal somitogene-

sis. Ultraviolet irradiated-notochordless *Xenopus* embryos [7] and notochordectomized *axolotl* embryos [8] both develop

normal somite files.

- (4) Both *Xenopus* and the axolotl, in common with some other vertebrates (e.g., shark), reduce their anterior-most somites. Figure 8 displays the degeneration of anterior *Xenopus* somites.

Differentiation

Although several important characteristics of somite differentiation differ, one key feature is similar: Actin and myosin differentiation (e.g., mRNA accumulation) is coordinated (Fig. 9a).

DIFFERENCES BETWEEN *XENOPUS* AND AXOLOTL SOMITOGENESIS

Morphogenesis

A large number of key features differ between these species, including the following:

- (1) *Xenopus* somite precursor cells arise internally, whereas axolotl somite cells originate on the embryonic surface. Figure 10 illustrates those disparate origins.
- (2) Axolotl somite precursor cells organize as rosettes, which include a myocoel. *Xenopus* cells arrange parallel to one another, without a myocoel (see Fig. 5).
- (3) *Xenopus* myotomal cells rotate 90 degrees, as individual cells, during early somite morphogenesis. They do not fuse. Axolotl cells re-arrange (turn) and then fuse (see Fig. 5).
- (4) *Xenopus* myotomal cells are elongated, but do not fuse. Axolotl myocytes fuse and become multinucleated.
- (5) *Xenopus* somitic mesoderm segments into arrowhead units, whereas axolotl somites segment into rectangular blocks. Those features are easily recognized on recently hatched tadpoles.
- (6) *Xenopus laevis* myotomal myocyte nuclei go from being large and polyploid (up to octaploid) in the mononucleated embryonic myocytes to being small and diploid in the multinucleated myocytes after stage 51 [9]. Axolotl nuclei remain at a constant diploid size during all stages of myotomal myogenesis.
- (7) *Xenopus* muscle cells become electrically coupled early, compared to axolotl muscle cells. Blackshaw and Warner [10] examined the coupling of cells in the mesoderm during somite segmentation and myogenesis. The relevant findings are that (a) in both *Xenopus* and the axolotl, cells

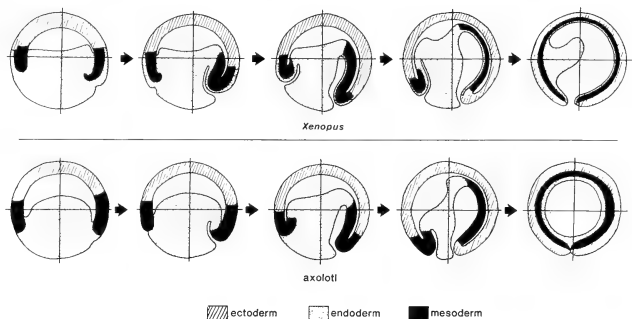


Fig. 10. Schematic diagrams of cross sections of gastrulae illustrating different location of mesoderm precursor cells in *Xenopus* and in the axolotl. *Xenopus* (top) mesoderm cells arise internally, whereas axolotl (bottom) mesoderm cells originate on the embryonic surface. This illustration is based upon data taken from Nieuwkoop and Florshutz [17], Keller [18], Vogt [19], and Smith and Malacinski [20].

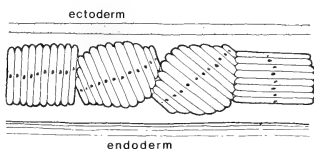
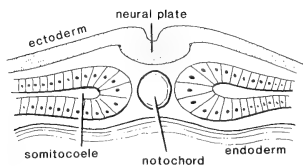
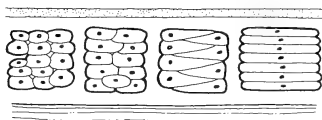
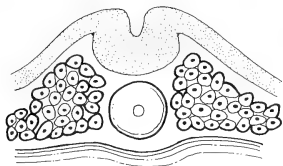
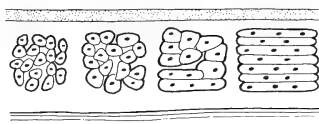
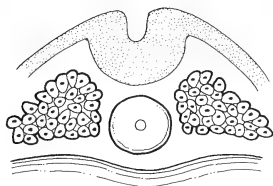
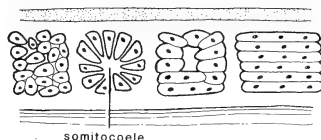
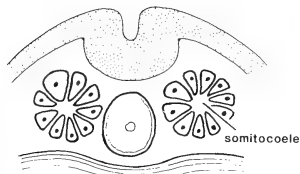
Xenopus laevis*Bombina variegata**Rana sphenocephala**Ambystoma mexicanum*

FIG. 11. Schematic illustration of somitogenesis in "intermediate" species.

in unsegmented mesoderm are electrically coupled; (b) in both species, coupling breaks down at the intersomitic borders during segmentation; and (c) after the

movements of segmentation, coupling is re-established in *Xenopus*, whereas in the axolotl the cells remain uncoupled. This pattern of electrical coupling is functionally

significant because in *Xenopus* it permits a coordinated contraction of myotome cells early in development at the 15 somite stage (st. 24), when only the first head somites are innervated. In the axolotl, in contrast, coordinated movements are possible only after approximately st. 32, when each myotome has been innervated.

Differentiation

Xenopus embryos accumulate actin and myosin mRNA relatively early (late gastrulation). Axolotl embryos accumulate those mRNAs later (head process stage). The data included in Figure 9 illustrate those differences in actin/myosin mRNA accumulation patterns.

INTERMEDIATE SOMITOGENESIS PATTERNS ARE DISPLAYED BY SOME SPECIES

Figure 11 shows that the pattern of somitogenesis varies widely among different species of amphibia. To illustrate this point the pattern of myotome development is focused on. *Xenopus* and the axolotl appear to display extremes in the range of myotome patterning. *Xenopus* primary myocytes rotate into place to form mononucleated myocytes within the myotomes. The axolotl forms multinucleated myocytes by the fusion of adjacent myocytes, starting at the medial quadrant of the somite. Between these two patterns intermediate modes of amphibian myotome patterning exist. For example, *Bombina* primary myocytes sort out and form mononucleated myocytes within each myotome. *Rana esculenta* myocytes sort out and fuse to form multinucleated myocytes within their myotome. The divergent patterns illustrated in Figure 11 illustrate the difficulty associated with attempting to formulate general rules or principles for amphibian somitogenesis.

ANOMALOUS CELL BEHAVIOR PATTERNS

Several features of amphibian somitogenesis are difficult to understand, especially in the context of a comparison between anurans and urodeles. Numerous questions arise, including the following:

- (1) Why do *Xenopus* cells rotate, rather than align parallel to the axis originally?
- (2) What is the advantage to developing mononucleated myocytes in embryonic myotomes as *Xenopus* does even though eventually, during the tadpole stages, all amphibians have multinucleated myotome myocytes?
- (3) Why does *Xenopus* presumptive somite mesoderm initiate muscle-specific actin and myosin synthesis as early as at gastrulation? In axolotl embryos those muscle-specific proteins don't appear until after somitogenesis (tailbud).

SIMILARITIES WITH AVIAN SOMITOGENESIS

It can be predicted from the foregoing discussion that if comparisons between amphibia can be drawn only at a superficial, and not necessarily very intellectually satisfying, level, contrasts with other species, such as avia, will be even more difficult. Indeed, that appears to be the case. Although, as mentioned previously, somitomeres can be recognized in virtually all vertebrates, the prominent myocoel in the chick somite contains mesenchymal cells, which are not seen in axolotl somites. The somite cells also appear to be more loosely packed in chick somites.

The formation of the cardiovascular system as well as axial structures which are clearly not important in either *Xenopus* or axolotl somitogenesis, appear to be involved, to one extent or another, in chick somite formation/differentiation [11]. Finally, in the chick embryo regression of the primitive streak, a process/structure having no homology in amphibia, plays an important role in somite formation [11].

UNRESOLVED ISSUES

Most of the descriptions of somitogenesis that employ conventional technology and that will be necessary as background information to fully understand the causative forces which drive somite cell behavior have been completed. As well, molecular probes for markers of embryonic muscle

differentiation are also available. The diligent efforts of several laboratories have contributed that background information.

Two areas of inquiry now require exploration. These include "genetics" and "cell biology."

Developmental genetics

Several questions associated with the genetic control of somite pattern formation call out for answers. These include the following:

- (1) How does gene expression regulate such pivotal events as muscle-cell-type determination, the timing of segmentation, and the selective commitment to death and degeneration of the anterior-most somites?
- (2) To what extent does zygotic gene activity (vs. maternally inherited gene products) control the early phases of somitogenesis (e.g., cell rearrangement and cell fusion)?
- (3) Are the regulatory elements responsible for the coordinate expression of the actin and myosin genes "cis" or "trans" acting?

Those questions will be very difficult to answer directly. The development of suitable amphibian genetic systems is hindered by a one year generation time. The use of gene injection approaches may prove useful. However, those approaches also will likely be of limited value due to the long generation time of most amphibian species, and the lack of candidate regulatory genes for injection.

More progress will no doubt be made in the near future with cell biology studies. Such studies can exploit many of the advantages of amphibian somitogenesis listed in the introduction.

Cell biology

Among the more relevant questions, which are likely to be amenable to experimentation in the near future are the following:

- (1) Does cell lineage or cell-cell interaction play the pivotal role in establishing the differentiation pattern of somites?
- (2) Do trunk and tail somites derive from separate cell lineages? Vital staining and transplantation experiments (e.g., [12]) indicate that axolotl tail muscles originate from the posterior medullary plate.

- (3) Do somite cells communicate with one another during cell rearrangement (e.g., via gap junctions)?
- (4) Are adhesive forces and physical tension actually involved in somite cell rearrangement?
- (5) Do dermatome and sclerotome cells behave independently of the myotome?

CONCLUDING REMARKS

The striking differences of several features of anuran and urodele somitogenesis solicit explanation. No doubt during evolution the patterns diverged considerably. What is surprising, however, is the extent to which several key features are different. The remodelling which occurred during evolution might appear to the experimentalist to be nonsensical. However, what no doubt matters to the embryo is that the changes which have been incorporated into the somite pattern do indeed work. *Xenopus* and the axolotl are concerned neither with maintaining their resemblance to related organisms nor with displaying common features to the researcher. The thought of serving as laboratory archetype species was not considered important by those species as they evolved different somite development pathways.

ACKNOWLEDGMENT

This research was supported in part by a grant from the Muscular Dystrophy Association and an NSF/KOSEF (INT 85-17743) Cooperative Research Program grant.

REFERENCES

- 1 Meinhardt, H. (1986) Models of segmentation. In "Somites in Developing Embryos". Ed. by R. Bellairs, D. A. Ede and J. W. Lash, Plenum Press, N. Y., pp. 179-189.
- 2 Jarvik, E. (1980) Basic Structure and Evolution of Vertebrates. Vol. 2. Academic Press, New York.
- 3 Duellman, W. E. and Trueb, L. (1986) Biology of Amphibians. McGraw-Hill Book Co., New York, pp. 437.
- 4 Nieuwkoop, P. D. and Sutasurya, L. A. (1979) Primordial Germ Cells in the Chordates. Cambridge Univ. Press, Cambridge.
- 5 Carroll, R. L. (1988) Vertebrate Paleontology and

- Evolution. Freeman & Co., New York.
- 6 Kaehn, K., Jacob, H. J., Christ, B., Hinrichsen, K. and Poelmann, R. E. (1988) The onset of myotome formation in the chick. *Anat. Embryol.*, **177**: 191–201.
 - 7 Youn, B. W. and Malacinski, G. M. (1981) Somatogenesis in the amphibian *Xenopus laevis*: Scanning electron microscopic analysis of intrasomitic cellular arrangements during somite rotation. *J. Embryol. Exp. Morphol.*, **64**: 23–43.
 - 8 Kitchen, J. C. (1949) The effects of notochordectomy in *Ambystoma mexicanum*. *J. Exp. Zool.*, **112**: 393–415.
 - 9 Kielbowna, L. (1966) Cytological and cytophotometrical studies on myogenesis in *Xenopus laevis* Daudin. *Zool. Pol.*, **17**: 247–258.
 - 10 Blackshaw, S. E. and Warner, A. E. (1976) Low resistance junctions between mesoderm cells during development of trunk muscles. *J. Physiol.*, **255**: 209–230.
 - 11 Bellairs, R. and Veini, M. (1984) Experimental analysis of control mechanisms in somite segmentation in avian embryos. II. Reduction of material in the gastrula stages of the chick. *J. Embryol. Exp. Morphol.*, **79**: 183–196.
 - 12 Ford, P. (1949) The origin of the segmental musculature of the tail of the Axolotl (*Ambystoma*). *Proc. Zool. Soc. Lond.*, **119**: 609–635.
 - 13 Jacobson, A. G. and Meier, S. (1986) Somitomeres: The primordial body segments. In "Somites in Developing Embryos". Ed. by R. Bellairs, D. A. Ede and J. W. Lash, Plenum Press, N. Y., pp. 1–16.
 - 14 Youn, B. W., Keller, R. E. and Malacinski, G. M. (1980) An atlas of notochord and somite morphogenesis in several anuran and urodelean amphibians. *J. Embryol. Exp. Morphol.*, **59**: 223–247.
 - 15 Youn, B. W. and Malacinski, G. M. (1981) Comparative analysis of amphibian somite morphogenesis: Cell rearrangement patterns during rosette formation and myoblast fusion. *J. Embryol. Exp. Morphol.*, **66**: 1–26.
 - 16 Nieuwkoop, P. D. and Faber, J. (1956) Normal tables of *Xenopus laevis* (Daudin). North Holland.
 - 17 Nieuwkoop, P. D. and Florshutz, P. (1950) Quelques caracteres speciaux de la gastrulation et de la neurulation de l'oeuf de *Xenopus laevis* Daud. et de quelques autres anoures. I. Etude descriptive. *Arch. Biol. (Liege)*, **61**: 113–150.
 - 18 Keller, R. E. (1976) Vital dye mapping of the gastrula and neurula of *Xenopus laevis*. II. Prospective areas and morphogenetic movements of the deep layer. *Dev. Biol.*, **51**: 118–137.
 - 19 Vogt, W. (1929) Gestaltungsanalyse am Amphibienkeim mit örtlicher Vitalfärbung. II. Gastrulation und Mesodermbildung bei Urodelen und Anuren. *Wilhelm Roux' Arch.*, **120**: 384–706.
 - 20 Smith, J. C. and Malacinski, G. M. (1983) The origin of the mesoderm in an anuran, *Xenopus laevis*, and a urodele, *Ambystoma mexicanum*. *Dev. Biol.*, **98**: 250–254.

REVIEW

Some Molecular Characteristics of Canine Mammary Tumours and Their Relationship to Biological Malignancy and Prognosis

WILHELM ENGSTRÖM, GUNNAR MÖLLERMARK¹,
LARS ERIK KÄNGSTRÖM² and OLLE LARSSON²

*Department of Pathology, Huddinge Hospital, S-141 86 Huddinge,
¹The Veterinary Hospital, Ljusnevägen 17, S-121 17 Johanneshov, and*

*²Department of Tumour Pathology, Karolinska Hospital,
S-104 01 Stockholm, Sweden*

ABSTRACT—This review has pointed at recent advances in three scientific areas that have only recently been applied to veterinary medicine. In it of particular interest is to unveil new molecular methods for the assessment of canine mammary tumours, since the limitations of the traditional histopathological measures are becoming more and more obvious. We summarize recent advances in the area of a) DNA-cytophotometry, b) determination of estrogen and EGF receptor content and c) oncogene expression and organization for the studies of canine mammary tumours. It is our belief that these areas will provide the breakthrough for a better and objective malignancy grading of this particular group of tumours.

INTRODUCTION

Mammary tumours rank second (behind skin tumours) as the most common neoplasm in dogs [1]. Furthermore, they are by far the most common tumour in the bitch. There is no indication of any geographical difference in frequency, and in fact, canine mammary tumours have been reported in all parts of the world. The assessment of prognosis in dogs with mammary tumours is still almost invariably based on clinical and morphological parameters. Morphologically these tumours are graded into histological classes. About 65% of the mammary tumours are considered to be benign mixed tumours, 25% are carcinomas and the rest are usually characterized as adenomas, myoepitheliomas and malignant mixed tumours [1].

However these classes do sometimes, but not always, differ in behaviour as reflected by the

progression of the disease and patient survival. This is hardly surprising since morphological features can not easily be determined in an objective and quantitative manner. Furthermore many tumours are morphologically heterogeneous and different morphological features are seen in different regions of the same tumour, which makes a morphological analysis even more difficult. Maybe — and this is one main weakness of the classical histopathology — the morphological features expressed by the tumour cells are quite unrelated to the biological properties that determine the malignant phenotype of the tumour.

Against this background it is highly desirable to explore whether criteria other than morphology can be used to assess canine mammary tumours and hence provide additional data for malignancy grading. This review has aimed at summarizing some recent attempts to develop such parameters. In particular we point at the application of cytophotometry, receptor biochemistry as well as

recently developed molecular biological techniques to clinical veterinary tumour pathology.

CYTOPHOTOMETRIC DETERMINATION OF DNA-CONTENT AND ITS RELATION TO CLINICAL PROGNOSIS

In a variety of human solid tumours, the relationship between gross ploidy level — as determined by intercellular distribution of nuclear DNA-content — and prognosis has been extensively studied [2]. For instance human carcinomas from four organs — prostate, breast, thyroid gland and kidney — can be classified into two major types on the basis of nuclear DNA-determinations namely the E-type and the A-type [2]. The E-type tumours contain the euploid — i.e. diploid or tetraploid — amount of DNA indicating no or only minor karyotypic modifications. In contrast A-type tumours contain clearly aneuploid DNA-contents indicating a high degree of karyotypic abnormality [2]. In large retrospective studies it was found that A-type tumours almost invariably progressed rapidly and killed the patients within a few years, while E-type tumours progressed slowly and only killed the patients after a very long time. Zetterberg and Auer [2] were able to show that E-type tumours were genetically stable in the sense that they rarely progressed into A-type tumours.

Very few attempts have been made to apply DNA-cytophotometry to clinical veterinary medicine. Only recently did Möllermark and coworkers [3] show that there seems to be a correlation between gross ploidy level and clinical prognosis in a series of canine mammary tumours. Out of 15 malignant mammary tumours 5 were found to be strictly diploid (type I as defined by Auer) and 10 were found to be clearly aneuploid (type IV as defined by Auer). By comparing the DNA-profiles with the clinical status one year after the operation it was found that 50% of the dogs with aneuploid tumours had been readmitted to hospital with tumour relapse within one year (Table 1). The time interval between first operation and tumour recurrence ranged from 2 to 10 months. The other 50% of the dogs with aneuploid tumours were clearly disease free one year after surgery. In contrast 100% of the patients with diploid DNA-

profile had survived without any clinical signs of tumour relapse during the one year follow up time. Furthermore Möllermark and coworkers [3] showed that there was no obvious correlation between DNA-profile and histological type. Nor was there any obvious correlation between histological type and prognosis. Thus, these data indicate that there exists a correlation between nuclear DNA-content of the tumour cells and patient survival. It was therefore concluded that DNA-measurements can give prognostic information in the individual dog above and beyond those obtained from clinical staging and morphological criteria.

ESTROGEN AND EGF RECEPTOR CONTENT IN CANINE MAMMARY TUMOURS

It has been known for some time that endocrine therapy affects the growth of human breast cancer. In such terms, breast cancer can be classified as estrogen receptor (ER) rich or poor on the basis of biochemical measurements of ER concentration. These two classes have distinct biological characteristics; the most important is that about 50% or more of ER-rich tumours respond to endocrine therapy whereas ER-poor tumours only rarely respond to such therapy. d'Arville and Pierrepoint [4] demonstrated that estrogen receptors could also be measured in canine mammary tumours. They showed that 52% of canine mammary adenocarcinomas were ER-positive, which is a figure that compares well with the situation in *Homo sapiens*.

More surprisingly, MacEwen *et al.* [5] found that 87% of benign lesions — usually fibroadenomas — were ER-positive. This is in sharp contrast to human fibroadenoma where only about 10% are ER-positive. Likewise with human sarcoma canine breast sarcomas were found to be ER-negative in 100% of the cases.

It can be envisaged that ER determinations can be introduced both as a prognostic parameter *per se* and as an instrument for selecting the appropriate therapy in the individual dog with mammary tumour. Recently, Nerukar *et al.* [6] showed that 70% of canine mammary tumours contain measurable quantities of EGF-receptor. However in 50%

of their material, there was an inverse relationship between EGF receptor and estrogen receptor content, which suggests that it is too early to draw conclusions concerning the clinical use of EGF-receptor determinations in the individual patient.

EXPRESSION AND ORGANISATION OF ONCOGENES IN CANINE TUMOURS

During the past decade we have experienced at least one major breakthrough in our understanding of the mechanisms of neoplastic transformation. The discovery of a group of genes — often denominated oncogenes — in mammalian cells have provided a new insight into the development of cancer. Oncogenes were first discovered in the genomes of acute transforming retroviruses. The protein products encoded by these viral oncogenes are responsible for the ability of such RNA tumour viruses to transform cells *in vitro* as well as in animals. Viral oncogenes (v-onc) were transduced from normal cellular genes (c-onc or protooncogenes), which are believed to play a pivotal role in the control of cellular growth and differentiation. Specific genetic alterations of protooncogenes which alter their coding potential or their regulation represent some of the critical progressive steps associated with neoplastic development.

The c-myc oncogene is conserved throughout development and is expressed in a large number of mammalian cell types. The protooncogene consists of three exons and the first of these consists of a large non-coding sequence in mice but contains an open reading frame in humans which may possess certain regulatory functions. The myc gene expression is controlled by two major transcription initiation sites and their promoters possess TATA sequence motifs. Under normal circumstances, myc transcripts are highly unstable with an estimated half life of 15–20 minutes. However the myc gene can be superinduced by protein synthesis inhibitors which implies that the gene is under some negative regulatory influence. Activation of the myc gene gives rise to a 62 kDa polypeptide product, which has been localized to the cell nucleus where it binds to DNA.

The activation of c-myc has been suggested to constitute a key step in the transition of cells from

quiescence to the cell cycle. Lymphocytes stimulated to divide by addition of plant lectins, or fibroblasts stimulated by platelet derived growth factor both show a transient increase in c-myc mRNA as an early event [7]. Elevated levels of myc transcript have been detected in both normal murine and normal human placenta [8] as well as in liver tissue after damage by chemicals or partial hepatectomy. Expression of c-myc is down regulated in some but not all differentiating cells [9].

Several molecular mechanisms have been identified in the deregulation of c-myc expression in tumour cell lines. These include gene amplification, mutation, rearrangement and increased production of transcript by promoter insertion [10]. The aberrant expression of the c-myc gene resulting in elevated levels of c-myc mRNA has been detected in a range of tumour cell lines and also in biopsies from primary human tumours.

The role for c-myc in development of human breast cancer has been extensively studied in the human. One of five breast cancer cell lines studied was found to have an amplified c-myc [11]. High levels of myc transcript were observed in several primary breast carcinomas examined [12]. In the largest material examined Callaghan and coworkers found that 32% of the breast cancers had a detectable c-myc amplification [13]. In addition they found a rearranged c-myc gene in 4% of the patients. However 10 out of 14 breast carcinomas examined had enhanced levels of c-myc-RNA, indicating that elevated levels of transcript also exist in tumours where the gene is unaltered.

We have recently examined the expression and organization of c-myc in canine mammary tumours. We found that only 8% of the dogs in our material had an elevated expression of c-myc, which is a considerably lower figure than in a comparable human material [14]. The expression of this oncogene was not accompanied by any rearrangement or amplification. In this respect canine mammary tumours resemble canine rhabdomyosarcoma, where an increased amount of myc transcript was observed in lieu of any detectable rearrangements of this gene [15]. In contrast, Katzir *et al.* [16] demonstrated a rearranged c-myc in the canine transmissible venereal tumour TVT. Southern blotting of an EcoRI digest revealed that

tumour DNA contained a 16.8 kB rearranged c-myc fragment in addition to the normal 15 and 7.5 kB fragments. When the structure of the cloned rearranged c-myc was compared to cloned normal c-myc, it was found that the rearrangement was due to insertion of a 1.8 kB DNA upstream of the first exon of c-myc. The inserted DNA was flanked by 10 bp direct repeats and contains a dA rich tail suggesting its origin from mRNA.

In conclusion, the remarkable conservation of the DNA-sequence of oncogenes across wide reaches of evolutionary time points to an essential role for their products in normal development. The control of cell division and differentiation are complex requiring the interaction of many different molecular mechanisms. The study of oncogenes allows the dissection of the growth control apparatus of the cell. It is within this molecular keyboard that cancer and several other diseases must begin. By understanding more about the constituent molecules, tools of diagnostic and therapeutic relevance will be uncovered over the next decade.

REFERENCES

- Moulton, J. E. (1978) *Tumours in Domestic Animals*. 2nd ed. UC Press, Berkeley, Los Angeles & London.
- Zetterberg, A. and Auer, G. (1984) *Genes and Cancer*. Alan Liss Inc., New York.
- Möllermark, G., Kängström, L. E., Eliasson, I., Barrios, C., Larsson, O., Azawedo, E. and Engström, W. (1988) Distribution of nuclear DNA-content in canine mammary tumours. *J. Small Animal Practice*, **29**: 309-314.
- d'Arville, C. N. and Pierrepont, C. G. (1979) The demonstration of estrogen, androgen and progesterone receptors in the cytosol fraction of canine mammary tumours. *Eur. J. Cancer*, **15**: 875-883.
- MacEwen, E. G., Partnial, A. K., Harvey, H. J. and Panko, W. B. (1982) Estrogen receptor in canine mammary tumours. *Cancer Res*, **42**: 2255-2259.
- Nerurkar, V. R., Seshadri, R., Mulherkar, R., Ischwad, I. S., Lahta, V. S. and Naik, S. N. (1987) Receptors for epidermal growth factor and estradiol in canine mammary tumors. *Int. J. Cancer*, **40**: 230-232.
- Kelly, K., Cochran, B. H., Stiles, C. D. and Leder, P. (1983) Cell specific regulation of the c-myc gene by lymphocyte mitogen and PDGF. *Cell*, **35**: 603-610.
- Pfeiffer Ohlsson, S., Grönsten, A. S., Rydnert, J., Goustin, A. S. and Ohlsson, R. (1984) Spatial and temporal pattern of cellular myc oncogene expression in developing human placenta. Implications for embryonic cell proliferation. *Cell*, **38**: 585-592.
- Schofield, P. N., Engström, W., Lee, A. J., Biddle, C. and Graham, C. F. (1987) Expression of c-myc during differentiation of the human teratocarcinoma cell line Tera 2. *J. Cell Sci.*, **88**: 57-64.
- Hamlyn, P. H. and Dyson, J. (1984) *Oncogenes*. In "Molecular Biology and Human Disease." Ed. by A. MacLeod and K. Sikora. Blackwells, Oxford. pp. 150-162.
- Kozbor, D. and Croce, C. (1987) Amplification of the myc oncogene in one of five breast carcinoma cell lines. *Cancer Res.*, **44**: 438-441.
- Slamon, D. J., de Kernion, J. B., Verma, I. M. and Cline, M. J. (1984) Expression of cellular oncogenes in human malignancies. *Science*, **224**: 256-262.
- Escot, C., Theillet, C., Lidereau, R., Spyrtas, F., Champens, M. H., Gest, J. and Callahan, R. (1986) Genetic alteration of the c-myc protooncogene in human primary breast carcinoma. *Proc. Natl. Acad. Sci. USA*, **83**: 4834-4838.
- Engström, W., Barrios, C., Azawedo, E., Möllermark, G., Kängström, L. E., Eliasson, I. and Larsson, O. (1981) Expression of c-myc in canine mammary tumours. *Anticancer Res.*, **7**: 1235-1238.
- Engström, W., Barrios, C., Willems, J., Möllermark, G., Kängström, L. E., Eliasson, I. and Larsson, O. (1988) Expression of the myc protooncogene in canine rhabdomyosarcoma. *Anticancer Res.*, **7**: 1109-1110.
- Katzir, N., Rechavi, G., Cohen, J. B., Unger, T., Simoni, F., Segal, S., Cohen, D. and Givol, D. (1985) Retroposon insertion into the cellular oncogene c-myc in canine transmissible venereal tumour. *Proc. Natl. Acad. Sci. USA*, **82**: 1054-1058.

Membrane Responses and Permeability Changes to Odorants in the Solitary Olfactory Receptor Cells of Newt

TAKASHI KURAHASHI and TATSUAKI SHIBUYA

*Institute of Biological Sciences, University of Tsukuba,
Tsukuba, Ibaraki 305, Japan*

ABSTRACT—The patch-clamp method was used to examine isolated olfactory receptor cells with whole-cell current- or voltage-clamp variation. Since these cells maintain their morphological characteristics, they can be easily distinguished from other kinds of cells under a phase-contrast microscope. The resting membrane potential was -41 mV ($n=70$). By depolarizing current injection (2 – 50 pA), at least an action potential was initiated. About ten percent of the cells discharged spikes repetitively due to the maintained membrane depolarization by injected current. Twenty two out of 78 cells showed obvious depolarized response to 10 mM amyl acetate. Eighty two percent of the cells showed the capacity for adaptation. When the odorant was applied to cells voltage-clamped at the resting potential, an inward current was elicited with increase in membrane permeability. The polarity of the odorant-induced current reversed at $+6$ mV (S.D. 2.2 mV; $n=6$).

The data of the present study indicate that odor stimulation possibly increases the ion permeability of the olfactory cell membranes and evokes depolarized response.

INTRODUCTION

The olfactory receptor cells of vertebrates respond with slow and graded depolarization to odor. These cells are primary sensory type cells having self-regenerating excitability on their membranes to discharge the spikes and spike conductive axons [1–3]. The function of the graded receptor potential is considered to be the triggering of the discharge of repetitive spikes to transmit olfactory information to the central nervous system [4–7].

For the generation mechanisms of the graded receptor potential, two different hypotheses have been proposed about whether the membrane permeability is changed [5–7] or not [8–10]. However, many of recent observations on the olfactory response support the former. The effects of the external ions on olfactory response had been studied in frog mucosa by recording EOG (electro-olfactogram) which is attributed to the olfactory receptor potential. In such experiments, the re-

sponse generation required external Na ions [11, 12]. More recent work on the membrane potential in intracellular response of the tiger salamander receptor potential indicated that the receptor potential reversed its polarity at about 0 mV [7]. Essentially the same has also been observed in solitary olfactory cell preparation from certain animals [13–15]. It thus appears that the receptor potential of olfactory receptor cells is generated by membrane ion permeability change, as has been found in the other sensory cells, such as retinal photoreceptor [16–18] and vestibular hair cell [19–21].

In the present study, membrane permeability change causing olfactory response were determined. To measure membrane conductance from such a small cell directly, a patch-clamp method [22, 23] was considered to be suitable. For its use, membrane surface was bared in the bath solution by mechanically dissociating the olfactory cells from the enzyme-treated olfactory mucosa of a newt for which such a process is easy and comparatively large olfactory cells can be obtained. Stable recording was frequently possible for such cells by a whole-cell variation of patch-clamp.

Accepted March 1, 1988

Received January 26, 1988

MATERIALS AND METHODS

Materials

The Japanese newts, *Triturus pyrrhogaster*, were used as materials (about 15 cm length). Though they usually live in water, olfactory response varies depending on whether they live in water or on land, as previously reported [24]. For specimens living in water, stimulation by volatile substance, such as the vapor of amyl acetate, failed to cause obvious EOG response. But after being transferred to land and kept there, response to this vapor became evident 2 to 4 days later. In the present study, to examine odor response to the volatile substances (n-amyl acetate, d-limonene), specimens having lived on land for such a period were used.

Isolation of olfactory cells

Dissociation of the olfactory mucosa was carried out as follows. Olfactory mucosa was removed from the olfactory cavity under ice-colded anesthesia, and cut into 4 to 8 pieces, each subsequently treated with 0.5-1% collagenase in Ca^{2+} and Mg^{2+} free solution (108 mM NaCl, 3.7 mM KCl, 1 mM NaH_2PO_4 , 0.5 mM NaHCO_3 , 1 mM Na pyruvate, 15 mM glucose, 2 mM HEPES, 0.001% phenol red, pH adjusted by NaOH to 7.4) for 5-10 min at 35°C. It was then mechanically dissociated by pipetting. Four millimolar CaCl_2 and 0.8 mM MgCl_2 were added into a solution containing the solitary cells to preserve their condition for a long time. This solution of 200 μl were introduced into a plastic Petri dish (35 mm in diameter, Falcon, 3001). The cells adhered to the bottom of the dish previously treated with a 1% concanavalin A (Sigma C2010) within about 10 min, and 2 ml of solution containing Ca^{2+} and Mg^{2+} was added. They remained alive for more than 3 days at a temperature of 4°C. Cells kept less than 10 hr in culture gave the best results.

Recordings

Electrical signals from the solitary cells were obtained with whole-cell recording configuration using a giga-seal suction pipette [22, 23]. The recording glass pipette (tip diameter 1-2 μm) was

filled with pseudo-intracellular medium (120 mM KCl, 2 mM HEPES, 5 mM EGTA, 0.001% phenol red, pH adjusted to 7.4 by KOH, final K^+ concentration, 132 mM; pipette resistance: 10-20 M Ω). The recording electrode was connected to the patch-clamp amplifier (Nihon Kohden, S-3666) with an Ag-AgCl wire.

The recording was conducted as follows. The recording mode of the amplifier was made "search" (by this mode, the clamped pipette voltage is slowly adjusted automatically with the current through the pipette being 0 pA), and the recording pipette was brought into contact with the bath solution. The junction potential was artificially corrected at a pipette voltage of 0 mV and the current through the pipette, 0 pA.

The pipette was carefully attached to the cell membrane under the phase-contrast microscope (Olympus, IMT-2: 600 \times) using a micro-manipulator (Narishige, MO-103), while voltage pulses of 0.5 mV (50 msec duration) were applied continuously (interval 300 msec) to monitor seal resistance at "cell-attached" configuration. Contact between the pipette and cell membrane was verified by a slight decrease in the current amplitude through the pipette (about half), and a negative pressure of 10-50 cm-H $_2\text{O}$ was then applied to the inside of the pipette. This immediately led to high seal (>1 G Ω).

Further pulse-like negative pressure was applied to rupture the patch membrane. When the pipette was clamped at 0 mV, the shift of the patch-clamp variation, from the "cell attached" to the "whole-cell" recording configuration, was confirmed by the observation of an instant large (a few hundred pA) outward current.

In this study, the recording pipette was always placed on the dendrite. If the pipette was placed only on the cell body occupied by a large nucleus having very hard membrane, the patch membrane was difficult to rupture.

The bath solution at the recording consisted of: 110 mM NaCl, 3.7 mM KCl, 3 mM CaCl_2 , 1 mM MgCl_2 , 1 mM Na pyruvate, 15 mM Glucose, 2 mM HEPES, 0.001% phenol red; pH adjusted by NaOH to 7.4.

Electrical signals were monitored with an oscilloscope (Nihon Kohden, VC-9) and on a chart

recorder (Nihon Kohden, RM-25) at real time, and stored in magnetic tape using FM tape recorder (TEAC, R-60 or R-100). At the same time, the signals were digitized by a 12 bit resolution of analog and digital converter (Neolog, PCN-2198) and taken into the micro-computer (NEC, PC9801VM) and stored in a floppy or hard disk as a directory in the operating system (Microsoft, MS-DOS).

Odor stimulation

n-Amyl acetate (Wako) or D-limonene (Tokyo Kasei, D-p-mentha-1, 8-diene) was used in this study as odorant. A micro glass pipette (tip diameter 1-10 μm) was used to chemically stimulate the solitary cells. The solution which filled the stimulus pipette was made by dissolving the odor substance in the bath solution. The tip of the pipette was situated at near the apical dendritic portion of the recorded cell in the solution (within 20 μm in distance), and the stimulus solution in the pipette was ejected toward the cell from the tip with small pressure. The tail opening of the stimulus pipette was connected to the air-pressure system with a solenoid valve. A timer (Omron, TDF) or micro-computer (NEC, PC9801VM) was used to regulate the period of time this valve was open.

Various amino acids (Ala, Arg, Glu) known to be taste substances were also used in the same manner. All the experiments were performed at 15°C.

RESULTS

Morphology of solitary olfactory cells

Following dissociation, the cells in the culture dish contained olfactory receptor-, supporting-, basal- and respiratory epithelial cells, all identified morphologically in the intact olfactory mucosa of newt [24, 25]. Among them, the olfactory receptor cells could be easily recognized by morphological characteristics under a phase-contrast microscope. Figure 1 shows a micrograph of an isolated olfactory receptor cell. The cell had a soma of 15 μm diameter (horizontal axis) and showed a bipolar morphology. One process was a dendrite (about 2

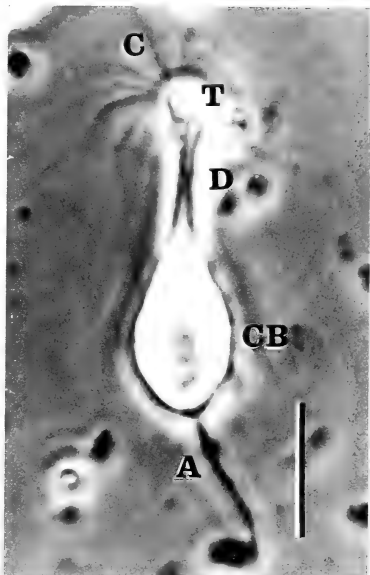


Fig. 1. Phase-contrast micrograph of solitary olfactory receptor cell. The cell was mechanically isolated from collagenase-treated olfactory mucosa of newt. Abbreviations; A; axon, C; olfactory cilia, T; terminal swelling, D; dendrite, CB; cell body. Calibration bar, 20 μm .

μm in diameter) and another an axon. The apical dendrite became swollen (called olfactory knob or terminal swelling) and from it, several cilia (more than 10 in number) extended. Each cilium waved randomly in the solution. The receptor cells in the intact olfactory mucosa were noted to have essentially the same features [26], except that the axon was lost during dissociation protocol. Mean cell body size of the solitary olfactory receptor cells was $21.0 \times 15.1 \mu\text{m}$ (longitudinal axis \times horizontal axis; $n=21$).

Among the solitary olfactory cells, those with no cilia were frequently observed. It could not be confirmed whether the loss of cilia resulted from dissociation, or was intrinsic morphological feature. Such cells failed to respond remarkably to 10

mM amyl acetate stimuli (0/18), and thus were not used in subsequent experiments.

Resting potential and spike discharge

Following establishment of the whole-cell recording configuration, the recording mode was switched from the voltage-clamp to current-clamp (0 pA) so that the pipette voltage would indicate the resting membrane potential (-41 ± 7 mV; mean \pm S.D., $n=70$). Sometimes, polarization at rest gradually increased by about 10 mV and becoming stable after a few minutes. The noise level at rest varied according to the cell. In some cell (about 10%), a spike was discharged on the steep potential drift toward the positive direction. Even for cells at rest from which spikes were not discharged, depolarization due to injected current

initiated spikes. Figure 2 shows an example of the spike discharge due to the injection of current into the solitary cell. At a current of 2 pA (1 sec in duration), the cell membrane was depolarized and on which, two spikes were generated (Fig. 2a, 2.0 Hz in frequency). At 4 pA and 6 pA, spike frequency increased (Fig. 2b, c). Frequency obtained as inverse of the interval between first and second discharge were 5.3 Hz and 8.0 Hz, respectively.

Of 70 cells examined, however, those showing such repetitive discharges were quite few (about 10%), even at large current (more than 50 pA). On most case, only one spike was observed at initial depolarization caused by the current.

Response to odor stimulation

When an odorant was applied to the current-clamped cell (0 pA), remarkable response was sometimes observed. Figure 3 shows an example of response to the 100 μ M n-amyl acetate stimulus. One second application of the odorant depolarized the membrane, generating a spike (Fig. 3a). For 3 sec application, the depolarized slow potential (peak magnitude: 23 mV) became clearer, and

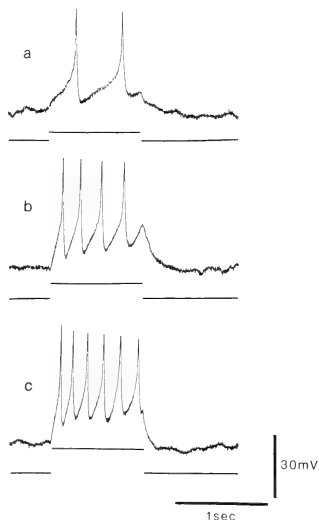


FIG. 2. Repetitive spike discharges caused by the injected current. The data was recorded under current clamp (0 pA). Upper trace of each pairs of record indicate the membrane potential and lower indicate the injected current. The duration of the injected current was 1 sec and the amounts were 2 pA (a), 4 pA (b) and 6 pA (c). The resting membrane potential of this cell was -54 mV.

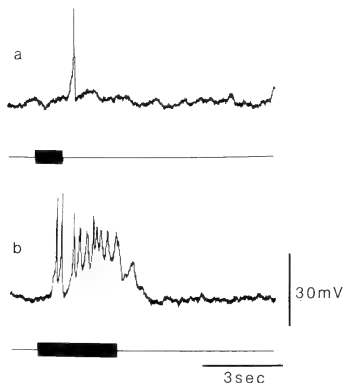


FIG. 3. Odor response in the solitary olfactory receptor cell. The odorant used was 100 μ M n-amyl acetate. The recording was made by current-clamp. Lower trace indicates odor stimulation. Duration of stimulation, a; 1 sec, b; 3 sec.

spikes were frequently seen (Fig. 3b).

At a concentration of 10 mM, depolarized potential became greater, exceeding that at 100 μ M, and the rising phase became steeper (compare Fig. 3 with Figs. 4, 5 and 6).

The response of 73 cells possessing moving olfactory cilia were examined with 10 mM n-amyl acetate. The amplitude or time course of the response varied from cell to cell. The depolarized response of 22 cells was obvious due to their large amplitude (>10 mV) and fast rising phase (>10 mV/sec). However, most of the cells failed to discharge spikes, as evident from the results of Figs. 4, 5 and 6.

Similar depolarized response was seen for d-limonene (1 μ l/ml, not dissolved completely). No remarkable response could be detected on using certain amino acids (10 mM Ala, 4 cell; 10 mM Arg, 8 cells; 10 mM Glu, 2 cells).

Response could usually be recorded for more than 10 min without remarkable change in amplitude and in time course. Sometimes, it gradually decreased during the recording from the time when whole-cell recording configuration was established, and then disappeared after a few minutes. This would not likely be due to membrane deterioration, since the voltage-gated ion conductance, such as delayed rectifier K current, could be recorded even after odor response disappeared. No further attention was given to this matter, in this study.

Time course of odor response to prolonged stimulation

Olfactory cells are generally considered to become adapted to the stimulus. For example, EOG response shows time-dependent decline in amplitude during the prolonged stimulation [27, 28]. A single unit spike response by most cells show essentially the same pattern [29, 30]. To determine if solitary cells respond in the same way, responses to prolonged stimulus (3–9 sec, 10 mM n-amyl acetate) were examined under the current-clamp mode.

Fourteen out of 18 cells showed "phasic/tonic response". Figure 4 shows a typical time course of this response. When stimulus was applied, the membrane started to depolarize within a second,

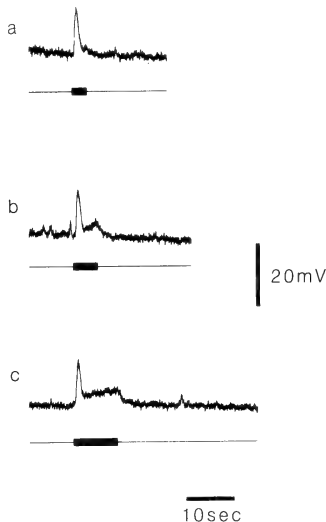


Fig. 4. Time course of the "phasic/tonic-response". Odor stimulus was 10 mM n-amyl acetate. Duration of stimulus, a; 3 sec, b; 5 sec, c; 9 sec.

and 0.5 sec later, the magnitude of response became maximum (15 mV in amplitude). Instantly, the membrane started to repolarize, though the stimulation was not terminated. But the membrane did not return to the resting level. It slowly returned after stopping the stimulation. Peak amplitude or time course of the phasic component of response was independent of the stimulus period from 3 sec to 9 sec, as illustrated in Fig. 4 a, b and c. Statistically, the mean duration of the phasic component from such cells was 3.5 sec (standard deviation (S.D.) = 1.6 sec).

Three cells of response did not decline during stimulation, even for a period of 9 sec. Figure 5A shows an example of the response from such a cell. In contrast to the response of Fig. 4, the peak value of the depolarized response was maintained during 3 sec of stimulation without significant decline (Fig. 5Aa). At 5 and 9 sec (Fig. 5Ab, Ac, respectively), the response was maintained for a

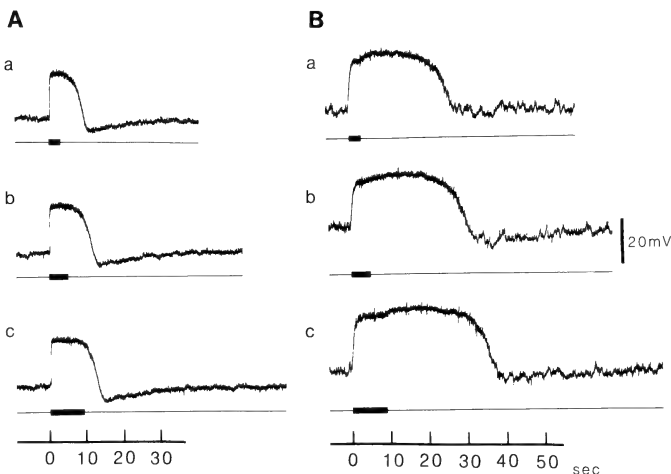


FIG. 5. Time course of the "Maintained-response". Odor stimulus was 10 mM *n*-amyl acetate. Data shown at A and B were obtained from two different cells. Duration of stimulus, a; 3 sec, b; 5 sec, c; 9 sec. Scale represented at bottom indicate the time from the initiation of stimulation.

greater period. As can be seen from Fig. 5A, after terminating the stimulus, the membrane instantly started to repolarize. But in one of the 3 cells, the depolarized response was maintained for more than 20 sec even after removing the stimulus (Fig. 5B).

The response pattern in one out of 18 cells was quite different from those in Figs. 4 and 5. The time course of the response is represented at Fig. 6. During stimulus application, although some depolarization occurred (about 5 mV), no significant response was seen. However, following 3 sec of stimulation, the membrane became depolarized (Fig. 6a). The response reached a peak value (30 mV in amplitude) and slowly returned to the resting level. Even for prolonged periods of 5 sec and 9 sec, the membrane depolarized after stopping the stimulation (Fig. 6 b and c). It thus seems unlikely that the latency of the depolarized response results from delayed application of the stimulus solution from the pipette tip to the cell. The response may belong to the category of "Off-

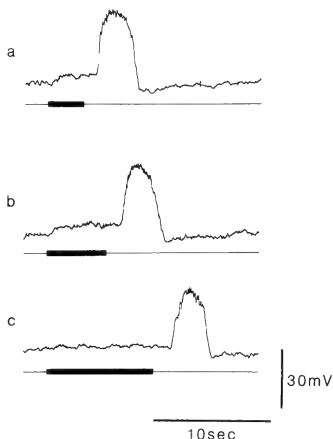


FIG. 6. Time course of the "Off-response". Odor stimulus was 10 mM *n*-amyl acetate. Duration of stimulation, a; 3 sec, b; 5 sec, c; 9 sec.

response".

Odorant-induced current under voltage-clamp condition

Under the voltage-clamp condition, stimulation elicited an inward current (odorant-induced current). Figure 7A shows an example of current induced by 10 mM n-amyl acetate. The membrane was clamped at -34.2 mV which was close to the resting potential, and the stimulant was applied to the cell for a second. The inward current observed was about 70 pA.

Figure 7B shows two types of different time courses of odorant-induced current for long lasting pulses. At 3 sec of stimulation to the cell in Fig. 7Ba, which showed a phasic time course under the current-clamp similar to the response in Fig. 4, the inward current observed was transiently activated and declined instantly during stimulation. Fig. 7B

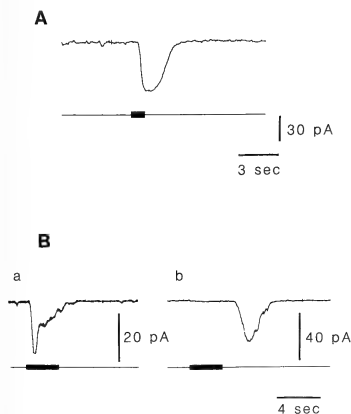


Fig. 7. Odorant-induced current. Odor stimulus was 10 mM n-amyl acetate. Each record was obtained under voltage-clamp condition. The downward deflection of the current trace indicate the inward flux. A; Current induced by the short pulse. Duration, 1 sec. The holding potential was equal to the resting potential. B; Current traces induced by long-lasting pulses (3 sec). a; The cell examined showed a "Phasic-response" pattern under current-clamp condition. b; The cell showed a "Off-response" under current-clamp.

b shows the time course of odorant-induced current from a cell which showed "Off-response". The current started to activate after the stimulus was terminated.

Assuming the current to be carried by ions through the membrane, its amplitude should depend on the membrane potential. Figure 8 shows the effect of membrane polarization on odorant-induced current. When a cell was voltage-clamped at -40 mV, 10 mM n-amyl acetate caused an inward current of about 24 pA. As the membrane potential shifted in a positive direction, the current amplitude decreased. Further depolarization to 10

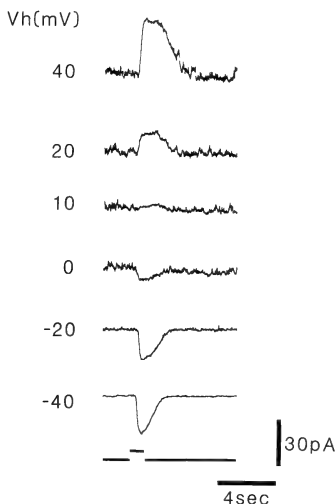


Fig. 8. Voltage dependence of the odorant-induced current. The number at left of each trace indicate the holding potential (Vh). The experiment was performed from hyperpolarized potential to the positive. Interval of each stimulation was more than 20 sec. Odor stimulus was 10 mM n-amyl acetate. Timing of the stimulus pulse is indicated at the bottom.

mV reversed the current polarity to outward.

The current-voltage (I-V) relationship of a membrane was plotted in the presence (1) and

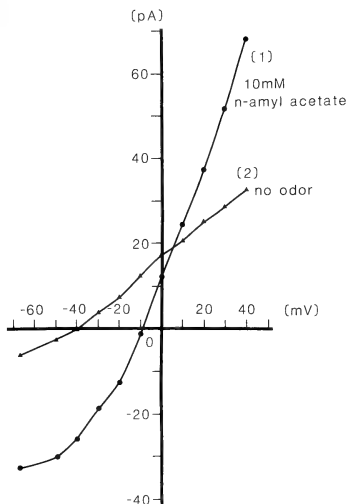


Fig. 9. Current-voltage (I-V) relation of the membrane in presence (1) and absence (2) of odorant. The absolute value of the membrane current (ordinate) were plotted against the voltage (abscissa) from Fig. 8. Plots at curve (2) was obtained at before stimulus applying, and curve (1) was obtained at the peak of the odorant-induced current. The slope resistances of the curve (2) calculated at below -40 mV and at 0 mV were 4.8 and 2.4 G Ω , respectively. And that of curve (1) was 800 M Ω at 0 mV.

absence (2) of an odorant (Fig. 9). The slope of the curve 1 was steeper than that of curve 2 in the range -50 mV to $+40$ mV, indicating membrane conductance to increase by application of amyl acetate.

The I-V relation of odorant-activated conductance was determined by subtraction of these two curves (Fig. 10). Polarity reversal was noted at about $+7$ mV. The I-V relation of conductance showed remarkable non-linearity, and outward rectification was observed. In a large hyperpolarized potential region (below -50 mV), the curve slope was negative.

These experiments were performed on 6 different cells all showing obvious depolarized response

under the current-clamp condition. The mean value of the reversal potential was 6.2 ± 2.2 mV, and the slope conductance at the reversal potential was 3.14 ± 1.59 nS. The potential level at which the cell membrane showed non-linearity varied according to the cell (from -50 to -20 mV). No cell had reversed current polarity at a hyperpola-

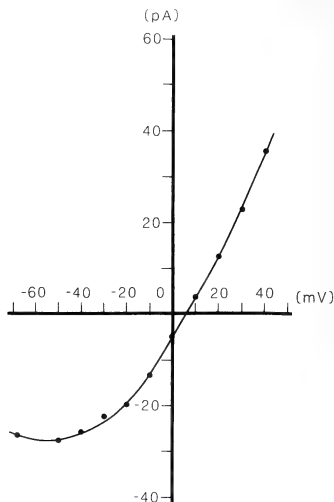


Fig. 10. I-V relation of odorant-activated conductance.

The curve was obtained by subtraction of two curve in Fig. 9. The crossing point between the I-V curve and the abscissa means a reversal potential of the conductance, which is noted at $+7$ mV.

rized potential, even at -100 mV.

DISCUSSION

The data of the present study clearly indicated that the olfactory receptor potential was caused by increase in the membrane permeability, using a solitary olfactory cell preparation and patch-clamp method.

The resting membrane potential of solitary cells was -41 mV, as measured immediately following

rupture of the patch membrane. This value is close to that for the intact olfactory cells in certain animals [1, 2, 4-7] or for solitary olfactory cells isolated from the tiger salamander [14, 15].

It is generally believed that the resting membrane potential of neurons is close to the equilibrium potential of K^+ . Under the present experimental conditions, concentration of extracellular K ion ($[K^+]_o$) was 3.7 mM. $[K^+]_i$ could not be determined exactly, however, when a whole-cell variation of patch-clamp method is used, the intracellular solution is known to be substitute by the pipette solution [22, 23] within a few minutes [31], and thus $[K^+]_i$ was considered to be 132 mM. In such an ionic environment, the equilibrium potential of K ions was predicted at -90 mV with a Nernst equation. Though the membrane was sometimes gradually hyperpolarized from an initial value (mean -41 mV) with time, the degree of shift was less than 10 mV and the membrane potential never reached -90 mV. Consequently, in olfactory receptor cells, it does not seem likely that the resting membrane potential is determined solely by the distribution of K ion across the membrane. The matter remains to be clarified.

It has been reported, in the intact cells of newt olfactory mucosa, that stimulation by *n*-amyl acetate or *D*-limonene used in this study evokes EOG or single unit response [24, 25]. The odor concentration in the present study was $100 \mu\text{M}$ – 10 mM dissolving in water. The threshold of intact olfactory cell response to the waterborne amyl acetate stimuli was about $100 \mu\text{M}$, for frog [7] and tiger salamander [32]. Thus the odor concentration used here was considered to be in the physiological range.

Though 10 mM amyl acetate was sufficient to induce response in salamander olfactory mucosa, not all the solitary cells were responded at this concentration, the probability being 1/3.5. This indicates that the cell sensitivity varies from cell to cell, and is quite consistent with the characteristics of intact olfactory cells [33–35].

It is generally known that olfactory receptor cells discharge repetitive spikes, the frequency being in proportion to the membrane depolarization [1–3, 5, 6]. Receptor potential increased in amplitude with odor concentration [7], and thus

spike frequency reflect strength of the stimulus (concentration of the odorant). Similar spike generation was observed after injecting a current into a minor group of solitary cells as illustrated in Fig. 2. In contrast, most of cell discharged only a single spike, even at a large (10 – 50 pA) and long (1 sec) current. Also in solitary olfactory cells from the tiger salamander, only a few spike were generated at the first rising phase of depolarization brought about by injected current or odor stimulation [15]. Dissociation may be correlated to lose of ability to discharge spikes repetitively.

Up to this point, it has been assumed that olfactory receptor cells adapt to long lasting stimulation [27–30]. Eighty two percent (14/17; cell showing "Off-response" not included) of depolarized response in solitary olfactory receptor cells showed time dependent decrease within 9 sec of stimulation (Fig. 4), and odorant-induced inward currents recorded from such cells also showed the transient time course (Fig. 7B a). These findings agree well those for EOG or single unit response. The phasic component of solitary cells was terminated at about 3.5 sec following the initial rising. This value is close to that for the decreasing time course of intact receptor potential of tiger salamander (3–6 sec, assumed from ref. [30]).

The receptor potential or isolated odorant-induced current was recorded in this study, and thus the present results indicate that there may be possibly an adaptation mechanism in the process of transduction between the receptor (odorant binding) site on a cell membrane and the transduction system. Recently, in a divalent cations- (Ca^{2+} and Mg^{2+}) free medium, cells found not to adapt significantly [36]. Considering the time-dependent kinetics of the phasic response and the effects of extracellular divalent cations, influx of divalent cations may reasonably be considered to affect the process of transduction.

The responses from minor cell did not decline during stimulation. Moreover, response was maintained for more than 20 sec following termination of the stimulus. This was also observed for intact cells [30].

One cell showed "Off-response", and its odorant-induced current was also activated after terminating the stimulus. In the frog, a strong odor

stimulus has been reported to evoke "Off" negative EOG response, indicating possibly the existence of cells which depolarize with stimulus termination [28]. The present observations on "Off-response" may support this possibility.

Trotter and MacLeod [7] found by an intracellular recording method, that the receptor potential of *in situ* salamander olfactory cells reverses its polarity at about 0 mV. Recently, the patch-clamp method was used to examine isolated olfactory cells from various species and voltage dependence of the odorant-evoked depolarized response [15] or odorant-induced current [13, 14] was analyzed. The results indicated the reversal potential to be near 0 mV. The reversal potential of odorant-induced current observed was +6 mV, which is quite close to the value found in previous studies.

This value was essentially the same among different cells (S.D. = 2.2 mV; $n=6$). This observation suggests that the certain ionic mechanism involves the receptor potential. Recently, Kurahashi and Shibuya [37] calculated the permeability ratios of the odorant-activated conductance to the alkali metal ions from reverse values for various ionic environments using the Goldman-Hodgkin-Katz equation. Na^+ and K^+ were found to have essentially the same permeability. Under the present experimental condition, the environments of both extra- and intracellular sides of cell membranes were filled by Na^+ and almost isotonic K^+ , respectively. Thus, the reversal potential may quite reasonably be concluded to be near the 0 mV.

The I-V relation of odorant-activated conductance showed remarkably non-linearity in the hyperpolarized potential region (Fig. 10). There are two possible explanations for this. The first, odorant-activated conductance itself may have a non-linear I-V relation. And secondly, inward current through the other ionic channel (e.g. voltage- or calcium-activated channel in cell membrane [38-41]) activated by hyperpolarization may be blocked by odor stimulation. For example, glutamate-induced conductance in retinal horizontal cells in goldfish shows similar non-linear I-V relation. This non-linearity is due to dual effect of the glutamate on the horizontal cell membrane. These are (1) activation of the Glu-activated chan-

nel and (2) blocking effect on the anomalous rectifier K channel [42, 43]. But the second possibility does not seem applicable to the non-linear I-V relation of the odorant-activated conductance, since olfactory cell membranes showed high input resistance at the hyperpolarized potential region about more than a few $\text{G}\Omega$ and no significant inward rectification was observed (Fig. 9). Thus, odorant-activated conductance itself appears to have a non-linear I-V relation. In addition, the time course of current also depended on membrane potential. As the membrane became depolarized, the current continued for a longer period of time. This may also indicate possible voltage-dependent kinetics of odorant-activated conductance.

Similar rectification has been reported for various ion channels, the most remarkable observation being that cyclic nucleotide-activated conductance on olfactory cilia, a candidate for the chemotransduction system, showed similar voltage dependence in normal Ringer's solution [44]. For the cyclic nucleotide-activated channel, the cyclic GMP-activated channel on the outer segment of rod photoreceptor cells is well known. This channel also shows a non-linear I-V relation in normal Ringer's solution resembling the I-V relation of the odorant-activated conductance observed in the present study [45]. There are some similarities between odorant-activated conductance and cyclic nucleotide channel. Significant information should be obtained from further comparison of the characteristics of odorant-activated conductance and of cyclic nucleotide conductance.

ACKNOWLEDGMENT

The authors wish to thank Professor Akimichi Kaneko and Dr. Masao Tachibana, Department of Information Physiology, National Institute for Physiological Sciences, for their valuable advice and discussion. Thanks are also to Associate professor Takehiko Saito, Institute of Biological Sciences, University of Tsukuba, for his various comments on the manuscript. This work was partially supported by the Program of Special Research Project on Instinct, University of Tsukuba, and a Grant-in-Aid for Olfaction Research from Takasago corporation.

REFERENCES

- 1 Masukawa, L. M., Kauer, J. S. and Shepherd, G. M. (1983) Intracellular recordings from two cell types in an *in vitro* preparation of the salamander olfactory epithelium. *Neurosci. Lett.*, **35**: 59–64.
- 2 Masukawa, L. M., Hedlund, B. and Shepherd, G. M. (1985) Electrophysiological properties of identified cells in the *in vitro* olfactory epithelium of tiger salamander. *J. Neurosci.*, **5**: 128–135.
- 3 Hedlund, B., Masukawa, L. M. and Shepherd, G. M. (1987) Excitable properties of olfactory receptor neurons. *J. Neurosci.*, **7**: 2338–2343.
- 4 Getchell, T. V. (1977) Analysis of intracellular recordings from salamander olfactory epithelium. *Brain Res.*, **123**: 275–286.
- 5 Suzuki, N. (1977) Intracellular responses of lamprey olfactory receptors to current and chemical stimulation. In "Food intake and chemical stimulation". Ed. by Y. Katsuki, M. Sato, S. F. Takagi and Y. Oomura, Univ. of Tokyo press, Tokyo, pp. 13–22.
- 6 Suzuki, N. (1982) Responses of olfactory receptor cells to electrical and chemical stimulation. In "Chemoreception of fishes". Ed. by T. J. Hara, Elsevier Scientific Publishing Company, Amsterdam, pp. 93–108.
- 7 Trotier, D. and MacLeod, P. (1983) Intracellular recordings from salamander olfactory receptor cells. *Brain Res.*, **268**: 225–237.
- 8 Kashiwayanagi, M. and Kurihara, K. (1984) Neuroblastoma cell as model for olfactory cell: Mechanism of depolarization in response to various odorants. *Brain Res.*, **293**: 251–258.
- 9 Kashiwayanagi, M. and Kurihara, K. (1985) Evidence for nonreceptor odor discrimination using neuroblastoma cells as a model for olfactory cells. *Brain Res.*, **359**: 97–103.
- 10 Kashiwayanagi, M. and Kurihara, K. (1987) Cell suspensions from porcine olfactory mucosa. Changes in membrane potential and membrane fluidity in response to various odorants. *J. Gen. Physiol.*, **89**: 443–457.
- 11 Takagi, S. F., Wyse, G. A., Kitamura, H. and Ito, K. (1969) The roles of sodium and potassium ions in the generation of the electro-olfactogram. *J. Gen. Physiol.*, **51**: 552–578.
- 12 Takagi, S. F., Kitamura, H., Imai, K. and Takeuchi, H. (1969) Further studies on the roles of sodium and potassium in the generation of the electro-olfactogram. Effect of mono-, di-, and trivalent cations. *J. Gen. Physiol.*, **53**: 115–130.
- 13 Kurahashi, T. and Shibuya, T. (1986) The odor responses and odor-induced current in the solitary olfactory receptor cells isolated from newts. *Proc. Jpn. Symp. Taste and Smell*, **20**: 33–36.
- 14 Trotier, D. (1986) A patch-clamp analysis of membrane currents in salamander olfactory receptor cells. *Pflüg. Arch.*, **407**: 589–595.
- 15 Anderson, P. A. and Hamilton, K. A. (1987) Intracellular recordings from isolated salamander olfactory receptor neurons. *Neurosci.*, **21**: 167–173.
- 16 Fesenko, E. E., Kolesnikov, S. S. and Lyubarsky, A. L. (1985) Induction by cyclic GMP of cationic conductance in plasma membrane of retinal rod outer segment. *Nature*, **313**: 310–313.
- 17 Haynes, L. W. and Yau, K.-W. (1987) Single cyclic GMP-activated channel activity in excised patches of outer segment membrane. *Nature*, **321**: 66–70.
- 18 Zimmerman, A. L. and Baylor, D. A. (1987) Cyclic GMP-sensitive conductance of retinal rods consists of aqueous pores. *Nature*, **321**: 70–72.
- 19 Ohmori, H. (1984) Mechano-electrical transducer has discrete conductances in the vestibular hair cell. *Proc. Natl. Acad. Sci.*, **81**: 1888–1891.
- 20 Ohmori, H. (1985) Mechano-electrical transduction currents in isolated vestibular hair cells of the chick. *J. Physiol.*, **359**: 189–217.
- 21 Ohmori, H. (1987) Gating properties of the mechano-electrical transducer channel in the dissociated vestibular hair cell of the chick. *J. Physiol.*, **387**: 589–609.
- 22 Hamill, O. P., Marty, A., Neher, E., Sakmann, B. and Sigworth, F. J. (1981) Improved patch-clamp techniques for high-resolution current recording from cells and cell-free membrane patches. *Pflüg. Arch.*, **391**: 85–100.
- 23 Sakmann, B. and Neher, B. (1983) Single-channel recording. Plenum press, New York.
- 24 Shibuya, T. and Takagi, S. F. (1963) Electrical response and growth of olfactory cilia of the olfactory epithelium of the newt in water and on land. *J. Gen. Physiol.*, **47**: 71–82.
- 25 Shibuya, T. and Tonosaki, K. (1971) Electrical responses of single olfactory receptor cells in some vertebrates. In "Olfaction and taste IV". Ed. by D. Schneider, Wissenschaftliche Verlagsgesellschaft MBH, Stuttgart, pp. 102–108.
- 26 Graziadei, P. (1971) The olfactory mucosa of vertebrates. In "Handbook of sensory physiology IV". Ed. by L. M. Beidler, Springer, Berlin, pp. 27–58.
- 27 Ottoson, D. (1956) Analysis of the electrical activity of the olfactory epithelium. *Acta Physiol. Scand.*, **35**: 1–83.
- 28 Takagi, S. F. and Shibuya, T. (1959) 'On' and 'Off' responses of the olfactory epithelium. *Nature*, **184**: 60.
- 29 Shibuya, T. and Shibuya, S. (1963) Olfactory epithelium: Unitary responses in the tortoise. *Science*, **140**: 495–496.
- 30 Getchell, T. V. and Shepherd, G. M. (1978) Adaptive properties of olfactory receptors analysed with odour pulses of varying durations. *J. Physiol.*, **282**:

- 541-560.
- 31 Kaneko, A. and Tachibana, M. (1986) Effect of γ -aminobutyric acid on isolated cone photoreceptors of the turtle retina. *J. Physiol.*, **373**: 443-461.
- 32 Arzt, A. H., Silver, L. S., Mason, J. R. and Clark, L. (1986) Olfactory responses of aquatic and terrestrial tiger salamanders to airborne and waterborne stimuli. *J. Comp. Physiol. A*, **158**: 479-487.
- 33 Mathews, D. (1972) Response patterns of single neurons in the tortoise olfactory epithelium and olfactory bulb. *J. Gen. Physiol.*, **60**: 166-180.
- 34 Baylin, F. (1979) Temporal patterns and selectivity in the unitary responses of olfactory receptors in the tiger salamander to odor stimulation. *J. Gen. Physiol.*, **74**: 17-36.
- 35 Sicard, G. and Holley, A. (1984) Receptor cell responses to odorants: Similarities and differences among odorants. *Brain Res.*, **292**: 283-296.
- 36 Kurahashi, T. and Shibuya, T. (1987) Adaptation of odor response in the olfactory receptor cells may be controlled by influx of extracellular divalent cations. *Zool. Sci.*, **4**: 964.
- 37 Kurahashi, T. and Shibuya, T. (1987) Cation selectivity of the chemo-electrical transduction channel in the olfactory receptor cells. *Proc. Jpn. Symp. Taste and Smell*, **21**: 133-136.
- 38 Kurahashi, T. and Shibuya, T. (1986) Membrane ionic currents in the solitary olfactory receptor cells of newt. *Zool. Sci.*, **3**: 982.
- 39 Maue, R. A. and Dionne, V. E. (1987) Patch-clamp studies of isolated mouse olfactory receptor neurons. *J. Gen. Physiol.*, **90**: 95-125.
- 40 Maue, R. A. and Dionne, V. E. (1987) Preparation of isolated mouse olfactory receptor neurons. *Pflug. Arch.*, **409**: 244-250.
- 41 Firestein, S. and Werblin, F. S. (1987) Gated current in isolated olfactory receptor neurons of the larval tiger salamander. *Proc. Natl. Acad. Sci.*, **84**: 6269-6296.
- 42 Tachibana, M. (1985) Permeability changes by L-glutamate in solitary retinal horizontal cells isolated from *Carassius auratus*. *J. Physiol.*, **358**: 153-167.
- 43 Kaneko, A. and Tachibana, M. (1985) Effects of L-glutamate on the anomalous rectifier potassium current in horizontal cells of *Carassius auratus* retina. *J. Physiol.*, **358**: 169-182.
- 44 Nakamura, T. and Gold, G. H. (1987) A cyclic nucleotide-gated conductance in olfactory cilia. *Nature*, **325**: 442-444.
- 45 Matthews, G. (1986) Comparison of the light-sensitive and cyclic GMP-sensitive conductances of the rod photoreceptor: Noise characteristics. *J. Neurosci.*, **6**: 2521-2526.

Immunofluorescent Staining of Visual Cells from Various Species by Mouse Monoclonal Antibodies against Bovine Rhodopsin

SHINRI HORIUCHI, HIROSHI KITANI¹, YUTAKA KOSHIDA,
FUMIO TOKUNAGA² and TAKUJI TAKEUCHI³

Department of Biology, College of General Education, Osaka University,
Toyonaka, Osaka 560, ²Department of Physics and ³Biological
Institute, Faculty of Science, Tohoku University,
Aobayama, Sendai, Miyagi 980, Japan

ABSTRACT—The fluorescent-isothiocyanate (FITC) indirect immunofluorescence method using three monoclonal antibodies against bovine rhodopsin was applied to polyethylene glycol-embedded sections of buffered formalin-fixed retinæ from bovine, cat, chicken, sparrow, bullfrog, and Japanese newt. The rod outer segments of retina in the bovine were labeled by all three antibodies, but only two of the antibodies were similarly reactive in the other five species. Except for the rod outer segments, neither cells nor other cell segments in the retinæ from the six species examined were labeled by any of the antibodies. Based on the results of FITC staining, similarities of epitopes recognized by the antibodies in these vertebrate retinæ are discussed.

INTRODUCTION

Monoclonal antibodies against visual pigments have been obtained in several laboratories [1-6]. These antibodies have been found useful for studying the structural and functional domains of visual pigments of the retina and also for distinguishing or identifying *in situ* the pigments, for such studies are practically difficult by ordinary methods of protein chemistry or biophysics.

Recently we prepared three monoclonal antibodies against bovine rhodopsin, the rod visual pigment mediating twilight vision [7, 8]; and in the present work, we employed them in the FITC indirect immunofluorescence method to learn what parts and kinds of cells in the vertebrate retinæ would be labeled by these antibodies, and also to examine similarities of epitopes recognized by these antibodies in different vertebrate retinæ.

MATERIALS AND METHODS

Monoclonal antibodies were raised against bovine rhodopsin purified by con A-Sepharose column chromatography, and three clones producing anti-rhodopsin antibodies, termed Rh29, 112, and 311, were prepared according to the standard method [9]. Their preparation and characterization were described elsewhere [7, 8], but in brief as follows: all three antibodies were found exclusively to be IgG and were specific to both bovine rhodopsin and its protein portion, opsin, although Rh311 showed more specificity to the former than the latter, and Rh29 did contrary specificity.

Retinæ were obtained from the eyeballs of the following adult vertebrates: bovine, cat, chicken, sparrow (*Passer montanus saturatus*), bullfrog (*Rana catesbeiana*), and Japanese newt (*Cynopus pyrrhogaster*). Because both amphibians show the retinomotor phenomenon, they were kept for more than 12 hr in the dark to obtain dark-adapted retinæ before they were sacrificed.

The retinæ were fixed in chilled 3.5% formalin in 0.1 M phosphate buffer (PB, pH 7.2) for 4 hr, rinsed in 0.1 M PB (pH 7.2) at 4°C overnight to

Accepted March 2, 1988

Received December 18, 1987

¹ Present address: Laboratory of Cell Biology, Riken, Tsukuba Lifescience Center, Institute of Physical and Chemical Research, Tsukuba, Ibaraki 305, Japan

remove completely the formaldehyde, and then embedded in polyethylene glycol (PEG, m.w. 1000) after having been passed through a graded series of PEG at 37°C. Sections, 4 μ m thick, were prepared from retinae in PEG by a rotary microtome at 2°C and mounted on non-fluorescent, ovalbuminized glass slides. After PEG was removed by distilled water, the sections, still attached to the slides, were rinsed in 0.1 M phosphate-buffered saline (PBS, pH 7.2), incubated with one of the anti-rhodopsin antibodies at 37°C for 30 min, washed by passage through three baths of cold PBS, and then incubated at 37°C for 30 min with FITC-conjugated goat antibody against mouse IgG (25 μ g/ml, Tago Burlingame, Calif.), which was used as the second antibody. Sections were counter-stained by 0.01% Evans blue in PBS for 2 min, mounted in 80% non-fluorescent glycerol in PBS, and observed under a fluorescence microscope (Olympus, BH-2-RFK, Tokyo) first with a BV excitation system and later with a phase-contrast optical system.

RESULTS AND DISCUSSION

Figure 1A shows a fluorescence photomicrograph of a part of a bovine retina immunologically stained with Rh311 as the monoclonal antibody; and Figure 1B, a phase-contrast image of the same field observed in Figure 1A, in order to identify the source of the fluorescence. We found that rod outer segments were FITC-stained, while rod inner segments and other kinds of cells found among the rod cells were unreactive. Most of these negative cells were regarded as cone cells, because their shape was quite different from that of rod cells. In the so-called rod retina of such animals as ungulate and carnivorous mammals, cone cells are few in number and difficult to distinguish in sections treated by ordinary histological methods, because both types of visual cells are stained

indiscriminately. But the present immunological staining allows the distinguishing of cone cells from rod cells in these mammalian retinae. In fact, similar results were obtained from the cat retina. In the sparrow retina as well as in the chicken eye, the number of rod cells was actually smaller (Fig. 2B) than that in the bovine or cat retina, but only rod outer segments were found FITC-stained (Fig. 2A). In the dark-adapted retina of both bullfrog and Japanese newt, rod cells were located in front of cone cells, and these two kinds of visual cells were unmistakably distinguished from each other by their shapes and locations in the layer of the neural retina, as shown in Figure 3B. FITC-fluorescence was present in rod outer segments, but no fluorescence was detected in cone outer segments of the retina (Fig. 3A). Both rod and cone inner segments were stained by Evans blue, while the pigment epithelium of the retina was stained by neither FITC nor Evans blue in any of the vertebrate species examined.

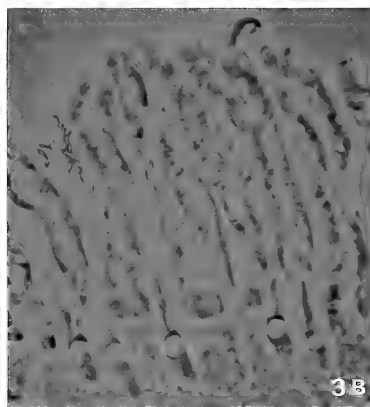
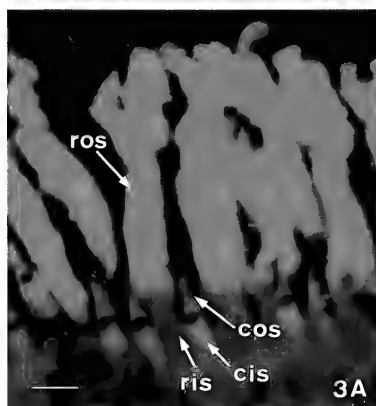
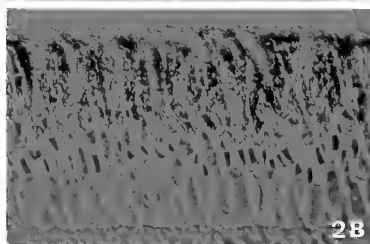
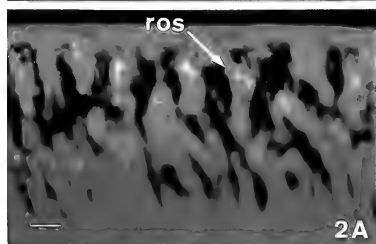
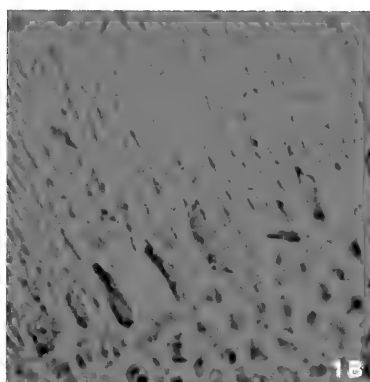
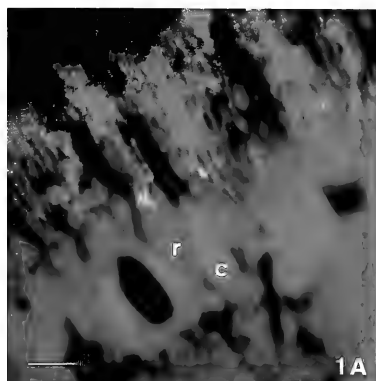
In the bovine retina, FITC-fluorescence was observed in rod outer segments with all three anti-rhodopsin antibodies although the fluorescence intensities were different among the antibodies employed. In the cat, chicken, sparrow, bullfrog, and Japanese newt retina, both Rh29 and 311 distinctly labeled rod outer segments, while Rh112 failed to bind to them. Again, FITC-fluorescence intensities differed with the antibodies employed and also with vertebrate species examined. There was a tendency for the FITC-fluorescence to be more intense when Rh311 was applied, as compared with Rh29.

The present findings, that is, both Rh311 and 29 labeled rod outer segments in all vertebrate species examined, would indicate that the epitopes recognized by both Rh311 and 29 are identical or very similar in rhodopsins of these six vertebrate species. Similar findings for cone visual pigments mediating color vision were obtained by Szél *et al.*

FIG. 1. Fluorescence photomicrograph of bovine retina stained with anti-rhodopsin antibody Rh311 and Evans blue (A) and its phase-contrast image (B). r: rod cell, c: cone cell. Bar: 10 μ m.

FIG. 2. Fluorescence photomicrograph of sparrow retina stained with Rh311 and Evans blue (A) and its phase-contrast image (B). ros: rod outer segment. Bar: 10 μ m.

FIG. 3. Fluorescence photomicrograph of bullfrog retina stained with Rh311 and Evans blue (A) and its phase-contrast image (B). ros: rod outer segment, ris: rod inner segment, cos: cone outer segment, cis: cone inner segment. Bar: 10 μ m.



[6]. They used monoclonal antibodies raised against a crude photoreceptor-membrane suspension from chicken retinae and found that one of their antibodies specifically labeled outer segments of both double cone and one type of single cone cells in the chicken retina and several types of cone cells in the retinae from monkey, pigeon, turtle, frog, and other species as well, but not outer segments of rod cell of retinae from these animals including the chicken. We presume that the epitopes recognized by the antibodies against bovine rhodopsin have been well-preserved, reflecting a conserved molecular structure that has descended from the ancestral to the current rhodopsin, irrespective of the phylogenical diversity of vertebrate species. Nathans *et al.* [10] carried out the isolation and sequencing of genomic and DNA clones which encoded three kinds of human cone visual pigments, and found that these deduced amino acid sequences showed $41 \pm 1\%$ identity with human rhodopsin, while bovine rhodopsin showed 94% identity with human one. Takao *et al.* [11] revealed that bovine opsin cDNA showed 87% for the deduced amino acid sequence with chicken opsin gene. It seems acceptable that rhodopsin and cone visual pigments have descended along separate lines, and our findings, that is, antibodies against bovine rhodopsin labeled rod cells in species other than the bovine, but not cone cells in this species, would be consistent with the results of these sequence identities cited above.

REFERENCES

- 1 Mackenzie, D. and Molday, R. S. (1982) Organization of rhodopsin and a high molecular weight glycoprotein in rod photoreceptor disc membranes using monoclonal antibodies. *J. Biol. Chem.*, **257**: 7100-7105.
- 2 Fekete, D. M. and Branstable, C. J. (1983) The subcellular localization of rat photoreceptor-specific antigens. *J. Neurocytol.*, **12**: 785-803.
- 3 Molday, R. S. and Mackenzie, D. (1983) Monoclonal antibodies to rhodopsin: characterization, cross-reactivity and application as structural probes. *Biochemistry*, **22**: 653-660.
- 4 Witt, P. L., Hamm, H. E. and Bownds, M. D. (1984) Preparation and characterization of monoclonal antibodies to several frog rod outer segment proteins. *J. Gen. Physiol.*, **84**: 251-263.
- 5 Molday, R. S. and Mackenzie, D. (1985) Inhibition of monoclonal antibody binding and proteolysis by light-induced phosphorylation of rhodopsin. *Biochemistry*, **24**: 776-781.
- 6 Szél, A., Takacs, L., Monostori, É., Diamantstein, T., Vigh-Teichmann, I. and Röhlich, P. (1986) Monoclonal antibody-recognizing cone visual pigment. *Exp. Eye Res.*, **43**: 871-883.
- 7 Tokunaga, F., Iwasa, T., Takao, M., Sato, S. and Takeuchi, T. (1989) Preparation and properties of mouse monoclonal antibodies against bovine rhodopsin. *Zool. Sci.*, **6**, 167-171.
- 8 Tokunaga, F., Takao, T., Iwasa, T., Koike, S., Sato, S., Takeuchi, T., Kitani, H., Horiuchi, S. and Koshida, Y. (1987) Anti-bovine rhodopsin monoclonal antibodies. In "Retinal Proteins", Ed. by Y. A. Ovchinnikov, VNU Science Press, pp. 145-152.
- 9 Oi, V. T. and Herzenberg, L. A. (1980) Immunoglobulin-producing hybrid cell lines. In "Selected Methods in Cellular Immunology", Ed. by B. B. Mishell and S. M. Shiigi, W. H. Freeman & Co., pp. 351-372.
- 10 Nathans, J., Thomas, D. and Hogness, D. S. (1986) Molecular genetics of human color vision: The genes encoding blue, green, and red pigments. *Science*, **232**: 193-202.
- 11 Takao, M., Yasui, A. and Tokunaga, F. (1988) Isolation and sequence determination of the chicken rhodopsin gene. *Vision Res.*, **28**, 471-480.

Cell Cycle in the Epidermis during Larval Instars of the Saturniid Moth *Samia cynthia ricini* (Lep.)

KIYOSHI MINATO

Laboratory of Phenogenetics, The National Institute of
Genetics, Mishima, Shizuoka 411, Japan

ABSTRACT—The cyclic patterns of DNA synthesis and mitosis of cells in the epidermis and other tissues of the Saturniid moth *Samia cynthia ricini* during the third and fourth larval instars were investigated. During both instars, epidermal cells divided as a wave in the middle of the “feeding” phase, just before synchronous DNA synthesis in this tissue. Studies on epidermal cells labelled with [^3H]thymidine showed that the wave of mitosis in the fourth instar followed after DNA replication in the third instar. Thus the cell cycle in the epidermis of this insect during larval instars has an unusually long (48 hr) pre-mitotic (G_2) phase and possibly a relatively short post-mitotic (G_1) phase. The significance of this long G_2 phase is discussed.

INTRODUCTION

In most eucaryotic cells, the stage of DNA synthesis (S) is followed somewhat autonomously by mitosis (M) after a relatively short (usually several hours) pre-mitotic (G_2) phase and the cells, then, remain in the post-mitotic (G_1) phase for a relatively long or indefinite time until DNA synthesis begins again. But the cells in mouse ear epidermis [1] and some cells in some other tissues of numerous animals and plants have a relatively long G_2 phase or arrested in G_2 indefinitely [2-7].

In insects, cells with a long G_2 phase have been found in the follicular epithelium of Hymenoptera larvae in diapause [8], the imaginal disc of Lepidoptera [9] and Diptera [10-12], and the fat body of Orthoptera [13]. As to the integumental epidermis of insects, I [14] and Kato [15] suggested existence of a long G_2 phase extending over larval molt cycles of *Samia cynthia* and *Bombyx mori*, respectively. Recently, Besson-Lavoignet and Delachambre [16] reported the general existence of cells in the epidermis of *Tenebrio molitor* (Coleoptera), in which cells stayed in G_2 except for a brief mitotic period in each instar. Epidermal cells with a long G_2 phase have also been found during the

last larval instar of *Manduca* (Lepidoptera) [17] and pupal stage in *Galleria* (Lepidoptera) [18].

In my previous study [14] as mentioned above, larval epidermal cells of *Samia cynthia ricini* divided in a wave in the middle of the “feeding” phase of the fourth instar not after, but just before synchronous DNA synthesis, suggesting the DNA synthesis for this division occurring in the previous instar and, hence, the existence of cells with a long G_2 phase. If the epidermal cells of *Samia* actually have a long G_2 phase during larval molt cycles, they are comparable to the epidermal cells of *Tenebrio* larvae. In this work, since the physiological significance of a long G_2 is interesting, I confirm that at least a high proportion of cell population in the epidermal cells of *Samia* larvae have a long G_2 phase by studies on their DNA synthesis and mitosis during the third and fourth larval instars.

MATERIALS AND METHODS

Animals Third and fourth (penultimate) instar larvae of *Samia cynthia ricini*, which have been maintained for many generations in this laboratory, were used. They were reared on the leaves of *Ricini communis* at 25°C. Under these conditions, the animals developed very uniformly through an instar stage, when collected within a few hours

after each ecdysis. The third and fourth instars both lasted about 3 days, and consisted of a two-day "feeding" phase and a one-day "pause" phase, during which they remained motionless and a new cuticle was secreted under the old cuticle. The duration of each instar (including the fifth (final) one) and the change of body weight during development are shown schematically in Figure 1.

Injection The animals were anesthetized with ether and test compounds were injected through a 0.25 ml hypodermic syringe with a 0.2 inch needle into a cut made with scissors at the dorso-lateral part in the abdominal third to fourth intersegmental membrane. The wound was then promptly sealed with melted paraffin. [^3H]thymidine (Daiichi Chem. Ltd., 5.0 Ci/mM) as a solution of 500 $\mu\text{Ci}/\text{ml}$ in 0.9% NaCl was injected at a dose of 10 $\mu\text{Ci}/\text{gm}$ body weight. Colchicine (Ciba Pharm. Inc.) was injected as a solution of 500 $\mu\text{g}/\text{ml}$ in 0.9% NaCl at a dose of 10 $\mu\text{g}/\text{gm}$ body weight.

Fixation and sectioning The animals were anesthetized with ether, pinned upside down on a dissection plate, opened along the midventral line, prefixed for 10 min. with FAAW (formaldehyde 2, acetic 1, 70% ethanol 3, and water 3, v/v). The second to fifth abdominal segments were then cut

out and fixed overnight in the same fixative in vials. The fixed materials were dehydrated and embedded in paraffin by the standard procedure. Longitudinal and vertical sections of the dermis including other tissues were cut at 5 μm thickness for autoradiography and 7.5 μm thickness for histological examination. Deparaffinized preparations were stained with Meyer's Haematoxylin-Eosin unless otherwise stated.

Autoradiography Autoradiographs were developed with emulsion (Konishiroku Photo Ind. Ltd.) and exposed for a week in the dark. Sections were stained with Feulgen's solution before dipping or with Haematoxylin-Eosin after autoradiography.

DNA synthesis [^3H]thymidine was injected into groups of three larvae at various times during the third and fourth (penultimate) instars. Ninety minutes later, the animals were killed, fixed and sectioned, and the incorporation of thymidine into tissues of dorso-lateral parts of the second to fifth abdominal segments were determined by autoradiography. Since, almost all radioactivity was found in the nuclei, it seemed to indicate DNA synthesis in the cell. However, [^3H]thymidine incorporation by nuclei decreased intensely with

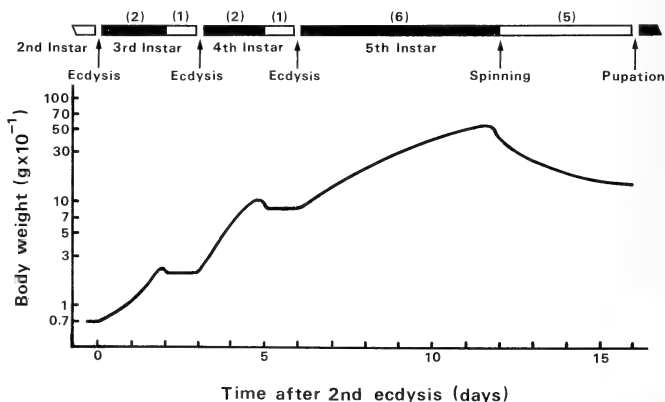


Fig. 1. Durations of various phases of development of *Samia* larvae at 25°C and associated change in body weight. Numbers in parentheses indicate durations in days. Closed bars indicate "feeding" phases and open bars indicate "pause" or "spinning" phases, respectively.

the distance from the injected point, resulting in the highly gradiental patterns of incorporation, which made the quantitative evaluation of results

difficult. Consequently, the ratio of incorporated cells was expressed with symbols rather than actual numbers.

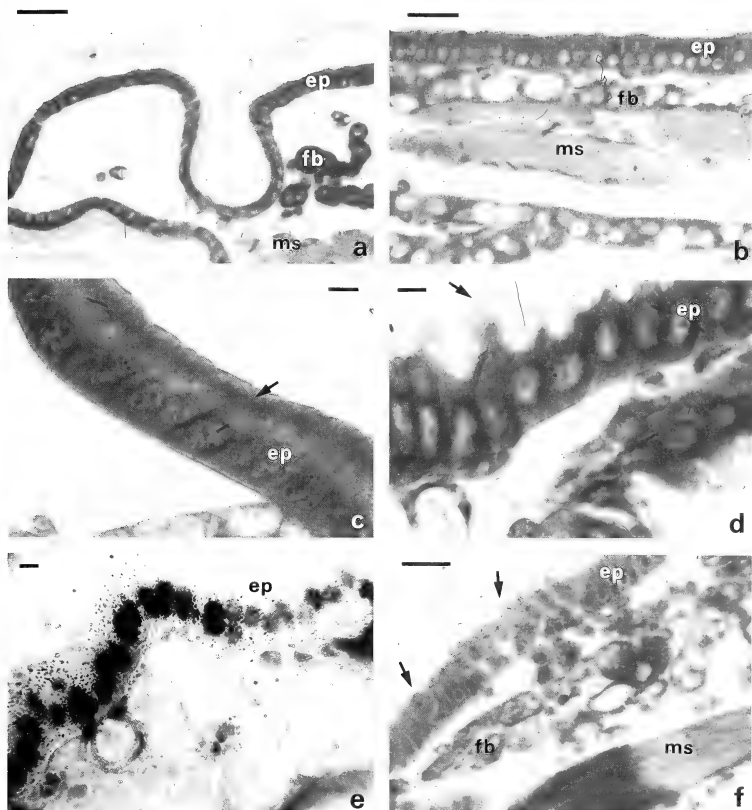


FIG. 2. Longitudinal cross sections of epidermal cells during the 4th-larval instar of *Samia*. a: Immediately after the 3rd ecdysis, the layer of epidermal cells is flattened. b: Early in the middle of the "feeding" phase, the epidermal cells are columnar with basal nuclei. c: At the end of the "feeding" phase, the layer of epidermal cells is thickest and shows a continuous strongly stained band (arrow) on the cuticular side. d: During the "pause" phase, a layer of newly secreted cuticle (arrow) with many folds is seen outside of cells. e: Near the end of the "feeding" phase, many epidermal cells are heavily labelled with $[^3\text{H}]$ thymidine. f: Epidermal cells arrested at metaphase (arrows) by colchicine treatment for 4 hr are slightly displaced from the single layer of cells. All preparations were stained with Haematoxylin-Eosin except (e) (Feulgen Staining). ep: epidermis, fb: fat body, ms: muscle. Bars indicate $10\text{ }\mu\text{m}$ (in c, d, and e) and $50\text{ }\mu\text{m}$ (in a, b, and f), respectively.

Mitosis In the fourth instar, colchicine was injected into groups of three larvae at various times after the third ecdysis, and 4 hours later, the animals were killed, fixed and sectioned, and numbers of metaphase figures in each tissue were scored. The mitotic cells in the epidermis were easily distinguishable from others, as round cells with central condensed chromosomes and no nuclear membrane, that were slightly displaced from the single layer of cells (Fig. 2f). In the third instar, the mitotic frequency was scored as the cells at the metaphase and anaphase of division cycle without colchicine treatment, in the same preparations as used for determination of DNA synthesis.

RESULTS

Histological changes of epidermal cells during larval instars

The histological changes of epidermal cells during the fourth larval instar were examined. The histological changes during the two-day "feeding" phase and one-day "pause" phase were as follows.

Early "feeding" phase Immediately after the third ecdysis, epidermal cells were small and were arranged in a single flattened layer just beneath the cuticle (Fig. 2a). Subsequently they gradually increased in size and became taller and columnar.

Middle "feeding" phase The cells became larger and more columnar with nuclei located near the basement membrane (Fig. 2b). Then they temporarily lost columnar nature and became slightly piled up each other here and there in the layer, possibly reflecting cell movement associated with mitotic events (see below).

Late "feeding" phase The epidermal cells became much larger and more columnar. Then a more densely stainable region appeared first around the nuclei situating near the basement membrane and later toward the cuticular side of the cells. Finally, the densely stained regions of neighboring cells joined forming a band just beneath the cuticle (Fig. 2c). This stainable region of the cells and its movement to the cuticular side seemed to reflect the synthesis of new cuticular material and preparation for its secretion.

"Pause" phase A thin layer of newly secreted

cuticle began to appear outside the cells under the old cuticle, which had already detached from the cells (apolysis). The new cuticular layer and, hence, the cell membrane just beneath it, had many folds, apparently in preparation for enlargement of the body during the next instar (Fig. 2d). This new layer of cuticle gradually thickened with decrease in the stainable region of the cells. The cells themselves also gradually became smaller and flattened. At the last of this phase, the size and features of the epidermal cells became similar to those of epidermal cells at the beginning of the instar.

Patterns of changes in DNA synthesis and mitosis of the epidermis and other tissues during the fourth instar

DNA synthesis The results showed that various tissues showed distinct patterns of DNA synthesis during the instar (Table 1). In some tissues thymidine was incorporated only in specified periods of the instar, while in other tissues, it seemed to be incorporated continuously throughout the instar. Moreover among tissues in which DNA synthesis was restricted to a certain period, the time of this period differed: the fat body, branched trachea, and abdominal muscle incorporated thymidine mainly in the first-half of "feeding" phase (although the fat body showed some incorporation during the "pause" phase also), whereas the epidermis incorporated thymidine mainly in the last-half and especially toward the end of the "feeding" phase. The midgut and silk gland incorporated thymidine at a nearly constant rate at all times examined, including the "pause".

Detailed examination of the epidermis showed that a little incorporation (into less than 10% of the cells) occurred in the first-half of the "feeding" phase from 12 to 24 hr after ecdysis. The incorporation in this period was, however, seen mainly in cells of the inter-segmental membrane region. In the last-half of the "feeding" phase, more epidermal cells incorporated thymidine: 28, 32, and 36 hr after ecdysis, 10 to 50% of the cells incorporated thymidine, although during this period, most of cells were labelled only lightly. In the last ten hours of the "feeding" phase, 40, 44, and 48 hr after ecdysis, epidermal cells incorpo-

TABLE 1. [^3H]Thymidine incorporation into various tissues and mitotic frequency in the epidermis of *Samia cynthia ricini* at various times during the fourth instar^a

Tissue	Time after 3rd ecdysis (hours)													
	4	8	12	16	20	24	28	32	36	40	44	48	52	56
"feeding" ^a / "pause".....													
Epidermis	-	-	±	+	+	+	+	(++)	(+++)	+++	+++	+++	-	-
Mitosis (%) ^b		0		4		14	24	14	4		0			0
Fat body	-	+	++	++	+	(+)	(+)	±	-	-	-	-	-	+
Trachea	-	+	+++	++++	++++	++++	++++	(+)	(+)	(±)	(±)	-	-	-
Muscle	+++	++++	++++	++++	++++	++++	++++	(+++)	-	-	-	-	-	-
Midgut	++	++	++	++	++	++	++	+	+			++	+	+
Silk gland	++	++	++	++				+	+			++	+	+

^aResults are based on the proportion of cells with incorporated [^3H]thymidine except those for the midgut and silk gland. Symbols indicate respectively: -; 0%; ±; 0-5%; +; 5-10%; ++; 10-30%; +++; 30-50%; ++++; more than 50% of cells with incorporated [^3H]thymidine. Symbols in parenthesis show the cells labelled only lightly with isotope. In the midgut and silk gland, symbols indicate the percentage area in which isotope was incorporated in the large nucleus.

^bNumbers represent percentages of metaphase figures accumulated after colchicine treatment for 4 hours.

rated thymidine most actively: at least 30%, and at most more than 80% of the cells were heavily labelled with radioactivity (Fig. 2e). This active incorporation of thymidine into the epidermis stopped abruptly as the animals entering the "pause", and thereafter no incorporation was seen for one day.

Mitosis The results in Table 1 show that mitosis in the epidermis occurred as an enough frequent wave with a maximum in about the middle of the "feeding" phase or 16 to 36 hr after ecdysis: 16, 24, 28, 32, and 36 hr after ecdysis, 4, 14, 24, 14, and 4%, respectively, of the cells were arrested in metaphase by colchicine treatment for 4 hr (cumulatively, the mitotic cells in the wave amounted to at least 68% of the cells), and no mitoses were seen in other periods of the instar. Unexpectedly, this mitotic wave was just before the period of the most active DNA synthesis in the epidermis, which occurred 40 to 48 hr after ecdysis. Although DNA synthesis was seen also before or during the mitotic wave in some epidermal cells, either the proportion of these cells was small (less than 10% of heavily labelled cells of the total cells) or the extent of thymidine incorporation was yet low (in 10 to 50% of the cells, but labelled only lightly). Thus, in most epidermal cells, the period of mitosis seemed to occur before that of DNA synthesis in the instar. In other tissues, such as the fat body,

muscle, and trachea, mitosis was seen in about the middle of "feeding", but occurred after DNA synthesis in these tissues (data not shown).

Considering the cyclical growth of tissues and cells during larval instars, a similar inverted relation between DNA synthesis and mitosis in the epidermis may be expected in the third instar. Then the DNA synthesis for the mitotic wave in the middle of the "feeding" phase in the fourth instar may occur in the third instar. If this is so, the cell cycle of the epidermis of *Samia* may have an unusually long pre-mitotic (G_2) phase (about 48 hr) and a relatively short post-mitotic (G_1) phase. To test this possibility, I examined the temporal patterns of DNA synthesis and mitosis during the third instar.

Temporal patterns of DNA synthesis and mitosis in the epidermis and other tissues during the third instar

DNA synthesis Results showed that the patterns of incorporation of [3 H]thymidine into various tissues were similar to those in the fourth instar (Table 2). Also in this stage, the epidermis showed the incorporation mainly in the last-half of "feeding" phase, most actively at the last 10 hr of it.

Mitosis As in the fourth instar, epidermal cells in the third instar divided as a wave during the

TABLE 2. [3 H]Thymidine incorporation and mitotic frequency of various tissues of *Samia cynthia ricini* at various times during the third instar

Tissue	Time after 2nd ecdysis (hours)								
	"feeding" -----								/"...pause"...
	6	12	18	24	30	36	42	48	54
Epidermis	—	—	+	(++)	(+++)	++++	+++++	+	—
Mitosis (%) ^a	0	0.1	0.8	1.7	2.3	0.4	—	0	—
Fat body	+	+++	(+)	(±)	—	—	—	—	+
Mitosis (%)	0	0.1	0.2	0.4	0.3	0.1	—	0	—
Trachea	—	++	++++	(+++)	(++)	—	—	—	—
Mitosis (%)	0	0.4	0.5	2.0	1.9	0.4	—	0	—
Muscle	+++++	+++++	(++)	(+)	(±)	—	—	—	—
Mitosis (%)	0	0.1	0.1	0.1	0.7	0.7	—	3.3	—
Midgut	++	+++	+++	++	++	++	++	++	++

^aNumbers represent percentages of mitotic (metaphase and anaphase) cells in tissues without colchicine treatment. Other explanations are as for Table 1.

middle of the "feeding" phase, before the period of most active DNA synthesis, and no cell division was seen at other times during the instar (Table 2). The frequency of mitosis in the wave cannot be compared directly to that in the fourth instar, because the frequency in the third instar was measured without the accumulation of mitotic cells by colchicine treatment contrary to that in the fourth instar and we have few informations about the mitotic time of insect cells necessary for the comparison of values between the two instars. It is, however, notable, that, except for the actual size, the features and time of presence of the wave in the third instar are similar to those in the fourth instar.

Cells of the fat body, trachea and muscle also divided in the middle of the "feeding" phase (although the muscle cells divided somewhat later than in the fourth instar), and cell divisions in these tissues occurred after DNA synthesis as in the fourth instar. In the midgut, no mitotic cells were found throughout the instar: the tissues seemed to grow through endoreduplication throughout the larval most cycle.

Thus similar patterns of DNA synthesis and mitosis in various tissues were found in the third and fourth instars. In both instars, the mitotic wave occurred just before synchronous DNA synthesis in the epidermis. This suggests that the DNA synthesis for the mitotic wave in the fourth instar occurred in the third instar.

Relation between the times of DNA synthesis and mitosis of epidermal cells during larval molt cycles

If DNA synthesis for mitosis of the epidermis in the fourth instar occurs in the third instar, [^3H]thymidine injected into the third instar larvae should be detected in the mitotic figures seen in the fourth instar, whereas [^3H]thymidine injected before the mitotic wave in the fourth instar should not be detected in mitotic figures in the fourth instar.

Fifteen larvae in the third instar, 44 hr after the second ecdysis, were used to examine this hypothesis. Nine larvae were promptly given an injection of [^3H]thymidine. When they entered the fourth instar, three larvae each were treated with colchicine at an appropriate time during the mitotic period, and killed two hours later. After fixation and sectioning, incorporation of [^3H]thymidine in arrested metaphase figures in the epidermis was examined.

Groups of 3 of the other 6 larvae that were not treated with [^3H]thymidine during the third instar were treated with [^3H]thymidine two or three times at 6 hr intervals from 14 to 26 hr after ecdysis in the fourth instar. Six hours after the last injection, they were treated with colchicine, and two hours later were killed for examination of [^3H]thymidine incorporation into metaphase figures in the epidermis and other tissues.

The experimental scheme and its results are

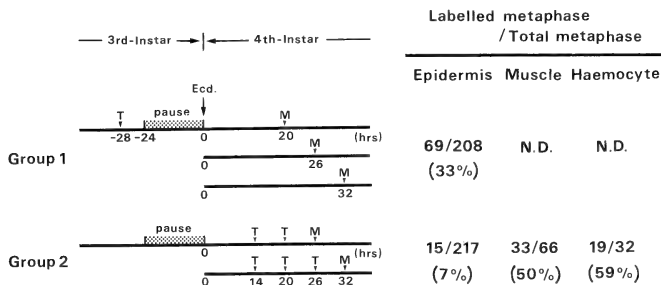


FIG. 3. Experimental design for thymidine labelling of metaphase figures and results. T: Time of thymidine injections. M: Time of counting of labelled metaphase after treatment with colchicine for two hours.

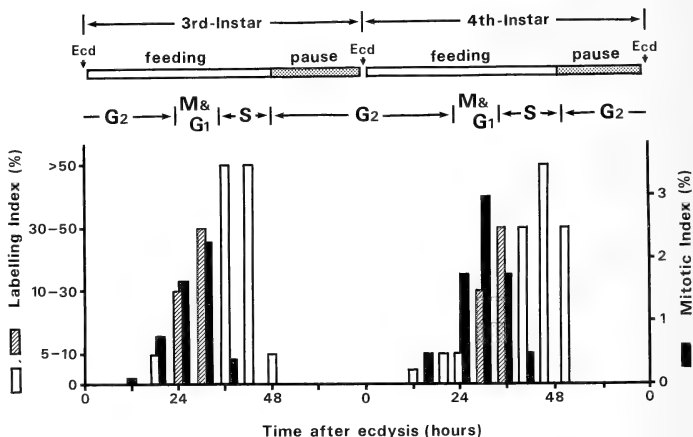


FIG. 4. Schematic representation of DNA synthetic and mitotic frequencies of epidermal cells during the 3rd and 4th instars. Data are from Table 1 and 2. Hatched and open bars indicate the labelling index with $[^3\text{H}]$ thymidine; hatched bars show only light labelling in most cells while open bars show heavy labelling of cells. Closed bars indicate the mitotic index; values in the 4th instar were tentatively corrected assuming that the mitotic time was 30 min; hence, the frequencies in the 3rd and 4th instars cannot be directly compared with each other.

shown in Figure 3, in which the results at different sampling times in each experimental group were expressed together because of virtually no difference between them. In larvae received only a single injection of $[^3\text{H}]$ thymidine later in the third instar, a high proportion of the epidermal cells at metaphase in the fourth instar were labelled. In contrast, in animals in which $[^3\text{H}]$ thymidine was injected at intervals before the mitotic wave during the fourth instar, few epidermal cells were labelled, although high proportions of muscle cells and hemocytes were labelled.

The above findings indicate that in at least rather high proportions of epidermal cells, DNA synthesis for the mitotic wave in the fourth instar occurs in the third instar. The patterns of DNA synthesis and mitosis in the epidermis in the third and fourth instars are shown schematically in Figure 4. Then, a large portion of cell populations in the epidermis in most larval instars probably have an unusually long G_2 phase (about 48 hr) extending over molt cycles and, possibly, a relatively short G_1 phase

between cell division and DNA synthesis in each instar.

DISCUSSION

The temporal patterns of DNA synthesis in various tissues during larval instars in insects have been investigated in two species of Saturniid silkmoths *Samia cynthia* and *Antheraea polyphemus* [19], in *Bombyx mori* [20] and a cricket *Gryllus bimaculatus* [21], in which many tissues synthesized DNA only during restricted periods of each instar and, on the other hand, other tissues synthesized DNA continuously throughout the instar. The present results are similar to those of Krishnakumaran *et al.* [19] on *Samia cynthia ricini* at the same larval instar. In both studies, tissues such as the epidermis, fat body, muscle, and trachea synthesized DNA only during restricted periods of the fourth instar. However, there were some differences between the two studies: whereas the above four tissues synthesized DNA late in the

instar in their report, the three tissues except for the epidermis synthesized DNA earlier in the instar in the present study. This discrepancy may be due to different durations of the fourth instar (7 days in their report contrary to 3 days in the present study).

The present work showed that at least large proportions of cell populations of *Samia* epidermis have a long G_2 phase (about 48 hr) and, possibly a relatively short G_1 phase in the third and fourth larval instars. The finding are enough comparable to those of the larval epidermis in *Tenebrio* [16]. As to the role of cells with a long or blocked G_2 phase, those in mouse ear epidermis etc., which represent only a small fraction (2–10%) of cells, are thought to be as "ready reserves" of mitotically competent cells for wound healing or regeneration of tissues [17]. The role of long G_2 cells in insects may also be the same as above, as suggested in the imaginal disc of Diptera [11]. However, the proportion of long G_2 cells in the imaginal disc or integumental epidermis of insects seems to be too high only for the function of "ready reserves" of mitotic competent cells for wound healing. Moreover, in *Samia* epidermis, mitosis was not stimulated around wounds made with scissors during a possible G_2 phase (preliminary experiment).

Besson-Lavoignet and Delachambre [16] suggested that a long and blocked in G_2 epidermal cells before synthesis of the pupal cuticle in *Tenebrio* may lengthen the duration between the "covert" differentiation (reprogramming during DNA synthesis) and "overt" differentiation (expression of the new program after mitosis) proposed in "quantal mitosis" theory [22]. If such is the case, the long G_2 phase found in the epidermis even during the third to fourth instar of *Samia*, the duration of which is thought to be little involved in the process of reprogramming, may occur only as preparative events for the following passages.

In general, insect cells with a long G_2 phase are physiologically active during the phase as especially seen in the active secretion of the cuticle in the epidermis, whereas G_2 blocked cells in other animals and plants are physiologically less active. On the other hand, many secretory cells such as mammalian liver, insect fat body, silk glands and salivary glands are known to have high ploidy.

Therefore, the long G_2 (or tetraploid) phase of the larval epidermis of insects including *Samia* may arise from any polyploid advantage associated with the secretion of the cuticle. Moreover, the larval epidermal cells of *Samia* stopped synchronous DNA synthesis abruptly as the animals entered the "pause" phase and immediately began to secrete the new cuticle. This gave me an impression that the cell division of the epidermal cells might be temporarily postponed until the next instar (or, hence, the presence of a long G_2) for the necessity of the urgent secretion of the cuticle. The above two reasons for the existence of long G_2 cell cycle are not exclusive to each other, but could be even cooperative to each other working together, which could make insects develop more efficiently during their larval stages. The epidermal cells of Hemimetabolous insects such as *Oncopeltus* (Hemiptera) [23] and *Scistocerca* (Orthoptera) [13] are known to have normal long G_1 cell cycle, whereas the epidermal cells (including imaginal ones) of Holometabolous insects such as Diptera [10–12], Coleoptera [16], and Lepidoptera [9, 17, 18] have long G_2 cell cycle. Therefore, if the above two reasons are the cases either singly or together, the long G_2 cell cycle in the epidermis of insects may be an evolutionarily more advanced form of development.

ACKNOWLEDGMENT

The author thanks Prof. H. Ishizaki, Faculty of Science, Nagoya University, for constant guidance during this work. He also thanks Prof. Y. Kuroda, National Institute of Genetics, Mishima, for critical reading of the manuscript. This is contribution No.1738 from the National Institute of Genetics, Mishima, Japan.

REFERENCES

- 1 Gelfant, S. (1962) Initiation of mitosis in relation to the cell division cycle. *Exp. Cell Res.*, **26**: 395–403.
- 2 Pederson, J. and Hoffman, J. (1970) G_2 -population cells in mouse kidney and duodenum and their behavior during the cell division cycle. *Exp. Cell Res.*, **59**: 32–36.
- 3 Gelfant, S. (1977) A new concept of tissue and tumor cell proliferation. *Cancer Res.*, **37**: 3845–3862.
- 4 Baguna, J. (1974) Dramatic mitotic response in

- planarians after feeding, and a hypothesis for the control mechanism (1). *J. Exp. Zool.*, **190**: 117-122.
- 5 Campbell, R. D. and David, C. N. (1974) Cell cycle kinetics and development of *Hydra attenuate*. II. Interstitial cells. *J. Cell Sci.*, **16**: 349-358.
- 6 Cameron, I. L. and Bols, N. C. (1975) Effect of cell population density on G₂ arrest in *Tetrahymena*. *J. Cell Biol.*, **67**: 518-522.
- 7 Van't Hof, J. (1966) Experimental control of DNA synthesizing and dividing cells in excised root tips of *Pisum*. *Am. J. Bot.*, **53**: 970-976.
- 8 Zielinska, Z. M. and Grzelakowska, B. (1965) Folate derivatives in the metabolism of insect. I. Mitoses in cells of the follicular epithelium as evoked in *Acantholyda nemoralis* Thoms. by folate and its 4-aminoanalogue. *J. Ins. Physiol.*, **11**: 405-411.
- 9 Löbbecke, E. A. (1969) Autoradiographische Bestimmung der DNS-Synthese-Dauer von Zellen der Flügelimaginalanlage von *Ephestia kühniella* Z. Wilhelm Roux' Archiv., **162**: 1-18.
- 10 Van Der Vant, J. J. L. and Spreij, T. E. (1976) DNA content in imaginal disc cells of *Calliphora erythrocephala* (Meigen). *Neth. J. Zool.*, **26**: 432-434.
- 11 Fain, M. J. and Stevens, B. (1982) Alterations in the cell cycle of *Drosophila* imaginal disc cells precede metamorphosis. *Dev. Biol.*, **92**: 247-258.
- 12 Graves, B. J. and Schubiger, G. (1982) Cell cycle changes during growth and differentiation of imaginal leg discs in *Drosophila melanogaster*. *Dev. Biol.*, **93**: 104-110.
- 13 Fontana, F. (1974) Cytophotometric studies on the nuclear DNA content in somatic tissues of *Sciotocerca gregaria* Forskal (Acrididae: Orthoptera). *Caryologia*, **27**: 73-82.
- 14 Minato, K. (1966) Proliferation of the epidermal cells in the fourth-instar larva of Eri-silkworm. *Jap. J. exp. Morph.*, **20**: 118 (In Japanese).
- 15 Kato, Y. and Oba, T. (1977) Temporal patterns of changes in mitotic frequency in the epidermis and other larval tissues of *Bombyx mori*. *J. Ins. Physiol.*, **23**: 1095-1098.
- 16 Besson-Lavoignet, M. and Delachambre, J. (1981) The epidermal cell cycle during the metamorphosis of *Tenebrio molitor* L. (Insecta Coleoptera). *Dev. Biol.*, **83**: 255-265.
- 17 Dyer, K. A., Thornhill, W. B. and Riddiford, L. M. (1981) DNA synthesis during the change to pupal commitment of *Manduca* epidermis. *Dev. Biol.*, **84**: 425-431.
- 18 Wolbert, P. and Kubbies, M. (1983) The cell cycle of epidermal cells during reprogramming in the pupa of *Galleria*. *J. Ins. Physiol.*, **29**: 787-794.
- 19 Krishnakumaran, A., Berry, S. J., Oberander, H. and Schneiderman, H. A. (1967) Nucleic acid synthesis during insect development. II. Control of DNA synthesis in the *Cecropia* silk worm and other Saturniid moths. *J. Ins. Physiol.*, **13**: 1-57.
- 20 Akai, H. and Park, K. J. (1971) Nucleic acid synthesis in various tissues during the larval molting cycle of *Bombyx mori*. L. (Lepidoptera: Bombycidae). *Appl. Ent. Zool.*, **6**: 63-66.
- 21 Romer, F. and Eisenbeis, I. (1983) DNA content and synthesis in several tissues and variation of molting hormone-level in *Gryllus bimaculatus* DEG (Ensifera, Insecta). *Z. Naturforsch.*, **38c**: 112-125.
- 22 Holtzer, H., Weintraub, H. and Mochan, B. (1972) The cell cycle, cell lineages, and cell differentiation. In "Current Topics in Developmental Biology". Ed. by A. A. Moscona and A. Monroy, Academic Press, New York, pp. 229-256.
- 23 Lawrence, P. A. (1968) Mitosis and the cell cycle in the metamorphic moult of the milkweed bug, *Oncopeltus fasciatus*. A autoradiographic study. *J. Cell Sci.*, **3**: 391-404.

Axopodial Contraction Evoked by Electrical Stimulation and its Ultrastructural Analysis in a Heliozoan *Echinospaerium*

YOSHINOBU SHIGENAKA, KAZUhide YANO¹
and MASAKO IMADA

*Laboratories of Cell Biology, Faculty of Integrated Arts and
Sciences, Hiroshima University, Hiroshima 730, Japan*

ABSTRACT—Certain degree of electrical stimulation (1 V/5 mm, 1 sec, rectangular wave) given by extra-cellularly applied electrodes was found to cause contraction of heliozoan axopodia according to Pflüger's law of polar excitation; the axopodia extending toward the cathode always contracted just when the electricity was turned on, but those toward the anode contracted just when the electricity was turned off. Furthermore, the axopodial contraction induced by electrical stimulation was observed in K^+ -free or Mg^{2+} -free saline solution but not in the Ca^{2+} -free medium or in the presence of Ca^{2+} channel inhibitor such as Mn^{2+} ions. Electron microscopy of the axopodia which contracted by electrical stimulation revealed that the axonemal microtubules often folded at several points because of the omnipresence of contractile tubules (16 to 23 nm in diameter) inside the axopodium. Furthermore, elongated tubular vesicles (35 to 90 nm in diameter) were found to run longitudinally in the axopodium, suggesting that they might be related to the conveyance of excitatory information.

INTRODUCTION

A large and multi-nucleated heliozoan, *Echinospaerium akamae* [1], possesses hundreds of needle-like projections termed axopodia which are radiating from the spherical cell body. By using the axopodia, the organisms catch small-sized protozoans such as *Tetrahymena* and *Chilomonas*, pull them toward the cell body surface, and finally ingest them into the cytoplasm by the process of phagocytosis.

According to Suzaki *et al.* [2], the prey organism adhering to an axopodium is conveyed to the proximal region of axopodium by one of the following two ways or by a combination of them: The first one is termed "axopodial contraction" (2 mm/sec in velocity) and characterized by rapid contraction of the axopodia to convey the prey to the cell body surface. On the other hand, the

second one is termed "axopodial flow", by which the prey attached to an axopodium is transported toward the cell surface by means other than axopodial contraction. In this second case, intra-axopodial particles which are featured by saltatory movement [3-6] also become to demonstrate the one-directional movement toward the proximal end of axopodium.

The above-mentioned axopodial contraction is considered not to be induced only by instantaneous degradation of axonemal microtubules and tension of axopodial membrane. The third contractile elements, X-bodies [7] or recently named contractile tubules [8], are the most important candidate which causes the axopodial contraction. In conjunction with this, localization of calcium has been investigated during axopodial contraction [9] and microtubular disassembly [10]. Thus far, however, the direct evidence of calcium influx resulting in microtubular disassembly or axopodial contraction has not been obtained. At this point, we found that the electrical stimulation could induce the axopodial contraction, which might be attributed to the electrically-induced ex-

Accepted April 11, 1988

Received March 11, 1988

¹ Present address: Sohgo Biomedical Laboratories, Inc., 1361-1 Matoba, Kawagoe-shi, Saitama-ken 350, Japan.

citation of plasma membrane. By using this system, therefore, the present study aimed to know whether or not the axopodial contraction is caused by the calcium influx through the plasma membrane, especially axopodial membrane. As the results, the calcium influx, in addition to intracellular discharge of reserved calcium, was found to be indispensable for inducing the axopodial contraction. Furthermore, electron microscopy revealed that the contractile tubules are running unevenly in the axopodium but in parallel with the axonemal microtubules, and that there are some tubular vesicles which might be related to the conveyance of excitatory information.

MATERIALS AND METHODS

Live samples of a multinucleated heliozoan *Echinopharium akamae* [1] were collected from the reservoir at Yoshinaga cho, Wake-gun, Okayama-ken, Japan by courtesy of Dr. T. Suzuki. They were cultured in 0.01% Knop solution at $22 \pm 1^\circ\text{C}$. Small-sized ciliates and flagellates (*Tetrahymena*, *Chilomonas* and so on) were provided as food organisms. Prior to every experiment, the cultured organisms were washed with a standard saline solution containing 0.2 mM CaCl_2 , 0.2 mM KCl, 0.05 mM MgCl_2 and 1 mM Tris-HCl buffer (pH 7.2).

Ca^{2+} -free, K^+ -free and Mg^{2+} -free saline solutions were examined for their effects on the electrically-induced axopodial contraction. By using Ca^{2+} channel inhibitor such as Mn^{2+} ions [11, 12], moreover, the relationship was examined between calcium channel and the contractility of axopodia.

Prior to experiment, the organisms were maintained in the experimental solutions to make them adapted to the solution. For the electrical stimulation, a specially-devised chamber was used as shown in Figure 1. Two electrodes were made of platinum wire (0.5 mm in diameter) and set in parallel with each other (5 mm in distance). In the midst of this chamber, a heliozoan cell to be tested was put with some quantity of experimental solution and covered with a cover slip. Following that, it was necessary to wait for 5 min or more in order to get fully recovered axopodia. The organism was stimulated by using an electric stimulation appa-

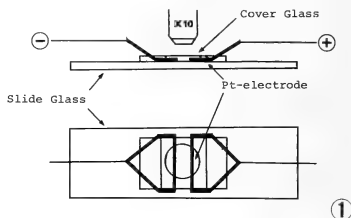


Fig. 1. Schematic figures of the chamber which was used for electrical stimulation. A heliozoan cell was put in the midst of space between the two parallel platinum electrodes.

ratus (Nihon Kohden, MSE-3); some rectangular pulses were employed with the duration of 1 sec and the voltage intensity ranging from 0.1 to 2.0 V at the step of 0.1 V.

For electron microscopy, control and electrically-stimulated (1.0 V/5 mm, rectangular wave, 1 sec) organisms were prefixed for 1 min with 3% glutaraldehyde fixative containing 0.01 mM MgSO_4 , 1 mM sucrose, 0.25 mg/ml ruthenium red and 24 mM cacodylate buffer (pH 7.2), rinsed with the same buffer as in the fixative for 10 min, and post-fixed with 1% OsO_4 fixative containing 0.01 mM MgSO_4 , 1 mM sucrose and 24 mM cacodylate buffer (pH 7.2) for 30 min. Following the post-fixation, the samples were rinsed with the same buffer, dehydrated with a graded series of ethyl alcohol, and embedded into Spurr's low viscosity embedding medium. Ultra-thin sections were prepared by using glass knives loaded onto the ultramicrotome (Proter-Blum, type MT-1), stained doubly with 3% uranyl acetate solution for 10 min and with Reynolds' lead citrate for 3 min. Subsequent observation was made with a transmission electron microscope (JEOL, Type JEM-100S) at the accelerating voltage of 100 kV.

RESULTS

Electrical stimulation was found to induce the axopodial contraction only at the limited range of voltage. In the standard saline solution containing 0.2 mM CaCl_2 , 0.2 mM KCl, 0.05 mM MgCl_2 and 1 mM Tris-HCl buffer (pH 7.2), the axopodial

contraction was evoked only at the stimulation intensity of 0.8 to 1.1 V/5 mm. At the intensity less than 0.8 V/5 mm, any changes of the organisms were not observed. At the intensity more than 1.1 V/5 mm, on the other hand, contraction or severe damage of the cell body was induced without showing axopodial contraction.

When applied by an appropriate electrical stimulation (1.0 V/5 mm, 1 sec, rectangular wave), the heliozoan axopodia were found to contract in accordance to Pflüger's law of polar excitation. That is to say, the axopodia extending toward the cathode always contracted just when the electricity was turned on (Fig. 2), but those toward the anode contracted just when the electricity was turned off. From the analysis of 16 mm cine films, this kind of contraction was shown to finish within 40 msec. Moreover, the axopodia often folded instan-

taneously with such an electrical stimulation as shown in Figure 2b.

Next, the inhibitory effect was examined on the axopodial contraction induced by electrical stimulation (0.8 to 1.0 V/5 mm). In this case, axopodial contraction was checked only at the cathodal side, because the subsequent contraction at the anodal side was considered to be affected by the primarily occurred excitation at the cathodal side. The results are shown in Table 1. In K^+ -free or Mg^{2+} -free saline solution, the axopodial contraction always occurred as well as in the control saline solution (SS) when stimulated electrically. On the other hand, the axopodia did not contract in the case of Ca^{2+} -free or Mn^{2+} -containing SS.

Electron micrographs shown in Figures 3 and 4 are from the organisms fixed just after they were stimulated electrically, demonstrating that the axonemal microtubules were folded at the points indicated by arrows or an arrow-head. In particular, Figure 4 demonstrates the wavy and just disassembling microtubules of axoneme.

When observed the ultra-thin sections of axopodia of a control organism, the bundle of contractile tubules (16 to 23 nm in diameter) is unevenly distributed in the axopodium as shown in a longitudinal (Fig. 5) and a cross (Fig. 6) sections. If these tubules correspond to the true contractile elements of axopodia, the instantaneous contraction of these elements should often bring about the folding of axonemal microtubules because of their omnipresence in the axopodium.

When viewed the longitudinally sectioned axopodia at a higher magnification (Figs. 7, 8), the axonemal microtubules run in parallel with each other and connected tightly by a number of links or bridges, suggesting that they apt to be folded when the axopodia contract. On the other hand, the contractile tubules appeared to be twisted with each other without being linked by bridges. Presumably, this means that the contractile tubules might generate the intensive force as they contract.

In addition to the axonemal microtubules and contractile tubules, the present study has revealed that there are some elongated vesicles or tubules (35 to 90 nm in diameter) which are extending longitudinally along the axopodial axis and sometimes contain various sizes of inclusions as shown

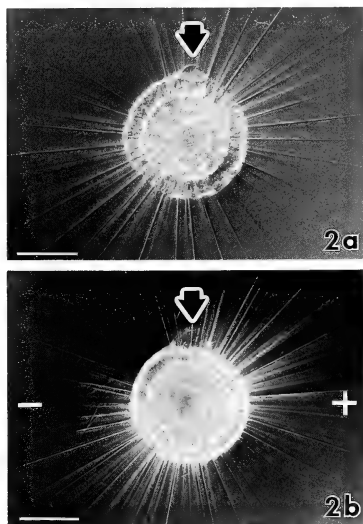


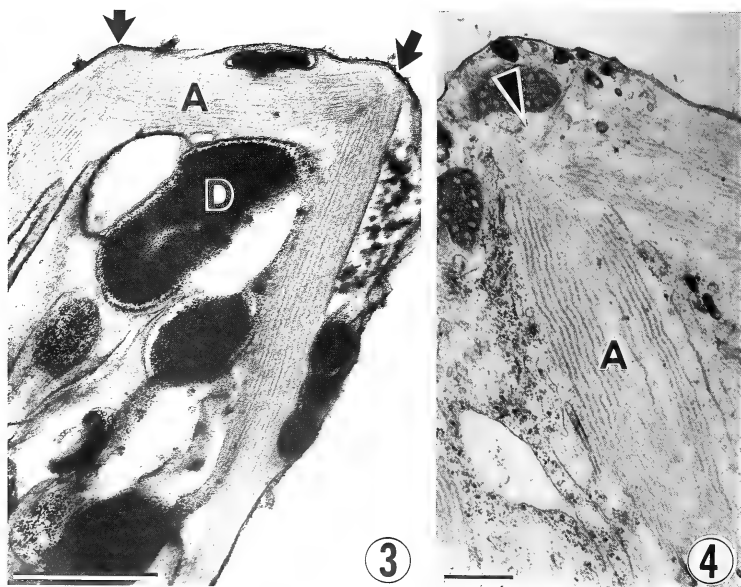
Fig. 2. Light micrographs of a heliozoan *Echinopharium akamae*, showing a control organism (a) and the same one (b) which was stimulated electrically. In b, the picture was taken just when the switch was on. The contractile vacuoles are indicated by arrows. Bar, 100 μ m.

TABLE 1. Effects of various solutions on the axopodial contraction induced by electrical stimulation

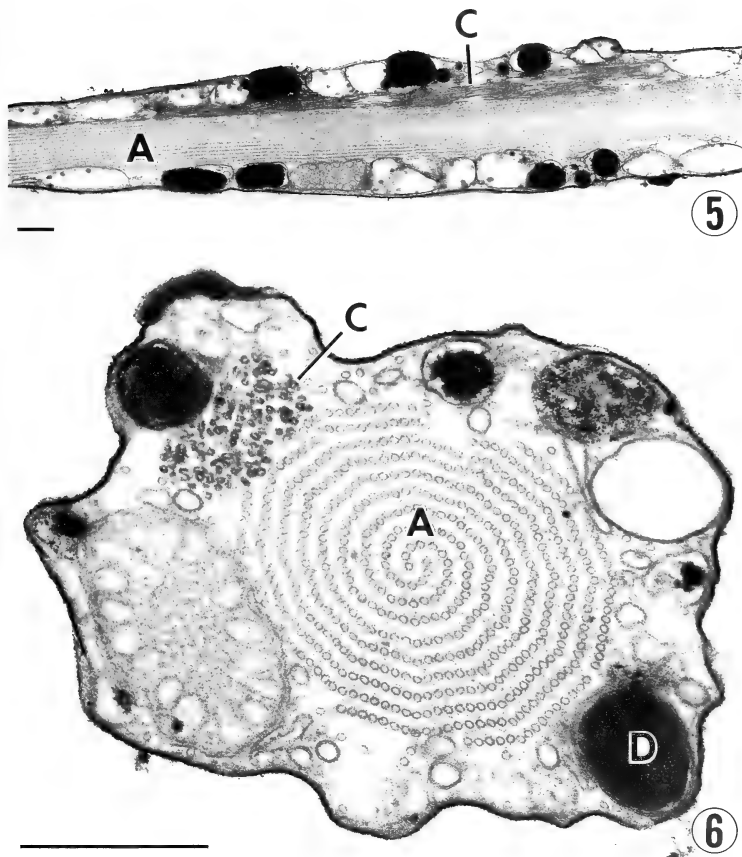
Test solution	Contraction
Standard saline solution (SS)*	+++
K ⁺ -free SS	+++
Ca ²⁺ -free SS	—
Mg ²⁺ -free SS	+++
Mn ²⁺ -containing SS**	—

*Standard saline solution: 0.2 mM CaCl₂, 0.2 mM KCl, 0.05 mM MgCl₂ and 1 mM Tris-HCl (pH 7.2)

**MnCl₂ was dissolved to make 1 mM at the final concentration.



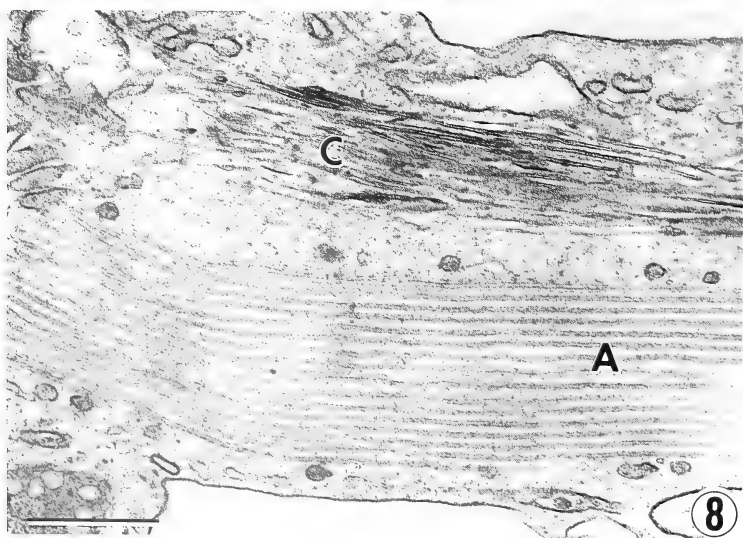
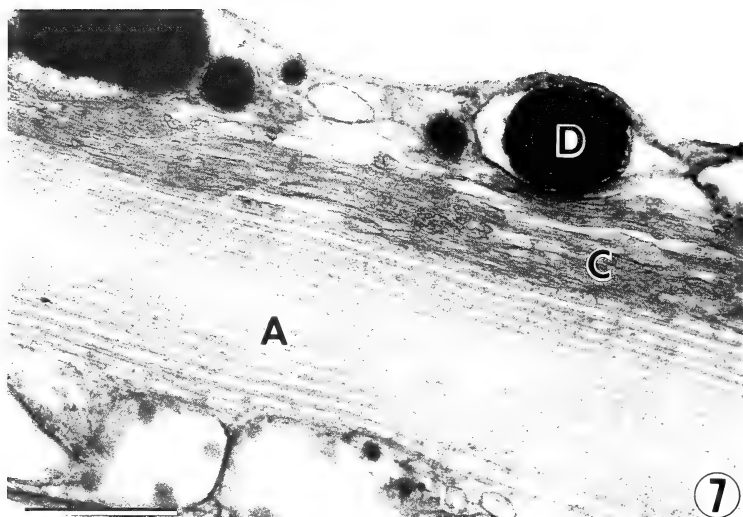
FIGS. 3 and 4. Electron micrographs of the sections through the axonemal microtubules (A) which were folded at the points indicated by arrows or an arrow head. D, an electron-dense body bound by a membrane. Bar, 0.5 μ m.

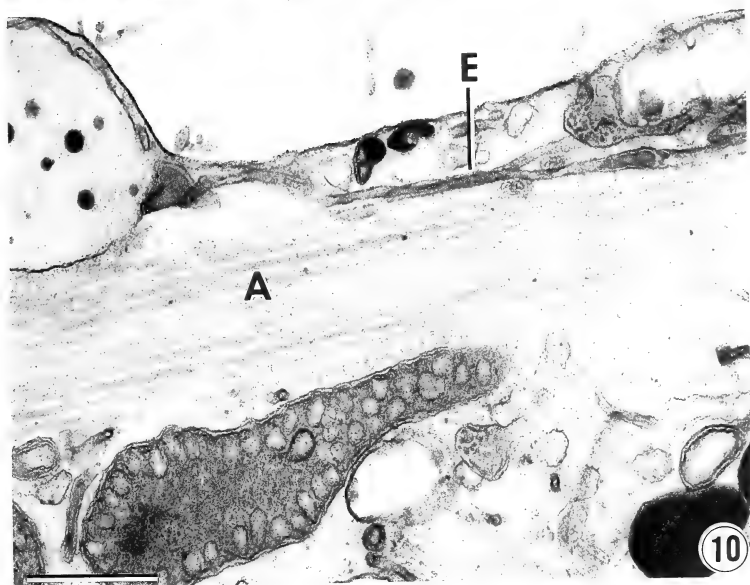
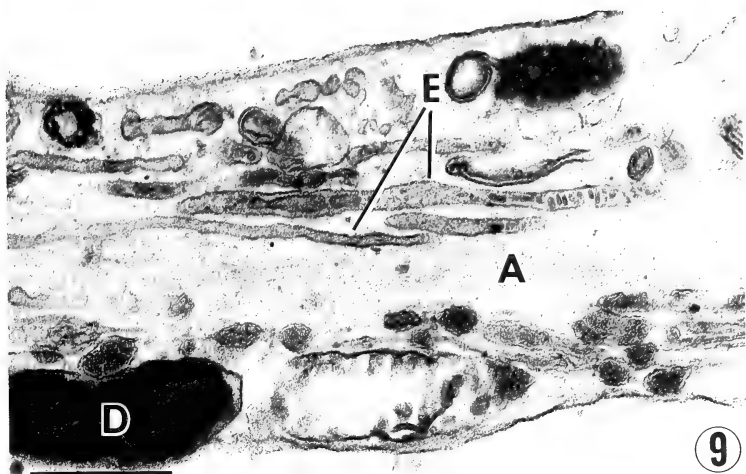


FIGS. 5 and 6. Electron micrographs of longitudinal (Fig. 5) and cross (Fig. 6) sections through the axopodia, showing axonemal microtubules (A), contractile tubules (C) and an electron-dense body (D). Bar, $0.5 \mu\text{m}$.

FIGS. 7 and 8. Electron micrographs of longitudinal sections through the middle (Fig. 7) and proximal (Fig. 8) regions of axopodia, showing axonemal microtubules (A), contractile tubules (C) and an electron-dense body (D). Bar, $0.5 \mu\text{m}$. (in page 50)

FIGS. 9 and 10. Electron micrographs of the longitudinal sections through the middle (Fig. 9) and proximal (Fig. 10) regions of axopodia, showing axonemal microtubules (A), elongated vesicles (E) and an electron-dense body (D). Bar, $0.5 \mu\text{m}$. (in page 51)





in Figures 9 and 10.

DISCUSSION

Up to the present, axopodial contraction has been reported also in other Actinopods such as *Ciliophrys* [13], *Heterophrys* [14] and *Actinophrys* [15]. Davidson [13, 14] has described that the axopodial rapid contraction can be induced also by mechanical stimulation in *Ciliophrys* and *Heterophrys*. In *Actinophrys* and *Echinospaerium*, however, the mechanical stimulation is known not to induce the axopodial contraction [2, 15, 16]. On the other hand, Suzaki *et al.* [2] have suggested that there are chemical receptors which can recognize the prey organisms on the axopodial membrane, because the albumin-coated carmine particles can induce the rapid contraction of axopodia as well as in food organisms.

From the present experiment on the electrical stimulation, the excitation of axopodial membrane can be considered to bring about just when the axopodia contract by the attachment of prey organisms to the axopodial membrane. Probably, the axopodial contraction is dependent on the extracellular Ca^{2+} ions, being attributed to the influx of Ca^{2+} ions through the Ca^{2+} channels of axopodial membrane. Moreover, the Ca^{2+} influx might be accompanied by generation of action potential, because the action potential has already been recognized in *Echinospaerium* by Nishi *et al.* [17].

Jahn [18] has reported that the direct current induces the contraction of protoplasm in various kinds of protozoans, and that the first contraction occurs at anodal side in the most of cases and the degree of this contraction is always larger than that occurred at the cathodal side. As the examples, there are *Paramecium* [19–21], *Spirostomum* [22–24], and *Stentor* and *Blepharisma* [24]. In particular, Etienne [22] has found that the contraction of *Spirostomum* is induced also in Ca^{2+} -free solution, and that the intracellular free Ca^{2+} ions increase in concentration when the organism contracts. From these results, he has concluded that the contraction of *Spirostomum* is attributed mainly to the discharge of Ca^{2+} ions which bind to the intracellular vesicles. In case of the present species, however,

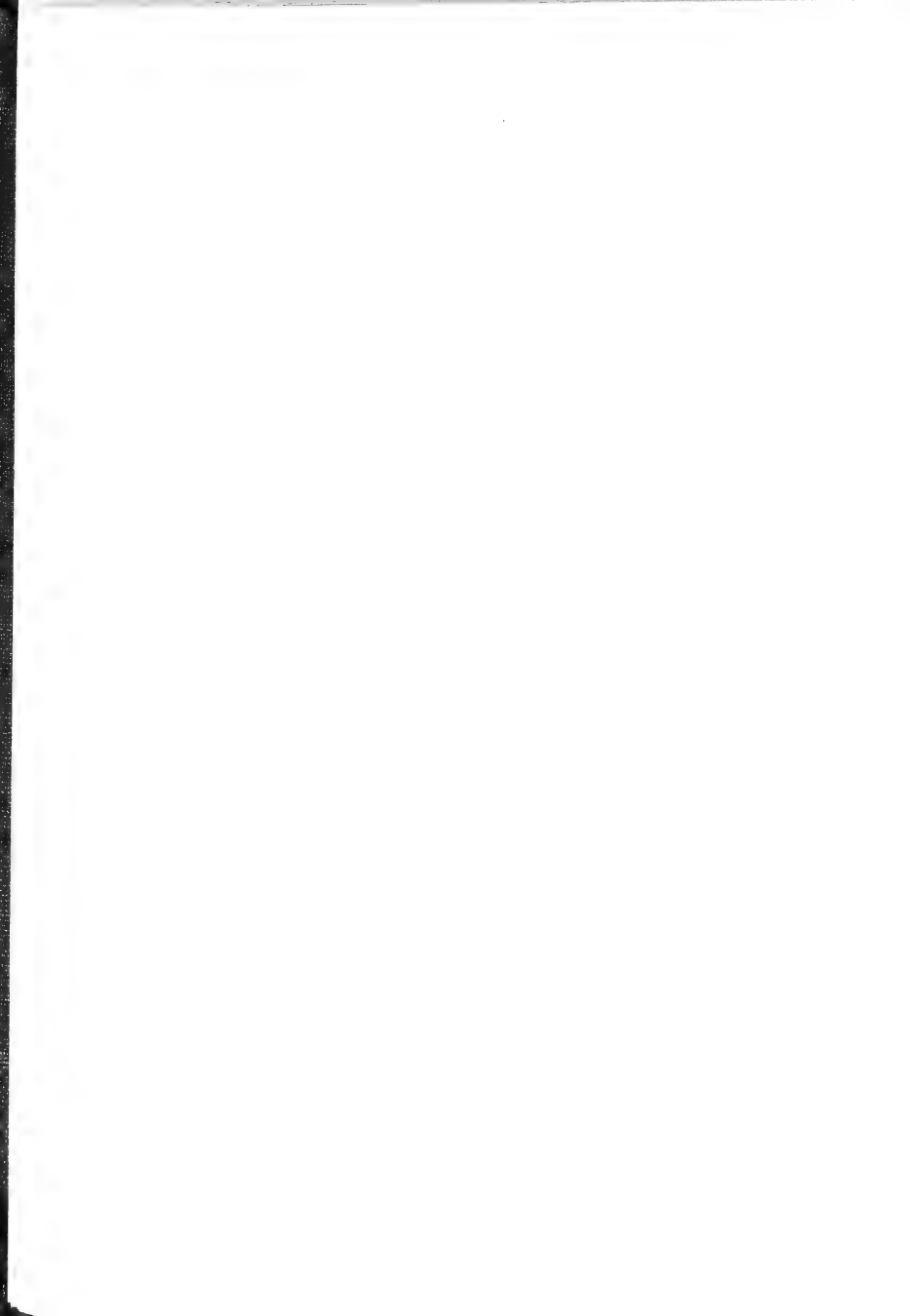
an appropriate electrical stimulation is considered to bring about the excitation of axopodial membrane which results into Ca^{2+} influx through the membrane and subsequent contraction of contractile tubules, although the discharge of Ca^{2+} ions from the intra-axopodial vesicles cannot be neglected as suggested by Matsuoka and Shigenaka [9, 10].

Suzaki *et al.* [2] have considered that the rapid contraction of heliozoan axopodia is not caused simply by disassembly of axonemal microtubules and tension of axopodial membrane, but that the candidate for the contractile elements might be X bodies [7]. Lately the X bodies are renamed contractile tubules by Matsuoka *et al.* [8]. From the present data, the Ca^{2+} influx induced by electrical stimulation is considered to induce the contraction of these contractile tubules directly, resulting into contraction or folding of axopodia. At this moment, the bundle of axonemal microtubules, which is undoubtedly the main cytoskeleton of axopodium, might be enforced to be folded at several points and finally to disassemble probably because of discharge of Ca^{2+} ions.

REFERENCES

- 1 Shigenaka, Y., Watanabe, K. and Suzaki, T. (1980) Taxonomic studies on the two heliozoans, *Echinospaerium akamae* sp. nov. and *Echinospaerium ikachiensis* sp. nov. *Annot. Zool. Japon.*, **53**: 103–119.
- 2 Suzaki, T., Shigenaka, Y., Watanabe, S. and Toyohara, A. (1980) Food capture and ingestion in the large heliozoan, *Echinospaerium nucleofilum*. *J. Cell Sci.*, **42**: 61–79.
- 3 Shigenaka, Y., Watanabe, K. and Kaneda, M. (1974) Degrading and stabilizing effects of Mg^{2+} ions on microtubule-containing axopodia. *Exp. Cell Res.*, **85**: 391–398.
- 4 Edds, K. T. (1975) Motility in *Echinospaerium nucleofilum*. I. An analysis of particle motions in the axopodia and a direct test of the involvement of the axoneme. *J. Cell Biol.*, **66**: 145–155.
- 5 Troyer, D. (1975) Possible involvement of the plasma membrane in saltatory particle movement in heliozoan axopods. *Nature*, **254**: 696–698.
- 6 Suzaki, T. and Shigenaka, Y. (1982) Intra-axopodial particle movement and axopodial surface motility in *Echinospaerium akamae*. In "Biological Functions of Microtubules and Related Structure". Ed. by H. Sakai, H. Mohri and G. G. Borisov,

- Academic Press, Tokyo, pp. 91-103.
- 7 Shigenaka, Y. and Kaneda, M. (1979) Studies on the cell fusion of heliozoans. IV. An electron microscopical study on the fusion process accompanied with axopodial degradation. *Annot. Zool. Japon.*, **52**: 28-39.
 - 8 Matsuoka, T., Shigenaka, Y. and Naitoh, Y. (1985) A model of contractile tubules showing how they contract in the heliozoan *Echinospaerium*. *Cell Struct. Funct.*, **10**: 63-70.
 - 9 Matsuoka, T. and Shigenaka, Y. (1984) Localization of calcium during axopodial contraction in heliozoan, *Echinospaerium akamae*. *Biomed. Res.*, **5**: 425-432.
 - 10 Matsuoka, T. and Shigenaka, Y. (1985) Calcium localization during microtubular disassembly in heliozoan cells. *J. Electron Microsc.*, **34**: 33-37.
 - 11 Hagiwara, S. and Nakajima, S. (1966) Differences in Na and Ca spikes as examined by application of tetrodotoxin, procaine and manganese ions. *J. Gen. Physiol.*, **49**: 793-806.
 - 12 Hagiwara, S. and Byerly, L. (1981) Membrane biophysics of calcium currents. *Fed. Proc.*, **40**: 2220-2225.
 - 13 Davidson, L. (1969) The ultrastructure and motile behavior of the marine helioflagellate *Ciliophrys* sp. *J. Protozool.*, **16** (Suppl.): 14.
 - 14 Davidson, L. (1973) Contractile axopodia of the centrohelidan heliozoan *Heterophrys marina*. *J. Cell Biol.*, **59**: 71a.
 - 15 Ockleford, C. D. and Tucker, J. B. (1973) Growth, breakdown, repair, and rapid contraction of microtubular axopodia in the heliozoan *Actinophrys sol*. *J. Ultrastruct. Res.*, **44**: 369-387.
 - 16 Kitching, J. A. (1960) Responses of the heliozoan *Actinophrys sol* to prey, to mechanical stimulation, and to solutions of proteins and certain other substances. *J. Exp. Biol.*, **37**: 407-416.
 - 17 Nishi, T., Kobayashi, M. and Shigenaka, Y. (1986) Membrane activity and its correlation with vacuolar contraction in the heliozoan *Echinospaerium*. *J. Exp. Zool.*, **239**: 175-182.
 - 18 Jahn, T. L. (1966) Contraction of protoplasm. II. Theory: Anodal vs. cathodal in relation to calcium. *J. Cell. Physiol.*, **68**: 135-148.
 - 19 Hisada, M. (1952) Induction of contraction in *Paramecium* by electric current. *Annot. Zool. Japon.*, **25**: 415-419.
 - 20 Kamada, T. and Kinoshita, H. (1945) Protoplasmic contraction of *Paramecium*. *Proc. Japan Acad.*, **21**: 349-358.
 - 21 Miller, D. M., Jahn, T. L. and Fonseca, J. R. (1968) Anodal contraction of *Paramecium* protoplasm. *J. Protozool.*, **15**: 493-497.
 - 22 Ettienne, E. M. (1970) Control of contractility in *Spirostomum* by dissociated calcium ions. *J. Gen. Physiol.*, **56**: 168-179.
 - 23 Jones, A. R., Jahn, T. L. and Fonseca, J. R. (1966) Contraction of protoplasm. I. Cinematographic analysis of the anodally stimulated contraction of *Spirostomum ambiguum*. *J. Cell. Physiol.*, **68**: 127-134.
 - 24 Jones, A. R., Jahn, T. L. and Fonseca, J. R. (1970) Contraction of protoplasm. III. Cinematographic analysis of the contraction of some heterotrichs. *J. Cell. Physiol.*, **75**: 1-8.



A Comparative Study of 40S Ribosomal Proteins in *Artemia salina* and Rat Liver: Peptide Analysis by Limited Proteolysis and Sodium Dodecyl Sulfate Acrylamide Gel Electrophoresis

NAOYA KENMOCHI¹ and KIKUO OGATA²

Department of Biochemistry, Niigata University
School of Medicine, Niigata 951, Japan

ABSTRACT—Forty-S ribosomal proteins of *Artemia salina* were compared with those of rat liver by using a convenient method for peptide mapping of proteins. Cyanogen bromide, α -chymotrypsin and papain were used as cleavage reagents for peptide mapping. The cleavage products were analyzed by sodium dodecyl sulfate (SDS) polyacrylamide gel electrophoresis and the pattern of peptide fragments of *Artemia* ribosomal proteins were compared with those of rat liver. There were some similarities between the peptide patterns of *Artemia* and rat liver in 8 out of 12 ribosomal proteins examined (S2, S4, S6, S7, S8, S9, S20 and S23), and 5 of those proteins (S2, S4, S6, S7 and S8) were very similar. Although this method has some limitations when it comes to analyzing homology between distinct proteins, the results suggest that some 40S ribosomal proteins are highly resistant to the evolutionary changes from *Artemia salina* to rat liver.

INTRODUCTION

Eukaryotic ribosomes contain about 70 species of structural proteins and the proteins are generally well conserved during evolution. Delaunay *et al.* [1], using two-dimensional gel electrophoresis, showed that the proteins were conserved among mammals, birds and reptiles. More careful analyses of the proteins on two-dimensional gel slabs by Ramjoué and Gordon [2], however, indicated that 7 proteins in 40S subunits and 17 in 60S subunits of rat liver were different from those of chick liver. Kuter and Rodgers [3] compared the electrophoretic patterns of ribosomal proteins from HeLa, Syrian, chick embryo and Novikoff hepatoma cells

on two-dimensional gel slabs and showed that approximately 10 chick specific proteins exist. In our previous study on ribosomal proteins of *Artemia salina* [4], 40S and 60S ribosomal basic proteins were identified and compared with those of rat liver using two-dimensional gel electrophoresis. There were some differences between the proteins of the two species, although ribosomal proteins were more conservative than most other proteins during evolution. We showed a correspondence between most individual 40S proteins of *Artemia salina* and those of rat liver. On the other hand, it was rather difficult to show a correspondence between the 60S proteins of the two species. But among all the proteins analyzed, only the S9 spot completely overlapped in both species using two different gel systems of two-dimensional gel electrophoresis. Therefore, other methods are required to analyze the individual ribosomal proteins in order to demonstrate a more accurate correspondence between ribosomal proteins of the two species.

Peptide mapping, using either chemical or en-

Accepted May 9, 1988

Received February 16, 1988

¹ Present address and reprint request: Facilities for Comparative Medicine & Animal Experimentation, Niigata University School of Medicine, Niigata 951, Japan.

² Present address: Institute for Gene Expression, Dobashi Kyouritu Hospital, Dobashi 3-1, Matuyama 790, Japan.

zymic degradative techniques, is a valuable tool for establishing structural similarities between polypeptides. Cleveland *et al.* [5] developed a technique for obtaining partial peptide maps of purified proteins by enzymatic digestion. They used three enzyme (chymotrypsin, *Staphylococcus aureus* protease and papain) as cleavage reagents. Subsequently, Lam and Kasper [6] employed three chemical reagents (cyanogen bromide, formic acid and hydroxylamine) and three enzymes (α -chymotrypsin, trypsin and *S. aureus* protease) as cleavage reagents and demonstrated close sequence homology between two phosphoproteins of microsomal membrane. In the present work, we compared 40S ribosomal proteins of *Artemia salina* with those of rat liver by peptide mapping using cyanogen bromide, α -chymotrypsin and papain as cleavage reagents and suggest that some of the 40S ribosomal proteins are highly conserved during evolution.

MATERIALS AND METHODS

Separation of ribosomal proteins of Artemia salina and rat liver 40S subunits

Artemia salina and rat liver 40S ribosomal proteins were prepared as described previously [4, 7]. The proteins in 40S ribosomes were separated by using two-dimensional acrylamide gel electrophoresis in a basic-acidic gel system [8]. After staining the two-dimensional gel slabs with Coomassie brilliant blue, the individual protein spots were cut out and trimmed to a cylindrical shape (4 mm diameter \times 1 mm thick).

Peptide mapping by cyanogen bromide cleavage

According to the method of Lam and Kasper [6], the cylindrical gel pieces which contained individual 40S proteins of *Artemia salina* and rat liver were shaken in 1 ml of 75% formic acid containing 20 mg of cyanogen bromide for 20 hr. The gels were then neutralized by several changes of 1 M Tris and subsequently shaken in 1 ml of buffer containing 3% SDS (w/v), 5% 2-mercaptoethanol (v/v), 20% glycerol (v/v) and 80 mM Tris-HCl, pH 6.8 for 30 min at room temperature. Then the gels were loaded into the sample

wells of a stacking gel and the SDS slab gel electrophoresis containing 18% acrylamide was carried out as described previously [4]. The staining patterns of the peptide fragments with Coomassie brilliant blue were analyzed.

Peptide mapping by enzymatic cleavage

For enzymatic cleavage, 40S ribosomal proteins of *Artemia salina* and rat liver were first labeled with ^{125}I as described previously [4]. Subsequently, the labeled proteins were separated by two-dimensional gel electrophoresis and the labeled spots were cut out from the gels as described above. Partial enzymatic cleavage on SDS gels was carried out according to Lam and Kasper [6]. The cylindrical gel pieces containing labeled 40S proteins were shaken in 1 ml of buffer A consisting of 0.1% SDS, 1 mM EDTA, 20% glycerol and 80 mM Tris-HCl, pH 6.8 for 30 min at room temperature. The gels were loaded into the sample wells of a stacking gel and 20 μl of buffer A containing 20 μg of α -chymotrypsin or 0.3 μg of papain (Worthington Biochemical Corp.) were added to each well. Digestion proceeded in the stacking gel during the subsequent electrophoresis in the SDS slab gel as described above. The gel slabs were dried and exposed to Fuji X-ray film.

RESULTS

Peptide mapping

The basic proteins of *Artemia salina* and rat liver 40S subunits were subjected to two-dimensional acrylamide gel electrophoresis and stained with Coomassie brilliant blue (Fig. 1). The staining patterns of the proteins from the two species were comparable but only the spots of S8 and S9 completely overlapped in the two species. The individual protein spots were cut out from the gel slabs and cleaved chemically or enzymatically followed by SDS slab gel electrophoresis.

For chemical cleavage, cyanogen bromide was used. Since ribosomal proteins had only a small number of methionine residues that were cleavage sites of cyanogen bromide, this reagent was suitable as a cleavage reagent only for the peptide mapping of proteins with higher molecular weights

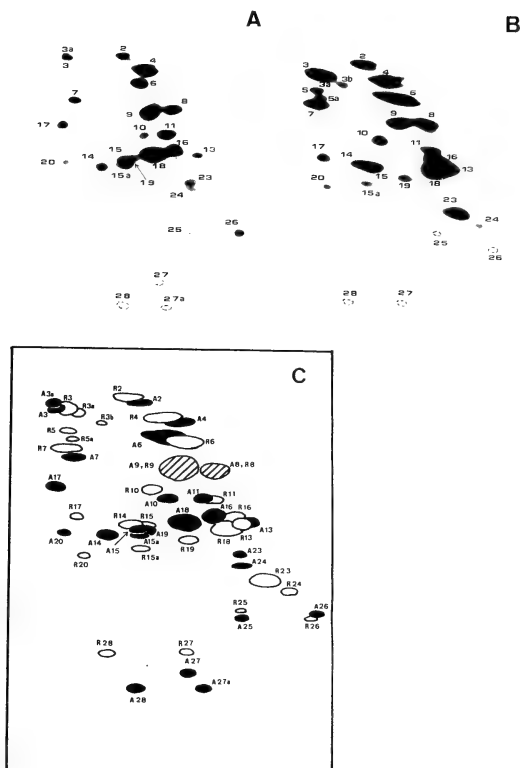


Fig. 1. Two-dimensional gel electrophoretograms of *Artemia salina* and rat liver 40S proteins. The electrophoretic conditions were according to Lastick and McConkey [8]. A, *Artemia* 40S proteins; B, rat liver 40S proteins; C, scheme of a two-dimensional gel electrophoretogram of a mixture of 40S proteins of both species. In A and B, the dotted circles represent faint spots. In C, the solid circles represent *Artemia* proteins (initial A), the open circles represent rat liver proteins (initial R), and the hatched circles represent overlapping spots in *Artemia* and rat liver on a two-dimensional gel.

(>25,000 daltons). For enzymatic cleavage, relatively large amounts of α -chymotrypsin and papain were used. When the enzymatic cleavage products were electrophoresed and stained with Coomassie brilliant blue, spots of the enzyme interfered with analyses of the peptide patterns.

So ^{125}I -labeled ribosomal proteins were used and the cleavage products were analyzed by autoradiography. Papain or α -chymotrypsin was suitable not only for peptide mapping of ribosomal proteins of high molecular weight but also for those of low molecular weight since these enzymes

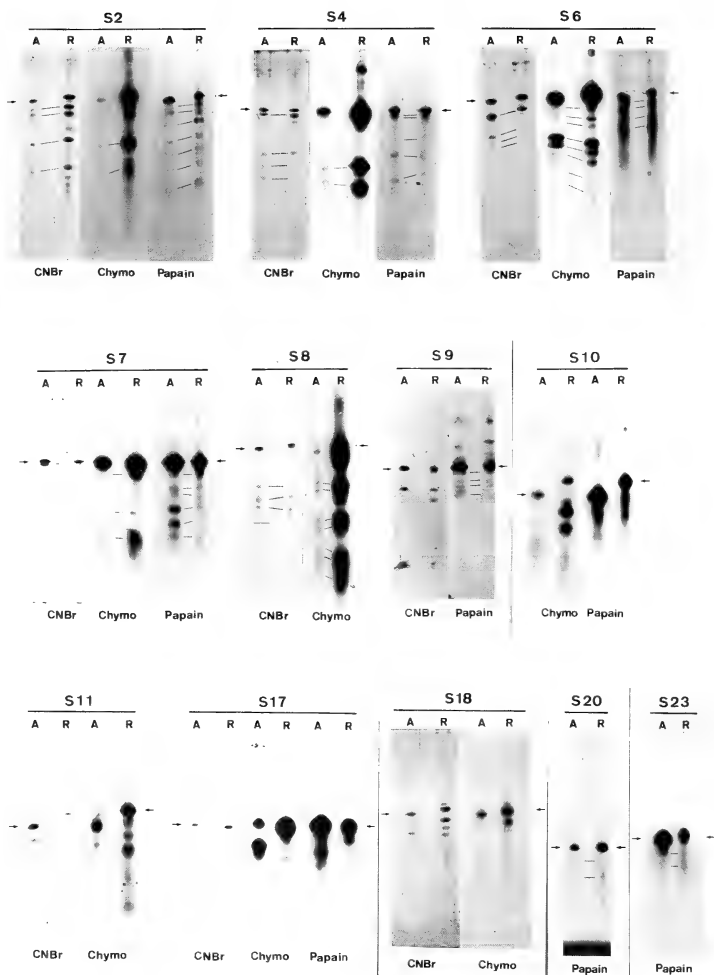


FIG. 2. Peptide maps comparing *Artemia salina* and rat liver 40S proteins. The individual 40S proteins were cut out from a two-dimensional gel and cleaved by cyanogen bromide (CNBr), α -chymotrypsin (Chymo), or papain as described in MATERIALS AND METHODS. A and R represent *Artemia* and rat liver proteins, respectively. The arrows show the position of the uncleaved protein. Pairs of cleaved products which probably correspond in the two species are indicated by dotted lines.

had more cleavage sites in ribosomal proteins as compared with cyanogen bromide. Peptide fragments were detected with a high degree of sensitivity by the use of autoradiography, although a considerable amount of undigested protein remained (Fig. 2).

Comparisons of individual 40S proteins of Artemia salina and rat liver

In S2 and S4, the patterns of the peptide fragments cleaved by cyanogen bromide, α -chymotrypsin or papain were very similar in both species. In S6, which is considered to have a significant role in protein synthesis because rat liver S6 was phosphorylated [9, 10] or cross-linked to mRNA in polysomes [11], the patterns of the peptide fragments were comparable in the two species but were less similar than that of S2 or S4. These results may have reflected a slight difference in the molecular weight of S6; i.e., 29,000 for *Artemia salina* and 31,000 for rat liver. As for S7, patterns from digestion with α -chymotrypsin or papain were comparable. There was only one

product in the case of cyanogen bromide cleavage since the molecular weight of S7 was low (22,000) compared with the other proteins mentioned above, but the positions of the cleavage product on the SDS gel slab were similar. S8 and S9 of both *Artemia salina* and rat liver completely overlapped on the two-dimensional gel slab (Fig. 1), and the peptide maps of S8 by cyanogen bromide or α -chymotrypsin were comparable in the two species. The large difference in the intensity of the two lanes is due to differences in labeling efficiency. In contrast, the maps of S9 by cyanogen bromide or α -chymotrypsin were not so comparable although their molecular weights were identical to each other [4]. There was no product by cyanogen bromide cleavage for S10, although some similarities were detected in maps by papain cleavage but not in those by α -chymotrypsin. As for S11, located close to each other on the two-dimensional gel slabs (Fig. 1), the peptide maps by cyanogen bromide and α -chymotrypsin cleavage differed in the two species. *Artemia* S11 may not correspond to that of rat liver. In S17, the maps by cyanogen

TABLE 1. Similarities between *Artemia* and rat liver 40S proteins as estimated by peptide mapping analyses. The results of peptide mapping were compared in the two species (Fig. 2) and the extent of correspondence was divided into 4 classes: —, no correspondence in the cleaved products of the two species; \pm , ambiguous correspondence; +, some correspondence pairs; ++, high correspondence (correspondence in size and intensity observed in more than 3 fragments).

	Molecular weight		Correspondence		
	<i>Artemia</i>	Rat liver	CNBr	Chymotrypsin	Papain
S2	29,000	31,000	++	+	++
S4	28,500	28,000	++	+	++
S6	29,000	31,000	+	++	+
S7	22,000	22,000	+	+	+
S8	25,000	27,000	+	+	n.d.*
S9	23,000	23,000	\pm	n.d.	+
S10	17,000	19,000	n.d.	—	\pm
S11	16,000	19,000	—	—	n.d.
S17	17,000	16,000	—	\pm	\pm
S18	17,000	17,000	—	—	n.d.
S20	14,500	14,500	n.d.	n.d.	+
S23	16,000	16,000	n.d.	n.d.	+

*n.d.: not determined

bromide cleavage differed and those by α -chymotrypsin and papain cleavage were ambiguous. The maps by cyanogen bromide and α -chymotrypsin cleavage differed in S18 of the two species but another protein may have contaminated the cylindrical gel piece of rat liver S18 when the spot was cut out from the two-dimensional gel slab. Some similarities in S20 and S23 were observed in peptide maps by papain cleavage. These results mentioned above are summarized in Table I.

DISCUSSION

The results shown in Table I indicate that 5 proteins, S2, S4, S6, S7 and S8 are correspond well and 3 proteins, S9, S20 and S23 are comparable to some extent in the two species. In another experiment, we compared the amino acid compositions of the individual 40S proteins of *Artemia salina* with those of rat liver and found that 10 of them (S2, S3, S4, S6, S7, S8, S15a, S16, S17 and S18) appeared to be strongly related in the two species [12]. These findings demonstrate the conservative properties of ribosomal proteins during the evolution of animal species, especially for 5 proteins, S2, S4, S6, S7 and S8, although further investigation is required for the other proteins in order to reveal an appropriate correspondence.

Recent experiments involving the cDNA sequences of various ribosomal proteins reveal the conservation of ribosomal proteins among different species [13-16]. Although the analyses of cDNA sequences of *Artemia salina* and rat liver ribosomal proteins are considered to be critical to determining the precise correspondence between the two species, it seems impractical at present, especially when a number of organisms are to be compared. Therefore, the peptide mapping analyses presented here is quite convenient and useful in comparing the structural homology between the ribosomal proteins of different species.

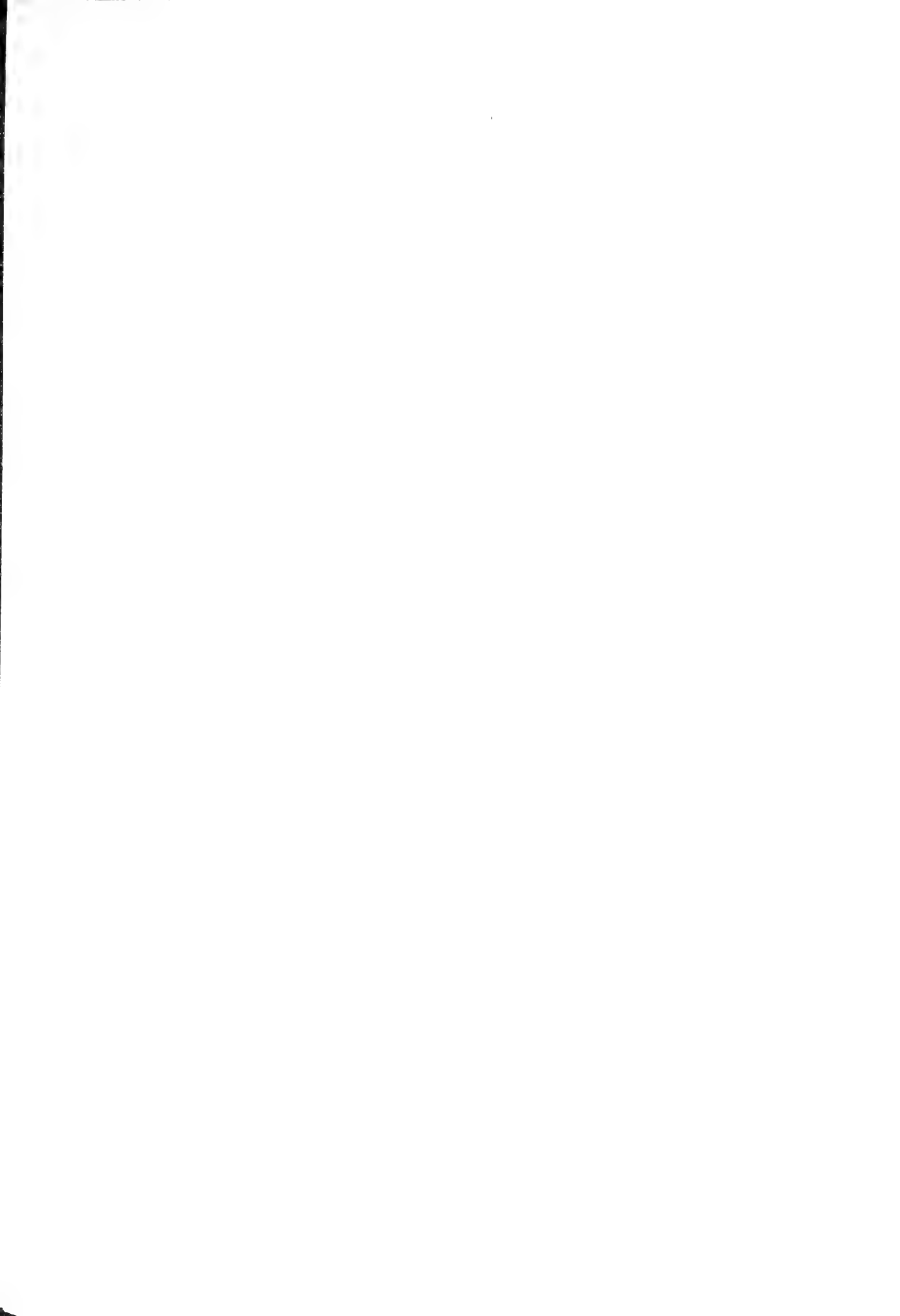
ACKNOWLEDGMENT

We thank Dr. Shoji Odani for his discussions and critical reading of this manuscript.

REFERENCES

- 1 Delaunay, J., Creusot, F. and Schapira, G. (1973) Evolution of ribosomal proteins. *Eur. J. Biochem.*, **39**: 305-312.
- 2 Ramjoué, H.-P. R. and Gordon, J. (1977) Evolutionary microdivergence of chick and rat liver ribosomal proteins. *J. Biol. Chem.*, **252**: 9065-9070.
- 3 Kuter, R. L. and Rodgers, A. (1974) Ribosomal protein differences between animal cells. *Exp. Cell Res.*, **87**: 186-194.
- 4 Kenmochi, N., Tsurugi, K. and Ogata, K. (1981) Analyses of 40S and 60S ribosomal proteins of *Artemia salina* with two-or "three-dimensional" acrylamide gel electrophoresis and comparisons with rat liver 40S and 60S proteins. *J. Biochem.*, **89**: 1293-1308.
- 5 Cleveland, D. W., Fischer, S. G., Kirschner, M. W. and Laemmli, U. K. (1977) Peptide mapping by limited proteolysis in sodium dodecyl sulfate and analysis by gel electrophoresis. *J. Biol. Chem.*, **252**: 1102-1106.
- 6 Lam, K. S. and Kasper, C. B. (1980) Sequence homology analysis of a heterogeneous protein population by chemical and enzymic digestion using a two-dimensional sodium dodecyl sulfate-polyacrylamide gel system. *Anal. Biochem.*, **108**: 220-226.
- 7 Terao, K. and Ogata, K. (1975) Studies on structural proteins of the rat liver ribosomes. *Biochim. Biophys. Acta.*, **402**: 214-229.
- 8 Lastick, S. M. and McConkey, E. H. (1976) Exchange and stability of HeLa ribosomal proteins *in vivo*. *J. Biol. Chem.*, **251**: 2867-2875.
- 9 Gressner, A. M. and Wool, I. G. (1974) The phosphorylation of liver ribosomal proteins *in vivo*. *J. Biol. Chem.*, **249**: 6917-6925.
- 10 Thomas, G., Siegmund, M. and Gordon, J. (1979) Multiple phosphorylation of ribosomal protein S6 during transition of quiescent 3T3 cells into early G1, and cellular compartmentalization of the phosphate donor. *Proc. Natl Acad. Sci. USA*, **76**: 3952-3956.
- 11 Takahashi, Y. and Ogata, K. (1981) Ribosomal proteins cross-linked to natural mRNA by UV irradiation of rat liver polysomes. *J. Biochem.*, **90**: 1549-1552.
- 12 Odani, S., Kenmochi, N. and Ogata, K. (1988) A comparative study on 40S ribosomal proteins of *Artemia salina* and rat liver: Micro analysis of amino acid composition by HPLC. *J. Biochem.*, **103**: 872-877.
- 13 Tanaka, T., Kuwano, Y., Ishikawa, K. and Ogata, K. (1985) Nucleotide sequence of cloned cDNA specific for rat ribosomal protein S11. *J. Biol. Chem.*, **260**: 6329-6333.

- 14 Nakanishi, O., Oyanagi, M., Kuwano, Y., Tanaka, T., Nakayama, T., Mitsui, H., Nabeshima, Y. and Ogata, K. (1985) Molecular cloning and nucleotide sequences of cDNAs specific for rat liver ribosomal proteins S17 and L30. *Gene*, **35**: 289-296.
- 15 Tanaka, T., Wakasugi, K., Kuwano, Y., Ishikawa, K. and Ogata, K. (1986) Nucleotide sequence of cloned cDNA specific for rat ribosomal protein L35a. *Eur. J. Biochem.*, **154**: 523-527.
- 16 Tanaka, T., Ishikawa, K. and Ogata, K. (1986) On the sequence homology of the ribosomal proteins, *Escherichia coli* S11, yeast rp59 and Chinese hamster S14. *FEBS Lett.*, **202**: 295-297.



Stimulating Effect of Dimethylsulfoxide on Unfertilized Eggs of the Echiuroid, *Urechis unicinctus*

EIGORO TAZAWA, AKIKO FUJIWARA¹ and IKUO YASUMASU¹

Biological Institute, Faculty of Literature and Science, Yokohama City University,
22-2 Seto, Kanazawa-Ku, Yokohama 236 and ¹Department of Biology,
School of Education, Waseda University, 1-6-1 Nishiwaseda,
Shinjuku-Ku, Tokyo 160, Japan

ABSTRACT—Dimethylsulfoxide (DMSO) stimulated eggs of the echiuroid, *Urechis unicinctus*, to induce fertilization membrane formation. At concentrations of DMSO between 2 and 4%, the number of eggs with fertilization membranes in normal artificial sea water increased in relation to its concentration and at above 5%, almost all eggs (more than 80%) underwent fertilization membrane formation. The stimulating effect of DMSO on echiuroid eggs was enhanced by an incubation in an ice bath. DMSO at 3%, which induced fertilization membrane formation only in about 30% eggs at room temperature, was enough to induce the formation in more than 70% eggs in an ice bath. The concentrations of DMSO to cause fertilization membrane formation were lower in Ca^{2+} free artificial sea water than in normal one. Acid production (pH decrease in external medium), which was induced by insemination, occurred in a short period after DMSO addition. Fertilization membrane formation and acid production caused by DMSO were inhibited, to some extent, by verapamil. DMSO also made the respiration of eggs sensitive to 2,4-dinitrophenol (DNP). This change in the sensitivity of respiration to DNP is also induced in echiuroid eggs following insemination.

INTRODUCTION

It has been demonstrated that dimethylsulfoxide (DMSO) stimulates Friend erythroleukemia cells to induce their cell differentiation [1-5]. This induction of cell differentiation by DMSO has been reported to be due to Ca^{2+} influx [6] or intracellular Ca^{2+} translocation [7] in Friend erythroleukemia cells. It has also been found that DMSO-treatment of sea urchin eggs followed by the cold treatment causes fertilization membrane formation and induction of cyanide-insensitive respiration [8]. Fertilization membrane formation induced by DMSO in sea urchin eggs is inhibited by verapamil, a Ca^{2+} antagonist, but Ca^{2+} in extracellular medium is not necessary for DMSO to stimulate sea urchin eggs [8]. Verapamil is known to block not only Ca^{2+} transport in plasma membrane through Ca^{2+} channels [9] but also Ca^{2+} mobilization in intracellular organelles [10,

11]. Thus, the activation by DMSO of sea urchin eggs seems to depend on DMSO-induced change in intracellular Ca^{2+} localization, which is sensitive to verapamil.

In the present study, we found that echiuroid eggs were activated by DMSO without any incubation in an ice bath, to undergo fertilization membrane formation, acid production, and change in the sensitivity of respiration to an uncoupler of oxidative phosphorylation, 2,4-dinitrophenol, in a similar manner to those activated by sperm [12-14].

MATERIAL AND METHODS

Handling eggs Gametes of echiuroid, *Urechis unicinctus*, were used as materials. Animals were collected at Choshi, Chiba Prefecture, and kept in a temperature-controlled and aerated sea water tank until use. Eggs, as well as sperm, were obtained from the storage organs, which were isolated from the body. Eggs or dry sperm, which were released from the isolated storage

organs, were stored in a Petridish at 4°C until use. The eggs thus stored were washed twice with artificial sea water (ASW) 20 min before use. Eggs thus stored at 4°C were found to be fertilizable at least for two days and were able to develop normally, whereas eggs suspended in natural sea water or ASW and kept at 4°C were fertilizable for one day at most. In the present study, the eggs were used within 4 hr. The results obtained in eggs thus stored for 24 hr were completely the same as obtained in fresh eggs. Otherwise specified, the eggs were suspended in ASW. Eggs were also suspended in Ca^{2+} free artificial sea water (Ca^{2+} free ASW) containing 5 mM glycoetherdiamine-N, N, N', N'-tetraacetic acid (EGTA), after they were washed three times with Ca^{2+} free ASW.

Treatment of eggs with DMSO To 2 ml egg suspension (0.5% v/v) in normal or Ca^{2+} free ASW, DMSO was added to make its final concentrations between 0.5% and 6%. The suspension was usually incubated for 60 min at room temperature (20°C \pm 1.5°C). In some experiments, an incubation of egg suspension in an ice bath was performed following DMSO addition. Incubation was terminated by adding 200 μl of ASW containing 0.5% formaldehyde (v/v) to 2 ml suspension. Another addition of A23187 at final concentration of 10 μM was performed 60 min after DMSO addition and the incubation was terminated 10 min after adding A23187. DMSO addition was also performed in egg suspension containing verapamil (final concentrations: 25–150 μM). Verapamil was added to egg suspension 5 min before DMSO addition and the incubation was terminated 10, 30, 60 and 120 min after DMSO addition. Then, the number of eggs with fertilization membranes was estimated by a light microscope. Verapamil and A23187 were dissolved in DMSO. Concentration of the stock solutions were 60 mM for verapamil and 4 mM for A23187. Final concentration of DMSO, added to egg suspension as the solvent of these compounds, were 0.25% at most, and were lower than those to exert an effect on eggs.

Estimation of pH change Change in pH was estimated by a glass electrode pH meter (Model HM-5A, Toa Electronics Ltd, Tokyo) and

recorder (056 Hitachi Co., Tokyo) equipped with a voltage compensating circuit. The pH change was estimated in 10 ml suspension of unfertilized eggs (5% v/v) in ASW containing 5 mM Tris HCl buffer pH 8.2 (to avoid drastic change in pH). Dry sperm (2 μl) or DMSO was added to an egg suspension of unfertilized eggs and pH change was recorded. The record of pH change caused by adding dry sperm or DMSO was also obtained in egg suspension to which verapamil had been added prior to addition of dry sperm or DMSO. After the estimation of pH change, a known amount of 0.1 N HCl was added for the calibration of the system. In control experiments, changes of pH in suspensions of fertilized eggs (5% v/v) were estimated following the additions of dry sperm, DMSO and verapamil, respectively. Small values of pH change thus obtained in the suspension of fertilized eggs were subtracted from those obtained in unfertilized egg suspensions.

Measurement of the rate of respiration

Concentration of oxygen in 2 ml of 5% egg suspension (v/v) in a closed vessel kept at 20°C was monitored by an oxygen electrode (Yellow Springs Co.) and recorded by a recorder (SP-H6P Rikendenshi Co., Ltd.). From the record obtained, the rate of respiration was calculated. The rate of respiration is expressed as nmole O_2 /min/ml packed egg volume. 2,4-Dinitrophenol (DNP), dissolved in ASW (2 mM), was added to the egg suspension in the closed vessel through a small hole in the stopper with which the vessel was closed. The respiratory rate was estimated 10 min after DMSO addition. DNP addition was performed 10 min after adding DMSO, and the respiratory rate was estimated 1 min after adding DNP. Na-cyanide, dissolved in distilled water (0.1 M), was also added to egg suspension in the same manner to DNP addition.

Reagents Dimethylsulfoxide (DMSO, more than 99.5%) was the product of Pierce Chem. Corp., IL. Verapamil was obtained from Sigma Chem. Corp., MO. 2,4-Dinitrophenol (DNP) and Na-cyanide were purchased from Kanto Chem., Tokyo. Normal and Ca^{2+} free artificial sea water were the products of Jamarin Lab., Osaka.

RESULTS

As shown in Figure 1, dimethylsulfoxide (DMSO) stimulated echiuroid eggs in normal and Ca^{2+} free ASW to induce formation of fertilization membrane. At concentrations of DMSO between 2 and 5%, the percentage of egg which

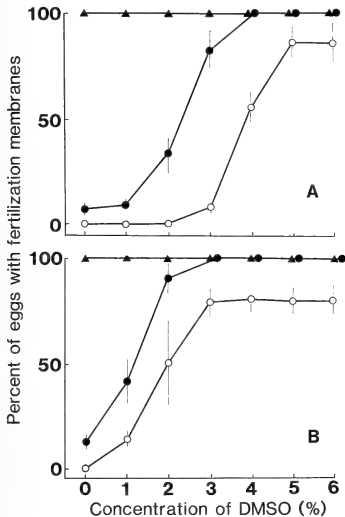


Fig. 1. Stimulating effect of DMSO on echiuroid eggs. Experiments were performed in normal ASW (A) and in Ca^{2+} free ASW (B). Percentages of eggs with fertilization membranes (the activated eggs) were estimated after an incubation for 60 min from the time of DMSO addition at room temperature (about 20°C) (○) and also in an ice bath (●). Another addition of A23187 (10 μM in final concentration) was performed 60 min after DMSO addition and incubated for another 10 min. Percentages of the activated eggs, stimulated by DMSO and the then by A23187, were estimated 70 min after DMSO addition (▲). Without A23187 addition, the percentages of activated eggs 70 min after DMSO addition were the same as observed 60 min after DMSO addition. Each value in the figure is the mean of 3 experiments on egg of different batches. Bar shows standard error of the mean (SEM).

underwent fertilization membrane formation in normal ASW increased in relation to DMSO concentration. The percentages were around 80% at concentrations of DMSO between 5 and 6% (Fig. 1A). About 80% eggs underwent fertilization membrane formation, when DMSO concentration was 12%. These suggest that DMSO exerted the maximum stimulating effects at above 5%. Eggs with fertilization membranes are referred hereafter to the activated eggs. Almost all eggs, which had indentations, became evidently spherical during exposure of them to DMSO at above 2%.

In Ca^{2+} free ASW, DMSO induced formation of fertilization membranes, which were apparently the same in their structures as formed in normal ASW. As shown in Figure 1B, the numbers of the activated eggs obtained by the treatment with DMSO at concentrations between 1 and 4% were larger than in normal ASW. For instance, 3% DMSO induced fertilization membrane formation in about 80% eggs in Ca^{2+} free ASW and less than 30% in normal ASW. DMSO at 2% hardly caused fertilization membrane formation in normal ASW (Fig. 1A) but induced it in appreciable number of eggs in Ca^{2+} free ASW (Fig. 1B). As shown in Figure 1, DMSO exerted maximum stimulating effects on these eggs at concentrations above 3% in the absence of Ca^{2+} and above 5% in its presence. These suggest that external Ca^{2+} in media surrounding eggs is not indispensable and rather inhibitory for DMSO to induce fertilization membrane formation in echiuroid eggs.

In Ca^{2+} free ASW, as well as in normal ASW, a small number of eggs failed to form fertilization membrane, even when they were treated with DMSO at high concentrations that exerted maximum stimulating effects (Fig. 1A and B). Those eggs, which did not respond to DMSO, were able to form the membranes, when another addition of A23187 was performed (Fig. 1).

An incubation of the egg suspension in an ice bath following addition of DMSO made the number of the activated eggs larger than at room temperature (at about 20°C) as shown in Figure 1. The minimum concentrations to exert maximum stimulating effect in the cold were 4% in ASW and 3% in Ca^{2+} free ASW, which were somewhat lower than at room temperature, respectively.

Furthermore, at the concentrations to exert maximum effect in the cold, DMSO treatment was able to activate nearly 100% eggs, though DMSO without the cold treatment was able to induce fertilization membrane formation in about 80% eggs at most. Incubation of eggs in an ice bath made them more sensitive to DMSO.

Without DMSO treatment, an incubation in the cold was found to induce fertilization membrane formation in a small number of eggs (Fig. 1). The same has also been reported in sea urchin eggs [18]. In sea urchin eggs, an incubation in the cold is found to be necessary for DMSO to induce fertilization membrane formation [8]. In this previous paper, we have postulated that the systems to induce fertilization membrane formation in sea urchin eggs, which are stimulated by DMSO, differ from those affected by the cold treatment [8].

Probably, fertilization membrane formation in echiuroid eggs is achieved by activation of both systems in the same manner as in sea urchin eggs. In echiuroid eggs, contribution of DMSO-stimulated systems to fertilization membrane formation seems to be higher than in sea urchin eggs.

As shown in Figure 2, verapamil concentration-dependently caused a delay of fertilization membrane formation in eggs kept in normal ASW at room temperature (Fig. 2A). The same was true in Ca^{2+} free ASW (Fig. 2B). Verapamil also caused a delay of fertilization membrane formation induced by the treatment with DMSO in the cold (Fig. 2C). On the basis of known efficacies of verapamil [10, 11], it is assumed that DMSO stimulate verapamil-sensitive Ca^{2+} mobilization in Ca^{2+} storage organelles to activate echiuroid eggs.

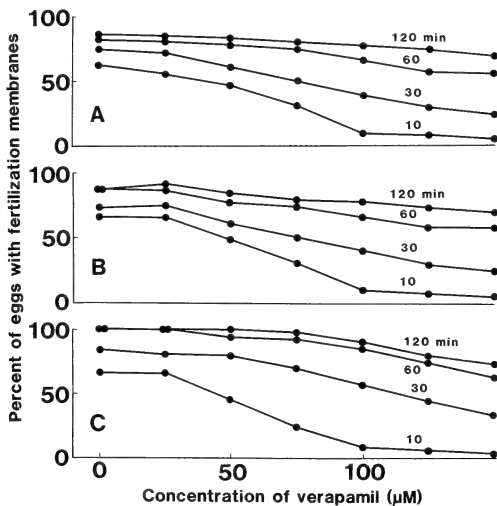


FIG. 2. Inhibitory effect of verapamil on DMSO-induced fertilization membrane formation. Percentages of eggs with fertilization membranes stimulated by DMSO (5%) in normal ASW, shown in A, and in Ca^{2+} free ASW, shown in B, were estimated 10, 30, 60 and 120 min after DMSO addition. Percentages of the activated eggs in normal ASW obtained by 5% DMSO treatment followed by an incubation in an ice bath are shown in C. Verapamil was added 5 min before DMSO addition. The times in min after DMSO addition are shown in the figure. The values shown are typical among 4 experiments on eggs of different batches.

As shown in Figure 3A, an addition of 2 μ l dry sperm to 10 ml egg suspension (5% v/v) kept at 20°C resulted in acid production (pH decrease in external medium). Acid production was turned off within 5 min from the time of sperm addition. At the time when acid production was turned off, less than 30% eggs formed fertilization membranes. DMSO addition (5% in final concentration) to egg suspension, as well as addition of 10 μ M A23187 (data not shown), also caused acid production, which was turned off during the formation of fertilization membranes (Fig. 3B). Acid production, resulting from the stimulation by DMSO, or

by sperm, seems to be evoked prior to the onset of fertilization membrane formation and turned off before the formation is accomplished. As also shown in Figure 3B with dotted line, an addition of 1% DMSO, which did not induce fertilization membrane formation, also caused acid production, even though the rate of acid production was quite low. Acid production is probably induced even in eggs which are insufficiently stimulated by DMSO.

The amount of produced acid and the number of activated eggs increased in relation to DMSO concentrations (Fig. 4). DMSO induced a production of considerable amount of acid even at concentrations lower than 2%, which were not enough

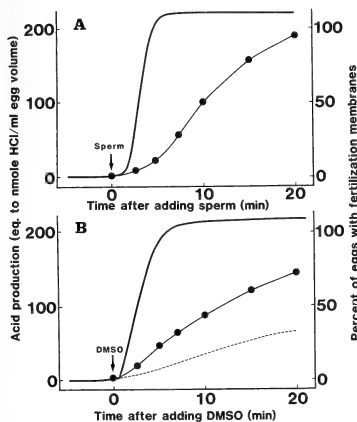


Fig. 3. Acid production induced by sperm and DMSO in echiuroid eggs. Thick lines show changes in the amount of acid (equivalent to nmole HCl/ml egg volume) produced following addition of sperm (2 μ l per 5 ml egg suspension) in A and following DMSO addition (5% in final concentration) in B. Thin lines and solid circles (—●—) show the changes in the number of eggs with fertilization membranes following additions of sperm (A) and DMSO (B). Dotted line in B indicates the change in the amount of produced acid in eggs following adding 1% DMSO, with which fertilization membrane formation is not induced in any eggs. These experiments were done in normal ASW. Essentially the same was also obtained by DMSO addition in Ca^{2+} free ASW (data not shown). The values shown are typical among 3 experiments.

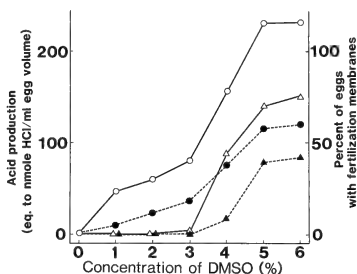


Fig. 4. The amounts of produced acid and the percentages of eggs with fertilization membranes following DMSO addition. The amounts of produced acid (nmole equivalent to HCl/ml of egg volume): —○— and the percentages of eggs with fertilization membranes (the activated eggs): —△— were estimated 20 and 30 min after DMSO addition, respectively. These values obtained in egg suspensions to which verapamil (150 μ M) is added 5 min prior to DMSO addition are shown with solid symbols and dotted lines (—●—: amount of produced acid, —▲—: percentages of eggs with fertilization membranes). Percentage of the activated eggs, obtained 30 min after DMSO addition, was slightly lower than that 60 min after the addition. Acid production was turned off about 10 min after DMSO addition in the presence of verapamil and within 5 min in its absence. Hence, the amount of acid estimated 20 min after the addition is whole amount of produced acid. The amounts of produced acid estimated 20 min after adding DMSO and verapamil in fertilized eggs, which were quite small, were subtracted from the values thus obtained in unfertilized eggs, respectively. These are typical among 3 experiments.

to cause fertilization membrane formation. In the presence of $150 \mu\text{M}$ verapamil, acid production and fertilization membrane formation were inhibited, as shown in Figure 4. Acid production induced by DMSO at 1 and 2%, at which fertilization membrane formation was hardly induced, was also blocked by verapamil. These suggest that acid production is Ca^{2+} -dependent, either directly or indirectly, and is not always accompanied by the formation of fertilization membranes.

The respiratory rates in unfertilized eggs, as well as in fertilized ones (10 min after fertilization), were estimated 10 min after DMSO addition. As shown in Figure 5, the rate of respiration in unfertilized eggs was the same as in fertilized eggs. An addition of 2,4-dinitrophenol (DNP) at 2×10^{-4} M markedly enhanced the rate in fertilized eggs but failed to elevate it in unfertilized eggs. These are in well agreement with the previous reports [12–14]. Fertilization makes the respiration in

echiuroid eggs sensitive to DNP. The respiratory rates in fertilized eggs estimated in the presence and absence of DNP were hardly altered by DMSO addition. DMSO did not cause any change in the sensitivity of respiration to DNP in fertilized eggs. In unfertilized eggs, DMSO did not cause any change in the respiratory rate but enhanced the rate of respiration in the presence of DMSO in a similar manner to that of fertilized eggs. DMSO at 1 and 2% hardly induced fertilization membrane formation but made the respiration sensitive to DNP.

DMSO-treated unfertilized eggs did not exhibit any cyanide-insensitive respiration (data not shown). Sea urchin eggs have been found to exhibit cyanide-insensitive respiration following DMSO treatment in a similar manner to that observed following fertilization [8]. The respiration in echinoid eggs before and after fertilization has also been found to be completely inhibited by cyanide [12–14]. Echinoid eggs seem to have no respiratory system to exhibit cyanide-insensitive respiration upon egg activation.

DISCUSSION

In the present study, it was found that fertilization membrane formation and acid production occurred in echinoid eggs following the treatment by DMSO in almost the same manner to those induced by insemination. Following DMSO-treatment, the respiratory rate hardly changed but the response of respiration to an uncoupler of oxidative phosphorylation, DNP, was altered in the same manner as observed following fertilization [12–14]. These indicate that DMSO stimulates echinoid eggs to activate cell functions, which also become active following fertilization.

The formation of fertilization membrane induced by DMSO in echinoid eggs was inhibited by verapamil, a Ca^{2+} antagonist. It is probable that DMSO-induced fertilization membrane formation is due to an increase in cytosolic Ca^{2+} concentration. Probably, an increase in cytosolic Ca^{2+} concentration also activates, either directly or indirectly, the cell functions in eggs, such as acid production and respiration.

In Ca^{2+} free ASW, DMSO induced fertilization

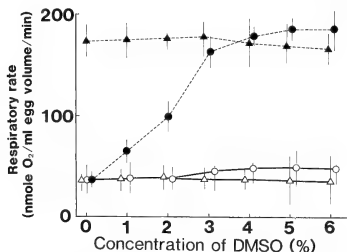


Fig. 5. Effects of DMSO on the respiration of unfertilized and fertilized eggs. The respiratory rates in fertilized and unfertilized eggs were estimated 1 min before and after adding DNP (2×10^{-4} in final concentration), which was introduced 10 min after addition of DMSO (5% in final concentration). The values shown are the respiratory rates calculated on the basis of tracing records of oxygen concentrations in egg suspensions 1 min before (Δ ; fertilized eggs; \circ : unfertilized eggs) and after DNP addition (\blacktriangle : fertilized eggs; \bullet : unfertilized eggs). The respiratory rates obtained in the presence of DNP are also identified with dotted lines. Fertilized eggs were those obtained 5 min after insemination. The mean of fertilization rate, obtained at 60 min after insemination in three batches used in the experiments shown in the figure, was $96.7 \pm 2.45\%$. Each value is the mean of 3 experiments. Bar indicates SEM.

membrane formation, which was inhibited by verapamil. Verapamil is also known to block Ca^{2+} mobilization in intracellular organelles [10, 11]. Hence, it is probable that DMSO induced Ca^{2+} mobilization in organelles elevates cytosolic Ca^{2+} concentration to a sufficient level for egg activation to occur in Ca^{2+} free ASW. In the presence of external Ca^{2+} , Ca^{2+} uptake through Ca^{2+} channels in plasma membrane is also one of the systems to elevate the level of cytosolic Ca^{2+} . If DMSO activates Ca^{2+} channels in plasma membrane in echiuroid eggs, Ca^{2+} influx probably causes an increase in cytosolic Ca^{2+} concentration. In sea urchin sperm, the acrosome reaction, which solely depends on Ca^{2+} influx through Ca^{2+} channels in plasma membrane [15, 16], has been found to be induced by DMSO treatment only in media containing Ca^{2+} [17]. This suggests that Ca^{2+} influx into sperm is induced by DMSO. In echiuroid eggs, however, the minimum concentrations of DMSO for the activation of almost all eggs were higher in the presence of external Ca^{2+} than in its absence. External Ca^{2+} seems to be rather inhibitory for DMSO to activate echiuroid eggs. Thus, Ca^{2+} influx into echiuroid eggs does not seem to contribute to the egg activation caused by DMSO, even if it may be induced by DMSO in a similar manner to that in sea urchin sperm. It remains unknown at present why external Ca^{2+} is rather inhibitory for DMSO to activate echiuroid eggs.

In sea urchin eggs, DMSO-caused formation of fertilization membranes occurs in Ca^{2+} free ASW and is inhibited by verapamil in a similar manner to that in echiuroid eggs, though it does not occur unless DMSO-treated eggs are incubated in an ice bath [8]. In echiuroid eggs, concentrations of DMSO enough to activate eggs were quite lower in the cold than at room temperature. Sensitivity of echiuroid eggs to DMSO also becomes high in the cold. Hence, the stimulation by DMSO of echiuroid eggs is assumed to occur in essentially the same manner as that of sea urchin eggs. Failure of DMSO to activate sea urchin eggs at room temperature is probably due to their lower sensitivity to this compound than that of echiuroid eggs. Indeed, the concentration of DMSO sufficient for the fertilization membrane formation in sea urchin eggs in the cold is around 5% [8] and is

evidently higher than those for the activation of echiuroid eggs (about 3% in the cold).

Low sensitivity to DMSO of sea urchin eggs, especially at room temperature, does not seem to be due to the permeability of DMSO into eggs. In the cold, shrinkage of sea urchin eggs is observed for a while following the addition of 7% DMSO (about 1 M), which makes media surrounding eggs hypertonic, but does not occur at room temperature [8]. Penetration of DMSO seems to occur instantly at room temperature, at which DMSO fails to stimulate sea urchin eggs.

Without DMSO treatment, the incubation in an ice bath results in the formation of fertilization membranes in a small number of echiuroid eggs. The same has been found in sea urchin eggs [8]. Thus, it is probable that Ca^{2+} mobilization in intracellular Ca^{2+} stores in eggs is stimulated by the cold treatment. The cold treatment of eggs probably causes a decrease in the activity of Ca^{2+} -ATPase in intracellular organelles, a Ca^{2+} pump in Ca^{2+} stores, and reduces the rate of mitochondrial respiration which forms H^+ gradient in mitochondria. Thus, Ca^{2+} uptake due to Ca^{2+} pump in intracellular Ca^{2+} stores and H^+ gradient-mediated Ca^{2+} uptake in mitochondria are assumed to decrease in their rates at low temperature. If Ca^{2+} transport through Ca^{2+} channels in these organelles is hardly reduced in its rate by the cold treatment, decrease in the rates of Ca^{2+} uptake in these organelles at low temperature probably enhances apparent rate of Ca^{2+} release from these organelles, to cause a considerable increase in cytosolic Ca^{2+} . Provided that DMSO stimulates Ca^{2+} release from these organelles, the level of cytosolic Ca^{2+} in DMSO treated eggs becomes higher at low temperature than at room temperature. Probably, an increase in cytosolic Ca^{2+} level, thus induced by DMSO treatment and the incubation in the cold, causes Ca^{2+} dependent activation of cell functions in eggs of echiuroid, as well as in those of sea urchin.

ACKNOWLEDGMENT

This work was supported by grant-in-aid from Waseda University, No. 61A-73 and 62A-80.

REFERENCES

- 1 Friend, C., Scher, W., Holland, J. G. and Sato, U. (1971) Hemoglobin synthesis in murine virus-induced leukemic cells in vitro: Stimulation of erythroid differentiation by dimethyl sulfoxide. *Proc. Natl. Acad. Sci. USA*, **68**: 378-382.
- 2 Ostertag, W., Moederis, H., Steinheider, G., Klug, N. and Dube, S. (1972) Synthesis of mouse hemoglobin and globin mRNA in leukemic cell cultures. *Nature, New Biol.*, **239**: 231-234.
- 3 Ross, J., Ikawa, Y. and Leder, P. (1972) Globin messenger RNA induction during erythroid differentiation of cultured leukemia cells. *Proc. Natl. Acad. Sci. USA*, **69**: 3620-3623.
- 4 Shibuya, T. and Mak, T. W. (1983) Isolation and induction erythroleukemic cell line with properties of erythroid progenitor burst-forming cell (BFU-E) and erythroid precursor cell (CFU-E). *Proc. Natl. Acad. Sci. USA*, **80**: 3721-3725.
- 5 Mishina, Y. and Obinata, M. (1985) Induction of commitment of murine erythroleukemia cells (TSA8) to CFU-E with DMSO. *Exp. Cell Res.*, **162**: 319-325.
- 6 Levenson, R., Housman, D. and Cantley, L. (1980) Amiloride inhibits murine erythroleukemia cell differentiation: Evidence for a Ca^{2+} requirement for commitment. *Proc. Natl. Acad. Sci. USA*, **77**: 5948-5952.
- 7 Sawyer, S. T. and Krants, S. B. (1984) Erythropoietin stimulates $^{45}Ca^{2+}$ uptake in friend virus-induced erythroid cells. *J. Biol. Chem.*, **259**: 2769-2774.
- 8 Fujiwara, A., Asami, K. and Yasumasu, I. (1987) Induction of fertilization membrane formation and cyanide-insensitive respiration in sea urchin eggs by the treatment with dimethylsulfoxide followed by an incubation in an ice bath. *Dev. Growth Differ.*, **29**: 13-23.
- 9 Fleckenstein, A. (1963) Metabolic aspects of the excitation contraction coupling. In "The cellular functions of membrane transport. Symposium of the Society General Physiologist in Woods Hole, Mass., Sept. 4-7". Ed. by J. F. Hoffmann, eds. Prentice-Hall, Englewood Cliffs. N. J. pp. 71-93.
- 10 Wang, T., Tosi, L.-I. and Schwartz, A. (1984) Effects of verapamil, diltiazem, nisoldipine and felodipine on sarco plasmic reticulum. *Eur. J. Pharmacol.*, **100**: 253-261.
- 11 Broekemeier, K. M., Schmid, P. C., Schmid, H. H. O. and Pfeiffer, D. R. (1985) Effects of phospholipase A₂ inhibitors on ruthenium red-induced Ca^{2+} release from mitochondria. *J. Biol. Chem.*, **260**: 105-113.
- 12 Fujiwara, A., Kusunoki, K., Tazawa, E. and Yasumasu, I. (1983) Stimulation of unfertilized eggs of the Echiurid, *Urechis unicinctus* by polyamines. *Dev. Growth Differ.*, **25**: 445-452.
- 13 Fujiwara, A., Tazawa, E., Hino, A., Asami, K. and Yasumasu, I. (1986) Respiration in eggs of the Echiurid, *Urechis unicinctus*, before and after fertilization. *Dev. Growth Differ.*, **28**: 431-442.
- 14 Yasumasu, I., Hino, A., Fujiwara, A., Tazawa, E., Nemoto, S. and Asami, K. (1988) Fertilization-induced change in the respiratory rate in eggs of several marine invertebrates. *J. Comp. Biochem. Physiol.*, **90B**: 69-75.
- 15 Collins, F. and Epel, D. (1977) The role of calcium ions in the acrosome reaction of sea urchin sperm. *Exp. Cell Res.*, **106**: 211-222.
- 16 Schackmann, R. W. and Shapiro, B. M. (1981) A partial sequence of ionic changes associated with the acrosome reaction of *Strongylocentrotus purpuratus*. *Dev. Biol.*, **65**: 483-495.
- 17 Mikami-Takei, K., Fujiwara, A. and Yasumasu, I. (1988) The acrosome reaction induced by dimethylsulfoxide in sea urchin sperm. *Dev. Growth Differ.*, (in press).
- 18 Kojima, M. (1967) *Jap. J. Exp. Morphol.*, **10**: 91 (Abstract in Japanese).

Sexual Dimorphism in the Genital Tubercle of the Duck: Analysis by Sex-steroid Administration and Steroid Autoradiography

HIDEHO UCHIYAMA and TAKEO MIZUNO

*Zoological Institute, Faculty of Science, University of Tokyo,
Hongo 7-3-1, Bunkyo-ku, Tokyo 113, Japan*

ABSTRACT—The development of the genital tubercle of the duck was studied by steroid autoradiography and administration of various sex-steroids and sex-steroid-inhibitors. Steroid autoradiography revealed that androgen receptors were present only in the mesenchyme of both male and female genital tubercles after day 8. Estrogen receptors were detected also in the mesenchyme of both male and female genital tubercles after day 9. Androgens promoted the growth of the male genital tubercle weakly when administered either on day 8, 12, or 16 of incubation. A large dose of cyproterone acetate had little effect on the male genital tubercle. Estrogens induced the regression of the male genital tubercle when administered either on day 8, 12, or 16. In such genital tubercles, incomplete histogenesis and many dying cells were marked. Tamoxifen significantly inhibited the regression of the female genital tubercle when administered before day 12 but hardly after day 14.

The results suggest that the regression of the female genital tubercle is induced by estrogens via estrogen receptors in the mesenchyme, and that a period from day 12 to 14 is critical when estrogens act on the mesenchyme to induce the regression, and that androgens are dispensable for the growth and histogenesis of the male genital tubercle in spite of the presence of abundant androgen receptors, at least until day 20.

INTRODUCTION

Sexual dimorphism of the genital tubercle of the duck becomes first manifest at about day 11 of incubation [1, 2]. After that, the male genital tubercle grows spirally, and histogenesis of tissues such as *Corpus fibrolymphatica*, cavernous bodies, *Ligamentum elasticum*, a spiral ligament, or *Pars glandularis phalli*, a blind duct, proceeds. In contrast, the female genital tubercle arrests growth and differentiation, then begins to regress, presumably due to the arrest of mitoses and the occasional cell deaths [2].

It has been shown that male duck embryos treated with estrogen at an early stage acquire female-type genital tubercles, and that embryos gonadectomized with X-rays acquire male-type genital tubercles [1, 3]. From these results, it has been believed that the male type is a "neutral"

type, and the female type is induced by estrogens. Furthermore, the genital tubercles develop into the male type when isolated before day 9 and cultured *in vitro* in a hormone-free medium, but develop or regress according to the sex of the donor when isolated after day 10 [4], suggesting that whether a genital tubercle is to develop into male type or female is determined before day 10.

To verify these ideas and analyze mechanisms of hormone action, we administered various sex-steroids and sex-steroid-inhibitors, and described their effects quantitatively and histologically. We also studied the ontogeny of sex-steroid-receptors in the genital tubercle with steroid autoradiography. Results were discussed in consideration of the plasma concentration of sex-steroids in the duck embryo [5].

MATERIALS AND METHODS

Fertilized eggs of Pekin and Aokubi ducks were incubated in a humidified atmosphere at 37.5°C.

Embryos were staged according to Kaltofen [6]. Histological procedures are presented elsewhere [2].

Administration of sex-steroids and sex-steroid-inhibitors

Various doses of testosterone propionate, β -estradiol benzoate, estrone, progesterone, tamoxifen citrate (all from Sigma, U.S.A.), 5α -dihydrotestosterone (Tokyo Kasei Kogyo, Japan) and cyproterone acetate (kindly presented by Dr. F. Neumann of Schering A. G., Berlin, to Dr. I. Lasnitzki of Strangeways Research Laboratory, Cambridge, U.K.) were dissolved or suspended in 50 μ l of sesame oil (Nakarai, Japan) and injected into the air chamber of the egg with 0.25 ml tuberculin syringe through a small hole opened on the shell. In case of higher doses than 1 mg of hormone/egg, hormones were suspended in 100 μ l of sesame oil and applied. The hole was sealed with a cellophane tape, and the egg was returned to an incubator. In the first set of experiments, the effects of sex steroids and sex-steroid-inhibitors were studied. Those drugs were applied at day 7 or 12 of incubation, and the effect was measured at day 20. In the second set of experiments, responsive periods to androgens and estrogens were studied. Application of hormones and measurement of the effect were done at various stages as presented in the results.

Measurement of the effect of hormones

Genital tubercles were dissected from hormone-administered-embryos, fixed overnight in Bouin's fluid and transferred to 70% ethanol. Effect of hormones on the genital tubercle was described by two parameters. *Length of the genital tubercle* (defined in Fig. 1a) was marked on a sheet of paper with dividers and measured with an ocular micrometer graduated in 0.1 mm under a dissecting microscope. *Rotation angle of the seminal groove* was approximated to the nearest angle in the scale dividing 360° into 16 steps under the dissecting microscope. After these measurements, some genital tubercles were studied histologically, or dehydrated with graded ethanol series, transferred to isoamyl acetate, critical point dried, mounted onto aluminum stubs, coated with gold,

and examined with a Hitachi S430 scanning electron microscope.

Steroid autoradiography

The method of Takeda *et al.* [7] was modified a little. Pieces of the genital tubercle cut frontally into smaller than 1 mm cube were attached to a Millipore filter (pore size 1.2 μ m), and placed with the filter on a stainless grid in a small glass dish and incubated with about 1.5 ml of phenol red-free medium 199 (Sigma, U.S.A.) containing 2.5 μ Ci/ml of [1, 2, 6, 7- 3 H] testosterone (Amersham, U.K., specific activity 91.7 Ci/mmol) or 2.5 μ Ci/ml of [2, 4, 6, 7- 3 H] estradiol (Amersham, U.K., specific activity 85–100 Ci/mmol), supplemented with antibiotics (penicillin 100 U/ml, streptomycin 100 μ g/ml, and fungisone 0.25 μ g/ml, GIBCO, U.S.A.) for 12 hr at 37.5°C in a moist atmosphere of 50% O_2 , 5% CO_2 , and 45% air. Phenol red-free medium was used for fear that phenol red may compete with ^3H -estradiol to estrogen receptors [8]. Competition experiments were carried out by the simultaneous addition of 100 fold molar excess of unlabeled dihydrotestosterone, estradiol benzoate, progesterone, or hydrocortisone in the medium. After the incubation, tissue pieces were washed in three exchanges of about 50 ml Tyrode's solution for 3 to 4 hr at room temperature, embedded in Tissue Tek II (Miles Laboratories, U.S.A.) or 60% carboxymethyl cellulose in deionized water, and frozen in liquid isopentane cooled with liquid nitrogen, and stored at -80°C . Frozen pieces were cut at 5 μ m in a Cryocut II microtome (American Optical, U.S.A.) at -23 to -25°C , and thaw-mounted onto a slide glass coated with Kodak NTB3 photographic emulsion [9]. Slides were usually exposed for one to three months at 4°C , then fixed in 70% ethanol, washed in distilled water, developed with Kodak D19 developer and stained with hematoxylin. Tissue Tek II often caused terrible background grains, although the histological features were better than those embedded in carboxymethyl cellulose paste. A cell was considered to have incorporated the labeled hormone if the number of grains on the nucleus was statistically higher in normal distribution ($p < 0.5\%$) than the number of background grains in 25 μm^2 of extracellular space in the same

section, since $25 \mu\text{m}^2$ corresponded to the mean area of a nucleus in the section. In each specimen, a representative section was chosen and silver grains were counted for more than 100 nuclei and 100 background squares.

Identification of the sex of embryos

The sex of embryos was determined by the macroscopical observation of the gonad. This method was applied for embryos older than 11 days, and was also available for embryos administered with sex-steroids. The sex of embryos before day 10 was determined by the sex chromosomes. Dissociated cells from a fragment of the tail of the embryo was obtained by treatment of 0.05% trypsin and 0.02% EDTA (GIBCO, U.S.A.). These cells were cultured at 10^5 cells/ml in medium 199 supplemented with 10% fetal calf serum in a humidified atmosphere of 5% CO_2 and 95% air at 37.5°C . Two days later, colcemid solution (GIBCO) was added at final concentration of $1 \mu\text{g}/\text{ml}$.

Cells were further incubated for 6 hr at 37.5°C , then collected with trypsin-EDTA, washed with Hanks' balanced salt solution, and fixed in acetic acid-methanol mixture (1:3). A few drops of this solution were dried on a slide glass. The preparation was stained with Giemsa (Merck), and observed at magnification of $\times 1500$. Criteria for the identification of sex chromosomes according to Gasc [10] were used.

RESULTS

1. Effects of various steroids on the development of the genital tubercle

The results are summarized in Table 1. The description of the effect written below is on the results when hormones were applied at day 7 unless otherwise stated.

TABLE 1. Length and rotation angle of the genital tubercle of hormone-treated-embryos at day 20

Hormones	Day of administration	Male		Female	
		Length (mm)	Angle ($^\circ$)	Length (mm)	Angle ($^\circ$)
None (normal)		$2.30^a \pm 0.18^b$ (23) ^c	326 ± 36 (20)	0.65 ± 0.11 (17)	0 ± 0 (4)
Sesame oil (control)	7	2.31 ± 0.15 (10)	331 ± 18 (10)	0.63 ± 0.15 (9)	0 ± 0 (9)
DHT 0.1 mg	7	2.78 ± 0.22 (4)**	344 ± 34 (4)	0.59 ± 0.11 (8)	0 ± 0 (8)
0.1 mg	12	2.48 ± 0.25 (4)	265 ± 29 (4)**	0.73 ± 0.15 (3)	0 ± 0 (3)
TP 0.1 mg	7	2.37 ± 0.06 (3)	293 ± 23 (3)	0.70 ± 0.16 (4)	0 ± 0 (4)
0.3 mg	7	2.84 ± 0.36 (7)**	317 ± 32 (7)	1.25 ± 0.52 (6)**	34 ± 12 (6)
CA 2 mg	7	2.10 ± 0.18 (4)	360 ± 32 (4)	0.96 ± 0.23 (5)*	68 ± 63 (6)*
2 mg	12	2.37 ± 0.27 (6)	365 ± 34 (6)	0.70 ± 0.16 (5)	0 ± 0 (5)
PRG 0.1 mg	7	2.23 ± 0.15 (4)	338 ± 181 (4)	0.66 ± 0.09 (9)	0 ± 0 (6)
E1 0.1 mg	7	2.08 ± 0.45 (4)	281 ± 99 (4)	0.50 ± 0 (4)	0 ± 0 (4)
TAM 0.1 mg	7	1.70 ± 0.10 (3)**	284 ± 20 (5)**	1.23 ± 0.25 (3)**	173 ± 79 (3)**
0.3 mg	7	ND	ND	1.40 ± 0.23 (4)**	221 ± 47 (4)**
0.5 mg	7	ND	ND	1.45 ± 0.24 (4)**	252 ± 41 (5)**
EB 0.002 mg	7	1.88 ± 0.42 (7)**	277 ± 83 (7)*	ND	ND
0.01 mg	7	1.53 ± 0.66 (6)*	203 ± 110 (6)**	ND	ND
0.05 mg	7	1.00 ± 0.70 (6)**	104 ± 108 (5)**	0.60 ± 0.2 (6)	0 ± 0 (6)
0.1 mg	7	0.54 ± 0.23 (7)**	0 ± 0 (5)**	0.53 ± 0.15 (4)	0 ± 0 (4)

a, mean; b, SD; c, number of cases; * and **, significant ($P < 5\%$) and highly significant ($P < 1\%$) deviation from control by Mann-Whitney's U test, respectively. Abbreviations; DHT, dihydrotestosterone; TP, testosterone propionate; CA, cyproterone acetate; PRG, progesterone; E1, Estrone; TAM, tamoxifen citrate; EB, estradiol benzoate; ND, not determined.

Male genital tubercle

Androgens, 5 α -dihydrotestosterone (0.1 mg/egg) and testosterone propionate (0.3 mg/egg), promoted the elongation of the male genital tubercle weakly. Rotation angle was little different from control when these androgens were applied at day 7, but became smaller when dihydrotestosterone was applied at day 12.

Cyproterone acetate (anti-androgen, 2 mg/egg) slightly inhibited the elongation of the genital

tubercle when applied at day 7. At the same time, the growth of the embryo itself was also inhibited. The embryos at day 20 weighed just about half of normal, and were also a little less advanced in the developmental stage. However, rotation angle and histological features of the genital tubercle of these embryos were little different from those of control male genital tubercles. When administered at day 12, cyproterone acetate had no effect.

Estrone (0.1 mg/egg) and tamoxifen (anti-

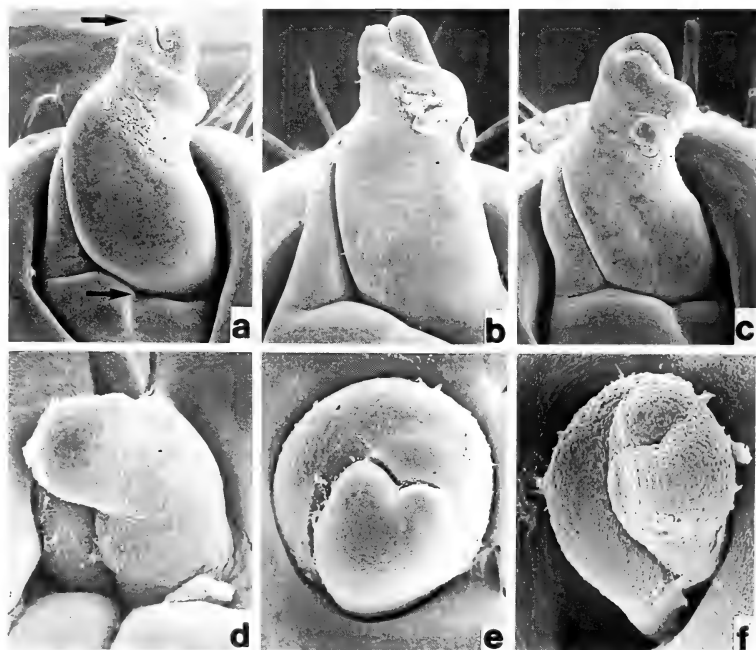


Fig. 1. Scanning electron micrographs of the genital tubercle. Age is 20 days unless otherwise indicated. Anterior is to the top. (a) A normal male genital tubercle. Length of the genital tubercle was measured as the distance between two arrows. Rotation angle of the seminal groove in this specimen was approximated to 360°. $\times 34$. (b) A genital tubercle of a male embryo injected with 0.3 mg of dihydrotestosterone at day 16. Growth is promoted. $\times 34$. (c) A genital tubercle of a female embryo injected with 0.5 mg of tamoxifen at day 7. Size being a little smaller, morphology is quite similar to the normal male one. $\times 41$. (d) A normal female genital tubercle. $\times 92$. (e) A genital tubercle of a male embryo injected with 0.1 mg of estradiol benzoate at day 16. The spiral morphogenesis is arrested in the state at day 16. $\times 88$. (f) A genital tubercle of a female embryo injected with 0.3 mg of dihydrotestosterone at day 12 and examined at day 16. The spiral morphogenesis is recognized. $\times 92$.

estrogen, 0.1 mg/egg) slightly inhibited the growth of the genital tubercle. Estradiol benzoate significantly provoked the regression of the male genital tubercle dose-dependently. At 0.1 mg/egg, the genital tubercle regressed just as much as in the normal female.

Progesterone (0.1 mg/egg) was ineffective.

Female genital tubercle

Tamoxifen significantly inhibited the regression of the female genital tubercle dose-dependently (Fig. 1c). At 0.3 mg/egg, rotation angle restored up to 85%, while length restored up to 64% of that in the normal male, respectively.

Estrone (0.1 mg/egg) and estradiol benzoate (0.1 mg/egg) promoted the regression. Consequently, the genital tubercle became even smaller than control.

Dihydrotestosterone and testosterone propionate (0.1 mg/egg) had no effect on the female genital tubercle, whereas testosterone propionate (0.3 mg/egg) and cyproterone acetate (2 mg/egg) weakly inhibited the regression.

Progesterone (0.1 mg/egg) was ineffective.

2. Responsive periods of the genital tubercle to sex-steroids and tamoxifen

Androgen and estrogen

Dihydrotestosterone (0.3 mg/egg) or estradiol benzoate (0.1 mg/egg) was injected into the egg at day 8, 12, or 16, and the genital tubercle was examined 4 days after the injection. Dihydrotestosterone promoted the growth of the male genital tubercle in all periods examined. It became long and thick, within which the hypertrophy of the connective tissue was marked (Fig. 2b). The female genital tubercle, when dihydrotestosterone was administered at day 8 and 12, was inhibited to regress and developed male-type characters in gross morphology (Fig. 1f), but was not inhibited to regress when dihydrotestosterone was administered at day 16 (data not shown).

Estradiol benzoate caused the arrest of development of the male genital tubercle in gross morphology at the stage of injection in all periods examined (Fig. 1e). Such genital tubercles had chromopyknotic cells scattered among peculiarly

sparse mesenchymal cells (Fig. 2e, 2f). These pyknotic cells constituted about 1 to 8% of total mesenchymal cells in a random microscopical field, and were most prominent around the blind duct. The regression of the female genital tubercle was also promoted by estradiol benzoate in all periods examined.

Tamoxifen

Tamoxifen (1 mg/egg) was applied from day 9 to 14 of incubation, and the effect was measured at day 20 (Table 2). Tamoxifen inhibited the regression of the female genital tubercle when injected before day 12 but hardly after day 14. Even twice dose of tamoxifen failed to inhibit the regression after day 14.

3. Sex-steroid target tissues in the genital tubercle.

Genital tubercles at day 8, 9, 10, 11, 12, 16, and 20 were isolated and incubated *in vitro* with [3 H]-testosterone or [3 H]-estradiol, and processed for steroid autoradiography. The results are summarized in Tables 3 and 4.

Androgen receptors were detected consistently in the mesenchyme of both male and female genital tubercles at all stages examined (Fig. 3a, b). The epidermis, the urethral plate, and the blind duct were always negative. The distribution of androgen receptors was limited to the mesenchyme of the urethral folds until day 9, then spreads to all over the mesenchyme of the genital tubercle. However, fibrolymphatic bodies of the male genital tubercle were most heavily labeled. After day 12, the proportion of labeled cells in the mesenchyme was over 80% in the male and 30–50% in the female. Simultaneous addition of 100 fold molar excess of dihydrotestosterone greatly reduced the grains on the nucleus (Fig. 3c).

Estrogen receptors were detected also in the mesenchyme of both male and female genital tubercles after day 9 (Fig. 3d, e), and especially prominent in the dermal region and around the blind duct of the male genital tubercle including *Suspensorium phalli*, where cells are densely packed in the collagenous matrix. The epidermis, the urethral plate, and the blind duct were also always negative. The proportion of labeled cells in the mesenchyme after day 12 was about 50% in the



TABLE 2. Rotation angle of the genital tubercle of tamoxifen-treated-embryos at day 20

Day of administration	Dose	Rotation angle (°)	
		Male	Female
9	1 mg	259 ^a ± 23 ^b (4) ^c	243 ± 11 (4)
10	1 mg	277 ± 27 (6)	284 ± 27 (3)
11	1 mg	275 ± 18 (7)	241 ± 27 (3)
12	1 mg	272 ± 29 (6)	254 ± 27 (3)
13	1 mg	304 ± 29 (4)	90 ± 0 (4)*
13	2 mg	ND	101 ± 99 (4)
14	1 mg	304 ± 11 (6)	45 ± 52 (4)**
14	2 mg	ND	0 ± 0 (8)

a, mean; b, SD; c, number of cases; ND, not determined; * and **, significant ($P < 5\%$) and highly significant ($P < 1\%$) difference between male and female by Mann-Whitney's U test.

TABLE 3. Ontogeny of sex-steroid-receptors in the genital tubercle

Day		8	9	10	11	12	16	20
ER	Epithelium	male	—	—	—	—	—	—
		female	—	—	—	—	—	—
	Mesenchyme	male	—	+	++	++	++	++
		female	—	+	++	+	+	+
AR	Epithelium	male	—	—	—	ND	—	—
		female	—	—	—	ND	—	—
	Mesenchyme	male	+	+	+++	ND	+++	+++
		female	+	+	++	ND	++	+

—, +, ++, +++; the proportion of receptor-positive-cells were $< 1\%$, $5\% \leq$, $35\% <$ and 70% , respectively; ND, not determined; ER, estrogen receptor; AR, androgen receptor.

FIG. 2. Histology of the genital tubercle of 20-days embryos. Anterior is to the top. Azan staining. Magnification is $\times 640$ in (f), and $\times 54$ in the others. (a) A cross section of a normal male genital tubercle. B: blind duct; E: elastic ligament; F: fibrolymphatic bodies; S: *Suspensorium phalli*. (b) A cross section of a genital tubercle of a male embryo injected with 0.3 mg of dihydrotestosterone at day 16. The hypertrophy of the connective tissue is marked. (c) A cross section of a genital tubercle of a male embryo injected with 2 mg of cyproterone acetate at day 7. The histology is almost identical to that in normal male. (d) A cross section of a genital tubercle of a female embryo injected with 0.3 mg of tamoxifen at day 7. The mesenchyme has differentiated into fibrolymphatic bodies and the blind duct is the normal male type. (e) A genital tubercle of a male embryo injected with 0.1 mg of estradiol benzoate at day 16. The mesenchyme is sparse and fibrolymphatic bodies are incomplete. (f) Enlarged view of the mesenchyme in (e). Many pyknotic cells (arrowheads) are observed.

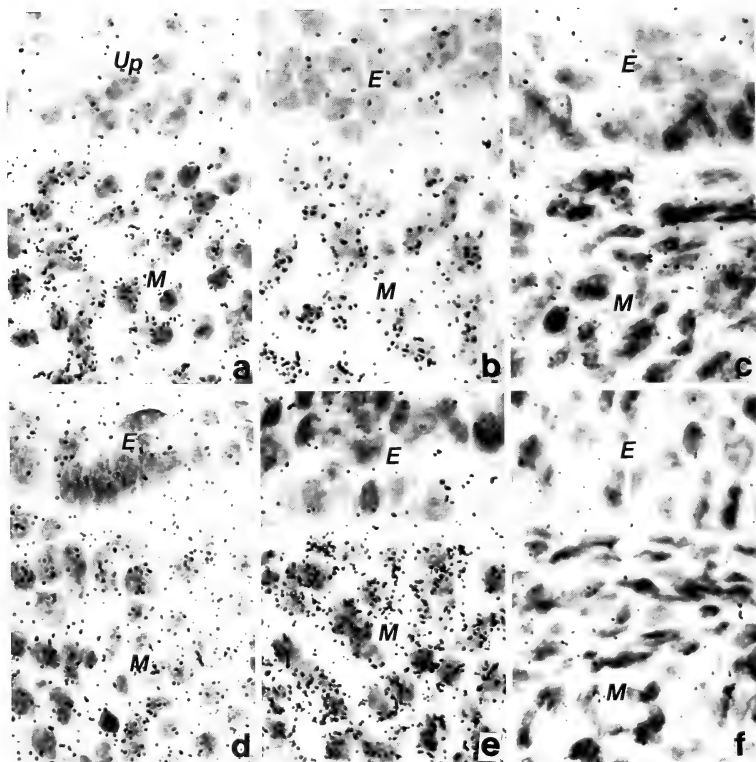


FIG. 3. Steroid autoradiography with $[^3\text{H}]$ -testosterone or $[^3\text{H}]$ -estradiol. Sections were counterstained with hematoxylin. $\times 840$. E: epidermis; M: mesenchyme. Up: urethral plate. (a) Male genital tubercle at day 9 incorporating $[^3\text{H}]$ -testosterone. More than half number of mesenchymal cells are labeled. Urethral plate is negative. (b) Male genital tubercle at day 16 incorporating $[^3\text{H}]$ -testosterone. Grains are seen on the mesenchymal cell nuclei, but not on the epidermal cell nuclei. (c) Male genital tubercle at day 18 in a competition experiment of $[^3\text{H}]$ -testosterone with 100-fold molar excess of unlabeled dihydrotestosterone. Note that grains on the nuclei were abolished. (d) Female genital tubercle at day 11 incorporating $[^3\text{H}]$ -estradiol. Some mesenchymal cell nuclei are labeled (have more than eight grains in this section) while the epidermal cell nuclei are negative. (e) Male genital tubercle at day 18 incorporating $[^3\text{H}]$ -estradiol. Mesenchymal cells are intensely labeled while the epidermis is negative. (f) Male genital tubercle at day 18 in a competition experiment of $[^3\text{H}]$ -estradiol with 100-fold molar excess of estradiol benzoate. Grains on the nuclei were greatly reduced.

TABLE 4. Competition experiments in steroid autoradiography

Labeled hormone	Unlabeled hormone	Sepecimen	Receptor-positive-cells in the mesenchyme (%)
$[^3\text{H}]$ -testosterone	only	male, day 16	80
	+ 100 \times dihydrotestosterone	male, day 20	2
	+ 100 \times estradiol benzoate	male, day 20	58
	+ 100 \times progesterone	male, day 17	59
$[^3\text{H}]$ -estradiol	only	male, day 20	47
	+ 100 \times dihydrotestosterone	male, day 20	32
	+ 100 \times estradiol benzoate	male, day 20	3
	+ 100 \times progesterone	male, day 17	33
	+ 100 \times hydrocortisone	male, day 17	25

male and 15–30% in the female. Thus, labeled cells were a minority in the female genital tubercle. In the male genital tubercle, the sum of the numbers of androgen- and estrogen-receptor-positive-cells exceeds the number of total mesenchymal cells after day 12, indicating that some cells have both receptors. Simultaneous addition of 100 fold molar excess of estradiol benzoate greatly reduced the grains on the nucleus (Fig. 3f).

DISCUSSION

In the previous works on the secondary sexual dimorphism in the duck embryo, the effect of castration and administration of sex-steroids on the development of the genital tubercle was described qualitatively [1, 3, 4]. We studied quantitatively the effect of sex-steroids on the development of the genital tubercle, taking care not to give hormones at excessive doses. Our results also demonstrated the responsiveness of the genital tubercle both to androgen and to estrogen. In addition, we used sex-steroid-inhibitors. The results fortified the idea that the male-type genital tubercle does not require sex-steroids for the growth and differentiation whereas the female-type genital tubercle is induced by estrogens. Furthermore, steroid autoradiography revealed that androgen and estrogen receptors are present in the genital tubercle during the hormone-responsive-period, suggesting that sex-steroids affect the development of the genital tubercle directly.

Estrogen action in the genital tubercle

Estradiol benzoate caused the regression of the male genital tubercle at very small doses (less than 0.01 mg/egg), and tamoxifen effectively inhibited the regression of the female genital tubercle, suggesting that estrogen, and especially estradiol is mainly responsible for the regression of the genital tubercle in the female embryo. This regression is characterized by the arrest of mitoses and the occasional cell death [2]. These features were also observed in the estrogen-treated male genital tubercle. Also in our preliminary study of the tissue culture of the genital tubercle, estrogens suppressed mitoses and increased pyknotic cells (data not shown). Therefore we assume that the arrest of mitoses and cell death are provoked directly by estrogens. It has been reported that tamoxifen has weak estrogenic activity in avian embryos [11]. This can explain the weak inhibition of growth of the male genital tubercle by tamoxifen.

The female genital tubercle before day 12, by the application of tamoxifen, could grow and differentiate into unambiguously male-type genital tubercle. However, tamoxifen could not inhibit the regression effectively when applied after day 14, suggesting that a period from day 12 to 14 is critical for the regression by estrogens. After this period, proliferation and differentiation in the female genital tubercle could hardly occur even in the presence of tamoxifen. From the results of Wolff and Wolff [4] that the genital tubercle isolated at as early as day 10 and cultured *in vitro*

with an estrogen-free medium developed or regressed according to the sex of the donor, the regression of the female genital tubercle is probably triggered before day 10. However, our results suggest that the regression is not irreversible before day 12. The regression of the female genital tubercle isolated after day 10 in the culture conditions may be explained as an autonomous regression by estrogens which was present in the explant itself.

Plasma estradiol in the duck embryo is detected consistently only in the female from day 15 to 26 [5]. As to younger embryos, there are not reports at present. However, in the chick and the quail embryos, the synthesis of estrogen in the ovaries is much greater than in the testes before day 6 when the gonad is sexually indifferent [12, 13]. Therefore, we deduce that the ovaries of young duck embryos also synthesize estrogens before the morphological differentiation of the gonad, that is, well before day 10.

Androgen action in the genital tubercle

Androgen promoted the elongation of the male genital tubercle when applied at day 7. Elongation and histogenesis were both promoted when applied at day 16. It is not known whether these effects are due only to the elevated proliferation or due also to the promotion of differentiation. In our preliminary study of the tissue culture of the genital tubercle, androgens promoted mitoses (data not shown), suggesting that the elevation of mitotic activity is induced directly by androgens. Androgens reduced the rotation angle of the seminal groove when applied at day 12. Excessive proliferation in the mesenchyme may interfere with the normal spiral morphogenesis.

Cyproterone acetate inhibited the growth of the embryo as well as that of the genital tubercle when applied at day 7. However, the histogenesis in the resulting genital tubercle was not perturbed. Furthermore, cyproterone acetate had no effect when applied at day 12. Therefore, androgens are not considered indispensable for the development of the male genital tubercle at least until day 20.

Dihydrotestosterone was more effective than testosterone propionate. The male genital tubercle may have weak 5 α -reductase activity, and that

dihydrotestosterone may be responsible for the androgenic action as in the mammalian genital tubercle [14].

In the present study, relatively high dose of androgens (more than 0.1 mg/egg) was required to promote the growth as compared to estradiol benzoate (less than 0.01 mg/egg) to induce the regression. According to Gasc and Thibier [15], the concentration of testosterone in the plasma of the chick embryo which was injected with 1 mg of testosterone propionate into the allantois at day 14 was 73 times higher than that in the control embryo at days 15-16, decreased sharply and was only 17 times at day 20. Since duck eggs (about 80 g) are bigger than chick eggs (about 50 g) and the air chamber is usually distant from the embryo, 0.1 mg/egg of androgens is not considered to be an excessively high dose. However, the regression of the female genital tubercle was weakly inhibited by 0.3 mg/egg of androgens and 2 mg/egg of cytototone acetate. This may be caused by the competition between the applied androgen or androgen-inhibitor and the endogenous estrogens to estrogen receptors in the female genital tubercle.

Plasma testosterone in the male embryo is not detected on day 15, and gradually increases from day 19 until day 26 [5]. Therefore androgens probably act after the initial phase of growth and histogenesis of the male genital tubercle.

Ontogeny of androgen and estrogen receptors

Steroid autoradiography revealed that mesenchymal cells of the male and female genital tubercle have androgen and estrogen binding sites at most stages studied. Since most of the radio-labeled steroids bound to the nuclei as commonly shown in other organs with steroid autoradiography [7, 16, 17], and the silver grains on the nucleus greatly reduced only when the tritiated hormone was competed with the same unlabeled hormone, we believe that labeled cells possess androgen or estrogen receptors. Both receptors were precociously present by day 8 or 9 which is about two to three days before the manifestation of the sexual dimorphism, and the receptors were distributed only in the mesenchyme. These two features coincide with the results of the steroid auto-

radiography applied to the urogenital tract of the chick embryo [17].

The proportion of estrogen-receptor-positive cells was somewhat lower in the female than in the male after day 12. These cells in the female genital tubercle are expected to degenerate gradually under the presence of estrogens. In addition, the result that the estrogen-receptor-positive cells was rather the minority in the female genital tubercle can explain why the regression of the genital tubercle in the female duck is incomplete.

ACKNOWLEDGMENT

We thank Dr. Shigeo Takeuchi for a critical reading of the manuscript. We also are indebted to Dr. Hiroyuki Takeda for expert assistance with steroid autoradiography.

REFERENCES

- Wolff, Em. (1950) La différenciation sexuelle normale et le conditionnement hormonal des caractères sexuels somatiques précoces, tubercule génital et syrinx chez l'embryon de canard. *Bull. Biol. Fr. Belg.*, **84**: 121-193.
- Uchiyama, H. and Mizuno, T. (1988) Sexual dimorphism in the genital tubercle of the duck: Studies on the normal development and histogenesis. *Zool. Sci.*, **5**: 823-832.
- Wolff, Et. and Wolff, Em. (1951) The effects of castration on bird embryos. *J. Exp. Zool.*, **116**: 59-98.
- Wolff, Em. and Wolff, Et. (1952) Sur la différenciation in vitro du tubercule génital de l'embryon de canard. *C. R. Soc. Biol.*, **146**: 492-493.
- Tanabe, Y., Yano, T. and Nakamura, T. (1983) Steroid hormone synthesis and secretion by testes, ovary, and adrenals of embryonic and post-embryonic ducks. *Gen. Comp. Endocrinol.*, **49**: 144-153.
- Kaltofen, R. S. (1971) Embryonic Development in the Eggs of the Pekin Duck. Center for Agricultural Publishing and Documentation, Wageningen.
- Takeda, H., Mizuno, T. and Lasnitzki, I. (1985) Autoradiographic studies of androgen-binding sites in the rat urogenital sinus and postnatal prostate. *J. Endocrinol.*, **104**: 87-92.
- Berthois, Y., Katzenellenbogen, J. A. and Katzenellenbogen, B. S. (1986) Phenol red in tissue culture media is a weak estrogen: Implications concerning the study of estrogen-responsive cells in culture. *Proc. Natl. Acad. Sci. USA*, **83**: 2496-2500.
- Stumpf, W. E. and Sar, M. (1975) Autoradiographic techniques for localizing steroid hormones. *Methods in Enzymology*, **36**: 135-156.
- Gasc, J.-M. (1973) Sur les résultats d'une technique d'identification précoce du sexe génotypique des embryons d'oiseaux. *C. R. Acad. Sci.*, **277**: 1925-1928.
- Scheib, D. and Baulieu, E.-E. (1981) Action antagoniste du tamoxifène sur la différenciation normale des gonades femelles de l'embryon de Caille. *C. R. Acad. Dci. Serie III*, **293**: 513-518.
- Scheib, D., Guichard, A., Mignot, Th.-M. and Reyss-Brion, M. (1985) Early sex differences in hormonal potentialities of gonads from quail embryos with a sex-linked pigmentation marker: An in vitro radioimmunoassay study. *Gen. Comp. Endocrinol.*, **60**: 266-272.
- Woods, J. E. and Earton, L. H. (1978) The synthesis of estrogens in the gonads of the chick embryo. *Gen. Comp. Endocrinol.*, **36**: 360-370.
- Imperato-McGinley, J., Guerrero, L., Gautier, T. and Peterson, R. (1974) Steroid 5 α -reductase deficiency in man: and inherited form of male pseudohermaphroditism. *Science*, **186**: 1213-1215.
- Gasc, J.-M. and Thibier, M. (1979) Plasma testosterone concentration in control and testosterone-treated chick embryos. *Experientia*, **35**: 1411-1412.
- Buell, R. H. and Tremblay, G. (1985) Autoradiographic demonstration of estrogen binding in human breast cancer after in vitro incubation. *Cancer Res.*, **45**: 4278-4284.
- Gasc, J.-M. and Stumpf, W. E. (1981) Sexual differentiation of the urogenital tract in the chicken embryo: autoradiographic localization of sex-steroid target cells during development. *J. Embryol. Exp. Morphol.*, **63**: 207-223.



***In vitro* Measurements of Calcium Influx into Isolated Goldfish Scales in Reference to the Effects of Putative Fish Calcemic Hormones**

YASUAKI TAKAGI, TETSUYA HIRANO¹, and Juro Yamada

Faculty of Fisheries, Hokkaido University, Hakodate 041, and

¹*Ocean Research Institute, University of Tokyo,
Nakano, Tokyo 164, Japan*

ABSTRACT—Calcium influx into the goldfish scale was measured by incubating individual scales in fish saline containing ⁴⁵Ca. The influx was proportional to the calcium concentration of the incubation medium and was not affected by the presence of 0.1 mM KCN. The influx into the scale taken from fish acclimatized to low temperature (8°C) was significantly lower than that into scale taken from fish acclimatized to 25°C. The influx into the scales of starved fish was not significantly different from that in normally fed fish. On the other hand, when fish were starved in deionized water after removal of all scales from one side of the body, the influx into the remaining scales was significantly greater than that into the scales of the intact fish starved in tap water. Extract of the corpuscles of Stannius from mature chum salmon, salmon prolactin or eel calcitonin did not affect the influx when added to the incubation medium. Thus, calcium influx into the isolated scale seems to be a passive process affected by the condition of the fish.

INTRODUCTION

Teleost fish scales, containing a large quantity of calcium, serve as an important internal calcium reservoir together with the bone [1, 2]. It is well known that some teleosts can survive under acalcic conditions; European eels survive and maintain the plasma calcium concentration in deionized water without food for several weeks [3-6]. Goldfish reared in deionized water and fed on a diet deficient in calcium and phosphorus can survive for at least 4 weeks with even higher plasma calcium levels than are seen in control fish [7]. In order to maintain plasma calcium concentration at a constant level, these fish must mobilize calcium from internal sources such as bones, scales or soft tissues, since passive loss of calcium from the body surface is inevitable.

Compared with bones, scales seem to have more labile calcium. Goldfish scales show greater turnover rate of ⁴⁵Ca than the bone [8]. Estrogen

injection to goldfish and killifish induces mobilization of scale calcium but not bone calcium into plasma [9]. Scales are resorbed when goldfish are starved [10, 11], or when precocious male parr of masu salmon reach sexual maturity [12].

In the present study, calcium influx into the scales of goldfish (*Carassius auratus*) was measured by incubating individual scales in fish saline containing ⁴⁵Ca, and effects of rearing conditions and of some putative calcemic hormones were examined.

MATERIALS AND METHODS

Fish

Immature goldfish (*Carassius auratus*), weighing 5-20 gm, were obtained from a commercial dealer or from a laboratory stock at Faculty of Fisheries of Hokkaido University in Hakodate. They were kept in tap water (Ca: 0.1 mM) at 25°C and fed a commercial carp or trout chow (Nihon Haigo Shiryō) at a rate of 3% of body weight per day, unless otherwise indicated.

Measurement of calcium influx into scales

Scales were removed from the fish using a fine forceps. They were individually incubated in 0.1 ml fish saline containing $0.2 \mu\text{Ci/ml } ^{45}\text{Ca}$, by shaking in a water bath at 25°C for up to 4 hr. Fish saline was composed of 135 mM NaCl, 2.5 mM KCl, 1.5 mM CaCl_2 , 2.0 mM KH_2PO_4 , 1.0 mM MgSO_4 , 10 mM NaHCO_3 , 10 mM N-2-hydroxyethylpiperazine-N-2-ethanesulfonic acid (HEPES) and 5 mM glucose. In some experiments, concentrations of CaCl_2 and KH_2PO_4 were modified from 1.5 mM to 0.5 or 3.5 mM and from 1.0 mM to 0.5 or 4.0 mM, respectively. The pH was adjusted to 7.4 with NaOH. After incubation, scales were briefly rinsed in saline and their outlines were sketched under a light microscope using a drawing device. They were then dried at 90°C for 24 hr and solubilized in a mixture of perchloric acid and hydrogen peroxide (1:1) or in "Soluen" (Packard Instrument), and their radioactivity was counted using a liquid scintillation counter (Aloka LSC-673 or Packard Tri-carb 300). Calcium influx into the scale was expressed as mean \pm S.E.M. (nmol/cm² or nmol/mg dry weight). Concentrations of calcium in the fish saline and in the aquarium water were measured by atomic absorption photometry (Hitachi 518 or Hitachi 180-50).

Experiments

In the first series of experiments, effects of rearing conditions on calcium influx into the scale were examined. For each group, 5-8 fish were used, and one scale per fish was taken from the midportion of the row under the lateral line. All scales were incubated in a standard saline at 25°C . The first experiment examined the effect of rearing temperature. Fish were reared in tap water at 8 or 25°C for 14 days. Although all fish were given a diet at a rate of 3% of body weight per day, the fish kept at 8°C ingested only 0.6% of their body weight. In the second experiment, fish were starved for 30 days in tap water at 25°C . Control fish were fed at a rate of 3% of body weight. In the third experiment, fish were subjected to calcium deficiency in both diet and environment. Experimental fish reared in deionized water were separated into two groups: one group remained

intact and the other group had one side of the body descaled. Control fish were reared in tap water. Both control and experimental fish were starved during the 15-day experiment.

In the next series of experiments, *in vitro* effects of an extract of the corpuscles of Stannius from mature female chum salmon (sCS extract), chum salmon prolactin and eel calcitonin were examined. The sCS extract was prepared as follows. Frozen tissue was homogenized in 0.9% NaCl (100 mg/ml). After centrifugation at 20000 rpm for 10 min, the supernatant was stored at -20°C until use. An extract of the body kidney was similarly prepared. The sCS extract or kidney extract was added to the incubation medium at a final concentration of 1 mg/ml. The chum salmon prolactin (sPRL), from Prof. Hiroshi Kawauchi, Kitasato University, was added to the incubation medium at a concentration of $1 \mu\text{g/ml}$. Eel calcitonin (Elcatonin, Toyo Jozo) was added to the medium at a concentration of 0.1 U/ml. In this series of experiments, all control and appropriate experimental scales were taken from same fish, which were reared in tap water at 25°C and fed a diet at a rate of 3% of their body weight per day.

RESULTS

The calcium influx into the scale incubated in standard fish saline was almost linear over a period of 4 hr (Fig. 1). The influx during the first 2 hr

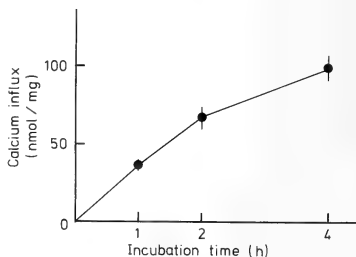
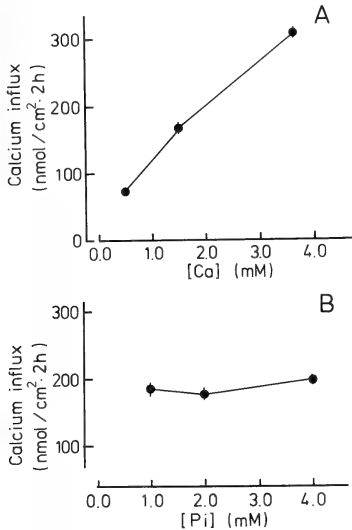


Fig. 1. Cumulative influx of calcium as measured by ^{45}Ca accumulation in scales incubated in standard fish saline at 25°C . Scales were removed from the fed fish reared in tapwater at 25°C . Each point is mean of 5 scales; vertical bars represent S.E.M.

(171.3 ± 4.5 nmol/cm², $n=7$) was not affected by the addition of 0.1 mM KCN in the incubation medium (182.6 ± 9.4 nmol/cm², $n=8$).



The calcium influx during 2 hr was proportional to the calcium concentration of the medium, when the inorganic phosphate concentration was kept at a constant level of 2.0 mM (Fig. 2A). On the other hand, the influx was not affected by changes of the inorganic phosphate concentration at a constant calcium concentration of 1.5 mM (Fig. 2B).

Table 1 summarizes the calcium influx during 2 hr into the scale taken from fish reared under various conditions. The calcium influx was significantly lower in the scales taken from fish reared in tap water at 8°C for 14 days (about 85%) than in those from fish acclimatized to 25°C. When the fish were starved for 30 days in tap water, the calcium influx was not significantly different from the control value in fed fish. On the other hand, when the fish were starved in deionized water for 15 days after removal of all the scales from one side of the body, the calcium influx into the remaining scales was significantly greater than that

FIG. 2. Calcium influx as a function of calcium (A) or phosphate (B) concentration of the incubation medium. Phosphate concentration in experiment A was kept at 2.0 mM and calcium concentration in experiment B at 1.5 mM. Scales were removed from the fed fish reared in tapwater at 25°C, and incubated at 25°C. Each point is mean of 8 scales; vertical bars represent S.E.M.

TABLE 1. Calcium influx into scales taken from fish reared under various conditions

Condition	Period of rearing (days)	Influx (nmol/cm ² ·2 hr)
Control ^{a)}	14	190.8 ± 5.4 (6)
Low temperature (8°C)	14	164.9 ± 6.7* (7)
Control ^{a)}	30	161.9 ± 6.6 (7)
Starved	30	143.9 ± 7.0 (7)
TW, intact ^{b)}	15	166.4 ± 5.7 (5)
DW, intact ^{b)}	15	192.3 ± 10.1 (7)
DW, descaled ^{b)}	15	207.0 ± 3.8** (6)

Mean ± S.E.M. (number of fish)

* Significantly different ($P < 0.05$) from the control group.

** Significantly different ($P < 0.01$) from TW, intact group.

a) Control fish were reared in tap water at 25°C and fed at a rate of 3% of the body weight per day.

b) Fish were reared at 25°C and starved during the experiment.

TW, tap water; DW, deionized water.

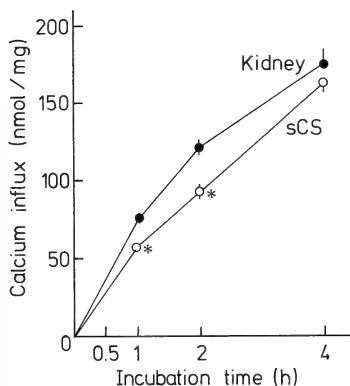


FIG. 3. Cumulative influx of calcium as measured by ^{45}Ca accumulation in scales incubated in standard fish saline at 25°C , in the presence of extract of salmon corpuscles of Stannius (sCS, 1 mg/ml) or of kidney extract (1 mg/ml). Scales were removed from the fed fish reared in tap water at 25°C . Each point is mean of 5 scales; vertical bars represent S.E.M. *Significantly ($P < 0.01$) different from kidney extract group.

TABLE 2. *In vitro* effect of extract of salmon corpuscles of Stannius (sCS) on calcium influx into scales incubated for 4 hr

Medium Ca	Tissue extract ^{a)}	Influx (nmol/mg·4 hr)
0.5 mM	kidney	79.7 ± 4.4
	sCS	79.8 ± 7.7
4.0 mM	kidney	156.1 ± 17.6
	sCS	153.1 ± 3.6

Mean \pm S.E.M. (n=5)

a) Extract of the body kidney of chum salmon or corpuscles of Stannius (sCS) was added to the medium at a concentration of 1 mg/ml. Scales were removed from fed fish reared in tap water at 25°C .

TABLE 3. *In vitro* effects of salmon prolactin (sPRL) and eel calcitonin (eCT) on calcium influx into scales incubated for 1 hr

Medium Ca	Hormone ^{a)}	Influx (nmol/mg·hr)
0.5 mM	Control	23.2 ± 1.2
	sPRL	19.7 ± 1.4
	eCT	25.0 ± 1.5
1.5 mM	Control	37.3 ± 1.2
	sPRL	$46.0 \pm 2.5^*$
	eCT	48.4 ± 5.6
4.0 mM	Control	68.9 ± 7.0
	sPRL	79.0 ± 8.8
	eCT	69.8 ± 7.3

Mean \pm S.E.M. (n=5)

* Significantly different from control ($P < 0.05$).

a) 1 $\mu\text{g/ml}$ sPRL or 0.1 U/ml eCT was added to the medium. Scales were removed from fed fish reared in tap water at 25°C .

TABLE 4. *In vitro* effect of salmon prolactin (sPRL) on calcium influx into the scales incubated for 4 hr

Medium Ca	Group	Influx (nmol/mg·4 hr)
0.5 mM	Control	70.1 ± 5.8
	sPRL ^{a)}	64.0 ± 4.5
1.5 mM	Control	80.6 ± 3.8
	sPRL	99.1 ± 8.2
4.0 mM	Control	128.0 ± 10.1
	sPRL	112.2 ± 3.0

Mean ± S.E.M. (n=5)

a) 1 µg/ml sPRL was added to the medium.

Scales were removed from fed fish reared in tap water at 25°C.

to the scales taken from the intact fish starved in tap water. The influx into the scales taken from the intact fish starved in deionized water tended to be greater than that in intact fish in tap water, but the difference was not significant.

Figure 3 shows the effect of sCS extract on calcium influx into the scale taken from the fed fish reared in tap water and incubated in standard saline. The influx was significantly ($P < 0.01$) reduced after 1- and 2-hr incubation with sCS extract compared with that seen in scales incubated with kidney extract, whereas no significant effect was observed after 4 hr. When sCS extract was added to either high calcium (4.0 mM) or low calcium (0.5 mM) medium and scales were incubated for 4 hr, no significant difference was observed between the scales incubated with sCS extract and those with kidney extract (Table 2).

One hour incubation with sPRL or eCT added to saline with various calcium concentrations did not affect the calcium influx into the scales taken from the fed fish reared in tap water, except for a significant ($P < 0.05$) increase when incubated in the standard saline (Ca: 1.5 mM) with sPRL (Table 3). However, when scales were incubated for 4 hr with sPRL, no significant effect was observed at any calcium concentrations (Table 4).

DISCUSSION

The presence of diffusible (or labile) and non-diffusible (or stable) calcium has been shown in bones and scales of an acellular boned fish, *Fundulus*

kansae [13] and also in goldfish scales [8]. During short-term incubation as was employed in this study, calcium appears to be incorporated into the diffusible pool. The calcium influx was not affected in the presence of KCN but was proportional to the calcium concentration in the incubation medium, suggesting that the calcium influx is a passive process. This is in accord with earlier studies using avian or mammalian bones. Scarpace and Neuman [14, 15] suggested that the calcium influx into the chick calvaria is a passive process; the flux was proportional to the calcium concentration of the incubation medium and to the absolute temperature/viscosity, and ouabain and carbonyl cyanide *m*-chloro phenyl hydrazine (CCCP), an uncoupler of oxydative phosphorylation, were without effect. Furthermore, Neuman *et al.* [16] showed that calcium influx into rat pup calvaria or to adult mouse calvaria was not directly linked to ATP levels of the bone cells.

Calcium influx into the goldfish scale was affected by rearing conditions; the flux decreased significantly when the fish were reared at low water temperature, whereas it increased significantly when the fish were starved in deionized water after removal of all the scales from one side of the body. The intact fish starved in deionized water showed a similar tendency. Fish acclimatized to low temperature did not feed actively, and little weight gain was seen as compared with the control fish (data not shown), suggesting their low metabolic activity. Both descaled and intact fish starved in deionized water showed a decrease in their scale

calcium content compared with intact fish starved in tap water (unpublished data). This suggests that fish starved in deionized water mobilized scale calcium to maintain plasma calcium concentration or to compensate for the shortage of calcium in the environmental water. These changes in the condition of the fish may affect the size of labile calcium pool of the scale, resulting in modification of calcium influx. Seasonal change in the size of the labile calcium pool of the scales and bones was shown in *F. kansae* by Brehe and Fleming [13].

The corpuscles of Stannius are unique in holostean and teleostean fishes and are considered endocrine glands producing a hypocalcemic hormone [17, 18]. Prolactin is likely to function as a hypercalcemic hormone in teleosts; injection of mammalian prolactin induces hypercalcemia in some species such as killifish, *Fundulus heteroclitus*, [19, 20], tilapia, *Oreochromis mossambicus*, [21, 22] or stickleback, *Gasterosteus aculeatus* [22]. Calcitonin is a major hypocalcemic hormone in mammals, but its effects in fish are inconsistent. Some investigators reported hypocalcemia after injection of calcitonin in some fishes [23–25], while others found no effect on plasma calcium level [26–28]. Little is known about the effects of these possibly calcemic hormones on fish bones or scales. When corpuscles of Stannius were removed from the European eel, the degree of mineralization of the vertebrae increased along with plasma calcium level [29]. Mammalian prolactin increased calcium content of bones and scales in tilapia [21, 22]. Calcitonin increased the degree of mineralization of the bones in European eels [25], although no effect was seen on the calcium and phosphate contents of the bones and scales in tilapia [26]. In the present study, none of these calcemic hormones affected the calcium influx into the goldfish scale *in vitro*. Since influx appears to be passive, it is possible that these calcemic hormones do not control the influx directly but control indirectly through effects on plasma calcium level. However, in the present study, only one dose of each hormone was used, and all scales were taken from fish reared in tap water and fed normally at 25°C. Further studies are required using different doses of the hormones under different experimental conditions to investigate the mechanisms controlling

calcium influx into the fish scale.

ACKNOWLEDGMENTS

We are grateful to Dr. Masaharu Iguchi, Faculty of Fisheries, Hokkaido University, Dr. Tsuyosi Ogasawara and Ms. Sanae Hasegawa, Ocean Research Institute, University of Tokyo, for their invaluable discussion. We are also grateful to Prof. Howard A. Bern, University of California, Berkeley, for critical reading of the paper. Thanks are also due to Prof. Hiroshi Kawauchi, School of Fisheries, Kitasato University for his generous gift of salmon prolactin. This work was supported in part by Cooperative Program (No. 84127) provided by the Ocean Research Institute, University of Tokyo, to YT and also by grants-in-aid from the Ministry of Education, Science and Culture to TH.

REFERENCES

- 1 Simkiss, K. (1973) Calcium metabolism of fish in relation to aging. In "Aging of Fish". Ed. by T. B. Bagenal, Gresham Press, Surrey, pp. 1–12.
- 2 Dacke, C. G. (1979) Calcium Regulation In Submammalian Vertebrates. Academic Press, London, 222 pp.
- 3 Henderson, I. W. and Chester Jones, I. (1967) Endocrine influences of the net external fluxes of sodium and potassium in the European eel (*Anguilla anguilla* L.). J. Endocrinol., **37**: 319–325.
- 4 Olivereau, M., Chambolle, P. and Dubourg, P. (1981) Ultrastructural changes in the calcium-sensitive (PAS-positive) cells of the pars intermedia of eels kept in deionized water and normal and concentrated sea water. Cell Tissue Res., **219**: 9–26.
- 5 Olivereau, M. and Olivereau, J. (1982) Calcium-sensitive cells of the pars intermedia and osmotic balance in the eel. I. Responses to changes in the environmental calcium and magnesium. Cell Tissue Res., **222**: 231–241.
- 6 Olivereau, M. and Olivereau, J. (1982) Calcium-sensitive cells of the pars intermedia and osmotic balance in the eel. II. Response to calcium-free sea water. Cell Tissue Res., **225**: 487–496.
- 7 Yamane, S., Iguchi, M., Ogasawara, T. and Nakamura, Y. (1982) Effects of blockage of exogenous calcium and phosphorus on the calcium regulatory systems in goldfish. Comp. Biochem. Physiol., **72A**: 709–713.
- 8 Ichii, T. and Mugiya, Y. (1983) Comparative aspects of calcium dynamics in calcified tissues in the goldfish *Carassius auratus*. Bull. Jap. Soc. Sci. Fish., **49**: 1039–1044.
- 9 Mugiya, Y. and Watabe, N. (1977) Studies on fish scale formation and resorption - II. Effect of estradiol on calcium homeostasis and skeletal tissue

- resorption in the goldfish, *Carassius auratus*, and the killifish, *Fundulus heteroclitus*. *Comp. Biochem. Physiol.*, **57A**: 197-202.
- 10 Yamada, J. (1956) On the mechanism of the appearance of the scale structure. VI. Some observations associating with the absorption of scale in the goldfish. *Bull. Fac. Fish. Hokkaido Univ.*, **7**: 202-207.
 - 11 Ikeda, Y., Ozaki, H. and Yasuda, H. (1974) The effects of starvation and reduced diet on the growth of scales in goldfish. *Bull. Jap. Soc. Sci. Fish.*, **40**: 859-868.
 - 12 Ouchi, K., Yamada, J. and Kosaka, S. (1972) On the resorption of scales and associated cells in precocious male parr of the masu salmon (*Oncorhynchus masou*). *Bull. Jap. Soc. Sci. Fish.*, **38**: 423-430.
 - 13 Brehe, J. E. and Fleming, W. R. (1976) Calcium mobilization from acellular bone and effects of hypophysectomy on calcium metabolism in *Fundulus kansae*. *J. Comp. Physiol.*, **110**: 159-169.
 - 14 Scarpace, P. J. and Neuman, W. F. (1973) Quantitation of Ca^{2+} fluxes in chick calvaria. *Biochim. Biophys. Acta*, **323**: 267-275.
 - 15 Scarpace, P. J. and Neuman, W. F. (1976) The blood: bone disequilibrium. II. Evidence against the active accumulation of calcium or phosphate into the bone extracellular fluid. *Calcif. Tissue Res.*, **20**: 151-158.
 - 16 Neuman, W. F., Neuman, M. W. and Meyers, C. R. (1979) Blood: bone disequilibrium. III. Linkage between cell energetics and Ca fluxes. *Am. J. Physiol.*, **236**: C244-C248.
 - 17 Sokabe, H. (1982) Role of the corpuscles of Stannius on calcium regulation in the teleosts. In "Comparative Endocrinology of Calcium Regulation". Ed. by C. Oguro and P. K. T. Pang, Japan Sci. Soc. Press, Tokyo, pp. 137-142.
 - 18 Wendelaar Bonga, S. E. and Pang, P. K. T. (1986) Stannius Corpuscles. In "Vertebrate Endocrinology: Fundamentals and Biomedical Implications" vol. 1. Ed. by P. K. T. Pang and M. P. Schreibman, Academic Press, New York, pp. 439-464.
 - 19 Pang, P. K. T., Schreibman, M. P., Balbontin, F. and Pang, R. K. (1978) Prolactin and pituitary control of calcium regulation in the killifish, *Fundulus heteroclitus*. *Gen. Comp. Endocrinol.*, **36**: 306-316.
 - 20 Pang, P. K. T. (1981) Hypercalcemic effects of ovine prolactin on intact killifish, *Fundulus heteroclitus*, subjected to different environmental calcium challenges. *Gen. Comp. Endocrinol.*, **44**: 252-255.
 - 21 Wendelaar Bonga, S. E. and Flik, G. (1982) Prolactin and calcium metabolism in a teleost fish, *Sarotherodon mossambicus*. In "Comparative Endocrinology of Calcium Regulation". Ed. by C. Oguro and P. K. T. Pang, Japan Sci. Soc. Press, Tokyo, pp. 21-26.
 - 22 Flik, G., Fenwick, J. C., Kolar, Z., Mayer-Gostan, N. and Wendelaar Bonga, S. E. (1986) Effects of ovine prolactin on calcium uptake and distribution in *Oreochromis mossambicus*. *Am. J. Physiol.*, **250**: R161-R166.
 - 23 Chan, D. K. O., Chester Jones, I. and Smith, R. N. (1968) The effect of mammalian calcitonin on the plasma levels of calcium and inorganic phosphate in the European eel (*Anguilla anguilla* L.). *Gen. Comp. Endocrinol.*, **11**: 243-254.
 - 24 Wendelaar Bonga, S. E. (1981) Effect of synthetic salmon calcitonin on protein-bound and free plasma calcium in the teleost *Gasterosteus aculeatus*. *Gen. Comp. Endocrinol.*, **43**: 123-126.
 - 25 Lopez, E., Peignoux-Deville, J., Lallier, F., Martelly, E. and Milet, C. (1976) Effects of calcitonin and ultimobranchialectomy (UBX) on calcium and bone metabolism in the eel, *Anguilla anguilla* L. *Calcif. Tissue Res.*, **20**: 173-186.
 - 26 Wendelaar Bonga, S. E. and Lammers, P. I. (1982) Effects of calcitonin on ultrastructure and mineral content of bone and scales of the cichlid teleost *Sarotherodon mossambicus*. *Gen. Comp. Endocrinol.*, **48**: 60-70.
 - 27 Hirano, T., Hasegawa, S., Yamauchi, H. and Orimo, Y. (1981) Further studies on the absence of hypocalcemic effects of eel calcitonin in the eel, *Anguilla japonica*. *Gen. Comp. Endocrinol.*, **43**: 42-50.
 - 28 Bjornsson, Th. B. and Deftos, L. J. (1985) Plasma calcium and calcitonin in the marine teleost, *Gadus morhua*. *Comp. Biochem. Physiol.*, **81A**: 593-596.
 - 29 Lopez, E. (1970) L'os cellulaire d'un poisson téléostéen (*Anguilla anguilla* L.). II. Action de l'ablation des corpuscules de Stannius. *Z. Zellforsch.*, **109**: 566-572.



Role of Internalization of Follicle-Stimulating Hormone (FSH)-Receptor Complex on Down-regulation of FSH Receptor in Mouse Sertoli Cells

AKITOSHI SHIMIZU

Hayashibara Biochemical Laboratory Inc, Fujisaki Institute,
Okayama 675-1, Japan

ABSTRACT—The role of internalization of FSH-FSH receptor complexes on down-regulation of cell-surface FSH receptors was studied in cultured mouse Sertoli cells using NaN_3 as an inhibitor of internalization. After maintaining in the medium (F12/DME) for 4 days, Sertoli cells were cultured for 8 days throughout or 4 plus 4 days combinations of one of the following media: 1) F12/DME (control group), 2) F12/DME for the first 4 days, then F12/DME containing 5 $\mu\text{g/ml}$ FSH for the following 4 days (down-regulated group), 3) F12/DME, then F12/DME containing 5 $\mu\text{g/ml}$ FSH and 10^{-5} , 10^{-4} or 10^{-3} M NaN_3 , or 4) F12/DME containing FSH and NaN_3 , then F12/DME containing FSH. After these cultures Sertoli cells were incubated with ^{131}I -FSH, and surface, internalized and degraded radioactivities were measured. In addition, Sertoli cells were pulse-labeled with ^{131}I -FSH and cold chase study was performed in order to estimate the effect of FSH on the rate constants of internalization (k_i) and degradation (k_d). It was found that surface and internalized radioactivities were decreased by exogenous FSH and the decrease was reversibly suppressed by coexistence of NaN_3 . In contrast, degraded radioactivity was increased by exogenous FSH and this increase was also suppressed by NaN_3 . Moreover, both k_i and k_d of down-regulated group were significantly larger than those of control group (k_i , 6.94×10^{-2} vs. $4.11 \times 10^{-2} \text{ min}^{-1}$; k_d , 6.61×10^{-3} vs. $9.01 \times 10^{-3} \text{ min}^{-1}$, respectively). These results indicate that down-regulation of cell-surface FSH-receptors may be due to the translocation of surface receptors into the cells and hence the decrease in the number of available surface receptors.

INTRODUCTION

It is well established that in the testis follicle-stimulating hormone (FSH) initially binds to cell-surface FSH receptors of Sertoli cells [1-4], and, therefore, the endocrine activity of Sertoli cells is dependent not only on the plasma levels of FSH but also on the number of FSH receptors on the membrane. Concerning the regulation of FSH receptors, O'Shaughnessy and Brown [5] and Francis *et al.* [6] reported that in immature and adult male rats exogenously administered large amount of FSH acted to decrease the number of FSH receptor. In our recent studies, hypophysectomy induced a significant increase in the number of FSH receptors in mouse Sertoli cells *in vitro* and the hypophysectomy-induced increase of

FSH receptors was suppressed by exogenous administration of FSH [7, 8]. For the possible mechanism of this FSH-induced down-regulation of FSH receptors in mouse Sertoli cells, we have proposed a hypothesis that internalization of FSH-FSH receptor complexes is an important regulatory process of down-regulation. Internalization of FSH-FSH receptor complexes has been reported previously in the rat [9] or the pig [10]. In mouse Sertoli cells, we have recently observed the internalization of FSH-FSH receptor complexes morphologically [11] and physiologically (unpublished observations). The primary aim of the present study is to verify the above-mentioned hypothesis. For this purpose, we have applied two approaches in this study as follows: 1) investigation of the effects of NaN_3 , an inhibitor of internalization, on FSH-induced down-regulation of FSH receptors, and 2) direct comparison of the rate constants of internalization between control and down-

Accepted March 1, 1988

Received February 8, 1988

regulated mouse Sertoli cells.

MATERIALS AND METHODS

Hormones and other chemicals

Highly purified rat FSH (NIADDK-rat FSH I-4) was supplied by the National Institute of Arthritis, Diabetes, Digestive and Kidney Diseases (NIADDK) and was radioiodinated with ^{131}I (Na ^{131}I , Radiochemical Centre, Amersham) by the lactoperoxidase method as described previously [11, 12]. The specific radioactivity of the radioiodinated rat FSH (^{131}I -FSH) was about 25 $\mu\text{Ci}/\mu\text{g}$. Porcine FSH (NIH-FSH-P2) was provided by the National Institutes of Health, Md. Collagenase-dispase was purchased from Boehringer-Mannheim (Mannheim, West Germany), and NaN_3 , from Kanto Chemical Co. (Tokyo, Japan). Ham's F-12 nutrient mixture and Dulbecco's Modified Eagle's Medium (1:1, vol/vol) (F12/DME), soybean trypsin inhibitor, insulin, transferrin, epidermal growth factor and gentamycin were the products of Sigma Chemical Co. (St. Louis, MO).

Animals

Male C57BL/6Ncrj mice maintained in this laboratory were used. They were housed in a temperature-controlled room under daily photoperiods of 12 hr-light (lights on, 06:00–18:00 hr) and 12 hr-darkness with free access to laboratory chow (CA-1, Japan Clea Inc.) and tap water.

Primary Sertoli cell culture

Sertoli cells were isolated from the testes of 2-month-old mice according to the method of Nakhla *et al.* [13]. Briefly, the testes were decapsulated in F12/DME medium and the tubules were dispersed in F12/DME containing 0.05% (wt/vol) collagenase-dispase and 0.005% (wt/vol) soybean trypsin inhibitor. After incubation for 10 min with constant agitation at room temperature, the tubules were allowed to settle by unit gravity. The interstitial, myoid and germ cells in suspension were discarded, and the remaining tubules were washed for three times with F12/DME medium. After washing, the tubules were cut into about 2-mm segments with scissors and treated

again with the collagenase-dispase mixture for 15 min at room temperature. Then the cell suspension was passed through a 102- μm mesh nylon cloth, and centrifuged at 800 $\times g$ for 4 min. The sediments were quickly washed with F12/DME, and plated in Corning tissue culture 24-well micro plate (Corning Glass Works, Corning, NY) in F12/DME medium supplemented with insulin (10 $\mu\text{g}/\text{ml}$), transferrin (5 $\mu\text{g}/\text{ml}$), epidermal growth factor (2.5 ng/ml) and gentamycin (20 $\mu\text{g}/\text{ml}$). The cells were cultured at 32°C in humidified atmosphere of 95% air and 5% CO_2 at a density of 5×10^5 cells/well (4.4×10^5 cells/cm 2). The culture medium was changed at 48-hr intervals. All assay procedures as described below were performed in the wells.

Analysis of surface, internalized and degraded radioactivities

After incubation with ^{131}I -FSH, radioactivity associated with Sertoli cells were counted as surface, internalized and degraded radioactivities by the method to be reported in a separate paper. Briefly, Sertoli cells in each well were pretreated with F12/DME containing 2% BSA and incubated with F12/DME containing 2.8 ng of ^{131}I -FSH (5.6 ng/ml) at 32°C. Incubation time was 10 min when cold chase was performed after incubation. Otherwise, incubation was carried out for 60 or 180 min. Cold chase was performed at 32°C for 0, 5, 10, 15 or 20 min. Either incubation media (incubation time was 60 or 18 min) or cold chase media were subjected to 20% trichloroacetic acid treatment for 4 hr at 4°C and centrifuged at 12,000 $\times g$ for 30 min. The radioactivities of supernatant and precipitate were counted as degraded and dissociated radioactivities, respectively. On the other hand, all the Sertoli cells were treated with 0.2 M acetic acid containing 0.5 M NaCl (pH 2.5) for 10 min at 4°C and the radioactivity released into the acidic medium was counted as surface radioactivity. Finally, Sertoli cells were incubated with 1 N NaOH for 2 hr at room temperature, and the radioactivity contained in the basic medium was counted as internalized radioactivity. Non-specific binding was measured by incubation of Sertoli cells with ^{131}I -FSH and an excess of unlabeled FSH (25 μg NIH-FSH-P2).

Effect of FSH on radioactivity associated with cultured Sertoli cells

At first, Sertoli cells were cultured in F12/DME, and then were cultured in F12/DME containing 2.5 μ g of FSH (NIH-FSH-P2) (5 μ g/ml) for the last 1, 2, 4 or 6 days. Total period of any culture was 10 days. After culture, the medium was aspirated out and Sertoli cells were treated with 0.2 M acetic acid containing 0.5 M NaCl (pH 2.5) in order to dissociate hormones bound to surface receptors. Then the cells were treated with 2% BSA and incubated with 2.8 ng of 131 I-FSH (5.6 ng/ml) for 180 min at 32°C. After rinse to remove unbound hormone, Sertoli cells were incubated with 1 N NaOH for 2 hr at room temperature and the radioactivity of the basic medium was counted.

Effects of various concentrations of NaN_3 on internalization and degradation of 131 I-FSH

After 12 days of incubation in F12/DME without NaN_3 , Sertoli cells were preincubated with F12/DME containing various concentrations of NaN_3 for 30 min at 32°C. Thereafter Sertoli cells were pretreated with 2% BSA, and incubated for 60 min at 32°C with 131 I-FSH and NaN_3 of which concentration was the same as that used for preincubation. Dissociated, surface, internalized and degraded radioactivities were measured by the method described above.

Effects of NaN_3 on FSH-induced down-regulation of FSH receptors

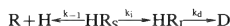
Eight culture plates of Sertoli cells were prepared for the following four experimental groups. 1) control group; one plate of Sertoli cells maintained in F12/DME for 12 days, 2) down-regulated group; one plate maintained in F12/DME for the first 8 days and in F12/DME containing 2.5 μ g FSH (5 μ g/ml) for the last 4 days, 3) internalization-inhibited group; three plates maintained in F12/DME for the first 8 days and in F12/DME containing 2.5 μ g FSH (5 μ g/ml) and 10^{-5} , 10^{-4} or 10^{-3} M NaN_3 for the last 4 days, 4) FSH-retreated group; three plates first maintained in F12/DME for 4 days and in F12/DME containing 2.5 μ g FSH (5 μ g/ml) and 10^{-5} , 10^{-4} or 10^{-3} M NaN_3 for the next 4 days, and finally cultured in F12/DME

containing 2.5 μ g FSH (5 μ g/ml) for the last 4 days. After culture, Sertoli cells in wells were rinsed with 0.2 M acetic acid, pretreated with 2% BSA and incubated with 131 I-FSH. Dissociated, surface, internalized and degraded radioactivities were counted in each well as described above.

Measurement of the rate constants of dissociation, internalization and degradation

Sertoli cells were maintained in F12/DME for 8 days, and then cultured in F12/DME (control group) or F12/DME containing 2.5 μ g FSH (5 μ g/ml) (down-regulated group) for 4 days. Thereafter Sertoli cells were subjected to 0.2 M acetic acid and 2% BSA. After the incubation with 131 I-FSH, cold chase was performed and dissociated, surface, internalized and degraded radioactivities were counted.

In our separated study a kinetic model for internalization and degradation of hormone under the condition of cold chase was demonstrated as follows:



where unoccupied surface receptor, free hormone, hormone-receptor complex on the cell surface, hormone-receptor complex in the cell and degradation product are designated as R, H, HR_S , HR_I and D, respectively. The rate constants of dissociation, internalization and degradation are denoted as k_{-1} , k_i and k_d , respectively. According to this kinetic model, the concentration of H ($[H]_t$), HR_S ($[\text{HR}_S]_t$) and HR_I ($[\text{HR}_I]_t$) at time "t" will be represented as follows:

$$[\text{HR}_S]_t = [\text{HR}_S]_0 e^{-(k_{-1} + k_i)t} \quad (1)$$

$$[H]_t = \frac{k_{-1}}{k_{-1} + k_i} ([\text{HR}_S]_0 - [\text{HR}_S]_t) \quad (2)$$

$$[\text{HR}_I]_t = \frac{k_i [\text{HR}_S]_0}{k_{-1} + k_i - k_d} (e^{-k_d t} - e^{-(k_{-1} + k_i)t}) + [\text{HR}_I]_0 e^{-k_d t} \quad (3)$$

Rate constants of dissociation, internalization and degradation were calculated by Equations 1 to 3. Equations 1 and 2 will be rewritten as follows:

$$\ln[\text{HR}_S]_t = -(k_{-1} + k_i)t + \ln[\text{HR}_S]_0 \quad (4)$$

$$k_{-1} = \frac{(k_{-1} + k_i)[H]_t}{[\text{HR}_S]_0 - [\text{HR}_S]_t} \quad (5)$$

Equation 4 predicts that a regression line can be

drawn on semi-log plot for $[HR_s]_t$ against cold chase time and the slope of the line will give a value for $k_{-1} + k_i$. Besides, if the value of $k_{-1} + k_i$, dissociated radioactivity, initial surface radioactivity ($[HR_s]_0$) and surface radioactivity are substituted into Equation 5, we can obtain the value of k_{-1} and, simultaneously, k_i . The value of k_d can be calculated by Newton method substituting value of k_{-1} , k_i , $[HR_s]_0$, $[HR_i]_0$ (initial internalized radioactivity) and $[HR_i]_t$ into Equation 3. In addition, on the basis of these three rate constants, 99% clearance time of surface radioactivity and internalized radioactivity were simulated.

Statistical analyses

All data were expressed as the mean and standard error of four determinations. In the study of effects of NaN_3 on FSH-induced down-regulation of FSH receptor, the homoscedasticity among groups was analyzed by Bartlett's method. The data which represented the heteroscedasticity were subjected to logarithmic transformation for the analysis of differences between the means of two groups (applied for the data for Fig. 3 only). The transformed data were again analyzed by Bartlett's method for homoscedasticity. The differences between the means of two groups were analyzed by Duncan's new multiple range test after single-classification analysis of variance. The significance of regression and the difference between two regression coefficients were analyzed by F-test [14].

RESULTS

Effect of FSH on the binding of ^{131}I -FSH to Sertoli cells

When Sertoli cells were cultured in F12/DME for 10 days, the ratio of surface radioactivity to total radioactivity added was $1.06 \pm 0.10\%$ (mean \pm S.E.). However, if Sertoli cells were cultured in F12/DME containing FSH for the last few days of culture, the ratio decreased according to the length of culture in the presence of FSH (Fig. 1). When Sertoli cells were cultured in FSH-containing medium for the last 4 days, the ratio of surface radioactivity was $0.52 \pm 0.14\%$. When Sertoli cells were cultured in the medium containing FSH for

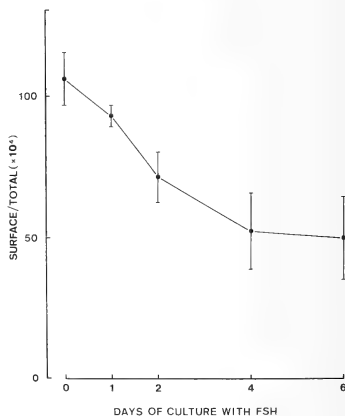


FIG. 1. FSH-induced down-regulation of cell-surface FSH receptors on cultured Sertoli cells. Sertoli cells were cultured for a total of 10 days. At first Sertoli cells were cultured in F12/DME and then in F12/DME containing $2.5 \mu\text{g}$ FSH ($5 \mu\text{g/ml}$) for the last 1, 2, 4 or 6 days. After the culture, Sertoli cells were rinsed with 0.2 M acetic acid ($\text{pH } 2.5$), incubated with $2.8 \text{ ng } ^{131}\text{I}$ -FSH for 180 min at 32°C and surface radioactivity was counted as described in "Materials and Methods". The radioactivity was represented as the ratio to total radioactivity of ^{131}I -FSH added in incubation medium.

the last 6 days, further significant decrease was not observed ($0.50 \pm 0.14\%$).

Effect of NaN_3 on internalization of ^{131}I -FSH

In order to demonstrate the effect of NaN_3 on internalization of ^{131}I -FSH in cultured Sertoli cells, percentage of surface radioactivity (the ratio of surface radioactivity to the sum of surface, internalized and degraded radioactivities) was measured in the presence of various concentrations of NaN_3 . Percentage of surface radioactivity showed a sigmoid increase along with the increase in NaN_3 concentration (Fig. 2). When no NaN_3 was added to the incubation medium, percentage of surface radioactivity was $11.0 \pm 4.0\%$. At the concentration more than 10^{-4} M NaN_3 percentage of surface radioactivity was almost constant ($67.0 \pm 7.0\%$ at 10^{-4} M , $73.7 \pm 4.5\%$ at 10^{-3} M). The sum of

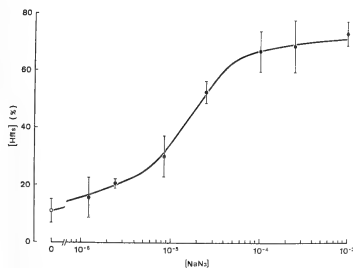


Fig. 2. Effects of $\text{Na}_2\text{S}_2\text{O}_3$ on surface radioactivity of Sertoli cells. Sertoli cells maintained in F12/DME for 4 days were pretreated with F12/DME containing various concentrations of $\text{Na}_2\text{S}_2\text{O}_3$ for 30 min at 32°C . Then Sertoli cells were incubated with F12/DME containing 2.8 ng of ^{125}I -FSH and $\text{Na}_2\text{S}_2\text{O}_3$ of which concentration was the same as that used for pretreatment, and surface, internalized and degraded radioactivities were counted as described in "Materials and Methods". Surface radioactivity was represented as percentage of surface radioactivity to the sum of surface, internalized and degraded radioactivities.

surface, internalized and degraded radioactivities was nearly constant regardless of the concentration of $\text{Na}_2\text{S}_2\text{O}_3$ (data not shown). The range of the sum was 2598 to 2811 cpm which corresponded with 4.3 to 4.7% of total radioactivity added to the incubation medium.

Effects of $\text{Na}_2\text{S}_2\text{O}_3$ on FSH-induced down-regulation of FSH receptors

Down-regulated group showed significantly smaller ratio of surface radioactivity to total radioactivity ($0.12 \pm 0.04\%$) than that of control group ($1.21 \pm 0.39\%$) (Fig. 3). On the other hand, the ratio of internalization-inhibited groups (10^{-4} M and 10^{-3} M $\text{Na}_2\text{S}_2\text{O}_3$) was significantly greater than that of down-regulated group and did not show any significant differences from the control value ($0.08 \pm 0.15\%$ and $0.82 \pm 0.27\%$, 10^{-4} M and 10^{-3} M $\text{Na}_2\text{S}_2\text{O}_3$, respectively). In FSH-retreated group (FSH + 10^{-5} , 10^{-4} or 10^{-3} M $\text{Na}_2\text{S}_2\text{O}_3$ followed by treatment of FSH alone) the ratio became significantly smaller than that of control group (0.12 ± 0.03 , 0.11 ± 0.03 and $0.23 \pm 0.08\%$;

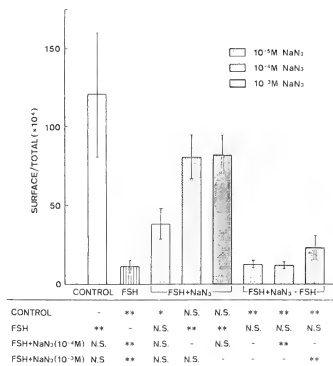


Fig. 3. Effect of $\text{Na}_2\text{S}_2\text{O}_3$ on FSH-induced down-regulation of Sertoli cells: surface radioactivity. Down-regulation was induced by treatment with 2.5 μg FSH ($5 \mu\text{g}/\text{ml}$) in the medium. Then the effect of various concentrations of $\text{Na}_2\text{S}_2\text{O}_3$ on surface radioactivity and the reversibility of the effect of $\text{Na}_2\text{S}_2\text{O}_3$ (designated as FSH+ $\text{Na}_2\text{S}_2\text{O}_3$ -FSH) were investigated as described in "Materials and Methods". For the analysis of differences between the means of two groups, data were subjected to logarithmic transformation. Thereafter, single-classification analysis of variance and Duncan's new multiple range test was performed. The results are shown in the lower part of the figure. * $P < 0.05$; ** $P < 0.01$; N.S., not significant.

10^{-5} , 10^{-4} and 10^{-3} M $\text{Na}_2\text{S}_2\text{O}_3$, respectively). Differences in the ratio of FSH-retreated groups from internalization-inhibited groups were statistically significant in either $\text{Na}_2\text{S}_2\text{O}_3$ concentrations of 10^{-4} or 10^{-3} M.

In internalized radioactivity (Fig. 4), we observed similar effects of FSH and $\text{Na}_2\text{S}_2\text{O}_3$ as in the case of surface radioactivity described above. Down-regulated groups showed significantly smaller ratio of the radioactivity to total radioactivity ($0.49 \pm 0.07\%$) than that of control group ($1.28 \pm 0.14\%$), and the decrease induced by FSH was suppressed by concomitant incubation with $\text{Na}_2\text{S}_2\text{O}_3$ (10^{-4} M, $1.07 \pm 0.06\%$; 10^{-3} M, $0.94 \pm 0.13\%$). By FSH treatment after FSH+ $\text{Na}_2\text{S}_2\text{O}_3$ treatment (FSH-retreated group), the ratio of internalized radioactivity to total radioactivity became statisti-

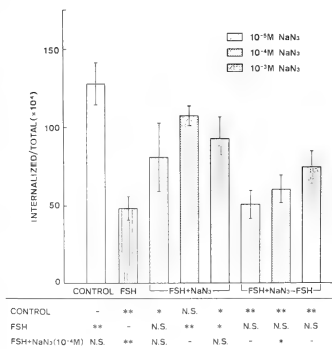


Fig. 4. Effect of $\text{Na}_2\text{S}_2\text{O}_3$ on FSH-induced down-regulation of Sertoli cells: internalized radioactivity. Down-regulation was induced by $2.5 \mu\text{g}$ FSH ($5 \mu\text{g}/\text{ml}$) in the medium. Then the effect of various concentrations of $\text{Na}_2\text{S}_2\text{O}_3$ on internalized radioactivity and the reversibility of the effect of $\text{Na}_2\text{S}_2\text{O}_3$ (designated as $\text{FSH} + \text{Na}_2\text{S}_2\text{O}_3 \rightarrow \text{FSH}$) were investigated as described in "Materials and Methods". Significance of the differences between two groups analyzed by Duncan's new multiple range test after single-classification analysis of variance as shown in the lower part of the figure. * $P < 0.05$; ** $P < 0.01$; N.S., not significant.

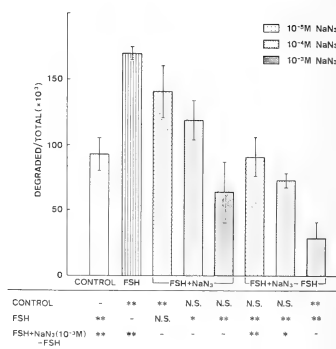


Fig. 5. Effect of $\text{Na}_2\text{S}_2\text{O}_3$ on FSH-induced down-regulation of Sertoli cells: degraded radioactivity. Down-regulation was induced by treatment with $2.5 \mu\text{g}$ FSH ($5 \mu\text{g}/\text{ml}$) in the medium. Then, the effect of various concentrations of $\text{Na}_2\text{S}_2\text{O}_3$ on degraded radioactivity and the reversibility of the effect of $\text{Na}_2\text{S}_2\text{O}_3$ (designated as $\text{FSH} + \text{Na}_2\text{S}_2\text{O}_3 \rightarrow \text{FSH}$) were investigated as described in "Materials and Methods". Significance of the differences between two groups analyzed by Duncan's new multiple range test after single-classification analysis of variance is shown in the lower part of the figure. * $P < 0.05$; ** $P < 0.01$; N.S., not significant.

cally not significant as compared to that of down-regulated group. In FSH-retreated groups the ratio tended to increase along with the rise in $\text{Na}_2\text{S}_2\text{O}_3$ concentration (10^{-5} M, $0.51 \pm 0.09\%$; 10^{-4} M, $0.06 \pm 0.08\%$; 10^{-3} M, $0.75 \pm 0.9\%$).

The effects on $\text{Na}_2\text{S}_2\text{O}_3$ on degraded radioactivity were generally reciprocal to those on surface and internalized radioactivities (Fig. 5). Down-regulated group showed significantly greater ratio of degraded radioactivity to total radioactivity ($17.00 \pm 0.52\%$) than control group ($10.06 \pm 1.30\%$). When Sertoli cells were incubated with FSH and various concentrations of $\text{Na}_2\text{S}_2\text{O}_3$, degraded radioactivity decreased in $\text{Na}_2\text{S}_2\text{O}_3$ dose-dependent fashion. The difference from down-regulated group was statistically significant at 10^{-4} M $\text{Na}_2\text{S}_2\text{O}_3$ ($11.96 \pm 1.46\%$, $P < 0.05$) or 10^{-3} M ($6.49 \pm 2.31\%$, $P < 0.01$). FSH-retreated groups also showed $\text{Na}_2\text{S}_2\text{O}_3$ dose-dependent decrease in the ratio of radioactivity, similar to the decrease in

internalization-inhibited groups. However, the ratios in FSH-retreated groups were smaller than those of internalization-inhibited groups (10^{-5} M, $9.18 \pm 1.39\%$; 10^{-4} M, $7.41 \pm 0.47\%$; 10^{-3} M, $2.90 \pm 1.22\%$) and were decidedly smaller than that of down-regulated group.

Effects of $\text{Na}_2\text{S}_2\text{O}_3$ and FSH on relative change of surface radioactivity

Table 1 shows the relative amount of surface radioactivity. The ratio of surface radioactivity to internalized radioactivity (S/I), the ratio of surface radioactivity to the sum of surface and internalized radioactivities (S/S+I) and the ratio of surface radioactivity of the sum of surface, internalized and degraded radioactivities (S/S+I+D) were calculated in control, down-regulated, internalization-inhibited ($\text{FSH} + 10^{-3}$ M $\text{Na}_2\text{S}_2\text{O}_3$) and FSH-retreated ($\text{FSH} + 10^{-3}$ M $\text{Na}_2\text{S}_2\text{O}_3 \rightarrow \text{FSH}$) groups. All the three relative amounts showed a similar

TABLE 1. Effect of FSH and NaN_3 on relative amount of surface radioactivity

Culture condition	Relative amount of surface radioactivity (%)		
	S	S	S
	I	S+I	S+I+D
control	89.8 ± 19.5*	45.8 ± 5.0	9.56 ± 1.60
FSH	22.7 ± 9.6 ^a	17.2 ± 5.7 ^a	0.67 ± 0.33 ^a
FSH + NaN_3 (10^{-3} M)	86.5 ± 7.5	46.1 ± 2.3	11.09 ± 1.70
FSH + NaN_3 (10^{-3} M) → FSH	28.4 ± 6.1 ^a	21.6 ± 6.1 ^a	6.34 ± 0.63 ^b

After culture in various conditions, Sertoli cells were incubated with 2.8 ng ^{131}I -FSH and surface (S), internalized (I) and degraded (D) radioactivities were measured by the method described in "Materials and Methods".

* Mean ± S.E. (n=4).

a) Significantly different from values of both "control" and "FSH + NaN_3 (10^{-3} M)" (internalization-inhibited) groups, $P < 0.01$.

b) Significantly different from value of "FSH + NaN_3 (10^{-3} M)" (internalization-inhibited) group, $P < 0.05$.

group-to-group relation. The ratios of internalization-inhibited group were similar to the control values. All the values of both down-regulated and FSH-retreated groups were significantly smaller than the matched values of control and internalization-inhibited groups, except the difference in ratio $\text{S}/\text{S}+\text{I}+\text{D}$ between FSH-retreated and control groups.

Effect of FSH on rate constants of internalization and degradation

In order to calculate the rate of internalization, regression lines on semi-log plots were drawn for percentage of surface radioactivity against cold chase time (Fig. 6). Both in control and down-regulated groups, a regression line was obtained. The equations of the two regression lines were calculated to be $\ln[\text{HR}_s]_c = -4.174875 \times 10^{-2}t + \ln 80.36807$ for control group and $\ln[\text{HR}_s]_d = -7.028035 \times 10^{-2}t + \ln 68.132562$ for down-regulated group. Rate constants of dissociation and internalization were calculated as described in "Materials and Methods". Rate constant of internalization of down-regulated group ($6.94 \times 10^{-2} \pm 1.54 \times 10^{-3} \text{ min}^{-1}$) was significantly larger than that of control group ($4.11 \times 10^{-2} \pm 2.42 \times 10^{-3} \text{ min}^{-1}$). On the other hand, any significant difference in rate constant of dissociation was not recognized between control and down-regulated groups ($8.97 \times 10^{-4} \pm 8.42 \times 10^{-5} \text{ min}^{-1}$ and $6.11 \times 10^{-4} \pm 8.29 \times 10^{-5}$

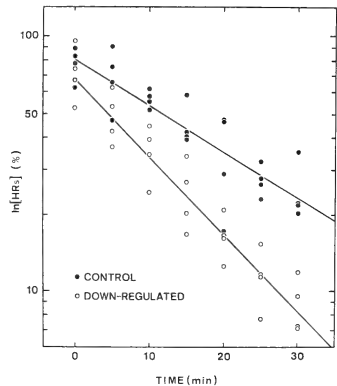


Fig. 6. Semi-log plots of surface radioactivity against cold chase time. Sertoli cells were cultured in F12/DME with (○) or without (●) FSH ($5 \mu\text{g}/\text{ml}$) for 4 days. After rinse with 0.2 M acetic acid, Sertoli cells were incubated with 2.8 ng of ^{131}I -FSH and cold chase was performed. Thereafter, dissociated, surface, internalized and degraded radioactivities were counted as described in "Materials and Methods".

min^{-1} , respectively). Finally, rate constants of degradation of control and down-regulated groups were calculated. The value was $6.61 \times 10^{-3} \pm 9.97$

$\times 10^{-5} \text{ min}^{-1}$ and $9.01 \times 10^{-3} \pm 9.57 \times 10^{-5} \text{ min}^{-1}$ in control and down-regulated group, respectively, and the difference between the two groups was statistically significant.

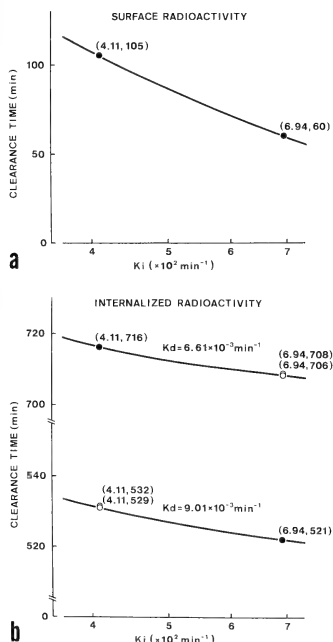


Fig. 7. Simulation of 99% clearance time of surface (a) and internalized (b) radioactivities. Values in parentheses represent the coordinates (readings of abscissa and ordinate each). Clearance time of both control and down-regulated group (●), and that of hypothetical state (○) were calculated by the use of parameters for initial radioactivity as follows: for control group and hypothetical state (upper coordinates), $[\text{HR}_S]_0 = 80.37\%$, $[\text{HR}_I]_0 = 19.63\%$; for down-regulated group and hypothetical state (lower coordinates), $[\text{HR}_S]_0 = 68.13\%$, $[\text{HR}_I]_0 = 31.67\%$. Other parameters used in this simulation were as follows: $k_{-1} = 6.11 \times 10^{-4} \text{ min}^{-1}$, $k_i = 4.11 \times 10^{-2}$ or $6.94 \times 10^{-2} \text{ min}^{-1}$, $k_d = 6.61 \times 10^{-3}$ or $9.01 \times 10^{-3} \text{ min}^{-1}$.

Simulation of clearance time of surface and internalized radioactivities

Ninety-nine percent clearance time of surface and internalized radioactivities is presented in Figure 7. The clearance time of surface radioactivity of control group ($k_i = 4.11 \times 10^{-2} \text{ min}^{-1}$) was 105 min and that of down-regulated group ($k_i = 6.94 \times 10^{-2} \text{ min}^{-1}$) was 60 min, being 57.1% of the value of control group (Fig. 7a). On the other hand, the clearance time of internalized radioactivity of control group ($k_i = 4.11 \times 10^{-2} \text{ min}^{-1}$, $k_d = 6.61 \times 10^{-3} \text{ min}^{-1}$) was 716 min and down-regulated group ($k_i = 6.94 \times 10^{-2} \text{ min}^{-1}$, $k_d = 9.01 \times 10^{-3} \text{ min}^{-1}$) was 521 min, being 72.8% of that of control group (Fig. 7b). Effect of difference of initial radioactivity ($[\text{HR}_S]_0$, $[\text{HR}_I]_0$) on the clearance time was only meager (when $k_i = 4.11 \times 10^{-2} \text{ min}^{-1}$ and $k_d = 9.01 \times 10^{-3} \text{ min}^{-1}$, 532 min vs. 529 min, at $[\text{HR}_S]_0 = 80.37\%$ and $[\text{HR}_I]_0 = 19.63\%$ vs. $[\text{HR}_S]_0 = 68.13\%$ and $[\text{HR}_I]_0 = 31.87\%$, respectively; when $k_i = 6.94 \times 10^{-2} \text{ min}^{-1}$ and $k_d = 6.61 \times 10^{-3} \text{ min}^{-1}$, 708 min vs. 706 min, at $[\text{HR}_S]_0 = 80.37\%$ and $[\text{HR}_I]_0 = 19.63\%$ vs. $[\text{HR}_S]_0 = 68.13\%$ and $[\text{HR}_I]_0 = 31.87\%$, respectively). The influence of k_i on the clearance time of internalized radioactivity was calculated to be 4.1 to 5.6%, and that of k_d , 94.4 to 95.9%, indicating that the effect of k_d was far greater than the effect of k_i .

DISCUSSION

A few possible mechanisms for the ligand-induced down-regulation of surface receptors may generally be conjectured as follows: 1) suppression of receptor synthesis (e.g. LH receptors in the rat granulosa cells [15]), 2) acceleration of receptor degradation (e.g. insulin receptors in 3T3-C2 mouse fibroblast [16]), and 3) acceleration of receptor internalization (e.g. LH receptors in MA-10 mouse Leydig tumor cells [17], calcitonin receptors in T 47D human breast cancer cells [18]). Of these mechanisms, suppression of receptor synthesis and acceleration of receptor degradation induce a decrease in the number of total receptors in the cells. Because down-regulation of receptors results in a decrease in the number of surface receptors, it may not always be accompanied by a decrease in the

total number of receptors. In fact, the evidence showing that neither the rate of synthesis nor the rate of degradation of total receptors was altered during down-regulation of surface receptors has been afforded for insulin receptors of chick liver cells [19]. Therefore, the change in the rate of internalization has been paid much attention in the present study.

In order to verify the hypothesis that down-regulation of FSH receptors might be related to internalization of FSH-FSH receptor complexes, the effects of inhibitor of internalization on down-regulation were examined, and internalization rate constants were compared between control and down-regulated groups. At first, the effect of FSH added to the culture medium on the decrease of surface binding of ^{131}I -FSH in cultured Sertoli cells was confirmed. The result coincides well with our previous findings *in vivo* [7, 8]. Then, NaN_3 was used as an inhibitor of internalization of hormone-receptor complexes. NaN_3 chelates heme a of cytochrome c oxidase and serves as a potent inhibitor of electron transport system. Since internalization is carried out by receptor-mediated endocytosis [11, 20, 21] which is an energy dependent process [22–25], NaN_3 inhibits internalization of hormone-receptor complexes in dose-dependent manner as observed in the present study.

The treatment with NaN_3 was effective in decreasing the effects of exogenous FSH, which were observed as the decrease of not only surface radioactivity and internalized radioactivities and the increase of degraded radioactivity. Internalized radioactivity measured represents the difference between net internalized radioactivity and degraded radioactivity dissipated to the medium from Sertoli cells. Because the source of degraded radioactivity is surface radioactivity, the increase of the former by exogenous FSH treatment indicates the increase in internalization of receptor-bound hormone and degradation of the internalized hormone. However, the release of internalized radioactivity as degraded products seems to be not effective as compared to the incorporation of surface radioactivity, because relative amount of surface radioactivity (S/I and S/S+I) was decreased by FSH treatment.

The effect of NaN_3 was general suppression of

these FSH-induced changes in radioactivities, in support of our hypothesis that down-regulation of FSH receptor is due to internalization of FSH-FSH receptor complexes. The result of FSH-retreatment experiment revealed that the effect of NaN_3 was reversible as concerns surface and internalized radioactivities and, hence, the suppression of FSH-induced down-regulation by NaN_3 was not due to the toxic effect of NaN_3 on Sertoli cells. In contrast, the reversibility of NaN_3 effect on degraded radioactivity was not observed. The rise of intracellular pH by NaN_3 may be the reason of this discrepancy, because in this conjunction Carpenter *et al.* [26] and Seglen *et al.* [27] reported that NH_4Cl or chloroquine which is known to rise intracellular pH caused malfunction of lysosomes, and Hendy *et al.* [28] found that 1 to 2 weeks was necessary to restore the initial lysosome activity after chloroquine treatment. In the present study, degraded radioactivity was measured 4 days after NaN_3 treatment. Therefore, the restoration of lysosome activity might be still incomplete in FSH-retreated group and degraded radioactivity of FSH-retreated group could not reach the level of down-regulated group. Besides, degraded radioactivity of FSH-retreated group tended to decrease along with the increase in concentration of NaN_3 and internalized radioactivity reciprocally tended to show an increase. These results may indicate that once damaged lysosome could not degrade internalized hormone normally. Nevertheless, relative amount of surface radioactivity (S/S+I+D) showed a reversibility of NaN_3 treatment. This is because the accumulation of internalized radioactivity compensated the loss of degraded radioactivity.

We have proposed in a separate paper a kinetic model for internalization and degradation of ^{131}I -FSH after binding to surface receptors. In this kinetic model the deviation of algebraic functions for concentration of $[\text{HR}_s]_t$, $[\text{HR}_i]_t$ and $[\text{D}]_t$ was performed without presupposition that reactions were in the steady-state. Therefore, we could calculate the rate constants of internalization and degradation covering all the possible processes of the reaction. In the present study, the rate constant of internalization was shown to increase by exogenous FSH. This kinetic result and the effects of NaN_3 strongly support our hypothesis that

down-regulation of FSH receptors is due to internalization of FSH-FSH receptor complexes. The present results accord well with the findings in other systems that the reduction of surface receptor number was induced by the acceleration of internalization [19, 29, 30].

Ninety-nine percent clearance time represents the period of time the cells will require to decrease their total radioactivity to 1% at the time of cold chase. The present study showed that 99% clearance time of both surface radioactivity and internalized radioactivity in down-regulated group was decreased, and the rate of decrease of clearance time of surface radioactivity was greater than that of internalized radioactivity (57.1% vs. 72.8% of the control value), and that the rate constant of degradation was increased in down-regulated group, but was smaller than the rate constant of internalization (168.9% vs. 136.3%; $k_i^{\text{down-regulated}}/k_i^{\text{control}}$ vs. $k_d^{\text{down-regulated}}/k_d^{\text{control}}$, respectively). Besides, relative amount of surface radioactivity in Sertoli cells was decreased in down-regulated group. These data indicate that internalization of surface hormone was much accelerated than degradation of internalized hormone by exogenous FSH.

Some investigators have reported that internalized receptors would be recycled back to the cell surface and that the rate of recycling is slower than the rate of internalization [31-35]. Recently, Saez *et al.* [10] demonstrated the possibility of recycling of FSH receptors in pig Sertoli cells. Although recycling of FSH receptors might have taken place in the present systems, our kinetic model did not deal with this possibility.

Acceleration of internalization by exogenous FSH may lead the intracellular accumulation of FSH receptors. If recycling of internalized receptors may occur very slowly in comparison with the rate of internalization, this would cause a decrease in the number of surface receptors. On the other hand, it was shown that the rate constant of degradation did not affect the change in surface radioactivity but the change in internalized radioactivity and its clearance time (unpublished observation). Clearance time of internalized radioactivity depends on the rate constants of both internalization and degradation, while the present

simulation study revealed that clearance time of internalized radioactivity was mainly related with the rate constant of degradation (Fig. 7). Therefore, the increase of degradation rate constant by exogenous FSH seems to induce a reduction in clearance time of internalized radioactivity which may indicate the acceleration of scavenging of internalized hormone out of Sertoli cells.

ACKNOWLEDGMENT

The author is grateful to Professor Seiichi Kawashima of Hiroshima University for his advice during the course of this study and kind help in preparing the manuscript. This work was supported in part by a Grant-in-Aid from the Ministry of Education, Science and Culture, Japan (No.62480023 awarded to Dr. S. Kawashima).

Thanks are also due to Dr. S. Raiti and the Pituitary Hormone Distribution Program, the National Institute of Arthritis, Diabetes, Digestive and Kidney Diseases (NIADDK) for kind supply of rat gonadotropins. Porcine FSH was also provided by the National Institutes of Health, Bethesda, Md.

REFERENCES

- 1 Mancini, R. E., Castro, A. E. and Seiguer, A. C. (1967) Histologic localization of follicle-stimulating and luteinizing hormone in the rat testes. *J. Histochem. Cytochem.*, **15**: 516-525.
- 2 Castro, A. E., Alonso, A. and Mancini, R. E. (1972) Localization of follicle-stimulating and luteinizing hormones in the rat testis using immunohistological tests. *J. Endocrinol.*, **52**: 129-136.
- 3 Fritz, I. B. (1978) Sites of action of androgens and follicle stimulating hormone on cells of the seminiferous tubule. In "Biochemical Actions of Hormones." Ed. by G. Litwack, Academic Press, New York, vol. 5, pp. 249-281.
- 4 Risbridger, G. P., Hodgson, Y. M. and de Kretser, D. M. (1981) Mechanism of action of gonadotropins on the testis. In "The Testis." Ed. by H. Burger and D. de Kretser, Raven Press, New York, pp. 195-212.
- 5 O'Shaughnessy, P. J. and Brown, P. S. (1978) Reduction in FSH receptors in the rat testis by injection of homologous hormones. *Mol. Cell. Endocrinol.*, **12**: 9-15.
- 6 Francis, G. L., Brown, T. J. and Bercu, B. B. (1981) Control of Sertoli cell response to FSH: Regulation by homologous hormone exposure. *Biol. Reprod.*, **24**: 955-961.
- 7 Tsutsui, K., Shimizu, A., Kawamoto, K. and

- Kawashima, S. (1983) Changes of testicular follicle-stimulating hormone receptor during maturation and after hypophysectomy in some vertebrates. In "Recent Trends in Life Sciences". Ed. by A. Gopalakrishna, S. B. Singh and A. K. Saxena, Manu Publications, Kanpur, India, pp. 93-102.
- 8 Tsutsui, K., Shimizu, A., Kawamoto, K. and Kawashima, S. (1985) Developmental changes in the binding of FSH to the testicular preparations of mice and the effects of hypophysectomy and administration of FSH on the binding. *Endocrinology*, **117**: 2534-2543.
- 9 Fletcher, P. W. and Reichert, Jr., L. E. (1984) Cellular processing of follicle-stimulating hormone by Sertoli cells in serum-free culture. *Mol. Cell. Endocrinol.*, **34**: 39-49.
- 10 Saez, J. M. and Jaillard, C. (1986) Processing of follitropin and its receptor by cultured pig Sertoli cells: effect of monensin. *Eur. J. Biochem.*, **158**: 91-97.
- 11 Shimizu, A., Tsutsui, K. and Kawashima, S. (1987) Autoradiographic study of binding and internalization of follicle-stimulating hormone in the mouse testis minces *in vitro*. *Endocrinol. Japon.*, **34**: 431-442.
- 12 Tsutsui, K. and Ishii, S. (1978) Effects of follicle-stimulating hormone and testosterone on receptors of follicle-stimulating hormone in the testis of the immature Japanese quail. *Gen. Com. Endocrinol.*, **36**: 297-305.
- 13 Nakhla, A. M., Mather, J. P., Janne, O. A. and Bardin, C. W. (1984) Estrogen and androgen receptors in Sertoli, Leydig, myoid and epithelial cells: effects of time in culture and cell density. *Endocrinology*, **115**: 121-128.
- 14 Sokal, R. R. (1973) Regression analysis. In "Introduction to Biostatistics". Ed. by R. R. Sokal, W. H. Freeman & Co., San Francisco, pp. 277-317.
- 15 Schwall, R. H. and Erickson, G. F. (1984) Inhibition of synthesis of luteinizing hormone (LH) receptors by a down-regulating dose of LH. *Endocrinology*, **114**: 1114-1123.
- 16 Knutson, V. P., Ronnett, G. V. and Lane, M. D. (1982) Control of insulin receptor level in 3T3 cells: Effect of insulin-induced down-regulation and dexamethasone-induced up-regulation on rate of receptor inactivation. *Proc. Natl. Acad. Sci. USA*, **79**: 2822-2826.
- 17 Lloyd, C. E. and Ascoli, M. (1983) On the mechanisms involved in the regulation of the cell-surface receptors for human chorionadotropin and mouse epidermal growth factor in cultured Leydig tumor cells. *J. Cell Biol.*, **96**: 521-526.
- 18 Findlay, D. M. and Martin, T. J. (1984) Relationship between internalization and calcitonin-induced receptor loss in T 47D cells. *Endocrinology*, **115**: 78-83.
- 19 Krupp, M. and Lane, M. D. (1981) On the mechanism of ligand-induced down-regulation of insulin receptor level in the liver cell. *J. Biol. Chem.*, **256**: 1689-1694.
- 20 Goldstein, J. L., Anderson, R. G. W. and Brown, M. S. (1979) Coated pits, coated vesicle and receptor mediated endocytosis. *Nature*, **279**: 679-685.
- 21 Willingham, M. C. and Pastan, I. (1980) The receptosome: an intermediate organelle of receptor mediated endocytosis in cultured fibroblasts. *Cell*, **27**: 67-77.
- 22 Ascoli, M. and Puett, D. (1978) Degradation of receptor bound human choriogonadotropin by murine Leydig tumor cells. *J. Biol. Chem.*, **253**: 4892-4899.
- 23 Ascoli, M. (1982) Internalization and degradation of receptor-bound human chorionadotropin in Leydig tumor cells. *J. Biol. Chem.*, **257**: 13306-13311.
- 24 Wiley, H. S. and Cunningham, D. D. (1982) The endocytotic rate constant: a cellular parameter for quantitating receptor-mediated endocytosis. *J. Biol. Chem.*, **257**: 4222-4229.
- 25 Standaert, M. L. and Pollet, R. J. (1984) Equilibrium model for insulin-induced receptor down-regulation: regulation of insulin receptors in differentiated BC3H-1 myocytes. *J. Biol. Chem.*, **259**: 2346-2354.
- 26 Carpenter, G. and Cohen, S. (1976) ¹²⁵I-labeled human epidermal growth factor: binding, internalization and degradation in human fibroblasts. *J. Cell Biol.*, **71**: 159-171.
- 27 Seglen, P. O. and Reith, A. (1976) Ammonia inhibition of protein degradation in isolated rat hepatocytes. *Exp. Cell Res.*, **100**: 276-280.
- 28 Hendy, R. J., Abraham, R. and Grasso, P. (1969) The effect of chloroquine on rat heart lysosomes. *J. Ultrastruct. Res.*, **29**: 485-495.
- 29 Lloyd, C. E. and Ascoli, M. (1983) On the mechanisms involved in the regulation of the cell-surface receptors for human chorionadotropin and mouse epidermal growth factor in cultured Leydig tumor cells. *J. Cell Biol.*, **96**: 521-526.
- 30 Findlay, D. M. and Martin, T. J. (1984) Relationship between internalization and calcitonin induced receptor loss in T 47D cells. *Endocrinology*, **115**: 78-83.
- 31 Fehlmann, M., Carpentier, J.-L., Obberghen, E. V., Freychet, P., Thamm, P., Saunders, D., Brandenburg, D. and Orci, L. (1982) Internalized insulin receptors are recycled to the cell surface in rat hepatocytes. *Proc. Natl. Acad. Sci. USA*, **79**: 5921-5925.
- 32 Krupp, M. N. and Lane, M. D. (1982) Evidence for different pathways for the degradation of insulin and

- insulin receptor in the chick liver cell. *J. Biol. Chem.*, **257**: 1372-1377.
- 33 Knutson, V. P., Ronnett, G. V. and Lane, M. D. (1983) Rapid, reversible internalization of cell surface insulin receptors: correlation with insulin-induced down-regulation. *J. Biol. Chem.*, **258**: 12139-12142.
- 34 Peterson, S. W., Miller, A. L., Kelleher, R. S. and Murray, E. F. (1983) Insulin receptor down regulation in human erythrocytes. *J. Biol. Chem.*, **258**: 9605-9607.
- 35 Carpentier, J.-L., Dayer, J.-M., Lang, U., Silverman, R., Orci, L. and Gorden, P. (1984) Down-regulation and recycling of insulin receptors: effect of monensin on IM-9 lymphocytes and U-937 monocyte-like cells. *J. Biol. Chem.*, **259**: 14190-14195.

Causal Analysis of the Development of Uterine Adenomyosis in Mice

TAKAO MORI and HIROSHI NAGASAWA¹

*Zoological Institute, Faculty of Science, University of Tokyo,
Bunkyo-ku, Tokyo 113 and ¹Experimental Animal Research
Laboratory, Meiji University, Tama-ku,
Kawasaki, Kanagawa 214, Japan*

ABSTRACT—Mechanisms of the development of uterine adenomyosis were examined in female SHN mice from various points of view. Treatments with prolactin during neonate (1–14 days of age) and youth (40–79 days of age) induced a high incidence of adenomyosis. On the other hand, transitory withdrawal of ovaries during youth suppressed the spontaneous development of adenomyosis with age, which indicates the presence of a critical period for the genesis of this lesion. Associated with the development of adenomyosis, uteri showed a marked accumulation of collagen, irregularities in myometrial organization, degeneration of smooth muscle cells, conspicuous development and dilatation of vascular network and cystic hyperplasia of uterine glands with a high mitotic rate. These changes are the limiting factors for the genesis of adenomyosis. The possible relevance of these results to the hormonal environment is discussed.

INTRODUCTION

Uterine adenomyosis, which occurs spontaneously in human and experimental animals with age [1–3], is an abnormal growth of glands and stroma into and beyond the smooth muscle layers of the uterus. Lipschütz *et al.* [4] and Ostrander *et al.* [5] suggest that an imbalance involving high levels of progesterone is primarily needed to bring about adenomyosis. Meanwhile, isografting of pituitary gland into mice has been found to accelerate this lesion. This induction system implies a key role of prolactin in the genesis of uterine adenomyosis, although ovarian sex steroids (oestrogen and progesterone) participate in this process [6–11]. Furthermore, the spontaneous development of adenomyosis with age can be prevented by administration of bromocriptine (CB-154), a potent suppressor of pituitary prolactin release, during youth [7, 12]. These results indicate that a certain hormonal milieu associated with a high circulating levels of prolactin during

youth is a limiting factor for the development of adenomyosis at advanced age.

The symptoms ascribed to human adenomyosis are pain, especially with menstrual periods, cramps, and abnormally prolonged and profuse bleeding, while this lesion is also considered to be one of the causes of sterility in human and animals [13, 14]. Thus, it is worthwhile to elucidate the mechanisms of the development of adenomyosis in an animal model for the management, therapy and prophylaxis of this lesion in human.

The goals of the present studies are (1) to examine the contribution of prolactin, (2) to reveal the histopathological changes of endometrium and myometrium and (3) to analyze the proliferative activity of uterine tissues, in the development of adenomyosis in female mouse model.

MATERIALS AND METHODS

Animals

Female mice of the SHN strain housed in a temperature- ($25 \pm 0.5^\circ\text{C}$) and light-controlled (12 hr/day) animal room were used. Throughout the

Accepted May 12, 1988

Received April 14, 1988

experiments, mice were kept 4 to 5 in a solid-bottom cage (32×21×14 cm) with wood shavings and provided with a commercial diet and tap water *ad libitum*.

Experiment I

Mice were divided into 4 groups. The 1st group was subcutaneously injected with 0.5 μ g mouse prolactin donated by Dr. Parlow (AFP-4111-E) dissolved in 0.02 ml phosphate buffer saline daily for 14 days from the day of birth and the 2nd group was injected with 5 IU prolactin (bovine, Teikoku Hormone Mfg. Co. Ltd., Tokyo) dissolved in 0.1 ml physiological saline for 40 days beginning on 40 days of age. The 3rd and the 4th groups were given the corresponding vehicles only as the controls of the 1st and the 2nd experimental groups, respectively. Data of these controls were pooled in Results, because of no differences between groups. All mice were killed at 80 days of age. Each group consisted of 7-11 mice.

Uteri were fixed in Bouin's fluid, dehydrated in alcohol, embedded in paraffin and sectioned at 7 μ m. The sections were stained with haematoxylin-eosin. The statistical significance of difference between groups in the incidence of adenomyosis was evaluated by the χ^2 -test with Yate's correction.

Experiment II

Mice were divided into 5 groups as shown in Figure 1. The 1st and the 2nd groups (Groups A

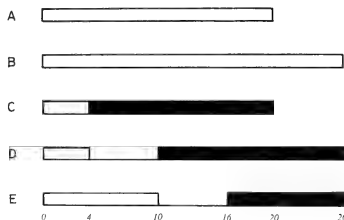


FIG. 1. Experimental schedules of Experiment II. Weeks in age are presented under the figure. Open bars: periods during which mice have ovaries *in situ*; dark bars: periods during which mice have ovarian grafts under abdominal skin; lines: periods during which mice are deficient of ovaries.

and B) were maintained with no treatment and killed at 20 and 26 weeks of age, respectively. The 3rd group (Group C) was ovariectomized at 4 weeks of age and simultaneously isografted with an ovary from 4-week-old mouse each under the abdominal skin. The 4th and the 5th groups (Groups D and E) were ovariectomized at 4 and 10 weeks of age, respectively, and transplanted with single ovaries from 4-week-old mice each under the abdominal skin 6 weeks after ovariectomy. The last three groups (Groups C, D and E) were killed 16 weeks after the transplantation of ovaries. Each group consisted of 12-21 mice.

Uteri, ovaries and ovarian grafts were fixed in Bouin's fluid and prepared as 7 μ m sections by a standard method. The sections were stained with haematoxylin-eosin. The statistical significance of difference between groups in the incidence of adenomyosis was evaluated by the χ^2 -test with Yate's correction.

Experiment III

Each mouse was given a single anterior pituitary gland or a piece of submaxillary gland from age-matched normal male mouse in the lumen of the right uterine horn at 5 weeks of age according to the method reported previously [9] and killed, 5 mice each, at 6, 9 and 12 weeks after the grafting.

Uteri were removed, fixed in Bouin's fluid, embedded in paraffin, and cut into 7 μ m transverse sections. In order to examine collagen accumulation, slides were stained with Masson's trichrome method.

Experiment IV

In order to examine the changes of the architecture of vascular network in the uterus bearing adenomyosis, mice were given single anterior pituitary glands each in the lumina of the right uterine horns at 5 weeks of age and killed 7 weeks after the grafting. Mice receiving the submaxillary isografts were also killed at 12 weeks of age as the control.

At autopsy, 6 experimental mice developing the subserosal nodules in uterus, an advanced state of adenomyosis, and 6 control mice showing no nodule formation were perfused with India ink through the left carotid artery under the nembutal

anaesthesia. Immediately after the perfusion, uteri were fixed in Telly's solution for one day. The specimens were kept in acetone for two days, dehydrated in alcohol and then immersed in toluene for the whole-mount preparation.

Experiment V

Five mice were given single anterior pituitary glands each in the lumina of the right uterine horns at 5 weeks of age and killed 8–9 weeks later. Five control mice receiving the submaxillary isografts were killed between 13 and 14 weeks of age. Beginning on 6–7 weeks after grafting, all mice were examined the vaginal smears and killed on the day of oestrus. Five hours before autopsy, mice were given single subcutaneous injections of colchicine (0.1 mg/0.1 ml physiological saline/20 g body weight).

Uteri were fixed in Bouin's fluid and prepared as 7 μ m sections by a standard method. The sections were stained with haematoxylin-eosin. In order to examine the mitotic activity among luminal and gland epithelial cells, stromal cells and smooth muscle cells of the inner and the outer layers in the middle region of the uterine horns, 5 sections were randomly sampled and colchicine-arrested mitoses were counted in about 500 cells of each tissue per section. The mitotic rate was calculated as a percentage of dividing cells for 5 hr. All slides were examined without knowledge of treatment. The statistical significance of the difference between groups was evaluated by Student's *t*-test.

Experiment VI

Five experimental mice received single anterior pituitary glands each in the lumina of the right uterine horns at 5 weeks of age and killed 5 weeks later. Five control mice receiving the submaxillary isografts were killed at 10 weeks of age.

Uteri were fixed in Bouin's fluid for one day, dehydrated in alcohol, embedded in paraffin and sectioned at 7 μ m. Immunocytochemical demonstration of prolactin was carried out by avidin-biotin-peroxidase complex (ABC) method [15], using rabbit antiserum to mouse prolactin donated by Dr. Parlow (AFP-131078) and Vectastain ABC kit (Vector Lab. Inc., Burlingame, USA). Peroxidase activity was demonstrated by the reaction with 3,3'-diaminobenzidine tetrahydrochloride. The immunocytochemical assays were controlled by sections overlaid with normal rabbit serum or Tris buffer instead of the primary antibody, which showed no immunoreactive staining. In order to check the antigen specificity, the primary antibody was absorbed with mouse prolactin as reported by Tsubura *et al.* [16]. Immunoreactivity was completely abolished by the absorption.

RESULTS

Experiment I

As shown in Table 1, treatments with prolactin during neonate (1–14 days of age) and youth (40–79 days of age) significantly increased the incidence of adenomyosis as compared to the control.

TABLE 1. Incidence of adenomyosis in SHN mice treated with prolactin during neonate and youth

Treatment (age)	No. of mice	No. and % of mice showing adenomyosis
Prolactin (1–14 days)	7	5 (71.4%) ^b
Prolactin (40–79 days)	9	6 (66.7%) ^b
Vehicle ^a (1–14 and 40–79 days)	20	4 (20.0%)

^aEleven out of 20 mice were injected with phosphate buffer saline during 1–14 days of age and the remaining nine mice were given physiological saline during 40–79 days of age.

^bDiffers from the control, $P < 0.05$.

TABLE 2. Incidence of adenomyosis in SHN mice after temporary removal of ovaries

Group ^a	No. of mice	Incidence of adenomyosis (%)	No. of mice bearing adenomyosis and ovaries with no corpora lutea/ No. of mice bearing adenomyosis	No. of mice bearing no adenomyosis and ovaries with no corpora lutea/ No. of mice bearing no adenomyosis
A	21	61.9 ^{b,c}	0/13	0/8
B	12	100.0 ^{b,d,e}	0/12	—
C	20	60.0 ^{d,f}	0/12	2/8
D	21	23.8 ^{c,e,f,g}	0/5	3/16
E	18	66.7 ^g	1/12	1/6

^aSee Fig. 1. for details of treatment.Incidences which have the same superscripts are significantly different from each other (^{b,c,d,f} $P < 0.05$;^g $P < 0.02$; ^e $P < 0.001$).

Experiment II

The results are summarized in Table 2. Adenomyosis developed spontaneously in intact female mice by 20 weeks of age (Group A) and its incidence significantly increased 6 weeks later (Group B).

In 20-week-old mice ovariectomized at 4 weeks of age and simultaneously given ovarian isografts (Group C), the incidence of adenomyosis was comparable to that of the intact 20-week-old controls but was lower than that of the intact 26-week-old controls. However, in 26-week-old mice ovariectomized at 4 weeks of age and given ovarian isografts at 10 weeks of age (Group D), the development of adenomyosis was significantly reduced by the removal of ovaries for 6 weeks when compared with those in the intact controls at 20 weeks of age. By contrast, the deficiency of ovaries between 10 and 16 weeks of age (Group E) resulted in no difference in the incidence of adenomyosis from that of 20-week-old intact controls. The incidences of adenomyosis in these last 2 groups (D and E) were significantly lower than that in the 26-week-old intact controls.

As shown in Table 2, the ovaries of almost all mice developing adenomyosis contained various sizes of follicles and a few corpora lutea. On the other hand, the mice bearing ovarian grafts with follicles but lack of corpora lutea showed no sign of the development of adenomyosis in their hypoplastic uteri.

Experiment III

As shown in Figure 2, mice showed a marked

accumulation of collagen in the inner circular smooth muscle layer, while not so much in the outer longitudinal smooth muscle layer 9 weeks after the pituitary grafting. The inner myometrium was interrupted by collagen and individual and groups of muscle cells became encased in collagen. In addition, collagen accumulation was also conspicuous in the stroma adjacent to the inner myometrium which contained the invasion of endometrium. Twelve weeks after the pituitary grafting, the inner and the outer smooth muscle layers were highly disorganized by a marked infiltration of collagen. However, in mice at 6 weeks after the pituitary grafting, a relatively large amount of collagen was found only in the connective tissue space between the inner and the outer muscle layers and in the submyometrial region of the stroma. There was no accumulation of collagen among the luminal epithelial cells.

When compared to pituitary-grafted mice, collagen accumulation in the control mice was limited, in which a relatively small amount of collagen distributed evenly throughout all tissues except for the epithelium. However, the amount of collagen became conspicuous in the uteri of control mice at 12 weeks of age, especially in the inner smooth muscle layers which, sometimes, contained an early stage of adenomyotic changes.

Experiment IV

In the pituitary-grafted mice bearing adenomyotic changes, the uterus showed a disintegration of myometrium due to derangement and involution of smooth muscle cells (Fig. 3) unlike the well-regulated bundles densely packed with smooth

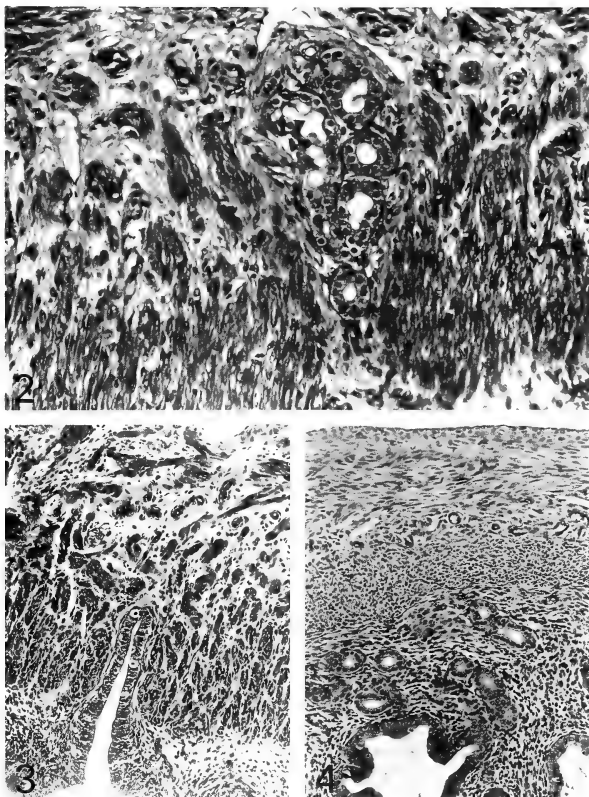


FIG. 2. Uterus of a 14-week-old mouse given a single pituitary isograft at 5 weeks of age. Note accumulation of collagen in the connective tissue space between the inner and the outer smooth muscle layers, and in the inner layer. Individual and groups of muscle cells become encased in the collagen and ectopic glands are also enclosed by the collagen. $\times 410$

FIG. 3. Uterus of a 12-week-old mouse given a single pituitary isograft at 5 weeks of age. Note the disintegration of myometrium due to the derangement and involution of smooth muscle cells. $\times 120$

FIG. 4. Uterus of a 12-week-old mouse given a submaxillary isograft at 5 weeks of age. Note well-regulated myometrium packed densely with smooth muscle cells. $\times 120$

muscle cells in the control mice receiving the isograft of submaxillary gland (Fig. 4).

Associated with the changes of myometrium, a marked development and dilatation of the blood

vessels were observed in the connective tissue space between the inner and the outer muscle layers of the pituitary-grafted mice with adenomyotic changes (Fig. 5), but not in the controls. In

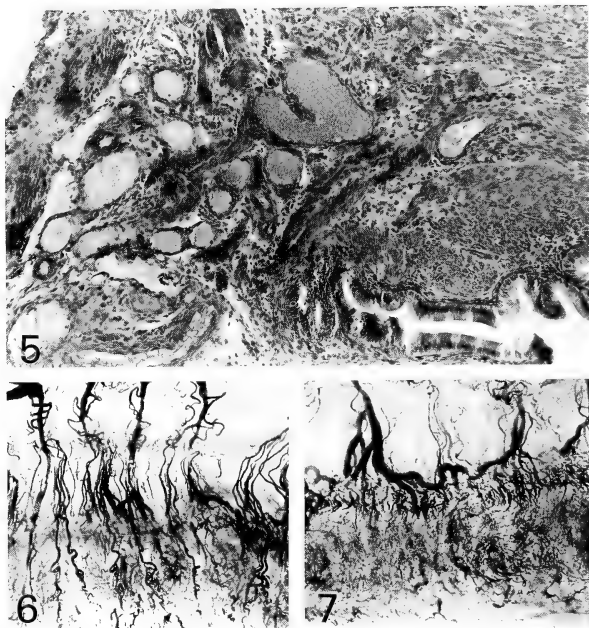


FIG. 5. Uterus of a 12-week-old mouse given a single pituitary isograft at 5 weeks of age. Note dilated blood vessels in the connective tissue space between the inner and the outer muscle layers. $\times 120$

FIG. 6. Uterus of a 12-week-old mouse given a single pituitary isograft at 5 weeks of age. Note straight penetration of the blood vessels across the myometrium. $\times 10$

FIG. 7. Uterus of a 12-week-old mouse given a submaxillary isograft at 5 weeks of age. Note complex vascularization in uterus. The picture of capillary network comes out of focus because of winding pattern of the vascularization. $\times 10$

the pituitary-grafted mice, the blood vessels run straight across the myometrium showing disintegration of muscular-bundles (Fig. 6), when compared with the controls in which thin blood vessels run winding and the running pattern of the capillary network were hard to follow by a fixed focus (Fig. 7).

Experiment V

The high mitotic rates were observed in the epithelial cells of uterine glands and stromal cells

of pituitary-grafted mice (Table 3). Furthermore, the mitotic rate of the luminal epithelial cells in the pituitary-grafted mice was slightly high as compared to that in the control. By contrast, the significantly larger numbers of mitotic figures were found in smooth muscle cells of the myometrium in the control mice than in the pituitary-grafted mice with adenomyotic changes.

Experiment VI

Both in the experimental and the control mice,

TABLE 3. Mitotic activity of uteri in mice with isografts of pituitary (PT) or submaxillary (SM) glands (Mean \pm SEM)

Group	Luminal epithelial cells	Gland epithelial cells	Stromal cells	Smooth muscle cells of inner myometrium	Smooth muscle cells of outer myometrium
PT	4.81 \pm 0.78	4.65 \pm 0.30	3.53 \pm 0.22	0.49 \pm 0.11	0.46 \pm 0.17
SM	3.33 \pm 0.25	2.42 \pm 0.23	1.80 \pm 0.19	2.22 \pm 0.40	1.77 \pm 0.08
Significance	P > 0.05	P < 0.05	P < 0.05	P < 0.01	P < 0.001

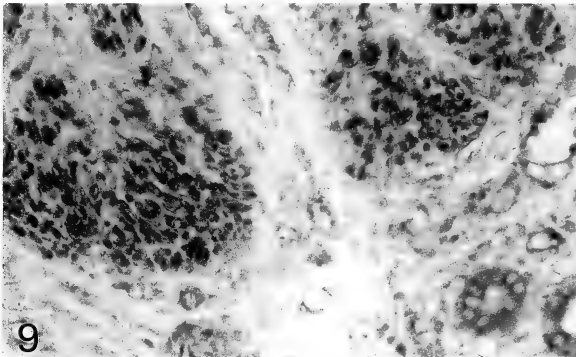


FIG. 8. Uterus of a 10-week-old mouse given a single pituitary isograft at 5 weeks of age. The section is stained immunocytochemically for prolactin. Some cells of luminal and gland epithelium are stained and the positive cells are intermixed with unstained cells. $\times 410$

FIG. 9. Uterus of a 10-week-old mouse given a single pituitary isograft at 5 weeks of age. The section is stained immunocytochemically for prolactin. Smooth muscle cells of the inner myometrium are stained. $\times 410$

immunocytochemically positive staining of prolactin by ABC method was found in uterine tissues such as luminal and glandular epithelial cells (Fig. 8), and inner and outer myometrial cells (Fig. 9), but not in stromal fibroblasts. There was little difference in the prolactin staining pattern of uterus between the pituitary-grafted mice with adenomyosis and the control, except that the former showed consistent and strongly positive reaction.

DISCUSSION

Treatments with prolactin during neonate and youth resulted in an early development of adenomyosis, indicating that prolactin plays a key role in the development of this lesion. In rats treated neonatally with prolactin, the serum and pituitary levels of prolactin were similar to those in the control at early pro-oestrus but were significantly higher than the controls on the 2nd day of dioestrus [17]. The results of ovariectomy and replacement with ovarian graft on uterine adenomyosis suggest that in mice ovarian hormones during youth also participates in the development of adenomyosis, and that there is a critical period in this process. In addition, the result of the presence of corpora lutea in grafted ovaries of mice developing adenomyosis stresses an important participation of progesterone in this process. Ostrander *et al.* [5] claimed that progesterone is a limiting factor for the genesis of adenomyosis, since continuous progesterone treatment results in the development of adenomyosis in ovariectomized mice. However, Mori *et al.* [8] have reported that the treatment with progesterone alone does not produce adenomyotic changes in the ovariectomized and pituitary-grafted mice, but progesterone treatment in combination with oestrogen results in the development of this lesion. While progesterone treatment accelerated the appearance of adenomyosis in the intact mice, progesterone in combination with prolactin further enhanced the effect of progesterone, such as subserosal nodule formation [18]. Moreover, the previous finding that spontaneous development of adenomyosis is completely inhibited by CB-154 treatment during a limited period of early postnatal life [7, 12] clearly indicates an important contribution of prolactin to the genesis

of adenomyosis. From these results, it is plausible that the initiation or the development of adenomyosis is primarily induced by prolactin, and the progression of the lesion is dependent upon progesterone together with oestrogen. This hypothesis would be supported by the intimate relationship between progesterone and prolactin; prolactin can stimulate functional development of corpora lutea, leading to progesterone secretion. It has been reported that in mice pituitary grafting induces the elevation of prolactin levels within 3 weeks to the levels during pregnancy associated with an increase in serum progesterone levels [11].

In the studies of the histogenesis of adenomyosis [6, 19, 20], early sign of the adenomyotic changes is reported to be the infiltration of stromal fibroblasts into the inner myometrium. Since the invasion is observed mainly along the blood vessels throughout the myometrium, aberrant endometrial tissue is often associated with dilated blood vessels. It was also pointed out that hypertrophy and hyperplasia of uterine vessels might play an important role in the development of adenomyosis [5, 21]. The present results of whole-mount preparation clearly show that adenomyotic change of uterus was often associated with both a marked dilatation and straight penetration of the blood vessels, which may be due to the physical damage of the muscle layer. In intact mice without adenomyosis, well-organized muscle bundles prevent the proliferation of the endometrial tissues and make the winding pattern of the running of blood vessels.

Ostrander *et al.* [5] have claimed that collagen accumulation is associated with the development of adenomyosis. The present data indicate that an increasing collagen accumulation with age demarcated the myometrium, leading to a massive destruction of the smooth muscle layer. It is revealed that collagen accumulation within the inner circular smooth muscle layer occurs after continuous oestrogen exposure [5]. Since the disintegration of the myometrium due to the involution and distorted polarity of smooth muscle cells are reported to be responsible for the invasion of endometrial tissues into the musculature [6, 20], it is evident that collagen accumulation is one of the causes of the disintegration of the myometrium.

The present results on the mitotic rate showed a

high proliferative activity in the epithelial cells of uterine glands and stromal cells, while not in myometrial cells, in the pituitary grafted-mice. This may reflect the degeneration of the muscular tissues by the pituitary grafting. The cells of both uterine glands and muscle layers showed the positive reaction in prolactin-immunocytochemical staining. Thus, the present findings imply that the disintegration of the myometrium produced by a low mitotic activity and a high proliferative activity of the uterine glands as well as stromal cells are ascribable to the invasion of endometrial tissues into the musculature, which is induced primarily by prolactin.

In conclusion, the present and the previous findings in our laboratories suggest that a hormonal environment induced by pituitary grafting has two effects on the uterine tissues: one is the trophic effect on the proliferation of uterine gland cells and stromal cells, and another is the inhibitory effect on the proliferation of smooth muscle cells.

ACKNOWLEDGMENTS

We thank Dr. A. F. Parlow, Pituitary Hormone & Antiserum Center, Harbor-UCLA Medical Center, Torrance, CA, USA, for mouse prolactin and its antiserum. This work was supported by Grants-in-Aid for Fundamental Scientific Research to TM (No. 60540478) and to HN (No. 60560292) from the Ministry of Education, Science and Culture, Japan.

REFERENCES

- Mody, J. K. (1963) Structural changes in the ovaries of IF mice due to age and various other states: Demonstration of spontaneous pseudopregnancy in grouped virgins. *Anat. Rec.*, **145**: 439-447.
- McCann, T. O. and Myers, R. E. (1970) Endometriosis in rhesus monkey. *Am. J. Obstet. Gynecol.*, **106**: 516-523.
- Blaustein, A. (1977) *Pathology of the Female Genital Tract*. Springer-Verlag, New York, Heidelberg, Berlin, p. 404.
- Lipschütz, A., Iglesias, R., Panasevich, V. I. and Salinas, S. (1967) Pathological changes induced in the uterus of mice with the prolonged administration of progesterone and 19-nor-contraceptives. *Brit. J. Cancer*, **21**: 160-165.
- Ostrander, P. L., Mills, K. T. and Bern, H. A. (1985) Longterm responses of the mouse uterus to neonatal diethylstilbestrol treatment and to later sex hormone exposure. *J. Natl. Cancer Inst.*, **74**: 121-135.
- Mori, T. and Nagasawa, H. (1983) Mechanisms of development of prolactin-induced adenomyosis in mice. *Acta Anat.*, **116**: 46-54.
- Mori, T. and Nagasawa, H. (1984) Alteration of the development of mammary hyperplastic alveolar nodules and uterine adenomyosis in SHN mice by different schedules of treatment with CB-154. *Acta Endocrinol.*, **107**: 245-249.
- Mori, T., Nagasawa, H. and Takahashi, S. (1981) The induction of adenomyosis in mice by intrauterine pituitary isografts. *Life Sci.*, **29**: 1277-1282.
- Mori, T., Nagasawa, H. and Nakajima, Y. (1982) Strain-difference in the induction of adenomyosis by intrauterine pituitary grafting in mice. *Lab. Anim. Sci.*, **32**: 40-41.
- Huseby, R. A. and Thurlow, S. (1982) Effects of prenatal exposure of mice to "low-dose" diethylstilbestrol and the development of adenomyosis associated with evidence of hyperprolactinemia. *Am. J. Obstet. Gynecol.*, **144**: 939-949.
- Huseby, R. A., Soares, M. J. and Talamantes, F. (1985) Ectopic pituitary grafts in mice: Hormone levels, effects of fertility, and the development of adenomyosis uteri, prolactinomas, and mammary carcinomas. *Endocrinology*, **116**: 1440-1448.
- Nagasawa, H. and Mori, T. (1982) Stimulation of mammary tumorigenesis and suppression of uterine adenomyosis by temporary inhibition of pituitary prolactin secretion during youth in mice. *Proc. Soc. Exp. Biol. Med.*, **171**: 164-167.
- Emge, L. A. (1962) The elusive adenomyosis of the uterus: Its historical past and its present state of recognition. *Am. J. Obstet. Gynecol.*, **83**: 1541-1563.
- Mori, T. and Nagasawa, H. (1984) Reproductive outcome in mice with experimentally induced-adenomyosis. *IRCS Med. Sci.*, **12**: 413.
- Hsu, S.-M., Raine, L. and Fanger, H. (1981) A comparative study of the peroxidase-antiperoxidase method and an avidin-biotin complex method for studying polypeptide hormones with radioimmunoassay antibodies. *Am. J. Clin. Path.*, **75**: 734-738.
- Tsubura, A., Morii, S., Mori, T. and Nagasawa, H. (1986) Immunoreactive prolactin in mouse urethral glands. *Acta Anat.*, **126**: 263-265.
- Nagasawa, H., Yanai, R., Kikuyama, S. and Mori, J. (1973) Effect of neonatal administration of prolactin on pituitary secretion of prolactin and gonadotrophins in adult female rats. *J. Endocrinol.*, **59**: 377-378.
- Nagasawa, H., Ishida, M. and Mori, T. (1987) Effects of treatment with prolactin or progesterone on the coincidence of mammary tumors and uterine adenomyosis in young SHN mice. *Lab. Anim. Sci.*,

- 37: 200-201.
- 19 Mori, T., Ohta, Y. and Nagasawa, H. (1984) Ultrastructural changes in uterine myometrium of mice with experimentally-induced adenomyosis. *Experientia*, **40**: 1385-1387.
- 20 Ohta, Y., Mori, T. and Nagasawa, H. (1985) Ultrastructural changes of endometrium and myometrium during development of adenomyosis in mice with ectopic pituitary transplants. *Zool. Sci.*, **2**: 239-247.
- 21 Schwarz, O. H. and Sherman, A. (1950) Hyperplasia of the endometrium, its relationship to hypertrophy and hyperplasia of the uterine vessels. *Am. J. Obstet. Gynecol.*, **59**: 1330-1345.

Neuroendocrine Regulation of the Development of Seasonal Morphs in the Asian Comma Butterfly, *Polygonia c-aureum* L.: Stage-dependent Changes in the Activity of Summer-morph-producing Hormone of the Brain-extracts

TADAKATSU MASAKI, KATSUHIKO ENDO¹
and KANJI KUMAGAI²

*Environmental Biology Laboratory, Biological Institute,
Faculty of Science, Yamaguchi University, Yamaguchi 753,
and ²Biological Institute, Faculty of Liberal Arts,
Yamaguchi University, Yamaguchi 753, Japan*

ABSTRACT—In the Asian comma butterfly, *Polygonia c-aureum* L., a physiological mechanism underlying the photoperiodic control of seasonal morphs involves a neuroendocrine system secreting summer-morph-producing hormone (SMPH). The SMPH extractable with 2% NaCl and precipitable by ammonium sulfate is thought to be a peptide hormone since it was inactivated by trypsin-hydrolysis. In the brains of long-day insects (LD-insects: summer-morph producers), SMPH-activity was low through the early and middle 5th instar, but peaked on the last day of the 5th instar (the pharate pupal stage). The activity once dropped on the day of larval-pupal ecdysis, but rose again gradually toward the end of the pupal stage. In contrast, in the brains of short-day insects (SD-insects: autumn-morph producers), it was low, but rose gradually through the 5th instar larval and pupal stages. The SMPH-responsiveness of SD-pupae may be high at hours after larval-pupal ecdysis, but drop drastically on the next day, at which ecdysteroids for adult development appeared in the hemolymph. In addition, ecdysteroids may be involved in the endocrine mechanism controlling seasonal-morph development in *P. c-aureum*.

The results suggest that both production and secretion of the SMPH seem to be enhanced to occur by long-days in *P. c-aureum*. Furthermore, *Polygonia* pupae may develop into summer morphs when they are exposed to the SMPH at an earlier pupal stage than the exposure to the hemolymph ecdysteroids.

INTRODUCTION

The Asian comma butterfly, *Polygonia c-aureum* L., exhibits seasonal dimorphism, i.e., summer and autumn morphs. Development of the seasonal morphs is governed by photoperiod and temperature existing during the larval stages [1, 2].

A physiological system underlying the photoperiodic control of seasonal-morph development involves a neuroendocrine system secreting a summer-morph producing hormone (SMPH) in the

early pupal stage [1].

In summer-morph producers (long-day pupae: LD-pupae), the SMPH is produced in the neurosecretory cells, conveyed along axons and secreted from corpora cardiaca and/or corpora allata into hemolymph. But, the LD-pupae produced autumn-morph butterflies as the autumn-morph producers (short-day pupae: SD-pupae) did when the brains (or the medial neurosecretory cells) were removed surgically on the day of larval-pupal ecdysis [3, 4].

The SMPH was shown to be present in both brains of LD- and SD-pupae and was concluded as being a peptide hormone of almost the same size as a factor responsible for SMPH-activity in the

Accepted April 13, 1988

Received February 20, 1988

¹ To whom reprints should be requested.

brain-extracts of the silkworm, *Bombyx mori* (M.W. about 4,500) [5, 6].

In addition, ecdysteroids forcing pupae to undergo metamorphosis were shown to play a significant role in seasonal-morph development of the three species of butterflies, *Araschnia burejana* [7], *A. levana* [8] and *Lycaena phlaeas daimio* [9].

The present study was designed to know how the SMPH-activity changes stage-dependently in the brains of the 5th instar larvae and pupae of *P. c-aureum*. In addition, the SMPH-responsiveness and the effect of 20-hydroxyecdysone-injection on the seasonal-morph development were also examined using SD-pupae (autumn-morph producers).

MATERIALS AND METHODS

Animals Larvae of *P. c-aureum* were held in a transparent plastic container of $\phi 9 \times 5 \text{ cm}^3$ or $19 \times 13 \times 5 \text{ cm}^3$ and exposed to long-day conditions alternating periods of 16-hr light and 8-hr dark (16L-8D) or to short-day conditions of 8L-16D. The rearing containers were placed in cabinets with constant temperature (20°C or 25°C) and illuminated by two 20-W white fluorescent tubes, which were controlled by a 24-hour time-switch. In the light period, light intensity was provided at about 500 lux to the rearing containers. Larvae were fed on leaves of *Humulus japonicus* and fresh leaves were provided daily. Under long-day conditions, larvae and pupae all developed into butterflies of summer morphs, whereas, under short-day conditions, they all developed into autumn-morph butterflies.

Quantitative analysis of hemolymph ecdysteroids Five μl of hemolymph was collected from each insects. Ecdysteroids of each sample were extracted with 400 μl methanol and were quantified against ecdysone obtained from Sigma Chemical Co. (St. Louis, U.S.A.), using the radioimmunoassay method [9]. Antiserum against 20-hydroxyecdysone from Rhoto Pharmaceutical (Osaka, Japan) was obtained from the Meguro Institute (Osaka, Japan). This antiserum exhibits almost 5-fold stronger cross reactivity against 20-hydroxyecdysone than that against ecdysone.

Radioactive ecdysone (23,24-H(N)-ecdysone (80 Ci/mmol) was obtained from New England Nuclear (Boston, U.S.A.).

Extraction of SMPH Brains were obtained from SD- and LD-pupae by dissection in saline (0.9% NaCl) and stored at -85°C . One hundred brains were grouped, homogenized with a Teflon homogenizer in ice-cold acetone (a total volume of ca 0.6 ml), washed 2 times in 80% ethanol (a total volume of ca 0.6 ml) and extracted 2 times with 2% NaCl (a total volume of 0.5 ml) at 0°C . At each step, insoluble materials were removed off by centrifugation at $12,000 \times g$ for 30 min at 4°C . The brain-extracts of 2% NaCl were heated in a boiling-water bath for 5 min, rapidly cooled and centrifuged at $12,000 \times g$ for 10 min. The supernatant was added with 100% trichloroacetic acid up to 10% (v/v) to precipitate the factor and centrifuged at $12,000 \times g$ for 10 min. The precipitate was washed with diethylether (a total volume of ca 0.5 ml), dissolved in saline (0.9% NaCl) and stored at -85°C . The solution was used as a crude SMPH fraction.

Decerebration Zero-day-old SD-pupae (4 to 12 hr after larval-pupal ecdysis) were chilled in an ice-bath and the brains were removed through an incision at the dorso-posterior region of the head-capsule using fine forceps. The wound was sealed with melted paraffin.

Injection of 20-hydroxyecdysone Five μl saline with/without 0.5 or 1.0 μg of 20-hydroxyecdysone, obtained from Rhoto Pharmaceutical (Osaka, Japan), was injected into the abdomen of 0-day-old SD-pupae. The injection was made through a dorso-lateral intersegmental region between the 6th and 7th abdominal segments and the wound was sealed with melted paraffin. The recipient pupae were allowed to develop at 25°C .

Bioassay of SMPH Five μl of samples with/without brain-extracts (5- or 10-brain equivalents) were injected into the abdomen of 0-day-old female SD-pupae (4 to 12 hr after larval-pupal ecdysis). The injection was made through a dorso-

lateral intersegmental region between the 6th and 7th abdominal segments and the recipient pupae were allowed to develop at 25°C.

On the day of emergence, butterflies developed from the recipient pupae were caught and classified into one of grades 0–4. The classification was made on a gradient of the ventral-side color of the female wings [5]. An average grade score (AGS) for summer morphs, on which SMPH-activity of the sample was evaluated, was obtained from the response of 6–20 insects.

RESULTS

Stage-dependent changes in SMPH-activity of the brain-extracts of SD- and LD-insects

To know how the SMPH-activity in the brains of SD- and LD-insects changes stage-dependently in *P. c-aureum*, brain-extracts (2% NaCl) were provided from each 300 of different/definite stages of the 5th-instar larvae and pupae, and of 10-brain equivalents were injected into the abdomen of 0-day-old SD-pupae.

In the brain-extracts of autumn-morph produc-

ers (SD-insects), the SMPH-activity was low through the 5th instar larval stage (AGS 0.8–1.0), but rose gradually as the days went on in the pupal stage (AGS 1.6 on day 4). The activity was also low (AGS 0.5–0.9) through the early and middle 5th instar in the extracts of summer-morph producers (LD-insects), but formed a peak (AGS 1.7) on the last day of the 5th instar (the pharate pupal stage). Once it lowered (AGS 0.7), thereafter, on the day of larval-pupal ecdysis (day 0), but rose quickly and reached a maximum level (AGS 3.3) 4 days after larval-pupal ecdysis (Fig. 1).

The results indicate in *P. c-aureum* that both production and secretion of SMPH may be enhanced to occur by long days, on which the SMPH-activity in the brains of LD-insects seems to fluctuate in the late 5th-instar larval and pupal stages.

Stage-dependent changes in titer of the hemolymph ecdysteroids during the last larval and pupal stages

Ecdysteroids were thought to force pupae to undergo pupal-adult metamorphosis in *P. c-aureum*.

To know how the titer of hemolymph ecdysteroids changes during the last larval and pupal

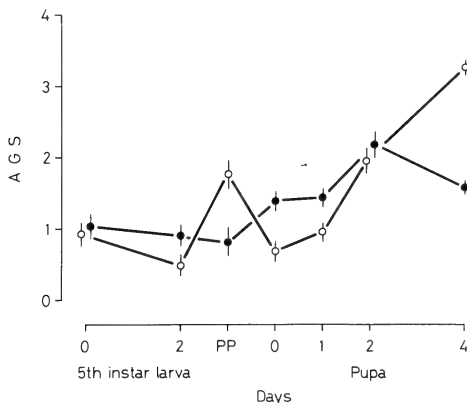


Fig. 1. Stage-dependent changes of the average grade scores (AGS) for summer morphs in the brain-extracts of LD-(open circles) and SD-insects (solid circles). Thin straight lines show the standard error of AGS scores, respectively. PP shows the pharate pupal stage (day 3 of the 5th instar at 25°C).

stages, 5 μ l of hemolymph was collected from each 5 SD- and each 5 LD-insects of different/definite stages, respectively. The stages examining the titer of hemolymph ecdysteroids were changed depending on the groups from the day of the 4th larval-larval ecdysis to the 7th day after larval-pupal ecdysis at 1-day intervals. The titer of ecdysteroids present in the samples were quantified by radioimmunoassay.

LD- and SD-insects showed almost the same fluctuation patterns in titer of the hemolymph ecdysteroids through the 5th-instar larval and pupal stages. The titer remained at a low level through the early and middle 5th instar (0.006–0.06 ng/ μ l), but formed a small peak (0.3 ng/ μ l in LD- and 0.8 ng/ μ l in SD-insects) on the last day of the 5th instar (the pharate-pupal stage). Once the titer lowered (0.1–0.2 ng/ μ l), thereafter, on the first day of larval-pupal ecdysis (day 0), but it rose again on day 1 and formed a large peak for adult development on day 2 (26.6 ng/ μ l in LD- and 17.3 ng/ μ l in SD-insects). Thereafter, it lowered quickly and reached almost the same level as the low titer of

the early 5th instar larvae (Fig. 2).

Stage-dependent change in the SMPH-responsiveness of SD-pupae

To know how the SMPH-responsiveness of SD-pupae changes during the pupal stage in *P. c-aureum*, the brain-extracts of 2% NaCl were provided from 1,000 brains of SD-pupae and of 10-brain equivalents were injected into the abdomen of SD-pupae at different/definite stages.

Zero-day-old SD-pupae treated with the extracts showed a strong reactivity and all produced summer-morph butterflies of grade 4 (AGS 4.0). However, treated with the extracts on days following the day of larval-pupal ecdysis, SD-pupae were all judged as developing into butterflies of autumn morphs (AGS 0–0.4) (Fig. 2).

SD-pupae seemed to have a high reactivity against the SMPH at hours following larval-pupal ecdysis. But, they may lost the reactivity quickly when ecdysteroids appear in pupal hemolymph.

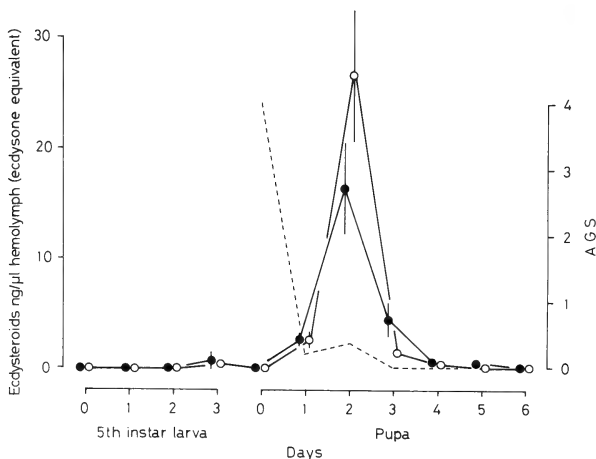


Fig. 2. Stage-dependent changes in titer of the hemolymph ecdysteroids of LD- (open circles) and SD-insects (solid circles) with the standard error (thin straight lines). A edged/broken line shows the reactions of SD-pupae (AGS) to the injection of a crude-SMPH fraction.

Effects of decerebration and/or 20-hydroxyecdysone-injection on the seasonal-morph development in SD-pupae

To determine whether or not ecdysteroids are involved in the endocrine system controlling the seasonal-morph development in *P. c-aureum*, 5 μ l saline with/without 0.5 μ g or 1.0 μ g of 20-hydroxyecdysone was injected into the abdomen of 0-day-old brained and 0-day-old decerebrated SD-pupae along with a SMPH-active fraction through Sephadex G-50 [6]. The treated pupae were allowed to develop at 25°C.

When injected with either the saline containing 20-hydroxyecdysone or the Sephadex G-50/SMPH-active fraction on the first day of larval-pupal ecdysis, both brained (unoperated) and decerebrated SD-pupae equally produced butterflies having characteristics of the summer morphs. In contrast, decerebrated and sham-operated SD-pupae developed without the injection all produced autumn-morph butterflies of grade 0 as the control SD-pupae did.

The results indicate that both SMPH and ecdysteroids seem to play significant roles in the development of summer morphs. But, the SD-pupae treated with 20-hydroxyecdysone were seen to produce summer-morph or intermediate-morph butterflies without the assistance of their brains.

DISCUSSION

The *Polygonia* mechanism underlying the photoperiodic control of seasonal-morph development involves a neuroendocrine factor producing summer morphs (SMPH) [1-4].

The activity of SMPH was detected from both brain-extracts of 0-day-old LD-pupae and 0-day-old SD-pupae of *P. c-aureum*. The SMPH was shown to be extractable with 2% NaCl and precipitable by raising either the concentrations of ammonium sulfate or trichloroacetic acid in the extracts [5]. In addition, the SMPH was thought to be a peptide showing almost the same physicochemical characteristics as the small prothoracicotropic hormone (small PTTH) of *P. c-aureum*. But, the factor showing SMPH-activity was judged as being different from the small PTTH since they

were separated by reversed-phase HPLC [6].

The SMPH synthesized in the brains of SD-insects may be a small amount, but accumulated through the 5th instar larval and pupal stages without secretion. In contrast, in LD-insects, both synthesis and secretion of the SMPH are thought to be enhanced to occur by long days, on which the SMPH-activity in the brains of LD-insects are seen to fluctuate during the 5th-instar larval and pupal stages. That is, the SMPH-synthesis enhanced by long days may be started from the late 5th-instar larval stage so that the SMPH-activity in the brains of LD-insects reaches a peak at the pharate pupal stage. In addition, the secretion of SMPH may be also enhanced to occur by long days and it may be started just before (or at) larval-pupal ecdysis. Thereafter, the lowering of SMPH-activity caused by the secretion may occur in the brains of LD-pupae until it reaches one twentieth of the activity of the brains of 0-day-old SD-pupae. But, the SMPH-activity in the pupal brains rises again quickly 2 or 3 days later, at which the SMPH-secretion is thought to be stopped in LD-insects.

Summer-morph producers (LD-pupae) were shown to produce autumn-morph butterflies when the brains (or medial neurosecretory cells) were extirpated within 20 hr after larval-pupal ecdysis at 20°C, indicating that the summer-morph development was determined by the SMPH which the brains of LD-insects secreted mainly at hours following larval-pupal ecdysis [3]. The hypothesis was also supported by another evidence that the SMPH-reactivity of SD-pupae was high at hours following larval-pupal ecdysis. But, the SD-pupae lost the SMPH-reactivity on the next day with the appearance of hemolymph ecdysteroids for pupal-adult metamorphosis.

Ecdysteroids appearing in the hemolymph of *Polygonia* pupae is thought to play a significant role in the determination of seasonal morph development as has been demonstrated in several other butterflies, i.e. *A. burejana* [6], *A. levana* [7] and *L. phlaeas daimio* [9]. However, the role of ecdysteroids played in seasonal-morph development may vary according to the butterfly species since the development of seasonal morphs were shown to be determined only by controlling the timing of ecdysteroid release in the nymphalid

TABLE 1. Effects of the injection of SMPH and 20-hydroxyecdysone on seasonal-morph development of *Polygonia* decerebrated pupae

Treatment and injected materials	No.	No. of butterflies classified into grades:					AGS
		0	1	2	3	4	
Control	16	16	0	0	0	0	0.0
Sham operation	9	9	0	0	0	0	0.0
Decerebration	9	9	0	0	0	0	0.0
Decerebration and SMPH-injection	10	2	4	4	0	0	1.2
Decerebration and 20-OH-Ecdy. injection (0.5 μ g)	10	0	5	3	2	0	1.7
20-OH-Ecdy. injection 0.5 μ g	18	2	3	9	1	3	2.0
1.0 μ g	8	0	1	5	2	0	2.1

Recipients were all 0-day-old SD-pupae (4–12 hr after larval-pupal ecdysis). Sham operation shows SD-pupae whose head-capsules were incised in the same manner as those of decerebrated SD-pupae. "SMPH-injection" shows SD-pupae injected with a *Polygonia* Sephadex G-50/SMPH-active fraction [6], whereas "20-OH-Ecdy. injection" represents SD-pupae injected with 20-hydroxyecdysone.

butterflies, *A. burejana* and *A. levana*. In contrast, in the small copper butterfly, *L. phlaeas daimio*, a cerebral factor causing the wing to be brownish was shown to play a significant role in the summer-morph development of LD-pupae. But, when applied to newly ecdysed LD- and SD-pupae, ecdysteroids shifted their wings to be reddish (spring) type.

From these lines of evidence, it may be concluded that, in *P. c-aureum*, both SMPH and ecdysteroids are important for the development of summer morphs, respectively. But, the action of 20-hydroxyecdysone in the summer-morph development is thought to be different from that of the SMPH since AGS scores in the 20-hydroxyecdysone-treated SD-insects was not risen by increasing the doses of 20-hydroxyecdysone injection (0.5 to 1.0 μ g) (Table 1) in contrast to those which were obtained from SD-pupae treated with the Sephadex G-50/SMPH-active fraction [6]. Furthermore, it may be that ecdysteroids appearing in pupal hemolymph drop the SMPH-responsiveness drastically in SD-pupae of *P. c-aureum*.

We still left open an interesting question as to how ecdysteroids act on 0-day-old SD-pupae to

produce SD-pupa-originated summer-morph butterflies. The questions may be solved in a course of further study about the endocrine mechanism determining the development of seasonal morphs in *P. c-aureum*.

ACKNOWLEDGMENT

The authors wish to express their sincere gratitude to Professor A. Okajima and to Professor Y. Chiba of Yamaguchi University for advice and valuable suggestions during the course of this work. Thanks are also due to Professor S. Y. Takahashi of Yamaguchi University for his counsel and advice in preparing this manuscript. This work was supported in part by a grant from the Ministry of Education, Science and Culture of Japan (No. 6154052).

REFERENCES

- 1 Fukuda, S. and Endo, K. (1966) Hormonal control of the development of seasonal morphs in the butterfly, *Polygonia c-aureum* L. Proc. Japan Acad., 42: 1082–1087.
- 2 Hidaka, T. and Takahashi, H. (1967) Temperature condition and maternal effect as modifying factor in the photoperiodic control of seasonal forms in *Polygonia c-aureum* (Lepidoptera, Nymphalidae). Annot. Zool. Japan, 40: 200–204.

- 3 Endo, K. (1972) Activation of corpora allata in relation to ovarian maturation in the seasonal forms of the butterfly, *Polygonia c-aureum* L. Dev. Growth Differ., **14**: 263-274.
- 4 Endo, K. (1984) Neuroendocrine regulation of the development of seasonal forms of the Asian comma butterfly, *Polygonia c-aureum* L. Dev. Growth Differ., **26**: 217-222.
- 5 Endo, K., Masaki, T. and Kumagai, K. (1988) Neuroendocrine regulation of the development of seasonal morphs in the Asian comma butterfly, *Polygonia c-aureum* L.: Difference in activity of summer-morph-producing hormone from brain-extracts of long-day and short-day pupae. Zool. Sci., **5**: 145-152.
- 6 Masaki, T., Endo, K. and Kumagai, K. (1988) Neuroendocrine regulation of the development of seasonal morphs in the Asian comma butterfly, *Polygonia c-aureum* L.: Is the factor producing summer morphs (SMPH) identical to the small prothoracicotropic hormone (4K-PTTH)? Zool. Sci., **5**: 1051-1057.
- 7 Keino, H. and Endo, K. (1973) Studies of the determination of the seasonal forms in the butterfly, *Araschnia burejana* Bermer. Zool. Mag., **82**: 48-52 (in Japanese with English summary).
- 8 Koch, P. B. and Bückmann, D. (1987) Hormonal control of seasonal morphs by the timing of ecdysteroids release in *Araschnia levana* L. (Nymphalidae: Lepidoptera). J. Insect Physiol., **33**: 823-829.
- 9 Endo, K. and Kamata, Y. (1985) Hormonal control of seasonal-morph determination in the small copper butterfly, *Lycaena phlaeas daimio* Seitz. J. Insect Physiol., **31**: 701-706.
- 10 Borst, D. W. and O'Conner, J. D. (1972) Arthropod molting hormone: radioimmune assay. Science, **178**: 418-419.



Qualitative and Quantitative Analysis of Juvenile Hormone in the Larvae of the Silkworm, *Bombyx mori*

MAYUMI KIMURA², SHO SAKURAI³, TAMOTSU NAKAMACHI,

MAYUMI NARIKI, SHINYA NIIMI, TETSUYA OHTAKI,

YOSHINORI FUJIMOTO¹, FUMIKO HATA¹

and NOBUO IKEKAWA¹

*Department of Biology, Faculty of Science, Kanazawa University, Kanazawa 920,
and ¹Department of Chemistry, Faculty of Science, Tokyo Institute
of Technology, Meguro, Tokyo 152, Japan*

ABSTRACT—Juvenile hormone (JH) in either whole body or hemolymph of newly molted fifth instar larvae of the silkworm, *Bombyx mori*, was identified by a selected ion monitoring method in gas chromatography-mass spectroscopy (GC-MS). JH was separated successively by solvent extraction, column chromatography, thin-layer chromatography and high performance liquid chromatography. The data indicated that major JH is JH I and JH II is minor. JH III was found in only a trace amount. Rabbit anti-JH I antiserum was prepared and used for radioimmunoassay to quantify the JH in hemolymph and culture medium after incubation of corpora allata. JH amount in hemolymph, determined by RIA, was in good accordance with those by GC-MS analysis and bioassay, indicating that RIA is useful to study the JH titer in hemolymph.

INTRODUCTION

Juvenile hormone (JH), secreted from corpus allatum (CA), participates with moulting hormone, ecdysone, in the hormonal control of post-embryonic development in insects [1]. This indicates the importance of determining precisely the changes in the titer of those two hormones in hemolymph. Development of radioimmunoassay (RIA) provides a simple method to measure quantitatively a minute amount of hormones. RIA has been used to determine the amount of ecdysteroids in various sources including hemolymph. RIA of JH has been developed by several groups [2-5] but useful only for quantitation of JH in culture medium after incubation of CA [4]. Recently,

Plantevin *et al.* [6] determined the change in JH titer in hemolymph using RIA but their method contains many steps including partial purification of JH by column chromatography and chemical derivatization of JH into JH-diol. We thus attempted to develop a simple method using RIA to quantify JH in hemolymph without purification or derivatization.

When JH is assayed by RIA, it is indispensable to know the JH species in the samples because the specificity of anti-JH antiserum extremely varies in different JHs [3-5]. In *Bombyx*, however, the JHs have not yet been identified. Therefore, we first tried to identify JHs in the silkworm and those produced by CA. We then attempted to prepare antiserum against JH I which was determined to be the main JH in *Bombyx*.

MATERIALS AND METHODS

Animals

Larvae of the silkworm, *Bombyx mori* (J 124×C

Accepted April 30, 1988

Received March 1, 1988

² Present address: Division of Biocybernetics, Institute for Medical and Dental Engineering, Tokyo Medical and Dental University, Kanda-Surugadai, Chiyoda, Tokyo 101.

³ To whom correspondence should be addressed.

124), were reared on fresh mulberry leaves or an artificial diet (Silkmate 2M, Nihon Nosan Kogyo K.K., Yokohama) at 25°C under LD 12:12 [7].

Hormones and Chemicals

Juvenile hormone I, II, and III (JH I, II, III) were purchased from Sigma (St. Louis). ^3H -JH I (15.5 Ci/mmol), ^3H -JH III (11.0 Ci/mmol) and $^{14}\text{CH}_3$ -methionine (51.4 mCi/mmol) were purchased from New England Nuclear (Boston). All the JH sample except for RIA were dissolved in distilled hexane, filled with nitrogen gas and stored at -80°C.

JH extraction from whole animals

A radioactive dilution method [8] was employed to extract JH. Newly molted 5th instar larvae (1731 g) were stored at -20°C. Larvae were homogenized in a brender with 300 ml diethyl ether and 60 g anhydrous sodium sulfate for every 120 g of larvae. Homogenate was shaken for 2 hr and filtered through a glass filter. Concentration of the filtrate *in vacuo* gave a green oil. The oily material was dissolved in diethyl ether (30 ml for every 60 g of oil) and added with -80°C cold methanol (40 ml) to make a precipitation which was removed by filtration. The filtrate was evaporated and added with 25000 cpm of ^3H -JH I (0.47 ng) and III (0.6 ng), respectively. The residue dissolved in hexane was applied to Florisil column chromatography (2.6×40 cm) equilibrated with hexane and eluted with 5% ethyl acetate/hexane. The radioactive fractions were combined, evaporated, dissolved in methanol and applied to reversed-phase column chromatography (RP-8, Lober type B, Merck) and eluted with 5% water/methanol to remove polar materials. The radioactive fractions were combined and evaporated *in vacuo* (67.2 mg). The residue was subjected to silica gel thin-layer chromatography (TLC) (0.25 mm thick, precoated plate, Kiesel gel 60, Merck) developed with hexane/ethyl acetate (2:1) (R_f for JH I=0.65). The radioactive zone was scraped, extracted, evaporated and applied on the second TLC (Aluminum oxide, type E, Merck) developed with hexane/ethyl acetate (8:1) (R_f for JH I=0.56) and the radioactive zone was once applied on reversed-phase TLC (RP-8, Merck) developed

with methanol/water (19:1) (R_f for JH I=0.49). The yield after the third TLC was 1.2 mg. The samples were dissolved in hexane for HPLC purification.

JH extraction from hemolymph

Hemolymph (33 ml) was collected into an ice-cold tube through incisions on prolegs of 185 newly molted 5th instar larvae. The same volume of hexane, and 0.05 μCi JH I and 0.05 μCi JH III were added, centrifuged for 5 min and upper phase was collected. The aqueous phase was further extracted twice with the same volume of hexane and upper phase was separated, combined and evaporated *in vacuo*. The oily residue was applied on a column (1.6×5 cm) of 10 g alumina (activated 300, Nakarai, Tokyo) equilibrated with hexane. Elution was performed stepwisely in order of 10 ml hexane, 10 ml hexane/benzene (4:1), 10 ml×3 of benzene and 10 ml×3 of benzene/ethyl acetate (9:1). The radioactive fractions were combined, evaporated and dissolved in hexane for HPLC purification.

High performance liquid chromatography (HPLC)

JH was further purified on a Zorbax-SIL column, 250×4.6 mm (Shimadzu), eluted with 10% diethyl ether in 50% water saturated n-hexane at a flow rate of 1 ml/min. The elution was monitored by an UV absorbance at 225 nm. The fractions containing JHs were combined, evaporated and dissolved in hexane for gas chromatography-mass spectroscopic (GC-MS) analysis.

GC-MS analysis

The purified biological samples was subjected to GC-MS analysis (Shimadzu LKB 9000S). Ionization (70 eV) was performed by electron impact and the column was 1% OV-17 on Shimalite w (1 m×4 mm i.d.), carrier, helium gas (30 ml/min), column temperature, 170°C, injector temperature, 260°C, and ion source temperature, 290°C.

Incubation of CA with $^{14}\text{CH}_3$ -methionine and purification of radioactive JHs

CA of newly molted 5th instar larvae were rinsed in insect Ringer's solution and Grace's medium minus methionine. Every 10 CA were

incubated with 1.54 μ Ci of 14 C-methionine in 90 μ l Judy's medium [9] containing 10% fetal bovine serum (FBS) at 30°C for 10 hr. The medium after incubation was added with one volume of water and extracted with two volumes of hexane. After three times extraction, hexane layer was combined and evaporated. The residue dissolved in ethyl acetate was applied on 0.25 mm precoated silica gel TLC plate (Kiesel gel 60, Merck) and developed with hexane/ethyl acetate (4:1). The radioactive zone was scraped, extracted and subjected to HPLC analysis. Fractions were collected every 0.5 min and radioactivity in an aliquot of each fraction was counted. To convert JH into JH-diol, the radioactive fractions of HPLC corresponding to JH I, II and III were combined, evaporated, dissolved in 400 μ l tetrahydrofuran (THF), added with 100 μ l 0.1 M perchloric acid and incubated for 4 hr at room temperature. The reaction mixture was neutralized with saturated NaHCO₃ solution and directly applied on silica gel TLC which was developed with hexane/ethyl acetate (1:1) to separate JH-diols (R_f for JH I-diol = 0.53). The wide zone containing all the diols was extracted and subjected to reversed-phase HPLC analysis using a column of Zorbax ODS (250 \times 4.6 mm), eluted with 40% water/acetonitrile at a flow rate of 1 ml/min.

Incubation of CA

For RIA determination of JH in medium, 3 pairs of CA of newly molted 5th instar larvae were incubated in 150 μ l Grace's insect culture medium (Gibco, Long Island) supplemented with 10% FBS at 25°C for 10 hr. After incubation, the medium was directly used as a sample for RIA.

Preparation of anti-JH antiserum

Protein-JH complex, used for immunization, was prepared according to Baehr *et al.* [3] with a minor modification. JH I (20 mg) in 0.4 ml methanol was added with 0.64 ml 2N-NaOH in 50% methanol aqueous and the mixture was stirred overnight at room temperature. The reaction mixture was titrated to pH 5 with 2N-HCl, extracted with ethyl acetate, and the extract was washed with water, dried with anhydrous sodium sulfate and evaporated. The residue containing JH

acid was subjected to the following reaction without purification. The residue (20 mg) was dissolved in 0.3 ml dioxane, added with 0.2 mM N-hydroxysuccinimide (NHS) and 0.2 mM N-ethyl-N'-(3-dimethylaminopropyl)-carbodiimide-hydrochloride and stirred overnight. The reaction mixture was applied on silica gel TLC plate and developed with benzene/ethyl acetate (5:1) (R_f for JH I acid = 0.26; R_f for JH I-NHS = 0.49) to separate JH I-NHS from JH acid. Structure of JH I-NHS (21 mg) was confirmed by 1 H-NMR spectroscopy (60 MHz, Hitachi HR-24). Human serum albumin (HSA, 45.45 mg) in 1.33 ml water was added to 10 mg JH I-NHS in 1.67 ml THF and the pH of the reaction mixture was adjusted to 9-10 with saturated sodium carbonate. The solution was stirred overnight at room temperature and dialyzed against phosphate buffered saline (PBS, 0.05 M phosphate buffer, 0.15 M NaCl, pH 7.4) overnight with the buffer solution being changed every 3 hr. The solution was lyophilized and used as an antigen. The HSA-JH complex was emulsified with Freund's complete adjuvant and injected into rabbits every 5 weeks.

RIA protocol

RIA was performed according to Granger *et al.* [4] and Granger and Goodman [10]. The antiserum and labeled ligand were diluted with 0.1 M phosphate buffer, pH 7.2, containing 0.1% bovine serum albumin, 0.1% rabbit immunoglobulin (Sigma) and 0.1% sodium azide. Standard JHs were dissolved in methanol and 50 μ l of the solution was placed in micro test tube precoated with 10% polyethylene glycol (MW 20000, Calbiochem) [11] and the solvent was evaporated *in vacuo*. JH in each tube was dissolved again in 50 μ l of the above phosphate buffer and added with 50 μ l diluted antiserum and 50 μ l ligand solution (approximately 6000 cpm of 3 H-JH I). After incubation for 16 hr at 4°C, precipitation was made with ammonium sulfate, suspended in Aquasol II (New England Nuclear, Boston) and the radioactivity was counted [12].

RESULTS

Identification of juvenile hormone in whole larvae

Figure 1 shows a typical HPLC separation of JHs from whole body. The fractions corresponding to JH-I, II and III were collected and subjected to GC-MS analysis. The electron-impact mass spectra of the authentic samples exhibited ion peaks at m/z : JH I, 294 (M^+ , very weak), 209 (24%), 149 (58%), 114 (52%), 95 (100%); JH II: 280 (M^+ , very weak), 195 (24%), 135 (43%), 114 (42%), 81 (100%); JH III (M^+ , very weak), 195 (17%), 135 (52%), 81 (100%). Among these ions, ions of m/z 95 and 209 for JH I and m/z 81 and 135 for JH II and III were predetermined as the monitoring ions, since these ions distinguish the methyl blanching pattern of JHs. The mass fragmentograms are presented in Figure 2a. Selected-ion monitoring (SIM) analysis of the fraction corresponding to JH I clearly showed peaks m/z 95 and 209 at the retention time (4.0 min) of JH I. Similar analysis of the fraction corresponding to JH II showed peaks of m/z 81 and 135 at the retention time (3.1 min) of JH II. However, SIM analysis of the fraction corresponding to JH III failed to detect the ions of JH III.

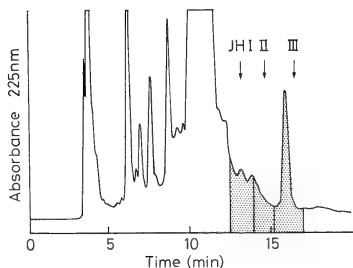


Fig. 1. Normal-phase HPLC separation of the extract of whole body from newly molted 5th instar larvae. The arrows indicate the elution times of radioactive JH I, II and III. The shaded fractions were separately collected. HPLC conditions: 250×4.6 mm Zorbax-Sil column, mobile phase 10% diethyl ether in hexane, flow rate, 1 ml/min.

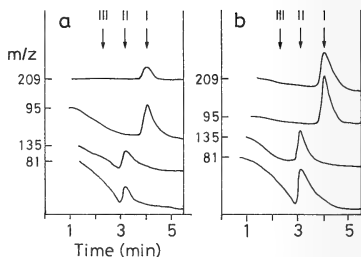


Fig. 2. Selected-ion monitoring chromatograms in GC-MS analysis of (a) purified JH extract of whole body, and (b) extract of hemolymph from newly molted 5th instar larvae. Conditions: $1 \text{ m} \times 4 \text{ mm}$ 1% OV-17 on Shimalite w, 170°C , He carrier at 30 ml/min, ionization voltage at 70 eV. I, II and III indicate the retention times of standard JH I, II and III, respectively.

Identification of juvenile hormone in larval hemolymph

JH in hemolymph was purified by HPLC and the fractions corresponding to standard JHs are subjected to SIM analysis. As shown in Figure 2b, JH I and II were detected. According to the comparison of the peak area with those of standard JH I and II, the amount of JH-I and II were estimated to be 10.6 ng (36.3 pmol) and 1.8 ng (6.4 pmol) in one ml, respectively. Since JH III was not detected in the electron impact SIM analysis, we used chemical ionization for the SIM analysis of the HPLC fraction corresponding to JH III. By this analysis, JH III was identified but the amount was just detectable and thus the exact amount was not calculated.

Identification of juvenile hormone produced by CA in vitro

To identify JH that CA secrete *in vitro*, 60 pairs of CA were incubated with $^{14}\text{CH}_3$ -methionine. After incubation, the medium was extracted and applied to HPLC with three standard JHs. Radio-HPLC analysis (Fig. 3) indicated that the major JH was JH I and the minor one was JH II. No radioactivity was found in the fraction corresponding to JH III. The radioactive materials migrating with standard JH I and II were converted into

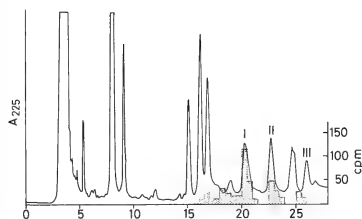


FIG. 3. Radio-HPLC analysis of JHs produced by *Bombyx* CA, cultured with [^{14}C]-methionine. Standard JH I, II and III were added prior to the HPLC run. Shaded histogram corresponds to radioactivity of each fraction collected every 0.5 min. Mobile phase, 7.5% ethyl ether in hexane. Other HPLC conditions as for Fig. 1.

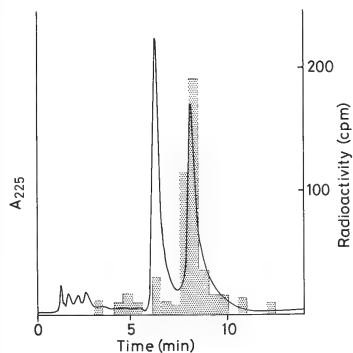


FIG. 4. Radio-reversed-phase HPLC of the JH-diol. Radioactive fractions in Fig. 3 converted into the JH-diol and applied on RPHPLC. Shaded histogram corresponds to radioactivity in each fraction collected every 0.5 min. Solid line indicates the UV absorbance at 225 nm of standard JH II diol (5.3 min) and JH I diol (8.0 min). HPLC conditions: 250 \times 4.6 mm Zorbax ODS column, mobile phase 40% water in acetonitrile; flow rate, 1 ml/min.

JH-diol. Reversed-phase HPLC analysis of the diol revealed that CA produced JH I and II (Fig. 4).

According to the peak area of the radioactivity in Figure 4, the amount of JH I was approximately 10

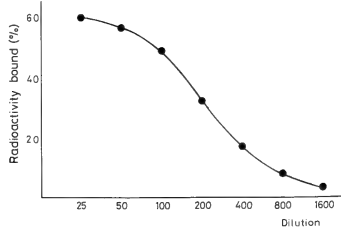


FIG. 5. Titration curve of the antiserum. [^3H]-JH I was incubated with serial dilutions of the antisera. The percentage of ligand bound was measured by the RIA protocol.

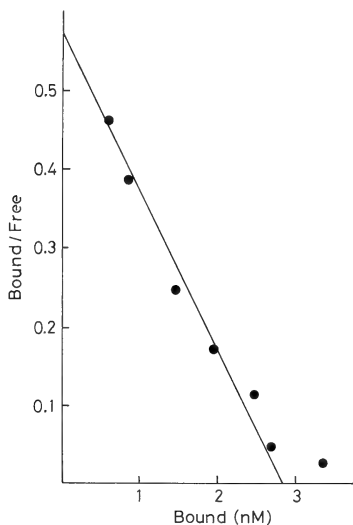


FIG. 6. Scatchard plot for the binding of JH I in the JH I RIA. The hormone bound after correction for non-specific binding is shown.

times as much as JH II (0.23 pmol JH I and 0.022 pmol JH II/pair).

Preparation of anti-JH-I antiserum and radioimmunoassay

JH-I was demonstrated to be the major JH in

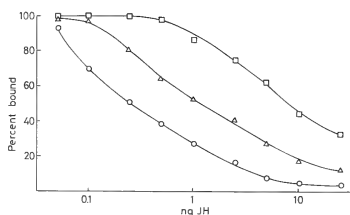


Fig. 7. Competitive binding analysis of the specificity of the JH I RIA for JH I (circles), II (triangles) and III (squares).

Bombyx larvae as mentioned above. In addition, JH I is the most active among JHs in several assays using lepidopteran larvae [13, 14]. Thus we attempted to prepare anti-JH I antiserum. First, the titer of the antiserum was determined. When the antiserum was diluted by 150 times, the serum bound approximately 40% of the total amount of labeled ligand (^3H -JH I) (Fig. 5).

Scatchard plot analysis of the data obtained from equilibrium binding of JH I in the assay system revealed a K_d of $4.56 \times 10^{-9} \text{ M}$ as determined by linear regression analysis of data after correction for nonspecific binding (Fig. 6).

The cross reactivity of the antibody with different homologs was determined. The competition curves (Fig. 7) showed that JH II and III exhibited cross reactivities of 20.4 and 3.2%, respectively. The cross reactivity of JH I acid was 100% (not shown in Fig. 7).

RIA determination of the amount of JH in biological samples

The amount of JH produced by CA *in vitro* was quantitated by RIA using our antiserum. When the incubation medium was directly used as a sample solution, the average amount of JH produced by one pair of CA for 10 hr was determined to be $415 \pm 91 \text{ pg}$ JH I equivalents in three different determinations.

Next we attempted to determine the JH concentration in hemolymph of newly molted 5th instar larvae by RIA. In preliminary experiments, an extract of hemolymph with organic solvent was used as a sample for RIA. The extract was found,

however, not to be suitable since the back ground level of such samples was approximately 50% of the total radioactivity that was bound in the assay system. Therefore, we tried to directly use the larval serum as a sample for RIA. According to this assay method, JH titer in hemolymph was determined to be $17.8 \pm 2.8 \text{ ng}$ JH I equivalent/ml in 6 different determinations.

DISCUSSION

The present study revealed that the major JH in *Bombyx mori* (J124×C124) is JH I and JH II is minor. *In vitro* incubation of CA also demonstrated that JH I was major and JH II was minor and the ratio of JH I/II was 10.5 according to the incorporation of radioactivity. Occurrence of JH III in *Bombyx* 5th instar larvae has been determined by Plantevin *et al.* [6]. In the present study, JH III was detected from extracts of hemolymph but the amount was only minute. These data are similar to those of JH composition in the lepidopteran larvae, i.e., *Bombyx mori* [6], *Hyalophora cecropia* [8], *Vanessa io* [8], *Heliothis virescens* [13] and *Manduca sexta* [14], in which JH I is the most abundant.

JH concentration in hemolymph of newly molted 5th instar larvae was previously determined to be 23 ng by bioassay using *Galleria* pupae [12]. Amounts of JH I and II in hemolymph determined by GC-MS 10.6 and 1.8 ng/ml. The loss during extraction and purification being taken into the consideration, the amount, 10.6 ng JH I seems not to be so far from the data obtained by bioassay.

The antiserum that we prepared distinguished JH I from JH II and III. JH II and III exhibited cross reactivities of approximately 20 and 3%, respectively. This specificity is similar to the antisera prepared by different authors [3, 4]. This means that our antiserum is useful to quantify JH in biological samples since JH I is the most potential among JHs in lepidopteran larvae [16, 17]. K_d value of our antiserum ($4.56 \times 10^{-9} \text{ M}$) is a little larger than that in other reports ($1.8 \times 10^{-9} \text{ M}$, [3]; $1.56 \times 10^{-9} \text{ M}$, [4]). However, the minimum detectable amount was estimated to be 25 pg JH I. This sensitivity seemed sufficient for JH RIA. In fact, JH concentration in hemolymph of newly

molted 5th instar larvae were determined to be 17.8 ng JH I equivalents in one ml, which is in good accordance with that obtained by bioassay [12].

In the present study, the JH species in *Bombyx* was identified and the simple method of JH RIA was thus established. Determination of changes in CA activity and JH titer in hemolymph through the larval and pupal stage are under the progress.

REFERENCES

- Riddiford, L. M. (1975) Hormonal action at the cellular level. In "Comprehensive Insect Physiology, Biochemistry, and Pharmacology vol. 7". Ed. by G. A. Kerkut and L. I. Gilbert, Pergamon Press, New York, pp. 37-84.
- Lauer, R. C., Solomon, P. H., Nakanishi, K. and Erlanger, B. F. (1974) Antibodies to insect C16-juvenile hormone. *Experientia*, **30**: 558-559.
- Baehr, J. C., Pradelles, Ph., Lebreux, C., Cassier, P. and Dray, F. (1976) A simple and sensitive radioimmunoassay of insect juvenile hormone using an iodinated tracer. *FEBS lett.*, **69**: 123-128.
- Granger, N. A., Bollenbacher, W. E., Vince, R., Gilbert, L. I., Baehr, J. C. and Dray, F. (1979) *In vitro* biosynthesis of juvenile hormone by the larval corpora allata of *Manduca sexta*: Quantification by radioimmunoassay. *Moll. Cell. Endocrinol.*, **16**: 1-17.
- Strambi, C., Strambi, A., Reggi, M. L., Hirn, M. H. and de Laage, M. A. (1981) Radioimmunoassay of insect juvenile hormone and of their diol derivatives. *Eur. J. Biochem.*, **118**: 401-406.
- Plantévin, G., Bosquet, G., Calvez, B. and Nardon, C. (1987) Relationship between juvenile hormone levels and synthesis of major hemolymph proteins in *Bombyx mori* larvae. *Comp. Biochem. Physiol.*, **86B**: 501-507.
- Sakurai, S. (1983) Temporal organization of endocrine events underlying larval-larval ecdysis in the silkworm, *Bombyx mori*. *J. Insect Physiol.*, **29**: 919-923.
- Trautmann, K. H., Suchy, M., Masner, P., Wipf, K. H. and Schuler, A. (1976) Isolation and identification of juvenile hormones by means of a radioactive isotope dilution method: Evidence for JH III in eight species from four orders. In "The Juvenile Hormone". Ed. by L. I. Gilbert, Plenum Press, New York, pp. 118-130.
- Judy, K. J., Schooly, D. A., Hall, M. S., Bergot, B. J. and Siddall, J. B. (1973) Chemical structure and absolute configuration of a juvenile hormone from grasshopper corpora allata *in vitro*. *Life Sci.*, **13**: 1511-1516.
- Granger, N. A. and Goodman, W. G. (1983) Juvenile hormone radioimmunoassays-theory and practice. *Insect Biochem.*, **13**: 333-340.
- Giese, Ch., Spindler, K. D. and Emmerrich, H. (1977) The solubility of insect juvenile hormone in aqueous solutions and its absorption by glassware and plastics. *Z. Naturforsch.*, **32c**: 158-160.
- Sakurai, S. (1984) Temporal organization of endocrine events underlying larval-pupal metamorphosis in the silkworm, *Bombyx mori*. *J. Insect Physiol.*, **30**: 657-664.
- Bergot, B. J., Ratcliff, M. and Schooly, D. A. (1981) Method for quantitative determination of the four known juvenile hormones in insect tissue using gas chromatography-mass spectroscopy. *J. Chromatogr.*, **204**: 231-244.
- Baker, F. C., Tsai, L. W., Reuter, C. C. and Schooly, D. A. (1987) *In vitro* fluctuation of JH, JH acid, and ecdysteroid titer, and JH esterase activity, during development of fifth stadium *Manduca sexta*. *Insect Biochem.*, **17**: 989-996.
- Bergot, B. J., Schooly, D. A., Chippendale, G. M. and Yin, C. M. (1976) Juvenile hormone titer determinations in the southwestern corn borer, *Diatraea grandisella*, by electron capture-gas chromatography. *Life Sci.*, **18**: 811-820.
- Ohtaki, T., Kiguchi, K., Akai, H. and Mori, K. (1972) Juvenile hormone and synthetic analogues: II. Novel substances with high juvenile hormone activity. *Appl. Ent. Zool.*, **7**: 161-167.
- Fain, M. J. and Riddiford, L. M. (1975) Juvenile hormone titers in the hemolymph during late larval development of the tobacco hornworm, *Manduca sexta* (L.). *Biol. Bull.*, **149**: 506-521.



Circadian Periodicity in Termination of Photorefractoriness in the Female Yellow-throated Sparrow, *Gymnorhis xanthocollis*

ANAND S. DIXIT and PRABHA D. TEWARY

*Department of Zoology, Banaras Hindu University,
Varanasi-221005, India*

ABSTRACT—Photorefractory female yellow-throated sparrows, when treated with six weeks of short days (8L:16D), showed redevelopment of gonad on their return to long days (15L:9D) whereas short days treatment of five weeks failed to break the photorefractoriness observed in this species. An endogenous circadian rhythm appears to be involved in the termination of photorefractoriness in this bird as 6-hr main photophase, when coupled with dark phases of 6, 18, 30, 42, 54 or 66-hr under various resonance light cycles, failed to terminate the photorefractoriness in cycles of 12-(6L:6D), 36-(6L:30D) and 60 hr (6L:54D) but terminated it in the cycles of 24-(6L:18D), 48-(6L:42D) and 72 hr (6L:66D). These results are consistent with the Bünning hypothesis or external coincidence model.

INTRODUCTION

In many photoperiodic birds each period of gonadal growth and development, whether induced by natural or artificial long days, is followed by rapid collapse of the gonad. Thereafter, the birds enter in a state of unresponsiveness, during which no known pattern of stimulatory photoperiodic regime can stimulate their gonad, which has come to be known as photorefractoriness. This post breeding phenomenon was apparently first described by Riley [1] and reviewed by Farner and Lewis [2], Lofts and Murton [3], Wingfield [4], Follett and Nicholls [5], Nicholls *et al.* [6]. The etiology of photorefractoriness is still a matter of dispute among the avian biologists. However, there are reports that the short days treatment for sufficient period can break the photorefractoriness to let the bird to require the capacity to respond to long days [7-9].

One of the powerful methods for testing the involvement of circadian rhythmicity in the measurement of daylength in photoperiodic response is that of resonance light cycles, first introduced by Nanda and Hamner [10]. In resonance

light cycles, a short fixed photophase (6-8 hr) is usually combined with varying durations of dark phases, such that the period (T) of the light/dark cycle is lengthened systematically by 12-hr increments, such as 12-(6L:6D), 24-(6L:18D), 36-(6L:30D), 48-(6L:42D), 60-(6L:54D) and 72 hr (6L:66D). Such resonance experimental protocol has been used to demonstrate that some birds monitor the seasonal changes in daylength by using their circadian system as photoperiodic clock [11].

Circadian rhythms have been shown to be involved in photoperiodic time measurement during the termination of photorefractoriness in some male birds [8, 9, 12, 13]. Whether this timing mechanism is operative in all the photoperiodic birds and in both sexes is still inconclusive since the number of species exposed to Nanda-Hamner protocol is so few, generally only the males have been investigated, and usually studies have been mainly confined to temperate zone birds. To our knowledge, this type of study has not been published using any female tropical or subtropical photoperiodic avian species. In order to test the generality of circadian rhythmicity in avian photoperiodic time measurement, it is necessary to study more avian species especially the female of previously examined species [14]. Therefore, we report here the results of the experiments designed to investi-

gate if the photorefractoriness can be terminated by short day treatment and if a circadian rhythm is involved in photoperiodic time measurement during the termination and maintenance of photorefractory period in the subtropical, female yellow-throated sparrow.

MATERIALS AND METHODS

Adult female yellow-throated sparrows, a non-migratory bird [15], were caught locally at Varanasi in the fall of 1982 and kept in an outdoor aviary. The average body weight of the birds at the time of capture was 18.50 ± 0.50 g. They were first brought indoors and allowed to acclimate to laboratory conditions for a fortnight. There they were subjected to natural variations of temperature, photoperiod and humidity which were 11–23°C, 10.50 hr/day and 58–91% respectively. Acclimatized birds were then maintained on a short daily light regime of 8-hr light and 16-hr darkness (8L:16D) for 8 weeks to eliminate photorefractoriness if they had any in nature and to make them photosensitive. Such photosensitive birds, having ovary of minimum weight ($OW = \text{ca. } 4 \text{ mg}$), were exposed to long days (15L:9D). They were laparotomised (surgical opening of abdominal wall between last two ribs) at monthly intervals to examine ovarian condition. Under this treatment, there was ovarian growth followed by regression and onset of photorefractoriness in a total duration of 150 days. After five months exposure to long days, all the birds were found in a state of complete ovarian regression and, thus, were in the photorefractory period of their gonadal cycle [16].

These photorefractory birds were then used for subsequent experiments.

Experiment I

The photorefractory birds were divided into one control (C) and two experimental (G_1 and G_2) groups of four birds each. The control group was maintained under long days (15L:9D) while birds of group G_1 and G_2 were transferred to short day (8L:16D) treatments for five or six weeks, respectively, and then returned to long days for 30 days. This was done to examine if photorefractoriness could be terminated by short days and also how much exposure to short days was sufficient to break the photorefractoriness in this species.

Experiment II

The photorefractory birds were divided into seven groups (one control and six experimental) and exposed to various resonance light cycles for 60 days as shown in Table 1. All the birds were laparotomised at the end of 60 days and were found having regressed ovaries. These birds were returned to long days (15L:9D) for 35 days and then laparotomised to examine in which group the photorefractoriness had been broken.

The ovarian weight was assessed before each transfer and at the end of the experiment by comparing the size of the ovary *in situ* with standard series of ovaries of known weights. The error inherent in this method may be $\pm 15\%$. Light proof wooden boxes containing these birds were lit by 20 W fluorescent tubes providing light intensity of about 400 lux at perch level. The first experimental photophase in all treatments com-

TABLE 1. Details of the resonance light cycle and one control

Group	Light schedule	Period of cycle (hour)	Light/dark ratio	Number of birds per group	
				Initial	Final
C	15L: 9D	24	1:1.6	5	5
G_{12}	6L: 6D	12	1:1	4	4
G_{24}	6L:18D	24	1:3	5	4
G_{36}	6L:30D	36	1:5	5	4
G_{48}	6L:42D	48	1:7	4	4
G_{60}	6L:54D	60	1:9	4	4
G_{72}	6L:66D	72	1:11	4	4

menced at 06:00 hr as it had during the pretreatment period. The food and water were freely available and were resupplied only during the light phase of the treatment. The temperature of the photoperiodic chambers was not regulated closely but it did not vary more than 2°C from the temperature of the bird room, which varied between $11\text{--}39^{\circ}\text{C}$ during the experiments.

The data obtained from both experiments were subsequently subjected to 'Analysis of Variance'. Supplemented Neuman Keuls' Multiple Range 't' test was employed at significance levels of 0.05 and 0.01 to ascertain the differences among mean values [17]. The data from the birds that died during the experiments were not included in statistical analysis.

RESULTS

Experiment I

A significant variation ($F=1024.22$; $P<0.001$) in ovarian weight of short day treated photorefractory birds was observed under long days. The data presented in Figure 1 suggest that short day (8L:16D) treatment of six weeks to yellow-throated sparrows is sufficient to break the photo-

refractoriness and the birds regrow their ovaries ($\text{OW}=17.00\pm 0.05\text{ mg}$; $P<0.01$) upon their return to long days in a duration of 30 days. On the other hand, five weeks of short days could not terminate photorefractoriness and the birds maintained their regressed ovaries ($\text{OW}=4.00\pm 0.00\text{ mg}$). The birds of control group, continued under long days, maintained photorefractoriness till the end of the experiment ($\text{OW}=4.00\pm 0.00\text{ mg}$).

Experiment II

The results obtained from the resonance experiments are presented in Figure 2. ANOVA exhibited significant variation ($F=956.79$, $P<0.001$) in ovarian weight in the birds under long days, that were previously exposed to various resonance light cycles. The regressed condition of the ovaries ($\text{OW}=4.00\pm 0.00\text{ mg}$) was maintained in the birds of control group held under long days throughout the course of experiment, indicating the persistence of photorefractoriness. A significant ovarian growth ($P<0.001$) was observed in the photorefractory birds previously exposed to the cycles of 24 ($\text{OW}=33.50\pm 0.86\text{ mg}$), 48 ($\text{OW}=31.00\pm 0.57\text{ mg}$) and 72 hr ($\text{OW}=29.50\pm 0.50\text{ mg}$), whereas those under the cycles of 12, 36 and 60 hr maintained the regressed ovaries ($\text{OW}=4.00\pm 0.00\text{ mg}$) upon their return to long days. Average ovarian weight in the birds previously included in cycles of 24 (6L:18D), 48 (6L:42D) and 72 hr (6L:66D) were significantly ($P<0.001$) greater than that of birds in cycles of 12 (6L:6D), 36 (6L:30D) and 60 hr (6L:54D) and in control group. The mean ovarian weight of the birds in cycle of 24 hr was significantly greater ($P<0.01$) than that of the birds in cycles of 48 and 72 hr. Further, a significant ($P<0.05$) difference in ovarian response of the birds was apparent between the cycles of 48 and 72 hr.

DISCUSSION

The results obtained from the experiment I suggest that short days treatment of six weeks to yellow-throated sparrow is sufficient to break the photorefractoriness induced by long days and such birds show redevelopment of their ovaries upon

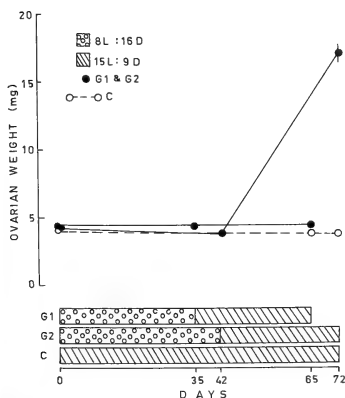


FIG. 1. Termination of photorefractoriness in *Gymnorhis xanthocolis* by short days (8L:16D).

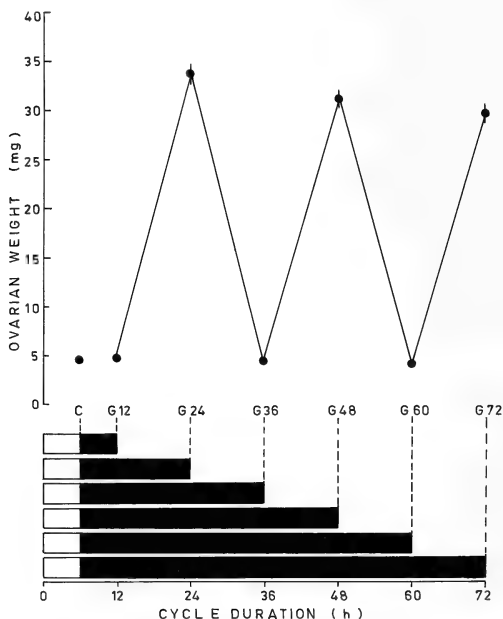


FIG. 2. Effect of resonance light cycles in termination and maintenance of the photorefractory period in *Gymnorhis xanthocolis*. The light dark cycles are represented as bars. The closed bars represent the different duration of dark phases following a 6 hr main photophase. A control group (15L:9D) is represented by C. ● indicates the mean ovarian weight for each group. Vertical bars represent the standard error if it does not fall within the point symbol.

subjecting them to long photoperiod. This is in agreement with the report that short days somehow terminate photorefractoriness and make the birds photosensitive [3, 7, 18, 19]. The number of short days required to dissipate photorefractoriness seems to be species specific. However, in general, six to eight weeks treatment of short days terminates photorefractoriness by making birds sensitive to photostimulation [20]. Although short days terminate the photorefractory period, how this treatment alters neuroendocrine gonadal activity seems to be unknown and leads our attention towards the involvement of circadian mechanism(s).

The effectiveness of various resonance light cycles in maintaining as well as in breaking refractory period is shown in Figure 2. The ovarian growth, under long days, is evident in the birds previously exposed to the cycles of 24 (6L:18D), 48 (6L:42D) and 72 hr (6L:66D), whereas it fails to occur in the birds previously subjected to the cycles of 12 (6L:6D), 36 (6L:30D) and 60 hr (6L:54D). It has already been discussed in earlier experiment that short days treatment for six weeks terminates photorefractoriness in this species. Thus, the cycles of 24, 48 and 72 hr acted as short days; these cycles terminated the refractory period and resulted in photosensitivity of the birds to long days.

On the other hand, 12, 36, and 60 hr cycles maintained the refractoriness, i.e., these cycles acted as long days despite the fact that birds under any of the above resonance light cycles had received only one 6 hr of light per cycle. It clearly indicates that neither the absolute duration of light or dark nor the ratio of the two is requisite for the termination of photorefractoriness in this species (Table 1).

These results are consistent with the Bünning hypothesis [21] or external coincidence model and suggest that an endogenous rhythm with a period of about 24 hr is involved in photoperiodic time measurement during the termination and maintenance of photorefractoriness in yellow-throated sparrows. Each circadian rhythm consists of two phases. First phase is photoinensitive or non-photoinducible while latter is photosensitive or photoinducible phase. According to the external coincidence model, first light entrains the circadian rhythm of responsiveness to itself and second, when external light is coincident or noncoincident with the photosensitive phase of that rhythm which it is entraining, the bird will interpret the photoperiod as a long or short day, respectively.

This model predicts that termination of the photorefractory period depended on the lack of coincidence of light with photosensitive (or photoinducible) phase of circadian rhythm existing within the bird [22, 23]. If we put our data within the frame work of the external coincidence model, it is found that in cycles of 24, 48 and 72 hr light is restricted only to photoinensitive phase and does not coincide with the photosensitive phase of an endogenous circadian rhythm. Thus, these cycles behave like short days and break the photorefractoriness in this species. On the other hand, since light coincides with the photosensitive phase of circadian rhythm in cycles of 12, 36 and 60 hr duration, so these cycles behave as long days and fail to terminate refractoriness, as is evident in the birds of control group maintained under long days.

These results on yellow-throated sparrows clearly follow those obtained for the termination of refractory period in white-crowned (*Zonotrichia leucophrys gambelii*) and golden-crowned (*Zonotrichia albicollis*) sparrows [9, 12]; house finch (*Carpodacus mexicanus*) [8] and house sparrow (*Passer domesticus*) [24].

Conclusively, six weeks of short days treatment could prove to be prerequisite for termination of photorefractoriness and restoration of photosensitivity in yellow-throated sparrow. Further, the results from present study provide evidence that females, like males of photoperiodic species, use circadian rhythm to measure the photoperiodic time during maintenance as well as termination of photorefractoriness.

ACKNOWLEDGMENTS

The work was financially supported by research associateship and senior research fellowship of CSIR, New Delhi to Dr. Anand S. Dixit.

REFERENCES

1. Riley, G. M. (1936) Light regulation of sexual activity in the male sparrow, *Passer domesticus*. Proc. Soc. Exp. Biol. Med., 34: 331-332.
2. Farner, D. S. and Lewis, R. A. (1971) Photoperiodism and reproductive cycle in birds. In "Photophysiology". Ed. by A. C. Giese, Academic Press, N. Y. and London, pp. 325-370.
3. Lofts, B. and Murton, R. K. (1968) Photoperiodic and physiological adaptations regulating avian breeding cycles and their ecological significance. J. Zool., 155: 327-394.
4. Wingfield, J. C. (1983) Environmental and endocrine control of avian reproduction: An ecological approach. In "Avian Endocrinology". Ed. by S. Mikami, K. Homma and M. Wada, Japan. Sci. Soc. Press, Tokyo, and Springer-Verlag, Berlin, Heidelberg and N.Y., pp. 263-288.
5. Follett, B. K. and Nicholls, T. J. (1984) Photorefractoriness in Japanese quail: Possible involvement of the thyroid gland. J. Exp. Zool., 232: 573-580.
6. Nicholls, T. J., Goldsmith, A. R. and Dawson, D. (1984) Photorefractoriness in European starlings: Associated hypothalamic changes and the involvement of thyroid hormones and prolactin. J. Exp. Zool., 232: 567-572.
7. Farner, D. S. and Follett, B. K. (1966) Light and other environmental factors affecting avian reproduction. J. Anim. Sci., 25: 90-118.
8. Hamner, W. M. (1968) The photorefractory period of the house finch. Ecology, 49: 211-227.
9. Turek, F. W. (1972) Circadian involvement in termination of the refractory period in two sparrows. Science, 178: 1172-1173.
10. Nanda, K. R. and Hamner, K. C. (1958) Studies on the nature of the endogenous rhythm affecting photoperiodic responses of *Bioloxi soyabean*. Bot.

- Gaz., **120**: 14-15.
- 11 Tewary, P. D., Dixit, A. S. and Kumar, V. (1984) Circadian rhythmicity and initiation of reproductive functions in female passerines. *Physiol. Zool.*, **57**: 563-566.
 - 12 Sansum, E. L. and King, J. R. (1975) Photorefractoriness in a sparrow: Phase of circadian photosensitivity elucidated by skeleton photoperiods. *J. Comp. Physiol.*, **98**: 183-188.
 - 13 Kumar, V. and Tewary, P. D. (1984) Circadian rhythmicity and the termination of photorefractoriness in the blackheaded bunting. *Condor*, **86**: 27-29.
 - 14 Turek, F. W. and Campbell, C. S. (1979) Photoperiodic regulation of neuroendocrine-gonadal activity. *Biol. Reprod.*, **20**: 32-50.
 - 15 Ali, S. and Ripley, D. S. (1983) *Handbook of the Birds of India and Pakistan* (Compact edition). Oxford Univ. Press, Bombay, London & N.Y.
 - 16 Tewary, P. D. and Dixit, A. S. (1986) Photoperiodic regulation of reproduction in subtropical yellow-throated sparrow (*Gymnorhis xanthocollis*). *Condor*, **88**: 70-73.
 - 17 Bruning, J. L. and Kintz, B. L. (1977) *Computational Handbook of Statistics* (Second edition). Glenview, Illinois.
 - 18 Turek, F. W. (1975) The termination of the avian photorefractory period and the subsequent gonadal response. *Gen. Comp. Endocrinol.*, **26**: 562-564.
 - 19 Tewary, P. D. and Dixit, A. S. (1983) Photoperiodic control of the ovarian cycle in the rosefinch, *Carpodacus erythrinus*. *J. Exp. Zool.*, **228**: 537-542.
 - 20 Wingfield, J. C. and Farner, D. S. (1980) Control of seasonal reproduction in temperate zone birds. *Prog. Reprod. Biol.*, **5**: 62-101.
 - 21 Bünning, E. (1973) *The Physiological Clock* (Third edition). Univ. Press Ltd., Springer Verlag, N. Y., Heidelberg & Berlin.
 - 22 Farner, D. S. (1975) Photoperiodic control in the secretion of gonadotropins in birds. *Am. Zool.*, **15**: 117-135.
 - 23 Turek, F. W. (1978) Diurnal rhythms and the seasonal reproductive cycle in birds. In "Environmental Endocrinology". Ed. by I. Assenmacher and D. S. Farner, Springer Verlag, N. Y., pp. 263-288.
 - 24 Murton, R. K., Lofts, B. and Westwood, N. J. (1970) Manipulation of photorefractoriness in the house sparrow, *Passer domesticus* by circadian light regimes. *Gen. Comp. Endocrinol.*, **14**: 107-113.

Circadian Rhythms in Locomotor Activity of the Hagfish, *Eptatretus burgeri* (IV). The Effect of Eye-Ablation

HIROSHI KABASAWA and SADAKO OOKA-SOUDA¹

*Keikey Aburatsubo Marine Park Aquarium, 1082 Koajiro, Misaki-machi,
Miura-shi, Kanagawa 238-02, and ¹Atomigakuen Junior College,
1-5-2 Otsuka, Bunkyo-ku, Tokyo 112, Japan*

ABSTRACT—The locomotor activity in the hagfish, *Eptatretus burgeri*, was recorded by means of an infra-red light-photocell system. The signals generated when the animal crossed the infra-red beam were relayed to an event recorder. Eye-ablated animals kept in constant darkness exhibited a free-running rhythm of swimming activity. This indicated that the circadian rhythm does not depend on presence of the eye. The motor activity in the sham-operated animals occurred only in the first two thirds of the dark period under 12L:12D, and the activity pattern adapted to the new light regimen under the light-dark reversal as it did in intact animals. In eye-ablated animals, the motor activity occurred not only in the dark period, but also it ran into the light period as if it were a free-running rhythm in constant darkness. It was found that one of the most important factors affecting such nocturnal rhythms was optically perceived peripheral lighting information.

INTRODUCTION

Eptatretus burgeri is nocturnally active in a natural environment [1]. The animal kept in constant darkness displays a distinct free-running rhythm. Swimming activity under a 12L:12D light program occurred only in the first 2/3 of the dark period. When the light-dark cycle was reversed by doubling the first dark phase, the time necessary to adapt to the new dark period was about a week [1]. These facts indicate that the nocturnal activity rhythm in the hagfish is correlated to the ambient light-dark cycle. Aside from the eye, the animal might have other photoreceptors in the skin [2]. The eye in the hagfish is morphologically in an advanced stage of reduction; it lines under and free from the skin, and it has no lens [3]. The optic nerve is underdeveloped and relays to the brain [4].

The present study aims to clarify the effect of eye-ablation on the circadian rhythm in locomotor activity. The eyeless animals were kept under conditions of constant darkness, 12L:12D and the

reversal of the light-dark cycle.

MATERIALS AND METHODS

Locomotor activity in the hagfish was recorded by means of an infra-red light-photocell system. The details of the procedure were described previously [1].

The collected animals were kept in a large aquarium to acclimatize under a 12L:12D light program for one or two weeks. The individuals used for the eye-ablation were lightly anesthetized with MS222, and then the eyeballs were removed by cutting at the base with iridectomy scissors. The skin was resewn. The operation was the same for the sham-operated animals except that the eyes were left intact. The experiments were carried out during August-December. The water temperature was kept constant at 15°C with cooling system. The source of illumination in the otherwise dark room was a 15W fluorescent lamp which presented 670 lux at the bottom of the aquarium. This value was estimated to be the same as at 25 m depth on a fine day in the open sea. Each experiment was done with one individual of the hagfish in an aquarium. The individuals used for these experi-

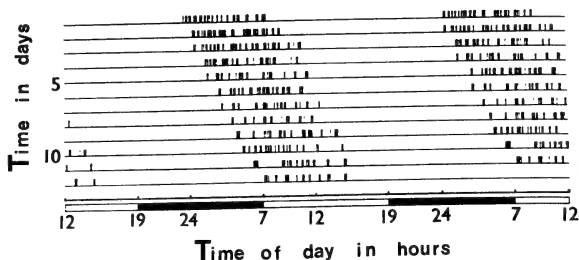


FIG. 1. Circadian rhythm of activity recorded in a sham-operated hagfish kept in constant darkness. Original record plotted twice. The activity displays a free-running rhythm like as an intact one does.

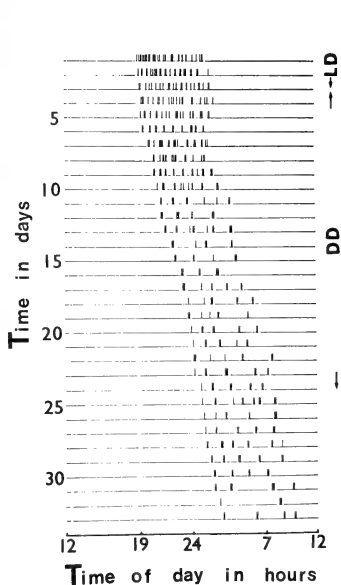


FIG. 2. Activity rhythm recorded in an eye-ablated hagfish kept in constant darkness. The activity displays also a free-running without the eye.

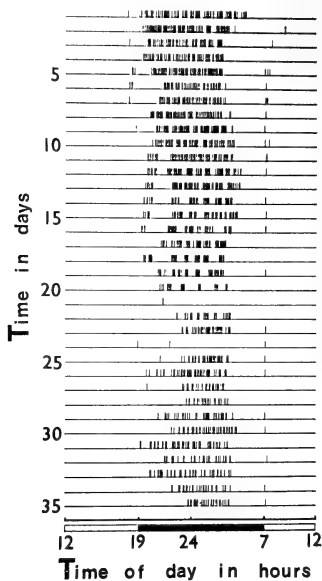


FIG. 3. In a sham-operated hagfish in 12L:12D. The activity phase is restricted within the dark period. Temporal activation occurs at the light-dark turning points.

ments were follows; 3 sham-operated animals (S.O.A.) and 6 eye-ablated animals (E.A.A.) for constant darkness experiment, 3 S.O.A. and 7 E.A.A. for 12L:12D experiment, and 2 S.O.A. and 4 E.A.A. for the 12L:12D-reversal experiment.

RESULTS

The swimming activity of the sham-operated animals under constant darkness presented a clear free-running rhythm similar to the intact animals (Fig. 1). The eye-ablated animals in same constant darkness also presented a free-running rhythm (Fig. 2). This indicates that a free-running rhythm in darkness in the hagfish is independent of the presence of the eye. The intact animal in a 12L:12D light program has a nocturnally dark-active rhythm of swimming, and the activity is distinctly confined to the first two thirds of the dark time [1]. The activity pattern in the sham-operated animals in this experiment resembled that of the intact hagfish except that some activity began at the beginning of the light period (Fig. 3). The eye-ablated animal under 12L:12D had a free-running active phase not only in the dark period but also in the light period with no influence of the established light-dark schedule (Figs. 4 and 5). The temporal activity illustrated in Figure 4 which occurred at the initiation of the light period sug-

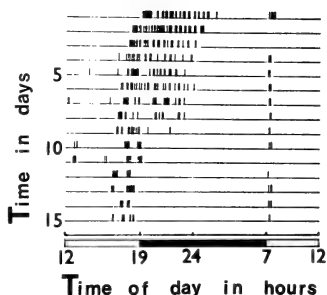


FIG. 4. In an eye-ablated hagfish in 12L:12D. The phase overruns the dark period.

gests that the eyeless animal had other photoreceptors responding to the peripheral light stimuli. In the reversed light-dark cycle, the intact animal achieved the phase shift of activity to the new dark period [1]. The sham-operated animal in this experiment also exhibited the phase shift in the reversal program (Fig. 6). The free-running activity in the eye-ablated animal under the same reversal program occurred not only in the dark period but also ran into the light period without shifting phase, in this way it resembled the free-running which the intact animals displays in constant darkness (Fig. 7). The temporal activity at

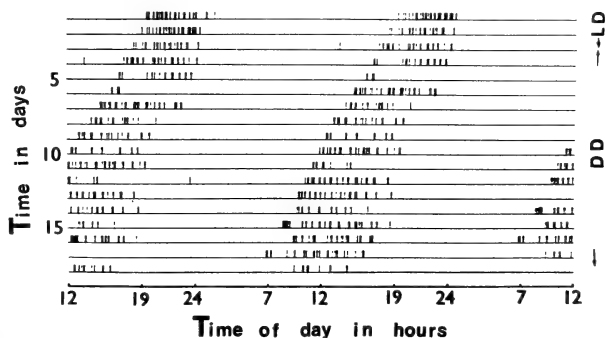


FIG. 5. Twice plotted view of the original record in an eye-ablated hagfish kept in 12L:12D. The activity phase is independent of light-dark cycle, and it seems to be a free-running rhythm.

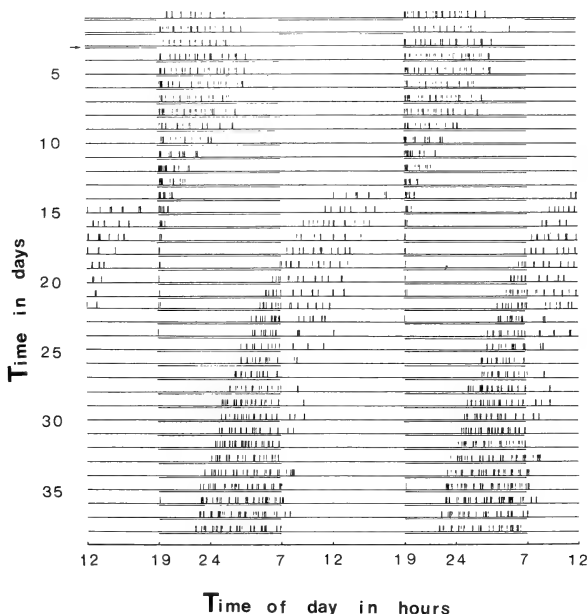


FIG. 6. The phase shift of activity in a sham-operated hagfish in reversed light-dark cycle which is achieved by doubling the first dark time. Underline shows light time. The activity shifts to the new dark period.

the onset of lighting also appeared in the animal.

DISCUSSION

Fernholm and Holmberg [3] have pointed out that the eye structure of *Eptatretus burgeri* shows several signs of degeneration: The eye is situated beneath an unpigmented patch of the skin, it has a retina, but it lacks a lens.

The eye-ablated animals both under 12L:12D and under the reversal of it displayed a free-running rhythm in locomotor activity, being independent of the outside light-dark cycles. These facts indicate that the activity rhythm is under the influence of external photoperiodic factors and the

eye plays an important part of a photo-transducer for the activity rhythm. Kusunoki and Amemiya [4] have investigated on the pathway of retinal fiber projection in *Eptatretus burgeri* by means of the transport of HRP. They found that the fibers reached the ventral surface of hypothalamus from the eye. Kobayashi [5] has reported on the action potentials recorded from the rudimentary eye of *Myxine garmani*. The authors also have observed action potentials from the eye of *Eptatretus burgeri* (unpublished). The eyeless hagfish displays a temporal activity at the dark-light turning point. This activity seems to be a photo-reflex whose activation occurred through the other photoreceptors than the eye.

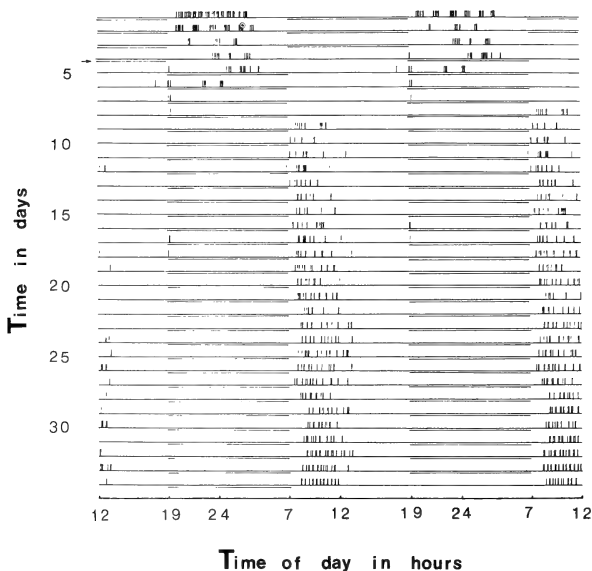


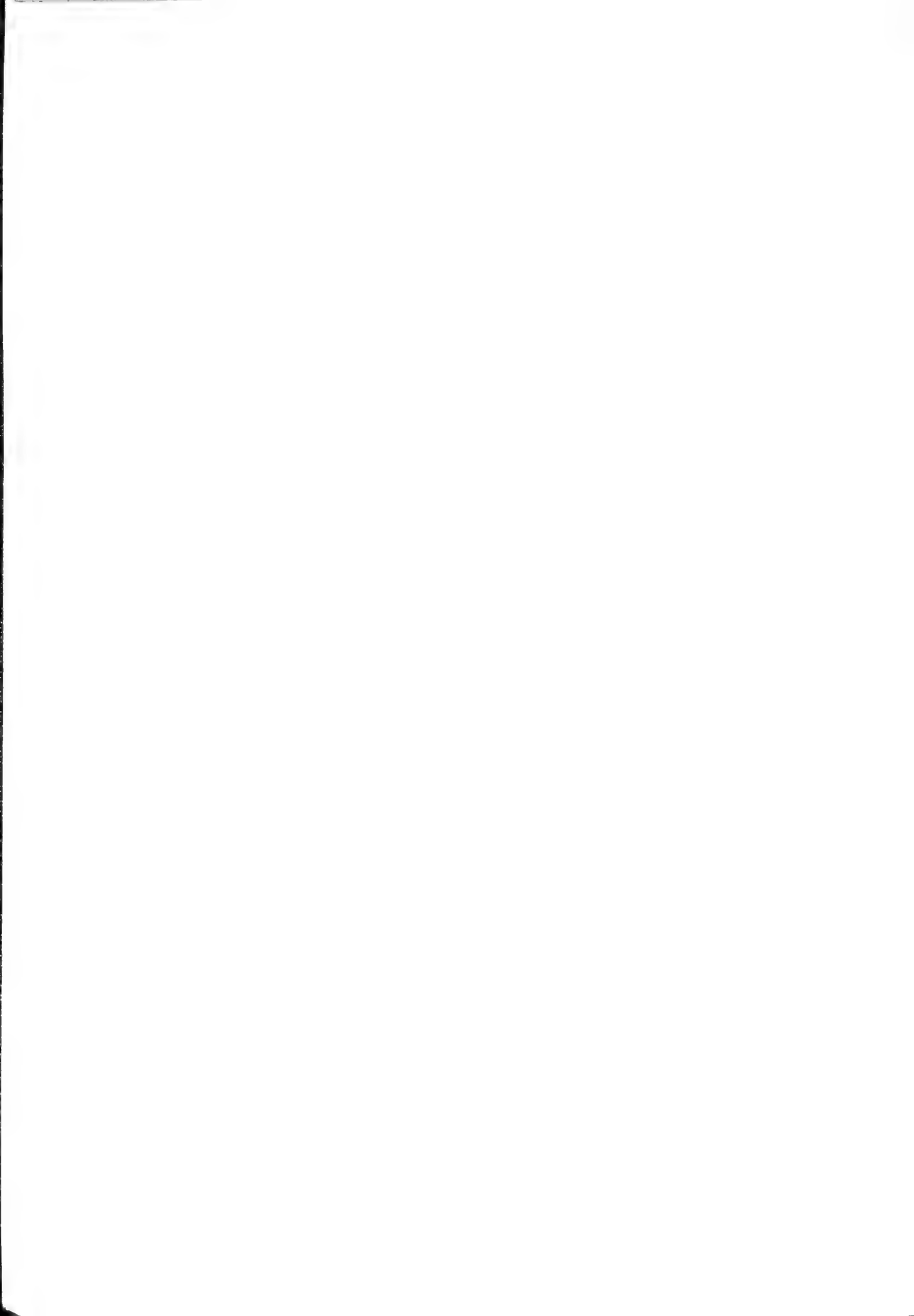
FIG. 7. Free-running activity in an eye-ablated hagfish in reversed light-dark cycle which is achieved by doubling the first dark time. The activity is independent of the reversal.

ACKNOWLEDGMENT

All these experiments were performed at Misaki Marine Biological Station, University of Tokyo. The authors are indebted to Prof. A. Gorbman, University of Washington, for critical reading the manuscript.

REFERENCES

- 1 Ooka-Souda, S., Kabasawa, H. and Kinoshita, S. (1985) Circadian rhythms in locomotor activity in the hagfish, *Eptatretus burgeri*, and effect of reversal of light-dark cycle. *Zool. Sci.*, **2**: 749-754.
- 2 Newth, D. R. and Rose, M. D. (1955) On the reaction to light of *Myxine glutinosa* L.. *J. Exp. Biol.*, **32**: 4-21.
- 3 Fernholm, B. and Holmberg, K. (1975) The eyes in three genera of hagfish (*Eptatretus*, *Paramyxine* and *Myxine*)—a case of degenerative evolution. *Vision Res.*, **15**: 253-259.
- 4 Kusunoki, T. and Amemiya, F. (1983) Retinal projections in the hagfish, *Eptatretus burgeri*. *Brain Res.*, **262**: 295-298.
- 5 Kobayashi, H. (1963) Preliminary report on the action potentials recorded from the rudimentary eye of hagfish, *Myxine garmani*. *Zool. Mag.*, **72**: 6-12.



Lordosis-inhibiting Pathway in the Lateral Hypothalamus: Medial Forebrain Bundle (MFB) Transection

KOREHITO YAMANOUCHI¹ and YASUMASA ARAI²

*Department of Anatomy, Juntendo University School of Medicine,
Hongo, Bunkyo-ku, Tokyo 113, Japan*

ABSTRACT—In order to clarify the lordosis inhibiting pathway, five types of half-dome cuts were made at the level of the suprachiasmatic nucleus or the premammillary nucleus in ovariectomized rats. Then, female sexual behaviors were tested following the treatment with estradiol benzoate (EB) and progesterone (P). Castrated and sham-operated control females showed low levels of lordosis activity when primed with 0.2 μ g EB and P. In contrast, the females with bilateral cuts located in and/or lateral to the supraoptic nucleus (VLC) showed high levels of lordosis response. Receptivity of females with bilateral cuts located dorsal to the VLC (DLC-I), a medial cut at the suprachiasmatic nucleus level (VMC-I), a medial cut (VMC-II) or bilateral dorsolateral cuts (DLC-II) at the premammillary nucleus level was low, being comparable to that of controls. When EB was given in a subthreshold range (0.5 μ g), lordosis activity was still significantly lower in these females than the females with VLC. Since the area of VLC corresponds to the site of passing the medial forebrain bundle, the facilitatory effect of VLC may be due to removal of the lordosis inhibiting influence of the medial forebrain bundle in female rats.

INTRODUCTION

Female sexual behaviors are regulated by dual systems, facilitatory and inhibitory ones in the forebrain [1]. For the facilitatory system the ventromedial hypothalamus is believed to be a main source of signals, because destruction of the ventromedial hypothalamic nucleus (VMN) suppressed lordosis [2-5], whereas electrical stimulation [6] or implantation of crystalline estrogen into the VMN [7] potentiated the display of lordosis. On the other hand, the septum plays an inhibitory role in lordosis regulation [1, 8, 9]. The inhibitory signals from the septum are thought to go down to the lower brain stem through the preoptic area, since the horizontal cut to the ventral septum markedly facilitated lordosis and soliciting behavior [10, 11]. A similar facilitatory effect has been reported in the rats with lesions of the

preoptic area (POA) [12-15].

The central gray of the midbrain, especially the dorsolateral central gray, has been reported to be a focus of the ventromedial hypothalamic influence [16]. However, the pathway of the septal lordosis inhibiting influence and its projecting focus have not been investigated yet. In this experiment, in order to clarify this inhibitory pathway, sexual behaviors were examined in estrogen- and progesterone-primed ovariectomized rats after the fibers which pass the hypothalamus were cut.

MATERIALS AND METHODS

Wistar female rats (210-250 g) housed under a controlled photoperiod (14:10 hr, light:dark) and temperature (24-25°C) were castrated and subjected to brain surgery. Five different types of neural transection were made stereotactically at the level of the suprachiasmatic nucleus or the premammillary nucleus by means of Halász knife under ether anesthesia (see Fig. 1). An incisor bar being set at 5 mm below the interaural line, a Halász knife (1.0×2.0 mm blade) was lowered 9 mm from the bregma level bilaterally at the point

Accepted April 11, 1988

Received October 27, 1987

¹ Present address: Department of Basic Human Sciences, Waseda University School of Human Sciences, 2-579-15 Mikajima, Tokorozawa, Saitama 359, Japan.

² To whom requests of reprints should be addressed.

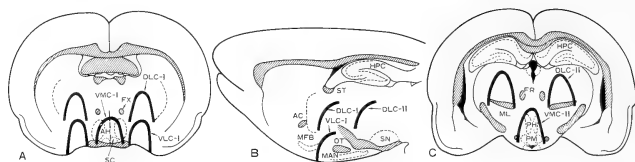


FIG. 1. Schematic representations of half-dome cuts in frontal section at the level of the suprachiasmatic nucleus (A) and the premammillary nucleus (C), and sagittal section at the level of the medial amygdaloid nucleus (B). In the suprachiasmatic level, ventromedial (VMC-I), ventrolateral (VLC) or dorsolateral cuts (DLC-I) were made. In the premammillary nucleus level, dorsolateral (DLC-I) or ventromedial (VMC-II) cut was made. Abbreviations: AC, anterior commissure; AH, anterior hypothalamic nucleus; FR, fasciculus retroflexus; FX, fornix; HPC, hippocampus; MAN, medial amygdaloid nucleus; MFB, medial forebrain bundle; ML, medial lemniscus; OT, optic tract; PH, posterior hypothalamic nucleus; PM, premammillary nucleus; SC, suprachiasmatic nucleus;

1.5 mm posterior to the bregma and 2 mm lateral to the midline, and then, was turned 180° anteriorly in order to transect the medial forebrain bundle at the level of the suprachiasmatic uncus (ventrolateral cut I, VLC-I). A similar type of half-dome cut was at the midline level (ventromedial cut I, VMC-I). Another half-dome cut at the level of the suprachiasmatic nucleus was made bilaterally 2 mm upper to the VLC (dorsolateral cut I, DLC-I). At the level of the premammillary nucleus, a Hálasz knife, having a 1.5×2 mm blade, was placed at the point 3.5 mm posterior to the bregma, 2 mm lateral to the midline and lowered to the point 7 mm below the bregma level and then rotated 180° anteriorly (dorsolateral cut II, DLC-II). A similar type of a half-dome cut was made at the midline level (ventromedial cut II, VMC-II). In addition, castrated and castrated sham-operated controls were made. In the sham-operated groups, the Hálasz knife was lowered to the same level of VLC-I without rotation.

Two to 3 weeks after the operation, the first behavioral test was started. All females were treated with 0.2 µg estradiol benzoate (EB, dissolved in 0.1 ml sesame oil) daily for 3 days and 0.5 mg progesterone (P, in 0.1 ml oil) on the fourth day 4–6 hr before the behavioral test. The second and the third tests were carried out at two-week intervals with higher doses of EB, 0.5 and 2.0 µg. In the behavioral tests, each experimental female was placed in an observation cage with two vigorous males and lordosis quotient (LQ, number of

lordosis/10 mounts, ×100) was recorded. The presence or absence of soliciting behaviors (ear wiggling and hopping) was also recorded in each animal. The animals were sacrificed at the end of the test series. Each brain was removed and fixed in 10% formalin solution. Then, frozen sections stained with cresylechtviolet were made in order to determine the precise location of the cuts.

LQs were analyzed using the F-test and then by t-test or Cochran Cox method. For comparison of the incidence of lordosis or soliciting behaviors among the groups, χ^2 -test with Yates' correction was used.

RESULTS

In the first test, lordotic activity was very low in all groups treated with 0.2 µg EB except females with the VLC (see Fig. 2). In the VLC group, 12 out of 14 females displayed lordosis with the mean LQ 73.6 ± 9.7 and 10 females showed ear-wiggling. However, none of 6 VMC-II and 10 DLC-II females exhibited female sexual behavior. When the dose of EB was increased to 0.5 µg in the second test, 7 out of 11 control females displayed lordosis and the mean LQ was 42.7 ± 12.9 . Ear-wiggling and hopping were observed in 4 control females. The mean LQs of the sham-operated, VMC-I, and DLC-I females were comparable to that of controls. In the VLC group, the mean LQ was 85.7 ± 9.7 and 11 out of 14 VLC females showed both ear-wiggling and hopping. In con-

trast, only 3 out of 10 DLC-II animals displayed lordosis with the mean LQ 19.0 ± 10.4 . In the third test with treatments of $2 \mu\text{g}$ EB-P, high scores of LQ were obtained in all groups except DLC-II group (see Fig. 2). In the DLC-II group, lordotic activity was lower than that of controls, the mean LQ being 45.0 ± 14.2 .

Histological examinations showed that VLC, VMC-I and DLC-I were seen at the level of the supra-chiasmatic nucleus. The cuts of the VLC were located in and/or just lateral to the supraoptic nucleus (Fig. 3). In VLC females except 3 animals, the cuts caused small damage in the lateral part of the supraoptic nucleus. DLC-I was seen above

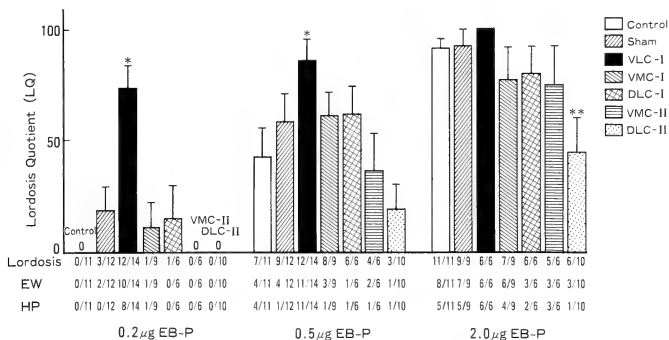


FIG. 2. Lordosis quotient (LQ) and incidence of lordosis, earwigging (EW) and hopping (HP) in the three tests. Animals were treated with 0.5–2 μg estradiol benzoate (EB) for 3 successive days and 0.5 mg progesterone (P). VMC-I, VMC-II; ventromedial cut I, II, VLC; ventrolateral cut, DLC-I, II; dorsolateral cut I, II. * $P < 0.05$, vs other groups. ** $P < 0.05$ vs control.

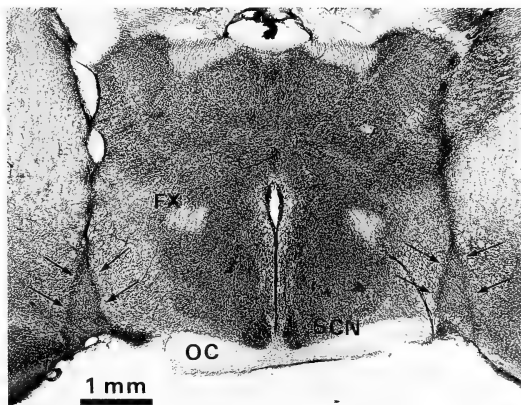


FIG. 3. Photomicrograph of a representative frontal section at the level of supra-chiasmatic nucleus in a female with ventrolateral cuts (VLC). Arrows indicate VLC. FX, fornix. OC, optic chiasma. (Cresylechtviolet stain).

the level of the fornix between the medial part of the globus pallidus and the lateral part of the ventral thalamus. In the VMC-I group, anterior end of halfdome cuts seemed to be located just anterior to the suprachiasmatic nucleus. VMC-II and DLC-II were seen at the level of the posterior end of the VMN and the premmammillary nucleus. In the DLC-II group, cuts were located above the level of the medial lemniscus and lateral to the fasciculus retroflexus. VMC-II were located inside of the right and left fiber bundles of fornix at the level of the premmammillary nucleus.

DISCUSSION

At the level of the suprachiasmatic nucleus, VLC significantly facilitated lordosis behavior, but DLC-I located more dorsal than VLC, or VMC had no marked influence on induction of female sexual behavior. Since the area affected by VLC corresponds to the site where fibers of the medial forebrain bundle (MFB) run [17], the MFB is considered to play an important role in sending inhibitory signals for lordosis. Destruction of the lateral septum potentiated lordosis in not only female rats [8] but also male rats [18, 19]. This suggests that the septum exerts an inhibitory influence on lordosis mediating system. Horizontal cuts at the border between the septum and the preoptic area (POA) also enhanced lordosis and soliciting behaviors both in female [10, 20] and male [21, 22]. Furthermore, there is evidence suggesting that ventrolateral outputs of the septum send the inhibitory signals, because only bilateral ventrolateral horizontal cuts enhanced lordotic activity, but dorsal, posterior or ventromedial cuts had no effect [1]. The facilitatory effect of preoptic lesions on lordosis response [4, 12, 13, 20] may be as a result of interruption of these descending inhibitory fibers from the septum. Anatomical study using tritium labeled amino acid method suggests that a large number of fibers leave the septum at the ventrolateral part and participate in the MFB [23]. These septal fibers then go down in the ventromedial part of the MFB at the level of the optic chiasma [23] which is almost identical to the area transected by VLC in the present study. Modianos *et al.* [24] reported that lesions of the

MFB at the level of the anterior hypothalamus did not change postoperative EB threshold for induction of lordosis, but prolonged lordotic activity after the treatment with progesterone. In the previous experiment, however, EB threshold was significantly lowered without progesterone treatment by ventral horizontal cuts of the septum, suggesting that septal inhibitory influence is estrogen-sensitive [10]. The present study with MFB cuts are also consistent with this observation.

On the other hand, dorsolateral cuts at the premmammillary level (DLC-II) decreased lordotic activity. Since the lateral outputs of the VMN converging onto the midbrain central gray area considered to play a facilitatory role in regulating lordosis [25], DLC-II in the present study may transect these VMN projecting fibers to the midbrain central gray. Consistent with this results, there is a report that bilateral knife cuts in a transverse plane transecting lateral running axons from the VMN severely reduced lordosis response [26]. Therefore, the facilitatory influence of the VMH and inhibitory influence of the septum which descend to the lower brain stem may operate independently [27, 28]. It is needed to clarify a possible contact point of these inhibitory and facilitatory influences in lordosis regulating system in the lower brain stem.

ACKNOWLEDGMENT

This study was supported by Grants-in-Aid from the Ministry of Education, Science and Culture of Japan.

REFERENCES

1. Yamanouchi, K., Matsumoto, A. and Arai, Y. (1985) Neural and hormonal control of lordosis behavior. *Zool. Sci.*, 2: 617-627.
2. Malsbury, C. W., L.-M. Kow and Pfaff, D. W. (1977) Effects of medial hypothalamic lesions on the lordosis response and other behaviors in female golden hamsters. *Physiol. Behav.*, 19: 223-237.
3. Mathews, D. and Edwards, D. A. (1977) Involvement of the ventromedial and anterior hypothalamic nuclei in the hormonal induction of receptivity in the female rat. *Physiol. Behav.*, 19: 159-164.
4. Pfaff, D. W. and Sakuma, Y. (1979) Deficit in the lordosis reflex of female rats caused by lesions in the

- ventromedial nucleus of the hypothalamus. *J. Physiol. (Lond.)*, **288**: 203-210.
- 5 Okada, R., Watanabe, H., Yamanouchi, K. and Arai, K. (1980) Recovery of sexual receptivity in female rats with lesions of ventromedial hypothalamus. *Exp. Neurol.*, **68**: 595-600.
 - 6 Pfaff, D. W. and Sakuma, Y. (1979) Facilitation of the lordosis reflex of female rats from the ventromedial nucleus of the hypothalamus. *J. Physiol. (Lond.)*, **288**: 186-202.
 - 7 Barfield, R. J. and Chen, J. J. (1977) Activation of estrous behavior in ovariectomized rats by intracerebral implants of estradiol benzoate. *Endocrinology*, **101**: 1716-1725.
 - 8 Nance, D. W., Shryne, J. and Gorski, R. A. (1975) Effects of septal lesions on behavioral sensitivity of female rats to gonadal hormones. *Horm. Behav.*, **6**: 59-64.
 - 9 Zasorin, N., Malsbury, C. and Pfaff, D. W. (1975) Suppression of lordosis in the hormone-primed female hamster by electrical stimulation of the septal area. *Physiol. Behav.*, **14**: 595-599.
 - 10 Yamanouchi, K. and Arai, Y. (1977) Possible inhibitory role of the dorsal inputs to the preoptic area and hypothalamus in regulating female sexual behavior in the female rat. *Brain. Res.*, **127**: 296-301.
 - 11 Yamanouchi, K. and Arai, Y. (1978) Lordosis behavior in male rats: Effect of deafferentation in the preoptic area and hypothalamus. *J. Endocrinol.*, **76**: 381-382.
 - 12 Nance, D. M., Christensen, L. W., Shryne, J. and Gorski, R. A. (1977) Modifications in gonadotropin control and reproductive behavior in the female rat by hypothalamic and preoptic lesions. *Brain. Res. Bull.*, **2**: 307-312.
 - 13 Powers, B. and Valenstein, E. S. (1972) Sexual receptivity: Facilitation by medial preoptic lesions in female rat. *Science*, **175**: 1003-1005.
 - 14 Rodriguez-Sierra, J. F. and Terasawa, E. (1979) Lesions of the preoptic area facilitate lordosis behavior in male and female guinea pigs. *Brain. Res. Bull.*, **4**: 513-517.
 - 15 Yamanouchi, K., Watanabe, H., Okada, R. and Arai, Y. (1983) Forebrain lordosis inhibiting system and serotonin neuron in female rats: Effects of p-chloroamphetamine. *Endocrinol. Japon.*, **29**: 469-474.
 - 16 Sakuma, Y. and Pfaff, D. W. (1981) Electrophysiologic determination of projection from ventromedial hypothalamus to midbrain central gray: Differences between female and male rats. *Brain Res.*, **225**: 184-188.
 - 17 Nieuwenhuis, R., Geeraedts, L. M. G. and Veen-
ing, J. G. (1982) The medial forebrain bundle of the rat. I. General introduction. *J. Comp. Neurol.*, **206**: 49-81.
 - 18 Nance, D. W., Shryne, J. and Gorski, R. A. (1974) Septal lesions: Effects on lordosis behavior and pattern of gonadotropin release. *Horm. Behav.*, **5**: 73-81.
 - 19 Kondo, Y., Shinoda, A., Yamanouchi, K. and Arai, Y. (1986) Role of septum and preoptic area in regulating masculine and feminine sexual behaviors in male rats. *Abst. 1st. Int. Congr. Neuroendocrinology*, p. 108.
 - 20 Yamanouchi, K. and Arai, Y. (1983) Forebrain and lower brainstem participation in facilitatory and inhibitory regulation of the display of lordosis in female rats. *Physiol. Behav.*, **30**: 155-159.
 - 21 Yamanouchi, K. and Arai, Y. (1975) Female lordosis pattern in the male rat induced by estrogen and progesterone: Effect of interruption of the dorsal inputs to the preoptic area and hypothalamus. *Endocrinol. Japon.*, **22**: 243-246.
 - 22 Yamanouchi, K. and Arai, Y. (1985) Presence of a neural mechanism for the expression of female sexual behaviors in the male rat brain. *Neuroendocrinology*, **40**: 393-397.
 - 23 Veening, J. G., Swanson, L. W., Cowan, M. W., Nieuwenhuis, R. and Geeredts, M. G. (1982) The medial forebrain bundle of the rat. II. An autoradiographic study of the topography of the major descending and ascending components. *J. Comp. Neurol.*, **206**: 82-108.
 - 24 Modianos, D. T., Delia, H. and Pfaff, D. W. (1976) Lordosis in female rats following medial forebrain bundle lesions. *Behav. Biol.*, **18**: 135-141.
 - 25 Pfaff, D. W. (1980) Estrogens and Brain Function; Neural Analysis of a Hormone-Controlled Mammalian Reproductive Behavior. Springer-Verlag, New York.
 - 26 Manogue, K. R., Kow, L.-M. and Pfaff, D. W. (1980) Selective brain stem transections affecting reproductive behavior of female rats: The role of hypothalamic output to the midbrain. *Horm. Behav.*, **14**: 377-302.
 - 27 Yamanouchi, K. (1980) Inhibitory and facilitatory neural mechanisms involved in the regulation of lordosis behavior in female rats: Effects of dual cuts in the preoptic area and hypothalamus. *Physiol. Behav.*, **25**: 721-725.
 - 28 King, T. R. and Nance, D. W. (1985) The effects of unilateral frontolateral hypothalamic knife cuts and asymmetrical unilateral septal lesions of lordosis behavior of rats. *Physiol. Behav.*, **35**: 955-959.



Systematic Study of a Paedomorphic Derivative Hydrozoan *Eugymnanthea* (Thecata-Leptomedusae)

SHIN KUBOTA

*Zoological Institute, Faculty of Science, Hokkaido University
Sapporo 060, Japan*

ABSTRACT—The Italian *Eugymnanthea* medusae collected in 1985 were morphologically compared with the Japanese *Eugymnanthea* medusae. The absence of manubrium and/or the greater number of statoliths per statocyst, nearly always distinguish the Italian morph from the Japanese one. These two morphs of *Eugymnanthea* also differ in main attachment sites of polyps to their host bivalves, moreover they seem to be reproductively isolated. Therefore, they are referable to two species and it is probable that the populations in Japan are not the result of a recent artificial introduction of the Italian morph. The possibility of the origin of *Eugymnanthea* by parallel and/or convergent evolution is mentioned.

INTRODUCTION

The genus *Eugymnanthea*, one of the bivalve-inhabiting hydroids, is characterized by an abortive mature medusa without tentacles. This genus is monotypic, and contains the two subspecies *E. inquilina inquilina* Palombi, 1935 and *E. i. japonica* Kubota, 1979. The nominotypical subspecies was based on morphology of the polyp and the mature medusa from Naples, Italy, by Palombi [1, cf. 4], with which *E. polimanti* Cerruti, 1941 from Taranto, Italy, is synonymous [2-6]. *E. i. inquilina* has so far been collected only from the coasts of Italy [cf. 6], while *E. i. japonica* has been collected only from Japanese waters [4, 7-9].

In the medusae of Japanese *Eugymnanthea*, the number of statocysts and marginal warts and the position of these at the umbrellar margin are varied and 44 different types have been distinguished [7]. However, the diagnostic characters of this subspecies, presence of a manubrium and the possession of one statolith per statocyst, have proven to be very stable in every population studied ([4, 7, 8] and Kubota, unpublished data).

No extensive study of morphological variation in the Mediterranean *Eugymnanthea* has been made until now. The purpose of the present study is to

reevaluate the taxonomic status of the two subspecies of *Eugymnanthea* as well as to deduce their origin [cf. 10]. Questions addressed include, how variable is the morphology of the medusa of the Mediterranean *Eugymnanthea*? Are there any biological differences other than the morphology between the Mediterranean and the Oriental *Eugymnanthea*? Are there any bivalve-inhabiting hydroids other than the genus *Eugymnanthea* in the Mediterranean? With these questions in mind, the author examined seven bivalve species obtained from coasts of Italy, including the type locality of *E. i. inquilina*. All bivalve-inhabiting hydroids discovered on this occasion were examined.

MATERIALS AND METHODS

A total of 680 bivalve specimens of seven species were obtained in Italy during the period from September 24 to October 15, 1985. Among them, 157 mussel specimens harbored commensal polyps. Many of these polyps, particularly those with medusa buds, were cultured in covered 60 cc polystyrene vessels, and 160 medusae were obtained. All these medusae were examined within a day after liberation. Besides them, 16 1-day old living medusae from La Spezia were examined in Sapporo, Japan - four females, four males, six spent specimens, and two abnormal ones. These

originated from eight mussel specimens that were reared in the laboratory at $22 \pm 1^\circ\text{C}$ in filtered seawater from Oshoro Bay, Hokkaido, and fed with *Artemia* nauplii for about a month after carrying them back to Japan. The other seven additional medusae, which were more than 2 days old, having survived being liberated from their polyps removed from several hosts from La Spezia on the way to Japan, were also examined. They were spent medusae. The measurements given below are mean \pm SD with ranges in parentheses.

RESULTS AND DISCUSSION

Distribution of bivalve-inhabiting hydroids in Italy

From eight localities in Italy (Fig. 1), 591 specimens of *Mytilus edulis galloprovincialis* were obtained. In addition, a total of 81 specimens of six bivalve species purchased at the seafood market of Pozzuoli (Fig. 1: 2) were examined. These included 31 specimens of *Donax trunculus*, 24 of *Venerupis rhomboides*, 10 of *Callista chione*, 4 of *Acanthocardia tuberculata*, 8 of *Lithophaga lithophaga*, and 4 of *Venus verrucosa*.

Eugymnanthea was found to be associated with

M. e. galloprovincialis from the four localities, Ischia Is., Pozzuoli, Taranto, and La Spezia (Fig. 1: 1–3, 8), but no bivalve-inhabiting hydroids were found from the localities Ancona, Venice, Trieste, or Pontetto (Fig. 1: 4–7). *Eugymnanthea* may be the commonest bivalve-inhabiting hydroid distributed along the coast of Italy.

Association rate and attachment site of *Eugymnanthea* polyps

Of the 591 mussel specimens examined, 149 (25.2%) harbored *Eugymnanthea* polyps. At Ischia Is. and Pontetto the mussels were attached to exposed intertidal rocks and were small in size. The mussels from Venice and Ancona grew larger, attaching to some artificial substrata such as a floating dock, a wooden pile, and a concrete quay or block. Other mussels examined were cultured ones and also large in size. The specimens from Pozzuoli were purchased at the seafood market of Pozzuoli and those from La Spezia and Trieste were purchased in Genoa. At Taranto, cultured mussels were collected in up to several meters of water. Relating these environmental conditions to some extent, at Pozzuoli, Taranto, and La Spezia the association rate of *Eugymnanthea* with mussels was high (61.9–86.2%), while at Ischia Is. it was very low (1.4%) (Table 1).

The polyps were usually found on both sides of the mantle and on the visceral mass, often attached to the labial palp and the foot of the host, but were rarely found on the gill even when a large number of polyps were associated with a host (Table 2). At Taranto, where the polyps were most frequently attached to the gill of the hosts, only a very small number of polyps were found at the base of the outer gill of the mussels – they were rarely found elsewhere on the gill.

Crowell [3] reported that no polyps of *Eugymnanthea* were attached to the gill of *M. e. galloprovincialis* from Naples, Italy. In the same paper he also reported that polyps were never found on the gill of *Venerupis decussata*, *Cardium tuberculatum*, *C. edule*, and *Ostrea* sp. from Naples, Italy. Cerruti [2] also observed that *Eugymnanthea* polyps lived on the mantle, labial palp, and visceral mass, but never on the gill of *M. e. galloprovincialis* from Taranto, Italy. Only Palombi [1] has previously

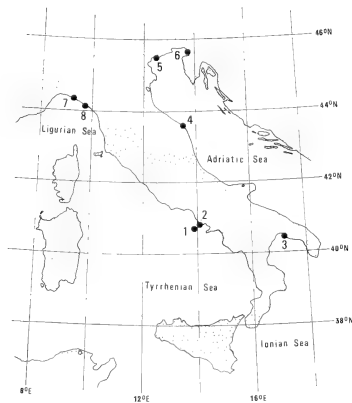


FIG. 1. Map showing the eight localities in Italy (1–8, see Table 1) where *Mytilus edulis galloprovincialis* was collected.

TABLE 1. Collection data of materials

Locality, code no. in Fig. 1	Date of obtaining mussels	Size* and number of mussels		Number of medusae (number of hosts) examined
		examined	associated with <i>Eugymnanthea</i>	
Ischia Is., 1	24-29-IX	31.6±5.7 (17-46), 142	33.0±0 2	2♀♀ (1)
Pozzuoli, 2	31-IX	57.8±6.2 (42-72), 97	58.8±5.6 (45-72), 60	23♂♂+30♀♀+32 (31)
Taranto, 3	9-X	53.2±6.6 (39-64), 29	52.1±6.3 (39-60), 25	12♀♀+21 (14)
Ancona, 4	12-X	62.8±11.9 (41-85), 35	0	0 (0)
Venice, 5	13-X	44.5±7.1 (31-74), 106	0	0 (0)
Trieste, 6	14-X	74.9±6.7 (62-96), 49	0	0 (0)
Pontetto, 7	14-X	33.0±3.4 (27-42), 43	0	0 (0)
La Spezia, 8	15-X	55.1±7.1 (38-69), 90	54.6±7.1 (38-67), 62	(8♂♂+16♀♀+32 (21)

* Mean±SD and range of the antero-posterior axis of *Mytilus edulis galloprovincialis*, in mm.

TABLE 2. Attaching site of the polyp of the Italian *Eugymnanthea*, showing frequency of bivalve specimens harboring polyps on five body portions of *Mytilus edulis galloprovincialis*

Locality	No. of bivalve specimens examined	Frequency (%) on:				
		Labial palp	Mantle	Gill	Visceral mass	Foot
Ischia Is.	2	0	100	0	100	50.0
Pozzuoli	60	51.7	83.3	1.7	65.0	6.7
Taranto	25	32.0	92.0	20.0	100	8.0
La Spezia	49	73.5	65.3	4.1	83.7	12.2
	136	55.1	78.7	5.9	78.7	9.6

found *Eugymnanthea* polyps attached to the gill of *V. decussata* from Naples, Italy.

In contrast to the absence or very rare attachment of *Eugymnanthea* polyps on the gill of *M. e. galloprovincialis* in Italy, the Japanese polyps usually attach to the gill of this mussel as well as to its mantle and visceral mass (see Table 1 in [7]). Moreover, many polyps are found on the gill of this host, attaching to any part of the gill. Furthermore, the Japanese polyps often attach to the gill of other bivalve species such as *Crassostrea gigas* and *Chlamys farreri* (see also Table 1 in [7]). Therefore, a marked difference was detected between the Italian and the Japanese *Eugymnanthea* polyps with respect to main attachment sites to their host bivalve species, especially mussels and oysters.

Morphological difference of medusae between the two Eugymnanthea morphs

Medusa buds were being produced in most of the bivalve specimens harboring polyps from Italy: that is, in 73% of the specimens from Pozzuoli, 88% from Taranto, and in all the specimens from Ischia Is. Such reproductive polyps were found to be small in number in every host. After removing all medusa bud-bearing polyps from every host specimens, these were reared in the vessel filled with ambient seawater at room temperature. Only one to nine medusae were obtained from each host, and a total of 183 medusan individuals originating from 67 mussel specimens could be examined (cf. Table 1). Both male and female *Eugymnanthea* colonies were found together in five mussel specimens.

The Italian and the Japanese *Eugymnanthea* medusae appear to be distinguishable by two characters: presence or absence of the manubrium and the number of statoliths per statocyst [4, 7, 8]. It was the main purpose of the present study to

reexamine medusae of the Italian *Eugymnanthea* in order to verify this, because it seemed possible that medusae with manubrium and/or a small number of statoliths might also occur in Italy. In the Taranto population of the Italian *Eugymnanthea*, Cerruti [2] has already observed that statocysts sometimes contain only one statolith. For that reason and with attention to the variability of these two characters, many medusae of *Eugymnanthea* from coasts of Italy were examined in the present study, and they were morphologically compared with the Japanese *Eugymnanthea* medusae which were well studied by the author ([4, 7-9] and unpublished data).

It was found that the manubrium was absent in almost all of the Italian specimens examined. Only seven out of 183 medusae had the manubrium. These were two medusae from Pozzuoli and five from La Spezia, and two of them were males. This is the first time that medusae with a manubrium have been found in Italy.

Eugymnanthea medusae usually have eight statocysts. Among the 170 medusae examined, two from Pozzuoli and four from La Spezia had seven statocysts (Fig. 2, A-D), one female from La Spezia had nine (Fig. 2, Q), and one male from Pozzuoli had ten (Fig. 2, R). The statocysts were

oval in shape, measuring 58 ± 9 ($36-72$) \times 39 ± 7 ($20-48$) μm ($N=21$) in diameter in five living medusae from La Spezia (observed in Sapporo). Most of these statocysts contained more than two statoliths, 4 ± 1 ($2-6$), while one large statocyst, $96 \times 48 \mu\text{m}$ in diameter, contained seven. The variation range of the number of statoliths per statocyst was 0-9 in a total of 183 medusae examined. Most of the statocysts contained two or three statoliths, this included 77.3% of 481 statocysts found in 60 females, 75.3% of 247 statocysts in 31 males, and 68.8% of 734 statocysts in the other 92 spent medusae (Table 3). Only 9.6% of these 1462 statocysts in 183 medusae contained one or no statolith. This result, together with the former observations made by Cerruti [2] and Uchida [11], indicates that statocysts in the Italian *Eugymnanthea* usually contain more than two statoliths. Excluding a few abnormal medusae, a medusa of the Italian *Eugymnanthea* had 21 ± 6 ($8-41$) statoliths ($N=170$). Among these medusae, 20.6% had 8-16 statoliths. Even the six medusae with a manubrium usually had more than 16 statoliths per specimen, that is 14, 17, 20, 23, 26 and 37, respectively. The other medusa with a manubrium had 17 statoliths although a part of the umbrellar margin was damaged and only six statocysts were

TABLE 3. Frequency distribution of the number of statoliths per statocyst in the Italian *Eugymnanthea*

Locality	No. of medusae, (no. of hosts), and no. of statocysts examined		Frequency distribution of statocysts possessing the following number of statoliths per statocyst:									
			0	1	2	3	4	5	6	7	8	9
Ischia Is.	2 ♀ ♀ (1)	16			6	4	6					
Pozzuoli	30 ♀ ♀ (15)	240	3	23	107	91	16					
Taranto	12 ♀ ♀ (7)	96		13	28	41	11	3				
La Spezia	16 ♀ ♀ (9)	129	1	4	38	57	16	8	5			
Pozzuoli	23 ♂ ♂ (11)	185		6	62	80	23	12	2			
La Spezia	8 ♂ ♂ (7)	62		2	25	19	13	2		1		
Pozzuoli	32	(21) 255		51	108	77	15	2	1	1		
Taranto	21	(12) 168		29	66	45	18	6	4			
La Spezia	30	(13) 247		8	85	78	44	19	9	3		1
La Spezia	9*	(-) 64		1	20	26	9	5	2	1		
	183	(67) 1462	4	137	545	518	171	57	23	6	0	1

* Two abnormal medusae (not shown in Fig. 3) and seven spent medusae more than 2 days old.

found.

The number of marginal warts per specimen was usually eight in both sexes: among 170 medusae, 139 had eight marginal warts (Fig. 2, C, D, L-O, Q, R), six had four (Fig. 2, E, F), five had five (Fig. 2, G), nine had six (Fig. 2, H-J), ten had seven (Fig. 2, A, B, K), and one had nine (Fig. 2, P). The perradial marginal warts were always larger than the others.

Eighteen types of medusa were discriminated according to the combination of the number of statocysts per specimen (7-10), the number of marginal warts per specimen (4-9), and the position of these warts and statocysts at the umbrellar margin (Fig. 2, A-R). Besides these 18 types, four

abnormal types were found: two were relatively regular (Fig. 2, S, T) but the others were irregular in the arrangement of radial canals. The type with eight statocysts and eight marginal warts, both of which were regularly arranged (Fig. 2, O), was most common, appearing in 77.1% of the 170 specimens examined. It is conceivable that this is the basic type of the Italian *Eugymnanthea* as is the case in the Japanese *Eugymnanthea* [cf. 7]. The modifications from this basic type were due partly to the formation of statocysts at the interradii (Fig. 2, C, E, H, M) and due partly to the formation of marginal warts at adradial (Fig. 2, L, P). The total number of morphological types of medusa in the Italian *Eugymnanthea* (18) was less than that in the

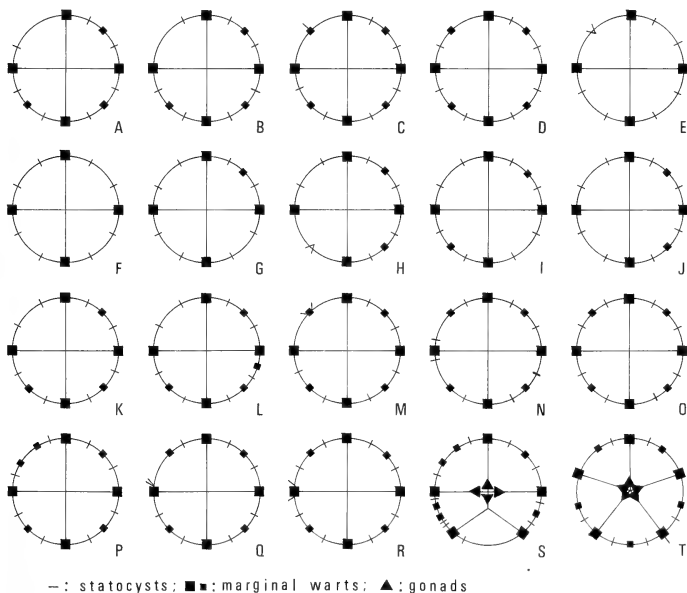


Fig. 2. Schematic illustration of 18 types of medusa of the Italian *Eugymnanthea* (A-R) and two abnormal types (S, T). A-D: Four types with seven statocysts and seven or eight marginal warts; E-P: 12 types with eight statocysts and four to nine marginal warts; Q: A type with nine statocysts and eight marginal warts; R: A type with ten statocysts and eight marginal warts; S: An abnormal type in which one radial canal is bifurcated; T: An abnormal type with five radial canals and five gonads.

Japanese *Eugymnanthea* (44) because the number of statocysts per specimen of the former was nearly constant, as is described above.

In three medusae from La Spezia two or three of the gonads were connected to each other by a thread-like structure.

Five medusae without manubrium from La Spezia were reared in the laboratory in Sapporo. They survived up to nine days. During this short life span, (1) the size of umbrella (Fig. 3) increased slightly, measuring up to 1.5 mm in diameter and 1.4 mm in height; (2) the mesoglea, particularly at the apex of the umbrella, thickened, measuring up to 0.6 mm; (3) the nematocysts on the exumbrella nearly disappeared; (4) the marginal warts produced at other than the perradii were often difficult to observe; (5) the manubrium was never produced; and (6) the number of statoliths per statocyst did not change. (For these reasons, seven spent medusae from La Spezia that were more than 2 days old were included in Table 3.)

It is confirmed from the above examination that medusae of the Italian *Eugymnanthea* do not possess the manubrium, and they have many statoliths. Such characteristics of the Italian *Eugymnanthea* medusae are in striking contrast to the

Japanese ones [cf. 4, 7, 8]. Consequently, the manubrium and the number of statoliths are ascertained to be reliable characters by which nearly every individual specimen of *Eugymnanthea* can be referred to one of the two morphs. Medusae without manubrium and with a small number of statoliths or with manubrium and many statoliths were very rare in any population of *Eugymnanthea* so far been examined. Not all the morphological characters of the medusa reduce simultaneously in *Eugymnanthea*.

It should be noted here that Brinckmann-Voss [12] made an extensive faunal survey of hydromedusae in the Gulf of Naples during 1958-1963, but no free *Eugymnanthea* medusae were found in plankton.

Kinship test

In order to test the kinship between the Italian and the Japanese *Eugymnanthea*, a total of four 1 day old male *Eugymnanthea* medusae from La Spezia, Italy, were crossed with a total of five 1 day old female *Eugymnanthea* medusae from Shimizu, Shizuoka Pref., central Japan, during December 24-30, 1985 in Sapporo. Each of the four pairs were put into a covered 60 cc polystyrene vessel filled with seawater from Oshoro, Hokkaido for one to several days. (In one case, as is described below, two females were crossed with one male.) As to the collection data and the result of the conspecific cross test of this Japanese *Eugymnanthea*, see paper [9].

Many embryos resulted from one cross, but all of them disappeared on the third day after the onset of the experiment. It is possible that these larvae were produced parthenogenetically [cf. 9]. In this case a female specimen [8(host number)-2(medusa number) (see paper [9])] was crossed with one male. In the other three cases, no larvae appeared (in each case, one or two females such as 5-2+1-5, 2-7, and 6-5 were crossed with one male).

This cross test suggests that reproductive isolation might be present between the Italian and the Japanese *Eugymnanthea*. The reciprocal cross test, female Italian *Eugymnanthea* × male Japanese *Eugymnanthea*, and the conspecific cross test of the Italian *Eugymnanthea* were unable to

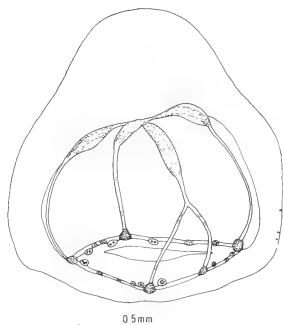


FIG. 3. Side view of a 5 day old spent male medusa of *Eugymnanthea* from La Spezia, slightly squashed, drawn from life using a drawing apparatus and compound microscope. Note the thick mesoglea at the apex of the umbrella, presence of only three nematocysts on the exumbrella, possession of many statoliths, and branching of one radial canal (cf. Fig. 2, S).

conduct in Sapporo.

Concluding remarks

It is generally accepted that *Mytilus edulis galloprovincialis* in Japan was introduced sometime after 1925, possibly from Europe [cf. 5]. This bivalve species is the preferred host for *Eugymnanthea* in both Italy and Japan [2-4, 6-9]. Taking this into account, it is possible that the Mediterranean *Eugymnanthea* invaded Japanese waters together with its bivalve host [cf. 5]. However, this may not have taken place, judging from the following knowledge clarified in the present study: (1) the mature medusae are morphologically different between the Italian morph and the Japanese morph; (2) the morphology of the Italian medusa did not change easily when the polyps were reared in seawater in Hokkaido, Japan (for a month); (3) main attachment sites of the polyps to their host bivalve species are different; (4) a reproductive isolation might be present; and (5) their geographical distribution seems to be disjunct. Therefore, they are referable to two species rather than the two subspecies so far been assigned to. The origin of these two paedomorphic derivative hydrozoans might be explained by parallel or convergent evolution [cf. 10].

It should be noted that the polypoid species, *Anthohydra psammobionta* Salvini-Plawen and Rao, 1973 was described from Little Andaman Is., Bay of Bengal, India [13]. It lives in the interstium of the mesopsammon in the intertidal zone. Although *Anthohydra* was provisionally included in the family Olindiasidae by Bouillon [14], Salvini-Plawen [15] considered *Anthohydra* to be synonymous with *Eugymnanthea*. "*E. psammobionta*" is not commensal to bivalves, and a possible origin of this species might be also by parallel or convergent evolution. Further biological studies on these peculiar hydrozoan species will shed light on their origin and systematics.

ACKNOWLEDGMENTS

I wish to express my cordial gratitude to Dr. Mayumi Yamada, Professor Emeritus of Hokkaido University, Dr. Claudia Mills, Friday Harbor Laboratories, University of Washington, and Dr. Ferdinando Boero, University of Lecce, for their critical reading of the manu-

script. Special gratitude is due to Dr. Ferdinando Boero for his kindness in providing facilities, particularly the laboratory of the Zoological Institute of the University of Genoa at Pontetto where I was able to rear the specimens from La Spezia, and for helping me in general to obtain materials in Italy. Cordial thanks should be extended to the many colleagues who attended the 1st International Workshop of the Hydrozoan Zoologist Association held at Ischia Is. in Italy in 1985, for they kindly collected mussels there for me. I am also indebted to the staff and researchers of the Laboratorio di Ecologia del Benthos della Stazione Zoologica di Napoli, at Ischia Is. in Naples, those of the Istituto Sperimentale Talassografico del C.N.R. in Taranto, and those of the Istituto di Ricerche sulla Pesca Marittima del C.N.R. in Ancona. I am much obliged to Dr. Tadashige Habe, Tokai University, for identification of the bivalves from Pozzuoli, Italy.

REFERENCES

- 1 Palombi, A. (1935) *Eugymnanthea inquilina* nuova leptomedusa derivante da un atecato idroide ospite intero di *Tapes decussatus* L. Pubbl. Staz. Zool. Napoli, 15: 159-168.
- 2 Cerruti, A. (1941) *Mytilhydra polimantii* n. gen., n. sp. idroide vivente sul mantello dei mitili. Riv. Biol., 32: 3-20.
- 3 Crowell, S. (1957) *Eugymnanthea*, a commensal hydroid living in pelecypods. Pubbl. Staz. Zool. Napoli, 30: 162-167.
- 4 Kubota, S. (1979) Occurrence of a commensal hydroid *Eugymnanthea inquilina* Palombi from Japan. J. Fac. Sci. Hokkaido Univ., Ser. VI, Zool., 21: 396-406.
- 5 Kubota, S. (1983) Studies on life history and systematics of the Japanese commensal hydroids living in bivalves, with some reference to their evolution. J. Fac. Sci. Hokkaido Univ., Ser. VI, Zool., 23: 296-402, pl. X.
- 6 Morri, C. (1981) Idrozoi lagunari. Guide per il riconoscimento delle specie animali delle acque lagunari e costiere italiane. 6. Collana del progetto finalizzato "Promozione della qualità dell'ambiente", serie AQ/1/94. C.N.R., Roma: 1-105.
- 7 Kubota, S. (1985) Systematic study on a bivalve-inhabiting hydroid *Eugymnanthea inquilina japonica* Kubota from central Japan. J. Fac. Sci. Hokkaido Univ., Ser. VI, Zool., 24: 70-85.
- 8 Kubota, S. (1987) Occurrence of a bivalve-inhabiting hydroid *Eugymnanthea inquilina japonica* Kubota from Okinawa Island, southwest of Japan, with notes on parthenogenesis. Galaxea, 6: 31-34.
- 9 Kubota, S. (1987) Parthenogenesis and crossability among bivalve-inhabiting hydroids in Japan. Proc. Jpn. Soc. syst. Zool., 35: 6-18.

- 10 Kubota, S. (1987) The origin and systematics of four Japanese bivalve-inhabiting hydroids. In "Modern trends in systematics, ecology, and evolution of hydroids and hydromedusae". Ed. by J. Bouillon, F. Boero, F. Cicogna and R. F. S. Cornelius, Oxford University Press, London. pp. 274-287.
- 11 Uchida, T. (1964) Medusae of *Eugymnanthea*, an epizoic hydroid. Publ. Seto. mar. biol. Lab., 12: 101-107.
- 12 Brinckmann-Voss, A. (1987) Seasonal distribution of hydromedusae (Cnidaria, Hydrozoa) from the Gulf of Naples and vicinity, with observations on sexual and asexual reproduction in some species. In "Modern trends in systematics, ecology, and evolution of hydroids and hydromedusae". Ed. by J. Bouillon, F. Boero, F. Cicogna and R. F. S. Cornelius, Oxford University Press, London. pp. 133-141.
- 13 Salvini-Plawen, L. v. and Rao, G. C. (1973) On three new mesopsammobiotic representatives from the Bay of Bengal: species of *Anthohydra* gen. nov. (Hydrozoa) and of *Pseudovermis* (Gastropoda). Z. Morph. Tiere, 74: 231-240.
- 14 Bouillon, J. (1985) Essai de classification des Hydroméduses (Hydrozoa-Cnidaria). Indo-Malay. Zool., 1: 29-243.
- 15 Salvini-Plawen, L. v. (1987) Mesopsammic Cnidaria from Plymouth (with systematic notes). J. mar. biol. Ass. U. K., 67: 623-637.

Eight Species of the Subgenus *Drosophila* (Diptera: Drosophilidae) from Guangdong Province, Southern China

MASANORI J. TODA and TONG XU PENG¹

*Institute of Low Temperature Science, Hokkaido University,
Sapporo 060, Japan, and ¹Guangdong Institute of
Entomology, Guangzhou, China*

ABSTRACT—Six new and two known species of the subgenus *Drosophila* are reported from Guangdong, China. A new species-group, the *Drosophila quadrisetata* species-group, is established by one known and two new species.

INTRODUCTION

Up to the present, no drosophilid species has been reported from Guangdong Province, China. In order to fill the lack of knowledge on its drosophilid fauna, we have been making a faunal survey since 1985. As the first report this paper deals with six new and two known species of the subgenus *Drosophila*. The information on other known species will be reported elsewhere.

All the holotypes and a part of paratypes are deposited in the Guangdong Institute of Entomology, Guangzhou, China, and the remaining paratypes in the Entomological Institute, Hokkaido University, Sapporo, Japan.

D. polychaeta Species-group

D. polychaeta species-group, Sturtevant, 1942, Univ. Texas Publ., 4213: 31.

Diagnosis. Reddish brown species (*D. asper* Lin et Tseng, 1971 blackish brown) with 3 pairs of postsutural dorsocentral bristles and without prominent acrostichal bristles between dorsocentral lines. C-index *ca.* 1.8 to 2.1 (*ca.* 3.1 in *D. kashimirensis* Kumar et Gupta, 1985) and 4V-index *ca.* 2.0 to 2.3. Aedeagus usually T-shaped in lateral view. Surstylus dorsally with more or less

pubescent flap. The last two characters were confirmed in *D. polychaeta* Patterson et Wheeler, 1942, *D. daruma* Okada, 1956, *D. bivibrissae* Toda, 1988 and *D. latifshahi* Gupta et Ray-Chaudhuri, 1970.

Drosophila (Drosophila) latifshahi Gupta et Ray-Chaudhuri (Figs. 1-4)

Drosophila (Scaptodrosophila) latifshahi Gupta et Ray-Chaudhuri, 1970 [1]: 67.

Diagnosis. ♂ fore tarsus anteriorly with long recurved hairs. Epandrium caudo-subapically with acute projection (Fig. 1). Surstylus with small, slightly pubescent flap on dorsal margin (Fig. 1). Ovipositor with *ca.* 3 long bristle-like discal teeth and longest ultimate marginal tooth (Fig. 4).

♂, ♀. Body length, ♂ *ca.* 2.3 mm (range: 2.17-2.52), ♀ *ca.* 3.0 mm (2.89-3.29). Thorax length (including scutellum), ♂ *ca.* 1.0 mm (0.96-1.12), ♀ *ca.* 1.2 mm (1.12-1.28).

Head: Eye brownish red with thick pile. Antenna dark brown. Arista with *ca.* 5 (5-6) upper and *ca.* 2 (2-3) lower long branches in addition to large terminal fork. Frons slightly narrower than 1/2 of head width (mean=0.48, 0.46-0.49, measured at level of anterior ocellus), dark brown, anteriorly with frontal hairs; inside margins of ocelli darker; periorbit paler. Anterior reclinate orbital *ca.* 3/7 (0.43, 0.36-0.53) length of

posterior reclinate; proclinate *ca.* 2/3 (0.67, 0.62–0.75) length of posterior reclinate. Face dark brown; carina broad. Clypeus dark brown. Cheek dark brown, *ca.* 1/5 (0.21, 0.17–0.23) as broad as maximum diameter of eye. Second oral *ca.* 7/10 (0.70, 0.53–0.80) length of vibrissa. Palpus dark brown, club-shaped, with several long setae.

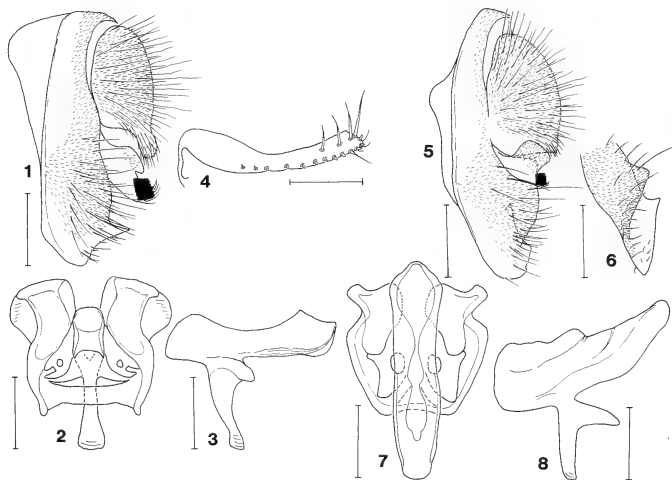
Thorax brown; episternum darker. Humeral 2, subequal. One extra pair of dorsocentrals present in front of usual anteriors. Several bristles in row of dorsocentrals and in 1st row lateral to dorsocentrals somewhat longer than other acrostichal hairs. First dorsocentral *ca.* 2/5 (0.40, 0.32–0.49), 2nd *ca.* 7/10 (0.69, 0.61–0.77) length of 3rd; length distance from 1st to 2nd *ca.* 1/3 (0.32, 0.25–0.41), distance from 2nd to 3rd *ca.* 1/2 (0.48, 0.41–0.54) cross distance between 2nds. Prescutellars absent. Acrostichal hairs in 6 rows. Anterior scutellar *ca.* 9/10 (0.91, 0.80–0.99) length of posterior; posteriors nearer to each other than to anterior. Sterno-index *ca.* 0.8 (0.68–0.95).

Legs brown. Preapicals on all tibiae; apicals on fore and mid tibiae. Fore metatarsus as long as 3 succeeding tarsal joints together; mid and hind metatarsi as long as rest together.

Wing hyaline, somewhat fuscous. Veins dark brown; cross veins clear. R_{2+3} slightly curved to costa at tip; R_{4+5} and M nearly parallel. C1-bristles 2, subequal. Wing indices: C *ca.* 1.9 (1.79–2.06), 4V *ca.* 2.3 (2.03–2.45), 4C *ca.* 1.4 (1.30–1.50), 5x *ca.* 1.6 (1.23–2.00), Ac *ca.* 2.7 (2.46–2.87), C3-fringe *ca.* 0.9 (0.79–0.90). Haltere dark grayish brown.

Abdomen: Tergites dark brown; 1st and antero-medial part of 2nd and 3rd yellowish. Sternites pale brown, quadrate, broader than long; ♂ 3rd to 5th large.

Periphallic organs (Fig. 1): Epandrium pubescent except ventral and anterior portions, with *ca.* 34 bristles in lower part and several small setae on lower margin. Surstylus narrow, triangular, with *ca.* 6 long, slightly curved primary teeth on distal



FIGS. 1–4. *Drosophila (Drosophila) latifshahi* Gupta et Ray-Chaudhuri, 1970. 1: Periphallic organs. 2: Phallic organs. 3: Aedeagus (lateral view). 4: Ovipositor. (Scale-line=0.1 mm.)

FIGS. 5–8. *Drosophila (Drosophila) daruma* Okada, 1956. 5: Periphallic organs. 6: Lower part of epandrium (caudal view). 7: Phallic organs. 8: Aedeagus (lateral view). (Scale-line=0.1 mm.)

margin and several recurved spines at caudoventral corner. Cercus separate from epandrium, oval, elongate below, pubescent except ventral portion, with ca. 66 bristles and tuft of short setae on lower elongation.

Phallic organs (Figs. 2, 3): Aedeagal apodeme ca. 1/2 as long as aedeagus. Anterior paramere tiny, circular, without sensilla. Posterior paramere absent. Novasternum quadrate, without submedian spines; hypandrium large, somewhat quadrate, laterally with flap.

♀ reproductive organs: Ovipositor (Fig. 4) slender, proximally broader, with ca. 13 small marginal teeth, ca. 3 short terminal and 1 long subterminal hairs; basal ithmus narrow, ca. 1/5 as long as ovipositor. Spermatheca unsclerotized.

Specimens examined. China: 18 ♂, 41 ♀, Nankunshan, Guangdong Province, 27, 28. VIII. 1987, ex trap (K. Beppu).

Distribution. India, Bangladesh; China (n. loc. rec.): Guangdong.

Relationship. Gupta and Ray-Chaudhuri [1] described this species as a member of the subgenus *Scaptodrosophila*. However, this species should belong to the *polychaeta* species-group of the subgenus *Drosophila* in having 3 pairs of dorsocentral bristles and ♂ genitalia characteristic to this species-group. This species is clearly distinguishable from other members of the *polychaeta* species-group by the diagnostic characters.

***Drosophila (Drosophila) daruma* Okada**
(Figs. 5–8)

Drosophila (Drosophila) daruma Okada, 1956, Syst. Study: 155.

Diagnosis. Caudal margin of lower epandrial part expanding triangularly; toe not pointed, but with acute corner on inner side (Figs. 5, 6). Surstylus triangular, dorsally with large, quadrate, pubescent flap, and with 5 primary teeth in straight row on lower distal margin (Fig. 5). Cercus narrowly fused to epandrium at middle (Fig. 5).

♂. Body length ca. 2.8 mm. Thorax length ca. 1.2 mm (1.20–1.23).

Head: Arista with 5 upper and 2 lower long branches in addition to large terminal fork. Frons slightly narrower than 1/2 of head width (0.47,

0.45–0.48), dark brown; inside margins of ocelli darker; periorbit paler. Anterior reclinate orbital ca. 4/9 (0.44, 0.43–0.45) length of posterior reclinate; proclinate ca. 5/7 (0.72, 0.71–0.72) length of posterior reclinate. Face dark brown; carina broad. Cheek dark brown, ca. 1/5 (0.21, 0.20–0.21) as broad as maximum diameter of eye. Second oral ca. 5/6 (0.82, 0.81–0.83) length of vibrissa.

Thorax: Humerals 2, subequal. One extra pair of dorsocentrals present in front of usual anteriors. Several bristles in row of dorsocentrals and in 1st row lateral to dorsocentrals somewhat longer than other acrostichal hairs. First dorsocentral ca. 2/5 (0.40, 0.38–0.41), 2nd ca. 5/7 (0.73) length of 3rd; length distance from 1st to 2nd ca. 1/4 (0.25), distance from 2nd to 3rd ca. 3/7 (0.43, 0.42–0.43) cross distance between 2nds. Acrostichal hairs in 8 rows. Anterior scutellar ca. 9/10 (0.90, 0.88–0.92) length of posterior; posteriors nearer to each other than to anterior. Sterno-index ca. 0.8 (0.77–0.83).

Leg: Fore metatarsus as long as 3 succeeding tarsal joints together; mid and hind metatarsi as long as rest together.

Wing: Veins brown. R_{2+3} nearly straight; R_{4+5} and M nearly parallel. C1-bristles 2, subequal. Wing indices: C ca. 2.1 (2.05–2.12), 4V ca. 2.0 (1.97–2.01), 4C ca. 1.2 (1.21–1.26), 5x ca. 1.4 (1.30–1.52), Ac ca. 2.7 (2.58–2.85), C3-fringe ca. 0.8 (0.82–0.86). Haltere dark grayish brown.

Abdomen: Sternites quadrate, broader than long.

Periphallallic organs (Figs. 5, 6): Epandrium pubescent except ventral and anterior portions, with ca. 23 bristles in lower part, narrow in submedian to upper part. Surstylus with several recurved setae at caudoventral corner. Cercus oval, pubescent except ventral portion.

Phallic organs (Figs. 7, 8): Aedeagus T-shaped in lateral view, dorsally broad, ventrally somewhat flat; apodeme ca. 1/3 as long as aedeagus. Novasternum somewhat quadrate; hypandrium slightly serrate on inner margin.

Specimens examined. China: 2 ♂, Dinghushan, Guangdong Province, 21. VIII. 1987, ex trap (K. Beppu).

Distribution. Korea, Japan, Bonin Is., Ryukyu Is., Malaya, Borneo, India; China: Taiwan,

Guangdong (n. loc. rec.).

Relationship. This species is somewhat related to *D. bivibrissae* in having surstylus dorsally with large, quadrate, pubescent flap, but clearly distinguishable from the latter by the other diagnostic characters.

D. quadrisetata Species-group

Diagnosis. Dull brown species with 4 pairs of dorsocentral bristles and prominent acrostichal bristles between dorsocentral lines. C-index *ca.* 2.4 to 3.6 and 4V-index *ca.* 1.7 to 1.8. Cercus separate from epandrium. Aedeagus large, curved ventrad.

This newly established species-group consists of *D. quadrisetata* Takada, Beppu et Toda, 1979 and the following two new species. *D. quadrisetata* was previously included in the *polychaeta* species-group [2], because of having extra pairs of dorsocentrals. However, this species and the following two new species resemble the *D. robusta* species-group, especially *D. neokadai* Kaneko et Takada, 1966 and *D. okadai* Takada, 1959, rather than the *polychaeta* species-group in the body color, the morphology of aedeagus and the larger values of C-index, although clearly distinguished from the *robusta* species-group by the presence of extra dorsocentrals and cercus separate from epandrium. Therefore, these three species are considered to form a separate species-group probably intermediate between the *polychaeta* and the *robusta* species-group.

Drosophila (Drosophila) beppui sp. nov.

(Figs. 9–14)

Diagnosis. ♂ palpus modified, apically much broadened and with flat undersurface (Fig. 9). Epandrium moderate in width, slightly broader below; toe round (Fig. 10). Ovipositor subapically much broad, with *ca.* 22 black, stout teeth in irregular rows and 1 short subterminal hair (Fig. 13).

♂, ♀. Body length, ♂ *ca.* 2.4 mm (2.19–2.70), ♀ *ca.* 2.6 mm (2.38–2.98). Thorax length, ♂ *ca.* 0.9 mm (0.88–1.07), ♀ *ca.* 1.0 mm (0.84–1.07).

Head: Eye brownish red, with thick pile.

Antenna dark grayish brown. Arista with *ca.* 4 (2–5) upper and *ca.* 1 (1–2) lower small branches in addition to terminal fork. Frons *ca.* 1/2 (0.51, 0.49–0.54) as wide as head, grayish brown, anteriorly with a few frontal hairs; ocellar triangle and its surrounding area darker. Anterior reclinate orbital *ca.* 2/5 (0.39, 0.31–0.52) length of posterior reclinate; proclinate *ca.* 3/5 (0.61, 0.49–0.85) length of posterior reclinate. Face pale brown; carina broad. Clypeus dark brown. Cheek pale brown, *ca.* 1/4 (0.25, 0.21–0.27) as broad as maximum diameter of eye. Second oral minute. Palpus pale brown, with numerous setae.

Thorax pale brown; median line and posteromedian portion of mesoscutum and scutellum darker. Humerals 2; upper one longer. Two extra pairs of dorsocentrals present in front of usual ones; 1st pair located before transverse suture, 2nd slightly posterior to suture. Two pairs of acrostichal bristles present between dorsocentral lines, arranged somewhat irregularly. Relative lengths of dorsocentrals and acrostichal bristles to 4th dorsocentral: 1st dorsocentral *ca.* 3/5 (0.59, 0.53–0.65), 2nd *ca.* 1/2 (0.50, 0.33–0.64), 3rd *ca.* 7/10 (0.69, 0.61–0.76), anterior acrostichal bristle *ca.* 2/5 (0.41, 0.33–0.48), posterior *ca.* 4/9 (0.45, 0.38–0.57). Length distance from 1st dorsocentral to 2nd *ca.* 4/7 (0.57, 0.43–0.64), distance from 2nd to 3rd *ca.* 4/9 (0.47, 0.34–0.67), distance from 3rd to 4th *ca.* 1/2 (0.50, 0.44–0.57) cross distance between 3rds. Acrostichal hairs sparse, in *ca.* 4 irregular rows. Anterior scutellar *ca.* 9/10 (0.90, 0.82–0.97) length of posterior; posteriors nearer to each other than to anterior. Sterno-index *ca.* 0.6 (0.45–0.75).

Legs pale brown. Preapicals on all tibiae; apicals on fore and mid tibiae. Fore metatarsus as long as rest of tarsal joints together; mid and hind metatarsi longer than rest together.

Wing hyaline, slightly fuscous. Veins grayish brown; cross veins clear. R_{2+3} nearly straight; R_{4+5} and M nearly parallel. C1-bristles 2, subequal. Wing indices: C *ca.* 2.7 (2.38–2.92), 4V *ca.* 1.8 (1.69–2.05), 4C *ca.* 0.9 (0.88–1.01), 5x *ca.* 1.3 (1.05–1.62), Ac *ca.* 2.4 (2.12–2.79), C3-fringe *ca.* 0.8 (0.71–0.81). Haltere pale brown; stalk anteriorly darker.

Abdomen: Tergites nearly entirely dark

brown. Sternites pale gray, quadrate, broader than long; ♂ 3rd to 5th large.

Periphallic organs (Fig. 10): Epandrium pubescent on middle to upper caudal half, with ca. 1 bristle in middle part and ca. 6 in lower part. Surstylus quadrate, broad, distally narrowing, with ca. 9 primary teeth in straight row on distal margin, ca. 3 spines on lower outer surface and several small bristles at caudoventral corner. Cercus oval, entirely pubescent, with ca. 32 long bristles and tuft of several short bristles on caudoventral apex.

Phallic organs (Figs. 11, 12): Aedeagus basally bilobed and expanded anteriorly, with 1 pair of dark-colored dorsal ridges and vertical rod; apodeme short, ca. 1/3 as long as aedeagus. Anterior and posterior parameres absent. Novasternum without submedian spines; ventral fragma arc-shaped; hypandrium large, quadrate, with sharp ridge starting from lateral corner.

♀ reproductive organs: Basal ithmus of ovipositor narrow, sinuate, ca. 1/2 as long as ovipositor (Fig. 13). Spermatheca (Fig. 14) elongate, conical, apically slightly indented, basally horizontally wrinkled; introvert deep.

Holotype ♂, China: Nankunshan, Guangdong Province, 28. VIII. 1987, ex trap (K. Beppu).

Paratypes, China: 1 ♂, 2 ♀, same data as holotype; 4 ♂, 4 ♀, same data except 27. VIII. 1987.

Distribution. China: Guangdong.

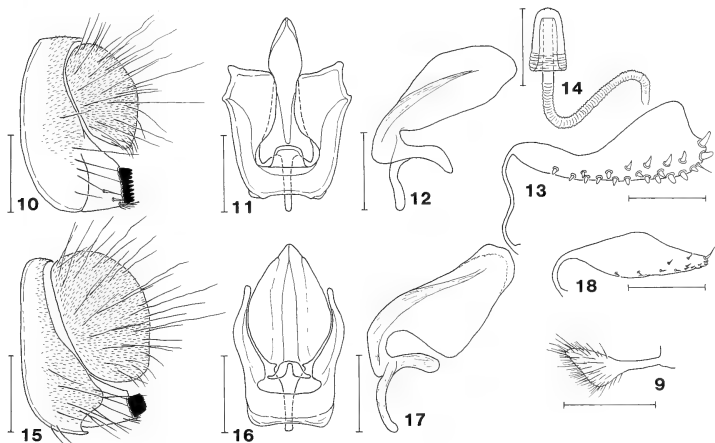
Relationship. This species is somewhat close to *D. quadrisetata*, but easily distinguishable from the latter by the diagnostic characters.

Remarks. This species is named in honor of our colleague, Dr. K. Beppu, Shinshu University, who provided us with the material.

Drosophila (Drosophila) potamophila sp. nov.
(Figs. 15–18)

Diagnosis. Epandrium narrow in submedian to upper part, broad below; caudal margin of lower part sigmoidal; toe pointed (Fig. 15). Ovipositor slender, apically somewhat truncate, with 1 stout apical tooth, ca. 12 minute marginal teeth in somewhat irregular rows and ca. 2 small discal teeth (Fig. 18). Spermatheca unsclerotized.

The characters such as eye, antenna, frons, clypeus, acrostichal hairs and so on are same as in



Figs. 9–14. *Drosophila (Drosophila) beppui* sp. nov. 9: ♂ palpus. 10: Periphallic organs. 11: Phallic organs. 12: Aedeagus (lateral view). 13: Ovipositor. 14: Spermatheca. (Scale-line=0.1 mm.)

Figs. 15–18. *Drosophila (Drosophila) potamophila* sp. nov. 15: Periphallic organs. 16: Phallic organs. 17: Aedeagus (lateral view). 18: Ovipositor. (Scale-line=0.1 mm.)

the foregoing species, *D. beppui*, and not referred to in the following description.

♂, ♀. Body length, ♂ *ca.* 2.4 mm (2.22–2.49), ♀ *ca.* 2.5 mm (2.21–2.94). Thorax length, ♂ *ca.* 1.0 mm (0.89–1.08), ♀ *ca.* 1.0 mm (0.90–1.10).

Head: Arista with *ca.* 4 (3–5) upper and 2 lower small branches. Periorbit darker than frons. Anterior reclinate orbital *ca.* 4/9 (0.46, 0.39–0.53) length of posterior reclinate; proclinate *ca.* 5/9 (0.53, 0.47–0.57) length of posterior reclinate. Face grayish brown. Cheek grayish brown, *ca.* 2/7 (0.27, 0.23–0.32) as broad as maximum diameter of eye. Palpus dark gray, club-shaped, with several long and numerous small setae.

Thorax grayish brown. Humerals 2, subequal. Second pair of dorsocentrals located beside suture. One or 2 pairs of acrostichal bristles present; anterior pair between 1st dorsocentrals, posterior pair (if present) between 2nd dorsocentrals. Relative lengths of dorsocentrals and acrostichal bristles to 4th dorsocentral: 1st dorsocentral *ca.* 5/8 (0.62, 0.57–0.68), 2nd *ca.* 5/8 (0.63, 0.49–0.68), 3rd *ca.* 3/4 (0.74, 0.67–0.81), anterior acrostichal bristle *ca.* 1/2 (0.51, 0.43–0.60), posterior (if present) *ca.* 1/2 (0.50, 0.38–0.64). Length distance from 1st dorsocentral to 2nd *ca.* 1/2 (0.52, 0.48–0.61), distance from 2nd to 3rd *ca.* 3/5 (0.59, 0.52–0.65), distance from 3rd to 4th *ca.* 1/2 (0.52, 0.46–0.58) cross distance between 3rds. Anterior scutellar *ca.* 9/10 (0.92, 0.74–1.06) length of posterior. Sterno-index *ca.* 0.7 (0.56–0.91).

Legs grayish brown.

Wing fuscous. Veins dark brown. R_{2+3} slightly curved to costa at tip. Wing indices: C *ca.* 2.4 (2.14–2.77), 4V *ca.* 1.8 (1.59–2.05), 4C *ca.* 1.0 (0.88–1.16), 5x *ca.* 1.4 (1.26–1.60), Ac *ca.* 2.2 (1.96–2.45), C3-fringe *ca.* 0.9 (0.82–0.95). Haltere grayish brown.

Abdomen: Tergites nearly entirely dark grayish brown. Sternites grayish brown.

Periphallic organs (Fig. 15): Epandrium pubescent except anterior margin, with *ca.* 12 bristles in lower part. Surstylus quadrate, distally narrowing, with *ca.* 8 primary teeth in straight row on distal margin and several small bristles at caudoventral corner. Cercus with *ca.* 42 bristles.

Phallic organs (Figs. 16, 17): Aedeagus broad in both ventral and lateral views. Ventral fragma

quadrate; hypandrium large, triangular.

♀ reproductive organs: Basal ithmus of ovipositor *ca.* 1/4 as long as ovipositor (Fig. 18).

Holotype ♂, China: Dinghushan, Guangdong Province, 3. IX. 1987, ex trap (K. Beppu).

Paratypes, China: 1 ♂, 1 ♀, same data as holotype; 1 ♂, 2 ♀, same data except 21. VIII. 1987, 2 ♂, 6 ♀, Nankunshan, Guangdong Province, 27, 28. VIII. 1987, ex trap (K. Beppu).

Distribution. China: Guangdong.

Relationship. This species is somewhat similar to the foregoing species, *D. beppui*, but clearly distinguishable from the latter by the diagnostic characters.

D. histrio Species-group

D. histrio species-group, Okada, 1966, Bull. Brit. Mus. (Nat. Hist.) Ent. Suppl., 6: 99.

Drosophila (Drosophila) liae sp. nov.

(Figs. 19–24)

Diagnosis. Thoracic pleura dark brown; episternum paler below. Aedeagus apically with 1 pair of small, acute, thorn-like projections (Figs. 20, 21). Anterior paramere absent (Fig. 20). Hypandrial process elongate, distally expanded triangularly, somewhat irregularly serrate on margin (Fig. 22).

♂, ♀. Body length, ♀ *ca.* 2.2 mm. Thorax length *ca.* 1.0 mm.

Head: Eye orange red, with pile. Antenna with 2nd joint dark brown and 3rd grayish. Arista with 6 or 7 upper and 3 lower branches in addition to terminal fork. Frons *ca.* 4/9 (0.45, 0.43–0.46) as wide as head, orange brown, anteriorly with a few frontal hairs; periorbit and ocellar triangle darker, especially on inside margins of ocelli. Anterior reclinate orbital *ca.* 3/8 (0.39, 0.36–0.41) length of posterior reclinate; proclinate *ca.* 4/7 (0.57, 0.52–0.62) length of posterior reclinate. Face brown; carina high, narrow. Clypeus dark brown. Cheek yellowish brown, narrower than 1/10 of maximum diameter of eye (0.09, 0.08–0.09). Second oral *ca.* 5/6 (0.83, 0.67–0.98) length of vibrissa. Palpus pale brown, club-shaped, with several prominent setae on apical to lateral margin, in ♂ with numer-

ous small setae on ventral surface.

Thorax: Mesoscutum orange brown; scutellum yellowish brown. Humerals 2, subequal. Acrostichal hairs in 6 rows. Anterior dorsocentral *ca.* 5/9 (0.55) length of posterior; length distance of dorsocentrals *ca.* 1/2 (0.50, 0.46–0.53) cross distance. Posterior scutellars equidistant to each other and to anterior. Sterno-index *ca.* 0.5 (0.52–0.55); mid sternopleural *ca.* 1.3 (1.31–1.32) times longer than anterior.

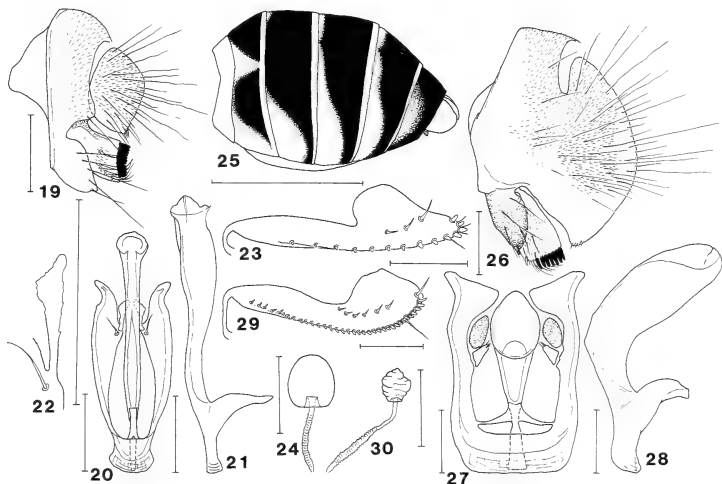
Legs pale brown. Preapicals on all tibiae; apicals on fore and mid tibiae. Fore metatarsus slightly longer than 2 succeeding tarsal joints together; mid and hind metatarsi slightly longer than 3 succeeding joints together.

Wing hyaline, slightly fuscous. Veins brown; anterior cross vein clear; posterior clouded. R_{2+3} slightly curved to costa at tip; R_{4+5} and M nearly parallel. C1-bristles 2; ventral one somewhat weak. Wing indices: C *ca.* 3.3 (3.22–3.31), 4V *ca.*

1.6 (1.51–1.68), 4C *ca.* 0.7 (0.67–0.73), 5x *ca.* 1.3 (1.31–1.35), Ac *ca.* 2.4 (2.37–2.44), C3-fringe *ca.* 0.5 (0.51–0.57). Haltere white; stalk anteriorly dark gray.

Abdomen: Tergites yellow; 2nd to 5th each with medially interrupted, laterally forward extending, dark brown, caudal band. Sternites pale yellow.

Periphallic organs (Fig. 19): Epandrium pubescent mediocaudally to dorsally, constricted deeply at base of surstylus, with 1 bristle in middle part and 5 in lower part; heel present; toe somewhat pointed. Surstylus quadrate, broad, medially slightly pubescent, with 11 primary teeth in slightly concave row on distal margin, 4 spines on outer surface and many curved setae on inner surface. Cercus oval, pubescent except ventral portion, separate from epandrium, with *ca.* 28 bristles and tuft of a few short bristles at caudoventral, somewhat pointed corner.



FIGS. 19–24. *Drosophila (Drosophila) liae* sp. nov. 19: Periphallic organs. 20: Phallic organs. 21: Aedeagus (lateral view). 22: Hypandrial process and submedian spine. 23: Ovipositor. 24: Spermatheca. (Scale-line=0.1 mm.)
FIGS. 25–30. *Drosophila (Drosophila) fluvialis* sp. nov. 25: ♂ abdomen. 26: Periphallic organs. 27: Phallic organs. 28: Aedeagus (lateral view). 29: Ovipositor. 30: Spermatheca. (Scale-line=1 mm in 25, 0.1 mm in 26–30.)

Phallic organs (Figs. 20–22): Aedeagus slender, basally with vertical rod; apodeme short, *ca.* 1/3 as long as aedeagus. Posterior paramere absent. Novasternum narrow, long, with 1 pair of submedian spines at bases of hypandrial processes; median notch deep, wide.

♀ reproductive organs: Ovipositor (Fig. 23) dorso-submedially expanded, apically round, with 3 bristle-like discal, *ca.* 14 apically round, marginal teeth, 3 short terminal and 1 subterminal hairs; basal ithmus narrow, short. Spermatheca (Fig. 24) ellipsoidal; introvert shallow, *ca.* 1/5 height of outer capsule; duct distally expanded.

Holotype ♂, China: Conghua, Guangdong Province, 27. I. 1987, by sweeping on forest floor (M. J. Toda).

Paratype, China: 1♀, Dinghushan, Guangdong Province, 24. I. 1987, by sweeping on forest floor (M. J. Toda).

Distribution. China: Guangdong.

Relationship. This species is closely related to *D. trisetosa* Okada, 1966, but readily distinguishable from the latter by the diagnostic characters.

Remarks. This species is named in honor of Dr. Li Ying Li, the director of the Guangdong Institute of Entomology, who understood and promoted this study.

Ungrouped Species

Drosophila (Drosophila) fluvialis sp. nov. (Figs. 25–30)

Diagnosis. Third to 6th abdominal tergites each with medially uninterrupted and broad, laterally narrowing blackish brown, caudal band (Fig. 25). Cercus fused broadly to epandrium (Fig. 26). Aedeagus large, curved ventrad, with vertical rod (Fig. 28). Anterior paramere narrowly separate from novasternum, triangular, apically with *ca.* 3 sensilla (Fig. 27). Finely pubescent, oval hypandrial plate present posteriorly to anterior paramere, separate from novasternum (Fig. 27).

♂, ♀. Body length, ♀ *ca.* 3.1 mm (2.70–3.36), ♀ *ca.* 3.2 mm (3.01–3.36). Thorax length, ♂ *ca.* 1.4 mm (1.27–1.57), ♀ *ca.* 1.5 mm (1.34–1.55).

Head: Eye brownish red, with thick pile. Second joint of antenna dark grayish brown; 3rd

dark gray. Arista with 3 upper and 1 or 2 lower branches in addition to terminal fork. Frons *ca.* 1/2 (0.49, 0.47–0.51) as wide as head, brown, anteriorly with frontal hairs; ocellar triangle darker. Anterior reclinate orbital *ca.* 1/3 (0.35, 0.25–0.46) length of posterior reclinate; proclinate *ca.* 6/7 (0.86, 0.75–0.94) length of posterior reclinate. Face brownish yellow, medially whitish; carina high, broad. Clypeus brown. Cheek brownish yellow, dark gray below eye and on anteroventral margin, *ca.* 1/4 (0.25, 0.21–0.26) as broad as maximum diameter of eye. Second oral *ca.* 2/5 (0.40, 0.29–0.52) length of vibrissa. Palpus grayish yellow, with several long setae.

Thorax: Mesoscutum grayish brown, medially darker; scutellum dark grayish brown; thoracic pleura grayish yellow. Humerals 2; upper one longer. Acrostichal hairs in 6 somewhat irregular rows. Anterior dorsocentral *ca.* 2/3 (0.65, 0.59–0.67) length of posterior; length distance of dorsocentrals *ca.* 3/8 (0.38, 0.34–0.42) cross distance. Anterior scutellar *ca.* 8/9 (0.89, 0.83–0.95) length of posterior; posteriors nearer to each other than to anterior. Sterno-index *ca.* 0.7 (0.63–0.77).

Legs grayish yellow; fore tibia and tarsus blackish. Preapicals on all tibiae; apicals on fore and mid tibiae. All metatarsi much longer than rest of tarsal joints together. ♂ fore tarsus anteriorly with many erected hairs.

Wing hyaline. Veins dark brown; cross veins clear. R_{2+3} slightly curved to costa at tip; R_{4+5} and M nearly parallel. C1-bristle 1. Wing indices: C *ca.* 3.0 (2.74–3.62), 4V *ca.* 1.9 (1.77–2.06), 4C *ca.* 0.9 (0.71–0.94), 5x *ca.* 1.3 (1.06–1.35), Ac *ca.* 2.1 (1.97–2.35), C3-fringe *ca.* 0.9 (0.83–0.93). Haltere pale grayish brown; anterior side of stalk darker.

Abdomen (Fig. 25): Tergites yellow; 2nd with 1 pair of large, triangular, blackish brown patches. Sternites pale yellow, quadrate; ♂ 5th longer than broad, concave on caudal margin.

Periphallallic organs (Fig. 26): Epandrium yellow, broad, pubescent caudally and dorsally, with *ca.* 5 bristles in middle to upper part; lower blackish, narrow, apically pointed, with *ca.* 6 bristles. Surstylus quadrate, pubescent on medial to ventral outer surface, with 7 primary teeth in straight row on distal margin, 2 straight spines on

outer surface and numerous recurved spines at caudoventral corner and on inner surface. Cercus large, oval, pubescent medially to dorsally, with ca. 40 bristles; ventral part bare except for tuft of short bristles on caudoventral apex.

Phallic organs (Figs. 27, 28): Aedeagal apodeme ca. 1/4 as long as aedeagus. Posterior paramere absent. Novasternum quadrate, longer than broad, without submedian spines.

♀ reproductive organs: Ovipositor (Fig. 29) subapically broad, with ca. 6 discal, ca. 36 marginal teeth and subterminal hair; ultimate marginal tooth long, bristle-like; basal ithmus narrow, ca. 1/5 as long as ovipositor. Spermatheca (Fig. 30) small, less sclerotized, irregularly wrinkled and shaped; introvert very shallow.

Holotype ♂, China: Nankunshan, Guangdong Province, 28. VIII. 1987, ex trap (K. Beppu).

Paratypes, China: 9 ♂, 25 ♀, same data as holotype; 1 ♂, 1 ♀, same data except 27. VIII. 1987.

Distribution. China: Guangdong.

Relationship. The large, ventrad curved aedeagus and the cercus fused to epandrium suggest the relationship to the *robusta* species-group. However, the abdominal color pattern, the morphology of anterior paramere, the presence of characteristic hypandrial plate and the small, less sclerotized spermatheca are inconsistent with the characters of the latter group.

***Drosophila (Drosophila) wakahamai* sp. nov.**

(Figs. 31–36)

Diagnosis. Arista with 3 upper and 1 lower long branches in addition to large terminal fork. Longest axis of eye oblique to body axis. Wing entirely brownish fuscous. Epandrial toe truncate, with ca. 6 short bristles (Fig. 31). Decasternum triangular and with lateral short arms (Fig. 32). Aedeagus bilobed but with apical fusion (Fig. 33). Ventral fragma triangular, basally tapering and with narrow elongation, distally overlapping with hypandrium (Fig. 33).

♂, ♀. Body length, ♂ ca. 2.9 mm (2.43–3.50), ♀ ca. 3.0 mm (2.84–3.24). Thorax length, ♂ ca. 1.2 mm (1.00–1.34), ♀ ca. 1.2 mm (1.16–1.33).

Head: Eye dark brownish red, with thick pile. Second joint of antenna dark brown; 3rd gray. Frons slightly wider than 1/2 of head width (0.51, 0.50–0.51), dark brown, anteriorly with frontal hairs; ocellar triangle and periorbit darker. Anterior reclinate orbital ca. 3/10 (0.31, 0.25–0.35) length of posterior reclinate; proclinate ca. 2/3 (0.68, 0.62–0.72) length of posterior reclinate. Face dark brown, paler below; carina high, broad. Clypeus dark brown. Cheek dark brown, ca. 1/4 (0.27, 0.23–0.30) as broad as maximum diameter of eye. Second oral small. Palpus grayish brown, with a few prominent setae.

Thorax: Mesoscutum dark brown, with 1 pair of broad, darker bands between dorsocentrals; scutellum blackish brown, anteromedially paler; thoracic pleura dark brown, with diffuse, darker patch on episternum. Humerals 2, subequal. Acrostichal hairs in 6 rows. Anterior dorsocentral ca. 2/3 (0.65, 0.59–0.72) length of posterior; length distance of dorsocentrals ca. 1/2 (0.48, 0.40–0.56) cross distance. Anterior scutellar as long as posterior (1.00, 0.93–1.06); posteriors nearer to each other than to anterior. Sterno-index ca. 0.7 (0.60–0.85).

Legs brown. Preapicals on all tibiae; apicals on fore and mid tibiae. Fore metatarsus as long as rest of tarsal joints together; mid and hind metatarsi slightly longer than rest together.

Wing apically somewhat pointed. Veins dark brown; cross veins clear. R_{2+3} slightly curved to costa at tip; R_{4+5} and M nearly parallel. C1-bristles 2; lower one thin. Wing indices: C ca. 3.7 (3.53–3.79), 4V ca. 1.5 (1.41–1.56), 4C ca. 0.7 (0.64–0.71), 5x ca. 1.3 (1.05–1.50), Ac ca. 1.7 (1.59–1.91), C3-fringe ca. 0.4 (0.32–0.45). Haltere dark grayish brown.

Abdomen: Tergites nearly entirely blackish brown, each anterolaterally somewhat paler. Sternites pale grayish brown, longer than broad.

Periphallallic organs (Figs. 31, 32): Epandrium pubescent caudally and dorsally, broad medially, narrow below, with ca. 1 (0–2) bristle in upper part and ca. 2 in middle part; heel prominent. Surstylus blackish brown, narrow proximally, broad distally, with ca. 8 primary teeth in concave row on distal margin and several setae at caudoventral corner and on inner surface. Cercus oval, fused to

epandrium, pubescent medially to dorsally, with ca. 42 (33–47) bristles.

Phallic organs (Figs. 33, 34): Aedeagal apodeme as long as aedeagus. Anterior paramere attached to aedeagus, ventrally pubescent, with a few small warts on apical inner surface. Posterior paramere absent. Novasternum without submedian spines; hypandrium somewhat quadrate.

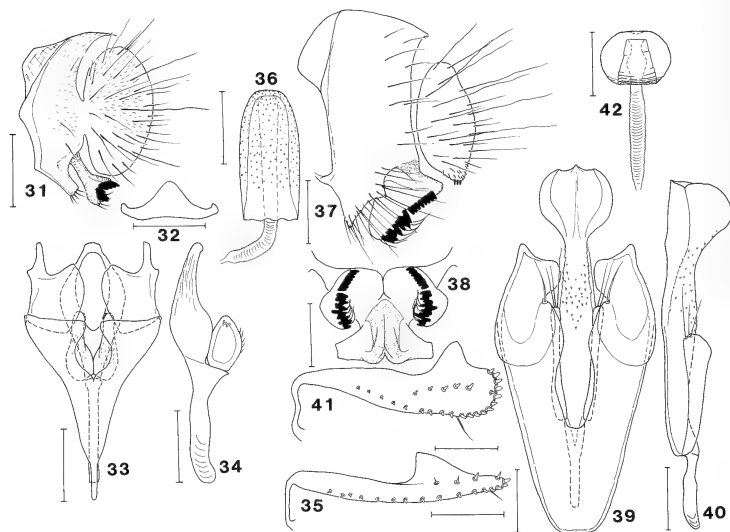
♀ reproductive organs: Ovipositor (Fig. 35) narrow, dorso-subapically expanded triangularly, with ca. 3 apically pointed discal, ca. 17 marginal teeth and subterminal hair; ultimate marginal tooth only apically pointed, other marginals apically round; basal ithmus narrow, ca. 1/5 as long as ovipositor. Spermatheca (Fig. 36) large, long, sinuate on basal margin, with numerous small warts on upper 3/4 outer capsule; introvert wide and deep.

Holotype ♂, China: Nankunshan, Guangdong Province, 28. VIII. 1987, ex trap (K. Beppu).

Paratypes, China: 1 ♂, same data as holotype; 3 ♂, 3 ♀, Dinghushan, Guangdong Province, 22. VIII, 3, 4. IX. 1987, ex traps (K. Beppu).

Distribution. China: Guangdong.

Relationship. This species is conspecific or very close to *Drosophila (Drosophila)* sp. a reported by Takada and Wakahama [3]. According to their description, though not referring to the phallic organs, there are slight differences only in the number of bristles on epandrium and the morphology of decasternum between the two forms. Although Takada and Wakahama [3] thought that their form "probably belongs to the *robusta* group", the present species is quite unique in the subgenus *Drosophila*, having the diagnostic characters different from any species-groups of this



FIGS. 31–36. *Drosophila (Drosophila) wakahamai* sp. nov. 31: Peripheral phallic organs. 32: Decasternum. 33: Phallic organs. 34: Aedeagus and anterior paramere (lateral view). 35: Ovipositor. 36: Spermatheca. (Scale-line = 0.1 mm.)

FIGS. 37–42. *Drosophila (Drosophila) guangdongensis* sp. nov. 37: Peripheral phallic organs. 38: Surstylus and decasternum. 39: Phallic organs. 40: Aedeagus and anterior paramere (lateral view). 41: Ovipositor. 42: Spermatheca. (Scale-line = 0.1 mm.)

subgenus. However, the cercus fused to epandrium and the absence of submedian spines on novasternum indicate at least the relationship to the *virilis-repleta* Radiation [4].

Remarks. This species is named in honor of Dr. K. Wakahama, Shimane University.

Drosophila (Drosophila) guangdongensis sp. nov.
(Figs. 37–42).

Diagnosis. Eye bare. Cross veins clear. ♂ abdominal tergites entirely black except for 1st and anterior part of 2nd. ♀ tergites yellow; 2nd with medially interrupted, narrow, dark brown, caudal band; 3rd to 6th each with medially uninterrupted, narrow, caudal band. Surstylus with ca. 8 moderate teeth in straight row on upper half distal margin, ca. 15 larger teeth in irregular rows on lower half (Fig. 37). Aedeagus long, distally bilobed and swollen (Figs. 39, 40). Anterior paramere long, slender, apically with 3 long bristles, basally attached to aedeagus (Fig. 40).

♂, ♀. Body length, ♂ ca. 3.0 mm (2.63–3.19), ♀ ca. 3.2 mm (3.01–3.33). Thorax length, ♂ ca. 1.4 mm (1.25–1.46), ♀ ca. 1.6 mm (1.57–1.79).

Head: Eye orange red. Antenna grayish yellow. Arista with ca. 5 (4–6) upper and 3 lower branches in addition to terminal fork. Frons slightly narrower than 1/2 of head width (0.48, 0.47–0.50), orange yellow, anteriorly with frontal hairs; inside margins of ocelli darker; periorbit paler. Anterior reclinate orbital ca. 3/7 (0.43, 0.34–0.55) length of posterior reclinate; proclinate ca. 7/9 (0.77, 0.72–0.87) length of posterior reclinate. Face orange yellow; carina pale, high, narrow. Clypeus brownish yellow. Cheek orange yellow, ca. 1/5 (0.19, 0.16–0.21) as broad as maximum diameter of eye. Second oral small. Palpus grayish yellow, with a few prominent setae.

Thorax brownish yellow. Humeral 2, subequal. Acrostichal hairs in ca. 10 irregular rows. Anterior dorsocentral ca. 5/9 (0.54, 0.50–0.65) length of posterior; length distance of dorsocentrals ca. 3/10 (0.30, 0.24–0.37) cross distance. Anterior scutellar ca. 8/9 (0.89, 0.81–0.93) length of posterior; posteriors nearer to each other than to anterior. Sterno-index ca. 0.7 (0.63–0.76).

Legs yellow. Preapicals small, but present on

all tibiae; apicals on fore and mid tibiae. Fore metatarsus as long as 2 succeeding tarsal joints together; mid as long as 3 succeeding together; hind as long as rest together.

Wing hyaline. Veins yellow. R_{2+3} slightly curved to costa at tip; R_{4+5} and M slightly convergent distally. C1-bristle 1. Wing indices: C ca. 3.1 (2.96–3.35), 4V ca. 1.7 (1.56–1.73), 4C ca. 0.8 (0.73–0.82), 5x ca. 1.4 (1.21–1.65), Ac ca. 2.4 (2.13–2.59), C3-fringe ca. 0.7 (0.62–0.73). Haltere grayish pale yellow.

Abdomen: Sternites grayish pale yellow; ♂ 5th broader than long.

Periphallic organs (Figs. 37, 38): Epandrium broad, with ca. 8 bristles in upper to middle part and ca. 23 in lower part; lower part triangular, curved inward, apically pointed, with rectangular corner on caudal margin; heel prominent, pointed. Surstylus broad, with several curved spines on ventral inner surface; upper part fused basally to epandrium, distally to decasternum. Decasternum composed of dark median plate and lateral broad arms. Cercus somewhat narrow, with ca. 26 bristles; caudoventral corner somewhat pointed, with 3 stout short spines and several small spines.

Phallic organs (Figs. 39, 40): Aedeagus with numerous spinules on submedian ventral to lateral surface; apodeme short, ca. 3/10 as long as aedeagus. Posterior paramere absent. Novasternum long, basally narrowing, with 1 pair of submedian spines at apices of U-shaped hypandrial plates; median notch deep, narrow.

♀ reproductive organs: Ovipositor (Fig. 41) apically quadrate, dorso-subapically expanded triangularly, with ca. 5 discal, ca. 21 marginal teeth and subterminal hair; basal ithmus narrow, somewhat sinuate, ca. 1/4 as long as ovipositor. Spermatheca (Fig. 42) spherical, apically shallowly indented, basally slightly wrinkled; introvert deep, distally narrowing, basally wrinkled; duct expanded medially and distally in introvert.

Holotype ♂, China: Dinghushan, Guangdong Province, 20–28. V. 1986, ex trap (T. X. Peng).

Paratypes, China: 38♂, 39♀, same data as holotype.

Distribution. China: Guangdong.

Relationship. This species seems to have some affinities to the *D. quinaria* species-group in the

arrangement of teeth on surstylus and the morphology of phallic organs, but clearly differs from the latter group in having the clear cross veins, the bare eye and the neither spotted nor medially interrupted caudal bands on 3rd to 6th abdominal tergites.

ACKNOWLEDGMENTS

We wish to thank Mr. L. Xie, the Guangdong Institute of Entomology, and Mr. Y. C. Zhang for their help in collecting the samples. This work was supported by Grants-in-Aid for Overseas Scientific Survey from the Ministry of Education, Science and Culture, Japan (Nos. 60041061, 61043056, 62041085).

REFERENCES

- 1 Gupta, J. P. and Ray-Chaudhuri, S. P. (1970) Some new and unrecorded species of *Drosophila* (Diptera: Drosophilidae) from India. Proc. R. Entomol. Soc. Lond., B, **39**: 57-72.
- 2 Takada, H., Beppu, K. and Toda, M. J. (1979) *Drosophila* Survey of Hokkaido, XXXVI. New and unrecorded species of Drosophilidae. J. Fac. Gen. Ed., Sapporo Univ., **14**: 105-129.
- 3 Takada, H. and Wakahama, K. I. (1967) A *Drosophila* survey in Okinawa Main Island. Annot. Zool. Japon., **40**: 55-60.
- 4 Throckmorton, L. H. (1975) The phylogeny, ecology, and geography of *Drosophila*. In "Handbook of Genetics, Vol. III". Ed. by R. C. King, Plenum Publ., New York, pp. 421-469.

[COMMUNICATION]

Preparation and Properties of Monoclonal Antibodies against Bovine Rhodopsin

FUMIO TOKUNAGA, TATSUO IWASA, MASASHI TAKAO,
SEIJI SATO^{1,2} and TAKUJI TAKEUCHI¹

*Department of Physics, and ¹Biological Institute,
Faculty of Science, Tohoku University,
Aobayama, Sendai, Miyagi 980, Japan*

ABSTRACT—Monoclonal antibodies against bovine rhodopsin were prepared. Bovine rhodopsin was purified by Con A sepharose chromatography and used as an antigen. Three cell lines which produced anti-rhodopsin antibody (Rh29, Rh112 and Rh311) were isolated.

The Rh29 showed greater affinity to opsin than rhodopsin, while Rh311 exhibited greater affinity to rhodopsin than opsin. The Rh112 showed almost the same affinity to rhodopsin and opsin. This difference in the affinity suggests that these monoclonal antibodies obtained in the present study bind to the different parts of rhodopsin molecule.

The Rh29 binds with rhodopsins of carp and octopus, but weakly with that of chicken. The Rh311 binds also with chicken and octopus rhodopsins, and very weakly with carp rhodopsin. These results indicate that some parts are conserved in vertebrate rhodopsin molecules and in some of invertebrate visual pigments in the process of evolution.

INTRODUCTION

Animals possess different visual pigments from species to species. A number of species of animals have color vision which is based on several different kinds of photoreceptive pigments in the retina. Southern blot hybridization experiments with cDNA of bovine rhodopsin as a probe have shown that homologous sequences of DNA were present in the genomic DNAs from vertebrates to chlamydomonas [1]. Therefore, amino acid sequen-

ces of visual pigments, at least in part, are assumed to be conserved in the evolution process. We attempted to examine this assumption with monoclonal antibodies raised against bovine rhodopsin.

Monoclonal antibodies have been used for various researches since Köhler and Milstein [2] introduced the technique. Monoclonal antibodies are powerful probes not only for the histochemical researches but also for clarifying the relationship among proteins in various species of animals in evolution. Monoclonal antibodies against visual pigments have been isolated in some laboratories [3-8]. They showed localization of visual pigments in retinas, cross-reactivity of the monoclonal antibodies with visual pigments of different species of vertebrates and specification of visual cell types. We prepared monoclonal antibodies against bovine rhodopsin and investigated the cross-reactivities of them with rhodopsin of vertebrates (chicken, carp), molluscs (octopus) and arthropods (locust, crayfish).

MATERIALS AND METHODS

Chemicals Con A sepharose was purchased from Pharmacia, Ammonyx LO, Gunze Sangyo Inc.; α -D-Methylmannoside, Sigma; Freund's complete adjuvant, DIFCO laboratories; RPMI 1640, Flow laboratories; HRPO-conjugated anti-mouse IgG, DAKO; Fetal calf serum, Dainippon; Normal goat serum, Rockland. The other

Accepted March 9, 1988

Received December 17, 1987

² Present address: Itoham Foods Inc. Mita, Meguro-ku, Tokyo 153, Japan

chemicals in special grade were purchased from Wako.

Preparation of antigens Rod outer segments were prepared from bovine retinas according to the procedure described by Papermaster *et al.* [9]. Rhodopsin was extracted from the rod outer segments by 1.4% Ammonyx LO in 10 mM HEPES buffer (pH 7.0) containing 3 mM $MgCl_2$. The extracted rhodopsin was charged on the Con A sepharose column (2×5 cm) and was eluted by 10 mM HEPES buffer (pH 7.0) containing 3 mM $MgCl_2$, 1.4% Ammonyx LO and 1% α -D-methylmannoside. The purified rhodopsin was used as an antigen. After the rhodopsin was bleached by irradiation with white light (>370 nm, Toshiba L-39) from a projector lamp (1 KW), it was used as opsin without further preparation. For solid phase enzyme-linked immunosorbent assay (ELISA), outer segment fraction of visual cells of chicken and carp were prepared from the retinas by the similar method as bovine rod outer segment membrane. Octopus microvilli fraction was prepared by the method reported by Shichida *et al.* [10]. Rhabdomes of locust and crayfish were prepared by sucrose flotation from isolated retinas [11].

Preparation of monoclonal antibodies On day 0 mice were injected intraperitoneally with 100 μ g of the purified rhodopsin in 0.5 ml Hanks' BSS (0.8% NaCl, 0.04% $CaCl_2$, 0.02% $MgSO_4 \cdot 7H_2O$, 0.0006% $Na_2HPO_4 \cdot 2H_2O$, 0.006% KH_2PO_4 , 0.1% glucose, 0.035% $NaHCO_3$) with an equal amount of Freund's complete adjuvant. On day 14, animals were again injected with the antigen (the same amount as day 0). On day 35 the titer of antiserum was checked. On day 42 a booster injection was carried out with 10 μ g of the antigen in BSS. On day 45 spleen cells were obtained from the animals. Cultured P6 ($\times 63Ag$ 8. 6. 5. 13) mouse myeloma cells (gift from Dr. J. A. Brumbaugh, University of Nebraska) were harvested and washed. A suspension of the spleen cells was prepared and washed 3 times in serum free medium (RPMI 1640, Flow laboratories). P6 cells (2×10^7) and spleen cells (1×10^8) were mixed in a 50 ml centrifuge tube and centrifuged at 1,500 rpm

for 10 min. The pellet was kept at $37^\circ C$ in a water bath. One ml of warm 50% polyethyleneglycol (1500) in RPMI 1640 was added to the pellet over 1 min period. The cells were gently stirred during the addition. One ml of the warm serum free-medium was slowly added. More 7 ml was added and cells were stirred over 2–3 min period during the addition. The suspension was centrifuged and the supernatant was removed. Ten ml of warm medium (RPMI 1640 with 15% fetal calf serum, FCS) was added and stirred. Twenty ml of warm medium with FCS was further added. Cells were inoculated into wells of 96-well plates and incubated in a CO_2 -incubator. On day 1, 0.1 ml of HAT medium (100 μ M hypoxanthine, 0.4 μ M aminopterin, 16 μ M thymidine in 15% FCS, 85% RPMI 1640) was added to each well. On days 2, 3, 5, 8, 11 and then every 3 days, a half of the culture medium in the well was exchanged. Supernate of each well with colonies was examined for antibody secretion by the dot-immunobinding assay [12]. Cells in the wells which contained an antibody were transferred to 24-well tissue-culture plates. Subsequently, they were cloned on 96-well tissue-culture plates. Three cell lines were shown to produce the anti-bovine rhodopsin antibodies.

Enzyme-linked immunosorbent assay (ELISA) Each 50 μ l of serially diluted suspension of outer segment, microvilli or rhabdome membrane was placed in a well of a 96-well microtiter plate and incubated for 2 hr at $37^\circ C$ for immobilization. The wells were rinsed with TBS (Tris buffer saline; 50 mM Tris buffer, 200 mM NaCl, pH 7.4) and coated with 100 μ l of blocking solution (TBS containing 3% bovine serum albumin, 1% normal goat serum) followed by incubation for 30 min. After the solution was removed, 50 μ l of monoclonal antibody (50 ng), which was purified by protein A sepharose column (Bio Rad) and whose concentration was estimated by UV absorbance at 280 nm (A_{280} , mg/ml = 1.4) [13] was added and incubated for 1 hr. The wells were washed with Tw-TBS (TBS containing 0.05% Tween 20) and treated for 1 hr with 50 μ l of second antibodies, horseradish peroxidase (HRPO)-conjugated rabbit antibodies against mouse immunoglobulin (DAKO) diluted in Tw-TBS at a

concentration of 1 $\mu\text{g}/\text{ml}$. Above reactions were carried out at 37°C. After washing the wells thoroughly with Tw-TBS, 100 μl of HRPO indicator (o-phenylenediamine; 0.4 mg/ml) and H_2O_2 (0.01%) were added. The reaction was terminated after 30 min by the addition of 100 μl of 2N H_2SO_4 and absorbance at 492 nm was measured.

Immunoblot staining Proteins in the purified photoreceptor membranes or the purified bovine rhodopsin were developed on 10% polyacrylamide SDS slab gel by electrophoresis. The proteins in slab gel were electrically transferred onto nitrocellulose filters in a transfer chamber (Bio Rad) containing 25 mM Tris/192 mM glycine, pH 8.3 and 20% methanol. The nitrocellulose filters were stained by amidoblack (0.1%) or washed several times with TBS followed by incubation with an anti-rhodopsin antibody solution. The filters were further incubated with HRPO-conjugated anti-mouse goat IgG (1/500 sol. in TBS, DAKO), and developed by H_2O_2 (0.005%) and 3, 3'-diaminobenzidine tetrahydrochloride (0.2 mg/ml) after several washes with TBS.

RESULTS AND DISCUSSION

Cells of three lines produced anti-rhodopsin monoclonal antibodies. These monoclonal antibodies were designated as Rh29, Rh112 and Rh311. Immunoglobulin class of Rh29, Rh112 or Rh311 was determined as IgG by ELISA method using the rabbit immunoglobulines against mouse IgA, IgG and IgM.

Specificity of the monoclonal antibody to bovine rhodopsin was confirmed as follows. Rhodopsin in 10 mM HEPES buffer with 1.4% Ammonyx LO was immobilized on wells and then the wells were treated serially with the monoclonal antibodies and with HRPO-conjugated anti-mouse antibodies. The result showed that antibodies obviously bind to the immobilized antigens as compared to non-specific mouse IgG. They were further investigated by immunoblotting. Proteins were extracted from bovine rod outer segment membranes with 0.1% digitonin and were developed on 10% SDS slab gel. The proteins in the gel were transferred to nitrocellulose membrane.

Rh29 detected bands at ca. 40 and 80 kDa on the membrane. No other bands were observed in Figure 1a, though several other bands can be seen in Figure 1b. The 40 and 80 kDa bands are at the same positions with Con A-purified rhodopsin. Thus, we concluded that these two bands are rhodopsin monomer and dimer. The other antibodies, Rh112 and Rh311, did not react with any band. This may be accounted for that the antibodies have an affinity to the conformation of rhodopsin which easily denatured by SDS.

The antigenicity of the purified rhodopsin was tested by means of the ELISA where series of the diluted antigen was immobilized (Fig. 2). Each antibody demonstrated different characters with respect to the effect of bleaching. Rh29 reacted with the bleached rhodopsin more extensively than unbleached one (Fig. 2a). On the antigenicity to Rh112, both bleached and unbleached rhodopsin exhibited the same extent of affinity (Fig. 2b). Rhodopsin had the ability to bind to Rh311, but bleached rhodopsin lost the ability (Fig. 2c).

Cross-reaction of these antibodies was also

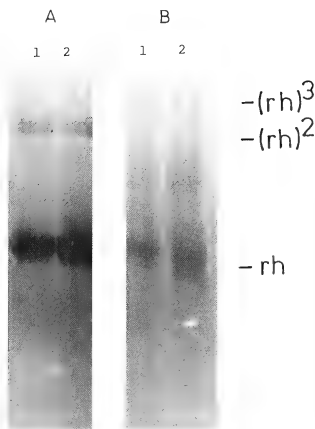


Fig. 1. Western blotting of proteins extracted from bovine rod outer segment membrane with 0.1% digitonin. A; stained by Rh29. B; stained by amidoblack. 1; 11.2 μg rhodopsin. 2; 22.4 μg rhodopsin.

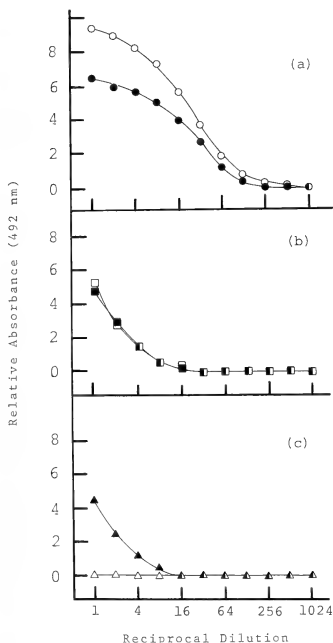


FIG. 2. Affinity of the antibodies (a: Rh29, b: Rh112, c: Rh311) to rhodopsin (closed symbols) and opsin (open symbols). The purified rhodopsin and opsin prepared by irradiating the rhodopsin were diluted and subjected to ELISA. Horseradish peroxidase-conjugated anti-mouse goat IgG was used as a second antibody. The reactivity was monitored by absorbance increase at 492 nm due to decomposition of o-phenylenediamine.

examined with isolated visual cell outer segment membranes of chicken and carp, and microvilli of octopus (Fig. 3). Rh29 reacted strongly with carp and octopus membranes, but very weakly with chicken membrane. Our preliminary results showed that the epitope of Rh29 is located around the amino acid sequence from 20th to 30th of bovine rhodopsin. Only 26th amino acid residue of chicken (tyrosine) is different from bovine (alanine) in this region [14]. This replacement of

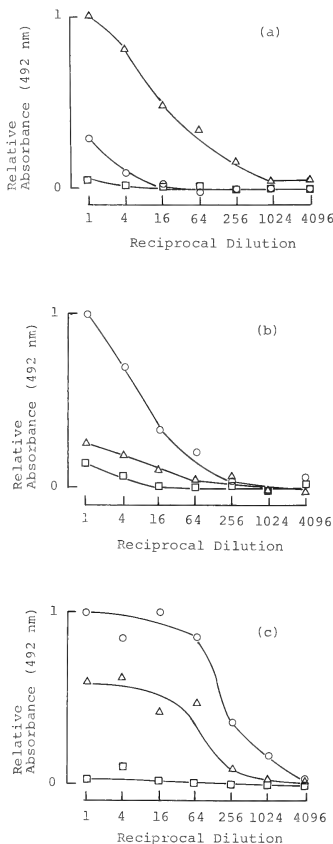


FIG. 3. Cross-reactivity of the antibodies to photoreceptor membranes of animals. a: chicken, b: carp and c: octopus. \circ : Rh29, \square : Rh112, \triangle : Rh311.

amino acid residue may affect the affinity of Rh29. Rh311 also reacts with chicken and octopus membranes, and very weakly with carp membrane. This result indicates that Rh311 recognizes a part of rhodopsin different from the recognition site of Rh29, though both antibodies bind to the surface

of bovine rhodopsin inside the disks (Takao *et al.*, in preparation). Rh112 reacted scarcely with the membranes that we examined; no reaction was observed in some cases.

In the case of locust, on the other hand, all of our monoclonal antibodies showed very low affinity close to non-specific binding. We also examined the cross-reactivity of Rh 29 with crayfish rhodome membrane by immunoblotting. Rh 29 did not show the binding ability.

The binding sites of Rh29 and Rh311 seem to be conserved among vertebrates and molluscs in the process of evolution. However, these antibodies did not react with visual pigments of locust and crayfish. The amino acid sequence of *Drosophila* rhodopsin has been shown to significantly different from that of mammalian rhodopsin [15-18]. Therefore, it seems reasonable that these antibodies do not react with arthropod visual pigments.

ACKNOWLEDGMENT

We thank Prof. Takehiko Tachibana (Institute for Tuberculosis and Cancer, Tohoku University) for gift of anti-mouse-IgA, -IgG and -IgM goat antibodies. This research was supported in part by Grant-in-Aid to F.T. (5821002, 59106004, 59123001, 60115001, 61107006) and to T.I. (60780292) from the Ministry of Education, Science and Culture.

REFERENCES

- 1 Martin, R. L., Wood, C., Baehr, W. and Applebury, M. L. (1986) *Science*, **232**: 1266-1269.
- 2 Köhler, G. and Milstein, C. (1975) *Nature*, **256**: 495-497.
- 3 Mackenzie, D. and Molday, R. S. (1982) *J. Biol. Chem.*, **257**: 7100-7105.
- 4 Fekete, D. M. and Branstable, C. J. (1983) *J. Neurocytol.*, **12**: 785-803.
- 5 Molday, R. S. and Mackenzie, D. (1983) *Biochemistry*, **22**: 653-660.
- 6 Witt, P. L., Hamm, H. E. and Bownds, M. D. (1984) *J. Gen. Physiol.*, **84**: 251-263.
- 7 Molday, R. S. and Mackenzie, D. (1985) *Biochemistry*, **24**: 776-781.
- 8 Szel, A., Takacs, L., Monostori, E., Diamantstein, T., Vigh-Teichmann, I. and Rohlich, P. (1986) *Exp. Eye Res.*, **43**: 871-883.
- 9 Papermaster, D. S. and Dreyer, W. J. (1974) *Biochemistry*, **13**: 2438-2444.
- 10 Shichida, Y., Tokunaga, F. and Yoshizawa, T. (1978) *Biochim. Biophys. Acta*, **504**: 413-430.
- 11 Larrivee, D. and Goldsmith, T. H. (1982) In "Methods in Enzymol. Vol. 81". Ed. by L. Packer, Academic Press, New York, pp. 34-37.
- 12 Hawkes, R., Niday, E. and Gordon, J. (1982) *Anal. Biochem.*, **119**: 142-147.
- 13 Ohara, J. and Watanabe, T. (1982) In "Hybridoma and monoclonal antibody". (In Japanese) Ed. by T. Watanabe, R & D Planning, Tokyo, pp. 13.
- 14 Takao, M., Yasui, A. and Tokunaga, F. (1988) *Vision Res.*, **28**: 471-480.
- 15 O'Tousa, J. E., Baehr, W., Martin, R. L., Hirsh, J., Pak, W. L. and Applebury, M. L. (1985) *Cell*, **40**: 839-850.
- 16 Zuker, C. S., Cowman, A. F. and Rubin, G. M. (1985) *Cell*, **40**: 851-858.
- 17 Cowman, A. F., Zuker, C. S. and Rubin, G. M. (1986) *Cell*, **44**: 705-710.
- 18 Fryxell, K. J. and Meyerowitz, E. M. (1987) *EMBO J.*, **6**: 443-451.



[COMMUNICATION]

Occurrence of Biliverdin IX α in the Gallbladder Bile of Hagfish, *Eptatretus burgeri*

TADASHI SAKAI, NOBUYUKI TABATA and MASAHITO SUIKO¹

Department of Fisheries, and ¹Agricultural Chemistry, Faculty of Agriculture,
Miyazaki University, Miyazaki City, Miyazaki 889-21, Japan

ABSTRACT—The gallbladder bile of hagfish, *Eptatretus burgeri*, was analyzed by thin layer chromatography (TLC) and high performance liquid chromatography (HPLC). TLC showed one blue, one red and several yellow bands. Pigments extracted from the blue band were analyzed by HPLC. Only one peak appeared. Judging from the absorbances at 436 and 650 nm, the pigment in this peak may be biliverdin IX isomer. The retention time of this peak was equal to that of authentic biliverdin IX α . The blue pigment in the peak was reduced with NaBH₄ and analyzed by HPLC. The retention time of reduced pigment was same as that of authentic bilirubin IX α . The blue pigment was methylated with BF₃-methanol and analyzed by HPLC. The retention time of the methylated pigment was similar to that of synthesized biliverdin IX α dimethyl ester. These results indicate that this blue pigment is biliverdin IX α and that only α isomer exists as biliverdin IX isomer. This fact strongly suggests that heme oxygenase exists in hagfish.

INTRODUCTION

In animals having hemoglobin in the blood, a large amount of the protein is degraded to bile pigments every day. Biliverdin is the bile pigment first produced by the degradation of heme [1, 2]. Until Schmid and his associates discovered the presence of heme oxygenase in microsomes of spleen and liver [3, 4], the biochemical mechanism of heme metabolism has remained obscure. Now it is generally accepted that microsomal heme oxygenase plays a key role in the physiological catabolism

of heme in mammals, birds, reptiles, and amphibians [5]. In fish and cyclostomes, however, occurrence of the enzyme has remained uncertain. In fish several enzymic activities in microsomal membranes, such as mixed-function oxidases, cannot be detected when assayed under the conditions used for mammalian enzymes because these activities are much lower than those of mammals [6]. Probably for the same reason, heme oxygenase activity cannot be detected in the liver of yellowtail *Seriola quinqueradiata* and hagfish *Eptatretus burgeri* (Sakai *et al.*, unpublished). Because it is well known that only biliverdin IX α is produced when heme is cleaved by heme oxygenase but all 4 isomers of biliverdin IX are produced when heme is cleaved nonenzymatically [7], the nature of the bile pigments in the bile of fish has been examined to elucidate the occurrence of heme oxygenase. Heme oxygenase may exist in fish because there is only the α -isomer in the bile of several fish studied [8, 9]. In cyclostomes, however, even the identity of the pigments in the bile has been unclear until now. It is well known that hemoglobin is in the blood of cyclostomes but not in blood prochorodates [10]. It is of interest whether heme oxygenase exists in cyclostomes. Therefore, we undertook the present study.

The blue pigment in the bile of hagfish, a cyclostome, was analyzed by thin layer chromatography (TLC) and high performance liquid chromatography (HPLC). Reduced and demethylated derivatives of the pigment were also analyzed by HPLC. Results of these analyses indicate that there is only the α -isomer of biliverdin IX in the

bile of hagfish. This fact strongly suggests that heme oxygenase exists in hagfish.

MATERIALS AND METHODS

Materials

Hagfish (average body weight 157 g) were caught in Nobeoka Bay in Miyazaki Prefecture on June 18 and 19, 1987. Reagents used were biliverdin IX_α from Porphyrin Products, bilirubin IX_α from Sigma Chemical Company, hemin and BF₃-methanol from Wako Pure Chemical Industry Ltd., and pre-coated silica gel plates and NaBH₄ from E. Merck. Other reagents were of analytical grade.

Bile collection

Fish were anesthetized with ethylcarbamate. The gallbladder was exposed through mid ventral incision. The contents of the gallbladder were aspirated and transferred to ice-cooled tube in the dark. Samples were stored at -80°C until analyzed.

TLC analysis

The bile samples obtained were directly applied to a pre-coated silica gel plate. TLC was carried out using two solvent systems, chloroform-methanol-water (65:35:8) until solvent ran 3–5 cm and then chloroform-methanol-water (40:9:1) until 13–15 cm. The blue band was scraped from the plate. Blue pigment was extracted with methanol and directly analyzed by HPLC.

Synthesis of 4 isomers of biliverdin IX from hemin and methylation of bile pigments

Verdohemochrome was prepared by the Method of Bonnett and McDonagh [11]. The crude verdohemochrome obtained was dissolved in 0.1 M KOH/anhydrous methanol and methylated with BF₃-methanol. The crude dimethyl esters of 4 biliverdin IX isomers were purified by the method of Yamaguchi [12]. Each isomer purified was analyzed by proton nuclear magnetic resonance spectroscopy (NMR). NMR chromatograms of 4 isomers were similar to those reported by Bonnett and McDonagh [11]. Blue pigment

extracted was also methylated with BF₃-methanol and analyzed by HPLC.

HPLC analysis

Analytical conditions were as follows. Column: Waters μ -Bondapak C18 (0.39×30 cm). Flow rate: 1 ml/min. Detection wavelengths: 436 and 650 nm. Solvent system: Initial mobile phase was methanol-5% acetic acid solution (60:40) then the amount of methanol was linearly increased from 60% to 90% over 20 min and held at 90% for 15 min. Column temperature: 40°C. HPLC analysis of dimethyl esters of biliverdin IX isomers was carried out by the same procedures as mentioned above except that the detection wavelengths were 365 and 436 nm and the solvent system used was methanol-water (80:20).

RESULTS

Figure 1 shows the TLC pattern of bile pigments in the bile of normal hagfish. One red band, some yellow bands and only one blue band appeared. Judging from the color, the blue band may contain biliverdin IX isomers.



FIG. 1. TLC chromatogram of the bile of hagfish. Analytical conditions are described in Materials and Methods.

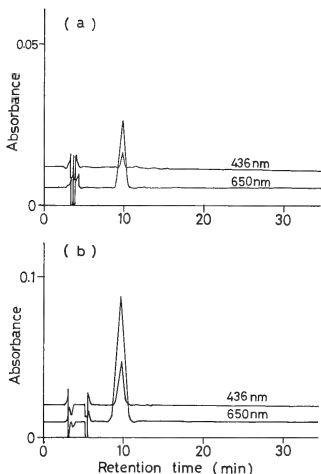


FIG. 2. HPLC chromatograms of the blue pigment extracted from blue band in TLC (a) and authentic biliverdin IX_a (b). Analytical conditions are described in Materials and Methods.

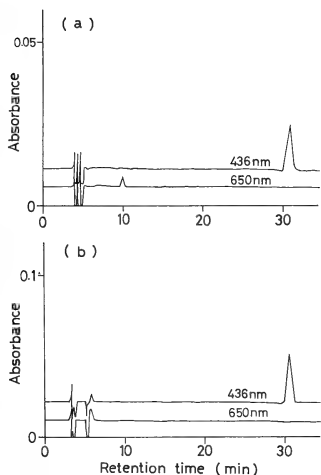


Figure 2a shows the HPLC chromatogram of bile pigments in the blue band. Only one peak appeared. Judging from the absorbances at 436 and 650 nm, the pigment in the peak seems to be one of biliverdin IX isomers. The retention time of this pigment was equal to that of biliverdin IX_a (Fig. 2b).

The pigment in the blue band was reduced with NaBH₄ and directly analyzed by HPLC. The HPLC chromatogram is illustrated in Fig. 3a. The pigment was changed by reduction. The retention time of reduced pigment was equal to that of bilirubin IX_a (Fig. 3b).

Figure 4 shows the HPLC chromatogram of dimethylesters of the blue pigment and 4 biliverdin

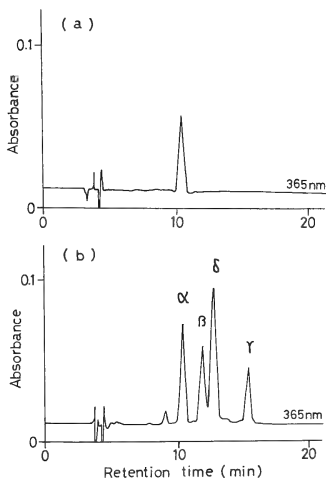


FIG. 4. HPLC chromatograms of dimethyl ester of the blue pigment (a) and those of 4 biliverdin IX isomers (b). Peak α, β, γ, and δ are responsible for dimethyl esters of biliverdin IX_a, IX_b, IX_γ, and IX_δ, respectively. Analytical conditions and synthesis method of biliverdin IX isomers are described in Materials and Methods.

FIG. 3. HPLC chromatograms of the blue pigment reduced with NaBH₄ (a) and authentic bilirubin IX_a (b). Analytical conditions are described in Materials and Methods.

IX isomers. Retention time of dimethyl ester of the blue pigment was equal to that of dimethyl-ester of the α -isomer.

These results indicate that the blue pigment is biliverdin IX $_{\alpha}$ and that only α -isomer exists as biliverdin IX isomer in the bile of hagfish.

DISCUSSION

As shown in Figure 4b, when heme was cleaved nonenzymatically, all biliverdin IX isomers were produced. However, there is only α -isomer in the bile of hagfish. This fact strongly suggests that in hagfish heme is cleaved enzymatically; accordingly heme oxygenase appears to exist in hagfish.

Along with hemoglobin, there are many biomolecules that have heme as a prosthetic group, therefore, animal without hemoglobin in the blood need to catabolize heme to bile pigments. In mammals, however, more than 90% of endogenous heme degraded to bile pigments is known to be derived from hemoglobin [13]. Animals that have hemoglobin in the blood require a heme-catabolizing enzyme, namely heme oxygenase, because they must degrade much more heme to bile pigments than animals without hemoglobin. In this connection, we examined pigments of the squid *Dorteuthis bleekeri* whose liver is colored green indicating that the causative pigments are a mixture of 4 biliverdin IX isomers (Sakai *et al.*, un-published). This finding suggests that heme, that is probably derived from feed, was cleaved nonenzymatically in these squid. Because animals lacking hemoglobin as respiratory pigment need not degrade a large amount of heme, they may not require a heme-cleaving enzyme. Prochordates belong to a phylum related to, more primitive than cyclostomes. They have no hemoglobin in the blood, and therefore they may lack a heme oxygenase. Although cyclostomes have a blood hemoglobin, some biochemical properties of this molecule, such as molecular weight, differ from those of higher vertebrates [14]. Cyclostomes

must continually cleave a large amount of heme, much of which is derived from hemoglobin. In the present study we have shown that heme-catabolizing enzyme, namely heme oxygenase, probably exists in Myxini. Therefore, heme oxygenase may be considered typical of all vertebrate animals.

ACKNOWLEDGMENT

We thank Mr. T. Michishita, Fisheries Laboratory of our University, for supplying hagfish. We also thank Dr. T. Suzuki, Faculty of Pharmaceutical Science, Teikyo University, who kindly measured NMR spectra of dimethyl esters of 4 biliverdin IX isomers.

REFERENCES

- McDonagh, A. F. (1979) In "The Porphyrins". Ed. by D. Dolphin, Academic Press, New York, Vol. 6 pp. 293-491.
- Colleran, E. and Heirwegh, K. P. M. (1979) *Comp. Biochem. Physiol.*, **64B**: 133-139.
- Tenhunen, R., Marver, H. S. and Schmid, R. (1968) *Proc. Natl. Acad. Sci. U.S.A.*, **61**: 748-755.
- Tenhunen, R., Marver, H. S. and Schmid, R. (1969) *J. Biol. Chem.*, **244**: 6388-6394.
- Schmid, R. (1977) *Trans. Assoc. Am. Physicians*, **89**: 64-76.
- Chambers, J. E. and Yarbrough, J. D. (1976) *Comp. Biochem. Physiol.*, **55C**: 77-84.
- Kikuchi, G. and Yoshida, T. (1983) *Mol. Cell. Biochem.*, **53**: 163-183.
- McDonagh, A. F. and Palma, L. A. (1982) *Comp. Biochem. Physiol.*, **73B**: 501-507.
- Sakai, T., Suiko, M. and Sakaguchi, H. (1985) *Nippon Suisan Gakkaishi*, **51**: 1871-1874.
- Fingerman, M. (1981) *Animal Diversity*, CBS College Publishing, New York, 3rd ed.
- Bonnett, R. and McDonagh, A. F. (1970) *J. Chem. Soc. Chem. Comm.*, 237-240.
- Yamaguchi, T. (1980) *Ochanomizu Igaku Zasshi*, **28**: 231-244 (in Japanese).
- Harri, J. W. and Kellermeyer, R. W. (1979) *The Red Cell*. Harvard Univ. Press, Cambridge.
- Bannai, S., Sugita, Y. and Yoneyama, Y. (1972) *J. Biol. Chem.*, **249**: 505-510.

[COMMUNICATION]

The Stimulatory Effect of 2-Deoxyecdysone on Spermiogenesis of the Diapausing Cabbage Armyworm, *Mamestra brassicae* (Lepidoptera : Noctuidae), *in vitro*

TOSHIAKI SHIMIZU and EIJI OHNISHI¹

Laboratory of Biologically Active Natural Products, Division of
Entomology, National Institute of Agro-Environmental Sciences,
Kannondai 3-1-1, Yatabe, Tsukuba, Ibaraki 305, and

¹Department of Biology, Faculty of Science,
Nagoya University, Chikusa, Nagoya 464, Japan

ABSTRACT—Testes obtained from the diapausing pupae of *Mamestra brassicae* were cultivated in Grace's medium containing 2-deoxyecdysone, which was previously detected from testis culture medium. 2-Deoxyecdysone induced spermiogenesis in cultivated testes. The elucidation of activity of 2-deoxyecdysteroids is discussed.

INTRODUCTION

The ovaries of *Bombyx mori* accumulate several ecdysteroids (oecdysteroids) characteristic to the ovaries and eggs [1]. These ecdysteroids were isolated from the ovaries and purified to a chromatographically pure state. Recently Ohnishi [2] revealed that 2-deoxyecdysone, one of the major ecdysteroids in *Bombyx mori*, has about 1/5 the activity of ecdysone on ovarian development.

As for the testicular ecdysteroids, Loeb *et al.* [3] reported that there is extensive ecdysteroid synthesis and release by isolated testes of late last-instar larvae of the tobacco budworm, *Heliothis virescens*. Shimizu *et al.* [4] also reported that the cultured testis of *Mamestra brassicae* releases into the medium approximately 3 as much of RIA detectable ecdysteroids than those contained in intact testis during a 24 hr period. Identical results were obtained with 2-deoxyecdysone, ecdysone

and 20-hydroxyecdysone by high-performance liquid chromatography (HPLC) and by the RIA system. However, it is not clear whether ecdysteroids produced by the testes functionally stimulate spermatocyst differentiation, especially spermatocyst mitosis and spermiogenesis.

In the present study, the stimulatory effect of 2-deoxyecdysone on spermiogenesis of the diapausing cabbage armyworm, *Mamestra brassicae* was examined, *in vitro*.

MATERIALS and METHODS

Insects Larvae of the cabbage armyworm, *Mamestra brassicae* were reared on an artificial diet [5] at 20°C under a 12 hr light and 12 hr dark (12L-12D) photoperiod to obtain diapausing pupae. Day 0 to day 3 pupae were used in the present experiments.

Culture methods The general culture methods used in the experiments were the same as those described previously [6]. Seven days after the onset of cultivation the cultivated testes were torn open to examine the developmental status of spermatocysts, which were classified into 3 grades; spherical spermatocysts, pyriform spermatocysts and elongated spermatocysts.

Culture media 2-Deoxyecdysone was dis-

solved in 99% ethanol and added to Grace's medium so as to make the final concentrations of the hormone 10 $\mu\text{g}/\text{ml}$ and 1 $\mu\text{g}/\text{ml}$. As control media, Grace's medium containing 0.5% and 0.05% ethanol, respectively were used.

Chemicals 2-Deoxyecdysone was extracted and purified from the ovaries of *Bombyx mori* [1]. This compound was purified with HPLC and contained less than 1% of 2, 22-dideoxy-20-hydroxyecdysone. Grace's culture medium was obtained from GIBCO (Grand Island, New York, USA).

RESULTS AND DISCUSSION

In a medium containing 2-deoxyecdysone 1 $\mu\text{g}/\text{ml}$, the elongation of spermatocysts was observed 5 to 7 days after the initiation of culture (Table 1) (Fig. 1). In the control, spermiogenesis

generally was not induced in Grace's medium containing 0.5 and 0.05% ethanol, but in a few case spermiogenesis was observed in the both media (Table 1). Since the elongation of spermatocysts occurred in the ruptured testis in Grace's medium without hormones [7], the development of cysts seems to be due to artificial injury effects on intact testis. In a control medium containing 0.5% ethanol, degenerated spermatocysts were observed. The developments of spermatocysts were inhibited in the medium containing 10 $\mu\text{g}/\text{ml}$ of 2-deoxyecdysone as compared with that of lower concentration of hormone. Since this medium contains 0.5% ethanol, the inhibitory effect might be caused by added ethanol, and not caused by the higher concentrations of the hormone, since the degenerated spermatocysts were observed in a 0.5% ethanol added control. By Kambyzellis and Williams [8], the addition of certain organic solvents apparently damaged the

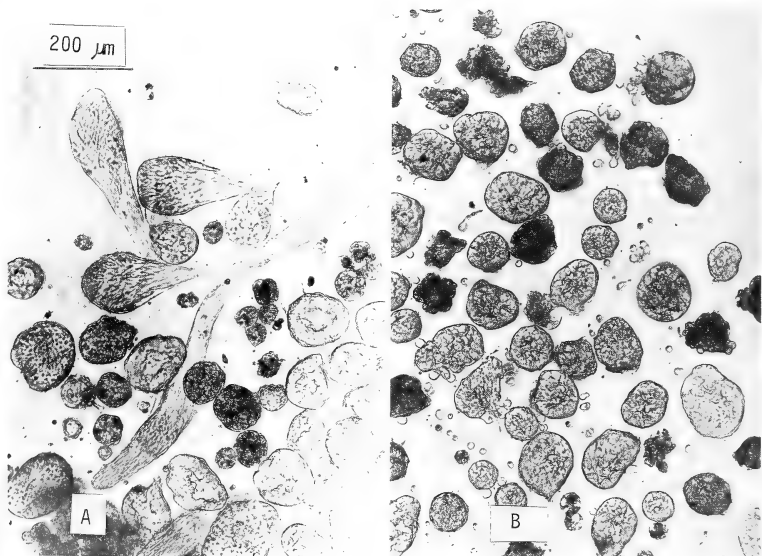


FIG. 1. Spermatocysts of *M. brassicae* 7 days after the onset of cultivation of intact testes in Grace's medium with 1 $\mu\text{g}/\text{ml}$ of 2-deoxyecdysone (A) and without any hormones (B).

TABLE 1. The stimulatory effect of 2-deoxyecdysone on spermiogenesis of cultivated testis of the cabbage armyworm, *Memestra brassicae*, *in vitro*

Treatment	Concentr.	No. of exp.	No. of cultures*	
			Spermiogenesis appearance	Per cent (%)
2-Deoxyecdysone	10 μ g/ml	16	11	68.8
	1 μ g/ml	19	15	78.9
Control (ethanol)	0.5%	20	2	10.0
	0.05%	10	1	10.0

*Testes were cultivated for 7 days with 50 μ l of Grace's medium containing 2-deoxyecdysone, then ruptured to examine the status of spermatocysts.

testis walls and thereby the deleterious developments of spermatocysts were observed.

The formation of a cell sheet from the testis and the development of the spermiduct were observed in the medium containing 10 μ g/ml of 20-hydroxyecdysone [9, 10], but they were not observed in the medium containing 10 μ g/ml of 2-deoxyecdysone.

Although 1 μ g/ml of 2-deoxyecdysone contains less than 10 ng/ml of 2, 22-dideoxy-20-hydroxyecdysone, this ecdysteroid might have no effect on the induction of spermiogenesis at these low concentrations. In the *Bombyx* ovarian development, this compound had negligible activity up to the dose of 36 μ g per abdomen [2]. The cultured *Mamestra brassicae* testis released RIA responsive ecdysteroids, and their retention times in HPLC were identical with 2-deoxyecdysone, ecdysone and 20-hydroxyecdysone [4]. The level of this 2-deoxyecdysone detected by HPLC followed by RIA of resulting fractions was considerably higher. However, the detectability of 2-deoxyecdysone with ecdysone antibody of RIA used is low [11]. Therefore, the quantity of ecdysteroid does not appear at the actual concentrations. The quantity of actual ecdysteroid is higher than peak of 2-deoxyecdysone (see [4]).

In ovarian development, 2-deoxyecdysone had about 1/5 of the activity of ovarian development compared with ecdysone, indicating that the hydroxy group at C-2 has a significant effect [2]. Previously we reported that ecdysone (α -type) was effective for the induction of spermiogenesis [6]; and in the present experiment, 2-deoxyecdysone induced spermiogenesis. From these results,

ecdysteroid with structures like ecdysone and 2-deoxyecdysone have gonadotropic action (2-deoxyecdysone is converted to ecdysone in according to Kappler *et al.* [12]). Thus, studies focusing on the elucidation of activity of 2-deoxy type ecdysone for spermiogenesis of *Mamestra brassicae* may be interesting.

ACKNOWLEDGMENTS

The authors thank Dr. H. Oberlander, USDA, for his critical reading of the manuscript.

REFERENCES

- Ohnishi, E., Mizuno, T., Ikekawa, N. and Ikeda, T. (1981) *Insect Biochem.*, **11**: 155-159.
- Ohnishi, E. (1987) *Zool. Sci.*, **4**: 315-321.
- Loeb, M. J., Woods, C. W., Brandt, T. P. and Borokov, A. B. (1982) *Science*, **218**: 896-898.
- Shimizu, T., Moribayashi, A. and Agui, N. (1985) *Appl. Ent. Zool.*, **20**: 56-61.
- Shimizu, T., and Fukami, J. (1983) *Appl. Ent. Zool.*, **18**: 554-557.
- Shimizu, T., and Yagi, S. (1982) *Appl. Ent. Zool.*, **17**: 385-392.
- Shimizu, T., and Yagi, S. (1978) *Appl. Ent. Zool.*, **13**: 278-282.
- Kambysellis, M. and Williams, C. M. (1971) *Biol. Bull.*, **141**: 541-552.
- Shimizu, T. (1986) *Zool. Sci.*, **3**: 207-209.
- Shimizu, T. (1986) *Zool. Sci.*, **3**: 309-314.
- Gilbert, L. I., Goodman, W. and Bollenbacher, W. E. (1977) "International Review of Biochemistry". Vol. 14, Ed., by Goodwin, T. W., University Press, p. 1.
- Kappler, C., Kabbouh, M., Durst, F. and Hoffman, J. A. (1986) *Insect Biochem.*, **16**: 25-32.



[COMMUNICATION]

Interbreeding Experiments of the Two Forms of *Macrophthalmus japonicus* (Crustacea: Brachyura: Ocypodidae)

KEIJI WADA

*Seto Marine Biological Laboratory, Kyoto University,
Shirahama, Wakayama 649-22, Japan*

ABSTRACT—Virgin females of the two forms of *Macrophthalmus japonicus* were housed separately with males of the same form and males of the opposite form. Ovigerous females occurred in both cases. Eggs of all the females confined with males of the same form developed successfully, whereas eggs of some females with males of the opposite form did not.

INTRODUCTION

Macrophthalmus japonicus (De Haan) is a common ocypodid crab inhabiting intertidal mud flats of the Japanese coast. This species consists of two forms (Forms V and L) which differ conspicuously in male waving displays [1]. Although the two forms are very similar in appearance, differences in some morphological characters have also been described [1]. Furthermore, where the two forms occur sympatrically, pair formation is confined to members of the same form [2], suggesting that premating isolating mechanisms exist. But their separation might also occur because of postmating barriers. Such data are important not only to determine the status of the two forms but also to understand the nature of the isolating mechanisms. In this study, virgin females of each form were confined with males of the same and the opposite forms to determine whether females became ovigerous, and if so, whether their eggs developed successfully.

MATERIALS AND METHODS

In the autumn of 1984 and 1985, small (8–10 mm

in carapace width: CW) immature females of both forms of *Macrophthalmus japonicus* (N=50 Form V; N=42 Form L) were collected from their habitats in Shirahama (33°41' N, 135°22' E). The females of each form were raised in a tank (59 × 98 × 40 cm high) to maturity, isolated from males. In the tank, mud was laid in the depth of 7–10 cm. Sea water continuously dripped from one side of the tank to a drain on the other. No tidal cycle was provided, and light and water temperature were not controlled. For the tank, 18–20 g of assorted fish food "pellet" was scattered over the mud 1 or 2 times a week. When these females became mature as shown by their CW (15.5–22.0 mm, Form V; 12.4–17.9 mm, Form L) and widened abdomen, they were used for experiments. Identification of each form was based upon interform morphological differences shown by Wada [1].

Two series of experiments were carried out: those with Form V females (Apr. 20-Jul. 26, 1985) and those with Form L females (May 9-Jul. 26, 1986). In each series, 2–4 females were kept in each of 5 tanks (each: 30 × 42 × 30 cm high). Males of both forms were collected from their habitats in Shirahama, and 2–3 Form V males (15.7–24.3 mm CW) were kept with females in each of Tanks 1–2 and 2–4 Form L males (16.1–22.2 mm CW) in each of Tanks 3–4. All the males were larger in CW than the smallest crabs observed waving in the field (Shirahama). No male was introduced into Tank 5. Each tank contained a muddy beach, sloping from ca. 15 cm in depth at the rear to ca. 1 cm at the front. Sea water continuously dripped from one side of the tank to a drain on the other. No tidal cycle was provided. Water temperature

Accepted March 1, 1988

Received January 22, 1988

was not controlled, but was measured at intervals of 3–5 days. For each tank, 2–3 g of assorted fish food "pellet" was scattered over the mud 2 times a week. Crabs in the tank were examined once weekly to tally the number of crabs, to measure the CW of each female, and to note whether any females became ovigerous. When females were ovigerous, some eggs of each female were extracted and their developmental stage was determined under a binocular microscope following the procedure adopted by Fukui and Wada [3] as: (1) stage I: newly deposited, filled with yolk; (2) stage II: a yolk-free part present; (3) stage III: eye pigment visible. All the crabs held in tanks could not always be captured. Size differences among females in each tank were larger in the experiment with Form V females than in the experiment with Form L females. Hence, each female in each tank could be specified according to her size in the former experiment, but not in the latter. At the end of the experiment, all the crabs in tanks were captured and their CW were measured.

RESULTS

Monthly values of water temperature in the tank during the experiment were almost the same between 1985 and 1986 (Table 1). Sizes (CW) of the crabs at the start and the end of the experiment were summarized in Table 2. In both series of experiment, sizes of the males were similar between the two forms, with Form V being slightly larger than Form L. Between the two series of

experiment, the CW of the males of the same form was almost the same. The CW of the females did not differ significantly among three groups (Tanks 1–2, Tanks 3–4, and Tank 5) at the start and at the end of both series of experiment (1985 start: $F=0.427$, $P>0.25$; 1985 end: $F=1.684$, $P>0.25$; 1986 start: $F=0.046$, $P>0.25$; 1986 end: $F=0.398$, $P>0.25$).

Form V ovigerous females were found in June and July (Table 3). In June, 2 of 4 females confined with Form V males (Tanks 1–2) and 2 of 4 females confined with Form L males (Tanks 3–4) became ovigerous. Eggs of the former developed to stage II or III, but eggs of the latter remained at Stage I. In July, 3 of 4 females in Tanks 1–2 and 3 of 5 females in Tanks 3–4 bore eggs, and eggs of all the females developed to Stage II or III. None of the females kept isolated from males (Tank 5) became ovigerous.

Form L ovigerous females were found in all of Tanks 1–5 (Table 4). Eggs of females confined

TABLE 1. Sea water temperature ($^{\circ}\text{C}$) in the tank during the experiment period

		N	$\bar{x} \pm \text{SD}$	Range
1985	April	3	18.0 ± 1.0	17.0–19.0
	May	7	20.1 ± 1.5	17.0–21.5
	June	8	23.2 ± 1.6	21.0–25.0
	July	10	26.7 ± 1.1	24.0–28.0
1986	May	9	19.8 ± 1.1	17.9–21.5
	June	11	22.4 ± 1.3	20.1–24.2
	July	8	26.2 ± 1.2	24.3–27.9

TABLE 2. Carapace widths (mm) of the crabs in each of three groups (Tanks 1–2, 3–4 and 5) at the start and the end of the experiment period

		$\hat{\delta}\hat{\delta}$ (Form V)		$\hat{\delta}\hat{\delta}$ (Form L)		$\hat{\sigma}\hat{\sigma}$					
		Tanks 1–2		Tands 3–4		Tanks 1–2		Tanks 3–4		Tank 5	
		N	$\bar{x} \pm \text{SD}$	N	$\bar{x} \pm \text{SD}$	N	$\bar{x} \pm \text{SD}$	N	$\bar{x} \pm \text{SD}$	N	$\bar{x} \pm \text{SD}$
1985 ($\hat{\sigma}\hat{\sigma}$: Form V)											
Apr. 20		6	20.0±3.2	6	17.0±1.9	4	17.1±2.2	4	17.6±1.1	2	16.4±0.2
Jul. 26		5	24.5±0.6	7	21.5±1.4	4	22.2±0.9	4	22.9±0.3	2	23.2±1.0
1986 ($\hat{\sigma}\hat{\sigma}$: Form L)											
May 9		4	20.1±1.3	4	18.2±1.5	6	14.9±0.8	6	15.0±1.4	3	14.8±0.7
Jul. 26		5	22.4±1.1	4	20.2±1.4	7	17.4±0.8	6	17.9±0.9	4	17.7±1.1

TABLE 3. Results of experiments with Form V females

		Date																
Tank	Crabs	Apr.	May		June							Jul.						
		20	7	8	21	22	29	7	8	14	22	27	30	5	12	19	26	
1	V♂♂	3				3		3		3	3		3	3	3	3	3	
	♀♀1	N	N			N		I		II	III		N	I	II	N	N	
	♀♀2	N	N			N		N		I	II		N	I	II	N	N	
2	V♂♂	3	2		3	3		2		2	2		2	2	2	2	2	
	♀♀3	N	N			N		N		N	N		N	N	N	N	I	
	♀♀4								N	N	N		I	II	III	N	N	
3	L♂♂	3				3		3		3	3		3	3	3	3	3	
	♀♀5	N	N			N		N		N	I		N	N	D			
	♀♀6	N	N			N		N		N	N		N	I	II	III	N	
4	♀♀7															N	N	
	L♂♂	3	2		3	3		4		4	4		4	4	4	4	4	
	♀♀8	N	N			N		N		N	N		N	N	I	III	N	
5	♀♀9	N	N			N		I		I	I		N	I	I	III	N	
	♀♀10	N				N	N											
	♀♀11	N		D														
	♀♀12								N	N	N	D						
	♀♀13									N	N		N	N	N	N	N	
	♀♀14											N	N	N	N	N	N	

Sequential changes in ovigerous conditions of each female and in the number of males found in each tank are shown. I, II and III represent bearing eggs of Stages I, II and III, respectively. For details of Stages I-III, see text. N: non-ovigerous; D: death.

TABLE 4. Results of experiments with Form L females

Tank	Crabs	Date												
		May			June				Jul.					
		9	23	31	7	9	14	21	24	28	5	13	19	26
1	V♂♂	2	2	2	2		2	1		3	3	3	3	3
	♀♀N	3	2	2	2	1	3	2	2	3	4	2	3	2
	I							1		1				
2	V♂♂	2	2	2	2		2	2		2	2	2	2	2
	♀♀N	3		2	3		2	1	1	2	3	4	4	5
	I		1					1						
3	L♂♂	2	1	2	2		2	2		2	2	2	2	2
	♀♀N	3	3	1	1		1	1			2	2	3	2
	I			1				1		1		1		1
4	II				1									
	III						1				1			
	L♂♂	2	2	2	2		2	2		2	2	1	2	2
	♀♀N	3	2	3	2		2		1	1	1	1	1	1
	I				1			1				1		2
5	II									1			2	
	III									1	2			
	♀♀N	3	2	3	1	3	4	2	1	4	3	4	1	3
	I											1	1	

Sequential changes in the number of ovigerous and non-ovigerous females and males found in each tank are shown. I, II, III and N are the same as in Table 3.

with Form L males (Tanks 3-4) exhibited Stage I in 10 cases, Stage II in 4 cases and Stage III in 5 cases, whereas eggs of females confined with Form V males (Tanks 1-2) were at stage I in all 4 cases. In Tank 5 only one female became ovigerous, with its eggs remaining at Stage I.

DISCUSSION

Some of Form L females confined with Form V males became ovigerous, and all of their eggs remained at Stage I. This is in contrast with the case of Form L females with males of the same form, in which the eggs in all Stages I-III were recognized. Also, Form V females confined with Form L males became ovigerous, but in 2 of the 5 cases their eggs did not develop beyond Stage I, whereas all ovigerous Form V females with males of the same form had eggs which developed to Stage II or III. These results show that even when the two forms are forced to pair, they are reproductively isolated from each other to a certain degree, confirming that they are distinct species.

Inviability of eggs of the females exposed to males of the different form may result because: (1) copulation and insemination did not occur; (2) insemination occurred but sperm were immobilized or rendered inviable before fertilization; or (3) development of fertilized eggs ceased. Compared with the females isolated from males (Tank 5), the females kept with males of the different form became ovigerous with more frequency. It is improbable that egg extrusion by females is induced by interactions with males other than copulation. Hence copulation and insemination probably occurred between the sexes of different

forms, though I never observed copulations during the course of experiment. If so, postmating isolating mechanisms such as (2) or (3) above, may be responsible for differences in egg development.

On the other hand, some of Form V females that mated with Form L males bore eggs which successfully developed to Stage III, though the eggs of Form L females that mated with Form V males never developed beyond Stage I. This fact means that postmating reproductive isolation between the two forms is incomplete, to the extent that one cross (Form V female x Form L male) might result in viable hybrids. To determine the nature of reproductive isolation in more detail, it is necessary to investigate the survival [4] and fertility [5, 6] of the hybrids.

ACKNOWLEDGMENTS

Messrs. C. Araga, M. Ohta and Y. Fukui helped raise crabs, for which I am most grateful. Critical comments on earlier drafts were provided by Drs. M. Salmon and E. Harada. This work was supported in part by a Grant-in-Aid for Special Project Research on Biological Aspects of Optimal Strategy and Social Structure from the Japan Ministry of Education, Science and Culture.

REFERENCES

- 1 Wada, K. (1978) *Publ. Seto Mar. Biol. Lab.*, **24**: 327-340.
- 2 Wada, K. (1984) *J. Ethol.*, **2**: 7-10.
- 3 Fukui, Y. and Wada, K. (1986) *Mar. Ecol. Prog. Ser.*, **30**: 229-241.
- 4 Salmon, M., Hyatt, G., McCarthy, K. and Costlow, J. D. Jr. (1978) *Z. Tierpsychol.*, **48**: 251-276.
- 5 Lucas, J. S. (1970) *J. Zool., Lond.*, **160**: 267-278.
- 6 Salmon, M. and Hyatt, G. W. (1979) *Mar. Behav. Physiol.*, **6**: 197-209.

[COMMUNICATION]

**Effects of Thyroid and Gonadal Hormones *in vitro*
on Hepatic Succinate Dehydrogenase Activity
of the Teleost, *Anabas testudineus* (Bloch)**

M. C. SUBASH PETER and OOMMEN V. OOMMEN

*Department of Zoology, University of Kerala, Kariavattom,
Trivandrum 695 581, India*

ABSTRACT—Administration of L-thyroxine (T_4) or triiodo-L-thyronine (T_3) *in vitro* significantly stimulated succinate dehydrogenase (SDH) activity at 1 and 10 μ M concentrations and inhibited it at 100 μ M concentration. Addition of T_4 or T_3 to mitochondria isolated from thiouracil-treated specimens produced a stimulation of SDH activity only at 100 μ M concentration. The addition of 1 and 100 μ M testosterone into the reaction mixture caused significant increase in hepatic SDH activity and that of estradiol-17 β inhibited the enzyme activity significantly. It was observed that T_3 -stimulated or testosterone-induced hepatic SDH activity was prevented by both protein synthesis inhibitors when added together. It is suggested that thyroid and gonadal hormones influence the activity of this oxidative enzyme in *Anabas testudineus* by a mechanism sensitive to the action of actinomycin D or chloramphenicol.

INTRODUCTION

It has been recently reported that in some lower vertebrates thyroid and gonadal hormones influence the oxidative metabolism by altering the enzyme activity [1-4]. However, very little is known about the role of these hormones on oxidative metabolism in fishes [5, 6]. Currently it has been reported in *Anabas testudineus* that administration of T_3 *in vivo* stimulated the activities of cytochrome oxidase and α -glycerophosphate dehydrogenase and thereby the oxidative metabolism [3]. However, T_3 administration *in vivo* was not reported to influence hepatic SDH activity in the previous study. Peter and Oommen observed a

stimulatory effect of oxidative metabolism in *Anabas* by the administration of testosterone *in vivo*, but the hepatic SDH activity was found unaltered (unpublished data). They also found that estradiol-17 β administration in *Anabas* inhibited hepatic SDH activity, despite the increased mitochondrial respiration. SDH is a marker enzyme of Krebs's cycle and its activity indicates the level of oxidative metabolism. Therefore, in order to find out direct effects of thyroid and gonadal hormones on hepatic mitochondrial enzymes, we have investigated the effects of these hormones *in vitro* with or without protein synthesis inhibitors on hepatic SDH activity in *Anabas testudineus*, as most of the actions of thyroid and steroid hormones are reported to be due to the stimulated synthesis of the particular enzymatic proteins [7, 8].

MATERIALS AND METHODS

Healthy adult fish weighing 40 ± 5 g were used for the present study, which were fed with fish feed every other day. Two sets of experiments were conducted. The first set comprised four groups of fish having six each. The first three groups comprised female and the fourth group comprised male fish only. The fish were sacrificed by decapitation and the liver tissue was excised. The chilled liver was weighed, homogenised and centrifuged in Beckman J2 21 centrifuge at 4°C to isolate mitochondria [9]. Mitochondrial fraction obtained was washed twice and suspended in 0.25 M sucrose

solution. The purity and structural integrity of mitochondrial preparations were tested by assaying p/o ratio and a value of 1.6 ± 0.2 was obtained, when succinate was used as substrate. Mitochondria were isolated from all groups of normal fish and from the second group which was pretreated with thiouracil, an antithyroidal drug (1 mg i. p. over 15 days).

The second set of experiment comprised three groups of fish. First and third groups were females and second group comprised males. Mitochondria prepared from the first group were treated with 2 μ g actinomycin D or 4 μ g chloramphenicol (Sigma Chemical Co., USA) alone or with 1 μ M T_3 . Mitochondria from the second group were treated with 2 μ g actinomycin D or 4 μ g chloramphenicol alone or with 1 μ M testosterone. Mitochondria prepared from the third group were treated with the same dose of inhibitors alone or with 5 μ M estradiol-17 β . Doses of hormones were selected from the previous studies.

The activity of SDH was assayed spectrophotometrically using phenazine methosulphate and 2, 6 dichlorophenolindophenol as electron acceptors in a B and L Spectronic 2000 spectrophotometer at 25°C [10]. The assay reaction mixture contained 100 μ mol KH_2PO_4 (pH 7.6), 3 μ mol KCN, 0.75 μ mol $CaCl_2$, 0.04 μ mol succinate and 1 mg PMS in a total volume of 3 ml. Different concentrations viz., 1.0, 10 and 100 μ M of T_4 , T_3 , and testosterone (Sigma Chemicals Co., USA) and 0.5, 5 and 50 μ M concentrations of estradiol-17 β (Ovocyclin, CIBA-GEIGY, Bombay) were added to the reaction mixture. Mitochondria of around 0.5 mg protein were allowed to incubate with the hormone for 1 min and the decrease in absorbance was measured at 600 nm after adding the reaction mixture. Proper control experiments were also done with hormone vehicles as well as drug vehicles. The specific activity of SDH was expressed as μ mol DCIP reduced/min/mg mitochondrial protein. Protein was estimated by Biuret reaction [11]. Statistical analysis of the data done by one way classification of analysis of variance [12].

RESULTS AND DISCUSSION

Addition of 1 μ M and 10 μ M concentrations of

T_3 or T_4 , *in vitro*, significantly stimulated SDH activity of normal liver mitochondria. However, 100 μ M concentrations of both the hormones inhibited hepatic SDH activity (Fig. 1). It may be suggested that *in vitro* administration of low doses of thyroid hormones stimulate SDH activity despite its unaltered activity by *in vivo* administration as reported previously [3]. It has been known that hormone doses higher than the circulating levels are necessary for eliciting the thyroid hormone-mediated responses in fishes [5]. Therefore, the low doses of hormones used in the present study seem to be physiological. The inhibitory effect observed by 100 μ M dose may be due to the high concentration of hormones. It is interesting to note that, when comparing the effects of thyroid hormones on SDH and other enzyme activities studied earlier [3], T_3 is more potent than T_4 as has been reported earlier in fishes [13]. Though the SDH activity of mitochondria prepared from thiouracil-treated specimens showed little effect with 1 and 10 μ M T_3 or T_4 , the enzyme activity was found significantly stimulated at 100 μ M concentration (Fig. 2). This suggests that the stimulation of SDH activity in the mitochondria may be achieved only by high concentrations of thyroid hormones in

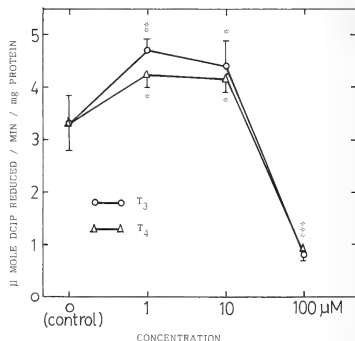


Fig. 1. Effects of T_3 and T_4 *in vitro* on normal hepatic mitochondrial SDH activity. The control reaction mixture was added with equal volume of hormone vehicle (alkaline saline, pH 9.0) For details of reaction mixture contents see Materials and Methods. * $P < 0.05$, ** $P < 0.005$, *** $P < 0.001$.

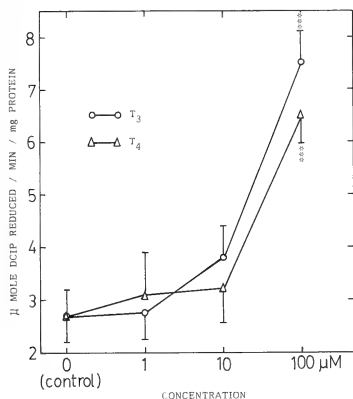


FIG. 2. Effects of T_3 and T_4 *in vitro* on SDH activity of hepatic mitochondria which were isolated from thiouracil-treated (chemically thyroidectomised) fish. The control reaction mixture was added with equal volume of hormone vehicle (alkaline saline, pH 9.0). For details of reaction mixture contents see Materials and Methods. *** $P < 0.001$.

thiouracil-treated specimens which were deprived of thyroid hormones due to chemical thyroidectomy. This has been reported in the case of a reptile, where high doses of thyroid hormones were required to produce the effects *in vivo*, if injected into the thyroidectomised lizards [4]. Peter and Oommen observed that thyroid hormones or thiouracil treatment *in vivo* have produced no change in hepatic SDH activity in *Anabas* (unpublished data). Therefore, the present study helps to suggest the possibility that thyroid hormones significantly stimulate the activity of hepatic SDH and thereby oxidative metabolism *in vitro* in *Anabas*, since mitochondrion has been considered as a possible subcellular locus of thyroid hormone action in view of the crucial role of the mitochondria in energy metabolism [14]. The earlier reports on the administration of T_3 *in vivo* on hepatic SDH activity in *Anabas* [3] and the present *in vitro* observations on hepatic SDH activity are found to be consistent with the suggestion that the mechanism of action of hor-

mones *in vitro* and *in vivo* may not be the same as a few workers have reported the significant differences between the two [15]. Therefore, it can be assumed that there is some kind of discrepancy existing between the *in vitro* and *in vivo* action of the same hormone in fish.

It has been observed that 1 and 100 μM concentrations of testosterone produced significant stimulation on the hepatic SDH activity (Fig. 3) suggesting the stimulatory effect of testosterone *in vitro* on hepatic oxidative metabolism, though a decrease in activity was observed at 10 μM concentration level. The observed decrease in SDH activity at 1 min time by 10 μM testosterone concentration could probably be due to a dose-dependent effect of hormone, since the inhibition was recovered to a stimulation after a long incubation of 5 min time (data not shown). It appears that testosterone administration *in vitro* stimulates hepatic oxidative metabolism in *Anabas* despite its lack of effect on hepatic SDH activity, when administered *in vivo* (unpublished data). It has been reported that administration of testoster-

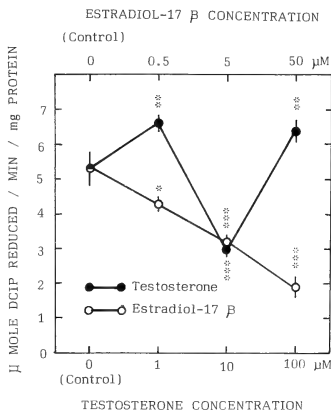


FIG. 3. Effects of various concentrations of testosterone and estradiol-17 β *in vitro* on hepatic mitochondrial SDH activity. The control reaction mixture was added with equal volume of hormone vehicle (ethanol). For details of reaction mixture contents see Materials and Methods. * $P < 0.05$, *** $P < 0.001$.

one *in vitro* stimulated oxidative metabolism in isolated tissues of a reptile *Calotes versicolor*, which was found to be temperature dependent [16].

It was observed in the present study that T_3 -induced stimulation in the activity of hepatic SDH was prevented by $2 \mu\text{g}$ actinomycin D or $4 \mu\text{g}$ chloramphenicol, when compared to drug-treated controls, indicating that thyroid hormone-induced oxidative metabolism *in vitro* in *Anabas* might be brought about by increased protein synthesis at the mitochondrial level. In the absence of T_3 , addition of actinomycin D, while significantly inhibited SDH activity, that of chloramphenicol had no effect (Fig. 4). This observation confirms our

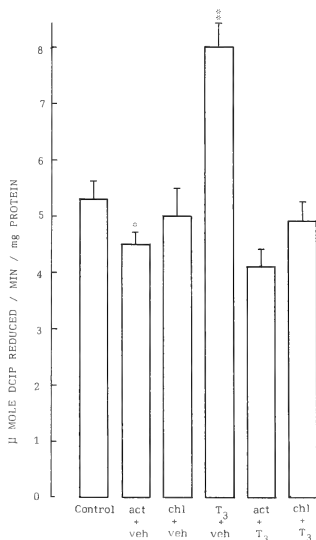


Fig. 4. Effects of actinomycin D and chloramphenicol with or without T_3 *in vitro* on hepatic mitochondrial SDH activity. The control reaction mixture received drug vehicle (ethanol plus distilled water) as well as hormone vehicle (alkaline saline, pH 9.0). act = actinomycin D, $2 \mu\text{g}/\text{assay}$; T_3 , $1 \mu\text{M}/\text{assay}$; veh = vehicle; chl = chloramphenicol, $4 \mu\text{g}/\text{assay}$. For details of reaction mixture contents see Materials and Methods. * $P < 0.05$, ** $P < 0.005$.

earlier report that *in vivo* administration of actinomycin D inhibited and chloramphenicol produced no effect on hepatic SDH activity in *Anabas* [17]. This could be probably due to the discrepancy in potential capacity of both the inhibitors to inhibit protein synthesis, as chloramphenicol prevents the mitochondrial peptidyl transfer at the level of translation, while actinomycin D inhibits protein synthesis at the transcriptional and translational levels.

It was also noticed that testosterone-stimulated increase in hepatic SDH was prevented by the inhibitors when compared to the drug-treated controls (Fig. 5). Therefore, it can be suggested that in *Anabas* also the primary site of thyroid and gonadal steroid hormone action could be at the genetic transcriptional levels as evidenced by the inhibition of hormone-induced enzyme activity by actinomycin D. Chloramphenicol, when administered with estradiol- 17β prevented the estradiol-inhibited hepatic SDH activity. It is presumed that protein synthesis inhibitors prevented the action of

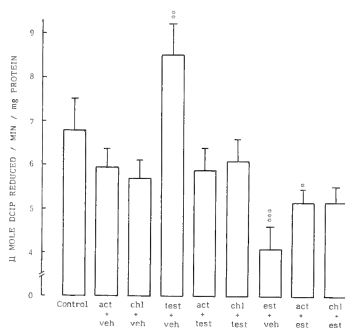


Fig. 5. Effects of actinomycin D and chloramphenicol with or without testosterone or estradiol- 17β *in vitro* on hepatic mitochondrial SDH activity. The control reaction mixture was added with equal volume of drug vehicle (ethanol plus distilled water) as well as hormone vehicle (ethanol). act = actinomycin D, $2 \mu\text{g}/\text{assay}$; chl = chloramphenicol, $4 \mu\text{g}/\text{assay}$; test = testosterone, $1 \mu\text{M}$; est = estradiol- 17β , $5 \mu\text{M}$; veh = vehicle. For details of reaction mixture contents see Materials and Methods. * $P < 0.05$, ** $P < 0.005$, *** $P < 0.001$.

estrogen as has been reported earlier in rat [18].

The present study for the first time at the mitochondrial level clearly demonstrate in a teleostean fish that T_3 - or testosterone-stimulated oxidative metabolism *in vitro* could be due to a mechanism sensitive to the action of actinomycin D and chloramphenicol as evidenced by the suppression of T_3 - or testosterone-stimulated hepatic SDH activity by these protein synthesis inhibitors.

ACKNOWLEDGMENTS

We are grateful to the Ministry of Science and Technology, New Delhi (Scheme HCS/DST/1110/81) for financial assistance and the Head, Dept. of Zoology, University of Kerala, for laboratory facilities.

REFERENCES

- Oommen, O. V. (1980) J. Anim. Morphol. Physiol., **27**: 124-131.
- Oommen, O. V. (1981) Comp. Physiol. Ecol., **6**: 95-98.
- Peter, M. C. S. and Oommen, O. V. (1987) J. Reprod. Biol. Comp. Endocrinol., **7**: 53-60.
- Oommen, O. V. and Sreedevamma, K. K. (1988) Gen. Comp. Endocrinol., **69**: 391-398.
- Plisetskaya, E., Woo, N. Y. S. and Murat, J. C. (1983) Comp. Biochem. Physiol., **74**: 179-187.
- Matty, A. J. and Lone, K. P. (1983) In "Fish Energetics: New Perspectives". Ed. by P. Tytler and P. Calow, Croom Helm, London, pp. 185-209.
- Gorbman, A. (1978) In "The Thyroid Gland". Ed. by S. C. Werner and S. H. Ingbar, Harper and Row, Maryland, pp. 22-30.
- Litwack, G. and Singer, S. (1972) In "Biochemical Actions of Hormones". Ed. by G. Litwack, vol. II, Academic Press, New York, pp. 114-165.
- Johnson, D. and Lardy, H. (1967) Meth. Enzymol., **10**: 694-696.
- Arrigoni, O. and Singer, T. P. (1962) Nature, **193**: 1256-1258.
- Gornall, A. G., Bardwill, C. J. and David, M. M. (1949) J. Biol. Chem., **177**: 751-766.
- Snedecor, G. W. and Cochran, W. G. (1967) Statistical Methods. Oxford and IBH Publishing Company, Bombay.
- Leloup, J. and Luze, A. D. (1985) In "The Endocrine System and the Environment". Ed. by B. K. Follett., S. Ishii and A. Chandola, Springer Verlag, Berlin, pp. 23-32.
- Sterling, K. (1979) New Engl. J. Med., **300**: 117-123.
- Gordon, A., Surks, M. I. and Oppenheimer, J. H. (1973) Acta Endocrinol., **72**: 684-696.
- Oommen, O. V. (1985) Indian J. Comp. Anim. Physiol., **3**: 9-11.
- Oommen, O. V. and Peter, M. C. S. (1987) Physiologist, **30**: 127.
- Ui, H. and Mueller, G. C. (1963) Proc. Natl. Acad. Sci. USA, **50**: 256-260.

[COMMUNICATION]

Lack of Influence of Photoperiod on the Brood Interval of the Guppy (*Poecilia reticulata*)

ANGUS D. MUNRO

*Department of Zoology, The National University,
Kent Ridge, Singapore 0511*

ABSTRACT—Domesticated and feral female guppies were isolated under a variety of photoperiods (3L21D, 8L16D, 12L12D, 16L8D and 24L0D), and the time interval between two successive parturitions recorded. Contrary to earlier reports, there was no evidence for an inverse relationship between photoperiod and the brood interval.

INTRODUCTION

Annual changes in daylength have been implicated in the regulation of seasonal breeding in several species of teleosts (reviewed by [1-3]), including some species of live-bearing poeciliids (e.g. [4]; reviewed by [5]).

In the case of poeciliids, the time interval between successive broods (brood interval) has been found to change with season, being shortest in summer [6, 7], and it has been suggested that this is in response to changes in photoperiod. Thus, Scrimshaw [8] reports that the brood interval may be "as low as 21 days" in guppies kept under constant light, compared to the usual of "30 days or more"; although he considered that superfoetation occurred at such short brood intervals, this was apparently solely on the basis of the dissection of pregnant females rather than the pattern of their births [9]. Subsequently, Kujala [10] also reported that long daylengths (18L6D) reduced the brood interval; furthermore, he noted that the fry were born prematurely under these long photoperiods.

A survey of published data suggests a linear negative relationship between daylength and duration of the brood interval (reviewed by [5]). Such an effect is difficult to explain using any of the accepted photoperiodic-clock mechanisms (hour-glass or resonance models, for example). This suggests that, if the brood interval is indeed directly dependent upon photoperiod, then a novel control mechanism would have to be modelled to explain such a relationship between the reported brood intervals and photoperiod [5].

In view of the scattered observations of previous reports, the present study aimed to systematically investigate any apparent relationship between brood interval and daylength using a wider range of photoperiods. Factors other than photoperiod have been shown to influence the duration of the brood interval in poeciliids, and thus must be taken into consideration when designing an experiment. Commercially-bred guppies have been subject to a relatively large number of generations of artificial selection; hence females from a feral population, first introduced to Singapore about fifty years ago [11], have also been examined. Apart from genetic influences [12] and temperature [13], the nutritional status of the mother has also been found to influence the brood interval: poor food supplies prolong the brood interval, apparently through retarding oocyte recruitment [12-14].

MATERIALS AND METHODS

Pregnant red-tailed blonde guppies were pur-

Accepted May 18, 1988

Received April 5, 1988

chased from Ang Brothers' Fish Farm (Chua Chu Kang Rd., Singapore), and feral females caught from a stream near Thomson Rd., Singapore. The fish were individually isolated in glass jars containing approximately 3 litres of 20% artificial sea-water supplemented with vitamins (SeaVita; Waterlife Research Ltd., Heathrow, U.K.). The jars were placed in basins of water maintained at 26–27°C by electric heaters, and kept under natural photoperiod (12L12D) using 40 W fluorescent tubes suspended 40 cm above. The fish were fed once daily *ad libitum* with a commercial flake food and partial water changes were made at regular intervals.

The fish were checked twice daily for births. As soon as a female was found to have given birth, she was transferred to one of the five photoperiods tested (3L21D, 8L16D, 12L12D, 16L8D or 24L0D); again, the jars were kept in heated baths in a light-tight chamber provided with a 40 W fluorescent tube. An appropriate (red-tailed blonde or feral) male was generally placed in with each female for four to seven days following each birth: the presence or absence of a male at this time was subsequently found to have no effect on

brood interval. The fish were again checked twice daily for births, except for those under 3L21D which were only checked once daily, during 'lights on', when they and the other groups were also fed and maintained.

RESULTS

'Control' fish, kept under 12L12D, showed a broad range of brood intervals: 22 to 32 days for red-tailed blondes and 23 to 36 days for feral guppies (Fig. 1). The frequency distribution of brood intervals for the 12L12D treatment showed no significant departure from normality ($P > 0.05$: Kolmogorov-Smirnov one-sample test [15]) for either red-tailed blonde or feral guppies.

The four other photoperiods tested did not influence (t-test: $P > 0.10$ for all comparisons) the duration of the brood interval of either red-tailed blonde or feral guppies (Table 1). Again, the pooled data (i.e. for all photoperiod regimes) showed no significant departure from normality ($P > 0.05$: Kolmogorov-Smirnov one-sample test) for either type guppy.

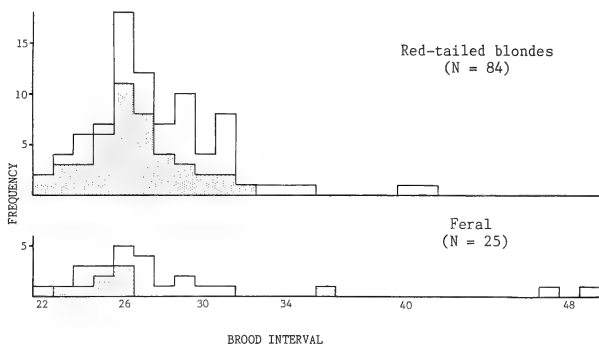


FIG. 1. Frequency distribution of brood intervals for the pooled data for all photoperiods for red-tailed blonde (above) and feral guppies (below); in each case, the stippled area shows the results for the control (12L12D) group alone.

TABLE 1. The brood intervals of guppies kept under different photoperiods

	Photoperiod	Interval between broods	
		Mean \pm S.D.; range (N)*	
Red-tailed blondes	3L21D	28.7 \pm 2.8;	23-31 (9)
	8L16D	27.5 \pm 2.1;	25-31 (12)
	12L12D	26.5 \pm 2.2;	22-32 (46)
	16L 8D	31.0 \pm 5.9;	24-41 (9)
	24L 0D	29.1 \pm 3.9;	24-35 (8)
	Overall	27.8 \pm 4.2;	22-41 (84)
Feral	3L21D	26.8 \pm 3.1;	24-31 (4)
	8L16D	27.5 \pm 2.6;	24-30 (4)
	12L12D	26.4 \pm 4.0;	23-36 (8)
	16L 8D	26.6 \pm 2.7;	22-29 (5)
	24L 0D	37.5 \pm 12.2;	26-49 (4)
	Overall	28.4 \pm 6.7;	22-49 (25)

*(N)=number of guppies tested

DISCUSSION

At 12L12D, the lengths of the brood intervals of feral and cultured females are similar, although relatively variable. The observed variability is consistent with the figures given by several other workers (e.g. [7, 10]), and is presumably a consequence of variability in the timing of fertilisation of the eggs, rather than in the development rates of the individual embryos ([13], Munro *et al.*, unpublished). However, there was no evidence for a positive-skewing of the pattern of births, such as was found by Snelson *et al.* [13] in *Poecilia latipinna*; the present results, showing a normal distribution of brood intervals, are thus in agreement with other reports for *P. reticulata* [7, 16].

There was no evidence in the present study for a inverse relationship between photoperiod and the length of the first experimental brood interval in either feral or a cultured variety of guppy. From the more limited data available, this also applies to the second and third cycles in red-tailed blondes, where there is a close correlation with the duration of the first cycle under a given photoperiod (Munro, unpublished). The failure of both cultured (red-tailed blonde) and feral guppies to show

a photoperiodic response suggests that the present negative results are not an artefact of artificial selection.

The failure to demonstrate an effect of photoperiod stands in contrast to the findings of Scrimshaw [8] and Kujala [10], who both report that long photoperiods lead to the early birth of premature fry. The cause of this disparity is not apparent: the only obvious difference between these earlier studies and the present one is that the female guppies used here were kept in 33% seawater rather than freshwater. There would appear to be no published studies on the effect of salinity on the duration of gestation, so that one possibility is that increased salinity may over-ride any effects of photoperiod. Whilst other workers have noted that the brood interval tends to be shorter in summer in poeciliids, they do not state whether the difference is statistically significant; and they either provide little information about holding conditions [6, 7], or else maintained the fish under constant laboratory conditions of photoperiod and temperature [17]. In such cases, other external factors may be involved—for example, food quantity or quality [12-14].

ACKNOWLEDGMENTS

I would like to thank the National University for its financial support (RP123/84); and two anonymous referees for their constructive comments.

REFERENCES

- 1 de Vlaming, V. L. (1972) *J. Fish Biol.*, **4**: 131-140.
- 2 Lam, T. J. (1983) In "Fish Physiology", Vol. 9B. Ed. by W. S. Hoar, D. J. Randall and E. M. Donaldson, Academic Press, New York, pp. 65-116.
- 3 Munro, A. P. Scott, A. P. and Lam, T. J. (1989) Environmental Control of Teleost Reproduction. CRC Press, Boca Raton, in press.
- 4 Nishi, K. (1981) *Bull. Fac. Fish. Hokkaido Univ.*, **32**: 211-220.
- 5 Munro, A. D. (1989) In [3].
- 6 Turner, C. L. (1937) *Biol. Bull.*, **72**: 145-164.
- 7 Rosenthal, H. L. (1952) *Biol. Bull.*, **102**: 30-38.
- 8 Scrimshaw, N. S. (1944) *Copeia*, **1944**: 180-183.
- 9 Rosenthal, H. L. (1955) *Copeia*, **1955**: 52-53.
- 10 Kujala, G. A. (1978) *Gen. Comp. Endocrinol.*, **36**: 286-296.
- 11 Alfred, E. R. (1966) *Zool. Verhandl.*, **78**: 1-68.
- 12 Reznick, D. N. (1980) Ph. D. Thesis, Univ. Pennsylvania, Philadelphia.
- 13 Snelson, F. F., Wetherington, J. D. and Large, H. L. (1986) *Copeia*, **1986**: 295-304.
- 14 Thibault, R. E. and Schultz, R. J. (1978) *Evolution*, **32**: 320-333.
- 15 Sokal, R. R. and Rohlf, F. J. (1969) *Biometry*. W. H. Freeman, San Francisco.
- 16 Reznick, personal communication cited in [12].
- 17 Billard, R. and Breton, B. (1981) *Cah. Lab. Montereau*, **12**: 43-56.

INSTRUCTIONS TO AUTHORS

ZOOLOGICAL SCIENCE publishes contributions, written in English, in the form of (1) Reviews, (2) Articles, and (3) Communications of material requiring prompt publication. A *Review* is usually invited by the Editors. Those who submit reviews should consult with the Editor-in-Chief or the Managing Editor in advance. *Articles* of less than 6 printed pages and *Communications* less than 3 printed pages will be published free of charge. Charges will be made for extra pages (7,000 yen/page). A *Communication* cannot exceed 4 printed pages. No charge will be imposed for invited reviews up to 15 printed pages. No free reprints of Articles and Communications are available. To the author of an invited review 50 reprints are provided gratis. Submission of papers from nonmembers of the Society is welcome. However, page charges (7,000 yen/page) will be made to nonmembers.

A. SUBMISSION OF MANUSCRIPT

The manuscript should be submitted in triplicate, one original and two copies, each including all illustrations. Rough copies of line drawings and graphs may accompany the manuscript copies, but the two copies of continuous-tone prints (photomicrographs, etc.) should be as informative as the original. The manuscript should be sent to:

Dr. CHITARU OGURO, Managing Editor,
ZOOLOGICAL SCIENCE, Department of Biology,
Faculty of Science, Toyama University,
Toyama 930, Japan.

B. CONDITIONS

All manuscripts are subjected to editorial review. A manuscript which has been published or of which a substantial portion has been published elsewhere will not be accepted. It is the author's responsibility to obtain permission to reproduce illustrations, tables, etc. from other publications. Accepted papers become the permanent property of ZOOLOGICAL SCIENCE and may not be reproduced by any means, in whole or in part, without the written consent of both the Zoological

Society of Japan and the author(s) of the article in question.

C. ORGANIZATION OF MANUSCRIPT

The desirable style of the organization of an original paper is as follows: (1) Title, Author(s) and Affiliation (2) Abstract (3) Introduction (4) Materials and Methods (5) Results (6) Discussion (7) Acknowledgments (8) References (9) Tables (10) Illustrations and Legends (11) Footnotes. The author is not obliged to adhere rigidly to this organization. He or she may modify the style when such modification makes the presentation clearer and more effective. In a Communication, combination of some of these sections is recommended. There is no restriction on the style of review articles.

D. FORM OF MANUSCRIPT

Manuscripts should be typewritten and double spaced throughout on one side of white type-writing paper with 2.5 cm margins on all sides. Abstract not exceeding 250 words, tables, figure legends and footnotes should be typed on separate sheets. All manuscript sheets must be numbered successively. The use of footnotes to the text is not recommended.

1. Title page

The first page of manuscript should contain title, authors' names and addresses of university or institution, abbreviated form of title (40 characters or less, including spaces), and name and address for correspondence. Authors with different affiliations should be identified by the use of the same superscript on name and affiliation. If one or more of the authors has changed his or her address since the work was carried out, the present address(es) to be published should be indicated in a footnote. In addition, a sub-field of submitted papers to be used as heading of an issue may be indicated in the first page. Authors are encouraged to choose one of the following: physiology, cell biology, molecular biology, genetics, immunology, biochemistry, developmental biology, reproductive biology,

endocrinology, behavior biology, ecology, phylogeny, taxonomy, or others (specify). However, the Editors are responsible for the choice and arrangement of headings.

2. Introduction

This section should clearly describe the objectives of the study, and provide enough background information to make it clear why the study was undertaken. Lengthy reviews of past literature are discouraged.

3. Materials and Methods

This section should provide the reader with all the information that will make it possible to repeat the work. For modification of published methodology, only the modification needs to be described with reference to the source of the method.

4. Results

Results should be presented referring to tables and figures, without discussion.

5. Discussion

The Discussion should include a concise statement of the principal findings, a discussion of the validity of the observations, a discussion of the findings in the light of other published works dealing with the same subject, and a discussion of the significance of the work. Redundant repetition of material in Introduction and Results, and extensive discussion of the literature are discouraged.

6. Statistical analysis

Statistical analysis of the data using appropriate methods is mandatory and the method(s) used must be cited.

7. References

References should be cited in the text by an Arabic numeral in square parentheses and listed at the end of the paper in numerical order. For example:

- 1 Takewaki, K. (1931) Oestrus cycle of female rat in parabiotic union with male. *J. Fac. Sci. Imp. Univ. Tokyo, Sec. IV*, 2: 353-356.
- 2 Shima, A., Ikenaga, M., Nikaido, O., Takabe, H. and Egami, N. (1981) Photoreactivation of ultraviolet light-induced damage in cultured fish cells as revealed by increased colony forming ability and decreased content of pyrimidine dimers. *Photochem. Photobiol.*, 33: 313-316.
- 3 Hubel, O. and Wiesel, T. N. (1986) The

functional architecture of the striated cortex. In "Physiological and Biochemical Aspects of Nervous Integration". Ed. by F. D. Carlson, Prentice-Hall, New Jersey, pp. 153-161.

- 4 Campbell, R. C. (1974) *Statistics for Biologists*. Cambridge Univ. Press, London, 2nd ed., pp. 59-61.

Titles of cited papers may be omitted in Reviews and Communications. The source of reference should be given following the commonly accepted abbreviations for journal titles (e.g., refer to 'International List of Periodical Title Abbreviations'). The use of "in preparation", "submitted for publication" or "personal communication" is not allowed in the reference list. "Unpublished data" and "Personal communication" should appear parenthetically following the name(s) in the text. Text citations to references with three or more authors should be styled as, e.g., Everett *et al.* [7].

E. ABBREVIATIONS

Abbreviations of measurement units, quantity units, chemical names and other technical terms in the body of the paper should be used after they are defined clearly in the place they first appear in the text. However, abbreviations that would be recognized by scientists outside the author's field may be used without definition, such as SD, SE, DNA, RNA, ATP, ADP, AMP, EDTA, UV, and CoA. The metric system should be used for all measurements, and metric abbreviations (Table)

Table. Abbreviations for units of measure which may be used without definition

Length:	km, m, cm, mm, μ m, nm, pm, etc.
Area:	km^2 , m^2 , cm^2 , mm^2 , μm^2 , nm^2 , pm^2 , etc.
Volume:	km^3 , m^3 , cm^3 , mm^3 , μm^3 , nm^3 , pm^3 , kl, liter (always spellout), ml, μ l, nl, etc.
Weight:	kg, g, mg, μ g, ng, pg, etc.
Concentration:	M, mM, μ M, nM, %, g/l, mg/l, μ g/l, etc.
Time:	hr, min, sec, msec, μ sec, etc.
Other units:	A, W, C, atm, cal, kcal, R, Ci, cpm, dB, v, Hz, lx, \times g, rpm, S, J, IU, etc.

should, in general, be expressed in lower case without periods.

F. PREPARATIONS OF TABLES

Tables should only include essential data needed to show important points in the text. Each table should be typed on a separate sheet of paper and must have an explanatory title and sufficient explanatory material. All tables should be referred to in the text, and their approximate position indicated in the margin of manuscript.

G. PREPARATION OF ILLUSTRATIONS

All figures should be appropriately lettered and labelled with letters and numbers that will be at least 1.5 mm high in the final reproduction. Note the conventions for abbreviations used in the journal so that usage in illustrations and text is consistent. All figures should be referred to in the text and numbered consecutively (Fig. 1, Fig. 2, etc.). The figures must be identified on the reverse side with the author's name, the figure number and the orientation of the figure (top and bottom). The preferred location of the figures should be indicated in the margin of the manuscript. Illustrations that are substandard will be returned, delaying publication. Illustrations in color may be published at the author's expense.

1. Line drawings and graphs

Original artwork of high quality, glossy prints mounted on appropriate mounting card (less than 25×38 cm) should be submitted for reproduction. Author(s) may indicate size preference by making on the back of figures, such as "Do not reduce", "Two-column width" (no wider than 14.5 cm), or "One-column width" (no wider than 7 cm). Lines must be dark and sharply drawn. Solid black, white, or bold designs should be used for histograms. Xerox or any other copying mean may be used for the two review copies.

2. Continuous-tone prints

Three sets of continuous-tone prints (photomicrographs, etc.) must be submitted. One set for reproduction should be mounted on appropriate mounting card, and the other two for reviewers may be unmounted prints. Xerox or similar copies of photomicrographs are not acceptable for review purposes. The continuous-tone prints should be submitted preferably at the exact magnification which is to be used in the published papers and trimmed to conform to the page size (in no case should it exceed 14.5×20 cm). Press-on numbers should be applied to the lower right corner of individual prints. Letters (a, b, c, etc.) should be used for multiple parts of a single figure. If important structures will be covered by use of the lower right corner, identification may be applied in the lower left corner.

Reproduction of color photographs will have to be approved by the Editors. The extra costs of color reproduction will be charged to the authors.

3. Figure legends

Each figure should be accompanied by a title and an explanatory legend. The legends for several figures may be typed on the same sheet of paper. Sufficient detail should be given in the legend to make it intelligible without reference to the text.

H. PROOF AND REPRINTS

A galley proof and reprint order will be sent to the submitting author. The first proofreading is the author's responsibility, and the proof should be returned within 72 hours from the date of receipt (by air mail from outside Japan). The minimum quantity for a reprint order is fifty. Manuscript, tables and illustrations will be discarded after the editorial use unless their return is requested when the manuscript is accepted for publication.

ERRATUM

In the Author Index of Vol. 5, No. 6, page 1358,
'Yagi, S.....1247' was not printed. Please add this
after Yada, 'T.....1311'.

Development Growth & Differentiation

Published Bimonthly by the Japanese Society of
Developmental Biologists
Distributed by Business Center for Academic
Societies Japan, Academic Press, Inc.

Papers in Vol. 31, No. 1. (February 1989)

1. **REVIEW:** C. E. Somers and B. M. Shapiro: Insights into the molecular mechanisms involved in sea urchin fertilization envelope assembly.
2. **REVIEW:** H. Fukuda and H. Kobayashi: Dynamic organization of the cytoskeleton during tracheary-element differentiation.
3. A. Nicotra, A. Serafino and M. Arizzi: Deprenyl, an inhibitor of monoamine oxidase B, delays the first two mitotic cycles of sea urchin eggs.
4. Y. Kadokawa, I. Fuketa, A. Nose, M. Takeichi and N. Nakatsuji: Expression pattern of E- and P-cadherin in mouse embryos and uteri during the periimplantation period.
5. M. Iwami, A. Kawakami, H. Ishizaki, S. Y. Takahashi, T. Adachi, Y. Suzuki, H. Nagasawa and A. Suzuki: Cloning of a gene encoding bombyxin, an insulin-like brain secretory peptide of the silkworm *Bombyx mori* with prothoracicotrophic activity.
6. T. Iwamatsu: Exocysis of cortical alveoli and its initiation time in medaka eggs induced by microinjection of various agents.
7. T. Iwamatsu and T. Ohta: Effects of forskolin on fine structures of medaka follicles.
8. S. Ito and K. Shimamoto: Fertilization potential of the medaka egg.
9. H. Kobayashi, T. Watanabe, N. Terashita, S. Handa and N. Furuno: Vertebral abnormalities following heat shock in *Xenopus* embryos.
10. K. W. Makabe and N. Satoh: Temporal expression of nuosen heavy chain gene during ascidian embryogenesis.
11. H. Nakayama, H. Kuroda, J. Fujita, X.-M. Ru and Y. Kitamura: Kidney proximal tubule cells originate from approximately four progenitor cells and make distinct patches in mouse aggregation
12. S. Yamaguchi, J. L. Hedrick and C. Katagiri: The synthesis and localization of envelope glycoproteins in oocytes of *Xenopus laevis* using immunocytochemical methods.
13. W. K. Morishige and A. M. Montes: The effect of corticosterone on the growth of perinatal rat lung fibroblasts in culture: modulation by the extracellular matrix.

Development, Growth and Differentiation (ISSN 0012-1592) is published bimonthly by The Japanese Society of Developmental Biologists, Department of Developmental Biology, Mitsubishi Kasei Institute of Life Science, Minami-ootani 11, Machida, Tokyo 194, Japan. 1989: Volume 31. Annual subscription for vol. 31, 1989: U. S. \$ 136.00, U. S. and Canada: U. S. \$ 150.00, All other countries except Japan. All prices include postage, handling and air speed delivery except Japan. Second class postage paid at Jamaica, N.Y. 11431, U. S. A.

Outside Japan: Send subscription orders and notices of change of address to Academic Press, Inc., Journal Subscription Fulfillment Department, 6277 Sea Harbor Drive, Orlando, FL 32887, U. S. A. Send notices of change of address at least 6-8 weeks in advance. Please include both old and new addresses. U. S. A. POSTMASTER: Send changes of address to *Development, Growth and Differentiation*, Academic Press, Inc., Journal Subscription Fulfillment Department, 6277 Sea Harbor Drive, Orlando, FL 32887, U. S. A.

In Japan: Send nonmember subscription orders and notices of change of address to Business Center for Academic Societies Japan, 16-3, Hongo 6-chome, Bunkyo-ku, Tokyo 113, Japan. Send inquiries about membership to Business Center for Academic Societies Japan, 4-16, Yayoi 2-chome, Bunkyo-ku, Tokyo 113, Japan.

Air freight and mailing in the U. S. A. by Publications Expediting, Inc., 200 Meacham Avenue, Elmont, NY 11003, U. S. A.

NARISHIGE

THE ULTIMATE NAME IN MICROMANIPULATION

OUR NEW MODELS MO-102 and MO-103
MAKE PRECISION MICROMANIPULATION SO EASY!

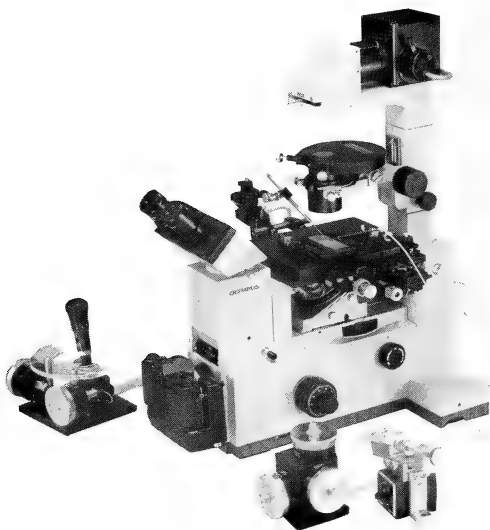


(Photo: by courtesy of Olympus Optical CO., LTD.)

SOME FEATURES of MO-102 and MO-103:

- * The manipulator head is so small that it can be mounted directly on the microscope stage. There is no need for a bulky stand.
- * Hydraulic remote control ensures totally vibration-free operation.
- * 3-D movements achieved with a single joystick.

Micromanipulators Microelectrode pullers Stereotaxic instruments



**NARISHIGE SCIENTIFIC INSTRUMENT
LABORATORY CO., LTD.**

4-9-28, Kasuya, Setagaya-ku, Tokyo 157 JAPAN
Telephone: 03-308-8233 Telex: NARISHG J27781

(Contents continued from back cover)

Shimizu, A.: Role of internalization of follicle-stimulating hormone (FSH)-receptor complex on down-regulation of FSH receptor in mouse Sertoli cells	91
Mori, T. and H. Nagasawa: Causal analysis of the development of uterine adenomyosis in mice	103
Masaki, T., K. Endo, and K. Kumagai: Neuroendocrine regulation of the development of seasonal morphs in the Asian comma butterfly, <i>Polygonia c-aureum</i> L.: Stage-dependent changes in the activity of summer-morph-producing hormone of the brain-extracts	113
Kimura, M., S. Sakurai, T. Nakamachi, M. Nariki, S. Niimi, T. Ohtaki, Y. Fujimoto, F. Hata, and N. Ikekawa: Qualitative and quantitative analysis of juvenile hormone in the larvae of the silkworm, <i>Bombyx mori</i>	121
Dixit, A. S. and P. D. Tewary: Circadian periodicity in termination of photorefractoriness in the female yellow-throated sparrow, <i>Gymnorhis xanthocollis</i>	129
Peter, M. C. S. and O. V. Oommen: Effects of thyroid and gonadal hormones <i>in vitro</i> on hepatic succinate dehydrogenase activity of the teleost, <i>Anabas testudineus</i> (Bloch) (COMMUNICATION)	185
Behavior Biology	
Kabasawa, H. and S. Ooka-Souda: Circadian rhythms in locomotor activity of the hagfish, <i>Eptatretus burgeri</i> (IV). The effect of eye-ablation	135
Yamanouchi, K. and Y. Arai: Lordosis-inhibiting pathway in the lateral hypothalamus: Medial forebrain bundle (MFB) transection	141
Munro, A. D.: Lack of influence of photoperiod on the brood interval of the guppy (<i>Poecilia reticulata</i>) (COMMUNICATION)	191
Taxonomy and Systematics	
Kubota, S.: Systematic study of a paedomorphic derivative hydrozoan <i>Eugymnanthea</i> (Thecata-Leptomedusae)	147
Toda, M. J. and T. X. Peng: Eight species of the subgenus <i>Drosophila</i> (Diptera: Drosophilidae) from Guangdong Province, southern China	155
Instructions to Authors	195
Erratum	198

ZOOLOGICAL SCIENCE

VOLUME 6 NUMBER 1

FEBRUARY 1989

CONTENTS

REVIEWS

- Malacinski, G. M., A. W. Neff, G. Radice and H.-M. Chung: Amphibian somite development: contrasts of morphogenetic and molecular differentiation patterns between the laboratory archetype species *Xenopus* (anuran) and Axolotl (urodele) 1
- Engström, W., G. Möllermark, L. E. Kängström and O. Larsson: Some molecular characteristics of canine mammary tumours and their relationship to biological malignancy and prognosis 15

ORIGINAL PAPERS

Physiology

- Kurahashi, T. and T. Shibuya: Membrane responses and permeability changes to odorants in the solitary olfactory receptor cells of newt 19
- Horiuchi, S., H. Kitani, Y. Koshida, F. Tokunaga, and T. Takeuchi: Immunofluorescent staining of visual cells from various species by monoclonal antibodies against bovine rhodopsin 31
- Minato, K.: Cell cycle in the epidermis during larval instars of the saturniid moth *Samia cynthia ricini* (Lep.) 35
- Tokunaga, F., T. Iwasa, M. Takao, S. Sato, and T. Takeuchi: Preparation and properties of anti-bovine rhodopsin monoclonal antibodies (COMMUNICATION) 167

Cell Biology

- Shigenaka, Y., K. Yano, and M. Imada: Axopodial contraction evoked by electrical stimulation and its ultrastructural analysis in a heliozoan *Echinophaeurum* 45

Biochemistry

- Kenmochi, N. and K. Ogata: A comparative study of 40S ribosomal proteins in *Artemia salina* and rat liver: Peptide analysis by limited proteolysis and sodium dodecyl sulfate acrylamide gel electrophoresis 55
- Sakai, T., N. Tabata, and M. Suiko: Occurrence of biliverdin IX_α in the gallbladder bile of hagfish, *Eptatretus burgeri* (COMMUNICATION) 173

Developmental Biology

- Tazawa, E., A. Fujiwara, and I. Yasumasu: Stimulating effect of dimethylsulfoxide on unfertilized eggs of the echinuroid, *Urechis unicinctus* 63
- Uchiyama, H. and T. Mizuno: Sexual dimorphism in the genital tubercle of the duck: Analysis by sex-steroid administration and steroid autoradiography 71
- Shimizu, T. and E. Ohnishi: The stimulatory effect of 2-deoxyecdysone on spermiogenesis of the diapausing cabbage armyworm, *Mamestra brassicae* (Lepidoptera: Noctuidae), *in vitro* (COMMUNICATION) 177
- Wada, K.: Interbreeding experiments of the two forms of *Macrophthalmus japonicus* (Crustacea: Brachyura: Ocypodidae) (COMMUNICATION) 181

Endocrinology

- Takagi, Y., T. Hirano, and J. Yamada: *In vitro* measurements of calcium influx into isolated goldfish scales in reference to the effects of putative fish calcemic hormones 83

(Contents continued on inside back cover)

INDEXED IN:

Current Contents/LS and AB & ES,
Science Citation Index,
ISI Online Database,
CABS Database, INFOBIB

Issued on February 15

Printed by Daigaku Printing Co., Ltd.,
Hiroshima, Japan

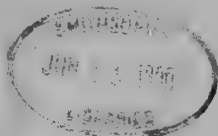
Vol. 6 No. 2

April 1989

ZOOLOGICAL SCIENCE

An International Journal

PHYSIOLOGY
CELL and MOLECULAR BIOLOGY
GENETICS
IMMUNOLOGY
BIOCHEMISTRY
DEVELOPMENTAL BIOLOGY
REPRODUCTIVE BIOLOGY
ENDOCRINOLOGY
BEHAVIOR BIOLOGY
ENVIRONMENTAL BIOLOGY
ECOLOGY and TAXONOMY



published by Zoological Society of Japan

distributed by Business Center for Academic Societies Japan
VSP, Zeist, The Netherlands

ISSN 0289-0003

QL
1
2864
NH

ZOOLOGICAL SCIENCE

The Official Journal of the Zoological Society of Japan

Editor-in-Chief:

Hideshi Kobayashi (Tokyo)

Managing Editor:

Chitaru Oguro (Toyama)

Assistant Editors:

Yuichi Sasayama (Toyama)

Hitoshi Michibata (Toyama)

Miëko Komatsu (Toyama)

The Zoological Society of Japan:

Toshin-building, Hongo 2-27-2, Bunkyo-ku,
Tokyo 113, Japan. Tel. (03) 814-5675

Officers:

President: Nobuo Egami (Tokyo)

Secretary: Hideo Namiki (Tokyo)

Treasurer: Tadakazu Ohoka (Tokyo)

Librarian: Masatsune Takeda (Tokyo)

Editorial Board:

Howard A. Bern (Berkeley)

Horst Grunz (Essen)

Susumu Ishii (Tokyo)

Koscak Maruyama (Chiba)

Kazuo Moriawaki (Mishima)

Hidemi Sato (Nagoya)

Ryuzo Yanagimachi (Honolulu)

Walter Bock (New York)

Robert B. Hill (Kingston)

Seiichiro Kawashima (Tokyo)

Roger Milkman (Okazaki)

Tokindo S. Okada (Okazaki)

Hiroshi Watanabe (Tokyo)

Aubrey Gorbman (Seattle)

Yukio Hiramoto (Chiba)

Yukiaki Kuroda (Mishima)

Hiromichi Morita (Fukuoka)

Andreas Oksche (Giessen)

Mayumi Yamada (Sapporo)

ZOOLOGICAL SCIENCE is devoted to publication of original articles, reviews and communications in the broad field of Zoology. The journal was founded in 1984 as a result of unification of Zoological Magazine (1888-1983) and Annotationes Zoologicae Japonenses (1897-1983), the former official journals of the Zoological Society of Japan. ZOOLOGICAL SCIENCE appears bimonthly. An annual volume consists of six numbers of more than 1100 pages including an issue containing abstracts of papers presented at the annual meeting of the Zoological Society of Japan.

MANUSCRIPTS OFFERED FOR CONSIDERATION AND CORRESPONDENCE CONCERNING EDITORIAL MATTERS should be sent to:

Dr. Chitaru Oguro, Managing Editor, Zoological Science, Department of Biology, Faculty of Science, Toyama University, Toyama 930, Japan, in accordance with the instructions to authors which appear in the first issue of each volume. Copies of instructions to authors will be sent upon request.

SUBSCRIPTIONS. ZOOLOGICAL SCIENCE is distributed free of charge to the members, both domestic and foreign, of the Zoological Society of Japan. To non-member subscribers within Japan, it is distributed by Business Center for Academic Societies Japan, 6-16-3 Hongo, Bunkyo-ku, Tokyo 113. Subscriptions outside Japan should be ordered from the sole agent, VSP, Utrechtseweg 62, 3704 HE Zeist (postal address: P. O. Box 346, 3700 AH Zeist), The Netherlands. Subscription rates will be provided on request to these agents. New subscriptions and renewals begin with the first issue of the current volume.

All rights reserved. No part of this publication may be reproduced or stored in a retrieval system in any form or by any means, without permission in writing from the copyright holder.

© Copyright 1989, The Zoological Society of Japan

[Publication of Zoological Science has been supported in part by a Grant-in-Aid for
Publication of Scientific Research Results from the Ministry of Education, Science
and Culture, Japan.]

REVIEW

Evolution of the Development and Larval Types in Asteroids

CHITARU OGURO

*Department of Biology, Faculty of Science, Toyama University,
Toyama 930, Japan*



I. INTRODUCTION

What form is the most primitive type of sea-stars and what group is the most advanced has been a long-lasting dispute which remains unsettled. More than half century ago, vehement discussions were held among Bather [1-3], Gemmill [4], MacBride [5-7] and Mortensen [8, 9] on the ancestral type of sea-stars and whether the brachiolaria is a primitive type of sea-star larva or not. Discussion was held on Nature as a stage for the battle. In fact, Mortensen [9] stated "to protest against the character of his unprovoked attack on me". Mortensen took the position that the brachiolaria is a secondarily specialized larval type. Therefore, he is of the opinion that the sucker of the brachiolaria is not a vestigial organ of a fixed stage of ancestral echinoderms. In contrast to the view of Mortensen, Gemmill [4] and MacBride [5-7] convinced that the sucker of the brachiolaria is a typical ancestral feature, and therefore the brachiolaria is a primitive type of sea-star larvae. These contrasting ideas on the phyletic nature of the larval type led to different views on the primitive types of the asteroid species or groups. There is no doubt that Gemmill and MacBride believed that astropectinid and luidid species, in which the larvae bear no sucker, are advanced types of sea-stars. Mortensen believed, as a matter of course, that the species belonging to the Astropectinidae and Luidiidae, are more primitive than species of the other groups

which give rise the brachiolaria with a sucker [9, 10].

Thereafter, not much discussion has been held on the phyletic rank of the Orders of asteroids, although many ideas and revised schemes have been put forth on the relative positions in the higher taxa of asteroids or related groups.

Based on the comparative morphology of existent and extinct species of asteroids and their presumable relatives, Fell [11] proposed a scheme for the possible evolutionary process of asteroids. According to this scheme, Asteroidea and Ophiuroidea rose from a common ancestor, the Somasteroidea, from which he illustrated the transition to modern asteroids through the Platyasterida. Since then, contemporary systematists adopted basically this scheme for asteroid systematics and evolution [12-17].

It is not the primary object of this article to illustrate the evolution of asteroids themselves. Therefore, further discussion on this problem will not take place here. However, it is to be noted that Blake [18] gave a novel idea on the systematics of Asteroidea based on the detailed comparative anatomy in existent and extinct specimens. He noted "No living sea star is primitive in the sense of being close to ancestral sea stars and other echinoderm groups: the Paxillosida, which commonly has been considered primitive, is here considered to be specialized."

Table 1 shows some of the different schemes of the systematic arrangement of Asteroidea (existent groups only are shown).

TABLE 1. Systematic arrangement of sea-stars by selected authors

Fell and Pawson (1966) [12]		Nichols (1969) [14]	
Class Stelleroidea		Class Asteroidea	
Subclass	Somasteroidea	Subclass	Somasteroidea
Subclass	Asteroidea	Subclass	Euasteroidea
Order	Platyasterida	Order	Platyasterida
—	Phanerozonida	—	Phanerozonida
—	Spinulosida	—	Spinulosida
—	Euclasterida	—	Euclasterida
—	Forcipulatida	—	Forcipulatida
Subclass	Ophiuroidea		
Downey (1973) [16]		Blake (1987) [18]	
Class Asteroidea		Class Asterozoa	
Order	Platyasterida	Superorder	Forcipulatacea
—	Paxillosida	Order	Brisingida
—	Valvatida	—	Forcipulatida
—	Spinulosida	Superorder	Valvatacea
—	Forcipulatida	Order	Valvatida
—	Zorocallida	—	Notomyotida
—	Euclasterida	—	Paxillosida
		Superorder	Spinulosacea
		—	Valvatida
		—	Spinulosida

II. DEVELOPMENTAL TYPES

Before going on to discuss the evolution of larval types of asteroids, it would be helpful to give a brief survey for understanding the discussion on the development of asteroids and its classification. Development of the sea-star is classified into four types by what type of larvae appear, as shown in Figure 1 [19, 20].

a. Indirect type of development

In this type of development, the larva passes through two apparently different stages, viz. bipinnaria and brachiolaria (Fig. 1, I-1~I-4). Slightly after the commencement of gastrulation, the tip of the archenteron bulges laterally. These bulges become coelomic pouches. The coelomic pouches are separated from the archenteron and differentiated, each into an anterior coelom and a posterior coelom. The archenteron differentiates into a larval esophagus, stomach and intestine. The

mouth opens at the ventro-anterior portion of the larva and the blastopore becomes the anus.

Along with the internal changes noted above, several projections appear at the anterior and lateral portions of the larval body. These projections are called the bipinnarian arms and the larvae bearing the bipinnarian arms are called bipinnariae (Fig. 1, I-2). Two heavily ciliated bands, preoral and postoral, appear in the anterior and posterior portions, the former being called the preoral ciliary band, and the latter, the postoral ciliary band.

Bipinnariae feed on planktonic algae and grow for a certain period of time. The full grown bipinnaria bears five pairs of bipinnarian arms. Then three new processes are formed on the anterior part of the bipinnaria. They are different from the bipinnarian arms since they contain a part of the coeloms inside. The larvae with brachiolar arms are called brachiolariae (Fig. 1, I-3). In the majority of the brachiolaria, a sucker which was one the foci of the discussion among Bather,

Gemmill, MacBride and Mortensen, as described before, is formed among the brachiolar arms. During the later bipinnarian stage and the brachiolarian stage, organogenesis proceeds inside the larval body for the adult structure. In the late brachiolaria, the adult rudiment is formed on the posterior portion of the larval body. Close to the metamorphic climax, the anterior portion of the larval body begins to degenerate and the brachiolaria sinks to the substratum. The sucker, together with the papillae on the brachiolar arms, functions to fix to the substratum. The eggs of the species of the indirect type are poor yolky and small (120~250 μm in diameter).

Thus, the indirect type of development is characterized by two larval types, feeding bipinnaria and feeding brachiolaria. The following are some of the species having this type of development: *Culcita novaeguineae* [21], *Archaster typicus* [10], *Lincxia laevigata* [21], *Porania pulvillus* [22], *Stichaster australis* [23], *Acanthaster planci* [24], *Acanthaster brevispinus* [25], *Asterina pectinifera* [26, 27], *Coscinaster calamaria* [23], *Asterias rubens* [28].

The term "development with bipinnaria and brachiolaria" is suggested instead of the indirect type of development to show more clearly the larval types to pass [29, 30]

b. Direct type of development

In this type of development, the larva passes through only 1 stage, the brachiolaria (Fig. 1, D-1~D-3). However, the shape of the brachiolaria of this developmental type is quite different from that of the indirect type.

After passing through the gastrula stage, the blastopore closes. The external form does not change for a certain period of time. Then it takes a bilobed form. This larva possesses no functional digestive system and is lecithotrophic. However, internal organogenesis proceeds as in the bipinnaria of the indirect type. One projection emerges from the anterior portion and two projections from the ventro-anterior portions of the larva. As a result, the larva takes a sort of snow-man shape (Fig. 1, D-2). These three projections are the brachiolar arms since they are lined with embryonic coelom, although they are different in form from the brachiolaria in the indirect develop-

ment. A sucker (fixing disk) appears among the brachiolar arms. Tips of the brachiolar arms and the sucker bear an adhesive apparatus and are utilized for fixing to the substratum as in the brachiolaria of the indirect type.

It is noteworthy that the eggs of the species having the direct type are rich in yolk and large (>400 μm). The larval mouth and anus are not formed and the brachiolaria of the direct type is a non-feeding larva, as noted before. After a certain period of time as a free-swimming larva, the adult rudiment appears in the posterior portion. During the metamorphic climax, the anterior portion is absorbed into the posterior portion, the adult rudiment.

The species noted below are some of the representatives having the direct type of development.

Mediaster aequalis [31], *Certanardoa semiregularis* [32], *Henricia sanguinolenta* [33], *Crossaster papposus* [34], *Solaster endeca* [35], *Asterina gibbosa* [36], *Asterina coronata* [37], *Asterina minor* [38], *Pteraster tessellatus* [39], *Leptasterias hexactis* [40].

The term "development with brachiolaria" is suggested instead of the direct type of development [29, 30].

c. Nonbrachiolarian type of development

In contrast to the case of the direct type of development, which lacks the bipinnaria stage, the nonbrachiolarian type of development does not pass through the brachiolarian stage during larval development (Fig. 1, NB-1~NB-3). In this developmental type, metamorphosis takes place while the bipinnaria is still planktonic. Internal organogenesis proceeds for the adult structure in the metamorphosing bipinnaria as in the brachiolaria in the indirect and direct types. However, metamorphosing larvae do not bear brachiolar arms and suckers which would appear in the brachiolaria, utilized for the settlement of metamorphosing brachiolaria to the substratum.

The following species are known to occur with this type of development. *Luidia ciliaris* [41], *Luidia sarsi* [42], *Luidia quinaria* [43], *Astropecten irregularis* [44], *Astropecten aranciaceus* [45], *Astropecten scoparius* [19]. Eggs of these species are poor yolky and small (<250 μm).

BIPINNARIA BRACHIOLARIA

INDIRECT

I-1



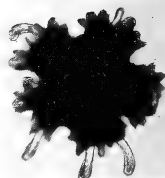
I-2



I-3

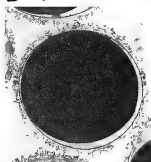


I-4

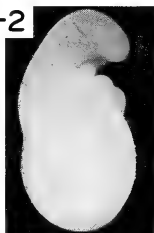


NONBRACHIOLARIAN DIRECT

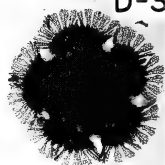
D-1



D-2



D-3



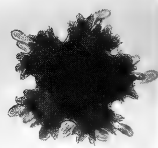
NB-1



NB-2



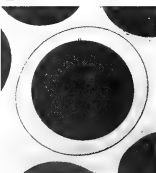
NB-3



BARREL-SHAPED LARVA

WITH BARREL-SHAPED LARVA

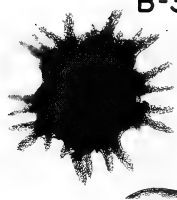
B-1



B-2



B-3



It is of interest that all species having the non-brachiolarian type of development belong to the family Luidiidae and Astropectinidae. No species belonging to groups other than Luidiidae and Astropectinidae are known to have the non-brachiolarian type of development. The fact that the nonbrachiolarian type occurs in very limited systematic groups shows that at least some of the developmental types are intimately related to the systematic position in sea-stars. This might give a logical base for discussing the evolution of the larval type of sea-stars.

The term "development with bipinnaria only" is suggested instead of the nonbrachiolarian type of development to show more clearly the larval type to pass [29, 30].

d. Development with barrel-shaped larva

Two types of sea-star larvae, bipinnaria and brachiolaria, the latter having two forms, had been known until the barrel-shaped larva was discovered in *Astropecten latespinosus* by Komatsu [46]. In this species, the embryos reach the gastrula stage after passing through the wrinkled blastula and then the blastopore closes. Neither the larval mouth nor anus opens. Until the commencement of metamorphosis, the larvae retain their barrel-shape or ovoid shape without emerging brachiolar arms and suckers (Fig. 1, B-2). Therefore, the term, barrel-shaped larva, was given to this type of sea-star larva.

The barrel-shaped larvae are planktonic and swim with the cilia which uniformly cover the entire surface of the larval body. However, the internal organogenesis of the adult organs proceeds as in the brachiolaria of the direct type. The adult rudiment appears on the posterior portion of the barrel-shaped larva when metamorphosis begins. Metamorphosing larvae sink to the substratum as the anterior portion of the larva begins to degenerate and be absorbed into the posterior

portion. Details of the morphology of the barrel-shaped larva of *Astropecten latespinosus* has been recently described [20].

This type of development has so far been observed in only three species, *Astropecten latespinosus* [46], *Astropecten gisselbrechti* [48] and *Ctenopleura fisheri* [49]. It is of considerable interest that all three species belong to the family Astropectinidae. This gives another cue to discuss the evolution of sea-star larva as will be described later.

III. RELATION BETWEEN DEVELOPMENTAL TYPE AND SYSTEMATIC POSITION

Development of the sea-stars has been reported in more than one hundred species, including fragmentary observations. However, details of development from fertilization through metamorphosis have been known in only about thirty species. Although nothing has been known on the development of species belonging to Zorocallida and Eulasterida, knowledge on the development of some representatives in the other five orders (according to Downey's system) is available to some extent.

Table 2 shows the relationship between developmental types and systematic groups. As is apparent from this table, the indirect and direct types of development occur in four Orders (Paxillosida, Valvatida, Spinulosida, and Forcipulatida). Therefore, these two types have no intimate relation to the systematic position of sea-stars.

This is well exemplified in the development of species belonging to the subfamily Asterininae, whose development has been fairly well documented. The direct development has been reported in *Asterina gibbosa* [36], *Patiriella exigua* [8], *Asterina coronata japonica* [37], *Patiriella vivipara* [50], *Asterina batheri* [47], *Asterina minor* [38]. Two asterinid species, *Patiria minata* [51] and

FIG. 1. Four developmental types of asteroids and their typical larvae shown by photographs of stages to pass through. I-1~I-4, Indirect type: I-1, Fertilized ova; I-2, Bipinnaria; I-3, Brachiolaria; I-4, Newly metamorphosed juvenile. D-1~D-3, Direct type: D-1, Fertilized ova; D-2, Brachiolaria; D-3, Newly metamorphosed juvenile. NB-1~NB-3, Nonbrachiolarian type: NB-1, Fertilized ova; NB-2, Bipinnaria; NB-3, Newly metamorphosed juvenile. B-1~B-3, Development with barrel-shaped larva: B-1, Fertilized ova; B-2, Barrel-shaped larva; B-3, Newly metamorphosed juvenile.

TABLE 2. Relationship between developmental type and systematic group (after Downey [16])

Developmental type	Larval type	Order	Remarks
Indirect	Bipinnaria & brachiolaria	Paxillosida Valvatida Spinulosida Forcipulatida	except Astropectinidae
Direct	Brachiolaria	Paxillosida Valvatida Spinulosida Forcipulatida	except Astropectinidae
Nonbrachiolarian	Bipinnaria	Platyasterida Paxillosida	Astropectinidae only
With barrel-shaped larva	Barrel-shaped larva	Paxillosida	Astropectinidae only

TABLE 3. Relation between egg size and developmental type in asterinid species

Species	Egg diameter (μm)	Developmental type
<i>Asterina pectinifera</i>	170	Indirect
<i>Patiria miniata</i>	185	Indirect
<i>Asterina coronata japonica</i>	420	Direct
<i>A. batheri</i>	430	Direct
<i>A. minor</i>	435	Direct
<i>A. burtoni</i>	450-500	Direct
<i>A. gibbosa</i>	500	Direct
<i>A. pseudoxigua pacifica</i>	700	Direct

Asterina pectinifera [27], undergo the indirect development. Thus, these two types of development occur in species belonging to a subfamily and even to a genus (*Asterina*).

Questions arise on aspects of two separate ways of development, direct or indirect, in the asterinid species. Size or quantity of yolk content in the egg has been suggested as a primary factor to determine the type of development in echinoderms [40, 52]. Development of the asterinid species seems not to be precluded from this general rule, as shown in Table 3.

It is obvious from this table that eggs less than 200 μm in diameter take the indirect type and those larger than 400 μm in diameter develop through the direct type. It is clear that taking either the indirect or the direct type depends upon the size of the egg. Systematic position contributes

nothing to this dichotomous choice.

In contrast to the situation in the indirect and direct types, the nonbrachiolarian type of development occurs in a very limited group of sea-stars (viz. in 2 families, Astropectinidae and Luidiidae). As well, development with the barrel-shaped larva has been reported only in Astropectinidae. It is therefore reasonable to conclude that these 2 developmental types are linked to the systematic position of the species.

IV. EVOLUTION OF THE DEVELOPMENT AND LARVAL TYPES

The term "dipleurula" was first proposed for a hypothetical common ancestor of Echinoderm. It is bilaterally symmetrical organism with a simple digestive tract and a pair of hydrocoel, each having

a hydropore. The whole body is covered by cilia or a single loop ciliary band which encircles the body. As is assumed from the bilateral organization, the "dipleurula" was put as having a bottom creeping nature. However, no one today believes such an organism is an ancestor of existent echinoderms. Instead, "dipleurula" is now given as a type of basic echinoderm larva from which most of the various later larvae are derived.

It has been well accepted that basic types of marine invertebrates produce a large number of poor yolky eggs and emerged larvae are feeding and pelagic [53]. In fact, poor yolky eggs of small size are most commonly observed in marine invertebrates. On the other hand, marine invertebrates adapted to deep sea or high latitude produce a small number of yolky and large eggs [52]. This is understood to be the most economical and efficient way in reproductive strategy, with a limited total energy in a severe environment.

If reproductive strategy of echinoderms, including asteroids, takes place along this general line, the most basic type of echinoderm eggs should be poor yolky and of small size. As well, larvae emerged from such eggs are feeding and pelagic. The basic pattern of this larva should follow the basic design of the dipleurula, even the dipleurula is purely imaginary.

According to this concept, the indirect or the nonbrachiolarian development must be of the basic pattern in sea-star development. As a consequence, the direct type of development is denoted as differentiated or advanced as shown in Figure 2.

As described before, the indirect and direct types are commonly found and not linked to the systematic position of species. Thus, it is understandable that A→B transition could have occurred. Actually, the final larval form before the initiation of metamorphosis in either type is the brachiolaria, which bear a sucker and adhesive

papillae on the brachiolar arms.

In the indirect type, poor yolky eggs give rise to planktonotrophic bipinnariae, which feed on planktonic algae and grow into a different type of larvae, brachiolariae which furnish with structures necessary to complete metamorphosis. On the other hand, larvae emerged from yolky eggs grow without feeding, but use the deposited yolk material for energy and constructive sources [54, 55]. Thus, the bipinnaria stage in the indirect type is a necessary stage to nurse the larvae to grow to a certain stage in which they are prepared enough for taking on metamorphosis. In large and yolky eggs, this trophogenic and growing stage has been omitted. In fact, some authors have called the direct development a shortened or abbreviated development [8, 56]. This is of course based on the concept that the original type of sea-star development passes through the two-step larval stage, but the later trophogenic stage retrogressed as they become acquired yolk material. Strathmann also suggested that the ancestral echinoderm had feeding larva [57].

The next question is which type is more primitive or basic in sea-star development, the indirect or the nonbrachiolarian type. If one takes a position for accepting that the dipleurula type larva is more basic, although no known echinoderm has only a dipleurula type as pointed out by Nichols [14], the conclusion is narrowed to the idea that the nonbrachiolarian type is the more basic. In the nonbrachiolarian type of development, the larva is of only one type, which is of dipleurula type, while the indirect type bears two types of larvae. This conclusion is fortified by the following:

(1) As noted earlier, Paxillosida and Platysteirida have been generally considered as primitive groups among existent asteroids. The fact that the nonbrachiolarian development occurs only in Astropectinidae (Paxillosida) and Luidiidae

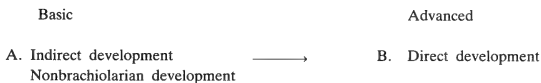


Fig. 2. A possible transition of the developmental type in association with the change from poor yolky eggs to yolky eggs.

(Platyasterida) may indicate that this developmental type is the most primitive, which has been persistently conserved in these primitive groups of sea-stars.

(2) The brachiolar larvae of both the direct type and indirect type species take a specialized form preparing for metamorphosis by having a central sucker and adhesive papillae on the brachiolar arms, although different in contour. It can thus be recognized that brachiolaria is a larval form which is designed to accomplish metamorphosis by settling on the substratum, furnished with a specialized fixing apparatus.

One may intend to believe that the bipinnaria of the nonbrachiolarian type is a larval form with degenerated fixing apparatuses by an adaptation to a mud or fine sand bottom [7]. However, it does not seem to be correct. In *Astropecten scoparius* and *Luidia quinaria*, the larvae in the late stages of metamorphosis and juveniles just after the completion of metamorphosis are furnished with suckered tube-feet, although the adult tube-feet are suckerless. They utilize these tube-feet to fix to the substratum [19, 43]. Thus, the fixing apparatus is so necessary for the metamorphosing larvae of these astropectinid and luidiid species, as well as in all species of the other sea-star groups. Therefore, it is hardly acceptable that the fixing apparatus has degenerated by adaptation of the metamorphosing larvae to a mud or sand bottom. In contrast, suckerless tube-feet of the adult may be attributable to a result of the adaptation of the adult to mud or sand substrata.

This means, for one thing, that the fixing apparatus of the metamorphosing larvae is of a later

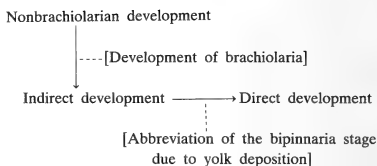


FIG. 3. Evolution of developmental type and factors or phenomena involved.

character, acquired in advanced groups of sea-stars, to ensure efficient progress of metamorphosis. Thus, the step is shown in Figure 3.

Discussion has so far been concerned to three types of development and two types of larvae (bipinnaria and brachiolaria). However, further questions should be presented on the status of the barrel-shaped larva and development with the barrel-shaped larva.

As described before, this type of larva has been found only in species belonging to the family Astropectinidae. Furthermore, all other species of Astropectinidae described so far develop through the nonbrachiolarian type. These facts suggest an intimate affinity between the nonbrachiolarian development and the development with the barrel-shaped larva. In fact, it was pointed out that early formation of the madreporic plate and precocious tube-feet formation in the metamorphosing larvae are characteristic features occurring only in these 2 developmental types [19, 20, 43, 46, 48, 49].

These facts all indicate that the development of barrel-shaped larva is a modification of the nonbrachiolarian type of development as suggested by

TABLE 4. Relation between the egg size and developmental types in astropectinid species

Species	Egg diameter (μm)	Developmental type
<i>Astropecten polyacanthus</i>	160	Nonbrachiolarian
<i>A. aranciacus</i>	200	Nonbrachiolarian
<i>A. irregularis</i>	210	Nonbrachiolarian
<i>A. scoparius</i>	230	Nonbrachiolarian
<i>A. latespinosus</i>	300	With barrel-shaped larva
<i>A. gisselbrechti</i>	350	With barrel-shaped larva
<i>Ctenopleura fisheri</i>	460	With barrel-shaped larva

Komatsu and Nojima [48]. Furthermore, it is extended to the idea that the barrel-shaped larva is a modified bipinnaria of the nonbrachiolarian type.

It is of special interest that the size (yolk content) seems here again to be the most decisive factor for having either type of larva in astropectinid species as shown in Table 4.

A conclusion is drawn from this table that eggs larger than 300 μm in diameter develop through the barrel-shaped larva and smaller than that through the bipinnaria of the nonbrachiolarian type. As suggested before, it is now reasonable to conclude that the barrel-shaped larva is a modified bipinnaria of the nonbrachiolarian type, brought about by yolk deposition. This leads to the scheme shown in Figure 4.

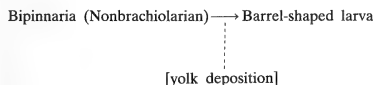


FIG. 4. Transition of the larval type in association with yolk deposition in astropectinid species.

Affinity between the barrel-shaped larva and the brachiolaria of the direct type may be of special interest, since they resemble each other in external form.

It seems that acquisition of the oval shape is a basic feature in larvae emerged from yolky eggs in echinoderms, since this can be seen in species in other Classes, too. Here only few representatives are listed in Table 5.

As described before, transition from the indirect type to the direct type, due to the yolk deposition,

brought about an oval or snow man-shaped, brachiolaria. If the same could happen in the nonbrachiolarian type, yolk deposition would cause transition from the bipinnaria to an oval shaped larva. However, in primitive sea-stars, which develop through nonbrachiolarian development, an ability to develop brachiolar arms and fixing apparatus has not yet been evolved. The resultant larva is presumed to be an oval without brachiolar arms and sucker. Of course, this is nothing but the barrel-shaped larva.

This idea is in perfectly conformity with the facts shown in Table 4, indicating that smaller eggs pass through the nonbrachiolarian development while larger eggs emerge the barrel-shaped larva.

Therefore, the barrel-shaped larva and the brachiolaria of the direct type should be placed in very distant positions, although they resemble each other in a sense. Figure 5 shows the integrated construction of a possible evolutionary process of larval types together with developmental types.

The following is a summary of the discussion described above. The most primitive type of development is the nonbrachiolarian development which can now be observed only in luidid (Platyasterida) and astropectinid (Paxillosida) species (Fig. 5, 2~4). The only larva appearing in this developmental type is the bipinnaria. As a result of yolk accumulation in some species of this group by adaptive promotion to certain environmental conditions, the bipinnaria is transformed into the barrel-shaped larva, which is a fundamental form of yolky and non-feeding echinoderm larva (Fig. 5, 5~7). This is one line of changes in larval form and developmental types occurring in a limited primitive groups. A common feature found in

TABLE 5. Some representatives of oval shaped larvae with rich yolk in 3 other echinoderm Classes

Ophiuroidea	<i>Ophiolepis cincta</i> Mortensen, 1921 [8]
	<i>Amphioplus abditus</i> Hendler, 1977 [58]
Echinoidea	<i>Heliocidarid erythrogramma</i> Mortensen, 1921 [8]
	<i>Asthenosoma iijimai</i> Amemiya & Tsuchiya, 1979 [59]
Holothuroidea	<i>Cucumaria echinata</i> Ohshima, 1921 [60]
	<i>Scoliodotella uchidai</i> Oguro, 1971 [61]

these larvae is lacking in the specialized fixing apparatus that can appear in more advanced groups. They utilize their tube-feet, which are precociously formed in metamorphosing larvae, for fixing to the substratum during metamorphosis.

Additionally, more advanced sea-star groups come to have more advanced type of larva furnished with fixing apparatuses for settlement to the substratum at metamorphosis. This advanced larval type is called the brachiolaria. As a result, these species come to have a two-step larval stage,

one for growing and the other preparing for metamorphosis (Fig. 5, 8~11).

However, if yolk deposition occurs by taking an advantage in reproductive strategy, abbreviation of the growing stages occurs. The resulting larvae are inevitably oval (Fig. 5, 12~14). They are different from the barrel-shaped larva by being furnished with a specialized fixing apparatus. Thus, brachiolaria of the direct type should be the most specialized type among sea-star larvae. The contents are illustrated in Figure 5.

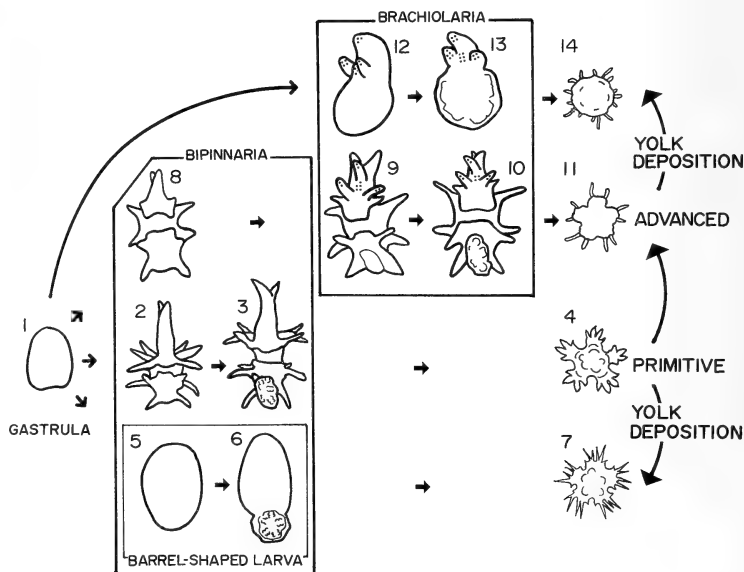


FIG. 5. A scheme showing the possible process of evolution of the larval type and developmental type. From left to right, the actual developmental process.

1~4. Primitive or basic process of development (nonbrachiolarian development), occurring only in species belonging to Luidiidae and Astropectinidae.

1, 5~7. Development (development with barrel-shaped larva) derived from [1~4] (nonbrachiolarian development) by yolk deposition in the egg, occurring only in species belonging to Astropectinidae.

1, 8~11. Advanced developmental process (indirect development) with the evolution of specialized type of larva (brachiolaria), which is furnished with fixing apparatuses. Dotted areas show the presence of fixing apparatus.

1, 12~14. Development (direct development) derived from [1, 8~11]. Abbreviation of the growing stage (bipinnaria) is consequent on the yolk deposition in the egg. Dotted areas show the presence of the fixing apparatus.

ACKNOWLEDGMENTS

The author wishes to express his cordial thanks to Dr. Miéko Komatsu for her helpful discussion and for providing photographs used in this article.

REFERENCES

- 1 Bather, F. A. (1921) *Nature*, **108** (2719): 459-460.
- 2 Bather, F. A. (1921) *Nature*, **108** (2721): 530.
- 3 Bather, F. A. (1923) *Nature*, **111** (2786): 397.
- 4 Gemmill, J. F. (1923) *Nature*, **111** (2776): 48.
- 5 MacBride, E. W. (1921) *Nature*, **108** (2721): 530.
- 6 MacBride, E. W. (1923) *Nature*, **111** (2776): 47.
- 7 MacBride, E. W. (1923) *Nature*, **111** (2784): 323-324.
- 8 Mortensen, Th. (1921) *Studies on the Development and Larval Forms of Echinoderms*. G. E. C. Gad., Copenhagen
- 9 Mortensen, Th. (1923) *Nature*, **111** (2784): 322-323.
- 10 Mortensen, Th. (1931) *Kgl. Dansk. Vidensk. Selsk. Skr., Naturvid. Math. Afd., ser. 9*, **4** (1): 1-39.
- 11 Fell, B. H. (1963) *Phil. Trans. Roy. Soc. London*, **B246**: 381-435.
- 12 Fell, B. H. and Pawson, D. L. (1966) In "Physiology of Echinodermata". Ed. by R. A. Boolootian, John Wiley & Sons, N. Y., pp. 1-48.
- 13 Spencer, W. K. (1951) *Phil. Trans. Roy. Soc. London*, **B235**: 87-129.
- 14 Nichols, D. (1969) *Echinoderms*. Hutchinson Univ. Lib., London
- 15 Clark, A. M. and Rowe, F. W. E. (1971) *Shallow Water Indo-Pacific Echinoderms*. Trustees British Mus. (Nat. Hist.), London
- 16 Downey, M. E. (1973) *Smithsonian Contr. Zool.*, **126**: 1-158.
- 17 McNight, D. G. (1975) *J. Roy. Soc. New Zealand*, **5**: 13-19.
- 18 Blake, D. B. (1987) *J. Nat. Hist.*, **21**: 481-528.
- 19 Oguro, C., Komatsu, M. and Kano, Y. T. (1976) *Biol. Bull.*, **151**: 560-573.
- 20 Komatsu, M., Murase, M. and Oguro, C. (1988) In "Echinoderm Biology". Ed. by R. D. Burke, P. V. Mladenov, P. Lambert and R. L. Parsley, A. A. Balkema, Rotterdam, pp. 241-246.
- 21 Yamaguchi, M. (1973) In "Biology and Geology of Coral Reefs, II". Ed. by O. Jones and R. Endean, Academic Press, N. Y., pp. 369-387.
- 22 Gemmill, J. F. (1915) *Quart. J. Microsc. Sci.*, **61**: 27-50.
- 23 Barker, M. F. (1978) *Biol. Bull.*, **144**: 1-11.
- 24 Henderson, J. A. and Lucas, J. S. (1971) *Nature*, **232**: 655-657.
- 25 Lucas, J. S. and Jones, M. M. (1976) *Nature*, **263**: 409-412.
- 26 Komatsu, M. (1984) *Zool. Sci.*, **1**: 942.
- 27 Komatsu, M. (1988) In "Development of Invertebrates, II". Ed. by K. Dan *et al.*, Baifukan, Tokyo, pp. 339-356.
- 28 Gemmill, J. F. (1914) *Phil. Trans. Roy. Soc. London*, **B205**: 213-294.
- 29 Oguro, C., Komatsu, M. and Kano, Y. T. (1988) In "Echinoderm Biology". Ed. by R. D. Burke, P. V. Mladenov, P. Lambert and R. L. Parsley, A. A. Balkema, Rotterdam, pp. 267-272.
- 30 Chia, F. S., Oguro, C. and Komatsu, M. (1989)
- 31 Birkeland, C., Chia, F. S. and Strathmann, R. R. (1971) *Biol. Bull.*, **141**: 99-108.
- 32 Hayashi, R. and Komatsu, M. (1971) *Proc. Japn. Soc. Syst. Zool.*, **7**: 74-80.
- 33 Masterman, A. T. (1902) *Trans. Roy. Soc. Edinburgh*, **40**: 373-418.
- 34 Gemmill, J. F. (1920) *Quart. J. Microsc. Sci.*, **64**: 155-189.
- 35 Gemmill, J. F. (1912) *Trans. Zool. Soc. London*, **20**: 1-71.
- 36 MacBride, E. W. (1896) *Quart. J. Microsc. Sci.*, **38**: 339-441.
- 37 Komatsu, M. (1975) *Proc. Japn. Soc. Syst. Zool.*, **11**: 42-48.
- 38 Komatsu, M., Kano, Y. T., Yoshizawa, H., Akabane, S. and Oguro, C. (1979) *Biol. Bull.*, **157**: 258-274.
- 39 Chia, F. S. (1966) *Proc. Calif. Acad. Sci.*, **34**: 505-510.
- 40 Chia, F. S. (1968) *Acta Zool.*, **49**: 321-364.
- 41 Mortensen, Th. (1938) *Kgl. Dansk. Vidensk. Selsk. Skr., Naturvid. Math. Afd., ser. 9*, **7** (3): 1-45.
- 42 Wilson, D. P. (1978) *J. Mar. Biol. Assoc., U. K.*, **58**: 467-478.
- 43 Komatsu, M., Oguro, C. and Kano, Y. T. (1982) In "Echinodermata". Ed. by J. M. Lawrence, A. A. Balkema, Rotterdam, pp. 497-503.
- 44 Newth, H. G. (1925) *Quart. J. Microsc. Sci.*, **69**: 519-554.
- 45 Hörstadius, S. (1939) *Pubbl. Staz. Zool. Napoli*, **17**: 221-312.
- 46 Komatsu, M. (1975) *Biol. Bull.*, **148**: 49-59.
- 47 Kano, Y. T. and Komatsu, M. (1978) *Develop. Growth and Differ.*, **20**: 107-144.
- 48 Komatsu, M. and Nojima, S. (1985) *Pacific Sci.*, **39**: 274-282.
- 49 Komatsu, M. (1982) *Marine Biol.*, **66**: 199-205.
- 50 Chia, F. S. (1976) *Amer. Zool.*, **16**: 181.
- 51 Cameron, R. A. and Holland, N. D. (1983) *Cell Tiss. Res.*, **234**: 193-200.
- 52 Emlet, B. R., McEdward, L. R. and Strathmann, R. R. (1987) In "Echinoderm Studies, 2". Ed. by M. Jangoux and J. M. Lawrence, A. A. Balkema,

- Rotterdam, pp. 55-136.
- 53 Thorson, G. (1950) *Biol. Rev.*, **25**: 1-45.
- 54 Lawrence, J. M., McClintock, J. B. and Guille, A. (1984) *Internat. J. Invert. Repr. Develop.*, **7**: 249-259.
- 55 Turner, J. M. and Rutherford, J. C. (1976) *J. Exp. Mar. Biol. Ecol.*, **24**: 49-60.
- 56 Hyman, L. H. (1955) *The Invertebrates. IV. Echinodermata*. McGraw-Hill, N. Y.
- 57 Strathmann, R. R. (1975) *Amer. Zool.*, **15**: 717-730.
- 58 Hendler, G. (1977) *Biol. Bull.*, **152**: 51-63.
- 59 Amemiya, S. and Tsuchiya, T. (1979) *Marine Biol.*, **52**: 93-96.
- 60 Ohshima, H. (1921) *Quart. J. Microsc. Sci.*, **65**: 173-246.
- 61 Oguro, C. (1976) *Proc. Japn. Soc. Syst. Zool.*, **12**: 58-64.

REVIEW

Cellular Aspects of Oocyte Growth in Teleosts

KELLY SELMAN¹ and ROBIN A. WALLACE^{1,2}

¹*Department of Anatomy and Cell Biology, College of Medicine,
University of Florida, Gainesville, Florida, 32610, and* ²*Whitney
Laboratory, St Augustine, Florida, 32086, U. S. A.*

ABSTRACT—In teleosts, the transformation of oogonia into oocytes apparently occurs within the germinal regions of the luminal epithelium of the ovary. As observed to particular advantage in syngnathans, prefollicle cells surround each oocyte, which is arrested in meiotic prophase, and the entire oocyte-follicle cell complex buds off the germinal nest as a primordial follicle. Oocyte growth within the follicle is due, to some extent, to the accumulation of normal cytoplasmic components; however, the preponderant mechanisms that contribute to oocyte growth are the endogenous synthesis of cortical alveoli, the accumulation of hepatically derived yolk protein (vitellogenesis) and in some (particularly marine) teleosts, a pronounced water uptake, which occurs concomitant with the resumption of meiosis (oocyte maturation). Our current understanding of these events is discussed and a new perspective on oocyte staging is presented, which is based on data indicating that the cellular events of oocyte growth do not sequentially replace one another, but rather are initiated sequentially and remain active throughout oocyte development.

INTRODUCTION

The production of viable eggs is obviously needed for species survival. Interest in teleost reproduction, therefore, has increased in recent years as teleosts have become appreciated for a number of commercial reasons. Frequently it is desirable to know the reproductive condition of a population of fish and this is often monitored either by representative sampling of individual fish or, in large fish, by a relatively simple biopsy through the genital pore (e.g., [1]). In either case, a knowledge of oocyte development is a prerequisite for a proper evaluation of reproductive condition and several staging systems have been used for different teleosts [2-8]. We have previously given a detailed review of the events of teleost oocyte growth and development [9] and will here simply summarize the various sequential processes involved along with related considerations,

emphasizing some of the newer information that has recently emerged. This review paper is intended to supplement the several monographs on various aspects of oocyte growth that have been published in the last few years [10-22] and will not attempt to cover endocrinological aspects of oocyte growth and maturation (for which, see [23]). In summarizing the cellular events of oocyte growth, examples will be drawn from the prevailing literature on a variety of teleosts, with some bias toward a few species that we have investigated in our own laboratories.

OOGENESIS AND FOLLICULOGENESIS

Apparently, oogonia can be found throughout the life of the female in most teleosts. These mitotically dividing cells represent a stem-cell population that gives rise to oocytes and ultimately to eggs. Discrepancies exist in the literature concerning the location of oogonia within the ovary, the seasonality of oogonial proliferation and the

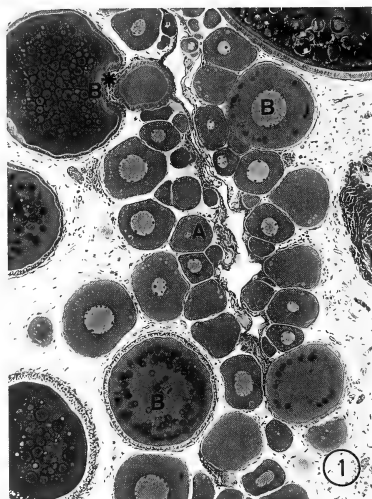


FIG. 1. Light micrograph of a section through an ovigerous fold of the ovary of the killifish, *Fundulus heteroclitus*, showing randomly arranged follicles in different stages of development. A, primary growth stage; B, B¹, B*, early, mid, and late cortical alveolus stages respectively; C, vitellogenic stage. Tissue was embedded in Histo-resin and the section was stained with toluidine blue. $\times 80$.

timing of oogenesis *per se* [24]. In mature ("ripe") ovaries of many fish, oocytes of variable size are randomly distributed (Fig. 1) and oögonia and early oocytes occur in nests embedded in the wall of ovigerous lamellae [8, 25–27]. Because of their small size, they are hard to locate and thus many conclusions in the literature regarding oogenesis may be compromised by periodic observational difficulties. A particularly useful adult material for studying oögonia and early oocyte stages is provided by syngnathans (pipefish and seahorse), where a sequential pattern of follicle development is observed. In the pipefish, *Syngnathus scovelli*, this pattern begins at the "germinal ridge", with a gradient of follicles of increasing developmental age extending to the mature edge (Fig. 2, [7, 28]).

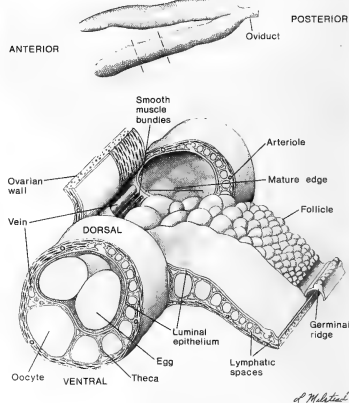
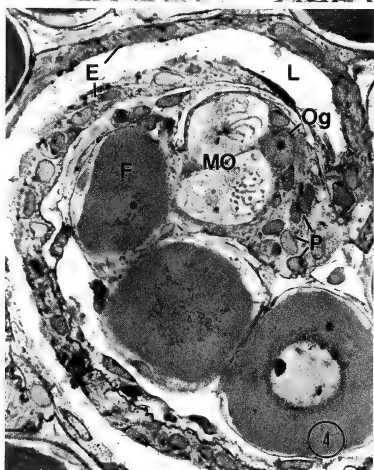
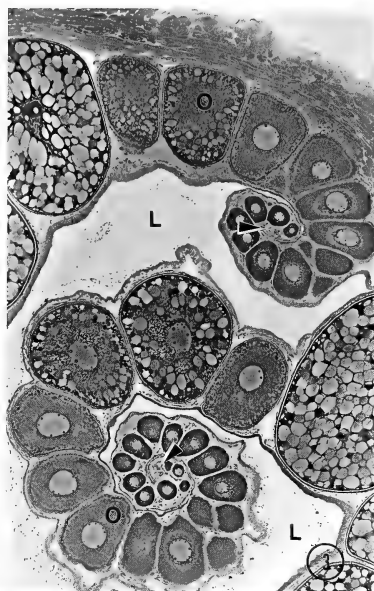


FIG. 2. Schematic summary of the ovary of the pipefish, *Syngnathus scovelli*. The upper diagram indicates the paired ovaries which join to give rise to the oviduct. The dashed line indicates a segment of the ovary that is enlarged in the lower diagram maintaining *in situ* relations. The middle section of the ovary has been unfurled to allow visualization of the follicles and ovarian lumen. Note that a strip of luminal epithelium has been removed except near the germinal ridge along with the underlying connective tissue elements to visualize the follicle progression in the ovarian sheet. The association of the luminal epithelium with the germinal ridge is indicated. The germinal ridge in the reflected segment of the luminal epithelium depicts early follicles in various stages of separation. The sandwichlike nature of the ovary is apparent in the unfurled region with follicles lying between the ovarian wall and the luminal epithelium. This diagram highlights features of the ovary and is not drawn fully to scale. From Begovac and Wallace [28].

In the seahorse, *Hippocampus erectus*, each of the ovaries has two germinal ridges, which run the length of the ovary on opposite sides of the ovarian sheet, and sequentially developing follicles arising from each grow towards a shared mature region (Fig. 3). In both cases, the germinal ridges contain



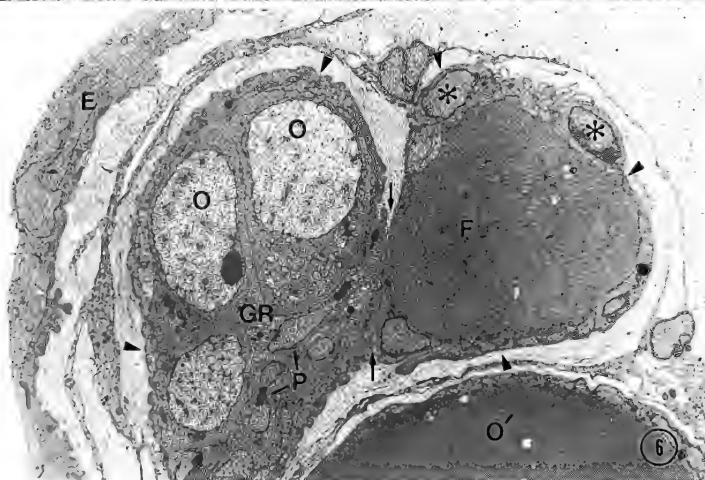
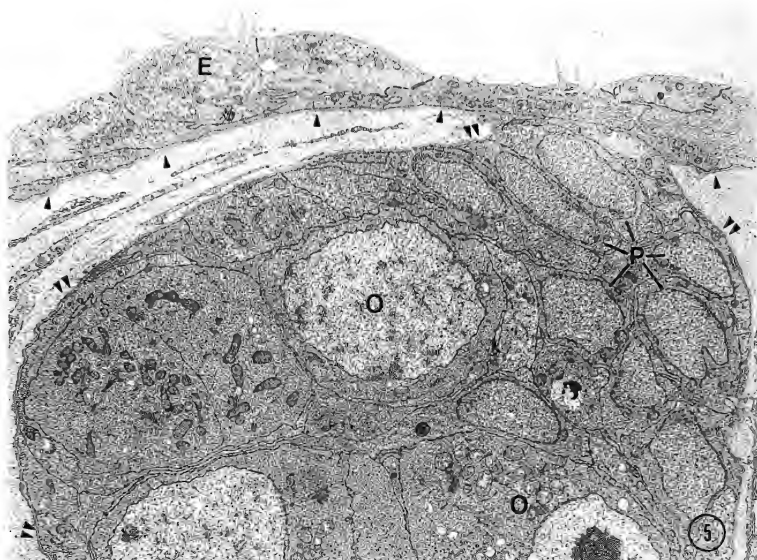
the germinal cells (oogonia and oocytes up to early diplotene) together with somatic prefollicle cells (Figs. 4–6) and, because of the exceptional accessibility of the germinal ridges, syngnathans are well suited for studies on the early events of oogenesis.

Until quite recently, the origin of germ cells and pre-follicle cells in teleosts has been speculative, being based primarily on light microscopic observations (e.g., [27, 29–31]). These studies suggested that germ cells were derived from the germinal (luminal or coelomic) epithelium or the underlying connective tissue cells. A more recent ultrastructural study of the killifish, *Fundulus heteroclitus*, suggested the latter [32]. Both mesenchymal and epithelial cells have also been purported to give rise to the prefollicle cells in a variety of fish. Recent ultrastructural studies on *S. scovelli*, however, have indicated that oogonia, the earliest oocytes, and the prefollicle cells are all derived from the luminal epithelium, i.e., they reside within an outpocketing of this ovarian compartment [28]. Figure 5 supports the notion of a single compartment and reveals that the basal lamina surrounding the germinal ridge is continuous with the basal lamina underlying the luminal epithelium.

The transformation of oogonia to oocytes is referred to as oogenesis. In syngnathans, oocytes are formed from oogonia within the germinal ridge as they enter the early stages of meiotic prophase (Fig. 4). During this period, DNA replication occurs (pre-leptotene), homologous chromosomes pair and begin to condense (leptotene, zygotene), these pairs subsequently shorten and thicken to

FIG. 3. Light micrograph of part of a transverse section through the ovary of the seahorse, *Hippocampus erectus*, showing two germinal ridges (arrowheads) and sequentially arranged growing follicles arising from each. O, oocytes; L, ovarian lumen. Tissue was embedded in Historesin and the section was stained with toluidine blue. $\times 95$.

FIG. 4. Light micrograph of a section through a germinal ridge region of an ovary from *H. erectus*. Within the germinal ridge prefollicle cells (P), an oogonium (Og) and meiotic oocytes (MO) with visible chromosomes are apparent. F, developing follicle that has already separated from the germinal ridge; L, ovarian lumen; E, luminal epithelium. Tissue was prepared as for Fig. 3. $\times 950$.



form synaptonemal complexes (pachytene), and finally the chromosomes take on a "lampbrush" configuration (diplotene), which is sometimes difficult to detect in routine histological preparations. Collectively, these events are referred to as the "chromatin nucleolus stage of primary oocyte growth". We have found that soon after the pipefish oocyte enters diplotene, it becomes enveloped by a continuous layer of follicle cells prior to leaving the germinal ridge (Fig. 6). Arrested in late diplotene of first meiotic prophase, the oocyte then begins an extensive period of growth concomitant with the differentiation of its follicular components and this is generally called the "perinucleolus stage of primary oocyte growth".

Soon after arrest in prophase, ribosomal genes are amplified and multiple nucleoli appear, although some alterations of this process have been described [33]. Although the size and morphology of the multiple nucleoli are variable amongst teleosts, their presence appears to be universal; they usually lie in the peripheral region of the enlarging oocyte nucleus, which is from this point on generally referred to as the "germinal vesicle" (Fig. 7). At this stage, the lampbrush configuration of the chromosomes becomes more apparent, indicating prominent transcription of heterogeneous RNA in addition to the ribosomal RNA provided by the multiple nucleoli [34]. The former is processed into poly(A)-containing RNA, the so-called "maternal message" (mRNA), as it moves from the germinal vesicle into the cytoplasm. Where quantified, the amount of maternal mRNA that is found in full-grown oocytes is already present by the end of primary oocyte growth [34, 35]. Aggregations of basophilic or electron dense material (nuage) is apparent in the perinuclear cytoplasm and has been shown to contain ribonucleoprotein [36, 37].

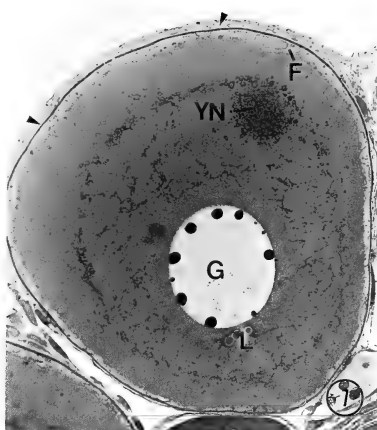
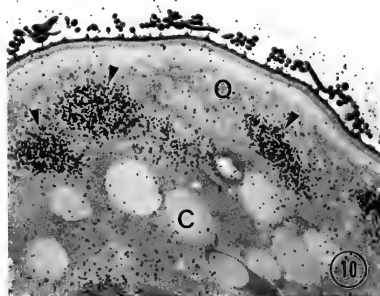
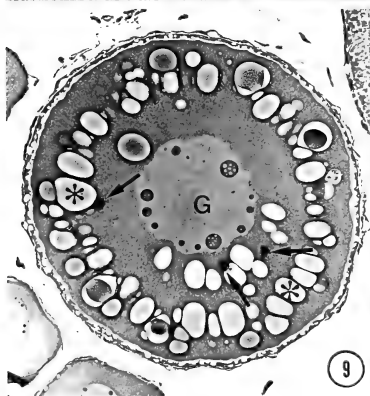
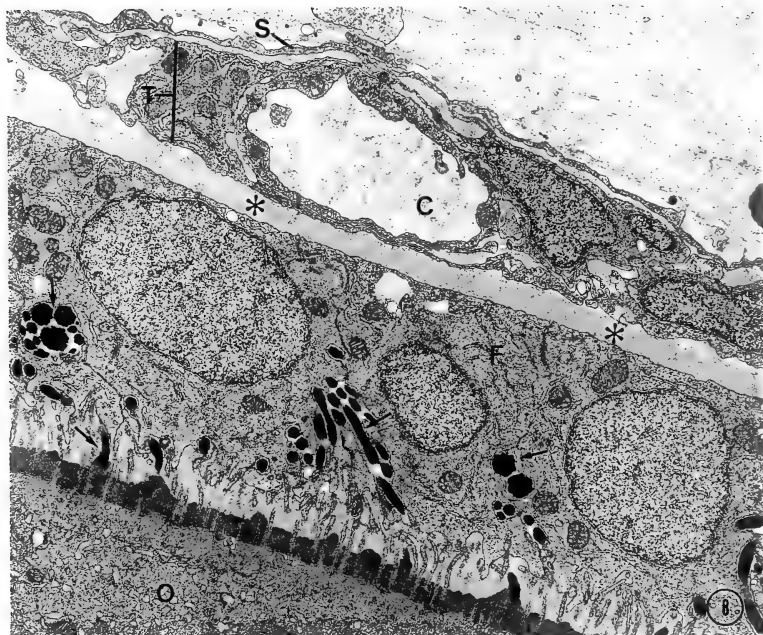


FIG. 7. Light micrograph of a section through a follicle in the perinucleolus stage of primary oocyte growth from the seahorse, *H. erectus*. The oocyte contains a distinct yolk nucleus (YN) and multiple nucleoli (G) are visible at the periphery of the germinal vesicle (G). A darkly stained basement membrane (arrowheads) separates the follicle cells (F) from the remaining follicular investments. L, lipid droplets. Tissue was embedded in Histo-resin and the section was stained with toluidine blue. $\times 565$.

A rather prominent feature of this stage is the formation of the "yolk nucleus" or "Balbani body" (Fig. 7), which was first described in teleosts by Hubbard [38]. At the ultrastructural level, this variably sized structure appears to be composed of aggregations of ribonucleoprotein particles associated with a heterogeneous population of cytoplasmic organelles, such as mitochondria, multivesicu-

FIG. 5. Electron micrograph of part of the germinal ridge from *S. scovelli*. Note that the basal lamina (single arrowheads) underlying the luminal epithelial cells (E) is continuous with the basal lamina (double arrowheads) that completely surrounds the germinal ridge. Groups of oocytes (O) and prefollicle cells (P) can be seen within the germinal ridge. $\times 5,700$. From Begovac and Wallace [28].

FIG. 6. Electron micrograph of an early follicle (F) separating from the germinal ridge (GR) in the ovary of *S. scovelli*. Definitive follicle cells (*) surround the oocyte as it "pinches" away (arrows) from the ridge. The basal lamina (arrowheads) can be followed and seen to enclose the entire germinal ridge and young follicle. Within the germinal ridge, prefollicle cells (P) and meiotic oocytes (O) are evident. E, luminal epithelium; O', an oocyte in a definitive follicle of the early follicle progression. $\times 18,500$. From Begovac and Wallace [28].



lar bodies, endoplasmic reticulum, and Golgi elements (see review by Guraya [39]). The Balbiani body initially forms in a juxtanuclear position and subsequently migrates to the oocyte periphery where it disperses into small fragments [40, 41]. These events have been followed in living oocytes by vitally staining with rhodamine 123 or acridine orange, which indicate mitochondria- and lysosome-related structures, respectively [7]. Although the existence of the Balbiani body is well documented, its functional significance is not fully understood, but most opinion suggests it is involved in the extensive fabrication of organelles that occurs during primary oocyte growth [39].

By the end of the primary growth stage a multilayered follicle has formed (Fig. 8). The follicle consists of a) an oocyte surrounded by a sheath of follicle (or granulosa) cells that rests on a prominent basal lamina, b) a vascularized thecal layer containing capillaries within a connective tissue meshwork, and c) a thin surface epithelium, in which the cells are connected by occluding junctions that prevent the diffusion of macromolecular material from the ovarian lumen into the follicle or vice versa. In many teleosts, formation of the vitelline envelope (variously referred to as the zona pellucida, zona radiata, chorion, or primary envelope) begins during the perinucleolus stage of oocyte growth and electron-dense material is observed at the ultrastructural level to be accumulating between short microvilli that project from the oocyte surface towards the overlying follicle cells (see Fig. 19a below).

During the primary growth stage in most teleosts, the oocyte grows from a diameter of approximately 10–20 μm at leptotene to a diameter ranging from 100–200 μm . The elaboration of normal cytoplasmic organelles and the accumulation of huge amounts (for a single cell) of cytoplasmic RNAs and proteins is responsible for approximately a thousand-fold increase in oocyte volume and a noticeable decrease in nucleocytoplasmic ratio. It is important to realize, however, that ovaries containing oocytes only in the primary growth stage are still relatively small, having gonadosomatic indices of <2 , and thus these ovaries are generally perceived as immature.

CORTICAL ALVEOLUS STAGE

The first distinct cytoplasmic structures that are uniquely associated with teleost oocytes at the light microscopic level are the cortical alveoli (Fig. 9), sometimes referred to as "yolk vesicles", "cortical vesicles", "intravesicular yolk", "endogenous yolk", and a variety of other terms [42, 43]. Initially, these spherical structures appear circumferentially at various depths in the cytoplasm (depending on species) and generally stain for both protein and carbohydrate [42]. As they enlarge to a size sometimes in excess of 50 μm in diameter, the cortical alveoli become more difficult to preserve during routine tissue preparation for microscopy, and in suboptimally fixed oocytes they often lose their staining properties and appear empty (vacuolar). By the end of this stage, cortical

FIG. 8. Low power electron micrograph of the follicle wall and underlying oocyte (O) from *F. heteroclitus*. The follicle is covered by a surface epithelium (S) made of squamous epithelial cells that are connected by tight junctions. The theca (T) consists of a network of capillaries (C) within a connective tissue stroma and is separated from the follicle cells (F) by a distinct basal lamina (*). Note the electron-dense fibrils (arrows) lying within spaces between adjacent follicle cells and attaching to the outer region of the developing vitelline envelope (V). $\times 8,830$.

FIG. 9. Light micrograph of a section through a cortical alveolus-stage follicle from *F. heteroclitus*. Multiple nucleoli are apparent within the germinal vesicle (G) and variable-size cortical alveoli (*) are randomly arranged within the oocyte. Lipid droplets (arrows) are readily distinguished from the cortical alveoli because the fixation solution contained osmium tetroxide. Tissue was embedded in JB-4 resin and the section was stained with toluidine blue. $\times 130$.

FIG. 10. Autoradiograph of a cortical alveolus-stage follicle that was incubated for 12 hr in fish saline containing 100 $\mu\text{Ci/ml}$ [^3H]glucose followed by a 12 hr incubation in fish saline containing an excess of unlabeled glucose. The endogenous synthesis of a cortical alveolus glycoconjugate is indicated by the high concentration of grains over cortical alveoli (C) that were formed prior to exposure to [^3H]glucose. Tissue was embedded in Epon, the slide was exposed for 7 days prior to development and was subsequently stained with toluidine blue. $\times 690$.

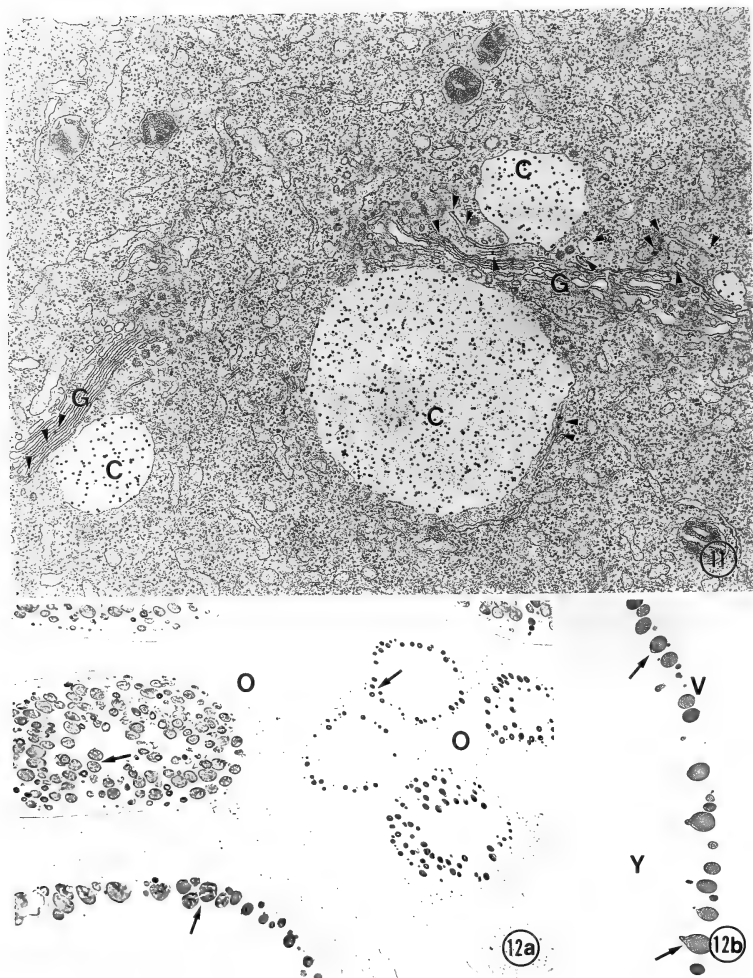


FIG. 11. Electron micrograph of a cortical alveolus-stage oocyte from *F. heteroclitus* that demonstrates immunoreactivity within Golgi complexes (G) and cortical alveoli (C) after treatment with an antibody raised against a component of cortical alveoli. The section was first treated with antiserum raised against a >200-kDa glycoconjugate that was derived from a cortical alveolus-stage oocyte and then secondarily treated with Protein

alveoli almost entirely fill the oocyte cytoplasm (Fig. 1), but in subsequent stages they continue to form and are displaced to the periphery of the oocyte by yolk protein, which accumulates centripetally [9, 42–44]. As a response to fertilization [45–48], cortical alveoli release their contents from the egg surface, and hence are homologous to “cortical granules” that are ubiquitous in eggs of other vertebrates and invertebrates [49]. Cortical alveoli, therefore, do not contain yolk (utilized by the embryo for nutrition) and should never be referred to in any way as yolk inclusions.

The formation of cortical alveoli has been examined in developing oocytes of a variety of teleosts and a common conclusion from these studies is that a carbohydrate-containing component of these vesicular structures is endogenously produced [43]. Recent studies have shown that cortical alveoli in several unrelated fish contain lectins with specific sugar-binding properties [50–52], the functions of which are unknown. Early reports had shown that oocytes of the zebrafish (*Brachydanio rerio*) synthesized a glycoprotein component of cortical alveoli [53, 54] and this has been followed more recently by a similar finding for the killifish, *F. heteroclitus* [42]. Autoradiographs (Fig. 10) made of follicles incubated in the presence of [^3H]glucose indicate that a carbohydrate component of cortical alveoli is endogenously produced within cortical alveolus-stage oocytes [42], and ultrastructural studies implicate the Golgi and/or the endoplasmic reticulum in this process [40, 42, 55–58]. This can be seen in Figure 11, where the Golgi complex and associated vesicles reveal immunocytochemical labeling with antibody directed against a >200-kDa glycoconjugate present within cortical alveoli [43]. Antibodies raised against purified ovarian lectins [52] and against cortical alveolus-derived glycoconjugates [43, 59] have been used to definitively establish the related-

ness of cortical alveoli present in eggs with what have generally been called “yolk vesicles” in early oocytes (Fig. 12). Taken together these studies indicate that yolk vesicles and cortical alveoli are identical in structure and composition and lead us to suggest that the term “yolk vesicle” not be used in future publications [43].

The most detailed analyses of cortical alveoli have been made by Inoue and colleagues [60, 61] for eggs of the rainbow trout, *Salmo gairdneri*. These investigators found the major cortical alveolus-associated component to be an unusual 200-kDa polysialoglycoprotein that has a core made of 25 tandem repeating tridecapeptide units with 0-linked glycan side chains composed of large blocks of sialic acid. They have also demonstrated that after fertilization and the concomitant exocytosis of cortical alveoli, the 200-kDa polysialoglycoprotein depolymerizes to 9-kDa subunits [62].

VITELLOGENESIS

Since yolk proteins contribute >80–90% of the dry weight of eggs in most lower vertebrates, including teleosts, vitellogenesis represents a major aspect of oocyte growth [17]. Many studies conducted primarily on amphibians and birds have indicated that the sequence of events that exclusively contributes to vitellogenesis involves 1) the hepatic synthesis and secretion of vitellogenin, the yolk protein precursor, in response to circulating estrogen, 2) the delivery of vitellogenin via the maternal circulation to the surface of the growing oocyte, 3) selective uptake of vitellogenin by receptor-mediated endocytosis, and 4) cytoplasmic translocation of vitellogenin to forming yolk bodies concomitant with proteolytic cleavage of vitellogenin into the polypeptide subunits of the yolk proteins, lipovitellin and phosvitin [17]. Some complexity has been introduced into this general

A-gold. Arrowheads indicate immunoreactivity within Golgi saccules. $\times 23,520$.

FIG. 12. The relationship of cortical alveoli (“yolk vesicles”) in oocytes and cortical alveoli in eggs. These sections were embedded in Histo-resin prior to treatment with antibodies. a: Light micrograph of a section through the ovary of *F. heteroclitus* that was treated with anti-cortical alveolus antibody (see above) followed by treatment with horseradish peroxidase-labeled secondary antibody. Peroxidase reaction product is visible only within the cortical alveoli [“yolk vesicles” (arrows)] of various size oocytes and is not present in smaller (pre-cortical alveolus-stage) oocytes (O). $\times 80$. b: This section through an egg of *F. heteroclitus* demonstrates immunoreactivity only in the cortical alveoli (arrows). V, vitelline envelope; Y, yolk mass. $\times 85$.

scheme in recent years with the realization that vitellogenin in some species may be encoded by multiple, closely related genes [63, 64], so that multiple, closely related yolk polypeptides may accumulate in the oocyte [65, 66].

The biochemical and cytological details of vitellogenesis in fish have not been as forthcoming. But, since this subject was last reviewed [9–11, 16], previously unemphasized or new observations have been made. Vitellogenin has been identified in the plasma or serum from females or estrogen-treated males of a variety of teleosts (Fig. 13, [44, 67–81]) and a partial characterization has been

made of vitellogenin in trout [82]. Extracellular tracers have been used to follow protein transport from the perifollicular capillaries to the oocyte surface via patent intercellular channels of the follicular epithelium (Fig. 8, [44, 83–85]) and vitellogenin transport to forming yolk bodies has been documented [44, 83]. Figure 14 is an electron micrograph of the surface of a vitellogenic oocyte and reveals much pinocytotic activity, which is typical of the oocyte during this stage of growth. One study that has attempted to demonstrate selective uptake of vitellogenin by trout oocytes *in vitro* [86] is unconvincing when the results are recalculated on a molar basis [17] and the only demonstration of selective uptake in teleosts is a recent report by Tyler *et al.* [87] in which they observe that *in vitro* rates of vitellogenin uptake in the rainbow trout, *S. gairdneri*, are comparable to those observed for the amphibian, *Xenopus laevis*. Using [32 P]vitellogenin, Wallace and Begovac [88] have shown that vitellogenin gives rise to at least the phosvitin polypeptides in *F. heteroclitus*, and more recently Tyler *et al.* [81] demonstrated in *S. gairdneri* that both lipovitellin and phosvitin are vitellogenin-derived. However, several studies also exist that claim vitellogenin is not processed into smaller yolk polypeptides after being taken up by the teleost oocyte [89, 90 (but see 91), 92]. Several descriptive studies in teleosts have documented that multivesicular (or lysosome-like) bodies are prominent within oocytes when vitel-

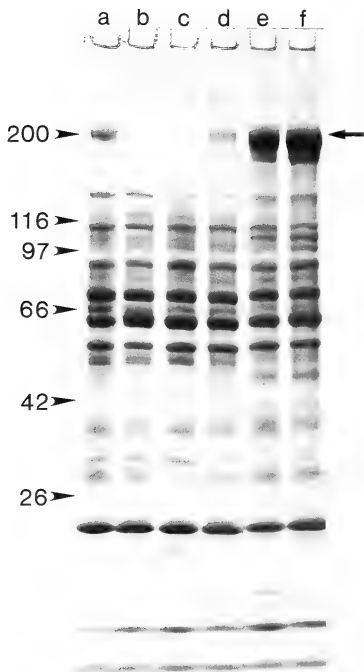


FIG. 13. Estrogen induction of vitellogenin in male *F. heteroclitus*. Plasma from female (lane a), male (lane b) and estrogen-treated males (lanes c-f) were analyzed by SDS-polyacrylamide gel electrophoresis on linear gradient gels (6.93–20.44% acrylamide). Estrogen-treated males, maintained at 28–30°C, were given a single injection of 20 μ g 17 β -estradiol dissolved in 20 μ l peanut oil 6 hr (lane c), 12 hr (lane d), 24 hr (lane e) and 72 hr (lane f) prior to bleeding. All fish were injected with 0.1 ml aprotinin solution (17 trypsin inhibitor units/ml) 15 min prior to bleeding to suppress proteolysis during blood collection. The 200-kDa polypeptide, vitellogenin (arrow), is present in female (lane a) but not male (lane b) plasma and is apparent in males 12 hr after estrogen administration (lane d). Molecular mass values are indicated in kDa on the left. Each lane contains 1 μ l plasma.

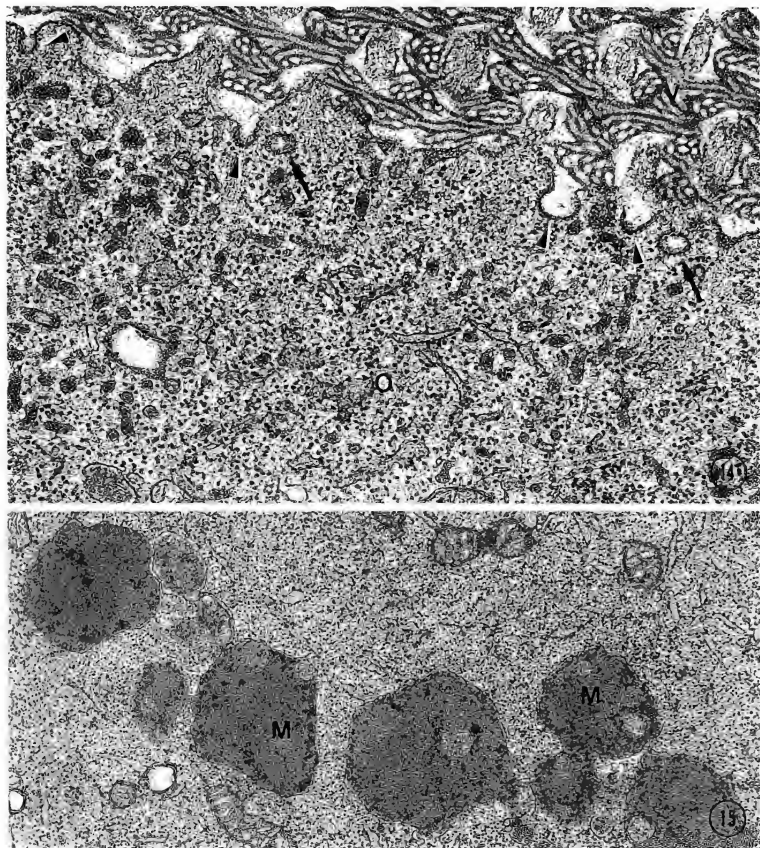


FIG. 14. Electron micrograph of the surface of an oocyte (O) from an early vitellogenic follicle from the sheephead minnow, *Cyprinodon variegatus*, showing abundant endocytotic activity. Coated pits (arrowheads), coated vesicles (arrows) and smooth-surfaced tubules are numerous at the oocyte surface. V, vitelline envelope. $\times 35,280$. From Selman and Wallace [83].

FIG. 15. Multivesicular-like bodies (M) in the cytoplasm of a cortical alveolus-stage oocyte from *C. variegatus* that was injected with the electron dense tracer iron dextran, 20 hr prior to sacrifice. The exogenous tracer was removed from the maternal circulation via endocytosis at the oocyte surface and subsequently translocated to multivesicular-like bodies within the oocyte. The dense particulate matter within these bodies is iron dextran. $\times 20,000$.

logenesis begins and that these structures disappear as yolk bodies accumulate within growing oocytes (Fig. 15, [7, 83, 93]). More detailed studies in *X. laevis* have demonstrated that multivesicular bodies do indeed play a key role in vitellogenin processing within oocytes [94, 95]. Clearly, the major areas requiring further inves-

tigation in teleosts are the selective uptake, translocation, and processing of vitellogenin. The development of appropriate culture procedures and methods of removing the surface epithelium from ovarian follicles will be a prerequisite for such studies.

Yolk proteins of several teleosts have been

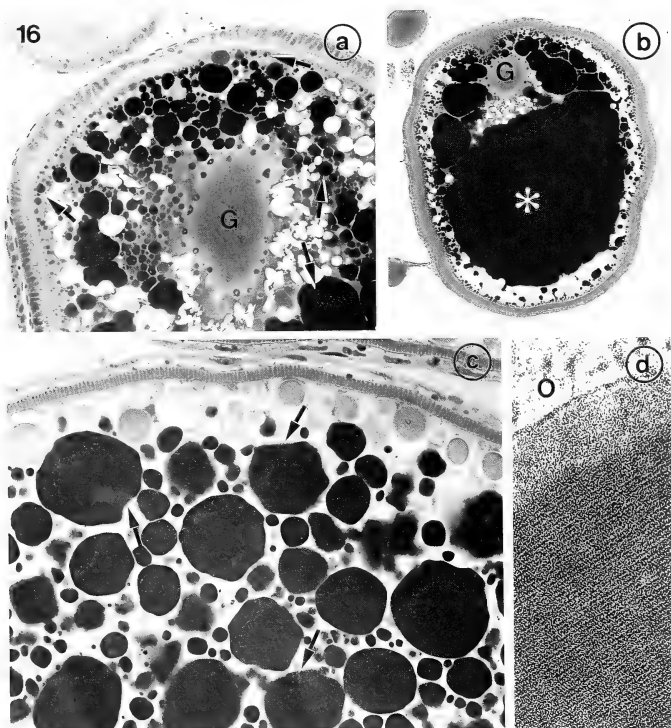


FIG. 16. Yolk accumulation within yolk spheres (panel a) that coalesce to form a continuous mass of fluid yolk (panel b) and within platelets (panel c) that have a crystalline core (panel d). Panels a, b: These sections of mid- and late vitellogenic follicles, respectively, from *C. variegatus* show fluid yolk bodies (arrows) in various states of fusion. Note the central mass of fluid yolk (*) occupying much of the ooplasm in the oocyte in panel b. G, germinal vesicle. Panel a: $\times 215$; Panel b: $\times 62$. Panel c: This section through a mid-vitellogenic follicle from the zebrafish, *Brachydanio rerio*, reveals numerous yolk platelets of variable size (arrows). $\times 572$. Panel d: This electron micrograph shows the crystalline core of a yolk platelet from the mullet, *Mugil cephalus*. O, ooplasm. $\times 108,000$.

isolated and/or partially characterized in recent years, primarily by gel electrophoretic and chromatographic procedures [68, 78, 80, 88, 96–98]. A detailed comparative study by Lange and colleagues [99, 100] has documented that the yolk proteins of two freshwater teleosts, as well as several other actinopterygians [101, 102] are present in platelets (Fig. 16c, d) comprised of an orthorhombic crystalline structure, as is found in all other anamniotes except cyclostomes. A unique feature of many teleosts is that yolk proteins accumulate in fluid-filled yolk spheres or "yolk globules" (Fig. 16a), rather than crystalline platelets [103]. These yolk spheres may either maintain their integrity throughout oocyte growth [104] or fuse centripetally to form a continuous mass of fluid yolk (Fig. 16b, [9]), a process that confers on many teleost eggs their characteristic transparency. This fusion can occur relatively soon after the initial formation of yolk spheres, as in sticklebacks and pipefish (our unpublished observations), during the later stages of vitellogenesis as in the sheepshead minnow, *Cyprinodon variegatus* [9], or during maturation as in those teleosts that have pelagic eggs [105–107]. As a consequence of yolk fusion, the ooplasm is displaced into a peripheral rim surrounding the yolk mass (Fig. 16b).

MATURATION

The following events characterize the resumption of meiosis that occurs during oocyte maturation: a) the germinal vesicle migrates towards the periphery of the oocyte and the nuclear envelope dissociates; b) the chromosomes condense and proceed to first meiotic metaphase, followed by the elimination of the first polar body; and c) the remaining chromosomes then proceed to the second meiotic metaphase, where they arrest once again [108]. In teleosts, as in other vertebrates, once this second arrest occurs (and not before), the oocyte has become "mature" and fertilizable, and now can correctly be called an egg. Ovulation of the oocyte usually occurs towards the end of the maturation process. In recent years, studies on oocyte maturation, especially in amphibians, have given considerable attention to the sequence of

cytoplasmic events responsible for the reinitiation of meiosis and to the waxing and waning of cytoplasmic factors responsible for nuclear and chromosomal behavior during this stage [109, 110]. Aside from hormonal signals associated with oocyte maturation [13, 19], virtually nothing is known about similar processes in teleosts.

In most animals, oocytes reach their final size during vitellogenesis and undergo maturation and ovulation, after an appropriate hormonal stimulus. This is the situation for most freshwater teleosts. Oocyte maturation in teleosts is usually quite rapid and accomplished within 24 hr (depending on species, temperature, etc.). In some, particularly marine teleosts, there is also an enormous volume increase due to rapid water uptake, which occurs concomitant with oocyte maturation [9]. Measurements made by Fulton [105] on two dozen different marine teleosts indicated increases in oocyte volume during maturation ranging from three- to four-fold. More recently, several authors have noticed that ovarian hydration occurs either after injection of maturation-inducing hormones to gravid fish ([111], see also references in [9]) or during the normal course of oocyte maturation [112–114]. Correlated with hydration were increases in total K^+ [111, 113] and in protein dephosphorylation [114].

Maturation accompanied by normal hydration has also been achieved *in vitro* for oocytes isolated from a variety of fish (Fig. 17, [115, 116]). Observations initially made on *F. heteroclitus* indicated that proteolysis of yolk proteins also occurs during maturation *in vivo* or *in vitro* (Fig. 18, [88, 97]). Greeley *et al.* [116] subsequently surveyed a variety of teleosts whose oocytes increased in volume from 0% to 643% and found that the extent of yolk proteolysis correlated well with the extent of oocyte hydration. More recently, we demonstrated that oocyte maturation could be dissociated from hydration but not proteolysis by incubating steroid-treated follicles of *F. heteroclitus* in paraffin oil [117]. Thus, hydration is unnecessary for maturation and proteolysis, but the dependence of hydration on maturation or proteolysis is as yet uncertain.

In summary, for some teleosts oocyte hydration during maturation accounts for up to 86% of the

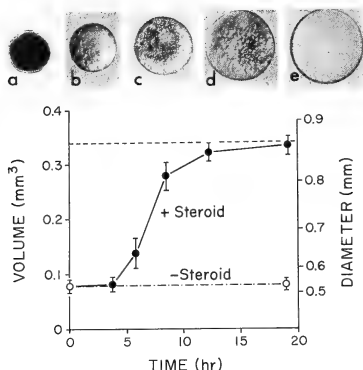


FIG. 17. Size change which occurs in the oocytes of the cunner, *Tautoglabrus adspersus*, during maturation. The largest follicles present in the ovary were incubated at 20°C in the presence (solid line) or absence (stippled line) of maturation-inducing steroid. Each point represents the average size of 10 follicles \pm SD. Dashed horizontal line at 0.87 mm indicates the average size of 10 eggs collected from the ovarian lumen. Photomicrographs at top depict the appearance of individual follicles with diameters of (a) 0.50 mm, (b) 0.55 mm, (c) 0.67 mm (GV apparent near center), (d) 0.82 mm (GV approaching animal pole) and (e) 0.85 mm (GV no longer apparent and ooplasm has clarified). Adapted from Wallace and Selman [9].

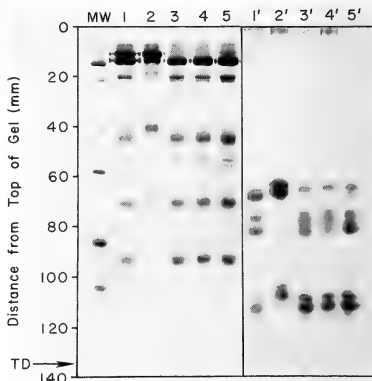
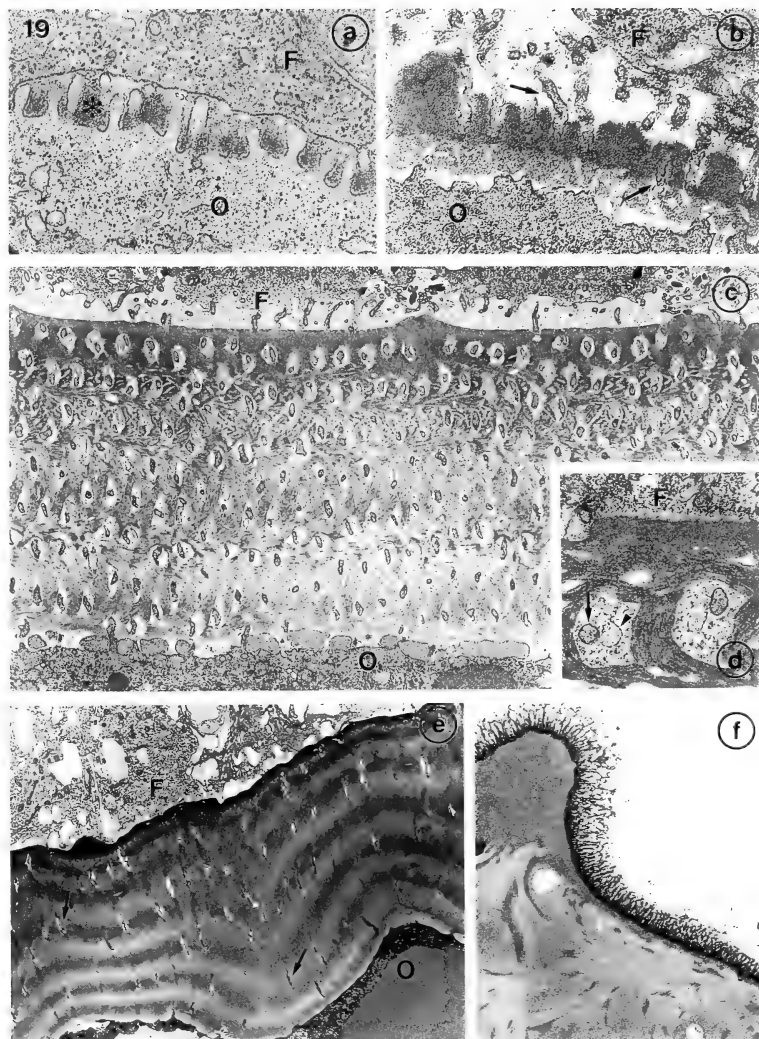


FIG. 18. SDS-polyacrylamide electrophoresis on 12% gels of the major proteins present in extracts of ovary (lanes 1 and 1'), prematurational (post-vitellogenic) follicles (lanes 2 and 2'), postmaturation follicles matured *in vivo* (lanes 3 and 3') or *in vitro* (lanes 4 and 4') and ovulated eggs (lanes 5 and 5'). Lanes 1-5 represent samples containing approximately 50 μ g protein and are stained with Coomassie Blue, as is the first lane that indicates molecular mass standards (92.5, 66.2, 45.0, 31.0, 21.0 and 14.4 kDa from top to bottom respectively). Lanes 1-5 represent samples containing approximately 100 μ g protein electrophoresed under identical conditions but stained with Stains-all to demonstrate acidic phosphoproteins. From Wallace and Begovac [88].

final egg size. As a consequence, such eggs are rendered buoyant in sea water [105] and thus become widely dispersed. It appears that the accumulation of K^+ and/or protein dephosphory-

lation may contribute the osmotic effectors involved in this remarkable phenomenon. The occurrence of yolk protein proteolysis during oocyte maturation helps to explain the presence of

FIG. 19. Vitelline envelope formation in *F. heteroclitus*. Panel a: Electron-dense envelope material (*) begins to accumulate between microvilli that extend from the surface of the oocyte (O) towards the overlying follicle cells (F) within a primary growth stage follicle. $\times 42,000$. Panel b: Envelope material continues to accrue and become bilaminar in appearance as oocyte growth continues. Microvillar processes (arrows) extending both from the oocyte (O) and follicle cells (F) can be seen penetrating the developing envelope. $\times 29,700$. Panel c: The vitelline envelope in this late vitellogenic follicle has greatly increased in size and complexity and has become multilaminar. Microvillar processes from both the oocyte (O) and follicle cells (F) are apparent within patent pore canals that traverse the developing vitelline envelope. $\times 5,280$. Panel d: Higher power electron micrograph demonstrating pore canals that contain both oocyte (arrow) and follicle cell (arrowhead) processes. F indicates cytoplasm of a follicle cell. $\times 22,400$. Panel e: The vitelline envelope in this late maturational follicle has undergone compaction and has become more homogenous in appearance. The pore canals (arrows) become narrower as the microvillar process from both the oocyte (O) and follicle cells (F) begin to retract. $\times 2,950$. Panel f: The outer region of the vitelline envelope (chorion) from a mature egg displays a filamentous coat. $\times 10,500$.



unusual yolk protein polypeptides present in the eggs of many, particularly marine teleosts [17]. However, the molecular and physiological mechanisms responsible for oocyte hydration during maturation remain to be elucidated.

OTHER CELLULAR ASPECTS OF OOCYTE GROWTH

Vitelline envelope formation

The vitelline envelope begins to form during the perinucleolus stage of oocyte growth and continues to increase in size and differentiate throughout the remainder of the oocyte growth stages (Fig. 19). As envelope material continues to accrue extracellularly, the microvillar processes extending from both the oocyte and follicle cells increase in length and reside within pore canals that penetrate the enlarging envelope. Gap junctions have been identified between microvillar processes of both cell types on the distal side of the vitelline envelope [8, 118–120]. As the follicle grows, the vitelline envelope becomes highly ordered and architecturally complex; particularly good descriptions of this process are provided by Azevedo [2], Wourms [3], Ulrich [57], Anderson [121], Busson-Mabillot [122], Riehl [123], and Stehr and Hawkes [124]. Most studies on the vitelline envelope are of a morphological nature, but several recent reports have described the biochemical composition of these intricate structures [125–127]. One important unanswered question regarding the vitelline envelope in teleosts is which cells, the oocyte and/or the follicle cells, are synthesizing its components? Immunochemical studies in the medaka, *Oryzias latipes*, indicate that the liver contributes to its formation, at least in this species [128].

Lipid formation

In most teleosts, lipid bodies first appear in cortical alveolus-stage oocytes, where they reside in the perinuclear ooplasm (Fig. 20). Lipid continues to amass throughout most of oocyte growth and more variation occurs in this process among fish species than for previously mentioned events. Examples can be cited ranging from fish eggs

devoid of lipid droplets, such as in the cunner, *Tautoglabrus adspersus* [9, 129], to gravid ovaries of the gourami, *Trichogaster cosbyi*, in which 37% of the weight is wax ester [130, 131]. The latter fish is typical of the bubble nest builders, which spawn buoyant eggs in fresh water [132]. It should be noted that lipid is frequently hard to detect in histological preparations since it is dissolved during routine histological processing of tissue. Thus, unless fixatives are used that specifically retain lipids (e.g., osmium tetroxide (Fig. 9)), it is difficult to distinguish lipid droplets from vacuolar appearing cortical alveoli (Fig. 20).



FIG. 20. Light micrograph of a section through a cortical alveolus-stage follicle from *F. heteroclitus*. This tissue was fixed in a solution that did not contain osmium tetroxide and thus it is difficult to distinguish the lipid droplets (arrowheads) from cortical alveoli (*) because the contents of both are leached out during tissue preparation (compare with Fig. 9). Although much lipid is located in a perinuclear position, lipid bodies that are more randomly arranged throughout the ooplasm are difficult to distinguish. This section was stained with toluidine blue. $\times 180$.

Determination of egg size

The final egg size can vary considerably among teleosts, the extremes for North American waters ranging from less than 0.3-mm diameter for the sea perch, *Cymatogaster aggregatus* [133], up to 30-mm diameter for the marine catfish, *Bagre marinus*

[134]. The most effective way to achieve disparate egg size would be to modify yolk accumulation or hydration. The published pictures of *C. aggregatus* eggs seem to indicate that oocytes do not advance beyond the cortical alveolus-stage, i.e., neither vitellogenesis or terminal hydration during maturation take place [135, 136]. If so, it would be interesting to explore whether these animals have lost the capacity to make vitellogenin or whether oocyte sequestration is deficient. The available evidence for *B. marinus* is inconclusive, but it would appear that its eggs are fully yolked, i.e., they are opaque and do not display the transparent quality of eggs that have undergone enlargement due to hydration.

A NEW PERSPECTIVE OF OOCYTE STAGES

Many staging systems of oocyte development focus on a specific event (or events) that characterizes a certain size range of oocytes with the implication being that only within this size class of oocytes does the specific event (or events) occur. As we have learned more about the cellular and biochemical processes that are involved in oocyte growth and have developed procedures to quantify such events, it has become quite apparent that the synthesis or accumulation of various materials is not necessarily stage-specific, as is implied by most oocyte staging systems. Some examples are:

1) For years it was widely held that lampbrush chromosomes were engaged in the synthesis of maternal mRNA only during the later part of primary oocyte growth, when such chromosomes are readily perceived and by the end of which the full complement of maternal mRNA has accumulated [137]. Nevertheless, in *X. laevis* lampbrush chromosomes have been demonstrated in late vitellogenic oocytes [138] and poly(A)-containing RNA continues to be synthesized in the absence of long-term accumulation throughout oocyte growth, suggesting that the level of maternal mRNA present at various stages of oocyte growth is the result of synthesis combined, in later stages, with turnover [139].

2) Vitelline envelope formation begins during the primary growth stage and appears to continue throughout the rest of oocyte growth (Fig. 19).

3) [^3H]Glucose has been found to label exclusively the glycoconjugate present in *F. heteroclitus* cortical alveoli during short-term pulse experiments, as demonstrated by autoradiographic (Fig. 10) and electrophoretic procedures [42]. When follicles of various sizes were incubated for short periods with [^3H]glucose, incorporation was greatest in cortical alveolus-stage oocytes for results expressed on a per volume basis [42], as expected from microscopic impressions. However, when the results were expressed on a per follicle basis, absolute rates of incorporation were found to be greater in vitellogenic and maturation-stage oocytes (Fig. 21). The massive accumulation of yolk protein and water during these later stages thus subjectively appeared to relegate the synthesis of cortical alveolus material to a trivial or nonexistent process when perceived cytologically.

4) The sequestration of vitellogenin has been found to occur not only during vitellogenesis *per se*, but also during at least the first part of maturation in both amphibians [140] and fish (Fig. 21, [44]). Pinocytotic activity is apparent at the oocyte surface throughout vitellogenesis and early maturation and the protein content of developing oocytes continues to increase concomitant with maturation [97].

Because of these and other observations, we would like to advance the notion that physiological events do not sequentially replace one another during oocyte growth, but rather that these events are sequentially initiated and, once initiated, remain active throughout oocyte development (Fig. 21). Oocyte growth and all the processes previously initiated may accelerate or slow down due to a regimen of hormonal clues, or even turn off during atresia, but overall oocyte development is considered to comprise a cascade of cellular processes that occur during meiotic arrest. Oocyte maturation appears to represent a true change in oocyte physiology since after germinal vesicle breakdown, surface projections from the oocyte retract and endocytosis no longer continues [97, 140] as the oocyte finally ovulates from its follicular investments and changes into an egg.

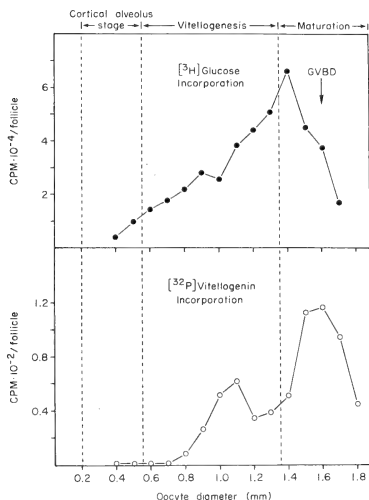


FIG. 21. Cortical alveoli formation and vitellogenesis. Top panel: Incorporation of [³H]glucose into TCA-precipitable material in different sized follicles from *F. heteroclitus* that were incubated for 12 hr in fish saline containing [³H]glucose, followed by a 12 hr incubation in saline solution alone. The data are expressed as cpm/follicle and indicate that a glycoconjugate component of cortical alveoli is made throughout vitellogenesis and early maturation. Adapted from Selman *et al.* [42]. Lower panel: Distribution of *F. heteroclitus* [³²P]vitellogenin within different sized follicles 20 hr after injection into a single female. Sequestration of vitellogenin occurs during vitellogenesis and continues through early maturation. Adapted from Selman and Wallace [44].

ACKNOWLEDGMENTS

Current personal research cited by the authors was supported by N. S. F. Grant Nos. DCB-8401647 to KS and DCB-8511260 to RAW.

REFERENCES

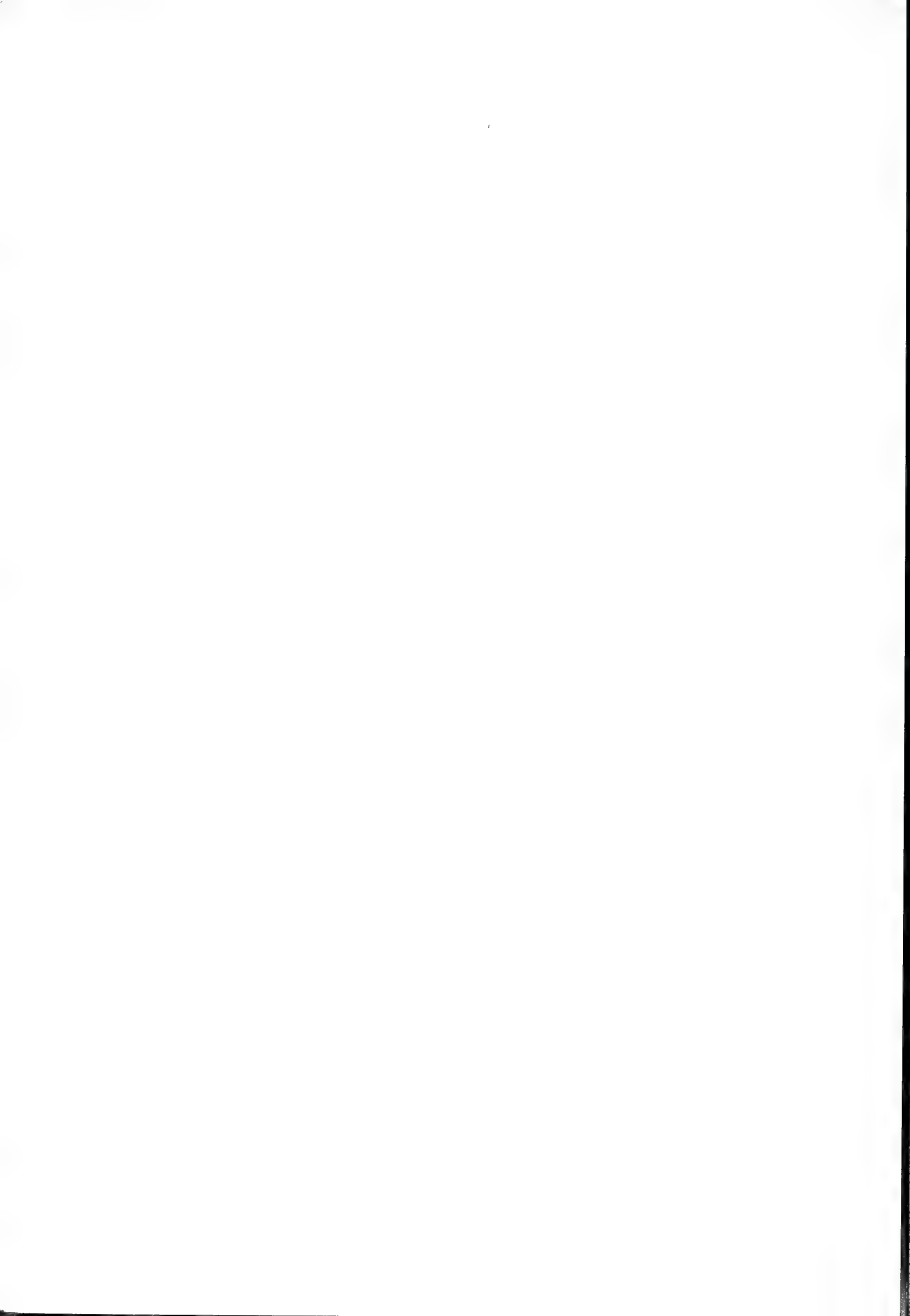
- 1 Kuo, C. M., Nash, C. E. and Shehadeh, Z. H. (1974) *Aquaculture*, **3**: 1-14.
- 2 Azevedo, C. (1974) *J. Microsc. (Paris)*, **21**: 43-54.

- 3 Wourms, J. P. (1976) *Develop. Biol.*, **50**: 338-354.
- 4 Shackley, S. E. and King, P. E. (1977) *Cell Tissue Res.*, **181**: 105-128.
- 5 Forberg, K. G. (1982) *J. Fish Biol.*, **20**: 143-154.
- 6 Selman, K. and Wallace, R. A. (1986) *Amer. Zool.*, **26**: 173-192.
- 7 Begovac, P. C. and Wallace, R. A. (1988) *J. Morphol.*, **197**: 353-369.
- 8 Iwamatsu, I., Ohta, T., Oshima, E. and Sakai, N. (1988) *Zool. Sci.*, **5**: 353-373.
- 9 Wallace, R. A. and Selman, K. (1981) *Amer. Zool.*, **21**: 325-343.
- 10 Wiegand, M. D. (1982) In "Reproductive Physiology of Fish". Ed. by C. J. J. Richter and H. J. T. Goos, Pudoc, Wageningen, pp. 136-146.
- 11 de Vlaming, V. (1983) In "Control Processes in Fish Physiology". Ed. by J. C. Rankin, T. J. Pitcher and R. T. Duggan, Croom Helm, London, pp. 176-99.
- 12 Fostier, A., Jalabert, B., Billard, R., Breton, B. and Zohar, Y. (1983) In "Fish Physiology. Vol IX/A: Reproduction/Endocrine Tissues and Hormones". Ed. by W. S. Hoar, D. J. Randall and E. M. Donaldson, Academic Press, New York, pp. 277-372.
- 13 Goetz, F. W. (1983) In "Fish Physiology. Vol IX/B: Reproduction/Behavior and Fertility Control". Ed. by W. S. Hoar, D. J. Randall and E. M. Donaldson, Academic Press, New York, pp. 117-170.
- 14 Idler, D. R. and Ng, T. B. (1983) In "Fish Physiology. Vol IX/A: Reproduction/Endocrine Tissues and Hormones". Ed. by W. S. Hoar, D. J. Randall and E. M. Donaldson, Academic Press, New York, pp. 187-221.
- 15 Nagahama, Y. (1983) In "Fish Physiology. Vol IX/A: Reproduction/Endocrine Tissues and Hormones". Ed. by W. S. Hoar, D. H. Randall and E. M. Donaldson, Academic Press, New York, pp. 223-275.
- 16 Ng, T. B. and Idler, D. R. (1983) In "Fish Physiology. Vol IX/A: Reproduction/Endocrine Tissues and Hormones". Ed. by W. S. Hoar, D. H. Randall and E. M. Donaldson, Academic Press, New York, pp. 373-404.
- 17 Wallace, R. A. (1985) In "Developmental Biology, Vol. 1. Oogenesis". Ed. by L. W. Browder, Plenum Press, New York, pp. 127-177.
- 18 Guraya, S. S. (1986) *The Cell and Molecular Biology of Fish Oogenesis. Monographs in Developmental Biology*, Vol. 18, Ed. by H. W. Sauer, Karger, Basel, pp. 1-223.
- 19 Nagahama, Y. (1987) In "Hormones and Reproduction in Fishes, Amphibians and Reptiles". Ed. by D. O. Norris and R. E. Jones, Plenum Press, New York, pp. 171-202.

- 20 Nagahama, Y. (1987) *Zool. Sci.*, **4**: 209-222.
- 21 Scott, A. P. (1987) In "Fundamentals of Comparative Vertebrate Endocrinology". Ed. by I. Chester-Jones, P. M. Ingleton and J. G. Phillips, Plenum Press, New York, pp. 223-256.
- 22 Scott, A. P. and Canario, A. V. M. (1987) In "Reproductive Physiology of Fish". Ed. by D. R. Idler, L. W. Crim and J. M. Walsh, Marine Sciences Research Laboratory, St. John's, Newfoundland, pp. 224-234.
- 23 Idler, D. R., Crim, L. W. and Walsh, J. M. (Eds.) (1987) "Reproductive Physiology of Fish". Marine Sciences Research Laboratory, St. John's, Newfoundland, pp. 1-336.
- 24 Tokarz, R. R. (1978) In "The Vertebrate Ovary". Ed. by R. E. Jones, Plenum Press, New York, pp. 145-179.
- 25 Yamamoto, K. (1962) *Annot. Zool. Japon.*, **35**: 156-161.
- 26 Yamazaki, F. (1956) *Mem. Fac. Fish., Hokkaido Univ.*, **13**: 1-64.
- 27 Braekvelt, C. R. and McMillan, D. B. (1967) *J. Morphol.*, **123**: 373-396.
- 28 Begovac, P. C. and Wallace, R. A. (1987) *J. Morphol.*, **193**: 117-133.
- 29 Bullough, W. S. (1942) *J. Endocrinol.*, **3**: 211-219.
- 30 Mendoza, G. (1943) *Biol. Bull.*, **84**: 87-97.
- 31 Lehri, G. K. (1968) *Acta Anat.*, **69**: 105-124.
- 32 Brummett, A. R., Dumont, J. N. and Larkin, J. R. (1982) *J. Morphol.*, **173**: 1-16.
- 33 Monaco, P. J., Rasch, E. M. and Balsano, J. S. (1981) *Histochem. J.*, **13**: 747-761.
- 34 Anderson, D. M. and Smith, L. D. (1978) *Develop. Biol.*, **67**: 274-285.
- 35 Golden, L., Schafer, U. and Rosbash, M. (1980) *Cell*, **22**: 835-844.
- 36 Riehl, R. (1978) *Cytobiol.*, **17**: 137-145.
- 37 Azevedo, C. (1984) *Cell Tiss. Res.*, **238**: 121-128.
- 38 Hubbard, J. W. (1894) *Proc. Amer. Phil. Soc.*, **33**: 74-83.
- 39 Guraya, S. S. (1979) *Int. Rev. Cytol.*, **59**: 249-321.
- 40 Beams, H. W. and Kessel, R. G. (1973) *Am. J. Anat.*, **136**: 105-122.
- 41 Thomas, P. C. and Sathyanesan, A. G. (1985) *Mikroskopie*, **42**: 281-286.
- 42 Selman, K., Wallace, R. A. and Barr, V. (1986) *J. Exp. Zool.*, **239**: 277-288.
- 43 Selman, K., Wallace, R. A. and Barr, V. (1988) *J. Exp. Zool.*, **246**: 42-56.
- 44 Selman, K. and Wallace, R. A. (1983) *J. Exp. Zool.*, **226**: 441-457.
- 45 Yamamoto, T. (1961) *Int. Rev. Cytol.*, **12**: 361-405.
- 46 Hart, N. H. and Yu, S.-F. (1980) *J. Exp. Zool.*, **213**: 137-159.
- 47 Brummett, A. R. and Dumont, J. N. (1981) *J. Exp. Zool.*, **216**: 63-79.
- 48 Kobayashi, W. (1985) *J. Fac. Sci., Hokkaido Univ. Ser. VI*, **24**: 87-102.
- 49 Schuel, H. (1985) In "Biology of Fertilization, Vol. 3". Ed. by C. B. Metz and A. Monroy, Academic Press, New York, pp. 1-43.
- 50 Krajhanzl, A., Nosek, J., Habrova, V. and Kocourek, J. (1984) *Histochem. J.*, **16**: 432-434.
- 51 Krajhanzl, A., Nosek, J., Monsigny, M. and Kocourek, J. (1984) *Histochem. J.*, **16**: 426-429.
- 52 Nosek, J. (1984) *Histochem. J.*, **16**: 435-437.
- 53 te Heesen, D. and Engles, W. (1973) *Wilhelm Roux Arch. Entwmech. Org.*, **173**: 46-59.
- 54 te Heesen, D. (1977) *Zool. Jahr. Anat. Bd.*, **97**: 566-582.
- 55 Droller, M. J. and Roth, T. F. (1966) *J. Cell Biol.*, **28**: 209-232.
- 56 Anderson, E. (1968) *J. Morphol.*, **125**: 23-60.
- 57 Ulrich, E. (1969) *J. Microsc. (Paris)*, **8**: 447-478.
- 58 Wegmann, I. and Götting, K. J. (1971) *Z. Zellforsch.*, **119**: 405-433.
- 59 Masuda, K., Iuchi, I., Iwamori, M., Nagai, Y. and Yamagami, K. (1986) *J. Exp. Zool.*, **238**: 261-265.
- 60 Kitajima, K., Inoue, Y. and Inoue, S. (1986) *J. Biol. Chem.*, **261**: 5262-5269.
- 61 Inoue, S., Kitajima, K., Inoue, Y. and Kudo, S. (1987) *Develop. Biol.*, **123**: 442-454.
- 62 Inoue, S. and Inoue, Y. (1986) *J. Biol. Chem.*, **261**: 5256-5261.
- 63 Wahli, W., Dawid, I. B., Wyler, T., Jaggi, R. B., Weber, R. and Ryffel, G. U. (1979) *Cell*, **16**: 535-549.
- 64 Wahli, W., Dawid, I. B., Ryffel, G. U. and Weber, R. (1981) *Science*, **212**: 298-304.
- 65 Wiley, H. S. and Wallace, R. A. (1981) *J. Biol. Chem.*, **256**: 8626-8634.
- 66 Wallace, R. A. and Morgan, J. P. (1986) *Biochem. J.*, **240**: 871-878.
- 67 Korsgaard, B., Emmersen, J. and Petersen, I. (1983) *Gen. Comp. Endocrinol.*, **50**: 11-17.
- 68 Hara, A., Matsubara, T., Saneyoshi, M. and Takano, K. (1984) *Bull. Fac. Fish., Hokkaido Univ.*, **35**: 144-153.
- 69 Maitre, J. L., Le Guellec, C., Derrien, S., Tenniswood, M. and Valotaire, Y. (1985) *Can. J. Biochem. Cell Biol.*, **63**: 982-987.
- 70 So, Y. P., Idler, D. R. and Hwang, S. J. (1985) *Comp. Biochem. Physiol.*, **81B**: 63-71.
- 71 Sumpter, J. P. (1985) In "Current trends in Comparative Endocrinology". Ed. by B. Lofis and W. N. Holmes, Hong Kong Univ. Press, Hong Kong, pp. 355-357.
- 72 Copeland, P. A., Sumpter, J. P., Walker, T. K. and Croft, M. (1986) *Comp. Biochem. Physiol.*

- 83B**: 487-493.
- 73 Fukayama, S., Takahashi, H., Matsubara, T. and Hara, A. (1986) *Comp. Biochem. Physiol.*, **84A**: 45-48.
 - 74 Hara, A., Takemura, A., Matsubara, T. and Takano, K. (1986) *Bull. Fac. Fish., Hokkaido Univ.*, **37**: 101-110.
 - 75 Korsgaard, B., Mommsen, T. P. and Saunders, R. L. (1986) *Gen. Comp. Endocrinol.*, **62**: 193-201.
 - 76 Tam, W. H., Roy, R. J. J. and Makaran, R. (1986) *Can. J. Zool.*, **64**: 744-751.
 - 77 Babin, P. J. (1987) *Biochem. J.*, **246**: 425-429.
 - 78 Covens, M., Covens, L., Ollevier, F. and De Loof, A. (1987) *Comp. Biochem. Physiol.*, **88B**: 75-80.
 - 79 Hamazaki, T. S., Iuchi, I. and Yamagami, K. (1987) *J. Exp. Zool.*, **242**: 333-346.
 - 80 Hara, A. (1987) *Mem. Fac. Fish., Hokkaido Univ.*, **34**: 1-59.
 - 81 Tyler, C. R., Sumpter, J. P. and Bromage, N. R. (1988) *J. Exp. Zool.*, **246**: 171-179.
 - 82 Norberg, B. and Haux, C. (1985) *Comp. Biochem. Physiol.*, **81B**: 869-876.
 - 83 Selman, K. and Wallace, R. A. (1982) *Tissue Cell*, **4**: 555-571.
 - 84 Abraham, M., Hilge, V., Lison, S. and Tibika, H. (1984) *Cell Tiss. Res.*, **235**: 403-410.
 - 85 Parmentier, H. K., van den Boogaart, J. G. M. and Timmermans, L. P. M. (1985) *Cell Tiss. Res.*, **242**: 75-81.
 - 86 Campbell, C. M. and Jalabert, B. (1979) *Ann. biol. Anim. Biochim. Biophys.*, **19**: 429-437.
 - 87 Tyler, C. R., Sumpter, J. P. and Bromage, N. R. (1987) In "Reproductive Physiology of Fish". Ed. by D. R. Idler, L. W. Crim and J. M. Walsh. Marine Sciences Research Laboratory, St. John's, Newfoundland, p. 221.
 - 88 Wallace, R. A. and Begovac, P. C. (1985) *J. Biol. Chem.*, **260**: 11268-11274.
 - 89 Skinner, E. R. and Rogie, A. (1978) *Protides Biol. Fluids*, **25**: 491-494.
 - 90 Hori, S. H., Kodama, T. and Tanahashi, K. (1979) *Gen. Comp. Endocrinol.*, **37**: 306-320.
 - 91 de Vlaming, V., Wiley, H. S., Delahunty, G. and Wallace, R. A. (1980) *Comp. Biochem. Physiol.*, **67B**: 613-623.
 - 92 Hara, A., Yamauchi, K. and Hirai, H. (1980) *Comp. Biochem. Physiol.*, **84B**: 315-320.
 - 93 Busson-Mabillot, S. (1984) *Biol. Cell.*, **51**: 53-66.
 - 94 Wall, D. A. and Meleka, I. (1985) *J. Cell Biol.*, **101**: 1651-1664.
 - 95 Wall, D. A. and Patel, S. (1987) *Develop. Biol.*, **119**: 275-289.
 - 96 Shigaura, H. T. and Haschemeyer, A. V. (1985) *Comp. Biochem. Physiol.*, **80B**: 935-939.
 - 97 Wallace, R. A. and Selman, K. (1985) *Develop. Biol.*, **110**: 492-498.
 - 98 McCollum, K., Gregory, D., Williams, B. and Taborsky, G. (1986) *Comp. Biochem. Physiol.*, **84B**: 151-157.
 - 99 Lange, R. H., Richter, H-P., Riehl, R., Zierold, K., Trandabura, T. and Magdowski, G. (1983) *J. Ultrastruct. Res.*, **83**: 122-140.
 - 100 Lange, R. H. (1985) *Int. Rev. Cytol.*, **97**: 133-181.
 - 101 Lange, R. H., Grodzinski, Z., and Kilarski, W. (1982) *Cell Tiss. Res.*, **222**: 159-165.
 - 102 Lange, R. H. and Kilarski, W. (1986) *Tissue Cell*, **18**: 117-124.
 - 103 Grodzinski, Z. (1954) *Bl. Folia Morphol. (Warsaw)*, **13**: 13-36.
 - 104 Yamamoto, K. (1957) *Bull. Fac. Fish., Hokkaido Univ.*, **8**: 270-277.
 - 105 Fulton, T. W. (1898) *Fish. Bd. Scotland 16th Ann. Rep.*, Part 3: 83-134.
 - 106 Yamamoto, K. (1957) *J. Fac. Sci., Hokkaido Univ. Ser. VI*, **13**: 344-351.
 - 107 Oshiro, T. and Hibiya, T. (1982) *Bull. Jap. Soc. Sci. Fish.*, **48**: 391-399.
 - 108 Schuetz, A. W. (1985) In "Developmental Biology, Vol. 1. Oogenesis". Ed. by L. W. Browder, Plenum Press, New York, pp. 3-83.
 - 109 Masui, Y. and Clarke, H. J. (1979) *Int. Rev. Cytol.*, **57**: 185-282.
 - 110 Maller, J. L. (1985) In "Developmental Biology, Vol. 1. Oogenesis". Ed. by L. W. Browder, Plenum Press, New York, pp. 289-311.
 - 111 Watanabe, W. O. and Kuo, C-M. (1986) *J. Fish Biol.*, **28**: 425-437.
 - 112 Craik, J. C. A. (1982) *Comp. Biochem. Physiol.*, **72B**: 507-510.
 - 113 Craik, J. C. A. and Harvey, S. M. (1984) *J. Fish Biol.*, **24**: 599-610.
 - 114 Craik, J. C. A. and Harvey, S. M. (1986) *Mar. Biol.*, **90**: 285-289.
 - 115 Wallace, R. A. and Selman, K. (1979) *J. Fish Biol.*, **14**: 551-564.
 - 116 Greeley, M. S., Jr., Calder, D. R. and Wallace, R. A. (1986) *Comp. Biochem. Physiol.*, **84B**: 1-9.
 - 117 McPherson, R., Greeley, M. S., Jr. and Wallace, R. A. (1987) In "Reproductive Physiology of Fish". Ed. by D. R. Idler, L. W. Crim and J. M. Walsh, Marine Sciences Research Laboratory, St. John's, Newfoundland, p. 265.
 - 118 Toshimori, K. and Yasuzumi, F. (1979) *J. Ultrastruct. Res.*, **67**: 73-78.
 - 119 Kessel, R. G., Tung, H. N., Roberts, R. and Beams, H. W. (1985) *J. Submicrosc. Cytol.*, **17**: 239-253.
 - 120 Kobayashi, W. (1985) *Develop. Growth Differ.*, **27**: 553-561.
 - 121 Anderson, E. (1967) *J. Cell Biol.*, **35**: 193-212.

- 122 Busson-Mabillot, S. (1973) *J. Microsc.*, **18**: 23-44.
- 123 Riehl, R. (1977) *Zool. Anz.*, **199**: 121-139.
- 124 Stehr, C. M. and Hawkes, J. W. (1983) *J. Morphol.*, **178**: 267-284.
- 125 Hamazaki, T., Iuchi, I. and Yamagami, K. (1985) *J. Exp. Zool.*, **235**: 269-279.
- 126 Begovac, P. C. and Wallace, R. A. (1989) *J. Exp. Zool.* (in press).
- 127 Cotelli, F., Andronico, F., Brivio, M., and Lamia, C. L. (1988) *J. Ultrastruct. Mol. Struct. Res.*, **99**: 70-78.
- 128 Hamazaki, T. S., Iuchi, I. and Yamagami, K. (1987) *J. Exp. Zool.*, **242**: 343-349.
- 129 Kuntz, A. and Radcliffe, L. (1917) *Bull. U. S. Bur. Fish.*, **35**: 89-134.
- 130 Sand, D. M., Hehl, J. L. and Schlenk, H. (1969) *Biochemistry*, **8**: 4851-4854.
- 131 Kaitaranta, J. K. and Ackman, R. G. (1981) *Comp. Biochem. Physiol.*, **69B**: 725-729.
- 132 Breder, C. M. and Rosen, D. E. (1966) "Modes of Reproduction in Fishes". Natural History Press, Garden City, New York, pp. 1-94.
- 133 Eigenmann, C. H. (1892) *Bull. U. S. Fish Comm.*, **12**: 401-478.
- 134 Gudger, E. W. (1918) *Carnegie Inst. Wash. Publ.*, **252**: 25-52.
- 145 Turner, C. L. (1938) *J. Morphol.*, **62**: 351-373.
- 136 Wiebe, J. P. (1968) *Can. J. Zool.*, **46**: 1221-1234.
- 137 Smith, L. D. and Richter, J. D. (1985) In "Biology of Fertilization. Vol. 1. Model Systems and Oogenesis". Ed. by C. B. Metz and A. Monroy, Academic Press, New York, pp. 141-188.
- 138 Martin, K., Osheim, Y. N., Beyer, A. L. and Miller, O. J. (1980) In "Results and Problems of Cell Differentiation. Vol XI. Differentiation and Neoplasia". Ed. by R. G. McKinnell, Springer-Verlag, Berlin, pp. 37-44.
- 139 Dolecki, G. J. and Smith, L. D. (1979) *Develop. Biol.*, **69**: 217-236.
- 140 Schuetz, A. W., Wallace, R. A. and Dumont, J. N. (1974) *J. Cell Biol.*, **61**: 26-34.



Autonomic Innervation of Intra- and Extra-Cranial Arteries in the Amphibia

TAKASUKE TAGAWA, ATSUSHI ISHIKAWA, WANAN CHUAN SU
and KIYOSHI OKAMOTO

*Department of Anatomy, Fukuoka University School of Medicine,
Jonan-ku, Fukuoka 814-01, Japan*

ABSTRACT—The pattern of adrenergic and cholinergic innervation in the intra- and extra-cranial arteries of the internal carotid and vertebro-basilar systems was investigated using histochemical techniques in three amphibian species, the Japanese toad, the clawed toad and the leopard frog. As a common feature among these three anuran species, the adrenergic and cholinergic innervation density in the major cerebral artery system was low when compared with the extra-cranial internal carotid artery. In the Japanese toad the adrenergic and cholinergic nerve supply to the two cerebral artery systems was more predominant in the internal carotid system than in the vertebro-basilar system. It was similar in the leopard frog. Adrenergic nerve plexuses in the major cerebral arteries in the Japanese toad were dense compared with those in the leopard frog, but the density of cholinergic nerve plexuses was quite similar in both species. In the clawed toad the nerve fibers showing catecholamine fluorescence or acetylcholin-esterase (AChE) activity were not observed in any pial arteries, except for very few aminergic and AChE-positive fibers in the cerebral carotid artery. The direct innervation by the adrenergic and cholinergic nerves of central origin was demonstrated in the intracerebral small vessels of the clawed toad.

INTRODUCTION

In mammalian cerebral vasculature, dual innervation by both sympathetic adrenergic and parasympathetic cholinergic fibers has been found histochemically [1-6]. Pharmacological and physiological studies have also shown vasomotor roles of these two populations of nerves on the cerebral vasculature [5-10]. In a previous series of histochemical studies in our laboratory, a unique aminergic and cholinergic innervation has been found in the cerebral blood vessels in a variety of submammalian species [11-15]. In the bullfrog, the major cerebral arteries are innervated only by the adrenergic fibers [14]. Besides this report, the innervation of amphibian cerebral vasculature has not been intensively studied using histochemical techniques. Here we report the distribution of aminergic and cholinergic nerves surrounding the cerebral blood vessels of three anuran species

other than bullfrog.

MATERIALS AND METHODS

Thirty clawed toads (*Xenopus laevis*), 20 Japanese toads (*Bufo japonicus*) and 30 leopard frogs (*Rana nigromaculata*) were used in this study. The Falck-Hillarp formaldehyde fluorescence technique [16] and the direct coloring thiocholine method [17] were used for demonstrating the aminergic and cholinergic nerve fibers, respectively.

The animals were anesthetized with ethyl ether, perfused through the aorta with Ringer's solution and decapitated. For whole-mount preparations, the common carotid, intra-cranial carotid, extra-cranial carotid and cerebral arteries were carefully dissected out from the cervical regions and brain respectively. The materials were either stretched over nonfluorescent glass slides, transferred to a desiccator and vacuum dried over P_2O_5 for 1 hr, or fixed with 4% buffered formaldehyde (pH 7.2) for 30 min at 4°C. For sectioning, small blocks of

brain tissue were quickly frozen in isopentane chilled with dry ice, and 15 μ m sections were cryostat sectioned, mounted on glass slides, and fixed with 4% cold formaldehyde for 30 min. Other blocks were freeze-dried.

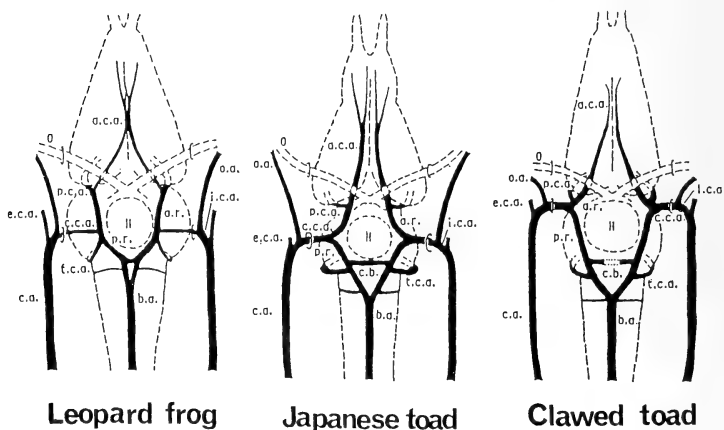
For demonstration of aminergic nerves, the air-dried materials and freeze-dried blocks were treated for 1 hr at 80°C with formaldehyde vapor from paraformaldehyde. The blocks were then infiltrated with paraffin and cut into 15 μ m sections. For cholinergic nerves, the whole-mount preparations fixed in formaldehyde and cryostat sections were maintained in Karnovsky's medium without acetylthiocholine iodide for 30 min at 4°C and then incubated in the complete medium, containing 2×10^{-4} M tetraisopropylpyrophosphoramide as a nonspecific cholinesterase inhibitor, for 1 to 5 hr at 20°C.

RESULTS

A schematic illustration of the cerebral artery systems in the leopard frog, Japanese toad and clawed toad is shown in Figure 1. A characteristic feature of their cerebral vascular anatomy is the well-developed posterior cerebral artery (PCA) arising from the anterior ramus (AR), with an ill-developed middle cerebral artery, regarded as a small branch of the anterior cerebral artery (ACA). In addition, the anterior communicating artery is filamentous or even completely absent, resulting in an incomplete circle of Willis in most cases.

Aminergic innervation

Dense plexuses of catecholaminergic nerve fibers, composed of thin fibers in a complicated meshwork, were found throughout the walls of the common and extra-cranial internal carotid arteries



①

FIG. 1. Diagrams of the arterial supply to the ventral surface of the brain in three species of amphibians. O, optic nerve; H, hypophysis; c.a., common carotid artery; i.c.a., internal carotid artery; e.c.a., external carotid artery; o.a., ophthalmic artery; c.c.a., cerebral carotid artery; a.r., anterior ramus; p.r., posterior ramus; p.c.a., posterior cerebral artery; a.c.a., anterior cerebral artery; t.c.a., tecto-cerebellar artery; b.a., basilar artery; c.b., posterior communicating branch.

(COCA, eICA) of the Japanese toad and leopard frog (Fig. 2). Nerve plexuses in the clawed toad COCA and eICA also demonstrated a plexiform appearance, but appeared to be less rich, and were organized in an elongated meshwork along the vascular axis (Fig. 3).

In the major cerebral arteries of the internal

carotid system (ICS) of the Japanese toad, the cerebral carotid artery (CCA) and AR were furnished with well-developed plexuses of adrenergic nerve fibers which were similar in density and meshwork construction to those seen in the COCA and eICA (Fig. 4). The PCA and ACA, were also richly supplied with adrenergic nerve fibers. In the

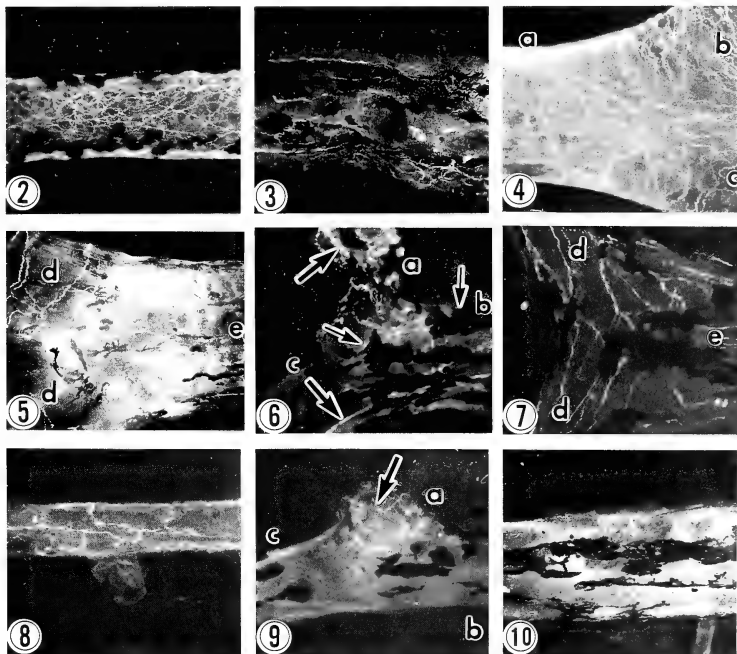


FIG. 2. Adrenergic innervation of common carotid artery in leopard frog. $\times 108$

FIG. 3. Adrenergic innervation of common carotid artery in clawed toad. $\times 108$

FIG. 4. Adrenergic innervation of cerebral carotid artery (a), anterior ramus (b) and posterior ramus (c) in Japanese toad. $\times 108$

FIG. 5. Adrenergic innervation of posterior ramus (d) and basilar artery (e) in Japanese toad. $\times 108$

FIG. 6. Adrenergic innervation of cerebral carotid artery (a), anterior ramus (b) and posterior ramus (c) in leopard frog. Arrows indicate the melanocyte. $\times 108$

FIG. 7. Adrenergic innervation of posterior ramus (d) and basilar artery (e) in leopard frog. $\times 108$

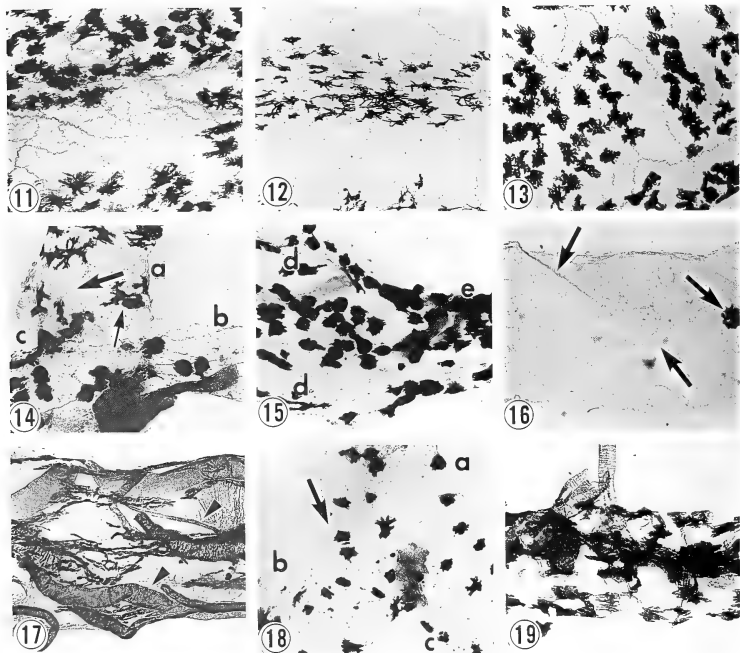
FIG. 8. Adrenergic innervation of anterior cerebral artery in leopard frog. $\times 108$

FIG. 9. Adrenergic innervation of cerebral carotid artery (a), anterior ramus (b) and posterior ramus (c) in clawed toad. Adrenergic fibers (arrow) are indicated in the cerebral carotid artery. $\times 108$

FIG. 10. Adrenergic innervation of basilar artery in clawed toad. $\times 108$

major cerebral arteries of the vertebro-basilar system (VBS), the density of nerve plexuses was not so high as in the ICS; a moderate number of adrenergic nerve fibers formed wide networks along the walls of the PR and basilar artery (BA) (Fig. 5).

The density of adrenergic innervation in the cerebral artery system of the leopard frog was low compared with the Japanese toad: nerve plexuses of the CCA, AR, PCA, PR and distal portion of the BA demonstrated approximately the same density and distribution as those observed in the



- FIG. 11. Cholinergic innervation of common carotid artery in leopard frog. $\times 108$
 FIG. 12. Cholinergic innervation of common carotid artery in Japanese toad. $\times 108$
 FIG. 13. Cholinergic innervation of common carotid artery in clawed toad. $\times 108$
 FIG. 14. Cholinergic innervation of cerebral carotid artery (a), anterior ramus (b) and posterior ramus (c) in leopard frog. Thick arrow indicates the cholinergic fibers and thin arrow, the melanocyte.
 FIG. 15. Cholinergic innervation of posterior ramus (d) and basilar artery (e) in leopard frog. $\times 108$
 FIG. 16. Cholinergic innervation of cerebral carotid artery in Japanese toad. Thick arrows indicate the cholinergic fibers and thin arrow, the melanocyte. $\times 108$
 FIG. 17. Cholinergic innervation of basilar artery and its small branches in Japanese toad. Relatively heavy AChE-activities on the walls of the small arteries are indicated by arrowheads. $\times 108$
 FIG. 18. Cholinergic innervation of cerebral carotid artery (a), anterior ramus (b) and posterior ramus (c) in clawed toad. AChE-positive fibers (arrow) are indicated in the cerebral carotid alone. $\times 108$
 FIG. 19. Cholinergic innervation of basilar artery in clawed toad. $\times 108$

Japanese toad PR and BA (Figs. 6 and 7). The ACA and proximal portion of the BA of this frog were very poorly supplied by or sometimes devoid of adrenergic nerve fibers (Fig. 8). In the clawed toad, no adrenergic nerve fibers were demonstrated in the pial arteries, except for only a few fluorescent fibers in the CCA (Figs. 9 and 10).

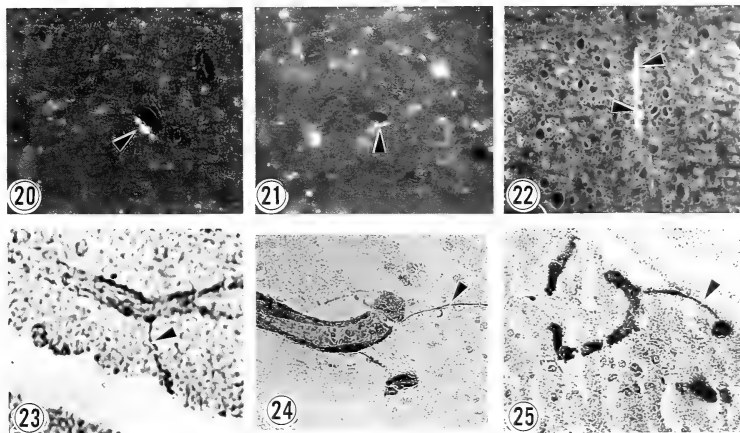
Cholinergic innervation

The COCA and eICA of the leopard frog possessed dense cholinergic nerve plexuses with a similar density and distribution to the adrenergic nerve plexuses (Fig. 11). Cholinergic nerve plexuses in the Japanese toad and the clawed toad COCA and eICA were also well organized, but they were more course than those in the leopard frog (Figs. 12 and 13).

The pattern of cholinergic innervation in the major cerebral arteries of the leopard frog corresponded well with the pattern of adrenergic innervation. A moderate number of nerve fibers positive for acetylcholinesterase (AChE) were found along the walls of the CCA, AR, PCA, PR

and distal portion of the BA (Figs. 14 and 15). The ACA and proximal portion of the BA received only a scarce supply of nerve fibers, with a low AChE activity. In the Japanese toad, the cholinergic nerve fibers surrounding the major cerebral arteries were distinctly fewer than the adrenergic nerves. Nerve fibers with very low AChE activity were sparsely distributed along the walls of the CCA, AR and PR (Fig. 16). In the remaining major cerebral arteries, AChE-positive nerve fibers were few or completely absent (Fig. 17). In the clawed toad, the distribution pattern of cholinergic nerve fibers was essentially the same as that of adrenergic nerve fibers and only a few AChE-positive fibers were observed in the CCA alone (Figs. 18 and 19).

It was apparent from the cross sections (Figs. 20–25) that capillaries and arterioles within the brain parenchyma are directly innervated by adrenergic and cholinergic nerve fibers. The direct adrenergic and cholinergic innervations of intraparenchymal small blood vessels were found in all of the species examined, and were often encoun-



Figs. 20–25. Cross sections of capillaries and arterioles in the brain parenchyma. Adrenergic fibers (arrowhead) in the vessel wall in leopard frog (Fig. 20. $\times 150$), Japanese toad (Fig. 21. $\times 150$) and clawed toad (Fig. 22. $\times 108$). Cholinergic fibers (arrowhead) running with the small blood vessels in leopard frog (Fig. 23. $\times 200$), Japanese toad (Fig. 24. $\times 200$) and clawed toad (Fig. 25. $\times 200$).

tered in the blood vessels supplying the diencephalon.

DISCUSSION

In mammals, the eICA, a major artery supplying blood to the cerebral circulation, has sparse adrenergic and cholinergic nerve plexuses, but the plexuses become dense rapidly as the ICA enters the cranial cavity [18]. In amphibian species studied, thus far ([14] and present findings) the eICA is more densely innervated by both adrenergic and cholinergic nerve fibers than the major cerebral arteries, or the mammalian eICA. Further, the innervation density of these two types of nerves in the amphibian eICA is high as compared with that in the corresponding artery of mammals. This suggests the significance of neurogenic vasomotor control in the amphibian eICA.

In our previous study, rich adrenergic innervation with no AChE-positive fibers has been found in the cerebral arteries of the bullfrog [14]. This innervation pattern cannot be regarded as a common feature of amphibian cerebrovascular innervation, since the present study has shown the presence of AChE-positive fibers in the major cerebral arteries of the clawed toad, Japanese toad and leopard frog.

In various mammalian species, adrenergic and cholinergic nerve fibers richly innervate the major cerebral arteries with approximately the same density [1-6, 19]. The dual innervation by adrenergic and cholinergic nerves has also been demonstrated in the cerebral arteries of the turtle [11], snake [12] and domestic fowl [13]. Unlike the mammals, the cerebrovascular innervation of these submammalian species is characterized by an unbalanced innervation with fewer cholinergic nerve fibers. In amphibians, although the density and distribution of cerebral perivascular adrenergic and cholinergic nerve fibers varies considerably from species to species, the adrenergic innervation usually predominates. Furthermore, the major cerebral arteries of the lamprey are innervated solely with serotonergic nerve fibers [15]. From these histochemical studies ([11-15] and present findings), we could assume an evolutionary trend that

aminergic fibers appeared earlier than cholinergic fibers in cerebral vascular autonomic innervation. In visceral and cardiovascular autonomic innervation, however, it was oppositely argued that cholinergic fibers appeared earlier than aminergic fibers [20].

It is generally accepted in various vertebrates that sympathetic adrenergic nerves surrounding the major cerebral arteries penetrate into the brain parenchyma along vascular branches to innervate the small intracerebral blood vessels [1-4, 11-14, 18, 19]. The innervation of small blood vessels within brain parenchyma by peripheral cholinergic nerves has also been confirmed in bats [19]. In addition, the existence of central adrenergic and cholinergic innervation has been demonstrated histochemically or ultrastructurally in the intracerebral capillaries and arterioles of laboratory mammals, with a combination of ganglionectomy or denervation technique [21-27]. Similar findings have also been noted in some submammalian species [11-15]. In the present study, dual adrenergic and cholinergic innervation has been observed in the small arteries and capillaries supplying the brain parenchyma, especially the diencephalon, in all the anuran species examined. Although we did not approach to the origin of these fluorescent and AChE-positive nerve fibers with ganglionectomy and denervation treatment in the present study, the absence of aminergic and AChE-positive nerve fibers in the major cerebral arteries of the clawed toad indicates that the aminergic and AChE-positive fibers innervating the intraparenchymal small vessels of this toad are of central origin.

A clear species difference is observed in the innervation density of adrenergic and cholinergic nerves in the amphibian cerebral artery system. This may reflect the uniqueness of adrenergic and cholinergic mechanisms operating in the cerebral circulation of respective amphibian species. Besides these classical neurotransmitters, our preliminary immunohistochemical study has also demonstrated the existence of nerve fibers containing vasoactive peptides, such as substance P, neurokinin A, calcitonin gene-related peptide and vasoactive intestinal polypeptide, in the major cerebral arteries of the bullfrog (Tagawa *et al.*, unpublished

data). The functional involvement of catecholamines, acetylcholine and different kinds of vasoactive peptides within cerebral perivascular nerves is not known in amphibia, and even in laboratory mammals it is still a matter of speculation. In order to explore the neurogenic control mechanisms in the amphibian cerebral circulation, it is necessary to resolve the interaction among these neurotransmitters and putative neurotransmitters.

REFERENCES

- 1 Shenk, E. A. and Badawi, A. E. L. (1968) Dual innervation of arteries and arterioles. A histochemical study. *Z. Zellforsch.*, **91**: 170-177.
- 2 Nelson, E. and Rennels, M. (1970) Innervation of intracranial arteries. *Brain*, **93**: 475-490.
- 3 Motavkin, P. A. and Dovish, T. V. (1971) Histochemical characteristics of acetylcholinesterase of the nerves innervating the brain vessels. *Acta Morphol. Acad. Sci. Hung.*, **19**: 159-173.
- 4 Peerless, S. J. and Yasargil, M. G. (1971) Adrenergic innervation of the cerebral blood vessels in the rabbit. *J. Neurosurg.*, **35**: 148-154.
- 5 Owman, Ch., Edvinsson, L. and Nielsen, K. C. (1974) Autonomic neuroreceptor mechanisms in brain vessels. *Blood vessels*, **11**: 2-31.
- 6 Edvinsson, L. (1975) Neurogenic mechanisms in the cerebrovascular bed. Autonomic nerves, amine receptors and their effects on cerebral blood flow. *Acta Physiol. Scand. (Suppl.)*, **427**: 1-35.
- 7 Mchedlishvili, G. I. and Nikolaishvili, L. S. (1970) Evidence of a cholinergic nervous mechanism mediating the autoregulatory dilation of the cerebral blood vessels. *Pflügers Arch.*, **315**: 27-37.
- 8 Nielsen, K. C. and Owman, Ch. (1971) Contractile response and amine receptor mechanisms in isolated middle cerebral artery of the cat. *Brain Res.*, **27**: 33-42.
- 9 Edvinsson, L., Nielsen, K. C., Owman, Ch. and West, K. A. (1937b) Evidence of vasoconstrictor sympathetic nerves in brain vessels of mice. *Neurol. (Mineap.)*, **23**: 73-77.
- 10 Matsuda, M., Meyer, J. S., Deshmukh, V. D. and Tagashima, Y. (1976) Effect of acetylcholine on cerebral circulation. *J. Neurosurg.*, **45**: 423-431.
- 11 Iijima, T. (1977a) A histochemical study of the innervation of cerebral blood vessels in the turtle. *J. Comp. Neur.*, **176**: 307-314.
- 12 Iijima, T., Wasano, T., Tagawa, T. and Ando, K. (1977b) A histochemical study of the innervation of cerebral blood vessels in the snake. *Cell Tissue Res.*, **179**: 143-155.
- 13 Tagawa, T., Ando, K. and Wasano, T. (1979a) A histochemical study of the innervation of the cerebral vessels in the domestic fowl. *Cell Tissue Res.*, **198**: 43-51.
- 14 Tagawa, T., Ando, K., Wasano, T. and Iijima, T. (1979b) A histochemical study on the innervation of cerebral blood vessels in the bullfrog. *J. Comp. Neur.*, **183**: 25-32.
- 15 Iijima, T. and Wasano, T. (1980) A histochemical and ultrastructural study of serotonin-containing nerves in cerebral blood vessels of the lamprey. *Anat. Rec.*, **198**: 671-680.
- 16 Falck, B. (1962) Observation on the possibilities of the cellular localization of monoamines by a fluorescence method. *Acta Physiol. Scand.*, **56**: 1-24.
- 17 Karnovsky, M. J. and Root, L. (1964) A "direct-coloring" thiocholine method for cholinesterases. *J. Histochem. Cytochem.*, **12**: 219-221.
- 18 Wasano, T. (1980) Morphology and implication of the vasomotor control of the cerebral vessels. *Med. Bull. Fukuoka Univ.*, **7**: 139-158.
- 19 Ando, K. (1981) A histochemical study on the innervation of the cerebral blood vessels in bats. *Cell Tissue Res.*, **217**: 55-64.
- 20 Burnstock, G. (1969) Evolution of the autonomic innervation of visceral and cardiovascular systems in vertebrates. *Pharmacol. Rev.*, **21**: 247-324.
- 21 Falck, B., Mchedlishvili, G. I. and Owman, Ch. (1965) Histochemical demonstration of adrenergic nerves in cortex-pia of rabbit. *Acta Pharmacol. Toxicol.*, **23**: 133-142.
- 22 Hartman, B. K., Zide, D. and Udenfriend, S. (1972) The use of dopaminohydroxylase as a marker for the central noradrenergic nervous system in rat brain. *Proc. Natl. Acad. Sci. USA*, **69**: 2722-2746.
- 23 Edvinsson, L., Lindvall, M., Nielsen, K. C. and Owman, Ch. (1973a) Are brain vessels innervated also by central (nonsympathetic) adrenergic neurons? *Brain Res.*, **63**: 496-499.
- 24 Raichle, M. E., Hartman, B. K., Eichling, J. O. and Sharpe, L. G. (1975) Central noradrenergic regulation of cerebral blood flow and vascular permeability. *Proc. Natl. Acad. Sci. USA*, **72**: 3726-3730.
- 25 Rennels, M. L. and Nelson, E. (1975) Capillary innervation in the mammalian central nervous system. An electron microscopic demonstration (1). *Am. J. Anat.*, **144**: 233-241.
- 26 Rosendorff, C., Mitchell, G., Striven, D. R. L. and Shapiro, C. (1976) Evidence for a dual innervation affecting local blood flow in the hypothalamus of the conscious rabbit. *Circul. Res.*, **38**: 140-145.
- 27 Itakura, T., Yamamoto, K., Tohyama, M. and Shimizu, N. (1977) Central dual innervation of arterioles and capillaries in the brain. *Stroke*, **8**: 360-365.



Growth-Related Biometrical and Biochemical studies of the Compound Eye of the Crab, *Hemigrapsus sanguineus*

EISUKE EGUCHI, KENTARO ARIKAWA, SATOMI ISHIBASHI,

TATSUO SUZUKI¹ and V. BENNO MEYER-ROCHOW²

Department of Biology, Yokohama City University, Kanazawa-ku, Yokohama 236,

¹Department of Pharmacology, Hyogo Medical College, Nishinomiya,

Hyogo 663, Japan, and ²Department of Biological Sciences,

Waikato University, Hamilton, New Zealand

ABSTRACT—In the crab, *Hemigrapsus sanguineus*, increase in body size follows an isometric growth pattern. All parameters such as eye stalk length, number of ommatidia, diameters of ommatidial facets, length and width of compound eye, rhabdom lengths, and chromophore content exhibit a linear relationship with carapace width ranging from approximately 5–31 mm. Eye width increases at a greater rate than eye length. The compound eye growth is accompanied by a narrowing of interommatidial angles, which is likely to lead to a foveal region and improves resolution in the eye of bigger specimens. The volume of retina per a compound eye increases rather exponentially than linearly. The circadian change in rhabdom occupation ratio, the diameter of microvilli as well as the intramembranous particle density are all independent of crab body size. Calculations of the amounts of visual pigment show that in larger crabs extra-rhabdomic chromophore levels are higher than in smaller crabs. The precise location and the function of the extra-rhabdomic chromophore remain enigmatic. A study on regional morphological differences in ommatidial organization indicated that the medial region where the facets are the smallest may be the most probable site of the development of new ommatidia with each moult.

INTRODUCTION

In a series of papers dealing with the structure and function of the compound eye of the crab, *Hemigrapsus sanguineus*, we have already communicated two findings: 1) structure, function and rhodopsin content change in a daily rhythm showing an approximately eightfold increase in rhabdom volume at night over that of daytime which is paralleled by electrophysiological and biochemical parameters [1]. 2) The reported changes in rhabdom size and rhodopsin content are circadian in nature and governed by an internal clock, continuing under the condition of continuous darkness [2].

All experiments mentioned above were carried out on adult crabs with carapace widths of 20–25 mm. On the other hand, age-related structural

changes in the eye of decapod crustaceans have been reported [3–5], and it is felt that for a deeper understanding of the significance of vision in *H. sanguineus* an appreciation of growth-related phenomena is of considerable importance.

Therefore, in this paper, we report data on biometrical investigations of the growth of the compound eye based on measurements of external and internal eye dimensions such as diameter, number of facets, length of retinula layer etc in relation to the crab's body growth. Reference is also made to regional morphological differences of ommatidia in the compound eye. Parallel to the biometrical study a quantitative analysis of visual pigments, measured by HPLC, is also presented.

To date, only a few papers have addressed the question of relative growth of the compound eyes of arthropods (*Limulus*: [6], crayfish: [7–10], insects: [11–13]), and to the best of our knowledge no paper as yet has dealt with the growth of the eye of brachyuran crabs. Since daily changes in rhab-

dom volume and function—at least in the adult have been reported from brachyura other than *H. sanguineus*, as well [14–16], this paper is intended to provide a basis for future comparative studies on growth and age-related phenomena.

MATERIALS AND METHODS

Animals

Hemigrapsus sanguineus crabs of both sexes (carapace width 3–35 mm) were collected at the sea shore in Nojima Park, Yokohama City, Japan. Following collection or maintenance in the laboratory at 10°C under a light dark regime of 12 LD (L = 9:00–21:00 at 2000 lux) the measurements described below were carried out.

Measurements

The parts of the crab's body and the compound eye used in the measurements, are diagrammatically illustrated in Figure 1. They are 1) carapace length, 2) carapace width, 3) body thickness, 4) eye stalk length, 5) eye stalk width, 6) compound

eye length, 7) compound eye width, 8) number or ommatidia. 9) diameter of ommatidial facet (four different regions per eye), 10) rhabdom length, 11) the volume of retina in a compound eye, 12) the ratio (%) of rhabdom volume to volume of retinula per ommatidium (=rhabdom occupation ratio, ROR), 13) the volume of rhabdom in a compound eye, 14) amount (pmol) of visual pigment chromophore as determined by high pressure liquid-chromatography, 15) interommatidial angle.

1) to 3) were measured with a caliper while 4) to 7) were measured with an ocular micrometer attached to a dissecting binocular microscope.

For counting the number of ommatidia, the compound eye including eye stalk was fixed for 2–3 days at 4°C in 2.0% glutaraldehyde 2.0% paraformaldehyde buffered to a pH of 7.3 with 0.1 M cacodylate solution. After washing with the same buffer solution, the eye preparation was decalcified with 5% acetic acid in 70% ethanol for 1 day. The softened eye preparation was then treated with a 1% chlorinated lime solution to dissolve all tissue other than the cornea and the exo-cuticle. After washing with water, the preparation was cut

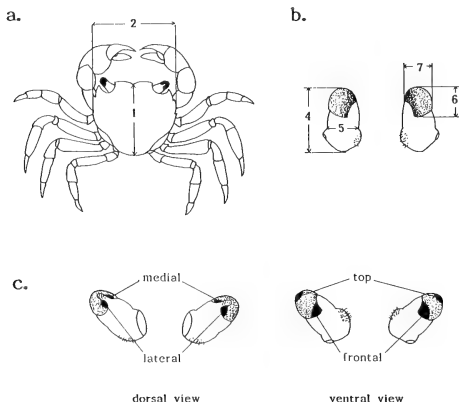


FIG. 1. Measured parts of the crab body and eye: a) carapace length (1), carapace width (CW)(2) and body thickness (3, not shown). b) eye stalk length (4), eye stalk width (5), compound eye length (6) and compound eye width (7). c) The four regions in which the facet sizes were measured are indicated by medial, lateral, top and ventral designations.

into several smaller pieces and mounted on a slide glass.

Diameter of an ommatidial facet i.e. the longest diagonal distance (line) on the outer surface of a facet (an ommatidial cornea), was measured on 10 randomly selected ommatidia in four different regions (frontal, top, lateral and medial) (Fig. 1c). The rhabdom length was measured from longitudinal sections of 20 μm in thickness of the frontal region of the eye. In order to determine the volume of retina, the area of the retinal layer (from the proximal end of the crystalline cone to the basement membrane=rhabdom length) of each longitudinal section was measured by an image analyzing system connected to a computer (NEC 9801E). The retinal areas, thus obtained from each section, were integrated through the entire series of sections of one whole eye.

All crabs used for ROR and chromophore measurements had been kept under the 12LD environment described above for at least two weeks prior to experiments. Day (15:00) and night (3:00) crabs, each 5 individuals of 6 groups according to CW sizes were measured. The measurements by HPLC were carried out on individually isolated compound eyes, and the procedures for the quantification of the amount of the visual pigment chromophore (11-*cis*- and all-*trans*-retinal) by HPLC were the same as reported previously [1]. The ROR of individual ommatidial retinulae was measured from light micrographs featuring cross sections through 16–20 ommatidia of the "forward looking" eye region at the nuclear layer of the retinula cells.

The volume of the rhabdom in a compound eye was calculated from the data of the ROR and the volume of retina, and the measurements were made at 6 points of CW from 7.5–29 mm of 5 individuals each.

The interommatidial angles were measured in the top region of a compound eye where the ommatidia are bigger than those in any other region. The measurements were made on longitudinal sections of compound eyes from a total of 24 individuals of different CW sizes.

RESULTS

Growth pattern

Generally, animal growth when plotted on the ordinate against time on the abscissa, fits a sigmoidal curve. If the shape of the body and the relative dimensions of any part of the body remain constant as the animal grows, a linear growth relationship can be expressed by the equation, $y = ax + b$ which is termed "isometric function" [17].

If, however, growth affects different parts of the body at different times, and growth rates are not constant, then we deal with allometric growth patterns which can be expressed by the general equation $y = cx^k + d$ [17]. It has to be born in mind that with regard to the compound eye the two growth patterns can exist side by side to varying degrees; eye length, for example, may show a linear growth relationship, whereas the volume of retina may not [6].

A total of 285 crabs of various sizes was used in the present investigation. Strong linear correlations ($r > 0.99$) and, thus, isometric growth patterns were observed between i) carapace width and carapace length (Fig. 2), ii) carapace width and body thickness and iii) carapace length and body thickness. Therefore, all of the following results were diagrammed against the carapace width (CW) as a parameter of body size on the abscissa. No sexual differences were noticed in any of the measurements and the assumption is made that increased growth is a reflection of increased age, though the precise moult stage cannot be deter-

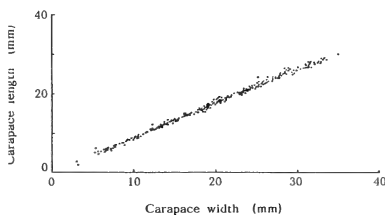


FIG. 2. Relation between carapace length and CW. As no sexual difference was apparent, the data were pooled. The number of measured animal, $n = 295$; correlation coefficient, $r = 0.998$.

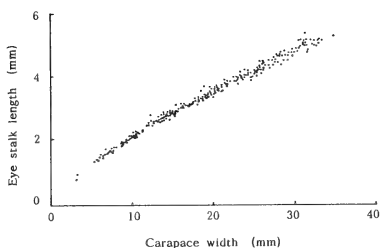


FIG. 3. Relative growth of the eye stalk length. No difference was observed between right and left. $n=291$; $r=0.995$.

mined by this method [9].

Eye stalk and the compound eye

Eye stalk length (Fig. 3), eye stalk width and compound eye length (Fig. 4) all show strong isometric growth correlations ($r > 0.99$) with the CW, and compound eye width (Fig. 6) also shows a high correlation ($r > 0.98$) with CW. The eye-stalk length (y_1) and the compound eye length (y_2) can be approximated by the following isometric equation ($CW = x$ mm);

$$y_1 \text{ (mm)} = 0.15x + 0.77$$

$$y_2 \text{ (mm)} = 0.03x + 0.75$$

The ratio (r_1) of the relative length of the compound eye to the length of eye stalk can be expressed as the following,

$$\frac{y_2}{y_1} = r_1 = \frac{0.03x + 0.75}{0.15x + 0.77} = 0.2 + \frac{0.62}{0.15x + 0.75}$$

From this equation, it is clear that the bigger x becomes, the more closely the ratio approaches to 0.2, which is seemingly identical to the asymptote of the curve shown in Figure 5.

The compound eye width (y_3) to the CW (x) can be approximated also by an isometric equation,

$$y_3 \text{ (mm)} = 0.05x + 0.54$$

It is apparent from the comparison of Figures 4 and 6 that at the smaller CW (10.5 mm), the compound eye length, y_2 , is longer than the eye width. As the crab's body (CW) grows bigger,

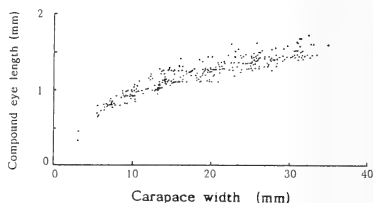


FIG. 4. Compound eye length to CW. $n=293$; $r=0.990$.

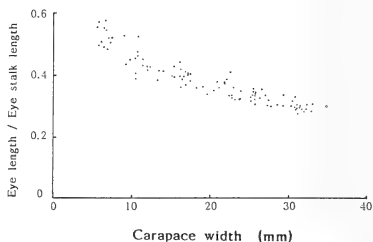


FIG. 5. Relative length of compound eye length to eye stalk length.

however, the eye width grows comparatively much faster than the eye length, and at a CW of 10.5 mm, the eye width reaches the same value (1.0 mm) as that of the eye length; after that eye width is longer than eye length. This relation is clearly shown in Figure 7 illustrating the ratio of compound eye width (y_3) to compound eye length (y_2). Mathematically the ratio (r_2) is expressed as follows;

$$\frac{y_3}{y_2} = r_2 = \frac{0.05x + 0.54}{0.03x + 0.75} = 1.7 + \frac{0.69}{0.03x + 0.75}$$

This means that the ratio is getting closer to 1.7 when x is sufficiently large.

Number and diameter of ommatidial facets

The number of ommatidia was counted in bilateral eyes of 43 crabs of both sexes possessing CW of 5–33 mm. The ommatidial numbers (y_4) increase linearly with CW ($r=0.93$), which is approximated by the equation;

$$y_4 = 144x + 1680.$$

A crab with a CW of 5 mm (referred to as "5 mm crab" in the following) has about 2400 ommatidia while a 30 mm crab has about 6000 ommatidia (Fig. 8). Assuming linear growth, this means that for each mm increase in CW, 144 extra ommatidia develop. Neither sexual differences nor differences between left and right eyes were observed with regard to the number of ommatidia.

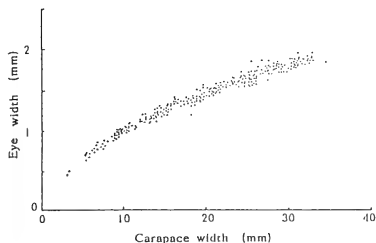


FIG. 6. Compound eye width to CW. $n=248$; $r=0.980$.

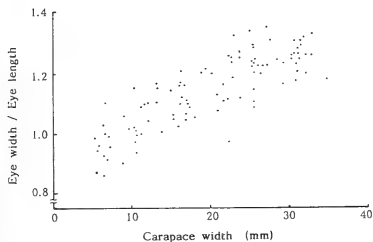


FIG. 7. Ratio of compound eye width to compound eye length to CW. $n=100$.

The diameter of an ommatidial facet (an ommatidial cornea) was measured in the four different regions of the compound eye. As shown in Figure 9, the crabs were divided into 6 group (3–10 individuals each) according to their CW lengths from 5–31 mm. The results showed a linear increase with CW, and the diameter (y_5) is

expressed as;

$y_5 (\mu) = 0.76x + b$ (b is different according to the region, but an average of b of the four regions = 24). All four regions show almost the same growth rate (0.76), and no compound eye show the obvious shape change as reported in *Palaemonetes* [4]. Compared to the other three regions, in which facets were regular, only in the medial region the facets were significantly smaller (Fig. 9) and sometimes even irregular in shape and arrangement.

The interommatidial angle in the top region of the compound eye decreases linearly (in the range $10 < x < 33$) with increasing growth of CW (Fig. 10), and the angle (y_6) is expressed by equation;

$$y_6 (\text{deg}) = -0.55x + 2.7$$

Interommatidial angles at CW smaller than 10 show a large deviations and range from 2.9 to 4.7.

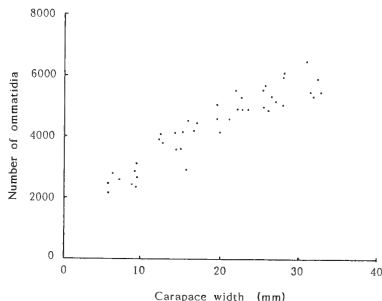


FIG. 8. Number of ommatidia in a compound eye to CW. $n=43$.

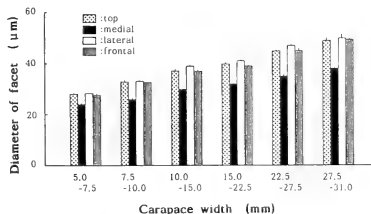


FIG. 9. Diameters of ommatidial facets to CW (each column based on measurements of 3–10 animals).

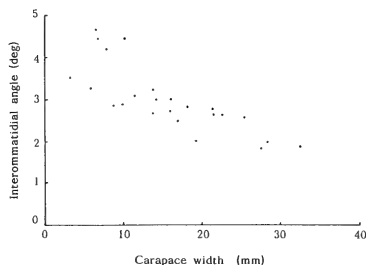


FIG. 10. Relationship between interommatidial angle and CW in the top region of the eye. $n=24$.

Rhabdom size, volume of retina and chromophore contents

Basic ommatidial organization in *H. sanguineus* was found to be in accordance with [18], but in addition we have already reported that in individuals of 20–25 mm CW the rhabdom occupation

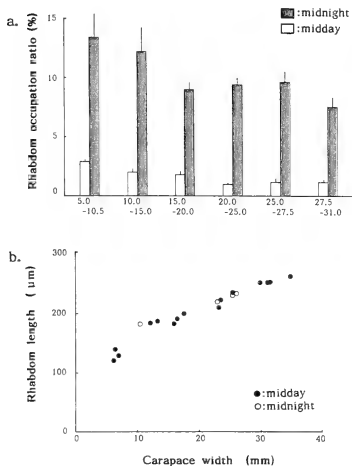


FIG. 11. Rhabdom structure. a) Rhabdom occupation ratio (%). Each column is based on 5 individuals each. b) Rhabdom length increases linearly with the growth of CW. $n=19$.

ratio (ROR) shows a remarkable 8 fold size difference between night and day [1]. The present results (Fig. 11a) show that day-night change of ROR occurs regardless of their body sizes. In small crabs compared to larger ones, ROR values are slightly higher but the ratio of the daily change of the ROR is lower.

Rhabdom length of a 10 mm crab and a 30 mm crab are ca. $150 \mu\text{m}$ and ca. $240 \mu\text{m}$, respectively (Fig. 11b). At least in the frontal region of the compound eye in the range of CW (x) >10 , rhabdom lengths (y_7) can be expressed by the equation;

$$y_7 (\mu\text{m}) = 4x + 132$$

This means $4 \mu\text{m}$ increase with each 1 mm increase in CW. In contrast to the situation of the decapod crustaceans *Panulirus longipes* and *Jasus edwardsii*

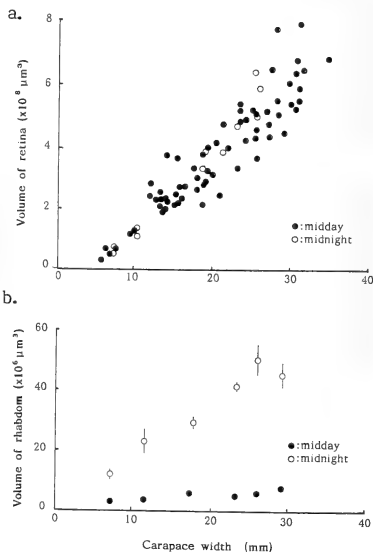


FIG. 12. The volumes of retina and rhabdom in a compound eye at midday and midnight a) The volume of the retina with growth of CW. $n=79$. b) Change in the volume of rhabdom calculated from the data of ROR and the volume of retina.

[3, 19], where the profiles of transversely sectioned rhabdoms change dramatically with age, the rhabdom of *H. sanguineus* was found to be columnar in all size-classes studied.

The increase of the volume of retina in a compound eye is shown in Figure 12. Mathematically the volume of the retina is expressed by the product of an ommatidial reticular volume and the number of ommatidia in a compound eye. An ommatidial reticular volume is obtained by the product of area of a cross sectioned ommatidial retinula and the length of the reticular layer. The length of the rhabdom layer in the frontal layer of a compound eye was given by y_7 . The length in that region is the longest of all, so that the averaged length of a rhabdom of the whole eye is approximately one half of y_7 . The radius of a cross sectioned ommatidial retinula is approximated by $1/2$ of the diameter of a facet (y_5) as determined by the light microscopic observations. Therefore the volume of retina (y_8) is expressed by;

$$y_8(\mu^3) = \pi \left(\frac{y_5}{2} \right)^2 \frac{y_7}{2} y_4$$

y_8 should increase not linearly but exponentially with CW. The values in Figure 12a are distributed in a wider range. The volume of retina (y_8) calculated from the equation at $x=10, 20$ and 30 (mm) for example, and compared with the averages of measured values respectively were the following (the latter in the parentheses); x (mm)=10, y (μ^3)= 2.1×10^8 (1.2×10^8); x (mm)=20, y (μ^3)= 5.8×10^8 (3.3×10^8); x (mm)=30, y (μ^3)= 13.0×10^8 (6.1×10^8). The comparison shows that the theoretical values and the measured ones agree reasonably well.

The ROR value remains constant along the entire longitudinal axis of the ommatidia in the crab [1], so that the volume of the rhabdom can be calculated from the data of ROR and the volume of retina. Although the ROR value is slightly higher in the smaller crabs, the volume of the rhabdom at midnight (Fig. 12b) shows a similar tendency to the volume of the retina (Fig. 12a). It should be noted that the volume of the rhabdom at midday stays nearly the same all through the different CWs examined.

The amount of chromophore (11-*cis*- and all-*trans*-retinal) within a compound eye was mea-

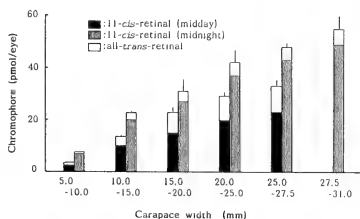


Fig. 13. Change in chromophore contents to CW. Each column is based on 5 individuals each.

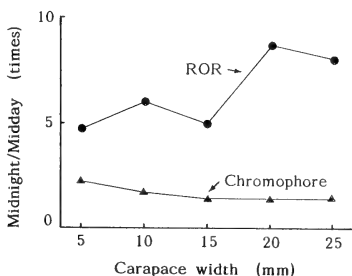


Fig. 14. Comparison between ratios of ROR and chromophore content of day and night eyes. The greater the difference between these two values, the greater the ratio of the extrarhabdomeric chromophore in the compound eyes; the latter is indisputably higher in the larger crabs. Each point represents values obtained from 5 individuals.

sured by HPLC at both midnight and midday. As shown in Figure 13, the amount of chromophore both at midnight and midday linearly increases with the CW. The quantity (y_9 , pmol) of the total chromophore (11-*cis*- and all-*trans*-retinal) at midnight can be expressed by the equation;

$$y_9 \text{ (pmol)} = 1.2x + 9 \quad (10 < x < 31)$$

and that at midday (y_{10}) by;

$$y_{10} \text{ (pmol)} = 1.2x + 2 \quad (5 < x < 27.5)$$

The gradient coefficients of both equations are the same which means that the size/chromophore content function has the same form, but is shifted only on the chromophore content axis with light adapta-

tion/dark adaptation. The fact that the relative amount of all-*trans*-retinal increases at midday indicates that the duration of light-exposure is responsible for the considerable increase of metarhodopsin with all-*trans*-retinal.

DISCUSSION

Relative growth of the body

The various size parameters of the crab *H. sanguineus* such as carapace length, carapace width and body thickness all showed strong linear positive correlations to each other (Fig. 2). The growth is isometric so that the general appearance of the large crab is identical to that of the small one except for the overall size difference. The largest crab which was found in the course of this study had a CW of 41 mm; this could be the final size of the species.

Compound eye, rhabdom and chromophore

The length of the eye stalk, and length and width of a compound eye increase linearly with CW ($r = 0.995$ (Fig. 3)). As the growth rate (the gradient coefficient of the isometric equation) of compound eye width (y_3) is greater than that of compound eye length, the compound eye becomes wider and flatter as the crab grows. The change is accompanied by a narrowing of the interommatidial angle especially in the top region of a compound eye, which should give the eye of grown individuals sharper vision (improved acuity) than that of smaller individuals.

It has already been documented that the rhabdom occupation ratio (ROR) of the crab eye changes between day and night: in 20–25 mm crabs the night rhabdom is 8 times larger than the day rhabdom [1]. The present results shown in Fig. 11a indicate that this daily change in ROR occurs irrespective of crab body size though day and night ROR-values are both slightly higher in the smaller crabs. This fact may suggest that the rhabdoms have to maintain a certain size to ensure certain visual capacities.

It should be noteworthy that the daily changes in the amounts of chromophore (Fig. 13) as well as the change in ROR occurred in crabs of any size

examined. As the measurements by HPLC were done on a whole compound eye, it is unclear how much (%) of the chromophore exists in the rhabdom or in the reticular cell cytoplasm.

We reported previously that a considerable amount of chromophore (both 11-*cis*- and all-*trans*-retinal) should exist outside the rhabdom at least for some time during the day [1]. It was found from preliminary observations that the density of intramembranous particles (IMP) by freeze-fracture (ca. 2000 at midnight and ca. 3000 at midday) and the diameter of a rhabdomeric microvillus (ca. 0.8 μm) are not dependent on CW. It follows from these findings that the content of the extra-rhabdomeric chromophore must be higher in the larger crabs than in the smaller ones because the ratios of night/day changes of ROR and chromophore for a 5 mm crab are 4.7 and 2.2 respectively, whereas corresponding figures for a 20 mm crab are 8.7 and 1.6 (Fig. 14). The function as well as the precise location of such seemingly extra-rhabdomeric chromophore remain unknown.

Ommatidia and their regional differences

In *H. sanguineus* the number of ommatidia is about 2400 in 5 mm crabs and about 6000 in 30 mm crabs. Parallel with the increase in the ommatidial number (Fig. 8), the individual ommatidium increases in size (Fig. 9). Rather similar results have been reported in some insects [11–13], crustacea [7, 8] and *Limulus* [6]. A recent report of the crayfish *Procambarus clarkii* [10], however, stated that the total number of corneal facets did not linearly increase with body length whereas the facet size did. In *H. sanguineus* it appears that both diameter of a facet and number of facets increase linearly with CW (Figs. 8 and 9), while interommatidial angles of the frontal region in particular do the reverse (Fig. 10).

In general, the increase of facet sizes means an increase of light sensitivity, and the decrease of interommatidial angle means an increase of resolution [20]. Optically, the compound eye of *H. sanguineus* is of the apposition type. The resolving power (highest spatial frequency, R) is given by the following equation [20];

$$R = \frac{1}{2\Delta\phi}$$

$\Delta\phi$ is the interommatidial angle in radian. Therefore it can be said that the bigger *H. sanguineus* grows, the better its resolution and its sensitivity become.

The eye parameter, $p = A\Delta\phi$ defines how close the resolving power of an apposition eye approaches the diffraction limit (A is a diameter (μm) of the aperture of an optical system = a diameter of an ommatidial facet in this paper) [21]. If p is 0.25, the eye's resolving power reaches its diffraction limit. The eye parameters calculated for $CW = 5.0$ – 7.5 and 27.5 – 31.0 (from the data shown in Figs. 9 and 10) are 1.96 and 1.72 respectively. This means that the eye is still far from the diffraction limit.

An increase in the number of ommatidia with body size indicates, of course, that new ommatidia are added at each moult. In Myriapoda, a new row of ocelli is added at each moult so that by counting the rows it is possible to determine the moult stage [22]. Similarly, the eye of many insect nymphs grow by addition of new ommatidia to the anterior or antero-dorsal eye margin [23]. In *H. sanguineus* the medial region in which facet sizes are significantly smaller than those in the rest of the eye could be the most obvious candidate for the region of the development of new ommatidia at the moult. A similar region, termed "rostrad" was identified in the eye of the freshwater crayfish *Astacus fluviatilis* [8].

In general, regional differences of a compound eye favour the formation of so-called "acute zones" or "foveae" known from a few other compound eyes [24]. Measurements of the interommatidial angle and other parameters of the eye of *H. sanguineus* indicate that the "fovea" defined as the area of most acute vision develops as the animal grows, and that it is confined to the zone between the frontal and top regions (Figs. 9 and 10) where facet sizes are relatively large. In eyes of flies a very similar location has been identified [25]. Ultrastructural changes of the developing ommatidia and the physiological significance of the reported regional differences of ommatidial structure are currently under investigation.

ACKNOWLEDGMENTS

This research was supported in part by Grants-in-Aid for Scientific Research from the Ministry of Education, Science and Culture of Japan.

REFERENCES

1. Arikawa, K., Kawamata, K., Suzuki, T. and Eguchi, E. (1987) Daily changes of structure, function and rhodopsin content in the compound eye of the crab *Hemigrapsus sanguineus*. *J. Comp. Physiol.*, **161**:161–174.
2. Arikawa, K., Morikawa, Y., Suzuki, T. and Eguchi, E. (1988) Intrinsic control of rhabdom size and rhodopsin contents in the crab compound eye by circadian biological clock. *Experientia*, **44**: 219–220.
3. Meyer-Rochow, V. B. (1975) Larval and adult eye of the western rock lobster (*Panulirus longipes*). *Cell. Tissue Res.*, **162**:439–457.
4. Land, M. F. (1981) Optical mechanisms in the higher crustacea with a comment on their evolutionary origins. In "Sense Organs". Ed. by M. S. Laverack and D. J. Casens, Blachie Publ., Glasgow, pp. 31–48.
5. Nilsson, D. E., Hallberg, E. and Elofsson, R. (1986) The ontogenetic development of refracting superposition eyes in crustaceans: transformation of optical design. *Tissue & Cell*, **18**:509–519.
6. Waterman, T. H. (1954) Relative growth and the compound eye in Xiphosura. *J. Morphol.*, **95**:125–158.
7. Parker, G. H. (1895) The retina and optic ganglia in decapods, especially in *Astacus*. *Mitt. Zool. Stat. Neapel*, **12**:1–73.
8. Bernhards, H. (1916) Der Bau des Komplexauges von *Astacus fluviatilis* (*Potamobius astacus* L.). Ein Beitrag zur Morphologie der Decapoden. *Z. Wiss. Zool.*, **116**:649–707.
9. Shelton, P. M. J., Shelton, R. G. J. and Richards, P. R. (1981) Eye development in relation to moult stage in the European lobster *Homarus gammarus* (L.). *J. Cons. int. Explor. Mer.*, **39**:239–243.
10. Tokarski, T. R. and Hafner, G. S. (1984) Regional morphological variations within the crayfish eye. *Cell. Tissue Res.*, **235**:387–392.
11. Bernstein, S. and Finn, C. (1971) Ant compound eye: Size-related ommatidium differences within a single wood ant nest. *Experientia*, **27**:708–710.
12. Sherk, T. E. (1978) Development of the compound eyes of dragonflies (Odonata). II Development of the larval compound eyes. *J. Exp. Zool.*, **203**:47–60.
13. Sherk, T. E. (1978) Development of the compound eyes of dragonflies (Odonata). III Adult compound eyes. *J. Exp. Zool.*, **203**:61–80.

- 14 Nüssel, D. R. and Waterman, T. H. (1979) Massive diurnal modulated photoreceptor membrane turnover in crab light and dark adaptation. *J. Comp. Physiol.*, **131**:205-216.
- 15 Stowe, S. (1981) Effects of illumination changes on rhabdom synthesis in a crab. *J. Comp. Physiol.*, **142**:19-25.
- 16 Toh, Y. and Waterman, T. H. (1982) Diurnal changes in compound eye fine structure in the blue crab *Callinectes*. 1. Differences between noon and midnight retinas on an LD 11:13 cycle. *J. Ultrastruct. Res.*, **78**:40-59.
- 17 Kermack, K. A. and Haldane, J. B. S. (1959) Organic correlation and allometry. *Biometrika*, **37**:30-41.
- 18 Shukolyukov, S. A., Kalishevich, O. O., Polyanovsky, A. D. and Gribakin, F. G. (1984) Vision in the crab *Hemigrapsus sanguineus*: spectral sensitivity and ommatidium fine structure. *Mar. Biol. (Vladivostok)*, **2**:53-59.
- 19 Meyer-Rochow, V. B. and Tiang, K. M. (1984) The eye of *Jasus edwardsii* (Crustacea, Decapoda, Palinuridae): electrophysiology, histology, and behaviour. *Zoologica*, **45**:1-61.
- 20 Land, M. F. (1981) Optics and vision in invertebrates. In "Handbook of sensory physiology, Vol. VII/6B". Ed. by H. Autrum, Springer, Berlin/Heidelberg/New York, pp. 471-594.
- 21 Snyder, A. W. (1977) Acuity of compound eyes: physical limitations and design. *J. Comp. Physiol.*, **116**:161-182.
- 22 Vachon, M. (1947) Contribution à l'étude de développement postembryonnaire de *Pachybolus ligatus* Voges. Les étages de la croissance. *Annls. Sci. nat. (Zool.)*, **11**:109-121.
- 23 Meinertzhagen, I. A. (1973) Development of the compound eye and optic lobes in insects. In "Developmental Neurobiology of Arthropods". Ed. by D. Young, Cambridge Univ. Press, London/New York, pp. 51-104.
- 24 Stavenga, D. G. (1979) Pseudopupils of compound eyes. In "Handbook of Sensory Physiology, Vol. VII/6A". Ed. by H. Autrum, Springer, Berlin/Heidelberg/New York, pp. 357-439.
- 25 Land, M. F. and Eckert, H. (1985) Maps of the acute zone of fly eyes. *J. Comp. Physiol.*, **156**:525-538.

Effect of Calcium Ionophore A23187 upon the Rate of Leukotriene C₄ Production and the Cellular Morphology in Highly Purified Mouse Peritoneal Macrophages Cultured *in vitro*

CHIKASHI TACHI and URIEL ZOR¹

Zoological Institute, Faculty of Science, University of Tokyo, Bunkyo-ku, Tokyo 113, Japan, and ¹Department of Hormone Research, Weizmann Institute of Science, Rehovot, Israel

ABSTRACT—When the highly purified mouse peritoneal macrophages cultured *in vitro*, were exposed to calcium ionophore, A23187, at a concentration of 0.5 $\mu\text{g/ml}$ for 1.5–2.0 hr under alkaline conditions (pH 7.6–8.0) of the medium, the rate of leukotriene C₄ (LTC₄) production by these cells was enhanced approximately by 100 times. The amount of LTC₄ produced was measured by assaying the total amount of cysteinyl leukotrienes released into the medium: the newly developed monoclonal antibodies (supplied by Dr. F. Kohen, Dept. Hormone Res. Weizmann Inst., Rehovot, Israel), specific to cyteinyl leukotrienes were used for the purpose. Concomitantly, the ionophore transformed the macrophages of rounded cellular shape to assume the strongly elongated cellular morphology. Causal relationship between the two phenomena, however, remains to be investigated.

INTRODUCTION

In 1980, Samuelsson *et al.* [1, 2] introduced the term, leukotriene, to describe a family of compounds which are metabolites of arachidonic acid, produced via 5-lipoxygenase pathway and contain conjugated triene. Elucidation of the molecular structures of various leukotrienes opened an entirely new perspectives to the understanding of the mechanisms which underlie the functions of leukocytes, the regulation of the activities of smooth muscles, the pathogenesis of inflammation, allergy, asthma etc. (for reviews see [3–9]).

Leukotriene C₄ (LTC₄ in the following) is the first peptidolipid of the family to be synthesized in the pathway and an important component of SRS (slow reacting substance) and/or SRS-A (slow reacting substance of anaphylaxis) [3]. Both the peritoneal [10, 11] and the alveolar [12] macrophages cultured *in vitro* have been shown to produce LTC₄ in response to the stimulation by

calcium ionophore A23187 [10–12]. Dependence of LTC₄ production upon the intracellular high concentration of Ca²⁺, i.e., [Ca²⁺]_i, has been demonstrated in cultured leukemic basophils [13]; hydrocortisone reduces antigen-induced elevation of [Ca²⁺]_i and, as its consequence, the rate of LTC₄ production in these cells.

On the other hand, it has been known that cytoplasm of macrophages contains calcium-sensitive protein component, gelsolin, which is probably responsible for the regulation of the cytoskeletal organization of the cells [14–16], and that macrophages change their shape according to their functional states or to the modulation of environmental conditions (for reviews see [17, 18]). It might be possible, therefore, that the stimulation of LTC₄ production by calcium ionophore in the cultured macrophages, is correlated with the morphological changes of the cells.

To answer the question, we assayed the rate of LTC₄ production in the highly purified peritoneal macrophages of the mouse using newly developed monoclonal antibodies specific against cysteinyl leukotrienes, and, at the same time, observed the

changes in the cellular morphology of the same cells. The results will be described in this paper. Summarized account of the findings were presented in abstract form [19].

MATERIALS AND METHODS

Animals

Adult mice of BALB/c (H-2^d) and C3H/HeJ (H-2^k) strains were purchased from a local dealer (Nippon Clea & Co., Ltd., Tokyo, Japan). They had been kept under regulated temperature (25°C) and illumination cycles (12 hr dark and 12 hr light per day), until the day of the experiments. Both male and female mice were used; they were 8–10 weeks old and the female mice were in diestrus of the estrous cycle at the time of the experiments.

Compounds and reagents

Tritium-labelled leukotriene C₄ (specific activity, 39 Ci/mMol) purchased from Amersham Japan & Co., Ltd. (Tokyo, Japan), was diluted with 50% ethanol to give a final concentration of 1.0 μ Ci/ml. Unlabelled LTC₄ (Wako Pure Chemical Industries & Co., Ltd., Osaka, Japan) was dissolved in double distilled water. Stock solution of calcium ionophore A23187 (Sigma Chemical & Co., Ltd., St. Louis, Mo, USA) was prepared by dissolving the compound in dimethyl sulfoxide (DMSO; Wako Pure Chemical Industries & Co., Ltd., Osaka, Japan) at a concentration of 500 μ g/ml. Sterilized Ficoll-Hypaque solution ($d=1.090\pm0.001$) was purchased from Otsuka Assay Laboratories (Tokushima-shi, Japan).

Antibodies and antibody solution

Since LTC₄ may be rapidly converted into LTD₄ and LTE₄ by macrophages *in vitro*, as recently shown in the rat [20, 21], the amount of the three cysteinyl leukotrienes in the medium will have to be assayed simultaneously in order to assess correctly the rate of LTC₄ production by these cells. The monoclonal antibodies against the cysteinyl leukotrienes were generously supplied from Dr. F. Kohen, Department of Hormone Research, Weizmann Institute of Science, Rehovot, Israel: the antibodies react with LTC₄ (100%), LTD₄

(105%), and LTE₄ (77%) at a 50% saturation level of binding (F. Kohen, 1988, personal communication).

The stock solution of the antibodies was prepared by dissolving freeze-dried IgG in phosphate buffered saline containing heat-inactivated horse serum at a concentration of 3% (abbreviated in the following as PBS-HS/3), and stored at -20°C. Immediately before use, an aliquot of the stock solution was diluted with PBS-HS/3 to an appropriate level of the titre.

Macrophages

Macrophages were collected from peritoneal exudate of the mice following injection of Earl's minimum essential medium (MEM) containing heparin at a concentration of 30 units/ml [22]. The highly purified macrophage cell cultures were prepared, according to the procedures described elsewhere [23, 24], as follows. The lavage was layered onto a Ficoll-Hypaque gradient [25] and centrifuged at approximately 1200 \times g. A band formed between the lavage and Ficoll-Hypaque contains white cells including macrophages. The cells were removed, suspended in MEM fortified with foetal calf serum at a concentration of 20% (abbreviated in the following as MEM-FCS/20), and plated onto Falcon dishes. They were incubated for 1.0 hr at 37°C under an atmosphere of 5% CO₂ and 95% air. At the end of the incubation, the non-adherent cells were removed by decanting the medium. Then fresh MEM-FCS/20 was added to the cells. The medium, MEM-FCS/20, was used at the initial phase of the culture, because the presence of FCS at relatively high concentrations (20–40%) in the medium limits the adherence of B-lymphocytes to the culture dishes [26]. The remaining cells after the wash, were incubated for another 1 hr. Then the medium was replaced with fresh MEM-FCS/10. The incubation was continued for another 16 hr. Decantation of the medium with the detached cells, and replacement with the fresh FCS-MEM/10 were done as before. The cells removed from the dish at each step, mainly consisted of lymphocytes and dead macrophages; the number of the removed cells decreased sharply as the procedures were repeated. At the end of 16 hours' incubation, approximately

20% of the cells present in the original suspension, remained firmly adhered to the bottom surface of the dish: those cells represented very pure population of peritoneal macrophages. They were incubated in fresh MEM-FCS/10 for additional 24–48 hr to "stabilize" them under an atmosphere of 2–3% CO₂ and 97–98% air. Immediately before the start of the experiments where the rates of LTC₄ production were assayed, the medium was replaced with the freshly prepared MEM containing 4 mM cysteine without addition of FCS; the macrophages were incubated in the assay medium, either with or without the ionophore, for 1.5–2.0 hr under an atmosphere of 2–3% CO₂ and 97–98% air.

Radioimmunoassay procedure for LTC₄

One tenth ml of the sample solution to be assayed was mixed with an equal amount of the antibody solution and incubated at 0°C for 30 min. At the end of the incubation, 0.1 ml of ³H-LTC₄ solution containing 7 nCi of the isotope in 50% ethanol-PBS, was added to the mixture, and had been stood at 4°C for overnight [27]. Free LTC₄ was removed by adding 0.2 ml of dextran-charcoal [27, 28], and by centrifugation at 15,000 rpm for 3 min. The radioactivity was measured by means of liquid scintillation counting.

Counting of macrophages according to their cell shape

The cells were fixed with 3.5% formaldehyde in 1/15 M phosphate buffer (pH 7.4), and stained with Giemsa's. The stained dishes were mounted on a projection microscope, and the magnified images were projected onto a digitizer tablet (model DT 1000, Watanabe Sokki, Tokyo, Japan). Then, the number of the cells of the elongated, or the rounded morphology was differentially counted. The acquisition and the processing of the data from the digitizer tablet were carried out by a personal computer (PC-9801, NEC, Tokyo, Japan) using a software package written by one of the authors [29].

RESULTS

Slightly alkaline conditions (pH 7.6–8.0) of the

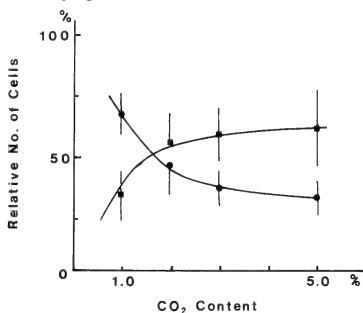


Fig. 1. Percentage of the macrophages in culture with the elongated (■), and the rounded (●) morphology according to the different CO₂ content of the atmosphere. The highly purified phagocytes had been cultured for 24 hr under the designated atmospheric conditions before counting. Each value plotted is the mean of at least 5 independent experiments; vertical bars indicate the standard deviation.

medium which had been kept under an atmosphere containing less than 5% CO₂, caused rounding of the macrophages (Fig. 1). In order to obtain macrophage population where the proportion of the rounded cells, was close to 0.5, CO₂ content of the atmosphere under which incubation was carried out, was kept at a low level of about 2%, throughout the following experiments.

We measured, as stated in Materials and Methods, the rate of LTC₄ production by assaying the rate of the release of the total cysteinyl leukotrienes into the medium using the monoclonal antibodies specific for the peptidolipids. While the antibodies we used, reacted with LTE₄ less strongly than they did so with the other two cysteinyl compounds (see Materials and Methods), the amount of LTE₄ produced by the macrophages under the presently-employed conditions is expected to be negligibly low, owing to the presence of cysteine in the medium: cysteine added to the medium at a concentration of 2 mM, has been shown to inhibit the activity of LTD₄-metabolizing enzyme in the peritoneal macrophages of the rat, by approximately 90% [21]. Therefore, it is perfectly safe and appropriate, as done in the follow-

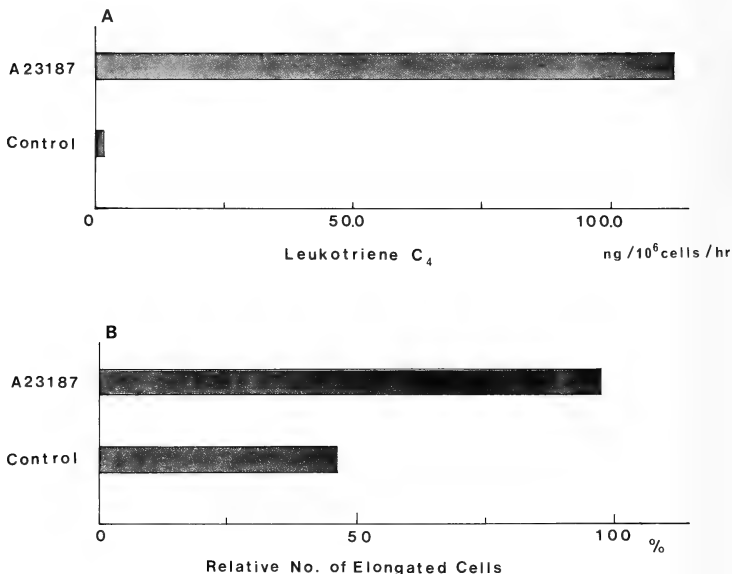


FIG. 2. Effects of calcium ionophore, A23187, upon the rate of LTC₄ production (A) and the cellular morphology (B) in the highly purified macrophages cultured *in vitro*. Concentration of the ionophore was 0.5 μ g/ml. The rate of LTC₄ production was calculated, as described in Materials and Methods, on the basis of the values obtained by assaying the total amount of cysteinyl leukotrienes released into the medium during the entire course of 1.5–2.0 hr's incubation period.

ing, to refer to the combined rate of the release of the cysteinyl leukotrienes as representing that of the production of LTC₄ by the cells.

Thus, the highly purified peritoneal macrophages of the mouse in the unstimulated state, under the culture conditions we employed, produced LTC₄ at the rate of 1–3 ng/10⁶ cells per hour (Fig. 2A).

However, exposure of the cells to calcium ionophore, A23187, at a concentration of 0.5 μ g/ml, for 90–120 min caused approximately hundredfold increase in the rate (Fig. 2A). At the same time, the treatment induced the nearly complete transformation of the macrophages of the rounded cellular shape into the ones with elongated morphology (Figs. 2B, 3).

At 1.0 μ g/ml, the ionophore was highly toxic to the cells, and the cells were almost totally disrupted at the end of the 2 hr's incubation period.

At the concentrations below 0.5 μ g/ml, the effect of the ionophore rapidly decreased in the dose dependent-manner.

DISCUSSION

The present report demonstrated that calcium ionophore, A23187, brought about the transformation of the cellular morphology in the macrophages of rounded shape and caused them to assume highly elongated form under the alkaline conditions (pH 7.6–8.0) of the medium, while the same treatment induced approximately hundred-

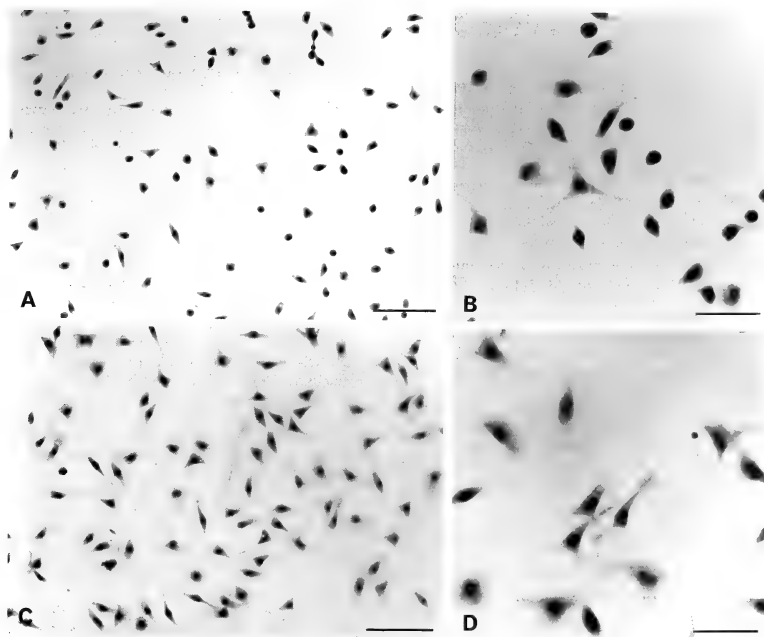


Fig. 3. Photomicrographs showing the appearance of the highly purified macrophages without (A & B) and with (C & D) the ionophore (0.5 $\mu\text{g/ml}$) treatment. The concentration of the ionophore, and the duration of the incubation period are as described in the legend for Fig. 2. In B and D, the cells are shown at high magnification. Scale indicates 20 μm in A and C, 10 μm in B and D.

fold increase in the rate of LTC₄ production by these cells.

K. Carr and I. Carr [30] analyzed by means of light microscopy, microcinematography and scanning electron microscopy, the morphological properties of the mouse peritoneal macrophages cultured *in vitro*. As a result of their studies, they concluded that the processes passed through by the macrophages in culture, may be divided into 4 consecutive stages, i.e., stages of 1) adhesion, 2) flattening, 3) movement and 4) extension. They suggested, on the basis of microcinematographic studies, that while the moderately elongated cells were moving, the fully extended cells were not

actively motile and probably represented a post-motile stage of the cells [30]. Their observations indicated also that the stimulated macrophages attained the fully extended stage earlier in the culture than the non-stimulated ones [30].

The sequence of events followed by the mouse peritoneal macrophages during settlement *in vitro*, under the culture conditions we employed, coincided very well with the description made by K. Carr and I. Carr [30].

Effect of pH upon the spreading (a condition similar to, but probably not identical with the flattening mentioned above) of macrophages in culture was studied by Rabinovitch and DeStepha-

no [31]; they showed that acidic pH of the medium induced spreading of the cells. As described in the present report, the elongation of the macrophages, too, took place under acidic pH while the rounding was caused under alkaline pH of the medium. It might be possible that the spreading and the elongation of macrophages share common cytoskeletal mechanisms underlying the morphological changes.

Relatively little is known about the effects of calcium ionophore upon the cellular shape. Recently, Stanisstreet and Smedley [32] examined the morphological changes of the cells in *Xenopus* embryos following the local application of the ionophore; they found that the treatment caused strong rounding, rather than elongation, of the cells. The cause for the discrepancy between our results and theirs is not known.

Causal relationship between the morphological transformation of the macrophages and the increased rate of LTC₄ production remains to be investigated. Since many of the biological actions of LTC₄ and its metabolites are directed toward or mediated by the smooth muscle cells (for reviews see [4, 5, 9]), it might be possible that LTC₄ and its derivatives produced by the macrophages under the stimulation of A23187, in turn, would affect, either by themselves or in cooperation with PAF (platelet activating factor) [33, 34], the contractile elements in the cells, leading to the changes of their shape. Different mechanisms, however, would have to be postulated for the morphological changes induced by A23187 in the amphibian embryonic cells and those in the mouse macrophages, to account for the discrepancy between our results and those obtained by Stanisstreet and Smedley [32].

Question remains, furthermore, with regard to the relevance of the present findings to the elongation of the macrophages attained spontaneously in culture, or to the physiological processes taking place *in vivo*.

ACKNOWLEDGMENTS

We are much indebted to Drs. F. Kohen and S. Moshonof, Dept. Hormone Res., Weizmann Inst. of Science, Rehovot, Israel, for generous supply of the monoclonal antibodies against cysteinyl leukotrienes.

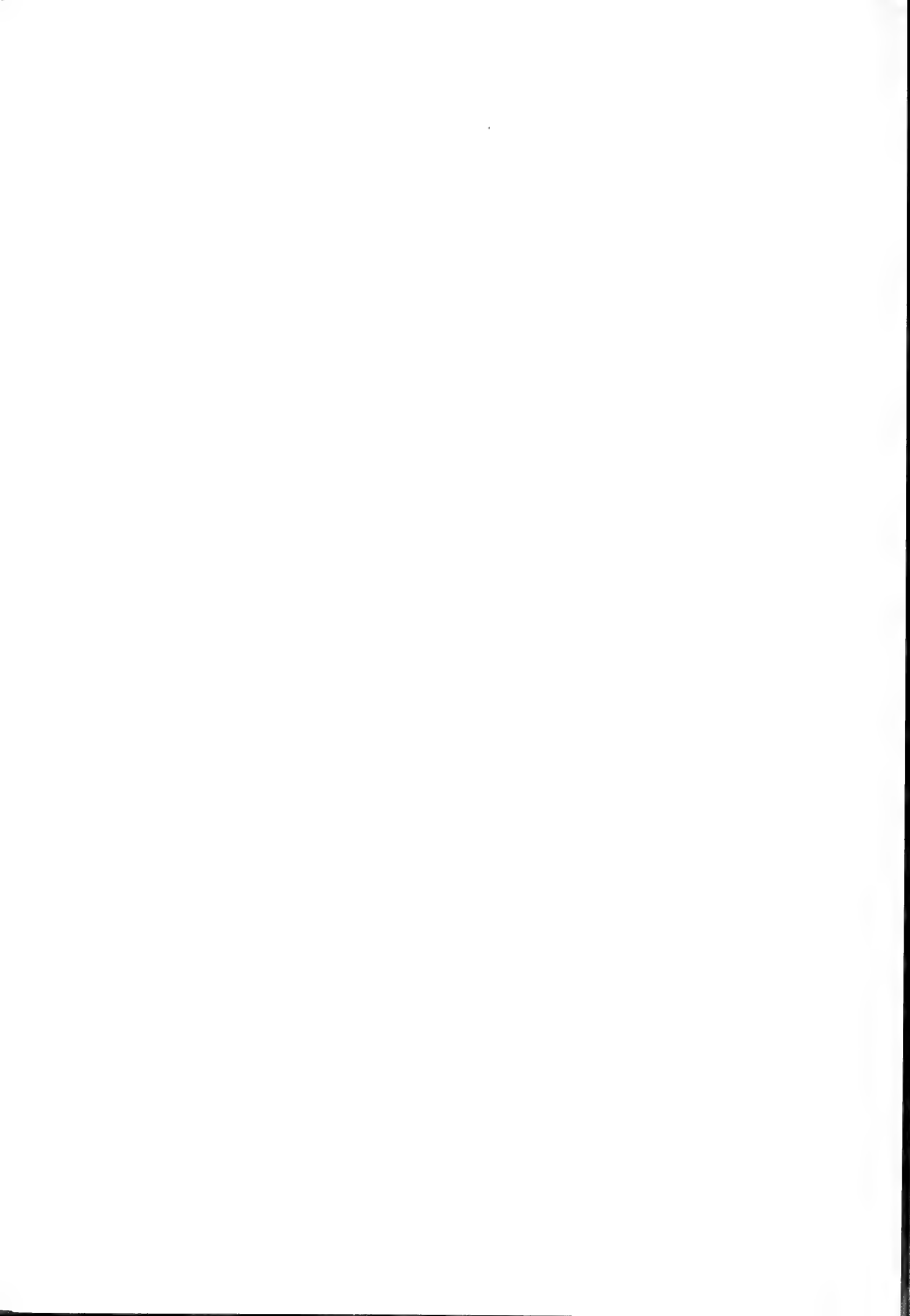
The work was supported in part by grant to C. Tachi from the Ministry of Education, Japan (No. 62109006). C. Tachi is Visiting Professor of Embryology, Dept. Anatomy, Tokyo Medical College, Shinjuku-ku, Tokyo, Japan.

U. Zor had been on the leave of absence from Dept. Hormone Res., Weizmann Inst. (1986.3 - 1986.5), where he is incumbent of W. B. Graham Professorial Chair of Pharmacology.

REFERENCES

- Samuelsson, B., Borgeat, P., Hammerstrom, S. and Murphy, R. C. (1979) Introduction of a nomenclature: leukotrienes. *Prostaglandins*, **17**: 785-787.
- Samuelsson, B. and Hammerstrom, S. (1980) Nomenclature for leukotriene. *Prostaglandins*, **19**: 645-648.
- Samuelsson, B. and Hammerstrom, S. (1982) Leukotrienes: a novel group of biologically active compounds. *Vitam. Horm.*, **39**: 1-30.
- Piper, P. J. (1983) Pharmacology of leukotrienes. *Brit. Med. Bull.*, **39**: 255-259.
- Piper, P. J. (1984) Formation and actions of leukotrienes. *Physiol. Rev.*, **64**: 744-761.
- Lewis, R. A. and Austen, K. F. (1984) The biologically active leukotrienes. *J. Clin. Invest.*, **73**: 889-897.
- Ford-Hutchinson, A. W. (1985) Leukotrienes: their formation and role as inflammatory mediators. *Fed. Proc.*, **44**: 25-29.
- Salmon, J. A. and Higgs, G. A. (1987) Prostaglandins and leukotrienes as inflammatory mediators. *Brit. Med. Bull.*, **43**: 285-296.
- Piper, P. J. and Samhoun, M. W. (1987) Leukotrienes. *Brit. Med. Bull.*, **43**: 445-459.
- Bach, M. K. and Brashler, J. R. (1978) Ionophore A23187-induced production of slow reacting substance of anaphylaxis (SRS-A) by rat peritoneal cells *in vitro*: evidence for production by mononuclear cells. *J. Immunol.*, **120**: 998-1005.
- Bach, M. K., Brashler, J. R., Brooks, C. D. and Neerken, A. J. (1979) Slow reacting substances: comparison of some properties of human lung SRS-A and two distinct fractions from ionophore-induced rat mononuclear cell SRS. *J. Immunol.*, **122**: 160-165.
- Rankin, J. A., Hitchcock, M., Merrill, W., Bach, M. K., Brashler, J. R. and Askenase, P. W. (1982) IgE-dependent release of leukotriene C₄ from alveolar macrophages. *Nature*, **297**: 329-331.
- Zor, U., Her, E., Talmon, J., Kohen, F., Harell, T., Moshonov, S. and Rivnay, B. (1987) Hydrocortisone inhibits antigen-induced rise in intracellular free calcium concentration and abolishes leukotriene C₄ production in leukemic basophils. *Prosta-*

- glandins, **34**: 29-40.
- 14 Stossel, T. P. and Hartwig, J. H. (1976) Interactions of actin, myosin, and a new actin-binding protein of rabbit pulmonary macrophages. *J. Cell Biol.*, **68**: 602-612.
- 15 Yin, H. L. and Stossel, T. P. (1979) Control of cytoplasmic actin gel-sol transformation by gelsolin, a calcium dependent regulatory protein. *Nature (Lond.)*, **281**: 583-586.
- 16 Stossel, T. P., Hartwig, J. H., Yin, H. C. and Davies, W. A. (1979) Actin-binding protein. In "Cell Motility". Ed. by S. Hatano, H. Ishikawa and H. Sato., Univ. Tokyo Press, Tokyo, pp. 189-210.
- 17 Carr, I. (1973) The Macrophage. Academic Press, London.
- 18 Cohn, Z. (1975) Macrophage physiology. *Fed. Proc.*, **34**: 1725-1729.
- 19 Tachi, C. and Zor, U. (1986) Possible correlation between the production of leukotriene C₄ and cytoskeletal organization in mouse peritoneal macrophages cultured *in vitro*. *Zool. Sci.*, **3**: 1011 (abstract).
- 20 Nagaoka, I. & Yamashita, I. (1987) Conversion of leukotriene C₄ to leukotriene D₄ by a cell-surface enzyme of rat macrophages. *Biochem. Biophys. Res. Comm.*, **147**: 282-287.
- 21 Nagaoka, I. & Yamashita, I. (1987) Studies on the leukotriene D₄-metabolizing enzyme of rat leukocytes, which catalyzes the conversion of leukotriene D₄ to leukotriene E₄. *Biophys. Acta*, **922**: 8-17.
- 22 Tachi, C., Tachi, S., Knyszynski, A., and H. R. Lindner (1981) Possible involvement of macrophages in embryo-maternal relationships during ovum implantation in the rat. *J. Exp. Zool.*, **217**: 81-92.
- 23 Tachi, C. (1988) Cellular mechanisms of the interactions between blastocysts and macrophages co-cultured *in vitro*. *Proc. 2nd Ann. Meeting Japan Assoc. Basic Reprod. Immunol.*, 71-75.
- 24 Tachi, C. and Tachi, S. (1988) The role of macrophages in the maternal recognition of pregnancy. *J. Reprod. Fert., suppl.*, **37**: 63-68.
- 25 Mantovani, A. (1981) Adherence to microexudate-coated plastic. In "Manual of Macrophage Methodology". Ed. by H. B. Herscovitz, H. T. Holden, J. A. Bellanti and A. Ghafter, Marcel Dekker Inc., New York, pp. 69-74.
- 26 Pennline, K. J. (1981) Adherence to plastic or glass surfaces. In "Manual of Macrophage Methodology". Ed. by H. B. Herscovitz, H. T. Holden, J. A. Bellanti, A. Ghafter, Marcel Dekker Inc., New York, pp. 63-68.
- 27 Denzlinger, C., Guhlmann, A., Scheuber, P. H., Wilker, D., Hammer, D. K. and Keppler, D. (1986) Metabolism and analysis of cysterinyl leukotrienes in the monkey. *J. Biol. Chem.*, **261**: 15601-15606.
- 28 Murphy, B. E. P. (1967) Some studies of the protein-binding of steroids and their application to the routine micro and ultramicro measurement of various steroids in body fluids by competitive protein-binding radioassay. *J. Clin. Endocr.*, **27**: 973-990.
- 29 Tachi, C. (1985) Mechanisms underlying regulation of local immune responses in the uterus during early gestation of eutherian mammals. I. Distribution of immuno-competent cells which bind anti-IgG antibodies in the post-nidatory uterus of the mouse. *Zool. Sci.*, **2**: 341-348.
- 30 Carr, K. and Carr, I. (1970) How cells settle on glass: a study by light and scanning electron microscopy of some properties of normal and stimulated macrophages. *Z. Zellforsch.*, **105**: 234-241.
- 31 Rabinovitch, M. and DeStefano, M. J. (1973) Macrophage spreading *in vitro*. I. Inducers of spreading. *Exptl Cell Res.*, **77**: 323-334.
- 32 Stanisstreet, M. and Smedley, M. J. (1986) Ionophore-induced cell shape changes in *Xenopus* early embryos. *Cytobios*, **46**: 155-165.
- 33 Snyder, F. (1985) Chemical and biochemical aspects of platelet-activating factor: a novel class of acetylated ether-linked choline-phospholipids. *Med. Res. Rev.*, **5**: 107-140.
- 34 Vargrafit, B. B. and Braquet, P. G. (1987) PAF-acether tody - relevance for acute experimental anaphylaxis. *Brit. Med. Bull.*, **43**: 312-335.



Fine Structure of the Lingual Dorsal Epithelium in the Bullfrog, *Rana catesbeiana*

SHIN-ICHI IWASAKI and KAN KOBAYASHI

Department of Anatomy, School of Dentistry at Niigata,
The Nippon Dental University, Niigata 951, Japan

ABSTRACT—The structure of the lingual dorsal epithelial cells in the bullfrog, *Rana catesbeiana*, was investigated by light and transmission electron microscopy. Differences in the thickness of the epithelium were detected between the top and the base of each filiform papilla. Granular cells were located over all of the papillar epithelium, and these cells contained many electron-dense granules plus a few electron-lucent vacuoles, which may be a secretory form of the electron-dense granules in the cytoplasm on the free-surface side. There were a few mucus cells, the cytoplasm of which was filled almost completely with mucus granules. Ciliated cells were scattered among these granular cells.

INTRODUCTION

There have been many studies on the ultrastructure of the lingual taste organs or the sensory papillae of anurans [1-10]. However, of these reports, only a few describe aspects of the lingual epithelium other than the sensory papillae [8-10]. In particular, histological aspects of the lingual dorsal epithelium of anurans have been almost completely ignored.

In our recent study [8] using the scanning electron microscope, we showed that filiform papillae were distributed compactly over the entire dorsum of *Rana catesbeiana*, and that fine plicated structures, or microridges, were widely distributed on the surface of these papillar epithelial cells. In the present study, light and transmission electron microscopy were used to investigate the structure of the tongue of *Rana catesbeiana*.

MATERIALS AND METHODS

Five males and five females of the adult *Rana catesbeiana* were obtained commercially and used in the present study. Under MS-222 anesthesia, the animals were perfused from the heart with 1/2 Karnovsky solution which contained 2.5% glutar-

aldehyde and 2% paraformaldehyde in cacodylate buffer (pH 7.4). The tongues were then removed and refixed in the same solution for a few hr. After rinsing in 0.1 M cacodylate buffer, specimens were postfixed in phosphate-buffered 1% osmium tetroxide solution [11] at 4°C for 1.5 hr. This procedure was followed by dehydration, Epon-Araldite embedding, ultrathin sectioning, and U-Pb double staining. The specimens were then observed under a transmission electron microscope (Hitachi H-500, JEOL JEM-1200EX). Semi-thin sections of Epon-Araldite embedded specimens were stained with 0.2% toluidine blue in 2.5% Na₂CO₃. Micrographs of the sections taken with a light microscope (Olympus BH-2) were compared with the transmission electron micrographs.

RESULTS

The epithelium which forms the upper part of the filiform papillae was revealed by light microscopy to be thicker than that forming the basal part. The former was composed of stratified columnar cells, while the latter was composed of simple columnar and/or cuboidal cells. In the upper region of the filiform papillae, a relatively large number of mucus cells were seen in comparison to the basal part of the filiform papillae. The connective tissue and the smooth muscle penetrated deeply into the center of each papilla (Fig. 1).

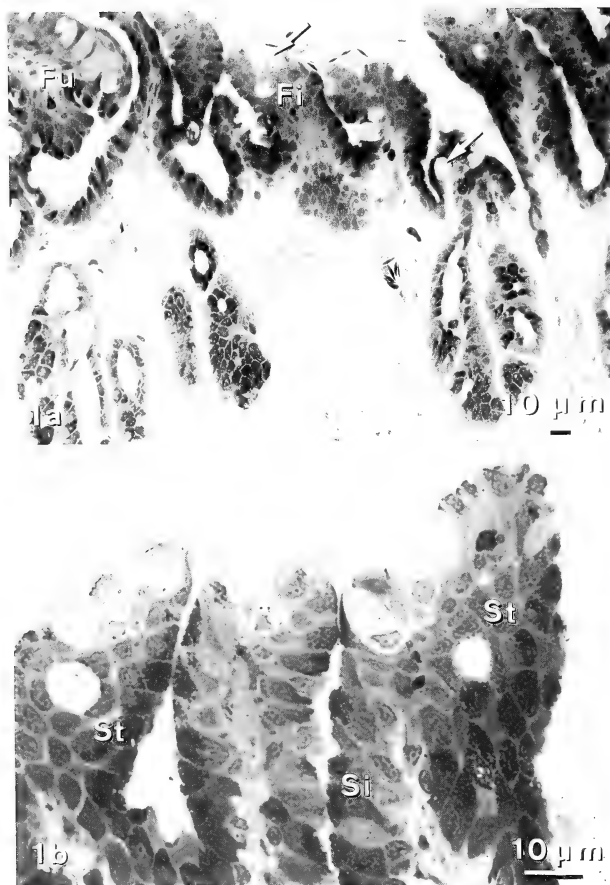


FIG. 1. Light micrograph of the lingual dorsal mucosa of the frog, *Rana catesbeiana*, embedded in Epon-Araldite. a. Filiform papillae (Fi) and fungiform papilla (Fu) are observed. Arrows show mucus cells. A large portion of the epithelium is composed of granular cells and ciliated cells, but they are not distinguishable from each other at this magnification. b. The upper area of filiform papillae. A large part of the top area of papillar epithelium consists of stratified columnar cells (St). The rest consists of simple columnar and/or cuboidal cells (Si).

Transmission electron microscopy of the stratified columnar epithelium in the upper portion of the filiform papillae revealed the presence of cells

that contained a large number of electron-dense, round granules (Fig. 2). Some of the cells not only contained these round granules but also a few,

electron-lucent vacuoles. The nucleus was located basally, and rough-surfaced endoplasmic reticulum was well-developed in the perikaryon (Fig. 2). The columnar and/or cuboidal cells of the epithelium at the base of the filiform papillae also contained a large number of electron-dense granules. The same cells often contained a small number of electron-lucent vacuoles. The nucleus was located basally, and rough-surfaced endoplasmic reticulum was well-developed in the perikaryon. In both the upper and the basal regions of the filiform papillae, microridges were widely distributed on the free-surface side of the epithelial cell. The cell surfaces which faced adjacent cells bore abundant cellular processes (Fig. 2). At higher magnification, the electron-dense granules were observed to consist of randomly packed tubules, or in some instances, appeared to show polygonal packing. The diameter of each tubule was 30–40 m μ . Endoplasmic reticulum and free ribosomes were dispersed in the cytoplasm around the electron-dense granules (Fig. 3). In some

cases, an image showing that the electron-lucent vacuole seemed to take in electron-dense granules was observed. The tubular structures in the electron-dense granules might be lost in this process (Fig. 4). In some granular cells, the contents of the electron-lucent vacuoles were likely to be lost by exocytosis (Fig. 5).

Large cells, in which almost all the cytoplasm was filled with mucus, were scattered among the electron-dense granular cells (Fig. 6). There were more of these large mucus cells in the upper portion of the filiform papillae than in the base (Fig. 1)

Ciliated cells were scattered among the granular cells in the filiform papillar epithelium. The ciliated cells had cilia and microvilli on their free exterior surfaces. The nucleus was located basally. Just beneath the free surface of the cells, basal bodies could be recognized. Ciliary rootlets were distributed throughout the cytoplasm. Free ribosomes and endoplasmic reticulum were seen mainly in the perikaryon (Figs. 7 and 8).

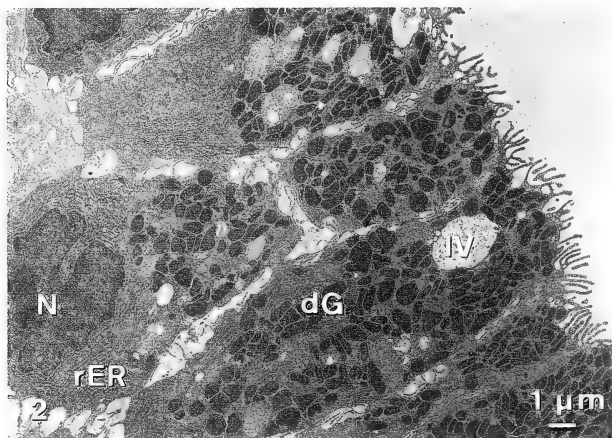


Fig. 2. Transmission electron micrograph of the epithelial cells in the upper part of a lingual filiform papilla from *R. catesbeiana*. Nucleus (N) is located basally. Rough-surfaced endoplasmic reticulum (rER) is well-developed in the perikaryon. A large part of the cytoplasm of each cell is occupied by many electron-dense granules (dG). An electron-lucent vacuole (IV), which seems to be the secretory form of electron-dense granules, is seen just beneath the free-surface of the cell.

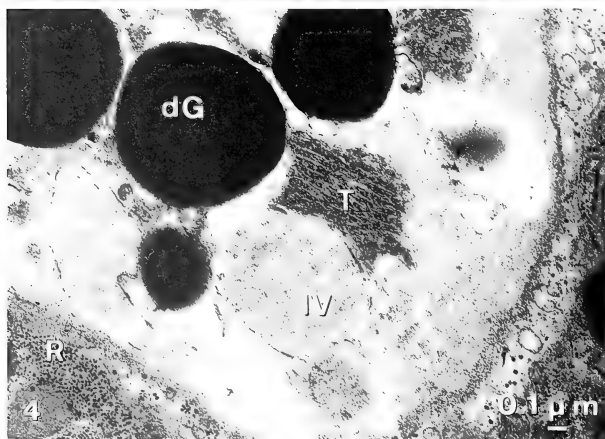
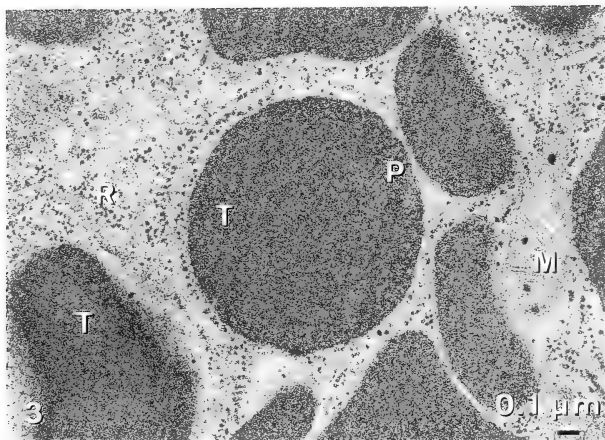


FIG. 3. Higher magnification of electron-dense granules. These granules consist of randomly packaged tubules (T) which in some instances, show polygonal packing (P). The diameter of tubules is 30-40 μm .

FIG. 4. Transmission electron micrograph showing the process in which the electron-lucent vacuole (IV) seems to take in the electron-dense granules (dG). T: tubular structure of the collapsing electron-dense granules, R: ribosomes.

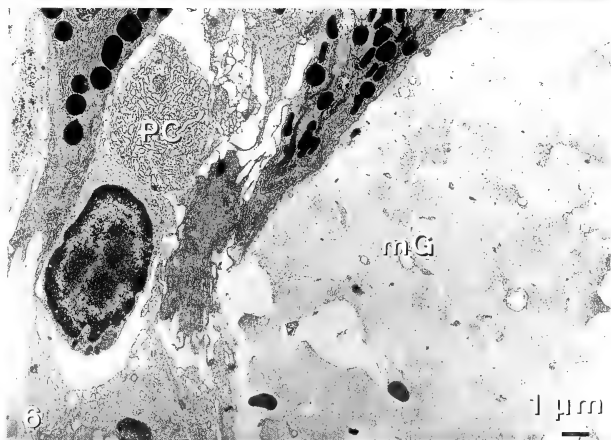


FIG. 5. Transmission electron micrograph of electron-lucent vacuoles (IV) just beneath the free surface of the cell. The contents of vacuoles were likely to be discharged into the oral cavity (OC) by exocytosis. dG: electron-dense granule.

FIG. 6. Transmission electron micrograph of a mucus cell; almost all the cytoplasm is filled with mucus granules (mG) and a plasma cell (PC).

On very rare occasions, cells were observed which originated from the epithelium but which lacked electron-dense granules, mucus granules,

and cilia (Fig. 9). In these cells, the nucleus was basally located, and mitochondria, free ribosomes, and glycogen granules were abundantly scattered

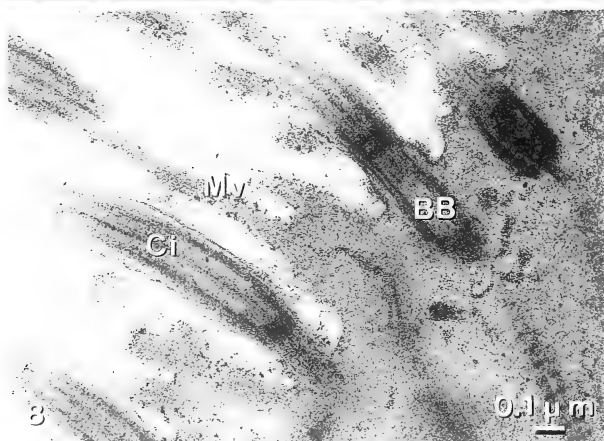
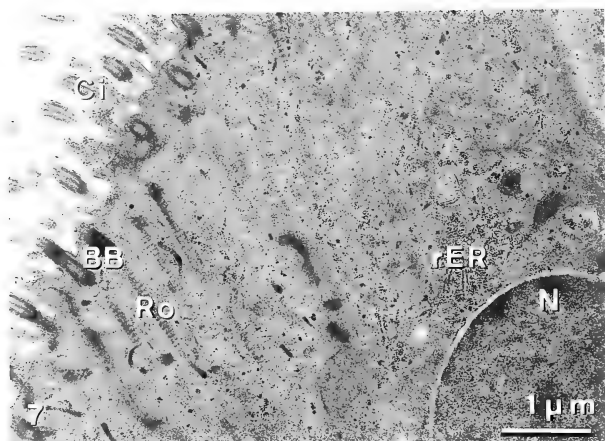


FIG. 7. Transmission electron micrograph of a ciliated cell. Nucleus (N) is located basally. Basal bodies (BB) can be recognized just beneath the free-surface of the cell. Ciliary rootlets (Ro) are distributed in the cytoplasm. Rough-surfaced endoplasmic reticulum (rER) are seen mainly in the perikaryon. Ci: cilia.

FIG. 8. Higher magnification of the free-surface side of a ciliated cell. Microvilli (Mv) are scattered among cilia (Ci). BB: basal bodies.

in the cytoplasm (Fig. 10). The mitochondria contained some intramitochondrial granules. A few electron-dense bodies, which were probably

the basal bodies, were present within the cells on the free-surface side in the cytoplasm. Filamentous structures were recognized through-

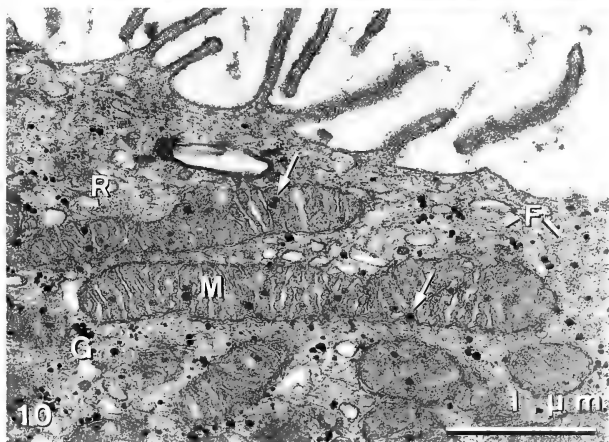
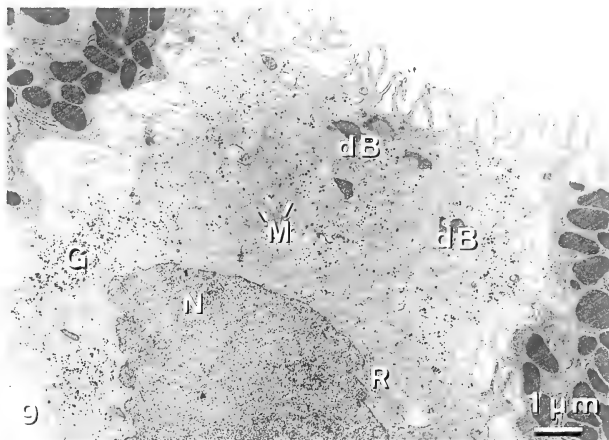


FIG. 9. Transmission electron micrograph of a cell without electron-dense granules, mucus granules, or cilia. The nucleus (N) is located basally. Mitochondria (M) and glycogen granules (G) are distributed throughout the cytoplasm. Free ribosomes (R) are seen mainly in the perikaryon. Dense bodies (dB) are located on the free-surface side.

FIG. 10. Higher magnification of the free-surface side of the cytoplasm of a cell which contains no electron-dense granules, mucus granules, or cilia. Mitochondria (M) contain intramitochondrial granules (arrows). Glycogen granules (G) and free ribosomes (R) can be recognized in the cytoplasm. Filamentous structures (F) are seen throughout the cytoplasm.

out the cytoplasmic matrix at higher magnification. Microvilli on the free-surfaces of cells and cellular processes on the surfaces which faced adjacent cells were well-developed (Figs. 9 and 10).

A very small number of plasma cells, which originated from the connective tissue, were seen within the epithelium (Fig. 6).

DISCUSSION

There are two possible explanations for the presence of electron-dense granules in the whole papillar epithelium: one is that they may be immature forms of mucus granules, and the other is that they may be analogous to serous granules found in the salivary glands of higher organisms [12-14]. However, it appears that the electron-dense granules are unrelated to the mucus granules because we found no evidence of any transitional stages existing between the electron-dense granules and the mucus granules.

It is well known that in the salivary glands of mammals, the secretion or discharge of the contents of serous granules occurs through exocytosis, involving the fusion of the granule membrane with the plasma membrane at the lumen or intercellular canaliculus, followed by the opening of the fused portion [15]. In the present study, direct discharge of the contents of electron-dense granules into the oral cavity was not obvious. Instead, it seems likely that after some electron-dense granules aggregate to form an electron-lucent vacuoles, the contents of the electron-lucent vacuoles are discharged into the oral cavity by exocytosis. This scheme for secretion of the contents of the granules is very similar to the rapid secretion of the contents of serous granules in the salivary glands of mammals, as it occurs after stimulation with pharmacologic agents [15, 16].

It has been reported in the mouse [17] and the rat [18], that secretory granules of the submandibular gland of newborns contain tubular structures. In the present study of the bullfrog tongue, we found that the secretory granules of the cells within the lingual dorsal epithelium contained tubular structures similar to those found in the submandibular glands of newborn mice. Based on the time at which the tubular structures appear,

Yohro [17] assumed that they were related to secretory activity. Therefore, the analogous structures observed in the lingual epithelial cells of bullfrogs may be involved in the active secretion of granules.

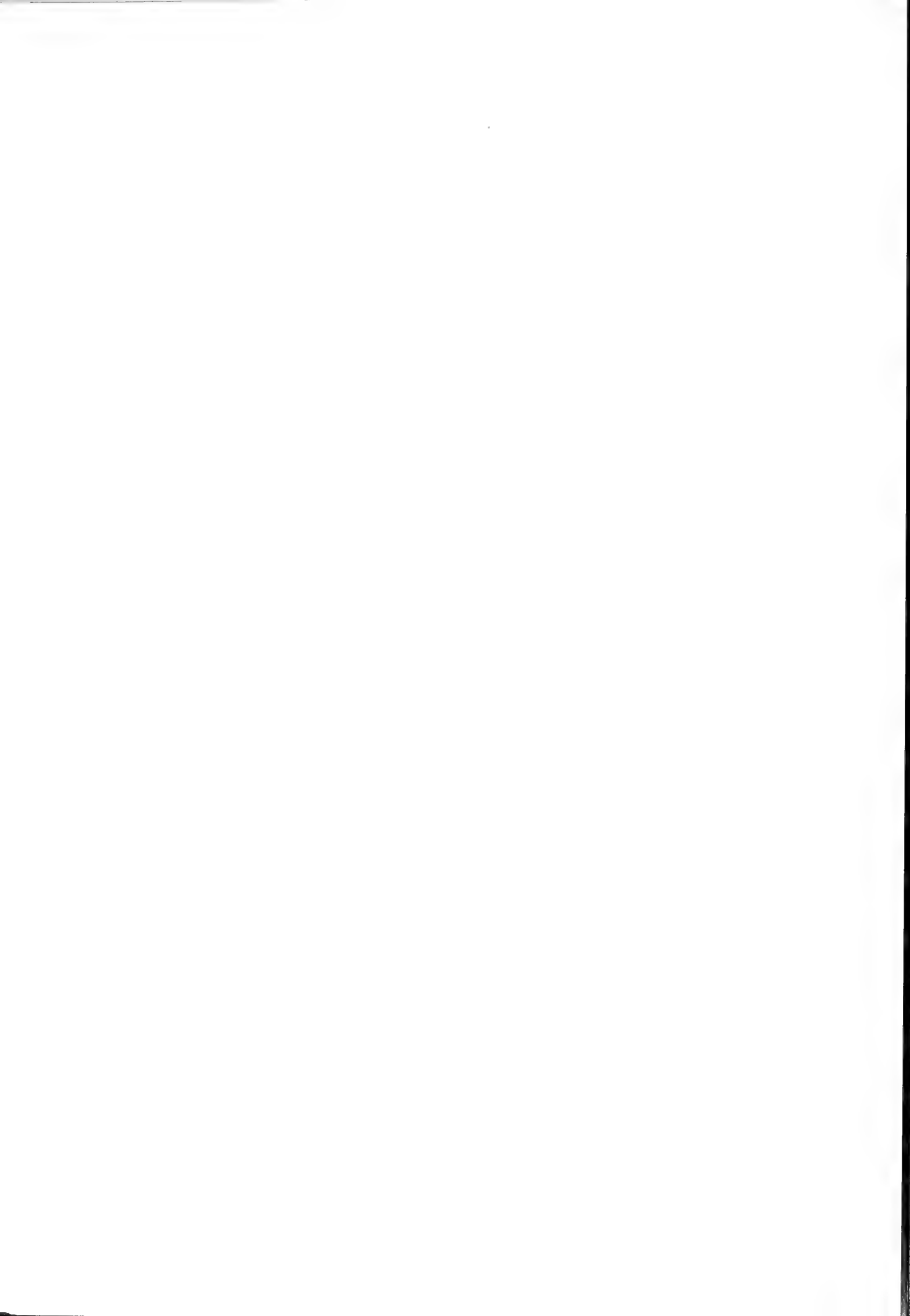
A very small number of cells without electron-dense granules, mucus granules, or cilia was found within the epithelium. However, these cells contain a lot of mitochondria throughout their cytoplasm, and have many microvilli on their free-surface. These structural features are very similar to those of the flask cells or mitochondria-rich cells [19-21]. The mitochondria-rich cells of amphibian skin epithelium have been implicated in the mechanism for passive chloride conductance across the skin [22-24]. There is a possibility that the mucosal epithelium of the frog tongue also plays the same role as the skin in passive chloride conductance.

In previous studies with the scanning electron microscope [9], microridges were found to be widely distributed on the filiform papillar surface of the bullfrog tongue. The present study indicates that the electron-dense granular cells have microridges on their free-surfaces, and cellular processes [25] on the surfaces which face adjacent cells. There are no significant differences between these structures except for whether or not they face adjacent cells. By scanning electron microscopic observation [9], they are clearly different from microvilli. These cellular processes seem to function as connecting structures between adjacent cells, while the microridges on the free-surface probably facilitate the spreading and holding of mucus [26].

REFERENCES

- 1 Uga, S. and Hama, K. (1967) Electron microscopic studies on the synaptic region of the taste organ of carps and frogs. *J. Electron Microsc.*, **16**: 269-276.
- 2 Graziadei, P. P. C. (1969) The ultrastructure of vertebrate taste buds. In "Olfaction and Taste". Ed. by C. Pfaffman, Rockefeller Univ. Press, New York, pp. 315-330.
- 3 Graziadei, P. P. C. and DeHan, R. S. (1971) The ultrastructure of frogs' taste organs. *Acta Anat.*, **80**: 563-603.
- 4 Sensaas, L. J. (1971) The fine structure of fungiform papillae and epithelium of the tongue of a

- South American toad, *Calyptocephalella gayi*. Am. J. Anat., **131**: 443-462.
- 5 Hirata, K. and Nada, O. (1975) A monoamine in the gustatory cell of the frog's taste organ—a fluorescence histochemical and electron microscopic study. Cell Tissue Res., **159**: 101-108.
- 6 Düring, M. v. and Andres, K. H. (1976) The ultrastructure of taste and touch receptors of frog's taste organ. Cell Tissue Res., **169**: 185-198.
- 7 Jaeger, C. B. and Hillman, D. E. (1976) Morphology of gustatory organs. In "Frog Neurobiology". Ed. by R. Linal and W. Precht, Springer-Verlag, Berlin/Heidelberg/New York/Tokyo, pp. 558-606.
- 8 Gubo, G., Lametschwandtnr, A., Simonsberger, P. and Adam, H. (1978) Licht- und rasterelktronenmikroskopische Untersuchungen an Gaumen und Zunge der Gelbbauchunke, *Bombina variegata* L. Anat. Anz., **114**: 169-178.
- 9 Iwasaki, S. and Sakata, K. (1985) Fine structure of the lingual dorsal surface of the bullfrog. Okajimas Folia Anat. Jpn., **61**: 437-450.
- 10 Iwasaki, S., Miyata, K. and Kobayashi, K. (1986) Studies on the fine structure of the lingual dorsal surface in the frog, *Rana nigromaculata*. Zool Sci., **3**: 265-272.
- 11 Millonig, G. (1961) Advantages of a phosphate buffer for OsO_4 solutions in fixation. J. Appl. Physics, **32**: 1637.
- 12 Hand, A. R. (1971) Morphology and cytochemistry of Golgi apparatus of rat salivary gland acinar cells. Am. J. Anat., **130**: 141-158.
- 13 Riva, A. and Riva-Testa, F. (1973) Fine structure of acinar cells of human parotid gland. Anat. Rec., **176**: 149-166.
- 14 Ichikawa, M. and Ichikawa, A. (1977) Light and electron microscopic histochemistry of the serous secretory granules in the salivary glandular cells of the mongolian gerbil (*Mongolian meridianus*) and rhesus monkey (*Macaca irus*). Anat. Rec., **189**: 125-140.
- 15 Hand, A. R. (1980) Salivary glands. In "Orban's Oral Histology and Embryology". Ed. by S. N. Bhaskar, C. V. Mosby Co., St. Louis, pp. 336-370.
- 16 Amsterdam, A., Ohad, I. and Schramm, M. (1969) Dynamic changes in the ultrastructure of the acinar cell of the rat parotid gland during the secretory cycle. J. Cell Biol., **41**: 753-773.
- 17 Yohro, T. (1970) Development of secretory units of mouse submandibular gland. Z. Zellforsch., **110**: 173-184.
- 18 Kim, S. K., Han, S. S. and Nasjleti, C. E. (1970) The fine structure of secretory granules in submandibular glands of the rat during early postnatal development. Anat. Rec., **168**: 463-476.
- 19 Whitear, M. (1977) A functional comparison between the epidermis of fish and of amphibian. In "Comparative Biology of Skin". Ed. by R. I. C. Spearman, Academic Press, London/New York, pp. 291-313.
- 20 Ilic, V. and Brown, D. (1980) Modification of mitochondria-rich cells in different ionic conditions: Changes in cell morphology and cell number in the skin of *Xenopus laevis*. Anat. Rec., **196**: 153-161.
- 21 Robinson, D. H. and Heintzelman, M. B. (1987) Morphology of ventral epidermis of *Rana catesbeiana* during metamorphosis. Anat. Rec., **217**: 305-317.
- 22 Voute, C. L. and Meier, W. (1978) The mitochondria-rich cell of frog skin as a hormone sensitive "shunt path". J. Membr. Biol., **40S**: 141-165.
- 23 Foskett, J. K. and Ussing, H. H. (1986) Localization of chloride conductance to mitochondria-rich cells in frog skin epithelium. J. Membr. Biol., **91**: 251-258.
- 24 Katz, U. and Gabbay, S. (1988) Mitochondria-rich cells and carbonic anhydrase content of toad skin epithelium. Cell Tissue Res., **251**: 425-431.
- 25 Krstic, R. V. (1979) "Ultrastructure of the Mammalian Cell". Springer-Verlag, Berlin/Heidelberg/New York/Tokyo, pp. 238-239.
- 26 Sperry, D. G. and Wassersug, R. J. (1976) A proposed function for microridges on epithelial cells. Anat. Rec., **185**: 253-258.



Hemoglobins from the Two Closely Related Clams *Barbatia lima* and *Barbatia virescens*. Comparison of Their Subunit Structures and N-terminal Sequence of the Unusual Two-Domain Chain

TOMOHIKO SUZUKI¹, MAKOTO SHIBA, TAKAHIRO FURUKOHI
and MICHİYORI KOBAYASHI²

Department of Biology, Faculty of Science, Kochi University, Kochi 780,
and ²Department of Biology, Faculty of Science,
Niigata University, Niigata 880, Japan

ABSTRACT—The intracellular hemoglobins were isolated from the two closely related arcid clams *Barbatia lima* and *Barbatia virescens*, respectively, and their subunit structures were compared in detail.

B. virescens hemoglobin on Ultrogel AcA44 column had a single peak corresponding to the molecular weight (*M_r*) of 30,000. The hemoglobin was separated by high-performance liquid chromatography (HPLC) into two chains (I and II) with *M_r* 16,000, suggesting the heterodimeric structure. N-Terminal 20 residues of chain I showed homology (35% identity) with those of *Anadara* homodimeric hemoglobins.

On the other hand, *B. lima* hemoglobin on Ultrogel AcA44 column had two peaks, a polymeric hemoglobin eluted in the void volume of the column and a *M_r* 60,000 hemoglobin. The polymeric hemoglobin on HPLC eluted as a single peak, and the *M_r* was estimated to be 32,000 by sodium dodecyl sulfate-polyacrylamide gel electrophoresis in the presence of a reducing agent. Therefore, it was suggested that the constituent chain of polymeric hemoglobin has an unusual two-domain structure with two hemes per chain. The *M_r* 60,000 hemoglobin was separated by HPLC into two major chains (A and B) with *M_r* 16,000 suggesting the tetrameric structure (A₂ B₂). These structural features of *B. lima* hemoglobins were similar to those of *B. reeveana* [1].

N-Terminal sequences of 36 residues of each domain of *B. lima* two-domain chain were determined from three CNBr fragments. N-Terminus of the chain was blocked by an acetyl group, and the second domain appeared to start at methionine residue. The sequence homology between domains were very high; 27 out of 36 residues (75%) were identical. We propose from these results that the two-domain chain resulted from gene duplication and the following loss of a stop codon.

INTRODUCTION

Several taxodont(arcid) and heterodont clams have hemoglobins in circulating erythrocytes [2]. Usually, their quaternary structure is dimeric or tetrameric, but the subunit assembly has been shown to be quite different from that of vertebrate tetrameric hemoglobin [3]. Like tetrameric hemoglobin, the dimeric hemoglobin shows a

cooperativity [2]. It is also noted that the clam hemoglobins have an N-terminal extension of amino acid sequence which forms an additional helix (namely pre-A helix) [3].

Recently, Grinich and Terwilliger [1, 4] found that the arcid clam *Barbatia reeveana* has not only a tetrameric hemoglobin but also a polymeric hemoglobin in erythrocytes. Furthermore they showed that the polymeric hemoglobin appeared to be composed of unusual two-domain polypeptide chains with two hemes. Riggs *et al.* [5] reported the partial amino acid sequence (the first 129 residues of domain 1 and the middle 108

Accepted June 25, 1988

Received May 23, 1988

¹ To whom all correspondence should be addressed.

residues of domain 2) of *B. reeveana* two-domain hemoglobin by cDNA sequencing.

In this paper, we report the subunit structures of hemoglobins from *Barbatia lima* and *Barbatia virescens*. It will be shown that these closely related clams have quite different hemoglobins. We also report the N-terminal sequences of 36 residues of each domain of *B. lima* two-domain hemoglobin.

MATERIALS AND METHODS

B. lima and *B. virescens* were collected from rocks near Usa, Kochi, Japan. *B. lima* is a open-sea type species, while *B. virescens* is a bay-type species. They have a similar shell but are distinguished by the hinge line and the interior color of shell.

The red cells were washed three times with 3% (w/v) NaCl and lysed with ice-cold 1 mM phosphate buffer (pH 7.2). The hemolysate was centrifuged at 15,000 rpm for 15 min, and the supernatant was immediately applied to the column of Ultrogel AcA 44 equilibrated with 0.1 M phosphate buffer (pH 7.2).

B. virescens hemoglobin passed through a gel filtration column was applied to a DEAE-cellulose column equilibrated with 20 mM Tris-HCl (pH 8.0) and eluted with a linear gradient of 0 to 40 mM NaCl in the same buffer.

B. lima polymeric hemoglobin, which is eluted in the void volume of the gel filtration column (Fig. 1B), was applied to a DEAE-cellulose column equilibrated with 20 mM Tris-HCl (pH 8.0) containing 0.1 mM dithiothreitol (DTT) and eluted with a linear gradient of 0 to 0.1 M NaCl in the same buffer. *B. lima* Mr 60,000 hemoglobin, which corresponds to the latter peak in Fig. 1B, was also applied to a DEAE-cellulose column equilibrated with 20 mM Tris-HCl (pH 9.4) and eluted with a linear gradient of 20 mM Tris-HCl (pH 9.4) to 20 mM Tris-HCl (pH 8.0).

The constituent polypeptide chains of hemoglobin were separated by high performance liquid chromatography (HPLC, Hitachi 655) on a C₁₈- μ Bondapak column (Waters) using a solvent system as described by Shelton *et al.* [6], or on a Lichrosorb RP2 column using a solvent system by

Ashauer *et al.* [7].

Sodium dodecyl sulfate-polyacrylamide gel electrophoresis (SDS-PAGE) was carried out in 15% acrylamide containing 0.1% SDS and 0.375 M Tris-HCl (pH 8.9). Samples containing 2.5% SDS and 5% 2-mercaptoethanol were incubated at 100°C for 5 min before electrophoresis.

CNBr cleavage of *B. lima* two-domain hemoglobin (370 nmoles) was performed in 70% formic acid with a 200-fold excess of CNBr over methionine at 37°C for 20 hr, and the CNBr peptides were fractionated by a Sephadex G-50 column (1.6 \times 100 cm) equilibrated with 8.7% (v/v) acetic acid / 2.5% formic acid. The peptides were purified further by HPLC on a Cosmosil 5C₁₈-300 column (Nakarai Chemicals Ltd.) with a linear gradient of 2 to 80% acetonitrile in 0.1% trifluoroacetic acid (TFA). Two CNBr fragments, CN1 and CN3, were further digested with trypsin (Worthington) in 0.1 M ammonium bicarbonate at 37°C for 2 hr at an enzyme-to-substrate ratio of 1/50 (w/w). The tryptic peptides were purified by HPLC using the same conditions as described above. The subpeptide CN1T1 was digested with lysyl endopeptidase (Wako) in 10 mM Tris-HCl (pH 8.9) at 37°C for 2 hr at an enzyme-to-substrate ratio of 1/200, and the resultant peptides (CN1T1L1 and CN1T1L2) were separated by HPLC. To remove the acylamino-acid, CN1T1L1 was digested further with acylamino-acid-releasing enzyme (0.025 units) (Takara) in 5 mM phosphate buffer (pH 7.2) containing 2-mercaptoethanol at 37°C for 2 hr.

B. lima two-domain hemoglobin (50 nmoles) was also digested with lysyl endopeptidase at 37°C for 2.2 hr, and the peptides were purified by HPLC.

Proteins and peptides were hydrolyzed with TFA/HCl (1/2, v/v) containing 0.02% phenol at 170°C for 30 min in evacuated sealed tubes. Amino acid analysis was performed in Hitachi 835-50 amino acid analyzer.

The amino acid sequence was determined by the manual Edman method with modification [8, 9]. Phenylthiohydantoin amino acid derivatives were identified by HPLC on a Cosmosil 5PTH column (Nakarai Chemicals Ltd.) with isocratic elution.

The primary peptides were numbered from the

amino-terminus, and the subpeptides are numbered in order within the parent peptide. In this paper, the prefix CN indicates a cyanogen bromide peptide; T, a tryptic peptide; L, a lysyl endopeptidase peptide; and A, an acylamino-acid-releasing enzyme peptide.

RESULTS

Gel filtration profiles of *B. virescens* and *B. lima* red cell hemolysates are shown in Figs. 1A and 1B, respectively. *B. virescens* hemoglobin had a single peak corresponding to the molecular weight (M_r) of 30,000, while *B. lima* hemoglobin had two peaks; one is a polymeric hemoglobin eluted in the void volume of the column and the other is a M_r 60,000 hemoglobin. Although we did not estimate the M_r of polymeric hemoglobin of *B. lima*, Grinich and Terwilliger [1] reported the value of 430,000 to the polymeric hemoglobin of *B. reeveana*.

DEAE-cellulose chromatography of *B. virescens* M_r 30,000 hemoglobin and *B. lima* polymeric and M_r 60,000 hemoglobins gave one major peak containing heme, respectively (Figs. 2A-C).

Figure 3 shows the SDS-PAGE patterns of reduced hemoglobins from *B. virescens* and *B. lima*. The hemolysate and purified hemoglobin (lanes 1 and 2) of *B. virescens* gave a single band (M_r 16,000). On the other hand, the hemolysate (lane 3) of *B. lima* gave two bands (M_r s 32,000 and 16,000), which corresponded to polymeric (lane 4) and M_r 60,000 (lane 5) hemoglobins, respectively.

B. virescens hemoglobin was separated by HPLC into two constituent polypeptide chains (I and II) in equimolar proportions (Fig. 4A). Amino acid compositions of isolated chains are shown in Table I. N-Terminal sequence (20 residues) of chain I was determined to be Pro-Ser-Val-Ala-Ala-Ala-Val-Ser-Ala-Val-Thr-Asn-Lys-Asp-Val-Ala-Gln-Glu-Ile-Trp- by manual Edman degradation, but that of chain II was not detected, suggesting that N-terminus is blocked. The M_r s of chains I and II were estimated to be 16,000 by SDS-PAGE. Based on gel filtration, DEAE-cellulose chromatography and SDS-PAGE, we concluded that *B. virescens* hemoglobin has a heterodimeric structure.

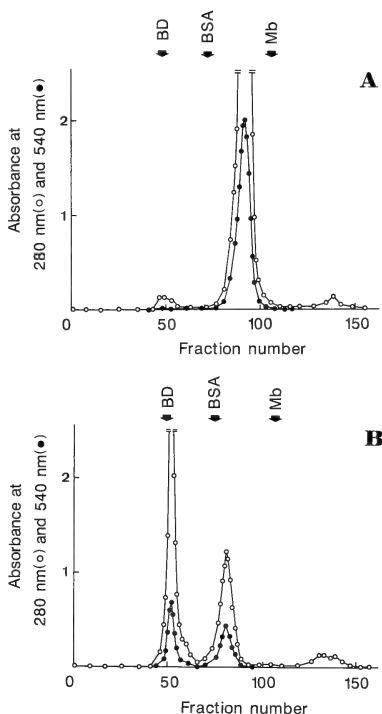


Fig. 1. (A) Gel filtration on Ultrogel AcA 44 of *B. virescens* red cell hemolysate. The column (3×100 cm) was equilibrated with 0.1 M phosphate buffer (pH 7.2). Fraction size, 5 ml/tube. BD, blue dextran; BSA, bovine serum albumin; Mb, sperm whale myoglobin. (B) Gel filtration on Ultrogel AcA 44 of *Barbatia lima* red cell hemolysate. Conditions are as for (A).

B. lima M_r 60,000 hemoglobin was separated by HPLC into two major chains (A and B) and a minor chain (A') as shown in Fig. 4B. Amino acid composition of chain A' was very similar to that of chain A (Table 1), suggesting that chain A' is a hetero-type of chain A. No N-terminal residue of all the chains was detected by manual Edman method. The M_r s of chains were determined to be

16,000 by SDS-PAGE. Based on gel filtration, DEAE-cellulose chromatography and SDS-PAGE, we concluded that *B. lima* Mr 60,000 hemoglobin has a heterotetrameric structure (A_2B_2).

B. lima polymeric hemoglobin was purified by HPLC on a Lichrosorb RP2 column (Fig. 4C) or a C₁₈- μ Bondapak column (data not shown). In each case, only one polypeptide chain (P) was eluted. No N-terminal residue was detected by manual Edman method. The Mr of chain P was determined

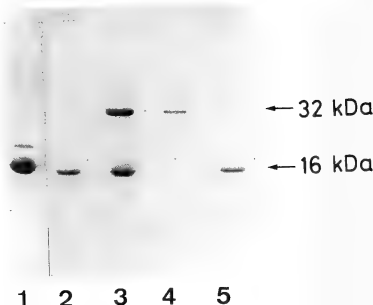
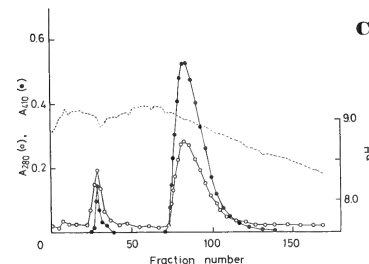
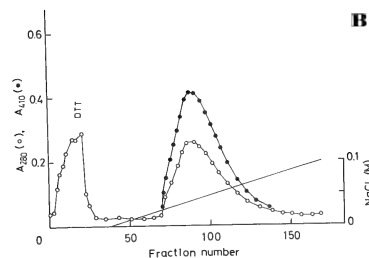
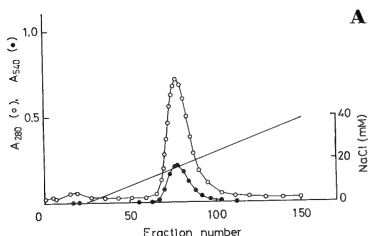


FIG. 3. SDS-PAGE patterns of reduced *Barbatia* hemoglobins. Lane 1, red cell hemolysate of *B. virescens*; 2, purified hemoglobin (Fig. 1A) of *B. virescens*; 3, red cell hemolysate of *B. lima*; 4, polymeric hemoglobin (Fig. 1B) of *B. lima*; 5, Mr 60,000 hemoglobin (Fig. 1B) of *B. lima*.

to be 32,000 by SDS-PAGE in the presence of reducing agent, which is two times as large as that of a typical globin subunit. Therefore we concluded that *B. lima* polymeric hemoglobin consists of one major chain and that the chain has an unusual two-domain structure with two hemes, like *B. reeveana* polymeric hemoglobin [1].

B. lima two-domain chain was cleaved with CNBr, and the CNBr peptides were fractionated by Sephadex G-50 chromatography (Fig. 5). Three peptides, CN1 (25 residues), CN2 (11 re-

FIG. 2. (A) DEAE-cellulose chromatography of *B. virescens* Mr 30,000 hemoglobin. The column (1.3 \times 10 cm) was equilibrated with 20 mM Tris-HCl (pH 8.0) and eluted with a linear gradient of 0 to 40 mM NaCl in the same buffer. Fraction size, 5 ml/tube. (B) DEAE-cellulose chromatography of *B. lima* polymeric hemoglobin. The column (1.3 \times 10 cm) was equilibrated with 20 mM Tris-HCl (pH 8.0) containing 0.1 mM DTT and eluted with a linear gradient of 0 to 0.1 M NaCl in the same buffer. The sample was reduced with 2 mM DTT before chromatography. Fraction size, 5 ml/tube. (C) DEAE-cellulose chromatography of *B. lima* Mr 60,000 hemoglobin. The column (1.3 \times 10 cm) was equilibrated with 20 mM Tris-HCl (pH 9.4) and eluted with a linear gradient of 20 mM Tris-HCl (pH 9.4) to 20 mM Tris-HCl (pH 8.0). Fraction size, 5 ml/tube.

sides) and CN3 (36 residues), were purified further by HPLC (Fig. 6). CN1 with blocked N-terminal residue was placed at the N-terminus of the whole protein. CN3 had strong sequence homology with CN1, therefore, we placed CN3 at the N-terminus of the second domain. With the aid of sequence homology, CN2 was placed behind CN1.

An N-terminal acetyl group was determined as dansylacetylhydrazine [8], using the peptide CN1.

CN1 and CN3 were digested with trypsin, and the tryptic peptides were purified by HPLC (Fig. 7). CN1 produced three tryptic peptides, CN1T1 with blocked N-terminus, CN1T2 and CN1T3 with

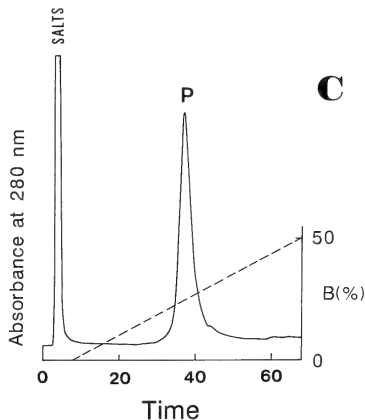
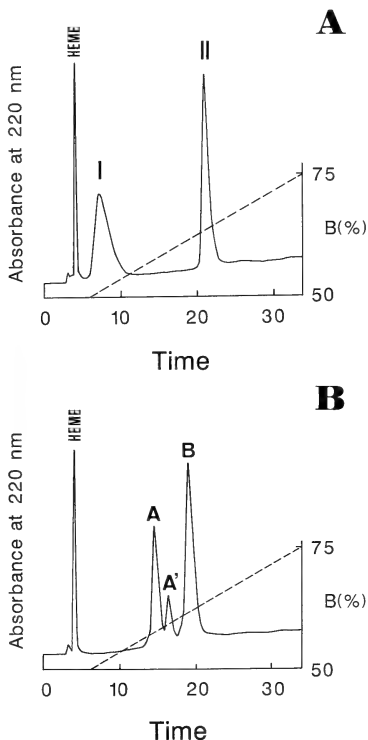


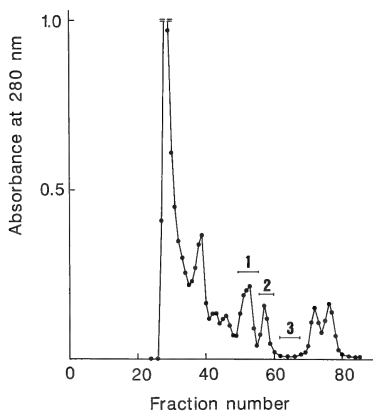
Fig. 4. (A) Separation of globin chains of *B. virescens* hemoglobin by HPLC. The column (C_{18} - μ Bondapak) was equilibrated with 50% solvent A/50% solvent B and eluted with a linear gradient of 50 to 75% solvent B over 25 min. Solvent A in volume %, 80:5:15:0.1:0.05 of 0.15 M NaClO_4 : methanol: acetonitrile: 85% H_3PO_4 : nonylamine. Solvent B, 20:5:75:0.1:0.05 of the same components. Flow rate, 1 ml/min. (B) Separation of globin chains of *B. lima* Mr 60,000 hemoglobin by HPLC. Conditions are as for (A). (C) Separation of globin chain of *B. lima* polymeric hemoglobin by HPLC. Heme was removed before HPLC, and the apoprotein was reduced with 10 mM DTT. The column (Lichrosorb RP2) was equilibrated with solvent A and eluted with a linear gradient of 0 to 100% solvent B over 60 min. Solvent A, 50 mM ammonium acetate containing 5% HCOOH and 15% acetonitrile. Solvent B, 50 mM ammonium acetate containing 5% HCOOH and 70% acetonitrile. Flow rate, 0.7 ml/min.

homoserine residue. Therefore we aligned them in the order CN1T1-CN1T2-CN1T3. CN1T1 was digested further with lysyl endopeptidase, and the N-terminal peptide CN1T1L1 was isolated. Since the N-terminus of CN1T1L1 is blocked by an acetyl group, we digested this peptide with acyl-amino-acid-releasing enzyme to remove the acyl-amino acid (acetyls erine) and then sequenced the resultant peptide without trouble. CN3 produced

TABLE 1. Amino acid compositions of constituent chains of *Barbatia* hemoglobins

	<i>B. virescens</i> Dimeric		<i>B. lima</i> Tetrameric		<i>B. lima</i> Polymeric	
	I	II	A	A'	B	P
Asp	16.6	18.6	16.6	16.2	18.9	43.4
Thr	6.3	3.7	8.8	8.3	5.6	9.0
Ser	9.5	9.0	9.8	10.9	8.7	6.2
Glu	15.6	11.8	13.6	14.0	8.5	31.1
Pro	5.9	3.8	3.0	3.4	4.7	8.7
Gly	6.9	9.7	12.5	12.8	7.4	19.8
Ala	12.7	15.5	11.9	13.5	22.6	23.1
Cys	0.0	0.3	0.9	1.1	1.3	1.8
Val	10.6	8.2	8.5	7.9	9.3	24.8
Met	5.6	2.8	6.7	6.0	4.7	6.0
Ile	5.2	7.3	5.9	5.6	5.2	14.2
Leu	14.6	18.3	16.5	15.6	15.8	33.2
Tyr	1.9	5.6	1.2	1.8	4.3	3.1
Phe	8.7	5.8	7.4	7.2	6.3	10.4
Lys	11.5	15.0	11.1	10.1	12.1	29.4
His	2.0	3.1	2.5	2.9	3.1	6.9
Arg	10.5	5.9	8.0	7.8	6.8	18.7
Trp	N.D.	N.D.	N.D.	N.D.	N.D.	N.D.
Total	144	144	145	145	145	290
SDQ	43.3	83.4	50.9	42.0	131.3	98.9

N.D. not determined.



five tryptic peptides. Since we determined the first 14 residues of CN3 by the direct sequencing, CN1T1 and CN1T2 were easily placed in this region. CN3T5 with homoserine residue was placed at the C-terminus, and the remaining two peptides (CN3T3 and CN3T4) were aligned by the homology with CN1.

B. lima two-domain chain was also digested with lysyl endopeptidase, and the N-terminal peptides L1 and L2 of second domain were purified by HPLC (Fig. 8).

The amino acid compositions of peptides are

FIG. 5. Gel filtration on Sephadex G50 of CNBr fragments of *B. lima* two-domain hemoglobin. The column (1.6×100 cm) was equilibrated with 8.7% acetic acid/2.5% formic acid. Three fractions (1, 2 and 3) were pooled, respectively. Fraction size, 2 ml/tube.

shown in Table 2.

The amino acid sequence was mainly determined from the tryptic peptides of CNBr fragments. The procedures used for sequence determination are summarized in Fig. 9. N-Terminal Ser of domain 1 was determined from amino acid composition of the peptide CNITIL1. Val-Met at positions 24–25 (domain 1), Leu-Met at 35–36 (domain 1), Lys at 30 (domain 2) and Leu-Met at 35–36 (domain 2) were determined from amino acid compositions of peptides and specificity of CNBr cleavage or trypsin. Heterogeneity was found at positions 10 (Thr and Ala) and 29 (Arg and Lys) of domain 2. In each case, the former amino acid in parentheses was obtained at high yield.

DISCUSSION

One of the recent topics on molluscan hemoglobins was the finding of polymeric hemoglobin (M_r 430,000) in the circulating erythrocytes of *B. reeveana* [1]. The hemoglobin was not only the largest intracellular hemoglobin so far known, but also consisted of unusual two-domain polypeptide chains (M_r 32,000–34,000). In order to elucidate the physiological role and evolutionary origin of the unusual two-domain chain, we examined the subunit structures of the hemoglobins from *B. lima* and *B. virescens* in detail.

B. virescens contained only a heterodimeric hemoglobin consisting of myoglobin-like subunits. This seems rather unique, since many arcids such as *Anadara* [10, 11] and *Scapharca* [12] contain both homodimeric and tetrameric hemoglobins. Besides *B. virescens*, a heterodimeric hemoglobin is occurred only in the clam *Noetia ponderosa* [13] and might represent a prototype of tetrameric hemoglobin. The two constituent chains, I and II, of *B. virescens* hemoglobin have rather different

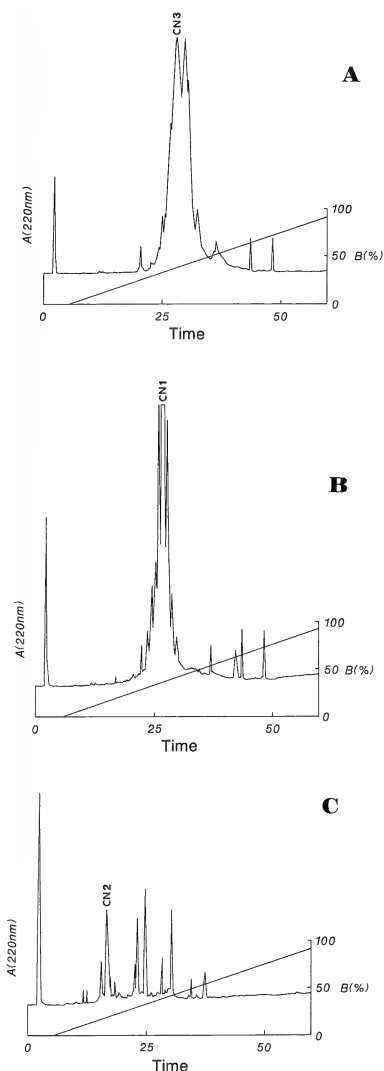


Fig. 6. HPLC purification of CNBr fragments of *B. lima* two-domain hemoglobin. The column (Cosmosil 5C₁₈-300) was equilibrated with solvent A (2% acetonitrile in 0.1% TFA) and eluted with a linear gradient of 0 to 100% solvent B (80% acetonitrile in 0.1% TFA) over 60 min. Flow rate, 1 ml/min. A, fraction 1 in Fig. 5; B, fraction 2; C, fraction 3.

TABLE 2. Amino acid compositions of CNBr, trypsin and lysyl endopeptidase

	CN1	CN1T1	CN1TIL1	CN1TIL2	CN1T2	CN1T3	CN2
Asp	4.0(4)	2.0(2)	1.0(1)	1.1(1)	1.0(1)	1.0(1)	2.0(2)
Thr	1.7(2)	0.9(1)		1.0(1)		0.8(1)	
Ser	1.6(2)	0.9(1)	0.9(1)			0.8(1)	
Glu	4.1(4)	3.9(4)	1.0(1)	3.1(3)			1.1(1)
Gly							2.7(3)
Ala	1.1(1)	1.0(1)		1.1(1)			0.9(1)
Cys							
Val	3.0(3)	1.9(2)	1.0(1)	1.1(1)		1.0(1)	1.0(1)
Met							
Ile	1.8(2)	0.9(1)		1.0(1)	0.9(1)		
Leu	1.1(1)				1.0(1)		1.2(1)
Tyr							
Phe							
Lys	1.9(2)	1.9(2)	1.0(1)	1.1(1)			
His							
Arg	1.0(1)				0.9(1)		1.1(1)
Pro	1.0(1)	1.0(1)		1.0(1)			
Trp	+ (1)					+ (1)	
Hse**	+ (1)					+ (1)	+ (1)
Total	25	15	5	10	4	6	11
Position	D1 [‡]	D1	D1	D1	D1	D1	D1
	1-25	1-15	1-5	6-15	16-19	20-25	26-36
Yield(%)	37.6	37.2	37.0	37.0	37.2	27.7	12.1

*Due to heterogeneity. **Homoserine. [‡]Domain 1. [§]Domain 2.

amino acid compositions; the S₄Q value [14] of chain I is 43.3 and that of chain II is 83.4, suggesting that they have rather different amino acid sequences. N-Terminal 20 residues of chain I shows homology (35% identity) with those of homodimeric chains from *Anadara* [11] and *Scapharca* [12], but shows little homology with the polymeric chain from *B. lima* (see Table 3).

B. virescens hemoglobin tended to polymerize. For example, when the aged sample was applied to the gel filtration column under the same conditions shown in Figure 1, several aggregates with higher *Mr* were newly emerged (data not shown). But HPLC analyses of the aggregates in the presence of a reducing agent gave the same elution profile as shown in Figure 4A. Since there is no cysteine residue in chain I, that in chain II must be responsible for the polymerization of *B. virescens* hemoglobin.

B. virescens chain I seems to contain only two histidine residues, which most likely correspond to the proximal and distal histidines (Table 1). Compared with vertebrate hemoglobins, molluscan globins have a low histidine content; *Anadara* dimeric and tetrameric hemoglobins have 2-3 histidines per chain [11]; *Scapharca* dimeric hemoglobin, 2 histidines [12]; *Aplysia* myoglobin, one histidine [15]; and *Dolabella* myoglobin, one histidine [8].

On the other hand, *B. lima* contained tetrameric and polymeric hemoglobins, like *B. reeveana* [4]. The tetrameric hemoglobin was composed of two myoglobin-like chains (A and B), while the polymeric hemoglobin was composed of unusual two-domain polypeptide chain (P). The amino acid compositions of chains A, B and P were rather different, the S₄Q values being 50.9, 131.3 and 98.9, respectively (Table 1). Chain B was especially rich in alanine and had lower content of glutamic

peptides of *Barbatia lima* two-domain hemoglobin

CN3	CN3T1	CN3T2	CN3T3	CN3T4	CN3T5	CN3T6	L1	L2
4.1(4)		1.1(1)		1.9(2)	2.0(2)	1.0(1)	1.1(1)	1.2(1)
2.2(2.5)*	0.9(1)	0.7(0.5)*		0.9(1)	0.9(1)		1.6(2)	0.9(1)
5.6(6)	1.0(1)	2.8(3)		1.1(1)	1.2(1)	0.9(1)	4.1(4)	3.9(4)
4.0(4)	1.0(1)		1.0(1)	1.2(1)	1.2(1)	1.0(1)	1.1(1)	1.2(1)
2.4(2.5)*		1.2(1.5)*		1.0(1)	1.0(1)		1.2(1)	1.9(2)
3.6(4)	1.0(1)	1.0(1)		0.8(1)	0.9(1)	1.0(1)	2.0(2)	2.0(2)
							0.8(1)	0.9(1)
2.5(3)		1.0(1)	0.9(1)	0.8(1)	0.8(1)		0.9(1)	0.9(1)
2.3(2)			1.0(1)			1.0(1)		
2.5(2.5)*		1.0(1)		1.1(1)	1.9(2)		1.1(1)	1.2(1)
2.5(2.5)*	1.0(1)		1.0(1)	0.8(1)			1.0(1)	1.0(1)
0.9(1)		0.9(1)					1.1(1)	1.0(1)
+ (1)				+ (1)	+ (1)			
+ (1)						+ (1)		
36	5	10	4	11	11	6	16	16
D2#	D2	D2	D2	D2	D2	D2	D2	D2
1-36	1-5	6-15	16-19	20-30	20-30	31-36	0-15	0-15
38.9	22.5	26.0	22.5	11.5	4.6	6.9	27.7	11.9

acid. The composition of chain A resembled that of *B. virescens* chain I, except glycine residue. Calculated from the *Mr* 32,000 of chain P, the chain has about 290 amino acids, just two times as many as typical globin.

The physiological role of *B. lima* two-domain hemoglobin is uncertain. Although *Barbatia* two-domain chain surely has two oxygen-binding sites [5] and can bind oxygen [4], the oxyhemoglobin isolated undergoes very rapid autoxidation and tends to precipitate. Although the two-domain hemoglobin is also found in the hemolymph of the water fleas *Daphnia* and *Moina* [16], unlike *Barbatia* two-domain hemoglobin, *Daphnia* hemoglobin is very resistant to autoxidation (Suzuki and Kobayashi, unpublished result). Therefore *Barbatia* two-domain hemoglobin seems to be rather disadvantageous as oxygen carrier protein.

To examine the evolutionary origin of two-

domain hemoglobin, we determined the N-terminal sequence of 36 residues of each domain of *B. lima* chain P. The partial sequences are aligned with that of *B. reeveana* domain 1 [5] in Figure 9. Of the three sequences, 24 out of 36 residues (67%) appear to be invariant, the highest homology being found between *B. lima* domain 1 and *B. reeveana* domain 1 (83% identity). The sequence homology between *B. lima* two domains was also high (75% identity). The presence of N-terminal Met of *B. reeveana* domain I is not sure, due to DNA sequencing. N-Terminus of *B. lima* domain 1 was blocked by an acetyl group, and the second domain appeared to start at methionine residue. From these results, it seems that *Barbatia* two-domain chain resulted from gene duplication and the following loss of a stop codon of the first domain.

We have shown that the two closely related

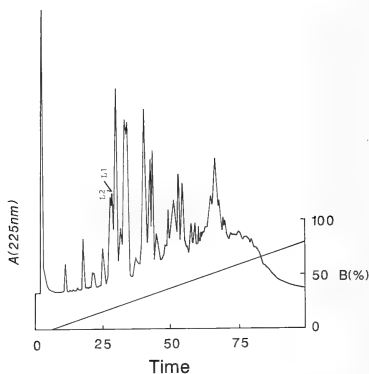
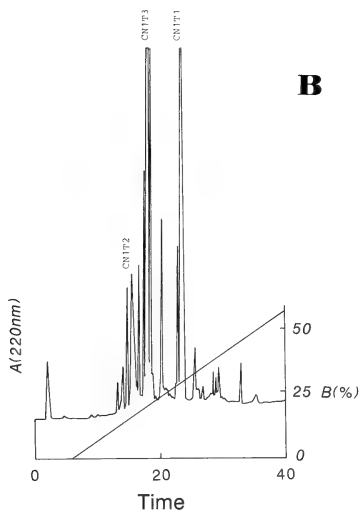
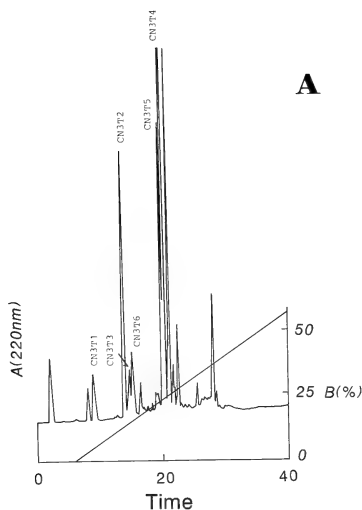


FIG. 8. HPLC separation of lysyl endopeptidase peptides of *B. lima* two-domain hemoglobin. Conditions are as for Fig. 6.

clams *B. virescens* and *B. lima* have quite different types of hemoglobins. It is usual that the closely related species have a similar hemoglobin in sequence and also in quaternary structure. For example, the related clams *Anadara trapezia*, *Anadara broughtonii* and *Scapharca inaequivalvis* have both dimeric and tetrameric hemoglobins, the sequence homology between corresponding chains being very high (over 85%) [11]; the related sea hares *Aplysia* and *Dolabella* have a monomeric myoglobin, the sequence homology being over 70% [8]. However, the S4Q values (Table 1) of *B. virescens* and *B. lima* chains do not suggest strong sequence homology between any chains. At present, we have no idea to explain this unusual phenomenon. But it is likely that this results from a taxonomical confusion.

N-Terminal amino acid sequences of invertebrate hemoglobins are compared in Table 3, which includes those of the phylum Echinodermata (sea cucumbers *Molpadia* [17] and *Paracaudina* (Suzuki, unpublished)), of Annelida (sea worms *Glycera*

FIG. 7. HPLC separation of tryptic peptides of *B. lima* CN3 (A) and CN1 (B). Conditions are as for Fig. 6.

TABLE 3. N-Terminal sequences of invertebrate hemoglobins

		-10	-5	0	5	10	15
		pre A					A
Vertebrata	Human tetramer beta (18)			V H L T P E E K S A V T A L W G K			
	Lamprey monomer (18)			P I V D S G S V A P L S A A E K T K I R S A W A P			
Echinodermata	<i>Molpadia</i> D (17)			Ac-G Q(T S A F Q S V G D L T L A E K D L I R S T W D N			
	<i>Paracaudina</i> I (unpublished)			Ac-G G T L A I Q S H G D L T L A Q K K I V R K T W H Q			
Annelida	<i>Glycera</i> monomer (18)			G L S A A Q R Q V I A A T W K D			
	<i>Tylorhynchus</i> IIA (9)			S S D H C G P L Q R L K V K Q Q W A K			
	<i>Lumbricus</i> I (19)			E C L V T E G L K V K L Q W A S			
	<i>Pheretima</i> I (unpublished)			D C N T L K R F K V K H Q W Q Q			
Vestimentifera	<i>Lamellibrachia</i> II-I (unpublished)			D C N I L Q R L K V K M Q W A K			
Arthropoda	<i>Chironomus</i> I (18)			G P S G D Q I A A A K A S W N T			
	<i>Artemia</i> domain E1 (20)			E R V D P I T G L S G L E K N A I L D T W G K			
	<i>Moita</i> domain 2 (unpublished)			A P E D L V D P E T R L S G I H K			
Mollusca	<i>Anadara</i> tetramer beta (11)			Ac-S T V A E L A N A V V S N A D Q K D L L R L S W G V			
	dimer (11)			P S V Q D A A A Q L T A D V K K D L R D S W K V			
	<i>Barbatia virescens</i> dimer I (This work)			P S V --- A A A V S A V T N K D V A Q E I W			
	<i>Barbatia reeveana</i> domain 1 (5)			(M) S V S A K L D E V T Q P A N K N L I R S T W N M			
	<i>Barbatia lima</i> domain 1 (This work)			Ac-S V E D K I E E V T Q P A N K N L I R S T W N V			
	domain 2 (This work)			M G V T E R I E E V T Q P A N K G L I R E T W N I			
	<i>Calyptogenia</i> chain I (unpublished)			V S A N D I K N V Q - D T W G K			
	chain II (unpublished)			V S Q A D I A A V Q - T S W R R			

Ac, an acetyl group. Helical segments by Chou and Fasman method [21] are marked by ...

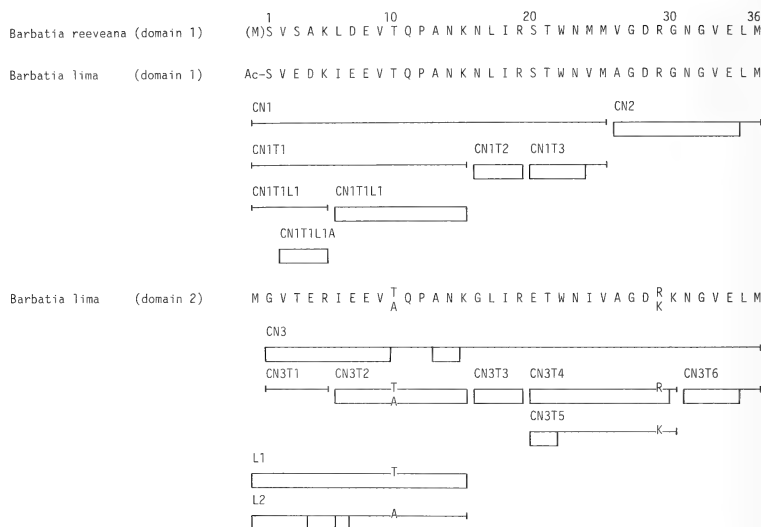


Fig. 9. Summary of data to establish the N-terminal sequences of 37 residues of each domain of *B. lima* two-domain hemoglobin. Manual Edman degradation (\square) was employed for sequence determination. The domain 1 sequence of *B. reeveana* hemoglobin [5] is aligned together. CN, a CNBr peptide; T, a tryptic peptide; L, a lysyl endopeptidase peptide; A, a acylamino-acid-releasing enzyme peptide.

[18] and *Tylorrhynchus* [9], and earthworms *Lumbricus* [19] and *Pheretima* (Suzuki, unpublished), of Vestimentifera (the deep-sea cold seep tube worm *Lamellibrachia* sp. (undescribed) (Suzuki, Takagi and Ohta, unpublished), of Arthropoda (*Chironomus* [18], *Artemia* [20] and *Moina* (Suzuki and Kobayashi, unpublished)) and of Mollusca (*Anadara* [11], *Barbatia* (this work, [5]) and the deep-sea cold seep clam *Calyplogena soyoeae* (Suzuki, Takagi and Ohta, unpublished)). These sequences were aligned by two conservative residues, Lys at position 7 (A5) and Trp at 14 (A12). As shown in Table 3, many invertebrate sequences have the N-terminal extension (pre-A segment) when compared with most of vertebrate globins. Since the extension of *Scapharca* hemoglobin has been shown to form an additional helix (pre-A helix), we examined the secondary structure of

N-terminal sequences of invertebrate hemoglobins by Chou-Fasman method [21]. Consequently, A-helix was predicted to most of all globins, and the pre A-helix was also predicted to the globins from *Molpadia*, *Moina*, *Anadara* and *Barbatia*. Anyway, the pre-A segment, which is distributed widely in invertebrate hemoglobin sequences, might represent a prototype of globin sequence.

ACKNOWLEDGMENTS

We are indebted to Mr Zenji Imoto for the supply of *B. lima*.

REFERENCES

- 1 Grinich, N. P. and Terwilliger, R. C. (1980) The quaternary structure of an unusually high mol. wt intracellular hemoglobin from the bivalve mollusc

- Barbatia reeveana*. Biochem. J., **189**, 1-8.
- 2 Terwilliger, R. C. and Terwilliger, N. B. (1985) Molluscan hemoglobins. Comp. Biochem. Physiol., **81B**, 255-261.
 - 3 Royer Jr., W. E., Love, W. E. and Fenderson, F. F. Cooperative dimeric and tetrameric clam haemoglobins are novel assemblages of myoglobin folds. (1985) Nature, **316**, 277-280.
 - 4 Grinich, N. P. Terwilliger, R. C. and Terwilliger, N. B. (1986) Oxygen equilibria and structural characteristics of the tetrameric and polymeric intracellular hemoglobins from the bivalve mollusc *Barbatia reeveana*. J. Comp. Physiol., **B 156**, 675-682.
 - 5 Riggs, A. F., Riggs, C. K., Lin, R.-J. and Domdey, H. (1986) Cloning of the cDNA for the globin from the clam, *Barbatia reeveana*. In "Invertebrate Oxygen Carriers". Ed. by B. Linzen, Springer-Verlag, Berlin/Heidelberg, pp. 473-476.
 - 6 Shelton, J. B., Shelton, J. R., Schroeder, W. A. and DeSimone, J. (1982) Detection of Hb-Papio B, a slight mutation of the baboon beta chain, by high performance liquid chromatography. Hemoglobin, **6**, 451-464.
 - 7 Ashauer, H., Weber, R. E. and Braunitzer, G. (1985) The primary structure of the hemoglobin of the dog fish shark (*Squalus acanthias*). Biol. Chem. Hoppe-Seyler, **366**, 589-599.
 - 8 Suzuki, T. (1986) Amino acid sequence of myoglobin from the mollusc *Dolabella auricularia*. J. Biol. Chem., **261**, 3692-3699.
 - 9 Suzuki, T. and Gotoh, T. (1986) The complete amino acid sequence of giant multisubunit hemoglobin from the polychaete *Tylorhynchus heterochaetus*. J. Biol. Chem., **261**, 9257-9267.
 - 10 Furuta, H., Ohe, M. and Kajita, A. (1977) Subunit structures of hemoglobins from erythrocytes of the blood clam, *Anadara broughtonii*. J. Biochem., **82**, 1723-1730.
 - 11 Gilbert, A. T. and Thompson, E. O. P. (1985) Amino acid sequence of the beta-chain of the tetrameric hemoglobin of the bivalve mollusc, *Anadara trapezia*. Aust. J. Biol. Sci., **38**, 221-236.
 - 12 Petruzzelli, R., Goffredo, B. M., Barra, D., Bossa, F., Boffi, A., Verzili, D., Ascoli, F. and Chiancone, E. (1985) Amino acid sequence of the cooperative homodimeric hemoglobin from the mollusc *Scapharca inaequivalvis* and topology of the intersubunit contacts. FEBS Lett., **184**, 328-332.
 - 13 San George, R. C., and Nagel, R. L. (1985) Dimeric hemoglobins from the acid blood clam, *Noetia ponderosa*. J. Biol. Chem., **260**, 4331-4337.
 - 14 Cornish-Bowden, A. (1983) The amino acid compositions of proteins are correlated with their molecular sizes. Biochem. J., **213**, 271-274.
 - 15 Suzuki, T., Takagi, T., and Shikama, K. (1981) Amino acid sequence of myoglobin from the mollusc *Aplysia kuroda*. Biochim. Biophys. Acta, **669**, 79-83.
 - 16 Kobayashi, M. and Hoshi, T. (1984) Analysis of respiratory role of haemoglobin in *Daphnia magna*. Zool. Sci., **1**, 523-532.
 - 17 Mauri, F. C. (1985) Ph. D. Dissertation, University of Texas, Austin, Texas.
 - 18 Kleinschmidt, T. and Sgouros, J. G. (1987) Hemoglobin sequences. Biol. Chem. Hoppe-Seyler, **368**, 579-615.
 - 19 Shishikura, F., Snow, J. W., Gotoh, T., Vinogradov, S. N. and Walz, D. A. (1987) Amino acid sequence of the monomer subunit of the extracellular hemoglobin of *Lumbricus terrestris*. J. Biol. Chem., **262**, 3123-3131.
 - 20 Moens, L., Van Hauwaert, M. L., Geelen, D., Verpooten, G. and Van Beeumen, J. (1986) The amino acid sequence of a structural unit isolated from the high molecular weight globin chains of *Artemia* sp. In "Invertebrate Oxygen Carrier". Ed. by B. Linzen, Springer-Verlag/Berlin/Heidelberg, pp. 81-84.
 - 21 Chou, P. Y. and Fasman, G. D. (1978) Empirical predictions of protein conformation. Ann. Rev. Biochem., **47**, 251-276.



Pepsinogen-Like Immunoreactivity in Ascidian Stomach and Intestine: Immunohistochemical and Biochemical Study

SADAO YASUGI¹, TAKASHI MATSUNAGA¹ and TAKEO MIZUNO^{1,2,3}

¹Zoological Institute, Faculty of Science, University of Tokyo, Tokyo 113,
and ²Misaki Marine Biological Station, Faculty of Science,
University of Tokyo, Miura, Kanagawa 238-02, Japan

ABSTRACT—The reactivity of epithelial cells of digestive tract of 5 species of ascidians against antisera to an adult chicken pepsinogen (ACPg) and to an embryonic chicken pepsinogen (ECPg) was examined by indirect immunofluorescence. Stomach and intestinal epithelial cells were reactive to anti-ACPg antiserum. The localization of reactive cells in the stomach coincided with that of chief cell population which was alkaline phosphatase-positive. The protease activity of ascidian stomach was so weak that we could not conceive that immunoreactive substances possess peptic activity. From the results, it was suggested that the substances fulfill a function different from that of digestive enzyme, and in the course of evolution to vertebrates, the substances acquired the active site in the molecule and came to work as digestive enzyme.

INTRODUCTION

Pepsinogens are the zymogens of pepsins, digestive enzymes produced and secreted by stomach epithelial cells of vertebrates [1]. The molecular characteristics of pepsinogens and their genes have been well studied in mammals and birds, and the evolutionary course of pepsinogen genes has been suggested [2, 3]. However the origin and evolution of pepsinogens in lower vertebrates have scarcely been studied. In previous papers [4, 5], we reported the existence of pepsinogens immunologically related to an adult-type chicken pepsinogen (ACPg) in stomach gland cells of all adult vertebrate species examined, and of pepsinogens related to an embryonic chicken pepsinogen (ECPg) which is a prochymosin-type pepsinogen [3] in those of adult teleosts and elasmobranchs. These observations suggest that the ACPg-type and ECPg-type pepsinogens appeared early in the history of vertebrates, and in primitive groups such as teleosts and elasmobranchs these pepsinogens are

co-expressed in the adult stomach, but in higher vertebrates the ACPg-type pepsinogen is predominant in adult stomach, and ECPg-type pepsinogen is expressed only during embryonic period.

We thought it interesting to seek the origin of these vertebrate pepsinogens in protochordates, the direct ancestral form of vertebrates. In this report, the presence of immunoreactive substances in the stomach and intestinal epithelial cells of adult ascidians was demonstrated. The localization pattern of immunoreactive substances in the stomach coincided with the compartmentation of epithelial cells [6, 7] and with the distribution of alkaline phosphatase activity. The stomach extract of ascidian *Styela plicata* possessed no or very low protease activity. Based on these facts, possible function of immunoreactive substances and their relations to the vertebrate pepsinogens will be discussed.

MATERIALS AND METHODS

Materials

Adult ascidians, *Styela plicata*, *Styela clava*, *Holocynthia hilgendorfi*, *Ciona savignyi*, and *Ascidia zara*, were collected at the Misaki Marine

Accepted May 27, 1988

Received April 25, 1988

³ Present address: Faculty of Pharmaceutical Sciences, Teikyo University, Sagamikomachi, Kanagawa 199-01, Japan

Biological Station, University of Tokyo.

Methods

Indirect immunofluorescence [8] was carried out as described [4] with tissues fixed in ice-cold 95% ethanol. The antisera used were polyclonal anti-serum against purified adult chicken pepsinogen (anti-ACPg) [9] and against purified embryonic chicken pepsinogen (anti-ECPg) [10], both raised in the rabbits. That these antisera are specific to each antigen was confirmed by immunofluorescence

and immunoblotting [11]. Protease activity of crude extract of *Styela plicata* stomach against bovine hemoglobin was assayed by the method of Anson [12], with pH range of 2.0 to 8.0. Protease activity after electrophoresis on the polyacrylamide gel without SDS (zymogram) was visualized by the method of Samloff and Townes [13], and immunoblotting was carried out by the method described [14]. Histochemistry for alkaline phosphatase, acid phosphatase and nonspecific esterase was done according to the method described [15].

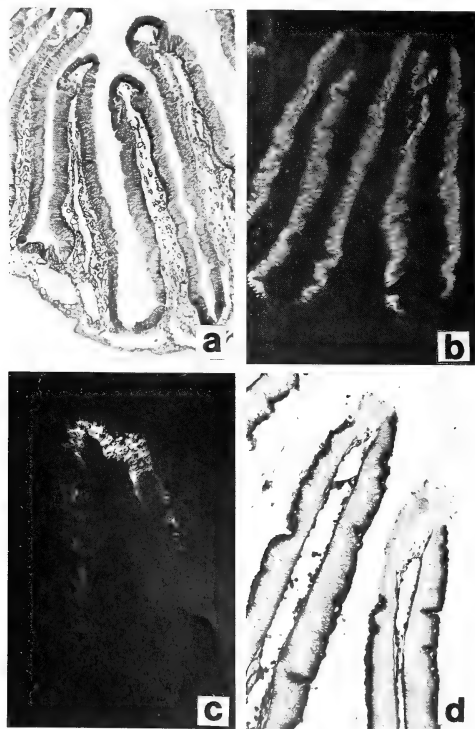


FIG. 1. Stomach of *Styela plicata*. (a) Normal histology (PAS-HX, $\times 63$). (b) Indirect immunofluorescence with anti-ECPg. Note the absence of fluorescence at crypt and villus-top ($\times 63$). (c) Indirect immunofluorescence with anti-ACPg. Only villus-top cells are reactive ($\times 250$). (d) Alkaline phosphatase histochemistry. Villus-top cells are negative ($\times 125$).

RESULTS

Immunocytochemical study

Digestive tract of five ascidian species was examined by indirect immunofluorescence with anti-ACPg- and anti-ECPg-antisera. Results are shown in Figures. 1 to 3 and Table 1.

In all species examined, the reactivity to anti-

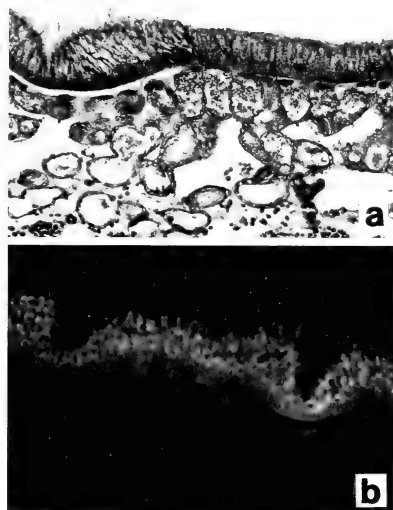


FIG. 2. Normal histology (a) and indirect immunofluorescence with anti-ECPg (b) of *Styela plicata* intestine ($\times 175$).

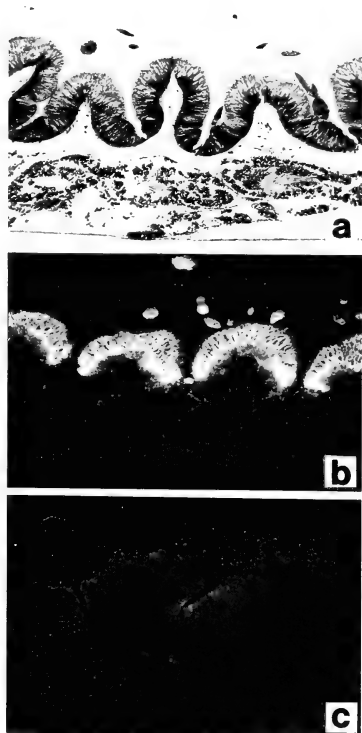


FIG. 3. Stomach of *Ciona savignyi* ($\times 125$). (a) Normal histology. (b) Indirect immunofluorescence with anti-ECPg. Cryptic part is negative. (c) Indirect immunofluorescence with anti-ACPg.

TABLE 1. Reactivity of epithelial cells of stomach villi of ascidians to anti-ECPg and anti-ACPg

Order	Genus and species	anti-ECPg			anti-ACPg		
		crypt	middle	top	crypt	middle	top
Pleurogona	<i>Styela plicata</i>	—	+	—	—	—	+
	<i>Styela clava</i>	—	+	—	—	—	±
	<i>Holocynthia hilgendorfi</i>	—	+	—	—	—	±
Enterogona	<i>Ciona savignyi</i>	—	+	+	—	—	—
	<i>Ascidia zara</i>	—	+	+	—	—	—

+ positive, ± weak or occasional, — negative

ECPg was found in stomach and intestinal epithelial cells. In the stomach, the localization of anti-ECPg-reactive cells differed between *Pleurogona* species and *Enterogona* species (Table 1). In the former, the stomach has long villi (Fig. 1a) and epithelial cells intermediate between villus-top and crypt were reactive to the anti-ECPg antiserum (Fig. 1b), while in the latter all epithelial cells of short villi (Fig. 3a) except those of crypt were reactive (Fig. 3b). Intestinal epithelial cells were always reactive to the anti-ECPg antiserum (Fig. 2a, b). In the digestive organs other than the stomach and intestine, only small number of gland cells of endostyle showed very weak fluorescence when they were treated with anti-ECPg.

Villus-top cells of the stomach of *Pleurogona* species were often weakly reactive to anti-ACPg (Fig. 1c) while stomach epithelial cells of *Enterogona* species showed virtually no reactivity against anti-ACPg (Fig. 3c).

Alkaline phosphatase histochemistry

To examine the possible functional significance of cells immunoreactive to anti-ECPg in ascidian digestive tract, we studied alkaline phosphatase activity of the stomach and intestine of *Styela plicata*. Alkaline phosphatase activity was demonstrated on apical part of epithelial cells of the stomach (Fig. 1d) and intestine, and the localization of alkaline phosphatase-positive cells coin-

cided with that of anti-ECPg-positive cells, the cells of cryptic part and villus-top being negative to alkaline phosphatase. Acid phosphatase and non-specific esterase were not detected in the stomach or intestine.

Protease activity in crude extract of Styela plicata stomach

Next, we examined whether anti-ECPg-reactive substances have protease activity or not. We measured protease activity in crude extract of the stomach at various pHs against hemoglobin or albumin as substrate. The results are summarized in Table 2, in which protease activity of smooth dogfish is also cited as a reference. From the Table it is obvious that protease activity of *Styela* stomach is very low compared to that of dogfish; it is about 1/500 of that of dogfish. There is no pH-dependency and substrate-dependency. When the activity was measured at 15°C or 20°C, no increase in activity was observed, and the activity was not inhibited by pepstatin, a specific inhibitor of acid proteases (data not shown). On the zymogram made with 10% polyacrylamide gel without SDS, we could not detect the band of activity (Fig. 4) nor the immunoreactive band after immunoblotting (data not shown). We also measured the activity in whole homogenate or supernatant after extraction with several kinds of detergent, such as SDS, Tween 20 or NP40, but the results were

TABLE 2. Protease activity in stomach extract of *Styela plicata* and smooth dogfish at 37°C

Animal	Substrate	pH	Specific activity (units/mg protein)
<i>S. plicata</i>	Hemoglobin	2.0	0.010
		3.0	0.018
		4.0	0.003
		5.0	0.004
		6.0	0.001
		7.0	0.005
		8.0	0
	Albumin	3.0	0.002
		7.0	0.002
Smooth dogfish	Hemoglobin	2.0	9.6
		8.0	0

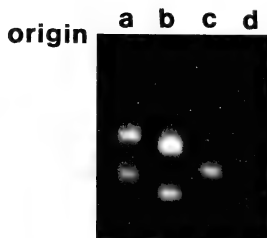


FIG. 4. Zymogram for acid protease (pH 2.0) in crude extract of the stomach taken from mouse (lane a), chicken (lane b), smooth dogfish (lane c) and *Styela plicata* (lane d). After electrophoresis, gel was immersed in hemoglobin solution (pH 2.0) and then incubated at 37°C for 1 hr. Hemoglobin was stained with amidoblack. The sites of acid protease activity appear as white bands.

always the same as in the case of extraction without detergent (data not shown).

DISCUSSION

It is well known that vertebrate stomachs have pepsinogens as proenzymes for digestion under acidic conditions [1]. We have demonstrated that vertebrate stomachs produce at least one pepsinogen species which is immunologically related [4]. This pepsinogen is called "adult-type" since it is detectable by the antiserum raised against ACPg [9]. Moreover, stomach epithelial cells of adult teleosts and elasmobranchs have pepsinogen immunoreactive to the antiserum against ECPg [5].

In the present study, we found that anti-ECPg-reactive substances exist in epithelial cells of the stomach and intestine of all ascidian species examined. Their localization in the stomach is interesting from the point of view of function and compartmentation of epithelial cells. The compartments of epithelial cells in ascidian stomach were studied by Ermak [6, 7], by autoradiography with tritiated thymidine. The author revealed that there exist two types in stomach epithelial cells; chief cell population and mucous cell populations. Each population has its germinal zone. In Phleobranchs such as *Ciona*, mucous cell population is confined in one part of stomach, but in Styelids

mucous cell populations exist on each villus-top. Our immunocytochemical observations clearly demonstrated that cells in chief cell population except its germinal zone are reactive to anti-ECPg (Fig. 1b). These cells possess also alkaline phosphatase activity. These results indicate that chief cell population is different from mucous cell population not only in cell kinetic properties but also functionally.

Although it is presumed that anti-ECPg-reactive substances in chief cell population have some functional significance, we detected only very low protease activity in stomach extract. As for the protease activity of ascidian stomach, Ikeda *et al.* [16] reported considerable activity in *Microcosmus* stomach at pH 3.6 against hemoglobin. However, Giraud and Yeomans [17] stated that protochordate (*Polycarpa*) stomach does not contain measurable amount of pepsinogen. We measured the protease activity against hemoglobin or albumin at wide range of pH (2.0–8.0) but the values of specific activity were 1/500 to 1/5000 of those of vertebrate stomachs. It may be nevertheless possible that anti-ECPg-reactive substances in ascidians are acid proteases, and that their proteolytic nature is different from that of vertebrate acid proteases. But we have at present no convincing data to support the idea that the pepsinogen-like substances in ascidians play definite role in ascidian digestion.

Thus the function of anti-ECPg-reactive substances is not clear at present, but we can imagine as a tentative hypothesis possible relation of the substances and vertebrate ECPg-like pepsinogens as follows: The anti-ECPg-reactive substances in ascidians fulfill a non-digestive function, and in the evolutionary course to vertebrates, these substances came to possess protease activity presumably by acquiring the active site in the molecules. To test this hypothesis, we have to clone the gene for ECPg-like molecule in ascidians and compare its structure with ECPg gene which has already been cloned [18], with special attention to the base sequence of active center that is well conserved in vertebrate pepsinogens. In this regards, our cDNA probe of ECPg [3] will be helpful.

The presence of anti-ACPg-reactive substance in mucous cell population of *Styela plicata* is very

curious, and it deserves further studies. In adult teleosts and elasmobranchs, single cells seemed to produce ECPg- and ACPg-like pepsinogens at the same time [5]. The segregation of cell types reactive to two antisera in the ascidian stomach raised a possibility that ECPg-like and ACPg-like molecules were produced in different cell population in vertebrate ancestor. This problem, as well as the fact that anti-ECPg-reactive substances exist also in intestinal epithelial cells of ascidians, is very important in elucidating the origin and evolution of stomachs in vertebrates.

ACKNOWLEDGMENTS

The authors are grateful to the Staff of the Misaki Marine Biological Station for providing the materials used in the present study. They are indebted to Dr. N. Sensui for valuable discussions. The work was supported in part by the Grant-in-Aid of the Ministry of Education, Science and Culture of Japan.

REFERENCES

- Vonk, H. J. and Western, J. R. H. (1984) Comparative Biochemistry and Physiology of Enzyme Digestion. Academic Press, New York.
- Kageyama, T. and Takahashi, K. (1985) Monkey pepsinogens and pepsins. VII. Analysis of the activation process and determination of the NH₂-terminal 60-residue sequence of Japanese monkey progastricsin, and molecular evolution of pepsinogens. *J. Biochem.*, **97**: 1235-1246.
- Hayashi, K., Agata, K., Mochii, M., Yasugi, S., Eguchi, G. and Mizuno, T. (1988) Molecular cloning and the nucleotide sequence of cDNA for embryonic chicken pepsinogen: Phylogenetic relationship with chymosin. *J. Biochem.*, **103**: 290-296.
- Yasugi, S. (1987) Pepsinogen-like immunoreactivity among vertebrates: Occurrence of common antigenicity to an anti-chicken pepsinogen antiserum in stomach gland cells of vertebrates. *Comp. Biochem. Physiol.*, **86B**: 675-680.
- Yasugi, S., Matsunaga, T. and Mizuno, T. (1988) Presence of pepsinogens immunoreactive to anti-embryonic chicken pepsinogen antiserum in fish stomachs: Possible ancestor molecules of chymosin of higher vertebrates. *Comp. Biochem. Physiol.*, **91A**: 565-569.
- Ermak, T. H. (1975) Cell proliferation in the digestive tract of *Stryela clava* (Urochordata:Ascidacea) as revealed by autoradiography with tritiated thymidine. *J. Exp. Zool.*, **194**: 449-466.
- Ermak, T. H. (1981) A comparison of cell proliferation patterns in the digestive tract of ascidians. *J. Exp. Zool.*, **217**: 325-339.
- Sainte-Marie, G. (1962) A paraffin embedding technique for studies employing immunofluorescence. *J. Histochem. Cytochem.*, **10**: 250-256.
- Esumi, H., Yasugi, S., Mizuno, T. and Fujiki, H. (1980) Purification and characterization of a pepsinogen and its pepsin from proventriculus of the Japanese quail. *Biochim. Biophys. Acta*, **511**: 363-370.
- Yasugi, S. and Mizuno, T. (1981) Purification and characterization of embryonic chicken pepsinogen, unique pepsinogen with large molecular weight. *J. Biochem.*, **89**: 311-315.
- Yasugi, S., Hayashi, K., Takiguchi, K., Mizuno, T., Mochii, M., Kodama, R., Agata, K. and Eguchi, G. (1987) Immunological relationships among embryonic and adult chicken pepsinogens: A study with monoclonal and polyclonal antibodies. *Develop. Growth and Differ.*, **29**: 85-91.
- Anson, M. L. (1939) The estimation of pepsin, trypsin, papain, and cathepsin with hemoglobin. *J. Gen. Physiol.*, **22**: 79-89.
- Samloff, I. M. and Townes, P. L. (1970) Electrophoretic heterogeneity and relationships of pepsinogens in human urine, serum and gastric mucosa. *Gastroenterology*, **58**: 462-471.
- Towbin, H., Staehelin, T. and Gordon, J. (1979) Electrophoretic transfer of proteins from polyacrylamide gels to nitrocellulose sheets: Procedures and some applications. *Proc. Natl. Acad. Sci., U. S. A.*, **76**: 4350-4354.
- Lojda, Z., Gossrau, R. and Schiebler, T. H. (1979) *Enzyme Histochemistry*. Springer Verlag, Berlin/Heidelberg/New York.
- Ikeda, T., Watabe, S., Yago, N. and Horiuchi, S. (1986) Comparative biochemistry of acid proteinase from animal origins. *Comp. Biochem. Physiol.*, **83B**: 725-730.
- Giraud, A. S. and Yeomans, N. D. (1982) Comparative distribution of pepsinogen in the chordate gastric mucosa from representatives of five classes. *Comp. Biochem. Physiol.*, **72B**: 145-147.
- Hayashi, K., Yasugi, S. and Mizuno, T. (1988) Isolation and structural analysis of embryonic chicken pepsinogen: Avian homologue of prochymosin gene. *Biochem. Biophys. Res. Commun.*, **152**: 776-782.

Effects of Vanadium Ions in Different Oxidation States on Myosin ATPase Extracted from the Solitary Ascidian, *Halocynthia roretzi* (Drasche)

HITOSHI MICHIBATA, YUTAKA ZENKO, KENJI YAMADA, MASATO HASEGAWA,
TATSURO TERADA¹ and TAKAHARU NUMAKUANI²

Biological Institute, Faculty of Science, Toyama University, Toyama 930,

¹*Department of Chemistry, Toyama College of Technology, Toyama 930-11,*

and ²*Marine Biological Station, Tohoku University, Asamushi, Aomori 039-34, Japan*

ABSTRACT—Some ascidians are known to accumulate vanadium ion within their tissues by 10^6 -fold as that in sea water and store the metal ion in its reduced tetravalent and/or trivalent states. It is also well known that phosphoenzymes are inhibited by pentavalent vanadium ion over a range of 10 nM to 1 mM. In the present experiment we have therefore examined the effects of vanadium ions in different oxidation states on the activity of myosin ATPase extracted from the mantle of the ascidian, *Halocynthia roretzi*, in order to know the mechanism for protectin phosphoenzymes against inhibition by the massive amounts of vanadium ion within their tissues. The activity of myosin ATPase was inhibited by pentavalent vanadium ion but was not inhibited by tetravalent or trivalent vanadium ion. The addition of 5 mM ascorbic acid, which is known to reduce pentavalent vanadium ion to tetravalent state, to the reaction mixture reduced the inhibitory effect of pentavalent vanadium ion on the ATPase. Based on the results, one of the reasons that the ATPase within the ascidian is not inhibited *in vivo*, in spite of the high level of vanadium within ascidian tissues, may be that the pentavalent vanadium ion which is accumulated from sea water is readily reduced to the tetravalent and/or trivalent oxidation states by the endogenous reducing substances in ascidian tissues.

INTRODUCTION

Since it has been demonstrated that a physiological concentration of pentavalent vanadium ions causes inhibition of $\text{Na}^+\text{-K}^+\text{-ATPase}$ [1, 2], the effects of vanadium ions on various enzymes have been studied by many investigators [cf. 3, 4]. Ascidians are known to accumulate very high levels of vanadium within their tissues [5-10], at concentrations that are, in some cases, much higher than those that are able to inhibit the activity of phosphoenzymes [4]. When actomyosin ATPase, extracted from several species of ascidians, was allowed to react with pentavalent vanadium ions *in vitro*, it was found that the vanadium ions, at concentrations of 10 μM to 100 μM , caused an

apparent inhibition of ATPase activity [11].

Ascidians must, however, have an efficient mechanism for protecting phosphoenzymes against inhibition by the massive amounts of vanadium ions within their tissues, but there are no reports of such a mechanism.

In this study, we have examined the effects of vanadium ions in different oxidation states on the activity of myosin ATPase, extracted from the ascidian mantle, having chosen this enzyme as representative of ascidian phosphoenzymes.

MATERIALS AND METHODS

Halocynthia roretzi (Stolidobranchia) were purchased from a fisherman at Asamushi, Aomori, Japan. Myosin was prepared from the mantle by the method of Obinata *et al.* [12].

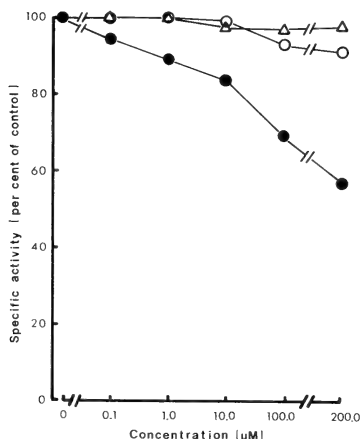
Each reaction mixture (1 ml) contained 20 mM

Tris-maleic acid buffer (pH 8.0), 120 mM KCl, 10 mM CaCl_2 , 0.5 mM ADP, and myosin (200 μg protein/ml reaction mixture). Vanadium ions were added to the reaction mixture by dilution from concentrated stock solutions which were prepared just before use. The mixture was preincubated without ATP for 15 min at 25°C , then the reaction was started by addition of a solution of ATP (final concentration of ATP was 1 mM). The reaction was terminated by the addition of 1 ml of ice-cold 20% trichloroacetic acid. All assay were carried out in triplicate. Liberated inorganic phosphate (Pi) was measured by the method of Allen [13]. Protein was determined, using Coomassie brilliant blue, with bovine serum albumin as standard [14].

To examine the effects of vanadium ions in different oxidation states on the myosin ATPase, the following compounds were tested; $\text{Na}_3\text{VO}_4(\text{V})$, $\text{VOSO}_4(\text{IV})$, and $\text{VCl}_3(\text{III})$. Experiments were also carried out in the presence of 5 mM ascorbic acid, as a reducing agent. This agent was added to the reaction mixture at the same time as the pentavalent vanadium compound was added.

RESULTS

The specific activity of myosin ATPase,



obtained from the mantle of the ascidian, was about $1.89 \mu\text{moles Pi/mg protein/min}$. This activity tended to decrease gradually with storage.

The degree of inhibition of ATPase activity by vanadium compounds was expressed as the per cent of the initial control value which corre-

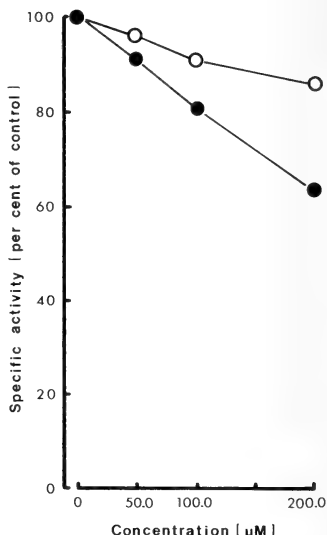


FIGURE 2. Diminution of the inhibitory effect of pentavalent vanadium ions by ascorbic acid. ●: Na_3VO_4 ; ○: $\text{Na}_3\text{VO}_4 + 5 \text{ mM Ascorbic acid}$. 5 mM ascorbic acid was added to the reaction mixture at the same time as the pentavalent vanadium compound was added. The data points shown are the averages of triplicate determinations. The initial control value of 100% corresponds to liberation of $0.54 \mu\text{ moles Pi/mg protein/min}$.

FIGURE 1. Effects of vanadium ions in different oxidation states on myosin ATPase extracted from *Halocynthia roretzi*. ●: $\text{Na}_3\text{VO}_4(\text{V}^{+5})$; ○: $\text{VOSO}_4(\text{V}^{+4})$; △: $\text{VCl}_3(\text{V}^{+3})$. The data points shown are the averages of triplicate determinations. The initial control value of 100% corresponds to liberation of $1.89 \mu\text{ moles Pi/mg protein/min}$.

sponded to the liberation of $1.89 \mu\text{moles Pi/mg protein/min}$, as shown in Figure 1. The results clearly demonstrated that pentavalent vanadium ions, at a concentration of $100 \mu\text{M}$, are a powerful inhibitor of the myosin ATPase extracted from the ascidian mantle. The half-maximum inhibition of activity was seen at approximately $200 \mu\text{M}$ vanadium ion(V). In contrast to this result, tetravalent and trivalent vanadium ions, in the same range of concentrations, had little or no inhibitory effect on the enzymatic activity. Maximum values of only 8.2% and 2.6% inhibition were observed when $200 \mu\text{M}$ tetravalent and trivalent vanadium ions, respectively, were included in the reaction mixture.

Ascorbic acid is known to reduce pentavalent vanadium ions to the tetravalent state under physiological conditions [15]. Therefore, we examined whether the addition of ascorbic acid to the reaction mixture could diminish the inhibitory effect of pentavalent vanadium ions on the enzymatic activity. Figure 2 shows that 5 mM ascorbic acid can clearly diminish the inhibitory effect of pentavalent vanadium ions. Two hundreds μM pentavalent ion reduced the activity of myosin ATPase by about 37% in this experiment, while in the presence of 5 mM ascorbic acid, the same concentration of pentavalent vanadium ions reduced the activity by only 14.8%.

DISCUSSION

In spite of a massive accumulation of vanadium within ascidian tissues [5-10], at concentrations that are thousands to million times higher than those that can inhibit ATPases [1, 2], ascidians are able to protect their enzymes from the inhibitory effects of vanadium. The present results demonstrate that the activity of the ascidian myosin ATPase is inhibited only by pentavalent vanadium ions, and is not inhibited by tetravalent and trivalent vanadium ions (Fig. 1). In other words, the enzyme are not subject to the inhibition by vanadium so long as the oxidation state of vanadium ions is not pentavalent even so ascidians contain high levels of vanadium ions within their tissues. It has been known, in fact, that the oxidation state of the vanadium ions that are stored within ascidian tissues is tetravalent and/or trivalent [5, 9, 16-22]

although the vanadium ions dissolved in sea water is in the pentavalent state [23].

Ascorbic acid [24, 25], glutathione [4, 26], cysteine [27], and NADH [28], which are common to cells, have been known to be able to reduce pentavalent vanadium ions to tetravalent vanadium ions *in vitro*, which suggests that these reducing agents are involved in oxidation-reduction reactions of vanadium ions *in vivo*. It is, therefore, probable that endogenous reducing agents such as the ascorbic acid in the ascidian tissues change the oxidation state of the vanadium ions and keep vanadium ions in reduced states. The presence of such reduced vanadium ions would explain why ascidian phosphoenzymes are not subject to the inhibitory effects of the vanadium within their tissues.

Although free tetravalent vanadium ions are oxidized to pentavalent vanadium ions within a few minutes in aqueous solution at neutral pH, the tetravalent ions are stable in combination with various cellular components [29]. In fact, the results obtained from the present experiments show a clear difference between the effect of pentavalent vanadium ions and that of tetravalent vanadium ions on the activity of myosin ATPase (Fig. 1), and imply that the tetravalent vanadium ions are also stabilized in the present assay system. The partial inhibitory effect exerted by the tetravalent vanadium ions may depend on the partial oxidation of these ions to pentavalent vanadium ions in the reaction mixture.

Furthermore, it is known that trivalent vanadium ions are appreciably hydrolyzed below pH 2.2 but above that pH they dimerize and precipitate. Thus, it is probable that a water-soluble species does not exist under neutral and basic conditions in a simple aqueous solution [30]. However, the actual chemical forms of vanadium ions in complex solutions, such as the reaction mixture described in MATERIALS AND METHODS, are little understood. Since the trivalent vanadium ions have no inhibitory effect on the activity of the ATPase, it is unlikely that the trivalent vanadium ions are quickly oxidized to the tetravalent and/or pentavalent form. However, if the trivalent vanadium ions dimerize and precipitate immediately after addition to the medium, this

result can be explained. There is also another possibility: the trivalent vanadium ions may be able to maintain their oxidation state by complexing with some molecules in the reaction mixture. In such case, the trivalent vanadium ions themselves would have no effect on the enzymatic activity. The actual behaviour of trivalent vanadium ions in the reaction mixture is, however, unknown at the present time.

As described above, ascidians contain the vanadium ions in tetravalent and/or trivalent state [5, 9, 16–22]. We have isolated a vanadium-binding substance (Vanadobin) from the blood cells of *Ascidia sydneiensis samea*, which substance can maintain the vanadium ions in reducing form of tetravalent state both under aerobic and anaerobic conditions [21]. However, the corresponding substance to keep the vanadium ions in trivalent state in ascidian tissues is not yet extracted.

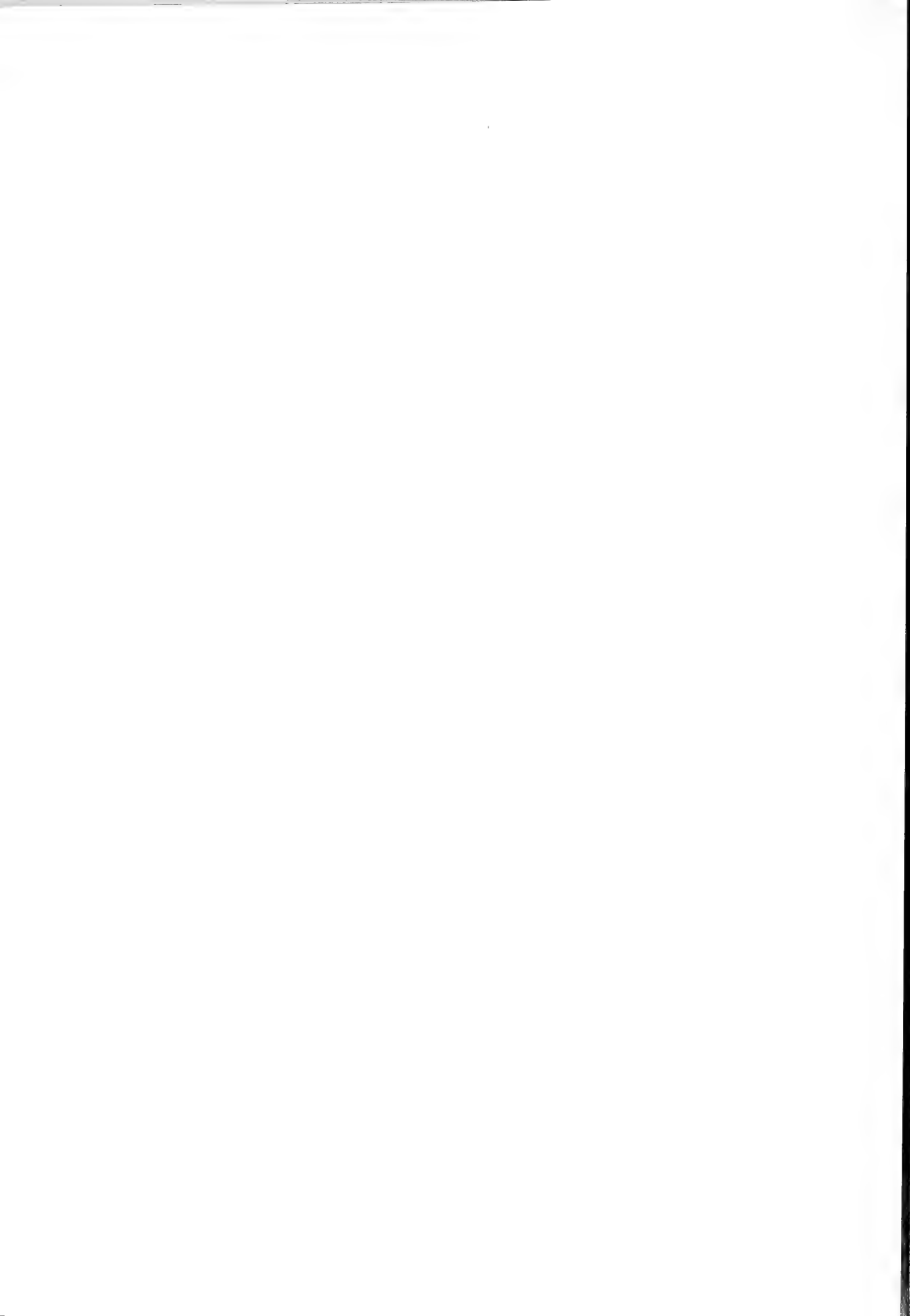
ACKNOWLEDGMENTS

We are grateful to the staff of Asamushi Marine Biological Station, Tohoku University, for providing many conveniences. We also wish to express our cordial thanks to Professor Hiromu Sakurai of the University of Tokushima and to Dr. William E. Robinson of the New England Aquarium for valuable discussion and comments. This work was supported by a Grant-in-Aid from the Ministry of Education, Sciences and Culture, Japan to H. M., and was also supported partially by a grant from the Cooperative Program provided by the Ocean Research Institute of the University of Tokyo.

REFERENCES

- Cantley, L. C. Jr., Josephson, L., Warner, R., Yanagisawa, M., Lechene, C. and Guidotti, G. (1977) Vanadate is a potent (Na, K)-ATPase inhibitor found in ATP derived from muscle. *J. Biol. Chem.*, **252**: 7421–7423.
- Beaugé, L. A. and Glynn, I. M. (1977) A modifier of $(\text{Na}^+ + \text{K}^+)\text{ATPase}$ in commercial ATP. *Nature*, **268**: 355–356.
- Simons, T. J. B. (1979) Vanadate- a new tool for biologists. *Nature*, **281**: 337–338.
- Macara, I. G. (1980) Vanadium- an element in search of a role. *Trends Biochem. Sci.*, **5**: 92–94.
- Swinehart, J. H., Biggs, W. R., Halko, D. J. and Schroeder, N. C. (1974) The vanadium and selected metal contents of some ascidians. *Biol. Bull.*, **146**: 305–312.
- Goodbody, I. (1974) The physiology of ascidians. *Adv. Mar. Biol.*, **12**: 1–149.
- Biggs, W. R. and Swinehart, J. H. (1976) Vanadium in selected biological systems. In "Metal Ions in Biological Systems. Vol. 6". Ed. by H. Sigel, Marcel Dekker, New York, pp. 141–196.
- Macara, I. G., McLeod, G. C. and Kustin, K. (1979) Tunichromes and metal ion accumulation in tunicate blood cells. *Comp. Biochem. Physiol.*, **63B**: 299–302.
- Hawkins, C. J., Parry, D. L., Kott, P. and Swinehart, J. H. (1983) Vanadium content and oxidation state related to ascidian phylogeny. *Comp. Biochem. Physiol.*, **76B**: 555–558.
- Michibata, H., Terada, T., Anada, N., Yamakawa, K. and Numakunai, T. (1986) The accumulation and distribution of vanadium, iron, and manganese in some solitary ascidians. *Biol. Bull.*, **171**: 672–681.
- Michibata, H., Nishiyama, I., Gualtieri, R. and de Vincenzi, M. (1985) Inhibition by vanadate of actomyosin ATPase extracted from ascidians. *Comp. Biochem. Physiol.*, **80B**: 247–250.
- Obinata, T., Ooi, A. and Takano-Ohmuro, H. (1983) Myosin and actin from ascidian smooth muscle and their interaction. *Comp. Biochem. Physiol.*, **76B**: 437–442.
- Allen, R. J. L. (1940) The estimation of phosphorus. *Biochem. J.*, **34**: 858–865.
- Bradford, M. M. (1976) A rapid and sensitive method for the quantitation of microgram quantities of protein utilizing the principle of protein-dye binding. *Anal. Biochem.*, **72**: 248–254.
- Sakurai, H. personal communication.
- Tullius, T. D., Gillum, W. O., Carlson, R. M. K. and Hodgson, K. O. (1980) Structural study of the vanadium complex in living ascidian blood cells by X-ray absorption spectrometry. *J. Am. Chem. Soc.*, **102**: 5670–5676.
- Hawkins, C. J., Parry, D. L. and Pierce, C. (1980) Chemistry of the blood of the ascidian *Podoclavella moluccensis*. *Biol. Bull.*, **159**: 669–680.
- Dingley, A. L., Kustin, K., Macara, I. G. and McLeod, G. C. (1981) Accumulation of vanadium by tunicate blood cells occurs via specific anion transport system. *Biochim. Biophys. Acta*, **649**: 493–502.
- Bell, M. V., Pirie, B. J. S., McPhail, D. B., Goodman, B. A., Falk-Petersen, I.-B. and Sargent, J. R. (1982) Contents of vanadium and sulphur in the blood cells of *Ascidia mentula* and *Ascidia aspersa*. *J. Mar. Biol. Ass. U. K.*, **62**: 709–716.
- Frank, P., Carlson, R. M. K. and Hodgson, K. O. (1986) Vanadyl ion EPR as a noninvasive probe of pH in intact vanadocytes from *Ascidia ceratodes*. *Inorg. Chem.*, **25**: 470–478.

- 21 Michibata, H., Miyamoto, T. and Sakurai, H. (1986) Purification of vanadium binding substance from the blood cells of the tunicate, *Ascidia sydneiensis samea*. *Biochem. Biophys. Res. Commun.*, **141**: 251-257.
- 22 Michibata, H., Hirata, J., Uesaka, M., Numakunai, T. and Sakurai, H. (1987) Separation of vanadocytes: determination and characterization of vanadium ion in the separated blood cells of the ascidian, *Ascidia ahodori*. *J. Exp. Zool.*, **244**: 33-38.
- 23 McLeod, G. C., Ladd, K. V., Kustin, K. and Toppen, D. L. (1975) Extraction of vanadium(V) from seawater by tunicates: a revision of concepts. *Limnol. Oceanogr.*, **20**: 491-493.
- 24 Schmitz, W., Scholz, H., Erdmann, E., Krawietz, W. and Werdan, K. (1982) Effect of vanadium in the +5, +4 and +3 oxidation states on cardiac force of contraction, adenylate cyclase and (Na^+ + K^+)-ATPase activity. *Biochem. Pharmacol.*, **31**: 3853-3860.
- 25 Kustin, K. and Toppen, D. L. (1973) Reduction of vanadium(V) by L-ascorbic acid. *Inorg. Chem.*, **12**: 1404-1407.
- 26 Legrum, W. (1986) The mode of reduction of vanadate(+V) to oxovanadium (+IV) by glutathione and cysteine. *Toxicol.*, **42**: 281-289.
- 27 Sakurai, H., Shimomura, S. and Ishizu, K. (1981) Reduction of vanadate(V) to oxovanadium(IV) by cysteine and mechanism and structure of the oxovanadium(IV)-cysteine complex subsequently formed. *Inorg. Chim. Acta*, **55**: L67-L69.
- 28 Ramasarma, T., MacKellar, W. C. and Crane, F. L. (1981) Vanadate-stimulated NADH oxidation in plasma membrane. *Biochim. Biophys. Acta*, **646**: 88-98.
- 29 Macara, I. G., Kustin, K. and Cantley, L. C. Jr. (1980) Gultathione reduces cytoplasmic vanadate. Mechanism and physiological implications. *Biochim. Biophys. Acta*, **629**: 95-106.
- 30 Kustin, K. and Macra, I. G. (1982) The new biochemistry of vanadium. *Comments Inorg. Chem.*, **2**: 1-22.



The 5S RNA Binding Protein of *Artemia salina* Ribosomes: Identification and Immunological Comparison with That of Rat Liver

NAOYA KENMOCHI¹ and KIKUO OGATA²

Department of Biochemistry, Niigata University School
of Medicine, Niigata 951, Japan

ABSTRACT—The ribonucleoprotein complex between 5S RNA and its binding protein of *Artemia salina* ribosomes was released from 60S subunits with 25 mM EDTA. The protein component of the complex was found to contain a single ribosomal protein which seemed to correspond to rat liver ribosomal protein L5 in two-dimensional gel electrophoresis. We therefore designated the 5S RNA binding protein of *Artemia salina* as *Artemia* L5 (AL5) when compared with rat liver L5. The molecular weight of AL5 was about 34,000 in SDS-polyacrylamide gel electrophoresis and was similar to rat liver L5. The 5S RNA-AL5 complexes were injected into rabbits intradermally, and antisera against AL5 were obtained. Cross-reactivity of the anti-AL5 with rat liver 60S proteins was examined by immunoblotting and the anti-AL5 was found to cross-react with rat liver L5. This result indicated that *Artemia* and rat liver L5 share immunological determinants. These results suggest that 5S RNA binding proteins are probably conserved during the evolution of eukaryotic cells and may play a significant role in ribosomes.

INTRODUCTION

Ribonucleoprotein complexes between 5S RNAs and their binding proteins have been released from both prokaryotic and eukaryotic ribosomes [1-5]. The structure of 5S RNAs is well known, but the role of 5S RNA-protein complex is not yet known except for the functions of tRNA binding [6] and subunit association [7]. However, our studies on rat liver 5S RNA-protein complex have revealed that the protein moiety of the complex (rat liver L5) cross-linked to poly A⁺ mRNA in the polysome and to globin mRNA in the 80S initiation complex by ultraviolet irradiation [8, 9],

and cross-linked to proteins S4 and S25 by treatment of 80S ribosomes with 2 iminothiolane [10]. These results suggest that rat liver 5S RNA-L5 complex is located at the boundary between the large and the small subunits and interacts with mRNA.

Three ribosomal proteins (EL5, EL18, EL25) in *E. coli* and one each in yeast (YL3) and in rat liver (L5) are known to bind to 5S RNA [3-5]. In a study of the amino acid sequence of YL3 in yeast, Yaguchi *et al.* [11] indicated that a single large eukaryotic 5S RNA binding protein may have evolved through a fusion of genes for the multiple 5S RNA binding proteins in prokaryotes. This is an interesting suggestion concerning the evolution of ribosomal proteins.

In the present work we identified the 5S RNA binding protein of *Artemia salina* ribosomes and compared it to that of rat liver. Furthermore, the immunological homology between the proteins of *Artemia salina* and rat liver was examined by using the antibody against the 5S RNA binding protein of *Artemia* ribosomes.

Accepted April 26, 1988

Received May 27, 1988

¹ Present address and reprint request: Facilities for Comparative Medicine and Animal Experimentation, Niigata University School of Medicine, Niigata 951, Japan.

² Present address: Institute for Gene Expression, Dobashi Kyoritsu Hospital, Dobashi 3-1, Matsuyama 790, Japan.

MATERIALS AND METHODS

Preparation of the 5S RNA-protein complex from Artemia ribosomes

Ribosomes were prepared as described previously [12] and large amount of 60S subunits were obtained by means of zonal centrifugation originally described by Sherton *et al.* [13]. About 1 g of ribosomal pellet was suspended in 100 ml of a high-salt buffer containing 20 mM Tris/HCl (pH 7.8), 0.5 M KCl, 3 mM MgCl₂, 20 mM 2-mercaptoethanol and 9% sucrose and sedimented through a 13–37% hyperbolic sucrose density gradient in the high-salt buffer at 13,500 rpm for 18 hr in a Hitachi RPZ 35T rotor at 18°C. The resulting profile of absorbance at 260 nm is shown in Figure 1. Fractions of 60S subunits were collected and pelleted by centrifugation at 130,000×g for 15 hr.

The 5S RNA-protein complex was prepared from 60S subunits by suspending the pellet in 25 mM EDTA followed by centrifugation according to Terao *et al.* [5]. About 1.6 mg of ribonucleoprotein was obtained from 1 g of *Artemia* ribosomes.

Electrophoretic analysis of the 5S RNA-protein complex and its binding protein

Disc gel electrophoresis of the 5S RNA-protein complex was carried out as described previously [14]. Two-dimensional gel electrophoresis of the 5S RNA binding protein was performed in an acidic-SDS gel system according to the method of Madjar *et al.* [15] with slight modification. The protein sample was dissolved in buffer consisting of 8 M urea, 1% 2-mercaptoethanol and 10 mM bis-Tris/acetic acid (pH 4.0) and applied to disc gel containing 4% acrylamide, 0.1% N, N'-tetramethylethylenediamine (TEMED), 8 M urea

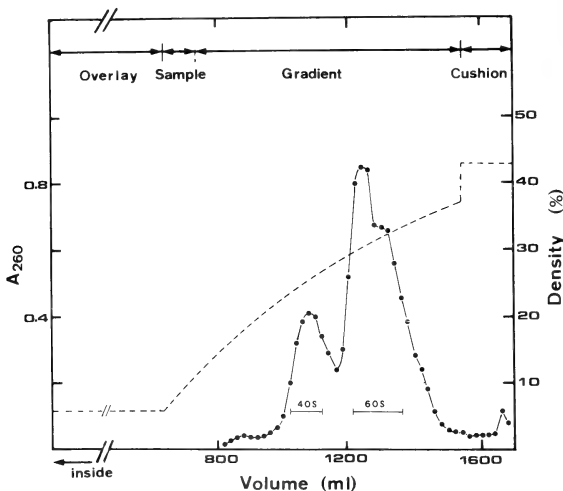


Fig. 1. Sedimentation profile of ribosomal subunits of *Artemia salina* in a zonal rotor. Ribosomal subunits (about 1 g) were separated by centrifugation for 18 hr at 13,500 rpm in a Hitachi RPZ 35T rotor at 18°C using a 13 to 37% hyperbolic sucrose density gradient in the high salt buffer described in MATERIALS AND METHODS. Fractions of 60S subunits (150 ml) were collected and about 400 mg of 60S subunits were recovered. The interrupted lines indicate densities of sucrose; 5.8% as to "overlay", 5.8–13% linear gradient as to "sample", 43% as to "cushion".

and 40 mM bis-Tris/acetic acid (pH 5.0). The upper and lower electrode buffers, which contained 10 mM bis-Tris, were adjusted to pH 4.0 and pH 6.0 with acetic acid, respectively. Electrophoresis in the first dimension was run at 150 V for 6 hr. After the gel was incubated in dialyzing buffer consisting of 6 M urea, 1% SDS and 40 mM bis-Tris/acetic acid (pH 6.0), the second dimensional SDS-polyacrylamide gel electrophoresis was carried out in the manner described previously [12].

Preparation of antibodies against the 5S RNA-protein complex

Antisera against *Artemia* 5S RNA-protein complexes were raised in rabbits by injecting the complexes intradermally with complete Freund's adjuvant (1:1 vol). Rabbits were injected with 0.3–0.5 mg of the complexes every two weeks and the total amount of antigen injected into one animal over the whole immunization period was 0.9 mg of protein. Immunoglobulins were precipitated from antisera at 40% saturation with ammonium sulfate and the IgG fractions were purified by DEAE-cellulose column chromatography. ^{125}I -labeled IgG was prepared with the Bolton-Hunter ^{125}I reagent (2,000 Ci/mmol) from New England Nuclear.

Immunoblotting procedures

Sixty S ribosomal proteins separated by two-dimensional acidic-SDS acrylamide gel electrophoresis were transferred to a nitrocellulose membrane sheet essentially according to the method of Towbin *et al.* [16]. Blotting was performed under a constant 200 mA current for 20 hr at room temperature in buffer containing 25 mM Tris, 192 mM glycine and 20% methanol at pH 8.2. The sheet was then soaked in 2% BSA (bovine serum albumin) in PBS (0.15 M NaCl and 10 mM sodium phosphate buffer, pH 7.2) for 2 hr. ^{125}I -labeled IgG (5×10^5 cpm) was added to 5 ml of 2% BSA in PBS and incubated with the sheet for 4 hr at room temperature. The membrane sheet was washed in 2% BSA in PBS for 5 min and rinsed twice with PBS. The sheet was air dried and autoradiographed with Fuji X-ray film for 18–48 hr.

RESULTS

Analysis of the 5S RNA-protein complex by disc gel electrophoresis

As previously observed with yeast and rat liver ribosomes [4, 5], the 5S RNA-protein complex was released from *Artemia* 60S ribosomes with 25 mM EDTA. The split-7S fraction released from EDTA-treated *Artemia* 60S ribosomes was analyzed by disc gel electrophoresis and compared with that from rat liver (Fig. 2). The split-7S fraction of *Artemia salina* contained two components and one of them was shown to be a ribonucleoprotein complex by staining the gel with Coomassie brilliant blue. The two components corresponded to rat liver 5S RNA-protein complex and free 5S RNA, respectively. SDS gel electrophoresis of the ribonucleoprotein complex showed that the complex consisted of two components: 5S ribosomal

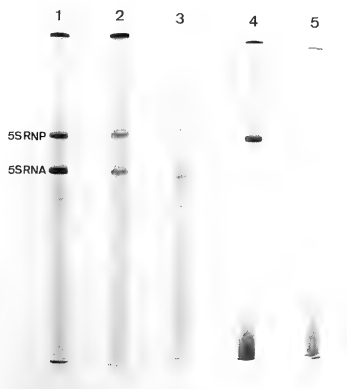


Fig. 2. Disc gel electrophoresis of the split-7S fraction released from *Artemia* and rat liver 60S ribosomes with 25 mM EDTA. Gels were stained with Azur B (lanes 1–3) or with Coomassie brilliant blue (lanes 4 and 5). Lanes 1 and 4; the split-7S fraction from *Artemia* 60S ribosomes, lanes 2 and 5; those from rat liver 60S ribosomes, lane 3; rat liver 5S RNA. "5S RNP" and "5S RNA" indicated the positions of rat liver 5S RNA-protein complex and 5S RNA, respectively.

RNA and a single ribosomal protein (data not shown). Thus, similarly to rat liver and yeast ribosomes, the 5S RNA-protein complex is released from *Artemia* 60S ribosomes with 25 mM EDTA and may contain a single ribosomal protein.

Two dimensional gel electrophoresis of the 5S RNA binding protein

Two dimensional gel electrophoresis was carried out to identify the 5S RNA binding protein of *Artemia* ribosomes. As shown in Figure 3, a single ribosomal protein spot is almost undetectable in the EDTA-treated 50S ribosomes but exists in the split-7S fraction. This protein seemed to correspond to rat liver ribosomal protein L5 (5S RNA binding protein) on the two dimensional gel slab, so we designated this protein *Artemia* L5 (AL5). The molecular weight of this protein is found to be about 34,000 by SDS gel electrophoresis, and this is the same as that of rat L5.

Characterization of the antibody against the 5S RNA-AL5 complex

In *E. coli* ribosomes, antibodies against each ribosomal protein have proved very useful in studying their functions [17, 18]. On the other hand, few antibodies against ribosomal proteins were able to be obtained in eukaryotic ribosomes. Therefore, we tried to obtain an antibody against *Artemia* L5 and intended to examine the function of the 5S RNA-protein complex by using the antibody. The 5S RNA-AL5 complexes were injected into rabbits intradermally and the antisera were obtained. In a series of preliminary experiments, the antisera were assayed for the formation of a precipitin line by Ouchterlony double diffusion with the 5S RNA-AL5 complex, the protein AL5, total proteins from *Artemia* 60S ribosomes or 40S ribosomes, and RNAs from *Artemia* 60S ribosomes. In the results the antisera cross-reacted with the 5S RNA-AL5 complex, the protein AL5 and total proteins from 60S ribosomes, but not with the others (data not shown). These results indicate that this antisera are specific for the protein moiety of the 5S RNA-protein complex.

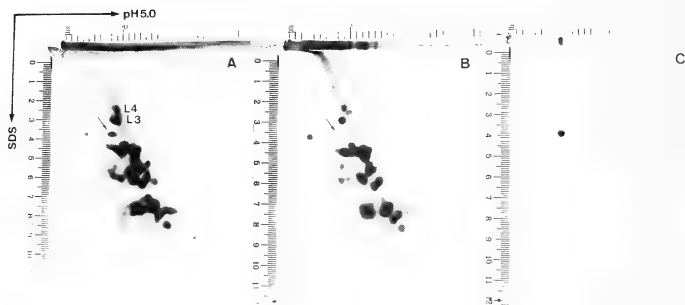


FIG. 3. Analysis of the protein of the split-7S fraction by two-dimensional gel electrophoresis. *Artemia* 60S ribosomal proteins (A), the core-50S ribosomal proteins derived from *Artemia* 60S ribosomes with 25 mM EDTA treatment (B) and protein of the split-7S fraction released from *Artemia* 60S ribosomes (C). Electrophoresis was run at pH 5.0 in the first dimension and in the presence of SDS in the second. The arrow shows the *Artemia* L5.

To show the specificity of the antibody, immunoblotting was carried out. Sixty S proteins of *Artemia* ribosomes separated by two dimensional gel electrophoresis were transferred to a nitrocellulose

sheet and ^{125}I -labeled IgG from the antisera was treated. As shown in Figure 4, this antibody cross-reacted with AL5 only.

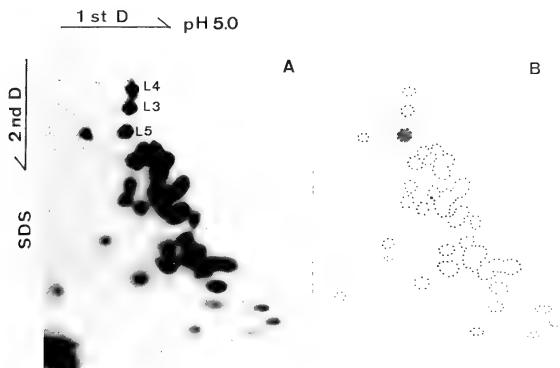


FIG. 4. Two-dimensional gel electrophoretogram of *Artemia* 60S ribosomal proteins (A) and autoradiogram by immunoblotting (B). Sixty S ribosomal proteins separated by two-dimensional acidic-SDS acrylamide gel electrophoresis were transferred to a nitrocellulose membrane sheet and the sheet was treated with ^{125}I -labeled IgG (5×10^5 cpm) and then autoradiographed.

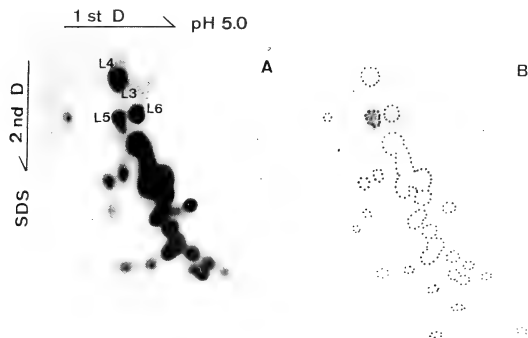


FIG. 5. Cross-reactivity of anti-AL5 with rat liver 60S ribosomal proteins by immunoblotting. Rat liver 60S ribosomal proteins were separated by acidic-SDS two-dimensional gel electrophoresis (A) and transferred to a nitrocellulose membrane sheet. The sheet was treated with ^{125}I -labeled anti-AL5 IgG (5×10^5 cpm) and then subjected to autoradiography (B).

Immunological homology between Artemia and rat liver L5

The cross-reactivity of anti-AL5 with rat liver 60S proteins was then examined by immunoblotting as described above. As shown in Figure 5, anti-AL5 was found to cross-react with a single protein of rat liver 60S proteins. This protein was L5, which was the 5S RNA binding protein of rat liver ribosomes. This indicates that *Artemia* and rat liver L5 share immunological determinants. Although correspondence between individual 60S proteins of *Artemia* and rat liver was very difficult to find [12], the protein L5 is shown to be highly conserved between the two species.

DISCUSSION

The 5S RNA binding protein of *Artemia* ribosomes (AL5) was a basic protein with a molecular weight of about 34,000, apparently the third largest protein component in the 60S ribosomal subunit. It was located in the same position as rat liver L5 on the two-dimensional gels. In our previous study on *Artemia* ribosomal proteins by two dimensional gel electrophoresis [12], we were unable to exactly detect AL5 which corresponded to rat liver L5 on the two dimensional gel slab. We detected only a faint spot of AL5 on the two dimensional gel slab. The basic-acidic and the basic-SDS gel systems were formerly used, where the first dimensional electrophoresis was run at pH 8.6. But in the present work, the protein corresponding to rat liver L5 was detected with the acidic-SDS gel system. Fabijanski and Pellegrini pointed out that many ribosomal proteins were only slightly soluble at pH 8.6 without thiol reducing agents [19]. Therefore, they used the acidic gel (pH 5.0) for the first dimension. In yeast ribosomes, the 5S RNA binding protein was largely insoluble in the first dimensional buffer at pH 8.6 and most of the protein remained trapped at the origin [4]. Consequently, AL5 also seemed to be insoluble and unable to be detected in the previous gel systems as in the case of yeast ribosomes.

In *E. coli* ribosomes, antibodies to each ribosomal protein were very useful in elucidating their functions [17, 18], but in the case of eukaryotic

ribosomes few antibodies against each ribosomal protein were available because of the difficulty of obtaining sufficient pure proteins for immunization. We succeeded in obtaining the antibody against AL5 in the present work, so the antibody would become an effective means to clarify the function of the 5S RNA-protein complex. At first we showed that there exists an immunological homology between *Artemia* and rat liver L5 by immunoblotting. As to the amino acid sequences of the 5S RNA binding proteins, Tamura *et al.* [20] showed that 18 residues of amino acids in the N-terminal region and 28 in the C-terminal of rat liver L5 were identical with those of yeast YL3 (5S RNA binding protein). Both their results and ours indicate that a 5S RNA binding protein is probably conserved during the evolution of yeast to mammalian cells. After analyzing the amino acid sequences of YL3, Yaguchi *et al.* [11] suggested that the single large eukaryotic 5S RNA binding protein might have evolved through a fusion of genes for the multiple 5S RNA binding proteins in prokaryotes. Analysis of the amino acid sequences of AL5 is required to clarify this point of view.

Fabijanski and Pellegrini [19] indicated that rat liver L5 was located at or near the P site in affinity labeling experiments. Uchiumi *et al.* [10] showed that rat liver L5 cross-linked to S4 and S25 at the interface between the small and large subunits. Rat liver L5 may be located near the initiation region of 40S subunits in the 80S couples since S4 and S25 appeared to cross-link to eIF-3 [21, 22]. Concerning the location of *Artemia* L5 on ribosomes, the ability of the anti-AL5 to bind to the ribosomes or their subunits was examined and it was proved that the anti-AL5 did not react to 80S ribosomes but to 60S subunits [23]. Consequently, *Artemia* L5 is probably located at the interface between the two subunits as rat liver L5 and may play a significant role in protein synthesis at or near the initiation region of ribosomes.

ACKNOWLEDGMENTS

We thank Mr. Y. Maeda for excellent technical assistance in the immunization of rabbits. We also thank Dr. N. Sato for encouragement and support during the course of this work.

REFERENCES

- 1 Blobel, G. (1971) Isolation of a 5S RNA-protein complex from mammalian ribosomes. *Proc. Natl. Acad. Sci. USA*, **68**: 1881-1885.
- 2 Erdmann, V. A. (1976) Structure and function of 5S and 5.8S RNA. *Progr. Nucleic Acid Res. Mol. Biol.*, **18**: 45-90.
- 3 Garret, R. A., Douthwaite, S. and Noller, H. F. (1981) Structure and role of 5S RNA-protein complexes in protein biosynthesis. *Trends Biochem. Sci.*, **6**: 137-139.
- 4 Nazar, R. N., Yaguchi, M., Willick, G. E., Rollin, C. F. and Roy, C. (1979) The 5-S RNA binding protein from yeast (*Saccharomyces cerevisiae*) ribosomes. *Eur. J. Biochem.*, **102**: 573-582.
- 5 Terao, K., Takahashi, Y. and Ogata, K. (1975) Differences between the protein moieties of active subunits and EDTA-treated subunits of rat liver ribosomes with specific references to a 5S rRNA-protein complex. *Biochim. Biophys. Acta*, **402**: 230-237.
- 6 Erdmann, V. A., Sprinzl, M. and Pongs, O. (1973) The involvement of 5S RNA in the binding of tRNA to ribosomes. *Biochem. Biophys. Res. Commun.*, **54**: 942-947.
- 7 Azad, A. A. and Lane, B. G. (1973) A possible role for 5S rRNA as a bridge between ribosomal subunits. *Can. J. Biochem.*, **51**: 1669-1672.
- 8 Takahashi, Y. and Ogata, K. (1981) Ribosomal proteins cross-linked to natural mRNA by UV irradiation of rat liver polysomes. *J. Biochem.*, **90**: 1549-1552.
- 9 Takahashi, Y. and Ogata, K. (1985) Attachment of the 5'-terminal portion of globin mRNAs to 5S-RNA L5-protein in the 80S initiation complex. *Eur. J. Biochem.*, **152**: 279-286.
- 10 Uchiumi, T., Kikuchi, M. and Ogata, K. (1986) Cross-linking study of protein neighborhoods at the subunit interface of rat liver ribosomes with 2-iminothiolane. *J. Biol. Chem.*, **261**: 9663-9667.
- 11 Yaguchi, M., Rollin, C. F., Roy, C. and Nazar, R. N. (1984) The 5S RNA binding protein from yeast (*Saccharomyces cerevisiae*) ribosomes. *Eur. J. Biochem.*, **139**: 451-457.
- 12 Kenmochi, N., Tsurugi, K. and Ogata, K. (1981) Analyses of 40S and 60S ribosomal proteins of *Artemia salina* with two- or "three-dimensional" acrylamide gel electrophoresis and comparisons with rat liver 40S and 60S proteins. *J. Biochem.*, **89**: 1293-1308.
- 13 Sherton, C. C., Camelli, R. F. and Wool, I. G. (1974) Separation of large quantities of eukaryotic ribosomal subunits by zonal ultracentrifugation. *Methods in Enzymology*, **30**: 354-367.
- 14 Terao, K., Uchiumi, T. and Ogata, K. (1980) Cross-linking of L5 protein to 5S RNA in rat liver 60S subunits by ultraviolet irradiation. *Biochim. Biophys. Acta*, **609**: 306-312.
- 15 Madjar, J. J., Michel, S., Cozzone, A. J. and Reboud, J. P. (1979) A method to identify individual proteins in four different two-dimensional gel electrophoresis systems: Application to *Escherichia coli* ribosomal proteins. *Anal. Biochem.*, **92**: 174-182.
- 16 Towbin, H., Staehelin, T. and Gordon, J. (1979) Electrophoretic transfer of proteins from polyacrylamide gels to nitrocellulose sheets: Procedure and some applications. *Proc. Natl. Acad. Sci. USA*, **76**: 4350-4354.
- 17 Stöffler, G. (1974) Structure and function of the *Escherichia coli* ribosome: Immunochemical analysis. In "Ribosomes". Ed. by M. Nomura, A. Tissieres and P. Lengyel, Cold Spring Harbor Laboratory, New York, pp. 615-667.
- 18 Wittmann, H. G. (1976) Structure, function and evolution of ribosomes. *Eur. J. Biochem.*, **61**: 1-13.
- 19 Fabijanski, S. and Pellegrini, M. (1981) Identification of proteins at the peptidyl-tRNA binding site of rat liver ribosomes. *Mol. Gen. Genet.*, **184**: 551-556.
- 20 Tamura, S., Kuwano, Y., Nakayama, T., Tanaka, S., Tanaka, T. and Ogata, K. (1987) Molecular cloning and nucleotide sequence of cDNA specific for rat ribosomal protein L5. *Eur. J. Biochem.*, **168**: 83-87.
- 21 Westermann, P. and Nygård, O. (1983) The spatial arrangement of the complex between eukaryotic initiation factor eIF-3 and 40S ribosomal subunit. *Biochim. Biophys. Acta*, **741**: 103-108.
- 22 Tolan, D. R., Hershey, J. W. B. and Traut, R. R. (1983) Crosslinking of eukaryotic initiation factor eIF3 to the 40S ribosomal subunit from rabbit reticulocytes. *Biochimie (Paris)*, **65**: 427-436.
- 23 Kenmochi, N., Takahashi, Y. and Sato, N. L. (1989) Effects of antibody to 5S RNA-binding protein on protein synthesis in *Artemia salina* ribosomes. *Biochem. J.*, **259**: 277-281.



Arthropod Immune System. II. encapsulation of Implanted Nerve Cord and "Plain Gut" Surgical Suture by Granulocytes of *Blattella germanica* (L.) (Dictyoptera: Blattellidae)

SUNG S. HAN¹ and AYODHYA P. GUPTA²

Department of Entomology and Economic Zoology, New Jersey Agricultural
Experiment Station, Cook College, Rutgers University,
New Brunswick, New Jersey 08903, USA

ABSTRACT—In the German cockroach, *Blattella germanica* only the granulocyte (GR) encapsulates the nerve cord implants from the American cockroach and "plain gut" surgical suture implants in the abdominal hemocoel. Encapsulation commences about 40 min after implantation and is completed in 10 days. The completed capsule is often 6.5 μ m thick, consists of inner and outer regions, which together are composed of about 20 layers, and a 64 nm thick outer sheath; the latter when completed, does not show any further attachment of GRs to it, and in fact marks the end of encapsulation. Early on in capsule formation, the innermost GR layer of the inner region seems to secrete melanin, and later other layers produce random melanin deposits in the entire capsule. It seems that in this cockroach, the GR provides both the phenols and the phenol-oxidizing enzyme to produce melanization. Desmosome-like-, intermediate-, B-type gap, and septate cell junctions are present, the latter reported for the first time.

INTRODUCTION

Encapsulation of foreign or nonself tissue is a cellular reaction that is accomplished by plasmotocytes (PLs) and/or granulocytes (GRs), previously referred to as immunocytes [1, 2], because of their ability to distinguish between self and nonself tissues. Several aspects of this cellular immune reaction vary in different insects and are controversial [2, 3]. For example, the structural changes in the immunocytes during capsule formation, including the degree of flattening, necrosis, and the formation of membrane-bounded granules vary in different insects. Similarly, there are differences in the immunocytes of the middle and the outer regions in terms of the occurrence of gap junctions, desmosomes, microtubules, and mitochondria. Furthermore, the degree of melani-

nization and the hemocytic origin of the phenols and the phenoloxidase that produce melanization are controversial, because, in addition to the GRs, coagulocytes and oenocytoids have been reported to provide both these compounds [4, 5].

Although encapsulation in the German cockroach, *Blattella germanica* has not been previously reported, it has been described in the American cockroach, *Periplaneta americana* [6-11]. According to Ennesser and Nappi [10], both the immunocytes (PLs and GRs) participate in capsule formation in *P. americana*, the GRs playing the major role. During an investigation of the immune system of *B. germanica*, we noticed several specific differences in the encapsulation process in this species from those in the American cockroach. For example, only the GRs form the capsule in *B. germanica*. Furthermore, early on in capsule formation, one layer of GRs secretes melanin and later other layers produce scattered melanin deposits in the entire capsule; the completed capsule has an outer sheath that shows no further attachment of GRs to it. In addition, the capsule has desmosome-like-, intermediate-, gap- and septate

Accepted June 22, 1988

Received March 24, 1988

¹ Present Address: Department of Plant Protection, Kangwon National University, Kangwon, South Korea.

² To whom reprint requests should be addressed.

junctions. In this paper, we present these details of encapsulation and point out the significant differences from those in the American cockroach.

MATERIALS AND METHODS

Adult males of *B. germanica* from colonies, maintained at $28 \pm 2^\circ\text{C}$ on Purina laboratory chow and water, were used. After implantation, the insects were kept separately.

Implantation and fixation of implants

We implanted 1mm-long pieces of fixed (surface-altered) and unfixed nerve cord from *Periplaneta americana* and commercially available pieces of "plain gut" (sterile, absorbable surgical suture) (Ethicon, Inc., Somerville, NJ). Surface alteration was carried out by fixing in 2.5% glutaraldehyde in 0.1 M sodium cacodylate buffer (pH 7.4) for 1.5 hr and in 1% buffered osmium tetroxide for 1.5 hr. After rinsing the fixed and unfixed nerve cords and unfixed gut pieces in sterilized buffer for 1 hr, we implanted them in the abdominal hemocoel through an incision in the intersegmental membrane between the first and second abdominal tergites. The insects were temporarily immobilized with CO_2 prior to the implantation procedure. All instruments involved in surgery were sterilized and the abdomens of the host insects cleaned with 70% ethanol. Some of the implants from the host insects at 10, 20, 40 min, 1, 2, 4, 8, 16 hr and 1, 3, 10, and 20 day intervals (ages) were placed in 2.5% glutaraldehyde at 4°C , and others in a mixture of 4% tannic acid and 2.5% glutaraldehyde (1:1) in 0.1 M cacodylate buffer (pH 7.4), containing 0.13 M sucrose, at room temperature. They were then washed in buffer for 1 hr, placed in 1% buffered osmium tetroxide for 1.5 hr, washed again in buffer, dehydrated through a graded ethanol series, and embedded in Epon-Araldite mixture. The sections, stained in uranyl acetate and lead citrate, were observed in a Philips 300 electron microscope.

Freeze fracture and etching

One to 7 days after implantation, the implants were fixed *in situ* with 2.5% glutaraldehyde in 0.1

M cacodylate buffer for 1 hr, rinsed in 30% glycerol buffer and kept at 4°C . The implants were placed on standard gold disc and quickly frozen in melting Freon 22 at -160°C for 10 sec and then quickly transferred to liquid nitrogen. Platinum-carbon replicas of etched specimens were produced in a Blazer High Vacuum Freeze-Etch Unit BAF 301 at a temperature of -100°C and a vacuum of 2×10^{-6} Torr [12]. Clean replicas were observed in a Philips 300 electron microscope.

The total (THC) and differential (DHC) hemocyte counts were determined according to the technique by Chiang *et al.* [13].

RESULTS

We have reported elsewhere [13, 14] that, in addition to the 2 major immunocytes (plasmacytes (PLs) and granulocytes (GRs)), the German cockroach possesses prohemocytes, oenocytoids, adipohemocytes, and spherulocytes. We identified these hemocytes according to Gupta's [15-17] classification.

Normal and activated granulocytes

Normal or resting (unactivated) GR (Figs. 1 and 2) is a flattened, discoid cell, and contains, among other organelles, microtubules that are arranged in the form of bundles in its peripheral region in the plane of flattening. The activated (postimplantation) GRs (Figs. 3 and 4) show different ultrastructural details; they are characterized by irregular outline, presence of numerous cytoplasmic extensions, and pronounced development of peripheral microtubules (Figs. 3, 4 and 17).

Encapsulation

In *B. germanica*, only GRs participate in capsule formation, which commences about 40 min after implantation, and is completed in 10 days. Because the reactions of the GRs to both the nerve cord and the artificial gut implants were very similar, we have presented the encapsulation of only the nerve cord implants.

Encapsulation begins with the lysis of some GRs. On the surface of 40 min to 8 hr old implants, we noticed flattening and lysis of some GRs (Fig. 3); lysis is evidenced by the presence of

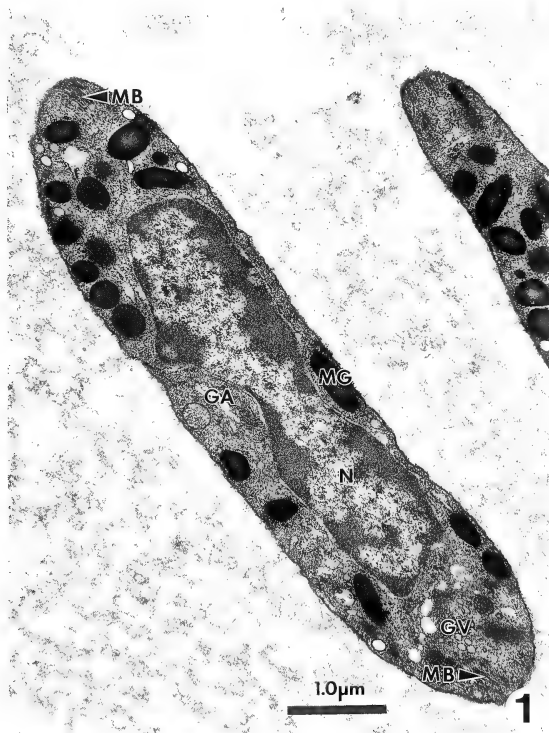


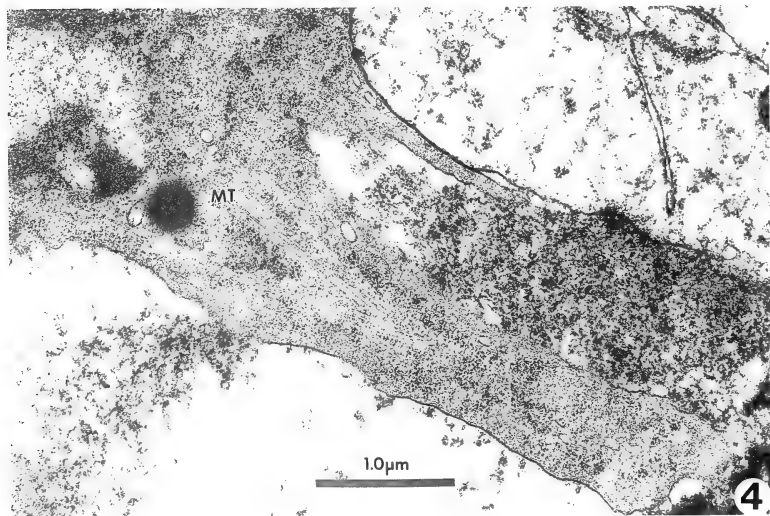
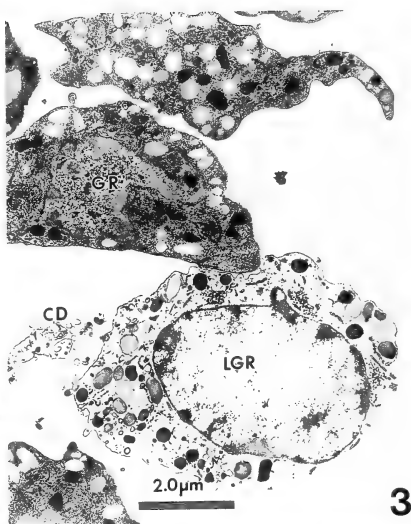
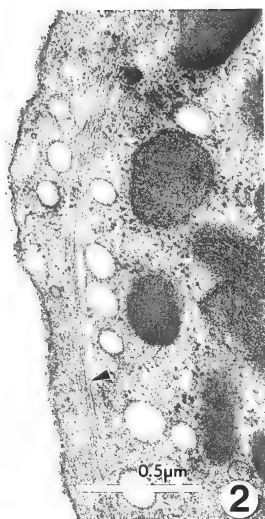
FIG. 1. Cross section of a normal or resting (unactivated) granulocyte (GR), showing membrane-bounded structureless granules (MG), microtubule bundles (arrow head, MB) in apical region, Golgi apparatus (GA), Golgi vesicles (GV) and nucleus (N).

lysosomes, free nuclei, mitochondria, smooth endoplasmic reticulum (Fig. 6), microvesicles, granules, and other cell debris.

The completed capsule (Fig. 18) consists of an inner and an outer region in this roach, the latter being externally limited by a sheath. No further attachment of GRs to the sheath occurs. The structural equivalent of the outer region of other insect capsules is not formed in the capsule of *B. germanica*.

The inner region

The inner region is completed any time between 8 hours to 3 days in various specimens. It is about $4\text{ }\mu\text{m}$ thick and generally shows 6–9 layers (Fig. 7), the first or innermost of which is consistently covered with a coating of melanin that appears as 2 sublayers, on its inner and outer surfaces, each sublayer being 50 nm thick in cross section. The GRs forming the innermost layer are considerably



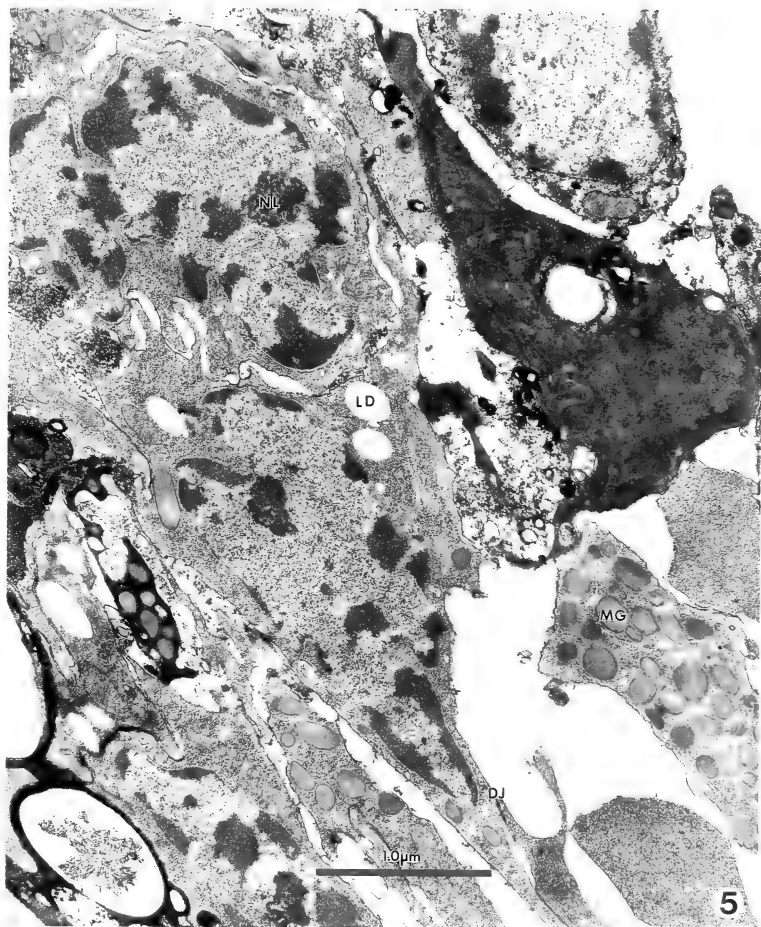
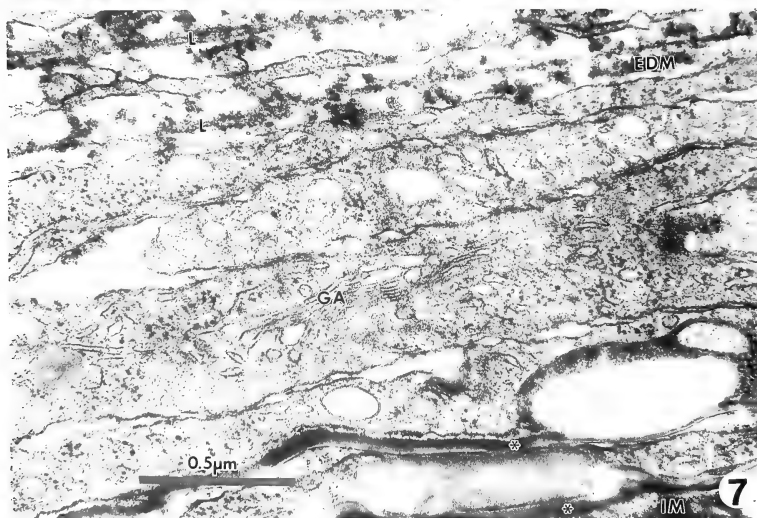
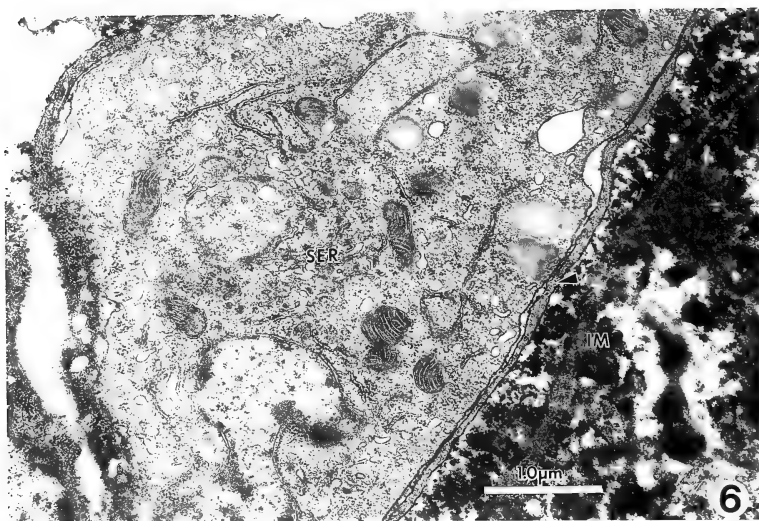


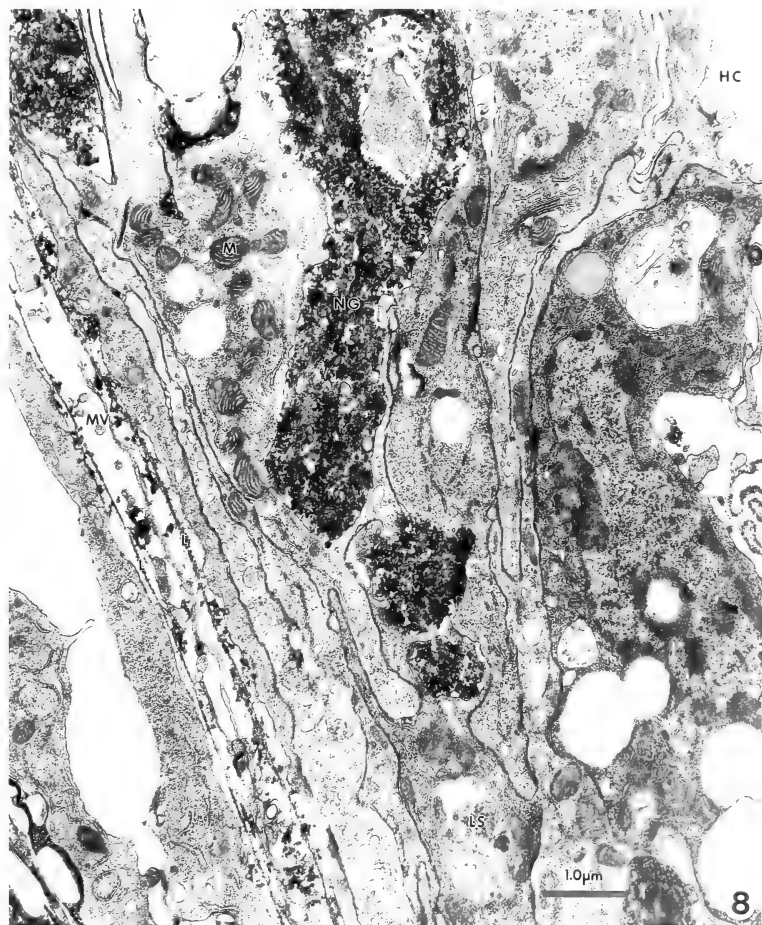
FIG. 5. Section of an 8 hr old capsule showing, loosely aggregated GRs. Note some degenerated GRs, membrane-bounded structureless granules (MG), nucleolus (NL), lipid droplet (LD), and desmosome-like junctions (DJ).

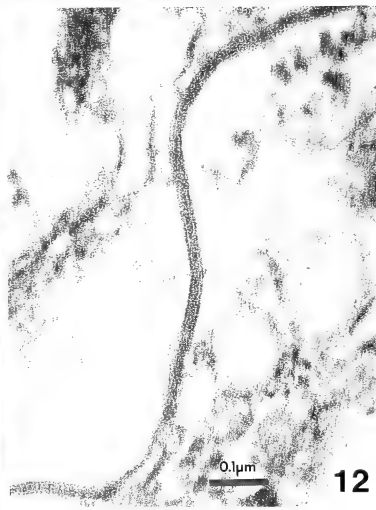
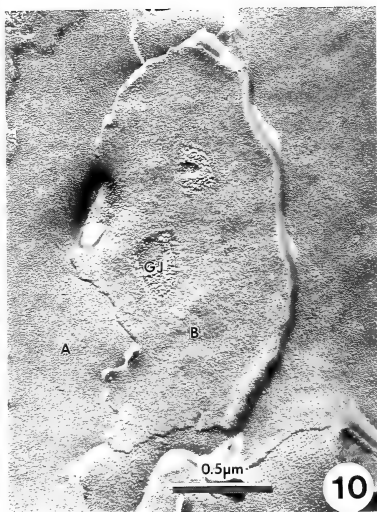
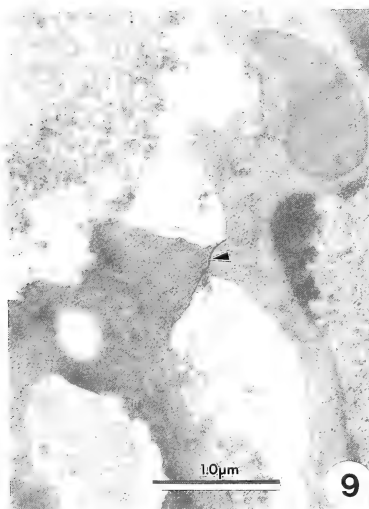
FIG. 2. Section of a normal GR along its plane of flattening, showing microtubule bundle (arrow head) close to the plasma membrane in the plane of flattening.

FIG. 3. Section of an activated GRs 40 min after implantation. Note the irregular outline of GR and features of lysis in them. CD=cell debris; LGR=lysed GR.

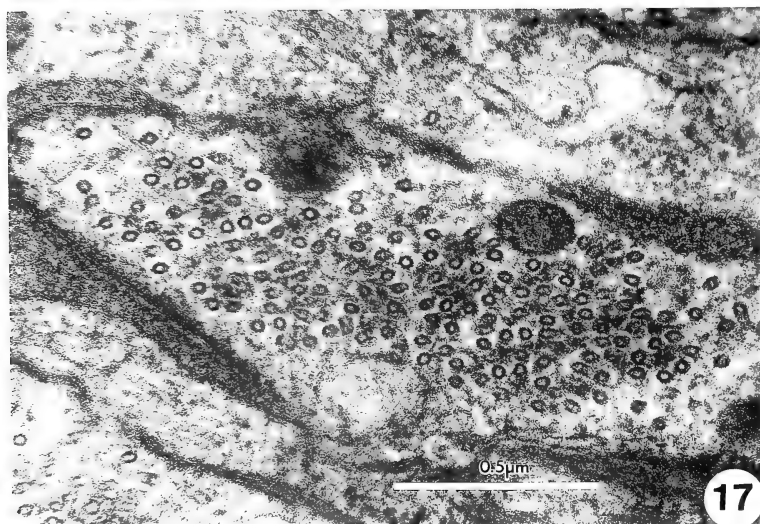
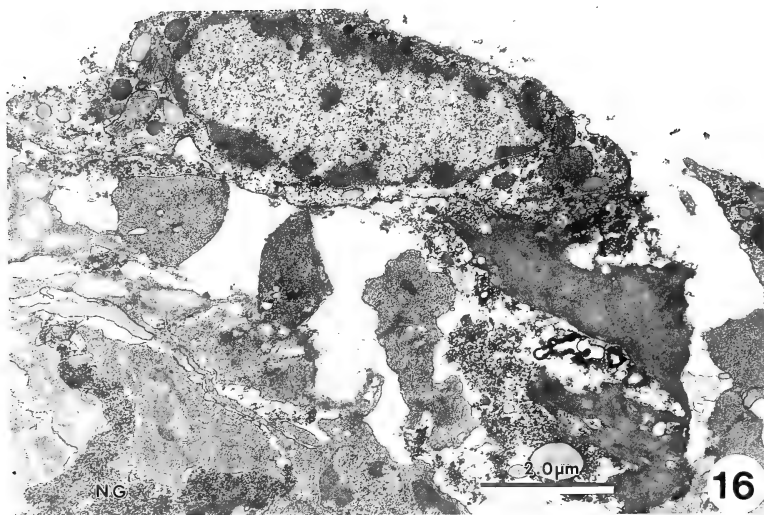
FIG. 4. Section of an activated GR 8 hr after implantation, showing cytoplasmic extensions and pronounced development of microtubules (MT).











flattened and show several structural changes. For example, the Golgi apparatus is well developed, and the number and the electron density of the membrane-bounded granules are reduced. In addition, microvesicles exocytosed from intact cells and mitochondria are also visible (Fig. 8). The plasma membranes of cells are not obscured.

External to the innermost layer are 4 other layers (2nd–5th), whose ultrastructural changes resemble those of the innermost layer, except that they lack the melanin sublayers. These 5 layers are surrounded by 2 (18–23 nm thick) laminae (Fig. 7), which appear to be composed of amorphous coagulated hemolymph. Between the 2 laminae is a GR layer represented by fragments of electron-dense material. In the next 3–4 layers (6th–9th),

the GRs are less compactly arranged, but ultrastructurally resemble the preceding 5 layers. The 9th, or both the 8th and 9th, layers show necrotic GRs (Fig. 8). Desmosome-like-, B-type (=E-type) gap-, septate-, and intermediate cell junctions are found in this region (Figs. 5, 9, 10, 13–15); the gap junctions occur less frequently in the inner region than in the outer region, and the septate junctions are very few in this region and absent in the outer region.

The outer region

The outer region is completed in a 3–5 day old capsule. It is about 2.5 μm thick and separated from the inner region by a narrow band (in which distinct layering is obscure) of loosely aggregated

Fig. 6. Section of an 8 hr old capsule, showing attachment of GRs to the implant at the beginning of encapsulation. Note a very thin peripheral cytoplasm (arrow head) against the implant (IM). SER=smooth endoplasmic reticulum.

Fig. 7. Section of a 3 day old capsule, showing the inner region. Note that the innermost layer of this region is covered with a melanin sublayer (*) on its inner and outer surfaces. External to the innermost layer are 4 other layers and 2 (18–23 nm thick) laminae (L) surrounding the 5 layers. Between the 2 laminae is a GR layer with some electron-dense materials (EDM). Note necrotic GRs in the following 2 layers. GA=Golgi apparatus; IM=implant.

Fig. 8. Micrograph showing GRs in a 3 day old capsule. In the region of the capsule facing the hemocoel (HC), the GRs are less compactly arranged. Note necrotic GRs (NG), several vacuoles, and lysosomes (LS), and well-developed Golgi apparatus, mitochondria (M), laminae (L), RER, and microvesicles (MV) exocytosed from intact cells.

Fig. 9. Section of a 3 day old capsule, showing gap junction (arrow head) in the inner region. Whenever GRs first contact each other, they generally form gap junctions.

Fig. 10. Freeze fracture and etching of the inner region of a 3 day old capsule, showing gap junctions (GJ). Of the 2 B-type (=E-type) junctions, one shows greater dispersion of the particles. A=A (=P) fracture face; B=B (=E) fracture face.

Fig. 11. Freeze fracture and etching of the outer region of a 3 day old capsule, showing gap junction. The intramembranous particles on the B (=E) fracture face are 20 nm in diameter, and their number is approximately $640/\mu\text{m}^2$.

Fig. 12. Section of a 3 day old capsule, showing gap junction in the outer region. Plasma membrane of the GR is 7.5 nm thick and is distinguishable as 2 electron-dense layers and 1 electron-lucent region between the 2 layers, the thicknesses of the 2 layers and the electron-lucent region being 2.5 nm; that of the intercellular space between the 2 GRs forming the gap junction is also 2.5 nm.

Fig. 13. Section of a 3 day old capsule's inner region, showing septate junction (arrow heads). The separation of the membranes within the junctional region is about 3.5 nm wide and the septa are often about 15 nm wide but may vary in width. NG=necrotic GR.

Fig. 14. Section of the inner region of a 3 day old capsule, showing intermediate junction (IJ). The 2 adjacent plasma membranes run parallel to each other, the electron-lucent space between them always being 9 nm wide.

Fig. 15. Freeze fracture and etching of the inner region of a 3 day old capsule, showing septate junction. The septate junction reveals rows of particles (8–14 nm in dia.) on the A (=P) face and corresponding furrows (6 nm wide, 16 nm center to center) on the B (=E) face.

Fig. 16. Section of a 5 day old capsule, showing the outer region, which is formed by continuous layering of GRs, and is separated from the inner region by a band of loosely aggregated necrotic GRs (NG).

Fig. 17. Section of a 10 day old, completed capsule, showing the cytoplasm of GR with pronounced development of microtubules.

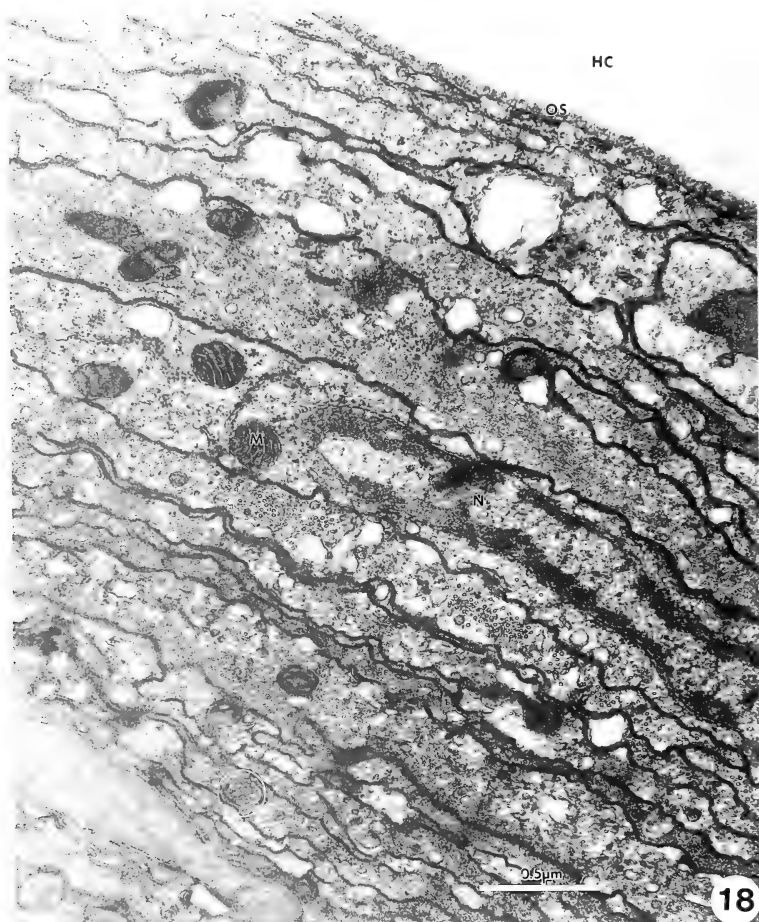


FIG. 18. Section of a 10 day old, completed capsule. It is about 6.5 μm thick. Numerous microtubules, but few mitochondria (M) and RER, and flattened nuclei (N) are seen. The outer sheath (OS) surrounding the capsule is 64 nm thick. HC=hemocoel; multivesicular body in white circle.

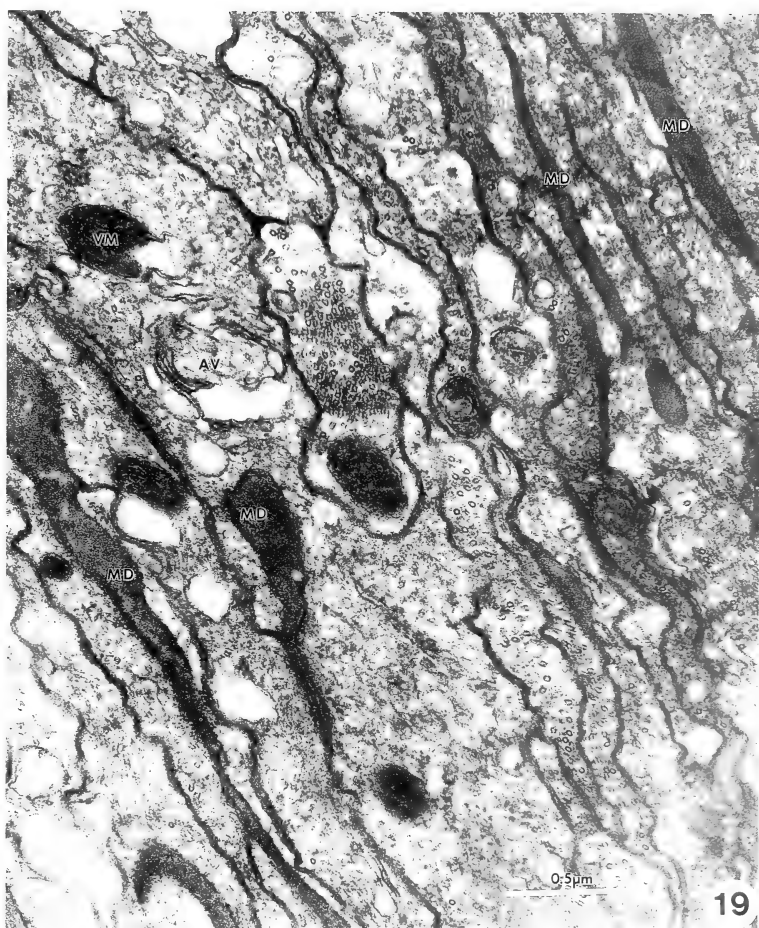


FIG. 19. Section of a 10 day old, completed capsule, showing random deposits of melanin (MD), RER, vacuolated mitochondria (VM), and autophagic vacuoles (AV).

necrotic GRs (Fig. 16); this band of loosely packed GRs is marked by nuclei and other cell remnants.

The first 4-5 layers of the outer region are visible in a 3 day old capsule and consist of GRs that essentially show the same structural details as those of the inner region. Gap junctions are frequently found in the capsule at this stage (Figs. 11 and 12).

The outer region is completed by deposition of additional 4-5 layers of GRs, which are extremely flattened and marked by pronounced development of microtubules (Fig. 17). The granules and the Golgi apparatus gradually disappear, and very few mitochondria and RER are visible. At this stage of capsule formation, the innermost layer and the 2 amorphous laminae of the inner region become indistinguishable. Autophagic vacuoles, large lipid vacuoles, masses of endoplasmic reticulum, vacuolated mitochondria, fragmented nuclei, randomly scattered melanin deposits, and cell remnants are commonly found throughout the capsule (Figs. 18 and 19), and the plasma membranes of the GRs are highly electron dense. No septate junctions were observed.

The completed (10 day old) capsule as a whole (Figs. 18 and 19) is very compact, consists of about 20 layers in some regions of the implant, and is about 6.5 μm thick. The most characteristic feature of the capsule is the presence of 64 nm thick outer sheath that marks the end of encapsulation. No further attachment of GRs to the sheath occurs. The general features of a finished capsule include numerous microtubules, free ribosomes, few mitochondria and RER, and randomly distributed melanin deposits throughout the capsule. Golgi apparatus and granules are rarely observed. Only gap cell junctions are found in the outer region of the completed capsule. At no stage of the capsule formation did we notice the "cylinder inclusions" that had been observed in the capsule of *P. americana* [10, 18].

DISCUSSION

Most of the general discussion on encapsulation pertaining to other insects has been previously reviewed by Gupta [2, 17]. Although, there is disagreement among insect hematologists as to the

number of hemocyte types and their identification in various insects [17], the immunocytes (PLs and GRs) that participate in immunorecognition and encapsulation are generally recognizable in light, scanning, and transmission electron microscopical examinations. In the present study, we did not find any plasmatocytes participating in capsule formation. Why the PLs do not participate in capsule formation may be related to the absence of peripheral microtubules in these cells [20]. Both altered (fixed) and unaltered (unfixed) xenogeneic implants produced similar reaction.

Initial immunocyte response to the implant

Apparently, capsule formation both commences and is completed much earlier in *P. americana* (Blattoidea: Blattidae) than in *B. germanica* (Blattoidea: Blattellidae). Ennesser and Nappi [10] reported that capsule formation in *P. americana* commences 10 min postimplantation, and is completed in about 40 min. In *B. germanica*, we noticed first signs of aggregation of GRs on the implant 40 min postimplantation, and it took about 10 days for the capsule to be completed. Whether this differential cellular reaction between the two species of cockroaches is due to taxonomic differences (the two species belonging to two different families), or that the immunocytes in the German cockroach are less reactive to the foreign tissue than those of the American cockroach, is difficult to explain. This difference in response does not seem to be due to lower total (THC) and differential (DHC) counts of hemocytes, because we did not find any significant differences in the THCs and DHCs of GRs of the two species [13 and unpublished observation]. At any rate, it is hard to imagine that the slow and delayed hemocytic reaction to the implants is an efficient or beneficial immune reaction from the standpoint of survival of the cockroach; this prompted us to investigate whether a much faster rate of phagocytic reaction, being often the first line of defense, compensates for the much slower process of encapsulation. Our preliminary results of the rate of phagocytosis of injected microspheres suggest that this indeed is the case (unpublished observation).

Number of cell layers

Cellular capsules vary in terms of the structural changes in the immunocytes that take part in capsule formation and the number of cell layers (regions) in the completed capsule. Baerwald [18] reported a range of 20-75 layers in various insects. In many insects, the layers of the inner region show flattened and necrotic PLs and/or GRs. In *B. germanica*, the most characteristic features of the inner region are the presence of the 2 sublayers of melanin on the inner and outer surfaces of the first or innermost layer of GRs and the 2 laminae, which disappear later in the completed capsule.

Melanization and sources of melanin

Although Ennesser and Nappi [10] only occasionally observed melanin layers in the *P. americana* capsules, we consistently found the 2 sublayers of melanin in the innermost layer of the inner region during the initial stages of encapsulation and numerous randomly distributed melanin deposits in various parts of the 10 day old completed capsules in *B. germanica*. The question whether melanization originates in the inanimate foreign tissue or in the host's immunocytes is still debated, although it has been reported in many cases that the immunocytes provide both the phenolic substrate and the phenol-oxidizing enzymes [see 2, 17 for review]. It should be stated, however, that the hemocytic origin of both the phenols and the phenoloxidases continues to be controversial. Furthermore, in addition to GRs and/or PLs, coagulocytes and oenocytoids have been reported by one author or another to provide both the substrate and the enzyme [4, 5], although Gupta [1] did not find tyrosinase in the oenocytoids of another cockroach, *Gromphadorhina portentosa*.

Our present studies suggest that in *B. germanica* both the phenols and phenoloxidase are supplied by the GRs, because we noticed the melanin sublayers even in the capsules around the artificial gut implants, which would be the most unlikely sources of these compounds. Indeed, Schmit *et al.* [5] have demonstrated the presence of melanin precursors in the GRs of *Galleria mellonella*. However, the possibility that the hemolymph could be the source of the phenols and the phenol-

oxidase that produced the melanization cannot be ignored.

Lysis and other structural changes in granulocytes

That encapsulation commences with the lysis of GRs has been reported by many authors. Apart from the general flattening of the immunocytes forming the capsules, several other changes have been described in them [see 2, 3, 17 for review]. We also noticed lysing GRs on the surface of the implant and the 2 (18-23 nm thick) laminae surrounding the 5th layer of the inner region. We consistently observed these laminae, which, as far we know, have not been reported in the capsules of other insects. They seem to be transient structures, because they gradually disappear as the capsule formation progresses and are generally absent in the fully formed, 10 day old capsules. Their function remains unknown.

The pronounced development of microtubules in the GRs forming the capsule has been reported in other insects and is prominent in those of *B. germanica*. François [19] has shown numerous microtubules and desmosomes in 7 day old capsules of *Thermobia domestica*. According to Baerwald [18], the microtubules in the marginal bundles are presumably associated with desmosomes. We have reported elsewhere [20] that the pronounced development of microtubules is characteristic of activated GRs and that these organelles are absent in the PLs.

Functional significance of cell junctions in capsule formation

The presence of the intermediate-, desmosome-like-, gap-, and the septate junctions in the capsules seems to be functionally significant. On the basis of the known functions of these cell junctions in vertebrate tissue, we propose that they perform two most important functions in the formation of the capsules: 1) the gap junctions provide cell-to-cell communication during coupling of the GRs to form the various layers and 2) the desmosome-like- and septate junctions anchor the layer-forming GRs mechanically.

Gupta [2] has briefly summarized some of the literature on gap cell junctions in some arthropods. The presence of gap junctions in capsules is impor-

tant, because during capsule formation, these junctions probably assist the enveloping GRs to recognize one another and thus interact more effectively in forming the capsule. In fact, Caveney and Berdan [21] have suggested rapid *de novo* formation of gap junctions in the hemocytic capsule of *P. americana*. It is conceivable that coupling through gap junctions enables the GRs in *B. germanica* to set up a pathway for communication among the cells of various layers by establishing gradients of ion concentrations along the width of the capsule, for, according to Alberts *et al.* [22], "any of these gradients could serve as a reference system for the determination of the relative cell position," thus instructing each GR to attach in a certain position.

Although experimental demonstration of GR-to-GR communication through gap junctions in the capsules in *B. germanica* remains to be established, Caveney and Berdan [21] have shown that carboxy fluorescein, when microinjected into 72 hr old hemocytic capsule of *P. americana*, "moved readily from cell to cell," via the gap junctions. Furthermore, cell-to-cell communication has been reported in cultured multicell spheroids of mammary tumor cells of the marshall rat [23]. These authors reported that 2 days after the formation of the spheroids, the pores in the gap junctions apparently closed (indicated by the fact that injected Lucifer yellow dye was retained in the injected cell and did not spread to other cells of the spheroid). Gupta [2] suggested that if a similar cessation of cell-to-cell communication occurred during the capsule formation in arthropods, it would explain the progressive retardation of the attachment of immunocytes to the capsule as its thickness increases. The existence of such a mechanism remains to be confirmed, however.

In the very few arthropods in which the gap junction particles had been studied by the early 1970s, they were generally reported to be located on the extracellular E (=B) fracture face, and therefore, Flower [24] designated these gap junctions as "inverted type," with reference to the mammalian gap junctions, in which the location of the particles is reversed (i.e. on the cytoplasmic P (=A) fracture face). Thus, Staehelin [25] and Baerwald [8] suggested that the extracellular E-

type gap junctions may be characteristic of arthropods, although such junctions have also been found in the coelenterate, *Hydra* [26]. The nematode, *Trichinella spiralis* [27] and some mollusks [28, 29], on the other hand, have P-type gap junctions. In view of this, Gupta [2] suggested that probably the E-type represents the most primitive stage, while the P-type is a more advanced type that originated before the evolution of the arthropods, in which both P- and E-types are present. Indeed P-type junctions are now known to be present in several arthropods [30-32]. We counted about $640/\mu\text{m}^2$ such intramembranous particles (connexons) on the E fracture face in the capsule of *B. germanica*. According to Baerwald [18], gap junctions are more numerous in the deeper layers of *P. americana* capsules. Our observations in *B. germanica* support this.

The desmosome-like- and septate junctions probably help maintain the structural integrity of the capsule. Desmosomes are known to anchor cells together and are most abundant in tissues (e.g. cardiac muscle, skin, and neck of uterus) that are subject to severe mechanical stress [22]. Desmosomes have been reported in the capsules of *Carausius morosus*, *Locusta migratoria*, *Melolontha melolontha*, *P. americana* and *G. mellonella*, and gap junctions only in *Ephestia kuehniella* and *P. americana* [18].

We report for the first time the presence of septate junctions in the capsule of *B. germanica* by both thin section and freeze-fracture methods. We should mention, however, that Grimstone *et al.* [33], in their Figure 13, have mentioned "transverse striations in intercellular material." We have reported the details of the septate junctions elsewhere [34].

Continuation and cessation of layering in capsule formation

The mechanisms, involved in the maintenance of continuous layering in the capsule and its cessation when the capsule has been completed, remain conjectural. Grimstone *et al.* [33] suggested that as each layer is formed, the surface properties of the plasma membrane of the cells forming the capsule changes, as a result of which they are recognized as nonself tissue and in turn attract new cells. Amir-

ante [35] hypothesized that as hemocytes adhere to the foreign tissue, they form "new acceptors" (some sort of lectin receptors) on their plasma membranes that attract the lectins on the plasma membranes of other hemocytes, which then form the next layer. We have suggested above the possible role of gap junctions in establishing a continuous ion gradient, which might promote continuous positioning of GRs on the developing capsule.

Whatever the mechanism(s), it must cease to operate when the capsule reaches a certain thickness or age, because no further attachment of immunocytes occurs. In fact, this cessation of attachment is not abrupt, but seems to occur gradually. How this mechanism is turned off in other insects is unknown. In *B. germanica*, the completed capsule has an outer sheath, which, because it is composed of the host material, seems to render the capsule as a soft tissue, and no further immunoreaction among the GRs occurs. It must also act as a barrier and interrupt the cell-to-cell communication through the gap junctions. Because we found this sheath only when we allowed encapsulation to proceed at least until 10 days, it is likely that it was missed in the capsules of other insects that were not allowed to fully mature.

ACKNOWLEDGMENTS

This paper is the New Jersey Agricultural Experiment Station Publication No. D-08125-14-87, supported by state funds, U.S. Hatch funds, Korean Science and Engineering Foundation grant to SSH, and C. and J. Busch Award of Rutgers University to APG. Sung-Sik Han was on sabbatic leave from Kangwon National University, South Korea, during the completion of this work. We thank Roy Baerwald for his comments on septate junctions and Ann S. Chiang for his technical assistance in THC and DHC counts.

REFERENCES

- Gupta, A. P. (1985) The identity of the so-called crescent cell in the hemolymph of the cockroach, *Gromphadorhina portenosia* (Schaum) (Diptera: Blaberidae). *Cytologia*, **50**: 739-746.
- Gupta, A. P. (1986) Arthropod immunocytes: Identification, structure, functions and analogies to the functions of vertebrate B- and T-lymphocytes. In "Hemocytic and Humoral Immunity in Arthropods". Ed. by A. P. Gupta, John Wiley & Sons, New York, pp. 3-59.
- Gupta, A. P. (1986) Hemocytic and Humoral Immunity in Arthropods. John Wiley & Sons, New York.
- Neuwirth, M. (1973) The structure of the hemocytes of *Galleria mellonella* (Lepidoptera). *J. Morphol.*, **139**: 105-124.
- Schmit, A. R., Rowley, A. F. and Ratcliffe, N. A. (1977) The role of *Galleria mellonella* hemocytes in melanin formation. *J. Invertebr. Pathol.*, **29**: 232-234.
- Mercer, E. H. and Nicholas, W. L. (1967) The ultrastructure of the capsule of the larval stages of *Moniliformis dubius* (Acanthocephala) in the cockroach *Periplaneta americana*. *Parasitology*, **57**: 169-174.
- Peterson, L. G. (1968) Cellular immune responses of insects to foreign tissue implants. Ph. D. Thesis, University of Illinois, Urbana, Illinois.
- Baerwald, R. J. (1975) Inverted gap and other cell junctions in cockroach hemocyte capsule: A thin section and freeze-fracture study. *Tissue Cell*, **7**: 575-585.
- Lackie, A. M. (1979) Cellular recognition of foreignness in 2 insect species, the American cockroach and the desert locust. *Immunology*, **36**: 909-1007.
- Ennesser, C. A. and Nappi, A. J. (1984) Ultrastructural study of the encapsulation response of the American cockroach, *Periplaneta americana*. *J. Ultrastruct. Res.*, **87**: 31-45.
- Lackie, A. M., Tackle, G. B. and Tetley, L. (1985) Hemocytic encapsulation in the locust *Schistocerca gregaria* and the cockroach *Periplaneta americana*. *Cell Tissue Res.*, **240**: 343-351.
- Staehelin, L. A. (1982) Freeze-fracture and freeze-etch electron microscopy of chloroplast membranes. In "Methods in Chloroplast Molecular Biology". Ed. by M. Edelman, R. B. Hallick and N. H. Chua, Elsevier Biomedical Press, Amsterdam, New York, Oxford, pp. 821-833.
- Chiang, A. S., Gupta, A. P. and Han, S. S. (1988) Arthropod immune system. I. Comparative light and electron microscope account of immunocytes and other hemocytes of *Blattella germanica* (Diptera: Blattellidae). *J. Morphol.*, **198**: 257-267.
- Hazarika, L. K. and Gupta, A. P. (1987) Variation in hemocyte populations during various developmental stages of *Blattella germanica* (L.) (Diptera: Blattellidae). *Zool. Sci.*, **4**: 307-313.
- Gupta, A. P. (1979) Identification key for hemocyte types in hanging-drop preparation. In "Insect Hemocytes". Ed. by A. P. Gupta, Cambridge Univ. Press, Cambridge, pp. 527-529.
- Gupta, A. P. (1979) Hemocyte types: Their structure, synonymies, interrelationships, and taxonomic

- significance. In "Insect Hemocytes". Ed by A. P. Gupta, Cambridge Univ. Press, Cambridge, pp. 85-127.
- 17 Gupta, A. P. (1985) Cellular elements in the hemolymph. In "Comprehensive Insect Physiology, Biochemistry and Pharmacology, Vol. 3". Ed. by G. A. Kerkut and L. I. Gilbert, Pergamon Press, Oxford, pp. 401-451.
 - 18 Baerwald, R. J. (1979) Fine structure of hemocyte membranes and intercellular junctions formed during hemocyte encapsulation. In "Insect Hemocytes". Ed. by A. P. Gupta, Cambridge University Press, Cambridge, pp. 155-188.
 - 19 François, J. (1975) L'encapsulation hémocytaire expérimentale chez le lépidoptère *Thermobia domestica*. J. Insect Physiol., **21**: 1535-1546.
 - 20 Han, S. S. and Gupta, A. P. (1988) Arthropod immune system. V. Activated immunocytes (granulocytes) of the German cockroach, *Blattella germanica* (L.) (Dictyoptera: Blattellidae) show increased number of microtubules and nuclear pores during immune reaction to foreign tissue. Cell Struct. Funct., **13**: 333-343.
 - 21 Caveney, S. and Berdan, R. (1982) Selectivity in junctional coupling between cells of insect tissue. In "Insect Ultrastructure, Vol. 1". Ed. by R. C. King and H. Akai, Plenum Press, New York, pp. 434-465.
 - 22 Alberts, B., Bray, D., Lewis, J., Raff, M., Robert, K. and Watson, J. D. (1983) Molecular Biology of the Cell. Garland Publishing, New York.
 - 23 Brummer, F. and Hulser, D. F. (1982) Gap junctions in multicell spheroids. Zeiss Inf., **1**: 34-38.
 - 24 Flower, N. E. (1972) A new junctional structure in the epithelia of insects of the order Dictyoptera. J. Cell Sci., **10**: 683-691.
 - 25 Staehelin, L. A. (1974) Structure and function of intercellular junctions. Int. Rev. Cytol., **39**: 191-283.
 - 26 Wood, R. L. (1977) The cell junctions of *Hydra* as viewed by freeze-fracture replication. J. Ultrastruct. Res., **58**: 299-315.
 - 27 Wright, K. A. and Lee, D. L. (1984) Membrane specializations in a nematode revealed by freeze-fracture technique. Zeiss Inf., **3**: 35-39.
 - 28 Flower, N. E. (1971) Septate and gap junctions between the epithelial cells of an invertebrate, the Mollusc *Cominella maculosa*. J. Ultrastruct. Res., **37**: 259-268.
 - 29 Gilula, N. P. and Satir, P. (1971) Septate and gap junctions in molluscan gill epithelium. J. Cell Biol., **51**: 869-872.
 - 30 Peracchia, C. (1974) Excitable membrane ultrastructure. I. Freeze-fracture of crayfish axons. J. Cell Biol., **61**: 107-122.
 - 31 Shaw, S. R. and Stowe, S. (1982) Freeze-fracture evidence for gap junctions connecting the axon terminals of dipteran photoreceptors. J. Cell Sci., **53**: 115-141.
 - 32 St. Marie, R. L. and Carlson, S. D. (1982) Synaptic vesicle activity in stimulated and unstimulated photoreceptor axons in the housefly: A freeze-fracture study. J. Neurocytol., **11**: 747-761.
 - 33 Grimstone, A. V., Rotheram, S. and Salt, G. (1967) An electron microscope study of capsule formation by insect blood cell. J. Cell Sci., **2**: 281-292.
 - 34 Gupta, A. P. and Han, S. S. (1988) Arthropod immune system. III. Septate junctions in the hemocytic capsule of the German cockroach, *Blattella germanica* (L.) (Dictyoptera: Blattellidae). Tissue Cell, **20**: 629-634.
 - 35 Amirante, G. A. (1986) Cellular immune responses in crustaceans. In "Hemocytic and Humoral Immunity in Arthropods". Ed. by A. P. Gupta, John Wiley & Sons, New York, pp. 61-73.

Effects of Foodstuffs on Intestinal Length in Larvae of *Rhacophorus arboreus* (Anura: Rhacophoridae)

SHINRI HORIUCHI¹ and YUTAKA KOSHIDA

Department of Biology, College of General Education,
Osaka University, Toyonaka, Osaka 560, Japan

ABSTRACT—Correlation between foodstuffs and intestinal length was examined in larvae of *Rhacophorus arboreus* (Anura: Rhacophoridae). The larva, being heterophagous, has a tube-like intestine provided with neither epithelial outfoldings nor villi, and intestinal length is found to be a good morphological index of digestive and absorptive functions of the intestine. The results obtained were summarized as follows: The grown larva fed on boiled spinach had an intestine more than 1.5 times as long as that of a grown larva fed on scrambled eggs. Change of diet from the scrambled eggs to boiled spinach triggered intestinal lengthening in the egg-fed larvae, whose intestine had hardly elongated; and in 4 days after the change of diet, intestinal length became almost equal to that of the larvae fed on boiled spinach from the beginning. The intestinal length of the larvae was proportional to the number of intestinal epithelial cells, irrespective of their diets and developmental ages before the metamorphic climax. Incorporation of [³H]thymidine into DNA of intestinal epithelial cells was the highest in larvae 2 days after the change of diet, but the incorporation was low in larvae whose diet was not changed. These data suggested strongly that many intestinal epithelial cells entered the S-phase of the cell cycle after the change of diet. Labeled mitotic index of intestinal epithelial cells showed a peak at 12 hr after [³H]thymidine administration in the diet-changed larvae. The intestinal lengthening after the change of diet would be brought by approximately 50% of the intestinal epithelial cells having divided once and followed by recovery of their cell size.

INTRODUCTION

It has been often cited in textbooks [1-3] that in general the intestine of plant eaters is longer than that of flesh eaters from teleosts to mammals, although there are many exceptions. In fact, recently Iwata [4] reported that *Carassius auratus grandoculis*, a carnivorous teleost, had the shortest intestine when compared with two herbivorous species, *C. auratus cuvieri* and *Hypophthalmichthys molitrix*. Altig and Kelly [5] compared the length, diameter, and other characteristics of the intestine in anuran larvae among 13 species belonging to 11 genera, and ascertained that the larvae thought to be carnivorous had a shorter and less voluminous intestine than the larvae thought to be herbivorous. Plant food, particularly cellu-

lose, may be difficult to be digested and its products also difficult to be absorbed in vertebrates, so that intestinal lengthening, often accompanied by outfoldings and/or projections of intestinal lining, is believed, at least in part, to represent a functional adaptation to the problems of plant food digestion. However, we have few experimental findings of any correlation between feeding habits and intestinal area capable of absorption in vertebrates, except for experiments with anuran larvae. Oshima's preliminary experiment was cited in Ichikawa's textbook [6] as a personal communication showing that larvae of *Rana nigromaculata* fed on herbivorous diet had a longer intestine than the larvae fed on carnivorous one; and Janes [7] using *R. sylvatica* reported results similar to those of Oshima's experiment. In order to detect whether or not the area of intestinal epithelium actually correlates with the type of foodstuff ingested, a detailed re-examination should be carried out. The present paper deals

Accepted June 21, 1988

Received December 15, 1987

¹ To whom all correspondence should be addressed.

with the results obtained and conclusions drawn from this re-examination.

MATERIALS AND METHODS

Experimental animal

Based on our previous experiences, we used larvae of the Japanese green frog *Rhacophorus arboreus* as an adequate experimental animal because larvae of this frog, having a smoothly lined tube-like intestine, are heterophagous; and the larvae grow not only healthily but in synchronously during the development even under various laboratory conditions. Eggs of the frog are enveloped in a foamy substance and lie scattered in a mass numbering 400–500. Egg-masses hanging on twigs above marshes were collected at Kiyotaki hill near Kyoto in June during its breeding season, and the eggs were made to hatch out in a moist chamber in the laboratory. Under natural field conditions the larvae hatch out in the mass that has become semi-fluid in about one-third of its inner part, gather together in this semi-fluid environment, and then fall into the water by tearing through the lower end of the semi-fluid portion. However, in the laboratory we obtained the hatch-out larvae by stirring the mass gently in tap water.

We set up every series of experiments with the larvae obtained from one egg-mass that was laid by one female, although 2–3 males were usually involved with the spawning.

Feeding and diets

Feeding of the larvae was started at Iwasawa-Kawasaki stage 36 [8], which begins 4–5 days after hatching when the larvae first exhibit food-searching behavior. The change of diet from the carnivorous to the herbivorous was made at 11–25 days after the initiation of feeding, when the larvae had grown, at room temperature (20–30°C), to stage 38. About 100 young larvae were kept in a plastic aquarium with 4.5 liter of dechlorinated tap water; when they grew up to stage 35–36, the number was reduced to about 50 in order to eliminate the so-called “crowding effect” [9–10]. The tap water of each aquarium was made fresh once a day and the larvae were allowed to feed *ad*

libitum.

Frozen boiled spinach bought from a local market was thawed and chopped finely into pieces about 1–2 mm long for the herbivorous diet; and hens' whole eggs were scrambled in a pan without using any cooking oil for the carnivorous diet. Scrambled eggs containing cellulose were prepared by mixing cellulose powder (Type C 300 mesh, Toyo Roshi Co. Ltd., Tokyo) in the eggs before cooking, and cellulose contents were expressed as cellulose powder dry weight in per cent in egg (wet weight).

Morphological measurements, histological examination, and cell counting

Every experimental measurement was provided by 4–10 larvae chosen at random and the data measured were expressed by sample average with its standard deviation. The body length was calipered as the length from snout to vent. After the whole digestive tract was removed from the body cavity onto a piece of moistened filter paper, the tract was uncoiled and laid straight along a ruler by cutting the mesentery. The intestinal length from the esophagus orifice to the posterior end of rectum was measured with the ruler. The intestine of the larva was coiled into a double helix-like structure, which consisted of both descending and ascending coils with the turning point of coils lying midway between esophagus and rectum.

As soon as the measurement of intestinal length was completed, a 10 mm piece of intestine was cut out from 15 to 5 mm anterior to the turning point, which was easily distinguishable, irrespective of larval stage and feeding condition. The piece was fixed in Bouin's fluid modified by Lillie, embedded in paraplast, sectioned at a thickness of 5–8 μ m, and finally stained with Ehrlich's hematoxylin and eosin for histological examination.

The remainder of the intestine was used for determination of total number of epithelial cells. The determination procedures were as follows: The intestine was put into a tube with 4 ml of ice-chilled homogenizing solution which contained 10 mM ethylenediamine tetra-acetic acid and 1% citric acid. After a drop of octyl alcohol was added to prevent foaming during homogenization, the intestine was homogenized for 15–30 sec in a

Polytron (Kinematica G.m.b.H., Luzern) equipped with a 10 mm diameter crushing shaft. The homogenate was shaken for 2-3 sec by a thermomixer (Taiyo Mixer OT-1, Taiyo Bussan Co., Tokyo). A 0.5 ml aliquot of the homogenate was mixed with the same volume of staining solution (0.1% crystal violet in 0.1 M citric acid) and shaken well again by the thermomixer, after which a drop of the mixture was mounted on a Thoma's hemocytometer (Erma Optical Works Ltd., Tokyo) for cell counting. The nucleus of the epithelial cell, being the major one in the intestinal cell preparations, was easily distinguished by its elliptic shape from other nuclei, such as the elongated nucleus of smooth muscle cells, small and condensed nuclei of connective tissue cells, and the round flat nucleus of the red blood cells. Counting of epithelial cell number was carried out on 2 aliquots of the homogenate prepared from each of the larvae. The total number of epithelial cells in the whole intestine (A) was estimated by the following formula:

$$A = 4 \times 10^4 \times a \times b \times 1/(b-10)$$

where a is the average number of epithelial cells contained in 10^{-4} ml and b is the intestinal length expressed in mm. The term $1/(b-10)$ is included to compensate for the length of intestine (10 mm) removed for histological examination; and the factor 4×10^4 , to arrive at the number of epithelial cells in the total volume of homogenate (4 ml).

Tritiated thymidine administration, radioactivity measurement, and autoradiography

In order to elucidate intestinal cell proliferation, we carried out cell kinetics studies using [3 H]thymidine as a DNA precursor. After the larvae were anesthetized by immersion in a 0.05% aqueous solution of tricaine (ethyl m-aminobenzoate methanesulfonic acid), each of them was administered 1 μ l of physiological saline solution containing 0.5 μ Ci of [3 H]thymidine (sp. act. 10.9 Ci/mM, Radiochemical Centre, Amersham, Buckinghamshire) by intraperitoneal injection through tail muscles using a micro-syringe (Hamilton microliter syringe 710) equipped with a repeating dispenser (Hamilton Pb600-1, Hamilton Co., Reno, Nevada).

We removed intestines from the larvae adminis-

tered [methyl- 3 H]thymidine (abbreviated [3 H]Tdr hereafter) after the lapse of the desired time. The intestine removed was measured for its total length, and one piece 10 mm in length was extirpated from near the turning point for autoradiography, as was described above. The remaining intestine was used for determination of both epithelial cell number and [3 H]Tdr incorporation into DNA of the cell nucleus.

[3 H]Tdr incorporation was expressed as cpm of tritium per 10^6 epithelial cells, and the radioactivity was measured by the filter disk method as follows: A 100- μ l aliquot of the cell homogenate was dripped by a micropipet (Gilson Pipetman P-200) onto a filter disk (Whatman 3MM) 24 mm in diameter. The filter disks were air-dried, treated sequentially in a beaker with ice-chilled 10% and 5% TCA for 30 min each, washed at room temperature in absolute ethanol 2-3 times for about 20 min in total, and finally rinsed in ethyl ether for 5 min. After the ethyl ether had completely evaporated, the filter disk was placed in a vial with 2.5 ml of scintillation mixture (PCS: Amersham Japan, Tokyo), and the radioactivity was measured in a liquid scintillation counter (Beckman LS8000, Beckman Japan, Tokyo). Two filter disks were prepared for radioactivity measurement from each cell homogenate.

For autoradiography, we used the dipping method to determine labeled mitotic index of intestinal epithelial cells in larvae administered [3 H]Tdr. Paraplast sections of the intestine, 5 μ m thick, prepared as mentioned above, were deparaplasted, hydrated, and finally dipped into autoradiographic emulsion, Sakura NR-M2 (Konika, the former Konishiroku Photo Industry, Tokyo). Being exposed for 3 weeks below 5°C, the emulsion was developed with Kodak D19b developer. A diluted Ehrlich's hematoxylin or Mayer's carmalum staining solution was applied for cytological examination after photographic development.

RESULTS AND DISCUSSION

Larval development

Larvae of *Rhacophorus arboreus* obtained from one egg-mass were divided into two groups. The

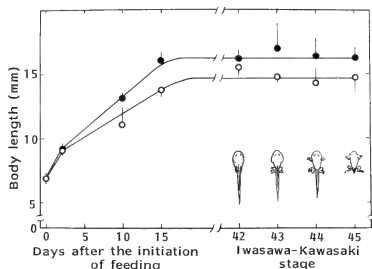


FIG. 1. Time courses of body lengthening in herbivorous (●) and carnivorous larvae (○). Bars show standard deviation.

larvae of one group were fed on the boiled spinach (herbivorous larvae, for short, hereafter); and those of the other group, the scrambled eggs (carnivorous larvae, hereafter). Figure 1 shows the change in body length with development in both herbivorous and carnivorous larvae. The trunk elongated in both larvae for about 2 weeks after the initiation of feeding, then hardly underwent further elongation. Both larvae grew similarly and metamorphosed into froglets in the laboratory, as would be expected in the field. It was convenient to show larval ages by days after hatching or after the initiation of feeding in the early larval phase. However, the expression by Iwasawa-Kawasaki stage [8] was convenient in the late larval phase, because the larvae became less syn-

chronized in their development after the stage 42 (metamorphic climax). From these preliminary surveys, we analyzed diet effects on the intestinal epithelium.

Intestine and diets

Figure 2 shows the change in intestinal length with development in both herbivorous and carnivorous larvae. Three phases were distinguished in the curves of Figure 2: the lengthening phase, in which the intestine elongated rapidly for about 2 weeks after the initiation of feeding; the plateau phase, in which the intestine practically ceased to elongate and which followed the lengthening phase and lasted for more than 2 weeks; and the shorten-

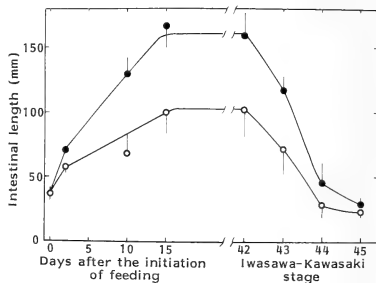


FIG. 2. Time course of intestinal lengthening in herbivorous (●) and carnivorous larvae (○). Bars show standard deviation.

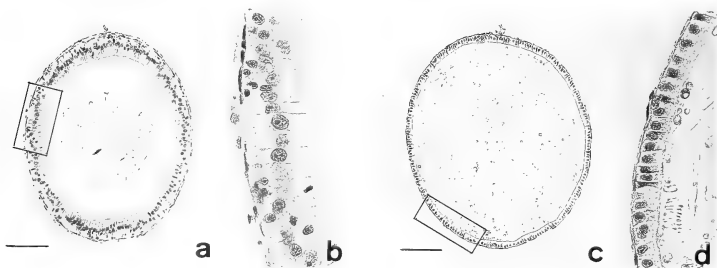


FIG. 3. Transverse-section of intestine. a: a carnivorous larva 20 days after the initiation of feeding. Scale bar represents 100 μ m. b: High-power view of the area outlined in a. c: a herbivorous larva 20 days after the initiation of feeding. Scale bar represents 100 μ m. d: High-power view of the area outlined in c.

ing phase, in which the intestine shortened and which began from the metamorphic climax. The herbivorous larvae had a longer intestine than the carnivorous larvae, and the average intestinal length of the former larvae reached a value more than 1.5 times greater as that of the latter larvae at the plateau phase.

As depicted in Figure 3, no significant difference in diameter of intestine was found between herbivorous and carnivorous larvae at the plateau phase. In both larvae the intestine was tube-like in the one cell-thick epithelium and having neither villi nor outfoldings of intestinal lining were observed. The epithelium was composed of columnar cells in carnivorous larvae (Fig. 3a and b), but cuboidal cells in herbivorous ones (Fig. 3c and d); although the reason for this difference of cell type was unsolved. A considerable amount of indigestible material remained in the feces of herbivorous larvae, while few undigested remnants were found in feces of carnivorous ones. We concluded that boiled spinach was more difficult to be digested than the scrambled eggs and that cellulose may be the main indigestible substance in the herbivorous diet.

As intestinal epithelium is the most responsible tissue for digestion and absorption of the food, the total number of epithelial cells in it may be regarded as an index of these functions. Figure 4 shows how the total epithelial cell number of intestine changed with development in both her-

bitorous and carnivorous larvae. These intestines were the same ones measured for Figure 2. The patterns of curves for herbivorous larvae depicted in Figures 2 and 4 were similar to each other.

As shown in Figure 5, in both herbivorous and carnivorous larvae, the ratio of epithelial cell number to length of intestine, increasing very slowly for several days after the initiation of feeding, became practically constant at least for about 2 weeks (constant phase), and then increased drastically after the metamorphic climax. Before the metamorphic climax, the intestine of the larvae was tube-like with a uniform diameter; and, accordingly, an increase in this ratio was regarded as a decrease in cell size. However, after outfoldings of epithelial lining began to develop, accompanied with other intestinal changes that occur during the transformation from larva to adult, an increase in this ratio could be regarded as a decrease in the cell size and/or an increase in the cell number. Thus, we carried out diet-change experiments with the larvae in this constant phase in which intestinal lengthening was ascribed to an increase in epithelial cell number.

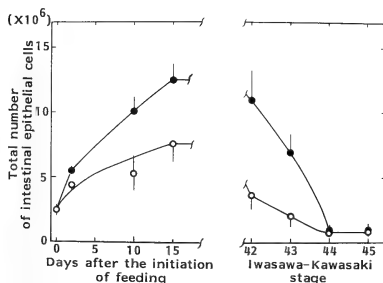


FIG. 4. Time courses of total number of intestinal epithelial cells in herbivorous (●) and carnivorous larvae (○). Bars show standard deviation.

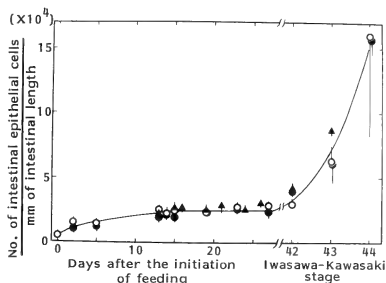


FIG. 5. Time courses of intestinal epithelial cell number per unit length of intestine in herbivorous (●), carnivorous (○) and diet-changed larvae (▲). Bars show standard deviation.

Intestinal lengthening by change of diet

The larvae obtained from one egg-mass were divided into three groups. Larvae of the first group were fed on the herbivorous diet; and larvae of the second group, on the carnivorous diet. But larvae

TABLE 1. comparison of intestinal length in larvae under various feeding conditions

Experimental schedules of feeding	Larva	Intestinal length (mm) at day 25
<p>The diagram shows a timeline from hatching to day 25. A break occurs between day 5 and day 15. At day 20, an arrow points up to the timeline, indicating a diet change from carnivorous to herbivorous. The timeline ends at day 25.</p>	Carnivorous larvae	58.5 ± 14.3
	Diet-changed larvae	75.8 ± 14.7
	Diet-changed larvae	91.0 ± 11.3
	Herbivorous larvae	93.8 ± 4.3

Arrows show change of diet from the carnivorous to the herbivorous.

of the third group were fed on the carnivorous diet for 12 days at least until they had grown to the constant phase shown in Figure 5, and then the diet was changed from the carnivorous to the herbivorous (diet-changed larvae, for short, hereafter). In Table 1, data are given of intestinal length in larvae obtained from a series of experiments. The intestine of diet-changed larvae began to elongate after the change of diet; and in 4 days, on the average, their intestinal length became almost equal to that of herbivorous larvae.

If cellulose, an indigestible substance in the diet, is responsible for the intestinal lengthening in herbivorous larvae, it would be expected that larvae fed on a carnivorous diet mixed with cellulose would have a longer intestine than the ordinary carnivorous larvae. Thus, we examined the effects of cellulose on intestinal lengthening. The larvae hatched out from one egg-mass were divided into four groups. The larvae of one group were fed on the ordinary carnivorous diet, i.e., scrambled eggs only; while the larvae of the other three groups were fed on scrambled eggs containing 5%, 10%, and 20% cellulose, respectively. Results shown in Figure 6 were as was to be expected. The larvae fed on the ordinary carnivorous diet had the shortest intestine; and the intestines were longer with the amount of cellulose in their diets, although the ratio was not directly proportional.

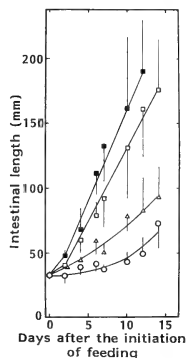


FIG. 6. Comparison of intestinal lengthening among the larvae fed on carnivorous diets containing 0% (○), 5% (△), 10% (□), or 20% (■) cellulose. Bars show standard deviation.

Epithelial cell proliferation triggered by change of diet

To elucidate intestinal lengthening brought about by the change of diet, [^3H]Tdr was administered to the larvae 1, 2, 3, 4, 5, and 10 days after change of diet from the carnivorous to the herbivorous, and also to both herbivorous and carnivorous larvae as controls. The amount of [^3H]Tdr incorporated into DNA of intestinal epithelial cells 1 hr after administration was the highest in the larvae 2 days after the change of diet (Fig. 7),

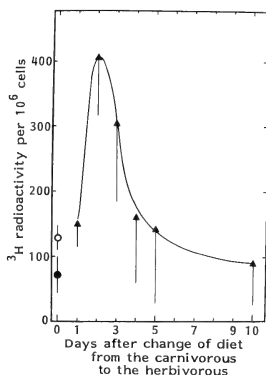


Fig. 7. ^3H Tdr incorporation into DNA of intestinal epithelial cells 1 hr after administration in herbivorous (\bullet), carnivorous (\circ), and diet-changed larvae (\blacktriangle). Bars show standard deviation.

apparently indicating that the number of cells entering the S-phase of the cell cycle was the highest in the intestine 2 days after change of diet from the carnivorous to the herbivorous.

Next, the labeled mitotic index was determined for the intestinal epithelial cells in larvae that had been administered ^3H Tdr at 48 hr after the change of diet. A peak of labeled mitotic index was seen at about 12 hr after ^3H Tdr administration, and no second peak was found for 36 hr following the first peak (Fig. 8).

As was shown in Table 1, the intestine of larvae 4 days after the change of diet from the carnivorous to the herbivorous became approximately 1.5 times as long as that of carnivorous larvae and practically equal to that of herbivorous larvae. This intestinal lengthening would be brought about if approximately 50% of the intestinal epithelial cells divided once and then regained their original size. As found in Figure 7 ^3H Tdr incorporation into the cells of carnivorous larvae was about one-third that of diet-changed larvae at their highest level of incorporation, that is, at day 2. This may mean that the labeling index of intestinal epithelial cells in the diet-changed larvae at day 2 was about 3 times as high as that of carnivorous

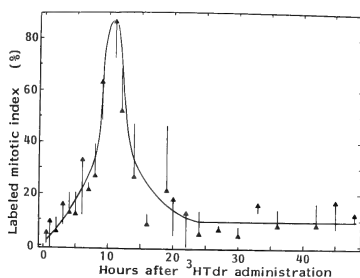


Fig. 8. Time course of labeled mitotic index of intestinal epithelial cells in the larvae injected with ^3H Tdr 48 hr after change of diet from the carnivorous to the herbivorous. Bars show standard deviation.

larvae. The labeling index of the latter larvae measured about 7%, so 20% may be reasonably regarded as the estimated value of the labeling index for the former larvae. If the total number of intestinal epithelial cells which multiplied during the 4 days after the change of diet is expressed as a term of integration along the time course curve of the labeling index, and if 20% is taken as its peak in the time course curve, the above-mentioned speculation is acceptable. That is, it can be reasonably understood that approximately 50% of the intestinal epithelial cells had divided once for the intestinal lengthening in the larvae after the change of diet. If indeed only the half of the epithelial cells were triggered to divide once by the change of diet, which cells of the entire population were destined to proliferate? These problems are still unsolved, but intestinal length of the herbivorous larva, that is, about 1.5 times the intestinal length of the carnivorous larva, may be the maximal length capable of being held within the abdominal cavity of the diet-changed larva.

ACKNOWLEDGMENTS

We are indebted to Dr. Toshiteru Morita, the present Professor of Biology of our College and the former Head of Laboratory of Biophysics, Aichi Cancer Center Research Institute, Nagoya, for his valuable suggestions and for the use of radioisotope facilities of his laboratory when he was at the Institute, and also to Ms. Kazumi

Tsutsui who assisted us in many ways throughout this work.

REFERENCES

- 1 Iijima, I. (1918) An Manual of Zoology (in Japanese). Dainippon Tosho Ltd., Tokyo.
- 2 Waterman, A. J. (1971) Chordate Structure and Function. The Macmillan Co., New York.
- 3 Romer, A. S. and Parsons, T. S. (1977) The Vertebrate Body. 5th ed. W. B. Saunders Co., Philadelphia/London.
- 4 Iwata, K. (1977) Morphological and physiological studies on the phytoplankton feeders of cyprinids. II—Developmental changes of assimilation efficiency in terms of carbon, estimated by using ^{14}C -labeled green algae in *Carassius auratus cuvieri*, *Hypophthalmichthys molitrix* and *C. auratus grandoculis* (in Japanese with English abstract). Jap. J. Limnol., **38**: 19–32.
- 5 Altig, R. and Kelly, J. P. (1974) Indices of feeding in anuran tadpoles as indicated by gut characteristics. Herpetologica, **30**: 200–203.
- 6 Ichikawa, M. (1939) Experimental Embryology, vol. 2, (in Japanese), Kobundo Ltd., Tokyo.
- 7 Janes, R. G. (1939) Studies on the amphibian digestive system. IV. The effect of diet on the small intestine of *Rana sylvatica*. Copeia, **1939**: 134–140.
- 8 Iwasawa, H. and Kawasaki, N. (1979) Normal stages of development of the Japanese green frog *Rhacophorus arboreus* (Okada et Kawano) (in Japanese with English abstract). Jpn. J. Herpetol., **8**: 22–35.
- 9 Rose, S. M. (1960) Feedback mechanism of growth control in tadpoles. Ecology, **41**: 188–199.
- 10 Gromko, M. H., Mason, F. S. and Smith-Gill, S. J. (1973) Analysis of the crowding effect in *Rana pipiens* tadpoles. J. Exp. Zool., **186**: 63–72.
- 11 Sokol, A. (1984) Plasticity in the fine timing of metamorphosis in tadpoles of the Hylid frog, *Litorina ewingi*. Copeia, **1984**: 868–873.

Effect of Zinc Ion on Formation of the Fertilization Membrane in Sea Urchin Eggs

SHOGO NAKAMURA, CHIKA OHMI and MANABU K. KOJIMA

*Department of Biology, Faculty of Science,
Toyama University, Toyama 930, Japan*

ABSTRACT—The effect of Zn^{2+} on the formation of the fertilization membrane was observed in eggs of the sea urchin, *Anthocidaris crassispina*. When the eggs were transferred into sea water containing more than $5 \mu M Zn^{2+}$ within 10 sec after insemination, formation of the fertilization membrane was inhibited. This inhibition was irreversible. Although the time of the first cleavage was delayed in a dose-dependent fashion, cleavage occurred normally in the presence of up to $1 mM Zn^{2+}$. Electron microscopic examinations revealed that the exocytosis of cortical granules progressed. However, the elevation and the hardening of the vitelline layer were blocked by more $5 \mu M Zn^{2+}$.

INTRODUCTION

When sea urchin eggs are fertilized or artificially activated, cortical granules, which are located beneath the plasma membrane, are exocytotically discharged and cortical granule components are released into the perivitelline space. Some of the components hydrate and elevate the fertilization membrane, while others are incorporated into the fertilization membrane to make it thick and tough. Thus the fertilization membrane is formed around the eggs [see references for review 1, 6].

It is well known that Zn^{2+} inhibits the formation of the fertilization membrane [2, 4, 7]. However, the mechanism of the inhibition by Zn^{2+} is unknown. Moreover, not much is known about the mechanism of the fertilization membrane formation itself. We consider that clarifying the inhibitory mechanism by Zn^{2+} may provide information concerning the mechanism of formation of the fertilization membrane. As our first step, we observed in detail the effect of Zn^{2+} on formation of the fertilization membrane. The results suggest that Zn^{2+} inhibits the elevation and hardening of the fertilization membrane occurring after the cortical reaction in the process of the fertilization membrane formation.

MATERIALS AND METHODS

Gametes from the sea urchin, *Anthocidaris crassispina*, were collected by intracoelomic stimulation with 0.5 M KCl. Sperm was kept 'dry' in a refrigerator until use; eggs were spawned into filtered sea water, and washed three times by sedimentation. Experiments were done at 25–29°C.

Small amounts of Zn^{2+} from a stock solution (100 mM $ZnCl_2$) in deionized water were added to the experimental sea water. The eggs were transferred to the sea water containing Zn^{2+} 10–60 sec after insemination.

Formation of the fertilization membrane was observed with an inverted microscope (Olympus CK-2). Micrographs were taken on Fuji Neopan F film.

Eggs for electron microscopy were fixed in 2% glutaraldehyde in 80% sea water (pH 7.0), and post-fixed in 1% OsO_4 in 50 mM sodium cacodylate (pH 7.2). After dehydration through an ethanol series, they were infiltrated and embedded in epoxy resin (Epok 812, Oken Shoji Co., Ltd., Tokyo). Ultrathin sections were stained with uranyl acetate and Reynold's lead citrate and examined with a JEOL 100C electron microscope operated at 80 kV.

RESULTS AND DISCUSSION

The eggs of *Anthodiaris crassispina* were treated with various concentrations of Zn^{2+} from 10, 30 and 60 sec after insemination. Figure 1 shows the

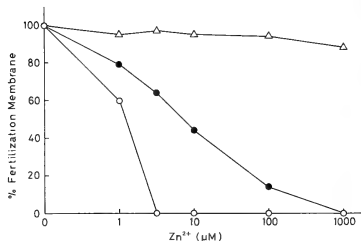


Fig. 1. Effect of Zn^{2+} on formation of the fertilization membrane in *Anthodiaris crassispina* eggs. At 10 sec (○), 30 sec (●), or 60 sec (△) after insemination, the eggs were transferred into sea water containing various concentrations of Zn^{2+} .

effects of increasing Zn^{2+} -concentration on formation of the fertilization membrane. Although the rate of inhibition varied from experiment to experiment, formation of the fertilization membrane was completely prevented when more than 5 μM Zn^{2+} was applied within 10 sec after insemination (Figs. 1 and 2b). This inhibition was irreversible. When eggs without a fertilization membrane in 5 μM Zn^{2+} -containing sea water were removed and placed in fresh sea water, they could not form a fertilization membrane. The surfaces of the eggs in Zn^{2+} -containing sea water were rougher than those of unfertilized eggs in normal sea water (Fig. 2b, c).

To confirm that fertilization occurred in the eggs without a fertilization membrane in Zn^{2+} -containing sea water, we measured percentage of cleavage in those eggs (Fig. 3). The time of the first cleavage was delayed by Zn^{2+} in a dose-dependent manner, but cleavage occurred normal-

dependent manner, but cleavage occurred normally in the presence of up to 1 mM Zn^{2+} . For

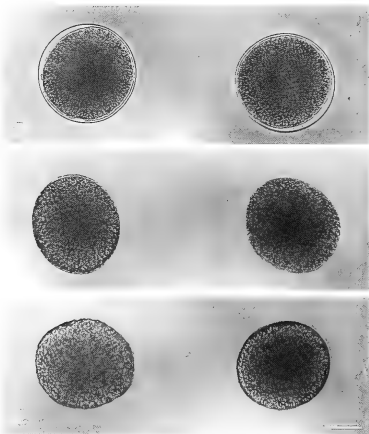


Fig. 2. Formation of the fertilization membrane in eggs treated or untreated with Zn^{2+} . (a) Control, (b) 5 μM , and (c) 1 mM Zn^{2+} . Bar, 50 μm .

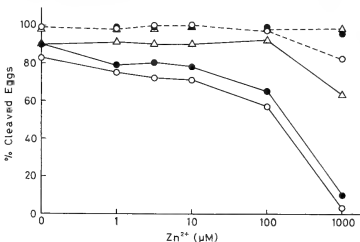
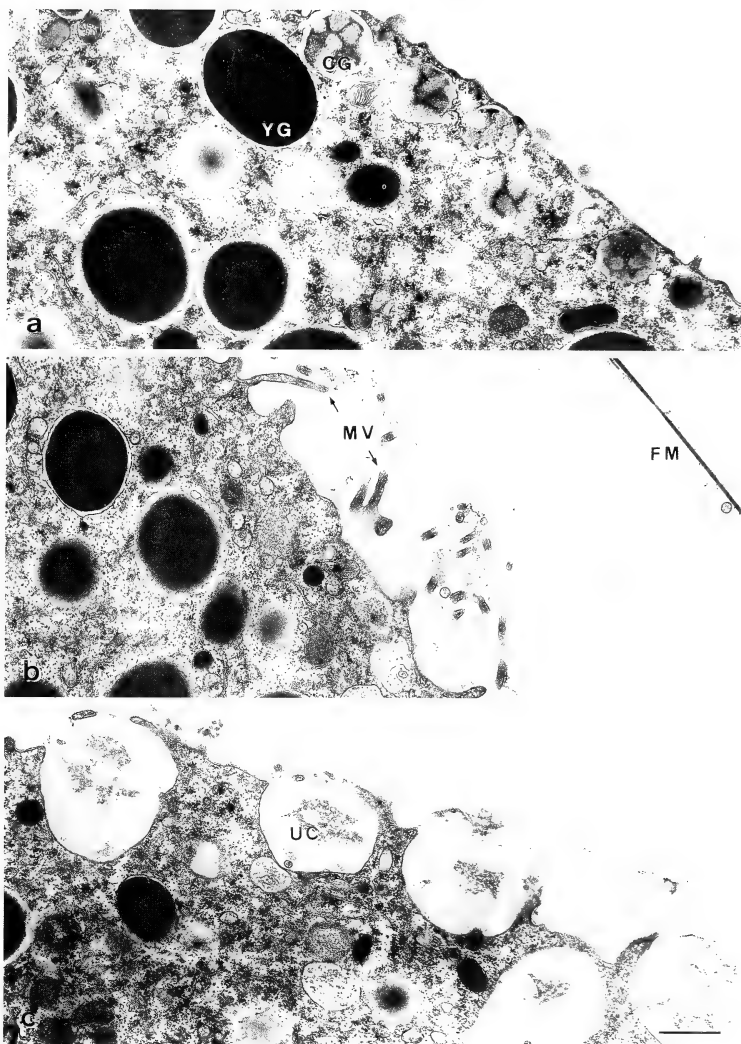


Fig. 3. Percentage of cleaved eggs in the presence of various concentrations of Zn^{2+} . At 10 sec (○), 30 sec (●), or 60 sec (△) after insemination, the eggs were transferred into sea water containing Zn^{2+} . The percentage was measured at 55 min (solid line) and 65 min (dotted line) after insemination.

Fig. 4. Electron micrographs of sea urchin eggs. The eggs were fixed at 10 min after insemination. An unfertilized egg (a), a fertilized egg (b), and a fertilized egg treated with 5 μM Zn^{2+} from 10 sec after insemination (c). CG, cortical granule; FM, fertilization membrane; MV, microvillus; YG, yolk granule; UC, undispersed contents of cortical granule. Bar, 1 μm .



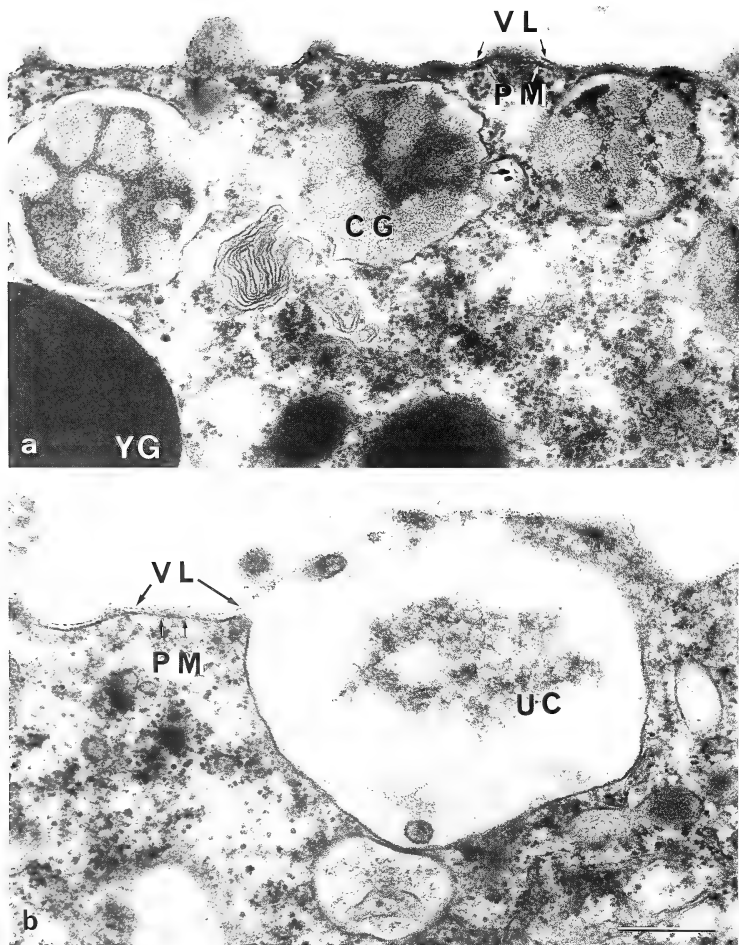


FIG. 5. High-magnification views of portions of the eggs shown in Fig. 4 (a) and (c). (a) Unfertilized egg, and (b) Z^{2+} -treated egg. CG, cortical granule; VL, vitelline layer; PM, plasma membrane; YG, yolk granule; UC, undispersed contents of cortical granule. Bar, $0.5 \mu\text{m}$.

ly in the presence of up to 1 mM Zn^{2+} . For example, 3% of eggs transferred into 1 mM Zn^{2+} -containing sea water within 10 sec after insemination cleaved by 55 min after insemination, but the rate of cleavage had recovered to 82% by 65 min after insemination. This result shows that fertilization occurred normally in Zn^{2+} -treated eggs.

Next, we examined by electron microscopy whether the cortical granules react normally in eggs treated with Zn^{2+} (Figs. 4 and 5). Exocytosis of cortical granules occurred in Zn^{2+} -containing sea water (Figs. 4c and 5b), i.e., the membrane of cortical granules fused with the plasma membrane of the egg and the contents were released out of the egg. However, dispersion of the contents was incomplete, and part of them were undispersed by 10 min after insemination. Moreover, detachment of the vitelline layer from the plasma membrane and hardening of the vitelline layer were blocked by more than 5 μ M Zn^{2+} . This resulted in rupture of the vitelline layer by the pressure from influx of water into the perivitelline space or swelling of the cortical granule components. The undispersed contents may relate to the detachment and hardening of the vitelline layer.

In normal formation of the fertilization membrane, the following processes occur [1, 6]. (a) Intracellular concentration of free Ca^{2+} is increased by fertilization or artificial activation. (b) This Ca^{2+} triggers the cortical granule exocytosis. (c) Proteases in the cortical granules break the attachment between the vitelline layer and the plasma membrane of the eggs. (d) The vitelline layer is elevated by hydration and/or osmotic effects resulting from the secretion of cortical granule contents. (e) The vitelline layer is hardened through cross-linkage and structuralization with cortical granule-derived proteins, such as ovoperoxidase [1, 6] and proteolisin [8]. The results we obtained in this study suggest that Zn^{2+} inhibits steps (c), (d) and (e) in the process of formation of the fertilization membrane.

Zn^{2+} is a potent animalizing agent in sea urchin embryos. However, we do not know how animalization is induced by Zn^{2+} . Lallier [3] suggested that when Zn^{2+} binds to proteins, their structure and biochemical properties may become altered, so that abnormal development occurs. In fertiliza-

tion membrane formation, Zn^{2+} may exert the same effect on proteins. We are now searching Zn^{2+} -binding protein in the cortical granule components of unfertilized eggs. In addition, Zn^{2+} has an affinity for -SH groups, and action of Zn^{2+} on the enzymes whose activity depends on -SH groups has also been suggested [5]. It should be noted that -SH groups may play an important role in the elevation and the hardening of the vitelline layer.

ACKNOWLEDGMENTS

We are grateful to Dr. K. Aketa (Hokkaido University) for his critical reading of this manuscript. We also thank Drs. R. Kamiya, S. Higashi-Fujime and S. Asakura (Nagoya University) for their help in electron microscopy.

REFERENCES

1. Kay, E. S. and Shapiro, B. M. (1985) The formation of the fertilization membrane of the sea urchin egg. In "Biology of Fertilization, Vol. 3". Ed. by C. B. Metz, and A. Monroy, Academic Press, New York, pp. 45-80.
2. Kobayashi, N. (1971) Fertilized sea urchin eggs as an indicator material for marine pollution bioassay, preliminary experiments. Publ. Seto Mar. Biol. Lab., **18**: 379-406.
3. Lallier, R. (1975) Animalization and vegetalization. In "The Sea Urchin Embryo: Biochemistry and Morphogenesis." Ed. by G. Cizhak, Springer-Verlag/Berlin/Heidelberg/New York, pp. 473-509.
4. Murakami, H., Hayakawa, M., Fujii, T., Hara, T., Itami, Y., Kishida, A. and Nishida, I. (1976) The effects of heavy metals on developing sea urchin eggs. Okayama Igakkai Zasshi, **88**: 39-50. (in Japanese)
5. Rulon, O. (1955) Developmental modifications in the sand dollar caused by zinc chloride and prevented by glutathione. Biol. Bull., **109**: 316-327.
6. Schuel, H. (1985) Functions of egg cortical granules. In "Biology of Fertilization, Vol. 3". Ed. by C. B. Metz, and A. Monroy, Academic Press, New York, pp. 1-43.
7. Sugiyama, M. (1949) Studies on the artificial parthenogenesis of the sea urchin eggs. VIII. Effect of heavy metal ions on membrane formation. Zool. Mag. (Tokyo), **58**: 137-138. (in Japanese)
8. Weidman, P. J., Kay, E. S. and Shapiro, B. M. (1985) Assembly of the sea urchin fertilization membrane: Isolation of proteolisin, a calcium-dependent ovoperoxidase binding protein. J. Cell Biol., **100**: 938-946.



Molecular- and Immuno-histochemical Study on Expressions of Vasopressin and Oxytocin Genes Following Water Deprivation

SUSUMU HYODO¹, MORIYUKI SATO² and AKIHISA URANO¹

Department of Regulation Biology, Faculty of Science, Saitama University,
Urawa, Saitama 338, and ²Tokyo Research Laboratories,
Kyowa Hakko Kogyo Co., Machida, Tokyo 194, Japan

ABSTRACT—We investigated the effects of 1 to 7 day water deprivation on expressions of vasopressin (AVP) and oxytocin (OXT) genes in neurosecretory neurons of the supraoptic (SON) and the paraventricular (PVN) nuclei in rats with the oligonucleotide-mRNA *in situ* hybridization (ISH) and the immunohistochemical avidin-biotin-peroxidase complex methods. Autoradiographic hybridization signals that indicate the localization of AVP mRNA were significantly increased in both nuclei after 4 day water deprivation. The water deprivation induced a rapid and marked increase in signals for OXT mRNA especially in the SON. Meanwhile, immunoreactivity of AVP neurons in the mirror image sections of those used for ISH was promptly decreased in both the SON and the PVN after day 1 of the treatment. Stainability of immunoreactive OXT neurons in the PVN was also reduced but after day 4, while the number of stained OXT neurons in the SON was decreased after day 4. Significant hypertrophy was first found in both AVP and OXT neurons in the PVN after day 2 and then in the SON after day 4. The present results thus indicate that both supraoptic and paraventricular AVP neurons are responsible for adapting to water deprivation, and that OXT neurons, especially supraoptic ones, may have some physiological role in the early phase of response to water deprivation. Paraventricular AVP neurons may be more sensitive to water deprivation than to sodium loading by which the elevation of AVP mRNA level in the PVN was not so conspicuous as that in the SON in our previous study.

INTRODUCTION

Arginine vasopressin (AVP) and oxytocin (OXT) are mammalian neurohypophysial hormones synthesized in the hypothalamic magnocellular neurosecretory neurons. AVP has important roles in regulation of plasma osmolality and blood pressure, although any roles of OXT in homeostatic regulation are not clear. In the previous study, we examined effects of sodium loading on AVP and OXT gene expressions with cellular and immunocytochemical changes of neurosecretory neurons in the supraoptic (SON) and the paraventricular (PVN) nuclei by applying the oligonucleotide-mRNA *in situ* hybridization (ISH) and the immunohistochemical methods [1]. After sodium loading, the AVP mRNA level was

markedly increased in supraoptic AVP neurons, while the increase in the AVP mRNA level in the PVN was much less than that in the SON. Hypertrophy of AVP neurons was also marked in the SON [1]. On the other hand, it is well known that neurosecretory neurons are responsive not only to sodium loading but also to water deprivation. Although there is no detailed analysis of the effects of water deprivation on expressions of AVP and OXT genes, the AVP mRNA levels in both the SON and the PVN were actually increased after 4 day water deprivation [2, 3]. These results suggest that responses of supraoptic and paraventricular neurosecretory neurons to water deprivation differ from those to sodium loading mentioned above.

The OXT mRNA level was increased rapidly and conspicuously in both the SON and the PVN after sodium loading [1]. OXT release was also stimulated after sodium loading [4, 5]. In addition, water deprivation elevated plasma OXT concentrations [6]. The OXT content in the neurohy-

Accepted May 27, 1988

Received April 5, 1988

¹ Present address: Ocean Research Institute, University of Tokyo, Nakano, Tokyo 164, Japan.

pophysis was decreased not only by sodium loading but also by water deprivation [7]. These results indicate that OXT neurons are also responsive to water deprivation other than sodium loading. However, changes in the OXT mRNA level after water deprivation have not been investigated yet.

In the present study, effects of water deprivation on the levels of AVP and OXT mRNAs in magnocellular neurons of the rat hypothalamus were examined by the ISH method using synthetic oligonucleotide probes following the time course for 1 to 7 days. Mirror image sections were immunohistochemically stained, and stainability and sizes of single AVP and OXT immunoreactive (ir) neurons were determined for better understanding of synthetic activity. Present results were compared with those of the previous sodium loading study [1]. Preliminary results appeared elsewhere [8].

MATERIALS AND METHODS

Animals

Male Wistar-Imamichi rats (Imamichi Institute for Animal Reproduction, 140–160 g) were housed in individual cages with 14 L:10 D light schedule. Animals were allowed free access to tap water and standard laboratory chow (Charles River) for at least 5 days prior to the start of the treatment. They were divided into 5 experimental groups, each of them included 7 rats, and were deprived of water for 0, 1, 2, 4 and 7 days prior to sacrifice. Urine samples were collected daily, their volumes were measured, and they were kept at -20°C until measurements of osmolalities and Na^{+} concentrations. The animals were killed by decapitation between 10:00 to 12:00 to avoid possible circadian fluctuations in AVP and OXT gene expressions [9]. Their hypothalami and pituitaries were immediately removed and were immersed in a fixative solution containing 2% paraformaldehyde, 1% glutaraldehyde and 1% picric acid in 0.05 M phosphate buffer (pH 7.3). At the same time, blood was collected and centrifuged. Plasma samples were stored at -20°C . Plasma and urine Na^{+} concentrations were measured later with an atomic absorption spectrometer (Hitachi 180–50). Their osmolality were measured with a vapor

pressure osmometer (Wescor 5500).

In situ hybridization and quantitation of autoradiographic signals

The individual tissues were paraffin-sectioned, divided into several groups, and were processed for *in situ* hybridization and immunohistochemistry. The precise procedures for tissue preparation and ISH were described previously [10]. Three types of 22mer synthetic deoxyoligonucleotide probes, complementary to the loci of rat mRNAs encoding AVP (2–9), AVP-neurophysin (NP) (1–8) and OXT-NP (1–8), were used in this study. A mixture of the AVP and AVP-NP probes was used as a mixed probe for ISH study of AVP mRNA, since the mixed probe could markedly improve hybridization sensitivity [10]. Thus, we tried to detect changes in AVP mRNA, if occur, in parvocellular AVP neurons in the suprachiasmatic nucleus (SCN) and the parvocellular part of the PVN. The precise procedure for semiquantitative expression of hybridization signals was described previously [1]. In brief, the numbers of autoradiographic silver grains in $100\text{ }\mu\text{m} \times 100\text{ }\mu\text{m}$ squares settled in each of the SON and the PVN were counted. Then the numbers of grains in the areas adjacent to the SON and the PVN, that is, the background levels, were counted, and were subtracted from the corresponding values in the SON and the PVN. Thereafter, the single-cellular numbers of grains were calculated by dividing the specific numbers of silver grains by the numbers of immunoreactive neurons within the $100\text{ }\mu\text{m} \times 100\text{ }\mu\text{m}$ squares.

Immunohistochemistry

The mirror image sections to those used for grain counting were immunohistochemically stained by the avidin-biotin-peroxidase complex (ABC) method, the detailed procedure of which was described previously [11]. Specificity tests of immunohistochemistry were also described previously [2, 10]. In this study, primary antisera were used as follows: rabbit anti-AVP (UCB-Bioproducts) was diluted 1:32000 with phosphate buffered saline containing 0.5% bovine serum albumin (PBS-BSA, pH 7.6) and rabbit anti-OXT (a gift from Professor S. Kawashima, Hiroshima

University) was diluted 1:20000 with PBS-BSA. These values for dilution of the antisera, with which tissue sections from normal rats were

stained half-maximally, were determined by serial dilution experiments [1].

Intensity of immunohistochemical stainability in

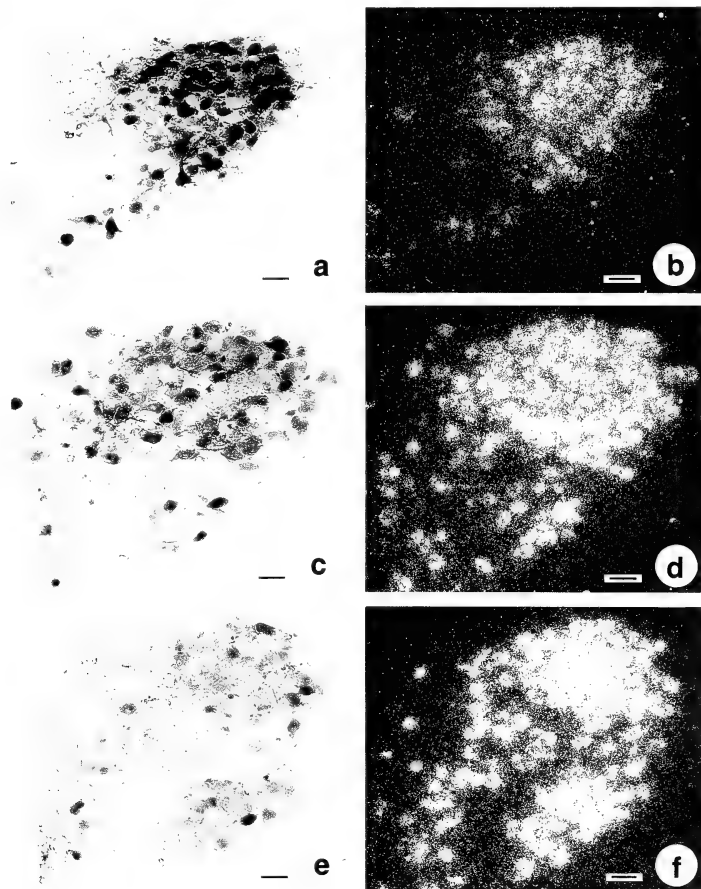


FIG. 1. AVP immunoreactive (ir) neurons and hybridization signals for the AVP mRNA in the PVN of normal (a, b), 4-day (c, d) and 7-day (e, f) water deprived rats in mirror image sections. Note that the density of silver grains over the PVN of the water deprived rats (d, f) is higher than that in the control rat (b). On the contrary, stainability of ir-AVP neurons in the water deprived rats (c, e) is reduced from that in the control rat (a). Scale bar, 50 μ m. Dark-field photomicrographs for ISH.

each magnocellular neuron was scored according to the following criteria: not stained, weakly stained, medially stained and heavily stained, by consulting to the arbitrarily selected standard sections. Immunoreactivity in each of the SON and the PVN was shown by the percentage of the number of ir-neurons to that of total magnocellular neurons, and the percentages of weakly, medially and heavily stained neurons in either ir-AVP or ir-OXT neurons. In addition, after depicting the outline of individual ir-neurons with a camera lucida, their cellular areas were determined with a tablet digitizer-microcomputer system.

RESULTS

Autoradiographic signals of the mixed AVP

probe and the OXT-NP probe were densely localized over the magnocellular neurons in the SON, the PVN and several accessory magnocellular nuclei, as was previously described [10]. The localization of hybridization signals was consistent with the immunohistochemical distribution of corresponding neurohypophysial hormones. The ventral region of the SON and the dorsolateral region of the posterior magnocellular PVN were predominantly composed of ir-AVP neurons, and the mixed AVP probe was localized in these regions (Fig. 1). While, the dorsal region of the SON and the ventromedial region of the posterior magnocellular PVN were mainly ir-OXT neurons, coinciding well with the localization of the OXT-NP probe. Hybridization signals in the SCN were only slightly above the background, and were not

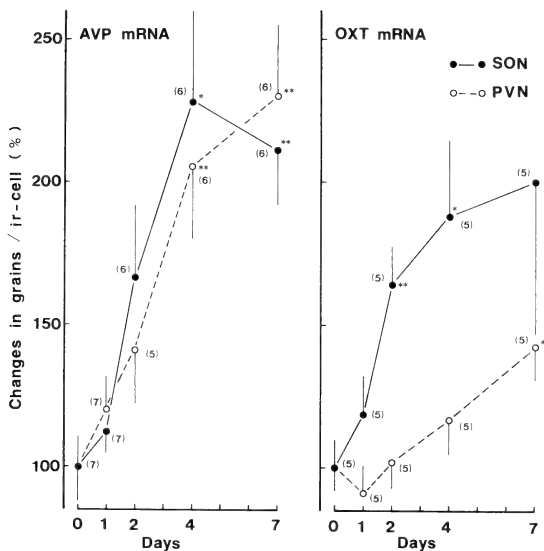


Fig. 2. Effects of water deprivation on the AVP and OXT mRNA levels in the SON and the PVN. The mRNA levels are expressed relatively as percent changes compared to the level of day 0. The numbers of silver grains/ir-cell on day 0 are: AVP mRNA in the SON, 45.8 ± 7.2 ; AVP mRNA in the PVN, 95.7 ± 10.8 ; OXT mRNA in the SON, 15.9 ± 1.6 ; OXT mRNA in the PVN, 42.7 ± 3.7 . Each point represents the mean \pm S.E.. The number of animals is given in parentheses. *, $p < 0.05$; **, $p < 0.01$; by the t-test compared to day 0.

noticeable in the parvocellular part of the PVN.

AVP neurons

The density of autoradiographic signals for the AVP mRNA was markedly increased in both the SON and the PVN by the water deprivation (Figs. 1 and 2). The increase became statistically significant after day 4 of the treatment.

The percentage of heavily stained neurons in ir-AVP ones was markedly decreased in the PVN after day 1 and in the SON at day 1 and after day 4 (Figs. 1 and 3). Medially stained neurons were somewhat decreased, and weakly stained neurons were increased in the PVN, while medially stained neurons were increased in the SON by day 7 (Fig. 3). Significant hypertrophy of ir-AVP neurons was observed in the PVN after day 2 and in the SON after day 4. The hypertrophy of paraventricular neurons was more conspicuous than that of supraoptic neurons (Fig. 4).

The density of silver grains in the SCN was not changed noticeably by the water deprivation.

OXT neurons

The density of hybridization signals for the OXT mRNA was rapidly increased and attained to a submaximal level in the SON on day 2 of water deprivation (Fig. 2). On the other hand, the increase in the hybridization signals in the PVN was much smaller than that in the SON and was significant only by day 7.

The percentage of the number of ir-OXT neurons to total magnocellular neurons in the SON was decreased after day 4, while medially stained neurons were increased after day 4 (Fig. 5). The percentage of heavily stained neurons was decreased in the PVN after day 4 (Fig. 5). Significant hypertrophy of ir-OXT neurons was observed in the PVN after day 2 and in the SON after day 4 (Fig. 4).

Neurohypophysis

Although immunoreactivity of the neurohypophysis was not analyzed quantitatively, it

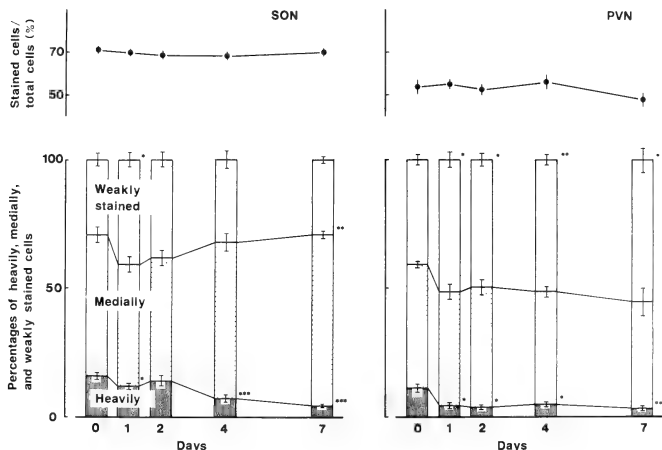


Fig. 3. Effects of water deprivation on the percentages of immunoreactive (ir) AVP neurons to total magnocellular neurons, and the percentages of heavily stained, medially stained and weakly stained AVP neurons per total ir-AVP neurons in the SON and the PVN. Each point represents the mean \pm S.E. ($n=7$). *, $p<0.05$; **, $p<0.01$; ***, $p<0.001$; by the t-test compared to day 0.

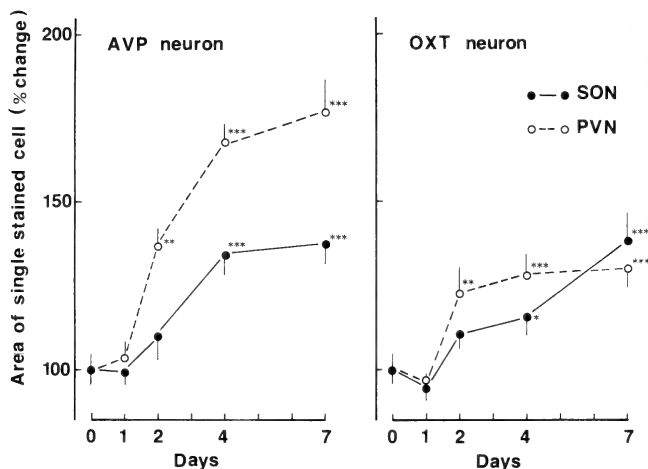


Fig. 4. Effects of water deprivation on sizes of the AVP and OXT immunoreactive neurons in the SON and the PVN. The values of cell areas ($\times 10^{-4} \text{mm}^2$) on day 0 are: AVP neurons in the SON, 3.16 ± 0.14 ; AVP neurons in the PVN, 3.25 ± 0.16 ; OXT neurons in the SON, 3.00 ± 0.14 ; OXT neurons in the PVN, 3.04 ± 0.13 . Each point represents the mean \pm S.E. ($n=7$). *, $p<0.05$; **, $p<0.01$; ***, $p<0.001$; by the t-test compared to day 0.

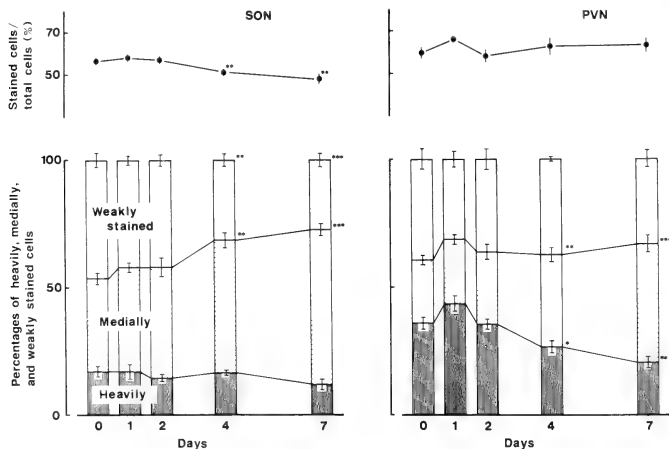


Fig. 5. Effects of water deprivation on the percentages of immunoreactive (ir) OXT neurons to total magnocellular neurons, and the percentages of heavily stained, medially stained and weakly stained OXT neurons per total ir-OXT neurons in the SON and the PVN. Each point represents the mean \pm S.E. ($n=7$). *, $p<0.05$; **, $p<0.01$; ***, $p<0.001$; by the t-test compared to day 0.

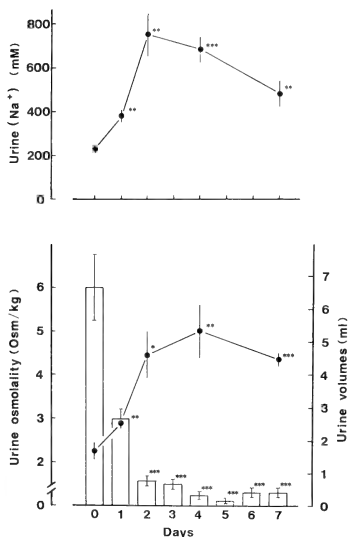


Fig. 6. Changes in urine osmolality, urine [Na⁺] and urine volume (open bars) by water deprivation. Each point represents the mean \pm S.E. (n=7). *, p < 0.05; **, p < 0.01; ***, p < 0.001; by the t-test compared to day 0.

appeared that AVP immunoreactivity was markedly decreased after 4 day water deprivation, indicating depletion of a stored pool of AVP.

Changes in plasma and urine by water deprivation

The urine volumes were drastically decreased by the water deprivation (Fig. 6). The plasma osmolality and the plasma Na⁺ concentration were gradually increased (Fig. 7). The increases in plasma osmolality and Na⁺ concentration after the water deprivation were less conspicuous compared with those after sodium loading [1]. On the contrary, the urine osmolality and the urine Na⁺ concentration were drastically increased and attained to maximal levels within 2 days after the onset of the water deprivation (Fig. 6). These facts indicate that the water deprived animals were exposed to severe hypovolemic stimulation, as was

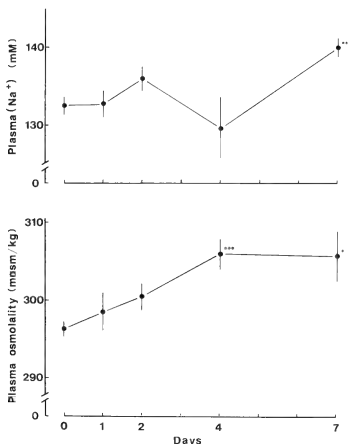


Fig. 7. Changes in plasma osmolality and plasma [Na⁺] by water deprivation. Each point represents the mean \pm S.E. (n=7). *, p < 0.05; **, p < 0.01; *** p < 0.001; by the t-test compared to day 0.

reported by Elkinton and Taffel [12], and that the observed cellular and molecular changes are partly induced by hypovolemic stimulation, although the involvement of osmotic stimulation cannot be excluded.

DISCUSSION

The present study showed that the AVP and OXT mRNA levels in magnocellular neurons in the SON and the PVN were elevated by the water deprivation, indicating that the water deprivation stimulated transcription of the genes encoding neurohypophysial hormones. Since the water deprivation simultaneously induced significant hypertrophy of both AVP and OXT neurons, translation rates of both AVP and OXT mRNAs to AVP and OXT precursors may be also increased by water deprivation. This possibility is supported by several facts on neurosecretory cells that a few day water deprivation elicited an increase in amino acid incorporation [13], and increases in nuclear and nucleolar diameters and dilation of endoplas-

mic reticulum [14]. Nevertheless, drastic reduction in stainability of ir-AVP neurons was observed in both the SON and the PVN, suggesting a rapid transport of newly synthesized AVP to the neurohypophysis where AVP may be instantaneously liberated. Transportation and releases of OXT may be lesser than those of AVP, since comparable reduction in OXT stainability was not observed in ir-OXT neurons and the neurohypophysis.

The conspicuous increase in the AVP mRNA level was observed in both the SON and the PVN after the water deprivation. In contrast, the increase in the AVP mRNA level in the PVN was gradual and much less than that in the SON after the sodium loading [1]. Similarly, a significant increase in incorporation of methionine into peptides was observed in both the SON and the PVN after water deprivation [13], while a significant increase in incorporation of cytidine into RNA and that of tyrosine into peptides in response to sodium loading were demonstrated in the SON, but not in the PVN [15, 16]. These results suggest that AVP neurons in both the SON and the PVN are sensitive to hypovolemic stimulation, and that supraoptic AVP neurons are more responsible for osmotic or sodium regulation than paraventricular ones.

Although the increase in the AVP mRNA level were similar in the SON and the PVN, the hypertrophy of paraventricular AVP neurons was more conspicuous than that of supraoptic AVP neurons. Furthermore, the reduction in stainability of ir-AVP neurons was also marked in the PVN. These results show the possibility that the release of AVP from axon terminals of paraventricular AVP neurons are more active than that from axon terminals of supraoptic AVP neurons.

In the present study, the noticeably dense localization of signals for the AVP mRNA and the change in the density were observed in the magnocellular part of the PVN, but not in the parvocellular part of the PVN. AVP and corticotropin-releasing factor coexist in parvocellular neurosecretory neurons in the PVN which project to the external zone of the median eminence [17]. They act synergistically to release corticotropin from the anterior pituitary [18]. Adrenalectomy resulted in increases in the AVP levels in the

median eminence and the portal plasma [19, 20]. In contrast to water deprivation, the AVP mRNA levels in adrenalectomized rats are conspicuously increased only in the parvocellular part of the PVN, but not in the magnocellular part of the PVN [21]. Therefore, it is probable that the rats used in the present study were not exposed to a so-called stress that was followed by changes in the hypothalamo-pituitary-adrenal axis.

The OXT mRNA level was increased by the water deprivation. Hypertrophy and the reduction in stainability of ir-OXT neurons were also observed in the present study. Meanwhile, water deprivation led to an increase in the plasma OXT level [6]. OXT have been implicated in the control of renal functions [4]. These results suggest that OXT neurons have some physiological role in homeostatic responses to overcome water deprivation. Although the increase in the OXT mRNA level was observed in both the SON and the PVN, the increase in supraoptic OXT neurons was more rapid and conspicuous than that in paraventricular OXT neurons. This fact suggests that supraoptic OXT neurons are involved in the early phase of physiological responses to water deprivation. However, the reason for the above difference between paraventricular and supraoptic OXT neurons remains to be clarified.

ACKNOWLEDGMENTS

The authors would like to thank Drs. T. Hirano and T. Ogasawara and Ms. S. Hasegawa, Ocean Research Institute of the University of Tokyo, for the use of an atomic absorption spectrometer and an osmometer, and Prof. S. Kawashima, Hiroshima University, for providing the antiserum to oxytocin.

REFERENCES

- 1 Hyodo, S., Fujiwara, M., Sato, M. and Urano, A. (1988) Molecular- and immuno-histochemical study on expressions of vasopressin and oxytocin genes following sodium loading. *Zool. Sci.*, 5: 1033-1042.
- 2 Nojiri, H., Sato, M. and Urano, A. (1986) Increase in the vasopressin mRNA levels in the magnocellular neurosecretory neurons of water-deprived rats: *in situ* hybridization study with the use of synthetic oligonucleotide probe. *Zool. Sci.*, 3: 345-350.
- 3 Uhl, G. R., Zingg, H. H., and Habener, J. F. (1985) Vasopressin mRNA *in situ* hybridization:

- localization and regulation studied with oligonucleotide cDNA probes in normal and Brattleboro rat hypothalamus. *Proc. Natl. Acad. Sci. USA*, **82**: 5555-5559.
- 4 Balment, R. J., Brimble, M. J. and Forsling, M. L. (1980) Release of oxytocin induced by salt loading and its influence on renal excretion in the male rat. *J. Physiol.*, **308**: 439-449.
- 5 Brimble, M. J., Dyball, R. E. J. and Forsling, M. L. (1978) Oxytocin release following osmotic activation of oxytocin neurons in the paraventricular and supraoptic nuclei. *J. Physiol.*, **278**: 69-78.
- 6 Dogterom, J., Van Wimersma Greidanus, T. J. B. and Swaab, D. F. (1977) Evidence for the release of vasopressin and oxytocin into cerebrospinal fluid: measurements in plasma and CSF of intact and hypophysectomized rats. *Neuroendocrinology*, **24**: 108-118.
- 7 Jones, C. W. and Pickering, B. T. (1969) Comparison of the effects of water deprivation and sodium chloride imbibition on the hormone content of the neurohypophysis of the rat. *J. Physiol.*, **203**: 449-458.
- 8 Urano, A., Hyodo, S. and Sato, M. (1987) *In situ* hybridization study of neurohypophyseal hormone mRNAs. In "Proceedings of the 10th international symposium of neurosecretion". Ed. by B. T. Pickering, J. B. Wakerley and A. J. S. Summerlee, Plenum, New York/London, pp. 43-51.
- 9 Uhl, G. R. and Reppert, S. M. (1986) Suprachiasmatic nucleus vasopressin messenger RNA: circadian variation in normal and Brattleboro rats. *Science*, **232**: 390-393.
- 10 Hyodo, S., Fujiwara, M., Kozono, S., Sato, M. and Urano, A. (1988) Development of an *in situ* hybridization method for neurohypophyseal hormone mRNAs using synthetic oligonucleotide probes. *Zool. Sci.*, **5**: 397-406.
- 11 Jokura, Y. and Urano, A. (1985) Projections of luteinizing hormone-releasing hormone and vasotocin fibers to the anterior part of the preoptic nucleus in the toad, *Bufo japonicus*. *Gen. Comp. Endocrinol.*, **60**: 390-397.
- 12 Elkinton, J. R. and Taffel, M. (1942) Prolonged water deprivation in the dog. *J. Clin. Invest.*, **21**: 787-794.
- 13 Lepeit, P., Lestage, P., Gauquelin, G., Vitte, P. A., Debilly, G., Gharib, C., Jouvet, M. and Bobillier, P. (1985) Differential effects of chronic dehydration on protein synthesis in neurons of the rat hypothalamus. *Neurosci. Lett.*, **62**: 13-18.
- 14 Rechardt, L. (1969) Electron microscopic and histochemical observations on the supraoptic nucleus of normal and dehydrated rats. *Acta Physiol. Scand. Suppl.*, **329**: 1-79.
- 15 George, J. M. (1973) Localization in hypothalamus of increased incorporation of ^3H cytidine into RNA in response to oral hypertonic saline. *Endocrinology*, **92**: 1550-1555.
- 16 Murray, M. (1967) Effects of dehydration on incorporation of ^3H -tyrosine by some hypothalamic neurons in the rat. *Exp. Neurol.*, **19**: 212-231.
- 17 Kiss, J. Z., Mezey, E. and Skirboll, L. (1984) Corticotropin-releasing factor-immunoreactive neurons of the paraventricular nucleus become vasopressin positive after adrenalectomy. *Proc. Natl. Acad. Sci. USA*, **81**: 1854-1858.
- 18 Gillies, G. E., Linton, E. A. and Lowry, P. J. (1982) Corticotropin releasing activity of the new CRF is potentiated several times by vasopressin. *Nature*, **299**: 355-357.
- 19 Koenig, J. I., Meltzer, H. Y., Devane, G. D. and Gudelsky, G. A. (1986) The concentration of arginine vasopressin in pituitary stalk plasma of the rat after adrenalectomy or morphine. *Endocrinology*, **118**: 2534-2539.
- 20 Robinson, A. G., Seif, S. M., Verbalis, J. G. and Brownstein, M. J. (1983) Quantitation of changes in the content of neurohypophyseal peptides in hypothalamic nuclei after adrenalectomy. *Neuroendocrinology*, **36**: 347-350.
- 21 Scott Young III, W., Mezey, E. and Siegel, R. E. (1986) Vasopressin and oxytocin mRNAs in adrenalectomized and Brattleboro rats: analysis by quantitative *in situ* hybridization histochemistry. *Mol. Brain Res.*, **1**: 231-241.



Pituitary Hormone-Dependent Aldosterone Secretion in *Xenopus laevis*

SHAWICHI IWAMURO, NAOKO MAMIYA
and SAKAÉ KIKUYAMA

Department of Biology, School of Education, Waseda University,
Shinjuku-ku, Tokyo 169, Japan

ABSTRACT—Involvement of pituitary hormones in aldosterone secretion in *Xenopus laevis* was investigated. Both hypophysectomy and distalobectomy reduced plasma aldosterone concentration. However, the aldosterone levels were higher in the animals retaining neurointermediate lobe than those lacking total hypophysis. Neurointermediate lobe homogenate was as potent as anterior lobe homogenate in elevating aldosterone levels in hypophysectomized toads. Administration of adrenocorticotrophic hormone (ACTH) to intact or distalobectomized animals increased plasma concentrations of aldosterone dose-dependently. Response to ACTH was smaller in distalobectomized animals than in intact ones. α -Melanocyte-stimulating hormone did not affect aldosterone levels in hypophysectomized toads. Both arginine vasotocin (AVT) and mesotocin (MT) were effective in elevating aldosterone levels in hypophysectomized animals, AVT being more potent than MT. The pituitary gland of *X. laevis* seems to contain multiple principles which affect aldosterone secretion.

INTRODUCTION

It has been reported that renin-angiotensin system is operating to regulate aldosterone secretion in amphibians as in other vertebrates [1]. However, aldosterone secretion seems to be also under pituitary control. Many investigators have observed that adrenocorticotrophic hormone (ACTH) stimulates aldosterone secretion in anurans [2-8] and urodeles [9, 10]. On the other hand, the evidence has accumulated that in mammals non-ACTH peptides of pituitary origin have an aldosterone-releasing activity [11-14].

This study was designed 1) to confirm the effect of ACTH on the release of aldosterone, 2) to compare the effect of removal of the total hypophysis with that of removal of the anterior lobe on aldosterone secretion and 3) to examine the aldosterone-releasing activity of anterior and neurointermediate lobes as well as that of main neurointermediate lobe hormones, namely α -melanocyte-

stimulating hormone (α -MSH) and arginine vasotocin (AVT) and mesotocin (MT), using clawed toads, *Xenopus laevis* juveniles.

MATERIALS AND METHODS

Animals

Xenopus laevis juveniles weighing about 8 g were used. They were kept under an artificial daylight regime getting illumination from 8:00 to 20:00 hr each day and were maintained at $22 \pm 2^\circ\text{C}$. They were fed every other day, the water being changed prior to the feeding.

Hypophysectomy

The toads were anesthetized by immersion in the water containing MS 222. Hypophysectomy was performed by a transpalatine approach. After the epithelial covering of the palate was cut and retracted, a U-shape cut was made through sphenoid bone by a small surgical knife and the flap of the bone was deflected, the brain-pituitary region being exposed. Either the whole pituitary or the anterior pituitary was taken out with fine forceps.

Administration of hormones

Porcine ACTH and α -MSH were purchased from Sigma. AVT and MT were obtained from Bachem. Each hormone was dissolved in frog Ringer's solution. 50 μ l of the solution was injected into the dorsal lymph sac. All injections were performed at 9–11 a.m. Anterior and neurointermediate lobes from *X. laevis* or *Rana catesbeiana* were separately homogenized in frog Ringer's solution. The homogenate was also injected as described above.

Collection of plasma samples

Blood was collected into heparinized glass tubes by heart puncture. Collection was finished within 2 min to avoid elevation of aldosterone levels due to blood taking [15].

Aldosterone radioimmunoassay

Aldosterone in each plasma sample (50 μ l) was extracted with 1.0 ml of methylene chloride. 800 μ l of the methylene chloride layer was transferred to a glass tube and evaporated by a stream of nitrogen gas. The evaporated samples were diluted in 1.0 ml of 0.05 M potassium phosphate buffer (pH 7.4) containing 0.15 M NaCl, 0.1% NaN₃, and 0.5% BSA (diluent). The aliquot (0.2 ml) was mixed with 0.1 ml of antialdosterone serum (Miles-Yeda) which had been reconstituted and diluted 1:7 with diluent. The cross reactivity of various steroids with the antibody was below 0.1%. After incubation for 30 min at room temperature, 8,000 dpm of ³H-aldosterone (New England Nuclear Co., 72 Ci/mmol) in 50 μ l of diluent was added and the tubes were incubated at 4°C overnight. After incubation, 0.1 ml dextran-coated charcoal (0.1% dextran T-70, 0.5% charcoal in diluent) was added and samples were mixed on a Vortex mixer. The radioactivity of an aliquot (0.25 ml) of the supernatant was counted in scintillant (1 liter of Triton-X100, 2 liters of toluene, 12 g PPO, 600 mg POPOP). The intraassay coefficient of variation was 9% and interassay coefficient of variation was 10%. The sensitivity of the assay defined as twice the standard deviation at zero dose was 6.7 pg/tube.

RESULTS

As illustrated in Figure 1, complete decline of aldosterone levels was observed by 24 hr after hypophysectomy. Effects of hypophysectomy and of distalobectomy on aldosterone levels were studied. Both hypophysectomized and distalobectomized animals exhibited low concentrations of plasma aldosterone when measured 5 days after operation. In the totally hypophysectomized animals, however, aldosterone levels were lower

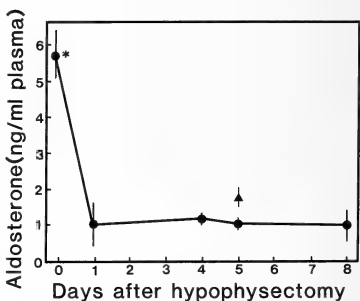


Fig. 1. Effect of hypophysectomy on plasma aldosterone levels in *X. laevis*. The value for totally hypophysectomized animals (●) is significantly different from the value for distalobectomized ones (▲) when compared 5 days after operation ($P < 0.01$, Student's *t*-test). Each point and vertical line represent mean of 5 determinations and SEM, respectively. *The value is significantly different from other values at 1% level (analysis of variance).

than in the distalobectomized ones (Fig. 1). Effect of ACTH on aldosterone levels in distalobectomized and intact animals was studied. In both cases, aldosterone peak was seen 20 min after injection. In distalobectomized animals, the levels became as low as the initial levels when 24 hr elapsed after injection (Fig. 2). As shown in Figure 3, aldosterone levels elevated according to the amount of ACTH injected. It was revealed that responsiveness to ACTH was smaller in distalobectomized animals than in intact ones. Treatment with homogenate of neurointermediate lobe as well as homogenate of the anterior lobe from

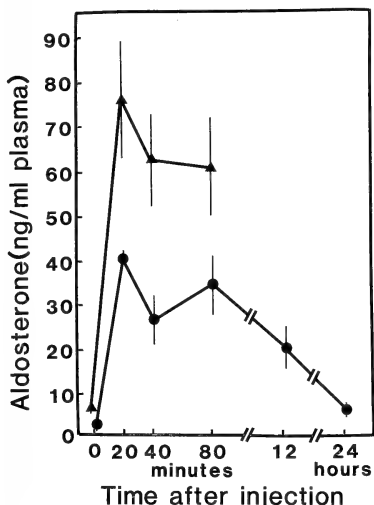
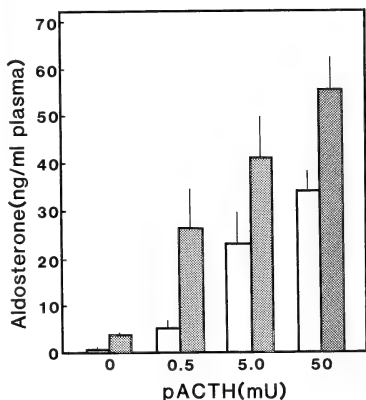


FIG. 2. Time course of response to ACTH. Distalobectomized (●) or intact (▲) animals received 50 mU ACTH. At the indicated time after injection, plasma samples were prepared for aldosterone assay. Each point and vertical line represent mean of 5 determinations and SEM, respectively.



bullfrogs and *X. laevis* resulted in the elevation of aldosterone levels to a similar extent (Fig. 4). In order to ascertain whether α -MSH, AVT, and MT have any influence upon aldosterone secretion, these hormones were separately injected to hypophysectomized animals. α -MSH (250 ng) showed little effect during the period of 20–80 min after injection (Fig. 5). Neither lower nor higher

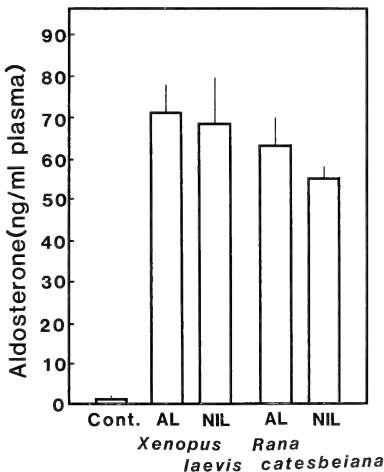


FIG. 4. Effect of pituitary homogenate on aldosterone levels in hypophysectomized *X. laevis*. Test samples were obtained from anterior lobes (AL) and neurointermediate lobes (NIL) of *X. laevis* and *Rana catesbeiana*. Each homogenate injected contained 25 μ g protein. Each column and vertical bar represent mean of 5 determinations and SEM, respectively. The values for treated groups are significantly different from the value for controls at 1% level (analysis of variance).

FIG. 3. Effect of ACTH on plasma aldosterone levels in intact and distalobectomized *X. laevis*. Various doses of ACTH as indicated were given to the animals. Blood samples were collected 20 min after injection. Each column and vertical bar represent mean of 5 determinations and SEM, respectively. The value for intact animals is significantly different from the value for distalobectomized animals treated similarly at 1% level (Student's *t*-test).

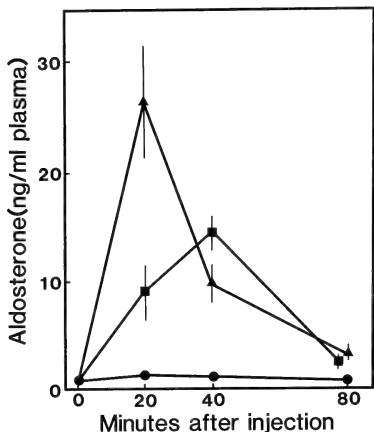


Fig. 5. Time course of response to neurointermediate lobe hormones. Hypophysectomized *X. laevis* received 250 ng α -MSH (●), 14 ng AVT (▲) and 140 ng MT (■). Blood samples were collected at the indicated time after injection. Each point and vertical line represent mean of 5 determinations and SEM, respectively.

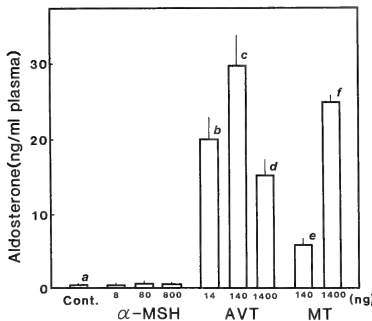


Fig. 6. Effect of neurointermediate lobe hormones on aldosterone levels in hypophysectomized *X. laevis*. Animals received injection of Ringer's solution, α -MSH, AVT or MT. Blood samples were prepared 20 min after injection. Each column and vertical bar represent mean of 5 determination and SEM, respectively. Significance of difference: a vs b, a vs c, a vs d, a vs f, c vs d, and e vs f, $P < 0.01$ (analysis of variance).

dose of α -MSH affected aldosterone levels as determined 20 min after injection (Fig. 6). On the other hand, both AVT and MT elevated aldosterone levels markedly. The peak was observed 20 min after injection in the case of AVT and 40 min after injection in the case of MT (Fig. 5). The aldosterone-releasing activity of AVT was more prominent than that of MT. In the case of AVT, the largest dose (1400 ng) tested was less effective than a smaller dose (140 ng) (Fig. 6).

DISCUSSION

It was confirmed that ACTH is a powerful aldosterone-release stimulator in *X. laevis*. In the intact animal, ACTH produced quantitatively greater response of interrenals than the same hormone when administered to the animals lacking the anterior lobe. In the iguanid lizard, Daugherty and Callard [16] observed that in hypophysectomized animals, the adrenal response to ACTH is slow and small as compared with the response in intact animals. They assumed that the poor response in hypophysectomized specimens is due to the decline of the entire level of steroidogenic activity which is dependent on ACTH and the absence of other pituitary hormones to act synergistically with ACTH.

In the present experiment, aldosterone levels were markedly lowered by the removal of the distal lobe of the pituitary gland as well as the removal of the total pituitary gland, the levels being lower in the case of removal of the total hypophysis than in the case of removal of the anterior lobe only. This indicates that some hormonal factor(s) released from the neurointermediate lobe has a stimulatory, though minor, effect on aldosterone release. According to Le Boulenger *et al.* [17], there was no significant difference in corticosterone levels between totally hypophysectomized and distalobectomized frogs (*Rana esculenta*). It was demonstrated that the neurointermediate lobe homogenate was as potent as the anterior lobe homogenate in elevating plasma aldosterone levels. Delarue *et al.* [3] have also reported that the intermediate lobe homogenate caused a considerable increase in aldosterone release from interrenal fragments of *Rana ridibunda*.

in vitro. They assumed that ACTH which is detectable in pars intermedia by means of radioimmunoassay [18] is responsible for the elevation of aldosterone secretion. Recently, Leboulenger *et al.* [19] have reported that *Rana ridibunda* interrenals respond to α -MSH, desacetyl α -MSH and γ -MSH to release corticoids *in vitro*. In the present experiment, α -MSH exhibited no aldosterone-releasing activity in *Xenopus*. On the other hand, AVT increased aldosterone levels markedly. Hanke and Masor [20] have observed that AVT stimulates the *in vitro* release of both aldosterone and corticosterone from the interrenal tissue according to the concentrations (1-100 ng/ml), suggesting that the posterior lobe hormone acts directly on the interrenal tissue. According to our data, higher dose (1400 ng) of AVT was not so effective as the lower one (140 ng). This might happen if AVT acts *in vivo* to enhance aldosterone release on one hand directly and suppress on the other indirectly, the effective dose-range for each action being different. In fact, it is known that administration of vasopressin in human and several animal species suppresses renin secretion, consequently inhibiting aldosterone secretion [21]. In the present experiment, it was found that another neurohypophyseal hormone, MT is also effective in increasing aldosterone levels in hypophysectomized toads. We have tested only α -MSH and two neurohypophyseal hormones for their aldosterone-releasing activity so far. It is a matter of further investigation to separate aldosterone-releasing principles from the neurointermediate lobe as well as the anterior lobe of the amphibian pituitary gland and to clarify their mode of action.

ACKNOWLEDGMENTS

This study was supported by Grants-in-Aid from the Ministry of Education, Science and Culture, Japan and a research grant from Waseda University to S.K.

REFERENCES

- 1 Nishimura, H. (1980) Evolution of renin-angiotensin system. In "Evolution of Vertebrate Endocrine System". Ed. by P. K. T. Pang and A. Epplé, Texas Tech Press, Lubbock, pp. 373-404.
- 2 Johnston, C. I., Davis, J. O., Wright, F. S. and Howards, S. S. (1967) Effects of renin and ACTH on adrenal steroid secretion in the American bullfrog. *Am. J. Physiol.*, **213**: 393-399.
- 3 Delarue, C., Tonon, M. C., Leboulenger, F., Jegou, S., Leroux, P. and Vaudry, H. (1979) *In vitro* study of frog (*Rana ridibunda* Pallas) interrenal function by use of a simplified perfusion system. II. Influence of adrenocorticotropin upon aldosterone production. *Gen. Comp. Endocrinol.*, **38**: 399-409.
- 4 Leboulenger, F., Delarue, C., Tonon, M. C., Jegou, S. and Vaudry, H. (1979) *In vitro* study of frog (*Rana ridibunda* Pallas) interrenal function by use of a simplified perfusion system. I. Influence of adrenocorticotropin upon corticosterone release. *Gen. Comp. Endocrinol.*, **36**: 327-338.
- 5 Maser, C., Janssens, P. A. and Hanke, W. (1982) Stimulation of interrenal secretion in amphibia. I. Direct effects of electrolyte concentration on steroid release. *Gen. Comp. Endocrinol.*, **47**: 458-466.
- 6 Krug, E. C., Honn, K. V., Battista, J. and Nicoll, C. S. (1983) Corticosteroids in serum of *Rana catesbeiana* during development and metamorphosis. *Gen. Comp. Endocrinol.*, **52**: 232-241.
- 7 Kikuyama, S., Suzuki, M. R. and Iwamuro, S. (1986) Elevation of plasma aldosterone levels of tadpole at metamorphic climax. *Gen. Comp. Endocrinol.*, **63**: 186-190.
- 8 Thurmond, W., Kloas, W. and Hanke, W. (1986) Circadian rhythm of interrenal activity in *Xenopus laevis*. *Gen. Comp. Endocrinol.*, **61**: 260-271.
- 9 Mazzi, V., Colucci, D., Andreoletti, G. E. and Velano, C. (1984) ACTH dependency of aldosterone increment in the newt *Triturus cristatus carnifex* Laur. *Fisiologia e Genetica*, **118**: 339-343.
- 10 De Ruyter, M. L. and Stiffler, D. F. (1986) Interrenal function in larval *Ambystoma tigrinum*. II. Control of aldosterone secretion and electrolyte balance by ACTH. *Gen. Comp. Endocrinol.*, **62**: 298-305.
- 11 Vinson, G. P., Whitehouse, B. J., Dell, A., Etinen, T. and Morris, H. R. (1980) Characterization of an adrenal zona glomerulosa-stimulating component of posterior pituitary extracts as α -MSH. *Nature*, **284**: 464-467.
- 12 Matsuoka, H., Mulrow, P. J., Franco-Saenz, R. and Li, C. H. (1981) Effects of α -lipotropin and β -lipotropin-derived peptides on aldosterone production in the rat adrenal gland. *J. Clin. Invest.*, **68**: 752-759.
- 13 Gullner, H. G. and Gill Jr. J. R. (1983) Beta endorphin selectively stimulates aldosterone secretion in hypophysectomized, nephrectomized dogs. *J. Clin. Invest.*, **71**: 124-128.
- 14 Shenker, Y., Villareal, J. Z., Sider, R. S. and Grekin, J. (1985) α -Melanocyte-stimulating hormone stimulation of aldosterone secretion in

- hypophysectomized rats. *Endocrinology*, **116**: 138-141.
- 15 Le Boulenger, F., Delarue, C., Belanger, A., Netchitailo, P., Leroux, P., Jegou, S., Tonon, M. C. and Vaudry, H. (1982) Direct radioimmunoassays for plasma corticosterone and aldosterone in frog. I. Validation of methods and evidence for daily rhythms in a natural environment. *Gen. Comp. Endocrinol.*, **46**: 521-532.
- 16 Daugherty, D. R. and Callard, I. P. (1972) Plasma corticosterone levels in the male iguanid lizard *Sceloporus cyanogenys* under various physiological conditions. *Gen. Comp. Endocrinol.*, **19**: 69-79.
- 17 Le Boulenger, F., Trochard, M. C., Morin, J. P., Dupont, W., Vaudry, H. and Vaillant, R. (1977) Dosage par radiocompetition de la corticostérone plasmatique chez la Grenouille verte *Rana esculenta* L. *J. Physiol. (Paris)*, **73**: 73-83.
- 18 Vaudry, H., Vague, P., Dupont, W., Le Boulenger, F. and Vaillant, R. (1975) A radioimmunoassay for plasma corticotropin in frogs (*Rana esculenta* L.). *Gen. Comp. Endocrinol.*, **25**: 313-322.
- 19 Le Boulenger, F., Lihmann, I., Netchitailo, P., Delarue, C., Perroteau, I., Ling, N., and Vaudry, H. (1986) *In vitro* study of frog (*Rana ridibunda pallas*) interrenal function by use of a simplified perfusion system. *Gen. Comp. Endocrinol.*, **61**: 187-196.
- 20 Hanke, W. and Maser, C. (1985) Regulation of interrenal function in Amphibians. In "Current Trends in Comparative Endocrinology vol. 1". Ed. B. Lofts, and W. N. Holmes, Hong Kong Univ. Press, Hong Kong, pp. 447-449.
- 21 Reid, L. A. (1983) Salt and water regulation. In "Brain Peptides". Ed. by D. T. Krieger, M. J. Brownstein, and J. B. Martin, John Wiley and Sons, New York, pp. 333-347.

Effects of Post-Weaning Differential Housing on Serum Testosterone Levels in Male Mice throughout Aging

SATOSHI KOIKE¹ and TETSUO NOUMURA

*Department of Regulation Biology, Faculty of Science,
Saitama University, Urawa, Saitama 338, Japan*

ABSTRACT—The influence of differential housing (1, 2, 5 or 10 per cage) on serum testosterone (T) levels was studied in male ICR mice from 21 days to 550 days of age. In socially-housed individuals, the circulating T levels were lowered with increasing group size from 60 to 200 days of age. Peak T levels in groups of 2, 5 and 10 males were 5.55, 4.09 and 2.65 ng/ml, respectively. However, individual T levels showed great variations ranging from 1.67 to 20.49 ng/ml within a cage. Suppressive effect was exclusively focused on a few members in each cage, and intensified with increasing group size throughout 200 days of age. But the difference of serum T levels among different group sizes and the individual variations within a cage were gradually decreased with age since 300 days of age. On the other hand, singly-housed individuals showed different age-associated changes in serum T levels from those of socially-housed ones. These results suggest that (1) testicular endocrine function may be greatly influenced by grouping size from sexually maturing period through adult life in male mice, (2) this effect is concentrated on a few members within a cage, and (3) singly-housing condition may be qualitatively different from socially-housing condition.

INTRODUCTION

There are many reports for age-associated changes in endocrine functions in mice [1-5]. Most of them reported the increase in reproductive functions and in circulating levels of sex steroids during sexually maturing period, and the decrease in the senescent and old age. Machida *et al.* [6] determined plasma testosterone levels over almost the whole range of the life span of male mice of their ICR colony.

On the other hand, it is known that the size of group in gregarious species plays very important roles on their body growth, physiological and psychological conditions [7-13]. In laboratory mice, body weight gain was decreased with increasing population density [7-9] and the onset of puberty was delayed [14, 15]. For relationship between group sizes and endocrine functions in male mice, many investigators have reported that the functions of hypothalamic-pituitary-gonadal

axis were decreased with increasing population size, but those of hypothalamic-pituitary-adrenocortical axis were increased [12, 13, 16].

In the present paper, we examined the influence of housing conditions with different group sizes (1, 2, 5 and 10 per cage) on serum testosterone levels in male mice from juvenile to senescent period.

MATERIALS AND METHODS

Animals

Mice were raised from a randomly bred ICR strain colony maintained in the animal room of the Department of Regulation Biology in the Saitama University. The day when litters were found was designated as day 1 of life for the pups. At 21 days of age, male mice were weaned and randomly divided into groups of 1, 2, 5 and 10 per cage (15 × 22 × 12 cm plastic cage with a wire cover). All animals were maintained in a temperature (21 ± 1°C)—and humidity (50% relative humidity)—controlled animal room with a light cycle of 14 hr of light/10 hr of dark (lights on at 0600). Mouse chow (Charles River CRF-1) and water were pro-

Accepted June 22, 1988

Received May 12, 1988

¹ Present address: Upjohn Pharmaceuticals Limited, Tsukuba, Ibaraki 300-42, Japan.

vided *ad libitum*. In this colony of the ICR mouse, the mean life span was around 450 days for male animals maintained in group-housing, two to ten per cage. On socially-housing groups, the members of each group were shared to two subgroups, social dominance (D) or subordination (S) in each cage, according to observation of wounding and coat conditions.

Testosterone determination

Blood samples were collected into non-heparinized syringes by cardiac puncture under ether anesthesia at the appropriate age (21, 30, 60, 90, 120, 150, 200, 300 and 550 days of age, respectively) between the hours of 1100 and 1300 in order to control for diurnal fluctuations in hormone levels, immediately centrifuged twice at 3,000 rpm for 10 min, and then the serum was separated and stored at -20°C until assayed.

Serum testosterone (T) levels were determined by a radioimmunoassay. The antiserum (against testosterone-11 α -succ-BSA, Teikoku Hormone Mfg. Co., Ltd.) used reacted with testosterone, 5 α -dihydrotestosterone, androstenedione, androstenediol and other steroids to the extent of 100, 13.5, 2.24, 1.39 and less than 0.2%, respectively. Therefore, chromatographic separation of DHT from T after extraction was not carried out. In order to examine the accuracy of the method, various quantities of nonradioactive T were added to serum obtained from female mice and assayed as references. This gave the recovery of 94%. Precision of the method was ascertained by calculating a coefficient of variation. The interassay variation was 5.26% and the intrassay variation was 5.39%. The least detectable T dose in the assay was 4.0 pg/tube. Individual T value was the mean of duplicate determinations and was expressed as nanograms per milliliter of serum.

The mean T values were calculated in each group size and each subgroup, respectively. Statistical comparisons were performed either by Student's *t*-test or by Aspin Welch's *t*-test. Significant levels were $P < 0.05$.

RESULTS

Serum T values of each male from 30 to 550 days

of age were shown in Figure 1. In both singly-housed and socially-housed mice, considerable individual variation in serum T levels was observed at most ages. In particular, a wide range of individual variation was 0.20–18.07 at 150 days for 1 per cage, 2.03–11.22 at 60 days for 2 per cage, 1.67–20.49 at 150 days for 5 per cage, and 0.78–8.85 ng/ml at 90 days of age for 10 mice per cage.

The mean values of serum T concentration were shown in Table 1 and Figure 2. In all groups, the mean T values raised linearly from 21 to 60 days of age, but the rate of increase varied with group sizes. Singly-housed males took two peaks on the mean T level; the first peak value was 3.22 ± 0.73 ng/ml at 60 days and the second, a higher peak level was 6.70 ± 1.66 ng/ml at 120 days of age. Age-associated changes of T levels in singly-housed males were different from socially-housed ones, which took one peak, from 21 through 120 days of age. But age-associated changes in singly-housed ones were similar to those in 2-males group after 150 days old. In socially-housed males, the circulating T levels tended to be lowered with increasing group size from 30 through 90 days of age and the peak level did in a similar manner (5.55 ng/ml for 2-males at 60 days, 4.09 ng/ml for 5-males at 60 days, 2.65 ng/ml for 10-males at 90 days of age). So, age-associated changes in serum T levels showed characteristic of each group size throughout 200 days of age, but at 300 and 550 days of age there were not so much differences among different group sizes except for a lower level in 10-males group at 550 days old.

In socially-housed mice, a rough correlation was shown between social structure and serum T level in male mice within a cage. The mean T level of dominant male was higher than the average T concentration of the subordinates. Then, it was examined whether age-associated patterns of serum T levels differ between subgroups. Age-associated changes of mean T levels of every subgroups in each group size were shown in Figure 3. In all groups, the mean T values of the dominants were remarkably raised between 30 and 60 days of age, and then held at high levels. Age-associated patterns were characteristic in each group size. In 2-males, serum T achieved to peak levels 7.43 ± 1.36 ng/ml at 60 days and gradually

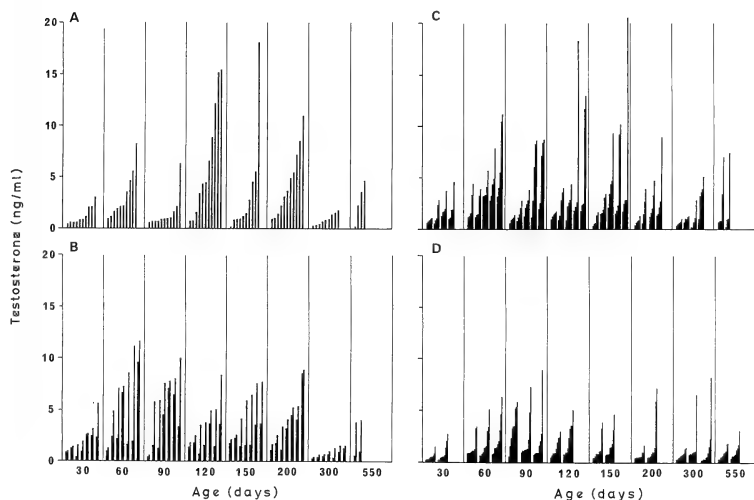


Fig. 1. Individual serum testosterone levels in male mice maintained in different grouping sizes. A: One-male. B: 2-males. C: 5-males. D: 10-males. One column showed one male. In 2-, 5- and 10-males group, each cage was showed as one block consisted of two, five and ten columns, respectively. Some blocks consisted of 4 and 9 columns in 5- and 10-males group at 300 and 550 days of age, respectively, because one male died just before the sacrificed day.

TABLE 1. Serum testosterone levels of male mice housed in different group sizes from 21 days of age.

Serum testosterone values at 21 days of age represented the result for assays of serum in a litter unit of male pups obtained from 4 mothers.

Mice per cage	Age in days								
	21	30	60	90	120	150	200	300	550
1 (11) ^a	0.41 ^b ±0.02	1.21 ±0.28 (10) ^c	3.22 ±0.73 (10)	1.53 ±0.50 (11)	6.70 ±1.66 (11)	3.66 ±1.69 (10)	4.52 ±0.99 (11)	0.91 ±0.18 (9)	2.69 ±0.95 (4)
2 (7)	0.41 ±0.02	2.04 ±0.36 (14)	5.55 ±1.02 (14)	5.11 ^{**} ±0.85 (14)	3.20 ±0.54 (14)	3.50 ±0.68 (14)	4.00 ±0.65 (14)	0.85 ±0.12 (14)	2.39 ±0.92 (4)
5 (5)	0.41 ±0.02	1.66 ±0.23 (20)	4.09 ±0.52 (25)	3.26 ±0.56 (25)	3.70 ±0.88 (24)	3.82 ±0.88 (25)	2.21 ±0.46 (19)	1.51 ±0.32 (20)	2.47 ±0.94 (9)
10 (3)	0.41 ±0.02	0.78 ^{††} ±0.15 ^{§§} (20)	1.96 ^{††} ±0.27 ^{§§} (30)	2.65 ^{††} ±0.41 (28)	1.93 [*] ±0.28 [†] (20)	1.59 ^{††} ±0.29 [§] (19)	1.38 ^{**} ±0.41 ^{††} (20)	1.30 ±0.34 (28)	1.07 ±0.16 (19)

a Number of cages

b Mean ± SE (ng/ml)

c Number of mice

*** Significantly different from 1 mouse per cage (* $p < 0.05$, ** $p < 0.01$)

†,†† Significantly different from 2 mice per cage († $p < 0.05$, †† $p < 0.01$)

§,§§ Significantly different from 5 mice per cage (§ $p < 0.05$, §§ $p < 0.01$)

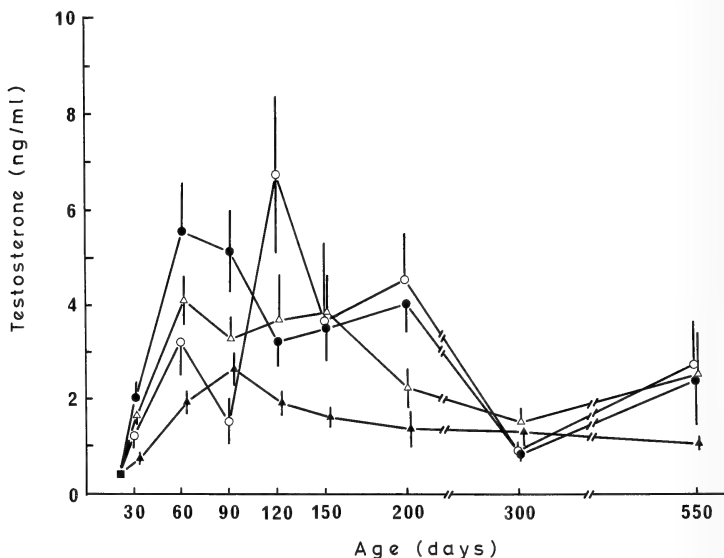


Fig. 2. Age-associated changes in serum testosterone levels of male mice from weaning to senescent ages when maintained in differently housing conditions. Each point showed mean testosterone levels and vertical bar showed standard error of the mean. Statistical significance represented Table 1. Open circle (○), closed circle (●), open triangle (△) and closed triangle (▲) expressed one-, two-, five- and ten-males group, respectively.

decreased through 300 days but increased again at 550 days. In 5-males, serum T levels showed a similar pattern to those in 2-males but the second, higher peak level appeared at 150 days (9.04 ± 2.70 ng/ml). In 10-males, serum T increased linearly through 90 days to peak levels of 6.43 ± 0.72 ng/ml, and continued second high levels of about 4 ng/ml between 200 and 300 days, but decreased again to 2.24 ± 0.43 ng/ml at 550 days.

T levels of the subordinates took much lower values compared with those of the dominants since 30 days of age. In the subordinates in 2-males serum T levels showed age-associated changes through 200 days and then decreased to less than 1 ng/ml since 300 days; peak levels taken at 60 and 200 days were 3.68 ± 1.22 and 3.53 ± 1.00 ng/ml, respectively. In 5-males, T levels of the subordin-

ates gradually decreased from 60 days through 550 days with the peak levels of 3.03 ± 0.30 ng/ml at 60 days of age. The subordinates in 10-males had peak T levels of 1.83 ± 0.24 ng/ml at 90 days and had low levels as 1 ng/ml since 200 days of age.

DISCUSSION

In this study, it is suggested that the post-weaning housing conditions may influence serum T levels in male mice through 200 days of age. From puberty to adult, the circulating T levels in both the average and the peak values were lowered with increasing group size. In 10-males group, the age when serum T reached the first peak values delayed. These results are partially consistent with the previous findings. Jean-Faucher *et al.* [15]

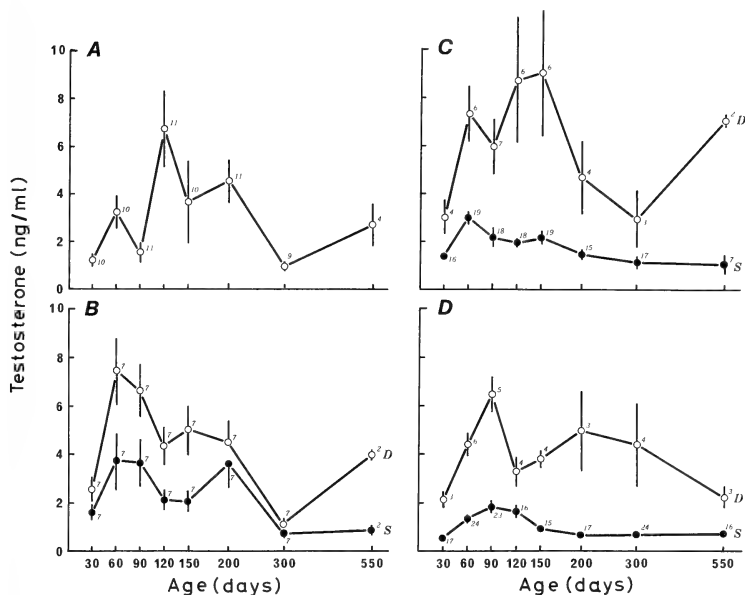


Fig. 3. Age-associated changes in serum testosterone levels between dominants (D) and subordinates (S) in differently housing male mice. A: One-male. B: 2-males. C: 5-males. D: 10-males. Each point showed mean testosterone levels and vertical bar showed standard error of the mean. The number on each point showed number of mice classified into dominance and subordination.

Statistically significant difference between D and S represented 120, 150 and 550 days in 2-males, from 60 to 120 and 550 days in 5-males, and from 30 to 150 and 550 days of age in 10-males.

reported that plasma T levels were lowered with increasing group size from weaning to 50 days but increased at 60 and 90 days in female-containing male groups, and Christian [12, 17] suggested that functions of hypothalamic-pituitary-testicular axis were decreased with increasing population size and population density in the small mammals. On the other hand, there is a suggestion that reduction of circulating T level might be partially related to increases in plasma ACTH and adrenocortical hormones which would be caused by the social stress within a group [16]. From this point, group size might influence the degree of stress within a group to affect serum T levels.

The reduction of mean serum T level with

increasing group size was caused largely by the decrease in serum T level of the subordinates to which belonged the most part of group, and there was the extreme decrease in a few members within subordinates. The degree of decrease in serum T levels of the subordinates was enhanced with increasing grouping size, because serum T level was higher in 2-males than in 5- and 10-males, respectively and because the subordinates of 5-males were higher T levels than those of 10-males, respectively. However, testicular functions in members of the dominance would be stimulated by an increase in groups size because they kept greatly higher T level compared with those of the subordinates in all ages. These results suggest that

suppressive effects on testicular function are intensified with increasing group size and then confined to a few members within a group. On the other hand, such considerable individual variation was reported previously by Machida *et al.* [6] in ICR males maintained four to six per cage. They suggested that marked individual variation in plasma T titers seemed to be related to the social dominance/subordinate rank within a group. Social dominant-subordinate relationship was not examined in detail in the present experiment, but both individual growth and serum T variation were observed over a wide range. Thus, these may be referred to the establishment of social hierarchy.

In 10-males group, there were linear increases in serum T from 30 to 90 days of age. These results suggest that the onset of puberty, as shown by the first peak of serum T level, delayed in all members of a group. From this point, suppressive effects on testicular function may cover all individuals of a population under the overcrowding condition such as 10-males per cage.

The result that the differences of serum T among groups decreased with aging since 300 days is consistent with previous reports [1, 6]. This decrease of difference may be caused by a lowering of testicular activity with age. However, there were still many differences within cages in all socially-housing groups after 300 days of age, much the same as before 200 days. This suggests that the suppressive effect due to housing condition is unevenly distributed among individuals within a cage through life span and that some males may keep high testicular activities, even at the highest density of 10 per cage, and some males may be consistently suppressed.

Mean T level at 550 days was higher than that at 300 days of age in all grouping sizes. In the colony of the ICR mouse used in this experiment, the last tenth survival day was 380, 520, 540 and 550 for 1-, 2-, 5- and 10-males, respectively. Therefore, testosterone secretion in male mice that survived until 550 days of age might not reduce. Rothstein [18] reviewed that there were no changes in plasma levels of T between the adult (8–11 months) males and the healthy old (29–31 months) males in C57BL/6J mice. These results suggest that the healthy senescent males may maintain the same

ability of hormone secretion from their testes as the adult males.

Age-associated changes in serum T of singly-housing males were extremely different from those of group-housing males from 30 through 150 days of age. This suggests that individual-housing may be a special condition different from group-housing. Brain and Nowell [16, 19] reported that isolation increased in pituitary-gonadal function and declined in pituitary-adrenal function. Our methods were different from their methods which transferred from grouping to isolating condition in the adulthood. But our results are consistent with their results in respect that isolating condition causes the endocrine functions different from those of grouping one.

Finally, in both singly-housed and socially-housed male mice, marked individual variation in serum T levels was observed. Vom Saal *et al.* [20] found that in male mice there was a relationship between intrauterine proximity to female fetuses, prenatal titers of estradiol, and adult morphology and behavior. It is possible that the occurrence of considerable individual variation in serum T levels is related to the effects of prior intrauterine position during prenatal development, other than to the inheritance. Research is required to examine this relationship.

ACKNOWLEDGMENTS

This work was supported in part by a Grant for Life Science Research Project "Discovery of Factors Regulating Aging" from the Institute of Physical and Chemical Research to T.N.

REFERENCES

- 1 McKinney, T. D. and Desjardins, C. (1973) Post-natal development of the testis, fighting behavior, and fertility in house mice. *Biol. Reprod.*, **9**: 279–294.
- 2 Barkley, M. S. and Goldman, B. D. (1977) A quantitative study of serum testosterone, sex accessory organ growth, and the development of intermale aggression in the mouse. *Horm. Behav.*, **8**: 208–218.
- 3 Finch, C. E., Jones, V., Wisner, Jr., J. R., Shaha, Y. N., de Vellis, J. S. and Swerdloff, R. S. (1977) Hormone production by the pituitary and testes of male C57BL/6J mice during aging. *Endocrinology*, **101**: 1310–1317.

- 4 Jean-Faucher, Ch., Berger, M., de Turckheim, M., Veyssiere, G. and Jean, Cl. (1978) Developmental patterns of plasma and testicular testosterone in mice from birth to adulthood. *Acta Endocrinol.*, **89**: 780-788.
- 5 Coquelin, A. and Desjardins, C. (1982) Luteinizing hormone and testosterone secretion in young and old male mice. *Amer. J. Physiol.*, **243**: E257-263.
- 6 Machida, T., Yonezawa, Y. and Noumura, T. (1981) Age-associated changes in plasma testosterone levels in male mice and their relation to social dominance or subordination. *Horm. Behav.*, **15**: 238-245.
- 7 Takeda, M. (1959) Effects of population density on the growth and reproduction in mouse -I. Different number of animals in same space (different density). *Bull. Exp. Anim.*, **8**: 101-104.
- 8 Takeda, M. (1959) Effects of population density on the growth and reproduction in mouse -II. Same number of animals in different space (different density). *Bull. Exp. Anim.*, **8**: 104-106.
- 9 Takeda, M. (1959) Effects of population density on the growth and reproduction in mouse -III. Different number of animals in different space (same density). *Bull. Exp. Anim.*, **8**: 182-183.
- 10 Rowe, F. P. (1963) Population studies of the house-mouse. *Ann. Appl. Biol.*, **51**: 348-350.
- 11 Christian, J. J. (1968) Social subordination, population density, and mammalian evolution. *Science*, **168**: 84-90.
- 12 Christian, J. J. (1971) Population density and reproductive efficiency. *Biol. Reprod.*, **4**: 248-294.
- 13 Andrews, R. V. (1979) The physiology of crowding. *Comp. Biochem. Physiol.*, **63A**: 1-6.
- 14 McKinney, T. D. and Desjardins, C. (1973) Inter-male stimuli and testicular function in adult and immature house mice. *Biol. Reprod.*, **9**: 370-378.
- 15 Jean-Faucher, Ch., Berger, M., de Turckheim, M., Veyssiere, G. and Jean, Cl. (1981) Effects of dense housing on the growth of the reproductive organs, plasma testosterone levels and fertility of male mice. *J. Endocrinol.*, **90**: 397-402.
- 16 Brain, P. F. and Nowell, N. W. (1970) The effects of differential grouping on endocrine function of mature male albino mice. *Physiol. Behav.*, **5**: 907-910.
- 17 Christian, J. J. (1955) Effect of population size on the adrenal glands and reproductive organs of male mice in populations of fixed size. *Amer. J. Physiol.*, **182**: 292-300.
- 18 Rothstein, M. (1982) Testosterone. In "Biochemical Approaches to Aging". Ed. by M. Rothstein, Academic Press, New York, pp. 286-290.
- 19 Brain, P. F. and Nowell, N. W. (1971) Isolation versus grouping effects on adrenal and gonadal function in albino mice. *Gen. Comp. Endocrinol.*, **16**: 149-154.
- 20 Vom Saal, F. S., Grant, W. H., McMullen, C. W. and Laves, K. S. (1983) High fetal estrogen concentrations: Correlation with increased adult sexual activity and decreased aggression in male mice. *Science*, **220**: 1306-1309.



Erythrocyte Diapedesis in Anterior Pituitary Hemorrhage after Intraperitoneal Injection of Hypertonic Solution in Mice

YASUO KOBAYASHI and CHIE IGA

*Department of Biology, Faculty of Science,
Okayama University, Okayama 700, Japan*

ABSTRACT—Initial changes of hemorrhage occurring in the anterior pituitary of mice received ip injection of 9% NaCl at a dose of 0.03 ml/g body weight were investigated with the electron microscope. The sinusoidal capillaries were distended and filled with erythrocytes after 10 min of the injection. Extravasation of red blood cells took place without distinct injury to the endothelium, being involved in a mechanism known as diapedesis. Two types of passages traversing the endothelium were distinguished in this erythrocyte diapedesis: through the large endothelial gaps up to 1 μ m in diameter, and the other of, predominantly, through the occluding junctions of adjacent cells of the endothelium. In the latter case, the red blood cell showed thread-like configuration in the middle of the cell body when migrating across the endothelial tight junction. In addition the erythrocyte migration through the zonula occludens of the marginal cells with no obvious structural injury was encountered. The intercellular junctions of the endothelium as well as those of the marginal cells of the anterior pituitary may be provided with the zonula occludens which is very leaky in structure.

INTRODUCTION

Our previous study has demonstrated that hypertonic solution induced acute and intense hemorrhage into the anterior pituitary in mice [1]. This incidental heavy bleeding occurred exclusively in the anterior pituitary 10 min after ip injection of hypertonic solutions of electrolytes or non-electrolytes. No hemorrhage was observed in other endocrine glands and visceral organs so far investigated histologically [1].

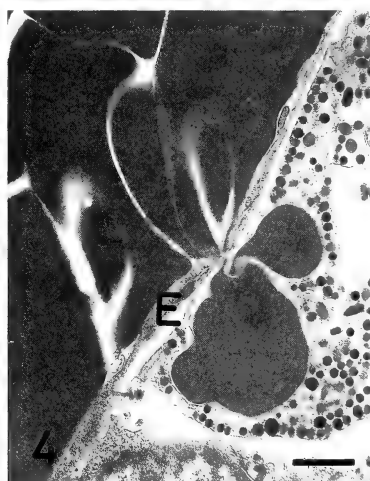
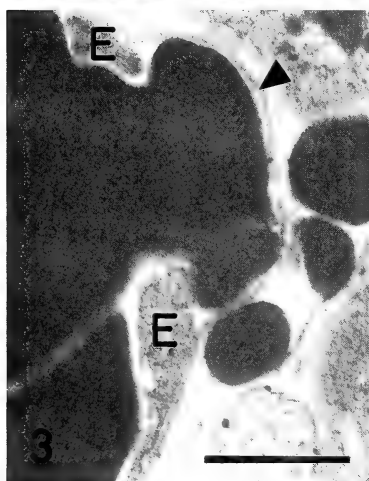
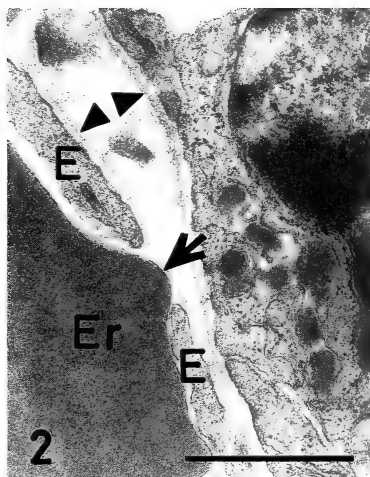
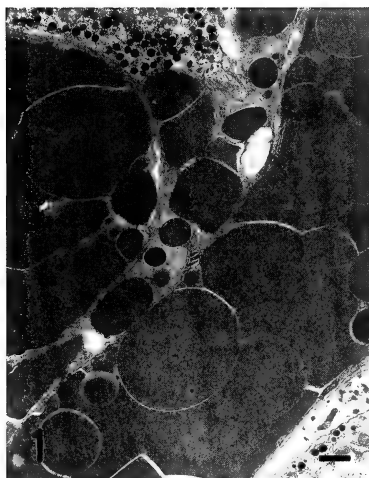
Ultrastructural studies on experimental hemorrhage in endocrine glands and some organs have been reported. Leakage of red blood cells through the capillary wall of the anterior pituitary after electrolytic destruction of pituitary stalk [2], hemorrhagic necrosis (apoplexy) by acrylonitrile in the adrenals [3], extravasation of erythrocytes in the adrenal cortex after chronic ACTH stimulation [4] and fragmented erythrocytes in the mesangium of the rabbit kidney after the Shwartzman reaction [5]. In these studies, however, no ultrastructural

findings for the initial changes of erythrocyte extravasation have been illustrated. Therefore, the present electron microscopic study was designed to elucidate the changes at the beginning of the migration of red blood cells across the endothelium in this acute pituitary hemorrhage in mice.

The results disclosed a fact that this anterior pituitary hemorrhage is involved in "diapedesis", a mechanism by which extravasation of red blood cells takes place without structural destruction of the endothelial cells.

MATERIALS AND METHODS

Male mice of the Jcl/ICR strain were housed in air-conditioned room ($21 \pm 1^\circ\text{C}$) with lights on from 7:00 to 21:00 hr. They were fed on standard laboratory chow and were allowed free access to tap water. Ten animals at 8 weeks of age received a single ip injection of 9% NaCl at a dose of 0.03 ml/g body weight. They were sacrificed by decapitation 10 or 20 min after the injection. The pituitary glands were removed and fixed with 2.5% glutaraldehyde in 0.1 M phosphate buffer (pH 7.2) followed by buffered 1% OsO_4 for 1 hr each.



Specimens were dehydrated and embedded in Quetol 812. Parasagittal ultrathin sections were stained with uranyl acetate and lead citrate, and examined with an 11-E Hitachi Electron Microscope.

RESULTS

The anterior pituitary showed acute hemorrhage 10 min after the ip injection of 9% NaCl at a dose of 0.03 ml/g body weight. However, the administration of hypertonic solution via the tail vein under ether anesthesia at the same dose failed to cause pituitary hemorrhage. Sinusoidal blood capillaries appeared to be dilated and filled with red blood cells showing apparent congestion in the anterior pituitary after the ip injection of 9% NaCl (Fig. 1). Despite such expansion of blood vessels any lesions or discontinuities of the vasculature were not observed. Nevertheless, there was massive extravasation of red blood cells from capillaries into the intercellular space of the parenchymal cells of the anterior lobe (Fig. 1).

In the extravasation of erythrocytes there seemed to be two passages across the endothelial cells in this anterior pituitary hemorrhage. In the first type of migration, erythrocytes moved through endothelial gaps and/or endothelial stomata. The small extrusion of erythrocytes was inserted into the endothelial gaps which were invested with the basal lamina (Fig. 2). Successively, large endothelial gaps, approximately 1 μ m in diameter, permitted emigration of erythrocytes whose outline appearing a mushroom-like protrusion into the pericapillary space, and the basal lamina still remained its structural integrity covering the de-

formed erythrocytes (Fig. 3). At this stage visible structural damage of the endothelial cells was not encountered.

In the second type of extravasation, rather predominant, erythrocytes migrated through the intercellular tight junction between adjacent endothelial cells (Figs. 4 and 5). The most characteristic feature of the migrating red blood cells was an extremely irregular configuration of the cell when pushed it through the junction. Constriction of the erythrocyte by the endothelial junction was so tight that the migrating cell body at the level of the junction was extremely thin and thread-like contour of less than 100 μ m in diameter (Figs. 4 and 5). Extravasated erythrocytes adhered directly to the parenchymal glandular cells without intervening basal laminae.

Subsequently some blood capillaries contained almost no cellular components of the blood, whereas their endothelial cells were intact in fine structure (Fig. 6). Close examination revealed that the narrow pericapillary space was provided with a double structure of the continuous basal laminae (Fig. 6, inset). The extravasated erythrocytes had a tendency to gather in groups forming a number of massive conglomerates among the parenchymal glandular cells. These erythrocytes moved, without exception, towards the hypophyseal residual lumen after 20 min of the injection (Fig. 7). The conglomerates crept into the intercellular space of the marginal cells whose apical zone was provided with distinct tight junctions (Fig. 7). Eventually the erythrocytes of conglomerates began to migrate into the Rathke's residual lumen through the zonula occludens of the marginal cells (Fig. 8). As was the case of erythro-

FIG. 1. Extravasation of fragmented erythrocytes into the intercellular space of the parenchymal cells between two blood capillaries filled with red blood cells 10 min after ip injection of 9% NaCl. No visible structural lesion of endothelial cells is evident. Scale bar: 1 μ m.

FIG. 2. A small protrusion (arrow) of erythrocytes (Er) penetrating into the endothelial gaps (or stomata) 10 min after 9% NaCl injection. The opposing two basal laminae (arrow heads) in the pericapillary space are intact. E, endothelial cells. Scale bar: 1 μ m.

FIG. 3. Dilated endothelial gaps through which migration of red blood cells showing mushroom-like-extrusion that is invested with intact basal lamina (arrow head) after 10 min of 9% NaCl injection. E, endothelial cells. Scale bar: 1 μ m.

FIG. 4. Red blood cells emerging from capillaries through the endothelial junctions 10 min after 9% NaCl injection. Irregular shape of erythrocyte showing thread-like configuration at the level of the junction. No structural destruction of endothelial cells (E). Scale bar: 1 μ m.

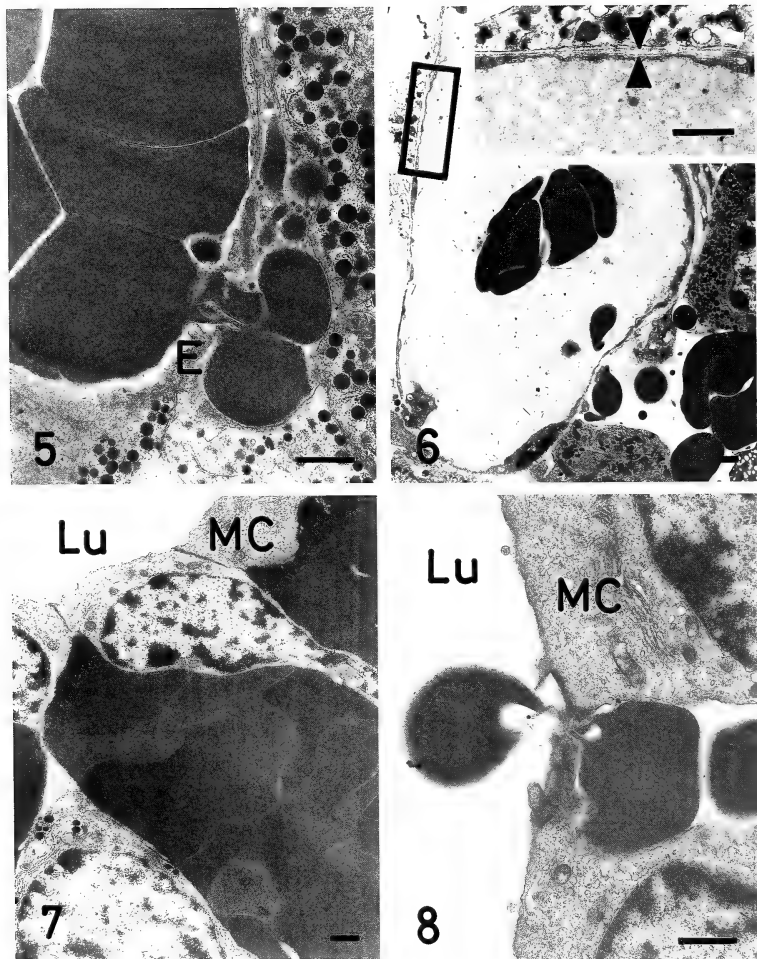


FIG. 5. Another erythrocyte emigration through endothelial junctions 10 min after 9% NaCl injection. Note the extreme constriction of the cell body when passing through the junction. E, endothelial cells. Scale bar: $1\ \mu\text{m}$.
 FIG. 6. Blood capillary without structural lesion and its lumen containing little cellular components 20 min after 9% NaCl injection. Scale bar: $1\ \mu\text{m}$. *Inset*, Higher magnification of a portion of pericapillary space supported by two intact basal laminae (arrow heads). Scale bar: $1\ \mu\text{m}$.

cytes diapedesis (Figs. 4 and 5), the traversing erythrocytes squeezed through the tight junction of marginal cells and showed thread-like configuration in the middle of the cell body (Fig. 8). Additionally the maximum extent of hemorrhage into the anterior pituitary was observed 12 hr after the injection of hypertonic solution and lasted for approximately 3 days [1].

DISCUSSION

Hemorrhage from pituitary adenoma is known as "pituitary apoplexy", a clinical condition that has been first described by Bleibtreu in 1905 [6]. Many factors and possible mechanism by which hemorrhage could occur in pituitary adenoma have been proposed in cases including bromocriptine therapy [7, 8], radiation therapy [9], anticoagulant therapy [10], atherosclerotic embolization [11, 12], thrombosis of the hypophyseal portal vein [13], induction of ovulation [14], head trauma [15], spontaneous necrosis of pituitary tumors [16], carotid angiography [17], arteriography [18] and pre-operative test for pituitary function [19]. The pathogenesis of pituitary apoplexy may not be uniform, but individual cases are probably caused by different mechanism [8]. Whatever the mechanisms are involved, pituitary apoplexy is a life-threatening disorder that requires prompt medical treatment to avoid catastrophe [12]. To obtain an awareness of predisposing factors it seems necessary to establish an experimental system which mimics human pituitary apoplexy. In this regard, our previous studies have demonstrated acute and intense hemorrhage occurring exclusively in the anterior pituitary after ip injection of hypertonic solutions in the conscious mouse [1]. The present electron microscopic study has accumulated an additional evidence that anterior pituitary hemorrhage occurs without obvious destruction of sinusoidal blood capillaries, that is a mechanism known as diapedesis. Up to date no reports have been available dealing with the ear-

liest ultrastructural changes in the erythrocyte diapedesis of either pituitaries or other endocrine glands. Electrolytic destruction of the pituitary stalk resulted in the disrupted capillary walls followed by the leakage of red blood cells and platelets in the pituitary of the rat [2]. Acrylonitrile administration [3] and chronic ACTH stimulation [4] caused hemorrhage into the adrenal cortical zone in rats but no initial changes of erythrocyte extravasation were illustrated.

Under the present experimental conditions the observed erythrocyte diapedesis in the anterior pituitary can be accounted for by postulating the two passages of traversing endothelial cells: through the large endothelial gaps up to 1 μ m in diameter, and through the occluding intercellular junctions between adjacent endothelial cells. The fenestrated capillaries of the endocrine gland type, unlike sinusoids of the hepatic type, are not provided with the large endothelial gaps. Thus these endothelial gaps observed were formed under the present experimental conditions. It is suggested, therefore, that the presence of large endothelial gaps may represent a modification of endothelial junctions as reported after leukotriene B₄ treatment in leukocyte diapedesis in the rabbit [20]. Alternatively, another possibility that endothelial fenestrae, a regular feature of endocrine glands, gather and fuse together to form large endothelial gaps or stomata under the given conditions should be considered. In fact the expansion of stomata is now believed to be a cause of diapedesis in cases including hemorrhagic infarct in the lung, scurvy, purpura, leukemia, vicarious menstruation and toxipathic jaundice.

The second passage of erythrocytes for diapedesis occurred, predominantly, through the endothelial tight junction between adjacent cells (Figs. 4 and 5). In general, the zonula occludens is impermeable for free migration of substances along the intercellular space [21]. However, the junctional complex differs in precise arrangement from one organ to another. The proximal convo-

Fig. 7. Large conglomerates of erythrocytes locating beneath the marginal cells (MC) 20 min after 9% NaCl injection. Lu, hypophyseal lumen. Scale bar: 1 μ m.

Fig. 8. Extreme constriction of red blood cells migrating into the hypophyseal lumen through the tight junction of marginal cells (MC). Scale bar: 1 μ m.

luted tubule of the mouse kidney has a "very leaky epithelium" provided with the zonula occludens consisting in most places of only one junctional strand [22]. Further, the presence of "maculae occludentes" rather than "zonulae occludentes" has been demonstrated in the mouse cardiac muscle [23]. Although general features of the endothelial junctions of endocrine glands are not known, it is considered that erythrocyte diapedesis through endothelial junctions in the anterior pituitary after hypertonic solution administration may be ascribed to structural variations of the junctional complex of either "leaky" structure of the zonulae occludentes or the "maculae occludentes".

One of the interesting findings in this pituitary hemorrhage is the erythrocyte migration into the hypophyseal lumen through tight junctions of the marginal cells which are thought to be provided with a epithelial type of zonulae occludentes. Thus, the zonulae occludentes of the marginal cells may be made up of one or two junctional strands like those of the proximal tubules of the mouse kidney [22]. The similar configuration of red blood cells during the migration through the tight junctions of endothelial cells (Figs. 4 and 5) and of marginal cells (Fig. 8) favors the assumption that both of the tight junctions may belong to the type of zonulae occludentes of leaky in structure. The structural relationship between the endothelial tight junction and the endothelial gaps (or stomata) in diapedesis remains unclear. Further work is required to establish the fine structure and function of endothelial cell junctions of the anterior pituitary.

REFERENCES

- Kobayashi, Y., Masuda, A. and Kumazawa, T. (1982) Hypertonic solutions induce hemorrhage in the anterior pituitary in mice. *Endocrinol. Japon.*, **29**: 647-652.
- Kovacs, K., Horvath, E., Bilbail, J. M., Nagy, E., Domokos, L. and Laszlo, F. A. (1977) Adenohypophysial necrosis in rats following destruction of the pituitary stalk. *Exp. Path.*, **14**: S.243-251.
- Szabo, S., Hüttner, I., Kovacs, K., Horvath, E., Szabo, D. and Horner, H. C. (1980) Pathogenesis of experimental adrenal hemorrhagic necrosis ("Apoplexy"): Ultrastructural, biochemical, neuropharmacologic and blood coagulation studies with acrylonitrile in the rat. *Lab. Invest.*, **42**: 533-546.
- Pudney, J., Price, G. M., Whitehouse, B. J. and Vinson, G. P. (1984) Effects of chronic ACTH stimulation on the morphology of the rat adrenal cortex. *Anat. Rec.*, **210**: 603-615.
- Watanabe, T. and Tanaka, K. (1977) Electron microscopic observations of the kidney in the generalized Schwartzman reaction. *Virchows Arch. A Path. Anat. Histol.*, **374**: 183-196.
- Bleibtreu, L. (1905) Ein Fall von Akromegalie (Zerstörung der Hypophysis durch Blutung), *Munch Med. Wochenschr.*, **41**: 2079-2080.
- Wakai, S., Fukushima, T., Teramoto, A. and Sano, K. (1981) Pituitary apoplexy: Its incidence and clinical significance. *J. Neurosurg.*, **55**: 187-193.
- Yamaji, T., Ishibashi, M., Kosaka, K., Fukushima, T., Hori, T., Manaka, S. and Sano, K. (1981) Pituitary apoplexy in acromegaly during bromocriptine therapy. *Acta Endocrinol.*, **98**: 171-177.
- Weisberg, L. A. (1977) Pituitary apoplexy: Association of degenerative change in pituitary adenoma with radiotherapy and detection by cerebral computed tomography. *Am. J. Med.*, **63**: 109-115.
- Rovit, R. L. and Fein, J. M. (1972) Pituitary apoplexy: A review and reappraisal. *J. Neurosurg.*, **37**: 280-288.
- Sussman, E. B. and Porro, R. S. (1974) Pituitary apoplexy: The role of atheromatous emboli. *Stroke*, **5**: 318-323.
- Reid, R. L., Quigley, M. E. and Yen, S. S. C. (1985) Pituitary apoplexy: A review. *Arch Neurol.*, **42**: 712-719.
- Locke, S. and Tyler, H. R. (1961) Pituitary apoplexy: Report of two cases, with pathological verification. *Am. J. Med.*, **30**: 643-648.
- Nagulesparan, M. and Roper, J. (1978) Haemorrhage into the anterior pituitary during pregnancy after induction of ovulation with clomiphene. *Br. J. Obstet. Gynaecol.*, **85**: 153-155.
- Holness, R. O., Ogundimu, F. A. and Langille, R. A. (1983) Pituitary apoplexy following closed head trauma. Case report. *J. Neurosurg.*, **59**: 677-679.
- Müller-Jensen, A. and Lüdecke, D. (1981) Clinical aspects of spontaneous necrosis of pituitary tumors (pituitary apoplexy). *J. Neurol.*, **224**: 267-271.
- Reichenthal, E., Manor, R. S. and Shalit, M. N. (1980) Pituitary apoplexy during carotid angiography. *Acta Neurochirurgica*, **54**: 251-255.
- Ebersold, M. J., Laws, E. R. Jr., Scheithauer, B. S., Randall, R. V. (1983) Pituitary apoplexy treated by transphenoidal surgery. A clinico-pathological and immunocytochemical study. *J. Neurosurg.*, **58**: 315-320.
- Bernstein, M., Hegele, A., Gentili, F., Brothers,

- M., Holgate, R., Sturtridge, W. and Deck, J. (1984) Pituitary apoplexy associated with a triple bolus test. Case report. *J. Neurosurg.*, **61**: 586-590.
- 20 Thureson-Klein, A., Hedqvist, P. and Lindbom, L. (1986) Leukocytes diapedesis and plasma extravasation after leukotriene B₄: Lack of structural injury to the endothelium. *Tissue and Cell*, **18**: 1-12.
- 21 Farquhar, M. G. and Palade, G. E. (1963) Junctional complexes in various epithelia. *J. Cell Biol.*, **17**: 375-412.
- 22 Claude, P. and Goodenough, D. A. (1973) Fracture faces of zonulae occludentes from "tight" and "leaky" epithelia. *J. Cell Biol.*, **58**: 390-400.
- 23 Karnovsky, M. J. (1967) The ultrastructural basis of capillary permeability studied with peroxidase as a tracer. *J. Cell Biol.*, **35**: 213-236.



Circadian Rhythm of Locomotor Activity in a Teleost, *Silurus asotus*

MITSUO TABATA, MAUNG MINH-NYO, HIROSHI NIWA
and MIKIO OGURI

Laboratory of Fish Biology, School of Agriculture, Nagoya University,
Chikusa, Nagoya 464, Japan

ABSTRACT—Circadian locomotor activities were examined in the nocturnal catfish, *Silurus asotus*. Under constant darkness (DD), the overt rhythm of locomotor activity lasted, in most cases, for 5–10 days, then disappeared. The ratio of fish with circadian activity under DD was higher (approximately 94%) than those under the other experimental conditions described below. Persistence of circadian activity for 5–10 days and subsequent arrhythmicity were also found under constant light (LL). τ value and total amount of locomotor activity tended to decrease with an increase in light intensity. Under the condition of dark pulses (DP), the circadian activity was observed but not prominent as those in DD. The participation of intrinsic rhythmicity on diel locomotor activity was examined by delaying and advancing the LD phases. Resynchronization to the new LD cycle was attained within 1–2 days. In conclusion, the data suggest that, despite the high ratio of fish with intrinsic rhythmicity of locomotor activity, the timing mechanism for diel locomotor activity is fundamentally dependent on the external LD cycles.

INTRODUCTION

Although the circadian rhythm of locomotor activity is well established in mammals [1], birds [2] and reptiles [3], it is not fully documented and still controversial in fish. The existence of circadian rhythm in fish has been demonstrated under constant light and darkness [4–13], whereas other fish display arrhythmicity [14–17].

The persistence of circadian locomotor activity in many fish under constant conditions is relatively low compared with that in higher vertebrates. Overt rhythm of locomotor activities in some fish disappears within several days after imposition of constant conditions [18–21]. Moreover, inter- and/or intra-individual variability has also been demonstrated [21–23].

In order to gain a better understanding of the circadian system of the catfish, *Silurus asotus*, the following experiments were performed. The rhythmicity of circadian locomotor activity was

measured under three different conditions; constant darkness (DD), constant light (LL) and dark pulses (DP). The circadian rule [24, 25] was tested by measuring period length (τ) and total amount of activity under different intensities of constant light. The participation of intrinsic rhythmicity on the diel locomotor activity was examined by shifting the LD phase.

MATERIALS AND METHODS

Catfish of 21–33 cm in total length and 90–215 gm in body weight were used. They were caught in local rivers of Aichi prefecture during May to October in 1985–1987 and kept in laboratory tank. All fish were placed in an acclimatized tank under 12 hr light and 12 hr dark (LD12:12, L=100 lx, D=complete darkness) at 20°C before the experiments.

Fluorescent light (regulatory fluorescent lamp, National, NQ-21550) was set above the tank as the light source for the L phase of the light regime of LD12:12. A heat absorbing filter was placed in front of the light source. Light intensity was

adjusted with neutral density filters (Lee filters). Attenuation by a filter was 1 log unit. The light intensity without neutral density filters, measured at the water surface of the experimental tank, was adjusted to 100 lx.

Measurement for locomotor activity was carried out on individual catfish in a tank (30×30×45 cm) of which the aerated water depth was 10 cm. The tank was placed in a light proof chamber. All experiments were performed at water temperature of 20°C. Locomotor activity was detected by an infrared sensor (Omron, E3D-10M2) set at both sides of the tank. When the fish swims in front of the sensor, the interruption of the infrared light beam was recorded as one count. The shallow water depth was employed to minimize activities outside the infrared light beam (3-5 cm in diameter). Count numbers exceeding 4/sec were cancelled because high frequency counts might be caused by tail beats or small, incomplete intersections of the light beam. Activities were recorded for more than 17 days. Catfish were randomly fed live 1-2 goldfishes once a day, but not fed under constant conditions. All data were recorded by an event recorder (Shinwa Riken, SAC-10P). Simultaneously, counted numbers for each hr were stored in a microcomputer (NEC, PC-8801).

At the end of the experiment, data were converted to periodogram for each animal. Period lengths of the recorded locomotor activity and their statistical significance relative to random "noise" in the time-series data records were determined by the periodogram [26]. In the present study, circadian activity was determined by 95% confidence limit.

Experiment 1. Circadian rhythm of locomotor activity under constant darkness (DD)

This experiment was designed to determine whether a catfish has endogenous locomotor activity under DD condition. Sixteen intact animals were used in this experiment. They were exposed for at least a week to LD12:12 (L=100 lx, D=complete darkness) during the period of entrainment. After the entraining period, locomotor activity of individual fish was recorded under DD for 10-22 consecutive days.

Experiment 2. Circadian rhythm of locomotor activity under constant light (LL)

The purpose of this experiment was to investigate the intrinsic locomotor activity under LL condition. In addition, it was designed to test the so-called circadian rule with respect to the period length of free-running (τ) and the total amount of locomotor activity (mean count/day) [24, 25]. Thirty-two fish were used in this experiment. Entraining conditions to the LD cycle were the same as experiment 1.

Locomotor activities were measured under 4 different intensities of light; 0.01, 0.1, 1 and 10 lx. To exclude after-effects [27, 28], all experimental animals were pre-exposed to the same LD cycle (L=100 lx, D=complete darkness) for one week before exposure to each of the 4 LL intensities. After entrainment, fish were exposed to constant light for 10-22 days. To test the circadian rule on the relationship between τ and light intensity a completely randomized design was employed. Four groups of fish (6 fish each), each exposed to 1 of 4 given LL intensities, were used for the analysis. Each fish represents 1 replication. To examine the relationship between total locomotor activity and light intensity, the data from fish that mentioned above were used for analysis. The animals were divided into 4 groups (6 fish each), each corresponding to a given light intensity. Each fish represents 1 replication. The locomotor activity was measured for 5 days and averaged. The results were analyzed by the paired t-test.

Experiment 3. Circadian rhythm of locomotor activity under repeated dark pulses (DP)

This experiment was designed to observe the effect of dark pulses (DP) on locomotor activity. Dark pulses are thought to enhance free-running rhythmicity and reduce the rapid disassociation of the multi-oscillatory circadian system in some fish [20]. Dark pulses were composed of 15 min of complete darkness alternating with 45 min light (L=100 lx) (LD 0.75:0.25). The experimental period lasted for 10-22 days. Eight fish were used in this experiment. Entraining conditions before exposure to dark pulses were the same as those in experiment 1.

Experiment 4. Shifting of the LD phase

Shifting the LD cycle was employed to examine the contribution of endogenous mechanisms on diel locomotor activity. The initial light phase started at 6:00 and ended at 18:00. The LD cycles continued for at least a week. Then the LD cycle was delayed for 6 hrs by lengthening the dark phase 6 hrs and changing the time of light-on and -off to 12:00 and 24:00, respectively. After the phase shift of the LD cycle, locomotor activity of the fish was recorded for another 9 days. Then, the LD cycle was advanced 6 hrs by shortening dark phase 6 hrs returning the light-on and -off times to 6:00 and 18:00 again. Then, locomotor activity was recorded for another 8 days. Two different intensities (0.1, 100 lx) for the light phase were used in the shifting experiment. This experiment was performed using 7 fish.

RESULTS

Experiment 1. Circadian rhythm of locomotor activity under DD

All fish showed active behavior in the dark when they were subjected to the LD cycles. The catfish displayed continuous activity mostly after the offset of light which ended after the onset of light. With imposition of constant darkness, the animal lost synchrony with the previous LD cycle and freeran as shown in Figure 1. Most catfish showed overt circadian rhythmicity for 5–10 days as shown in this fish. Although instability of free-running activity may be a common feature in catfish, it was lasted for, in a few cases, more than 20 days. The persistence of circadian rhythmicity of catfish was longer when compared with other species of fish.

τ values, measured in a total of 15 animals by periodogram analysis in which transient cycles were excluded, were between 22.5 and 27.3 hr (24.64 ± 0.38 hr, mean \pm SEM). The occurrence ratio of fish with circadian rhythmicity under the DD was approximately 94% (15/16).

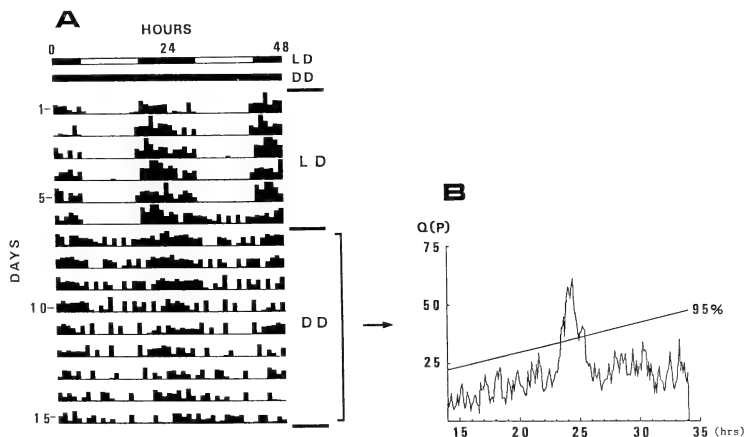


FIG. 1. A record of locomotor activity in a catfish kept under LD 12:12 (100:0 lx) and constant darkness (DD). White and dark bars at the top of the panel represent L and D phases. B. Periodogram derived from analysis of the actogram under constant darkness (DD). The Q(p) values in the periodogram above the 95% confidence limit (slanted line) are significantly different from random noise. The record was double plotted for clarity.

Experiment 2. Circadian rhythm of locomotor activity under LL

A total of 32 intact catfish was used in the LL experiments, using 4 different intensities of white light. As shown in an example record in Figure 2, rhythmicity of locomotor activity was detected when animals were subjected to LL ($L=10$ lx). The circadian rhythm in the actograms seemed less clear in LL compared to those in DD. The ratio of fish with circadian rhythmicity for all light intensities was approximately 75%. Overall τ values were between 20.1 to 27.0 hr. The values were calculated from data collected for 5–10 days in which transient cycles were excluded.

The relationship between light intensity in LL and τ value is shown in Figure 3. The dependence of τ on intensity was demonstrated. Although a pair of τ values between 0.1 and 1 lx was insignificant, those of the other pairs (0.01 and 0.1 lx, 1 and 10 lx) were significantly different ($p < 0.001$, $p < 0.05$). The data suggest that the correlation of τ and light intensity is negative.

The relation between different light intensities

and mean locomotor activity is shown in Figure 4. It was observed that only a pair of results between 0.01 and 10 lx was significantly different ($p < 0.01$). However, there was a tendency that mean locomotor activity decreased with an increase of light intensity.

Experiment 3. Circadian locomotor activity under DP

The circadian locomotor activity was detected under DP, but not prominent as those in DD. As shown in Figure 5, circadian activity was not clear by visual inspection of this actogram but it was detected by the periodogram. Six out of eight animals showed circadian rhythmicity under the condition of dark pulses. The total τ values, which were analyzed without transient cycle, were between 20.9 and 27.5 hr (24.71 ± 1.07 hr, mean \pm SEM).

Experiment 4. Shifting the LD phase

As described above all fish showed typical active behavior in the dark under the LD cycles. After the LD cycle was delayed 6 hr at day 10 (Fig. 6),

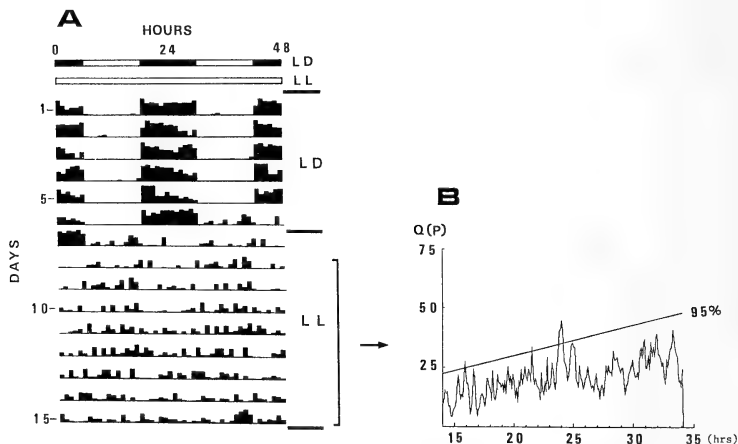


Fig. 2. A. An example of locomotor activity in a catfish held under LD 12:12 (100:0 lx) and constant light (LL, $L=10$ lx). B. Periodogram derived from analysis of the actogram under constant light. Other features are as described in Fig. 1.

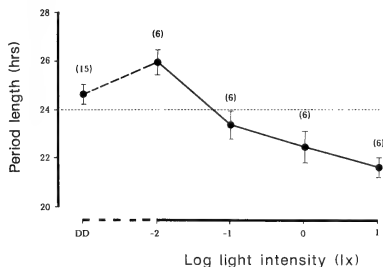


FIG. 3. Relationship between mean free-running period (τ) during 5–10 days and intensity of continuous illumination (lx) in catfish. Closed circles represent the τ means and vertical lines indicate the SEM. Numbers in parentheses indicate the number of fish used. Values for DD were derived from experiment 1.

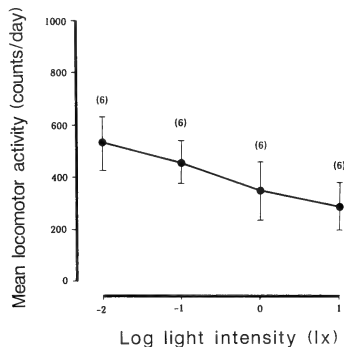


FIG. 4. Relationship between mean amount of locomotor activity and intensity of continuous illumination (lx) in catfish. Closed circles indicate the mean locomotor activity and vertical lines represent the SEM. Numbers in parenthesis indicate the number of fish used.

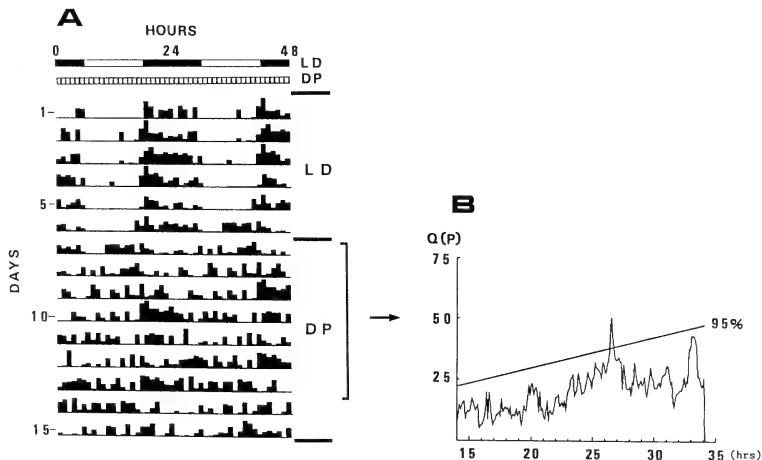


FIG. 5. A. An example of locomotor activity of a catfish kept under LD 12:12 (100 lx), then exposed to dark pulses (LD 0.75:0.25, L=100 and D=0 lx). B. Periodogram derived from analysis of the actogram under dark pulses. Other features are as described in Fig. 1.

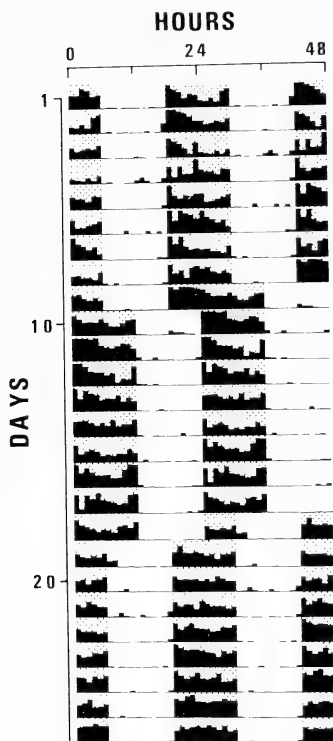


FIG. 6. Double plot of locomotor activity of a catfish in response to a phase shift of LD 12:12 (L=100 lx). Shaded areas indicate the D phase.

the animal displayed locomotor activity during the prolonged dark phase. Small amount of activities were observed during the initial day of the newly changed light phase comparable to that during the period corresponding to the previous dark phase. However, a stable nocturnal pattern was quickly achieved. Resynchronized activities to the phase shifted LD cycles were observed afterwards. After 8 days, the LD cycle was shifted again by advancing the LD regime 6 hr. After the phase shift some

locomotor activity was observed during the new light phase on the first day. Locomotor activity ceased after a few hrs. However, the activity was completely synchronized to the new LD cycles for the subsequent days.

The same protocol was conducted using a different light intensity during the L phase (0.1 lx). As shown in Figure 6, all actograms revealed a similar pattern of behavior indicating small amounts of transient activity during the light phase immediately after changing the LD regime.

The requirement of resynchronization to the new LD cycles was 1-2 days in the shifting experiments under the intensity of both 0.1 and 100 lx. The same period of transient cycles following the delay and advance of the LD phase (symmetry-effects) were apparent.

DISCUSSION

Despite the fact that endogenous locomotor activity is prolonged, lasting for 100-300 cycles in some higher vertebrates [29, 30], instability of free-running activity is commonly observed in many species of fish. The circadian activity pattern in fish is labile and fades-out easily. Moreover, intra- and inter-individual variations in activity rhythms appears to be common in fish [21-23]. Although the ratio of fish with circadian rhythmicity under constant conditions was higher in catfish than in other species of fish [4-13], similar characteristics of instability of the circadian rhythm of locomotor activity reported in many other fish were observed. One of the reasons for the unstable nature of the rhythm in fish is thought to be the multiple components of the locomotor activity system [31, 32]. In contrast to fish, only a single criterion of behavior is observed in the circadian or entrained activity in higher vertebrates [33]. It has been documented that, under LL conditions, τ depends on the intensity of light. According to the so-called Aschoff's rule [24, 25], termed by Pittendrigh [27], τ decreases but total amount of activity increases with increased intensities in light active animals, whereas the relationship is reversed in night active animals. According to this rule the definition for teleosts has been contradicted. Electric fish, *Gymnorhamphichthys hypostomus* [34],

killifish, *Fundulus heteroclitus* [7], cyprinid, *Leucaspis delinatus* [35], and diurnal juvenile pink salmon, *Onchorhynchus gorbuscha* [21] obey this rule, but not the lake chub, *Couesius plumbeus* [31] or nocturnal juvenile pink salmon [21]. There are also several other exceptions to this rule in other species of animals [36]. Instead of grouping data from nocturnal and diurnal animals for analysis, Pittendrigh and Daan [37], proposed that τ is lengthened in LL with increasing light intensity in species with $\tau_{DD} < 24$ hr, while it is shortened in species with $\tau_{DD} > 24$ hr (cf. [36]). In a strict sense, the results obtained in the present experiment do not obey Aschoff's rule, but fit the modified Aschoff's rule with respect to τ and total amount of activity.

Arrhythmicity or extinction of a rhythm occurs in many fish when they are kept under constant conditions. These characteristics of circadian activity are thought to be associated with a multi-oscillator system in some species of fish. The circadian system of these fish is considered to be composed of two or more groups of loosely coupled oscillators synchronized to dawn and dusk [22, 38–40]. If a fish is kept under constant conditions, the oscillators are uncoupled, resulting in free-run with their own periods of activity. This could cause arrhythmicity or disappearance of circadian rhythms. If disassociation of the loosely coupled oscillators could be prevented in some way, intrinsic activity might appear in fish. Based on this hypothesis, Eriksson & van Veen [20] applied a light and dark regime of LD 0.75:0.25 instead of LL or DD. This procedure stabilized and prolonged the free-running rhythm in the brown bullhead. However, in our experiment, a 15 min dark pulse every hour did not stabilize or prolong circadian activity. Rather, it caused an opposite effect on locomotor activity of the catfish. The frequency of circadian activity under the dark pulses decreased compared to that of DD. This indicates that (1) dark pulsing causes a dissociation of the oscillators that control circadian activity or (2) possible existence of a circadian organization in catfish differing from a multi-oscillator system.

LD cycle is an effective entraining agent in many species of fish, resulting in diurnal, nocturnal and/or crepuscular patterns of behavior. The endoge-

nous nature of these diel locomotor activities, however, has not been characterized well. When endogenous factors are strongly associated with the timing mechanism under LD condition, delaying or advancing the LD regime causes the appearance of several transient cycles. Duration of transient period is known to depend on the direction of the LD shift. It is generally shorter for delay-shift compared to advance-shift. If several days are required for an animal to synchronize to a new LD cycle, the timing mechanism of locomotor activity has an endogenous component [24, 41]. On the other hand, if an animal synchronizes to a new LD cycle within a day, activities may be exogenously controlled [2, 24, 41]. The endogenous control in fish, examined by shifting the LD regime, has been shown in hagfish, *Eptatretus burgeri* [11], swell shark, *Cephaloscyllium ventriosum* [5], and river chub, *Zacco temminckii* (Tabata and Minh-Nyo, unpublished). On the other hand, exogenous control of locomotor activities has been demonstrated in horn shark, *Heterodontus francisci* [5], juvenile pink salmon, [21], juvenile American shad, *Alosa sapidissima* [15], Atlantic salmon parr, *Salmo salar* [42] and Ayu, *Plecoglossus altivelis* (Tabata and Minh-Nyo, unpublished). In the present study, resynchronization to a new LD cycle following a shift in either direction was attained after 1–2 transient cycles. This was observed with both intensities of light (0.1 and 100 lx). The weaker intensity used in the present experiment (0.1 lx) is strong enough to be sensed by the lateral eye and the pineal organ but is not an effective stimulus for the extra-retinal and nonpineal photoreceptors which are associated with the 24 hr locomotor activity of catfish [43]. Hence, despite the high ratio of fish with circadian activity observed under both constant light and darkness conditions, it is suggested that the timing mechanism for diel locomotor activity of the catfish is, fundamentally, based on external LD cycles perceived by the lateral eyes and the pineal organ.

Parametric and nonparametric effects may be mediated by different photoreceptors as described by Underwood and Menaker [44]. Catfish possess three or more photoreceptors which are involved in eliciting locomotor activity and entrainment [43,

45]. Moreover, the contribution of photoreceptors to photoreception is also species-dependent (Tabata *et al.*, unpublished). Additional studies are needed to determine whether differences in receptor mechanisms are responsible for the τ values observed under different light intensities of constant illumination.

ACKNOWLEDGMENTS

The authors are grateful to Prof. T. Oishi of Nara Women's University for his helpful discussion of the manuscript. We wish to thank Prof. T. I. Koike of Univ. Arkansas for Med. Sci. for reading the manuscript.

REFERENCES

- 1 Moore-Ede, M. C., Sulzman, F. M. and Fuller, C. A. (1982) In "The Clocks That Time Us". A Commonwealth Fund Book. Harvard Univ. Press. Cambridge/Massachusetts/London, pp. 30-151.
- 2 Gwinner, E. (1975) Circadian and circannual rhythms in birds. In "Avian Biology, Vol. 5". Ed. by D. S. Farner and J. R. King. Academic Press, New York/San Francisco/London, pp. 221-285.
- 3 Underwood, H. (1977) Circadian organization in lizards: The role of the pineal organ. *Science*, **195**: 587-589.
- 4 Lissmann, H. W. and Schwassmann, H. O. (1965) Activity rhythm of an electric fish, *Gymnorhamphichthys hypostomus*. *Z. Verh. Physiol.*, **51**: 153-170.
- 5 Nelson, D. R. and Johnson, R. H. (1970) Diel activity rhythms in the nocturnal bottom dwelling sharks *Heterodontus francisci* and *Cephaloscyllium ventriosum*. *Copeia*, **4**: 732-739.
- 6 Nishi, G. (1980) Locomotor activity rhythms in two gobies, *Eleotriodes wardi* and *Amblyeleotris japonica*, under experimental conditions. *Inst. Oceanic Res. & Develop. Tokai Univ. Notes*, **2**: 69-87. (In Japanese).
- 7 Kavaliers, M. (1980) Social groupings and circadian activity of the killifish, *Fundulus heteroclitus*. *Biol. Bull.*, **158**: 69-76.
- 8 Kavaliers, M. (1980) Circadian locomotor activity rhythms of the burbot, *Lota lota*: seasonal differences in period length and the effect of pinealectomy. *J. Comp. Physiol.*, **136**: 215-218.
- 9 Kavaliers, M. (1980) Circadian activity of the white sucker, *Catostomus commersoni*: comparison of individual and shoaling fish. *Can. J. Zool.*, **58**: 1399-1403.
- 10 Ueda, M. and Oishi, T. (1982) Circadian oviposition rhythm and locomotor activity in the Medaka, *Oryzias latipes*. *J. interdiscipl. Cycle Res.*, **6**: 131-140.
- 11 Ooka-Souda, S., Kabasawa, H. and Kinoshita, S. (1985) Circadian rhythms in locomotor activity in the hagfish, *Eptatretus burgeri*, and the effect of reversal of light-dark cycle. *Zool. Sci.*, **2**: 749-754.
- 12 Tabata, M. (1986) Circadian rhythms and the pineal organ of fishes. *Dobutsu Seiri*, **3**(4): 103-112. (In Japanese).
- 13 Garg, S. K. and Sundararaj, B. I. (1986) Role of pineal in the regulation of some aspects of circadian rhythmicity in the catfish, *Heteropneustes fossilis* (Bloch). *Chronobiol.*, **3**: 1-11.
- 14 Richardson, N. E. and McCleave, J. D. (1974) Locomotor activity rhythms of juvenile Atlantic salmon (*Salmo salar*) in various light conditions. *Biol. Bull.*, **147**: 422-432.
- 15 Katz, H. M. (1978) Circadian rhythms in juvenile American shad, *Alosa sapidissima*. *J. Fish Biol.*, **12**: 609-614.
- 16 Mashiko, K. (1979) The light intensity as a key factor controlling nocturnal action in the catfish, *Pseudobagrus aurantiacus*. *Japan. J. Ichthyol.*, **25**(4): 251-258.
- 17 Goudie, C. A., Davis, K. B. and Simco, B. A. (1983) Influence of the eyes and pineal gland on locomotor activity patterns of channel catfish, *Ictalurus punctatus*. *Physiol. Zool.*, **56**(1): 10-17.
- 18 Davis, R. E. (1963) Daily 'predawn' peak of locomotion in bluegill and largemouth bass. *Anim. Behav.*, **12**: 272-283.
- 19 Stickney, A. P. (1972) The locomotor activity of juvenile herring (*Clupea harengus harengus* L.) in response to changes in illumination. *Ecology*, **53**: 438-445.
- 20 Eriksson, L.-O. and van Veen, T. (1980) Circadian rhythms in the brown bullhead, *Ictalurus nebulosus* (Teleostei). Evidence for an endogenous rhythm in feeding, locomotor, and reaction time behaviour. *Can. J. Zool.*, **58**: 1899-1907.
- 21 Godin, J.-G. J. (1981) Circadian rhythm of swimming activity in juvenile pink salmon (*Oncorhynchus gorbuscha*). *Mar. Biol.*, **64**: 341-349.
- 22 Eriksson, L.-O. (1978) Nocturnalism versus diurnalism-dualism within fish individuals. In "Rhythmic Activity of Fishes". Ed. by J. E. Thorpe, Academic Press, London/New York/San Francisco, pp. 69-89.
- 23 Müller, K. (1978) The flexibility of the circadian system of fish at different latitudes. In "Rhythmic Activity of Fishes". Ed. by J. E. Thorpe. Academic Press. London New York San Francisco, pp. 91-129.
- 24 Aschoff, J. (1960) Exogenous and endogenous components in circadian rhythms. In "Biological clocks". Cold Spring Harbor Symp. Quant. Biol.,

- 25: 11-28.
- 25 Aschoff, J. (1965) The phase angle difference in circadian periodicity. In "Circadian Clock". Ed. by J. Aschoff, North Holland, Amsterdam, pp. 262-276.
- 26 Sokolove, P. G. and Bushell, W. N. (1978) The chi square periodogram: Its utility for analysis of circadian rhythms. *J. theor. Biol.*, **72**: 131-160.
- 27 Pittendrigh, C. S. (1960) Circadian rhythms and circadian organization. Cold Spring Harbor Symp. Quant. Biol., **25**: 159-184.
- 28 Pittendrigh, C. S. and Daan, S. (1976) A functional analysis of circadian pacemakers in nocturnal rodents. I. The stability and lability of spontaneous frequency. *J. Comp. Physiol.*, **106**: 223-252.
- 29 Eskin, A. (1971) Some properties of the system controlling the circadian activity rhythms of sparrows. In "Biochronometry". Ed. by M. Menaker. Natl. Acad. Sci., Washington, pp. 55-80.
- 30 Hoffmann, K. (1971) Splitting of the circadian rhythm as a function of light intensity. In "Biochronometry". Ed. by M. Menaker. Natl. Acad. Sci., Washington, pp. 134-150.
- 31 Kavaliers, M. (1978) The role of photoperiod and twilight in the control of locomotory rhythms in the lake chub, *Couesius plumbeus*. Ph. D. Thesis, University of Alberta, Edmonton.
- 32 Weber, D. N. and Spielgr, R. E. (1987) Effects of the light-dark cycle and scheduled feeding on behavioral and reproductive rhythms of the cyprinodont fish, Medaka, *Oryzias latipes*. *Experientia*, **43**: 621-624.
- 33 Enright, J. T. (1970) Ecological aspects of endogenous rhythmicity. *Ann. Rev. Ecol. Syst.*, **1**: 221-238.
- 34 Schwassmann, H. O. (1971) Circadian activity patterns in gymnotid fish. In "Biochronometry". Ed. by M. Menaker. Natl. Acad. Sci., Washington, pp. 186-199.
- 35 Siegmund, R. and Wolff, D. L. (1973) Circadian-Rhythmik und Gruppenverhalten bei *Leucaspis delineatus* (Pisces, Cyprinidae). *Experientia*, **29**: 54-58.
- 36 Aschoff, J. (1979) Circadian rhythms: influences of internal and external factors on the period measured in constant conditions. *Z. Tierpsychol.*, **49**: 225-249.
- 37 Pittendrigh, C. S. and Daan, S. (1976) A functional analysis of circadian pacemakers in nocturnal rodents. IV. Entrainment: Pacemaker as clock. *J. Comp. Physiol.*, **106**: 291-331.
- 38 Andreasson, S. (1973) Seasonal changes in diel activity of *Cottus poecilopus* Heckel and *C. gobio* (Pisces) at the arctic circle. *Oikos*, **24**: 16-23.
- 39 Eriksson, L.-O. (1973) Spring inversion of the diel rhythm of locomotor activity in young sea-going brown trout, *Salmo trutta trutta* L., and Atlantic salmon, *Salmo salar* L. *Aquilo. Ser. Zool.*, **14**: 68-79.
- 40 Kavaliers, M. (1978) Seasonal changes in the circadian activity period of lake chub, *Couesius plumbeus*. *Can. J. Zool.*, **56**: 2591-2596.
- 41 Bünning, E. (1973) *The Physiological Clock*. Springer-Verlag, New York, 3rd ed., pp. 89-115.
- 42 Varanelli, C. C. and McCleave, J. D. (1974) Locomotor activity of Atlantic salmon parr (*Salmo trutta* L.) in various light conditions and in weak magnetic fields. *Anim. Behav.*, **22**: 178-186.
- 43 Tabata, M., Minh-Nyo, M. and Oguri, M. (1988) Involvement of retinal and extraretinal photoreceptors in the mediation of nocturnal locomotor activity rhythms in the catfish, *Silurus asotus*. *Exp. Biol.*, **47**: 219-225.
- 44 Underwood, H. and Menaker, M. (1976) Extraretinal photoreception in lizards. *Photochem. Photobiol.*, **25**: 227-243.
- 45 Tabata, M., Minh-Nyo, M. and Oguri, M. (1988) Threshold of retinal and extraretinal photoreceptors measured by photobehavioral response in catfish, *Silurus asotus*. *J. Comp. Physiol.*, **164**: 797-803.



Cestode Parasites of Some Taiwanese Shrews

ISAMU SAWADA and MASASHI HARADA¹*Biological Laboratory, Nara Sangyo University, Nara 636, and*¹*Laboratory of Experimental Animals, Osaka City University
Medical School, Osaka 545, Japan*

ABSTRACT—Five new species of hymenolepidid and one new species of dilepidid cestodes were obtained through the examination of 15 shrews belonging to four species of four genera, collected in three regions of Taiwan from October 7 to 9, 1986. *Vampirolepis formosana* sp. n. from *Anourosorex squamipes yamashinai* is related to but differs from *V. montana* and *V. molus* in the shape of rostellar hooks. *Vampirolepis magnihamata* sp. n. from *A. squamipes yamashinai* is related to but differs from *V. macroselidarum*, *V. neomidis* and *V. stefanskii* in the size and shape of rostellar hooks. *Vampirolepis sunci* sp. n. from *Suncus myosurus swinhoei* is related to but differs from *V. amamiensis* in the size and shape of rostellar hooks, and the size of embryonic hooks. *Vampirolepis sessilihamata* sp. n. from *S. myosurus swinhoei* is related to but differs from *V. bahli* in the shape of rostellar hooks. *Vampirolepis gracilistrobila* sp. n. from *S. myosurus swinhoei* is related to but differs from *V. notoensis* in the size of strobila, the number of rostellar hooks, the position of genital pores and the form of ovary. *Choanotaenia (Choanotaenia) tubirostellata* sp. n. from *A. squamipes yamashinai* is related to but differs from *C. (C.) sciuricola* in the size of rostellum, the number of rostellar hooks and the size of onchospheres.

INTRODUCTION

The cestode parasites of shrews in Taiwan have been unknown the most part except one by Olsen and Kuntze (1978) [1], who described *Staphylocystis (Staphylocystis) suncuensis* from *Suncus murinus* collected at Wu Shi, Nantou Hsien. So far no attempt have been made to study the cestode parasites of shrews, although they are quite common in Taiwan. It is the purpose of this paper to give a preliminary note of the cestode parasites obtained from shrews in Taiwan. More complete information on these helminths will be published at a later date.

MATERIALS AND METHODS

A total of 15 shrews were captured by trap at Nantou and Taoyuan Hsiens from October 7 to 9, 1986. The shrews were autopsied immediately

after capture and their intestinal tracts were fixed in Carnoy's fluid and brought to Japan. After being soaked in 45% acetic acid for five hr for expanding, they were cut open in 70% alcohol and examined for cestodes. The cestodes obtained were stored in 70% alcohol. The morphological features of scoleces, eggs and a part of mature segments were observed under the interference contrast light microscope. The strobilae were stained with alcohol-hydrochloride-carmin, dehydrated in alcohol, cleared in xylene, and mounted in Canada balsam. Measurements are given in millimetres.

RESULTS

Localities of the shrews and their cestodes obtained are shown in Figure 1 and Table 1. The cestodes found were as follows: *Vampirolepis formosana* sp. n., *V. magnihamata* sp. n., *V. sunci* sp. n., *V. sessilihamata* sp. n., *V. gracilistrobila* sp. n. and *Choanotaenia (Choanotaenia) tubirostellata* sp. n..

Accepted May 27, 1988

Received April 2, 1988

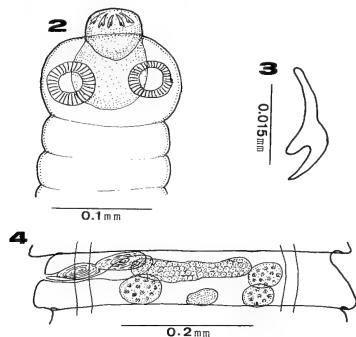


Fig. 1. Map showing the collection sites of shrews. For the locality, see Table 1.

Vampirelepis Spassky, 1954
Vampirelepis formosana sp. n.
 (Figs. 2-4)

One Yamashinai's mole-shrew, *Anourosorex squamipes yamashinai*, captured at Kunyan, Lenai Hsiang, Nantou Hsien on October 7, 1986, contained two specimens of the present new species. They were fully mature, but not gravid.

Description: Small-sized hymenolepidid; strobila length 15-19 and 0.4-0.6 width. Metamerism distinct, craspedote, margins slightly serrate. Scolex nearly tetragonal, 0.140-0.273 long by 0.154-0.175 wide. Rostellum oval or spherical, 0.070-0.091 long by 0.063-0.091 wide, armed with a single row of 28-30 chela-shaped hooks. Hooks



Figs. 2-4. *Vampirelepis formosana* sp. n. 2: Scolex. 3: Rostellar hook. 4: Mature segment, ventral view.

measuring 0.021; handle comparatively long, guard round at its end, remarkably shorter than blade; blade sharp at its end, curved toward guard. Rostellar sac oval, 0.120-0.126 long by 0.019-0.098 wide. Suckers discoid, unarmed, 0.084-0.091 in diameter. Neck absent.

Genital pores unilateral, located a little anterior to middle of segment margins. Testes three in number, subspherical, 0.056-0.063 by 0.028-0.035, situated in the posterior field of segment and arranged triangularly, one poral and two aporal. Vagina opening in genital atrium, posterior to cirrus sac, passing behind cirrus sac, gradually expanding into voluminous seminal receptacle measuring 0.035-0.053 long by 0.025 wide. Ovary transversely elongated, 0.070-0.091 across, situated in anterior field of segment. Vitelline gland compact, 0.035-0.063 long by 0.028-0.035 wide, situated near midline in space between poral and aporal testes, posterior to ovary.

Host: *Anourosorex squamipes yamashinai* Kudoda.

Site of infection: Small intestine.

Locality and date: Kunyan, Lenai Hsiang, Nantou Hsien; October 7, 1986.

Type specimen: Holotype: NSU Lab. Coll. No. 8901.

Remarks: The present new species closely resembles *Vampirelepis montana* Crusz and Sanmugasunderam, 1971 from *Suncus murinus montanus* [2] and *V. molus* Srivastava and Capoor, 1979 from *Crocidura murianus* [3] in the number of rostellar hooks, furthermore, it closely resembles the latter in the length of rostellar hooks (Table 2). However, it differs from the above-mentioned two cestodes in the shape of rostellar hooks (Fig. 5).



Fig. 5. Rostellar hooks of closely related species. A: *V. montana*. B: *V. olus*.

TABLE 1. Shrews examined and their cestode parasites in Taiwan in 1986

Serial No. of locality in Fig. 1	Locality	Date	Shrew species	No. of shrew		Cestode species
				examined	infected	
1	Kunyan, Lenai Hsiang Nantou Hsien	Oct. 7	<i>Soriculus fumidus</i> <i>Anourosorex squamipes yamashinai</i>	2 3	0 { 1 1 }	<i>Vampirolepis formosana</i> s. n. <i>V. magnihamata</i> sp. n.
2	Tsuifeng, Lenai Hsiang, Nantou, Hsien	Oct. 8	<i>A. squamipes yamashinai</i>	6	{ 6 1 }	<i>Choanotaenia (Choanotaenia) tubirostellata</i> sp. n. * <i>C. (C.) tubirostellata</i> sp. n. <i>V. magnihamata</i> sp. n.
3	Kuamin Tsun, Kuanyin Hsiang, Taoyuan Hsien	Oct. 9	<i>Crociodura tanakae</i> <i>Suncus myosurus swinhoei</i>	1 3	{ 1 1 }	juvenile (unidentified) * <i>V. sessilihamata</i> sp. n. <i>V. gracilistrobila</i> sp. n. <i>V. sunci</i> sp. n.

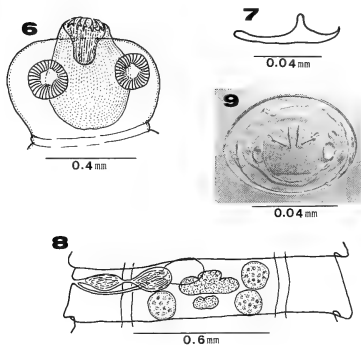
* double infection

TABLE 2. Comparison of closely related species armed with 24-32 rostellar hooks

Species	Rostellar hook		Host species
	No.	length	
<i>V. montana</i>	24-28	0.0553-0.065	<i>Suncus murinus nonianus</i>
<i>V. molis</i>	26-32	0.015-0.019	<i>Crociodura murianus</i>
<i>V. formosana</i> sp. n.	28-30	0.021	<i>Anourosorex squamipes yamashinai</i>

Vampirolepis magnihmata sp. n.
(Figs. 6–9)

On October 7, 1986, one Yamashina's mole-shrew, *A. squamipes yamashinai*, was captured at Kunyan, Lenai Hsiang, Nantou Hsien. The shrew was found infected with six mature specimens of this cestode.



FIGS. 6–9. *Vampirolepis magnihmata* sp. n. 6: Scolex. 7: Rostellar hook. 8: Mature segment, ventral view. 9: Egg.

Description: Medium-sized hymenolepidid; worm length 46–60; maximum width 1.2–1.7. Metamerism distinct, margins serrate. Segments wider than long. Scolex 0.154–0.277 long by 0.140–0.207 wide, set off from strobila. Rostellum mushroom-shaped, 0.207–0.387 long by 0.083–0.161 wide, armed with a single row of 16–18 hooks measuring 0.063–0.070. Hook handle slightly long; guard round at its end, making a right angle with handle; blade remarkably curved and sharp at its end. Rostellar sac large and pyriform, 0.434–0.448 long by 0.343–0.350 wide. Suckers discoid, 0.154–0.277 long by 0.140–0.207 wide. Neck absent.

Genital pores unilateral, located at anterior 1/3 of segment margins. Testes three in number, spherical or oval, arranged triangularly. Cirrus sac pyriform, 0.175–0.245 long by 0.063–0.070 wide, extending beyond longitudinal osmoregulatory

canals. Internal seminal vesicle 0.091–0.112 long by 0.056–0.063 wide. External seminal vesicle oval, 0.210–0.238 long by 0.077–0.091 wide. Vagina opening in genital strium, extending medially, then enlarging, and forming voluminous seminal receptacle measuring 0.196–0.245 long by 0.190–0.245 wide. Ovary transversely elongate, trilobate in mature segment, 0.077–0.084 wide. Vitelline gland weakly developed, bilobate, 0.056–0.098 by 0.042–0.056, situated near middle in space between poral and aporal testes, just posterior to ovary. Eggs oval or spherical, 0.070–0.081 by 0.053–0.063, surrounded by four thin envelopes, with smooth surface. Onchospheres spherical, 0.039 by 0.028–0.030; embryonic hooks 0.011 long.

Host: *Anourosorex squamipes yamashinai* Kuroda.

Site of infection: Small intestine.

Localities and date: Kunyan, Lenai Hsiang, Nantou Hsien: October 7, 1986 and Tsuifeng, Lenai Hsiang, Nantou, Hsien: October 8, 1986.

Type specimen: Holotype: NSU Lab. Coll. No. 8902; Paratypes: No. 8903.

Remarks: About 20 species of the *Vampirolepis* have been recorded from the Soricidae. Of these, the species armed with 15–22 rostellar hooks are *V. macroscelidarum* (Baer, 1926) [4], *V. neomidis* (Baer, 1931) [5] and *V. stefanski* (Zarnowki, 1954) [6]. The present new species differs from any of them in the size and shape of rostellar hooks (Table 3 and Fig. 10).

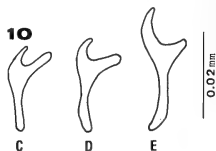


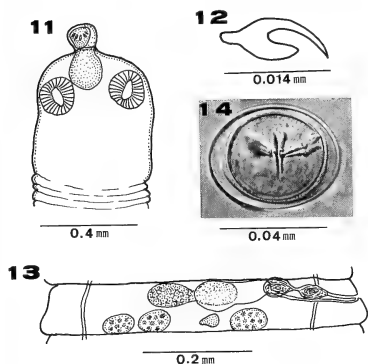
FIG. 10. Rostellar hooks of closely related species. C: *V. macroscelidarum*. D: *V. neomidis*. E: *V. stefanski*.

Vampirolepis sunci sp. n.
(Figs. 11–44)

On October 9, 1986, three brown musk shrews, *Suncus myosurus swinhoei* were captured at Kua-

TABLE 3. Comparison of closely related species armed with 15–22 rostellar hooks

Cestode species	Rostellar hook		Host species
	No.	length	
<i>V. macroscelidarum</i>	20	0.019	<i>Macroscelides brachyrynchus</i>
<i>V. neomidis</i>	18	0.022	<i>Neomys fodiens</i>
<i>V. stefanskii</i>	15–22	0.028–0.032	<i>Sorex araneus</i>
<i>V. magnihamata</i> sp. n.	16–18	0.063–0.070	<i>Anourosorex squamipes yamashinai</i>



FIGS. 11–14. *Vampirolepis sunci* sp. n. 11: Scolex. 12: Rostellar hook. 13: Mature segment, dorsal view. 14: Egg.

nyin Tsun, Kuanyin Hsiang, Taoyuan Hsien. One of them harbored a specimen of this cestode.

Description: Small-sized hymenolepidid: mature strobila length 18 and maximum width 0.6. Metamerism distinct, margins serrate. Segments wider than long. Scolex 0.415 long by 0.484 wide, not demarcated from neck. Rostellum pyriform, 0.070 long by 0.055 wide, armed with a single circle of 16 thorn-shaped hooks measuring 0.014 long. Hook handle short; guard bluntly round at its end, shorter than blade; blade remarkably slender, sharp at its end. Rostellar sac elongate, 0.194 long by 0.221 wide. Suckers discoid, 0.138 by 0.111. Neck absent.

Genital pores unilateral, situated in middle or a little posterior to middle of segment margins.

Testes three in number, oval, 0.124–0.166 by 0.069–0.124, arranged in a transverse row, one poral and two aporal. Cirrus sac pyriform, 0.152–0.194 long by 0.055 wide, extending beyond longitudinal osmoregulatory canals. Internal seminal vesicle measuring 0.111–0.124 long by 0.055 wide and external seminal vesicle 0.180–0.193 long by 0.042–0.055 wide. Seminal receptacle large, dorsal to ovary, measuring 0.346 long by 0.124 wide. Vitelline gland weakly developed, 0.138 by 0.042, situated in posterior field of segment. Ovary transversely elongate, bilobate, 0.194–0.207 across. Eggs oval or spherical 0.042–0.053 long by 0.039 wide, surrounded by four thin envelopes. Onchosphered spherical, 0.028–0.032 in diameter; embryonic hooks 0.018 long.

Host: *Suncus myosurus swinhoei* (Blyth)

Site of infection: Small intestine.

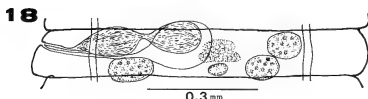
Locality and date: Kuanyin Tsun, Kuanyin Hsiang, Taoyuan Hsien; October 9, 1986.

Type specimen: Holotype: NSU Lab. Coll. No. 8904.

Remarks: *Vampirolepis sunci* sp. n. most closely resembles *V. amamiensis* Sawada, 1986 [7] from *Crociodura horsfieldi watasei* in the number of rostellar hooks and the size of strobila. However, this species is distinguished from *V. amamiensis* by the smaller rostellar hooks (0.014 vs. 0.018), the shape of rostellar hooks (Fig. 15) and the longer embryonic hooks (0.018 vs. 0.011).

Vampirolepis sessilihamata sp. n.
(Figs. 16–19)

On October 9, 1986, three brown musk shrews, *Suncus myosurus swinhoei*, were captured at Kuanyin Tsun, Kuanyin Hsiang, Taoyuan Hsien and

FIG. 15. Rostellar hook of *V. amamiensis*.FIGS. 16-19. *Vampirolepis sessilihamata* sp. n. 16: Scolex. 17: Rostellar hook 18: Mature segment, ventral view. 19: Egg.

were examined for cestodes. A large number of specimens of this cestode and the following *V. gracilistrobila* sp. n. were found in one of three shrews.

Description: Small-sized hymenolepidid; mature strobila with gravid segments, 15-35 in length by 0.8-0.9 in maximum width. Metamerism distinct, craspedote, margins slightly serrate. Mature and gravid segments markedly wider than long. Scolex 0.245 long by 0.350 wide, not distinctly set off from neck. Rostellum spherical, 0.056-0.063 in diameter, armed with a single circle of 10 thorn-shaped hooks measuring 0.018 long. Hook handle remarkably short, guard prominent, round at its end, shorter than blade; blade sharp at its end, curved toward guard. Rostellar sac slightly elongate, 0.168 by 0.105-0.119, extending past posterior margin of suckers. Suckers discoid, 0.126-0.133 in diameter.

Genital pores unilateral, located a little anterior to middle of segment margin. Testes three in number, ovoid, 0.091-0.098 long by 0.056-0.083 wide, arranged in a form of triangle, one poral and two aporal. Cirrus sac cylindrical, 0.161-0.210 long by 0.042-0.047 wide, extending beyond longitudinal osmoregulatory canals. Internal seminal vesicle 0.119-0.133 long by 0.042-0.056 wide, occupying almost whole of cirrus sac. External seminal vesicle 0.105-0.140 long by 0.049-0.077 wide. Ovary irregularly lobate, 0.056-0.077 by 0.028-0.035. Seminal receptacle well developed, 0.077-0.091 long by 0.049-0.056 wide. Vitelline gland weakly developed, compact, 0.028-0.042 by 0.021. Gravid uterus filling entire segment. Eggs slightly ovoid, 0.056-0.063 by 0.049-0.056, by four thin envelopes, with smooth surface. Onchospheres spherical, 0.032-0.035 in diameter; embryonic hooks 0.014-0.016 long.

Host: *Suncus myosurus swinhoei* (Blyth).

Site of infection: Small intestine.

Locality and date: Kuanyin Tsun, Kuanyin Hsiang, Taoyuan Hsien: October 9, 1986.

Type specimen: Holotype: NSU Lab. Coll. No. 8905; Paratypes No. 8906.

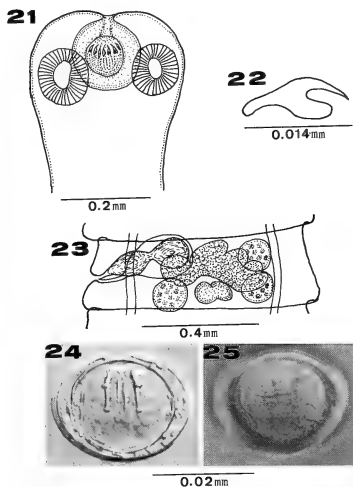
Remarks: In possessing ten rostellar hooks among the species of *Vampirolepis* occurring in Soricidae, this new species is related to the following six species; *V. parva* (Rausch and Kuns, 1950) [8], *V. blarinae* (Rausch and Kuns, 1950) [8], *V. lineola* (Oswald, 1951) [9], *V. virilis* (Voge, 1955) [10], *V. bahli* (Singh, 1958) [11] and *V. petrodromi* (Baer, 1933) [12]. Of these, this new cestode closely resembles *V. bahli* in the length of rostellar hooks. However, it differs from *V. bahli* in the shape of rostellar hooks (Fig. 20).

FIG. 20. Comparison of rostellar hook shapes among seven species of cestodes. F: *V. parva*. G: *V. blarinae*. H: *V. lineola*. I: *V. virilis*. J: *V. bahli*. K: *V. sessilihamata* sp. n. L: *V. petrodromi*.

Vampirolepis gracilistrobila sp. n.

(Figs. 21–25)

Description: Small-sized hymenolepidid; worm length 25–30 and maximum width 0.7–0.8. Metamerism distinct, segment margin slightly serrate. Mature gravid segments wider than long. Scolex round, 0.140–0.280 long by 0.252–0.315 wide, not sharply demarcated from neck region. Rostellum spherical, 0.070 long by 0.084 wide, armed with a single row of 33 thorn-shaped hooks measuring 0.014 long. Hook handle short; guard prominent, round at its end, shorter than blade; blade sharp at its end. Rostellar sac spherical, 0.140 in diameter, extending nearly to posterior margin of suckers. Suckers discoid, 0.098–0.105 in diameter.



FIGS. 21–25. *Vampirolepis gracilistrobila* sp. n. 21: Scolex. 22: Rostellar hook. 23: Mature segment, ventral view. 24: Egg. 25: Surface of egg, showing polar filaments.

Genital pore unilateral and located a little posterior to middle of segment margins. Testes three in number, subspherical, 0.070–0.077 long

by 0.056–0.063 wide, arranged in a form of triangle, one poral and two aporal. Cirrus sac cylindrical, 0.084–0.091 long by 0.014–0.021 wide, extending beyond longitudinal osmoregulatory canals. Internal seminal vesicle 0.077–0.084 long by 0.014–0.021 wide, occupying almost whole of cirrus sac. External seminal vesicle 0.077–0.084 long by 0.035–0.049 wide. Seminal receptacle well developed, 0.070–0.105 long by 0.056–0.084 wide. Ovary penta- or hexa-lobate, 0.053–0.063 across. Uterus arising directly from ovarian lobes as a lobe sac, gradually enlarging, filling all available space in senile segments. Eggs subspherical, 0.046 long by 0.032–0.035 wide, with at each pole a round projection provided with polar filaments. Onchospheres spherical, 0.025–0.032 in diameter; embryonic hooks 0.014 long.

Host: *Suncus myosurus swinhoei* (Blyth).

Site of infection: Small intestine.

Locality and date: Kuanyin Tsun, Kuanyin Hsiang, Taoyuan Hsien; October 9, 1986.

Type specimen: Holotype: NSU Lab. Coll. No. 8907; Paratypes: 8908.

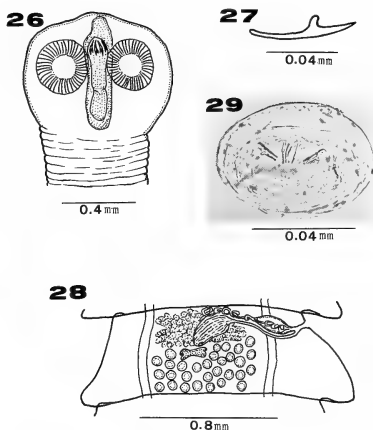
Remarks: The present new species most closely resembles *V. notoensis* Sawada, 1986 [7] from *Crociodura dsinezumi chisai* in the size and form of rostellar hooks, and the arrangement of testes. However, it differs from *V. notoensis* in the larger size of strobila (25–32 long by 0.7–0.8 wide vs. 4.5 long by 0.5 wide), the larger number of rostellar hooks (33 vs. 23), the position of genital pores (located a little posterior to middle of segment vs. located a little anterior) and the form of ovary (penta- or hexa-lobate vs. transversely elongate and bilobate).

Choanotaenia Railliet, 1896*Choanotaenia* (*Choanotaenia*) *tubirostellata* sp. n.

(Figs. 26–29)

A large number of specimens of this cestode were obtained from six *Yamashina's* mole-shrews, *Anourosorex squamipes yamashinai*, captured at Tsuifeng, Lenai Hsiang Nantou Hsien, on October 8, 1986.

Description: Medium-sized dilepidid, mature worm length 34–39 and maximum width 1.4–1.6. Anterior segments much broader than long, but



FIGS. 26-29. *Choanotaenia (Choanotaenia) tubirostellata* sp. n. 26: Scolex. 27: Rostellar hook. 28: Mature segment, dorsal view. 29: Egg.

gradually proportion reversed, posterior ones being much longer than broad. Scolex spherical, 0.567–0.692 long by 0.830–1.042 wide, distinctly set off from neck. Suckers round, 0.249–0.290 in diameter. Rostellum cylindrical, 0.401 long by 0.097–0.111 wide, armed with a single row of 18 hooks measuring 0.060–0.063 long. Hook handle slender; guard small, round at its end, remarkably shorter than blade; blade sharp at its end. Rostellar sac cylindrical, extending beyond posterior margins of suckers, measuring 0.443–0.484 long by 0.166–0.193 wide.

Genital pores irregularly alternate, located at extreme anterior margins of segment. Testes oval or spherical, numbering about 29–32, lying in posterior half of segment. Vas deferens much coiled, located in anterior field of segment, and joining to posterior edge of cirrus sac. Cirrus sac pyriform, 0.105 long by 0.035 wide. Cirrus unarmed. Ovary well developed, irregularly lobate, composed of a number of follicles, pretesticular, lying in anterior field of segment, measuring 0.252–0.259 across. Vagina opening just posterior to genital atrium, extending to median field, parallel to cirrus sac, then enlarging, forming a seminal

receptacle measuring 0.180–0.249 long by 0.063 wide. Vitelline gland weakly developed, bilobate, 0.105–0.133 long by 0.028–0.035 wide, situated posterior to ovary. Eggs subspherical 0.053–0.074 long by 0.028–0.035 wide, surrounded by four thin envelopes. Onchospheres subspherical, 0.028–0.035 long by 0.018–0.021 wide; embryonic hooks 0.011–0.014 long.

Host: *Anourosorex squamipes yamashinai* Kuroda.

Site of infection: Small intestine.

Locality and date: Tsuifeng, Lenai Hsiang, Nantou Hsien, October 8, 1986.

Type specimen: Holotype: NSU Lab. Coll. No. 8909; Paratypes No. 8910.

Remarks: So far as known to the authors, five species of *Choanotaenia* (*Choanotaenia*) Matevossian, 1954 have been recorded from mammals: *C. (C.) nebraskensis* Hansen, 1950 [13], *C. (C.) peromysci* (Erickson, 1938) [14], *C. (C.) sciuriola* Harwood et Cooke, 1949 [15], *C. (C.) scutigera* (Duj., 1845) [16] and *C. (C.) spermophilus* (McLeod, 1933) [17]. The present new species most closely resembles *C. (C.) sciuricola* from *Sciurus niger* in the shape of rostellar hooks and the number of testes. However, it differs from *C. (C.) sciuricola* in the larger rostellum (0.507–0.692 long by 0.830–1.043 wide vs. 0.26 long by 0.32 wide), the smaller number of rostellar hooks (18 vs. 22), the longer rostellar hooks (0.060–0.063 vs. 0.038) and the smaller onchospheres (0.028–0.035 by 0.018–0.021 vs. 0.0547).

ACKNOWLEDGMENTS

The authors are grateful to Mr. Ho-mu-Lin, Taiwan Provincial Institute of Infectious Disease, for generous assistance in collecting shrews on Taiwan.

REFERENCES

- Olsen, O. W. and Kuntz, R. E. (1978) *Staphylocystis (Staphylocystis) suncusensis* sp. n. (Cestoda: Hymenolepididae) from the musk shrew, *Suncus murinus* (Soricidae), from Taiwan, with a key to the known species of *Staphylocystis* Villot, 1877. Proc. Helminthol. Soc. Wash., 45: 182–189.
- Crusz, H. and Sanmugasunderam, V. (1971) Parasites of the relict fauna of Ceylon. II. New species of cyclophyllidean cestodes from small hillvertebrates.

- Ann. Parasitol. Hum. Comp., **46**: 575-588.
- 3 Srivastava, A. K. and Capoor, V. N. (1979) On a new cestode, *Vampirolepis molus* sp. n. Helminthologia, **16**: 195-198.
 - 4 Baer, J. G. (1926) Contribution to the helminth fauna of South Africa. Mammalian cestodes. Union S. Afr., Dept. Agric. 11th and 12th. Rep. Dir. Vet. Ed. Res. Pretoria, pp. 61-136.
 - 5 Baer, J. G. (1931) Helminthes nouveaux parasites de la Musaraigne d'eau, *Neomys fodiens* Pall. Un nouveau genre de Trématode provoquant des lésions dans le rein de la Taupe. (Notes préliminaires). Actes Soc. helvét. sc. nat., pp. 338-340, La Chaux-de-Fonds.
 - 6 Zarnowski, E. (1954) A new tapeworm *Hymenolepis stefanskii* sp. n. from the common shrew, *Sorex araneus* (in Polish with English summary). Parasit. Polon., **1**: 313-328.
 - 7 Sawada, I. (1986) Two new species of the *Vampirolepis* (Cestoda: Hymenolepidae) from Japanese shrews. Jpn. J. Parasitol., **35**: 171-174.
 - 8 Rausch, R. and Kuns, M. L. (1950) Studies on some North American shrew cestodes. J. Parasitol., **35**: 433-438.
 - 9 Oswald, V. H. (1951) Three new hymenolepidid cestodes from the smoky shrew, *Sorex fumeus* Miller. J. Parasitol., **37**: 573-576.
 - 10 Voge, M. (1955) *Hymenolepis virilis* n. sp., a cestode from the shrew *Sorex trowbridgei* in California. J. Parasitol., **41**: 270-272.
 - 11 Singh, K. S. (1958) *Hymenolepis bahli* n. sp. from grey musk shrew, *Crocidura caerulea* (Kerr, 1792) Paters, 1870 from India. J. Parasitol., **44**: 446-448.
 - 12 Baer, J. G. (1933) Contribution à l'étude de la faune helminthologique africaine. Rev. Suisse Zool., **40**: 31-84.
 - 13 Hansen, M. F. (1950) A new dilepidid tapeworm and notes on other tapeworms of rodents. Am. Midl. Nat., **43**: 471-479.
 - 14 Erickson, A. D. (1938) Parasites of some Minnesota Cricetidae and Zapodidae and a host catalogue of helminth parasites of native American mice. Am. Midl. Nat., **20**: 575-589.
 - 15 Harwood, P. D. and Cooke, V. (1949) The helminths from a heavily parasitized fox squirrel, *Sciurus niger*. Ohio J. Sci., **49**: 146-148.
 - 16 Dujardin, F. (1845) Histoire Naturelle des Helminthes ou Vers Intestinaux. Paris, xvi + 654.
 - 17 McLeod, J. A. (1933) A parasitological survey of the genus *Citellus* in Manitoba. Canad. J. Res. Sect., D., Zool. Sci., **9**: 108-127.



***Nautilina calyptogenicola*, a New Genus and Species of Parasitic
Polychaete on a Vesicomysid Bivalve from the Japan Trench,
Representative of a New Family Nautilinidae**

TOMOYUKI MIURA¹ and LUCIEN LAUBIER²

Faculty of Fisheries, Kagoshima University,
Kagoshima 890, Japan, and ²IFREMER, 66 avenue
d'Iéna, 75116 Paris, France

ABSTRACT—A polychaete species was found in the mantle cavity of the giant deep-sea clam, *Calyptogena phaseoliformis* collected from the cold-seep zone of the Japan Trench at a depth of 5960 m. Although the new species recalls species of the families Levidoridae and Calamyzidae in the simplified body, the presence of subbiramous parapodia and the absence of achaetous peristomial rings in the new species lead us to propose the erection of a new family. *Nautilina calyptogenicola*, a new genus and species, is described as a representative of a new family Nautilinidae.

INTRODUCTION

An aberrant polychaete species was found in the mantle cavity of the giant deep-sea clam, *Calyptogena phaseoliformis* Métivier *et al.* 1986 [1], collected from the landward wall of the Japan Trench at a depth of 5960 m by the French submersible "Nautile" in the course of the French-Japanese project KAICO [2]. This species has a simplified body with similar body segments and resembles that of the family Calamyzidae Hartmann-Schröder, 1971 [3], a parasitic worm on ampharetid polychaetes, and that of the Levidoridae Perkins, 1987 [4], but is not thought to belong to these families particularly due to the differences in the cephalic region and the parapodia. In consequence of the comparison of this species with those of other polychaete families, the erection of a new family is proposed in this study.

The types are deposited in the Muséum National d'Histoire Naturelle, Paris (MNHN) and the National Science Museum, Tokyo (NSMT).

Nautilinidae, new family

Type genus: *Nautilina*, new genus, with type species *N. calyptogenicola*, new species, by monotype.

Diagnosis: Body long, vermiform, tapering posteriorly with numerous setigerous segments; body in cross-section flattened ventrally and strongly arched dorsally. Segmentation distinct. Prostomium with 2 pairs of antennae, without eyes. Foregut with muscular proventriculus. Achaetous peristomial ring absent. All segments setigerous. Buccal opening situated between prostomium and first setiger. Parapodia of one type, subbiramous with reduced notopodia and well developed neuropodia supported by a single neuroacicula. Setae consisting of simple, smooth and slightly curved hooks. Pygidium simple and cylindrical without appendages.

Remarks: *Calamyzas amphictenicola* Arwidson, 1932 [5], still known as the single species of the family Calamyzidae and ectoparasitic on ampharetid polychaetes [6], resembles the species of the new family in the cross-section of the body and the parapodial structure. The resemblance of the two families may be due to a convergence in the ectoparasitic life. *C. amphictenicola* lacks prostomial antennae and has compound setae,

Accepted June 3, 1988

Received March 19, 1988

¹ To whom all correspondence should be addressed.

while *Nautilina calyptogenicola* g. sp. n. bears 4 prostomial antennae and has simple setae. The species of the Levidoridae also resembles *N. calyptogenicola* g. sp. n. in having a similar foregut with a muscular proventriculus and a semi-circular cross-section of the body. However, *N. calyptogenicola* g. sp. n. lacks the achaetous peristomial rings which are characteristic for a species of the Levidoridae. The new family is also characterized by the presence of 2 pairs of prostomial antennae and the absence of eyes instead of the exclusive presence of 2 pairs of eyes in the Levidoridae (including one pair of lensed eyes recalling those of Syllidae). The setal structure is also different in these two families. The setae of the new family are simple and unidentate without any sculptures on their surface, while those of Levidoridae are sometimes bidentate with serrations on subterminal ends.

Although families such as Spintheridae, Acrocirridae, Sphaerodoridae and Pilargidae contain species with strongly curved hooks [7], their hooks are compound in their structure when neuropodial or are positioned on the notopodia and differ from those of the new family, which are simple ventral hooks.

The presence of a muscular proventriculus in the new family suggests close relationship with the Syllidae, as in the case of the Levidoridae [4]. However, the absence of achaetous peristomial rings and the possession of the subbiramous parapodia in *N. calyptogenicola* g. sp. n. are negative for the close relationship between these families. The 4 prostomial antennae and the subbiramous structure of parapodia of the new family may be important and significant characters to elucidate the phylogenetic relation with other polychaete families, especially with those of the order Phyllodocida. Further discussion on the taxonomical position of the new family should be retaken after the finding of more species belonging to this family.

Nautilina, new genus

Diagnosis: Body flattened ventrally and strongly arched dorsally. Prostomium globular with 2 pairs of antennae, without eyes. Muscular proventricu-

lus present. Peristomium inconspicuous: achaetous peristomial ring absent. Parapodia subbiramous with dorsal and ventral cirri; notopodium supported by a single notoaciculum within swollen base of dorsal cirrus; neuropodium with a single neuroaciculum. Single projected hook and several developing embedded hooks present on each setal lobe. Pygidium simple and cylindrical.

Etymology: The genus is named in the honor of the French submersible "Nautil" which collected the bivalve host of that parasitic polychaete during KAIKO expedition phase 2 in July, 1985.

Nautilina calyptogenicola, new species (Fig. 1)

Materials: Holotype (MNHN UC86), complete, separated in 3 pieces, Landward wall of the Japan Trench, 40°06.3'N, 144°10.6'E, 5960 m, 31 July 1985, French submersible "Nautil" Dive KD-18, collected from the mantle cavity of *Calyptogena phaseoliformis*.

Paratypes (NSMT-Pol. P-251), a complete specimen separated in 2 pieces, an anterior and a posterior fragment, Japan Trench, 35°54.2'N, 142°30.7'E, 5640–5695 m, 22 July 1985, Dive KD-14, collected with *C. phaseoliformis*.

Measurements: Holotype separated in 3 parts, 20 mm long (7.4+8.4+4.2 mm), 2.4 mm wide including parapodia, with 68 setigers (22+25+21). Complete paratype separated in 2 parts, 32.4 mm long (22.0+10.4 mm), 4.2 mm wide, with 62 setigers (35+27).

Description: Body long, vermiform, flattened ventrally and strongly arched dorsally, with ventral longitudinal groove (Fig. 1a, e). Integument smooth. Specimens preserved in alcohol pale or colorless.

Prostomium globular with antero- and posteroventral pairs of very short cirreiform antennae, without eyes or other appendages (Fig. 1b, c). Achaetous peristomial ring absent. Mouth opening situated between prostomium and first setiger, with one rounded posterior and two rectangular buccal peristomial lobes (maybe eversible), without jaws or paragnaths (Fig. 1c). Foregut with well-developed muscular part (maybe proventriculus), without tubiform chiti-

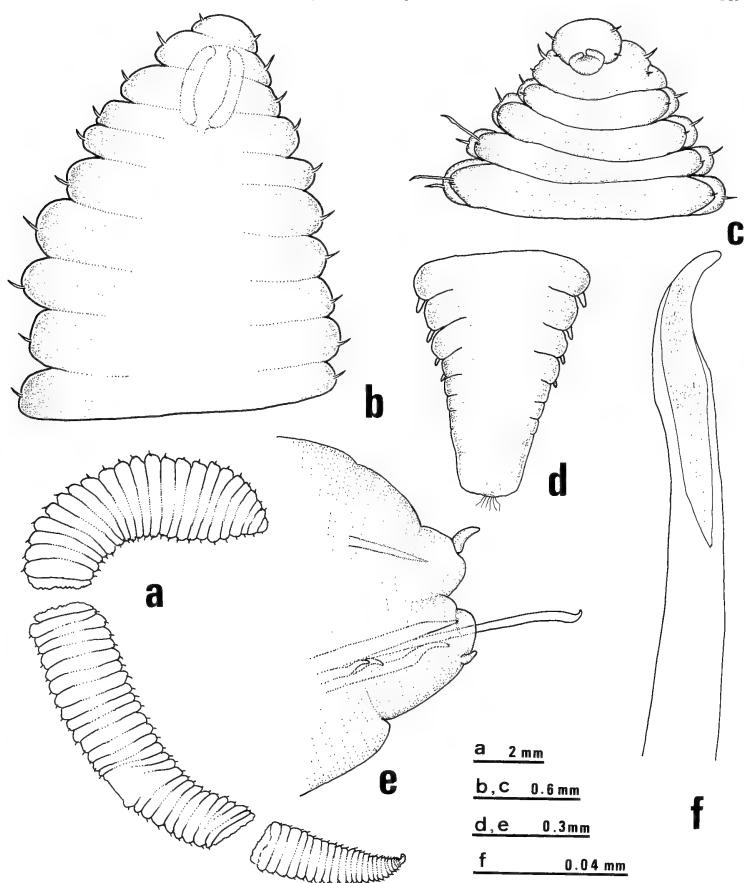


FIG. 1. *Nautilina calyptogenicola* g. sp. n. (holotype): a, Whole body, dorsal view; b, Anterior end, dorsal view; c, Same, ventral view; d, Pygidium, dorsal view; e, Parapodium 10, anterior, view; f, Hook.

nous pharynx.

Parapodia subbiramous throughout body, with dorsal and ventral cirri; dorsal cirri more than 3 times as long as ventral one; bases of dorsal cirri swollen, forming globular pads containing embed-

ded notoacacula; ventral cirri present on ventral bases of setal lobes, supported by stout embedded neuroacacula; setal lobes globular, of same size as dorsal pads (Fig. 1e).

Setae consisting of simple ventral hooks only;

single hook projected from each setal lobe; several developing hooks embedded around neuroacacula. Hooks simple, stout and strongly curved on distal end; cortex and medulla well defined on distal half (Fig. 1f).

Pygidium cylindrical with anus on distal end, without anal cirri (Fig. 1d).

Etymology: The specific name is derived from the generic name, *Calypptogena*, of the host bivalve species.

ACKNOWLEDGMENTS

The authors wish to thank Dr. Suguru Ohta of Ocean Research Institute, University of Tokyo and Dr. Michel Segonzac of CENTOB, Brest for their sorting and the transmission of the material for study.

REFERENCES

- 1 Métivier, B., Okutani, T. and Ohta, S. (1986) *Calypptogena* (*Ectenagena*) *phaseoliformis* n. sp., an unusual vesicomyid bivalve collected by the submersible Nautile from abyssal depths of the Japan and Kurile Trenches. *Venus* (Japan. J. Malacol.), **45**(3): 161–168.
- 2 Laubier, L., Ohta, S. and Sibuet, M. (1986) Découverte de communautés animales profondes durant la campagne franco-japonaise KAICO de plongées dans les fosses de subduction autour du Japon. *C. R. Acad. Sci., Paris, Ser. III*, **303**(2): 25–29.
- 3 Hartmann-Schröder, G. (1971) Annelida, Borstenwürmer, Polychaeta. *Tierwelt Dtl.*, **58**: 1–594.
- 4 Perkins, T. H. (1987) Levidoridae (Polychaeta), new family, with descriptions of two new species of *Levidorum* from Florida. *Bull. Biol. Soc. Wash.*, **7**: 162–168.
- 5 Arwidsson, I. (1932) *Calamyzas amphictenicola*, ein ektoparasitischer Verwandter der Sylliden. *Zool. Bid. Uppsala*, **14**: 153–218.
- 6 Fauchald, K. (1977) The polychaete worms. Definitions and keys to the orders, families and genera. *Nat. Hist. Mus. Los Angeles Ctry., Sci. Ser.*, **28**: 1–190.
- 7 Pettibone, M. H. (1982) Annelida, Polychaeta. In "Synopsis and Classification of Living Organisms. Vol. 2". Ed. by S. P. Parker *et al.*, McGraw-Hill, New York. pp. 1–43.

A Proposal of Establishing Tribes for the Family Drosophilidae with Key to Tribes and Genera (Diptera)

TOYOHI OKADA

Gotokuji 2-30-18, Setagaya, Tokyo 154, Japan

ABSTRACT—Subdivision into tribes of the family Drosophilidae is attempted. Establishment of two tribes, Steganini and Leucophengini, for the subfamily Steganinae and five tribes, Microdrosophilini, Hypselethyrini, Colocasiomyini, Dettopsomyini and Drosophilini, for Drosophilinae is proposed.

INTRODUCTION

By the end of 1984, 62 genera of the family Drosophilidae were recorded by Wheeler [1], including one fossil and five ungrouped into subfamilies. Since then, one genus, *Thyreocephala*, was added by myself [2], which was, however, synonymized with *Mulgravea* Bock by myself [3], and two fossil genera, *Miomysia* and *Protochymomyza*, by Grimaldi [4]. The genus *Drosophilella* Duda was recently synonymized with *Colocasiomyia* de Meijere by myself [5]. The genera *Atele-drosophila* Hardy and *Nudidrosophila* Hardy were treated as distinct genera according to Wheeler [6], although they were synonymized with *Drosophila* s. str. by Kaneshiro [7] because their females are not distinguishable from the latter.

To recognize tribe, a subordinate category of family or subfamily, is a general rule especially in large families of insects. No explicit subdivision of the family Drosophilidae has, however, been attempted before the present proposal, although an implicit subdivision into "Drosophiloids" and "Scaptomyzoids (as Scaptoids)" was made for endemic Hawaiian Drosophilidae by Throckmorton [8]. The inference that drosophilid taxonomy is highly developed might be accepted mostly at the level below species group.

METHODS

The descriptions of the tribes with diagnoses of

involving genera are given by a form of key. For establishing the tribes and constructing the key, following fourteen diagnostic characters (n=14: A-N) each divided into two states (0: presumed plesiomorph; 1, presumed apomorph) are taken into consideration, supplemented by some additional special characters.

Eye bare (A=0) or piled (a=1).

Arista plumose (B=0) or bare or pubescent (b=1).

Ocellars inside (C=0) or outside (c=1) ocellar triangle.

Postverticals present (D=0) or absent (d=1).

Carina undeveloped (E=0) or developed (e=1).

Anterior reclinate orbital large (F=0) or fine (f=1).

Posterior reclinate orbital nearer to inner vertical than to proclinate (G=0) or nearer to proclinate than to inner vertical (g=1).

Prescutellars developed (H=0) or absent (h=1).

Anterior dorsocentral nearer to scutellum than to suture (I=0) or nearer to suture than to scutellum (i=1).

Acrostichal hairs in more than 8 rows (J=0) or 8 or less than 8 rows (j=1).

Lateral scutellars convergent or parallel (K=0) or divergent (k=1).

Second costal break shallow (L=0) or deep (l=1).

Second costal lappet small (M=0) or large (m=1).

Discal and second basal cells separated (N=0)

Accepted June 21, 1988

Received April 23, 1988

TABLE 1. $n(\text{characters}) \times t(\text{taxa})$ matrix

Taxa Genus	A	B	C	D	E	F	G	H	I	J	K	L	M	N
Steganinae														
1. Steganini														
†Electrophortica	0	0	0	0	0	0	0	0	0	1 ₅	1	0	0	0
Soederbomia	NC	0	NC	NC	0	0	0	0	0	0	NC	0	0	0
Pyrgometopa	NC	0	NC	NC	0	NC	0	NC	NC	NC	NC	0	0	0
Eostegana	0	0	0	0	1	0	0	0	0	0	1	0	0	0
Stegana	0	0	0	0	1	0	0	0	0	0	1	0	0	0
Amiota	0	0	0	0	1	0	0	0	0	0	1	0	0	0
Crincosia	0	1	1 ₉	1 ₉	0	0	0	0	0	0	1	0	0	0
Apenthecia	0	1	0	0	0	1 ₁₀	0	0	0	0	1	0	0	0
Mayagueza	0	1	0	0	0	0	0	0	0	0	1	0	0	0
Cacoxenus	0	1	0	0	1 ₈	0	0	0	0	0	1	0	0	0
Gitona	0	1	0	0	1	0	0	0	0	1 ₁₁	1	0	0	0
2. Leucophengini														2
Acletoxenus	0	1	NC	0	1	0	0	0	0	0	0	0	0	1
Luzonimyia	0	1	1	0	1	0	0	0	0	0	1 ₁₄	0	0	1
Leucophenga	0	0 ₁₃	0	0	1	0	0	0	0	0	1	0	0	1
Paraleucophenga	0	0	0	0	1	0	0	0	0	0	1	0	0	1
Pseudiasata	0	1	1	0	0 ₁₂	0	0	0	0	0	0	0	0	1
Trachyleucophenga	NC	0 ₁₆	NC	0	0	0	0	0	NC	NC	NC	0	0	1
Pararhinoleucophenga	0	0	0	0	0	0	0	0	0	0	1	0	0	1
Rhinoleucophenga	0	0	0	0	0	0	0	0	0	0	1	0	0	1
Drosophilinae														
1. Microdrosophilini														
Microdrosophila	1	0	0	0	0	1	1	1	1	1	1	1	0	1
2. Hypselothyriini														
Hypselothyrea	1 ₂₅	0	0	1	1 ₂₅	1	1	1	1	1	0	0	0	1
Tambourella	0 ₂₅	0	0	1	0 ₂₅	1	1	1	1	1	0	0	0	1
Sphaerogastrella	0	0	0	1	0 ₂₄	1	1	1	1	1	1 ₂₆	0	0	1
Liodrosophila	0 ₂₈	0	0	0	1	1	1	1	1	1	1	0	0	1
Lissocephala	1 ₂₈	0	0	0	1	1	1	1	1	1	1	0	0	1
Mulgravea	1	0	0	0	0 ₂₇	1	1	1	1	1	1 ₂₉	0	0	1
Paraliodrosophila	1	0	NC	NC	0	NC	1	NC	NC	1	0	0	0	1

TABLE 1. (continued)

Taxa Genus	Characters													
	A	B	C	D	E	F	G	H	I	J	K	L	M	N
3. Colocasiomyini														
Calodrosophila	1	0 ³¹	1	0	1	1	1	1	0 ³¹	1	0	0	0	1
Colocasiomyia	1	1	1	0	1	1	1	1	1	1	0	0	0	1
Nesiodrosophila	1	0	1	0	0 ³⁰	0 ³⁰	1	1	1	1	1 ³⁰	0	0	1
Jeannelopsis	1	0	1	0	0	0	1	1	1	1	1	0	0	1
4. Dettopsomyini			21										21-2	
Mycodrosophila	0 ³³	0	0	0	0	1	1	1	0	1	1	1	1	1
Styloptera	1	0	1 ³⁴	0	0	0	1	1	1	1	1	0	1	1
Dettopsomyia	1	0	0	0	1	1	1	1	1 ³⁵	1	1	1	1	1
Paramycodrosophila	1	0	0	0	0 ³⁵	1	1	1	0 ³⁵	1	1	1	1	1
5. Drosophilini												22	22	
Dicladochaeta	NC	1	NC	0	NC	1	1	NC	1	1	NC	0	0	1
Baeodrosophila	1	1 ³⁷	1	0	0	1	1	0	0	1	1	0	0	1
Sphyrnoceps	NC	0	NC	NC	0	1	1	1	NC	1	NC	0	0	1
Cladochaeta	0	0	0	0	0	1	1	1	0	1	0	0	0	1
†Miomyia	0 ⁴¹	0	0	NC	0	1	1	1	0	NC	NC	0	0	1
Diathoneura	1	0	0	0 ⁴³	0	1	1	1	1	1	0	0	0	1
Neotanygastrella	1	0	0	1	0	1	1	1	0	1	1	0	0	1
Ateledrosophila	1	0	NC	0	1 ³⁹	1	1	1	0	1	1	0	0	1
Nudidrosophila	1	0	1	0	0	0	0	0	0	1	1	0	0	1
Zygothrica	1	0	0	0	1	1	1	1	0	1	0 ⁴⁶	0	0	1
Collessia	1	0	0	0	1	1	1	1	0	1	1	0	0	1
Phorticella	1	0	0	0	1	1 ³⁶	1	1	0	1	1	0	0	1
Grimshawomyia	1	0	0	0	0 ⁴⁹	0	1	1	1 ⁴⁹	1	1	0	0	1
Celidosoma	NC	0	0	0	1	0	1	1	0	1	NC	0	0	1
†Protochymomyza	0	0	0	0	1	0	1	1	0	1	1 ⁵²	0	0	1
Chymomyza	0 ⁵¹	0	0	0	1	0	1	1	0 ⁵¹	1	0	0	0	1
Titanochaeta	1	0	0	0	1 ⁵⁰	0	1	1	1	1	1	0	0	1
Balara	0	0	0	0	0	0	1	0 ⁵³	0	0	0	0	0	1
Samoaia	1	0	0	0	0	0	1	1	1	1	1	0	0	1
Scaptomyza	1	0	0	0	0	0	1	1	1 ⁵⁴	1	1	0	0	1
Marquesia	NC	0	NC	0	0	0	1	1	0	1	NC	0	0	1
Neorhynoleucophenga	0 ⁵⁷	0	NC	0	0	0	1	1	NC	1	NC	0	1	1

TABLE 1. (continued)

Taxa Genus	A	B	C	D	E	F	G	H	I	J	K	L	M	N
Zaprius	1	0	0	0	0	0	0	1	0	1	0	0	0	1
Drosophila	1	0	0	0	0	0	1	1	0	1	0	0	0	1
Ungrouped genera														
Apachrochaeta	0	0	NC	0	0	NC	1	NC	0	NC	NC	0	0	1
Laccodrosophila	1	0	NC	0	0	0	0	0	0	NC	NC	0	0	1
Pseudocacoxenus	NC	1	NC	NC	0	NC	NC	0	1	NC	NC	0	0	1
Zapriothrica	NC	1	0	0	NC	1	1	1	0	NC	NC	0	0	1

0, Presumed plesiomorph; 1, presumed apomorph; NC, no comparison; †, fossil genus; numerical figure interceding a longitudinal line, order of key couplet.

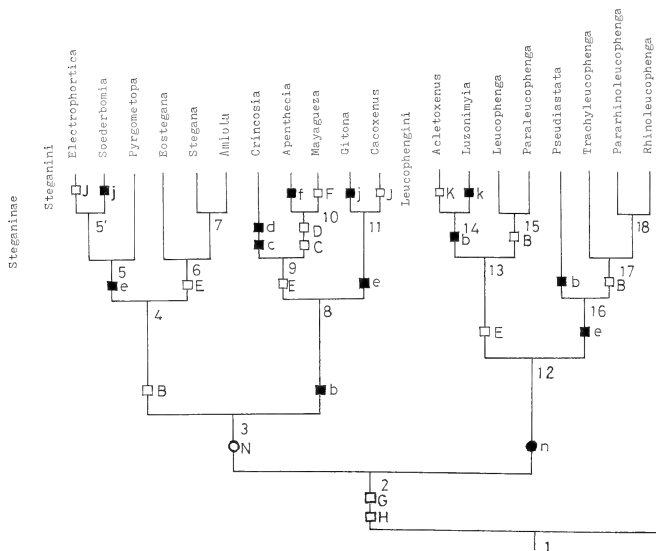
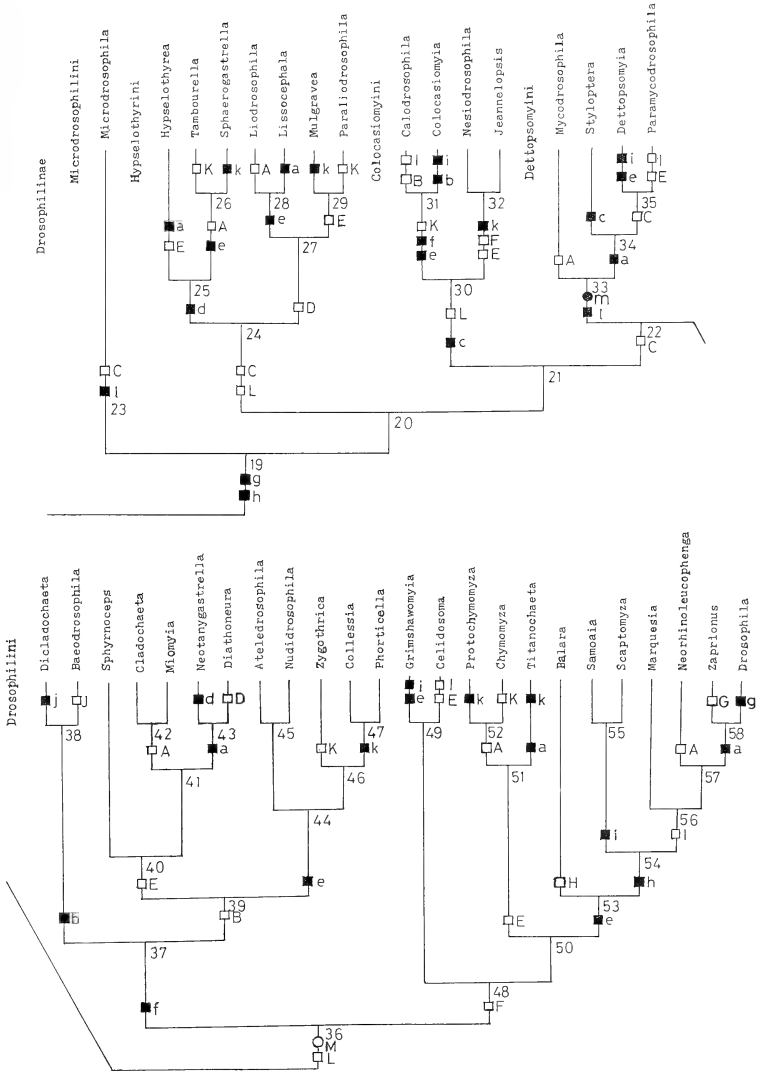


FIG. 1. Diagrams to show the key to tribes and genera of the family Drosophiliidae. Alphabetical signs: Presumed plesiomorphous (large letters) and apomorphous states (small letters) of diagnostic characters; open and solid circles: plesiomorphs and apomorphs, respectively, appearing only once in the key; open and solid squares: plesiomorphs and apomorphs, respectively, repeatedly appearing in the key; numerical figures at the branching points of diagrams: orders of key couplets.



or confluent ($n=1$).

From the $n \times X$ matrix (Table 1), a key is constructed by means of "even dichotomous diagram method" [9]. The result is expressed also by key diagrams (Fig. 1), which may enable one to find the relationships of the tribes more easily.

Samples of some genera unknown to me were borrowed from various investigators and institutions: Dr. Ben Brugge, University of Amsterdam (*Colocasiomyia*). Dr. Don Colles, C.S.I.R.O., Canberra (*Luzonimyia*, *Crincosia*, *Balara*), Dr. K. Y. Kaneshiro, University of Hawaii (*Grimshawomyia*, *Titanochaeta*, *Samoaia*), and Dr. D. A. Grimaldi, American Museum of Natural History, New York (*Cladochaeta*, *Diathoneura*).

RESULTS

Family Drosophilidae

1. Posterior reclinate orbital nearer to inner vertical than to proclinate (G); prescutellars developed (H); tibiae and tarsi of mid and hind legs with dense rows of short bristles.Subfamily Steganinae.2.
- Posterior reclinate orbital nearer to proclinate than to inner vertical (g, excl. *Zaprionus* s. str.); prescutellars usually absent (h); tibiae and tarsi of mid and hind legs without dense rows of short bristles.Subfamily Drosophilinae.19.

Subfamily Steganinae

2. Discal and second basal cells separated (N)....Tribe 1. Steganini3.
- Discal and second basal cells confluent (n)....Tribe 2. Leucophengini12.

Tribe 1. Steganini Okada, n.

Type genus: *Stegana* Meigen

3. Arista usually plumose (B).....4.
- Arista usually bare or pubescent (b).8.
4. Carina developed (e).5.
- Carina undeveloped (E).6.
5. Dorsocentrals in 2 pairs; R_{2+3} much waved; frons caudally protruded.
-Genus *Pyrgometopa* Kertész
- Dorsocentrals in 1 pair; R_{2+3} not waved;

frons caudally not protruded.....5'.

- 5'. Acrostichal hairs in 8 or less than 8 rows (j).
-Genus *Soederbomia* Hendel
- Acrostichal hairs in more than 8 rows (J).
-Genus *Electrophortica* Hendel
6. Ac-index less than 4.0; wing maculated.
-Genus *Eostegana* Hendel
- Ac-index more than 4.0; wing not maculated7.
7. Mid tibia usually with stout bristles above.
-Genus *Stegana* Meigen
- Mid tibia without stout bristles above.
-Genus *Amiota* Loew
8. Carina undeveloped (E).9.
- Carina developed (e).11.
9. Ocellars outside ocellar triangle (c); postverticals absent (d).Genus *Crincosia* Bock
- Ocellars inside ocellar triangle (C); postverticals present (D).10.
10. Anterior reclinate orbital fine (f).
-Genus *Apenthesia* Tsacas
- Anterior reclinate orbital large (F).
-Genus *Mayagueza* Wheeler
11. Acrostichal hairs in 8 or less than 8 rows (j).
-Genus *Gitona* Meigen
- Acrostichal hairs in more than 8 rows (J).
-Genus *Cacoxenus* Loew

Tribe 2. Leucophengini Okada, n.

Type genus: *Leucophenga* Mik

12. Carina undeveloped (E).13.
- Carina developed (e).16.
13. Arista pubescent (b).14.
- Arista plumose (B).15.
14. Lateral scutellars divergent or parallel (K); ocellae absent.
-Genus *Acletoxenus* Frauenfeld
- Lateral scutellars convergent (k); ocellars present, though minute.
-Genus *Luzonimyia* Malloch
15. Excessive small scutellars absent.
-Genus *Leucophenga* Mik
- Excessive small scutellars usually presentGenus *Paraleucophenga* Hendel
16. Arista pubescent (b)16.
- Arista plumose (B).17.

17. Frons punctured.
 Genus *Trachyleucophenga* Hendel
 — Frons not punctured.18.
18. Vein M curved to R_{4+5} distally.
 Genus *Pararhinoleucophenga* Hendel
 — Veins R_{4+5} and M divergent distally.
 Genus *Rhinoleucophenga* Hendel
- Subfamily Drosophilinae
19. Periorbit broadened anteriorly; second costal break deep (l); frons not glossy; ocellars inside ocellar triangle (C). Tribe 1. Microdrosophilini.23.
 — Periorbit not broadened anteriorly.20.
20. Frons glossy; second costal break shallow (L); ocellars inside ocellar triangle (C). Tribe 2. Hypselothyriini.24.
 — Frons not glossy.21.
21. Ocellars outside ocellar triangle (c); second costal break shallow (L). Tribe 3. Colocasiomyini.30.
 — Ocellars usually inside ocellar triangle (C). ...
 22.
22. Second costal break deep (l; excl. *Styloptera*); second costal lappet usually large (m). Tribe 4. Dettopsomyini.33.
 — Second costal break shallow (L); second costal lappet Small (M). Tribe 5. Drosophilini.36.
- Tribe 1. Microdrosophilini Okada, n.
 Type genus: *Microdrosophila* Malloch
23. Monotypic.
 Genus *Microdrosophila* Malloch
- Tribe 2. Hypselothyriini Okada, n.
 Type genus: *Hypselothyrea* de Meijere
24. Postverticals absent (d).25.
 — Postverticals present (D).27.
25. Carina undeveloped (E); eye piled (a).
 Genus *Hypselothyrea* de Meijere
 — Carina developed (e); eye bare (A).26.
26. Lateral scutellars convergent (K) or parallel.
 Genus *Tambourella* Wheeler
 — Lateral scutellars divergent (k).
 Genus *Sphaerogastrella* Duda
27. Carina developed (e).28.
 — Carina undeveloped (E).29.
28. Eye bare (A); fore femur with a row of small spicules inside. ... Genus *Liiodrosophila* Duda
 — Eye piled (a); fore femur without spicules inside. Genus *Lissocephala* Malloch
29. Lateral scutellars divergent (k).
 Genus *Mulgravea* Bock
 — Lateral scutellars convergent (K).
 Genus *Paraliiodrosophila* Duda
- Tribe 3. Colocasiomyini Okada, n.
 Type genus: *Colocasiomyia* de Meijere
30. Carina developed (e); anterior reclinate orbital fine (f); lateral scutellars convergent or parallel (K).31.
 — Carina undeveloped (E); anterior reclinate orbital large (F); lateral scutellars divergent (k).32.
31. Arista plumose (B); anterior dorsocentrals nearer to scutellum than to suture (I).
 Genus *Calodrosophila* Wheeler & Takada
 — Arista usually pubescent (b); anterior dorsocentrals nearer to suture than to scutellum (i). Genus *Colocasiomyia* de Meijere
32. Wing not crispy; R_{2+3} apically gently curved to costa.
 Genus *Nesiodrosophila* Wheeler & Takada
 — Wing crispy; R_{2+3} apically strongly curved to costa. Genus *Jeannelopsis* Séguy
- Tribe 4. Dettopsomyini Okada, n.
 Type genus: *Dettopsomyia* Lamb
33. Eye bare (A); anterior dorsocentral minute or absent. Genus *Mycodrosophila* Oldenberg
 — Eye piled (a); anterior dorsocentral large. 34.
34. Ocellars outside ocellar triangle (c); anterior reclinate orbital behind proclinate.
 Genus *Styloptera* Duda
 — Ocellars inside ocellar triangle (C); anterior reclinate orbital slightly before proclinate.35.
35. Carina developed (e); anterior dorsocentrals nearer to suture than to scutellum (i).
 Genus *Dettopsomyia* Lamb

- Carina undeveloped (E); anterior dorsocentrals nearer to scutellum than to suture (I). Genus *Paramycodrosophila* Duda

Tribe 5. Drosophilini Okada, n.

Type genus: *Drosophila* Fallén

- 36. Anterior reclinate orbital fine (f).37.
- Anterior reclinate orbital large (F).48.
- 37. Arista pubescent (b) or with a few branches.38.
- Arista plumose (B).39.
- 38. Acrostichal hairs in 2 rows (j).38.
- Genus *Di cladochaeta* Malloch
- Acrostichal hairs in more than 8 rows (J).
- Genus *Baeodrosophila* Wheeler & Takada
- 39. Carina undeveloped (E).40.
- Carina developed (e).44.
- 40. Head much broader than thorax.
- Genus *Sphyrnoceps* de Meijere
- Head not broader than thorax.41.
- 41. Eye bare (A).42.
- Eye piled (a).43.
- 42. Arista without lower branches.
- Genus *Cladochaeta* Coquillett
- Arista with 2 lower branches.
- Genus *Miomyia* Grimaldi
- 43. Postverticals absent (d); body slender.
- Genus *Neotanygastrella* Duda
- Postverticals present (D); body thick.
- Genus *Diaethoneura* Duda
- 44. Arista inserted near apex of 3rd antennal joint.45.
- Arista inserted near base of 3rd antennal joint.46.
- 45. Arista without upper branches; orbitals present.
- Genus *Ateledrosophila* Hardy (♂)
- Arista with upper branches; orbitals absent.
- Genus *Nudidrosophila* Hardy (♂)
- 46. Lateral scutellars convergent or parallel (K); proboscis long.
- Genus *Zygothrica* Wiedemann
- Lateral scutellars divergent (k); proboscis not very long.47.
- 47. Mesoscutum without white longitudinal stripes; R_{4+5} and M divergent distally.
- Genus *Collessia* Bock
- Mesoscutum with white longitudinal stripes; R_{4+5} and M parallel distally.
- Genus *Phorticella* Duda
- 48. Second antennal joint protruded anteriorly below.49.
- Second antennal joint not protruded anteriorly below.50.
- 49. Carina developed (e); anterior dorsocentrals nearer to suture than to scutellum (i); wing markings distinct.
- Genus *Grimshawomyia* Hardy
- Carina undeveloped (E); anterior dorsocentrals nearer to scutellum than to suture (I); wing dark brown, basally hyaline.
- Genus *Celidosoma* Hardy
- 50. Carina undeveloped (E).51.
- Carina developed (e).53.
- 51. Eye entirely or nearly bare (A); anterior dorsocentrals nearer to scutellum than to suture (I); anterior reclinate orbital before proclinate; arista with branches.52.
- Eye piled (a); anterior dorsocentrals nearer to suture than to scutellum (i); lateral scutellars divergent (k); anterior reclinate orbital behind proclinate; arista without lower branches.
- Genus *Titanochaeta* Knab
- 52. Lateral scutellars convergent (K).
- Genus *Chymomyza* Czerny
- Lateral scutellars divergent (k).
- Genus *Protochymomyza* Grimaldi
- 53. Prescutellars present (H); dorsocentrals in 3 pairs.
- Genus *Balara* Bock
- Prescutellars usually absent (h); dorsocentrals in 2, 3, or 4 pairs.54.
- 54. Anterior dorsocentral nearer to suture than to scutellum (i).55.
- Anterior dorsocentral nearer to scutellum than to suture (I).56.
- 55. Dorsocentrals in 3 pairs, body stout.
- Genus *Samoia* Malloch
- Dorsocentrals in 2 pairs; body slender.
- Genus *Scaptomyza* Hardy
- 56. Dorsocentrals in 4 pairs; lower margin of gena densely haired.
- Genus *Malquessia* Malloch
- Dorsocentrals usually in 2 pairs; lower margin of gena not densely haired.57.

57. Eye nearly bare (A).....
..... Genus *Neorhinoleucophenga* Duda
— Eye piled (a).....58.
58. Mesoscutum with white longitudinal stripes;
posterior reclinate orbital usually nearer to
inner vertical than to proclinate (G).
..... Genus *Zaprionus* Coquillett
— Mesoscutum without white longitudinal
stripes; posterior reclinate orbital nearer to
proclinate than to inner vertical (g).
..... Genus *Drosophila* Fallén

Ungrouped Genera

1. Arista plumose (B).....2.
— Arista pubescent (b).3.
2. Eye bare (A). ... Genus *Apachrochaeta* Duda
— Eye piled (a). Genus *Laccodrosophila* Duda
3. Prescutellars present though weak (H);
anterior dorsocentral nearer to suture than to
scutellum (i). Genus *Pseudocacoxenus* Duda
— Prescutellars absent (h); anterior dor-
socentral nearer to scutellum than to suture
(I). Genus *Zapriothrica* Wheeler

ACKNOWLEDGMENTS

My sincere thanks are due for the loan of material and valuable information to Dr. Ian R. Bock, La Trobe University, Victoria, Dr. Ben Brugge, University of Amsterdam, Dr. Don H. Colles, C. S. I. R. O., Canberra, Dr. David A. Grimaldi, American Museum of Natural History, New York, Dr. D. Elmo Hardy, University of Hawaii, Honolulu, Dr. Kenneth I. Kaneshiro, University of Hawaii, Honolulu, Dr. Wayne N. Mathis, Smithsonian Institution, Washington, and Dr. Francisca C. do

Val, University of São Paulo.

I deeply thanks Dr. Marshall R. Wheeler, University of Texas, Austin, for reading manuscript.

REFERENCES

1. Wheeler, M. R. (1986) Additions to the catalog or the World's Drosophilidae. In "The Genetics and Biology of Drosophila" Ed. by M. Ashburner, H. L. Carson and J. N. Thompson Jr., Academic Press, London, pp. 395-409.
2. Okada, T. (1985) The genus *Lissocephala* Malloch and an allied new genus of Southeast Asia and New Guinea (Diptera, Drosophilidae). Kontyû, Tokyo, 53: 335-345.
3. Okada, T. (1987) Note on the genus *Mulgravea* (Diptera, Drosophilidae). Kontyû, Tokyo, 55: 187.
4. Grimaldi, D. A. (1987) Amber fossil Drosophilidae (Diptera), with particular reference to the Hispaniolan taxa. Am. Mus. Novit., 2880: 1-23.
5. Okada, T. (1988) Taxonomic note on *Colocasiomyia cristata* de Meijere with generic synonymy (Diptera, Drosophilidae). Proc. Jap. Soc. syst. Zool., 37: 34-39.
6. Wheeler, M. R. (1981) The Drosophilidae, taxonomic overview. In "The Genetics and Biology of Drosophila" Ed. by M. Ashburner, H. L. Carson and J. N. Thompson Jr. Academic Press, London, pp. 1-57.
7. Kaneshiro, K. Y. (1976) A revision of generic concepts in the biosystematics of Hawaiian Drosophilidae. Proc. Hawaii Ent. Soc., 22: 255-278.
8. Throckmorton, L. H. (1966) The relationships of the endemic Hawaiian Drosophilidae. Univ. Texas Publ., 6615: 335-396.
9. Okada, T. (1977) The automatic construction of keys. Jap. Soc. syst. Zool. Circular, 50: 6-11 (in Japanese).



Systematic Position and Biology of *Pectinatella gelatinosa* Oka (Bryozoa: Phylactolaemata) with the Description of a New Genus

SHUZITU ODA¹ and HIDEO MUKAI²

Biology Laboratory, Rikkyo University, Ikebukuro, Tokyo 171,

and ²Department of Biology, Faculty of Education,

Gunma University, Maebashi, Gunma 371, Japan

ABSTRACT—The biology of "*Pectinatella*" *gelatinosa* is reviewed, and it is proposed to establish the new genus *Asajirella* for *Pectinatella gelatinosa* Oka, 1891. The new genus is closely related to *Lophopodella*, but differing from it in forming composite colonies and nearly square saddle-shaped statoblasts. *Asajirella*, together with *Lophopodella* and *Lophopus*, should be placed in the Lophopodiidae, and is regarded as the most specialized genus of these three. A discussion on the phylogenetic relations among higher phylactolaemates is also given. The families Pectinatellidae and Cristatellidae are closely related to each other, but they are distantly related to the Lophopodiidae.

INTRODUCTION

Pectinatella gelatinosa was originally described by Oka [1] in 1891 based on the material obtained from Shinji Pond on the campus of the Imperial University of Tokyo. At that time, he assigned this species to the genus *Pectinatella* based on the massive growth form of the colony, the copious hyaline gelatinous nature of ectocyst, and the formation of saddle-shaped floatable statoblasts with marginal hooks. These characteristics are shared with the previously characterized species, *P. magnifica* (Leidy), the other member of the Pectinatellidae. However, recent studies on the histological and histochemical features of the epidermis [2], the morphology of the statoblasts [3, 4], the growth pattern of colonies [5], and the karyotype [6] all indicate that *P. gelatinosa* is more closely related to *Lophopodella*, especially *L. carteri* (Hyatt), than to *P. magnifica*. On the other hand, the species in question is different from *Lophopodella* in some other important characteristics. Therefore, it is reasonable to establish a new genus for *P. gelatinosa*.

In this paper, descriptions of the new genus and the biology of "*gelatinosa*" are given, and a discussion on the phylogenetic relationship among higher phylactolaemates is also comprised.

SYSTEMATIC ACCOUNT

Asajirella gen. nov.

The colony proper is massive and oval in outline, with a dichotomously branched, sac-like cystidal wall; no septa between the cystids; ectocyst copious, colorless, hyaline and gelatinous, covering thinly even the dorsal side of the cystid, and forming a common base for many colonies; polypides most crowded in the periphery of the colony; digestive tract straight when retracted; statoblast (floatoblast only) large and nearly square to somewhat oblong with rounded corners as it lies flat, curved in two axes like a saddle, with numerous minute marginal hooks, and non-buoyant unless dried; larvae bear as a rule two polypides.

This new genus is diagnostically distinguished from *Pectinatella* Leidy, 1851 [7] in forming sac-like colonies and non-buoyant floatoblasts, and from *Lophopodella* Rousselet, 1904 [8] in forming large gelatinous aggregation of colonies and nearly square saddle-shaped floatoblasts. As will be

Accepted June 22, 1988

Received May 6, 1988

¹ Present address: 5-27-15 Kugayama, Suginami-ku, Tokyo 168, Japan.

discussed below in detail, this new genus is more closely related to *Lophopodella* than to *Pectinatella*, and should be placed in the family Lophopodidae.

Etymology: This genus name is named after Asajiro Oka (1868–1944), who was one of the excellent zoologists, and who first studied freshwater bryozoans in Japan, with a diminutive, -ella.

Type species: *Pectinatella gelatinosa* Oka, 1891.

Asajirella gelatinosa (Oka, 1891), comb. nov.

Pectinatella gelatinosa Oka, 1891 [1]; Toriumi, 1941 [9]; Toriumi, 1956 [10]; Lacourt, 1968 [11].

Pectinatella burmanica Annandale, 1908 [12].

For the time being, this is the only species belonging to the genus *Asajirella*.

BIOLOGY OF *Asajirella gelatinosa*

Colony

A colony or zoarium is externally circular to somewhat oval, measuring about 1.5–2.5 cm in diameter. There are no septa between zooids, and the cystids of all zooids are united to form colonial wall (or coenocelial endocyst) enclosing a common body cavity in which polypides are suspended. Polypides are most crowded along the margin of

the colony, and arranged with their oral or ventral side facing outward. In the central part of the colony, functional polypides are scarce, and some club-shaped protrusions, which represent the cystids of degenerated polypides, are present (Fig. 1A). The colony is sac-like, with the conically protruding basal wall, so that the polypides can retract with their digestive tracts straight.

When the colony is observed from the underside, the dichotomous branching pattern of radially-arranged short branches, with some deep constrictions between them, is clear. The budding zone is restricted to the basal margin of the colony or to the ventral side of marginal zooids. Along the basal submarginal zone of the colony, there are some adhesive pads or attachment organs of the colony consisting of specialized epidermal cells, the alveolar cells [2, 13].

The ectocyst is colorless, hyaline and gelatinous. It is thick basally, and covers the surface of the colony in a thin coat. As a rule, the copious ectocyst makes a common base for many colonies (Fig. 1B). The composite colonies often reach about 15 cm across and 30 cm long.

Polypide

The polypide is essentially the same in gross morphology with those of other species, but it is the largest in phylactolaemates, measuring about 5

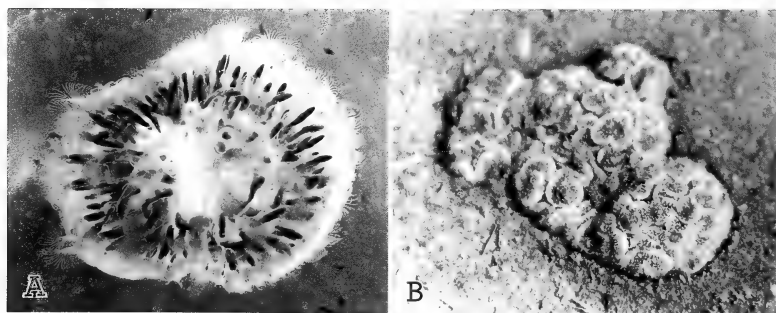


FIG. 1. Colonies of *Asajirella gelatinosa* gen. et comb. nov. A. Single colony, about 1 cm in diameter. Functional polypides are crowded along the periphery; several club-shaped cystids of degenerated polypides are seen in the central part. This colony was collected from a pond on the Imperial Villa of Katsura, Kyoto. B. Massive gelatinous aggregation of colonies, about 25 cm long, growing at the bottom of water in Lake Ezu, Kumamoto.

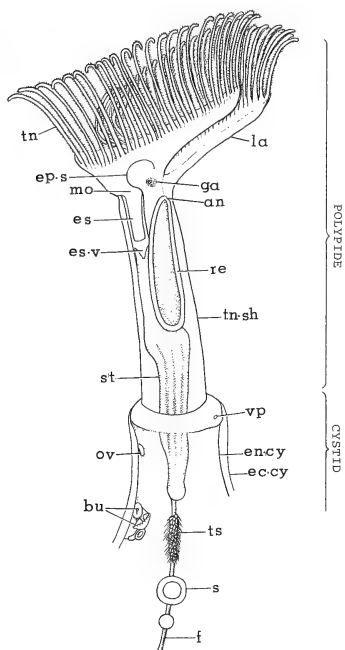


Fig. 2. Diagrammatic representation of the polypide of *Asajirella gelatinosa*. Retractive muscles are not shown; the collar-like distal part of the cystid is shown. an, anus; bu, bud; ec.cy, ectocyst; en.cy, endocyst; ep.s, epistome; es, esophagus; es.v, esophageal valve; f, funiculus; ga, ganglion; la, lophophore-arm; mo, mouth; ov, ovary; re, rectum; s, statoblast; st, stomach; tn, tentacle; tn.sh, tentacular sheath; ts, testis; vp, vestibular pore.

mm in length (Fig. 2). The digestive tract is Y-shaped in side view. The lophophore is horseshoe-shaped, bearing long, ciliated tentacles along its margin. The number of tentacles is mostly 90–98 [1], ranging from 75 to 106 [10]. When expanded, all parts of the digestive tract in grown polypides are wholly surrounded by the tentacular sheath, but in younger polypides a posterior portion of the stomach remains within the cystidal tube projecting above the body of the

colony. The digestive tracts are almost straight even when retracted. Oda [14] found that a sudden retraction of polypides causes the ejection of coelomic fluid, together with a number of coelomic corpuscles and spermatozoa, through the vestibular pore at the dorsal upper margin of the cystidal tube. For histological and histochemical features of the polypide, see Oka [1] and Mukai [15], respectively. A double monster with completely separate polypides, belonging to the oral type, has been reported [16, 17].

Statoblast

Only the floatoblast is produced (Fig. 3A). It is somewhat oblong or nearly quadrate with rounded corners, measuring about 1.5×1.3 mm in size and about 0.3 mm in thickness [1]. The cystigenic or dorsal side and the deutoplasmic or ventral side can be distinguished. The annulus has double curvature like a saddle. On the cystigenic side, it is convex along the major axis and concave along the minor axis. Both surfaces of the statoblast are beautifully marked into hexagonal meshes, the diameter of which decreases as one approaches the center. The central capsular area, the so-called

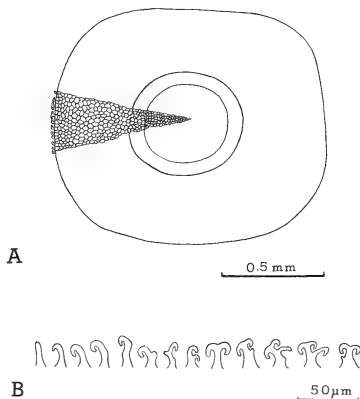


Fig. 3. Statoblast of *Asajirella gelatinosa*. A. Cystigenic side of a statoblast. B. Various types of hooks emerging from the rim of the deutoplasmic valve.

fenestra [18], is oval on the cystigenic side and circular on the deutoplasmic side. The statoblast does not float unless it is dried. Once dried, however, the float chambers of the annulus are filled with air and the statoblast floats on the surface of the water with the cystigenic side up.

The shell consists of two valves, which are separated from each other when the statoblast germinates. When flattened, the cystigenic valve is oval and the deutoplasmic valve is circular, the diameter of the latter being intermediate between the length and width of the former [3]. Numerous minute hooks are present around the margin of the deutoplasmic valve. They rise from the edge of the valve, and have no direct connection with the central part. The shape of the hooks varies widely; some of them are complex, while others are simpler (Fig. 3B).

In cross-section, the shell is found to consist of three layers, from within to the outside, the inner chitinous layer representing the capsule, the outer chitinous layer forming the walls of the float chambers, and the basophilic layer covering the surface of the statoblasts [3]. The latter two layers enveloping the central capsule form periblast [18]. When the statoblast is treated with 10 M KOH at room temperature, the periblast is separated into two valves, cystigenic and deutoplasmic, leaving the capsule intact and the germinal mass within the capsule still viable [19]. Each lateral wall between float chambers is provided with one small pore which is simple in structure [3]. The formation of the shell and its architecture have been studied by transmission as well as scanning electron microscopy [4, 20].

The germinal mass is composed of two parts, an outer layer of epidermal cells and an inner mass of yolk cells. The yolk granules are uniformly small and oval with a length of about $2\ \mu\text{m}$ [3]. The yolk cells have been studied histochemically [21] and electron microscopically [22, 23].

In nature, young colonies appear from overwintered statoblasts in early summer. The colonies produce numerous statoblasts from mid-summer to autumn. Mature statoblasts are set free from the funiculus and accumulate in the coelom (Fig. 4). The statoblasts are released after the disintegration of colonies in late autumn, when they are

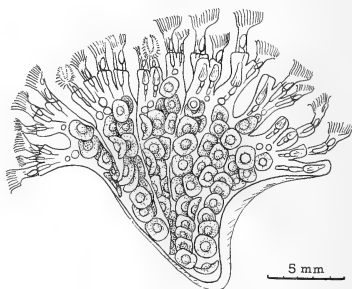


Fig. 4. Ventral view of a colony of *Asajirella gelatinosa* collected from Furutone-numa, Chiba Pref., in late autumn. The coelom is full of mature statoblasts.

in a dormant state [24]. These statoblasts survive the winter and germinate in the early summer of the following year.

Sexual reproduction

Oka [1] described the ovary, but no testis. The testis was found first by Oka and Oda [25]. Spermatozoa have been illustrated in Oda and Nakamura [26], and oogenesis has been studied by Tajima *et al.* [27]. According to Annandale [28], in Lower Burma many larvae were produced. In Japan, Oda and Nakamura [26] found only four larvae among a number of colonies obtained from Furutone-numa (Chiba Pref.) in August, 1962. The larva is oval or spherical, about 1.2 mm in diameter, and has two grown buds of slightly different sizes. At Tataru-numa (Gunma Pref.), both testes and ovaries are produced in the summer season, but no larvae have been found [13, 24]. Therefore, at least in Japan, sexual reproduction of the present species seems to be very limited.

Budding and colony formation

The budding zone is located on the ventral wall of the zooid. Blastogenesis has been studied in detail by Oka [1]. Mukai *et al.* [5, 13] studied the mode of budding and colony formation, starting from the ancestrula germinated from a statoblast. As a rule, the ancestrula produces three buds, and each of the subsequent zooids produces two buds,

not simultaneously but successively. The paired buds are located bilaterally relative to the median sagittal plane of the mother. A left bud always produces its first bud to the right, and vice versa. As daughter zooids separate rather laterally away from their mother zooids, thus leaving traces of dichotomous branching, a young colony is fan-shaped with zooids and buds occupying the peripheral arc. Subsequently, the colony becomes semicircular and then circular. With continued budding, the colony becomes oval in outline and is eventually divided into two or more small colonies.

Karyotype

Five different karyotypes have been found in germinating statoblasts obtained from Tataranuma. The five karyotypes are consistent in having 18 chromosomes, showing that the $2n$ is 18 [6].

Distributions

The present species has been recorded from Japan [1], Burma, India [12, 28], Java [29], Korea [30] and Taiwan [31].

Within Japan, this species has been distributed widely in the southern half [10]. A number of localities have been recorded in the Kanto district, but at the present time we can find no colonies in the city of Tokyo. Mukai [21] reported the abundant occurrence of colonies in Tataranuma (a pond), Gunma Pref., and most recent studies have utilized material collected at this pond. More recently, the occurrence of this species has been known in Lake Ezu, Kumamoto Pref. [32], a pond in Mitsuikaido, Ibaraki Pref. [33], a reservoir in Kurashiki, Okayama Pref. (personal communication of 1986 from Dr. Kuniyasu Satoh, Kawasaki Medical College), Isanuma, Saitama Pref. and a pond on the Imperial Villa of Katsura, Kyoto [34].

PHYLOGENETIC RELATIONSHIPS OF HIGHER PHYLACTOLAEMATES

Lophopus, *Lophopodella* and *Asajirella* have several characteristics in common, e.g., sac-like colonies with the convex basal wall [5, 35]; ectocyst covering the whole cystids; PAS-negative vacuolar cells and PAS-positive alveolar cells in the

epidermis [2]; non-buoyant floatoblasts with a three-layered shell and small yolk granules [3, 4]; and larvae with two grown buds [26, 36]. Moreover, *Lophopodella* and *Asajirella* have similar karyotypes [6]. Therefore, these three genera should be placed in the same family, the Lophopodidae.

The genus *Lophopus* consists of a single species, *L. crystallinus* (Pallas), in which the colony is semicircular [35] and the statoblast is spindle-shaped with pointed ends [3]. In *Lophopodella*, individual colonies are separated and statoblasts are generally elliptical with marginal hooked spines. *Asajirella* produces aggregations of colonies and nearly quadrate statoblasts with minute hooks around the margin of the deutoplasmic valve. Thus, *Lophopus* seems to represent the least specialized type and *Asajirella* seems to be the most specialized in the Lophopodidae.

The genus *Lophopodella* comprises four distinct species: *L. capensis* (Sollas), *L. thomasi* Rousset, *L. carteri* (Hyatt), and *L. pectinatelliformis* Lacourt. A series of changes in the number and position of the spines can be seen among these species. The statoblasts of *L. capensis* have a single hooked spine at both ends [4, 37], and those of *L. thomasi* are furnished with 3 or 4 hooked spines at both ends [4, 8, 37]. Statoblasts of *L. carteri* show markedly seasonal changes [38]. The number of hooked spines at one end is usually 6 to 16, but varies from 1 to 25. The dimensional outline of the statoblast proper also changes from spindle to elliptical to square and then circular as the number of spines increases. This variation depends mainly on the water temperature [38, 39]. At high temperatures (up to 30°C) the statoblasts are spindle-shaped with one to a few spines at both ends. The number of spines definitely increases with decreasing temperature. Statoblasts nearly circular in shape and bearing large numbers of spines along the entire border are formed at 10°C. The spindle-shaped statoblasts with one spine at both ends resemble those of *L. capensis*, and the spindle-shaped statoblasts with a few spines at both ends resemble those of *L. thomasi*. The statoblasts of *L. pectinatelliformis* are ellipsoidal in shape and have a number of minute anchor-like hooks emerging from the entire borders of both

valves [11, 40], thus more or less resembling the circular statoblasts with numerous spines of *L. carteri*. Accordingly, *L. pectinatelliformis* should be an intermediate between *L. carteri* and *A. gelatinosa* in terms of statoblast morphology.

The genus *Pectinatella* was established by Leidy [7], and now comprises an only species, *P. magnifica* (Leidy), which was originally described as *Cristatella magnifica* Leidy [41]. *Cristatella* also currently comprises a single species, *C. mucedo* Cuvier. In these two genera (and species), the colony is flat so that the digestive tracts of the polypides, when retracted, are folded characteristically [5], and the ectocyst covers only the basal wall [2]. Their statoblasts are buoyant with the annulus developed more voluminously on the cystigenic valve than on the deutoplasmic valve, and no distinction between the capsule and the periblast is possible [3]. Their larvae have generally four grown buds [see 42-44]. In these respects, these two genera are clearly distinguished from the

members of the Lophopodidae. In some respects *Asajirella* does resemble *Pectinatella*. In both genera, colonies form massive aggregates, and statoblasts are saddle-shaped. These resemblances seem to be superficial without phylogenetic significance.

In *Pectinatella*, the colony is rosette-shaped and radially branched or lobulated; a number of colonies form a huge gelatinous mass. The statoblast of this genus is somewhat oblong in outline, saddle-shaped, and bears spines emerging only from the cystigenic valve. On the other hand, the colony of *Cristatella* is worm-like in shape and not lobulated. Its statoblast is circular with the equatorial annulus borne entirely on the cystigenic valve and spines arising from both valves. On account of these marked differences, *Pectinatella* and *Cristatella* should be placed in different families, Pectinatellidae and Cristatellidae, respectively. The family Pectinatellidae was erected by Lacourt [11] to comprehend both *Pectinatella mag-*

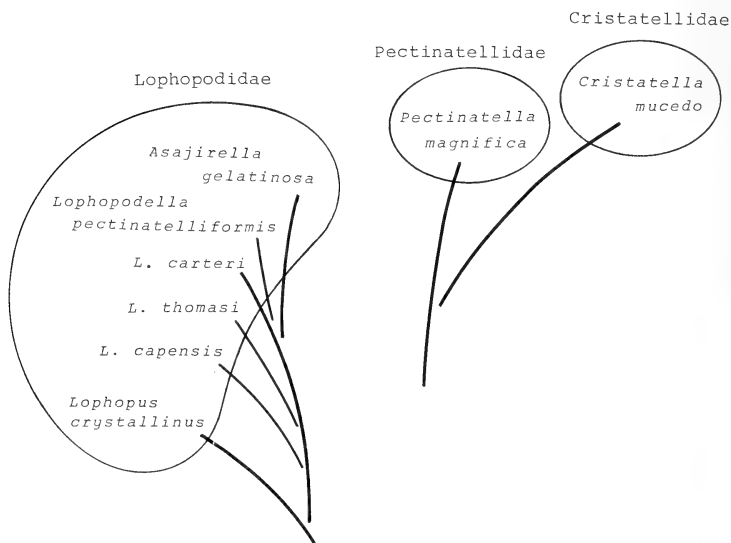


FIG. 5. Phylogeny of higher phylactolaemates.

nifica and "P." *gelatinosa*, but now this family should be amended to comprise only a single species, *P. magnifica*. The Cristatellidae seem to be more specialized than the Pectinatellidae.

On the basis of the above discussion, we propose a phylogenetic relationship of higher phylactolaemates in Figure 5. Our proposition is essentially consistent with that presented by Mukai [44], but is different in some important points from those by Toriumi [45] and Lacourt [11].

ACKNOWLEDGMENTS

We would like to dedicate the present paper to the late Professor Hidemitsu Oka, under whose guidance we started our research activity. Thanks are also due to Dr. Tsukané Yamasaki of Tokyo Metropolitan University for his critical reading of the manuscript. The present work was supported in part by a Grant-in-Aid for Scientific Research from the Ministry Education, Science and Culture, Japan.

REFERENCES

- Oka, A. (1891) Observations on fresh-water Polyzoa (*Pectinatella gelatinosa* nov. sp.). J. Coll. Sci. Imp. Univ. Tokyo, 4: 89–150.
- Mukai, H. and Oda, S. (1980) Histological and histochemical studies on the epidermal system of higher phylactolaemate bryozoans. Annot. Zool. Japon., 53: 1–7.
- Mukai, H. and Oda, S. (1980) comparative studies on the statoblasts of higher phylactolaemate bryozoans. J. Morphol., 165: 131–155.
- Oda, S. and Mukai, H. (1985) Fine surface structure of the statoblasts of higher phylactolaemate bryozoans. In "Bryozoa: Ordovician to Recent" Ed. by C. Nielsen and G. P. Larwood, Olsen and Olsen, Fredensborg, pp. 233–244.
- Mukai, H., Fukushima, M. and Jinbo, Y. (1987) Characterization of the form and growth pattern of colonies in several freshwater bryozoans. J. Morphol., 192: 161–179.
- Backus, B. T. and Mukai, H. (1987) Chromosomal heteromorphism in a Japanese population of *Pectinatella gelatinosa* and karyotypic comparison with some other phylactolaemate bryozoans. Genetica, 73: 189–196.
- Leidy, J. (1851) Some American fresh-water Bryozoa. Proc. Acad. Natl. Sci. Philad., 5: 320–322.
- Rousselet, C. F. (1904) On a new fresh-water Polyzoan from Rhodesia, *Lophopodella thomasi* gen. et sp. nov. J. Quekett Micr. Club, Ser. 2, 9: 45–56.
- Toriumi, M. (1941) Studies on freshwater Bryozoa, I. Sci. Rep. Tohoku Imp. Univ., Ser. 4, 16: 193–215.
- Toriumi, M. (1956) Taxonomical study on fresh-water Bryozoa, XV. *Pectinatella gelatinosa* Oka. Sci. Rep. Tohoku Univ., Ser. 4, 22: 29–33.
- Lacourt, A. M. (1968) A monograph of the fresh-water Bryozoa-Phylactolaemata. Zool. Verh. Utigeg. Rijksmus Natl. Hist. Leiden, 93: 1–159.
- Annandale, N. (1908) Three Indian Phylactolaemata. Rec. Ind. Mus., 2: 168–174.
- Mukai, H., Karasawa, T. and Matsumoto, Y. (1979) Field and laboratory studies on the growth of *Pectinatella gelatinosa* Oka, a freshwater bryozoan. Sci. Rep. Fac. Educ. Gunma Univ., 28: 27–57.
- Oda, S. (1958) On the outflow of the blood in colonies of freshwater Bryozoa. Kagaku (Tokyo), 28: 37. (In Japanese).
- Mukai, H. (1974) A histochemical study of a freshwater bryozoan, *Pectinatella gelatinosa*. Annot. Zool. Japon., 47: 91–102.
- Oda, S. (1954) On the double monsters of polypides in freshwater Bryozoa. Coll. Breed. (Tokyo), 16: 15–18. (In Japanese with English abstract).
- Oda, S. and Nakamura, R. M. (1973) The occurrence of double polypides in freshwater Bryozoa. In "Living and Fossil Bryozoa". Ed. by G. P. Larwood, Academic Press, London, pp. 523–528.
- Wood, T. S. (1979) Significance of morphological features in bryozoan statoblasts. In "Advances in Bryozoology". Ed. by G. P. Larwood and M. B. Abbott, Academic Press, London, pp. 59–73.
- Mukai, H. (1977) Effects of chemical pretreatment on the germination of statoblasts of the freshwater bryozoan, *Pectinatella gelatinosa*. Biol. Zbl., 96: 19–31.
- Tajima, I. (1980) Electron microscope studies on the statoblasts of a fresh-water bryozoan, *Pectinatella gelatinosa*, II. Changes in fine structure of cystigenous cells during statoblast formation. Zool. Mag. (Tokyo), 89: 26–40. (In Japanese with English abstract).
- Mukai, H. (1973) Histological and histochemical studies on the formation of statoblasts of a freshwater bryozoan, *Pectinatella gelatinosa*. J. Morphol., 141: 411–426.
- Tajima, I. and Mukai, H. (1975) Electron microscope studies on the statoblasts of a fresh-water bryozoan, *Pectinatella gelatinosa*, I. Vitellogenesis in the "yolk cell" during statoblast formation. Zool. Mag. (Tokyo), 84: 205–216. (In Japanese with English abstract).
- Terakado, K. and Mukai, H. (1978) Ultrastructural studies on the formation of yolk granules in the statoblast of a fresh-water bryozoan, *Pectinatella gelatinosa*. J. Morphol., 156: 317–338.
- Mukai, H. (1974) Germination of the statoblasts of

- a fresh-water bryozoan, *Pectinatella gelatinosa*. J. Exp. Zool., **187**: 27-40.
- 25 Oka, H. and Oda, S. (1948) Observations on fresh-water Bryozoa, with special reference to their reproduction. Coll. Breed. (Tokyo), **10**: 39-48. (In Japanese).
- 26 Oda, S. and Nakamura, R. M. (1980) Sexual reproduction in *Pectinatella gelatinosa*, a freshwater bryozoan. Proc. Jap. Soc. syst. Zool., **9**: 38-44.
- 27 Tajima, I., Inoue, S. and Gopal Dutt, N. H. (1984) Oogenesis in the freshwater bryozoan, *Pectinatella gelatinosa*: light microscopy. Z. Mikrosk.-Anat. Forsch. (Leipzig), **98**: 193-197.
- 28 Annandale, N. (1910) Materials for a revision of the phylactolaematous Polyzoa of India. Rec. Ind. Mus., **5**: 37-57.
- 29 Vorstman, A. G. (1928) Some freshwater Bryozoa of West Java. Treubia, **10**: 1-14.
- 30 Toriumi, M. (1941) Studies on freshwater Bryozoa, II. Freshwater Bryozoa of Korea. Sci. Rep. Tohoku Imp. Univ., Ser. 4, **16**: 413-425.
- 31 Toriumi, M. (1942) Studies on freshwater Bryozoa, IV. Freshwater Bryozoa of Formosa. Sci. Rep. Tohoku Imp. Univ., Ser. 4, **17**: 207-214.
- 32 Koumori, T. (1984) Appearance of *Pectinatella gelatinosa*, a freshwater bryozoan, in Lake Ezu, Kumamoto. Mogura (Kumamoto), **11**: 74-78 (In Japanese).
- 33 Oda, S. and Horikoshi, I. (1986) Massive colonies of *Pectinatella magnifica*, a freshwater bryozoan, occurring in a pond of Yoshino Park, Mitsuikaido, Ibaraki Prefecture. Coll. Breed. (Tokyo), **48**: 218-222. (In Japanese).
- 34 Oda, S. (1987) *Pectinatella galatinosa*, a freshwater bryozoan, occurring on the Imperial Villa of Katsura, Kyoto. Iden (Tokyo), **41**: 65-72. (In Japanese).
- 35 Marcus, E. (1934) Über *Lophopus crystallinus* (Pall.). Zool. Jahrb. Anat. Ont. Tiere, **58**: 501-606.
- 36 Oda, S. (1961) Relation between asexual and sexual reproduction in freshwater Bryozoa. Bull. Mar. Biol. Stat. Asamushi, **10**: 111-116.
- 37 Hastings, A. B. (1929) Phylactolaematous Polyzoa from the "Pans" of the transvaal. Ann. Mag. Natl. Hist., Ser. 10, **3**: 129-137.
- 38 Oda, S. (1955) Variability of the statoblasts in *Lophopodella carteri*. Sci. Rep. Tokyo kyoiku Dai., Sec. B, **8**: 1-22.
- 39 Oda, S. (1963) Factors causing variation in the statoblasts in *Lophopodella*. Proc. 16th Int. Congr. Zool. (Washington D. C.), **1**: 35.
- 40 Lacourt, A. M. (1959) *Lophopodella pectinatelliformis* nov. spec. (Bryozoa-Phylactolaemata). Zool. Mededelingen, **36**: 273-274.
- 41 Leidy, T. (1851) On *Cristatella magnifica*, n. sp. Proc. Acad. Natl. Sci. Philad., **5**: 265-266.
- 42 Oda, S. (1974) *Pectinatella magnifica* occurring in Lake Shoji, Japan. Proc. Jap. Soc. syst. Zool., **10**: 31-39.
- 43 Oda, S. (1961) Observations on *Cristatella mucedo* Cuvier. Coll. Breed. (Tokyo), **23**: 39-44. (In Japanese with English abstract).
- 44 Mukai, H. (1982) Development of freshwater bryozoans (Phylactolaemata). In "Developmental Biology of Freshwater Invertebrates". Ed. by F. W. Harrison and R. R. Cowden, Alan R. Liss Inc., New York, pp. 535-576.
- 45 Toriumi, M. (1956) Taxonomical study on freshwater Bryozoa. XVII. General consideration: Interspecific relation of described species and phylogenetic consideration. Sci. Rep. Tohoku Univ., Ser. 4, **22**: 57-88.

Phylogenetic Relationships among Seven Taxa of the Japanese Microtine Voles Revealed by Karyological and Biochemical Techniques

IKUYA YOSHIDA¹, YOSHITAKA OBARA² and NORIMASA MATSUOKA

Department of Biology, Faculty of Science,
Hirotsuki University, Hirotsuki 036, Japan

ABSTRACT—Chromosomes and 15 different protein systems of seven taxa of the Japanese microtine voles were examined to establish their phylogenetic relationships, making use of differential staining and protein electrophoretic techniques. While interspecific variations in the size of C-bands were observed only in the Y chromosomes, a highly homologous G-banding pattern as well as the karyotypic similarity were found among the microtine taxa examined, indicating that all of the microtine taxa here dealt with are regarded to be closely related to each other. The biochemical dendrogram for the seven taxa constructed from the Nei's genetic distances between taxa by using the UPGMA clustering method showed that the seven microtine taxa could be classified into three groups, though the differences of the D values were small in general, and this classification was well consistent with the karyological evidence of the interspecific Y-chromosome variations and their geographic distribution pattern. Furthermore, the electrophoretic results indicated that the *andersoni* complex should be classified not as a member of the genus *Aschizomys* or *Eothenomys*, but as that of the genus *Clethrionomys*, and that both *andersoni* and *niigatae* may still be at the subspecies level from their high genetic similarity. Phylogenetic relationships among the Japanese microtine voles are discussed in some detail from karyological and biochemical viewpoints.

INTRODUCTION

Ever since the first description of *Evotomys* (= *Clethrionomys*) *smithii*, *E. bedfordiae*, *E. andersoni* and *E. mikado* [1, 2], taxonomy of the Japanese microtine voles has been studied by many workers mainly from a morphological standpoint [3-9]. However, in spite of the extensive examination on the phylogeny of these microtine voles, their phylogenetic relationships are still in a great controversy.

While the voles of Hokkaido and its adjacent islands have been classified into either two species [9-11], three species [12-14] or five species [15, 16], the voles of Honshu, Shikoku and Kyushu into either two species [9, 14, 17] or five species [5, 6,

15, 18] excluding *Microtus montebelli*. On the other hand, four different views on the generic allocation of *andersoni* have been proposed on the basis of the traditional taxonomic criteria such as dental and skull systems: *andersoni* should be included in either the genus *Clethrionomys* [14, 17], the genus *Aschizomys* [5], the subgenus *Aschizomys* of the genus *Clethrionomys* [6], or the genus *Eothenomys* [9]. The specific (and even generic) allocation of *andersoni* has still remained indistinct and unresolved.

In the last decade, chromosome banding and protein electrophoretic techniques have provided much relevant, in some cases critical, information on the phylogenetic relationships in various groups of mammals [19-22]. As to the Japanese microtine species, no systematic investigation on the chromosome banding pattern as well as on the electrophoretic analysis of proteins has been made so far, except for a couple of case reports on the chromosome banding analysis [23-25]. In this study, we have attempted to establish the phy-

Accepted June 22, 1988

Received April 2, 1988

¹ Present address: Chromosome Research Unit, Faculty of Science, Hokkaido University, Sapporo 060, Japan.

² To whom reprint requests should be addressed.

logenetic relationships among the Japanese microtine species by using chromosome banding and protein electrophoretic techniques.

MATERIALS AND METHODS

Animals

A total of 72 specimens from seven microtine taxa were examined in this study. They were all trapped alive at various localities of Honshu, Hokkaido and Rishiri Island. For nomenclature of the voles studied here the taxonomic system of Corbet [14] was adopted. Triplet and doublet of alphabets in parentheses show abbreviations for their scientific names.

Clethrionomys rutilus mikado (Crm): Mt. Petegari (1050 m), Hokkaido (♂ 0, ♀ 2); *C. rex* (Cre): Rishiri Shrine and Kanrosen, Rishiri Is. (♂ 4, ♀ 4); *C. rufocanus sikotanensis* (Crs): Rishiri Shrine, Rishiri Is. (♂ 2, ♀ 0); *C. rufocanus bedfordiae* (Crb): Mt. Petegari (1050 m), Shojiyama, Yunotai and Miyauta, Hokkaido (♂ 13, ♀ 11); *C. andersoni andersoni* (Caa): Mt. Iwaki, Zatōishi and Ainai, Aomori Pref., Nagabashiri, Akita Pref., Asahi-kousen, Yamagata Pref. (♂ 16, ♀ 9); *C. andersoni niigatae* (Can): Jumonjitoge (2050 m), Saitama Pref. (♂ 2, ♀ 2); *Eothenomys smithi* (Es): Nanzawakousen and Nezame, Nagano Pref., Eiheiiji and Heisenji, Fukui Pref. (♂ 5, ♀ 2). All of the animals examined are preserved as standard museum specimens (skin with skull) or formalin-fixed specimens in the Department of Biology, Faculty of Science, Hirosaki University, Hirosaki.

Chromosome preparation

Metaphase chromosomes were obtained from the femoral bone marrow cells of the chloroform-anesthetized specimens. The procedure for chromosome preparation was almost the same as that previously described [26, 27]. For G- and C-band staining, the ASG [28] and BSG [29] methods were adopted. Analytical data on the conventionally-stained and G- and C-banded karyotypes are summarized in Table 1.

Electrophoresis

Five different tissues (kidney, liver, intestine,

pancreas and skeletal muscle) which had been stored at -80°C were used for the electrophoretic study. The procedures for tissue preparation and polyacrylamide gel electrophoresis were almost the same as those described by Matsuoka [30, 31]. The following 14 different enzymes and general proteins (non-enzymatic proteins) were assayed, using supernatants of tissue homogenates: α -glycerophosphate dehydrogenase (α -GPDH), glucose-6-phosphate dehydrogenase (G6PD), hexose-6-phosphate dehydrogenase (H6PD), lactate dehydrogenase (LDH), malate dehydrogenase (MDH), octanol dehydrogenase (ODH), 6-phosphogluconate dehydrogenase (6-PGD), xanthine dehydrogenase (XDH), superoxide dismutase (SOD), hexokinase (HK), aspartate aminotransferase (AAT), esterase (EST), amylase (AMY), leucine amino peptidase (LAP), and general protein (GP). G6PD, H6PD, LDH, ODH, 6-PGD, HK and AAT were assayed with the extract of the kidney; α -GPDH, MDH, XDH and SOD with that of the liver; AMY and LAP with that of the intestine and pancreas, and EST and GP with that of the skeletal muscle. As three enzymes (EST, LAP and AMY) and GP showed many polymorphic bands, these were assayed using a vertical slab gel apparatus (gel plate measured $1 \times 160 \times 140$ mm with 8–20 sample slots). For other enzymes a disc gel apparatus ($3 \times 11 \times 75$ mm plastic column) was used. The stain mixtures for LDH and 6-PGD were prepared according to Shaw and Prasad [32] and that for α -GPDH according to Ayala *et al.* [33]. Stain recipes for other enzymes were those described previously [31, 34, 35]. GP was stained with Coomassie Brilliant Blue R-250 by the method of Matsuoka *et al.* [36].

RESULTS

Karyological analysis

All of the seven taxa of microtines examined had the diploid number of 56 (Table 1). A conventional karyotype of Caa is presented in Figure 1a as a standard karyotype representing these microtines. The karyotype consisted of 26 pairs of acrocentrics of gradually decreasing size, one pair of the small-

TABLE 1. Analytic and cytologic data on the seven taxa of the Japanese red-backed voles examined in the present study

Species	No. of cells karyotyped			NFA	2n	Sex chromosome	
	Conv.	ASG	BSG			X	Y
<i>Clethrionomys rutilus mikado</i>	8	5	5	56	56	A	M*
<i>C. rex</i>	23	16	8	56	56	A	A
<i>C. rufocanus sikotanensis</i>	13	14	6	56	56	A	A
<i>C. r. bedfordiae</i>	48	57	24	56	56	A	A
<i>C. andersoni andersoni</i>	65	41	30	56	56	A	M
<i>C. a. niigatae</i>	18	15	14	56	56	A	M
<i>Eothenomys smithi</i>	15	12	11	56	56	A	St

* Shimba *et al.* [41], Tsuchiya and Yoshida [44] and Tsuchiya [37]. A, acrocentric; M, metacentric; St, subtelocentric; Conv., conventional staining; ASG, G-banding; BSG, C-banding; NFA, fundamental number of autosomes; 2n, diploid number of chromosomes.

lest metacentrics and the XY chromosomes. Small but easily detectable short arms were found only in the pair No. 3 which can be regarded as acrocentric judging from its arm ratio, 9.87 ± 0.71 , though Tsuchiya [37] thought this chromosome to be subtelocentric. Thus, the NFA of Caa should be 56. Similar pattern of the small short arms was observed in all of the remaining taxa. Their autosomal constitution was almost identical with that of Caa, and hence their NFA was 56 in all the taxa examined (Table 1). The interspecific difference in the length and morphology of chromosomes was found only in the Y chromosomes. The X chromosomes were all acrocentrics of the same length.

A G-banded karyotype of Caa is presented in Figure 1b. Chromosomes are arranged according to the numbering system proposed by Gamperl [38] who has described the G- and C-banding patterns of the grey red-backed vole, *C. rufocanus*, and the bank vole, *C. glareolus*. As clarified in the previous report [25], the G-banding pattern of Caa is almost identical with that of these continental species. So, making this karyotype of G-bands standard, detailed pair matching analysis of G-banding pattern was made among the seven taxa (Fig. 2). As clearly demonstrated in the composite karyotype, almost perfect G-band homology was obtained in all the chromosome complements including the X chromosomes among the seven taxa,

reflecting their phylogenetic kinship. The C-bands of Caa were all centromeric except for the Y chromosome which was entirely heterochromatic along its arms (Fig. 1b, insertion). There was no significant difference in the G- and C-banding patterns among the seven taxa, except for their Y chromosomes. The Y chromosomes showed distinct interspecific variations in their G- and C-banding patterns, but no detectable variation at the intraspecific or subspecies level (Fig. 3). On the basis of the size and morphology of the Y chromosomes the microtine taxa under present study could be classified into three groups as follows: *andersoni*-type carrying a metacentric Y (Caa and Can), *rufocanus*-type carrying an acrocentric one (Crb, Crs and Cre) and *smithi*-type carrying a subtelocentric one (Es). The rates of the Ys to the Xs ($Y/X \pm SD$) were 0.28 ± 0.02 in Crs, 0.28 ± 0.03 in Crs, 0.30 ± 0.03 in Crb, 0.28 ± 0.03 in Caa, 0.27 ± 0.05 in Can and 0.41 ± 0.05 in Es. Thus, the Y chromosomes correspond to 27–30% of the X chromosomes in length except for Es, in which the Y was about 41% of its X chromosome length.

Electrophoretic analysis

From the electrophoretic patterns of 14 different enzymes and general protein observed in and among the seven taxa of microtines, we assumed 26 genetic loci (Table 2). The major features of

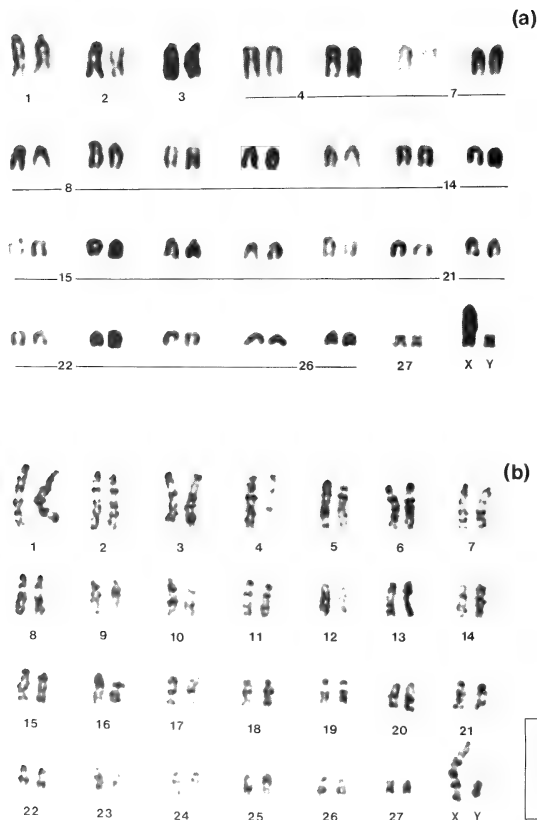


FIG. 1. Conventional (a) and G-banded (b) karyotypes of a male Japanese red-backed vole, *Clethrionomys a. andersoni*.

variation in these proteins are summarized as follows.

Eight enzymes: α -GPDH, G6PD, H6PD, ODH, 6-PGD, XDH, HK and AAT exhibited a single band of activity and they were all monomorphic.

The bands of individual enzymes showed the same electrophoretic mobility in the seven taxa.

LDH showed five-banded pattern in all taxa. As this enzyme is known to be a tetrameric protein, the five bands could be interpreted as five different



FIG. 2. Pair-matching of G-banded haploid chromosomes from each of seven taxa of the Japanese red-backed voles. From left to right; *Clethrionomys rutilus mikado*, *C. rex*, *C. rufocanus sikotanensis*, *C. r. bedfordiae*, *C. andersoni andersoni*, *C. a. niigatae* and *Eothenomys smithi*.

tetramers consisting of two polypeptides produced by two codominant alleles at two different loci (LDH-1 and LDH-2). Each of these bands showed the same mobility in all taxa and the two loci were

monomorphic in each taxon.

MDH showed two active bands, of which the faster band was markedly high in activity. These two bands were interpreted as the products of two

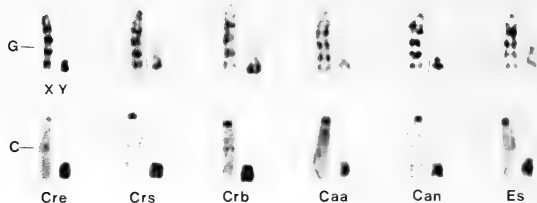


FIG. 3. G-banded (G) and C-banded (C) sex chromosomes, X and Y, of the seven taxa of the Japanese red-backed voles.

different loci (MDH-1 and MDH-2) in the light of other electrophoretic studies of various animal groups. Each of these two bands also showed the same mobility in all of the taxa. The two loci were also monomorphic in each taxon.

SOD consisted of three bands with the highest activity in the fastest band. These were interpreted as the products of three different loci (SOD-1, SOD-2 and SOD-3) in the light of the electrophoretic studies of sea-urchins [31, 34, 35]. The bands of SOD-1 and SOD-2 in *Es* showed the faster mobilities than those of other taxa, but the band of SOD-3 had the same mobility in all the taxa. These three loci were monomorphic in each taxon.

EST activity was detected as several bands which were grouped into two zones. The slow zone (EST-1) consisted of a single faint band and was monomorphic. While the fast zone (EST-2) showed high genetic variability in *Crb*, *Crm* and *Es*, it was monomorphic in the remaining four taxa.

LAP showed only a single active band in *Crm*, but in the remaining six taxa the enzyme consistently appeared as two active bands. These band patterns were interpreted to be controlled by two different loci (LAP-1 and LAP-2). LAP-1 was polymorphic in four taxa (*Crb*, *Cre*, *Caa* and *Es*) and LAP-2 in three taxa (*Crb*, *Caa* and *Es*).

AMY activity was detected as one to two bands.

It was polymorphic within each of four taxa (*Crb*, *Caa*, *Can* and *Es*), and furthermore it also showed considerable variations among taxa.

In GP, six to ten bands were obtained in each taxon. These were assumed to be products of six different loci (GP-1~GP-6) from the electrophoretic mobilities of these bands. Four of them (GP-1, GP-2, GP-4 and GP-6) could be presumed to be commonly possessed by all taxa, but the others (GP-3 and GP-5) were considered to be specific only to certain given taxa. Polymorphic band patterns were observed in GP-3 of *Crs*, in GP-5 of *Crb* and in GP-4 of *Caa* and *Can*.

The allele frequencies for all loci in these seven taxa are given in Table 2. In this table, it was assumed that the bands showing the same electrophoretic mobility between taxa in a given locus are products of the same alleles. Based on these data, the genetic identity (I) and genetic distance (D) between each taxon were calculated by the method of Nei [39]. Table 3 represents the matrices of I and D values between all pairs of the taxa examined. As evident from this table, the I value between *Caa* and *Can*, which allopatrically inhabit the hilly countries of northern Honshu (Tohoku district) and the high mountains (more than 2,000 m above the sea level) of central Honshu (Kanto and Chubu districts), respectively, is the highest (I = 0.951). The I values between *Crb*, *Crs*, *Cre* and *Crm*, all of which are distributed in Hokkaido and

TABLE 2. Allele frequencies at various genetic loci in the seven taxa of microtines

Locus	Crn	Cre	Crn	Crb	Caa	Can	Es
α -GPDH	a	a	a	a	a	a	a
G6PD	a	a	a	a	a	a	a
H6PD	a	a	a	a	a	a	a
ODH	a	a	a	a	a	a	a
6-PGD	a	a	a	a	a	a	a
XDH	a	a	a	a	a	a	a
HK	a	a	a	a	a	a	a
AAT	a	a	a	a	a	a	a
LDH-1	a	a	a	a	a	a	a
LDH-2	a	a	a	a	a	a	a
MDH-1	a	a	a	a	a	a	a
MDH-2	a	a	a	a	a	a	a
SOD-1	a	a	a	a	a	a	b
SOD-2	a	a	a	a	a	a	b
SOD-3	a	a	a	a	a	a	a
EST-1	a	b	b	c	c	c	c(0.71) d(0.29)
EST-2	b(0.50) c(0.50)	e	b	a(0.02) b(0.38) c(0.08) d(0.06) e(0.44) f(0.02)	e	e	c(0.29) e(0.71)
LAP-1	f	d(0.29) e(0.71)	f	a(0.05) d(0.62) f(0.33)	b(0.86) d(0.14)	b	c(0.14) d(0.43) f(0.43)
LAP-2	—	b	b	b(0.43) c(0.57)	a(0.14) b(0.86)	b	d(0.57) e(0.43)
AMY	b	e	h	f(0.39) g(0.11) h(0.50)	a(0.47) c(0.53)	a(0.50) c(0.50)	b(0.21) d(0.29) e(0.50)
GP-1	a	a	a	a	a	a	a
GP-2	a	a	a	a	a	a	a
GP-3	b	b	a(0.50) b(0.50)	b	—	—	—
GP-4	a	a	a	a	a(0.79) b(0.21)	a(0.50) b(0.50)	a
GP-5	a	d	—	b(0.04) c(0.96)	—	—	d
GP-6	a	a	a	a	a	b	a

Alleles are correspondingly lettered from "a", this being the allele of lowest mobility. The value in parenthesis represents the frequency of each allele in taxon. The scientific name of each taxon is shown as abbreviation described in Materials and Methods.

its neighbouring islands, are relatively high with the range of 0.803~0.895. On the other hand, the I values between Es and the six taxa of the genus *Clethrionomys* are in the range of 0.713~0.792 and lower than the values mentioned above. Figure 4 shows the biochemical dendrogram for the

seven taxa constructed from the genetic distance matrix of Table 3 using the unweighted pair-group arithmetic average (UPGMA) clustering method of Sneath and Sokal [40]. The biochemical dendrogram indicates the following: (1) The seven taxa studied here are divided into three clusters.

TABLE 3. Genetic identities (above diagonal) and genetic distances (below diagonal) between the seven taxa of microtines

Taxa	Crm	Cre	Crs	Crb	Caa	Can	Es
Crm	—	0.803	0.824	0.844	0.769	0.713	0.736
Cre	0.219	—	0.842	0.855	0.823	0.771	0.789
Crs	0.194	0.172	—	0.895	0.816	0.763	0.713
Crb	0.170	0.157	0.111	—	0.891	0.829	0.783
Caa	0.263	0.195	0.203	0.115	—	0.951	0.792
Can	0.338	0.260	0.270	0.188	0.050	—	0.729
ES	0.307	0.237	0.338	0.245	0.233	0.316	—

The scientific name of each taxon is shown as abbreviation described in Materials and Methods.

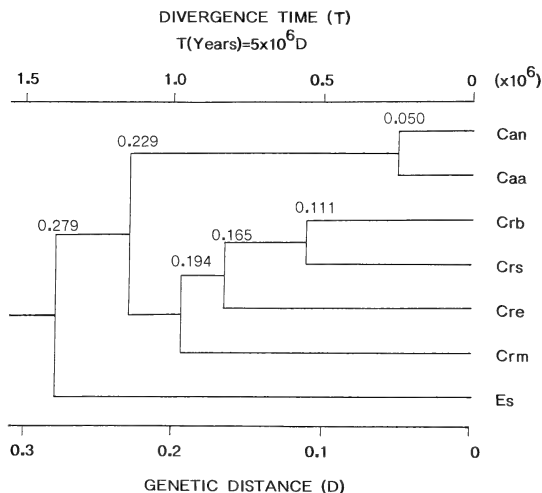


FIG. 4. A biochemal dendrogram showing the phylogenetic relationships among the seven taxa of the Japanese microtine voles.

The first cluster consisted of two *andersoni* subspecies (Caa and Can), the second cluster four taxa (Crb, Crs, Cre and Crm), and the third cluster only Es. (2) Of the seven taxa, Caa and Can of the first cluster is the most closely related to each other ($D=0.050$). (3) In the second cluster, Crb and Crs are the most closely related to each other ($D=0.111$), and Cre is more closely related to Crb and

Crs than Crm. However, the differences of the D values are small in all pair-groups of these four taxa. (4) Es is slightly differentiated from the first and second clusters, and the mean D value between Es and two large clusters consisting of six taxa of the genus *Clethrionomys* is 0.279.

The proportion of polymorphic loci (P) in each taxon was as follows: 4.0% for Crm and Crs, 3.8%

for Cre, 19.2% for Crb, 16.7% for Caa, 8.3% for Can and 20.0% for Es. The mean value of P was 10.9%. The expected mean heterozygosity per locus (H) in each taxon was as follows: 2.0% for Crm and Crs, 1.6% for Cre, 8.9% for Crb, 5.5% for Caa, 4.2% for Can and 10.2% for Es. The mean value of H was 4.9%.

DISCUSSION

The karyotypes of the seven taxa of microtines here studied were essentially identical, except for the Y chromosome of Can, to those of the previous observation [37, 41–44]. The Y chromosomes of the *andersoni* complex were metacentric in both Caa and Can, as far as the present specimens are concerned. Hsu and Benirschke [42] regarded the Y chromosome of Can as the smallest metacentric element, but Tsuchiya [37] as an acrocentric one. Our finding is, therefore, consistent with the former view. These facts may be suggestive of the polymorphic nature of the Y chromosome of this taxon, just indicating an additional case of the parallelism of the Y chromosome variability reported in three *Clethrionomys* species; *C. glareolus*, *C. rutilus* and *C. rufocanus* [45]. However, it is still uncertain whether the Y chromosome variants have been established as the interpopulation polymorphism or not. Further examination of the specimens from various localities is necessary for elucidation of this subject. The Y chromosome of Cre showed a similar but somewhat indistinct variation: it was regarded as a subtelocentric element by Tsuchiya [37], and as an acrocentric one in the present specimens. Further, he is of opinion that the X chromosomes of Cre, Caa and Es are subtelocentric. But they were all acrocentric in the present study (Fig. 3). These minor discrepancies may be not essential but attributable to the technical matters or how to set up the criteria for chromosome morphology.

As shown by the composite karyotype of Figure 2, the seven taxa studied are almost identical to each other in their G- and C-banding pattern as well as in their conventional karyotypes, though their Y chromosomes showed three types of interspecific variations; *andersoni*-type, *rufocanus*-type and *smithi*-type (Table 1 and Fig. 3). These

findings plainly signify that all of these microtines are the descendants from a common ancestral form, and with the only exception of Y chromosome, no karyotypic differentiation has proceeded in the course of phenotypic differentiation. As clearly demonstrated from the pair-matching analysis of G-bands between Caa and *C. rufocanus* from near Gallivare, Sweden [38], the red-backed voles of Japan could be closely related to the grey red-backed vole, *C. rufocanus* which is widely but sporadically distributed from Scandinavia to Siberia, Sakhalin and Hokkaido. In view of these facts, it may be most likely that the seven taxa of microtines studied have derived from a *rufocanus*-like ancestor of the Eurasian continent.

The biochemical dendrogram (Fig. 4) demonstrated that the seven taxa of microtine voles are genetically divided into three groups. This relationship is well consistent with their distribution in Japan: Caa and Can are distributed in northern and central Honshu, Crs, Crb, Cre and Crm are endemic to Hokkaido and its neighbouring islands, and Es inhabits Kyushu, Shikoku and southwestern Honshu. Further, the biochemical dendrogram consisting of three clusters is also consistent with the morphological variations of their Y chromosomes: metacentric in the first cluster, acrocentric in the second one and subtelocentric in the third one. The present electrophoretic results seem to be compatible, in a broad sense, with the taxonomic system of Imaizumi [15] based on the phenotypic characters. He classified, in the light of the rooting pattern of molars, these microtine taxa into three different genera: the genus *Aschizomys* including Caa and Can, the genus *Clethrionomys* including Crs, Crb, Cre and Crm, and the genus *Eothenomys* including Es. However, this classification is out of harmony, in a strict sense, with our taxonomic system in some respects. He regarded *andersoni* and *niigatae* as two distinct species of the genus *Aschizomys*. As already mentioned, the D value between the two taxa is markedly low ($D=0.050$) and comparable to the D values observed between conspecific geographic populations in many other animals [46–48]. Judging from their highly close similarity at molecular and chromosomal level, *andersoni* and *niigatae* should be considered as two subspecies of the same

species. Further, the mean D value ($D=0.229$) between the *andersoni* complex (Caa and Can) and the four taxa of red-backed voles (Crs, Crb, Cre and Crm) is much lower than the D values reported between different genera of many other animals and rather at the subspecies or closely related species level [46–48]. Since they are also very similar to each other in phenotypic and karyological aspects, these microtine taxa should be considered as the congeneric members of *Clethrionomys*, as proposed by Corbet [14].

In the cluster consisting of the *rufocanus* complex (Crb and Crs), Cre and Crm, Crb has the closest affinity with Crs and the D value between them is the lowest ($D=0.111$), which is comparable to the D values observed between subspecies of many other animals [46–48]. Taking their distribution areas and high genetic similarity into consideration, it seems very reasonable to regard the insular (Rishiri Island) taxon Crs and the mainland (Hokkaido) taxon Crb as conspecific, though these two have been regarded as distinct species by Imaizumi [15]. It is clear from the electrophoretic results that Crm had already differentiated prior to the evolutionary divergence of the *rufocanus* complex and Cre. These biochemical findings may substantiate the phenotypic evidence that Crm significantly differs in the molar pattern as well as in the body size from *rufocanus* complex and Cre. However, the high I values found between these four taxa strongly suggest that *rufocanus*, *rex* and *rutilus* are distinct but closely related species each other.

With respect to the taxonomic allocation of the *andersoni* complex (Caa and Can), Aimi [9] proposed that *andersoni* (including *niigatae*) should be referred to the genus *Eothenomys* on the basis of the craniometry and the occlusal pattern of molars. If *andersoni* and *smithi* are congeneric with each other, then *rufocanus*, *rex* and *rutilus* also must necessarily be included in the genus *Eothenomys*, judging from the biochemical dendrogram shown in Figure 4. But, the view that the *rufocanus*-group must be included in the genus *Eothenomys* may be hard to accept even from usual taxonomic criteria because of the clear difference in rooting of the cheek-teeth. On the whole, our classification system as to the generic allocation of the *andersoni*

complex is consistent not with that of Aimi [9], but with that of Corbet [14] who classified the *andersoni* complex as a member of the genus *Clethrionomys*. According to Corbet [14], the *Eothenomys* species closely resemble *Clethrionomys*, only being distinguished mainly by the absence of rooting of the cheek-teeth even in old age. Further, the *Eothenomys* species are distributed mainly in China, and quite rarely in the Korean Peninsula and Japan, and the *Clethrionomys* species are widely distributed to the northern regions of the Eurasian Continent. Thus, it would be most probable that the genus *Eothenomys* might have diverged from the red-backed voles, *Clethrionomys*, by modifying the rooting pattern of molars somewhere in the Eurasian Continent and the ancestral population of Es might have migrated into Japan through a southern route, or the Korean Peninsula. The genetic differentiation of the genus *Eothenomys* from the lineage of the genus *Clethrionomys* may well be reflected in our biochemical dendrogram.

In general, biochemical dendrogram shows not only the phylogenetic relationships, but also the sequence of evolutionary divergence. According to Nei [49], genetic distance (D) corresponds well with the divergence time (T) from the common ancestor, and T of two taxa can be estimated by $T = 5 \times 10^6 D$ (year). Applying this equation to our biochemical dendrogram, each divergence time may be calculated as follows: 1.4 million years (MY) for *Eothenomys* and *Clethrionomys*, 1.1–1.2 MY for the two large groups of *Clethrionomys*, 0.5–1.0 MY for the four taxa of *Clethrionomys* endemic to Hokkaido, and 0.25 MY for the two *andersoni* subspecies.

For further clarification of the phylogenetic relationships among the Japanese microtine voles, it would be needed to synthetically examine the chromosomes, genetic distances and the phenotypic characters of all the taxa including *C. montanus*, *C. imaizumii* and *E. kageus* which could not be dealt with in this study.

ACKNOWLEDGMENTS

The authors wish to express their gratitude to Dr. M. Yoshiyuki, National Science Museum, Tokyo, for her

cooperation in identifying the microtine voles examined. Our gratitude is also extended to Professor K. Saitoh, Hirosaki University, Hirosaki, for his valuable suggestions and encouragement throughout this work, and for critically reading the manuscript. Our thanks are also due to Professor M. Takahashi, Marine Biomedical Institute, Sapporo, Medical College, Rishiri Island, Hokkaido, Dr. N. Takada, Fukui Medical College, Fukui, Mr. A. Abe, Hirosaki High School, Hirosaki, Mr. M. Mukohyama, San-nohe High School, San-nohe, Aomori Pref., Mr. K. Machida, Saitama Museum of Natural History, Chichibu, Mr. Y. Nagao, Hokkaido Government Office, Sapporo, Mr. N. Nishizawa, Asahi-cho, Yamagata Pref., for their help in collecting the research materials.

REFERENCES

- 1 Thomas, O. (1905) On some new Japanese mammals presented to the British Museum by Mr. R. Gordon-Smith. *Ann. Mag. Nat. Hist.*, Ser. 7., **15**: 487-495.
- 2 Thomas, O. (1905) Abstract. *Proc. Zool. Soc. London*, **23**: 18-19.
- 3 Hinton, M. A. C. (1926) Monograph of the voles and lemmings (Microtinae), living and extinct. Vol. 1, pp. 246-248, 257-262, 437-438. British Museum (N. H.), London.
- 4 Kuroda, N. (1931) A new locality and scientific name of red-backed vole, *Eoatomys niigatae*. *Zool. Mag.*, **43**: 661-666 (in Japanese).
- 5 Imaizumi, Y. (1960) Coloured illustrations of the mammals of Japan. pp. 128-139. Hoikusha, Tokyo. (in Japanese).
- 6 Jameson, E. W. Jr. (1961) Relationships of the red-backed voles of Japan. *Pacific Sci.*, **15**: 594-604.
- 7 Miyao, T., Morozumi, T., Hanamura, H., Akahane, H. and Sakai, A. (1964) Small mammals on Mt. Yatsugatake in Honshu. III. Smith's red-backed vole (*Eothenomys smithi*) in the subalpine forest zone on Mt. Yatsugatake. *Zool. Mag.*, **73**: 189-195 (in Japanese with English summary).
- 8 Tanaka, R. (1971) A research into variation in molar and external features among a population of the Smith's red-backed vole for elucidation of its systematic rank. *Japn. J. Zool.*, **16**: 163-176.
- 9 Aimi, M. (1980) A revised classification of the Japanese red-backed voles. *Mem. Fac. Sci. Kyoto Univ.*, Ser. Biol., **8**: 35-84.
- 10 Ota, K. (1956) The Muridae of the islands adjacent to Hokkaido. *Mem. Fac. Agr. Hokkaido Univ.*, **2**: 123-136 (in Japanese with English summary).
- 11 Abe, H. (1968) Growth and development in two forms of *Clethrionomys*. I. External characters, body weight, sexual maturity and behaviour. *Bull. Hokkaido Forest Exp. Station*, No. 6: 69-89 (in Japanese with English summary).
- 12 Abe, H. (1973) Growth and development in two forms of *Clethrionomys*. II. Tooth characters with special reference to phylogenetic relationships. *J. Fac. Agr. Hokkaido Univ.*, **57**: 229-254.
- 13 Abe, H. (1973) Growth and development in two forms of *Clethrionomys*. III. Cranial characters, with special reference to phylogenetic relationships. *J. Fac. Agr. Hokkaido Univ.*, **57**: 255-274.
- 14 Corbet, G. B. (1978) The mammals of the Palearctic region: A taxonomic review. Cornell Univ. Press, London-Ithaca, pp. 97-100.
- 15 Imaizumi, Y. (1979) Classification of the Japanese myomorphs. *Nat. Anim.*, **9**: 2-6 (in Japanese).
- 16 Imaizumi, Y. (1972) Land mammals of the Hidaka Mountains, Hokkaido, Japan, with special reference to the origin of an endemic species of the genus *Clethrionomys*. *Mem. Natl. Sci. Mus. (Tokyo)*, **5**: 131-149 (in Japanese with English summary).
- 17 Tokuda, M. (1941) A revised monograph of the Japanese and Manchou-Korean Muridae. Biogeographica, Transact. Biogeogr. Soc. Japan, **4**: 1-156.
- 18 Imaizumi, Y. (1971) A new vole of the *Clethrionomys rufocanus* group from Rishiri Island, Japan. *J. Mammal. Soc. Japan*, **5**: 99-103.
- 19 Greenbaum, I. F. (1981) Genetic interactions between hybridizing cytotypes of the tent-making bat (*Uroderma bilobatum*). *Evolution*, **35**: 306-321.
- 20 Bohlin, R. G. and Zimmerman, E. G. (1982) Genic differentiation of two chromosomal races of the *Geomys bursarius* complex. *J. Mammal.*, **63**: 218-228.
- 21 Hafner, J. C., Hafner, D. J., Patton, J. L. and Smith, M. F. (1983) Contact zones and the genetics of differentiation in the pocket gopher *Thomomys bottae* (Rodentia: Geomyidae). *Syst. Zool.*, **32**: 1-20.
- 22 Gothran, E. G. and Smith, M. H. (1983) Chromosomal and genic divergence in mammals. *Syst. Zool.*, **32**: 360-368.
- 23 Yamakage, K., Nakayashiki, N., Hasegawa, J. and Obara, Y. (1985) G-, C- and N-banding patterns on the chromosomes of the Japanese grass vole, *Microtus montebelli montebelli*, with special attention to the karyotypic comparison with the root vole, *M. oeconomus*. *J. Mammal. Soc. Japan*, **10**: 209-220 (in Japanese with English summary).
- 24 Obara, Y. and Yoshida, I. (1985) A case of X-autosome translocation in the Japanese red-backed vole, *Clethrionomys andersoni andersoni*. *Chrom. Inf. Serv.*, **39**: 3-5.
- 25 Obara, Y. (1986) G-band homology between the Japanese red-backed vole, *Clethrionomys a. andersoni* and the grey red-backed vole, *C. rufocanus*. *Chrom. Inf. Serv.*, **40**: 7-9.
- 26 Obara, Y. (1982) Comparative analysis of

- karyotypes in the Japanese mustelids, *Mustela nivalis namiyei* and *M. erminea nippon*. J. Mammal. Soc. Japan, **9**: 59-69.
- 27 Saitoh, M. and Obara, Y. (1986) Chromosome banding patterns in five intraspecific taxa of the large Japanese field mouse, *Apodemus speciosus*. Zool. Sci., **3**: 785-792.
 - 28 Sumner, A. T., Evans, H. J. and Buckland, R. A. (1971) New technique for distinguishing between human chromosomes. Nature New Biol., **232**: 31-32.
 - 29 Sumner, A. T. (1972) A simple technique for demonstrating centromeric heterochromatin. Exptl. Cell Res., **75**: 304-306.
 - 30 Matsuoka, N. (1981) Phylogenetic relationships among five species of starfish of the genus *Asterina*: An electrophoretic study. Comp. Biochem. Physiol., **70B**: 739-743.
 - 31 Matsuoka, N. (1985) Biochemical Phylogeny of the sea-urchins of the family Toxopneustidae. Comp. Biochem. Physiol., **80B**: 767-771.
 - 32 Shaw, C. R. and Prasad, R. (1970) Starch gel electrophoresis of enzymes: A compilation of recipes. Biochem. Genet., **4**: 297-320.
 - 33 Ayala, F. J., Powell, J. R., Tracey, M. L., Mourão, C. A. and Pérez-Salas, S. (1972) Enzyme variability in the *Drosophila willistoni* group. IV. Genetic variation in natural populations of *Drosophila willistoni*. Genetics, **70**: 113-139.
 - 34 Matsuoka, N. (1987) Biochemical study on the taxonomic situation of the sea-urchin, *Pseudocentrotus depressus*. Zool. Sci., **4**: 339-347.
 - 35 Matsuoka, N. and Suzuki, H. (1987) Electrophoretic study on the taxonomic relationship of the two morphologically very similar sea-urchins, *Echinostrephus aciculatus* and *E. molaris*. Comp. Biochem. Physiol., **88B**: 637-641.
 - 36 Matsuoka, N., Ohnishi, K., Takahashi, T., Oka, K. and Hori, S. H. (1983) Evidence for the homology of hexose 6-phosphate dehydrogenase and glucose 6-phosphate dehydrogenase: Comparison of the amino acid compositions. Comp. Biochem. Physiol., **76B**: 811-816.
 - 37 Tsuchiya, K. (1981) On the chromosome variations in Japanese cricetid and murid rodents. Honyurui Kagaku, **42**: 51-58 (in Japanese).
 - 38 Gamperl, R. (1982) Chromosomal evolution in the genus *Clethrionomys*. Genetica, **57**: 193-197.
 - 39 Nei, M. (1972) Genetic distance between populations. Amer. Natur., **106**: 283-292.
 - 40 Sneath, P. H. A. and Sokal, P. R. (1973) Numerical Taxonomy. Freeman, San Francisco.
 - 41 Shimba, H., Ito, M., Obara, Y., Kohno, S. and Kobayashi, T. (1969) A preliminary survey of the chromosomes in field mice, *Apodemus* and *Clethrionomys*. J. Fac. Sci. Hokkaido Univ., Ser. 6, Zool., **17**: 257-262.
 - 42 Hsu, T. C. and Benirschke, K. (1974) An Atlas of Mammalian Chromosomes. Vol. 8., Folio 370, 371. Springer-Verlag, New York/Heidelberg/Berlin.
 - 43 Sonta, S., Hayata, I. and Kobayashi, T. (1971) A chromosome survey of the red-backed mouse, *Clethrionomys rufocanus bedfordiae*, in Hokkaido, with a note of a karyotypically abnormal specimen. Proc. Japan Acad., **47**: 679-682.
 - 44 Tsuchiya, K. and Yoshida, T. H. (1971) Chromosome survey of small mammals in Japan. Ann. Rep. Natl. Inst. Genet., **21**: 54-55.
 - 45 Vorontsov, N. N., Lyapunova, E. A., Borissov, Y. M. and Dovgal, V. E. (1980) Variability of sex chromosomes in mammals. Genetica, **52/53**: 361-372.
 - 46 Avise, J. C. (1976) Genetic differentiation during speciation. In "Molecular Evolution" Ed. by F. J. Ayala, Sinauer Associates, Massachusetts, pp. 106-122.
 - 47 Ferguson, A. (1980) Biochemical Systematics and Evolution. Blackie, Glasgow.
 - 48 Ayala, F. J. (1982) Population and Evolutionary Genetics: A Primer. The Benjamin/Cummings Publishing Company, California.
 - 49 Nei, M. (1975) Molecular Population Genetics and Evolution. North-Holland, Amsterdam.

[COMMUNICATION]

**Karyotype of the Loggerhead Turtle,
Caretta caretta, from Japan**

NAOKI KAMEZAKI

*Department of Zoology, Faculty of Science, Kyoto University,
Sakyo, Kyoto 606, Japan*

ABSTRACT—The karyotype of the loggerhead turtle, *Caretta caretta*, from Japan was studied by bone marrow-Giemsa staining technique. This species has $2n=56$ homologous chromosomes, consisting of 12 metacentric, 2 submetacentric, 6 subtelocentric, 12 acrocentric macroelements and 24 micro-elements in a graded series. Comparison of the present karyotype with other cheloniid species confirmed the strong chromosomal conservativeness within the family.

INTRODUCTION

The karyotype of the loggerhead turtle, *Caretta caretta* was studied first by Nakamura [1]. He reported that the chromosome number of this species from Shirahama, Kii Peninsula, Japan was 51 in the female and 52 in the male showing the sex chromosome heteromorphism. Later, Nakamura [2] checked a larger sample and corrected the number to be 57 in the female and 58 in the male. On the other hand, Bickham [3] and Bickham and Carr [4] noted that the turtle from unknown localities had 56 chromosomes without providing detailed description of the karyotype. The differences between the results of Nakamura [1, 2] and of later authors [3, 4] might indicate the existence of intraspecific chromosome variation within *Caretta caretta*. However, the other possibility is that Nakamura miscounted chromosome numbers, since he employed testis-sectioning methods which sometimes provide wrong data [5]. In order to test Nakamura's data, I reinvestigated the karyotype of the sample from Kii Peninsula, by bone marrow-

air dry method.

MATERIALS AND METHODS

Four hatchlings (one male and three females) were used. The mother turtles were caught from the coastal waters of Kushimoto, Kii Peninsula, and oviposited in captivity.

The hatchlings were injected with 0.1 ml of colchicine solution ($1 \mu\text{g/ml}$) per gram of body weight. Twenty hr after the injection, the femur bone marrows were taken out, treated with hypotonic solution following Ota *et al.* [6] and fixed in Carnoy's solution. Metaphase chromosome spreads were obtained by an air-dry method stained with 2% Giemsa solution. Each specimen was sexed by microscopic examination of gonadal sections.

RESULTS AND DISCUSSION

Twelve cells from a male and six from three females exhibited $2n=56$ chromosomes in a graded series. Of these, pairs 2, 6, 8-10 and 13 were regarded as metacentric, pair 1 submetacentric, pairs 3, 12 and 14 subtelocentric, and pairs 4, 5, 7, 11, 15 and 16 acrocentric elements. The remainders were classified as microchromosomes. No sex chromosome heteromorphism was evident in either sex (Fig. 1).

The chromosome number of the present sample agrees with that reported by Bickham [3] or Bickham and Carr [4], but considerably differs from those reported by Nakamura [1, 2], although there is only a little distance between each locali-

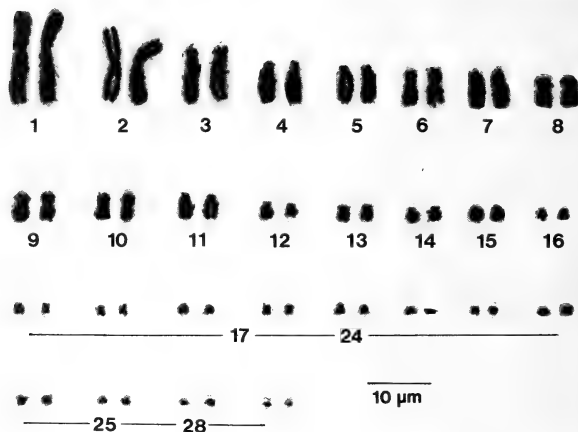


FIG. 1. Karyotype of a female *Caretta caretta* from Kii, Japan.

ties. Thus, it is highly probable that the chromosome numbers provided by Nakamura [1, 2] were in reality incorrect due to the unreliable method he adopted.

Several authors postulated that the pattern of karyotypic variation in the suborder Cryptodira is basically conservative, and that all or most of the species within a family appear karyotypically identical [4, 7]. The karyotype of *Caretta caretta* seems to agree with those of *Chelonia mydas* and *Lepidochelys olivacea* reported by Bickham *et al.* [8] and Bhunya and Mohanty-Hejmadi [9], respectively. The close resemblance among karyotypes of these sea turtle species belonging to different genera seem to support the above assumption. Even so, however, it is required to examine the other three chelonid species [10], whose karyological data are presently unavailable, to draw a conclusion upon the variability of the karyotype in this family.

ACKNOWLEDGMENTS

I thank I. Miyawaki of Kushimoto Marine Parks

Center for providing samples, M. Tasumi for facilities, S. Ishihara for literature and H. Ota for comments on this manuscript.

REFERENCES

- 1 Nakamura, K. (1937) Jap. J. Genet., **13**: 240.
- 2 Nakamura, K. (1949) La Kromosomo, **5-6**: 205-213.
- 3 Bickham, J. W. (1981) Science, **212**: 1291-1293.
- 4 Bickham, J. W. and Carr, J. L. (1983) Copeia, **1983**: 918-932.
- 5 Gorman, G. C. (1973) In "Cytotaxonomy and Vertebrate Evolution". Ed. by A. B. Chiarelli and E. Capanna, Academic Press, New York, pp. 349-424.
- 6 Ota, H., Matsui, M., Hikida, T. and Tanaka, S. (1987) Experientia, **43**: 924-925.
- 7 Bickham, J. W. (1983) In "Chromosomes in Evolution of Eukaryotic Groups, vol. 2". Ed. by A. K. Sharma and A. Sharma, CRC Press, Inc., Boca Raton, Florida, pp. 14-36.
- 8 Bickham, J. W., Bjørndal, K. A., Haiduk, M. W. and Rainey, W. E. (1980) Copeia, **1980**: 540-543.
- 9 Bhunya, S. P. and Mohanty-Hejmadi, P. (1986) Chrom. Inf. Serv., **40**: 12-14.
- 10 Pritchard, P. C. H. (1979) Encyclopedia of Turtles. T. F. H. Publ., Neptune, N. J.

[COMMUNICATION]

Immunohistochemical Demonstration of Calcitonin Gene-Related Peptide in the Ultimobranchial Gland of Some Lower Vertebrates and in the Nervous Tissues of Some Invertebrates

YUICHI SASAYAMA, KOUHEI MATSUDA, CHITARU OGURO
and AKIRA KAMBEGAWA¹

Department of Biology, Faculty of Science, Toyama University, Toyama 930,
and ¹Department of Obstetrics and Gynecology, Faculty of Medicine,
Teikyo University, Tokyo 173, Japan

ABSTRACT—Calcitonin gene-related peptide (CGRP) was detected immunohistochemically in the ultimobranchial gland of 2 species of cartilaginous fish and 3 species of frog, and in the nervous tissues of one species each of earthworm and sea-squirt.

INTRODUCTION

Calcitonin is a hormone secreted from the C-cells of the thyroid gland in mammals or from the ultimobranchial gland (UBG) in lower vertebrates. Recently, it was shown that the rat and human calcitonin genes encode a peptide other than calcitonin: calcitonin gene-related peptide (CGRP) [1-3]. This peptide has been identified immunochemically and immunohistochemically in the C-cells of the rat thyroid gland [4-6]. It is well known that the parenchymal cells of the UBG are embryologically homologous to the C-cells of the thyroid. However, it has not yet been determined whether the UBG is capable of producing CGRP. On the other hand, it has been reported that in some invertebrates, immunoreactive calcitonin exists in nervous tissues [7, 8]. This fact suggests that invertebrates may also possess the calcitonin gene that encodes CGRP. In the present study, therefore, an attempt was made to detect CGRP

immunohistochemically in the UBG of some lower vertebrates and in nervous tissues of some invertebrates.

MATERIALS AND METHODS

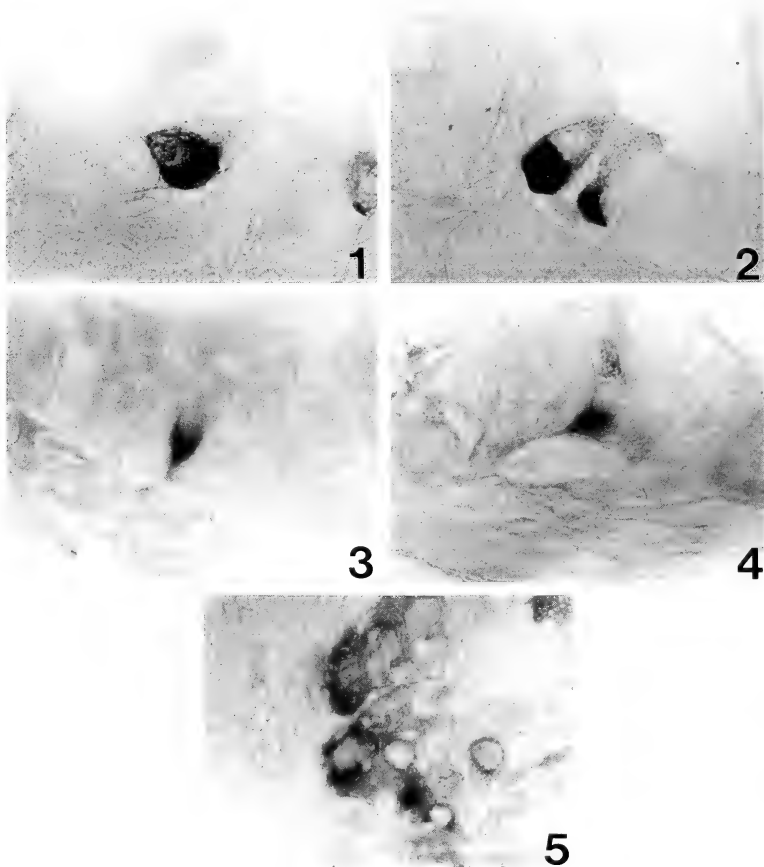
Twelve species of lower vertebrates examined. These were stingray (*Dasyatis akajei*) and guitarfish (*Rhinobatos schlegelii*) as representative cartilaginous fish, goldfish (*Carassius auratus*) as a representative bony fish, frogs (*Rana rugosa*, *R. nigromaculata*, and *R. catesbeiana*) and a newt (*Cynops pyrrhogaster*) as representative amphibians, snakes (*Rhabdophis tigrinus* and *Elaphe quadrivirgata*) and a lizard (*Takydromus tachydromoides*) as representative reptiles, and chicken (*Gallus domesticus*) as a representative bird. Furthermore, the earthworm (*Pheretima communissima*), an annelid, and the sea-squirt (*Styela plicata*), a protochordate were examined as representative invertebrates.

The UBG of lower vertebrates, the ventral nervous chain in the earthworm, and the neural complex of the sea-squirt were fixed in Bouin's solution (without acetic acid) for 5 hr, then dehydrated and embedded in paraffin. These were then sectioned at 6 μ m according to routine procedures.

The double peroxidase-antiperoxidase (PAP) method was applied for the detection of CGRP.

Rabbit anti-rat CGRP antiserum (Amersham; diluted 1:900) was used as a primary antiserum at room temperature for 12 hr. Then, sections were incubated with anti-rabbit IgG porcine serum (1:20; Dako) and PAP (1:50; Dako), respectively

for 30 min, in that order. Subsequently, anti-rabbit IgG and PAP were applied again, respectively for 30 min, in order to reinforce the reaction. Finally, the sections were treated with 0.05 M Tris-HCl buffer (pH 7.6) containing 3, 3'-



FIGS. 1-5. CGRP immunoreactive cells in the UBG of some vertebrate species demonstrated by the PAP method. $\times 1120$. Fig. 1. The sting-ray (*Dasyatis akajei*). Fig. 2. The guitar-fish (*Rhinobatos schlegelii*). Fig. 3. The frog (*Rana rugosa*). Fig. 4. The frog (*Rana nigromaculata*). Fig. 5. The frog (*Rana catesbeiana*).

diaminobenzidine tetrahydrochloride and H_2O_2 solution.

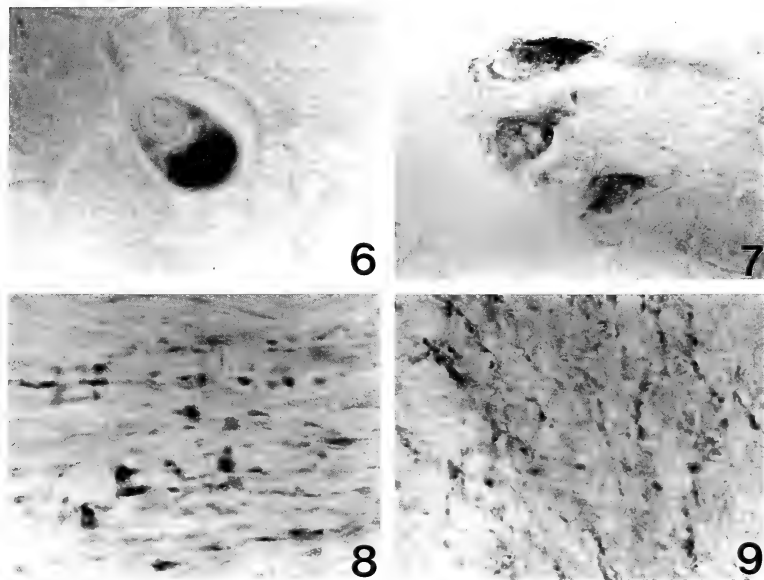
The specificity was checked using primary anti-serum inactivated by the addition of an excess amount of synthetic rat CGRP ($7.7 \mu\text{g/ml}$ of the diluted antiserum). Furthermore, it was confirmed that the potency of the anti-CGRP antiserum was not damaged by incubation with synthetic salmon calcitonin ($1.25 \mu\text{g/ml}$). This result implies that anti-CGRP antiserum does not cross-react with calcitonin.

RESULTS AND DISCUSSION

CGRP immunoreactivity was detected in the UBG of the 2 species of cartilaginous fish and 3 species of frog, among the vertebrates examined.

In other vertebrates examined in this study, no positive reaction was obtained in their UBG.

In the stingray and the guitar-fish, the UBG was composed of small follicles. The CGRP-immunoreactive cells were found dotted within the follicle wall (Figs. 1 and 2). In the latter species, the number of positive cells was rather smaller than in the former species. There was a tendency that in both species, the basal portion of positive cells was stained more strongly. In the frogs, the UBG was composed of a few follicles of various sizes. A few of the follicle cells located at the periphery of the gland reacted with the antiserum (Figs. 3–5). The number of positive cells in the UBG differed from species to species among these frogs, being more abundant in *R. rugosa* than in other 2 species. Also in the frog UBG, there was a



FIGS. 6–9. CGRP immunoreactivity in the nervous tissue of some invertebrate species demonstrated by the PAP method. Fig. 6. Cell in the ventral nervous chain of the earthworm (*Pheretima communissima*). Fig. 7. Cells in the cerebral ganglion of the sea-squirt (*Styela plicata*). Fig. 8. Immunoreactive axons in the earthworm (*Pheretima communissima*). Fig. 9. Immunoreactive axons in the sea-squirt (*Styela plicata*).

tendency for the basal portion of positive cells to be stained more strongly. These results show that the UBG in some species of lower vertebrates is capable of generating CGRP, as in the C-cells of higher vertebrates. In rats, it has been reported that CGRP is released at a rate similar to that of calcitonin [4]. Therefore, it seems that the amount of CGRP elaborated in the UBG of lower vertebrates is fairly small, even though it exhibits a positive reaction by the double PAP method. On the other hand, the physiological role CGRP present in C-cells has not yet been clarified. Also in the UBG of some lower vertebrates, its biological significance is unclear at the present time.

In the earthworm and the sea-squirt, CGRP immunoreactivity was detected in a few neurons of the nervous tissue. In the earthworm, the immunoreactive cells were found dotted within the

in these 2 species, many neuronal axons were also clearly stained (Figs. 8 and 9). Figure 10 shows schematically the location of the positive cells and axons. In rats, it has been reported that CGRP is also distributed in the brain in addition to the UBG. In the brain, this peptide is thought to play an important role as a neuromodulator [2]. Consequently, in the nervous tissues of some invertebrates, this putative function of CGRP may also apply.

The results obtained in the present study suggest a possibility that CGRP might have been encoded in the calcitonin gene at a fairly early stage of animal evolution. However, the problem of species specificity of the anti-CGRP antiserum used in the present study still remains. In order to generalize the significance of the present results, much more work needs to be done.

ACKNOWLEDGMENTS

We wish to express our sincere thanks to Dr. H. Michibata for kindly supplying the sea-squirts. The present study was supported in part by the Toyama Prefecture Centennial Foundation.

REFERENCES

- 1 Amara, S. G., Jonas, V., Rosenfeld, M. G., Ong, E. S. and Evans, R. M. (1982) *Nature*, **298**: 240-244.
- 2 Rosenfeld, M. G., Mermod, J.-J., Amara, S. G., Swanson, L. W., Sawchenko, P. E., Rivier, J., Vale, W. W. and Evans, R. M. (1983) *Nature*, **304**: 129-135.
- 3 Morris, H. R., Panico, M., Etienne, T., Tippins, J., Girgis, S. I. and MacIntyre, I. (1984) *Nature*, **308**: 746-748.
- 4 Cooper, C. W., Borosky, S. A. and Peng, T.-C. (1980) *Proc. Soc. Exp. Biol. Med.*, **180**: 562-566.
- 5 Lee, Y., Kawai, Y., Shiosaka, S., Takami, K., Kiyama, H., Hillyard, C. J., Girgis, S., MacIntyre, I., Emson, P. C. and Tohyama, M. (1985) *Brain Res.*, **330**: 194-196.
- 6 Lee, Y., Takami, K., Kawai, Y., Girgis, S. I., Hillyard, C. J., MacIntyre, I., Emson, P. C. and Tohyama, M. (1985) *Neuroscience*, **15**: 1227-1237.
- 7 Girgis, S. I., Galan, F., Arnett, T. R., Rogers, R. M., Bone, Q., Ravazzola, M. and MacIntyre, I. (1980) *J. Endocrinol.*, **8**: 375-382.
- 8 Fritsch, H. A. R., Van Noorden, S. and Pearce, A. G. E. (1979) *Cell Tiss. Res.*, **202**: 263-274.

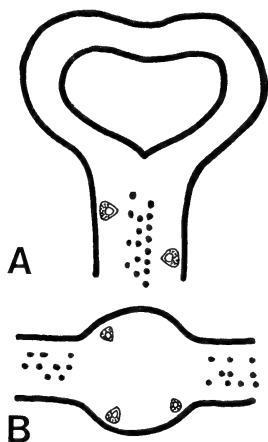


Fig. 10. Schematic drawings showing location of the CGRP immunoreactive cells and axons in the nervous tissues of the earthworm (A) and the sea-squirt (B).

peripheral region of the ventral nervous chain (Fig. 6). In the sea-squirt, the immunoreactive cells were found scattered in the peripheral portion of the cerebral ganglion (Fig. 7). It was noted that

[COMMUNICATION]

Dual Photobehavioral Response in Catfish

MITSUO TABATA and MAUNG MINH-NYO

*Laboratory of Fish Biology, School of Agriculture,
Nagoya University, Chikusa, Nagoya 464, Japan*

ABSTRACT—Photobehavioral responses were measured in respect to the length of dark adaptation in the catfish, *Silurus asotus*. The light stimulation had dual effect on the activities, inhibition and excitation with the period of dark adaptation for less than 4 hr and for more than 5 hr, respectively. The excitatory photobehavioral responses were assessed for the measurement of light threshold.

INTRODUCTION

It has been generally accepted that the photoreception of most fishes is mediated by retinal and extraretinal photoreceptor organs. The extraretinal photoreception is well known to be mediated mainly by the pineal organ in many fishes [1-3], while extraretinal and nonpineal photoreception is also suggested in several fishes [4-8]. These photoreceptor organs receive ambient light information to give rise to various physiological, biochemical and behavioral activities. However, little is known about the threshold of these organs of individual fishes, probably due to lack of a common indicator for the measurement.

Locomotor activity is used as one of indicators for the comparative study of light sensitivity of fishes [9-11]. The activity pattern, however, seems to depend on the species, age and various experimental conditions of light. The present study was conducted to observe properties of photobehavioral responses in catfish, *Silurus asotus*, in respect to behavioral pattern along with dark adaptation. Then, the suitability of the responses for the measurement of light threshold was assessed.

MATERIALS AND METHODS

Catfish of both sexes, ranging from 17-30 cm in body length and 80-200 gm in body weight, were obtained from a fish firm in Aichi prefecture at the period from June to November of 1986-1987. Totally 20 catfish were used.

Before commencement of experiment, the fish was acclimatized for 7-10 days in a tank (56×40×36 cm) with a light regime of 12 hr light and 12 hr dark (LD12:12, L=100 lx) at 20°C. Lights were on either from 6:00 to 18:00 or from 18:00 to 6:00. The latter light schedule was mainly used to obtain long dark adaptation. Determination of photobehavioral response was carried out in a single catfish kept in an experimental tank (40×30×30 cm). For the fish being kept under L phase the dark adaptation started immediately after it was transferred to the experimental tank. On the other hand, for the fish being transferred from D phase the dark adaptation has started at lights off of acclimatizing tank. The transfer of catfish to experimental tank did not largely effect on the amount of activity. This was previously ascertained by comparing activities of dark adapted fish for 5 hr in the experimental tank to that of transferred fish which has been dark adapted for 5 hr in the acclimatizing tank. Both showed nearly the same amount of activities. It was considered that the possible effect of circadian rhythmicity on the locomotor activities could be eliminated by observing dark adapted fish for more than 12 hr.

Fish activities were measured with electropotential method which was first described by Spoor *et al.* [12]. Locomotion of fish in the tank elicited electrical potential changes depending on the

magnitude of the activities. These were detected by placing a pair of Ag-AgCl or stainless steel electrodes at each end of the tank. The maximum amplitude of the potential changes was approximately 300 mV. The amount of activity of the fish was expressed by counting potentials exceeding 50 mV.

Xenon lamp was used for examining activity pattern and the threshold of photobehavioral responses. The light intensity without neutral density filters was 6.8×10^3 lx measured at the surface of water. The intensity was controlled by neutral density filters with a step of 0.3 log unit which was placed in the light pathway. Diffused light was given to illuminate whole body of the fish with almost equal intensity.

RESULTS AND DISCUSSION

The catfish, in most cases, showed continuous, rapid and vigorous movement immediately after it was kept in darkness. This high activity gradually decreased with the time of dark adaptation. To investigate the effect of light on the activity of catfish different periods of dark adaptation, the fish were kept under darkness for 1–15 hr depending on individuals. After different period of dark adaptation, light stimulation (100 lx) was applied on each fish for 10 min. In each trial, activity during each 10 min before and after light stimulation was measured. On exposure of light to the fish adapted for 1 hr, for example, brief but rapid movement was followed by a quiescent state

during the light stimulation (Fig. 1, A). Conversely, when the fish was kept under darkness for longer period (5 hr), the movement during darkness became less active compared to that of 1 hr (Fig. 1, B). The fish displayed only limited movement, occasionally it nearly came to rest. However, when the light stimulation with the same intensity was delivered to this fish, the locomotor activities increased gradually and lasted during light stimulation. These records indicate that, even with the same intensity, the light had a different effect on the activity of fish, which seemed to depend on the length of dark adaptation.

To clarify the relationship between activity pattern and period of dark adaptation, activities for 10 min in the light phase ($L=10$ min) versus that of light and previous dark phase ($L+D=20$ min) was investigated. The result of relative locomotor activity is shown in Figure 2. In this figure, values less than 50% represent an inhibitory effect of light on activity, whereas those of more than 50% represent an excitatory effect. It is evident from this result that when dark adaptation was less than 4 hr, fish displayed inhibitory locomotor activity, whereas excitatory locomotor activity occurred when dark adapted for more than 5 hr. The excitatory effect of light on activity can be observed in animals which were dark adapted even for more than 10 hr.

The intensity of the light stimulus used in the present experiment was strong enough to produce distinct dual responses of catfish. Moreover,

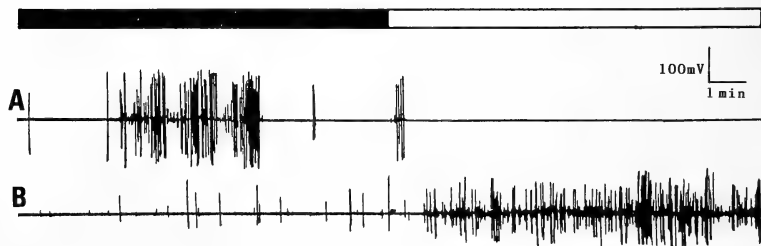


Fig. 1. Photobehavioral responses of catfish before and after the transition of light on (open bar). In A, stimulation was given after dark adaptation for 1 hr, whereas after 5 hr for B.

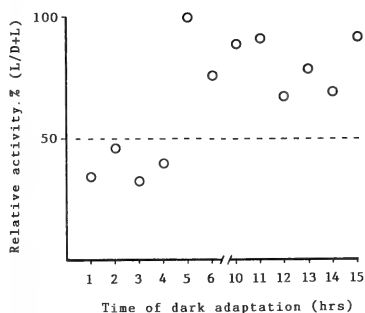


FIG. 2. Result of relative activity measured after different period of dark adaptation. Relative activity was obtained from values in light (10 min) versus those of dark plus light (20 min). Each circle represents mean value of 4 different animals.

stimulus duration was longer as 10 min. These were employed to know the basic properties of response to light for decreasing the variation of movement due to occasional random activities. In the next experiment, therefore, fish were stimulated by light of weak intensity of 1 min duration in order to determine whether excitatory property can be observed in catfish which was dark adapted for more than 5 hr. As shown in Figure 3, the property of excitation by light was observed.

Increased light intensity from 5.4×10^{-5} to 2.2×10^{-4} lx resulted in increased excitatory activity. The latency for responses at the onset of light decreased with increasing light intensity. These results may indicate that excitatory property of locomotor activity can be used as an indicator to measure the threshold photobehavioral response.

Using this photobehavioral response as an indicator, light threshold of locomotor activity of dark adapted fish for 5 hr was measured in 5 catfish. In this experiment, stimulation was composed of 30 sec light followed by 30 sec darkness as a recovery period. The stimulation was repeatedly delivered to the quiescent fish by changing intensity. If no activities of fish occurred, the intensity was increased with an increment of 0.3 log unit until the photobehavioral response was observed. When response occurred, this intensity was determined as the threshold for induced locomotor activity. As a result, the average threshold of photobehavioral response measured in 5 catfish was 1.2×10^{-4} lx. This value was comparable to the data obtained by the holding method in catfish [13].

Among the fishes, several investigators have demonstrated the threshold of photobehavioral response by using various indicators. The results were dependent upon many factors, such as species, age and criterion of the experiment. In adult lamprey, *Lampetra planeri*, the threshold for



FIG. 3. Photobehavioral responses to different light intensities of white light (1 min) obtained after dark adapted for 5 hr. A; 5.4×10^{-5} lx, B; 1.1×10^{-4} lx, C; 2.2×10^{-4} lx.

swimming activity was $2.7\text{--}10.7$ lx [14], whereas $5.4\text{--}54$ lx for photokinesis in larva [10]. Moreover, even in the same species, different values were obtained in flatfish larvae, *Pleuronectes platessa* L., $10^{-6}\text{--}10^{-4}$ lx for negative phototaxis and $10^{-2}\text{--}1$ lx for positive phototaxis. These might be attributed to the retinal input [15]. On the other hand, little is known on the threshold of blinded fish required to elicit the photobehavioral response. In blinded minnows, *Phoxinus laevis*, the threshold for photobehavioral responses was less than 1.7×10^{-2} lx [16]. However, the pineal photosensitivity has been demonstrated by electrophysiologically in many fishes, in which wide range of thresholds can be seen as in the order of $10^{-4}\text{--}10^{-1}$ lx corrected with the attenuation by tissue absorbance in front of the pineal [17].

In the present experiment, consideration of phototactic and photokinetic responses were not examined in respect to the excitatory activity. However, the excitatory activity elicited by light stimulation may not be related with phototaxis, since diffused light stimulation was delivered to illuminate the whole body of the animal with equal intensity. Thus, the excitatory activity may be classified as one of photokinetic responses. The photokinetic responses are defined as the direction in which the animal moves is at random. The speed or frequency of movement is dependent on the intensity of stimulation (ortho-kinesis), and the frequency or amount of turning is similarly dependent (kino-kinesis). On the other hand, the biological meaning of dual photobehavioral response in darkness for the nocturnal catfish remains to be elucidated.

Since the locomotor activity of fishes is mediated by, at least three types of photoreceptor organs, such as lateral eyes, pineal organ and extraretinal nonpineal photoreceptor(s) [18], the present result of excitatory photobehavioral responses could be available for the threshold measurement of these organs [13].

ACKNOWLEDGMENTS

The authors are indebted to Prof. Mikio Oguri for his critical reading of the manuscript.

REFERENCES

1. Dodt, E. and Meissl, H. (1982) The pineal and parietal organs of lower vertebrates. *Experientia*, **38**: 996-1000.
2. Hartwig, H. G. and Oksche, A. (1982) Neurobiological aspects of extraretinal photoreceptive systems: Structure and function. *Experientia*, **38**: 991-996.
3. Tabata, M. (1982) Persistence of pineal photosensory function in blinded cave fish, *Astyanax mexicanus*. *Comp. Biochem. Physiol.*, **73A**: 125-127.
4. von Frisch, K. (1911) Beiträge zur Physiologie der Pigment-zellen in der Fischhaut. *Pflügers Arch ges Physiol.*, **138**: 319-387.
5. van Veen, Th., Hartwig, H.-G. and Müller, K. (1976) Light-dependent motor activity and photonegative behavior in the eel (*Anguilla anguilla* L.). Evidence for extraretinal and extraretinal photoreception. *J. Comp. Physiol.*, **111**: 209-219.
6. Kavaliers, M. (1980) Retinal and extraretinal entrainment action spectra for the activity rhythms of the lake chub, *Couesius plumbeus*. *Behav. Neural Biol.*, **30**: 56-67.
7. Kavaliers, M. (1981) Circadian rhythm of nonpineal extraretinal photosensitivity in a teleost fish, the lake chub, *Couesius plumbeus*. *J. Exp. Zool.*, **216**: 7-11.
8. Underwood, H. and Groos, G. (1982) Vertebrate circadian rhythms; retinal and extraretinal photoreception. *Experientia*, **38**: 1013-1021.
9. Newth, D. R. and Ross, D. M. (1955) On the reaction to light of *Myxine glutinosa* L. *J. Exp. Biol.*, **32**: 4-21.
10. Jones, F. R. H. (1955) Photokinesis in the ammocoete larvae of the lamprey. *J. Exp. Biol.*, **32**: 492-503.
11. Wales, W. (1975) Extraretinal photosensitivity in fish larvae. In "Visions in Fishes". Ed by M. A. Ali, NATO-ASI Series, Plenum, New York, pp. 445-450.
12. Spoor, W. A., Neaheisel, T. W. and Drummond, R. A. (1971) An electrode chamber for recording respiratory and movements of free-swimming animals. *Trans. Amer. Fish. Soc.*, **100**: 22-28.
13. Tabata, M., Minh-Nyo, M. and Oguri, M. (1988) Threshold of retinal and extraretinal photoreceptors measured by photobehavioral response in catfish, *Silurus asotus*. *J. Comp. Physiol.*, **164**: 797-803.
14. Steven, D. M. (1950) Some properties of the photoreceptors of the brook lamprey. *J. Exp. Biol.*, **32**: 22-38.
15. Blaxter, J. H. S. (1969) Visual thresholds and spectral sensitivity of flatfish larvae. *J. Exp. Biol.*, **51**: 221-230.
16. Scharrer, E. (1928) Die Lichtempfindlichkeit blinder Elritzen (Untersuchungen über das Zwischenhirn

- der Fische). Z. Vergl. Physiol., 7: 1-38.
- 17 Meissl, H. and Dodt, E. (1981) Comparative physiology of pineal photoreceptor organs. In "The Pineal Organ: Photobiology-Biochemistry-Endocrinology" Ed. by A. Oksche, and P. Pevét, Elsevier/North-Holland Biomedical Press, Amsterdam/New York/Oxford, pp. 61-80.
- 18 Tabata, M., Minh-Nyo, M. and Oguri, M. (1988) Involvement of retinal and extraretinal photoreceptors in the mediation of nocturnal locomotor activity rhythms in the catfish, *Silurus asotus*. Exp. Biol., 47: 219-225.



ERRATA

- #1. In the article of Volume 6, Number 1, pp. 35-44 entitled "Cell Cycle in the Epidermis during Larval Instars of the Saturniid Moth *Samia cynthia ricini* (Lep.)" by KIYOSHI MINATO, the running headline on odd number pages was misprinted.
It should read, 'Eri-silkworm Epidermal Cell Cycle'.
- #2. In the article of Volume 6, Number 1, pp. 135-139 entitled "Circadian Rhythms in Locomotor Activity of the Hagfish, *Eptatretus burgeri* (IV). The Effect of Eye-Ablation" by HIROSHI KABASAWA and SADAOKA OOKA-SOUDA, some figures are erroneously placed.
Fig. 1 and Fig. 5 should be exchanged each other, and similarly, Fig. 6 and Fig. 7 should be exchanged. The figure legends stay as they are. Thus, correct arrangement of figures will appear as follows.

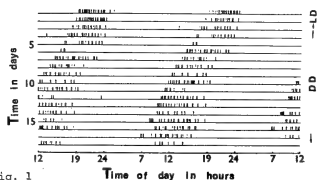


Fig. 1

Fig. 1. Circadian rhythm of activity recorded in a sham-operated hagfish kept in constant darkness. Original record plotted twice. The activity displays a free-running rhythm like an intact one does.

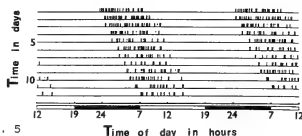


Fig. 5

Fig. 5. Twice plotted view of the original record in an eye-ablated hagfish kept in 12L:12D. The activity phase is independent of light-dark cycle, and it seems to be a free-running rhythm.

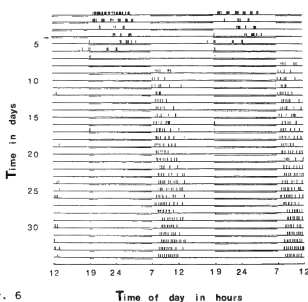


Fig. 6

Fig. 6. The phase shift of activity in a sham-operated hagfish in reversed light-dark cycle which is achieved by doubling the first dark time. Underline shows light time. The activity shifts to the new dark period.

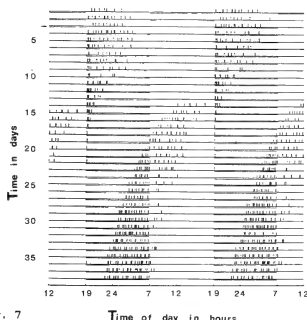


Fig. 7

Fig. 7. Free-running activity in an eye-ablated hagfish in reversed light-dark cycle which is achieved by doubling the first dark time. The activity is independent of the reversal.

Development Growth & Differentiation

Published Bimonthly by the Japanese Society of
Developmental Biologists
Distributed by Business Center for Academic
Societies Japan, Academic Press, Inc.

Papers in Vol. 31, No. 2. (April 1989)

14. **REVIEW:** G. Giudice: Heat shock proteins in sea urchin embryos.
15. H. Fukamachi and Y. S. Kim: Glandular structure formation of LS174T human colon cancer cells cultured with collagen gels.
16. T. Hirohama, H. Uemura, S. Nakamura, M. Naruse and T. Aoto: Ultrastructure and atrial natriuretic peptide (ANP)-like immunoreactivity of cardiocytes in the larval, metamorphosing and adult specimens of the Japanese toad, *Bufo japonicus formosus*.
17. R. Murakami, M. Suzuki, K. Fujii and I. Yamaoka: Organization of actin filaments and zonula adherens during somitogenesis in the chick embryo.
18. S. Amemiya: Development of the basal lamina and its role in migration and pattern formation of primary mesenchyme cells in sea urchin embryos.
19. H. Takasaki and H. Konishi: Dorsal blastomeres in the equatorial region of the 32-cell *Xenopus* embryo autonomously produce progeny committed to the organizer.
20. R. J. Hauptman, B. A. Perry and D. G. Capco: A freeze-sectioning method for preparation of the detergent-resistant cytoskeleton identifies stage-specific cytoskeletal proteins and associated mRNA in *Xenopus* oocytes and embryos.
21. B. Dale, B. Hagström and L. Santella: Partially fertilized sea urchin eggs: an electrophysiological and morphological study.
22. K. Mitsunaga, A. Fujiwara, Y. Fujino and I. Yasumasu: Changes in the activities of H, K-ATPase and Na, K-ATPase in cultured cells derived from micromeres of sea urchin embryos with special reference to their roles in spicule rod formation.
23. M. Nakamura, M. Komukai, R. Matsuda, S. Okinaga and K. Arai: Stimulation of tubulin synthesis by lactate in isolated spermatogenic cells.
24. H. Mizoguchi, A. Fujiwara and I. Yasumasu: Synthesis of collagen-like proteins in embryonic organs of the sea urchin, *Hemicentrotus pulcherrimus*.

Development, Growth and Differentiation (ISSN 0012-1592) is published bimonthly by The Japanese Society of Developmental Biologists, Department of Developmental Biology, Mitsubishi Kasei Institute of Life Science, Minami-ootani 11, Machida, Tokyo 194, Japan. 1989: Volume 31. Annual subscription for vol. 31, 1989: U. S. \$ 136.00, U. S. and Canada: U. S. \$ 150.00, All other countries except Japan. All prices include postage, handling and air speed delivery except Japan. Second class postage paid at Jamaica, N.Y. 11431, U. S. A.

Outside Japan: Send subscription orders and notices of change of address to Academic Press, Inc., Journal Subscription Fulfillment Department, 6277 Sea Harbor Drive, Orlando, FL 32887, U. S. A. Send notices of change of address at least 6-8 weeks in advance. Please include both old and new addresses. U. S. A. POSTMASTER: Send changes of address to *Development, Growth and Differentiation*, Academic Press, Inc., Journal Subscription Fulfillment Department, 6277 Sea Harbor Drive, Orlando, FL 32887, U. S. A.

In Japan: Send nonmember subscription orders and notices of change of address to Business Center for Academic Societies Japan, 16-3, Hongo 6-chome, Bunkyo-ku, Tokyo 113, Japan. Send inquiries about membership to Business Center for Academic Societies Japan, 4-16, Yayoi 2-chome, Bunkyo-ku, Tokyo 113, Japan.

Air freight and mailing in the U. S. A. by Publications Expediting, Inc., 200 Meacham Avenue, Elmont, NY 11003, U. S. A.

Sophisticated Balance between Safety and Centrifugation Capability without Compromise.

**Centrifuge in
Integrated with A
Refrigerator**

**Extra-Quiet
Operation**

**Ease of Loading/
Unloading
The Rotors**

**Quick Start/
Quick Stop**

High Quality

**Triple Safety
Design**

**Corrosion
Resistance**



**HIGH SPEED
REFRIGERATED
MICRO CENTRIFUGE**

MODEL MR-150

TOMY CORPORATION

1002 SOLEIL NARIMASU BLDG., 31-8, NARIMASU 1-CHOME,
ITABASHI-KU, TOKYO 175 JAPAN
TEL:(03)976-3411 TLX:02723111 TOMYCO J
CABLE:TOMYSHO TOKYO FAX:(GIII GII)(03)930-7010

TOMY SEIKO CO., LTD.

2-2-12, ASAHICHO NERIMA-KU, TOKYO 176 JAPAN
TEL:(03)976-3111

SOLE AGENT

MANUFACTURER

NARISHIGE

THE ULTIMATE NAME IN MICROMANIPULATION

OUR NEW MODELS MO-102 and MO-103
MAKE PRECISION MICROMANIPULATION SO EASY!

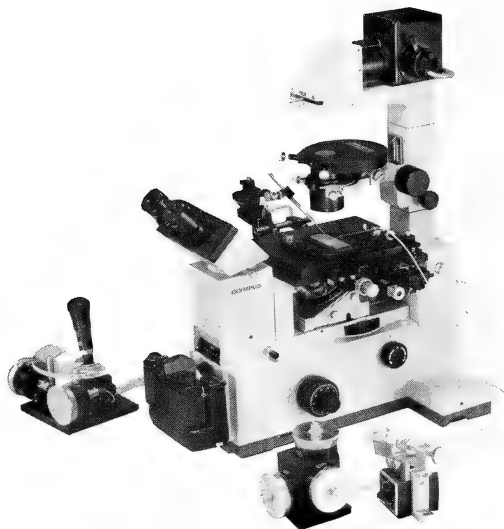


(Photo: by courtesy of Olympus Optical CO., LTD.)

SOME FEATURES of MO-102 and MO-103:

- * The manipulator head is so small that it can be mounted directly on the microscope stage. There is no need for a bulky stand.
- * Hydraulic remote control ensures totally vibration-free operation.
- * 3-D movements achieved with a single joystick.

Micromanipulators Microelectrode pullers Stereotaxic instruments



**NARISHIGE SCIENTIFIC INSTRUMENT
LABORATORY CO., LTD.**

4-9-28, Kasuya, Setagaya-ku, Tokyo 157 JAPAN
Telephone: 03-308-8233 Telex: NARISHG J27781

(Contents continued from back cover)

following water deprivation	335
Iwamuro, S., N. Mamiya and S. Kikuyama: Pituitary hormone-dependent aldosterone secretion in <i>Xenopus laevis</i>	345
Koike, S. and T. Noumura: Effects of post- weaning differential housing on serum testo- sterone levels in male mice throughout aging	351
Kobayashi, Y. and C. Iga: Erythrocyte di- apedesis in anterior pituitary hemorrhage after intraperitoneal injection of hypertonic solution in mice	359
Sasayama, Y., K. Matsuda, C. Oguro and A. Kambegawa: Immunohistochemical dem- onstration of calcitonin gene-related peptide in the ultimobranchial gland of some lower vertebrates and in the nervous tissues of some invertebrates (COMMUNICATION)	423

Behavior Biology

Tabata, M., M. Minh-Nyo, H. Niwa and M. Oguri: Circadian rhythm of locomotor activity in a teleost, <i>Silurus asotus</i>	367
---------------------------------------------------------------------------------------------------------------------------------------	-----

Tabata, M. and M. Minh-Nyo: Dual photo- behavioral response in catfish (COM- MUNICATION)	427
------------------------------------------------------------------------------------------------------	-----

Taxonomy and Systematics

Sawada, I. and M. Harada: Cestode parasites of some Taiwanese shrews	377
Miura, T. and L. Laubier: <i>Nautilina calypto- genicola</i> , a new genus and species of parasitic polychaete on a vesicomid bivalve from the Japan Trench, representative of a new family Nautilinidae	387
Okada, T.: A proposal of establishing tribes for the family Drosophilidae with key to tribes and genera (Diptera)	391
Oda, S. and H. Mukai: Systematic position and biology of <i>Pectinatella gelatinosa</i> Oka (Bryozoa: Phylactolaemata) with the de- scription of a new genus	401
Yoshida, I., Y. Obara and N. Matsuoka: Phylogenetic relationships among seven taxa of the Japanese microtine voles revealed by karyological and biochemical techniques	409
Erratum	433

ZOOLOGICAL SCIENCE

VOLUME 6 NUMBER 2

APRIL 1989

CONTENTS

REVIEWS

- Oguro, C.: Evolution of the development and larval types in asteroids 199
- Selman, K. and R. A. Wallace: Cellular aspects of oocyte growth in teleosts 211

ORIGINAL PAPERS

Physiology

- Tagawa, T., A. Ishikawa, W. C. Su and K. Okamoto: Autonomic innervation of intra- and extra-cranial arteries in the amphibia 233
- Eguchi, E., K. Arikawa, S. Ishibashi, T. Suzuki and V. B. Meyer-Rochow: Growth-related biometrical and biochemical studies of the compound eye of the crab, *Hemigrapsus sanguineus* 241

Cell Biology

- Tachi, C. and U. Zor: Effect of calcium ionophore A23187 upon the rate of leukotriene C₄ production and the cellular morphology in highly purified mouse peritoneal macrophages cultured *in vitro* 251
- Iwasaki, S. and K. Kobayashi: Fine structure of the lingual dorsal epithelium in the bullfrog, *Rana catesbeiana* 259

Biochemistry

- Suzuki, T., M. Shiba, T. Furukohri and M. Kobayashi: Hemoglobins from the two closely related clams *Barbatia lima* and *Barbatia virescens*. Comparison of their subunit structures and N-terminal sequence of the unusual two-domain chain 269
- Yasugi, S., T. Matsunaga and T. Mizuno: Pepsinogen-like immunoreactivity in ascidian stomach and intestine: Immuno-

histochemical and biochemical study 283

- Michibata, H., Y. Zenko, K. Yamada, M. Hasegawa, T. Terada and T. Numakunai: Effects of vanadium ions in different oxidation states on myosin ATPase extracted from the solitary ascidian, *Halocythia roretzi* (Drasche) 289
- Kenmochi, N. and K. Ogata: The 5S RNA binding protein of *Artemia salina* ribosomes: Identification and immunological comparison with that of rat liver 295

Genetics

- Kamezaki, N.: Karyotype of the loggerhead turtle, *Caretta caretta*, from Japna (COMMUNICATION) 421

Immunology

- Han, S. S. and A. P. Gupta: Arthropod immune system. II. Encapsulation of implanted nerve cord and "plain gut" surgical suture by granulocytes of *Blattella germanica* (L.) (Dictyoptera: Blattellidae) 303

Developmental Biology

- Horiuchi, S. and Y. Koshida: Effects of food-stuffs on intestinal length in larvae of *Rhacophorus arboreus* (Anura: Rhacophoridae) 321
- Nakamura, S., C. Ohmi and M. K. Kojima: Effects of zinc ion on formation of the fertilization membrane in sea urchin eggs 329

Endocrinology

- Hyodo, S., M. Sato and A. Urano: Molecular- and immuno-histochemical study on expressions of vasopressin and oxytocin genes

(Contents continued on inside back cover)

INDEXED IN:

Current Contents/LS and AB & ES,
Science Citation Index,
ISI Online Database,
CABS Database, INFOBIB

Issued on April 15

Printed by Daigaku Letterpress Co., Ltd.,
Hiroshima, Japan

QL
1
Z864
NH
6 No. 3

June 1989

ZOOLOGICAL SCIENCE

An International Journal

PHYSIOLOGY
CELL and MOLECULAR BIOLOGY
GENETICS
IMMUNOLOGY
BIOCHEMISTRY
DEVELOPMENTAL BIOLOGY
REPRODUCTIVE BIOLOGY
ENDOCRINOLOGY
BEHAVIOR BIOLOGY
ENVIRONMENTAL BIOLOGY
ECOLOGY and TAXONOMY

published by Zoological Society of Japan

distributed by Business Center for Academic Societies Japan
VSP, Zeist, The Netherlands

ISSN 0289-0003

ZOOLOGICAL SCIENCE

The Official Journal of the Zoological Society of Japan

Editor-in-Chief:

Hideshi Kobayashi (Tokyo)

Managing Editor:

Chitaru Oguro (Toyama)

Assistant Editors:

Yuichi Sasayama (Toyama)

Hitoshi Michibata (Toyama)

Miëko Komatsu (Toyama)

Editorial Board:

Howard A. Bern (Berkeley)

Horst Grunz (Essen)

Susumu Ishii (Tokyo)

John M. Lawrence (Tampa)

Hiromichi Morita (Fukuoka)

Andreas Oksche (Giessen)

Mayumi Yamada (Sapporo)

Walter Bock (New York)

Robert B. Hill (Kingston)

Seiichiro Kawashima (Tokyo)

Koscak Maruyama (Chiba)

Kazuo Moriwaki (Mishima)

Hidemi Sato (Nagoya)

Ryuzo Yanagimachi (Honolulu)

Aubrey Gorbman (Seattle)

Yukio Hiramoto (Chiba)

Yukiaki Kuroda (Mishima)

Roger Milkman (Okazaki)

Tokindo S. Okada (Okazaki)

Hiroshi Watanabe (Tokyo)

The Zoological Society of Japan:

Toshin-building, Hongo 2-27-2, Bunkyo-ku,
Tokyo 113, Japan. Tel. (03) 814-5675

Officers:

President: Nobuo Egami (Tokyo)

Secretary: Hideo Namiki (Tokyo)

Treasurer: Tadakazu Ohoka (Tokyo)

Librarian: Masatsune Takeda (Tokyo)

ZOOLOGICAL SCIENCE is devoted to publication of original articles, reviews and communications in the broad field of Zoology. The journal was founded in 1984 as a result of unification of Zoological Magazine (1888-1983) and Annotationes Zoologicae Japonenses (1897-1983), the former official journals of the Zoological Society of Japan. ZOOLOGICAL SCIENCE appears bimonthly. An annual volume consists of six numbers of more than 1100 pages including an issue containing abstracts of papers presented at the annual meeting of the Zoological Society of Japan.

MANUSCRIPTS OFFERED FOR CONSIDERATION AND CORRESPONDENCE CONCERNING EDITORIAL MATTERS should be sent to:

Dr. Chitaru Oguro, Managing Editor, Zoological Science, Department of Biology, Faculty of Science, Toyama University, Toyama 930, Japan, in accordance with the instructions to authors which appear in the first issue of each volume. Copies of instructions to authors will be sent upon request.

SUBSCRIPTIONS. ZOOLOGICAL SCIENCE is distributed free of charge to the members, both domestic and foreign, of the Zoological Society of Japan. To non-member subscribers within Japan, it is distributed by Business Center for Academic Societies Japan, 6-16-3 Hongo, Bunkyo-ku, Tokyo 113. Subscriptions outside Japan should be ordered from the sole agent, VSP, Utrechtseweg 62, 3704 HE Zeist (postal address: P. O. Box 346, 3700 AH Zeist), The Netherlands. Subscription rates will be provided on request to these agents. New subscriptions and renewals begin with the first issue of the current volume.

All rights reserved. No part of this publication may be reproduced or stored in a retrieval system in any form or by any means, without permission in writing from the copyright holder.

© Copyright 1989, The Zoological Society of Japan

[Publication of Zoological Science has been supported in part by a Grant-in-Aid for
Publication of Scientific Research Results from the Ministry of Education, Science
and Culture, Japan.]

OBITUARY

**Masao Yoshida (1926-1988)**

On 29 November 1988, Professor Masao Yoshida of Okayama University died of bronchial pneumonia resulting from a pharyngeal tumor, at the age of 62. All who are familiar with his scientific work or who had the good fortune to experience his kindness and warmth, were deeply shocked to hear of his loss.

Professor Yoshida was born in Kobe on 23 August 1926. Because his father, a banker, was transferred abroad soon after his birth, he spent his early years in the United States and China, four years in New York and six years in Shanghai. After graduating from the Second High School in Sendai in 1949, he entered the Zoological Institute of the Faculty of Science at the University of Tokyo. There he became a student of the late Professor Kiyoshi Takewaki and pursued studies on the ovulation of the anthomedusa (*Spirocodon saltatrix*) and the maturation of the sea urchin (*Diadema setosum*) at the Misaki Marine Biological Station. These studies had a profound influence on his academic career; he came to love the study of marine invertebrates and he was never far from the seaside throughout the rest of his life. After graduation from the University in 1950, he continued his post-graduate work at Misaki. In 1951 he was appointed to the position of research associate at the University of Tokyo, serving at the Marine Biological Station.

The years between 1956 and 1960 were spent at a research associate in the laboratory of Professor N. Millott at Bedford College of the University of London, where he devoted himself to studies on the extraocular photoreception of sea urchins. His most significant accomplishments were the demonstration of direct photoreception of sea urchin chromatophores and the clarification of dermal photoreception mediating shadow reaction through photosensitive neurons in the superficial nervous system.

After returning from London, he became an associate professor of Biology at Tamano Marine Biological Laboratory (now Ushimado Marine Biological Laboratory) of Okayama University where he was responsible for marine biology curricula designed especially for the training of biology students. In 1967 he was promoted to full professor at the same university and nominated Director of the

Laboratory. In the years to follow, he and his students conducted extensive and comprehensive studies on the photoreception of both *Spirocodon* and the starfish (*Asterias amurensis*). The results of these studies revealed the presence of a retinol-like substance in the ocelli of *Spirocodon*, in addition to a relationship between the role of starfish ocelli and the nervous system in determining the direction of locomotion. In 1972 he won the Zoological Society of Japan Prize for excellence in his studies on the photoreception of lower invertebrates.

Professor Yoshida's later work was devoted mainly to the study of the functional structure necessary for cell photosensitivity and for photoreceptors in various invertebrates (anthomedusan, scyphomedusan, cubomedusan, starfish, cuttlefish, ascidian, arrow-worm, holothurian, amphioxus), especially from an evolutionary aspect. Some of the results were summarized in his reviews (e.g., "Photoreception and Vision in Invertebrates" ed. by M. A. Ali, pp. 727-771, Plenum, 1984). It should be also noted that he was never interested merely in structure throughout his later studies, but always took a great interest in the general biological phenomena involved in photoreception such as light-controlled spawning, oriented light reaction, and circadian rhythm. Throughout these studies, he guided and gave direction to many students.

In 1982 Professor Yoshida was elected to a member of the Board of Okayama University and in 1985 he was appointed Dean of the Faculty of Science in the University; he participated directly in the administrative planning and development of the University until 1987. In 1985-1986 he served as Chairman of the Council of Japanese National Marine and Inland Water Biological Stations where he expended great effort in implementing a credit exchange program (for laboratory work in marine biology) among universities in Japan. From 1985 until his death, he served as President of the Japan Society for General and Comparative Physiology. During his presidency, he spent a great deal of time managing the Society and prearranging the 3rd International Congress of Comparative Biochemistry and Physiology which will be held at Tokyo in 1991 under the sponsorship of the Society, in spite of suffering from ill health. Professor Yoshida also contributed much to the Zoological Society of Japan as an active member of the Board for many years.

With time, Professor Yoshida assumed increasing responsibilities for his scientific studies, for his University, and for his students. Just as Professor Yoshida's contributions have made a lasting impression on zoology, his personality made an indelible impression on those who knew him. These fond and lasting memories of Professor Yoshida sustain us as we reflect on his untimely death and our grievous loss. His cheerful smile in the photograph will never fail to recall these memories to our mind.

TSUNEO YAMAGUCHI
Department of Biology
Faculty of Science
Okayama University

REVIEW

Hormonal Regulation of Sodium Absorption and Chloride Secretion Across the Lower Intestines of Birds

ERIK SKADHAUGE

*Department of Animal Physiology and Biochemistry,
The Royal Veterinary and Agricultural University,
Copenhagen, Denmark*

ABSTRACT—NaCl depletion, which is accompanied by a marked increase in plasma level of aldosterone, augments Na-absorption 100-fold in the coprodeum of the hen. A Cl-secretion induced by theophylline after amiloride treatment is similarly augmented 8-fold. The increased Na-absorption is caused by augmented specific Na-permeability of the apical membrane, whereas changes of basolateral ATPase activity and cellular mitochondrial content are limited. Extra-cellular recording with the vibrating micro-probe demonstrates that both normal Na-absorption and theophylline-induced Cl-secretion takes place from cells at the villi. Evidence for special cells having a particularly high rate of transport was not found. NaCl-depletion induced, with a time course of several days, and partly mimicked by external aldosterone, densely packed microvilli of the apical surface, and emergence of "chloride-cells". The late adaptation of Na-absorption is probably induced by the enlargement of the apical surface area by the microvilli. This enlargement may also induce more Cl-channels responsible for the Cl-secretion after cAMP induction. The "chloride-cell" phenomenon may express local ion trapping.

The colonic tissue of the hen is different in having both microvilli and "chloride-cells" at both high and low NaCl-intake and no time dependent adaptations extending more than 24 hr.

INTRODUCTION

Absorption of Na and Cl ions takes place across the colon (rectum) and coprodeum of terrestrial seed-eating birds, as the domestic fowl, the galah (*Cacatua roseicapilla*) and the emu (*Dromaius novaehollandiae*). The main function of these organs is to store ureteral urine and faeces until voiding/defaecation occurs. During this storage both solutes and water may pass across the gut wall. Our investigations have shown that the NaCl absorption across the coprodeum and colon is profoundly influenced by the NaCl-content of the diet. The NaCl-absorption is correlated to the plasma level of aldosterone, and can be induced by injection of this hormone. The coprodeum shows

one of the largest changes in net rate of Na-absorption as a function of the NaCl content of the diet, and the colon undergoes a marked change in Na-transport pattern. On a low-NaCl diet the colonic Na-transport is totally inhibited by amiloride and not stimulated by glucose and amino acids on the luminal side, whereas on a high-NaCl diet (low plasma concentration of aldosterone) the epithelium becomes insensitive to amiloride. The sodium transport is now stimulated by low luminal concentrations of hexoses and/or amino acids. Our studies have also shown that coprodeum and colon exert an important influence on final NaCl and water reabsorption from faeces and ureteral urine when several species of seed-eating birds are exposed to either dehydration and/or lack of NaCl [1-4].

Birds with nasal salt glands, at least the domestic

duck [15] and the gull (*Larus glaucescens*) [6] seem, however, to have a much smaller range of regulation of the NaCl uptake by the lower gut. This may also apply to desert birds which have a diet containing more than "adequate salt" [7].

CHARACTERISTICS OF COPRODEAL AND COLONIC TRANSPORT IN VITRO IN THE DOMESTIC FOWL

Both coprodeum and colon are easy to mount in conventional Ussing-chambers in either Krebs-phosphate or bicarbonate buffer. Under these conditions these tissues maintain a stable and long-lasting short-circuit current (SCC) equivalent to the net transport of ions.

Epithelia from fowls on a low-NaCl diet exhibit a net rate of Na absorption (difference between isotope fluxes in the two directions) which is nearly equal to the SCC, and a flux ratio for chloride which is near unity [8]. This Na-transport is completely suppressed by 10^{-4} M amiloride, a competitive blocker of Na-entry across the apical membrane in high-resistance epithelia. The epithelia of the fowl are among the most sensitive to amiloride [9]. In some preparations amiloride treatment results in a negative current, undoubtedly caused by H^+ or K^+ secretion. On a high-NaCl diet Na-transport of coprodeum and SCC are nearly completely suppressed whereas colonic Na-absorption remains high provided low concentrations of either hexoses or amino acids are present of the mucosal side. The dietary effects described have been demonstrated to be caused specifically by NaCl [8, 10]. In the first study wheat and barley (which has a low NaCl content) were used with and without addition of NaCl in the drinking water, in the second a complete diet was prepared with and without addition of 1% NaCl.

An interesting question is which level of NaCl is recognized by the bird as "high" NaCl and "low" NaCl, and at which level of intake the switchover takes place. Experiments by Arnason and Skadhauge (in preparation) demonstrated that decreasing NaCl content of the diet caused a rising amiloride-sensitive SCC in colon and coprodeum without conspicuous changes in the plasma concentrations of corticosterone, arginine vasotocin

and prolactin. The transport parameters of the lower gut were, however, well correlated to the plasma level of aldosterone. Only very high levels of NaCl intake caused an osmotic stress which raised plasma osmolality and NaCl concentrations and induced increases in arginine vasotocin and prolactin concentrations. These increased hormone concentrations did not cause any conspicuous response of colonic and coprodeal Na-transport patterns. The intestinal transport parameters at 6 levels of NaCl intake are shown in Figures 1 and 2. These studies were carried out in tissues of adult birds with the mucosal sheets stripped of the underline muscle layer. Except for the testing of effects of amino acids essential similar effects of reducing NaCl content of the diet was found in younger birds with unstripped colon [11-13].

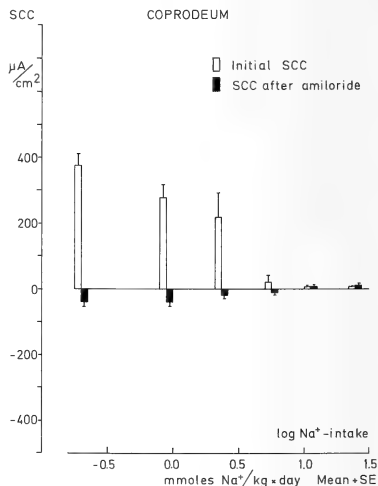


Fig. 1. Coprodeal short-circuit current as a function of NaCl-intake. The short-circuit current (near equal to net Na-transport) is suppressed by higher levels of stable NaCl-intake. The SCC is fully suppressed by amiloride. Simultaneous measurements of plasma aldosterone (not shown on figure) follow the initial SCC closely indicating that Na-transport is largely regulated by aldosterone. (From Arnason and Skadhauge, in preparation).

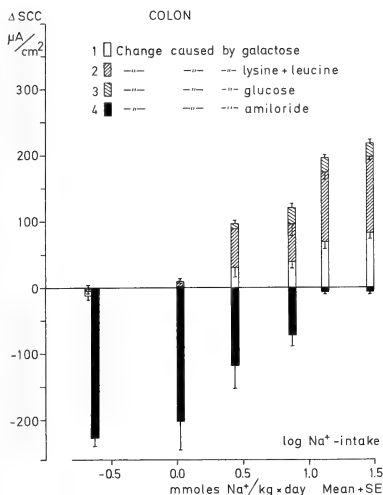


Fig. 2. Colonic short-circuit current as a function of NaCl-intake. The figure reports Δ SCC caused by hexoses (galactose and glucose), amino acids (lysine and leucine), and amiloride. It will appear that at a low NaCl-intake this epithelium has a large fully amiloride-suppressible SCC (Na-transport) which gradually disappears at higher intakes of NaCl and is replaced by a non-electrolyte-stimulated Na-transport. The net Na-transport (near equal to total length of the bars) remains nearly constant throughout the entire range of NaCl-intake. This switch-over of transport pattern is fairly closely related to plasma level of aldosterone (not shown on figure), but not to plasma concentrations of corticosterone, arginine, vasotocin and prolactin (From Arnason and Skadhauge, in preparation).

NaCl DEPLETION AND REPLETION: STUDIES OF THE TIME COURSE

Switching from a high to a low NaCl diet (NaCl depletion) resulted in a gradual increase in plasma concentration of aldosterone and over a week a slow increase in SCC of coprodeum and the amiloride sensitive-component of colonic NaCl absorption. Abrupt shift from low-NaCl diet to high-NaCl diet (acute resalination) resulted within a day in total suppression of Na absorption and

plasma aldosterone in coprodeum and a switch-over to the amiloride independent hexose/amino acid stimulated Na-transport in colon. These results were interpreted to indicate that the slow NaCl depletion over a week caused a gradual activation of an aldosterone stimulated Na-transport [10, 3, 14]. The rapid effects of resalination (immediate fall in SCC) were interpreted as originating from a closure of apical Na-channels caused by an absence of aldosterone, since the acute resalination led to fast NaCl-repletion. The difference during depletion between colon and coprodeum might indicate differing organ sensitivities. The experiment with different stable levels of NaCl (previous section) points also to aldosterone as the main hormonal mediator. It was therefore our expectation that external aldosterone injection to birds on high-NaCl diet could mimic the low-NaCl transport pattern. This was however, to our surprise, not the case. External injections of aldosterone could only cause approximately 20% of the increase in SCC induced by low-NaCl diet in coprodeum. The colonic transport pattern changed more dramatically, suggesting that aldosterone might be the major regulator of Na-transport in this epithelium.

A major step forward in deciding whether or not the major mediator was aldosterone was achieved by injecting aldosterone during the first 24 hr of acute resalination [15]. Resalination, which would normally reduce the SCC to zero, now allowed full maintenance of the low-NaCl SCC after aldosterone injection rather than the low response seen after giving external aldosterone over 24 hr to birds on chronic high-NaCl diet. This experiments show that aldosterone, and aldosterone alone, can cause the maintenance of a very high rate of Na absorption. It is therefore not necessary to invoke other possible regulating factors such as reduced extracellular volume, etc. and important effects of other hormones are also likely to be excluded. How long will the "low-NaCl mode" of the cells continue if the aldosterone injection (over 24 hr) is delayed further and further from the time of acute resalination? This question was studied by Claus *et al.* [16]. We observed that the SCC induced by the aldosterone became smaller and smaller, from about 400 to 100 μ Amp/cm² over a period of 4-6

days. It is thus apparent that the aldosterone-inducible sodium transport decays.

It appears here that the aldosterone inducible sodium transport decays from the "low-NaCl mode" to "high-NaCl mode" over 4–6 days. It should be emphasized that in contrast to coprodeum the colon does not show this decay phenomenon. If the aldosterone level is kept continuously high by repeated injection over several days simultaneously with resalination the SCC is maintained at a relatively high level [17]. These findings are shown in Figure 3.

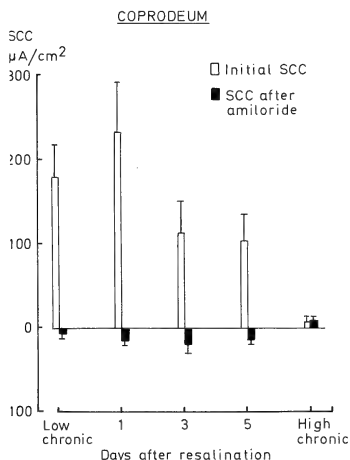


Fig. 3. Coprodeal short-circuit current after resalination of low-NaCl diet adapted birds during prolonged injections of aldosterone. A supramaximal dose of aldosterone was injected from 1–5 days simultaneously with switch-over from low- to high-NaCl diet. (Means \pm SE are reported) [17]. Aldosterone will appear to be able to partially maintain the high SCC characteristic of low NaCl-adaptation. The level is only 60–70%, but still more than double of the SCC inducible over 24 hr in birds chronically exposed to a high-NaCl diet (not shown on figure).

It therefore appears that there are pronounced differences in apparent sensitivity to aldosterone between coprodeum and colon and there is an

intriguing NaCl depletion/resalination difference in the apparent sensitivity of the coprodeum, which most likely involves very prolonged (more than 24 hr) actions of the hormone. In order to investigate these adaptations further it would seem important to study the effect of aldosterone on cellular transport parameters in these epithelia and the possible role of development of different cell types.

CELLULAR MECHANISMS OF ACTION OF ALDOSTERONE IN THE HEN COPRODEUM

Early anatomical studies indicated that adaptation to high or low NaCl diet did not cause measurable changes at the light microscopy level in coprodeal and colonic structure [2] but toluidine staining of ultra-thin sections and freeze-fracture revealed, on low-NaCl diet, a special cell type which might be mitochondria-rich and which had rod-shaped particles in the apical membrane. The emergence of such cells under prolonged aldosterone action might be responsible for the apparently higher sensitivity to aldosterone when the coprodeum is in the "low-NaCl mode". Such cells might also have a higher Na-transport capacity (higher mitochondrial content), higher apical Na-permeability and higher ouabain-inhibitable basolateral membrane-located Na-K-ATPase activity/pump sites. We have made some studies on the coprodeum which led us to conclude, first, that the major adaptation lies in augmentation of apical permeability to Na and second, that there seems to be a special class of transporting cells. The first of these conclusions seems to hold, the second not.

Early investigation by Bindslev [18] provided strong semi-quantitative evidence for a major augmentation of the Na-permeability of the apical membrane induced by a low-NaCl diet. This was shown by the so-called Schultz-Curran influx technique and by measuring dilution potentials. The former technique involves measuring rapid uptake (within a minute) of labelled Na from the mucosal side into the cells. An extracellular volume-marker corrects for the Na-isotope remaining extracellularly. The latter technique follows the diffusion potential of Na out of/into the cells after

inactivation of the basolateral Na-pump by ouabain. The dilution potential was large, 16–18 mV, in epithelia from low-NaCl diet birds, but low (around 2 mV) in epithelia from birds on a high-NaCl diet. The specificity of this effect for Na was demonstrated by amiloride (10^{-4} M).

More quantitative studies of the Na-permeability of the apical membrane of coprodeum, involving depolarization of the basolateral membrane with a high K-concentration and measurement of rapid voltage-current relations before and after addition of 10^{-4} M amiloride to the mucosal side, were carried out by Clauss *et al.* [19]. So-called “instantaneous” values were obtained when the voltage deflection after (bipolar) squarewave changes of current are measured within a few milliseconds. These reflect the intracellular Na-activity immediately inside the apical membrane in the short period before the

electrical events modify the intracellular concentration of this ion. These experiments confirm the high apical Na-permeability of low-NaCl diet birds, and show a non-detectable permeability in high-NaCl birds. Aldosterone and dexamethasone treatments partially restore the Na-permeability of the apical membrane. These data taken together reveal a straight line relationship between SCC and apical Na-permeability (also with SCC before basolateral depolarization) (Fig. 4) demonstrating beyond doubt that the effect of aldosterone is insertion of new Na-channels into the apical membrane. There was no detectable difference in intracellular Na activity showing that the transcellular “flush-through” of Na is regulated by other signals than intracellular Na-activity.

The possible mitochondrial and basolateral adaptation was explored by analysis of the content of succinyl-dehydrogenase and K-activated oua-

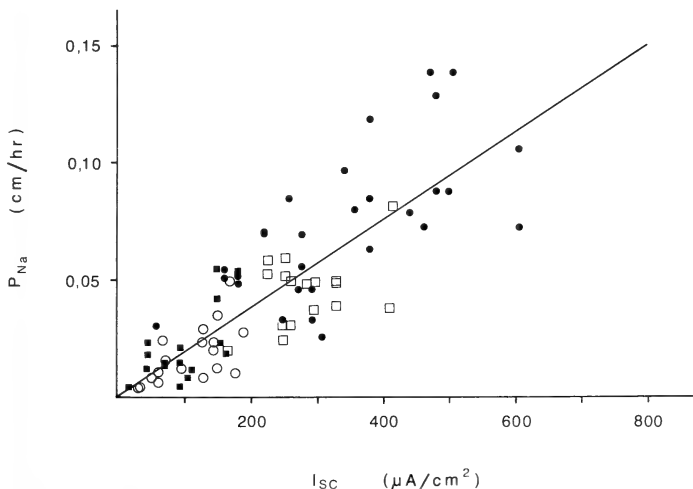


Fig. 4. Correlation of apical Na-permeability with initial short-circuit current. The figure is based on apical current-voltage relations from serosal-depolarised (high K) hen coprodeum. The Na permeability (P_{Na}) is related to the short-circuit current (I_{SC}) of the epithelium before depolarization. The tissues are from birds on a low-NaCl diet (filled circles) and low-NaCl diet birds exposed to spironolactone (open squares), and high-NaCl diet birds exposed to aldosterone (filled squares) and dexamethasone (open circles) [19]. The figure demonstrates beyond doubt that a high transcellular Na-flux involves an opening of apical Na-channels.

bain sensitive paranitrophenylphosphatase, respectively. From low- to high-NaCl diet the former was reduced by only 23%, the latter by 48% [20].

These observations indicate a much less pronounced adaptation than the huge (100-fold) change in amiloride-sensitive net Na-absorption.

"CHLORIDE CELLS" AND PRESENCE OF MICROVILLI

In the course of a histochemical analysis of the location of the K-dependent paranitrophenylphosphatase, which showed no cellular heterogeneity [21], we found a morphological difference between high- and low-NaCl diet birds. There were no apical microvilli in the coprodeum of the high-NaCl birds whereas on low-NaCl diet the apical membrane was densely packed with microvilli. Scanning electronmicroscopy revealed that these microvilli were evenly distributed from cell to cell

but with some minor differences. We were furthermore able to demonstrate that aldosterone injection over 2, 4 and 6 days into birds on high-NaCl diet caused a gradual increase in the density and height of these microvilli under all experimental conditions tested. Furthermore, the microvilli were observed to regress over 3–5 days after acute resalination as did the aldosterone-induced Na-transport and a theophylline-induced Cl-secretion (vide infra).

In other experiments we have shown that the coprodeum can secrete Cl under the influence of increased cAMP and that this effect is increased eightfold in low-NaCl diet compared with high-NaCl diet animals [22]. Furthermore after resalination this Cl secretion decayed over a period of 3 to 4 days. The chloride secretion augmented by a low-NaCl diet was also apparent in the study of six levels of NaCl intake by Arnason and Skadhauge (in prep.) (Fig. 5). We therefore hypothesize that the emergence of apical microvilli

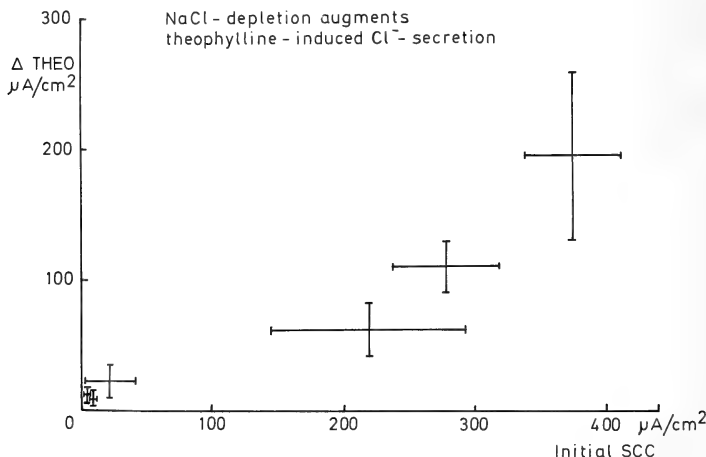


FIG. 5. The relation between short-circuit current and theophylline induced chloride secretion. The figure is obtained from coprodeal measurements in the same study as Figures 1 and 2. The high short-circuit current (higher Na-absorption) induced by low NaCl-intake is matched by a high rise of SCC after treatment with amiloride followed by the phosphodiesterase inhibitor theophylline (which increases the level of cAMP). Other experiments [22] proved that the theophylline-induced rise in SCC is caused by Cl-secretion, which occurs from the same villar areas as normal Na-absorption [12]. Means \pm SE are reported.

in the coprodeum augments the apical surface area and that this enlarges the number of possible Na-channels which will be open when aldosterone is present. This explains why the coprodeum responds more slowly during NaCl depletion than does the colon which has microvilli all the time. This possibly also explains the "staircase" stimulation of SCC seen in the coprodeum after acute resalination [16].

Recent experiments using the vibrating microprobe [23] have further demonstrated that the villi of the coprodeum are sites for both normal Na-absorption and theophylline-induced Cl-secretion. The spatial resolution of the probe-approximately 10 μ m equal to the width of the cells (in the horizontal direction, that is along the surface of the epithelium)-did, however, not disclose different sites for Na-absorption and Cl-secretion. We have accordingly, so far, no positive evidence for the occurrence of "super-cells" for either normal Na-absorption or secretagogue-induced Cl-secretion.

ACKNOWLEDGMENTS

It is a great pleasure to acknowledge the collaboration of S. S. Arnason (Iceland), W. Clauss (F.R.G.), V. Dantzer (DK), K. Holtug (DK), A. Shipley (U.S.A.) and D. H. Thomas (U.K.). S.S.A. was supported by Leo Research Foundation and Eivind Eckbos Legat. W.C. and D.H.T. received NATO grants. Economic support was provided by the Danish Research Councils (Natural Science, and Veterinary and Agricultural), Leo Research Foundation, the NOVO Foundation and the Velux (1981) Foundation. Aldosterone was a gift from Ciba-Geigy, amiloride from Merck, Sharp and Dohme.

This manuscript is in part adapted from a lecture given in Babraham, Cambridge, September 1987.

REFERENCES

- Skadhauge, E. (1977) Excretion in lower vertebrates: Function of gut, cloaca and bladder in modifying the composition of the urine. *Fed. Proc.*, **36**: 2487-2492.
- Skadhauge, E. (1981) Osmoregulation in Birds. Springer-Verlag, Berlin/Heidelberg/New York, 203 pp.
- Skadhauge, E., Clauss, W., Arnason, S. S. and Thomas, D. H. (1985) Mineralocorticoid regulation of lower intestinal ion transport. In "Transport Processes, Iono- and Osmoregulation". Ed. by R. Gilles and M. Gilles-Baillien, Springer-Verlag, Berlin/Heidelberg/New York, pp. 118-133.
- Thomas, D. H. (1982) Salt and water excretion by birds: The lower intestine as an integrator of renal and intestinal excretion. *Comp. Biochem. Physiol.*, **71A**: 527-535.
- Skadhauge, E., Munck, B. G. and Rice, G. E. (1984) Regulation of NaCl and water absorption in duck intestine. In "Lecture Notes on Coastal and Estuarine Studies, Vol. 9. Osmoregulation in Estuarine and Marine Animals". Ed. by A. Pegueux, R. Gilles and L. Bolis. Springer-Verlag, Berlin/Heidelberg/New York/Tokyo, pp. 132-142.
- Goldstein, D. L., Hughes, M. R. and Braun, E. J. (1986) Role of the lower intestine in the adaptation of gulls (*Larus glaucescens*) to sea water. *J. exp. Biol.*, **123**: 345-357.
- Thomas, D. H., Pinshow, B. and Degen, A. (1984) Renal and lower intestinal contributions to the water economy of desert-dwelling phasianid birds: Comparison of free-living and captive chukars and sand partridges. *Physiol. Zool.*, **57**: 128-136.
- Choshniak, I., Munck, B. G. and Skadhauge, E. (1977) Sodium chloride transport across the chicken coprodeum. Basic characteristics and dependence on sodium chloride intake. *J. Physiol. (Lond.)*, **271**: 489-504.
- Cuthbert, A. W., Edwardson, J. M., Bindeslev, N. and Skadhauge, E. (1982) Identification of potential components of the transport mechanism for Na⁺ in the hen colon and coprodeum. *Pflügers Arch.*, **392**: 347-351.
- Skadhauge, E., Thomas, D. H., Chadwick, A. and Jallageas, M. (1983) Time course of adaptation to low and high NaCl diets in the domestic fowl: Effects on electrolyte excretion and on plasma hormone levels (aldosterone, corticosterone and prolactin). *Pflügers Arch.*, **39**: 301-307.
- Grubb, B. R. and Bentley, P. J. (1987) Aldosterone-induced, amiloride-inhibitable short-circuit current in the avian ileum. *Am. J. Physiol.*, **253**: G211-G216.
- Grubb, B. R. and Bentley, P. J. (1988) Relationship of transmural electrical parameters to the luminal Na concentration in the colon of the fowl (*Gallus domesticus*). *J. Comp. Physiol.*, **158B**: 19-24.
- Grubb, B. R., Driscoll, S. M. and Bentley, P. J. (1987) Electrical PD, short-circuit current and fluxes of Na and Cl across avian intestine. *J. Comp. Physiol.*, **157B**: 181-186.
- Thomas, D. H. and Skadhauge, E. (1982) The course of adaptation to low and high NaCl diets in the domestic fowl: Effects on electrical behaviour of isolated epithelia from the lower intestine. *Pflügers Arch.*, **395**: 165-170.
- Skadhauge, E. (1983) Temporal adaptation and hormonal regulation of sodium transport in the

- avian intestine. In "Intestinal Transport: Fundamental and Comparative Aspects". Ed. by M. Gilles-Baillien and R. Gilles, Springer-Verlag, Berlin/Heidelberg/New York, pp. 284-294.
- 16 Clauss, W., Arnason, S. S., Munck, B. G. and Skadhauge, E. (1984) Aldosterone-induced sodium transport in lower intestine. Effect of varying NaCl-intake. *Pflügers Arch.*, **401**: 354-360.
 - 17 Arnason, S. S. and Skadhauge, E. (1985) Effects of prolonged injections of aldosterone during resalination on coprodeal short-circuit current (SCC) of the domestic hen. *Acta Physiol. Scand.*, **123**: 50A.
 - 18 Bindslev, N. (1979) Sodium transport in the hen lower intestine. Induction of sodium sites in the brush border by a low sodium diet. *J. Physiol. (Lond.)*, **288**: 449-466.
 - 19 Clauss, W., Durr, J. E., Guth, D. and Skadhauge, E. (1987) Effects of adrenal steroids on Na-transport in the lower intestine (coprodeum) of the hen. *J. Membrane Biol.*, **96**: 1241-152.
 - 20 Dantzer, V., Møller, O. and Skadhauge, E. (1988) Morphological and enzymic adaptation to aldosterone of the epithelium of the caudal hindgut of the hen. *J. Physiol. (Lond.)*, **396**: 30P.
 - 21 Møller, O., Dantzer, V. and Skadhauge, E. (1989) Salt transport related changes in the hen lower intestinal tract. A morphological and histochemical study. *Biol. Cell.*, **66** (In press).
 - 22 Clauss, W., Dantzer, V. and Skadhauge, E. (1988) A low-salt diet facilitates Cl secretion in hen lower intestine. *J. Membrane Biol.*, **102**: 83-96.
 - 23 Holtug, K., Skadhauge, E. and Shipley, A. (1988) Localization of sodium absorption and chloride secretion in a villar epithelium. *Gastroenterology*, **94A**: 191.

REVIEW

Transgenic Fish: Biological and Technical Problems

KENJIRO OZATO, KOJI INOUE¹ and YUKO WAKAMATSU

Biological Laboratory, Yoshida College, Kyoto University, Kyoto 606,
and ¹Central Research Laboratory, Nippon Suisan Kaisha,
Hachioji, Tokyo 192, Japan

INTRODUCTION

Explosive progress in genetic engineering in the 1970's made it possible to isolate eukaryotic genes and resulted in the accumulation of an enormous amount of information on their structure and function through *in vitro* experiments. The *in vitro* study, alone, however, can not be the basis for conclusions, because genes exist and function in living individuals. Early in the 1980's revolutionary technique was developed to introduce isolated genes into living animals and investigate their function *in vivo*. This technique is the microinjection of foreign genes into eggs and production of animal lines carrying the injected genes. Individuals carrying such foreign genes are called "transgenic" animals and have been produced in various species: *C. elegans* [1], *Drosophila* [2, 3], sea urchin [4-13], amphibians [14-19], mice [20, see for review 21], and farm mammals [22, 23]. This technique has been particularly well established in mice and *Drosophila*, and used as a practical tool for studying genetic processes in developmental biology, immunology, neurobiology and oncology, and for producing new experimental animals useful in biological and medical research. Application of the transgenic technique to fish began only a few years ago and has not yet proves entirely successful, although interest in this area has been increasing. A review on the initial research period was published in 1987 [24]. In the period since that appeared, the gene transfer technique in fish has made remarkable progress

and has been shown to be applicable to a number of problems of fisheries science and basic biology. Here, we review the current state of transgenic research in fish. First, a brief description on the characteristics of fish in transgenic experiments and four lines of research in fisheries science and basic biology are provided. Then the usefulness of the medaka for studying gene expression in development is described referring to the authors' recent investigations.

I. CHARACTERISTICS OF TRANSGENIC RESEARCH IN FISH

Table 1 summarizes 12 published reports on transgenic fish prepared by 11 groups [24-35]. Ten of these [24-33] are concerned with fisheries science, and seven of them [24-30] dealing with growth promotion of fish by introduction of mammalian growth hormone genes. The other two reports are also concerned with the methodology which appears to be designed for growth promotion [32, 33]. Transgenic animals carrying foreign growth hormone genes have been produced in mice [36] and domestic mammals such as rabbits, sheep and pigs [22, 23]. The "super mouse" produced by introduction of the rat growth hormone genes was about twice as large as a normal mouse [36]. One experiment proposes to provide salmon with the low-temperature resistance to be able to live in icy water by introduction of the anti-freeze protein gene [31]. This type of experiment aimed at endowing animals with resistance to their environment and to enlarging their habitats is unique to fish. Only two reports are concerned with basic

TABLE 1. Studies

Field	Purpose	Species	Gene
Fisheries science	Growth promotion	Trout	hGH cDNA
		♂ Tilapia	rGH
		Loach	hGH
		Catfish	♂
		Goldfish	♂
	Low-temperature resistance	Salmon	fAFP
	Method	Salmon	<i>E. coli</i> β -gal
		Goldfish	<i>E. coli</i> neo
Developmental genetics	Insertional mutagenesis	Zebrafish	<i>E. coli</i> <i>hygro</i>
Developmental biology	Developmental gene expression	Medaka	c δ CR

hGH: human growth hormone gene

rGH: rat growth hormone gene

fAFP: flounder antifreeze protein gene

 β -gal: β -galactosidase gene

neo: neomycin resistant gene

hygro: hygromycin resistant gene

mMT: mouse metallothionein-I gene

c δ CR: chicken δ -crystallin gene

biology, developmental genetics and developmental biology using small fresh water fish [34, 35]. Thus, current transgenic research in fish is mostly devoted to fisheries science and is seen as one of the aquatic biotechnologies for the breeding of economically important fish. This situation in fish is in contrast to that of other animals in which the research is founded primarily on basic biology.

No fish gene or promoter has yet been used except for the antifreeze protein gene. This reflects that molecular biology of fish genes is still quite weak and there are few fish genes and promoters usable for transgenic experiments.

Techniques for transgenic experiments in mice have been developed through three steps, integration into the host chromosome, expression, and germ-line transmission of foreign genes early in the

1980's [21]. No single experiment has yet combined all three steps in fish. Many experiments remain at the first step of integration, and only a few proceed to expression or germ-line transmission. In Table 1, foreign genes which were injected into eggs and detected in embryos, fry, or adult tissues are counted as "integrated". However, the possibility that the injected genes replicated extrachromosomally can not be excluded. Extrachromosomal replication has been reported in *C. elegans*, sea urchin, and amphibians, although rarely in mice [21].

Fish have many distinctive biological features which characterize the transgenic experiments done on them.

(1) Fish generally undergo external fertilization. This makes embryological experiments easy, re-

TABLE 2. Microinjection of foreign

Species [Reference]	Stage	Dealing with chorion	Injection site	DNA size (kb)	DNA form
Trout [25, 26]	1-cell	2 step	Cytoplasm		Linear
Salmon [31]	1-cell	Micropyle	Cytoplasm	7.8	Linear
Zebrafish [34]	1~4-cell	Dechoriation	Cytoplasm	5.2	Linear
Medaka [35]	Oocyte	—	Germinal vesicle	14.4	Circular
Mouse [37]	1-cell	—	Male pronucleus	0.7~50	Linear

on transgenic fish

Promoter	Integration	Expression	Transmission	Year	Reference
SV40	○		○	1986 '88	[25, 26]
mMT	○			1987	[24]
mMT	○			1988	[27]
mMT	○			1986	[28]
mMT	○			1988	[29]
mMT	○			1985	[30]
	○			1988	[31]
mMT	○	○		1988	[32]
mMT	○	○		1988	[33]
SV40	○		○	1988	[34]
	○	○		1986	[35]

quiring no complex manipulations such as the culture of eggs and transfer of eggs into foster mothers which are essential in mice. In eggs of some fish species which have the transparent chorion it is easy to observe developing embryos and perform experimental manipulations on them during embryogenesis.

(2) In mice, microinjection of DNA is carried out into the male pronucleus of fertilized eggs using a few hundred copies of genes per egg. However, optical recognition of the nucleus is difficult in fish fertilized eggs. The microinjection in fish is usually done into the egg cytoplasm and the quantity of genes required for injection is enormous, a few hundred million copies per egg in some cases [26]. Cytoplasmic injection is much easier and less injurious to development so that the survival rate of injected embryos is much higher in fish than in mice (Table 2). One exception to the cytoplasmic injection is the case of the medaka

[35]. Here, microinjection is made into the germinal vesicle of oocytes which is clearly recognizable under a microscope.

(3) The tough chorion of many fish has required the devising of special methods of inserting microneedles into eggs. In rainbow trout and salmon eggs, an opening is made by a thick needle before the insertion of a microneedle [25, 32]. In Atlantic salmon and tilapia, a microneedle can be inserted through the micropyle, an opening for sperm penetration at fertilization [27, 31]. The chorion of goldfish and loach eggs is removed by trypsin digestion [28, 30] and that of zebrafish eggs manually with forceps [34]. In some species such as salmon and trout, the chorion is opaque and the penetration of a microneedle into the cytoplasm is difficult to confirm [25]. In contrast, the process of microinjection can be easily observed in medaka and zebrafish eggs because of their transparency [34, 35].

genes into fish eggs

Injected gene copies	Injection volume	Survival rate (%)	Integration rate (%)	Gene copies /cell	Mosaicism
200 pg (2×10^5)	20 nl	77 (hatching)	75 (embryo)		+
10^6	2~3 nl	80 (fly)	7 (fly)	1	
30 pg	300 pl	16 (fly)	5 (adult)	<1	+
$5 \times 10^3 \sim 10^4$	10~20 pl	50 (embryo)	50 (embryo)	1~100	+
540	2 pl	19 (fetus)	25 (fetus)		+

II. TRANSGENIC FISH RESEARCH IN FISHERIES SCIENCE AND BASIC BIOLOGY

Current transgenic fish research is being directed toward the areas of growth promotion, low-temperature resistance, insertional mutagenesis, and developmental gene expression (Table 1). In this section, we describe the present state of these four lines of research by selecting typical experiments and examining their data which are summarized in Table 2. Data on transgenic mice [37] are also indicated for comparison.

a. Growth promotion

Investigations by Chourrout *et al.* [25, 26] are a typical study on growth promotion of fish using gene transfer of mammalian growth hormone genes. This French group reported integration of mammalian growth hormone cDNA in rainbow trout in 1986 [25]. In their experiments, ova and sperm collected from 3- or 4-year-old adult rainbow trout were artificially fertilized. Eggs were microinjected at the cytoplasm of the animal pole in the interval from about 2 to 6 hr after fertilization when eggs were in the stage between formation of the embryonic disc and prior to first cleavage. To overcome hardness of the chorion, they devised a two-step method of microinjection: the chorion was first drilled with a micropipette of 50 μm diameter to make a 100 μm slot, through which a 10 μm microneedle was inserted to the cytoplasm. Through this, 20 nl of solution containing 200 pg DNA of the SV40 promoter-human growth hormone fusion gene was injected in five seconds. By this method, 30 eggs could be treated per hour. The survival rate of injected embryos at hatching was 77% and foreign DNA was detected at considerably high rates, in 75% of survivors when linearized plasmids were used and 40% when circular ones were used. In mice, integration of foreign genes was not efficient when genes were injected into the cytoplasm [21]. The high integration rate in rainbow trout may be due to injection of a large quantity of DNA.

More recently, this same group [26] reported that 60% of eggs injected with 200 million copies of mammalian growth hormone genes gave rise to adult fish and more than 50% of them retained the

foreign genes. Eight of fifteen males analyzed transmitted the foreign genes to about 20% of their offspring. From these data, they suggested that the integration of the plasmid in the parental genome was mosaic and happened at an early developmental stage. No growth hormone could be detected in any of the fish examined in this experiment. Thus, the success of the French group in introduction and germ-line transfer of foreign genes into rainbow trout opened the way to producing transgenic animals of economically important fish.

b. Low-temperature resistance

The antifreeze protein (AFP) gene is the only fish gene which has been used for transgenic experiments in fish. The winter flounder living in icy waters of the polar sea avoids freezing of its blood and can survive even at sub-zero temperatures by producing a set of antifreeze proteins. In contrast, salmon and other salmonids which lack this gene cannot live at such extremely low temperatures [31, 38]. Two groups in the United States and Canada have attempted to introduce the AFP gene into fish cells or embryos to improve the freezing resistance of these latter species.

AFPs of winter flounder appear in the serum in autumn and disappear in spring under natural conditions. Huang *et al.* [39] of Johns Hopkins University were able to induce synthesis of AFP mRNA in this fish in summer by exposing them to a low temperature. A similar cold induction of the mRNA was also found *in vitro* in liver tissues and isolated liver nuclei. On the background of these basic studies, they introduced the cloned AFP gene into cell lines from other species, rainbow trout, bluegill, and salmon, and observed the gene expression in these cells by detecting AFP mRNA synthesis. This finding that the cloned AFP gene can be introduced and expressed in fish cells derived from other species gives promise of the possibility of producing transgenic fish with this gene. In transgenic mice, many successful experiments have been based on data of gene transfer and expression at the cellular level *in vitro*.

Fletcher *et al.* [31] of the Canadian group attempted to introduce the AFP gene cloned from winter flounder into Atlantic salmon. They de-

vised an ingenious method for microinjection in which microneedles 3 to 5 μm in diameter were inserted into eggs through the micropyle. The micropyle locates near the egg nuclear area within 3 hr after fertilization. A similar method for microinjection was used in tilapia eggs [27]. Fletcher and his colleagues [31] injected 2 to 3 nl of DNA solution containing 10^6 copies of linearized plasmids into eggs 2 hr after fertilization. This number of gene copies is quite small in comparison with that used in rainbow trout by Chourrout *et al.* [25, 26]. Microinjection to the nuclear region through the micropyle may be an efficient method in eggs with a hard chorion.

About 80% of the 1800 injected eggs survived to hatching. When 30 fingerlings were analyzed 8 months after hatching, the AFP gene was detected in 2 of them, showing that the winter flounder AFP gene could be introduced into Atlantic salmon. Expression of this gene in the salmon has not yet been examined, but the researchers will analyze the expression by determining whether the AFP is in the serum when the fish grow to an appropriate size. This group also introduced the flounder AFP-*Drosophila* heat shock promoter (Hsp-70) fusion gene into *Drosophila* using the P element and detected the AFP in the hemolymph [40].

Thus the AFP gene of winter flounder is a fish gene which is well characterized by its structure, nature of product proteins, and introduction and expression in cell lines and individuals of other species. These factors assure that the AFP gene will be the focus of transgenic fish research in future.

c. Insertional mutagenesis

Zebrafish are small freshwater fish which have many advantages as experimental animals: a short generation time of only 3 to 4 months; mature females lay several hundred eggs at weekly intervals; transparency of eggs; synchronous division of blastomeres; rapid development, hatching within 3 days [41, 42]. A group at University of Oregon has performed extensive studies on the genetics, neurobiology, and developmental biology of zebrafish [42]. In 1981, Streisinger *et al.* [43] developed a simple method to produce homozygotes in zebrafish by inducing artificial parthenogenesis;

this makes them unique experimental animals for vertebrate genetics. Recently, Kimmel and Warga [42] traced the developmental fate of blastomeres at the cleavage stage by injecting dyes and learned that the fate of an embryonic cell was not determined until the gastrula stage. These significant findings in vertebrate development were possible by taking advantage of the large and transparent blastomeres in zebrafish eggs which can be manipulated experimentally during development. Thus, the biological characteristics of zebrafish make them attractive material for transgenic experiments.

Insertion of foreign genes into the host chromosomes is known to produce recessive or dominant mutations, at least in more than several percent of transgenic mice [21]. Some insertional mutations cause developmental abnormality including limb deformity [44]. Insertional mutations produced by transgenic techniques are now becoming a potent tool for genetic analysis of development in vertebrates which lack appropriate developmental mutants.

Stuart *et al.* [34] of the Oregon group introduced foreign genes into zebrafish in order to generate stable lines of transgenic fish carrying insertional mutations. In their experiments, fertilized zebrafish eggs at the 1-, 2-, and 4-cell stages within 1 hr after fertilization were dechorionated manually and injected with a 300 μl solution containing 30 μg DNA at a concentration of 0.1 mg/ml into the cytoplasm. The volume of injection was estimated by adding 2% phenol red to the solution. The DNA was a linearized form of the 5.2 kb bacterial plasmid, SV40-hygro, containing the hygromycin resistant gene linked to the SV40 promoter. The plasmid was expected to produce hygromycin phosphotransferase in the host and thereby enable antibiotic selection of transgenic fish. Thus, 200 embryos could be treated daily. In transgenic experiments, usually 1-cell stage embryos are used in order to introduce foreign DNA into all the descendant cells. It may be due to the rapid development of zebrafish that the 2- and 4-cell stage embryos as well as the 1-cell stage were used for microinjection, in spite of the risk of reducing the efficiency of introduction. The foreign gene could be detected in most of the injected fish at 3

weeks of age, but in only about 5% of fish at 4 months when their fins were analyzed. When 20 fin-positive fish were crossed with uninjected fish, one fish transmitted the foreign sequences to approximately 20% of the F_1 offspring. In the second outcrossed generation produced using one of the F_1 fish carrying the foreign sequences, nine out of eighteen (50%) F_2 progeny inherited the sequences. Thus, Stuart *et al.* [34] showed that the foreign gene introduced into zebrafish embryos could be transmitted to subsequent generations in a Mendelian fashion. No expression of the introduced gene could be detected.

d. Developmental gene expression

Animal development is accomplished as the result of sequential gene expression during embryogenesis, which is regulated in a temporal- and tissue-specific manner. The transgenic technique is the most powerful tool for elucidating the regulatory mechanism of gene expression in development. Using transgenic fish we have investigated the expression of a vertebrate crystallin gene, and this is described in the next section.

III. MEDAKA AS A MODEL SYSTEM

a. Microinjection into the oocyte nucleus

The medaka is a small, egg-laying freshwater teleost which is widely used as a laboratory animal [45]. It is the only fish species in which several inbred strains have been established [46]. The oogenesis, fertilization, and embryonic development of this species have been extensively studied. Table 3 summarizes biological characters of the medaka in relation to transgenic experiments. The 3 cm long size medaka falls into the smallest group of vertebrates known. The generation time is short, 2 to 3 months, comparable with that of zebrafish and mice. The spawning is daily and year-round under artificial conditions, and the timing of spawning can be controlled by light conditions during a 24-hr period. In addition, the transparency of eggs is distinct advantage for embryological manipulations.

When we started experiments of transgenic fish using the medaka in 1982, the first problem we had to resolve was hardness of the chorion and difficulty in optical recognition of the nucleus in fertilized eggs. We solved this by using oocytes in place of fertilized eggs: the chorion of medaka oocytes is

TABLE 3. Medaka as a material for transgenic fish

Strain	Orange-red-colored Wild type
Inbred strain	Present (only one in a fish)
Life span	2 years
Sex maturation	3 months
Total length	3 cm
Spawning	year-round
Spawning cycle	24 hr
Days for hatching	10 days
Diameter of eggs	1 mm
Transparency of eggs	Transparent
Chorion	Hard
Diameter of oocytes	1 mm
Diameter of germinal vesicles	100 μ m
Culture of oocytes	Possible
Chromosome number	48
Genome size	20% of mammals

soft and the large nucleus (germinal vesicle) is recognizable at some stages of maturation.

In our experiments, the cultivated orange-red-colored strain of the medaka (*Oryzias latipes*) was bred under controlled lighting arrangements (14 hr light and 10 hr darkness) at 26°C. The medaka spawned at the beginning of lighting. Nine hr before the anticipated time of ovulation, oocytes which are to be ovulated the next time are in the prophase of the second meiotic division. They are 900 to 1000 μm in diameter and have nuclei (germinal vesicles) 120–150 μm in diameter at the animal pole in the transparent cytoplasm (Fig. 2). To obtain these oocytes for microinjection in the early morning, the time of lighting was set at 16:00 (Fig. 1). Around this time, females with eggs in their abdomen were isolated. These females were expected to have oocytes to be laid the next day because the ovulation cycle of the medaka is 24 hr. At 6:00 o'clock the next morning (10 hr before the

anticipated time of ovulation), intrafollicular oocytes were taken out and put into Earle's 199 medium supplemented with 2% bovine serum albumin and 17.8 mM NaHCO_3 (pH 8.0) [47]. Oocytes were placed in a glass apparatus made on

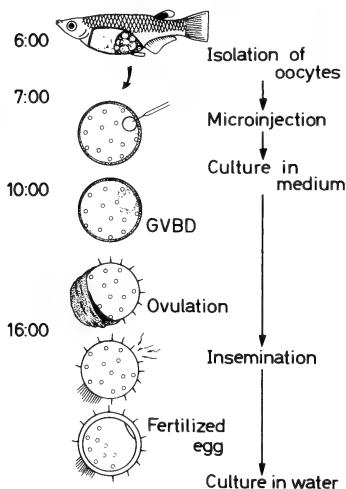


FIG. 1. Time schedule for microinjection to the medaka oocyte nucleus (germinal vesicle). Fish are bred under controlled lighting arrangements (14 hr light and 10 hr darkness). The time of lighting is set at 16:00. GVBD, germinal vesicle breakdown.

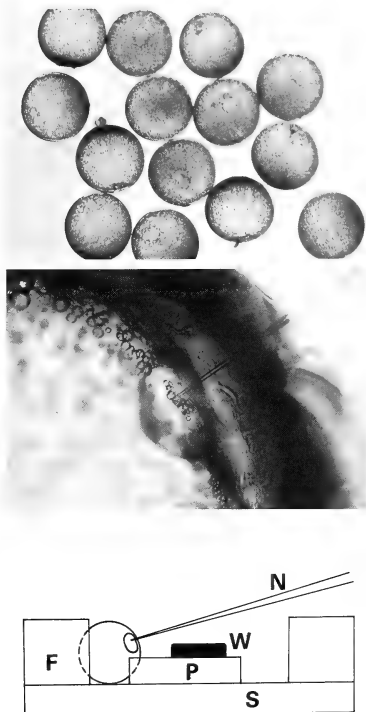


FIG. 2. Nuclear microinjection in medaka oocytes. Upper frame: Medaka oocytes 8 hr before ovulation. $\times 15$. Middle frame: Insertion of a microneedle into the nucleus (germinal vesicle). $\times 185$. Lower frame: Fixation and orientation of oocytes. Medaka oocytes are fixed in a direction where the nucleus and microneedle are opposite each other. F, glass frame; N, microneedle; P, glass plate; S, slide glass; W, metal for weight.

a slide glass which was filled with the medium, and were fixed in a direction where the nucleus and microneedle were opposite to each other (Fig. 2). Microinjection was carried out under a microscope of 100 magnification using microneedles with sharpened tips of 3–4 μm in inner diameter (Fig. 2). The volume of injection was estimated by the degree of swelling of the nucleus. The solution was injected until the moment that the nucleus began to swell. At this point, the injection volume was 20–30 pl and injection of larger volume than this resulted in degeneration of embryos before the blastula stage. With maturation of oocytes in the medium, the nucleus gradually became flat, causing breakdown of the nuclear membrane and hampering microinjection into the nucleus. The time for microinjection was thus limited to about 2 hr during which 60–100 oocytes could be treated. The injected oocytes were cultured in the same medium at 26°C for about 8 hr until the anticipated time of ovulation (16:00). Some of mature oocytes lost their follicles during the culture; in these remaining, follicles were removed manually with fine forceps. The oocytes were then inseminated with a sperm suspension. Rate of fertilization was about 70%. Fertilized eggs were incubated separately in distilled water in small plastic wells at 26°C.

b. Foreign gene transfer and expression

Crystallins are major soluble proteins of the vertebrate lens (48, 49), and are of 4 types: α -, β -, γ -, and δ -crystallin. α -, β -, and γ -crystallin are present in fish, amphibians, and mammals. In reptiles and birds, γ -crystallin is replaced by δ -crystallin. To study regulation of gene expression of vertebrate crystallin genes, we introduced the chicken δ -crystallin gene into medaka embryos. Since fish do not naturally have the δ -crystallin gene, introduction of this gene may be advantageous to study the state and expression of a foreign gene in medaka embryos. In addition, this gene has been qualified well in that it is expressed in a tissue specific manner in mouse cells [50, 51], transgenic mice [52], and chimeric mice [53]. The plasmid used for microinjection, p δ C-1B, consisted of 11.4 kb chicken δ -crystallin sequences and 3.0 kb pAT153 sequences. About 5×10^3 – 10^4 copies of the circular plasmid in 10–20 pl of 0.1 mM Tris and 0.01 mM EDTA solution containing DNA at 10 $\mu\text{g}/\text{ml}$ were microinjected into each nucleus. The gene copies injected were fewer than is other fish experiments adopting cytoplasmic injection.

Analysis of introduction and expression of the foreign gene was carried out on 7-day-old embryos.

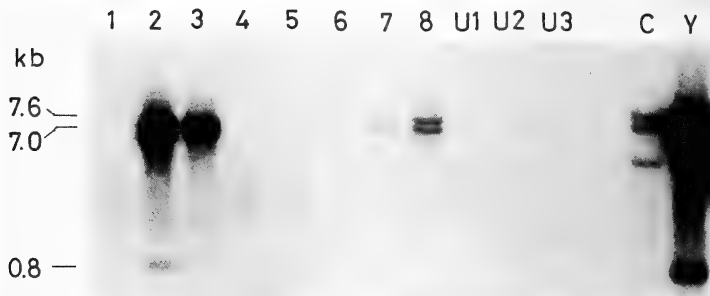


FIG. 3. Detection of the chicken δ -crystallin gene from medaka embryos by Southern blot analysis. Lanes 1–8, Microinjected medaka embryos; U1–U3, Uninjected medaka embryos; C, A 15-day-old chick embryo; Y, A mouse teratocarcinoma cell line carrying 500 copies of p δ C-1B sequences per cell. Molecular sizes are shown in kb on the left.

9 10 11 12 13 14 15 16 17 18 19 20 21 22 23 24 U4 U5 CL



FIG. 4. Detection of the chicken δ -crystallin from medaka embryos by immunoblot analysis. Lanes 9–24, Microinjected medaka embryos; U4–U5, Uninjected medaka embryos; CL, the lens from a 15-day-old chick embryo. Molecular sizes are shown in kDa on the right.

About 50% of the injected oocytes developed normally to this stage. This survival rate is rather low compared with that in many other cases using cytoplasmic injection. By Southern blot analysis, δ -crystallin sequence could be detected in about half of the embryos examined (Fig. 3). The average copies of δ -crystallin gene per cell in individual medaka embryos varied considerably from 1 to 100. By immunoblot analysis, δ -crystallin was detected in 30% of the embryos examined and the content varied in each embryo (Fig. 4). Thus, it was shown by biochemical analysis that the chicken δ -crystallin gene was introduced and expressed in medaka embryos.

In order to investigate tissue-specific expression of the foreign gene, histological localization of the sequence and its product protein was examined by DNA-DNA *in situ* hybridization and immunohistological staining, respectively. On the histological distribution, the sequence was detected in nuclei of all tissues (Fig. 5a); however, the frequency of nuclei with the sequence was not 100%, but 50% or less. Thus, δ -crystallin gene-carrying and non-carrying cells were distributed mosaically in every tissue. This mosaicism suggests that incorporation of the microinjected gene into the genome took place at the 2-cell stage or later, and that multiple copies of the chicken δ -crystallin sequences were

stably inherited by the descendant cells. The mosaicism is also found in trout [26] and zebrafish [34], and is not rare even in transgenic mice produced by microinjection into the pronucleus at 1-cell stage [21].

On the tissue specificity of gene expression, the δ -crystallin was expressed in the retina, brain, spinal cord, muscle, gill, and gut, but rarely expressed in the lens where the gene primarily should be expressed (Fig. 5b). One possible reason for the broad tissue-specificity is that the gene expression is subject to a temporal regulation during embryonic development and that the stage chosen for analysis might be inappropriate. In fact, the lens formation is already completed in 7-day old embryos and thus the gene expression may be detected in earlier embryonic stages. When several stages of embryos were examined from 2- to 7-day old, the gene expression in the lens was restricted to 3-day old embryos and was found neither before nor after this stage [54]. Thus, it was shown that tissue specific expression of the chicken δ -crystallin gene depended on the stage of development and was regulated temporally in medaka embryos.

Comparing Figures 5a and 5b, which represent adjacent sections, it is evident that δ -crystallin was not detected in all the cells carrying this gene. This

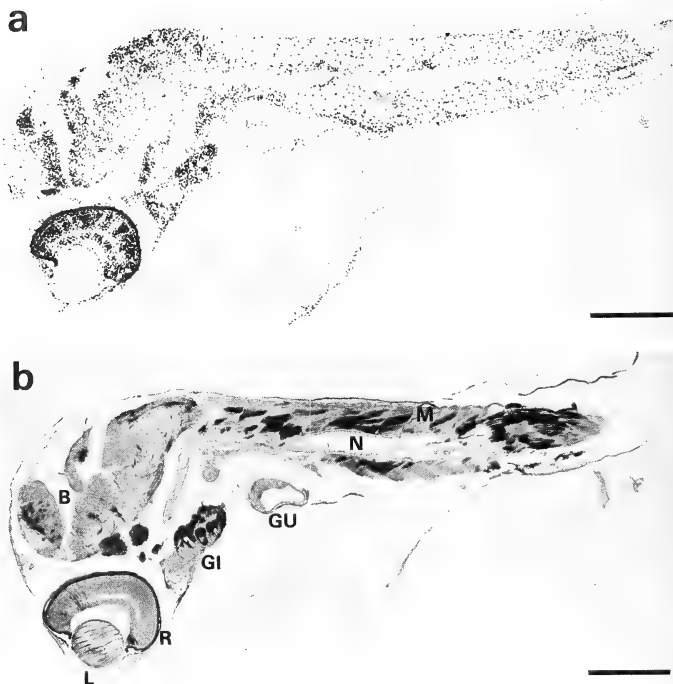


FIG. 5. Histological distribution of chicken δ -crystallin gene and its product protein. (a) DNA-DNA *in situ* hybridization. This plane of the section passes through the lens. The bar represents 500 μ m. (b) Immunohistological staining. This section is a few sections distant laterally from (a). B, brain; GI, gill; GU, gut; L, lens; M, muscle; N, notochord; R, retina. The bar represents 500 μ m.

apparently stochastic expression of foreign genes is not an uncommon phenomenon in transgenic mice [21].

Our experiments indicate that the medaka offers many advantages for transgenic fish research, that is, capability of nuclear microinjection, relatively high survival rates of injected embryos, and efficient introduction and expression of foreign genes. Furthermore, it was demonstrated that expression of the chicken gene introduced was regulated in a tissue- and temporal-specific man-

ner. All these facts show that the medaka is a potent experimental system for studying gene expression during vertebrate development.

IV. CONCLUSION

1) Current studies on transgenic fish are being carried out in connection with growth promotion and low-temperature resistance, insertional mutagenesis, and gene expression in development.

2) Techniques for transgenic experiments in fish

are not yet established as they are in *Drosophila* and mice. Introduction of foreign genes has been accomplished in many fish species, but the expression and germ-line transmission of these genes has been successful in only a few cases.

3) Many problems such as variation in copies of integrated genes, mosaicism in integration, and variation in efficiency of gene expression are present in transgenic fish as they are in transgenic mice, although these problems may be inherent in the transgenic technique when it is currently applied.

4) Most genes used for producing transgenic fish are derived from mammals. Future progress in transgenic fish studies will depend on the cloning of fish genes and the development of promoter/enhancer sequences suitable for the expression of fish genes.

5) The medaka, a small freshwater fish, is one of the most promising materials for transgenic research in fish.

ACKNOWLEDGMENTS

This review was written on the basis of the work supported in part by grants from the Ministry of Education, Science and Culture (Nos. 62619503 and 63619503) and the Fisheries Agency, Japan.

REFERENCES

- 1 Stinchcomb, D. T., Shaw, J. E., Carr, S. H. and Hirsh, D. (1985) Extrachromosomal DNA transformation of *Caenorhabditis elegans*. *Mol. Cell. Biol.*, **5**: 3484-3496.
- 2 Spradling, A. C. and Rubin, G. M. (1982) Transposition of cloned P-elements into *Drosophila* germ line chromosomes. *Science*, **218**: 341-347.
- 3 Rubin, G. M. and Spradling, A. C. (1982) Genetic transformation of *Drosophila* with transposable element vectors. *Science*, **218**: 348-353.
- 4 McMahon, A. P., Novak, T. J., Britten, R. J. and Davidson, E. H. (1984) Inducible expression of a cloned heat shock fusion gene in sea urchin embryos. *Proc. Natl. Acad. Sci. USA*, **81**: 7490-7494.
- 5 McMahon, A. P., Flytzanis, C. N., Hough-Evans, B. R., Katula, K. S., Britten, R. J. and Davidson, E. H. (1985) Introduction of cloned DNA into sea urchin egg cytoplasm: replication and persistence during embryogenesis. *Dev. Biol.*, **108**: 420-430.
- 6 Flytzanis, C. N., McMahon, A. P., Hough-Evans, B. R., Katula, K. S., Britten, R. J. and Davidson, E. H. (1985) Persistence and integration of cloned DNA in postembryonic sea urchins. *Dev. Biol.*, **108**: 431-442.
- 7 Colin, A. M., Catlin, T. L., Kidson, S. H. and Maxson, R. (1987) Closely linked early and late H2B histone genes are differentially expressed after microinjection into sea urchin zygotes. *Proc. Natl. Acad. Sci. USA*, **85**: 507-510.
- 8 Flytzanis, C. N., Britten, R. J. and Davidson, E. H. (1987) Ontogenic activation of a fusion gene introduced into the sea urchin egg. *Proc. Natl. Acad. Sci. USA*, **84**: 151-155.
- 9 Hough-Evans, B. R., Franks, R. R., Cameron, R. A., Britten, R. J. and Davidson, E. H. (1987) Correct cell type-specific expression of a fusion gene injected into sea urchin eggs. *Dev. Biol.*, **121**: 576-579.
- 10 Katula, K. S., Hough-Evans, B. R., Britten, R. J. and Davidson, E. H. (1987) Ontogenic expression of a Cyt:actin fusion gene injected into sea urchin eggs. *Development*, **101**: 437-447.
- 11 Franks, R. R., Hough-Evans, B. R., Britten, R. J. and Davidson, E. H. (1988) Spatially deranged though temporally correct expression of a *Strongylocentrotus purpuratus* actin gene fusion in transgenic embryos of a different sea urchin family. *Genes & Dev.*, **2**: 1-12.
- 12 Franks, R. R., Hough-Evans, B. R., Britten, R. J. and Davidson, E. H. (1988) Direct introduction of cloned DNA into the sea urchin zygote nucleus, and fate of injected DNA. *Development*, **102**: 287-299.
- 13 Vitelli, L., Kemler, I., Lauber, B., Birnstiel, M. L. and Busslinger, M. (1988) Developmental regulation of microinjected histone genes in sea urchin embryos. *Dev. Biol.*, **127**: 54-63.
- 14 Rusconi, S. and Schaffner, W. (1981) Transformation of frog embryos with a rabbit β -globin gene. *Proc. Natl. Acad. Sci. USA*, **78**: 5051-5055.
- 15 Etkin, L. D. (1982) Analysis of the mechanisms involved in gene regulation and cell differentiation by microinjection of purified genes and somatic cell nuclei into amphibian oocytes and eggs. *Differentiation*, **21**: 149-159.
- 16 Bendig, M. M. and Williams, J. G. (1983) Replication and expression of *Xenopus laevis* genes injected into fertilized *Xenopus* eggs. *Proc. Natl. Acad. Sci. USA*, **80**: 6197-6201.
- 17 Etkin, L. D. and Pearman, B. (1987) Distribution, expression and germ-line transmission of exogenous DNA sequences following microinjection into *Xenopus laevis* eggs. *Development*, **99**: 15-23.
- 18 Etkin, L. D., Pearman, B., Roberts, M. and Bektesh, S. L. (1984) Replication, integration and expression of exogenous DNA injected into fertilized

- eggs of *Xenopus laevis*. *Differentiation*, **26**: 194–202.
- 19 Wilson, C., Cross, G. S. and Woodland, H. R. (1986) Tissue specific expression of actin genes injected into *Xenopus* embryos. *Cell*, **47**: 589–599.
- 20 Gordon, J. W., Scangos, G. A., Plotkin, D. J., Barbosa, J. A. and Ruddle, F. H. (1980) Genetic transformation of mouse embryos by microinjection of purified DNA. *Proc. Natl. Acad. Sci. USA*, **77**: 7380–7384.
- 21 Palmiter, R. D. and Brinster, R. L. (1986) Germ-line transformation of mice. *Ann. Rev. Genet.*, **20**: 465–499.
- 22 Hammer, R. E., Pursel, V. G., Rexroad, C. E. Jr., Wall, R. J., Bolt, D. J., Ebert, K. M., Palmiter, R. D. and Brinster, R. L. (1985) Production of transgenic rabbits, sheep and pigs by microinjection. *Nature*, **315**: 680–683.
- 23 Brem, G., Brenig, B., Goodman, H. M., Selden, R. C., Graf, F., Kruff, B., Springmann, K., Hondele, J., Meyer, J., Winnacker, E.-L. and Kräusslich, H. (1985) Production of transgenic mice, rabbits and pigs by microinjection into pronuclei. *Zuchthygiene*, **20**: 251–252.
- 24 Maclean, N., Penman, D. and Zhu, Z. (1987) Introduction of novel genes into fish. *Bio/Technology*, **5**: 257–261.
- 25 Chourrout, D., Guyomard, R. and Houdebine L. M. (1986) High efficiency gene transfer in rainbow trout (*Salmo gairdneri* Rich.) by microinjection into egg cytoplasm. *Aquaculture*, **51**: 143–150.
- 26 Chourrout, D., Guyomard, R., Leroux, C., Pourrain, F. and Houdebine, L. M. (1988) Integration and germ-line transmission of foreign genes in trout after injection into the egg cytoplasm. *J. Cell. Biochem., Suppl.* **12B**: 188.
- 27 Brem, G., Brenig, B., Hörstgen-Schwark, G. and Winnacker, E.-L. (1988) Gene transfer in tilapia (*Oreochromis niloticus*). *Aquaculture*, **68**: 209–219.
- 28 Zhu, Z., Xu, K., Li, G., Xie, Y. and He, L. (1986) Biological effects of human growth hormone gene microinjected into the fertilized eggs of loach *Misgurnus anguillicaudatus* (Cantor). *Kexue Tongbao*, **31**: 988–990.
- 29 Dunham, R. A. and Eash, J. (1987) Transfer of the metallothionein-human growth hormone fusion gene into channel catfish. *Trans. Amer. Fisheries Soc.*, **116**: 87–91.
- 30 Zhu, Z., Li, G., He, L. and Chen, S. (1985) Novel gene transfer into the fertilized eggs of goldfish (*Carassius auratus* L. 1758). *Z. angew. Ichthyol.*, **1**: 31–34.
- 31 Fletcher, G. L., Shears, M. A., King, M. J., Davies, P. L., and Hew, C. L. (1988) Evidence for antifreeze protein gene transfer in Atlantic salmon (*Salmo salar*). *Can. J. Fish Aquat. Sci.*, **45**: 352–357.
- 32 McEvoy, T. G., Stack, M., Keane, B., Barry, T., Sreenan, J. M. and Gannon, F. (1988) The expression of a foreign gene in salmon embryos. *Aquaculture*, **68**: 27–38.
- 33 Yoon, S. J., Liu, Z., Kapuscinski, A. R., Hackett, P. B., Faras, A. and Guise, K. S. (1988) Successful gene transfer in fish. *J. Cell. Biochem, Suppl.* **12B**: 190.
- 34 Stuart, G. W., McMurray J. V. and Westerfield, M. (1988) Replication, integration and stable germ-line transmission of foreign sequences injected into early zebrafish embryos. *Development*, **103**: 403–412.
- 35 Ozato, K., Kondoh, H., Inohara, H., Iwamatsu, T., Wakamatsu, Y. and Okada, T. S. (1986) Production of transgenic fish: introduction and expression of chicken δ -crystallin gene in medaka embryos. *Cell Differ.*, **19**: 237–244.
- 36 Palmiter, R. D., Brinster, R. L., Hammer, R. E., Trumbauer, M. E., Rosenfeld, M. G., Birnberg, N. C., and Evans, R. M. (1982) Dramatic growth of mice that develop from eggs microinjected with metallothionein-growth hormone fusion genes. *Nature*, **300**: 611–615.
- 37 Brinster, R. L., Chen, H. Y., Trumbauer, M. E., Yagle, M. K. and Palmiter, R. D. (1985) Factors affecting the efficiency of introducing foreign DNA into mice by microinjecting eggs. *Proc. Natl. Acad. Sci. USA*, **82**: 4438–4442.
- 38 Hew, C. L. and Fletcher, G. L. (1985) Biochemical adaptation to the freezing environment—structure, biosynthesis and regulation of fish antifreeze polypeptides. In “Circulation, Respiration and Metabolism”, Ed. by R. Gilles, Springer-Verlag, Berlin, pp. 553–563.
- 39 Huang, R. C., Gourlie, B. and Price, J. (1987) Winter flounder antifreeze protein genes: demonstration of a cold-inducible promoter and gene transfer to other species. *Fed. Proc.*, **46**: 2039.
- 40 Rancourt, D. E., Walker, V. K. and Davies, P. L. (1988) Chimaeric fish antifreeze protein genes in transgenic *Drosophila*. *J. Cell. Biochem, Suppl.* **12B**: 193.
- 41 Laale, H. W. (1977) The biology and use of zebrafish, *Brachydanio rerio* in fisheries research. A literature review. *J. Fish Biol.*, **10**: 121–173.
- 42 Kimmel, C. B. and Warga, R. M. (1988) Cell lineage and developmental potential of cells in the zebrafish embryo. *Trends in Genetics*, **4**: 68–74.
- 43 Streisinger, G., Walker, C., Dower, N., Knauber, D. and Singer, F. (1981) Production of clones of homozygous diploid zebrafish (*Brachydanio rerio*). *Nature*, **291**: 293–296.
- 44 Woychik, R. P., Stewart, T. A., Davis, L. G., D'Eustachio, P. and Leder, P. (1985) An inherited limb deformity created by insertional mutagenesis in a transgenic mouse. *Nature*, **318**: 36–40.

- 45 Yamamoto, T. (1975) Medaka (Killifish). Biology and Strains. Keigaku Publ. Co., Tokyo.
- 46 Hyodo-Taguchi, Y. and Egami, N. (1985) Establishment of inbred strains of the medaka *Oryzias latipes* and the usefulness of the strains for biomedical research. Zool. Sci., **2**: 305-316.
- 47 Iwamatsu, T. (1974) Studies on oocyte maturation of the medaka, *Oryzias latipes*. II. Effects of several steroids and calcium ions and the role of follicle cells on *in vitro* maturation. Annot. Zool. Jpn., **47**: 30-42.
- 48 Clayton, R. M. (1974) Comparative aspects of lens proteins. In "The Eye, Vol. 5". Ed. by H. Davson and L. T. Graham, Academic Press, London, pp. 399-494.
- 49 Piatigorsky, J. (1984) Lens crystallins and their gene families. Cell, **38**: 620-621.
- 50 Kondoh, H., Yasuda, K. and Okada, T. S. (1983) Tissue-specific expression of a cloned chick δ -crystallin gene in mouse cells. Nature., **301**: 440-442.
- 51 Hayashi, S., Kondoh, H., Yasuda, K., Soma, G., Ikawa, Y. and Okada, T. S. (1985) Tissue-specific regulation of a chicken δ -crystallin gene in mouse cells: involvement of the 5' end region. EMBO J., **4**: 2201-2207.
- 52 Kondoh, H., Katoh, K., Takahashi, Y., Fujisawa, H., Yokoyama, M., Kimura, S., Katsuki, M., Saito, M., Nomura, T. Hiramoto, Y. and Okada, T. S. (1987) Specific expression of the chicken δ -crystallin gene in the lens and the pyramidal neurons of the piriform cortex in transgenic mice. Dev. Biol., **120**: 177-185.
- 53 Takahashi, Y., Hanaoka, K., Hayasaka, M., Katoh, K., Kato, Y., Okada, T. S. and Kondoh, H. (1988) Embryonic stem cell-mediated transfer and correct regulation of the chicken δ -crystallin gene in developing mouse embryos. Development, **102**: 259-269.
- 54 Inoue, K., Ozato, K., Kondoh, H., Wakamatsu, Y., Fujita, T. and Okada, T. S. (1989) Stage-dependent expression of the chicken δ -crystallin gene in transgenic fish embryos. Cell Differ. in press.

References added at proof stage: Rokkones, E., Ales-trøm, P., Skjervold, H. and Gautvik, K. M. (1989) Microinjection and expression of a mouse metallothionein fusion gene in fertilized salmonid eggs. J. Comp. Physiol. B **158**: 751-758.



Electrophysiological Identification of Neuronal Pathway to the Prothoracic Gland and the Change in Electrical Activities of the Prothoracic Gland Innervating Neurones During Larval Development of a Moth, *Mamestra brassicae*

AKIRA OKAJIMA and MASAO WATANABE

Department of Biology, Faculty of Liberal Arts,
Yamaguchi University, Yamaguchi 753, Japan

ABSTRACT—The neuronal connections between the prothoracic gland and the central nervous system were characterised electrophysiologically in larvae of the moth, *Mamestra brassicae*. Three nerves innervate the prothoracic gland and all contain both efferent and afferent activities. The activity of one of the efferent neurosecretory neurones showed remarkable changes during the course of development, its firing frequency varying inversely with ecdysteroid titer in the haemolymph. This neurosecretory neurone possibly inhibits prothoracic gland activity.

INTRODUCTION

The nervous connections between the prothoracic gland (PTG) and the central nervous system have been described in various insect orders using anatomical and histological techniques. The results in lepidopterous insects are fairly uniform [1-6]. The PTG is innervated by the suboesophageal, prothoracic and mesothoracic ganglia. Electron-microscopic studies have shown that a neurosecretory axon enters the gland and makes intimate contact with the gland cells. However the detailed descriptions of the neuroglandular junction do not agree [3, 7-9].

Experimental approaches to analysing the functions of this innervation have been made mainly by the surgical techniques; transections of the ventral nerve cord or the nerves to PTG and extirpations and implantations of various ganglia or PTG [6, 10-13]. Among these, Mala and Sehna [13], using surgical operations on head-ligated *Galleria* larvae, showed that PTG activity was inhibited by the prothoracic and mesothoracic ganglia and accelerated by the suboesophageal ganglion, in contrast to the results of Alexander [11] who proposed that

the suboesophageal ganglion was inhibitory to the PTG. Delayed pupal ecdysis occurring after transection of the ventral nerve cord was explained by Edwards [10] and Alexander [11] as a result of alteration in proprioceptive inputs to the ganglia which regulate the PTG activity.

In a different order of insect, in *Periplaneta*, Richter and Gersch [14] have shown a positive correlation between the level of electrical activity of PTG nerve and the ecdysteroid titer in the haemolymph during the course of development in the last larval instar.

The electrophysiological experiments reported here have used the isolated ganglia-gland preparation in order to obtain direct evidence of the various pathways of the neuronal connections to PTG from the ventral ganglia and to plot the change of electrical activities of the PTG innervating neurones in relation to the stage of development in last instar larvae of *Mamestra brassicae*. As well, cobalt staining and electronmicroscopic observations reveal more about the projections of the PTG nerves.

MATERIALS AND METHODS

Larvae of *Mamestra brassicae* were reared on an artificial diet [15] at $23^{\circ}\pm 1^{\circ}\text{C}$ under long day

photoperiod (16L, 8D). Under these conditions, last instar larva showed a transparent ventral epidermis as a first detectable sign of the transformation to the pharate pupal period 5 days after the last larval moulting. After a further 5 or 6 days they developed to the pupa. Female larvae were used throughout this experiment.

The preparation consisted of the isolated ganglionic chain from brain to mesothoracic ganglion connected by one, or in some cases 2 nerves to the PTG. Electrophysiological recordings were made from this *in vitro* preparation. Extracellular potential changes at one or two sites on a single nerve were recorded by the oil-gap method using the chamber as shown in Figure 1. Width of oil-gap was 300 μ m, and volume of each saline pool was about 100 μ l.

Composition of the physiological saline was 30

mM KCl, 4 mM NaCl, 4 mM CaCl_2 , 15 mM MgCl_2 , 40 mM trehalose, 120 mM glucose and 5 mM KH_2PO_4 - K_2HPO_4 buffer, pH 6.5 (total 300 milliosmolar), modified from Jungreis, Jatlow and Wyatt [16] to fit their results on trehalose composition in the haemolymph of *Hyalophora cecropia*.

Cobalt back-fills from PTG nerves were performed to elucidate the projections of the PTG nerves within the ganglia. The ganglia were immersed in Grace insect medium (GIBCO) while the cut end of a nerve was immersed in 5% CoCl_2 for over 12 hr at 5°C. Cobalt-filled ganglia were silver intensified and prepared for whole mount viewing [17].

For electronmicroscopic examination of the nerve-gland contact, the PTG and PTG nerve were isolated and fixed with a mixture of 2.5% glutaraldehyde and 1% osmium tetroxide in 0.1 M cacodylate buffer (pH 7.4) for 2 hr at 0°C. After washing in the same buffer, the preparation was dehydrated through graded concentrations of ethanol followed by propylene oxide and embedded in epon resin. Thin sections were stained with uranyl acetate and lead citrate and examined with Hitachi H 500H electronmicroscope at 75 kV.

RESULTS

Anatomy of the nervous connections

Figure 2 shows a diagrammatic representation of the nervous connections between PTG and central nervous system as seen in the last instar larvae of *Mamestra brassicae*. Configuration of the nervous network in this species is known to be fairly similar to that in *Antheraea pernyi* [3] and that in *Papilio demoleus* [6], although in the former two species the glandular cells of PTG are not packed in a flat mass as observed in *Mamestra brassicae* but are held fairly loosely. Five nerves shown in the figure were designated as N1 through N5 as in the papers cited above. Thin nerve branches of about 10 μ m in diameter were found to contact the PTG (b2, b4, c5 in Fig. 2).

Histology of PTG innervating neurones

Cobalt backfills from the nerves N2 and N4 were performed to trace the PTG innervating neurones

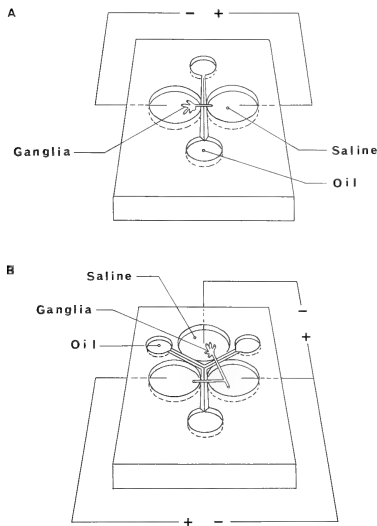


FIG. 1. Semi-diagrammatic representation of the oil-gap chambers used for recording electrical activities from PTG nerves. A, a single oil-gap; B, dual oil-gaps for studying the direction of impulse conduction.

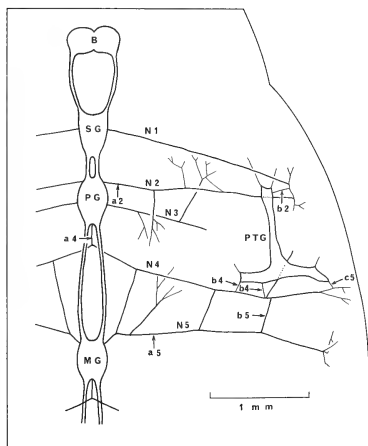


Fig. 2. Diagrammatic representation of the nervous connections between the prothoracic gland and the central nervous system in the larva of *Mamestra brassicae*. Arrows+codes a2, a4, etc. give the position of recording electrodes in the experiments shown in Figures. 5 and 6. B, brain; SG, suboesophageal ganglion; PG, prothoracic ganglion; MG, mesothoracic ganglion; PTG, prothoracic gland; N1-N5, nerves to prothoracic gland.

to their cell bodies located in the prothoracic ganglion. In the case of perfusion of nerve N2, one large cell located on the dorsomedial side of the ganglion was stained easily and quickly (Fig. 3A). The shapes of the cell body and the dendritic field were always the same regardless of whether the perfusions were made from any single N2 nerve or simultaneously from both N2s (as in Fig. 3A).

Similarly in the case of N4 (Fig. 3B), two large cells located on the ventrolateral side of each ganglionic hemisphere could be the PTG innervating neurones recorded from this nerve. All four of these cells in the prothoracic ganglion could be stained by perfusion of either nerve N4, although the amount of staining was different in the cells of the two sides. These results from *Mamestra brassicae* correspond to those from *Galleria mellonella* [18]. The one dorsomedial cell from the nerve N2 and four ventrolateral cells from the nerve N4

found here are analogous to their group 12 and group 3 neurones respectively.

The ultrastructure of nerve N4 was examined at two sites. The micrograph Figure 4A was obtained from about half way between prothoracic ganglion and PTG and that shown in Figure 4B was taken just at the entry point of thin nerve branch from the nerve N4 to the PTG. The thin nerve bundle in photograph B contains one neurosecretory axon. These neurosecretory axons contain dense-core granules ranging from 1000 to 2000 Å in diameter.

Identification of the neuronal pathways

Electrophysiological recording is indispensable for obtaining conclusive evidence for the innervation of the PTG. Typical electrical activities of PTG nerves, recorded by the oil-gap method, from the nerves N2, N4 and N5 are shown in Figure 5 and 6. In these recordings, the gap electrode placed on the nerve nearer to the ganglion was connected to the cathodic input of the oscilloscope, so that the efferent activity showed a positive first deflection while afferent activity had a negative one. Direction of impulse conduction was also determined by comparing the timing of the impulses arriving at the two electrodes (see Figs. 5 and 6).

Both efferent and afferent activities were observed in nerves N2, N4 and N5. Both fast and slow types of efferent activities can be seen in each upper trace of Fig. 5 recorded from PTG nerve close to the ganglion. The fast activity is similar in shape to the potentials recorded from the motor nerve of this preparation using the same oil-gap. The slow activity was similar to that recorded from the anterior *Corpora cardiaca* nerve from brain of this preparation. Therefore the slow type of efferent activity could be neurosecretory. Further evidence to support this was observed by electronmicroscopy (Fig. 4).

No quantitative analysis was made to determine whether the difference in shape of recorded potentials was attributable to duration of the action potential or to its conduction velocity. Comparison of the recordings from different electrodes revealed that there is one efferent neurone of neurosecretory type in nerve N2, and four neurosecretory neurones in nerve N4. It is impor-

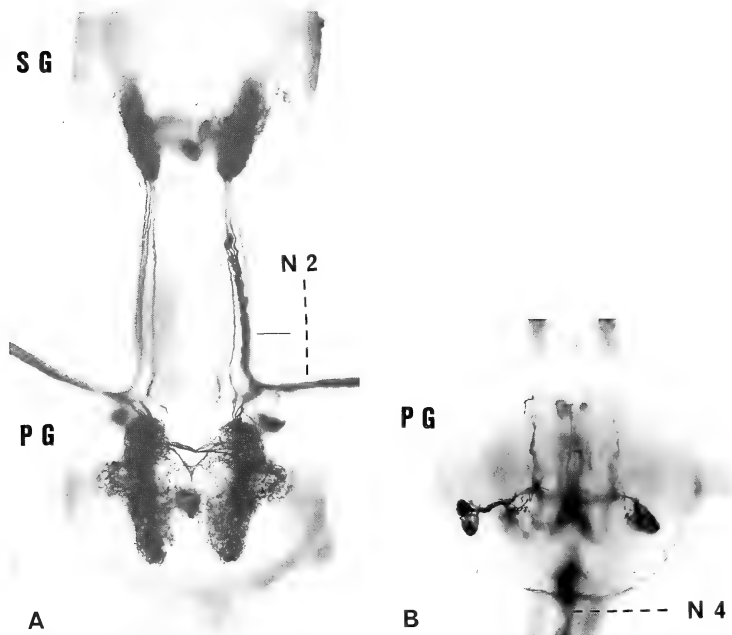


FIG. 3. Photomicrographs of the ganglia stained by cobalt filling method. View from dorsal. A: Filling from the nerve N2. B: Filling from the nerve N4. SG; subesophageal ganglion. PG; prothoracic ganglion.

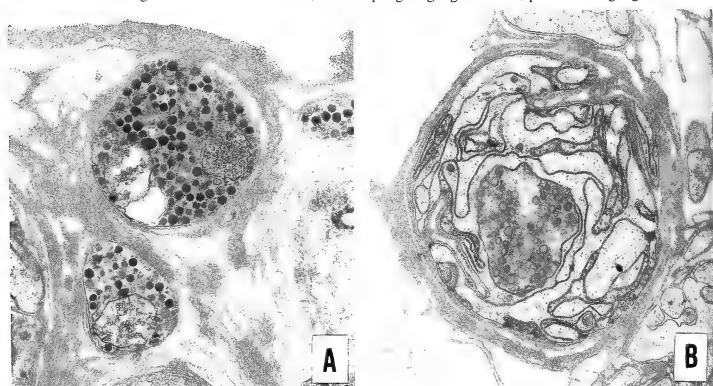


FIG. 4. Electron micrographs of the nerve N4. See text for the position of the sections. A: $\times 12000$. B: $\times 14000$.

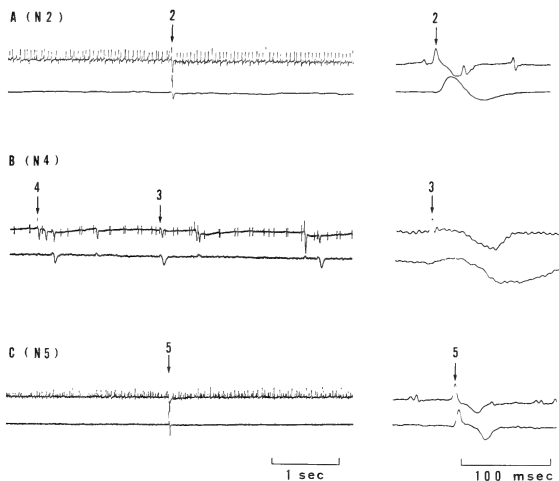


FIG. 5. Simultaneous recordings of the electrical activities at two different places on a single nerve tract to PTG. Efferent electrical activities observed in N2, N4 and N5 are shown in A, B and C respectively. In the nerve N2 or N4 (A, B) one of the pair of oil-gap electrodes was situated at the nearest region of the nerve to the ganglion (upper trace), and the other was at a thin nerve branch just before PTG (lower trace). The positions of two oil-gaps in each nerve (N2, N4) are labelled in Figure 2 as a2 or a4 and b2 or left b4 respectively. In the case of nerve N5 (C), two oil-gaps were situated at positions b5 (upper trace) and c5 (lower trace) in Figure 2. Faster sweep recordings are shown in each case, and amplitudes of potential were adjusted separately in each recording. The routes of impulse conduction of individual neurones indicated by each number are summarized in Figure 7.

tant to note here that the efferent activity in the thin nerves just in front of PTG was consistently of the slow neurosecretory type as is seen in the lower traces in each part of Figure 5. This figure also shows that all slow type activity arising in nerve N2 is conducted to PTG. In contrast, in nerve N4 some slow type activity arrives at the PTG (arrow 3) but, as well, some is conducted to an unknown target in the lateral part of the body (arrow 4).

Simultaneous recordings from the bilateral parts of nerves clearly showed the bilateral synchronization in the slow efferent activity in every type of PTG innervating neurone examined in this material.

It is important to note here that number of slow units recorded from nerves N2 and N4 and their bilateral synchronization fit well with the findings obtained from cobalt backfills (Fig. 2). Compari-

son of the results obtained from electrophysiological recordings with those of cobalt backfilling thus suggest that action potentials synchronous in both N2 all arise from the dorsomedial cell which innervates the PTG.

Determination of the course of innervation of the PTG from the suboesophageal ganglion was not successful, because the spontaneous activities of this nerve N1 were not usually observed in the isolated preparation.

Afferent activity arriving at the prothoracic ganglion was observed in nerves N2, N4 and N5 as shown in Figure 6. These afferent electrical activities were of the slow type and frequently showed a compound shape. In nerve N4, one type of afferent activity generated in PTG was recorded at the thin nerve from PTG (arrow 9 in B). Another type of afferent activity was generated at certain points

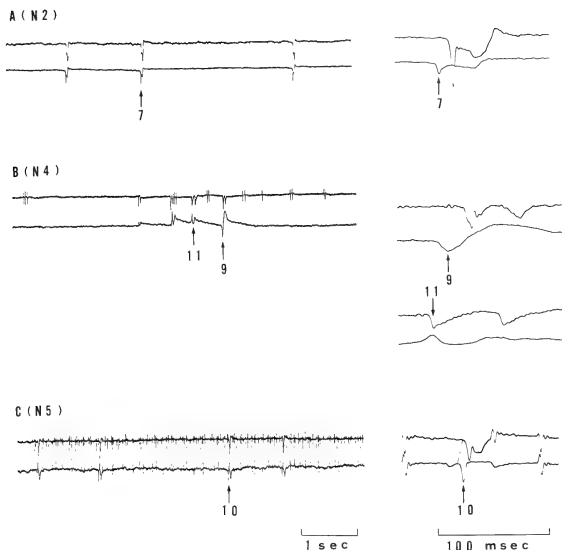


FIG. 6. Simultaneous recordings of the electrical activity at two different places of a single nerve tract to PTG. Afferent electrical activities observed in N2, N4 and N5 are shown A, B and C respectively. In the nerves N2 or N4 (A, B) one of the pair of oil-gap electrodes was situated at the nearest region of the nerve to the ganglion (upper trace), and the other was at thin nerve branch just before PTG (lower trace). The positions of two oil-gaps in each nerve (N2, N4) are labelled in Figure 2 as a-2 or a4 and b2 or right b4 respectively. In the case of nerve N5 (C), two oil-gaps were situated at positions a5 (upper trace) and b5 (lower trace). Recordings at two different sweep speed are shown in each case, and amplitudes of the potential were adjusted separately in each recording. The routes of conduction of individual neurones indicated by each number are summarized in Figure 7.

of the PTG nerve network (arrow 11 in B). We confirmed that the generation sites of afferent activities within the nerve network were localized to the specific regions of branching into two nerves by shifting the position of the oil-gap or cutting the nerve tract in various places. Every type of neuronal pathway described above (Figs. 1 and 6) is shown diagrammatically in Figure 7. Some other neurones identified by similar recordings are also shown in these figures (neurone number; 1, 6, 8).

Change in activity of PTG neurones during larval development

As described above the frontal part of the

ganglionic chain was isolated with both N4 nerves connected with PTG. The isolated preparation was placed in the oil-gap chamber so that the two N4 nerves crossed over the oil-gap. This chamber was placed in a gas mixture containing 95% O₂ and 5% CO₂. Temperature was adjusted to $23 \pm 1^\circ\text{C}$. In this condition, spontaneous electrical activity continued for over 24 hr. However recordings 1-2 hr after isolation proved best for following the marked change in nervous activity during the different stage of larval development. Saline composition, especially the amount of sugar, was also important as will be discussed later. The firing frequency of slow efferent activity was measured

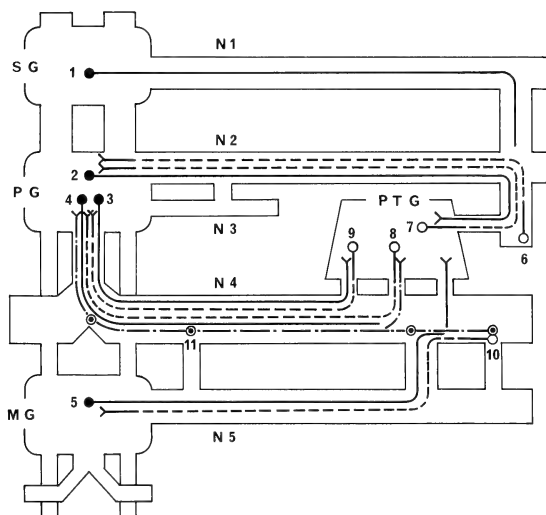


Fig. 7. Diagrammatically summarized representation of the neuronal pathways between the prothoracic gland and central ganglia. SG, subesophageal ganglion; PG, prothoracic ganglion; MG, mesothoracic ganglion; PTG, prothoracic gland. Generation site of efferent activity; ●, generation site of afferent activity; ○, routes of conduction of efferent activity; —, routes of conduction of afferent activity; ----, terminal region of neuronal conduction; —<, . Among afferent neurones, several neurones having generation sites within nerve N4 are shown together as a single dotted line (----) with four double circles (⊙). Numbers shown beside the generation sites of neuronal activities are those indicated by arrows in the recordings of Figures 5 and 6.

for 10 min at one hr after the isolation which was done at 6 ± 2 hr after the onset of light in LD16:8 and a typical result is shown in Figure 8. Although there is a large scatter in individual values, it can be clearly seen that the frequency of slow efferent activity declines with the progress of the larval development. Perceptible decrease in frequency was visible at day 3 and fell markedly by day 5, the stage of development where transparent ventral epidermis was visible. The frequency remained low for 3 days and finally the activity stopped at day 8 and 9.

The change in ecdysteroid titers during development, determined in this material by Agui and Hiruma [19] and by us as will be reported in the following paper shows a clear inverse relationship to the change of electrical activity of nerve N4 in

Figure 8. The one exception is day 9. This result strongly suggests that the activity of nerve N4 is inhibitory to the ecdysteroid synthesis or release at PTG.

DISCUSSION

Using electrophysiological techniques the present study has directly demonstrated the existence of various neuronal connections between prothoracic ganglion and PTG. The electrical activities of individual neurones could be determined separately by external electrodes in an oil-gap chamber. This could be done because the nerves innervating the PTG contain only a small number of neurones and these fire with extremely low frequency. Although exclusively spontaneous potential

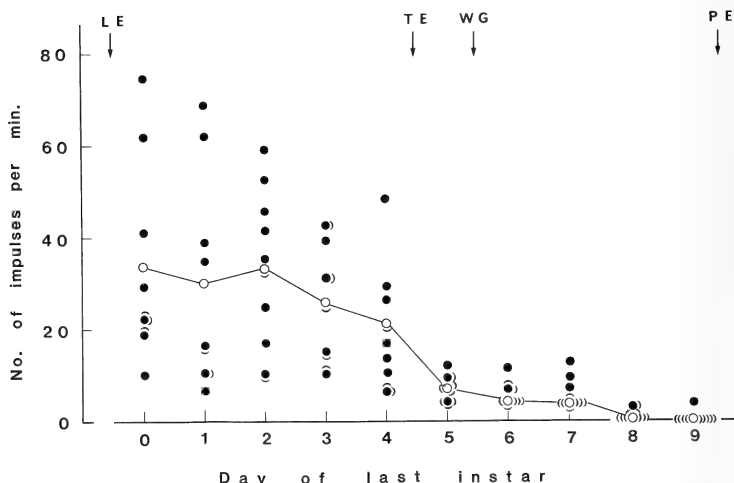


Fig. 8. Electrical activity of PTG nerve N4 at different stages of development in the last larval instar. Black circles show the individual values of determination (overlapping points are shown by semicircles) and white circle is a mean of these values. The following developmental stages are indicated; LE: Larval ecdysis, TE: Transparent ventral epidermis, WG: Wandering to the ground, PE: Pupal ecdysis.

changes were observed throughout the experiment, chemical stimulation of the ganglion by adding K-rich external medium did not reveal additional neurone units innervating PTG.

All PTG innervating neurones appear to be neurosecretory. Their electrical activities were of the slow type similar to the brain neurosecretory neurones and their axons contained the dense-core neurosecretory granules. Singh and Sehna [18] have suggested that of the dorsomedial cells in each thoracic ganglion of *Galleria mellonella*, one (group 12) could correspond to the unpaired medial neurone which has been shown to produce octopamine [20] and azan stainable ventrolateral cells (group 3) could be homologous to the bursicon producing cells described in *Manduca sexta* [21]. Taghert and Truman [22] showed that the dorsolateral, but not ventrolateral, bluish cells in the thoracic and ventral ganglia contained the bursicon like substances. However, because there are fairly large differences between both species in

terms of the number and orientation of the nerve cells within the ganglia and the map of the nerve tracts, the idea of Singh and Sehna [18] should not be disregarded.

As is clearly demonstrated in this study, the frequency of the spontaneous electrical activities of the nerve N4 shows an inverse relationship to the ecdysteroid titer during the course of the larval development. This result is opposite to that obtained in *Periplaneta americana* by Richter and Gersch [14]. The discrepancy could arise from the difference in insect order but also it is possible that the neurones concerned in both cases could be of different type and show the opposite performance. In fact, antagonistic dual regulation of PTG by two types of neurones has been proposed on the bases of the results obtained from surgical experiments [13].

We must be extremely careful in comparing the PTG regulation machinery established by using the isolated preparation with the real regulation

mechanisms in normal intact material. The reason is that saline used here for the external medium of isolated preparation was the same one without regard to the developmental stage of the animals. Composition of the haemolymph of lepidopterous insects has been described to alter significantly according to the larval development [23, 24]. And indeed the frequency of electrical activities of PTG innervating neurones has been known to change dramatically depending on the composition of the external medium. The important question is whether the changes of electrical activity during development are purely the outcome of the development of innate activity of the central nervous system or else the expression of an activity level resulting from changes in specific chemical condition of the haemolymph and preserved for some hours after the isolation in the saline. This is the main theme of further work concerned with the feedback mechanisms involving the afferent neurone activity which is generated by the influence of the specific chemical constituents in the external medium.

ACKNOWLEDGMENTS

We wish to thank Dr. N. Agui, the National Institute of Health, for his technical advice on rearing method and teaching published information on this field of study, and Dr. T. Goto, Mie University, for his kind help on electronmicroscope study. We wish to thank Dr. J. Kien, University of Regensburg, for critical reading of the manuscript.

REFERENCES

- Williams, C. M. (1948) Extrinsic control of morphogenesis as illustrated in the metamorphosis of insects. *Growth Symp.*, **12**: 61-74.
- Herman, W. S. and Gilbert, L. I. (1966) The neuroendocrine system of *Hyalophora cecropia* (L.) (Lepidoptera: Saturniidae). I. The anatomy and histology of the ecdysial glands. *Gen. Comp. Endocr.*, **7**: 275-291.
- Beauraton, J. (1968) Etude ultrastructurale et cytochimique des glandes prothoraciques de vers a soie aux quatrieme et ciquieme ages larvaires. II. Let cellules interstitielles et les fibres nerveuses. *J. Ultrastruct. Res.*, **23**: 499-515.
- Srivastava, K. P. and Singh, H. H. (1968) On the innervation of the prothoracic glands in *Papilio demoleus* L. (Lepidoptera). *Experientia*, **24**: 838-839.
- Singh, Y. N. (1975) The anatomy and innervation of the ecdysial glands of the mature larvae of cester silk moth, *Philosamia ricini* Hutt. *Experientia*, **31**: 40-42.
- Srivastava, K. P., Tiwari, R. K. and Kumar, P. (1977) Effect of sectioning of the prothoracic gland nerves in the larva of the lemon-butterfly, *Papilio demoleus* L. *Experientia*, **33**: 98-99.
- Hintze-Podufal, Ch. (1970) The innervation of the prothoracic glands of *Cerura vinula* L. (Lepidoptera). *Experientia*, **26**: 1269-1271.
- Gersch, M., Birkenbeil, H. and Ude, J. (1975) Ultrastructure of the prothoracic gland cells of the last instar of *Galleria mellonella* in relation to the rate of development. *Cell Tiss. Res.*, **160**: 389-397.
- Benedeczy, I., Mala, J. and Sehnal, F. (1980) Ultrastructural study on the innervation of prothoracic glands in *Galleria mellonella*. *Gen. Comp. Endocr.*, **41**: 400-407.
- Edwards, J. S. (1966) Neural control of metamorphosis in *Galleria mellonella* (Lepidoptera). *J. Insect Physiol.*, **12**: 1423-1433.
- Alexander, N. J. (1970) A regulatory mechanism of ecdysone release in *Galleria mellonella*. *J. Insect Physiol.*, **16**: 271-276.
- Mala, J., Granger, N. A. and Sehnal, F. (1977) Control of prothoracic gland activity in larvae of *Galleria mellonella*. *J. Insect Physiol.*, **23**: 309-316.
- Mala, J. and Sehnal, F. (1978) Role of the nerve cord in the control of prothoracic glands in *Galleria mellonella* L. *Experientia*, **39**: 1233-1235.
- Richter, K. and Gersch, M. (1983) Electrophysiological evidence of nervous involvement in the control of the prothoracic gland in *Periplaneta americana*. *Experientia*, **39**: 917-918.
- Agui, N., Ogura, N. and Okawara, M. (1975) Rearing of cabbage armyworm, *Mamestra brassicae* L. (Lepidoptera: Noctuidae) and some lepidopterous larvae on artificial diet. *Appl. Ent. Zool.*, **19**: 91-96.
- Jungreis, A. M., Jatlow, P. and Wyatt, G. R. (1973) Inorganic ion composition of haemolymph of the cecropia silkworm: Changes with diet and ontogeny. *J. Insect Physiol.*, **19**: 225-233.
- Bacon, J. and Altman, J. S. (1977) A silver intensification method for cobalt-filled neurones in whole mount preparations. *Brain Res.*, **138**: 359-363.
- Singh, H. H. and Sehnal, F. (1979) Lack of specific neurons in the ventral nerve cord for the control of prothoracic gland. *Experientia*, **35**: 1117-1119.
- Agui, N. and Hiruma, K. (1982) Ecdysteroid titer and its critical period during larval and pupal ecdysis in the cabbage armyworm, *Mamestra brassicae* L. (Lepidoptera: Noctuidae). *Appl. Ent. Zool.*, **17**: 144-146.

- 20 Evans, P. D. and O'Shea. (1977) An octopaminergic neurone modulates neuromuscular transmission in the locust. *Nature*, **270**: 257-259.
- 21 Truman, J. W. (1973) Physiology of insect ecdysis. III. Relationship between the hormonal control of eclosion and of tanning in the tobacco hornworm, *Manduca sexta*. *J. Exp. Biol.*, **58**: 821-829.
- 22 Taghert, P. H. and Truman, J. W. (1982) Identification of the bursicon-containing neurones in abdominal ganglia of the tobacco horn worm, *Manduca sexta*. *J. Exp. Biol.*, **98**: 385-401.
- 23 Wyatt, G. R. (1961) The biochemistry of insect hemolymph. *Ann. Rev. Entomol.*, **6**: 75-102.
- 24 Florkin, M. and Jeuniaux, C. (1974) Haemolymph: Composition. In "Physiology of Insecta, Vol. 5". Ed. by M. Rockstein, Academic Press, New York, pp. 255-307.

Flash-Induced Depression of the ERP under the Ca^{2+} -Free Condition in the Octopus Retina

KOHZOH OHTSU

*Ushimado Marine Laboratory, Okayama University,
Ushimada, Okayama 701-43, Japan*

ABSTRACT—Effects of Ca^{2+} on the octopus photoreceptor cells were investigated, taking advantage of the early receptor potential (ERP) closely concerned with conformation of the photoreceptor rhabdomeric membrane. In Ca^{2+} -free artificial sea water (ASW), the ERP evoked by the first test flash was normal but those by the following test flashes were almost depressed (flash-induced depression, FID). Recovery usually took 30–60 min in the dark, but was greatly enhanced within 5 min by an addition of Ca^{2+} of more than 5×10^{-4} M. If Na^+ , in addition to Ca^{2+} , was freed from the ASW after previously loading Ca^{2+} into the photoreceptor cells by irradiating with test flashes in Na^+ -free ASW, however, the FID was extremely weakened, suggesting weak (or almost no) Na-Ca exchange due to a lack of counter ion, Na^+ . Alkali earth metals, Sr^{2+} and Ba^{2+} could substitute for Ca^{2+} regarding the FID. Higher concentrations of Zn^{2+} could also prevent the retina from an FID, but even in normal ASW it strongly suppressed the late receptor potential (LRP), while Sr^{2+} and Ba^{2+} showed no particular inhibitory effect on the LRP. Imipramine (or decipramine), an antidepressant and N-ethyl maleimide, an SH-reagent, also strongly suppressed the LRP. Such agents, including Zn^{2+} , also abolished the FID under a Ca^{2+} -free condition, suggesting that there might be some common mechanisms between the FID and the LRP.

INTRODUCTION

The early receptor potential (ERP) is an electrical voltage due to charge displacement occurring within the visual pigment (VP) protein, when it absorbs photons and changes the conformation [1–3]. The generation mechanism is quite different from that of the late receptor potential (LRP) attributed to ion conductance changes of the photoreceptor membrane. The ERP is thus a physicochemical voltage and shows waveforms and polarities characteristic of various photoproducts of rhodopsin (R) [3, 4]. In the octopus, photon absorption of R produces a vitreous-side positive ERP and that of metarhodopsin (M), a vitreous-side negative ERP in the transretinal recording configuration [5, 6]. Furthermore, the amplitude of the ERP is linearly proportional to the photon number absorbed by the VP molecule, allowing rough estimation of the VP content existing in the

retina [7, 8].

Ca^{2+} has been suggested to play significant roles in visual excitation and adaptation processes [9–13]. In the course of experiments designed to investigate the roles of Ca^{2+} in the photoreceptor membrane, it was found that by lowering the external Ca^{2+} , ERP generation was drastically suppressed, following the first test flash which produced a normal ERP. Because of its physicochemical nature, an ERP can even be recorded in a fixed retina with formaldehyde or glutaraldehyde [1, 3, 14] and has so far been considered to be tolerant of changing ion composition in external bathing media. However, the ERP is an electrical event closely related to the structure of the microvillous membrane of the photoreceptor [1, 4, 15]. It is therefore suggested from the susceptibility of the retina to Ca^{2+} that the conformation of the photoreceptor membrane might be seriously affected by external Ca^{2+} . In this experiment, the effects of various divalent cations and some drugs on the ERP were further investigated to reveal the actions of Ca^{2+} in the functions of photoreceptor

membrane.

MATERIALS AND METHODS

The retina of *Octopus ocellatus* Gray was studied by recording the ERP transretinally. Animals were dark-adapted for more than 4 hr in an aerated container prior to the experiments.

The methods for electrical recording are described elsewhere [6]. Briefly, after removing the anterior half of the eye, the eye-cup preparation was pinned scleral-side down to a rubber sheet, through which a hole was made to allow insertion of an L-shaped glass tubing with an internal diameter of 3 mm. The glass tubing served as the recording electrode, through which slight suction was applied to secure electrical isolation. The indifferent electrode was placed on the vitreous side, out of the light path. Both electrodes consisted of chlorided silver plates and were light-shielded by black lacquer. Electrical responses were amplified via a DC/AC-coupled preamplifier and finally displayed on an oscilloscope with the vitreous-side positive deflection being upward.

Test solutions were circulated through the experimental chamber making use of the floating force of air bubbles supplied from an air pump via a cooling unit which kept the temperature at 10°C. The pH values were adjusted by either NaHCO₃ 6 mM or Tris-buffer (30 mM) to 7.7–8.2.

To evoke the ERP and LRP, a violet or an orange flash was derived from a strobe and passed through a heat-absorbing filter and then a wide-band spectral filter (Toshiba V-DIB), $\lambda_{\text{max}}=396$ nm, half-band width=75 nm or VO-57, >570 nm). The violet and orange flashes were exclusively used to generate vitreous-positive ERP due to R and vitreous-negative ERP due to M [5, 6]. Unless otherwise stated, the violet flash was used.

Monochromatic lights supplied from a grating-type monochromator equipped with xenon arc lamp (2kW) were admitted to the retina at a slightly oblique angle and used for adaptive irradiation or photoconversion of R to M.

RESULTS

Amplitudes of ERPs in normal artificial sea

water (ASW) hardly changed throughout the experiment, except at extremely early or late stages of experiment. The ERP, in response to the first test flash, is slightly attenuated in its peak by the LRP rising subsequent to its onset with reversed polarity (Fig. 1A left). Upon the second flash shortly after the first one, the ERP reveals its peak because of a prolonged latency of the LRP due to light adaptation (Fig. 1A, right). The peak of ERP becomes attenuated again in parallel with the recovery of the LRP as dark adaptation proceeds (Fig. 1B, C).

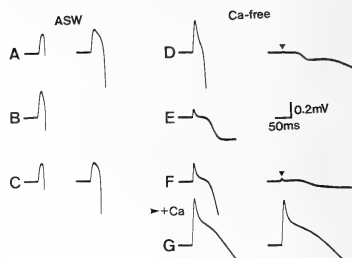


FIG. 1. ERPs in normal ASW and Ca²⁺-free ASW.

The ERPs were evoked by paired violet test flashes spaced 30 sec except B and E, where single test flashes were used. (left column) A: ERPs after 30 min incubation in ASW. B: an ERP 5 min after A. C: ERPs 30 min after B. (right column) D: ERP with striking FID 45 min after incubation in Ca²⁺-free ASW. E, F: 10 min (E) and 40 min (F) after D. Note slow recovery of the ERPs in the dark. G: ERPs without FID 15 min after an addition of CaCl₂ (10 mM). The retinæ were kept dark for inter-flash intervals in this Figure and in the following Figures.

In Ca²⁺-free ASW, the ERP in response to the first test flash is normal (Fig. 1D, left) but that to the second test flash is almost absent (Fig. 1D, right). This phenomenon occurred at Ca²⁺ concentration less than 10⁻⁴ M and will be called hereafter flash-induced depression (FID). The ERPs recover very slowly in the dark (Fig. 1E, F) but the response to the second flash is still depressed (Fig. 1F right). Usually it takes about an hour for full recovery without an addition of EGTA (1 mM). If EGTA was added to chelate the Ca²⁺,

recovery was often incomplete. However, recovery is greatly enhanced by an addition of CaCl_2 more than 5×10^{-4} M, resulting in no further FID (Fig. 1G). Almost complete recovery was usually attained within 5 min, probably the time when Ca^{2+} could penetrate the rhabdomeric layer.

The FID does not occur quite instantaneously after the first flash but it takes more than 30 msec to be completely depressed. In the ERPs evoked by paired flashes, responses to the second flashes become obviously smaller after 30 msec and abolished after 100 msec (Fig. 2A-B).

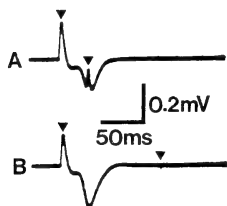


Fig. 2. ERPs (arrow heads) evoked by paired flashes spaced 30 msec (A) and 100 msec (B). The LRP is partially suppressed by gaseous CO_2 (deficient O_2) and further attenuated here by extremely short time constant of the amplifier system to reveal the ERPs in response to the second flashes.

As described above, an ERP is direct result of the conformation change occurring during photoconversion of the VP molecule. If the ability for photoconversion were damaged through the irradiation in Ca^{2+} -free ASW, depression of the ERP could occur. This possibility, however, is excluded in view of the results in Figure 3.

Paired violet flashes spaced 30 sec in Ca^{2+} -free ASW similarly induce FID (Fig. 3A). An orange test flash evokes only a residual amplitude of the ERP (Fig. 3B), indicating no appreciable amount of M photoconverted from R by the preceding paired flashes. After irradiation with monochromatic light of 470 nm which converts a bulk of R to M, the ERPs induced by orange test flashes, although residual, reverse their polarity (Fig. 3C). If the depression is released by an addition of CaCl_2 , vitreous-negative and positive

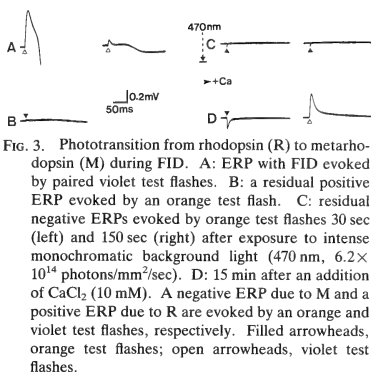


Fig. 3. Phototransition from rhodopsin (R) to metarhodopsin (M) during FID. A: ERP with FID evoked by paired violet test flashes. B: a residual positive ERP evoked by an orange test flash. C: residual negative ERPs evoked by orange test flashes 30 sec (left) and 150 sec (right) after exposure to intense monochromatic background light (470 nm, 6.2×10^{14} photons/mm²/sec). D: 15 min after an addition of CaCl_2 (10 mM). A negative ERP due to M and a positive ERP due to R are evoked by an orange and violet test flashes, respectively. Filled arrowheads, orange test flashes; open arrowheads, violet test flashes.

ERP originating in M and R appear in response to orange and violet test flashes, respectively (Fig. 3D). These results clearly show that even in the period of the FID with almost no ERP, photoconversion between R and M can be achieved and also that the conformation of the VP molecule is well preserved. The mechanism for FID cannot therefore be attributed to loss of the VP conformation.

An FID is induced normally even if the retina is subjected to paired flashes in Na^+ -free ASW and then transferred into Ca^{2+} -free ASW (Fig. 4A, B). If the retina is immersed in not only Ca^{2+} - but Na^+ -free ASW after being submitted to the same flashes in the same solution described above, however, almost no FID and an incomplete FID are observed 15 min and 30 min after the immersion, respectively (Fig. 4C-E). A similar result was obtained without the paired flashes when Ca^{2+} -ionophore (A23187, 50 μM) was added to Na^+ -free ASW, indicating loading of Ca^{2+} into the photoreceptor cells by the paired flashes in Na^+ -free ASW. On the other hand, immersing the retina directly in $\text{Na}^+/\text{Ca}^{2+}$ -free ASW without incubation in Na^+ -free ASW and paired flashes results in a transient FID which recovers within a few minutes (Fig. 4F, G). Prolonged incubation in the same solution again resulted in a transient FID. Thus, a divalent cation, Ca^{2+} , seems to play a significant role in stabilizing the ERP.

Another divalent cation, Zn^{2+} exerts somewhat

different effects from Ca^{2+} (Fig. 5). The ERP appears normal in ASW containing 1 mM of ZnCl_2 (Zn-ASW) (Fig. 5A). After irradiation with a monochromatic wavelength of light (600 nm) and then changing the bathing solution from Zn-ASW to Ca^{2+} -free ASW containing ZnCl_2 (Ca-free/Zn-

ASW), however, only a very weak FID occurs even after considerable incubation in the second solution (Fig. 5B, C). An addition of CaCl_2 completely diminishes the FID (Fig. 5D). If paired test flashes and monochromatic irradiation are omitted, however, an FID occurs in the following

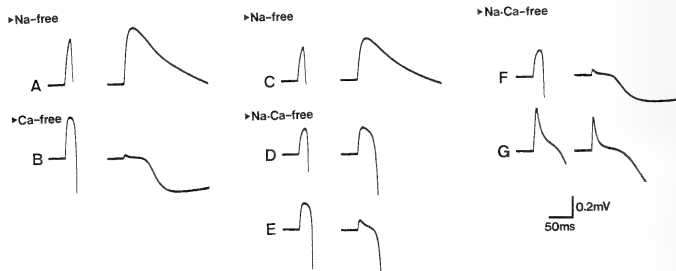


FIG. 4. FIDs in Ca^{2+} -free ASW and $\text{Na}^+/\text{Ca}^{2+}$ -free ASW. (left column) A: ERPs evoked by paired flashes 60 min after incubation in Na^+ -free ASW. B: ERPs with striking FID 15 min after changing Na^+ -free ASW for Ca^{2+} -free ASW. (middle column) C: ERPs in the same situation as A. D: ERPs without detectable FID 15 min after changing Na^+ -free ASW for $\text{Na}^+/\text{Ca}^{2+}$ -free ASW. E: ERPs with partially developed FID after 30 min incubation in $\text{Na}^+/\text{Ca}^{2+}$ -free ASW. A lack of Na^+ in the second solution results in incomplete FID. (right column) F: ERPs with transient FID after 60 min in $\text{Na}^+/\text{Ca}^{2+}$ -free ASW. G: ERPs 3 min after F. The ERPs recover from FID within a few minutes.

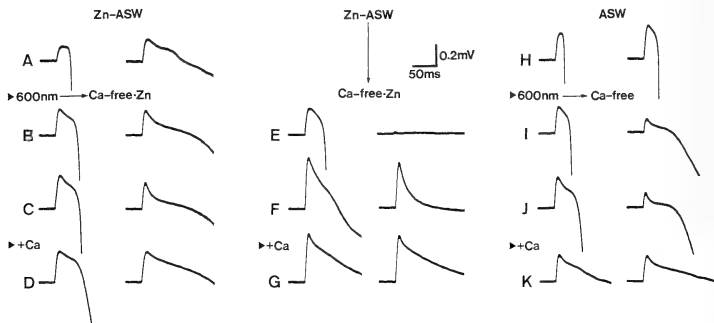


FIG. 5. Effects of Zn^{2+} on FID. The ERPs were evoked by paired flashes spaced 30 sec. (left column) A: ERPs in ASW containing 1 mM ZnCl_2 (Zn-ASW). After recording A, the solution was changed within 3 min for Ca^{2+} -free ASW containing 1 mM ZnCl_2 (Ca-free/Zn) following 60 sec irradiation with 600 nm monochromatic light (2.9×10^{14} photons/mm²/sec). B, C: ERPs without detectable FID 20 min (B) and 35 min (C) after changing the solution. D: ERPs after an addition of CaCl_2 (10 mM). (middle column) The retina was incubated in Zn-ASW for 20 min without test flashes and irradiation with the 600 nm light and then the solution was changed for Ca^{2+} -free/Zn. E: ERPs with striking FID 20 min after changing the solution. F: Recovered ERPs from the FID 35 min after changing the solution. G: ERPs with no FID after an addition of CaCl_2 (10 mM). (right column) Recording situation, same as the left column but with no added ZnCl_2 . For explanation, see text.

Ca-free/Zn-ASW (Fig. 5E) but recovers within a few minutes (Fig. 5F). In the same series of experiments as the left column in Figure 5 but with no added Zn^{2+} , the FID also occurs, although the reduction rates are much smaller (Fig. 5H-K). The smaller reduction was generally the case, for which exhaustive irradiation was performed.

Among other divalent cations tested, alkali earth metals, Sr^{2+} and Ba^{2+} can prevent the retina from the FID while Co^{2+} cannot (Fig. 6A-C). In higher concentrations, Zn^{2+} has an effect similar to that of Sr^{2+} and Ba^{2+} (Fig. 6D), being somewhat different from the result in Figure 5 (E-G), where an FID, although transiently, occurred. However, Zn^{2+} , as can be seen from strikingly prolonged latency of the negative-going LRP in Figure 6D, strongly suppresses the LRP, while Sr^{2+} and Ba^{2+} added in normal ASW did not seem to have any inhibitory effect. A notch denoted by an arrow head (Fig. 6D) was probably a part of an LRP and was frequently observed in conditions where the LRP was strongly suppressed. The generation mechanism is as yet unknown.

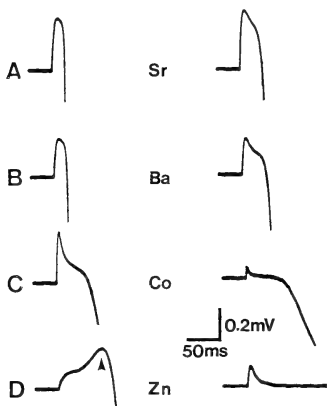


FIG. 6. Effects of some other divalent cations on the ERPs. Responses were evoked by paired test flashes spaced 30 sec. A: 10 mM SrCl_2 in ASW. B: 10 mM BaCl_2 in ASW. C: 10 mM CoCl_2 in ASW. D: 4 mM ZnCl_2 in ASW. Arrowhead in D, a part of LRP. For explanation, see text.

Imipramine and decipramine which are suggested to be ATPase and calmodulin inhibitors [16], could abolish the FID under the Ca^{2+} -free condition (Fig. 7A, B) and also inhibit the LRP strongly in normal ASW, as does Zn^{2+} (Fig. 7C, D). A more specific calmodulin inhibitor, N-(6-aminohexyl)-5-chloro-1-naphthalenesulfonamide (W7) [17], however, was not effective as imipramine, decipramine and Zn^{2+} on the FID and LRP (data, not shown), suggesting no direct involvement of calmodulin in the FID and LRP.

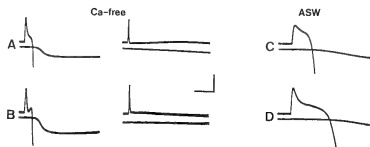


FIG. 7. Effects of imipramine and decipramine on the FID. Upper traces, high gain recordings of the ERPs; lower traces, low gain recordings showing waveforms of the LRPs. A, B: ERPs and LRPs evoked by paired test flashes in Ca^{2+} -free ASW containing 5×10^{-4} M imipramine (A) or decipramine (B). No FID is observed in A and B. C, D: ERPs and LRPs in normal ASW containing 1 mM imipramine (C) or decipramine (D). Note strongly suppressed LRPs. Calibration: 125 msec in A and B, 50 msec in C and D; 0.2 mV in upper traces of A-D, 20 mV in lower traces of A-C and 10 mV in a lower trace of D.

DISCUSSION

Generation of the FID in the Ca^{2+} -free condition was quite unexpected because of its physicochemical nature. However, the ERP generation seriously depends on the arrangement and orientation of the VP molecule in the rhabdomeric membrane [4]. If the retina is warmed up to 60°C and then cooled down to room temperature, the ERP can no longer be recorded due to disarrangement of the VP molecule spanning across the photoreceptor membrane [18]. If the VP molecule is dislodged from the rhabdomeric membrane, they can no longer contribute to the ERP recorded by conventional methods [15]. This could be one of possible reasons for FID.

Other possible reasons for ERP regression are

as follows. (1) The VP molecule is broken down by a strong flash under the Ca^{2+} -free condition and thus the function is lost. (2) Membrane resistance around the VP molecule is extremely reduced so that the ERP current is almost shunted down, resulting in a residual ERP in the transretinal recording configuration. The first possibility is easily excluded because of the facts described in Figure 3, wherein photoconversion from R to M, the most principal nature of VP is preserved in the Ca^{2+} -free condition. However, there seems to be no choice regarding other possibilities as yet. Further study should be performed to take any of them or other possible explanations. It is at least concluded that Ca^{2+} is necessary for preservation of the ERP.

An FID could be induced at concentrations of less than 10^{-4} M of Ca^{2+} , but under such concentrations of Ca^{2+} , the ERP evoked by the first test flash was normal. In the resting stage, intracellular concentration of Ca^{2+} is kept extremely low about 10^{-6} – 10^{-7} M, much lower than 10^{-4} M [13, 19]. It follows from a series of facts, especially those in Figures 1 and 4, that the FID might occur because the needs for intracellular Ca^{2+} induced following the first flash were not fulfilled by the Ca^{2+} which could flow into the photoreceptor cells if the retina were in normal ASW.

As illustrated in Figure 4, striking differences were found between perfusions with Na^+ -free ASW and $\text{Na}^+/\text{Ca}^{2+}$ -free ASW after the same treatment. This is best interpreted in view of Na-Ca exchange reported in both vertebrate [10, 20, 21] and invertebrate [9, 22] photoreceptors. According to Takagi (personal communication) ion channels of the octopus photoreceptors are cation channels. The Ca^{2+} should therefore flow into the photoreceptor cells by the paired flashes given in Na^+ -free ASW. If, thereafter, the retina is transferred to Ca^{2+} -free ASW, Ca^{2+} loaded intracellularly is probably pumped out by active Na-Ca exchange, so FID occurs. However, if the retina is transferred to $\text{Na}^+/\text{Ca}^{2+}$ -free ASW, instead of Ca^{2+} -free ASW (Fig. 4, middle column), Ca^{2+} cannot be pumped out because of a lack of its counter ion, Na^+ . If the retina is immersed directly into $\text{Na}^+/\text{Ca}^{2+}$ -free ASW without previously being subjected to test flashes in Na^+ -free

ASW (Fig. 4, left column), a FID occurs probably because of the lack of previous loading of Ca^{2+} but recovers within several minutes, probably because of weak (or nearly absent) Na-Ca exchange and following Ca^{2+} -release from the intracellular Ca^{2+} -store as suggested in *Limulus* ventral photoreceptors [23]. It thus appears likely that Ca^{2+} flows into the photoreceptors through the channels opened following light exposure and functions inside the cells.

Effects of Zn^{2+} (Fig. 5) are also well interpreted by the Na-Ca exchange mechanism. The Zn^{2+} probably intrudes the cells through channels opened by the paired flashes and the 600 nm irradiation in Zn-ASW (Fig. 5). Inside the cells, two possible functions of Zn^{2+} are considered, i.e., Zn^{2+} might play the role of Ca^{2+} or alternatively suppress pumping out of Ca^{2+} by inhibiting Ca-ATPase [24, 25], both resulting in prevention of the retina from FID. On the other hand, it seems that Sr^{2+} and Ba^{2+} simply substitute for Ca^{2+} because they showed no special inhibitory effect on the LRP in the normal ASW.

It is very interesting that such agents as formaldehyde, glutaraldehyde, N-ethyl (or methyl) maleimide, decipramine, imipramine, gaseous CO_2 (deficient O_2) and Zn^{2+} which strongly inhibit or completely abolish an LRP, could also abolish an FID. Except for the former two, the others are relatively mild agents and not considered to be lethal to living cells, e.g., Zn^{2+} , imipramine and decipramine are ATPase inhibitors and N-ethyl (or methyl) maleimide is an SH reagent which could inhibit various enzymatic activities. Gaseous CO_2 could inhibit biological activities by suppressing metabolism. It is therefore inferred from the parallel between the FID and LRP that FID generation might be attributed to a biological cascade somewhat similar to the mechanism generating the LRP. The fact that an FID takes 30 msec or more to occur (Fig. 2) indicates not a physicochemical but a biological nature of the mechanism for the FID. The exact mechanism by which the FID is generated, however, remains to be determined.

The series of evidences described above, might suggest an internal release of Ca^{2+} from the rhabdomeric membrane. In ASW with a millimo-

lar concentration of Ca^{2+} , however, released Ca^{2+} is rapidly recombined inside the membrane forced by an internal increase of Ca^{2+} intruding the photoreceptor cells from the extracellular space following test stimuli, resulting in no FID. It thus appears likely that Ca^{2+} functions to keep the conformation of the rhabdomeric membrane, which generates the ERP and LRP.

ACKNOWLEDGMENTS

This work was supported in part by a Grant-in-Aid for Scientific Research (No. 62304008) from the Ministry of Education, Science and Culture of Japan.

REFERENCES

- Brindley, G. S. and Gardner-Medwin, A. R. (1966) The origin of the early receptor potential of the retina. *J. Physiol.*, **182**: 185-194.
- Cone, R. A. (1967) Early receptor potential: photo-reversible charge displacement in rhodopsin. *Science*, **155**: 1128-1131.
- Hagins, W. A. and McGaughy, R. E. (1967) Molecular and thermal origins of fast photoelectric effects in the squid retina. *Science*, **157**: 813-816.
- Cone, R. A. and Pak, W. L. (1971) The early receptor potential. In "Handbook of Sensory Physiology". Ed. by W. R. Loewenstein, Springer-Verlag, Berlin, pp. 345-365.
- Tsukahara, Y. and Tasaki, K. (1972) Dark recovery of ERP in isolated octopus retina. *Tohoku J. Exp. Med.*, **108**: 97-98.
- Ohtsu, K. and Kito, Y. (1985) A photoproduct with 13-cis retinal generated by irradiation with violet light in the octopus retina. *Vision Res.*, **25**: 775-779.
- Cone, R. A. (1964) Early receptor potential of the vertebrate retina. *Nature*, **204**: 736-739.
- Cone, R. A. and Cobbs, W. H. (1969) Rhodopsin cycle in the living eye of the rat. *Nature*, **221**: 820-822.
- Lisman, J. E. and Brown, J. E. (1972) The effects of intracellular iontophoretic injection of calcium and sodium ions on the light response of *Limulus* ventral photoreceptors. *J. Gen. Physiol.*, **59**: 701-719.
- Bader, C. R., Baumann, F. and Bertrand, D. (1976) Role of intracellular calcium and sodium in light adaptation in the retina of the honey bee drone (*Apis mellifera*, L.). *J. Gen. Physiol.*, **67**: 475-491.
- Hermolin, J., Karell, M. A., Hamm, H. E. and Bownds, M. D. (1982) Calcium and cyclic GMP regulation of light-sensitive protein phosphorylation in frog photoreceptor membranes. *J. Gen. Physiol.*, **79**: 633-655.
- Bolsover, S. R. and Brown, J. E. (1985) Calcium ion, an intracellular messenger of light adaptation, also participates in excitation of *Limulus* Photoreceptors. *J. Physiol.*, **364**: 381-393.
- Levy, S. and Fein, A. (1985) Relationship between light sensitivity and intracellular free Ca concentration in *Limulus* ventral photoreceptors: a quantitative study using Ca-selective microelectrodes. *J. Gen. Physiol.*, **85**: 805-841.
- Arden, G. B., Bridges, C. D. B., Ikeda, H. and Siegel, I. M. (1968) Mode of generation of the early receptor potential. *Vision Res.*, **8**: 3-24.
- Hagins, W. A. and McGaughy, R. E. (1968) Membrane origin of the fast photovoltage of squid retina. *Science*, **159**: 213-215.
- Lavoie, P.-A. and Tiberi, M. (1986) Inhibition of fast axonal transport in bullfrog nerves by dibenzazepine and dibenzocycloheptadiene calmodulin inhibitors. *J. Neurobiol.*, **17**: 681-695.
- Tanaka, T., Ohmura, T. and Hidaka, H. (1982) Hydrophobic interaction of the Ca^{2+} -calmodulin complex with calmodulin antagonists: naphthalene-sulfonamide derivatives. *Mol. Pharmacol.*, **22**: 403-407.
- Cone, R. A. and Brown, P. K. (1967) Dependence of the early receptor potential on the orientation of rhodopsin. *Science*, **156**: 536.
- MuNaughton, P. A., Cervetto, L. and Nunn, B. J. (1986) Measurement of the intracellular free calcium concentration in salamander rods. *Nature*, **322**: 261-263.
- Yau, K.-W. and Nakatani, K. (1984) Electrogenic Na-Ca exchange in retinal rod outer segment. *Nature*, **311**: 661-663.
- Hodgkin, A. L., MuNaughton, P. A. and Nunn, B. J. (1987) Measurement of sodium-calcium exchange in salamander rods. *J. Physiol.*, **391**: 347-370.
- Minke, B. and Tsacopoulos, M. (1986) Light induced sodium dependent accumulation of calcium and potassium in the extracellular space of bee retina. *Vision Res.*, **26**: 679-690.
- Brown, J. E. and Blinks, J. R. (1974) Changes in intracellular free calcium concentration during illumination of invertebrate photoreceptors: detection with aequorin. *J. Gen. Physiol.*, **64**: 643-665.
- Bettger, W. J. and O'Dell, B. L. (1981) A critical physiological role of zinc in the structure and function of biomembranes. *Life Sci.*, **28**: 1425-1438.
- Brewer, G. J., Aster, J. C., Knutsen, C. A. and Kruckeberg, W. C. (1979) Zinc inhibition of calmodulin: a proposed molecular mechanism of zinc action on cellular functions. *Amer. J. Hematol.*, **7**: 53-60.



Mechanisms of Skin Coloration and Its Changes in the Blue-Green Damselfish, *Chromis viridis*

RYOZO FUJII, HIROAKI KASUKAWA¹, KAZUYUKI MIYAJI,
and NORIKO OSHIMA²

Department of Biology, Faculty of Science,
Toho University, Funabashi 274, Japan

ABSTRACT—Mechanism of light reflection from the skin of the blue-green damselfish, *Chromis viridis*, was investigated. A chromatophore unit, consisting of a melanophore, a number of iridophores, and, if present, a few xanthophores in this order from the bottom to the top was found in the dermis. The iridophores could be categorized into motile and non-motile types. The former iridophores usually assumed a blue or greenish color, while the latter did yellowish tints mainly. The motile and non-motile iridophores were found to be assembled above the cell body and the surrounding dendrite zone, respectively, of the melanophore. The greenish hue of the skin was thus shown to be due to a mixed effect of various colors from different areas. Role of xanthophores or melanophores in producing delicate skin hues was also explained.

INTRODUCTION

Chromatophores are predominantly responsible for the skin coloration in fishes [1, 2]. Among chromatophore sorts, the iridophores are known to function to reflect or scatter incident light to produce brighter tone of the integument. Silvery or metallic tone seen in many species has adequately been explained by the presence of such cells [3, 4]. Usually, stacks of parallel reflecting platelets with a high refractive index are present in the iridophores. More frequently, those platelets were found to exist almost parallel to the surface of the skin [5, 6]. The platelets in the cell had almost the same thickness, and the distance between adjacent platelets was also uniform. When the optical thickness of the platelets and that of the cytoplasm intervening adjacent platelets were practically the same, the light reflection became so efficient that the phenomenon has been explained as the result of multilayered thin-film interference of the ideal type. Above-mentioned metallic glit-

ters are the good examples.

Recently, on the other hand, iridophores of a different type were found, in which the reflecting platelets were very thin and the reflection occurred as a results of non-ideal multilayer interference. Net reflectance was rather low. However, "purer" color, namely the higher "chroma" in terms of the Munsell color system, can be produced. Thus, the characteristic hue of the blue damselfish, *Chrysiptera cyanea*, could properly be explained by such a phenomenon [7, 8].

Iridophores have long been thought to be physiologically inactive, i.e. being without motility. Recently, however, "motile" iridophores have been reported to exist in few fish species. The materials were the neon tetra, *Paracheirodon innesi*, [9], the blue damselfish, *Chrysiptera cyanea*, [7, 10], and the freshwater goby, *Obontobutis obscura*, [11]. The motile iridophores of the latter species were dendritic, in which small reflecting platelets aggregated or dispersed in response to certain stimuli. Thus, they resembled the leucophores very well. In the blue damselfish, on the other hand, the iridophores were of the round type, and played an active role not only in the manifestation of the brilliant cobalt-blue coloration, but also in the color changes [8]. The color

Accepted August 3, 1988

Received June 23, 1988

¹ Present address: Terumo Corp., Shibuyaku, Tokyo 151, Japan.

² To whom reprint requests should be addressed.

changes in the damselfish were due to the continuous shift of spectral peak of reflected light from the cells, caused by the parallel increase or decrease in the distance between the platelets.

Quite recently, in the scalychick damselfish (*Pomacentrus lepidogenys*), which manifested normally a greenish tone, we found two types of iridophores: cells assuming the analogous configuration with those in the blue damselfish, and dendritic ones [12]. The greenish tone of the skin has been shown to be resulted from the mixed effects of different colors displayed by the two types of iridophores. Since both types of iridophores were non-motile, the melanophore motility may play a primary role in the physiological color changes of this fish species.

The blue green damselfish, *Chromis viridis*, usually assume greenish tone, but change their hue to a certain degree under various conditions. In the present study, therefore, we have tried to know the mechanisms by which their colors are generated and how the color can be changed.

MATERIALS AND METHODS

The blue-green damselfish, *Chromis viridis*, (synonym: *C. caeruleus*; "deba-suzumedei" in Japanese name) was used. This species is widely distributed from Amamioshima to the Western Pacific. They dwell in shallow lagoons. Youngs inhabit in the vicinity of live branching corals, and adult forms tend to form larger schools near the sea surface.

Pieces of dorsal fin from an adult fish having body lengths between 30 and 60 mm were excised in a physiological solution of the following composition (mM): NaCl 125.3, KCl 2.7, CaCl₂ 1.8, MgCl₂ 1.8, D-glucose 5.6, Tris-HCl buffer 5.0 (pH 7.2). Split fin preparations were prepared according to the method originally described by Fujii [12].

In order to measure the spectrum of reflected light from an excised live skin piece, the Spectro-Multichannel Photo-Detector System (MCPD-100, Otsuka Electronics, Osaka) was employed. Being equipped with a quartz fiber-optics and a halogen lamp as a light source, this apparatus enables us to measure almost instantaneously the

spectral reflectance from 350 to 800 nm [8]. The area subjected for measurement was about 1 mm², and the sampling time was set to be 500 msec.

In addition to the spectral reflectance characteristics of a live material, those of an individual iridophore on an enlarged photographic color print was also examined. Color films of the reversal type (Ektachrome 100, Eastman Kodak, Rochester, N.Y.) were used, and the prints at a final magnification of 250 processed by a local photographic laboratory were employed. An area of about 1.5 mm², i.e. a little smaller than that occupied by an iridophore, was measured at a sampling time of 800 msec.

In order to study the osmotic effects on the spectral reflectance characteristics of the iridophores, bathing media having various osmolarities were used. Such a solution was prepared by increasing or decreasing the NaCl concentration in the primary saline (125.3 mM) to 170, 150, 100 or 80 mM. In these solutions, the concentrations of components other than NaCl were left unchanged.

The drugs used were norepinephrine hydrochloride (Sankyo, Tokyo), isoproterenol hydrochloride (Nikken Chemicals, Tokyo) and isoxsuprine hydrochloride (Daiichi Seiyaku, Tokyo). A precise description on the mechanism by which these substances act on the chromatophores of this species will be put forward elsewhere in conjunction with the nervous and endocrine regulation of the cells (Oshima *et al.*, to be published).

In some experiments, K⁺-rich saline was used to stimulate chromatonic nerves to release adrenergic neuro-transmitter [13]. For this purpose, a saline containing 50 mM K⁺ was used, in which the Na⁺ concentration was compensatorily decreased.

All the experiments were performed at room temperature between 20 and 25°C.

RESULTS

Dermal chromatophore unit

By the conventional transmission light microscopy, melanophores and xanthophores were easily observable (Fig. 1D-F). In addition, a number of small iridophores were clearly recognizable by an incident light illumination (Fig. 1A-C). All

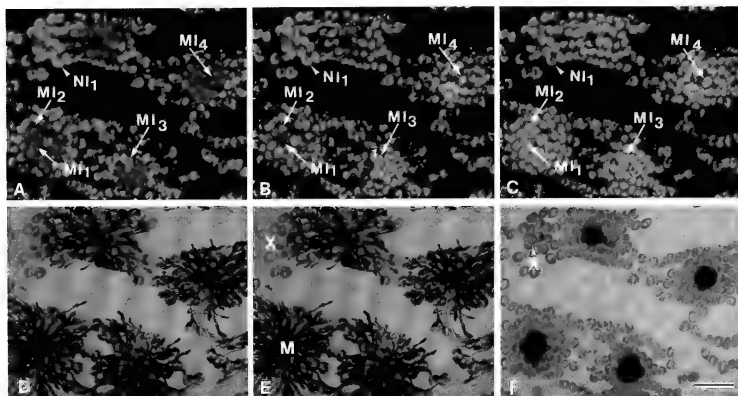


FIG. 1. Photomicrographs of three kinds of chromatophores constituting chromatophore units in the dermis of the blue-green damselfish, *Chromis viridis*. All photographs were taken on the same field on a split dorsal-fin piece. The responses of light-reflecting chromatophores (iridophores) were examined under dark-field epi-illumination (A, B and C), while those of the light-absorbing chromatophores (melanophores and xanthophores) were followed by the transmission optics (D, E and F). A and D: 5 min after the application of 5×10^{-6} M isoproterenol. B and E: Equilibrated in physiological saline. C and F: 5 min after the application of 5×10^{-6} M norepinephrine. Motile iridophores were classified into four subtypes (MI₁-MI₄) according to the ranges of the spectral peak shift inducible by alpha and/or beta adrenergic stimuli. Iridophores of the non-motile type are categorized into two subtypes (NI₁ and NI₂) according to the position of spectral reflectance peaks. NI₁: Non-motile iridophores reflecting yellowish rays. The non-motile iridophores showing greenish color (NI₂) are not included in this series of photomicrographs. For details of the classification of the iridophores, see text and Table 1. M: melanophore. X: xanthophore. A xanthophore in which the yellow pigment was maximally dispersed or aggregated, was seen in E or F, respectively. Scale bar: 50 μ m.

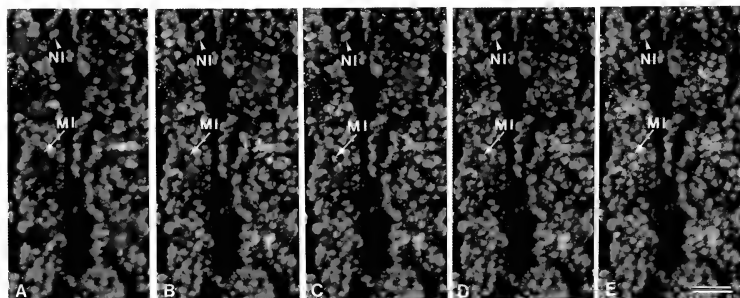


FIG. 2. Photomicrographs showing five states of iridophores in the same microscopic field under different osmotic conditions. An arrow-head and an arrow in each print indicate representatively an iridophore of the non-motile type (NI) and that of the motile type (MI), respectively. A and B: 5 min after equilibration in hypertonic saline of 371.8 mOsm (A) and 331.8 mOsm (B), respectively. C: Equilibrated in normal physiological saline (282.4 mOsm). D and E: 5 min after equilibration in hypotonic saline of 231.8 mOsm (D) and 191.8 mOsm (E), respectively. Scale bar: 50 μ m.

these chromatophores constituting the chromatophore unit were present in the dermis.

Melanophores having overall diameters from 100 to 150 μm were distributed in a layer deeper than other chromatophores. Like in the blue damselfish, *Chrysiptera cyanea* [8], peripheral halves of their cellular processes were commonly inserted into the space among iridophores.

Being present in a layer just above the layer of the melanophore, iridophores were found mostly in groups within rather restricted areas of the integument, i.e., the areas approximately overlying the melanophores. According to their physiological properties, the iridophores were first categorized into two types, i.e. the motile and non-motile iridophores. The former ones were responsive to adrenergic stimulants by changing their light-reflecting characteristics, while the latter were not. It was found that the motile iridophores were predominantly localized above the cell body of the melanophore. Surrounding the islet of the motile cells, on the other hand, the non-motile iridophores were found to exist on the area where dendritic processes of the melanophore developed (Fig. 1).

About 30 motile cells occupied a circular area having diameter of about 70 μm . Such assemblages distributed at intervals of about 150 μm , forming a polka-dotted blueish pattern against yellowish background. The motile cells accounted for about 60% of the total iridophores (Figs. 1 and 2). In spite of the apparent difference in physiological properties, morphological features of both types of iridophores were quite similar even at the fine structural levels: Being round or somewhat ellipsoidal, the cell of either type contained a nucleus located in its apical part, from where several piles of the light-reflecting platelets disposed radially (Fig. 3). Observations at higher magnifications revealed that the reflecting platelets were not more than 5 nm thick.

Xanthophores were present in the uppermost layer of the dermis. They were dendritic, and their overall diameter was from 40 to 60 μm . Like the melanophores, they were responsive to adrenergic stimuli, although the rate of the response was rather limited.

A melanophore, several iridophores and a few

xanthophores in this order from the bottom to the skin surface from a kind of dermal chromatophore unit. Sometimes, xanthophores were lacking. Being composed of only two sorts of chromatophores in that case, the unit was of very simple type.

Light reflection from the skin

Live specimen of the present species normally assumes greenish hue, and the spectral peak of light reflected from the dorso-lateral surface was near 550 nm. After decapitation, the trunk skin became darker quickly, as observed in many other fish species.

This phenomenon is apparently caused by the dispersion of pigmentary organelles in melanophores and xanthophores. Current studies have indicated that such a response is primarily due to the loss of tonic influences on the chromatophores of the sympathetic nervous system [2, 14, 15]. In a skin piece excised in physiological saline, the pigment dispersion naturally takes place and is maintained, since the chromatophores are free from the central nervous influences. In split dorsal-fin piece of the present material, too, the decrease in the light reflectance was confirmed.

When such a preparation was treated with nor-epinephrine or K^+ -rich saline, the spectral reflectance peak of the preparation shifted towards longer wavelength up to about 575 nm (yellowish green or near yellow tone) (Fig. 4). As will precisely be described elsewhere (Oshima *et al.*, to be published), such effects have been shown to be mediated by alpha adrenoceptors possessed by the chromatophores.

The change in the spectral characteristics during the recovery process from the maximally stimulated stage was then followed. In a typical series of measurements displayed in Figure 4, a beta adrenergic agent, isoproterenol, was employed to accelerate the change. As the skin became darker, the spectral peak shifted towards the shorter wavelength. Usually, there were plural spectral peaks on the curves for intermediate degrees of the response (Fig. 4E, F, G and H). Such peaks were recognizable around 550 nm (green), 515 nm (blue-green) or 465 nm (blue). The occurrence of such plural peaks on a spectral curve may be due to

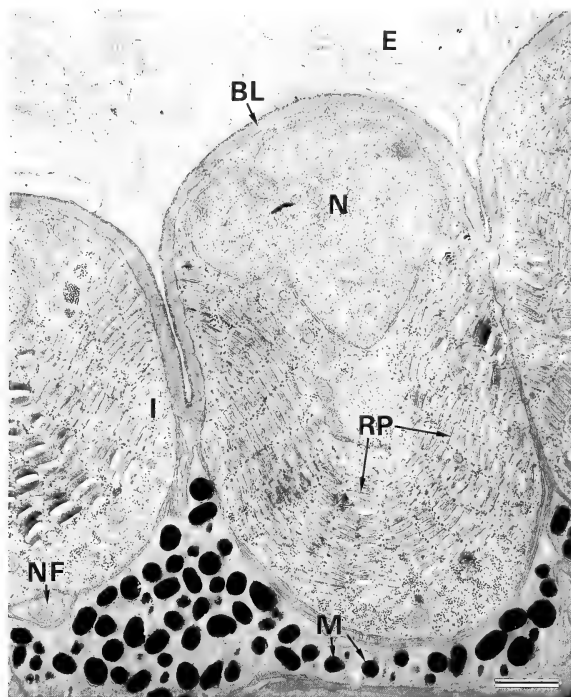


FIG. 3. Electron-micrograph showing iridophores and adjacent structures in the skin of the blue-green damselfish. Interradial membrane of the dorsal fin was sectioned almost perpendicularly to the surface of the skin. E: epidermis, BL: basal lamina, N: nucleus, I: iridophore, M: melanosome in melanophore, RP: reflecting platelets, NF: nerve fiber. Scale bar: $1\ \mu\text{m}$.

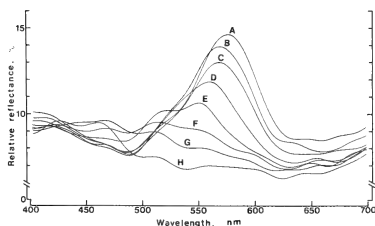


FIG. 4. Typical consecutive recordings of spectral reflectance change due to the response of integumentary chromatophores to beta-adrenergic stimulation. Dorsal skin piece was used. Curve A was recorded 5 min after the application of 50-mM K^+ -Ringer, which brought about alpha adrenergic response at a maximal level. The wave peak situated around 575 nm. Curves B through H were obtained at 44, 62, 92, 101, 116, 139 and 166 sec, respectively, after changing the irrigating saline to 5×10^{-6} M isoproterenol. Peak on curve B or C stood near 567 nm, but it moved to 557 as seen in curve D. With the progress of the response, the peak shifted gradually to shorter wavelength region, and the peak became lower and complicated.

the summed effect of several different spectra from a number of iridophores, since the area being measured included many of them.

In order to study the light-reflecting property of a single iridophore, a small circular area just to cover a cell on a photographic color print was then subjected to the spectral reflectance measurements. The motile cells were thus classified into four subtypes, i.e. MI₁-MI₄, according to the tints when they were equilibrated in the saline, and also to the ranges of spectral peak shift inducible by alpha- or beta-agonists (Table 1). The non-motile cells, on the other hand, were categorizable into two subtypes, i.e. NI₁ and NI₂, by the position of the wave peaks (cf. also Fig. 1). As the representatives of such spectral curves, those of MI₂ and NI₁ were exhibited in Figure 5. The results of the quantitative analyses on all the iridophores are summarized in Table 1. The results indicate, for example, that the iridophores reflecting blue tint in the saline (MI₁) was not affected by the beta adrenergic agent, but the peak was moved to green by the alpha agonist. Conversely, MI₃ and MI₄ were only responsive to beta agonists, while the cells designated as MI₂ were responsive to the agonists of both sorts. Those agents, however, had no influences on the non-motile iridophores (NI₁ and NI₂).

It may be noticed that iridophores are partly covered with peripheral portions of the mela-

nophore dendrites. Thus, either the incident lights into or the reflected ones from the iridophores should be interfered at least in part, when melanophore inclusions were dispersed far into the

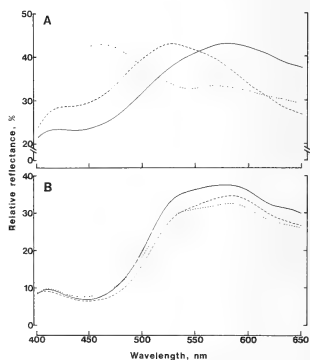


FIG. 5. Typical examples of spectral reflectance characteristics of a single iridophore on a color photomicrograph as measured and recorded with the MCPD system. A: motile iridophore of MI₂ type. B: non-motile iridophore of NI₁ type. Broken line represents spectrum obtained in physiological saline, where the peak stands at about 526 nm. Spectral curves with a solid and dotted line were recorded 5 min after the application with 50-mM K⁺-saline and 5×10^{-6} M isoproterenol, respectively.

TABLE 1. Effects of beta- and alpha-adrenergic stimuli on the spectral peak wavelength reflected from a single motile or non-motile iridophore of the blue-green demselfish, *Chromis viridis*

Type of iridophore ¹	Mean peak wavelength \pm SE (nm)			No. of measurements
	Ringer	Beta-stimulus ²	Alpha-stimulus ³	
MI ₁	473.6 \pm 4.12	471.6 \pm 4.96	532.4 \pm 4.61 ⁴	5
MI ₂	526.0 \pm 9.14	469.4 \pm 0.60 ⁴	584.4 \pm 2.71 ⁴	5
MI ₃	578.3 \pm 1.61	521.9 \pm 2.60 ⁴	581.4 \pm 1.45	7
MI ₄	529.2 \pm 2.75	463.9 \pm 1.92 ⁴	537.8 \pm 4.92	10
NI ₁	582.3 \pm 2.02	582.1 \pm 1.92	586.0 \pm 3.33	8
NI ₂	542.3 \pm 4.06	541.7 \pm 4.15	540.6 \pm 4.55	7

¹ Motile and non-motile iridophores are categorized into four (MI₁-MI₄) and two subtypes (NI₁ and NI₂), respectively. For further details, see text.

² 5×10^{-6} M isoxsuprine was used.

³ 50-mM K⁺-Ringer was used.

⁴ Significant at $P < 0.01$ when compared with the mean value obtained in the physiological saline.

peripheral cytoplasm of the dendrites.

Although being strongly concerned with the light-to-dark change of the skin, i.e. the "value" in terms of the Munsell color system, the melanophores were not directly responsible for the spectral changes. Xanthophores, on the other hand, should somewhat be involved in the revelation of yellowish hue of the integument, especially by their being underlaid with iridophores (Fig. 1).

Osmotic effects on iridophore reflectivity

Changes in the tonicity of bathing medium gave rise to a shift of the spectral peak of light reflectance of iridophores. When the skin piece was equilibrated in the normal saline (282.4 mOsm), the motile iridophores (MI) exhibited green hue, while the non-motile ones (NI) reflected yellow rays, as exhibited in Figure 2. When the medium was replaced with a hypertonic saline of 381.8 mOsm, however, the color reflected from the motile and non-motile iridophores changed to blue and green hue, respectively. Evidently, the spectral peak changed towards the shorter or longer wavelengths when the tonicity of the medium became higher or lower. Spectral peaks from two types of iridophores shifted concomitantly under such conditions. These changes were reversible. In solution having osmolarities higher or lower than those mentioned above, both the rate and the degree of the response were more pronounced. Within the range of reversibility, the maximal or minimal wavelength attainable in the solution of

low or high tonicity was around 610 or 460 nm, respectively.

Color distributions among iridophores

It has just been shown that, although the blue-green damselfish normally display greenish hue, the colors exhibited by individual iridophores are variable.

The gross ratio of the areas occupied by three groups of iridophores displaying different hues, i.e. "blue", "green" and "yellow", within the domain of a melanophore was estimated under three different conditions (Fig. 6). In physiological saline, the ratio of "blue": "green": "yellow" was roughly 1:4:2. When a beta agonist, isoxsuprine, was applied, the ratio of the blue area increased. By an alpha agonist, norepinephrine, on the other hand, the ratio of green and yellow areas increased, while the blue part lost its proportion. The changes in the ratio of differently colored areas should be caused by the activities of the motile iridophores which account for about 60% of iridophores.

DISCUSSION

In the blue-green damselfish, *Chromis viridis*, with which the present work has been performed, both the motile and non-motile iridophores were found in the dermis. This situation is different from those in other pomacentrid fishes studied thus far. In the blue damselfish, *Chrysiptera*

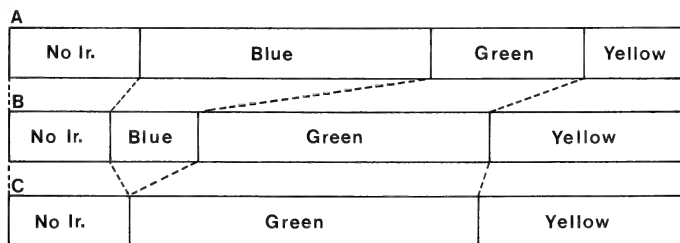


FIG. 6. Rough estimation of the ratios of areas of blue, green and yellow tints displayed by a number of iridophores within the domain of a melanophore. A: 5 min after the application of 5×10^{-6} M isoxsuprine, a beta agonist. B: Equilibrated in physiological saline. C: 5 min after the application of 5×10^{-6} M norepinephrine, an alpha agonist. No Ir.: Area where no iridophores were present. A mean value of 9 measurements on different animals is shown in each bar.

cyanea, for instance, all the iridophores were shown to be motile and play a predominant role in color changes [7, 8]. Contrarily, all of them in the scalycheek damselfish, *Pomacentrus lepidogenys*, were disclosed to be non-motile [12].

It was found in the present material that a melanophore, dozens of iridophores, and, if present, a few xanthophores constitute a dermal chromatophore unit. The motile iridophores existing over the perikaryon of the melanophore display variable hues from blue to green, whereas the non-motile iridophores surrounding the islet of the motile ones exhibit green or yellow color. The characteristic greenish hue of the integument must therefore be attributable to a mixed effect of those different colors. Such a mechanism of revelation of skin color is similar to that in the scalycheek damselfish, although the spectral reflectance peak in the latter species did not shift [12].

In the present material, the skin hue changed within the visual range of the spectrum, i.e. between blue green and yellowish green. The changes may predominantly be due to the spectral peak shift of the reflected light from the motile iridophores. When an excised skin piece was treated with adrenergic beta agonists, furthermore, the skin color could be brought even to dark blue or dark blue-green. At that time, the peak of the spectrum reflected from the motile iridophores was shifted towards shorter wavelength region (Table 1). Conversely, all the iridophores exhibited green or yellowish green hue, like when the isolated skin piece was treated with alpha agonistic amines. Thus, the mechanism of skin color change in this species may appropriately be likened to the repainting of many small divisions of a certain color with those of another color on a pointillistically painted picture.

In *Hyla* tree frog and *Anolis* lizard, the motility of the melanophore in the dermal chromatophore unit is considered to play a predominant role in the adaptive change of skin color between green and dark brown [16, 17]. In fish, on the other hand, the melanophore in the unit does not take such a primary role in the changes of hue, although the changes of the darkness, or the "value" in the Munsell color system, are primarily dependent on their motility [2]. Recently, for instance, such a

role of the melanophore has clearly been demonstrated in a pomacentrid, the scalycheek damselfish [12].

In the blue-green damselfish, too, the primary function of the melanophores may be to change skin darkness, like in other fish [18]. In addition, they may be useful to absorb light-rays transmitted through the iridophores which overlie them. Like in the blue damselfish [8], such a situation may be useful for realizing purer coloration, or higher "chroma" in terms of the Munsell color system, of the skin.

Through the intracellular aggregation or dispersion of yellow-colored organelles, xanthophores are certainly responsible for changing yellowish component of the integumental hue. Thus, the delicately manifested coloration as well as its subtle changes observable in the skin of this species should be due to the cooperative effects of those three kinds of chromatophores.

Fine structural features of the iridophores of the present species resemble well those of the blue damselfish [7]. It is therefore conceivable that the same mechanism of light reflection proposed for the blue damselfish [8] applies to the present species. That is, the color reflected from the iridophore must be dependent on the difference in the optical thickness of the periodical unit constituting a pile of reflecting platelets, i.e. a platelet and a sheet of cytoplasm sandwiched between two adjacent platelets [6, 8]. In motile cells, the distance between platelets changes actively in response to nervous or hormonal cues. Incidentally, the physiological and pharmacological analyses of the regulatory system for the movements of chromatophores comprizing the motile iridophores will precisely be presented elsewhere (Oshima *et al.*, to be published).

Changes in the osmolarity of bathing medium resulted in the changes of reflective properties of iridophores: The consequent changes in the cellular volume should have led to a passive increase or decrease in the distance between platelets. Such a phenomenon was observed both in the motile and in the non-motile iridophores. As the definitive name naturally implies, on the other hand, the non-motile iridophores are refractory to the physiologically active regulatory factors. At present, we do not

know why the non-motile cells are unresponsive. Presumably, cellular receptors involved in regulatory signal transduction are lacking. An alternative explanation is that the defect is deep in the intracellular motile mechanism, which has lately been disclosed to be of the tubulin-dynein type [10]. Until the present time, however, we could not detect any morphological difference between the active and the quiescent ones. Further studies are needed to obtain more detailed information on the presence as well as the characterization of membrane receptors or the intracellular machinery in these small cells.

Another point of interest in relation to the responsiveness of iridophores is the fact that only the cells above the perikaryon of a melanophore were found to be motile. Could the motility be induced, if a non-motile cell is transferred on the melanophore perikaryon? Does the motile cell lose its activity, when it is brought out of the melanophore domain? The neurotransmitter substances released more thickly over the melanophore perikaryon might have trophic effects on the responsiveness of iridophores nearby. In any case, such problems should be important for further understanding of the mechanisms of coloration as well as of the pattern formation of the skin.

Finally, we like to consider briefly as to whether a damselfish perceives such a polka-dotted pattern in the skin of other individuals as it actually exhibits or as being homogeneously colored. The question has naturally been arisen since an individual should recognize others including those of the same species through the visual means. Each iridophore has a diameter of only about 10 μm . The size should be too small to be discriminated by the lateral eye. As seen in Figure 1, about 30 motile iridophores constitute an islet of blue-to-green hue. In the skin, such islets distribute at intervals of about 150 μm . The diameter of the eye is not more than 2 mm. Preliminary histological examinations showed that the average distance between adjacent cones was a little less than 10 μm . Therefore, the minimal visual angle calculated on the basis of the geometry was about 0.4°. In order to discriminate two dots 150 μm apart among others, the observer fish must approach the others nearer than 20 mm, even when we assume

that the eye is near-sighted as to be able to focus upon the object at such a short distance, and further that the light paths inside the eye do not suffer from optical disturbances of any sorts. Believably, the fish can recognize others from much longer way off by perceiving them as a greenish colored entity. Results of histological observations on the lateral eye will separately be presented in reference to the visual acuity and the visual communication among individuals elsewhere (Fujii *et al.*, unpublished data).

ACKNOWLEDGMENTS

To authors thank Professor H. Ida, School of Fisheries Sciences, Kitasato University, Iwate, for identifying the present material. This work was supported in part by a grant from the Ito Foundation for the Promotion of Ichthyological Research to N.O. and by those from the Ministry of Education, Science and Culture of Japan to R.F. and to N.O.

REFERENCES

1. Fujii, R. (1969) Chromatophores and pigments. In "Fish Physiology". Ed. by W. S. Hoar and D. J. Randall, Vol. 3, Academic Press, New York, pp. 307-353.
2. Fujii, R. and Oshima, N. (1969) Control of chromatophore movements in teleost fishes. *Zool. Sci.*, **3**: 13-47.
3. Denton, E. J. and Nicol, J. A. C. (1965) Reflexion of light by external surface of the herring, *Clupea harengus*. *J. Mar. Biol. Assoc. U.K.*, **45**: 711-738.
4. Denton, E. J. and Land, M. F. (1971) Mechanism of reflexion in silvery layers of fish and cephalopods. *Proc. Roy. Soc. London, B*, **178**: 43-61.
5. Kawaguti, S. and Kamishima, Y. (1966) A supplementary note on the iridophore of the Japanese porgy. *Biol. J. Okayama Univ.*, **12**: 57-60.
6. Land, M. F. (1972) The physics and biology of animal reflectors. *Progr. Biophys. Molec. Biol.*, **24**: 75-106.
7. Oshima, N., Sato, M., Kumazawa, T., Okeda, N., Kasukawa, H. and Fujii, R. (1985) Motile iridophores play the leading role in damselfish coloration. In "Pigmentation 1985: Biological, Molecular and Clinical Aspects of Pigmentation". Ed. by J. Bagnara, S. N. Klaus, E. Paul, and M. Scharf, Univ. Tokyo Press, Tokyo, pp. 241-246.
8. Kasukawa, H., Oshima, N. and Fujii, R. (1987) Mechanism of light reflection in blue damselfish motile iridophores. *Zool. Sci.*, **4**: 245-259.

- 9 Lythgoe, J. N. and Shand, J. (1982) Changes in spectral reflexions from the iridophores of the neon tetra. *J. Physiol.*, **325**: 23–34.
- 10 Oshima, N. and Fujii, R. (1987) Motile mechanism of blue damselfish (*Chrysiptera cyanea*) iridophores. *Cell Motility & Cytoskeleton*, **8**: 85–90.
- 11 Iga, T. and Matsuno, A. (1986) Motile iridophores of a freshwater goby, *Odontobutis obscura*. *Cell Tiss. Res.*, **244**: 165–171.
- 12 Kasukawa, H. and Oshima, N. (1987) Divisionistic generation of skin hue and the change of shade in the scalycheek damselfish, *Pomacentrus lepidogenys*. *Pigment Cell Res.*, **1**: 152–157.
- 13 Fujii, R. (1959) Mechanism of ionic action in the melanophore system of fish. I. Melanophore-concentrating action of potassium and some other ions. *Annot. Zool. Japon.*, **32**: 47–58.
- 14 Fujii, R. and Novales, R. R. (1969) The nervous mechanisms controlling pigment aggregation in *Fundulus melanophores*. *Comp. Biochem. Physiol.*, **29**: 109–124.
- 15 Fujii, R. and Miyashita, Y. (1976) Receptor mechanisms in fish chromatophores—I. Alpha nature of adrenoceptors mediating melanosome aggregation in guppy melanophores. *Comp. Biochem. Physiol.*, **51C**: 171–178.
- 16 Bagnara, J. T., Taylor, J. D. and Hadley, M. E. (1968) The dermal chromatophore unit. *J. Cell Biol.*, **38**: 67–79.
- 17 Taylor, J. D. and Hadley, M. E. (1970) Chromatophores and color change in the lizard, *Anolis carolinensis*. *Z. Zellforsch.*, **104**: 282–294.
- 18 Kasukawa, H., Sugimoto, M., Oshima, N. and Fujii, R. (1985) Control of chromatophore movements in dermal chromatic units of blue damselfish—I. The melanophore. *Comp. Biochem. Physiol.*, **81C**: 57–60.

Filaments in the Cells of Frog Taste Organ

YUKO SUZUKI and MASAKO TAKEDA

*Department of Oral Anatomy, Higashi-Nippon-Gekuen University,
School of Dentistry, Ishikari-Tobetsu, Hokkaido 061-02, Japan*

ABSTRACT—The filaments in the cells of frog taste organ were investigated by conventional electron microscopy, fluorescent microscopy using phalloidin, and immunohistochemistry using anti-keratin, anti-NSE and anti-S-100 protein antibodies. The apical cytoplasm of taste and supporting cells contained thin and straight filaments (6 nm in diameter) which were composed of f-actin, as detected by fluorescein labeled phalloidin binding. Other regions of taste and supporting cells contained numerous bundles of filaments (10 nm in diameter) extending from desmosomes. The 10 nm filaments were also observed in the basal cells. The present immunohistochemical study using antikeratin antibodies verified that these 10 nm filaments were composed of keratin protein. Polyclonal and KL-1 monoclonal antibodies against keratin reacted with the taste and basal cells, and EAB 902 reacted with the taste and supporting cells. These antibodies also reacted with the ciliated and epithelial cells surrounding the taste organ. PKK-1 antikeratin antibody reacted with the ciliated and epithelial cells, but did not react with the taste organ. Moreover, anti-NSE and anti-S-100 protein antisera reacted with the basal cells in the taste organ. We concluded that all types of cells in the frog taste organ, including basal cells, might originate from the epithelial cells rather than the neural crest cells, because of the presence of keratin protein. It also appeared that keratin subtypes differed between taste organ cells and surrounding epithelial cells, and among each type of cell in the taste organ.

INTRODUCTION

The taste organ of frogs is a disc-like shape, located at the top of fungiform papillae which are found on the dorsal surface of tongue. This organ has been widely used in electrophysiological and ultrastructural studies of taste sensation [1-5]. Many ultrastructural studies have revealed that the cells of the frog taste organ are classified into three types: taste, supporting, and basal cells [1-4]. The presence of abundant filaments in these cells has been described [2, 3], but little is yet known about the chemical nature of filament proteins.

It has been reported that mammalian taste bud cells contain thin filaments (6 nm in diameter) in the microvilli and intermediate filaments (10 nm diameter) throughout the cytoplasm [6]. Recent fluorescent and immunohistochemical studies have shown that the 6 nm filaments in the taste bud cells of rabbit and mice are made of f-actin [7, 8], while the 10 nm filaments in the taste bud cells of mice

are formed by keratin [9].

Because keratin has been regarded as a marker protein for epithelial origin [10], some authors have suggested that the taste bud cells of the rat and mouse originate from the epithelial cells [9, 11]. However, Grover-Johnson and Farbman [12] have suggested that the basal cells of the catfish taste buds do not originate from the epidermis, but rather from the neural crest. In the frog taste organ, the basal cells have been identified as monoamine-containing cells similar to those of catfish [3, 13]. Düring and Andres [2] have reported that the basal cell of frogs are similar to Merkel cells in the epidermis, which have a mechanoreceptive function. The Merkel cells were shown to contain neuron specific enolase (NSE) [14], Met-enkephalin [15], vasoactive intestinal polypeptide (VIP) [16], and serotonin [17]; thus, it has been suggested that Merkel cells originate from the neural crest. On the other hand, the fact that Merkel cells can be stained with antikeratin antibodies has supported their epithelial origin rather than their neural crest origin [18, 19].

In the present study, the characteristics of the

filaments in the frog taste organ were examined by conventional electron microscopy, fluorescent microscopy using phalloidin, and immunostaining using antikeratin, anti-NSE, and anti-S-100 protein antibodies. It was of particular interest to clarify whether frog taste organs originate from epithelial cells or neural crest cells.

MATERIALS AND METHODS

The tongues of frog, *Rana catesbeiana*, were removed and cut into small blocks. The tissues were immersed into a cacodylate buffered (pH 7.4) ice-cold mixture of 2% glutaraldehyde and 2% paraformaldehyde for 3 hr, and were postfixed in 1% OsO_4 for 1 hr. The tissues were dehydrated in ethanol and embedded in Epok 812. Ultrathin sections were cut, stained with uranyl acetate followed by lead citrate, and examined under a Hitachi H-500 electron microscope. Thick sections were stained with toluidine blue for light microscopic examination.

For fluorescent microscopy, the tissues were fixed in 4% paraformaldehyde dissolved in phosphate-buffered saline (PBS), and rinsed overnight at 4°C in PBS containing 10% sucrose. The serial cryostat sections (10 μm thickness) were made. The sections were treated with FITC-labeled phalloidin (Sigma, 33 ng in each section) for 30 min at room temperature. They were rinsed in PBS, mounted with glycerin, and examined under a fluorescence microscope. Some sections were stained with hematoxylin-eosin and examined under a light microscope.

For immunohistochemistry, the tissues were fixed for 2 hr in either Bouin's fluid without acetic acid or phosphate-buffered 10% formalin, and then embedded in paraffin. Sections 5 μm thick were made; after deparaffinization and rehydration, the sections were treated with 3% H_2O_2 for 10 min. The sections were incubated with several primary antibodies (dilution, 1:100–1:500) for 1 hr at room temperature. They were washed in PBS for 20 min and incubated for 1 hr in peroxidase-labeled swine anti-rabbit immunoglobulin (dilution 1:200, Dako) if the primary antibodies were raised in rabbit. In cases where primary antibodies were raised in mouse, the sections were treated

with rabbit anti-mouse immunoglobulin (Dako) for 30 min, rinsed well, and treated with peroxidase-anti-peroxidase complex (Dako) for 30 min. The sections were immersed in diaminobenzidine solution for 5 min to visualize the binding of the antibody. The primary antibodies used were as follows: (a) polyclonal anti-keratin antiserum obtained from bovine muzzle epidermis (Dako), which reacts with keratin polypeptides of 58, 56, and 52 kd and weakly reacts with 60, 51, and 48 kd keratin polypeptides; (b) KL-1 monoclonal anti-keratin antibody obtained from human keratinocyte (Immunotech), which reacts with 56 kd keratin polypeptide; (c) EAB 902 anti-keratin antibody obtained from human hepatocellular carcinoma cells (Enzo Biochem. Inc.), which reacts with 54 kd keratin polypeptide; (d) PKK-1 anti-keratin antibody obtained from a pig kidney epithelial cell line (Labsystem), which reacts with keratin polypeptides of 40, 45, and 52.5 kd; (e) anti-bovine NSE antiserum (Dako); and (f) anti-bovine S-100 protein antiserum (Advance). In control experiments, normal rabbit serum and mouse ascites were used instead of the polyclonal and monoclonal antibodies, respectively.

RESULTS

The disc shaped frog taste organs, located at the top of fungiform papillae, were surrounded by ciliated cells that in turn were surrounded by epithelial cells. The cell types in the taste organ could be classified into three types: supporting, taste, and basal cells. The supporting cells were arranged in one layer at the apical one-third of the taste organ. They were cylindrical in shape and their subnuclear cytoplasm formed very thin processes which terminated among the taste cells. The taste cells were spindle shaped, and occupied the lower two-thirds of the taste organ. Their thin apical processes were elongated between the supporting cells to the surface, while their basal processes were attached to the basal lamina (Fig. 1). The basal cells were located only in the basal portion of the periphery of the taste organ, and their thin processes were extended along the basal lamina toward the center of the taste organ.

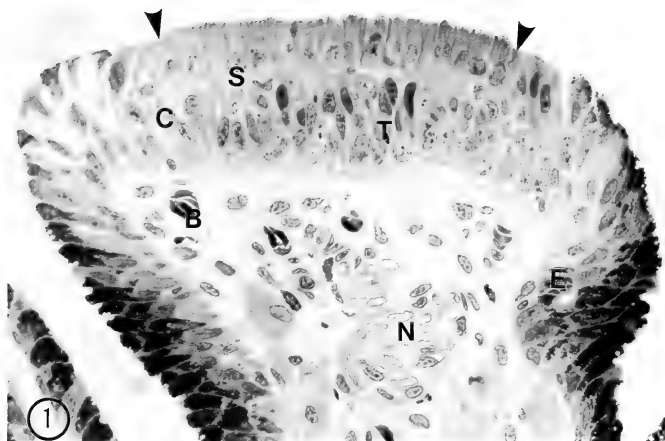
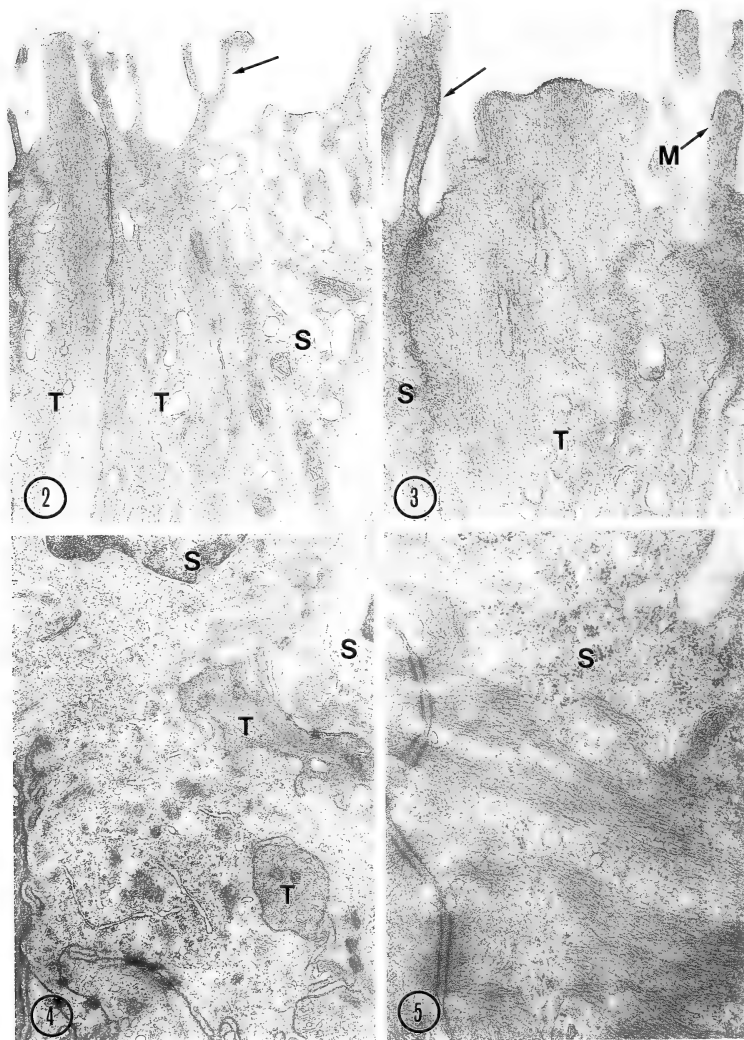


FIG. 1. A light micrograph of a longitudinal section of a frog fungiform papillae stained by toluidine blue. The supporting cells (S) are arranged in one layer. The taste cells (T) are occupied in lower two-thirds of taste organ and protrude their cytoplasm between the supporting cells. The basal cells are not distinguished from other types of cells by this staining method. Arrowheads indicate the border of taste organ. C: ciliated cells, E: epithelial cells, B: blood vessel, N: nerve bundles. $\times 450$.

Electron microscopy

The apical cytoplasm of taste cells, which contained smooth endoplasmic reticulum and microtubules, terminated in rod-shaped processes or microvilli (Fig. 2). A bundle of straight, thin filaments (6 nm in diameter) filled rod-shaped processes and microvilli. Those filaments in parallel alignment were bound to the cell membrane at one end; the other end extended down-ward about 2–3 μm into the apical cytoplasm of the taste cells (Fig. 3). The supporting cells had many secretory granules in the apical cytoplasm. They terminated in microvilli which were smaller than the microvilli of the taste cells (Figs. 2 and 3). The subnuclear cytoplasm of supporting cells, which formed irregular thin processes, was filled by numerous bundles of filaments which were 10 nm in diameter (Fig. 4). The 10 nm filaments extended from the well developed desmosomes and wove into the cytoplasm (Fig. 5). The subnuclear cytoplasm of the taste cells was also composed of thin cell processes extending to the basal lamina. The 10 nm filaments aggregated

to form thick bundles, filled thin processes, and connected to the basal lamina via half desmosomes (Fig. 6). The 10 nm filaments were also distributed in the supranuclear cytoplasm and the region surrounding the nucleus, although they were fewer than those in the subnuclear cytoplasm. In the basal cytoplasm of taste cells, many cored vesicles (60–100 nm in diameter) were found accumulated in the cytoplasm facing junctions with the nerve terminals of the afferent synapses (Fig. 6, inset). The basal cells possessed ovoid shaped nuclei. Their cytoplasm contained fewer 10 nm filaments than the other types of cells. The filaments were not aggregated into bundles, but were arranged in reticular patterns. Desmosomes were few in number and poorly developed. Cored vesicles (50–100 nm in diameter) were also present in the basal cells—similar to the taste cells—but synapses with nerve terminals were not observed (Fig. 7). The epithelial cells in the fungiform papillae were non-keratinized and contained numerous bundles of filaments which were 10 nm in diameter.



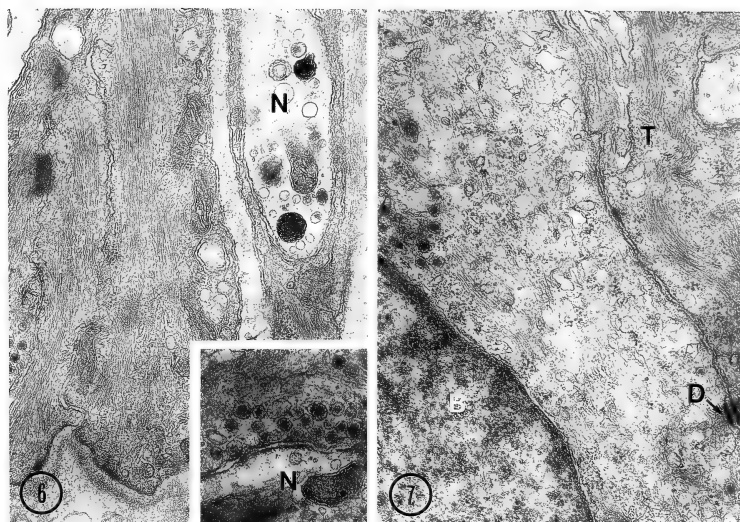


FIG. 6. The basal region of taste cells. The cytoplasm are filled by the thick bundles of 10 nm filaments. N: nerve terminal. $\times 27,000$. inset: A synapse between the taste cell and afferent nerve terminal (N). Abundant dense-cored vesicles of 60–100 nm in diameter are accumulating along the nerve terminal. $\times 46,000$.

FIG. 7. The basal cell (B) in the periphery of a taste organ. The cytoplasm is less distributed by 10 nm filaments than the taste cells (T). A small desmosome (D) is seen between the basal cells and the taste cells. Many dense-cored vesicles of 50–100 nm in diameter are seen in the cytoplasm. $\times 34,000$.

Fluorescent microscopy

After the application of FITC-labeled phalloidin, fluorescence was observed in the apical region of the taste organ, the surface of ciliated cells, and the muscle fibers in the connective tissue of fungiform papillae. The epithelial cells showed no reaction (Fig. 8a, b). In the taste organ, strong-

ly fluorescent dots were observed in the apical regions of taste cells; supporting cells were also observed to be weakly fluorescent between the strongly fluorescent dots (Fig. 8c).

Immunohistochemistry

Polyclonal antibody against keratin generated from the bovine muzzle stained the basal region

FIG. 2. An electron micrograph of the apical region of a taste organ. The taste cells (T) terminate in rod-shaped processes or microvilli. The supporting cells (S) terminate in thin processes (arrow) and contain many secretory granules in the apical cytoplasm. $\times 24,000$.

FIG. 3. Higher magnification of the apical region of taste (T) and supporting (S) cells. Note the bundles of filaments of 6 nm diameter with parallel alignment in the rod-shaped processes and microvilli (M) of taste cells. A few of 6 nm filaments are seen in thin processes of supporting cells (arrow). $\times 52,000$.

FIG. 4. The subnuclear cytoplasm of the supporting cells (S) showing irregularly branched processes which are connected with the neighboring supporting cells or taste cells (T) by many desmosomes. Numerous bundles of the 10 nm filaments are distributed in the cytoplasm. $\times 13,000$.

FIG. 5. The well-developed desmosomes in the supporting cells (S). The 10 nm filaments extending from desmosomes are interwoven and wound in the cytoplasm. $\times 39,000$.

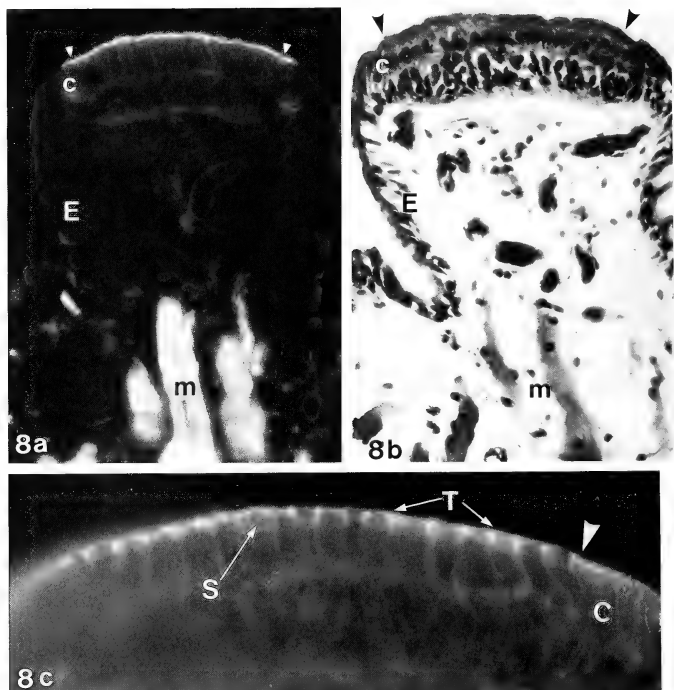


Fig. 8. (a) Fluorescence micrograph of fungiform papillae after the application of FITC-labeled phalloidin and (b) the corresponding light micrograph. The reactions are seen in the apical region of taste organ and in ciliated cells (C). The epithelial cells (E) show negative stain. The bundles of muscle fibers (m) in connective tissue exhibit the strong positive reaction. Arrowheads indicate the border of taste organ. $\times 300$ (a, b). (c) Higher magnification of apical region of taste organ after the application of FITC-labeled phalloidin. Apical cytoplasm of taste cells (T) are strongly positive, which form the fluorescent dots in the surface of taste organ. The supporting cells (S) show a weak reaction. C: ciliated cells. An arrow indicates the border of taste organ. $\times 600$.

of taste organ, which comprises the subnuclear cytoplasm of taste cells. Similarly the ciliated and epithelial cells surrounding the taste organ were stained by the polyclonal antibody. This antibody stained weakly in middle region of taste organ, which comprise the subnuclear cytoplasm of supporting cells and the region surrounding the nucleus of taste cells. The upper region of taste organ, which comprise the supranuclear cytoplasm of

both the supporting and taste cells showed no detectable staining (Fig. 9). In the section though the edge of taste organ, ovoid-shaped basal cells were stained with polyclonal antibody (Fig. 10). Control experiment exhibited no detectable staining in epithelial cells, ciliated cells and any type of taste organ cells (Fig. 11).

KL-1 monoclonal anti-keratin antibody stained the basal region of taste organ, ciliated and epithe-

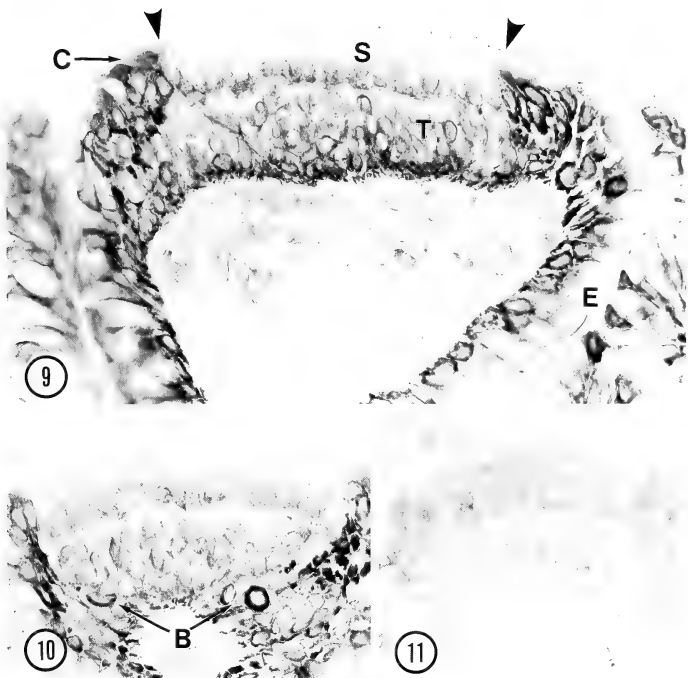


FIG. 9. The immunoreaction with polyclonal antikeratin antiserum from bovine muzzle in fungiform papillae. The basal region of taste organ consisting of the subnuclear cytoplasm of taste cells (T), ciliated cells (C) and epithelial cells (E) are stained. The reaction is weak in the subnuclear cytoplasm of supporting cells (S) and in the region surrounding the nucleus of taste cells. The reaction is absent in the supranuclear cytoplasm of supporting, taste and epithelial cells. Arrowheads indicate the border of taste organ. $\times 400$.

FIG. 10. The immunoreaction with polyclonal antikeratin antiserum from bovine muzzle in the edge of taste organ. Three ovoid shaped keratin immunoreactive cells are seen in the base of taste organ, which show the characteristics of the basal cells (B). $\times 340$.

FIG. 11. The control specimens using normal rabbit serum. Staining is not detected in the taste organ and ciliated and epithelial cells. $\times 250$.

lial cells (Fig. 12). The basal cells were also stained by KL-1 antibody (Fig. 13). EAB 902 monoclonal anti-keratin antibody exhibited the staining of the subnuclear cytoplasm of supporting cells in the taste organ (Fig. 14). This antibody gave no staining of the basal cells, but basal region of taste organ, ciliated and epithelial cells were stained.

PKK-1 monoclonal antibody reacted with none of the taste organ cell types, but reacted with ciliated and epithelial cells (Fig. 15). Control specimen using mouse ascites exhibited no detectable staining in tongue sections.

Furthermore, the basal cells reacted with anti-NSE antiserum (Fig. 16) and anti-S-100 protein

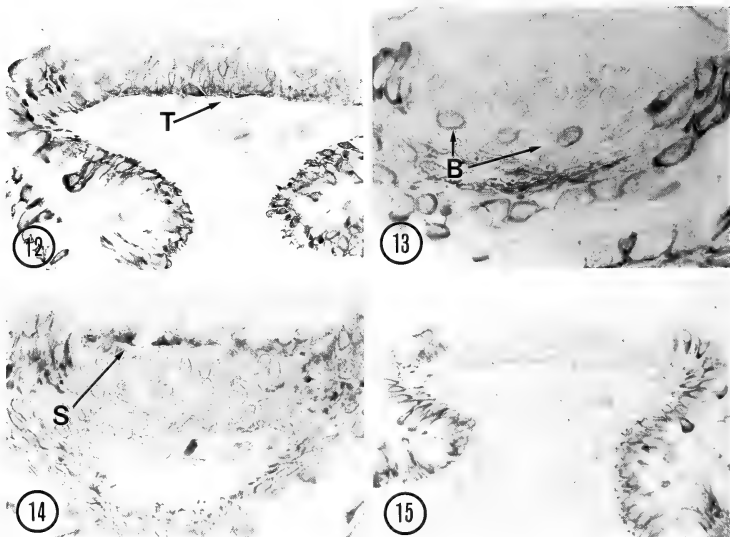


FIG. 12. The immunoreaction with monoclonal antikeratin antibody KL-1 in fungiform papillae. The staining is seen in the base of taste organ (T), ciliated and epithelial cells. $\times 200$.

FIG. 13. The immunoreaction with monoclonal antikeratin antibody KL-1 in the edge of taste organ indicates the immunostaining for keratins of three basal cells (B). $\times 480$.

FIG. 14. The immunoreaction with monoclonal antikeratin antibody EAB 902 in the edge of taste organ. The strong reaction is seen in the subnuclear cytoplasm of supporting cells (S). $\times 440$.

FIG. 15. The immunoreaction with monoclonal antikeratin antibody PKK-1 in fungiform papillae. The taste organ is not stained, but ciliated and epithelial cells are stained. $\times 340$.

TABLE 1. Reactivity of antikeratin antibodies on the taste, supporting and basal cells of taste organ and the ciliated and epithelial cells in fungiform papillae

Antibodies	Immunogenic preparation (Keratin subunit)	Staining				
		Taste Cell	Supporting Cell	Basal Cell	Ciliated Cell	Epithelial Cell
Polyclonal	Bovine muzzle epidermis (52, 56, 58 kD)	+	±	+	+	+
Monoclonal						
KL-1	Human keratinocyte (56 kD)	+	±	+	+	+
EAB 902	Human hepatocellular carcinoma (54 kD)	+	+	—	+	+
PKK 1	Pig kidney epithelial cell line (40, 45, 52.5 kD)	—	—	—	+	+

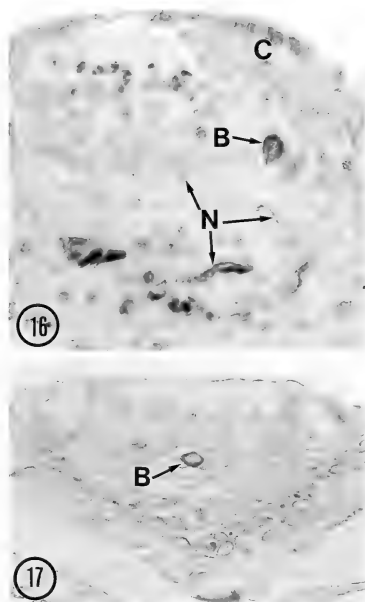


FIG. 16. The immunoreaction for NSE in fungiform papillae. A basal cell (B) in the taste organ and the nerve fibers (N) in the connective tissue are strongly reacted. The ciliated cells (C) and the small area of middle region of taste organ are weakly stained. $\times 480$.

FIG. 17. The immunoreaction for S-100 protein in fungiform papillae. A basal cell (B) in the taste organ shows moderate staining. $\times 420$.

antisera (Fig. 17). The immunostained basal cells were identified as ovoid cells in the section through the edge of the taste organ. The nerve fibers in the connective tissues of fungiform papillae strongly reacted with anti-NSE antiserum. The small area of middle region of taste organ and the ciliated cells were weakly reacted with anti-NSE antiserum, but they were negative for anti S-100 protein antiserum (Figs. 16, 17).

DISCUSSION

In the frog taste organ, it can be regarded that the 6 nm filaments in the apical cytoplasm of taste and supporting cells are formed of f-actin, judging from the characteristic binding of FITC-labeled phalloidin. Similar actin filaments have been observed in mammalian taste bud cells and intestinal epithelial cells [8, 20]. The present study revealed that a greater number of filaments existed in the rod-shaped processes and the microvilli of taste cells than in the supporting cells. This suggests that the actin filaments are related to the support of the taste cell membrane where the reception of taste stimulus may occur [5]. Furthermore, this study also suggested the presence of actin filaments in the apex of ciliated cells. This may be related with the presence of rootlets in the base of cilia; the rootlets have been reported as having striated structures [21].

The 10 nm filaments studied in the thin sections were distributed more densely in the subnuclear cytoplasm of the supporting and taste cells than in other regions of both cells or than in the basal cells. The subnuclear parts of both cells was thin and irregularly formed, and thus the framework of 10 nm filaments might be required to support their structures. The present immunohistochemical study verified that these 10 nm filaments were composed of keratin proteins. Since all the cell types in the frog taste organ as well as the epithelial cells involved keratins, all the cell types in the frog taste organ may originate from the epithelial cells. Keratin represents a family of about 20 polypeptides that are differentially expressed in different epithelial tissues. The present tests with antikeratin antibodies with various molecular weights indicated differences in immunostaining between the taste organ and the surrounding epithelial cells, and among the cell types in the taste organ. PKK-1 antibody reacted with the epithelial cells, but did not react with the taste organ. Lane [22] has reported that monoclonal antibodies generated against cytoskeleton extracts from PtK₁ cells, which demonstrate the presence of a simple epithelium antigenic determinant, reacted with the taste bud cells in the rat and mouse, but not with the surrounding epithelium. It

is likely that different subtypes of keratin protein may exist in the frog taste organ and the epithelial cells.

Furthermore, in the taste organ, polyclonal and KL-1 antibodies stained with both the taste cells and the basal cells, but weak in the supporting cells; while EAB 902 antibody reacted with the taste and supporting cells, but not with the basal cells. It appears that the differences among keratin subtypes also exist among the cells types of the taste organ.

The antikeratin antibodies used in the present study showed no detectable reaction of keratins in the supranuclear cytoplasm of supporting, epithelial and taste cells. In the light and electron microscopic observation, both the supporting and epithelial cells contained numerous secretory granules in their supranuclear cytoplasm, thus the keratin filaments may not be involved in these regions. In contrast, taste cells contain 10 nm filaments in the supranuclear cytoplasm. These filaments may be composed of keratin protein rather than other types of intermediate filament proteins. It is likely that different keratin subtypes exist in the supranuclear cytoplasm of taste cells as observed among the taste organ cells types.

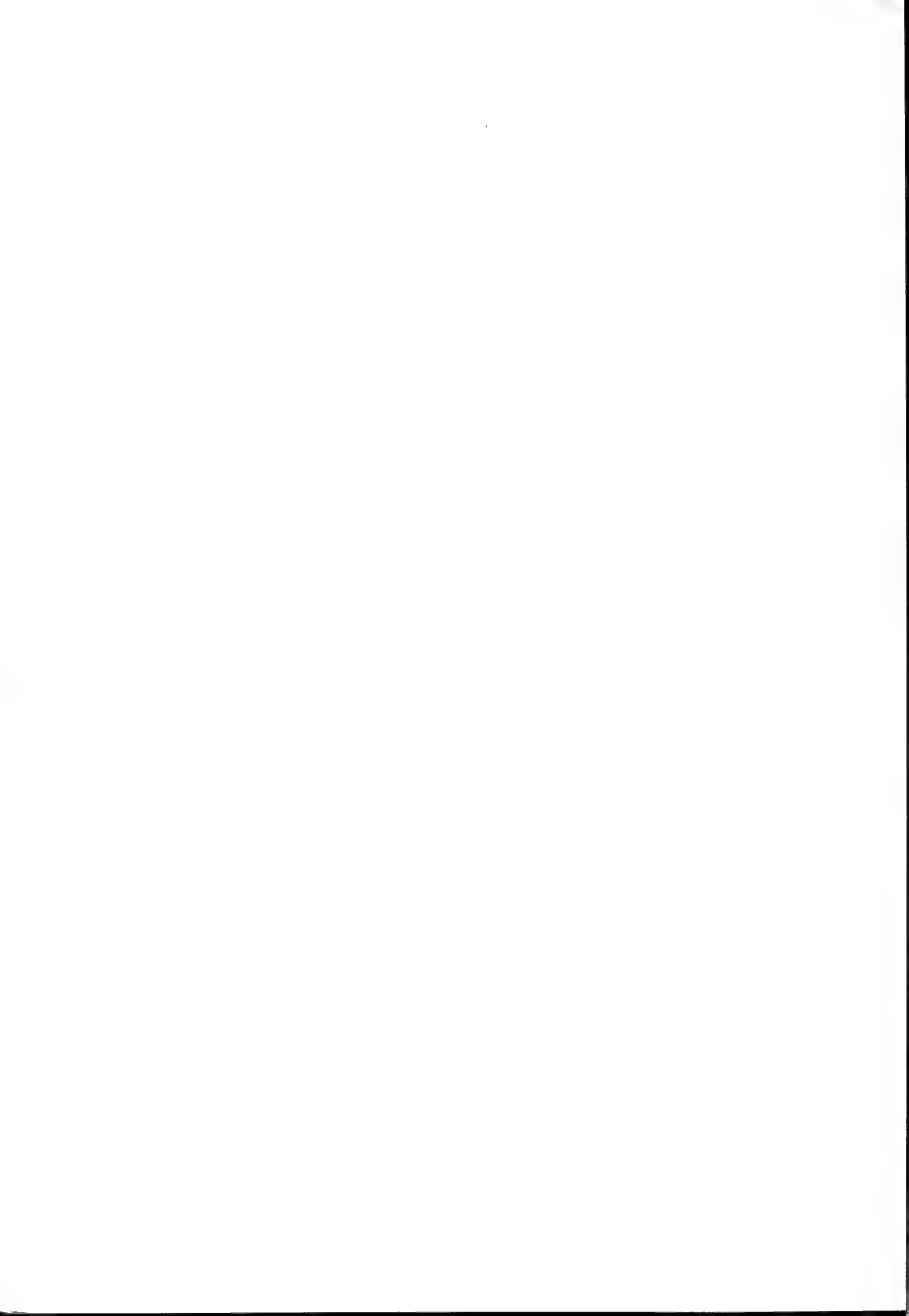
The coexistence of keratins, NSE, and S-100 protein observed in the basal cells may not be a discrepancy. Although it has been considered that NSE is the specific marker for neuronal cells and cells derived from the neural crest [23], and likewise, S-100 protein for Schwann cells and glia cells [24], recent immunohistochemical studies have shown the presence of both of them in several non-neuronal cells. S-100 protein has been detected in Langerhans cells in the skin [25], reticular cells [26], chondrocytes [27] and parathyroid gland cells [28]. Also, the presence of both keratin and NSE has been reported in Merkel cells [14, 18, 19] and insulin secreting islet cells [29]. It appears that NSE and S-100 protein are not always specific markers for neural crest origin. Therefore, it is reasonable that the basal cells in the taste organ are of epithelial origin rather than of neural crest origin, because of the presence of keratin protein. The function of the basal cells is unclear; they are not considered to be undifferentiated stem cells, such as the basal cells in mammalian taste buds.

Probably, the basal cells may play a significant role in taste stimulus reception together with the taste cells, although the possibility as mechanoreceptors cannot be excluded as suggested by some authors [2, 4, 13].

REFERENCES

1. Graziadei, P. P. C. and DeHan, R. S. (1971) The ultrastructure of frog's taste organ. *Acta Anat. (Basel)*, **80**: 563-603.
2. Düring, M. V. and Andres, K. H. (1976) The ultrastructure of taste and touch receptors of frog's taste organ. *Cell Tiss. Res.*, **165**: 185-198.
3. Jaeger, C. B. and Hillman, D. E. (1976) Morphology of gustatory organs. In "Frog Neurobiology". ed. by R. Llinas and W. Precht, Springer, Berlin, pp 585-606.
4. Toyoshima, K., Honda, E., Nakahara, S. and Shimamura, A. (1984) Ultrastructural and histochemical changes in the frog taste organ following denervation. *Arch. histol. Jap.*, **47**: 31-42.
5. Avenet, P. and Lindemann, B. (1987) Patch-clamp study of isolated taste receptor cells of the frog. *J. Membrane Biol.*, **97**: 223-240.
6. Takeda, M. (1982) Electron microscopy of taste buds. *Higashi Nippon Gakuen Dent. J.*, **1**: 1-17. (In Japanese)
7. Hirakawa, Y. and Nomura, H. (1986) F-actin bundles in the microvilli of taste bud cells. The Matsu-moto Shigaku, **12**: 42-45. (In Japanese)
8. Takeda, M., Obara, M. and Suzuki, Y. (1986) Filaments in the apical cytoplasm of taste bud cells. *Jap. J. Oral Biol.*, **28**: Supple. pp 178.
9. Takeda, M., Obara, N. and Suzuki, Y. (1988) Intermediate filaments in mouse taste bud cells. *Arch. Histol. Cytol.*, **51**: 99-108.
10. Sun, T. T., Eichner, R., Nelson, W. G., Tseng, S. C. G., Weiss, R. A., Jarvinen, M. and Woodcock-Mitchell, J. (1983) Keratin classes: Molecular markers for different types of epithelial differentiation. *J. Invest. Derm.*, **81**: 109-115.
11. Kim, H. M., Hwang, S. M., Ko, J. S. and Lee, Z. H. (1986) Immunohistochemical localization of keratin in the taste buds of rat vallate papillae. *Arch. Oral Biol.*, **31**: 419-412.
12. Grover-Johnson, N. and Farbman, A. I. (1976) Fine structure of taste buds in the barbels of the catfish, *Ictalurus punctatus*. *Cell Tiss. Res.*, **169**: 395-403.
13. Goossens, N. and Vandenbergh, M. P. (1974) The basal cells in the papillae fungiformes of the tongue of the common frog, *Rana temporaria*, L. *Arch. histol. Jap.*, **36**: 173-179.
14. Gu, J., Polak, J. M., Tapia, F. J., Marangos, P. J.

- and Pearse, A. G. E. (1981) Neuron-specific enolase in the Merkel cells of mammalian skin. The use of specific antibody as a simple and reliable histologic marker. *Am. J. Pathol.*, **104**: 63-68.
- 15 Hartschuh, W., Weihe, E., Bucher, M., Hemsteadler, V., Feurle, G. E. and Forsmann, W. G. (1979) Met-Enkephalin-like immunoreactivity in Merkel cells. *Cell Tiss. Res.*, **201**: 343-348.
- 16 Hartschuh, W., Reinecke, M., Weihe, E. and Yanaihara, N. (1984) VIP-immunoreactivity in the skin of various mammals: immunohistochemical, radioimmunological and experimental evidence for a dual localization in cutaneous nerves and Merkel cells. *Peptides*, **5**: 239-245.
- 17 Zaccane, G. (1986) Neuron-specific enolase and serotonin in the merkel cells of conger-eel (*Conger conger*) epidermis. An immunohistochemical study. *Histochemistry*, **85**: 29-34.
- 18 Saurat, J. H., Didierjean, L., Skalli, O., Siegenthaler, G. and Gabbiani, G. (1984) The intermediate filament proteins or rabbit normal epidermal Merkel cells are cytokeratins. *J. Invest., Dermatol.*, **83**: 431-435.
- 19 Ness, K. H., Morton, T. H. and Dale, B. A. (1986) Identification of Merkel cells in oral epithelium using antikeratin and anti-neuroendocrine monoclonal antibodies. *J. Dent. Res.*, **66**: 1154-1158.
- 20 Ishikawa, H., Bischoff, R. and Holzer, H. (1969) Formation of arrowhead complexes with heavy meromyosin in a variety of cell types. *J. Cell Biol.*, **43**: 312-328.
- 21 Stenssas, L. J. (1971) The fine structure of fungiform papillae and epithelium of tongue of a south american toad, *Calyptocephalla gayi*. *Amer. J. Anat.*, **131**: 443-462.
- 22 Lane, E. B. (1982) Monoclonal antibodies provide specific intramolecular markers for the study of epithelial tonofilament organization. *J. Cell Biol.*, **92**: 665-673.
- 23 Pearse, A. G. E. (1975) Neurocristopathy, neuroendocrine pathology and the APUD concept. *Z. Krebsforsch.*, **84**: 1-18.
- 24 Moore, B. W. (1965) Soluble protein characteristic of the nervous system. *Biochem Biophys Res. Commun.*, **19**: 739-744.
- 25 Cocchia, D., Michetti, F. and Donato, R. (1981) Immunochemical and immunocytochemical localization of S-100 antigen in normal human skin. *Nature*, **294**: 85-87.
- 26 Takahashi, K., Yamaguchi, H., Ishizeki, J., Nakajima, T. and Nakazato, Y. (1981) Immunohistochemical and immunoelectron microscopic localization of S-100 protein in the interdigitating reticulum cell of the human lymph nodes. *Virchows Arch. [Cell Pathol.]*, **37**: 125-135.
- 27 Stefansson, K., Wollman, R. L., Moore, B. W. and Arnason, B. G. (1982) S-100 protein in human chondrocytes. *Nature*, **295**: 63-64.
- 28 Zabel, M. and Dierel, M. (1987) S-100 protein and neuron-specific enolase in parathyroid gland and C-cells of the thyroid. *Histochemistry*, **86**: 389-392.
- 29 Schubart, U. K. and Fields, K. L. (1984) Identification of a calcium-regulated insulinoma cell phosphoprotein as an islet cell keratin. *J. Cell Biol.*, **98**: 1001-1009.



Use of the Laser Microbeam for Preserving Frozen *Drosophila* Embryos

YUKIAKI KURODA¹, YUKO TAKADA and TAKAHIRO KASUYA²

Laboratory of Phenogenetics, Department of Ontogenetics, National Institute of Genetics, Mishima 411, and ²Microbeam Physics Laboratory, The Institute of Physical and Chemical Research, Wako 351-01, Japan

ABSTRACT—The possibility of using the laser microbeam to preserve early embryos of *Drosophila melanogaster* at -196°C was examined. To date, the most difficult problem encountered in freezing *Drosophila* embryos has involved the method by which a protective agent is introduced into the eggs through the vitelline membrane. In the present study, a UV laser microbeam was applied to inflict breaks or cuts on the micropile of the eggs in order to allow protective glycerol to enter. Specifically, the laser was directed against the micropile of dechorionated eggs, after which the eggs were incubated at 25°C in Medium K-17 supplemented with fetal bovine serum and glycerol. Following a 1–24 hr incubation, the eggs were frozen rapidly at -196°C in liquid nitrogen. After at least another 24 hr, the eggs were thawed and incubated in a physiological salt solution at 25°C . A few of the eggs hatched, and the larvae grew to adult flies. Glycerol incorporation was confirmed by staining the eggs with neutral red. The survival rate of frozen, irradiated eggs increased upon incubation with glycerol for at least 16 hr. The stage and site of eggs to be laser irradiated, the conditions of incubation, and the rates of freezing and thawing are now under investigation so as to yield a larger number of viable eggs.

INTRODUCTION

Drosophila has always been one of the most widely and commonly used systems in genetics. Recently, it has become an useful tool in addressing the broader problems of developmental and molecular biology, and behavioral and population genetics as well. Currently, a tremendous number of wild-type and mutant strains of *Drosophila* are being maintained in the laboratories of universities and institutes throughout the world. Most stock cultures of *Drosophila* are kept at temperatures of 25°C or slightly lower. They are maintained by mating male and female flies, and rearing hatched larvae on agar in bottles. The day-to-day operation for maintaining these stocks entails enormous cost, labor, and time.

On the other hand, microorganisms, cultured cells [1], sperm [2] and ovum [3] can be maintained simply by freezing at subzero temperatures. More

complex organisms such as mammalian embryos at the early stage of development can also be frozen at subzero temperature [4]. To freeze these organisms, the introduction of a protective agent such as dimethyl sulfoxide (DMSO), or glycerol is essential to prevent intracellular ice-crystal formation which destroys the organella.

Drosophila eggs are surrounded by two distinct membranes, the chorion and the vitelline membrane. The chorion is easily removed by immersing eggs in sodium hypochloride solution. The vitelline membrane, however, is very tolerant to chemicals, and prevents protective agents from entering the eggs.

In the present study an attempt was made to use the laser microbeam for punching small holes on the vitelline membrane and permitting the protective agent to enter the eggs.

MATERIALS AND METHODS

Preparation of dechorionated eggs

Eggs were collected from adult flies of the

Accepted August 3, 1988

Received March 23, 1988

¹ To whom reprint requests should be addressed.

wild-type Oregon-R strain of *Drosophila melanogaster* reared on the standard cornmeal-sugar-agar medium. The eggs were dechorionated by treatment with 3% sodium hypochloride solution for 6 min, whereupon they were washed with distilled water, and transferred to a physiological salt solution (0.7 g NaCl, 0.02 g KCl, 0.002 g $\text{CaCl}_2 \cdot 2\text{H}_2\text{O}$, 0.01 g $\text{MgCl}_2 \cdot 6\text{H}_2\text{O}$, 0.005 g NaHCO_3 , 0.02 g $\text{NaH}_2\text{PO}_4 \cdot 2\text{H}_2\text{O}$ and 0.08 g glucose in 100 ml of distilled water). The developmental stages of dechorionated eggs were readily observed through the transparent vitelline membrane using a binocular microscope. Some experiments were carried out with eggs at a wider range of developmental stages from St. 1 to St. 13. Other experiments were carried out with eggs of the same general developmental stage according to the Bownes' stages [5].

Laser microbeam irradiation

Eggs of the appropriate developmental stage

were transferred to a thick plastic slide plate ($74 \times 32 \times 3.2$ mm), containing in a $20 \text{ mm} \times 20 \text{ mm}$ area at the center grooves 0.5 mm wide and 0.5 mm deep. The eggs were arranged tandemly in these grooves. A small drop of either the physiological salt solution or culture medium was then added, and the slide was covered with a glass cover slip (Matsunami Glass, $24 \text{ mm} \times 32 \text{ mm}$; 0.13–0.17 mm thick). This was placed on the stage of a microscope which had been incorporated into a laser microinjector system [6] (Fig. 1). The third-harmonic wave of a Nd:YAG laser (wavelength = 355 nm, pulse duration: 5 ns) was employed for irradiation. A laser beam with a spot size of $0.5 \mu\text{m}$ was focused through an incident-light microscope objective (Carl Zeiss, Ultrafluor $32\times$) onto the micropile of each egg. This particular target was chosen, because it was an extra-embryonic part of the egg and irradiating it was thought to have a minimal effect on the embryos. Several shots of laser pulses, each of about $10 \mu\text{J}$ energy, were

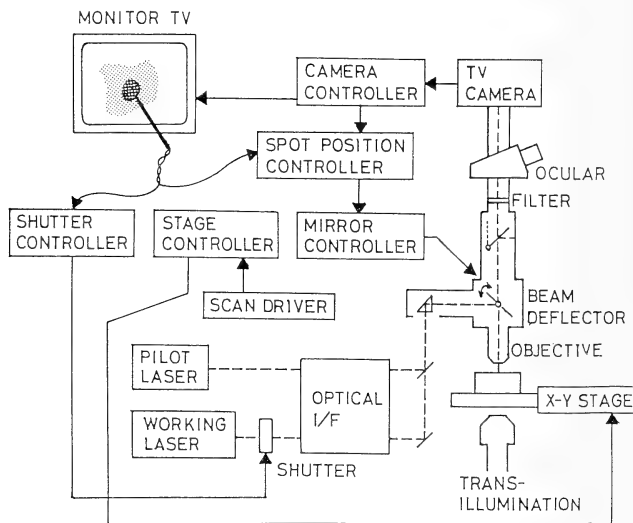


Fig. 1. Diagrammatic representation of electric and optical arrangement of UV laser microbeam for irradiating *Drosophila* eggs.

delivered into a small spot of a micrometer size on the micropile of eggs. Exact aiming was accomplished by pointing the target image on TV monitor screen with a light pen.

Incorporation of glycerol

The slide plates with the irradiated eggs were dipped in a 100 mm petri dish containing 15% glycerol in culture medium. The eggs were then liberated from the slide plate by a pipette, and incubated at 25°C in order to permit glycerol to enter. The culture medium consisted of Medium K-17 [7, 8], supplemented with 10% or 15% fetal bovine serum (GIBCO Laboratories). Entry of glycerol was verified by adding 0.001% neutral red to the culture medium and observing for its uptake by the embryos under a binocular microscope.

Freezing eggs at -196°C

Treated eggs were transferred to small glass vials (15×40 mm) containing 3 ml of 15% glycerol in culture fluid. The glass vials were rapidly frozen at -196°C in a liquid nitrogen container (Dia Cryogenic Co., DC Type). No attempt was made to freeze eggs gradually by using a programming freezer.

Survival assays of frozen eggs

Frozen eggs in the glass vials were thawed in warm water. The eggs were transferred to 35 mm petri dishes containing a physiological salt solu-

tion, and incubated at 25°C. The eggs were kept under observation to see whether they developed and hatched. The larvae were then transferred to the standard agar medium and allowed to develop into adult flies.

RESULTS

Effect of laser irradiation on survival of eggs

Dechoriation of eggs had some effect on hatchability. When these eggs were incubated in a physiological salt solution at 25°C, hatchability was reduced (Table 1). The reduction in hatchability of dechorionated eggs was dependent on the developmental stage of the eggs preceding incubation.

Eggs dechorionated during the early stages of development were affected more severely than those dechorionated during the late stages. The duration of incubation in the physiological salt solution may have had something to do with this effect.

Table 1 shows that when eggs at a wider range of developmental stages (St. 1 to St. 13) was irradiated by laser microbeam as described under Materials and Methods, the hatchability was 26.1% in physiological salt solution. On the other hand, a similar mixed population irradiated by the laser showed a hatchability of 46.9% in Medium K-17 supplemented with 15% fetal bovine serum and

TABLE 1. Effect of laser irradiation on survival of *Drosophila* eggs

Laser irradiation	Incubation medium	Stage of eggs ^b	No. of eggs irradiated	No. of eggs hatched	Hatchability (%)
—	PSS ^a	St. 1–2	1,477	219	14.8
—	PSS	St. 3–6	2,188	397	18.1
—	PSS	St. 7–10	13,808	1,725	12.5
—	PSS	St. 11–13	1,164	618	53.1
—	PSS	St. 14–	1,429	1,080	75.6
+	PSS	St. 1–13	115	30	26.1
+	Medium K-17 +15% FBS ^c +15% glycerol	St. 1–13	143	67	46.9

^a PSS: Physiological salt solution (see Materials and Methods).

^b Bownes' developmental stage of *Drosophila melanogaster* [5].

^c FBS: Fetal bovine serum.

15% glycerol. Thus, it was decided to include K-17 supplemented medium in subsequent experiments in order to enhance the viability of the eggs.

Uptake of protective agents by the eggs

For maintaining the viability of eggs at subzero temperatures, it was necessary to introduce an agent to protect against ice-crystal formation in the egg cytoplasm. In the present experiment, 15% glycerol was used as the protective agent. Laser-irradiated eggs were incubated in Medium K-17

supplemented with 15% fetal bovine serum and 15% glycerol. Neutral red was also included in the medium as a visual indicator of the embryonic uptake of the smaller glycerol molecule. Following incubation for 2, 3, 4 or 16 hr, the eggs were examined for the presence of neutral red under a binocular microscope. The results are shown in Table 2. Irradiated eggs were stained with neutral red from the anterior end through the micropile which had been the target of the laser (Fig. 2).

Following two hr of incubation, strongly or

TABLE 2. Stainability of laser-irradiated *Drosophila* eggs with neutral red

Laser irradiation	Time of incubation (hr)	Stage of embryos	No. of embryos irradiated	Stainability			
				++ ^a	+ ^b	± ^c	— ^d
—	16	St. 1-13	180	0(0%)	0(0%)	0(0%)	180(0%)
+	2	St. 1-13	105	9(8.6%)	13(12.4%)	12(11.4%)	71(67.6%)
+	3	St. 1-13	132	8(6.1%)	15(11.4%)	20(15.1%)	89(67.4%)
+	4	St. 1-13	132	12(9.0%)	17(12.9%)	29(22.0%)	74(56.1%)
+	16	St. 1-13	143	15(10.5%)	85(59.4%)	30(20.3%)	13(9.1%)

^a ++: Strongly stained. ^b +: Moderately stained. ^c ±: Faintly stained. ^d —: No stained.

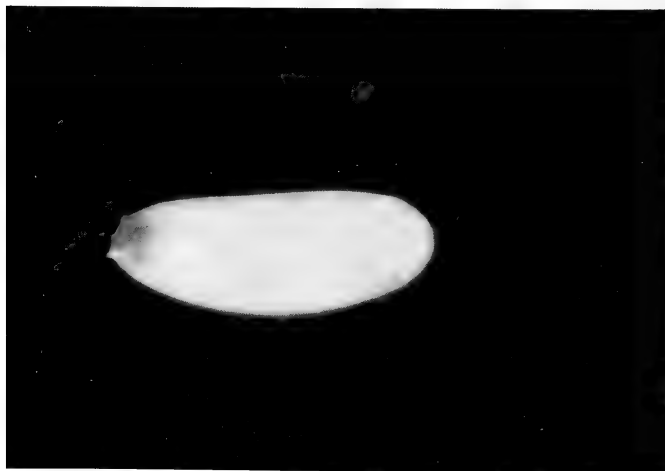


FIG. 2. A *Drosophila* egg irradiated at the micropile by laser microbeam, and incubated in culture medium supplemented with 15% glycerol and 0.001% neutral red for 2 hr.



FIG. 3. *Drosophila* eggs irradiated at the micropile by laser microbeam, and incubated in culture medium supplemented with 15% glycerol and 0.001% neutral red for 16 hr.

TABLE 3. Survival and growth of laser-irradiated *Drosophila* eggs after freezing and thawing

Laser irradiation	Incubation		Stage of eggs	No. of eggs	No. of larvae hatched	No. of adults
	Medium	Time (hr)				
—	Medium K-17 +15%FBS +15%glycerol	16	St. 1-13	1,000	0	0
+	Medium K-17 +15%FBS +15%glycerol	1	St. 1-13	151	1	0
+	„	1.5	St. 1-13	178	2	0
+	„	2	St. 1-13	107	0	0
+	„	3	St. 1-13	51	0	0
+	Medium K-17 +15%FBS +15%glycerol	1	St. 1-13	62	0	0
+	„	2	St. 1-13	113	3	0
+	„	3	St. 1-13	52	0	0
+	„	4	St. 1-13	54	0	0
+	„	5	St. 1-13	62	0	0
+	„	16	St. 1-13	46	0	0
+	„	24	St. 1-13	126	5	2 (♂)
+	Medium K-17 +15%glycerol	16	St. 1-13	43	3	1 (♀)
+	PSS+15%glycerol	0.5	St. 1-13	44	1	0

FBS: Fetal bovine serum. PSS: Physiological salt solution.

moderately stained eggs comprised approximately one fifth of the total number of irradiated eggs. From this point on, the percentage of stained eggs increased gradually as the incubation time was prolonged. When a similarly irradiated mixed population eggs at a wider range of developmental stages (st. 1—St. 13) was incubated, their embryonic development proceeded, and some of the eggs hatched. During the course of development, the neutral red was distributed unevenly within the embryo and was found to be concentrated in specific tissues and organs, such as the mid-gut, muscle, and nervous system (Fig. 3). On the contrary, no uptake of neutral red was found in non-irradiated control eggs after incubation for 16 hr.

These results indicate that certain substances may be effectively introduced into embryos by irradiating the micropile with lasers.

Freezing and thawing of eggs

Laser-irradiated eggs were incubated in Medium K-17 supplemented with 15% fetal bovine serum and 15% glycerol for various periods of time at 25°C. They were then transferred to glass vials containing the same medium and glycerol, and frozen rapidly at -196°C in liquid nitrogen. After at least 24 hr, the eggs were thawed quickly in warm water and incubated in physiological salt solution at 25°C. Table 3 shows the results of this experiment. Nonirradiated control eggs did not hatch following the freeze-thaw process. On the other hand, laser-irradiated eggs were able to hatch, albeit at a very low rate. The larvae, however, were unable to mature into adult flies when they were transferred to the standard agar medium, if they were incubated for less than 2 hr in glycerol-supplemented medium before freezing.

It was exciting to note that 5 of 126 irradiated eggs and subsequently frozen eggs hatched, and that two of the larvae subsequently grew into male flies. These males came from eggs which had been incubated in the glycerol supplemented medium for 24 hr prior to freezing. This indicates that higher survivability may be achieved by extending the incubation time with the glycerol supplemented medium prior to freezing. The preliminary experiment showed that these males were

fertile and produced normal F₁ flies when they were mated with females from the wild-type Oregon-R strain. In a separate experiment, it was noted that a 16 hr incubation in serum-free medium with glycerol also improved the hatchability of the eggs and the survivability of the larvae (Table 3).

DISCUSSION

Laser-irradiated *Drosophila* eggs which had been frozen at -196°C were able to hatch into larvae capable of growing into adult flies, although the rate was very low. This study may be the first reporting of a successful method for ensuring the survival of *Drosophila* eggs following freezing at -196°C. Exposure of the eggs to laser irradiation produced breaks and cuts on the micropile from which the protective agent glycerol was able to seep inside. It was shown that the visual indicator neutral red entered the egg cytoplasm from the anterior end and gradually diffused to other parts of the embryo. Glycerol and neutral red are highly soluble in water. The embryonic uptake of neutral red suggested that glycerol with one third molecular weight of neutral red may be effectively introduced into embryos irradiated with lasers. Since the maturation of hatched larvae from these eggs appeared to be dependent on the incubation time with glycerol prior to freezing, it can be hypothesized that glycerol takes at least 16 hr to diffuse throughout the egg from the micropile wound.

It takes the fertilized egg of *Drosophila* about 10 days at 25°C to develop into the adult fly. At lower temperatures, the speed of development slows down, and the life cycle lengthens. In many laboratories, some of the *Drosophila* stocks are maintained at 18°C. This saves the cost and the labor for maintenance. At even lower nonfreezing temperatures, certain stocks can be maintained for a fairly long time. These low temperatures, however, may have harmful effects on the physiological condition, metabolism, and function of *Drosophila*. On the other hand, freezing at -196°C is known to have no detectable effect on cultured cells, germ cells and early embryos of mammals [1-4]. This may be due to several factors including the short time required to pass through the critical

temperatures of -15°C to -20°C and the prevention of ice-crystal formation, dehydratation and concentration of electrolytes by added protective agents such as glycerol or dimethyl sulfoxide. Glycerol is nontoxic, and miscible with electrolytes, lipids, inorganic and organic compounds in the egg cytoplasm. Most significantly, glycerol or its related substances occur naturally in the insect egg cytoplasm. Dimethyl sulfoxide, on the other hand, is more toxic than glycerol, and does not appear to be suitable when organisms have to be incubated for relatively long periods to ensure adequate uptake.

In the present study, the hatching rate of eggs and the maturation rate of larvae were still very low following the laser irradiation-freezing process. The morphological, genetical and cytological examinations should be carried out on flies grown from larvae which were frozen at -196°C . Many problems need to be solved in order to improve these rates. The appropriate stage and site of eggs for laser-irradiation, the temperature at which incubation is carried out in glycerol medium, the speed of freezing and thawing, and the incubation media before and after freezing are all now undergoing further investigation.

ACKNOWLEDGMENTS

The laser irradiation experiments in the present study were all performed at the Institute of Physical and

Chemical Research employing the model system of microinjector provided by Hitachi Co. Ltd. The authors are grateful to Dr. Raleigh W. Hankins, Hoken Kagaku Laboratory, for his critical reading of this manuscript. One of the author (Y.K.) files this report as the contribution No. 1758 from the National Institute of Genetics, Mishima, Shizuoka, Japan.

REFERENCES

- 1 Scherer, W. F. and Hoogasian, A. C. (1954) Preservation at subzero temperatures of mouse fibroblasts (strain L) and human epithelial cells (strain HeLa). *Proc. Soc. Exp. Biol. Med.*, **87**: 480-487.
- 2 Polge, C., Smith, A. U. and Parker, A. S. (1949) Revival of spermatozoa after vitrification and dehydration at low temperatures. *Nature*, **164**: 666.
- 3 Parker, A. S. (1957) Viability of ovarian tissue after freezing. *Proc. Roy. Soc., London, SB*, **147**: 520-528.
- 4 Whittingham, D. G., Leibo, S. P. and Mazur, P. (1972) Survival of mouse embryos frozen to -196°C and -269°C . *Science*, **178**: 411-414.
- 5 Bownes, M. (1975) A photographic study of development in the living embryo of *Drosophila melanogaster*. *J. Embryol. Exp. Morphol.*, **33**: 789-801.
- 6 Tsukakoshi, M., Kurata, S., Nomiyama, Y., Ikawa, Y. and Kasuya, T. (1984) A novel method of DNA transfection by laser microbeam cell surgery. *App. Phys. B*, **35**: 135-140.
- 7 Kuroda, Y. (1974) Studies on *Drosophila* embryonic cells *in vitro*. I. Characterization of cell types in culture. *Develop. Growth Differ.*, **16**: 55-66.
- 8 Kuroda, Y. (1974) Spermatogenesis in pharate adult testes of *Drosophila* in tissue cultures without ecdysterones. *J. Insect Physiol.*, **20**: 637-640.



Comparison of Two Lectins Isolated from *Xenopus* Cortical Granules

NORIO YOSHIZAKI

*Department of Biology, Faculty of General Education,
Gifu University, Gifu 501-11, Japan*

ABSTRACT—Two cortical granule lectins (CGLs) of *Xenopus laevis* were compared by PAGE, immunodiffusion, immunoblot, atomic absorption and amino acid analysis. The CGL was released following activation of coelomic eggs by electric stimuli and purified by affinity chromatography with immobilized melibiose. On PAGE in native condition, the purified CGL existed in two different molecular forms, CGL-1 and CGL-2. The two were isolated electrophoretically from polyacrylamide gel. The CGLs had the following characteristics in common: (1) the specific activity of hemagglutination; (2) the specific binding to galactosides; (3) a calcium requirement; (4) calcium content of 5.69–7.24 mole per 10^5 g protein, and (5) antigenicity to an antiserum raised against CGL-1. Differing characteristics included: (1) the molecular weights of the subunits (42 kDa and 46 kDa for CGL-1, and 39–46 kDa for CGL-2); (2) the pI value of the native lectins (4.55 for CGL-1 and 4.70 for CGL-2); (3) the isofocusing pattern of the subunits, and (4) the amino acid composition, such that the amount of tyrosine is less but that of valin and tryptophan greater in CGL-2 than in CGL-1. So CGL-1 and CGL-2 differ in their particular combination of subunits, each of which is heterogeneous in size, charge and amino acid sequence.

INTRODUCTION

Upon fertilization in *Xenopus laevis*, cortical granule materials released into the perivitelline space pass through the vitelline coat and interact with a prefertilization layer produced by the oviduct to form a fertilization (F) layer [1–4]. The F layer is assumed to be a “macromolecular block” that functions as a polyspermy block [5] and that enables the normal development of an embryo by producing turgid pressure in the perivitelline space [7]. Lectin (CGL) activity to form the F layer has been detected in an exudate of cortical granules [7, 8]. The CGL has also been shown histologically to be localized in the cortical granules and in the F layer [9].

The CGL is a major component of the cortical granule exudate [10]. It is apparent by polyacrylamide gel electrophoresis of native lectin that CGL is a mixture of two lectins, CGL-1 and CGL-2, the molecular weights of which are 539 kDa and 655

kDa, respectively [7]. Extensive biochemical characterization has been made of this mixture on the assumption that the two lectins are “size isomers” [7, 11]. In the present report, the author describes the isolation of the individual lectins and compare their biochemical natures. These two lectins share several characteristics but are different in their combination of subunit components, each of which is heterogeneous.

MATERIALS AND METHODS

Isolation and purification of the lectin

Xenopus laevis were purchased from a dealer in Hamamatsu. Coelomic eggs were obtained by ligating the uppermost portion of the oviduct of anesthetized females in an ice bath and inducing ovulation by injection of 1,000 IU of the gonadotropic hormone Gonatropin (Teikoku Zoki Co.) into the females. The coelomic eggs were washed several times in De Boer solution (110 mM NaCl, 1.3 mM KCl, 1.3 mM CaCl_2 , adjusted to pH 7.4 with NaHCO_3) and artificially activated with a 100

V AC current for 5 sec.

The cortical granule exudate obtained was dialyzed overnight against distilled water, freeze-dried and dissolved in TCS (10 mM Tris-HCl, 1 mM CaCl_2 , 150 mM NaCl, pH 7.4). Insoluble substances were removed by centrifugation at $7,000 \times g$ for 15 min (4°C). The supernatant was fractionated on an affinity column according to the method of Roberson and Barondes [12]. The supernatant was loaded over a 5-ml column of aminoethylated polyacrylamide gel conjugated with melibiose (Pierce Chemical Co.) and equilibrated with TCS. Materials were eluted at a flow rate of 20 ml/hr and fractions of 2 ml were collected. The column was washed with TCS extensively until the absorption at 280 nm decreased to the basal level and then the cortical granule lectins (CGLs) were eluted with TCS containing 0.3 M galactose. Fractions of CGLs were pooled, dialyzed against De Boer solution overnight, concentrated, and subjected to 5% polyacrylamide slab gel electrophoresis (PAGE) by the method of Davis [13]. Sections of 3 mm width at $\text{Rf}=0.155$ and 0.111 for the CGL-1 and CGL-2, respectively, were scraped off and cut into several pieces. Each lectin was extracted electrophoretically from the pieces of gel into 2.5 mM Tris-HCl buffer, pH 8.3, in a Max-Yield Protein Concentrator (Atto Co.) at 5 W for 2.5 hr. At the time of chemical and biochemical analyses, the lectins were further dialyzed overnight against distilled water.

Hemagglutination assay

Agglutination assays were done in microtiter V plates using serial two-fold dilutions of the test materials. Defibrinated rabbit erythrocytes were purchased from Japan Biological Material Center (Nagoya) and washed 3 times in VS (10 mM Veronal-HCl, 150 mM NaCl, 1 mM CaCl_2 , 1 mM MgCl_2 , pH 7.4). Each well contained 25 μl of the CGL diluted in VS, 25 μl of VS, and 50 μl of rabbit erythrocytes (10% in volume) in VS. The erythrocytes were added last, after which the plates were shaken vigorously. Agglutination was determined after 90 min. For sugar inhibition experiments, the sugar in question was diluted to appropriate concentrations in VS and added in place of the VS. For metal activation experiments, all the materials

were prepared in Ca- and Mg-free VS (CMFVS): the metal chloride in question was dissolved in CMFVS, the erythrocytes were washed in CMFVS, and the CGLs were treated once with 2 mM EDTA at room temperature for 3 hr and dialyzed extensively against CMFVS.

Electrophoresis

The method for PAGE of the native material was outlined in the *Purification* section. Slab sodium dodecyl sulfate (SDS)-PAGE in 15% gel was carried out as described by Laemmli [14]. The molecular weights of the subunit proteins were estimated from a calibration curve obtained with the standard proteins in the MW-SDS-200 kit (Sigma).

Native proteins were isofocused on a polyacrylamide gel of "Ampholine PAG plates" (LKB Instruments) at pH 4.0–6.5 according to the instruction manual. The proteins denatured in 8 M urea, were isofocused in the presence of mercaptoethanol according to the method of O'Farrell [15]. The gels were stained with Coomassie blue. Silver staining was also done to check the purity of the isolated lectins.

Immunodiffusion and immunoblot

Purified CGL-1 was emulsified in Freund's complete adjuvant to be injected into rabbits by the subcutaneous route. Immunodiffusion in two dimensions was performed in a 1% agarose gel containing 50 mM NaCl, 25 mM Tris, 10 mM maleic acid and 0.5 mM EDTA. For immunoblot analyses, the lectins were electrophoresed in 5.6% native polyacrylamide gel and electroblotted to nitrocellulose membranes. The membranes were blocked overnight in a phosphate-buffered saline solution (PBS, pH 7.2) containing 10% normal sheep serum and 4% bovine serum albumin (BSA), treated with an antiserum diluted to 1/50 in PBS containing 4% BSA for 1 hr, and treated with horseradish peroxidase (HRP)-conjugated sheep antirabbit IgG for 1 hr according to the method of Smith [16]. A control experiment was made by treating the membranes with non-immune rabbit serum in place of the antiserum. The method of Adams [17] was used to detect HRP.

Chemical methods

Protein was determined by the method of Smith *et al.* [18] using bicinchoninic acid with BSA as a standard.

Calcium content in the CGLs was determined by an atomic absorption spectrophotometric method with an atomic absorption spectrometer (Hitachi, 180-70).

For amino acid analyses, CGLs dialyzed against distilled water were hydrolyzed in vacuo in 6 N HCl at 110°C for 24 hr and the amino acid content was determined by a JEOL amino acid analyzer, JLC-6AH. The amount of tryptophan was determined by procedure of Edelhoch [19].

RESULTS

Electrophoretic behaviour of the cortical granule lectins

The lectin purified by affinity chromatography was a mixture of two lectins (CGL-1 and CGL-2), as can be seen in the PAGE pattern of native



FIG. 1. PAGE (6.5%) of native cortical granule lectin (CGL). Samples of 20 μ g of protein from CGL (A) purified by affinity chromatography and of approximately same amount of CGL-1 (B) and CGL-2 (C) obtained as an electrophoretic extract from the corresponding portion of lane A on 5% gel were subjected to electrophoresis. Faint bands are thought to be an aggregation of the lectins.

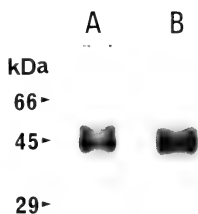


FIG. 2. SDS-PAGE of denatured CGL-1 (A) and CGL-2 (B). Subunit proteins of CGL-1 are concentrated in the bands corresponding to 42 kDa and 46 kDa whereas those of CGL-2 are distributed between 39 kDa and 46 kDa.

proteins (Fig. 1A). Occasionally more proteins, which should be an aggregation of the above-mentioned lectins, appeared near the origin of a gel. The CGL-1 and CGL-2 were obtained separately by electrophoretically removing them from the corresponding part of the gel (Fig. 1B and C). On SDS-PAGE of the lectins after denaturing, the subunits of CGL-1 were concentrated in the bands corresponding to molecular weights of 42 kDa and 46 kDa, whereas those of CGL-2 were distributed evenly between 39 kDa and 46 kDa, suggesting that the CGL-1 and CGL-2 were different in the subunit composition (Fig. 2).

The lectins isofocused in native condition showed that the pI value of CGL-1 is 4.55 and that of CGL-2 is 4.70 (Fig. 3). When the lectins denatured in urea were isofocused, approximately eleven components ranging from pI 4.30 to 5.00 were observed, eight of which are major bands ranging from pI 4.40 to 4.70 and three of which are less intense [11]. Although the number of component species was the same in both lectins, the four components of CGL-2 with pI values from 4.55 to 4.70 became more intensely stained than those of CGL-1 (Fig. 4). This means that both lectins consist of the same components but the number of individual components differs.

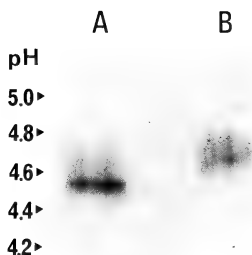


FIG. 3. Isoelectric focusing in a polyacrylamide gel of native CGL-1 (A) and CGL-2 (B). The pI value is 4.55 for CGL-1 and 4.70 for CGL-2.

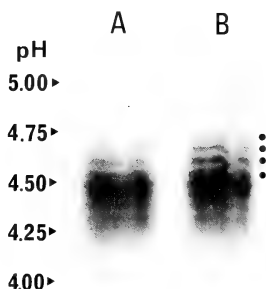


FIG. 4. Isoelectric focusing in a polyacrylamide gel of denatured CGL-1 (A) and CGL-2 (B). Both lectins are composed of the same subunit proteins. Note that the subunits (marked with dots) from pI 4.55 to 4.70 in the case of CGL-2 are stained more intensely than those in that of CGL-1.

Immunodiffusion and immunoblot

Purified CGL-1 gave a single precipitin line in double-diffusion experiments using an antiserum against the CGL-1. The CGL-2 cross-reacted with the antiserum and no spur was observed in the precipitin line (Fig. 5). When this antiserum was applied to a nitrocellulose membrane on which a mixture of the lectins was westernblotted and the membrane was subjected to an HRP reaction,



FIG. 5. Immunodiffusion agarose plate stained with Coomassie blue. CGL-1 (A) forms a precipitin line with an antiserum (B) raised against CGL-1. CGL-2 (C) cross-reacts with the antiserum but there is no spur. D, non-immune serum.



FIG. 6. Immunoblot test of the lectin. Nitrocellulose membranes on which the affinity-purified lectins are westernblotted were treated with the antiserum and subjected to the HRP reaction (A). Each lectin is stained in proportion to its amount (cf., lane A in Fig. 1). The control membrane (B) treated with the non-immune serum was printed heavily to show the location of lectins.

CGL-1 and CGL-2 were each stained at an intensity approximately parallel to the amount (Fig. 6).

Hemagglutination activity

The hemagglutination activity of the two lectins was compared using serial two-fold dilutions of the lectins in microtiter plates. The minimal concentration of each lectin at which hemagglutination occurred was 13.3 ng/ml (mean of two experiments) for CGL-1 and 6.2 ng/ml for CGL-2.

Although the minimal concentration of CGL-1 was twice that of CGL-2, the difference was insignificant considering that it appeared in one dilution step after 13–16 steps of dilution. Thus the specific hemagglutination activity per protein amount seems to be the same for each lectin.

Effect of saccharides on hemagglutination activity

The saccharide specificity of the lectins was investigated by inhibiting the hemagglutinating reaction with various sugars in serial two-fold dilution. The hemagglutination activity of the

TABLE 1. Effect of metal chlorides on CGL activity: minimal concentration (mM) restoring hemagglutination activity of EDTA-treated lectins (400 ng/ml)

Cations	CGL-1*		CGL-2*	
Zn	0.14	(0.29)	0.29	(0.29)
Co	9.4	(9.4)	18.8	(18.8)
Fe	0.58	(1.17)	1.17	(1.17)
Cu	0.14	(0.14)	0.14	(0.14)
Ni	1.17	(2.35)	4.7	(4.7)
Mg	>150	(>150)	>150	(>150)
Mn	>150	(>150)	>150	(>150)
Ca	0.07	(>150)	0.04	(>150)

* Numbers in parentheses are minimal concentrations of cations to cause hemagglutination in the absence of EDTA-treated lectins.

TABLE 2. Amino acid composition of CGL-1 and CGL-2

Amino acids	CGL-1	CGL-2	CGL-2/CGL-1
Asp	13.3*	12.8*	1.0
Thr	5.3	5.5	1.0
Ser	8.2	7.9	1.0
Glu	8.0	8.1	1.0
Pro	4.5	4.7	1.0
Gly	10.7	10.7	1.0
Ala	6.6	6.2	0.9
Cys	1.8	1.9	1.1
Val	2.1	3.0	1.4
Met	1.4	1.4	1.0
Ileu	2.2	2.4	1.1
Leu	6.3	6.0	1.0
Tyr	10.2	8.0	0.8
Phe	6.1	6.7	1.1
His	1.2	1.2	1.0
Lys	4.4	4.6	1.0
Try**	4.2	5.2	1.2
Arg	3.5	3.5	1.0

* Expressed as residues per 100 residues.

** According to Edelhoch (1967).

lectins was inhibited by α -lactose, β -lactose, methyl- α -galactoside, D-galactose, melibiose, and methyl- β -galactoside in this order, but not inhibited by D-glucose, D-mannose, L-fucose, acetylgalactosamine and acetylglucosamine. The difference between CGL-1 and CGL-2 with respect to the minimal concentration of the sugars to inhibit the lectin activity was insignificant.

Effect of metals on hemagglutination activity

EDTA-treated lectins displayed no hemagglutination activity. To define which metal is involved in the lectin activity, various metal chlorides in serial two-fold dilutions were added to hemagglutination plates containing EDTA-treated lectins. Since some of the metals used have the power to agglutinate erythrocytes in themselves, the metals were also tested under the same conditions but without lectins as a control. As shown in Table 1, Ca chloride effectively restored the activity of EDTA-treated lectins, but Zn, Co, Fe, Cu, Ni, Mg, and Mn chlorides did not. The difference between CGL-1 and CGL-2 with respect to the effect of metals was insignificant.

Calcium content of the lectins

The calcium content was determined by an atomic absorption method. The molar concentration per 10^5 g protein was 5.69 ± 1.10 (mean \pm SD, $n=3$) for CGL-1 and 7.24 ± 1.75 for CGL-2. Thus the difference between CGL-1 and CGL-2 in calcium content per protein amount was insignificant.

Amino acid composition of the lectins

The amino acid composition of CGL-1 and CGL-2 is presented in Table 2. The amount of tyrosine is less but the amounts of valine and tryptophan more in CGL-2 than in CGL-1. Other amino acids are present in both lectins in nearly the same amounts. This pattern of amino acid composition was obtained by a duplicate experiment with different lots of the lectins.

DISCUSSION

The CGLs purified by affinity chromatography separate into CGL-1 and CGL-2, molecular weights of which are 539 kDa and 655 kDa in

PAGE analysis of native proteins [7]. The two lectins thus isolated shared the following characteristics: specific activity of hemagglutination, the specific galactosides to which they bind, a calcium requirement, calcium content, and antigenicity toward an antiserum raised against the CGL-1. On the other hand, they differed in their structures, evidenced by their isoelectric points in a native condition, the SDS-PAGE patterns, and in their amino acid compositions. Analysis of the lectins in a denatured condition by isoelectric focusing showed that CGL-2 has more subunits at pI 4.55–4.70 than does CGL-1. Therefore, CGL-1 and CGL-2 differ in the combination of subunits, each of which is heterogeneous in size, charge and amino acid sequence. Then the term "size isomer" which is used by Nishihara *et al.* [7] is not adequate to figure out the relationship of CGL-1 and CGL-2.

The amino acid sequence heterogeneity of subunits was indicated in the present study by the difference of the amino acid composition such that the amount of tyrosine is less but that of valine and tryptophan greater in CGL-2 than in CGL-1. Although Chamow and Hedrick [11] indicated significant amino acid homology of subunits by peptide mapping of subunits separated by isoelectric focusing, small difference of the amino acid sequence may not be represented by the peptide mapping.

The CGL studied is a metalloglycoprotein composed of 84% protein, 15.8% carbohydrate, and 0.19% calcium [7]. Although thorough analysis of the carbohydrates was not done in this study, CGL-1 and CGL-2 possessed at least the same amount of neutral sugars (unpubl.). The high amount of carbohydrate in CGL may make it impossible to calculate the exact number of subunits. As mentioned above, both lectins were composed of heterogeneous subunits. Chamow and Hedrick [11] have suggested that 10–12 subunits comprise the native molecule of CGL-1, based on SDS-PAGE analysis of the lectins after removing *N*-linked oligosaccharides.

In the unfertilized eggs, CGL is localized in the cortical granules and in the fertilized eggs it is located predominantly in the fertilization (F) layer and the perivitelline space [9]; when combined

with its ligand in the prefertilization layer, it forms the F layer [3, 8] and makes the egg impenetrable to sperm [20]. When the location of CGL was reexamined by immunofluorescent staining using the antiserum raised against CGL-1, a significant area of cytoplasm outside the cortical granules was also stained, indicating the presence of some sort of lectin (unpublished observation). This may not signify the presence of CGL in the ground cytoplasm, since lectins have been described in the eggs, embryos and adult liver of *Xenopus* and other amphibians [12, 21, 22, 23] and extensive amino acid sequence homologies were observed among animal lectins [24]. Thus heterogeneous lectins may be present in *Xenopus* eggs.

An intriguing point concerning CGL is its clearly established function, for the functions of many of the lectins identified are mostly a matter of speculation. However, the molecular mechanism by which sperm are blocked at the vitelline coat is yet unknown. The CGL may construct a physical barrier by means of the F layer, or may hide moieties of the vitelline coat the sperm bind on. It may decrease sperm accessibility to the eggs by binding to sperm membranes, as was suggested by sperm agglutination experiments (unpubl.), or may inactivate the molecules in the sperm or the egg which induce the secretion of the acrosomal enzyme needed to make a hole in the vitelline coat. To clarify the molecular mechanism, it is required merely to clarify the characteristics of the ligand molecules which are produced at the pars recta of the oviduct [4] and included in the prefertilization layer of the egg [3, 25].

ACKNOWLEDGMENTS

The author thanks Dr. Chitaru Oguro, Toyama University for measuring the calcium content and reading through the manuscript.

REFERENCES

- Grey, R. D., Wolf, D. P. and Hedrick, J. L. (1974) Formation and structure of the fertilization envelope in *Xenopus laevis*. *Devel. Biol.*, **36**: 44-61.
- Wolf, D. P. (1974) On the contents of the cortical granules from *Xenopus laevis* eggs. *Develop. Biol.*, **38**: 14-29.
- Yoshizaki, N. and Katagiri, Ch. (1984) Necessity of oviducal pars recta secretions for the formation of the fertilization layer in *Xenopus laevis*. *Zool. Sci.*, **1**: 255-264.
- Yoshizaki, N. (1985) Fine structure of oviducal epithelium of *Xenopus laevis* in relation to its role in secreting egg envelopes. *J. Morph.*, **184**: 155-169.
- Wyrick, R. E., Nishihara, T. and Hedrick, J. L. (1974) Agglutination of jelly coat and cortical granule components and the block to polyspermy in the amphibian *Xenopus laevis*. *Proc. Natl. Acad. Sci. USA*, **71**: 2067-2071.
- Nishihara, T. and Hedrick, J. L. (1977) A molecular mechanism for envelope elevation at fertilization. *Fed. Proc.*, **36**: 811.
- Nishihara, T., Wyrick, R. E., Working, P. K., Chen, Y. H. and Hedrick, J. L. (1986) Isolation and characterization of a lectin from the cortical granules of *Xenopus laevis* eggs. *Biochemistry*, **25**: 6013-6020.
- Yoshizaki, N. (1986) Properties of the cortical granule lectin isolated from *Xenopus* eggs. *Develop. Growth Differ.*, **28**: 275-283.
- Greve, L. C. and Hedrick, J. L. (1978) An immunocytochemical localization of the cortical granule lectin in fertilized and unfertilized eggs of *Xenopus laevis*. *Gamete Res.*, **1**: 13-18.
- Greve, L. C., Prody, G. A. and Hedrick, J. L. (1985) N-acetyl- β -D-glucosaminidase activity in the cortical granules of *Xenopus laevis* eggs. *Gamete Res.*, **12**: 305-312.
- Chamow, S. M. and Hedrick, J. L. (1986) Subunit structure of a cortical granule lectin involved in the block to polyspermy in *Xenopus laevis*. *FEBS Letters*, **206**: 353-357.
- Roberson, M. M. and Barondes, S. H. (1982) Lectin from embryos and oocytes of *Xenopus laevis*. *J. Biol. Chem.*, **257**: 7520-7524.
- Davis, B. J. (1964) Disc electrophoresis. II. Methods and application to serum proteins. *Ann. N. Y. Acad. Sci.*, **121**: 404-427.
- Laemmli, U. K. (1970). Cleavage of structural proteins during the assembly of the head of bacteriophage T4. *Nature*, **227**: 680-685.
- O'Farrell, P. H. (1975) High resolution two-dimensional electrophoresis of proteins. *J. Biol. Chem.*, **250**: 4007-4021.
- Smith, J. C. (1987) A mesoderm-inducing factor is produced by a *Xenopus* cell line. *Development*, **99**: 3-14.
- Adams, J. C. (1981) Heavy metal intensification of DAB-based HRP reaction product. *J. Histochem. Cytochem.*, **29**: 775.
- Smith, P. K., Krohn, R. I., Hermanson, G. Y., Mallia, A. K., Gartner, F. H., Provenzano, M. D., Fujimoto, E. K., Goeke, N. M., Olson, B. J. and

- Klenk, D. C. (1975) Measurement of protein using bicinchoninic acid. *Anal. Biochem.*, **150**: 76-85.
- 19 Edelhoch, H. (1967) Spectroscopic determination of tryptophan and tyrosine in proteins. *Biochemistry*, **6**: 1948-1954.
- 20 Grey, R. D., Working, P. K. and Hedrick, J. L. (1976) Evidence that the fertilization envelope blocks sperm entry in eggs of *Xenopus laevis*: Interaction of sperm with isolated envelopes. *Devel. Biol.*, **54**: 52-60.
- 21 Nitta, K., Takayanagi, G. and Kawauchi, H. (1984) Reactivity of lectin from *Xenopus laevis* eggs towards tumor cells and human erythrocytes. *Chem. Pharm. Bull.*, **32**: 2325-2332.
- 22 Sakakibara, F., Takayanagi, G., Kawauchi, H., Watanabe, K. and Hakomori, S. (1976) An anti-A-like lectin of *Rana catesbeiana* eggs showing unusual reactivity. *Biochem. Biophys. Acta*, **444**: 386-395.
- 23 Sakakibara, F., Kawauchi, H., Takayanagi, G. and Tse, H. (1979) Egg lectin of *Rana japonica* and its receptor glycoprotein of Ehrlich tumor cells. *Cancer Res.*, **39**: 1347-1352.
- 24 Paroutaud, P., Levi, G., Teichberg, V. I. and Strosberg, A. D. (1987) Extensive amino acid sequence homologies between animal lectins. *Proc. Natl. Acad. Sci. USA*, **84**: 6345-6348.
- 25 Yoshizaki, N. (1984) Immunoelectron microscopic demonstration of the pre-fertilization layer in *Xenopus* eggs. *Develop. Growth Differ.*, **26**: 191-195.

Studies on Embryonic Diapause in the *pnd* Mutant of the Silkworm, *Bombyx mori*: Characterization of Protein Synthesis during Early Development¹

HARUYUKI SONOBE

Department of Biology, Faculty of Science,
Konan University, Kobe 658, Japan

ABSTRACT—In the *pnd* mutant of the silkworm, *Bombyx mori*, developmental changes in the rate of protein synthesis were analyzed in homozygous, non-diapause type embryos, and in heterozygous, diapause type embryos. In the homozygotes, two distinct peaks of incorporation of [³H]amino acid mixture into protein were detected. These peaks corresponded to the stage of cellular blastoderm and the stage of organogenesis. The first peak in protein synthesis around the cellular blastoderm stage appeared in the heterozygotes as well as in the homozygotes. However, a second slight rise in protein synthesis was detected at the middle stage of gastrulation in the heterozygotes. In the two types of embryos, the first peak in protein synthesis, at the cellular blastoderm stage, occurred without elevation of RNA synthesis. In contrast, the second peak in protein synthesis was accompanied by an increase in the rate of RNA synthesis. These results suggest that protein synthesis prior to gastrulation is to be ascribed to maternal RNAs (probably mRNAs), however, beginning with the early gastrula stage, embryonic development involves predominantly the expression of embryonic genes. This inference was also supported by an inhibitor experiment by using actinomycin D. The results obtained are discussed in relation to the possible role of the *pnd*⁺ gene in the decrease in protein synthesis at the onset of embryonic diapause.

INTRODUCTION

The *Bombyx* silkworm produces two types of embryos, which are called non-diapause and diapause. Embryos of the former type develop continuously, and larvae hatch about 12 days after oviposition. However, embryos of the latter type cease development at a late stage of gastrulation and enter diapause. The embryonic diapause is preconditioned by a proteinaceous hormone, called diapause factor or diapause hormone, during oogenesis at the pharate adult stage [1-5]. Then diapause is triggered by the activity of a *pnd*⁺ gene (the wild type allele of the pigmented and non-diapausing egg gene) at the early-middle gastrula stage and the embryo enters diapause at the late gastrula [6]. Thus, two factors, the hormonal factor during oogenesis and the genetic factor

during embryogenesis, are required for the onset of embryonic diapause in the silkworm [6-10].

The homozygous embryo of the *pnd* mutant of the silkworm never enters diapause, owing to a genetic defect of the *pnd*⁺ gene, but the embryonic defect caused by the *pnd* mutation is repairable after fertilization by the action of the paternal *pnd*⁺ gene [6-10]. Recently, a putative *pnd*⁺ gene-specific protein was identified by use of two-dimensional gel electrophoresis [10]. In the course of biochemical studies of genetic control of embryonic diapause in the *pnd* mutant, we demonstrated that two distinct peaks of protein synthesis are detectable, and that these correspond to the stages of cellular blastoderm and organogenesis in the non-diapause type of embryo, but the diapause type of embryo does not exhibit the peak of protein synthesis that corresponds to the stage of organogenesis [10].

The purpose of this study is to characterize the stage-specific alterations in protein synthesis. I thus compared the changing pattern of protein

Accepted July 29, 1988

Received June 11, 1988

¹ "Studies on embryonic diapause in the *pnd* mutant of the silkworm, *Bombyx mori*. VI."

synthesis with that of RNA synthesis during early development, and then examined the effect of actinomycin D, a general inhibitor of RNA synthesis, on protein synthesis at various times during embryogenesis.

MATERIALS AND METHODS

Female moths of the homozygous *pnd* mutant of the silkworm, *Bombyx mori*, were used to obtain eggs. The female moths had been incubated at 25°C under continuous illumination during their embryonic development (for details, see [6, 8–10]). When these females were mated with males homozygous for *pnd*, the resulting embryos (homozygotes) were of the non-diapause type. On the other hand, when the homozygous female moths were mated with wild type males (Chinese No. 124 in this experiment), all of the resulting embryos (heterozygotes) were of the diapause type. These non-diapause and diapause eggs were used to analyze the patterns of RNA and protein synthesis. In order to sample closely synchronized eggs, the period of oviposition was limited to within 3 hr. The eggs were timed from the mid-point of the collection so that the starting material consisted of 0 ± 1.5 hr-old-eggs. The eggs collected were aged at 25°C until they attained the desired age for the experiments.

The changes in total RNA content during early development were determined as follows. At the appropriated developmental stages, 200 eggs were homogenized in 50 mM Tris-HCl buffer (pH 7.5) containing 10 mM $MgCl_2$, and the homogenate was centrifuged for 5 min at 800 rpm (Hitachi, 05 PR) to remove egg debris. Then an ice cold trichloroacetic acid (TCA) solution was added to aliquots of the supernatant to make a final concentration of 5%. The mixture was then maintained at 0°C for 30 min. TCA-insoluble material was collected and then treated with ethanol-ether (1:1, v/v) at 50°C to remove lipids. The RNA fraction was isolated according to the Schmidt and Thannhauser procedure [11]. The RNA was quantitated colorimetrically with the orcinol reagent [12]. The results were calculated to express the total RNA content per eggs.

The extent of incorporation of labelled precursors

was used as an estimation of the rate of RNA and protein synthesis. At the appropriate developmental stages in early embryogenesis, each egg was injected with 10 nl of [5,6- 3H]uridine (specific activity, 48 Ci/mmol, Amersham) or [3H]amino acid mixture (1 mCi/ml, TRK. 550, Amersham) according to the method of injection described in the previous paper [6]. Eggs injected with the labelled precursor were incubated in a humid chamber for 3 hr at 25°C. The incorporation was stopped by freezing the eggs at -70°C. The presence of label in protein was determined according to the method described by Sonobe and Otake [10]. Incorporation of [3H]uridine into acid insoluble material was determined by the method of Kress [13]. Over 95% of the [3H]uridine label incorporated into this fraction was in RNA (unpublished data). Radiactivity was assayed in toluene-based scintillator with an Aloka scintillation counter using an external standard to determine quenching. Eggs of known developmental stage were injected with actinomycin D (10 nl/egg) at a predetermined concentration (see Results). The degree of inhibition of RNA and protein synthesis by the actinomycin D treatment was calculated by taking the mean rate of incorporation of tritium-labelled precursor observed in treated eggs as a percentage of the mean rate of incorporation of control eggs. Results are the means of determinations made in three separate experiments.

RESULTS

Changes in rate of protein synthesis during early development

Figure 1 shows the incorporation of [3H]amino acid mixture into protein at different stages of embryogenesis. The first peak in protein synthesis was detected at the stage of cellular blastoderm (12-hr embryo). The rates of protein synthesis in the homozygotes and the heterozygotes were essentially identical throughout the stages of syncytial blastoderm (3-hr embryo), cellular blastoderm, and early gastrula (24-hr embryo). However, these rates became significantly different in the middle stage of gastrulation (36-hr

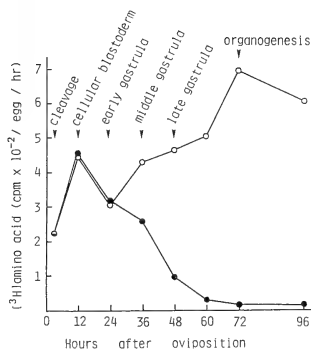


Fig. 1. Incorporation of $[^3\text{H}]$ amino acid mixture into protein at different stages of early development in the homozygotes and heterozygotes of the *pnd* mutant. \circ — \circ , homozygotes; \bullet — \bullet , heterozygotes. Eggs were injected with 10 nCi $[^3\text{H}]$ amino acid mixture, and incubated for 3 hr at 25°C. The acid insoluble material was collected on glass micro-fiber filters (GF/C, Whatman), and the radioactivity was counted. The stages of embryogenesis are based on Sonobe *et al.* [6].

embryo). In the homozygotes, protein synthesis increased gradually during the period which encompasses both the late stage of gastrulation (48-hr embryo) and the early stage of organogenesis (72-hr embryo). This second increase in protein synthesis lasted throughout organogenesis. On the other hand, in the heterozygotes the rate of protein synthesis decreased gradually after cellular blastoderm, although a small shoulder was detected at the middle stage of gastrulation. It finally fell to a trace amount at 3 days after oviposition, and this level was maintained thereafter, suggesting that the heterozygotes entered diapause. The pattern of incorporation of $[^3\text{H}]$ amino acid mixture into protein (Fig. 1) was almost the same as that of $[^{35}\text{S}]$ methionine [10].

Changes in RNA content and the rate of RNA synthesis during early development

Figure 2 shows changes in the amounts of total RNA at different stages of early embryogenesis in the homozygotes and heterozygotes. In the two

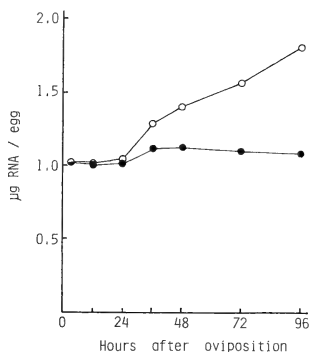


Fig. 2. Changes in the amounts of total RNA at different stages of early development in the homozygotes and heterozygotes of the *pnd* mutant. \circ — \circ , homozygotes; \bullet — \bullet , heterozygotes. The RNA fraction was isolated according to the Schmidt and Thannhauser procedure. The RNA was quantitated calorimetrically with the orcinol reagent. For further details, see text.

types of embryos, the RNA content remained low (about 1 $\mu\text{g}/\text{egg}$) until 24 hr after oviposition. In the homozygotes, the RNA content began to elevate linearly from 36 hr after oviposition. However, the heterozygotes showed only a slight rise in RNA content at 36 hr after oviposition and maintained this low level thereafter.

Figure 3 shows the pattern of incorporation of $[^3\text{H}]$ uridine into total RNA at different stages of embryogenesis in the homozygotes and heterozygotes. In the homozygous embryos, the incorporation of $[^3\text{H}]$ uridine remained low for 12 hr after oviposition. At the beginning of gastrulation the incorporation increased steadily until 60 hr after oviposition. The rate of uridine incorporation decreased gradually at the stage of organogenesis. In the heterozygous embryos, the rate of incorporation of $[^3\text{H}]$ uridine increased for the first 24 hr in the same manner as in the homozygotes. However, after 24 hr the rate decreased gradually, and it fell to a trace amount at 4 days after oviposition. The rates of uridine incorporation by

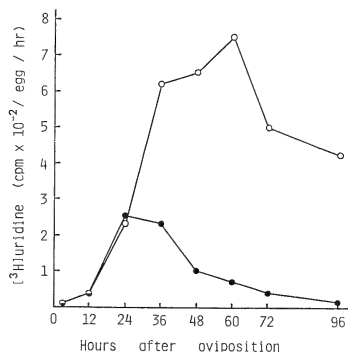


FIG. 3. Incorporation of [^3H]uridine into RNA at different stages of early development in the homozygotes and heterozygotes of the *pnd* mutant. \circ — \circ , homozygotes; \bullet — \bullet , heterozygotes. Eggs were injected with 10 nCi [^3H]uridine, and incubated for 3 hr at 25°C. The acid insoluble material was collected on glass microfiber filters (GF/C, Whatman), and the radioactivity was counted.

the homozygotes and the heterozygotes differed appreciably from 36 hr to 96 hr after oviposition. The patterns of RNA synthesis in the homozygous and heterozygous *pnd* mutant embryos were essentially the same as those in the non-diapause and diapause embryos of the wild type silkworm, respectively. However, in the wild type the dividing point in RNA synthesis between the non-diapause eggs and diapause eggs was at 24 hr after oviposition [14], whereas, in the *pnd* mutant the dividing point was at 36 hr.

Effect of actinomycin D on RNA and protein synthesis

The effect of actinomycin D on RNA and protein synthesis was examined in homozygous and heterozygous embryos. Preliminary experiments were carried out with 36-hr homozygotes. First, the relationship between the duration of actinomycin D treatment and the extent of inhibition of [^3H]uridine incorporation was examined in the 36-hr homozygotes (Table 1). The table shows that a treatment of 3 hr or longer almost completely inhibited RNA synthesis. Second, the effect of increasing doses of actinomycin D on incorporation of [^3H]uridine was examined in the 36-hr homozygotes (Fig. 4). The embryos were injected with 0.25 to 10 ng actinomycin D and then 3 hr later with 10 nCi [^3H]uridine. Increasing doses of actinomycin D progressively inhibited RNA synthesis. Approximately 82% inhibition was achieved with a dose of 5 ng per egg. Increasing the dose to greater than 5 ng per egg modified the level of incorporation only slightly. Therefore, the dose of 5 ng of actinomycin D per egg was used in subsequent experiments. Finally, the optimum duration of actinomycin D treatment for the inhibition of [^3H]amino acid mixture incorporation was determined in the 36-hr homozygotes. Figure 5 shows that the extent of inhibition increased proportionally with the duration of treatment, but leveled off at 10 hr treatment. The maximum level of inhibition of protein synthesis was about 40%.

On the basis of these preliminary experiments, the effect of actinomycin D on protein synthesis was examined at different stages in early

TABLE 1. The effect of duration of exposure to actinomycin D on RNA synthesis. The 36-hr homozygotes received 5 ng actinomycin D per egg. At timed intervals after injection of the inhibitor, the eggs were injected with 10 nCi [^3H]uridine. After 3 hr, the rate of label into RNA of eggs was determined. Control eggs received injections of insect saline followed by [^3H]uridine

Time of exposure to actinomycin D (hr)	Inhibition of incorporation (%)
1	51.4
3	80.2
6	82.2

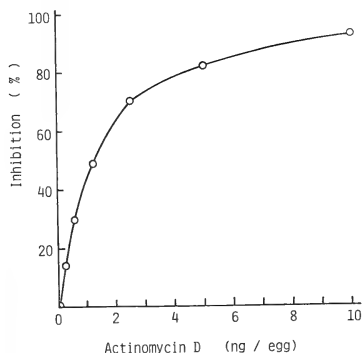


FIG. 4. Effects of concentration of actinomycin D on incorporation of $[^3\text{H}]$ uridine into RNA. The 36-hr homozygous embryos of the *pnd* mutant were injected with actinomycin D, and then 3 hr later with 10 nCi $[^3\text{H}]$ uridine. After 3 hr the incorporation of label into acid insoluble material of the eggs was determined. Control eggs received injection of insect saline and then $[^3\text{H}]$ uridine.

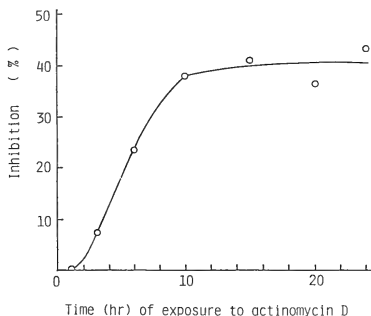


FIG. 5. Effects of duration of exposure to actinomycin D on protein synthesis. The 36-hr homozygotes received 5 ng actinomycin D per egg. At timed intervals after injection of inhibitor, the eggs were injected 10 nCi $[^3\text{H}]$ amino acid mixture. After 3 hr, incorporation of label into acid insoluble material was determined. Control eggs received injection of insect saline and then $[^3\text{H}]$ amino acid mixture.

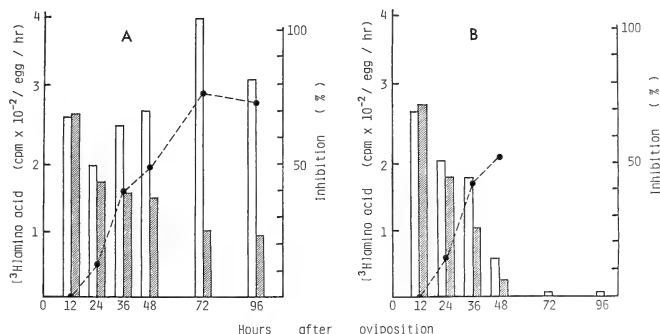


FIG. 6. Effect of actinomycin D on protein synthesis at different stages of early development in the homozygote and heterozygote of the *pnd* mutant. (A), homozygote; (B), heterozygote. ▨ , incorporation of $[^3\text{H}]$ amino acid mixture into protein in actinomycin D-treated eggs; \square , control eggs; \bullet — \bullet , inhibition (%) of incorporation. Eggs were injected with 5 ng actinomycin D, and then 10 hr later with 10 nCi $[^3\text{H}]$ amino acid mixture. After an additional 3 hr the incorporation of label into acid insoluble material was determined. Control eggs received injection of insect saline and then $[^3\text{H}]$ amino acid mixture.

embryogenesis. Five ng of actinomycin D per egg was administered to the eggs at timed stages 10 hr before the injection of [3 H]amino acid mixture. As shown in Figure 6 (A, B), the appearance of the first peak of protein synthesis was prevented by actinomycin D in the homozygotes or heterozygotes. However, when homozygotes after the middle gastrula stage were treated with actinomycin D, the rate of inhibition increased gradually with embryonic development, and the inhibitory effect reached a plateau of approximately 75% inhibition at 72 hr after oviposition (Fig. 6A). Thus the second peak of protein synthesis did not occur in the homozygotes. In the heterozygotes after the gastrula stage, the extent of inhibition of synthesis by actinomycin D was similar to that in the homozygotes until 48 hr after oviposition (Fig. 6B). However, the rate of inhibition was difficult to measure in the 72- and 96-hr heterozygotes, because only trace amounts of [3 H]amino acid were continued to be incorporated into protein in the control embryos at these times (Fig. 6B).

DISCUSSION

As shown in Figure 3, in the two types of embryos; the homozygotes and heterozygotes for the *pnd* gene, the beginning of incorporation of [3 H]uridine seemed to be synchronized with the onset of gastrulation. After that, in the homozygotes the incorporation increased gradually as embryogenesis proceeded. However, the incorporation in the heterozygotes decreased gradually for the middle stage of gastrulation. It was not possible to determine absolute rates of RNA synthesis without measuring the specific activities of the precursor pool [15]. However, in present experiments the incorporation patterns may give a reasonable measure of these rates, since they correspond nearly to the increasing content of RNA (Figs. 2 and 3).

From a comparison of the changing patterns of RNA synthesis with those of protein synthesis (Fig. 1 and 3), it is clear that protein synthesis around the cellular blastoderm stage is not dependent on synthesis of new RNA. This fact agrees with the result indicating that the occurrence of the first peak of protein synthesis was not affected at

all by the actinomycin D (Fig. 6 A, B). Furthermore, there was no appreciable difference between unfertilized eggs and 12-hr-fertilized eggs in the pattern of two-dimensional gel electrophoresis of proteins newly synthesized (unpublished data, refer to [10]). From these data, it is suggested that the first peak of protein synthesis may be ascribed to maternal mRNA. This inference is not contradictory to the investigations of Fujii and Kawaguchi [16] and Saito *et al.* [17], in which they have shown that the maternal mRNAs exist in the unfertilized silkworm eggs and may contribute to protein synthesis in early embryonic development. Furthermore, it has been reported that in other insects (e.g. *Drosophila* and *Smittia* embryos) early embryogenesis until blastoderm stage is independent of embryonic transcripts [18–20]. Contribution of maternal mRNA to early embryogenesis is also well known in other organisms besides insects [21].

On the other hand, the rate of protein synthesis after the early gastrula stage nearly paralleled the rate of RNA synthesis in both the homozygotes and heterozygotes (compare Fig. 1 with Fig. 3). Also, the effect of actinomycin D on protein synthesis increased gradually after the early gastrula stage (Fig. 6 A, B). These results suggest strongly that a decrease in the rate of protein synthesis in the heterozygote is caused by inhibition at the transcriptional level; that is, embryonic gene activity is needed for continuation of embryogenesis after the gastrula stage. Therefore, it is supposed that the *pnd*⁺ gene might take part in blocking the process of transcription of embryonic genes at the onset of diapause.

We have previously demonstrated in the heterozygote that although the rate of synthesis of most proteins falls off as the embryo begins to enter diapause, the synthesis of a *pnd*⁺ gene-specific protein and some diapause-associated proteins is especially enhanced at this time [10]. Therefore, the temporary rise in RNA synthesis in the 24- to 36-hr heterozygote (Fig. 3) may contribute to the production of mRNAs which correspond to the *pnd*⁺ gene-specific protein and some diapause-associated proteins, and then cause the appearance of the small shoulder in protein synthesis at about 36 hr after oviposition (Fig. 1). These proteins,

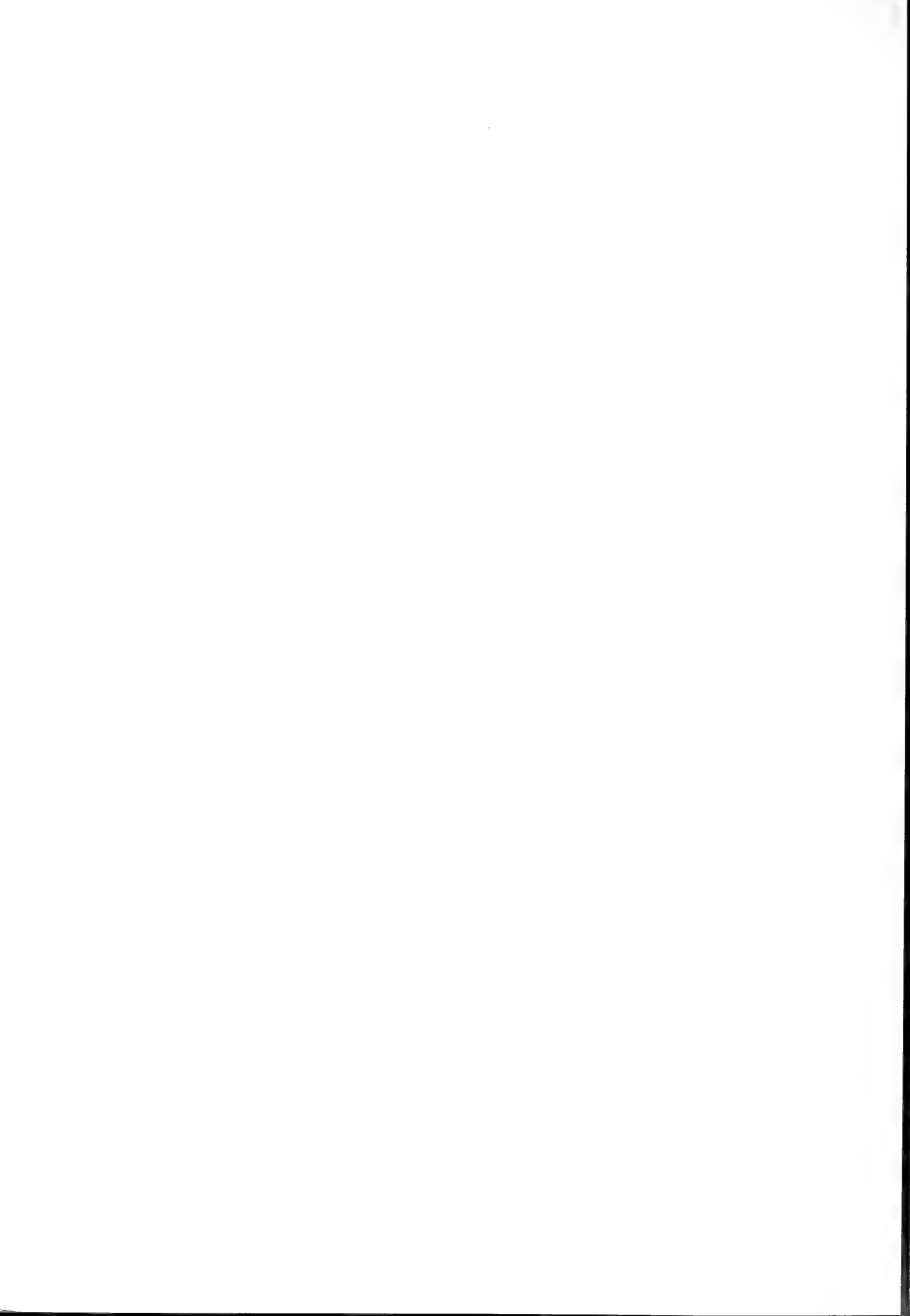
which are specific to the heterozygote, may control some biochemical events related to the initiation of diapause, such as the decrease in oxygen consumption [9], the decrease in DNA synthesis [6] and the decrease in protein synthesis (Fig. 1) due to the inhibition of transcription of embryonic genes (Fig. 3). More detailed analysis of the control mechanism in these stages is now under way.

ACKNOWLEDGMENTS

The author wishes to thank Mr. Y. Yamagiwa for his skillful technical assistance. Thanks are also due to Dr. H. S. Forrest of the University of Texas at Austin for his critical reading of the manuscript. The present study was supported in part by Grants-in-Aid for Scientific Research (Nos. 61540536 and 62304018) from The Ministry of Education, Science and Culture of Japan.

REFERENCES

- 1 Fukuda, S. (1951) The production of the diapause eggs by transplanting the subesophageal ganglion in the silkworm. *Proc. Japan Acad.*, **27**: 672-677.
- 2 Sonobe, H. and Ohnishi, E. (1971) Silkworm *Bombyx mori* L.: Nature of diapause factor. *Science*, **174**: 835-838.
- 3 Sonobe, H. (1974) The diapause factor from the silkworm, *Bombyx mori* L.: purification and inactivation experiments. *Dev. Growth and Differ.*, **16**: 147-159.
- 4 Yamashita, O. and Hasegawa, K. (1985) Embryonic diapause. In "Comprehensive Insect Physiology, Biochemistry and Pharmacology". Ed. by G. A. Kerkut and L. I. Gilbert, Pergamon Press, London, Vol. 1, pp. 407-434.
- 5 Matsutani, K. and Sonobe, H. (1987) Control of diapause factor secretion from the subesophageal ganglion in the silkworm, *Bombyx mori*: the roles of the protocerebrum and tritocerebrum. *J. Insect Physiol.*, **33**: 279-285.
- 6 Sonobe, H., Maotani, K. and Nakajima, H. (1986) Studies on embryonic diapause in the *pnd* mutant of the silkworm, *Bombyx mori*: Genetic control of embryogenesis. *J. Insect Physiol.*, **32**: 215-220.
- 7 Katsumata, F. (1968) Non-maternal inheritance in voltinism, observed in the crossing experiments between Indonesian polyvoltine and Japanese bivoltine race of the silkworm, *Bombyx mori* L. *Seri. Sci. Jpn.*, **37**: 453-461.
- 8 Sonobe, H. (1984) Studies on embryonic diapause in the *pnd* mutant of the silkworm, *Bombyx mori*. I. Responsiveness of the ovaries to the diapause factor. *Mem. Konan Univ., Sci. Ser.*, **35**: 95-103.
- 9 Sonobe, H. and Okada, Y. (1984) Studies on embryonic diapause of the *pnd* mutant of the silkworm, *Bombyx mori*. III. Accumulation of alanine in the diapause eggs. *Roux's Arch. Dev. Biol.*, **193**: 414-417.
- 10 Sonobe, H. and Odake, H. (1986) Studies on embryonic diapause in the *pnd* mutant of the silkworm, *Bombyx mori*. V. Identification of a *pnd*⁺ gene-specific protein. *Roux's Arch. Dev. Biol.*, **195**: 229-235.
- 11 Schmidt, G. and Thannhauser, S. G. (1945) A method for the determination of deoxyribonucleic acid, ribonucleic acid, and phospho-proteins in animal tissues. *J. Biol. Chem.*, **161**: 83-89.
- 12 Brown, A. H. (1946) Determination of pentose in the presence of large quantities of glucose. *Arch. Biochem.*, **11**: 269-278.
- 13 Kress, H. (1977) Transcriptional control of developmental processes by ecdysone in *Drosophila virilis* salivary glands. *Roux's Arch. Dev. Biol.*, **182**: 107-116.
- 14 Kurata, S., Koga, K. and Sakaguchi, B. (1979) RNA content and RNA synthesis in diapause and non-diapause eggs of *Bombyx mori*. *Insect Biochem.*, **9**: 107-109.
- 15 Anderson, K. V. and Lengyel, J. A. (1979) Rates of synthesis of major classes of RNA in *Drosophila* embryos. *Dev. Biol.*, **70**: 217-231.
- 16 Fujii, H. and Kawaguchi, Y. (1982) Maternal mRNA in an unfertilized egg of *Bombyx mori*. *J. Seri. Sci. Jpn.*, **51**: 503-509.
- 17 Saito, A., Sugimoto, K., Koga, K. and Sakaguchi, B. (1985) *In vitro* translation of RNA from unfertilized and fertilized eggs of *Bombyx mori*. *Comp. Biochem. Physiol.*, **82B**: 51-53.
- 18 Gutzeit, H. O. (1980) Expression of the zygotic genome in blastoderm stages of *Drosophila*: analysis of a specific protein. *Roux's Arch. Dev. Biol.*, **188**: 153-156.
- 19 Jäckle, H. and Kalthoff, K. (1981) Proteins foretelling head or abdomen development in the embryo of *Smittia* spec. (Chironomidae, Diptera). *Devel. Biol.*, **85**: 287-298.
- 20 Sander, K., Gutzeit, H. O. and Jäckle, H. (1985) Insect Embryogenesis: Morphology, Physiology, Genetical and Molecular Aspects. In "Comprehensive Insect Physiology, Biochemistry and Pharmacology". Ed. by G. A. Kerkut and L. I. Gilbert, Pergamon Press, London, Vol. 1, pp. 319-385.
- 21 Davidson, E. H. (1986) *Gene Activity in Early Development*, Academic Press, New York, 3rd ed., pp. 45-191.



Spontaneous Release of B Lymphocyte-Enhancing Factors for Growth and Differentiation by YH-1 Cells in Serum-Free Culture Media —Identification of Interleukin 1 Activities

YASUJI OKAI¹ and SHIGEAKI ISHIZAKA²

Tokyo Research Labs., Kyowa Hakko Kogyo Co., Machida 194,
and ²3rd Department of Internal Medicine,
Nara Medical College, Kashiwara 634, Japan

ABSTRACT—The partially purified fraction of the serum-free culture medium conditioned by a human embryo fibroblast cell strain (YH-1) significantly enhanced proliferative responses and polyclonal antibody (immunoglobulin M and G) production by murine and human B lymphocytes. This fraction did not show significant interleukin 2 or interferon activity. The B cell-enhancing activity by the YH-1 fibroblast-derived fraction was almost completely inactivated by the treatment with the antisera against human interleukin 1 α and β . In addition, thymocyte proliferative responses by this fraction were also suppressed by the same antisera. These results indicate that the factors released from YH-1 cells are similar to interleukin 1. The biological significance of this finding is discussed from the viewpoint the immunological regulation between fibroblasts and lymphocytes.

INTRODUCTION

In a series of our recent reports, we have described the identification of fibroblast-derived thymocyte-activating factors (FTAFs), which stimulate thymocyte proliferation and cytotoxic T cell functions [1-4]. Partially purified FTAFs were found to have stimulatory effect on biochemical functions in casein-induced murine peritoneal granulocytes [5]. However, the effect on B cell growth and differentiation by the fibroblast-derived factors have not yet been analyzed.

The present study deals with the identification of the stimulating activities on proliferation and antibody production of B lymphocytes in the serum-free culture media of YH-1 cells. Experimental results suggest that YH-1 cells release factors that stimulate proliferative responses and immunoglobulin synthesis of murine and human B lymphocytes. These activities were inactivated by the

treatment with antibodies against interleukin 1 α and β , but not by those against interleukin 2 or interferon β . The biological significance of fibroblast-derived cytokines in the regulation for lymphocyte proliferation and differentiation is discussed.

MATERIALS AND METHODS

Cell culture and preparation of the culture media

A human embryo fibroblast cell strain (YH-1) was kindly donated from Dr. S. Gotoh (University of Occupational and Environmental Health, School of Medicine, Kitakyushu, Japan). This cell strain was established from an embryo dermal tissue as described previously [7]. The cells were grown in Eagle minimum essential medium (MEM, Nissui Seiyaku G., Tokyo) supplemented with 10% fetal bovine serum (FBS, Gibco, Gland Island biological Lab., New York) in 5% CO₂ and 95% air at 37°C. The confluent cells (7×10^6 cells/150 cm² flask) were cultured in 50 ml of serum-free MEM and the medium was changed with serum-free medium supplemented with soy

Accepted August 30, 1988

Received July 22, 1988

¹ Present address: Department of Molecular Genetics, Beckman Research Institute of the City of Hope, Duarte, California 91010, USA

been trypsin inhibitor (2 µg/ml, Sigma) to protect endogenous protease actions in every 2 days during a week. During this culture, the cell viability was not changed significantly.

Partial purification of B cell-activating factors

The pooled culture media (1L) were mixed with two volumes of saturated ammonium sulphate and kept overnight at 4°C. The precipitate was spun down, dissolved with 5 ml of 10 mM phosphate-buffered saline (PBS, pH 7.2), applied on a Sephadex G-100 column (Pharmacia, 1.8×48 cm) and eluted with the same buffer (PBS) in 5 ml fractions. Active fractions were recovered and used for the experiments.

Assay for thymocyte proliferative response

Thymocyte proliferative response was assayed by the previous method [2]. Thymocytes (5×10^5) from C3H/He mice (10 weeks, Shizuoka Experimental Animal Lab.) were suspended in RPMI 1640 medium supplemented with 10% FBS and added with 0.1 ml of test solution and Concanavalin A (Sigma Chemical Co., 5 µg/ml). Two days after the cell culture, the cells were further cultured for 18 hr with the medium containing 0.5 µCi of [3 H]TdR (5 Ci/mmol, Radiochemical Centre, England). The cell culture was stopped with 10% trichloroacetic acid (TCA) and TCA-insoluble materials were collected on a Whatman GF/C membrane filter. After the membrane was washed with 5% TCA and ethanol, it was dried and the radioactivity of the membrane was counted in a Beckman Scintillation counter.

Assay for antibody production by B lymphocytes

For antibody production, splenocytes from DBA/2 mice (10 weeks old, Shizuoka Experimental Animal Lab.) and healthy human peripheral blood lymphocytes were used. Human lymphocytes were prepared by centrifugation with a Ficoll-Paque gradient (Pharmacia). Splenocytes and human lymphocytes (1×10^6) were suspended in 0.1 ml of RPMI 1640 medium supplemented with 10% FBS and cultured with 0.1 ml of test solution in 5% CO₂ and 95% air at 37°C for 4 days (murine cells) or 7 days (human cells). The number of antibody-forming cells was determined

by the protein A-plaque assay as follows; 25 µl of lymphocyte suspension, 25 µl of a 1:8 suspension of protein A-coupled SRBC, 25 µl of 1:11 dilution of anti-mouse Ig M and Ig G serum (Littion Bionetics, Kensington, USA) or antihuman Ig M and Ig G serum (Dako, Copenhagen, Denmark: 60-fold dilution) and 25 µl of guinea pig complement (60-fold dilution) were added to 0.5% agar (Difco) (0.2 ml) containing 0.05% DEAE dextran (Pharmacia). The mixture was placed on Petri dishes, covered with a coverglass, incubated at 37°C for 4 hr and the number of plaque-forming cells (PFC) were counted as the mean and standard error of four assays. E. coli lipopolysaccharide (LPS, Sigma Chemical Co.) and Pokeweed mitogen (PWM, Funakoshi Chemical Co.) were used for positive controls of murine and human antibody production.

Assay for proliferative responses of B lymphocytes

Murine B lymphocytes were prepared from splenocytes of C57BL/6 nu/nu mice (7–8 weeks, Shizuoka Experimental Animal Lab.). Human B lymphocytes were prepared by T cell rosette formation technique by mixing human peripheral blood lymphocyte (1×10^7 /ml) with SRBC (2×10^9 /ml) in FBS and successive centrifugations ($60 \times g$ for 10 min and $400 \times g$ for 30 min) in a Ficoll-paque gradient. Murine or human B cells (1×10^5) were suspended in 0.1 ml RPMI 1640 medium-10% FBS, added with 0.1 ml test solution and cultured for 2 days (murine cells) or 3 days (human cells) in 5% CO₂ and 95% air at 37°C. After the cells were labeled with 1 µCi of [3 H]TdR (5 Ci/mmol) for 18 hr, the cells were harvested on a GF/C membrane filter and the radioactivity was counted as described in thymocyte proliferative assay.

Assay for interleukin 2 (IL 2) activity

Assay for IL 2 activity was carried out by the previous method [2]. C3H/He splenocytes were cultured in RPMI 1640 medium supplemented with 10% FBS at a cell concentration of 10^7 /ml for 2 days in the presence of Concanavalin A (2.5 µg/ml) and washed three times with RPMI 1640 medium supplemented with α -methyl-D-mannoside (Sigma Chemical Co., 10 mg/ml). Washed blast

cells (2.5×10^6) were cultured in 0.1 ml of RPMI 1640 medium-10% FBS and 0.1 ml of test solution in the presence of α methyl-D-mannoside (10 mg/ml) for 1 day. The cells were labeled with 0.5 μ Ci of [3 H]TdR for further 18 hr and the radioactivity into cells was counted as in thymocyte proliferative assay. Human IL 2 and its antibody were purchased from Genzyme Co. (Boston).

Assay for IFN activity

Interferon (IFN) activity was assayed by the previous method [3]. Human amnion cells, Wish (2×10^4) were cultured in 0.1 ml of MEM-10% FBS for 4 days at 37°C in 5% CO₂ and 95% air. The confluent cells were treated with vesicular stomatitis virus (VSV) as a challenge virus, supplemented with 0.1 ml of test solution and incubated for 24 hr at 37°C in 5% CO₂ and 95% air. After the medium was removed. The cells were fixed, stained with crystal violet and its absorbance was measured at 550 nm in a Hitachi spectrophotometer. As a positive control, recombinant human IFN β (Kyowa Hakko Kogyo Co.) was used and

monoclonal antibody against IFN β was purchased from Paesel GmbH & Co. (Frankfurt).

RESULTS

As can be seen in Figure 1, the major Ig M-producing activity was observed in the fractions at 30–70 KDa and minor activities were detected in the fractions at void volume and at less than 2 KDa (Fig. 1). The considerable activity at void volume was shifted to the position at 30–70 KDa by a treatment with a high salt treatment (1–2 M NaCl) suggesting that the activity at void volume is derived from polymerization of 30–70 KDa activity or complex with other molecules. In addition, the activity at around 2 KDa in Figure 1 seems to be degradative products of 30–70 KDa activity by endogenous protease(s), since the considerable activity at 30–70 KDa fraction from Sephadex G-100 chromatography converted into smaller molecular weights when it was kept standing at 37°C for several hrs (data not shown). Then the authors focussed the 30–70 KDa fraction in Figure

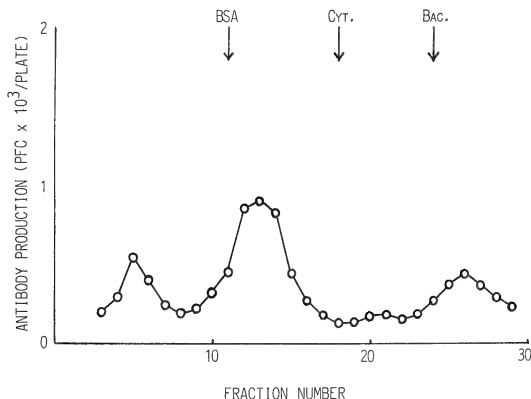


FIG. 1. YH-1 cells release enhancing factors for Ig M production in murine lymphocytes. Serum-free culture media of YH-1 cells were concentrated, applied to a Sephadex G-100 column and Ig M producing activity in each eluting fraction was assayed as described in materials and methods. Each point in the figure shows the average plaque-forming cell numbers of four assays. Upper arrows represent the positions of molecular weight markers; Bovine serum albumin (67 kDa), cytochrome C (13 kDa) and bacitracin (1.5 kDa) from the left to the right.

1. The fraction also caused stimulatory effects on Ig G production in murine lymphocytes, although it showed weaker activity than that of lipopolysaccharide (LPS)-treated cells (Table 1).

TABLE 1. Polyclonal murine IgG producing activity by fibroblast-derived fraction

Volume of fraction	IgG producing activity (PFC/10 ⁵ cells)
None	10 ± 1
10 μ l	24 ± 3
50 μ l	59 ± 4
LPS (25 μ g/ml)	174 ± 14

Fibroblast-derived factors are derived from the fraction No. 12–14 in Figure 1. The values in the table show the mean and standard errors of 4 assays.

Next, we analyzed the effects of this fraction on the proliferative responses in B lymphocytes from C57 BL/6 nu/nu mice. As summarized in Table 2, this fraction considerably stimulated [³H]TdR incorporation into B lymphocytes of nude mice as compared with the negative control experiment. This result indicates that this fraction can stimulate not only antibody production, but also B cell proliferation.

TABLE 2. Stimulation of proliferative response of murine B cells by fibroblast-derived factors

Volume of fraction	[³ H]TdR Incorporation (CPM/10 ⁵ cells)	S.I.
None	585 ± 52	1.0
10 μ l	1648 ± 78	2.8
50 μ l	3460 ± 224	5.9
LPS (25 μ g/ml)	4680 ± 306	8.0

B lymphocytes were prepared from C57 BL/6 nu/nu mouse. Fibroblast-derived factors are same as in Table 1. The values in the table show the mean and standard error of triplicate assays. S.I.: stimulation index.

To investigate the effect of this fraction on human B cells, we analyzed the ability of this fraction on the antibody production in human peripheral blood lymphocytes. When the fraction

was added to the human lymphocyte culture, both the Ig M and Ig G production were significantly enhanced as compared with the negative control, but lower than that of pokeweed mitogen (PWM)-stimulated lymphocytes (Table 3).

Furthermore, we studied the effect of this fraction on the proliferation of human B lymphocytes. As shown in Table 4, the fraction considerably stimulated [³H]TdR incorporation into the cells. These results suggest that the serum-free culture medium contains B cell-activating factors, which enhance growth and differentiation of murine and human B lymphocytes.

The relationship between fibroblast-derived activity and other well-known B cell-activating factors such as IL 2 and IFN [8, 9] was studied. We

TABLE 3. Effect of fibroblast-derived factors on Antibody production in human lymphocytes

Volume of fraction	Antibody-producing activity (PFC/10 ⁵ cells)	
	IgG	IgM
None	5 ± 3	6 ± 2
25 μ l	35 ± 5	13 ± 4
50 μ l	56 ± 10	18 ± 5
PWM (100 μ g/ml)	245 ± 33	185 ± 16

Human lymphocytes were prepared from peripheral bloods as described in Materials and Methods. Fibroblast-derived factors are same as in Table 1. The number of PFC shows the mean and standard error of four assays.

TABLE 4. Effect of fibroblast-derived factors on proliferative response of human B cells

Volume of fraction	[³ H]TdR Incorporation (CPM/10 ⁵ cells)	S.I.
None	982 ± 89	1.0
25 μ l	2320 ± 396	2.4
50 μ l	4468 ± 803	4.5
PWM (100 μ g/ml)	6480 ± 1109	6.6

Human B lymphocytes were prepared from human peripheral blood lymphocytes as described in Materials and Methods. Fibroblast-derived factors are same as in Table 1. The value in the table indicates the mean and standard error of triplicate assays. S.I.: Stimulation Index.

assayed IL 2 activity in fibroblast-derived fraction by T cell blast assay. Human IL 2 showed the stimulatory effect on [^3H]TdR incorporation into T cell blasts and thymocytes (Fig. 2). However, fibroblast-derived fraction enhanced [^3H]TdR in-

corporation into thymocytes, but not into T cell blasts (Fig. 2), indicating that YH-1 cells does not secrete IL 2 activity. Furthermore, IFN activity was measured by an assay system of virus-infected amnion cells. As can be seen Figure 3, a treatment of amnion cells with IFN β protected the virus-induced cells lysis in a dose-dependent manner, but fibroblast-derived fraction could not exhibit any antiviral activities. This finding suggests that YH-1 cell-derived fraction does not contain IFN activity.

Finally, the relationship between FTAFs [1-5] and B cell stimulating activity in YH-1 cell-derived fraction was studied. YH-1 cell-derived fraction showed a stimulating activity for thymocyte proliferation (Fig. 2). Since interleukin 1 (IL 1) shows the similar activity for thymocyte proliferation [10],

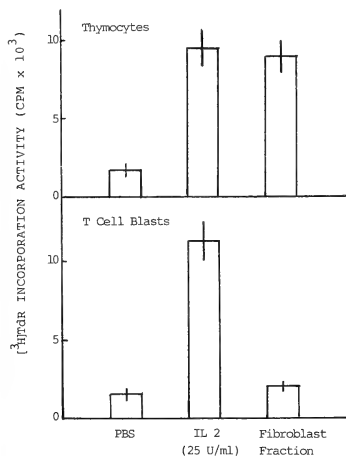


FIG. 2. Fibroblast-derived fraction does not contain IL 2 activity. Upper panel shows Con A-thymocyte proliferation activities treated with PBS, recombinant IL 2 and fibroblast-derived fraction (fraction 12-14 in Fig. 1). Lower panel represents IL 2-dependent [^3H]TdR incorporation into T cell blasts of the same test solutions as in upper panel. Histogram and bar exhibits the mean and standard error of triplicate assays in each test solution.

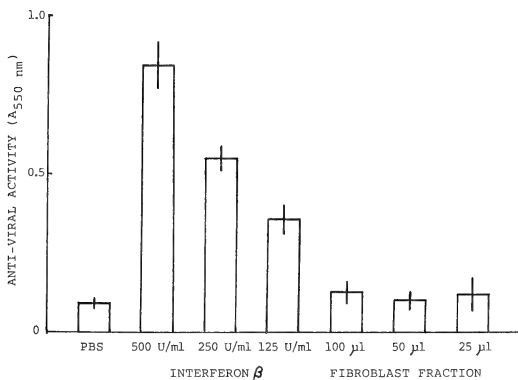


FIG. 3. significant IFN activity is not detected in fibroblast-derived fraction. Histograms and bars represent the mean and standard errors of antiviral activities by PBS, interferon β and fibroblast-derived fraction (fraction 12-14 in Fig. 1), which show the absorbance at 550 nm of the viable cells stained with crystal violet on the cultured plate.

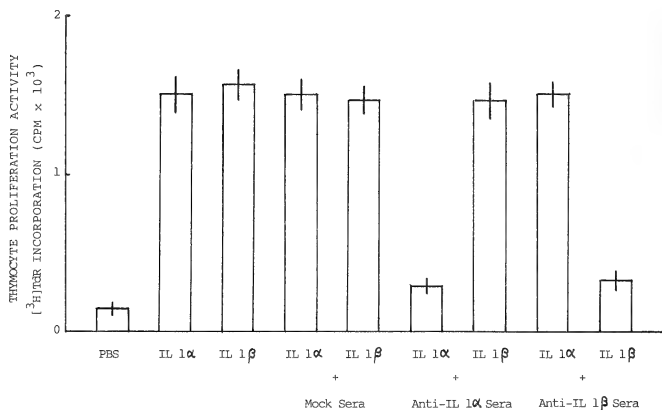


Fig. 4. Antisera against IL 1 α or β selectively inhibit thymocyte proliferation induced by IL 1 α or β . 50 μ l of mock rabbit sera or rabbit antisera against IL 1 α or β were diluted to 1:50 fold with PBS, mixed with 50 μ l of IL 1-containing solution, incubated for 3 hr at 37°C and added to thymocyte culture system. IL 1 concentration was adjusted to a final concentration at 20 U/ml. Histogram and bar show the mean and standard error of triplicate assays.

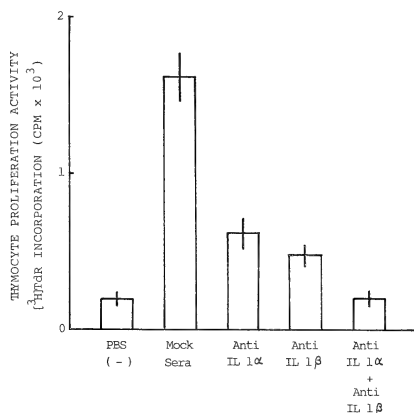


Fig. 5. Antisera against IL 1 inactivate thymocyte proliferation activity induced by YH-1 cell-derived fraction. 50 μ l of mock antisera or 1:50 diluted antisera against IL 1 α or β was mixed with 50 μ l of YH-1 cell-derived fraction (fraction 12-14 in Fig. 1), incubated for 3 hr at 37°C and added to murine thymocytes. Histogram and bar show the mean and standard error of [3H]TdR incorporation activity into thymocytes of triplicate assays.

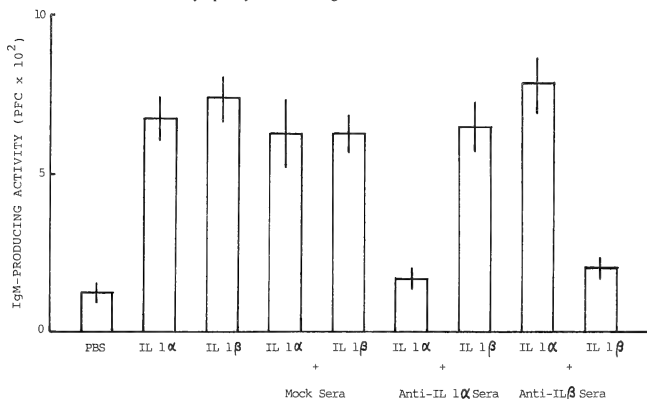


FIG. 6. Antisera against IL 1 α or β selectively block antibody production in murine splenocytes induced by IL 1 α or β . Effect of antisera against IL 1 α or β on IL 1-induced Ig M production in murine splenocytes was analyzed. Mock rabbit sera or rabbit antisera against IL 1 were diluted to 1:50 fold with PBS, mixed with IL 1-containing solution, incubated for 3 hr at 37°C and added to murine splenocyte culture system. A final concentration of human recombinant IL 1 α or β was adjusted to 20 U/ml. Histogram and bar show the mean and standard error of plaque-forming cell numbers in 4 assays.

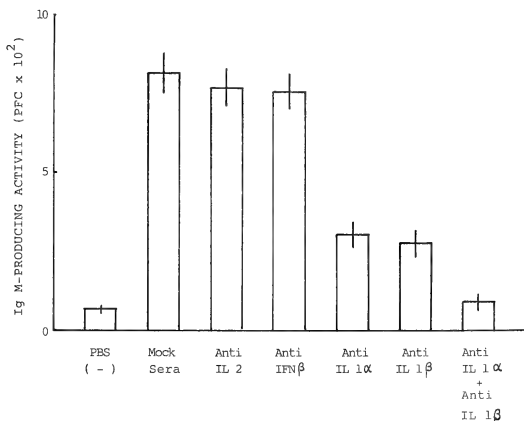


FIG. 7. Antisera against IL 1 cause inhibitory effects on enhancing activity by YH-1 cell-derived fraction in antibody production of murine splenocytes. 50 μ l of monoclonal antibodies (20 μ g/ml) against IL 2 or IFN or 50 μ l of 1:50 diluted antisera against IL 1 α or β , was mixed with 50 μ l of fibroblast-derived fraction (fraction 12-14 in Fig. 1), incubated for 3 hr at 37°C and added to the murine splenocyte culture (final volume: 200 μ l). Ig M-producing activity was assayed by protein A-PFC method using 25 μ l of splenocyte suspension as described in materials and methods. Histogram and bar represent the mean and standard error of four assays.

the effect of antisera against IL 1 on thymocyte proliferation induced by YH-1 cell-derived fraction was analyzed. These antibodies could selectively block the IL 1 α and β -dependent [3 H]TdR incorporation into thymocytes (Fi. 4). Thymocyte proliferative response by fibroblast-derived fraction was significantly suppressed by the antisera against IL 1 α or β . In addition, an additive inhibitory effect was observed by the treatment with combined these antibodies (Fig. 5).

As a parallel experiment, the authors studied the effect of these antisera on mouse polyclonal Ig M production by IL 1 or YH-1 cell-derived fraction. As indicated in Figure 6, these antisera selectively blocked polyclonal Ig M production in murine B cells induced by IL 1 α or β and a drastic inhibition was observed by the treatment with combined antisera. Furthermore, the enhancing activity to the Ig M production by the YH-1-derived fraction was inactivated in a similar fashion by the same antisera as mentioned above, but not antibodies against IL 2 or IFN β (Fig. 7). These results indicate that YH-1 cell-derived B cell-enhancing activities are responsible for IL 1 or IL 1-like factors similar to FTAFs reported previously [1-5].

DISCUSSION

It has been reported that B cell proliferation and differentiation are regulated by the soluble factors derived macrophages and T cells [8, 9]. These soluble factors are functionally derived into two groups: one, the B cell differentiation factor (BCGF), which is involved in B cell proliferation; and the other, the B cell differentiation factor (BCDF), responsible for maturation of activated B cells into immunoglobulin-secreting cells [8, 9]. This classification should need to be reevaluated by the recent gene cloning study of various lymphokines by the following facts. B cell stimulating factor (BSF 1), now termed IL 4, shows several BCGF activities and it differentiates LPS-treated B cells into Ig G1 and Ig E plasma cells [10, 11]. BCGF II or T cell replacing factor (TRF), which is named IL 5, exhibits inducing activities of Ig M secretion by BGL 1 tumor cell line and of anti DNP-Ig G by DNP-primed B cells [12, 13].

However, these lymphokines are T cell products. Other lymphokine, BSF 2 (IL 6) was originally found in the culture supernatant of T cell lines which stimulates Ig synthesis in antigen-stimulated B cells without inducing cell proliferation [14]. Interestingly, this lymphokine is identical to interferon β 2 which is induced in human diploid fibroblasts stimulated with poly(I):poly (C), [15]. In the present study, the authors could not find significant IFN activity in the culture medium of the fibroblast cell strain, YH-1 as described in the experimental results. As other B cell stimulating lymphokine, IL 2 has been known [8, 9]. However, IL 2 activity was not detected in the YH-1 cell-derived fraction.

We consider that FTAFs and B cell stimulating activity from YH-1 cells are identical to IL 1. Because both activities were inactivated almost completely by a treatment with the mixed antibodies against IL 1 α and β .

Recently, it has been reported that human FS-4 fibroblasts induce membrane-associated IL 1 but not soluble IL 1 by tumor necrosis factor and that untreated cells contained no demonstrable IL 1 α mRNA and very low level of IL 1 β mRNA [16]. Although FS-4 cells did not release soluble IL 1 activity, (J. Vilček personal communication), YH-1 cells released soluble IL 1 activities as mentioned above. Although reasons for this discrepancy are not clear at present, the following possibility may be considered. Since the considerable thymocyte proliferating activity contained in fetal bovine serum supplemented with the culture medium, it is difficult to separate clearly spontaneously releasing IL 1 activity from serum-derived activity. Then, to remove serum-derived activity, we depleted the serum from the culture medium of confluent YH-1 cells. Under this condition, the confluent cells survived during several changes with serum-free culture medium and released the clearly significant IL 1 activity as mentioned above. Interestingly, this activity was detected in the presence of protease inhibitor such as soy bean trypsin inhibitor in the culture medium, but not observed in the absence of protease inhibitor (data not shown). Possibly, although these cells secrete significant IL 1, its activity apparently disappear by the action of the endogenous protease(s) from cells in the abs-

ence of the protease inhibitor.

Other interesting phenomena were observed with respect to the molecular weights of FTAFs from YH-1 cells. Previously, we showed that YH-1 cells secrete FTAFs and their secretion was enhanced by a treatment with a phorbol ester [4] or tumor virus [2, 5] under a relatively high serum condition, which were characterized to be 10–20 KDa proteins or glycoproteins. However, under a serum-free condition, the major FTAFs exhibited the larger molecular weight at more than 30 KDa and 10–20 KDa factors could not be detected in the previous (6) and present report. In addition, there is a dominant activity of 30–40 KDa FTAF in the extracellular matrix fraction of transformed YH-1 cells [3]. These findings suggest that YH-1 cells seem to release different molecular weight FTAFs under different culture conditions.

At last, we discuss the other important significance of the present report. Previously some researchers suggested the important role of fibroblasts in B cell survival, growth and its cloning efficiency, but its mechanism remained unknown. For example, 3T3 murine fibroblasts supports a high efficient cloning for hapten-specific B lymphocytes and much more enhanced B cell activation induced by IL 2 [17]. Possibly, one of the reasons for the feeder layer effect of fibroblast on B cell functions may be associated with the soluble IL released from fibroblasts.

ACKNOWLEDGMENTS

We would like to thank Dr. U. Yasasita (University of Occupational and Environmental Health, School of Medicine, Kitakyushu) for generous gift for antibodies against IL 1 and Dr. K. Kobayashi (Department of Pediatrics, Yamaguchi University, School of Medicine) for critical reading of this manuscript.

REFERENCES

- Okai, Y., Tashiro, H. and Yamashita, U. (1982) 3T3 fibroblasts are stimulated by 12-O-tetradecanoylphorbol-13-acetate to produce thymocyte-activating factors. *FEBS Lett.*, **142**: 93–95.
- Okai, Y., Gotoh, S. and Yamashita, U. (1985) Thymocyte-activating factors from SV40-transformed human embryo fibroblasts. *Immunol. Lett.*, **9**: 153–159.
- Okai, Y. (1985) Large-molecular weight thymocyte-activating factors in extracellular matrix of SV40-transformed human embryo fibroblasts. *Immunol. Lett.*, **11**: 63–68.
- Okai, Y. and Yamashita, U. (1986) Human embryo fibroblast cell line produces thymocyte-activating factors to induce cytotoxic T lymphocytes. *Zool. Sci.*, **3**: 765.
- Okai, Y. and Yamashita, U. (1987) Different inducing activities for cytotoxic T cells by heterogeneous thymocyte-activating factors from SV40-transformed human embryo fibroblasts. *Immunol. Lett.*, **14**: 1–7.
- Okai, Y. (1986) Enhancing factors for granulocyte functions from a human embryo fibroblast cell strain. *Zool. Sci.*, **3**: 627–631.
- Yanagisawa, K., Suenaga, Y., Nishio, K. and Gotoh, S. (1983) Establishment of a human diploid strain. *J. Univ. Occup. Environ. Health.*, **5**: 49–54.
- Haward, M. and Paul, W. E. (1983) Regulation of B cell growth and differentiation by soluble factors. *Ann. Rev. Immunol.*, **1**: 307–333.
- Jelinek, D. F. and Lipsky, P. E. (1987) Regulation of human B lymphocyte activation, proliferation and differentiation. *Advances in Immunology*, **40**: 1–59.
- Noma, Y., Sideras, P., Naito, T., Bergstedt-Lindquist, S., Azuma, C., Severinson, E., Tanabe, T., Kinashi, T., Matsuda, F., Yaoita, Y. and Honjo, T. (1986) Cloning of cDNA encoding the murine IgG1 induction factor by a novel strategy using SP6 promoter. *Nature*, **319**: 640–645.
- Yokota, T., Otsuka, T., Mosmann, T., Banchereau, J., DeFrance, T., Blanchard, D., De Vries JE, Lee, F. and Arai, K. (1986) Isolation and characterization of a human interleukin cDNA clone, homologous to mouse B-cell stimulatory factor 1, that expresses B-cell- and T-cell-stimulating activities. *Proc. Natl. Acad. Sci. USA*, **83**: 5894–5898.
- Tanabe, T., Konishi, M., Mizuta, T., Noma, T. and Honjo, T. (1987) Molecular cloning and structure of the human interleukin-5 gene. *J. Biol. Chem.*, **262**: 16580–16584.
- Harada, N., Kikuchi, Y., Tominaga, A., Takaki, S. and Takatsu, K. (1985) BCGF II activity on activated B cells of a purified murine T cell-repressing factor (TRF) from a T cell hybridoma (B15K12). *J. Immunol.*, **134**: 3944–3951.
- Hirano, T., Yasukawa, K., Harada, H., Taga, T., Watanabe, Y., Matsuda, T., Kashiwamura, S., Nakajima, K., Koyama, S., Sakiyama, F., Matsui, H., Takahara, Y., Taniguchi, T. and Kishimoto, T. (1986) Complementary DNA for a novel human interleukin (BSF-2) that induced B lymphocytes to produce immunoglobulin. *Nature*, **324**: 73–76.
- Sehgal, P. B., May, L. T., Tamm, I. and Vilček (1987) Human 2 interferon and B-cell differentia-

- tion factor BSF-2 are identical. *Science*, 731-732.
- 16 Le, J., Weinstein, D. Gubler, U. and Vilc  k, J. (1987) Induction of membrane-associated interleukin 1 by tumor necrosis factor in human fibroblasts. *J. Immunol.*, **138**: 2137-2142.
- 17 Pike, B. L. and Nossal, G. J. V. (1985) A high-efficiency cloning system for single hapten-specific B lymphocytes that is suitable for assay of putative growth and differentiation factors. *Proc. Natl. Acad. Sci. USA.*, **82**: 3395-3399.

Control of Cuticle Formation in Wing Epidermal Cells of the Fleshfly, *Sarcophaga bullata*

MAROKO MYOHARA^{1,2} and JUDITH H. WILLIS

Department of Entomology, University of Illinois,
Urbana, Illinois 61801, U.S.A.

ABSTRACT—Insect wing epidermis forms either pupal type or adult type cuticle depending on its developmental stage. To study the control of this stage-specific cuticle formation, we examined the type of cuticle formed by wing discs or pupal wings transplanted into larvae or pupae and subjected to larval-pupal and/or pupal-adult metamorphosis. Following transplantation into larvae, the type of cuticle formed by wing discs and by pupal wings was always the same; both formed only pupal cuticle if recovered from their hosts immediately after larval-pupal metamorphosis, and formed both pupal and adult cuticles if recovered from the hosts after pupal-adult metamorphosis was completed. On the other hand, following transplantation into pupae, the type of cuticle formed by wing discs and by pupal wings was different; wing discs formed only adult cuticle along with the pupal-adult metamorphosis of the hosts, whereas pupal wings formed both pupal and adult cuticles under the same condition. Wings transplanted from late prepupae into pupae also formed both pupal and adult cuticles. These results demonstrate that the type of cuticle formed by wing epidermis depends not only on hormonal conditions but also on the developmental stage of the epidermal cells.

INTRODUCTION

During the course of holometabolous insect development, epidermal cells form several cuticles, i.e., larval cuticles, one per instar, as well as pupal and adult cuticles. Epidermal cells of imaginal discs, undifferentiated larval structures determined to form specific adult structures such as eyes and wings, form two cuticles. The first, the pupal cuticle, is deposited immediately after larval-pupal apolysis, and the second, the adult cuticle, is deposited after pupal-adult apolysis. There must be mechanisms that specify the correct temporal sequence of the type of cuticle formed.

It has been generally accepted that insect metamorphosis is controlled by the joint action of two hormone classes, ecdysteroids and juvenoids. Schneiderman [1] has claimed that temporal determination of cuticle type secreted by an insect

epidermal cell depends solely upon local hormonal conditions. One of the experimental results supporting this view is that larval epidermis deposits adult cuticle instead of pupal cuticle when it is transplanted into a pupa and exposed to the hormonal condition of pupal-adult metamorphosis [2, 3]. However, the phenomenon is not universal; the omission of pupal stage was not induced in transplantations of *Samia* larval integument and of *Ephesia* wing discs into the pupae [4, 5], suggesting that the control of cuticle formation at metamorphosis cannot be fully explained by the hormonal condition alone.

In this study, transplantation experiments were carried out with wing imaginal discs, prepupal wings and pupal wings of the fleshfly, *Sarcophaga bullata*, to learn if different types of cuticles would be formed by epidermal cells of different stages under the same hormonal condition. We chose to use *Sarcophaga* rather than *Drosophila* for the following reasons. First, because of its large size, recovering the implants after metamorphosis was easier; second, because of its slow developmental rate, the developmental stage of donors and hosts could be determined more accurately.

Accepted August 3, 1988

Received June 23, 1988

¹ Present Address: National Institute of Sericultural and Entomological Science, Tsukuba 305, Japan.

² To whom reprint requests should be addressed.

MATERIALS AND METHODS

The stages of donors and hosts employed in this study are listed in Table 1. Postfeeding third (final) instar larvae were used as larval hosts and as donors of wing imaginal discs. To obtain prepupae or pupae of a precise stage, white prepupae were collected and kept at 24°C until they reached the desired stage (see [6], for terminology). The white prepupal stage begins immediately after pupariation. Discs and wings were dissected in sterilized insect Ringer's solution [7] and kept in it until all tissues needed for a given experiment were collected. A whole disc or wing was implanted into a host animal with a glass injection needle. Prior to implantation, larval hosts were anesthetized on ice for several minutes.

For examination of the formed cuticle(s), implanted tissues were recovered from the hosts either after larval-pupal metamorphosis (2 days after pupariation), or from late pharate adults (12–13 days after pupariation, i.e. 1–2 days prior to adult eclosion). The recovered tissues were fixed with Bouin's solution, embedded in Paraplast tissue embedding medium (Monoject Scientific, St. Louis), sectioned at 4–5 µm, and stained with Cason's Stain [8], a variant of Mallory's triple stain containing 0.5% phosphotungstic acid, 1% orange G, 0.5% aniline blue, and 1.5% acid fuchsin.

The type of cuticle formed by implanted tissues was determined according to its color, shape, and

location in the implant. Pupal cuticle was uniformly stained a pale lilac and appeared as a thin smooth layer without any projecting structures. It was located generally inside the recovered wing discs. (The implanted imaginal discs failed to evaginate and secreted cuticle interiorly.) On those recovered wings that had evaginated prior to implantation (prepupal or pupal wings), pupal cuticle formed most often on their outer surfaces. Adult cuticle appeared as a thick multicolored layer stained in red, blue, orange and yellow, with many projecting structures such as hairs or bristles, known to be adult specific.

RESULTS

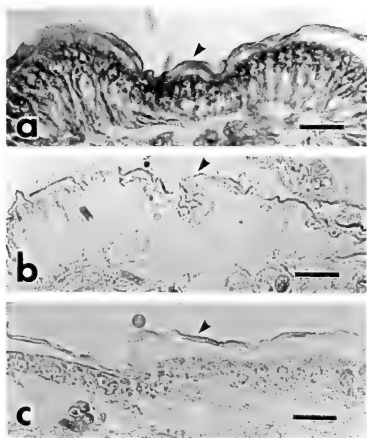
Transplantations of wing epidermis into larvae

To compare the responses of larval and pupal epidermis to a larval-pupal metamorphic challenge, we first transplanted wing discs and pupal wings into postfeeding third instar larvae, and recovered them when the hosts become pupae, 2 days after pupariation. The wing discs and pupal wings responded to this hormonal challenge in a same way; only pupal cuticle was found (Fig. 1 and Table 2, a). The pupal wings had secreted only the slightest trace of cuticle at the time of implantation. The pupal cuticle observed in the recovered pupal wings was no thicker than that secreted by transplanted wing discs.

TABLE 1. Stages of donors and hosts

Stage	Time after pupariation (white prepupa), at 24°C	Other remarks ¹
Larva	—	Postfeeding third instar larva, 1–2 days before pupariation
Early prepupa	3–5 hr	—
Late prepupa	17–18 hr	2–3 hr before beginning of larval-pupal apolysis
Pupa (for implantation)	28–30 hr	Immediately after completion of larval-pupal apolysis
(for recovery)	2 days	1 day before beginning of pupal-adult apolysis
Adult	12–13 days	Pharate adult, 1–2 days before eclosion

¹ From Fraenkel and Bhaskaran [6].



The type of cuticle formed by wing discs and pupal wings was also similar when recovery of implants was carried out after the hosts had developed to the adult stage; both pupal and adult cuticles were always found (Fig. 2 and Table 2, b). Again, the thicknesses of the pupal cuticle formed by wing discs and by pupal wings were comparable. Similar results were obtained from the transplantation experiments using prepupal wings (Table 2, b).

Transplantations of wing epidermis into pupae

To compare the responses of larval and pupal

FIG. 1. Pupal cuticle formed by a wing disc (a) and a pupal wing (b) that was transplanted into a larva and recovered after larval-pupal metamorphosis of the host. Pupal cuticle of a wing of host animal at the time of recovery, 2 days after pupariation, is shown in c. Each arrowhead indicates pupal cuticle, each bar represents 20 μ m.

TABLE 2. Transplantation of wing epidermis in *Sarcophaga bullata*

Exp.	Stage ¹ of host at the time of		Stage ¹ of donor	Number of tissues		Type of cuticle formed ³
	implantation	recovery		implanted	recovered ²	
(a)	Larva	Pupa	Larva	8	5	P
			Pupa	15	5	P
(b)	Larva	Adult	Larva	20	15	P+A
			Early prepupa	10	2	P+A
			Late prepupa	10	10	P+A
			Pupa	20	5	P+A
(c)	Early prepupa	Adult	Larva	7	4	P+A
			Early prepupa	8	6	P+A
			Late prepupa	8	6	P+A
			Pupa	10	10	P+A
(d)	Late prepupa	Adult	Larva	22	10	A
			Early prepupa	8	6	P+A
			Late prepupa	8	6	P+A
			Pupa	10	8	P+A
(e)	Pupa	Adult	Larva	9	3	A
			Early prepupa	10	3	A
			Late prepupa	8	3	P+A
			Pupa	10	8	P+A

¹ See Table 1, for detail.

² Not all implants could be recovered because some hosts died before reaching the stage of recovery.

³ P, pupal cuticle; A, adult cuticle.

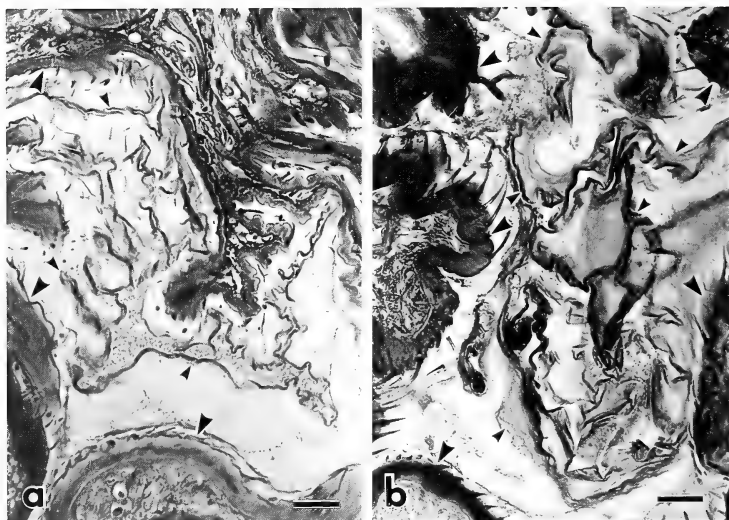


FIG. 2. Cuticles formed by tissues that were transplanted into larvae and recovered after pupal-adult metamorphosis of the hosts. Transplanted wing discs (a) as well as pupal wings (b) formed both pupal cuticle (small arrowheads) and adult cuticle (large arrowheads). The thickness of the cuticle is a function of the obliqueness of the cut. Each bar represents 20 μ m.

epidermis to a pupal-adult metamorphic challenge, we next transplanted wing discs and pupal wings into pupae, and recovered them when the hosts had completed adult development. In this case, wing discs and pupal wings responded differently to the hormonal challenge; the wing discs formed only adult cuticle, whereas pupal wings formed both pupal and adult cuticles (Fig. 3 and Table 2, e). The pupal cuticles formed by pupal wings implanted into pupae were not thinner than those formed by the pupal wings implanted into larvae.

This result indicates that the wing discs, but not the pupal wings, of *Sarcophaga bullata* can omit the formation of pupal cuticle, under appropriate hormonal conditions. To learn at what stage the wing epidermis becomes incapable of omitting pupal cuticle formation, we transplanted wings from early and late prepupae into pupal hosts. As shown in Table 2e, the wings from early prepupae

(3–5 hr after pupariation) formed only adult cuticle as transplanted wing discs did, but the wings from late prepupae (17–18 hr after pupariation) formed both pupal and adult cuticles, failing to omit the pupal stage.

Transplantations of wing epidermis into prepupae

The results described above indicate that there is a transition in the response of wing epidermis to a pupal-adult metamorphic challenge during the period between the early and late prepupal stages, suggesting that an event(s) which changes the nature of the epidermal cells takes place during the course of prepupal development. There also was a difference in the environment during a larval-pupal and a pupal-adult molt. These inferences were supported by experiments in which wing discs were implanted into prepupae of different ages and recovered when the hosts became adults.

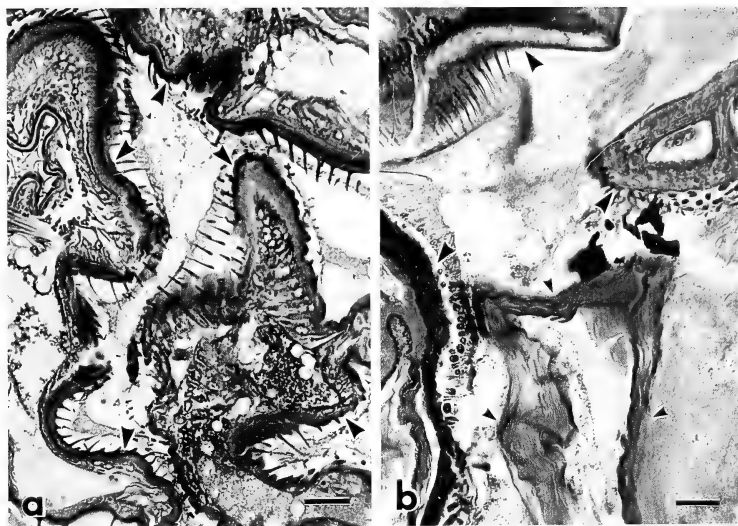


FIG. 3. Cuticles formed by tissues that were transplanted into pupae and recovered after pupal-adult metamorphosis of the hosts. Transplanted wing discs (a) formed only adult cuticle (large arrowheads), whereas pupal wings (b) formed both pupal cuticle (small arrowheads) and adult cuticle. Each bar represents 20 μ m.

Both pupal and adult cuticles were formed by wing discs implanted into early prepupae (Table 2, c), whereas only adult cuticle with little or no trace of pupal cuticle was formed by wing discs implanted into late prepupae (Table 2, d). When prepupal or pupal wings instead of wing discs were transplanted into early or late prepupae, both pupal and adult cuticles were always formed (Table 2, c, d).

DISCUSSION

Our results show that both the developmental stage of the epidermis and the environment to which it is exposed affect its differentiation.

Immature wing tissue, ranging in age from late larval (imaginal discs) to early pupal, formed both pupal and adult cuticles when implanted into larvae which were allowed to develop normally to the adult.

Differences between hosts at different developmental stages were apparent when only a single metamorphic transition occurred. Wing discs formed only pupal cuticle after the host underwent a larval-pupal molt and formed only adult cuticle after pupal-adult development. Although it is tempting to suggest that the presence of juvenile hormone in the larva accounts for this difference, this is unlikely to be the cause. Wing tissues of the ages used in this study are insensitive to juvenoids (see [9] for review and discussion).

The different response of imaginal discs to the two different host environments is reminiscent of the results obtained with cultured wing discs from the lepidoptera *Ephestia kuhniella* [5]. It was observed that wing discs could be directed to form either pupal or adult-like cuticles solely by manipulating the concentration and duration of ecdysteroid exposure. In the present situation, the

adult cuticles made by transplanted wing discs of *Sarcophaga* are unambiguously adult for they have numerous hairs, a characteristic found only in adult cuticles.

Ecdysteroid titers for *Sarcophaga bullata* [10] reveal a gradual rise in the late last instar and a brief plateau. This rise is assumed to initiate the processes culminating in pupariation. A sharp peak, lasting about a day, occurs at the time of pupariation and is believed to control pupation. The ecdysteroid titer begins to rise again a few hours later, at the time larval-pupal apolysis begins (20 hr after pupariation), and remains at high levels for several days. This prolonged presence of ecdysteroid is assumed to be responsible for pupal-adult apolysis and adult morphogenesis. The results from the present study indicate that wing discs respond to the larval peak of ecdysteroid with pupal cuticle formation and to the prolonged presence of ecdysteroid of the pupal-adult transition by adult cuticle formation. This is in contrast to the situation in *Drosophila melanogaster* where only traces of cuticulin but no well developed cuticle is deposited in the continuous presence of ecdysteroids [11, 12]. Whether the differences found for the two species are due to phylogeny or to the differences between culturing *in vivo* and *in vitro* remains unknown.

We found that young pupal wings form only pupal cuticles when implanted into larval hosts and recovered at the time of pupation, while they form both pupal and adult cuticles when implanted into pupal hosts which subsequently undergo metamorphosis. Here the difference may reside in the duration of incubation and length of exposure to ecdysteroids.

Our experiments show clearly that developmental stage influences the response of the wing epidermis to different hormonal environments. We have defined the critical period for the donor wings to be able to form both pupal and adult cuticles after transplantation into pupal hosts. It occurs between 5 and 17 hr after pupariation. Initiation of deposition of pupal cuticle may be the key event. Even though cuticle was not visible with the light microscope in wings from animals 17 hr after puparium formation, we suspect it was present. In *Drosophila* cuticulin (outer epicuticle)

deposition coincides with disc evagination [12]. By the time of anterior apolysis (4–6 hr after pupariation in *Drosophila* [6]), cuticulin is present in most regions [12]. Anterior apolysis in *Sarcophaga bullata* begins at 20 hr [6]. Hence it is likely that by 17–18 hr (our late prepupae) cuticle formation would be underway, and wing tissues from these animals form both pupal and adult cuticles in pupal hosts.

ACKNOWLEDGMENTS

We are grateful to Drs. Tetsuya Ohtaki, Masukichi Okada, Koji Myohara and James Nardi for their helpful comments on this study. We thank Dr. Nardi for teaching one of us (M.M.) the transplantation technique. This work was supported by Grant AG 00248 from the U. S. National Institutes of Health.

REFERENCES

- 1 Schneiderman, H. A. (1976) New ways to probe pattern formation and determination in insects. Symp. Roy. Ent. Soc. London, 8: 3–34.
- 2 Nayer, K. K. (1954) Metamorphosis in the integument of caterpillars with omission of the pupal stage. Proc. Roy. Entomol. Soc. London, Ser. A, 29: 129–134.
- 3 Williams, C. M. (1961) The juvenile hormone. II. Its rôle in the endocrine control of molting, pupation, and adult development in the cecropia silkworm. Biol. Bull., 121: 572–584.
- 4 Kato, Y. (1973) Can larval epidermis omit the secretion of a pupal cuticle in a saturniid moth, *Samia cynthia ricini*? J. Insect Physiol., 19: 495–504.
- 5 Nardi, J. B. and Willis, J. H. (1979) Control of cuticle formation by wing imaginal discs *in vitro*. Develop. Biol., 68: 381–395.
- 6 Fraenkel, G. and Bhaskaran, G. (1973) Pupariation and pupation in cyclorhaphous flies (Diptera): Terminology and interpretation. Ann. Entomol. Soc. Amer., 66: 418–422.
- 7 Ephrussi, B. and Beadle, G. W. (1936) A technique of transplantation for *Drosophila*. Am. Naturalist, 70: 218–225.
- 8 Cason, J. E. (1950) A rapid one-step Mallory-Heidenhain stain for connective tissue. Stain Technol., 25: 225–226.
- 9 Sehna, F. and Zdarek, J. (1976) Action of juvenoids on the metamorphosis of cyclorhaphous diptera. J. Insect Physiol., 22: 673–682.
- 10 Zdarek, J. (1985) Regulation of pupariation in flies. In "Comprehensive Insect Physiology Biochemistry and Pharmacology". Ed. by G. A. Kerkut and L. I.

- Gilbert, Pergamon Press, Oxford, Vol. 8, pp. 301-333.
- 11 Doctor, J., Fristrom, D., and Fristrom, J. W. (1985) The pupal cuticle of *Drosophila*: Biphasic synthesis of pupal cuticle proteins *in vivo* and *in vitro* in response to 20-hydroxyecdysone. *J. Cell Biol.*, **101**: 189-200.
- 12 Fristrom, D. and Liebrich, W. (1986) The hormonal coordination of cuticulin deposition and morphogenesis in *Drosophila* imaginal discs *in vivo* and *in vitro*. *Develop. Biol.*, **114**: 1-11.



Studies on the Sawfly, *Athalia rosae* (Insecta, Hymenoptera, Tenthredinidae).

I. General Biology

MASAMI SAWA, AKIHIRO FUKUNAGA¹, TIKAHIKO NAITO²
and KUGAO OISHI^{3,4}

Division of Science of Biological Resources, Graduate School of Science and Technology, Kobe University, Nada, Kobe 657, ¹Laboratory of Biology, Osaka City University Medical School, Abeno, Osaka 545, ²Laboratory of Entomology, Faculty of Agriculture, Kobe University, Nada, Kobe 657, and ³Department of Biology, Faculty of Science, Kobe University, Nada, Kobe 657, Japan

ABSTRACT—We have chosen *Athalia rosae* as an experimental material for studies on developmental biology of Hymenopteran insects. Parthenogenetic male production (arrhenotoky) and non-reductional maturation division in these males are among the most interesting basic biological phenomena associated with this insect group. We describe here the general biology of *A. rosae* relevant to the future works. *A. rosae* can be reared in laboratory throughout the year if kept at 25°C under 16 hr light-8 hr dark condition. Embryonic development takes about 5 days and larval development takes about 9 days in the female (6 instars) and 8 days in the male (5 instars). Mature larvae dig into the soil and construct cocoons. The pupal period lasts about 10 days in the female and 11 days in the male, both including 5-day prepupal stage. Eclosed adults stay in the cocoon for a day, then come out and mate within the next day. Females live up to two weeks and each lays up to 100 eggs. A brief account of stock maintenance, and description of adult internal reproductive organs are also given.

INTRODUCTION

Hymenopterans are a unique group of insects in which parthenogenetic male production (arrhenotoky) is almost universal. The group thus provides an opportunity for studies on the mechanism of egg activation and embryonic development without fertilization. Males are generally haploid and their maturation division is non-reductional. Non-reductional maturation division is observed even in the artificially obtained diploid and triploid males [1-3, Naito and Suzuki, unpubl.]: that is, the system also provides an important tool for studies on the mechanism of reduction division.

Developmental and/or genetic studies of Hymenopteran insects in most cases have utilized the species in the Suborder Apocrita [4-7]. We have chosen *Athalia rosae* (Tenthredinidae, Suborder Symphyta) as an experimental material. The species represents a primitive form in Hymenopteran insects, and hence the results obtained with this species may provide a basis for understanding evolutionary aspects of Hymenopteran biology. Mature unfertilized eggs of this species and others in the Family Tenthredinidae can be explanted from the adult female and placed on a wet filter paper where they are activated and begin development [8]. These eggs have proven to be extremely amenable to experimental manipulations such as microinjection and ligation. The species can be reared easily in the laboratory throughout the year. Here we describe general biology of *A. rosae* as relevant to results to be presented later.

Accepted August 19, 1988

Received July 5, 1988

⁴ To whom all correspondence should be addressed.

OBSERVATION

Life cycle

The larvae of the Family Tenthredinidae generally resemble to those of the Order Lepidoptera and feed on leaves of various plants. They can be serious pests in the forest, in the garden and in the farm fields. *A. rosae* larvae feed on cruciferous plants. In the field, *A. rosae* may be found from the late spring, and throughout the summer to the fall, usually producing 5–6 generations in the area around Kobe. During the winter they hibernate as prepupae. In the laboratory, *A. rosae* can be reared throughout the year if kept at 25°C under 16 hr light-8 hr dark condition. Under these conditions one generation takes about 25 days. Representative photographs of *A. rosae* and a general developmental timetable are shown in Figures 1–4. Unless otherwise specified, descriptions below apply to stocks maintained for more than six months in the laboratory.

Embryogenesis takes about 5 days (Figs. 2 and 3). The embryo is sufficiently transparent so that development can be followed easily under the microscope. Mature eggs measure about 800 μm in length and 350 μm in diameter and can be handled easily for such manipulations as ligation and microinjection. Embryogenesis can be followed either in eggs removed from the leaves in which they are deposited by females (male and

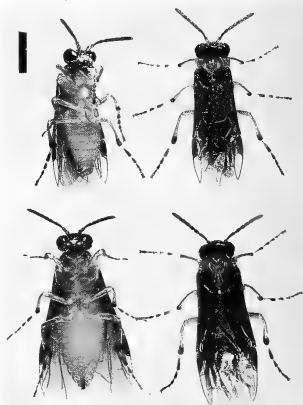


Fig. 1. Adult males (top) and females (bottom) of *A. rosae*. Bar, 2 mm.

female embryos) or in mature unfertilized eggs dissected out of the ovary and activated by various means [8, 9]. This latter characteristic allows the investigator to study the embryonic development of embryos of known (male) sex.

Larval development takes about 9 days (6 instars) in the female and 8 days (5 instars) in the male (Fig. 2). The larvae, caterpillar like in mor-

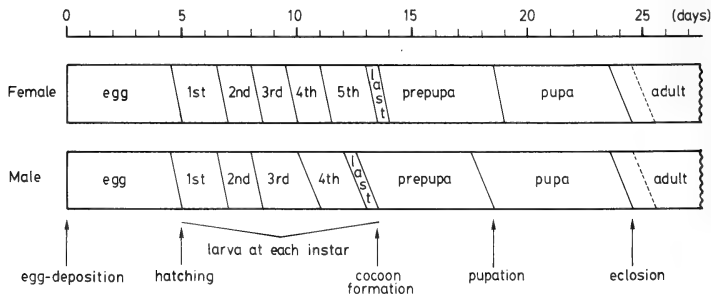


Fig. 2. Life cycle of *A. rosae*. last, last instar larva. Note females have 6 larval instars while males have 5. Prepupal period is 5 days both in females and males.

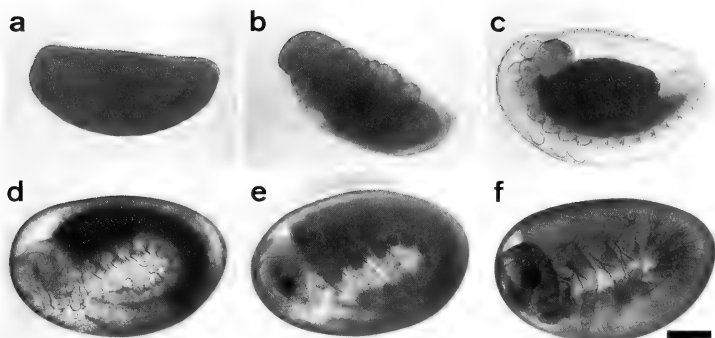


FIG. 3. Embryonic development in *A. rosae* males. Mature unfertilized eggs dissected from ovaries of unmated females were activated by placing on wet filter paper (see text). a, 0 hr; b, 24 hr; c, 48 hr; d, 72 hr; e, 96 hr; and f, 120 hr. Bar, 200 μ m. Photographs were taken of living specimens placed under a compound microscope. The anterior end of the embryo is at the left and the dorsal side is at the top.

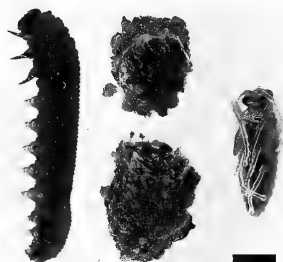


FIG. 4. A fourth instar male larva (left) and a broken cocoon (middle) from which a male pupa (right) was taken out. Bar, 2 mm.

phology (Fig. 4), are pale black in color in the early instars, become pure black in the fourth instar and blue-black in the last instar. Larvae feed actively on leaves of cruciferous plants except for the last instar larvae which feed little. During the fourth instar, the fat body begins to grow rapidly. Two size classes become apparent in the last instar larvae: the large females and smaller males. The last instar larvae leave the plant and dig into the

soil where they construct cocoons, of two size classes. Within the cocoon the larva forms a prepupa (about 5 days both in the female and the male), and then a pupa (about 5 days in the female and 6 days in the male) (Figs. 2 and 4). Old prepupae or pupae can be removed from the cocoons and placed on a wet filter paper in a small petri dish where their development to adulthood can be followed directly.

Under laboratory condition, embryonic, larval, prepupal and pupal development takes about 25 days (Fig. 2). The eclosed adult remains in the cocoon for a day, then opens a small hole at the anterior pole, and comes out of the cocoon and out of the soil. Adult females are about 8 mm in length, and males about 6 mm (Fig. 1). Females mate within a day after emergence and start laying eggs the next day. Both females and males, if fed on diluted honey, live about two weeks, and individual females lay up to 100 eggs. Well-fed females or wild-caught females may lay more eggs. Young adult females have well developed fat bodies, while older ones apparently use up the reservoir. Adult males, on the other hand, have very small fat bodies even when they are young.

Apart from the difference in size and from the

obvious difference in the external genital structure morphology (Fig. 1), there is only one clear external sexual dimorphic character: the ratio of head width and body length. The distance between two compound eyes is narrower in the haploid male than in the diploid female (Fig. 1).

Maintenance of stock

Since *A. rosae* is introduced as a new experimental material for developmental studies, it is useful to describe briefly the maintenance of stocks. *A. rosae* is distributed widely in the palaearctic area [10]. Stocks are started from wild-caught adult females or female and male larvae. Wild-collected females are nearly always mated and, when provided with fresh young leaves of cruciferous plants, may lay several scores of eggs. Adult females fed diluted honey live longer and lay more eggs. When embryos hatch, they should be provided with fresh young leaves. *Raphanus sativus* [Cruciferae (Brassicaceae)] has proven a convenient species for rearing stocks. It is easy to cultivate, and if covered with shade in the summer and cultivated in a glass house in the winter, it can supply fresh young leaves year-round. Several square plastic garden pots should be sufficient to provide enough leaves unless large-scale rearing of *A. rosae* is attempted. Obviously it is essential to place the pots in a frame with fine net to prevent access of wild sawflies to the plants. We have tested several cultivars of *R. sativus*, and found that those of which leaves bear fine hairs on the surface are not liked by *A. rosae* adult females. Apparently they have some difficulty in laying eggs on such leaves.

Adults are handled with the help of an insect suction tube or they can be anesthetized with ether. Adult females and males are placed in a glass jar with a plastic foam top plug inside of which is placed a small glass vial with fresh leaves for egg deposition (Fig. 5). Eggs are deposited individually in the leaf just inside the lower surface along the edge. A low-magnification lens is sufficient to detect the slightly bulging areas where the eggs are deposited. If the leaves get spoiled before eggs complete embryonic development, the eggs should be removed and placed on a wet filter paper. In the laboratory it is easiest to rear *A.*



Fig. 5. Rearing of *A. rosae* in the laboratory. Left: Adult females and males are placed in a glass jar in which fresh young leaves of *Raphanus sativus* and a wad of tissue paper soaked with diluted honey are provided. Right: Larvae are reared in a plastic container. Fresh *R. sativus* leaves are placed on a sheet of wet filter paper. Larvae are transferred to a new container daily. A small petri dish is provided when larvae become last instar. Bar, 5 cm.

rosae larvae in a plastic container with a sheet of wet filter paper on top of which fresh leaves are placed (Fig. 5). This allows larvae to be transferred easily as needed when changing the leaves. When larvae reach the last instar, they are transferred to a small shallow container such as a small petri dish (diameter 45 mm) containing sterilized mixture of sand and soil (Fig. 5). They crawl into this and there construct cocoons. Several days after cocoons are formed, the cocoons either dug out or within the container may be transferred to a refrigerator (4°C) to slow down development. Such cultures, apparently mimicking hibernation in nature, may be kept refrigerated for at least a month without any harmful results.

Sex in *A. rosae* is determined by a single-locus multiple-allele system: hemizygous and homozygous (homoallelic) conditions produce haploid and diploid males, respectively, and heterozygous condition results in females [3]. It is thus advisable that as many stocks of independent origins as possible be established first, and crosses be made between females and males from different parents to prevent extinction of stocks due to production of too few females.

When stocks are maintained for generations in the laboratory as described above, females appear to gradually lose their sex appeal and matings, both single-pair and mass, may become increasingly difficult. Males remain potentially active since, if provided with young females obtained from wild-caught larvae, they eagerly try to copulate. Leaves of *Clerodendron trichotomum* (Verbenaceae), for example, produce a dramatic effect. Apparently leaves of this plant attract both female and male adults. They stay on the leaf for as long as an hour and engage in what appears to be a chewing and sucking action and then males begin to court females. Interestingly, females do not lay eggs nor larvae feed on this plant. Discovery of the effect of *C. trichotomum* is fortuitous and no systematic search for plants with similar effects nor for the active substance has yet been made. Leaves of *C. trichotomum*, wrapped individually and kept frozen at -20°C , are as effective as fresh leaves.

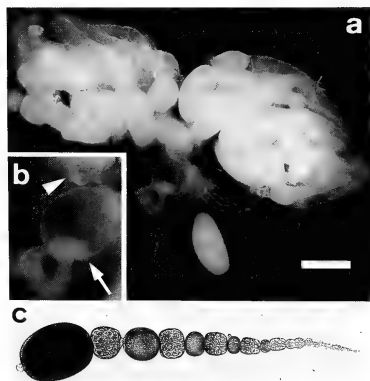


FIG. 6. Adult female internal reproductive organs of *A. rosae*. a, Fresh specimen seen under a dissecting microscope showing a pair of ovaries and other organs. Bar, 500 μm . b, An enlarged portion of (a). Arrowhead, seminal receptacle; Arrow, accessory gland. c, Fresh specimen of an ovariole seen under a compound microscope. At the far left is a growing oocyte to which a group of nurse cells (second from the left) is connected. Younger stages of oocyte-nurse cell complexes are seen to extend to the right.

Adult female internal reproductive organs

Adult female internal reproductive organs of *A. rosae* are composed of a paired ovaries and lateral oviducts, a common oviduct, a seminal receptacle, and an accessory gland (Fig. 6a). The exact number of ovarioles per ovary varies, but averages about 14. An ovariole contains germ cells and somatic cells at the extreme anterior end and follicles (egg chambers) of progressively advanced stages along the rest of its length. The average number of follicles per ovariole is about 10 in newly eclosed females. Few mature eggs are observed until the third day of adult life (second day after their appearance from the cocoons). Clearly, not all the follicles recognizable in the ovaries of newly eclosed females become mature eggs. Only three or so per ovariole actually mature and are laid (a female lays up to some 100 eggs). As a follicle grows in the ovariole, the chamber

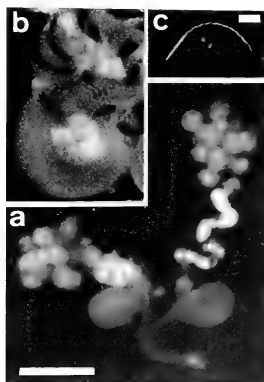


FIG. 7. Adult male internal reproductive organs of *A. rosae*. a, Fresh specimen seen under a dissecting microscope showing paired testes, spermathecae, and accessory glands, and a pair of lateral and a common ejaculatory ducts. The group of cells surrounding the spermatheca at the right is removed to show the detail. Bar, 500 μm . b, Fresh specimen of sperm bundles taken out from the spermatheca seen under a compound microscope with dark-field illumination. c, Fresh specimen of free sperm (dark-field). Bar, 10 μm .

containing the oocyte seemingly separates from the one containing nurse cells, although actually maintaining the passage between them (Fig. 6c). The seminal receptacle of a mated female contains a large number of individual and moving sperm. A portion of this organ is sclerotized and bears cuticular denticles (Fig. 6b). The accessory gland is a round-shaped heavily muscled organ containing a transparent and very viscous material apparently secreted from a pair of structures attached to it (Fig. 6b). Function of this organ is unknown, but conceivably it has something to do with egg deposition and protection of the eggs deposited. It is, however, not essential for egg development, as mature unfertilized eggs, explanted from the ovary and placed on a wet filter paper, can start and complete development.

Adult male internal reproductive organs

Adult male internal reproductive organs of *A. rosae* are composed of paired testes, sperm ducts, spermathecae, and accessory glands, and a pair of lateral and a common ejaculatory duct (Fig. 7a). Each testis consists of a central sphere with several smaller surrounding spheres attached to it. In young males, the surrounding smaller spheres are slightly constricted at their equators. Active spermatogenesis is taking place in this "double" structure. Within a few days this "double" structure is lost and the smaller spheres become "single" spheres. They become progressively empty. The spermatheca is an extensively folded structure covered by a mass of yellowish-colored relatively large cells (Fig. 7a), filled with bundles of sperm (Fig. 7b), which opens into the accessory gland (Fig. 7a). A sperm is about 55 μm in length, of which 15 μm is the head and 40 μm is the tail. The tail has a spiral or screw shape, is curved (Fig. 7c), and shows screw-motion, rather than beating or undulating motion, along its length. Sperm bundles dissected from spermatheca in 0.15 M saline solution show little movement at first, but begin to move their tails within a few min.

DISCUSSION

Since *A. rosae* is here introduced as a new experimental organism, some of the merits of the

system and the aims and plans of our future studies should be mentioned.

Most Hymenopterans produce males by arrhenotoky [1, 2]. Nevertheless, artificial activation of mature unfertilized eggs explanted from the ovary has been successfully carried out in only a small number of species. Unfertilized eggs of *Pimpla turionellae* (Ichneumonidae, Apocrita), dissected from ovaries, can be activated by passage through narrow capillary tubing [6, 11]. Examples of egg activation by similar "mechanical stress" have been noted in several Apocritan species [6, 7, 12]. Recently, cold shock and incubation in hypertonic solution have been reported to activate non-mechanically stressed eggs of *Campoletis sonorensis* (Ichneumonidae) [12].

On the other hand, in more than 200 species of sawflies of Tenthredinidae (Symphyta) examined including *A. rosae*, it has been shown that unfertilized eggs taken out from ovaries can be activated by simply placing them on a filter paper soaked with water [8]. Usefulness of the system common in Tenthredinidae species is obvious. The eggs are easily activated *in vitro*, which means it is possible to obtain a large number of exactly timed developing embryos (of known sex, male, if necessary). Along with the ease in handling these eggs by various means including microinjection, molecular dissection of the processes of egg activation and also of the (sex-specific) events in early embryogenesis might be approached with relative ease. Because of the ease in handling mature unfertilized eggs, possibilities of artificial fertilization and even of artificial induction of thelytoky [1, 2, 13], which is known in some Hymenopteran species [1, 2, 14], can be examined. Various agents, chemical or otherwise, can be applied at various stages and their possible effects on nuclear division and fusion examined.

We have chosen *A. rosae* as an experimental material because, in addition to the features noted above, stocks are easily maintained in the laboratory which is essential for genetic studies, and it also has a simple "single-locus multiple-allele" sex determination system (see Maintenance of stock). Diploid and even triploid males can be obtained easily in *A. rosae*, and these males produce diploid and triploid sperm, respectively [3, Naito and

Suzuki, unpubl.). Clearly sperm maturation division is non-reductional, and thus the genes involved in the process are active in females but not in males.

At the moment we have but one spontaneous color mutant arisen, and our knowledge on the formal genetics of *A. rosae* is practically nil. It might be expected, however, that such important genes as those involved in sex determination and those in cell division are evolutionally conserved. We can then, for the time being, make use of such genes cloned in other species, and, by using them as probes, may be able to "pick up" homologous genes in *A. rosae*.

ACKNOWLEDGMENTS

We thank Dr. S. J. Counce of Duke University for critically reading the manuscript.

REFERENCES

- White, M. J. D. (1973) Animal Cytology and Evolution. 3rd. ed. Cambridge Univ. Press, London.
- Suomalainen, E., Saura, A. and Lokki, J. (1987) Cytology and Evolution in Parthenogenesis. CRC Press, Boca Raton.
- Naito, T. and Suzuki, H. (1985) Sex determination in sawflies (Hymenoptera). Jpn. J. Genet., **60**: 646. (Abstract, in Japanese)
- Cassidy, J. D. (1975) The parasitoid wasps, *Habrobracon* and *Mormoniella*. In "Handbook of Genetics". Vol. 3, Ed. by R. C. King, Plenum Press, New York, pp. 173-223.
- Rothenbuhler, W. C. (1975) The honey bee, *Apis mellifera*. In "Handbook of Genetics". Vol. 3, Ed. by R. C. King. Plenum Press, New York, pp. 165-172.
- Went, D. F. (1982) Egg activation and parthenogenetic reproduction in insects. Biol. Rev., **57**: 319-344.
- Sander, K. (1985) Fertilization and egg cell activation in insects. In "Biology of Fertilization". Vol. 2, Ed. by C. H. Metz and A. Monroy. Academic Press, Orlando, pp. 409-430.
- Naito, T. (1982) Chromosome number differentiation in sawflies and its systematic implication. (Hymenoptera, Tenthredinidae). Kontyû (Tokyo), **50**: 569-587.
- Sawa, M. and Oishi, K. (1989) Studies on the sawfly, *Athalia rosae* (Insecta, Hymenoptera, Tenthredinidae) II. Experimental activation of mature unfertilized eggs. Zool. Sci., **6**: 549-556.
- Benson, R. B. (1962) A revision of the athalini (Hymenoptera-Tenthredinidae). Bull. British Mus. (Nat. Hist.) Entomology, **2**: 333-382.
- Went, D. F. and Krause, G. (1973) Normal development of mechanically activated, unaided eggs of an endoparasitic Hymenopteran. Nature (Lond.), **244**: 454-455.
- Vinson, S. B. and Jang, H.-S. (1987) Activation of *Camponotus sonorensis* (Hymenoptera: Ichneumonidae) eggs by artificial means. Ann. Entomol. Soc. Am., **80**: 486-489.
- Lamb, R. Y. and Willey, R. B. (1987) Cytological mechanisms of thelytokous parthenogenesis in insects. Genome, **29**: 367-369.
- Maeta, Y., Kubota, N. and Sakagami, S. F. (1987) *Nomada japonica* as a thelytokous cleptoparasitic bee, with notes on egg size and egg complement in some cleptoparasitic bees. Kontyû (Tokyo), **55**: 21-31.



Studies on the Sawfly, *Athalia rosae* (Insecta, Hymenoptera, Tenthredinidae). II. Experimental Activation of Mature Unfertilized Eggs

MASAMI SAWA and KUGAO OISHI^{1,2}

Division of Science of Biological Resources, Graduate School of Science and Technology, Kobe University, Nada, Kobe 657, and

¹*Department of Biology, Faculty of Science, Kobe University, Nada, Kobe 657, Japan*

ABSTRACT—Mature unfertilized eggs (primary oocytes arrested at metaphase of the first meiotic division) of *Athalia rosae* can be explanted from ovaries and placed on a filter paper soaked with distilled water, or submerged in distilled water where they are activated and start complete embryonic development. Eggs placed and kept in a saline solution (0.15 M NaCl) are not activated, show no signs of development and deteriorate after a few hours. However once activated in distilled water for 20 min, eggs can then be placed in saline solution and development continues. This 20-min period corresponds to the time required by the arrested metaphase nucleus to proceed to telophase. Various ions as well as osmolality are involved in this egg activation process in varying capacities. Other treatments such as brief desiccation, passage through narrow capillary tubing, pricking with a glass needle or lowering pH of the solution are also found to be effective in activating the eggs to various degrees.

INTRODUCTION

Studies on the process of egg activation in insects appear to be still in the infant stage (for reviews see [1-3]). Parthenogenetic species, especially arrhenotokous ones, provide useful material for pursuing such studies since in these species both fertilized and unfertilized eggs develop and comparisons can be made between them. Information may be obtained with respect to the common and unique events associated with both or each of the processes.

Hymenopterans are one of the most successful groups of insects in terms of the number of species included. Most Hymenopterans show arrhenotokous, and a few thelytokous, reproduction [4, 5]. In view of the extraordinary success of this group of insects, we believe that Hymenopterans are the material of choice for studies on the mechanism of egg activation.

Experimental egg activation in this group has been studied using species of the suborder Apocrita. It should be pointed out that the development of unfertilized eggs in arrhenotokous Hymenopterans applies normally only to the laid eggs and not to the unlaid eggs dissected from ovaries. Mechanical deformation [6, 7] as well as cold shock and incubation in hypertonic solution [7] have been shown to induce egg activation in unlaid mature unfertilized eggs of two ichneumonid wasp species.

We have chosen the sawfly, *Athalia rosae*, a species belonging to the lower suborder, Symphyta, as experimental material. Mature unfertilized eggs dissected from ovaries of the sawflies of Tenthredinidae (Symphyta) can be activated to develop if they are placed on a filter paper soaked with distilled water [8]. We have examined the system in some detail and describe here the effects of various treatments on egg activation.

MATERIALS AND METHODS

Stocks of *Athalia rosae* were maintained in the laboratory as described previously [9]. Unmated

Accepted August 19, 1988

Received July 5, 1988

² To whom all correspondence should be addressed.

females were severed at the thorax-abdomen junction. The abdomen was then dissected in distilled water or in various solutions. Mature unfertilized eggs thus obtained provided material for the present study.

Eggs were either placed on a filter paper soaked with distilled water in a small petri dish (diameter 43 mm, depth 12 mm), or submerged in distilled water or various solutions in a small covered watch glass (diameter 70 mm, depth in the center 5 mm), and incubated at room temperature (ca. 25°C). Eggs placed in watch glasses can be directly observed under the dissecting microscope and the development can be followed with living specimens [9].

Feulgen staining of the eggs and embryos was done as follows. Eggs were fixed in an FAA solution (95% ethanol: 50% acetic acid: formalin = 2:0.5:0.2) at 4°C overnight, washed 4 times, each for 30 min, in 70% ethanol, and dechorionated under the dissecting microscope using sharp tungsten needles. The chorion of *A. rosae* egg is thin and soft and can be removed only after proper fixation. The eggs were then washed in 3 changes of distilled water, hydrolysed in 1N HCl for 5 min at room temperature and then in 1N HCl for 10 min at 60°C, and washed in 3 changes of ice-cold distilled water. They were stained with Schiff's solution (Merck) for 1 hr at room temperature, washed briefly in 5% acetic acid and in 2 changes of 95% ethanol, and dehydrated in 99% ethanol for 15 min and then in 2 changes of 100% ethanol, each for 20 min. Dehydrated eggs were cleared of yolk in toluene, placed on a microscope slide between strips of cover slip as spacers, and mounted with Bioleite (Oken, Tokyo).

RESULTS

We first confirmed the observation made previously by Naito [8], that mature unfertilized eggs dissected from ovaries of *Athalia rosae* and placed on a filter paper soaked with distilled water developed normally. Most eggs completed embryonic development in 5 days and hatched [9]. To make various treatments on the eggs and observations on developing embryos much easier, we submerged eggs in distilled water in a small

watch glass. Most eggs began development and many nearly completed embryonic development, though development was retarded by a couple of days. Only a few, however, actually hatched. This is most probably due to the limited supply of oxygen available to developing embryos when they are kept submerged in water, since eggs kept submerged for one to two days, if transferred to wet filter paper, developed normally and hatched.

When examined under the compound microscope, the eggs kept on a wet filter paper developed to blastoderm in about 12–13 hr, while those kept submerged in water did so in about 14–15 hr. Since blastoderm formation can easily be recognized under the dissecting microscope when a little practice is exercised, we took this developmental stage, determined at 15–18 hr, as the criterion for successful egg activation for our further examinations.

Number of mature eggs per female of various ages and their ability to be activated

Figure 1a shows the average number of mature

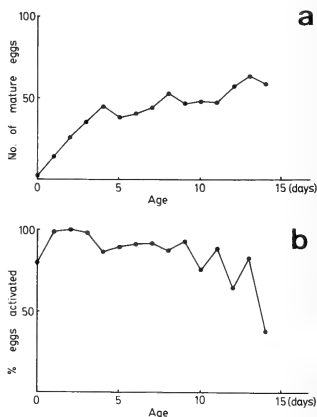


FIG. 1. Average number of mature eggs per female at various ages in days (a), and per cent of the eggs activated and developed to blastoderm in distilled water (b). Females within 24 hr after emergence from the cocoon are shown as 0-day old.

eggs an unmated female carries at various ages in days. Females within 24 hr of emergence from the cocoons (that is, within 48 hr post-eclosion, as they remain for a day after eclosion in the cocoon, see Sawa *et al.* [9] for general description of development of *A. rosae*) are shown here as 0 day of age. Day 0 females have few mature eggs (average 2 mature eggs per female). The number of mature eggs increases rapidly with the age of females, reaching a maximum of some 45 in 4-day females, stays more or less at the same number for about a week, and increases again to a maximum of about 65 in 13-day females. In these studies females were fed on diluted honey but were not provided with *Raphanus* leaves on which they lay eggs [9]. Females under these conditions do not lay any eggs. No apparent degeneration of the eggs accumulated in the ovary was observed in a 2-week period.

Mature eggs were dissected from ovaries and submerged in distilled water in watch glasses as above, and the numbers of eggs developed to blastoderm were determined. Figure 1b shows the results in per cent of the eggs so developed. Eighty to 100% of the eggs from 0-9 day-old females were activated and formed complete blastoderm. The frequency of activated eggs then began to fall as the females became older. All subsequent experiments presented below were thus done with eggs dissected from females 6-8 days old.

Time required for egg activation

We observed that eggs dissected out and placed in a saline solution (0.15 M NaCl) were not activated. Such eggs formed many vacuoles in their interiors after a few hr and deteriorated. If eggs

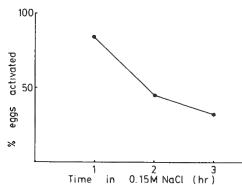


Fig. 2. Per cent of eggs activated and developed to blastoderm in distilled water after various periods of time in 0.15 M NaCl.

were transferred to distilled water within 1 hr, however, they were activated and developed to blastoderm normally (Fig. 2).

To determine the time required for activation by exposure to water, unmated females were dissected in the saline solution and the eggs were kept submerged. Batches of eggs were transferred to distilled water, kept there for various periods of time, then returned to the saline solution, and observed for the formation of blastoderm (Fig. 3). If the eggs were kept in distilled water for 20 min or more, nearly all the eggs were activated and continued development even upon return to the saline solution. The initial event of egg activation is thus completed irreversibly within 20 min. The saline solution, although it prevents eggs from activation, apparently does not interfere with the development once eggs are activated. Some embryos were transferred to filter paper wet with distilled water after 20 hr in saline and most of them completed embryonic development and hatched.

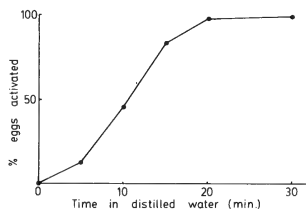


Fig. 3. Per cent of eggs activated and developed to blastoderm when eggs are dissected in 0.15 M NaCl, transferred to distilled water for various periods of time, and then returned to 0.15 M NaCl.

Some mature unfertilized eggs were fixed immediately upon dissection from the ovary, Feulgen stained, and examined under the compound microscope (Fig. 4a and b). The egg nucleus is located just below the dorsal surface at about a quarter of the egg length from the anterior end. Clearly the "mature unfertilized egg" is the primary oocyte in which the nucleus is arrested at metaphase of the first meiotic division. The same meiotic figure was observed in the eggs dissected and kept in the

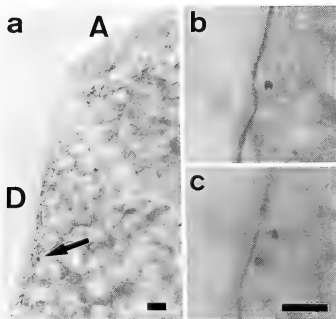


FIG. 4. a, A mature egg fixed immediately after dissection from ovary and Feulgen stained. A, anterior end; D, dorsal side of the egg. Arrow indicates a nucleus at metaphase of first meiotic division. b, Same sample as in (a) photographed at higher magnification. Magnification as in (c). c, An egg dissected from ovary, placed in distilled water for 20 min, and fixed and Feulgen stained. Note that the nucleus is now at telophase of the first meiotic division. Bar, 10 μ m.

saline solution for an hr. Arrest was released when "the egg" was transferred to distilled water and the nuclear division proceeded to telophase in 20 min (Fig. 4c). This is probably the cytological basis of irreversible egg activation. The spindle of meiotic division was oriented more or less parallel to the dorsal surface of the egg and never perpendicular.

Effects of ions and of osmolality on egg activation

The simple saline solution used above prevented activation of the eggs. Four kinds of salts, NaCl, KCl, CaCl_2 and MgCl_2 , most often used in various physiological salt solutions and in tissue culture media, were examined at various concentrations for their effects on egg activation (Fig. 5). Eggs were dissected out and kept submerged in the test solution. NaCl was most effective in preventing the eggs from activation. No eggs developed to blastoderm when placed in 0.1 M NaCl (200 mOsm), while about 80% of the eggs developed to this stage in 0.1 M KCl (200 mOsm). Complete inhibition of egg activation in KCl was achieved only at 0.3 M (600 mOsm). CaCl_2 and MgCl_2 were similar in their effects: nearly all the eggs de-

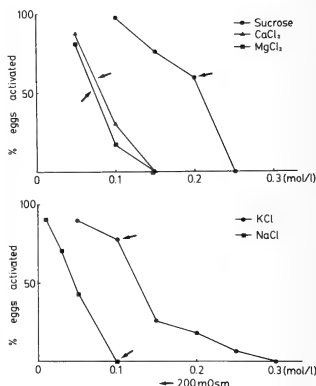


FIG. 5. Effects of various ions and sucrose at different concentrations on egg activation. Mature eggs were dissected from ovary, submerged in each solution, and observed for development to blastoderm.

veloped in 0.05 M solutions (130 mOsm), and some 25% developed in 0.1 M solutions (260 mOsm), while none developed in 0.15 M solutions (390 mOsm).

Sucrose was included in these examinations (Fig. 5) because the solution is often used to hold cells and other biological materials temporarily when necessary to avoid the effect of ions. More than 50% of the eggs developed in 0.2 M (200 mOsm) solution but none in 0.25 M solution. Clearly osmolality has an important influence on egg activation. It is also clear, however, that it is not the only factor involved.

Other treatments effective in egg activation

Unexpectedly we noted that eggs could develop in 0.15 M NaCl if they were removed from the solution, desiccated briefly, and then returned to the saline. Eggs were taken out of the saline solution, placed on a piece of double-stick tape on the microscopic slide, desiccated by touching them with a piece of filter paper, and left there for various periods of time (Table 1). Even brief treatments up to 3 min were effective: when desiccated for 3 min, some 30% of the eggs were

TABLE 1. Effect of desiccation on egg activation

	Desiccation period (min)			
	3	5	10	15
No. of eggs treated	75	60	60	56
No. of eggs activated	22	7	1	0
% Activation	29	12	2	0

activated and developed. Longer treatments simply resulted in deterioration of the eggs. Desiccation for shorter periods might be more effective. These studies, however, were made as a preliminary for studies in which further treatments such as microinjection were attempted for which a three-min period was necessary as a minimum time [10].

Suspecting now that almost any treatment might result in egg activation, we examined several of the treatments known to be effective in activating the eggs of various organisms. Eggs were dissected from ovaries in 0.15 M NaCl, exposed to various treatments, and observed for blastoderm formation.

It has been known that the eggs dissected from ovaries of *Pimpla turionellae* (Hymenoptera) can be activated mechanically by passing them through a narrow capillary tubing [2, 6]. Table 2 shows the results of similar treatment of *A. rosae* eggs. Eggs in batches of 50 were passed through glass capillary tubings of various sizes made by pulling commercially available capillary tubing (Drummond, Microcaps 25 μ l) with a vetical pipet puller (Narishige, Tokyo, PB-7). Eggs in the saline solution were first sucked half way up the capillary tube by the action of 10 ml syringe via a connecting plastic tubing and then gently blown out by disconnecting and reconnecting the plastic tubing to the opposite end and applying pressure. The best results in egg activation were obtained with capillaries through which one-third to one-half the number of the eggs examined passed without bursting, where egg activation of the total intact eggs could reach more than 80%. These embryos, when transferred after they formed blastoderm and placed on filter paper wet with distilled water, developed normally and hatched.

Pricking unfertilized eggs with a needle results in

TABLE 2. Effects of passage through capillary tubings on egg activation

No. of eggs passed through capillary tubings of various sizes	No. of eggs passed without bursting	No. of eggs activated
50	44	1
50	43	0
50	42	0
50	39	1
50	39	3
50	37	8
50	29	0
50	28	5
50	25	0
50	24	0
50	22	11
50	17	14
50	15	4
50	5	0
50	3	0

TABLE 3. Effects of pricking on egg activation

Site of pricking	No. of eggs treated	No. of eggs activated	% Activation
anterior pole	200	41	21
posterior pole	200	38	19
mid-ventral	100	24	24
mid-dorsal	100	16	16

parthenogenetic development in various organisms [4, 5]. Eggs of *A. rosae* were similarly treated (Table 3). Eggs in saline solution were held by using a holding pipet connected through a plastic tubing to a 10 ml syringe and a glass needle was inserted at various places. Glass needles were prepared by pulling off the Drummond Microcaps, 25 μ l, using a Narishige vertical pipet puller. Egg activation was observed in some 20% of the eggs so treated regardless of the site of pricking.

Lowering the pH in the egg interior has been implicated to be a cause of androgenesis and gynogenesis in the silkworm [11]. We examined the possible effect of pH of the solution in which eggs were placed (Table 4). Eggs dissected and placed in 0.15 M phosphate buffer (ca. 300 mOsm) were not activated at pH 7.0 and 8.0 but nearly

TABLE 4. Effects of pH on egg activation

pH	No. of eggs treated	No. of eggs activated	% Activation
0.15 M Phosphate buffer			
5.8	196	114	58
7.0	192	0	0
8.0	204	0	0
0.15 M Citrate buffer			
4.0	176	85	48
5.0	187	154	82
6.0	142	44	31

60% of them were activated at 5.8. Since the pH value 5.8 is the lower limit of phosphate buffer, we repeated the examination with 0.15 M citrate buffer. About 30% of the eggs were activated at pH 6.0, while more than 80% were activated at 5.0. At pH 4.0, the rate of activation went down and only about 50% were activated. Embryos developed normally and hatched when transferred at the blastoderm stage to filter paper wet with distilled water.

DISCUSSION

Unmated *A. rosae* females were fed on diluted honey but were not provided with leaves of cruciferous plants on which they lay eggs and the progeny larvae feed. Under these conditions females do not lay any eggs, but accumulate mature eggs (primary oocytes arrested at metaphase of the first meiotic division). Since the average number of ovarioles per ovary in this species is 14 [9], the results indicate that on an average about 2 follicles (egg chambers) per ovariole mature in 4 days (Fig. 1). If females are allowed to lay eggs, each lays up to about 100 in a 2-week period [9], indicating that on an average 3 follicles can potentially mature. Whether the decrease in the rate of activation in eggs obtained from older females (Fig. 1) means that the eggs can be held in the ovary in physiologically healthy conditions only for about 10 days is an open question.

Ambient osmolality has been related to egg activation in several insect species, e.g., *Mycophila speyeri* (Diptera) [12], *Drosophila melanogaster* (Diptera) [13], *Psychoda cinerea* and a *Smittia*

spec. (diptera) [14], and *Campoletis sonorensis* (Hymenoptera) [7]. Most probably, however, various ions contribute in varying capacities and the effect of osmolality is not the simple sum. Effects of mixing and balancing these ions remain to be examined. Treatments such as mechanical deformation, pricking and desiccation are also effective in activating eggs. Common to these treatments seems to be that they all cause damage to the egg surface. This principle may also apply to the results of various ions and osmolality, and of ambient pH, although in much more subtle ways. Taken together, one possible way of explaining the present results may be to assume that the eggs are activated by changes in the egg surface membrane potential.

Egg activation has been defined in various ways, and not in all cases have those "activated" eggs developed any further than beyond the blastoderm formation [1]. It should be emphasized that egg activation induced *in vitro* in the present system leads to normal development, both embryonic and postembryonic.

Sander [14] has shown that in *Psychoda cinerea*, eggs exposed to tap water for 5 min or longer can then be returned to Grace's cell culture medium, which itself does not allow egg activation, where they continue development. In the present study we have shown that the *A. rosae* eggs, if exposed to distilled water for 20 min, are activated and then continue development upon return to 0.15 M NaCl which itself does not allow egg activation, and also that the egg nucleus arrested at metaphase of the first meiotic division is derepressed and proceeds to telophase in this 20 min period in distilled water.

We have noted that the spindle of meiotic division in these parthenogenetically activated eggs is oriented more or less parallel to the long axis and along the dorsal surface of the egg (Fig. 4c) and is never perpendicular. This contrasts strongly with the general observation that the nuclei produced by meiotic divisions lie in a line at right angles to the long axis of an egg [1]. Two questions arise and remain to be examined: (1) Which one of the two products of the first meiotic division (or of the products of the second meiotic division) contributes to the embryonic develop-

ment? Is it always, for example, the anterior-most nucleus or is it the one which happens to be the inner-most? This may have some important implications for the occurrence of rare thelytokous reproduction in this species [10]. (2) Is the same spindle orientation observed in fertilized eggs?

The *A. rosae* system used here is the one in which eggs are shown to be activable by the widest range of means in insects so far examined. Since in the present results some 15–25% of the eggs pricked in 0.15 M NaCl solution were activated, it might be possible to inject various substances into the egg and see if they cause increase or decrease in the rate of egg activation. Great ease in *A. rosae* eggs in handlings such as microinjection should provide means to study various possibilities. Fine structural and molecular biological studies, both appear to be feasible in the present system since exactly timed mature oocytes as well as embryos are available, may be made in this connection.

The *A. rosae* system permits investigations on various substances or factors involved not only in the processes of egg activation as discussed above but also those in fertilization as well as in egg maturation. Although no eggs bathed in 0.15 M NaCl solution in which sperm were suspended developed in our initial attempt, attempts to induce *in vitro* fertilization by sperm injection have been successful [10].

Whether cytoplasmic factors such as the maturation promoting factor (MPF) present in mature oocytes of various vertebrate and echinoderm species (e.g., [15, 16]) exist in insects might also be investigated in the *A. rosae* system. It should be interesting to see if this non-species-specific MPF can induce germinal vesicle breakdown in *A. rosae* and if so, whether precociously "matured" eggs can be activated *in vitro*. The timetable for various maternal gene products essential for early morphogenetic development to be localized within the frame of egg architecture might then hopefully be studied. Comparative studies examining common and unique processes among insects, other non-vertebrates and vertebrates should be quite rewarding.

ACKNOWLEDGMENTS

We thank Dr. S. J. Counce of Duke University for critically reading the manuscript.

REFERENCES

- 1 Counce, S. J. (1973) The causal analysis of insect embryogenesis. In "Developmental Systems: Insects". Vol. 2. Ed. by S. J. Counce and C. H. Waddington, Academic Press, London and New York, pp. 1–156.
- 2 Went, D. F. (1982) Egg activation and parthenogenetic reproduction in insects. *Biol. Rev.*, **57**: 319–344.
- 3 Sander, K. (1985) Fertilization and egg cell activation in insects. In "Biology of Fertilization". Vol. 2. Ed. by C. H. Metz and A. Monroy, Academic Press, Orlando, pp. 409–430.
- 4 White, M. J. D. (1973) *Animal Cytology and Evolution*. 3rd edition. Cambridge Univ. Press, London.
- 5 Suomalainen, E., Saura, A. and Lokki, J. (1987) *Cytology and Evolution in Parthenogenesis*. CRC Press, Boca Raton.
- 6 Went, D. F. and Krause, G. (1973) Normal development of mechanically activated, unaided eggs of an endoparasitic Hymenopteran. *Nature (Lond.)*, **244**: 454–455.
- 7 Vinson, S. B. and Jang, H.-S. (1987) Activation of *Campoletis sonorensis* (Hymenoptera: Ichneumonidae) eggs by artificial means. *Ann. Entomol. Soc. Am.*, **80**: 486–489.
- 8 Naito, T. (1982) Chromosome number differentiation in sawflies and its systematic implication. (Hymenoptera, Tenthredinidae). *Kontyû (Tokyo)*, **50**: 569–587.
- 9 Sawa, M., Fukunaga, A., Naito, T. and Oishi, K. (1989) Studies on the sawfly, *Athalia rosae* (Insecta, Hymenoptera, Tenthredinidae). I. General biology. *Zool. Sci.*, **6**: 541–547.
- 10 Sawa, M. and Oishi, K. (1989) Studies on the sawfly, *Athalia rosae* (Insecta, Hymenoptera, Tenthredinidae). III. Fertilization by sperm injection. *Zool. Sci.*, **6**: 557–563.
- 11 Li, W. Q., Abe, S. and Sakaguchi, B. (1988) Induction of androgenesis, gynogenesis and mosaic by treatment with CO₂ gas derived from dry ice. *J. Seric. Sci. Jpn.*, **57**: 43–48 (In Japanese with English summary).
- 12 Nicklas, R. B. (1960) The chromosome cycle of a primitive cecidomyiid *Mycophila speyeri*. *Chromosoma*, **11**: 402–418.
- 13 Mahowald, A. P., Gorlaski, C. D. and Caulton, J. H. (1983) *In vitro* activation of *Drosophila* eggs.

- Devl. Biol., **98**: 437-445.
- 14 Sander, K. (1985) Experimental egg activation in lower dipterans (*Psychoda*, *Smittia*) by low osmolality. *Int. J. Invert. Reprod. Dev.*, **8**: 175-183.
- 15 Masui, Y. and Clarke, H. J. (1979) Oocyte maturation. *Int. Rev. Cytol.*, **57**: 185-282.
- 16 Sorensen, R. A., Cyert, M. S. and Pedersen, R. A. (1985) Active maturation-promoting factor is present in mature mouse oocytes. *J. Cell Biol.*, **100**: 1637-1640.

Studies on the Sawfly, *Athalia rosae* (Insecta, Hymenoptera, Tenthredinidae). III. Fertilization by Sperm Injection

MASAMI SAWA and KUGAO OISHI^{1,2}

Division of Science of Biological Resources, Graduate School of Science and Technology, Kobe University, and ¹Department of Biology, Faculty of Science, Kobe University, Nada, Kobe 657, Japan

ABSTRACT—Mature unfertilized eggs of *Athalia rosae* (Hymenoptera, Tenthredinidae) dissected from ovaries of unmated adult females were injected with sperm obtained from spermathecae of adult males. If the eggs are fertilized they would develop to females, and if not, to haploid parthenogenetic males. By employing a color mutant, *yfb*, with which we can recognize the phenotypes *yfb/yfb*, *yfb/+*, *+/+*, *yfb* and *+*, we obtained *yfb/+* female adults in up to 10% of the total number of eggs injected. Mature unfertilized eggs of these females were parthenogenetically activated and they developed to *yfb* (haploid) and *+* (haploid) males, confirming that these females derived from fertilized eggs. In rare occasions, the sperm injection resulted in the production of possible *yfb* ↔ *+* chimeric males, in which both egg nucleus and sperm nucleus separately participated in development.

INTRODUCTION

Examination of individual steps of gamete maturation and fertilization processes have long been a subject of intensive research in various animal species (for recent reviews see [1]). Progress in studies on insect fertilization, however, has been very slow apparently because of so many technical difficulties encountered in insects (for a recent review see [2]). It seems that diversity rather than generality has been emphasized in insect systems. This may be justifiably so considering the number of species included in this group (some 70% of the total number of species in the entire animal kingdom), and the great diversity in their habitats. Still it seems important to search for an insect system where studies on fertilization can be made to some extent in comparable terms with the results obtained in other groups of animals.

We report here the results of our initial attempts to this end, employing *Athalia rosae* (Hymenoptera, Tenthredinidae) as an experimental material. One powerful technique adopted in recent years in studies on individual steps towards karyogamy is

the direct injection of sperm into eggs in such diverse groups of animals as echinoderms [3], amphibians [4, 5], mammals [6-8], and even between groups [9]. Our results show that fertilization can take place in mature unfertilized eggs of *A. rosae* injected with sperm and that it results in the production of adults.

MATERIALS AND METHODS

Athalia rosae stocks

General description of development and methods of rearing for *A. rosae* are to be found in Sawa *et al.* [10]. In the present study, eggs and sperm from wildtype stocks and stocks of a color mutant, yellow fat body (*yfb*), were used.

The mutant *yfb* is spontaneous in origin and was found in 1986 while rearing wild-collected *A. rosae* in the laboratory of Dr. T. Naito, Laboratory of Entomology, Faculty of Agriculture, Kobe University, who kindly provided it to us. Detailed studies on this mutant have not yet been made. Only a brief description is thus given below.

Normally fat body tissues begin extensive growth in the fourth instar larvae in both females and males, maintain their prominence throughout

Accepted August 19, 1988

Received July 5, 1988

² To whom all correspondence should be addressed.

late larval, prepupal and pupal stages, and lose their massive volume in adults. The shrinkage in mass is already apparent in males on the first day of adult life, but in females it becomes apparent only after about a week. In wildtype individuals, fat body cells are green in color in larvae and prepupae, become greenish yellow in early-to-mid pupae and gradually turn yellow in late pupae, and are pale yellow in adults. Homozygous *yfb/yfb* females and hemizygous *yfb* males have fat body cells bright yellow in color in late larval, prepupal and early-to-mid pupal development, but the color fades gradually and becomes yellow in late pupae and pale yellow in adults. This difference in color between the wildtype and the *yfb* fat body cells shows through the integument when the cuticle is not extensively pigmented, namely in the last instar larvae and in the early-to-mid stage pupae. Heterozygous *yfb/+* females have fat body cells slightly greenish yellow in color which later become pale yellow. *yfb/+* and *+/+* cannot be distinguished externally in the last instar larvae, but can be done at the pupal stage. When examining live whole specimens externally, the best time to differentiate *yfb/yfb*, *yfb/+*, and *+/+* or *yfb* and *+* is the mid-pupal stage (2–3 days after pupation or 7–8 days after cocoon formation), at which time they can be distinguished quite easily

(Fig. 1).

Injection of eggs

Unmated 6–8 day old adult females can each supply about 40–50 mature unfertilized eggs for experimentation [11]. Adult females were dissected in 0.15 M NaCl on a depression slide and mature eggs were transferred to a new slide with fresh saline solution. Egg activation does not occur in this solution, and the eggs can sit there for one hr without losing the ability to be activated when transferred in distilled water [11]. Five eggs at a time were placed on a piece of double-stick tape attached to a microscopic slide, arranged in a row with a blunt dissection needle with their posterior ends to the left, and desiccated by touching carefully with a piece of Kimwipe. The eggs then attach firmly to the tape without applying any pressure. The slide was then placed on the stage of an inverted microscope (Olympus, IMT-2) provided with a joystick micromanipulator (Narishige, Tokyo, MN-151, and the pipet holder substituted to that of Leitz).

Adult males, about a week old, were dissected in the saline solution, or other solutions as indicated in results (Table 1) on a depression slide and sperm bundles carefully squeezed out from the spermathecae and transferred to a shallow de-

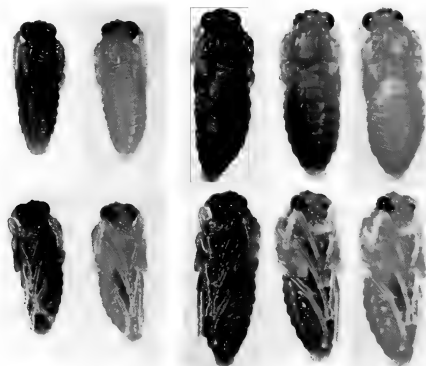


FIG. 1. Phenotypes of *yfb* mutant in males (left: *+* and *yfb*) and females (right: *+/+*, *yfb/+* and *yfb/yfb*) at mid-pupal stage.

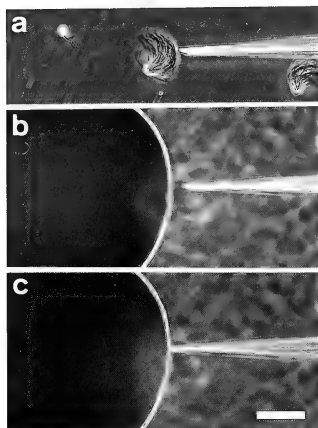


FIG. 2. Sperm bundles being dispersed by injection pipet (a), and an egg before (b) and after (c) the insertion of injection pipet. Background in (b) and (c) shows the double-stick tape on which the egg is attached. Bar, 50 μ m.



FIG. 3. Phenotypes of + (left), *yfb* (right) and probable *yfb*/ \leftrightarrow (center) chimeric male at mid-pupal stage. Note that *yfb*/ \leftrightarrow has the color seen in heterozygous *yfb*/ \leftrightarrow females (compare with Fig. 1).

pression slide with fresh solution. The slide was placed on the stage of the inverted microscope, next to the slide on which eggs were attached.

The eggs within one hr in the saline solution

were processed as above and injected within three min after drying. Drying eggs itself causes egg activation, but such treatment for more than three min is quite deleterious [11]. The sperm preparation was used for injection within one hr.

Injection was carried out at a magnification of 300 \times under phase contrast optics. The sperm, mostly still in variously-sized bundles, were dispersed as much as possible by flushing them in and out of the injection pipet several times (Fig. 2). Then the sperm, up to two dozen each, were sucked into the injection pipet, and were injected into individual eggs at the anterior pole just below the egg surface. Immediately after injection of the five eggs completed within three min, drops of silicone oil (Shin Etsu, Tokyo, FL-100, 1,000 c.s.) or distilled water were placed over the eggs. The eggs were then gently removed from the tape by using a blunt dissection needle, and transferred by Pasteur pipet to a piece of filter paper wet with distilled water placed in a small petri dish (diameter 43 mm, depth 12 mm). Silicone was removed four days later, one day before the eggs were to hatch, by flushing distilled water over the eggs and gently rubbing the eggs against filter paper. Once freed of oil in a small petri dish the eggs sank down to the bottom and were then placed on a new filter paper freshly wet with distilled water. With practice, up to 50 eggs per hr and some 200 eggs per day can be injected.

Instruments for injection

Injection pipets were made by pulling glass capillary tubing (Drummond, Microcaps 25 μ m, 65 mm in length, 0.97 mm in outer diameter and 0.69 mm in inner diameter) in a vertical pipet puller (Narishige, PB-7). Pipet pulling was done in two steps. The first step was with the No. 1 heater adjustment control at 50 and with one light weight. This gave a tapered region about 4 mm in length. The second step was with the No. 2 heater adjustment control at 900 and with one light weight. This pulled off the capillary and gave the second tapered region to the sealed tip about 2 mm each in length. The pulled pipet was then mounted on a rotating diamond grinding wheel (Narishige, EG-4) at an angle of 30°. The wheel was run with the adjustment control at 55. Distilled water was

dripped onto it during the operation. The pipet was slowly lowered, and as the tip was ground and an opening was made, distilled water came up in the pipet, and when it reached about 1 mm in height the pipet was lifted. The pipet was then removed, connected to a 10 ml plastic disposable syringe through a Tygone plastic tubing, cleaned by sucking distilled water, coated with Sigmacote (Sigma), and then kept in a clean plastic box on modelling clay until use.

The pipet, with the tip opening about 5 μ m in diameter, was fitted firmly to a Leitz pipet holder attached to a joystick micromanipulator and connected to Tygone plastic tubing and to a 10 ml plastic disposable syringe. Midway along the tubing metal joint having three openings with taps was

placed. No liquid was filled into the pipet and the whole operation was carried out directly under the air pressure provided by the syringe. Just before injection operation the pipet was rinsed extensively with the solution in which sperm were held.

RESULTS

Mature unfertilized eggs were dissected from ovaries of unmated adult females and injected at their anterior ends with sperm obtained from spermathecae of adult males. Sperm bundles from spermathecae were dispersed as much as possible to produce free individual sperm by pipetting and up to two dozen of sperm were injected to each egg. In preliminary experiments (Table 1, Exp. 1

TABLE 1. Results of sperm injection into unfertilized eggs

	No. of eggs injected	No. larvae hatched	No. pupae	Pupal phenotype*			
				♀		♂	
				yfb/+	+/+ or yfb/yfb	+ or yfb	yfb/+
Sperm suspended in 0.15 M NaCl solution: +/+ eggs injected with yfb sperm:							
Exp. 1	750 (100)	192 (25.6)	115 (15.3)	1 (0.1)	3	110	1
Exp. 2	500 (100)	—	107 (21.4)	0	0	106	1
Sperm suspended in 0.1 M NaCl solution: yfb/yfb eggs injected with + sperm:							
Exp. 3	180 (100)	63 (35.0)	44 (24.4)	2 (1.1)	0	42	0
Sperm suspended in 0.01 M NaCl solution: yfb/yfb eggs injected with + sperm:							
Exp. 4	220 (100)	139 (63.2)	54 (24.5)	14 (6.4)	1	39	0
Sperm suspended in distilled water: yfb/yfb eggs injected with + sperm:							
Exp. 5	49 (100)	19 (38.8)	14 (28.6)	5 (10.2)	0	9	0
Exp. 6	50 (100)	33 (66.0)	22 (44.0)	5 (10.0)	0	17	0
Exp. 7	55 (100)	25 (45.5)	13 (23.6)	4 (7.3)	0	9	0
Exp. 8	45 (100)	23 (51.1)	12 (26.7)	5 (11.1)	0	7	0

Results for Exp. 1-4 are the totals of several replications, and those for Exp. 5-8 are individual replications, respectively.

*see text for explanation.

and 2), eggs from wildtype (+/+) females were injected with sperm from *yfb* males suspended in 0.15 M NaCl. In Exp. 1, injected eggs were covered with silicone oil immediately and then placed on wet filter paper until just before the larvae hatched; in Exp. 2 injected eggs were simply covered with distilled water and placed on wet filter paper. In Exp. 1, 750 eggs were injected, and of these, 192 hatched and 115 developed to the mid-pupal stage; almost all of the latter became adults. Of the 115 mid-pupae examined, 110 were parthenogenetic males having wildtype (+) color as expected. Five exceptional individuals were obtained: one female with the color of the heterozygote *yfb*+, three wildtype-colored (+/+) females, and one male having the color characteristic of heterozygous *yfb*+ females (Fig. 3). In Exp. 2, 500 eggs were injected and of these 107 developed to the mid-pupal stage, almost all of which became adults. Of the 107 mid-pupae examined, one was an exceptional male having the color similar to heterozygous *yfb*+ females.

The single female with the color heterozygous for *yfb* obtained in the present study is apparently the product of fertilization. The female was aged for a few days and her eggs were dissected and activated in distilled water. Thirty *yfb* males and 25+ males were obtained indicating that the female was in fact *yfb*+: namely, syngamy and karyogamy did take place between an injected sperm and the egg nucleus.

The three wildtype-colored females probably resulted from the fusion of two of the four nuclei produced by maturation division. In the few years previous to the time the mutant *yfb* became available we had experienced in rare occasions the appearance of females from eggs parthenogenetically activated. We had considered the possibility of rare thelytokous reproduction in this species, but could not eliminate the possibility of contamination since the observation had been made in a casual way. While maintaining the *yfb* stocks we made in various occasions small scale experiments and activated *in vitro* the eggs from *yfb*+ females. Homozygous *yfb/yfb* and +/+ and heterozygous *yfb*+ females appeared in a sporadic manner. On average, one such individual appeared per several hundred eggs activated. Thus, thelytokous repro-

duction, although rare, does occur in this species.

The two exceptional males having the color similar to heterozygous *yfb*+ females were of normal haploid male body size. Diploid males which can be obtained readily in this species by repeated brother-sister matings [12], have a size just between haploid males and diploid females [Naito *et al.* unpublished]. Our explanation for these exceptional males is thus that they are chimeras (*yfb*↔+) in which both a haploid egg nucleus (+) and a haploid sperm nucleus or nuclei (*yfb*) contributed separately to development. If the nuclei do not mingle extensively before the blastoderm is formed, as in *Drosophila* [13], the heterozygous color in these males would mean that the mutant is non-autonomous in action. Preliminary observations on *yfb*+/+ and *yfb/yfb*+ triploid females obtained in separate mating experiments indicate that they can be distinguished by external inspection at the mid-pupal stage if individuals of exactly the same age are examined. Most probably, then, the number of sperm which contributed to the formation of the chimeric males above is just one.

Encouraged with the above results, efforts were concentrated on increasing the rate of fertilization. Since there appeared to be no significant difference in results between the injected eggs covered with silicone and with distilled water, in all subsequent experiments, injected eggs were simply covered with distilled water. Also in the following experiments eggs from *yfb/yfb* females were injected with sperm from + males, so that heterozygous *yfb*+ individuals resulting from fertilization could be distinguished among *yfb* at the last instar larval stage (see MATERIALS AND METHODS).

Sperm bundles were suspended in different concentrations of NaCl and in distilled water (Table 1, Exp. 3-8). As the concentration decreased sperm bundles became increasingly difficult to handle as they became progressively more sticky. On the other hand, less pipetting was required to obtain individual sperm. Best results for fertilization were obtained when sperm were suspended in distilled water (Exp. 5-8), where some 10% of the injected eggs developed as fertilized females. Seven females out of 19 obtained in Exp. 5-8 were

progeny tested and each and every one of them produced both *yfb* and + males.

Sperm bundles in distilled water were quite sticky and the whole handling required some effort and patience. Although the rate of fertilization was somewhat lower (6.4%), the injection procedure was far much easier with sperm suspended in 0.01 M NaCl (Exp. 4). With sperm suspended in a higher concentration of 0.1 M NaCl (Exp. 3), the rate of fertilization became considerably lower (1%) although it was still significantly higher than the case with sperm suspended in 0.15 M NaCl (Exp. 1 and 2).

DISCUSSION

We have succeeded in producing fertilization *in vitro* by sperm injection and resultant adult individuals in *Athalia rosae*. This is, to our knowledge, the first successful attempt of such kind in insects, and along with other features described previously [10, 11] should add to the usefulness of this species as an experimental material for developmental studies.

In the present study eggs were dried, attached to the tape on a slide, injected with sperm, and covered with distilled water. Drying the eggs itself causes egg activation [11]. Although eggs are prevented from activation in the saline solution, the eggs in solution are activated if pricked by a needle [11]. Pricking the dried eggs is probably also effective in activation. Thus, in the present study three stimuli for egg activation were given: drying, pricking and exposure to distilled water. Under these conditions it is difficult to ascertain the possible effect of sperm on egg activation. It is possible that the presence of sperm itself in an egg has no effect on activation. Activation of sperm-injected eggs in mammals appears to occur by the injection process (pricking) itself [14].

We have concentrated on producing, as a result of fertilization *in vitro* by means of sperm injection, pupae (to recognize marker mutant phenotype) and the adults (to do progeny testing), and left other aspects being actively investigated in other animal groups (for reviews see [1]) such as the process of transformation of sperm head to male pronucleus for future study. This is partly because

of the difficulty in obtaining, at the moment, properly fixed and stained preparations for such studies. The present results have shown that the sperm suspended in progressively more hypotonic solutions resulted upon injection in more and more successful cases of fertilization. It is likely, thus, that the sperm plasma membrane needs to be at least partially damaged in order for a sperm to become a male pronucleus. This is in accordance with the results in other animal species in which pretreatment of sperm by sonication or by suspending in Triton X-100 proved a necessary step (e.g., [5-7, 9]).

Nor did we examine possible effects of the number of sperm injected into each egg. The polyspermic injection used here was simply based on the fact that in *Apis mellifera* (Hymenoptera), polyspermy is normal [15]. Questions such as whether polyspermy is the rule in normal fertilization of *A. rosae* and, if so, how many of them or of those artificially introduced become pronuclei all remain to be elucidated. Although the present results do not tell us anything about the process of sperm capacitation, if it exists in insects, it is clear that the sperm still in bundles in male spermathecae have, if suspended in hypotonic solutions and injected into eggs, an ability to fertilize the egg.

In the *yfb/+* females obtained in the present study, karyogamy must have taken place between a single female pronucleus and a single male pronucleus. A possibility remains, however, that additional sperm might also have participated in development albeit in a small fraction of the body, and the *yfb/+* individuals could have been the *yfb/+ ↔ yfb* or + chimeras. We did obtain two probable *yfb ↔ +* chimeras (Exp. 1 and 2). It would be of considerable interest to see if chimeric development would prevail in the eggs injected with sperm at, for example, the posterior end.

By employing direct sperm injection, we were able to circumvent various difficulties inherent to most insect systems such as sperm transfer, storage, release, and egg penetration. The present technique thus provides an interesting possibility for studies on inter-specific hybridization. Can the sperm from only distantly related species become male pronuclei upon injection into *A. rosae* eggs? There should be an egg cytoplasmic factor(s) re-

sponsible for the sperm-to-pronucleus transformation and the non-species-specific nature has been shown in between human and frog [9]. Observations on karyogamy in eggs injected with sperm from different species may also be used as a means to ascertain the relatedness between the species.

Among three closely-related species of *Athalia*, *A. rosae*, *A. lugens* and *A. japonica*, inter-specific copulation takes place under the laboratory conditions but no hybrids are produced (Sawa *et al.* unpublished observation). It would be of interest to see by sperm injection if inter-specific fertilization can take place and can lead to the production of hybrids or if inter-specific chimeras can be produced.

The technique would also provide a means for other aspects of development to be studied. Diploid and even triploid males can be produced easily in *A. rosae* by repeated brother-sister matings and their maturation division is also non-reductional ([12] and their unpublished results). It might be possible to produce, for example, diploid female-diploid male chimeras, and to examine if, for example, non-reductional maturation division characteristic of males is a cell-autonomous feature. With the *A. rosae* system as explored here, many developmental and genetic questions not only those specific to this species or to Hymenoptera or insects but also those more general in nature may be asked and may be expected to be answered.

ACKNOWLEDGMENTS

We thank Dr. T. Naito for kindly supplying us the *yfb* mutant stock. We are indebted to Dr. S. J. Counce of Duke University for her critical reading of the manuscript.

REFERENCES

- Metz, C. H. and Monroy, A. eds. (1985) *Biology of Fertilization*. Vols. 1-3. Academic Press, Orlando.
- Sander, K. (1985) Fertilization and egg cell activation in insects. In "Biology of Fertilization". Vol. 2. Ed. by C. H. Metz and A. Monroy, Academic Press, Orlando, pp. 409-430.
- Hiramoto, Y. (1962) Microinjection of the live spermatozoa into sea urchin eggs. *Exp. Cell Res.*, **27**: 416-426.
- Brun, R. B. (1974) Studies on fertilization in *Xenopus laevis*. *Biol. Reprod.*, **11**: 513-518.
- Moriya, M. and Katagiri, Ch. (1976) Microinjection of toad sperm into oocytes undergoing maturation division. *Dev. Growth Differ.*, **18**: 349-356.
- Uehara, T. and Yanagimachi, R. (1976) Microsurgical injection of spermatozoa into hamster eggs with subsequent transformation of sperm nuclei into male pronuclei. *Biol. Reprod.*, **15**: 467-470.
- Thadani, V. M. (1980) A study of hetero-specific sperm-egg interactions in the rat, mouse, and deer mouse using *in vitro* fertilization and sperm injection. *J. Exp. Zool.*, **212**: 435-453.
- Markert, C. L. (1983) Fertilization of mammalian eggs by sperm injection. *J. Exp. Zool.*, **228**: 195-201.
- Ohsumi, K., Katagiri, Ch. and Yanagimachi, R. (1986) Development of pronuclei from human spermatozoa injected microsurgically into frog (*Xenopus*) eggs. *J. Exp. Zool.*, **237**: 319-325.
- Sawa, M., Fukunaga, A., Naito, T. and Oishi, K. (1989) Studies on the sawfly, *Athalia rosae* (Insecta, Hymenoptera, Tenthredinidae). I. General biology. *Zool. Sci.*, **6**: 541-547.
- Sawa, M. and Oishi, K. (1989) Studies on the sawfly, *Athalia rosae* (Insecta, Hymenoptera, Tenthredinidae). II. Experimental activation of mature unfertilized eggs. *Zool. Sci.*, **6**: 549-556.
- Naito, T. and Suzuki, H. (1985) Sex determination in sawflies (Hymenoptera). *Jpn. J. Genet.*, **60**: 646 (Abstract, in Japanese).
- Hall, J. C., Gelbart, W. M. and Kankel, D. R. (1976) Mosaic systems. In "The Genetics and Biology of *Drosophila*". Vol. 1a. Ed. by M. Ashburner and E. Novitski, Academic Press, London, pp. 265-314.
- Uehara, T. and Yanagimachi, R. (1977) Activation of hamster eggs by pricking. *J. Exp. Zool.*, **199**: 269-274.
- DuPraw, E. J. (1967) The honeybee embryo. In "Methods in Developmental Biology". Ed. by F. H. Wilt and N. K. Wessells, Thomas Y. Crowell Co., New York, pp. 183-217.



Photoperiod during Post-Embryonic Development Affects Some Parameters of Adult Circadian Rhythm in the Cricket, *Gryllus bimaculatus*

KENJI TOMIOKA and YOSHIHIKO CHIBA

*Environmental Biology Laboratory, Biological Institute, Faculty of Science,
Yamaguchi University, Yamaguchi 753, Japan*

ABSTRACT—Adult male cricket, *Gryllus bimaculatus* exhibits a nocturnal circadian locomotor rhythm but with a small activity peak at lights-on. Effect, on the adult locomotor rhythm, of the ratio of light to dark phase (L/D-ratio) of the 24 hr light to dark (LD) cycle was investigated using animals reared under either of the three LD cycles, i.e. LD8:16, LD12:12 or LD16:8. Activity pattern differed from each other depending on the preceding LD conditions in which the animal was reared. The length of the nocturnal activity phase which was about 12 hr in the standard lighting condition, LD12:12, shortened to about 8 hr in LD16:8 but never lengthened more than 12 hr even in LD8:16 with the longest dark phase. This fact suggests that the maximal length of the nocturnal activity may be homostatically regulated to be 12 hr. Some animals showed an enhanced lights-on peak which made activity pattern almost diurnal. The number of animal with the enhanced lights-on peak was greater in LDs other than LD12:12. In the constant darkness, freerunning periods and the ratio of the activity phase to the rest phase (α/ρ -ratio) were affected greatly by the preceding LD-ratio. Average freerunning period of the animal reared in LD16:8 was 24.49 ± 0.49 (S.D.) hr, significantly longer than about 23.8 hr of animals reared in other LDs. The α/ρ -ratio changed in inversely proportional to the L/D-ratio: 1.29 ± 0.52 (S.D.), 0.94 ± 0.28 (S.D.) and 0.88 ± 0.33 (S.D.) in LD8:16, LD12:12 and LD16:8, respectively. Possible physiological mechanisms and biological role of the lability in the cricket circadian rhythm are discussed.

Abbreviations and terms used in the present paper:

α	Length of activity phase
DD	Constant darkness
JST	Japanese standard time
LD12:12	Repeated alternation of 12 hr of light phase with 12 hr of dark phase
L/D-ratio	Ratio of light period to dark period
LL	Constant light
ρ	Length of inactive phase

INTRODUCTION

It has been generally accepted that the freerunning period of the circadian rhythm is genetically determined. This concept has been developed by experiment with *Drosophila melanogaster* in which the mutants of circadian periodicity has been found [1]. However, there are lines of evidence that the light to dark (LD) cycle greatly affects the period and the waveform of the circadian rhythm. Pittendrigh and Daan [2] reported that, in some

nocturnal rodents, the circadian waveform and the freerunning period were altered by the ratio of light to dark period (L/D-ratio) of a 24 hr LD cycle. In insects some profound studies have been made about the effect of non-24 hr LD cycles on the circadian activity rhythm. Page and Block [3] showed that the freerunning period of the cockroach (*Leucophaea maderae*) reared under LD11:11 or LD13:13 differed significantly from that of the animal reared under LD12:12. In the same insect, Roberts [4] demonstrated that the circadian period is systematically affected by high frequency LD cycle according to the L/D-ratio in each cycle.

It is well known that insects have a characteristic phenomenon of the photoperiodism such as diapause or seasonal polymorphism as a response to the L/D-ratio in the 24 hr LD cycle [5]. Although some researches [6-9] have been done to clarify the relationship between the photoperiodic clock controlling the photoperiodism and the circadian clock, little is known about the effect of L/D-ratio in 24 hr LD cycle on the circadian rhythm. The present experiment was designed to analyse the effect of L/D-ratio of 24 hr LD on the circadian locomotor rhythm of the cricket (*Gryllus bimaculatus*).

MATERIALS AND METHODS

All experiments were carried out with adult male crickets, *Gryllus bimaculatus*. They were reared from the egg stage under constant temperature of $26 \pm 0.5^\circ\text{C}$ and either of the three different light (L)-dark(D) cycles, i.e. 8 hr light to 16 hr dark (LD8:16, L:10⁰⁰-18⁰⁰ Japanese standard time(JST)), LD12:12 (L:06⁰⁰-18⁰⁰, JST) and LD16:8 (L:04⁰⁰-20⁰⁰, JST). In all rearing conditions they became to adult undergoing 8 molts, and the length of nymphal stage was about 60 days.

To investigate effects of the L/D-ratio of 24 hr light cycle during the post-embryonic development on the adult circadian rhythm, locomotor activities of adult males were recorded individually by an actograph with a rocking substratum whose movement caused by a moving animal was sensed by a magnetic lead switch connected to an event recorder and a digital printer logging a total number of movement at a 30 min interval. Food and water were given *ad libitum*. Light cycle was given by the two 10 W fluorescent lamps which were hanged from the ceiling of the environment controlled room. The distance between the activity chamber and the lamp was about 1 m and the light intensities were 90-100 lux at the level of activity chambers. Event records of individuals were cut into 24 hr strips and pasted one below the other in chronological order in the conventional manner.

Quantitative data were analyzed statistically using a NEC personal computer (PC-9801). The freerunning period under constant darkness (DD) was calculated by the chi-square periodogram

method [10]. The duration of active (α) and inactive (ρ) phases were obtained from the averaged activity histogram for 10 successive days, which was calculated at the freerunning period: the active and rest phases were designated as the portion where the activity was above or below, respectively, the arithmetic mean.

RESULTS

Effect of the L/D-ratio of the 24 hr light cycle during the post-embryonic development on the adult circadian locomotor rhythm were investigated in a total of 68 males: 20 of LD8:16, 19 of LD12:12 and 29 of LD16:8. As the first step, the activity pattern under the LD condition was examined. The animals were recorded individually in the LD condition, in which they had been reared, for at least 10 days. Figure 1 gives examples of event recorder tracings of animals from the three groups.

In LD conditions, most animals exhibited essentially nocturnal activity peaking just after lights-off but with small peak at lights-on (Fig. 1) as have been reported previously for LD12:12 [11]. In some animals, however, the lights-on peak was greater and longer than the lights-off, nocturnal peak, making an almost diurnal pattern (Fig. 1D). The occurrence of the enhanced lights-on peak was least frequent in LD12:12 and most in LD16:8 animals (Table 1). In the ensuing DD the lights-on peak rapidly became smaller (Fig. 1D) or disappeared (Fig. 1A), indicating that it is mainly a positive masking effect of light as is discussed in detail in the previous paper [12].

The temporal distribution of the activity over 24 hr was different among the groups. As shown in Figure 2, amount of activity of the lights-on peaks in LD16:8 group showed the activity concentrated in the first 4 hr of dark phase, while other group animals exhibited prolonged lights-off activity continuing for about 12 hr (Figs. 1 and 2). One notable fact is that the offset of nocturnal activity of LD8:16 group did not coincide the lights-off but preceded it by about 4 hr (Figs. 1A and 2A). Number of animals showing anticipatory activity which occurred just before lights-off was increased with lengthening the scotophase: 5, 4, 1 animals in

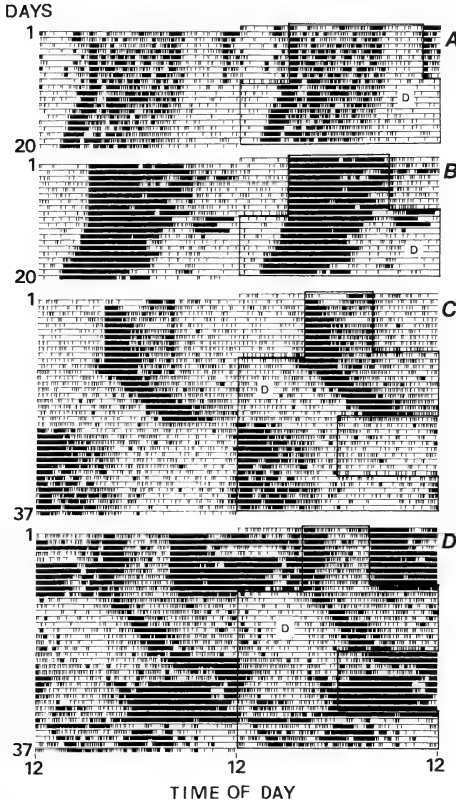


FIG. 1. Double plotted activity records of 4 adult male crickets under various L/D-ratio in 24 hr light cycle and constant darkness. Lighting conditions are indicated in the right half of the figure: blackets, indicated by a small D, show a dark fraction. Animals were reared either of the three LD cycles, i.e. LD8:16 (A), 12:12 (B) or 16:8 (C, D). At the beginning of the record, the animals were entrained for 10–11 days by the LD cycle in which they were reared, then transferred to DD. Remarkable differences are seen in the freerunning period and in the length of the activity phase of the freerunning rhythm among the animal groups reared in different L/D-ratios. Animals from LD 16:8 group (C and D) were further entrained by LD12:12 for 10 days and thereafter transferred to DD. Second freerunning period seems to differ from the first one in C. In D, the enhanced lights-on peak forms predominantly diurnal activity pattern in LD condition. However, it disappeared immediately after transferred into DD, suggesting that it is a positive masking effect.

LD8:16, LD12:12 and LD16:8, respectively (Table 1).

Effects of LD during post-embryonic development on the parameters of the circadian rhythm can be examined by recording the locomotor activity under the DD condition. Representative freerunning locomotor rhythms were given in Figure 1. As the results, consistent differences in some circadian parameters were revealed among

the three groups (Table 2). The α/p -ratio was significantly larger in LD8:16 group animals averaging 1.29 than in other two groups ($P < 0.01$, t -test). The ratio in LD16:8 group was not significantly but slightly smaller than that in LD12:12 group. Therefore, the α/p -ratio appears to change depending on the previous L/D-ratio: active phase was longer when animals had experienced longer scotophase. The freerunning period is the most remarkably affected parameter, averaging 24.49 ± 0.49 (S.D.) hr in LD16:8 group significantly longer than 23.87 ± 0.18 (S.D.) hr and 23.76 ± 0.13 (S.D.) hr detected in LD8:16 and LD 12:12 groups, respectively ($P < 0.01$, t -test). The latter two did not show significant difference, however.

Ten of LD16:8 animals freerunning in DD were further entrained by LD12:12 to investigate effects of photoperiod on the adult circadian rhythm. After 10 days of entrainment, the animals were transferred again into DD. A representative result is shown in Figure 1C. They synchronized to

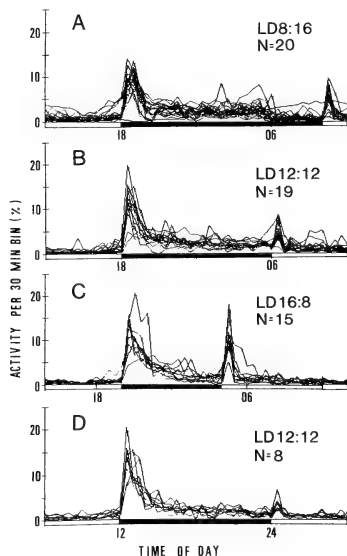


FIG. 2. Daily distribution of activity of adult male crickets under LD cycle with various L/D-ratio. Each line represents an activity pattern of individual animal. Animals with predominantly diurnal activity pattern were excluded from the analysis in LD16:8 group (C, D), since they disturbed the visual estimation of the nocturnal activity. The value of each 30 min bin of a single animal is obtained by summing the activity in that time over 5 cycles and by expressing it as a percentage of the total activity. Black and white bars under each panel indicate dark and light phase, respectively. A, B and C show the pattern in LD under which the animals were reared. D represents the activity pattern of the LD16:8 animals entrained by LD12:12 as adult.

TABLE 1. Effects of L/D-ratio of 24 hr LD cycle on the entrained circadian locomotor rhythm

Animal group	LD cycle	N	Animals with	
			anticipatory activity	enhanced lights-on peak
LD 8:16	LD 8:16	20	5 (25) ^b	7 (35)
LD12:12	LD12:12	19	4 (21)	4 (21)
LD16:8	LD16:8	29	1 (3)	14 (48)
	LD12:12 ^a	10	0 (0)	2 (20)

^a Ten animals of LD 16:8 group were entrained LD12:12 after 10 days of freerun in DD.

^b Numerals in brackets indicate the percentage of the animals.

TABLE 2. Effects of photoperiod of 24 hr LD cycle on the freerunning period and α/ρ -ratio

Animal group	Preceding LD cycle	N	Freerunning period	α/ρ -ratio
LD 8:16	LD 8:16	20	23.87 \pm 0.18	1.29 \pm 0.52
LD12:12	LD12:12	19	23.76 \pm 0.13	0.94 \pm 0.28
LD16: 8	LD16: 8	29	24.49 \pm 0.49	0.88 \pm 0.33
	LD12:12 ^a	10	24.14 \pm 0.52	1.25 \pm 0.29

^a Ten animals of LD 16:8 group were transferred from DD to LD12:12 lasting for 10 days followed by the second DD.

LD12:12 and the activity pattern became to be similar to that of LD12:12 group animals (Fig. 2D). In the ensuing DD, the freerunning period averaging 24.14 \pm 0.52 (S.D.) hr is shorter than that in the first DD following LD16:8 ($P < 0.05$, two tailed t -test), but still significantly longer than that of the other two groups in DD ($P < 0.05$, t -test). The α/ρ -ratio averaging 1.25 \pm 0.29 was larger than that in the first DD averaging 0.88 \pm 0.33 ($P < 0.01$, t -test).

DISCUSSION

We have found that the exposure of cricket nymphs to the 24 hr light cycles of various L/D-ratio affected substantially the freerunning period and the α/ρ -ratio of the adult locomotor rhythm: The freerunning period was significantly longer and the α/ρ -ratio was smaller in LD16:8 group than other LDs with shorter photoperiod. Unlike the nocturnal rodents [2], the L/D-ratio dependency in the freerunning period and α/ρ -ratio obeys the Aschoff's circadian rule [13] stating that the frequency which is the reverse of the period and the α/ρ -ratio change in parallel with each other. In the nocturnal rodents, *Peromyscus leucopus* and *Mus musculus*, the long photoperiod shortened the freerunning period in the ensuing DD [2]. Pittendrigh and Daan [2] emphasized the non-parametric effect of light to explain their results on the rodents, which is contradict to the expectation based on the effect of constant light, i.e. lengthening the freerunning period. The possibility of the involvement of the non-parametric effect in the cricket's case may be implied by the fact that it plays major role in entrainment by forcing the rhythm to

phase-shift (in other words, by temporal lengthening or shortening the rhythm's period) [12]. If this is true, the nature of the underlying pacemaker, such as the phase response curve to the light pulse, may differ from that of the nocturnal rodents. It is more plausible explanation at present, however, that the photoperiod dependency of the freerunning period is caused by the parametric effect of long light pulse on the rhythm, since the constant light has been found to lengthen the freerunning period [11]. Further critical experiment with skeleton photoperiods would be needed to solve the issue about the parametric and non-parametric effects of light.

There is some evidence suggesting that the effect of L/D-ratio occurs at the pacemaker level. From a series of experiments, it has been shown that the cricket circadian pacemaker is located in the lamina-medulla part of the optic lobe, regulating the locomotor rhythm through a neural pathway [14, 15]. The efferent neural activity of the optic lobe as an output of the pacemaker exhibited the circadian rhythm with a ratio of subjective-night to -day changing as a function of the L/D-ratio of 24 hr LD cycle in the rearing condition (Tomioka and Chiba, in preparation).

Anticipatory activities were sometimes observed in animals reared in shorter photoperiods, whose freerunning period in DD was shorter than that of LD16:8 animals (Table 1). This observation is well explained by the empirical rule that the shorter period of the circadian rhythm exhibits more positive phase angle relation to the environmental cycle [16].

Between LD8:16 and LD12:12 groups, the freerunning periods in DD and the length of

activity phase in the LD condition did not differ significantly. Standard deviations for the freerunning period of these two groups were very small (up to 0.18). These facts reminiscent of the statement by Pittendrigh and Cardalora [17] that freerunning period was regulated homeostatically in the cockroach, *Leucophaea maderae*. The freerunning period value of about 23.8 hr and the length value of activity phase of 12 hr, shown by animals reared in LD8:16, may be the lowest and the upper limit, respectively, of homeostatic range.

An important question should be addressed, as to whether the photoperiod dependent changes in freerunning period and α/p -ratio are temporal (after-effects) or permanent. They are after-effects in the nocturnal rodents [2]. But, in the cockroach, *Leucophaea maderae*, the effect of the different length of LD cycle on the freerunning period was maintained for at least 5 months, suggesting that the effect would be permanent [18]. In our cricket, the effect of photoperiod seems to be rather temporal. This statement is based on the fact that only 10 cycles of LD12:12 during adult stage still can alter the freerunning period in the animals raised under LD16:8 (Fig. 1C, D). However, the freerunning period after reentrainment, showing an intermediate value between the initial freerunning period and that of LD12:12 group animals, may suggest that the effect of the photoperiod during post-embryonic development still remained and interacted with that during adult stage.

There are at least two points one can argue for the biological significance of the lability of the freerunning period and the α/p -ratio in this cricket. In the natural field, the cricket activity may depend on temperature to some extent as suggested by Lohr and Wiedenmann [19]. Our results suggest that the photoperiod as well may have important role in the regulation of the temporal activity pattern. The other possible significance of the lability may be its involvement in the photoperiodic time measurement, although no photoperiodism has been known in this particular cricket species. Some models, such as the external and internal coincidence models, developed so far for the photoperiodic time measurement, include a circadian oscillator(s) more or less rigid in frequency

and waveform [6, 7]. Unlike the oscillator(s) in these models, the α/p -ratio of the cricket oscillator changes as a function of the L/D-ratio. This may open up another possibility that the oscillator itself is a device to measure the photoperiod. Further studies are required to determine the sensitive stage for the photoperiodic control of the circadian parameter and the number of cycles needed for the pacemaker to adapt to the new L/D-ratio.

ACKNOWLEDGMENTS

We are grateful to Mr. Tadakatsu Masaki for computer programming. This work was supported in part by Grants-in-Aid for Scientific Research from the Ministry of Education, Science and Culture of Japan.

REFERENCES

- 1 Konopka, R. and Benzer, S. (1971) Clock mutants of *Drosophila melanogaster*. *Proc. Natl. Acad. Sci. U.S.A.*, **68**: 2112-2116.
- 2 Pittendrigh, C. S. and Daan, S. (1976) A functional analysis of circadian pacemakers in nocturnal rodents. I. The stability and lability of spontaneous frequency. *J. Comp. Physiol.*, **106**: 223-252.
- 3 Page, T. L. and Block, G. D. (1980) Circadian rhythmicity in cockroaches: Effects of early post-embryonic development and ageing. *Physiol. Entomol.*, **5**: 271-281.
- 4 Roberts, S. K. (1982) Circadian periodicity in cockroaches altered by high frequency light-dark cycle. *J. Comp. Physiol.*, **146**: 255-259.
- 5 Beck, S. D. (1980) *Insect Photoperiodism*. Academic Press, New York, 2nd ed.
- 6 Pittendrigh, C. S. and Minis, D. H. (1964) The entrainment of circadian oscillations by light and their role as photoperiodic clocks. *Amer. Nat.*, **98**: 261-294.
- 7 Tychchenko, V. B. (1966) Two-oscillator model of the physiological mechanism of insect photoperiodic reaction. *Z. Obshch. Biol.*, **27**: 209-222 (in Russian)
- 8 Takeda, M. (1986) A circadian clock controlling cricket photoperiodism: a resonance effect? *J. Insect Physiol.*, **32**: 557-560.
- 9 Nakahama, K., Nakaoka, S. and Endo, K. (1986) Time-measurement system underlying the photoperiodic control of pupal diapause in the swallowtail, *Papilio xuthus* L.: A trial for the application of the external coincidence mode. *Zool. Sci.*, **3**: 837-846.
- 10 Sokolove, P. G. and Bushell, W. N. (1978) The chi-square periodogram: its utility for analysis of

- circadian rhythms. *J. Theor. Biol.*, **72**: 131-160.
- 11 Tomioka, K. and Chiba, Y. (1982) Post-embryonic development of circadian rhythm in the cricket, *Gryllus bimaculatus*: A rhythm reversal. *J. Comp. Physiol.*, **147**: 299-307.
 - 12 Tomioka, K. and Chiba, Y. (1987) Entrainment of cricket circadian locomotor rhythm after 6-hour phase shifts of light dark cycle. *Zool. Sci.*, **4**: 535-542.
 - 13 Aschoff, J. (1960) Exogenous and endogenous components in circadian rhythms. Cold Spring Harbor Symp. Quant. Biol., **25**: 11-27.
 - 14 Tomioka, K. and Chiba, Y. (1984) Effects of nymphal stage optic nerve severance or optic lobe removal on the circadian locomotor rhythm of the cricket, *Gryllus bimaculatus*. *Zool. Sci.*, **1**: 385-394.
 - 15 Tomioka, K. and Chiba, Y. (1986) Circadian rhythm in the neurally isolated lamina-medulla-complex of the cricket, *Gryllus bimaculatus*. *J. Insect Physiol.*, **32**: 747-755.
 - 16 Aschoff, J. (1981) Freerunning and entrained circadian rhythms. In "Handbook of Behavioral Neurobiology". Ed. by J. Aschoff, vol. 4. Biological Rhythms. Plenum Press, New York, London, pp. 81-93.
 - 17 Pittendrigh, C. S. and Caldarola, P. C. (1973) General homeostasis of the frequency of circadian oscillations. *Proc. Natl. Acad. Sci. U.S.A.*, **70**: 2697-2701.
 - 18 Page, T. L. (1982) Transplantation of the cockroach circadian pacemaker. *Science*, **216**: 73-75.
 - 19 Loher, W. and Wiedenmann, G. (1981) Temperature-dependent changes in circadian patterns of cricket premating behaviour. *Physiol. Entomol.*, **6**: 35-43.



Excessive Transitory Migration of Guppy Populations. II. Analysis of Possible Conspecific-Following Tendency

MUNETAKA WATANABE and HARUE TERAMI

Department of Biology, College of Liberal Arts and Sciences,
Okayama University, Okayama 700, Japan

ABSTRACT—The mechanism of the excessive transitory migration of guppy population, a fact that a population put in one of two compartments halved with a slitted septum once migrates excessively to the other compartment, was examined in relation to fish's conspecific-following tendency. For a comparative study two other fish, medaka and goldfish, were also examined. The degree of conspecific-following tendency of fish was estimated by comparing the runs, a succession of identical symbols; the distribution of length of the run of one-directioned slit-passing by guppies showed no significant difference from that in the random number series (the one-sample runs test). A direct recording of time of the slit-passing by guppies with an oscillograph clarified that they passed at intervals of fairly long time, often containing occasional opposite-directioned passing, in a strong contrast to a rapid succession of the same-directioned slit-passing in the conspecific-following goldfish. These results suggest that a conspecific-following tendency in fish is not the main cause of the excessive transitory migration.

INTRODUCTION

We previously reported that, when a population of guppies was put into one of two compartments in a tank halved with a septum having a small slit, the population gradually approached an equal distribution between both compartments after an excessive transitory migration (abbreviated, E.T.M.) to the other compartment [1]. In an attempt to explain the behavioral mechanism the first supposition that their avoidance of the environment polluted with fish's excretions was rejected by the experimental fact that the population migrated even from clean water to polluted environment.

Many fish follow their conspecifics [2-5]. Radakov [6] showed in the observation of the feeding behavior of pollock, that fish may choose a particular spot not because they have seen food there, but because one or several specimens have gone in that direction. This following tendency of fish may cause the excessive transitory migration.

The present work will analyze in details the second supposition that guppies might exhibit the excessive migration due to their possible following, in comparison with other two fish species.

MATERIALS AND METHODS

Experimental fish was the guppy *Poecilia reticulata* of 2.80 ± 0.40 cm in total length. Only females were used because a population of the same-sized male individuals could not be easily obtained due to a large variation of tail length. For a comparative study, the medaka *Oryzias latipes* of 2.50 ± 0.35 cm and the goldfish *Carassius auratus* of 5.12 ± 0.80 cm were also used. The former fish is of a family related to the guppy and much resembles to it in size and shape. The latter fish has a strong conspecific-following tendency.

Several days before the experiments, populations of 40 fish were isolated from the breeding aquaria and placed in rearing tanks. Throughout the present study the populations were not mixed with one another. Water temperature was maintained within a range between 23.0 and 27.0°C.

Further details of method will be described

under each section.

RESULTS

Analysis by comparison of the runs

Method An experimental tank ($60 \times 25 \times 25$ cm deep for guppy and medaka; $90 \times 25 \times 25$ cm for goldfish) was divided into two equal compartments with an opaque white plastic septum having a vertical slit 25×2 cm. The slit was closed with a plastic plate until the onset of the experiment. A group of fish was introduced into the left (starting) compartment of an experimental tank. The number of fish in a population was 80 or 60 in trials for ascertaining the E.T.M. in the guppy, while 40 in trials for comparison between the guppy, medaka and goldfish. After acclimation to the tank for 15 min the plate was quietly pulled up. The number of fish passing through the slit from the left to the right compartments and *vice versa* was recorded for 30 min. Ten populations were observed and the number of fish in the left compartment at the end of every one-minute interval was calculated. The degree of conspecific-following tendency of fish was estimated by comparing the number of runs. A run is defined as a succession of identical symbol [7]. Here, we dealt the run of the direction of slit-passing, i.e. left-to-right and right-to-left. Whether the order of the direction is random or not was statistically tested by the one-sample runs test [7].

In addition, the distribution of the length of the runs of one-directioned passing in each fish species was compared with that of the random number series.

Results The number of guppies introduced into the left compartment decreased rapidly, and the population gradually approached a balance of equal distribution between both compartments after an excessive transitory migration (E.T.M.) to the other compartment. The E.T.M. was so striking that in a specimen using 80 fish, all but 3 fish migrated to the opposite compartment in 5 min. The E.T.M. was reproducible in 4 consecutive trials even at an interval as short as 30 min (Fig. 1). Figures 2a and 2b are the records of

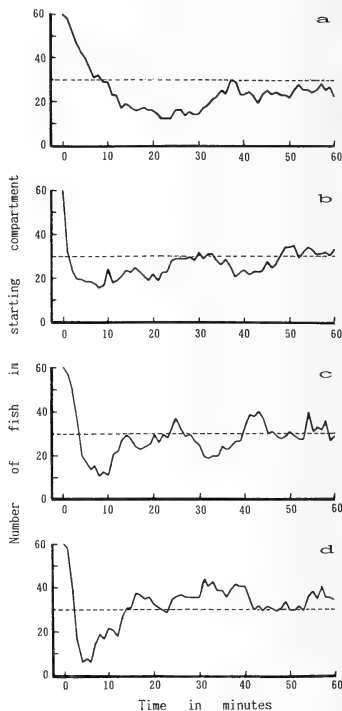


Fig. 1. Migration of guppies through a slit from the starting compartment, to which 60 fish were initially introduced, to the other one. a~d are a series of 4 consecutive trials using a population at a 30 min interval. Note the reproducibility of an excessive transitory migration (E.T.M.).

slit-passing by 40-fish populations of the medaka and goldfish respectively. Because an expression by median value would cancel rapid changes in each of 10 trials, these figures are based on the records of a single trial of moderate trend. The medaka populations showed an E.T.M. (Fig. 2a) in a similar manner as the guppy (Fig. 1), although their slit-passing was rather active, but the goldfish behaved in a quite different manner from the other

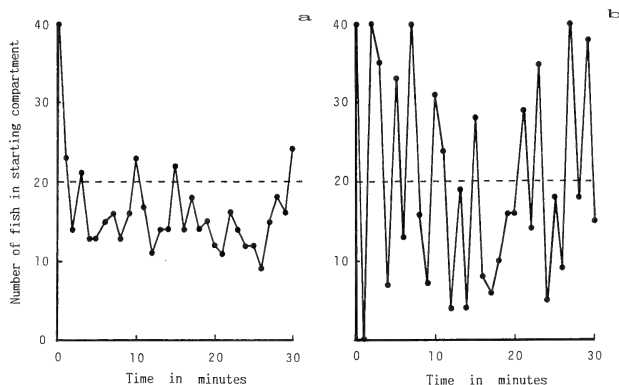


FIG. 2. Migration of the medaka and goldfish through a slit. a: medaka. b: goldfish. Note the repetition of alternate migration to either compartment in the goldfish.

two species: all the fish promptly aggregated alternately in either compartment at intervals of a few minutes (Fig. 2b), not only at the initial phase, but throughout the observation time. The total number of either left-to-right or right-to-left slit-passing in 10 populations of each of the three species was counted (Table 1). The guppy and medaka populations passed the slit 9.9 and 13.5 times in average per min respectively, while in the goldfish the mean of slit-passing was 46.5.

In addition, the total number of runs of either left-to-right or right-to-left slit-passing was also counted for each fish (Table 1). To judge whether the order of the direction of slit-passing was random or not, the one-sample runs test was used [7].

As for the guppy and medaka, a null-hypothesis of randomness of the order was not rejected at 5% significance level ($z=1.321$ and $1.575 < 1.96$, respectively). In the goldfish, however, the runs test clarified that the distribution of the run of the same-directioned slit-passing was quite different from the randomness ($z=24.5$, $p < 0.001$). Moreover, the runs of slit-passing in 10 populations of each species were grouped into 5 classes of the length of 1 to 4, 5 to 9, 10 to 19, 20 to 29 and 30 to 40 (Table 2). In the guppy and medaka populations there were no runs longer than 20, while the runs of over 30 often appeared in the goldfish.

The relative frequency of the runs of each class to the total number of runs was calculated, and on

TABLE 1. The number of the slit-passing and the number of the run of one-directioned slit-passing by the guppy, medaka and goldfish. The number of the run of one-directioned slit-passing was compared with that of same-signed (odd or even) figures in the random number series (the one-sample runs test). z is the statistic in the test of randomness of the order of left-to-right and right-to-left slit-passing by fish

Fish	Number of Populations	Number of slit-passing			Total of runs	Statistic $ z $
		Left-to-right	Right-to-left	Total		
Guppy	10	1617	1352	2971	1369	1.321
Medaka	10	2154	1903	4057	1860	1.575
Goldfish	10	7108	6861	13929	2108	26.145 *

* $P < 0.001$

TABLE 2. The distribution of length of the runs of the same-directioned slit-passing for 30 min in 10 populations of the guppy, medaka and goldfish

Fish	Length of runs					Total of runs
	1~4	5~9	10~19	20~29	30~40	
Guppy	1248	106	15	—	—	1369
Medaka	1676	171	13	—	—	1860
Goldfish	1373	276	255	110	94	2108

the other hand, all runs of the same-signed (odd or even) figures in the random number series of 5,000 figures were counted and grouped into the five classes, and the relative frequency was calculated (Fig. 3). The distribution of the runs by either the

guppy or medaka are very similar to that of the random number series, and the runs of the length of 10 or more are so few as below 1% in both the fish, in a great contrast to more than 30% in the goldfish.

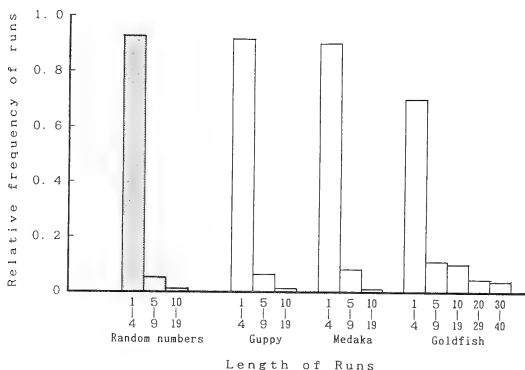


FIG. 3. The relative frequency of length of runs of the same-directioned slit-passing by the guppy, medaka and goldfish populations in comparison with that of runs of the same-signed (odd or even) figures in the random number series. Note the resemblance of the distribution of the run in guppy and medaka to that in the random number series.

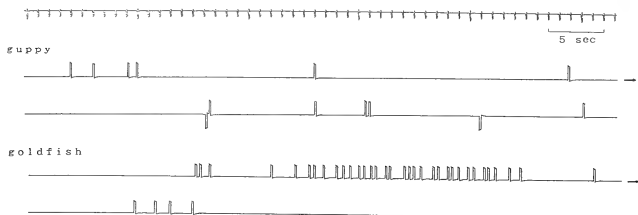


FIG. 4. The oscillographic records of slit-passing by the guppy and goldfish during about 100 sec from the onset of the experiment. \neg representing left-right passing, \neg right-left one. Note fairly long intervals of passing in the guppy.

Analysis by an oscillographic recording

Method Another recording method was used for directly measuring the intervals of slit-passing. Switch devices were interposed in the circuit of a dual channel pen-recorder (Nihon Kohden RM-20) at a chart speed of 6.0 mm per sec. The observer noted the time of slit-passing of fish in left-to-right direction by pushing a switch, and the time of passing in the opposite direction by pushing another one.

Results Guppies did not pass the slit in succession in so short time, in a strong contrast to the rapid succession of the passing by goldfish. Figure 4 is an oscillogram recorded during about 100 sec from the onset of experiment in a specimen of either species. Here, the slit-passing by guppies occurred at so long interval as several seconds in spite of frequent repetition of one-directioned passing owing to the initial phase of the trial, while the goldfish passed the slit in so many as 30 individuals during 20 sec.

DISCUSSION

In the previous paper [1] we rejected a working hypothesis that guppy's avoidance of polluted environment would be a cause of the excessive transitory migration, by an experiment in which populations put in the clean-water circulating compartment excessively migrated to the polluted-water circulating one.

Schooling of fish has been noticed by many workers [2] and the role of vision in the fish schooling has been stressed since Parr's pioneer work on mackerel [8]. We also showed experimentally that vision is the main sensory cue in the excessive transitory migration [1].

If fish's conspecific-following tendency is a cause of E.T.M., the successive passing of a certain direction would be frequent, accordingly the frequency of runs of slit-passing in the same direction would be significantly different from randomness.

But, the runs test did not reject the null hypothesis that the order of left-to-right and right-to-left slit-passing in the guppy and medaka is random (Table 1), and the distribution of the length of their runs is very much like that of odd and even numbers in the random number series (Fig. 3).

The oscillographic record offered a direct evidence that the guppy has not a conspecific-following tendency. If this fish had the tendency, a frequent successive slit-passing would be recorded, as in goldfish. The guppy, however, passed at intervals of a fairly long time, often containing occasional opposite-directioned passing.

If the following between conspecifics is the cause of the E.T.M., the excessive migration is expected to occur throughout the whole observation period as goldfish did. But this migration occurs only in the initial phase. From the present results the main cause of the excessive transitory migration must be investigated from another point of view.

REFERENCES

1. Watanabe, M. (1981) Excessive transitory migration of guppy populations. I. Analysis of sensory cues and mechanisms. *Zool. Mag.*, **90**: 33-38.
2. Radakov, D. V. (1973) Schooling in the ecology of fish. A Halsted Press Book, John Wiley & Sons, New York.
3. Shaw, E. (1960) The development of schooling behavior in fishes. *Physiol. Zool.*, **33**: 79-86.
4. Shaw, E. (1961) The development of schooling behavior in fishes. II. *Physiol. Zool.*, **34**: 263-272.
5. Yamagishi, H., Nakamura, M. and Fukuhara, O. (1978) Behavioral studies on school of fishes II. Leading-following relationship of the immature yellowtail, *Seriola quinqueradiata* Temminck et Schlegel in captivity. *Zool. Mag.*, **87**: 125-131.
6. Radakov, D. V. (1958) Adaptive value of the schooling behavior of young pollock *Pollackius virens* (L.). *Voprosy Ikhtologii*. No. 11.
7. Siegel, S. (1956) Nonparametric Statistics for the Behavioral Science. McGraw-Hill, London.
8. Parr, A. E. (1927) A contribution to the theoretical analysis of the schooling behavior of fishes. *Occ. Pap. Bingham Oceanogr. Colln.*, **1**.



Two New Species of the Genus *Diploproctodaeum* (Trematoda: Lepocreadiidae: Diploproctodaeinae), with Some Comments on Species in the Subfamily Diploproctodaeinae, from Japanese Marine Fishes

TAKASHI SHIMAZU

Nagano-ken Junior College, Nagano 380, Japan

ABSTRACT—Two new species of the trematode genus, *Diploproctodaeum* La Rue, 1926 (Lepocreadiidae: Diploproctodaeinae), are described and illustrated from Japanese marine fishes. *Diploproctodaeum hakofugu* sp. n. from the intestine of *Ostracion immaculatus* (Teleostei: Ostraciidae) differs from all the previously known species of the genus and *Diploproctodaeoides soleaticus* Reimer, 1981, chiefly in a much more lobed ovary. *Diploproctodaeum oviforme* sp. n. from the intestine of *Lactoria diaphanus* (Ostraciidae) is separated from the most closely allied species, *D. hakofugu*, chiefly by the ventral sucker being much smaller than the oral sucker and pharynx. Some morphological and systematic comments are given on Japanese species in the subfamily Diploproctodaeinae Park, 1939. *Diploporus* Ozaki, 1928, is reduced to a synonym partly of *Diploproctodaeum* and partly of *Bianium* Stunkard, 1930. *B. holocentri* Yamaguti, 1942, is considered synonymous with *B. hemistoma* (Ozaki, 1928) Yamaguti, 1934.

INTRODUCTION

Shimazu and Nagasawa [1] reported three specimens of a trematode as *Bianium cryptostoma* (Ozaki, 1928) Manter, 1940 [sic] (Lepocreadiidae: Diploproctodaeinae), from *Ostracion immaculatus* from Moroiso Bay, Misaki, Kanagawa Prefecture, Japan. (They gave the host name as "*Lactoria cubicus*" in error). A closer examination of them and additional specimens has shown that the trematode represents a new species of *Diploproctodaeum* La Rue, 1926, in the same subfamily. Another new species of the same genus has also been found out in the course of this study. This paper describes these two new species and incidentally presents some morphological and taxonomic comments on other Japanese species in the subfamily from examination of their museum specimens.

MATERIALS AND METHODS

Two worms were newly obtained from the intestine of *O. immaculatus* taken in Moroiso Bay in July, 1987. They were fixed in Nozawa's fluid without flattening, made into serial paraffin sections (transverse, 15 μ m) and stained with Delafield's hematoxylin and eosin. Museum specimens were received already stained and whole-mounted in Canada balsam by various methods. The specimens studied are deposited at the National Science Museum, Tokyo (NSMT), and the Meguro Parasitological Museum (MPM), Tokyo. Measurements (length by width) are given in millimeters unless otherwise stated.

RESULTS AND DISCUSSION
Diploproctodaeum hakofugu sp. n.
(Figs. 1-5)

Bianium cryptostoma

[2] of Shimazu and Nagasawa, 1985 [1], p. 11.

Material studied. All the specimens examined were obtained from the intestine of *Ostracion immaculatus*, as follows.

1) Lot 1. 3 gravid whole-mounts (NSMT-PI 2878) of *B. cryptostoma* of Shimazu and Nagasawa [1] from Moroiso Bay, Misaki, Kanagawa Prefec-

ture, on July 18, 1983.

2) Lot 2. 2 sectioned gravid worms (NSMT-PI 3118) from the same locality on July 21, 1987.

3) Lot 3. 6 gravid whole-mounts (MPM Coll. No. 20469) collected by Kamegai from Kuruwa, Kanagawa Prefecture, on October 3 and November 25, 1984.

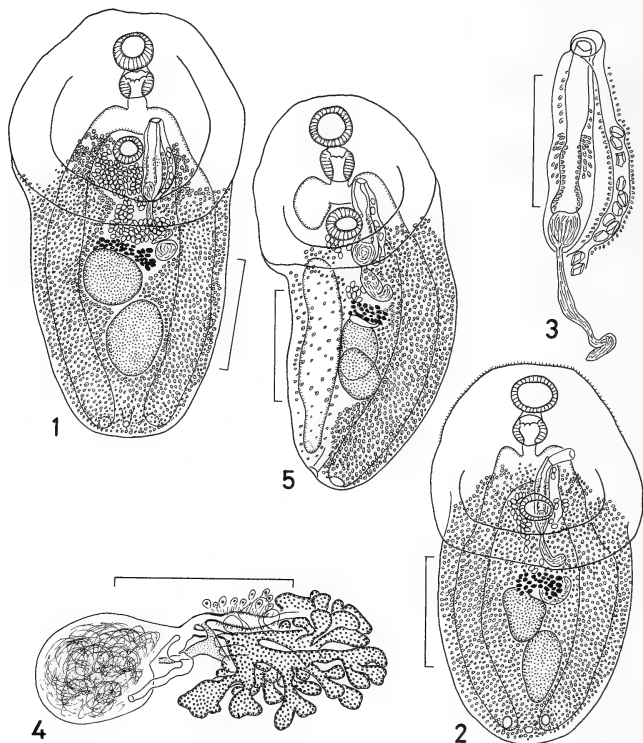
4) Lot 4. 5 gravid whole-mounts (MPM Coll. No. 20508) collected by him from the same locality

on December 5, 1987.

5) Lot 5. 2 gravid whole-mounts (NSMT-PI 970) collected by Machida from Nan'yofukaura, Ehime Prefecture, on May 22, 1972.

6) Lot 6. 1 immature and 5 gravid whole-mounts (NSMT-PI 1509 and 1647) collected by him from Nishidomari, Tsushima, Nagasaki Prefecture, on July 12, 1973, and April 27, 1974.

7) Lot 7. 1 gravid whole-mount (NSMT-PI



FIGS. 1-5. *Diploproctodaeum hakofugu* sp. n. from *Ostracion immaculatus*. 1. Entire worm, holotype, ventral view. 2. Entire worm, paratype, ventral view, showing more anteriorly distributed vitellaria. 3. Terminal genitalia, holotype, ventral view. 4. Ovarian complex, paratype, dorsal view. 5. Entire worm, paratype, ventral view, showing malformed intestine and vitellaria in right half of body. (Scale bars: 1 mm in Figs. 1-2 and 5; 0.5 mm in Figs. 3-4.)

1747) collected by him from Tanegashima, Kagoshima Prefecture, on November 24, 1974.

8) Lot 8. 8 gravid whole-mounts (NSMT-PI 2787) collected by him from Haneji, Okinawa Prefecture, on May 20, 1983.

9) Lot 9. 2 gravid whole-mounts (NSMT-PI 3282) collected by him from Owase, Mie Prefecture, on October 13, 1986.

Description. 24 better-prepared gravid whole-mounts measured (Figs. 1-4). Trematoda: Lepocreadiidae: Diploproctodaeinae: *Diploproctodaeum*. Body sometimes truncate on its anterior tip, 2.60-5.80 by 1.20-2.50; anterior glandular portion of body scoop-shaped, with its thick lateral edges united posteriorly, orbicular to ovate, lacking unicellular glands in central part, wider than hindbody, 1.20-2.40 by 1.20-2.90, 38-46% of total body length; forebody 1.04-1.80 long, 26-40% of total body length; hindbody subcylindrical. Tegumental spines minute, seen on ventral side of body anterior to intestinal bifurcation. Eyespot pigments not seen. Oral sucker subterminal, ventral, 0.27-0.51 by 0.28-0.61. Prepharynx short. Pharynx almost as large as oral sucker, 0.21-0.35 by 0.24-0.43, with well-developed circular muscle bearing 8 protuberances at its anterior end. Esophagus short, bifurcating in front of ventral sucker; intestines thick, opening outside through separate, ventral or dorsal anal one on each side of excretory pore. Ventral sucker small, 0.24-0.43 by 0.30-0.47, located at about anterior one-third of body in anterior glandular portion of body; sucker width ratio 1:0.74-0.91 (1:1.11 as an exception); ratio of ventral sucker width to pharynx width 1:0.88-1.00 (1:1.33 as an exception).

Testes almost entire, a little diagonal, close together or slightly overlapping, in middle one-third of hindbody; anterior one globular to somewhat elongated, 0.51-0.86 by 0.43-0.79; posterior one usually longitudinally elongated, 0.67-1.02 by 0.35-0.71. Cirrus pouch club-shaped, thin-walled, 0.61-1.20 by 0.12-0.23, extending midway between ventral sucker and ovary; internal seminal vesicle ellipsoidal, 0.08-0.39 by 0.08-0.23; pars prostatica claviform, elongated, possibly bipartite (proximal portion with more finely granular internal cells; and distal, with more coarsely); a short duct surrounded by larger gland cells present be-

tween pars prostatica and ejaculatory duct; ejaculatory duct and cirrus thick, about half as long as cirrus pouch, protrusible; external seminal vesicle curved, reaching ovary, lying free in parenchyma. Genital atrium small, shallow. Genital pore ventral to shoulder of left intestine. Ovary deeply multilobed (or almost multibranched, counted to as many as 60-80 lobes in some specimens), compactly massed, median, immediately pretesticular, wider than long, 0.16-0.59 by 0.31-0.94. Seminal receptacle oval, sinistral to sinistrodorsal to ovary, 0.23-0.47 in diameter. Laurer's canal running backward, opening dorsal to seminal receptacle. Ootype-complex anterodorsal to dorsal to ovary. Uterus arranged in a few intercecal folds, preovarian; metraterm well-developed, surrounded by small gland cells, almost as long as cirrus pouch, 0.55-0.79 long. Eggs many, thin-shelled, operculate, not embryonated, 60-74 by 38-50 μ m (slightly collapsed) in balsam. Vitelline follicles small, filling all available space (even over testes and seminal receptacle) in hindbody, usually distributed anteriorly to level of ventral sucker and separated anteriorly, or rarely reaching to bifurcal level and confluent anteriorly. Excretory vesicle tubular, extending to near bifurcal level; excretory pore postero-ventral or -dorsal.

Type host. *Ostracion immaculatus* (Teleostei: Ostraciidae).

Site of infection. Intestine.

Localities. Morois Bay, Misaki, Kanagawa Prefecture (type locality); Kuruwa, Kanagawa Prefecture; Owase, Mie Prefecture; Nan'yofukura, Ehime Prefecture; Nishidomari, Tsushima, Nagasaki Prefecture; Tanegashima, Kagoshima Prefecture; and Haneji, Okinawa Prefecture.

Specimens. NSMT-PI 2878 (holotype); and NSMT-PI 970, 1509, 1647, 1747, 2787, 2878, 3118 and 3282, and MPM Coll. Nos. 20469 and 20508 (30 paratypes).

Remarks. One specimen of lot 4 had a teratological variation in the intestine (Fig. 5). The right intestinal trunk was partly broken off immediately after descending from the shoulder. The vitelline follicles in the right half of the body were poorly developed and thinly distributed. These anomalies may be unrelated to injury.

Discussion. This trematode belongs in *Diplo-*

proctodaeum La Rue, 1926 [3], because (1) the anterior glandular portion of the body is scoop-shaped with its thick lateral folds united posteriorly; (2) the intestines with no blind anterior process open outside through respective ani; (3) the ventral sucker is simple; (4) the testes are only slightly oblique; (5) the genital pore is just bifurcal; (6) the ovary is pretesticular; and (7) the vitellaria are abundant, filling the hindbody.

Diploproctodaeum consists of seven species: *D. haustum* (MacCallum, 1919) La Rue, 1926 (type species) [3]; *D. cryptostoma* (Ozaki, 1926) Sogandares-Bernal et Hutton, 1958 [4]; *D. longipygum* Oshmarin, Mamaev et Parukhin, 1961 [5], or *Diploproctodaeoides l.* (Oshmarin et al., 1961) Reimer, 1981 [6]; *D. macracetabulum* Oshmarin et al., 1961 [5], or *Diploproctodaeoides m.* (Oshmarin et al., 1961) Reimer, 1981 [6]; *D. ghanensis* [sic] (Fischthal et Thomas, 1970) Nasir, 1976 [7]; *D. plataxi* Mamaev, 1970 [8], or *Diploproctodaeoides p.* (Mamaev, 1970) Reimer, 1981 [6]; and *D. chelonodoni* Parukhin, 1979 [9]. *Diploproctodaeum hakofugu* sp. n. is different from *D. haustum* [6, 10, 11], *D. cryptostoma* [12, this paper] and *D. macracetabulum* [5] mainly in having the ventral sucker being distinctly smaller than the oral sucker and pharynx and the ovary being much more lobate. This new species appears most closely similar to *D. ghanense* out of the other four, but differs from it [13, 14] in a much larger body, tegumental spines confined to the prebifurcal part of the body instead of distributed posteriorly to the testicular region, and a much more lobed ovary (15–18 lobes in *D. ghanense* [14]). If the lateral folds of the anterior glandular portion of the body are separated posteriorly in *D. ghanense* (see below), this characteristic readily distinguishes it from the new species. The much more lobed ovary separates the new species from the remaining three [5, 8, 9]. Furthermore, the new species is different from *Diploproctodaeoides soleaticus* Reimer, 1981 [6], in the ventral sucker being smaller than the oral sucker and pharynx, more posteriorly located testes, a much longer cirrus pouch, a much more lobed ovary and larger eggs. The new species is named after the Japanese name of the host fish.

Ozaki's collection deposited at the MPM,

Tokyo, includes three gravid whole-mounts (MPM Coll. No. 30014) obtained from *O. immaculatus* from Goza, Mie Prefecture (other data not given). These are also assigned to the new species.

Diploproctodaeum oviforme sp. n.

(Fig. 6)

Material studied. 3 gravid whole-mounts (NSMT-PI 1688) collected by Machida from the intestine of *Lactoria diaphanus* from Tanegashima, Kagoshima Prefecture, on November 9, 1974.

Description. 3 gravid whole-mounts measured (Fig. 6). Similar to the foregoing species in morphology. Body oval to oblong, 2.40–2.90 by 1.10–2.00; anterior glandular region of body scoop-shaped, small, not prominent, slightly narrower than hindbody, 1.10–1.70 by 1.00–1.70, 46–58% of total body length; forebody 0.90–1.26 long, 37–43% of total body length. Tegumental spines not seen. Eyespot pigments not seen. Oral sucker large, 0.31–0.43 by 0.39–0.47. Prepharynx short. Pharynx large, 0.27–0.33 by 0.34–0.55, with well-developed circular muscle bearing 8 protuberances. Esophagus short. Ventral sucker small, 0.21–0.27 by 0.27–0.33; sucker width ratio 1:0.70–0.71; ratio of ventral sucker width pharynx width 1:0.59–0.81.

Testes subglobular, slightly diagonal; anterior one 0.31–0.35 by 0.35–0.40; posterior one 0.51–0.63 by 0.32–0.40. Cirrus pouch 0.47–0.79 by 0.24–0.27; internal seminal vesicle 0.16–0.20 long; pars prostatica club-shaped, 0.11–0.20 long; ejaculatory duct and cirrus 0.20–0.43 long; external seminal vesicle 0.40–0.55 long. Genital pore bifurcal, median in holotype, but sinistrosmedian in 2 paratypes. Genital atrium not seen. Ovary multi-branched, 0.20–0.24 by 0.31–0.71. Seminal receptacle elliptical, 0.31 by 0.18–0.20. Laurer's canal running posteriorly. Metratrum 0.51–0.95 long. Eggs 60–64 by 40–46 μ m (a little collapsed) in balsam. Vitelline follicles small, distributed anteriorly to level of ventral sucker. Excretory vesicle not worked out; excretory pore postero-ventral or -dorsal.

Type host. *Lactoria diaphanus* (Ostraciidae).

Site of infection. Intestine.

Type locality. Tanegashima, Kagoshima Pre-

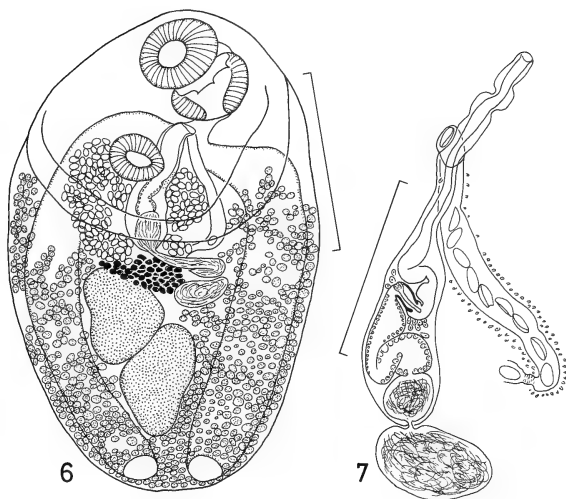


FIG. 6. *Diploproctodaeum oviforme* sp. n. from *Lactoria diaphanus*, entire worm, holotype, ventral view.

FIG. 7. *Bianium hemistoma* (Ozaki, 1928) Yamaguti, 1934, from *Takifugu vermicularis*, terminal genitalia, ventral view.

(Scale bars: 1 mm in Fig. 6; 0.5 mm in Fig. 7.)

ecture.

Specimens. NSMT-PI 1688 (holotype and 2 paratypes).

Discussion. *Diploproctodaeum oviforme* sp. n. is closest to the foregoing species but distinguishable from it mainly by the ventral sucker being much smaller than the oral sucker and pharynx, a smaller body and a smaller anterior glandular portion of the body.

Japanese species in the subfamily Diploproctodaeinae

Systematic discussion. The subfamily Diploproctodaeinae Park, 1939 [15], comprises eight genera: *Diploproctodaeum* La Rue, 1926 [3]; *Bianium* Stunkard, 1930 [16]; *Diplocreadium* Park, 1939 [15]; *Anterovitellosum* Gupta, 1967 [17]; *Caecobiporus* Mamaev, 1970 [8]; *Diploproctia* Mamaev, 1970 [8]; *Cotylcreadium* Madhavi,

1972 [18]; and *Diploproctodaeoides* Reimer, 1981 [6]. The following is a discussion on *Diploproctodaeum* and *Bianium*. The validity of the six others also seems to need studying critically.

Sogandares-Bernal and Hutton [4] concluded that there is not a single character to distinguish *Bianium* from *Diploproctodaenum* and so these two genera are generically identical, after they compared MacCallum's [10] type material of *Diploproctodaenum haustum* (type species) [3] with their material of *Bianium plicitum* (Linton, 1928) Stunkard, 1931 (type species) [19]. Besides, they declared that the two species (*D. hemistoma* Ozaki, 1928, and *D. cryptostoma* Ozaki, 1928) in *Diploporus* Ozaki, 1928 [12], are congeneric with *D. haustum*. Stunkard [19] stated that (1) *Bianium* differs from *Diploporus* in shape and proportions of the body; (2) in *Diploporus* the ventrally curved sides of the anterior glandular portion of the body are continued medially to form a conspicuous fold.

similar to that of *Diploproctodaeum*, but such a structure is not present in *Bianium*; (3) the suckers are closer together in *Bianium* and the preacetabular portion of the body is relatively much smaller; (4) in *Bianium* the testes are not situated so obliquely as in *Diploporus*, and in fully mature worms they are distinctly lobed; and (5) the vitelline follicles and the seminal receptacle are much larger in *Bianium*. La Rue [3] defined the anterior glandular portion as spoon- or scoop-shaped in *D. haustrum*. When he erected a new genus, *Diploporus*, for the two new species, Ozaki [12] described and illustrated the portion as shovel- or scoop-shaped in the generic diagnosis and *D. hemistoma*. He said that this genus differs from *Diploproctodaeum* in the oblique position of the testes, the shape of the ovary and the submedian position of the genital pore. Later, Yamaguti [20] indicated that in his own material of *D. hemistoma*, the lateral edges of the portion turn ventrad and approach each other but do not fuse at all. According to him [11, 20], *Diploporus* and *Bianium* are synonyms, and the proper generic name is *Bianium* because *Diploporus* is preoccupied. I think that the morphology of the portion can safely separate these three genera from one another. It seems that the above mentioned other features [12, 19] offer less important generic differences. Some authors [21] have taken it into consideration whether the vitellaria commence anteriorly at the level of or behind or in front of the ventral sucker. This anterior limit, however, varying largely even in a single species (see this paper), is probably of no generic significance.

I consider that *Diploproctodaeum* and *Bianium* are similar but distinct: In the former, the lateral folds of the anterior glandular portion of the body are united posteriorly; but in the latter, separated. The present study has shown that the lateral folds are fused in *D. cryptostoma*, but separated in *D. hemistoma* (see below). *Diploporus* [12] is synonymous partly with *Diploproctodaeum* and partly with *Bianium*. The combinations, *Diploproctodaeum cryptostoma* (Ozaki, 1928) Sogandares-Bernal et Hutton, 1958 [4], and *Bianium hemistoma* (Ozaki, 1928) Yamaguti, 1934 [20], for the two species are accepted.

Reimer [6] created *Diploproctodaeoides* for *Diplo-*

proctodaeum longipygum Oshmarin *et al.*, 1961 [5] (type species), and other three species (see above). He distinguished this genus from *Diploproctodaeum* by the anterior glandular portion of the body with a thick edge being flattened and only slightly raised above the flat hindbody, the esophagus being short or absent, and the ovary being lobed or follicular (in his new species, *D. soleaticus*, with 10 to 12 follicles). In the case of *D. haustrum*, the ovary is said to be entire [10, Fig. 47] to variously lobed (7 gravid whole-mounts of Yamaguti [11], MPM Coll. No. 15088; [22]). These two genera are possibly synonyms. Nasir's [7] combination, *D. ghanensis*, for *B. ghanensis* [13], seems to be problematical, because it has not yet been clarified whether the lateral folds are united or separated posteriorly in this species. The description on them (fused) by Fischthal and Thomas [13] is inconsistent with that (may or may not be united) by Nasir and Gomez [14].

From Japanese waters have so far been recorded the following five species of two genera in the subfamily Diploproctodaeinae.

1. Genus *Bianium* Stunkard, 1930

- Bianium* Stunkard, 1930 [16], p. 363 (type species, *Psilostomum plicatum* Linton, 1928 [19]).
Diploporus Ozaki, 1928 [12], preoccupied, partim, pp. 24–25 (type species, *D. hemistoma* Ozaki, 1928, by subsequent designation).
Diploporetta Strand, 1942 [23], renamed, partim, p. 387 (type species, not designated).
Amarocotyle Travassos, Freitas et Bührnheim, 1965 [24], p. 70 (type species, *A. simonei* Travassos *et al.*, 1965).

1-1. *B. hemistoma* (Ozaki, 1928) Yamaguti, 1934 (Fig. 7)

- Diploporus hemistoma* Ozaki, 1928 [12], pp. 25–29, figs. 13–15.
Bianium hemistoma: Yamaguti, 1934 [20], pp. 525–526.
Bianium holocentri Yamaguti, 1942 [25], pp. 357–359, fig. 14.
Diploporetta hemistoma: Strand, 1942 [23], p. 387.
Bianium hemistomum: Manter, 1947 [26], p. 280.
Diploproctodaeum hemistoma: Sogandares-Bernal and Hutton, 1958 [4], p. 566.
Diploproctodaeum holocentri: Sogandares-Bernal and Hutton, 1958 [4], p. 566.

Material studied. 1) Lot 1. 17 gravid whole-

mounts of "*Maculifer*" from *Takifugu pardalis* (= *Spheroides p.*) (Teleostei: Tetraodontidae) and 3 sectioned gravid specimens of "*Hemistomum*" (unpublished?, MPM Coll. No. 30016) in Ozaki's collection (other data not given).

2) Lot 2. 1 gravid whole-mount of *B. hemistoma* (MPM Coll. No. 22212) of Yamaguti [20] from the intestine of *Spheroides* sp. from Tokoname (Ise Bay), Aichi Prefecture, on April 19, 1929.

3) Lot 3. 2 immature whole-mounts (MPM Coll. No. 22208) in Yamaguti's collection from the intestine of *T. pardalis* from Hamajima, Mie Prefecture on April 14, 1941. (These were identified as *Bianium* on the label by Sh. Kamegai on April 19, 1972).

4) Lot 4. 6 gravid whole-mounts (MPM Coll. No. 22206) of *B. hemistoma* in the same collection from the intestine of *Spheroides* sp. from Shibukawa (prefecture unknown) on April 29, 1957.

5) Lot 5. 1 gravid whole-mount (NSMT-PI 2879) of *B. hemistoma* of Shimazu and Nagasawa [1] from the intestine of *T. pardalis* from Moroiso Bay on October 16, 1978.

6) Lot 6. 26 immature and 35 gravid whole-mounts (NSMT-PI 3119–3120) collected by Ogawa from the intestine of the same species of fish from Hagi, Yamaguchi Prefecture, on May 20 and 22, 1986.

7) Lot 7. 3 immature and 6 gravid whole-mounts (NSMT-PI 3121) collected by him from the intestine of the same species of fish from Nomo, Nagasaki Prefecture, on June 18, 1986.

8) Lot 8. 18 gravid whole-mounts (NSMT-PI 3123) collected by him from the intestine of *T. poecilnotus* from Nomo on June 19, 1986.

9) Lot 9. 3 immature and 41 gravid whole-mounts (NSMT-PI 3122) collected by him from the intestine of the same species of fish from Hagi on April 21, 1987.

10) Lot 10. 6 immature and 87 gravid whole-mounts (NSMT-PI 3124–3126) collected by him from the intestine of *T. vermicularis* from Hagi on May 20–21, 1986, and April 21, 1987.

11) Lot 11. 8 immature and 10 gravid whole-mounts (MPM Coll. No. 22205) of *B. hemistoma* in Yamaguti's collection from *T. niphobles* from Tokoname on April 15, 1941.

12) Lot 12. 1 gravid whole-mount (NSMT-PI

3127) collected by Ogawa from the intestine of the same species of fish from Hagi on April 22, 1987.

13) Lot 13. 11 (9 whole-mounted and 2 sectioned) gravid specimens (NSMT-PI 3128–3129) found in the intestine of the same species of fish from Moroiso Bay on July 22–23, 1987.

14) Lot 14. 1 gravid whole-mount (MPM Coll. No. 22213) of *B. hemistoma* in Yamaguti's collection from the intestine of *Stephanolepis cirrhifer* (Monacanthidae) from Tarumi, Hyogo Prefecture, on August 27, 1936.

15) Lot 15. 24 gravid whole-mounts (NSMT-PI 1013) collected by Machida from the intestine of the same species of fish from Nan'yofukaura on May 25, 1972.

16) Lot 16. 1 gravid whole-mount (holotype and only specimen, MPM Coll. No. 22207) of *B. holocentri* of Yamaguti [25] from the intestine of *Holocentrus spinosissimus* [= *Adioryx* s.] (Holocentridae) from Tokushima, Tokushima Prefecture, on July 5, 1940.

Description. Ozaki [12] published a full description of this species. He described and illustrated the anterior glandular portion of the body as dilated and shovel- or spoon-shaped. However, Yamaguti [11, 20, 27] pointed out that the lateral edges of the portion are completely separated posteriorly from each other, which has been confirmed by the present examination. The following concerns lots 1–15. Fine eyespot pigments were dispersed on each side of the pharynx. The oral sucker was always smaller than the ventral sucker, the sucker width ratio being 1:1.31–1.80. In a few specimens of lot 10, a considerable atrophy was seen in either one or both testes, and the male terminal duct and cirrus pouch were lacking in their anterior parts in one specimen. Shimazu and Nagasawa's [1] pluglike structure was present in the sheathlike proximalmost part of the ejaculatory duct in all the specimens examined with a few exceptions (Fig. 7). The pars prostatica was elastic and appeared to be bipartite: The proximal portion had more finely granular internal cells; and the distal, more coarsely. The male terminal duct (ejaculatory duct and cirrus) was long, invaginating or evaginating, and sometimes much convoluted. The vitelline follicles were distributed anteriorly to the ventral sucker zone in most of the

specimens examined; but in some specimens of lots 5, 9 and 13, they extended anteriorly farther than it along each side of the ventral sucker to almost the pharyngeal level and occasionally were confluent in front of the ventral sucker. Eggs measured 60–76 by 32–47 μm in balsam. Lot 16 was described in detail by Yamaguti [25]. The present reexamination has shown that in it, the pluglike structure is present as well, and the male terminal duct is a little shorter and more straight than in the others.

Discussion. Ozaki [12] described this species from the intestine of *S. pardalis* from Takamatsu, Kagawa Prefecture. He deposited the holotype (No. p. 283) at the Zoological Institute, Science Faculty, Tokyo Imperial University, but most presumably it has already been lost. It is uncertain whether lot 1 is part of the type material. Yamaguti [20] obtained the species (lot 2) from the intestine of various species of *Spheroides* from Mutu, Toyama and Ise bays and the Inland Sea. Later, he [27] briefly described it from *S. pardalis* (other data not given). His specimens have not yet been specified. Shimazu and Nagasawa [1] recorded it (lot 5) from the same species of fish from Moroiso Bay, Misaki.

Ozaki [12] described the vitelline follicles as commencing from the level of the genital pore (or just behind the ventral sucker). Yamaguti [27] observed that they begin in the ventral sucker zone in the majority of cases, and occasionally a little in front of it. He [25] proposed a new species, *B. holocentri* (lot 16), distinguishing it from the most closely related species, *B. hemistoma*, by the anterior extent of the vitellaria (reaching anteriorly to the pharyngeal level, Fig. 14, instead of to the ventral sucker level [12]) and the egg size (66–72 by 39–42 μm instead of 74–81 by 48–52 μm [12]). Stating that no differential character can be found in the anterior extent of the vitellaria between *B. holocentri* and *B. hemistoma* and that the egg size is very variable in other species of *Bianium*, Caballero *et al.* [28] considered that *B. holocentri* is synonymous with *B. hemistoma*. According to Sogandares-Bernal and Hutton [29] and Gupta [30], however, *B. holocentri* is valid, and they [28] apparently confused the anterior parenchymal gland cells figured by Ozaki [12] with the vitelline follicles. The sucker width ratio is 1:1.87 (calcu-

lated from Yamaguti [25] in *B. holocentri*. In *B. hemistoma*, the ratio is 1:1.31–1.80 (this paper); the eggs are 66–72 by 33–39 μm in life [27] and 60–76 by 32–47 μm in balsam (this paper); and sometimes the vitellaria extend anteriorly as far as the pharyngeal level and are confluent in front of the ventral sucker (this paper). The male terminal duct in *B. holocentri* is a little shorter and more straight than in *B. hemistoma*. These differences are very slight. I concur with Caballero *et al.* [28] in reducing *B. holocentri* to a synonym of *B. hemistoma*.

2. Genus *Diploproctodaeum* La Rue, 1926

Diploproctodaeum La Rue, 1926 [3], p. 208 (type species, *Hemistomum haustum* MacCallum, 1919 [3]).
Diploporus Ozaki, 1928 [12], preoccupied, partim, pp. 24–25 (type species, *D. hemistoma* Ozaki, 1928, by subsequent designation).
Diploporetta Strand, 1942 [23], renamed, partim, p. 387 (type species, not designated).

2-1. *D. cryptostoma* (Ozaki, 1928) Sogandares-Bernal et Hutton, 1958

Diploporus cryptostoma Ozaki, 1928 [12], pp. 30–32, figs. 16–17.
Bianium cryptostoma: Yamaguti, 1934 [20], pp. 525–526; Manter, 1940 [2], p. 377.
Diploporetta cryptostoma: Strand, 1942 [23], p. 387.
Bianium cryptostomum: Manter, 1947 [26], p. 280.
Diploproctodaeum cryptostoma: Sogandares-Bernal and Hutton, 1958 [4], p. 566.

Material studied. 1) Lot 1. 17 gravid whole-mounts of "*Diploproctodaeum*" and 3 sectioned gravid specimens of "*Hemistomum*" (unpublished?, MPM Coll. No. 30015) in Ozaki's collection (other data not given).

2) Lot 2. 2 sectioned gravid specimens (unpublished, MPM Coll. No. 22209) of *B. cryptostoma* in Yamaguti's collection from the intestine of *Spheroides* sp. on October 14 and 24, 1936 (locality not given).

3) Lot 3. 1 or 2 sectioned gravid specimens (unpublished, MPM Coll. No. 22210) of *B. cryptostoma* in the same collection from the intestine of *Spheroides* sp. from Maisaka, Shizuoka Prefecture, on April 12 (year not given).

4) Lot 4. 4 gravid whole-mounts (unpublished,

MPM Coll. No. 22211) of *B. cryptostoma* in the same collection from the intestine of *Canthigaster rivulata* (Tetraodontidae) from Katase, Kanagawa Prefecture, on June 7, 1958.

Description. The present examination has verified Ozaki's [12] observation that the lateral edges of the anterior glandular portion of the body are united posteriorly. The following supplements his original description: fine eyespot pigments dispersed in forebody; prepharynx short; oral sucker usually slightly larger than ventral sucker; sucker width ratio 1:0.9–1.09; esophagus short; internal seminal vesicle elliptical; pars prostatica globular; pluglike structure absent in proximal part of ejaculatory duct; ejaculatory duct and cirrus thick, straight, protrusible; genital pore sinistrosymmetric, bifurcal or a little posterior to it; ovarian lobes numbering to about 30; eggs in uterus measuring 67–80 by 40–47 μ m in balsam; and vitellaria distributed anteriorly to ventral sucker level to midpharyngeal level, may or may not be confluent in front of ventral sucker.

Discussion. This species has previously been described as *Diploporus cryptostoma* only once by Ozaki [12] from egg-bearing worms found in the intestine of *Spheroides pardalis* from Takamatsu, Kagawa Prefecture. He missed the egg size out of his description. According to him, the species was found together with *B. hemistoma*, but much less frequently, in the fish. Most probably the holotype (No. p. 284) deposited by him at the Zoological Institute, Science Faculty, Tokyo Imperial University, has already been lost. It is uncertain whether lot 1 is the component of the type series. Shimazu and Nagasawa's [1] trematode of *B. cryptostoma* has been described as a new species (see above).

Yamaguti evidently obtained the trematode that he identified as *B. cryptostoma* at least once as late as 1936 and subsequently at least twice. Nevertheless he did not mention a word about this species in his publications somehow. The combination for the species, *B. cryptostoma*, which Manter [2] used as well, is due to Yamaguti [20], because he first made *Diploporus* a synonym of *Bianium*.

In this species the lateral edges of the anterior glandular portion of the body are united posteriorly. I agree with Sogandares-Bernal and Hutton [4]

who transferred the species from *Diploporus* to *Diploproctodaeum* as *D. cryptostoma* (Ozaki, 1928). Manter [26] listed a new combination, *B. cryptostomum* (Ozaki, 1928), for the species, which accordingly is untenable.

2-2. *D. hakofugu* sp. n.

See this paper.

2-3. *D. oviforme* sp. n.

See this paper.

2-4. *Diploproctodaeum* sp. of Machida (1986)

Machida [31] obtained this trematode from the intestine of *Aluterus monoceros* and *A. scriptus* (Monacanthidae) from southern Japanese waters. He assumed it to be *D. haustum*. It may possibly be that he had more than one species. There has not yet appeared a full description of the trematode.

ACKNOWLEDGMENTS

I wish to thank the following persons for kindly permitting me to study their unpublished specimens or lending me the specimens or both: Mr. Shunya Kamagai, the MPM, Tokyo; Dr. Masaaki Machida, the NSNT; and Dr. Kazuo Ogawa, University of Tokyo, Tokyo. Thanks are also due to Dr. Makoto Shimizu, University of Tokyo, for providing me with the fish examined; and Dr. L. Margolis, Pacific Biological Station, Nanaimo, Canada, for the photocopy of the reference.

REFERENCES

- 1 Shimazu, T. and Nagasawa, K. (1985) Trematodes of marine fishes from Moroto Bay, Misaki, Kanagawa Prefecture, Japan. J. Nagano-ken Jun. Coll., (40): 7–15.
- 2 Manter, H. W. (1940) Digenetic trematodes of fishes from the Galapagos Islands and the neighboring Pacific. Rep. Allan Hancock Pacific Exped. (1932–1938), 2: 325–497.
- 3 La Rue, G. R. (1926) A trematode with two ani. J. Parasitol., 12: 207–209.
- 4 Sogandares-Bernal, F. and Hutton, R. F. (1958) The status of the trematode genus *Bianium* Stunkard, 1930, a synonym of *Diploproctodaeum* La Rue, 1926. J. Parasitol., 44: 566.
- 5 Oshmarin, P. G., Mamaev, Yu. L. and Parukhin, A. M. (1961) New species of trematodes of the family Diploproctodaeidae Ozaki, 1928. Helmintho-

- logia, 3: 254-260. (In Russian with English summary)
- 6 Reimer, L. W. (1981) *Lepocreadiidae* (Digenea) aus Fischen der Küste von Moçambique. *Angew. Parasitol.*, 22: 204-212.
 - 7 Nasir, P. (1976) Morfologia comparada de genitalia terminal en cuatro especies de trematodos digeneticos (*Lepocreadiidae*). In "Resúmenes de Trabajos Libres. Congreso (IV) Latinoamericano de Parasitología, etc., San José, Costa Rica, 7-11 Dec., 1976". Federación Latinoamericana de Parasitólogos; Asociación Costarricense de Microbiología y Parasitología, Costa Rica, p. 77. Cited by *Helminthol. Abst.*, Ser. A (1977), 46: 759-760.
 - 8 Mamaev, Yu. L. (1970) [Helminths of some commercial fishes in the Gulf of Tonkin.] In "[Helminths of Animals of South-Eastern Asia]". Ed. by P. G. Oshmarin, Yu. L. Mamaev and B. I. Lebedev. Izdatel'stvo AN SSSR, Moskva, pp. 127-190. (In Russian)
 - 9 Parukhin, A. M. (1979) New species of trematodes of fishes from the Indian Ocean and the Red Sea. *Parazitologiya*, 13: 639-643. (In Russian with English summary)
 - 10 MacCallum, G. A. (1919) Notes on the genus *Telorchis* and other trematodes. *Zoopathologica*, 1: 77-98 (1918).
 - 11 Yamaguti, S. (1970) *Digenetic Trematodes of Hawaiian Fishes*. Keigaku Publishing, Tokyo, 436 pp.
 - 12 Ozaki, Y. (1928) On some trematodes with anus. *Jpn. J. Zool.*, 2: 5-33.
 - 13 Fischthal, J. H. and Thomas, J. D. (1970) Digenetic trematodes of marine fishes from Ghana: Family *Lepocreadiidae*. *J. Helminthol.*, 44: 365-386.
 - 14 Nasir, P. and Gomez, Y. (1977) Digenetic trematodes from Venezuelan marine fishes. *Riv. Parasitol.*, 38: 53-73.
 - 15 Park, J. T. (1939) Fish trematodes from Työsen. II. Some new digenetic trematode parasites from marine fishes. *Keizyō J. Med.*, 10: 7-18, pl. 2.
 - 16 Stunkard, H. W. (1930) Another trematode with two anal openings. *Anat. Rec.*, 47: 363.
 - 17 Gupta, A. N. (1967) *Anterovitellosus indicum* gen. et sp. n., from globe fish *Tetraodon viridipunctatus* (Gunther [sic]) from India, with discussion on its systematic position in the subfamily *Diploproctodaeinae* Park, 1939. *Ciencia, Méx.*, 25: 215-218.
 - 18 Madhavi, R. (1972) Digenetic trematodes from marine fishes of Waltair coast, Bay of Bengal. I. Family *Lepocreadiidae*. *J. Parasitol.*, 58: 217-225.
 - 19 Stunkard, H. W. (1931) Further observations on the occurrence of anal openings in digenetic trematodes. *Z. Parasitenkd.*, 3: 713-725.
 - 20 Yamaguti, S. (1934) Studies on the helminth fauna of Japan. Part 2. Trematodes of fishes, I. *Jpn. J. Zool.*, 5: 249-541.
 - 21 Yamaguti, S. (1971) Synopsis of Digenetic Trematodes of Vertebrates. Keigaku Publishing, Tokyo, 2 vols., 1074 pp., 349 pls.
 - 22 Nahhas, F. M. and Cable, R. M. (1964) Digenetic and aspidogastroid trematodes from marine fishes of Curaçao and Jamaica. *Tulane Stud. Zool.*, 11: 169-228.
 - 23 Strand, E. (1942) Miscellanea nomenclatorica zoologica et palaeontologica. X. *Folia Zool. Hydrobiol.*, Riga, 11: 386-402. (In German)
 - 24 Travassos, L. P., Teixeira de Freitas, J. F. and Bühlheim, P. F. (1965) Trematódeos de peixes do litoral capixaba: *Amarocotyle simonei* gen. n., sp. n., parasito de baiacu. *Atas Soc. Biol. Rio de Janeiro*, 9: 69-73.
 - 25 Yamaguti, S. (1942) Studies on the helminth fauna of Japan. Part 39. Trematodes of fishes mainly from Naha. *Trans. Biogeogr. Soc. Jpn.*, 3: 329-398, pl. 24.
 - 26 Manter, H. W. (1947) The digenetic trematodes of marine fishes of Tortugas, Florida. *Am. Midl. Natur.*, 38: 257-416.
 - 27 Yamaguti, S. (1951) Studies on the helminth fauna of Japan. Part 48. Trematodes of fishes, X. *Arb. Med. Fak. Okayama*, 7: 315-334, pls. 1-2.
 - 28 Caballero y C., E. C., Bravo-Hollis, M. and Grocott, R. G. (1952) Helmintos de la República de Panamá. III. Tres trematódeos de peces marinos con descripción de una nueva especie. *Ann. Inst. Biol. Méx.*, 23: 167-180.
 - 29 Sogandares-Bernal, F. and Hutton, R. F. (1959) Studies on helminth parasites from the coast of Florida. III. Digenetic trematodes of marine fishes from Tampa and Boca Ciega bays. *J. Parasitol.*, 45: 337-346.
 - 30 Gupta, A. N. (1968) Studies on the genus *Bianium* Trematoda (Digenea) with description of three new species and discussion on status of genera *Diploproctodaeum* La Rue, 1926, *Bianium* Stunkard, 1930, and *Diplocreadium* Park, 1939. *Jpn. J. Parasitol.*, 17: 139-148.
 - 31 Machida, M. (1986) Trematodes from fishes of the genus *Aluterus* in Japanese waters. *Jpn. J. Parasitol.*, 35 (Suppl.): 140. (In Japanese)

Electrophoretic Study on the Phylogenetic Relationships among Six Species of Sea-Urchins of the Family Echinometridae Found in the Japanese Waters

NORIMASA MATSUOKA¹ and HIROBUMI SUZUKI²

Department of Biology, Faculty of Science, Hirosaki University,
Hirosaki 036, Japan

ABSTRACT—The family Echinometridae of the order Echinoida found in the Japanese waters is represented by six sea-urchin species belonging to the five different genera. They are *Anthocardia crassispina*, *Echinometra mathaei*, *Echinostrephus aciculatus*, *Echinostrephus molaris*, *Heterocentrotus mammillatus* and *Colobocentrotus mertensii*. The phylogenetic and evolutionary relationships among these six members of this family were investigated by electrophoretic analyses of 18 different enzymes. The biochemical dendrogram for the six species constructed from the Nei's genetic distances between species for 26 genetic loci showed the following: (1) *H. mammillatus* and *C. mertensii* are largely genetically differentiated from the other four species, and these two species are considered to be more primitive sea-urchins among echinometrids from the molecular estimation of their divergence time. (2) *A. crassispina* endemic to Japan is more closely related to *Echinometra* than to *Echinostrephus*, and it is estimated that *Anthocardia* has speciated in relatively recent geological age of the late Pliocene. (3) The two morphologically very similar species of *Echinostrephus* (*E. aciculatus* and *E. molaris*) are little genetically differentiated from each other, and therefore these two may belong to one and the same species. These electrophoretic results are discussed through the detailed comparison with other molecular and non-molecular results.

INTRODUCTION

The echinoid fauna of the seas around Japan is remarkably abundant and about 160 species have been ascertained by Shigei [1]. Under such richness in forms, the taxonomy of the echinoids has been extensively studied from the morphological and/or paleontological standpoints [1-4]. However, many unresolved problems concerning the phylogenetic and evolutionary relationships among echinoids still remain [4]. For a elucidation of these problems, it is necessary to introduce actively the different methods from the traditional and usual morphological method (e.g., biochemical or cytogenetical approach) into the echinoid taxonomy. We have been investigating the phylogenetic relationships among echinoids found in

the seas around Japan by the electrophoretic analyses of various enzymes and by the immunological techniques such as enzyme inhibition test [5-11]. Such molecular approaches make possible for us to estimate the phylogenetic relationships among taxa and their evolutionary process quantitatively with the common parameters such as enzymes or DNA, and they have been providing much valuable, and in some cases critical, information on the field of echinoid taxonomy. In the previous papers, one of the present authors (N.M.) reported on the biochemical systematics of the sea-urchins of the two families, Toxopneustidae and Strongylocentrotidae, of the order Echinoida by the electrophoretic analyses of various enzymes [7, 9]. Another large family of the order Echinoida is the Echinometridae and the phylogeny within this family has not yet been examined biochemically. In the present study, we therefore have attempted an electrophoretic study to clarify the phylogenetic relationships among the members of the family Echinometridae.

Accepted August 3, 1988

Received June 24, 1988

¹ To whom reprint requests should be addressed.

² Present Address: Research Department, Olympus Optical Co., Ltd., Ishikawa-cho, Hachioji 192, Japan.

At present, the family Echinometridae in the seas around Japan is represented by six species belonging to five genera. They are *Echinostrephus aciculatus* A. Agassiz, *E. molaris* (Blainville), *Anthocidaris crassispina* (A. Agassiz), *Echinometra mathaei* (Blainville), *Heterocentrotus mammillatus* (Linnaeus) and *Colobocentrotus mertensii* Brandt [1]. *A. crassispina* is an endemic Japanese species, but the other five species are widely distributed over the tropical and subtropical regions of the Indo-West Pacific, all of which are commonly found in shallow water. The Echinometridae is a tropical family and distinguished morphologically from other families of the order Echinoida by the valve of globiferous pedicellariae, the body skeleton of first larval stage and the optical crystal axis of calcite of coronal plate [4]. Although each of the five genera of this family is characterized by the highly specialized external form, it is considerably difficult to establish their phylogenetic relationships or the sequence of their evolutionary divergence by the morphological criteria. Further, there is little quantitative information available concerning the genetic differentiation among these members of this family.

In this paper, we report on the results of an electrophoretic investigation designed to clarify the phylogenetic relationships among the six members of the family Echinometridae found in the Japanese waters.

MATERIALS AND METHODS

Sea-urchins

The sea-urchins examined in this study were the six species belonging to the five different genera of the family Echinometridae: *Anthocidaris crassispina*, *Echinometra mathaei*, *Echinostrephus aciculatus*, *Echinostrephus molaris*, *Heterocentrotus mammillatus* and *Colobocentrotus mertensii*. The specimens of *A. crassispina* were the same as those used in our previous population genetic study [11]: 118 individuals were collected from the six different localities (Fukaura, Aomori Pref.; Noto, Ishikawa Pref.; Tsuruga, Fukui Pref.; Misaki, Kanagawa Pref.; Shirahama, Wakayama Pref. and Tanegashima, Kagoshima Pref.) from July 1983 to

August 1986. More recently, it has been found that on Okinawan reef flats *E. mathaei* consists of four different types (A, B, C, and D-types) and they are distinguishable by color pattern of spines, shape of spicules, distribution pattern and habitat preference, etc. each other [12, 13]. In this study, we used 10 individuals of A-type of *E. mathaei*, which were collected from Minatogawa in the main land of Okinawa Pref. in March 1986. *E. aciculatus* and *E. molaris* were the same as those used in our previous electrophoretic study [10]: the former was collected from Kushimoto and Shirahama of Wakayama Pref. in August, 1983 and 1984, and the latter from Sesoko-jima of Okinawa Pref. in July 1983 and February 1986. The number of individuals examined was 32 for *E. aciculatus* and 14 for *E. molaris*. *H. mammillatus* was collected from the coast near the Sesoko Marine Science Center, the University of the Ryukyus, in Sesoko-jima of Okinawa Pref. in July 1983. The number of individuals examined was 4. *C. mertensii* was collected from two different localities: 2 individuals from Izeiki and Kubota in the northeast coast of Tanegashima, Kagoshima Pref., in August 1985, and 3 individuals from Uka in the northern coast of the main land of Okinawa Pref. in February 1986. Immediately after collection, the guts and gonads were extracted from these specimens and exhaustively washed in filtered sea-water. They were then frozen on dry ice and transported to the laboratory at Hirotsuki University, where they were stored at -80°C until used.

Electrophoresis

Electrophoresis was performed on 7.5% polyacrylamide gels by the method of Davis [14] using a disc gel apparatus consisted of 12 plastic columns (the size of one column: $3 \times 11 \times 75$ mm) as described previously [7, 10]: About 0.2 g of gut or gonad was separately homogenized using a small polyethylene homogenizer of the Potter-Elvehjem type with 3 vols of cold 20 mM phosphate buffer (pH 7.0) containing 0.1 M KCl and 1 mM EDTA in an ice-water bath. After centrifugation at 10,000 rpm for 10 min, 0.04–0.1 ml of the clear supernatant was used for polyacrylamide gel electrophoresis. After electrophoresis, the gels were stained for the following 18 different enzymes:

alcohol dehydrogenase (ADH), glucose-6-phosphate dehydrogenase (G6PD), hexose-6-phosphate dehydrogenase (H6PD), hydroxybutyrate dehydrogenase (HBDH), malate dehydrogenase (MDH), malic enzyme (ME), nothing dehydrogenase (NDH), octanol dehydrogenase (ODH), sorbitol dehydrogenase (SDH), xanthine dehydrogenase (XDH), superoxide dismutase (SOD), hexokinase (HK), aspartate aminotransferase (AAT), alkaline phosphatase (ALK), esterase (EST), peroxidase (PO), amylase (AMY) and leucine amino peptidase (LAP). Five enzymes (G6PD, H6PD, HK, AAT and ALK) were assayed with the supernatant of homogenate of the gonad, and the remaining 13 enzymes with that of the gut. Stain recipes for these enzymes have been described previously [7, 9, 10].

RESULTS

The electrophoretic patterns of the 18 different enzymes observed in the 6 sea-urchin species of the family Echinometridae are diagrammatically

shown in Figure 1. From these band patterns, we assumed 26 genetic loci. The major features of variation in the 18 enzymes are summarized as follows.

Eight enzymes (ADH, G6PD, H6PD, HBDH, HK, NDH, SDH and XDH) exhibited a single band of activity and were monomorphic, all but NDH and XDH varying interspecifically. In the course of this study, ADH could not be scored in *C. mertensii*, though the cause of this enzymatic inactivity was not known.

PO in *E. mathaei*, AAT in the two *Echino-strephus* species and ALK in the five species except *C. mertensii* showed double-banded phenotypes. These three enzymes in the other species showed single-banded phenotypes. The two and one band pattern in these enzymes were interpreted as the products of different alleles at a single locus. These enzymes were monomorphic in each species.

ME consistently appeared as two active bands, of which the faster band showed higher activity. The mobilities of the two bands in *H. mammillatus*

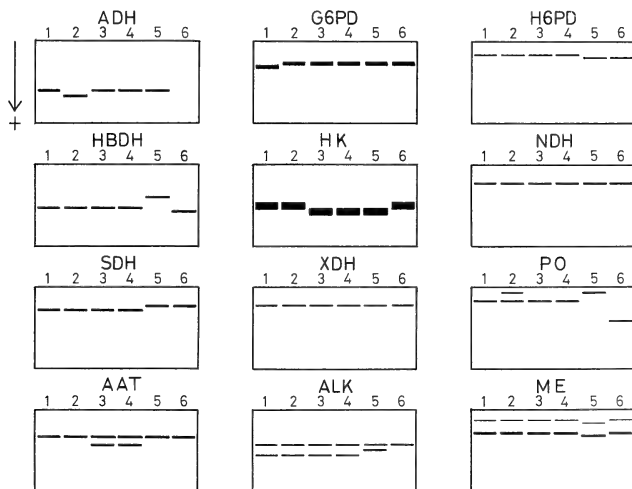


FIG. 1-a.

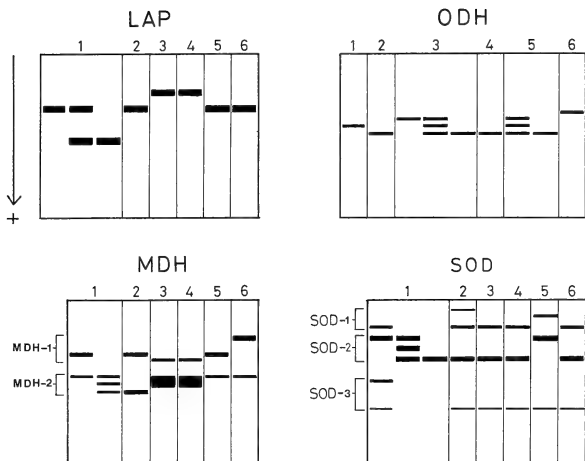


FIG. 1-b.

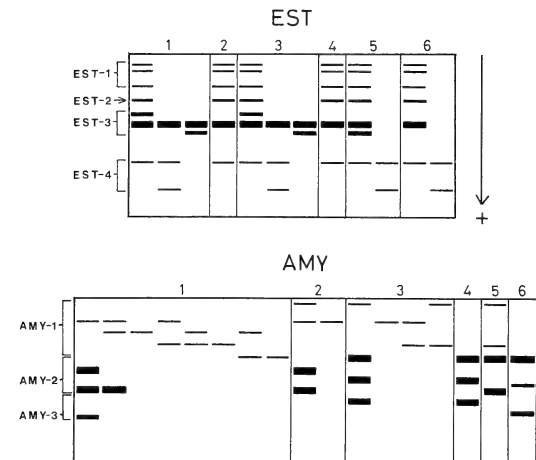


FIG. 1-c.

FIG. 1. a-c. Electrophoretic patterns of 18 different enzymes in six species of sea-urchins of the family Echinometridae. For each enzyme the origin is at the top and the direction of mobility toward the bottom. Presumptive genetic loci are numbered downwards from 1, starting with that nearest the origin (i.e., of lowest electrophoretic mobility). 1=*Anthocidaris crassispina*, 2=*Echinometra mathaei*, 3=*Echinostrephus aciculatus*, 4=*Echinostrephus molaris*, 5=*Heterocentrotus mammillatus*, 6=*Colobocentrotus mertensii*.

Analysis by an oscillographic recording

Method Another recording method was used for directly measuring the intervals of slit-passing. Switch devices were interposed in the circuit of a dual channel pen-recorder (Nihon Kohden RM-20) at a chart speed of 6.0 mm per sec. The observer noted the time of slit-passing of fish in left-to-right direction by pushing a switch, and the time of passing in the opposite direction by pushing another one.

Results Guppies did not pass the slit in succession in so short time, in a strong contrast to the rapid succession of the passing by goldfish. Figure 4 is an oscillogram recorded during about 100 sec from the onset of experiment in a specimen of either species. Here, the slit-passing by guppies occurred at so long interval as several seconds in spite of frequent repetition of one-directioned passing owing to the initial phase of the trial, while the goldfish passed the slit in so many as 30 individuals during 20 sec.

DISCUSSION

In the previous paper [1] we rejected a working hypothesis that guppy's avoidance of polluted environment would be a cause of the excessive transitory migration, by an experiment in which populations put in the clean-water circulating compartment excessively migrated to the polluted-water circulating one.

Schooling of fish has been noticed by many workers [2] and the role of vision in the fish schooling has been stressed since Parr's pioneer work on mackerel [8]. We also showed experimentally that vision is the main sensory cue in the excessive transitory migration [1].

If fish's conspecific-following tendency is a cause of E.T.M., the successive passing of a certain direction would be frequent, accordingly the frequency of runs of slit-passing in the same direction would be significantly different from randomness.

But, the runs test did not reject the null hypothesis that the order of left-to-right and right-to-left slit-passing in the guppy and medaka is random (Table 1), and the distribution of the length of their runs is very much like that of odd and even numbers in the random number series (Fig. 3).

The oscillographic record offered a direct evidence that the guppy has not a conspecific-following tendency. If this fish had the tendency, a frequent successive slit-passing would be recorded, as in goldfish. The guppy, however, passed at intervals of a fairly long time, often containing occasional opposite-directioned passing.

If the following between conspecifics is the cause of the E.T.M., the excessive migration is expected to occur throughout the whole observation period as goldfish did. But this migration occurs only in the initial phase. From the present results the main cause of the excessive transitory migration must be investigated from another point of view.

REFERENCES

- 1 Watanabe, M. (1981) Excessive transitory migration of guppy populations. I. Analysis of sensory cues and mechanisms. *Zool. Mag.*, **90**: 33-38.
- 2 Radakov, D. V. (1973) Schooling in the ecology of fish. A Halsted Press Book, John Wiley & Sons, New York.
- 3 Shaw, E. (1960) The development of schooling behavior in fishes. *Physiol. Zool.*, **33**: 79-86.
- 4 Shaw, E. (1961) The development of schooling behavior in fishes. II. *Physiol. Zool.*, **34**: 263-272.
- 5 Yamagishi, H., Nakamura, M. and Fukuhara, O. (1978) Behavioral studies on school of fishes II. Leading-following relationship of the immature yellowtail, *Seriola quinqueradiata* Temminck et Schlegel in captivity. *Zool. Mag.*, **87**: 125-131.
- 6 Radakov, D. V. (1958) Adaptive value of the schooling behavior of young pollock *Pollackius virens* (L.). *Voprosy Ikhtologii*. No. 11.
- 7 Siegel, S. (1956) Nonparametric Statistics for the Behavioral Science. McGraw-Hill, London.
- 8 Parr, A. E. (1927) A contribution to the theoretical analysis of the schooling behavior of fishes. *Occ. Pap. Bingham Oceanogr. Colln.*, **1**.



Two New Species of the Genus *Diploproctodaeum* (Trematoda: Lepocreadiidae: Diploproctodaeinae), with Some Comments on Species in the Subfamily Diploproctodaeinae, from Japanese Marine Fishes

TAKASHI SHIMAZU

Nagano-ken Junior College, Nagano 380, Japan

ABSTRACT—Two new species of the trematode genus, *Diploproctodaeum* La Rue, 1926 (Lepocreadiidae: Diploproctodaeinae), are described and illustrated from Japanese marine fishes. *Diploproctodaeum hakofugu* sp. n. from the intestine of *Ostracion immaculatus* (Teleostei: Ostraciidae) differs from all the previously known species of the genus and *Diploproctodaeoides soleaticus* Reimer, 1981, chiefly in a much more lobed ovary. *Diploproctodaeum oviforme* sp. n. from the intestine of *Lactoria diaphanus* (Ostraciidae) is separated from the most closely allied species, *D. hakofugu*, chiefly by the ventral sucker being much smaller than the oral sucker and pharynx. Some morphological and systematic comments are given on Japanese species in the subfamily Diploproctodaeinae Park, 1939. *Diploporus* Ozaki, 1928, is reduced to a synonym partly of *Diploproctodaeum* and partly of *Bianium* Stunkard, 1930. *B. holocentri* Yamaguti, 1942, is considered synonymous with *B. hemistoma* (Ozaki, 1928) Yamaguti, 1934.

INTRODUCTION

Shimazu and Nagasawa [1] reported three specimens of a trematode as *Bianium cryptostoma* (Ozaki, 1928) Manter, 1940 [sic] (Lepocreadiidae: Diploproctodaeinae), from *Ostracion immaculatus* from Moroiso Bay, Misaki, Kanagawa Prefecture, Japan. (They gave the host name as "*Lactoria cubicus*" in error). A closer examination of them and additional specimens has shown that the trematode represents a new species of *Diploproctodaeum* La Rue, 1926, in the same subfamily. Another new species of the same genus has also been found out in the course of this study. This paper describes these two new species and incidentally presents some morphological and taxonomic comments on other Japanese species in the subfamily from examination of their museum specimens.

MATERIALS AND METHODS

Two worms were newly obtained from the intes-

tine of *O. immaculatus* taken in Moroiso Bay in July, 1987. They were fixed in Nozawa's fluid without flattening, made into serial paraffin sections (transverse, 15 μ m) and stained with Delafield's hematoxylin and eosin. Museum specimens were received already stained and whole-mounted in Canada balsam by various methods. The specimens studied are deposited at the National Science Museum, Tokyo (NSMT), and the Meguro Parasitological Museum (MPM), Tokyo. Measurements (length by width) are given in millimeters unless otherwise stated.

RESULTS AND DISCUSSION

Diploproctodaeum hakofugu sp. n.

(Figs. 1-5)

Bianium cryptostoma

[2] of Shimazu and Nagasawa, 1985 [1], p. 11.

Material studied. All the specimens examined were obtained from the intestine of *Ostracion immaculatus*, as follows.

1) Lot 1. 3 gravid whole-mounts (NSMT-PI 2878) of *B. cryptostoma* of Shimazu and Nagasawa [1] from Moroiso Bay, Misaki, Kanagawa Prefec-

ture, on July 18, 1983.

2) Lot 2. 2 sectioned gravid worms (NSMT-PI 3118) from the same locality on July 21, 1987.

3) Lot 3. 6 gravid whole-mounts (MPM Coll. No. 20469) collected by Kamegai from Kuruwa, Kanagawa Prefecture, on October 3 and November 25, 1984.

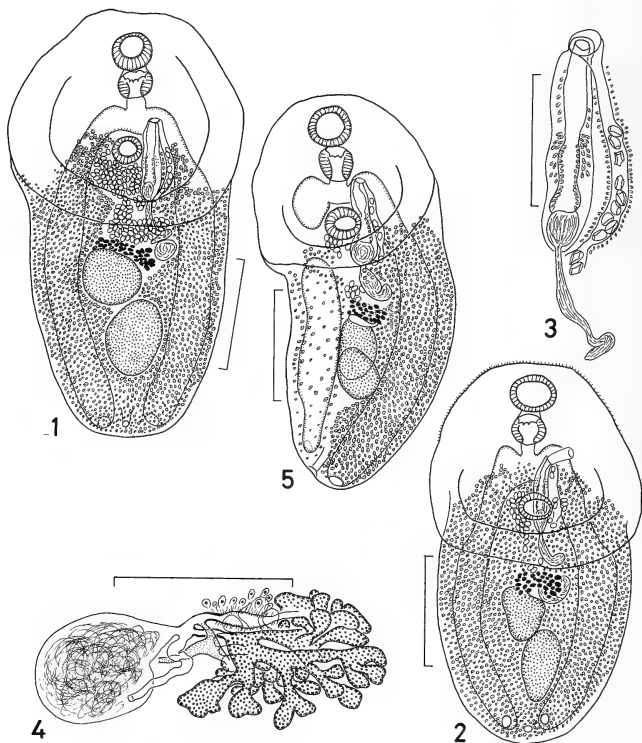
4) Lot 4. 5 gravid whole-mounts (MPM Coll. No. 20508) collected by him from the same locality

on December 5, 1987.

5) Lot 5. 2 gravid whole-mounts (NSMT-PI 970) collected by Machida from Nan'yofukaura, Ehime Prefecture, on May 22, 1972.

6) Lot 6. 1 immature and 5 gravid whole-mounts (NSMT-PI 1509 and 1647) collected by him from Nishidomari, Tsushima, Nagasaki Prefecture, on July 12, 1973, and April 27, 1974.

7) Lot 7. 1 gravid whole-mount (NSMT-PI



FIGS. 1-5. *Diploproctodaeum hakofugu* sp. n. from *Ostracion immaculatus*. 1. Entire worm, holotype, ventral view. 2. Entire worm, paratype, ventral view, showing more anteriorly distributed vitellaria. 3. Terminal genitalia, holotype, ventral view. 4. Ovarian complex, paratype, dorsal view. 5. Entire worm, paratype, ventral view, showing malformed intestine and vitellaria in right half of body. (Scale bars: 1 mm in Figs. 1-2 and 5; 0.5 mm in Figs. 3-4.)

1747) collected by him from Tanegashima, Kagoshima Prefecture, on November 24, 1974.

8) Lot 8. 8 gravid whole-mounts (NSMT-PI 2787) collected by him from Haneji, Okinawa Prefecture, on May 20, 1983.

9) Lot 9. 2 gravid whole-mounts (NSMT-PI 3282) collected by him from Owase, Mie Prefecture, on October 13, 1986.

Description. 24 better-prepared gravid whole-mounts measured (Figs. 1–4). Trematoda: Lepocreadiidae: Diploproctodaeinae: *Diploproctodaeum*. Body sometimes truncate on its anterior tip, 2.60–5.80 by 1.20–2.50; anterior glandular portion of body scoop-shaped, with its thick lateral edges united posteriorly, orbicular to ovate, lacking unicellular glands in central part, wider than hindbody, 1.20–2.40 by 1.20–2.90, 38–46% of total body length; forebody 1.04–1.80 long, 26–40% of total body length; hindbody subcylindrical. Tegumental spines minute, seen on ventral side of body anterior to intestinal bifurcation. Eyespot pigments not seen. Oral sucker subterminal, ventral, 0.27–0.51 by 0.28–0.61. Prepharynx short. Pharynx almost as large as oral sucker, 0.21–0.35 by 0.24–0.43, with well-developed circular muscle bearing 8 protuberances at its anterior end. Esophagus short, bifurcating in front of ventral sucker; intestines thick, opening outside through separate, ventral or dorsal and one on each side of excretory pore. Ventral sucker small, 0.24–0.43 by 0.30–0.47, located at about anterior one-third of body in anterior glandular portion of body; sucker width ratio 1:0.74–0.91 (1:1.11 as an exception); ratio of ventral sucker width to pharynx width 1:0.88–1.00 (1:1.33 as an exception).

Testes almost entire, a little diagonal, close together or slightly overlapping, in middle one-third of hindbody; anterior one globular to somewhat elongated, 0.51–0.86 by 0.43–0.79; posterior one usually longitudinally elongated, 0.67–1.02 by 0.35–0.71. Cirrus pouch club-shaped, thin-walled, 0.61–1.20 by 0.12–0.23, extending midway between ventral sucker and ovary; internal seminal vesicle ellipsoidal, 0.08–0.39 by 0.08–0.23; pars prostatica claviform, elongated, possibly bipartite (proximal portion with more finely granular internal cells; and distal, with more coarsely); a short duct surrounded by larger gland cells present be-

tween pars prostatica and ejaculatory duct; ejaculatory duct and cirrus thick, about half as long as cirrus pouch, protrusible; external seminal vesicle curved, reaching ovary, lying free in parenchyma. Genital atrium small, shallow. Genital pore ventral to shoulder of left intestine. Ovary deeply multilobed (or almost multibranched, counted to as many as 60–80 lobes in some specimens), compactly massed, median, immediately pretesticular, wider than long, 0.16–0.59 by 0.31–0.94. Seminal receptacle oval, sinistral to sinistrodorsal to ovary, 0.23–0.47 in diameter. Laurer's canal running backward, opening dorsal to seminal receptacle. Ootype-complex anterodorsal to dorsal to ovary. Uterus arranged in a few intercecal folds, preovarian; metraterm well-developed, surrounded by small gland cells, almost as long as cirrus pouch, 0.55–0.79 long. Eggs many, thin-shelled, operculate, not embryonated, 60–74 by 38–50 μ m (slightly collapsed) in balsam. Vitelline follicles small, filling all available space (even over testes and seminal receptacle) in hindbody, usually distributed anteriorly to level of ventral sucker and separated anteriorly, or rarely reaching to bifurcal level and confluent anteriorly. Excretory vesicle tubular, extending to near bifurcal level; excretory pore postero-ventral or -dorsal.

Type host. *Ostracion immaculatus* (Teleostei: Ostraciidae).

Site of infection. Intestine.

Localities. Moroiso Bay, Misaki, Kanagawa Prefecture (type locality); Kuruwa, Kanagawa Prefecture; Owase, Mie Prefecture; Nan'yofukaura, Ehime Prefecture; Nishidomari, Tsushima, Nagasaki Prefecture; Tanegashima, Kagoshima Prefecture; and Haneji, Okinawa Prefecture.

Specimens. NSMT-PI 2878 (holotype); and NSMT-PI 970, 1509, 1647, 1747, 2787, 2878, 3118 and 3282, and MPM Coll. Nos. 20469 and 20508 (30 paratypes).

Remarks. One specimen of lot 4 had a teratological variation in the intestine (Fig. 5). The right intestinal trunk was partly broken off immediately after descending from the shoulder. The vitelline follicles in the right half of the body were poorly developed and thinly distributed. These anomalies may be unrelated to injury.

Discussion. This trematode belongs in *Diplo-*

proctodaeum La Rue, 1926 [3], because (1) the anterior glandular portion of the body is scoop-shaped with its thick lateral folds united posteriorly; (2) the intestines with no blind anterior process open outside through respective ani; (3) the ventral sucker is simple; (4) the testes are only slightly oblique; (5) the genital pore is just bifurcal; (6) the ovary is pretesticular; and (7) the vitellaria are abundant, filling the hindbody.

Diploproctodaeum consists of seven species: *D. haustum* (MacCallum, 1919) La Rue, 1926 (type species) [3]; *D. cryptostoma* (Ozaki, 1928) Sogandares-Bernal et Hutton, 1958 [4]; *D. longipygum* Oshmarin, Mamaev et Parukhin, 1961 [5], or *Diploproctodaeoides l.* (Oshmarin et al., 1961) Reimer, 1981 [6]; *D. macracetabulum* Oshmarin et al., 1961 [5], or *Diploproctodaeoides m.* (Oshmarin et al., 1961) Reimer, 1981 [6]; *D. ghanensis* [sic] (Fischthal et Thomas, 1970) Nasir, 1976 [7]; *D. plataxi* Mamaev, 1970 [8], or *Diploproctodaeoides p.* (Mamaev, 1970) Reimer, 1981 [6]; and *D. chelonodoni* Parukhin, 1979 [9]. *Diploproctodaeum hakofugu* sp. n. is different from *D. haustum* [6, 10, 11], *D. cryptostoma* [12, this paper] and *D. macracetabulum* [5] mainly in having the ventral sucker being distinctly smaller than the oral sucker and pharynx and the ovary being much more lobate. This new species appears most closely similar to *D. ghanense* out of the other four, but differs from it [13, 14] in a much larger body, tegumental spines confined to the prebifurcal part of the body instead of distributed posteriorly to the testicular region, and a much more lobed ovary (15–18 lobes in *D. ghanense* [14]). If the lateral folds of the anterior glandular portion of the body are separated posteriorly in *D. ghanense* (see below), this characteristic readily distinguishes it from the new species. The much more lobed ovary separates the new species from the remaining three [5, 8, 9]. Furthermore, the new species is different from *Diploproctodaeoides soleaticus* Reimer, 1981 [6], in the ventral sucker being smaller than the oral sucker and pharynx, more posteriorly located testes, a much longer cirrus pouch, a much more lobed ovary and larger eggs. The new species is named after the Japanese name of the host fish.

Ozaki's collection deposited at the MPM,

Tokyo, includes three gravid whole-mounts (MPM Coll. No. 30014) obtained from *O. immaculatus* from Goza, Mie Prefecture (other data not given). These are also assigned to the new species.

Diploproctodaeum oviforme sp. n.

(Fig. 6)

Material studied. 3 gravid whole-mounts (NSMT-PI 1688) collected by Machida from the intestine of *Lactoria diaphanus* from Tanegashima, Kagoshima Prefecture, on November 9, 1974.

Description. 3 gravid whole-mounts measured (Fig. 6). Similar to the foregoing species in morphology. Body oval to oblong, 2.40–2.90 by 1.10–2.00; anterior glandular region of body scoop-shaped, small, not prominent, slightly narrower than hindbody, 1.10–1.70 by 1.00–1.70, 46–58% of total body length; forebody 0.90–1.26 long, 37–43% of total body length. Tegumental spines not seen. Eyespot pigments not seen. Oral sucker large, 0.31–0.43 by 0.39–0.47. Prepharynx short. Pharynx large, 0.27–0.33 by 0.34–0.55, with well-developed circular muscle bearing 8 protuberances. Esophagus short. Ventral sucker small, 0.21–0.27 by 0.27–0.33; sucker width ratio 1:0.70–0.71; ratio of ventral sucker width pharynx width 1:0.59–0.81.

Testes subglobular, slightly diagonal; anterior one 0.31–0.35 by 0.35–0.40; posterior one 0.51–0.63 by 0.32–0.40. Cirrus pouch 0.47–0.79 by 0.24–0.27; internal seminal vesicle 0.16–0.20 long; pars prostatica club-shaped, 0.11–0.20 long; ejaculatory duct and cirrus 0.20–0.43 long; external seminal vesicle 0.40–0.55 long. Genital pore bifurcal, median in holotype, but sinistrosmedian in 2 paratypes. Genital atrium not seen. Ovary multi-branched, 0.20–0.24 by 0.31–0.71. Seminal receptacle elliptical, 0.31 by 0.18–0.20. Laurer's canal running posteriorly. Metraterm 0.51–0.95 long. Eggs 60–64 by 40–46 μ m (a little collapsed) in balsam. Vitelline follicles small, distributed anteriorly to level of ventral sucker. Excretory vesicle not worked out; excretory pore postero-ventral or -dorsal.

Type host. *Lactoria diaphanus* (Ostraciidae).

Site of infection. Intestine.

Type locality. Tanegashima, Kagoshima Pre-

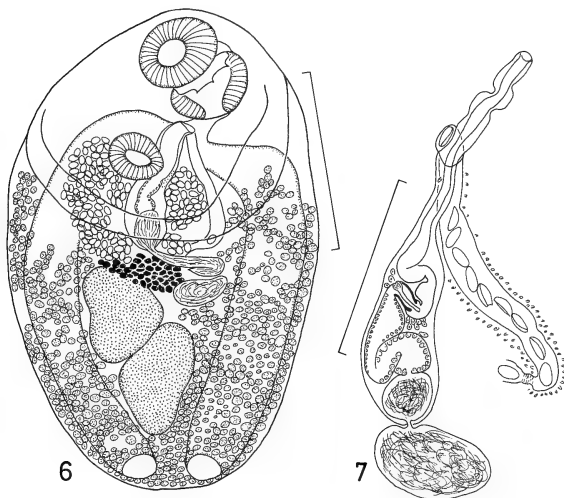


FIG. 6. *Diploproctodaeum oviforme* sp. n. from *Lactoria diaphanus*, entire worm, holotype, ventral view.

FIG. 7. *Bianium hemistoma* (Ozaki, 1928) Yamaguti, 1934, from *Takifugu vermicularis*, terminal genitalia, ventral view.

(Scale bars: 1 mm in Fig. 6; 0.5 mm in Fig. 7.)

feature.

Specimens. NSMT-PI 1688 (holotype and 2 paratypes).

Discussion. *Diploproctodaenum oviforme* sp. n. is closest to the foregoing species but distinguishable from it mainly by the ventral sucker being much smaller than the oral sucker and pharynx, a smaller body and a smaller anterior glandular portion of the body.

Japanese species in the subfamily Diploproctodaeinae

Systematic discussion. The subfamily Diploproctodaeinae Park, 1939 [15], comprises eight genera: *Diploproctodaeum* La Rue, 1926 [3]; *Bianium* Stunkard, 1930 [16]; *Diplocreadium* Park, 1939 [15]; *Anterovitellosum* Gupta, 1967 [17]; *Caecobiporus* Mamaev, 1970 [8]; *Diploproctia* Mamaev, 1970 [8]; *Cotylcreadium* Madhavi.

1972 [18]; and *Diploproctodaeoides* Reimer, 1981 [6]. The following is a discussion on *Diploproctodaeum* and *Bianium*. The validity of the six others also seems to need studying critically.

Sogandares-Bernal and Hutton [4] concluded that there is not a single character to distinguish *Bianium* from *Diploproctodaenum* and so these two genera are generically identical, after they compared MacCallum's [10] type material of *Diploproctodaenum haustum* (type species) [3] with their material of *Bianium plicatum* (Linton, 1928) Stunkard, 1931 (type species) [19]. Besides, they declared that the two species (*D. hemistoma* Ozaki, 1928, and *D. cryptostoma* Ozaki, 1928) in *Diploporus* Ozaki, 1928 [12], are congeneric with *D. haustum*. Stunkard [19] stated that (1) *Bianium* differs from *Diploporus* in shape and proportions of the body; (2) in *Diploporus* the ventrally curved sides of the anterior glandular portion of the body are continued medially to form a conspicuous fold.

similar to that of *Diploproctodaeum*, but such a structure is not present in *Bianium*; (3) the suckers are closer together in *Bianium* and the preacetabular portion of the body is relatively much smaller; (4) in *Bianium* the testes are not situated so obliquely as in *Diploporus*, and in fully mature worms they are distinctly lobed; and (5) the vitelline follicles and the seminal receptacle are much larger in *Bianium*. La Rue [3] defined the anterior glandular portion as spoon- or scoop-shaped in *D. haustrum*. When he erected a new genus, *Diploporus*, for the two new species, Ozaki [12] described and illustrated the portion as shovel- or scoop-shaped in the generic diagnosis and *D. hemistoma*. He said that this genus differs from *Diploproctodaeum* in the oblique position of the testes, the shape of the ovary and the submedian position of the genital pore. Later, Yamaguti [20] indicated that in his own material of *D. hemistoma*, the lateral edges of the portion turn ventrad and approach each other but do not fuse at all. According to him [11, 20], *Diploporus* and *Bianium* are synonyms, and the proper generic name is *Bianium* because *Diploporus* is preoccupied. I think that the morphology of the portion can safely separate these three genera from one another. It seems that the above mentioned other features [12, 19] offer less important generic differences. Some authors [21] have taken it into consideration whether the vitellaria commence anteriorly at the level of or behind or in front of the ventral sucker. This anterior limit, however, varying largely even in a single species (see this paper), is probably of no generic significance.

I consider that *Diploproctodaeum* and *Bianium* are similar but distinct: In the former, the lateral folds of the anterior glandular portion of the body are united posteriorly; but in the latter, separated. The present study has shown that the lateral folds are fused in *D. cryptostoma*, but separated in *D. hemistoma* (see below). *Diploporus* [12] is synonymous partly with *Diploproctodaeum* and partly with *Bianium*. The combinations, *Diploproctodaeum cryptostoma* (Ozaki, 1928) Sogandares-Bernal et Hutton, 1958 [4], and *Bianium hemistoma* (Ozaki, 1928) Yamaguti, 1934 [20], for the two species are accepted.

Reimer [6] created *Diploproctodaeoides* for *Diplo-*

proctodaeum longipygum Oshmarin *et al.*, 1961 [5] (type species), and other three species (see above). He distinguished this genus from *Diploproctodaeum* by the anterior glandular portion of the body with a thick edge being flattened and only slightly raised above the flat hindbody, the esophagus being short or absent, and the ovary being lobed or follicular (in his new species, *D. soleaticus*, with 10 to 12 follicles). In the case of *D. haustrum*, the ovary is said to be entire [10, Fig. 47] to variously lobed (7 gravid whole-mounts of Yamaguti [11], MPM Coll. No. 15088; [22]). These two genera are possibly synonyms. Nasir's [7] combination, *D. ghanensis*, for *B. ghanensis* [13], seems to be problematical, because it has not yet been clarified whether the lateral folds are united or separated posteriorly in this species. The description on them (fused) by Fischthal and Thomas [13] is inconsistent with that (may or may not be united) by Nasir and Gomez [14].

From Japanese waters have so far been recorded the following five species of two genera in the subfamily Diploproctodaeinae.

1. Genus *Bianium* Stunkard, 1930

- Bianium* Stunkard, 1930 [16], p. 363 (type species, *Psilostomum plicatum* Linton, 1928 [19]).
- Diploporus* Ozaki, 1928 [12], preoccupied, partim, pp. 24–25 (type species, *D. hemistoma* Ozaki, 1928, by subsequent designation).
- Diploporeta* Strand, 1942 [23], renamed, partim, p. 387 (type species, not designated).
- Amarocotyle* Travassos, Freitas et Bührnheim, 1965 [24], p. 70 (type species, *A. simonei* Travassos *et al.*, 1965).

1-1. *B. hemistoma* (Ozaki, 1928) Yamaguti, 1934 (Fig. 7)

- Diploporus hemistoma* Ozaki, 1928 [12], pp. 25–29, figs. 13–15.
- Bianium hemistoma*: Yamaguti, 1934 [20], pp. 525–526.
- Bianium holocentri* Yamaguti, 1942 [25], pp. 357–359, fig. 14.
- Diploporeta hemistoma*: Strand, 1942 [23], p. 387.
- Bianium hemistomum*: Manter, 1947 [26], p. 280.
- Diploproctodaeum hemistoma*: Sogandares-Bernal and Hutton, 1958 [4], p. 566.
- Diploproctodaeum holocentri*: Sogandares-Bernal and Hutton, 1958 [4], p. 566.

Material studied. 1) Lot 1. 17 gravid whole-

mounts of "*Maculifer*" from *Takifugu pardalis* (= *Spheroides p.*) (Teleostei: Tetraodontidae) and 3 sectioned gravid specimens of "*Hemistomum*" (unpublished?, MPM Coll. No. 30016) in Ozaki's collection (other data not given).

2) Lot 2. 1 gravid whole-mount of *B. hemistoma* (MPM Coll. No. 22212) of Yamaguti [20] from the intestine of *Spheroides* sp. from Tokoname (Ise Bay), Aichi Prefecture, on April 19, 1929.

3) Lot 3. 2 immature whole-mounts (MPM Coll. No. 22208) in Yamaguti's collection from the intestine of *T. pardalis* from Hamajima, Mie Prefecture on April 14, 1941. (These were identified as *Bianium* on the label by Sh. Kamegai on April 19, 1972).

4) Lot 4. 6 gravid whole-mounts (MPM Coll. No. 22206) of *B. hemistoma* in the same collection from the intestine of *Spheroides* sp. from Shibukawa (prefecture unknown) on April 29, 1957.

5) Lot 5. 1 gravid whole-mount (NSMT-PI 2879) of *B. hemistoma* of Shimazu and Nagasawa [1] from the intestine of *T. pardalis* from Moroiso Bay on October 16, 1978.

6) Lot 6. 26 immature and 35 gravid whole-mounts (NSMT-PI 3119–3120) collected by Ogawa from the intestine of the same species of fish from Hagi, Yamaguchi Prefecture, on May 20 and 22, 1986.

7) Lot 7. 3 immature and 6 gravid whole-mounts (NSMT-PI 3121) collected by him from the intestine of the same species of fish from Nomo, Nagasaki Prefecture, on June 18, 1986.

8) Lot 8. 18 gravid whole-mounts (NSMT-PI 3123) collected by him from the intestine of *T. poecilonotus* from Nomo on June 19, 1986.

9) Lot 9. 3 immature and 41 gravid whole-mounts (NSMT-PI 3122) collected by him from the intestine of the same species of fish from Hagi on April 21, 1987.

10) Lot 10. 6 immature and 87 gravid whole-mounts (NSMT-PI 3124–3126) collected by him from the intestine of *T. vermicularis* from Hagi on May 20–21, 1986, and April 21, 1987.

11) Lot 11. 8 immature and 10 gravid whole-mounts (MPM Coll. No. 22205) of *B. hemistoma* in Yamaguti's collection from *T. niphobles* from Tokoname on April 15, 1941.

12) Lot 12. 1 gravid whole-mount (NSMT-PI

3127) collected by Ogawa from the intestine of the same species of fish from Hagi on April 22, 1987.

13) Lot 13. 11 (9 whole-mounted and 2 sectioned) gravid specimens (NSMT-PI 3128–3129) found in the intestine of the same species of fish from Moroiso Bay on July 22–23, 1987.

14) Lot 14. 1 gravid whole-mount (MPM Coll. No. 22213) of *B. hemistoma* in Yamaguti's collection from the intestine of *Stephanolepis cirrhifer* (Monacanthidae) from Tarumi, Hyogo Prefecture, on August 27, 1936.

15) Lot 15. 24 gravid whole-mounts (NSMT-PI 1013) collected by Machida from the intestine of the same species of fish from Nan'yofukaura on May 25, 1972.

16) Lot 16. 1 gravid whole-mount (holotype and only specimen, MPM Coll. No. 22207) of *B. holocentri* of Yamaguti [25] from the intestine of *Holocentrus spinosissimus* [= *Adioryx s.*] (Holocentridae) from Tokushima, Tokushima Prefecture, on July 5, 1940.

Description. Ozaki [12] published a full description of this species. He described and illustrated the anterior glandular portion of the body as dilated and shovel- or spoon-shaped. However, Yamaguti [11, 20, 27] pointed out that the lateral edges of the portion are completely separated posteriorly from each other, which has been confirmed by the present examination. The following concerns lots 1–15. Fine eyespot pigments were dispersed on each side of the pharynx. The oral sucker was always smaller than the ventral sucker, the sucker width ratio being 1:1.31–1.80. In a few specimens of lot 10, a considerable atrophy was seen in either one or both testes, and the male terminal duct and cirrus pouch were lacking in their anterior parts in one specimen. Shimazu and Nagasawa's [1] pluglike structure was present in the sheathlike proximalmost part of the ejaculatory duct in all the specimens examined with a few exceptions (Fig. 7). The pars prostatica was elastic and appeared to be bipartite: The proximal portion had more finely granular internal cells; and the distal, more coarsely. The male terminal duct (ejaculatory duct and cirrus) was long, invaginating or evaginating, and sometimes much convoluted. The vitelline follicles were distributed anteriorly to the ventral sucker zone in most of the

specimens examined; but in some specimens of lots 5, 9 and 13, they extended anteriorly farther than it along each side of the ventral sucker to almost the pharyngeal level and occasionally were confluent in front of the ventral sucker. Eggs measured 60–76 by 32–47 μm in balsam. Lot 16 was described in detail by Yamaguti [25]. The present reexamination has shown that in it, the pluglike structure is present as well, and the male terminal duct is a little shorter and more straight than in the others.

Discussion. Ozaki [12] described this species from the intestine of *S. pardalis* from Takamatsu, Kagawa Prefecture. He deposited the holotype (No. p. 283) at the Zoological Institute, Science Faculty, Tokyo Imperial University, but most presumably it has already been lost. It is uncertain whether lot 1 is part of the type material. Yamaguti [20] obtained the species (lot 2) from the intestine of various species of *Spheroides* from Mutu, Toyama and Ise bays and the Inland Sea. Later, he [27] briefly described it from *S. pardalis* (other data not given). His specimens have not yet been specified. Shimazu and Nagasawa [1] recorded it (lot 5) from the same species of fish from Moroiso Bay, Misaki.

Ozaki [12] described the vitelline follicles as commencing from the level of the genital pore (or just behind the ventral sucker). Yamaguti [27] observed that they begin in the ventral sucker zone in the majority of cases, and occasionally a little in front of it. He [25] proposed a new species, *B. holocentri* (lot 16), distinguishing it from the most closely related species, *B. hemistoma*, by the anterior extent of the vitellaria (reaching anteriorly to the pharyngeal level, Fig. 14, instead of to the ventral sucker level [12]) and the egg size (66–72 by 39–42 μm instead of 74–81 by 48–52 μm [12]). Stating that no differential character can be found in the anterior extent of the vitellaria between *B. holocentri* and *B. hemistoma* and that the egg size is very variable in other species of *Bianium*, Caballero *et al.* [28] considered that *B. holocentri* is synonymous with *B. hemistoma*. According to Sogandares-Bernal and Hutton [29] and Gupta [30], however, *B. holocentri* is valid, and they [28] apparently confused the anterior parenchymal gland cells figured by Ozaki [12] with the vitelline follicles. The sucker width ratio is 1:1.87 (calcu-

lated from Yamaguti [25] in *B. holocentri*. In *B. hemistoma*, the ratio is 1:1.31–1.80 (this paper); the eggs are 66–72 by 33–39 μm in life [27] and 60–76 by 32–47 μm in balsam (this paper); and sometimes the vitellaria extend anteriorly as far as the pharyngeal level and are confluent in front of the ventral sucker (this paper). The male terminal duct in *B. holocentri* is a little shorter and more straight than in *B. hemistoma*. These differences are very slight. I concur with Caballero *et al.* [28] in reducing *B. holocentri* to a synonym of *B. hemistoma*.

2. Genus *Diploproctodaeum* La Rue, 1926

Diploproctodaeum La Rue, 1926 [3], p. 208 (type species, *Hemistomum haustum* MacCallum, 1919 [3]).
Diploporus Ozaki, 1928 [12], preoccupied, partim, pp. 24–25 (type species, *D. hemistoma* Ozaki, 1928, by subsequent designation).
Diploporetta Strand, 1942 [23], renamed, partim, p. 387 (type species, not designated).

2-1. *D. cryptostoma* (Ozaki, 1928) Sogandares-Bernal *et* Hutton, 1958

Diploporus cryptostoma Ozaki, 1928 [12], pp. 30–32, figs. 16–17.
Bianium cryptostoma: Yamaguti, 1934 [20], pp. 525–526; Manter, 1940 [2], p. 377.
Diploporetta cryptostoma: Strand, 1942 [23], p. 387.
Bianium cryptostomum: Manter, 1947 [26], p. 280.
Diploproctodaeum cryptostoma: Sogandares-Bernal and Hutton, 1958 [4], p. 566.

Material studied. 1) Lot 1. 17 gravid whole-mounts of “*Diploproctodaeum*” and 3 sectioned gravid specimens of “*Hemistomum*” (unpublished?, MPM Coll. No. 30015) in Ozaki’s collection (other data not given).

2) Lot 2. 2 sectioned gravid specimens (unpublished, MPM Coll. No. 22209) of *B. cryptostoma* in Yamaguti’s collection from the intestine of *Spheroides* sp. on October 14 and 24, 1936 (locality not given).

3) Lot 3. 1 or 2 sectioned gravid specimens (unpublished, MPM Coll. No. 22210) of *B. cryptostoma* in the same collection from the intestine of *Spheroides* sp. from Maisaka, Shizuoka Prefecture, on April 12 (year not given).

4) Lot 4. 4 gravid whole-mounts (unpublished,

MPM Coll. No. 22211) of *B. cryptostoma* in the same collection from the intestine of *Canthigaster rivulata* (Tetraodontidae) from Katase, Kanagawa Prefecture, on June 7, 1958.

Description. The present examination has verified Ozaki's [12] observation that the lateral edges of the anterior glandular portion of the body are united posteriorly. The following supplements his original description: fine eyespot pigments dispersed in forebody; prepharynx short; oral sucker usually slightly larger than ventral sucker; sucker width ratio 1:0.9–1.09; esophagus short; internal seminal vesicle elliptical; pars prostatica globular; pluglike structure absent in proximal part of ejaculatory duct; ejaculatory duct and cirrus thick, straight, protrusible; genital pore sinistrosymmetric, bifurcal or a little posterior to it; ovarian lobes numbering to about 30; eggs in uterus measuring 67–80 by 40–47 μm in balsam; and vitellaria distributed anteriorly to ventral sucker level to midpharyngeal level, may or may not be confluent in front of ventral sucker.

Discussion. This species has previously been described as *Diploporus cryptostoma* only once by Ozaki [12] from egg-bearing worms found in the intestine of *Spheroides pardalis* from Takamatsu, Kagawa Prefecture. He missed the egg size out of his description. According to him, the species was found together with *B. hemistoma*, but much less frequently, in the fish. Most probably the holotype (No. p. 284) deposited by him at the Zoological Institute, Science Faculty, Tokyo Imperial University, has already been lost. It is uncertain whether lot 1 is the component of the type series. Shimazu and Nagasawa's [1] trematode of *B. cryptostoma* has been described as a new species (see above).

Yamaguti evidently obtained the trematode that he identified as *B. cryptostoma* at least once as late as 1936 and subsequently at least twice. Nevertheless he did not mention a word about this species in his publications somehow. The combination for the species, *B. cryptostoma*, which Manter [2] used as well, is due to Yamaguti [20], because he first made *Diploporus* a synonym of *Bianium*.

In this species the lateral edges of the anterior glandular portion of the body are united posteriorly. I agree with Sogandares-Bernal and Hutton [4]

who transferred the species from *Diploporus* to *Diploproctodaeum* as *D. cryptostoma* (Ozaki, 1928). Manter [26] listed a new combination, *B. cryptostomum* (Ozaki, 1928), for the species, which accordingly is untenable.

2-2. *D. hakofugu* sp. n.

See this paper.

2-3. *D. oviforme* sp. n.

See this paper.

2-4. *Diploproctodaeum* sp. of Machida (1986)

Machida [31] obtained this trematode from the intestine of *Aluterus monoceros* and *A. scriptus* (Monacanthidae) from southern Japanese waters. He assumed it to be *D. haustorium*. It may possibly be that he had more than one species. There has not yet appeared a full description of the trematode.

ACKNOWLEDGMENTS

I wish to thank the following persons for kindly permitting me to study their unpublished specimens or lending me the specimens or both: Mr. Shunya Kamagai, the MPM, Tokyo; Dr. Masaaki Machida, the NSNT; and Dr. Kazuo Ogawa, University of Tokyo, Tokyo. Thanks are also due to Dr. Makoto Shimizu, University of Tokyo, for providing me with the fish examined; and Dr. L. Margolis, Pacific Biological Station, Nanaimo, Canada, for the photocopy of the reference.

REFERENCES

- Shimazu, T. and Nagasawa, K. (1985) Trematodes of marine fishes from Morois Bay, Misaki, Kanagawa Prefecture, Japan. *J. Nagano-ken Jun. Coll.*, (40): 7–15.
- Manter, H. W. (1940) Digenetic trematodes of fishes from the Galapagos Islands and the neighboring Pacific. *Rep. Allan Hancock Pacific Exped.* (1932–1938), 2: 325–497.
- La Rue, G. R. (1926) A trematode with two ani. *J. Parasitol.*, 12: 207–209.
- Sogandares-Bernal, F. and Hutton, R. F. (1958) The status of the trematode genus *Bianium* Stunkard, 1930, a synonym of *Diploproctodaeum* La Rue, 1926. *J. Parasitol.*, 44: 566.
- Oshmarin, P. G., Mamaev, Yu. L. and Parukhin, A. M. (1961) New species of trematodes of the family Diploproctodaeidae Ozaki, 1928. *Helmintho-*

- logia, 3: 254-260. (In Russian with English summary)
- 6 Reimer, L. W. (1981) Lepocreadiidae (Digenea) aus Fischen der Küste von Moçambique. *Angew. Parasitol.*, **22**: 204-212.
 - 7 Nasir, P. (1976) Morfologia comparada de genitalia terminal en cuatro especies de trematodos digeneticos (Lepocreadiidae). In "Resumen de Trabajos Libres. Congreso (IV) Latinoamericano de Parasitología, etc.", San José, Costa Rica, 7-11 Dec., 1976". Federación Latinoamericana de Parasitólogos; Asociación Costarricense de Microbiología y Parasitología, Costa Rica, p. 77. Cited by Helminthol. Abst., Ser. A (1977), **46**: 759-760.
 - 8 Mamaev, Yu. L. (1970) [Helminths of some commercial fishes in the Gulf of Tonkin.] In "[Helminths of Animals of South-Eastern Asia]". Ed. by P. G. Oshmarin, Yu. L. Mamaev and B. I. Lebedev, Izdatel'stvo AN SSSR, Moskva, pp. 127-190. (In Russian)
 - 9 Parukhin, A. M. (1979) New species of trematodes of fishes from the Indian Ocean and the Red Sea. *Parazitologiya*, **13**: 639-643. (In Russian with English summary)
 - 10 MacCallum, G. A. (1919) Notes on the genus *Telorchis* and other trematodes. *Zoopathologica*, **1**: 77-98 (1918).
 - 11 Yamaguti, S. (1970) Digenetic Trematodes of Hawaiian Fishes. Keigaku Publishing, Tokyo, 436 pp.
 - 12 Ozaki, Y. (1928) On some trematodes with anus. *Jpn. J. Zool.*, **2**: 5-33.
 - 13 Fischthal, J. H. and Thomas, J. D. (1970) Digenetic trematodes of marine fishes from Ghana: Family Lepocreadiidae. *J. Helminthol.*, **44**: 365-386.
 - 14 Nasir, P. and Gomez, Y. (1977) Digenetic trematodes from Venezuelan marine fishes. *Riv. Parasitol.*, **38**: 53-73.
 - 15 Park, J. T. (1939) Fish trematodes from Työsen. II. Some new digenetic trematode parasites from marine fishes. *Keizyō J. Med.*, **10**: 7-18, pl. 2.
 - 16 Stunkard, H. W. (1930) Another trematode with two anal openings. *Anat. Rec.*, **47**: 363.
 - 17 Gupta, A. N. (1967) *Anterovitellosus indicum* gen. et sp. n., from globe fish *Tetraodon viridipunctatus* (Günther [sic]) from India, with discussion on its systematic position in the subfamily Diploproctodaeinae Park, 1939. *Ciencia, Méx.*, **25**: 215-218.
 - 18 Madhavi, R. (1972) Digenetic trematodes from marine fishes of Waltair coast, Bay of Bengal. I. Family Lepocreadiidae. *J. Parasitol.*, **58**: 217-225.
 - 19 Stunkard, H. W. (1931) Further observations on the occurrence of anal openings in digenetic trematodes. *Z. Parasitenkd.*, **3**: 713-725.
 - 20 Yamaguti, S. (1934) Studies on the helminth fauna of Japan. Part 2. Trematodes of fishes, I. *Jpn. J. Zool.*, **5**: 249-541.
 - 21 Yamaguti, S. (1971) Synopsis of Digenetic Trematodes of Vertebrates. Keigaku Publishing, Tokyo, 2 vols., 1074 pp., 349 pls.
 - 22 Nahhas, F. M. and Cable, R. M. (1964) Digenetic and aspidogastriid trematodes from marine fishes of Curaçao and Jamaica. *Tulane Stud. Zool.*, **11**: 169-228.
 - 23 Strand, E. (1942) Miscellanea nomenclatorica zoologica et palaeontologica. X. *Folia Zool. Hydrobiol.*, Riga, **11**: 386-402. (In German)
 - 24 Travassos, L. P., Teixeira de Freitas, J. F. and Bühn-heim, P. F. (1965) Trematódeos de peixes do litoral capixaba: *Amarocotyle simonei* gen. n., sp. n., parasito de baiacu. *Atas Soc. Biol. Rio de Janeiro*, **9**: 69-73.
 - 25 Yamaguti, S. (1942) Studies on the helminth fauna of Japan. Part 39. Trematodes of fishes mainly from Naha. *Trans. Biogeogr. Soc. Jpn.*, **3**: 329-398, pl. 24.
 - 26 Manter, H. W. (1947) The digenetic trematodes of marine fishes of Tortugas, Florida. *Am. Midl. Natur.*, **38**: 257-416.
 - 27 Yamaguti, S. (1951) Studies on the helminth fauna of Japan. Part 48. Trematodes of fishes, X. *Arb. Med. Fak. Okayama*, **7**: 315-334, pls. 1-2.
 - 28 Caballero y C., E. C., Bravo-Hollis, M. and Grocott, R. G. (1952) Helminths of la República de Panamá. III. Tres trematódeos de peces marinos con descripción de una nueva especie. *Ann. Inst. Biol. Méx.*, **23**: 167-180.
 - 29 Sogandares-Bernal, F. and Hutton, R. F. (1959) Studies on helminth parasites from the coast of Florida. III. Digenetic trematodes of marine fishes from Tampa and Boca Ciega bays. *J. Parasitol.*, **45**: 337-346.
 - 30 Gupta, A. N. (1968) Studies on the genus *Bianium* Trematoda (Digenea) with description of three new species and discussion on status of genera *Diploproctodaeum* La Rue, 1926, *Bianium* Stunkard, 1930, and *Diplocreadium* Park, 1939. *Jpn. J. Parasitol.*, **17**: 139-148.
 - 31 Machida, M. (1986) Trematodes from fishes of the genus *Aluterus* in Japanese waters. *Jpn. J. Parasitol.*, **35** (Suppl.): 140. (In Japanese)

Electrophoretic Study on the Phylogenetic Relationships among Six Species of Sea-Urchins of the Family Echinometridae Found in the Japanese Waters

NORIMASA MATSUOKA¹ and HIROBUMI SUZUKI²

Department of Biology, Faculty of Science, Hirosaki University,
Hirosaki 036, Japan

ABSTRACT—The family Echinometridae of the order Echinoida found in the Japanese waters is represented by six sea-urchin species belonging to the five different genera. They are *Anthocardis crassispina*, *Echinometra mathaei*, *Echinostrephus aciculatus*, *Echinostrephus molaris*, *Heterocentrotus mammillatus* and *Colobocentrotus mertensii*. The phylogenetic and evolutionary relationships among these six members of this family were investigated by electrophoretic analyses of 18 different enzymes. The biochemical dendrogram for the six species constructed from the Nei's genetic distances between species for 26 genetic loci showed the following: (1) *H. mammillatus* and *C. mertensii* are largely genetically differentiated from the other four species, and these two species are considered to be more primitive sea-urchins among echinometrids from the molecular estimation of their divergence time. (2) *A. crassispina* endemic to Japan is more closely related to *Echinometra* than to *Echinostrephus*, and it is estimated that *Anthocardis* has speciated in relatively recent geological age of the late Pliocene. (3) The two morphologically very similar species of *Echinostrephus* (*E. aciculatus* and *E. molaris*) are little genetically differentiated from each other, and therefore these two may belong to one and the same species. These electrophoretic results are discussed through the detailed comparison with other molecular and non-molecular results.

INTRODUCTION

The echinoid fauna of the seas around Japan is remarkably abundant and about 160 species have been ascertained by Shigei [1]. Under such richness in forms, the taxonomy of the echinoids has been extensively studied from the morphological and/or paleontological standpoints [1-4]. However, many unresolved problems concerning the phylogenetic and evolutionary relationships among echinoids still remain [4]. For a elucidation of these problems, it is necessary to introduce actively the different methods from the traditional and usual morphological method (e.g., biochemical or cytogenetical approach) into the echinoid taxonomy. We have been investigating the phylogenetic relationships among echinoids found in

the seas around Japan by the electrophoretic analyses of various enzymes and by the immunological techniques such as enzyme inhibition test [5-11]. Such molecular approaches make possible for us to estimate the phylogenetic relationships among taxa and their evolutionary process quantitatively with the common parameters such as enzymes or DNA, and they have been providing much valuable, and in some cases critical, information on the field of echinoid taxonomy. In the previous papers, one of the present authors (N.M.) reported on the biochemical systematics of the sea-urchins of the two families, Toxopneustidae and Strongylocentrotidae, of the order Echinoida by the electrophoretic analyses of various enzymes [7, 9]. Another large family of the order Echinoida is the Echinometridae and the phylogeny within this family has not yet been examined biochemically. In the present study, we therefore have attempted an electrophoretic study to clarify the phylogenetic relationships among the members of the family Echinometridae.

Accepted August 3, 1988

Received June 24, 1988

¹ To whom reprint requests should be addressed.

² Present Address: Research Department, Olympus Optical Co., Ltd., Ishikawa-cho, Hachioji 192, Japan.

At present, the family Echinometridae in the seas around Japan is represented by six species belonging to five genera. They are *Echinostrephus aciculatus* A. Agassiz, *E. molaris* (Blainville), *Anthocidaris crassispina* (A. Agassiz), *Echinometra mathaei* (Blainville), *Heterocentrotus mammillatus* (Linnaeus) and *Colobocentrotus mertensii* Brandt [1]. *A. crassispina* is an endemic Japanese species, but the other five species are widely distributed over the tropical and subtropical regions of the Indo-West Pacific, all of which are commonly found in shallow water. The Echinometridae is a tropical family and distinguished morphologically from other families of the order Echinoida by the valve of globiferous pedicellariae, the body skeleton of first larval stage and the optical crystal axis of calcite of coronal plate [4]. Although each of the five genera of this family is characterized by the highly specialized external form, it is considerably difficult to establish their phylogenetic relationships or the sequence of their evolutionary divergence by the morphological criteria. Further, there is little quantitative information available concerning the genetic differentiation among these members of this family.

In this paper, we report on the results of an electrophoretic investigation designed to clarify the phylogenetic relationships among the six members of the family Echinometridae found in the Japanese waters.

MATERIALS AND METHODS

Sea-urchins

The sea-urchins examined in this study were the six species belonging to the five different genera of the family Echinometridae: *Anthocidaris crassispina*, *Echinometra mathaei*, *Echinostrephus aciculatus*, *Echinostrephus molaris*, *Heterocentrotus mammillatus* and *Colobocentrotus mertensii*. The specimens of *A. crassispina* were the same as those used in our previous population genetic study [11]: 118 individuals were collected from the six different localities (Fukaura, Aomori Pref.; Noto, Ishikawa Pref.; Tsuruga, Fukui Pref.; Misaki, Kanagawa Pref.; Shirahama, Wakayama Pref. and Tanegashima, Kagoshima Pref.) from July 1983 to

August 1986. More recently, it has been found that on Okinawan reef flats *E. mathaei* consists of four different types (A, B, C, and D-types) and they are distinguishable by color pattern of spines, shape of spicules, distribution pattern and habitat preference, etc. each other [12, 13]. In this study, we used 10 individuals of A-type of *E. mathaei*, which were collected from Minatogawa in the main land of Okinawa Pref. in March 1986. *E. aciculatus* and *E. molaris* were the same as those used in our previous electrophoretic study [10]: the former was collected from Kushimoto and Shirahama of Wakayama Pref. in August, 1983 and 1984, and the latter from Sesoko-jima of Okinawa Pref. in July 1983 and February 1986. The number of individuals examined was 32 for *E. aciculatus* and 14 for *E. molaris*. *H. mammillatus* was collected from the coast near the Sesoko Marine Science Center, the University of the Ryukyus, in Sesoko-jima of Okinawa Pref. in July 1983. The number of individuals examined was 4. *C. mertensii* was collected from two different localities: 2 individuals from Izeki and Kubota in the northeast coast of Tanegashima, Kagoshima Pref., in August 1985, and 3 individuals from Uka in the northern coast of the main land of Okinawa Pref. in February 1986. Immediately after collection, the guts and gonads were extracted from these specimens and exhaustively washed in filtered sea-water. They were then frozen on dry ice and transported to the laboratory at Hiroaki University, where they were stored at -80°C until used.

Electrophoresis

Electrophoresis was performed on 7.5% polyacrylamide gels by the method of Davis [14] using a disc gel apparatus consisted of 12 plastic columns (the size of one column: $3 \times 11 \times 75$ mm) as described previously [7, 10]: About 0.2 g of gut or gonad was separately homogenized using a small polyethylene homogenizer of the Potter-Elvehjem type with 3 vols of cold 20 mM phosphate buffer (pH 7.0) containing 0.1 M KCl and 1 mM EDTA in an ice-water bath. After centrifugation at 10,000 rpm for 10 min, 0.04–0.1 ml of the clear supernatant was used for polyacrylamide gel electrophoresis. After electrophoresis, the gels were stained for the following 18 different enzymes:

alcohol dehydrogenase (ADH), glucose-6-phosphate dehydrogenase (G6PD), hexose-6-phosphate dehydrogenase (H6PD), hydroxybutyrate dehydrogenase (HBDH), malate dehydrogenase (MDH), malic enzyme (ME), nothing dehydrogenase (NDH), octanol dehydrogenase (ODH), sorbitol dehydrogenase (SDH), xanthine dehydrogenase (XDH), superoxide dismutase (SOD), hexokinase (HK), aspartate aminotransferase (AAT), alkaline phosphatase (ALK), esterase (EST), peroxidase (PO), amylase (AMY) and leucine amino peptidase (LAP). Five enzymes (G6PD, H6PD, HK, AAT and ALK) were assayed with the supernatant of homogenate of the gonad, and the remaining 13 enzymes with that of the gut. Stain recipes for these enzymes have been described previously [7, 9, 10].

RESULTS

The electrophoretic patterns of the 18 different enzymes observed in the 6 sea-urchin species of the family Echinometridae are diagrammatically

shown in Figure 1. From these band patterns, we assumed 26 genetic loci. The major features of variation in the 18 enzymes are summarized as follows.

Eight enzymes (ADH, G6PD, H6PD, HBDH, HK, NDH, SDH and XDH) exhibited a single band of activity and were monomorphic, all but NDH and XDH varying interspecifically. In the course of this study, ADH could not be scored in *C. mertensii*, though the cause of this enzymatic inactivity was not known.

PO in *E. mathaei*, AAT in the two *Echinostrephus* species and ALK in the five species except *C. mertensii* showed double-banded phenotypes. These three enzymes in the other species showed single-banded phenotypes. The two and one band pattern in these enzymes were interpreted as the products of different alleles at a single locus. These enzymes were monomorphic in each species.

ME consistently appeared as two active bands, of which the faster band showed higher activity. The mobilities of the two bands in *H. mammillatus*

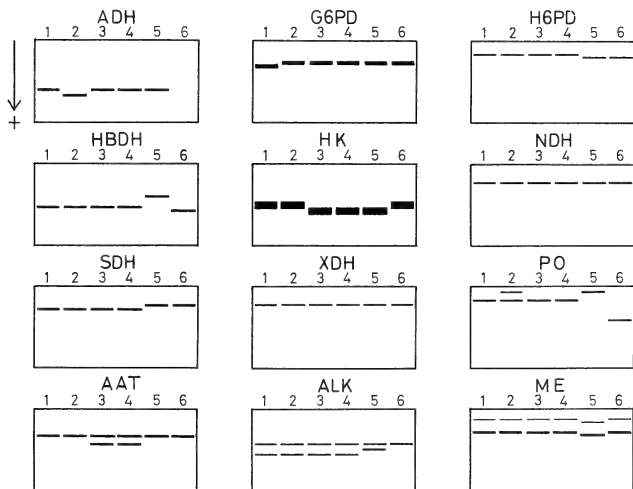


FIG. 1-a.

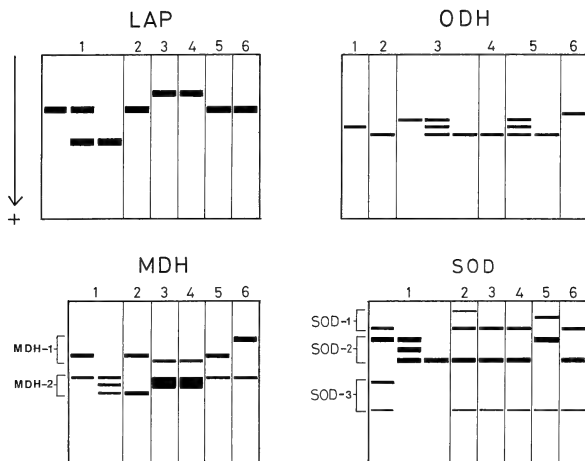


FIG. 1-b.

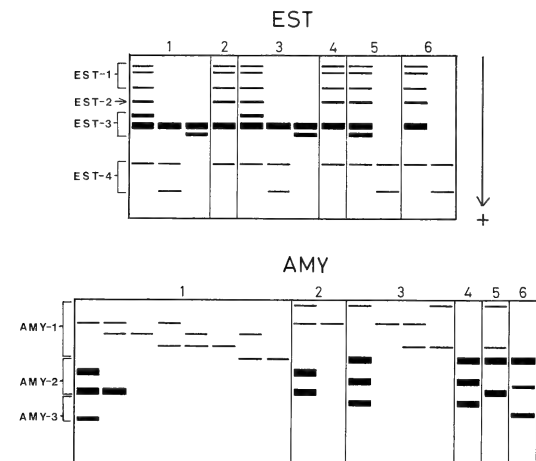


FIG. 1-c.

FIG. 1. a-c. Electrophoretic patterns of 18 different enzymes in six species of sea-urchins of the family Echinometridae. For each enzyme the origin is at the top and the direction of mobility toward the bottom. Presumptive genetic loci are numbered downwards from 1, starting with that nearest the origin (i.e., of lowest electrophoretic mobility). 1=*Anthocidaris crassispina*, 2=*Echinometra mathaei*, 3=*Echinostrephus aciculatus*, 4=*Echinostrephus molaris*, 5=*Heterocentrotus mamillatus*, 6=*Colobocentrotus mertensii*.

[COMMUNICATION]

Immunohistochemical Study of the Ultimobranchial Gland in Chum Salmon Fry

YUICHI SASAYAMA, KOUHEI MATSUDA, CHITARU OGURO
and AKIRA KAMBEGAWA¹

Department of Biology, Faculty of Science, Toyama University, Toyama 930, and

¹Department of Obstetrics and Gynecology, Faculty of Medicine,
Teikyo University, Tokyo 173, Japan

ABSTRACT—The ultimobranchial gland (UBG) in fry of the chum salmon, *Onchorhynchus keta*, was studied immunohistochemically using the peroxidase-anti-peroxidase method. In the embryo at 3 days before hatching, some of the parenchymal cells of the gland showed a weak immunoreaction to anti-salmon calcitonin antiserum. These calcitonin-immunoreactive cells gradually increased in both number and stainability during larval development. In these fry, however, the scales and hard bones on which calcitonin might act have not yet formed. The significance of calcitonin production in salmon fry is discussed.

INTRODUCTION

In mammals, calcitonin is a hormone that controls the mineralization of bones by depressing the resorption of calcium from hard tissues. It is well known that this action of calcitonin is more prominent in young animals than in old ones. In teleosts, calcitonin is secreted from the ultimobranchial gland (UBG). In this animal group, however, the physiological role of the UBG is in dispute because no clear conclusions have been obtained so far in spite of various studies [1]. In the present investigation, the UBG of fry of the chum salmon, *Onchorhynchus keta*, was examined immunohistochemically, in order to obtain fundamental data for elucidating the function of the teleost UBG.

MATERIALS AND METHODS

The fry were collected at the Jintsuu-gawa Salmon Hatchery once a week for 4 months from December, 1985, to March, 1986. The sampling was performed on individuals from 3 days before hatching up to the time of fry-liberation at 11 weeks after hatching. The individuals obtained were fixed in Bouin's solution without acetic acid for 5 hr on a shaker. The anterior part of the body of each specimen was cut off, then dehydrated and embedded in paraffin, followed by sectioning at a thickness of 6 μ m. On mounting the serial sections on slide glasses, the region that was considered to include the UBG was divided into 2 groups, each group including an equal proportion of the tissue from one individual [2]. Initially, on the slide glass, the exact location of the UBG was examined in one group by staining with Delafield's hematoxylin and eosin. Then, the other group was subjected to immunohistochemical examination for detection of immunoreactive calcitonin using the peroxidase-antiperoxidase (PAP) method of Sternberger [3].

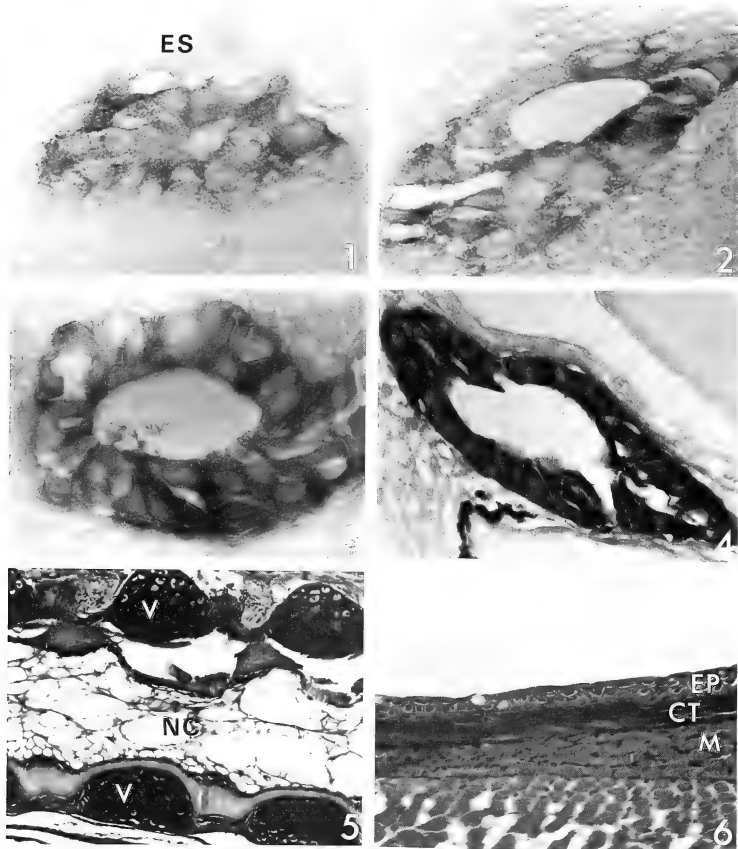
Immunohistochemical procedures were done as follows. Anti-calcitonin antiserum was raised in rabbits by injections of synthetic salmon calcitonin (Teikokuzoki)-BSA conjugate. Sections were incubated with the antiserum (diluted 1:20,000) for 12 hr at room temperature. The sites of antigen-antibody reaction were localized using anti-rabbit

IgG porcine serum (1:20; Dako) for 30 min followed by incubation with PAP (1:50; Dako) for 30 min. Finally, sections were treated with 0.05 M Tris-HCl buffer (pH 7.6) containing 3,3'-diaminobenzidine tetrahydrochloride-H₂O₂ solution. The specificity was checked using normal rabbit serum in place of the primary antiserum, and using primary antiserum inactivated by addition of an excess amount of synthetic salmon calcitonin

(1.25 µg/ml of anti-calcitonin antiserum).

RESULTS

In the embryo at 3 days before hatching, the UBG has already differentiated bilaterally just beneath the esophagus, appearing as two cell masses. Some of the parenchymal cells showed a weak immunoreaction to the anti-calcitonin anti-



serum (Fig. 1). In the emerged sac fry (so-called alevin), the UBG assumes a follicular arrangement. Until 4 weeks after hatching, the gland showed immunoreactivity in some parenchymal cells of UBG (Fig. 2). At 5 and 6 weeks after hatching, the immunoreactivity of the UBG became intensely. Until this time, sac fry remained lying on the artificial incubation bed. At 7 weeks after hatching, however, they sometimes showed more active movement. At this stage, most of the parenchymal cells of UBG were stained (Fig. 3). Between 8 and 9 weeks, artificial fry-food was given to fry which were able to swim more briskly. Until that time, the yolk sac had been almost exhausted. The UBG at these stages, which looked like a flat bag, exhibited strong immunoreaction (Fig. 4). There was no difference in stainability among the parenchymal cells themselves. Subsequently, the immunoreactivity of UBG remained unchanged until at least 11 weeks, when the fry were released into the sea.

DISCUSSION

The present study clarified that the UBG of the chum salmon produces immunoreactive calcitonin before hatching. Furthermore, it was shown that the number and stainability of calcitonin-immunoreactive cells increased gradually with growth of the fry. On the other hand, in the chick [4] and the snake [5, 6], it is known that the UBG is active only for a very short period around hatching. In the chick, it has been considered that the changes in blood pH accompanying the alteration in the breathing method at hatching may act as a trigger for increasing the activity of the UBG [4]. However, chum salmon juveniles respire not

through gills but the body surface from the embryonic period until the start of swimming. Therefore, it seems that in chum salmon fry, commencement of calcitonin production is not related to the change in breathing method.

On the other hand, in the rat [7], the frog and the salamander [8], it has been reported that the UBG is activated gradually with embryonic or larval development. In the amphibians, it has been suggested that the time of commencement of calcitonin production is related to bone growth. In teleosts, it has been shown that a highly active site of calcium metabolism is the scales [9]. Furthermore, it has been reported that in one kind of cichlid fish, synthetic salmon calcitonin stimulated the growth of skeletal bone and scales [10]. In chum salmon fry, however, no formation of either hard bones or scales was recognized, at least during the present observation period (Figs. 5 and 6). Therefore, it seems that in chum salmon fry, commencement of calcitonin production is not directly connected with the construction of hard tissues. In *Onchorynchum masou*, it is known that the scales are formed at the parr stage [11]. However, it is probable that the UBG accelerates the intake of calcium from the yolk or food into the growing cartilaginous skeleton. Alternatively, the UBG may suppress the reabsorption of calcium once it has been deposited in the parts that will develop into hard tissues at a later stage. Furthermore, there is also possibility that the UBG may not secrete the hormone until a suitable time.

ACKNOWLEDGMENTS

We wish to express our sincere thanks to Mr. Y. Tsuno, the Toyama Prefectural Fisheries Experiment

- FIG. 1. The ultimobranchial gland (UBG), composed of cellular masses at 3 days before hatching in a chum salmon embryo. Only some of the parenchymal cells exhibit a weak immunoreaction to the anti-salmon antiserum. ES: esophagus. PAP staining. $\times 1120$.
- FIG. 2. UBG, showing a follicular structure at 4 weeks after hatching. The calcitonin-immunoreactivity of some positive cells is still weak. PAP staining. $\times 1120$.
- FIG. 3. UBG, showing gradual increases in the immunoreactivity at 7 weeks after hatching. Most of the parenchymal cells are positive. PAP staining. $\times 860$.
- FIG. 4. UBG, showing a strong immunoreaction at 9 weeks after hatching. PAP staining. $\times 620$.
- FIG. 5. Sagittal section of the vertebral bones of a juvenile at 11 weeks after hatching. Note that the bones are composed of cartilaginous cells. V, vertebral bone; NC, notochord. HE staining. $\times 110$.
- FIG. 6. Sagittal section of the skin of a juvenile at 11 weeks after hatching. Note that the scales have not yet formed. EP, epidermis; CT, connective tissue; M, muscle. HE staining. $\times 220$.

Station, and to Mr. S. Matushima, Jintsuu-gawa Salmon Hatchery, for their kind cooperation on this work. The present study was supported in part by the Toyama Prefecture Centennial Foundation.

REFERENCES

- 1 Pang, P. K. T., Kenny, A. D. and Oguro, C. (1980) In "Evolution of Vertebrate Endocrine Systems". Ed. by P. K. T. Pang and A. Epplé, Texas Tech. Press, Lubbock, pp. 323-356.
- 2 Sasayama, Y., Matsuda, K., Oguro, C. and Kambe-gawa, A. (1986) *Zool. Sci.*, **3**: 911-914.
- 3 Sternberger, L. A. (1979) *Immunocytochemistry*, John Wiley and Sons, New York, 2nd ed.
- 4 Taylor, T. G., Balderstone, O., Baimbridge, K. G. and Lewis, P. E. (1975) In "Calcium-Regulating Hormones". Ed. by R. V. Talmage, M. Owen and J. A. Parsons, American Elsevier Publ., New York, pp. 116-118.
- 5 Yoshizawa, H., Suzuki, K., Yoshihara, M., Sasayama, Y. and Oguro, C. (1985) *Proc. 10th Ann. Meet. Jap. Soc. Comp. Endocrinol.*, Tokyo, Japan, p. 46.
- 6 Yoshihara, M., Uchiyama, M., Murakami, T., Ishizuka, K., Aoki, S., Itokuwa, S., Yoshizawa, H. and Oguro, C. (1986) *Proc. 11th Ann. Meet. Jap. Soc. Comp. Endocrinol.*, Tokyo Japan, p. 13.
- 7 Nitta, K., Kito, S., Kubota, Y., Girgis, S. I., Hill-yard, C. J., MacIntyre, I. and Inagaki, S. (1986) *Histochemistry*, **84**: 139-143.
- 8 Sasayama, Y., Matsuda, K., Oguro, C. and Kambe-gawa, A. (1985) *Zool. Sci.*, **2**: 977.
- 9 Mugiya, Y. and Watabe, N. (1977) *Comp. Biochem. Physiol.*, **57A**: 197-202.
- 10 Wendelaar Bonga, S. E. and Lammers, P. I. (1982) *Gen. Comp. Endocrinol.*, **48**: 60-70.
- 11 Kubo, T. (1980) *Sci. Rep. Hokkaido Salmon Hatchery*, **34**: 1-95. (in Japanese with English abstract)

[COMMUNICATION]

Calcitonin-Immunoreactive Cells found in the Extra-Ultimobranchial Areas of the Salamander, *Hynobius nigrescens*, during Larval Development

KOUHEI MATSUDA, YUICHI SASAYAMA, CHITARU OGURO
and AKIRA KAMBEGAWA¹

Department of Biology, Faculty of Science, Toyama University, Toyama 930, and

¹Department of Obstetrics and Gynecology, Faculty of Medicine,
Teikyo University, Tokyo 173, Japan

ABSTRACT—In the larva of the salamander, *Hynobius nigrescens*, calcitonin-immunoreactive cells were found dispersed in the epithelia of the pharynx, esophagus and the approach to the trachea, in addition to the ultimobranchial gland (UBG), where cells are known to normally exist. The time of appearance of the cells in the extra-UBG areas during larval development was synchronized with that of cells in the UBG. The total number of calcitonin-immunoreactive cells found in the extra-UBG areas was comparable to that of the cells composing the UBG.

INTRODUCTION

Calcitonin is a hormone secreted from the C-cells of the thyroid gland in mammals, or from the ultimobranchial gland (UBG) in sub-mammalian vertebrates. Recently, however, immunochemical and immunohistochemical studies have revealed that calcitonin exists in various tissues, for example, the nervous system [1-4], pituitary gland [5], cerebrospinal fluid [6], lung [7], digestive tract [8] and prostate gland [9]. These facts suggest that calcitonin present in areas other than the thyroid gland or the UBG may have some unknown roles, which are different from its original function of lowering the serum calcium level. Recently, we reported that in the salamander, *Hynobius nigrescens*, calcitonin-immunoreactive

cells are also distributed in the brain [10].

In the present study, calcitonin-immunoreactivity was also detected in the upper part of the digestive tract and the approach to the trachea in this salamander. The biological significance of this finding is discussed here.

MATERIALS AND METHODS

The eggs of salamander, *Hynobius nigrescens*, were collected in the mountainous area of Toyama Prefecture in March, 1985. They hatched out in April and had completed metamorphosis by July or August. The temperature was controlled so that it was close to that their native habitat (12-22°C). *Tubifex* worms or pieces of porcine liver were given as food. Developmental stages were determined according to Sawano's criteria for *Hynobius lichenatus* [11].

The larvae were fixed in Bouin's solution without acetic acid for 5 hr on a shaker. These materials were then dehydrated, embedded in paraffin and cut at a thickness of 6 µm. On mounting the sections on slide glasses, the region considered to include the UBG and various other tissues, was divided into 2 groups of specimens, each slide group including an equal proportion of tissues [12]. One group was subjected to immuno-histochemical examination. The other group was used to clarify the exact location of the calcitonin-

immunoreactive cells by staining with Delafield's hematoxylin and eosin.

The peroxidase-antiperoxidase method (PAP) of Sternberger [13] was used for detection of calcitonin. Anti-calcitonin antiserum was raised in rabbits by injections of synthetic salmon calcitonin (Teikokuzoki)-BSA conjugate. Sections were incubated with the primary antiserum (diluted 1:20,000) for 24 hr at room temperature. Then, those were treated with anti-rabbit IgG porcine serum (1:20; Dako) for 30 min. Subsequently, the sections were incubated with PAP (1:50; Dako). Finally, those were treated with 0.05 M Tris-HCl buffer (pH 7.6) containing 3,3'-diaminobenzidine

tetrahydrochloride and H_2O_2 solution. The specificity was checked using normal rabbit serum in place of the primary antiserum, and using primary antiserum inactivated by the addition of an excess amount of synthetic salmon calcitonin (1.25 $\mu\text{g/ml}$ of anti-calcitonin antiserum).

RESULTS AND DISCUSSION

At stage 45, when hind-limb primordia protrude outside the body, calcitonin-immunoreactive cells of extra-UBG areas were present in the epithelium of the pharynx (Fig. 1). At a slightly later stage (stage 47), these cells were also recognized in the

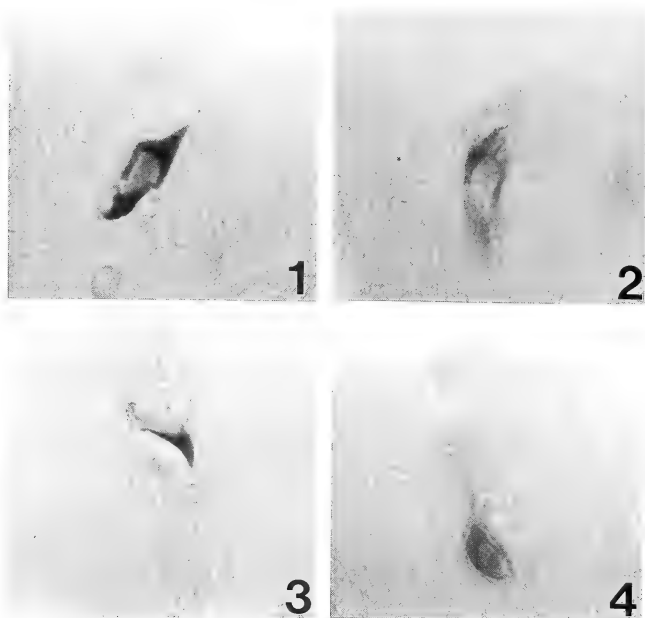


Fig. 1. Calcitonin-immunoreactive cell (iCT cell) present in the epithelium of the pharynx in the larva of a salamander at stage 45. PAP staining. $\times 1,120$.

Figs. 2 and 3. iCT cells present in the epithelia of the esophagus and the trachea, in that order, in salamander larvae at stage 47. PAP staining. $\times 1,120$.

Fig. 4. iCT cell present in the epithelium of the stomach in a metamorphosed salamander. PAP staining. $\times 1,120$.

epithelia of the esophagus and trachea (Figs. 2 and 3). In individuals just after metamorphosis, such cells were also found in the upper part of the stomach (Fig. 4). The time of occurrence of these positive cells was synchronized with that of the cells in the UBG (stage 45) [12]. In this salamander, it is known that the UBG differentiates from the pharyngeal floor at stage 40 just after hatching [12]. Therefore, it is probable that some of the calcitonin-producing cells, which become located in the UBG, are intermingled in the digestive tract and trachea. However, this phenomenon seems to be a normal process in this salamander, since positive cells were found in all individuals examined. The locations of calcitonin-immunoreactive cells present in extra-UBG areas are drawn schematically in Figure 5.

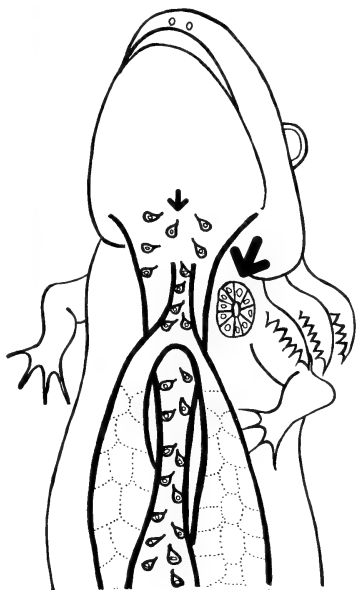


FIG. 5. Schematic drawing of the location of iCT cells in the larva of the salamander. Large arrow: UBG; small arrow: iCT cells distributed in extra-UBG areas.

In the present study, the numbers of calcitonin-immunoreactive cells in the UBG and extra-UBG areas were examined by counting their nuclei in the slide group subjected to immunohistochemical examination (Fig. 6). The number of these cells in the UBG was around 100 in the first half of metamorphosis (stage 47–57). Thereafter, the cells showed an acute increase in the latter half of metamorphosis (stages 60–66), and attained about 700 in individuals just after metamorphosis. On the other hand, also in extra-UBG areas, the number of these cells showed a change similar to that as seen in the UBG. Furthermore, the number sometimes exceeded the value for the UBG in the latter half of metamorphosis and in young individuals. In this salamander, it has been reported that hypocalcemic activity in the UBG is extremely low in comparison with other vertebrates [14]. Therefore, there is a possibility that these calcitonin-immunoreactive cells present in extra-UBG areas compensate for the paucity of UBG function.

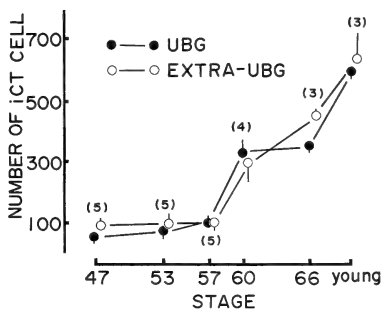


FIG. 6. Changes in the numbers of iCT cells in the UBG and extra-UBG areas during larval development of the salamander. The figures in parentheses show the numbers of animals examined. Vertical lines represent \pm SE.

On the other hand, it is known that in the monkey, the taste buds are distributed not only in the oral cavity but also in the entrance of the larynx and the upper part of the esophagus [15]. It is considered that these cells obtain information

for the opening and shutting of the larynx and esophagus when food passes through. In mammals, it has been discussed that calcitonin may participate in the control of gastrin and hydrochloric acid secretion in the stomach [16]. Therefore, it is interesting to speculate that in this salamander also, calcitonin-immunoreactive cells distributed in extra-UBG areas may act as receptors for certain digestive processes.

ACKNOWLEDGMENTS

The present study was supported in part by the Toyama Prefecture Centennial Foundation.

REFERENCES

- 1 Fischer, J. A., Tobler, P. H., Kaufmann, M., Born, W., Henke, H., Cooper, P. E., Sagar, S. M. and Martin, J. B. (1981) *Proc. Natl. Acad. Sci. USA*, **78**: 7801-7805.
- 2 Yui, R., Yamada, Y., Kayamori, R. and Fujita, T. (1981) *Biomedical Res.*, **2**: 208-216.
- 3 Girgis, S. I., Galan Galan, F., Arnett, T. R., Rogers, R. M., Bone, Q., Ravazzola, M. and MacIntyre, I. (1980) *J. Endocrinol.*, **87**: 375-382.
- 4 Fritsch, H. A. R., Van Noorden, S. and Pearce, A. G. E. (1979) *Cell Tiss. Res.*, **202**: 263-274.
- 5 Defetos, L. J., Burton, D., Bone, H. G., Catherwood, B. D., Parthemore, J. G., Moore, R. Y., Minick, S. and Guillemain, R. (1978) *Life Sci.*, **23**: 743-748.
- 6 Saggese, G., Bertelloni, S., Baronecelli, G. I., Abadessa, A., Macchia, P. and Battone, U. (1986) *Hormone Res.*, **23**: 177-180.
- 7 Galan Galan, F., Rogers, R. M., Girgis, S. I., Arnett, T. R., Ravazzola, M., Orci, L. and MacIntyre, I. (1981) *Acta Endocrinol.*, **97**: 427-432.
- 8 Fritsch, H. A. R., Van Noorden, S. and Pearce, A. G. E. (1982) *Cell Tiss. Res.*, **223**: 369-402.
- 9 DiSant'Agnese, P. A. (1986) *Arch. Pathol. Lab. Med.*, **110**: 412-415.
- 10 Sasayama, Y., Matsuda, K., Oguro, C. and Kambe-gawa, A. (1986) *Proc. 10th Ann. Meet. Jap. Soc. Comp. Endocrinol.*, Tokyo, Japan, p. 5.
- 11 Sawano, J. (1947) Normal table of the development of *Hynobius lichenatus*. Tsuru Publ., Sapporo. (In Japanese)
- 12 Sasayama, Y., Matsuda, K., Oguro, C. and Kambe-gawa, A. (1986) *Zool. Sci.*, **3**: 911-914.
- 13 Sternberger, L. A. (1979) *Immunocytochemistry*. John Wiley and Sons, New York, 2nd ed.
- 14 Oguro, C., Tarui, H. and Sasayama, Y. (1983) *Gen. Comp. Endocrinol.*, **51**: 272-277.
- 15 Khaisman, E. B. (1976) *Acta Anat.*, **95**: 101-115.
- 16 Chiba, T., Taminato, T., Kadowaki, S., Goto, Y., Mori, K., Seino, Y., Abe, H., Chihara, K., Matsukura, S., Fujita, T. and Kondo, T. (1980) *Gut*, **21**: 94-97.

[COMMUNICATION]

Juvenile Hormone Levels in *Bombyx* Larvae and Their Impairment after Treatment with an Imidazole Derivative KK-42

HIROMU AKAI and HEINZ REMBOLD¹

Sericultural Experiment Station, Ministry of Agriculture, Forestry and Fisheries, Tsukuba 305, Japan, and ¹Max-Planck-Institute for Biochemistry, 8033 Martinsried bei München, German Federal Republic

ABSTRACT—JH titers during the penultimate and last larval instars were identified and quantified by combined GC-selected ion monitoring MS. During the penultimate instar, considerable amounts of JH 1 and JH 2 were detected but JH 3 was undetectable. By contrast, neither JH 1 nor JH 2 was detectable in last larval instar, whereas JH 3 was noted about 3 days before spinning and also present during spinning period.

Treatment with KK-42 at the start of the 4th instar caused JH throughout this instar to disappear in any measurable amount; 99% of the treated larvae did not molt into the 5th larval instar but pupated precociously.

INTRODUCTION

Post-embryonic development of insects is regulated by two hormones, ecdysone and juvenile hormone (JH). Various morphogenetic processes are controlled by changes in the titers of these hormones. Recently, the changes in ecdysteroid titers in *Bombyx* larvae were measured in detail by radioimmunoassay [1]. Information on the pattern of ecdysteroid titer should provide a background for hormonal manipulations that affect larval and pupal molts. Freshly ecdysed last instar larvae with suitable amounts of ecdysteroids easily induced an extra larval molt (Akai, *et al.*, in preparation).

The data on ecdysteroid titer also clarified that not only development but other events in the

insect life cycle are hormonally regulated. For example, the spinning of *Bombyx* larvae in the final instar is initiated by an increase in the ecdysteroid titer, and a decrease in titer terminates the spinning behavior [2]. Non-spinning larvae treated with JH analogue can be induced to spin with peroral administration of ecdysteroid [3]. However, the role of JH in the regulation of spinning is not fully known because the titer of this hormone in *Bombyx* was measured only by a radioimmunoassay [4, 5] and definite proof of JH was lacking.

Two imidazol compounds frequently induce precocious metamorphosis in *Bombyx mori* [6, 7]. These chemicals have been suspected to possess anti-JH activity, as they are known in a number of other compounds. In our recent experiments, however, we found that the ecdysteroid titers in the hemolymph of the last instar larvae were remarkably inhibited by topical application of the imidazole derivative KK-42 [8]. Ultrastructural difference between normal and KK-42 treated prothoracic gland cells were also detected [9]. Therefore, this chemical actually seems to be an anti-ecdysteroid, although there is no evidence yet that it shows an antagonistic effect against JH.

In this short report we describe changes in the JH titer during the penultimate and last larval instars, and demonstrate that JH penultimate instar larvae becomes undetectable after the topical application of KK-42.

MATERIALS AND METHODS

Experimental animals

Larvae of the hybride N 140×X 145 were reared on an artificial diet (Kuwano-hana) at 25°C and a 12D:12L photoperiod. Under these conditions, their feeding period in the penultimate (4th) instar lasted 4 days, and in the last (5th) larval instar about 7 days. The larval molting period took one and a half days and pupation occurred on the 11th days of the last instar.

Surgical method and application of anti-JH substance

Allatectomy was performed on larval molting at the very end of the penultimate instar according to the method described by Kiguchi and Riddiford [10]. The imidazole compound KK-42 (obtained from Dr. E. Kuwano) was dissolved in acetone and 2 μ l of the solution with 5 μ g KK-42 was topically applied to each newly ecdysed 5th-instar larva.

Hemolymph collection

Duplicate samples of 100 μ l hemolymph were added to 2 ml methanol containing ethyl ester of JH 1 as internal standard. Samples from normal larvae were prepared at 1 day intervals from day 0 of the 4th instar to newly molted pupa, whereas allatectomized larvae were analysed only on day 3 of the 5th instar. The same amounts of hemolymph were also collected throughout the penultimate instar of the KK-42-treated larvae.

JH measurements

Hemolymph (100 μ l) was dropped into methanol (2 ml) which also contained the ethyl ester homologues of JH 1 and 3 (5 pmol) as internal standards. The samples were diluted with the same volume of 0.34 M aqueous NaCl. After centrifugation, the supernatant was processed as described by Rembold and Lackner [11]. After derivatisation of JH and the internal JH-ethyl standards to their 10-dimethyl (nonafluorohexyl) rilyloxy-11-methoxy derivatives, they were identified and quantified by combined GC-selected ion monitoring MS. The limit of detection was 0.01

pmol/0.1 ml hemolymph sample.

RESULTS AND DISCUSSION

Three types of JH were measured in the penultimate and final larval instars. During the penultimate instar, considerable amounts of JH 1 and JH 2 were detected (Fig. 1) but JH 3 was undetectable, the latter fact being an indication that its total quantity per sample was less than 0.01 pmol. By contrast, neither JH 1 nor JH 2 was detectable in last larval instar, (i.e., there was less than 0.05 pmol per sample), whereas JH 3 noted about 3 days before spinning (day 3 of the instar) and was also present during the spinning period (Fig. 1). JH 1 and JH 2 were present at these times in trace amounts but JH 1 titers rose steeply after pupal ecdysis.

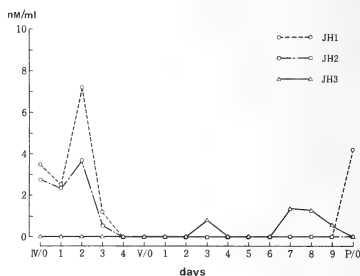


FIG. 1. Comparative levels of JH 1, JH 2 and JH 3 in the hemolymph in *Mombyx mori*. IV and V: larval instars; P: pupal stage.

These data are similar in quantity with those of JH titers in *Galleria*, but in the latter two JHs are still high during the molt from the penultimate to the last instar larva and there is only one increase of JH titer in the last larval instar. All three JHs appear important in *Manduca* and *Bombyx* whereas *Galleria* normally contains nearly exclusively JH2. That the JH in *Bombyx* comes from the corpora allata was demonstrated in allatectomized larvae. Only negligible traces of JH were detected in the last instar larvae that had been allatectomized at the end of 4th instar (Table 1).

TABLE 1. Levels of JH 1, JH 2 and JH 3 on day 3 of the 5th instar in larvae allatectomized at the end of the 4th instar

Experiment	No. of samples	Total pmol per 100 μ l hemolymph		
		JH 1	JH 2	JH 3
Control	17	—	—	—
	18	trace	trace	0.16
Allatectomized	33	—	—	trace
	34	—	—	—

TABLE 2. Levels of JH 1, JH 2 and JH 3 from the 4th instar in larvae treated with KK-42 on day 0 of 4th instar

Stage	No. of samples	Total pmol per 100 μ l hemolymph		
		JH 1	JH 2	JH 3
Day 1 of 4th instar	35	—	—	—
	36	—	—	—
2 "	37	—	—	—
	38	—	—	—
3 "	39	—	—	—
	40	—	—	—
4 "	41	—	—	—
	42	—	—	—
5 "	43	—	—	—
	44	—	—	—

Treatment with KK-42 at the start of the 4th instar caused JH throughout this instar to disappear in any measurable amount (Table 2); 99% of the treated larvae did not molt into the 5th larval instar but pupated precociously.

Preocious pupation with KK-42 is associated with a suppression of the ecdysteroid titer for the 6 days preceding spinning; the pattern is the same as in the normal final instar (Kiuchi *et al.*, 1985). Our present study complements these results and reveals that in the penultimate instar larvae treated with KK-42 the titers of both ecdysteroids and JH approach levels typical for the precocious pupation.

The effect of KK-42 on the titer of both ecdysteroids and JH indicate that this and similar compounds may act on the brain-centered regulation of hormone production.

ACKNOWLEDGMENTS

We thank Dr. F. Sehnal and Dr. M. Kiuchi for their supports. We also thank Mrs. S. Kopp for technical assistance in preparing and measuring the analysis.

REFERENCES

- Kiuchi, M. (1987) Doctoral thesis at Hokkaido University.
- Kiuchi, M. and Akai, H. (1987) Abstract of Kanto Branch of Japanese Soc. of Sericul. Sci., **38**, p. 35.
- Akai, H., Takabayashi, K. and Kiuchi, M. (1988) *J. Seric. Sci. Jpn.* **57**: 341-344.
- Plantevin, G., Bosquet, G., Galvez, B. and Nardon, C. (1987) *J. Insect Physiol.*, **86**: 501-507.
- Niimi, S., Sakurai, S., Nariki, M., Kimura, M. and Ohtaki, T. (1987) *Proc. 1st Cong. Asia & Oceania Soc. Comp. Endocr.*, 230-231.
- Akai, H., Kimura, K., Kiuchi, M. and Shibukawa, A. (1984) *J. Seric. Sci. Jpn.*, **53**: 545-546.
- Kiuchi, M., Kimura, K. and Akai, H. (1985) *J.*

- Seric. Sci. Jpn., **54**: 77-81.
- 8 Kiuchi, M. and Akai, H. (1988) In "Invertebrate and Fish Tissue Culture". Ed. by Kuroda, Japan Scientific Societies Press, Tokyo, pp. 60-64.
 - 9 Akai, H. and Kiuchi, M. (1987) Proc. 1st Cong. Asia & Oceania Soc. Comp. Endocr., 240-241.
 - 10 Kiguchi, K. and Riddiford, L. M. (1978) J. Insect Physiol., **24**: 673-680.
 - 11 Rembold, H. and Lackner, B. (1985) J. Chromatogr., **232**: 355-361.
 - 12 Rembold, H. and Lackner, B. (1987) Insect Biochem., **17**: 997-1001.
 - 13 Baker, F. C., Tsai, L. W., Reuter, C. C. and Schooley, D. A. (1987) Insect Biochem., **17**: 989-996.

Development Growth & Differentiation

Published Bimonthly by the Japanese Society of
Developmental Biologists
Distributed by Business Center for Academic
Societies Japan, Academic Press, Inc.

Papers in Vol. 31, No. 3. (June 1989)

25. **REVIEW:** M. Wakahara: Specification and establishment of dorsal-ventral polarity in eggs and embryos of *Xenopus laevis*.
26. K. Hashimoto and N. Nakatsuji: Formation of the primitive streak and mesoderm cells in mouse embryos —Detailed scanning electron microscopical study.
27. Y. G. Watanabe: Differentiation of striated muscle fibers in monolayer cultures of rat anterior pituitary.
28. M. Sousa and C. Azevedo: Ultrastructural localization of calcium in the acrosome and jelly coat of starfish gametes.
29. M. Yamaguchi, M. Kurita and N. Suzuki: Induction of the acrosome reaction of *Hemicentrotus pulcherrimus* spermatozoa by the egg jelly molecules, fucose-rich glycoconjugate and sperm-activating peptide I.
30. M. Medina and C. G. Vallejo: The maternal origin of acid hydrolases in *Drosophila* and their relation with yolk degradation.
31. A. Shinagawa, S. Konno, Y. Yoshimoto and Y. Hiramoto: Nuclear involvement in localization of the initiation site of surface contraction waves in *Xenopus* eggs.
32. N. Usui and M. Yoneda: Regional response to cytochalasin B of the equatorial cell cortex in sea-urchin eggs during the first mitosis.
33. P. Andreuccetti: Ultrastructural observations of the germ plasm in the lizard *Podarcis sicula*.
34. H. R. Eistetter: Pluripotent embryonal stem cell lines can be established from disaggregated mouse morulae.
35. T. Shimizu: Asymmetric segregation and polarized redistribution of pole plasm during early cleavages in the *Tubifex* embryo: Role of actin networks and mitotic apparatus.
36. D. Petrey, D. Buster, K. K. Donato and H. Anderson: Injection of antibodies into grasshopper eggs as a method for studying embryonic development.
37. H. Fukamachi and Y. S. Kim: Importance of desmosome formation for glandular organization of LS174T human colon cancer cells in organ culture.

Development, Growth and Differentiation (ISSN 0012-1592) is published bimonthly by The Japanese Society of Developmental Biologists, Department of Developmental Biology, Mitsubishi Kasei Institute of Life Science, Minami-ootani 11, Machida, Tokyo 194, Japan. 1989: Volume 31. Annual subscription for Vol. 31, 1989: U. S. \$ 136.00, U. S. and Canada: U. S. \$ 150.00, all other countries except Japan. All prices include postage, handling and air speed delivery except Japan. Second class postage paid at Jamaica, N.Y. 11431, U. S. A.

Outside Japan: Send subscription orders and notices of change of address to Academic Press, Inc., Journal Subscription Fulfillment Department, 1 East First Street, Duluth, MN 55802, U. S. A. Send notices of change of address at least 6-8 weeks in advance. Please include both old and new addresses. U. S. A. POSTMASTER: Send changes of address to *Development, Growth and Differentiation*, Academic Press, Inc., Journal Subscription Fulfillment Department, 1 East First Street, Duluth, MN 55802, U. S. A.

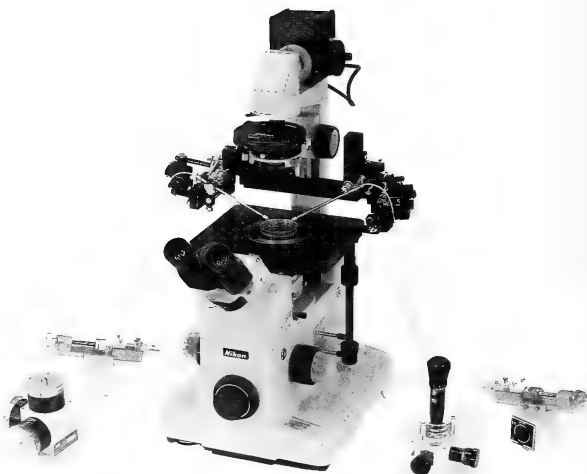
In Japan: Send nonmember subscription orders and notices of change of address to Business Center for Academic Societies Japan, 16-3, Hongo 6-chome, Bunkyo-ku, Tokyo 113, Japan. Send inquiries about membership to Business Center for Academic Societies Japan, 4-16, Yayoi 2-chome, Bunkyo-ku, Tokyo 113, Japan.

Air freight and mailing in the U. S. A. by Publications Expediting, Inc., 200 Meacham Avenue, Elmont, NY 11003, U. S. A.

NARISHIGE

THE ULTIMATE NAME IN MICROMANIPULATION

OUR NEW MODELS **WR-88** and **MO-102M**
MAKE PRECISION MICROMANIPULATION SO EASY!



SOME FEATURES of THE WR-88 WATER ROBOT MICROMANIPULATOR (3-DIMENSIONAL)

- * Drift-free, the new WR-88 has a DRIFT movement of less than 2 microns.
- * The new WR-88 has a SMOOTH MICRODRIVE MECHANISM.
- * An Aqua Purificate remote control ensures totally vibration-free operation.



NARISHIGE SCIENTIFIC INSTRUMENT LAB.

9-28 KASUYA 4-CHOME SETAGAYA-KU, TOKYO 157, JAPAN
PHONE (INT-L) 81-308-8233, FAX (INT-L) 81-3-308-2005
CABLE : NARISHIGE LABO, TELEX, NARISHIGE J27781

THE BOTANICAL MAGAZINE TOKYO

An international journal for plant sciences published quarterly by the Botanical Society of Japan. For a century, the journal has continuously published outstanding papers by Japanese as well as foreign botanical scientists. Contributors to the journal are not limited to the members of the Society and their papers are accepted by paying the page charge.

Papers in a Recent Issue:

- HORI, Y.: Life History and Population Dynamics of the Japanese Yam, *Dioscorea japonica* Thunb.
II. Adaptive Significance of the Emergence Mode
KUROIWA, H.: Ultrastructural Examination of Embryogenesis in *Crepis capillaris* (L.) Wallr.: 1.
The Synergid before and after Pollination
HIZUME, M., A. OHGIKU AND A. TANAKA: Chromosome Banding in the Genus *Pinus*. II.
Interspecific Variation of Fluorescent Banding Patterns in *P. densiflora* and *P. thunbergii*
SAKANISHI, Y., Y. YOKOHAMA AND Y. ARUGA: Seasonal Changes of Photosynthetic Activity of a
Brown Alga *Ecklonia cava* Kjellman
SUZUKI, K. AND K. YANAGISAWA: Environmental Factors Inducing Sexual Development in *Dictyo-
stelium discoideum*
NAKATSUBO, T., Y. TAKAMINE AND Y. INO: Response Patterns of Net Photosynthesis to Moisture of
Mosses in Xeric Habitats
HOZUMI, K.: Biomass Duration in Growth Models
BHADULA, S.K. AND V.K. SAWNEY: Protein Analysis of Floral Organs of Some Members of
Solanaceae
YAMAMOTO, S.: Gap Dynamics in Climax *Fagus crenata* Forests
YAMAKURA, T.: A Further Analysis of the Quasi-1/2 Power Law of Tree Height in Stratified Forest
Communities
AOKI, I.: Entropy Budget of Conifer Branches
TERASAKA, O. AND T. NIITSU: Peculiar Spindle Configuration in the Pollen Tube Revealed by the
Anti-Tubulin Immunofluorescence Method

Order form

Send to

THE BOTANICAL SOCIETY OF JAPAN

Toshin Building
Hongo 2-27-2, Bunkyo-ku,
Tokyo 113, Japan

THE BOTANICAL MAGAZINE, TOKYO

☐ Individuals: ¥ 7,000 p.a.

☐ Institutions: ¥ 17,500 p.a.

Name (Please print): _____

Address: _____

Date: _____ Signature: _____

Sophisticated Balance between Safety and Centrifugation Capability without Compromise.

Centrifuge in
Integrated with A
Refrigerator

Extra-Quiet
Operation

Ease of Loading/
Unloading
The Rotors

Quick Start/
Quick Stop

High Quality

Triple Safety
Design

Corrosion
Resistance



HIGH SPEED
REFRIGERATED
MICRO CENTRIFUGE

MODEL MR-150

TOMY CORPORATION

1002 SOLEIL NARIMASU BLDG. 31-8, NARIMASU 1-CHOME,
ITABASHI-KU, TOKYO 175 JAPAN
TEL:(03)976-3411 TLX:02723111 TOMYCO J
CABLE:TOMYSHO TOKYO FAX:(GIII GII)(03)930-7010

SOLE AGENT

TOMY SEIKO CO., LTD.

2-2-12, ASAHICHO NERIMA-KU, TOKYO 176 JAPAN
TEL:(03)976-3111

MANUFACTURER

(Contents continued from back cover)

Kambegawa: Immunohistochemical study of the ultimobranchial gland in chum salmon fry (COMMUNICATION)	607
Matsuda, K., Y. Sasayama, C. Oguro and A. Kambegawa: Calcitonin-immunoreactive cells found in the extra-ultimobranchial areas of the salamander, <i>Hynobius nigrescens</i> , during larval development (COMMUNICATION)	611
Akai, H. and Rembold: Juvenile hormone levels in <i>Bombyx</i> larvae and their impairment after treatment with an imidazole derivative KK-42 (COMMUNICATION) ..	615

Behavior Biology

Tomioka, K. and Y. Chiba: Photoperiod during post-embryonic development affects some parameters of adult circadian rhythm in the cricket, <i>Gryllus bimaculatus</i>	565
----------------------------------------------------------------------------------------------------------------------------------------------------------------------------	-----

Watanabe, M. and H. Terami: Excessive transitory migration of guppy populations. II. Analysis of possible conspecific-following tendency	573
------------------------------------------------------------------------------------------------------------------------------------------------	-----

Systematics and Taxonomy

Shimazu, T.: Two new species of the genus <i>Diploproctodaeum</i> (Trematoda: Lepocreadiidae: Diploproctodaeinae), with some comments on species in the subfamily Diploproctodaeinae, from Japanese marine fishes	579
Matsuoka, N. and H. Suzuki: Electrophoretic study on the phylogenetic relationships among six species of sea-urchins of the family Echinometridae found in the Japanese waters	589

ZOOLOGICAL SCIENCE

VOLUME 6 NUMBER 3

JUNE 1989

CONTENTS

Obituary435

REVIEWS

Skadhauge, E.: Hormonal regulation of sodium absorption and chloride secretion across the lower intestines of birds437

Ozato, K., K. Inoue and Y. Wakamatsu: Transgenic fish: biological and technical problems445

ORIGINAL PAPERS

Physiology

Okajima, A. and M. Watanabe: Electrophysiological identification of neuronal pathway to the prothoracic gland and the change in electrical activities of the prothoracic gland innervating neurones during larval development of a moth, *Mamestra brassicae*459

Ohtsu, K.: Flash-induced depression of the ERP under the Ca^{2+} -free condition in the octopus retina469

Fujii, R., H. Kasukawa, K. Miyaji and N. Oshima: Mechanisms of skin coloration and its changes in the blue-green damselfish, *Chromis viridis*477

Cell Biology

Suzuki, Y. and M. Takeda: Filaments in the cells of frog taste organ487

Kuroda, Y., Y. Takada and T. Kasuya: Use of the laser microbeam for preserving frozen *Drosophila* embryos499

Sugino, Y. M. and M. Ishikawa: The intercellular bridge of a blood cell in the ascidian, *Ciona savignyi* (COMMUNICATION) ..599

Okai, Y.: A human embryo fibroblast-derived peptide suppresses the formyl-Met-Leu-Phe (FMLP)-induced activation in hu-

man polymorphonuclear leukocytes (COMMUNICATION)603

Biochemistry

Yoshizaki, N.: Comparison of two lectins isolated from *Xenopus* cortical granules507

Sonobe, H.: Studies on embryonic diapause in the *pnd* mutant of the silkworm, *Bombyx mori*: characterization of protein synthesis during early development515

Immunology

Okai, Y. and S. Ishizaka: Spontaneous release of B lymphocyte-enhancing factors for growth and differentiation by YH-1 cells in serum-free culture media-Identification of interleukin 1 activities523

Developmental Biology

Myohara, M. and J. H. Willis: Control of cuticle formation in wing epidermal cells of the fleshfly, *Sarcophaga bullata*533

Sawa, M., A. Fukunaga, T. Naito and K. Oishi: Studies on the sawfly, *Athalia rosae* (Insecta, Hymenoptera, Tenthredinidae). I. General biology541

Sawa, M. and K. Oishi: Studies on the sawfly, *Athalia rosae* (Insecta, Hymenoptera, Tenthredinidae). II. Experimental activation of mature unfertilized eggs549

Sawa, M. and K. Oishi: Studies on the sawfly, *Athalia rosae* (Insecta, Hymenoptera, Tenthredinidae). III. Fertilization by sperm injection557

Endocrinology

Sasayama, Y., K. Matsuda, C. Oguro and A.

(Contents continued on inside back cover)

INDEXED IN:

Current Contents/LS and AB & ES,
Science Citation Index,
ISI Online Database,
CABS Database, INFOBIB

Issued on June 15

Printed by Daigaku Letterpress Co., Ltd.,
Hiroshima, Japan

Vol. 6 No. 4

August 1989

ZOOLOGICAL SCIENCE

An International Journal

PHYSIOLOGY
CELL and MOLECULAR BIOLOGY
GENETICS
IMMUNOLOGY
BIOCHEMISTRY
DEVELOPMENTAL BIOLOGY
REPRODUCTIVE BIOLOGY
ENDOCRINOLOGY
BEHAVIOR BIOLOGY
ENVIRONMENTAL BIOLOGY
ECOLOGY and TAXONOMY

published by Zoological Society of Japan

distributed by Business Center for Academic Societies Japan
VSP, Zeist, The Netherlands

ISSN 0289-0003

ZOOLOGICAL SCIENCE

The Official Journal of the Zoological Society of Japan

Editor-in-Chief:

Hideshi Kobayashi (Tokyo)

Managing Editor:

Chitaru Oguro (Toyama)

Assistant Editors:

Yuichi Sasayama (Toyama)

Hitoshi Michibata (Toyama)

Miëko Komatsu (Toyama)

The Zoological Society of Japan:

Toshin-building, Hongo 2-27-2, Bunkyo-ku,
Tokyo 113, Japan. Tel. (03) 814-5675

Officers:

President: Nobuo Egami (Tokyo)

Secretary: Hideo Namiki (Tokyo)

Treasurer: Tadakazu Ohoka (Tokyo)

Librarian: Masatsune Takeda (Tokyo)

Editorial Board:

Howard A. Bern (Berkeley)

Horst Grunz (Essen)

Susumu Ishii (Tokyo)

John M. Lawrence (Tampa)

Hiromichi Morita (Fukuoka)

Andreas Oksche (Giessen)

Mayumi Yamada (Sapporo)

Walter Bock (New York)

Robert B. Hill (Kingston)

Seiichi Kawashima (Tokyo)

Koscak Maruyama (Chiba)

Kazuo Moriwaki (Mishima)

Hidemi Sato (Nagoya)

Ryuzo Yanagimachi (Honolulu)

Aubrey Gorbman (Seattle)

Yukio Hiramoto (Chiba)

Yukiaki Kuroda (Mishima)

Roger Milkman (Okazaki)

Tokindo S. Okada (Okazaki)

Hiroshi Watanabe (Tokyo)

ZOOLOGICAL SCIENCE is devoted to publication of original articles, reviews and communications in the broad field of Zoology. The journal was founded in 1984 as a result of unification of Zoological Magazine (1888-1983) and Annotationes Zoologicae Japonenses (1897-1983), the former official journals of the Zoological Society of Japan. ZOOLOGICAL SCIENCE appears bimonthly. An annual volume consists of six numbers of more than 1100 pages including an issue containing abstracts of papers presented at the annual meeting of the Zoological Society of Japan.

MANUSCRIPTS OFFERED FOR CONSIDERATION AND CORRESPONDENCE CONCERNING EDITORIAL MATTERS should be sent to:

Dr. Chitaru Oguro, Managing Editor, Zoological Science, Department of Biology, Faculty of Science, Toyama University, Toyama 930, Japan, in accordance with the instructions to authors which appear in the first issue of each volume. Copies of instructions to authors will be sent upon request.

SUBSCRIPTIONS. ZOOLOGICAL SCIENCE is distributed free of charge to the members, both domestic and foreign, of the Zoological Society of Japan. To non-member subscribers within Japan, it is distributed by Business Center for Academic Societies Japan, 6-16-3 Hongo, Bunkyo-ku, Tokyo 113. Subscriptions outside Japan should be ordered from the sole agent, VSP, Utrechtseweg 62, 3704 HE Zeist (postal address: P. O. Box 346, 3700 AH Zeist), The Netherlands. Subscription rates will be provided on request to these agents. New subscriptions and renewals begin with the first issue of the current volume.

All rights reserved. No part of this publication may be reproduced or stored in a retrieval system in any form or by any means, without permission in writing from the copyright holder.

© Copyright 1989, The Zoological Society of Japan

[Publication of Zoological Science has been supported in part by a Grant-in-Aid for
Publication of Scientific Research Results from the Ministry of Education, Science
and Culture, Japan.]

OBITUARY

**Denzaburo Miyadi (1901-1988)**

Denzaburo Miyadi, Professor Emeritus of Kyoto University, passed away at the age of 87 during the early hours of 20 October 1988 at a hospital in Kyoto, following a long illness. His death occurred only a few hours after that of his beloved wife, Sugako, who was also ill in bed in the same room of the hospital. He was undoubtedly one of Japan's most eminent ecologists, and his far ranging contributions encompassed various aspects of ecology, biogeography, and taxonomy.

Miyadi was born in Innoshima, a small island in the Seto Inland Sea. After an education at Seishikan Middle School in Fukuyama and the Sixth Higher School in Okayama, he entered the Imperial University of Tokyo (now the University of Tokyo) in 1922, where he read zoology and studied fish physiology under Professor Naohide Yatsu.

Following his graduation in 1925, he was appointed Lecturer at the Otsu Hydrobiological Station, College of Science, Kyoto Imperial University (now Kyoto University), where Masuzo Uéno was on the staff. His long university career began here with research on the benthic fauna of lakes. Presumably, this decision was inspired by the distinguished zoologist, Tamiji Kawamura, then Professor of the Department of Zoology in Kyoto, and author of an outstanding book on freshwater biology, later renowned as Kawamura's *Freshwater Biology*. Miyadi's great enthusiasm for research resulted in him soon publishing a series of papers on the benthic fauna of lakes in Japan and adjacent areas, from the Kuril Islands to Formosa. Through the comparison of benthic faunas, he proposed basic criteria which served to characterize and classify the lakes in the Far East. This study was the first comparative hydrobiological study performed outside Europe and North America, where the field was already fairly established. For this pioneering work he was awarded a D.Sc. from Kyoto Imperial University. Subsequently, he began taxonomic and biogeographical research on freshwater fishes and molluscs, and published the first faunal records of the freshwater fishes in both the Kyoto and Shinshu districts, and also studies on the distribution and endemism of several molluscs and mysids.

In 1936, he was promoted to Associate Professor of the Seto Marine Biological Laboratory of Kyoto Imperial University. While at this marine facility, he extended his work to include the benthic fauna of shallow bays along the Japanese coast. Using a similar analysis to that applied to benthic lake fauna, in collaboration with Tetsuo Masui, Tadashige Habe and others, he developed the concept of "the degree of embayment" as an indication of the ecological state of a bay. His association with freshwater biology during this period, however, remained intact. Together with Masuzo Uéno, Masatake Yamazaki and others, he joined a biological expedition to the Manchurian region of northeastern China, which was at that time occupied by Japan. His published findings from this expedition included papers on amphibians, fishes, crabs and leeches.

Fortunately, Miyadi was not called up for military service during the Second World War, and in 1942 he succeeded Professor Tamiji Kawamura in the chair of Physiology and Ecology at the Department of Zoology of the College of Science of Kyoto Imperial University. In this capacity he continued his work on marine communities in shallow coastal areas in collaboration with his research fellows and students. In later years, however, he placed more importance on enabling his students to perform their own research utilizing financial support which he had secured from outside the university. This was possibly partly due to his increasing involvement in administrative duties which deprived him of time to conduct his own research, but more likely because he came to believe that the field of ecology could be advanced by tackling problems related directly to human society, during which process the students could also be trained.

In 1951, Miyadi initiated a study of the ecology of the Ayu fish, *Plecoglossus altivelis*, at the request of the Fisheries Department of Kyoto Prefectural Government. He was requested to ascertain the optimal density for release of young of this highly appreciated food and sport fish into rivers. A succession of students joined the research group for this study, and the description of the territorial social structure of this fish was one of the important early results. It was Miyadi himself who introduced SCUBA equipment of the original Cousteau type for underwater observation early in this study. This SCUBA equipment was later utilized even more extensively in an ecological study of *Zostera* beds, which he initiated in 1952 with financial support from the Fisheries Agency of the Ministry of Agriculture. Students were also part of this research group and the detailed community structure was clarified, providing confirmation of the role of the beds as a nursery ground for some important commercial fishes. For the study of the Japanese monkey, *Macaca fuscata*, which was started in 1948 by one of his students in Kyushu and later attracted many students, he also drew upon various sources of financial support. This study became famous for its fascinating discoveries on the social structure and behaviour of this primate, and later evolved into inspired research on various primates at places all over the world. Miyadi's chief virtue was his ability to attract students of varied disciplines to join his research groups and promote an exchange of ideas on the various problems and to work in collaboration to solve them.

In 1958, on behalf of Shimane Prefectural Government, Miyadi recommended an ecological investigation of Lake Naka-umi and its adjacent areas, shallow brackish waters which at that time were planned to be turned into a freshwater reservoir and be partly reclaimed. Scientists from various fields of aquatic biology were invited to participate in the survey and greatly advanced the knowledge of the biology of the lake. The results contributed to the appraisal of the project, which has just recently been suspended for an unlimited period. Likewise, in 1962, at the request of the Biwa-ko Office of the Ministry of Construction, he began a survey of Lake Biwa-ko, with over fifty participating scientists, which resulted in the first integrative biological investigation of this lake.

From 1961 to 1963, he was Dean of the Faculty of Science (formerly College of Science) of Kyoto University, and, from 1946 until his retirement in 1964, Director of the Seto Marine Biological Laboratory. In 1951, he was elected to the Science Council of Japan and was an active participant until 1963. In addition, he served as President of the Ecological Society of Japan from 1960 to 1971, and also

served as Director of the Japan Monkey Center, a private research body, in the founding and establishment of which he played a major role.

In his later years at the university, his personal interests extended into the examination of the sociological aspects of ecology. He concentrated on the study of the social structure and behaviour of animals and placed great emphasis on the study of the primates. Together with Kinji Imanishi, he founded the Laboratory of Physical Anthropology in the Department of Zoology, and also the Primate Research Institute of Kyoto University.

He invited many distinguished foreign scientists from different disciplines to his laboratory during the hard times in Japan which followed the war; among these visitors were Professor Sir Alister C. Hardy and Professor Eugene P. Odum. He also attended various international conferences held abroad, such as the Pan-Pacific Science Congress in Quezon City and the International Congress of Zoology in London. It was truly remarkable that at that time he also received an invitation from the Akademia Nauk of the U.S.S.R.

In his early days, Miyadi did not write textbooks, choosing instead to write chapters in many biological publications. However, in 1953, in joint authorship with Syuiti Mori, he published a small book on animal ecology, which is nowadays regarded as the pioneering introduction to this field in Japan, and greatly stimulated the ecology students of the day. Books he published later reflected his change in interest and were mostly concerned with the society and behaviour of animals, particularly of monkeys.

We do not know what Miyadi was like as a research worker in his early years, but we have heard an old captain of the Seto Marine Biological Laboratory talking of his experience: "He was 'greedy' in doing research. We were nearly killed on a boat by sweeping bullets from a U.S. fighter. He simply would not stop dredging." As a professor, he was warm, quiet and always generously prepared to listen to his students; we never heard him raise his voice. Rather, he was a man of relatively few, carefully chosen words, which conveyed the depth of his thought.

He was not a narrow-minded scientist. For some time, his poetic feeling led him to write Japanese short verses, haiku, that were shaded with zoological hues. His nom de plume, Hidei (the Chinese characters of this may also be pronounced in Japanese as Hidoro), was obviously adapted from the word hydrobiology, and in his later years he published his haikus in small books, accompanied by relevant essays. Here is one of them, which was composed by him upon the occasion of his retirement.

How cold does it make an aged midge feel
Off the water leaving a lake.

— Hidei

HIROYA KAWANABE

Department of Zoology
Kyoto University
and

EIJI HARADA

Seto Marine Biological Laboratory
Kyoto University



REVIEW

New Trends in the Regulation of the Gonadal Activity in Vertebrates: Paracrine and Autocrine Control

GIOVANNI CHIEFFI

*Istituto di Biologia, I Facoltà di Medicina e Chirurgia,
Università di Napoli, and Stazione Zoologica, Napoli, Italy*

INTRODUCTION

The gonadal function of vertebrates is regulated by an intricate interplay of exogenous and endogenous factors. As far as endogenous factors are concerned, neuroendocrine control of gonadal function has been largely investigated (see for review, Chieffi [1]). However interesting data were accumulating in the recent years in favour of a local control of both gonadal compartments, the germinative and endocrine. The term "ultrashort feed-back" was also used in this case. This term was introduced by Motta and coworkers [2] to explain the modulation of synthesis, storage and release of the hypothalamic releasing hormones by changes of their own titers in the general circulation. Therefore the term "ultrashort feedback" became misleading in case of a local control of gonadal activity, since this type of control does not use systemic circulation. It could be also suspected that part of the ultrashort feedback, as defined by Motta and coworkers [2], might correspond to local mechanisms of control. This hypothesis might be true especially in the case of hypothalamic releasing factors whose half life is known to be very short. Therefore I would suggest to keep the term "ultrashort feedback" for the endocrine autoregulation, i.e. via blood stream as it was first used, and to use the terms "autocrine" and "paracrine" (which are already used by several authors) controls for the local autoregulation.

Autocrine control occurs when one cell is able to

regulate its own functions using one of its secretory products. The substance produced within the cell acts through raising receptors and modulating the sensitivity of diverse biochemical processes to stimulation by other hormones (Fig. 1B).

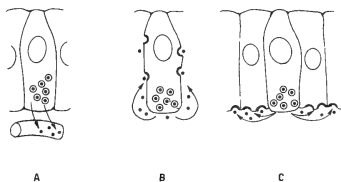


Fig. 1. Various types of cell to cell communications: endocrine (A), autocrine (B), paracrine (C). Chemical messengers are shown in latent form within the cell. Thickened regions of the cell membrane represent receptor sites; however receptors to some hormones may be intracellular.

Various lines of evidence indicate another type of local control as well, the so-called "paracrine control"; it became known as a generalized form of bioregulation whereby one cell in a tissue selectively influences the activity of an adjacent different cell type through the biosynthesis and release of chemical messengers which diffuse into the parenchyma and act specifically on neighbouring target cells. However, it should be remembered that a formal assignment of a paracrine regulatory role requires a substance to be present, locally biosynthesized, and to exert a receptor-mediated biological effect in the tissue in question (Fig. 1C).

In this review only selected aspects of this kind of regulation of gonadal activity will be taken into consideration. Paracrine and autocrine communications involve locally produced steroidal and nonsteroidal bioregulators. The list of candidates for involvement in gonadal paracrine and autocrine communications is growing rapidly as new factors are identified in the gonads or are shown to have direct effects *in vitro*.

TESTICULAR LOCAL CONTROL

As far as the testis is concerned, as in any organ or tissue containing different cell types, local coordination of the function of different cell types is fundamental to the efficient working of the organ.

Testis is a composite organ, whose specific components offer a valuable model to investigate possible cell to cell communication. Although testicular function drops following gonadotropins withdrawal, the reception, transmission and/or utilization of these pituitary signals must be locally modulated or mediated. Since heterogeneity of seminiferous tubules and adjacent interstitial cell function exists within the testis, local requirements for testosterone production cannot be satisfied by the circulating LH. Therefore local factors should provide appropriate modulation of androgen production.

Overview of mammals

An important impulse to the knowledge of testicular paracrinology was given by the technique of transillumination-assisted dissection of rat seminiferous tubules devised by Parvinen [3] and Parvinen and Ruokonen [4]. The embracement of the spermatogonia by a Sertoli cell from the onset until the end of spermatogenesis led to investigate the intimate exchange of information between the two cell types. The simplest function of physical and nutritional support for the growing spermatogonia attributed to the Sertoli cell turned into a number of unpredictable biochemical and metabolic events during spermatogenesis.

Figure 2 summarizes only some of the cyclical changes in Sertoli cell secretion in the rat that Sharpe [5] well defines as "the tip of the iceberg". In fact Sertoli cells secrete certainly numerous

proteins; the identity and function are still unknown for most of them.

Stages I-IV of spermatogenic cycle of the rat are characterized by a high concentration and responsiveness of FSH receptors. At stages IV-VI ceruloplasmin, a copper-transporting protein whose function is still vague, is detected at highest concentrations. At stage VI peaks also a protein of unknown function called "cyclic protein 2", while FSH receptors reach the lowest concentration. Maximal secretion of the androgen binding protein (ABP), along with the highest secretion of an aromatase inhibitor, occurs at stage VII when meiosis commences. Increase of the plasminogen activator, a protease, at stages VII and VIII seems to be related to spermiation, residual body ingestion and meiotic germ cell translocation. Finally, transferrin, an iron-transferring protein, is produced in large amounts from stage IX until XIV. During this period lipid accumulation is also observed in Sertoli cells (see for review, Sharpe [5]).

These are simply the most remarkable cyclic metabolic changes occurring in the Sertoli cell during spermatogenesis of the rat and likely represent the response to germ cell requirements.

It is worthy of notice that co-culture of Sertoli cells with pachytene spermatocytes stimulates Sertoli cells' ABP secretion [6]; however co-culture of Sertoli cells with spermatids does not stimulate ABP secretion [7] thus indicating the possible existence of specific "orders" sent by the germ cells to Sertoli cells at different stages of the spermatogenic cycle; Sertoli cells in turn trigger the spermatogenic events in appropriate succession.

Concomitantly, Sertoli cells interact with peritubular cells. The growth factor, somatomedin-C, present in the peritubular cells, has binding affinity for Sertoli cell receptors [8]. Sertoli cells also interact with Leydig cell directly and/or through peritubular cell mediation. Leydig cells are known to produce, besides testosterone and neurohypophysial-hormones like substance, a number of other hormones such as estrogens, prostaglandins, angiotensin, β -endorphin. According to Drummond *et al.* [9], testosterone regulates inhibin production by Sertoli cells. As regard to the paracrine-autocrine control of AVP-like peptide,

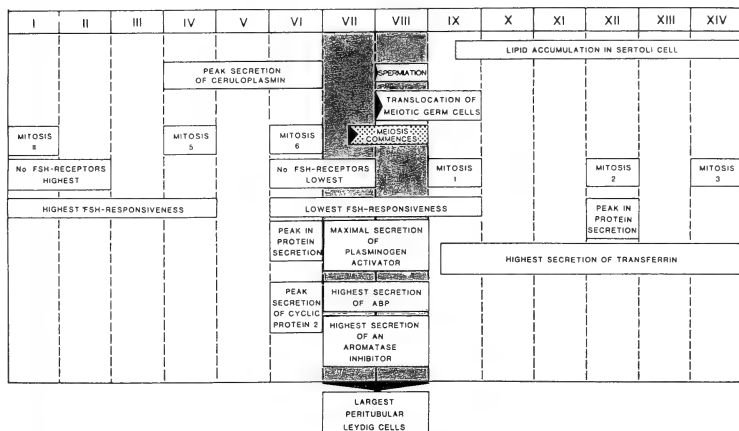


FIG. 2. Scheme of the major cyclical changes in Sertoli cell secretion in the rat. Spermatogenic cycle lasts 12 day and is divided into 14 stages (I-XIV). The shaded area (stages VII and VIII) corresponds to the most androgen dependent period of the spermatogenic cycle (Sharpe [5]).

Kasson *et al.* [10] propose that pituitary LH interacts with specific receptors on Leydig cell membranes activating cholesterol side-chain cleavage enzyme, 17 α -hydroxylase and 17, 20-desmolase thus increasing testosterone production. This is locally regulated by an AVP-like peptide which binds to specific receptors on Leydig cells increasing progesterone biosynthesis but decreasing androgen secretion affecting 17 α -hydroxylase and 17, 20-desmolase activities (Fig. 3).

Testosterone is the main hormone which acting

on Sertoli cells drives spermatogenesis. There are many convincing evidences for a local regulation of testosterone secretion by Sertoli cells. The first and the most thoroughly investigated factor, probably produced by Sertoli cells, is a LHRH-like factor. This differs from hypothalamic LHRH and stimulates Leydig cell testosterone production via pathways different from those utilized by LH (see for review, Sharpe [5]). Recently, a number of factors different from LHRH-like substances have been claimed to exert stimulatory effect on rat Leydig cell testosterone production, at least *in vitro* [11-16].

Very recently, Hsueh *et al.* [17] have shown that inhibin related gene products synthesized by Sertoli cells may form heterodimers or homodimers to serve intragonadal paracrine signals in the modulation of LH-stimulated androgen biosynthesis. It has been shown that $\alpha\beta$ heterodimer of inhibin enhances LH-stimulated androgen production by primary cultures of neonatal testicular cells. In contrast $\beta\beta$ homodimer of inhibin suppresses Leydig cell androgen production at all doses of LH tested. When both heterodimer and homodimer

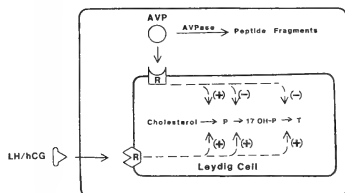


FIG. 3. Paracrine-autocrine control of androgen biosynthesis by AVP as an intratesticular hormone (Kasson *et al.* [10]).

tion of the testicular 17β -hydroxysteroid dehydrogenase *in vitro* by androgens in the rat testis. It was then reported by Naessany *et al.* [20] that physiological concentrations of testosterone were ineffective in inducing inhibition of testosterone production by whole testis in organ culture. Using a different experimental model, i.e. the fetal testicular suspension, Pointis *et al.* [21] demonstrated that doses of testosterone and DHT in the same range (20 times greater than that found in the male fetal circulation) do exert a local negative autocrine control. The higher activity of DHT compared to testosterone suggests that aromatization is not a prerequisite for androgen action. This autocrine control might explain the decrease of circulating testosterone during late fetal life [22].

Nonmammalian vertebrates.

Ho *et al.* [23] obtained an indirect evidence of a local control of testis function by estrogens in the anadromous lamprey *Petromyzon marinus*. They did not detect androgen specific binding in the testicular subcellular fractions, while definite estrogen binding activities were demonstrated both in the cytosol and nuclear extract of the testis.

Elasmobranchs show some interesting features. Although Leydig cells have been considered as estrogen target in *Squalus acanthias*, Sertoli cells are the more likely responsible for both androgen and estrogen biosynthesis than the Leydig cells [24]. Consequently, in my opinion, control of the Sertoli cells might be autocrine. Sourdain *et al.* [25] have suggested on the basis of different sex steroid concentrations in the different zones of *Scylliorhinus canicula* testis that the germ cells must influence the steroidogenesis of Sertoli cells.

In *Torpedo ocellata* and *Torpedo marmorata*, where Leydig cells are well developed [26, 27], estradiol provokes plasma androgen increase either in intact or in hypophysectomized animals [28]. Thus estrogen in *Torpedo* has a different effect than found in mammals. Conversely, a GnRH analog (buserelin) induces plasma androgen increase in hypophysectomized animals in short term treatment [28] (Fig. 6) in accordance with the results available in rats (see for review, Sharpe [5]). Since irGnRH has been found in dogfish plasma [29], it remains to be established

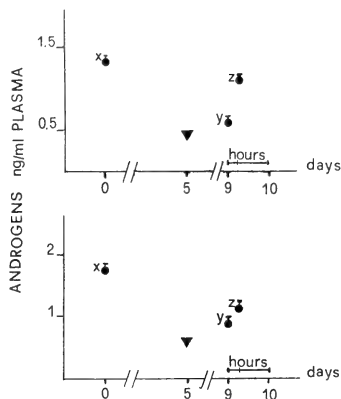


Fig. 6. Direct effect of a GnRH analog (buserelin) on the androgen production by the testis of hypophysectomized *Torpedo*. Animals were blood sampled before hypophysectomy and after 6 hr from a single intratesticular injection of buserelin. (▼) indicates the time of hypophysectomy. Androgen concentration decreases after hypophysectomy (x vs y: $p < 0.01$) and increases significantly (y vs z: $p < 0.01$) after buserelin treatment. The two panels are representative of two experiments (Fasano *et al.* [28]).

whether GnRH-like peptides share local regulation.

Among teleosts the steroidogenic activity of *Gobius paganellus* does not seem to be locally regulated neither by estradiol nor by GnRH analog (buserelin) (Pierantoni *et al.*, unpubl. data). In fact both substances were ineffective in inducing changes in androgen secretion. Anyway more species and hormones need to be investigated before excluding a possible local control of testicular activity in teleosts.

More thoroughly studied is the local control of testis in amphibians. Rastogi *et al.* [30] were the first to show that androgens control the formation of spermatids and play a synergistic role in enhancing the pituitary gonadotropin influence on spermatogonial proliferation in *Rana esculenta* (Fig. 7). These early data have been later interpreted as an example of local regulation [31]. Mak *et al.* [32]

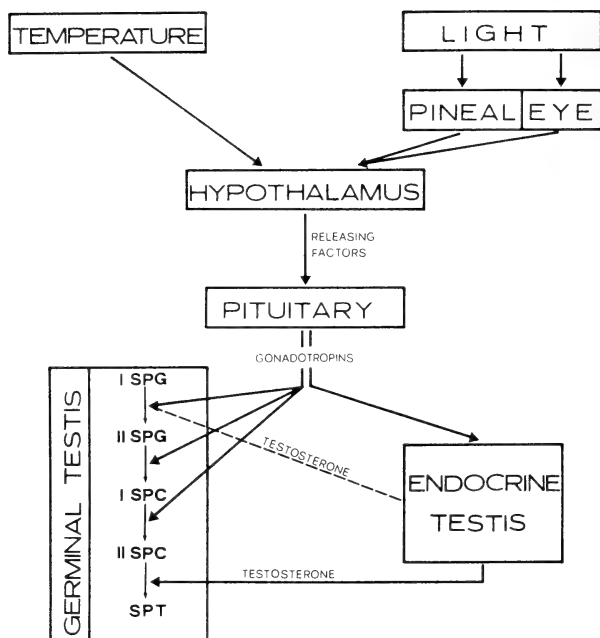


FIG. 7. A generalized scheme depicting the major relationships between the ambient cues, hypothalamus, pituitary, pineal, eye, and endocrine tissue of the testis, involved in the control of spermatogenesis in *Rana esculenta* (Rastogi *et al.* [30]).

consider estrogens to be somehow involved in regulating the secretory activity of the Leydig cells in *Necturus* testis. Since the high level of testicular aromatase seems to be associated exclusively with the Leydig cells and estrogen binding activity is located mainly in the region of differentiating or fully differentiated Leydig cells, accordingly to my presentation, the local feedback mechanism of estrogen in *Necturus* should be considered as autocrine. Thereafter Pierantoni *et al.* [32] have shown in *Rana esculenta* that estradiol peaks at the time of the year when androgens are at baseline values. Furthermore the same research group has shown that estradiol inhibits androgen production by the testis *in vitro*, while preincubation with testoster-

one or DHT enhanced o-LH stimulated androgen secretion suggesting that steroids may regulate their own intratesticular levels without passing into the blood stream. The inhibitory action of estradiol in *Rana esculenta* is supported by the finding of estrogen binding activity sharing features of estrogen receptors in the testis [34].

Like mammals, *Xenopus laevis* Sertoli cells communicate with germ cells at least at specific stages of spermatogenesis [35]. The leptotene to elongating spermatid stages appear to be independent of substances produced solely by Sertoli cells. In fact spermatocytes developed *in vitro* into four spermatids as well as preleptotene spermatocytes developed into zygotene. In contrast, the develop-

ment of the spermatogonia to meiotic prophase and the transformation of spermatids into spermatozoa seem to require Sertoli cell-specific secretory products since these processes did not occur in culture.

Among nonsteroidal bioregulators, the indole amines, melatonin and serotonin, did not induce any changes in androgen production *in vitro* in *Rana esculenta* [32]. However, numerous studies *in vivo* and *in vitro* have hypothesized a local control exerted by GnRH-like material either on steroidogenesis [31, 36, 37] (Fig. 8) or on spermatogonial multiplication of the frog [38] (Fig. 9). Very recently GnRH-like material has been demonstrated in the frog testes by radioimmunoassay, immunocytochemistry [40] and HPLC purification (Cariello *et al.*, unpubl. data). The immunohistochemical staining found in Sertoli cells and in the interstitial tissue suggests multiple sites of release or uptake for GnRH-like factors. The seasonal changes in testicular irGnRH appear independent of the seasonal changes in gonadal weight and are in accordance with the androgen and spermatogenic annual profiles. In fact in *Rana esculenta* androgen production starts to increase in autumn [31, 41, 42], when irGnRH is high in the testis. The second increase of irGnRH in spring coincides with the initiation of a new wave of spermatogenesis [30]. It is interesting to note that irGnRH reaches its nadir in February when the

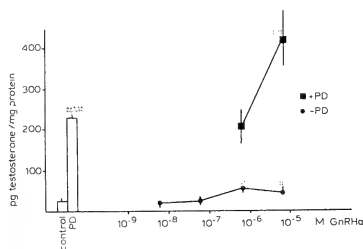


Fig. 8. Direct effect of a GnRH analog (buserelin) on the androgen production by the testis of *Rana esculenta*. 8×10^{-7} M buserelin incubated testes show a significant increase of basal androgen output. 8×10^{-5} M buserelin induces a further significant increase in pars distalis (PD) stimulated testis (Pierantoni *et al.* [31]).

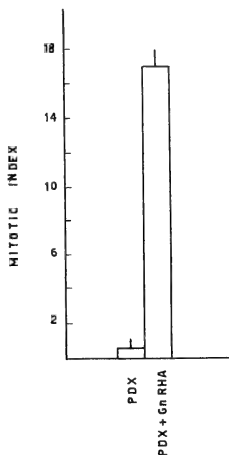


Fig. 9. Direct stimulatory effect of a GnRH analog (buserelin) on spermatogonial multiplication of hypophysectomized (PDX) *Rana esculenta* (Minucci *et al.* [38]).

mitotic index of the primary spermatogonia is at the lowest [43].

Risley *et al.* [44] have recently demonstrated that "a critical factor" in the *in vitro* maintenance of *Xenopus* spermatogenesis appears to be the preservation of testicular organization since isolated spermatogonia and late spermatids fail to progress in either serum-supplemented or serum-free media, whereas intermediate stages of spermatogenesis continue to develop in testis fragments cultured in serum-free media. These observations strongly suggest that local regulatory factors do exist in amphibian testis.

For reptiles, we have only indirect evidence of a local control of the testicular activity. Mak *et al.* [45] have identified an estrogen-binding macromolecule in the testis of the fresh-water turtle *Chrysemys picta*, suggesting the idea that testis is an important target of estrogen action. The temporal dissociation between the plasma and testis levels of testosterone in the garter snake *Thamnophis sirtalis* strongly suggests a local control of

spermatogenesis [46].

Ciarcia and Botte [47] have shown the presence of GnRH-like material in the testis of *Podarcis s. sicula* throughout the year, except summer when testosterone is at its nadir [48]. Andò *et al.* [49] have given an indirect evidence of the inhibitory role of estradiol on androgen biosynthesis by the testis of *Podarcis s. sicula*. In fact testosterone reaches its baseline value at the time when both estradiol and progesterone reach the highest value. Furthermore the progesterone/17 α -hydroxyprogesterone ratio increases indicating an inhibition of the 17 α -hydroxylase activity. However it should be demonstrated whether the inhibitory effect of estradiol is direct or mediated by the pituitary.

No information is available yet for the local control of testicular activity in birds.

OVARIAN LOCAL CONTROL

The composite structure of the ovary represents another example of intriguing communications between different cell compartments. The ovarian follicle, the functional unit of the ovary, is composed of two principal cell systems, the theca and the granulosa, whose growth, development and secretion are under the endocrine control by FSH and LH. However their function is also regulated by paracrine and autocrine secretion of steroidal and nonsteroidal bioproducts.

Overview of mammals

It is well known that in mammals steroid biosynthesis by granulosa cells requires their interaction with neighbouring theca cells. Androstenedione and testosterone from theca cells cross the basal membrane, enter the granulosa layer and accumulate in follicular fluid. Granulosa cells metabolize androgens to 5 α -reduced androgens, estradiol and catechol estrogens. The androgens produced by theca cells exert important paracrine action on granulosa cell differentiation inducing the transformation of the immature granulosa cells into fully immature counterpart.

Testosterone and androstenedione are converted by the aromatizing enzymes of mature granulosa cells into estrogens which reduce the

potential for direct androgenic action. On the other hand 5 α -reduced androgen metabolites may act as aromatase inhibitors hence suppressing estrogen biosynthesis (see for review, Hsueh *et al.* [50]).

Local regulation of folliculogenesis and ovulation is also modulated by nonsteroidal substances like proteins, secreted by the granulosa cells (see for review, Tsafiri [51]). The list of these substances is growing rapidly. In fact candidates involved in intraovarian paracrine communications include inhibin, plasminogen activator, oocyte maturation inhibitor, relaxin, epidermal growth factor (EGF), transforming growth factors (TGFs), insulin-like growth factors (IGFs), fibroblast growth factors (FGFs), various proteases and protease/substrate inhibitors, components of the extracellular matrix such as fibronectin, oxytocin-vasopressin, opiates, GnRH-like peptides, prostaglandins, etc. However the most well known proteins secreted by the granulosa cells are inhibin, plasminogen activator, oocyte maturation inhibitor and relaxin.

Dimers of inhibin subunits synthesized by granulosa cells modulate androgen secretion by theca-interstitial cells *in vitro* [16]. $\alpha\beta$ heterodimer and $\beta\beta$ homodimer do not affect androgen biosynthesis by themselves. However when given with LH they do affect androgen biosynthesis *in vitro*: $\alpha\beta$ heterodimer further enhances LH-stimulated androgen secretion by theca-interstitial cells, whereas $\beta\beta$ homodimer suppresses LH action. When $\alpha\beta$ heterodimer and $\beta\beta$ homodimer are given together, they antagonize each other's action (Fig. 10A). Mismatching experiments show that increasing doses of $\alpha\beta$ heterodimer or $\beta\beta$ homodimer enhanced or inhibited respectively LH-stimulated androgen secretion (Fig. 10B).

Hence, similarly to the testis, also in the case of the ovary, besides the long feedback between ovarian androgen producing and pituitary LH-secreting cells, there exists an additional feedback axis between FSH-secreting and inhibin-producing cells. A paracrine control between granulosa and theca cells further mediates the cross-communications between the two axis (Fig. 11).

Plasmin, which is produced by the action of plasminogen activator, seems to intervene in de-

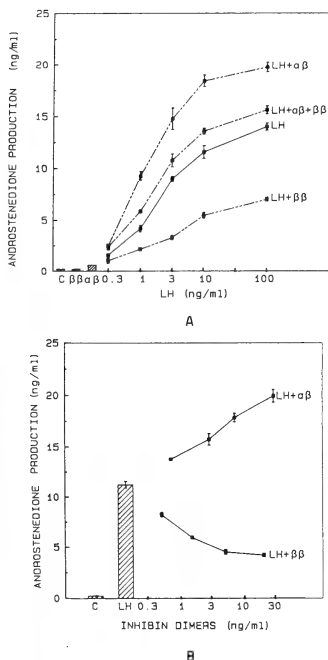


FIG. 10. Modulatory effect of inhibin dimers on LH-stimulated androgen production by cultured ovarian theca-interstitial cells of the rat. A, Modulatory effect of inhibin dimers on increasing doses of LH. B, Mismatching experiments using increasing doses of inhibin dimers (Hsueh *et al.* [17]).

creasing follicle wall strength leading to ovulation [52].

Prostaglandins, as the plasminogen activator, are also important secretory products of granulosa cells; they play a remarkable role in follicular maturation and ovulation since inhibitors of their synthesis prevent ovulation (see for review, Hsueh *et al.* [50]). Proteoglycans have been identified in the follicular fluid. They seem to be linked to the ovulation processes through increasing the viscosity of the fluid and consequently the intrafollicular pressure [53]. Relaxin, a characteristic product of the corpus luteum, is also produced by granulosa cells [54]. Too *et al.* [55] reported that relaxin stimulates granulosa cell production of plasminogen activator.

Another proposed protein produced by granulosa cells is the oocyte maturation inhibitor (OMI). OMI likely maintains the oocyte in a resting state until LH surge stimulates folliculogenesis (see for review, Hsueh [50]).

The mitogenic effect of FSH and estradiol on granulosa cells might be mediated by locally induced growth factors (EGF, IGF, etc.). In fact neither FSH nor estradiol exert mitogenic effect *in vitro*, which they do *in vivo* (see for review, Hsueh *et al.* [50]).

As regard to the intraovarian autocrine communications, Hsueh [50] has shown that estrogens stimulate granulosa cell mitoses and enhance FSH and LH action. Furthermore the still debated theory explaining how "dominant" follicles are selected to ovulate in the mammalian menstrual cycle, suggests that will be the follicle more rapidly

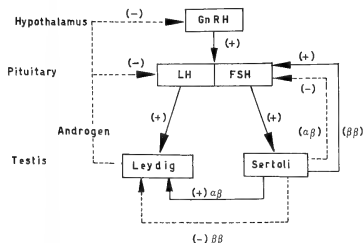


FIG. 11. Diagram of the hypothalamic-pituitary-ovarian feedback mechanisms. Based on findings of paracrine and endocrine actions of heterodimer of inhibin subunits, the cross-communication between two hypothalamic-pituitary ovarian feedback axes can be postulated. LH stimulates theca cell production of androgens, which exert negative feedback on LH release, whereas FSH stimulates granulosa cell production of inhibin, which suppresses FSH release but enhances the LH stimulation of theca cell androgen biosynthesis. In addition, LH may also stimulate granulosa cell inhibin production in mature follicles. Likewise, the $\beta\beta$ homodimer of inhibin may antagonize the action of the $\alpha\beta$ heterodimer of inhibin (Hsueh *et al.* [17]).

increasing its estrogen production to be favoured through the activation of an autocrine feedback. The selected follicles owing to their estrogen production, reduce both systemic and intrafollicular FSH, therefore the maturation of the not selected follicles fail to occur (see for review, Hsueh *et al.* [50]). They undergo atresia since they are not longer able to produce enough estrogens following FSH decline. It is not known how the selected follicles may continue to grow despite declining FSH levels (Fig. 12).

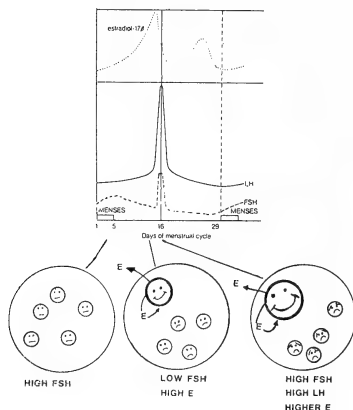


FIG. 12. Autocrine control of estrogen biosynthesis in the ovary. The "dominant follicle" is selected through the activation of an autocrine feedback (lower diagram). Upper panel, hormone profile during human menstrual cycle (Hsueh *et al.* [50]).

Autocrine control of estrogens also reflects the increased progesterone production by granulosa cells [56, 57]. Also in this case estrogens act locally enhancing the sensitivity of granulosa cells to pituitary gonadotropins.

Luteal cell progesterone biosynthesis represents another clear example of an intraovarian control mechanism. Rothchild [58] has shown the stimulatory effect of progesterone on its own secretion in hypophysectomized rats. This hypothesis has been supported by the finding of specific receptors in rat

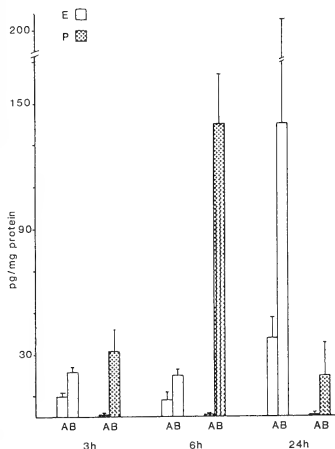
granulosa cells [59, 60]. Progesterone receptors have been demonstrated also in the ovary of guinea pig, rabbit, cow and human [61–63].

Ovarian GnRH deserves a particular mention, since it can act at the autocrine as well as the paracrine levels. Although the production of this peptide by the ovary has not yet been demonstrated with certainty, specific high affinity GnRH binding sites have been identified in luteal, thecal and granulosa cells at all stages of cellular differentiation [64–66]. Among the multiple effects detected, I will cite both inhibition and stimulation of steroidogenesis according to the maturational stages of the follicles, the maturation of follicle-enclosed rat oocyte *in vitro*, the induction of ovulation in hypophysectomized rats, the inhibition of FSH stimulation of cAMP production, the inhibition of ovarian luteal functions in women as well as in non pregnant and pregnant rats (see for review, Hsueh *et al.*, [50]).

Nonmammalian vertebrates

No data are available for the intraovarian control of either steroidogenesis or oogenesis in cyclostomes and elasmobranchs. In the remaining vertebrate classes the theca-granulosa communication is well known, as well as the progesterone and $17\alpha, 20\beta$ diOH-progesterone induced maturational process of the oocyte in amphibians and teleosts (see for review, Chieffi and Pierantoni [67]). Recently in amphibians Schuetz and Lessman [68] studied the role of the follicle wall in ovulation and progesterone production in the frog *Rana pipiens*. Follicles deprived of the surface epithelium and the theca accumulated less progesterone than intact follicles. Furthermore outer surface epithelium plays some role in the pituitary-induced ovulation. In fact the "contractions" of the follicle wall are dependent upon the presence of the surface epithelium. These observations emphasize the interaction of the cellular layers of the follicle.

Estradiol exerts an important role in regulating progesterone synthesis as it has been shown by Lin and Schuetz [69, 70] in *Rana pipiens*. *In vitro* experiments demonstrated unequivocally that estrogen has an inhibitory effect on pituitary-induced progesterone biosynthesis and consequently on the oocyte maturation. Interesting



enough is the peak of progesterone level in the ovary when estradiol value decreases in the annual cycle of *Rana esculenta* [71]. Furthermore *in vitro* experiments show that oLH-stimulated oocytes produced estradiol which in turn inhibits progesterone biosynthesis (Fig. 13).

GnRH does not affect ovarian steroidogenesis or oocyte maturation *in vitro* in *Rana catesbeiana* and *Rana pipiens* [72]. However in *Rana esculenta* GnRH does seem to influence the ovarian function. In fact, injections of GnRH induce a signi-

FIG. 13. Modulatory effect of estradiol (E) on progesterone (P) output by cultured minced ovaries of *Rana esculenta*. Minced ovaries containing 1 mm follicles were incubated for 3, 6 and 24 hr in absence (A) and in presence (B) of 20 μg of oLH. Progesterone decreases after 24 hr incubation; concomitantly estradiol increase in oLH stimulated tubes indicating the inhibitory role of estradiol on progesterone production (Pierantoni *et al.* [71]).

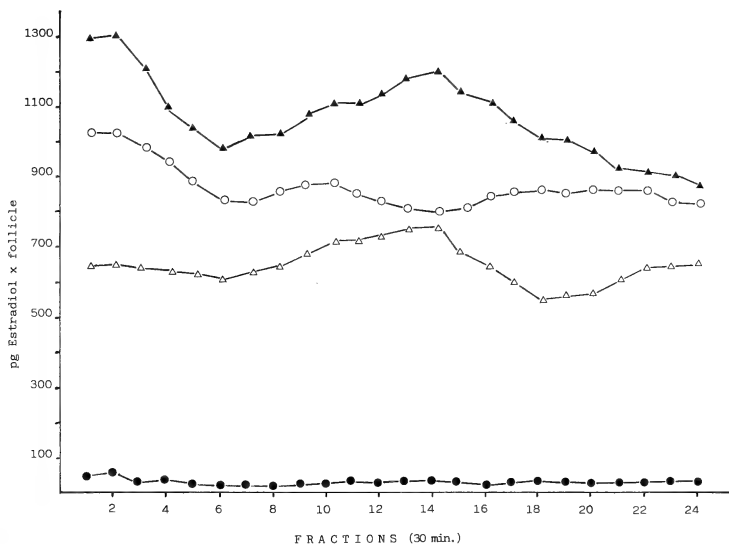


FIG. 14. Direct effect of mammalian GnRH on estradiol output by superfused ovarian follicles of *Rana esculenta*. Secretion rates of estradiol from small sized follicles (●) and continuously superfused ones with 100 ng/ml mammalian GnRH (○), homologous pituitary (▲) and mammalian GnRH plus homologous pituitary (△). Data represent averages for five females in July (Zerani *et al.* [73]).

ficant increase of plasma estradiol in hypophysectomized animals [36]. *In vitro* superfusion system confirms that GnRH acts directly on ovarian steroidogenesis as indicated by high estradiol concentrations found in the culture medium of early (~ 1 mm) vitellogenic follicles [73] (Fig. 14).

An inhibition of progesterone output induced by GnRH has been shown in *Rana esculenta* minced ovaries by Varriale *et al.* [74]. Discrepancies between the above quoted data may be explained either by interspecific differences or by differences in the experimental design. In fact, the size of the follicles used and the dose of peptide tested may account for discrepant results.

Sauropsida have been rather neglected so far. Among the few studies carried out, I mention the stimulation of progesterone output by the lizard *Podarcis s. sicula* follicles due to GnRH [74] and the stimulation *in vitro* by GnRH [75] (Fig. 15) and androgen [76] on progesterone production by chicken granulosa cells. It appears therefore that progesterone production may also be influenced by intraovarian steroidal and nonsteroidal environ-

of research is accumulating which helps in filling in the wide gaps in our knowledge of the local control of gonadal activity.

- 2) Although normal gonadal function ceases when gonadotropin support is withdrawn, local mechanisms, both paracrine and autocrine, subserve, mediate or modulate the action of gonadotropins according to local requirements.
- 3) In response to gonadotropin secretion, various gonadal compartments interact in highly integrated manner not only to modulate steroid secretion, but also to ensure the regular succession of gametogenic events.
- 4) We know for sure that gonadal activity is responsive to environmental and neuroendocrine factors, but only now we start to consider that these factors need for their goal also paracrine and autocrine regulation (Fig. 16).
- 5) Although the majority of the research in this field deals with mammals, the growing literature shows that not only local regulation occurs in nonmammalian vertebrates, but also that different mechanisms might modulate locally gonadal activity.

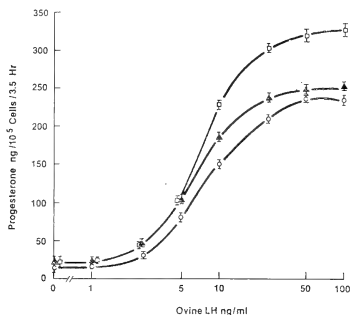


Fig. 15. Effect of GnRH on oLH induced progesterone production in granulosa cells of laying hens. Control ○; GnRH 10^{-8} △; GnRH 10^{-6} □ (Hertelendy *et al.* [75]).

CONCLUDING REMARKS

- 1) The science of "paracrinology" and "autocri-

REFERENCES

- 1 Chieffi, G. (1984) *Boll. Zool.*, **51**: 205-222.
- 2 Motta, M., Fraschini, F. and Martini, L. (1969) In "Frontiers in Neuroendocrinology". Ed. by W. F. Ganong and L. Martini, Oxford University Press, Oxford, pp. 211-253.
- 3 Parvinen, M. (1982) *Endocrin. Rev.*, **3**: 404-417.
- 4 Parvinen, M. and Ruokonen, A. (1982) *J. Androl.*, **3**: 211-220.
- 5 Sharpe, R. M. (1986) *Clin. Endocrin. Metab.*, **15**: 185-207.
- 6 Vinko, K. K., Suominen, J. J. O. and Parvinen, M. (1984) *Biol. Reprod.*, **31**: 383-389.
- 7 Galdieri, M., Monaco, I. and Stefanini, M. (1984) *J. Androl.*, **5**: 409-415.
- 8 Tres, L. L., Smith, E. P., Van Wyk, J. J. and Kierszenbaum, A. L. (1986) *Exp. Cell Res.*, **162**: 33-50.
- 9 Drummond, A. E., Rybridger, G. P. and De Kretser, D. M. (1988) *Proc. 5th European Workshop on the Molecular and Cellular Endocrinology of the Testis*, Brighton, U. K., 13-16 April, p. A4.
- 10 Kasson, B. G., Adashi, E. Y. and Hsueh, A. J. W. (1986) *Endocr. Rev.*, **7**: 156-168.

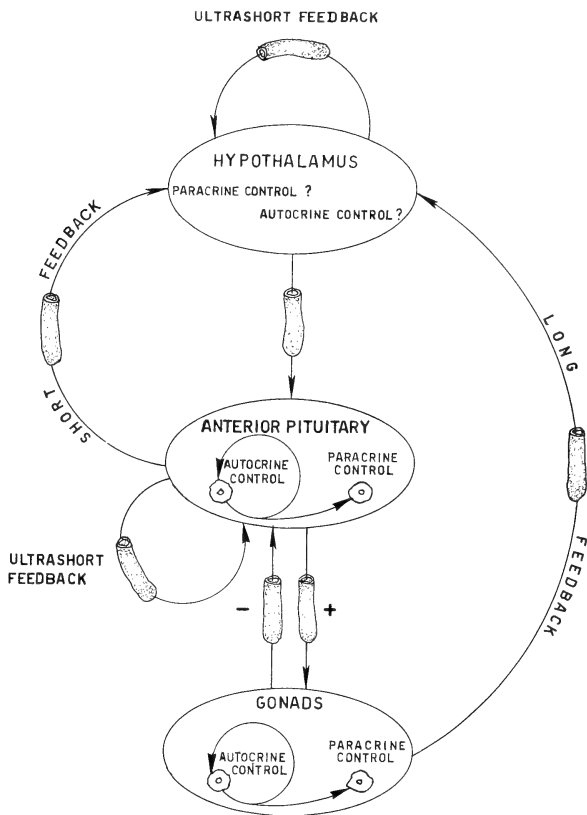


FIG. 16. The up-to-date scheme of the endogenous mechanisms modulating gonadal activity.

- 11 Grotjan, H. E. and Heindel, J. J. (1982) *Ann. N. Y. Acad. Sci.*, **383**: 456-457.
- 12 Sharpe, R. M. and Rommerts, F. F. G. (1983) In "Regulation of target cell responsiveness". Ed. by K. M. McKerns, Plenum Press, New York, pp. 267-290.
- 13 Parvinen, M., Nikula, H. and Huhtaniemi, I. (1984) *Mol. Cell. Endocrinol.*, **37**: 331-336.
- 14 Sharpe, R. M. and Cooper, I. (1984) *Mol. Cell. Endocrinol.*, **37**: 159-168.
- 15 Verhoeven, G. and Cailleau, J. (1985) *Mol. Cell. Endocrinol.*, **40**: 57-68.
- 16 Janecki, A., Jakubowiak, A. and Lukaszyk, A. (1985) *Mol. Cell. Endocrinol.*, **42**: 235-243.
- 17 Hsueh, A. J. W., Dahl, K. D., Vaughan, J., Tucker, E., Rivier, J., Bardin, C. W. and Vale, W. (1987) *Proc. Natl. Acad. Sci. USA*, **84**: 5082-5086.
- 18 Lee, W., Schwall, R. Mason, A. J. and Mather, J. P. (1988) *Proc. 5th European Workshop on the Molecular and Cellular Endocrinology of the Testis*,

- Brighton, U. K., 12-16 April, p. A1.
- 19 Murolo, E. P. and Payne, A. H. (1976) *Biochem. Biophys. Acta*, **450**: 89-100.
- 20 Naessens, S., Habert, R. and Picon, R. J. (1981) *J. Endocrinol.*, **88**: 359-366.
- 21 Pointis, G., Latreille, M. T. and Cedard, L. (1984) *Experientia*, **40**: 756-757.
- 22 Pointis, G., Latreille, M. T. and Cedard, L. (1980) *J. Endocrinol.*, **86**: 483-488.
- 23 Ho, S. M., Press, D., Chang, L. C. and Sower, S. (1987) *Gen. Comp. Endocrinol.*, **67**: 119-125.
- 24 Callard, G. V. and Mak, P. (1985) *Proc. Natl. Acad. Sci. USA*, **82**: 1336-1340.
- 25 Sourdaire, P., Garnier, D. H. and Jegou, B. (1988) *Proc. 14th Conference of European Comparative Endocrinologists, Salzburg (Austria)*, 11-16 September, p. 52.
- 26 Chieffi, G., Della Corte, F. and Botte, V. (1961) *Boll. Zool.*, **28**: 211-217.
- 27 Della Corte, F., Botte, V. and Chieffi, G. (1961) *Atti Soc. Pelorit. sci. fis. mat. nat.*, **7**: 393-397.
- 28 Fasano, S., Pierantoni, R. and Chieffi, G. (1988) *Quad. Anat. Prat.*, **44** suppl.: 119.
- 29 Powell, R. C., Millar, R. P. and King, J. A. (1986) *Gen. Comp. Endocrinol.*, **63**: 77-85.
- 30 Rastogi, R. K., Iela, L., Saxena, P. K. and Chieffi, G. (1976) *J. Exp. Zool.*, **196**: 151-166.
- 31 Pierantoni, R., Fasano, S., Di Matteo, L., Minucci, S., Varriale, B. and Chieffi, G. (1984) *Mol. Cell. Endocrinol.*, **38**: 215-219.
- 32 Mak, P., Callard, I. P. and Callard, G. V. (1983) *Biol. Reprod.*, **28**: 261-270.
- 33 Pierantoni, R., Varriale, B., Minucci, S., Di Matteo, L., Fasano, S., D'Antonio, M. and Chieffi, G. (1986) *Gen. Comp. Endocrinol.*, **64**: 405-410.
- 34 Fasano, S., Pierantoni, R., Minucci, S., Di Matteo, L., Varriale, B. and Chieffi, G. (1986) *Trends Life Sci.*, **1**: 141-144.
- 35 Risley, M. S. (1983) *Gam. Res.*, **4**: 331-346.
- 36 Segal, S. J. and Adejuwon, C. A. (1979) *Biol. Bull.*, **157**: 393-394.
- 37 Zerani, M., Gobetti, A., Bellini Cardellini, L., Pozzonetti Magni, A. and Botte, V. (1986) *Boll. Zool.*, **53**: 46.
- 38 Minucci, S., Di Matteo, L., Pierantoni, R., Varriale, B., Rastogi, R. K. and Chieffi, G. (1986) *Endocrinology*, **119**: 731-736.
- 39 Di Matteo, L., Minucci, S., Fasano, S., Pierantoni, R., Varriale, B. and Chieffi, G. (1988) *Endocrinology*, **122**: 62-67.
- 40 Fasano, S., Minucci, S., Pierantoni, R., Fasolo, A., Di Matteo, L., Basile, C., Varriale, B. and Chieffi, G. (1974) *Ster. Lip. Res.*, **5**: 42-48.
- 41 D'Istria, M., Delrio, G., Botte, V. and Chieffi, G. (1974) *Ster. Lip. Res.*, **5**: 42-48.
- 42 Varriale, B., Pierantoni, R., Di Matteo, L., Minucci, S., Fasano, S., D'Antonio, M. and Chieffi, G. (1986) *Gen. Comp. Endocrinol.*, **64**: 401-404.
- 43 Rastogi, R. K., Chieffi, G., Iela, L., Di Meglio, M., Vitiello Izzo, I. and Di Matteo, L. (1985) In "Current Trends in Comparative Endocrinology". Ed. by B. Lofis and W. N. Holmes, Hong Kong Univ. Press, Hong Kong, pp. 251-252.
- 44 Risley, M. S., Miller, A. and Bumcrot, D. A. (1987) *Biol. Reprod.*, **36**: 985-997.
- 45 Mak, P., Ho, S. M. and Callard, I. P. (1983) *Gen. Comp. Endocrinol.*, **52**: 182-189.
- 46 Weil, M. R. (1985) *Comp. Bioch. Physiol.* **81A**: 585-587.
- 47 Ciarcia, G. and Botte, V. (1988) *Rend. Accad. Naz. Lincei, Cl. Sci. fis. mat. nat.*, *in press*.
- 48 Ciarcia, G., Angelini, F., Polzonetti, A., Zerani, M. and Botte, V. (1986) In "Endocrine Regulations as Adaptive Mechanisms to the Environment". Ed. by I. Assenmacher and J. Boissin, CNRS, Paris, pp. 95-102.
- 49 Andò, S., Ciarcia, G., Panno, M. L., Angelini, F., Aquila, S., D'Uva, V. and Botte, V. (1988) *Proc. 14th Conference of European Comparative Endocrinologists, Salzburg (Austria)*, 11-16 September, p. 49.
- 50 Hsueh, A. J. W., Adashi, E. Y., Jones, P. B. C. and Welsh, T. H. (1984) *Endocr. Rev.*, **5**: 76-127.
- 51 Tsafirri, A. (1987) In "The Physiology of Reproduction". Ed. by E. Knobil and J. D. Neill, Raven, New York, pp. 527-565.
- 52 Beers, W. H. (1975) *Cell*, **6**: 379-386.
- 53 Yanagishita, M., Rodbard, D. and Haschall, V. C. (1979) *J. Biol. Chem.*, **254**: 911-920.
- 54 Loeken, M. R., Channing, C. P., D'Elletto, R. and Weiss, G. (1983) *Endocrinology*, **112**: 769-771.
- 55 Too, C. K. L., Weiss, R. T. J. and Bryant-Greenwood, G. D. (1982) *Endocrinology*, **111**: 1424-1426.
- 56 Richards, J. S., Jonassen, J. A., Rolfes, A. I., Kersey, K. and Reichert Jr., L. E. (1979) *Endocrinology*, **104**: 765-773.
- 57 Rani, C. S. S., Salhanick, A. R. and Armstrong, D. T. (1981) *Endocrinology*, **108**: 1379-1385.
- 58 Rothchild, I. (1981) *Rec. Progr. Horm. Res.*, **37**: 183-298.
- 59 Schreiber, J. R. and Erickson, G. F. (1979) *Steroids*, **34**: 459-469.
- 60 Naess, O. (1981) *Acta Endocrinol.*, **98**: 288-294.
- 61 Philibert, D., Ojasoo, T. and Raynaud, J. P. (1977) *Endocrinology*, **101**: 1850-1861.
- 62 Jacobs, B. R., Suchocki, S. and Smith, R. G. (1980) *Am. J. Obstet. Gynecol.*, **138**: 332-336.
- 64 Harwood, J. P., Clayton, R. N. and Catt, K. J. (1980) *Endocrinology*, **107**: 407-413.

- 65 Harwood, J. P., Clayton, R. N., Chen, T. T., Knox, G. and Catt, K. J. (1980) *Endocrinology*, **107**: 414-421.
- 66 Pelletier, G., Seguin, C., Dube, D. and St.-Arnaud, R. (1982) *Biol. Reprod. suppl.*, **26**: 151A.
- 67 Chieffi, G. and Pierantoni, R. (1987). In "Hormones and Reproduction in Fishes, Amphibians and Reptiles". Ed. by D. O. Norris and R. E. Jones, Plenum, New York and London, pp. 117-144.
- 68 Schuetz, A. W. and Lessman, C. (1982) *Differentiation*, **22**: 79-84.
- 69 Lin, Y. W. P. and Schuetz, A. W. (1983) *J. Exp. Zool.*, **226**: 281-291.
- 70 Lin, Y. W. P. and Schuetz, A. W. (1985) *Gen. Comp. Endocrinol.* **58**: 421-435.
- 71 Pierantoni, R., Varriale, B., Fasono, S., Minucci, S., Di Matteo, L. and Chieffi, G. (1987) *Gen. Comp. Endocrinol.*, **67**: 163-168.
- 72 Hubbard, G. M. and Licht, P. (1985) *Gen. Comp. Endocrinol.*, **60**: 154-161.
- 73 Zerani, M., Gobetti, A., Carnevali, O., Polzonetti Magni, A. and Botte, V. (1987) *Gen. Comp. Endocrinol.*, **66**: 8-9.
- 74 Varriale, B., Pierantoni, R., Di Matteo, S., Minucci, S. and Chieffi, G. (1986) *Boll. Zool.*, **53**: 381-383.
- 75 Hertelendy, F., Lintner, F., Asem, E. K. and Raab, B. (1982) *Gen. Comp. Endocrinol.*, **48**: 117-122.
- 76 Phillips, A., Scanes, C. G. and Hahn, D. W. (1985) *Comp. Biochem. Physiol.*, **81A**: 847-852.



REVIEW

New Aspects of Accumulation and Reduction of Vanadium Ions in Ascidians, Based on Concerted Investigation from Both a Chemical and Biological Viewpoint

HITOSHI MICHIBATA

*Biological Institute, Faculty of Science,
Toyama University, Toyama 930, Japan*

ABSTRACT—Ever since high levels of vanadium was found unexpectedly in the blood cells of ascidians about 80 years ago, the mechanism of accumulation and the function of this metal in blood cells have been absorbed the interest of not only chemists but also biologists from various fields including analytical chemistry, coordination chemistry, physiology and biochemistry. Recently, this phenomenon has been the focus of concerted investigation from both a chemical and biological viewpoint. Here we summarize the most recent findings with special reference to data obtained by a combination technique involving cell fractionation for purification of a specific type of blood cell, neutron activation analysis for vanadium determination, and ESR (electron spin resonance) spectrometry for determination of chemical forms of vanadium in the blood cells.

INTRODUCTION

It was found unexpectedly by Henze about 80 years ago that ascidians contained a high level of vanadium in their blood cells [1, 2]. Many analytical chemists subsequently showed an interest, and analyzed the metal contents of species belonging to all three ascidian suborders (the Aplousobranchia, Phlebobranchia and Stolidobranchia) using newer analytical techniques [3-25]. The resulting data have shown that several species in the suborder Aplousobranchia generally have a high vanadium content, and that a significant amount of vanadium is likewise found in representatives of the Phlebobranchia, whereas species of the suborder Stolidobranchia contain relatively smaller amounts of vanadium, but a high level of iron. Webb [5] first pointed out that high concentrations of vanadium in ascidian species were correlated with certain evolutionary traits in the class Ascidiacea; he also predicted that the presence of vanadium was a primitive characteristic which had

been lost in the more specialized families, based on earlier data on the vanadium and iron contents of ascidians already examined. Endean [26, 27] reported that ascidian species belonging to the Pyuridae concentrated iron instead of vanadium. He assumed that since the ascidians are an intermediate group between the invertebrates and vertebrates, the animals were the key for resolving how transition metals were selected by organisms. Swinehart *et al.* [22] also suggested that these species might indeed represent animals that were in transition between the vanadium and iron "users". This proposal has brought particular interest from a wide area of investigation.

REEXAMINATION OF METAL CONTENTS WITH NEUTRON ACTIVATION ANALYSIS

We have also taken interest in the fact that the ascidians are the only organisms in animal kingdom to accumulate vanadium at a high level. Although animal feeding studies has suggested that the vanadium is an essential element for living organisms [28] and biochemical studies revealed

accidentally that vanadium in a V oxidation state was a potent inhibitor of Na-K-ATPase [29, 30], its physiological roles have not yet been clarified in detail. The use of ascidians, which accumulate high levels of vanadium, as study materials would be valuable for helping to resolve the mechanism of metal accumulation against a concentration gradient as high as seven orders of magnitude, as will be mentioned below. For studying this problem, we were fortunate to have access to neutron activation analysis which is the most sensitive technique for detection of vanadium (Fig. 1), and was available at the Institute for Atomic Energy of Rikkyo University. At the commencement of the study, we first intended to re-determine the vanadium content in several tissues of ascidians employing the same analytical method of the neutron activation analysis and the same pretreatments used for the determination. The data obtained from 15 species of solitary ascidian belonging to

the suborders Phlebobranchia and Stolidobranchia agreed substantially with previous reports of high vanadium levels in the family Ascidiidae, the highest amounts being present in blood cells. However, in contrast with former studies, it is important to note that significant levels of vanadium were detected in all tissues of all species, even those belonging to the suborder Stolidobranchia, and that the content of iron did not vary sharply between the two suborders studied, in contrast with vanadium content. In other words, we cannot conclude that the relative concentrations of two metals in different ascidian subfamilies reflects phylogeny [31].

Although niobium (Nb) [32, 33], titanium (Ti) [6, 13], chromium (Cr) [13, 34] and tantalum (Ta) [33] have been reported to be present in ascidian tissues besides vanadium, the reproducibility of data indicating the presence of these metals in ascidians has been poor up to the present time.

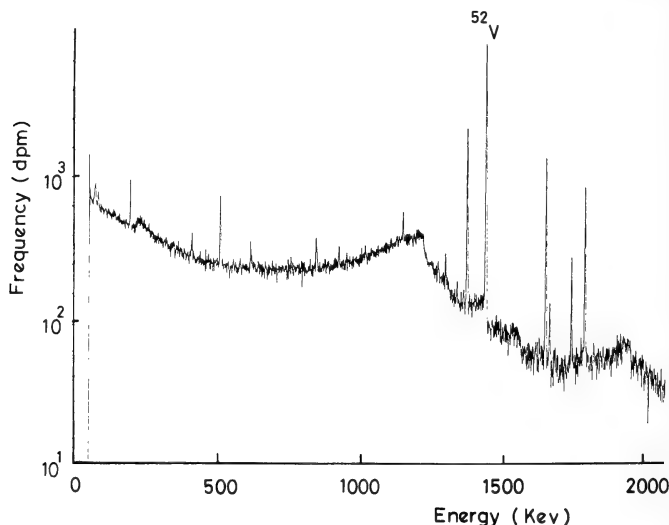


Fig. 1. γ -ray spectrometry of ascidian blood cells after irradiation with thermal neutrons at the Institute for Atomic Energy, Rikkyo University. Clear photopeak of ^{52}V , produced in the irradiated sample, can be seen.

COMBINATION TECHNIQUES OF CELL FRACTIONATION AND NEUTRON ACTIVATION ANALYSIS FOR IDENTIFICATION OF TRUE VANADOCYTES

Seawater is reported to contain dissolved vanadium ion at a concentration of 35 nM [35, 36], yet some ascidians accumulate the ion in their blood cells to a maximum concentration of 150 mM [31, 37, unpubl. data], which is more than four million times higher than that in seawater. Ascidian blood cells are classified into six to nine types based on their morphology [26, 27, 38, 39]. Among these, the morula cells (Fig. 2A), light green in color and containing several vacuoles, have been thought to be involved in the accumulation of vanadium ion and have called "vanadocytes" [5, 11, 16, 27], since the color of the cells resembles that of vanadium complex, and dense granules are observed in the cells after fixation with osmium tetroxide, which may be deposits of vanadium [16, 17, 19, 27, 40, 41]. Several investigators using X-ray microanalysis have claimed recently that the morula cells contain little or no vanadium ion. Mainly de Vincentiis's group found more vanadium ion associated with the vacuolar membranes of granular amoebocytes, signet ring cells, and compartment cells than in the vacuoles of the morula cells of *Phallusia mammillata* and *Ciona intestinalis*. Morula cells of *P. mammillata* contained very little or no vanadium ion, and granular amoebocytes of *C. intestinalis* contained more vanadium ion than

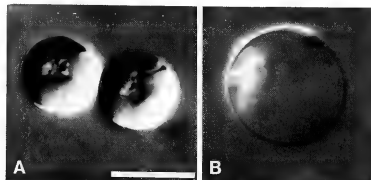


FIG. 2. Differential interference contrast photomicrographs of morula cells (A) and signet ring cell (B) in *Ascidia ahodori*. Morula cell appears typical berry-like shape. Signet ring cell is characterized by a single and fluid filled vacuole which displaced the nucleus and cytoplasm to the periphery of the cell. Scale bar indicates 10 μ m.

the morula cells [42–47]. Ultrastructural observation, however, can only provide limited data on which blood cells are the true vanadocytes because of artifacts resulting from the preparation method.

Therefore, we have attempted to identify the vanadocytes among several kinds of blood cell using a combination techniques consisting of Ficoll density gradient centrifugation and neutron activation analysis. Each kind of blood cell has a specific gravity, and consequently, a pure subpopulation of a single type of blood cell can form a separate layer depending on its specific gravity after density gradient centrifugation on Ficoll type 400, as shown in Figure 3. Each subpopulation is subjected to analysis of its vanadium content by neutron activation analysis. Following this tech-

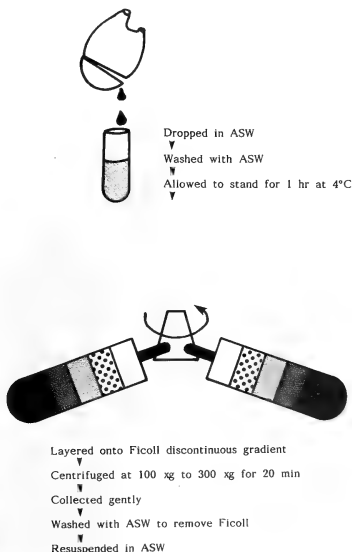


FIG. 3. Experimental scheme for density gradient centrifugation in order to obtain a pure subpopulation of each blood cell type. Ficoll type 400 was dissolved in the artificial seawater (ASW) at four different concentrations and discontinuous density gradients were prepared. Then, the cells were layered onto the gradients and were centrifuged.

nique, blood cells were partitioned into four discrete layers: Layer 1 contained a relatively small number of compartment cells and amoebocytes. Layer 2 contained mostly compartment cells (84.2%). Layer 3 contained more than 90% morula cells. Layer 4 contained 67% morula cells and 31% signet ring cells. Neutron activation analysis revealed that the vanadium level was highest in layer 4. The pattern of distribution of vanadium was compared with those of the blood cells in Figure 4. This pattern was very similar to that of the signet ring cells, but was clearly different from that of the morula cells and the other cell types. In other words, it was apparent that the vanadocytes are the signet ring cells, not the morula cells. The signet ring cell has a single, large fluid-filled vacuole containing granules, as shown in Figure 2B. The nucleus and cytoplasm are displaced by the vacuole to the periphery, giving the cell its characteristic signet ring-like appearance [48].

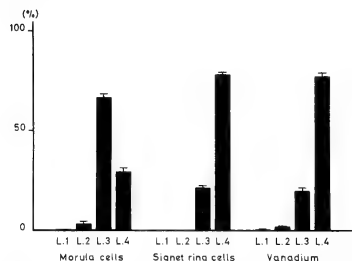


FIG. 4. Comparison of the patterns of distribution of morula cells and signet ring cells with that of vanadium ions after density gradient centrifugation. The pattern of distribution of vanadium is similar to that of signet ring cells but is different from that of morula cells.

CHEMICAL FORMS OF VANADIUM IN ASCIDIAN BLOOD CELLS

The chemical form of vanadium present in ascidian blood cells have long been a subject of discussion. Following Henze's reports [1, 2], it was believed that the vanadium was present in the form of a nitrogenous compound including sulfuric acid, well known as haemovanadin [12, 19, 49]. Recently,

it has become clear that the vanadium ion in seawater is the vanadate(V) anion [50] whereas that in ascidian blood cells is reduced to vanadyl cations, VO^{2+} and/or V^{3+} [22, 48, 51–58]. Therefore, it can be assumed that some reducing agents for reducing of vanadate ion to vanadyl form must exist in the blood cells. Several years ago Kustin's group reported the successful isolation of a reducing agent from the blood cells of *Ascidia nigra* and *Ciona intestinalis* under a reducing atmosphere [37, 59]. This substance, named tunichrome, can readily reduced vanadate ion to vanadyl ion and is also able to reduce Fe(III) to Fe(II) *in vitro*. Thereafter, Nakanishi and his co-workers directed their attention to this substance and isolated a tunichrome B-1 from the blood cells of *Ascidia nigra* under argon gas by means of centrifugal counter-current chromatography. They have verified that tunichrome B-1 consists of three alanine residues and that the reducing property is due to the presence of pyrogallol subunits, which are known to reduce vanadate(V) to vanadyl(IV) and to form complexes [60, 61]. Furthermore, this substance has been reported to emit a specific autonomous fluorescence at 532 nm and 581 nm upon excitation with blue-violet light at 488 nm, and consequently, it has been suggested that the intensity of fluorescence is indicative of the concentration of vanadium ion in blood cells because both tunichrome and vanadium have been presumed to be present at approximately equimolar concentrations based on the stoichiometry of the reaction of vanadium with tunichrome purified from *A. nigra* *in vitro*. Spectrofluorometric analysis revealed that the concentration of tunichrome was highest in morula cells, followed by compartment cells and signet ring cells in that orders. Therefore, it was believed that the vanadium concentrations occurred in the same order, i.e., the morula cell was the so-called vanadocyte [62, 63].

If tunichrome is involved in the accumulation and reduction of vanadium ion in ascidian blood cells, it necessary to confirm that vanadocytes do in fact contain both tunichrome and vanadium. As mentioned above, we have already proved that morula cells contain no vanadium, whereas signet ring cells contain a very high level of vanadium ion in the case of *A. ahodori* [48]. In order to verify

the participation of tunichrome in the accumulation of vanadium ion from seawater and its reduction in ascidian blood cells, we examined whether the signet ring cells, newly identified as vanadocytes, emit autonomous fluorescence due to the tunichrome. In recent experiments, we found that the morula cells, compartment cells and the orange pigment cells emitted autonomous fluorescence after excitation with blue-violet light, composed of line spectra at 405 nm and 435 nm and a wide spectrum at 490 nm. The fluorescence emitted from the morula cell was absorbed by an O515 barrier filter, indicating that its wavelength was longer than 515 nm. The compartment cell and orange pigment cell emitted a fluorescence longer than 475 nm and 530 nm, respectively. However, no fluorescence due to the tunichrome was detected from the signet ring cell as shown in Figure 5 [64]. The same results were obtained in a different ascidian species, *A. sydneiensis samea* [65]. At the present time, therefore, it is doubtful whether tunichrome participates in the accumulation and reduction of vanadium ion in ascidian blood cells.

VANADIUM-BINDING SUBSTANCE (VANADOBIN) EXTRACTED FROM ASCIDIAN BLOOD CELLS

On the other hand, as we have considered that the vanadium must be present as some type of complex in ascidian blood cells, we attempted to extract and purify a vanadium-binding substance from the blood cells of *Ascidia sydneiensis samea* by a combination of techniques including chromatography, neutron activation analysis and electron spin resonance spectrometry (ESR). Through this approach, we succeeded in obtaining the vanadium-binding substance by chromatographies on Sephadex G-25 and SE-cellulose under the low pH conditions [57]. This substance, named vanadobin, is colorless and can maintain the vanadium ion in the vanadyl form (VO(IV)) even under aerobic conditions. Moreover, it has an affinity for exogenous vanadate ion(V) and contains a reducing sugar. The most recent experiments have revealed that vanadobin is detectable in the signet ring cells [unpubl. data].

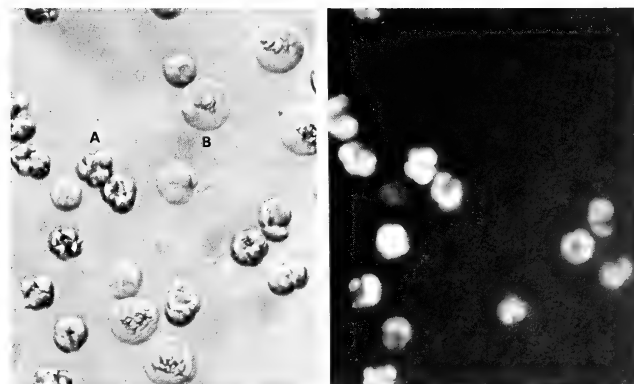


Fig. 5. Blood cells of *Ascidia ahodori* observed with a light (left) and a fluorescence microscope (right). Morula cell (A) emitted fluorescence due to tunichrome upon excitation with blue-violet light but signet ring cell (B) did not fluoresce.

NEW PHYSICAL TECHNIQUES FOR RESOLVING THE CHEMICAL FORM OF VANADIUM IN BLOOD CELLS

New physical technology, including EXAFS (extended X-ray absorption fine structure), ESR and SQUID (superconducting quantum interference device), may provide new information on chemical structure of vanadium in ascidian blood cells. These techniques have an advantage in that they can determine the intracellular oxidation state of vanadium non-invasively. Although many investigators have detected the IV oxidation state of vanadium in the blood cells using ESR spectrometry (Fig. 6) [22, 48, 54–58], whether the IV oxidation state is predominant remains unsolved. Hawkins *et al.* [55] mentioned that the Aplousobranchia had vanadium ion in the oxovanadium(IV) form, whereas the Phlebobranchia contained vanadium ion in the trivalent(III) state. Dingley *et al.* [53] reported that about 4% of the total vanadium in the cells existed in the vanadyl form. Recently, Hodgson's group, using EXAFS, has reported that the vanadium exists in the III oxidation state and binds only with water molecules in blood cells [51, 66]. Measurements with SQUID have also revealed that the predominant species of vanadium is that in the III oxidation state in blood cells of *Ascidia nigra* [67]. Views are still divided regarding the chemical forms and oxidation states of vanadium in ascidian blood cells.

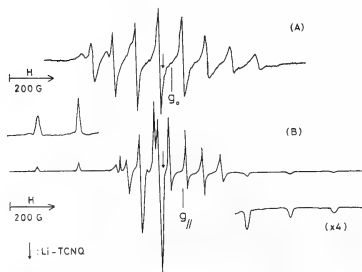


Fig. 6. ESR spectra characteristic of oxovanadium (IV) observed in the blood cells of *Ascidia ahodori*, which were measured at room temperature (A) and at 77K (B).

Besides the blood cells, vanadyl ions have been detected in the branchial basket of *Ascidia ahodori* by ESR spectrometry. Furthermore, it was observed that exogenous vanadate ions were reduced to the vanadyl form upon incubation with fragments of branchial basket, suggesting that the branchial basket may be the first organ to reduce vanadium ion, and that the reduced ion is then transferred to the blood cells [68].

PROBLEM OF LOW pH IN VANADOCYTES

The mechanism of accumulation of high levels of vanadium in ascidian blood cells has been considered to be associated with a very low pH value within the cells [5, 11, 13, 23, 26, 40, 49, 54, 69, 70]. The intracellular pH of vanadocytes has, however, been disputed. Following Henze's discovery of 1N acidity in ascidian blood cells [1, 2], 1.83 N sulfuric acid and 0.39 N acid were measured by titration method of the acid liberated upon cytolysis of the blood cells of *Phallusia mammillata* [5] and *Pyura stolonifera* [26], respectively. Dingley *et al.* [71] and Agudelo *et al.* [72] recently claimed that the methods used previously gave spurious results when applied to ascidian blood cells. They mentioned that the intracellular pH was neutral on the basis of measurements made by a new technique with improved trans-membrane equilibrium of ^{14}C -labeled methylamine. Hawkins *et al.* [73, 74] also found a neutral pH value using a non-invasive probe based on the chemical shift of ^{31}P -NMR (nuclear magnetic resonance). Conversely, Frank *et al.* [56] reported a blood cell of pH value of 1.8 based on a new finding that the ESR line width reflected accurately the intracellular pH, a method which was also non-invasive. These previous studies focused on the greenish-hued morula cells, considered to be vanadocytes, but these, of course, were not separated from the other blood cells. We believe that one of the reasons for the variation in pH values reported for ascidian blood cells is probably the measurement of pH without cell fractionation. In other words, one blood cell type among several must have a highly acidic solution within its vacuole, where the vanadium ions would be present in a reduced state. The combined technique involving cell fractionation by density

gradient centrifugation, a microelectrode for pH measurement and neutron activation analysis for vanadium measurement revealed that the signet ring cells had a low pH of 2.6 under both aerobic and anaerobic conditions and contained a high amount of vanadium in *Ascidia ahodori* [unpubl. data]. Using X-ray microanalysis with electron microscopy, Bell *et al.* [54] and de Vincentiis's group [42–46] reported the coexistence of sulfur with vanadium in blood cells. It is within the bounds of possibility that the accumulation and reduction of vanadium ion is carried out in the presence of sulfuric acid in the blood cells. Whether the vanadocyte, or more precisely speaking, the vacuole fluid of the vanadocyte, has a low pH is still a matter to be resolved in order to account for the mechanism of accumulation and reduction of vanadium ions in ascidian blood cells.

FUNCTION OF VANADIUM CONTAINED IN BLOOD CELLS

The function of such a high concentration of vanadium in ascidian blood cells remains unexplained. Endean [26, 27, 75, 76] and Smith [77, 78] proposed that the cellulose of the tunic might be produced by vanadocytes. Carlisle [21] has suggested that vanadium-containing vanadocytes can reversibly trap oxygen under conditions of low oxygen tension. Swinehart *et al.* [22] suggested the acid-producing function of vanadium, and Rowley [79] has demonstrated that the vanadium contained in vacuole works as an antimicrobial agent. However, almost all of the proposals put forward have recently become doubtful on the basis of newer experimental evidence. We maintain that any proposals concerning the function of vanadium should be reconsidered in the light of current evidence.

It is well known that transition metals including vanadium have several oxidation states and easily form coordination complexes [80–85]. Therefore, these metals have been successively revealed to be involved in enzymatic reactions and reduction-oxidation reactions in living organisms [86–89]. For example, vanadium functions as an active center in bromoperoxidase, extracted from marine algae [90, 91], and in nitrogenase purified from

bacteria [92–94]. Vanadium complex, named amavadin, was isolated from fly agaric [95]. It becomes clear that vanadium exerts an insulin-like effect on adipocytes and diabetic rats [96, 97] and inhibitory effect on carcinogenesis [98]. Moreover, the oxidation states and ionic forms of vanadium are known to be readily changeable by ascorbic acid, glutathione, cysteine and NADH (reduced nicotinamide adenine dinucleotide) [99–103], substances which are common to all living organisms.

CONCLUSION

The fact that some ascidians accumulate vanadium ion to a level exceeding four million times that present in seawater is a remarkable phenomenon. Resolution of the above issues would be a shortcut to clarifying the mechanism of accumulation of trace elements across bio-membranes and the function of transition metals in the other organisms as well as ascidians. Interdisciplinary investigation, based on marine biology, physiology, biochemistry, bioinorganic chemistry and the chemistry of natural products, are absolutely necessary for achieving these aims.

ACKNOWLEDGMENTS

I would like to express my hearty thanks to my associates for their friendly assistance and to Dr. Noriyuki Satoh, Kyoto University, for many stimulating discussion. Particular thanks are due to the staff of marine biological stations of the Asamushi, Tohoku University, the Ushimado, Okayama University, and the Misaki, University of Tokyo. This work was supported in part by a Grant-in-Aid from the Ministry of Education, Science and Culture, Japan and was also supported financially by the Japan Securities Scholarship Foundation and the Ito Science Foundation. A part of this paper was announced at the Japan-U.S. Cooperative Seminar on the theme, "Developmental Biology of the Ascidian", which was held on Aug. 22–27, 1988 at Asamushi, Aomori, Japan.

REFERENCES

- 1 Henze, M. (1911) Hoppe-Seyler's Z. Physiol. Chem., 72: 494–501.
- 2 Henze, M. (1912) Hoppe-Seyler's Z. Physiol. Chem., 79: 215–228.
- 3 Cantacuzène, J. and Tchekirian, A. (1932) Compt.

- Rend. Acad. Sci. Paris, **195**: 846-849.
- 4 Vinogradov, A. P. (1934) C. R. Acad. Sci. U.R.S.S., **3**: 454-459.
- 5 Webb, D. A. (1939) J. Exp. Biol., **16**: 499-523.
- 6 Noddack, I. and Noddack, W. (1939) Arkiv Zool., **32**: 1-35.
- 7 Kobayashi, S. (1935) Sci. Rep. Tohoku Univ. 4th Ser., **18**: 185-193.
- 8 Bertrand, D. (1950) Bull. Am. Mus. Natl. Hist., **94**: 403-455.
- 9 Goldberg, E. D., McBlair, W. and Taylor, K. M. (1951) Biol. Bull., **101**: 84-94.
- 10 Lybing, S. (1953) Arkiv Kemi, **6**: 261-269.
- 11 Boeri, E. and Ehrenberg, A. (1954) Arch. Biochem. Biophys., **50**: 404-416.
- 12 Webb, D. A. (1956) Publ. Staz. Zool. Napoli, **28**: 273-288.
- 13 Levine, E. P. (1961) Science, **133**: 1352-1353.
- 14 Bielig, H.-J., Jost, E., Pfleger, K., Rummel, W. and Seifen, E. (1961) Hoppe-Seyler's Z. Physiol. Chem., **325**: 122-131.
- 15 Kalk, M. (1963) Nature, **198**: 1010-1011.
- 16 Kalk, M. (1963) Quart. J. Microsc. Sci., **104**: 483-493.
- 17 Kalk, M. (1963) Acta Embryol. Morph. Exp., **6**: 289-303.
- 18 Ciereszko, L. S., Ciereszko, E. M., Harris, E. R. and Lane, C. A. (1963) Comp. Biochem. Physiol., **8**: 137-140.
- 19 Bielig, H.-J., Bayer, E., Dell, H.-D., Rohns, G., Möllinger, H. and Rüdiger, W. (1966) Protides Biol. Fluids, **14**: 197-204.
- 20 Rummel, W., Bielig, H.-J., Forth, W., Pfleger, K., Rüdiger, W. and Seifen, E. (1966) Protides Biol. Fluids, **14**: 205-210.
- 21 Carlisle, D. B. (1968) Proc. Roy. Soc., B, **171**: 31-42.
- 22 Swinehart, J. H., Biggs, W. R., Halko, D. J. and Schroeder, N. C. (1974) Biol. Bull., **146**: 302-312.
- 23 Danskin, G. P. (1978) Can. J. Zool., **56**: 547-551.
- 24 Botte, L. and Scippa, S. (1979) Annot. Zool. Japon., **52**: 188-190.
- 25 Michibata, H. (1984) Comp. Biochem. Physiol., **78A**: 285-288.
- 26 Endean, R. (1955) Austr. J. Mar. Freshwat. Res., **6**: 35-59.
- 27 Endean, R. (1960) Quart. J. Microsc. Sci., **101**: 177-197.
- 28 Schwarz, K. and Milne, D. B. (1971) Science, **174**: 426-428.
- 29 Cantley, L. C. Jr., Josephson, L., Warner, R., Yanagisawa, M., Lechene, C. and Guidotti, G. (1977) J. Biol. Chem., **252**: 7421-7423.
- 30 Beaugé, L. A. and Glynn, I. M. (1977) Nature, **268**: 355-356.
- 31 Michibata, H., Terada, T., Anada, N., Yamakawa, K. and Numakunai, T. (1986) Biol. Bull., **171**: 672-681.
- 32 Carlisle, D. B. (1958) Nature, **181**: 933.
- 33 Kokubu, N. and Hidaka, T. (1965) Nature, **205**: 1028-1029.
- 34 Botte, L., Scippa, S. and de Vincentiis, M. (1979) Dev. Growth Differ., **21**: 483-491.
- 35 Cole, P. C., Eckert, J. M. and Williams, K. L. (1983) Anal. Chim. Acta, **153**: 61-67.
- 36 Collier, R. W. (1984) Nature, **309**: 441-444.
- 37 Macara, I. G., McLeod, G. C. and Kustin, K. (1979) Comp. Biochem. Physiol., **63B**: 299-302.
- 38 Wright, R. K. (1981) In "Invertebrate blood cells" vol. 2. Ed. by Ratcliffe, N. A. and Rowley, A. F., Academic Press, London, pp. 565-626.
- 39 Rowley, A. F. (1981) J. Invertebrate Pathol., **37**: 91-100.
- 40 Henze, M. (1913) Hoppe-Seyler's Z. Physiol. Chem., **86**: 340-344.
- 41 Hecht, S. (1918) Am. J. Physiol., **45**: 157-187.
- 42 Botte, L. and Scippa, S. (1977) Experientia, **33**: 80-81.
- 43 Botte, L., Scippa, S. and de Vincentiis, M. (1979) Experientia, **35**: 1228-1230.
- 44 Scippa, S., Botte, L. and de Vincentiis, M. (1982) Acta Zool. (Stokh.), **63**: 121-131.
- 45 Scippa, S., Botte, L., Zierold, K. and de Vincentiis, M. (1985) Cell Tissue Res., **239**: 459-461.
- 46 Scippa, S., Zierold, K. and de Vincentiis, M. (1988) J. Submicrosc. Cytol. Pathol., **20**: 719-730.
- 47 Rowley, A. F. (1982) J. Mar. Biol. Ass., U.K., **62**: 607-620.
- 48 Michibata, H., Hirata, J., Uesaka, M., Numakunai, T. and Sakurai, H. (1987) J. Exp. Zool., **244**: 33-38.
- 49 Califano, L. and Boeri, E. (1950) J. Exp. Zool., **27**: 253-256.
- 50 McLeod, G. C., Ladd, K. V., Kustin, K. and Toppen, D. L. (1975) Limnol. Oceanogr., **20**: 491-493.
- 51 Tullius, T. D., Gillum, W. O., Carlson, R. M. K. and Hodgson, K. O. (1980) J. Am. Chem. Soc., **102**: 5670-5676.
- 52 Hawkins, C. J., Parry, D. L. and Pierce, C. (1980) Biol. Bull., **159**: 669-680.
- 53 Dingley, A. L., Kustin, K., Macara, I. G. and McLeod, G. C. (1981) Biochim. Biophys. Acta, **649**: 493-502.
- 54 Bell, M. V., Pirie, B. J. S., McPhail, D. B., Goodman, B. A., Falk-Petersen, I.-B. and Sargent, J. R. (1982) J. Mar. Biol. Ass., U.K., **62**: 709-716.
- 55 Hawkins, C. J., Kott, P., Parry, D. and Swinehart,

- J. H. (1983) *Comp. Biochem. Physiol.*, **76B**: 555-558.
- 56 Frank, P., Carlson, R. M. K. and Hodgson, K. O. (1986) *Inorg. Chem.*, **25**: 470-478.
- 57 Michibata, H., Miyamoto, T. and Sakurai, H. (1986) *Biochem. Biophys. Res. Commun.*, **141**: 251-257.
- 58 Sakurai, H., Hirata, J. and Michibata, H. (1987) *Biochem. Biophys. Res. Commun.*, **149**: 411-416.
- 59 Macara, I. G., McLeod, G. C. and Kustin, K. (1979) *Biochem. J.*, **181**: 457-465.
- 60 Bruening, R. C., Oltz, E. M., Furukawa, J., Nakanishi, K. and Kustin, K. (1985) *J. Am. Chem. Soc.*, **107**: 5298-5300.
- 61 Oltz, E. M., Bruening, R. C., Smith, M. J., Kustin, K. and Nakanishi, K. (1988) *J. Am. Chem. Soc.*, **110**: 6162-6172.
- 62 Robinson, W. E., Agudelo, M. I. and Kustin, K. (1984) *Comp. Biochem. Physiol.*, **78A**: 667-673.
- 63 Oltz, E. M. (1987) Ph. D. Thesis of Columbia Univ.
- 64 Michibata, H., Hirata, J., Terada, T. and Sakurai, H. (1988) *Experientia*, **44**: 906-907.
- 65 Michibata, H., Uyama, T. and Hirata, J. (1989) *Zool. Sci.*, in press.
- 66 Frank, P., Hedman, B., Carlson, R. M. K., Tyson, T. A., Roe, A. L. and Hodgson, K. O. (1987) *Biochemistry*, **26**: 4975-4979.
- 67 Lee, S., Kustin, K., Robinson, W. E., Frankel, R. B. and Spertalian, K. (1988) *J. Inorg. Biochem.*, **33**: 183-192.
- 68 Sakurai, H., Hirata, J. and Michibata, H. (1988) *Inorg. Chim. Acta*, **152**: 177-180.
- 69 Stoecker, D. (1980) *J. Exp. Mar. Biol. Ecol.*, **48**: 277-281.
- 70 Roman, D. A., Molina, J. and Rivera, L. (1988) *Biol. Bull.*, **175**: 154-166.
- 71 Dingley, A. L., Kustin, K., Macara, I. G., McLeod, G. C. and Roberts, M. F. (1982) *Biochim. Biophys. Acta*, **720**: 384-389.
- 72 Agudelo, M. I., Kustin, K. and McLeod, G. C. (1983) *Comp. Biochem. Physiol.*, **75A**: 211-214.
- 73 Hawkins, C. J., James, G. A., Parry, D. L., Swinehart, J. H. and Wood, A. L. (1983) *Comp. Biochem. Physiol.*, **76B**: 559-565.
- 74 Brand, S. G., Hawkins, C. J. and Parry, D. L. (1987) *Inorg. Chem.*, **26**: 627-629.
- 75 Endean, R. (1955) *Austr. J. Mar. Freshwat. Res.*, **6**: 139-156.
- 76 Endean, R. (1955) *Austr. J. Mar. Freshwat. Res.*, **6**: 157-164.
- 77 Smith, M. J. (1970) *Biol. Bull.*, **138**: 354-378.
- 78 Smith, M. J. (1970) *Biol. Bull.*, **138**: 379-388.
- 79 Rowley, A. F. (1983) *J. Exp. Zool.*, **227**: 319-322.
- 80 Rubinson, K. A. (1981) *Proc. Roy. Soc. London, B*, **212**: 65-84.
- 81 Chasteen, N. D. (1981) In "Biological magnetic resonance" vol. 3 Ed. by Berliner, L., and Reuben, J., Plenum Press, New York, pp. 53-119.
- 82 Kustin, K. and Macara, I. G. (1982) *Comments Inorg. Chem.*, **2**: 1-22.
- 83 Chasteen, N. D. (1983) *Structure Bonding*, **53**: 105-138.
- 84 Kustin, K. and McLeod, G. C. (1983) *Structure Bonding*, **53**: 139-160.
- 85 Boyd, D. W. and Kustin, K. (1985) *Adv. Inorg. Biochem.*, **6**: 311-365.
- 86 Macara, I. G. (1980) *Trends Biochem. Sci.*, **5**: 92-94.
- 87 Ramasarma, T. and Crane, F. L. (1981) *Cur. Topics Cell. Regul.*, **20**: 247-301.
- 88 Michibata, H., Nishiyama, I., Gualtieri, R. and de Vincentis, M. (1985) *Comp. Biochem. Physiol.*, **80B**: 247-250.
- 89 Michibata, H., Zenko, Y., Yamada, K., Hasegawa, M., Terada, T. and Numakunai, T. (1989) *Zool. Sci.*, **6**: 289-293.
- 90 de Boer, E., Tromp, M. G. M., Plat, H., Krenn, G. E. and Wever, R. (1986) *Biochim. Biophys. Acta*, **872**: 104-115.
- 91 de Boer, E., van Kooyk, Y., Tromp, M. G. M., Plat, H. and Wever, R. (1986) *Biochim. Biophys. Acta*, **869**: 48-53.
- 92 Robson, R. L., Eady, R. R., Richardson, T. H., Miller, R. W., Hawkins, M. and Postgate, J. R. (1986) *Nature*, **322**: 388-390.
- 93 Mornigstar, J. E., Johnson, M. K., Case, E. E. and Hales, B. J. (1987) *Biochemistry*, **26**: 1795-1800.
- 94 Kentemich, T., Danneberg, G., Hundeshagen, B. and Bothe, H. (1988) *FEMS Microbiol. Lett.*, **51**: 19-24.
- 95 Bayer, E., Koch, E. and Anderegg, G. (1987) *Angew. Chem. Int. Ed. Engl.*, **26**: 545-546.
- 96 Dubyak, G. R. and Kleinzeller, A. (1980) *J. Biol. Chem.*, **255**: 5306-5312.
- 97 Heyliger, C. E., Tahilian, A. G. and McNeill, J. H. (1985) *Science*, **227**: 1474-1477.
- 98 Thompson, H. J., Chasteen, N. D. and Meeker, L. D. (1984) *Carcinogenesis*, **5**: 849-851.
- 99 Kustin, K. and Toppen, D. L. (1973) *Inorg. Chem.*, **12**: 1404-1407.
- 100 Macara, I. G., Kustin, K. and Cantley, L. C. Jr. (1980) *Biochim. Biophys. Acta*, **629**: 95-106.
- 101 Ramasarma, T., MacKellar, W. C. and Crane, F. L. (1981) *Biochim. Biophys. Acta*, **646**: 88-98.
- 102 Sakurai, H., Shimomura, S. and Ishizu, K. (1981) *Inorg. Chim. Acta*, **55**: L67-L69.
- 103 Legrum, W. (1986) *Toxicology*, **42**: 281-289.



Oscillations of Membrane Potential and Membrane Resistance during the Cell Cycle in the Newt Egg Macromeres

ELJI SATO and SHIN-ICHI TAGAWA

Department of Environmental Science, Division of Graduate School of Science and Technology, and Department of Biology, Faculty of Science, Kumamoto University, Kumamoto 860, Japan

ABSTRACT—The electrical characteristics of macromeres in newt eggs at the morula stage were examined electrically during the cell cycle, and the negative membrane potential (E_m) and membrane resistance (R_m) were found to oscillate. For designation of the cell stage in the cell cycle, the time between cleavage-furrow formations was divided into 100 stages. The cell stage at which furrow formation occurred was designated St.50. The increase in R_m began from St.0 and reached a peak value at St.30. On the other hand, the membrane showed hyperpolarization from St.10 to St.40 and then showed depolarization. After furrow formation, R_m continued to decrease and reached a minimum value at St.60, after which the value increased and showed a small peak at St.80. The membrane continued to depolarize from St.40 and reached a plateau level at around St.60. To investigate the mechanism of these electrical changes, a $\text{Na}^+\text{-K}^+$ pump inhibitor and high- Ca^{2+} solution were perfused to the macromeres. Despite the inhibition of the $\text{Na}^+\text{-K}^+$ pump, the membrane was hyperpolarized during the furrow formation. Accordingly it appears that the $\text{Na}^+\text{-K}^+$ pump does not participate in the hyperpolarization of the membrane upon the furrow formation in macromeres. In high Ca^{2+} -application, the times of minimum R_m and the hyperpolarization of the membrane during the cell cycle did not always coincide with the time of furrow formation. Consequently it appears that these electrical and morphological changes are controlled by two mechanisms which are independent of each other and linked to the normal cell cycle.

INTRODUCTION

The execution of events in the cell-cycle has been studied from various aspects such as changes in intracellular pH [1-4], intracellular Ca^{2+} [5-10] and maturation promoting factor (MPF) [11-16]. In the present study, electrical measurement was applied to examine such cell-cycle phenomena. Among various electrophysiological approaches, oscillations in the membrane potential of amphibian eggs associated with fertilization have been described by many investigators [17-21, review 22]. They found that the membrane potential of the egg showed a general shift toward a hyperpolarized state at cleavage in *Xenopus laevis* [20, 21], *Rana pipiens* [23], and in *Cynops pyrrhogaster* [24, 25]. However, membrane potential and membrane resistance appeared to fluctuate during the

cell cycle [23] or the recording time appeared to be short compared with whole cell cycle. Even when this did not occur, these reports confirmed the values of electrical characteristics at fertilization [20, 21] or first and second cleavage [24, 25], and there were a number of obscure points, such as when the membrane resistance began to increase, when it began to decrease, when the membrane potential began to hyperpolarize, and when furrow formation was initiated during the observed changes in membrane resistance. Therefore, the present study was conducted to examine these electrical changes in detail and their changes with time during cell division, focusing particularly on the relationship between furrow formation and changes in membrane potential and membrane resistance. Moreover, in order to elucidate the mechanism of membrane hyperpolarization, it was examined whether the membrane during hyperpolarization was dependent not only on K^+ ion [3, 23, 25, 26] but also on the $\text{Na}^+\text{-K}^+$ pump.

Accepted October 12, 1988

Received August 4, 1988

MATERIALS AND METHODS

Macroblastomere cells were obtained from the blastocoel of eggs of the newt, *Cynops pyrrhogaster* in the morula stage (stage 7, 8) [29], by careful isolation with a hair-loop and placed in modified Holtfreter's solution (80 mM NaCl, 1.0 mM KCl, 1.2 mM CaCl_2 , 1.2 mM MgCl_2 , 0.36 mM NaHCO_3 , pH 7.4) on a Sylgard slab. The cell diameter of each isolated macromere was measured on a plastic dish coated with agar at the "rounding-up" stage when the macromere became spherical. For investigating the electrical characteristics of the membrane, two kinds of perfusion solution were used: 56.2 mM Ca^{2+} solution, in which all NaCl in modified Holtfreter's solution was substituted by CaCl_2 , and g-strophanthin (Merk) solution of various concentrations (0.03, 0.05, 0.10, 1.0 mM) added to modified Holtfreter's solution, for inhibition of the $\text{Na}^+ - \text{K}^+$ pump.

Electrical measurements were carried out using a current-clamp system (Fig. 1). The system was made by modifying the voltage-clamp system as described by Brown *et al.* [30]. For electrical recording, two glass microelectrodes filled with 3 M KCl were inserted into one macromere cell. One thick-walled electrode (resistance: 10 M Ω) was connected to a head amplifier (V) and the other thin-walled electrode (resistance: 2–3 M Ω) was connected to the output of a current-feedback amplifier (Vi) for current injection. The reference electrode was an Ag-AgCl wire immersed in 3 M KCl solution, connected to an agar bridge immersed in experimental medium. The other end of the Ag-AgCl wire was connected to a current-voltage converter for current monitoring and current feedback to the feedback amplifier (Vi). The outputs of the preamplifier (Vm) and current monitor (Im) were connected to a pen-recorder (NIHON KODEN RJG 4004).

For insertion of the two microelectrodes into the macroblastomere cell, one voltage-recording microelectrode was oscillated by a brief overcompensation of the electrode capacitance. This procedure was important for obtaining a more negative membrane potential, which appeared to be a real negative potential without any leakage.

In the present examination, depolarizing pulses

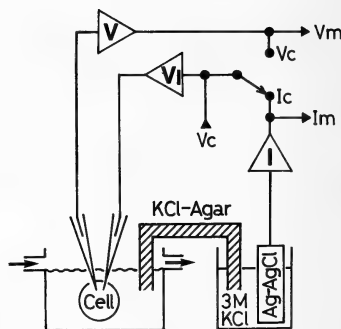


FIG. 1. Schematic representation of the circuits used for electrical measurements in current-clamp and voltage-clamp systems. In this experiment, all electrical recordings were performed under current-clamp conditions. The converted output (I_c) through the virtual ground (I) of the current-voltage converter was connected to an amplifier for current feedback (V_i) with a voltage command (V_c) pulse. V, voltage-follower for voltage recordings (Teledyne Philbrick 1332 operational amplifier). I_m , current monitor. V_c , under voltage-clamp conditions, the output of the voltage-follower was connected to the voltage-feedback amplifier (V_i). The other operational amplifier was an LF356, which was used on a glass-epoxy plate with 5-mm-wide print pattern.

(duration of current-pulses, 500 msec; pulse interval, 9 sec) were used for current injection because intense rectification was observed in hyperpolarizing pulses. The membrane resistances referred to in this series mean input membrane resistances measured by the depolarizing currents.

RESULTS

Timing of the cell cycle in relation to cell diameter

In order to identify the cell-cycle stage, the timing of one cell cycle in relation to various cell sizes was first measured. The cell diameters of the isolated macroblastomeres were examined on a plastic dish coated with agar at the "round-up" stage. The sizes of the macroblastomeres obtained from the blastocoel of morula-stage eggs usually ranged from 250 μm to 500 μm , as indicated in

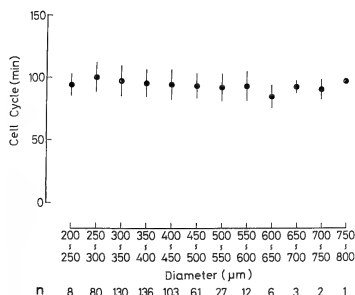


Fig. 2. The relationship between cell diameter (μm ; with standard deviations) and the timing of the cell cycle (min). n; numbers of samples.

Figure 2. Cells larger than $500\ \mu\text{m}$ were occasionally obtained at the early morula stage.

For identification of the cell-cycle stage, the first cleavage-furrow served as a convenient reference. Accordingly, the times of the cell cycle were calculated from the formation of the initial cleavage-furrow to that of the next cleavage-furrow. When the timing of the cell cycle was compared between 5 ranges of cell size from $250\text{--}300\ \mu\text{m}$ to $450\text{--}500\ \mu\text{m}$, the marked difference of the time was not found ($P < 0.05$). Consequently, the timing of the cell cycle in used macromeres were about 96 min ($n = 568$).

Timing of the cell cycle in relation to room temperature

Having established that one cell cycle took about 96 min in cells of various sizes, the dependence of cell-cycle timing on room temperature was then examined in order to identify the cell-cycle stages of cells used.

As shown in Figure 3, room temperature within a range of $22^\circ\text{C}\text{--}28^\circ\text{C}$ was classified into 4 ranges for convenience. The respective values of Q_{10} obtained were 1.16 between $22\text{--}24^\circ\text{C}$ (101 min) and $24\text{--}25^\circ\text{C}$ (97 min), and 1.37 between $22\text{--}24^\circ\text{C}$ and $26\text{--}28^\circ\text{C}$ (89 min). Consequently, at these room temperatures, the mean time of the cell cycle tended to decrease ($P < 0.5$). If the time from first furrow formation to second furrow formation was constant in relation to the room temperature and

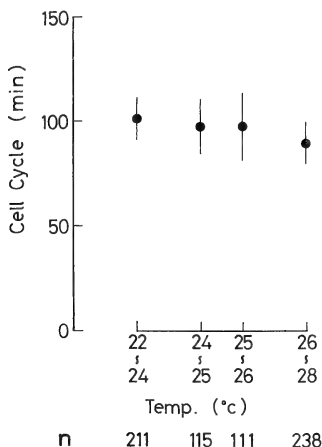


Fig. 3. The relationship between room temperature and the timing of the cell cycle. n; number of samples.

the cell sizes, an absolute time was able to designate the cell stage in the present study. However the mean time of the cell cycle was changed with the room temperature. Therefore, in the present paper, the time from first furrow formation to second furrow formation has been divided into a hundred stages, designated St.0 to St.100. The stage designations are as follows: st.50 is the start of furrow formation, and the "round-up" stage, for example, covers range from st.30 to st. 40 and the "relaxed" stage a range from st.40 to st. 45. These designations of cell stages are different from those used in previous reports [cf. 31].

Electrical measurement of the cell-division cycle

Recordings of changes in membrane potential and membrane resistance are shown in Figure 4. The time-markers in the uppermost trace (Time) correspond to the cell stages from St.0 to St.100 in these two records (Figs. 4A and B). The second traces (Im) show the intensities of the respective injected currents (A, 20 nA; B, 15 nA). The third traces (Vm) show the membrane potentials and

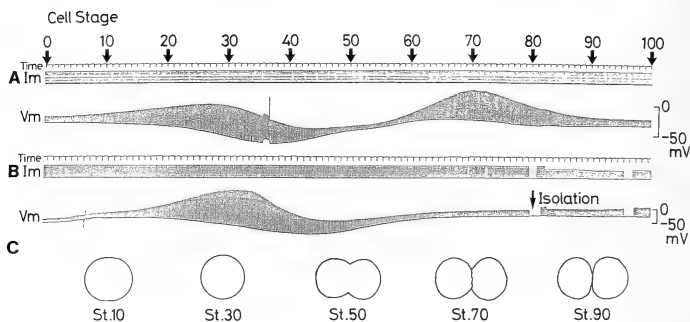


Fig. 4. Two typical recordings obtained during the cell cycle (A, B). The illustrations in C are morphological outlines of blastomere cells at each stage. I_m in A indicates the intensity of the injected current (20 nA constant). I_m in B is 15 nA. After the stimulation had been interrupted briefly near the arrow in B, the membrane resistance was slightly increased as a result of electrical uncoupling. The temperature was 26°C and the macromere sizes before cleavage were 500 μm (A) and 625 μm (B). The arrow in B indicates the separation of a daughter-cell by a hair-loop. The calibration of potential is indicates on the right.

membrane resistances. Figure 4C shows schematic drawings of the macroblastomere at St.10, St.30, St.50, St.70 and St.80, respectively.

As seen in Figure 4A, the membrane resistance began to increase at about St.5, and reached an initial peak resistance (2.2 M Ω) at about St.30. In parallel with this increase in membrane resistance, the membrane began to hyperpolarize at about St.10 and attained a maximum hyperpolarized potential (-75 mV) at St.35. Thus, the maximum hyperpolarization potential always appeared after the first maximum membrane resistance, the time lag being about 10 min in Figure 4A. After St.30, the membrane resistance began to decrease and reached a minimum value (0.29 M Ω) at St.53, subsequently increasing again and reaching a second peak (2.1 M Ω). After the maximum hyperpolarization, the membrane potential began to depolarize and reached a plateau of E_m (-36 mV) at about St.63. In the process of this depolarization, furrow formation occurred at St.50.

As seen in Figure 4B, the stage of maximum hyperpolarization potential (-84 mV) was St.44. Despite this similarity in the features of the change in membrane potential in Figure 4A and B, there was only one stage of maximum resistance (Fig. 4B). The membrane resistance began to show an increase at St.10 (0.54 M Ω) and reached maximum

R m (4.6 M Ω) at St.33, subsequently decreasing and reaching 0.89 M Ω at St.65.

The marked difference between Figures 4A and 4B was due to the changes in membrane resistance, that in Figure 4A having two peaks (St.20–St.40).

The changes in the mean membrane potentials and mean membrane resistances are shown in Figure 5. The membrane potential at St.0 was -53 ± 9 mV, and then the membrane became depolarized to -50 ± 11 mV at St.10. After St.10, hyperpolarization was seen, reaching a maximum of E_m at St.40 (-85 ± 8 mV). When the membrane potentials had reached a value of about 90% of the maximum (St.40), the cleavage-furrow was usually formed at St.50 (-75 ± 11 mV). After cleavage, the membrane potential reached a plateau at St.70 (-50 ± 11 mV). It thus appeared to be characteristic that the maximum hyperpolarized potential occurred within about 10 min after furrow-formation.

In parallel with these changes, the mean membrane resistance began to increase from St.0 (2.3 ± 0.9 M Ω) and then increased gradually to its maximum value (4.3 ± 2.3 M Ω) at St.30. After St.30, the average membrane resistance decreased to a minimum value (1.4 ± 0.7 M Ω) at St.60 through furrow-formation at St.50, close to the time when

the decreasing R_m crossed the depolarization of the membrane. After St.60, the membrane resistance increased gradually, and finally reached $2.8 \pm 1.4 \text{ M}\Omega$ at St.100, corresponding to the next St.0.

Thus, as shown in Figure 5, the average membrane resistances of the blastomere increased in two stages of the cell cycle and decreased to a minimum value at St.60, although the second increase at St.70–St.80 was not remarkable.

Application of two different Ca^{2+} -rich solutions

As shown in Figure 6A–D, 10 mM CaCl_2 solution was perfused for a 5-min period at various stages (A, St. 0; B, St.40; C, St.60; D, St.80), resulting in membrane resistance increases of 1.7-fold, 1.6-fold, 2.9-fold and 1.5-fold, respectively, in comparison with preperfusion values of 2.9, 4.4, 1.2 and 2.5 $\text{M}\Omega$, respectively. The values of the depolarized potential was from +12 to +14 mV in each case. Consequently, the depolarization produced by application of 10 mM Ca^{2+} solution suggested qualitatively that the membrane of the blastomere cell seemed to be most sensitive at

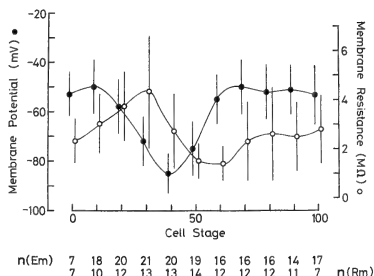


Fig. 5. Changes in the averaged membrane potential and membrane resistance, with standard deviations, during the cell cycle. n : numbers of samples.

about St.40 (Fig. 6A–D).

As shown in Figure 6E, 56.2 mM Ca^{2+} solution was applied for 5 min beginning at St.10, and the membrane potential was depolarized from -39 mV (St.10) to -24 mV after 2 min. Subsequently, the membrane potential gradually became hyperpolarized to -66 mV after 9 min, and was then

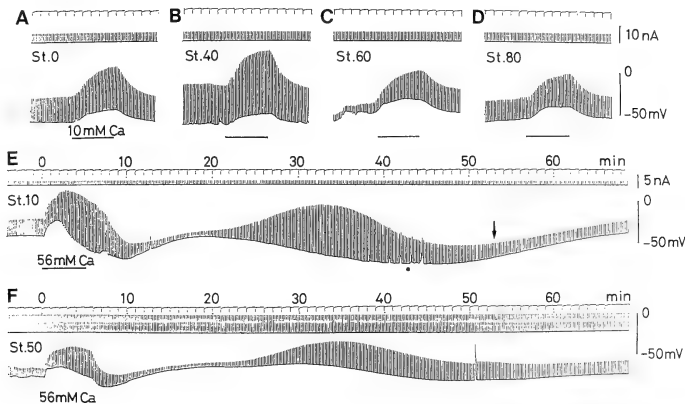


Fig. 6. The effects of Ca^{2+} -rich solutions on the membrane of blastomeres (A–D, 10 mM; E, F, 56 mM). The calibrations of current and voltage are indicated on the right. The electrical changes in E were recorded during a 113-min period from St. 10, whereas those in F were recorded during a 148-min period from st. 50. The macromere sizes were $406 \mu\text{m}$ in A–E, and $724 \mu\text{m}$ in F. The arrow head in E indicates the timing of furrow-formation. At 100 min in E, the daughter-cells sizes were $292 \mu\text{m}$ and $262 \mu\text{m}$. After 51 min in F, the daughter-cells were separated and their sizes were 527 and $513 \mu\text{m}$.

depolarized to -43 mV after 17 min. Meanwhile the membrane resistance increased from $4.0\text{ M}\Omega$ (St.10) to $11.3\text{ M}\Omega$ after 6 min, and then decreased $1.2\text{ M}\Omega$ after 17 min.

After the application of Ca^{2+} , the features of the electrical change during 20–68 min (Fig. 6E) were similar to those before and after furrow formation (Fig. 4B), i.e., the membrane resistance increased to $11.9\text{ M}\Omega$ after 34 min, and then decreased to $2.7\text{ M}\Omega$ after 62 min, followed by an increase to $4.3\text{ M}\Omega$ after 82 min, and a decrease from St.50 until 113 min. On the other hand, the membrane potential was -43 mV after 17 min, and then the membrane was hyperpolarized to -74 mV after 43 min. At 82 min after application, depolarization to -37 mV was seen, and 53 min after St.10, furrow formation occurred.

As shown in Figure 6F, 56.2 mM Ca^{2+} solution was applied for 5 min beginning at St.50, and then the membrane was depolarized from -69 mV (St.50) to -58 mV after 2 min. Subsequently the potential became gradually hyperpolarized to -80 mV after 7 min, and then depolarized to -58 mV after 18 min. Meanwhile, the membrane resistance increased from $0.51\text{ M}\Omega$ (St.50) to $1.57\text{ M}\Omega$ after 5 min, and then decreased to $0.25\text{ M}\Omega$ after 18 min. At 37 min after St.50, the membrane resistance increased to $1.61\text{ M}\Omega$, and then decreased to $0.79\text{ M}\Omega$ after 65 min. On the other hand, the membrane potential was -43 mV after 22 min, and then the membrane hyperpolarized to 74 mV after 48 min. At 90 min after application, depolarization to -37 mV was seen, and 148 min after St.50, furrow-formation occurred.

Consequently, the changes occurring in membrane potential and membrane resistance during 20–68 min after the application of 56 mM Ca^{2+} solution were similar to the electrical changes shown in Figure 4B. As shown in Figure 6E, furrow formation was observed 53 min after St.10, suggesting that the timing of furrow formation was delayed for 20 min by perfusion of the Ca^{2+} solution. On the other hand, as shown in Figure 6F, furrow formation was not observed 18 min and 65 min after St.50, but did occur 142 min after St.50. In other words, the timing of furrow formation was delayed for about 50 min due to perfusion of the Ca^{2+} solution. Then, in stead of the cell stage, the

times from the onset of the perfusion were used for staging the cell cycle. From the observation that cleavage furrow formation did not always occur when the membrane resistance was low and the membrane hyperpolarized, the respective mechanisms responsible for furrow formation and

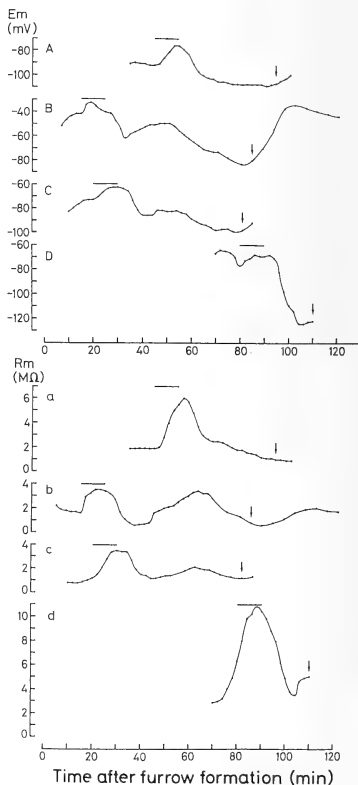


Fig. 7. The effects of $\text{Na}^+\text{-K}^+$ pump blocking by the $1\text{-mM g-strophanthin}$ for 10-min periods at various cells stages. The arrow indicate the timing of furrow-formation. The changes in the membrane potentials and membrane resistances in one recording are indicated separately in the top (A, B, C, D) and bottom (a, b, c, d) panels, respectively.

electrical changes were considered to be independent, but closely linked.

g-Strophanthin solution

The K^+ ion dependence of the membrane potential in macromeres has been previously investigated by many researchers [3, 23, 25–28]. In this study, we examined whether the Na^+-K^+ pump was present not only in whole egg [32] but also in macromeres from the blastocoel. Upon transient application of 1 mM *g-strophanthin* for 10 min, as indicated in Figure 7, the depolarized membrane potentials were 16 mV (A), 9 mV (B), 10 mV (C) and 9 mV (D), respectively, whereas the corresponding increases in membrane resistance were 4.1 M Ω (a), 1.9 M Ω (b), 2.3 M Ω (c) and 4.5 M Ω (d). After application, both types of electrical change became irregular in comparison with the normal ones, although furrow formation was not affected, as indicated by the arrows in Figure 7. In other word, the activity of the Na^+-K^+ pump was confirmed in the membrane of macromeres.

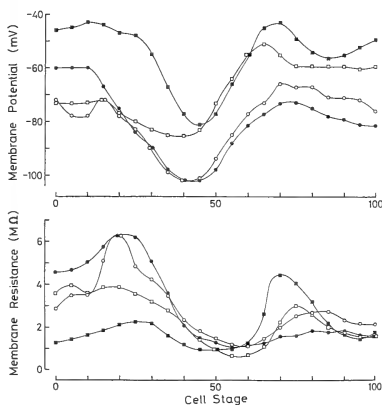


Fig. 8. The effects on the blastomere cell membrane of *g-strophanthin* solutions (0.03 mM, solid squares, 0.05 mM, solid circles; 0.1 mM, solid circles; 1 mM, clear circles). The membrane potential and membrane resistance are shown separately in the top and bottom panels, respectively.

In contrast with transient application of *g-strophanthin*, the oscillations in membrane resistance and membrane potential throughout the cell cycle were unaffected by long-term application, as shown in Figure 8. At various concentrations of the agent (0.03, 0.05, 0.1, 1 mM), the membrane was hyperpolarized up to -102 mV (0.1, 1.0 mM), -85 mV (0.05 mM) and -81 mV (0.03 mM) at about St.40 and the membrane resistance was increased in a range from 2.2 to 6.2 M Ω at about St.30. Thus the hyperpolarization potential was not influenced by inhibition of the activity of the Na^+-K^+ pump, and therefore it appeared that regulation of the membrane potential at cleavage was independent of the Na^+-K^+ pump.

DISCUSSION

In amphibian eggs, changes in the membrane potential and membrane resistance have been investigated electrophysiologically by many workers [1, 3, 17, 19–21, 23–28]. However it seems that previous investigators have generally concentrated on two main aspects, one being fertilization and additional cleavage, and the other first cleavage including aspects such as the formation of new membrane. In the present study, we restricted our investigation to oscillations in membrane parameters detected electrophysiologically during the cell cycle.

For the present purpose, we used macroblastomere cells from the blastocoel of *Cynops pyrrhogaster* egg instead of using the whole egg. This was because macromere cells seem to have uniform membrane quality without possessing certain factors such as pigments and "ion barrier" [24, 25], and also because the isolation of macromeres from the blastocoel is more convenient than obtaining pigmented macromeres from the whole egg. In spite of these advantages, this difference between unpigmented macromeres from the blastocoel and pigmented cells from the whole egg produced differences in the timing of cleavage. In pigmented cells, cleavage is seen at a time of high membrane resistance and before hyperpolarization in *Xenopus laevis* (3, 64-cell embryo; 20, 1st–5th cleavages; 21, 1st and 2nd cleavages). However in unpigmented cells from the blastocoel, cleavage

was visible as a furrow after maximum hyperpolarization. Accordingly, cleavage seems to occur later than that in pigmented macromeres. The differences in membrane resistance observed during St.60–80 (Fig. 4A and B) may be due to the presence of two kinds of macromere in the blastocoel. Thus, it may be necessary to conduct electrical examinations of vegetal blastomeres containing germ plasma situated around the vegetal pole [33, 34].

With the exception of the increase in membrane resistance during St.60–80, increases generally occurred between St.0 and St.30, as shown in Figure 5. Accordingly, it appears feasible to time furrow formation on the basis of the increase in membrane resistance, and it was revealed that preparation for the next cleavage was established at least by St.0. This consideration for furrow determination holds the similar views shown by Dettlaff units [35].

The relationships between Ca^{2+} ion and furrow formation have been reported in various aspects [5–9, 36]. Especially, it appears important whether the intracellular Ca^{2+} rises at the cleavage or not. However, in amphibian egg, there are no direct evidence for the distribution or sequential changes of the intracellular Ca^{2+} during the cleavage. If the concentration of the intracellular Ca^{2+} in amphibian egg was low at the furrow formation as well as sea urchin egg [37], the responsibility of the egg membrane to the extracellular Ca^{2+} appeared to change.

Upon application of 10 mM Ca^{2+} -rich solution, the membrane potential and membrane resistance of macromeres changed transiently. On the other hand, 56 mM Ca^{2+} -rich solution produced oscillations in membrane potential and membrane resistance during a 20-min period after application and beyond. Such electrical changes were similar to those observed in standard solution, as shown in Figure 4B. Accordingly, these oscillatory electrical changes in the membrane produced by application of Ca^{2+} solution strongly suggest that Ca^{2+} ion plays an important role in the cell cycle. Moreover, the mechanism which induces these oscillatory changes and the mechanism responsible for furrow formation appear to be independent of each other, since furrow formation did not occur

even 65 min after St.50, as seen in Figure 6F. The two mechanisms seem to be closely linked in the normal cell cycle, but separable by application of 56 mM Ca^{2+} solution. Thus it suggests that membrane possess the peculiar rhythm. This phenomenon coincides with the presence of autonomous cyclic activities in non-nucleate egg fragments of amphibian eggs [38–40]. Then, it will be necessary to measure electrophysiologically for the effects of the various inhibitors as colchicine and cytochalasin B in addition to test the non-nucleate egg fragment.

It have been reported that Em of the whole egg and macromere in *Cynops pyrrhogaster* was dependent on extracellular K^{+} -ion [3, 23, 25–28]. Moreover, it was reported that Na^{+} - K^{+} pump inhibitor decreased the membrane potential [32; 41, 42: neurula embryo]. However the effect of Na^{+} - K^{+} pump inhibitor on the hyperpolarization of the membrane at the cleavage was not examined without first cleavage [cf. 32].

The application of 1 mM g-strophanthin confirmed the transient responsiveness of the membrane to this agent in various cell stages. However, the results of g-strophanthin application throughout the cell cycle indicated that the hyperpolarizations of the membrane potential during furrow formation and the changes in membrane resistance are not influenced. Consequently, at least during one cell cycle, the function of the Na^{+} - K^{+} pump was found to be unnecessary for the complete passage of the cell cycle.

These facts that Em depend on external K^{+} -ion [3, 23, 25–28] and hyperpolarization of Em at cleavage need not Na^{+} - K^{+} pump in addition to the effect of high- Ca^{2+} ions on membrane suggest circumstantially the existence of Ca^{2+} -activated K^{+} conductance [43–45].

Recordings that have been reported up to now have been obtained over short periods or with an unstable membrane resistance due to fluctuations in the microelectrode current injection. In particular, the relation between membrane resistance and membrane potential has not been described in detail. In this study, it was revealed that the membrane resistance measured using the depolarizing current had at least one single peak of high resistance at St.30 in the cell cycle, and that the

hyperpolarized membrane potential was as large as about -90 mV. For future studies on the relation between nuclear division and membrane electrical oscillation in the cell cycle, observations using a dissecting microelectrode as well as detailed histological investigation, will be necessary.

ACKNOWLEDGMENTS

We thank Dr. Katsushi Morimoto for advice during the work. This work was supported partially by Grants-in-Aid for Scientific Research from the Ministry of Education, Science and Culture, Japan (No. 59740370 and No. 61740425).

REFERENCES

- Lee, S. C. and Steinhardt, R. A. (1981) Observations on intracellular pH during cleavage of eggs of *Xenopus laevis*. *J. Cell Biol.*, **91**: 414-419.
- Shen, S. S. and Steinhardt, R. A. (1978) Direct measurement of intracellular pH during metabolic derepression on of the sea urchin egg. *Nature*, **272**: 253-254.
- Clack, C. and Warner, A. E. (1973) Intracellular and intercellular potentials in the early amphibian embryo. *J. Physiol. (Lond.)*, **232**: 313-330.
- Slack, C., Warner, A. E. and Warren, R. L. (1973) The distribution of sodium and potassium in amphibian embryos during early development. *J. Physiol. (Lond.)* **232**: 297-312.
- Baker, P. F. and Warner, A. E. (1972) Intracellular calcium and cell cleavage in early embryos of *Xenopus laevis*. *J. Cell Biol.*, **53**: 579-581.
- Izant, J. G. (1983) The role of calcium ion during mitosis: calcium participates in the anaphase trigger. *Chromosoma*, **88**: 1-10.
- Poenie, M., Alderton, J., Tsien, R. and Steinhardt, R. A. (1985) Changes of free calcium levels with stages of the cell division cycle. *Nature*, **314**: 147-149.
- Poenie, M., Alderton, J., Steinhardt, R. and Tsien, R. (1986) Calcium rises abruptly and briefly throughout the cell at the onset of anaphase. *Science*, **233**: 886-889.
- Keith, C. H., Maxfield, F. R., and Shelanski, M. L. (1985) Intracellular free calcium levels are reduced in mitotic PtK2 epithelial cells. *Proc. Natl. Acad. Sci. U.S.A.*, **82**: 800-804.
- Keith, C. H., Ratan, R. Maxfield, F. R., Bajer, A. and Shelanski, M. L. (1985) Local cytoplasmic calcium gradients in living mitotic cells. *Nature*, **316**: 848-850.
- Masui, Y., and Markert, C. (1971) Cytoplasmic control of nuclear behavior during oocyte maturation of frog oocytes. *J. Exp. Zool.*, **177**: 129-146.
- Hara, K., Tydeman, P., and Kirschner, M. (1980) A cytoplasmic clock with the same period as the division cycle in *Xenopus* egg. *Proc. Natl. Acad. Sci. U.S.A.*, **77**: 462-466.
- Miake-Lye, R., and Kirschner, M. W. (1985) Induction of early mitotic events in a cell-free system. *Cell*, **41**: 165-175.
- Karsenti, E., Bravo, R., and Kirschner, M. (1987) Phosphorylation changes associated with the early cell cycle in *Xenopus* eggs. *Dev. Biol.*, **119**: 442-453.
- Labbe, J.-C., Picard, A., Karsenti, E., and Doree, M. (1988) An M-phase-specific protein kinase of *Xenopus* oocytes: partial purification and possible mechanism of its periodic activation. *Dev. Biol.*, **127**: 157-169.
- Gelerstein, S., Shapira, H., Dascal, N., Yekuel, R., and Oron, Y. (1988) Is a decrease in cyclic AMP a necessary and sufficient signal for maturation of amphibian oocytes?. *Dev. Biol.*, **127**: 25-32.
- Cross, N. L., and Elinson, R. P. (1980) A fast block to polyspermy in frogs mediated by changes in the membrane potential. *Dev. Biol.*, **75**: 187-198.
- Grey, R. D., Bastiani, M. J., Webb, D. J., and Schertel, E. R. (1982) An electrical block is required to prevent polyspermy in eggs fertilized by natural mating of *Xenopus laevis*. *Dev. Biol.*, **89**: 475-484.
- Iwao, Y. (1985) The membrane potential changes of amphibian eggs during species- and cross-fertilization. *Dev. Biol.*, **111**: 26-34.
- Webb, D. J. and Nuccitelli, R. (1981) Direct measurement of intracellular pH changes in *Xenopus* eggs at fertilization and cleavage. *J. Cell Biol.*, **91**: 562-567.
- Webb, D. J. and Nuccitelli, R. (1985) Fertilization potential and electrical properties of the *Xenopus laevis*. *Develop. Biol.*, **107**: 395-406.
- Hagiwara, S., and Jaffe, L. A. (1979) Electrical properties of egg cell membranes. *Annu. Rev. Biophys. Bioeng.*, **8**: 385-416.
- Woodward, D. J. (1968) Electrical signs of new membrane production during cleavage of *Rana pipiens* eggs. *J. Gen. Physiol.*, **52**: 509-531.
- Takahashi, M. and Ito, S. (1968) Electrophysiological studies on membrane formation during cleavage of the amphibian egg. *Zool. Mag. (Tokyo)*, **77**: 307-316.
- Ito, S. and Loewenstein, W. R. (1969) Ionic communication between early embryonic cells. *Dev. Biol.*, **19**: 228-243.
- DeLaat, S. W. and Bluemink, J. G. (1974) New membrane formation during cytokinesis in normal and cytochalasin-B-Treated eggs of *Xenopus laevis*. *J. Cell Biol.*, **60**: 529-540.

- 27 Ito, S. and Hori, N. (1966) Electrical characteristics of *Triturus* egg cells during cleavage. *J. Gen. Physiol.*, **49**: 1019-1027.
- 28 Kline, D., Robinson, K. R. and Nuccitelli, R. (1983) Ion currents and membrane domains in the cleaving *Xenopus* egg. *J. Cell Biol.*, **97**: 1753-1761.
- 29 Okada, Y. K. and Ichikawa, M. (1947) External stage criteria in the development of *Cynops pyrrhogaster*. *Jap. J. Exp. Morphol.*, **3**: 1-6. (In Japanese)
- 30 Brown, A. M., Tsuda, Y. and Wilson, D. L. (1983) A description of activation and conduction in calcium channels based on tail and turn-on current measurements in the snail. *J. Physiol. (Lond.)*, **344**: 549-583.
- 31 Ito, S., Sato, E. and Loewenstein, W. R. (1974) Studies on the formation of a permeable cell membrane junction. I. Coupling under various conditions of membrane contact. Effect of colchicine, cytochalasin B, dinitrophenol. *J. Membrane Biol.*, **19**: 305-338.
- 32 Ohara, A., Doida, Y., Murayama, K., Imaizumi, M., Marunaka, Y. and Kitasato, H. (1988) Na/K pump activity in the new membrane formed at first cleavage in *Cynops pyrrhogaster* eggs. *Dev. Biol.*, **126**: 331-336.
- 33 Ikenishi, K. (1982) A possibility of an *in vitro* differentiation of primordial germ cells (PGCs) from blastomeres containing "germinal plasma" of early cleavage stage in *Xenopus laevis*. *Develop., Growth and Differ.*, **17**: 101-110.
- 34 Kalt, M. R. (1973) Ultrastructural observations on the germ line of *Xenopus laevis*. *Z. Zellforsch.*, **138**: 41-62.
- 35 Selman, G. G. (1982) Determination of the first two cleavage furrows in developing eggs of *Triturus alpestris* compared with other forms. *Develop. Growth Differ.*, **24**: 1-6.
- 36 Timourian, H., Clothier, G., and Watchmaker, G. (1972) Cleavage furrow: Calcium as determinant of site. *Exptl. Cell Res.*, **75**: 296-298.
- 37 Suprynowicz, F. A., and Mazia, D. (1985) Fluctuation of the Ca^{2+} -sequestering activity of permeabilized sea urchin embryos during the cell cycle. *Proc. Natl. Acad. Sci. U.S.A.*, **82**: 2389-2393.
- 38 Sakai, M., and Kubota, H. Y. (1981) Cyclic surface changes in the non-nucleate egg fragment of *Xenopus laevis*. *Develop. Growth & Differ.*, **23**: 41-49.
- 39 Hara, K., Tydeman, P., and Kirschner, M. (1980) A cytoplasmic clock with the same period as the division cycle in *Xenopus* eggs. *Proc. Natl. Acad. Sci. U.S.A.*, **77**: 462-466.
- 40 Kobayakawa, Y. and Kubota, H. Y. (1981) Temporal pattern of cleavage and the onset of gastrulation in amphibian embryos developed from eggs with the reduced cytoplasm. *J. Embryol. Exp. Morphol.*, **62**: 83-94.
- 41 Blackshaw, S., and Warner, A. E. (1976) Alterations in resting membrane properties during neural plate stages of development of the nervous system. *J. Physiol. (Lond.)*, **255**: 231-247.
- 42 Bergman, C. and Bergman, J. (1981) Electrogenic responses induced by neutral amino acids in endoderm cells from *Xenopus* embryo. *J. Physiol. (Lond.)*, **318**: 259-278.
- 43 Miyazaki, S. and Igusa, Y. (1982) Ca-mediated activation of a K current at fertilization of golden hamster eggs. *Proc. Natl. Acad. Sci. U.S.A.*, **79**: 931-935.
- 44 Igusa, Y., and Miyazaki, S.-I. (1986) Periodic increase of cytoplasmic free calcium in fertilized hamster eggs measured with calcium-sensitive electrodes. *J. Physiol. (Lond.)*, **377**: 193-205.
- 45 Miyazaki, S.-I. (1988) Inositol 1,4,5-triphosphate-induced calcium release and guanine nucleotide-binding protein-mediated procalcium rises in golden hamster eggs. *J. Cell Biol.*, **106**: 345-353.

Mosaic Fate Mapping of the Behavioral and the Muscular Defects Induced by a *Drosophila* Mutation, *abnormal proboscis extension reflex C* (*aperC*)

KEN-ICHI KIMURA¹, TEIICHI TANIMURA²
and TATEO SHIMOZAWA³

Zoological Institute, Faculty of Science, Hokkaido University, Sapporo 060,
and ²Division of Behaviour and Neurobiology, National Institute
for Basic Biology, Okazaki 444, Japan

ABSTRACT—Mosaic analysis was applied to investigate whether the muscle degeneration induced by an X-linked mutation *aperC* is myogenic or neurogenic. The *aperC* mutation causes a progressive loss of the proboscis extension reflex to sugar stimulus. This behavioral defect is associated with the degeneration of a particular pair of muscles, the rostral protractors. Mosaic flies with mutant and wild-type tissues were produced by using an unstable ring-X chromosome. Both the behavioral defect and the muscle degeneration were examined after scoring the genotypes of the external structures of the mosaic flies. The behavioral defect in the mosaics correlated with the degeneration of the muscles. Over a half of the mosaics showed normal phenotypes in both the behavior and the muscles. Since very few mosaics showed hemilateral abnormality, the focus of the *aperC* mutation seems therefore to be submissive to the wild-type focus. The focus for the behavioral defect was located in the ventro-anterior region of the blastoderm fate map. The primary cause of the muscle degeneration of the *aperC* mutation must presumably therefore lie in the brain, not in the muscles.

INTRODUCTION

Hereditary muscular dystrophy covers a wide spectrum of muscle diseases both in vertebrates [1] and in invertebrates [2, 3]. The ultimate causes of muscular dystrophy have not yet been traced. Extensive studies have tried to determine whether the primary cause of muscular dystrophy in vertebrates is myogenic or neurogenic. For instance, cross innervation in the parabiosis of normal and dystrophic mice [4-6] and muscle transplantation between normal and dystrophic mice [7, 8] have been executed. The conclusions are diverse, however, and have led to difficulties in the inter-

pretation of the results. To overcome these difficulties, the mutant and the normal tissues must be juxtaposed at a very early stage of development. Peterson [9, 10] made a chimera mouse which was derived from the embryonic cell aggregation of normal and dystrophic mice. His chimera mosaic analysis indicates that some entirely extramuscular factors are primarily responsible for the muscle degeneration.

In *Drosophila melanogaster*, genetic mosaics with mutant and wild-type tissues can be produced by using an unstable ring-X chromosome. The internal anatomical site (focus) at which a mutant gene exerts its primary effect can be located on the blastoderm fate map by a statistical examination of the correlation between the genotypes of the external structures and the mutant phenotypes of the mosaics [11].

A recessive mutation, *abnormal proboscis extension reflex C* (*aperC*), causes degeneration of a pair of muscles, the rostral protractors which exert the force required for the proboscis extension reflex

Accepted November 17, 1988

Received July 18, 1988

Present Addresses: ¹Laboratory of Biology, Iwamizawa Campus, Hokkaido University of Education, Iwamizawa 068, Japan, ²Department of Biology, Faculty of Science, Fukuoka University, Fukuoka 814-01, Japan, ³Section of Sensory Information Processing, Research Institute of Applied Electricity, Hokkaido University, Sapporo 060, Japan

(PER) [12]. No muscle degeneration was seen in the newly eclosed mutants. The mutant muscles degenerate at advanced ages of eclosion. The muscle degeneration is influenced by temperature [3] and by the use or disuse of the muscle [13].

In this study, we applied the mosaic technique to investigate whether the muscle degeneration of the *aperC^{TF36}* mutation is of myogenic or neurogenic origin. The focus for the PER defect mapped on the blastoderm fate map suggests that the nervous system is the primary site of the cause of muscle degeneration.

MATERIALS AND METHODS

Flies

Fruit flies, *Drosophila melanogaster*, were reared on the usual cornmeal-yeast medium under constant illumination. The Canton-S strain was used as a wild-type. The *aperC^{TF36}* mutation isolated in our laboratory is recessive and is mapped at 0.4 of the X chromosome [12]. The wild-type, *aperC^{TF36}* mutant and mosaic flies were reared at 25°C until eclosion and kept at 20°C after eclosion. The *aperC^{TF36}* mutation is temperature sensitive [3]. The sensitive period is 2–3 days after eclosion. At 20°C, the loss of PER is almost complete, nor does PER recover at advanced stages.

Production of genetic mosaics

Gynandromorphs were produced by using the unstable ring-X chromosome, *In(1)w^{VC}*. The *aperC^{TF36}* mutant chromosome was marked with four recessive genes for surface structure. Mutant males of *y aperC^{TF36} w sn³ f^{6a}/B^SY* were crossed to females of *In(1)w^{VC}/y w spl* (for genetic symbols, see Lindsley and Grell [14]). Loss of the ring-X chromosome from a part of nuclei of the *In(1)w^{VC}/y aperC^{TF36} w sn³ f^{6a}* female zygotes at or after the first mitosis results in the genetic mosaics [11]. The mutant phenotype is expressed in the cell lineage with the male genotype (*y aperC^{TF36} w sn³ f^{6a}/0*) caused by a loss of the ring-X chromosome. The mutant phenotype is masked in the cell lineage with the female genotype (*In(1)w^{VC}/y aperC^{TF36} w sn³ f^{6a}*). Cell lineages with the male

genotype produce a white eye and yellow cuticle with singed-forked bristles. Those with the female genotype produce a variegated eye and wild-type cuticle and bristles.

Examination of the PER defect

Flies were starved for about 20 hr with free access to water. About 5 hr prior to the test, the flies were anesthetized by chilling. The mesonotum and wings were pasted on acryl board, ventral side up, with myristyl alcohol melted by a needle-shaped heater. All legs and proboscis were free to move. The fixed flies were kept in a moist chamber. A small hemispherule of test solution ejected on the tip of a hypodermic needle from a 1-ml plastic syringe was brought into contact with the prothoracic tarsi or proboscis labella. The flies were first satiated with distilled water. The PER was examined with 1 M sucrose solution.

Examination of the muscle degeneration

After the examination of the PER defect, the degeneration of the rostral protractors was observed by polarizing light microscopy. Flies were fixed in 70% alcohol, dehydrated in graded alcohol series, and cleared in methyl benzoate. The head was separated from the body and then mounted in Bioleite (Oken Shoji Co.). The preparations were viewed in a frontal plane under a polarizing light microscope or a dissecting microscope equipped with crossed-polarizers. The axis of the analyzer was perpendicularly crossed with that of polarizer. The midline of the fly's head was aligned along the bisector of the angle between polarizer and analyzer. Because of the birefringence of the contractile elements, the normal rostral protractors were seen brightly and the brightness was equal on both sides. If the muscles degenerated, the brightness weakened or disappeared (Fig. 1).

Mapping of the behavioral focus

Prior to the examination of the PER defect, each mosaic fly was immobilized by ice-chilling and the genotypes of the surface structure (landmarks) were scored according to the color of cuticle or eyes and the form of the bristles. If both the mutant and the wild-type cuticles were mixed

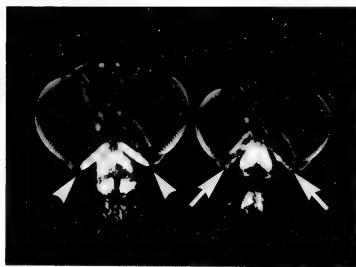


Fig. 1. Heads of *y aper^{CTF36} w sn³ f^{36a}* male in whole mount preparation under crossed polarizers. Left: 1 day after eclosion; arrowheads: rostral protractors with normal birefringence. Right: 5 days after eclosion; arrows: weakened birefringence of the muscles. Both at 25°C.

within a large structure, it was counted half as normal and half as mutant. The correlations between the genotypes of surface landmarks and the PER phenotypes were summarized into matrices.

The distance between two external structures on the blastoderm fate map is represented by the probability that the mosaic boundary passes between them. The unit of the distance on the blastoderm fate map is called a "sturt" [11, 15]. One sturt means that the genotypes of a pair of structures differ from one another in 1% of all the mosaics observed. As well as the distance between the two external sites, the distance between an external landmark and a behavioral focus can be calculated [11]. Distances between the focus for the PER defect and various surface landmarks were calculated. The submissive focus model in which the effect of a hemilateral mutant focus is masked by the wild-type focus on the other side of the mosaic fly [11] was applied. The focus for the PER defect was located on the blastoderm fate maps of Hotta and Benzer [11] and of Koana and Hotta [16].

RESULTS

Correlation between PER defect and muscle degeneration in the aper^{CTF36} mutant

The PER to the sugar stimulus and the birefrin-

gence of the rostral protractors examined in 50 wild-type flies were normal irrespective of ages.

The PER phenotypes of the *aper^{CTF36}* mutants were examined at various ages after eclosion. The mutants came to show a defective PER at advanced ages (Fig. 2). At day 3 of eclosion, all mutants extended the proboscis normally to the sugar stimulus. At day 5 about 60% of the mutants showed the PER defect. Later, most of the mutants showed the PER defect. By day 14, only a few had recovered the PER.

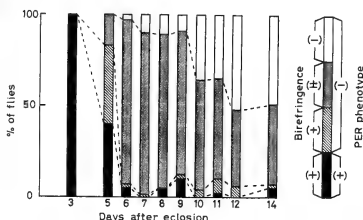


Fig. 2. Progression of the PER defect and the loss of birefringence of rostral protractors at 20°C. The column on the right indicates the category of the phenotypes. About 50 flies were examined for each column.

After the PER test, the birefringence of the rostral protractors of the mutant flies was examined (Fig. 2). All mutants which showed normal PER possessed the normal muscular birefringence. The degree of birefringence varied in the mutants with abnormal PER. The degree of birefringence was classified into three groups according to its brightness under the crossed polarizers; +): brightness is similar to that of the wild-type fly, -): brightness is absent or patchy if present, and ±): brightness is present but markedly weak compared with that of the wild-type fly. At day 5, about 67% of the PER defective mutants still showed normal birefringence (+). After that, the number of mutants with normal birefringence rapidly decreased, whereas the number of flies with no birefringence (-) increased. After day 6 of eclosion, the loss of the birefringence of the mutant's rostral protractors correlated with the PER defect. Most of the PER defective flies

showed abnormal birefringence ($-$ or \pm). Only a small percent of the PER defective flies showed normal birefringence ($+$). No differences were seen in the birefringence between the bilateral pair of the muscles.

Correlation between PER defect and muscle degeneration in the mosaic flies

The PER phenotypes of the mosaic flies correlated with the birefringences of the rostral protractors (Table 1). The PER phenotype and the birefringence were examined at 9–11 days after eclosion at 20°C. The mosaic flies showed either normal ($+$), weak (\pm) or no ($-$) birefringence in the rostral protractors. Weak (\pm) or no ($-$) birefringence were counted as abnormal. The mosaics with normal PER showed normal birefringence, whereas the mosaics with defective PER showed abnormal birefringence, although the correlation was not absolute. Of 207 mosaic flies, 144 showed normal PER, 62 showed defective PER and one fly extended the proboscis only on the right side of the body. Of 144 PER normal flies, 135 ones showed normal birefringence ($+$) and

only 9 showed abnormal birefringence. Out of 62 PER defective flies, only 3 demonstrated normal birefringence. The fly with the right-sided PER showed normal birefringence on the left side rostral protractor but no birefringence on its right side protractor. No other left-right asymmetries were observed in the PER defect or in the birefringence.

The head surfaces of 89 mosaics were solidly of either wild-type or mutant (Table 2A). The genotype of the head surface coincided with the PER phenotype in most mosaics. Of 46 mosaics whose head surface was entirely wild-type, all flies showed normal PER. Of 43 mosaics whose head surface was entirely mutant, 36 flies showed defective PER and 7 flies showed normal PER. The muscle birefringence also correlated with the genotype of head surface (Table 2B). Forty five of the 46 mosaics with the wild-type head surface showed normal birefringence and only one of them showed abnormal birefringence. Thirty seven mosaics out of 43 with the mutant head surface showed abnormal birefringence and 6 of them showed normal birefringence.

All the 14 mosaics whose head had a mosaic

TABLE 1. Correlation matrix between the PER phenotype and birefringence of the rostral protractors, in the *aperC^{TF36}* mosaics, 9–11 days after eclosion, 20°C

		PER phenotype	
		normal (wild)	abnormal (mutant)
Birefringence	normal (wild)	135	3
	abnormal (mutant)	9	59

TABLE 2. Correlation matrices between head surface genotype and the PER phenotype (A) and the muscle birefringence (B) in the *aperC^{TF36}* mosaics (A)

		Entire head cuticle	
		wild-type	mutant
PER Phenotype	normal (wild)	46	7
	abnormal (mutant)	0	36

		Entire head cuticle	
		wild-type	mutant
Birefringence	normal (wild)	45	6
	abnormal (mutant)	1	37

TABLE 3. Summary of focus mapping of the PER defect: Correlation matrices for 12 surface landmarks and fate map distances (\overline{Af})

Surface landmarks ¹	Correlation matrices*			Calculated distances in sturts [#]
	a_{11} b_{11}	a_{10} b_{10}	a_{00} b_{00}	
ANT	147 2.5	62.5 21.5	8.5 49	13.2
OC	151 2	54 15	13 56	12.8
PV	159 6	46 17	13 50	15.3
OV	153 9	48 19	17 45	19.2
PA	138 2	71 26	9 45	15.0
IV	153 5	50 20	15 48	17.1
PR	146.5 20.5	41 28.5	30.5 24	35.8
HU	127.5 23	63 28	27.5 22	33.9
ANP	97 7	97 46	24 20	31.4
ADC	110 15	78 39	30 19	35.3
LEG1	126 13	77 32	15 28	24.8
4t	122.5 41	70.5 25	25 7	43.3

¹abbreviations for surface landmarks: ANT, antenna; OC, ocellar bristle; PV, post vertical bristle; OV, outer vertical bristle; PA, palp; IV, inner vertical bristle; PR, proboscis; HU, humeral bristle; ANP, anterior notopleural bristle; ADC, anterior dorsocentral bristle; LEG1, foreleg; 4t, 4th abdominal tergite.

* a_{ij} and b_{kl} represent the number of flies classified in each category.

		A pair of surface landmarks, A and A'		
		Both wild-type	One wild one mutant	Both mutant
PER phenotype	normal	a_{11}	a_{10}	a_{00}
	abnormal	b_{11}	b_{10}	b_{00}

[#]Map distance \overline{Af} between the surface landmark (A) and the ipsilateral behavioral focus (\overline{f}) is calculated according to the submissive focus model [11].

$$\overline{Af} = (1 - \overline{AA'}) \times (a_{00}/(a_{00} + b_{00}) + b_{11}/(a_{11} + b_{11}))/2 \\ + \overline{AA'} \times b_{10}/(a_{10} + b_{10}),$$

where $\overline{AA'} = (a_{10} + b_{10})/\text{total number of mosaic flies}$.

boundary at the midline showed normal PER and normal birefringence on both sides of the rostral protractors.

Mapping the focus for the PER defect

The PER phenotype and the genotype of 12 pairs of surface landmarks were examined in 291 mosaic flies (Table 3). The PER of the mosaic fly was examined individually 7 days after eclosion, so as to minimize any error due to the incomplete penetrance of the mutation (data not shown).

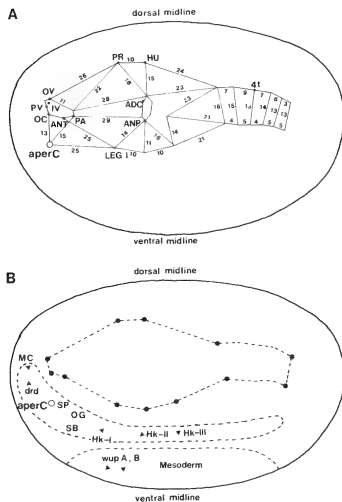


Fig. 3. A: the defective PER focus (open circle, *aperC*) of the *aperC*^{TF36} mutation on the blastoderm fate map redrawn from Hotta and Benzer [11]. For abbreviations of surface landmarks, see Table 3. B: the *aperC* focus on the fate map redrawn from Koana and Hotta [16]; the presumptive regions of the central nervous system and the mesodermal structures are inferred and shown with dotted line. Abbreviations: *drd*⁸, *drop-dead* focus; *Hk-I*, *Hk-II*, *Hk-III*⁹, *Hyperkinetic* leg shaking foci for pro-, meso-, and metathoracic legs respectively; *MC*¹, male courtship focus; *OG*², optic ganglion; *SB*³, subesophageal ganglion; *SP*⁴, supraesophageal ganglion; *wup-A*, *B*⁵, foci for two *wing-up* mutants. ⁸from Hotta and Benzer [11], ¹from Hotta and Benzer [23], ²from Kankel and Hall [17].

Seventy three flies showed the mutant phenotype in PER and 218 flies showed normal PER. The one fly with the right-sided PER was counted as a mutant. The correlation matrices between the genotypes of various surface landmarks and the PER phenotype of an individual suggest that the focus is located in the anterior region of the animal. The distances (Af) on the fate map between the PER focus (f) and a surface landmark (A) were calculated according to the submissive focus model [11]. The triangulate mapping located the focus for the PER defect in the antero-ventral region of the blastoderm fate map (Fig. 3).

DISCUSSION

Amongst our mosaic flies, the PER defect correlated with the loss of birefringence of the rostral protractors. The same correlation has been seen during the course of progression of the PER defect in the *aperC*^{TF36} mutant (Fig. 2 and [3]). These correlations indicate that the PER defect of the *aperC*^{TF36} mutation is caused by the degeneration of the muscles, or that the PER defect and the muscle degeneration result from a common but non-muscular cause. The behavioral focus for the PER defect and the focus for the muscle degeneration must be located on the same site of the blastoderm fate map. The focus of the PER defect suggests the site where the *aperC*^{TF36} mutation exerts its primary effect responsible for the muscle degeneration.

The phenotypes of the *aperC*^{TF36} (the PER defect and the muscle degeneration) closely correlated with the genotypes of the head cuticle in the mosaics whose entire head cuticle shows a solid genotype. However, there were several exceptional cases in which the genotype of head cuticle and the PER or muscle phenotype did not match. This indicates that the area of blastoderm which gives rise to the defect of the *aperC*^{TF36} mutation is close to, but distinct from the area which gives rise to the head cuticle.

Very few mosaics showed any hemilateral abnormality. The mosaic flies were either wild- or mutant type for the PER except for two cases out of 498. No other intermediate PER abnormality was found. Birefringence of the muscles in the

mosaics was also either wild- or mutant type with bilateral symmetry except for one out of 207. The phenotypic expression of the *aperC^{TF36}* mutation seems therefore to be an all or nothing event in an animal as a whole.

Homolateral expression in the mosaics led us to consider three possibilities for the focus which causes the defect of the *aperC^{TF36}* mutation: a single focus, two bilateral independent foci and two bilateral interacting foci. If the *aperC^{TF36}* defect is expressed by a single focus, the genotype of the focus is either mutant or wild-type with equal probability, and half the mosaic flies studied would show the mutant phenotype. Since 70% of the mosaics were wild-type in the PER and muscle birefringence, however, no single focus model is applicable. If two bilateral foci cause the defect independently on each side of the body, hemilateral abnormality should appear in proportion to the distance between the foci. The very low frequency of hemilateral abnormality may indicate that a pair of bilateral foci are independent but very close to the blastoderm midline. As this would be equivalent to a single unpaired focus on the midline, we can rule out the possibility of bilateral independent foci as well, since we found a much larger frequency of mosaics with the wild-type than those with the mutant phenotype. This is reinforced by the result that none of the mosaics whose head surface was separated into the wild-type and the mutant at the midline showed hemilateral abnormality. It is therefore plausible to suggest that the bilateral foci are interacting together to express a single phenotype in a fly as a whole.

When two bilaterally homologous PER foci are different in genotype, the interaction of both the mutant and the wild-type focus must result in either a tally mutant or a totally wild-type fly. The resultant phenotype depends on whether the mutant focus is submissive to or domineers over the wild-type focus [11]. Because the majority of the mosaic flies were wild-type, the *aperC^{TF36}* mutation focus is assumed to be submissive to the wild-type focus. The mutant phenotype results only when both of the bilateral foci are mutant.

Location of the *aperC^{TF36}* focus obtained from the submissive focus model suggests that the primary cause of the muscle degeneration lies in the

nervous system. The focus of the *aperC^{TF36}* was located in the ventro-anterior region of the blastoderm fate map. This region of the fate map corresponds to the brain of the adult fly [17]. A possible explanation for the submissiveness is that the normal side of the brain supplies a sufficient amount of a factor, e.g. of neuro-endocrine nature, which controls the posteclosional maintenance or maturation of the muscles.

It is unlikely that the muscle degeneration of the *aperC^{TF36}* mutation is myogenic. If the muscles with a mutant genotype degenerate of themselves, the hemilateral degeneration would appear frequently in the mosaics. We can find this case in the *heldup²* (*hdp²*) mutation, which causes a degeneration of flight muscles in the late pupal development. Quite a large proportion of the mosaics of the *hdp²* mutation have shown such hemilateral muscle degeneration [18]. The primary focus for *hdp²* degeneration was mapped on the ventral mesoderm of the presumptive musculature [18]. In contrast to this, hemilateral abnormality appeared very rarely in the *aperC^{TF36}* mosaics.

The homolateral expression in the mosaic may indicate a bilateral origin of the muscle: migration of precursor cells across the midline. As our present methods of examination of the birefringence and the PER may not be sensitive enough to detect the loss of half amount of muscles, the majority of the mosaics may have been allotted as normal although suffering from some myogenic degeneration. Cell lineage analysis by the mitotic recombination and a histochemical marker [19] implies that the rostral protractor is of unilateral origin, whereas many of the other head muscles are of bilateral origin.

We can not, of course, rule out the possibility that the primary focus of the *aperC^{TF36}* mutation is in the muscles per se, because location of a focus by triangulation in the anterior portion of the blastoderm is sensitive to statistical errors [20]. To obtain direct evidence, we must use histochemical markers to examine the genotypes of muscles [19, 21, 22] or of nervous tissues [17].

ACKNOWLEDGMENTS

We thank Mr. S. Fujiwara and Mr. A. Takahashi for their statistical help.

REFERENCES

- 1 Harris, J. B. (1979) Muscular dystrophy and other inherited diseases of skeletal muscle in animals. *Annu. Rev. N.Y. Acad. Sci.*, **317**: pp. 1-716.
- 2 Brenner, S. (1974) The genetics of *Caenorhabditis elegans*. *Genetics*, **77**: 71-94.
- 3 Kimura, K.-I., Shimozawa, T. and Tanimura, T. (1986) Muscle degeneration in the posteclosional development of a *Drosophila* mutant, *abnormal proboscis extension reflex C(aperC)*. *Dev. Biol.*, **117**: 194-203.
- 4 Douglas, W. B. (1975) Sciatic cross-reinnervation of normal and dystrophic muscle in parabiotic mice: Isometric contractile responses of reinnervated tibialis anticus and triceps surae. *Exp. Neurol.*, **48**: 647-663.
- 5 Law, P. K., Cosmos, E., Butler, J. and McComas, A. J. (1976) The absence of dystrophic characteristics in normal muscles successfully cross-reinnervated by nerves of dystrophic genotype: Physiological and cytochemical study of crossed solei of normal and dystrophic parabiotic mice. *Exp. Neurol.*, **51**: 1-21.
- 6 Law, P. K. (1977) "Myotrophic" influences on motoneurons of normal and dystrophic mice in parabiosis. *Exp. Neurol.*, **54**: 444-452.
- 7 Hironaka, T. and Miyata, Y. (1975) Transplantation of skeletal muscle in normal and dystrophic mice. *Exp. Neurol.*, **47**: 1-15.
- 8 Neerunjun, J. S. and Dubowitz, V. (1977) Regeneration of muscles transplanted between normal and dystrophic mice: A quantitative study of early transplants. *J. Anat.*, **124**: 459-467.
- 9 Peterson, A. C. (1974) Chimera mouse study shows absence of disease in genetically dystrophic muscle. *Nature*, **248**: 561-564.
- 10 Peterson, A. C. (1979) Mosaic analysis of dystrophic \leftrightarrow normal chimeras: An approach to mapping the site of gene expression. *Annu. Rev. N.Y. Acad. Sci.*, **317**: 630-648.
- 11 Hotta, Y. and Benzer, S. (1972) Mapping of behaviour in *Drosophila* mosaics. *Nature*, **240**: 527-535.
- 12 Kimura, K.-I., Shimozawa, T. and Tanimura, T. (1986) Isolation of *Drosophila* mutants with abnormal proboscis extension reflex. *J. Exp. Zool.*, **239**: 393-399.
- 13 Kimura, K.-I., Shimozawa, T. and Tanimura, T. (1987) Suppression of inherited muscle degeneration in a *Drosophila* mutant by mechanical and genetical immobilizations. *J. Neurogenet.*, **4**: 21-28.
- 14 Lindsley, D. L. and Grell, E. H. (1968) "Genetic variations of *Drosophila melanogaster*". Carnegie Inst. Washington Publ. No. 627.
- 15 Sturtevant, A. H. (1929) The claret mutant type of *Drosophila simulans*: A study of chromosome elimination and cell lineage. *Z. wiss. Zool.*, **135**: 325-356.
- 16 Koana, T. and Hotta, Y. (1978) Isolation and characterization of flightless mutants in *Drosophila melanogaster*. *J. Embryol. exp. Morph.*, **45**: 123-143.
- 17 Kankel, D. R. and Hall, J. C. (1976) Fate mapping of nervous system and other internal tissues in genetic mosaics of *Drosophila melanogaster*. *Dev. Biol.*, **48**: 1-24.
- 18 Deak, I. I. (1977) A histochemical study of the muscles of *Drosophila melanogaster*. *J. Morphol.*, **153**: 307-316.
- 19 Raghavan, K. V. and Pinto, L. (1985) The cell lineage of the muscles of the *Drosophila* head. *J. Embryol. exp. Morph.*, **85**: 285-294.
- 20 Hall, J. C. and Greenspan, R. J. (1979) Genetic analysis of *Drosophila* neurobiology. *Ann. Rev. Genet.*, **13**: 127-195.
- 21 Lawrence, P. A. (1981) A general cell marker for clonal analysis of *Drosophila* development. *J. Embryol. exp. Morph.*, **64**: 321-332.
- 22 Lawrence, P. A. and Johnston, P. (1986) Observations on cell lineage of internal organs of *Drosophila*. *J. Embryol. exp. Morph.*, **91**: 251-266.
- 23 Hotta, Y. and Benzer, S. (1976) Courtship in *Drosophila* mosaics: sex-specific foci for sequential action patterns. *Proc. Natl. Acad. Sci. USA.*, **73**: 4154-4158.

Sodium and Chloride Transport in the Lizard Duodenum

ANTHONIO LORENZO¹, PINO SANTANA, TOMAS GÓMEZ and PILAR BADIA

*Laboratorio de Fisiología Animal, Departamento de Biología Animal,
Facultad de Biología, Universidad de La Laguna, Tenerife, España*

ABSTRACT—The mechanisms by which Na and Cl ions are transported across the duodenal epithelium of the lizard *Gallotia galloti* were studied under voltage-clamped conditions. The lizard duodenum actively absorbed sodium and chloride with a ratio of approximately 2:1. In the absence of sodium, the short-circuit current (Isc) and net chloride flux ($J_{\text{net}}^{\text{Cl}}$) were abolished. In the absence of chloride, the net sodium flux ($J_{\text{net}}^{\text{Na}}$) was halved but the short-circuit current (Isc) was not changed significantly. Treatment with acetazolamide, amiloride, or disulfonic stilbene (DIDS) abolished the net chloride flux almost completely, whereas the Isc was not changed significantly. When ouabain was added to the serosal side, the short-circuit current and net fluxes of sodium and chloride were abolished. From an analysis of the effects of these inhibitors, a plausible model was developed to explain the characteristics of the sodium and chloride transport. It is proposed that the entry of sodium into the cell across the luminal membrane occurs via two pathways. A part of the Na^+ entry occurs through the Na^+/H^+ antiporter and a part through an electrogenic pathway. The entry of Cl^- across the apical membrane occurs through the $\text{Cl}^-/\text{HCO}_3^-$ antiport. Chloride seems to exit the cell by a diffusional process.

INTRODUCTION

Electrolyte transport across leaky epithelia such as the gallbladder, renal proximal tubule and small intestine has been studied extensively *in vivo* and *in vitro* by measuring electrical parameters and tracer fluxes [1-3]. Numerous studies have demonstrated an interdependence of net transepithelial Na^+ and Cl^- fluxes [4-7]. These results have been interpreted by the existence of direct coupling of Na^+ and Cl^- fluxes through a ternary-complex of Na^+ and Cl^- , and cotransporter at the apical membrane [2]. However, the other possibility of neutral, coupled NaCl transport resulting from the simultaneous operation of Na^+/H^+ and Cl^-/OH^- exchanges has been suggested [8-10]. These transport mechanisms have been studied specially in the small intestine of mammals and few references are found in reptilian intestine, where electrolyte transport has been studied especially in

the colon. Studies of the proximal and distal colon of *Testudo graeca* [11] have demonstrated that sodium and chloride are transported at a similar rate. Active transport of sodium and chloride ions has also been shown across the isolated turtle colon [12], lizard colon [13], and ileum [14].

The purpose of the present study was to investigate mechanisms of Cl^- and Na^+ transport across isolated lizard duodenum by measuring unidirectional sodium and chloride fluxes in presence of several inhibitors. The results suggest that about 50% of apical sodium entry results from amiloride sensitive Na^+/H^+ exchange and that of the other 50% of the sodium uptake is electrogenic. The entry of chloride into the cell across the luminal membrane results from a $\text{Cl}^-/\text{HCO}_3^-$ exchange.

MATERIALS AND METHODS

Animals and preparation

Experiments were performed on male and female *Gallotia galloti* lizards (mean body weight

Accepted November 21, 1988

Received July 12, 1988

¹ To whom reprint requests should be addressed.

30–40 g). They were killed by spinal transection and ileum was removed and placed in ice cold bathing solution gassed with 5% CO₂ in O₂. Duodenal mucosa was separated from underlying smooth muscle and was mounted in Ussing chambers with an exposed area of 0.21 cm². Chambers were water jacketed and the temperature was maintained at 30°C. The tissue was bathed on both sides with each experimental solution (4.0 ml).

Solutions

The bathing solution contained in mM: NaCl 107, KCl 4.5, NaHCO₃ 25, Na₂HPO₄ 1.8, NaH₂PO₄ 0.2, CaCl₂ 1.25, MgSO₄ 1.0 and glucose 5. The solution was gassed with 5% CO₂ in O₂ and pH of 7.4. In Na⁺-free solution, Na⁺ was replaced with choline. When Cl⁻-free solution was used, Cl⁻ was replaced with isothionate. HCO₃⁻-free solution was buffered with Hepes-Tris (pH=7.4) and gassed with pure O₂.

Electrical measurements

Agar bridges, 4% w/v made with bathing solution, were positioned near each of the tissues and at opposite ends of the chamber. Calomel electrodes and Ag/AgCl electrodes in saturated KCl were connected to the agar bridges to measure the transmural potential difference and to pass direct current, respectively. The tissue was continuously short circuited with an automatic computer controlled voltage clamp device (AC-Microclamp, Aachen, W. Germany). Algorithm A6 was utilized. Briefly, the procedure was as follows: after correcting for offset potential and solution resistance, direct current was applied to nullify the transmural potential difference. The necessary current (Isc) was corrected at a frequency of 4Hz. Every 5 sec, a 25 μ A pulse (1 sec duration) was alternately added, which was subtracted from the short-circuit current (Isc). After a 0.5 sec delay, the displacement in potential difference from zero caused by the pulse was measured. From the change in potential difference and pulse amplitude, tissue conductance (Gt) was calculated. The transmural open circuit potential difference (PD) was calculated from the Gt and Isc. All three parameters, Isc, Gt and PD were recorded by a digital printer at 1 min intervals. In addition, Isc

was continuously recorded on a chart recorder.

Unidirectional ion flux measurements

Twenty min after the tissue was mounted, isotopes (²²Na and ³⁶Cl) were added to the bathing solution on one side of the tissue. After additional 20 min, by which time isotope fluxes had reached a steady-state, samples were taken from the unlabelled side every 20 min. After each sampling, equal volume of cold solution was added to maintain the volume. The effects of inhibitors on ion fluxes were studied by comparing ion fluxes before (3 samples) and after (3 samples) addition of each inhibitor. Isotope activities were determined simultaneously by sequential counting in a Beckman liquid scintillation spectrometer (Nuclear Chicago, model Isocap-300). Unidirectional Na⁺ and Cl⁻ fluxes were calculated using standard equations [15]. The net residual ion flux (J_{net}^R) was calculated from the difference in Isc and net Na⁺ ($J_{net}^{Na^+}$) and Cl⁻ ($J_{net}^{Cl^-}$) fluxes ($J_{net}^R = \text{Isc} - (J_{net}^{Na^+} - J_{net}^{Cl^-})$).

Statistics

Results are given as the mean \pm one standard error of the mean (SEM). Significances of differences were tested using a two-tailed Student's *t*-test. Paired or unpaired tests were used.

Materials

Amiloride, acetazolamide, DIDS (4,4'-diisothio-cyanatostilbene-2,2'-disulfonic acid) and ouabain were obtained from Sigma Chemical (St. Louis). Radioisotopes (²²Na and ³⁶Cl) were obtained from New England Nuclear.

RESULTS

Electrical and flux measurements under standard conditions

The isolated duodenum was first incubated for 40 min (t_0 - t_{40}) under open-circuit conditions and then for 60 min (t_{40} - t_{100}) under short-circuit conditions (Fig. 1). Under open-circuit conditions the measured PD (serosa positive) and Gt and the calculated Isc were equal to the respective calculated PD and measured Gt and Isc under short-

circuit conditions. Thus the short-circuiting does not appear to affect the duodenum from lizards. Measurements of Na^+ and Cl^- fluxes across the short-circuited mucosa are given in Figure 1. Net fluxes of Na^+ and Cl^- were observed under short-circuited condition, whereas Na^+ absorption predominated. The $J_{\text{net}}^{\text{Na}}$ was already twice times the $J_{\text{net}}^{\text{Cl}}$ ($J_{\text{net}}^{\text{Na}} = 2.35 \pm 0.16$ and $J_{\text{net}}^{\text{Cl}} = 1.25 \pm 0.15 \mu\text{eq}/\text{cm}^2 \text{ h}$) and the difference between them was approximately equal to the Isc and the residual flux did not differ significantly from zero.

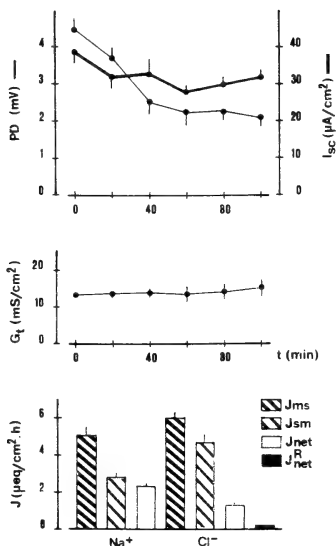


Fig. 1. Electrical characteristics and sodium and chloride fluxes in lizard duodenum under standard conditions. The bars represent SEM of 14 experiments.

Effects of substitutions on the electrical characteristics and ion fluxes

In order to test the coupling between sodium and chloride transport processes, Cl^- and Na^+ fluxes were determined in sodium-free and chloride-free Ringer solutions respectively. The tissue was first incubated in standard bathing solution in

order to obtain control values of electrical parameters and unidirectional fluxes. The tissue was then rinsed three times with either a Na^+ -free solution containing the normal concentration of Cl^- (114 mM) or a Cl^- -free solution containing the normal concentration of Na^+ (136 mM) and incubated until a new steady-state was obtained.

When Na ions were replaced with choline Isc and PD were decreased to zero ($\text{Isc} = -0.006 \pm 0.15 \mu\text{eq}/\text{cm}^2 \text{ h}$, $\text{PD} = -0.15 \pm 0.31 \text{ mV}$), the tissue conductance remaining unchanged ($G_t = 18.25 \pm 2.75 \text{ mS}/\text{cm}^2$). In contrast, the PD and Isc , in isothionate Ringer were not significantly different from control values ($\text{PD} = 3.26 \pm 0.35 \text{ mV}$, $\text{Isc} = 1.03 \pm 0.12 \mu\text{eq}/\text{cm}^2 \text{ h}$, $G_t = 11.45 \pm 2.80 \text{ mS}/\text{cm}^2$). Steady-state Na^+ and Cl^- fluxes in Cl^- -free and Na^+ -free Ringer's solution are given in Table 1. Na^+ replacement with choline (Na -free) abolished $J_{\text{net}}^{\text{Cl}}$ and Cl^- replacement with isothionate (Cl -free) halved $J_{\text{net}}^{\text{Na}}$. This appears to indicate that approximately 50% of the net sodium transport is coupled with the net Cl^- transport.

Effects of various inhibitors, acetazolamide, amiloride and ouabain, on ion fluxes

In order to determine whether NaCl absorption is via Na^+/Cl^- cotransport or $\text{Na}^+/\text{H}^+/\text{Cl}^-/\text{HCO}_3^-$ dual exchange system, the effects of acetazolamide, amiloride and ouabain on the Na^+ and Cl^- fluxes were investigated. The results are listed in Table 2. Working with HCO_3^- -free solutions, net sodium and chloride fluxes did not change significantly with respect to control solution. When acetazolamide was added to both mucosal and serosal bathing solutions (HCO_3^- -free), the net chloride transport was completely inhibited ($-0.47 \pm 0.18 \mu\text{eq}/\text{cm}^2 \text{ h}$) due to a decrease in the mucosa to serosa chloride flux. Net sodium transport was almost halved. The Isc , PD and G_t remained unchanged. This appears to indicate that chloride absorption is all via $\text{Cl}^-/\text{HCO}_3^-$ antiport and 50% of sodium absorption is via Na^+/H^+ antiport and the electrical parameters are due to the remaining 50% Na^+ transport.

The addition of amiloride (10^{-3} M) to the mucosal side (standard solution) revealed that this substance completely inhibited the net chloride transport ($0.07 \pm 0.17 \mu\text{eq}/\text{cm}^2 \text{ h}$) and halved the

TABLE 1. Effects of ion substitution on electrical

	J^{Na} (n=14)			J^{Cl} (n=13)		
	ms	sm	net	ms	sm	net
Control	5.5 \pm 0.57	3.2 \pm 0.31	2.29 \pm 0.17	6.27 \pm 0.36	5.11 \pm 0.47	1.16 \pm 0.16
Cl-free	4.30 \pm 0.60*	3.18 \pm 0.59	1.12 \pm 0.22*	—	—	—
Na-free	—	—	—	5.30 \pm 0.11 [†]	5.39 \pm 0.54	-0.09 \pm 0.15*

Values are means \pm SEM, n=number of tissues.

Ion fluxes and ISC are given in $\mu\text{eq}/\text{cm}^2$ h, PD in mV and Gt in mS/cm^2 h. Measurements were made before conditions the chloride ions of both sides of the tissue were replaced by isothionate; likewise, the sodium-Na-free conditions.

[†],* significant difference ($P < 0.05$, $P < 0.001$) respectively, with the control series according to t-test.

TABLE 2. Effects of acetazolamide, amiloride and ouabain

(n)	J^{Na}			J^{Cl}		
	ms	sm	net	ms	sm	net
(HCO_3^- -free) (10)	6.50 \pm 0.57	3.21 \pm 0.31	2.29 \pm 0.20	7.23 \pm 0.25	5.87 \pm 0.36	1.36 \pm 0.13
Acetazolamide (10)	4.50 \pm 0.30 [#]	3.60 \pm 0.38	0.90 \pm 0.12*	5.68 \pm 0.47 [#]	6.15 \pm 0.34	-0.47 \pm 0.18*
Control (14)	8.39 \pm 0.55	6.25 \pm 0.42	2.14 \pm 0.18	9.31 \pm 0.40	8.20 \pm 0.60	1.11 \pm 0.19
Amiloride (14)	7.50 \pm 0.49 [#]	6.25 \pm 0.30	1.15 \pm 0.15*	8.10 \pm 0.39 [†]	8.03 \pm 0.50	0.07 \pm 0.17*
Control (11)	5.60 \pm 0.40	3.10 \pm 0.61	2.50 \pm 0.21	6.32 \pm 0.35	5.46 \pm 0.41	0.86 \pm 0.16
Ouabain (11)	4.70 \pm 0.50 [#]	4.70 \pm 0.45 [†]	0.00 \pm 0.20*	5.20 \pm 0.13 [#]	5.38 \pm 0.32	-0.18 \pm 0.09*

Ion fluxes and I_{sc} are given in $\mu\text{eq}/\text{cm}^2$ h, PD in mV and Gt in mS/cm^2 . Measurements were made before and after Acetazolamide was added to the HCO_3^- -free bathing solution both sides of tissue. Amiloride and ouabain tively. Values are the mean \pm SEM.

[†],[#],* significant difference $P < 0.05$, $P < 0.01$, $P < 0.001$.

TABLE Effects of DIDS on ion fluxes

(n)	J^{Na}			J^{Cl}		
	ms	sm	net	ms	sm	net
Control (9)	6.25 \pm 0.68	3.90 \pm 0.43	2.35 \pm 0.25	6.32 \pm 0.48	5.02 \pm 0.89	1.30 \pm 0.34
DIDS (mucosa) (9)	4.08 \pm 0.37	2.67 \pm 0.25	1.41 \pm 0.15 [#]	4.96 \pm 0.41 [†]	4.78 \pm 0.79	0.18 \pm 0.30
Control (9)	6.70 \pm 0.56	4.20 \pm 0.28	2.50 \pm 0.21	6.15 \pm 0.42	5.20 \pm 0.63	0.95 \pm 0.25
DIDS (Serosa) (9)	5.60 \pm 0.28	3.40 \pm 0.43	2.20 \pm 0.17	6.08 \pm 0.43	5.16 \pm 0.45	0.91 \pm 0.20

Ion fluxes and I_{sc} are given in $\mu\text{eq}/\text{cm}^2$ h, PD in mV and Gt in mS/cm^2 . Measurements were made before and after Values are the mean \pm SEM.

[†],[#] significant difference ($P < 0.05$, $P < 0.01$) compared to control.

net sodium transport while I_{sc} , PD and Gt remained unchanged. This observation indicates that amiloride inhibits the $\text{Na}^+/\text{H}^+ - \text{Cl}^-/\text{HCO}_3^-$ dual exchange system across the apical membrane of the epithelial cell. The effects of ouabain (10^{-3}

M) added to the serosal side showed that sodium and chloride transport was dependent on the activity of the basolateral $\text{Na}^+ - \text{K}^+$ pump. As indicated in Table 2, the Na^+ and Cl^- transport and I_{sc} were all abolished.

characteristics and ion fluxes

(n=14)		
Isc	PD	Gt
1.24 ± 0.18	2.99 ± 0.15	12.07 ± 1.86
1.03 ± 0.12	3.26 ± 0.35	11.45 ± 2.80
-0.006 ± 0.15*	-0.15 ± 0.31*	18.15 ± 2.75

and after the substitution of the ion. Under the Cl-free ions were substituted in both media by choline under the

on ion fluxes in duodenum

Isc	Gt	PD
1.13 ± 0.15	12.15 ± 1.82	2.10 ± 0.28
1.07 ± 0.12	11.42 ± 2.02	2.22 ± 0.18
1.14 ± 0.12	13.15 ± 2.65	2.39 ± 0.23
1.10 ± 0.23	13.14 ± 1.67	2.27 ± 0.19
1.42 ± 0.30	17.68 ± 2.68	2.54 ± 0.23
0.49 ± 0.16*	26.00 ± 4.08	2.21 ± 0.22

the addition of inhibitors to the bathing solution. were only added to the mucosal and serosal side respec-

in duodenum

Isc	Gt	PD
1.23 ± 0.16	18.06 ± 2.06	1.92 ± 0.23
1.08 ± 1.12	21.56 ± 2.44	1.35 ± 0.19
1.26 ± 0.17	13.20 ± 1.99	2.21 ± 0.22
1.32 ± 0.23	15.54 ± 1.26	2.18 ± 0.30

the addition of inhibitor to the bathing solution.

Effects of DIDS on ion fluxes

The disulfonic stilbenes SITS and 4,4'-diisothiocyanatostilbene-2,2'-disulfonic acid (DIDS) have been utilized as anion exchange inhibitors [10]. To further differentiate the chloride transport across the brush-border membrane from that across the

basolateral membrane, we next examined the effects of DIDS on Na⁺ and Cl⁻ fluxes. As indicated in Table 3, after addition of 10⁻³ M DIDS to the mucosal bath, Isc, PD and Gt remained unchanged, but DIDS reduced the net flux of sodium by decreasing the m-s flux and abolished the net flux of chloride. These results suggest, as indicated above, that chloride absorption is via Cl⁻/HCO₃⁻ and a part of sodium absorption is via Na⁺/H⁺-Cl⁻/HCO₃⁻ dual exchange system. When DIDS was added to serosal side the mucosal to serosal chloride flux was not reduced at all (Table 3), suggesting that chloride exit does not occur through a Cl⁻/HCO₃⁻ exchange.

DISCUSSION

Several reports suggest an obligatory coupling of the transport of sodium and chloride across the brush-border membrane of leaky epithelia [1, 2, 6, 16-24]. Recently a significant contribution of a Na⁺/Cl⁻ cotransport mechanism to NaCl uptake across the intestinal brush-border membranes has been excluded in rat small intestine [9, 10]. The findings are, consistent with a double exchange of Na⁺ for H⁺ and Cl⁻ for OH⁻ (HCO₃⁻). On the other hand, studies performed in apical membrane of *Necturus* gallbladder [25] also support the hypothesis that NaCl entry results primarily from the operation of parallel Na⁺/H⁺ and Cl⁻/HCO₃⁻ exchanges, and not from a NaCl cotransport.

The importance of the present results lies in how they relate to the mechanism of NaCl entry into lizard duodenal epithelium. *Gallotia* duodenal mucosa *in vitro* develops a small transmural potential and high tissue conductance, which are characteristics of leaky epithelia. Under control conditions, duodenum actively absorbs sodium and chloride in a stoichiometric ratio of 2:1. These results differ from those described for other leaky epithelia, where the net fluxes of sodium and chloride are identical under the steady state [25, 26].

The discrepancy between the net sodium flux and the short circuit current may mean that a part of the net sodium transport is due to an electrically neutral mechanism or that other electrogenic

mechanism opposite in sign contributes to the Isc. When chloride was replaced with isothionate (Table 1) the J_{ms} and J_{net} of sodium were significantly reduced. It is important to point out that the net flux was not abolished but was, in fact reduced by 50%. When sodium was replaced by chloride, J_{ms}^{Cl} was reduced significantly; the amount of the reduction ($0.97 \mu\text{eq}/\text{cm}^2 \text{ h}$) was similar to the amount by which J_{ms}^{Na} was reduced ($1.2 \mu\text{eq}/\text{cm}^2 \text{ h}$) in the absence of chloride. These results indicate that a coupled transport exists, which accounts for approximately 50% of the net sodium transport and all of the net chloride transport. The fact that the I_{mc} was near zero in the absence of sodium seems to be consistent with the existence of a sodium electrogenic transport, responsible for the Isc.

One method of deciding whether the transport of NaCl is via Na^+/Cl^- cotransport or Na^+/H^+ $\text{Cl}^-/\text{HCO}_3^-$ dual exchange system would be to study the transport at zero CO_2 and HCO_3^- concentrations. The intracellular absence of HCO_3^- and H^+ would block the mechanisms of $\text{Cl}^-/\text{HCO}_3^-$ and Na^+/H^+ . Our results show that in HCO_3^- -free solution and in presence of acetazolamide, the net sodium flux was inhibited by 50% and the net chloride flux was abolished completely. Short circuit current was not affected by the acetazolamide. This suggests that all of the net chloride transport takes place via $\text{Cl}^-/\text{HCO}_3^-$ exchange and 50% of the sodium via Na^+/H^+ exchange.

Other evidence for $\text{Na}^+/\text{H}^+/\text{Cl}^-/\text{HCO}_3^-$ transport and against Na^+/Cl^- cotransport was the use of specific inhibitors such as amiloride and DIDS. Amiloride has been described as an inhibitor of the Na^+/H^+ antiporter for a wide variety of epithelia [27] and as an inhibitor of the sodium channels in the apical membrane of tight epithelia at lower concentration [28]. The addition of amiloride to the mucosal solution abolished the net chloride flux and halved the net sodium flux across the tissue. The PD and Isc were not significantly reduced. These results suggest that amiloride blocks the Na^+/H^+ antiporter, it would reduce the intracellular pH and abolishes the formation of HCO_3^- and therefore inhibits the $\text{Cl}^-/\text{HCO}_3^-$ transport system. Amiloride did not block the

electrogenic sodium transport since the Isc did not change.

The effects of DIDS support the hypothesis described above for NaCl transport mechanisms. DIDS has been reported as a potent inhibitor of the $\text{Cl}^-/\text{HCO}_3^-$ exchange in red blood cells [29] and in other cell types such as turtle bladder [30] and muscle fiber [31]. When DIDS was added to the mucosal side, the effect was similar that obtained after the treatment with amiloride; the net chloride flux was abolished and the net sodium flux was halved. If DIDS is a specific inhibitor of $\text{Cl}^-/\text{HCO}_3^-$, these results support the hypothesis that the mechanism of NaCl transport across lizard duodenum is via dual exchange mechanism of Na^+/H^+ and $\text{Cl}^-/\text{HCO}_3^-$, similar to the model proposed for human ileum [8], rat small intestine [10] and rat kidney [32].

The energy for entry of NaCl derives from two sources: the Na^+/K^+ ATPase, that allows a large potential energy to be made as the Na^+ gradient across the mucosal membrane and the other from the production of HCO_3^- and H^+ from CO_2 and H_2O inside the cell. If the production of H_2CO_3 ($\text{H}^+ + \text{HCO}_3^-$) is abolished by inhibiting carbonic anhydrase with acetazolamide, the $\text{Na}^+/\text{H}^+/\text{HCO}_3^-/\text{Cl}^-$ dual exchange system will be inhibited. If the Na^+/K^+ ATPase is blocked by ouabain, then all the Na^+ -dependent transport systems would cease since the blockage of the Na^+/K^+ pump would increase the intracellular Na^+ concentration. The increase in the intracellular Na^+ will inhibit both the electrogenic sodium transport and the Na^+/H^+ antiporter. The results obtained from ouabain treatment (Table 2) clearly indicate that sodium and chloride transport depends on Na^+/K^+ ATPase activity, which is consistent with a consideration cited above.

Figure 2 shows a possible model which could account for the various features observed in the present study. The entry of sodium into the cell across the luminal membrane occurs by two pathways. A part of the influxes occurs through the Na^+/H^+ antiporter and a part through an electrogenic conductive pathway. The second pathway may be responsible for the serosa-positivity of the PD under standard conditions. The chloride ion would enter across the brush border membrane in

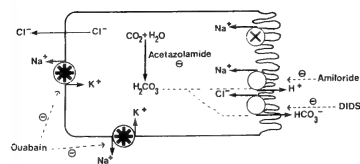


FIG. 2. Provisional model for ion movements across the lizard duodenum epithelium. For details see text.

exchange for bicarbonate. The Na^+/K^+ ATPase is responsible for sodium exit through the basolateral membrane. Since DIDS in serosal bathing solution did not reduce the chloride fluxes, chloride exit through the basolateral membrane does not seem to be via $\text{Cl}^-/\text{HCO}_3^-$ exchange but due to a passive diffusion. This model is similar to that for the ileum of lizard [14].

ACKNOWLEDGMENTS

This work is supported by research grant no. 3037-83/28-11-84 from the C.A.Y.C.Y.T. (Comisión Asesora de Investigación Científica y Técnica) M.E.C. España.

REFERENCES

- 1 Diamond, J. M. (1962) The reabsorptive function of the gallbladder. *J. Physiol. (London)*, **161**: 442-473.
- 2 Frizzell, R. A., Field, M. and Schultz, S. G. (1979a) Sodium-coupled chloride transport by epithelial tissues. *Am. J. Physiol.*, **236**: F1-F8.
- 3 Warnock, D. G. and Eveloff, J. (1982) NaCl entry mechanisms in the luminal membrane of the renal tubule. *Am. J. Physiol.*, **242**: F561-F574.
- 4 Field, M., Fromm, D. and McColl, I. (1971) Ion transport in rabbit ileal mucosa. I. Na and Cl fluxes and short-circuit current. *Am. J. Physiol.*, **220**: 1388-1396.
- 5 Frizzell, R. A., Dugas, M. C. and Schultz, S. G. (1975) Sodium chloride transport in rabbit gallbladder. *J. Gen. Physiol.*, **65**: 769-795.
- 6 Nellans, H. N., Frizzell, R. A. and Schultz, S. G. (1973) Coupled sodium-chloride influx across the brush border of rabbit ileum. *Am. J. Physiol.*, **225**: 467-475.
- 7 Nellans, H. N., Frizzell, R. A. and Schultz, S. G. (1974) Brush border processes and transepithelial Na and Cl transport by rabbit ileum. *Am. J. Physiol.*, **226**: 1131-1141.
- 8 Turnberg, L. A., Bieberdorf, F. A., Morawski, S.

G. and Fordtran, J. S. (1970) Interrelationships of chloride, bicarbonate, sodium and hydrogen transport in the human ileum. *J. Clin. Invest.*, **49**: 557-567.

- 9 Liedtke, C. M. and Hopfer, U. (1982) Mechanism of Cl translocation across small intestinal brush-border membrane. I. Absence of Na^+/Cl^- cotransport. *Am. J. Physiol.*, **242**: G263-G271.
- 10 Liedtke, C. M. and Hopfer, U. (1982) Mechanisms of Cl translocation across small intestinal brush-border membrane. II. Demonstration of Cl^-/OH^- exchange and Cl^- conductance. *Am. J. Physiol.*, **242**: G272-G280.
- 11 Hajjar, J. J. (1971) Ion transport in proximal and distal halves of turtle colon. *Comp. Biochem. Physiol.*, **40A**: 35-44.
- 12 Smith, P. L. and McCabe, R. D. (1984) Mechanism and regulation of transcellular potassium transport by turtle colon. *Am. J. Physiol.*, **247**: G445-G456.
- 13 Badía, P., Gómez, T., Díaz, M. and Lorenzo, A. (1987) Mechanisms of transport of Na^+ and Cl^- in the lizard colon. *Comp. Biochem. Physiol.*, **87A**: 883-887.
- 14 Badía, P., Lorenzo, A., Gómez, T. and Bolaños, A. (1988) Sodium chloride absorption across the ileal epithelium of the lizard *Gallotia galloti*. *J. Comp. Physiol.*, **157B**: 865-871.
- 15 Schultz, S. G. and Zalusky, R. (1964) Ion transport in isolated rabbit ileum. I. Short circuit current and Na fluxes. *J. Gen. Physiol.*, **47**: 567-583.
- 16 Cremaschi, D. and Henin, S. (1975) Na^+ and Cl^- transepithelial routes in rabbit gallbladder. *Pflügers Arch.*, **361**: 33-41.
- 17 Duffey, M. E., Turnheim, K., Krizzell, A. and Shultz, S. G. (1978) Intracellular chloride activities in rabbit gallbladder: direct evidence for the role of the sodium-gradient in energizing "uphill" chloride transport. *J. Membr. Biol.*, **42**: 229-245.
- 18 Duffey, M. E., Thompson, S. M., Frizzell, R. A. and Schultz, S. G. (1979) Intracellular chloride activities and active chloride absorption in the intestinal epithelium of the winter flounder. *J. Membr. Biol.*, **50**: 331-341.
- 19 Field, M. (1978) Some speculations on the coupling between sodium and chloride transport processes in mammalian and teleost intestine. In "Membrane Transport Processes, Vol. 1," Ed. by J. Hoffmann, Raven Press, New York, pp. 277-292.
- 20 Spring, K. R. and Kimura, G. (1978) Chloride reabsorption by renal proximal tubules of *Necturus*. *J. Membr. Biol.*, **38**: 233-254.
- 21 Armstrong, W. McD., Bixenman, W. R., Frey, K. F., García-Díaz, J. F., O'Regan, M. G. and Owens, J. L. (1979) Energetics of coupled Na and Cl entry into epithelial cells of bullfrog small intestine. *Biochem. Biophys. Acta*, **551**: 207-219.

- 22 Frizzell, R. A., Smith, P. L., Vosburgh, E. and Field, M. (1979) Coupled sodium chloride influx across brush border of flounder intestine. *J. Membr. Biol.*, **46**: 27-39.
- 23 Reus, L. Weinmann, S. A. (1979) Intracellular ionic activities and transmembrane electrochemical potential differences in gallbladder epithelium. *J. Membr. Biol.*, **49**: 345-362.
- 24 Ramos, M. M. P. and Ellory, J. C. (1981) Na and Cl transport across the isolated anterior intestine of the plaice *Pleuronectes platessa*. *J. Exp. Biol.*, **90**: 123-142.
- 25 Weinman, S. A. and Reuss, L. (1984) $\text{Na}^+\text{-H}^+$ exchange and Na^+ entry across the apical membrane of necturus gallbladder. *J. Gen. Physiol.*, **83**: 57-74.
- 26 Baerentsen, H. J., Giraldez, F. and Zeuthen, T. (1983) Influx mechanisms for Na^+ and Cl^- across the brush border membrane of leaky epithelia: a model and microelectrode study. *J. Membr. Biol.*, **75**: 205-218.
- 27 Benos, D. J. (1982) Amiloride: a molecular probe of sodium transport in tissues and cells. *Am. J. Physiol.*, **242**: C131-C145.
- 28 Frizzell, R. A., Koch, M. J. and Schultz, S. G. (1976) Ion transport by rabbit colon. I. Active and passive components. *J. Membr. Biol.*, **27**: 297-316.
- 29 Cabantchik, Z. I. and Rothstein, A. (1972) The nature of the membrane sites controlling anion permeability of human red blood cells as determined by studies with disulfonic stilbene derivatives. *J. Membr. Biol.*, **10**: 311-330.
- 30 Ehrenspeck, G. and Brodsky, W. A. (1976) Effects of 4-acetamido-4-isothiocyano-2,2-disulfonic stilbene on ion transport in turtle bladders. *Biochem. Biophys. Acta*, **419**: 555-558.
- 31 Boron, W. R., Russell, J. M. and Brodwick, M. S. (1978) Influence of cyclic AMP on intracellular pH regulation and chloride fluxes in barnacle muscle fibres. *Nature (London)*, **276**: 511-513.
- 32 Murer, H., Hopfer, U. and Kinne, R. (1976) Sodium/proton antiport in brush-border-membrane vesicles isolated from rat small intestine and kidney. *Biochem. J.*, **754**: 597-604.

New Morphological Aspects of the Brush Cells in the Main Excretory Ducts of the Rat Submandibular Glands

KAZUYOSHI HIGASHI, TOSHIAKI GOMI¹, MIYABI SOEDA,
SHOZO SASA, AKIHIKO KIMURA¹ and YASUHIRO KIKUCHI¹

*Department of Histology, Kanagawa Dental College, Inaoka-cho 82
Yokosuka 238, and ¹Department of Anatomy, School of Medicine,
Toho University, Tokyo 143, Japan*

ABSTRACT—The brush cells in the main excretory ducts (MED) of rat submandibular glands were observed by electron microscopy.

Characterized by long and thick microvilli, brush cells are scattered throughout the epithelium. The fine structures of the brush cells in this study are basically similar to those described in earlier studies. However, several brush cells concentric whorls of rER comprising several lamellae were observed at the juxtanuclear portion. The presence of these concentric whorls of rER alludes to the cellular activity of the brush cells. Moreover, several intranuclear inclusions were found in the nuclei of almost all the brush cells observed. Intranuclear inclusions in the brush cells have not been reported elsewhere in other organs or tissues so far investigated. Therefore, it seems that the brush cells in the MED of rat submandibular glands are characterized by the presence of intranuclear inclusions. In contrast, neither whorls of rER nor intranuclear inclusions are present in the epithelial cells of the MED. Therefore, we can assume that the brush cells have a different function from that of the epithelial cells.

INTRODUCTION

Rhodin and Dalhamn [1] once observed a new type of cell in the rat trachea which was characterized by long and thick microvilli on the luminal surface, and thus named them "brush cells". The peculiar structure of the microvilli allows for easy identification of the brush cells by electron microscopy. Besides microvilli, other characteristics of brush cells include (1) the extension of many bundles of filaments from the top of each microvilli to the supranuclear region, and (2) the presence of numerous vesicles and tubules between the bundles of filaments in the apical cytoplasm.

The brush cells are observed throughout the epithelia of the respiratory system, that is, from the respiratory mucosa of the nasal cavity [2] to the alveolar epithelium [3]. Further, these cells have been identified in the epithelia of the digestive tract, including in the main excretory duct of the

salivary glands [4, 5], the stomach [6, 7], the gallbladder [8, 9] and the colon [10]. In the MED of the salivary glands, the brush cells are known by other names, either as "tuft cells" [5] or "dark cells" [4, 11]. Various hypotheses concerning the function of brush cells are discussed. However, because of a scanty number of brush cells in the relevant organs and tissues, the structural details of the brush cells in relation to their function have not yet been established. Therefore, in the present study, we examined the fine structure of the brush cells in the MED of submandibular glands in rats.

MATERIALS AND METHODS

MED were obtained from ten adult (170–200 g) male Wistar rats. The rats were anesthetized with sodium pentobarbital (50 mg/kg, i.p.), and the submandibular glands were exposed, with the length of the MED extending distally about 1 cm from the hilus. The MED was then ligated at the end of its distal exposure, taking care to avoid applying unnecessary tension to it. The area from

the ligature to the hilus was removed and immersed in 2.5% cold buffered glutaraldehyde. The ducts were cut off near both ends, and the remains were cut into approximately 2 mm segments, kept in the same solution and used in this study. After 1 hr of fixation in glutaraldehyde, the specimens were rinsed in buffer and transferred to 1% cold

buffered osmium tetroxide, where the tissue was allowed to post-fix for 2 hr. Phosphate buffer at pH 7.4 was used to buffer the fixatives. Following dehydration, the specimens were embedded in spurr resin and sectioned for electron microscopy on an ultramicrotome. Ultra-thin sections were placed on uncoated copper grids and stained with

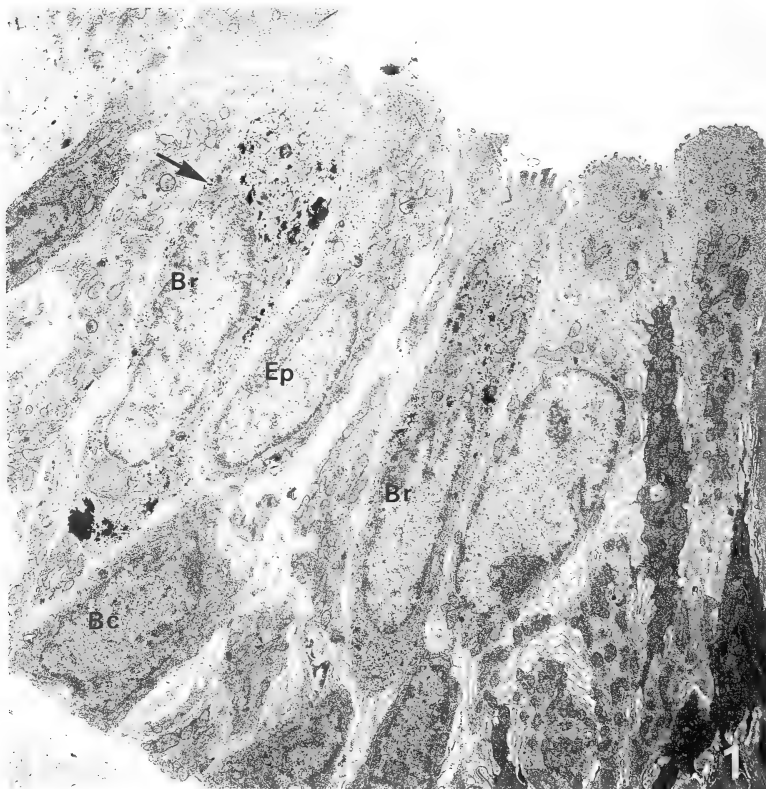


FIG. 1. MED in rat submandibular glands is composed of three cell types: epithelial cells (Ep), brush cells (Br) and basal cells (Bc). Brush cells have long, thick microvilli, bundles of filament extending from the top of microvilli to deep in the cytoplasm, many vesicles and glycogen granules. Concentric whorls of membranous structure and a well-developed rough surfaced endoplasmic reticulum (arrow) comprising several lamellae are seen around the irregular nucleus of the brush cell. $\times 6,000$.

uranyl acetate [12] and lead citrate [13], and examined using a JEM 100B electron microscope.

RESULTS

The main excretory ducts (MED) of the rat submandibular glands were composed of three cell types: epithelial cells, basal cells and brush cells (Fig. 1). The luminal surface of these cells frequently showed a bulbous expansion upon which short and stubby microvilli were present. The epithelial cells were predominant in number and made up of columnar cells. The nucleus was oval in shape containing a small nucleolus with a rounded appearance. Several basal cells, which had more electron-dense cytoplasm than other cell types, were situated under the epithelial cells and brush cells.

A total of 34 brush cells were examined in this study.

The brush cells were present between the epithelial cells and their microvilli were larger and more regularly spaced than those of the epithelial cells. The brush cells were easily distinguished from the surrounding epithelial cells in structure because of their long and regular arrangement microvilli. Desmosomes were present at the neck

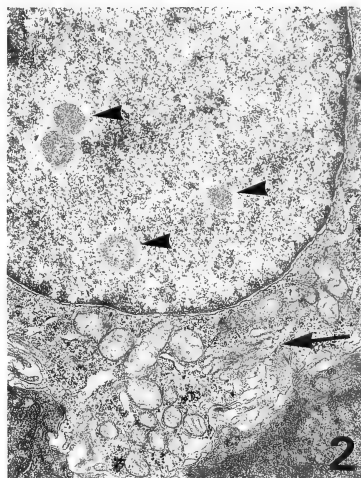


FIG. 2. Well-developed rough surfaced endoplasmic reticulum (arrow) is located in the basal portion, and several intranuclear inclusions (arrow heads) are seen in the nucleus of the brush cell. $\times 12,000$.

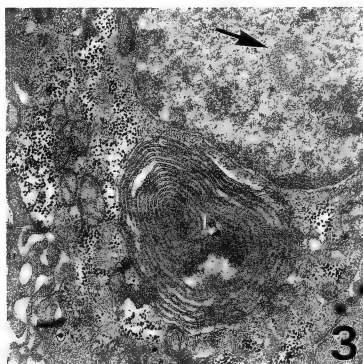


FIG. 3. Concentric whorls of membranous structure composed of several lamellae are seen in the basal portion of the brush cell. The intranuclear inclusion (arrow) is ring-shaped. $\times 18,000$.

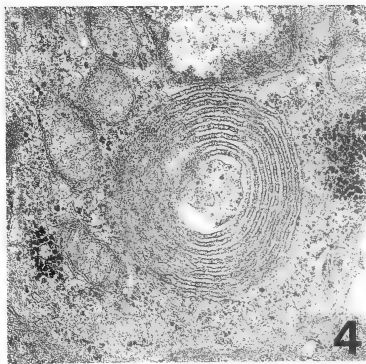


FIG. 4. Some ribosomes are attached to the inner- and outer-most lamellae of these membranous structures. $\times 37,000$.

portion which was narrower than the basal area of the brush cells. The bundles of filaments extended from the core of the distal end of the microvilli to the supranuclear region. A few long, thin cytoplasmic processes without filaments were present on the lateral border. There were no cell organelles in the free zone beneath the microvilli of the brush cells, except for a large number of electron-lucent vesicles among the filaments. These vesicles, having different diameters, were either oval or tortuous in shape. Several vesicles contained dense granules. The nucleus, having a small, dense nucleolus, was rather irregular in shape and situated in the basal half of the brush cell. The nuclei of almost all brush cells contained several intranuclear inclusions (Figs. 1, 2 and 3). These intranuclear inclusions were comprised of fine granules and were oval or ring-shaped, and easily distinguished from surrounding nuclear matrices and nucleoli. They had a lower electron-density than the nucleolus, and there was a halo between the nuclear matrix and the core of the intranuclear inclusion (Figs. 1, 2 and 3). No intranuclear inclusions were observed in any other cell type in the MED epithelium. Several lysosomes were located in the supranuclear region. Many mitochondria, rough surfaced endoplasmic reticulum (rER) in a short tubular form and numerous glycogen granules were scattered throughout the cytoplasm except in the apical part of the brush cells. Sometimes, rER with well-developed cisternae were observed in the cytoplasm near the nucleus (Figs. 1 and 2). In addition, concentric whorls of membranous structures composed of several lamellae were seen in the basal portion of some brush cells; such structures were seen in 5 out of 34 brush cells. Some ribosomes were attached to the inner- and outer-most lamellae of these structures (Figs. 1, 3 and 4). In contrast, epithelial cells had no whorls of membranous structures.

DISCUSSION

The epithelium contains three cell types: epithelial cells, basal cells and brush cells, in the MED of the salivary glands [5, 11]. Differences in the structures of these three cell types make them easy to distinguish from one another. The fine struc-

tures of the cells examined in the present study are basically similar to those described in earlier studies [3, 5, 6, 8, 9]. The brush cells in the MED of salivary glands have also been called various other names, such as tuft cells [5, 14] or dark cells [11, 14]. Accordingly the structures of those cells correspond to the characteristics of brush cells in other organs and tissues. The ultrastructural findings in earlier studies were confirmed in the present investigation.

Many authors have reported that various shapes of intranuclear inclusions, composed of fine granules or bundles of filaments, are contained in the cells of many organs and tissues, for example, in pancreatic islets cells [15], endocrine cells of stomach [16], adrenocortical cells [17] and acinar cells of the human salivary labial glands [18]. However, intranuclear inclusions were not mentioned in the brush cells observed in earlier studies. Intranuclear inclusions similar in structure to those we found in the brush cells of the submandibular glands have been previously described by Tandler *et al.* [18], who regarded them as peculiar to the nuclei of acinar secretory cells of the human salivary labial glands. According to Boquist [15], in pancreatic islets cells, intranuclear inclusions might play some role in cellular activity, or in cell renewal and division. In acinar cells of the human salivary labial gland, they might be related to the secretory cycle of the mucous cells, since they were found only in immature cells [18]. However, almost all brush cells in the MED have several intranuclear inclusions, while epithelial cells in the MED have none. In addition, these structures have not been reported in brush cells in other organs and tissues. Therefore, the presence of intranuclear inclusions in the brush cell of the MED seems to be related to the function of these brush cells. Moreover, the brush cells in the MED are most likely not immature, because the brush cells observed contain rich filaments and well-developed rER, which are not typical features of immature cells. This suggests that the brush cells in the MED of rat submandibular glands are characterized by the presence of these structures.

The concentric whorls of membranous structure in the present study may be a kind of rER, since they have some ribosomes in the most inner and

outer lamellae. Nickerson [19] described the formation of concentric whorls of rER in adenocortical cells of the mongolian gerbil, and states that the function of these rER is the saving of rER in adenocortical cells. Brush cells containing concentric whorls of rER have not been reported in earlier studies. Many brush cells having no concentric whorls of rER in the MED of the submandibular glands contain well-developed rER. Following the administration of pilocarpine in the rat submandibular gland, the brush cells reached the state of hyperergasia, and the concentric whorls of rER were not observed (unpubl. data). Therefore, it seems that well-developed rER in brush cells is referable to concentric whorls of rER, and the formation of concentric whorls of rER may be related to cellular activity.

Several hypotheses have been put forward as to the function of brush cells, including that they might be reabsorptive [6, 20], secretory [21] and/or chemoreceptive [9, 22]. Due to the presence of large numbers of vesicles and tubules arranged in rows between bundles of filaments, brush cells have been considered to have a reabsorptive function [6]. However, Luciano and Reale [8] showed that electron microscopic observations with horseradish peroxidases injected into the lumen of the gallbladder did not reveal tracers within the vesicles and tubules of the brush cells. On the other hand, Qvarnström and Hand [14] observed that when horseradish peroxidase was injected into the lumen of the MED of the submandibular gland, the brush cells were found to contain horseradish peroxidase in the cytoplasmic matrix, but not in vesicles, other cell organelles or the nucleus. Therefore, a reabsorptive function for these cells has been ruled out. A secretory function for brush cells may also be disregarded since they do not show the typical morphology of secretory cells, which consists of a prominent Golgi apparatus and secretory granules. In addition, the features of microvilli and bundles of filaments in the brush cells of the rat submandibular gland after the administration of pilocarpine and isoproterenol were changed. However, the endocytosis and exocytosis in the brush cells has not been confirmed. Following administration of those drugs, alterations in the components of saliva in the

submandibular gland were investigated (unpubl. data). In the trachea, Luciano *et al.* [23] observed brush cells with a nerve ending. Therefore, they consider the function of brush cells to be chemoreceptive. Such neural connections were not confirmed in this study; however, the brush cells in the MED of the rat submandibular glands may indeed have a chemoreceptive function, since their morphological features, including characteristic microvilli, bundles of filaments, and large number of vesicles are similar to those of taste bud type 1 sensory cells [24].

REFERENCES

- 1 Rhodin, J. and Dalhamn, T. (1956) Electron microscopy of the tracheal ciliated mucosa in rat. *Z. Zellforsch.*, **44**: 345-412.
- 2 Andres, K. H. (1969) Der olfaktorische Saum der Katze. *Z. Zellforsch.*, **96**: 250-274.
- 3 Gomi, T., Kimura, A., Tsuchiya, H., Hashimoto, T., Higashi, K. and Sasa, S. (1987) Electron microscopic observations of the alveolar brush cell of the Bullfrog. *Zool. Sci.*, **4**: 613-620.
- 4 Pinkstaff, C. A. (1980) The cytology of salivary glands. *Int. Rev. Cytol.*, **63**: 141-261.
- 5 Sato, A. (1982) Scanning and transmission electron microscopical study of the main excretory duct of the rat major salivary glands. *J. Kyusyu Dent. Soci.*, **36**: 610-631.
- 6 Isomäki, A. M. (1973) A new cell type (tuft cell) in the gastrointestinal mucosa of the rat. *Acta Path. Microbiol. Scand (Suppl.)*, **240**: 1-35.
- 7 Wattel, W. and Geuze, J. J. (1978) The cells of the rat gastric groove and cardia. *Cell Tiss. Res.*, **186**: 375-391.
- 8 Luciano, L. and Reale, E. (1979) A new morphological aspect of the brush cells of the mouse gallbladder epithelium. *Cell Tiss. Res.*, **201**: 37-44.
- 9 Higashi, K., Takano, K. and Sasa, S. (1982) Ultrastructural aspects of the brush cell in mouse gallbladder. *Zool. Mag.*, **91**: 158-164. (In Japanese with English abstract)
- 10 Silva, D. G. (1966) The fine structure of multivesicular cells with large microvilli in the epithelium of the mouse colon. *J. Ultrastruct. Res.*, **16**: 693-705.
- 11 Shackleford, J. M. and Schneyer, L. H. (1971) Ultrastructural aspects of the main excretory duct of rat submandibular gland. *Anat. Rec.*, **169**: 679-696.
- 12 Watson, M. L. (1958) Staining of tissue sections for electron microscopy with heavy metals. *J. Biophys. Biochem. Cytol.*, **4**: 475.

- 13 Reynold, E. S. (1963) The use of lead citrate at high pH as an electron microscopy. *J. Cell Biol.*, **17**: 208–212.
- 14 Qwarnström, E. E. and Hand, A. R. (1982) A light and electron microscopic study of the distribution and effects of water-soluble radiographic contrast medium after retrograde infusion into the rat submandibular gland. *Arch. oral Biol.*, **27**: 117–127.
- 15 Boquist, L. (1969) Intranuclear rods in pancreatic islets B-cells. *J. Cell Biol.*, **43**: 377–381.
- 16 Müller, O. and Ratzenhofer, M. (1971) Intranukleare Einschlüsse in endokrinen Zellen des Kaninchensmagens. *Z. Zellforsch.*, **117**: 526–536.
- 17 Weber, A., Whipp, S., Usenik, E. and Frommes, S. (1964) Structural changes in the nuclear body in the adrenal zona fasciculata of the calf following the administration of ACTH. *J. Ultrastruct. Res.*, **11**: 564–576.
- 18 Tandler, B., Denning, C. R., Mandel, L. D. and Kutscher, A. H. (1969) Ultrastructure of human labial salivary glands II. Intranuclear inclusions in the acinar secretory cells. *Z. Zellforsch.*, **94**: 555–564.
- 19 Nickerson, P. A. (1977) Formation of concentric whorls of rough endoplasmic reticulum in the adrenal gland of the mongolian gerbil. *J. Anat.*, **124**: 383–391.
- 20 Nevalainen, T. J. (1977) Ultrastructural characteristics of tuft cells in mouse gallbladder epithelium. *Acta Anat.*, **98**: 210–220.
- 21 Nabeyama, A. and Leblond, C. P. (1974) "Caveolated cells" characterized by deep surface invaginations and abundant filaments in mouse gastro-intestinal epithelia. *Am. J. Anat.*, **140**: 147–166.
- 22 Luciano, L. (1972) Die Feinstruktur der Gallenblase und der Gallengänge II. Das Epithel der extrahepatischen Gallengänge der Maus und der Ratte. *Z. Zellforsch.*, **135**: 103–114.
- 23 Luciano, L., Reale, E. and Ruska, H. (1968) Über eine glykogenhaltige Bürstenzelle im Rectum der Ratte. *Z. Zellforsch.*, **91**: 153–158.
- 24 Takeda, M. and Hoshino, T. (1975) Fine structure of taste buds in the rat. *Arch. histol. jap.*, **37**: 395–413.

Fine Structure of the Lingual Dorsal Epithelium of the Japanese Toad, *Bufo japonicus* (Anura: Bufonidae)

SHIN-ICHI IWASAKI, KEN MIYATA and KAN KOBAYASHI

*Department of Anatomy, School of Dentistry at Niigata,
The Nippon Dental University, Niigata 951, Japan*

ABSTRACT—The structure of the so-called "ridge-like papillae" of the lingual dorsal epithelium of the Japanese toad, *Bufo japonicus* was investigated by light and transmission electron microscopy. The top of each ridge-like papilla was composed of stratified columnar epithelium and its base was composed of simple columnar epithelium. The apical cells, which were located on the top of ridge-like papillae, contained a large number of mitochondria, free ribosomes and fibrous structures, and a small number of electron-dense, round granules and clear bodies. The nuclei were located in the basal part of apical cells. By contrast, cells that contained a large number of mucus granules were located at the base of the papillae. The nuclei were located in the basal part of cells. Rough-surfaced endoplasmic reticulum and Golgi apparatus were distributed in the perikaryal part of cytoplasm. Ciliated cells were also scattered at the base of the papillae. The nucleus was located in the basal region of these cells. Mitochondria and ribosomes were widely distributed in the cytoplasm. Basal bodies could be seen just beneath the free surface of the cells. In addition to these cells, a very small number of mitochondria-rich cells were located within the epithelium. Distinct, fine, cellular protrusions were distributed in a compact array on the free surface of these cells.

INTRODUCTION

We showed in our recent study [1], using the scanning electron microscope, that irregular, undulant structures or ridge-like papillae, which may be homologous to the filiform papillae of frogs, are distributed compactly over the entire dorsum of the tongue of *Bufo japonicus*. We also demonstrated that fine, plicated structures or microridges are widely distributed over the surface of these papillar epithelial cells. Furthermore, in *Bufo japonicus*, no ciliated cells were observed on the surface of the ridge-like papillae or in the surrounding areas of the sensory disc [1], while in *Rana*, many ciliated cells were seen on the surface of the filiform papillae and in the surrounding areas of the sensory discs [2, 3]. The purpose of the present study was to clarify the histological and cytological structure of the lingual epithelium of *Bufo japonicus* and to compare the results to those for *Rana* [4, 5]. Light and transmission electron

microscopy were used for this purpose.

MATERIALS AND METHODS

Five male and five female adult specimens of *Bufo japonicus* were obtained commercially and used in the present study. Under MS-222 anesthesia, the animals were perfused from the heart with 50% diluted Karnovsky solution that contained 2.5% glutaraldehyde and 2% paraformaldehyde in cacodylate buffer (pH 7.4). The tongues were then removed and refixed in the same solution for a few hr. After rinsing in 0.1 M cacodylate buffer, specimens were postfixed in phosphate-buffered 1% osmium tetroxide solution at 4°C for 1.5 hr. This procedure was followed by dehydration, Epon-Araldite embedding, ultrathin sectioning, and U-Pb double-staining. The specimens were then observed under a transmission electron microscope (Hitachi H-500 or JEOL JEM-1200EX). Thick sections from the blocks embedded in Epon-Araldite were stained with 0.2% toluidine blue in 2.5% Na₂CO₃. Micrographs of sections taken under a light microscope (Olympus

BH-2), were compared with the transmission electron micrographs.

RESULTS

The epithelium at the tip of the ridge-like papillae was thicker than that in the basal part, as revealed by light microscopy of sections of Epon-Araldite embedded material. The apical epithelium was composed of stratified columnar cells, whereas the basal epithelium was composed of simple columnar cells. Mucus granules, which stained densely with toluidine blue, were concentrated mainly at the base of the papillae and occupied about 60% to 70% of the epithelium. Connective tissue and smooth muscle penetrated deeply into the center of each papilla (Fig. 1).

Transmission electron microscopy of the stratified columnar epithelium in the apical portion of the papillae revealed apical cells which contained a small number of electron-dense, round granules just beneath the free surface. The size of each granule varied, however, with a maximum value of $0.7 \mu\text{m}$ in diameter or along the long axis. The nucleus was located in the basal part of each cell (Fig. 2). In addition to round granules which have very high electron-density, large numbers of mitochondria, free ribosomes, fibrous structures and a small number of clear bodies were present in the cytoplasm (Figs. 2, 3 and 4). The rough-surfaced endoplasmic reticulum and Golgi apparatus were well-developed in the perikaryal cytoplasm (Figs. 6 and 7). Microridges, which were clearly revealed by scanning electron microscopy [1], were widely distributed on the free surface of the apical cells. The cell surfaces facing adjacent cells bore many cellular processes (Figs. 2, 3 and 6). Underlying cells without free surfaces showed almost the same configurations as the cells located on the free-surface side. However, the number of round granules was reduced in the cells in this underlying area. Other kinds of cells could not be found at the top of the papillae. Tight and intermediate junctions were clearly visible between the adjacent cells that were located on the free-surface side. Desmosomes were widely distributed between the adjacent cells throughout the epithelium at the top of papillae (Figs. 3 and 5).

Most of the epithelium at the base of the papillae was composed only of mucus cells and ciliated cells (Fig. 8). A large part of the cytoplasm of mucus cells was filled with mucus granules of varying degrees of electron-density. The nucleus was located in the basal part of each cell. Rough-surfaced endoplasmic reticulum and Golgi apparatus were distributed mainly in the perikaryal cytoplasm of mucus cells. In some cells, microvilli on the free surface of cells were not very distinct (Fig. 9).

In ciliated cells, the nucleus was located in the basal region of each cell (Fig. 8). In the cytoplasm, mitochondria and ribosomes were widely distributed. A small number of electron-dense vesicles was seen. Basal bodies could be seen just beneath the free surface of the cells. Cilia and microvilli were located on the free surface. Tight junctions and desmosomes were intercalated on the adjacent surfaces of neighboring cells in both mucus and ciliated cells (Fig. 10).

In addition to these cells, a very small number of mitochondria-rich cells or flask cells were located within the epithelium. These cells were electron-lucent and contained many mitochondria and glycogen granules. However, they did not contain any secretory granules. Each such cell rested on the basal lamina, and its apical side reached the free surface against the oral cavity. Distinct, fine, cellular protrusions were distributed in a compact array on the free surface (Fig. 11).

In the intermediate region from the top to the base, the change in apical cells to mucus or ciliated cells was not drastic. The border between these two areas contained all types of cells, as observed under both the light and electron microscope (Figs. 1 and 2).

There were no histological differences between males and females with regard to the present results.

DISCUSSION

In mammals, almost all of the lingual epithelium is composed of stratified squamous epithelium, and various degrees of keratinization of the epithelium have been observed in some areas [6-8]. By contrast, no keratinization of any sort could be

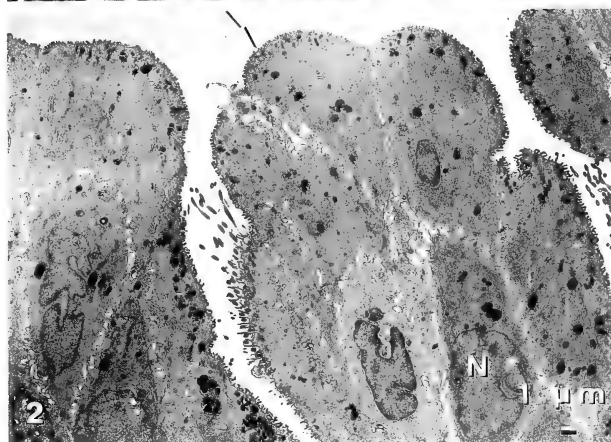
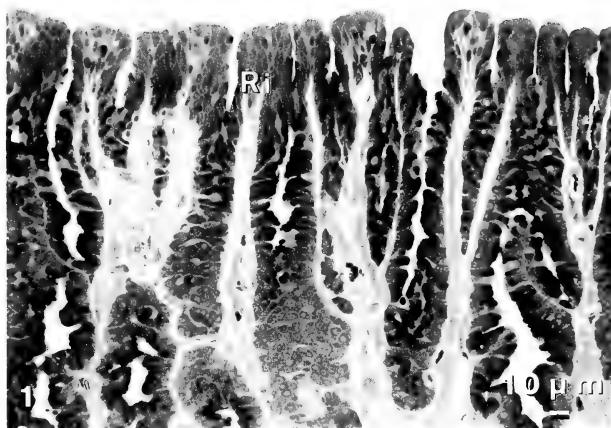


FIG. 1. Light micrograph of the lingual dorsal mucosa from a Japanese toad, *Bufo japonicus*, from Epon-Araldite embedded material. Ri: ridge-like papilla.

FIG. 2. Transmission electron micrograph of the apical cells in the epithelium from the tip of a ridge-like papilla in *Bufo japonicus*. N: nucleus. Arrow indicates microridges.

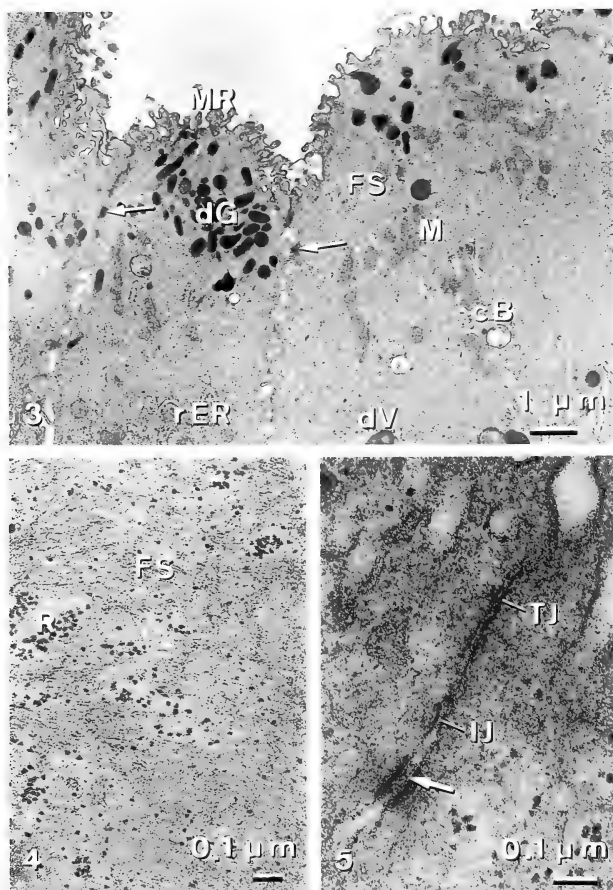
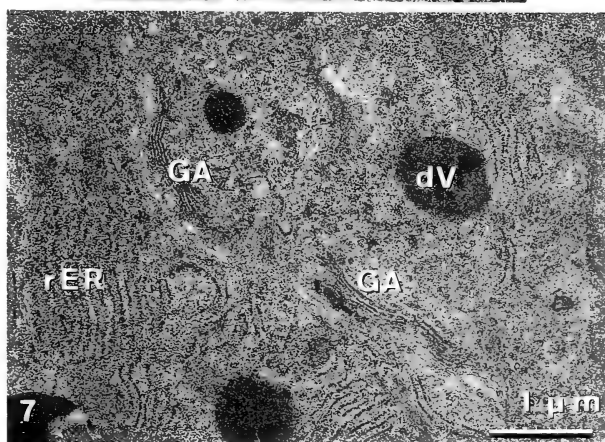
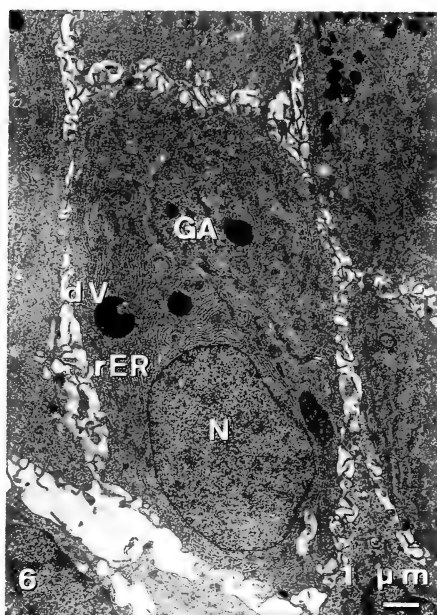


FIG. 3. Transmission electron micrograph of the epithelial cells at the tip of a ridge-like papilla. M: mitochondria, rER: rough-surfaced endoplasmic reticulum, MR: microvilli, FS: fibrous structure, dG: electron-dense, round granules, cB: electron-lucent bodies. Arrows indicate desmosomes.

FIG. 4. Higher magnification of the cytoplasm of an apical cell. FS: fibrous structure, R: ribosomes.

FIG. 5. Higher magnification of the junctional complex of the adjacent apical cells. TJ: tight junction, IJ: intermediate junction. Arrow indicates desmosome.



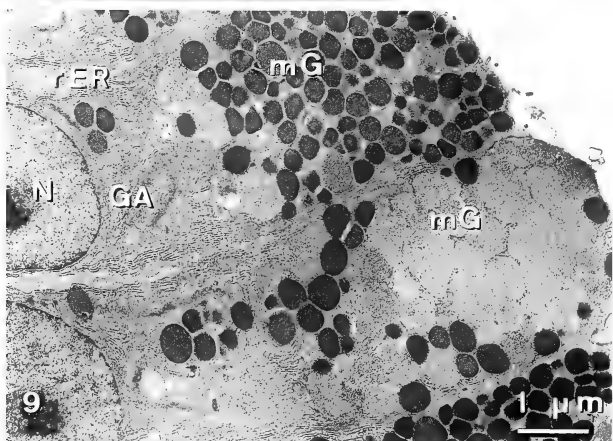
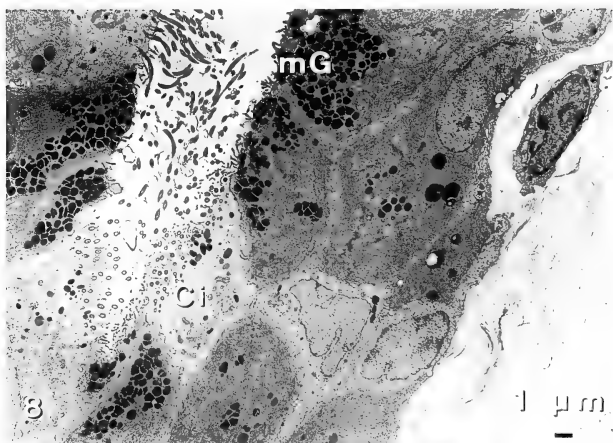


FIG. 8. Transmission electron micrograph of the epithelium of the basal part of a ridge-like papilla. mG: mucus granules, Ci: ciliated cell.

FIG. 9. Transmission electron micrograph of the mucus cells in the basal part of a ridge-like papilla. N: nucleus, rER: rough-surfaced endoplasmic reticulum, GA: Golgi apparatus, mG: mucus granules.

FIG. 6. Transmission electron micrograph of the basal area of the epithelial cells at the tip of a ridge-like papilla. N: nucleus, rER: rough-surfaced endoplasmic reticulum, GA: Golgi apparatus, dV: electron-dense vesicle.

FIG. 7. Higher magnification of the Golgi apparatus of the cell shown in Fig. 6. rER: rough-surfaced endoplasmic reticulum, GA: Golgi apparatus, dV: electron-dense vesicle.

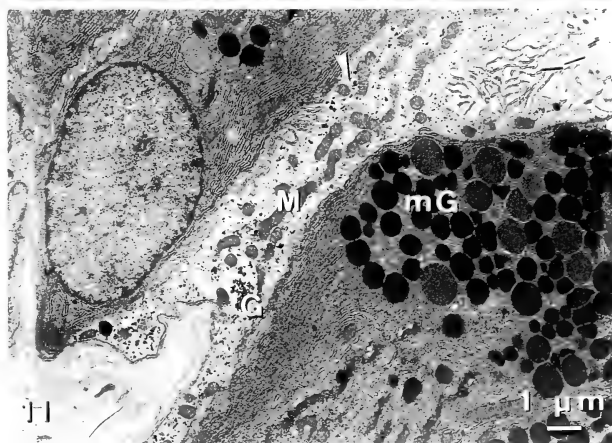
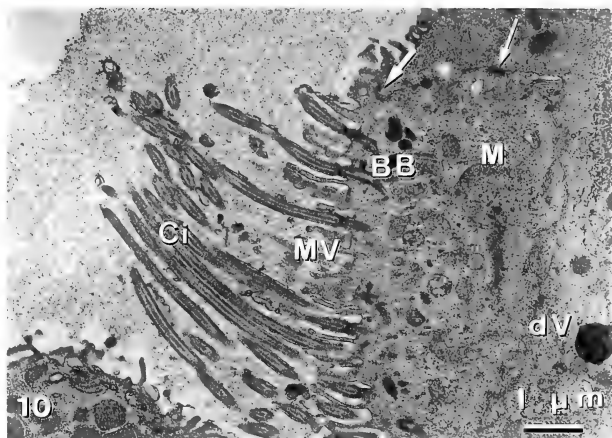


FIG. 10. Transmission electron micrograph of a ciliated cell in the basal part of a ridge-like papilla. M: mitochondria, Ci: cilia, MV: microvilli, BB: basal bodies, dV: electron-dense vesicles. Thick arrow indicates tight junction. Thin arrow indicates desmosome.

FIG. 11. Transmission electron micrograph of a mitochondria-rich cell (arrowhead) in the papillar epithelium. M: mitochondria, G: glycogen granules, mG: mucus granules. Arrow indicates long cellular protrusions.

recognized in the lingual epithelium of the toad. Instead, the epithelium was composed of several kinds of cells: electron-dense granular cells, mucus

cells, ciliated cells, and other cells. These observations imply that the lingual dorsal epithelium of toads may be composed of cells that are morpholog-

ically, rather similar to the epithelial cells of the mucosa located in the gastrointestinal tract and/or the trachea of mammals.

The present study revealed that the proportion of mucus cells in the epithelium of the toad tongue was obviously larger than that in the epithelium of the frog tongue [4]. This suggests that the epithelium of the toad tongue may be more important in the secretion of mucus than that of the frog tongue. The mucus granules are variable in density. Kurosumi *et al.* [9] point out that in rat jejunal epithelium, younger granules seem to be relatively denser; this is also the case in the epithelium of toad tongue.

There are some designations that can be attributed to the electron-dense granules found in the apical papillar epithelium, such as, the immature form of mucus granules [9], serous granules [10-12], and other different types of granules [13]. However, the exact nature of the granules could not be resolved from the morphological aspects described here and therefore, this problem remains to be elucidated.

A study by scanning electron microscopy [1] showed that ciliated cells were not found on the dorsal surface of the toad tongue. This result is coincident with the present observations that ciliary cells are located exclusively in the basal area of the papillae. The pattern of distribution of ciliary cells obviously differs between the lingual epithelia of the toad and the frog [3].

A very small number of mitochondria-rich cells or flask cells were found within the epithelium. The cells may very likely be the same kind of cells found in the epidermis of amphibia [14, 15]. Significantly developed cellular protrusions such as those found on the mitochondria-rich cells of the amphibian lingual epithelium in the present study have also been recognized under conditions of high salinity in the same sort of cell in the skin of *Xenopus* [16]. Fox [15] surmised that the flask cells may be involved in the elimination of bicarbonate [17] and in osmoregulation [18] because of their capacity to transport ions [19]. Thus, it is possible that the mitochondria-rich cells of the amphibian lingual epithelium may also have the capacity to transport ions.

REFERENCES

- 1 Iwasaki, S. and Kobayashi, K. (1988) Fine structure of the dorsal tongue surface in the Japanese toad, *Bufo japonicus* (Anura, Bufonidae). *Zool. Sci.*, **5**: 325-330.
- 2 Iwasaki, S. and Sakata, K. (1985) Fine structure of the lingual dorsal surface of the bullfrog. *Okajimas Folia Anat. Jpn.*, **61**: 437-450.
- 3 Iwasaki, S., Miyata, K. and Kobayashi, K. (1986) Studies on the fine structure of the lingual dorsal surface in the frog, *Rana nigromaculata*. *Zool. Sci.*, **3**: 265-272.
- 4 Iwasaki, S., Miyata, K. and Kobayashi, K. (1988) Fine structure of filiform papillar epithelium from the tongue of the frog, *Rana nigromaculata*. *Zool. Sci.*, **5**: 61-68.
- 5 Iwasaki, S. and Kobayashi, K. (1989) Fine structure of the lingual dorsal epithelium in the bullfrog, *Rana catesbeiana*. *Zool. Sci.*, **6**: 259-267.
- 6 Cane, A. K. and Spearman, R. I. C. (1969) The keratinized epithelium of the house-mouse (*Mus musculus*) tongue: its structure and histochemistry. *Arch. Oral Biol.*, **14**: 829-841.
- 7 Farbman, A. I. (1970) The dual pattern of keratinization in filiform papillae on rat tongue. *J. Anat.*, **106**: 233-242.
- 8 Iwasaki, S. and Miyata, K. (1985) Light and transmission electron microscopic study on the lingual dorsal epithelium of the musk shrew, *Suncus murinus*. *Okajimas Folia Anat. Jpn.*, **62**: 67-68.
- 9 Kurosumi, K., Shibuichi, I. and Tosaka, H. (1981) Ultrastructural studies on the secretory mechanism of goblet cells in the rat jejunal epithelium. *Arch. Histol. Jap.* **44**: 263-284.
- 10 Hand, A. R. (1971) Morphology and cytochemistry of the Golgi apparatus of rat salivary gland acinar cells. *Am. J. Anat.*, **130**: 141-158.
- 11 Riva, A. and Riva-Testa, F. (1973) Fine structure of acinar cells of human parotid gland. *Anat. Rec.*, **176**: 149-166.
- 12 Ichikawa, M. and Ichikawa, A. (1977) Light and electron microscopic histochemistry of the serous secretory glandular cells of the Mongolian gerbil (*Mongolian meridianus*) and rhesus monkey (*Macaca irus*). *Anat. Rec.*, **189**: 125-140.
- 13 Cheng, H. (1974) Origin, differentiation and renewal of the four main epithelial cell types in the mouse small intestine. IV. Paneth cells. *Am. J. Anat.*, **141**: 521-536.
- 14 Fox, H. (1983) The skin of *Ichthyophis* (Amphibia: Caecilia): an ultrastructural study. *J. Zool.*, **199**: 223-248.
- 15 Fox, H. (1986) The skin of amphibia, 5: Epidermis. In "Biology of the integument, 2: Vertebrates". Ed. by J. Bereiter-Hahn, A. G. Matoltsy and K. Sylvia-

- Richard, Springer-Verlag, Berlin/Heidelberg/New York/Tokyo, pp. 78-110.
- 16 Ilic, V. and Brown, D. (1980) Modification of mitochondria-rich cells in different ionic conditions: changes in cell morphology and cell number in the skin of *Xenopus laevis*. *Anat. Rec.*, **196**: 153-161.
- 17 Guardabassi, A., Campantico, E. and Olivero, M. (1972) Effect of environmental changes on the skin and pituitary of *Xenopus laevis* Daudin specimens treated and untreated with prolactin. *Monit. Zool. Ital.*, **6**: 129-146.
- 18 Lodi, G. (1971) Histoenzymologic characterization of the flask cells in the skin of the crested newt under normal and experimental conditions. *Atti. Accad. Sci. Torino Univ.*, **105**: 561-570.
- 19 Whitear, M. (1977) A functional comparison between the epidermis of fish and of amphibians. In "Comparative biology of skin. Symp. Zool. Soc. London, vol. 39". Ed. by R. I. C. Spearman, Academic Press, London/New York, pp. 291-313.



Synergistic Effects of Calyx Fluid and Venom of *Apanteles kariyai* (Hymenoptera: Braconidae) on the Granular Cells of *Pseudaletia separata* WALKER (Lepidoptera: Noctuidae)

HARUHISA WAGO and TOSHIHARU TANAKA¹

*Department of Bacteriology, Saitama Medical School,
Moroyama 350-04, Japan, and ¹Department of Entomology,
Texas A&M University, College Station, Texas 77843, USA*

ABSTRACT—This study describes some of the effects of calyx and venom fluids of *Apanteles kariyai* on the morphology and the filopodial function of *Pseudaletia separata* granular cells, using scanning electron microscopy and an *in vitro* incubation system. Calyx fluid contained virus-like particles, which were shown to be round or oval with a smooth surface and a size of about 225 nm in diameter under the scanning electron microscopy. When granular cells were incubated in the presence of either calyx or venom fluids, their filopodia elongated extensively at the cell periphery just like the control. However, incubation of cells with both calyx and venom fluids greatly inhibited filopodial elongation and further caused a remarkable cytolysis during the incubation time. Calyx fluid seems to require components of the venom fluid to have inhibitory effects on the initial cellular defence reaction of host larvae. In this paper, the possible roles of calyx and venom fluids in suppression of the hemocytic reaction of host will be discussed.

INTRODUCTION

Eggs and larvae of endoparasitoids normally complete development in the hemocoel of suitable hosts without triggering host cellular defence reactions such as encapsulation. In braconid parasitoids, calyx and venom fluids injected with eggs during oviposition and teratocytes derived from parasitoid serosal cells seem to be responsible for inhibition of host encapsulation. In the egg stage of parasitoid, the surface coat of egg [1], the calyx fluid and venom (alone or together) are apparently essential in evading the host defence system [2, 3], whereas in the larval stage teratocyte-derived substances in conjunction with calyx and venom fluids are involved in inhibition of hemocytic encapsulation [4]. However, the mechanism through which these inhibitory factors prevent the encapsulation of braconid parasitoids is unknown. In *A. kariyai*,

the eggs evade the cellular encapsulation through the activity of calyx and venom fluids and a coating of egg surface with venom fluid is important to depress the nonself recognition capacity of host hemocytes [3]. In addition, prevention of nonself recognition was suggested to be due to the inhibition of filopodial elongation of granular cells [5]. Since filopodial elongation of cells is an essential factor in the progress of cellular reactions such as phagocytosis or encapsulation [6], this study was undertaken to examine the effects of calyx fluid and venom of *A. kariyai* on the surface ultrastructure and filopodial function of granular cells of *P. separata* larvae using an *in vitro* incubation system.

MATERIALS AND METHODS

Insect cultures The braconid parasitoid, *Apanteles kariyai* was laboratory-reared on larvae of *Pseudaletia separata* maintained on the artificial medium described by Hattori and Atsushima [7] at $25 \pm 1^\circ\text{C}$ under a 16 hr light-8 hr dark photo-

periodic regime and fed a 30% sugar solution in the glass tube [3]. Host larvae were individually parasitized to avoid the superparasitism. About 100 host larvae were maintained in 200 ml flask under aseptic conditions until the fifth instar, then a group of 20–30 host larvae were separately reared in $15 \times 20 \times 5$ cm plastic case.

Collection of the hemocyte suspension from host larvae Hemolymph of 20 individuals of day 2-sixth instar larvae of *P. separata* was collected in a chilled small tube containing 1.5 ml of insect physiological saline (IPS; 150 mM NaCl, 5 mM KCl) with 0.1% phenylthiourea (PTU), and centrifuged at 600 rpm for 5 min at 4°C to obtain the hemocytes. After twice rinse of hemocytes in IPS at 4°C, hemocyte concentration was finally adjusted to 1×10^6 cells/ml with IPS. Observation of hemocyte suspension with 0.5% neutral red stain solution showed that the granular cells made up about 42.5% of the total hemocyte count.

Collection of calyx and venom fluid Calyx fluid and venom were individually collected from lateral oviduct and venom reservoir of female wasp using a binocular microscope as described previously [8]. Briefly, venom fluid was first collected by rupturing venom reservoirs in 3 μ l of IPS. Second, calyx fluid was collected from the lateral oviduct in 3 μ l of IPS and then centrifuged at 800 rpm for 3 min to remove eggs and cell debris. Since two microliter (1/3 female wasp equivalent for each) of their fluid is effective in *in vivo* inhibition of encapsulation ability against parasitoid eggs, this concentration was also used to treat the granular cells.

Treatment of incubated granular cells with the calyx fluid and venom First, hemocyte suspension collected as mentioned above was similarly spun and resuspended in an equal volume of cell-free plasma, which had been already collected in a cold-tube containing a few crystals of PTU. Hemocyte suspension (0.15 ml) was incubated at 4°C for 60 min to allow the granular cells to attach on a glass surface of 7×7 mm coverslip in each well of Lab-Tex 8-chamber slide, because a 4°C temperature inhibits the filopodial elongation of granular cells [9]. Thereafter, supernatant plasma was removed and gently rinsed with chilled IPS three times. Fifty μ l of each solution of venom,

calyx fluid, and a 1:1 mixture of calyx and venom fluids was respectively overlaid on the hemocyte monolayers, and further incubated at 25°C for 120 min. The cell viability at the onset of incubation was over 98% with 0.25% trypan blue. Following a 60- and 120-min incubation, the granular cells were processed as a scanning electron microscopic preparation for the observation of the surface ultrastructure.

Scanning electron microscopy (SEM) observation After a series of procedures for SEM, including fixation, dehydration in ethanol, critical point drying, and coating with platinum, which is the case with the previous method [10], the cell preparations were examined with the SEM (Hitachi S-550) at 20 kV to observe the surface ultrastructure of the granular cells and the calyx particles.

RESULTS AND DISCUSSION

Although it had been already shown by transmission electron microscopic observation that calyx fluid of *A. kariyai* contains a lot of particles, of which each envelope had several electron-dense cores [5], the shape of envelop was unclear. SEM observation showed that a calyx particle was round or oval with a smooth surface and size of about 225 nm in diameter (Fig. 1). Furthermore, attachment on the surface of granular cells seems to suggest that virus-like particles penetrate into the cell [11] and have some effect on the granular cell function.

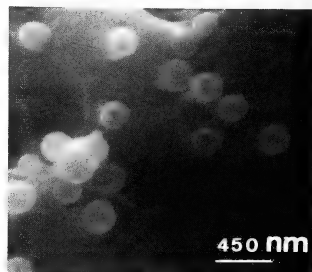


FIG. 1. Calyx particles under the SEM observation. Calyx particle was round or oval with a smooth surface and size of about 225 nm in diameter.

Granular cells are involved in the cellular reactions including phagocytosis and encapsulation in *P. separata* [5] like other lepidopterans [12], and possess many filopodia on the cell surface. Additionally, filopodial elongation of the cells are required for the progress of the initial cellular reactions against foreign substances [10, 13]. On the other hand, it is reported that both parasitization and manual injection of calyx and venom fluids of *Microplitis mediator* to host *P. separata* strongly suppress the filopodial elongation [5]. Conversely, although in the hemolymph of hosts parasitized by *A. kariyai*, suppression of filopodial elongation of granular cell was not evident, Sephadex particle encapsulation in the parasitized host was inhibited compared to controls [5]. In this study, degree of suppression of filopodium was expressed quantitatively by counting the number of elongated filopodia on the granular cell. Inhibitory effect of calyx and venom fluids on filopodial elongation, which was not apparent *in vivo* system, was observed *in vitro* system, although it was unclear whether concentration of calyx and venom fluids used was

suitable or not. Neither calyx fluid nor venom inhibited the filopodial elongation as compared to the control (Fig. 2). Moreover, most of granular cells attached to the coverslip with more than 20 filopodia extensively elongated (Fig. 3a, b) just as control (Fig. 3d). Conversely, elongation was remarkably inhibited in the presence of both calyx and venom fluids after a 60-min incubation (Figs. 2 and 3c). The cells were unable to elongate their filopodia on the surface at the periphery. Additionally, after a 60-min treatment of cells with calyx and venom fluids mixtures, about 4.8% of attached granular cells showed a great degree of cytolysis. As shown in Figure 4b and 4c, many granules in the cytoplasm were exposed outside and in the case of more damaged cells, only a sticky cytoskeleton component was observed. After a 120-min incubation in calyx and venom fluids, about 76% of cells showed a cellular damage. These results strongly suggested that the co-existence of calyx and venom fluids was important in affecting the host cellular reactions by the granular cells in *A. kariyai*-*P. separata* system.

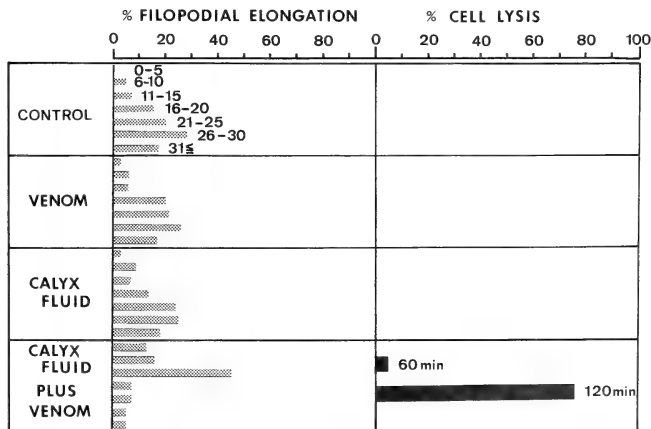


Fig. 2. Inhibition of filopodial elongation and the cytolysis of granular cells of *Pseudaletia separata* by the calyx fluid and/or venom of *Apanteles kariyai*. Granular cells of last instar host were attached on the cover-slip at 4°C for 60-min incubation. Fifty μ l of each solution of venom, calyx fluid, and a 1:1 mixture of calyx fluid and venom was respectively overlaid on the hemocyte monolayers. Then, filopodial elongation was examined under the SEM after a 60-min treatment, and cytolysis was also observed after a 60- and 120-min incubation.

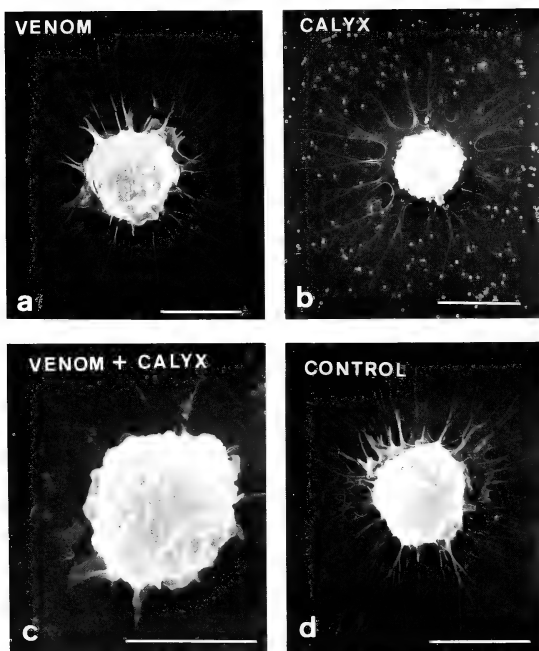


FIG. 3. Degree of inhibition of filopodial elongation in the presence of calyx fluid and/or venom of *A. kariyai*. Scale bar = 10 μm .

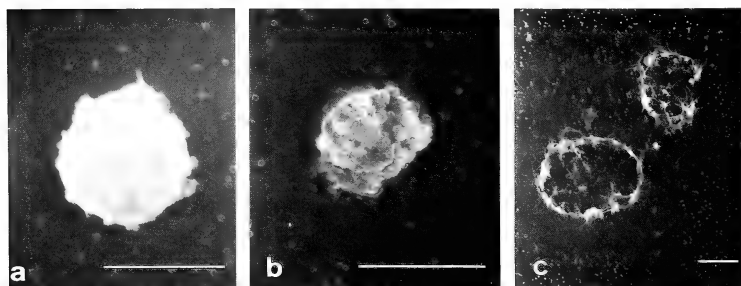


FIG. 4. Process of cytolysis of granular cells overlayed with calyx fluid and venom of *A. kariyai*. Filopodial elongation was, first of all, inhibited (a), then the intracellular granules were exposed outside (b), and finally the cytoskeletal components were only observed (c). Scale bar = 10 μm .

Rizki and Rizki [14] demonstrated that lamellocytes underwent a great morphological change and lost their adhesiveness in *Drosophila melanogaster* parasitized by *Leptopilina heterotoma*. These changes were induced by lamellocin contained in an accessory gland of the female reproductive system. Calyx and venom fluids also seem to give hemocytes an damage so that parasitoid eggs and larvae are not recognized as non-self material. Moreover, plasmatocytes of *Heliothis virescens* have recently been reported to be functionally interfered by the calyx virus of parasitoid *Camptoplex sonorensis* [15]. Calyx fluid injection caused a removal of approximate 75% of the circulating plasmatocytes [16]. Stoltz *et al.* [17] reported that polydnavirus from braconid wasp *Cotesia melanoscela*, required venom to penetrate into the host cells. In this sense, if venom which braconid parasitoid should possess had the similar composition to a wasp venom in the family of Vespidae [18] containing an enzyme such as phospholipase A₂ or hyaluronidase, its composition could influence the membrane of hemocytes and facilitate the introduction of calyx virus into the cytoplasm. It has been known that phospholipase A₂ catalyzes the hydrolysis of structural phospholipids via synergistic action with melittin [19], and hyaluronidase hydrolyzes mucopolysaccharide polymers consisting the bulk of animal connective tissue and opens passage for other venom components to diffuse through the host tissue matrix [20]. The possibility of such aspect is now being investigated. Since neither application of calyx fluid nor of venom alone induced the cytolysis of granular cells, virus-like particles of calyx fluid seems to require venom activity to alter granular cell function. In *A. kariyai*, it is unclear whether or not the number of granular cells, *in vivo*, decreases following parasitization or calyx-injection. This point is also under currently investigation.

ACKNOWLEDGMENTS

We thank Dr. B. A. Webb of Texas A & M University for critical reading of the manuscript.

REFERENCES

- 1 Davies, D. H. and Vinson S. B. (1986) Passive evasion by eggs of braconid parasitoid *Cardiophiles nigrisepe* of encapsulation *in vitro* by haemocytes of host *Heliothis virescens*. Possible role for fibrous layer in immunity. *J. Insect Physiol.*, **32**: 1003-1010.
- 2 Kitano, H. (1982) Effect of the venom of gregarious parasitoid *Apanteles glomeratus* on its hemocytic encapsulation by the host, *Pieris*. *J. Invertebr. Pathol.*, **40**: 61-67.
- 3 Tanaka, T. (1987) Effect of the venom of the endoparasitoid, *Apanteles kariyai* Watanabe, on the cellular defence reaction of the host, *Pseudaletia separata* Walker. *J. Insect Physiol.*, **33**: 413-420.
- 4 Tanaka, T. and Wago, H. (1989) Ultrastructural and functional maturation of teratocytes of *Apanteles kariyai*. *Arch. Insect Biochem. Physiol.*, (in press)
- 5 Tanaka, T. (1987) Morphological changes in haemocytes of the host, *Pseudaletia separata*, parasitized by *Microplitis mediator* or *Apanteles kariyai*. *Dev. Comp. Immunol.*, **11**: 57-67.
- 6 Wago, H. (1983) Cellular recognition of foreign materials by *Bombyx mori* phagocytes: II. Role of hemolymph and phagocyte filopodia in the cellular reactions. *Dev. Comp. Immunol.*, **7**: 199-208.
- 7 Hattori, M. and Atsushima, S. (1980) Mass-rearing of the cabbage armyworm, *Mamestra brassicae* Linne and the common armyworm, *Mythimna separata* Walker (Lepidoptera: Noctuidae) on a simple artificial diet. *Jap. J. Appl. Entomol. Zool.*, **24**: 36-38. (In Japanese)
- 8 Tanaka, T., Agui, N. and Hiruma, K. (1987) The parasitoid *Apanteles kariyai* inhibits pupation of its host, *Pseudaletia separata*, via disruption of prothoracicotropic hormone release. *Gen. Comp. Endocrinol.*, **67**: 364-374.
- 9 Wago, H. (1982) Regulatory effects of temperature and hemolymph on inhibition and enhancement of attachment and filopodial function of phagocytic granular cells of the silkworm, *Bombyx mori*. *Dev. Comp. Immunol.*, **6**: 231-241.
- 10 Wago, H. (1980) Humoral factors promoting the adhesive properties of the granular cells and plasmatocytes of the silkworm, *Bombyx mori* and their possible role in the initial cellular reactions. *Cell Immunol.*, **54**: 155-169.
- 11 Stoltz, D. B. and Faulkner, G. (1978) Apparent replication of an unusual virus-like particle in both a parasitoid wasp and its host. *Can. J. Microbiol.*, **24**: 1509-1514.
- 12 Wago, H. (1982) Cellular recognition of foreign materials by *Bombyx mori* phagocytes: I. Immunocompetent cells. *Dev. Comp. Immunol.*, **6**: 591-599.

- 13 Wago, H. (1984) *In vitro* evidence for the requirement of filopodial elongation for the progress of phagocytosis by phagocytic granular cells of the silkworm, *Bombyx mori*. Dev. Comp. Immunol., **8**: 7-14.
- 14 Rizki, R. M. and Rizki, T. M. (1984) Selective destruction of a host blood cell type by a parasitoid wasp. Proc. Natl. Acad. Sci. USA, **81**: 6154-6158.
- 15 Davies, D. H. and Vinson, S. B. (1988) Interference with function of plasmatocytes of *Heliothis virescens* *in vivo* by calyx fluid of the parasitoid *Campoletis sonorensis*. Cell Tissue Res., **251**: 467-475.
- 16 Davies, D. H., Strand, M. R. and Vinson, S. B. (1987) Changes in differential haemocyte count and *in vitro* behaviour of plasmatocytes from host *Heliothis virescens* caused by *Campoletis sonorensis* polydnavirus. J. Insect Physiol., **33**: 143-153.
- 17 Stoltz, D. B., Belland, E. R., Lucarotti, C. J. and MacKinnon, E. A. (1988) Venom promotes uncoating *in vitro* and persistence *in vivo* of DNA from a braconid polydnavirus. J. gen. Virol., **69**: 903-907.
- 18 Blum, M. S. (1981) Proteinaceous Venoms. In "Chemical Defenses of Arthropods". Ed. by M. S. Blum, Academic Press, New York, pp. 288-328.
- 19 O'Conner, R. and Peck, M. L. (1978) Venom of Apidae. In "Handbook of Experimental Pharmacology, 48. Arthropod Venoms". Ed. by S. Bettini, Springer-Verlag, Berlin, pp. 613-659.
- 20 Schmidt, J. O. (1982) Biochemistry of insect venom. Ann. Rev. Entomol., **27**: 339-368.

Spontaneous Mutations of Trichlorfon Resistance in the Nematode, *Caenorhabditis elegans*

RYUJI HOSONO, TOSHIHIRO SASSA and SIGERU KUNO

Department of Biochemistry, School of Medicine, Kanazawa University,
Kanazawa 920, Japan

ABSTRACT—Spontaneous trichlorfon-resistant mutations were isolated in *Caenorhabditis elegans* var. Bergerac and its derived mutator strains. Of these, six uncoordinated mutations were assigned by complementation analyses to the *unc-13(cn490)*, *unc-17(cn355)*, *unc-18(cn347)*, *unc-10(cn257)*, *unc-3(cn4146)* and *unc-41(cn252)* genes. Resistance of these mutations to acetylcholinesterase (AChE) inhibitors is partial, with the extent dependent on the mutations. These mutations fall into two classes based on acetylcholine (ACh) levels, that is, the normal ACh levels in *unc-10* and *unc-3* mutations and the abnormally high ACh levels in *unc-13*, *unc-17*, *unc-41* and *unc-18* mutations. Mutations in the latter gene groups are also accompanied by growth retardation and small body size in adulthood. Double mutants were constructed between the six trichlorfon-resistant strains together with the *cha-1-unc-17* complex gene alleles which are also resistant to trichlorfon. All doubles constructed between trichlorfon-resistant strains survived and their properties were studied.

INTRODUCTION

The presynaptic terminal liberates a neurotransmitter in response to depolarization [1]. However, little is known about the mechanism underlying the synthesis, storage and release of neurotransmitters. Acetylcholine (ACh) is one of the primary neurotransmitters. Although there are extensive studies on the synthetic enzyme choline acetyltransferase (ChAT) and the receptor functions of cholinergic neurons [1-3], there are few genetic studies on the profiles of ACh at the presynaptic terminal. The nematode *C. elegans* has several advantages as an experimental organism for genetic manipulations [4].

Johnson and Stretton [5] identified inhibitory and excitatory classes of ventral cord motoneurons in *Ascaris* and pointed out the possibility that ACh is the neurotransmitter used by the excitatory motoneurons. Because of its morphological similarity, ACh appears to be a neurotransmitter in the ventral cord neurons of *C. elegans* [6]. The complex gene *cha-1-unc-17* consists of at least two parts, the *cha-1* region and the *uch-17* region.

Although the *cha-1* encodes the structural gene for ChAT [7-9], the function of the *unc-17* region is obscure. Although ACh levels in the *cha-1* mutations decreased and were accompanied by a reduction in ChAT activity, ACh levels were abnormally high in the *unc-17* mutation in spite of normal ChAT activity [10]. We demonstrated the possibility that ACh of the mutant accumulates at the presynaptic terminal rather than at the synaptic gap. To identify additional genes that affect profiles of ACh, we carried out a further isolation of mutants. Alleles of the *cha-1-unc-17* complex gene are resistant to inhibitors of acetylcholinesterase (AChE). Therefore, we isolated resistants to trichlorfon, one of the potent AChE inhibitors.

For mutant screening, *C. elegans* var. Bergerac strain BO and its derived mutator strains were used instead of the var. Bristol strain N2 which has been well-characterized. BO and mutator strains produce spontaneous mutations at a high rate [11]. Many of these mutations appear to be brought about by the insertion of transposable element Tc1 into the gene which makes it possible to tag the gene with Tc1 as a probe [12, 13].

In *C. elegans*, the transposable element Tc1 was identified as a repetitive sequence [14-17]. It was found that in the *unc-22* [18] and *unc-54* genes [19,

20], the frequency of spontaneous mutation caused by TcI transposition was much higher in the BO than in the N2 strain. TcI has now become an useful tool for cloning *C. elegans* genes identified by insertional mutation as already successfully shown in the genes *unc-22* [13] and *lin-12* [12].

In an attempt to clone genes in the future, we have isolated the spontaneous mutants resistant to trichlorfon with BO and its derived mutator strains. Of the trichlorfon resistants isolated, the properties of six mutants are presented here.

MATERIALS AND METHODS

General handling Culturing, stock maintenance and genetic manipulation of *C. elegans* were performed as described by Brenner [4]. All experiments were carried out at 20°C unless otherwise noted.

Strains, genes, and alleles of *C. elegans* The gene alleles used are listed below by linkage groups. Positions of these genes on the *C. elegans* genetic map are shown in Figure 1. Standard nomenclature for *C. elegans* genotypes and phenotypes is used according Horvitz *et al.* [21].

LG I: *unc-13*(*cn490*, *e1019*), *dpy-5*(*e61*), *unc-63*(*e384*), *unc-11*(*e47*), *lin-6*(*e1416*),

unc-35(*e259*).

LG II: *dpy-10*(*jk64*)

LG III: *dpy-18*(*e364*), *unc-32*(*e189*), *unc-36*(*e251*), *unc-64*(*e246*)

LG IV: *cha-1*(*p1152*, *cn101*), *unc-17*(*e113*, *e245*, *cn355*), *unc-33*(*e204*), *dpy-13*(*e184*), *dpy-20*(*jk142*), *lin-1*(*e275*).

LG V: *dpy-11*(*e224*), *unc-42*(*e270*), *unc-23*(*e25*) *unc-41*(*e268*, *cn252*), *rol-3*(*e754*), *sma-1*(*e30*), *unc-65*(*e351*).

LG X: *unc-18*(*e81*, *cn347*, *md118*, *md120*, *md183*, *md193*), *unc-10*(*cn257*, *e1021*), *unc-3*(*cn4146*, *e151*), *lon-2*(*e678*), *dpy-6*(*e14*), *dpy-7*(*e88*), *mah-2*(*cn110*), *dpy-3*(*e27*), *unc-6*(*e78*), *unc-1*(*e74*, *e1598*), *unc-7*(*e5*)

Genetic properties of other strains used for three-factor crosses and the analysis of a TcI polymorphism associated with the *unc-18*(*cn347*) mutation are summarized in Table 1.

Isolation of trichlorfon-resistant mutants The *C. elegans* var. Bergerac strain BO and its derived mutator strains RW7097(*mut-6*) and RW7464(*mut-5*) were used for the resistant mutant isolation. The mutator strains RW7097 and RW7464 were generated from mutator/N2 hybrids as a TcI-transposing strain carrying only about 60 copies of TcI (I. Mori, personal communication).

Test animals were cultured at 16°C on 10 cm-diameter NGM plates and were washed off plates with M9 buffer immediately before food became exhausted. Collected animals were transferred to 5 cm-diameter NGM plates containing 0.1 mM trichlorfon and kept for 7 to 10 days. Animals that survived were picked up. Finally, one animal per test plate was selected as potentially resistant. The isolates were made congenic by 10 cycles of outcrossing with Bristol N2.

Drug sensitivity test Sensitivity of the animals to cholinergic reagents was tested in S medium or on NGM. Drugs were previously sterilized by filtration through 0.22 µm nitrocellulose filters. Behavioral analyses were mainly performed in a liquid medium while the survival test was on solid agar.

Preparation and assay of ChAT The method for the preparation and the determination of *C. elegans* ChAT has already been described else-

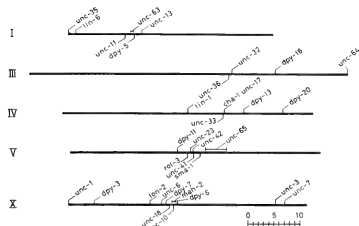


Fig. 1. Partial genetic maps of LG I, LG III, LG IV, LG V and LG X showing locations of the trichlorfon-resistant gene and some of the other markers used in this study.

Abbreviations: *unc*, uncoordinated^[4]; *sma*, small^[4]; *dpy*, dumpy^[4]; *rol*, roller^[4]; *lon*, long^[4]; *mah*, mahi^[8]; *cha*, choline acetyltransferase^[7].

TABLE 1. *C. elegans* strains used for a Tcl polymorphism associated with the *unc-18(cn347)* mutation

Strain	Genotype	Comments
TN347	<i>unc-18(cn347)</i>	Stable mutation
Tn3472	<i>unc-18(+)</i>	Intragenic revertant from TN347
TN3475	<i>unc-18(+)</i>	Intragenic revertant from TN347
TN1301	<i>unc-18(cn347)mah-2(cn110)</i>	Recombinant replaced DNA to the right of <i>unc-18</i>
TN1302	<i>mah-2(cn110)</i>	Recombinant replaced DNA to the left of <i>unc-18</i>
TN1303	<i>dpy-7(e88)</i>	Recombinant replaced DNA to the right of <i>unc-18</i>

All strains are primarily Bristol in chromosomal background.

where [7, 9, 22]. The procedures are briefly summarized as follows. Animals were washed extensively to remove bacterial contamination and suspended in extract buffer consisting of 100 mM Tricine (pH 8.0), 10 mM sodium thioglycollate, 1 mM phenanthroline, 1 mM EDTA, and 0.5 mM phenylmethyl-sulfonyl fluoride. The animals were ground to a fine powder in liquid nitrogen. After thawing, the preparation was used as a crude enzyme. The reaction mixture contained 50 mM Tricine (pH 8.0), 20 μ M neostigmine bromide, 0.1 mM dithiothreitol, 1 mM EDTA, 0.5 mM acetyl-CoA, 30 μ M choline, and 0.32 μ Ci [methyl-³H]-choline chloride. The reaction was initiated by the addition of the enzyme and incubated at 5°C for 40 to 60 min. Protein concentration was determined by using Coomassie Blue dye reagent with bovine serum albumin as a standard.

Choline and ACh levels The extraction and radiochemical assay of *C. elegans* choline and acetylcholine has been described previously [10, 23]. Briefly, the animals were lysed in a 1N-formic acid-acetone mixture, centrifuged at 1,000 \times g for 5 min whereupon the supernatant was evaporated to dryness under a stream of dry nitrogen. Dried samples were reconstituted with 0.1 N HCl. A 50 μ l portion of the sample was mixed with 60 μ l sodium tetraphenylboron. The organic phase was mixed with an equal volume of 0.4 M HCl and dried. Choline and ACh levels were measured radiometrically by the enzymatic conversion of choline to phosphorylcholine [23]. For choline and ACh assays, nematodes were grown on 10

cm-diameter petri dishes which contained the same components as the NGM agar but with more bacto-peptone (25 g/l). The dishes were allowed to grow about 0.2 g of *C. elegans*. Usually two dishes were used for one assay.

Southern blot hybridization The method for DNA extraction from nematodes has been described [24, 25]. Total genomic DNAs were digested with restriction enzymes and then electrophoresed on 1% agarose gels. Filter-transfer hybridizations were carried out by the methods of Southern [26]. A radiolabeled Tcl probe was prepared by nick translation [27].

Constructions of double mutants of trichlorfon resistant Double mutants were generated by a pairing combination of the following trichlorfon

resistants: *unc-13(cn490)*, *unc-41(cn252)*, *cha-1-unc-17(p1152, cn101, e113, e245, cn355)*, *unc-10(cn257)*, *unc-18(cn347, e81)* and *unc-3(cn4146)*. The *Dpy* mutation belonging to the same linkage group of either one of two trichlorfon-resistant genes was accompanied by the doubles as visible phenotypes. The construction of *dpy-13(e184) unc-17(e245) unc-18(cn347)* is described, as an example. *N2* males were mated with *dpy-13(e184) unc-17(e245)* hermaphrodites. The *dpy-13(e184)* mutation is semi-dominant, showing semi-*Dpy* phenotype in a *dpy-13/+* heterozygote. Semi-*Dpy* male progeny (*dpy-13-unc-17/+*) were mated with *unc-18(cn347)* hermaphrodites. Semi-*Dpy* hermaphrodites (*dpy-13-unc-17/+; +/unc-18*) were picked and the resultant *Dpy-Unc* progeny were randomly transferred to forty individual NGM

plates. The presence of the *unc-17* and *unc-18* mutations in the double mutants were tested by mating the Dpy-Unc hermaphrodites with *dpy-13(e184)-unc-17(e245)/+* males. If the double was viable, both Dpy-Unc and semi-Dpy-Unc males appeared on the same plates. If the double was undetectable, the experiments were repeated twice. If no double was detectable on 120 NGM plates, the double was concluded to be lethal.

Chemicals Trichlorfon [(2, 2, 2-trichloro-1-hydroxyethyl) phosphonic acid dimethyl ester], levamisole [L-[-]2, 3, 5, 6-tetrahydro-6-phenylimidazo[2, 1-b] thiazole], choline kinase (yeast) and AChE (electric eel, type V1-S) were purchased from Sigma. Aldicarb [2-methyl-2-(methylthio) propionaldehyde-O-(methylcarbamoyl) oxime] was provided by Union Carbide. [α - 32 P] dCTP (3000 Ci/mmol), nick translation system and (methyl- 3 H) choline chloride (180 Ci/nmole) were from Amersham. γ - 32 P] ATP (5209 Ci/nmole) was obtained from ICN Radiochemicals.

RESULTS

Effects of trichlorfon on *C. elegans* Prior to the resistant selection, the effects of trichlorfon on *C. elegans* were studied. Fourth larval (L4) animals were placed into S medium containing trichlorfon. Animals were not paralyzed instantaneously and it took several minutes to visualize abnormal phenotypes. L4 animals stopped their movement at around ten minutes in the presence of 10 mM trichlorfon but kept moving more than one hour in 1 mM of trichlorfon. The body of the paralyzed animals shrunk so much that the mouth part was often extruded. Animals exposed for one hour to 10 mM trichlorfon could recover gradually from the paralysis upon withdrawal of the drug. The recovered animals laid eggs and were indistinguishable from nontreated animals in morphology and movement.

When newly-hatched larvae were placed on plates of growth medium containing trichlorfon,

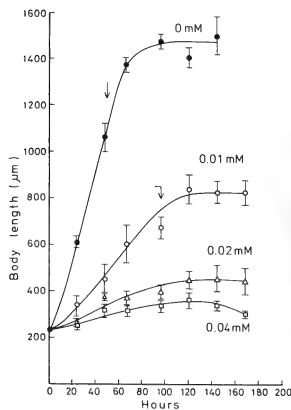


Figure 2 (A)

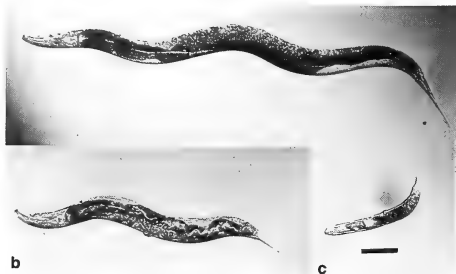


Figure 2 (B)

FIG. 2. Growth (A) and photographs (B) of hermaphrodites of *C. elegans* strain N2 grown in the presence of trichlorfon.

(A) Animals were grown on NGM at the indicated concentrations of trichlorfon.

S.D. is indicated by the vertical bar. Arrows indicate the time at which eggs were detected on test plates.

(B) Light micrographs of adult hermaphrodites cultured with 0 mM (a), 0.02 mM (b) and 0.04 mM (c) trichlorfon. Bar = 0.1 mm.

the growth of the animals was impaired according to levels of drug concentration. Although animals were able to grow slowly on NGM containing 0.01 mM trichlorfon, they were small in body size at adulthood (Fig. 2). Some animals produced a very small number of progeny in the presence of 0.02 mM but not 0.04 mM of trichlorfon.

Isolation of trichlorfon resistants

Trichlorfon-induced paralysis provides a convenient basis for the isolation of resistant mutants. We carried out a screening of spontaneous mutations of trichlorfon resistance with *C. elegans* var. Bergerac (strain BO) and the Bergerac-derived mutator strain RW7097 and RW7464. Each strain was cultured on 150 plates of 10 cm-diameter NGM, transferred to test plates containing trichlorfon and animals which survived were picked as described in MATERIALS AND METHODS. We obtained two resistant strains from BO, three resistants from RW7097, and two resistants from RW7464. All resistants were accompanied by uncoordinated phenotypes that were not segregated by extensive genetic studies.

Complementation tests and mapping Each mutation was assigned to a linkage group and the approximate locus was determined by a two-factor cross. Complementation tests were performed among uncoordinated mutations located near the locus on the same linkage group. Five mutations, *cn355*, *cn490*, *cn252*, *cn347*, *cn4146*, and *cn257* were assigned to genes that had been identified previously as *unc-17*, *unc-13*, *unc-41*, *unc-3*, and *unc-10*, respectively (Fig. 1), because no complementation was observed with the known mutant alleles at the respective gene. From the two- and three-factor crosses, one mutation *cn347* showed a tight linkage to *unc-18* (data not presented). Phenotypes of *cn347* and all the known mutations at the *unc-18* locus (*e81*, *md118*, *md120*, *md180*, *md193*) showed characteristics which were very similar to each other, i.e., kinky paralysis, slow growth, small body size in adulthood, and resistance to inhibitors of acetylcholinesterase. From these results, *cn347* is likely to be an allele of the *unc-18* gene. Complementation tests with *tra-1* males are in progress.

Evidence that the spontaneous mutants are induced by the insertion of Tcl Each of the six

mutants was grown on 100 plates of 10 cm-diameter NGM and inspected for the appearance of revertant strains showing the wild-type phenotype in movement. Wild-type revertants were obtained from six plates of *cn252* animals, four plates of *cn257* animals and forty-one plates of *cn347* animals. From the plates of *cn490*, *cn355* and *cn4146*, no revertant was found. These results suggest that at least three mutations are induced by the insertion of a transposable element.

To prove directly that the spontaneous mutations are associated with Tcl insertion, we examined Tcl polymorphisms of the *unc-18(cn347)* mutation (Fig. 3). Southern blot analyses revealed that DNA from the TN347 strain had a novel 6.8 kb Tcl-containing DNA fragment that was not seen in DNAs from the RW7097 and N2 strains. Two independent non-*unc-18* revertants of the *cn347* mutation did not have the band suggesting that Tcl inserted into the *unc-18* gene caused the *cn347* mutation. Furthermore, the *unc-18 mah-2* recombinant (TN1301) chromosome showed the 6.8 kb band while the *dpy-7 non-unc-18* recombinant (TN1303) chromosomes and *mah-2 non-unc-18* recombinant (TN1302) chromosomes did not. This also suggests that the novel 6.8 kb Tcl band is mapped between *dpy-7* and *mah-2*.

General properties of trichlorfon resistants

The morphology, movement, and touch response of the six isolated mutants are described. Typical body forms of the adult hermaphrodite are shown in Fig. 4. Body forms of the *unc-10(cn257)* and *unc-3(cn4146)* are fat but correspond to the wild type in body size. However, body sizes of the other four mutants are smaller. All resistant strains are able to lay eggs. Body shapes are clearly different from animals bearing mutations in muscle genes such as *unc-52* or *unc-54* whose body is relaxed and limp. Bodies of the resistants are kinky or coiled. A brief phenotypic description of the uncoordinated mutants has appeared elsewhere [28].

***unc-13(cn4146)*:** The animals are shrunken and have a fat body. The animals are defective in locomotion but respond with a slight movement of the head when the body is touched.

***unc-17(cn355)*:** The body of the mutant is thin and small as in the *unc-18(cn347)* mutation. The

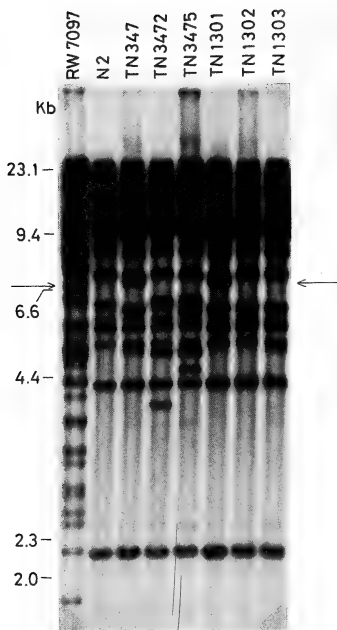


FIG. 3. A Tcl polymorphism associated with the *unc-18(cn347)* mutation. Strain TN347 contains the spontaneous *unc-18(cn347)* mutation crossed ten times into Bristol N2. Strains TN3472 and TN3475 are spontaneous wild-type revertants of *cn347*. Strain TN301 is a recombinant containing the *unc-18(cn347) mah-2(cn110)* mutations. TN1302 is a recombinant containing the *mah-2(cn110)* mutation that replaced DNA to the left of *unc-18*. TN1303 is a recombinant containing the *dpy-7(e88)* mutation that replaced DNA to the right of *unc-18*. DNAs from these strains were digested with BglII and analyzed as described in MATERIALS AND METHODS. Animals with the spontaneous *unc-18* mutation *cn347* have a unique band of approximately 6.8 kb as indicated by arrows. The plasmid pCe2002, which contains Tcl, was used as a hybridization probe. Relevant λ HindIII size standards (kb) are given to the left of the figure.



FIG. 4. Photomicrographs of adult hermaphrodites. Wild type (a), *unc-13(cn490)*(b), *unc-17(cn355)*(c), *unc-41(cn252)*(d), *unc-18(cn347)*(e), *unc-10(cn257)*(f), and *unc-3(cn4146)*(g). Bar=0.1 mm.

body is shrunken and often coil. The animals are able to locomote rather smoothly. Although the animals escape rapidly when touched on the tail region, the animals coiled up their bodies when their heads are stimulated.

unc-41(cn252): The animal bodies are thin and shrunken. The animals smoothly locomote forward and are able to move backward by a repeating pause and movement when stimulated on their heads.

unc-18(cn347): The body of the mutant is thin and small. The animals are so severely paralyzed that locomotion is defective. When touched on the body, the animal is almost totally unresponsive except for a slight movement of the head.

unc-10(cn257): The animals are weakly coiled but move forward smoothly. The animals move backward by sinusoidal their bodies steeply when stimulated on the head.

unc-3(cn4146): The animals are fat but normal in body size. Although the body is almost para-

lyzed, the animals can locomote forward.

Developmental growth The growth rate of the six mutants was compared (Fig. 5). All the mutants are smaller in adult body size than the wild type. The difference in body size of the remaining four mutations *unc-17(cn355)*, *unc-13(cn490)*, *unc-41(cn252)* and *unc-18(cn347)* are quite marked. As shown by the arrows in Figure 5, mutants containing *cn257* and *cn4146* start egg-laying at around 50 hours after hatching, corresponding to the wild-type animals. On the other hand, the egg-laying of the other four mutants is remarkably retarded though the extent is variable.

Sensitivity to cholinergic reagents Survival of the six mutants was tested in the presence of cholinergic reagents that cause nematocide and were originally used as an anthelmintic (Table 2). The antagonist, decamethonium did not inhibit nematode growth. No mutant was resistant to the cholinergic agonist, levamisole compared to the wild-type animals. Trichlorfon, neostigmine, eser-

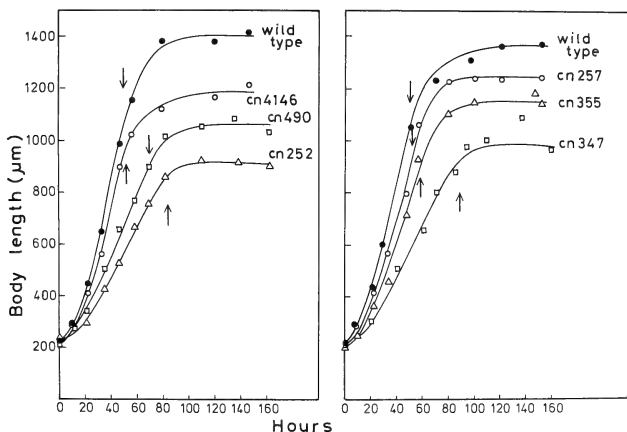


FIG. 5. Growth and egg-laying stage of each strain was prepared so that all worms hatched within a two-hour period. Worms were grown on NGM and at intervals, were suspended in one drop of M9 buffer. On a slideglass, worms were heated slightly and body length was measured with an eyepiece graticule. The mean value of seven worms is presented, but the bar for standard deviation is omitted. To determine the egg-laying stage, L4 larvae were transferred to 21 individual plates and inspected at two-hour intervals. The mean time is indicated by an arrow.

TABLE 2. The effect of cholinergic reagents on the growth of trichlorfon-resistant

Genotype	Trichlorfon mM	Growth on Aldicarb mM	Levamisole mM
Wild type	0.02	0.20	>0.30
<i>unc-13(cn490)</i>	0.10	>1.00	0.04
<i>unc-17(cn355)</i>	>0.30	>1.00	>0.30
<i>unc-41(cn252)</i>	0.20	>1.00	0.01
<i>unc-18(cn347)</i>	0.10	>1.00	0.01
<i>unc-10(cn257)</i>	0.10	>1.00	0.20
<i>unc-3(cn4146)</i>	0.04	0.80	>0.30

Three larvae were put onto NGM containing ten different concentrations of reagents (0, 0.01, 0.02, 0.04, 0.06, 0.08, 0.1, 0.15, 0.2 and 0.3 mM). Four different concentrations were further tested in the case of aldicarb at which the worm, in triplicate experiments, was able to produce F2 progeny within ten days.

ine, diisofluorophosphate, and aldicarb (2-methyl-2-(methoxythio) propionaldehyde-0-(methylcarbamoyl) oxine) are representative inhibitors to *C. elegans* AChE [29]. However, the extent of the effect on nematode growth is not always comparable to the degree of AChE inhibition. For example, 2 mM neostigmine and eserine did not influence nematode growth though they are potent inhibitors to AChE. At higher concentrations, the reagents caused *C. elegans* paralysis [8] and probably would inhibit growth. Of the mutants, the *cn355* animals were the strongest and the *cn4146* animals were the weakest in resistance to trichlorfon. The wild type animals were the most sensitive to aldicarb while the *cn4146* animals showed low significant resistance. The growth of *cn355* animals is not influenced by 1 mM aldicarb.

Other mutant strains are also able to make F2 progeny but their growth was greatly suppressed at a high concentration of aldicarb. Although aldicarb is a much weaker inhibitor of nematode growth than trichlorfon, the mutant show a pattern of sensitivity to aldicarb which is almost the same as that observed for trichlorfon. Therefore, the mutants were not specifically resistant to trichlorfon but probably resistant to AChE inhibitors.

ChAT activity, choline and ACh levels

Mutant alleles of the *cha-1 unc-17* complex gene were all resistant to AChE inhibitors. However, these alleles were greatly different each other in ChAT activity and ACh levels [10]. Accordingly, ChAT activity, choline and ACh levels of the six mutants were measured (Table 3). Choline levels were all normal (data not shown). ChAT activity

TABLE 3. ChAT activity and ACh levels in the trichlorfon-resistant strains

Genotype	ChAT activity (μ mol/h/mg protein)	ACh (nmol/mg protein)
Wild type	0.021 \pm 0.004	0.118 \pm 0.025
<i>unc-13(cn490)</i>	0.027 \pm 0.006	0.375 \pm 0.027
<i>unc-17(cn355)</i>	0.079 \pm 0.002	0.475 \pm 0.058
<i>unc-41(cn252)</i>	0.035 \pm 0.006	0.409 \pm 0.016
<i>unc-18(cn347)</i>	0.031 \pm 0.000	0.673 \pm 0.122
<i>unc-10(cn257)</i>	0.019 \pm 0.002	0.219 \pm 0.008
<i>unc-3(cn4146)</i>	0.023 \pm 0.002	0.119 \pm 0.026

Animals were grown at 20°C. Each value represents the mean \pm S.D. of three independent measurements of ChAT activity and of assays for ACh levels repeated three times.

was all within normal values, though the ChAT activity of *cn355* was about two times higher than that of the wild type as already reported with the other *unc-17* allele *e245* [10]. ACh levels of the remaining four mutants were abnormally high. All mutations showing high ACh levels were accompanied by abnormal development (Table 3 and Fig. 5). In the *unc-18* mutation, ACh levels are the highest and the developmental rate is the slowest of the six mutations. However, the extent of the retardation is different, irrespective of similar ACh levels in the *unc-17* and the *unc-41* mutations. A correlation between ACh levels and the extent of trichlorfon-resistance was not observed.

Double mutants between trichlorfon resistants

In order to test the interaction between the trichlorfon resistant mutations, we tried to construct double mutants of following mutations on different linkage groups: *unc-13(cn490)*, *cha-1(p1152, cn101)*, *unc-17(e113, e245, cn355)*, *unc-41(cn252)*, *unc-10(cn257)*, *unc-18(cn347, e81)* and *unc-3(cn4146)*. All possible combinations of doubles between them were detectable. However, the growth was poor in all the double mutants, especially in the *unc-17-unc-18* double mutations. To determine which gene was expressed in the doubles, ACh levels were followed (Table 4).

ACh of the double mutants *p1152 cn347*, that is, a combination of low and high ACh, was kept at high levels but lower than in the single *cn347* mutation. ACh levels were lower than expected in the double mutation *e245 cn257*, that is, the combination of normal and high ACh levels in the respective single mutation. In other double mutations, ACh levels are higher than additive levels of the single mutation. High ACh levels were maintained in the double mutants *e113 cn347*, *cn252 cn4146*, *cn252 cn257* and *cn490 cn4146* that were a combination of normal and high levels of ACh. The ACh levels in the double mutants *e245 cn490*, *e245 cn252*, *cn347 cn252* and *cn252 cn490* were much higher than in a single mutation.

DISCUSSION

To aid in understanding, the phenotypes of the six mutants mentioned above are summarized in Table 5. The six trichlorfon resistants all showed a similar kinky paralysis but were classified into two groups based on the other two phenotypes, development and ACh levels. In one group, the *unc-10* and the *unc-3* gene mutations were normal but in the other group, the *unc-13*, *unc-18*, *unc-41* and *unc-17* gene mutations were abnormal in de-

TABLE 4. ACh levels of double mutants of trichlorfon resistance

Genotype	ACh levels
	nmol/ mg protein
<i>dpy-13(e184)</i>	0.154 ± 0.052
<i>cha-1(p1152) dpy-13(e184) unc-18(cn347)</i>	0.502 ± 0.032
<i>unc-17(cn113) dpy-13(e184) unc-18(cn347)</i>	0.733 ± 0.046
<i>unc-17(cn245) dpy-13(e184) unc-13(cn490)</i>	1.77 ± 0.055
<i>unc-17(cn245) dpy-13(e184) unc-41(cn252)</i>	1.81 ± 0.145
<i>unc-17(cn245) dpy-13(e184) unc-10(cn257)</i>	0.347 ± 0.038
<i>unc-17(cn245) dpy-13(e184) unc-3(cn4146)</i>	0.777 ± 0.059
<i>dpy-11(e224)</i>	0.187 ± 0.024
<i>unc-41(cn252) dpy-11(e224) unc-18(cn347)</i>	1.48 ± 0.008
<i>unc-41(cn252) dpy-11(e224) unc-13(cn490)</i>	1.46 ± 0.176
<i>unc-41(cn252) dpy-11(e61) unc-3(cn4146)</i>	0.681 ± 0.008
<i>unc-41(cn252) dpy-11(e224) unc-10(cn257)</i>	0.632 ± 0.023
<i>dpy-5(e61)</i>	0.149 ± 0.042
<i>unc-13(cn490) dpy-5(e61) unc-3(cn4146)</i>	0.804 ± 0.053
<i>unc-13(cn490) dpy-5(e61) unc-10(cn257)</i>	0.896 ± 0.015

TABLE 5. Summary of phenotypes of six mutants

Matations	Development	Bahavior	Sensitivity to AChE inhibitors	ChAT activity	Choline levels	ACh levels
<i>unc-10(cn257), unc-3(cn4146)</i>	normal	kinky paralysis	resistant	normal	normal	normal
<i>unc-13(cn490), unc-41(cn252), unc-18(cn347), unc-17(cn355)</i>	slow growth, small and thin body	kinky paralysis	resistant	normal	normal	high

velopment and ACh levels. We are especially interested in mutations causing abnormal accumulation of ACh. Information on the localization of ACh at the synaptic level was scarce in *C. elegans*. Higher levels of ACh were also observed in the mutation of the *ace-2* gene that encodes one of three types of AChE [10]. However, ACh in this mutant may be accumulated at the synaptic gap because of a partial defect in ACh hydrolysis. This possibility is supported by the finding that the *ace-2* mutant is more sensitive to AChE inhibitors than wild-type animals. In contrast to the *ace-2* mutant, the *unc-17(e245)* mutant was resistant to AChE inhibitors and the ACh levels were no longer influenced by the addition of reagents. From these results, it is hypothesized that ACh in the mutant is not released into the synaptic gap [10]. From the similarity between the phenotypes of *unc-17(e245)* and *unc-13*, *unc-41*, and *unc-18* gene mutants, the functions of these genes might be partially overlapping. Indeed, ACh levels were higher in the four double mutants between these genes than in the respective single mutants. Therefore, ACh in the nematode might be accumulated by multiple pathways rather than by a single pathway. However, these pathways are not independent but might be interactive because the ACh levels in double mutants are much higher than additive levels. A major goal of our work is to elucidate the genetic basis of the synaptic transmission. Some insight into the molecular nature of the gene products may be very useful for accomplishing this. We have started and recently cloned the 6.8 kb BglIII DNA fragment including the *unc-18* gene (Fig. 3) into the plasmid pUC 18 (unpubl. results).

Morphological defects in neurons have been

revealed in the *unc-13* and *unc-3* gene mutants. In the *unc-13* mutations, some interneurons in the ventral cord had extraneous gap junctions to motorneurons in addition to normal neural connections (I. Maruyama, personal communication). In the *unc-3* mutations, the processes of the interneurons are disorganized along the cord leading to wrong synaptic inputs from the interneurons [30, 31]. It is probable that mutations showing abnormal accumulation of ACh are also defective in the function of motor neurons because about three-quarters of the neurones in the ventral nerve cord are occupied by cholinergic neurones in nematodes [5]. We cannot infer how the response to trichlorfon is controlled in the nematode because of limitations in the knowledge about the neuroanatomy or molecular defects of the mutant strains. It is possible that the response of these mutations to trichlorfon may be an indirect consequence of grosser cellular or subcellular defects. From preliminary work, we found that in doubles constructed with *cha-1*, *unc-18*, *unc-17*, *unc-13*, *unc-41*, *unc-3*, and *unc-10* mutations, the one with the phenotype of stronger trichlorfon resistance of the two was expressed in many cases, though the extent of the resistant was variable. However, any combination of *unc-17*, *unc-10* and *unc-13* mutations was no longer resistance to trichlorfon, suggesting the functional interactions of these genes.

We began this work with the hope of isolating spontaneous mutants of the *cha-1-unc-17* complex gene induced by the insertion of TcI. One allele of the *unc-17* region but no alleles of the *cha-1* region were isolated through this work. Recently, Dr. J. Rand also isolated spontaneous resistant mutants to the AChE inhibitor, aldicarb and found alleles of *unc-17* but no alleles of *cha-1*. One reason why

no spontaneous *cha-1* mutant can be found is that the site for the TcI insertion may be defective in the *cha-1* region. The frequencies of spontaneous TcI-induced mutations are not even throughout the chromosomal regions but greatly varied, e.g., the frequencies for the *unc-54*, *lin-12* and *unc-22* genes are 5×10^{-7} , 5×10^{-5} , 1×10^{-4} , respectively (see review by Herman and Shaw [11]). The other possibility is that the mutant induced by TcI insertion at the *cha-1* region is either lethal or the growth is too slow to detect in the screening. No null allele in the *C. elegans cha-1* gene has so far been isolated [9, 22]. Totally ChAT defective mutants may be lethal as seen in *Drosophila cha* mutants [32]. It may also be possible that the growth of the *cha-1* mutants induced by TcI insertion is so greatly affected that the mutants could not be detected from the screening plates. The screening method for trichlorfon resistants described here is not complete because most animals can recover from the inhibition when transferred under highly condensed states on the screening plates.

In this report, we presented a genetic analyses of six genes showing resistance to trichlorfon. The eleven remaining trichlorfon resistants isolated in this work were accompanied by marginal uncoordinated phenotypes and complemented the six gene mutants, indicating the presence of other genes resistant to AChE inhibitors in addition to the six described. We cannot predict how many genes affect the worm's response to AChE inhibitors. From the preliminary screening of uncoordinated mutants isolated in addition to the six genes, seven gene mutants were found to be resistant to AChE inhibitors: *unc-63*, *unc-11*, *unc-32*, *unc-36*, *unc-64*, *unc-65* and *unc-1* (J.M. RAND, personal communication). The mutations in the *unc-63*, *unc-11*, *unc-32*, *unc-36*, *unc-64*, *unc-65* and *unc-1* genes were also classified into two groups based on the body size of the mature animals: nearly normal (*unc-32*, *unc-36*, and *unc-65*) and small (*unc-63*, *unc-64*, *unc-11*, and *unc-1*). The latter group except for *unc-1* developed slowly. The *unc-1(e94)* mutation resulted in a small body but with normal development. Measurement of ACh levels in these mutants is in progress.

ACKNOWLEDGMENTS

We thank R. Kitamura and S. Matsudaira for technical help. We thank Y. Iida for guidance in the technique of Southern blotting. We thank A. M. Levitt and S. Emmons for sharing pCe2002 and pCe1012. For providing strains, we are grateful to P. Anderson, I. Mori, D. G. Moerman, R. H. Waterston, J. B. Rand and the *Caenorhabditis* Genetics Center, which is supported by a contract between the NIH and the Curators of the University of Missouri.

REFERENCES

- Reichard, L. F. and Kelly, R. B. (1983) A molecular description of nerve terminal function. *Annu. Rev. Biochem.*, **52**: 871-926.
- Miyamoto, M. D. (1978) The actions of cholinergic drugs on motor nerve terminals. *Pharmacol. Rev.*, **29**: 221-247.
- Tücek, S. (1985) Regulation of acetylcholine synthesis in the brain. *J. Neurochem.*, **44**: 11-24.
- Brenner, S. (1974) The genetics of *Caenorhabditis elegans*. *Genetics*, **77**: 71-94.
- Johnson, C. D. and Stretton, A. O. W. (1980) Neural control of locomotion in *Ascaris*: Anatomy, electrophysiology and biochemistry. 1 In "*Nematodes as biological models*". Ed. by B. Zuckerman, Academic Press, New York/London, pp. 159-195.
- White, J. G., Southgate, E., Thomson, J. N. and Brenner, S. (1986) The structure of the nervous system of the nematode *Caenorhabditis elegans*. *Phil. Trans. R. Soc. Lond. B*, **314**: 1-340.
- Rand, J. B. and Russell, R. L. (1984) Choline acetyltransferase-deficient mutants of the nematode *Caenorhabditis elegans*. *Genetics*, **106**: 227-248.
- Hosono, R., Kuno, S. and Midsukami, M. (1985) Temperature-sensitive mutation causing reversible paralysis in *Caenorhabditis elegans*. *J. Exp. Zool.*, **235**: 409-421.
- Sassa, T., Hosono, R. and Kuno, S. (1987) Choline acetyltransferase from a temperature-sensitive mutant of *C. elegans*. *Neurochem. Int.*, **11**: 323-329.
- Hosono, R., Sassa, T. and Kuno, S. (1987) Mutations affecting acetylcholine levels in the nematode *Caenorhabditis elegans*. *J. Neurochem.*, **49**: 1820-1823.
- Herman, R. K. and Shaw, J. E. (1987) The transposable genetic element TcI in the nematode *Caenorhabditis elegans*. *Trends Genet.*, **3**: 222-225.
- Greenwald, I. (1985) *lin-12*, a nematode homeotic gene, is homologous to a set of mammalian proteins that includes epidermal growth factor. *Cell*, **43**: 583-590.
- Moerman, D. G., Benian, G. M. and Waterston, R. H. (1986) Molecular cloning of the muscle gene

- unc-22* in *Caenorhabditis elegans* by Tc1 transposon tagging. Proc. Natl. Acad. Sci. USA, **83**: 2579-2583.
- 14 Rosenzweig, B., Liao, L. W. and Hirsh, D. (1983) Sequence of the *C. elegans* transposable element Tc1. Nucleic Acids Res., **11**: 4201-4209.
- 15 Rosenzweig, B., Liao, L. W. and Hirsh, D. (1983) Target sequences for the *C. elegans* transposable element Tc1. Nucleic Acids Res., **11**: 7137-7140.
- 16 Emmons, S. W., Yesner, L., Ruan, K. and Kastzenberg, D. (1983) Evidence for a transposon in *Caenorhabditis elegans*. Cell, **32**: 55-65.
- 17 Liao, L. W., Rosenzweig, B. and Hirsh, D. (1983) Analysis of a transposable element in *Caenorhabditis elegans*. Proc. Natl. Acad. Sci. USA, **80**: 3585-3589.
- 18 Moerman, D. G. and Waterston, R. H. (1984) Spontaneous unstable *unc-22* IV mutations in *C. elegans* var. Bergerac. Genetics, **108**: 859-877.
- 19 Eide, D. and Anderson, P. (1985) The gene structures of spontaneous mutations affecting a *Caenorhabditis elegans* myosin heavy chain gene. Genetics, **109**: 67-79.
- 20 Eide, D. and Anderson, P. (1985) Transposition of Tc1 in the nematode *Caenorhabditis elegans*. Proc. Natl. Acad. Sci. USA, **82**: 1756-1760.
- 21 Horvitz, H. R., Brenner, S., Hodgkin, J. and Herman, R. K. (1979) A uniform genetic nomenclature for the nematode *Caenorhabditis elegans*. Mol. Gen. Genet., **175**: 129-133.
- 22 Rand, J. B. and Russell, R. L. (1985) Properties and partial purification of choline acetyltransferase from the nematode *Caenorhabditis elegans*. J. Neurochem., **44**: 189-200.
- 23 McCaman, R. E. and Stetler, J. (1977) Radiochemical assay for ACh: modifications for sub-picomole measurements. J. Neurochem., **28**: 669-671.
- 24 Sulston, J. and Brenner, S. (1974) The DNA of *Caenorhabditis elegans*. Genetics, **77**: 95-104.
- 25 Emmons, S. W. and Yesner, L. (1984) High-frequency excision of transposable element Tc1 in the nematode *Caenorhabditis elegans* is limited to somatic cells. Cell, **36**: 599-605.
- 26 Southern, E. M. (1975) Detection of specific sequences among DNA fragments by gel electrophoresis. J. Mol. Biol., **98**: 503-517.
- 27 Rigby, P. W. J., Dieckmann, M., Rhodes, C. and Berg, P. (1977) Labeling deoxyribonucleic acid to high specific activity in vitro by nick translation with DNA polymerase I. J. Mol. Biol., **113**: 237-251.
- 28 Hodgkin, J. (1983) Male phenotypes and mating efficiency in *Caenorhabditis elegans*. Genetics, **103**: 43-64.
- 29 Johnson, C. D. and Russell, R. L. (1983) Multiple molecular forms of acetylcholinesterase in the nematode *Caenorhabditis elegans*. J. Neurochem., **41**: 30-46.
- 30 Herman, R. K. (1984) Analysis of genetic mosaics of the nematode *Caenorhabditis elegans*. Genetics, **108**: 165-180.
- 31 Herman, R. K. (1987) Mosaic analysis of two genes that affect nervous system structure in *Caenorhabditis elegans*. Genetics, **116**: 377-388.
- 32 Greenspan, R. J. (1980) Mutations of choline acetyltransferase and associated neural defects in *Drosophila melanogaster*. J. Comp. Physiol., **137**: 83-92.

Cytostatic Effect of the Cytoplasm of Mature Oocytes in the Newt, *Cynops pyrrhogaster*

TSUYOSHI SAWAI and KEIKO HIGUCHI

Department of Biology, Faculty of General Education,
Yamagata University, Yamagata 990, Japan

ABSTRACT—In anura, it has been known that the cytoplasm of mature oocytes possesses a specific factor to arrest nuclear division at metaphase. In the present study, we examined a similar effect of the cytoplasm in oocytes of a urodele, *Cynops pyrrhogaster*.

Eggs during the first cleavage were injected various amounts of the oocyte cytoplasm (50–200 nl) into the animal region of one of the two prospective blastomeres. The cytoplasm injection had no effect on the process of the first cleavage, but gave great influence for the subsequent divisions. In many cases, the second division of the cytoplasm-injected blastomeres was considerably delayed or completely arrested. Cytological examination revealed that chromosomes, spindle fibers or astral rays were frequently present in the uncleaved blastomeres.

These results strongly suggested that the mature oocyte of the newt also contained a cytoplasmic factor which could arrest the nuclear division at metaphase.

INTRODUCTION

It is a well known fact that the meiosis of fully mature oocytes is arrested at metaphase II in amphibia, as in many other vertebrates. Several hypotheses have been proposed to account for this phenomenon [1]. For instance, using eggs of anura, *Rana pipiens* [2, 3] and *Xenopus laevis* [4], Masui and his colleagues have shown that the metaphase arrest was caused by some cytoplasmic factor of the mature oocyte [2–4]. Their conclusion was based on the evidence that the nuclear division in recipient zygotes was arrested at metaphase when they were injected with the cytoplasm of unfertilized eggs. The unknown cytoplasmic component responsible for this effect was termed "cytostatic factor" (CSF). Recently, Newport and Kirschner [5] confirmed the existence of CSF in *Xenopus* eggs, and further they showed that CSF inhibited not only cleavage, but also DNA synthesis as well as cyclic changes of cytoplasmic activities such as surface contraction waves.

However, contradicting to these observations,

Chulitskaia and Feulgebauer [6] reported negative results of CSF in the eggs of *Rana temporaria* and *Acipenser stellatus* (sturgeon). In the present study, we report examination about the existence of the cytostatic factor in the cytoplasm of mature oocytes of a urodele, *Cynops pyrrhogaster*.

MATERIALS AND METHODS

Eggs of the newt, *Cynops pyrrhogaster*, were used as the experimental material. Spawning of fertilized eggs was induced by injecting about 80 i.u. of chorionic gonadotropin (Gonatoropin, Teikoku-Zoki Co., Japan) into the abdomen of females every other day. Unfertilized eggs were obtained by squeezing them out of the oviduct of females stimulated by hormone. The jelly coat of the egg was removed by treatment with 1.5% sodium thioglycollate (Wako Pure Chemical Institutes Ltd., Japan) dissolved in Holtfreter's saline solution (pH 10). The eggs with the vitelline membrane but without the jelly coat were put on a small depression of an agar gel (about 3%). They were operated in Ca-free Holtfreter's saline solution (pH 7.0) and then transferred to the standard Holtfreter's saline solution at room temperature (18–23°C).

Microinjection of the cytoplasm was carried out with a glass micropipette, the one end of which was drawn out into a capillary of about $50\text{ }\mu\text{m}$ inner diameter, and the other end of which was connected to a rubber tubing for applying a negative or positive pressure by mouth [7]. The volume of the injected cytoplasm was estimated from the calibration with the predetermined markers on the pipette.

For cytological observation, eggs were fixed in modified Smith's fixative for about one day; solution A (potassium bichromate, 0.5 g; water 87.5 ml) and solution B (40% formalin, 2.5 ml; glacial acetic acid, 10 ml) were prepared, and freshly mixed in the ratio of A:B=9:1 immediately before the application. A modification was made by adding glutaraldehyde up to 3% to the mixed solution. The fixed eggs were washed with running water for one to two days. They were then dehydrated in alcohol series and embedded in paraffin according to the usual way. Serial sections were made about $10\text{ }\mu\text{m}$ thickness. The sections were double stained with 1% acid fuchsin solution and 0.1% amino black which was dissolved in 7% acetate solution.

RESULTS

Eggs undergoing the first cleavage were used as recipients. They were arbitrarily classified into four stages according to the advance of the cleavage furrow (Fig. 1A-D); just after the onset of the formation of cleavage furrow (A), when the cleavage furrow came about half the way (B), when it encompassed the whole circumference of the egg

(C), and about 20 min before the onset of the second cleavage (D). At each stage, the cytoplasm from the unfertilized egg was injected into one side of the animal hemisphere separated by the cleavage furrow (one blastomere in the next two-cell stage). In control experiments, eggs were injected with the cytoplasm from fertilized eggs in the same way as described above. The volumes of the cytoplasm injected were approximately 50, 100, 150 or 200 nl. The cytoplasm injection had no effect on the progression of the first cleavage of the recipients, but greatly influenced the subsequent cleavage, especially in the experimental group.

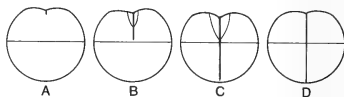


Fig. 1. Stages of recipient eggs classified by the extent of cleavage. (A) just, (B) about 45 min, (C) 90 min and (D) 110 min after the onset of the first cleavage. The stage D is about 20 min before the second cleavage.

In many cases of the group, the second or the third cleavage of the blastomere of the operated side was delayed in various extents compared with that of the unoperated side in which cleavage occurred at the normal time (Fig. 2A, B). Also, in many cases cleavage of the operated side was arrested (Fig. 2C). Disturbances of cleavage were ranked into four categories. To the first category belonged the cases in which the cleavage delay occurred within one cleavage cycle (delay within about 2 hr). These cases were included in the

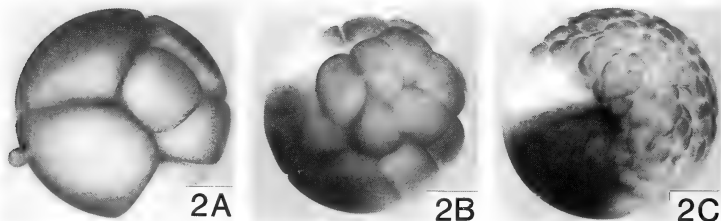


Fig. 2. Delay and arrest of division in the blastomere injected oocyte cytoplasm. (A) Delay of one cleavage cycle (operated blastomere; left 2 cells). (B) Delay of three cycle (left 2 cells). (C) Cleavage arrest. $\times 23$.

TABLE 1. Division of the blastomeres injected with oocyte cytoplasm during the first cleavage cycle

Volume injected (nl)	Stage of recipient	Results									
		Experiment					Control				
		Total no.	Normal	Delay	Arrest	% of arrest	Total no.	Normal	Delay	Arrest	% of arrest
50	A	48	25	4	19	40	10	10	0	0	0
	B	26	20	1	5	19	15	13	1	1	7
	C	31	22	2	7	23	18	15	1	2	11
	D	32	23	3	6	19	17	17	0	0	0
100	A	90	39	15	36	40	44	33	5	6	14
	B	116	38	21	57	49	47	31	8	8	17
	C	50	24	8	18	36	18	13	2	3	17
	D	47	24	8	15	31	26	21	2	3	12
150	A	50	16	4	30	60	49	41	2	6	12
	B	67	10	6	51	76	46	31	3	12	26
	C	42	6	5	31	74	34	24	4	6	18
	D	47	18	3	26	55	32	25	2	5	16
200	A	65	14	8	43	66	54	37	9	8	15
	B	85	11	8	66	78	58	47	4	7	12
	C	56	8	6	42	75	38	32	2	4	11
	D	39	12	4	23	59	21	16	1	4	19

See text further explanation.

TABLE 2. The relationship between the stage of recipient zygotes and the time of their cleavage-arrest

Stage of recipients	total no.*	Time of arrest		
		2nd cleavage	3rd cleavage	4th cleavage
A	128	119 (93%)	8 (6.3%)	1 (0.8%)
B	179	163 (91.1%)	13 (7.3%)	3 (1.7%)
C	100	77 (77%)	23 (23%)	0
D	70	33 (47%)	37 (53%)	0

*Sum of arrested cases in each stage in the Table 1.

normal category of Table 1, because this slight delay was probably not due to the effect of some cytoplasmic factor but the mechanical perturbation caused by the addition of the cytoplasm. The second category involved cases with the delay longer than one but shorter than three cleavage cycles (about 2-6 hr delay). In the third category, cases with the delay longer than three cycles were included (delay over 6 hr). This extended delay would be regarded as a temporary arrest caused by

the effect of a cytoplasmic factor. In the cases of the last category, cleavage was completely arrested during the entire period of observation, at least, until the time when control embryos reached morula to blastula stages. In Table 1, the third and the last groups were consolidated, because these prolonged but temporary arrests as well as complete arrests must be caused by the effect of a cytoplasmic factor. The frequency of cleavage inhibition increased proportionally with the in-

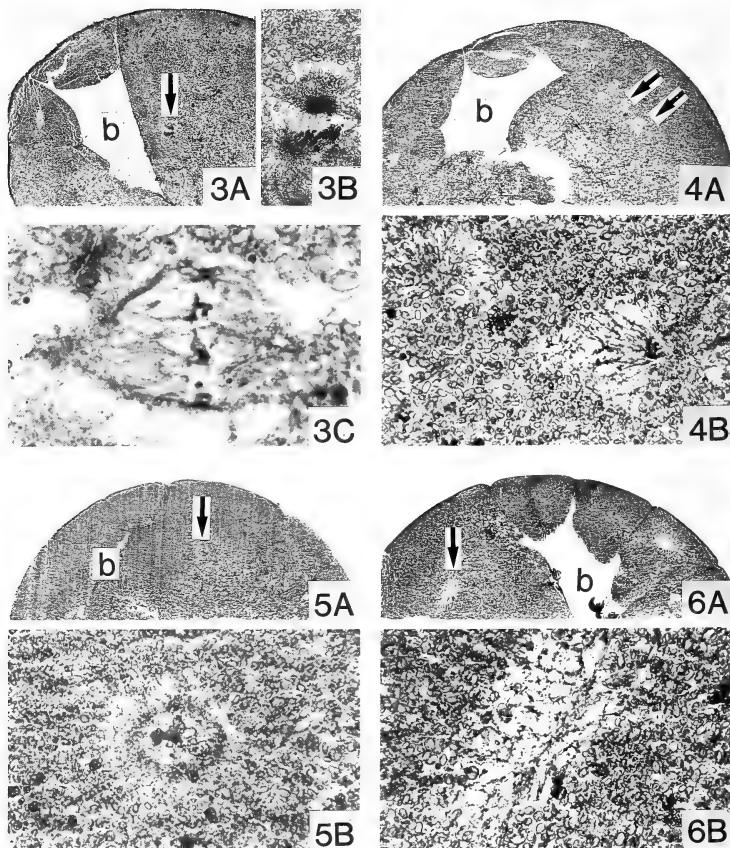


FIG. 3. (A) Anaphase mitotic figure in the cleavage-arrested blastomere (arrow) and (B) its high power observation. (C) Another example of mitotic figure in metaphase. b, blastocoel. A; $\times 45$. B; $\times 260$. C; $\times 400$.

FIG. 4. (A) Aster-like structure in the cleavage-arrested blastomere (arrow) and (B) its high power observation. A; $\times 36$. B; $\times 280$.

FIG. 5. (A) A structure seeming to be degenerated nucleus in the cleavage-arrested blastomere (arrow) and (B) its high power observation. A; $\times 40$. B; $\times 280$.

FIG. 6. (A) Fibrous structures in the cleavage-arrested blastomere (arrow) and (B) its high power observation. A; $\times 42$. B; $\times 260$.

crease of the injected volume of cytoplasm.

Table 2 shows the relationship between the stage of recipient eggs and the time of cleavage arrest. When the injection was carried out in the stage A and B, the arrest occurred at the second cleavage stage in almost all cases. In the injection in the stage C and D, however, the arrest occurred at the second cleavage stage in 77 and 47% of the cases respectively, and in the remaining cases, the arrest took place at the third cleavage stage.

Cleavage-arrested blastomeres were cytologically examined in 31 embryos, 15 examples of which were fixed when the unoperated half developed into 8 to 32 cells (8-12 hr after cytoplasm injection), and 16 examples were fixed at the morula to blastula stages (20-30 hr after cytoplasm injection) of the unoperated one. In 8 cases of the former group, spindle fibers and chromosomes were observed (Fig. 3). Four cases had one nucleus of interphase or telophase which was weakly stained in comparison to the normally dividing nucleus. And in remaining 3 cases, chromatin substance was not observed but fibrous structure resembled to the vestigial asters was observed (Fig. 4). In the latter fixation group, 3 cases involved a structure seeming to be karyomeres in indistinct feature (Fig. 5), 11 cases involved fibrous structures (Fig. 6), but remaining 2 cases involved neither chromatin-like substance nor fibrous structures.

DISCUSSION

The results of the present study strongly suggested that the oocyte cytoplasm of a urodele, *Cynops pyrrhogaster*, involved the cytotstatic factor (CSF) which was well known in the oocytes of anura, *Rana pipiens* [2, 3] and *Xenopus laevis* [4].

Concerning the relationship between the amount of injected cytoplasm and the effect of CSF on the recipient egg, the present results good agreed to the previous ones. About 60 nl in *Rana* [2] and 30 nl in *Xenopus* [4] were sufficient amount to arrest cleavage of the recipient in high percentage (about 90%). These quantities represented about 6% of the egg volume of respective species. In the present experiment using *Cynops*, the maximum amount of the injected cytoplasm (about 200 nl) represented roughly 6-7% of *Cynops* egg

volume, and arrested cleavage in about 70%.

In the present study, when the injection of the oocyte cytoplasm was made at late stage of the first cleavage, the cleavage arrest did not occur at the second cleavage stage but at the third stage, in half of cases. Similar results had been obtained in the studies with anuran eggs. In such cases, the second nuclear division would already proceeded to anaphase or telophase, and CSF influenced the next division. In fact, the cytokinesis of amphibian eggs could take place even after the mitotic apparatus was removed at metaphase to anaphase of karyokinesis, about 20 min before the appearance of furrow, in *Rana nigromaculata* [8].

In the cytological investigation, the previous experiments with anuran eggs showed that the karyokinesis of cleavage-arrested blastomeres was ceased at metaphase even after unoperated half developed into the blastula or the gastrula stage. In the present works with urodele eggs, mitotic figures were also found in the uncleaved blastomere which was fixed at 8 to 32 cells stage of the unoperated half. In the uncleaved blastomere which was fixed at the morula to the blastula stage, however, nuclei or mitotic figures could not be found. This discrepancy between the anura and the urodele would imply that, in the urodele, the mitotic apparatus of the cleavage-arrested blastomere gradually degenerated after the karyokinesis was ceased at metaphase.

It is also noted that the frequency of the delay or the arrest in the control experiment was about 10-20% in the case of *Cynops*, while its value was several percent in the case of anura. This disagreement might be caused by the difference of the volume of injected cytoplasm between the present experiment and the previous ones. Adding much cytoplasm, probably, gave perturbative effect on cleavage of recipients.

In the previous experiment, the injection of a large amount of the oocyte cytoplasm frequently resulted in cytolysis of the operated blastomere [4]. A similar phenomenon was also observed in the present experiment.

ACKNOWLEDGMENTS

We gratefully acknowledge Professor Y. Masui for his

valuable suggestion and reading of the manuscript.

REFERENCES

- 1 Masui, Y. (1985) Meiotic arrest in animal oocytes. In "Biology of fertilization". Vol. 1, Ed. by C. B. Metz, and A. Monroy, Academic Press, London, pp. 189-219.
- 2 Masui, Y. and Markert, C. L. (1971) Cytoplasmic control of nuclear behavior during meiotic maturation of frog oocytes. *J. Exp. Zool.*, **177**: 129-145.
- 3 Myerhof, P. G. and Masui, Y. (1979) Chromosome condensation activity in *Rana pipiens* eggs matured in vitro and in blastomeres arrested by cytotstatic factor (CSF). *Exp. Cell Res.* **123**: 345-353.
- 4 Myerhof, P. G. and Masui, Y. (1979) Properties of a cytotstatic factor from *Xenopus laevis* eggs. *Dev. Biol.*, **72**: 182-187.
- 5 Newport, J. W. and Kirschner, M. W. (1984) Regulation of the cell cycle during early *Xenopus* development. *Cell*, **37**: 731-742.
- 6 Chulitskaia, E. V. and Feulgengauer, P. E. (1977) A study of cytotstatic effect of the oocyte and mature egg cytoplasm in the common frog and sevruga. *Ontogenez*, **8**: 305-308. (In Russian)
- 7 Sawai, T. (1972) Roles of cortical and subcortical components in the cleavage furrow formation in amphibia. *J. Cell Sci.*, **11**: 543-556.
- 8 Kubota, T. (1966) Studies of the cleavage in the frog egg. I. On the temporal relation between furrow determination and nuclear division. *J. Exp. Biol.*, **44**: 543-552.

The Alkaline Substances and Other Constituents of Blastocoel Fluid of the Newt Embryo

TEZRO ASAO

*St. Marianna University, School of Medicine, Biological Laboratory,
Miyamae-ku, Kawasaki 213, Japan*

ABSTRACT—Blastocoel fluid of early gastrula of the newt, *Triturus pyrrhogaster*, was initially separated into four fractions by gel permeation chromatography. The estimation or characterization of the fractions was performed by infrared spectrometry or SDS-polyacrylamide gel electrophoresis. The alkalinity of blastocoel fluid (pH 8.83 to 9.19) was owing to the existence of ca. 40 mM of sodium bicarbonate and sodium carbonate. Blastocoel fluid also contained small, acidic molecular carbonates including amino acids, which seemed to buffer blastocoel fluid against salts of sodium carbonate. Over twenty kinds of protein were countable by silver stain method after SDS-PAGE. Concentration of inorganic ions was 72 mM in Na^+ , 6.9 mM in K^+ , and 1.3 mM in Ca^{++} .

INTRODUCTION

At the gastrula stage a dramatic change begins, namely, the presumptive mesodermal and endodermal tissues invaginate the blastocoelic cavity and form a double-ball type embryo. This is the beginning of morphogenesis. However, although many studies have been performed on the inductive experiments [1, 2], there is as yet little information concerning the blastocoel fluid of the newt embryo. Although the intercellular pH of the morulla embryo of *Xenopus* has been reported to be 8.4 [3], the blastocoel fluid of newt gastrula also has shown alkalinity in our preliminary experiments. The constituents of the blastocoel fluid of newt gastrula are analyzed and discussed in this paper.

MATERIALS AND METHODS

Newt eggs were obtained by injection of 50 μl gonadotropin solution per day (75 units, Teikoku-zoki Seiyaku, Tokyo) into female newts for five days. The female newts were commercially gathered at several places in the Tohoku districts. Eggs reached early gastrula on the third day at

18°C. Capsules of embryos were removed manually by gentle use of Wickel's scissors. The embryos were then set in small holes made on an agar bed in a glass dish. A micro-capillary tube connected to a micro-syringe handled by micro-manipulator was advanced into the blastocoel of early gastrula through a vitelline membrane and an outer blastoderm. Usually, at most 2 μl of blastocoel fluid was sucked out into the capillary tube per embryo by reversal usage of the syringe. The fluid was collected in a plastic micro-centrifuge tube with a cap. The tube was centrifuged at $1,800 \times g$ for five minutes. Supernatant was used as blastocoel fluid in the experiments leading to this paper. About 40 μl of mixed blastocoel fluid from different embryos was used to obtain a measurement by using a single complex micro-electrode (Microelectrode Company, New Hampshire, USA).

One hundred μl of mixed fluid was used in a measurement of inorganic ions analysis. Sodium and potassium ions were analyzed by atomic absorption spectrometry, calcium ions by ICP emission spectrometry, chlorine ions by ion chromatography.

The constituents of blastocoel fluid was analyzed by gel permeation chromatography, using Cellulofine GCL 25 superfine (Seikagaku Kogyo, Tokyo). The blastocoel fluid (0.3 ml) was applied to the column (1.5 cm \varnothing , 48 cm in length) and was

eluted out with distilled water at a velocity of 1 ml per 6 min. Each fraction (1 ml) was monitored at 200 nm and its pH was measured. The peak fractions in question were collected and lyophilized for infrared spectrometry or electrophoresis.

SDS-polyacrylamide gel electrophoresis was performed according to Laemmli [4], though with some modifications. Gradient slab gel ($14 \times 14 \times 0.1$ cm) was prepared from a stock solution of 30% acrylamide and 0.8% methylene bisacrylamide. The final concentration of separation gel were 0.375 M Tris-HCl containing 0.1% SDS (pH 8.8), and 7.5 to 18% acrylamide. The gel was polymerized by the addition of 0.025% tetramethylethylenediamine and 1% ammonium persulfate. The stacking gel concentration was 0.375 M Tris-HCl (pH 6.8), 0.1% SDS and 3.5% acrylamide. Each preparation in water (10 to 50 μ l) was mixed with an equal volume of the sample solution containing 0.125 M Tris-HCl (pH 6.8), 4% SDS, 0.002% bromophenol blue in ethanol, 10% β -mercaptoethanol and 20% glycerol. Proteins were completely dissociated by immersing the tubes in boiling water for three minutes. Electrophoresis was continued under constant current of 25 mA till the marker dye reached to 2 cm from the margin. The proteins in gel were detected by the silver stain method using a Silver Stain Kit (Wako Pure Chemical, Tokyo).

Infrared spectrometry of the lyophilized specimen at its third and fourth peaks were measured by the FT-IR diffuse reflectance method.

RESULTS

Blastocoel fluid was fairly alkaline. As shown in Table 1, pH values varied from 8.83 to 9.19. The variety of the pH values was not due to error in the

TABLE 1. pH values of blastocoel fluid

Group	pH (mean value \pm S.D.)
1	8.83 ± 0.05 (n=10)
2	9.01 ± 0.06 (n= 5)
3	9.19 ± 0.06 (n= 4)

Mixed blastocoel fluid (about 40 μ l) collected from about 30 embryos was used per a measurement of pH.

measurement, but to differences of habitat in the female newt group.

The inorganic ion contents in blastocoel fluid are shown in Table 2. Concentrations of sodium, potassium, and calcium ions were 72, 6.9 and 1.3 mM, respectively. Values of the concentrations of

TABLE 2. Inorganic cation and chlorine ion concentration of blastocoel fluid

Ion	Mean concentration (mM \pm S.D.)
Na ⁺	71.7 ± 2.2 (n=3)
K ⁺	6.9 ± 1.5 (n=2)
Ca ⁺⁺	1.2 ± 0.3 (n=2)
Cl ⁻	42.3 (n=1)

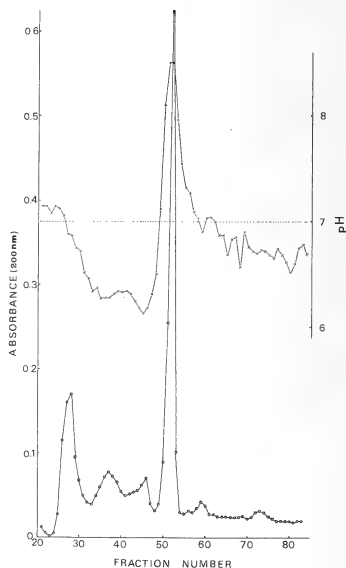


FIG. 1. Gel permeation chromatography of blastocoel fluid.

The gross blastocoel fluid (0.3 ml) was applied. The conditions of chromatography are mentioned in the text. Absorbance is indicated by a small circle and pH, by a cross. The fourth peak was alkaline while the second and third peaks were acidic.

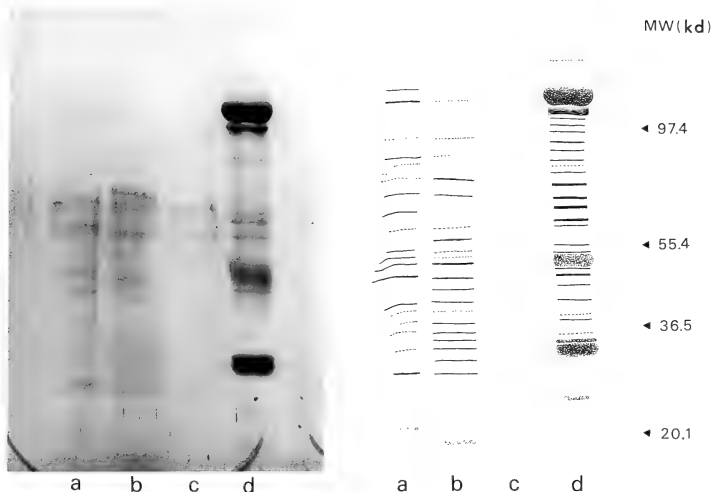


FIG. 2. Polyacrylamide gel electrophoresis in SDS (left), and sketches (right) of the gross blastocoel fluid, its subcomponents separated by chromatography and homogenate of embryo.

The lanes a, b, c and d are, gross blastocoel fluid, first peak, second peak in chromatography and homogenate of embryo, respectively. Two bands appeared commonly in the lanes a, b and c are contaminations from the reagents used.

potassium and calcium ions, however, had large standard deviations.

Gel permeation chromatography of the blastocoel fluid gave rise to four peaks (Fig. 1). As mentioned in the Methods and Materials section above, the first peak at void volume was further analyzed by SDS-polyacrylamide gel elec-

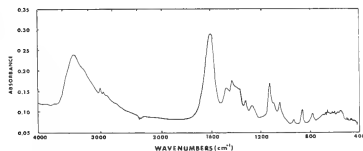


FIG. 3. Infrared spectrum of the third peak in chromatography.

Absorptions at 1400 and 1600 cm^{-1} revealed carbonic salts. A broad band of absorption from 2500 to 3600 cm^{-1} suggested the existence of NH or OH structure.

trophoresis. The pH measurement of each fraction showed that the second and third peaks were acidic, while the fourth peak was alkaline. The third and

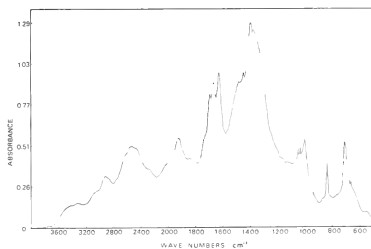


FIG. 4. Infrared spectrum of the fourth peak in chromatography.

The spectrum of the fourth peak was very similar to that of sodium bicarbonate but for the absorption at 1400 cm^{-1} .

fourth peaks were further analyzed by infrared spectrometry.

The SDS-polyacrylamide gel electrophoresis pattern of gross blastocoel fluid, together with the first and second peaks in chromatography and the homogenate of embryos are shown in Figure 2. From the electrophoresis band patterns of the first peak and the gross blastocoel fluid, at least twenty kinds of protein were possibly detected, of 17.6, 27, 29, 31, 33.5, 35.4, 37, 39, 40, 42, 44, 47.5, 49, 51, 53, 65.5, 72.5, 80.5, 89, 105 and 114×10^3 daltons, although some bands existed only in the gross blastocoel fluid. On the other hand, any bands were scarcely recognizable in the lane of the second peak.

Infrared spectrums of the third and fourth peaks are shown in Figures 3 and 4, respectively. Absorption at 780, 860, 930, 1045, 1122, 1267, 1317, 1427 and 1473 cm^{-1} were recorded in the third peak and in the fourth 700, 850, 1000, 1400, 1630, 1700, 1930, 2500-2600, and 2900 cm^{-1} .

DISCUSSION

The alkalinity of the blastocoel fluid of newt gastrula is possibly due to the existence of both sodium bicarbonate and sodium carbonate. The reasoning is as follows: firstly, the infrared spectrum of the fourth peak in gel permeation chromatography was similar to that of sodium bicarbonate, whose absorption peaks exist at 680, 820, 990, 1290, 1620, 1920, 2500 etc. cm^{-1} . On the other hand, the absorption peaks of sodium carbonate are at 700, 880, 1410-1450, 1780 etc. cm^{-1} . The spectrum of the mixture of these two salts was therefore closer to that of the fourth peak (see results). Secondly, the chromatography of the mixture of both salts under the same conditions could successfully simulate that of fourth peak in the elution pattern and the pH value of each of its fractions (Fig. 5). The sharpness of the peak is owing to the coexistence of other components, while the shift in the elution position seemed to be owing to the concentration of the applied salt mixture. In the case of sodium carbonate salt mixture, the higher the concentration of the applied sample was, the later was the elution order. Thirdly, the pH of blastocoel fluid is also simulated

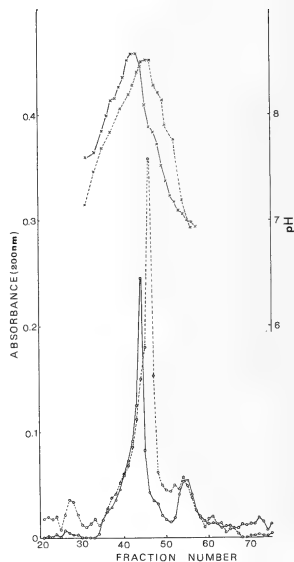


Fig. 5. Chromatography of a mixture of sodium bicarbonate and sodium carbonate.

The equal amount to blastocoel fluid in Fig. 1 (0.3 ml) of 30 mM each of sodium bicarbonate and sodium carbonate (solid line), and 50 mM each of the same compounds (dotted line) were applied. In both cases the salts were solved in 0.1 M sucrose solution. Sucrose was eluted out at fractions of number 53 to 56. The conditions of the chromatography were the same as those of Fig. 1.

by the mixture of equal amount of sodium bicarbonate and sodium carbonate. From the concentration of the total cation (ca. 80 mM) and chlorine ion (ca. 40 mM), actual concentration of each of these salts in blastocoel fluid was supposed to be near to 40 mM. In our preliminary observations of the embryos reared in the dilute Holtfreter's solution containing $0.1 \mu\text{M}$ antimycin for 24 hr, the blastocoel fluid turned to near neutral (pH 7.6), not but alkaline. This suggests that high concentration of sodium carbonate salts may have some relationship to the product of the respiration of embryos. Kostellow and Morrill have reported

that intracellular sodium moves to intercellular spaces to contribute to the developing blastocoel fluid with no significant change in potassium in the cells during pregastrular stage of *Rana pipiens* [5]. Such a phenomenon is also observed in the case of *Xenopus laevis* [6]. It is possibly supposed that carbon dioxide produced by the respiration of embryonic tissues moves to intercellular spaces and solves in water to combine with sodium to form sodium bicarbonate or sodium carbonate.

By infrared spectrometry, the third peak is supposed to contain the small molecular substances of carbonic and aminic structure. Several ninhydrin-positive spots were observed in our preliminary experiments of thin-layer chromatography of the gross specimen of blastocoel fluid. There may be present members of an amino acid group. These small, acidic molecules seemed to buffer blastocoel fluid against salts of sodium bicarbonate and sodium carbonate.

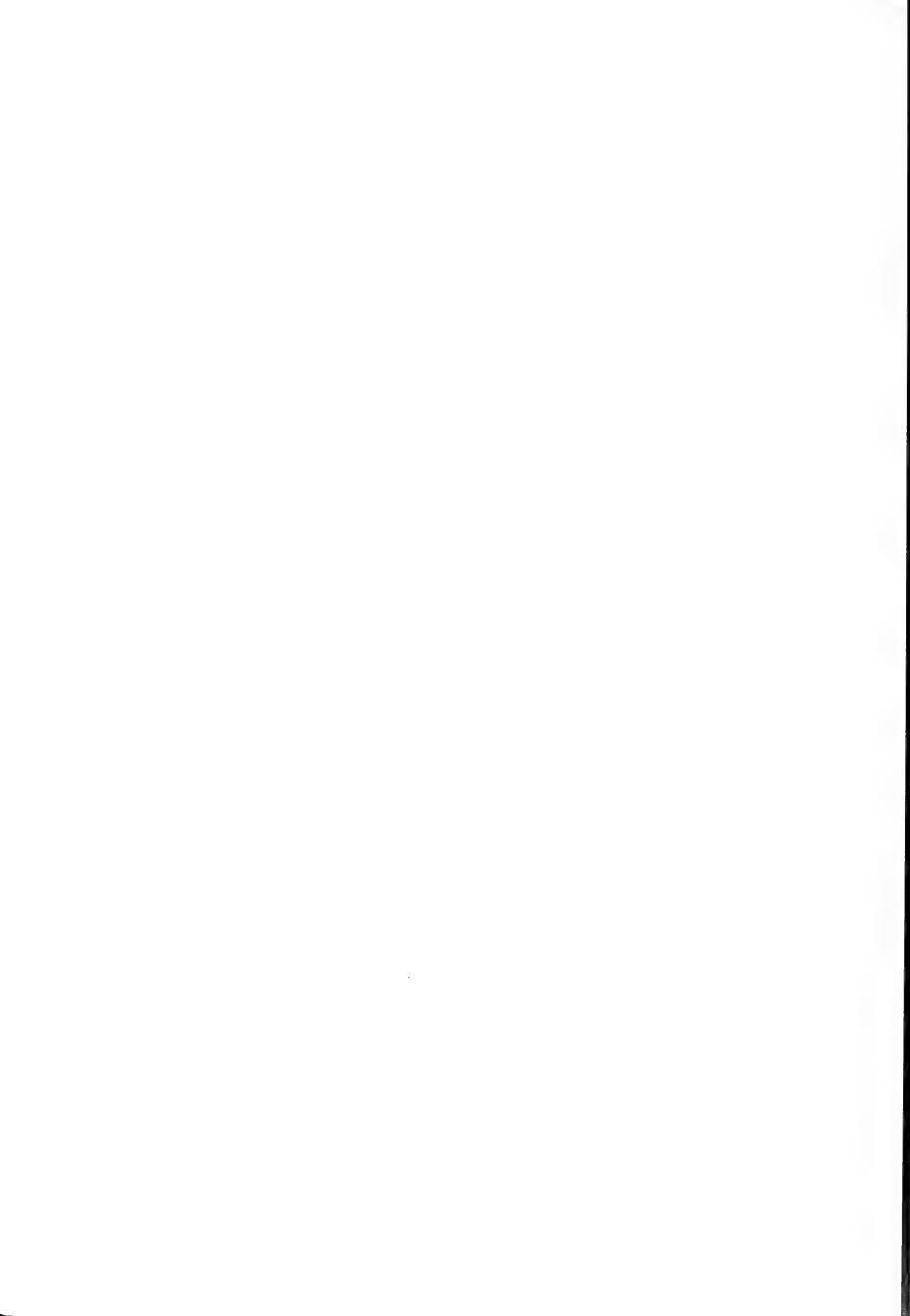
The electrophoretic patterns of the first peak of chromatography and the gross blastocoel fluid were clearly different from those of the homogenate moiety of embryos. The proteins were peculiar constituents of blastocoel fluid, and not cellular fragments contaminated when sucking the fluid from the blastocoel of the embryos. It should be said, however that the largest proteins of 108 and 115 kd were probably the main components of homogenate since they agreed in position in the electrophoresis profile. In any case, blastocoel fluid proved to contain many kinds of protein.

Here, when about 0.5 ml of blastocoel fluid was used, at least twenty bands could be counted. The electrophoretic band pattern also showed all the protein components eluted out in the first peak, while the other peaks contained no proteins at all.

Many experiments of early embryonic induction have been hitherto performed by the so-called sandwich method in neutral Ringer's solution as Holtfreter's solution. For the elucidation of the mechanism of primary induction, however, the pH factor may also have to be paid attention to together with inductor itself.

REFERENCES

1. Holtfreter, J. (1933) Nachweis der Induktionsfähigkeit abgetöteter Keimteile. Isolation- und Transplantationsversuche. Arch. EntwMech. Org., **128**: 584-633.
2. Saxén, L. (1961) Transfilter neural induction of Amphibian ectoderm. Develop. Biol., **3**: 140-152.
3. Turin, L. and Warner, A. E. (1980) Intracellular pH in early *Xenopus* embryos: its effect on current flow between blastomeres. J. Physiol., **300**: 489-504.
4. Laemmli, U. K. (1970) Cleavage of structural proteins during the assembly of the head of bacteriophage T4., Nature, **227**: 680-685.
5. Kostellow, A. B. and Morrill, G. A. (1967) Intracellular sodium ion concentration changes in the early amphibian embryo and the influence on nuclear metabolism. Exp. Cell Res., **50**: 639-644.
6. Slack, C. and Warner, A. E. and Warren, R. L. (1973) The distribution of sodium and potassium in amphibian embryos during early development. J. Physiol., **232**: 297-312.



Environmental Control of Gonadal Maturation in Laboratory-Reared Sea Urchins, *Anthocidaris crassispina* and *Hemicentrotus pulcherrimus*

KAZUHIRO SAKAIRI, MASAMICHI YAMAMOTO,

KOZO OHTSU and MASAO YOSHIDA

Ushimado Marine Laboratory, Okayama University,
Ushimado 701-43, Japan

ABSTRACT—Gametogenic processes in laboratory-reared sea urchins, *Anthocidaris crassispina* and *Hemicentrotus pulcherrimus*, were compared under different experimental environments. The juvenile sea urchins were obtained by artificial fertilization. After preparatory rearing for 3 months under continuous illumination at 20°C, the juveniles were divided into groups and kept under various light and temperature regimes. The stages in gonadal maturation were determined according to a histological standard. In *A. crassispina* kept at ambient temperatures, the gonads matured under both continuous light (LL) and continuous darkness (DD) simultaneously with those under ambient light (control). In *A. crassispina* kept under LL, the gonads matured at either constant 20 or 25°C earlier than those in the control but remained immature at 15°C. In *H. pulcherrimus* kept under LL, the gonads remained immature as long as the animals were kept at a constant temperature (15, 20, 25°C). If the water temperature was lowered stepwise from 25°C to 20°C and after a month to 15°C, the gonads matured about 3 months after the first temperature drop. The gonads of the fully grown sea urchins that had once experienced gonadal maturation in the outdoor tank showed the same response as those of the juveniles to the stepwise temperature drops. It is concluded from previous [18] and the present results that in *A. crassispina*, *H. pulcherrimus* and *Pseudocentrotus depressus*, the three sea urchin species common to shallow water along the Japanese coast, the environmental factor determining their breeding season is not light but water temperature.

INTRODUCTION

Most marine invertebrates living in the temperate zone generally show species-specific annual reproductive cycles. In field studies of many sea urchin species [1-11], various environmental factors such as photoperiods, temperatures, food supplies and the lunar cycle have been presumed to serve as environmental cues to synchronize their reproductive cycles. To know the actual environmental factor regulating the reproductive activity in the sea urchin, it is necessary to examine gonadal responses to artificially manipulated environments under which animals were kept for a long time. Such efforts have been made mostly in

Strongylocentrotus purpuratus [12-17]. Pearse and his colleagues have recently shown that the gametogenesis in that species is under photoperiodic control [16, 17].

We have started a series of long-term experiments on environmental control of gametogenesis in Japanese sea urchins. Since it has been reported in some echinoderms [13, 15, 22] that the annual reproductive calendar once set in the field persists long after the animals are transferred under experimental conditions, we have used juvenile sea urchins produced by artificial fertilization and reared under a constant laboratory environment until they are transferred to experimental conditions. In the preceding paper [18], we have demonstrated in *Pseudocentrotus depressus* and *Hemicentrotus pulcherrimus* that the gonad matured independently of photic conditions. In this

report, we present evidence that light is not a main environmental factor regulating the gonadal activity also in *Anthocidaris crassispina* and further that the reproductive cycle is controlled by water temperature in *A. crassispina* and *H. pulcherrimus*.

MATERIALS AND METHODS

Adult sea urchins

Adults of *Anthocidaris crassispina* and *Hemicentrotus pulcherrimus* were collected in the intertidal zone near the Ushimado Marine Laboratory, Okayama Prefecture in July and March, respectively. The breeding seasons of these species at that place are from June to August and from January to March, respectively.

Obtaining juvenile sea urchins

Embryos used in each series of experiments were obtained by artificial fertilization of gametes spawned from one male and one female. They were reared according to the method by Kakuda [19–21] after slight modifications, the details of which were described in the preceding paper [18]; briefly, the swimming larvae were fed with a diatom, *Chaetoceros gracilis*, and the metamorphosis was induced by giving plastic plates with a film of diatoms attaching on both surfaces (about 10 days and 15 days after fertilization for *A. crassispina* and *H. pulcherrimus*, respectively). The juveniles were kept at 20°C under continuous illumination of the ceiling lights until they were transferred into experimental environments.

Maintenance of sea urchins under experimental environments

When the juveniles had grown into a certain size range (about 90 days after fertilization; the test diameter were 4–10 mm and 4–7 mm in *A. crassispina* and *H. pulcherrimus*, respectively), they were divided into groups matched for similar size distributions, placed in plastic cages (30 cm in diameter), and transferred into experimental environments. Except for the control groups, we used indoor aquaria (120×65×45 cm), each equipped with a system to recirculate constant temperature

sea water. In the aquaria for constant temperature groups, the recirculating sea water at a constant temperature was continuously replaced little by little by new sea water. The aquaria for ambient temperature groups were continuously supplied with running sea water at the ambient temperatures. The illumination for continuous light (LL) was given by some 40 W fluorescent bulbs (about 2000 lux). The aquaria for constant darkness (DD) were made light-tight using opaque plastic boards. The lid of the aquaria for DD was opened briefly (less than 15 min) every 3 or 4 days at an unfixed time of the day for feeding and/or cleaning. The control groups were kept in an outdoor tank under the ambient light supplied continuously with running sea water at ambient temperatures. During the experiments the sea urchins were provided with an unlimited amount of food. They were fed with *Ulva pertusa* from March to October and some species of *Sargassum* (*S. horneri*, *S. serratifolium*, *S. tortile* etc.) from November to February. Feces and sediments were removed from the aquaria at least once a week.

Sampling

The test diameters and wet weights of all animals were periodically measured. Some randomly selected animals were dissected periodically for histological observations. The gonads were weighed and pieces were fixed in Bouin's solution. Paraffin-embedded gonadal tissues were sectioned and stained with haematoxylin and eosin. Since exact measuring of wet gonad weights is difficult and the gonadal indices (percentage of wet gonad weight in wet animal weight) do not fully correlate with the degree of gonadal maturity in small and rapidly growing sea urchin, we judged the degree of gonadal maturity in the histological sections according to the standard that was defined in the preceding paper [18] as shown schematically in Figure 1.

RESULTS

Anthocidaris crassispina

Figure 2 shows the results in the individuals derived from the zygotes fertilized on 7 July 1986

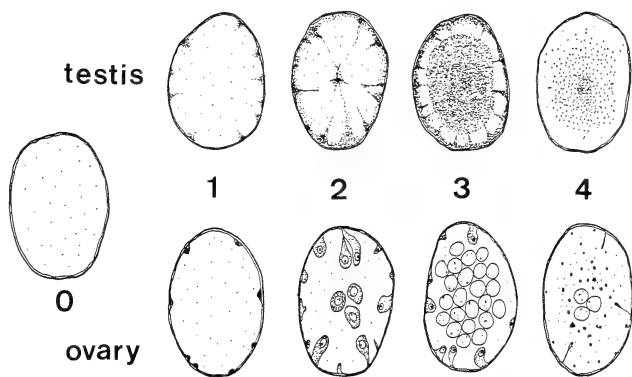


FIG. 1. Schematic representation of stages in the development of the sea urchin gonad.

Stage 0: No obvious germ cells are found and the gonadal sexes cannot be identified in the section.

Stage 1: Ovary—A few small oocytes are present in the periphery of the ovarian lobe. No large oocytes are found.

Testis—Small clusters of spermatogenic cells are present in the periphery of the testicular lobe.

Stage 2: Ovary—Many large oocytes with a prominent germinal vesicle are present in the ovarian wall. Some oocytes migrate toward the center of the ovarian lobe. No mature eggs are present.

Testis—The wall of the testicular lobe is lined with columns of spermatocytes. Small masses of spermatozoa are present in the center of the testicular lobe.

Stage 3: Ovary—Numerous mature eggs are present in the center of the ovarian lobe (ovarian cavity).

Testis—The space in the center of the testicular lobe (lumen) is filled with large numbers of spermatozoa.

Stage 4: Ovary—The ovarian cavity contains only a few relict eggs. Oocytes are few in the ovarian wall.

Testis—The lumen is almost empty with a few relict spermatozoa. Spermatogenic cells are few in the testicular wall.

and transferred into the experimental conditions on 24 September 1986. We tried to compare the processes of gonadal maturation among groups maintained under the following 6 environmental conditions: continuous light (LL), continuous darkness (DD) and ambient light (control) each at ambient temperatures, and constant 15°C, 20°C and 25°C each under LL. Since we had accidentally lost the group under DD at ambient temperatures, we partly repeated the experiments in 1987. In the repeated experiments, the juveniles derived from the zygotes fertilized on 9 July 1987 were placed under DD and ambient light (control) each at ambient temperatures on 22 September 1987. The results are shown in Figure 3. At the beginning of both series of experiments, the gonads were rudimentary and the sexes were unidenti-

fiable (stage 0) in each individual.

In the controls, the gonads reached the full maturity (stage 3) about one year after fertilization, a little earlier in 1986 than in 1987 (Figs. 2 and 3). In the groups kept under LL and DD at ambient temperatures, the gonads reached stage 3 at the same time as those in each control (Figs. 2 and 3). In all the three groups, the testes became ripe earlier than the ovaries.

In the groups kept at constant 20 and 25°C under LL, the gonads grew more rapidly and became mature about 3 months earlier than those in the control (Fig. 2). Although individuals kept at 25°C were unfortunately biased to male, there seems to be little difference in the rate of gonadal maturation between the groups kept at 20 and 25°C. In the group kept at 15°C under LL, no individuals

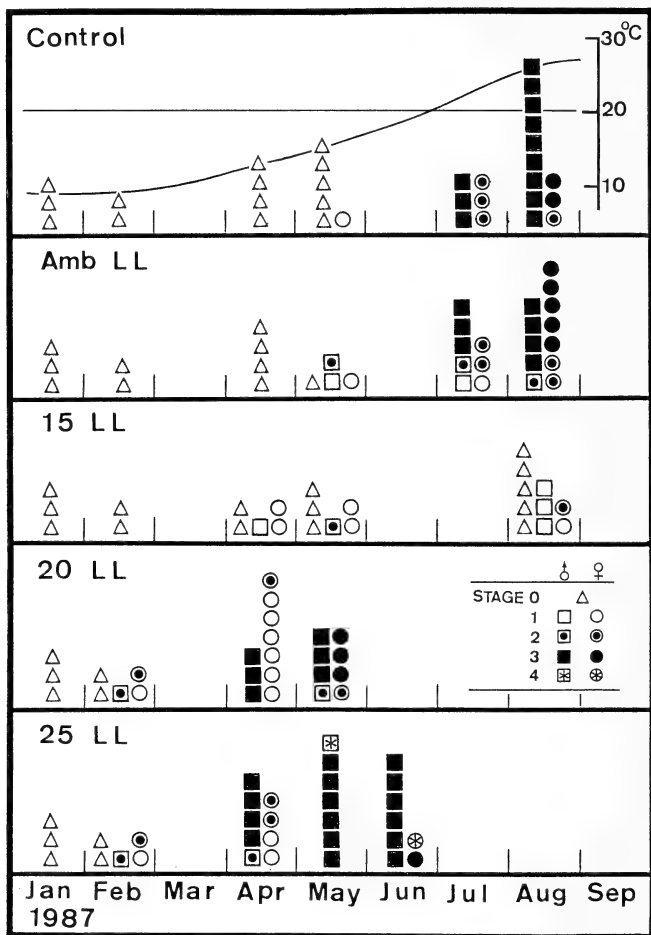


FIG. 2. The stages of the gonads of *Anthocidaris crassispina*. Each symbol represents one individual. Sea urchins were reared from zygotes of the same batch fertilized on 7 June 1986 and were kept under constant illumination at 20°C until they were transferred on September 1986 to one of the following experimental environments: ambient temperatures under ambient light (Control), and ambient temperatures (Amb LL), constant 15°C (15 LL), 20°C (20 LL) and 25°C (25 LL) under continuous light. The change in sea water temperature near the Ushimado Marine Laboratory is shown at the top.

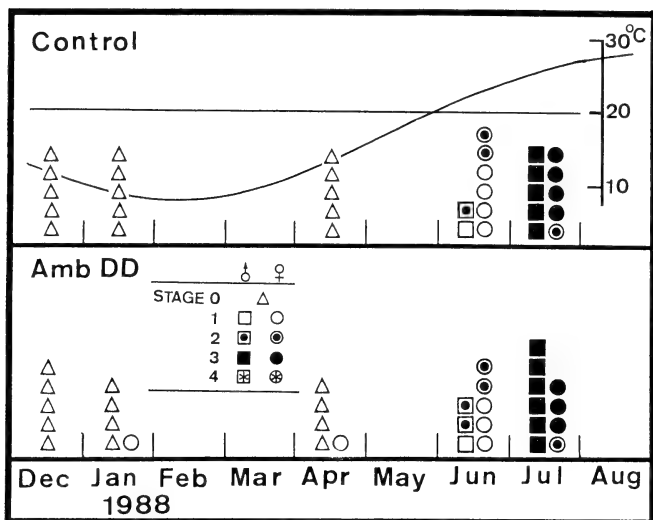


FIG. 3. The stages of the gonads of *Antohocidaris crassispina*. Each symbol represents one individual. Sea urchins were reared from zygotes of the same batch fertilized on 9 June 1987 and were kept under constant illumination at 20°C until they were transferred to ambient light at ambient temperatures (control) or to continuous darkness at ambient temperatures (Amb DD) on 22 September 1987. The change in sea water temperature near the Ushimado Marine Laboratory is shown at the top.

reached stage 3 and in a half of the individuals examined the gonadal sexes remained unidentifiable (stage 0) when the gonads in the control had matured (Fig. 2).

There was little difference in the growth rates among the two control groups and the groups kept under LL and DD at ambient temperature; mean test diameters one year after fertilization were 20–22 mm. The groups kept at 20 and 25°C grew more rapidly and the one kept at 15°C more slowly than the control; mean test diameters one year after fertilization were 31, 28 and 20 mm in 25, 20 and 15°C groups, respectively.

Hemicentrotus pulcherrimus

In the preceding paper [18] we have reported that in *H. pulcherrimus*, the gonads matured under LL as well as DD when the animals were kept at ambient temperatures but remained immature at

constant 20°C irrespective of the photic conditions tested. In the present experiments we examined the effects of three constant temperatures (15, 20 and 25°C) and a temperature drop from 25°C to 15°C on the gonadal maturation. In the experiments of the temperature drop, the water temperature was lowered stepwise from 25°C to 20°C and after a month to 15°C since the direct drop from 25°C to 15°C seemed harmful to the sea urchins. Except for the control groups that were kept under ambient light at ambient temperatures, all the experimental groups were maintained under LL.

Figure 4 shows the results of the experiment using the juveniles derived from zygotes fertilized on 22 March 1987 and transferred into the experimental conditions on 30 June 1987. At the beginning of the experiment animals were 4–7 mm in test diameter, the gonads were small and the sexes were unidentifiable (stage 0). In the control

group, the testes in most males reached the full maturity (stage 3) in December and the ovaries in most females in January. As long as the animals were kept at constant temperatures (15, 20, 25°C), however, the gonads did not mature; even gonadal sexes remained unidentifiable (stage 0) in more than a half of the individuals examined. In the experiments of the temperature drop, the water temperature was lowered from 25°C to 20°C on three different dates (20 August, 22 September and 8 January) and from 20°C to 15°C after a month or less. In the two groups where the temperature was lowered from 25°C to 20°C either on 22 September or 8 January, the testes and ovaries became ripe in almost all individuals about 3 months after the first temperature drop. In the group where the temperature was lowered on 20 August, the testes matured in November but the ovaries did not reach the full maturity (stage 3) though oocytes grew to some extents in many ovaries.

In *H. pulcherrimus*, the growth rates did not differ so largely among groups kept at different temperatures as seen in *A. crassispina*; the mean test diameters in January (10 months after fertilization) were 21, 23, 18 and 24 mm in 15, 20, 25°C groups and the control (ambient temperatures), respectively.

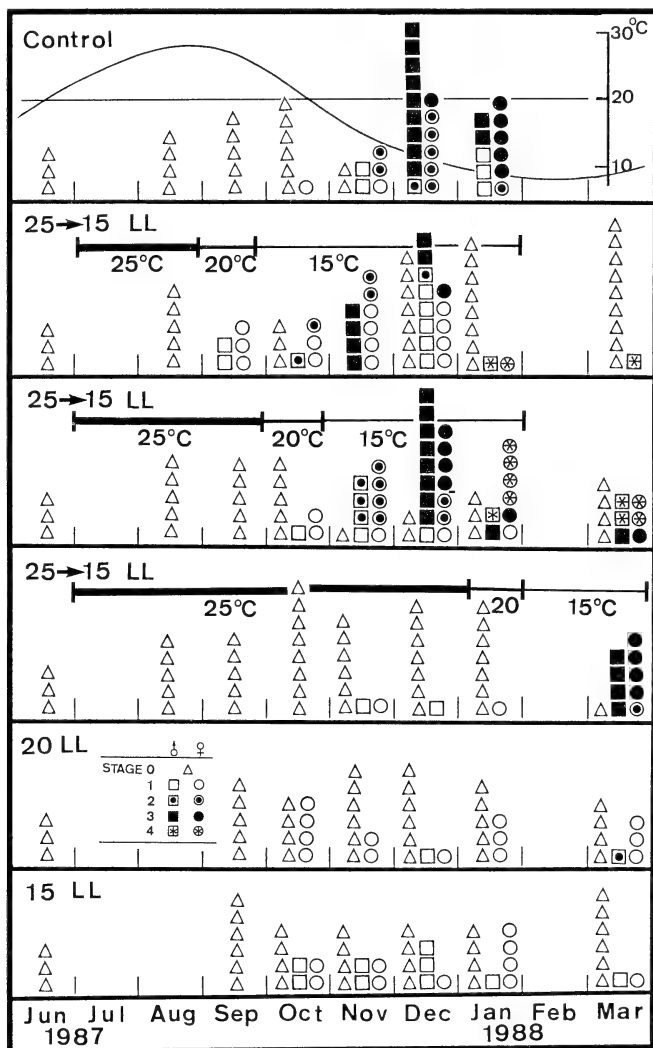
We examined whether or not the gonads in fully grown sea urchins were also responsive to the temperature drop using individuals that had once experienced gonadal maturation in the outdoor tank. The sea urchins were derived from the zygotes fertilized on 29 March 1986 and reared at 20°C under continuous illumination until they were transferred on 21 June 1986 into outdoor tanks that was supplied with running sea water of ambient temperatures. Their gonads were in the mature state (stage 3) from February to May 1987. On 20 May 1987, the sea urchins were divided into four groups; one was remained in the outdoor tank

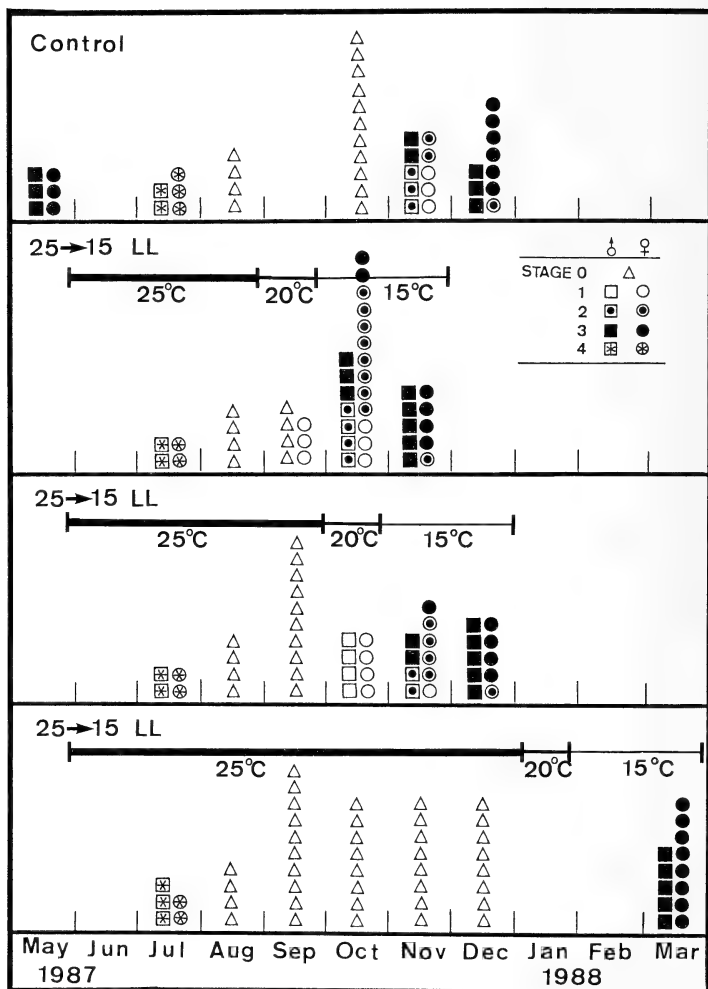
as a control and the other three were transferred into indoor aquaria maintained at constant 25°C under LL. At that time the sea urchins were 23–25 mm in test diameter. The gonads were in the post-spawned state (stage 4) in July and the gonadal sexes became unidentifiable (stage 0) in August though the gonads remained large in size with accumulation of nutritive materials. The gonads in all individuals remained in this state as long as the water temperature was maintained at 25°C (Fig. 5). The water temperature was lowered from 25°C to 20°C on three different dates (20 August, 22 September and 8 January) and from 20°C to 15°C after a month or less. The sea urchins grew to 27–30 mm in test diameter in January. In all the three groups, the testes and ovaries of almost all individuals fully matured 3 months after the first temperature drop (Fig. 5).

DISCUSSION

We have previously shown [18] that in *Pseudocentrotus depressus* kept at 20°C, the gonads reached full maturity within a year under all the photic conditions tested (LL, DD, and in-phase and out-of-phase photoperiods) and that in *Hemicentrotus pulcherrimus* kept under LL and DD at ambient temperatures, the gonads matured simultaneously with those of the control animals kept under the ambient photoperiod at ambient temperatures. In the present experiments, the gonads of *H. pulcherrimus* matured under LL after stepwise drops of temperature from 25°C to 15°C. In contrast to these two species, *Anthocidaris crassispina* has the breeding season in summer. In this species also, the gonads matured under DD as well as LL simultaneously with those of the control animals kept under the ambient photoperiod. These results strongly suggest that the photoperiod is not the environmental factor controlling the annual reproductive cycle in these three sea urchin

FIG. 4. The stages of the gonads of *Hemicentrotus pulcherrimus*. Each symbol represents one individual. Sea urchins were reared from zygotes of the same batch fertilized on 22 March 1987 and were kept under constant illumination at 20°C until they were transferred on 30 June 1987 to one of the following experimental conditions: ambient temperatures under ambient light (control), and constant 25°C (25→15 LL), 20°C (20 LL) and 15°C (15 LL) under continuous light. The water temperature for the 25°C groups (25→15 LL) were lowered to 15°C via a short interval of 20°C on three different dates. The change in sea water temperature near the Ushimado Marine Laboratory is shown at the top.





species.

In *A. crassispina*, the gonad became ripe at constant 20°C and 25°C but did not at 15°C. In *P. depressus*, which have mature gonads in fall in the field, the gonads reached maturity at constant 20°C [18]. The gonads of *H. pulcherrimus*, however, remained immature when the animals were kept at constant temperatures even if the temperature (15°C) fell in the range of that of the breeding season (winter); gametogenesis proceeded after the temperature was lowered from 25°C to 15°C. These results suggest that in these species warm water temperatures are generally necessary for some preparatory processes of gametogenesis, e.g., accumulation of nutritive materials in the gonad, and that there is a species specific temperature range that permits the progression of gametogenesis; water temperature such as 15°C may be too cold for the preparation of gonadal maturation. In *P. depressus* [18] and *A. crassispina*, the gonads matured even if individuals were kept under a constant environment (LL at 20°C) from the beginning of their lives. This fact indicates that no external cues are necessary for their gonads to start maturation. Also in *H. pulcherrimus* warm water temperature (20 and 25°C) may be necessary for some preparatory processes of gametogenesis. In the juveniles of *H. pulcherrimus* that had experienced warm water temperatures only for a relatively short period (2 months in 25°C and 1 month in 20°C), the ovaries could not reach the fully mature state (Fig. 4). Three months' stay in the warm temperatures may be too short for the ovaries to store enough nutritive materials, which may be more crucial for oogenesis than for spermatogenesis. In this species warm water temperatures may suppress the progression of gametogenesis. The gonadal maturation did not proceed when animals were kept in 20 or 25°C. Cochran and Engelmann [14] reported that the water temperature in excess of 17°C suppressed the gametogenesis in *S. purpuratus*.

The results shown in Figure 5 are practically

important. We can obtain gametes of *H. pulcherrimus* at any time of the year we want by transferring the sea urchins kept in warm water into cold water about three months before.

The response of the gonad to environmental conditions in *S. purpuratus* is in sharp contrast to those in our three Japanese sea urchins. *S. purpuratus* has mature gonads in winter along the Pacific coast of North America [2, 5]. Cochran and Engelmann [14] have reported that experimental temperature drops can not stimulate gametogenic activity of this sea urchin. Booloottian [12], Pearse *et al.* [16] and Bay-schmith and Pearse [17] have demonstrated that the gonad of *S. purpuratus* is under photoperiodic control; short day photoperiods induce gonadal maturation. Seasonal changes in sea water temperatures are small on the Pacific coast of North America; the monthly means of sea temperatures at Santa Cruz, California, where the experiments by Pearse' group [16, 17] were carried out, range 12 to 17°C [22]. In such an environment, not the water temperature but the photoperiod may become the main factor to control the annual reproductive cycle. It has been reported [22-24] that gametogenesis in two species of sea stars from the Pacific coast of California is also regulated by the photoperiod. Seasonal changes in sea temperature are more conspicuous along the coast of Japan than along the Pacific coast of North America; monthly means near the Ushimado Marine Laboratory range 9 to 26°C. In such an environment, not the changes in the photoperiod but in the water temperature may be important as the environmental factor to regulate the annual reproductive cycles of sea urchins.

ACKNOWLEDGMENTS

We thanks Messrs. Masao Isozaki and Waichiro Godo of this marine laboratory for their help in rearing and maintenance of sea urchins. This work was supported by a Grant-in-Aid for Special Project Research from the Ministry of Education, Science and Culture (No. 62124037).

Fig. 5. The stages of the gonads of *Hemicentrotus pulcherrimus*. Each symbol represents one individual. Sea urchins were reared from zygotes of the same batch fertilized on 29 March 1986 and kept in an outdoor tank from 30 June 1986 to 20 May 1987, when they were transferred to ambient temperatures under ambient light (control) or to 25°C under continuous light (25→15LL). The water temperature for the 25°C groups (25→15 LL) was lowered to 15°C via a short interval of 20°C on three different dates.

REFERENCES

- 1 Yoshida, M. (1952) Some observations on the maturation of the sea urchin, *Diadema setosum*. Annot. Zool. Japon., **25**: 265–271.
- 2 Boolootian, R. A. (1966) Reproductive physiology. In "Physiology of Echinodermata". Ed. by R. A. Boolootian, Interscience Publishers, New York/London/Sydney, pp. 465–486.
- 3 Holland, N. D. (1967) Gametogenesis during the annual reproductive cycle in a cidaroid sea urchin (*Stylodidaris affinis*). Biol. Bull., **133**: 578–590.
- 4 Pearse, J. S. (1969) Reproductive periodicities of Indo-Pacific invertebrates in the Gulf of Suez. II. The echinoid *Echinometra mathaei* (de Blainville). Bull. Mar. Sci., **19**: 580–613.
- 5 Gonor, J. J. (1973) Reproductive cycles in Oregon populations of the echinoid, *Strongylocentrotus purpuratus* (Stimpson) I. Annual gonad growth and ovarian gametogenic cycles. J. Exp. Mar. Biol. Ecol., **12**: 45–64.
- 6 Mori, T., Tsuchiya, T. and Amemiya, S. (1980) Annual gonadal variation in sea urchins of the order Echinothurioida and Echinoidea. Biol. Bull., **159**: 728–736.
- 7 Iliffe, T. M. and Pearse, J. S. (1982) Annual and lunar reproductive rhythms of the sea urchin, *Diadema antillarum* (Philippine) in Bermuda. Int. J. Invertebr. Reprod., **5**: 139–148.
- 8 Falk-Petersen, I. B. and Lønning, S. (1983) Reproductive cycles of two closely related sea urchin species, *Strongylocentrotus droevachiensis* and *S. pallidus*. Sarsia, **68**: 157–164.
- 9 Lessios, H. A. (1985) Annual reproductive periodicity in eight echinoid species on the Caribbean coast of Panama. In "Echinodermata". Ed. by B. F. Keegan and B. D. S. O'Connor, A. A. Balke-ma, Boston, pp. 302–211.
- 10 Nichols, D., Bishop, G. M. and Sime, A. A. T. (1985) Reproductive and nutritional periodicities in populations of the European sea urchin, *Echinus esculentus* (Echinodermata: Echinoidea) from the English channel. J. Mar. Biol. Ass. U. K., **65**: 203–220.
- 11 Hori, R., Phang, V. P. E. and Lam, T. J. (1987) Preliminary study on the pattern of gonadal development of the sea urchin, *Diadema setosum*, off the coast of Singapore. Zool. Sci., **4**: 665–673.
- 12 Boolootian, R. A. (1963) Response of the testes of purple sea urchins to variations in temperature and light. Nature, **197**: 403.
- 13 Boolootian, R. A. (1964) Die Bedeutung abiotischer Faktoren für die Gonadenentwicklung und Fortpflanzung mariner Evertrebraten. Helgolander wiss. Meeresuntersuch., **10**: 118–139.
- 14 Cochran, R. C. and Engelman, F. (1975) Environmental regulation of the annual reproductive season of *Strongylocentrotus purpuratus* (Stimpson). Biol. Bull., **148**: 393–401.
- 15 Leachy, P. S., Hough-Evans, B. R., Britten, R. J. and Davidson, E. (1981) Synchrony of oogenesis in laboratory-maintained and wild populations of the purple sea urchin (*Strongylocentrotus purpuratus*). J. Exp. Zool., **215**: 7–22.
- 16 Pearse, J. S., Pearse, V. B. and Davis, K. K. (1986) Photoperiodic regulation of gametogenesis and growth in the sea urchin *Strongylocentrotus purpuratus*. J. Exp. Zool., **237**: 107–118.
- 17 Bay-Schmith, E. and Pearse, J. S. (1987) Effect of fixed daylengths on the photoperiodic regulation of gametogenesis in the sea urchin *Strongylocentrotus purpuratus*. Int. J. Invertebr. Reprod. Dev., **11**: 287–294.
- 18 Yamamoto, M., Ishine, M. and Yoshida, M. (1988) Gonadal maturation independent of photic conditions in laboratory-reared sea urchins, *Pseudocentrotus depressus* and *Hemicentrotus pulcherrimus*. Zool. Sci., **5**: 979–988.
- 19 Kakuda, N. and Nakamura, T. (1975) Studies on the artificial seedling of the sea urchin. II. On the food for larvae of *Pseudocentrotus depressus*. The Aquiculture, **22**: 56–60. (In Japanese)
- 20 Kakuda, N. (1978) Studies on the artificial seedling of the sea urchin. III. On mass culture of pluteus larvae. The Aquiculture, **25**: 121–127. (In Japanese)
- 21 Kakuda, N. (1978) Studies on the artificial seedling of sea urchin. IV. On culture of juvenile sea urchins. The Aquiculture, **25**: 128–133. (In Japanese)
- 22 Pearse, J. S., Earnisse, D. J., Pearse, V. B. and Beauchamp, K. A. (1986) Photoperiodic regulation of gametogenesis in sea stars, with evidence for an annual calendar independent of fixed daylength. Amer. Zool., **26**: 417–431.
- 23 Pearse, J. S. and Beauchamp, K. A. (1986) Photoperiodic regulation in a brooding sea star from central California. Int. J. Invertebr. Reprod. Dev., **9**: 289–297.
- 24 Pearse, J. D. and Earnisse, J. D. (1982) Photoperiodic regulation of gametogenesis and gonadal growth in the sea star *Pisaster ochraceus*. Mar. Biol., **67**: 121–125.

In vitro Viability and Fertilizing Capacity of Guinea Fowl Spermatozoa

NOBORU FUJIHARA, HISAYOSHI NISHIYAMA¹

and OSAMU KOGA

Department of Animal Science, Kyushu University, Hakozaki, Fukuoka 812, and

¹Department of Animal Science, Kyushu Tokai University,
Kumamoto 869-14, Japan

ABSTRACT—*In vitro* viability and fertilizing capacity of guinea fowl spermatozoa were examined by the method of storing semen at 0°C (in ice). Freshly ejaculated undiluted guinea fowl spermatozoa survived for only three days, in clear contrast to those which were diluted with a phosphate buffer and retained their motility for up to ten days. The number of abnormal spermatozoa increased considerably during the period of preservation of undiluted semen. A relatively high fertility was obtained from both undiluted and diluted semen when they were inseminated shortly after collection and dilution. Duration of fertility of spermatozoa declined from 15 days to 11 days owing to the dilution of semen with the phosphate buffer. The fertilizing capacity of undiluted stored spermatozoa was severely impaired, and their duration of fertility was less than half of that of the diluted unstored ones. The damaged fertility and reduced duration of fertility of stored spermatozoa are likely to be associated with the increased number of deformed spermatozoa during storage.

INTRODUCTION

Male guinea fowl (*Numida meleagris*) have been reported to eject only a negligible amount of accessory reproductive fluid during ejaculation [1], though they possess a special tissue in the ventral cloaca [2] similar to the vascular tissue in roosters [3], the EGR (ejaculatory groove region) in drakes [4] and the TVP (tissue at the vicinity of the papilla of the ductus deferens) in male turkeys [5].

The above-mentioned male birds with the exception of guinea fowl, produce a lymph-like fluid in the cloacal region which is ejected concomitantly with semen during natural copulation and manual semen collection [4, 6–12]. The lymph-like fluid is sometimes called the accessory reproductive fluid in male birds. Roosters and male turkeys eject a tiny quantity of frothy fluid (foam) in addition to a considerable volume of the lymph-like fluid at the time of semen collection [12, 13]. Male quail have foam glands in the cloaca which

produce a foam that is ejected with semen at ejaculation [14–17]. In the male pigeon, on the other hand, little or no lymph-like fluid is added to the ejaculated semen (Fujihara, unpubl. data). These findings suggest that the chemical properties of ejaculated semen of male birds may be modified, depending upon the presence or absence of the fluid which is added to semen during copulation.

On the one hand, the seminal plasma amino acids and protein profiles of the guinea fowl have been shown to be similar to those reported for the chicken and turkey [18]. This result might be obtained from the analysis of cock and turkey semen which were collected without addition of the accessory reproductive fluid, suggesting the possibility that these semen samples might be identical in their components to the ductus deferens semen. In the previous report, however, we have confirmed that ejaculated guinea fowl semen were comparable in semen volume and sperm density to the ductus deferens semen [1]. These results lead us to infer that guinea fowl semen may be different in its quality from that of other

domestic poultry. The present study was undertaken in an attempt to see if guinea fowl spermatozoa have special features peculiar to this species, by examining for *in vitro* viability and fertilizing capacity of spermatozoa.

MATERIALS AND METHODS

Animals

Mature male and female guinea fowl were housed individually in wire cages similar to those used for the rearing of chicken hens, given food and water *ad libitum*, and subjected to a daily photoperiod of 14 hr light/10 hr dark. The diet used here were consisted of the same commercial feed as for laying hens. Egg production was recorded on a daily basis. Male birds were handled for several days prior to the experiment to accustom them to ejaculation by the manual massage method.

Semen samples

The lumbo-sacral massage method available for roosters as a one-man technique [19] was applied to obtain semen from male guinea fowl because we failed to induce male birds to copulate naturally. As guinea fowl semen were very small in volume, the operator aspirated the semen as it appeared at the tip of the copulatory appendage. Semen samples were collected from at least 6 males. Artificially collected semen were pooled immediately after collection and divided equally into two aliquots, one for the undiluted semen group and the other for semen diluted with a phosphate buffer [20] at a semen:extender ratio of 1:3. Sampled semen were placed in test tubes and covered with a piece of aluminum foil.

One part of each aliquot was used to inseminate females immediately after preparation, and the other part was stored in a thermos jar containing ice (0°C) for a given period of time.

Survivability of spermatozoa in vitro

To assess motility and viability of spermatozoa, an aliquot of sperm suspension stored at 0°C (in ice) was taken out at 24 hr intervals and the remainder of each sperm suspension was preserved

for further determination of motility and survival time of spermatozoa. Motility of stored spermatozoa was examined by the method of hanging-drop after warming an aliquot of semen to room temperature (24–27°C). The method used for sperm motility measurement was a microscopic visual score of 0 to 5, with 5 representing the highest motility [21]. Measurement of motility at regular intervals was continued until all spermatozoa halted their motile activity.

Morphology of spermatozoa

Morphology and percent abnormality of spermatozoa were determined at a given interval by the staining method described below. One drop of sperm suspension was spread over a slide glass with a coverslip. Spermatozoa smeared over the slide glass were immediately fixed for 1 to 3 hr in a vapor of formalin and then air-dried, after which spermatozoa were stained with carvol-fuchsin solution. Spermatozoan morphology was observed with a light microscope and photographed. Percent abnormality of spermatozoa was calculated by the number of spermatozoa over 1,000 sperm cells on the stained slide glass. Types of malformed spermatozoa were categorized according to the previous reports [10, 22, 23].

For scanning electron microscopy, one aliquot of sperm suspension stored in ice was taken out and washed twice with the phosphate buffer [20] then resuspended in the same buffer solution. A small quantity of sampled semen was dropped on a thin coverslip, spread over, fixed in a vapor of formalin as mentioned above, then air-dried at room temperature. Spermatozoa on the coverslip were further fixed in 2.5% glutaraldehyde in a phosphate buffer [24] for 2 hr at 4°C. The coverslip with spermatozoa was then washed twice with the phosphate buffer and dehydrated, using a graded ethyl alcohol series. The specimens were subsequently critical point-dried and then sputter-coated with gold palladium. Scanning electron micrographs were obtained using a Hitachi SSM-2 microscope operating at 20 Kv.

Fertilizing power of spermatozoa

Aliquots of freshly ejaculated semen, semen diluted 1:3 with the phosphate buffer and semen

stored at 0°C were used for examination of the fertilizing capacity of spermatozoa. Each type of semen sample was inseminated intravaginally, applying the same basic technique as used for chickens, with minor modifications. Briefly, pressure on the abdomen is applied by holding the female between the hands, the oviduct is everted with one hand and insemination carried out with the other. A tuberculin syringe (1.0 ml) calibrated to 0.01 ml divisions, connected with a piece of rubber tubing attached to the end of a syringe with a small glass semen holder (cannula) inserted into the vagina, has been used with success. The semen was most successfully deposited in the vagina at a depth of about 3 to 5 cm. The number of spermatozoa inseminated was adjusted to be equal to the various semen groups by controlling the volume of inseminated semen. Eggs were saved daily for a given period, beginning the second day following single insemination, and incubated weekly in a similar fashion to the method used for hen's eggs, followed by candling after 5 days of incubation. Eggs thought to be infertile were broken open and examined macroscopically for evidence of embryonic development. Duration of the fertility of spermatozoa was determined by mean values of the period (days) in which fertile eggs were produced.

Statistical analysis

The reproduction results, after transformation to arcsine values, were statistically analysed using analysis of variance. If these analyses for variance revealed significance, Student's *t*-test at $P:0.05$ was given [25].

RESULTS

In vitro survival time of spermatozoa

The results shown in Figure 1 reveal that freshly ejaculated undiluted spermatozoa of guinea fowl survived for three days, while those diluted with the phosphate buffer retained their motility for ten days. A definite difference between the two semen groups was also found in sperm motility. Spermatozoa suspended in the buffer solution maintained considerably higher motile activity through their

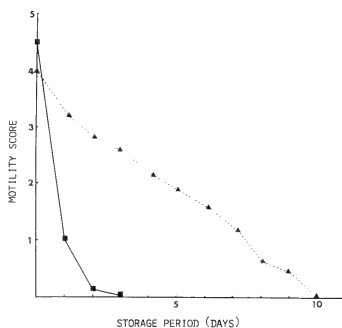


Fig. 1. Viability of guinea fowl spermatozoa preserved at 0°C.

■—■ Undiluted semen. ▲—▲ Semen diluted 1:3 with phosphate buffer.

survival, in clear contrast to the undiluted semen in which the motility of spermatozoa declined rapidly after one day of preservation at 0°C (in ice) (Fig. 1). The difference in sperm motility and survival time between undiluted and diluted semen samples was statistically significant ($P < 0.05$).

In the course of preservation of sperm suspension in ice, the number of abnormal spermatozoa in undiluted semen increased markedly: more than 80 percent of the spermatozoa were deformed at the end of the storage period. Percent abnormality of stored spermatozoa increased along with the prolonged preservation period: even in diluted semen, a considerable number of abnormal spermatozoa was observed towards the end of the preservation period.

Figure 2 shows the rate of deformed spermatozoa on the first day of preservation, being 70% in the undiluted semen group and 40% in the semen diluted (1:3) with the optimal diluter. The obvious difference between the two semen groups was statistically significant ($P < 0.05$). Most of the deformed spermatozoa observed at the beginning of storage were crooked-necked [23] or neck-bent [10] spermatozoa (Fig. 3). The deformed spermatozoa with crooked or bent necks were characterized by the fact that their heads and tails were so closely bent to each other on the middle-piece that they appeared as almost straight lines, just like

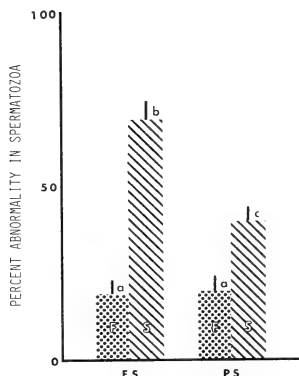


FIG. 2. Percentage of abnormal spermatozoa in fresh and stored guinea fowl semen.

ES, ejaculated semen; PS, semen diluted 1:3 with phosphate buffer. F, fresh semen; S, semen stored for 24 hr at 0°C. Values with different letters are significantly different ($P < 0.05$).

normal spermatozoa. The crooked-necked spermatozoa showed forward movement, just as normal ones did, and their motility and viability were

the same. The percentage of abnormal spermatozoa in semen increased with the lapse of storage time and its incidence was greater when semen was undiluted and stored than when it was diluted with the phosphate buffer (Fig. 2). Malformed spermatozoa other than the neck-bent ones, i.e. detached head, deformed mid-piece, abnormal tail [22] also increased in number with prolonging storage period. Another peculiarity to guinea fowl spermatozoa was that a small number of spermatozoa possessed swollen heads (Fig. 4). The general morphology of normal guinea fowl spermatozoa was quite similar to that of other domestic birds (Fig. 5).

Fertilizing capacity of spermatozoa

Table 1 shows that a relatively high fertility was obtained from both undiluted and diluted semen when inseminated shortly after collection and treatment, though there was no significant difference ($P > 0.05$) between the two semen types. One major difference between undiluted and diluted semen groups was seen in the duration of fertility, which was 15.2 days for undiluted semen and 10.9 days for diluted semen (Table 1). A statistical difference ($P < 0.05$) was found between the two semen samples.

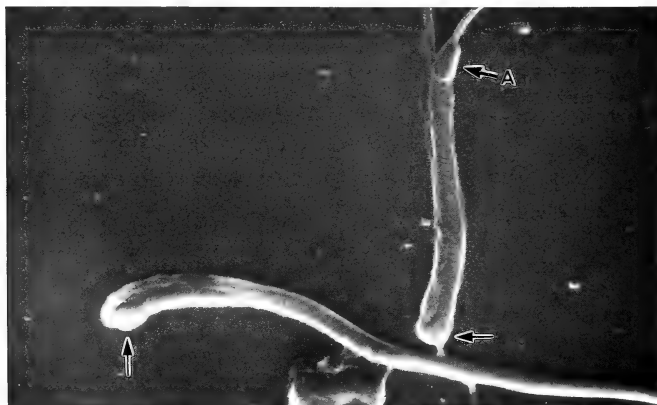


FIG. 3. Deformed guinea fowl spermatozoa with crooked neck (arrows). Note that the head and tail were so closely bent to each other upon middle-piece. A, acrosome. $\times 4750$.

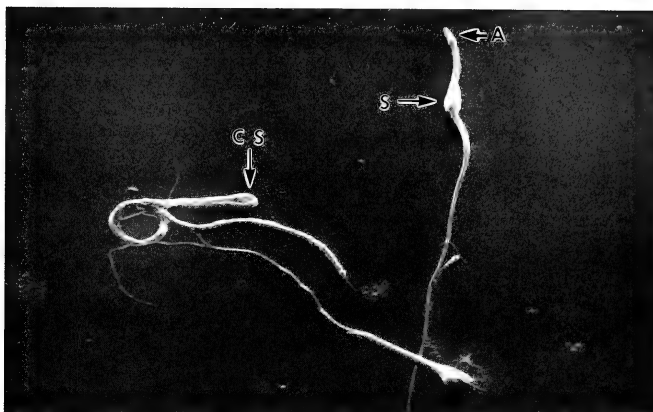


Fig. 4. Abnormal guinea fowl spermatozoa with crooked neck (CS), and swollen head (S). A, acrosome. $\times 1690$.

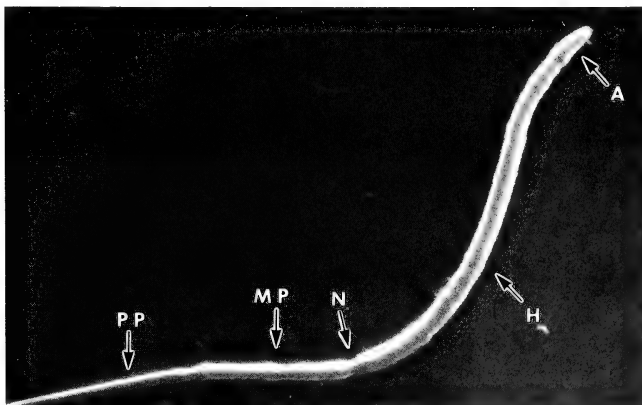


Fig. 5. Scanning electron micrograph showing morphologically normal guinea fowl spermatozoon. A, acrosome; H, head; MP, middle-piece; N, neck; PP, principal piece. $\times 5890$.

Compared to freshly ejaculated spermatozoa, the fertilizing capacity of undiluted and stored spermatozoa was severely impaired (Table 1). Even for semen extended with optimal buffer solution, the percentage of fertility was lower

when semen samples were preserved at a low temperature (0°C). Duration of fertility of diluted preserved spermatozoa (5.7 days) was half that of diluted unstored ones (10.9 days) (Table 1). Most of the females which received undiluted stored

TABLE 1. Percentage of fertile eggs after single insemination with fresh and stored semen of guinea fowl

Semen	No. of females inseminated	No. of sperm inseminated ($\times 10^6$)	Percent fertile (%)	Duration of fertility (Days)
Fresh				
Undiluted	6	68	68.3 ^a	15.2 ^a
Diluted*	8	64	66.8 ^a	10.9 ^b
Stored**				
Undiluted	6	62	3.7 ^b	1.2 ^b
Diluted*	6	62	44.8 ^a	5.7 ^a

*Semen were diluted with a phosphate buffer (1:3).

**Semen were stored for 24 hr in a thermos jar containing ice.

a,b Values within each column with different superscripts are significantly different ($P < 0.05$).

semen produced no fertile eggs after single insemination, thus resulting in very short duration of fertility on average. Semen diluted with the phosphate buffer and stored had considerably higher fertility (44.8%) than undiluted stored semen (3.7%), but duration of fertility (5.7 days) was reduced noticeably in comparison with unstored semen groups (10.9 days).

DISCUSSION

In vitro viability of undiluted guinea fowl spermatozoa was maintained for only three days, in clear contrast to those which were diluted with the phosphate buffer and retained their motility for up to ten days (Fig. 1). This suggested that freshly ejaculated undiluted guinea fowl spermatozoa were unable to withstand *in vitro* storage for a long period of time in comparison with spermatozoa from roosters, drakes and male turkeys in which spermatozoa survived for a considerable period of time even when their semen were not diluted with semen extender [26-28]. Judging from sperm motility and viability, guinea fowl spermatozoa seem to be quite different from those from other domestic birds. It is not known what factors are responsible for the shorter life span of undiluted spermatozoa of guinea fowl during storage.

As reported previously [1], only a negligible amount of the lymph-like fluid was added to guinea fowl semen at the time of ejaculation, indicating that ejaculated guinea fowl semen is

more or less comparable in its component to the ductus deferens semen. This means that the ductal spermatozoa of guinea fowl is strikingly poor in storability *in vitro*. Undiluted ductus deferens spermatozoa from male turkeys and drakes remained motile *in vitro* for a period ranging from 10 to 15 days, a period similar to those diluted with the accessory reproductive fluid and the phosphate buffer [27, 28].

Spermatozoa from the ductus deferens of pigeon and quail could not withstand *in vitro* storage when they were not diluted (Fujihara, unpubl. observation). These results indicate that spermatozoa from guinea fowl, quail and pigeon have some characteristics in their function which differ from spermatozoa from other domestic birds. The vas deferens fluid is considered in general to be an isotonic, physiological medium for spermatozoa, but if the frequency of ejaculation is not optimal, the chemical environment in the vas deferens is not likely to be ideal for the survival of spermatozoa [29]. The difference in life span of spermatozoa between guinea fowl (in this study) and other male birds may be attributed to the natural characteristics inherent in spermatozoa from the respective species of birds.

As for fertilizing capacity of spermatozoa, a few studies have centered on fertilizability of guinea fowl spermatozoa. The fertility (68.3%) of freshly ejaculated undiluted guinea fowl spermatozoa reported here was considerably lower than that (90%) reported previously [30]. This value was

also small in comparison with the fertility of spermatozoa from roosters, turkeys and drakes which have so far been reported by investigators. The lowered fertility of guinea fowl sperm in this study may be partly due to the small number of sperm inseminated. On the contrary, the duration of fertility (15.2 days) of guinea fowl spermatozoa described here was a little longer than the value reported by Belshaw [31] who noted seven days as the fertile period for guinea fowl spermatozoa.

On the other hand, undiluted stored guinea spermatozoa lost its fertilizing capacity after two days of preservation. Even semen extended with optimal buffer solution showed impaired fertility following preservation for 24 hr at a low temperature despite the fact that spermatozoa could remain motile for as long as ten days.

In the past, many attempts have been made to find diluent media, the ideal temperature for preservation and other physical conditions for the prolonged storage of avian semen. The best fertility results were always obtained when diluted semen was used within a very short time after collection. The reason for the rapid reduction in fertilizing ability of preserved avian sperm has yet to be clarified. For reviews of poultry semen preservation and factors affecting fertility with artificial insemination, the reader should refer to Cooper [32, 33], Lake [34-36] and Sexton [37].

Even in mammalian spermatozoa stored at a low temperature, fertility correlated very poorly with motility. Low temperature storage of liquid semen could yield spermatozoa of apparently good motility and percentage motile, but of low fertility [38].

From the morphological point of view, increased numbers of crooked-necked or bent-neck spermatozoa were observed in stored guinea fowl semen, as is also the case in semen from cocks [10, 23], drakes [27] and male turkeys [28]. Guinea fowl spermatozoa with bent-neck were still strongly motile, just like normal spermatozoa were, but incapable of fertilizing eggs. Higher incidence of deformed spermatozoa in guinea fowl semen stored *in vitro* was thought to be associated with lowered fertility. A similar phenomenon to this has been demonstrated in semen from drakes [27] and male turkeys [28]. Significant ($P < 0.01$) correlation has also been observed between crooked-

necked spermatozoa and fertility in chickens and turkeys [23, 39]. It is, thus, considered that in avian spermatozoa, motility score is a poor indicator of fertility, and that the number of abnormal spermatozoa may give a better indication of fertility than estimation of visual motility.

The reports on the fluid contained in ejaculated avian semen suggest that the lymph-like fluid and frothy fluid (foam) originated in the cloacal region of male birds may not always be indispensable for semen and spermatozoa. Based on these findings, guinea fowl and pigeon, which do not produce fluids in the cloacal region, may be considered to be unique in the production of semen and sperm physiology.

ACKNOWLEDGMENTS

The skilled technical assistance provided by Mr. N. Yoshihiro was greatly appreciated.

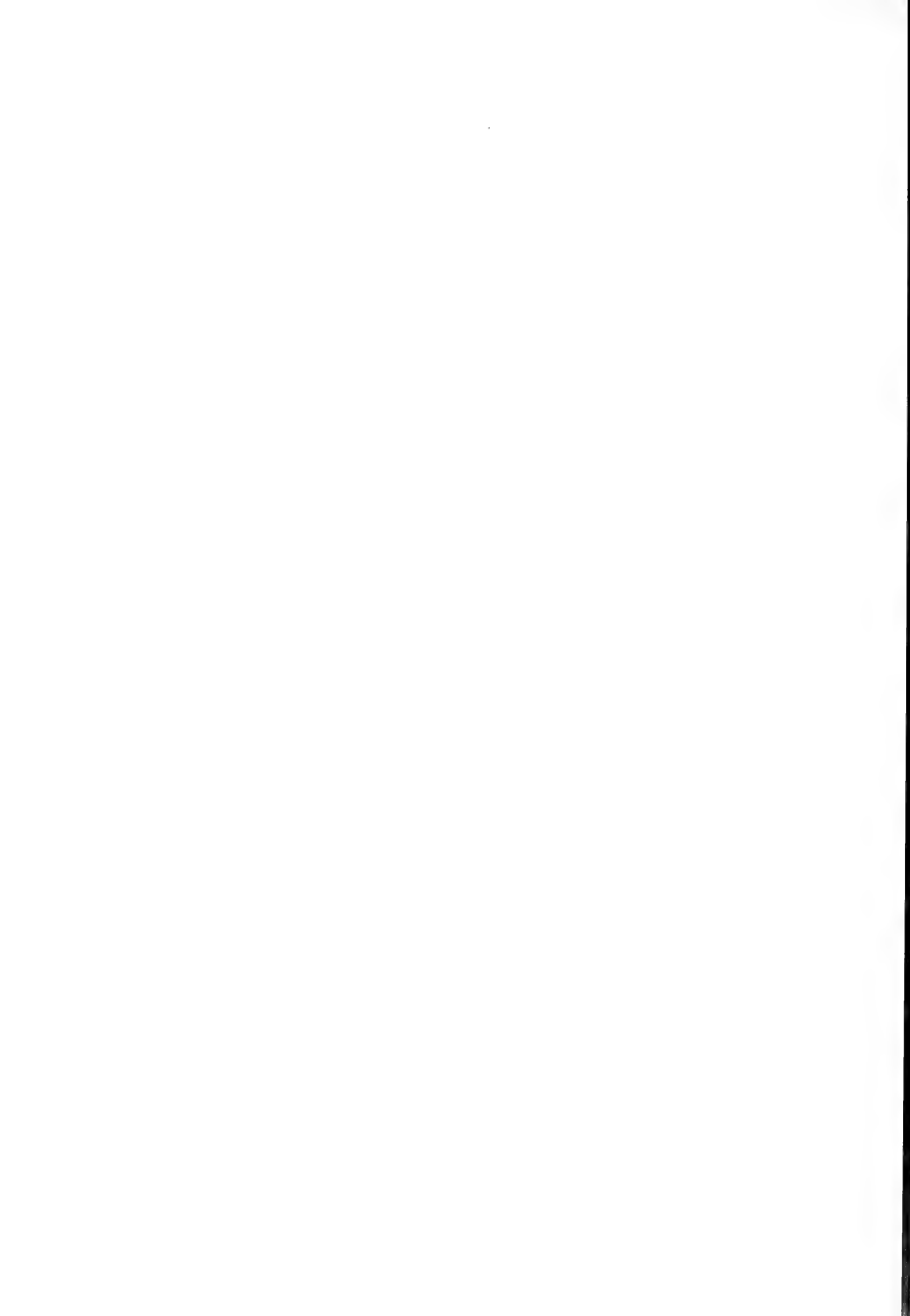
REFERENCES

- 1 Fujihara, N., Nishiyama, H. and Koga, O. (1986) Characteristics of artificially ejaculated and ductus deferens semen in the guinea-fowl. *Anim. Reprod. Sci.*, **12**: 69-74.
- 2 Fujihara, N., Nishiyama, H. and Koga, O. (1988) Anatomical features of cloacal region of male guinea fowl with special reference to the ejection of lymph-like fluid. *Anat. Anz. Jena*, **167**: 341-347.
- 3 Lake, P. E. and El Jack, M. H. (1966) The origin and composition of fowl semen. In "Physiology of the Domestic Fowl". Ed. by C. Horton-Smith and E. C. Amoroso, Oliver & Boyd, Edinburgh, pp. 44-51.
- 4 Nishiyama, H., Nakashima, N. and Fujihara, N. (1976) Studies on the accessory reproductive organs in the drake. 1. Addition to semen of the fluid from the ejaculatory groove region. *Poultry Sci.*, **55**: 234-242.
- 5 Fujihara, N., Nishiyama, H. and Koga, O. (1986) Localization of frothy fluid-producing region in the cloaca of male turkey. *Anat. Anz. Jena*, **162**: 359-366.
- 6 Nishiyama, H. (1955) Studies on the accessory reproductive organs in the cock. *J. Fac. Agr. Kyushu Univ.*, **10**: 277-306.
- 7 Nishiyama, H. (1961) On the quality and quantity of the cock semen obtained by different collection methods. *Mem. Fac. Agr. Kagoshima Univ.*, **4**: 43-50.

- 8 Nishiyama, H. and Fujishima, T. (1961) On the ejection of the accessory reproductive fluid of the cock during natural copulation. Mem. Fac. Agr. Kagoshima Univ., 4: 27-42.
- 9 Nishiyama, H. and Ogawa, K. (1961) On the function of the vascular body, an accessory reproductive organ, of the cock. Jap. J. Zootech. Sci., 32: 89-98.
- 10 Yamane, J., Tsukunaga, S. and Takahashi, T. (1966) "Hiroshima" method of artificial insemination of the domestic fowl. J. Fac. Fish. Anim. Husb. Hiroshima Univ., 6: 395-429.
- 11 Knight, C. E., Lucas, A. M. and Ringer, R. K. (1969) Anatomy of structures involved in the production of seminal fluid in the chicken. Poultry Sci., 48: 1830-1831. (Abstract)
- 12 Fujihara, N. and Nishiyama, H. (1984) Addition to semen of a fluid derived from the cloacal region by male turkeys. Poultry Sci., 63: 554-557.
- 13 Fujihara, N., Nishiyama, H. and Koga, O. (1985) The ejection of a frothy fluid from the cloacal region of rooster during manual semen collection. Can. J. Anim. Sci., 65: 985-988.
- 14 Ikeda, K. and Taji, K. (1954) On the foamy ejaculate of Japanese quail, *Coturnix coturnix japonica*. Sci. Rep. Matsuyama Agr. Coll., 13: 1-4.
- 15 Coil, W. H. and Wetherbee, D. K. (1959) Observations on the cloacal gland of the Eurasian quail, *Coturnix coturnix*. Ohio J. Sci., 59: 268-270.
- 16 Nagra, C. L., Meyer, R. K. and Bildstad, N. (1959) Cloacal glands in Japanese quail (*Coturnix coturnix japonica*): histogenesis and response to sex steroids. Anat. Rec., 133: 415. (Abstract)
- 17 Klemm, R. D., Knight, C. E. and Stein, S. (1973) Gross and microscopic morphology of the *glandula proctodealis* (foam gland) of *Coturnix c. japonica* (Aves). J. Morph., 141: 171-184.
- 18 Thurston, R. J., Hess, R. A., Hughes, B. L. and Froman, D. P. (1982) Seminal plasma free amino acids and seminal and blood plasma proteins of the guinea fowl (*Numidia meleagris*). Poultry Sci., 61: 1744-1747.
- 19 Bogdonoff, P. D. and Shaffner, C. S. (1954) The effect of pH on *in vitro* survival, metabolic activity, and fertilizing capacity of chicken semen. Poultry Sci., 33: 665-669.
- 20 Wilcox, F. H. and Shaffner, C. S. (1958) The effect of different handling methods and added fructose on the fertilizing ability of chicken spermatozoa after storage. Poultry Sci., 37: 1353-1357.
- 21 Wheeler, N. C. and Andrews, F. N. (1943) The influence of season on semen production in the domestic fowl. Poultry Sci., 22: 361-367.
- 22 Kamar, G. A. R. and Badreldin, A. L. (1959) Sperm morphology and viability. Acta anat., 39: 81-83.
- 23 Saeki, Y. (1960) Crooked-necked spermatozoa in relation to low fertility in the artificial insemination of fowl. Poultry Sci., 39: 1354-1361.
- 24 Millonig, G. (1961) Advantages of a phosphate buffer for OsO_4 solutions in fixation. J. Appl. Physics, 32: 1637. (Abstract)
- 25 Steel, R. G. D. and Torrie, J. H. (1980) Principles and Procedures of Statistics. A biometrical approach. McGraw-Hill, New York, 2nd ed., pp. 86-238.
- 26 Nishiyama, H. (1971) Studies on the artificial insemination in the domestic fowl. III. Sperm concentration of semen at collection and sperm-quality of the semen. Mem. Fac. Agr. Kagoshima Univ., 8: 355-366.
- 27 Fujihara, N. and Nishiyama, H. (1976) Studies on the accessory reproductive organs in the drake. 5. Effects of the fluid from the ejaculatory groove region on the spermatozoa of the drake. Poultry Sci., 55: 2415-2420.
- 28 Fujihara, N., Nishiyama, H. and Koga, O. (1987) Effect on turkey spermatozoa of a frothy fluid derived from the cloaca of a male turkey. Theriogenology, 28: 225-235.
- 29 Lake, P. E. (1966) Physiology and biochemistry of poultry semen. In "Advances in Reproductive Physiology". Ed. by A. McLaren, Logos Press, London, pp. 93-123.
- 30 Bahr, J. M. and Bakst, M. R. (1987) Poultry. In "Reproduction in Farm Animals". Ed. by E. S. E. Hafez, Lea & Febiger, Philadelphia, 5th ed., pp. 379-398.
- 31 Belshaw, R. H. H. (1985) Guinea Fowl of the World. Nimrod Book Services, Hampshire, pp. 55-112.
- 32 Cooper, D. M. (1965) Artificial insemination in poultry. World Poultry Sci. J., 21: 12-22.
- 33 Cooper, D. M. (1969) The use of artificial insemination in poultry breeding, the evaluation of semen and semen dilution and storage. In "The Fertility and Hatchability of the Hen's Egg". Ed. by T. C. Carter and B. M. Freeman, Oliver & Boyd, Edinburgh, pp. 31-44.
- 34 Lake, P. E. (1962) Artificial insemination in poultry. In "The Semen of Animals and Artificial Insemination". Ed. by J. R. Maule, Commonwealth Agr. Bureau, England, pp. 331-356.
- 35 Lake, P. E. (1978) The principles and practice of semen collection and preservation in birds. Symp. zool. Soc. Lond., 43: 31-49.
- 36 Lake, P. E. (1983) Factors affecting the fertility level in poultry, with special reference to artificial insemination. World Poultry Sci. J., 39: 106-117.
- 37 Sexton, T. J. (1979) Preservation of poultry semen—a review. In "Animal Reproduction". Ed. by H. W. Hawk, John Wiley & Sons, New York, pp. 159-170.
- 38 Robertson, L. and Watson, P. F. (1987) The effect

of egg yolk on the control of intracellular calcium in ram spermatozoa cooled and stored at 5°C. *Anim. Reprod. Sci.*, **15**: 177-187.

39 Saeki, Y. and Brown, K. I. (1962) Effect of abnormal spermatozoa on fertility and hatchability in the turkey. *Poultry Sci.*, **41**: 1096-1100.



**Stimulating Influence of Cerebral Ganglia on *in vitro*
Incorporation of Tritiated Leucine into Ovaries of
Eisenia fetida Sav. (Annelida: Oligochaeta)**

CLAUDE LATTAUD and ROGER MARCEL¹

*Laboratoire de Physiologie de la Reproduction, Université Pierre
et Marie Curie, 4 Place Jussieu Bât A, 75252 Paris Cedex 05, and*

¹*Laboratoire d'Endocrinologie Comparée des Invertébrés,
URA CNRS n° 59, Université des Sciences et
Techniques de Lille-Flandres-Artois, 59655
Villeneuve d'Ascq Cedex, France*

ABSTRACT—In sexually active *Eisenia fetida*, gametogeneses are controlled by a cerebral neurohormone. Present results show that the central nervous system (CNS, *i.e.* cerebral ganglia, the circum-oesophageal ring and the ventral nerve cord cut at clitellum level) stimulates the uptake of ³H-leucine by ovaries. Cultured together with CNS, ovaries incorporate twice as much ³H-leucine as when cultured alone. This protein synthesis is independent of the duration of the culture of explants, of their period of incubation with a precursor and of the concentration of this precursor. However, in culture *in vitro*, ovaries syntheses are low as the percentage of incorporation goes from 0.11% in isolated ovaries to 0.22% in ovaries associated with CNS. This confirms that in ovarian oocytes vitellogenesis is low. Among the different ganglia of CNS, the cerebral ganglia alone stimulate the incorporation of ³H-leucine with ovaries.

It is suggested that a same cerebral neurohormone is thought to control cephalic regeneration, clitellogenesis, testis differentiation and ovarian protein metabolism.

INTRODUCTION

During genital activity, the testicular tissues of *Eisenia fetida* secrete an androgen under the control of a neurohormone produced by the central nervous system (C.N.S.) [1, 2]. This hormone is synthesized by the cerebral ganglia [3, 4] which also induce the male and female gametogenetic activity in *Eisenia fetida* [5, 6] and in *Allolobophora icterica* [7]. Moreover, they control, by inhibition, the cephalic regeneration of *E. fetida* [8] and are necessary to the maintaining of clitellum turgescence in mature worms [9]. Several endocrine actions can therefore be attributed to cerebral ganglia in worms of the lumbricid oligochaetes [10]. A cerebral hormone controlling cephalic regeneration and clitellum turgescence has been isolated in *E. fetida* and partly purified

[11-14]. It is a peptidic substance [15] of a molecular weight between 1500 and 2000 [12]. In this species, a purified fraction from the brain stimulates the secretion of testicular androgen [16].

But, previous experiments of organotypic culture had shown that the survival time of a gonad associated to C.N.S. was always longer than that of a gonad cultured on its own. Besides its neurohormonal control of gametogeneses, the C.N.S. also seems to exert a sort of "trophic" effect on metabolism in gonad (testis or ovaries).

Before studying the ways the control mechanisms of gonad function we felt inclined to separate the different parameters. In order to achieve this goal, a simple biological test had first to be defined for the metabolic activity of gonads. The ovary, which does not require the presence of cerebral hormone for its differentiation, was chosen. A low vitellogenesis was found in growing oocytes, the vitelline material being composed of

protein granules together with glycogen particles and fat droplets [17]. This test measured the uptake of tritiated leucine by ovaries of *E. fetida*, cultured on their own or in association with C.N.S. (or different ganglia of C.N.S.).

MATERIALS AND METHODS

Experiments were done on sexually active *Eisenia fetida* Sav. Each culture, composed of 3 ovaries isolated or associated with 3 C.N.S. (i.e. cerebral ganglia, the circum-oesophageal nerve ring and the ventral nerve cord cut at the clitellum level), lasted 4 or 8 days. After culture, explants were incubated in a physiological medium with a radioactive amino-acid, leucine, for 1, 2 or 4 hr. When the ovaries and C.N.S. were associated, they would be incubated together or separately. The controls were composed of 3 ovaries associated with 3 muscle fragments and cultured in the same experimental condition. Ovaries and muscle fragments were then incubated together or separately with leucine. The quantity of muscle was roughly equal to that of a central nervous system. The culture technique and the medium composition have been previously described [18]. The physiological incubating medium was the Holtfreter solution at 8.77‰ (saline solution at 8.13‰ NaCl). This solution is isotonic with the coelomic fluid of *E. fetida*. The tritiated leucine (L-leucine ^3H , 3-4-5; specific activity 5550 GBq/mM; CEA, France) was added to the medium in the proportion of 370, 740 or 1480 kBq/ml of medium. Incubations were done in a Kotterman agitator for 2 hr at 20°C in eppendorf tubes containing 100 μl of solution. After incubation, explants were rinsed in Holtfreter physiological solution, in 3 successive baths of 10 min each at least to wash away the unincorporated leucine. They were then sonicated in the Holtfreter solution and treated in 20% trichloroacetic acid to precipitate the labelled proteins. Total hydrolysis of explants was done in 200 μl of Soluene (Packard). Five ml of scintillating liquid (insta-gel) was added to each sample. Radioactivity was measured by scintillating liquid spectrophotometry in an Inter technique SL 300 counter. In order to take into account the results of the first series, the subsequent experiments needed 4 to 8

days of culture followed by 1, 2 or 4 hr incubation in a medium with a ^3H -Leu concentration of 1110 kBq/ml of physiological solution.

In order to localize the origin of the C.N.S. activity, 3 ganglia of different levels (cerebral ganglia, C.G., sub-oesophageal ganglia, S.O.G., and ganglia of male genital segments, G.G. o and female G.G.o) were cultured with 3 ovaries for 4 days. In the end, each association was incubated for 1 hr in a tritiated leucine solution (1110 kBq/ml), then treated according to the conditions previously described made to measure radioactivity.

The values given by the radioactivity counter were normalized to 1 mg of wet weight for each sample and expressed in counts per minute (cpm). Before we weighed the explants. The average values obtained after weighing 10 organs were: C.N.S. (=C.G.+S.O.G.+ganglia of the first 13 segments)=1.3 mg; C.G.=0.2 mg; S.O.G.=G.G.o=G.G.o=0.1 mg; ovaries=0.1 mg; muscle fragment=1.3 mg. The mean of radioactivity measures on several explants was calculated for each experimental series together with standard deviation. Student's t-test was used to compare the different mean values. Results are shown in tables by + or - indicating that, in comparisons, the differences are significant or not for $p < 0.01$.

RESULTS

A. Measure of *in vitro* incorporation of ^3H -leucine with ovaries associated or not with C.N.S.

Comparison with controls (ovaries+muscles)

1. Explants cultured for 8 days, then incubated for 2 hr in tritiated leucine (concentrations 370, 740 or 1480 kBq/ml)

Results are presented in Table 1 and in Figures 1 and 2. The radioactivity of ovaries associated to C.N.S. (incubated together or separately, columns 2 and 3) was always superior to that of isolated ovaries (col. 1) at whatever concentration of ^3H -Leu (370 to 1480 kBq/ml). Indeed, for these different concentrations, radioactivity increased from 21200 to 66400 cpm/mg of wet weight isolated ovaries (col. 1) while it reached from 56000 to 178000 cpm/mg of wet weight of ovaries incubated with C.N.S. (col. 2) and from 52000 to 230000

TABLE 1. *In vitro* incorporation of ^3H -Leu at different concentrations with ovaries of *E. fetida* associated or not to central nervous system (controls: ovaries associated to muscle). Duration of culture: 8 days; incubation period: 2 hr. Results in cpm/mg wet weight

	Ovaries and CNS associated in culture				Ovaries and muscles associated in culture		
	Ovaries (1)	incubated together (2)	incubated separately		incubated together (5)	incubated separately	
			ovaries (3)	CNS (4)		ovaries (6)	Muscles (7)
370 kBq/ml	21200 ± 1000	56000 ± 150	52000 ± 100	4100 ± 10	27700 ± 100	25000 ± 1000	350 ± 40
	Comparisons with (1)	+	+		-	-	
	56200 ± 14000	74000 ± 500	54000 ± 11000	4300 ± 850	69800 ± 1800	67000 ± 4300	1800 ± 300
740 kBq/ml	66400 ± 18000	17800 ± 1000	232000 ± 150	18100 ± 100	133700 ± 3000	118700 ± 5400	1700 ± 400
	Comparisons with (1)	+	+		+	+	
	81480 kBq/ml						
81480 kBq/ml	Comparisons with (2)				+	+	
	Comparisons with (2)				+	+	
	Comparisons with (3)				+	+	

t-test: + = significant difference for $p < 0.01$; - = not significant difference.

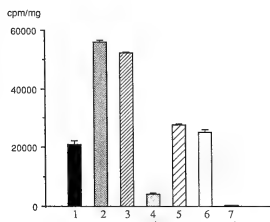


FIG. 1. *In vitro* incorporation of ^3H -Leu ovaries of *Eisenia fetida* associated or not to C.N.S. Duration of culture: 8d; incubation period: 2 hr in a physiological medium with ^3H -Leu (370 kBq/ml). 1: isolated ovaries. 2: ovaries and C.N.S. 3 and 4: ovaries and C.N.S. associated together and incubated separately (3: ovaries, 4: C.N.S.). 5: ovaries and muscle associated and incubated together. 6 and 7: ovaries associated to muscle and incubated separately (6: ovaries, 7: muscles). Ordinate: radioactivity expressed in cpm/mg wet weight.

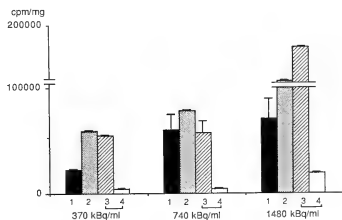


FIG. 2. *In vitro* incorporation of ^3H -Leu ovaries of *Eisenia fetida* associated or not to C.N.S. Duration of culture: 8 days; incubation period: 2 hr in a medium with ^3H -Leu at different concentrations (370, 740 or 1480 kBq/ml). For legend see Fig. 1.

cpm/mg of ovaries incubated independently of C.N.S. (col. 3). The comparison with results obtained in ovaries cultured on their own showed that difference were always significant ($p < 0.01$). It should be noted that in this experimental series (col. 3 and 4) the radioactivity measured in C.N.S. was 12 times below that measured in ovaries: the uptake of radioactive precursor by C.N.S. was small. So C.N.S. stimulate the uptake of ^3H -Leu by ovaries *in vitro* for an amino-acid concentration varying from 370 to 1480 kBq/ml of incubating medium. When ovaries cultured without C.N.S. were incubated with tritiated leucine at a concentration of 370 kBq/ml (i.e. 2×10^6 cpm in 100 μl solution), the radioactivity measured in an ovary of 0.1 mg was 2120 cpm, which corresponds to a low rate of uptake of tritiated leucine (0.11%). Spontaneous protein synthesis by ovaries were very low. In the presence of C.N.S., these protein syntheses correspond to an incorporation rate of 0.26% (col. 3) and of 0.28% (col. 2). Even under the influence of C.N.S., syntheses were still very low. For the same tritiated leucine concentrations, radioactivity in the controls (ovaries cultured and incubated with muscle fragments, col. 5) varied from 27200 to 133700 cpm/mg wet weight. When ovaries and muscles were incubated separately (col. 6) the counting revealed, according to concentration, an increase in radioactivity of 25000 to 118700 cpm/mg wet weight of ovaries and of 350 to 1700 cpm/mg wet weight of muscles. It can be observed that ^3H -Leu of 350 to 1700 cpm/mg wet weight of muscles. It can be observed that ^3H -leucine incorporation by muscle is very low and can be overlooked. Another conclusion is that muscle has no stimulating effect on the incorporation of this amino-acid with ovaries *in vitro*. Indeed, the radioactivity measured in control ovaries (col. 5 and 6) was almost always equal to that in isolated ovaries (col. 1). The differences observed are not significant, except in the experimental series in which the concentration of tritiated leucine is 1480 kBq/ml: the radioactivity of ovary-muscle associations (col. 5 and 6) represented twice (133700 and 118700 cpm/mg) that of isolated ovaries (66400 cpm/mg, col. 1). Nevertheless the Student's t-test revealed that the averages obtained in columns 5 and 6 differed significantly

($p < 0.05$) from those found in column 2 as well as in column 3. Therefore, even in this case, it can be said that muscle has no effect over ovary in culture; statistics confirm that muscle is a good control. Nevertheless the remarkable increase of incorporation by the ovary in this experimental series cannot be explained.

In later experiments, the control series, ovaries and muscle incubated separately (col. 6 and 7) will be suppressed. Indeed, in such experimental conditions, the radioactivity specific to muscle represents less than 3% of the total radioactivity and the sum of the radioactivities of ovaries and muscles is approximately equal to that measured in the ovary-muscle association (col. 5).

From the results of this experimental series, a protocole was chosen from the later series: concentration in ^3H -Leu, 1110 kBq/ml of medium; duration of cultures, 4 and 8 days; incubation period with a radioactive precursor, 1, 2, and 4 hr.

2. Explants cultured for 4 or 8 days, then incubated 1, 2, or 4 hours in a medium with tritiated leucine (concentration 1110 kBq/ml)

Culture and incubation time vary in this experimental series. Results are summed up in Table 2 and Figures 3 and 4. After 4 or 8 days in culture, explants are incubated 1, 2 or 4 hr in a physiological medium with ^3H -Leu (1110 kBq/ml). The radioactivity measured in explants (ovaries and C.N.S. incubated together, col. 3 and 4, or separately, col 5 and 6) is always superior to that found in isolated ovaries (col. 1 and 2). So when ovaries cultured separately for 4 days are incubated 1 to 4 hr in tritiated leucine, the radioactivity goes from 11400 to 46600 cpm/mg wet weight of ovaries (col. 1). In the same conditions, ovaries associated to C.N.S. reveal a radioactivity respectively 2 to 5 times greater, whether incubated together (col. 3) or separately (col. 5). Statistically, the differences are highly significant ($p < 0.01$) and similar to those obtained after 8 days in culture (col. 2, 4, and 6).

It can therefore be concluded that C.N.S. has a stimulating effect on the incorporation of tritiated leucine with ovaries *in vitro*, when explants cultured 4 or 8 days are then incubated for 1 to 4 hr with this amino-acid. It should be noted, without satisfactory explanation, that explants cultured for

TABLE 2. *In vitro* incorporation of ^3H -Leu (1110 kBq/ml) with ovaries of *Eisenia fetida* associated or not to central nervous system (controls: ovaries associated to muscle). Duration of culture: 4 or 8 days; incubation period: 1, 2 or 4 hr. Results in cpm/mg wet weight

Ovaries + CNS associated in culture										Ovaries + muscles associated in culture and incubated together									
Isolated ovaries		incubated together		incubated separately															
				ovaries		CNS													
4d		8d		4d		8d		4d		8d		4d		8d					
(1)		(2)		(3)		(4)		(5)		(6)		(7)		(8)		(9)		(10)	
1 hr	11400 ± 2600	24300 ± 7800	55900 ± 20000	43400 ± 12000	50500 ± 2000	38200 ± 19000	2800 ± 80	3400 ± 1200	13600 ± 5800	19300 ± 4600									
	Compa-	with (1)	+		+				-										
	rison	with (2)		+		+				-									
2hr	36800 ± 8700	16400 ± 6200	56800 ± 16700	40200 ± 3300	50400 ± 3800	49500 ± 7800	5200 ± 100	4200 ± 1800	21200 ± 7000	28200 ± 9700									
	Compa-	with (1)	+		+				-										
	rison	with (2)		+		+				-									
4 hr	46600 ± 13000	68700 ± 23000	79000 ± 20000	71500 ± 10600	79600 ± 42000	97300 ± 25000	8400 ± 1600	13800 ± 4000	43000 ± 15000	51500 ± 20000									
	compa-	with (1)	+		+				-										
	rison	with (2)		+		+				-									

t-test: + = significant difference for $p < 0.01$; - = not significant difference.

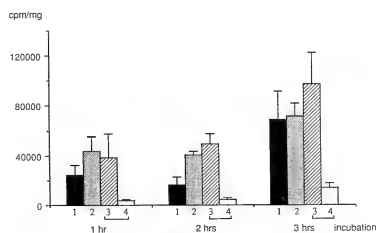


FIG. 3. *In vitro* incorporation of ^3H -Leu ovaries of *Eisenia fetida* associated or not to C.N.S. Duration of culture: 8 days; incubation period of 1, 2 or 4 hr (1110 kBq/ml of medium). For legend see Fig. 1.

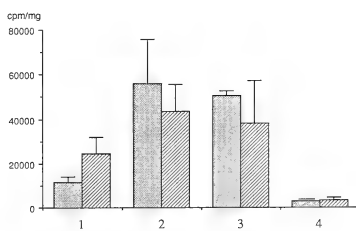


FIG. 4. *In vitro* incorporation of ^3H -Leu ovaries of *Eisenia fetida* associated or not to C.N.S. Duration of culture: 4 or 8 days; incubation period: 1 hr (1110 kBq/ml). Stippled columns: 4 days in culture; striped columns: 8 days in culture. For legend see Fig. 1.

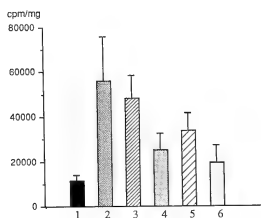


FIG. 5. *In vitro* incorporation of ^3H -Leu (1110 kBq/ml) by ovaries of *E. fetida* associated or not to different ganglia of C.N.S. In associations, ovaries and ganglia were incubated together. Duration of culture: 4 days; incubation period: 1 hr. 1: isolated ovaries; 2: ovaries + C.N.S.; 3: ovaries + C.G.; 4: ovaries + S.O.G.; 5: ovaries + G.G.o; 6: ovaries + G.G.o. Ordinate: radioactivity expressed in cpm/mg wet weight.

8 days do not incorporate a quantity of leucine strictly proportional to the incubation period.

On the other hand, in experimental series (col. 5 to 8) where ovaries are incubated independently of C.N.S. (col. 7 and 8) is low and clearly below (7 to 18 times) that measured in ovaries. It only represents 5 to 12% of the radioactivity of the ovaries and C.N.S. These results are comparable to those present in the previous paragraph (Table 1).

When ovaries and muscles, associated in culture (controls), are incubated together for 1, 2, or 4 hr with tritiated leucine (concentration: 1110 kBq/ml), radioactivity varies from 13600 to 43000 cpm/mg for 4 days in culture (col. 9) and from 19300 to 51500 cpm/mg for 8 days in culture (col. 10). Comparatively the radioactivity measured in isolated ovaries (col. 1 and 2) goes from 11400 to 46600 cpm/mg for 4 days in culture and from 24300 to 68700 cpm/mg for 8 days.

The analysis of previous series (Table 1, col. 7) having shown that the incorporation of tritiated leucine by muscles was negligible, the experiments recorded in Table 2, col. 9 and 10, take into account the ovary-muscle association. Considering that the differences between the mean values of the series 1 and 2, on the one hand, and 9 and 10 on the other hand are not significant, it can be

concluded that muscles have no effect on the incorporation of tritiated leucine with ovaries *in vitro*. These results thoroughly confirm those of previous series (paragraph 1) i.e. muscle is an excellent control. The homogeneity of results enable the selection of a culture duration of 4 days and an incubation period of 1 hr for all subsequent experiments. Moreover, the incorporation specific to C.N.S., on average less than 10% than the total incorporation, can be overlooked and the values which were considered would only concern ovaries + C.N.S. incubated together.

B. Measure of incorporation of tritiated leucine with ovaries *in vitro* associated to different ganglia of C.N.S.

The results presented in the Table 3, correspond to the following experimental conditions: 4 days in culture followed by 1 hr incubation in a physiological medium with ^3H -Leu (1110 kBq/ml). The radioactivities measured in association of ovaries with different parts of C.N.S. (C.G., S.O.G., G.G.o or G.G.o) are respectively of 48200, 25200, 33700 and 19200 cpm/mg wet weight (col. 3 to 6). These values should be compared to the radioactivity previously measured in isolated ovaries (11400 cpm/mg, col. 1) and in ovaries incubated with C.N.S. (55900 cpm/mg, col. 2) in identical experimental conditions. Only the radioactivity of ovary-C.G. associations (col. 3) is almost equal to that of ovaries cultured with C.N.S. (the difference between these values are not significant). On the other hand, it is clearly above that of isolated ovaries (col. 1) (difference highly significant). Besides, the difference between the values of radioactivity of ovaries associated to C.G. (col. 3) or to C.N.S. (col. 2) and that of ovaries associated to other nervous ganglia (S.O.G., col. 4; G.G.o, col. 5; G.G.o, col. 6) is equally significant. From these results we can conclude that in C.N.S., the C.G. alone stimulate the *in vitro* incorporation of tritiated leucine with ovaries.

On the contrary, it is difficult to explain the small difference of radioactivity of ovary-G.G.o. associations (col. 6) in relation to that of ovaries + G.G.o (col. 5) or S.O.G. (col. 4). The Student's t-test reveals that values do not differ significantly

TABLE 3. *In vitro* incorporation of ^3H -Leu (1110 kBq/ml) with ovaries of *Eisenia fetida* associated or not to different ganglia of central nervous system. Duration of culture: 4 days, incubation period: 1 hr. Results in cpm/mg wet weight

	Isolated ovaries (1)	Ovaries + CNS (2)	Ovaries + CG (3)	Ovaries + SOG (4)	Ovaries + GGo (5)	Ovaries + GGo (6)
	11400 ± 2600	55900 ± 20000	48200 ± 10500	25200 ± 7500	33700 ± 8000	19200 ± 8000
Comparisons	with (1)	+	+	+	+	—
	with (2)		—	+	+	+
	with (3)			+	+	+
	with (4)					—
	with (5)					—

t-test: + = significant difference for $p < 0.01$; — = not significant difference.

between them. Similarly, the difference between the radioactivity measured in ovaries + G.G.o (col. 6) and that of isolated ovaries (col. 1) is not significant. Finally, the difference between radioactivity values of these isolated ovaries and those of ovaries associated to C.G. (col. 3), S.O.G. (col. 4) or G.G.o (col. 5) is significant.

DISCUSSION

The present results clearly show the stimulating action of the central nervous system over the *in vitro* incorporation of tritiated leucine with ovaries. Indeed, the radioactivity measured in ovaries cultured with C.N.S. is about twice as much as that found in isolated ovaries, whatever the duration of culture (4 or 8 days), the incubation period (1, 2 or 4 hr) and the precursor concentration (370, 740 or 1480 kBq/ml of medium). However, the ovarian protein syntheses are low, as percentages of incorporation are about 0.27%, at the most, in presence of C.N.S. and about 0.11% for isolated ovaries. This confirms all cytological and cytochemical observations: ovarian oocytes reveal a low vitellogenesis because eggs of *Eisenia* are poor in yolk [19]. It is also interesting to note that the *in vitro* incorporation of ^3H -Leu with C.N.S. is very low and always below that of ovaries. Finally, in the same experimental conditions, the muscles represent an insignificant radioactivity which can be overlooked; they have no stimulating effect on the

incorporation of leucine by ovaries.

Among the different ganglia of C.N.S., only the cerebral ganglia exert some influence over the protein metabolism of ovaries. The responsible substance seems distributed according to a gradient of activity, from the C.G. to the ganglia of the 10th and 11th segment (testes level): it could diffuse within the C.N.S. from the C.G. which is the elaboration site. This would seem to confirm that the radioactivity measured in associations ovaries + S.O.G., ovaries + G.G.o or G.G.o is still quite important. Distantly acting ovaries (in the 13th segment) and mostly through the circulatory system, this substance could be akin to a neurohormone. This anteroposterior gradient in C.N.S. could be related to that experimentally established for the inhibition of cephalic regeneration [20]. Such a similar distribution could lead to presume that the trophic action revealed here, would be due to the same cerebral neurohormone, already well known in cephalic regeneration, male genital differentiation and clitellagenesis. However, before attempting to verify this hypothesis, it is necessary to confirm present results. For this purpose, an autoradiographic study is in process, to define the site of protein syntheses in the ovary.

ACKNOWLEDGMENTS

The authors wish to express their gratitude to Dr. J. C. Meusy and Dr. D. Soyeux (Université P. et M. Curie,

Paris) for their helpful advice and suggestions. Sincere thanks are also due to Dr. J. C. Challier (Université P. et M. Curie, Paris) for his critical comments on the figures, and to Mrs. F. Bonet (U.S.T. Lille-Flandres-Artois) for her skilful technical assistance and for typing the manuscript.

REFERENCES

- 1 Lattaud, C. (1974) Etude en culture organotypique du contrôle du sexe des gamétogénèses chez l'Annélide Oligochète *Eisenia foetida* f. *typica* Sav.; mise en évidence d'une action androgène des tissus testiculaires en présence du système nerveux central. C. R. Acad. Sci., D, **279**: 935-938.
- 2 Lattaud, C. (1975) Study of sex control of gametogenesis by organ culture in the Oligochaete Annelid *Eisenia foetida* f. *typica* Sav. In "Intersexuality in the Animal Kingdom". Springer-Verlag, Berlin/Heidelberg/New York, pp. 64-71.
- 3 Lattaud, C. (1980) Demonstration by organ culture of a cerebral hormone stimulating the secretion of testicular androgen in the oligochaete annelid, *Eisenia foetida* f. *typica* Sav. Int. J. Invert. Reprod., **2**: 23-26.
- 4 Lattaud, C. (1982) Stimulation *in vitro* de l'androgène testiculaire par l'hormone cérébrale chez l'annélide oligochète, *Eisenia foetida* f. *typica* Sav. Int. J. Invert. Reprod., **4**: 223-237.
- 5 Herlant-Meewis, H. (1959) Phénomènes neurosécroires et sexualité chez *Eisenia foetida*. C. R. Acad. Sci., **248**: 1405-1407.
- 6 Herlant-Meewis, H. (1967) Evolution de l'appareil génital d'*Eisenia foetida* au cours du jeûne, de la régénération postérieure et à la suite de l'ablation de ganglions nerveux. Ann. Soc. r. Zool. Belg., **96**: 189-240.
- 7 Saussey, M. (1963) Effects de la décérébration et de l'amputation caudale sur la spermatogénèse d'*Allobophora icterica* Sav. (Oligochète, Lumbicidae). C. R. Acad. Sci., **257**: 511-513.
- 8 Marcel, R. (1967) Rôle du système nerveux dans l'inhibition de la régénération antérieure chez *Eisenia foetida* f. *typica* Sav. (Annélide Oligochète). C. R. Acad. Sci., D, **265**: 693-694.
- 9 Berjon, J. J. (1965) Application de la culture organotypique sur milieux artificiels à la discrimination des fonctions endocrines des ganglions cérébroïdes du Lombricien *Eisenia foetida* (Sav.) C. R. Acad. Sci., D, **260**: 6216-6214.
- 10 Olive, P. J. W. and Clark, R. B. (1978) Physiology of reproduction, In "Physiology of Annelids". Ed. by P. J. Mill, Acad. Press, New York, pp. 271-368.
- 11 Marcel, R. and Cardon, C. (1974) Essais de purification du facteur inhibiteur de la régénération céphalique chez *Eisenia foetida* Sav. f. *typica* (Annélide Oligochète). C. R. Acad. Sci., D, **279**: 1545-1548.
- 12 Marcel, R. and Cardon, C. (1979) Partial purification and characterization of the peptide which inhibits cephalic regeneration in *Eisenia foetida* Sav. (Oligochaeta, Annelida). Comp. Biochem. Physiol., **63B**: 233-237.
- 13 Marcel, R. and Cardon, C. (1982) Régénération céphalique et clitelligenèse sont-elles gouvernées par la même neurohormone chez le Lombricien *Eisenia foetida*? J. Physiol., **78**: 574-578.
- 14 Marcel, R. and Cardon, C. (1983) Purification par chromatographie liquide à haute performance de la neurohormone cérébrale d'*Eisenia foetida* Sav. (Annélide Oligochète). Essai sur la régénération et la clitelligenèse. Reprod. Nutr. Dévelop., **23**: 1003-1009.
- 15 Cardon, C. and Marcel, R. (1976) Démonstration de la nature peptidique du facteur inhibiteur de la régénération céphalique chez le Lombricien *Eisenia foetida* Sav. f. *typica* (Annélide, Oligochète). C. R. Acad. Sci., D, **282**: 657-658.
- 16 Lattaud, C. et Marcel, R. (1983) Stimulation *in vitro* de la sécrétion de l'androgène testiculaire par une fraction purifiée de cerveaux chez *Eisenia foetida* f. *typica* Sav. (Annélide Oligochète). Can. J. Zool., **61**: 2399-2404.
- 17 Lechenault, H. (1968) Etude cytochimique et ultrastructurale de l'ovocyte d'*Eisenia foetida* Sav. Z. Zellforsch. mikr. Anat., **90**: 96-112.
- 18 Lattaud, C. (1976) Etude du contrôle du sexe des gamétogénèses au moyen de la culture organotypique chez un hermaphrodite à gonades séparées, l'Annélide Oligochète *Eisenia foetida* f. *typica* Sav. Bull. Soc. Zool. Fr., **101**: 1-7.
- 19 Dawidoff, C. (1959) Ontogenèse des Annélides. In "Traité de Zoologie (Dir. P. P. Grassé) T V f I", pp. 494-686.
- 20 Marcel, R. (1968) Effets inhibiteur et trophique dans la régénération céphalique de *Eisenia foetida* Sav. f. *typica* (Annélide Oligochète). Ann. Embryol. Morph., **1**: 417-425.

Uptake of 3,5,3'-L-Triiodothyronine into Bullfrog Red Blood Cells Mediated by Plasma Membrane Binding Sites

KIYOSHI YAMAUCHI, RYUYA HORIUCHI¹,

SAKUJI KOYA and HIROO TAKIKAWA

*Institute of Endocrinology, Gunma University,
Maebashi 371, Japan*

ABSTRACT—To examine the mechanism of thyroid hormone transport into the bullfrog red blood cells (RBCs), the uptake of 3,5,3'-L-triiodothyronine (T_3) into the intact RBCs of bullfrog and the binding of T_3 to the purified plasma membranes were studied. The specific T_3 uptake into the adult RBCs was saturable at a certain T_3 concentration and temperature-dependent showing maximum binding at 15°C. The uptake of iodothyronines into RBCs showed stereospecificity for T_3 ($T_3 \gg 3,5,3'$ -D-triiodothyronine = L-thyroxine). The nuclear uptake of T_3 was only a few percent of the cellular associated T_3 after incubating at 15°C for 1 hr. Monodansylcadaverine, an inhibitor of receptor-mediated endocytosis, blocked T_3 uptake into the adult RBCs even at 0°C, with a half maximal inhibitory concentration of 65 μ M. The effect of MDC strongly suggests that even at 0°C T_3 should enter bullfrog RBCs by receptor-mediated endocytosis. To clarify the presence of the T_3 binding sites on the plasma membranes, we purified the plasma membranes from adult RBCs. Scatchard analysis revealed the presence of two classes of T_3 binding sites on the plasma membrane: a high affinity-low capacity site (K_d : 36.0 ± 12.7 nM, MBC : 14.8 ± 6.7 fmol/ μ g protein), and a low affinity-high capacity site (K_d : 5.34 ± 1.54 μ M, MBC : 2.44 ± 0.51 pmol/ μ g). From these results it is suggested that T_3 initially binds to the specific binding sites on the cell surface of the bullfrog RBCs, and then enters the cells by receptor-mediated endocytosis.

INTRODUCTION

It has been indicated that the nuclei of tadpole red blood cells (RBCs) contain putative thyroid hormone receptors [1], and the number of the receptors increases corresponding to the enhancement of the 3,5,3'-L-triiodothyronine (T_3) concentration in plasma during metamorphosis and decreases after metamorphosis [2, 3]. These results suggest that T_3 might regulate the metabolism of the differentiated RBCs.

It is known that the plasma membranes from human [4, 5], rabbit [6] and rat RBCs [7] contain specific binding sites for T_3 . Further, in mammalian cells, many evidences have been accumulated that T_3 binding to the membrane associated pro-

teins on the cell surface should be the initial step in its actions on the target cells, and the uptake of T_3 into the cells might be mediated by endocytosis [8-12].

In the case of bullfrog RBCs, it was reported that T_3 , but not L-thyroxine (T_4), was transported into RBCs by a carrier mediated pathway that is not dependent on metabolic energy [13]. However, details of the thyroid hormone transport pathways into bullfrog RBCs are still unclear. In order to clarify this problem, the mechanism of T_3 uptake into the intact RBCs closely related to the plasma membranes was examined.

MATERIALS AND METHODS

Reagents [125 I] T_3 (3380 μ Ci/ μ g) was purchased from New England Nuclear (Boston, U.S.A.). T_3 , 3,5,3'-D-triiodothyronine (D- T_3), T_4 and Monodansylcadaverine (MDC) were purch-

Accepted September 19, 1988

Received June 10, 1988

¹ To whom reprint requests should be addressed.

ased from Sigma (St. Louis, U.S.A.). Dibutyl phthalate and Dinonyl phthalate were obtained from Eastman Kodak (Rochester, U.S.A.). MS-222 (tricaine methane sulfonate) was purchased from Sankyo (Tokyo, Japan).

Preparation of RBC *Rana catesbeiana* were collected from ponds in Misato, Saitama Pref., Japan. The adult frogs were anesthetized by immersing in 0.2% MS-222, and the heart areas were exposed. Blood samples were obtained by cardiac puncture with heparinized syringes. The RBCs were separated from plasma by centrifugation at $1,500 \times g$ for 15 min at 4°C , followed by washing three times with TNC buffer (15 mM Tris-HCl, 108 mM NaCl, 0.77 mM CaCl_2 ; pH 7.4). The number of RBCs was determined with a Coulter Counter (Coulter Electronics, U.S.A.).

Preparation of the plasma membranes of RBC The plasma membrane fractions of RBCs were obtained by osmotic lysis and discontinuous sucrose density gradient centrifugations according to the method of Okazaki *et al.* [14] with slight modifications. In brief, the washed RBCs were poured into 20 volumes of stirring ice-cold Solution A (10 mM Tris-HCl, 20 mM MgCl_2 and 5 mM dithiothreitol, pH 7.4). The nucleated RBC ghosts were then pelleted by centrifugation at $15,000 \times g$ for 20 min. After washing the ghosts several times with Solution A, the precipitate was resuspended in 5 volumes of Solution B (Solution A containing 50 mM sodium bisulfite) and sonicated. The resultant suspension was layered over a step gradient of 20% (w/w) and 60% sucrose, and then centrifuged at $80,000 \times g$ for 90 min. The membrane fraction at the interface of the sucrose solutions was further layered over a step gradient of 20%, 30%, 40%, 50% and 60% sucrose. After centrifugation at $80,000 \times g$ for 2 hr, the membrane fraction at the 40–50% sucrose was immediately used for [^{125}I]T₃ binding experiments. Protein content was determined by the method of Bradford [15] using bovine γ -globulin as the standard protein.

Uptake of [^{125}I]T₃ by intact cells RBCs (2.5×10^5 cells) were incubated in 250 μl of TNC buffer containing 0.1% glucose and 0.1 nM [^{125}I]T₃ in the presence or absence of 20 μM unlabeled T₃ at 15°C . Cellular bound [^{125}I]T₃ and free [^{125}I]T₃

were separated by the oil-centrifugation method according to Horiuchi *et al.* [10] with slight modifications. In brief, after incubation of RBCs with [^{125}I]T₃, 200 μl of the chilled cell suspension was applied on the top of a three-layer solution in an Eppendorf 400 μl micro test tube. The three-layer solutions from top to bottom consisted of 40 μl of dibutyl phthalate : dinonyl phthalate (6.5:3.5, v/v); 100 μl of the buffer containing 0.25 M sucrose, 0.5 mM CaCl_2 , and 10 mM Tris-HCl (pH 7.4); and 30 μl of dibutyl phthalate : dinonyl phthalate (8: 2, v/v), respectively. The cells and free [^{125}I]T₃ were immediately separated by centrifugation at $14,000 \times g$ for 2 min at 4°C . The tips of the tubes containing the cell pellet were cut off. The cellular [^{125}I]T₃ values were determined in a Beckman Gamma 8000 spectrometer. Non-specific [^{125}I]T₃ association with the cells calculated from the samples in the presence of 20 μM unlabeled T₃ was less than 5% of total [^{125}I]T₃ uptake.

Binding of [^{125}I]T₃ to nuclei of RBCs After incubation of RBCs with 0.2 nM [^{125}I]T₃ at 15°C for various periods, the cells were washed twice with TNC buffer, and the pellets were treated twice with 2 ml of the buffer containing 60 mM KCl, 15 mM NaCl, 0.5 mM spermidine, 0.15 mM spermine, 2 mM EDTA, 0.5 mM ethylene glycol bis(β -aminoethyl ether)-N,N,N',N'-tetraacetic acid, 15 mM 2-mercaptoethanol, and 0.5% Triton X-100 [16] at 0°C . The isolated nuclei were collected by centrifugation at $400 \times g$ for 5 min and [^{125}I]T₃ bound to the nuclei was determined.

Binding of [^{125}I]T₃ to plasma membranes The purified membranes (10 μg protein in 250 μl of TNC buffer) from bullfrog RBCs were incubated with 0.2 nM [^{125}I]T₃ in the presence of various concentrations of unlabeled T₃ at 15°C . After incubation, 50 μl of 5 mg/ml bovine γ -globulin and 300 μl of cold 12% polyethylene glycol 6000 in TNC buffer containing 0.2 M ZnCl_2 were added to the chilled incubation mixture. The resultant suspension was centrifuged at $1,500 \times g$ for 10 min at 4°C . The pellet was washed once with 2 ml of 6% polyethylene glycol containing 0.1 M ZnCl_2 , and bound [^{125}I]T₃ in the pellet and free [^{125}I]T₃ were determined. Non-specific binding calculated from the samples in the presence of 20 μM unlabeled T₃ was 40–50% of total binding, which was

subtracted from total binding. The values for the dissociation constant (K_d) and maximum binding capacity (MBC) were calculated from Scatchard plot by computer analysis according to the method of Rosenthal [17].

RESULTS

The characteristics of T₃ uptake into adult RBCs [¹²⁵I]T₃ uptake into adult RBCs at 15°C increased with time and reached a plateau after 15 min as shown in Figure 1A. The specific T₃ uptake was approximately 95% of the total uptake. As shown in Figure 2, the T₃ uptake was temperature-dependent showing maximum at 15°C, but it decreased to be 68% of the maximum uptake at 30°C. The [¹²⁵I]T₃ uptake into the nuclei was slow and only 2–3% of the total cellular [¹²⁵I]T₃ incubated at 15°C for 2 hr, and then the uptake gradually increased to 12% of the cellular

T₃ after 8 hr (Fig. 1B).

Figure 3 shows the competitive inhibition of [¹²⁵I]T₃ uptake into RBCs by the iodothyronines. The inhibition was stereospecific for T₃ and fifty percent of the specific cellular uptake of [¹²⁵I]T₃ was inhibited by 28 nM unlabeled T₃, 3.0 μM T₄ or 3.6 μM D-T₃. These results indicate that T₃ is stereospecifically transported into the bullfrog RBCs.

To examine the possibility of the receptor-mediated uptake of T₃ into bullfrog RBCs, the effect of MDC, an inhibitor of receptor-mediated endocytosis [9], on [¹²⁵I]T₃ uptake into RBCs was examined. As shown in Figure 4, the specific [¹²⁵I]T₃ uptake at 0°C was almost completely inhibited by MDC, and 50% of the specific [¹²⁵I]T₃ uptake was inhibited by 65 μM MDC. When incubated at 15°C for 30 min, similar results were obtained (data not shown).

The characteristics of T₃ binding to the plasma membranes of RBCs

Figure 1C shows that [¹²⁵I]T₃ binding to the purified plasma membranes at 15°C increased with time and reached a plateau after 30 min. [¹²⁵I]T₃ binding to the plasma membranes was specifically inhibited by unlabeled T₃. From the concentrations of unlabeled iodothyronines required to depress 50% of the specific

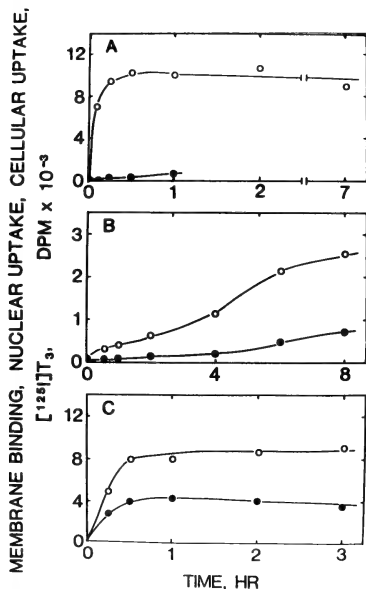


FIG. 1. Time course of [¹²⁵I]T₃ uptake into the bullfrog RBCs and its binding to the plasma membranes. (A) [¹²⁵I]T₃ uptake into the intact RBCs. Bullfrog RBCs (2.5×10^5 cells) were incubated with 0.1 nM [¹²⁵I]T₃ at 15°C for the indicated periods. The cellular uptake of [¹²⁵I]T₃ was determined by the oil-centrifugation method as described in "Materials and Methods". (B) [¹²⁵I]T₃ uptake into nuclei. Cells (2.5×10^5 cells) were incubated with 0.2 nM [¹²⁵I]T₃ at 15°C for the indicated periods. The nuclei were isolated and the radioactivity incorporated into the nuclei was determined as described in "Materials and Methods". (C) [¹²⁵I]T₃ binding to the plasma membranes. The purified plasma membranes (10 μg protein) from bullfrog RBCs were incubated with 0.2 nM [¹²⁵I]T₃ at 15°C. After washing the membranes with 6% polyethylene glycol, 0.1 M ZnCl₂ in TNC buffer, the bound [¹²⁵I]T₃ was determined as described in "Materials and Methods". (●—●): in the presence of 20 μM unlabeled T₃. (○—○): in the absence of unlabeled T₃. Each point in the figures represents the mean for triplicate tubes with a standard error less than 5%.

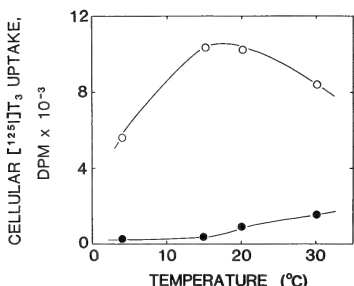


FIG. 2. Temperature-dependent uptake of $[^{125}\text{I}]\text{T}_3$ into the bullfrog RBCs. The bullfrog RBCs (2.5×10^5 cells) were incubated with 0.1 nM $[^{125}\text{I}]\text{T}_3$ for 30 min at 4, 15, 20 or 30°C with (●) or without (○) 20 μM of unlabeled T_3 . The cellular $[^{125}\text{I}]\text{T}_3$ uptake was determined as described in "Materials and Methods". Each point represents the mean for triplicate tubes with a standard error less than 5%.

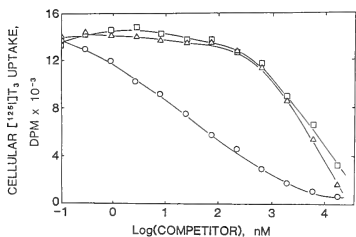


FIG. 3. Competitive inhibition of $[^{125}\text{I}]\text{T}_3$ uptake into bullfrog RBCs by various iodothyronine analogues. The bullfrog RBCs (2.5×10^5 cells) were incubated with 250 μl of 0.1 nM $[^{125}\text{I}]\text{T}_3$ for 30 min at 15°C in the presence of various concentrations of L- T_3 (○), T_4 (△) or D- T_3 (□), respectively. $[^{125}\text{I}]\text{T}_3$ uptake was determined as described in "Materials and Methods". Non-specific association was calculated to be 5% of total uptake from the samples with 20 μM unlabeled T_3 and was subtracted from total $[^{125}\text{I}]\text{T}_3$ uptake. Each point represents the mean for triplicate determinations with a standard error less than 5%.

binding of $[^{125}\text{I}]\text{T}_3$, it is roughly estimated that the affinities of D- T_3 and T_4 were 1/7 and 1/70 of T_3 , respectively (data not shown). A typical Scatchard plot of T_3 binding to RBC membranes at 15°C is

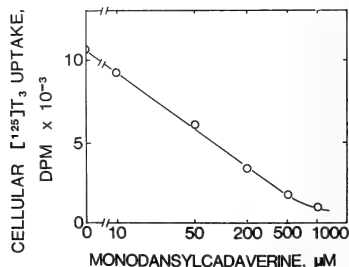


FIG. 4. Inhibition of $[^{125}\text{I}]\text{T}_3$ uptake into bullfrog RBCs by MDC. The bullfrog RBCs (2.5×10^5 cells) were incubated with 0.1 nM $[^{125}\text{I}]\text{T}_3$ in the presence of various concentrations of MDC for 3 hr at 0°C. Cellular associated $[^{125}\text{I}]\text{T}_3$ was determined by the oil-centrifugation method as described in "Materials and Methods". Each point is the mean for triplicate determinations with a standard error less than 10%. Non-specific association determined from the samples incubated with 20 μM T_3 was subtracted.

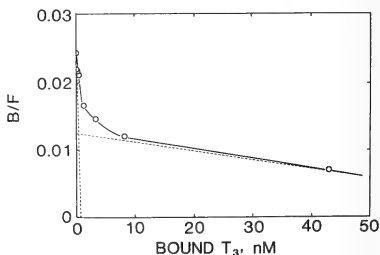


FIG. 5. Scatchard plot of T_3 binding to the plasma membranes of bullfrog RBCs. The membranes (10 μg protein) prepared from bullfrog RBCs were incubated with 0.2 nM $[^{125}\text{I}]\text{T}_3$ at 15°C for 2 hr in the presence of various concentrations of unlabeled T_3 . $[^{125}\text{I}]\text{T}_3$ binding to the membranes were determined by the method of centrifugation as described in "Materials and Methods". Each point represents the mean for triplicate determinations. The solid line is the theoretical curve analyzed by computer for two classes of binding sites according to Rothenthal [17]. The broken lines are the Scatchard plot resolved into two lines showing the high affinity-low capacity site and the low affinity-high capacity site.

shown in Figure 5, revealing the presence of two classes of binding sites. The mean values for

binding of [¹²⁵I]T₃, it is roughly estimated that the affinities of D-T₃ and T₄ were 1/7 and 1/70 of T₃, respectively (data not shown). A typical Scatchard plot of T₃ binding to RBC membranes at 15°C is shown in Figure 5, revealing the presence of two classes of binding sites. The mean values for dissociation constants (K_ds) and maximum binding capacities (MBCs) from three separated experiments were 36.0 ± 12.7 nM (K_{d1}) and 14.8 ± 6.7 fmol/μg protein (MBC₁) for a high affinity-low capacity site, and 5.34 ± 1.54 μM (K_{d2}) and 2.44 ± 0.51 pmol/μg protein (MBC₂) for a low affinity-high capacity site, respectively.

DISCUSSION

Recently much evidence has been accumulated showing that T₃ specific binding sites are on the plasma membranes of many mammalian cells. T₃ binding to the binding sites on the cell surface has been considered to be the initial step in T₃ actions on the target cells. However, in poikilothermal animals, the pathway of thyroid hormone from plasma into the cells is still unclear. The putative thyroid hormone receptors in the nuclei of hepatocytes from pre- and pro-metamorphic tadpoles have been characterized *in vitro* [18]. However, the prepared hepatocytes were proved to be heterogeneous. Further, the hepatocytes from the tadpole would be easily damaged by extensive perfusion. To clarify the thyroid hormone transport system on the cell surface, bullfrog RBCs could be a good model because the nuclear thyroid hormone receptors have been characterized in the RBCs of metamorphic tadpoles and adult frog [1-3], and the pure intact RBCs could be easily obtained by simple centrifugations. Furthermore, it was demonstrated by indirect immunofluorescent staining of blood smear that T₄ distributed not only in the plasma but within the RBCs, where it appeared at the edge of the nucleus and around the plasma membrane [19]. In this study, we demonstrated the presence of T₃ specific binding sites on the plasma membrane of bullfrog RBCs and further showed that receptor-mediated endocytosis might be the major pathway of the thyroid hormone uptake into bullfrog RBCs.

The uptake of T₃ into the intact bullfrog RBCs

was saturable, temperature-dependent and stereospecific, as shown in Figures 2 and 3. T₃ uptake into the cells was maximal at 15°C and the cellular uptake reached a plateau after 30 min at this temperature. Non-specific association was less than 5% of total cellular T₃, and 15% of the [¹²⁵I]T₃ added to the incubation medium was accumulated to RBCs under the experimental conditions (Fig. 1A). Considering that the separation of cellular associated T₃ and free T₃ in the incubation medium by the oil-centrifugation method is very rapid to be done within 30 sec, the dissociation of cellular [¹²⁵I]T₃ might be negligible during the experimental process. These data indicate that the T₃ uptake into RBCs is by active transport but not by simple diffusion.

However, the distribution of T₃ to the nuclei was small and slow: only 2-3% of cellular T₃ was distributed to the nuclei after 2 hr and the nuclear distribution was increased to 12% after 8 hr at 15°C. In the case of mammalian cells, the distribution of T₃ to the nuclei of GH₃ cells was reported to reach a plateau at 10% of the cellular T₃ within 1 hr [10]. These data suggest that the capacity of nuclear T₃ receptor is only a part of the whole cellular binding capacity of mammalian and also amphibian cells. The binding to the purified plasma membranes and the uptake into the intact cells are both stereospecific for T₃. The order of the stereospecificity of the uptake into the cells and the binding to the purified plasma membrane are similar (T₃ > D-T₃ ≥ L-T₄). These results might evidence that T₃ enters the cells after having bound to the T₃ specific binding sites on the plasma membrane.

In bullfrog tadpole RBCs, Galton *et al.* [13] reported the presence of a single, T₃ specific but energy-independent T₃ uptake pathway with a K_m of 50 nM from the kinetic analysis at 22°C. However, they did not attach importance to the binding sites on the cell surface. From the equilibrium binding of T₃ to the plasma membranes purified from RBCs, we showed the presence of two classes of binding sites: a high affinity-low capacity site (K_{d1}: 36 nM, MBC₁: 14.8 fmol/μg protein) and a low affinity-high capacity site (K_{d2}: 5.34 μM, MBC₂: 2.44 pmol/μg protein). Although a comparison of the K_d value of T₃ binding to the

plasma membrane with the K_m value of T_3 uptake is not warranted because they were obtained at the different conditions, the K_m value corresponded well with the K_d value in our study. Thus, the uptake of T_3 into bullfrog RBCs might occur via the high affinity-low capacity site on the plasma membrane. Considering that the affinity of the low affinity site is far weaker than those of thyroid hormone binding proteins in plasma [20], the contribution of the low affinity site on the T_3 uptake pathway of bullfrog RBCs could be little.

The binding of iodothyronines to the purified plasma membrane from bullfrog RBCs was stereospecific for T_3 and the affinity of L- T_4 was 1/70 of T_3 . In mammalian RBCs, the presence of two classes of T_3 binding sites on the plasma membranes from human [4] and rat RBCs [5] was reported. We also found that the stereospecificity and affinity of T_3 binding to bullfrog RBC membranes were similar to those of T_3 binding to the human RBC ghosts [21].

We showed a further link between the binding sites for T_3 on the plasma membranes and the uptake of T_3 into the intact RBCs. MDC is known to be an inhibitor of the internalization of α_2 -macroglobulin, epidermal growth factor or vesicular stomatitis virus into mouse fibroblasts [9]. MDC was also shown to inhibit internalization of T_3 bound to the plasma membrane into GH₃ cells, a rat pituitary tumor cell line [10], and mouse fibroblasts [11] with a half-maximal concentration of 29 and 90 μ M, respectively. However, MDC showed no effect on rat GH₃ cells treated at 0°C. In the case of bullfrog RBCs, as shown in Figure 4, MDC almost completely inhibited the cellular association of T_3 at 0°C with a half-maximal concentration of 65 μ M. A similar effect was seen when incubated at 15°C (data not shown). From these results, it was strongly suggested that the T_3 uptake into bullfrog RBCs was performed by receptor-mediated endocytosis even at 0°C. The difference between the feature in bullfrog and mammalian cells could partially depend on the components and fluidity of the plasma membranes. These results might support the probability that T_3 would be effective even at 0°C and this might be physiologically significant in poikilothermal animals including frogs.

In mammalian RBCs, we know the T_3 actions which are not mediated by nuclear receptors, such as the stimulation of glucose uptake [22], Ca^{2+} -ATPase activity [23], or the enhancement of oxygen consumption [24]. In the case of bullfrog RBCs, it was shown that the life span of the RBCs of tadpole form was shortened and the production of the RBCs of adult form was induced by *in vivo* treatment with T_4 [25]. Moreover, Thomas *et al.* [26] showed that T_3 induced the synthesis of T_3 receptors in RBC nuclei. We showed in this study the evidences indicating that T_3 is actively transported from plasma into RBCs, and strongly suggested the possibility of the receptor-mediated endocytosis of T_3 into RBCs. However, direct relevance of the T_3 actions of bullfrog RBCs and T_3 transport pathways, especially T_3 binding to the plasma membrane, is remained to be clarified in future.

ACKNOWLEDGMENTS

We are grateful to Prof. K. Wakabayashi for the computer analysis of Scatchard plot and Prof. T. Okazaki (Nippon Medical School) for his technical advice on membrane preparation from bullfrog RBCs.

REFERENCES

- 1 Galton, V. A. (1984) Putative nuclear triiodothyronine receptors in tadpole erythrocytes: Regulation of receptor number by thyroid hormone. *Endocrinology*, **114**: 735-742.
- 2 Moriya, T., Thomas, C. R. and Frieden, E. (1984) Increase in 3,5,3'-triiodothyronine (T_3)-binding sites in tadpole erythrocyte nuclei during spontaneous and T_3 -induced metamorphosis. *Endocrinology*, **114**: 170-175.
- 3 Galton, V. A. and Germain, D. L. ST. (1985) Putative nuclear triiodothyronine receptors in tadpole erythrocytes during metamorphic climax. *Endocrinology*, **116**: 99-104.
- 4 Holm, A.-C. and Jacquemin, C. (1979) Membrane transport of L-triiodothyronine by human red cell ghosts. *Biochem. Biophys. Res. Commun.*, **89**: 1006-1017.
- 5 Botta, J. A. and Farias, R. N. (1985) Solubilization of L-triiodothyronine binding site from human erythrocyte membrane. *Biochem. Biophys. Res. Commun.*, **133**: 442-448.
- 6 Singh, S. P., Carter, A. C., Kydd, D. M. and Costanzo, R. R. Jr. (1976) Interaction between thyroid

- hormones and erythrocyte membrane: Competitive inhibition of binding ¹³¹I-L-triiodothyronine and ¹³¹I-L-thyroxine by their analogs. *Endocrine. Res. Commun.*, **3**: 119-131.
- 7 Botta, J. A., Mendoza, D., Morero, R. D. and Farias, R. N. (1983) High affinity L-triiodothyronine binding sites on washed rat erythrocyte membranes. *J. Biol. Chem.*, **258**: 6690-6692.
- 8 Cheng, S.-y., Maxfield, F. R., Robbins, J., Willingham, M. C. and Pastan, I. (1980) Receptor-mediated uptake of 3,3',5-triiodo-L-thyronine by cultured fibroblasts. *Proc. Natl. Acad. Sci. USA*, **77**: 3425-3429.
- 9 Pastan, I. H. and Willingham, M. C. (1981) Receptor-mediated endocytosis of hormones in cultured cells. *Ann. Rev. Physiol.*, **43**: 239-250.
- 10 Horiuchi, R., Cheng, S.-y., Willingham, M. and Pastan, I. (1982) Inhibition of the nuclear entry of 3,3',5-triiodo-L-thyronine by monodansylcadaverine in GH₃ cells. *J. Biol. Chem.*, **257**: 3139-3144.
- 11 Cheng, S.-Y. (1983) Characterization of binding and uptake of 3,3',5-triiodo-L-thyronine in cultured mouse Fibroblast. *Endocrinology*, **112**: 1754-1762.
- 12 Pontecorvi, A. and Robbins, J. (1986) Energy-dependent uptake of 3,5,3'-triiodo-L-thyronine in rat skeletal muscle. *Endocrinology*, **119**: 2755-2761.
- 13 Galton, V. A., Germain, D. L. ST. and Whittemore, S. (1986) Cellular uptake of 3,5,3'-triiodothyronine and thyroxine by red blood and thymus cells. *Endocrinology*, **118**: 1918-1923.
- 14 Okazaki, T., Tamai, K. and Shukuya, R. (1984) Membrane proteins of the erythrocytes of bullfrog, *Rana catesbeiana*, and its tadpole. *Comp. Biochem. Physiol.*, **77B**: 131-134.
- 15 Bradford, M. M. (1976) A rapid and sensitive method for the quantitation of microgram quantities of protein utilizing the principle of protein-dye binding. *Anal. Biochem.*, **72**: 248-254.
- 16 Hewish, D. R. and Burgoyne, L. A. (1973) Chromatin sub-structure, the digestion of chromatin DNA at regularly spaced sites by a nuclear deoxyribonuclease. *Biochem. Biophys. Res. Commun.*, **52**: 504-510.
- 17 Rosenthal, H. E. (1967) A graphic method for the determination and presentation of binding parameters in a complex system. *Anal. Biochem.*, **20**: 525-532.
- 18 Galton, V. A. and Germain, D. S. (1985) Putative nuclear triiodothyronine receptors in tadpole liver during metamorphic climax. *Endocrinology*, **117**: 912-916.
- 19 Kaltenbach, J. C. (1982) Circulating thyroid hormone levels in amphibia. In "Phylogenic aspects of thyroid hormone action". (Institute of Endocrinology, Gunma Univ. eds) pp. 63-74.
- 20 Miyauchi, H., LaRochelle, F. T. J., Suzuki, M., Freeman, M. and Frieden, E. (1977) Studies on thyroid hormones and their binding in bullfrog tadpole plasma during metamorphosis. *Gen. Comp. Endocrinol.*, **33**: 254-266.
- 21 Yamauchi, K., Horiuchi, R. and Takikawa, H. (1989) Uptake of 3,5,3'-L-triiodothyronine in human erythrocytes. *J. Endocrinol.*, **121**: 585-591.
- 22 Snyder, L. M., Neri, L. L., Chung, S. K., Morinari, P. F. and Reddy, W. F. (1971) The variation of glucose metabolism in human erythrocytes in the presence of L-thyroxine. *Proc. Soc. Exp. Biol. Med.*, **138**: 1-3.
- 23 Davis, P. J. and Susan, D. B. (1981) In vitro stimulation of human red blood cell Ca²⁺-ATPase by thyroid hormone. *Biochem. Biophys. Res. Commun.*, **99**: 1073-1080.
- 24 Necheles, T. and Beutler, E. (1959) The effect of triiodothyronine on the oxidative metabolism of erythrocytes. I. cellular studies. *J. Clin. Invest.*, **38**: 788-797.
- 25 Forman, L. J. and Just, J. J. (1981) Cellular quantitation of hemoglobin transition during natural and thyroid-hormone-induced metamorphosis of the bullfrog *Rana catesbeiana*. *Gen. Comp. Endocrinol.*, **44**: 1-12.
- 26 Thomas, C. R., Drake, J. and Frieden, E. (1986) Receptor induction in tadpole erythrocytes by thyroid hormones *in vivo* and *in vitro*. In "Frontiers in Thyroidology". Volume 1, Ed. by G. Medeiros-Neto and E. Gaitan, Plenum Publ. Corp., New York, pp. 741-743.



**[³⁵S]-Sulphate Uptake by *Xenopus laevis* Cartilage:
The Influence of Plasma from the Growth
Hormone-Treated Animal**

TETSUYA KOBAYASHI, SAKAÉ KIKUYAMA¹, AKIHIDE KUME,
JIRO OKUMA and MUNEYOSHI OHKAWA

*Department of Biology, School of Education, Waseda University,
Shinjuku-ku, Tokyo 169, Japan*

ABSTRACT—Plasma samples prepared from hypophysectomized *Xenopus laevis* which had received ovine or bullfrog GH injections stimulate the uptake of [³⁵S]-sulphate by the xiphisternal cartilage from the hypophysectomized *Xenopus* juveniles *in vitro*. The stimulating effect of the plasma is dependent on the dosage of GH which had been given to the plasma donors. Addition of GH to the incubation medium does not affect the uptake of labeled sulphate by the cartilage. The results indicate that GH induces the factor(s) which acts on the tissue to stimulate growth in the toad.

INTRODUCTION

It is widely accepted that in mammals, the growth-stimulating effect of GH is mediated by GH-dependent serum factor(s), somatomedins or insulin-like growth factors [1-3]. In amphibians, the growth-promoting activity of GH has been assessed by the increase in body weight, body length, femur length [4-7] or by the enhancement of the uptake of labeled sulphate by the cartilage [8]. Hypophysectomy results in the retardation of body growth and the decline of the uptake of labeled sulphate by the cartilage, which are restored by the GH supplementation [8, 9]. However, there is not much information of the mediator of somatotrophic effect of GH in amphibians. The presence of somatomedin-like substance(s) in the serum of *Bufo marinus* has been evidenced immunologically by Daughaday *et al.* [10]. Rothstein *et al.* [11] demonstrated that administration of bovine GH to the hypophysectomized *Rana catesbeiana* increases the immunoreactive somatomedin C in the blood. In the present paper, we report that the plasma from the hypophysectomized *Xenopus laevis* treated with ovine or bullfrog GH

stimulates chondroitin sulphate synthesis in the xiphisternal cartilage *in vitro*, the stimulating effect of the plasma being dependent on the concentration of the plasma and the dosage of the hormone which had been given to the plasma donor, and that GH added to the plasma from the hypophysectomized animal does not affect the chondroitin sulphate synthesis in the cartilage.

MATERIALS AND METHODS

Animals

Juvenile African clawed toads, *Xenopus laevis* of both sexes were used. They were hypophysectomized and kept for 7 days in tap water at 22°C prior to the experiment. Food (*Tubifex*) was provided in surplus throughout the experiment.

Hormones and plasma samples

Ovine GH(NIH-GH-S11) was supplied from the NIH. Bullfrog GH was prepared as a by-product during purification of bullfrog prolactin [12] according to the method described elsewhere [13]. Each hormone was dissolved in 1% BSA and given to the hypophysectomized toad (about 20 g in body weight) intraperitoneally at 10-11 a.m. every other day for 5 days (3 injections in total). Daily

Accepted October 7, 1988

Received August 24, 1988

¹ To whom all correspondence should be addressed.

dose of GH was 5–20 μg per animal. Twenty hours after the last injection, the blood was collected in a heparinized tube by heart puncture. Plasma was separated by centrifugation. Approximately 300 μl of plasma from each animal was pooled and stored at -70°C until use.

Incorporation of [^{35}S]-sulphate into cartilage

Xiphisternal cartilage from hypophysectomized toads weighing about 8 g was dissected out and cut into 0.8–1.0 mm sections. Each sample consisting of cartilage sections from 2 animals was transferred to a glass vial containing 2 ml sterile 67% Eagle's MEM (Nissui Seiyaku Co.) supplemented with 18mM NaHCO_3 , 5 mM HEPES and 4 μCi of [^{35}S]-sulphate (carrier-free, Radiochemical Center, Amersham). To the medium, plasma from the hormone-treated or vehicle-injected animals, or plasma from vehicle-injected animals supplemented with GH was added as a test substance. Incubation was performed at 23°C in a Dubnoff-metabolic shaking incubator gassed with 95% O_2 –5% CO_2 . After incubation, the cartilage sections were immersed in boiling water for 10 min. Sections were then transferred into a small basket made of stainless steel and washed in saturated sodium sulphate, running water and distilled water. After drying in an oven at 55°C for 1 hr, the sections were weighed and solubilized in 250 μl of 98% formic acid at 110°C in glass vials with caps. After solubilization, 2.5 ml scintillation fluid was added to the vial. The radioactivity was measured in a liquid scintillation counter (Aloka, LSC-700). Analysis of the labeled cartilage revealed that about 60–80% of the label is incorporated into chondroitin sulphates [8].

RESULTS

The cartilage sections from the hypophysectomized *Xenopus laevis* were incubated for varying time at 23°C in the medium containing 10% plasma from the vehicle-injected animals (control) or ovine GH-treated animals. For the initial 5 hr of incubation, there was no difference in the uptake of the [^{35}S]-sulphate between the cartilage sections cultured in the medium containing the plasma from the GH-treated animals and those cultured in

the plasma from the vehicle-injected animals. At 20 hr of incubation, the uptake of [^{35}S]-sulphate by the cartilage sections cultured in the medium containing the plasma from the hormone-treated toads was more prominent than that by the cartilage sections cultured in the medium containing the plasma from the vehicle-injected toads (Fig. 1). In the subsequent experiments, the cartilage was incubated for 20 hr.

Effect of various concentrations of plasma from the ovine GH-treated animals and from the vehicle-injected animals on the uptake of [^{35}S]-sulphate by the cartilage was studied. The stimulating effect of the plasma from the GH-treated toads increased according to the amount of the plasma added to the medium. On the other hand, the uptake of the [^{35}S]-sulphate by the cartilage was scarcely affected by the concentration of the plasma from the vehicle-injected animals. In Figure 2, the uptake of [^{35}S]-sulphate by the cartilage in response to 2.5–10% plasma from the ovine

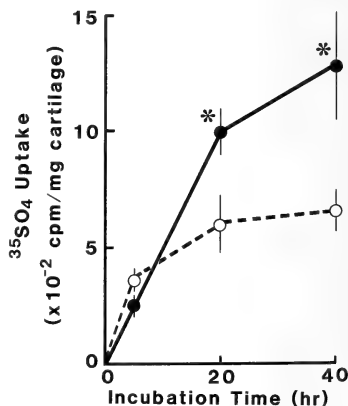


Fig. 1. Time course of the *in vitro* uptake of [^{35}S]-sulphate by the xiphisternal cartilage incubated in the medium containing 10% plasma from the ovine GH (10 $\mu\text{g}/\text{animal}$)-treated (●) or vehicle-injected (○) animals. Each point and vertical line represent the mean of 5 determinations and SEM, respectively.

*Statistically significant between the values for the 2 groups at $p < 0.05$ (analysis of variance).

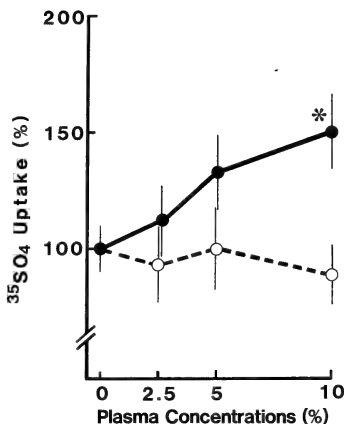


Fig. 2. Effect of various concentrations of the plasma from the ovine GH (10 μ g/animal)-treated toads (●) and from the vehicle-injected animals (○) on the uptake of [35 S]-sulphate by the xiphisternal cartilage *in vitro*. The uptake of [35 S]-sulphate by the cartilage incubated for 20 hr with increasing concentrations of plasma is expressed as the percentage of the value for the cartilage incubated in the medium containing no plasma. Each point and vertical line represent the mean of 5 determinations and SEM, respectively.

*Statistically significant between the values for the 2 groups at $p < 0.05$ (analysis of variance).

GH-treated and from the vehicle-injected animals is shown as the percentage of the value for the cartilage incubated in the medium containing no plasma. In the subsequent experiments, the medium containing 10% plasma was used unless

otherwise stated.

The cartilage from the hypophysectomized toads was incubated for 20 hr in the medium containing 10% plasma taken from the animals which had been treated with various doses of ovine or bullfrog GH. The uptake of [35 S]-sulphate by the cartilage was enhanced by the plasma according to the dosage of GH given to the donor of the plasma (Fig. 3A and B). In order to confirm that chon-

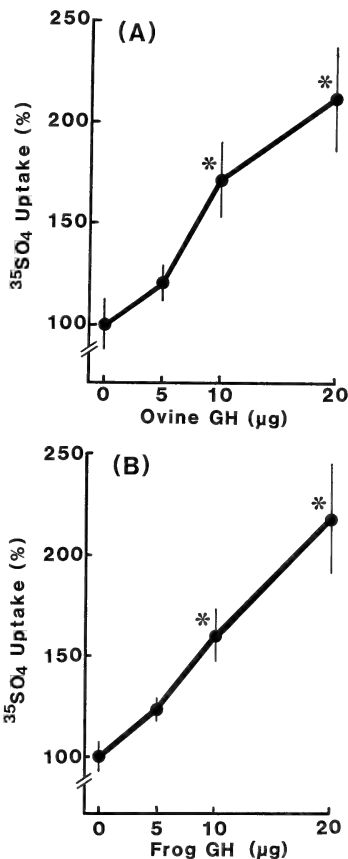


Fig. 3. Effect of plasma obtained from animals which had received various doses of ovine GH(A) or bullfrog GH(B) on the uptake of [35 S]-sulphate by the cartilage *in vitro*. The cartilage was incubated for 20 hr in the medium containing 10% plasma from the animals treated with 5–20 μ g/animal of GH. The [35 S]-sulphate uptake is expressed as the percentage of the control value (the uptake in the medium containing the plasma from the animals treated with vehicle only). Each point and vertical line represent the mean of 5 determinations and SEM, respectively.

*Significantly different from the control (0 dose) value at $p < 0.05$ (Student's *t*-test).

droitin sulphate synthesis in the cartilage of the donor of the plasma is also stimulated by GH, xiphisternal cartilage dissected out at the time of blood-taking was incubated in the medium containing [35 S]-sulphate for 12 hr. As shown in

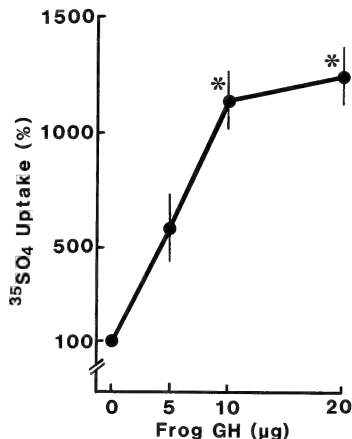


FIG. 4. *In vitro* uptake of [35 S]-sulphate by the xiphisternal cartilage from the animals which had received various doses of bullfrog GH. Incubation was performed for 12 hr according to the method of Ishii and Kikuyama [8]. [35 S]-sulphate uptake is expressed as the percentage of the control value. Each point and vertical line represent the mean of 5 determinations and SEM, respectively.

*Significantly different from the control (0 dose) value at $p < 0.01$ (Cochran-cox test).

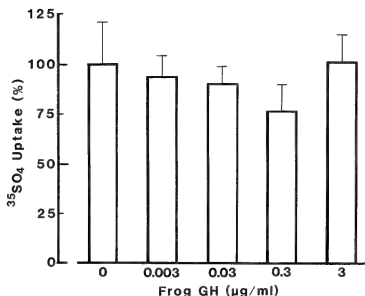


Figure 4, bullfrog GH administered *in vivo* caused a marked increase in the uptake of [35 S]-sulphate by the cartilage *in vitro*.

In the final experiment, effect of GH added in the medium on the [35 S]-sulphate uptake by the xiphisternal cartilage was studied. [35 S]-sulphate uptake by the cartilage incubated in the medium containing 10% plasma from the vehicle-injected animals was not affected by addition of 0.003–3 µg of bullfrog GH per ml of the medium (Fig. 5).

DISCUSSION

Several investigators have reported that amphibian GHs stimulate growth in amphibians [6–9]. This is the first report communicating that amphibian GH induces the plasma factor(s) which stimulates the synthesis of chondroitin sulphates in the cartilage as mammalian GHs do. In the present experiment, bullfrog GH and ovine GH exhibited an equipotent activity in inducing plasma factor(s) in *Xenopus laevis*. It has been known that amino acid composition of amphibian GHs closely resemble that of mammalian GHs [13, 14]. According to our analytical data, amino acid sequences of 40 residues of NH₂-terminal and of COOH-terminal of bullfrog GH have 73 and 68% identity with the comparable portions of ovine GH, respectively [13].

Shapiro and Pimstone [15] observed that the plasma from the normal *Xenopus laevis* as well as several nonmammalian vertebrates enhances [35 S]-sulphate uptake by the porcine cartilage *in vitro*. However, they did not show that the stimulating factor(s) in the plasma is dependent on GH. We have previously observed that hypophysectomy of *Xenopus laevis* juveniles brings about a marked decline of incorporation of [35 S]-sulphate into the xiphisternal cartilage and that injection of GH

FIG. 5. Effect of bullfrog GH added in the medium on the uptake of [35 S]-sulphate by the xiphisternal cartilage *in vitro*. The cartilage was incubated for 20 hr in the medium containing 10% plasma from the vehicle-injected animals in the presence of various amount of bullfrog GH. Each column and vertical bar represent the mean of 4 determinations and SEM, respectively. No significant difference between the values for any 2 groups (Duncan's multiple range test).

enhances the [^{35}S]-sulphate uptake by the cartilage dose-dependently [8]. The results of the present experiments indicate that the effect of GH on the cartilage is mediated by the plasma factor(s), because the stimulatory effect of the plasma was enhanced by GH which had been given to the plasma donors, while GH itself did not stimulate the *in vitro* [^{35}S]-sulphate uptake by the cartilage. In the present experiments, the maximum concentration of GH added to the incubation medium was 3 μg per ml. Plasma samples were obtained from the hypophysectomized animals which had received GH in total dose of 0.75–3 μg per g body weight. Therefore, the amount of GH added to the incubation medium containing the plasma from the hypophysectomized toads seems to be enough to substitute for the amount of GH existing in the incubation medium which contains 10% plasma from the GH-treated hypophysectomized animals. According to Van Buskirk *et al.* [16], hypophysectomy in *Rana catesbeiana* and *Rana pipiens* brings about the cessation of mitosis in the lens epithelium. Administration of GH reinitiates mitosis in the lens epithelium [17]. In organ cultures of lenses from the hypophysectomized frogs, the addition of serum from the hypophysectomized frogs treated with GH or normal frogs triggers cell division. However, the addition of serum from the hypophysectomized frogs does not stimulate cell proliferation. [18]. Rothstein *et al.* [11] demonstrated that immunoreactive somatomedin C existing in the serum of *Rana catesbeiana* was diminished by hypophysectomy and restored by GH administration and that administration of human somatomedin C to hypophysectomized bullfrogs induced mitosis in the lens epithelium. The results indicate that somatomedin C-like factor(s) mediates the GH-induced proliferation of the lens epithelium in bullfrogs. Although the presence of immunoreactive somatomedin C in amphibians is known only in two species such as *Rana catesbeiana* [11] and *Bufo marinus* [10], it is probable that the similar growth factor(s) mediates the action of GH in *Xenopus laevis* as observed in the present experiments.

ACKNOWLEDGMENTS

This research was supported by Grants-in-Aid from the Ministry of Education, Science and Culture of Japan to S.K. and by research grants from Waseda University to S.K. and T.K. The ovine GH was a gift from the National Hormone and Pituitary Program of the NIH. The authors thank to Drs. K. Yamamoto and K. Kawamura and Mr. S. Iwamuro of Waseda University for their help and advice.

REFERENCES

- 1 Daughaday, W. H., Hall, K., Raben, M. S., Salmon, W. D., Van den Brande, J. L. and Van Wyk, J. J. (1972) Somatomedin: Proposed designation for sulphation factor. *Nature*, **235**: 107.
- 2 Rinderknecht, E. and Humbel, R. E. (1976) Polypeptides with nonsuppressible insulin-like and cell-growth promoting activities in human serum: Isolation, chemical characterization, and some biological properties of forms I and II. *Proc. Natl. Acad. Sci. USA*, **73**: 2365–2369.
- 3 Van Wyk, J. J. (1984) The somatomedins: Biological actions and physiologic control mechanisms. In "Hormonal Proteins and Peptides". Ed. by C. H. Li, Academic Press, New York, Vol. XII, pp 81–125.
- 4 Zipser, R. D., Licht, P. and Bern, H. (1969) Comparative effect of mammalian prolactin and growth hormone on growth in the toads *Bufo boreas* and *Bufo marinus*. *Gen. Comp. Endocrinol.*, **13**: 382–391.
- 5 Brown, P. S. and Frye, B. E. (1969) Effect of hypophysectomy, prolactin and growth hormone on growth of postmetamorphic frogs. *Gen. Comp. Endocrinol.*, **13**: 139–145.
- 6 Nicoll, C. S. and Licht, P. (1971) Evolutionary biology of prolactin and somatotropins. II. Electrophoretic comparison of tetrapod somatotropins. *Gen. Comp. Endocrinol.*, **17**: 490–507.
- 7 Farmer, S. W., Licht, P. and Papkoff, H. (1977) Biological activity of bullfrog growth hormone in the rat and the bullfrog (*Rana catesbeiana*). *Endocrinology*, **101**: 1145–1150.
- 8 Ishii, T. and Kikuyama, S. (1984) Uptake of [^{35}S]sulphate by *Xenopus* cartilage: The influence of growth hormone and prolactin. *Zool. Sci.*, **1**: 609–615.
- 9 Kikuyama, S., Ishii, T., Kobayashi, T. and Yamamoto, K. (1984) Effect of growth hormone-containing fraction obtained from bullfrog hypophyses on growth of *Xenopus* juveniles. *Proc. Japan Acad.*, **60**: 69–72.
- 10 Daughaday, W. H., Kapadia, M., Yanow, C. E., Fabrick, K. and Mariz, I. K. (1985) Insulin-like

- growth factor I and II of nonmammalian sera. *Gen. Comp. Endocrinol.*, **59**: 316-325.
- 11 Rothstein, H., Van Wyk, J. J., Hayden, J. H., Gordon, S. R., Weinsieder, A. (1980) Somatomedin C: Restoration *in vivo* of cycle traverse in G0/G1 blocked cells of hypophysectomized animals. *Science*, **208**: 410-412.
 - 12 Yamamoto, K. and Kikuyama, S. (1981) Purification and properties of bullfrog prolactin. *Endocrinol. Japon.*, **28**: 59-64.
 - 13 Kobayashi, T., Kikuyama, S., Yasuda, A., Kawauchi, H., Yamaguchi, K. and Sano, H. (1987) Purification and properties of bullfrog growth hormone. *Proceedings of the First Congress of the Asia and Oceania Society for Comparative Endocrinology*, 33-34.
 - 14 Farmer, S. W., Papkoff, H. and Hayashida, T. (1976) Purification and properties of reptilian and amphibian growth hormone. *Endocrinology*, **99**: 692-700.
 - 15 Shapiro, B. and Pimstone, B. L. (1977) A phylogenetic study of sulphation factor activity in 26 species. *J. Endocrinol.* **74**: 129-135.
 - 16 Van Buskirk, R., Worgul, B. V., Rothstein, H. and Wainwright, N. (1975) Mitotic variations in the lens epithelium of the frog. *Gen. Comp. Endocrinol.*, **25**: 52-59.
 - 17 Wainwright, N., Rothstein, H. and Gordon, S. (1976) Mitotic variations in the lens epithelium of the frog IV. Studies with isolated anuran pituitary factors. *Growth*, **40**: 317-328.
 - 18 Wainwright, N., Hayden, John. and Rothstein, H. (1978) Total disappearance of cell proliferation in the lens of a hypophysectomized animal. *In vivo* and *in vitro* maintenance of inhibition with reversal by pituitary factors. *Cytobios*, **23**: 79-92.

Stimulation of Nuclear Volume Enlargement and Neuronal Process Growth by Estrogen in the Hypothalamic and Limbic Nuclei of the Rat

MASAYUKI UCHIBORI and SEIICHIRO KAWASHIMA¹

Zoological Laboratory, Suzugamine Women's College, Hiroshima 733, and

¹Zoological Institute, Faculty of Science, University of Tokyo, Tokyo 113, Japan

ABSTRACT—Effects of estradiol-17 β (E_2) on the growth of nuclear volume of the ventromedial nucleus (VMN), the suprachiasmatic nucleus (SCN) and the bed nucleus of the stria terminalis (STN), and the growth of neuronal process length in these nuclei were studied. Male and female rats of the Wistar/Tw strain were castrated on the day of birth (Day 1), and were given subcutaneous injections of 10 μ g E_2 daily for the first 10 postnatal days. They were killed on Days 11 and 31. E_2 treatment generally stimulated the growth of the nuclear volume and the neuronal process length in the VMN. However, the E_2 effect was not significant in the nuclear volume of the VMN in males on Day 31 and in the neuronal process length in females on Day 11. In the SCN, E_2 failed to stimulate the nuclear volume enlargement, but it was effective for the neuronal process elongation only on Day 31. In the STN, E_2 stimulated the growth of nuclear volume on Day 31 in males and on Day 11 in females and the neuronal process length on Day 11 in males. The present results showed that the E_2 effects were marked in the VMN but were less evident in the SCN and STN, and that the E_2 response in the nuclear volume in a nucleus was generally accompanied by a similar stimulatory effect of E_2 in the neuronal process growth in the nucleus, indicating that the nuclear volume enlargement is due, at least partly, to the neuronal process growth.

INTRODUCTION

Sexual dimorphism has been demonstrated in some discrete areas of the brain, such as an intensely staining area of the medial preoptic area, called the sexually dimorphic nucleus of the preoptic area (SDN-POA) [1-3], the ventromedial nucleus (VMN) [4], the medial nucleus of the amygdala [5] and the medial preoptic nucleus (MPN) in the rostroventral periventricular region of the POA [6, 7]. The volumes of the SDN-POA, VMN and amygdala nuclei in male rats were greater than those in females, and these nuclei in females grew to the male level by perinatal treatment with sex steroids [1, 3-5]. On the other hand, Ito *et al.* [7] reported that the volume of the MPN in female rats was greater than that of males and decreased to the male level by neonatal steroid treatment.

These morphological sexual dimorphisms in the

nuclear volume may be due to the differences in individual neuronal size, total number of neurons and/or neuronal density of the nuclei, which are induced by exposure to testicular androgen during the perinatal period. With regard to the sex steroidal influence on the neurogenesis for the sexual differentiation of the brain, Toran-Allerand [8, 9] studied neuronal process outgrowth in newborn mouse hypothalamus-POA in organotypic culture, and this was confirmed by our studies in monolayer culture of cells derived from the hypothalamus-POA of neonatal mice, fetal and neonatal rats [10-12]. *In vivo* studies also substantiated the findings of these *in vitro* effects of sex steroids. Hammer and Jacobson [13] reported that the dendritic extent and neuronal size in the SDN-POA were found to increase more in male rats than females during the first 10 postnatal days. Recently we found that subcutaneous injections of estradiol-17 β (E_2) for the first 10 postnatal days in both sexes of rats castrated on the day of birth increased both the nuclear volume and the total

process length of SDN-POA neurons at 11 and 31 days of age.

To afford further evidence for the steroidal effects on the development of sexual dimorphism in the rat brain, the effects of E_2 on the growth of nuclear volume and neuronal process length were quantitatively studied in the VMN, the suprachiasmatic nucleus (SCN) and the bed nucleus of the stria terminalis (STN).

MATERIALS AND METHODS

Male and female rats of the Wistar/Tw strain were castrated on the day of birth (Day 1) under hypothermal anesthesia. Subsequently they were subcutaneously injected with $10 \mu\text{g}$ E_2 (Sigma) dissolved in 0.02 ml sesame oil daily for the first 10 postnatal days. As controls castrated rats were given injections of 0.02 ml vehicle oil only. In the study of neuronal process length, sham-operated controls were also prepared. On Day 11 or 31 rats were subjected to intracardiac perfusion under ether anesthesia.

For the study of nuclear volume 10% formalin was used as perfusion fluid. The brains were removed and placed in 10% formalin for at least 5 days. Paraffin sections of the brains were cut frontally at $15 \mu\text{m}$ thickness, and every third sections were stained with cresyl violet (Nissl preparations). Representative profiles of the VMN, SCN and STN are shown in Figure 1. The outlines of these nuclei in both sides of the brain were traced in all the third sections with a camera lucida at $\times 98.5$ magnification. From the drawings, the nuclear area was measured with the aid of a tablet digitizer (Mutoh Industry Ltd.), and the nuclear volume (the mean of left and right nuclei) was calculated from the measurements.

The neuronal process length was measured using Golgi-stained preparations. Rats were anesthetized with ether and perfused with 0.9% NaCl followed by freshly prepared Golgi-Hortega fixative [14] consisting of potassium dichromate (5 g), chloral hydrate (5 g), formaldehyde (5 ml), 50% glutaraldehyde (5 ml), dimethyl sulfoxide (5 drops) and deionized water (100 ml). Brains were removed and placed in a fresh Golgi-Hortega fixative, which was changed daily for 4 days.

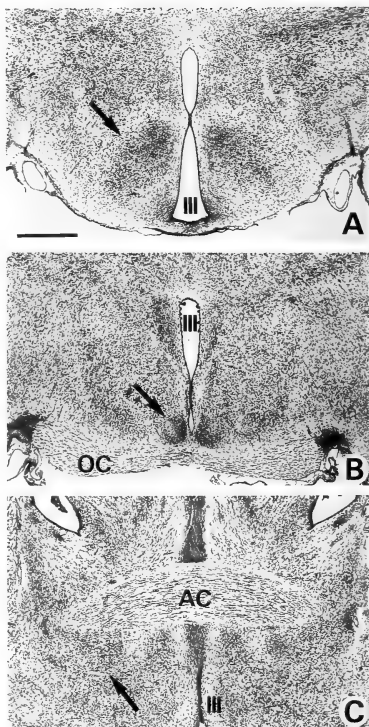


Fig. 1. Microphotographs of representative frontal sections in neonatally castrated control male rats on Day 31. Cresyl violet preparations. (A) ventromedial nucleus (VMN), (B) suprachiasmatic nucleus (SCN), (C) bed nucleus of the stria terminalis (STN). Arrows indicate these nuclei. AC, anterior commissure; OC, optic chiasm; III, third ventricle. Bar: $200 \mu\text{m}$.

Whole brain was then stained in 0.75% AgNO_3 for 4 days, embedded in celloidine and frontally sectioned at $120 \mu\text{m}$ thickness. Completely impregnated neurons (Fig. 2) in both sides of the VMN, SCN and STN in sham-operated and castrated control rats and E_2 -injected ones of both sexes were traced with a camera lucida at $\times 395$ mag-

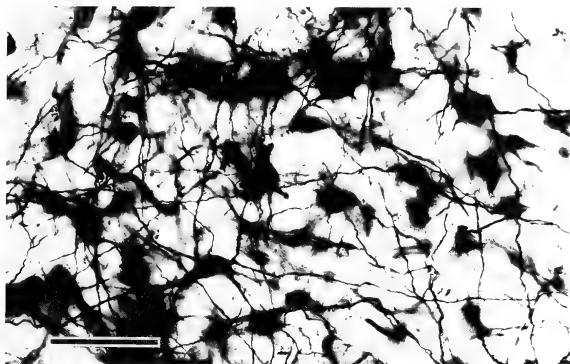


Fig. 2. A part of the VMN of an E_2 -injected male rat on Day 31. Golgi-stained preparation. Bar: 100 μ m.

nification. Total neuronal process length per neuron was measured using the tablet digitizer. The mean number of neurons measured per rat in the VMN, SCN and STN was 16.5, 7.8 and 17.7, respectively. As the double staining of the VMN, SCN and STN neurons by $AgNO_3$ and cresyl violet was unsuccessful, the area of measurement in a Golgi preparation was determined by referring to a separately stained Nissl preparation.

The results were analyzed by Mann-Whitney U-test.

RESULTS

Nuclear volume

Figures 3–5 show the effects of E_2 on the growth of nuclear volume of the VMN, SCN and STN. E_2 clearly increased the nuclear volume of the VMN in Day 11 rats of both sexes and in Day 31 females as compared to matched controls (all comparisons, $P < 0.05$). In Day 31 males, the E_2 effect on nuclear volume enlargement was statistically not significant (Fig. 3). The nuclear volume of the SCN in E_2 -treated rats tended to be greater than that of the controls, but the differences were statistically not significant (Fig. 4). The increase of the STN volume by E_2 treatment was detected in

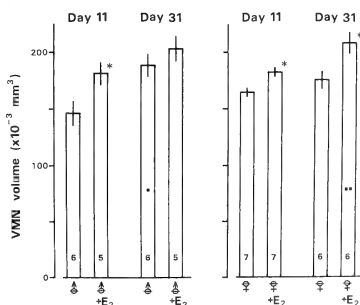


Fig. 3. Effects of estradiol-17 β (E_2) on the mean nuclear volume of the VMN in Day 11 and Day 31 rats. Numbers in columns indicate the numbers of rats measured. Vertical bars depict the standard errors of means. Significance of differences: E_2 -treated vs castrated control rats, * $P < 0.05$; Day 11 vs comparable group of Day 31, • $P < 0.05$, ** $P < 0.01$. Significant differences between male and matched female rats were not detected.

Day 31 males and in Day 11 females (both comparisons, $P < 0.05$) (Fig. 5).

Significant sex differences in the nuclear volume were rarely observed among groups. In the SCN of Day 31 E_2 -injected rats the nuclear volume was

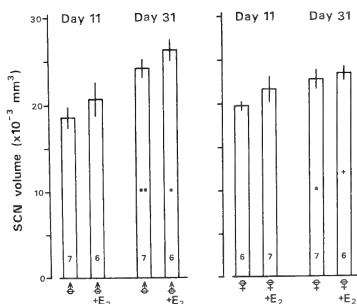


Fig. 4. Effects of E₂ on the mean nuclear volume of the SCN in Day 11 and Day 31 rats. Significance of differences: male vs matched female rats, *P<0.05; Day 11 vs comparable group of Day 31, ■P<0.05, ■P<0.01. Significant differences between E₂-treated and castrated control rats were not detected. For other explanations, refer to legend of Fig. 3.

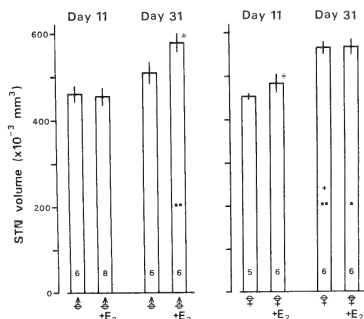


Fig. 5. Effects of E₂ on the mean nuclear volume of the STN in Day 11 and Day 31 rats. Significance of differences: E₂-treated vs castrated control rats, *P<0.05; male vs matched female rats, +P<0.05; Day 11 vs comparable group of Day 31, ■P<0.05, ■P<0.01. For other explanations, refer to legend of Fig. 3.

larger in males than females (P<0.05). While in the STN of Day 31 castrated controls it was smaller in males than females (P<0.05).

Age-related increase in the nuclear volume (Day 11 vs Day 31) was observed in the VMN of

castrated male control rats (P<0.05) and E₂-injected females (P<0.01). In the SCN and STN the nuclear volume on Day 31 was significantly larger than that on Day 11 in the following groups: in the SCN, castrated male controls (P<0.01); E₂-injected males (P<0.05); castrated female controls (P<0.05), and in the STN, E₂-injected males (P<0.01); castrated female controls (P<0.01); E₂-injected females (P<0.05).

Neuronal process length

The effects of E₂ on the growth of neuronal process length in the VMN, SCN and STN are shown in Figures 6–8. The neuronal process length in the VMN was greater in E₂-treated male rats than castrated controls on Days 11 and 31 and was also greater in E₂-treated female rats than castrated controls on Day 31 (all comparisons, P<0.01). Similar stimulatory effects of E₂ were detected in the SCN in Day 31 rats of both sexes (males, P<0.05; females, P<0.01) and in the STN in Day 11 males (P<0.05). When E₂-treated rats were compared with sham-operated controls, the neuronal process length in the VMN was greater in the former than the latter in Days 11 and 31 females (Day 11, P<0.01; Day 31, P<0.05), but in males such stimulatory effects of E₂ were not observed. The stimulatory effects of E₂ on the SCN neurons were observed only in Day 31 females (P<0.05). In the STN no positive E₂ response was found when E₂-treated rats were compared with sham-operated controls.

The neuronal process length of sham-operated controls was significantly greater than that of castrated controls in the VMN of Day 11 males (P<0.01) and in the STN of Days 11 and 31 males (both comparisons, P<0.05). However, in Day 11 females the neuronal process length was smaller in sham-operated controls than castrated controls (VMN, P<0.01; STN, P<0.05). No significant differences were found in the SCN.

The comparison of the neuronal process length in the VMN between males and females showed that it was significantly greater in males than females in sham-operated control and E₂-injected groups on Day 11 (P<0.001 and P<0.05, respectively), but on Day 31 the process length in males was smaller than that in females in sham-operated

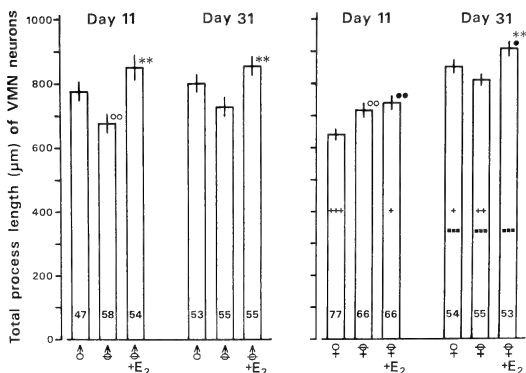


FIG. 6. Effects of E₂ on the mean total process length of neurons in the VMN in Day 11 and Day 31 rats. Numbers in columns indicate the numbers of neurons measured. Vertical bars depict the standard errors of means. Significance of differences: E₂-treated vs castrated control rats, **P<0.01; E₂-treated vs sham-operated control rats, •P<0.05, ••P<0.01; castrated vs sham-operated control rats, ○P<0.01; male vs matched female rats, +P<0.05, ++P<0.01, +++P<0.001; Day 11 vs comparable group of Day 31, ■■■P<0.001. ♂, ♀: sham-operated controls.

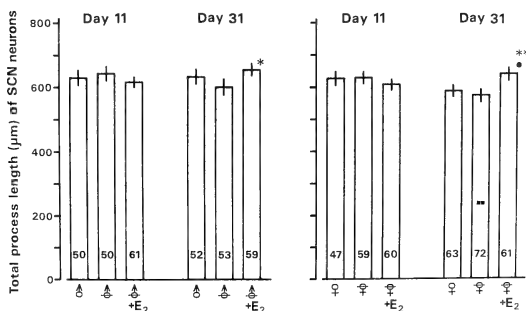


FIG. 7. Effects of E₂ on the mean total process length of neurons in the SCN in Day 11 and Day 31 rats. Significance of differences: E₂-treated vs castrated control rats, *P<0.05, **P<0.01; E₂-treated vs sham-operated control rats, •P<0.05; Day 11 vs comparable group of Day 31, ■P<0.01. Significant differences between castrated and sham-operated control rats, and between male and matched female rats were not detected. For other explanations, refer to legend of Fig. 6.

and castrated control groups (P<0.05 and P<0.01, respectively). In the SCN sex difference was not detected. In the STN, the neuronal process

length of males was significantly greater than that of females in sham-operated controls and E₂-injected rats on Day 11 (P<0.001 and P<0.05,

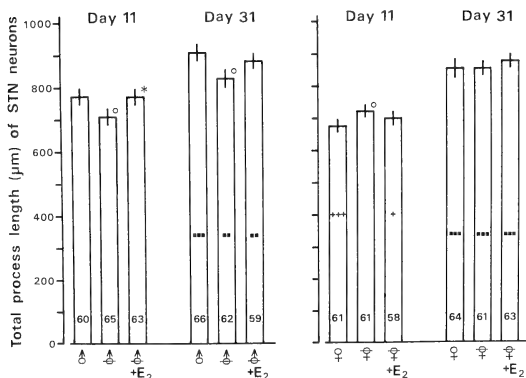


FIG. 8. Effects of E_2 on the mean total process length of neurons in the STN in Day 11 and Day 31 rats. Significance of differences: E_2 -treated vs castrated control rats, * $P < 0.05$; castrated vs sham-operated control rats, ○ $P < 0.05$; male vs matched female rats, + $P < 0.05$, +++ $P < 0.001$; Day 11 vs comparable group of Day 31, ** $P < 0.01$, *** $P < 0.001$. Significant differences between E_2 -treated and sham-operated control rats were not detected. For other explanations, refer to legend of Fig. 6.

respectively). Thus, sex difference in the neuronal process length in the VMN, SCN and STN was inconsistent, likewise in the nuclear volume.

Age-related increase in the neuronal process length (Day 11 vs Day 31) was evident in the female VMN and in the STN of both sexes in sham-operated and castrated controls and E_2 -injected groups (female VMN: all comparisons, $P < 0.001$; male STN: sham-operated controls, $P < 0.001$; castrated controls and E_2 -injected groups, $P < 0.01$; female STN: all comparisons, $P < 0.001$). In contrast, the neuronal process length in the SCN was smaller on Day 31 than Day 11 in castrated control females ($P < 0.01$).

DISCUSSION

In a previous paper we reported that neonatal injections of E_2 for 10 days clearly enhanced the growth of nuclear volume of the SDN-POA and neuronal process length in the SDN-POA in rats of both sexes [15]. These results supported the earlier findings *in vivo* [1] and *in vitro* [8–11].

The present results showing that the stimulatory

effects of E_2 on the growth of nuclear volume of the VMN were apparent and the sex difference in the VMN volume of neonatally castrated control rats was not detected are in conformity with the observations by Matsumoto and Arai [4]. They reported that the volume of the VMN of normal male rats was greater than that of normal female rats and that castration on the day of birth in male rats reduced the VMN volume to a level comparable to that of normal females. They concluded that the volume of the VMN is sexually dimorphic and is modified by steroids secreted from neonatal testes.

In the SCN and STN, the E_2 response was weak and the sex difference in the volume of those nuclei was not apparent. In an earlier report Gorski *et al.* [1] found that injection of testosterone propionate to neonatal female rats or castration of neonatal males had no significant effects on the volume of the SCN, when examined in adults, and that the SCN volume of adult males castrated neonatally did not differ from that of adult females injected neonatally with sesame oil. Our present results on the SCN seem to accord with their

findings. The nuclear volume of the medial nucleus of the amygdala is greater in adult male rats than females and its differentiation occurs during the early postnatal period under the influence of sex steroids [5]. While, in the lateral nucleus of the amygdala [5], neither sex difference in the nuclear volume nor steroidal response was demonstrated. It seems likely that sex difference is detectable in brain regions which are known to control reproductive functions.

The neuronal process length in the VMN of castrated male rats was significantly less on Day 11 as compared with that of sham-operated males, and significantly increased to the level of sham-operated controls by E_2 injection. In females the length was significantly greater in E_2 -injected groups than sham-operated controls. Accordingly, it is evident that the growth of neuronal process length in the VMN is enhanced by neonatal E_2 treatment. Small but significant increase of neuronal process length by E_2 injections in the SCN was observed on Day 31 but not on Day 11 in both sexes. In the STN significant increase in neuronal process length by E_2 treatment was detected only in castrated Day 11 male rats.

A certain parallelism between the neuronal process length and nuclear volume indicates that the increase in the neuronal process length by E_2 treatment is one of the factors involved in nuclear volume enlargement. However, the parallelism was not always observed. For example, the VMN volume in castrated control males was significantly larger on Day 31 than on Day 11, whereas the neuronal process length was not significantly different between Days 11 and 31. There may be some factors other than neuronal process elongation for nuclear volume enlargement.

A number of autoradiographic studies have demonstrated the accumulation of steroid hormones by neurons in the limbic and preoptic-hypothalamic structures. In adult females, a large number of neurons in the medial POA, VMN and STN were labelled with radioactive E_2 but scarcely in the SCN [16]. Testosterone-concentrating neurons were also reported in the medial POA, VMN and STN [17]. In 2-day-old female rats, Sheridan *et al.* [18] reported a topographic pattern of neuronal nuclear concentration of radioactive E_2 in these

regions similar to that in the adult. Sheridan *et al.* [19] further reported that the E_2 -concentrating neurons in 2-day-old female rats also concentrate testosterone. In autoradiographic study of the SDN-POA of adult rats, it was reported that for both sexes there was a greater percentage of labelled cells following E_2 exposure than following testosterone or dihydrotestosterone exposure, and the percentage of labelled cells in males following testosterone exposure was greater than that in females but such a sex difference was not found following E_2 or dihydrotestosterone exposure [20]. Our results that the nuclear volume of the SDN-POA and VMN and the neuronal process length in these nuclei markedly increased and those of the SCN showed little increase by neonatal E_2 treatment correspond well to the steroid-concentrating ability of neurons in these nuclei. However, the E_2 response of the STN failed to fit this conclusion, indicating that high steroid-concentrating ability is not always accompanied by morphological E_2 response as nuclear volume enlargement and neuronal process elongation.

ACKNOWLEDGMENTS

This work was supported in part by a Grant-in-Aid for Scientific Research from the Ministry of Education, Science and Culture, Japan (No. 62480023).

REFERENCES

- 1 Gorski, R. A., Gordon, J. H., Shryne, J. E. and Southam, A. M. (1978) Evidence for a morphological sex difference within the medial preoptic area of the rat brain. *Brain Res.*, **148**: 333-346.
- 2 Jacobson, C. D., Shryne, J. E., Shapiro, F. and Gorski, R. A. (1980) Ontogeny of the sexually dimorphic nucleus of the preoptic area. *J. Comp. Neurol.*, **193**: 541-548.
- 3 Döhler, K.-D., Coquelin, A., Davis, F., Hines, M., Shryne, J. E. and Gorski, R. A. (1982) Differentiation of the sexually dimorphic nucleus in the preoptic area of the rat brain is determined by the perinatal hormone environment. *Neurosci. Lett.*, **33**: 295-298.
- 4 Matsumoto, A. and Arai, Y. (1983) Sex difference in volume of the ventromedial nucleus of the hypothalamus in the rat. *Endocrinol. Japon.*, **30**: 277-280.
- 5 Mizukami, S., Nishizuka, M. and Arai, Y. (1983)

- Sexual difference in nuclear volume and its ontogeny in the rat amygdala. *Exp. Neurol.*, **79**: 569-575.
- 6 Bleier, R., Byne, W. and Siggelkow, I. (1982) Cytoarchitectonic sexual dimorphisms of the medial preoptic and anterior hypothalamic areas in guinea pig, rat, hamster, and mouse. *J. Comp. Neurol.*, **212**: 118-130.
- 7 Ito, S., Murakami, S., Yamanouchi, K. and Arai, Y. (1986) Perinatal androgen exposure decreases the size of the sexually dimorphic medial preoptic nucleus in the rat. *Proc. Japan Acad.*, **62(B)**: 408-411.
- 8 Toran-Allerand, C. D. (1976) Sex steroids and the development of the newborn mouse hypothalamus and preoptic area *in vitro*: implications for sexual differentiation. *Brain Res.*, **106**: 407-412.
- 9 Toran-Allerand, C. D. (1980) Sex steroids and the development of the newborn mouse hypothalamus and preoptic area *in vitro*. II. Morphological correlates and hormonal specificity. *Brain Res.*, **189**: 413-427.
- 10 Ohtani, R. and Kawashima, S. (1983) The effects of estradiol-17 β on the neuritic growth of neonatal mouse hypothalamus and preoptic area in primary culture. *Annot. Zool. Japon.*, **56**: 275-281.
- 11 Uchibori, M. and Kawashima, S. (1985) Effects of sex steroids on the growth of neuronal processes in neonatal rat hypothalamus-preoptic area and cerebral cortex in primary culture. *Int. J. Dev. Neurosci.*, **3**: 169-176.
- 12 Uchibori, M. and Kawashima, S. (1985) Stimulation of neuronal process growth by estradiol-17 β in dissociated cells from fetal rat hypothalamus-preoptic area. *Zool. Sci.*, **2**: 381-388.
- 13 Hammer, R. P., Jr. and Jacobson, C. D. (1984) Sex difference in dendritic development of the sexually dimorphic nucleus of the preoptic area in the rat. *Int. J. Dev. Neurosci.*, **2**: 77-85.
- 14 Stensaas, L. J. (1966) The development of hippocampal and dorsolateral pallial regions of the cerebral hemisphere in fetal rabbits. I. Fifteen millimeter stage, spongioblast morphology. *J. Comp. Neurol.*, **129**: 59-70.
- 15 Uchibori, M., Hayashibara, M. and Kawashima, S. (1986) Effects of estradiol-17 β on the growth of nuclear volume and neuronal processes in the sexually dimorphic nucleus of the preoptic area in neonatally gonadectomized rats. *J. Sci. Hiroshima Univ.*, **32**: 283-292.
- 16 Pfaff, D. and Keiner, M. (1973) Atlas of estradiol-concentrating cells in the central nervous system of the female rat. *J. Comp. Neurol.*, **151**: 121-158.
- 17 Sar, M. and Stumpf, W. E. (1975) Distribution of androgen-concentrating neurons in rat brain. In "Anatomical Neuroendocrinology". Ed. by W. E. Stumpf and L. D. Grant, Karger, Basel, pp. 120-133.
- 18 Sheridan, P. J., Sar, M. and Stumpf, W. E. (1974) Autoradiographic localization of ³H-estradiol or its metabolites in the central nervous system of the developing rat. *Endocrinology*, **94**: 1386-1390.
- 19 Sheridan, P. J., Sar, M. and Stumpf, W. E. (1975) Estrogen and androgen distribution in the brain of neonatal rats. In "Anatomical Neuroendocrinology". Ed. by W. E. Stumpf and L. D. Grant, Karger, Basel, pp. 134-141.
- 20 Jacobson, C. D., Arnold, A. P. and Gorski, R. A. (1987) Steroid autoradiography of the sexually dimorphic nucleus of the preoptic area. *Brain Res.*, **414**: 349-356.

Seasonal Changes of Triiodothyronine Binding to Piscine Ovarian Nuclei

GAURANGI MAITRA and SAMIR BHATTACHARYA¹

Department of Zoology, Visva-Bharati University
Santiniketan-731235, West Bengal, India

ABSTRACT—The pattern of ¹²⁵I-triiodothyronine (¹²⁵I-T₃) binding to the fairly pure oocytes nuclei preparation and plasma T₃ levels were studied in the seasonally breeding fresh water perch, *Anabas testudineus*. ¹²⁵I-T₃ binding affinity was found to remain fairly constant (K_a varied from 0.11 to 0.12 × 10⁹ M⁻¹) during the four reproductive phases while maximum binding capacity (MBC) altered significantly. The highest value was seen in the prespawning phase (MBC=4.13 p mole/mg DNA) and the lowest in postspawning phase (MBC=3.44 p mole/mg DNA). Plasma T₃ level was in a peak during prespawning (2.9 ng/ml) whereas it was the lowest in postspawning phase fish (0.92 ng/ml). Seasonal indices of plasma T₃ level and MBC suggest an autoregulation of T₃ binding site. Further evidences in support of this were obtained from fish treated with T₃, thiourea and thiouracil; T₃ increased ¹²⁵I-T₃ binding while antithyroid drugs decreased it significantly.

INTRODUCTION

Several reports support the involvement of thyroid in vertebrate reproduction including fishes [1-6]. Whether thyroid influences gonadal activity directly or indirectly is still unclear. In seasonally breeding lower vertebrates, such as fish, the gonadal cycle coincides with the thyroid cycle [7-9]. Thyroid influence on the piscine ovary has been viewed by some as an indirect one and suggested that thyroid hormone increased ovarian response to gonadotropin [10-12], while others indicated an individual effect of thyroid hormone on piscine ovary as ovarian metabolic activity considerably increased in *in vitro* [13-14]. Recently, we have reported high affinity, low capacity thyroid hormone binding sites in the nuclei of perch ovary [15]. This indicates that thyroid hormone has distinct physiological relevance in relation to reproduction. Since this perch is a seasonally breeding fish, it will be interesting to note the profile of triiodothyronine (T₃) binding to ovarian nuclei in relation to the seasonal reproduc-

tive cycle. The present report deals with the T₃ binding patterns in perch ovarian nuclei at four distinct reproductive phases and how this information leads to the revelation of autoregulation of ovarian thyroid hormone receptor.

MATERIALS AND METHODS

Anabas testudineus is a freshwater perch occurring commonly in India. Its reproductive cycle can be divided into four distinct phases: i) preparatory (February - April) ii) prespawning (May - June) iii) spawning (July - early September) and iv) postspawning (late September - January). Adult female perch (body wt. 20-25 g; length 10-12 cm) were collected at different reproductive phases from local ponds. Method used for the collection of blood and ovarian tissue were similar to a paper reported earlier [9]. Blood was collected from the caudal vein with 1 ml syringe (24 gauge needle), plasma was separated and stored at -20°C. Plasma T₃ level was determined by specific radioimmunoassay (RIA) after our earlier report [9].

Ovaries collected from perch belonging to different reproductive phases, and subjected to homogenization followed by isolation of nuclei [16] for its *in vitro* binding incubation. Procedures

Accepted October 31, 1988

Received August 16, 1988

¹ To whom reprint requests should be addressed.

followed for isolating the nuclei from perch ovary, its quantitation (as reflected by DNA concentration) and ^{125}I - T_3 binding assay were similar to our earlier report [15]. In the binding assay 80 μg DNA was incubated with 1.6 p mole of ^{125}I - T_3 (sp. activity 180.65 $\mu\text{Ci}/\mu\text{g}$, Bhabha Atomic Research Centre, India) in 500 μl binding incubation medium, with or without 400 p mole of cold T_3 . Specific binding was calculated by subtracting nonspecific binding and expressed as a percentage of total binding.

Adult female perch used for T_3 and thiourea treatment were acclimatized for 7 days, fed and maintained in a manner as described before [9]. Preparatory stage fish were selected for this experi-

ment as endogenous T_3 level was found to be low and thus response to exogenous T_3 by the ovary was expected to be better. T_3 , thiouracil and thiourea were injected separately and intramuscularly on the dorsal peduncle (100 ng/100 g body wt and 2 $\mu\text{g}/100\text{g}$ body wt respectively) for 7 days. Control group received saline (vehicle) in equal volume. Ovaries thereafter collected from treated and control groups, processed for obtaining nuclei receptor material and subjected to binding assay.

For *in vitro* T_3 treatment of perch ovarian tissue (from prespawning stage fish), oocytes were separated and incubated by following the procedure described earlier [17]. Incubations were made with T_3 (100 ng/incubation) or 0.6% saline for 6 hr and

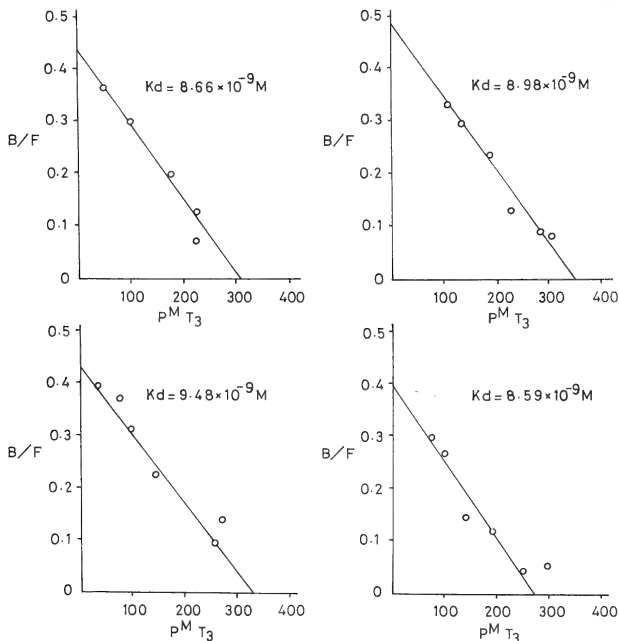


Fig. 1. Scatchard analysis of T_3 binding to ovarian nuclei in different seasons. Each point is the mean of 6 tests.

terminated by transferring them to an ice bed. The oocytes were immediately processed for nuclei isolation, extraction and binding assay. Student's *t*-test [18] was applied to analyse the data.

RESULTS

T₃ binding to perch ovarian nuclei of different reproductive phases was assessed by incubating 80 µg of DNA with increasing concentrations of radiolabeled T₃ (0.41 to 3.2 p mole) keeping other conditions constant. Scatchard analysis for the four reproductive phases shows that high affinity, low capacity T₃ binding sites for ovarian nuclei were clearly detectable in all stages. The K_a for different phases did not vary significantly (between 0.11 to 0.12 × 10⁹ M⁻¹, Fig. 1).

Maximum binding capacity (MBC) on the other hand, varied remarkably in different seasons (Table 1). MBC was the highest during prespawning and spawning phases, which was significantly reduced in the postspawning stage ($p < 0.02$ in comparison to prespawning) and this lower MBC continued till the preparatory stage. Table 1 also shows that the peak MBC values coincided with the peak seasonal plasma T₃ levels. This indicates that the amount of ovarian nuclear T₃ binding sites may be dependent on its own ligand level in the circulation. To investigate such a possibility, binding of T₃ to ovarian tissue of T₃ and thiourea treated fish was compared. Figure 2 demonstrates the results of this experiment. Treatment of T₃ increased its specific binding significantly ($p < 0.001$) while treatment with thyroid inhibitors, thiourea and thiouracil, decreased T₃ level remarkably ($p < 0.001$). To confirm this, oocytes were incubated *in vitro* with T₃ and nuclei isolated from them showed a comparable increase in T₃ binding over the control (Fig. 3).

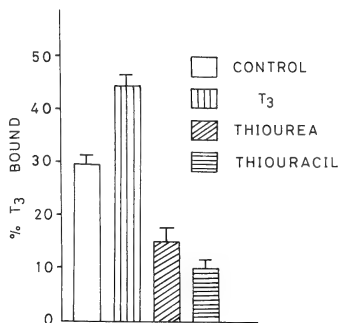


FIG. 2. Effect of T₃, thiourea and thiouracil on T₃ binding to perch ovarian nuclei. Vertical bar in each case represents mean for 3 tests (\pm SE).

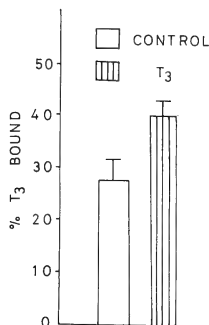


FIG. 3. *In vitro* incubation of perch oocytes with T₃. Vertical bar represents mean of 4 tests (\pm SE).

TABLE 1. Plasma T₃ levels and MBC in different seasons

Season	Plasma T ₃ level ^a ng/ml	Maximum binding ^b capacity p mol/mg DNA
Preparatory	1.70 \pm 0.04	3.813 \pm 0.91
Prespawning	2.90 \pm 0.28	4.313 \pm 0.71
Spawning	1.05 \pm 0.02	4.125 \pm 0.24
Postspawning	0.92 \pm 0.02	3.440 \pm 0.08

^{a,b} Mean \pm SE of 6 determinations.

DISCUSSION

The present work is an attempt to elucidate the seasonal profile of ovarian thyroid hormone receptor in a seasonally breeding teleost. Freshwater perch, *A. testudineus*, breeds once a year and that is during the monsoon or rainy season in India. To explain the physiological relevance of ovarian thyroid hormone receptor [15], a study in relation to reproductive cycle, which is categorised into four stages, appears to be important. Scatchard analysis of T_3 binding to the ovarian nuclei of perch from 4 reproductive phases indicates that affinity for binding sites remained almost unaltered as K_a values varied between 0.11 to $0.12 \times 10^9 M^{-1}$. This appears to be a little surprising since the size and weight of the perch ovary varied strikingly in different reproductive phases. But alteration of MBC in different reproductive phases correlates ovarian size and weight. MBC was found to be highest in prespawning fish ovarian nuclei. There was a significant drop in MBC in the ovarian nuclei of postspawning fish and a similar MBC value was obtained for preparatory stage fish. All these observations indicate that affinity of T_3 for the ovarian binding site does not alter in different phases of reproductive cycle while the amount of receptor occupancy has distinct variation.

Seasonal profile of plasma T_3 level in perch coincides with peak of MBC value, both are the highest in prespawning phase. Report from this laboratory indicates that reproductive metabolism of this perch was the highest in the prespawning, while it decreased, although not significantly, in the spawning phase, followed by a significant fall in the postspawning phase [19]. Plasma level and MBC of T_3 followed the same pattern. It has been suggested that temperature plays a important role in elevating plasma level of thyroid hormone in fish [20], whereas on the photoperiod there is no such report in fish. There is a considerable rise of temperature from preparatory to prespawning and in fact the highest temperature is recorded in May and June in this area of India. This particular environmental factor is also found to be very important in this perch, as keeping them at $30-35^\circ C$ regime not only enhanced thyroid hormone level but also induced gonadal maturation in pre-

paratory stage fish (data not shown). Hence it may be presumed that an increase in environmental temperature resulted higher plasma T_3 level and this in turn caused higher MBC in the prespawning fish.

To assess such possibility, perch of the preparatory stage were treated with T_3 , thiourea and thiouracil for 7 days. T_3 significantly increased the binding of $^{125}I-T_3$ while there was a remarkable drop in T_3 binding by thiourea and thiouracil in comparison with control. Treatment by thiourea resulted significant fall of thyroid hormone level in plasma (data not shown). Since *in vivo* experiments face a question of interference or mediation by some endogenous factor, an *in vitro* incubation of oocytes with T_3 was performed. Increase of $^{125}I-T_3$ binding to ovarian nuclei was again clear.

Evidences so far obtained from seasonal and experimental data provide two important information—1) a direct relation of thyroid with seasonal reproduction of perch 2) thyroid hormone regulates T_3 binding sites in the ovarian nuclei. These two information are relevant in assessing the thyroid function related to reproduction of teleostean fishes.

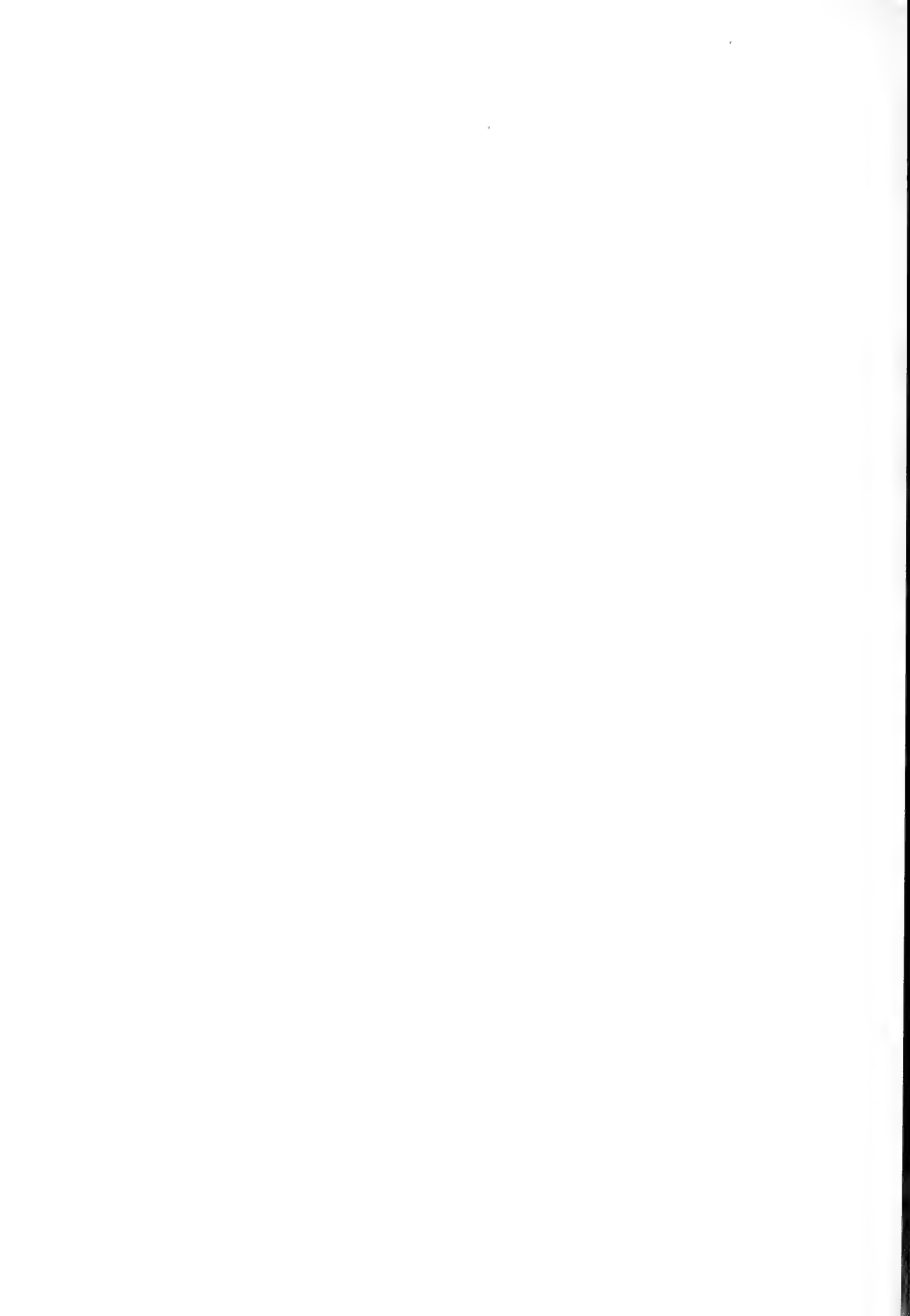
ACKNOWLEDGMENTS

This work was supported by fund from University Grants Commission, New Delhi, India. We wish to thank Dr. Md. Jamaluddin for constructive comments.

REFERENCES

- 1 Ball, J. N. (1960) Reproduction in female bony fishes. Symp. Zool. Soc. London, 1: 105-135.
- 2 Fontaine, Y. A. (1975) Hormones in fishes. In "Biochemical and Biophysical Perspectives in Marine Biology". Ed. by D. C. Malins and J. R. Sargents, Academic Press, Orlando, Vol. 2, pp. 139-212.
- 3 Bona-Gallo, A., Licht, P., Mackenzie, D. S. and Lofts, B. (1980) Annual cycles in levels of pituitary and plasma gonadotropin, gonadal steroids and thyroid activity in the Chinese cobra (*Naja naja*). Gen. Comp. Endocrinol., 42: 477-493.
- 4 Ingbar, S. H. and Woelbar, K. A. (1980) The Thyroid Gland. In "Textbook of Endocrinology". Ed. by R. H. Williams, Igakushoin/Saunders International Edition, Philadelphia/Tokyo, pp. 117-243.
- 5 Bhattacharya, S., Sen, S. and Deb, S. (1985) Hor-

- monal regulation of ovarian 17 β -hydroxy-steroid dehydrogenase in teleost. In "Current Trends in Comparative Endocrinology". Ed. by B. Lofis and W. N. Holmes, Hong Kong Univ. Press, Hong Kong, Vol. II, pp. 237-238.
- 6 Tasaki, Y., Inoue, M. and Ishii, S. (1986) Annual cycle of plasma thyroid hormone levels in the toad, *Bufo japonicus*. Gen. Comp. Endocrinol., **62**: 404-410.
 - 7 Ichikawa, M., Mori, T., Kawashima, S., Ueda, K. and Shirahata, S. (1974) Histological changes in the thyroid and internal tissue of kokanee (*Oncorhynchus nerka*) during sexual maturation and spawning. J. Fac. Sci. Univ. Tokyo, **4**: 175-182.
 - 8 White, B. and Henderson, N. E. (1977) Annual variations in the circulating levels of thyroid hormones in the brook trout, *Salvelinus fontinalis*, as measured by radioimmunoassay. Canad. J. Zool. **55**: 475-481.
 - 9 Chakraborti, P. and Bhattacharya, S. (1984) Plasma thyroxine levels in freshwater perch : Influence of season, gonadotropins and gonadal hormones. Gen. Comp. Endocrinol., **53**: 179-186.
 - 10 Hurlburt, M. E. (1977) Role of thyroid gland in ovarian maturation of the goldfish, *Carassius auratus* L. Canad. J. Zool., **55**: 1906-1913.
 - 11 Dettlaff, T. A. and Davydova, S. I. (1974) Effect of triiodothyronine on the ripening of oocytes in stellate sturgeon after action of low temperatures and reservation of females. Soc. J. Dev. Biol., **5**: 402-409.
 - 12 Dettlaff, T. A. and Davydova, S. I. (1979) Differential sensitivity of cells of follicular epithelium and oocytes in the stellate sturgeon to unfavourable conditions and correlating influence of triiodothyronine. Gen. Comp. Endocrinol., **39**: 229-232.
 - 13 Sen, S. and Bhattacharya, S. (1982) Hormonal influence on perch ovarian 17 β -hydroxysteroid dehydrogenase activity in *in vitro* system. Indian J. Exp. Biol., **20**: 664-667.
 - 14 Sen, S. and Bhattacharya, S. (1981) Role of thyroxine and gonadotropin on the mobilization of ovarian cholesterol in a teleost, *Anabas testudineus* (Bloch). Indian J. Exp. Biol., **19**: 408-412.
 - 15 Chakraborti, P., Maitra, G. and Bhattacharya, S. (1986) Binding of thyroid hormone to isolated ovarian nuclei from a freshwater perch, *Anabas testudineus*. Gen. Comp. Endocrinol., **62**: 239-246.
 - 16 Jackson, V. and Chalkey, R. (1974) Separation of newly synthesized nucleohistone by equilibrium centrifugation in calcium chloride. Biochemistry, **13**: 3952-3956.
 - 17 Deb, S., Jamaluddin, Md., Bhadra, R., Bhattacharya, S. and Datta, A. G. (1985) Bioassay of fish gonadotropin by ovarian mitochondrial cholesterol depletion. Gen. Comp. Endocrinol., **57**: 491-497.
 - 18 Snedecor, G. W. and Cochran, W. G. (1971) "Statistical Methods", 6th Ed. Iowa State University Press, Ames.
 - 19 Deb, S. and Bhattacharya, S. (1986) Circulatory cholesterol as an important source of substrate for piscine ovarian steroidogenesis. Indian J. Exp. Biol., **24**: 71-76.
 - 20 Leloup, J. and Deluze, A. (1985) Environmental effects of temperature and salinity on thyroid function in teleost fishes. In "Endocrine and the Environment". Ed. by B. K. Follett, S. Ishii and A. Chandra, Japan Sci. Soc. Press, Tokyo/Springer-Verlag, Berlin, pp. 23-32.



Age-Related Changes and Sex Difference in the Ultrastructure of Renal Glomerulus in Wistar/Tw Rats

WIN WIN YEE, SUMIO TAKAHASHI
and SEIICHIRO KAWASHIMA¹

Zoological Institute, Faculty of Science, Hiroshima University, Hiroshima 730, and

¹Zoological Institute, Faculty of Science, University of Tokyo, Tokyo 113, Japan

ABSTRACT—Changes in the renal glomerulus were electron microscopically examined in male and female rats of the Wistar/Tw strain at 1, 3, 6, 12 and 18 months of age. Initial lesions as focal thickening of the glomerular capillary basement membrane (GBM) and the fusion of glomerular epithelial cell foot processes (EpF) were encountered at 3 months in male and at 6 months in female rats. Twelve-month-old female rats showed focal thickening of the GBM with fusion of the EpF and the formation of vacuoles. At 18 months focal thickening of the GBM became segmental with fusion of the EpF and frequent occurrence of fusion of the mesangial matrix to the GBM. At 12 and 18 months, there were striking sex differences in the severity of the renal lesions. Only 12- and 18-month-old male rats showed extensive thickening of the GBM with nodular folds intermingled with massive mesangial matrix, extensive fusion, denudation of the EpF and degeneration of the epithelial cells.

INTRODUCTION

A marked increase in the water intake and urinary output with low electrolyte concentration was commonly observed in male rats of the Wistar/Tw strain maintained in our laboratories at the age of over 16 months [1-3]. These changes are correlated with histopathological changes of the kidney with about 70% of glomeruli degeneration [4]. We have recently light microscopically observed that 50% of the glomeruli was affected as early as at 3 months of age in male rats and more than 80% of the glomeruli, at 13 months. In contrast, in female rats the affected glomeruli were only about 40% at 9 months of age [5]. The retarded development of kidney lesions in female rats is well reflected by the changes in renal functions, that is, female rats of the Wistar/Tw strain develop polydipsia and polyuria at 19 months of age [6].

In electron microscopical study, we found degenerative changes in the epithelial cell cytoplasm

as bearing slender processes, extreme enlargement of the mesangium intermingled with glomerular basement membrane (GBM) and the cortical collecting tubules filled with electron dense material and with completely flattened epithelial cells in male rats at 18 months of age, while the renal structure of 3-month-old rats was mostly healthy. At 3 months a slight thickening of the GBM with some fusion of the epithelial cell foot processes (EpF) was present in a few scattered areas of the GBM, but the cortical collecting tubules were normal [7]. Several authors have already reported the age-related changes in other strains of rats characterized by the thickening of the GBM and the enlargement of mesangium area of male rats [8-10]. Our results are generally in harmony with theirs. However, as clear sex difference in renal histopathological changes was the feature of the Wistar/Tw strain, we attempted to extend our electron microscopical study focusing on the male-female difference of the glomerulus as a function of age. The understanding of the factors causing this sex difference may elucidate the aging processes of the kidney structure and function.

Accepted November 14, 1988

Received July 11, 1988

¹ To whom reprint requests should be addressed.

MATERIALS AND METHODS

Male and female rats of the Wistar/Tw strain were used in the present study. They were maintained in a temperature- and light-controlled room with free access to laboratory chow (CA-1, Japan Clea Inc.) and tap water. At 1, 3, 6, 12 and 18 months of age, five male and five female rats each were killed by decapitation. Both kidneys were quickly removed and weighed. Frontal slices about 1 mm thick were fixed in 2.5% glutaraldehyde and 4% paraformaldehyde in ice-cold 0.1 M cacodylate buffer at pH 7.4. Then, cortical parts of the kidney slices were cut into 1–2 mm blocks and fixed in the same fixative for 2 hr. The tissue blocks were washed with three or four changes of 0.1M cacodylate buffer containing 8% sucrose and post-fixed in 1% OsO_4 in the same buffer for 2 hr. All fixation procedures were performed at 4°C. After dehydration in a graded series of ethanol, the tissue blocks were embedded in low viscosity 'Spurr' resin (TAAB). Ten to fifteen blocks in each rat were used for electron microscopical observations. For the identification of glomerular-tubular orientation, 0.6–1 μm thick sections were cut and stained with toluidine blue. In some blocks of old rat kidneys, the glomeruli were absent and those blocks were not used for further observation.

From the blocks which showed renal corpuscles with vascular and urinary poles in thick sections, ultrathin sections were cut with an ultramicrotome (Ultratome Nova, LKB 2188). After staining with uranyl acetate and lead citrate, sections were examined with a JOEL 1200 EX electron microscope. Glomeruli were examined and 10–20 photographs were taken at the magnification of $\times 8000$. Semi-quantitative analyses of ultrastructural changes were carried out according to the method of Hayashida et al. [10] with some modifications. Outline of the analyses were briefly shown as follows:

(a) Thickness of GBM - In each rat, the thickness of GBM perpendicular to the basement membrane were measured at 100 points.

(b) Epithelial cells and their foot processes - Percent area of vacuoles in glomerular epithelial cell (GEC) cytoplasm was calculated in 50 GECs in a total of 400 μm^2 by point counting planimetry [11]. Size of vacuoles in each rat was randomly measured in 50 vacuoles. For the lesions of GEC foot processes, the indices of I-V as shown in Table 2 were recorded in each rat. GEC lesions such as the percent of the incidence of GEC cytoplasmic attachment to the GBM in the GECs and the cytoplasmic degeneration bearing vacuolation and slender processes were also used as parameters.

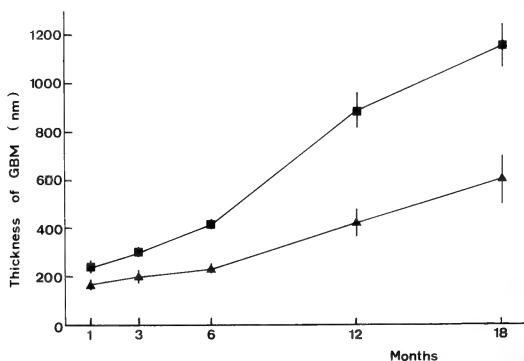


Fig. 1. Age-related changes in the thickness of GBM in male (■) and female (▲) rats. Vertical bars indicate standard errors of means (SEM). Each point depicts the mean of 5 rats.

(c) Mesangium - Indices were used for the lesions of the mesangium (Table 3).

Comparison between groups of male and female rats was made by Kruskal-Wallis test and Mann Whitney's U test.

RESULTS

Glomerular capillary basement membrane (GBM)

Age-related changes in the thickening of GBM in both sexes of rats are presented in Figure 1. The thickness of GBM increased as a function of age in both sexes. However, apparent sex difference was present. At 12 and 18 months of age, the GBM of male rats was about twice thicker than that of female rats ($P < 0.005$). The frequency of ultrastructural lesions in the GBM is shown in Table 1. Typical ultrastructural changes occurring in the GBM are shown in Figure 2. Two rats with focal thickening of lamina densa with three distinct layers and two other rats with segmentally thickened GBM without three distinct layers were found at 6 months. At 18 months of age all male rats showed extensive thickening with nodular foldings of GBM. However, female rats started showing focal thickening of lamina densa without three distinct layers of GBM at 12 months. Only at 18 months female rats showed obvious thickening

of GBM (Fig. 3a).

Glomerular epithelial cell (GEC)

Morphological changes of GEC cytoplasm include the increase in the area of vacuoles, the size of vacuoles, the attachment of GEC cytoplasm to the GBM and the degeneration of GEC cytoplasm (Figs. 4-6). The most widespread changes in both sexes of rats were the vacuolation in the rough endoplasmic reticulum in GEC cytoplasm (Figs. 3b and 7). The highest percentage and the biggest diameter of vacuoles were found in male rats at 12 months of age. However, 18-month-old male rats showed lower percentage of vacuoles with smaller diameter than 12-month-old ones (Figs. 7b and 8). In addition, the attachment of GEC cytoplasm to the GBM was observed in about 70 and 80% of the GECs in 12- and 18-month-old male rats, respectively (Fig. 6). Eighteen-month-old male rats showed degeneration of GEC cytoplasm in about 70% of the cells (Fig. 7b), while in female rats it was about 3% (Fig. 3 and 6).

Glomerular epithelial cell foot processes

Age-related changes of GEC foot process lesions were recorded as indices from I-V (Fig. 9) and the incidence of lesions in GEC foot processes in male and female rats is shown in Table 2. Frequent occurrence of focal and scattered fusion

TABLE 1. Frequency of ultrastructural lesions in GBM in male and female rats of various ages

Sex	Age in months	No. of rats	Normal	Lesion				
				I	II	III	IV	V
Male	1	5	4	1	—	—	—	—
	3	5	—	3	2	—	—	—
	6	5	—	1	2	2	—	—
	12	5	—	—	—	3	1	1
	18	5	—	—	—	—	1	4
Female	1	5	5	—	—	—	—	—
	3	5	4	1	—	—	—	—
	6	5	2	2	1	—	—	—
	12	5	—	1	2	2	—	—
	18	5	—	—	1	4	—	—

Lesion indices: I. Absence of significant ultrastructural abnormalities except focal and scattered thickening of lamina densa with distinct three layers. II. Focal thickening of lamina densa with distinct three layers. III. Segmental thickening of GBM without distinct three layers. IV. Thickening and folding of GBM. V. Extreme thickening and nodular folding of GBM.

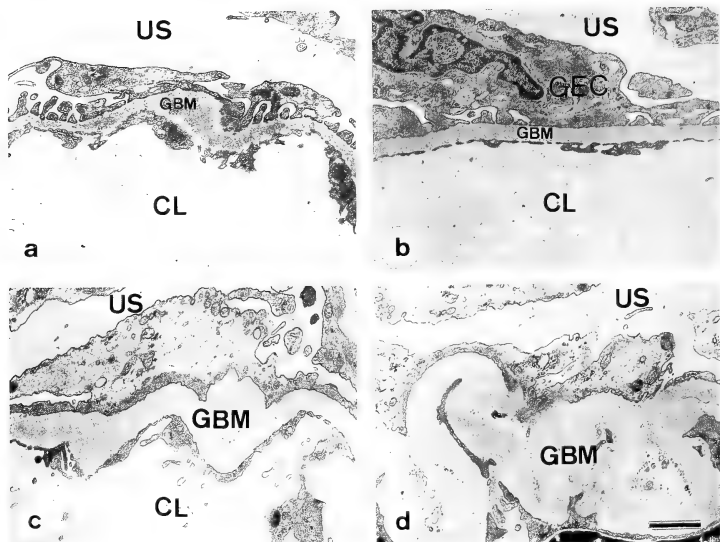


Fig. 2. Electron microphotographs illustrating lesions of II-V (refer to Table 1 for indices) in glomerular basement membrane (GBM). Bar: $1\mu\text{m}$. CL, capillary lumen; GEC, epithelial cell; US, urinary space.

- Focal thickening of lamina densa with three distinct layers (Lesion II).
- Thickening of GBM without three distinct layers (Lesion III).
- Thickening and folding of GBM (Lesion IV).
- Extreme thickening and nodular foldings of GBM (Lesion V).

of GEC foot processes were apparent at 3 months of age in male rats and total degeneration of GEC developed at 18 months in 2 out of 5 male rats. However, in female rats no severe changes were observed, except focal and segmental flattening of fused foot processes at 12 months of age.

Mesangium

Increase in amount of the mesangial matrix in male and female rats is shown in Table 3. Frequent occurrence of fusion of the mesangial matrix to the GBM was apparent in 6- and 12-month-old male and 12- and 18-month-old female rats. However, 2 out of 5 males at 12 months of age and all 18-month-old male rats showed massive mesan-

gial matrix. The massive mesangial matrix filled the glomerular capillary lumen which resulted in the obliteration of the lumen (Fig. 8a). In 18-month-old male rats the mesangial cell cytoplasm underwent shrinkage due to massive accumulation of the mesangial matrix (Fig. 8b).

Endothelial cell cytoplasm

One-, 3- and 6-month-old male rats and all female rats showed normal structure of the endothelial cell cytoplasm (Fig. 3). However, in 12- and 18-month-old male rats the numbers of thin layers of the endothelial cytoplasm and the fenestrae were reduced (Fig. 8).

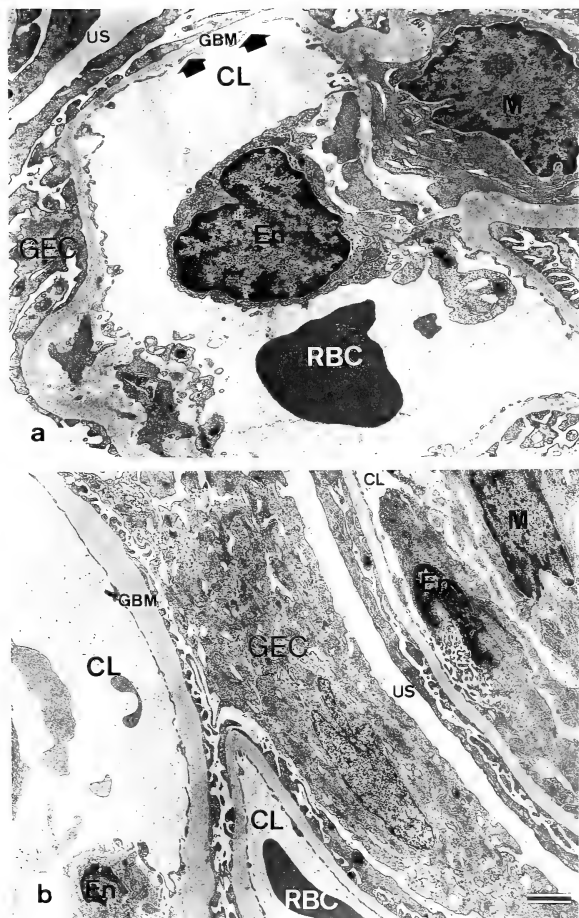


FIG. 3. Electron microphotographs of a part of glomerulus of an 18-month-old female rat. Bar: $1\mu\text{m}$. CL, capillary lumen; En, endothelial cell; GBM, glomerular basement membrane; GEC, epithelial cell; M, mesangial cell; RBC, red blood cell; US, urinary space.

a. Thickening of GBM with focal fusion of epithelial cell foot processes (arrows). Mesangial cell and endothelial cell show no significant abnormalities.

b. Vacuolation of the rough endoplasmic reticulum in the cytoplasm of glomerular epithelial cell.

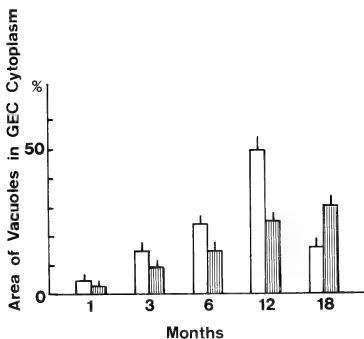


FIG. 4. Age-related changes in % area of vacuoles in GEC (glomerular epithelial cell) cytoplasm in male (open columns) and female (hatched columns) rats. Vertical bars indicate SEM. Each point depicts the mean of 5 rats.

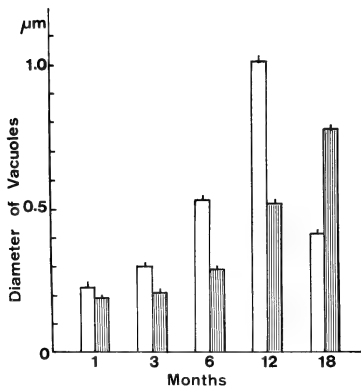


FIG. 5. Age-related changes in diameter of vacuoles in male (open columns) and female (hatched columns) rats. Each column shows the mean and SEM of 5 rats.

DISCUSSION

We have recently reported that the earliest ultrastructural changes of the renal glomerulus

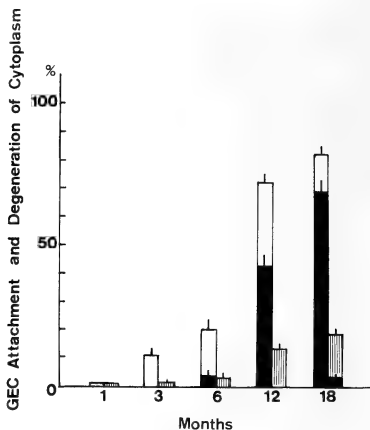


FIG. 6. Age-related changes of % GEC attachment to the GBM and degeneration of cytoplasm in male (open columns) and female (hatched columns) rats. The black columns indicate the degeneration of GEC cytoplasm. Each column shows the mean and SEM of 5 rats.

were observed in male Wistar/Tw rats at the age of 3 months. The changes were slight thickening of GBM, blurring of lamina densa and focal fusion of epithelial cell foot processes [7]. Similar morphological changes have been observed in Sprague-Dawley rats [8] and Wistar rats [9] at 6 months of age. Age-related changes in the kidney are characterized by the thickening of GBM [9, 10, 12] which was confirmed in our recent paper [7]. However, in Wistar/Tw male rats the thickness of GBM was about twice greater than in female rats at 12 and 18 months of age.

Kurtz and Feldman [13] and Walker [14] suggested that the epithelial cell foot processes manufacture a major proportion of GBM material and the changes of the GEC and GBM is interrelated [15]. Several authors have reported that GEC injury is associated with a number of experimental and clinical glomerular disease [16-21]. The age-related changes that occurred in the GBM and GEC and their foot processes were closely interrelated each other in Wistar/Tw rats and the changes were sexually different. Only male rats showed

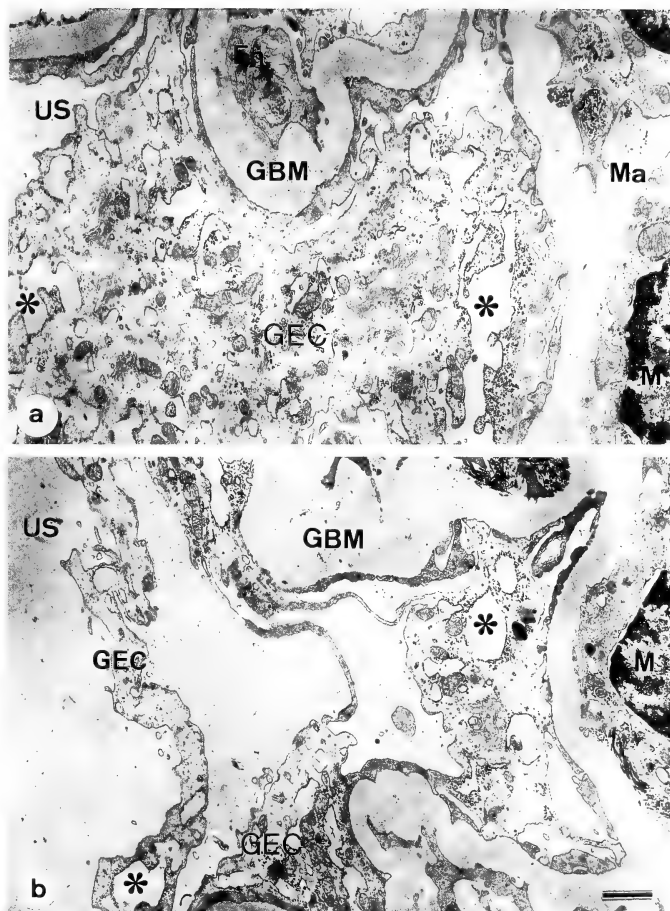


FIG. 7. Electron microphotographs of a part of glomerulus of an 18-month-old male rat. Bar: $1\ \mu\text{m}$. En, endothelial cell; GBM, glomerular basement membrane; GEC, epithelial cell; M, mesangial cell; Ma, mesangial matrix; US, urinary space.

- a. The cytoplasm of glomerular epithelial cell containing vacuoles of rough endoplasmic reticulum (asterisks).
- b. Attachment of epithelial cell cytoplasm to GBM and degeneration with vacuoles (asterisks).

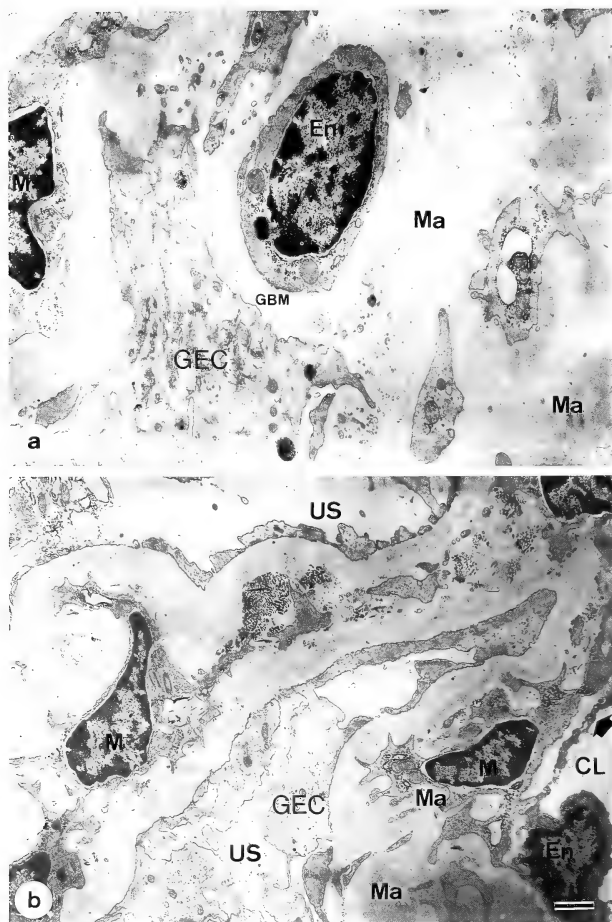


FIG. 8. Electron microphotographs of a part of the glomerulus of male rats at 12 (a) and 18 months (b) of age. Bar: 1 μ m. CL, capillary lumen; En, endothelial cell; GBM, glomerular basement membrane; GEC, epithelial cell; M, mesangial cell; Ma, mesangial matrix; US, urinary space.

a. Glomerular capillary lumen is filled with massive mesangium matrix and the endothelial cell is shrunken. Note disappearance of thin layer cytoplasm of the endothelial cell.

b. Mesangial and endothelial cell cytoplasm is shrunken by massive mesangium matrix. Note reduction of thin layer cytoplasm and fenestrae of the endothelial cell (arrow).

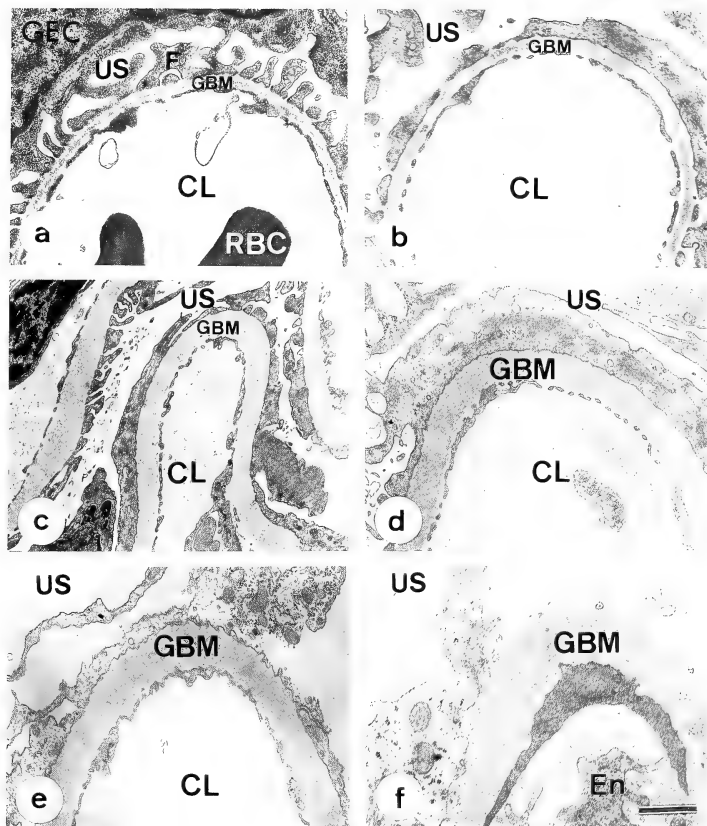


FIG. 9. Electron microphotographs illustrating lesions in the glomerular epithelial cell (GEC) foot processes. Bar: 1 μm . CL, capillary lumen; En, endothelial cell; F, foot process; GBM, glomerular basement membrane; GEC, epithelial cell; RBC, red blood cell; US, urinary space.

- Normal GEC foot processes.
- Lesion I: focal and scattered fusion of GEC foot processes.
- Lesion II: segmental flattening and extensive fusion of GEC foot processes.
- Lesion III: zonal fusion of GEC foot processes and attachment of GEC cytoplasm to GBM.
- Lesion IV: modest degeneration of GEC foot processes.
- Lesion V: total degeneration of GEC foot processes.

TABLE 2. Age-related changes in incidence of lesions in the glomerular epithelial cell (GEC) foot processes in male and female rats

Sex	Age in months	No. of rats	Normal	Lesion				
				I	II	III	IV	V
Male	1	5	4	1	—	—	—	—
	3	5	—	5	—	—	—	—
	6	5	—	1	4	—	—	—
	12	5	—	—	—	3	2	—
	18	5	—	—	—	1	2	2
Female	1	5	5	—	—	—	—	—
	3	5	4	1	—	—	—	—
	6	5	2	3	—	—	—	—
	12	5	—	2	3	—	—	—
	18	5	—	—	4	1	—	—

Lesion indices: I. Frequent occurrence of focal and scattered fusion of foot processes. II. Segmental flattening and extensive fusion of GEC foot processes. III. Zonal fusion of GEC foot processes and attachment of GEC cytoplasm to GBM. IV. Modest degenerative changes of GEC foot processes. V. Total degeneration of GEC foot processes.

TABLE 3. Age-related changes in mesangium in male and female rats

Sex	Age in months	No. of rats	Normal	Lesion			
				I	II	III	IV
Male	1	5	5	—	—	—	—
	3	5	—	4	1	—	—
	6	5	—	1	2	2	—
	12	5	—	—	—	3	2
	18	5	—	—	—	—	5
Female	1	5	5	—	—	—	—
	3	5	4	1	—	—	—
	6	5	2	2	1	—	—
	12	5	—	1	3	1	—
	18	5	—	—	1	4	—

Lesions indices: I. Focal occurrence of fusion of mesangial matrix to GBM. II. Frequent occurrence of fusion of mesangial matrix to GBM. III. Frequent occurrence of fusion of mesangial matrix to GBM with some accumulation of mesangial matrix. IV. Very frequent occurrence of fusion of mesangial matrix to GBM with massive accumulation of mesangial matrix.

huge vacuolation at 12 months with the attachment of GEC cytoplasm to the GBM and some 12-month-old and all 18-month-old rats showed the degeneration of GEC cytoplasm.

Enlargement of mesangium was frequently observed as age-related changes [8, 10]. However, Gray *et al.* [22] reported that there was no wide-

ning of the mesangial area in aged Sprague-Dawley rats. In the present study there was frequent occurrence of fusion of mesangial matrix to the GBM in both sexes which increased with age. Massive enlargement of mesangium was encountered only at 12- and 18-month-old male rats.

Kreisberg and Karnovsky [21] suggested that persistent injury to the epithelial cells could lead to the alteration in glomerular permeability which resulted in the accumulation of proteins in the mesangial area and could consequently lead to mesangial cell injury. In Wistar/Tw rats, while GEC cytoplasm started to degenerate at 12 months of age, huge mesangium accumulation occurred at more advanced ages. These findings support the view of Kreisberg and Karnovsky [21]. In addition, we found the reduction and disappearance of fenestrae and thin cytoplasm layer of endothelial cells at 12 and 18 months of age in male rats.

To conclude, the results of the present study indicate that the epithelial cell injury could lead not only to mesangial cell injury but also to endothelial cell injury, and that there is a clear sex difference in the age-related changes of the renal glomerulus at 12 and 18 months of age. In order to know the cause of this sex difference, the study on the influence of androgen on these changes is under way.

ACKNOWLEDGMENTS

This study was supported in part by Grants-in-Aid for Scientific Research from the Ministry of Education, Science and Culture, Japan (Nos. 62480023 and 63304008 to S.K.).

REFERENCES

- Kobayashi, Y. and Kawashima, S. (1980) Polydipsia and polyuria in aged male rats of the Wistar/Tw strain. *Proc. Japan Acad., Ser. B.*, **56**: 643-648.
- Kobayashi, Y. and Kawashima, S. (1984) Age-related changes in the water and electrolyte metabolism in male rats of the Wistar/Tw strain. *Exp. Gerontol.*, **19**: 107-113.
- Kawashima, S. and Kobayashi, Y. (1982) Morphometric study of the hypothalamo-neurohypophyseal system in aged rats. *J. Sci. Hiroshima Univ. Ser. B., Div. 1*, **30**: 229-242.
- Kobayashi, Y. and Kawashima, S. (1983) Histological changes in the kidney of aged rats of the Wistar/Tw strain showing polydipsia and polyuria. *J. Sci. Hiroshima Univ., Ser. B., Div. 1*, **31**: 149-154.
- Win Win Yee and Kawashima, S. (1987) Sex difference in the early histopathological changes of the kidney in Wistar/Tw rats. *Zool. Sci.*, **4**: 867-873.
- Kawashima, S., Kawamoto, K. and Kobayashi, Y. (1986) Aging of the hypothalamo-neurohypophyseal system and water metabolism in rats. *Zool. Sci.*, **3**: 227-244.
- Win Win Yee, Takahashi, S. and Kawashima, S. (1987) An ultrastructural study of renal glomerular capillaries and collecting tubules in aged male rats of the Wistar/Tw strain. *J. Sci. Hiroshima Univ., Ser. B., Div. 1*, **33**: 1-9.
- Couser, W. G. and Stilmant, M. M. (1975) Mesangial lesions and focal glomerular sclerosis in the aging rat. *Lab. Invest.*, **33**: 491-501.
- Hirokawa, K. (1975) Characterization of age-associated kidney disease in Wistar rats. *Mech. Ageing Dev.*, **4**: 301-316.
- Hayashida, M., Yu, B. P., Masoro, E. J., Iwasaki, K. and Ikeda, T. (1986) An electron microscopic examination of age-related changes in the rat kidney: the influence of diet. *Exp. Gerontol.*, **21**: 535-553.
- Weibel, E. R. (1969) Stereological principles for morphometry in electron microscopic cytology. *Int. Rev. Cytol.*, **26**: 235-302.
- Anderson, S. and Brenner, B. M. (1986) Effects of aging on the renal glomerulus. *Am. J. Med.*, **80**: 435-442.
- Kurtz, S. M. and Feldman, J. D. (1962) Experimental studies on the formation of glomerular basement membrane. *J. Ultrastruct. Res.*, **6**: 19-27.
- Walker, F. (1973) The origin, turnover and removal of glomerular basement membrane. *J. Path.*, **110**: 233-244.
- Venkatachalam, M. A., Cotran, R. S. and Karnovsky, M. J. (1970) An ultrastructural study of glomerular permeability in aminonucleoside nephrosis using catalase as a tracer protein. *J. Exp. Med.*, **132**: 1168-1180.
- Farquhar, M. G. and Palade, G. E. (1961) Glomerular permeability. II Ferritin transfer across the glomerular capillary wall in nephrotic rats. *J. Exp. Med.*, **114**: 699-715.
- Venkatachalam, M. A., Karnovsky, M. J. and Cotran, R. S. (1969) Glomerular permeability: Ultrastructural studies in experimental nephrosis using horseradish peroxidase as a tracer. *J. Exp. Med.*, **130**: 381-399.
- Messina, A., Davies, D. J., Dillane, P. C. and Ryan, G. B. (1987) Glomerular epithelial abnormalities associated with the onset of proteinuria in aminonucleoside nephrosis. *Am. J. Path.*, **126**: 220-229.
- Ryan, G. B. and Karnovsky, M. J. (1975) An ultrastructural study of the mechanisms of proteinuria in aminonucleoside nephrosis. *Kidney Int.*, **8**: 219-232.
- Kanwar, Y. S. and Rosenzweig, L. J. (1982) Altered glomerular permeability as a result of focal

- detachment of the visceral epithelium. *Kidney Int.*, **21**: 565-574.
- 21 Kreisberg, J. I. and Karnovsky, M. J. (1978) Focal glomerular sclerosis in the Fawn-Hooded rat. *Am. J. Path.*, **92**: 637-652.
- 22 Gray, J. E., Weaver, R. N. and Purmalis, A. (1974) Ultrastructural observations of chronic progressive nephrosis in the Sprague-Dawley rat. *Vet. Path.*, **11**: 153-164.

Cytological Differences in Early Germ Cells of the Three Genera of Grey Mulletts, *Mugil*, *Liza* and *Chelon* (Teleostei: Mugilidae)

SOLANGE BRUSLE

*Laboratoire de Biologie Marine, Faculté des Sciences
Université de Perpignan, Perpignan cédex, France*

ABSTRACT—A comparative study of the fine structure of early germ cells, primordial germ cells, oogonia and spermatogonia, of the three genera *Mugil*, *Liza* and *Chelon* of grey mullets has allowed the former to be separated from the other two genera.

INTRODUCTION

Among the most interesting works on the taxonomy of mugilids, we noticed those of Schultz [1], FAO [2], Thomson [3, 4] and Trewavas [5]. Several keys of determination for different species of grey mullets in the Mediterranean have been published by De Angelis [6], Tortonese [7], Ben Tuvia [8, 9], Farrugio [10], and Cambrony [11]. At present, six Mediterranean species were known:

Mugil cephalus cephalus (Linnaeus, 1758)—Clofnam 181.1.

Chelon labrosus (Risso, 1826)—Clofnam 101.21.

Liza (Liza) ramada (Risso, 1826)—Clofnam 181.3.1

Liza (Liza) aurata (Risso, 1810)—Clofnam 181.3.2.

Liza (Protomugil) saliens (Risso, 1810)—Clofnam 181.3.4.

Oedalechilus labeo (Cuvier, 1829)—Clofnam 101.4.1.

Specific differences in grey mullets concern morphological characteristics [4, 10, 12], morphometric [13] and anatomical evidences [4, 10, 14]. Moreover, research has been carried out in karyology [15], biology [16-18] and parasitology [19, 20]. The most interesting findings concern the genetic results in the field of blood proteins [21-

23], serous proteins [24], proteins of the cristallin lens [25] and enzymatic polymorphism [23, 26]. From all these results, differences have been established among the three genera *Mugil*, *Liza* and *Chelon* [4, 13]. No cytological information has been made in literature. A comparative study of gonadogenesis and gametogenesis in Mediterranean grey mullets [27] has allowed us to obtain ultrastructural knowledge on germ cells ranging from primordial germ cells [27, 28] to male [29] and female [30] gametes.

The present study therefore deals with the ultrastructure of the early germ cells in *Liza aurata*, *Mugil cephalus* and *Chelon labrosus* which are the most common species among the six known in Roussillon (Gulf of Lion).

MATERIALS AND METHODS

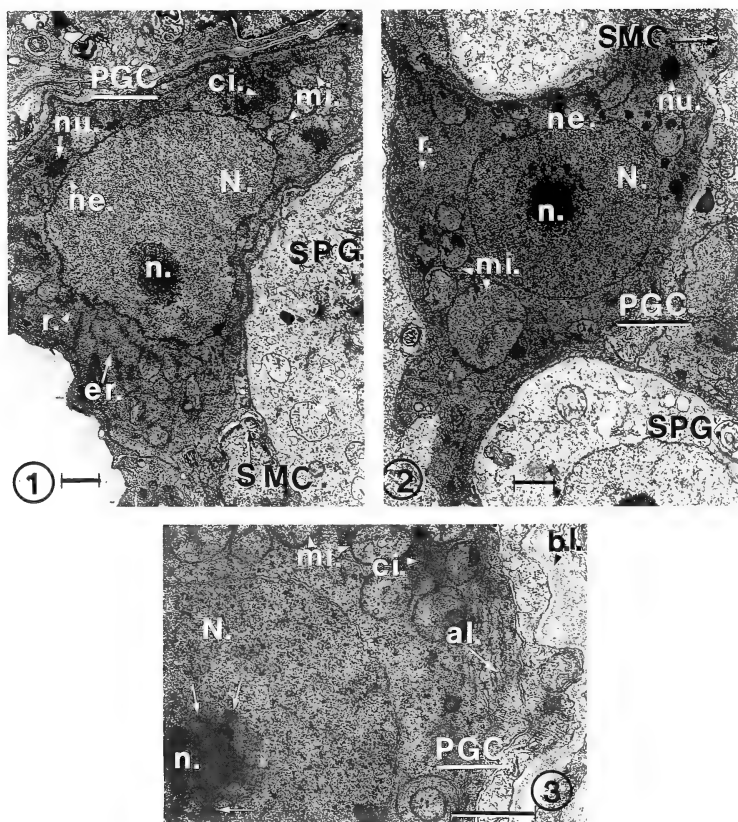
Juvenile grey mullets were caught by electric fishing in the brackish waters of Leucate, a Mediterranean lagoon and adult grey mullets by trawl in the Mediterranean Sea. Gonads were fixed for electron microscopy by the aid of conventional procedure previously reported [31].

RESULTS

Early germ cells, primordial germ cells (PGCs), oogonia and spermatogonia were examined in

Accepted October 24, 1988

Received July 13, 1988

FIG. 1. PGC in *Liza aurata*.FIG. 2. PGC in *Mugil cephalus*.FIG. 3. A part of a PGC in *M. cephalus*: annulated lamellae and granules (arrows) budded by fibrillar center of nucleolus.

- | | | | |
|-----|-------------------------|------|------------------------|
| al. | : annulated lamellae | nu. | : "nuage" |
| bl. | : basal lamina | OOG. | : Oogonium |
| ch. | : chromatin | PFC. | : Prefollicle cell |
| ci. | : "ciment" | PGC. | : Primordial germ cell |
| er. | : endoplasmic reticulum | r. | : ribosome |
| mi. | : mitochondria | SC. | : Sertoli cell |
| N. | : Nucleus | SMC. | : Somatic cell |
| n. | : nucleolus | SPG. | : Spermatogonium |
| ne. | : nuclear envelope | | |

The bar represents one micron in all micrographs.

three species of grey mullets, but results are given only for *Liza aurata* and *Mugil cephalus* because no significant differences were detected between *L. aurata* and *C. labrosus*. In *L. aurata*, 125 fish were studied from which micrographs of 71 PGCs, 64 oogonia and 90 spermatogonia were examined and in 82 samples of *M. cephalus*, micrographs of 53 PGCs, 52 oogonia and 52 spermatogonia were observed. These three cell types show the same ultrastructural features at every step of gametogenesis. PGCs developing to oogonia and spermatogonia were previously described [28] and are not noticed in this paper.

Primordial germ cells (PGCs)

PGCs (Figs. 1, 2) are oval-shaped undifferentiated cells [27], characterized by irregular outlines (which probably indicate amoeboid movements during migration to the gonadal anlage), a high nucleus to cell ratio about diameter ($N/C=0.39-0.40$), a heavy electron density (owing to a finely granular chromatin and many free ribosomes) and a small number of membrane organelles (endoplasmic reticulum and Golgi complexes). Mitochondria, few in number, are often found with "ciment" (cement) which is a dense fibrillar material (called "nuage" = halo when it is independent of mitochondria). The ciment [32, 33] migrates from the nucleus, is characteristic of germ cells and can also be called "germinal dense bodies" [34]. PGCs are, surrounded by somatic cells, characterized by a high nucleolus/cell, a dense chromatin lying along the inner membrane of the nuclear envelope and few membrane organelles. These cells are generally devoid of nucleoli.

PGCs show these typical characteristics in two species. The differences identified are related both to the sizes of the cell and mitochondria and to the structure of mitochondria. In *L. aurata* (Fig. 1), PGCs are $12.1\ \mu\text{m}$ (± 0.65) in length and $9.0\ \mu\text{m}$ (± 0.54) in width, and mitochondria are $0.66\ \mu\text{m}$ in diameter and display short cristae. In *M. cephalus* (Fig. 2), PGCs are smaller ($9.58\ \mu\text{m} \pm 0.63$ in length; $6.03\ \mu\text{m} \pm 0.63$ in width), mitochondria bigger ($0.7-1.2\ \mu\text{m}$) and mitochondrial cristae narrower than those of *L. aurata*. Moreover, the nuclear envelope of PGCs in *M. cephalus* is more regular (Fig. 2) than that of *L. aurata* (Fig. 1). At

last, in *M. cephalus*, rather voluminous granules in cortex of the nucleolus, budded by fibrillar center, and annulated lamellae in the cytoplasm can be observed (Fig. 3).

Oogonia

Oogonia (Figs. 4, 5) are oval or round cells characterized by regular outlines, a high nucleus to cell ratio (0.4) and a low electron density owing to a decrease in the number of ribosomes and a rather dispersed chromatin. "Ciment" and "nuage" are still recognized and the spherical nucleus is quite centrally located. There are more numerous membrane organelles than in PGCs. Prefollicle cells surrounding oogonia have already been noticed [35].

These general features of oogonia are seen both in *L. aurata* (Fig. 4) and in *M. cephalus* (Fig. 5) but, in the former species, oogonia are $14.3\ \mu\text{m}$ (± 1.05) in length and $11.34\ \mu\text{m}$ (± 1.62) in width, whereas they are $11.9\ \mu\text{m}$ (± 0.93) long and $9.36\ \mu\text{m}$ (± 0.75) wide in the latter species. Membrane organelles are more numerous in *L. aurata* than in *M. cephalus*. Moreover, the mitochondria in *L. aurata* are smaller ($0.66\ \mu\text{m}$ in diameter) with shorter cristae than those in *M. cephalus* ($0.8-1.5\ \mu\text{m}$ in diameter). Annulated lamellae are discernible in the oogonia of *M. cephalus*.

Spermatogonia

Spermatogonia (Figs. 6, 7) are oval-shaped cells characterized by quite regular outlines, and, like oogonia, have a high nucleus to cell ratio (0.39) and a low electron density. The oval-shaped nucleus is eccentric and the chromatin appears to be rather granular and dispersed, but small dense clumps with the nucleolus are found and packed along the inner nuclear membrane. Cytoplasmic characteristics are quite similar to those noted in oogonia. Sertoli cells surrounding spermatogonia are noticed as was accounted previously [27].

Spermatogonia show the same general characteristics in both species of grey mullets, but in *L. aurata* spermatogonia are $14.2\ \mu\text{m}$ (± 0.99) in length and $10.5\ \mu\text{m}$ (± 0.98) in width, and in *M. cephalus* they are $12.42\ \mu\text{m}$ (± 1.12) and $8.66\ \mu\text{m}$ (± 1.02) respectively. Differences in the membrane organelles of the two species, similar to

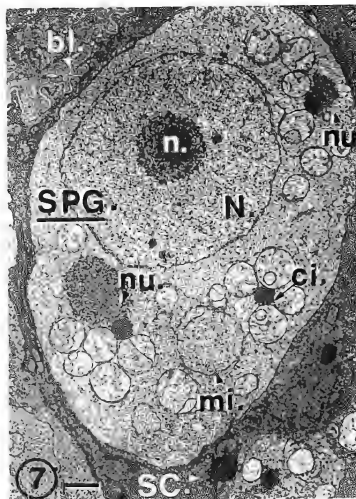
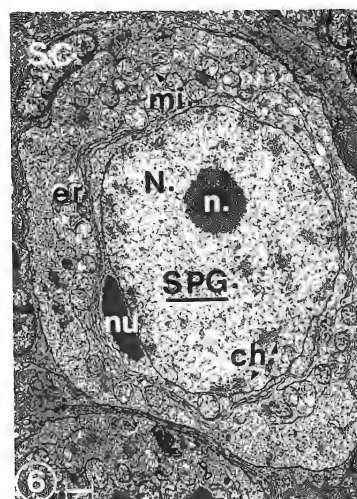
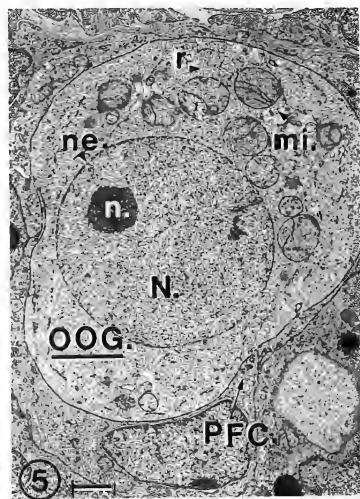
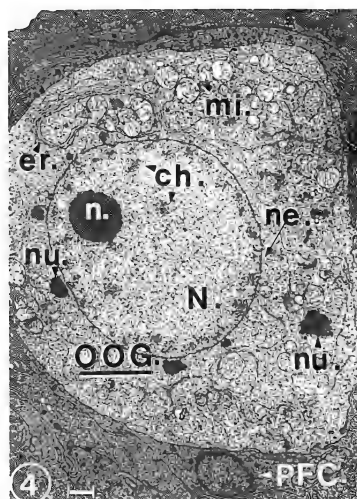


TABLE 1. Comparative study of early germ cells in *Liza aurata* and *Mugil cephalus*

		Likenesses	Differences		t	k
			<i>Liza aurata</i>	<i>Mugil cephalus</i>		
PGC	Morphology	-oval-shaped -heavy electron density -irregular outlines	-long: $12.1 \mu\text{m} \pm 0.65$ -wide: $9.0 \mu\text{m} \pm 0.54$	-long: $9.58 \mu\text{m} \pm 0.63$ -wide: $6.03 \mu\text{m} \pm 0.63$	26.7 25.2	
	Nucleus	-voluminous nucleus -N/C=0.39-0.40 -finely granular chromatin	-irregular envelope	-rather regular nuclear envelope -fibrillar center budding		122
	Cytoplasm	-numerous ribosomes -scarce membrane organelles -"nuage" and "ciment"	-mitochondria: diameter = $0.66 \mu\text{m}$	-mitochondria: diameter = $0.7-1.2 \mu\text{m}$ -narrow cristae -annulated lamellae		
	Morphology	-oval or round-shaped -low electron density -regular outlines	-long: $14.3 \mu\text{m} \pm 1.05$ -wide: $11.34 \mu\text{m} \pm 1.62$	-long: $11.9 \mu\text{m} \pm 0.93$ -wide: $9.36 \mu\text{m} \pm 0.75$	13.1 8.2	
OOGONIA	Nucleus	-round, central and voluminous nucleus -N/C=0.40 -granules of chromatin dispersed -regular outlines				114
	Cytoplasm	-ribosomes dispersed -"nuage" and "ciment"	-membrane organelles rather numerous -mitochondria: diameter = $0.66 \mu\text{m}$	-membrane organelles less numerous -annulated lamellae -mitochondria: diameter = $0.8-1.5 \mu\text{m}$ -narrow cristae		
SPERMATOGONIA	Morphology	-oval shaped -low electron density -rather regular outlines	-long: $14.2 \mu\text{m} \pm 0.99$ -wide: $10.5 \mu\text{m} \pm 0.98$	-long: $12.42 \mu\text{m} \pm 1.12$ -wide: $8.66 \mu\text{m} \pm 1.02$	9.4 10.7	
	Nucleus	-eccentric and voluminous nucleus -N/C=0.4 -granules of chromatin dispersed -"nuage" and "ciment"				140
	Cytoplasm	-ribosomes dispersed -"nuage" and "ciment"	-TER rather frequent -mitochondria (id. oogonia)	-GER infrequent -annulated lamellae -mitochondria (id. oogonia)		

t=student's parameter, k=degree of freedom

FIG. 4. Oogonium in *L. aurata*.FIG. 5. Oogonium in *M. cephalus*.FIG. 6. Spermatogonium in *L. aurata*.FIG. 7. Spermatogonium in *M. cephalus*.

The bar represents one micron in all micrographs.

those noted for oögonia, are discriminated in spermatogonia especially for the endoplasmic reticulum.

All these findings related to the three types of early germ cells in two species studied are summarized in the Table 1.

DISCUSSION

In the present work, ultrastructural features which allow the identification of PGCs, oögonia and spermatogonia were found to be similar in the three species of grey mullets. These three cell types show the same ultrastructural characteristics at every step of gametogenesis. As cell differentiation proceeds, changes in cell organelles are detected from primary cytes [27]. Therefore differences demonstrated between *M. cephalus* on the one hand and *L. aurata* and *C. Labrosus* on the other hand, are rather significant since they do not reflect physiological differences between cells. These differences are recognized in morphological (different sizes of cells, nuclei and mitochondria, shape of nuclear envelope), structural (granular cortex of the nucleolus, mitochondrial cristae) and quantitative (varying numbers of membrane organelles, especially for the endoplasmic reticulum, and presence or absence of annulated lamellae) evidences. Therefore, this study allows the genus *Mugil* to be separated from the other two genera *Liza* and *Chelon*, but there are no cytological criteria available to distinguish *Liza* from *Chelon*. Our results are in accordance with other works which have shown that the genus *Mugil* is quite different from the other two [13, 15, 36]. Especially, biochemical data showed not only this clear separation of the genus *Mugil* [22, 26], but also differences between *Liza* and *Chelon* [21] and the homogeneity of the genus *Liza* [26].

Cytological criteria to make comparisons between different genera or species are generally related to structural characteristics of differentiated cells such as spermatozoa [37, 38] or oocytes [39, 40]. In our previous examinations, significant differences were noted between the spermatozoa of *M. cephalus* and *L. aurata* [27] and between the oocytes of *L. aurata* and *C. labrosus* [30]. As for early germ cells, intergeneric or interspecific dif-

ferences have rarely been described. However, Hubert [41] showed differences in the features of the nucleoli in PGCs of species belonging to the genus *Lacerta* and Fujimoto *et al.* [42] distinguished the number of ribosomes of PGCs of man from those of rodents. Moreover, we recognized differences (size of cells and structure of mitochondria) in PGCs of teleosts *Serranus cabrilla* and *Serranus hepatus* [27]. To the best of our knowledge, these differences in early germ cells by means to distinguish between certain genera are shown in fish for the first time.

REFERENCES

- Schultz, L. P. (1946) A revision of the genera of mullets, fishes of the family Mugilidae, with descriptions of three new genera. Proc. U. S. Nat. Mus., **96**: 377-395.
- Fischer, W., Bauchot, M. L., Schneider, M. (rédacteurs) (1987) Fiches FAO d'identification des espèces pour les besoins de la pêche (Révision I). Méditerranée et Mer Noire. Zone de pêche 37. Volume II. Vertébrés.
- Thomson, J. M. (1966) The grey mullets. Oceanogr. Mar. Biol. Ann. Rev., **4**: 301-335.
- Thomson, J. M. (1981) The taxonomy of grey mullets. In "Aquaculture of Grey Mulletts". Ed. by O. Oren, Cambridge Univ. Press, pp. 1-15.
- Trewavas, E. (1973) Mugilidae. In "Catalogue des Poissons de l'Atlantique du Nord-Est et de la Méditerranée (CLOFNA)". Ed. by J. C. Hureau and Th. Mord, pp. 567-574.
- De Angelis, C. M. (1967) Osservazioni sulle specie del genere *Mugil* segnalate lungo le coste del Mediterraneo. Boll. pesca., piscicol. idrobiol., **22**: 5-35.
- Tortonese, E. (1972) I Mugilidi del bacino mediterraneo. Natura Soc. It. Sc. Nat., Museo Civ. Sc. Nat. e Acquario Civ., Milano, **61**: 231-236.
- Ben Tuvia, A. (1975) Mugilid fishes of the red sea with a key to the mediterranean and red sea species. Bamidgah, **27**: 14-20.
- Ben Tuvia, A. (1986) Mugilidae In "CLOFNA". Vol. III, pp. 1197-1204.
- Farrugio, H. (1977) Clés commentées pour la détermination des adultes et des alevins de Mugilidae de Tunisie. Cybium, **2**: 57-73.
- Cambrony, M. (1983) Recrutement et biologie des stades juvéniles de Mugilidae dans trois milieux lagunaires du Roussillon et du Narbonnais. Thèse Doct. 3ème cycle, Paris.
- Beaubrun, P. C. (1978) Catalogue raisonné des

- poissons des mers marocaines (3ème partie). Ordre des Mugiliformes. Bull. Inst. Pêches Marit. Maroc, **23**: 135-157.
- 13 Spain, A. V., Grant, C. J. and Sinclair, D. F. (1980) Phenotypic affinities of 11 species of australian mullet (Pisces: Mugilidae). Aust. J. Mar. Freshwater Res., **31**: 69-83.
 - 14 Figueiredo, M. J. and Silva, J. J. (1983) Preliminary experiments on the rearing of Mugilid fry from portuguese estuarine waters. Biol. Inst. Nac. Invest. Pescas, Lisboa, **10**: 51-63.
 - 15 Cataudella, S., Civitelli, M. V. and Capanna, E. (1974) Chromosome complements of the Mediterranean mullets (Pisces, Perciformes). Caryologia, **27**: 93-105.
 - 16 Quignard, J. P. and Farrugio, H. (1981) Age and growth of grey mullets. In "Aquaculture of Grey Mulletts". Ed. by O. H. Oren, Int. Biol. Programme, **26**, pp. 155-184.
 - 17 Bruslé, J. (1981) Sexuality and biology of reproduction in grey mullets. In "Aquaculture of Grey Mulletts". Ed. by O. H. Oren, Int. Biol. Programme, **26**, pp. 99-154.
 - 18 Whitfield, A. K. (1980) Distribution of fishes in the Mhlंगा estuary in relation to food resources. S. Afr. J. Zool., **15**: 159-165.
 - 19 Raibaut, A., Caillet, C. and Ben Hassine, O. K. (1978) *Colobomatus mugilis* n.sp. (Copepoda, Philichthyidae) parasite de poissons Mugilidés en Méditerranée occidentale. Bull. Soc. Zool. Fr., **103**: 449-457.
 - 20 Euzet, L. and Combes, C. (1980) Les problèmes de l'espèce chez les animaux parasites. Mem. Soc. Zool. Fr., **3**: 239-285.
 - 21 Perez, J. E. and Maclean, N. (1976) Multiple globins and haemoglobins in four species of grey mullet (Mugilidae, Teleostei). Comp. Biochem. Physiol., **53B**: 465-468.
 - 22 Callegarini, C. and Basaglia, F. (1978) Biochemical characteristics of mugilids in the lagoons of the Po delta. Boll. zool., **45**: 35-40.
 - 23 Carpené, E., Hakim, G. and Cortesi, P. (1983) Isoelectric focusing of lateral muscle myogen and haemoglobins of two species of mugilidae. Comp. Biochem. Physiol., **74 B**: 487-491.
 - 24 Senkevich, N. K. and Kulikova, N. I. (1970) Intraspecific differentiation of serum proteins in the blood of black sea mullets. J. Ichtyol., **10**: 538-544.
 - 25 Peterson, G. L. and Shehadeh, Z. H. (1971) Subpopulations of the hawaiian striped mullet *Mugil cephalus*: analysis of variations of nuclear eye-lens protein electropherograms and nuclear eye-lens weights. Mar. Biol., **11**: 52-60.
 - 26 Autem, M. and Bonhomme, F. (1980) Eléments de systématique chez les mugilidés de Méditerranée. Biochem. Syst. Ecol., **8**: 305-308.
 - 27 Bruslé, S. (1982) Contribution à la connaissance de la sexualité de Poissons Téléostéens marins gonochoriques (Mugilidés) et hermaphrodites (Serranidés). Thèse Doct. Etat, Perpignan.
 - 28 Bruslé, S. (1980) Etude ultrastructurale des cellules germinales primordiales et de leur différenciation chez *Mugil cephalus* L. 1758 (Teleostéen, Mugilidé). Bull. Ass. Ana., **64**: 207-216.
 - 29 Bruslé, S. (1981) Ultrastructure of spermiogenesis in *Liza aurata* Risso, 1810 (Teleostei, Mugilidae). Cell Tiss. Res., **217**: 415-424.
 - 30 Bruslé, S. (1985) The structure of oocytes and their envelopes in *Chelon labrosus* and *Liza aurata* (Teleostei, Mugilidae). Zool. Sci., **2**: 681-693.
 - 31 Bruslé, S. and Bruslé, J. (1978) An ultrastructural study of early germ cells in *Mugil (Liza) auratus* Risso, 1810 (Teleostei, Mugilidae). Ann. Biol. Anim. Bioch. Biophys., **18**: 1141-1153.
 - 32 Clerot, J. C. (1976) Les groupements mitochondriaux des auxocytes : structure, formation, composition, rôle dans la biogenèse des mitochondries. Thèse Doct. d'Etat, Paris XI.
 - 33 Azevedo, C. (1984) Development and ultrastructural autoradiographic studies of nucleolus-like bodies (nuages) in oocytes of a viviparous teleost (*Xiphophorus helleri*). Cell Tiss. Res., **238**: 121-128.
 - 34 Hamaguchi, S. (1985) Changes in the morphology of the germinal dense bodies in primordial germ cells of the teleost, *Oryzias latipes*. Cell Tiss. Res., **240**: 669-673.
 - 35 Bruslé, S. (1980) Fine structure of early previtellogenic oocytes in *Mugil (Liza) auratus* Risso, 1810 (Teleostei, Mugilidae). Cell Tiss. Res., **207**: 123-134.
 - 36 Cataudella, S. and Capanna, E. (1973) Chromosome complements of three species of Mugilidae (Pisces, Perciformes). Experientia, **29**: 489-491.
 - 37 Baccetti, B. (1970) Comparative spermatology. Acad. Press, N.Y.
 - 38 Mattei, X. (1969) Contribution à l'étude de la spermiogenèse et des spermatozoïdes de poissons par la méthode de la microscopie électronique. Thèse Doct. d'Etat, Sciences, Montpellier, AO 3363.
 - 39 Lonning, S. (1981) Comparative electron microscope studies of the chorion of the fish egg. Rapp. P. V. Réun. Cons. int. Explor. Mer., **178**: 560-564.
 - 40 Schmehl, M. K. and Graham, E. F. (1987) Comparative ultrastructure of the zona radiata from eggs of six species of Salmonids. Cell. Tiss. Res., **250**: 513-519.
 - 41 Hubert, J. (1974) Ultrastructure des gonocytes primordiaux du Lézard des murailles (*Lacerta muralis* Laur.) et du Lézard vert (*Lacerta viridis* Laur.). Comparaison avec le lézard vivipare (*Lacerta vivi-*

- para*) J. Arch. Anat. Hist. Emb. norm. et exp., **57**: 259–268.
- 42 Fujimoto, T., Miyayama, Y. and Fuyuta, M. (1977) The origin, migration and fine morphology of human primordial germ cells. Anat. Rec., **188**: 315–329.

[COMMUNICATION]

Calcium-Activated Neutral Protease Quickly Converts α -Connectin to β -Connectin in Chicken Breast Muscle Myofibrils

DI HUA HU, SUMIKO KIMURA, SEIICHI KAWASHIMA¹
and KOSCAK MARUYAMA

Department of Biology, Faculty of Science, Chiba University, Chiba 260, and

¹*Department of Biochemistry, Tokyo Metropolitan Institute of
Gerontology, Itabashi-ku, Tokyo 173, Japan*

ABSTRACT—Calcium activated neutral protease (CANP) quickly hydrolyzed α -connectin (2800 kDa) to β -connectin (2100 kDa) in chicken skeletal muscle myofibrils and the latter was slowly degraded to 1700 kDa and 400 kDa peptides. The 1700 kDa peptide was more slowly hydrolyzed to 1400 kDa peptide. The hydrolysis of nebulin by CANP was slower than that of α -connectin to β -connectin. The action of CANP on the isolated β -connectin was similar to that on β -connectin in myofibrils, but much less effective. E64c, a thiol protease inhibitor, completely inhibited the actions of CANP.

INTRODUCTION

Connectin (also called titin) is the largest protein (MW, 2800 k) in vertebrate skeletal muscle myofibrils (see [1] for a review) and nebulin (MW, 700 k) is the second largest protein [2]. These two proteins are more or less degraded in Duchenne dystrophy muscles [3, 4]. In normal skeletal muscles of the chicken or of the rabbit, there are always a small amount of β -connectin (also called T₂; MW, 2100 k) in addition to the mother molecule, α -connectin (also called T₁) (cf. [1]). In Duchenne dystrophic muscles, α -connectin was largely degraded to β -connectin [4]. It has been claimed that calcium-activated neutral protease (CANP; also called calpain) activity is increased in Duchenne dystrophic muscles [5]. Previously, however, it was reported that CANP rapidly

degraded nebulin, but not connectin [6].

In the present study, it was clearly shown that CANP quickly converted α -connectin to β -connectin that had been missed in the earlier investigation [6]. Nebulin was also hydrolyzed by CANP in agreement with the previous results [6], but not so effectively as α -connectin.

MATERIALS AND METHODS

Myofibrils were prepared from chicken breast muscle using a solution containing 50 mM KCl, 1 mM NaHCO₃ and 5 mM EGTA (pH 8.2). Finally, myofibrils were washed several times with 50 mM KCl. β -Connectin was isolated from chicken breast muscle as described before [7]. Calcium-activated neutral protease (CANP) was purified from rabbit skeletal muscle and required millimolar calcium ions for its full activity (mCANP; calpain II) [8]. The action of CANP was tested at 25°C in a solution containing myofibrils (approximately 5 mg/ml) or β -connectin (approximately 0.5 mg/ml), 3 mM CaCl₂, 50 mM NaCl and 20 mM Tris-HCl buffer, pH 7.5. The reaction was stopped by the addition of 1mM E64c and 5% SDS (final concentration). After boiled for 3 min followed by centrifugation for 10 min at $\times 15,000g$, the supernatant was subjected to SDS gel electrophoresis according to Weber and Osborn [9] using 1.8% polyacrylamide gels. E64c was kindly supplied from Taisho Pharm. Co., Ltd., Tokyo.

RESULTS AND DISCUSSION

When chicken breast muscle myofibrils were treated with CANP, 1: 100 by weight ratio, all the α -connectin was converted to β -connectin within 1 min at 25°C, and the β -connectin was slowly degraded to 1700 kDa peptide (Fig. 1a). After 1 hr, some β -connectin remained, 1700 kDa peptide was most abundant, and some 1400 kDa peptide was formed. Also, nebulin was rapidly degraded by CANP, disappeared completely within a few minutes of incubation, and smaller peptides were formed. After 1 hr, a distinct band of approximately 400 kDa appeared, and this 400 kDa peptide was one of the main hydrolytic products of β -connectin by trypsin or chymotrypsin ([10] cf. also, Fig. 3). On the other hand, myosin heavy chain was not appreciably hydrolyzed within 10 min (Fig. 1a).

It was not clear in Figure 1a whether the conversion of α -connectin to β -connectin was faster than the hydrolysis of nebulin or not. Under the conditions where a smaller amount of CANP was added to chicken breast muscle myofibrils (1:1000), it was revealed that α -connectin was more rapidly hydrolyzed to β -connectin than the proteolysis of nebulin (Fig. 1b). α -Connectin was largely degraded to β -connectin within 5 min, while nebulin was practically kept intact. The latter was hydrolyzed about 10 min after incubation when almost all the α -connectin was already gone.

The action of CANP was reduced in the absence of added Ca^{2+} (3 mM), as shown in Figure 2. With EGTA, the activity was to a small extent. However, it was completely inhibited by the addition of 1 mM E64c that specifically inhibits SH proteolytic enzymes [11], including CANP [12].

The action of CANP on the isolated β -connectin was examined. As seen in Figure 3a, CANP, 1:20 by weight ratio, slowly hydrolyzed β -connectin to 1700 kDa and 400 kDa peptides. The former was even more slowly converted to 1400 kDa peptide that appeared 30 min after incubation. These processes were also observed in the hydrolysis of β -connectin in myofibrils (Fig. 1). One of the reasons why isolated β -connectin was difficult to be attacked by CANP might be due to lateral association of β -connectin filaments *in vitro* [13]. The

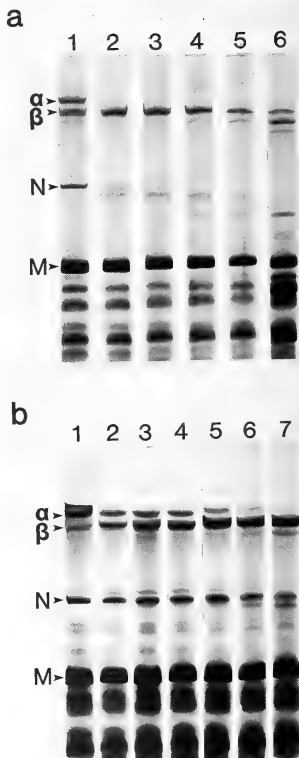


Fig. 1. Effects of calcium-activated neutral protease on the myofibrillar proteins of chicken breast muscle. Myofibrils, 5 mg/ml, were incubated with CANP (a, 1: 100 and b, 1: 1000 by weight ratio) in 50 mM NaCl, 3 mM CaCl_2 and 20 mM Tris-HCl buffer, pH 7.5 at 25°C. Reaction was stopped by adding 1 mM E64c and 5% SDS. SDS gel electrophoresis was carried out using 1.8% polyacrylamide gels [9]. The incubation time: a, 1, 0 time; 2, 1 min; 3, 2 min; 4, 5 min; 5, 10 min; 6, 60 min; b, 1, 0 time; 2, 30 sec; 3, 1 min; 4, 2 min; 5, 5 min; 6, 10 min; 7, 30 min. α , α -connectin; β , β -connectin; N, nebulin; M, myosin heavy chain.

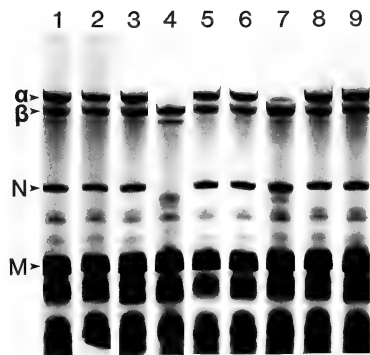


FIG. 2. Effects of various agents on the proteolysis of chicken breast muscle myofibrillar proteins by calcium-activated neutral protease. Conditions as in Fig. 1 except for the reaction time, 30 min in the presence of CANP, 1: 500 by weight ratio. 1, before incubation; 2, control after incubation; 3, CANP; 4, CANP+3 mM CaCl_2 ; 5, CANP+3 mM CaCl_2 +1 mM E64c; 6, 3 mM CaCl_2 +1 mM E64c; 7, 3 mM CaCl_2 ; 8, 5 mM EGTA; 9, 1 mM E64c.

action of CANP on β -connectin also required the presence of Ca^{2+} and was inhibited by E64c (Fig. 3b).

Chicken breast myofibrils tended to be degraded even when stored in 50 mM KCl and 1 mM NaHCO_3 at 0°C . Thus after 24 hr, α -connectin was considerably degraded to β -connectin while nebulin was hardly hydrolyzed (Fig. 4). Addition of 5 mM EGTA retarded this spontaneous breakdown of α -connectin, and that of 1 mM CaCl_2 greatly enhanced the hydrolysis. Also, E64c completely inhibited the degradation. These observations support that CANP may be mainly, if not solely, responsible for the spontaneous breakdown of α -connectin in isolated myofibrils.

The present work suggests that calcium-activated neutral protease play a role in the degradation of α -connectin and nebulin in Duchenne muscular dystrophy [3, 4]. However, since an endogenous CANP inhibitor exists in muscle cells [14, 15], the control mechanism of CANP activity

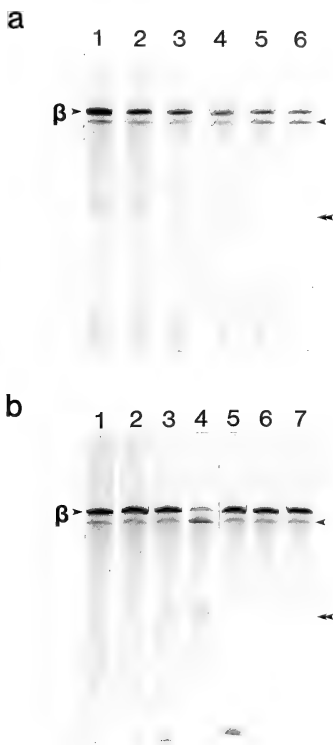


FIG. 3. Hydrolysis of isolated β -connectin by calcium-activated neutral protease. β -Connectin, 0.5 mg/ml was incubated with CANP, 1: 20 by weight ratio, in 0.3 M NaCl and 20 mM Tris buffer, pH 7.5, at 25°C . a, time course in the presence of 3 mM CaCl_2 . 1, 0 time; 2, 1 min; 3, 2 min; 4, 10 min; 5, 30 min; 6, 60 min. b, effects of various agents. Incubated for 30 min. 1, initial; 2, control after incubation; 3, CANP; 4, CANP+3 mM CaCl_2 ; 5, CANP+3 mM CaCl_2 +1 mM E64c; 6, 3 mM CaCl_2 +1 mM E64c; 7, 3 mM CaCl_2 . β , β -connectin; arrowheads, 1700 kDa peptide; double arrowheads, 400 kDa peptide.

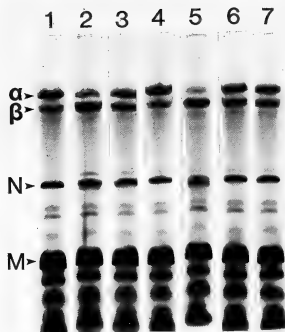


FIG. 4. Effects of various agents on the spontaneous breakdown of chicken breast muscle myofibrillar proteins when stored at 0°C. Myofibrils, 10 mg/ml, were kept for 24 hr at 0°C in 50 mM NaCl and 1 mM NaHCO₃. 1, before incubation; 2, control; 3, 5 mM EGTA; 4, 1 mM E64c; 5, 1 mM CaCl₂; 6, 1 mM E64c + 1 mM CaCl₂; 7, 1 mM E64c + 5 mM EGTA; α , α -connectin; β , β -connectin; N, nebulin; M, myosin heavy chain.

is rather complicated.

Finally, the disagreement of the present results with those of the previous report [6] should be explained. In the earlier investigation, SDS gel electrophoresis was performed using 3% polyacrylamide gels. Therefore, due to poorer resolution, α - and β -connectins were not properly distinguished. This was the reason why it was concluded that CANP did not hydrolyze connectin but did degrade nebulin in the previous study [6].

ACKNOWLEDGMENTS

This work was supported by grants from the Ministry of Education, Science and Culture, the Ministry of Health and Welfare (Japan) and Muscular Dystrophy Association.

REFERENCES

- 1 Maruyama, K. (1986) *Int. Rev. Cytol.*, **104**: 81–114.
- 2 Wang, K. and Williamson, C. L. (1980) *Proc. Natl. Acad. Sci. USA.*, **81**: 3685–3689.
- 3 Wood, D. S., Zeviani, M., Prella, A., Bonilla, E., Salviati, G., Miranda, A. F., Dimauro, S. and Rowland, L. P. (1987) *New Eng. J. Med.*, **316**: 106–108.
- 4 Sugita, H., Nonaka, I., Itoh, Y., Asakura, A., Hu, D. H., Kimura, S. and Maruyama, K. (1987) *Proc. Japn. Acad.*, **63B**: 107–110.
- 5 Obinata, T., Maruyama, K., Sugita, H., Kohama, K. and Ebashi, S. (1981) *Nerve & Muscle*, **4**: 456–488.
- 6 Maruyama, K., Kimura, M., Kimura, S., Ohashi, K., Suzuki, K. and Katunuma, N. (1981) *J. Biochem.*, **89**: 711–715.
- 7 Itoh, Y., Kimura, S., Suzuki, T., Ohashi, K. and Maruyama, K. (1986) *J. Biochem.*, **100**: 439–447.
- 8 Kawashima, S., Nomoto, M., Hayashi, M., Inomata, M., Nakamura, M. and Imahori, K. (1984) *J. Biochem.*, **95**: 95–101.
- 9 Weber, K. and Osborn, M. (1969) *J. Biol. Chem.*, **244**: 4406–4412.
- 10 Yoshidomi, H., Kimura, S. and Maruyama, K. (1984) *J. Biochem.*, **96**: 1947–1950.
- 11 Hanada, K., Tamai, M., Adachi, Oguma, K., Kashiwagi, K., Ohmura, S., Kominami, E., Towatari, T. and Katsunuma, N. (1983) In "Proteinase Inhibitors". Ed. by N. Katsunuma, H. Umezawa and H. Holzer, Jap. Sci. Soc. Press, Tokyo and Springer-Verlag, Berlin, pp. 25–36.
- 12 Sugita, H., Ishiura, S., Suzuki, K. and Imahori, K. (1980) *J. Biochem.*, **87**: 339–341.
- 13 Maruyama, K., Kimura, S., Yoshidomi, H., Sawada, H. and Kikuchi, M. (1984) *J. Biochem.*, **95**: 1424–1433.
- 14 Imahori, K., Suzuki, K. and Kawashima, S. (1983) In "Proteinase Inhibitors". Ed. by N. Katsunuma, H. Umezawa and H. Holzer, Jap. Sci. Soc. Press, Tokyo and Springer-Verlag, Berlin, pp. 173–180.
- 15 Murachi, T. (1983) *Trends in Biochem. Sci.*, **8**: 167–169.

[COMMUNICATION]

Transient Increase in Mitochondrial Protein Synthesis of Starfish Embryo before Gastrulation

TSUYOSHI KAWASHIMA and TOHRU NAKAZAWA¹

Department of Biology, Faculty of Science, Toho University,
Funabashi 274, Japan

ABSTRACT—A transient increase in protein synthesis *in vitro* was observed in mitochondrial fraction of starfish embryos at early gastrula stage. This stimulated activity was inhibited by chloramphenicol but not by cycloheximide. The purification of the protein synthesized in mitochondrial fraction was performed by column chromatography after labeling with [³H]-amino acids and the peak fraction of radioactivity was analyzed by SDS-polyacrylamide gel electrophoresis. The result shows that there was only three species of newly synthesized proteins in mitochondrial fraction of starfish embryos. The molecular weights of these proteins were estimated about 62, 54 and 47 kD respectively.

INTRODUCTION

The mechanism of differentiation at gastrulation of sea urchin embryos has not been elucidated yet. In a first step of this research, the effect of lithium chloride or other heavy metals had been examined. When embryos were treated with lithium chloride, invagination of archenteron at mesenchyme blastula stage was inhibited and the archenteron was turned inside out [1-4]. This type of gastrula embryos is called exogastrula. Some kinds of antibiotics were also responsible for the suppression of gastrulation. Chloramphenicol which is one of effective antibiotics for the induction of exogastrula [5-7] inhibits protein synthesis in prokaryote and mitochondria through the reaction with 70S ribosomes. In the previous paper, the relationship between the gastrulation of sea urchin embryo and mitochondrial protein synthesis was

examined. The protein synthetic activity *in vitro* was stimulated transiently at the mesenchyme blastula stage by the activation of peptide elongation factor in mitochondria [8]. In this paper, we examined characteristics of synthetic proteins in mitochondrial fraction of starfish embryos.

MATERIALS AND METHODS

Starfish embryos

Gonads were removed from the arms of mature starfish (*Asterina pectinifera*). The testes were placed on Petri dish on ice until used. The ovaries were removed and placed in a dish containing calcium-free sea water. After 30 min, the follicle-free ovaries were collected with nylon mesh, and washed twice with artificial sea water. Then the oocytes spawned by the addition of KCl were treated with 10⁻⁶ M 1-methyladenine. Over 95% of the oocytes showed germinal vesicle breakdown at 30 min after the treatment with 1-methyladenine. Then, the diluted sperm were added and fertilized eggs were cultured in filtered sea water at 18±2°C with gentle agitation.

Preparation of mitochondrial protein and column chromatography

The preparation of mitochondrial fraction and measurement of [³H]-amino acids incorporation were performed as the previous paper in sea urchin embryos [8].

The column chromatography was carried out at 4°C. After the treatment of [³H]-amino acids,

Accepted November 11, 1988

Received August 24, 1988

¹ To whom all correspondence should be addressed.

mitochondrial fraction was solubilized by the addition of 0.1 vol of 10% Triton X-100. The solution was filtered by TOYO-ultrafilter UP-20, size 43. Then the membrane was washed with buffer A consisted of 0.1 M NaCl and 50 mM Tris-HCl (pH 8.0) and the protein fraction obtained was concentrated to the volume of 1 ml. Thus the mitochondrial protein from 1 ml of packed cells was suspended in 1 ml of buffer A. The suspension was applied on a Sephadex G-100 column (15×300 mm) which was equilibrated and eluted with buffer A at a constant flow rate (8 ml per hour). Each 2 ml of the eluate was collected by a fraction collector. The 500 μ l of each fraction was added to 5 ml of AQUASOL-2 and the radioactivity was counted with a liquid scintillation counter (ALOKA LSC-700). Fractions at the peak of radioactivity were collected and concentrated by ultrafiltration. The sample was diluted with the same buffer and applied on a DEAE Sephadex A-50 column (15×300 mm). The elution was carried out by a linear gradient concentration of 0.1 M to 1.0 M NaCl in the buffer. The flow rate was 8 ml per hr and each 2 ml of fraction was collected. The incorporated radioactivity was counted.

SDS-polyacrylamide gel electrophoresis

SDS-polyacrylamide gel electrophoresis (SDS-PAGE) was performed according to the method of Laemmli [9], using 12.5% polyacrylamide gel.

Protein measurement was carried out according to the method of Lowry *et al.* [10], using the bovine serum albumin as standard.

RESULTS AND DISCUSSION

Protein synthetic activity in mitochondrial fraction of starfish embryo

Figure 1 shows *in vitro* incorporation of [3 H]-amino acids into the mitochondrial protein of developing starfish embryos in the presence or absence of chloramphenicol and cycloheximide. Protein synthetic activity in mitochondrial fraction was increased at the late blastula stage. The peak was observed at the early gastrula stage and the activity decreased to the low original level at the

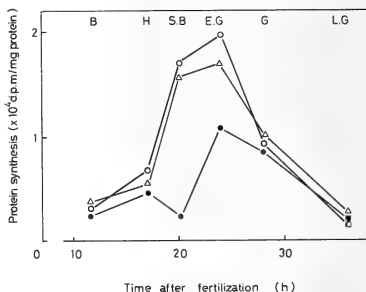


FIG. 1. Changes in [3 H]-amino acids incorporating activity into mitochondrial protein of starfish embryos during development. Reaction medium and procedures are described in text. Other additions are indicated as none (○), 100 μ M cycloheximide (△) and 100 μ M chloramphenicol (●). Characters in the uppermost part of the figure indicate stages of development: B, blastula; H, hatching; EG, early gastrula; G, gastrula and LG, late gastrula.

gastrula stage. The addition of 100 μ M chloramphenicol suppressed the protein synthesis between late blastula and early gastrula stage. In the case of sea urchin embryo, the addition of 35.5 μ M cycloheximide did not inhibit the protein synthesis in the mitochondria but rather stimulated [8]. In starfish embryos, the protein synthesis was not stimulated by cycloheximide. It seems that the stimulation of the protein synthesis in mitochondrial fraction may be regulated by different fashions between these two species.

Purification of the protein synthesized in mitochondrial fraction

To purify the protein synthesized in mitochondrial fraction, the mitochondrial fraction was incubated with [3 H]-amino acids, solubilized by Triton X-100, and applied on Sephadex G-100 and DEAE Sephadex A-50 columns. The elution pattern of the radiolabeled proteins by Sephadex G-100 column is shown in Figure 2. Although there was only one peak of the synthesized protein of mitochondrial fraction in the elution pattern of Sephadex G-100 column, several components were

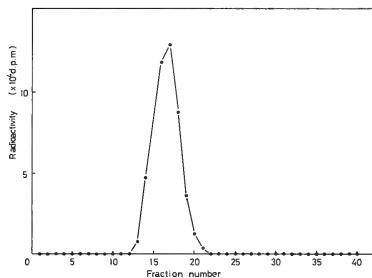


Fig. 2. Sephadex G-100 column chromatography. The mitochondrial fraction of starfish embryos was solubilized by Triton X-100 and loaded onto Sephadex G-100 column (15×300 mm). The column was eluted with buffer A (see text). Closed circle shows the elution pattern of the newly synthesized protein monitored by incorporated radioactivity.

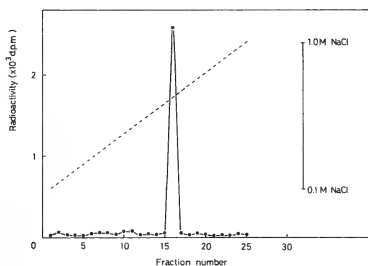


Fig. 3. DEAE Sephadex A-50 column chromatography. The peak fraction obtained from Sephadex G-100 was concentrated by ultrafiltration and applied on DEAE Sephadex A-50 column. The column was eluted with 0.1 to 1.0 M NaCl gradient. Closed circle shows the newly synthesized protein monitored by incorporated radioactivity (solid line). Broken line indicates NaCl concentrations.

recognized by SDS-polyacrylamide gel electrophoresis (Fig. 4-C). Then the Sephadex G-100 peak fractions were concentrated by ultrafiltration and eluted through a column of DEAE Sephadex A-50. As seen in Figure 3, the protein synthesized in mitochondrial fraction was eluted from the column at about 0.75 M NaCl. The peak of radioactivity was observed in only one fraction.

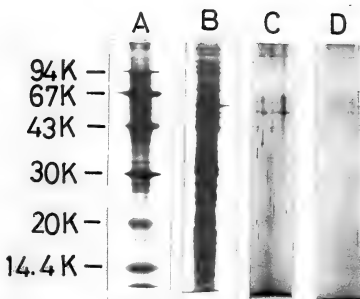


Fig. 4. Polyacrylamide gel electrophoresis of proteins from mitochondrial fraction at early gastrula stage of starfish embryos. Alphabet at the top of figure indicate as follows; A: low molecular weight standard, B: whole mitochondrial protein at early gastrula stage of starfish embryos, C: peak fraction of Sephadex G-100 column, D: peak fraction of DEAE Sephadex A-50 column.

Analysis of the purified protein by SDS-PAGE

The mitochondrial protein labeled with [3 H]-amino acids were examined by SDS-PAGE after the purification by two types of column chromatography. Figure 4 shows the results of SDS-PAGE using 12.5% polyacrylamide gel. When proteins from whole mitochondrial fraction at mesenchyme blastula stage was analyzed, many bands were observed (Fig. 4-B). In the peak fraction obtained from Sephadex G-100 column chromatography, three main and several minor bands were found in the high molecular weight region in SDS-PAGE (Fig. 4-C). After the DEAE Sephadex A-50 column chromatography, three major bands in SDS-PAGE were recognized in the peak fraction (Fig. 4-D). The molecular weight of these proteins were estimated as about 62, 54 and 47 kD, respectively. It has been known that the molecular weight of enzyme proteins located in mitochondria is in general 7.5 kD to 45 kD. Since all of proteins synthesized in mitochondria of starfish embryos had higher molecular weights

than that in general mitochondrial proteins, synthesized proteins might not be respiratory enzymes which have lower molecular weight. If the phenomenon observed in this paper were concerned with the multiplication of mitochondria itself, the synthesized proteins would be a constitutive protein of mitochondria

There are several recent indications for specific mitochondrial changes in morphology and functions during early development of animal embryos. In our previous paper, a transient increase in protein synthesis in mitochondria was observed in mesenchyme blastula of the sea urchin. In the mouse embryo, mitochondrial protein synthesis *in vitro* was also indicated during oogenesis and early embryogenesis [11, 12]. Furthermore, mitochondria might play an important role in the embryonic development of insects. It has been indicated that cytoplasmic factor in the polar region of insect embryos is encoded by mitochondrial genome. Mitochondria in the posterior pole of *Drosophila* eggs have been recognized to attach to polar granules which differentiate to primordial germ cell during development. As well as mitochondrial protein synthesis in starfish embryo, some sort of essential informations for embryonic differentiation might be stored or formed in mitochondria at

a certain stage of development in other kinds of embryo. The relationship between the transient increase of protein synthesis in mitochondria and differentiation of embryos should be analyzed furthermore.

REFERENCES

- 1 Herbst, C. (1892) Z. wiss. Zool., **55**: 446-518.
- 2 Lindahl, P. E. (1933) Wilhelm Roux' Arch. Entwickl.-mech. org., **128**: 661-664.
- 3 Bäckström, S. and Gustafson, T. (1953) Ark. Zool. Ser. 2, **6**: 185-188.
- 4 Mitsunaga, K., Fujiwara, A., Yoshimi, T. and Yasumasu, I. (1983) Develop. Growth and Differ., **25**: 249-260.
- 5 Hörstadius, S. (1963) Develop. Biol., **7**: 144-151.
- 6 Lallier, R. (1963) Exp. Cell Res., **29**: 119-127.
- 7 Fujiwara, A. and Yasumasu, I. (1974) Develop. Growth and Differ., **16**: 83-92.
- 8 Kawashima, T. and Nakazawa, T. (1988) Develop. Growth and Differ., **30**: 137-145.
- 9 Laemmli, U. K. (1970) Nature, **227**: 680-685.
- 10 Lowry, O. H., Rosenbrough N. J., Farr, A. L. and Randall, R. J. (1951) J. Biol. Chem., **193**: 265-275.
- 11 Cascio, S. M. and Wassarman, P. M. (1981) Develop. Biol., **83**: 166-172.
- 12 Pikó, L. and Chase, D. G. (1973) J. Cell Biol., **58**: 357-378.

[COMMUNICATION]

Immunohistochemical Studies of Juxtaglomerular Cells and the Corpuscles of Stannius in the Eel, *Anguilla japonica*

HISASHI TAZAWA, MAKIO MUKAI¹
and MIZUHO OGAWA²

Department of Biology, Faculty of Liberal Arts and Science,
Saitama University, Urawa 338, and ¹Department of Pathology,
Keio University School of Medicine, Shinano-machi,
Tokyo 160, Japan

ABSTRACT—The localization of immunoreactive renin in the juxtaglomerular cells (JGC) and the corpuscles of Stannius (CS) was investigated in the Japanese eel *Anguilla japonica*. Anti-serum against mouse submandibular gland renin raised in rabbits was used for the immunohistochemistry. Immunoreactive JGC were demonstrated in the wall of the glomerular afferent arterioles and the small arterial branches of the kidney. However, renin-immunoreactivity could not be detected in CS.

INTRODUCTION

The juxtaglomerular apparatus is not so well developed in non-mammalian vertebrates as in the mammals [1]. In the teleostean kidney, juxtaglomerular cells (JGC) have been observed in the walls of the renal arterioles and/or small arteries; macula densa and the extraglomerular mesangium are not found [2]. Localization of renin in the granules of JGC was first demonstrated in mammals by fluorescent antibody technique [3]. Although the JGC are known as renin-containing cells in mice [4, 5], rats [6, 7], and humans [8, 9], little recent information is available concerning the existence of renin-containing cells in non-mammalian kidneys [10]. However, renin-immunoreactive cells were recently demonstrated in the carp [11].

The corpuscles of Stannius (CS) are unique

endocrine glands of bony fishes. Since the removal of the CS was reported to induce hypercalcemia in the European eel [12], many investigations have indicated that the CS relate in calcium regulation in fishes [13]. The active principle of the CS has been termed hypocalcin [14] and several candidates for hypocalcin has been proposed: a small glycopeptide with a molecular weight of 3,000 [15], renin-like substance and/or angiotensin-like substance [16], acid stable protein with a molecular weight greater than 10,000 [17, 18], mammalian-PTH-like substance [19], and a glycoprotein with a molecular weight of 39,300 [20]. Histologically, granules in the CS cells are stained with Bowie's staining, which also stains granules in the JGC of the teleostean kidney [21, 22]. Renin-like activity was found in the CS of the carp and Japanese goosfish [23]. The amino acid sequences of angiotensin I (AI) obtained by incubating CS or kidney extracts with homologous plasma in chum salmon and the Japanese goosfish have identified [24, 25]. An angiotensin II-like substance, a member of the renin-angiotensin system, was found in the cells of CS of the rainbow trout immunohistochemically [26]. However, the presence of renin was not examined immunohistochemically in the CS.

In the present study, the presence of renin in the kidney and the CS of the Japanese eel, *Anguilla japonica* was studied by immunohistochemical methods.

Accepted September 24, 1988

Received June 7, 1988

² To whom reprint requests should be addressed.

MATERIALS AND METHODS

Japanese eels, *Anguilla japonica* were used. Fish were anesthetized by MS 222. The kidney tissue associated with the CS was fixed in Bouin's fluid for 2 hr, embedded in paraffin, and sectioned at 4 μ m. Rabbit anti-mouse submandibular gland renin antiserum was supplied through the courtesy of Prof. Kazuo Murakami, Institute of Applied Biochemistry, Tsukuba University [27, 28]. Its reliability was previously demonstrated in an immunohistochemical study [10, 11]. Immunohistochemical staining was carried out as previously described [29]. In brief, the sections were deparaffinized and hydrated, and then the endogenous peroxidase activity was blocked by exposure to methanol containing 0.2% H_2O_2 for 30 min. After being washed, the slides were incubated overnight with the antiserum diluted in phosphate-buffered saline to 1:500. The slides were then exposed to a biotinylated anti-rabbit immunoglobulin antiserum (dilution 1:500), avidin (dilution 1:1,000), and biotinylated horseradish peroxidase complex. The reagents were purchased from Vector Laboratories, Inc. (Vectastain, Burlingame, California). We developed the peroxidase reaction by incubating the slides in 0.5% H_2O_2 and 0.02% 3,3'-diaminobenzidine tetrahydrochloride for 10 min. Control sections were incubated with non-immune rabbit serum instead of anti-renin serum.

RESULTS AND DISCUSSION

The cells resembling JGC in the wall of the glomerular afferent arterioles and the small arterial branches in the eel kidney were intensely immunoreactive to anti-renin serum (Fig. 1). The immunoreactive JGC were located extensively and dispersedly in some portion in the afferent arterioles at the juxtaglomerular region and also in the small arterial branches locating apart from the vascular poles of glomeruli. They were detectable along the tunica media of the blood vessels (Fig. 2). The above features are consistent with those found in the previous investigations on the JGC of teleostean kidney [1].

A pair of eel CS were located on or in the ventral side of posterior kidney near its attachment

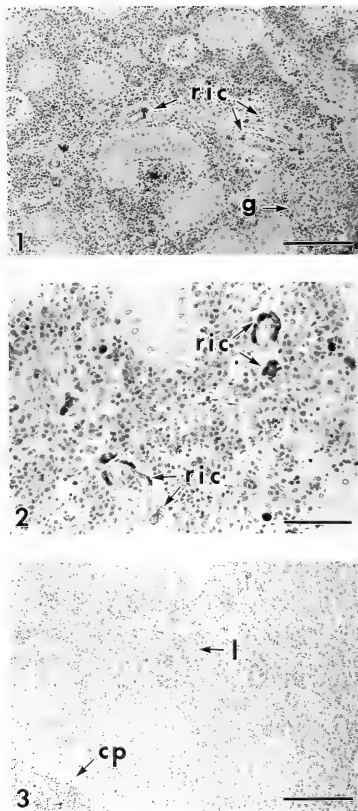


FIG. 1. Renin-immunoreactive cells (ric) resembling juxtaglomerular cells are observed in the wall of glomerular afferent arterioles and the small arterial branches of the kidney in the Japanese eel, *Anguilla japonica*. g: glomerulus. Scale, 100 μ m.

FIG. 2. High magnification of some renin-immunoreactive cells (ric) in the wall of glomerular afferent arterioles of eel kidney. Scale, 50 μ m.

FIG. 3. Corpuscles of Stannius of the Japanese eel. No renin-immunoreactive cells. l: lobule of CS. cp: capsule of the CS. Scale, 100 μ m.

to the posterior cardinal vein. No renin immunoreactivity was detected in the eel CS even though immunoreactivity occurs in the kidney tissue in the same section (Fig. 3). This result suggests that the eel CS do not contain any substances which react with anti-mouse submandibular gland renin serum.

Renin-like activity has been found in the CS of the carp and Japanese goosfish [23]. Moreover, both a homogenate of carp CS and angiotensin-like substances which were formed by incubating the eel CS extract with homologous plasma produced hypocalcemia in Japanese eel [16]. Further, [Asp¹, Val⁵, Asn⁹] AI and [Asn¹, Val⁵, Asn⁹] AI were obtained chemically by incubating the CS or the kidney extracts with homologous plasma in the chum salmon [24] and [Asn¹, Val⁵, His⁹] AI in Japanese goosfish [25]. However, renin-immunoreactivity of the CS could not be detected in the present study, even though the JGC of the kidney showed a positive reaction in the same section. It may be one of the possibilities that renin activity in the CS is too weak to be detected by the present immunohistochemical method. Moreover, the CS tissue, unlike the kidney, may require a different fixative for the best preservation of its cell inclusions. On the other hand, it was reported recently that the incubation of CS homogenate with homologous plasma did not result in any angiotensin-like peptides in the eel, *Anguilla australis* [30]. It is important to clarify whether renin is present in the CS or not. Therefore, further studies using different fixatives and antisera are required.

In the present investigation, it is evident that in the eel, the renin-immunoreactive cells resembling JGC are localized in the wall of the glomerular afferent arterioles and the small arterial branches of the kidney, but renin-immunoreactive cells are not detected in the CS.

ACKNOWLEDGMENTS

We are grateful for the generous gift of the anti-mouse submandibular gland renin serum by Prof. Kazuo Murakami, Institute of Applied Biochemistry, Tsukuba University, Japan. We wish also to express our gratitude to Prof. W. S. Hoar, University of British Columbia, for his critical reading of the manuscript.

REFERENCES

- 1 Sokabe, H. and Ogawa, M. (1974) *Inter. Rev. Cytol.*, **37**: 271-327.
- 2 Ogawa, M., Oguri, M., Sokabe, H. and Nishimura, H. (1972) *Gen. Comp. Endocrinol.*, Suppl. 3: 374-381.
- 3 Edelman, R. and Hartroft, P. M. (1961) *Circ. Res.*, **9**: 1069-1077.
- 4 Taugner, Ch., Poulsen, K., Hackenthal, E. and Taugner, R. (1979) *Histochemistry*, **62**: 19-27.
- 5 Tanaka, T., Gresik, E., Michelakis, A. and Barka, T. (1980) *J. Histochem. Cytochem.*, **28**: 1113-1118.
- 6 Taugner, R. and Hackenthal, E. (1981) *Histochemistry*, **72**: 499-509.
- 7 Taugner, R., Mannek, E., Nobiling, R., Buhrle, C. P., Hackenthal, E., Gauten, D., Inagami, T. and Schroder, H. (1984) *Histochemistry*, **81**: 39-45.
- 8 Amat, D., Camilleri, J. P., Phat, V. N., Bariety, J., Corvol, P. and Menard, J. (1981) *Virchow Arch. Pathol. Anat. Physiol. Klin. Med.*, **390**: 193-204.
- 9 Faraggiana, T., Gresik, E., Tanaka, T., Inagami, T. and Lupo, A. (1982) *J. Histochem. Cytochem.*, **30**: 459-465.
- 10 Kon, Y., Hashimoto, Y., Kitagawa, H., Kudo, N. and Murakami, K. (1986) *Jpn. J. Vet. Res.*, **34**: 111-123.
- 11 Kon, Y., Hashimoto, Y., Kitagawa, H. and Kudo, N. (1987) *Jpn. J. Vet. Sci.*, **49**: 323-331.
- 12 Fontaine, M. (1964) *C. R. Acad. Sci.*, **259**: 875-878.
- 13 Sokabe, H. (1982) In "Comparative Endocrinology of Calcium Regulation". Ed. by C. Oguro and P. K. T. Pang, Jap. Sci. Soc. Press, Tokyo, pp. 137-142.
- 14 Pang, P. K. T., Pang, R. K. and Sawyer, W. H. (1974) *Endocrinol.*, **94**: 548-555.
- 15 Ma, S. W. Y. and Copp, D. H. (1978) In "Comparative Endocrinology". Ed. by P. J. Gaillard and H. H. Boer, Elsevier/North Holland, Amsterdam, pp. 283-286.
- 16 Ogawa, M. and Sokabe, H. (1982) *Gen. Comp. Endocrinol.*, **47**: 36-41.
- 17 So, Y. P. and Fenwick, J. C. (1982) In "Comparative Endocrinology of Calcium Regulation". Ed. by C. Oguro and P. K. T. Pang, Jap. Sci. Soc. Press., Tokyo, pp. 161-165.
- 18 Fenwick, J. C. (1982) In "Comparative Endocrinology of Calcium Regulation". Ed. by C. Oguro and P. K. T. Pang, Jap. Sci. Soc. Press, Tokyo, pp. 167-172.
- 19 Milet, C., Hillyard, C. J., Martelly, E., Girgis, S., MacIntyre, I. and Lopez, E. (1980) *C. R. Acad. Sci., D*, **291**: 977-980.
- 20 Wagner, G. H., Hampson, M., Park, C. M. and Copp, D. H. (1986) *Gen. Comp. Endocrinol.*, **63**: 481-491.

- 21 Oguri, M. and Sokabe, H. (1968) Bull. Jap. Soc. Sci. Fish., **34**: 882-888.
- 22 Oguri, M. and Sokabe, H. (1974) Bull. Jap. Soc. Sci. Fish., **40**: 545-549.
- 23 Sokabe, H., Nishimura, H., Ogawa, M. and Oguri, M. (1970) Gen. Comp. Endocrinol., **14**: 510-516.
- 24 Takemoto, Y., Nakajima, T., Hasegawa, Y., Watanabe, T. X., Sokabe, H., Kumagai, S. and Sakakibara, S. (1983) Gen. Comp. Endocrinol., **51**: 219-227.
- 25 Hasegawa, Y., Watanabe, T. X., Nakajima, T. and Sokabe, H. (1984) Gen. Comp. Endocrinol., **54**: 264-269.
- 26 Yamada, C. and Kobayashi, H. (1987) Zool. Sci., **4**: 387-390.
- 27 Fukushi, T., Masuda, T., Imai, T., Sudoh, M., Kimura, S., Hirose, S. and Murakami, K. (1982) Biomed. Res., **3**: 534-540.
- 28 Hirose, S., Yamamoto, Y., Kim, S.-J., Tshuchiya, M. and Murakami, K. (1983) Biomed. Res., **4**: 591-596.
- 29 Mukai, M., Torikata, C., Hirose, S., Murakami, K. and Kageyama, K. (1984) Lab. Invest., **51**: 425-428.
- 30 Butkus, A., Roche, P. J., Fernley, R. T., Haralambidis, J., Penschow, J. D., Ryan, G. B., Trahair, J. F., Tregear, G. W. and Coghlan, J. P. (1987) Mol. Cell. Endocrinol., **54**: 123-133.

[COMMUNICATION]

**Possible Involvement of GABAergic Neurons in Regulation
of Diapause Hormone Secretion in the Silkworm,
*Bombyx mori***

ISAMU SHIMIZU, TOMOHIKO MATSUI and KOU HASEGAWA

*Research Section of Environmental Biology, Laboratory for
Plant Ecological Studies, Faculty of Science,
Kyoto University, Kyoto 606, Japan*

ABSTRACT—Injection of picrotoxin and bicuculline, blocking agents of GABA-mediated synaptic inhibition, into the silkworm pupae of non-diapause eggs producer induced diapause eggs. On the other hand injection of γ -aminobutyric acid (GABA) into diapause producers caused a production of non-diapause eggs. These two lines of evidence strongly suggest that GABAergic neurons are involved in the regulation of the diapause hormone secretion from the subesophageal ganglion of the silkworm.

INTRODUCTION

Insects enter diapause at various life stages characteristic of each species, which is governed by endocrine events [1, 2]. The silkworm, *Bombyx mori* is a typical insect species of embryonic diapause and the nature of the diapause has been well documented [3]. The embryonic diapause is determined by various environmental conditions which the mother moths have experienced during their embryonic and larval stages [4, 5]. The diapause hormone is secreted from neurosecretory cells located in the subesophageal ganglion (SG) of the diapause eggs producer during the pupal stage, acting on the developing ovaries and produces diapause eggs. In non-diapause eggs producer the secretion is blocked and the eggs laid become non-diapause [6-8]. Some pieces of evidence obtained by surgical experiments suggested that

brain (Br) of the silkworm controls the secretion of the diapause hormone from SG through subesophageal connective: in the pupa of diapause producer a stimulatory signal from Br brings about the release of the diapause hormone from SG and in non-diapause producer a repressive signal suppresses it [9-11]. However, the physiological mechanism controlling the secretion has not been revealed yet.

GABA functions as an inhibitory neurotransmitter in both vertebrate and invertebrate nervous systems and GABAergic neurons usually inhibit their targets by releasing the chemical transmitter (GABA) that opens chloride channels in the post-synaptic cells [12]. Several lines of evidence demonstrated that the inhibitory neurons play an important role in integrating overall level of neural activities. Picrotoxin and bicuculline are known to block selectively and reversibly the inhibitory synapses mediated by GABA [13]. These chemical agents are used often to probe the mechanism of the GABA-mediated synaptic inhibition [14]. Using these agents we obtained experimental results suggesting that GABAergic neurons are involved in the regulation of the diapause hormone secretion in the silkworm.

MATERIALS AND METHODS

The silkworm employed was a bivoltine race (*Daizo*), whose characteristics of the photo-

periodic response have been well documented elsewhere [15]. Two batches of female silkworms were destined to produce diapause eggs or non-diapause eggs by controlling the environmental conditions during their embryonic and larval stages [15]. Picrotoxin (Sigma) and GABA (Nakarai Chem. Ltd.) were dissolved in saline at the concentration of 30 $\mu\text{g}/10 \mu\text{l}$ and 10 $\text{mg}/10 \mu\text{l}$, respectively. Bicuculline (Sigma) was dissolved in ethylacetate at the concentration of 160 $\mu\text{g}/10 \mu\text{l}$. After ether anaesthesia injections of these test solutions into the abdominal segment of pupae were carried out using microsyringes. Injection of the agents did not affect the development of adults and ovaries.

Diapause eggs develop ommochrome pigments in serosa after oviposition. Usually the appearance of this pigment and an arrest of embryonic development are used as criterions for the embryonic diapause of the silkworm. Moths injected with picrotoxin or bicuculline laid only few eggs of their ovaries, and so we used following method to detect 3-hydroxykynurenine accumulated in eggs of ovary. After adult emergence ovaries were dissected out in saline and one of eight ovaioles was cutted out from the anterior to posterior end, putted on filter paper straightly in linear order, and all eggs were crushed completely without putting out of order. Then Ehrlich's diazo reagent was dropped upon the part of the filter paper into which the egg-extracts infiltrated and red coloration indicating the presence of 3-hydroxykynurenine was examined.

3-Hydroxykynurenine is a metabolic precursor of ommochrome pigments and the diapause hormone was reported to accelerate the accumulation of the amino acid in pupal ovaries [16]. Therefore the detection of 3-hydroxykynurenine accumulated in eggs using Ehrlich's diazo reaction has been carried out to see the commitment of the hormone to the developing eggs [17, 18]. We confirmed that eggs laid by diapause producers were positive (bright-red colour) to the reaction (the criterion was +++ or ++) and that eggs by non-diapause producers were slightly positive or negative (+ or -). The number and arrangement of diapause and non-diapause eggs in each ovariole were recorded.

RESULTS AND DISCUSSION

To see an involvement of GABAergic neurons in the diapause hormone secretion 90 μg of picrotoxin or 32 μg of bicuculline was injected into 4 day-old pupae of the non-diapause eggs producer (Table 1). Injection of these compounds caused continuous convulsions of pupal abdomen for 24–30 hr after the treatment, but scarcely affected the pupal development and almost all adult moths emerged 9–10 days after larval-pupal ecdysis. After adult ecdysis the diapause and non-diapause of eggs were examined by Ehrlich's diazo reaction according to the criteria as described above.

In non-injected control and saline injected control, all female moths had only non-diapause eggs. On the other hand, all animals injected with

TABLE 1. Production of diapause eggs in non-diapause eggs producers of the silkworm pupae by injection of picrotoxin or bicuculline

Injection	ND	Mixed	D	D%
	(-, +)	(- ~ +++)	(++, +++)	(++, +++/Total)
Control	20	0	0	0%
Saline (30 μl)	13	0	0	0%
Picrotoxin (90 μg)	0	13	0	53%
Ethylacetate (2 μl)	11	0	0	0%
Bicuculline (32 μg)	1	7	0	23%
GABA (10 mg)	12	0	0	0%

ND, Mixed and D represent the silkworm moths producing 100% non-diapause eggs, mixed eggs and 100% diapause eggs, respectively. 4 day-old pupae were used. Criterion (- ~ +++) represents the Ehrlich's diazo reaction. See the text in detail.

picrotoxin produced mixed batches of diapause and non-diapause eggs: the diapause percentage (eggs of +++ and ++ per total eggs examined) was 53%. There was no difference in the arrangement of diapause and non-diapause eggs in eight ovarioles of one moth. Dose response curve showed that injection of 15 μ g of picrotoxin was not effective dose to produce diapause eggs, but 30 μ g of the agent was effective (29% diapause). In every adult eggs of late (anterior) and middle part in each ovariole were positive to Ehrlich's reaction. On the other hand, injections into 0-3 day-old pupae produced the diapause eggs in the early (posterior) group. Bicuculline (32 μ g) of an antagonist of GABAergic neuron produced diapause eggs also, while ethylacetate (2 μ l) of the solvent did not affect the non-diapause production at all.

After surgical removal of SG from the pupae of non-diapause producer on the day of larval-pupal ecdysis picrotoxin was injected into the operated pupae of 4 day-old. However the injection of picrotoxin produced little diapause eggs. This showed that picrotoxin did not act directly on the ovary to make eggs diapause or not increase the content of 3-hydroxykynurenine in developing ovary. It is most likely that these agents act on the central nervous system of Br-SG. Injection of GABA into non-diapause eggs producers did not affect the non-diapause production.

From the observations obtained above we tentatively assumed that GABAergic inhibitory synapses function in the repression of the diapause hormone release from SG in non-diapause producers. Then GABA was injected into the pupae of diapause eggs producers in expectation of non-diapause eggs production (Table 2). Non-injected controls and saline-injected controls of 3 day-old

pupae did not produce any non-diapause egg. On the other hand injections of GABA (10 mg) into 20 pupae produced 12 moths of 100% diapause eggs and 8 moths of mixed type of diapause and non-diapause eggs. In this case the early and middle part of the ovariole became non-diapause. As the day of injection became late from 2 day to 5 day, non-diapause eggs zone of the animal in which it was effective went backward from early to late group of eggs. GABA injected was presumably effective as the synaptic inhibitor for about 24 hr after an injection before its degradation or absorption: production of non-diapause eggs by GABA may be due to a temporal repression of diapause hormone release through an inhibition of the neurosecretory cells. One mg of GABA was not effective dose, and injection of picrotoxin into diapause producers did not affect the diapause production at all.

It was suggested that series of functional components involved in the silkworm photoperiodic response, that is photoperiodic photoreceptor, clock and counter system, all reside in brain and that the hormonal-effector system is located in SG [11]. Fukuda and Takeuchi [7] concluded according to their detail histological studies that the diapause hormone was produced by a pair of neurosecretory cells located toward the ventral side of SG. They observed that the neurosecretory cells actively accumulated neurosecretory materials in non-diapause producers and released them in diapause producers. Our results obtained here suggested that the brain of the silkworm regulates the secretion of the diapause hormone from SG by innervation through GABAergic neurons and that the inhibitory regulation by the neurons is primary in the control of the hormone secretion. However

TABLE 2. Production of non-diapause eggs in diapause eggs producer of the silkworm pupae by injection of GABA

Injection	ND (-, +)	Mixed (- ~ + + +)	D (+, + +)	ND% (-, +/Total)
Control	0	0	16	0%
Saline (10 μ l)**	0	0	15	0%
Picrotoxin (90 μ g)*	0	0	16	0%
GABA (10 mg)**	0	8	12	15%

Injections were carried out using 3 day-old (*) and 4 day-old (**) pupae, respectively.

the problem whether the GABAergic neurons project to the neurosecretory cells directly or not remains to be open. In vertebrates GABAergic neurons have been reported to function in the neuroendocrine control of hormones [19]. This is the first report suggesting an involvement of GABAergic neurons in the endocrine control of insect hormones.

REFERENCES

- 1 Behrens, W. (1985) In "Environmental Physiology and Biochemistry of Insects". Ed. by K. H. Hoffman, Springer-Verg, Berlin/Heidelberg/New York/Tokyo, pp. 67-94.
- 2 Saunders, D. S. (1982) *Insects Clocks*. Pergamon Press, Oxford.
- 3 Yamashita, O. Yaginuma, T. and Hasegawa, K. (1981) *Entomol. Gen.*, **7**: 195-211.
- 4 Kogure, M. (1933) *J. Dep. Agr. Kyushu Univ.*, **4**: 1-93.
- 5 Shimizu, I. (1982) *J. Insect Physiol.*, **28**: 841-846.
- 6 Fukuda, S. (1951) *Proc. Japan Acad.*, **27**: 676-677.
- 7 Fukuda, S. and Takeuchi, S. (1967) *Embryologia*, **9**: 333-353.
- 8 Hasegawa, K. (1951) *Proc. Japan Acad.*, **27**: 667-671.
- 9 Fukuda, S. (1952) *Ann. Zool. Jap.*, **25**: 149-155.
- 10 Matsutani, K. and Sonobe, H. (1987) *J. Insect Physiol.*, **33**: 279-285.
- 11 Hasegawa, K. and Shimizu, I. (1987) *J. Insect Physiol.*, **33**: 959-966.
- 12 Gottlieb, D. I. (1988) *Scientific American*, **258**: 38-42.
- 13 Pichon, Y. (1974) In "The Physiology of Insecta (2nd ed.)". Ed. by M. Rockstein, Academic Press, New York/London, pp. 101-174.
- 14 Walddrop, B. Christensen T. A. and Hildebrand, G. (1987) *J. Comp. Physiol.*, **161**: 23-32.
- 15 Shimizu, I. and Hasegawa, K. (1988) *Physiol. Entomol.*, **13**: 81-88.
- 16 Yamashita, O. and Hasegawa, K. (1966) *J. Insect Physiol.*, **12**: 957-962.
- 17 Takeda, S. (1977) *Appl. Ent. Zool.*, **12**: 80-82.
- 18 Sonobe, H., Hiyama, Y. and Keino, H. (1977) *J. Insect Physiol.*, **23**: 633-637.
- 19 Yagi, K. and Sawaki, Y. (1978) *Neuroendocrinology*, **26**: 50-64.

[COMMUNICATION]

**Free-Running Locomotor Rhythms of
Feeding-Entrained Goldfish**

RICHARD E. SPIELER and JOHN J. CLOUGHERTY

*Milwaukee Public Museum, 800 West Wells St.,
Milwaukee, WI 53233, USA*

ABSTRACT—Groups of goldfish were held on a 12L:12D photoperiod and fed at one of four different circadian times (light onset at 6, 12, or 18 hr after light onset) for 46 days. The animals were then allowed to free-run on constant light or dark without food or disturbance for five days, and activity rhythms were remote monitored. Most groups maintained a circadian locomotor rhythm entrained to the approximate time of feeding. No consistent differences among fish on the different feeding regimes or between those on constant light or dark were noted.

INTRODUCTION

Meal-feeding a single daily meal can synchronize a host of daily rhythms in vertebrates including fishes. In many cases feeding is a more potent entrainer of the expressed rhythms (i.e., locomotor, circulating cortisol, agonistic behavior, etc.) than the light-dark cycle [1-3]. Whether meal-feeding is entraining an endogenous oscillator responsible for the expression of the rhythms is, however, not clear and may be species dependent. Previous research on the interrelationship of meal-feeding entrainment and the circadian locomotor rhythms of fishes have examined the feeding entrained rhythm in starved fish on a light-dark cycle [2] or examined the locomotor rhythm under conditions of constant light or dark while the animals continued to be fed [4, 5]. In either case, the fishes continued to receive a daily entraining stimulus and thus were not truly free-running. This study examined free-running locomotor

rhythms of feeding-entrained, starved goldfish on constant light or dark.

MATERIALS AND METHODS

Juvenile goldfish (body weight approximately 6 gm) of mixed sexes were obtained from a commercial supplier (Ozark Fisheries, Stoutland, MO) and placed in 18, 60-liter aquaria (12 fish/aquarium). Each aquarium received a continuous supply of filtered and aerated water ($13 \pm 2^\circ\text{C}$) and each had individual photoperiod control and was individually wired, via externally mounted ultrasound transducers, to an event recorder (Esterline Angus 2100). During periods of activity monitoring, disruption (activity) of a standing wave of ultrasound within an aquarium caused a change in voltage within a transceiver which was in turn recorded as an event. The event recorder totaled events per aquarium in 15 min blocks and these data were used in plotting rhythms and in statistical analysis. A more detailed description of the holding and recording equipment is given elsewhere [2].

The fish were held on a 12L:12D photoperiod and fed once daily (2.5% body weight - Biodiet, Bioproducts Inc. OR). All fish were fed at 1600 CST, however, the onset of light was staggered amongst the aquaria so that the fish received the food at one of four circadian times of day: light onset (0 hr), 6 hr after onset, 12 hr after onset, or 18 hr after onset. After 46 days on the feeding regime the fish were allowed to free-run under constant light (LL) or constant darkness (DD) (2

or 3 groups /each feeding regime) for 5 days. During this period the animals were not fed or disturbed (the aquarium room was not entered) and daily activity patterns were remote monitored.

The activity for the five day period was plotted for each tank and examined statistically by a Fourier time series analysis [6] and cosinor analysis [7]. One transceiver failed during the monitoring period and that tank was eliminated from the study.

RESULTS AND DISCUSSION

Total daily activity differed among days 1 through 5 in all tanks ($P < 0.01$, ANOVA-Day 1 > Day 4, 2, 3, 5 Tukey's Studentized range). This day-to-day difference in total activity produced some artifactual rhythms through the five day period in preliminary time series analysis. Therefore, mean daily activity for each tank was subtracted from the individual 15 min totals to yield a deviation about the daily mean per 15 min interval. These data were used, in turn, in subsequent analyses.

All tanks had highly significant rhythmic activity during the free-running period ($p < 0.01$, Fisher's Kappa and Bartlett's Kolmogorov-Smirnov tests). In the majority of cases a 24 hr rhythm was the predominant (12 groups) or secondary (3 groups) peak in the periodogram; only 2 groups lacked 24 hr intervals (Fourier time series analysis, unweighted). The mean acrophase of the five day period for the 17 groups ranged from $13:00 \pm 1.4$ (s.e.) to $22:54 \pm 1.0$ CST with an overall mean of $17:00 \pm 0.82$ (cosinor analysis); shortly after the acclimation feeding time (16:00). Likewise, a visual examination of the data reveals a peak of activity about the time of feeding, especially for the first two days of free-run, for most groups (Fig. 1). There were no consistent differences apparent, either visually or statistically, in rhythm phasing among the four feeding/light-dark regimes or the two free-running regimes (L:L or D:D).

Thus, meal-feeding does entrain the locomotor rhythm in goldfish and this circadian rhythm will free-run in the apparent absence of other obvious Zeitgebers (i.e., light-dark cycles, feeding, disturbance). Kavaliers [8], working with groups of

light-dark entrained goldfish on LL, has reported a free-running rhythm of about 24.5. The exact 24 hr rhythms recorded in our study are most likely due to the 15 min activity intervals used in the recording apparatus rather than the different entraining stimulus. As has been previously demonstrated in fishes [2, 4] and mammals [see 9] the onset of activity in this study anticipated the scheduled feeding (Fig. 1). In free-running rats it is mainly this anticipatory phase of the circadian locomotor rhythm that is entrained by meal-feeding; the remaining portion of the rhythm remains locked to the light-dark entrained oscillator [9, 10]. In contrast, with goldfish there is not an apparent splitting of the locomotor rhythm (this study) and it appears that the bulk of the activity is entrained to the time-of-feeding. We caution, however, that another study has demonstrated that the daily activity rhythm of a fish (Medaka) can be composed of component rhythms and these individual rhythms can be entrained to different environmental stimuli [3].

The mechanism whereby feeding entrains rhythms in fishes as well as mammals remains unresolved. At this time it does not appear to be a nutritional component of the diet. In previous research from this laboratory the absence of dietary tryptophan or tyrosine and phenylalanine did not affect the ability of meal-feeding to phase-shift locomotor activity in goldfish [11]. Although some other dietary constituent may play a role in meal-feeding entrainment, work with primates, fed intergastrially, has led to the conclusion that the diet *per se* is at best a weak synchronizer of circadian rhythms and that some aspect(s) of the pre-gastric feeding process is the major entraining stimulus [12]. The disturbance associated with feeding may play a role in the entrainment mechanism. A hypothesis supported in part by a study with fishes wherein feeding entrainment of anticipatory behavior could be altered by disturbance (feeding adjacent aquaria) [4]. Another aspect of the entraining mechanism is the social interaction induced in a feeding group. Social interaction does facilitate circadian activity and feeding in goldfish [8, 13]; and although preliminary research at this laboratory indicates single fish can be entrained to meal-feeding there

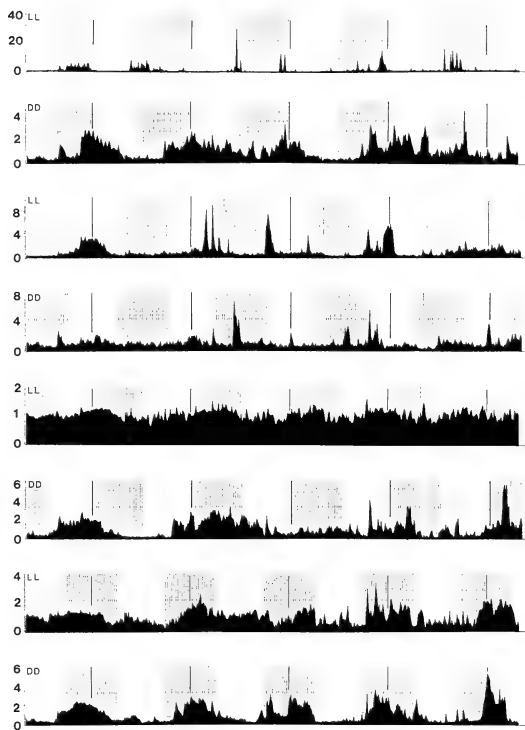


FIG. 1. Activity rhythms of eight groups of goldfish acclimated to 12L:12D and a single daily meal then allowed to free-run for five days without food on constant light (LL) or dark (DD). The vertical axis is percent of daily activity per 15 min interval. The shaded portions (vertical stippling) represent the dark portion of the acclimation light-dark cycle; the solid dark vertical lines represent the acclimation feeding times.

appears to be a strong reinforcing group influence on the length of time the activity rhythm will remain entrained to the feeding time in starved fish (Spieler *et al.*, unpubl.).

Also unresolved is the question of whether or not meal-feeding is entraining an endogenous oscillator in fishes. Previous studies [2, 3] as well as the present study support an entraining hypothesis; in the present study all groups remained

synchronized to the feeding time rather than undergoing differential phase shifts as would be anticipated if groups were using some aspect of the light-dark cycle to cue on and/or feeding induced rhythms were masking an endogenous locomotory rhythm. Further research is required, however, before the possibility that the animals are remembering the interval between a point on the endogenous oscillator(s) (presumably entrained by

the light-dark cycle) and the feeding time can be discounted.

ACKNOWLEDGMENTS

We thank Jay Beder and John Ottenweller for help with statistical analysis. The research was supported in part by National Institute of Environmental Health Sciences grant: ESO 4184.

REFERENCES

- 1 Moore-Ede, M. C., Sulzman, F. M. and Fuller, C. A. (1982) *The Clocks that Time Us*. Harvard University Press, Cambridge, MA, pp. 448.
- 2 Spieler, R. E. and Noeske, T. A. (1984) Effects of photoperiod and feeding schedule on diel variations of locomotor activity, cortisol and thyroxine in goldfish. *Trans. Am. Fish. Soc.*, **113**: 528-539.
- 3 Weber, D. N. and Spieler, R. E. (1987) Effects of the light-dark cycle and scheduled feeding on behavioral and reproductive rhythms of the cyprinodont fish, Medaka, *Oryzias latipes*. *Experientia*, **43**: 621-624.
- 4 Davis, R. E. and Bardach, J. E. (1965) Time-coordinated prefeeding activity in fish. *Anim. Behav.*, **13**: 154-162.
- 5 Zabka, H. and Siegmund, R. (1983) Tagesrhythmen der lokomotorischen Aktivität von Silberkarpfen (*Hypophthalmichthys molitrix*) unter labor- und paxisnahen Bedingungen. *Fischerei-Forschung, Wissenschaft. Schrift.*, **21**: 37-43.
- 6 SAS Institute Inc. (1984) *SAS/ETS User's Guide*, Version 5 Edition. Cary, NC: SAS Institute Inc., pp. 738.
- 7 Cornelissen, G., Halberg, F., Stebbings, J., Halberg, E., Carandente, F. and Hsi, B. (1980) Data acquisition and analysis by computers and pocket calculators. *La Ricerca Clin. Lab.*, **10**: 333-385.
- 8 Kavaliers, M. (1981) Period lengthening and disruption of socially facilitated circadian activity rhythms of goldfish by lithium. *Physiol. Behav.*, **27**: 625-628.
- 9 Boulos, Z. and Terman, M. (1980) Food availability and daily biological rhythms. *Neurosci. Biobehav. Rev.*, **4**: 119-131.
- 10 Aschoff, J. (1986) Anticipation of a daily meal: a process of "learning" due to entrainment. *Monitore Zool. Ital. (N.S.)*, **20**: 195-219.
- 11 Spieler, R. E., Noeske-Hallin, T. A., DeRosier, T. A. and Poston, H. A. (1987) Some dietary amino acids and meal-feeding phase shifts of locomotor activity. *Med. Sci. Res.*, **15**: 921-922.
- 12 Apelgren, K. N., Frim, D. M., Harling-Berg, C. J., Gander, P. H. and Moore-Ede, M. C. (1985) Effectiveness of cyclic intragastric feeding as a circadian zeitgeber in the squirrel monkey. *Physiol. Behav.*, **34**: 335-340.
- 13 Magurran, A. (1984) Gregarious goldfish. *New Scientist*, **103**: 32-33.

Development Growth & Differentiation

Published Bimonthly by the Japanese Society of
Developmental Biologists
Distributed by Business Center for Academic
Societies Japan, Academic Press, Inc.

Papers in Vol. 31, No. 4. (August 1989)

38. M. Yuge and K. Yamana: Regulation of the dorsal axial structures in cells in cell-deficient embryos of *Xenopus laevis*.
39. N. Yoshizaki: Immunoelectron microscopic demonstration of cortical granule lectins in coelomic, unfertilized and fertilized eggs of *Xenopus laevis*.
40. H. Tsujimura: Metamorphosis of wing motor system in the silk moth, *Bombyx mori*: Origin of wing motor neurons.
41. P. Sivasubramanian and D. R. Nässel: Sensory projections from ectopic appendages in an insect: Inherent specificity and influence of location.
42. S. Pelech, H. Paddon, L. Kwong and G. Weeks: Characterization of developmentally regulated cAMP/Ca²⁺-independent protein kinases from *Dictyostelium discoideum*.
43. B. W. Bisgrove and R. A. Raff: Evolutionary conservation of the larval serotonergic nervous system in a direct developing sea urchin.
44. M. Komukai, Y. Iizuka and I. Yasumasu: Synthesis of proteins enriched in Li⁺-induced vegetalized embryos of sea urchin during early development.

Abstracts of the papers presented at the 22nd Annual Meeting of the Japanese Society of Developmental Biologists, 1989

Author index of the papers presented at the 22nd Annual Meeting of the Japanese Society of Developmental Biologists, 1989

Development, Growth and Differentiation (ISSN 0012-1592) is published bimonthly by The Japanese Society of Developmental Biologists, Department of Developmental Biology, Mitsubishi Kasei Institute of Life Science, Minami-ootani 11, Machida, Tokyo 194, Japan. 1989: Volume 31. Annual subscription for Vol. 31, 1989: U. S. \$ 136.00, U. S. and Canada: U. S. \$ 150.00, all other countries except Japan. All prices include postage, handling and air speed delivery except Japan. Second class postage paid at Jamaica, N.Y. 11431, U. S. A.

Outside Japan: Send subscription orders and notices of change of address to Academic Press, Inc., Journal Subscription Fulfillment Department, 1 East First Street, Duluth, MN 55802, U. S. A. Send notices of change of address at least 6-8 weeks in advance. Please include both old and new addresses. U. S. A. POSTMASTER: Send changes of address to *Development, Growth and Differentiation*, Academic Press, Inc., Journal Subscription Fulfillment Department, 1 East First Street, Duluth, MN 55802, U. S. A.

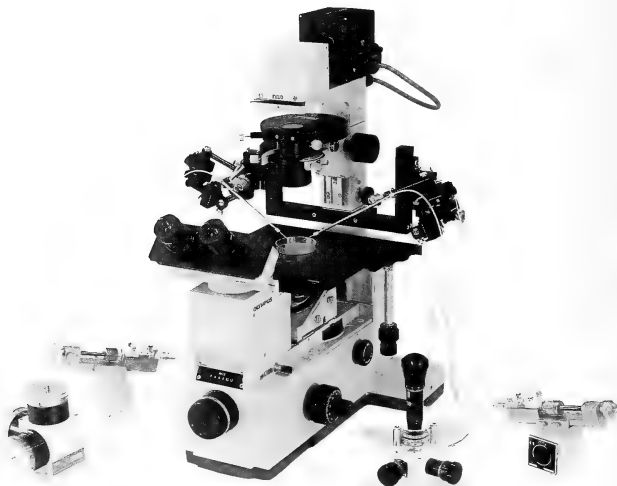
In Japan: Send nonmember subscription orders and notices of change of address to Business Center for Academic Societies Japan, 16-3, Hongo 6-chome, Bunkyo-ku, Tokyo 113, Japan. Send inquiries about membership to Business Center for Academic Societies Japan, 4-16, Yayoi 2-chome, Bunkyo-ku, Tokyo 113, Japan.

Air freight and mailing in the U. S. A. by Publications Expediting, Inc., 200 Meacham Avenue, Elmont, NY 11003, U. S. A.

NARISHIGE

THE ULTIMATE NAME IN MICROMANIPULATION

OUR NEW MODELS **WR-88** and **MO-102M**
MAKE PRECISION MICROMANIPULATION SO EASY!



SOME FEATURES of THE WR-88 WATER ROBOT MICROMANIPULATOR (3-DIMENSIONAL)

- * Drift-free, the new WR-88 has a DRIFT movement of less than 2 microns.
- * The new WR-88 has a SMOOTH MICRODRIVE MECHANISM.
- * An Aqua Purificate remote control ensures totally vibration-free operation.



NARISHIGE SCIENTIFIC INSTRUMENT LAB.

9-28 KASUYA 4-CHOME SETAGAYA-KU, TOKYO 157, JAPAN
PHONE (INT-L) 81-308-8233, FAX (INT-L) 81-3-308-2005
CABLE : NARISHIGE LABO, TELEX, NARISHIGE J27781

Sophisticated Balance between Safety and Centrifugation Capability without Compromise.

Centrifuge in
Integrated with A
Refrigerator

Extra-Quiet
Operation

Ease of Loading/
Unloading
The Rotors

Quick Start/
Quick Stop

High Quality

Triple Safety
Design

Corrosion
Resistance



HIGH SPEED
REFRIGERATED
MICRO CENTRIFUGE

MODEL MR-150

TOMY CORPORATION

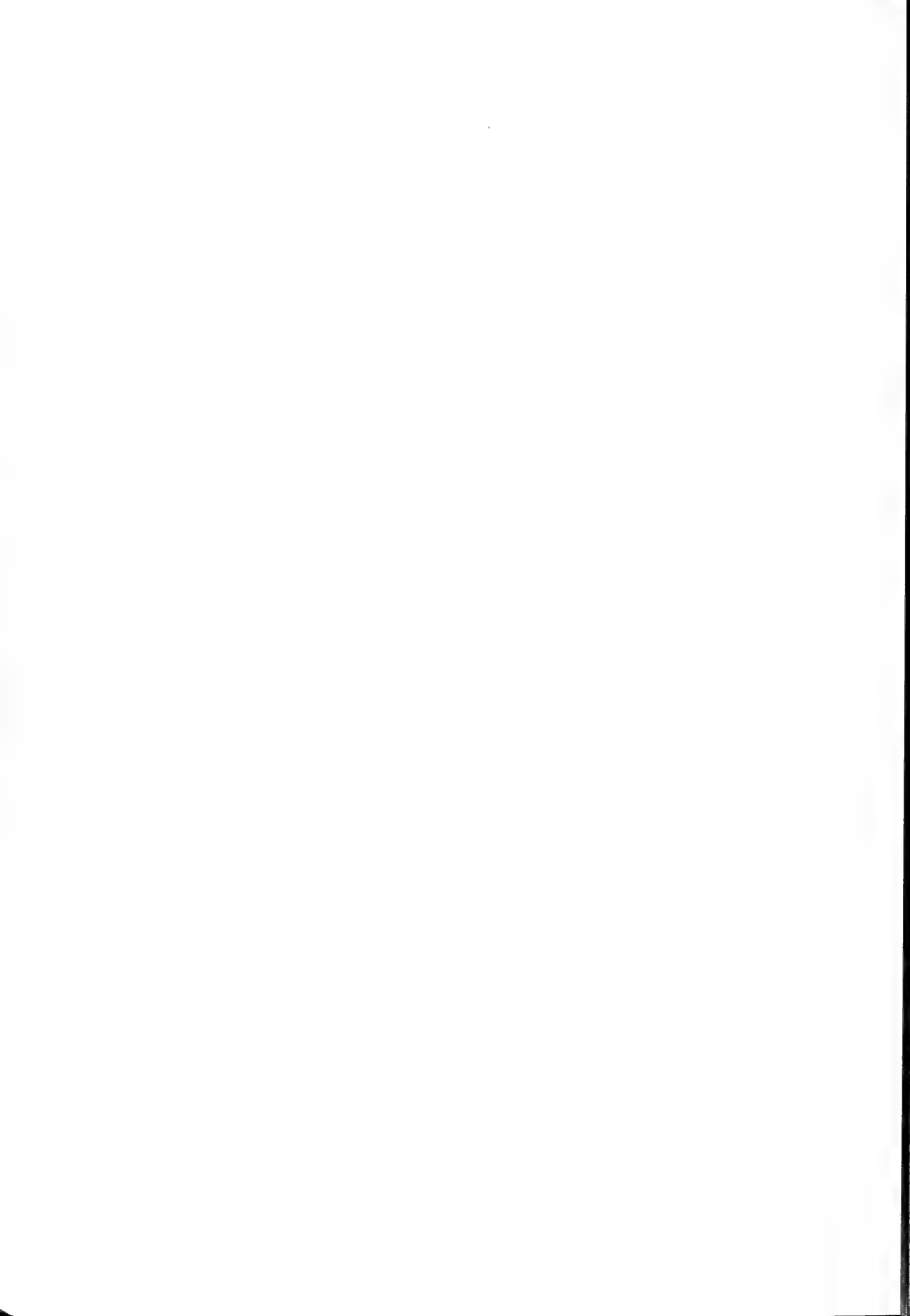
1002 SOLEIL NARIMASU BLDG., 31-8, NARIMASU 1-CHOME,
ITABASHI-KU, TOKYO 175 JAPAN
TEL:(03)976-3411 TLX:02723111 TOMYCO J
CABLE:TOMYSHO TOKYO FAX:(GIII G11)(03)930-7010

TOMY SEIKO CO., LTD.

2-2-12, ASAHICHO NERIMA-KU, TOKYO 176 JAPAN
TEL:(03)976-3111

SOLE AGENT

MANUFACTURER



(Contents continued from back cover)

- Lattaud, C. and R. Marcel: Stimulating influence of cerebral ganglia on *in vitro* incorporation of tritiated leucine into ovaries of *Eisenia fetida* Sav. (Annelida: Oligochaeta) 741

Endocrinology

- Yamauchi, K., R. Horiuchi, S. Koya and H. Takikawa: Uptake of 3,5,3'-L-triiodothyronine into bullfrog red blood cells mediated by plasma membrane binding sites .. 749
- Kobayashi, T., S. Kikuyama, A. Kume, J. Okuma and M. Ohkawa: [³⁵S]-sulphate uptake by *Xenopus laevis* cartilage: the influence of plasma from the growth hormone-treated animal 757
- Uchibori, M. and S. Kawashima: Stimulation of nuclear volume enlargement and neuronal process growth by estrogen in the hypothalamic and limbic nuclei of the rat 763
- Maitra, G. and S. Bhattacharya: Seasonal changes of triiodothyronine binding to piscine ovarian nuclei 771
- Tazawa, H., M. Mukai and M. Ogawa: Immunohistochemical studies of juxtaglomerular cells and the corpuscles of Stannius in the eel, *Anguilla japonica* (COMMUNICATION) 805

- Shimizu, I., T. Matsui and K. Hasegawa: Possible involvement of GABAergic neurons in regulation of diapause hormone secretion in the silkworm, *Bombyx mori* (COMMUNICATION) 809

Morphology

- Yee, Win Win, S. Takahashi and S. Kawashima: Age-related changes and sex difference in the ultrastructure of renal glomerulus in Wistar/Tw rats 777

Behavior Biology

- Spieler, R. E. and J. J. Clougherty: Free-running locomotor rhythms of feeding-entrained goldfish (COMMUNICATION) 813

Taxonomy

- Brusle, S.: Cytological differences in early germ cells of three genera of grey mullets, *Mugil*, *Liza* and *Chelon* (Teleostei: Mugilidae) 789

ZOOLOGICAL SCIENCE

VOLUME 6 NUMBER 4

AUGUST 1989

CONTENTS

Obituary 619

REVIEWS

Chieffi, G.: New trends in the regulation of the gonadal activity in vertebrates: paracrine and autocrine control 623

Michibata, H.: New aspects of accumulation and reduction of vanadium ions in ascidians, based on concerted investigation from both a chemical and biological viewpoint 639

ORIGINAL PAPERS

Physiology

Sato, E. and S. Tagawa: Oscillations of membrane potential and membrane resistance during the cell cycle in the newt egg macromeres 649

Kimura, K., T. Tanimura and T. Shimozawa: Mosaic fate mapping of the behavioral and the muscular defects induced by a *Drosophila* mutation, *abnormal proboscis extension reflex C (aperC)* 659

Lorenzo, A., P. Santana, T. Gómez and P. Badia: Sodium and chloride transport in the lizard duodenum 667

Cell Biology

Higashi, K., T. Gomi, M. Soeda, S. Sasa, A. Kimura and Y. Kikuchi: New morphological aspects of the brush cells in the main excretory ducts of the rat submandibular glands 675

Iwasaki, S., K. Miyata and K. Kobayashi: Fine structure of the lingual dorsal epithelium of the Japanese toad, *Bufo japonicus* (Anura: Bufonidae) 681

Wago, H. and T. Tanaka: Synergistic effects of calyx fluid and venom of *Apanteles kariyai*

Watanabe (Hymenoptera: Braconidae) on the granular cells of *Pseudaletia separata* Walker (Lepidoptera: Noctuidae) 797

Biochemistry

Hu, D. H., S. Kimura, S. Kawashima and K. Maruyama: Calcium-activated neutral protease quickly converts α -connectin to β -connectin in chicken breast muscle myofibrils (COMMUNICATION) 797

Genetics

Hosono, R., T. Sassa and S. Kuno: Spontaneous mutations of trichlorfon resistance in the nematode, *Caenorhabditis elegans* ... 697

Developmental Biology

Sawai, T. and K. Higuchi: Cytostatic effect of the cytoplasm of mature oocytes in the newt, *Cynops pyrrhogaster* 709

Asao, T.: The alkaline substances and other constituents of blastocoel fluid of the newt embryo 715

Sakairi, K., M. Yamamoto, K. Ohtsu and M. Yoshida: Environmental control of gonadal maturation in laboratory-reared sea urchins, *Anthocidaris crassispina* and *Hemacentrotus pulcherrimus* 721

Kawashima, T. and T. Nakazawa: Transient increase in mitochondrial protein synthesis of starfish embryo before gastrulation (COMMUNICATION) 801

Reproductive Biology

Fujiyama, N., H. Nishiyama and O. Koga: *In vitro* viability and fertilizing capacity of guinea fowl spermatozoa 731

(Contents continued on inside back cover)

INDEXED IN:

Current Contents/LS and AB & ES,
Science Citation Index,
ISI Online Database,
CABS Database, INFOBIB

Issued on August 15

Printed by Daigaku Letterpress Co., Ltd.,
Hiroshima, Japan

QL
1
28641
NH

5 No. 5

October 1989

ZOOLOGICAL SCIENCE

An International Journal

PHYSIOLOGY
CELL and MOLECULAR BIOLOGY
GENETICS
IMMUNOLOGY
BIOCHEMISTRY
DEVELOPMENTAL BIOLOGY
REPRODUCTIVE BIOLOGY
ENDOCRINOLOGY
BEHAVIOR BIOLOGY
ENVIRONMENTAL BIOLOGY
ECOLOGY and TAXONOMY

published by **Zoological Society of Japan**

distributed by **Business Center for Academic Societies Japan**
VSP, Zeist, The Netherlands

ISSN 0289-0003

ZOOLOGICAL SCIENCE

The Official Journal of the Zoological Society of Japan

Editor-in-Chief:

Hideshi Kobayashi (Tokyo)

Managing Editor:

Chitaru Oguro (Toyama)

Assistant Editors:

Yuichi Sasayama (Toyama)

Hitoshi Michibata (Toyama)

Miëko Komatsu (Toyama)

The Zoological Society of Japan:

Toshin-building, Hongo 2-27-2, Bunkyo-ku,
Tokyo 113, Japan. Tel. (03) 814-5675

Officers:

President: Nobuo Egami (Tokyo)

Secretary: Hideo Namiki (Tokyo)

Treasurer: Tadakazu Ohoka (Tokyo)

Librarian: Masatsune Takeda (Tokyo)

Editorial Board:

Howard A. Bern (Berkeley)

Horst Grunz (Essen)

Susumu Ishii (Tokyo)

John M. Lawrence (Tampa)

Hiromichi Morita (Fukuoka)

Andreas Oksche (Giessen)

Mayumi Yamada (Sapporo)

Walter Bock (New York)

Robert B. Hill (Kingston)

Seiichi Kawashima (Tokyo)

Kosac Maruyama (Chiba)

Kazuo Moriwaki (Mishima)

Hidemi Sato (Nagoya)

Ryuzo Yanagimachi (Honolulu)

Aubrey Gorbman (Seattle)

Yukio Hiramoto (Chiba)

Yukiaki Kuroda (Mishima)

Roger Milkman (Okazaki)

Tokindo S. Okada (Okazaki)

Hiroshi Watanabe (Tokyo)

ZOOLOGICAL SCIENCE is devoted to publication of original articles, reviews and communications in the broad field of Zoology. The journal was founded in 1984 as a result of unification of Zoological Magazine (1888-1983) and *Annotationes Zoologicae Japonenses* (1897-1983), the former official journals of the Zoological Society of Japan. ZOOLOGICAL SCIENCE appears bimonthly. An annual volume consists of six numbers of more than 1100 pages including an issue containing abstracts of papers presented at the annual meeting of the Zoological Society of Japan.

MANUSCRIPTS OFFERED FOR CONSIDERATION AND CORRESPONDENCE CONCERNING EDITORIAL MATTERS should be sent to:

Dr. Chitaru Oguro, Managing Editor, Zoological Science, Department of Biology, Faculty of Science, Toyama University, Toyama 930, Japan, in accordance with the instructions to authors which appear in the first issue of each volume. Copies of instructions to authors will be sent upon request.

SUBSCRIPTIONS. ZOOLOGICAL SCIENCE is distributed free of charge to the members, both domestic and foreign, of the Zoological Society of Japan. To non-member subscribers within Japan, it is distributed by Business Center for Academic Societies Japan, 6-16-3 Hongo, Bunkyo-ku, Tokyo 113. Subscriptions outside Japan should be ordered from the sole agent, VSP, Utrechtseweg 62, 3704 HE Zeist (postal address: P. O. Box 346, 3700 AH Zeist), The Netherlands. Subscription rates will be provided on request to these agents. New subscriptions and renewals begin with the first issue of the current volume.

All rights reserved. No part of this publication may be reproduced or stored in a retrieval system in any form or by any means, without permission in writing from the copyright holder.

© Copyright 1989, The Zoological Society of Japan

[Publication of Zoological Science has been supported in part by a Grant-in-Aid for
Publication of Scientific Research Results from the Ministry of Education, Science
and Culture, Japan.]

REVIEW

Nervous Organization of the Pineal Complex
in Lower VertebratesMANFRED UECK¹, KENJIRO WAKE² and HIDESHI KOBAYASHI³

*Institute of Anatomy and Cytobiology, Justus Liebig University,
63 Giessen, FRG, ²Department of Anatomy, Tokyo Medical
and Dental University, Bunkyo-ku, Tokyo 113, ³Research
Laboratory, Zenyaku Kogyo Co. Ltd.,
Nerima-ku, Tokyo 178, Japan*

ABSTRACT—The morphological and electrophysiological aspects of the neuronal organization of the pineal complex are reviewed in fishes and amphibians. In the frog pineal organ, two types of intrapineal neurons different in size and shape are distinguished using the AChE and NADPH-diaphorase methods: multipolar cells (the first cell type) interpreted as interneurons which receive inputs from a large number of photosensitive pinealocytes and transduce their responses to pseudounipolar cells (the second cell type) which send their axons to the brain. From this morphological perspective, the chromatic and achromatic responses obtained in the frog pineal complex are discussed. The distribution pattern of different types of nerve cells demonstrated by the AChE-method in the fish pineal complex varies widely not only between species but also regionally within the same pineal organ. Some unpublished results obtained from species which have not been investigated till now confirmed previous observations. In accordance with the results obtained by others in the retina, where more than twenty different types of amacrine cells and more than ten types of ganglion cells have been identified, our results indicate subpopulations of nerve cells in the fish pineal complex. Further investigations are necessary to complete our knowledge about the nervous organization in the fish pineal complex: this would be a precondition for a better understanding of the electrophysiological results.

INTRODUCTION

The pineal complex of non-mammalian vertebrates develops intracranially as a diencephalic evagination; additionally, in some fish species a parapineal organ exists [1-5] and in some anuran and reptilian species, a shift of part of the pineal anlage into the skin (frontal organ of the frog) or into a hole of the skull (parietal eye of the lizard) is observed [see 6-9]. The pineal complex is photosensitive and contains photoreceptive

pinealocytes interconnected with pineal nerve cells [see 10]. Light perception is not involved in vision; light-dependent impulses transduced by pinealofugal (afferent) fibres to di- and mesencephalic areas are involved in the entrainment of circadian and circannual pacemakers for the synchronization of rhythmic body functions (such as skin pigmentation, phototaxis, orientation, locomotory activity, metabolic and thermoregulatory responses and reproductive cycles) with the photoperiod of the environment. Direct light perception may also be involved in the regulation of melatonin synthesis in the pineal organ of lower vertebrates.

This short review deals mainly with the nervous organization of the pineal complex in fishes and amphibians. There is great variety of morphology

Received June 19, 1989

¹ To whom reprint requests should be addressed.

This review was written during the stay of MU as a Research Professor at the Tokyo Medical and Dental University.

and ultrastructure of the pineal complex between species of different vertebrate classes, and also within the same vertebrate class. Extensive morphological studies have been made on the frog pineal complex; therefore these results will be reviewed first and discussed with electrophysiological findings. In the second part morphological and electrophysiological data of the fish pineal complex will be reported including some of our unpublished results.

I. The nervous organization of the frog pineal complex

The frog pineal complex consists of the frontal organ and the pineal organ. The frontal organ is localized in the subcutis of the skin, the pineal organ is located intracranially and these organs are connected by the frontal nerve. A pineal tract leaves the dorsocaudal part of the pineal organ toward the brain [see 11]. The pineal parenchyma consists of pinealocytes, glial cells and nerve cells. The pinealocytes are photosensitive and possesses outer segment structures resembling retinal cones, but they are shorter in length because of a smaller number of disks [12-14]. The inner and outer segments of the pinealocytes protrude inversely and eversely directed into the pineal lumen, which is an outpocketing of the third ventricle. The pinealocytes are in synaptic ribbon contact with intrapineal nerve cells [11-14].

The visualization of the distribution pattern of pineal nerve cells and the demonstration of different types of nerve cells have been difficult for a long time, because a) unlike the retina the nervous organization of the pineal nerve cells is not in parallel layers and b) the silver impregnation technique successfully used in the retina does not work in the pineal organ. Pineal nerve cells are shown using methylene blue staining [15, 16], but a better understanding of the neural organization in the pineal complex was attained when an acetylcholinesterase (AChE) technique was histochemically applied. [17, 18]. Approximately 60 nerve cells in the frontal organ and 220-320 nerve cells in the pineal organ are counted. The dorsal wall of the pineal organ, where the pineal tract arises, contains three times more nerve cells than the ventral

wall. The nerve cells in the rostral part are bigger in size than in the caudal part. Two different types of nerve cells are observed: 1) big multipolar cells, localized more centrally in the frontal organ and within the parenchyma of the pineal organ, send their processes to different areas of the organ; they may be interneurons, and 2) smaller nerve cells with the appearance of pseudounipolar cells which send one process into the pineal tract. The ratio of the multipolar cells to the pseudounipolar cells is 1:4 for the frontal organ and 3:5 for the pineal organ. Additionally, 30-50 unipolar or pseudounipolar cells are clustered in juxtaposition with the pineal tract at the caudal end of the pineal organ, and another 30-50 neurons are scattered along the basis of the subcommissural organ. Some of these nerve cells each send a process toward the brain, but other neurons each send a process in the opposite direction, rostrally into the caudal part of the pineal organ via the pineal tract.

Electrophysiological studies of the pineal system in lower vertebrates have shown light-modulated electrical activity [see 19, 20]. A spontaneous activity of pineal nerve cells occurs in darkness and light changes the frequencies of this discharge. Constant illumination decreases the activity almost linearly with the logarithm of light intensity; a wide range of light intensity provides messages to the brain [21, 22]. The following two types of response are recorded using light flashes:

- 1) The chromatic response which consists of an opposed colour mechanism, i.e. an inhibition upon illumination by stimuli of short wavelengths and an excitation in response to light of longer wavelength. The net output depends on the balance between opposite inhibitory and excitatory processes in response to the particular spectral composition of the incident light [23]. The daily changes in spectral composition of light shift the chromatic response to another state of activation. It has been hypothesized that the nervous mechanism of such interactions in the pineal may be realized by two different receptor populations making synaptic contacts with a ganglion cell using inhibitory and excitatory transmitters [24]; another possibility would be that functionally polarized interneurons transfer information from one cone system to another [25].

2) The achromatic response which is characterized by a decrease of the firing rate or complete inhibition of the maintained discharge by light of all wavelengths; it is the most common response of the pineal. The achromatic response differs considerably from the chromatic response with respect to the absolute threshold, spectral sensitivity and the adaptation process. The lowermost light threshold of the achromatic response is of the same order as the light threshold of the frog retina; this indicates a highly developed nervous organization with a high degree of convergence of numerous sensory cells to one nerve cell [26].

A visual pigment with λ max 550–580 nm has been identified in the frontal organ [27] which is close to the sensitivity maximum of the achromatic response of pineal nerve fibres and, additionally, a visual pigment 502 in the pineal organ which is similar to that of accessory cones of the frog retina. A spectrosensitivity has been found to match the absorption spectrum of rhodopsin in the dark adapted pineal organ and of iodopsin in the light adapted pineal organ [28].

Illumination of the pineal complex of the frog evokes slow (graded) potential changes in addition to the spike activity of ganglion cells. The slow potentials may arise from ganglion cells as summated postsynaptic potentials or from photoreceptor cells as summated extracellular currents [29].

Pineal photoreceptors respond to light with a hyperpolarization of the membrane potentials as retinal photoreceptors do; this results in ganglion cell hyperpolarization and lowered spike activity. The depolarization of pineal photoreceptors in darkness results (as in the retina) in a continuous release of an excitatory transmitter, possibly L-glutamate or L-aspartate, from the pinealocytes to second-order neurons which cause a significant increase of neuronal cell firing. Taurine, by far the most abundant amino acid in pineal tissues, markedly decreased the spontaneous activity in half of the neurons tested, the remaining cells being unresponsive [30]. Almost all pineal neurons are inhibited by γ -aminobutyric acid (GABA); the GABA-induced inhibition interferes with the light-evoked inhibition of the ganglion cell activity, i.e. light reduced the strength of inhibition and shortened the effect of GABA. A major role

of GABAergic mechanisms in the ganglion cell output of pineal neurons is suggested [31]. In the retina GABA seems to be a neurotransmitter in H1 cone horizontal cells (goldfish) and in a class of amacrine cells (mammals) [32].

More recently morphological results have been published indicating a more complex photosensitive pineal system. On the basis of ultrastructural characteristics and of histochemical and immunohistochemical findings, three types of photoreceptor cells have been distinguished in the frog pineal complex [33]. Using an antiserum raised against the opsin of bovine rods [34, 35] the outer segments of one population of pinealocytes showed a positive reaction; they are rod-type. This has been an unexpected finding that cone-like outer segments reacted with antisera against rod pigment. However, the ultrastructure of cone outer segments characterized by a decreased number of membrane disks and a large surface toward the extracellular space is a less differentiated form of photoreceptor membrane multiplication and has nothing to do with type of the photopigment present therein [36]. The other pinealocytes are characterized by rhodopsin immunonegative outer segments; they are subdivided into two populations of cone-type pinealocytes: one cone-type contains a lipid droplet in its inner segment, the second cone-type pinealocyte possesses a small inner and outer segment, an electron-lucent perikaryon and a spherule-like axon terminal [33]. Demonstrating Ca^{++} -ATPase activity according to the histochemical and cytochemical technique of Ando *et al.* [37] the opsin-positive outer segments (rod-type) contain Ca^{++} -ATPase activity, the opsin-negative outer segments of cone-type pinealocytes containing a lipid droplet in their inner segment are Ca^{++} -ATPase negative [38].

Photosensitive pinealocytes differ also in the shape of their perikarya: slender-type (rod-like), spherical-type (cone-like) and double cone-type pinealocytes can be distinguished after staining with the NADPH-diaphorase technique according to Scherer-Singler [39], [40, 41]. Also the basal end-feet show differences in their length, distal ramification and in the number of boutons which are single, bouquet-like and cluster-like [40]. The ramified pinealocytes can contact several second-

order neurons, as Boycott [42] has shown for some cones of the retina.

The NADPH-diaphorase reaction demonstrates a fourth type of pinealocyte scattered in the basal part of the parenchyma; these cells obviously have no contact with the pineal lumen [40]. Pinealocytes with a reduced photosensitivity and a more pronounced secretory function seem to exist also in the frog pineal organ [40, 41], similarly to those described in the lamprey [43]. A fifth type of pinealocyte which sends a long axon-like process into the pineal tract has been described in fish pineal organ [44].

The ribbon synaptic contacts that exist between neighbouring photosensitive pinealocytes and between pinealocytes and neurons should also be taken into consideration [45]. Thus, the different types of photosensitive pinealocytes and their interrelationships should be taken into account when chromatic and achromatic responses are discussed on the basis of morphological findings.

The intrapineal neurons, described in detail with the AChE method [18], have recently been reinvestigated with tracer techniques and with the NADPH-diaphorase method (Fig. 1) and the results are interpreted differently. Eldred and Nolte [45] labeled not only the pseudounipolar cells but also the multipolar neurons by retrograde transport of either cobalt or horseradish peroxidase through the frontal nerve. They concluded from their results that both types of nerve cells in the frontal organ send an axon via the frontal

nerve to the brain. This result has been confirmed in other species of lower vertebrates [46]; the conclusion of the result led to diagrams of the nervous organization of the pineal complex in lower vertebrates which did not take interneurons into consideration [45]. Here, the achromatic and chromatic response of the pineal organ is explained as the result of an interaction between different types of photoreceptors and intrinsic secondary neurons [36].

The results obtained with the NADPH-diaphorase technique demonstrate clearly two different types of nerve cells [40, 47] and confirm the previous assumption of Wake *et al.* [18] of the existence of interneurons. The suggestion made on the basis of electrophysiological results, that the lowermost light threshold of the achromatic response indicates a highly developed nervous organization with a high degree of convergence of numerous sensory cells to one nerve cell [26, 48], is confirmed by the demonstration of big multipolar nerve cells, especially in the ventral wall of the organ, with the NADPH-diaphorase activity. These multipolar nerve cells send long processes, well documented in total preparations, in lateromedial and rostrocaudal directions ramifying and terminating in the so-called plexiform areas [40]. Plexiform areas are ultrastructurally well documented regions where terminals of pinealocytes and nerve cells are concentrated and in synaptic ribbon contact [11, 13, 14]. The NADPH-diaphorase positive end-feet of pinealocytes ter-

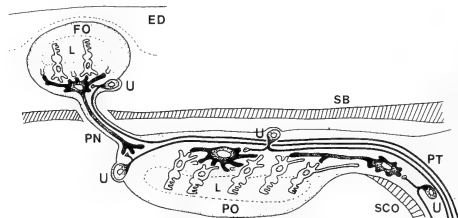


Fig. 1. Schematic drawing of characteristics of pineal nerve cells according to results obtained with the AChE-method and with the NADPH-diaphorase method. Multipolar nerve cells (black) are drawn as interneurons with relatively long processes; pseudounipolar cells (U) of the frontal organ (FO) and pineal organ (PO) send their axons to the brain. ED, epidermis; L, lumen; PN, pineal (frontal) nerve; PT, pineal tract; SB, cranial bone; SCO, subcommissural organ.

minate along the processes of the multipolar cells and in the plexiform areas at the ramified processes of the multipolar cells. Each multipolar cell sends its processes to different plexiform areas and the processes of several multipolar cells converge in each plexiform area. One multipolar cell is postsynaptic to synaptic ribbon synapses of a large number of pinealocytes in different areas of the organ. The pseudounipolar cells are localized adjacent to the plexiform areas; their perikarya and their axons which build up the pineal tract are not in contact with the end-feet of pinealocytes. Conventional synapses shown with an electron microscope and knobs of nerve fibres terminating at these pseudounipolar cells shown by silver impregnation techniques (Ueck and Ohba, unpubl. data) may indicate a presynaptic position of the multipolar cells to the pseudounipolar cells. Like the horizontal cells of the retina, the multipolar cells of the pineal complex receive information from a large number of photosensitive pinealocytes and they seem to transmit it to pseudounipolar cells in different plexiform areas. According to light microscopical findings, two types of multipolar cells may exist: in the first type perikarya and all the processes of these multipolar nerve cells are contacted by boutons of photoreceptor cells; in the second type of multipolar cells the perikarya and the proximal part of the processes are free of synaptic contacts and only distally a bouquet of boutons of pinealocytes contact the processes of the nerve cells. Therefore, each pseudounipolar cell can get information from several interneuronal multipolar cells terminating in the same plexiform area, and these multipolar cells may be of different types. In comparison with the retina which contains more than 20 types of amacrine cells and 10 types of third ganglion cells [49], the existence of subpopulations of multipolar cells and pseudounipolar cells in the pineal complex seems to be likely. Ekstroem *et al.* [50] described GABA-positive interneurons, and, additionally, GABA-positive neurons which send their axons to the brain in the pineal organ of the rainbow trout.

From the results of the study with NADPH-diaphorase activity [40, 41] it became clear that plexiform areas are important functional units of the pineal complex. The biggest plexiform area

exists at the rostral tip of the pineal organ. Using silver impregnation techniques (Ueck and Ohba, unpubl. data) a subdivision of the frontal nerve into three bundles was found before it enters the rostral tip of the pineal organ: the two lateral bundles run into the right and left ventrolateral wall of the pineal organ, the median bundle enters the pineal in its rostromedian part and some of its fibers ramify and terminate in the previously mentioned big plexiform area. From this result it is thought that processes of multipolar cells, localized within the frontal organ, reach the most rostrally localized plexiform area via the frontal nerve. This conclusion would explain the retrograde filling of multipolar cells with horseradish peroxidase in the frontal organ via the frontal nerve, but also confirm the multipolar cells as interneurons. Pineal multipolar cells with one long process beside shorter dendrites would resemble retinal horizontal cells (B-type) with an axon (telodendrite) which ends in an "axon terminal system". On the other hand, the telodendrite of retinal horizontal cells is in synaptic contact with rods, the other dendrites of these cells contact with cones; each cone synapses with 3 or 4 horizontal cells of A-type and B-type; A-type and B-type horizontal cells are unspecifically connected with all populations of cones. The "axon terminal system" of telodendrites of retinal horizontal cells, which are in contact with rods, is electrically independent of the rest of the horizontal cells [42]. The demonstration of rod-like and cone-like photosensitive pinealocytes in the frog pineal complex [33, 36] and the demonstration of the existence of a telodendritic process of pineal interneurons (multipolar cells) [40] is an interesting aspect for the discussion of the chromatic and achromatic responses.

Two results obtained with the AChE method [18] have been difficult to explain, but can now be discussed following the results obtained by the NADPH-diaphorase technique [40, 47]: 1) The dorsal wall of the frog pineal organ contains three times more nerve cells than the ventral wall. In total preparations, the NADPH-diaphorase method, which stains both cell types, pinealocytes and pineal nerve cells, demonstrates a greater number of pinealocytes by area in the pineal organ

in the ventral wall than in the dorsal wall. This means that a greater number of pinealocytes is correlated with a smaller number of nerve cells in the ventral wall in comparison with the dorsal wall (Fig. 2). But the large size of multipolar nerve cells, 20–30 μm in diameter, and their spreading of dendrites contacting a large number of pinealocytes is not so pronounced in the dorsal wall than in the ventral wall. Conversely, the number of pseudounipolar cells adjacent to the plexiform areas is much larger in the dorsal wall, where the pineal tract arises, than in the ventral wall. This difference in the nervous organization of the dorsal and ventral wall is an additional indirect indication

of the different functions of multipolar and pseudounipolar cells. 2) Further, as described above, some AChE-positive nerve cells, scattered around the pineal tract caudally to the pineal organ, send their processes toward the brain in the same way as the pseudounipolar cells, but other nerve cells send their processes in the opposite direction, via the pineal tract into the pineal organ. The latter may be interneurons, contacting not only photosensitive pinealocytes in the pineal organ, but also transmitting information outside the pineal organ to adjacent pseudounipolar cells.

II. The nervous organization of the fish pineal organ

The morphological characteristics of the fish pineal complex reveal striking differences between different species [4, 6]. The AChE method did not give such a clear picture of the nervous organization as it did in the frog [18]. The number, shape and distribution patterns of the intrapineal nerve cells vary widely, not only between different species [4], but also regionally within the same pineal organ. This structural variety makes it difficult to present a concept about the nervous organization at the moment. Therefore, published results are briefly referred to and our results obtained from species not previously described will be added (Figs. 3–6).

Wake [51] distinguished two different types of nerve cells on the basis of their size, intensity of AChE-activity and distribution pattern in the pineal organ of the goldfish, *Carassius auratus*: 1) large nerve cells with an extensive neuropil forma-

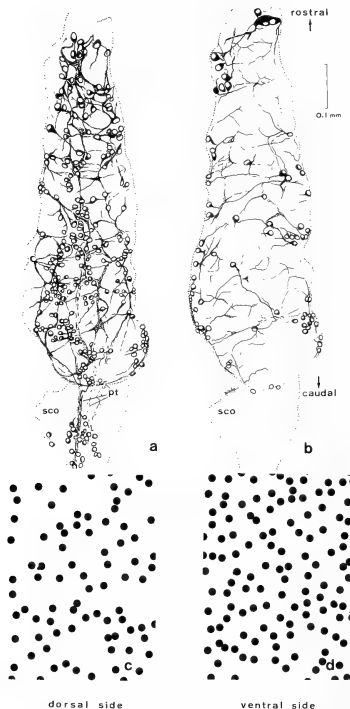


FIG. 2. a and b, Distribution of AChE-positive nerve cells in the dorsal (a) and ventral (b) walls of the pineal organ of *Rana ridibunda* [18]. The dorsal wall is more abundant in nerve cells than the ventral wall. A group of nerve cells is found in the area of the subcommissural organ (SCO); pt, pineal tract. c and d, Schematic drawing of the distribution patterns of the pinealocytes in the dorsal (c) and ventral (d) walls of the pineal organ; the number of pinealocytes by area is larger in the ventral (d) than in the dorsal wall (c). Drawings c and d were made from photographs with a final enlargement of $\times 1100$, which were taken from an *in toto* preparation of the pineal organ after histochemical visualization of the NADPH-diaphorase activity.

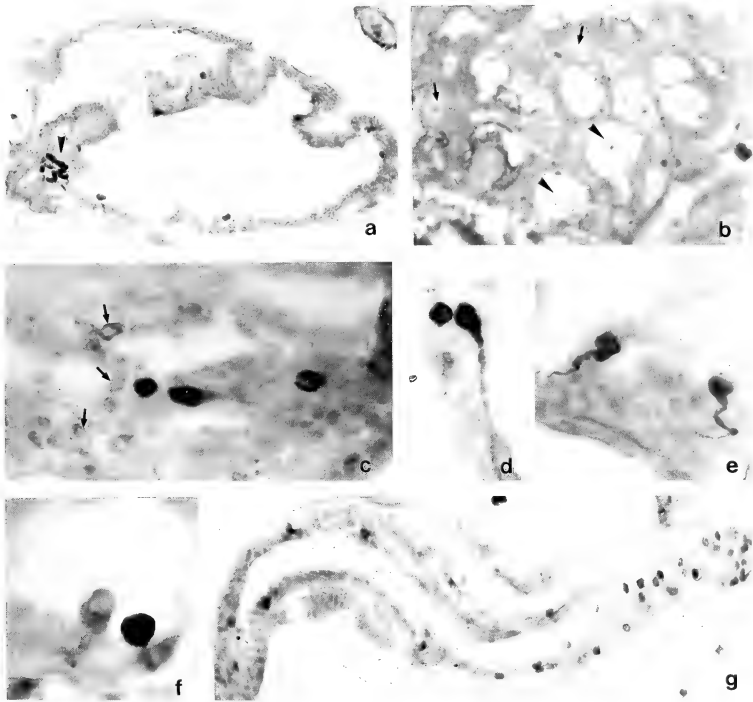


FIG. 3. *Fugu niphobles*. a, Ganglion-like concentration (\blacktriangle) of intensely stained AChE-positive nerve cells in the medio-rostral part of the pineal end-vesicle. $\times 120$. b, Ganglion-like area in a semithin section. Large nerve cells with a spherical nucleus (\blacktriangle) and smaller nerve cells with an oval nucleus (\blacktriangledown) are accumulated. $\times 1200$. c, In some regions of the pineal end-vesicle small faintly stained nerve cells (\blacktriangledown) can be recognized beside the bigger intensely stained nerve cells. $\times 490$. d-f, The large intensely stained nerve cells in the pineal end-vesicle possess a long axon-like process; their perikarya are intraparenchymal or protrude into the pineal lumen (f). d, e, f, $\times 490$. g, Pineal stalk; the number of intensely stained nerve cells by area increases in disto-proximal direction; the size of the nerve cells is smaller than in the pineal end-vesicle. g, $\times 240$.

tion, demonstrating a moderate AChE activity only in the rostro-lateral regions of the hammer-shaped pineal end-vesicle, and 2) intensely stained, small nerve cells located in the medio-rostral area of the pineal end-vesicle and along the entire length of the pineal stalk.

Additionally, faint staining of the inner segments of the photosensitive pinealocytes made

possible the estimation of the ratio of pinealocytes to nerve cells: approximately 50 pinealocytes are related to one large nerve cell in the pineal end-vesicle, and 3 to 4 pinealocytes to one AChE-positive nerve cell in the pineal stalk. Therefore, the size of the nerve cells is correlated with the number of pinealocytes in the surrounding area; however, it cannot be deduced that there are

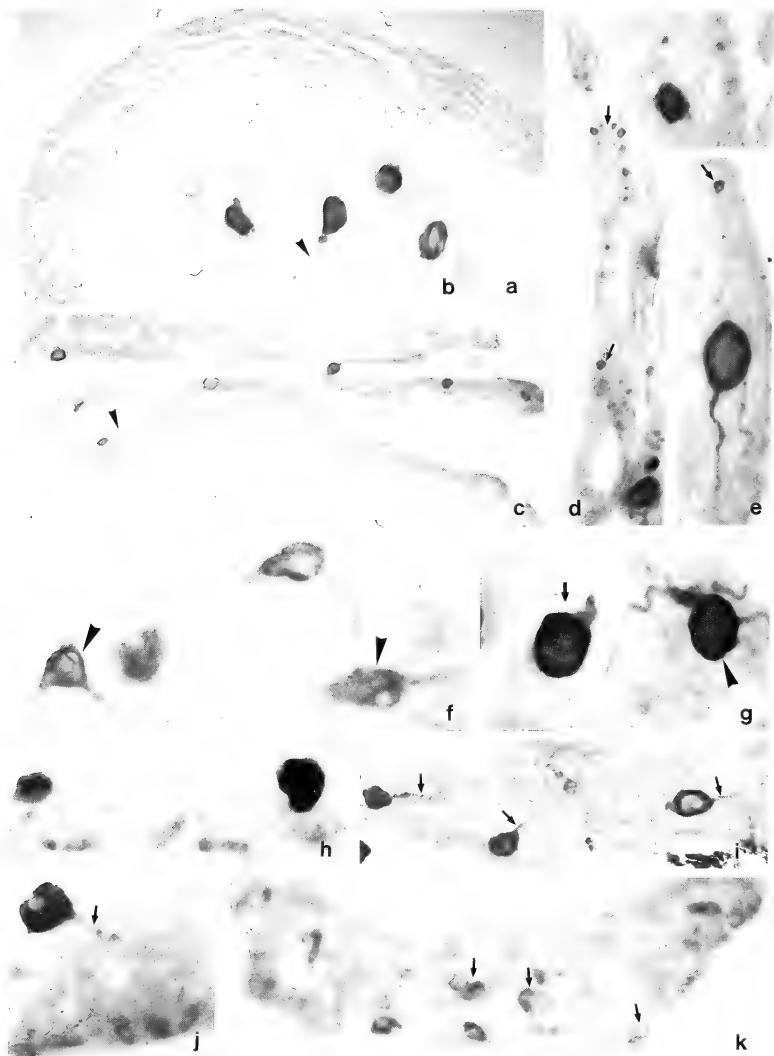


FIG. 4. (legends p. 827)

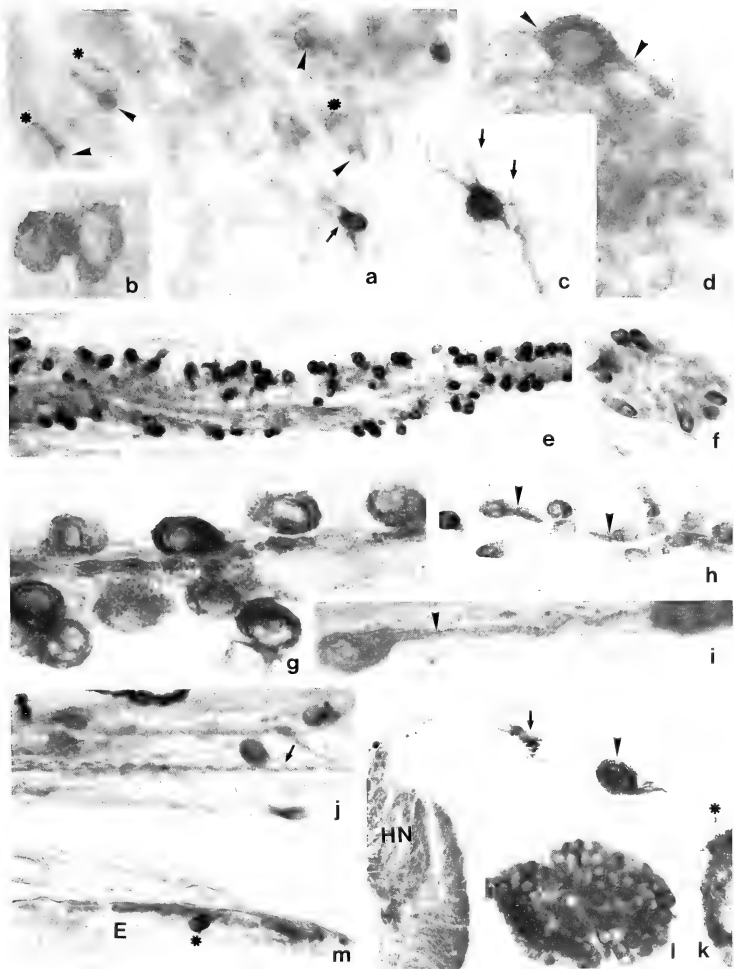


FIG. 5. (legends p. 827)

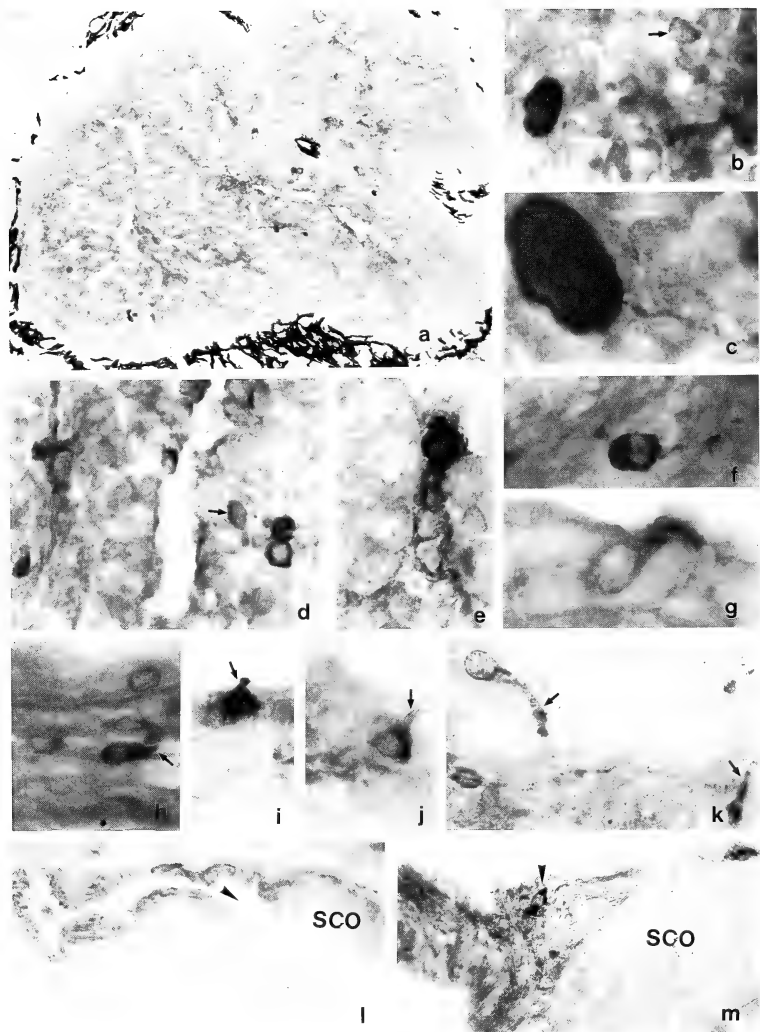


FIG. 6. (legends p. 827)

not—especially in the stalk area—two different types of AChE-positive nerve cells of similar size, because only the perikarya and not the cell processes are stained. Axons of pineal nerve cells are stained with silver impregnation technique [52]: long processes of nerve cells in the rostral part of the hammer-shaped pineal organ converge in a mediolateral direction into one lateral area on each side, an area where large bi- or multipolar cells are concentrated in the AChE-stained preparations. These two ganglion-like areas resemble the rostromedial ganglion described in the trout [2], in the rostro-ventral portion of the pineal end-vesicle of the minnow, *Phoxinus phoxinus* [53] and in *Fugu niphobles* (unpublished data) (Fig. 3a, b). In other fish species like *Fugu pardale* (Fig. 4a-e), *Scomber japonica* (Fig. 4f-k), the deep-sea fish *Helicolenus hilgendorfi* (Fig. 5a-m) and the shark *Triakis scyllia* (Fig. 6a-m), no ganglion-like accumulation of nerve cells exists, but large multipolar cells are scattered throughout the pineal end-vesicle. These large nerve cells are only in some areas surrounded by small nerve cells due to either difficulties in staining or to real regional

differences (Figs. 3c; 4d, e, h, j). The large intraparenchymal cells may be functionally comparable to the multipolar cells of the frog pineal complex [40, 41] (Figs. 3d-f; 4b, e, i, j; 5a; 6b, c-unipolar), (Fig. 6f-bipolar), (Figs. 4f, g; 5a, c; 6e-multipolar). However, the fact that unipolar, bipolar and multipolar cells are stained by horseradish peroxidase backfilling suggests an alternative conclusion [46].

The regional differences in the existence of small nerve cells may reflect functional zonation in the pineal organ (compare Figs. 3c and e; 4c and d). A zonation in the distribution pattern of nerve cells is described in the pineal organ of the pike, *Esox lucius*, [54, 55] where AChE-positive nerve cells are distributed in the rostral and proximal part of the pineal organ, whereas nerve cells are nearly absent and the photosensitive structures of the pinealocytes are reduced in the proximal part of the pineal end-vesicle. This kind of zonation does not seem to appear in other fish species [46, 51], but the regional differences in the number and shape of nerve cells are apparent. The small nerve cells, often localized at the basal side of the

Fig. 4. *Fugu pardale*. a, Sagittal section of the pineal end-vesicle. $\times 50$. b and c, Large, intensely stained AChE-positive nerve cells scattered within the parenchyma of the pineal end-vesicle. They show sometimes a long and thick axon-like process (\blacktriangle). b, $\times 475$; c, $\times 120$. d and e, In some regions of the pineal end-vesicle small nerve cells (\blacklozenge) are accumulated around a few large nerve cells. d, e, $\times 475$. f-k, *Scomber japonica*. As in *Fugu*, intensely stained big nerve cells—sometimes multipolar in appearance—(\blacktriangle) (f, g), sometimes with one axon-like process (\blacklozenge) (g, i, j). In some areas of the end-vesicle small, faintly stained small cells (\blacklozenge) are concentrated (k). f, g, h, $\times 475$; i, $\times 260$; j, k, $\times 475$.

Fig. 5. a-m. Pineal complex of the deep-sea fish *Helicolenus hilgendorfi* (Cottidae, Teleostei). a-d, AChE-positive nerve cells in the pineal end-vesicle. A few number of intensely stained multipolar cells (\blacklozenge) (a, c) and a large number of faintly stained cells with one (\blacktriangle) (a, b) or more (\blacklozenge) (d) processes which characteristically bend and return near to the perikarya (\ast) (a, b). c, Pinealocytes project (\blacklozenge) their processes toward the multipolar cells. a, $\times 475$; b, c, d, $\times 1200$. e-j, Transverse (e, g-j) and cross sections (f) of the long, thin pineal stalk; most of the nerve cells are intensely stained (e, f). Some nerve cells contain a long, thick, axon-like process (\blacktriangle) (h, i), but the process (\blacklozenge) which is sent by other nerve cells into the nerve fiber bundles, is thin (j). e, $\times 240$; f, $\times 475$; g, $\times 1200$; h, $\times 475$; i, $\times 1200$; j, $\times 475$. k and l, Parapineal organ (\blacktriangle) with a large number of AChE-positive nerve cells (l) lateral to the pineal tract (\blacklozenge) in a cross section of the diencephalon. HN, habenular nucleus. k, $\times 120$; l, $\times 475$. m, Some nerve cells (\ast) are scattered along the parapineal tract which connects the parapineal organ with the brain (see also k). E, ependyma of the third ventricle.

Fig. 6. Pineal organ of the shark, *Triakis scyllia* (Selachii). a, The spherical end-vesicle is surrounded by the cartilaginous skull and ramified pigment cells. $\times 120$. b-g, As in *Fugu* and *Scomber* large intensely stained AChE-positive nerve cells (b, c) and faintly stained small cells (\blacklozenge) (b, d) are distinguishable. The intensely stained cells show one (c), two (f) or more (e) processes. Some cells obviously send one process into the lumen of the end-vesicle (g). b, $\times 475$; c, $\times 1200$; d, e, f, $\times 475$; g, $\times 1200$. h-k, Nerve cells in the long, thin pineal stalk; they often send one process into the wide pineal lumen (\blacklozenge). h, $\times 475$; i, $\times 600$; j, k, $\times 475$. l, The proximal part of the pineal stalk has a broad connection with the third ventricle (\blacktriangle) at the rostral tip of the subcommissural organ (SCO). $\times 200$. m, Single nerve cells (\blacktriangle) are scattered along the pineal tract at the dorsal side of the subcommissural organ (SCO). $\times 1,200$.

parenchyma (Figs. 3c; 4e, h, j, k), may be comparable to the pseudounipolar cells of the frog pineal complex. But it is possible that not all pineal nerve cells are AChE-positive. A population of GABA-immunoreactive neurons has been described in the rostral portion of the pineal end-vesicle of the rainbow trout. Additionally, GABA-positive cells have been found in the pineal stalk [50]. An interesting finding is the description of intrapineal nerve cells in the goldfish at the ultrastructural level, containing dense-cored vesicles, 80–160 nm in diameter, in their perikarya and their processes [52, 56]. These nerve cells are in contact with synaptic ribbon synapses of pinealocytes at their perikarya and their processes [56]. Dense-cored granules are known in neuropeptide-containing amacrine cells of the retina [49]. Intrapineal neurons containing granules may be an indication of the existence of interneurons.

A large number of pinealocytes related to one large nerve cell shown in the pineal end-vesicle of the goldfish [51] may be a sign of a higher photosensitivity in this part of the pineal organ in comparison to the pineal stalk. Generally, a greater number of nerve cells per area exist in the pineal stalk compared to the pineal end-vesicle [2, 51] (compare Fig. 3a and g; Fig. 5a and e). A small number of pinealocytes is related to each of these small nerve cells in the stalk area [51], and different types of photosensitive pinealocytes are described [36]. These findings make it likely that the small nerve cells conduct more specific light responses to the brain.

The pineal lumen of most of the lower vertebrates is in direct contact with the third ventricle (Fig. 6l); thus it contains cerebrospinal fluid (CSF). CSF-contacting neurons have been demonstrated in the shark pineal organ [4] (Fig. 6g-k) and further results are described for *Fugu niphobles* (Fig. 3f), *Scomber japonica* (Fig. 4j) and *Fugu pardale* (Fig. 4b, c). CSF-contacting neurons are also described in the cartilaginous fish, *Chimaera monstrosa*. The processes of pinealocytes terminate at their perikarya. The axons of these CSF-contacting neurons extend toward the pineal stalk. These neurons are comparable to the Landolt's bipolars of the retina [57] and their function is supposed to be an integration of changes in the

composition of the pineal CSF and the photoreceptive activity of pinealocytes [36]. CSF-contacting neurons are also described in the rainbow trout by retrogradually labeling with horseradish peroxidase [58]. According to Ekstroem [58], they are second-order neurons receiving synaptic inputs from photosensitive pinealocytes and presynaptic to other neurons, and also send a long axon toward the brain. However, according to the same report, photosensitive pinealocytes also send a long process to the brain and other characteristics of CSF neurons are also true for pinealocytes [52, 59]. Further investigations seem to be necessary.

In general, the electrophysiological characteristics of the fish pineal complex are similar to those of the amphibians [19, 20, 25, 26, 48]. The photosensitive pinealocytes respond to light with a hyperpolarization whose amplitude correlated with intensity [60]. According to extracellular recordings, the trout pineal organ contains two kinds of photopigments [61]. The different response patterns of the pineal photoreceptors to bright flashes and to background illumination indicate the existence of several receptor types with rod- or cone-like characteristics in the teleostean pineal likely. Opsin immunoreactivity studies distinguished two different types of photoreceptors in the lamprey [see 36]. Visual adaptation is governed to a considerable extent by the photoreceptor cells themselves [62], but that does not exclude the involvement of pineal ganglion cells in the adaptation process [19]. A large number of photosensitive pinealocytes related to one nerve cell shown in the pineal end-vesicle of the goldfish are suggested to be an indication of a high degree of light sensitivity of this area [52]; in contrast, similar characteristics of the adaptation process in the dark of individual photosensitive pinealocytes and interneurons [62] supports the notion that the high light sensitivity of the pineal organ is not primarily due to a high convergence rate of photoreceptors onto centrally projecting ganglion cells, but mirrors the high sensitivity of individual pineal receptors [60]. Therefore, a clear discrepancy is obvious at moment between the morphological and electrophysiological findings in the explanation of the adaptation process.

In the goldfish, ganglion cells showed discharges

under conditions of steady illumination, both in dim and bright light; the response to light flashes was purely achromatic. The operating range of ganglion cells does not only depend on the absolute level of photoreceptor potentials: the most significant class of ganglion cells operates in a photopic-scotopic range with a nearly linear relationship between firing frequency and logarithm of background illumination, and the operating range of the other cell population is mainly at photopic levels of illumination [63, 64]. Possibly, both types of ganglion cells receive different inputs from other cells [63]. Morphological counting of 500 nerve cells and of only 310 nerve fibres in the pineal organ of the goldfish suggests the presence of interneurons [65]. Unfortunately only little is known about the possible presence of different neuronal populations in the pineal organ. In the rainbow trout, an intrapineal non-spiking interneuron exists that responds to light with a membrane hyperpolarization similar to that of photosensitive pinealocytes; there is a different decreasing response amplitude at higher light intensities between them. This may be due to a) interactions with other interneuronal types, b) a direct reciprocal innervation by ganglion cells or c) an effect of light adaptation by the previous light flash [60].

A small class of interneurons is described in *Phoxinus phoxinus* which exhibits a biphasic response pattern to light stimulation; the cells depolarize with dim light flashes and hyperpolarize with bright flashes. These cells do not show spike activity as ganglion cells, they have an atypical biphasic response pattern and they differ from photoreceptors in the voltage-intensity relation and likewise in the shape of the response. The spectral response curves peak at a wavelength different from that of photoreceptors, suggesting that this cell type receives complex receptor input. These cells provide further evidence of the presence of a differentiated network in the pineal tissue [66].

The nervous organization of the most primitive lamprey has been described by several investigators [26, 67-70]. Putative interneurons were not observed in the lamprey pineal [71]. However, Morita *et al.* [72] describe a special type of nerve cells responding to light stimuli exclusively with

off-discharges without spontaneous discharge.

Summarizing the morphological and electrophysiological results, there is evidence that the neuronal circuitry of the pineal complex in fish and amphibians exhibits a greater complexity than implied by the concept that signal transmission in the pineal organ is realized by a simple binauronal pathway from photoreceptors to ganglion cells. But we are far from understanding of the functional meaning of the species-dependent and the intraspecific regional differences of the nervous organization of the pineal complex.

ACKNOWLEDGMENTS

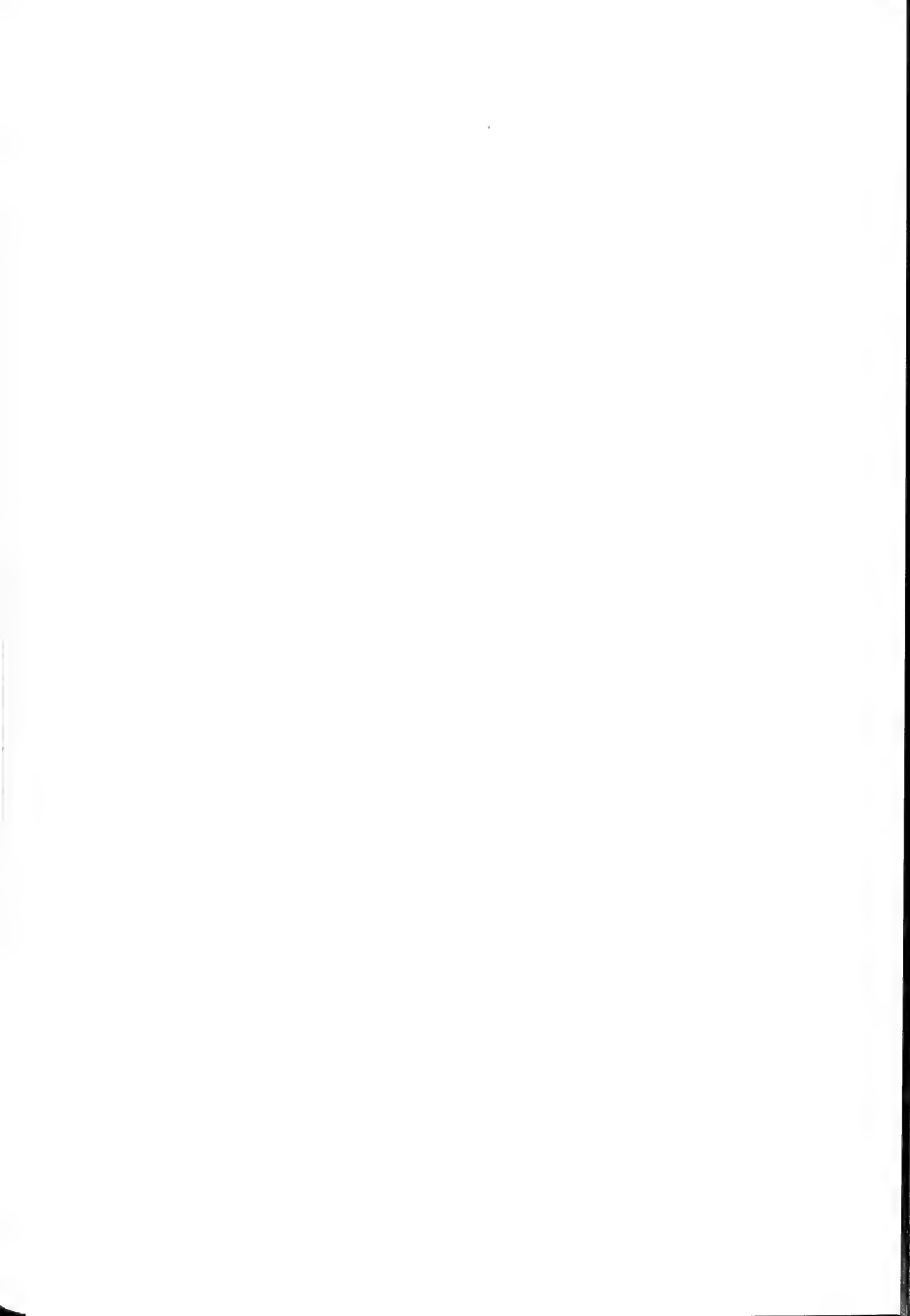
The original results on the fish pineal complex were obtained during the stay by M. Ueck as a Visiting Professor of the Japan Society for the Promotion of Science at Misaki Marine Biological Station of the University of Tokyo (Head: Prof. H. Kobayashi). The authors thanks R. Liesner and A. Hach for their skillful technical assistance.

REFERENCES

1. Ruedeberg, C. (1969) *Z. Zellforsch.*, **93**: 282-304.
2. Korf, H. W. (1974) *Cell Tissue Res.*, **155**: 475-489.
3. Meinil, A. and Collin J. P. (1971) *Z. Zellforsch.*, **117**: 354-380.
4. Ueck, M. and Kobayashi H. (1979) *Verh. Anat. Ges.*, **73**: 961-963.
5. Veen van Th. (1982) *Cell Tissue Res.*, **222**: 433-444.
6. Studnička, F. K. (1905) Die Parietallorgane. In "Lehrbuch der vergleichenden mikroskopischen Anatomie der Wirbeltiere, 5A". Ed. by A. Oepel, Gustav Fischer, Jena, pp. 1-254.
7. Ueck, M. (1974) *Fortschritte der Zoologie Bd. 22, Heft 2/3*. Gustav Fischer, Stuttgart, pp. 167-203.
8. Ueck, M. (1982) *Verh. Dtsch. Zool. Gesellsch. Hannover. Gustav Fischer, Stuttgart*, pp. 61-80.
9. Vollrath, L. (1981) The pineal gland. In "Handbuch der mikroskopischen Anatomie des Menschen. Band 6/7". Ed. by A. Oksche and L. Vollrath, Springer-Verlag, Berlin/Heidelberg/New York, pp. 1-665.
10. Collin, J. P. and Oksche, A. (1981) In "The Pineal Gland: Anatomy and Biochemistry". Ed. by R. J. Reiter, CRC Press, Boca Raton, pp. 27-67.
11. Ueck, M., Vaupel-von Harnack, M. and Morita, Y. (1971) *Z. Zellforsch.*, **116**: 250-274.
12. Eakin, R. M. and Westfall, J. A. (1961) *Embryologia (Nagoya)*, **6**: 84-98.

- 13 Oksche, A. and Vaupel-von Harnack (1963) *Z. Zellforsch.*, **59**: 230-288.
- 14 Oksche, A. and Vaupel-von Harnack, M. (1963) *Z. Zellforsch.*, **59**: 582-614.
- 15 Holmgren, N. (1918/1919) *Ark. Zool.*, **24**: 1-13.
- 16 Paul, E., Hartwig, H. G. and Oksche, A. (1971) *Z. Zellforsch.*, **112**: 466-493.
- 17 Ueck, M. and Kobayashi, H. (1972) *Z. Zellforsch.*, **129**: 140-160.
- 18 Wake, K., Ueck, M. and Oksche, A. (1974) *Cell Tissue Res.*, **154**: 423-442.
- 19 Dödt, E., Ueck, M. and Oksche, A. (1971) In "J. E. Purkinje Centenary Symposium, Prague 1969". Ed. by V. Kruta, Universita Jena Evangelisty Purkyne, Brno, pp. 253-278.
- 20 Dödt, E. (1973) In "Handbook of Sensory Physiology". VII/3B, Ed. by R. Jung, Springer-Verlag, Berlin/Heidelberg/New York, pp. 113-140.
- 21 Morita, Y. and Dödt, E. (1965) *Experientia* (Basel), **21**: 221-222.
- 22 Hamasaki, D. I. and Esserman, L. (1976) *J. Comp. Physiol.*, **109**: 279-285.
- 23 Meissl, H. and Donley, C. S. (1980) *Vision Res.*, **20**: 379-383.
- 24 Hamasaki, D. I. (1970) *Vision Res.*, **10**: 307-316.
- 25 Dödt, E. and Meissl, H. (1982) *Experientia*, **38**: 996-1000.
- 26 Morita, Y. (1975) In "Brain Endocrine Interaction II. The Ventricular System". Ed. by K. M. Knigge, D. E. Scott, H. Kobayashi and S. Ishii, Karger, Basel, pp. 376-387.
- 27 Hartwig, H. G. and Baumann, Ch. (1964) *Vision Res.*, **14**: 597-598.
- 28 Dödt, E. and Morita, Y. (1964) *Vision Res.*, **4**: 413-421.
- 29 Donley, C. S. and Meissl, H. (1979) *Vision Res.*, **19**: 1343-1349.
- 30 Meissl, H. and George, S. R. (1984) *Vision Res.*, **24**: 1727-1734.
- 31 Meissl, H. and George, S. R. (1985) *Brain Res.*, **332**: 39-46.
- 32 Ehinger, B. (1982) *Retina*, **2**: 305-321.
- 33 Vigh, B. and Vigh-Teichmann, I. (1986) *Arch. Histol. Jpn.*, **49**: 495-518.
- 34 Vigh, B. and Vigh-Teichmann, I. (1981) *Cell Tissue Res.*, **221**: 451-463.
- 35 Vigh, B., Vigh-Teichmann, I., Aros, B. and Oksche, A. (1985) *Cell Tissue Res.*, **240**: 143-148.
- 36 Vigh, B. and Vigh-Teichmann, I. (1988) *Pineal Research Reviews*, **6**, Alan R. Liss, Inc., New York, pp. 1-65.
- 37 Ueno, S., Bambauer, H. J., Umar, H. and Ueck, M. (1984) *Cell Tissue Res.*, **237**: 479-489.
- 38 Ueck, M., Umar, M., Umar, H. and Hach, A. (1987) In "Fundamentals and Clinics in Pineal Research". Ed. by G. P. Trentini, C. De Gaetani and P. Pévet, Sereno Symposia Publications, **44**, Raven Press, New York, pp. 53-56.
- 39 Scherer-Singler, U., Vincent, S. R., Kimura, H. and McGeer, E. G. (1983) *J. Neuroscience Methods*, **9**: 229-234.
- 40 Ueck, M., Sato, T., Ohba, S., Wake, K. and Kobayashi, H. (1989) In "Proceedings of the Internat. Symposium on Neurons and Paraneurons". Ed. by Fujita, *Arch. Histol. Cytol.* **52** (in press).
- 41 Sato, T. (1989) *Arch. Histol. Cytol.*, (in press)
- 42 Boycott, B. B. (1988) *Neuroscience Res.*, Suppl. **8**, Elsevier Scientific Publishers Ireland Ltd., pp. S97-S111.
- 43 Meinil, A. (1980) *Cell Tissue Res.*, **207**: 407-424.
- 44 Korf, H. W. and Ekstroem, P. (1987) In "Fundamentals and Clinics in Pineal Research". Ed. by G. P. Trentini, C. Gaetani, and P. Pévet, Sereno Symposia Publications, **44**, Raven Press, New York, pp. 35-47.
- 45 Eldred, W. D. and Nolte, J. (1981) *J. Comp. Neurology*, **203**: 269-295.
- 46 Ekstroem, P. and Korf, H. W. (1985) *Cell Tissue Res.*, **240**: 693-700.
- 47 Ueck, M., Sato, T. and Ohba, S. (1989) *Verh. Anat. Ges.*, **83**(Ulm), in press.
- 48 Meissl, H. and Dödt, E. (1981) In "The Pineal Organ: Photobiology-Biochronometry-Endocrinology". Ed. by A. Oksche and P. Pévet, Elsevier/North-Holland Biomedical Press, Amsterdam, pp. 61-80.
- 49 Rodieck, R. W. (1988) The primate retina. In "Comparative Primate Biology". **4**: Neuroscience, Alan R. Liss, Inc., New York, pp. 203-278.
- 50 Ekstroem, P., Veen van, Th., Bruun, A. and Ehinger, B. (1987) *Cell Tissue Res.*, **250**: 87-92.
- 51 Wake, K. (1973) *Z. Zellforsch.*, **145**: 287-298.
- 52 Ohba, S., Wake, K. and Ueck, M. (1979) *Progress in Brain Res.*, **52**: 93-96.
- 53 Vigh-Teichmann, I., Korf, H.-W., Oksche, A. and Vigh, B. (1982) *Cell Tissue Res.*, **227**: 351-369.
- 54 Falcón, J. (1979) *Ann. Biol. Anim. Bioch. Biophys.*, **19**(2A): 445-465.
- 55 Falcón, J. and Meissl, H. (1981) *J. Comp. Physiol.*, **144**: 127-137.
- 56 Ohba, S., Wake, K., Ohnishi, R. and Ueck, M. (1979) *Verh. Anat. Ges.*, **73**: 953-959.
- 57 Vigh-Teichmann, I. and Vigh, B. (1987) In "Functional Morphology of Neuroendocrine Systems". Ed. by B. Scharer, H.-W. Korf and H.-G. Hartwig, Springer-Verlag, Berlin/Heidelberg, p. 160.
- 58 Ekstroem, P. (1987) *J. Neuroscience*, **7**: 987-995.
- 59 McNulty, J. A. (1980) *Cell Tissue Res.*, **210**: 249-256.
- 60 Ekstroem, P. and Meissl, H. (1988) *Neuroscience*,

- 25: 1061-1070.
- 61 Meissl, H. and Ekstroem, P. (1988) *Neuroscience*, **25**: 1071-1076.
- 62 Meissl, H. and Ekstroem, P. (1988) *Vision Res.*, **28**: 49-56.
- 63 Meissl, H., Nakamura, T. and Thiele, G. (1986) *Comp. Biochem. Physiol.*, **84A**: 467-473.
- 64 Falcón, J. and Meissl, H. (1981) *J. Comp. Physiol.*, **144**: 127-137.
- 65 McNulty, J. A. (1981) *Canad. J. Zool.*, **59**: 1321-1325.
- 66 Nakamura, T., Thiele, G. and Meissl, H. (1986) *J. Comp. Physiol.*, **A159**: 325-330.
- 67 Collin, J. P. (1969) *J. Neuro-Visceral Relations*, **31**: 308-333.
- 68 Meiniel, A. and Collin, J.-P. (1971) *Z. Zellforsch.*, **117**: 354-380.
- 69 Cole, W. C. and Youson, J. H. (1982) *Amer. J. Anat.*, **165**: 131-163.
- 70 Morita, Y. and Dodt, E. (1973) *Nova Acta Leopoldina*, **38**: 331-339.
- 71 Pu, G. A. and Dowling, J. E. (1981) *J. Neurophysiol.*, **46**: 1018-1038.
- 72 Morita, Y., Tabata, M. and Tamotsu, S. (1985) *Neurosci. Res. (Suppl.)*, **2**: S79-S88.



REVIEW

**Bioelectric Control of Effector Responses in The Marine
Dinoflagellate, *Noctiluca miliaris***KAZUNORI OAMI¹ and YUTAKA NAITOH*Institute of Biological Sciences, University of Tsukuba,
Tsukuba 305, Japan*

INTRODUCTION

All animals exhibit effector activity in response to stimuli from their external and internal environments. In multicellular animals, stimulus energy is converted into a receptor potential at the receptor membrane of a sensory cell. The receptor potential produces a train of action potentials, the sensory information, across the membrane of the sensory nerve axon, adjacent to the receptor membrane. The sensory information travels along the axon to the central nervous system, where it is integrated by means of chemoelectrical interaction between many neurons. Integration of the sensory information results in the generation of action potential in the central nervous system. These potentials are sent down motor nerve axons to effector organs. Thus the effector responds appropriately to the sensory input. Membrane electrical events, therefore, play a major role in regulating effector activities in multicellular organisms. This is also true for unicellular organisms. Unicellular organisms, however, must perform all these functions within the confines of a single cell. Naitoh [1] reviewed how this is achieved in some protozoans. During the course of their evolution protozoans have come to possess multiple functions in their single membrane. For example, the *Paramecium* membrane produces receptor potentials in response to external stimuli, integrates the

potentials due to the isopotential nature of its protoplasm, and generates action potentials according to the integrated level of the membrane potential. The action potentials control the motility of the cilia, and thereby the swimming behavior of the *Paramecium*. It should be noted that these different membrane functions reside in different membrane areas respectively. For example, in a forward swimming cell, a depolarizing mechanoreceptor potential is generated at the membrane of anterior end in response to a collision with a mechanical obstacle. A Ca^{2+} action potential is generated exclusively at the membrane covering the cilia when it is depolarized electrotonically by this receptor potential. The action potential brings about a transient increase in Ca^{2+} concentration within the cilia to cause a transient ciliary reversal, which results in a transient backward swimming of the cell to avoid the mechanical obstacle.

Localized differentiation of the membrane electrogenic function within a single cell is also seen in multicellular organisms. For example, the axon hillock is a generation site of action potentials in a motor neuron [2], the distal end of some sensory nerve axons are generation site of receptor potentials etc. Therefore, studies on the localized differentiation of the membrane function and its biological significance in unicellular organisms can contribute greatly to our understanding of general principles of functional differentiation within single cell.

A large marine dinoflagellate *Noctiluca* exhibits two distinct kinds of effector activity, emission of light and motile response of its tentacle. In 1957

Received June 19, 1989¹ To whom all correspondence should be addressed.

Hisada* [3] of Tokyo University first recorded spontaneous membrane potential perturbations through a microelectrode inserted into *Noctiluca*. In 1960 Chang** [4] of the National Institute of Health, U.S.A. examined the electrophysiological properties of a non-luminescent form of *Noctiluca*. In his admirable series of papers appearing in Science [5-7], Eckert*** of Syracuse University presented some beautiful data on the bioelectric control of the bioluminescent flash in *Noctiluca*. His papers also attracted considerable attention because of his employment of sophisticated (at least at that time) electrophysiological and photo-sensing equipment. Sibaoka**** of Tohoku University had joined Eckert in 1966 to perform more detailed examinations of the membrane electrogenesis and its relation to the effector activity in *Noctiluca*. After his coming back to Japan, Sibaoka continued his studies on *Noctiluca* with his student Nawata. They proposed a H^+ -mediated coupling mechanism between the membrane electrogenesis and the luminescent flash [8]. They also examined the feeding behavior of *Noctiluca* and its electrophysiological correlates [9-11].

More recently Sibaoka's student Oami joined Naitoh at the University of Tsukuba to perform detailed examinations of the membrane electrogenesis in relation to flexion-extension of the tentacle. Oami and Naitoh have been obtaining various results, some of which are consistent with those obtained by previous workers, some not. They have proposed a new hypothesis for the bioelectric control of the tentacular movement in *Noctiluca* [12].

We will review the electrophysiological studies on *Noctiluca* with special reference to the control of its effector activity and related behavior by membrane electrogenesis. Readers can refer to a famous book by Harvey [13] for an understanding of bioluminescence in general. In 1966, Eckert [14] reviewed excitation and luminescence in *Noctiluca* based mainly on his experimental results.

Sibaoka [15] reviewed electrogenesis in *Noctiluca* in Japanese. Widder [16] reviewed bioluminescence excitation in a dinoflagellate *Pyrocystis* (see also Sweeney [17]).

MORPHOLOGY AND BEHAVIORS

Noctiluca has been classified as a protozoan belonging to the order Dinoflagellida. Recent detailed examinations of its life history revealed that *Noctiluca* produces flagellated gametes in a certain phase of its life cycle similarly to dinophycean algae [18]. Plant taxonomists, therefore, have politely invited *Noctiluca* to be a member of the plant kingdom.

Noctiluca is quasi-spherical, ranging from 300 to 600 μm in diameter (Fig. 1). The larger portion of the cell interior is a vacuole filled with sap having a specific weight a little lighter than that of sea water. The vacuole, therefore, serves as a float for the planktonic life of the cell. The vacuole is covered by a thin layer of protoplasm termed the perivacuolar cytoplasm. *Noctiluca*, therefore, has two protoplasmic membranes, one facing sea water (outer membrane) and the other facing the vacuolar sap (inner membrane).

The most prominent feature of this small animal is its emission of light in response to stimulus, though the biological significance of this remains obscure. *Noctiluca* together with its luminescent dinoflagellate (or dinophycean) relatives is responsible for the spooky glow surrounding you when you swim in the quiescent warm sea on a summer night. The flash mechanism resides in the cytoplasm as scattered small particles.

As shown in Figure 1, *Noctiluca* has a minute motile projection, a tentacle (about 300 μm in length and $6 \times 10 \mu m$ in its elliptical cross-section; tn), which is used for gathering and eating its food (mostly small algae such as *Dunaliella*). The tentacle traps the algae with its sticky tip as it beats slowly, then sharply bends at its proximal region so that the tip comes into contact with the cytostome (indicated by an arrowhead) located in the deepest portion of the sulcus (a longitudinal groove of the cell). The algae are then ingested into the food vacuole (fv) in the perinuclear cytoplasmic mass (cm) by phagocytosis at the cytostome. The cyto-

* Hisada moved to Hokkaido University in 1956.

** Chang moved to Sogang University, Seoul.

*** Eckert moved to UCLA in 1969 and passed away in 1986.

**** Sibaoka moved to Kyoritsu Women's College in 1985.

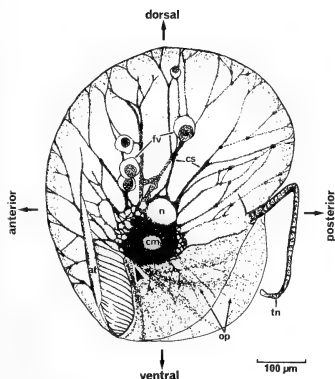


FIG. 1. Schematic drawing of lateral view of *Noctiluca*. at, apical trough; op, oral pouch (at and op form a longitudinal groove termed "sulcus"); tn, food-gathering tentacle; fv, food vacuole; cm, perinuclear cytoplasmic mass; n, nucleus; cs, cytoplasmic strand. A black arrowhead near cm indicates approximate location of the cytostome. From Nawata and Sibaoka [9].

plasmic mass contains a nucleus (n) and is connected with the perivacuolar cytoplasm by many fine cytoplasmic strands (cs). Cytoplasmic streaming towards or away from the cytostome is seen in association with its feeding behavior. The tentacle sometimes shows coiling.

EARLY ELECTROPHYSIOLOGICAL STUDIES

Summary of the first electrophysiological studies on Noctiluca by Hisada

In 1957 Hisada [3] had first recorded intracellular potentials through a microcapillary electrode inserted into *Noctiluca* (Fig. 2). Resting potential was about 50 mV negative to the external solution, when the cell was quiescent without showing tentacle movement. The electronegativity decreased with increasing external K^+ concentration as in most excitable cells, though the rate of decrease was about a half of that found in nerves and muscles (30 mV per unit decrease in logarithmic K^+ concentration).

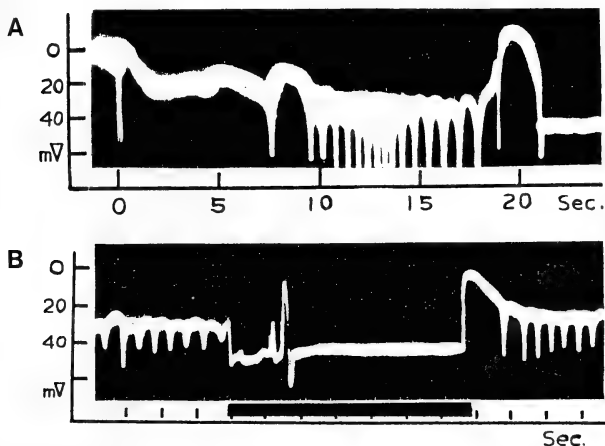


FIG. 2. A: The first records of intracellular spontaneous action potentials of *Noctiluca* correlated with tentacular activity. B: Inhibition of the spontaneous action potentials by injection of an inward current into the cell (period of the injection is indicated by a black bar below the potential record). From Hisada [3].

Trains of action potentials with varied repeating frequency (2–3 Hz at its maximum) were observed to be superimposed over a slowly fluctuating membrane potential. Strikingly, the polarity of the action potential was negative (hyperpolarizing) to the external solution, contrary to “conventional” depolarizing action potentials of nerves and muscles. Each action potential was always preceded by a depolarization of varied duration (Fig. 2A). The amplitude of the action potential was about 30 mV. More interestingly, a flexion of the tentacle was always accompanied by the hyperpolarizing action potential. Injection of an outward (depolarizing) current produced the action potential together with flexion of the tentacle upon its switching off. An inward (hyperpolarizing) current produced neither. Moreover, the repetitive action potentials were inhibited by inward current injection (Fig. 2B). Hisada could not detect the membrane potential change associated with the flash.

Summary of electrophysiological studies on Noctiluca by Chang

Chang [4] examined the electrophysiological characteristics of *Noctiluca* by employing fine glass capillary microelectrodes inserted into the flota-

tion vacuole and electronic equipment more sophisticated than those used by previous workers. In contrast to Hisada, no significant resting potential was observed. A hyperpolarizing action potential of all-or-none type was elicited when an inward current was injected into the vacuole and the resultant shift of the vacuolar potential (electric potential of the vacuolar sap with reference to the external solution) toward hyperpolarizing direction exceeded 100 mV (Fig. 3). The amplitude of the action potential was calculated by subtracting the Ohmic voltage shift across the membrane (i.e. current divided by electric conductance of the membrane at the peak of the action potential) from the potential shift at the peak of the action potential, and was found to be about 100 mV. The action potential was always accompanied by a conspicuous decrease in the membrane impedance within a suction hole of the experimental chamber by which the cell is arrested (about 3% of the total membrane area).

The action potential was little affected by changing ionic compositions in the external solution. This fact together with the unorthodox polarity of the action potential caused Chang to assume that the action potential might be generated in the membrane facing the vacuole.

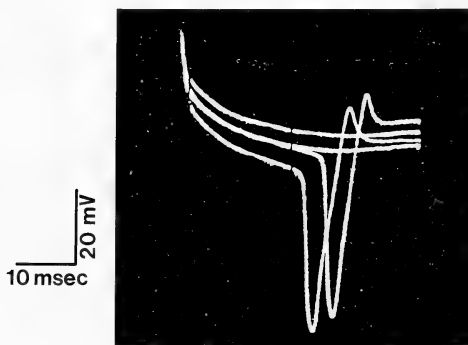


FIG. 3. Superimposed records of electric responses of *Noctiluca* to inward rectangular current pulses of four different intensities. A downward deflection of the trace corresponds to an increase in the negativity of vacuolar sap relative to the surrounding sea water. The base line of the potential trace is above the upper edge of the photograph, so it cannot be seen. From Chang [4], modified.

Membrane resistance and capacitance averaged $1.4 \times 10^3 \text{ ohm-cm}^2$ and $1.3 \text{ } \mu\text{F/cm}^2$ respectively when the cell was inactive.

Since Chang's specimens were a non-luminescent form, correlation of the action potential with the bioluminescent flash was not examined. Chang was, however, interested in flash control by membrane electrogenesis.

BIOELECTRIC CONTROL OF LIGHT EMISSION

Characteristics of the luminescent flash

Noctiluca emits light when it is stimulated mechanically, chemically, electrically or by some other means. The light flash is all-or-none and short-lived as it attains a peak amplitude 15 to 20 msec after onset, and decays to 50% in about the same time. The emission spectrum of the flash has a peak at a wavelength of 470 nm. Therefore, the flash is blue. Maximum light intensity of a single flash is about 1.5×10^{-22} watts and its total energy is about 4.1×10^{-10} joules (ca. 9.7×10^8 photons). The flash shows summation, potentiation and fatigue. For detailed kinetics of the flash see the review by Eckert [14].

Flash-triggering action potential

In a luminescent form of *Noctiluca*, Eckert [5] obtained a hyperpolarizing action potential similar to that obtained by Chang [4]. He employed a high-gain photomultiplier for monitoring the flash, and found that the flash was always preceded by the action potential by 2–3 msec (Fig. 4). Eckert, therefore, termed the action potential the "flash triggering action potential (FTP)".

Propagation of the FTP and the flash over the cell surface

Eckert [6] determined the conduction latency of the FTP by examining FTP-associated localized currents measured at three different membrane areas. One near the stimulation site, a second one 90 degree around the cell and a third one approximately opposite the stimulation site. As shown in Figure 5B, the latency for the peak of the membrane current was shortest with the electrode

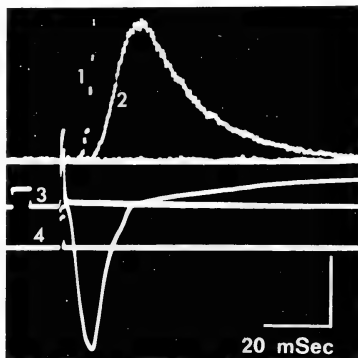


FIG. 4. The luminescent flash and the flash-triggering potential (FTP) of *Noctiluca*. Two sweeps of four traces each, one sweep with external stimulating current (monitored on trace 4) below threshold and a second sweep with suprathreshold current. The flash is converted into an electric signal by a photomultiplier and monitored on traces 1 and 2. Trace 1 is superimposed on trace 2 and displays the same signal at 20 times the gain of trace 2. Trace 3 displays the potential recorded with a microelectrode from the vacuole. Calibration pulse at beginning of this trace is 10 mV and 5 msec. Vertical calibration mark: 9×10^5 photons/msec for trace 1, 1.8×10^7 photons/msec for trace 2, 32 mV for trace 3, and 4×10^{-4} amp. for trace 4. From Eckert [5].

closest to the stimulus site and longest with the furthest one. From the latency difference between the two extreme recording sites the propagation velocity of the FTP along the circumference of the cell was estimated to be about 60 mm/sec. He also determined the light emission latency at three different cellular locations corresponding to the membrane areas where the conduction latency was measured. As shown in Figure 5A, emission latency was least when the recording location was next to the stimulus site and greatest when it was opposite the stimulus site. The propagation velocity calculated from the latency difference is almost identical with that of the FTP. These findings indicate that the flash initiated at the stimulation site spreads as the FTP spreads all over the cell.

Eckert [7] precisely examined localized sources of the flash on a highly magnified image of a

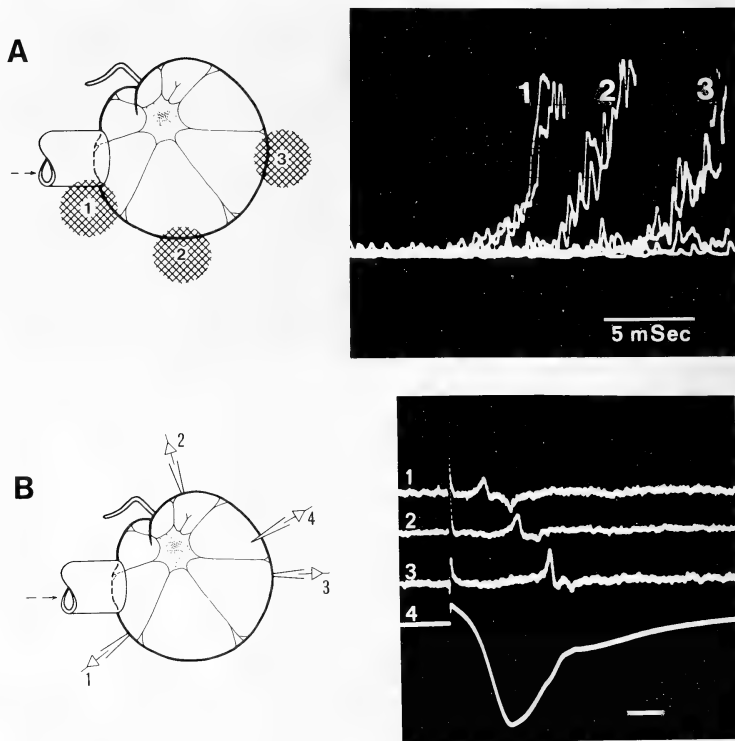


Fig. 5. Emission latency and conduction latency of the FTP in *Noctiluca*. A: Emission latencies from three restricted photometer fields at three different distances from the stimulus site. Photometer fields are indicated by shading with numbers on the left-hand diagram. 1; closest to the stimulus site, 2; about 90 degrees around the cell from the stimulus site, 3; opposite the stimulus site. The three traces with respective numbers on the right are high-gain photometer recordings of the flash from the photometer fields with corresponding numbers. B: Conduction latencies of the flash-triggering action potential. The potential is recorded through three extracellular suction electrodes placed at three different portions of the cell surface, which are shown on the left-hand diagram. Trace 4; The FTP recorded from the vacuole. The numbers beside the electrode diagrams and the traces correspond to those in A. From Eckert [6], modified.

flashing *Noctiluca* and found that fluorescent inclusions ranging from $0.5\text{--}1.5\text{ }\mu\text{m}$ in the perivacuolar cytoplasm were responsible for the flash. He termed a flash from each microsource a "micro-flash", and a flash from a whole cell, which is a

sum of all the microflashes, a "macroflash".

Generation site of the FTP

Eckert and Sibaoka [19] successfully recorded the FTP from the perinuclear cytoplasmic mass.

The FTP was diphasic in contrast to the monophasic FTP from the vacuole. This suggests a propagation of the FTP along the inner membrane. As a matter of fact, difference between the FTP recorded from the vacuole and that from the cytoplasmic mass, (which corresponds to the FTP recorded from the cytoplasm with reference to the vacuole) showed a depolarizing polarity similar to an orthodox action potential of general excitable cells. Thus it is concluded that the FTP is an orthodox action potential generated across the inner (vacuolar) membrane of *Noctiluca*.

Ionic mechanism of the FTP and coupling between the FTP and the flash

By making use of a pH-sensitive microelectrode inserted into the vacuole, Nawata and Sibaoka [20] determined the vacuolar pH to be as low as 3.5, a value similar to that obtained by previous workers

[21–23]. They also determined concentrations of major ions in the vacuolar sap, such as Na^+ , K^+ , Ca^{2+} , Mg^{2+} , NH_4^+ and Cl^- . Concentrations of these ions were almost identical with those in sea water except for the lower Mg^{2+} concentration and the presence of NH_4^+ ions.

Nawata and Sibaoka [8] injected HCl-glycine pH buffers with different pH values ranging from 2.5 to 3.7 into the vacuole. The buffer's volume was 10–30% of the vacuolar volume. The effects of vacuolar pH on the amplitude of the FTP were then examined. The lowering the pH increased the amplitude at a rate of 58 mV/unit pH change. Ion species concentrations in the vacuolar sap other than that of H^+ showed no conspicuous effects on the amplitude. These results indicated that the FTP was dependent on H^+ ions.

Using the procedures exploited by Fogel *et al.* [24] to extract the scintillons (luminescent parti-

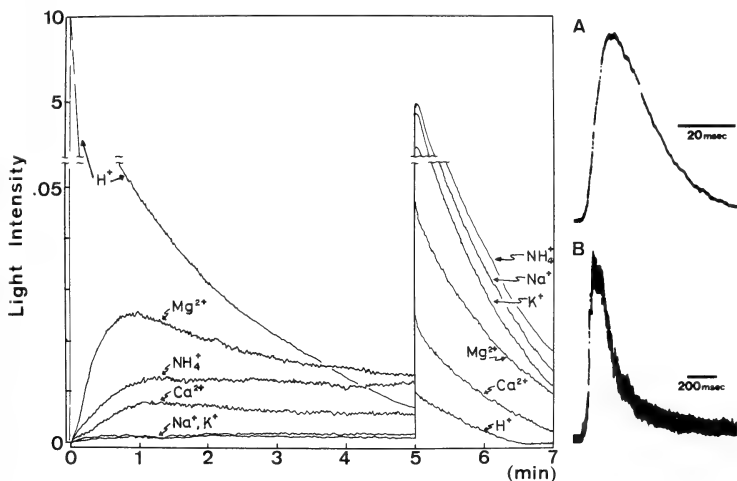


Fig. 6. Time-decay of the luminescence of the cell-free extract of *Noctiluca* after its activation. The extract was mixed with each of the various solutions with different cation species (H^+ , Mg^{2+} , NH_4^+ , Ca^{2+} , Na^+ and K^+) at time 0. The H^+ -containing solution (pH 5.1) was added 5 min after mixing. The light emission from the mixture was monitored. Ordinate: light intensity relative to the maximum intensity (regarded as 10) of the light emitted immediately after mixing the extract with the pH 5.1 solution. CRO-traces on the right of the figure are the flash from a living cell evoked by FTP (A), and that from the cell-free extract evoked by lowering pH to 5.1 (B). From Nawata and Sibaoka [8].

cles) of *Gonyaulax*, a relative of *Noctiluca*, Nawata and Sibaoka [8] prepared crude extracts of the luminescent particles of *Noctiluca*. The extract showed luminescence when the pH was lowered by mixing it with pH buffer (Fig. 6). Maximum light was obtained at pH 5.0–5.5. The peak wavelength of the emission spectrum was about 470 nm, the value identical with that of the flash in live specimens. Mixing of the extract with solutions containing Mg^{2+} , NH_4^+ , Ca^{2+} , Na^+ or K^+ produced no light emission except for a dim glow (less than 0.05% of the maximum light intensity).

These data strongly supported the hypothesis of the control of bioluminescence by membrane excitation. That is, voltage-sensitive H^+ channels in the inner membrane of *Noctiluca* are activated by a mechanoreceptor potential elicited in the inner membrane by a mechanical stimulus. H^+ in the vacuole diffuses down its electrochemical gradient through the activated channels into the cytoplasm, causing a lowering of the cytoplasmic pH. The lowered pH brings about activation of the flash mechanism in the cytoplasm, which, in turn, causes the flash. Hastings and his coworkers [25–27] had confidently predicted that *in vivo* flashing of *Gonyaulax* must be caused by H^+ movement into the scintillon in response to cellular excitation.

BIOELECTRIC CONTROL OF TENTACLE MOVEMENT

Tentacle regulating potentials

Flexion-extension of the tentacle occurs in close association with spontaneous membrane potential perturbations [3]. Eckert and Sibaoka [28] termed the potential perturbations "tentacle regulating potentials (TRPs)". The basic wave form of the TRPs consists of a slow depolarization to a level of -10 mV (pre-spike positive wave), a hyperpolarizing spike with a peak level of -85 mV (spike) and a more or less stable potential level of -45 to -60 mV (post-spike negative level). Recently Oami *et al.* [29] found that a depolarizing spike could be seen immediately before the slow depolarization, when the external Ca^{2+} concentration was lowered. The spike had been ignored by previous workers, since it is so obscure in normal sea water. Oami *et al.* [29] termed the depolarizing spike the "positive spike" and the hyperpolarizing spike the "negative spike" (Fig. 7). Recent voltage-clamp experiments [30] demonstrated that a transient small inward current corresponding to the positive spike was always evoked by a membrane depolarization even in normal sea water. The positive

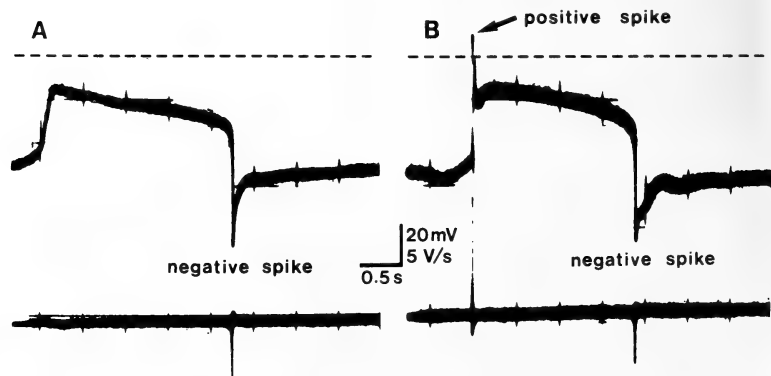


FIG. 7. The tentacle regulating potentials (TRPs) recorded through an electrode inserted into the flotation vacuole of *Noctiluca* in normal ASW (A) and in Ca-deprived ASW (B). Lower traces, first-order time derivatives of the potential shown in upper traces; dotted line, reference level for the potential. From Oami *et al.* [29].

spike, therefore, is a normal component of the TRPs.

Temporal correlation of the TRPs with the tentacle movement

Based on their simultaneous recordings of membrane potential and tentacle movement (Fig. 8), Eckert and Sibaoka [28] examined the temporal correlation of the TRPs with the tentacle movement. They found that the tentacle starts to flex within 1 sec after the beginning of the slow depolarization, and continues to flex throughout it. Extension of the tentacle takes place 1–2 sec after the negative spike. Recently we found a quick acceleration of the flexion to be associated with the negative spike [29, 31]. This finding is consistent with the early observation by Hisada [3]. Eckert and Sibaoka [28] overlooked the quick flexion. In their experiments, *Noctiluca* exhibited a rather long slow depolarization, during which the degree of the flexion reached its maximum. Therefore, enhancement of the flexion by the negative spike was obscure. Correlation of the positive spike with the tentacle movement has not yet been observed.

Generation site of the TRPs

Sibaoka and Eckert [32] pointed out that the unorthodox polarity of the TRPs could be seen as a conventional depolarizing spike with a plateau potential (such as a cardiac action potential) if the TRPs were assumed to be generated in the inner membrane. That is, the pre-spike positive wave bears similarity to a pace maker potential, while the negative spike and the post-spike negative level resemble a prolonged action potential. However, Oami *et al.* [29] found that the wave form of the TRPs recorded from the cytoplasmic compartment was identical with those recorded from the vacuole, but there was a small DC potential difference (20–30 mV) between these two potential records (Fig. 9). This indicates that the TRPs are generated in the outer membrane. Insertion of the electrode into the nucleus was a key technique for successful recording of the TRPs from the cytoplasmic compartment. Sibaoka and Eckert [32] also recorded the TRPs from the perinuclear cytoplasmic mass. The wave form of the TRPs was identical but smaller (1/2–1/4) in its

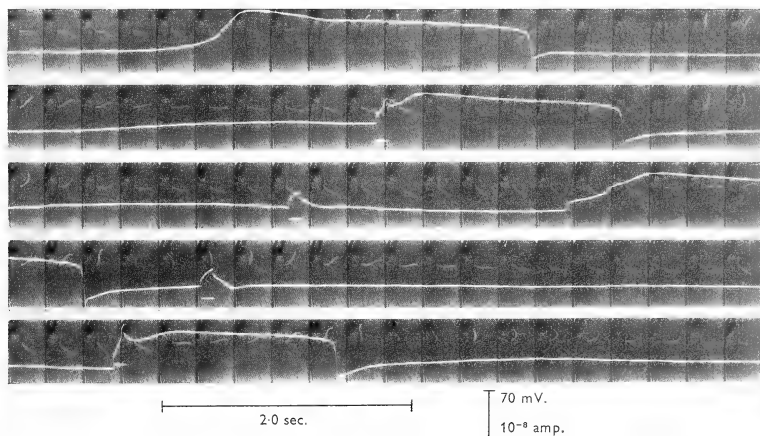


Fig. 8. Concurrent records of the tentacle regulating potentials and tentacle position in *Noctiluca*. Each frame was exposed stroboscopically at about 3/sec on continuously moving film. The potential trace was photographed from the face of a CRT. From Eckert and Sibaoka [28].

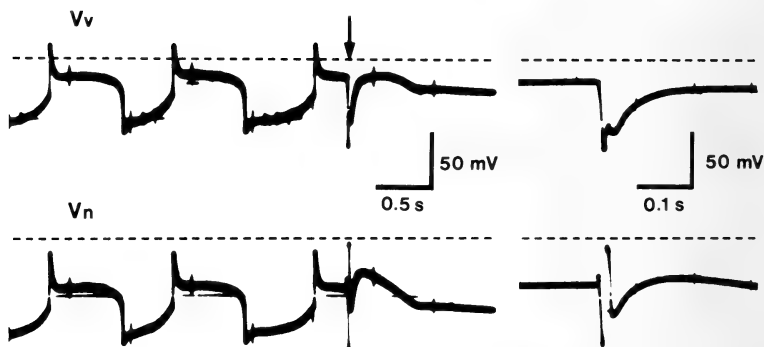


FIG. 9. Potential responses recorded simultaneously from the flotation vacuole (Vv) and from the nucleus (Vn) of a single specimen of *Noctiluca* in Ca-deprived ASW. The arrow on the Vv trace indicates the time when an inward current pulse was injected into the cell through the holding pipette to evoke a flash-triggering potential (FTP). The FTP recorded with a faster sweep (5 times as fast) is shown to the right of each trace. Dotted lines, reference levels for the potential. From Oami *et al.* [29].

amplitude than that recorded from the vacuole. We also obtained the TRPs with smaller amplitude when the electrode tip was outside the nucleus. In this state, the amplitude was unstable and became smaller with time probably due to encapsulation of the electrode tip by the streaming cytoplasm. The DC potential difference is assumed to be an algebraic sum of the potential difference across the nuclear membrane and that across the inner membrane.

Ionic mechanism for the TRPs

Oami *et al.* [29] examined effects on the TRPs of various kinds of ions in the external solution. Replacement of the standard solution with an experimental solution containing or deprived of certain kinds of ions quickly affected the TRPs. The speed of the effects of external ions on the TRPs also support the idea that the TRPs are generated across the outer membrane. The peak value of the positive spike increased with increasing external Na^+ concentration, and peak negativity of the negative spike increased with increasing external Cl^- concentration. Therefore, it can be said that the positive spike is Na^+ -dependent, and the negative spike Cl^- -dependent. Ionic mechanisms

for the slow depolarization and for the post-spike negative level remain unsolved. As already mentioned, the peak value of the positive spike increased with lowering external Ca^{2+} concentration. This indicates that Ca^{2+} is not a current carrier but a modifier of the Na^+ -dependent positive spike.

Localized distribution of the ionic channels

Sibaoka and Eckert [32] found a conspicuous decrease in the membrane impedance near the base of the tentacle in association with the negative spike (Fig. 10). Localized outward electric current accompanied by the negative spike was observed only through the membrane near the base of the tentacle. From these results, they concluded that the negative spike is generated exclusively at the base of the tentacle. Contrary to their results, we [33] demonstrated that the localized outward current was observed anywhere on the cell surface in association with the negative spike, though the current intensity was the largest around the base of the tentacle. This indicates that the TRPs are generated anywhere on the cell surface. Sibaoka and Eckert [32] used a suction pipette thinner than ours. It is presumable that a larger negative

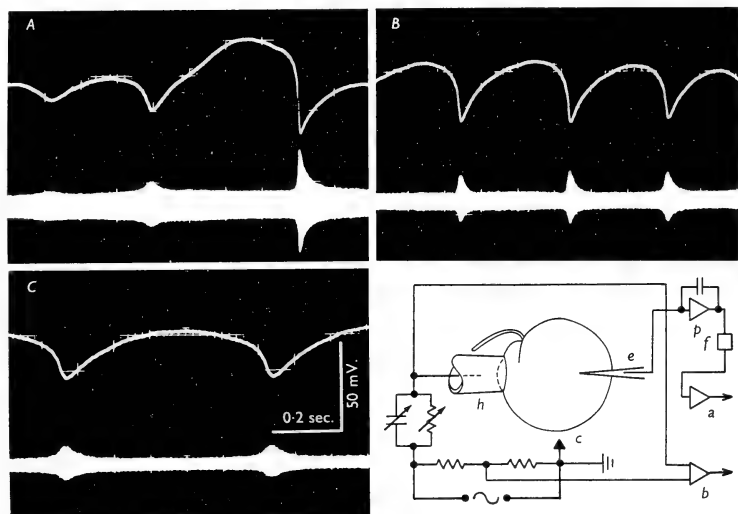


Fig. 10. Impedance changes associated with the negative spikes of the TRPs with three different patterns recorded in one and the same specimen. Upper trace: vacuolar potential. Lower trace: bridge balance. Increments in the trace width are proportional to the impedance change. Schematic of experimental set-up is shown in the bottom right: h, holding pipette having an internal diameter of about $100\ \mu\text{m}$; e, recording microelectrode; c, calomel electrode in sea-water bath; p, neutralized capacity unity-gain electrometer; f, high-cut filter. a, d.c. amplifier used for potential recordings. b, a.c. differential amplifier used for recording bridge balance. A 2000 Hz sine wave was applied to the bridge. From Sibaoka and Eckert [32].

pressure was needed to keep the membrane tight to the opening of a thinner suction pipette, therefore, the Cl^- channels in the membrane inside the pipette could have been injured by excessive stretching of the membrane. As a matter of fact, we failed to record the outward current, when we used a thinner suction pipette like theirs. In conclusion, the hyperpolarization-sensitive Cl^- channels responsible for the negative spike are present anywhere on the cell surface, but most densely clustered around the cytostome.

Oami and Naitoh [33] measured regional membrane impedance changes and localized inward membrane currents associated with the positive spike under Ca^{2+} deficient condition. They found that both impedance decrease and inward current were detected only when the suction pipette was

placed around the cytostome and the tentacle. Furthermore, the positive spike-associated localized membrane currents were always outward through the rest of the membrane. The outward current is a return current of the active inward current through the cytostome region. These results clearly indicate that the depolarization-sensitive Na^+ channels responsible for the positive spike are present restrictedly at the region around the cytostome.

Conduction of the negative spike over the cell surface

Presence of the hyperpolarization-sensitive Cl^- channels all over the cell surface implies a propagation of the negative spike over the cell surface. As a matter of fact, the localized current was

always diphasic. It was first positive then became negative when the suction electrode was around the cytostome, but was first negative then positive when the electrode was on the membrane distant from the cytostome [33]. Since the positive current is an active Cl^- current and the negative current is its passive return current, the positive-negative current sequence at the cytostome region corresponds to the generation of the negative spike and its subsequent propagation away to the aboral region. The negative-positive current sequence at the area distant from the cytostome corresponds to the approaching of the negative spike from the cytostome region and the subsequent generation of the spike in the area.

Voltage-sensitivity of the ionic channels

The outer membrane of *Noctiluca* produces the positive spike in response to an outward current when its membrane potential level has been more or less hyperpolarized, while it produces the negative spike in response to an inward current when the membrane potential level has been more or less depolarized [29]. Conventional two-microelectrode voltage clamp of *Noctiluca* [34] revealed that a step depolarization of the membrane from a holding potential of -80 mV produced a transient inward Na^+ current, which corresponds to the positive spike. The I-V relationship of the current was the so-called N-shape, which is common to other conventional excitable membranes with voltage-sensitive channels. Threshold voltage was about -50 mV and the reversal potential +25 mV. Inactivation of the current was depolarization-dependent. The steady state inactivation curve for the current was the typical S-shape. When the step depolarization was beyond 0 mV, a delayed outward current came to follow the Na^+ inward current. The ion species responsible for the outward current remain unidentified.

On the other hand, a step hyperpolarization of the outer membrane from a holding potential of -20 mV, produced a transient outward Cl^- current, which corresponds to the negative spike. The I-V relationship of the current showed a shape similar to that of the Na^+ inward current but rotated by 180 degrees. The threshold voltage was about -30 mV, and the reversal potential about -

90 mV. The current exhibited hyperpolarization-dependent steady state inactivation.

Modulation of the Na^+ channels by Ca^{2+}

As already mentioned, the positive spike becomes conspicuous when the external Ca^{2+} concentration is lowered. Under voltage clamp condition, the Na^+ inward current became larger and longer as the external Ca^{2+} concentration was lowered, while it became smaller and shorter as the Ca^{2+} concentration was raised. The increasing phase of the inward current was little affected, whereas its decreasing phase was prolonged by lowering the Ca^{2+} concentration. The threshold and reversal potential for the inward current were remained unchanged despite changes in the external Ca^{2+} concentration [30]. These data strongly suggest that external Ca^{2+} modifies the inactivation process of the voltage sensitive Na^+ channels, but not the activation process. Under high Ca^{2+} conditions, inactivation of the Na^+ channels is so fast and the Na^+ conductance increase so small that the positive spike becomes obscure. On the other hand, in low Ca^{2+} , the Na^+ channels are inactivated slowly, so the Na^+ conductance is allowed to become high enough to generate a conspicuous positive spike.

Factors affecting the contractile mechanism of the tentacle

External Ca^{2+} is required for the control of the tentacle movement by the TRPs [28, 29]. Ca^{2+} , therefore, seems to be involved in the activation of the contractile mechanism responsible for the tentacle movement. In order to investigate the intracellular chemical factors activating the contractile mechanism, Oami and Naitoh [12] examined the effects of various chemicals on the detergent-extracted, membrane-disrupted tentacle of *Noctiluca*. The extracted tentacle flexed when the pH of the reactivation medium was lowered (Fig. 11). Maximum flexion was seen at pH 4.0. The extracted tentacle sometimes flexed and coiled if the pH was lowered to below 5.5. Ca^{2+} was much less effective than H^+ in producing the flexion of the extracted tentacle. K^+ , Na^+ and Mg^{2+} were all ineffective in producing the flexion. Addition of ATP with Mg^{2+} or Ca^{2+} had no effect

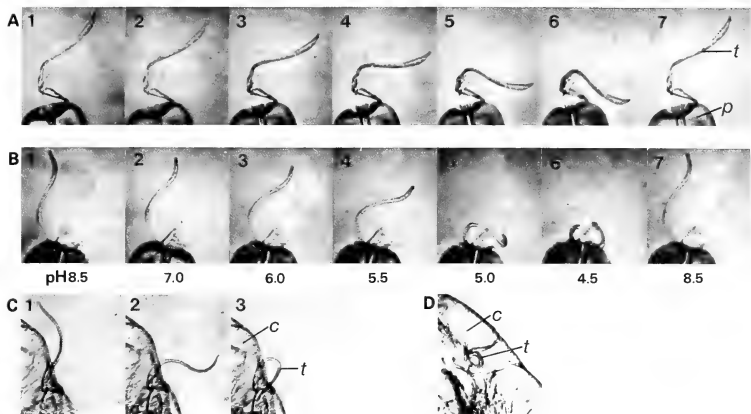


FIG. 11. A and B: Two typical examples of motile responses to H^+ ions in Triton X-100-extracted food-gathering tentacles of the marine dinoflagellate *Noctiluca*. Photographs are magnified images of an extracted tentacle videorecorded 10–20 sec after its subjection to various solutions with different pH values. An extracted tentacle (t) with its basal appendages was held at the tip of a suction pipette (p). After the pH of the reactivation medium had been lowered, the tentacle flexed in A (1–6), whereas in B it flexed (1–4) and finally coiled (5, 6). The tentacle resumed its original shape when the pH was raised again (compare 1 with 7 in both A and B). C: Photographs of a spontaneously moving tentacle of a live specimen of *Noctiluca* in artificial sea water (ASW). 1, extended; 2, half flexed; 3, completely flexed. c, cell body. D: A photograph of a coiled tentacle of a live specimen in Ca^{2+} -rich ASW. From Oami and Naitoh [12].

on the pH-dependent flexion. These results clearly indicate that the contractile mechanism in the tentacle is regulated and energized by H^+ .

The contractile mechanism of the tentacle resembles that of the contractile protein responsible for the contraction of the stalk in *Vorticella*, spasmin, in its ATP independence [35, 36]. However, spasmin is activated by Ca^{2+} as are many other contractile mechanisms. The H^+ -dependent contractile mechanism in the tentacle of *Noctiluca* is very unique among eucaryotic cells. The relationship between the fine structure and the flexion of the tentacle remains to be investigated.

The TRP-tentacle flexion coupling: A hypothesis

As already mentioned, the vacuolar pH is low enough (pH 3.5 [20]) to supply H^+ ions into cytoplasm for activation of H^+ -dependent luminescent mechanism [8]. Similarly, H^+ ions

must be supplied from the vacuole for activation of the H^+ -dependent flexion mechanism of the tentacle. Ca^{2+} requirement for the flexion of the tentacle implies involvement of Ca^{2+} in the release of H^+ from the vacuole into cytoplasm of the tentacle. Considering these facts together with electrophysiological evidence, Oami and Naitoh [12] proposed a hypothesis for the coupling mechanism between the TRPs and tentacle movements (Fig. 12). Depolarization-sensitive Ca channels are activated by a slow depolarization in the TRP (pre-spike positive wave) and causes Ca^{2+} influx into the cytoplasm of the tentacle. This increase in the cytoplasmic Ca^{2+} concentration activates a proton transport system in the inner membrane to convey H^+ ions from the vacuole into the cytoplasm. The lowered pH activates the H^+ -dependent contractile mechanism in the tentacle. Activation of the mechanism results in the

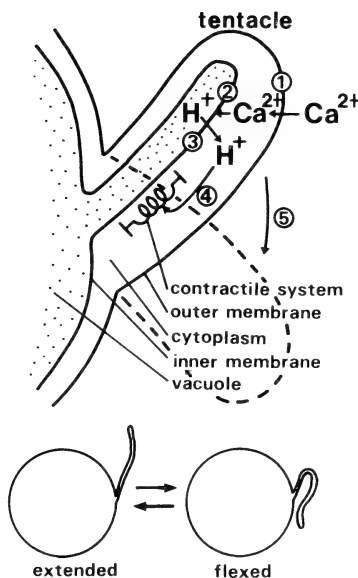


FIG. 12. Schematic representation of the proposed mechanism for bioelectrical control of movement of the food-gathering tentacle in a marine dinoflagellate *Noctiluca miliaris*. External Ca^{2+} is driven into the cytoplasm of the tentacle by a hyperpolarizing spike of the tentacle-regulating potentials [28, 29] through Ca^{2+} channels activated by a slow depolarization preceding the spike (1). The resultant increase in cytoplasmic Ca^{2+} concentration activates a H^+ transport system in the inner membrane facing the flotation vacuole (2). The transport system conveys H^+ from vacuole to the cytoplasm (3). The resultant increase in cytoplasmic H^+ concentration activates the H^+ -sensitive contractile system in the tentacle (4). The activation of the system results in flexion of the tentacle (5). The Ca^{2+} influx ceases when the hyperpolarizing spike terminates. Cytoplasmic Ca^{2+} concentration is decreased by pumping out or sequestering of Ca^{2+} . Thus the H^+ transport system is deactivated. Cytoplasmic H^+ concentration is decreased by pumping out of H^+ or by some other means (not yet identified). The contractile system is then deactivated. The tentacle extends owing to its elasticity. The lower insets show the positions of extended and flexed tentacles relative to the cell body. From Oami and Naitoh [12].

flexion of the tentacle. The tentacle, therefore, continues to flex during the slow depolarization. The rate of the Ca^{2+} influx is suddenly increased by the negative spike due to the increased driving force on Ca^{2+} ions. This causes a rapid increase in the cytoplasmic Ca^{2+} concentration, and in the H^+ concentration thereby. Thus an enhancement of the flexion takes place in association with the negative spike. Sustained hyperpolarization seen after the negative spike (post-spike negative level) causes deactivation of the Ca channels. The Ca^{2+} influx, therefore, ceases. Cytoplasmic Ca^{2+} ions are pumped out or sequestered to lower the cytoplasmic Ca^{2+} concentration back to its normal level. The H^+ transport system is thus deactivated. The cytoplasmic H^+ concentration is then lowered by the pumping out of H^+ ions or by some other means. The contractile system is then deactivated. The tentacle's extension then occurs due to its own elasticity.

BIOELECTRIC CONTROL OF FOOD INTAKE BEHAVIOR

Feeding behavior of *Noctiluca* and its correlation with the TRPs

Motile activity exhibited by *Noctiluca* during its feeding on green algae can be divided into two successive phases, 1) the food gathering phase, in which flexion and extension of the tentacle is repeated for trapping the algae, and 2) the food intake phase, which consists of an initial strong flexion of the tentacle so that its tip plus trapped algae touches the cytostome. Phagocytotic ingestion of the algae through the cytostome accompanied by vigorous cytoplasmic streaming towards the cytostome region then takes place.

During food-gathering, *Noctiluca* exhibits TRPs as described in previous sections. The potential pattern of the TRPs suddenly changes when *Noctiluca* initiates the food intake phase [10].

Experimental induction of the food intake behavior

Nawata and Sibaoka [9] looked for various chemical factors in the external solution which could induce food intake behavior in *Noctiluca*. Reduction of SO_4^{2-} concentration to less than 2

mM from its original 30 mM was most effective in inducing motile activity comparable with the food intake behavior. That is, *Noctiluca* showed cytoplasmic aggregation around the cytostome and subsequent formation of empty food vacuoles. A crude extract of the food algae was only 15% effective compared to the reduction of SO_4^{2-} . Reduced glutathione was as effective as the food extract. Some aminoacids, such as valine, methionine, triptophan, leucine, histidine and proline, induced the behavior in 40–0% of the cells examined. External Ca^{2+} , Mg^{2+} , and Cl^- ions were necessary for the induction of the food intake behavior.

The food intake behavior was also induced by pressing the tip of a glass capillary against the cell surface around the cytostome. The capillary was then engulfed by the cell (Fig. 13). Interestingly pressing the pipette against the cell surface other than the cytostome region was not effective in inducing the behavior.

Injection of an inward current into the vacuole also induced the food intake activity similar to lowering SO_4^{2-} concentration.

The food intake behavior and its electrophysiological correlates

Deprivation of SO_4^{2-} from the external solution caused a marked increase in the repetitive frequency of the negative spike and prolongation of the spike, and thereby a final sustained hyperpolarization [10]. The food intake behavior took place when the hyperpolarization exceeded -80 mV and lasted for more than 1 min. The reduced SO_4^{2-} -induced hyperpolarization shifted toward depolarizing direction if the external Cl^- concentration was lowered. This suggests Cl^- -dependence of the sustained hyperpolarization like the negative spike of TRPs.

A membrane hyperpolarization produced by an inward current injection induced the food intake behavior in normal ASW as well as in an ASW with lowered Cl^- concentration. Therefore, a membrane hyperpolarization is a primary cause for induction of the food intake behavior. However, a membrane hyperpolarization did not induce the food intake behavior when the external Ca^{2+} concentration was as low as 10^{-8} M. Na^+ , K^+ and

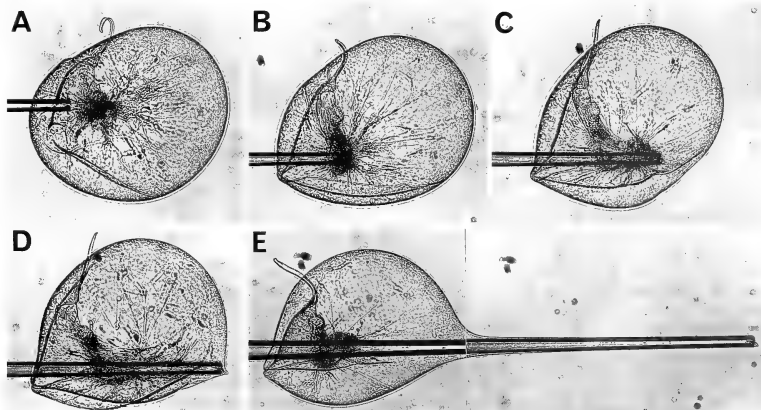


FIG. 13. A series of photomicrographs of a hungry *Noctiluca* swallowing a glass capillary. B, C, D, and E were taken at 5, 14, 17, and 24 min after taking A, respectively. A, tip of the capillary is pressed against the cytostome; B, swallowing of the capillary is initiated; C-D, swallowing is progressing; E, swallowing is at its maximum as the extended cell membrane pushes the capillary back toward the cytostome. Magnification in E is 85% of the others. From Nawata and Sibaoka [9].

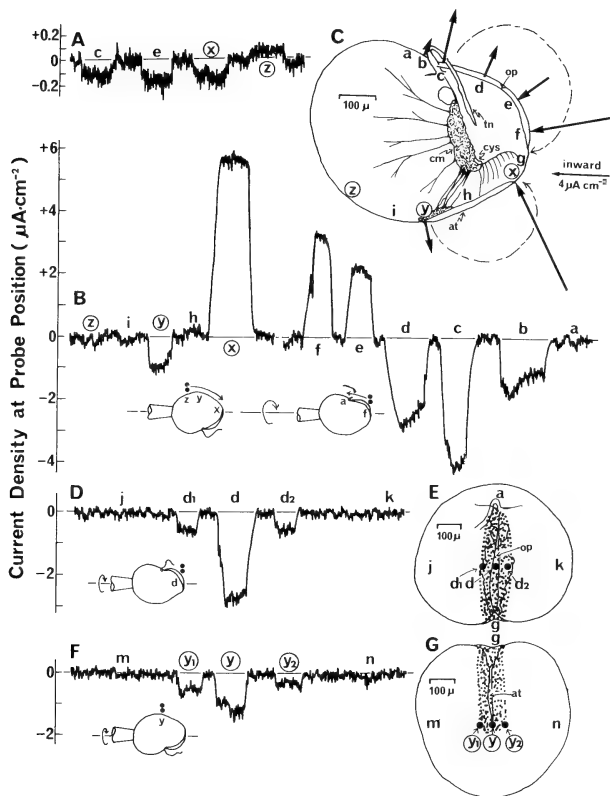


FIG. 14. Localized membrane currents associated with the feeding behavior in *Noctiluca* measured with a vibration current probe. Locations of the probe was indicated by small letters in the schematic drawings of the cell (C, E and G). Trace A: Current recorded before the food intake behavior is experimentally induced. Traces B, D, and F: Currents recorded 5 to 15 min after the food intake behavior-inducing solution was administered to the cell. B, current recorded along the sulcus; C, distribution pattern of currents along the sulcus depicted on the basis of B. Arrows toward the cell indicate inward currents and those away from the cell outward currents. The length of each arrow is proportional to the current density estimated at each position; D, current recorded across the oral pouch; E, current flowing region (dotted area) estimated from D and some other similar recordings; F, current recorded across the distal end of the apical trough. G, current flowing region (dotted area) estimated from F and others. Nawata and Sibaoka [11].

H⁺ concentration changes had no effect on the food intake behavior.

By employing a vibrating current probe, Nawata and Sibaoka [11] examined localized transmembrane ionic currents on different areas of the cell surface in relation to the feeding behavior. The current entered into the cell through the cytostome region, and it left the cell through both ends of the sulcus (Fig. 14). Current intensity was 7.5 $\mu\text{A}/\text{cm}^2$ at the proximal end of the apical trough during the sustained hyperpolarization. The current intensity decreased if Ca²⁺ and Na⁺ concentrations in the external solution were decreased. Therefore, the current is assumed to be carried by both Na⁺ and Ca²⁺.

Using data collected from the introduction of ⁴⁵Ca to *Noctiluca* during feeding behavior, Nawata and Sibaoka [11] calculated that Ca²⁺ concentration in the cytoplasmic compartment near the cytostome had risen to several μM during hyperpolarization over 1 min. Thus presumably, external Ca²⁺ is driven into the cytoplasm during the hyperpolarization, and regulates the cytoplasmic streaming essential for food ingestion. A role of Ca²⁺ in regulation of protoplasmic streaming and amoeboid movement has long been suggested by many authors [37–40].

DISCUSSION AND CONCLUSION

Control of different effectors, by separate mechanism

In *Noctiluca* the bioluminescent flash is controlled by the FTP generated across the inner membrane, whereas the tentacle movement is controlled by the TRPs generated across the outer membrane. The possession of two control methods for two different effector activities could minimize possible interference between the activities within the single cell. The control of different effector activities by separate mechanisms is also seen in some protozoans. For example, the carnivorous ciliate *Didinium* exhibits two kinds of effector activity, i.e. a ciliary motile response to a mechanical stimulus and extrusion of the extruding organelles in response to its food (mostly *Paramecium*) [41]. The ciliary response is controlled by

Ca²⁺-mediated electrogenesis across the surface membrane like *Paramecium* [1]. Whereas, the extrusion is controlled by a chemosensory mechanism in the tip of the proboscis independently of the electrogenesis across the surface membrane. *Vorticella* shows a ciliary motile response and a contraction of the cell in response to a mechanical stimulus. The ciliary response is controlled by the membrane electrogenesis like other ciliates, whereas the cellular contraction is independent of the membrane electrogenesis [42, 43].

Control of one effector by two separate mechanisms

Both the flash and the contractile mechanisms of *Noctiluca* are activated by H⁺ ions, which are supplied from the intracellular vacuole. It is interesting to note that the flash is always accompanied by an instantaneous coiling of the tentacle. The coiling is regarded as a strong flexion. The tightly coiled tentacle is useless for food-gathering. However, the coiled tentacle is certainly secure from damage caused by mechanical agitation, which triggers the FTP in nature. The tentacle plays a major role in the feeding behavior of *Noctiluca*. The H⁺-dependent contractile mechanism of the tentacle is precisely controlled by the TRPs through the mediation of Ca²⁺ when it exhibits feeding activity. However, when *Noctiluca* faces an emergency (eg. jostling by a big surf), H⁺ ions carried by the FTP directly activate the H⁺-dependent contractile mechanism to produce coiling of the tentacle.

Biological significances in the distribution of the ionic channels within a single membrane

In *Noctiluca* H⁺ channels responsible for the FTP are distributed all over the inner membrane. This distribution contributes to the propagation of the flash along the inner membrane from the stimulus site. The Cl[−] channels responsible for the negative spike are distributed all over the outer membrane, but the channel density is higher in the area around the tentacle than the rest of the membrane area. The denser distribution of the Cl[−] channels brings about a higher rate of Ca²⁺ influx into the tentacle for its rapid flexion. Overall distribution of the Cl[−] channels in the outer membrane somehow relates to the generation of

the sustained hyperpolarization, which initiates the food intake behavior. However, the biological significance of the localized distribution of the Na^+ channels, responsible for the positive spike around the tentacle region, remains to be investigated. The distribution of the ionic channels in a single membrane plays an important role in the precise control of the effector activity. This has been well documented in *Paramecium* and some other ciliate protozoans [1].

ACKNOWLEDGMENTS

We thank Dr. W. F. Cooper for reading the manuscript. We also thank the following organizations for their financial support: Mitsubishi Foundation, Nippon Petrochemical Co. Ltd., Honda Motors Research Institute, Ministry of Science, Culture and Education of Japan.

REFERENCES

- Naitoh, Y. (1982) In "Conduction and Behavior in 'Simple' Invertebrates". Ed. by G. A. B. Shelton, Clarendon Press, Oxford, pp. 1-48.
- Tauc, L. (1962) *J. Gen. Physiol.*, **45**: 1077-1097.
- Hisada, M. (1957) *J. Cell. Comp. Physiol.*, **50**: 57-71.
- Chang, J. J. (1960) *J. Cell. Comp. Physiol.*, **56**: 33-42.
- Eckert, R. (1965) *Science*, **147**: 1140-1142.
- Eckert, R. (1965) *Science*, **147**: 1142-1145.
- Eckert, R. (1966) *Science*, **151**: 349-352.
- Nawata, T. and Sibaoka, T. (1979) *J. Comp. Physiol.*, **134**: 137-149.
- Nawata, T. and Sibaoka, T. (1983) *Protoplasma*, **115**: 34-42.
- Nawata, T. and Sibaoka, T. (1986) *Zool. Sci.*, **3**: 49-58.
- Nawata, T. and Sibaoka, T. (1987) *Protoplasma*, **137**: 125-133.
- Oami, K. and Naitoh, Y. (1989) *J. Exp. Biol.*, (in press).
- Harvey, E. N. (1952) "Bioluminescence". Academic Press, New York.
- Eckert, R. (1966) In "Bioluminescence in Progress". Ed. by F. H. Johnson and Y. Haneda. Princeton Univ. Press, Princeton, pp. 269-300.
- Sibaoka, T. (1968) *Seitai no Kagaku*, **20**: 145-152 (In Japanese).
- Widder, E. A. and Case, J. F. (1981) In "Bioluminescence, Current Perspectives". Ed. by K. H. Nealson, Burgess Publ. Co., Minneapolis, pp. 125-132.
- Sweeney, B. M. (1987) In "The Biology of Dinoflagellates". Ed. by F. J. R. Taylor, Blackwell Scientific Publ., Oxford, pp. 269-281.
- Taylor, F. J. R. (1987) "The Biology of Dinoflagellates". Blackwell Scientific Publ., Oxford.
- Eckert, R. and Sibaoka, T. (1968) *J. Gen. Physiol.*, **52**: 258-282.
- Nawata, T. and Sibaoka, T. (1976) *Plant Cell Physiol.*, **17**: 265-272.
- Gross, F. (1934) *Arch. Protistenk.*, **83**: 178-196.
- Iida, T. T. and Iwata, K. S. (1943) *J. Fac. Sci. Univ. Tokyo*, IV, **6**: 175-178.
- Kesseler, H. (1966) *Veroeffentl. Inst. Meeresforsch. Bremerhaven*, **12**: 357-368.
- Fogel, M., Schmitter, R. E. and Hastings, J. W. (1972) *J. Cell. Sci.*, **11**: 305-317.
- Hastings, J. W., Vergin, M. and Desa, R. (1966) In "Bioluminescence in Progress". Ed. by F. A. Johnson and Y. Haneda, Princeton Univ. Press, Princeton, pp. 301-329.
- Hastings, J. W. (1968) *Ann. Rev. Biochem.*, **37**: 597-630.
- Fogel, M. and Hastings, J. W. (1972) *Proc. Natl. Acad. Sci. USA*, **69**: 690-693.
- Eckert, R. and Sibaoka, T. (1967) *J. Exp. Biol.*, **47**: 433-446.
- Oami, K., Sibaoka, T. and Naitoh, Y. (1988) *J. Comp. Physiol. A*, **162**: 179-185.
- Oami, K., Sibaoka, T. and Naitoh, Y. (1985) *Zool. Sci.*, **2**: 877.
- Oami, K. and Naitoh, Y. (1987) *Zool. Sci.*, **4**: 973.
- Sibaoka, T. and Eckert, R. (1967) *J. Exp. Biol.*, **47**: 447-459.
- Oami, K. and Naitoh, Y. (1988) *Zool. Sci.*, **5**: 1216.
- Oami, K., Sibaoka, T. and Naitoh, Y. (1984) *Zool. Sci.*, **1**: 879.
- Amos, W. B. (1971) *Nature, London*, **229**: 127-128.
- Amos, W. B., Routledge, L. M. and Yew, F. F. (1975) *J. Cell. Sci.*, **19**: 203-213.
- Jahn, T. L. and Bovee, E. C. (1969) *Physiol. Rev.*, **49**: 793-862.
- Kato, T. and Tonomura, J. (1977) *J. Biochem.*, **81**: 207-213.
- Allen, R. D. and Allen, N. S. (1978) *Ann. Rev. Biophys. Bioeng.*, **7**: 469-495.
- Kamiya, N. (1981) *Ann. Rev. Plant Physiol.*, **32**: 205-236.
- Hara, R., Asai, H. and Naitoh, Y. (1985) *J. Exp. Biol.*, **119**: 211-224.
- Shiono, H. and Naitoh, Y. (1977) *Zool. Mag. (Tokyo)*, **86**: 408.
- Shiono, H. and Naitoh, Y. (1978) *Zool. Mag. (Tokyo)*, **87**: 429.

The Inhibitory Control of Prothoracic Gland Activity by the Neurosecretory Neurones in a Moth, *Mamestra brassicae*

AKIRA OKAJIMA and KANJI KUMAGAI

Department of Biology, Faculty of Liberal Arts, Yamaguchi University,
Yamaguchi 753, Japan

ABSTRACT—The change in both the ecdysteroid titers in the haemolymph and the amount of ecdysteroids released from the prothoracic gland (PTG) *in vitro* during larval development were determined in *Mamestra brassicae*. These showed a clear inverse relationship to the efferent electrical activity in the PTG nerves, even in the detailed changes in each day during development. An exception was the final day of the last instar. This result suggests that, as well as the activating effect of prothoracicotropic hormone (PTTH), the PTG innervating neurosecretory neurones are possibly involved in the delicate inhibitory adjustment of the amount of ecdysteroids in the haemolymph. Here, the simultaneous determinations of the amount of ecdysteroids released from PTG and of the electrical activity of nerves by using the isolated preparation *in vitro*, provides direct evidence of the inhibitory effect of PTG innervating nerve on the PTG.

INTRODUCTION

Various types of PTG innervating neurones were described in the previous paper [1]; both histological and electrophysiological studies showed that they are neurosecretory. The electrical activities of one of PTG innervating nerves shows the remarkable changes during the course of development, its firing frequency varying inversely with the ecdysteroid titers in the haemolymph as examined by Agui and Hiruma [2]. These results and those from surgical experiments [3] have led to the suggestion that the function of this PTG innervating nerve is to inhibit the PTG.

To analyse accurately this inverse relationship between the electrical activity of the PTG innervating nerve and ecdysteroid titer in the haemolymph, it is important to reexamine the haemolymph ecdysteroid titers by using the same animals from our strain and reared under the same condition as was used for the measurement of the electrical activity. Also, it is better to use isolated preparations for determination of both the re-

leased ecdysteroids from PTG and the electrical activity of PTG innervating nerves. Therefore, the time change of the ability to synthesize ecdysteroid in the isolated PTG *in vitro* was determined. In this paper, the simultaneous determinations of the amount of released ecdysteroid from PTG and of the electrical activity of the PTG innervating neurones were made to obtain direct evidence for the nervous inhibition of the PTG activity.

MATERIALS AND METHODS

Larvae of *Mamestra brassicae* were reared on artificial diet [4] at $23^{\circ} \pm 1^{\circ}\text{C}$ under a long day photoperiod (16L, 8D). The time course of development of the last instar larva was the same as described in the previous paper [1]. The first day after ecdysis was designated day 0. Female larvae were used throughout this experiment.

Ecdysteroid titers in the haemolymph were determined by radioimmunoassay (RIA). Haemolymph collection was made four times in each day of larval development at 0:00, 6:00, 12:00 and 18:00, the middle of dark period being taken arbitrarily as 24:00 (0:00). Ten μl haemolymph was taken from each larvae, by making a small cut

on a proleg, and introduced into 400 μ l methanol. After mixing vigorously, this sample was centrifuged at 3000 g for 20 min, methanol in the supernatant was evaporated at 40°C, and the sample was stored frozen at -20°C. Before starting the RIA procedures, the dried sample was dissolved in 100 μ l borate buffer (pH 8.4). If necessary this solution was diluted to one tenth. Forty μ l of this solution were used as the biological sample in RIA.

The amount of ecdysteroids released from PTG *in vitro* was also determined by RIA. PTGs were extirpated from the larvae of various stages of last instar. The isolated PTGs were kept immersed in 100 μ l Grace's medium for about 1 hr. The necessity of the immersion of PTG in the culture medium will be described later. The PTGs were then transferred and incubated usually for 2 hr in 100 μ l new Grace's medium dropped on each compartment of an acrylic culture well (Falcon 3047, Becton Dickson & Co.). The culture wells were placed in a container which was filled with a gas mixture of O₂ 95% and CO₂ 5%, saturated with water vapor and kept at 23° ± 1°C. After the incubation, 40 μ l of the culture medium was collected and used as the biological sample in RIA. The culture method for the isolate ganglion-PTG preparation used for studying the ecdysteroid synthesis under the influence of PTG innervating nerves will be described later in the corresponding part of results.

RIA for ecdysteroids was performed according to Borst and O'Connor [5] using [23, 24-³H] ecdysone (ca. 70 Ci/mmol, New England Nuclear). The antiserum of ecdysterone (20-hydroxyecdysone, Rhoto Pharmaceutical, Osaka) was prepared in collaboration with Prof. E. Ohnishi, Nagoya University, Prof. N. Ikekawa, Tokyo Institute of Technology and Dr. K. Ozawa, Megro Institute (Osaka). Practical steps of RIA procedures were based on and modified from Bollenbacher *et al.* [6] which presented the systematic descriptions for the study of the synthetic ability of ecdysteroids by PTG *in vitro*. Antiserum was diluted to 1/3200 with 10% rabbit serum dissolved in the borate buffer so that about 50% of the radioactivity of labelled ecdysone was bound in the absence of unlabelled ecdysone. The labelled

ecdysone (ca. 8 nCi) in 80 μ l buffer and 50 μ l antiserum solution was added to each of a pair of 40 biological samples described above. Duplicated assays were performed for each sample. The mixture was stored at 4°C for 12-16 hr. After precipitation using ammonium sulfate, the precipitate was dissolved in 50 μ l distilled water and 400 μ l scintillation solution (ACS II, Amersham) was added. Radioactivity was determined using Packard scintillation counter (model 240 CL/CLD).

The standard curve for ecdysone (Sigma) was log-linear between 10 and 200 pg and that for 20-hydroxyecdysone (Rhoto Pharmaceutical) between 30 and 1000 pg. Therefore, in this experiment, the binding curve for ecdysone was exclusively used for both determinations of the haemolymph ecdysteroid and the secreted ecdysteroid from the PTG *in vitro*. All data were expressed as ecdysone equivalent, because the determinations in this experiment by RIA were based on the cross reactivity of the prepared antiserum with ecdysone, 20-hydroxyecdysone and other ecdysteroids.

RESULTS

Haemolymph ecdysteroid titers

Figure 1 shows the change in haemolymph ecdysteroid titer during development of the last instar larva. To show clearly the small change in ecdysteroid titer, the values from day 1 to day 7 were plotted separately with five fold magnification in the vertical scale. There are small peaks at each light period of day 3-6 which show gradual increase in magnitude with the progress of the development. It is difficult to assess directly which peak of haemolymph ecdysteroids is the stimulant for the appearance of transparent epidermis or for wondering behaviour to the ground. The highest peak prior to the pupal ecdysis was observable at 18:00 of day 8. Quantitative comparison between ecdysteroid titers in the haemolymph and the electrical activities of PTG innervating nerves during development will be given at the later section of results.

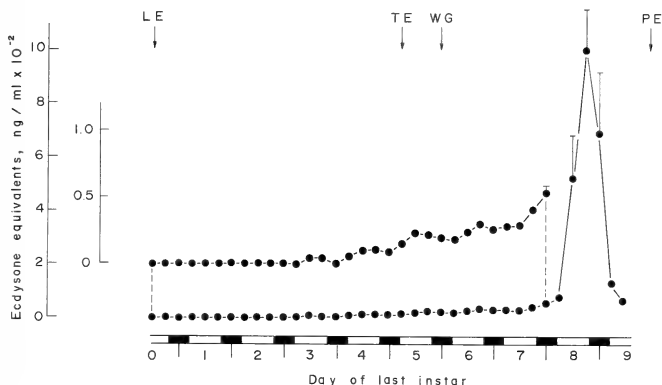


FIG. 1. Ecdysteroid titers in the haemolymph of *Mamestra brassicae* during the development of last instar larva. Each point is the mean (\pm SEM) of ten measurements. The following developmental stages are indicated by arrows: LE, larval ecdysis; TE, appearance of transparent ventral epidermis; WG, wandering to the ground; PE, pupal ecdysis. Light and dark periods in each day are shown at the lower part of the figure. See text for details of the representations of ecdysteroid titer from day 1 to day 7.

Released ecdysteroids from PTG *in vitro*

Time course of ecdysteroid synthesis by PTG *in vitro* was determined to find a convenient incubation condition for the study of the change in ability of the ecdysteroid synthesis during development.

PTGs were extirpated at 9:00–11:00 from day 8 last instar larva and then incubated in Grace's medium. The ecdysteroid titer determinations in Figure 1 suggest that the isolated PTG from the larvae of this stage would be sufficiently potent to produce the ecdysteroids under the influence of

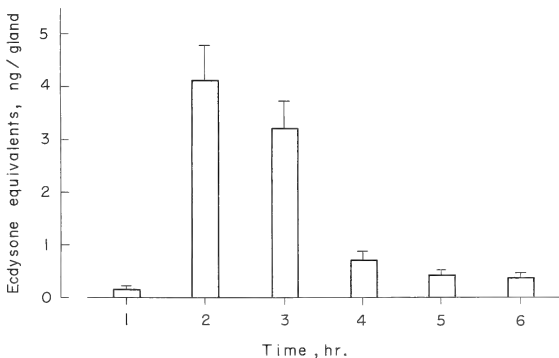


FIG. 2. Time course of the ability to synthesize ecdysteroid after incubation of PTG in the Grace's medium. Each point is the mean (\pm SEM) of ten measurements.

the prothoracicotrophic hormone (PTTH) in the haemolymph.

The amount of ecdysteroid released from PTG into the external medium every hour after the start of incubation was determined by RIA as shown in Figure 2. The ecdysteroid synthesis shown in this figure is limited to low values in the first 1 hr and elevated significantly in the succeeding 2 hr. The rate of ecdysteroid synthesis shows the marked decrease at 4 to 6 hr after the incubation, probably due to washing out the PTTH by the repeated changes of the external medium. The exact reasons for the limited synthesis in the first hour after incubation were difficult to find here physiologically.

In consideration of the time course of ecdysteroid synthesis shown in Figure 2, the following procedure was chosen for the determination of the change in ability of ecdysteroid synthesis during development. After incubation in the culture medium for about 1 hr, the PTGs were transferred and incubated in new Grace's medium for 2 hr, the external medium being used as a samples for RIA determination. In this series, PTG isolations were made at 9:00–11:00 from the larva of each development stage, and consequently incubated for 2

hr from 10:00–12:00 to 12:00–14:00.

The results in Figure 3 shows that a measurable amount of ecdysteroid synthesis is observable at day 3 and the values are increased by day 5 where the transparent epidermis was visible. The amounts of ecdysteroid synthesis remained fairly stable for 3 days from day 5 to day 7 increased significantly at day 8.

Comparison of ecdysteroid synthesis and electrical activity of nerves to PTG

It is important to compare three results; the ecdysteroid titers in the haemolymph (Fig. 1); ecdysteroid synthesis by PTG *in vitro* (Fig. 3); and electrical activities of the PTG innervating nerve (Fig. 8 in the previous paper [1]) during the larval development. These results are superimposed in Figure 4, where only data in Figure 1 obtained at 12:00 are plotted for better comparison.

There are clear parallels between the haemolymph ecdysteroids and the ecdysteroids synthesized *in vitro*, except that the rate of increase of the haemolymph ecdysteroids from day 7 to day 8 is about thirty times but only about two times in the latter case. This will be discussed below. The critical comparison of the absolute

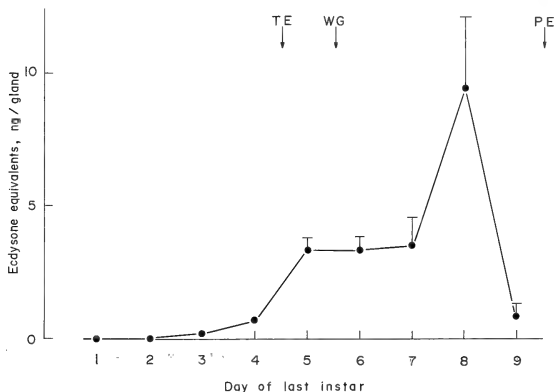


Fig. 3. Ecdysteroid synthesis by PTG *in vitro* during the development of last instar larva. Each point is the mean (\pm SEM) of ten measurements. Refer to Fig. 1 for explanation of the developmental stages shown at the upper part of the figure.

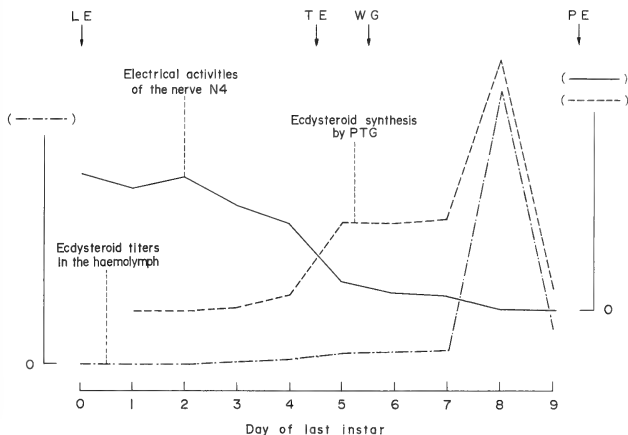


FIG. 4. Superimposed representation of ecdysteroid titers in the haemolymph (Fig. 1), ecdysteroid released from PTG *in vitro* (Fig. 3) and electrical activities of PTG innervating nerve N4 [1]. Refer to Fig. 1 for explanation of the developmental stages shown at the upper part of the figure.

values determined in both cases is difficult because the amount of haemolymph ecdysteroids cannot be compared directly with the values obtained using PTG preparation *in vitro*. In this connection, Warren *et al.* [7] published critical studies on the PTG activity of *Manduca sexta* with an important discussion of the results obtained from the RIA of released ecdysteroids in the culture medium from the isolated PTG.

Careful comparison in Figure 4 of the ability to synthesize ecdysteroid *in vitro* and the electrical activities of PTG innervating nerves in the isolated preparation indicate a clear inverse relationship even in the precise changes in each day during the development, day 9 being an exception. Detailed descriptions of the change of electrical activities each day have been given in the previous paper [1].

Inhibitory action of nerves to PTG on the ecdysteroid synthesis by PTG

The inverse relationship between electrical activity in nerve N4 to PTG and ecdysteroid synthesis by the PTG, as was demonstrated in the previous section of this paper as well as in the

previous paper [1], suggest that the activity of the nerve N4 is inhibitory to the ecdysteroid synthesis or release at PTG. This suggestion can be tested directly by simultaneous determination of released ecdysteroid from PTG and of electrical activities of nerves in the same preparation *in vitro*.

The preparations were isolated as the ganglionic chain from brain to mesothoracic ganglion connected with PTG by the nerve N4. In the first, the nerve N4 in the isolated preparation was placed on the oil gap as shown in Figure 1A of the previous paper [1] and the ganglion and the PTG were immersed separately in the two Grace's medium pools of the gap chamber. These oil-gap chambers were placed in a gas mixture as described above.

However, unexpected troubles occurred for two reasons. At first, after several min immersion of PTG in Grace's medium, there was enhanced afferent activity in the nerve N4 followed by the disappearance of the efferent activity generated at the prothoracic ganglion and conducted to PTG. Analysis of this phenomena will be made in the following paper. This problem was solved by replacing the physiological saline described in the

previous paper [1] with a K-rich saline with 70 mM KCl. With this medium, the efferent activity continued fairly well during at least half the period of PTG incubation in the Grace's medium.

Secondly, the rate of ecdysteroid synthesis by PTG in the oil-gap chamber was drastically reduced. This was due to chemical and/or physical disturbance by the paraffin oil on the synthetic activity of PTG and also to the difficulty of supplying oxygen to PTG in the incubation pool. This problem was reduced by using white vaseline instead of paraffin oil. Although the rate of ecdysteroid synthesis was reduced to about 1/5 in comparison with the case of the usual organ culture described above, the values obtained in the same experimental condition were fairly uniform.

The preparations were obtained from day 5 last instar larva. After the isolated preparations were arranged on the gap chamber in the improved manner and kept for 1 hr, the external medium was replaced by the new Grace's medium and the samples for RIA were collected after 2 hr incubation. Nervous activity was monitored during in-

cubation period. For the control determinations, contralateral PTGs with the connection of the nerve N4, severed just in front of prothoracic ganglion, were isolated from the same specimen used for the test above, and placed in the similar manner on the individual gap chambers. The efferent electrical activity was not routinely recorded from the nerve of this preparation.

The results are shown in Figure 5 where the rate of inhibition is expressed as a ratio divided by the value obtained from the control experiment. For comparison, ratios between right and left of a single pair of PTGs isolated from the connection with ganglia are also plotted. Thirty animals were used for each comparison; to help the immediate comparison in the figure the degree of inhibition was expressed by the number of animals showing the values which would fit the corresponding ranges of inhibition ratio. This figure shows that the action of the nerve N4 is inhibitory to the ecdysteroid synthesis at PTG. Although the small number of the preparations showed no inhibitory effect, this probably occurred by the injurious

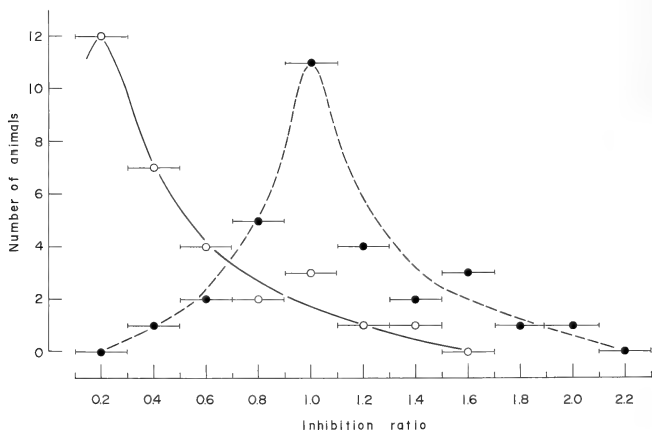


Fig. 5. Inhibitory effects of PTG innervating nerves on the rate of ecdysteroid synthesis by PTH. The rate of inhibition obtained by comparing the abilities of ecdysteroid synthesis in preparations both with and without PTH innervating nerves. The results obtained by the above determinations are plotted as white circles and those obtained by comparing the synthetic activities in both right and left PTGs of a single specimen as black circles. See the text for the explanation of the inhibition ratio.

effects on nerves or nerve junctions with PTG in the case of setting the isolated preparation on the gap chamber.

DISCUSSION

Based on the results suggested from the electrophysiological determinations in the first paper [1] of this series, the present work using RIA techniques was intended to establish the real function of the nerves to PTG with respect to the PTG activity. Direct determinations of the amounts of synthesized ecdysteroid under the influence of nerve N4 to the PTG clearly showed the inhibitory function of the PTG nerves on the PTG. This activity is assumed to be neurosecretory as described in the previous paper [1]. However, it is not yet clear whether the neurosecretory substance released into the PTG inhibits the synthetic or releasing process at PTG.

The high afferent electrical activity observed in nerve N4 shortly after the immersion of the isolated nervous system in Grace's medium and the following reduction in efferent activity is similar to changes already noticed during measurements of efferent activity during development. Here it was found that the firing frequency was greatly influenced by the chemical composition of the external medium [1]. Although the details of these phenomena will be described in the following paper, the results described above indicate that the main feedback machinery for monitoring the chemical condition of haemolymph must be contained in the ordinary isolated preparation of the nervous system.

The electrical activity of nerve N4 was found to show the remarkable changes with the progress of the larval development exactly related to the change in ecdysteroid synthetic or releasing activity at PTG. This result suggests that, as well as the activation effect of PTTH, the neurosecretory neurones, which directly innervate PTG, are involved in the precise adjustment of the amount of haemolymph ecdysteroids. These may regulate the appearance of the various important events of the development, like the wandering behaviour as has been analyzed in the lepidopterous larvae by Gilbert *et al.* [8], Dominick and Truman [9],

Fujishita *et al.* [10]. The exception observed at the final day of larval development to pupa probably means that the drastic decrement of the haemolymph ecdysteroids is solely governed by the chemical inactivation of ecdysteroids in the haemolymph. Similarly, the elevation to the extremely high level of haemolymph ecdysteroid titers just before pupal ecdysis (Fig. 1) may not be the consequence of regulation by the PTG innervating nerves.

ACKNOWLEDGMENTS

We wish to thank Dr. M. Fujishita, Nagoya University, for her technical support on radioimmunoassay. We also wish to thank Dr. J. Kien, University of Regensburg, for critical reading of the manuscript.

REFERENCES

- 1 Okajima, A. and Watanabe, M. (1989) Electrophysiological identification of neuronal pathways to the prothoracic gland and the change in electrical activities of the prothoracic gland innervating neurones during larval development of a moth, *Mamestra brassicae*. *Zool. Sci.*, **6**: 459-468.
- 2 Agui, N. and Hiruma, K. (1982) Ecdysteroid titer and its critical period during larval and pupal ecdysis in the cabbage armyworm, *Mamestra brassicae* L. (Lepidoptera: Noctuidae). *Appl. Ent. Zool.*, **17**: 144-146.
- 3 Mala, J. and Sehnal, F. (1978) Role of the nerve cord in the control of prothoracic glands in *Galleria mellonella* L. *Experientia*, **39**: 1233-1235.
- 4 Agui, N., Ogura, N. and Okawara, M. (1975) Rearing of cabbage armyworm, *Mamestra brassicae* L. and some Lepidopterous larvae on artificial diet. *Appl. Ent. Zool.*, **19**: 91-96.
- 5 Borst, D. W. and O'connor, J. D. (1974) Trace analysis of ecdysones by gas-liquid chromatography, radioimmunoassay and bioassay. *Steroids*, **24**: 637-656.
- 6 Bollenbacher, W. E., Agui, N., Granger, N. A. and Gilbert, L. I. (1979) *In vitro* activation of insect prothoracic glands by the prothoracicotrophic hormone. *Proc. Natl. Acad. Sci. USA*, **76**: 5148-5152.
- 7 Warren, J. T., Sakurai, S., Bountree, D. B., Gilbert, L. I., Lee, S. and Nakanishi, K. (1988) Regulation of the ecdysteroid titer of *Manduca sexta*: Reappraisal of the role of the prothoracic glands. *Proc. Natl. Acad. Sci. USA*, **85**: 958-962.
- 8 Gilbert, L. I., Bollenbacher, W. E., Agui, N., Granger, N. A., Sedlak, B. J., Gibbs, D. and Buys, C. M. (1984) The prothoracicotropes: Source of the

- prothoracicotropic hormone. Amer. Zool., **21**: 641-653.
- 9 Dominick, O. S. and Truman, J. W. (1984) The physiology of wandering behaviour in *Manduca sexta*. I. Temporal organization and the influence of the internal and external environments. J. Exp. Biol., **110**: 35-51.
- 10 Fujishita, M., Ohnishi, E. and Ishizaki, H. (1982) The role of ecdysteroids in the determination of gut-purge timing in the saturniid, *Samiaynthia ricini*. J. Insect Physiol., **28**: 961-967.

The Involvement of Interoceptive Chemosensory Activity in the Nervous Regulation of the Prothoracic Gland in a Moth, *Mamestra brassicae*

AKIRA OKAJIMA, KANJI KUMAGAI and NASAO WATANABE

Department of Biology, Faculty of Liberal Arts, Yamaguchi University,
Yamaguchi 753, Japan

ABSTRACT—Histidine-rich and trehalose-rich saline was applied to the isolated nervous system connected with the prothoracic gland (PTG) of the moth *Mamestra brassicae*. These salines produced a marked elevation of the afferent electrical activity in the nerve 4 to PTG and consequently a strong depression of the efferent activity. It is concluded that the afferent neurones in the nerve N4 are chemosensory and function as a sensor to monitor the histidine or trehalose concentration in the external medium. Further, the input from the afferent neurones must disinhibit the inhibitory function of the efferent neurones to PTG. The comparison these results with the determination of the change in sugar contents in the haemolymph during the larval development, suggests that it is the elevation of the trehalose concentration in the haemolymph during the progress of the development which, via the involvement of the afferents in N4, finally induces the accelerated ecdysteroid synthesis or release at PTG.

INTRODUCTION

In the preceding two papers [1, 2], it has been shown that the nerves to the PTG conduct both efferent and afferent electrical activity. From the measurements of efferent activity of nerves to PTG and the released ecdysteroids from PTG in the same isolated preparation, it was demonstrated that the efferent electrical activity of the nerve N4 inhibited the ecdysteroid synthesis or release at PTG.

The afferent electrical activity was shown to be generated at certain points of the nervous tract connected with PTG as well as at PTG itself [1]. An important suggestion as to its function was derived from the fact that the afferent electrical activity of the nerves was increased in response to some constituents in the Grace's medium [2] and net this activity appears to have an inhibitory influence on the generation of efferent activity.

The experiments reported here are intended to demonstrate chemoreceptive properties of the

afferent neurones, and to show their inhibitory influence on the efferent neurone which in turn inhibits the PTG activity. To examine possible physiological functions of the chemoreceptive activity of the afferent neurone, the changes in chemical constituents of the haemolymph, such as sugars, were measured during the larval development.

MATERIALS AND METHODS

Larvae of *Mamestra brassicae* were reared on artificial diet [3] at $23 \pm 1^\circ\text{C}$ under long day photoperiod (16L, 8D). Female larvae were used throughout this experiment.

Electrical activity of PTG innervating nerves was recorded as described in the previous paper [1]. The chemosensory region of the isolated nervous tract was stimulated by twice exchanging the external medium for the stimulant solution in the oil gap chamber. The change in electrical activities was recorded on tape recorder connected with the oscilloscope.

The chemosensory region of the nervous tract was prepared for histology using the modified

Bodian method.

For the determination of the change in sugar contents in the haemolymph during the larval development, 20 μ l haemolymph was taken from a larva by making small cut on the proleg. The haemolymph was introduced into a trichloroacetic acid solution to remove proteins. The total sugar contents of the supernatant were determined by the anthrone-H₂SO₄ method standardized with glucose. The trehalose content in the total sugar was estimated by comparing the results obtained from two different determinations of the reducing sugar contents in the total sugar by the Somogyi-Nelson method and of the trehalose contents in the total sugar by reversed-phase high-performance liquid chromatography.

RESULTS

Selection of chemically stimulative solutions

It was found in the preceding study of this series [2] that afferent activity in the nerve N4 was induced in response to the Grace's medium. The chemical constituents of Grace's medium are summarized in the right column of Table 1 while the left column shows the constituents of the normal saline used in this experiment. The main difference in the constituents of Grace's from

those of the normal saline is sucrose as disaccharide and various amino acids; another difference is in the osmotic concentrations.

The stimulative effects of hypertonic normal saline (370 m Osm) made up with excess glucose were tested and found to be practically negligible. Trehalose-rich, histidine-rich and K-rich salines were selected as the test solutions for chemical stimulation. The constituents of these solutions are shown in Table 1. Trehalose was selected as it is the main component of free sugars in the haemolymph of the preparation used here (See below). Histidine was selected as a common and representative amino acid in the haemolymph. The pH value of the histidine-rich saline was adjusted to 6.5 by mixing L-histidine and L-histidine-HCl solutions, in addition to the adjustment by the ordinary phosphate buffer.

Histology

Physiological techniques [1] have already shown that generation sites of afferent activity within the nerves to PTG are localized to specific regions of nerve branching. Whole mount histological preparations of the nerves to PTG were made to find the cell bodies of these afferent neurones. Figure 1 is the micrograph of the nervous tract to PTG as well as the locally enlarged one taken at the nerve branching just in front of PTG. Here, fairly large

TABLE 1. The chemical composition of various types of the saline used in this experiment. Concentrations of K-salts in the saline are shown as including the phosphate buffer (mM/l, pH 6.5)

	Glucose-rich normal saline	K-rich saline	Trehalose- rich saline	Histidine- rich saline	Grace's medium
K-salt	35	95	35	35	30
Na-salt	4	4	4	4	22
Ca-salt	4	4	4	4	7
Mg-salt	15	15	15	15	22
Mono-saccharide	160	40	0	0	4
Di-saccharide	0	0	160	0	80
Amino acid	0	0	0	160	70
Organic acid	0	0	0	0	9
Total milliosmolar concentration	300	300	300	300	366

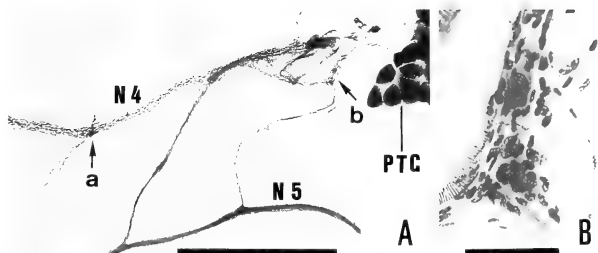


FIG. 1. Silver stained afferent neuron in the nervous tract N4 from prothoracic ganglion to PTG. For the size of cell body and nucleus, see text. A: Nervous tract to PTG; position of the cell body is shown by arrows (a, b). B: Enlargement of the position a in A. Scale bars in A and B are $500\text{ }\mu\text{m}$ and $50\text{ }\mu\text{m}$ respectively.

oval cell body can be seen among many glia cells, although its outline is not well distinct. The cell body was estimated from many preparations to be about $30\text{ }\mu\text{m}$ and $20\text{ }\mu\text{m}$ in apical and minor axes respectively. The nucleus was nearly a half the size of the cell body. This type of cell could be a chemosensory afferent neurone because, in many silver stained preparations of the nerve tract N4, it was the only clearly observable cell other than the glia cells seen. Distribution of the cell bodies of this type at the positions of each nerve branching of the nerve N4 was not perfectly consistent and consequently the number of cell bodies in each position ranged from zero, to one or two and some times three in different preparations. Total number of such cells in each preparation was about five. At least one cell body with the same shape could be seen at the surface of PTG tissues.

Stimulation of the chemosensory regions of the nerves to PTG

It has already been shown that the sites of generation of the afferent electrical activity are located both in the nerve N4 and in PTG itself [1]. The preparation used here to test chemical stimulation of these regions was the isolated ganglionic chain from brain to mesothoracic ganglion with the nerve N4. PTG was removed from the preparation because of the possibility that two chemosensory neurones with different physiological functions may exist within the nerves and PTG. Chemical stimulation of the PTG itself was not

studied here.

In recordings of the electrical activity, the nearest region of the nerve N4 to the prothoracic ganglion was placed in position on the oil-gap. Both ganglionic chain and nervous tract were immersed separately in two normal saline pools of the oil-gap chamber for 1 hr before the chemical stimulation. This chamber was placed in a gas mixture containing 95% O_2 and 5% CO_2 . Temperature was adjusted to $23^\circ \pm 1^\circ\text{C}$. For chemical stimulation, the normal saline in the one pool in which the nervous tract was immersed was replaced by a stimulant solution.

The effects of histidine-rich, trehalose-rich and K-rich salines are shown in Figures 2, 3 and 4, respectively. Each result is a representative example from several successful determinations.

Figure 2 shows the recordings of the electrical activity before and after the chemical stimulation as well as the wave forms of the efferent and afferent activity. The frequency histograms for both types of electrical activity recorded simultaneously from one nerve (N4) are also shown. Use of histidine-rich saline resulted in a remarkable augmentation of the afferent activity which appeared gradually and with long latency (lower histogram). This indicates that the afferent neurones in the nerves to PTG could be chemosensory in nature. Exact determination of the latency was difficult because the frequency of the electrical activity fluctuated during the period of determination even in the normal saline. Howev-

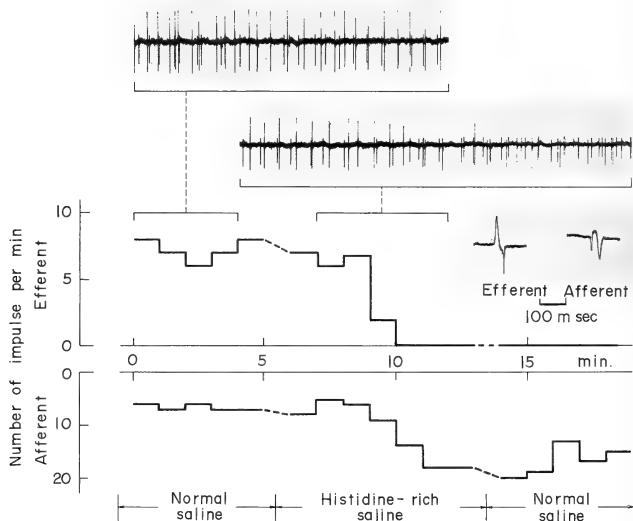


Fig. 2. Effects of histidine-rich saline applied to the nervous tract N4 from prothoracic ganglion to PTG. The period of application of various types of saline is shown in the lower part of the figure.

er, the extremely long latency observed in this sort of chemoreceptor is notable in comparison with the case of the chemical exteroceptors.

The upper histogram in Figure 2 also shows that the frequency of efferent activity decreased significantly and finally to zero as the afferent activity increased. The effects of histidine stimulation - high frequency of afferent activities and the following complete inhibition of efferent activity - continue usually for hours after a change back to normal saline. A serine-rich saline stimulated the afferent neurones similarly but to a lesser degree.

The stimulation effect of the trehalose-rich saline on the afferent neurones is shown by the frequency histograms in Fig. 3. The elevation of the afferent activity and resulting inhibition of the efferent activity were fundamentally the same as for histidine stimulation. Sucrose-rich saline (160 mM sucrose) was used for the chemical stimulation by another di-saccharide. This produced almost

the same effects as trehalose-rich saline.

It was difficult to determine accurately the threshold value for inducing a clear change in frequency of the afferent activity because of large individual differences and unstable firing during the determination. However the general estimation obtained from many preparations was that the threshold concentration for inducing a significant effect within 5 minutes was about 30 mM for both histidine-rich and trehalose-rich salines. The possibility that 160 mM histidine or trehalose in the saline could induce a nonspecific irritation to the neurones can be excluded; the normal glucose-rich saline containing 160 mM glucose produced the minimal level of afferent activity and haemolymph of lepidopterous insects contains fairly large amount of trehalose and amino acids [4, 5].

Figure 4 shows the effects of stimulation by the K-rich saline. There was an immediate change in frequency of afferent as well as efferent activity at

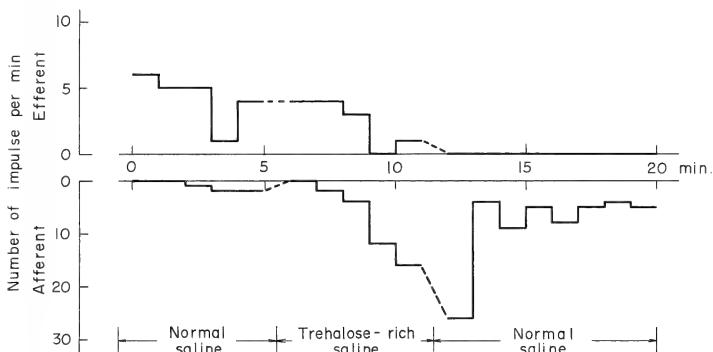


FIG. 3. Effects of trehalose-rich saline applied to the nervous tract N4 from prothoracic ganglion to PTG. Lower part of the figure drawn as in Fig. 2.

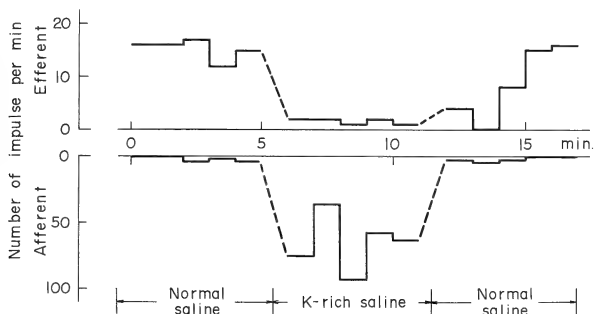


FIG. 4. Effects of K-rich saline applied to the nervous tract N4 from prothoracic ganglion to PTG. Lower part of the figure drawn as in Fig. 2.

the moment of application or removal of K-rich saline which clearly differed from the stimulation effect of histidine-rich or trehalose-rich salines. On removal of K-rich saline the efferent activity recovered from its inhibition within a few minutes after the fast return of the afferent activity to its normal level.

10^{-4} M juvenile hormone-II (JH-II) and 10^{-6} M or 10^{-8} M 20-hydroxyecdysone dissolved in the normal saline did not effect the afferent neurones (Fig. 5 shows JH saline). The histogram of the

afferent activity in this preparation always showed zero level. The frequencies of the afferent activity in the normal saline were low in almost all preparation as shown in Figures 2-5, and the normal saline used in this experiment was the best medium for keeping the afferent activity low.

The results presented here lead to the conclusion that the afferent neurones in the nervous tract N4 are chemosensory and work as sensors to monitor the concentration of the chemical composition of the external medium. In particular they

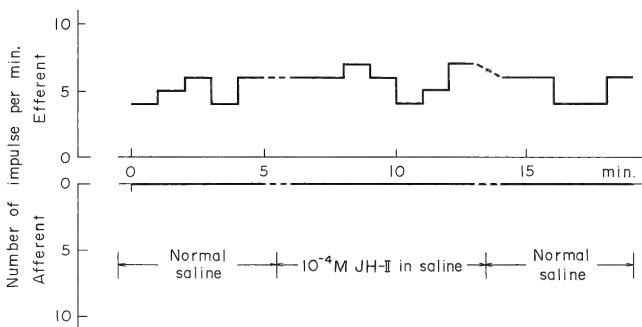


FIG. 5. Effects of JH containing saline applied to the nervous tract N4 from prothoracic ganglion to PTG. Lower part of the figure drawn as in Fig. 2.

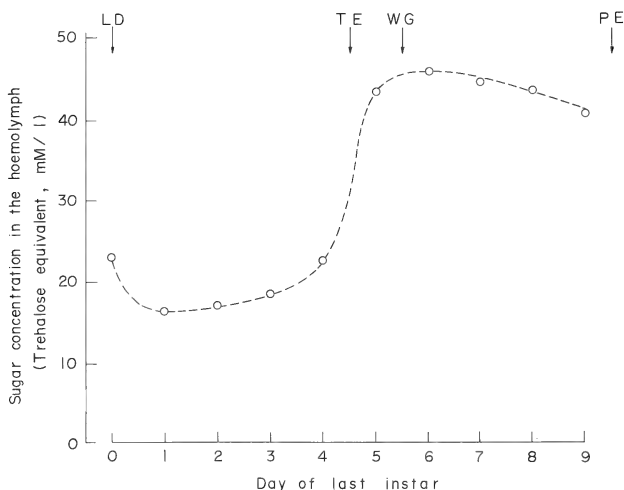


FIG. 6. The change of sugar content in the haemolymph during larval development. Sugar content was determined by the anthrone- H_2SO_4 method standardized with glucose but expressed in the figure by converting to the trehalose equivalents in mM/l. The following developmental stages are indicated by arrows: LE, larval ecdysis; TE, appearance of transparent epidermis; WG, wandering to the ground; PE, pupal ecdysis.

may sense the di-saccharides or amino acids. The input from the afferent neurones to the prothoracic ganglion inhibits the efferent activity to the

PTG, and as this efferent activity is inhibitory, afferent activity effectively disinhibits PTG activity.

Changes of sugar contents in the haemolymph during larval development

One typical example of six series of determinations is shown in Figure 6. Sugar contents in the haemolymph can be seen to increase sharply from day 4 to day 5 during which period the transparent epidermis appears, i.e. above 30 mM/l, the minimum required *in vitro* to produce activation of the afferent neurones. The trehalose content in the total sugar was determined in the day 4 larvae by the methods described above, and estimated to be greater than 95% of the total sugar in the haemolymph.

DISCUSSION

In the experiments reported here, the afferent neurones in the nerves to PTG were shown to be chemosensory neurones sensitive to the chemical constituents of the haemolymph. So far similar visceral chemosensory neurones have been described only in vertebrates [6]. In the larva or the pharate-pupa of lepidopterous insects, several authors have demonstrated the feedback influence of the released hormones on the central programs for the various types of the developmental events [7~10]. The effect of the hormones in these cases appeared to be directly on the central ganglia. The existence of chemosensory afferent neurones in the nervous network which is supplied directly by the haemolymph is important, because changes in the specific chemical constituents in the haemolymph can be checked and conducted quickly to the central nervous system.

It was demonstrated here that the elevation of afferent neurone activity induced by the chemical stimulation was followed by a marked inhibition of efferent neurone activity. Such response was observed to continue for hours after the removal of stimulant solution. This fact suggests that the level of efferent activity appearing in the isolated preparations from various stages of last instar larvae [1] is not purely the outcome of the development of innate activity of the central nervous system, but the expression of an activity resulting from changes in specific chemical condition of the haemolymph and preserved for longer time after the isolation in the saline. Further analysis by intracellular record-

ings and the electronmicroscopic study may be necessary to understand precisely the physiological mechanism of these unique chemosensory neurones and this modulating influence to the central ganglia as described in this paper.

The results obtained here, as well as those shown in the previous papers [1, 2] that the function of efferent neurone on PTG is inhibitory, indicate that the marked elevation of the trehalose concentration in the haemolymph to some critical value during the development may be a cause of the accelerated PTG activity. This speculation is supported well by the fact that the estimated threshold concentration for the trehalose stimulation is about 30 mM in the sensitive preparations and the trehalose concentration in the haemolymph exceed this threshold value during the period from day 4 to day 5. However we must be careful in extrapolating results from the isolated preparations to the normal situation.

Amino acid contents in the haemolymph were not determined. It seems premature to speculate on the overall function of the physiological responses induced by the individual amino acids. Although the biological functions of the amino acid sensitive neurones are not clear, the existence of the striking effects of amino acids, such as a histidine, on the afferent chemosensory neurones and of the consequent inhibition of the efferents to the PTG suggests they may act as regulators of PTG activity.

ACKNOWLEDGMENTS

We wish to thank Dr. J. Kien, University of Regensburg, for critical reading of the manuscript.

REFERENCES

- 1 Okajima, A. and Watanabe, M. (1989) Electrophysiological identification of neuronal pathways to the prothoracic gland and the change in electrical activities of the prothoracic gland innervating neurones during larval development of a moth, *Mamestra brassicae*. Zool. Sci., 6: 459-468.
- 2 Okajima, A. and Kumagai, K. (1989) The inhibitory control of prothoracic gland activity by the neurosecretory neurones in a moth, *Mamestra brassicae*. Zool. Sci., 6: 851-858.
- 3 Agui, N., Ogura, N. and Okawara, M. (1978) Rear-

- ing of cabbage armyworm, *Mamestra brassicae* L. (Lepidoptera: Noctuidae) and some lepidopterous larvae on artificial diet. Appl. Ent. Zool., **19**: 91-96.
- 4 Wyatt, G. R. (1961) The biochemistry of insect hemolymph. Ann. Rev. Entmol., **6**: 75-102.
 - 5 Florkin, M. and Jeuniaux, C. (1974) Haemolymph: Composition. In "Physiology of Insecta, vol. 5". Ed. by M. Rockstein, Academic Press, New York, pp. 255-307.
 - 6 Mei, N. (1983) Sensory structures in the viscera. In "Progress in sensory physiology, vol. 4". Ed. by D. Ottoson, Springer-Verlag, Berlin, pp. 1-42.
 - 7 Gilbert, L. I., Bollenbacher, W. E., Agui, N., Granger, N. A., Sedlak, B. J., Gibbs, D. and Buys, C. M. (1984) The prothoracicotropes: Source of the prothoracicotropic hormone. Amer. Zool., **21**: 641-653.
 - 8 Dominick, O. S. and Truman, J. W. (1984) The physiology of wandering behaviour in *Manduca sexta*. I. Temporal organization and the influence of the internal and external environments J. Exp. Biol., **110**: 35-51.
 - 9 Fujishita, M., Ohnishi, E. and Ishizaki, H. (1982) The role of ecdysteroids in the determination of gut-purge timing in the saturniid, *Samia synthia ricini*. J. Insect Physiol., **28**: 961-967.
 - 10 Truman, J. W. (1978) Hormonal release of stereotyped motor programs from the isolated nervous system of the cecropia silkworm. J. Exp. Biol., **74**: 151-173.

Visible Light Reception of Accessory Eye in the Giant Snail, *Achatina fulica*, as Revealed by an Electrophysiological Study

NOBUAKI TAMAMAKI¹

Department of Anatomy, Fukui Medical School,
Matsuoka, Fukui 910-11, Japan

ABSTRACT—Extracellular and intracellular recordings were made in the accessory eye of the giant snail, *Achatina fulica*, in order to compare its photoreceptor function with that of the main eye. Four types of ERGs were recorded through the suction electrode positioned at various locations in eye preparations. Recordings of the ERG mainly attributable to the accessory eye were accomplished by making fissure on the cornea. Intracellularly two types of receptor potentials with spiking and without spiking were recorded in the accessory and main eyes. With the HRP technique, it became apparent that the receptor potentials without spikes were evoked by photosensory cells type I in both eyes. Spectral sensitivity curve for the accessory and main eyes constructed with the criterion responses of ERGs and receptor potentials were similar. Both have a peak near 480 nm, and are not responsive to light having a wavelength greater than 750 nm.

These results, in combination with morphological data, lead me to conclude that the *Achatina* accessory eye may serve as a monitor of surrounding light intensity in a visible range.

INTRODUCTION

A sensory cell assembly called the accessory retina was first described in the eye of a slug, *Limax maximus*, by Henschman [1]. At present it is well known that such photoreceptor structures similar to that of *Limax maximus* widely occur in terrestrial slugs [2, 3]. Recently I found a relatively large accessory retina paired with a small lens in the eye of the African giant snail, *Achatina fulica* [4]. Because the *Achatina* accessory retina is histologically discontinuous from the main retina and is invariably paired with a small lens, I called the organ an accessory eye.

As for the function of the slug accessory retina, two hypotheses have been proposed. On the basis of morphological and behavioral observations,

Newell *et al.* [2] considered that the accessory retina of *Agriolimax reticulatus* is an infrared light receptor. Mainly from the morphological point of view, Kataoka [3] speculated that the sensory cells of the accessory retina in *Limax flavus* simply monitor the changes in light intensity.

Although a considerable amount of data on the morphology of accessory retinas in pulmonates has been accumulated, there is no information on their electrophysiological properties. The present paper deals with light-elicited electrical activity recorded extra- and intra-cellularly in the accessory eye of *Achatina fulica*. It focuses on the spectral sensitivity of its photosensory cells in comparison with that of sensory cells in the main eye.

MATERIALS AND METHODS

Experimental preparation

Adult African giant snail, *Achatina fulica*, collected in a suburb of Naha, Okinawa, were sent by air and kept in a terrarium. They were fed on lettuce and maintained in cyclic light (12L:12D) at

Accepted December 8, 1988

Received September 14, 1988

¹ Present address: Department of Neurobiology and Behavior, State University of New York at Stony Brook, Stony Brook, New York 11794, U.S.A. Reprint requests should be addressed to the address in Japan.

room temperature. The eye and its attached stump of optic nerve was cut away from the tentacular tissue under dim red light. The eye-optic nerve preparation was mounted on a small metal clamp in a dish containing a modified Ramsey's snail Ringer solution [5] maintained at approximately 25°C by circulating water at a constant temperature through a built-in glass coil. In such preparations normal electrical responses to photostimulation continued for up to 12 hr.

Electrophysiological recordings

Extracellular recordings were carried out with a glass suction electrode with a tip about 80 μm in diameter. The signal from the electrode were fed into a high input impedance preamplifier (Nihon Kodens MEZ-7101). The amplified signals were displayed on a digital storage oscilloscope (Hitachi VC-801L) and read on a chart recorder. The eye-optic nerve preparation obtained by cutting away the skin and musculature was held by sucking with the electrode under dim red light. After the specimen had been prepared, the eye was dark-adapted for at least one hour. Test flashes to evoke and record an electro-retino-gram (ERG) were 1 or 5 sec duration, 1 ($-\log I$) unit intensity and in steps of 50 nm from 400 nm to 800 nm in wavelength.

Intracellular recordings were made with micro-pipettes filled with 10% horseradish peroxidase (HRP, Sigma type VI) dissolved in 0.5 M KCl, 0.1 M tris buffer (pH 8.6). Electrode resistance was generally 40–80 M Ω . Signals from the electrode were fed into the pre-amplifier, the output of which was displayed on the digital storage oscilloscope or a chart recorder. The microelectrode was inserted into the cells through the opening formed in the cornea by removing the main lens. After the specimens had been prepared, the eye was dark adapted for at least 30 min. Test flashes were of 1 sec duration, 3 ($-\log I$) unit intensity and in steps of 50 nm from 400 nm to 800 nm in wavelength.

Cell identification

After recording the electrical phenomena, HRP was iontophoresed into the cells by introducing depolarizing current pulses (10 nA, 100 msec duration, 5 Hz, 10–20 min). The eye was allowed to

diffuse HRP for 60 min and was fixed in 2% glutaraldehyde containing 50 mM cacodylate buffer (pH 7.4) at 4°C. The prefixed sample was rinsed with the same buffer three times and incubated for 30 min at room temperature in the complete reagent containing 0.05% diaminobenzidine (DAB), 0.01% H_2O_2 and the same buffer [6]. The eye was postfixed in 1% OsO_4 for 2 hr, dehydrated, then embedded in Epon. Silver thin sections were contrasted with uranyl acetate and lead citrate.

Light stimulation

Light from a 150 W tungsten-bromide lamp (Iwasaki Electric Co.) was focused on the entrance slit of a prism-grating monochromator (Shimadzu RF-503), whose output was conducted to the preparation with a 5 mm diameter optical fiber. The stimulus intensity was controlled with a neutral density circular wedge and neutral density filters. The slit bandpass was 5 nm in the 400 to 600 nm range and 10 nm in the range 600 to 800 nm. The light intensity incident on the preparation was measured with a calibrated vacuum thermocouple (Japan Spectroscopic Co.) and a lock-in amplifier (NF Circuit Design Block LI-574). The maximum intensity, as indicated by 0 ($-\log I$) unit in the figures, was 6.5×10^{10} photons/cm 2 s. A schematic diagram of the experimental arrangement of optical stimulation and electrical recording systems is shown in Figure 1.

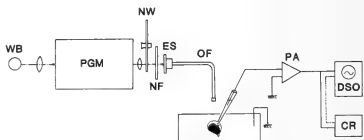


FIG. 1. Experimental arrangement of stimulating and recording systems. CR, chart recorder; DSO, digital storage oscilloscope; ES, electromechanical shutter; NF, neutral density filter; NW, neutral density circular wedge; OF, optical fiber; PGM, prism-grating monochromator; PA, preamplifier; WB, tungsten-bromide lamp.

RESULTS

The morphology of *Achatina* eye is shown in

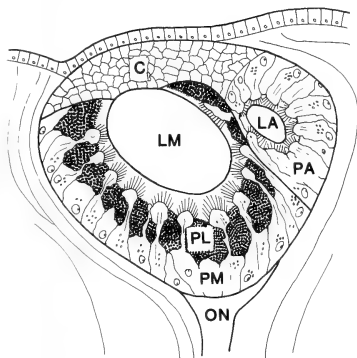


FIG. 2. Schematic drawing of *Achatina* eye. C, cornea; LA, lens of accessory eye; LM, lens of main eye; ON, optic nerve; PA, photosensory cells of accessory eye; PL, pigment cell layer; PM, photosensory cells of main eye.

Figure 2. The eyes of the adult snail are ovoid, about $200\text{ }\mu\text{m}$ wide and $250\text{ }\mu\text{m}$ long, and bear spheroidal main lenses. They are situated near the tips of two retractable ocular tentacles that can be extended nearly 2 cm in length. The accessory eye lies in an extension of the cornea and is always associated with a small lens. Both the main and accessory eyes are composed of two types of photoreceptor cells, type I and type II, and supporting cells. Many of these features have already been described [4]. A marked difference between the morphological appearance of the accessory and main eyes is that the former lacks the pigmented cell layer in the retina. This feature, in addition to the refractivity of the accessory lens, facilitates detection and manipulation of the accessory eye under the stereomicroscope.

General characteristics of electroretinograms

Responses recorded at three sites in the eye are shown in Figure 3. When the electrode was placed on the cornea, the electroretinogram (ERG) exhibited a biphasic negative potential consisting of a rapid fall followed by a slower potential change returning to the baseline (Fig. 3A), as commonly seen in molluscan and annelidan eyes [7-9]. When

the electrode was moved to the surface of the accessory eye the response was biphasic, comprising an initial rapid rising followed by a slow negative potential (Fig. 3B). When the electrode was set on the surface of the main eye, the ERG displayed similar waveform to the corneal ERG but had opposite polarity (Fig. 3C).

Except for the differences in amplitude, there were no change in the waveforms of these ERGs with stimulus light in the wavelength range from 400 to 700 nm. No response was evoked in either eye with light having a wavelength greater than 700 nm. From the waveforms of the ERGs and the spatial arrangement of the two kinds of eyes (Fig. 2), it was presumed that the initial rapid positive deflection in the Figure 3B biphasic ERGs originates in the accessory eye and the subsequent gradual negative potential change is due to the main eye. An attempt to eliminate the contribution of the main eye from the biphasic ERG was achieved by making a fissure on the cornea, and ERGs of the accessory eye were recorded (Fig. 3D). Examples of intensity-ERG amplitude double logarithmic plots are shown in Figure 4, where the amplitude data for the two retinas were obtained from ERGs as the difference between the baseline and the positive peak (Fig. 3C and 3D). The largest amplitude recorded on the main eye was about $800\text{ }\mu\text{V}$, and that of the accessory eye was about $560\text{ }\mu\text{V}$ with the flashes of 1 sec duration. These double logarithmic plots indicate that the intensity-amplitude relation is composed of two linear curves, steep and moderate. The inflection points fell on about 3 ($-\log 1$) unit.

ERG spectral sensitivity

In order to compare the spectral sensitivity of the accessory eye with that of the main eye, a spectral sensitivity curve was constructed. The ERG sensitivity was the relative intensity required to elicit the criterion amplitude of 0.1 mV at each wavelength. Figure 5A shows the spectral sensitivity curves obtained from each of 2 preparations of the main and accessory eye. The spectral sensitivity curves for both eyes exhibited a maximum at about 480 nm and corresponded well to the Dartnall nomograms [10] for a single visual pigment (Fig. 5B).

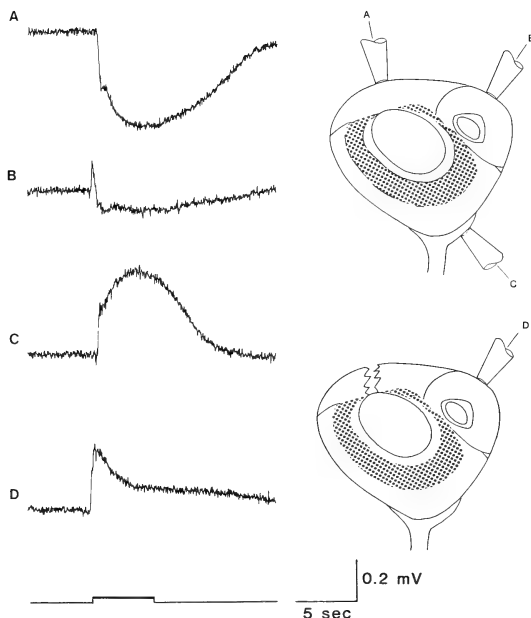


Fig. 3. Electrophoretograms recorded through the suction electrode placed at three sites. A, Recording on corneal surface; B, back of accessory eye; C, back of main eye; D, back of accessory eye after making a fissure on the cornea. Trace beneath D indicates the monitor of a 5 sec flash of 500 nm light at 6.5×10^7 photons/cm²·s ($-\log I = 3$). Right two drawings show their recording sites.

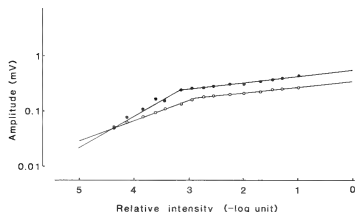


Fig. 4. Double logarithmic plots of ERG amplitude-intensity determined from the main eye (closed circles) and the accessory eye (open circles). Stimulus duration was 1 sec of 480 nm light. All data in each curve were recorded from a single preparation.

Intracellular responses

Intracellular recordings from the accessory eye gave two types of light responses (Fig. 6A). The first one was a simple depolarizing receptor potential. The majority of the recordings belonged to this type. These recordings were stable and were obtained from the same cells for up to two hours. The other type was a receptor potential, on which spike burst of the same polarity were superimposed (Fig. 6B). In the figure, the recording was initiated with injury spikes caused by the penetration of the microelectrode. There was only a slight chance of impaling such spiking cells and, in most cases, recordings for these cells failed to be

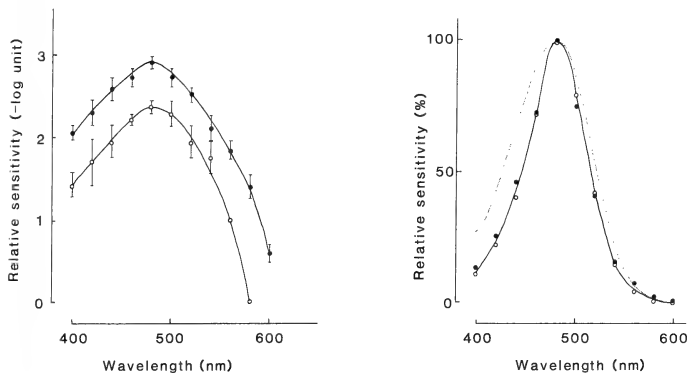


FIG. 5. Spectral sensitivity of the main eye (closed circles) and the accessory eye (open circles). Both curves represent the average of data from 2 preparations of each eye. Each stimulus duration was 1 sec. A, Relative sensitivity is the reciprocal of the light intensity required to elicit a 0.1 mV criterion response. B, Relative sensitivity is plotted in a percentage of the maximum sensitivity in A. Dotted line indicates the Darnall nomogram whose peak is at 480 nm.

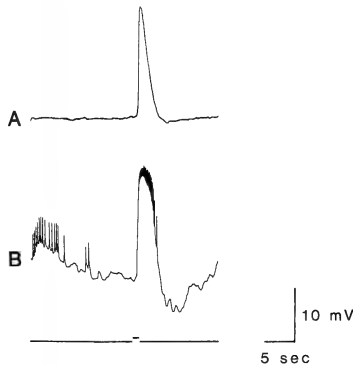


FIG. 6. Intracellularly recorded responses from photosensory cells of the accessory eye. Trace beneath B indicates the monitor of a 1 sec flash. The flash was 480 nm in wavelength and 1 ($-\log I$) unit intensity. A, Receptor potential without spikes. B, Receptor potential superimposed with spike burst. The recording is initiated with injury spikes.

obtained after a few minutes.

The two types of receptor potentials, with identical waveforms to those of the photosensory cells

of the accessory eye, were also recorded from the main eye. From the waveform alone it is difficult to tell which eye is evoking the receptor potential. With the HRP technique, the cells with simple receptor potentials were identified as photosensory cell type I in both eyes (Fig. 7). In the dark-adapted state, the resting potentials of photosensory cells in the two kinds of eyes lay between -50 and -60 mV. The potentials of photoinensitive cells, probably such as corneal and pigment cells, were -70 to -90 mV in both of the eyes.

Intensity-response characteristics of intracellular recordings

Figure 8 shows a sequence of receptor potentials, recorded at different intensities of light, from a type I photosensory cell of the accessory eye. At a high intensity (0, $-\log I$ unit), the flash elicits a large depolarizing potential which comes back to the base line through a short plateau and an after hyperpolarization. There was no overshooting in any cases. Attenuating the stimulus intensity (1 or 1.7, $-\log I$ unit), the amplitude of the receptor potentials successively decreases, and the repolarizing process turns out to be rapid and monophasic. Figure 9 shows examples of intensity-

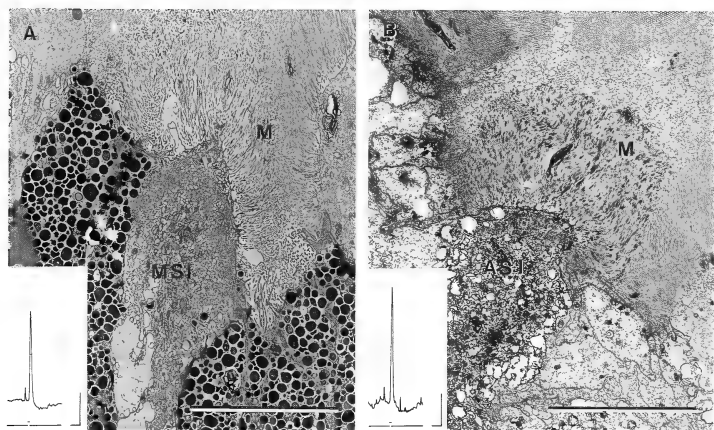


FIG. 7. Electron micrographs of sensory cells type I stained with HRP intracellularly. A, Sensory cell type I in main eye. MSI, sensory cell type I in main eye; M, microvilli. B, Sensory cell type I in accessory eye. ASI, sensory cell type I in accessory eye; M, microvilli. Calibration bars = $10 \mu\text{m}$. Each inset shows the receptor potential recorded from the sensory cell shown in the figure. Trace beneath the recording indicates the monitor of a 1 sec flash at 480 nm in wavelength and 3 ($-\log I$) unit intensity, and the calibration bars indicate 5 sec and 10 mV.

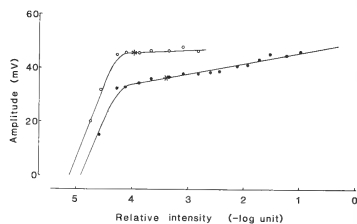
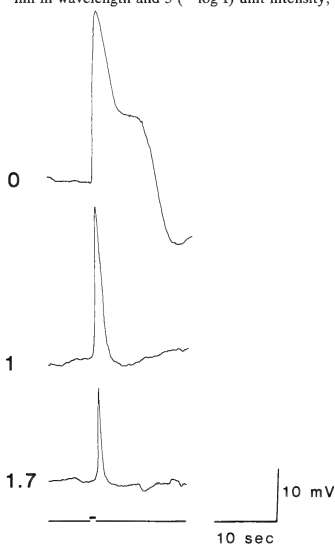


FIG. 9. Amplitude-log intensity curves for type I photo-sensory cells of the main (closed circles) and accessory (open circles) eyes. Flashes were 1 sec at 480 nm after the sensory cells were fully dark-adapted. All data in each curve were obtained from a single preparation. Asterisks on the curves indicate the point of each standard response respectively (see Results).

FIG. 8. Receptor potentials recorded from type I photo-sensory cells of the accessory eye at different light intensities. The number to the left of each recording indicates $-\log$ relative intensity for that response. Trace beneath the three recording indicates the monitor of a 1 sec flash at 480 nm in wavelength.

amplitude plots measured from type I cells in both of the eyes. The curves seem to show a higher part of the typical sigmoid intensity-response curves [11], where the amplitude of receptor potentials gradually increase as the light intensity increase.

Spectral sensitivity of photosensory cells

The sensitivity was the relative intensity required to evoke a criterion response. The criterion response was obtained as follows: As the intensity of the stimulus light increased, the spectral response curve at a constant photons of stimulus light, whose peak was found at 480 nm, became flat. When the receptor potentials of similar amplitudes (within a deviation range of 5 mV) were recorded in the range over 100 nm (it was from 420 nm to 520 nm), the amplitude at 480 nm was determined as a standard. For instance, the standard response of the samples used in Figure 9 fell on the asterisk in the figure. The criterion response was a half of the standard. Figure 10A shows the spectral sensitivity curve for type I sensory cells in both of the eyes. Open circles show data recorded from the type I cells of the accessory eye and filled circles are from those of the main eye. The sensitivity was also expressed as

a percentage of the maximum (Fig. 10B). The data for the curves were obtained from each of 3 preparations of main and accessory eye.

These show that the type I photosensory cells of both eyes exhibit the same spectral sensitivity peaking at 480 nm. The spectral sensitivity curve as well as in the case of the ERGs corresponds well to the Dartnall nomograms [10] for a single visual pigment. Although recordings on the other type of sensory cells, which may be type II sensory cells, were limited in number owing to the technical difficulty described above, the spectral response curves suggest that they may have a similar spectral sensitivity peak to the type I sensory cells. In all cases of both type of cells in the accessory and main eyes, no receptor potentials were evoked by stimulus light having a wavelength greater than 750 nm.

DISCUSSION

Since the accessory photosensory organ in pulmonate came to be known, two contradicting hypotheses (the infrared light receptor and the monitor of light intensity) have been proposed. The present study produced evidence of visible

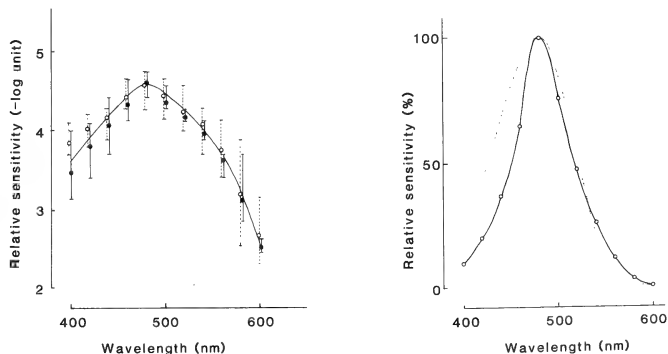


FIG. 10. Spectral sensitivity of type I sensory cells in the main and accessory eyes. Flashes were 1 sec in duration at various wavelengths and intensities. Data were obtained from each of 3 preparations of the main and accessory eye. Open circles are data recorded from the sensory cells of the accessory eye and closed circles are from those of the main eye. A, Relative sensitivity is the reciprocal of the light intensity required to elicit a criterion response (see Results). B, Relative sensitivity is plotted as a percentage of the maximum sensitivity in A. Dotted line indicates the Dartnall nomogram whose peak is at 480 nm.

light reception of the accessory eye by employing an electrophysiological technique. The electrical responses were recorded from the accessory eye with a suction electrode and a microelectrode, and each of them was compared with that from the main eye.

With a suction electrode, the ERGs of the accessory eye which were obtained by lesioning the cornea to convert the bipolar responses into monopolar ones were recorded, and the sensitivity peak was found at a similar wavelength to that of the main eye (480 nm). This sensitivity peaking wavelength was very close to those of other gastropods' eyes [8, 12–15]. It is unlikely that another peak of sensitivity will be found and the burst of spikes is caused in a range near infrared, since the suction electrode monitored the activity of the accessory eye as a whole in the 400 nm to 800 nm wavelength range.

The intracellular recordings from sensory cells in the accessory and main eyes were made with microelectrodes containing HRP in order to discriminate the activity of the each eye. Satisfactory recordings were obtained from type I sensory cells in both of the eyes. The recordings were used to construct the spectral sensitivity curve, whose sensitivity peak was found at 480 nm and coincided with the sensitivity peak of the ERGs. The other type of sensory cell, which may be sensory cell type II, also responded to visible range light. The accessory eye and the main eye of *Achatina fulica* were composed of only these two types of sensory cells in addition to the supporting cells in the main eye [4]. Two types of ganglion cells identified by some electrical properties may also be included in the main eye [16]. However, these are no longer any sensory cells to receive infrared light. If the accessory eye received infrared light, the main eye could also receive it because of the structural similarity of the sensory cells. Recently, in addition, rhodopsin and retinochrome were found in the accessory photosensory organ of *Limax flavus* [17, 18]. Therefore, in view of these facts, it is concluded that the accessory eye is a visible light receptor having a sensitivity maximum at 480 nm.

Other electrophysiological properties also support the above conclusion. The intensity-amplitude relationships of the ERGs (log-log

plots) were represented by two different components in the accessory eye, just as shown in the *Limax* main eye [5] and in the *Achatina* main eye [16]. The two components in the intensity-amplitude relations or in the dark adaptation curve are observed in the cases there are two kinds of photoreceptor cells with different sensitivity such as the cone and rod in vertebrate retina or the sensitivity is changed by the migration of screening pigment granules [19]. In the eye of *Achatina fulica*, pigment granules have been found only in supporting cells [4] and the position of pigment is unaffected by light. Therefore, these two components may also imply the existence of two types of sensory cells with different sensitivity in the accessory eye as well as the similarity between the two eyes.

In the construction of a spectral sensitivity curve, a standard response was adopted in order to obtain a criterion response immediately and to reduce the effects of the intracellular-recording conditions on relative sensitivity in each cell. Although the standard response is a value used tentatively, it was reliable in comparing the relative sensitivity and providing the evidence of visible light reception by the accessory eye.

As one of the other characteristics to advance speculation on the functions of the accessory eye,

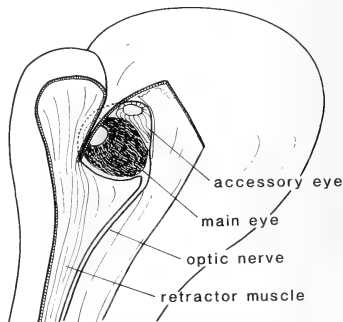


FIG. 11. Schematic diagram of the situation of the accessory and main eyes in a partially retracted optic tentacle. The eyeball was rotated about a right angle from the original situation in a fully extended tentacle.

there is the difference in the location of the two eyes. If the eye preparation is illuminated from a direction other than the pupillary opening of pigment cell layer in the main eye, the main eye may not perceive the illumination, even though the accessory eye perceives it well. Such a condition may occur in a partially retractor optic tentacle (Fig. 11). When a giant snail begins to crawl, it behaves as if it is looking around with the partially retracted optic tentacles (unpubl. data). Similar behavior was also observed in *Agriolimax reticulatus* [2]. In the partially retracted optic tentacles, the eyeball was rotated about a right angle and the pupillary opening of the main eye was masked by epidermal tissues, while the accessory eye might be exposed to environmental light as in the fully extended tentacles. Therefore, the accessory eye may function principally as a luminous intensity meter in the partially retracted tentacle.

REFERENCES

- Henchman, A. P. (1897) The eye of *Limax maximus*. Science, N. S. 5: 428-429.
- Newell, P. F. and Newell, G. E. (1968) The eye of the slug, *Agriolimax reticulatus*, Symp. Zool. Soc. London, 23: 97-111.
- Kataoka, S. (1977) Ultrastructure of the cornea and accessory retina in a slug, *Limax flavus* L. J. Ultrastr. Res. 60: 296-305.
- Tamamaki, N. and Kawai, K. (1983) Ultrastructure of the accessory eye of the giant snail, *Achatina fulica* (Gastropoda, Pulmonata). Zoomorphology, 102: 205-213.
- Suzuki, H., Watanabe, M., Tsukahara, Y. and Tasaki, K. (1979) Duplex system in the simple retina of gastropod mollusc, *Limax flavus* L. J. Comp. Physiol., 133: 125-130.
- Graham, R. C. and Karnovsky, M. J. (1966) The early stages of absorption of injected horseradish peroxidase in the proximal tubules of mouse kidney: ultrastructural cytochemistry by a new technique. J. Histochem. Cytochem., 14: 291-302.
- Gillary, H. L. (1970) Electrical responses from the eye of *Helix* to photic stimulation and simultaneous electrical stimulation on the optic nerve. Vision Res., 10: 977-991.
- Gillary, H. L. (1974) Light-evoked electrical potentials from the eye and optic nerve of *Strombus*: response waveform and spectral sensitivity. J. Exp. Biol., 60: 383-396.
- Wald, G. and Rayport, S. (1977) Vision in annelid worms. Science, 196: 1434-1439.
- Dartnall, H. J. A. (1953) The interpretation of spectral sensitivity curve. Brit. Med. Bull., 9: 23-30.
- Naka, K. I. and Rushton, W. A. H. (1966) Spontaneous potentials from colour units in the retina of fish (Cyprinidae). J. Physiol., 185: 536-555.
- Berg, E. V. and Schneider, G. (1972) The spectral sensitivity of the dark-adapted eye of *Helix pomatia* L. Vision Res., 12: 2151-2152.
- Dennis, M. J. (1967) Electrophysiology of the visual system in a nudibranch mollusc. J. Neurophysiol., 30: 1439-1465.
- Gillary, H. L. and Wolbarsht, M. L. (1967) Electrical responses from the eye of a land snail. Rev. Canad. Biol., 26: 125-134.
- Hughes, H. P. I. (1970) The spectral sensitivity and absolute threshold of *Onchidoris fusca* (Müller). J. Exp. Biol., 52: 609-618.
- Tasaki, K. and Suzuki, H. (1979) Duplex system in the retina of a gastropod mollusc, *Achatina fulica*. J. Physiol. Soc. Japan, 41: 346.
- Hara, T., Hara, R. and Takeuchi, J. (1967) Vision in octopus and squid. Nature, 214: 572-575.
- Ozaki, K., Hara, R. and Hara, T. (1983) Histochemical localization of retinochrome and rhodopsin studied by fluorescence microscopy. Cell Tissue Res., 233: 335-345.
- Bernhard, C. G. and Ottoson, D. (1964) Quantitative studies on pigment migration and light sensitivity in the compound eye at different light intensities. J. Gen. Physiol., 47: 465-478.



The Accessory Photosensory Organ of the Terrestrial Slug, *Limax flavus* L. (Gastropoda, Pulmonata): Morphological and Electrophysiological Study

NOBUAKI TAMAMAKI¹

Department of Anatomy, Fukui Medical School,
Matsuoka, Fukui 910-11, Japan

ABSTRACT—The accessory photosensory organ of the slug *Limax flavus* L., accessory eye was studied morphologically and electrophysiologically. The accessory eye is situated in the protuberance of the eyeball, and is separated by the septal structure from the main eye having a cavity of its own. One type of receptor potential was recorded intracellularly from sensory cells in the main eye and accessory eye, and identified with sensory cells type I by intracellular staining. The peaks of the spectral sensitivity curves of type I sensory cells in both eyes were found at 460 nm.

INTRODUCTION

An accessory photosensory organ called accessory retina or accessory eye was first described in the last century [1] and came to be known as common in some terrestrial slugs [2, 3] and also in a certain snail *Achatina fulica* [4]. The accessory photosensory organ of *Achatina fulica* had structure complex including an accessory lens and the septal structure between the two eyes, to call it an accessory eye. The fine structure of the accessory retina in *Limax flavus* has been closely studied [3], but the relationship between the main and accessory retina such as the septal structure, their cavities and lenses are still not clear in the slug.

As for the function of the slug accessory retina, two hypotheses, that it serving as a light intensity meter [3] and that it may be an infrared light receptor [2], have been proposed on the basis of morphological and behavioral studies. In order to know the function of the snail accessory photosensory organ, electrophysiological study was carried

out in *Achatina fulica* [5], and I obtained evidence of visible light reception by the accessory organ.

In this paper I consider the relationships between the main retina and the accessory retina in terrestrial slug, and report the evidence of visible light reception by the accessory organ in the terrestrial slug *Limax flavus* L.

MATERIALS AND METHODS

Animals and preparation for light and electron microscopy

Limax flavus slugs were collected in a suburb of Osaka and maintained in cyclic light (12L:12D) at room temperature. Tip of the optic tentacles were fixed in 2.5% glutaraldehyde containing 0.1 M phosphate buffer (pH 7.4). The eye and optic nerve were dissected free from the tentacular tissue, postfixed in 1% OsO₄ containing 0.1 M phosphate buffer (pH 7.4), dehydrated with an alcohol series and embedded in Spurr resin. Semi-thin sections were stained with toluidine blue and silver thin sections were contrasted with uranyl acetate and lead citrate.

Intracellular recording and intracellular staining with HRP

The eye and optic nerve were dissected free

Accepted November 18, 1988

Received September 14, 1988

¹ Present address: Department of Neurobiology and Behavior, State University of New York at Stony Brook, Stony Brook, New York 11794, U.S.A. Reprint requests should be addressed to the address in Japan.

from the tentacular tissue in snail Ringer's solution [6] and the preparation was mounted in an experiment chamber containing the Ringer's solution whose temperature was maintained at approximately 25°C. Stimulus light intensity was controlled with a neutral density circular wedge and neutral density filters. The maximum intensity of the stimulus light, indicated by 0 ($-\log I$ unit) in the figure, on the preparation was 6.5×10^{10} photons/cm² s with 5 nm bandpass. To obtain higher intensity in the near infrared region (600 to 800 nm), the slit bandpass was opened to 10 nm. These experimental arrangements for optical stimulation and electrical recording are reported previously [5].

After the specimens had been prepared, the eye was dark adapted for at least 30 min. Intracellular recordings were made with micropipettes filled with 10% HRP (Sigma type VI) dissolved in 0.5 M KCl, 0.1 M Tris. buffer (pH 8.6). Electrode resistance was generally 40–80 M Ω . The microelectrode was inserted into the cells through the opening formed in the cornea by removing the main lens. Test flashes were of 1 sec duration, 3 ($-\log I$) unit intensity and in steps of 50 nm from 400 nm to 800 nm in wavelength.

After recording electrical events, HRP was iontophoresed into cells, and HRP reaction was carried out following Graham-Karnovsky [7]. Details of these processes were also reported previously [5].

RESULTS

Light and electron microscopic observation of the relationship between the two retinas

The eyeball of the slug *Limax flavus* was shaped like a twisted pear and the accessory retina was situated in the protuberance which corresponded to the corner of the cornea (Fig. 1). In the figure, some distortion may be caused in the main retina by dehydration because of its large cavity and lens. The cavity of the main retina was occupied by the main lens and vitreous body into which the apical projections of sensory cells were projected. The cavity of the accessory retina is also occupied by a vitreous body and apical projections of its sensory

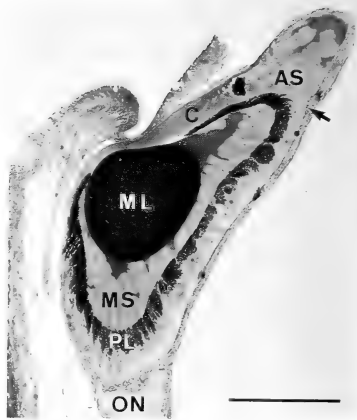
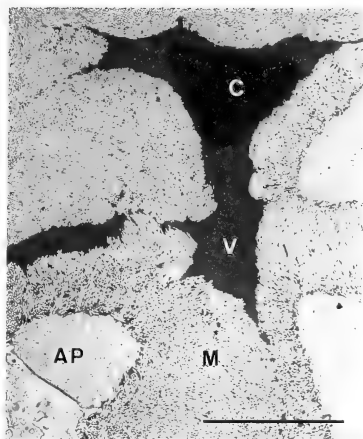


Fig. 1. Light micrograph of parasagittally sectioned eyeball. AS, sensory cells in accessory retina; C, cornea; ML, lens of main retina; MS, sensory cells in main retina; ON, optic nerve; PL, pigment layer; Arrow, indicating the location of septal structure. Calibration bar = 100 μ m.

cells. Some cores of the vitreous body which would grow into an accessory lens were sometimes contained in it (Fig. 2). As can be seen in Figure 1, the two cavities, i.e. of the main retina and the accessory retina, were separated by the cornea and the main retina. In some rare cases, in about one in ten eyeballs, partial destruction or emaciation of the cornea resulted in continuation of the two cavities. Therefore it is concluded that the cavities are ordinarily separated. Moreover the two retinas were separated by a septal structure composed of elongated cells (arrow in Figs. 1 and 3). The elongated cells contained some bundles of filaments (arrow in Fig. 3).

It is said that the main retina of the *Limax* eye are composed of two types of sensory cells [8, 9]. One of the two types of sensory cells is named sensory cell type I and characterized by aggregation of so-called photic vesicles [10], large cell body and long apical projection in the cavity. The other type of sensory cell is named sensory cell



type II. In addition to the main retina [8], the accessory retina of *Limax flavus* is also composed of two types of sensory cell, type I and type II [3]. The cell somata of these sensory cells are recognizable in Figure 3.

Intracellular recording

Resting potentials of photosensory cells were 50-60 mV, while photoinensitive cells were 70-90 mV. Only one type of receptor potentials were recorded stably from both the main and the accessory retina long enough that the spectral sensitivity curves could be constructed. The receptor potentials recorded from both retinas were similar

FIG. 2. Electron micrograph of core of vitreous body. AP, apical projection of type I sensory cell in the accessory retina; C, core of vitreous body; M, microvilli; V, vitreous body. Calibration bar = 10 μ m.

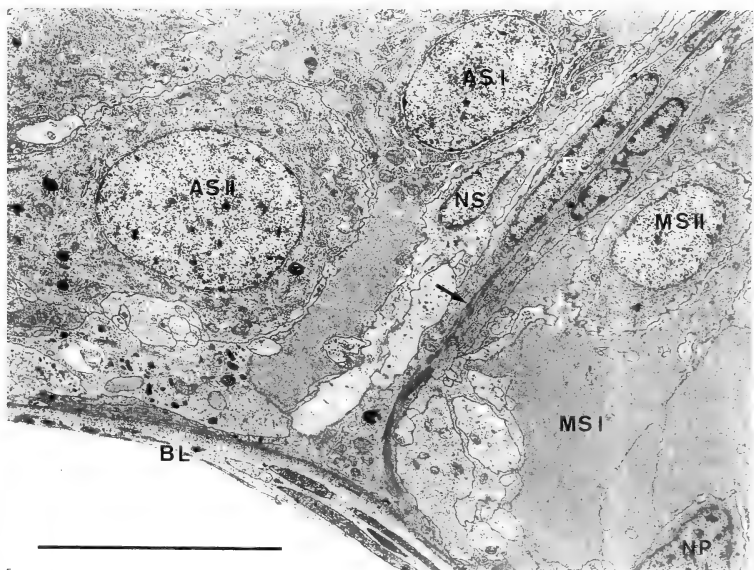


FIG. 3. Electron micrograph of septal structure between the two retinas. ASI, sensory cells type I in accessory retina; ASII, sensory cell type II in accessory retina; BL, basal lamina; EC, elongated cell; MSI, sensory cell type I in main retina; MSII, sensory cell type II in main retina; NP, nucleus of pigment cell; NS, nucleus of supporting cell in the accessory retina; Arrow, bundles of filaments. Calibration bar = 10 μ m.

graded depolarizations of as much as 40 mV, with no overshooting (Fig. 4). Therefore it was impossible to decide from which retina the responses were recorded by studying the waveform alone.

The amplitudes of these receptor potentials (from baseline to peak) were measured with stimulus lights of various wavelengths and intensities at intervals of 30 sec. Figure 5 shows the amplitude-

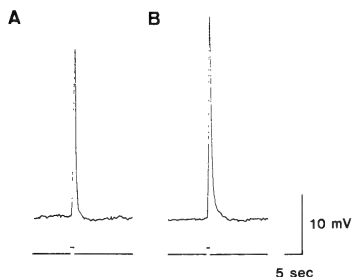


FIG. 4. Receptor potentials recorded from sensory cells in both retinas. A, receptor potential from a sensory cell in main retina. B, receptor potential from a sensory cell in accessory retina. Traces beneath the recording indicate the stimulus light of a 1 sec duration at 460 nm in wavelength and 2.14 ($-\log I$) unit intensity. Difference in the amplitudes of receptor potentials is due to the recording condition. Ultrastructural features of sensory cell in A and B are shown in Fig. 7A and B.

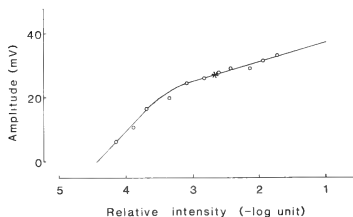


FIG. 5. Amplitude-log intensity curve for receptor potentials recorded from accessory retina. Flashes were 1 sec duration at 460 nm after the sensory cells were fully dark-adapted. All data were obtained from a single preparation. Asterisk indicates the standard response (see Results) of the preparation.

intensity plots of the receptor potentials elicited by the stimulus light of 460 nm in wavelength. Figure 6 shows the spectral sensitivity curve for the sensory cells in both retinas. The sensitivity was the relative intensity required to elicit a criterion response. The criterion response was obtained as follows: As the stimulus intensity increased, the spectral response curve at a constant photons of stimulus light, whose peak was found at 460 nm, became flat. When the receptor potentials for similar amplitudes (within a deviation range of 5 mV) were recorded in the range over 100 nm (it was from 400 to 500 nm), their amplitude at 460 nm was taken as the standard. The criterion response was a half of the standard. For instance, the standard response of the sample used in Figure 5 fell on the asterisk in the figure. The standard

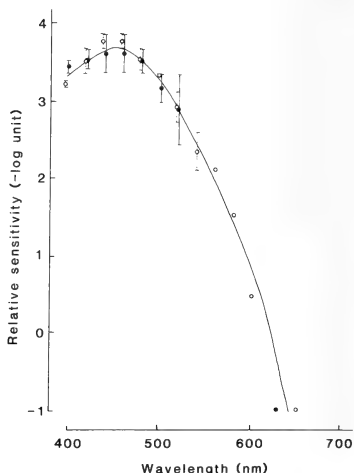


FIG. 6. Spectral sensitivity of type I sensory cells in the main and accessory retinas. Relative sensitivity is the reciprocal of the light intensity required to elicit the criterion response (see Results). Flashes were 1 sec in duration at various wavelengths and intensities. Open circles are the data obtained from accessory retina and filled circles are from main retina. These were obtained from each of 2 preparations of the main and accessory retina.

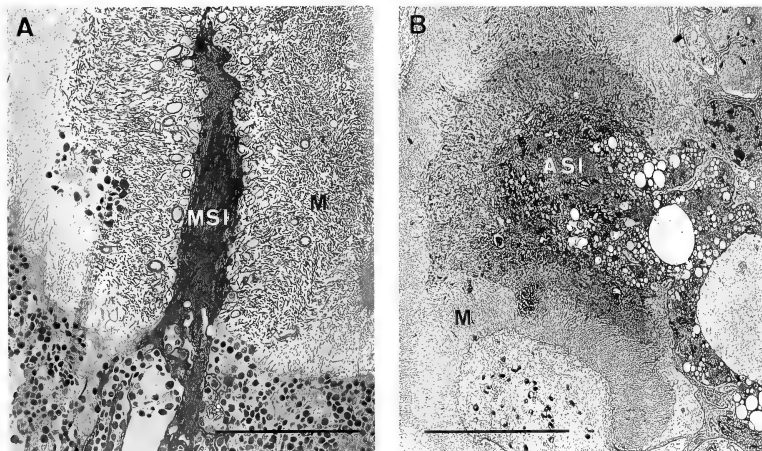


FIG. 7. Electron micrographs of sensory cell type I stained intracellularly with HRP. A, sensory cell type I in main retina. MSI, sensory cell type I in main retina; M, microvilli. B, sensory cell type I in accessory retina. ASI, sensory cell type I in accessory retina; M, microvilli. Receptor potential of each cell is shown in Fig. 4A and B. Calibration bar = 10 μ m.

response was 28 mV at 2.62 ($-\log I$) unit intensity. Therefore the criterion response was 14 mV. The sensory cells recorded in both retinas exhibit the same spectral sensitivity peaking at 460 nm. Open circles are data recorded from the accessory retina and filled circles are from the main retina. These were obtained from two preparations of each retina.

In no case was a receptor potential elicited by stimulus light having a wavelength greater than 700 nm, even if the stimulus intensity was -1 ($-\log I$) unit. After the recording, the sensory cells were labeled intracellularly with HRP and were confirmed as a sensory cell type I in the main retina (Fig. 7A) and a sensory cell type I in the accessory retina (Fig. 7B), respectively.

DISCUSSION

The accessory photosensory organ in the slug *Limax maximus* was first described by Henchman [1] and he used two terms, accessory retina and

accessory eye, for the organ in the report. But the following researchers hesitated to use the term accessory eye. For instance Smith [11] hesitated to use it because he could not find a septal structure between the two retinas in spite of the recognition of the discontinuity of the two cavities. In *Achatina fulica* these three items, accessory lens, septal structure and discontinuity of cavities, were stationary elements, which led me to call the organ an accessory eye [4]. This time I looked at the relationship of main retina to the accessory retina in *Limax flavus* and found a trace of lens and a septal structure as well as discontinuity of the two cavities. Concerning the accessory lens, the accessory retina in *Agriolimax reticulatus* was comparable to that of *Achatina fulica* (unpubl. data). It may be, therefore, preferable to revive the term accessory eye in slugs. I concluded that the situation and structure of the accessory eye in pulmonate was as follows. The accessory eye is situated in the corner of the cornea and discontinuous with the main eye. It is composed of two

types of sensory cells similar to those in the main eye and corneal cells or nonpigmented supporting cells.

The electrophysiological studies reported here showed that sensory cell type I in the accessory eye of the slug receives visible light similarly to the corresponding cell type in the main eye. In support of visible light reception by the accessory eye in *Limax flavus*, retinal pigments were detected with fluorescence microscopy [12]. Although the function of sensory cell type II in the accessory eye still remains unknown, structural similarity of sensory cell type II in the main and accessory eye may also exclude it from the candidate of infrared light receptor. The recording from the type II cells, anyhow, must be performed in the following study. The intensity-amplitude plots of the receptor potentials may present a higher part of the typical sigmoid curve [13]. Responses at lower light levels will be also the subjects of further studies. In the construction of a spectral sensitivity curve, a standard response was adopted in order to obtain a criterion response immediately and to reduce the effects of the intracellular-recording conditions on relative sensitivity in each cell. Although the standard response is a value used tentatively, it was reliable in comparing the relative sensitivity and providing the evidence of visible light reception by the accessory eye.

The work in this report showed that both sensory cells type I in the main and accessory eyes had a sensitivity peak at a wavelength of 460 nm, while the sensory cells type I in *Achatina fulica* had their peak at 480 nm [5] similarly to the peak of sensitivity in other gastropod eyes [14-18]. In another electrophysiological study of *Limax* main eye, the peak of spectral sensitivity at 460 nm was found in the light-adapted sample using spike discharge as the criterion response [6]. The report suggested that the sensitivity maximum for sensory cell type I is 480 nm and that for type II is 460 nm, which seems to be inconsistent with my data. The more close intracellular recording and HRP study will settle these inconsistency.

As one of the characteristics to advance speculation on the functions of the accessory eye, there is the difference in the location of the two eyes. The accessory eye is situated in the corner of the

cornea. If the eye preparation is illuminated from a direction other than the pupillary opening of pigment layer in the main eye, the main eye may not perceive the illumination, even though the accessory eye perceives it well. Such a condition was expected to occur in partially retracted optic tentacles and the accessory eye would be working specifically in these conditions [2, 5]. Newell and Newell observed the behavior of looking around with partially retracted optic tentacles in *Agriolimax reticulatus*. In the partially retracted optic tentacles, the eyeball was rotated about a right angle and the pupillary opening of the main eye was masked by epidermal tissues, while the accessory eye might be exposed to environmental light as in the fully extended tentacles. Therefore, the accessory eye may function principally as a luminous intensity meter in the partially retracted tentacle.

REFERENCES

1. Henchman, A. P. (1897) The eyes of *Limax maximus*. Science, N. S. 5: 428-429.
2. Newell, P. F. and Newell, G. E. (1968) The eye of the slug, *Agriolimax reticulatus* (Mull.). Symp. Zool. Soc. Lond. No. 23, 97-111.
3. Kataoka, S. (1977) Ultrastructure of the cornea and accessory retina in a slug, *Limax flavus* L. J. Ultrastr. Res., 60: 296-305.
4. Tamamaki, N. and Kawai, K. (1983) Ultrastructure of the accessory eye of the giant snail, *Achatina fulica* (Gastropoda, Pulmonata). Zoomorphology, 102: 205-213.
5. Tamamaki, N. (1989) Visible light reception of accessory eye in the giant snail *Achatina fulica*, as revealed by an electrophysiological study. Zool. Sci., 6:
6. Suzuki, H., Watanabe, M., Tsukahara, Y. and Tasaki, K. (1979) Duplex system in the simple retina of a gastropod mollusc, *Limax flavus* L., J. Comp. Physiol., 133: 125-130.
7. Graham, R. C. and Karnovsky, M. J. (1966) The early stages of absorption of injected horseradish peroxidase in the proximal tubules of mouse kidney: ultrastructural cytochemistry by a new technique. J. Histochem. Cytochem., 14: 291-302.
8. Kataoka, S. (1975) Fine structure of the retina of a slug, *Limax flavus* L. Vision Res., 15: 681-686.
9. Eakin, R. M. and Brandenburger, J. L. (1975) Retinal differences between light-tolerant and light-avoiding slugs (Mollusca: Pulmonata), J. Ultrastr.

- Res., **53**: 382-394.
- 10 Eakin, R. M. and Brandenburger, J. L. (1970) Osmic staining of amphibian and gastropod photoreceptors. *J. Ultrastr. Res.*, **30**: 619-640.
- 11 Smith, G. (1906) The eyes of certain pulmonate gastropods, with special reference to the neurofibrillae in *Limax maximus*. *Bull. Mus. Comp. Zool. Harvard Coll.*, **48**: 231-281.
- 12 Ozaki, K., Hara, R. and Hara, T. (1983) Histochemical localization of retinochrome and rhodopsin studied by fluorescence microscopy. *Cell Tissue Res.*, **233**: 335-345.
- 13 Naka, K. I. and Rushton, W. A. H. (1966) S-potentials from colour units in the retina of fish (Cyprinidae). *J. Physiol.*, **185**: 536-555.
- 14 Berg, E. and Schneider, G. (1972) The spectral sensitivity of the dark-adapted eye of *Helix pomatia* L. *Vision Res.*, **12**: 2151-2152.
- 15 Dennis, M. J. (1967) Electrophysiology of the visual system in a nudibranch mollusc. *J. Neurophysiol.*, **30**: 1439-1465.
- 16 Gillary, H. L. and Wolbarsht, M. L. (1967) Electrical responses from the eye of a land snail. *Rev. Cab. Biol.*, **26**: 125-134.
- 17 Gillary, H. L. (1974) Light-evoked electrical potentials from the eye and optic nerve of *Strombus*: response waveform and spectral sensitivity. *J. Exp. Biol.*, **60**: 383-396.
- 18 Hughes, H. P. I. (1970) The spectral sensitivity and absolute threshold of *Onchidoris fusca* (Muller). *J. Exp. Biol.*, **52**: 609-618.



Retinal Projections in the Himé Salmon (Landlocked Red Salmon, *Oncorhynchus nerka*)

TAKASHI SHIGA¹, YOSHITAKA OKA², MASAAHIKO SATOU,
NAOTO OKUMOTO³ and KAZUO UEDA

Zoological Institute, Faculty of Science, University of Tokyo,
Tokyo 113, and ³National Research Institute of Aquaculture,
Nikko Branch, Nikko 321-16, Japan

ABSTRACT—The retinofugal projections in the himé salmon (landlocked red salmon, *Oncorhynchus nerka*) were studied by means of the Fink-Heimer method, and the anterograde horseradish peroxidase and cobaltic-lysine methods. The major projections were found on the contralateral side in the nucleus anterioris periventricularis of the preoptic area, the nucleus opticus dorsomedialis, the nucleus commissuralis posterioris, the nucleus geniculatus lateralis, the nucleus opticus accessorius, the area pretectalis and the optic tectum. Direct retinal projections were not found within the nuclear boundaries of the area ventralis telencephali pars supracommissuralis and the nucleus preopticus periventricularis which are known to play important roles in sexual behavior.

INTRODUCTION

In the himé salmon (landlocked red salmon, *Oncorhynchus nerka*), Takeuchi *et al.* [1] have shown that the key stimulus for the male courtship behavior is visual. Newcomb *et al.* [2] have reached a similar conclusion in the rainbow trout. On the other hand, localized brain lesion and stimulation experiments have shown that several restricted regions within the telencephalic and preoptic areas including the area ventralis telencephali pars supracommissuralis and the neighboring posterior ventral telencephalon (Vs-pVv), and the nucleus preopticus periventricularis (NPP) of the medial preoptic area (MPOA) are involved in the sexual behavior of himé salmon [3-6] and other fish species [7-13]. To understand the visual information processing in the brain during the sexual behavior, it is indispensable, in the first place, to know the retinal projection areas and then the relationship between these areas and the

brain regions mentioned above which are supposed to be involved in the various aspects of the sexual behavior. In the present study, we examined the retinal projection areas of the himé salmon by means of Fink-Heimer method, and the anterograde HRP and cobaltic-lysine methods.

MATERIALS AND METHODS

Fish

We used 41 male and female himé salmon (landlocked red salmon, *Oncorhynchus nerka*). Twenty-one fish were 25.0-31.5 cm in body length and were captured at the mouth of a river flowing into Lake Chuzeji (Nikko City, Japan) in September and October, during a homeward migration about 3 years after hatching. Twenty fish were 20.0-34.0 cm in body length and were obtained from May to August in a pond of National Research Institute of Aquaculture, Nikko branch, where they had been cultured for about 3 years.

Fink-Heimer method

Nine fish were used. The fish were anesthetized by immersing them in a 0.03% tricaine methanesulfonate (MS 222) solution. The right eye was enucleated unilaterally and the orbit was

Accepted January 13, 1989

Received October 12, 1988

¹ Present address: Department of Anatomy, Yamagata University School of Medicine, Yamagata 990-23, Japan.

² To whom all correspondence should be addressed.

filled with vaseline and dental resin. The fish were allowed to survive for 12–32 days at 9°C.

After the survival period, the fish were anesthetized with 0.03% MS 222 and perfused through the conus arteriosus with 0.7% NaCl solution, followed by 10% formalin-saline. The brains were removed from the skull and were postfixed in 10% formalin containing 10% sucrose for more than two weeks at 4°C. The brains were embedded in egg yolk, serial frontal sections were cut at 30 μ m on a freezing microtome, and every fifth section was stained according to Ebbesson's modification of the Fink-Heimer method (Method 7 of [34]). The adjacent sections were stained with cresyl violet for histological identifications.

HRP method

Twenty-four fish were used. Eight to 20 μ l of 20–25% HRP (Toyobo, Grade I-C) were applied in four ways as follows. First group (two fish) received unilateral intraocular HRP injection using a microsyringe. In the remaining three groups (22 fish), the conjunctival membrane surrounding the eye was excised and the extraocular muscles were severed. After cutting the optic nerve close to the eye ball, the eye ball was removed. In the second group (two fish), a glass capillary with a tapered tip filled with the HRP solution was pricked into the proximal end of the cut optic nerve and the capillary was secured using vaseline and dental resin. In the third group (17 fish), the cut optic nerve was drawn into a polyethylene tube. Vaseline was used to secure the tube to the orbit, and the tube was filled with the HRP solution using a microsyringe. After filling the tube, the open end of the tube was sealed with vaseline and the orbit was covered with the dental resin. In the fourth group (three fish), a piece of Gelfoam (Japan Upjohn Ltd.) soaked in the HRP solution was placed on the cut end of the optic nerve and the orbit was filled with vaseline.

The fish were postoperatively maintained at 9°C. One to 14 days after the HRP-injection, they were reanesthetized with MS 222 and were perfused through the conus arteriosus with 0.7% NaCl solution containing 5 IU/ml heparin, followed by the primary fixative containing 1% paraformaldehyde and 1.25% glutaraldehyde in 0.1 M phosphate buffer (pH 7.4) and then the secondary

fixative containing 2.5% glutaraldehyde and 10% sucrose in 0.1 M phosphate buffer (pH 7.4). Immediately afterwards, the brains were dissected out and immersed in a 0.1 M phosphate buffer containing 30% sucrose for 12–24 hr. Serial frontal sections were cut at 40–60 μ m on a freezing microtome and mounted on gelatinized slides. The sections were processed using Mesulam's tetramethylbenzidine method [35] and were counterstained with neutral red.

Caobaltic-lysine method

Eight fish were used. Under the MS 222 anesthesia, 10–20 μ l of cobaltic lysine complex, prepared according to Görcs *et al.* [36], was applied unilaterally using the polyethylene tube in the same way as mentioned in the HRP method.

After the survival period between 7 and 14 days (at 9°C), the fish was decapitated. After dissecting out the brain, it was immersed in the 100 mM dibasic sodium phosphate solution saturated with H₂S for 20–30 min, fixed in 70% ethanol overnight, dehydrated, and embedded in paraffin. Serial frontal sections were cut at 40–50 μ m and mounted on gelatinized slide. The CoS precipitate was intensified using the sodium tungstate developer according to Görcs *et al.* [36], and the sections were counterstained with neutral red.

Nomenclature

The terminology of the brain areas and nuclei was mainly after Northcutt and Davis [37] for the telencephalon, and Billard and Peter [38] and Nieuwenhuys and Pouwels [39] for the diencephalon and the mesencephalon (except optic tectum). We used the terminology of Vanegas *et al.* [40] for the optic tectum.

ABBREVIATIONS

AP	area pretectalis
C	cerebellum
Dc	area dorsalis telencephali pars centralis
Dd	area dorsalis telencephali pars dorsalis
Did	area dorsalis telencephali pars lateralis dorsalis
Dlv	area dorsalis telencephali pars lateralis ventralis
Dm	area dorsalis telencephali pars medialis
Dp	area dorsalis telencephali pars posterioris
FDM	fasciculus dorsomedialis tractus optici

FR	fasciculus retroflexus
H	habenula
HOC	horizontal commissure
LI	lobus inferioris
LL	lemniscus lateralis
LPOA	lateral preoptic area
LV	nucleus lateralis valvulae
mOT	main optic tract
NAPv	nucleus anterioris periventricularis
NAT	nucleus anterior tuberis
NC	nucleus corticalis
NCP	nucleus commissuralis posterioris
NDL	nucleus dorsolateralis thalami
NDLI	nucleus diffusus lobi inferioris
NDM	nucleus dorsomedialis thalami
NDTL	nucleus diffusus tori lateralis
NE	nucleus entopeduncularis
NG	nucleus glomerulosus
NGL	nucleus geniculatus lateralis
NLTm	nucleus lateralis tuberis pars medialis
NNO	nucleus nervi oculomotorii
NOA	nucleus opticus accessorius
NODM	nucleus opticus dorsomedialis
NP	nucleus pretectalis
NPG	nucleus pregglomerulosus
NPO	nucleus preopticus
NPP	nucleus preopticus periventricularis
NPPv	nucleus posterioris periventricularis
NPT	nucleus posterior tuberis
NR	nucleus rotundus
NRL	nucleus recessus lateralis
NVM	nucleus ventromedialis thalami
NSV	nucleus saccus vasculosus
OB	olfactory bulb
OC	optic chiasm
ON	optic nerve
OT	optic tract
PC	posterior commissure
SAC	stratum album centrale
SFGS	stratum fibrosum et griseum superficiale
SGC	stratum griseum centrale
SM	stratum marginale
SO	stratum opticum
SPV	stratum periventriculare
SV	saccus vasculosus
TEL	telencephalon
TeO	optic tectum
TL	torus longitudinalis
TMC	tractus mesencephalocerebellaris anterior
TOA	tractus opticus accessorius
TOI	tractus opticus intermedius
TOL	tractus opticus lateralis
TOM	tractus opticus medialis
TS	torus semicircularis
Vp	area telencephali pars postcommissuralis

RESULTS

The retinal projections were examined in the present experiments using three different methods: the Fink-Heimer, HRP, and cobalt-lysine methods. Although the results obtained using these methods were essentially similar, the cobalt-filling method was most sensitive and revealed the most extensive retinal projections. Therefore, the following description is mainly based on the results obtained using the cobalt-filling method.

In the present study, cobalt-filled fibers of passage were characterized by a smooth, elongated appearance. Terminal areas were characterized by randomly oriented thin varicose fibers intermingled with granular profiles. The former probably represent terminal axonal arborizations in the plane of sectioning and the latter probably those oriented perpendicular to it. Although the final decision as to whether these profiles really represent synaptic terminals awaits examinations at the electron microscopic level, the present definition of the fibers of passage and terminals seems to be appropriate [see 19, 21, 27–33].

The retinal projections of the himé salmon were mostly contralateral, but sparse ipsilateral projections were also seen. Extensive contralateral projections in the diencephalon and mesencephalon were grouped into seven major terminal areas: NAPv of the POA, nucleus opticus dorsomedialis (NODM) of Ebesson [41], nucleus geniculatus lateralis (NGL), nucleus commissuralis posterioris (NCP), and nucleus opticus accessorius (NOA) of the diencephalon, and area pretectalis (AP) and optic tectum (TeO) of the mesencephalon.

Contralateral projections

Optic nerves, consisting of thick fibers, decussated at the optic chiasm (OC), and formed contralateral main optic tract (mOT) (Figs. 1A–D, 2). The main optic tract ran dorsocaudally toward the optic tectum, and at the level just rostral to the habenula, divided into three tracts; tractus opticus medialis (TOM), tractus opticus intermedius (TOI), and tractus opticus lateralis (TOL) (Figs. 1E, 3).

(1) POA and dorsal part of telencephalon

At the level of the rostral pole of the NAPv,

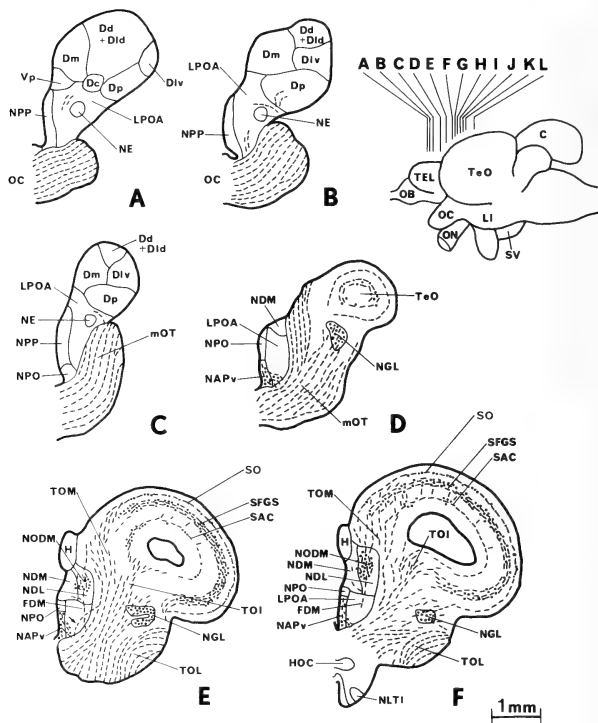


FIG. 1. Line drawings of frontal sections illustrating the retinal projections as determined using the cobaltic-lysine method. Dashes indicate cobalt-filled axons, while dots indicate cobalt-filled terminal fields. The inset shows the lateral view of the brain, and the levels of the sections are indicated.

several fine fibers branched from the main OT, ran dorsomedially in the ventral part of the LPOA, and terminated in the most rostral part of the NAPv (Figs. 1D, 4). Some of these fibers also terminated in the LPOA on the way to the NAPv. In some teleosts, this rostroventral part of the NAPv has been specifically named "the suprachiasmatic nucleus" [14, 19, 27]. After entering the NAPv, the fibers ran dorsocaudally along the ventricle and terminated in almost all parts of the NAPv (Fig. 1D-G). In the NPP and the NPO,

neither retinal fibers nor terminals were seen (Fig. 1A-G).

A few fine fibers were seen in the posterodorsal telencephalon (Dp) (Fig. 1B) and the lateral preoptic area near the nucleus entopeduncularis and lateral to the NPP (Fig. 1A-C).

(2) Other diencephalic and mesencephalic areas
A) Nucleus geniculatus lateralis (NGL)

At the level of the habenula (H), the main OT entered the most rostral part of the NGL (Fig. 1D). The retinal terminals were seen in almost

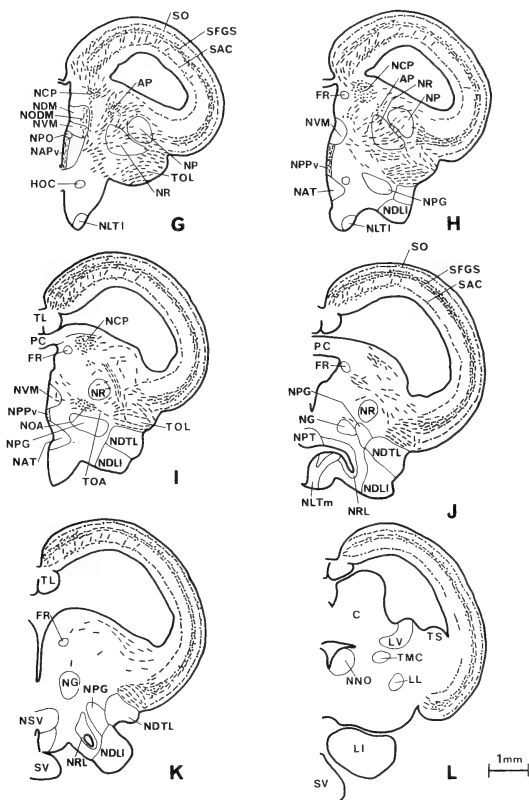


FIG. 1. Continued

entire part of the NGL, although the dorsolateral edge received heavier projections. In transverse sections both the NGL and the retinal terminal field appeared semilunar rostrally (Figs. 1D, 5A, B), U-shaped at the middle level with its opening facing medially (Figs. 1E, 3, 5C, D), and rectangular at the caudal level (Figs. 1F, 5E, F). Caudally, some fibers of the TOI passed through the NGL to enter the TeO. Recently, Braford and Northcutt

[14] renamed the NGL as the superficial pretectal parvocellular nucleus, because of its topography and the lack of projection to the telencephalon like the mammalian NGL.

B) Nucleus opticus dorsomedialis (NODM)

At more caudal level than the anterior margin of the NGL, a diffuse fiber bundle (fasciculus dorsomedialis tractus optici, FDM) branched from the medial margin of the TOM, ran dorsally through

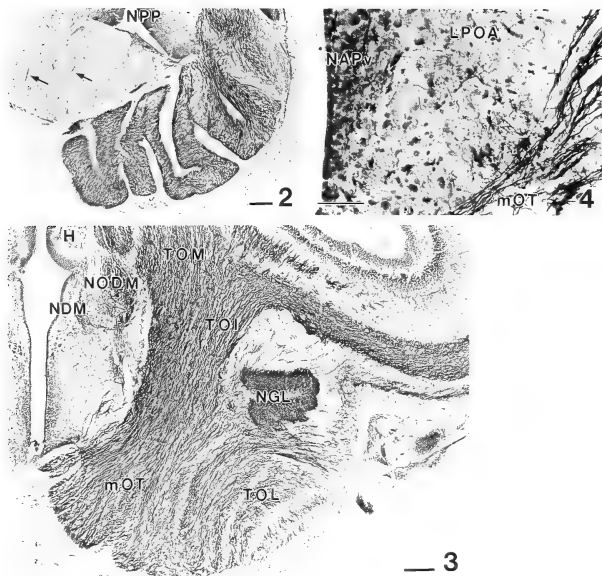


FIG. 2. Frontal section of the cobalt-filled optic nerve contralateral to the injection, at the level corresponding to that of Fig. 1A. A few cobalt-filled axons (arrows) also entered the ipsilateral optic nerve. Bar: 50 μ m.

FIG. 3. Frontal section through the rostral part of the habenula (H). The main optic tract (mOT) branched into the tractus opticus medialis (TOM), tractus opticus intermedius (TOI), and tractus opticus lateralis (TOL). Bar: 200 μ m.

FIG. 4. Frontal section through the rostral part of the nucleus anterioris periventricularis (NAPv), at the level corresponding to that of Fig. 1D. Some cobalt-filled axons branched from the main optic tract (mOT) to enter the NAPv through the lateral preoptic area (LPOA). 50 μ m.

the LPOA, to reach the nucleus dorsolateralis thalami (NDL), and made a major termination area there (Figs. 1E, 3, 6A, B). In addition, a small branch of the FDM also terminated in the lateral part of the nucleus dorsomedialis thalami (NDM) (Fig. 1E-G). At about the same level as the FDM branched from the TOM, thick fibers branched from the TOM, ran dorsolaterally in the LPOA just lateral to the NAPv, and rejoined the TOM (arrow in Fig. 1E). Some of these fibers branched dorsally to contribute to the FDM. Some terminals were also seen in the nucleus ventromedialis thalami (NVM) which appeared

ventral to the NDM at the caudal level of the habenula (Fig. 1G). These terminal areas ranging from the NDL to the lateral part of the NDM and the NVM seem to correspond collectively to the nucleus opticus dorsomedialis (NODM) of Ebbsen [41]. In the illustrations (Figs. 1, 3 and 6), the term "NODM" has been used in addition to "NDL", "NDM" and "NVM", to facilitate comparisons between Ebbsen's results [41] and ours. However, we should notice that the both nomenclatures are based on different criteria; the NODM of Ebbsen is a rather functional name, while the NDL, NDM and NVM are purely histological

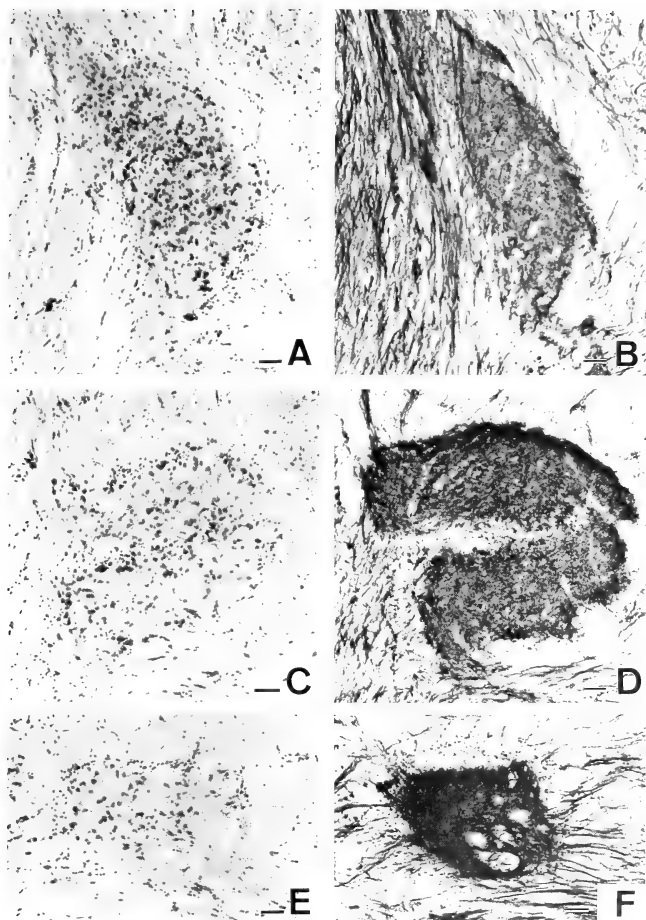


FIG. 5. Frontal sections of the Nissl-stained (A, C, E) and cobalt-labeled (B, D, F) nucleus geniculatus lateralis. A, B: rostral level, C, D: middle level, E, F: caudal level. Bar: 50 μ m.

ones. The NODM of the himé salmon continued caudally to the level just rostral to the posterior commissure (Figs. 1E-G, 7D). A small number of

fibers in the FDM ran dorsally through the NODM to enter the TeO, nucleus commissuralis posterioris and dorsal tegmentum (Fig. 1E-G).

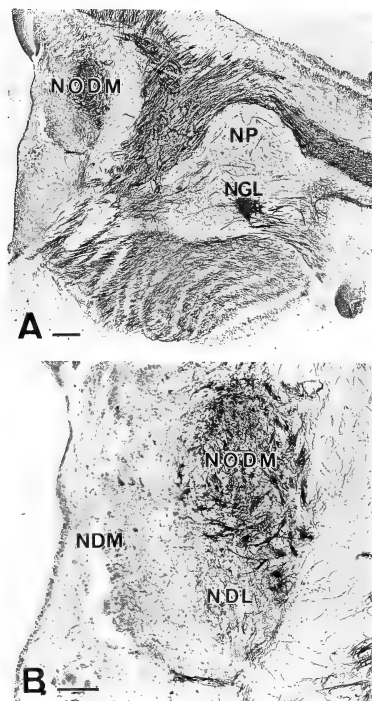


FIG. 6. A: Frontal section through the nucleus opticus dorsomedialis (NODM) and caudal part of the nucleus geniculatus lateralis (NGL). B: Higher magnification of the NODM shown in A. Cobalt-filled axon terminals of the NODM are distributed in the nucleus dorsolateralis thalami (NDL) and the lateral part of the nucleus dorsomedialis thalami (NDM). Bar: 200 μ m (A) and 50 μ m (B).

C) Nucleus commissuralis posterioris (NCP)

At the level caudal to the habenula, some fibers of the FDM ran through the NODM, entered the NCP, and terminated there (Figs. 1G-I, 7A, B). The NCP was located lateral to the fasciculus retroflexus (FR) and ventrolateral to the fibers of the posterior commissure, and was composed of sparsely distributed cells.

D) Nucleus posterioris periventricularis (NPPv)

At the level caudal to the horizontal commissure, the NAPv was gradually replaced caudally by the NPPv, which was situated dorsal to the nucleus anterior tuberculi (NAT) and ventral to the NVM. Some retinal fibers entered the NPPv after running through the NAPv, and terminated there (Figs. 1H, I, 7A, C).

E) Area pretectalis (AP)

At the level where the NGL disappeared and the NCP appeared, the TOI entered the AP (Figs. 1G, 7D). Although the majority of the TOI fibers passed through the AP to the tegmentum and the TeO, some of them formed patch-like terminal fields within the AP (Figs. 1G, H, 7E). In Nissl-stained preparations, the AP was composed of sparsely distributed cells and the nuclear boundary was obscure. The AP was delineated medially by the NODM, dorsomedially by the NCP, ventrally by the nucleus rotundus (NR) which was a globular nucleus of closely packed small cells, and ventrolaterally by the nucleus pretectalis (NP) which consisted of rather sparsely distributed large cells. Several discrete fiber bundles ran through the NR and the NP on their way to the TeO and the TOL, without terminating there (Figs. 1G-I, 7F). At the caudal part of the AP, a thick bundle connecting the AP and the TOL was seen dorsolateral to the NR (Fig. 1I, arrow in Fig. 7A).

F) Nucleus opticus accessorius (NOA)

A densely-packed fiber bundle (tractus opticus accessorius, TOA or basal optic tract) branched medially from the TOL and terminated in the area ventromedial to the NR and dorsal to the NPG (Figs. 1I, 7A). This area seems to correspond to the accessory or basal optic nucleus [15], although cells were scattered and the boundary was obscure in Nissl-stained preparations.

G) Optic tectum (TeO)

In the TeO, retinal fibers constituted three-layered terminal fields in the stratum opticum (SO), stratum fibrosum et griseum superficiale (SFGS) and stratum album centrale (SAC) (Figs. 1E-L, 8A). Small number of fibers in the SAC sometimes invaded the stratum periventriculare (SPV). Some fibers ran through the stratum griseum centrale (SGC) between the SAC and the SFGS (Fig. 8A-C). In the SO and SFGS, many

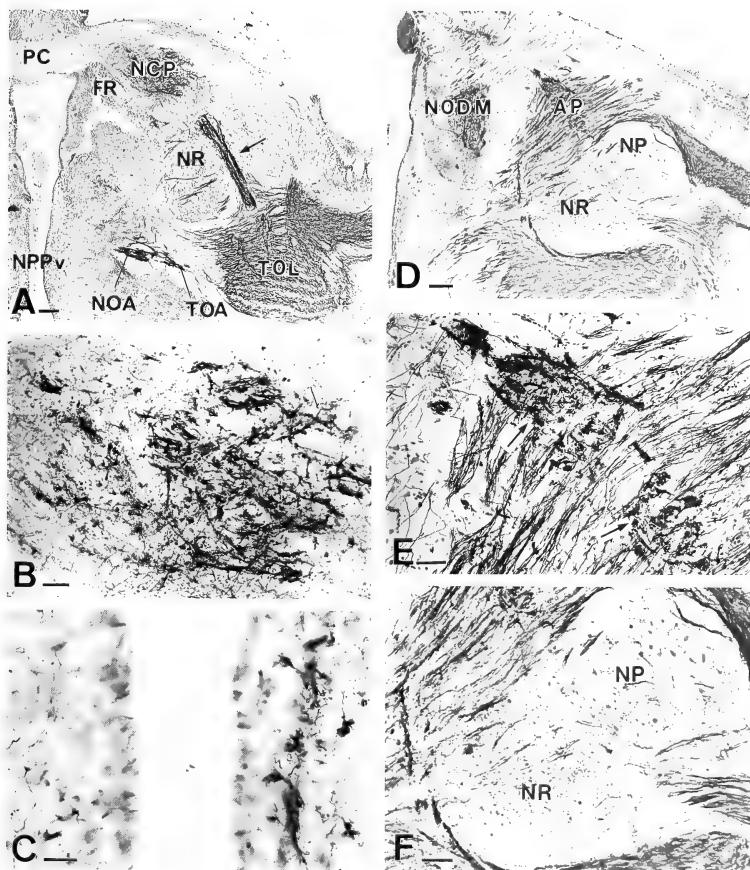


FIG. 7. A: Frontal section through the nucleus commissuralis posterioris (NCP), nucleus posterioris periventricularis (NPPv) and the nucleus opticus accessorius (NOA). A thick fiber bundle (arrow) connects the rostrally distributed area pretectalis (Fig. 7D) and the tractus opticus lateralis (TOL). B: Higher magnification of the terminal area in the NCP shown in A. C: Higher magnification of the axon terminals in the NPPv shown in A. D: Frontal section through the area pretectalis (AP) and the nucleus opticus dorsomedialis (NODM), at the level corresponding to that of Fig. 1G. E: Higher magnification of the AP shown in D. Cobalt-filled fibers formed patch-like terminal fields (arrows). F: Higher magnification of the nucleus rotundus (NR) and the nucleus pretectalis (NP) shown in D. Some cobalt-filled fibers passed through the NR and the NP. Bar: 200 μ m (A, D), 50 μ m (B, E) 20 μ m (C) and 100 μ m (F).

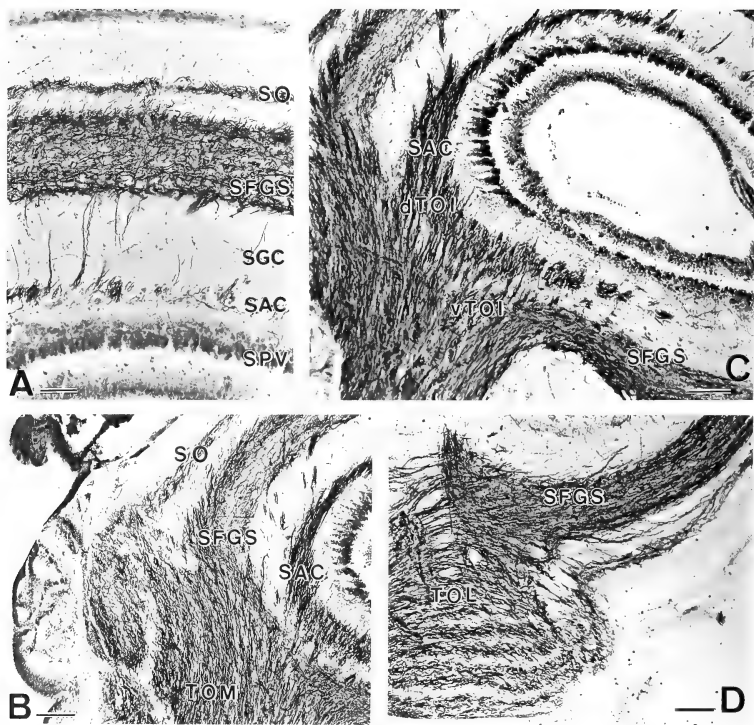


FIG. 8. Frontal sections showing the cobalt-filled axons and terminals in the optic tectum. A: Three-layered terminal fields in the stratum opticum (SO), stratum fibrosum et griseum superficiale (SFGS) and the stratum album centrale (SAC). B: The tractus opticus medialis (TOM) entered mainly the SO and the SFGS. C: The tractus opticus intermedius (TOI) branched into the dorsomedial (dTOL) and ventrolateral (vTOI) divisions. The dTOI mainly entered the SAC, while the vTOI mainly entered the SO and SFGS. D: The tractus opticus lateralis (TOL) entered mainly the SO and SFGS. Scale bar: 100 μ m (A), 20 μ m (B, C, D).

terminals were seen throughout the TeO. In the SAC, fibers and terminals were also distributed throughout the TeO, although more terminals were seen in the dorsomedial portion.

Fibers of the all three tracts (TOM, TOI, and TOL) contributed to these projections, although the course and the major stratum of termination were different among these tracts. The TOM entered the rostromedial portion of the TeO.

Majority of fibers in the TOM projected to the SO and SFGS, and some entered the SAC (Fig. 8B). The TOI was divided into the dorsomedial (dTOL) and ventrolateral (vTOI) branches at the entrance to the ventral portion of the TeO (Fig. 8C). The dorsomedial branch mainly entered the deep layer (SAC), while the ventrolateral branch ran through the tegmentum and mainly entered the intermediate layer (SFGS), and also made a minor projec-

tion to the deep layer (SAC). More caudally than the TOM and the TOI, the TOL entered the ventrolateral portion of the TeO. It terminated mainly in the SO and SFGS (Fig. 8D).

Ipsilateral projections

Ipsilateral retinal projections were observed in the NAPv, NODM, AP, NCP, and NOA, but not in the NGL and TeO, although they were fewer and sparser compared with the contralateral projections.

A few fibers were seen in the ipsilateral optic nerve at the optic chiasm (arrows in Fig. 2), which indicates the presence of retinal fibers running directly into the ipsilateral brain without decussating.

In the gray matter connecting both sides of the NAPv which made up the floor of the third ventricle, several recrossing fibers were seen running from the contralateral NAPv into the ipsilateral NAPv (arrowhead in Fig. 9). These recrossing fibers were seen rostrally from the level of the optic chiasm, and caudally to that of the horizontal commissure.

In the horizontal commissure, the posterior com-

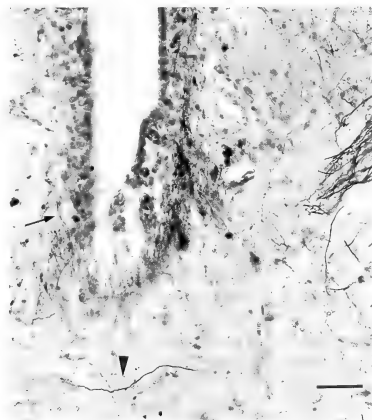


FIG. 9. Frontal section through the nucleus anterioris periventricularis (NAPv). Several cobalt-filled axons (arrowhead) recrossed to enter the NAPv (arrow) ipsilateral to the injected optic nerve. Scale bar: 50 μ m.

missure, and the intertectal commissure, however, such recrossing fibers were never seen.

Projection areas revealed by the Fink-Heimer and HRP methods

(1) Fink-Heimer method

In the POA, anterogradely degenerating fibers and terminals were observed in the LPOA lateral to the NAPv, but none of these degenerating fibers entered the NAPv. Similarly, degenerations were not observed in the LPOA lateral to the NPP where several cobalt-labeled fibers were seen.

Among the six major terminal areas in the diencephalon and midbrain revealed by the cobalt-filling method, many degenerating terminals were observed in the NODM, NCP, NGL, AP, and TeO, but only a few degenerating terminals were seen in the NOA.

A few silver grains were seen in the ipsilateral LPOA and NODM, indicating the presence of terminals. Since they were very sparsely distributed, it was often difficult to discriminate them from the background.

(2) HRP method

Among the four HRP-application methods, the method using the polyethylene tube revealed the most extensive retinal projections. In these materials, many HRP-labeled fibers were seen in all the major terminal areas shown by the cobalt-filling method. However, ipsilateral projections were never observed.

DISCUSSION

In the present study, the cobaltic-lysine method proved to be the most sensitive one, since the most extensive retinal projections were demonstrated by this method in comparison with the Fink-Heimer and HRP methods. Other similar cobalt-filling methods such as those using cobaltous-lysine [31–33] and cobalt chloride [30] have shown more extensive retinal projections than autoradiographic or anterograde degeneration methods in the goldfish, cichlid fish, and eel. Since it is not probable that the cobalt complex is transported transneuronally [31], the retinal projections shown in the present study can be regarded as truly primary projections.

In the himé salmon (the present study), the

NAPv received direct bilateral retinal projections, although the ipsilateral projections were scarce. In the LPOA lateral to the NPP, several retinal fibers of passage, not terminals, were recognized. In the NPP and the NPO, neither the retinal fibers nor the terminals were seen.

The direct retinal projection to the MPOA has so far been reported in many teleost species, but somewhat different results have been obtained depending on the species and the experimental methods.

It has been shown in some teleosts that the nucleus opticus hypothalami (NOH), which seems to correspond to the NAPv, or a part of the NAPv of the present study from the cytoarchitectural similarity, receive bilateral [14, 19, 23, 30], or contralateral [16, 22] retinal projections. It has also been reported that the region which might correspond to the NAPv of the present study receives bilateral [17, 21, 26] and contralateral [18, 25] retinal projections. The present study showed that there was no direct retinal projections to the NPO. It has, however, been shown in several teleosts that the nucleus opticus hypothalamicus, pars magnocellularis (NOHpm) or the nucleus preopticus pars magnocellularis (NPM), which seems to correspond to the NPO of the present study from the cytoarchitectural similarity, receives bilateral [23] or contralateral [16, 24] retinal projections.

Presence of direct retinal projections in the NPP seems to be still controversial. Reperant and Lemire [23] have reported in cyprinids the direct retinal projections in the "vicinity of the contralateral wall of the third ventricle" rostral to the NOHpm, which possibly corresponds to the NPP of the present study. In the goldfish, Springer and Gaffney [31] have found, using the cobaltous-lysine method, that the retinal projections to the POA are "far more complex than previously considered", and have reported four major fiber distributions (H1-H4) within the POA. It is inferred from their illustrations that the NPO and the NAPv, but not the NPP receive the direct bilateral retinal projections in the goldfish.

The retinal projections have been examined in many teleost species using the anterograde degeneration methods [14-26], autoradiographic

method [14, 17, 21-23, 26, 27], horseradish peroxidase (HRP) method [19, 21, 27-29] and cobalt-filling method [30-33]. In spite of some minor differences, there seems to be a general agreement that the optic tectum (TeO) receives a major retinal projection, and several diencephalic and mesencephalic areas receive some minor retinal projections. Although the cytoarchitecture of the telencephalon and the preoptic area is basically similar among teleosts, there are some interspecific variations in that of the diencephalon and the mesencephalon. In addition, the ambiguity of the cytoarchitectural description and the lack of uniformity of nomenclature have made it very difficult to compare retinal projections in the diencephalon and the mesencephalon among different teleost species. Therefore, we focus on the comparison of the retinal projections in areas other than the MPOA between *Salmo* and *Oncorhynchus*.

The retinal projections of the rainbow trout (*Salmo gairdneri*) have been studied using the Fink-Heimer and the autoradiographic methods [22]. The comparison of retinal projections between the rainbow trout and the himé salmon in the present study revealed the following similarities and differences. In both the rainbow trout and the himé salmon, the optic tract is divided into three bundles. Furthermore, the centrum opticum thalamicum (corresponding to the NODM of the present study), centrum opticum thalamopretectale (corresponding to the NCP of the present study), centrum opticum basale thalami (corresponding to the NOA of the present study), centrum opticum pretectale (corresponding to the AP of the present study), and TeO receive contralateral retinal projections.

On the contrary, there are several differences in the retinal projections between the two: (a) A few retinal fibers were seen in the Dp of the himé salmon, while no such fibers were described in the rainbow trout. (b) Sparse ipsilateral projections to the NODM, the NCP, and the AP were seen in the himé salmon, while the retinal projections of the rainbow trout were completely contralateral. (c) In the himé salmon, the retinal fibers in the SO, SFGS and SAC were seen throughout the TeO. In the rainbow trout, however, the retinal fibers in the SAC were restricted in the dorsomedial part of

the TeO, although those in the SO and SFGS were seen throughout the TeO. (d) In the rainbow trout, the centrum opticum laterale thalami, medial to the area thalamica lateralis which seems to correspond to the nucleus rotundus of the present study, receives contralateral retinal projections.

It is a future problem to know how the visual informations conveyed from the retina to the projection areas clarified in the present study reach the brain regions involved in the sexual behavior (Vs-pVv, NPP, etc.).

ACKNOWLEDGMENTS

The authors wish to thank the staff of the Lake Chuzenji Fishery Associations for providing the fish.

REFERENCES

- Takeuchi, H., Takei, K., Satou, M., Matsushima, T., Okumoto, N. and K. Ueda (1987) Visual cues as key stimuli for courtship behavior in male himé salmon (landlocked red salmon, *Oncorhynchus nerka*). *Anim. Behav.*, **35**: 936-939.
- Newcomb, C. P. and Hartman, G. F. (1980) Visual signals in the spawning behavior of rainbow trout. *Can. J. Zool.*, **58**: 1751-1757.
- Satou, M. (1987) A neuroethological study of reproductive behavior in the salmon. *Proceedings of the Third International Symposium on Reproductive Physiology of Fish*. 154-159.
- Satou, M., Oka, Y., Fujita, I., Koyama, Y., Shiga, T., Kusunoki, M., Matsushima, T. and Ueda, K. (1982) Effects of brain lesion and electrical stimulation on sexual behavior in himé salmon (land-locked red salmon, *Oncorhynchus nerka*). *Zool. Mag.*, **91**: 459.
- Satou, M., Oka, Y., Kusunoki, M., Matsushima, T., Kato, M., Fujita, I. and Ueda, K. (1984) Telencephalic and preoptic areas integrate sexual behavior in himé salmon (landlocked red salmon, *Oncorhynchus nerka*): Results of electrical brain stimulation experiments. *Physiol. Behav.*, **33**: 441-448.
- Satou, M. and Ueda, K. (1982) Brain mechanisms of salmon sexual behavior. In "Mechanisms of sexual behavior". Ed. by E. Ohnishi and T. Hisada, Sangyo-Tosho, Tokyo, pp. 5-19.
- Demski, L. S. and Knigge, K. M. (1971) The telencephalon and hypothalamus of the bluegill (*Lepomis macrochirus*): evoked feeding, aggressive and reproductive behavior with representative frontal sections. *J. Comp. Neurol.*, **143**: 1-16.
- Koyama, Y., Satou, M., Oka, Y. and Ueda, K. (1984) Involvement of the telencephalic hemispheres and the preoptic area in sexual behavior of the male goldfish, *Carassius auratus*: A brain-lesion study. *Behav. Neural. Biol.*, **40**: 70-86.
- Kyle, A. L. and Peter, R. E. (1982) Effects of forebrain lesions on spawning behavior in the male goldfish. *Physiol. Behav.*, **28**: 1103-1109.
- Kyle, A. L., Stacey, N. E. and Peter, R. E. (1982) Ventral telencephalic lesions: effects on bisexual behavior, activity, and olfaction in the male goldfish. *Behav. Neural. Biol.*, **36**: 229-241.
- Macey, M. J., Pickford, G. E. and Peter, R. E. (1974) Forebrain localization of the spawning reflex response to exogenous neurohypophyseal hormones in the killifish, *Fundulus heteroclitus*. *J. Exp. Zool.*, **190**: 269-280.
- Davis, R. E. and Kassel, J. (1983) Behavioral functions of the teleostean telencephalon. In "Fish Neurobiology, Vol. 2". Ed. by R. E. Davis and R. G. Northcutt, University of Michigan Press, Ann Arbor, pp. 237-264.
- Demski, L. S. (1983) Behavioral effects of electrical stimulation of the brain. In "Fish Neurobiology, Vol. 2". Ed. by R. E. Davis and R. G. Northcutt, Univ. of Michigan Press, Ann Arbor, pp. 317-360.
- Braford, Jr. M. and Northcutt, R. G. (1983) Organization of the diencephalon and pretectum of the ray-finned fishes. In "Fish Neurobiology, Vol. 2". Ed. by R. E. Davis and R. G. Northcutt, Univ. of Michigan Press, Ann Arbor, pp. 117-163.
- Campbell, C. B. G. and Ebbesson, S. O. E. (1969) The optic system of a teleost: *Holocentrus* re-examined. *Brain Behav. Evol.*, **2**: 415-430.
- Ebbesson, S. O. E. (1968) Retinal projections in two teleost fishes (*Opsanus tau* and *Gymnothorax funebris*). An experimental study with silver impregnation methods. *Brain Behav. Evol.*, **1**: 134-154.
- Ebbesson, S. O. E. and Ito, H. (1980) Bilateral retinal projections in the black piranha (*Serrasalminus niger*). *Cell Tissue Res.*, **213**: 483-495.
- Ebbesson, S. O. E. and O'Donnel, D. (1980) Retinal projections in the electric catfish (*Malapterurus electricus*). *Cell Tissue Res.*, **213**: 497-503.
- Fernald, R. D. (1982) Retinal projections in the African cichlid fish, *Haplochromis burtoni*. *J. Comp. Neurol.*, **206**: 379-389.
- Gulley, R. E., Cochran, M. and Ebbesson, S. O. E. (1975) The visual connections of the adult flatfish, *Achirus lineatus*. *J. Comp. Neurol.*, **162**: 309-320.
- Meyer, D. L. and Ebbesson, S. O. E. (1981) Retinofugal and retinopetal connections in the upside-down catfish (*Synodontis nigriventris*). *Cell Tissue Res.*, **218**: 389-401.
- Pinganaud, G. and Clairambault, P. (1979) The visual system of the trout *Salmo irideus* Gibb. A

- degeneration and radioautographic study. *J. Hirnforsch.*, **20**: 413-431.
- 23 Reperant, J. and Lemire, M. (1976) Retinal projections in cyprinid fishes: A degeneration and radioautographic study. *Brain Behav. Evol.*, **13**: 34-57.
 - 24 Sharma, S. C. (1972) The retinal projections in the goldfish. An experimental study. *Brain Res.*, **39**: 213-223.
 - 25 Vanegas, H. and Ebbesson, S. O. E. (1973) Retinal projection in the perch-like teleost *Eugerres plumieri*. *J. Comp. Neurol.*, **151**: 331-358.
 - 26 Voneida, T. J. and Sligar, C. M. (1976) A comparative neuroanatomic study of retinal projections in two fishes: *Astyanax hubbsi* (the blind cave fish), and *Astyanax mexicanus*. *J. Comp. Neurol.*, **165**: 89-106.
 - 27 Prasada Rao, P. D. and Sharma, S. C. (1982) Retinofugal pathways in juvenile and adult channel catfish, *Ictalurus (Ameiurus punctatus)*: An HRP and autoradiographic study. *J. Comp. Neurol.*, **210**: 37-48.
 - 28 Presson, J., Fernald, R. D. and Max, M. (1985) The organization of retinal projections to the diencephalon and pretectum in the cichlid fish, *Haplochromis burtoni*. *J. Comp. Neurol.*, **235**: 360-374.
 - 29 Rajendra Babu, P. and Prasada Rao, P. D. (1988) Retinal projections in the catfish, *Mystus vittatus* (Bloch) as revealed by tracer studies with horseradish peroxidase. *Cell Tissue Res.*, **253**: 259-262.
 - 30 Ekström, P. (1982) Retinofugal projections in the eel, *Anguilla anguilla* L. (Teleostei), visualized by cobalt-filling technique. *Cell Tissue Res.*, **225**: 507-524.
 - 31 Springer, A. D. and Gaffney, J. S. (1981) Retinal projections in the goldfish: a study using cobaltous-lysine. *J. Comp. Neurol.*, **203**: 401-424.
 - 32 Springer, A. D. and Mednick, A. S. (1985) Retinofugal and retinopetal projections in the cichlid fish *Astronotus ocellatus*. *J. Comp. Neurol.*, **236**: 179-196.
 - 33 Springer, A. D. and Mednick, A. S. (1985) Topography of the retinal projections to the superficial pretectal parvicellular nucleus of goldfish: A cobaltous-lysine study. *J. Comp. Neurol.*, **237**: 239-250.
 - 34 Ebbesson, S. O. E. (1970) The selective silver impregnation of degenerating axons and their synaptic endings in nonmammalian species. In "Contemporary research methods in neuroanatomy". Ed by W. J. H. Nauta and S. O. E. Ebbesson, Springer-Verlag, Berlin, pp. 132-161.
 - 35 Mesulam, M. M. (1978) Tetramethyl benzidine for horseradish peroxidase neurohistochemistry: A non-carcinogenic blue reaction-product with superior sensitivity for visualizing neural afferents and efferents. *J. Histochem. Cytochem.*, **26**: 106-117.
 - 36 Görös, T., Antal, M., Oláh, E. and Székely, G. (1979) An improved cobalt labeling technique with complex compounds. *Acta biol. Acad. Sci. hung.*, **30**: 79-86.
 - 37 Northcutt, R. G. and Davis, R. E. (1983) Telecephalic organization in ray-finned fishes. In "Fish Neurobiology. Vol. 2". Ed. by R. E. Davis and R. G. Northcutt, University of Michigan Press, Ann Arbor, pp. 203-236.
 - 38 Billard, R. and Peter, R. E. (1982) A stereotaxic atlas and technique for nuclei of the diencephalon of rainbow trout (*Salmo gairdneri*). *Reprod. Nutr. Develop.*, **22**: 1-25.
 - 39 Nieuwenhuys, R. and Pouwels, E. (1983) The brain stem of actinopterygian fishes. In "Fish Neurobiology, Vol. 1". Ed. by R. G. Northcutt and R. E. Davis, University of Michigan Press, Ann Arbor, pp. 25-88.
 - 40 Vanegas, H., Ebbesson, S. O. E. and Laufer, M. (1984) Morphological aspects of the teleostean optic tectum. In "Comparative Neurology of the Optic Tectum". Ed. by H. Vanegas, Plenum Press, New York/London, pp. 93-120.
 - 41 Ebbesson, S. O. E. (1972) A proposal for a common nomenclature for some optic nuclei in vertebrates and the evidence for a common origin of two such cell groups. *Brain Behav. Evol.*, **6**: 75-91.

Electron Microscopical and Histochemical Studies of the Spontaneous Tumors of *Xenopus laevis*

MAKOTO ASASHIMA, TSUTOMU OINUMA¹ and SHINJI KOMAZAKI²

Department of Biology, Yokohama City University, Kanazawa-ku, Yokohama 236,

¹Department of Anatomy, Miyazaki Medical School, Kiyotake, Miyazaki 889-16,

and ²Department of Anatomy, Saitama Medical School,
Moroyama, Saitama 350-04, Japan

ABSTRACT—Spontaneous tumors were found in eight *Xenopus laevis* (African clawed toads), and their various properties were studied. In five of the eight cases, the primary tumor appeared on the back and infiltrated the muscles of the abdomen and thighs. Destruction of muscle fibers by the tumor cells was observed. Virus particles were found in the middle and outer layers of the original tumor mass. They had apparently first appeared in the nucleus and then aggregated near the nuclear membrane, finally spilling out into the cytoplasm. Based on their movement from nucleus to cytoplasm and morphological form and size, the virus particles were presumed to be of the herpes type. DOPA tests revealed premelanophore cells, with tyrosinase activity but no melanin granules, in the tumors. The tumors appeared to consist of melanophoma cells and granules in different stages of differentiation. It was possible to transplant the tumors to normal toads, four out of fifteen becoming progressive.

INTRODUCTION

There are markedly fewer reports on spontaneous tumors in amphibians than in other vertebrates [1-3]. Lucké renal adenocarcinoma in *Rana pipiens* [4, 5] and Japanese newt papilloma in *Cynops pyrrhogaster* [6-8] have been investigated as amphibian tumors, but reports on other amphibian tumors have been sporadic.

Although African clawed toads (*Xenopus laevis*) are used as experimental animals world-wide, there have been few reports on tumors in this species [9-16].

At the rate of 10,000 per annum, we surveyed about 40,000 adult *X. laevis* breeding in an artificial pond between 1983 and 1986, and found eight large tumor-bearing toads. Examinations previous to this study had shown such tumors to be of melanophoma form and to contain virus particles [16]. Cell cultures derived from those tumors were established, and four cell lines containing both melanoma and neuroma cells had been obtained [15].

The eight tumor-bearing toads were used in the present study to further examine certain characteristics and properties of the tumors.

MATERIALS AND METHODS

Animal

Tumors were found in a total eight of 40,000 African clawed toads (*Xenopus laevis*) examined between 1983 and 1986. They were maintained at 20°C in a plastic aquarium until the time of autopsy [16]. Each toad, having a large tumor on its back, as shown in Figure 1, was anesthetized with MS-222 (Sankyo Co.) and subjected to gross biopsy.

Preparation for transmission electron microscopy

As shown in Figure 1, the original spontaneous tumor appeared under the skin of the back and infiltrated muscles of the abdomen and the right thigh. Tissue samples were taken from both the primary tumor and the infiltrated regions, and small blocks were prepared. For electron microscope examination, specimens were fixed in a buffered (0.05 M phosphate buffer, pH 7.2) 2.5% glutaraldehyde solution containing 2% paraform-

aldehyde and 0.1% picric acid, and embedded in Epon. Sections were stained with 2% uranyl acetate and lead citrate and examined with a JEM-100C electron microscope.

DOPA Test

Part of the tumor tissue was removed and sliced into sections approximately $3 \times 3 \times 1$ mm which were then fixed for 30 min in 5% formalin embedded in ice. They were rinsed in a 0.1 M phosphate buffer. Tyrosinase activity against 3,4-dihydroxyphenylalanine (L-DOPA) and L-tyrosine was examined histochemically in accordance with Lerner's method [17]. Incubation of the specimens in the reaction mixture was performed at 25°C. In the control experiments, either a substrate-free reaction mixture, heat-inactivated specimens (10 min in boiling water), or a reaction mixture to which 10 mM sodium diethyldithiocarbamate had been added as an inhibitor was used. After incubation, specimens were again fixed in Bouin's solution, embedded in paraffin, sectioned and counterstained with Körnechrot.

Transplantation Study

Fifteen unaffected normal control toads, 7 males and 8 females, were selected from the laboratory breeding colony as tumor transplant recipients. Their body surface was wiped with 70% ethanol.

Part of tumor tissue obtained from the original 8 affected toads was cut into 2 mm^3 cubes. Each cube was inserted into a small pocket created under the skin of a control toad's back with a sharp knife. After the operation, each recipient toad was covered with cotton gauze soaked in an antibiotic (Kanamycin-sulfate; Banyu Co., Tokyo) solution for a few days to protect the injured region from infection. They were then observed for 8 months.

RESULTS

Gross Observations

A spontaneous original tumor was found under the skin of the back, as shown in Figure 1, of five of the eight original toads, on the legs of two, and on the abdomen of one. In this study, only the tumors on the backs of the five toads were used as

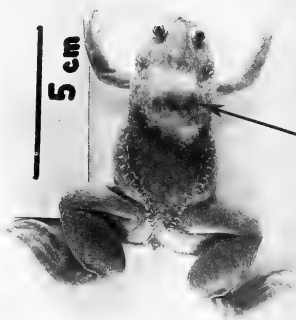


FIG. 1. Tumor-bearing *Xenopus*. The tumor (arrow) is seen on its back.

starting material. Vertical section specimens obtained from these five primary tumors demonstrated a thin cartilage plate connecting to the scapula. There were two layers of tumor tissue, one above and one below the cartilage. The five tumors did not remain within the primary region but infiltrated into muscles of such other regions as the abdominal wall (*m. obliquus externus*) and right thigh (*m. cruralis* and *m. gluteus magnus*).

Electron microscope observations

Presence of Virus Tumor tissue could be separated into three layers under low power magnification (Fig. 2A). The inner layer was necrotic but no virus particles could be seen in the observed cells (162 cells, 0%). Active tumor cells were found in the middle layer, and many (35 of 241 cells, 14.5%) contained virus particles. In the outer layer, tumor cells were narrower and more concentrated, but fewer (4 of 196 cells, 2.0%) contained virus particles than in the middle layer.

The virus particles in the middle layer were then examined at higher magnifications. They had first

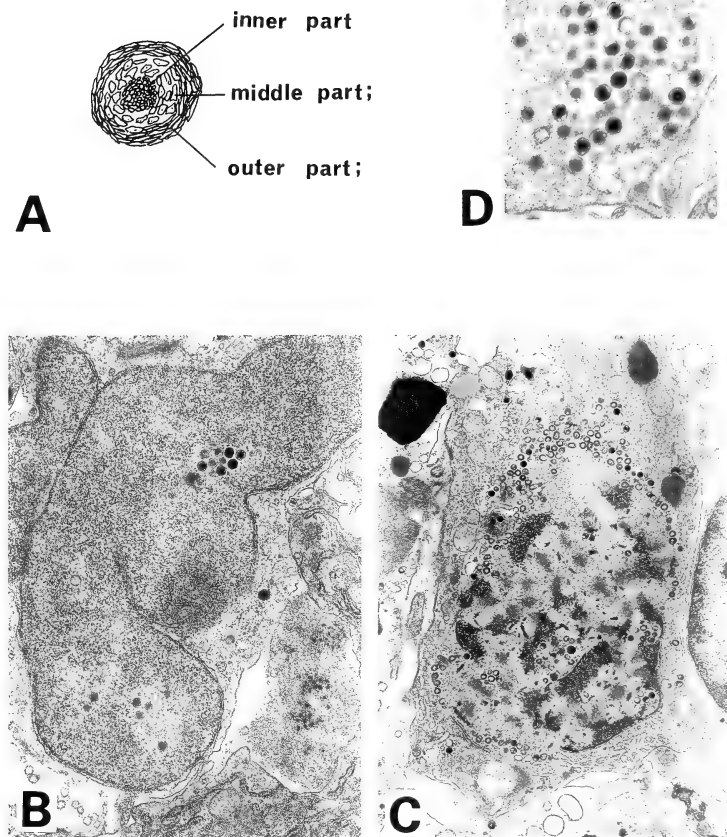


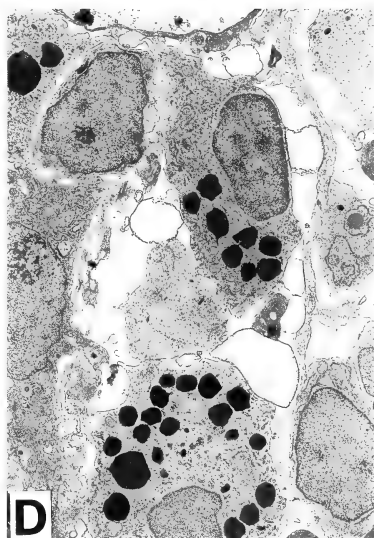
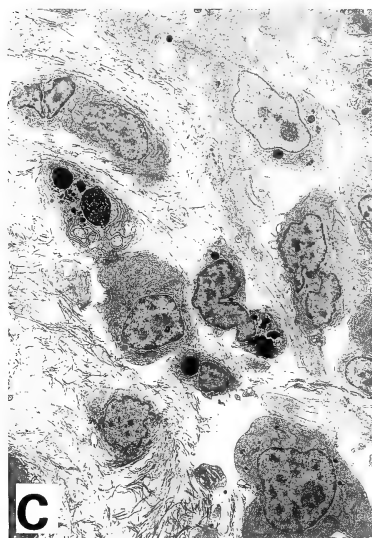
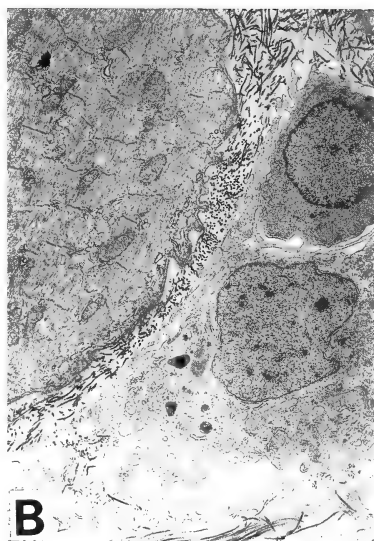
FIG. 2. Virus particles in tumor cells.

(A) Diagram of three layers of tumor mass containing virus particles ($\times 1.5$).

(B) Virus particles are first seen in the nucleus of tumor cells ($\times 13,700$).

(C) The particles have spilled out from the nucleus into the cytoplasm ($\times 9,100$).

(D) High magnification of virus particles found in *Xenopus* tumor cells ($\times 22,000$).



appeared in the nucleus (Fig. 2B). When they had filled the nucleus, they aggregated near the nuclear membrane and spilled out into the cytoplasm (Fig. 2C). The particles were about $0.15\ \mu\text{m}$ in diameter (Fig. 2D). Based on these observations, the virus observed in all five toads (100%) was presumed to be of the herpes type.

Infiltration of tumor cells Gross observation revealed the five back tumors to have infiltrated the abdomen and thighs. The process of infiltration was observed in the muscles of the thigh. The regular arrangement of striated muscle fibers was preserved in that region as yet not reached by tumor cells (Fig. 3A). Destruction of muscle fibers began at the point of intrusion of tumor cells into the muscle (Fig. 3B). Tumor cells moved through the connective tissue and they infiltrated into other tissues (Fig. 3C). Finally, only irregularly shaped tumor cells containing electron dense granules could be seen (Fig. 3D). Based on these observations, the tumor was thought to be malignant.

DOPA Test

A previous study had indicated that the tumors

were melanophoma-like because melanin granules had been observed in parts of the tumor mass. We therefore utilized the DOPA test to examine whether or not premelanophore cells which did not contain melanin granules, but had the ability to synthesize melanin, were present. Reaction-positive cells were detected as cell islands in tumor tissue when L-DOPA was used as a substrate (Fig. 4). Melanin granules were not seen in these cells. Some mature melanophores were seen near the positive cell islands, but such activity was not detected when L-tyrosine was used. In the control experiments, no reaction products were found.

Transplantation Study

Within eight months after tumor transplantation, swellings appeared on the backs of seven of the 15 toads. In four cases, the swellings grew to 0.5 cm in diameter during the first three months and to 0.9 cm within eight months. In the three other cases, the swellings grew to 0.5 cm during the first three months and then remained stable thereafter. With the transplants showing progressive growth in four toads, there was clear indica-

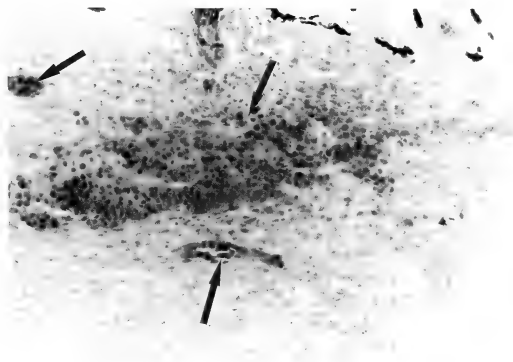


Fig. 4. Histological section of DOPA-positive cells (arrows) in tumor cells ($\times 150$).

Fig. 3. Degradation of muscle fibers by invading tumor cells.

(A) to (D) show progressive advancement of invasion by tumor cells. Normal regular microfilaments are destroyed in this penetration by tumor cells. magnification:

(A) $\times 2,200$ (B) $\times 5,6000$ (C) $\times 2,200$ (D) $\times 5,800$

tion that the tumors could be transplanted in normal toads.

DISCUSSION

There is a low frequency of spontaneous tumors in *Xenopus laevis*, only eight being found among 40,000 adult toads. Of the eight, five toads bearing tumors on their backs were subjected to biopsies. The tumors were found to be highly infiltrative, intruding from the primary region on the back into the muscles of the abdomen and the thighs. The process of tumor-cell infiltration into the muscles, resulting in destruction of muscle fibers, was observed. The muscle fibers dissolved into fragments and only their residue remained. Based on these observations, there was no doubt the tumor was malignant.

There have been no reports of such infiltration of tumors in amphibians. Lucké renal carcinoma cells proliferate and result in so-called renal adenocarcinoma [4, 5]. Epithelioma has been observed in the newt, *Cynops pyrrhogaster* [6, 8]. The cells of these tumors grow in the primary region of the tumor and do not infiltrate other tissues as in the manner of the *Xenopus* tumor.

In regard to tumors, virus particles are observed in some kinds of amphibians, such as *Rana pipiens* [4, 5, 18], *Xenopus laevis* [16, 19] and newt *Cynops pyrrhogaster* [6, 7, 20].

The inner layer of each primary tumor in our study was necrosed, but tumor cells in the middle layer appeared to be active, forming fibroblastic or moving cells. There was a high frequency of discovery of virus particles in this middle layer. Virus particles also were found in cells of the outer layer, but at a lower frequency.

In view of the preceding observations, we wondered what role the virus particles play. Did their presence lead to the necrosis of the inner layer and their own elimination, or are they responsible for the activity and condition of cells in the outer and, especially, middle layers? We do not know, but either could be possible.

The virus particles were observed to have first appeared in the nucleus. When the nucleus was filled, virus particles aggregated near the nuclear membrane and spilled out into the cytoplasm.

Virus particles were about 0.15 μ m in diameter. The movements, size and shape of the particles indicate the virus to likely be of the herpes type, resembling the herpes virus of Lucké renal adenocarcinoma [4, 5, 18].

We previously [16] found melanophores containing melanin granules in *Xenopus* tumor tissue, leading us to believe *Xenopus* tumors were similar to melanophoma. In this study, the tyrosinase activity of cells which did not contain melanin granules was examined by means of the DOPA test. Reaction products were detected in such cells. Hence, premelanophore cells with tyrosinase activity were involved in the tumor. Using the same type of tumor mass from *Xenopus*, Asashima *et al.* [15] have cultured cells for over 2 years and found four cell lines deriving from one of the *Xenopus* tumors.

Cells synthesizing melanin granules were found in only one of these cell lines. In a culture of these cells, the property of synthesizing melanin granules appeared after several weeks of subculture. The *Xenopus* tumors appeared to be multiple melanophomas which contained tumor cells in different stages of differentiation. Melanophoma (or melanoma) are rare in amphibians [21–23], so progress is expected in investigations of amphibian tumors with use of the *Xenopus* tumor.

In this study, tumor transplantation was partially successful: 7 out of 15 cases. Four of the transplants have been progressive for over eight months. This progressive nature of the *Xenopus* tumor may enable tumor transplantation and cell culture and prove to be a more satisfactory research material than the newt epithelioma. Further studies of the characterization and properties of the *Xenopus* tumor would be useful in the fields of biological and comparative tumors research [3, 24].

ACKNOWLEDGMENTS

This work was supported in part by a Grant-in-Aid for Cancer Research from the Ministry of Education, Culture and Science of Japan.

REFERENCES

- 1 Schlumberger, H. G. and Lucké, B. (1948) Tumors

- of fishes, amphibians, and reptiles. *Cancer Res.*, **8**: 657-753.
- 2 Balls, M. and Clothier, R. H. (1974) Spontaneous tumors in amphibia. A review. *Oncology*, **29**: 501-519.
 - 3 Asashima, M., Oinuma, T. and Meyer-Rochow, V. B. (1987) Tumors in amphibia. *Zool. Sci.*, **4**: 411-425.
 - 4 Mizell, M. (1969) State of the Art: Lucké renal adenocarcinoma. In "Biology of Amphibian Tumors". Ed. by M. Mizell, pp. 1-25. Springer-Verlag, New York.
 - 5 Rafferty, K. A. Jr. (1964) Kidney tumors of the leopard frog: A review. *Cancer Res.*, **24**: 169-185.
 - 6 Asashima, M. and Oinuma, T. (1982) Transplantation and injection of skin papilloma fragments in newts (*Cynops pyrrhogaster*). *J. Fac. Sci. Univ. Tokyo, Sec. IV*, **15**: 151-158.
 - 7 Asashima, M., Komazaki, S., Satou, C. and Oinuma, T. (1982) Seasonal and geographical changes of spontaneous skin papillomas in the Japanese newt *Cynops pyrrhogaster*. *Cancer Res.*, **42**: 3741-3746.
 - 8 Asashima, M., Oinuma, T., Matsuyama, H. and Nagano, M. (1985) Effects of temperature on papilloma growth in the newt, *Cynops pyrrhogaster*. *Cancer Res.*, **45**: 1198-1205.
 - 9 Elkan, E. (1960) Some interesting pathological cases in amphibia. *Proc. Zool. Soc., London*, **134**: 375-396.
 - 10 Elkan, E. (1963) Three different types of tumors in Salientia. *Cancer Res.*, **23**: 1641-1645.
 - 11 Reichenbach-Klinke, H. and Elkan, E. (1965) Principal Diseases of Lower Vertebrates. II. Diseases of Amphibians. Academic Press, New York, pp. 1-381.
 - 12 Elkan, E. (1968) Two cases of epithelial malignancy in Salientia. *J. Path. Bact.*, **96**: 496-499.
 - 13 Ruben, L. N., Balls, M., Stevens, J. and Rafferty, N. S. (1969) A new transmissible disease in the South African clawed toad, *Xenopus laevis*. *Oncology*, **23**: 228-237.
 - 14 Elkan, E. A. (1970) Spontaneous anaplastic metastasizing intestinal carcinoma in a South African clawed toad (*Xenopus laevis* DAUDIN). *J. Path. Bact.*, **100**: 205-207.
 - 15 Asashima, M., Sasaki, T. and Takuma, T. (1986) Long-term cultivation of cells derived from a *Xenopus laevis* tumor. *Proc. Japan Acad.*, **62**, Ser. B: 307-310.
 - 16 Oinuma, T., Seki, M. and Asashima, M. (1984) Histological and electron microscopical studies on neoplasia subcutaneously occurring in *Xenopus laevis*. *Proc. Japan Acad.*, **60**, Ser. B: 265-268.
 - 17 Lerner, A. B. (1955) Mammalian tyrosinase. In "Methods in Enzymology, Vol. II". Ed. by S. P. Colowick and N. O. Kaplan. Academic Press, New York, pp. 827-831.
 - 18 Naegele, R. F., Granoff, A. and Darlington, R. W. (1974) The presence of the Lucké herpes virus genome in induced tadpole tumors and its oncogenicity: Koch-Henle postulates fulfilled. *Proc. Natl. Acad. Sci.*, **71**: 830-834.
 - 19 Balls, M. and Ruben, L. N. (1968) Lymphoid tumors in amphibia. A review. *Prog. Exp. Tumor Res.*, **10**: 238-260.
 - 20 Pfeiffer, C. J., Nagai, T., Fujimura, M. and Tobe, T. (1979) Spontaneous regressive epitheliomas in the Japanese newt, *Cynops pyrrhogaster*. *Cancer Res.*, **39**: 1904-1910.
 - 21 Leone, V. G. and Zavanella, T. (1969) Some morphological and biological characteristics of a tumor of the newt, *Triturus cristatus* Laur. In "Biology of Amphibian Tumors". Ed. by M. Mizell, Springer-Verlag, New York, pp. 184-194.
 - 22 Rose, F. L. and Harshbarger, J. C. (1977) Neoplastic and possibly related skin lesions in neotenic salamanders from a sewage lagoon. *Science (Wash. D. C.)*, **196**: 315-317.
 - 23 Khudoley, V. V. and Mizgirev, I. V. (1980) On spontaneous skin tumors in Amphibia. *Neoplasma*, **27**: 289-293.
 - 24 Harshbarger, J. C., Charles, A. M. and Spero, P. M. (1981) Collection and analysis of neoplasms in sub-homeothermic animals from a phyletic point of view. In "Phyletic Approaches to Cancer". Ed. by C. J. Dawe, J. C. Harshbarger, S. Kondo, T. Sugimura and S. Takayama, Japan Sci. Soc. Press, Tokyo, pp. 357-384.



Annulate Lamellae in Prothoracic Gland Cells of Brainless Pupae of the Swallowtail, *Papilio xuthus* (Lepidoptera)

KANJI YASHIKA and PAULO H. HASHIMOTO¹

College of Bio-Medical Technology of Osaka University, Toyonaka 560,
and ¹Department of Anatomy, Osaka University Medical
School, Osaka 530, Japan

ABSTRACT—In 2 individuals out of 33 brain extirpated diapause pupae of the swallowtail, *Papilio xuthus*, the prothoracic gland cell (PGC) was particularly characterized by abundant annulate lamellae, of which some showed an unusual open flower arrangement. In addition, the cytoplasm contained numerous agranular membranes, which seemed to originate from the annulate lamellae and which were in close contact with dense masses that appeared to be liberated from large denser cytoplasmic spherules encapsulated by a nest of mitochondria. The PGC was also characterized by a multilobulated nucleus and remarkable perichromatin granules surrounded by massive condensed heterochromatin. These cytological features may account for the peculiar fact that some brainless pupae occasionally break their dormancy during a long storage period.

INTRODUCTION

Ultrastructural studies on insect prothoracic glands have been carried out on Lepidoptera [1-14], Diptera [15, 16] and Coleoptera [17, 18] as examples of holometabolous insects, and on Orthoptera [19], Dictyoptera [20, 21] and Hemiptera [see 22], as examples of hemimetabolous insects. In prothoracic gland cells (PGC's) of two species of silkworm, *Antheraea pernyi* and *Bombyx mori*, Beaulaton [6] observed annulate lamellae and their disorganization in the later half of the 4th larval period. Scharer [20] reported a cytomembrane system like annulate lamellae having a close relation to microtubules in cockroach PGC's.

In the previous paper [23], we reported a peculiar fact that 30% of artificial diapause pupae induced by a combined short day and brainless treatments could not maintain dormancy during a storage period as long as 8 months and occasionally differentiated into adults. Examining PGC's of

such brainless pupae under the light microscope, we found that 10% of the individuals showed cytological features which supported the conclusion that the dormant PGC's of brainless pupae had recovered their secretory activity. The recovery in diapause pupae of *Hyalophora cecropia* has been reported by McDaniel *et al.* [12], but fine structural detail in the spontaneous recovery of dormant PGC was unknown. The present study deals with electron microscope observations of the PGC's of brainless pupae of the swallowtail and reports that the annulate lamellae may be cytologically related to the secretory activity of the gland cell.

MATERIALS AND METHODS

Brainless pupae were prepared from the spring generation by rearing them in a dark room with only 7 hr of light every day throughout their whole embryonic and larval period. The brain together with the subesophageal ganglion was extirpated within 24 hr after pupation to ensure diapause. The wound was sealed immediately with melted paraffin as already reported [23]. A hundred

brainless pupae were prepared early in June, then stored in natural light at room temperature as long as 5 months until October. Starting from the 20th day after pupation, several samples were randomly selected every 20 days during the storage, and small pieces of the prothoracic segment containing one of the pair of prothoracic glands were fixed in 1/3 strength Karnovsky's aldehyde mixture diluted with 0.1 M phosphate buffer, pH 7.4. At the time of fixation, the pupal fat body was examined under the dissecting microscope to confirm that it was still in pupal form and had not initiated imaginal differentiation. The prothoracic glands were dissected out, immersed in fresh fixative for an hour, and then postfixed in 1% aqueous solution of osmium tetroxide for another hour. Thin plastic sections were cut with a Sorval MT-1 microtome and examined under Hitachi HU-11E electron microscope with acceleration voltage of 75 kv. Sections were stained with 2.5% aqueous uranyl acetate followed by 2.5% lead citrate.

RESULTS

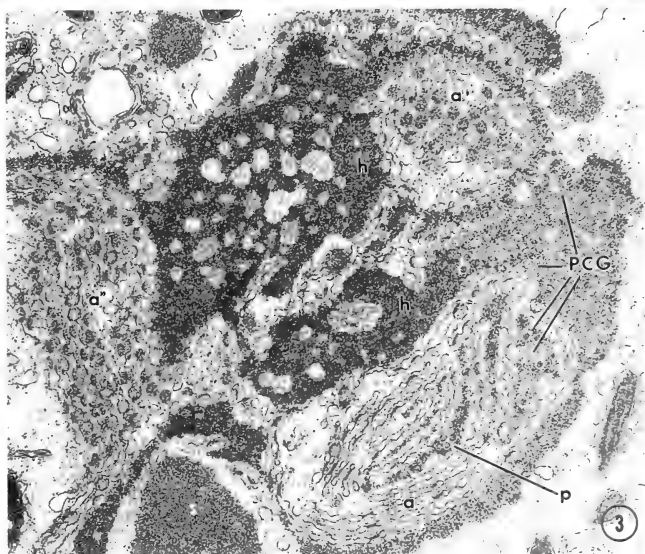
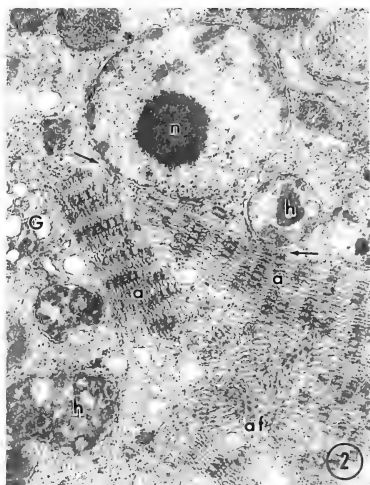
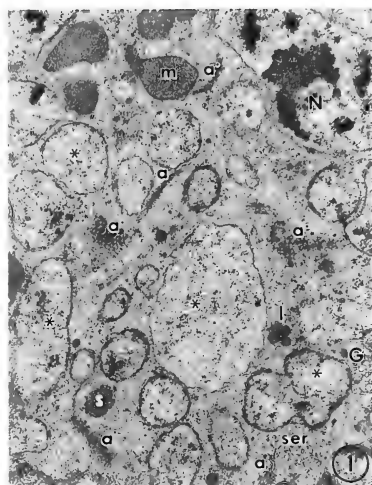
In the prothoracic glands of 2 individuals fixed on the 60th day and the 80th day after pupation, processes of the multilobulated nuclei were observed all over the cell, and annulate lamellae were conspicuous in almost all regions of the cytoplasm, especially around the nucleus (Fig. 1). They were arrayed in clusters of several or ten at most, having a length of more than 15 μ m. Except for a feature which will be mentioned below, the annulate lamellae in PGC's are essentially similar

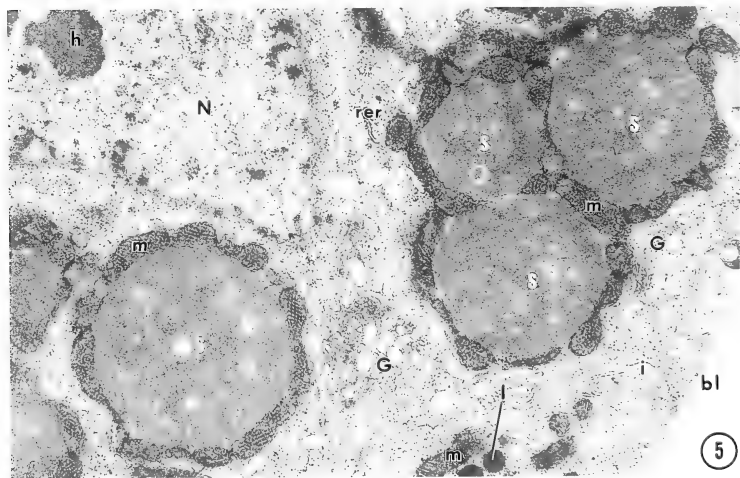
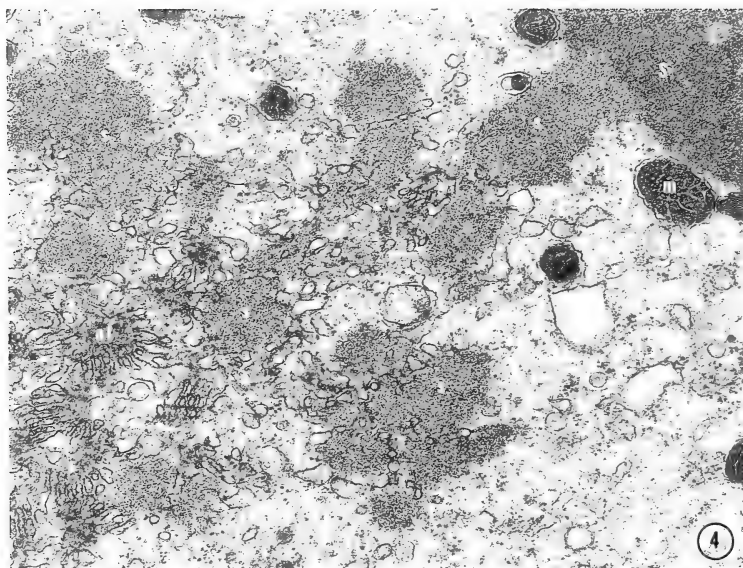
to those reported in oocytes and other tissues of many vertebrates and invertebrates [see 24]. The individual lamella consists of a pair of relatively parallel membranes, separated from each other by about 30–40 nm, and interrupted by pores about 60 nm in diameter (Figs. 2 and 3). The lamella lies in close contact with the outer nuclear membrane, from which it appears to originate (arrows in Fig. 2). Perichromatin granules surrounded by prominent halos were observed within dense heterochromatin masses (Fig. 3). A noticeable feature in the annulate lamellae, of the PGC's, is an appearance of an open flower with a central granular structure at the end of the stacks (Fig. 2). Numerous vesicular, agranular membranes are supplied from the open flower arrangement (af in Fig. 4) and have contact with masses of dense substance (s in Fig. 4) liberated from a denser granulo-filamentous cytoplasmic spherule encapsulated by a nest of mitochondria (S in Fig. 4). PGC's from the remaining individuals, on the other hand, showed rather quiescent looking (Fig. 5). The cytoplasm is essentially characterized by abundant ribosomes, and by sparse granular (RER) as well as agranular endoplasmic reticulum (SER). No annulate lamella nor agranular membrane system was observed. Nuclei are not much lobulated, and contain less heterochromatin with no perichromatin granules, in contrast with the cases of the other 2 pupae. Cytoplasmic spherules are tightly encapsulated by mitochondria, and do not show any morphological change to liberate dense masses into cytoplasm (Fig. 5).

FIG. 1. A prothoracic gland cell (PGC) in a pupa on the 60th day of diapause. Numerous profiles of cut processes (*) of the multilobulated nucleus (N) are visible. A few annulate lamellae cut normally (a) or tangentially (a') are observed. ser: smooth endoplasmic reticulum, G: Golgi complex, l: lysosomes, m: mitochondria, s: fragment of cytoplasmic spherule ($\times 12,000$).

FIG. 2. A PGC with conspicuous annulate lamellae (a) found in a limited pupa fixed on the 60th day of diapause. The plane of section cuts the annulate lamellae parallel to the axis of the stack. Perinuclear stacks appear to be continuous with the outer nuclear membrane (arrows). Another feature of annulate lamellae, of an appearance of open flower (af) with central dots, can be seen. Sections of nuclear processes with nucleolus (n), and those containing dense heterochromatin (h) can be seen. G: Golgi complex. ($\times 20,000$).

FIG. 3. A mass of annulate lamellae cut normally (a), tangentially (a') and obliquely (a"). Perichromatin granules (PGG) with remarkable halos are observed within dense heterochromatin. A PGC of an individual fixed on the 80th day of diapause. s: fragments of cytoplasmic spherule with lower density, h: mass of heterochromatin, p: nuclear pores cut to reveal the en face view ($\times 33,000$).





DISCUSSION

Although annulate lamellae have been described in adult somatic cells, they are more frequently observed in various rapidly growing, developing and differentiating cells. In many types of cells, annulate lamellae are formed in connection with or in close proximity to the nuclear membrane [24–29]. Another mode of formation has been described by Kessel and Beams [30] and by Halkka and Halkka [31], who noted annulate lamellae within dense masses in the oocyte cytoplasm of different species of dragonfly. Our observations, which showed annulate lamellae in close contact with the nuclear membrane, possibly support the former mode of formation. A marked concentric arrangement of annulate lamellae has been reported by Bawa in the Sertoli cells of the human testis [25], and by Harrison in the alligator and sea gull adrenal cortical cells [26]. Bawa [25] also observed another conspicuous type, the half-moon shaped paired annulate lamellae, in the Sertoli cells. Annulate lamellae in PGC's of the swallowtail showed another unusual type of arrangement, like an open flower with central dots.

Blazsek and Mala [9] observed extracellular micro vesicles at the time of cocoon formation in *Galleria mellonella*. Sedlak *et al.* [13] reported morphological changes of multivesicular sacs which occurred within cell cytoplasm and within intercellular spaces at the time of major ecdysone peak in *Manduca sexta*, suggesting that these sacs were likely involved in the packaging of a glandular product exocytosed into intercellular space. Gersh *et al.* [10] reported an increase in size of mitochondria in active PGC phase in *Galleria mellonella*. The extreme irregularity of multilobulated nuclear surface [1, 8, 13, 16], which were

often encountered in cases of our 2 pupae, too, may be interpreted as the induction of the transport of the nuclear material into cytoplasm. Regarding to the cytoplasmic agranular membrane system, which was also characteristic in our 2 pupae, Akai and Kiuchi [2] showed slit-like vesicles distributed in cytoplasm before the spinning stage in which ecdysone titers rapidly increase in *Bombyx mori*. McDaniel *et al.* [12] reported the filled vesicles at the periphery of PGC just prior to their secretion in *Hyalophora cecropia*. Takeda [14] and King *et al.* [16] suggested that ecdysone was synthesized by SER in *Monema flavescens* and in *Drosophila melanogaster*, respectively. The SER was thought to be the relation site for the side-chain alternation and hydroxylation of the cholesterol molecules in the course of the elaboration of ecdysone [14, 17]. SER has also been proposed as an important site of steroid hormone synthesis in vertebrates [32–34]. In our 2 individuals, PGC showed numerous agranular vesicular membrane system supplied by annulate lamellae, suggesting that the gland cells were in an active phase of hormone elaboration.

To our knowledge only two papers are concerned with the annulate lamella in the PGC's of insects. Beaulaton [6] reported the appearance of distinctive annulate lamellae in PGC's, which were taken from two different species of silkworm in the later half period of 4th instar larvae. Scharrer [20] observed a membrane system similar to annulate lamellae having a close relation to microtubules in the PGC's of freshly emerged cockroach. In *Xylenborus ferrugineus*, Chu *et al.* [18] reported an existence of many microtubules in PGC of pupae which contain high titers of ecdysteroid. However, whether the annulate lamellae and microtubules are in exact relation to secretory activity of the

Fig. 4. Substances with lower density (s) is liberated from a denser granulo-filamentous cytoplasmic spherule (S), which is surrounded by mitochondria (m), into cytoplasm to come in close contact with numerous agranular membranes supplied from annulate lamellae having an open flower arrangement with central dots (af). Eightieth day of diapause ($\times 35,000$).

Fig. 5. General profile of a PGC from one of the remaining 31 pupae. Numerous free ribosomes scatter in the cytoplasm, which has many dense spherules (S) surrounded by mitochondria (m). Agranular and granular endoplasmic reticula (rer) are sparse. No annulate lamella, whichever a stack or an open flower arrangement, has been observed in any case of the 31 pupae. Golgi complex (G) can be seen in this section but not frequently in other sections. Nucleus (N) is not so much lobulated as shown in Figs. 1 and 2. Eightieth day after pupation. l: lysosome, bl: basal lamina, i: infoldings of cell membrane ($\times 18,000$).

PGC remains an open question. McDaniel *et al.* [12] reported that the PGC's were filled with free ribosomes, but little RER and no SER in "dauer pupae" by brain extirpation and in "arrested pupae" by aminophilin, of *Hyalophora cecropia*. These characteristics are similar to those of PGC's of our remaining 31 pupae.

In our previous paper [23], large intracytoplasmic spherules in the PGC's of brainless swallowtail pupae were reported to be Feulgen positive, and encapsulated by a nest of mitochondria. They dissolve when larval brains were implanted or a crude extract of brain of *Bombyx mori* was injected into the brainless pupae. Even without any treatment, occasional individuals among a large number of brainless pupae showed dissolving spherules and vacuoles in their PGC [23]. This cytological figure, under the light microscope, presumably showed that the dormant PGC's had recovered their secretory activity previous to the imaginal differentiation, and could explain why some brainless pupae differentiated into adults during storage [23].

In the present report, numerous vesicular and agranular membranes which were shown to be derived from annulate lamellae came in contact with masses of substance liberated apparently from the large spherules. Nuclei of the PGC's with annulate lamellae also showed conspicuous intranuclear perichromatin granules. Reviewing these ultrastructural features in the swallowtail PGC's, we suggest that the formation of annulate lamellae might result from the manifestation of some genetic message stored in the nuclear perichromatin granules or in cytoplasmic spherules, and be related to the initial phase of the cell differentiation prior to the secretion of ecdysone.

REFERENCES

- 1 Akai, H., Sato, S. and Kobayashi, M. (1986) Ultrastructural changes of prothoracic gland during larval development of the silkworm, *Bombyx mori*. Bull. Sericultural Exp. Station (Tokyo), **30**: 341-359.
- 2 Akai, H. and Kiuchi, M. (1987) Regulation of secretory activity in the prothoracic gland of silkworm, *Bombyx mori*. Proc. Japan Soc. Comp. Endocrinol., **2**: 240-241.
- 3 Beaulaton, J. (1962) La morphologie du glycogène dans la glande prothoracique de *Philosamia cynthia* Drury, au cours de la diapause nymphale. J. Microscopie, **1**: 469-472.
- 4 Beaulaton, J. (1964) Evolution du chondriome dans la glande prothoracique du ver à soie tussor (*Antheraea pernyi* Guér.) au cours du cycle sécrétoire pendant les quatrième et cinquième stades larvaires. J. Microscopie, **3**: 167-184.
- 5 Beaulaton, J. A. (1968) Modifications ultrastructurales des cellules sécrétrices de la glande prothoracique de vers à soie au cours des deux derniers âges larvaires I. Le chondriome, et ses relations avec le réticulum agranulaire. J. Cell Biol., **39**: 501-525.
- 6 Beaulaton, J. (1968) Modifications ultrastructurales des cellules sécrétrices de la glande prothoracique de vers à soie, au cours des deux derniers âges larvaires III. Les lamelles annelées et leur dégradation. J. Microscopie, **7**: 895-906.
- 7 Beaulaton, J. (1968) Etude ultrastructurale et cytochimique des glandes prothoraciques de vers à soie aux quatrième et cinquième âges larvaires I. La tunica propria et ses relations avec les fibres conjonctives et les hémocytes. J. Ultrastruct. Res., **23**: 474-498.
- 8 Beaulaton, J. (1968) Etude ultrastructurale et cytochimique des glandes prothoraciques de vers à soie aux quatrième et cinquième âges larvaires III. Les cellules sécrétrices. J. Ultrastruct. Res., **23**: 516-536.
- 9 Blazsek, I. and Mala, J. (1978) Steroidtransport through the surface of the prothoracic gland cells *Galleria mellonella* L. Cell Tissue Res., **187**: 507-513.
- 10 Gersch, M., Birkenbeil, H. and Ude, J. (1975) Ultrastructure of the prothoracic gland cells of the last instar of *Galleria mellonella* in relation to the state of development. Cell Tissue Res., **160**: 389-397.
- 11 Hinze-Pondufal, C. (1971) Studies on the fine structure of prothoracic gland cells of *Cerura vinula* (Lepidoptera) (Basel). J. Zool. (Lond.), **164**: 425-428.
- 12 McDaniel, C. N., Johnson, E., Saum, T. and Berry, S. J. (1976) Ultrastructure of active and inhibited prothoracic glands. J. Insect Physiol., **22**: 473-481.
- 13 Sedlak, B. J., Marchione, L., Devorkin, B. and Davino, R. (1983) Correlations between endocrine gland ultrastructure and hormone titers in the fifth larval instar of *Manduca sexta*. Gen. Comp. Endocrinol., **52**: 291-310.
- 14 Takeda, N. (1976) Activatory mechanisms of the prothoracic glands of *Monema flavescens* (Lepidoptera) with special reference to the secretion of ecdysone. Biol. Bull., **150**: 500-521.
- 15 Aggarwal, S. K. and King, R. C. (1969) A compa-

- rative study of the ring glands from wild type and 1 (2)gl mutant *Drosophila melanogaster*. J. Morph., **129**: 171-200.
- 16 King, R. C., Aggarwal, S. K. and Bodenstein, D. (1966) The comparative submicroscopic morphology of the ring gland of *Drosophila melanogaster* during the second and third instars. Z. Zellforsch., **73**: 272-285.
 - 17 Romer, F. (1971) Die Prothorakaldrüsen der Larve von *Tenebrio molitor* L. (Tenebrionidae, Coleoptera) und ihre Veränderungen während eines Häutungszyklus. Z. Zellforsch., **122**: 425-455.
 - 18 Chu, H. M., Norris, D. M. and Rao, K. D. P. (1980) Ultrastructure of the prothoracic gland of variously aged female pupae of *Xylenborus ferrugineus* and associated ecdysteroid titers. Cell Tissue Res., **213**: 1-8.
 - 19 Maleville, P. A. (1978) Cytophysiologie de la glande prothoracique au cours de l'avant-dernier stade larvaire du grillon *Acheta domestica* L. et durant le cycle de régénération. Archives d'Anatomie Microscopique, **67**: 203-211.
 - 20 Scharrer, B. (1964) The fine structure of blattarian prothoracic glands. Z. Zellforsch., **64**: 301-326.
 - 21 Scharrer, B. (1966) Ultrastructural study of the regressing prothoracic glands of blattarian insects. Z. Zellforsch., **69**: 1-21.
 - 22 Herman, W. S. (1967) The ecdysial glands of arthropods. Int. Rev. Cytol., **22**: 269-347.
 - 23 Yashika, K. and Yoshizaki, K. (1967) A possible role of the brain hormone in the secretion of the prothoracic gland of swallowtail, *Papilio xuthus*. Jpn. J. Exp. Morph., **21**: 148-157.
 - 24 Kessel, R. G. (1968) Annulate lamellae. J. Ultrastruct. Res. Suppl. **10**: 1-82.
 - 25 Bawa, S. R. (1963) Fine structure of the Sertoli cell of the human testis. J. Ultrastruct. Res., **9**: 459-474.
 - 26 Harrison, G. A. (1966) Some observations on the presence of annulate lamellae in alligator and sea gull adrenal cortical cells. J. Ultrastruct. Res., **14**: 158-166.
 - 27 Kawabuchi, M. (1983) Complexes of annulate lamellae and nemaline bodies in soleplate nuclei in skeletal muscle fibers of the normal rat. Cell Tissue Res., **231**: 337-346.
 - 28 Kessel, R. G. (1985) The relationships of annulate lamellae, fibrogranular bodies, nucleolus, and polyribosomes during spermatogenesis in *Drosophila melanogaster*. J. Ultrastruct. Res., **91**: 183-191.
 - 29 Wischnitzer, S. (1970) The annulate lamellae. Int. Rev. Cytol., **27**: 65-100.
 - 30 Kessel, R. G. and Beams, H. W. (1969) Annulate lamellae and 'yolk nuclei' in oocytes of the dragonfly, *Liellula pulchella*. J. Cell Biol., **42**: 185-201.
 - 31 Halkka, L. and Halkka, O. (1977) Accumulation of gene products of the Dragonfly, *Cordulia aenea* II. Induction of annulate lamellae within dense masses during diapause. J. Cell Sci., **26**: 217-228.
 - 32 Christensen, A. K. and Fawcett, D. W. (1966) The fine structure of testicular interstitial cells in mice. Am. J. Anat., **118**: 551-572.
 - 33 Christensen, A. K. (1965) The fine structure of testicular interstitial cells in guinea pigs. J. Cell Biol., **26**: 911-935.
 - 34 Giacomelli, F., Wiener, J. and Spiro, D. (1965) Cytological alternations related to stimulation of the zona glomerulosa of the adrenal gland. J. Cell Biol., **26**: 499-522.



The Deep-Sea Tube Worm Hemoglobin: Subunit Structure and Phylogenetic Relationship with Annelid Hemoglobin

TOMOHIKO SUZUKI¹, TAKASHI TAKAGI², KAZUO OKUDA,
TAKAHIRO FURUKOHRI and SUGURU OHTA³

Department of Biology, Faculty of Science, Kochi University, Kochi 780,

²Biological Institute, Faculty of Science, Tohoku University,

*Sendai 980, and ³Ocean Research Institute, University
of Tokyo, Tokyo 164, Japan*

ABSTRACT—The deep-sea giant tube worm *Lamellibrachia* (the phylum Vestimentifera) contains two extracellular hemoglobins, a 3,000 kDa hemoglobin consisting of six chains (AI-VI) and a 440 kDa hemoglobin consisting of four chains (BI-IV) (Suzuki *et al.*, 1988, *Biochem. J.*, 255, 541-545). The subunit structures of the hemoglobins were investigated by polyacrylamide gel electrophoresis (PAGE). In sodium dodecyl sulfate (SDS), the unreduced 440 kDa hemoglobin dissociated into three subunits; two "myoglobin-like" monomers (BIII and BIV) and a disulfide-bonded dimer of chains BI and BII, while the 3,000 kDa hemoglobin dissociated into five subunits; two monomers (AIII and AIV), a disulfide-bonded dimer of chains AI and AII, and two 32-36 kDa linker subunits (AV and AVI). The dissociation pattern of 3,000 kDa hemoglobin resembles that of leech giant hemoglobin. A gel filtration study on the hemoglobins exposed to alkaline pH or 4 M urea showed that *Lamellibrachia* 3,000 kDa hemoglobin is much more susceptible to dissociation than 440 kDa hemoglobin. Furthermore, the 3,000 kDa hemoglobin is autooxidized about ten times faster than 440 kDa hemoglobin. These results suggest that the subunit assembly of 3,000 kDa hemoglobin is rather unstable. A molecular model, [(BI, BII, BIII)₂BIV]₄, for the subunit assembly of stable 440 kDa hemoglobin is proposed. Amino acid analyses of the isolated *Lamellibrachia* chains and structural comparison with annelid chains showed that chains AI, AII, AIII, BII and BIII have an additional free cysteine residue. This residue appears to be one of the most probable candidates for the sulfide binding site of the tube worm hemoglobin. Such a cysteine may be acquired by a molecular adaptation of hemoglobin, in order to transport sulfide to internal sulfide-oxidizing bacteria.

A phylogenetic tree was constructed from N-terminal partial sequences of 9 *Lamellibrachia* chains and 10 annelid chains. The tree showed that there are two distinct strains for the heme-containing globin chains of the phyla Vestimentifera and Annelida, consistent with our previous proposal that the vestimentiferan tube worms should be placed in the phylum Annelida (Suzuki *et al.*, 1988, *Biochem. J.* 255, 541-545).

INTRODUCTION

One of the recent, most exciting findings in biological fields was a discovery of the deep-sea hydrothermal or cold seep communities at a depth of 600-2500 m [1, 2], where the most conspicuous animals are the giant tube worms *Riftia* and *Lamellibrachia*, and the heterodont clam *Calyplogena*. Both animals are sustained by the mutual sym-

biosis with sulfide-oxidizing bacteria [3]. Although most of the animals in such communities were new to biologists, the tube worms, with an unique outward appearance such as the very long trunk region and the absence of a mouth, gut and anus, present a special interest in its taxonomic position. Very recently, Jones [4, 5] established a new phylum Vestimentifera for the deep-sea tube worms, *Riftia*, *Lamellibrachia*, *Escarpia*, *Tevnia*, *Oasisia* and *Ridgeia*.

The tube worms contain abundant extracellular hemoglobin, which is compatible with their high oxygen demand [6]. The hemoglobin also has a

Accepted January 4, 1989

Received November 17, 1988

¹ To whom all correspondence should be addressed.

special ability to bind sulfide, and transports it to internal bacterial symbionts [3, 7]. Interestingly, several biochemical analyses of this hemoglobin suggest that the tube worms are closely related to annelids [8–10].

In the previous report [8], we showed that the tube worm *Lamellibrachia* contains two extracellular hemoglobins, a 3,000 kDa hemoglobin and a 440 kDa hemoglobin, and that all the constituent chains are highly homologous with those of annelid giant hemoglobin. Here we report the electron microscopic appearance, subunit structure, dissociation property and autoxidation of the two *Lamellibrachia* hemoglobins. As a first step to understand the sulfide binding ability of this hemoglobin, we also determined the number of half-cystine residues of the isolated chains. Furthermore, a phylogenetic tree was constructed from 19 partial sequences of the tube worm and annelid hemoglobins, to elucidate the evolutionary position of the tube worms.

MATERIALS AND METHODS

Lamellibrachia sp. (undescribed) was collected from the cold-seep area located off Sagami Bay at a depth of 1,160 m, southeast of Hatsushima, Japan, by a Japanese submersible SHINKAI 2000 during November of 1987 [11].

Lamellibrachia hemoglobin was prepared according to the previous method [8].

Electron microscopy was carried out on the 3,000 kDa hemoglobin with a JEOL JEM 100U electron microscope. A solution of 1.5% potassium phosphotungstate was used for negative staining [9].

Sodium dodecyl sulfate-polyacrylamide gel electrophoresis (SDS-PAGE) was carried out in 15% acrylamide gel containing 0.087% bisacrylamide, 0.375 M Tris-HCl (pH 8.8) and 0.1% SDS. The samples were incubated in 0.75% SDS at 100°C for 5 min in the presence or absence of 2-mercaptoethanol, before electrophoresis.

Lamellibrachia hemoglobin, which had been exposed to an alkaline pH (in 0.4 NaHCO₃, pH 9.4, containing 4 mM EDTA) or 4 M urea (in 0.15 M phosphate buffer, pH 7.2) for 12 hr, was applied to a gel filtration column (Superose 12, 1×30 cm,

Pharmacia) equilibrated with 50 mM phosphate buffer, pH 7.2, containing 150 mM NaCl. The column was operated at a flow rate of 0.5 ml/min with a Hitachi 655 high-performance liquid chromatography (HPLC).

The constituent polypeptide chains of *Lamellibrachia* hemoglobin were isolated by reverse-phase HPLC as described previously [8]. The isolated chains were carboxymethylated [12] and subjected to amino acid analyzer (Hitachi 835).

Lamellibrachia chain AVI, which could not be recovered by HPLC, was prepared by extraction from SDS-PAGE according to the method of Tsugita [13]. A 500 pmoles of chain AVI was applied to an automated protein sequencer (Applied Biosystems 477A sequencer).

Autoxidation rate of *Lamellibrachia* oxyhemoglobin was measured in 0.1 M phosphate buffer, pH 7.4, at 37°C and under air saturated conditions [14]. An absorption change at 578 nm was monitored with a Hitachi 220A spectrophotometer.

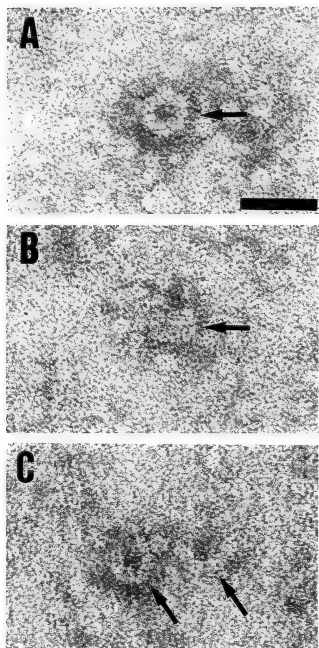
A phylogenetic tree was constructed from 19 partial sequences by an unweighted pair-group clustering method [15]. Calculation was carried out with a NEC PC-9801 personal computer.

RESULTS AND DISCUSSION

Subunit structure of Lamellibrachia hemoglobin.

Lamellibrachia contains two extracellular hemoglobins, a 3,000 kDa hemoglobin and a 440 kDa hemoglobin, which can be separated easily by gel filtration on a column of Sepharose CL-4B [8]. Electron micrographs of negatively stained 3,000 kDa hemoglobin are shown in Figure 1. Like the hemoglobins of annelids and other tube worms, a hexagonal bilayer structure was observed. The dimensions of *Lamellibrachia* 3,000 kDa hemoglobin were determined to be about 30×20 nm, which are very similar to those of annelid hemoglobin [22, 19]. However, the appearance of many incomplete structures such as those shown in Figure 1C suggests that this hemoglobin is unstable upon treatment with negative staining.

Figure 2 shows the SDS-PAGES of *Lamellibrachia* 3,000 kDa hemoglobin (lanes 1 and 2) and 440 kDa hemoglobin (lanes 3 and 4) in the pre-



sence or absence of a reducing agent. The unreduced 3,000 kDa hemoglobin dissociated in SDS into five subunits (lane 1): subunits A1 and A2 with an apparent molecular weight (M_r) of 16–17 kDa, subunit A3 with M_r 29 kDa, subunit A4 with M_r 30 kDa and subunit A5 with M_r 36 kDa. The reduced 3,000 kDa hemoglobin (lane 2) dissociated into chains AI–VI. The chain AV, which was recognized as a single band in the previous report [8], was separated further into two chains at this time. This is not surprising, because it is already known that there is a hetero-type of chain AV by reverse-phase HPLC, whose amino acid sequence differs slightly from that of chain AV [8]. Re-electrophoresis of unreduced subunits A1–5 in the presence of a reducing agent showed that the subunits A1, A2, A4 and A5 corresponded to chains AIII, AIV, AV and AVI, respectively, and that the subunit A3 dissociated further into chains AI and AII. Therefore, it can be concluded that the 3,000 kDa hemoglobin consists of two “myoglobin-like” monomers (chains AIII and AIV), a disulfide-bonded dimer of chains AI and AII, and two 32–36 kDa chains (AV and AVI) which may act as “linker proteins” in the assembly of the

FIG. 1. Electron micrographs of *Lamellibrachia* 3,000 kDa hemoglobin. A, top view; B, side view; C, incomplete molecule. Scale bar, 50 nm.

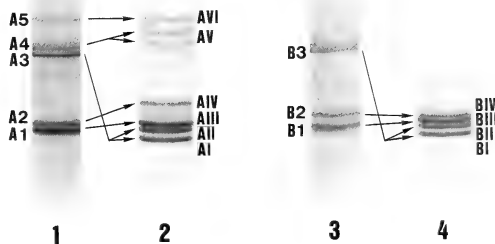


FIG. 2. SDS-PAGEs of *Lamellibrachia* 3,000 kDa (lanes 1 and 2) and 440 kDa (lanes 3 and 4) hemoglobins. Lanes 1 and 3, unreduced hemoglobin; lanes 2 and 4, reduced hemoglobin.

heme-containing chains [16, 17].

On the other hand, the unreduced 440 kDa hemoglobin dissociated in SDS into three subunits (lane 3): subunits B1 and B2 with *Mr* 16–18 kDa, and subunit B3 with *Mr* 29 kDa. The reduced 440 kDa hemoglobin dissociated into four chains BI–IV as reported previously [8]. Reverse-phase HPLC analyses and re-electrophoresis of unreduced subunits B1–3 in the presence of a reducing agent showed that the subunits B1 and B2 corresponded to chains BIII and BIV, respectively, and that the subunit B3 dissociated further into chains BI and BII. Therefore, it can be concluded that *Lamellibrachia* 440 kDa hemoglobin consists of two monomers (chains BIII and BIV) and a disulfide-bonded dimer of chains BI and BII.

It is of great interest to compare the subunit structure of *Lamellibrachia* hemoglobin with those of annelid hemoglobin. In most cases, annelid giant 3,000–4,000 kDa hemoglobin is composed of four subunits: a “myoglobin-like” monomer, a disulfide-bonded trimer and two 32–36 kDa chains [18]. This subunit structure appears to be very similar to that of *Lamellibrachia* 3,000 kDa hemoglobin, except for a difference in either “trimer” or “dimer”. Recent structural analyses of the hemoglobins from the polychaete *Tylorrhynchus* [19] and the oligochaete *Lumbricus* [20] showed that the trimeric subunit is linked by two inter-chain disulfide bridges, using four half-cystine residues located at NA4 and GH4 (see Fig. 5). Since *Lamellibrachia* chains lack the NA4-Cys (see Fig. 6, position 12 in this alignment), the trimer is not likely to be formed in *Lamellibrachia* hemoglobin. Of course, this speculation is based on the assumption that there is a structural similarity between annelid and *Lamellibrachia* hemoglobins. Thus, a disulfide-bonded dimer in *Lamellibrachia* hemoglobin can be considered as one of the variations of a molecular architecture for annelid-like hemoglobin, although it might affect on the stability of molecular assembly. The disulfide-bonded dimer is also found in the leech giant hemoglobin [18].

The 440 kDa hemoglobin, which is not a dissociated product of 3,000 kDa hemoglobin [8, 10], is unique to the deep-sea tube worms *Riftia* and *Lamellibrachia*. However, the subunit composition of the four heme-containing chains of *Lamel-*

librachia 440 kDa hemoglobin was the same as that of 3,000 kDa hemoglobin. This is consistent with the idea that the 440 kDa hemoglobin is a proto-type of 3,000 kDa hemoglobin [8].

It is also true that there is a slight, but significant difference in the ratio of heme-containing chains between the two tube worm hemoglobins. Reverse-phase HPLC analyses [8] showed that chains AI, AII, AIII and AIV of *Lamellibrachia* 3,000 kDa hemoglobin are present approximately in equimolar proportions, as in the case of *Tylorrhynchus* hemoglobin [21], while chains BI, BII, BIII and BIV of 440 kDa hemoglobin occur in a ratio of about 1:1:1:0.5. In *Tylorrhynchus* hemoglobin [21], a tetramer consisting of four chains in equimolar proportions is supposed to be a minimum structural entity. It is likely to take such a structure also in *Lamellibrachia* 3,000 kDa hemoglobin. For the subunit assembly of 440 kDa hemoglobin, however, we propose a rather different structure, in consideration of its chain ratio, as follows; $[(BI, BII, BIII)_2BIV]_4$. In this model, a trimer is composed of a disulfide-bonded dimer of chains BI and BII and a monomeric chain BIII, and two of the trimer are linked by chain BIV. Finally, the whole molecule is formed by four times of this structure. The calculated molecular mass for this model is 480 kDa, which is in good agreement with the observed value of 440 kDa.

As stated above, if the subunit assembly of 440 kDa hemoglobin is rather different from that of 3,000 kDa hemoglobin, a relatively large difference may be detected in several properties, such as stability and heme-heme interaction, between the two hemoglobins. Therefore we compared the dissociation property and autoxidation of both hemoglobins.

Figure 3 shows the results of gel filtration of *Lamellibrachia* intact hemoglobins (a1 and b1), the hemoglobins exposed to an alkaline pH (a2 and b2), and the hemoglobins exposed to 4 M urea (a3 and b3). At an alkaline pH (a2) and 4 M urea (a3), *Lamellibrachia* 3,000 kDa hemoglobin dissociated almost completely into two fractions 2 and 3, with *Mrs* of 60–70 kDa and 14–16 kDa, respectively. This dissociation pattern was very similar to those of annelid giant hemoglobins [16, 22]. On the other hand, *Lamellibrachia* 440 kDa hemoglo-

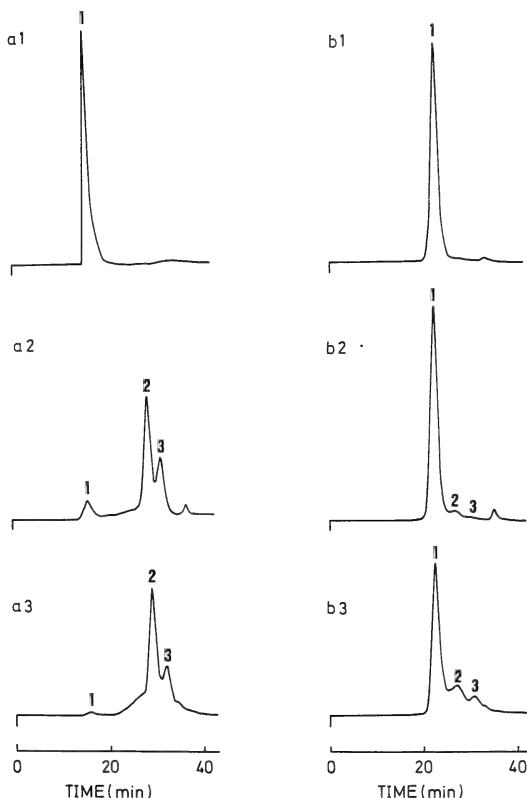


FIG. 3. Gel filtration of *Lamellibrachia* 3,000 kDa (a) and 440 kDa (b) hemoglobins. 1, intact hemoglobin; 2, hemoglobin exposed to an alkaline pH; 3, hemoglobin exposed to 4 M urea. The column (Superose 12, 1×30 cm) was equilibrated with 50 mM phosphate buffer (pH 7.2) containing 150 mM NaCl and eluted with the same buffer at a flow rate of 0.5 ml/min.

bin was very resistant to dissociation; only a small amount (at most 30%) of the dissociation products were observed by treatment with alkali (b2) and 4 M urea (b3), respectively. This different dissociation property of 3,000 kDa and 440 kDa hemoglobin is consistent with the idea that they have a different subunit assembly.

Figure 4 shows the first-order plots for the auto-oxidation of *Lamellibrachia* hemoglobins at pH 7.4 and 37°C. The plot for 440 kDa hemoglobin showed a straight line, and the first-order rate constant for autooxidation was determined to be 0.0026 h^{-1} , from its slope. On the other hand, the 3,000 kDa hemoglobin showed a biphasic auto-

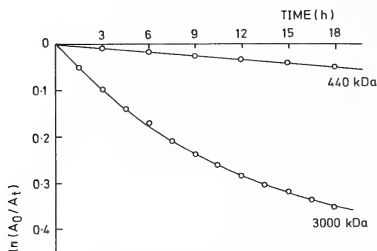


Fig. 4. The first-order plots of $\ln[(\text{HbO}_2)_0/(\text{HbO}_2)_t]$ vs. time t for autoxidation of *Lamellibrachia* oxyhemoglobins. Hemoglobin concentration, $20 \mu\text{M}$ as heme. Conditions, 37°C and pH 7.4.

oxidation curve, suggesting that there is a difference in the autoxidation rate of the subunits. The initial fast-phase rate constant was determined to be 0.031 h^{-1} , and the slow-phase rate was estimated tentatively to be 0.017 h^{-1} . These values are 7–12 times larger when compared with that of 440 kDa hemoglobin, indicating that the 3,000 kDa hemoglobin is rather unstable than 440 kDa hemoglobin. This might be attributed to a difference in subunit assembly of the two hemoglobins, as stated above, since both hemoglobins contain four heme-containing chains with homologous sequence [8]. The autoxidation rate of *Lamellibrachia* oxyhemoglobins at 37°C is comparable to that of human hemoglobin at the similar conditions [32]. This suggests that *Lamellibrachia* hemoglobin is enough stable to play as an oxygen carrier at a physiological temperature (about 3°C).

Half-cystine content of isolated chains of *Lamellibrachia* hemoglobins.

Arp and Childress [7] showed that the hemoglobin of the deep-sea tube worm *Riftia*, a phylogenetically related species with *Lamellibrachia*, has a special ability to bind sulfide, which is transported to internal bacterial symbionts. This seems to be one of the most important physiological roles of the tube worm hemoglobins. Like *Lamellibrachia*, *Riftia* contains two extracellular hemoglobins, a 3,000 kDa hemoglobin and a 400 kDa hemoglobin, both of which can bind sulfide (H_2S) [23]. However the sulfide binding site is not known as yet,

because no data are available for amino acid sequence and chain composition of *Riftia* hemoglobin.

A preliminary observation¹ suggested that *Lamellibrachia* hemoglobins also bind sulfide. We considered that one of the most probable candidates for sulfide binding site is a cysteine residue of heme-containing chains, and therefore determined the number of half-cystine residues of the isolated chains from amino acid analyses. As shown in Table 1, *Lamellibrachia* chains contained 2–4 half-cystine residues per molecule.

Here we should pay an attention to the structural homology between the tube worm and annelid hemoglobins. In terms of the location of half-cystine residues, the heme-containing chains of annelid hemoglobins so far sequenced can be classified into four groups I–IV, as shown in Figure 5. In all chains, an intrachain S-S bridge is formed between NA5-Cys and H8-Cys, and the remaining cysteine residues are all participating in interchain S-S bridge [19, 20]. Since the NA5-Cys is also present in all heme-containing chains of *Lamellibrachia* hemoglobins (see Figure 6, position 13 in this alignment), the same intrachain S-S bridge may be expected. In fact, amino acid sequencing of chain BIV shows the presence of H8-Cys (Takagi, Iwaasa, Ohta and Suzuki, unpubl. data) (see Fig. 5). Therefore, we estimated that two of the half-cystine residues of each chain were used for the formation of an intrachain S-S bridge. Furthermore, an interchain S-S bridge occurring between chains AI and AII, and also between chains BI and BII, needs one more half-cystine residue in each chain. Consequently, such estimation led us to conclude that chains AI, AII, AIII, BII and BIII have an additional free cysteine residue, which may be able to bind sulfide. The sequence analysis of chain BIII showed that it has cysteine residue at a unique position E18, where no cysteine residue is located in annelid hemoglobins (Suzuki, Takagi

¹ When we stored the purified *Lamellibrachia* hemoglobin at 4°C in a test tube with cap and opened it 6–7 days after, it smelled of mercaptan. The electrophoretic pattern (SDS-PAGE) of the stored hemoglobin was the same as that of freshly prepared sample, indicating that there is no change in the protein moiety during storage.

TABLE 1. Amino acid compositions of constituent polypeptide chains of *Lamellibrachia* hemoglobins. The number of half-cysteine residues estimated is shown in parentheses

A.A.	AI-1	AI-2	AII	AIII	AIV'	AIV	AV-1	AV-2	AVI	BI	BII	BIII	BIV
Cys*	3.4(4)	3.6(4)	3.4(4)	2.7(3)	1.6(2)	1.9(2)	9.8(10)	8.7(9)	N.D.	2.5(3)	3.4(4)	2.7(3)	1.7(2)
Asp	16.6	16.6	16.5	17.4	17.8	16.9	40.4	40.8	42.4	18.6	16.8	17.3	17.3
Thr	3.3	2.5	8.1	4.9	4.4	5.9	7.5	7.6	18.4	3.7	7.9	4.9	8.8
Ser	7.7	8.0	11.4	6.7	10.1	10.7	22.8	23.2	19.3	8.0	11.1	6.5	10.8
Glu	13.4	13.4	15.3	17.1	12.0	10.6	26.2	26.7	42.2	12.5	15.2	17.1	8.0
Pro	5.4	5.2	4.1	3.1	5.5	5.4	13.5	13.9	11.3	4.0	3.9	2.9	5.1
Gly	12.2	12.1	10.3	15.0	9.2	9.8	21.0	20.0	29.1	12.3	10.5	15.1	10.7
Ala	20.3	20.3	17.3	15.0	15.3	13.1	27.7	29.3	29.9	17.7	17.4	15.0	16.9
Val	8.4	8.2	8.9	10.8	9.9	9.5	20.2	20.3	20.9	8.2	9.0	11.0	8.7
Met	2.3	2.4	4.3	3.5	3.9	4.6	8.6	7.9	8.3	4.2	4.3	3.4	5.2
Ile	8.9	9.5	5.6	5.2	4.9	4.7	12.2	12.2	11.3	5.2	5.6	5.3	7.3
Leu	12.4	12.3	12.7	11.8	17.4	16.2	14.0	14.2	30.8	13.8	12.7	11.9	18.2
Tyr	2.6	2.9	0.0	3.1	4.1	4.8	8.3	6.9	6.0	2.2	0.0	3.0	2.9
Phe	6.3	6.4	8.9	6.1	7.7	7.7	12.4	12.6	11.8	10.8	9.2	6.2	7.0
Lys	6.2	6.1	3.2	5.2	3.3	4.5	17.6	17.9	8.7	10.5	3.7	5.2	7.8
His	5.9	6.0	4.8	7.9	11.6	11.4	10.7	11.0	16.2	3.5	4.6	8.0	4.0
Trp	N.D.	N.D.	N.D.	N.D.	N.D.	N.D.	N.D.	N.D.	N.D.	N.D.	N.D.	N.D.	N.D.
Arg	9.7	9.6	10.0	9.7	6.1	7.3	17.4	17.8	15.9	7.2	9.8	9.6	4.6
Total	145	145	145	145	145	145	290	290	323	145	145	145	145

*Determined as carboxymethylcysteine.

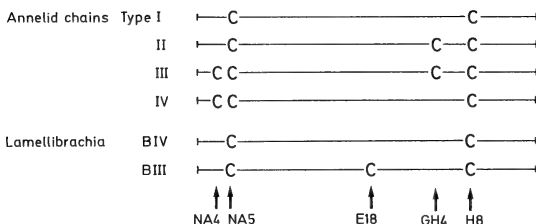


Fig. 5. Location of half-cysteine residues of heme-containing chains of annelid and tube worm hemoglobins.

and Ohta, unpubl. data) (see Fig. 5). It is likely that such a cysteine was acquired by a molecular adaptation of hemoglobin, in order to transport the sulfide to internal sulfide-oxidizing bacteria.

Amino acid sequence comparison and construction of a phylogenetic tree

In the previous report [8], we succeeded in isolating most of the chains of *Lamellibrachia* hemoglobins by reverse-phase HPLC and sequenced the N-terminal 20–40 residues. Chain AVI,

which was not recovered by HPLC, was extracted from SDS-PAGE and the N-terminal sequence was determined to be Phe-Ser-Thr-His-Leu-Asp-Thr-X-X-Val-X-Val-Gln-Asp-X-X-Phe by an automated protein sequencer.

N-Terminal amino acid sequences of all chains of *Lamellibrachia* hemoglobins are compared in Figure 6, with those of annelid giant hemoglobins. It has been already pointed out that the heme-containing chains of annelid hemoglobin can be separated two distinct groups [12, 24, 20]. Extend-

Strain A		10	20	30	34	
Lam. AI (ref.8)		T D C	G M L Q R I	K V K	Q Q W	A S V Y -- S S G
AIII & BIII (8)		Y E C	G P L Q R L	K V K	R Q W	A E A Y -- G S G
BI (8)		D C N	I L Q R L	K V K	M Q W	A K A Y -- G F G
Tyl. I (25)		T D C	G I L Q R I	K V K	Q Q W	A Q V Y -- S V G
IIA (12)		S S D	H C G P L Q R L	K V K	Q Q W	A K A Y -- G V G
Are. I (26)			D C G P L Q R L	K V K	H Q W	V Q V Y -- S G H
Lum. I (27)			E C L V T E G L	K V K	L Q W	A S A F -- G H A
II (20)		K K Q	C G V L E G L	K V K	S E W	G R A Y -- G S G
Phe. I (unpublished)			D C N T L K R F	K V K	H Q W	Q Q V F -- S G E
Strain B						
Lam. AII & BII (8)		S S N S	C T T E	D R R E M Q L M	W	A N V W S A Q F T
AIV (8)	S G N V A E A P K	H Y H	C S Y E D	D A E I V M R E	W	Y H V W -- G S G
AIV' (8)	S V A N A P K	H N H	C S Y E D	D A E I V M R E	W	Y H V W -- G S G
BIV (8)		S K F	C S E G	D A R I V I K Q	W	N Q I Y -- N
Tyl. IIB (28)		D D C	C S A A	D R H E V L D N	W	K G I V S A E F T
IIC (29)		D T C	C S I E D	D R R E V Q A L	W	R S I W S A E D T
Lum. III (20)		D E H E H C	C S E E D	D H R I V Q K Q	W	D I L W R D T E S
IV (20)		A D D E D C	C S Y E D	D R R E I R H I	W	D D V W S S S F T
Strain C						
Lam. AV (8)			A A V Q P L S V S D A M G A R V D A Q	--	A W R	
Lam. AVI (this work)			F S T H L D T X X V X V Q D X X F			

Fig. 6. Comparison of the N-terminal sequences of *Lamellibrachia* and annelid hemoglobins. The invariable residues are boxed. Lam., *Lamellibrachia*; Tyl., *Tylorrhynchus*; Are., *Arenicola*; Lum., *Lumbricus*; Phe., *Pheretima*.

ing this idea, we classified all the heme-containing chains of tube worm and annelid hemoglobins into two groups, strain A and strain B. Strain A contains the sequences of *Lamellibrachia* chains AI, AIII (BIII) and BI [8], of the polychaete *Tylorrhynchus* chains I and IIA [25, 12], of the polychaete *Arenicola* chain I [26], of the oligochaete *Lumbricus* chains I and II [27, 20] and of the oligochaete *Pheretima* chain I (Suzuki, unpubl. data). This group has five invariable residues, Cys-13, Lys-20, Val-21, Lys-22 and Trp-25. Strain B contains the sequences of *Lamellibrachia* chains AII (BII), AIV, AIV' (a hetero-type of AIV) and BIV [8], of *Tylorrhynchus* chains IIB and IIC [28, 29] and of *Lumbricus* chains III and IV [20]. This group has three invariable residues, Cys-13, Asp-17 and Trp-25.

In addition to the two strains, we propose a

"third" strain (strain C) for the constituent polypeptide chains of giant 3,000–4,000 kDa hemoglobin. This strain C includes the "linker proteins" with an unusual *Mr* 32–36 kDa [16, 17]. At present, only two sequence data (*Lamellibrachia* chains AV and AVI) shown in Figure 5, are available for strain C, but we now learn that *Lumbricus* chain V, belonging to strain C, has been sequenced partially (Vinogradov *et al.*, unpubl. data). In all cases, the proteins of strain C show a rather different amino acid sequence, and may have evolved from a different gene, compared with that of other heme-containing chains.

Many taxonomists agree that the worm-like animals such as annelids, pogonophores and deep-sea tube worms are closely related [see 9]. But recently, Jones [4, 5] placed the tube worms in a new phylum Vestimentifera. Inconsistent with

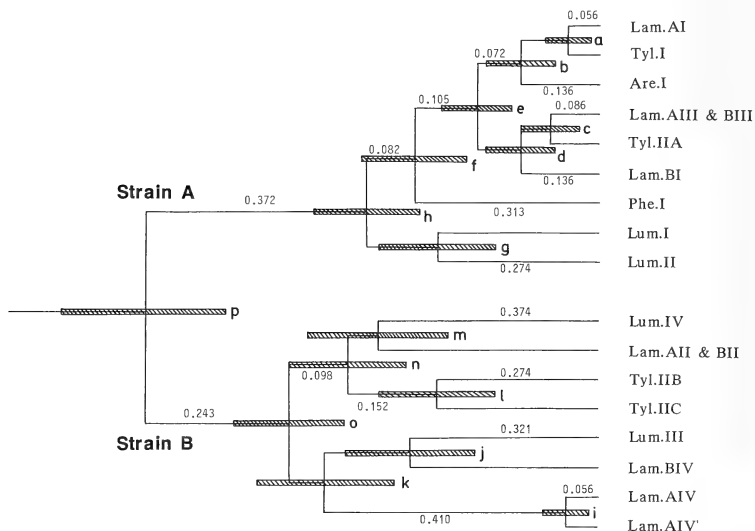


Fig. 7. A phylogenetic tree constructed from partial sequences of *Lamellibrachia* and annelid hemoglobins. The tree was constructed from Table II by an unweighted pair-group clustering method [15], using 19 amino acid residues common to all heme-containing chains (strains A and B) shown in Fig. 6. Standard errors at the branching points, a-p, are 0.039, 0.060, 0.050, 0.058, 0.063, 0.091, 0.098, 0.091, 0.039, 0.109, 0.122, 0.098, 0.121, 0.100, 0.094 and 0.104, respectively.

this, all of the biochemical data for the tube worm hemoglobin, such as electron microscopic appearance, subunit structure, chain composition and amino acid sequence, suggest that the tube worm is a member of annelids [8–10].

To make clear the taxonomical position of tube worms, we constructed a phylogenetic tree from the homology matrix of heme-containing chains shown in Table II. It is well known that the phylogenetic tree constructed from globin sequences shows a good correlation with that from classical taxonomy [30, 31]. The result is shown in Figure 7. The standard error is given at each branching point, to help evaluation of the tree. This pattern is essentially similar to that constructed from eight sequences of annelid hemoglobins [20], and suggests the following points. (i) There are two distinct globin strains A and B, which can be separated without any overlaps of standard errors, through the heme-containing chains of the phyla Vestimentifera and Annelida. Each strain may be produced by a gene duplication. (ii) A hemoglobin contains two chains in each of the two strains. Therefore, one more gene duplication is needed. After this process, the giant molecular architecture was constructed. (iii) The most closely related chains are *Lamellibrachia* AI and *Tylorrhynchus* I, *Lamellibrachia* AIV and AIV', and *Lamellibrachia* AIII(BIII) and *Tylorrhynchus* IIA. For example, 19 out of the N-terminal 22 residues are surprisingly identical between *Lamellibrachia* AI and *Tylorrhynchus* I. This indicates that there is a very close relationship between *Lamellibrachia* and *Tylorrhynchus*.

In conclusion, the phylogenetic tree shown in Figure 7 implies that the tube worm *Lamellibrachia* should be placed in the phylum Annelida, instead of the phylum Vestimentifera [4, 5]. The tube worms probably evolved in the deep-sea from other polychaetes, taking on a unique outward appearance, which is high adaptations for symbiosis with sulfide-binding bacteria.

ACKNOWLEDGMENTS

We thank Prof. S. N. Vinogradov of Wayne State University, Prof. T. Gotoh of Tokushima University, Prof. A. Kajita, Dr. K. Fushitani and Dr. Y. Igarashi of

Dokkyo University and Dr. Y. Machida of Kochi University for their interest during this work.

This work was partly supported by a Grant-in-Aid for scientific research from the Ministry of Education, Science and Culture of Japan (No. 63740417) to T. S.

REFERENCES

- 1 Corliss, J. B., Dymond, J., Gordon, L. I., Edmond, J. M., von Herzen, R. P., Ballard, R. D., Green, K., Williams, D., Bainbridge, A., Crane, K. and van Andel, T. H. (1979) Submarine thermal springs on the Galapagos Rift. *Science*, **203**: 1073–1083.
- 2 Ohta, S. and Laubier, L. (1987) Deep biological communities in the subduction zone of Japan from bottom photographs taken during "nautile" dives in the Kaiko project. *Earth Planet. Sci. Lett.*, **83**: 329–342.
- 3 Childress, J. J., Felbeck, H. and Somero, G. N. (1987) Symbiosis in the deep sea. *Scientific Amer.*, **256**: 106–112.
- 4 Jones, M. L. (1981) *Riftia pachyptila* Jones: Observations on the vestimentiferan worm from the Galapagos Rift. *Science*, **213**: 333–336.
- 5 Jones, M. L. (1985) On the Vestimentifera, new phylum: six new species, and other taxa, from hydrothermal vents and elsewhere. *Biol. Soc. Wash. Bull.*, **6**: 117–158.
- 6 Arp, A. J. and Childress, J. J. (1981) Blood function in the hydrothermal vent vestimentiferan tube worm. *Science*, **213**: 342–344.
- 7 Arp, A. J. and Childress, J. J. (1983) Sulfide binding by the blood of the hydrothermal vent tube worm *Riftia pachyptila*. *Science*, **219**: 295–297.
- 8 Suzuki, T., Takagi, T. and Ohta, S. (1988) N-Terminal amino acid sequence of the deep-sea tube worm haemoglobin remarkably resembles that of annelid haemoglobin. *Biochem. J.*, **255**: 541–545.
- 9 Terwilliger, R. C., Terwilliger, N. B. and Schabach, E. (1980) The structure of hemoglobin from an unusual deep sea worm (Vestimentifera) *Comp. Biochem. Physiol.*, **65B**: 531–535.
- 10 Terwilliger, R. C., Terwilliger, N. B., Bonaventura, C., Bonaventura, J. and Schabach, E. (1985) Structural and functional properties of hemoglobin from the vestimentiferan Pogonophora, *Lamellibrachia*. *Biochim. Biophys. Acta*, **829**: 27–33.
- 11 Ohta, S., Sakai, H., Taira, A., Ohwada, K., Ishii, T., Maeda, M., Fujioka, K., Saino, T., Kogure, K., Gamo, T., Shirayama, Y., Furuta, T., Ishizuka, T., Endow, K., Sumi, T., Hotta, H., Hashimoto, J., Handa, N., Masuzawa, T. and Horikoshi, M. (1987) Report on multi-disciplinary investigations of the *Calypotegna* communities at the Hatusushima site. *JAMSTECR Deepsea Res.*, **3**: 51–60 (in Japanese with English summary and legends).

- 12 Suzuki, T. and Gotoh, T. (1986) The complete amino acid sequence of giant multisubunit hemoglobin from the polychaete *Tylorhynchus heterochaetus*. *J. Biol. Chem.*, **261**: 9257–9267.
- 13 Tsugita, A. (1988) Purification of proteins. Kagaku To Seibutsu, **26**: 330–337 (in Japanese).
- 14 Suzuki, T. (1987) Autoxidation of oxymyoglobin with the distal(E7) glutamine. *Biochim. Biophys. Acta*, **914**: 170–176.
- 15 Nei, M., Stephens, J. C. and Saitou, N. (1985) Methods for computing the standard errors of branching points in an evolutionary tree and their application to molecular data from humans and apes. *Mol. Biol. Evol.*, **2**: 66–85.
- 16 Vinogradov, S. N., Lugo, S. D., Mainwaring, M. G., Kapp, O. H. and Crewe, A. V. (1986) Bracelet protein: A quaternary structure proposed for the giant extracellular hemoglobin of *Lumbricus terrestris*. *Proc. Natl. Acad. Sci. USA*, **83**: 8024–8038.
- 17 Mainwaring, M. G., Lugo, S. D., Fingal, R. A., Kapp, O. H. and Vinogradov, S. N. (1986) The dissociation of the extracellular hemoglobin of *Lumbricus terrestris* at acid pH and its reassociation at neutral pH. *J. Biol. Chem.*, **261**: 10899–10908.
- 18 Vinogradov, S. N. (1985) The structure of invertebrate extracellular hemoglobins (Erythrocrurins and Chlorocrurins). *Comp. Biochem. Physiol.*, **82B**: 1–15.
- 19 Suzuki, T., Kapp, O. H. and Gotoh, T. (1988) Novel S-S loops in the giant hemoglobin of *Tylorhynchus heterochaetus*. *J. Biol. Chem.*, **263**: 18524–18529.
- 20 Fushitani, K., Matsuura, M. S. A. and Riggs, A. F. (1988) The amino acid sequences of chains a, b, and c that form the trimer subunit of the extracellular hemoglobin from *Lumbricus terrestris*. *J. Biol. Chem.*, **263**: 6502–6517.
- 21 Suzuki, T. and Gotoh, T. (1986) Subunit assembly of giant haemoglobin from the polychaete *Tylorhynchus heterochaetus*. *J. Mol. Biol.*, **190**: 119–123.
- 22 Kapp, O. H., Polidori, G., Mainwaring, M. G., Crewe, A. V. and Vinogradov, S. N. (1984) The reassociation of *Lumbricus terrestris* hemoglobin dissociated at alkaline pH. *J. Biol. Chem.*, **259**: 628–639.
- 23 Arp, A. J. (1986) Sulfide-binding by an extracellular hemoglobin. In "Invertebrate Oxygen Carriers". Ed. by B. Linzen, Springer-Verlag, Berlin, 129–132.
- 24 Gotoh, T., Shishikura, F., Snow, J. W., Ereifej, K. and Vinogradov, S. N. (1987) Two globin strains in the giant annelid extracellular haemoglobins. *Biochem. J.* **241**: 441–445.
- 25 Suzuki, T., Takagi, T. and Gotoh, T. (1982) Amino acid sequence of the smallest polypeptide chain containing heme of extracellular hemoglobin from the polychaete *Tylorhynchus heterochaetus*. *Biochim. Biophys. Acta*, **708**: 253–258.
- 26 Sgourous, J., Kleinschmidt, T. and Braunitzer, G. (1986) A preliminary study of the hemoglobin of *Arenicola marina*. In "Invertebrate Oxygen Carriers". Ed. by B. Linzen, Springer-Verlag, Berlin, 73–76.
- 27 Shishikura, F., Snow, J. W., Gotoh, T., Vinogradov, S. N. and Walz, D. A. (1987) Amino acid sequence of the monomer subunit of the extracellular hemoglobin of *Lumbricus terrestris*. *J. Biol. Chem.*, **262**: 3123–3131.
- 28 Suzuki, T., Yasunaga, H., Furukohri, T., Nakamura, K. and Gotoh, T. (1985) Amino acid sequence of polypeptide chain IIB of extracellular hemoglobin from the polychaete *Tylorhynchus heterochaetus*. *J. Biol. Chem.*, **260**: 11481–11487.
- 29 Suzuki, T., Furukohri, T. and Gotoh, T. (1985) Subunit structure of extracellular hemoglobin from the polychaete *Tylorhynchus heterochaetus* and amino acid sequence of the constituent polypeptide chain (IIC). *J. Biol. Chem.*, **260**: 3145–3154.
- 30 Goodman, M., Moore, G. W. and Matsuda, G. (1975) Darwinian evolution in the genealogy of hemoglobin. *Nature*, **253**: 603–608.
- 31 Goodman, M., Pedwaydon, J., Czelusniak, J., Suzuki, T., Gotoh, T., Moens, L., Shishikura, F., Walz, D. and Vinogradov, N. (1988) An evolutionary tree for invertebrate globin sequences. *J. Mol. Evol.*, **27**: 236–249.
- 32 Mansouri, A. and Winterhalter, K. H. (1973) Nonequivalence of chains in hemoglobin oxidation. *Biochemistry*, **12**: 4946–4949.

Tibia to Femur Ratios of Unaltered and Regenerated Legs of the Stumpy Mutant of the German Cockroach

AKIRA TANAKA and MARY H. ROSS¹

Department of Biology, Nara Women's University, Nara 630, Japan, and

¹Department of Entomology, Virginia Polytechnic Institute and State University, Blacksburg, Virginia 24061, USA

ABSTRACT—In wild-type legs of the German cockroach, the ratio of tibia length to femur length (T/F ratio) is low in the foreleg, high in the hindleg, and intermediate in the midleg throughout nymphal instars up to the adult stage. After autotomy at the trochanterofemoral articulation, regenerates from foreleg coxae show intermediate T/F ratios between the normal foreleg and midleg, and those from the hindlegs, intermediate between the normal hindleg and midleg. Those from the midlegs are unaltered in the ratios. Similar studies were made on a mutant, stumpy (*sty*), which has shorter legs than wild type. The relative length of *sty* legs to wild-type legs was around 80%, showing some fluctuation with the stage and the type of legs. The T/F ratios of unoperated *sty* fore-, mid-, and hindleg were, respectively, similar to those of regenerated wild-type. This suggests that *sty* may have primitive legs that are not fully differentiated from midleg-like nonspecific forms. The T/F ratios of regenerated *sty* legs were similar to those of the unoperated *sty* when the legs were autotomized in early instars. When the legs were autotomized in middle and late instars, the ratios of *sty* regenerates increased in all legs. In the adult regenerates, the ratios of the *sty* fore-, mid-, and hindleg almost reached those of the *sty* midleg, *sty* hindleg, and wild-type hindleg, respectively.

INTRODUCTION

The fore-, mid- and hindleg of the German cockroach, *Blattella germanica* (L.), seem to be very similar in their gross morphology. Precise measurements, however, have revealed that the three legs differ from each other in the relative lengths of their segments: coxa, trochanter, femur, tibia and five tarsomeres [1]. In particular, the ratio of tibia length to femur length (T/F ratio) is quite different in the three legs. The ratio is low in the foreleg, high in the hindleg, and intermediate in the midleg throughout nymphal instars up to the adult stage [2].

When the legs of wild-type cockroaches were regenerated after autotomy at the trochanterofemoral articulation, some interesting facts were disclosed in the T/F ratios. In each nymphal instar and the adult stage, regenerates from foreleg coxae showed intermediate T/F ratios between the

normal foreleg and midleg, and those from the hindlegs, intermediate between the normal hindleg and midleg. Those from the midlegs were unaltered in the ratios [3]. In other words the T/F ratios of regenerates from the fore- and hindlegs converged to those of the midlegs, showing incomplete homeotic regeneration toward the midleg. This tendency suggested that the fore- and hindlegs were differentiated from midleg-like primitive forms during normal embryonic development.

Stumpy (*sty*) belongs to a group of mutants on chromosome 9 of the German cockroach that appear to have been highly conserved during the course of evolution [4]. The mutant is also of interest because it alters the shape of the entire body, including that of the legs [5]. The purpose of this study is to investigate the effects of *sty* on growth and development by (i) comparing the development of leg segments, specifically the femur and tibia, to that of wild type, and (ii) determining the effects of regeneration on the development of leg segments of the *sty* mutant.

MATERIALS AND METHODS

Selection of sty nymphs

The *sty* mutant is a simple autosomal recessive located on chromosome 9 [5]. Newly-hatched *sty* nymphs were obtained from oothecae produced by *sty/+* females that were mated to *sty/sty* males, because *sty/sty* females are almost sterile. Consequently, each ootheca about 50% *sty* and 50% phenotypically normal embryos. A *sty* nymph could be easily distinguished with its shorter legs from a phenotypically normal nymph as early as the 1st instar by simple inspection (Fig. 1). Only *sty* nymphs were selected for the present studies: regeneration experiments and control measurements. When the first operation was performed in the 1st instar, the detached legs were examined to ascertain whether they were really *sty* legs by measuring the lengths of femur and tibia (Fig. 2).



FIG. 1. First-instar nymphs: stumpy (*sty/sty*, left) and wild type (+/+, right). Note the short legs in the *sty* mutant.

Rearing and anesthetizing methods

Each 1st-instar *sty* nymph was isolated in a small plastic container (61 × 43 × 17 mm high, Sanplatec, No. 2), since it is known that operated nymphs are often attacked by others under group-rearing conditions. The container was transparent and the nymph could be easily inspected from the outside. A small piece of dog food and water was supplied *ad libitum*. The temperature was maintained at 25 ± 1°C throughout postembryonic development. Prior to each operation mentioned in the following

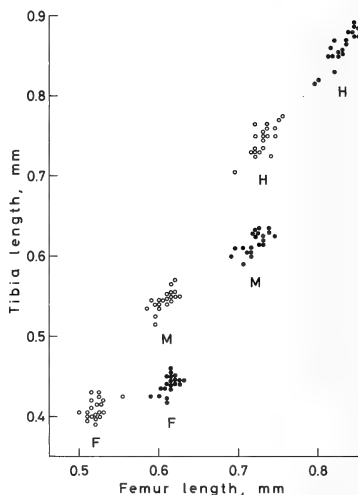


FIG. 2. Femur and tibia lengths of 1st-instar nymphs hatched from a single ootheca. A typical example of comparison between stumpy (*sty/sty*, open circles) and phenotypically normal (*sty/+*, filled circles): foreleg (F), midleg (M), and hindleg (H).

section, carbon dioxide was introduced from a cylinder to the container via a flexible tube. An anesthetized cockroach was carefully taken out, immediately subjected to the operation, and put back in the container before it recovered from anesthesia.

Trochanterofemoral autotomy

Repeated-regeneration experiments were carried out on each fore-, mid-, and hindleg of both sexes during each nymphal stadium. Only one leg was operated on in order to avoid possible complex interactions between operated legs. The leg was autotomized at the trochanterofemoral articulation by gentle pulling of the femur with fine forceps in order to minimize physiological damage. The first operation was performed on day 1 or 2 in the 1st instar before the regeneration critical period [6, 7] so that a regenerate appears in the 2nd instar. The regenerated leg was autotomized

again on day 1 or 2 in the 2nd instar. The same procedures were repeated in the following instars until the insect reached the adult stage. Operations were made always on the same leg of the same side of the body, usually the right side.

Size measurements

The maximal lengths of both the femur and tibia of all legs were measured along the median line of the segments as in previous studies [1, 3]. The measurements were carried out under a dissecting microscope equipped with a measuring apparatus (Kogaku Ltd.). The unit of measurement was 5 μ m. Data that appeared in Tanaka [2] and Tanaka *et al.* [1] were used as wild-type control measurements. The lengths of unoperated *sty* legs, usually from the right side of the body, were measured in every nymphal instar and the adult stage. No less than 40 insects (20 males and 20 females) were measured in each stadium, except: 31 in the 2nd, 35 in the 3rd instar. The lengths of regenerated *sty* legs were also measured. Regeneration experiments were initiated with no less than 40 insects (20 males and 20 females) in each series of fore-, mid-, and hindlegs, totaling more than 120 nymphs. Although the absolute lengths of the segments were slightly longer in females than in males in late nymphal instars and adults, no significant differences were detected between the sexes in the relative lengths so far calculated. Therefore, the values are given as combined totals of both sexes.

RESULTS

Effects of stumpy on the development of leg segments

The relative lengths of the stumpy (*sty/sty*) legs to the wild-type (+/+) legs are shown in Figure 3. Stumpy femurs (filled circles) were shorter than wild-type femurs throughout postembryonic development in all legs. The average values of relative femur lengths ranged from 75% to 85% of those of wild type, showing some minor fluctuation with the stage and the type of legs. Stumpy tibiae (open circles) were also shorter than wild-type tibiae throughout development of all legs. The

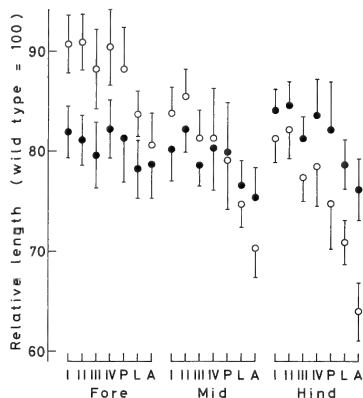


FIG. 3. Relative lengths of *sty* legs to wild-type legs: femur (filled circles) and tibia (open circles). Bars indicate standard deviation. I-IV, P, L, and A represents the 1st-4th, penultimate, last instar, and adult, respectively. No less than 40 insects were measured in each stadium, except: 31 in instar II, 35 in instar III.

relative lengths ranged from 64% to 91% to the wild type, showing more difference than the femur with the stage and the type of legs. The average values tended to decrease from foreleg to hindleg, and also from early instars to the adult stage. Figure 3 confirms that all *sty* legs are shorter than wild-type legs throughout development as far as the lengths of femur and tibia are concerned. It was also found that the variation in relative lengths is larger in the tibia than in the femur. The relative lengths of the foreleg were longer in the tibia than in the femur, and *vice versa* in those of the hindleg.

Figure 4 shows the ratios of tibia length to femur length of *sty* legs together with those of wild-type legs throughout postembryonic development. In wild-type legs, the T/F ratio is low in the foreleg, high in the hindleg, and intermediate in the midleg. The T/F ratios of the *sty* foreleg were consistently higher than those of the wild-type foreleg, showing intermediate ratios between the wild-type foreleg and wild-type midleg; 0.77-0.81 in the average ratios but varying a little with the stage.

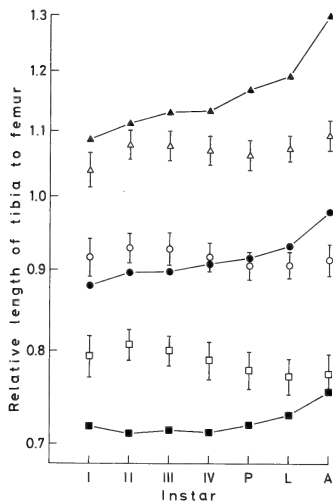


Fig. 4. Ratios of tibia length to femur length of *sty* legs: foreleg (open squares), midleg (open circles) and hindleg (open triangles). Bars indicate standard deviation. No less than 40 insects were measured in each stadium, except: 31 in instar II, 35 in instar III. The ratios of wild type are also marked: foreleg (filled squares), midleg (filled circles) and hindleg (filled triangles). Each symbol of the wild type represents the average of 40 legs; standard deviation is omitted. P, L, and A indicate penultimate, last instar, and adult, respectively.

This tendency of the ratios shifting to the midleg was stronger in early instars than in later instars. The T/F ratios of the *sty* midleg, ranging from 0.90 to 0.93 in the average, were almost unaltered from those of the wild-type midleg, showing a little higher ratios than those of wild-type in early instars and a little lower in later stages. The average ratios of the *sty* hindleg ranged from 1.04–1.09, varying a little with the stage. They were lower than those of the wild-type hindleg throughout postembryonic development, showing intermediate ratios between the wild-type midleg and wild-type hindleg. The extent of the shift toward the midleg was relatively small in early

instars and became larger as the stage advanced. The ratios of both *sty* foreleg and *sty* hindleg tended to converge toward those of the midleg in every nymphal instar and the adult stage. The ratios of all legs were closer to each other in *sty* than in wild type. The difference in the T/F ratio between the foreleg and hindleg was clearly smaller in *sty* (0.29 on the average of all stages) than in wild type (0.45).

Characteristics of regenerated sty leg segments

The number of instars of *sty* German cockroaches was usually six, as in the wild type. However, the number was increased to seven or eight when the leg was repeatedly autotomized. All the regenerated legs of *sty* had tetramerous tarsi, one tarsomere less as compared with normal pentamerous tarsi, as in the case of wild-type regenerates [3].

The relative lengths of regenerated *sty* legs to unoperated *sty* legs are shown in Figure 5. The relative lengths were calculated in the 2nd, 3rd, last (L) instar, and the adult stage (A). In the 4th and penultimate (P) instar, however, the lengths could not be appropriately compared with those of unoperated corresponding instars, because the extra instar(s) caused by repeated regeneration, *i.e.* instar(s) V (and VI), were inserted between the instars IV and P, which prevented accurate comparison between unaltered and regenerated *sty* during these middle stages. The average values of regenerated femur (filled circles) ranged from 73% to 87% of those of unoperated femur when compared in the 2nd, 3rd, last instar, and the adult stage. The relative lengths of regenerated tibia (open circles) also varied with the stage and the type of legs. The values were nearly equal to those of femur in the 2nd and 3rd instar, whereas they were considerably higher than those of femur in the last instar and the adult stage. Especially in the foreleg, tibia lengths showed almost full recovery after regeneration.

The relative lengths of *sty* regenerates, both femur and tibia, tended to decrease from instar II to III, and again from the last instar to the adult stage in each of the three legs. However, these tendencies are not authentic, because the number of instars increased by one or two with repeated

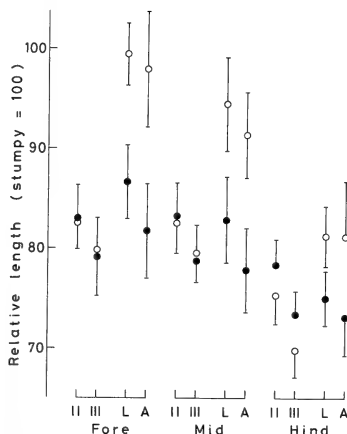


Fig. 5. Relative lengths of regenerated *sty* legs to unoperated *sty* legs: femur (filled circles) and tibia (open circles). Bars indicate standard deviation. The number of regenerates included in each symbol ranged from 31 to 41. II, III, L, and A represent the 2nd, 3rd, last instar, and adult, respectively. In the intermediate instars (IV-P), regenerated *sty* were not compared with unoperated *sty*, because the number of instars was increased with repeated regeneration and the additional instar(s), V (and VI), were inserted between IV and P, which prevented accurate comparison between regenerated and unoperated *sty* during these instars.

autotomy, and the extra instar(s) were inserted between instar IV and P, which affected the calculation of relative lengths compared to the wild type.

The T/F ratios of *sty* regenerates are shown in Figure 6 together with those of unaltered *sty* legs. The T/F ratio of the regenerated foreleg averaged about 0.80 in the 2nd instar; the value was almost equal to that of the unoperated control. The ratio, however, gradually increased and departed from that of the control in later instars. It finally reached 0.93 in the adult stage, a little higher than that of the midleg control. The ratio of the regenerated midleg in the 2nd instar was about 0.92, nearly equal to that of the uninjured control. The ratio also increased in later instars, reaching

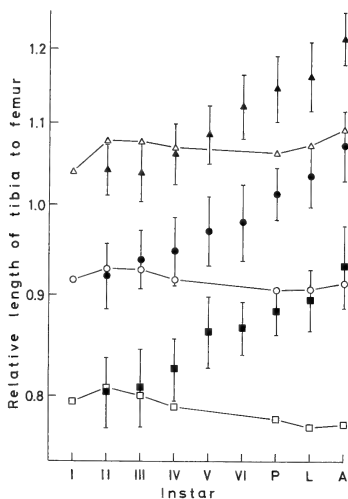


Fig. 6. Ratios of tibia length to femur length of *sty* regenerates: foreleg (filled squares), midleg (filled circles) and hindleg (filled triangles). Each symbol represents the average ratio of regenerates; the numbers ranged from 31 to 41, except 9-15 in the instar VI. Bars indicate standard deviation. The ratios of unoperated *sty* legs are also marked: foreleg (open squares), midleg (open circles) and hindleg (open triangles); standard deviation is omitted. Instar V includes that of VII- and VIII-instar type; instar VI, that of VIII-instar type. These instar types were not found in unoperated controls. P, L, and A indicate penultimate, last instar, and adult, respectively.

1.07 in the adult stage, almost that of the unoperated hindleg. The ratio of the regenerated hindleg was 1.04 in the 2nd instar, a little lower than that of the unaltered hindleg. However, it exceeded the control in the 5th instar, and reached 1.22 in the adult stage when the autotomy was performed in the last instar. The ratio in some late instars was almost as high as that of the wild-type hindleg.

DISCUSSION

Operation by autotomy necessitates carbon-

dioxide anesthesia. It has been found that the number of instars is increased not only by the repeated operation [3, 8] but also by repeated carbon-dioxide anesthesia [9, 10]. Accordingly, the increase of the number of instars observed in the regenerated *sty* larvae may be partly caused by carbon-dioxide anesthesia. Carbon dioxide also affects the T/F ratio. However, the effect is negligible, usually smaller than 0.01 in the ratio [10] as compared with the large differences in the ratio shown in Figures 4 and 6.

The T/F ratios of all legs of regenerated *sty*, unoperated *sty*, and unoperated wild-type are shown together in Figure 7. The ratios are presented in adjusted values in which the ratio of the wild-type midleg is chosen as a standard, since the midleg is considered to be an unmodified standard

leg [3]. First, it is noticeable that all the values concerning *sty*, irrespective of regenerated or unoperated, were plotted between those of the wild-type foreleg and wild-type hindleg throughout postembryonic development. In relation to that, the difference of the ratio between the foreleg and hindleg was smaller in *sty* than in wild type and smallest in regenerated *sty*. Second, the adjusted ratios of unoperated *sty* decreased consistently in all legs as development advanced, while those of regenerated *sty* increased.

Tanaka *et al.* [3] found that, in wild type, regenerates from the foreleg coxae show intermediate T/F ratios between the normal foreleg and midleg, and those from the hindlegs, intermediate between the normal hindleg and midleg. This convergence to the midleg was considered to be incomplete homeotic regeneration toward a midleg-like standard leg, from which the foreleg and hindleg are differentiated by some modifiers. The hypothesis that the midleg is a general type of leg seems comparable to the concept that a 'developmental sink' or 'ground state' is located in the mesothorax of *Drosophila* [11-14]. At the same time, it has been suggested that homeotic mutations found in *Drosophila* differ from the rather continuous alteration of characters such as the T/F ratio. Hence the analysis of the latter kind is also important to our understanding of developmental organization.

As we first expected, the T/F ratio of *sty* fore- and hindlegs showed convergence to that of the midleg. This implies that *sty* may have primitive legs that have not differentiated greatly from a midleg-like nonspecific form. This mutant also has shortened wings in adult males [5]. From a viewpoint that *sty* concerns the expression of a primitive developmental pathway, it is intriguing that the *sty* locus is included in the chromosome 9 gene cluster along with other primitive traits: prowling [15, 16], notched sternite [17, 18], miniature-wing [19], and maxillary-palp-elongate [20]. During the course of evolution, wild-type alleles of these genes seem to have suppressed primitive characters and modified the ancestral forms into the normal extant segments. It is of particular interest that *sty* has dual effects on both the dorsal (short wings in adult males) and ventral (short legs and

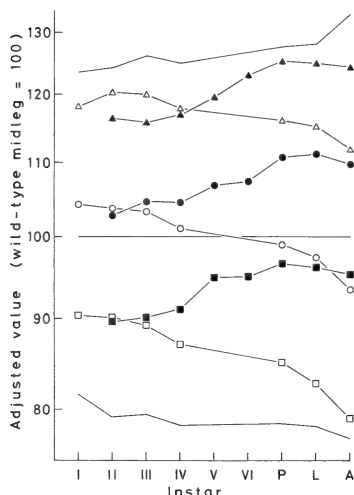


Fig. 7. Ratios of tibia length to femur length in adjusted values. The ratio of the wild-type midleg is regarded as the standard in each stage. Lowest line indicates the ratio of wild-type foreleg; highest line, that of wild-type hindleg. Unoperated *sty* foreleg (open squares), midleg (open circles) and hindleg (open triangles); regenerated *sty* foreleg (filled squares), midleg (filled circles) and hindleg (filled triangles).

converged T/F ratios) side of the thoracic segments as well as changing the entire form of the body. The locus acts as a simple recessive and may be a single gene that changes the entire shape of the body possibly through regulation of a number of structural genes.

ACKNOWLEDGMENTS

We thank Mrs. Nancy Boles for technical assistance and Dr. Bruce Wallace for valuable comments on the manuscript.

REFERENCES

- 1 Tanaka, A., Ogawa, E. and Ohtake, M. (1986) Relative growth of leg segments of the German cockroach, *Blattella germanica*. *Growth*, **50**: 273-286.
- 2 Tanaka, A. (1984) Relative growth between femur and tibia in the German cockroach, *Blattella germanica*. *Growth*, **48**: 278-296.
- 3 Tanaka, A., Ohtake-Hashiguchi, M. and Ogawa, E. (1987) Repeated regeneration of the German cockroach legs. *Growth*, **51**: 282-300.
- 4 Ross, M. H. and Cockran, D. G. (1975) The German cockroach, *Blattella germanica*. In "Handbook of Genetics, vol. 3". Ed. by R. C. King, Plenum Press, New York, pp. 35-62.
- 5 Ross, M. H. (1975) Genetic variability in the German cockroach. X. Genetics of pale purple, pearl, and stumpy. *J. Hered.*, **66**: 155-159.
- 6 O'Farrell, A. F. and Stock, A. (1953) Regeneration and the moulting cycle in *Blattella germanica* L. I. Single regeneration initiated during the first instar. *Aust. J. Biol. Sci.*, **6**: 485-500.
- 7 Kunkel, J. G. (1975) Cockroach molting. I. Temporal organization of events during molting cycle of *Blattella germanica* (L.). *Biol. Bull.*, **148**: 259-273.
- 8 O'Farrell, A. F., Stock, A. and Morgan, J. (1956) Regeneration and the moulting cycle in *Blattella germanica* L. IV. Single and repeated regeneration and metamorphosis. *Aust. J. Biol. Sci.*, **9**: 406-422.
- 9 Tanaka, A. (1982) Effects of carbon-dioxide anaesthesia on the number of instars, larval duration and adult body size of the German cockroach, *Blattella germanica*. *J. Insect Physiol.*, **28**: 813-821.
- 10 Tanaka, A. (1985) Further studies on the multiple effects of carbon dioxide anaesthesia in the German cockroach, *Blattella germanica*. *Growth*, **49**: 293-305.
- 11 Garcia-Bellido, A. (1975) Genetic control of wing disc development in *Drosophila*. In "Cell Patterning". Ciba Foundation Symposium 29, Elsevier, Amsterdam, pp. 161-182.
- 12 Garcia-Bellido, A. (1977) Homoeotic and atavic mutations in insects. *Amer. Zool.*, **17**: 613-629.
- 13 Lewis, E. B. (1978) A gene complex controlling segmentation in *Drosophila*. *Nature*, **276**: 565-570.
- 14 Struhl, G. (1982) Genes controlling segmental specification in the *Drosophila* thorax. *Proc. Natl. Acad. Sci.*, **79**: 7380-7384.
- 15 Ross, M. H. (1964) Pronotal wings in *Blattella germanica* (L.) and their possible evolutionary significance. *Amer. Mid. Nat.*, **71**: 161-180.
- 16 Ross, M. H. and Cochran, D. G. (1971) Cytology and genetics of a pronotal-wing trait in the German cockroach. *Can. J. Genet. Cytol.*, **13**: 522-535.
- 17 Ross, M. H. (1966) Notched sternite: a mutant of *Blattella germanica*, with possible implications for the homology and evolution of ventral abdominal structures. *Ann. ent. Soc. Amer.*, **59**: 473-484.
- 18 Ross, M. H. (1966) Embryonic appendages of the notched sternite mutant of *Blattella germanica*. *Ann. ent. Soc. Amer.*, **59**: 1160-1162.
- 19 Ross, M. H. and Keil, C. B. (1978) Genetic variability in the German cockroach. XI. Does chromosome 9 carry remnants of a primitive gene system? *J. Hered.*, **69**: 337-340.
- 20 Ross, M. H. and Tanaka, A. (1988) Genetic variability in the German cockroach. XII. A third mutant that suggests chromosome 9 carries a highly-conserved group of closely linked genes. *J. Hered.*, **79**: 439-443.



The Role of Sertoli Cells Adjacent to Efferent Ductules in Sperm Transport in *Rana porosa porosa*

TOHRU KOBAYASHI and HISAAKI IWASAWA

Biological Institute, Faculty of Science, Niigata University,
Niigata 950-21, Japan

ABSTRACT—Ultrastructural changes in Sertoli cells adjacent to efferent ductules were observed before and during sperm transport in *Rana porosa porosa*. In control frogs, the lumina of seminiferous tubules were not linked with the lumina of efferent ductules. Sertoli cells adjacent to efferent ductules were in close contact with the ductule cells, and no tubule lumen opened into the efferent ductules. After hCG treatment, dilation of the Sertoli cells was observed, and the lumina of seminiferous tubules and the lumina of efferent ductules were linked. Spermatozoa were then seen in the efferent ductules. Thus, the present observations indicate that Sertoli cells adjacent to efferent ductules act as a valve-like device for sperm transport from the seminiferous tubules to the efferent ductules in frogs.

INTRODUCTION

The significance of testicular contractile peritubular myoid cells in sperm transport has been pointed out in mammals. The intratesticular excurrent duct system is composed of the rete testis, tubuli recti and the terminal segment of the seminiferous tubules [1], and the last one acts as a valve-like device for the transport of sperm and fluid [2]. In anurans, however, little information has been available on the mechanism of sperm transport. Only a few electron microscopic studies have been performed on sperm release from Sertoli cells [3] and the intratesticular excurrent duct system [4, 5]. We carried out an ultrastructural study on the changes in seminiferous elements and intratesticular efferent ductules during gonadotropin-induced spermiogenesis. Particular emphasis was placed on Sertoli cells adjacent to efferent ductules, and their role in sperm transport is discussed.

MATERIALS AND METHODS

Adult males of *Rana porosa porosa* were collected in early November at Kurihashi, Saitama

Prefecture. The frogs were maintained at $18 \pm 1^\circ\text{C}$ with an artificial photoperiod of 12L:12D. Twenty-five frogs were divided into five groups, i.e., one initial control group, two saline-injected control groups and two gonadotropin-injected groups (sacrificed 20 or 45 min after the injection). In the injected control groups, a single injection of 0.7% saline was administered. Gonadotropin treatment consisted of a single injection of hCG (Puberogen, Sankyo Co., Ltd., Tokyo): 2.0 IU/g body weight.

In preparation for histological observation, the right testes and kidneys were fixed in Bouin's solution, embedded in Paraplast (Sherwood Medical, U.S.A.), and cut serially into 5 μm -thick transverse sections; the sections were then stained with Delafield's hematoxylin and eosin. For electron microscopy, the left testes were fixed for 2 hr in 1% glutaraldehyde-1% paraformaldehyde that had been adjusted to pH 7.2 with 0.07 M cacodylate buffer. After being rinsed in the buffer, they were postfixed in cold 1% OsO_4 for 2 hr, dehydrated through a series of ethanols, and embedded in epoxy resin. Thick sections were cut, stained with toluidine blue, and examined with a light microscope to identify sperm transport into efferent ductules. Gold to silver sections were cut with a Porter-Blum MT-1 ultramicrotome, stained with uranyl acetate and lead citrate, and examined with an H-300 electron microscope (Hitachi, Ltd.,

Japan).

From the electron microscopical observation, the number of dilated Sertoli cells adjacent to efferent ductules was recorded for each animal, i.e., the seminiferous tubules adjacent to efferent ductules were selected at random, and twenty Sertoli cells in this region were examined. From these results, the percentage of dilated Sertoli cells

was calculated for each group. The results obtained were tested for statistical significance using Student's *t*-test.

RESULTS

Light microscopical observations

In the control frogs, the seminiferous tubules

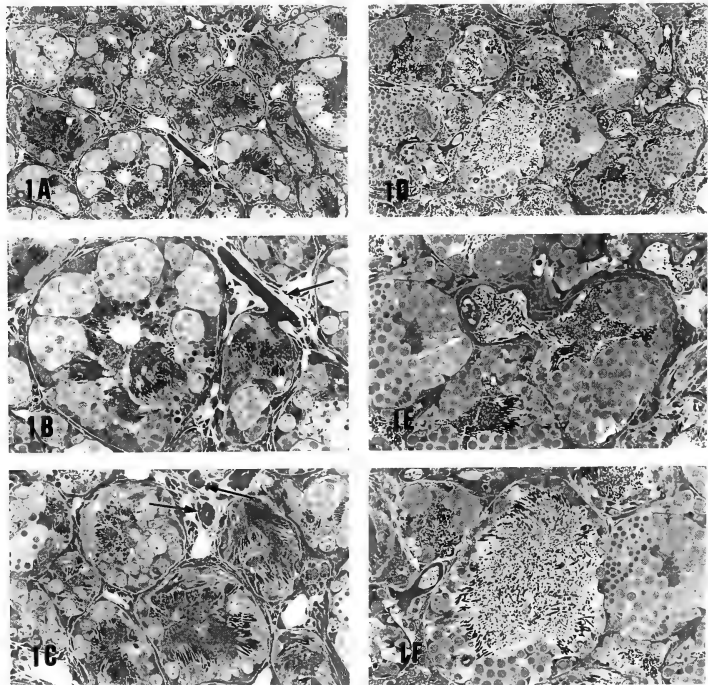
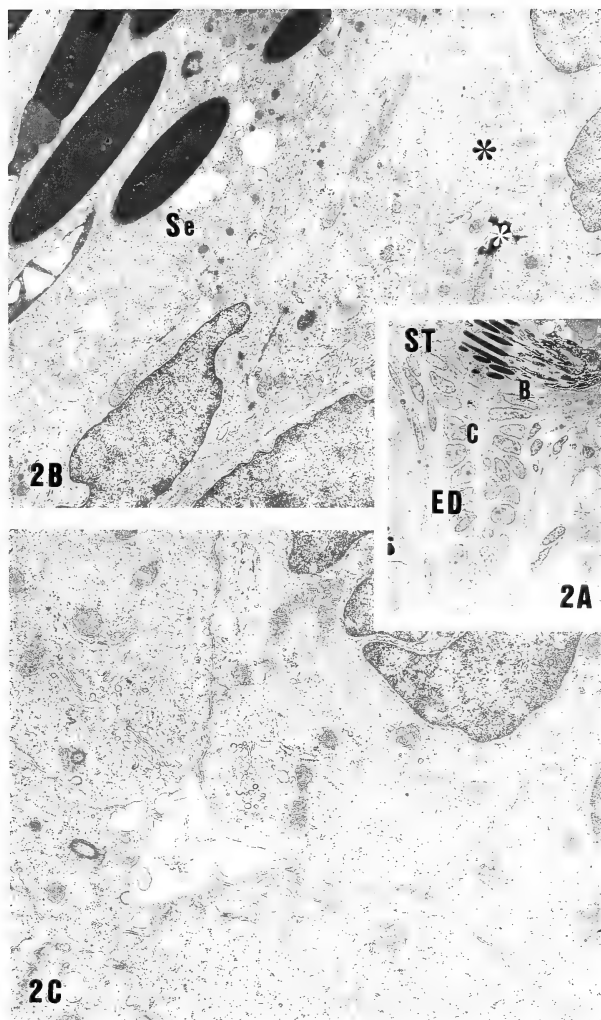


FIG. 1. Testicular histology at the time of spermiation induced by hCG treatment. arrow: intratesticular efferent ductules. A, B, C: control frogs. D, E, F: hCG-treated frogs 20 min after treatment. The release of numerous spermatozoa and their transport from the seminiferous tubules to the efferent ductules can be seen. A and D, $\times 105$, B, C, E and F, $\times 220$.

FIG. 2. A: The region adjoining the seminiferous tubule (ST) and the efferent ductule (ED) in the control. $\times 700$. B: Higher magnification of region B in Fig. 2A. Sertoli cells (Se) are in close contact with the cells of efferent ductules (*). $\times 72000$. C: Higher magnification of the region C in Fig. 2A showing the characteristic abundant filaments in the cells of the efferent ductules. $\times 13200$.



were filled with numerous spermatozoa and cysts of spermatogonia, spermatocytes, and spermatids. Spermatozoa were attached to the Sertoli cells, and free ones were hardly seen in the lumina of the tubule (Fig. 1A, C). Intratesticular efferent ductules were easily distinguished from other testicular components (Fig. 1B, C). The part of the efferent ductules adjacent to the seminiferous tubules was constricted and contained no spermatozoa in their small lumina (Fig. 1B). On the other hand, in the hCG-treated frogs, the lumina of seminiferous tubules were remarkably expanded, and numerous spermatozoa were observed in the lumina 20 min after injection (Fig. 1D, F). Furthermore, spermatozoa were frequently seen in the efferent ductules (Fig. 1E). The expansion of ductule lumina in which no spermatozoa were seen, was also observed. These changes were recognized in 40% of the planes of sections 20 min after hCG treatment and in almost all the planes of sections 45 min after treatment. The appearance of spermatozoa in the Wolffian duct was first recognized 20 min after hCG injection.

Ultrastructural observations

From light and electron microscopical observations, we determined that the intratesticular excurrent duct system is composed only of intratesticular efferent ductules (e.g., Fig. 2).

In the control frogs, Sertoli cells adjacent to efferent ductules were in close contact with the cells of efferent ductules, and no tubule lumen was linked with the small lumina of efferent ductules (Fig. 2B). The cells lining the small lumina of these efferent ductules were interdigitated (Fig. 2C).

When spermatozoa in the hCG-treated frogs were released from the Sertoli cells and observed in the efferent ductules, Sertoli cells adjacent to efferent ductules showed noticeable changes in structure, i.e., elongation of the cytoplasmic processes (Figs. 3A, 4) and dilation of the cell body (Fig. 3B). The percentage of dilated Sertoli cells in this region increased with time after hCG treatment ($p < 0.01$, Table 1). When the expansion of lumina was seen in the cells of efferent ductules, the protrusion of cytoplasmic processes into the lumina was observed (Fig. 5A). Furthermore,

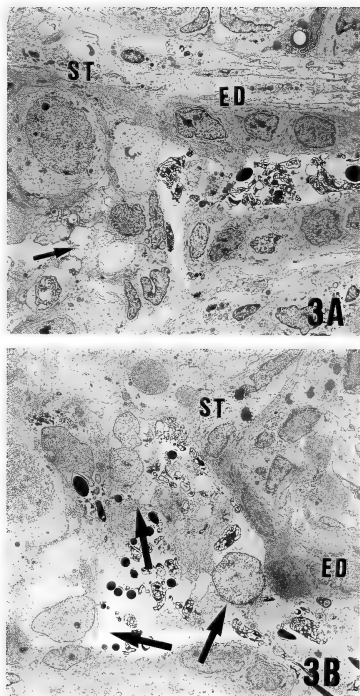


FIG. 3. The region adjoining the seminiferous tubule (ST) and the efferent ductule (ED) after hCG treatment. A: In the Sertoli cells, elongation of a cytoplasmic process (arrow) is observed. B: Arrows indicate dilated Sertoli cells. A, B, $\times 1300$.

these processes were often in contact with residual bodies (Fig. 5B). In the present study, however, phagocytosis of residual bodies by these cells was not seen. These changes are revealed schematically in Figure 6.

In the peritubular parts of the seminiferous tubules and efferent ductules, myoid-like cells and innervation were not observed.

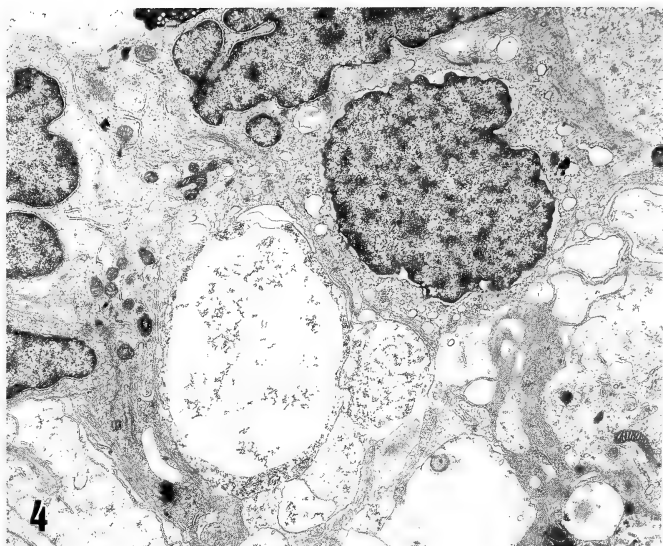


Fig. 4. Sertoli cells after hCG treatment. Sertoli cells show noticeable structural change. $\times 7400$.

TABLE 1. The percentage of dilated Sertoli cells in the region adjoining the seminiferous tubules and the efferent ductules

Group	Time after hCG treatment (min)		
	0	20	45
Control	13.3 ± 3.2	16.7 ± 5.2	6.3 ± 4.2
HCG-treatment	—	$40.4 \pm 7.3^*$	$76.9 \pm 6.8^*$

* $p < 0.01$ as compared with control value.

DISCUSSION

In anurans, numerous studies have been undertaken to determine the mechanism of spermiation [6]. However, there are few reports on the intratesticular excurrent duct system in the process of sperm transport from the seminiferous tubules to the efferent ductules.

In the present study, a remarkable expansion of the lumina of seminiferous tubules and the dilation

of Sertoli cells were seen after hCG-treatment. Shortly after, the release of sperm from the Sertoli cells was observed, and the dilation of the Sertoli cells adjacent to the efferent ductules caused a full opening of the lumina in both tubules and ductules (see Fig. 6).

It is known that a remarkable expansion of the lumina of seminiferous tubules at the time of spermiation indicates fluid accumulation [6]. In the present study, a remarkable expansion of the

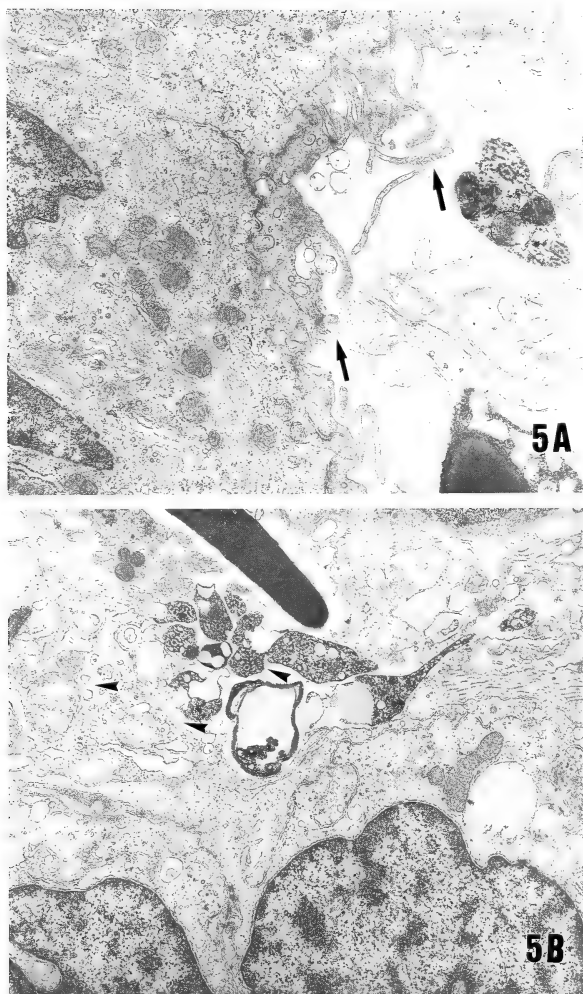


FIG. 5. The cells of the efferent ductules after hCG treatment. A: Arrows indicate the protrusion of cytoplasmic processes into the lumina. B: The cytoplasmic processes are in contact with residual bodies (arrowheads). A, B, $\times 143000$.

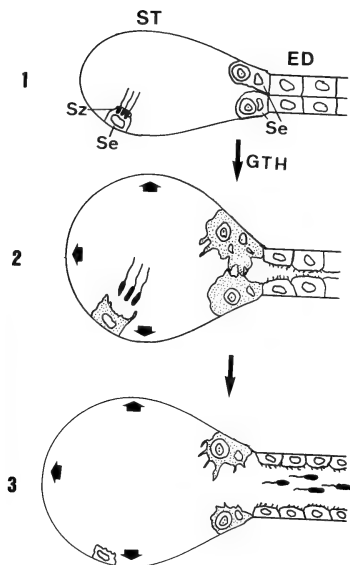


Fig. 6. Schematic representation of changes in the region adjoining the seminiferous tubules and the efferent ductules during sperm transport. This process is divided into three stages. ST: seminiferous tubule, ED: efferent ductule, Se: Sertoli cell, Sz: spermatozoa, GTH: gonadotropin. Stage 1: Seminiferous tubule and efferent ductule in the control are shown. Stage 2: After GTH treatment. Expansion of the seminiferous tubule (large arrows) and dilation of Sertoli cells are seen. Stage 3: Sertoli cells adjacent to the ED dilate, and the lumina of the ST and ED are linked. As a result, sperm transport from the ST to ED takes place.

lumina in seminiferous tubules was observed after hCG treatment. As mentioned above, fluid accumulation in the seminiferous tubules at the time of spermiation occurred simultaneously at the time of the dilation of Sertoli cells. Burgos and Vital-Calpe [3] indicated that fluid accumulation was caused by the dilation of sperm-supporting Sertoli cells at the time of spermiation. In young frogs, fluid accumulation is caused by the application of gonadotropin [7, 8]. In the present study, the

relation between the dilation of Sertoli cells and fluid accumulation in seminiferous tubules is not clear. Further study will be necessary with regard to the mechanism of fluid accumulation.

Burgos and Vital-Calpe [3] reported in *Bufo arenarum* that at the time of hCG-induced spermiation, the dilation of sperm-supporting Sertoli cells could be observed, with the consequence of sperm release from the Sertoli cells. In anurans, however, noticeable cytoplasmic changes are not known to occur in Sertoli cells except in those of the sperm-supporting type. In the present study, the changes in sperm-supporting Sertoli cells after hCG treatment are in accord with Burgos and Vital-Calpe [3]. Furthermore, the dilation of the Sertoli cells adjacent to efferent ductules after hCG treatment indicates that noticeable cytoplasmic changes also occur in Sertoli cells other than the sperm-supporting type. Our findings suggest that these cytoplasmic changes may be caused by gonadotropin treatment irrespective of the stages of the supporting germ cells.

In mammals, the intratesticular excurrent duct system is composed of the rete testis, tubuli recti, and the terminal segment of the seminiferous tubules [1]. The terminal segment of the seminiferous tubules is composed of modified Sertoli cells, and germ cells supported by Sertoli cells are not seen in this region. With regard to the function of the excurrent duct system during spermiation, Wrobel *et al.* [2] reported that in bulls, the terminal segment of the seminiferous tubules functions as a valve-like device to prevent a reflux of spermatozoa and tubuli rectes fluid under normal conditions. Although in anurans, there have been no suggestions as to the function of the excurrent duct system during spermiation, our observations suggest that the germ cell-supporting Sertoli cells adjacent to efferent ductules function as a valve-like device in the transport of spermatozoa which are released into the lumina of seminiferous tubules during spermiation.

With regard to the cells of efferent ductules, Unsicker [4] reported from electron microscopical observations in three anuran species that these cells were very filamentous and involved in mechanical support rather than serving as a contractile aid in sperm transport. Furthermore, innervation

in these peritubular tissues was not recognized [5]. In the present study, the cells of the efferent ductules were filamentous, and innervation in these peritubular tissues was not seen. From these facts, it is difficult to imagine that the cells of the efferent ductules are an active contractile aid to sperm transport in anurans. Therefore, we must conclude that the parts of intratesticular excurrent duct system involved in sperm transport in anurans differ from those in mammals.

In mammals, the epithelial cells of the intratesticular excurrent duct system phagocytose sperm material [2, 9, 10, 11]. From such observations, these investigators have suggested that the epithelial cells were capable of selectively disposing degraded sperm material. Although the processes of efferent ductule cells were frequently in contact with sperm residual bodies at the time of sperm transport in our study, we do not know whether or not efferent ductule cells phagocytose sperm residual bodies.

REFERENCES

- 1 Setchell, B. P. (1978) Fluid secretion and the entry of substances into the tubules. In: "The Mammalian Testes". Ed. by B. P. Setchell, Paul Elek Ltd., London, pp. 233-274.
- 2 Wrobel, K.-H., Sinowatz, F. and Mademann, R. (1982) The fine structure of the terminal segment of the bovine seminiferous tubule. *Cell Tissue Res.*, **225**: 29-44.
- 3 Burgos, M. H. and Vital-Calpe, R. (1967) The mechanism of spermiogenesis in the toad. *Am. J. Anat.*, **120**: 227-252.
- 4 Unsicker, K. (1975) Fine structure of the male genital tract and kidney in the anura *Xenopus laevis* Daudin, *Rana temporaria* L. and *Bufo bufo* L. under normal and experimental conditions. I. Testicular interstitial tissue and seminal efferent ducts. *Cell Tissue Res.*, **158**: 215-240.
- 5 Unsicker, K., Axelsson, S., Owman, C.-H. and Svensson, K. G. (1975) Innervation of the male genital tract and kidney in the Amphibia, *Xenopus laevis* Daudin, *Rana temporaria* L. and *Bufo bufo* L. *Cell Tissue Res.*, **160**: 453-484.
- 6 Lofts, B. (1974) Reproduction. In "Physiology of Amphibia Vol. II". Ed. by B. Lofts, Academic Press, New York, pp. 107-218.
- 7 Pizarro, N. Z. and Burgos, M. H. (1971) Action of FSH on the newly differentiated testis of *Bufo arenarum*. *Gen. Comp. Endocrinol.*, **3**: 644-648.
- 8 Iwasawa, H., Yamada, M. and Kobayashi, M. (1977) Response of immature testis to exogenous gonadotropins in young *Rana nigromaculata*. *Sci. Rep. Niigata Univ. Ser. D*, **14**: 15-20.
- 9 Dym, M. (1974) The fine structure of monkey Sertoli cells in the transitional zone at the junction of the seminiferous tubules with the tubuli recti. *Am. J. Anat.*, **140**: 1-26.
- 10 Sinowatz, F., Wrobel, K.-H., Sinowatz, S. and Kugler, P. (1979) Ultrastructural evidence for phagocytosis of spermatozoa in the bovine rete testis and testicular straight tubules. *J. Reprod. Fert.*, **57**: 1-4.
- 11 Murakami, M., Yokoyama, R., Nishida, T., Shimamoto, M. and Sato, H. (1988) Scanning and transmission electron microscope observations of the terminal segment of the cat seminiferous tubule: epithelial phagocytosis of spermatozoa and latex beads. *Arch. Histol. Cytol.*, **51**: 185-192.

Seasonal Changes in Ovarian Response to Photoperiods in Orange-Red Type Medaka¹

MASAHICO AWAJI and ISAO HANYU²

National Research Institute of Aquaculture, Fisheries Agency, Nansei, Mie 516-01, and

²Laboratory of Fish Physiology, Faculty of Agriculture, University of Tokyo,
Bunkyo, Tokyo 113, Japan

ABSTRACT—Three groups of orange-red type medaka, *Oryzias latipes*, were reared from October under different temperature-photoperiod regimes: natural condition, 18°C natural daylength and natural temperature 15L (15 hr of light/day). Pairs from these groups were periodically transferred to 18°C 15L or to 18°C 10L and kept separately. In natural condition group, ovaries of the fish transferred in mid- or late October kept immature even after one month under both regimes. In the fish transferred in late November or late December, ovarian growth and spawning were observed in about one month only under 18°C 15L. The fish transferred in early February matured in three weeks and spawned irrespective of photoperiod. Thus, ovarian refractoriness in autumn changed into long-daylength dependent maturation in winter, which was followed by photoperiod independent maturation in spring. In the fish transferred from 18°C natural daylength and natural temperature 15L in late December and early February, rapid ovarian growth occurred under 18°C 15L, but not under 18°C 10L. These results demonstrate that ovarian response to temperature-photoperiod conditions can be markedly influenced by environmental careers in medaka.

INTRODUCTION

Annual reproductive cycles of temperate-zone teleosts have been believed to depend upon seasonal changes in environmental factors such as photoperiod and water temperature. Effects of the environmental factors on the gonads have been studied in many fishes [1-5], and seasonal changes in gonadal responses have also been reported in cyprinids, gobiids and the stickleback [2, 6, 7].

Medaka, *Oryzias latipes*, is a small freshwater fish native to Japan and adjacent areas, and its spawning season extends from mid-April to early September [8-10]. Our previous study showed that only temperature rise in spring was necessary for the spawning season of medaka to begin and photoperiods had little effects on the gonadal growth [11]. The experiments started in late February, when yolk vesicle formation of ovaries had almost finished. In other seasons, however,

effects of temperature-photoperiod conditions on gonadal growth might be different from those in spring.

The present study was conducted to examine seasonal changes in effects of temperature-photoperiod regimes on gonadal growth of medaka, mainly for female. The fish were reared under natural condition or conditions with a warm temperature or with a long daylength. Part of them were transferred to long (18°C 15L) or short daylength (18°C 10L) condition almost monthly from October to February and gonadal responses were examined.

MATERIALS AND METHODS

Orange-red type medaka, *Oryzias latipes*, born in the preceding breeding season were obtained in Tokyo in July. They were kept in a circulating outdoor tank (90×180×50 cm) in University of Tokyo till experiments started and fed on tubifex (freshwater oligochaetes) to satiation. All experiments were carried out in Tokyo.

In October, the fish of 26 to 30 mm in standard

Accepted January 6, 1989

Received August 19, 1988

¹ Studies on the Reproductive Rhythms of Fishes-XXV.

length were divided into the following three experimental groups, i.e. natural condition, 18°C natural daylength and natural temperature 15L (15 hr of light/day). Natural condition group consisted of 200 fish of each sex, which were kept in another circulating outdoor tank from October 17 under natural temperature and daylength. For the 18°C natural daylength group, 110 fish of each sex were evenly distributed to 11 circulating glass-aquaria (30×45×30 cm) regulated at 18°C under natural daylength on October 29, when natural water temperature was around 18°C. For the natural temperature 15L group, 110 fish of each sex were transferred on October 17 to two light-proof circulating tanks (80×170×50 cm) given a photoperiod of 15L by two 20 W fluorescent lamps and no temperature regulation. The fluorescent lamps were placed 30 cm above the water surface. All experimental tanks and aquaria were provided with water plants, *Ceratophyllum demersum*.

Eight fish of each sex were monthly collected at random from each group to examine changes in gonadosomatic index (gonad weight×100/body weight: GSI). The fish were anesthetized with MS 222 and the body weights were measured. After decapitation, the gonads were taken out to measure their weights. Ovaries of three females from each group were dissociated in carp saline [12], and diameters of largest 50 oocytes were measured using a micrometer. Spawning was checked every week in 18°C and 15L groups by replacing water plants with artificial spawning beds for three days in aquaria or tanks after cleaning. If spawned during the three days, all eggs attached to the spawning beds or dropped on the bottom were counted.

From these three groups, 15 to 4 pairs were periodically transferred to 18°C 15L or to 18°C 10L and kept separately. In the natural condition group, this transfer was conducted monthly from mid-October to early February to a circulating glass-aquarium (30×45×30 cm) on each regime. The aquaria of each regime were placed in a light proof bath (90×180×50 cm) provided with two 20 W fluorescent lamps placed 15 cm above the water surface. In the 18°C natural daylength and natural temperature 15L groups, the transfer to the aquaria of the same type was conducted in late

December and early February. About half of the fish was randomly collected one month after the transfer. The rest was reared till mid-March and sacrificed. Changes in GSI and oocyte diameters were examined and spawning was checked in the same way as mentioned above.

RESULTS

Natural condition group

Under natural condition, average GSI of female gradually increased from 2% in October to 4% in March (Fig. 1), accompanied by slight increment of oocyte diameters (Fig. 2). In April female GSIs rose rapidly, and spawning began.

The transfers of the fish from natural condition

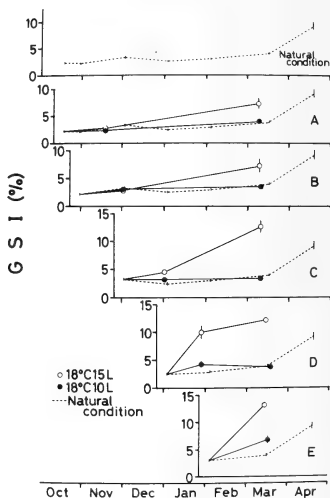


FIG. 1. Changes in gonadosomatic index (GSI) of female *Oryzias latipes* reared under natural condition, and transferred to 18°C 15L (15 hr of light/day) or to 18°C 10L. The transfer was conducted almost monthly from October to February. Solid lines in graphs A, B, C, D, E, indicate changes in GSIs of female transferred to 18°C 15L or to 18°C 10L. Dotted line in every graph shows GSI of female reared under natural condition.

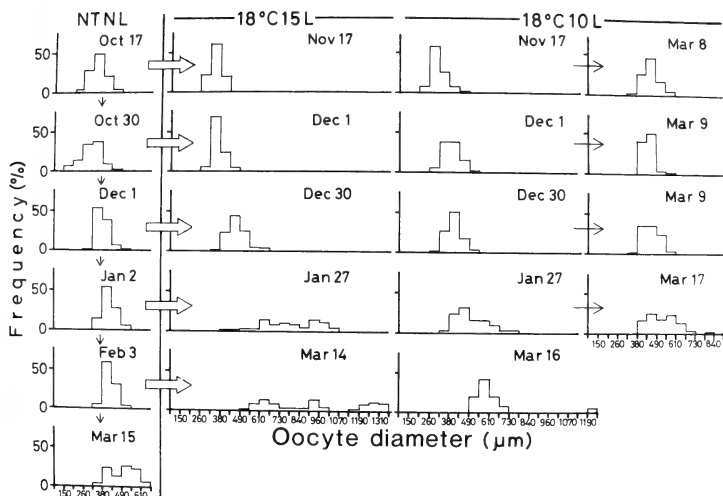


Fig. 2. Changes in distribution of oocyte diameters under natural condition (NTNL) and after the transfer to 18°C 15L or to 18°C 10L. The transfer was conducted almost monthly, and distributions of oocyte diameters under 18°C 15L or 18°C 10L were examined in one month and at the end (18°C 10L). Oocyte diameters under natural condition were examined within two days after the transfer.

to 18°C 15L or to 18°C 10L caused different responses in ovarian activity with time of transfer. When transferred in mid- or late October, ovarian growth was hardly observed during one month under both 18°C 15L and 18°C 10L. Under the long daylength, however, spawning started in January (Fig. 3) and GSI reached 7% in March (Fig. 1A, B). Under the short daylength, females did not mature until the end of the experiment with only slight increase in oocyte diameters (Fig. 2). Transfer in late November caused a little increase of GSI and oocyte growth under 18°C 15L in one month (Figs. 1C, 2), and resulted in active spawning from January (Fig. 3) and GSI of 12 to 13% in March (Fig. 1C). Under 18°C 10L, ovaries grew little until the end of the experiment (Figs. 1C, 2). Average GSI of the females transferred to 18°C 15L in late December increased to around 10% in one month (Fig. 1D), having oocytes large enough for ovulation (Fig. 2). Spawning began in

early February (Fig. 3). Under 18°C 10L, females showed some increase in GSI and in oocyte diameters, but ovaries were not fully mature even in mid-March (Figs. 1D, 2). When transferred in early February, spawning was observed under both 18°C 15L and 18°C 10L in three weeks (Fig. 3). In mid-March, average GSIs of long and short daylength regimes were 13% and 7%, respectively (Fig. 1E). Both exceeded the average GSI under natural condition (Cochran-Cox test, $p < 0.05$).

As for males, average GSIs under natural condition were about 1% from mid-October to early December, but decreased to about 0.7% in early January. Thereafter, GSI increased gradually to 0.9% in mid-March and 1.2% in mid-April. Male GSIs under 18°C 15L or 18°C 10L kept initial value of 1% when transferred in a season from mid-October to late November. Transfer in late December or early February caused increase in GSI to 1.1–1.3% in one month, also irrespective of

date		Oct.	Nov.	Dec.	Jan.	Feb.	Mar.															
		20	27	3	10	17	24	1	8	15	22	29	5	12	18	25	1	8	15	23		
Natural condition	18°C 15L	0	0	0	0	0	0	0	0	0	0	0	0	0	0	0	70	49	30	22	0	23
		(15)					(11)														(8)	
	18°C 10L	0	0	0	0	0	0	0	0	0	0	0	0	0	0	0	0	0	0	0	0	0
Oct. 17	NT 15L	0	0	0	0	0	0	0	0	0	0	0	0	0	0	0	0	0	0	0	0	0
		(15)					(10)														(5)	
Natural condition	18°C 15L	0	0	0	0	0	0	0	0	0	0	0	0	+	32	21	34	20	20	22	33	
		(15)					(10)														(5)	
	18°C 10L	0	0	0	0	0	0	0	0	0	0	0	0	0	0	0	0	0	0	0	0	0
Oct. 29	18°C NL	0	0	0	0	0	0	0	0	0	0	0	0	0	0	0	0	0	0	0	0	0
		(15)					(9)														(4)	
Natural condition	18°C 15L	0	0	0	0	0	0	0	0	0	0	0	0	0	+	105	143	127	123	162	114	141
		(15)																			(6)	
	18°C 10L	0	0	0	0	0	0	0	0	0	0	0	0	0	0	0	0	0	0	0	0	0
Nov. 30	18°C NL	0	0	0	0	0	0	0	0	0	0	0	0	0	0	0	0	0	0	0	0	0
		(15)																			(5)	
Natural condition	18°C 15L	0	0	0	0	0	0	0	0	0	0	0	0	0	0	74	166	121	110	97		
		(15)																			(9)	
	18°C 10L	0	0	0	0	0	0	0	0	0	0	0	0	0	0	0	0	0	0	0	0	0
Dec. 31	18°C NL	0	0	0	0	0	0	0	0	0	0	0	0	0	0	0	0	0	0	0	0	0
		(15)																			(9)	
Natural temp. 15L	18°C 15L	0	0	0	0	0	0	0	0	0	0	0	0	0	0	139	111	57	46	83		
		(15)																			(10)	
	18°C 10L	0	0	0	0	0	0	0	0	0	0	0	0	0	0	0	0	0	0	0	0	0
Dec. 31	18°C NL	0	0	0	0	0	0	0	0	0	0	0	0	0	0	0	0	0	0	0	0	0
		(15)																			(10)	
18°C Natural daylength	18°C 15L	0	0	0	0	0	0	0	0	0	0	0	0	0	0	104	78	101	129	122		
		(15)																			(9)	
	18°C 10L	0	0	0	0	0	0	0	0	0	0	0	0	0	0	0	0	0	0	0	0	0
Dec. 31	18°C NL	0	0	0	0	0	0	0	0	0	0	0	0	0	0	0	0	0	0	0	0	0
		(15)																			(10)	
Natural condition	18°C 15L	0	0	0	0	0	0	0	0	0	0	0	0	0	0	0	98	166				
		(7)																			(7)	
	18°C 10L	0	0	0	0	0	0	0	0	0	0	0	0	0	0	0	36	35				
Feb. 3	18°C NL	0	0	0	0	0	0	0	0	0	0	0	0	0	0	0	0	0	0	0	0	0
		(5)																			(5)	
Natural temp. 15L	18°C 15L	0	0	0	0	0	0	0	0	0	0	0	0	0	0	0	66	155				
		(4)																			(4)	
	18°C 10L	0	0	0	0	0	0	0	0	0	0	0	0	0	0	0	0	0	0	0	0	0
Feb. 3	18°C NL	0	0	0	0	0	0	0	0	0	0	0	0	0	0	0	0	0	0	0	0	0
		(4)																			(4)	
18°C Natural daylength	18°C 15L	0	0	0	0	0	0	0	0	0	0	0	0	0	0	0	28	71				
		(15)																			(15)	
	18°C 10L	0	0	0	0	0	0	0	0	0	0	0	0	0	0	0	0	0	0	0	0	0
Feb. 3	18°C NL	0	0	0	0	0	0	0	0	0	0	0	0	0	0	0	0	0	0	0	0	0
		(15)																			(15)	

FIG. 3. Total number of eggs spawned by *Oryzias latipes* during three days under various temperature photoperiod regimes. Date on the top indicates the middle day. Transfer dates are indicated between regimes. Number of female under each regime is shown in parenthesis. +, spawning was observed; NT15L, natural temperature-15L (15 hr of light/day); 18°C NL, 18°C-natural daylength.

photoperiod.

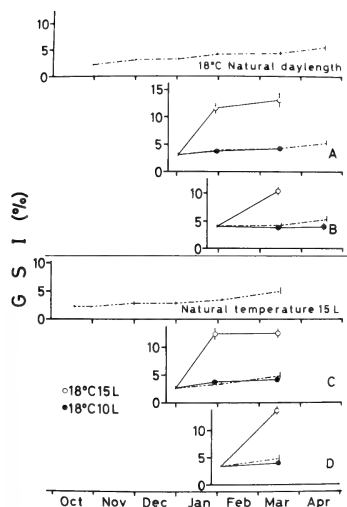
18°C natural daylength group

Average female GSI slowly increased from 2% in late October to 5% in mid-April (Fig. 4). Until mid-March, oocytes grew as gradually as in the natural condition group (Fig. 5), and no spawning was observed (Fig. 3). In mid-April some fish started spawning (data not shown), but rapid increase in average GSI shown under natural condition did not occur.

Transfer to 18°C 15L in late December brought about rapid ovarian growth. Average GSI reached 11% in one month (Fig. 4A) and spawning began in early February (Fig. 3). Average GSI kept high

until mid-March (Fig. 4A). Under 18°C 10L, average GSI increased only to 4% and kept the value till the end of the experiment (Fig. 4A). Oocyte diameters increased a little, but spawning was not observed (Figs. 3, 5). Transfer in early February had almost the same effect as in late December. Under long daylength, fish showed rapid ovarian growth (Fig. 4B) and spawning began in late February (Fig. 3). Under short daylength, average GSI kept low until mid-March (Fig. 4B) and oocyte diameters did not change much (Fig. 5). Minor spawning was observed in mid-February, but ceased in the next week (Fig. 3).

As for males, average GSIs kept high values over 1% under 18°C with natural daylength; 1% in



late October, 1.3% in late November, 1.2% in late December, 1% in early February and 1.2% in mid-April. Transfer to 18°C 15L in late December had no effect on average GSI. Under short daylength, however, GSI slightly decreased to around 1%. The transfer in early February caused GSI increase to 1.4% in mid-March, irrespective of photoperiod.

Natural temperature 15L group

Average GSI of female fish increased gradually from 2% in October to 5% in mid-March under 15L with natural water temperature (Fig. 4).

FIG. 4. Changes in gonadosomatic index (GSI) of female *Oryzias latipes* reared under 18°C natural daylength or natural temperature 15L, and transferred to 18°C 15L (15 hr of light/day) or to 18°C 10L. The transfer was conducted in late December (A, C) or early February (B, D). Solid lines in graphs A, B, C, D show changes in GSI of the fish transferred from 18°C natural daylength (A, B) or natural temperature 15L (C, D).

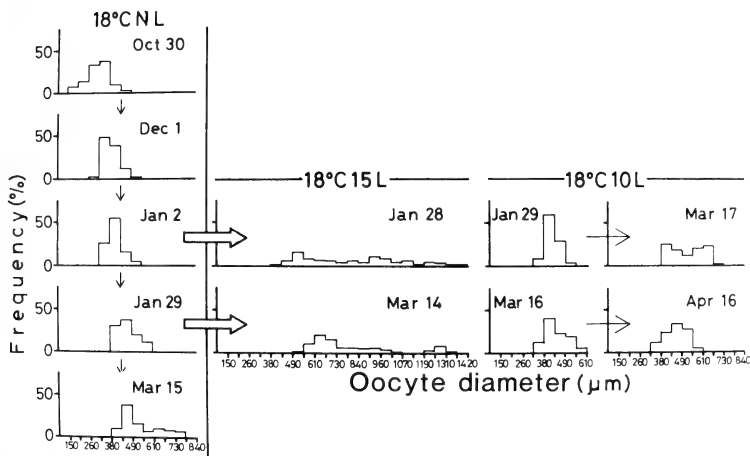


FIG. 5. Changes in distribution of oocyte diameters under 18°C natural daylength (18°C NL) and after the transfer to 18°C 15L or to 18°C 10L. The transfer was conducted in late December and early February, but distributions of oocyte diameters under 18°C NL was examined a few days earlier or later than the transfer. Distributions of oocyte diameters under 18°C 15L or 18°C 10L were examined in one month, and at the end (18°C 10L).

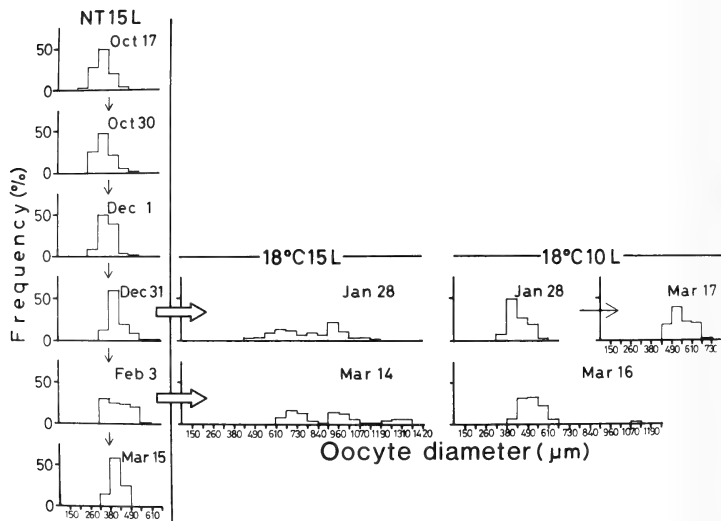


FIG. 6. Changes in distribution of oocyte diameters under natural temperature 15L (NT15L) and after the transfer to 18°C 15L or to 18°C 10L. The transfer was conducted in late December and early February. Distributions of oocyte diameters under 18°C 15L or 18°C 10L were examined in one month, and at the end (18°C 10L).

Oocytes grew slightly in accordance with the increase of GSI (Fig. 6). Spawning did not occur until the end of the experiment (Fig. 3).

When transferred to 18°C 15L in late December, average GSI of female increased rapidly and reached 13% in one month (Fig. 4C). Spawning began in early February (Fig. 3). Under 18°C 10L, however, GSIs kept as low as those of controls (Fig. 4C). Oocyte diameters increased a little by mid-March (Fig. 6), but no spawning was observed (Fig. 3). Transfer to 18°C 15L or to 10L in early February had almost the same effect as in late December (Figs. 4D, 6), except that spawning started under 15L in a shorter period or three weeks after the transfer (Fig. 3).

GSI of males under 15L with natural water temperature decreased slightly from 1% in mid-October to 0.8% in late December, but increased thereafter to 1% in mid-March. When transferred in late December to 18°C 15L or to 10L, male GSI

increased, reaching 1.3% and 1.1% respectively. Transfer to 18°C 10L in early February made male GSI decrease to 0.7%. Under 18°C 15L only two males survived, their GSIs being 1.5% and 0.5%.

DISCUSSION

In the natural condition group, ovarian responses of the medaka transferred to 18°C 15L or to 18°C 10L clearly changed with season. Although effects of temperature-photoperiod conditions on the ovarian activity of medaka have already been studied by several workers [9, 13–15], no one has reported seasonal change in ovarian response such as observed in the present study.

Ovarian unresponsiveness in autumn (Fig. 1A) is the same phenomenon as called refractoriness in wild-type medaka [13], *Notropis bifrenatus* [16] and *Heteropneustes fossilis* [17].

After the refractory period, the ovaries came to grow under long daylength. Results of the transfer from the natural condition to 18°C 15L in mid-October (Figs. 1A, 3) suggests that this change in ovarian response requires neither low temperature nor short daylength in winter. Similar results have been reported for wild type medaka [13] and *Notropis bifrenatus* [16].

Marked decline in ovarian photoperiodic response was observed in the natural condition group when transferred in early February. Though females of the 18°C natural daylength group or the natural temperature 15L group in early February had slightly larger oocytes than the natural condition group, they could not mature when transferred to 18°C 10L. Exposure to both low temperature and short daylength in winter seems to be necessary for the maturation independent of photoperiods.

In the natural condition group, the period between transfer to 18°C 15L and beginning of spawning shortened with approach of spring. Egami and Hosokawa [9] observed similar shortening of the period required for maturation in medaka transferred from natural water temperature to 23–26°C, though without photoperiod control, in seasons from autumn to spring. In our experiments, moreover, the females transferred from natural condition to 18°C 15L after late November reached higher GSIs than the females transferred in October, and GSIs of the females transferred from other experimental groups to 18°C 15L after late December were similarly higher than those of the females transferred from natural condition group in October. From these results, short daylength and/or low temperature in winter seem to be profitable for rapid ovarian growth and active spawning under 18°C 15L.

Testicular response to environmental alterations were different from that of ovaries. Seasonal changes in the response were not observed throughout the experiment. GSIs were kept at 1% or more under 18°C 15L or 18°C 10L, and in most cases photoperiods caused no difference in the testicular responses. In this study, however, only GSIs were considered. Histological observation will be necessary for further comments on testicular response.

Concerning environmental regulation of the spawning season of medaka, Awaji and Hanyu [11] showed that rapid gonadal growth and subsequent spawning in spring could be induced by raising water temperature over 14°C, irrespective of photoperiod, in the orange-red type medaka. This coincides with the present results. In the present study, in addition, temperature-photoperiod conditions necessary to induce rapid gonadal growth in medaka were shown to differ with maturational stages of the gonads or environmental career of the employed fish. Necessary period for maturation and average GSI of matured females also differed with these factors.

According to Yoshioka [13, 14, 18, 19], long daylength was necessary for maturation of wild type medaka in every season. Necessity of long daylength was also observed by Chan [15] in the orange-red type medaka. But Egami and Hosokawa [9] could induce ovarian maturation only by raising water temperature. Fish used in these studies were different from one another in its environmental career and the reproductive stage at the beginning of the experiments. On the other hand, Sawara and Egami [20] pointed out possible existence of racial difference in photoperiodic response of gonads in medaka. These circumstances make it difficult to generalize the environmental regulation of gonadal maturation in medaka. But as far as the orange-red type medaka cultured around Tokyo is concerned, environmental regulation of beginning of spawning season can be summarized as follows from the present study. Orange-red type medaka usually begins rapid gonadal growth and subsequent spawning in spring depending on rising water temperature, irrespective of photoperiod. Accidental warm temperature in winter will not induce rapid growth of young oocytes in the absence of long daylength. When ovarian development is delayed by some reasons, long daylength in spring will stimulate ovarian growth and lead to spawning in the regular season.

ACKNOWLEDGMENTS

The authors are grateful to Dr. K. Aida of University of Tokyo for advice during this work. Part of this study

was supported by a Grant-in-Aid for Scientific Research from the Ministry of Education, Science and Culture of Japan.

REFERENCES

- Crim, L. W. (1982) Environmental modulation of annual and daily rhythms associated with reproduction in teleost fishes. *Can. J. Fish. Aquat. Sci.*, **39**: 17-21.
- Hanyu, I., Asahina, K., Shimizu, A., Razani, H. and Kaneko, T. (1983) Environmental regulation of reproductive cycles in teleosts. *Proc. 2nd. N. Pac. Aquaculture Symp.*, 173-188.
- Peter, R. E. and Crim, L. W. (1979) Reproductive endocrinology of fishes: Gonadal cycles and gonadotropin in teleosts. *Ann. Rev. Physiol.*, **41**: 323-335.
- Peter, R. E. (1981) Gonadotropin secretion during reproductive cycles in teleosts: Influences of environmental factors. *Gen. Comp. Endocrinol.*, **45**: 294-305.
- de Vlaming, V. L. (1972) Environmental control of teleost reproductive cycles: a brief review. *J. Fish. Biol.*, **4**: 131-140.
- Kaneko, T. (1986) Studies on the reproductive cycles of the gobiid fishes. Dissertation for D. Agricul., Univ. of Tokyo.
- Baggerman, B. (1972) Photoperiodic responses in the stickleback and their control by a daily rhythm of photosensitivity. *Gen. Comp. Endocrinol.*, Suppl., **3**: 466-476.
- Awaji, M. and Hanyu, I. (1987) Annual reproductive cycle of the wild type medaka. *Nippon Suisan Gakkaishi*, **53**: 959-965.
- Egami, N. and Hosokawa, K. (1973) Responses of the gonads to environmental changes in the fish, *Oryzias latipes*. In "Responses of fish to environmental changes". Ed. by W. Chavin, Charles C. Thomas, Springfield, pp. 279-301.
- Yamamoto, K. and Yoshioka, H. (1964) Rhythm of development in the oocyte of the medaka, *Oryzias latipes*. *Bull. Fac. Fish., Hokkaido Univ.*, **15**: 5-24.
- Awaji, M. and Hanyu, I. (1988) Effects of water temperature and photoperiod on the beginning of spawning season in the orange-red type medaka. *Zool. Sci.*, **5**: 1059-1064.
- Kobayashi, M., Aida, K. and Hanyu, I. (1986) Annual changes in plasma levels of gonadotropin and steroid hormones in goldfish. *Nippon Suisan Gakkaishi*, **52**: 1153-1158.
- Yoshioka, H. (1966) On the effects of environmental factors upon the reproduction of fishes. 3. The occurrence and regulation of refractory period in the photoperiodic response of medaka, *Oryzias latipes*. *J. Hokkaido Univ. Education, Sec. II (B)*, **17**: 23-33.
- Yoshioka, H. (1970) On the effects of environmental factors upon the reproduction of fishes. IV. Effects of long photoperiod on the development of ovaries of adult medaka, *Oryzias latipes*, at low temperatures. *J. Hokkaido Univ. Education, Sec. II (B)*, **21**: 14-20.
- Chan, K. K.-S. (1976) A photosensitive daily rhythm in the female medaka, *Oryzias latipes*. *Can. J. Zool.*, **54**: 852-856.
- Harrington, Jr., R. W. (1957) Sexual photoperiodicity of the cyprinid fish, *Notropis bifrenatus* (Cope), in relation to the phases of its annual reproductive cycle. *J. Exp. Zool.*, **135**: 1-47.
- Sundararaj, B. J. and Vasal, S. (1976) Photoperiod and temperature control in the regulation of reproduction in the female catfish *Heteropneustes fossilis*. *J. Fish. Res. Board Can.*, **33**: 959-973.
- Yoshioka, H. (1962) On the effects of environmental factors upon the reproduction of fishes. I. The effects of day-length on the reproduction of the Japanese killifish, *Oryzias latipes*. *Bull. Fac. Fish., Hokkaido Univ.*, **13**: 123-141.
- Yoshioka, H. (1963) On the effects of environmental factors upon the reproduction of fishes. 2. Effects of short and long day-length on *Oryzias latipes* during spawning season. *Bull. Fac. Fish., Hokkaido Univ.*, **14**: 137-151.
- Sawara, Y. and Egami, N. (1977) Note on the differences in the response of the gonad to the photoperiod among populations of *Oryzias latipes* collected in different localities. *Annot. Zool. Japan*, **50**: 147-150.

Immunoreactive FMRFamide in the Nervous System of the Earthworm, *Eisenia foetida*

KEN FUJII, NAOSHI OHTA, TETSUO SASAKI, YOSHIYUKI SEKIZAWA

CHIFUMI YAMADA and HIDESHI KOBAYASHI

*Zenyaku Kogyo Co., Ltd., Research Laboratory,
Nerima-ku, Tokyo 178, Japan*

ABSTRACT—A number of large and small cells immunoreactive to FMRFamide (Phe-Met-Arg-Phe-NH₂) antiserum were found in the cerebral, subesophageal and segmental ganglia, and in the ganglia of the pharyngeal plexus of the earthworm, *Eisenia foetida*. The cerebral ganglion sends the immunoreactive fibers to the subesophageal ganglion through the pharyngeal connectives. The subesophageal ganglion projects the fibers to the segmental ganglia. From the cerebral and subesophageal ganglia, the nerve bundles containing immunoreactive nerve fibers proceed anteriorly towards the prostomium and the ventral region of the anterior segments, respectively. From the ganglia in the pharyngeal plexus, the immunoreactive fibers proceed towards the pharynx. From each segmental ganglion, three immunoreactive segmental nerve trunks emerge bilaterally and extend to the body wall. Then they run dorsally between the circular and longitudinal muscle layers of the body wall. Immunoreactive fibers were observed between the circular muscle layer and the epithelial cell layer of the skin. Furthermore, immunoreactive fibers were observed between the epithelial cell layer and the circular muscle layer of the alimentary canal. Immunoreactive products are occasionally present in contact with the blood vessels in the cerebral and subesophageal ganglia. FMRFamide seems to act both as a neurotransmitter or neuromodulator and as a neurohormone in the earthworm.

INTRODUCTION

Since Scharrer [1] first described neurosecretory cells in the central nervous system of the earthworm, many investigators have studied neurosecretion in the earthworm by cytological and physiological techniques. It has been suggested that some types of neurosecretory cell in the cerebral ganglion are involved in the growth and regeneration of nervous centers, in the reproduction of the earthworm [2], and in the regulation of the osmotic properties of the coelomic fluid in the earthworm [3, 4]. Biochemically, the occurrence of serotonin, dopamine, noradrenaline and octopamine has been established in the earthworm's central nervous system [5-8]. However, recent investigations in the earthworm have tended to concentrate on the search for biologically active peptides in the nervous system by predominantly

immunocytochemical techniques, which were developed primarily for vertebrate peptide hormones. For example, the following peptides have been found immunohistochemically in the earthworm's nervous system: pancreatic polypeptide (PP) and vasoactive intestinal peptide (VIP) [9], α -endorphin [10], β -endorphin [11], adrenocorticotrophic hormone (ACTH) [12], substance P (SP) [12, 13], Leu-enkephalin [13, 14], Met-enkephalin, human growth-hormone-releasing factor (h-GHRF), dynorphin [13], gastrin/cholecystokinin (CCK) [13-15], corticotropin-releasing factor (CRF) [13, 16], vasopressin (AVP) and oxytocin (OXT) [17]. Thus, the nervous system of the earthworm contains many biological active peptides previously identified in vertebrates.

FMRFamide (Phe-Met-Arg-Phe-NH₂) and its related peptides, which were first described in the clam *Macrocallista nimbosa* by Price and Greenberg [18, 19], have been detected chemically [20] and immunohistochemically not only in the molluscan nervous system [21-25], but also in the

nervous system of other species of invertebrates and vertebrates [25–27]. Thus, FMRFamide and its related peptides are widely distributed in invertebrates and vertebrates, but these compounds have not yet been examined in the earthworm.

This report describes the existence and distribution of FMRFamide-like immunoreactivity in the nervous system of the earthworm, *Eisenia foetida*.

MATERIALS AND METHODS

Adult earthworms, *Eisenia foetida*, were collected on the laboratory campus in May. The animals were cut into 4 or 5 pieces and fixed in Bouin's solution without acetic acid for 2–3 hr at room temperature. After fixation, the pieces were dehydrated through an ethanol series, cleared in

xylene, and embedded in paraffin. Serial frontal, sagittal and horizontal sections were cut at 6 μm thickness. Deparaffinized sections were immunostained by the peroxidase-antiperoxidase (PAP) method of Sternberger *et al.* [28]. To block the endogenous peroxidase activity, hydrated sections were soaked in 3% H_2O_2 in distilled water for 15 min and rinsed for 15 min in 0.01 M phosphate-buffered saline (PBS; pH 7.2). They were preincubated in 1% normal goat serum (Polysciences Inc., Warrington, Pennsylvania) in PBS for 30 min to remove background staining. The sections were then incubated with FMRFamide antiserum (1:4000; Immuno Nuclear Corp., Stillwater, Minnesota) overnight at 4°C. Subsequently, the sections were washed in PBS for 15 min and incubated with goat anti-rabbit IgG (1:200; Polysci-

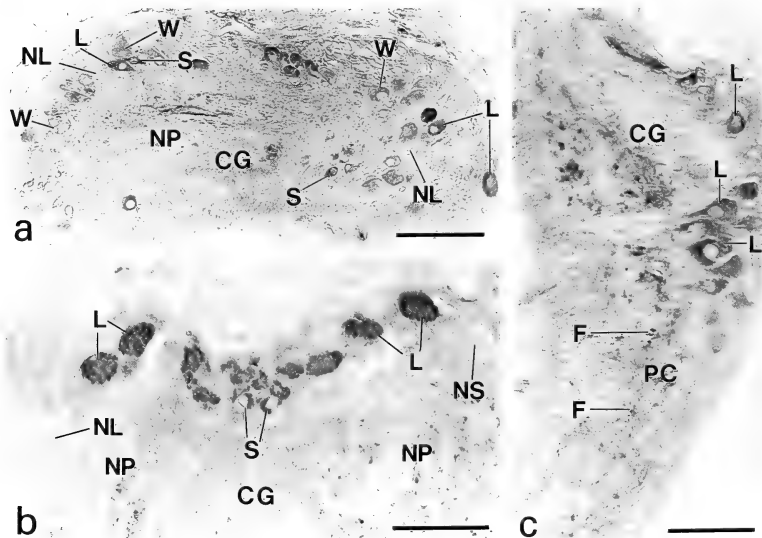


FIG. 1. a. Cross section of the earthworm, *Eisenia foetida*, through the dorso-posterior portion of the cerebral ganglion (CG), showing FMRFamide-like immunoreactive cells. b. Cross section through the anterior dorso-medial region of CG, showing a group of small cells (S) with FMRFamide-like immunoreactivity. A few large cells (L) are present on the both sides of the group. c. Cross section showing large cells (L) with FMRFamide-like immunoreactivity in the region of the CG, from which the pharyngeal connective (PC) emerges. F: immunoreactive fiber bundle, NL: non-immunoreactive cells, NP: neuropile, W: weakly immunoreactive cells. Scale: a: 100 μm , b: 50 μm , c: 50 μm .

ences Inc.) for 60 min. After the sections were washed in PBS for 15 min, they were incubated in PAP complex (1:100; Dako Corp., Copenhagen) for 30 min. Each incubation was performed in a moist chamber at room temperature. For the peroxidase reaction, slides were immersed in 0.02% 3, 3'-diaminobenzidine tetrahydrochloride (DAB; Wako Pure Chemicals, Osaka) in 0.05 M Tris-HCl buffer (pH 7.6) containing 0.005% H_2O_2 , for about 1-3 min, and then slides were washed in PBS and distilled water for 5 min each. The sections were dehydrated through an ethanol series, cleared in xylens, and mounted.

The specificity of the immunoreaction was checked for the various sections of the cerebral and subesophageal ganglia, the epidermal layer of

the skin and the alimentary canal, by the preabsorption test using the antiserum incubated for 24 hr with synthetic FMRFamide ($5 \mu\text{g/ml}$; Peptide Institute, Osaka, Japan).

RESULTS

The sections treated with FMRFamide antiserum preabsorbed with the antigen (FMRFamide) did not show any evidence of immunoreactivity in any tissues examined.

Cerebral ganglion

In the dorso-posterior portion of the cerebral ganglion, many large cells (approximately $20 \mu\text{m}$ in diameter) and small cells (approximately $10 \mu\text{m}$ in

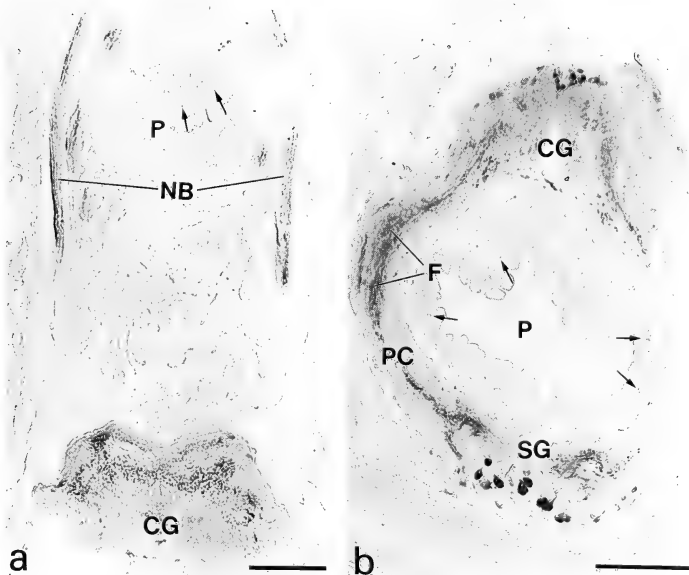


FIG. 2. a. Horizontal section showing FMRFamide-like immunoreactive nerve bundles (NB) proceeding anteriorly from the cerebral ganglion (CG) to the prostomium. b. Cross section showing the FMRFamide-like immunoreactive fibers (F) in the pharyngeal connective (PC). Arrows show immunoreactive products between the epithelial and circular muscle layers of the pharynx (P). SG: subesophageal ganglion. Scale, a: $150 \mu\text{m}$, b: $200 \mu\text{m}$.

diameter) immunoreacted strongly or weakly to FMRFamide antiserum (Fig. 1a). These cells were located predominantly near the surface of the cerebral ganglion. Among these immunoreactive cells, non-immunoreactive large and small cells of similar sizes were always present (Fig. 1a, b). Between the immunoreactive cells and the surface of the cerebral ganglion, many small non-immunoreactive cells (approximately $10\ \mu\text{m}$ in diameter) were present. Few immunoreactive large cells were also found in the anterior region, but none in the ventral region of the cerebral ganglion. In the dorso-anterior region, a few small immunoreactive cells (approximately $10\ \mu\text{m}$ in diameter) were gathered in a group in the median portion (Fig. 1b) and a few large immunoreactive cells (approximately $15\ \mu\text{m}$ in diameter) were distributed near both sides of the group (Fig. 1b). In addition, several large immunoreactive cells were

found bilaterally in the regions where the pharyngeal connectives emerged (Fig. 1c).

The nerve fibers of these immunoreactive cells proceeded first to the neuropile which was located in the middle portion of the cerebral ganglion (Fig. 1a). Two immunoreactive nerve bundles proceeded anteriorly from the ventral side of the cerebral ganglion to the prostomium (Fig. 2a). Other fibers proceeded to the subesophageal ganglion along the pharyngeal connectives (Figs. 1c, 2b). Immunoreactive products were occasionally present in contact with the blood vessels in the

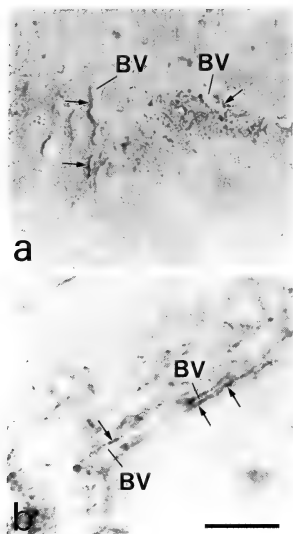


FIG. 3. a. Cross section of the cerebral ganglion. b. Cross section of the subesophageal ganglion. Arrows show FMRFamide-like immunoreactive products in close contact with blood vessels (BV). Scale, $50\ \mu\text{m}$.

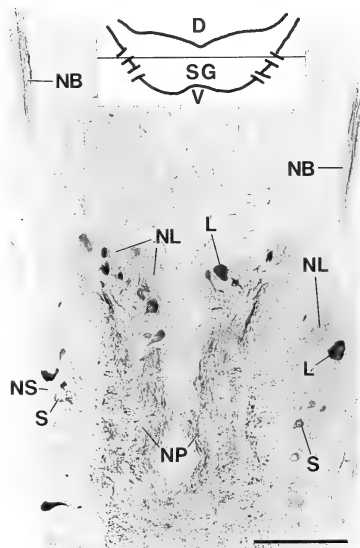


FIG. 4. Horizontal section of the subesophageal ganglion (SG) at the level shown in the inset. Immunoreactive and non-immunoreactive large and small cells are found. D: dorsal, L: immunoreactive large cells, NB: two nerve bundles containing immunoreactive nerve fibers which proceed towards the anterior segments. Two other bundles emerging from each side of the posterior region of SG are not shown in this figure. NL: non-immunoreactive large cells, NP: neuropile, NS: non-immunoreactive small cells, S: immunoreactive small cells, V: ventral. Scale, $100\ \mu\text{m}$.

neuropile of the cerebral ganglion (Fig. 3a).

Subesophageal ganglion

Many large nerve cells (approximately 15 μm in diameter) and small cells (approximately 10 μm in diameter) and their fibers in the subesophageal ganglion immunoreacted with FMRFamide antiserum (Figs. 2b, 4). The processes of the immunoreactive cells entered the neuropile in the middle portion of the ganglion and then proceeded posteriorly to join the ventral nerve cord (Fig. 4). Non-immunoreactive cells were also found in the ganglion (Fig. 4). From both sides of the anterior and posterior regions of the subesophageal ganglion, two thick immunoreactive nerve bundles emerged, respectively, and proceeded anteriorly towards the ventral region of the anterior segments (Fig. 4). Immunoreactive products were often present in close contact with blood vessels (Fig. 3b).

Pharyngeal plexus

FMRFamide-like immunoreactive cells (approximately 10 μm in diameter) were present in the ganglia of the pharyngeal plexus (Fig. 5a). Nerve tracts connecting these ganglia with the pharyngeal connectives were observed. The tracts contained

many immunoreactive fibers (Fig. 5b). Furthermore, it was observed that immunoreactive fibers proceeded anteriorly or posteriorly from the ganglia towards the pharynx (Fig. 5b).

Segmental ganglion and skin

FMRFamide-like immunoreactivity was observed in many large and small cells located bilaterally and ventrally in the ganglion of each segment. Figures 6a and 6b show the cross and horizontal sections, respectively, of the anterior sixth segment. From these cells, strong immunoreactive fibers proceeded to the neuropiles located on both sides of the central portion of the ventral nerve cord (Fig. 6a). Figure 7 shows the horizontal section cut through the neuropile shown in Figure 6a. The immunoreactive cells were observed in the peripheral region and two wide longitudinal immunoreactive nerve tracts were observed (Fig. 7). However, many non-immunoreactive cells were also found in the segmental ganglia (Fig. 7). The immunoreactive cell numbers in the segmental ganglia of the posterior region of the body were smaller than those in the anterior and the middle regions.

From each segmental ganglion, three nerve tracts containing immunoreactive fibers emerged

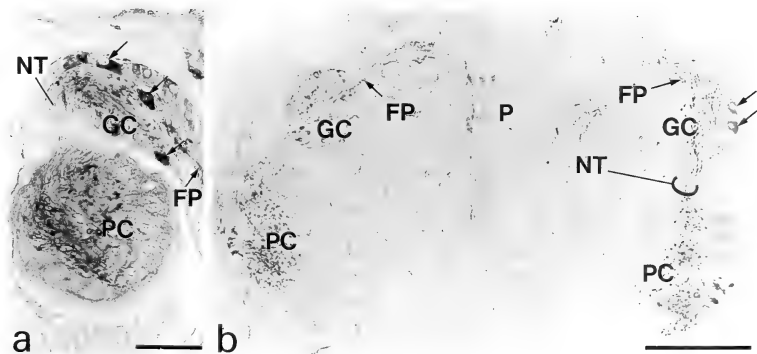


Fig. 5. Horizontal section of the pharyngeal plexus. a. Immunoreactive cells (arrows) in a ganglion (GC) of the pharyngeal plexus. b. Section showing the topographic relations between GC, pharyngeal connective (PC) and pharynx (P). Arrows show immunoreactive cells. FP, immunoreactive fiber bundles proceeding to the pharynx. NT: nerve tract containing immunoreactive fibers between GC and PC. Scale, a: 50 μm , b: 100 μm .

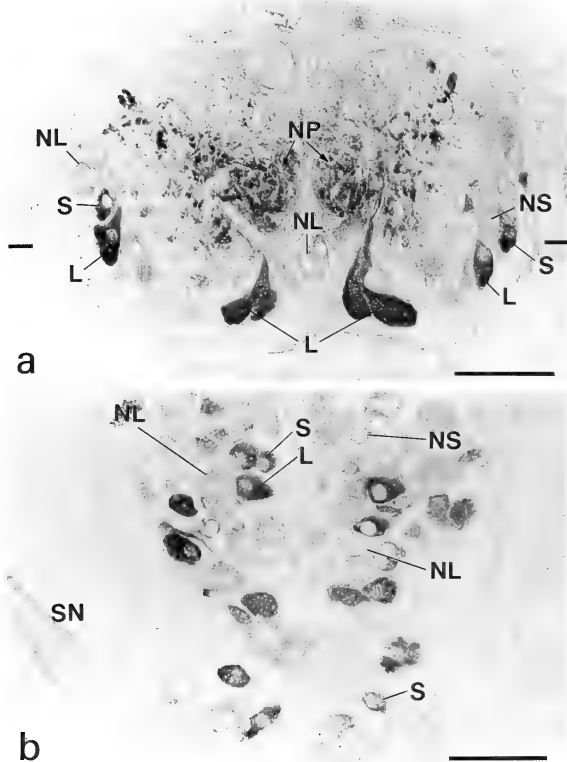


FIG. 6. a. Cross section of the 6th segment. b. Horizontal section of the ganglion of the 6th segment. The level at which the horizontal section was made is shown by bars at the margins of (a). L: immunoreactive large cells, NL: non-immunoreactive large cells, NP: neuropile, NS: non-immunoreactive small cells, S: immunoreactive small cells, SN: segmental nerve. Scale, 50 μ m.

bilaterally and extended as far as the body wall (Fig. 8a). Thus, three immunoreactive fiber tracts were clearly seen between the circular and longitudinal muscle layers of the body wall (Fig. 8b). The immunoreactive fibers in these tracts seem to branch off after they reach the body wall. Thus, there were many immunoreactive deposits indicat-

ing the immunoreactive fibers, between the circular muscle layer and the epidermal cell layer of the skin (Fig. 8b). The immunoreactive fibers were also found in the circular and longitudinal muscle layers (Fig. 8b). FMRamide-like immunoreactive cells were occasionally found between the epidermal cells of the skin (Fig. 8c).

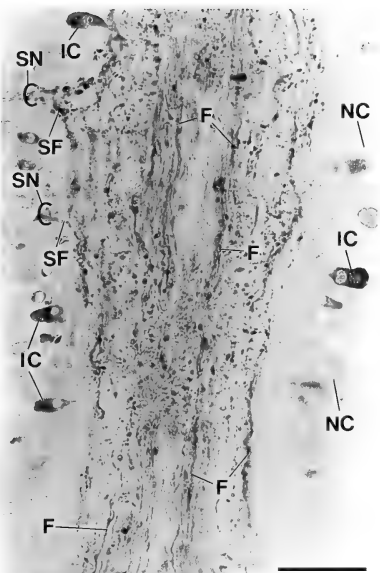


FIG. 7. Horizontal section of the ventral nerve cord of the segment in the latter half of the body, showing immunoreactive cells (IC) and two wide nerve tracts containing FMRFamide-like immunoreactive fibers (F). The section was made at the level of the neuropile shown in Fig. 6a. NC: non-immunoreactive cells, SF: immunoreactive fibers proceeding along segmental nerve (SN). Scale, 50 μ m.

DISCUSSION

The existence of immunoreactive FMRFamide-like peptides in the central nervous system has been studied phylogenetically in many animal species (see Introduction for references). In the case of annelids, however, there is only one relevant report and it describes the presence of FMRFamide-like immunoreactive cells in the brain and segmental ganglia of the medicinal leech [29]. The present study has revealed the dense distribution of FMRFamide-like immunoreactive nerve cells and fibers in the cerebral, subesophageal and segmental ganglia, and in the ganglia of the pharyngeal plexus in *Eisenia foetida*. These findings indicate that the earthworm possesses immunoreactive FMRFamide-nervous system, which is similar to the immunoreactive serotonin-nervous system [7, 8]. In addition, the presence of immunoreactive FMRFamide in the earthworm is considered to afford further evidence that FMRFamide-related peptides have had a long evolutionary history, since they are found in vertebrate nervous system [25].

In *E. foetida*, the immunoreactive nerve bundles proceeding from the cerebral ganglion towards the prostomium probably innervate peripheral organs of the anterior part of the body and release FMRFamide or related peptides as neurotransmitters or neuromodulators. The immunoreactive fibers proceeding ventro-posteriorly from the cerebral ganglion along the pharyngeal connectives may transfer information to the subesophageal ganglion, and further to the segmental ganglia directly or through the subesophageal ganglion. In the cerebral ganglion, there were cell groups consisting of small or large immunoreactive cells and they were located in different regions. At the present time, it is not known which cell types and groups extend their nerve fibers to the prostomium or the subesophageal ganglion.

The subesophageal ganglionic cells extend immunoreactive fibers towards the ventral region of the anterior segments. Further, the subesophageal ganglion projects immunoreactive fibers posteriorly towards the segmental ganglia. Thus, the immunoreactive fibers connect the subesophageal ganglion with the cerebral and segmental ganglia.

Alimentary canal

Immunoreactive nerve fibers were observed between the epithelial cell layer and the muscle layer of the pharynx (Fig. 9a), esophagus (Fig. 9b) and intestine (Fig. 9c). However, the numbers of immunoreactive deposits, which indicate the presence of immunoreactive fibers, were smaller in the anterior portion than the posterior portion of the pharynx (cf. Fig. 2a, b). Immunoreactive cells were occasionally found between the epithelial cells of the alimentary canal (Fig. 9b).

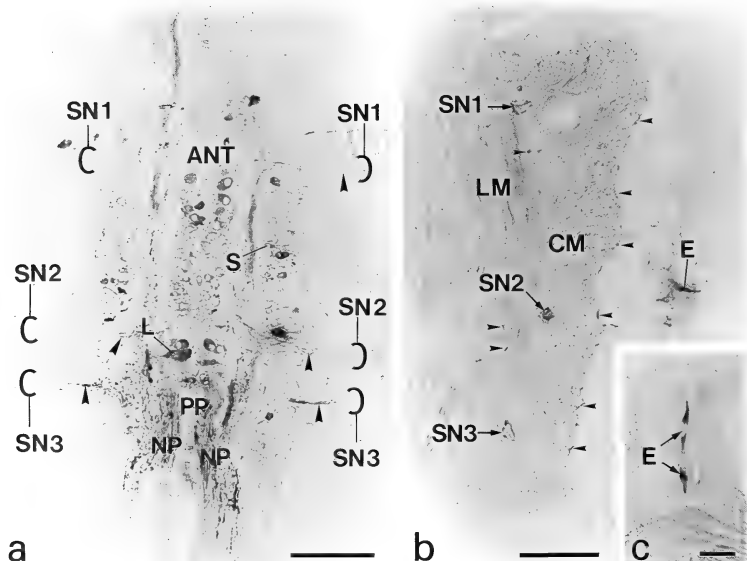


FIG. 8. a. Horizontal section of the segment in the latter half of the body. Three segmental nerve trunks (SN1, SN2, SN3) including immunoreactive fibers (arrow heads) extend to the body wall on both sides. The anterior part (ANT) is a cut at the same level as in Fig. 6b and the posterior part (PP) is a cut at the same level as in Fig. 7. b. Horizontal section of the skin of the anterior 8th segment, showing three segmental nerve tracts (SN1, SN2, SN3) including immunoreactive fibers. They were located between the circular (CM) and longitudinal (LM) muscle layers of the skin. c. Immunoreactive cells (E) between the epidermal cells of the skin near the rostral end of the body. L: immunoreactive large cells, NP: neuropile, S: immunoreactive small cells. Arrow heads: immunoreactive deposits. Scale: a: 100 μ m, b: 100 μ m, c: 20 μ m.

It is possible that information transfer may take place from the segmental ganglia to the sub-esophageal and cerebral ganglia through the immunoreactive FMRFamide fibers.

The immunoreactive fibers in the segmental nerve trunks proceeding to the body wall seem to innervate the epidermal cells and the circular and longitudinal muscles, as suggested earlier by electrophysiological studies [30]. It seems that immunoreactive FMRFamide fibers may be involved in the regulation of activities of the epidermal cells and the integumental muscles. Further, the immunoreactive cells found between the epidermal cells of the skin are most probably sensory cells.

The fibers immunoreactive to FMRFamide anti-serum in the pharynx must be derived from the ganglia of the pharyngeal plexus, since it has already been shown by anatomical and histological techniques that the pharynx is innervated by neurons in the ganglia of the pharyngeal plexus [30, 31].

The immunoreactive fiber connection between the ganglia of the pharyngeal plexus and the pharyngeal connectives may contribute to information exchange between them. Nervous connections between them have already been demonstrated by a silver nitrate impregnation technique [31]. The esophagus and the intestine seem to be

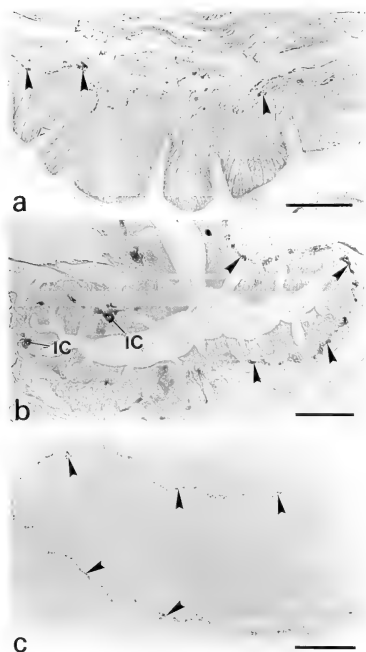


FIG. 9. Horizontal sections of the pharynx (a), esophagus (b) and intestine (c) showing FMRFamide-like immunoreactive nerve fibers (arrow heads) between the epithelial layer and the circular muscle layer. IC: immunoreactive cells. Scale: a: 50 μ m, b: 100 μ m, c: 100 μ m.

innervated by the immunoreactive fibers that originate in the subesophageal ganglion and the segmental ganglia, respectively. It has been shown electrophysiologically that nerve fibers proceed to those organs via the body wall and the septa [30].

Considering all the findings mentioned above, it is clear that immunoreactive FMRFamide-like peptides function as neurotransmitters or neuromodulators. However, they may also have neurohormonal functions, since we found immunoreactive products in close contact with the blood ves-

sels in the cerebral and subesophageal ganglia of *E. foetida*. Thus, our findings suggest that they can serve as neurotransmitters or neuromodulators in some cases and neurohormones in other cases, as discussed by other investigators [18, 21–27, 32–38].

In the present study, the immunoreactive nerve fibers originating from the segmental nerve trunks were found between the epithelial cell layer and the circular muscle layer of the alimentary canal. These findings suggest that immunoreactive FMRFamide is involved in the regulation of the activity of the epithelial cells of the alimentary canal.

It has been demonstrated that FMRFamide-like peptides are involved in cardiovascular control in molluscs [18, 38]. In the annelids, Kuhlman *et al.* [35] suggested that FMRFamide-like substances function in chemical transmission within the heart-beat system of the leech. Although we could not detect FMRFamide-like immunoreactive fibers in the heart of the earthworm, immunoreactive FMRFamide may affect the heart as a neurohormone after it has been released into the blood vessels.

As mentioned in the introduction, many neuropeptides, such as PP, VIP, α -endorphin, β -endorphin, ACTH, SP, Leu-enkephalin, Met-enkephalin, gastrin/CCK, CRF, h-GHRF, dynorphin, OXT and AVP, have been demonstrated immunohistochemically in the nervous system of the earthworm. We have added one more neuropeptide, FMRFamide-like substance, to those peptides found in the earthworm's nervous system. In the present study, we found many neurons non-immunoreactive to FMRFamide antiserum in all the ganglia. These neurons may contain serotonin, catecholamines or other peptides than immunoreactive FMRFamide. Physiological functions of these peptides are not clear at the present time.

REFERENCES

- 1 Scharrer, B. (1937) Über sekretorisch tätige Nervenzellen bei Wirbellosen Tieren. *Naturwissenschaften*, **25**: 131–138.
- 2 Herlant-Meeuwis, H. (1962) Neurosecretory phenomena during regeneration of nervous centres in

- Eisenia foetida*. In "Neurosecretion". Ed. by H. Heller and R. B. Clark, Academic Press, New York, pp. 267-274.
- 3 Takeuchi, N. (1980) Neuroendocrine control of hydration in megascolecid earthworms. *Comp. Biochem. Physiol.*, **67A**: 341-345.
 - 4 Takeuchi, N. (1980) Effects of brain removal on the osmotic and ionic concentrations of the coelomic fluid of earthworms placed in soil and salt solutions. *Comp. Biochem. Physiol.*, **67A**: 347-352.
 - 5 Welsh, J. H. (1970) Phylogenetic aspects of the distribution of biogenic amines. In "Biogenic Amines as Physiological Regulators". Ed. by J. J. Blum, Prentice-Hall, Englewood Cliffs, pp. 75-94.
 - 6 Parent, A. (1981) The anatomy of serotonin-containing neurons across phylogeny. In "Serotonin Neurotransmission and Behavior". Ed. by L. B. Jacobs and A. Gelperin, The MIT Press, Cambridge/London, pp. 3-34.
 - 7 Spörhase-Eichmann, U., Gras, H. and Schürmann, F. W. (1987) Patterns of serotonin-immunoreactive neurons in the central nervous system of the earthworm *Lumbricus terrestris* L. I. Ganglia of the ventral nerve cord. *Cell Tissue Res.*, **249**: 601-614.
 - 8 Spörhase-Eichmann, U., Gras, H. and Schürmann, F. W. (1987) Patterns of serotonin-immunoreactive neurons in the central nervous system of the earthworm *Lumbricus terrestris* L. II. Rostral and caudal ganglia. *Cell Tissue Res.*, **249**: 625-632.
 - 9 Sundler, F., Håkanson, R., Alumets, J. and Walles, B. (1977) Neuronal localization of pancreatic polypeptide (PP) and vasoactive intestinal peptide (VIP) immunoreactivity in the earthworm (*Lumbricus terrestris*). *Brain Res. Bulletin*, **2**: 61-65.
 - 10 Rémy, C. and Dubois, M. P. (1979) Localisation par immunofluorescence de peptides analogues à l' α -endorphine dans les ganglions infra-oesophagiens du lombricide *Dendrobaena subrubicunda* Eisen. *Experientia*, **35**: 137-138.
 - 11 Alumets, J., Håkanson, R., Sundler, F. and Thorell, J. (1979) Neuronal localization of immunoreactive enkephalin and β -endorphin in the earthworm. *Nature*, **279**: 805-806.
 - 12 Aros, B., Wenger, T., Vigh, B. and Vigh-Teichmann, I. (1980) Immunohistochemical localization of substance P and ACTH-like activity in the central nervous system of the earthworm *Lumbricus terrestris* L. *Acta Histochem.*, **66**: 262-268.
 - 13 Lkhider, M., Marcel, R. and Tramu, G. (1987) Etablissement d'une carte des neurones du cerveau d'*Eisenia foetida* (Annelide, Oligochète) contenant des substances immunologiquement apparentées à des peptides de vertébrés. *Gen. Comp. Endocrinol.*, **65**: 457-468.
 - 14 Takeuchi, N. (1987) Immunohistochemical localization of leu-enkephalin-like and gastrin/CCK-like peptides in the brain of earthworms. *Proc. 1st Congr., Asia and Oceania Soc. Comp. Endocrinol.* p. 131-132.
 - 15 Dhainaut-Courtois, N., Tramu, G., Marcel, R., Malecha, J., Verger-Bocquet, M., Andries, J. C., Masson, M., Selloum, L., Belemtougri, G. and Beauvillain, J. C. (1985) Cholecystokinin in the nervous systems of invertebrates and protochordates. *Ann. N. Y. Acad. Sci.*, **448**: 167-187.
 - 16 Rémy, C., Tramu, G. and Dubois, M. P. (1982) Immunohistological demonstration of a CRF-like material in the central nervous system of the annelid *Dendrobaena*. *Cell Tissue Res.*, **227**: 569-575.
 - 17 Kinoshita, K. and Kawashima, S. (1986) Differential localization of vasopressin- and oxytocin-immunoreactive cells and conventional neurosecretory cells in the ganglia of the earthworm *Pheretima hilgendorfi*. *J. Morphology*, **187**: 343-351.
 - 18 Price, D. A. and Greenberg, M. J. (1977a) Structure of a molluscan cardioexcitatory neuropeptide. *Science*, **197**: 670-671.
 - 19 Price, D. A. and Greenberg, M. J. (1977b) Purification and characterization of a cardioexcitatory neuropeptide from the central ganglia of a bivalve mollusc. *Prep. Biochem.*, **7**: 261-281.
 - 20 Price, D. A., Davies, N. W., Doble, K. E. and Greenberg, M. J. (1987) The variety and distribution of the FMRFamide-related peptides in molluscs. *Zool. Sci.*, **4**: 359-410.
 - 21 Schot, L. P. C. and Boer, H. H. (1982) Immunocytochemical demonstration of peptidergic cells in the pond snail *Lymnaea stagnalis* with an antiserum to the molluscan cardioactive tetrapeptide FMRFamide. *Cell Tissue Res.*, **225**: 347-354.
 - 22 Marchand, C. R., Wijdenes, J. and Schot, L. P. C. (1982) Localisation par la technique cyto-immuno-inzymologique d'un neuropeptide cardio-excitateur (le FMRF-amide) dans le collier nerveux péri-oesophagien d'*Helix aspersa* Müller (Gastéropode, pulmoné, stylomatophore). *C. R. Acad. Sc., Paris*, **294**: 39-44.
 - 23 Cardot, J. and Fellman, D. (1983) Immunofluorescent evidence of phenylalanyl methionyl arginyl phenylalanine amide-like peptide in the peripheral nervous system of the gastropod *Helix aspersa*. *Neurosci. Lett.*, **43**: 167-172.
 - 24 Takayanagi, H. and Takeda, N. (1987) FMRFamide immunoreactive neurons in the central nervous system of the snail, *Achatina fulica*. *Comp. Biochem. Physiol.*, **88A**: 263-268.
 - 25 Boer, H. H., Schot, L. P. C., Veenstra, J. A. and Reichelt, D. (1980) Immunocytochemical identification of neural elements in the central nervous systems of a snail, some insects, a fish, and a mammal with an antiserum to the molluscan cardio-excitatory tetrapeptide FMRFamide. *Cell Tissue Res.*, **213**:

- 21-27.
- 26 Jennings, J. B., Davenport, T. R. B. and Varndell, I. M. (1987) FMRFamide-like immunoreactivity and arylamidase activity in turbellarians and nemerteans - evidence for a novel neurovascular coordinating system in nemerteans. *Comp. Biochem. Physiol.*, **86C**: 425-430.
- 27 Greenberg, M. J., Price, D. A. and Lehman, H. K. (1985) FMRFamide-like peptides of molluscs and vertebrates: distribution and evidence of function. In "Neurosecretion and the Biology of Neuropeptides". Ed. by H. Kobayashi, H. A. Bern and A. Urano, Japan Sci. Soc. Press, Tokyo/Springer-Verlag, Berlin, pp. 370-376.
- 28 Sternberger, L. A., Hardy, P. H., Jr. Cuculis, J. J. and Meyer, H. G. (1970) The unlabeled antibody enzyme method of immunohistochemistry: preparation and properties of soluble antigen-antibody complex (horseradish peroxidase-anti-horseradish peroxidase) and its use in identification of spirochetes. *J. Histochem. Cytochem.*, **18**: 315-333.
- 29 Kuhlman, J. R., Li, C. and Calabrese, R. L. (1985a) FMRFamide-like substances in the leech. I. Immunocytochemical localization. *J. Neurosci.*, **5**: 2301-2309.
- 30 Millott, F. L. N. (1943) The visceral nervous system of the earthworm: I. Nerves controlling the tone of the alimentary canal. *Proc. Roy. Soc. London, Ser. B*, **131**: 271-295.
- 31 Chen, T. T. (1944) The morphology of the anterior autonomic nervous system of the earthworm, *Lumbricus terrestris* L. *J. Comp. Neurol.*, **80**: 191-209.
- 32 Veenstra, J. A. and Schooneveld, H. (1984) Immunocytochemical localization of neurons in the nervous system of the Colorado potato beetle with antisera against FMRFamide and bovine pancreatic polypeptide. *Cell Tissue Res.*, **235**: 303-308.
- 33 Weiss, S., Goldberg, J. I., Chohan, K. S., Stell, W. K., Drummond, G. I. and Lukowiak, K. (1984) Evidence for FMRF-amide as a neurotransmitter in the gill of *Aplysia californica*. *J. Neurosci.*, **4**: 1994-2000.
- 34 Watson, W. H., Groome, J. R., Chronwall, B. M., Bishop, J. and O'donohue, T. L. (1984) Presence and distribution of immunoreactive and bioactive FMRFamide-like peptides in the nervous system of the horseshoe crab, *Limulus polyphemus*. *Peptides*, **5**: 585-592.
- 35 Kuhlman, J. R., Li, C. and Calabrese, R. L. (1985b) FMRFamide-like substances in the leech. II. Bioactivity on the heartbeat system. *J. Neurosci.*, **5**: 2310-2317.
- 36 Carroll, L. S., Carrow, G. M. and Calabrese, R. L. (1986) Localization and release of FMRFamide-like immunoreactivity in the cerebral neuroendocrine system of *Manduca sexta*. *J. Exp. Biol.*, **126**: 1-14.
- 37 Brown, M. R. and Lea, A. O. (1988) FMRFamide- and adipokinetic hormone-like immunoreactivity in the nervous system of the mosquito, *Aedes aegypti*. *J. Comp. Neurol.*, **270**: 606-614.
- 38 Kobayashi, M. (1987) Innervation and control of the heart of a gastropod, *Rapana*. *Experientia*, **43**: 981-986.



Purification of Toad (*Bufo japonicus*) Gonadotropins and Development of Their Homologous Radioimmunoassays

KOJI TAKADA¹, MASANORI ITOH, HIROSHI NISHIO
and SUSUMU ISHII

Department of Biology, School of Education,
Waseda University, Tokyo 169, Japan

ABSTRACT—We obtained three gonadotropin fractions with different electrophoretic mobilities named B1D, B3D and B5D from a glycoprotein fraction of toad (*Bufo japonicus*) pituitaries by cation exchange chromatography using the fast protein liquid chromatography (FPLC) system, chromatofocusing and gel filtration using the FPLC system. Gonadotropin activity was monitored by two radioreceptor assay (RRA) systems, one using bullfrog testis and bullfrog LH as the source of receptor and radioligand respectively, and the other using toad testis and bullfrog FSH respectively. Although, LH/FSH specificity was not complete in these RRAs, the fraction B1D showed a higher potency in LH-RRA than in FSH-RRA, while B3D and B5D showed lower potencies in LH-RRA activity than in FSH-RRA. Furthermore, B1D had an activity to release androgen from the toad testis, while B3D and B5D had slight activities. All these fractions stimulated accumulation of cAMP in testis slices of the toad *in vitro*. These results suggest that B1D contains LH, and B3D and B5D contain FSH-like gonadotropin. SDS PAGE analysis in combination with immunoblot revealed that B1D was almost pure LH, but B3D seemed to be not homogeneous. Anti-B1D-serum and anti-B3D-serum were raised in rabbits, and radioimmunoassays (RIAs) for B1D and B3D were established. The cross reactivity of B3D and B5D in B1D-RIA was about 30% of B1D, while that of B1D in B3D-RIA was only 3% of B3D and B5D. These RIAs were sensitive enough to measure gonadotropins in plasma samples of *Bufo japonicus*.

INTRODUCTION

Purification of amphibian gonadotropins has been attempted in three species, *Rana catesbeiana*, [1-4], *Rana pipiens*, [5], *Ambystoma tigrinum*, [6]. However, precise chemical and biological properties have been studied only in the bullfrog, *Rana catesbeiana* [1-4, 7]. These investigators unanimously found two types of gonadotropins, acidic gonadotropin and basic gonadotropin. They identified the basic one as LH by its action in stimulating androgen release from the testis. Acidic gonadotropin was identified as FSH or FSH-like gonadotropin from its biological action [8] and receptor

binding properties [9]. Radioimmunoassays (RIAs) which are specific to each of these gonadotropins were established by Daniels *et al.* [10], Tanaka *et al.* [11] and Yoneyama and Ishii [12], and are being used for studies on the reproduction of the bullfrog.

Although toads of Bufonidae are as common as frogs of Ranidae, and widely used in studies of various fields of biology, we are completely ignorant about properties of toad gonadotropin. All of gonadotropin radioimmunoassay systems that we tested, including the bullfrog gonadotropin RIAs can not quantify toad gonadotropins with any great precision or sensitivity.

For these reasons, purification and characterization of toad (*Bufo japonicus*) gonadotropins were carried out. Furthermore, homologous RIAs for toad gonadotropins were developed.

Accepted January 4, 1989

Received December 8, 1988

¹ Present address: Department of Biochemistry, The Jikei University School of Medicine, Tokyo 105, Japan

MATERIALS AND METHODS

Purification and relative molecular mass (Mr) determination

About 8,000 acetone-dried pituitary glands of adult *Bufo japonicus* captured at the suburbs of Tokyo were used as starting material. A glycoprotein fraction was prepared from this using an ethanol precipitation method [4, 13].

The following three chromatographic steps were used for further purification: cation exchange chromatography with Mono S using the Pharmacia FPLC system, chromatofocusing, and gel filtration using the FPLC system. For the cation exchange chromatography, a Mono S HR10/10 column was equilibrated with 50 mM phosphate buffer (pH 7.4). The glycoprotein fraction was dissolved in the same buffer and divided into three aliquots. They were separately applied to the column. After washing with 40 ml of the equilibration buffer, the column was eluted with a 0 to 350 mM linear concentration gradient of NaCl. The flow rate was 4 ml/min. For chromatofocusing, PBE118 gel (Pharmacia) and 25 mM triethylamine-HCl buffer, pH 11, were used. The column (9 × 300 mm) was eluted with 45-fold diluted Pharmalyte (Pharmacia; pH range 8–10.5)-HCl buffer, pH 7.0. After the elution, the column was washed with 50 mM phosphate buffer, pH 7.0, containing 0.5 M NaCl. The flow rate was 18.4 ml/hr. The gel filtration was conducted with a Superose 12 column (HR10/30). The column was equilibrated and eluted with 50 mM phosphate buffer, pH 7.2, containing 0.15 M NaCl at a flow of 0.3 ml/min.

Mr values of native final products were estimated by comparing their elution volumes with those of standard proteins (104540 of Boehringer Mannheim) through the same Superose 12 column.

In addition to monitoring protein at 280 nm, the protein content of some fractions was determined by Folin reaction [14] using bovine serum albumin (fraction V, Wako) as the standard.

Radioreceptor assays

Two kinds of radioreceptor assay (RRA) were used for monitoring gonadotropin activity during

the course of purification and for quantifying the gonadotropins in the final products. One was frog LH-RRA (or LH-RRA) using a crude plasma membrane fraction of the bullfrog testis as the receptor and bullfrog LH (FL421B of Takada and Ishii [4]) for the radioligand. In this method, bullfrog LH is as 16 times potent as bullfrog FSH when compared at the 50% inhibition level [9]. Another method was heterologous frog FSH-RRA (or FSH-RRA) using a crude plasma membrane fraction of the testis of *Bufo japonicus* as the receptor and bullfrog FSH (FF1341B of Takada and Ishii, [4]) for the radioligand. We devised this assay method for this investigation, because it is more sensitive to toad FSH than toad LH. In this assay, bullfrog FSH is as four times potent as bullfrog LH. These assays were carried out according to Takada *et al.* [9] with the following modifications in the preparation of receptors: the testis homogenate was centrifuged at 1,000 g for 10 min at 4°C, and its supernatant was centrifuged again at 8,500 g for 10 min at 4°C; resulting pellet was resuspended at the final concentration of about 25 and 5 mg of the original tissue per 0.1 ml, in LH-RRA and FSH-RRA, respectively. A bullfrog hypophyseal glycoprotein fraction (FGS1, identical to HGP of Takada *et al.*, [9]) was used as the reference standard in both assays.

Bioassays

Minced testicular tissue of *Bufo japonicus* was incubated in modified Krebs Ringer bicarbonate with or without toad gonadotropins. The amount of 3'-5'-cyclic AMP (cAMP) accumulated in the tissue was determined by RIA as reported elsewhere [4]. Total androgen released from the tissue was determined by the RIA method for testosterone reported by Takada and Ishii [4] without separation of testosterone and 5 α -dihydrotestosterone.

Polyacrylamide gel electrophoresis

Polyacrylamide gel electrophoresis (PAGE) was performed by the method of Davis [15] on a vertical gel slab (1.0 mm thick, 85 mm horizontal and 50 mm vertical length) prepared in Tris-HCl buffer, pH 8.9, using Tris-glycine buffer, pH 8.3, in the reservoir. The concentration of the gel was

7.5%. Electrophoresis was performed first at 10 mA for 15 min and 15 mA for 34 min.

Sodium dodecyl sulphate polyacrylamide gel electrophoresis (SDS PAGE) was performed at 5 mA for 5 min and 10 mA for 120 min on a 0.2% SDS, 15% acrylamide slab gel, 1.0 mm thick, 85 mm horizontal and 70 mm vertical length. Details of the sample preparation and electrophoresis are described in Lugtenberg *et al.* [16]. SDS-7 (Sigma) was used as molecular weight markers.

Gels were stained with a silver stain kit (Kanto Chemical).

Amino acid composition

Two of the final products (B1D and B5D) were hydrolyzed in 6N HCl at 110°C for 24 hr. The hydrolysates were analyzed for amino acid composition by an automatic amino acid analyzer (Hitachi 835).

Antisera production and immunoblot

Antisera against two toad gonadotropin preparations were prepared by the method of Goudie *et al.* [17]. Briefly, B1D (0.15 mg) and B3D (0.15 mg) were used as antigens. They were emulsified with Freund's complete adjuvant. The emulsion containing 0.05 mg of hormone protein was directly injected into popliteal lymph nodes of each adult male rabbit. Two groups of three rabbits were used for immunization with B1D and B3D, respectively. After 25 days and 40 days, the same emulsion containing 0.1 mg of hormone was injected subcutaneously. A week after the last injection, the rabbits were bled. An anti-B1D-serum (L-2) and anti-B3D-serum (F-2) were selected among the sera raised and used for RIA and immunoblot, as they had the highest affinity against respective antigens. Antigenicity of purified toad gonadotropin was investigated by immunoblot [18] following SDS PAGE.

RIA protocol

Two radioimmunoassays, one for LH-like gonadotropin using ^{125}I -B1D and anti-B1D-serum (B1D-RIA), other for FSH-like gonadotropin using ^{125}I -B3D and anti-B3D-serum (B3D-RIA), were developed. Radioiodinations of gonadotropins were performed by the lactoperoxidase

method [9]. Samples were diluted to appropriate concentrations with 10 mM phosphate buffer-0.14 M NaCl, pH 7.4 (PBS) containing 0.2% Triton-X100 and 1% bovine serum albumin (RIA buffer A). The antisera were diluted with PBS containing 50 mM EDTA and 1% normal rabbit serum (RIA buffer B) to 1/10,000 for L-2 and 1/4,000 for F-2. Fifty microliters of each of the sample and anti-serum were mixed in an assay tube. Fifty microliters of the radioligand in the RIA buffer A (about 40,000 cpm) was added to the assay tube following 12 hr delay. Six hr after addition of the radioligand, 200 μl of a 1:60 dilution of goat anti-rabbit γ -globulin in the RIA buffer B containing 2% polyethylene glycol 6000 was added. The tubes were incubated for 12 hr, diluted with 500 μl of the chilled RIA buffer A, and centrifuged at 3,000 g for 45 min at 4°C. The supernatant was removed by aspiration and radioactivity in the pellet was measured. All RIA procedures except centrifugation were done at room temperature.

RIA validation

Specificity of RIAs was tested by assaying some vertebrate gonadotropin preparations. Rat LH and FSH used were rat LH-15 and rat FSH-14 from NIAMDD. Pregnant mares serum gonadotropin (PMSG, 1780 I.U./mg) and human chorionic gonadotropin (hCG, 2400 I.U./mg) were purchased from Sigma. Tuna and chicken pituitary glycoproteins (Tuna G.P. and chicken G.P.) were prepared according to Ando and Ishii [19] and Sakai and Ishii [20], respectively. Bullfrog LH and FSH were FL421B and FF1341B of Takada and Ishii [4]. *Bufo marinus* gonadotropins, putative LH (BmS4B) and FSH (BmS6B), were prepared by successive purification steps of precipitation in ethanol, an anion exchange chromatography and gel filtration from *Bufo marinus* pituitary glands (Takada and Ishii, unpubl.). The effect of plasma components other than gonadotropin on the assay result was studied by adding known amounts of gonadotropins dissolved in 0.025 ml of buffer to the same volume of a toad plasma sampled and measuring their recoveries by the RIAs. It was also studied by assaying a plasma sample from a male hypophysectomized toad collected in April.

RESULTS

Purification

Relative RRA and RIA potencies of the glycoprotein fraction (BAG11D in Table 1) were higher than those of acetone-dried powder (BA1D in Table 1), although recoveries of RRA potencies were as low as 20%. After the Mono S chromatography of BAG11D, both of LH and FSH RRA activities were detected in two closely associated protein peaks ranging between 73 and 98 ml of the elution volume (Fig. 1). Although there was a difference in the ratio of two RRA activities between the two peaks, we had to combine the peaks because of their close locations. The combined peaks were subjected to chromatofocusing. RRA activities were detected in four of resulting several protein peaks (Fig. 2). Elution volumes of the active peaks were 42 to 65 ml (Fr. 1), 66 to 90 ml (Fr. 2), 93 to 119 ml (Fr. 3) and 236 to 240 ml (Fr. 5). Levels of LH-RRA and FSH-RRA activities were similar in Frs. 1 and 2, while FSH-RRA activity exceeded LH-RRA activity clearly in Frs.

3 and 5. Frs. 1, 3 and 5 were further purified by gel filtration on Superose 12. The gel filtration of Fr. 1 yielded a single peak of both protein and RRA activities at the same location (M_r estimated to be 25,000), and hence the peak was recovered as one (B1D) of final products. Gel filtrations of Frs. 3 and 5 gave a large main protein peak (M_r being 28,000 and 20,000, respectively) and additional small ones. As RRA activities were detected only in the main peaks, the main peaks were recovered as final products (B3D for Fr. 3 and B5D for Fr. 5).

Biological potencies

The fraction B1D showed the highest LH-RRA activity which was as 3 to 4 fold potent as the fractions B3D and B5D (Table 1). In the FSH-RRA, B3D and B5D showed significantly higher activity than B1D. The activity ratio of FSH-RRA to LH-RRA was about one in B1D, while five to six in B3D and B5D.

Accumulation of cAMP in the testicular tissue of the toad *in vitro* was stimulated by all of B1D, B3D and B5D (Fig. 3). Stimulation by B1D at the dose

TABLE 1. Weight estimates of toad gonadotropins and comparison of their relative potency estimates of toad gonadotropins to bullfrog gonadotropins by radioreceptor assays and radioimmunoassays

	Yield ^c (mg)	Frog LH RRA Potency ^d (×FGS1)	Frog FSH RRA Potency (×FGS1)	FSH-RRA vs LH-RRA ratio ^e	B1D-RIA potency (×BA1D)	B3D-RIA potency (×BA1D)	B3D-RIA vs B1D-RIA ratio
BA1D ^a	(8850)	0.010	0.019	1.9	1.0	1.0	1.0
BAG11D ^b	(660)	0.023	0.057	2.5	5.96	10.2	1.72
B1D	19.7	1.0	0.94	0.94	25.8	1.59	0.062
B3D	2.40	0.30	1.6	5.3	9.56	51.9	5.43
B5D	0.26	0.23	1.5	6.5	7.57	44.5	5.88
bullfrog LH		17.2 ^f	3.5 ^g	0.20			
bullfrog FSH		1.1 ^g	14.8	13.0			

^a BA1D is an acetone-dried powder of the pituitary.

^b BAG11D is a glycoprotein preparation.

^c Dry weight only for BA1D and BAG11D. The other fraction protein contents in terms of the standard protein, bovine serum albumin.

^d Relative potency estimation in the parallel line assay was based on the method of Bliss [21]. Confidence limits were calculated but not shown.

^e Relative potency ratio of frog FSH-RRA to frog LH-RRA.

^f Data of Takada *et al.* [9].

^g Relative potency estimation was performed to compare at the 50% inhibition levels of bullfrog gonadotropins and FGS1, as their inhibition curves were not parallel.

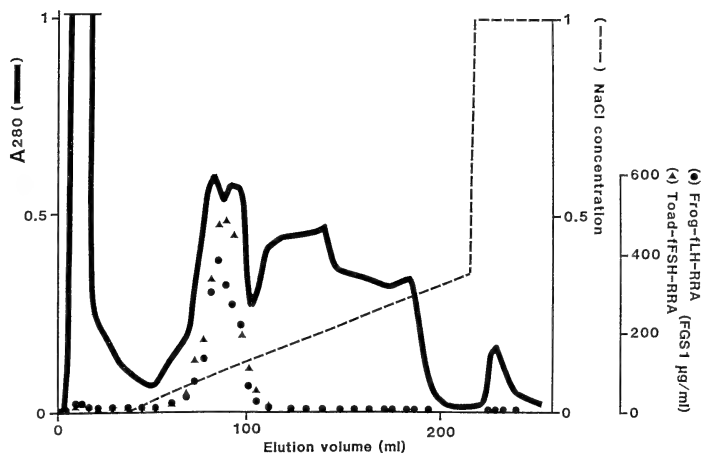


Fig. 1. Chromatography of *Bufo japonicus* adenohypophyseal glycoprotein (BAG11D) on Mono S. Optical absorbance at 280 nm is indicated by the thick line. The NaCl concentration is shown by the dotted line. Frog LH-RRA activity is depicted by circles, frog FSH-RRA activity by triangles.

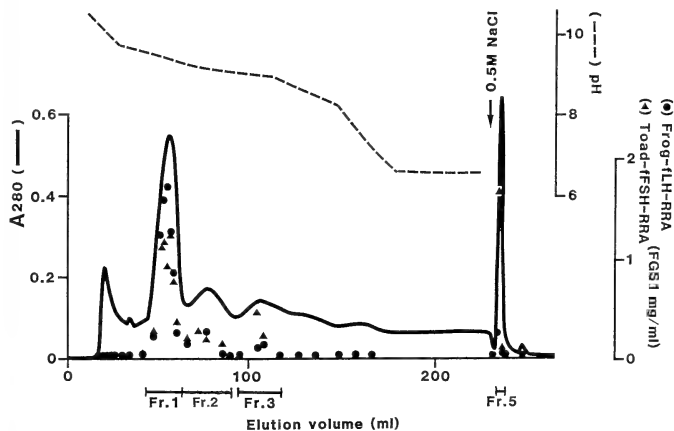


Fig. 2. Chromatofocusing of a RRA active fraction after Mono S chromatography. Optical absorbance at 280 nm is indicated by the thick line and pH by the dotted line. Frog LH-RRA activity is depicted by circles, frog FSH-RRA activity by triangles.

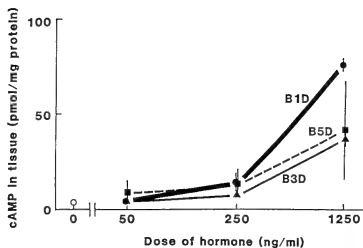


Fig. 3. Cyclic AMP accumulation in slices of *Bufo japonicus* testis treated with different doses of B1D, B3D and B5D *in vitro*. Each point indicates the mean cAMP accumulated in tissue of duplicate tubes and each vertical line represents the standard error.

of 1.25 $\mu\text{g/ml}$ was significantly higher than that by B3D at the same dose. At lower dose levels, there was no significant difference among fractions. *In vitro* androgen secretion was stimulated vigorously by B1D, but slightly by B3D and B5D at the highest dose level (Fig. 4).

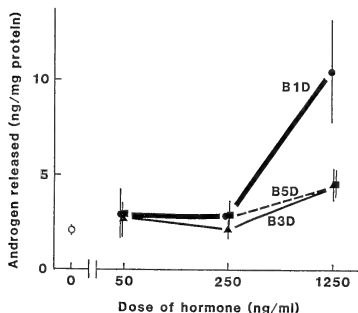


Fig. 4. *In vitro* release of androgen from *Bufo japonicus* testis treated with different doses of B1D, B3D and B5D. Each point indicates the mean androgen released from tissue of duplicate tubes and each vertical line represents the standard error.

PAGE and Immunoblot

The final products were analyzed by PAGE first without reduction. All the products consisted of

two bands or more. The stainability and mobility of the bands (a to d in Fig. 5) varied among the products.

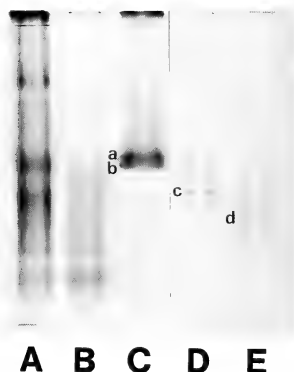


Fig. 5. PAGE of various preparations. A, BA1D (5 μg); B, BAG11D (1.2 μg); C, B1D (500 ng); D, B3D (500 ng); E, B5D (345 ng).

The SDS PAGE analysis was performed for B1D and B3D (Fig. 6). Two sharp and dense bands (a and b) were observed in B1D, while four faint bands (a', b', c and d) were found in B3D. Positions of a' and b' were close to those of a and b, respectively. M_r values estimated at the center

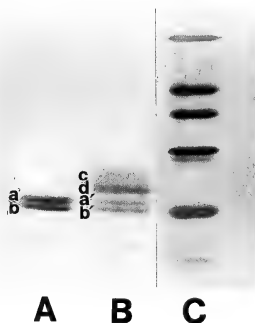


Fig. 6. SDS PAGE of toad gonadotropins. A, B1D (1 μg); B, B3D (1.75 μg); C, the molecular weight markers.

of each band were the followings: a, 20,700; b, 19,800; a', 20,600; b', 19,700; c, 24,500; d, 22,500.

In the immunoblot of SDS PAGE gels (Fig. 7), the anti-B1D-serum stained bands a and b of B1D densely, and bands a' and b' and d of B3D less densely. It did not stain band c of B3D at all. The anti-B3D-serum stained bands c and b' or its lower part of B3D densely. It slightly stained bands a and b of B1D, and did not stain band d of B3D.

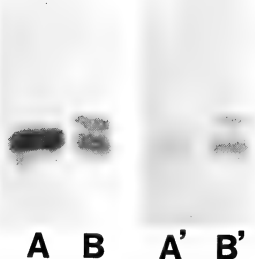


Fig. 7. Immunoblot of toad gonadotropins analyzed by SDS PAGE. A and A' B1D (500 ng); B and B' B3D (500 ng). A and B were stained by anti-B1D-serum, and A' and B' by anti-B3D-serum.

Amino acid composition

Amino acid compositions of fractions B1D and B5D are given in Table 2. Notably, B5D contained higher concentrations of glutamic acid plus glutamine and valine, but a lower concentration of phenylalanine than B1D. Contents of the other amino acid residues were almost identical.

Radioimmunoassays

We developed the following two assay systems: one using an anti-B1D-serum (L-2) and B1D for radioligand (abbreviated as B1D-RIA), and the other using an anti-B3D-serum (F-2) and B3D for radioligand (abbreviated as B3D-RIA). At dilutions of 1:10,000 for L-2 and 1:4,000 for F-2, about 20% of the radioligands were bound to the antibodies.

TABLE 2. Amino acid composition of toad gonadotropins

Amino acid ^a	B1D	B5D
Lys	9.7	8.5
His	3.4	3.6
Arg	4.0	3.5
Asx	11.1	10.9
Thr	9.6	10.0
Ser	8.6	7.5
Glx	6.2	7.9
Pro	7.0	7.1
Gly	3.4	4.2
Ala	7.6	6.6
Val	5.4	7.2
Met	2.7	1.8
Ile	5.3	5.1
Leu	6.6	7.6
Tyr	4.4	5.2
Phe	5.0	3.2

^a Residue per 100 residues. Uncertain estimates of Cys and Trp are omitted.

In both RIA systems, gonadotropin preparations of *Bufo japonicus*, *Bufo marinus* and *Rana catesbeiana* inhibited binding of the radioligands to antibodies at various rates and with different slopes of the inhibition curve, while none of gonadotropin preparations of mammals, a bird and a fish crossreacted (Fig. 8). LH or LH-like preparations of anurans were more potent to inhibit the binding than FSH or FSH-like preparations of them in B1D-RIA, while the FSH or FSH-like preparations were more potent than the LH or LH-like preparations in B3D-RIA. In B1D-RIA, the average inhibition potency of B5D was about 30% of the potency of B1D (Fig. 9a) In B5D-RIA, the average inhibition potency of B1D was as low as 3% as that of B5D (Fig. 9b).

The sensitivity, defined as the concentration of hormone to induce 2×standard error inhibition, and half-inhibition level were 0.05 and 1.88 ng/ml of the sample, respectively, for B1D-RIA, and 0.5 and 15.5 ng/ml, respectively, for B3D-RIA. Intra- and Inter-assay variation coefficients were 2.84 and 4.15%, respectively, for B1D-RIA, and 2.76 and 7.64%, respectively, for B3D-RIA.

As shown in Figure 9 a and b, plasma of an

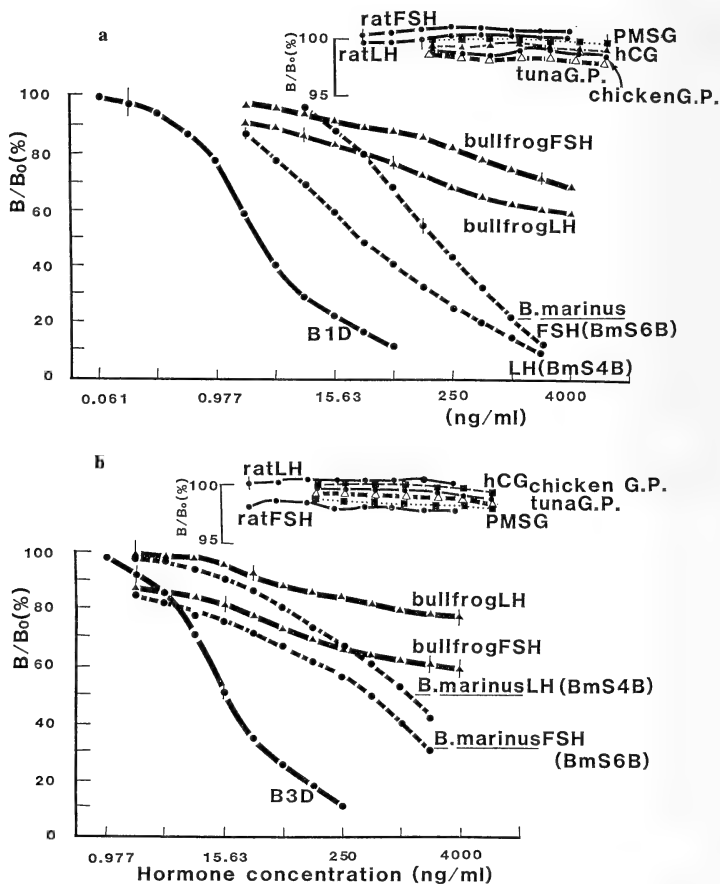


FIG. 8. Competition curves in RIA against (a) ^{125}I -toad LH, Fraction B1D, and (b) ^{125}I -toad FSH-like gonadotropin, Fraction B3D by gonadotropin preparations of various vertebrates. Curves for nonamphibian gonadotropins are indicated at the upper part of the figures with a different vertical-axis scale position. See text for details.

intact *Bufo japonicus* inhibited binding of radioligand in a parallel way with a *Bufo* gonadotropin, and plasma of a hypophysectomized *Bufo japonicus* slightly inhibited binding of radioligands in

both assays. In addition, experiments to know the effect of plasma components on the assay result were conducted by determining recoveries of B1D (0.056 to 0.442 ng) and B5D (0.261 to 6.32 ng)

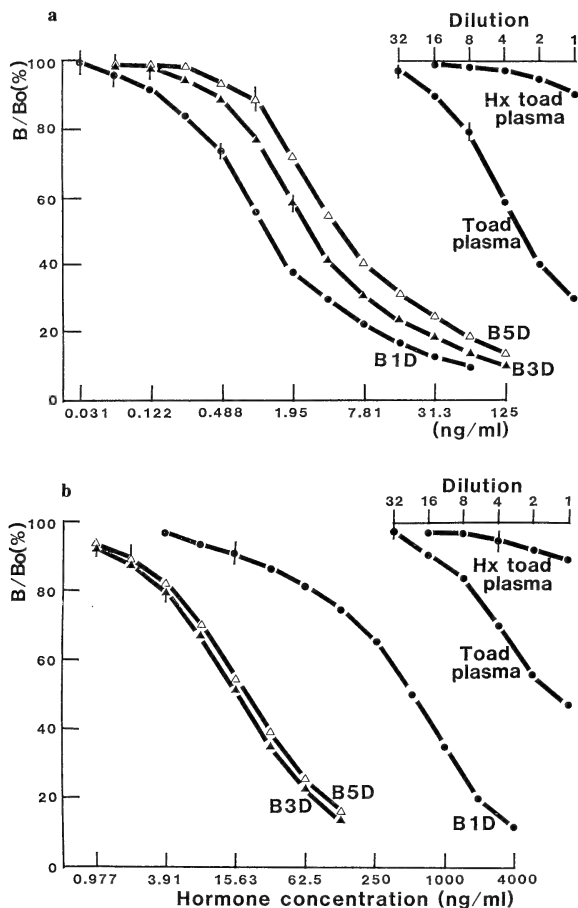


FIG. 9. Competition curves in RIA against (a) ^{125}I -toad LH, Fraction B1D, and (b) ^{125}I -toad FSH-like gonadotropin, Fraction B3D by different gonadotropin fractions of the toad and plasma samples of a normal intact (toad plasma) and hypophysectomized (Hx plasma) toads. B1D is toad LH, and B3D and B5D are toad FSH-like gonadotropin subspecies.

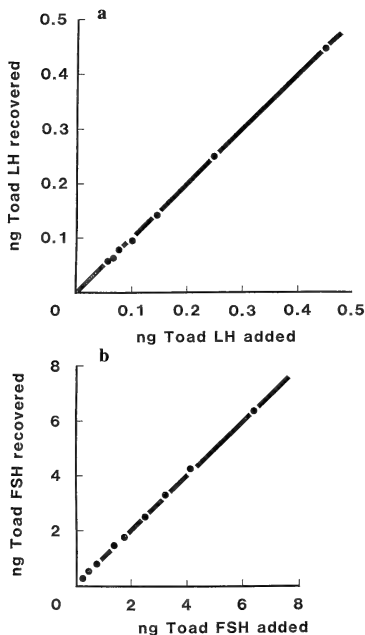


FIG. 10. Diagrams showing the relation between the amount of added hormones (horizontal axis) into plasma and the amount of recovered hormone from plasma (vertical axis) by RIA. The upper (a) and lower (b) figures are the LH- and FSH-RIAs, respectively. See text for details.

which were added into 1/2 diluted plasma samples (Fig. 10). The correlation analysis between amounts of hormones added and recovered resulted in the following formulas of regression lines and regression coefficients (r):

$$Y = 1.037X - 0.0317 \text{ and } r = 0.9995 \text{ for B1D-RIA and}$$

$$Y = 1.009X + 0.0573 \text{ and } r = 0.9991 \text{ for B3D-RIA.}$$

These parameters clearly show that there was practically no disturbance by plasma components in these assay systems.

DISCUSSION

It has been reported that the bullfrog as well as the other higher vertebrates has two sorts of pituitary gonadotropin, i.e. FSH and LH [1-4, 7]. One (B1D) of our final products of *Bufo* gonadotropins has characteristics of LH: it stimulated androgen release from the testis tissue *in vitro*, and showed similar receptor binding property to bullfrog LH. Behavior of B1D in the gel filtration and electrophoresis indicated that it is chemically homogeneous. Appearance of two bands after PAGE has been observed frequently in gonadotropins of other vertebrates, and is considered to represent dissociation of the hormone molecule into two subunits.

The remaining two of the final products, B3D and B5D, are similar or almost identical to each other in the biological, receptor binding and immunological properties, although they are electrophoretically different as revealed by the chromatofocusing and PAGE. Such a property has been known as a characteristic of gonadotropins and thyrotropin, and referred to "microheterogeneity". Accordingly, B3D and B5D are considered to be subspecies of a gonadotropin and belong to the same hormone species.

B3D and B5D are clearly distinct from B1D, *Bufo* LH, in all of the properties examined. For example, B3D and B5D showed clearly a higher RRA potency ratio (FSH-RRA/LH-RRA) than B1D, and this ratio is more similar to the ratio of bullfrog FSH than to that of bullfrog LH (Table 1). Furthermore, the anti-B3D-serum showed a higher affinity to B3D and B5D than B1D (Table 1), and also to bullfrog FSH than to bullfrog LH (Fig. 8). All these results suggest that the main component of B3D and B5D is FSH-like gonadotropin of *Bufo*. To confirm this, the establishment of specific biological assay for toad or anuran FSH is necessary.

There is a problem about the chemical homogeneity of B3D and presumably B5D also. Although they seemed to be homogeneous in mobilities in chromatographies and PAGE without reduction, B3D was dissociated into four bands after SDS PAGE. The immunoblot indicated that B3D contained three anti-B1D-serum positive

bands, two of them are indistinguishable from anti-B1D-serum positive bands, a and b, of B1D in their locations. These results suggest the contamination of B1D, LH, in B3D. However, the anti-B3D-serum only weakly stained a and b bands of B1D, while it stained the lower part of b' densely. Accordingly, at least the lower part of b' can not be a B1D component.

The resolution of B1D and B5D (or B3D) by the RRA is inferior to that by the RIAs. This is considered to be due to the intrinsic nature, i.e. incomplete LH/FSH specificity, of anuran gonadotropin receptors [9], and not to the cross contamination of two hormones. If we did collect more pituitaries, we could have improved the purity of B3D and B5D. However, 8,000 toads were the maximum number that was supposed not to affect the natural balance of the toad populations, although 8,000 were the minimum number for the isolation of gonadotropin.

The RIAs for *Bufo* LH and FSH developed have enough sensitivity to measure plasma gonadotropin levels of the toad, *Bufo japonicus*. Disturbance of the assay result by plasma components is low except for nondiluted or less diluted plasma samples. However, there is a problem in the LH/FSH specificity. The cross-reactivity to B5D (putative FSH) in B1D- or LH-RIA was high (30%), while that to LH in the putative FSH-RIA was low (3%). By applying these two RIAs to a single sample and incorporating the cross-reactivity values, we may calculate the true concentration of FSH and LH. Accordingly, these assays can be used now as an important tool for endocrinological studies of toad reproduction.

ACKNOWLEDGMENTS

This study was supported by a grant from Ministry of Education, Science and Culture, Japan. The authors are grateful to Drs. H. Hayashi, K. Iriyama and K. Murakami for the amino acid analyses, and colleagues of our laboratory in Waseda University for their assistance and suggestions. We also thank to Dr. A. F. Parlow and the Hormone Distribution Programs of the NIAMDD for their gifts of peptide hormones, and to Prof. M. Matsuda and Dr. Y. Yagi, Department of Biochemistry, The Jikei University School of Medicine, for their supports during the completion of the manuscript.

REFERENCES

- 1 Licht, P. and Papkoff, H. (1974) Separation of two distinct gonadotropins from the pituitary gland of the bullfrog *Rana catesbeiana*. *Endocrinology*, **94**: 1587-1594.
- 2 Takahashi, H. and Hanaoka, Y. (1981) Isolation and characterization of multiple components of basic gonadotropin from bullfrog (*Rana catesbeiana*) pituitary gland. *J. Biochem.*, **90**: 1333-1340.
- 3 Takahashi, H. and Hanaoka, Y. (1985) Characterization of bullfrog gonadotropin molecules in comparison with mammalian hormones. In "Current Trends in Comparative Endocrinology". Ed. by B. Lofth, and W. N. Holmes, Vol. 1, Hong Kong Univ. Press, Hong Kong, pp. 187-188.
- 4 Takada, K. and Ishii, S. (1984) Purification of bullfrog gonadotropins: presence of new subspecies of luteinizing hormone with high isoelectric points. *Zool. Sci.*, **1**: 617-629.
- 5 Farmer, S. W., Licht, P., Papkoff, H. and Daniels, E. L. (1977) Purification of gonadotropins in the Leopard Frog (*Rana pipiens*). *Gen. Comp. Endocrinol.*, **32**: 158-162.
- 6 Licht, P., Farmer, S. W. and Papkoff, H. (1975) The nature of the pituitary gonadotropins and their role in ovulation in a urodele amphibian (*Ambystoma tigrinum*). *Life Sci.*, **17**: 1049-1054.
- 7 Papkoff, H., Farmer, S. W. and Licht, P. (1976) Isolation and characterization of luteinizing hormone from amphibian (*Rana catesbeiana*) pituitaries. *Life Sci.*, **18**: 245-250.
- 8 Gavaud, J., Licht, P. and Papkoff, H. (1979) *In vitro* stimulation of cyclic-AMP production in *Rana catesbeiana* ovaries by homologous gonadotropins. *Gen. Comp. Endocrinol.*, **38**: 83-92.
- 9 Takada, K., Kubokawa, K. and Ishii, S. (1986) Specific gonadotropin binding sites in the bullfrog testis. *Gen. Comp. Endocrinol.*, **61**: 302-312.
- 10 Daniels, E. L., Licht, P., Farmer, S. W. and Papkoff, H. (1977) Immunochemical studies on the pituitary gonadotropins (FSH and LH) from the bullfrog, *Rana catesbeiana*. *Gen. Comp. Endocrinol.*, **32**: 146-157.
- 11 Tanaka, S., Hanaoka, Y. and Wakabayashi, K. (1983) A homologous radioimmunoassay for bullfrog basic gonadotropin. *Endocrinol. Japon.*, **30**: 71-78.
- 12 Yoneyama, H. and Ishii, S. (1985) Effects of mammalian luteinizing hormone-releasing hormone (LHRH) on releases of gonadotropin from adenohypophysis of male bullfrog *in vivo* and *in vitro*. *Zool. Sci.*, **2**: 979.
- 13 Stockell Hartree, A. and Cunningham, F. J. (1969) Purification of chicken pituitary follicle-stimulating

- hormone and luteinizing hormone. *J. Endocr.*, **43**: 609-616.
- 14 Lowry, O. H., Rosebrough, N. J., Farr, A. L. and Randall, R. J. (1951) Protein measurement with the Folin phenol reagent. *J. Biol. Chem.*, **193**: 265-275.
 - 15 Davis, B. J. (1964) Disk electrophoresis II. Method and application to human serum proteins. *Ann. N. Y. Acad. Sci.*, **121**: 404-427.
 - 16 Lugtenberg, B., Meijers, J., Peters, R., Hoek, P. and Alphen, L. (1975) Electrophoretic resolution of the 'major outer membrane protein' of *Escherichia coli* K12 into four bands. *FEBS Lett.*, **58**: 254-258.
 - 17 Goudie, R. B., Horne, C. H. W. and Wilkinson, P. C. (1966) A simple method for producing antibody specific to a single selected diffusible antigen. *Lancet*, **ii**: 1224-1226.
 - 18 Towbin, H., Staehelin, T. and Gordon, J. (1979) Electrophoretic transfer of proteins from polyacrylamide gels to nitrocellulose sheets: procedure and some applications. *Proc. Natl. Acad. Sci. USA*, **76**: 4350-4354.
 - 19 Ando, H. and Ishii, S. (1988) Separation of gonadotropic fractions with different species specificities from tuna pituitaries. *Gen. Comp. Endocrinol.*, **70**: 181-192.
 - 20 Sakai, H. and Ishii, S. (1980) Isolation and characterization of chicken follicle-stimulating hormone. *Gen. Comp. Endocrinol.*, **42**: 1-8.
 - 21 Bliss, C. I. (1952) "The Statistics of Bioassay". Academic Press, New York.

Excessive Transitory Migration of Guppy Populations.

III. Analysis of Perception of Swimming Space and a Mirror Effect

HARUE TERAMI and MUNETAKA WATANABE¹

*Department of Biology, College of Liberal Arts and Sciences,
Okayama University, Okayama 700, Japan*

ABSTRACT—In an aquarium halved with a slitted septum, a population of guppy put into one compartment moved excessively to the other compartment (the excessive transitory migration, E.T.M.) and gradually approached equal distribution. It was analyzed using a mirror whether the initial excessive migration and subsequent approach to final balance is performed by the information of real space or visual images of space. If the fish move according to the information by non-visual sense, their migration would be excessive referring to a balance level owing to the volume ratio between compartments. On the other hand, if they behave so due to visual informations, the initial migration and subsequent attainment to final balance would be performed referring to a balance expected from the ratio modified by a mirror image. Experiments showed that the population approached a balance expected from visual information, not that from real space. The information of the density of fish in the recovery to final balance was discussed in relation to the perception of real space or visual image of space.

INTRODUCTION

In an aquarium with a slitted septum, guppies put in one side move to the other side excessively, then they gradually reach an equal distribution. As they migrated from the clean water to polluted water with their excretions, the excessive migration could not be subjected to avoiding the substances [1]. Another supposition that they might exhibit the excessive migration due to their possible schooling tendency was also rejected by detailed analyses of both the distribution of runs of slit-passing and the oscillographic records [2]. We stated previously [1] that the avoidance from the pressure of excessive population might be one of the causes of excessive migration in the initial phase, because the fish which had been confined in a smaller space moved away more promptly.

In our recent trials, when an aquarium was unequally divided, the guppy population behaved

referring to a balanced state expected from the volume ratio between compartments. How does the guppy perceive the balance state? If the fish behave referring to an apparent extension of swimming space, when a mirror is placed in one compartment, they will respond to the space modified by the mirror, i.e. they will be in more number in the compartment with the mirror. If the fish perceive the real swimming space, they will react irrespective of the mirror.

In this paper we studied using a mirror the guppy's space perception by observing the initial migration and the subsequent recovery in an equal- and an unequal-divided tanks.

MATERIALS AND METHODS

Adult female guppies *Poecilia reticulata* used were of 2.8 ± 0.4 cm in total length, bred in our laboratory. Males were not used, since populations of uniform individuals could not be easily obtained because of a great variation in body-to-tail ratio. The guppies were kept in a white-graveled and plant-rooted aquarium. Several days

Accepted January 21, 1989

Received July 25, 1988

¹ To whom all correspondence should be addressed.

before the experiments, populations of 40 fish were isolated from the aquarium and placed in rearing tanks ($45 \times 25 \times 25$ cm deep). Water temperature was maintained within a range between 23.0 and 27.0°C . An experimental tank ($60 \times 25 \times 25$ cm deep) was halved with a white plastic septum having a vertical slit 25×2 cm. This size was large enough for the passage of the fish. The slit was closed with a plastic plate until the onset of the experiment. White papers were attached on the tank walls excepting the frontal wall for observation.

One group of 40 fish were introduced into the left compartment of an experimental tank. After acclimation to the tank for 15 min the plate was quietly pulled up. The number of fish passing through the slit from the left compartment to the right one and *vice versa* was recorded for 30 min. After the experiment, this data was used to calculate the number of fish in each compartment during 1-minute intervals. In Section 2, a mirror or a transparent glass plate was used.

Whether the migration to the other compartment is excessive or not was tested by the Wilcoxon one-sample signed-ranks test [3] using the median value of 10 data at each minute. In Section 1, when the difference between the minimum number observed and the number expected from the volume ratio of compartments, the migration was judged to be excessive. In Section 2 the difference between the minimum number and the number expected from the behavior by visual cue was tested.

What level the number of guppies finally approached was also examined by the same test between the final number observed and that expected. The median of the numbers of fish during the last 5 min of observation was used as the final number of fish. When the null hypothesis of no difference was not rejected, an approach to the expected level was admitted.

A mirror effect due to the reflection from the white paper attached on the glass walls was not observed in our experimental conditions, though, when singly put in, the guppy continued tenaciously to swim facing the glass walls.

RESULTS

Section I

Whether or not the initial migration is excessive in an unequal-divided tank was examined.

Experiment 1 An opaque plastic plate was put in the center of the right compartment, so that the volume ratio of the left compartment to the right one may become 2:1 (Fig. 1).

When a population of 40 fish was introduced into the left compartment, the fish immediately migrated to the right compartment.

The number of fish declined below the balance level 27 ($40 \times 2/3$) and reached 17.5. The deviation of the number 17.5 from 27 was significant ($p < 0.01$) (Table 1). Thus, the excessiveness of migration was confirmed even in an unequally divided tank.

The final number did not attain to 27 within 30

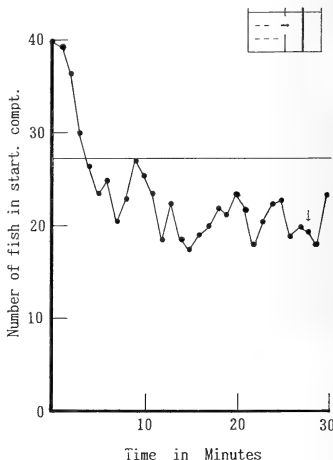


FIG. 1. Change of the number of fish in the left (starting) compartment in an aquarium, in which an opaque plastic plate was placed in the center of the right compartment. —: a level of volume ratio of left to right compartments. ↓ indicates the median of the numbers of fish during the last 5 min of observation. For details see text.

TABLE 1. The minium number observed and final number expected from volume ratio in the left (starting) compartment in Section 1

Expt. No.	Minimum number observed	Final number expected from volume ratio
Exp. 1 (Fig. 1)	17.5	27 (2.7011; <0.01)**
Exp. 2 (Fig. 2)	11.0	20 (2.1405; <0.05)*

The number in the parenthesis represents a statistic Z and significance level p in the Wilcoxon one-sample signed-ranks test between the observed minimum number and the final number expected from volume ratio. * and ** represent significance at 0.05 and 0.01, respectively.

TABLE 2. The final number observed and final number expected from volume ratio in the left (starting) compartment in Section 1

Expt. No.	Final number observed	Final number expected from volume ratio
Exp. 1 (Fig. 1)	19.5	27 (2.4879; <0.05)*
Exp. 2 (Fig. 2)	19.0	20 (0.2369; >0.80)

The number in the parenthesis represents a statistic Z and significance level p in the Wilcoxon one-sample signed-ranks test between the observed final number and the final number expected from volume ratio. Final number observed is the median of the numbers of fish during the last 5 min of observation. For details see text. * represents significance at 0.05.

min observation ($p < 0.05$) (Table 2).

Experiment 2 In an equal-divided tank, the number of fish in the left compartment once reached below the level of half number 20 (Fig. 2). The deviation of the minimum number of fish 11.0 from 20 was statistically significant ($p < 0.05$).

Then the population gradually approached a balance of equal number. The difference between the final number observed and 20 was not significant ($p > 0.80$).

Section II

This section was carried out to examine whether the attainment to final balance mainly depend upon visual or non-visual cue. Under a condition that the space is apparently modified with a mirror, if the fish behave according to visual informations, the final balance would be subject to a volume ratio expected from the modified space. On the other hand, if fish react to real space, the final distribution will approach a balance expected from a real volume ratio of compartments. The expected numbers are listed in Table 4.

Experiment 3 A large mirror was attached on

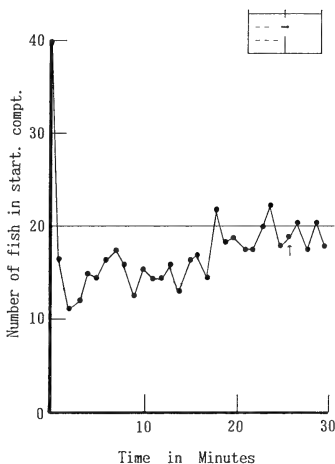
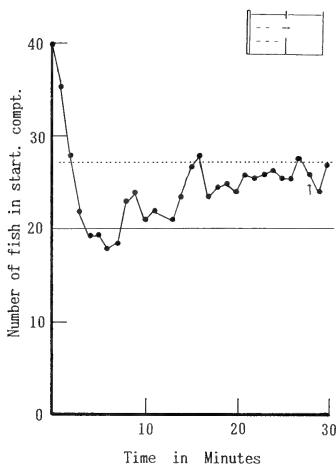


FIG. 2. Change of the number of fish in the left (starting) compartment in an equal-divided aquarium.



the left wall of the left compartment (Fig. 3). In this condition, while the compartment are spatially equal, the left (starting) compartment is visually twice as the right one.

Threat and other responses of fish to their own images in the mirror were scarcely observed. The minimum number in the left compartment was 18 (Table 3). This number differed nearly significantly at 0.05 from 27, a visually expected number.

The number of fish in the left compartment approached gradually 27 ($p > 0.50$) (Table 4), not 20 expected from spatial cue ($p < 0.05$).

Experiment 4 The mirror was attached on the right wall of the right compartment (Fig. 4). The apparent volume of the right compartment is twice as the left one.

The minimum number of fish was 5 (Table 3),

FIG. 3. Change of the number of fish in the left (starting) compartment. A mirror was attached on the left wall of the left compartment.: a level expected from visual cue.

TABLE 3. The minimum number observed and final number expected from visual cue in the left (starting) compartment in Section 2

Expt. No.	Minimum number observed	Final number expected from visual cue
Exp. 3 (Fig. 3)	18	27 (1.9545; ≈ 0.05)*
Exp. 4 (Fig. 4)	5	13 (2.6656; < 0.01)**
Exp. 5 (Fig. 5)	10.5	20 (2.6502; < 0.01)**
Exp. 6 (Fig. 6)	13.5	20 (2.0140; < 0.05)*

The number in the parenthesis represents a statistic Z and significance level p in the Wilcoxon one-sample signed-ranks test between the observed minimum number and the final number expected from visual cue. * and ** represent significance at 0.05 and 0.01, respectively.

TABLE 4. The final number observed and final numbers expected from visual and non-visual cues in the left (starting) compartment in Section 2

Expt. No.	Final number observed	Final number expected from	
		non-visual cue	visual cue
Exp. 3 (Fig. 3)	26.0	20 (2.4286; < 0.05)*	27 (0.6516; > 0.50)
Exp. 4 (Fig. 4)	10.5	20 (2.5471; < 0.05)*	13 (0.6625; > 0.50)
Exp. 5 (Fig. 5)	15.5	27 (2.8031; < 0.01)**	20 (1.8348; > 0.05)
Exp. 6 (Fig. 6)	18.5	27 (2.7011; < 0.01)**	20 (0.6625; > 0.50)

The number in the parenthesis represents a statistic Z and significance level p in the Wilcoxon one-sample signed-ranks test between the observed final number and the final number expected from visual and non-visual cues. For details see text. * and ** represent significance at 0.05 and 0.01, respectively.

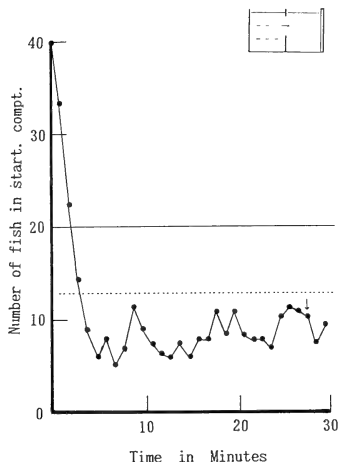


FIG. 4. Change of the number of fish in the left (starting) compartment. A mirror was attached on the right wall of the right compartment.

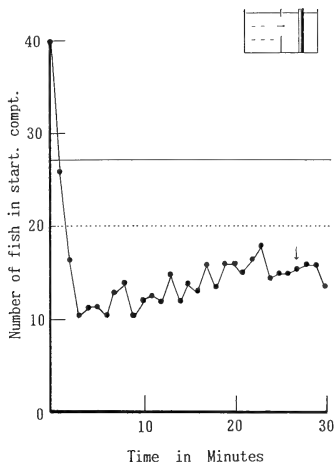


FIG. 5. Change of the number of fish in the left (starting) compartment. A mirror was placed in the center of the right compartment.

which is significantly smaller than a visually balanced number 13 ($p < 0.01$).

The difference of the final number 10.5 (Table 4) from 13 was not significant ($p > 0.50$), while that from the spatially expected 20 was significant ($p < 0.05$).

Experiment 5 The mirror was placed in the center of the right compartment (Fig. 5). The right compartment is visually the same as the left one, while spatially half.

The minimum number in the left was 10.5 (Table 3). The difference between 10.5 and a visually balanced number 20 was significant ($p < 0.01$).

The final number 15.5 (Table 4) was not significantly different from 20 ($p > 0.05$), but different from the spatially expected 27 ($p < 0.01$).

Experiment 6 A transparent glass plate was put in the center of the right compartment (Fig. 6). Here, the right compartment was visually equal to the left one, though spatially half.

The minimum number was 13.5 (Table 3), which was significantly different from the visually ex-

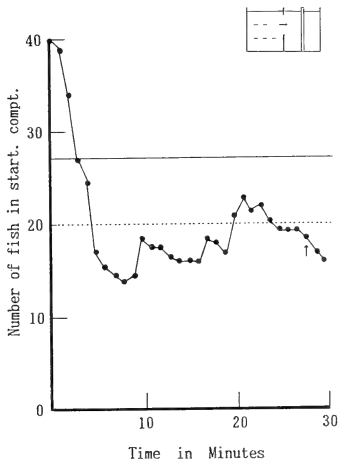


FIG. 6. Change of the number of fish in the left (starting) compartment. A transparent glass plate was placed in the center of the right compartment.

pected 20 ($p < 0.05$).

The final number 18.5 (Table 4) was of non-significant difference from 20 ($p > 0.50$), while significantly different from the spatially expected 27 ($p < 0.01$).

DISCUSSION

In a previous paper we concluded that the avoidance of pressure due to excessive fish density is one of the causes of E.T.M., because a guppy population confined in a small area more rapidly migrated and reached the half number level [1].

Many workers [4-8] noticed a spacing among fish individuals in the analysis of school formation since Parr's pioneer work [4]. Breder stated in 1954 that, there is a certain specified distance beyond which fish refuse to move any closer, and the regularity of spacing is brought about by an interaction of attraction and repulsion. While the attraction of fish to fish has been shown to operate by means of vision, the repulsion might work on a rather different basis. Operating at short distances, in addition to the visual component, other clues could include water movement, sound, odor and taste [5]. Symons [6] investigated the relationship between spacing and population density in the mummichog *Fundulus heteroclitus* and the stickleback *Gasterosteus aculeatus*, and reported that, when separated by 1 fish length, they spaced at random, but when within 1 fish length, they often became regularly spaced. Fenderson and Carpenter studied an interference in fish activity by the pressure due to social interaction: the salmon reared in hatchery where fish are confined at abnormally high density consumed less food than those reared in streams where population density is regulated by territorial dispersion [7]. Thus, fishes in general are apt to avoid so much pressure owing to population.

Section I obviously showed that guppy populations initially migrate excessively beyond the balance level expected from volume ratio between the left and right compartments, in either equally (Fig. 2) or unequally (Fig. 1) divided tank (Table 1).

Table 3 shows the statistical analyses of the difference between the minimum fish number and

the number expected from visual cue in Section II. The initial migration of fish populations to the other compartment was significantly excessive in all the experiments.

The excessive transitory migration exhibited a large variety of time. In Section 2, in some cases the population quickly attained to the level expected from visual cue (Figs. 3 and 6), and in some cases the attainment was much retarded (Figs. 4 and 5). It is noticeable that it behaved in relation to the level expected from visual cue, not the level from non-visual cue (Table 4).

A mirror was often used in the study of animal behavior [9-14]. Lissmann [9] demonstrated that Siamese fighting fish *Betta splendens* followed the movement of a mirror turned on a horizontal axis, and Tinbergen [10, 11] showed the threatening movement by a male stickleback to its own mirror image in an extensive study dealing with visual and non-visual social releasers. Dore *et al.* [14] reported on *Betta splendens* that a mirror presentation produced a large amount of display than a conspecific placed behind the glass partition, which in turn elicited more threat than an opponent in an actual fight. The above studies indicate that fish can identify its conspecifics due to mirror images.

As to the final number of fish in the starting compartment, in Experiments 3, 4, 5 and 6 the results supported the suggestion of superiority of visual information. Statistic analysis of the difference between observed and expected values of final number of fish is shown in Table 4, which indicates that the number of fish in the left compartment finally approached the value expected from visual cue, not the value expected from space cue.

In the tank in which an opaque septum was put in the center of the right compartment, the fish were finally distributed in 2:1 as expected from the volume ratio of compartments (Fig. 1). In an equal-divided tank (Fig. 2), the distribution was 1:1. So, in either case the final distribution was due to the volume ratio of the compartments.

When the mirror is placed in the left compartment (Fig. 3), the left one is visually twice as the right one in volume; the volume ratio between two compartments is visually 2:1. The experiment actually showed the fish distribution to be 2:1.

When the mirror was put in the right compartment (Fig. 4), the final distribution was 1:2. The results mean that the fish behave according to visual information of space.

In Figure 5, a mirror was in the center of the right compartment, so the real volume ratio was 2:1, but visually 1:1. The experimental result showed that the final distribution was 1:1. Next, when a transparent plate was put in place of the mirror, the real ratio was 2:1, but visually 1:1. The fish were finally distributed in 1:1. The above results again indicate that the fish react precisely to visual space rather than the real volume.

In Figure 4, however, there were twice number of fish in the right compartment as the left one, and accordingly the fish density was also twice. In Figure 5, as the images were in the mirror, the density of fish in the right part as a whole was twice as that of the left, while in Figure 6 the total density was the same as the left. These results suggest that the fish do not behave by recognizing their population density.

In both Figure 4 and Figure 5, however, the fish images are in the mirror. In the experiment the fish density actually was twice. Since the fish perceive the relative volume of compartments and decided their distribution, the fish must watch also the images of their own and conspecifics in the mirror. Nevertheless, they could be distributed precisely only according to the ratio of space. This contradiction could not be explained, because they perceive the space with their eyes, while they do the number of fish by the cue other than eyes, i.e. they might be able to assess the exact number of fish individuals by sound or water vibration without deception by the mirror.

Animals in general exhibit 'curiosity (exploratory nature)' [15] to a novel environment when they are newly exposed to it. Warren and Callagan discussed the curiosity in guppies using a bowl, the bottom of which was divided to outer and inner ring areas [15]. If each animal shows a response to unknown situation, some behaviors of an animal group may be explained as a result of summation of responses of individuals, thus the curiosity may also be a cause of the E.T.M. We are now planning an analysis to examine the above possibility in comparison between a condition of closing

the slit until onset of the trial and a condition of keeping fish's free passage through a slit until just before the trial. This may throw a light for further analysis of the excessive transitory migration.

ACKNOWLEDGMENTS

We are much thankful to Ms. Toshie Takahashi and Ms. Shikiko Takizawa for their assistances in carrying out the experiments.

REFERENCES

- 1 Watanabe, M. (1981) Excessive transitory migration of guppy populations. I. Analysis of sensory cues and mechanisms. *Zool. Mag.*, **90**: 33-38.
- 2 Watanabe, M. and Terami, H. (1988) Excessive transitory migration of guppy populations. II. Analysis of possible conspecific-following tendency. *Zool. Sci.*, **6**: 573-577.
- 3 Lehmann, E. L. (1975) Nonparametrics: Statistical methods based on the ranks. Holden-Day, Inc., San Francisco.
- 4 Parr, A. E. (1927) A contribution to the theoretical analysis of the schooling behavior of fishes. *Occas. Papers Bingham Oceanog. Coll.*, **1**: 1-32.
- 5 Breder, C. M. Jr. (1954) Equations descriptive of fish schools and other animal aggregations. *Ecology*, **35**: 361-370.
- 6 Symons, P. E. K. (1971) Spacing and density in schooling threespine sticklebacks (*Gasterosteus aculeatus*) and mummichog (*Fundulus heteroclitus*). *J. Fish. Res. Bd. Canada*, **28**: 999-1004.
- 7 Fenderson, O. C. and Carpenter, M. F. (1971) Effect of crowding on the behavior of juvenile hatchery and wild landlocked Atlantic salmon (*Salmo salar* L.). *Anim. Behav.*, **19**: 439-447.
- 8 Radakov, D. V. (1973) Schooling on the Ecology of Fish. John Wiley & Sons, New York.
- 9 Lissmann, H. W. (1932) Die Umwelt des Kampffisches (*Betta splendens* Regan). *Zeitschr. vergl. Physiol.*, **18**: 65-112.
- 10 Tinbergen, N. (1948) Social releasers and the experimental method required for their study. *Wilson Bull.*, **60**: 6-51.
- 11 Tinbergen, N. (1951) *The Study of Instinct*. Oxford Univ., Amen House, London, p. 114.
- 12 Rinc, A. (1976) Standardization of position and stability of display measures in Siamese fighting fish (*Betta splendens*). *Behav. Biol.*, **16**: 175-184.
- 13 Miley, W. M. and Burack, G. (1977) Strength of aggressive display in Siamese fighting fish (*Betta splendens*) toward a conspecific, an alien species (*Macropodus opercularis*), and a mirror image as

- affected by prior conspecific visual experience. Behav. Biol., **21**: 267-272.
- 14 Dore, F., Lefebvre, L. and Decharme, R. (1978) Threat display in *Betta splendens*: Effects of water condition and type of agonistic stimulation. Anim. Behav., **26**: 738-745.
- 15 Warren, E. W. and Callagan, S. (1976) The response of male guppies (*Poecilia reticulata*, Peters) to repeated exposure to an open field. Behav. Biol., **18**: 499-513.

Revision of *Molobratia* from Japan and Taiwan (Insecta, Diptera, Asilidae)¹

AKIRA NAGATOMI, HIROKI IMAIZUMI² and HISAKO NAGATOMI³

*Entomological Laboratory, Faculty of Agriculture, Kagoshima University,
Kagoshima 890, ²Kumamoto Business Office, Kyushu Sankyo Chemical Co.,
Tamana 865, and ³Biological Laboratory, Kagoshima
Women's College, Hayato 899-51, Japan*

ABSTRACT—Six species of *Molobratia* are now known from Japan (4 species) and Taiwan (2 species). *M. takasagense* is synonymized with *M. japonica* and one new species is added from Taiwan. It is found that aedeagus, horizontal branch of dorsodistal process in gonocoxite, male sternum 10, female tergum 8 and female sternum 8 vary in shape with species.

INTRODUCTION

Hull [1] erected the genus *Molobratia* and designated *Asilus teutonius* Linnaeus, 1767 as the type species, because the true type species of *Dasyopogon* Meigen, 1803 is not *teutonius*, but *Asilus diadema* Fabricius, 1781, by the designation of Latreille, 1810. *Selidopogon* Bezzi, 1902, whose type species is *diadema*, became a synonym of *Dasyopogon*.

From Japan, five described species of *Molobratia* were recorded (Bigot [2]; Matsumura [3]; Hradský [4]). One of them, *takasagense*, is here treated as a junior synonym of *japonica*. At present only one female specimen of *Molobratia* from Taiwan is on hand and this seems to represent a new species. The original description is copied as to *M. purpuripennis* (Matsumura) from Taiwan. Thus, four species from Japan and two species from Taiwan are now recorded as *Molobratia*.

Iwata and Nagatomi [5] treated *Molobratia japonica* and *M. sapporensis* as *Dasyopogon*, and recorded their prey: "The delicate wasps such as Ichneumonidae were principally seized" by *sapporensis*, and "The bees were mainly struck" by

japonica.

Richter (1968) and Weinberg (1970) put *egregia* Loew, 1869 from Transcaucasia and Caucasia into *Molobratia* (after Ionescu and Weinberg [6], p. 137). Weinberg [7] redescribed and illustrated *pekinensis* Bigot, 1878, whose type locality is northern China as *Molobratia*, based on the specimens from Kuantum, Fukien, China. Oldroyd [8] put *inopinata* Walker, 1860 and *inopportuna* Walker, 1860, both from Burma, into *Molobratia*. Unfortunately we have no specimens of *inopinata* and *inopportuna* and cannot compare them with the species from Japan and Taiwan.

PHYLOGENETICALLY RELATED GENERA OF MOLOBRATIA

What is the phylogenetically related genus or genera of *Molobratia*? According to Hull [9], it is *Leptarthrus* Stephens, 1829 (= *Isopogon* Loew, 1847), having two species from Europe. In the female tergum 9+10 of *Molobratia* and *Leptarthrus*, a circlet of rod-like spines are absent. On the basis of this character, Hull [9] put these two genera into the tribe Dioctrini. On the other hand, Theodor [10] (p. 27) mentioned that "The tribe Dioctrini of Hull is based on the absence of spines on tergite 9 (=tergum 9+10 or tergum 10 in our interpretation) of the female; however, spines are also absent in some species of other tribes which

Accepted January 12, 1989

Received September 5, 1988

¹ Studies of Diptera Collection in National Institute of Agro-Environmental Sciences, Tsukuba. No. 4.

belong to these tribes according to some very distinct characters, while other species have spines on tergite 9. *Dioctria* is here included in the Stenopogini, as this character does not seem to justify the establishment of a separate tribe." This statement may be correct, and the absence of the spines in question may occur secondarily within the same natural group, as pointed out already by Papavero [11, 12] and Theodor [13].

Lehr [14] still put *Molobratia* into the tribe Dioctrinini of the subfamily Stenopogoninae. However, *Molobratia* may belong to the tribe Dasypogonini (of the subfamily Dasypogoninae) which is characterized by the presence of a large twisted or sigmoid spine at the apex of fore tibia, although this spine rarely disappears individually or specifically (after Wood [15], p. 554). Theodor [10] (p. 171) mentioned that "This [=Dasypogonini] is probably an artificial group as the genera differ markedly in other characters and the spine on the fore tibiae also differs markedly in form and size and probably developed independently in different groups."

For separation of *Molobratia* from the related genera, see key to the genera by Engel [16] (pp. 437-438) ["*Dasypogon*" (= *Molobratia*); "*Selidopogon*" (= *Dasypogon*)]. Theodor [10] diagnosed the genera *Dasypogon*, *Saropogon* and *Parapharmartania*. Theodor [13] also described and illustrated the male genitalia of several genera of Dasypogonini, that is, *Dasypogon*, *Saropogon*, *Molobratia*, *Parapharmartania*, *Leptarthrus* and *Neolaparus*.

Molobratia is apparently nearer to *Dasypogon* and *Saropogon* than to *Leptarthrus*. In *Leptarthrus*, spur on fore tibia is bristle-like and antennal style is 2-segmented (after Papavero [12]). Lehr [14] and Papavero [12] put *Leptarthrus* into the tribe Isopogonini (of the subfamily Dasypogoninae).

Genus *Molobratia* Hull

Molobratia Hull, 1958, Proc. ent. Soc. Wash. 60: 251. Type species: *Asilus teutonius* Linnaeus, 1767 (from Europe), by original designation.
Dasypogon, authors, not Meigen, 1803.

Molobratia includes the following 11 species:

chujoi (Taiwan), *egregia* (Transcaucasia and Caucasia), *inopinata* (Burma), *inopportuna* (Burma), *japonica* (Japan), *kanoi* (Japan), *nipponi* (Japan: Okinawa I. and Amami Oshima), *pekinensis* (China), *purpuripennis* (Taiwan), *sap-porensis* (Japan) and *teutonius* (Europe and Turkey).

Molobratia differs from *Dasypogon* by having the following characters: (1) antennal style conical, tapering apically and with a terminal spinule, (2) antennal segment 3 with many stout hairs dorsally, (3) 4th posterior cell (=cell M₃) open, (4) fore basitarsus longer than mid or hind basitarsus, and (5) female tergum 9+10 without a circlet of rod-like spines. In *Dasypogon*, (1) antennal style cylindrical, not tapering apically and its apical concavity with a spinule, (2) antennal segment 3 bare or practically so dorsally, (3) 4th posterior cell closed, (4) fore basitarsus shorter than mid or hind basitarsus, and (5) female tergum 9+10 with a circlet of rod-like spines. (chiefly after Engel [16], p. 438)

Hull [9] (pp. 227-228) wrote that "Many species have been removed from the genus [*Dasypogon*] in recent years and it is probable that comparatively few species properly belong in *Dasypogon sensu stricto*.The species known to properly belong to *Dasypogon* are found in southern Europe and northwestern Africa."

Lehr [14] listed 15 species of *Dasypogon* which are distributed in Europe, North Africa and Asia (Israel, Turkey, and Iran). Weinberg [17-19] added 4 new species of *Dasypogon* from Yugoslavia, Greece, Transcaucasia and Mongolia respectively.

The diagnosis of *Molobratia* based on 5 species (from Japan and Taiwan) is given below. Head: Face without gibbosity, but more or less swollen especially near clypeus; hairs on face longer near clypeus, becoming shorter above and haired area nearly reaching to antennae; front with a tuft of hairs running longitudinally near each side; ocellar tubercle with 1 pair of longer and stouter hairs; antennal style conical or tapering apically and with a terminal spinule; antennal segment 3 with many strong hairs dorsally.

Thorax: Prosternum widely separated from propleura by membranous area; hairs are absent

on median stripe (except mid vitta) and on lateral stripes; *hm* 0, *npl* 2–12, *sa* 1–12, *pa* 1–7, *dc* 2–9, *sc* (on one side) 0–4, according to individual or species; *dc* postsutural (in *sapporensis*, rarely pre-sutural); antepnotum and propleura with strong hairs; metapleural fan weak and accompanied with pile; hypopleura and side of pronotum pilose.

Wing: Fourth posterior cell wide open and anal cell narrowly open or nearly closed.

Legs: Long and not very robust; fore basitarsus longer than mid or hind basitarsus; fore tibia with an apical process having a stout terminal spine directed inward and fore basitarsus with a knob, opposite fore tibial spine; fore tibial process with a row of strong hairs (which may become short in *chujoi*) along inner margin, and area at and before knob in basitarsus with denticles opposite process and spine; each femur with two dorsal setae (which are very short in *chujoi*) near apex and with several setae on other parts, but in *kanoi* dorsal setae near apex 3 (or so) in number.

Abdomen: Elongate, more or less slender; bristles are confined to sides of tergum 1.

Male genitalia (based on 4 Japanese species): Paired gonocoxites (excepting dorsodistal processes) wider than long; in gonocoxite, ventral surface except inner part and outer part of dorsal surface with strong long hairs; gonocoxite with a long dorsodistal process whose base has a vertical conical process directed upward, and with a flat distal inner ventral extension; ventral surface of gonocoxite more or less pointed at apex; in lateral view, dorsodistal process of gonocoxite bilobate and horizontal branch longer and wider than the vertical; gonostylus long, tapering apically, pointed dorsally at apex, and with a row of vertical dorsal hairs; gonocoxal apodeme rather long, but not extending beyond anterior margin of sternum 9 (= hypandrium); sternum 9 triangular, wider than long but comparatively long, and with a transverse row of hairs.

In aedeagus, dorsal and ventral plates form a sigmoid conical tube, having a posteroventral fin flattened laterally (in *japonica*, *nipponi* and *sapporensis*), whose size and shape vary with species, and apex of this tube is curved upward (in *japonica*, *kanoi* and *sapporensis*); in ventral or lateral view, base of tube (on one side) consisting of

dorsal outer and ventral inner processes; in dorsal view, paired dorsal outer processes forming a large V or U shape; anterior bar of aedeagus is flattened laterally and varies in size and shape with species.

Tergum 9 rather trapezoid, wider basally and covered with strong hairs (except base), some of which are bristle-like on outer margin; in *japonica*, *nipponi* and *sapporensis*, cerci except apical portions fused with each other; paired cerci rectangular and the middle of apical margin with a deep concavity; cerci with dorsal hairs; sternum 10 with a pair of elongate anterior sclerites which are widened and then pointed; apical (=posterior) margin of sternum 10 rounded or nearly straight and with hairs (except middle).

In the specimen of *nipponi*, the posteroventral fin of aedeagal tube is vertically divided into a pair. It is uncertain whether this separation is accidental or not. This fin is absent in *kanoi* (Fig. 22) and *teutonius* (see Fig. 216 in Theodor [13]).

Female terminalia (based on 4 Japanese species): The ovipositor may be composed of the segments 7–8 or 8. In *Leptarthrus*, the ovipositor is long and composed of the segments 6–8 (see Fig. 273 in Engel [16] and Fig. 213 in Oldroyd [20]). The tergum 9+10 is small and has no rod-like spines. In *Dasygogon*, a circlet of rod-like spines are present on tergum 9+10 (see Fig. 216 in Oldroyd [20] and Fig. 34 in Theodor [10]).

A pair of sclerotized cerci are usually separated, but sometimes fused with each other individually; each cercus roughly elliptic (except basal portion), longer than wide, and with strong hairs. Tergum 9+10 (or tergum 10) membranous, rectangular, and much wider than long. Sternum 10 composed of posterior trapezoid part having strong hairs and a pair of anterolateral bare darkened sclerites. Tergum 8 trapezoid, semicircular or its anterior margin with a wide and deep concavity according to species; tergum 8 except anterior part with dorsal hairs. Sternum 8 semicircular or roughly pentagonal according to species and with ventral hairs. Tergum 7 and sternum 7 rectangular, haired, and wider than tergum 8 and sternum 8; tergum 7 wider than sternum 7. Genital fork large and U-shaped.

Key (a) to species of *Molobratia* from Japan and Taiwan based on external characters

1. Legs and abdomen entirely dark brown to black 2
- Legs largely and abdomen partly yellowish (or reddish) brown 3
2. Face, cheek and base of proboscis with pale yellow hairs; legs with white and black hairs; sides of abdominal dorsum with long white hairs (after Matsumura [3]); (Taiwan) *M. purpuripennis*
- Hairs on head wholly black; legs without white hairs; hairs on abdomen (except cerci) wholly black; (Japan: Honshu) *M. kanoi*
3. Face at antenna much narrower than width of one eye (Figs. 21, 33); in fore and mid tibiae some setae longer than thicknesses of tibiae (as well as in hind tibia in *kanoi* and *sapporensis* [Figs. 43, 44]) 4
- Face at antenna about as wide as one eye; in fore and mid tibiae all setae shorter than thicknesses of tibiae as well as in hind tibia (Fig. 42); in sigmoid terminal spine of fore tibia, apical black part about 1/2 as long as basal yellowish brown part (Fig. 1) (as in *kanoi*); (Taiwan) *M. chujoi*
4. In sigmoid terminal spine of fore tibia, apical black part over 1/2 as long as basal yellowish brown part (Fig. 34) 5
- In sigmoid terminal spine of fore tibia, apical black part less than 1/2 as long as basal yellowish brown part (Fig. 24); face wider than in *sapporensis* (Fig. 21); (Japan: Okinawa I. and Amami Oshima) *M. nipponi*
5. Face wider than in *sapporensis*; humeral and posterior calli and scutellum may be brown (as in *nipponi*); abdominal tergum 1 yellowish brown (as in *nipponi*); no pale yellowish gray spots at postero-lateral corners of abdominal terga 2–6; scutellum with many hairs (as in *nipponi*); (Japan: Honshu, Shikoku and Kyushu) *M. japonica*
- Face narrower than in *japonica* (Fig. 33); humeral and posterior calli and scutellum dark brown to black; abdominal tergum 1 shining blue black; abdominal terga 2–6 with distinct pale yellowish gray pollinose spots at

posterolateral corners (as in *nipponi*); scutellum with no or few hairs; (Japan: Hokkaido, Honshu, Shikoku and Kyushu) *M. sapporensis*

Key (b) to species of *Molobratia* from Japan based on male genitalia

1. Posteroventral fin of aedeagal tube present (Figs. 9, 26, 36); cerci fused (except their apical portions) (Fig. 6); horizontal branch (in dorsodistal process of gonocoxite) with a minute apical seta (Figs. 8, 26, 35) 2
- Posteroventral fin of aedeagal tube absent (Figs. 20); each cercus apparently separate; horizontal branch (in dorsodistal process of gonocoxite) with two thicker apical teeth, of which dorsal one is pointed (Fig. 19) *M. kanoi*
2. Apex of aedeagal tube curved upward (Figs. 9, 36); posteroventral fin of aedeagal tube longer than in *nipponi* (Figs. 9, 36); anterior bar of aedeagus much narrower than in *nipponi* and not circular (Figs. 9, 36); horizontal branch in dorsodistal process of gonocoxite narrower than in *nipponi* at apical portion and without a sclerotized oblique line (Figs. 8, 35) 3
- Apex of aedeagal tube directed forward (Fig. 27); posteroventral fin of aedeagal tube shorter than in *japonica* and *sapporensis* (Fig. 27); anterior bar of aedeagus much wider than in *japonica* and *sapporensis* and somewhat circular (Fig. 27); horizontal branch in dorsodistal process of gonocoxite wider than in *japonica* and *sapporensis* at apical portion and with an oblique sclerotized line (Fig. 26) *M. nipponi*
3. Posteroventral fin of aedeagal tube bluntly pointed at anterodistal corner (Fig. 9); anterior bar of aedeagus in lateral view wider apically and then narrowed (Fig. 9) *M. japonica*
- Apical part of posteroventral fin in aedeagal tube wider than in *japonica* (Fig. 36); anterior bar of aedeagus without narrowed anterior (=apical) portion (except dorsal corner) (Fig. 36) *M. sapporensis*

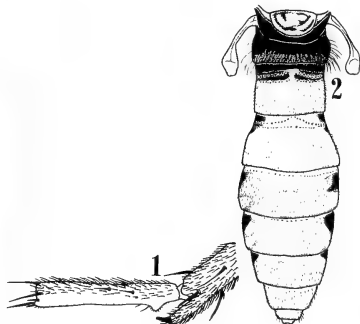
Key (c) to species of *Molobratria* from Japan
based on female terminalia

1. Tergum 8 much shorter than in *nipponi* and with anterior margin gently concave (Figs. 13, 39); sternum 8 rounded apically (Figs. 14, 40) 2
- Tergum 8 much longer than in *japonica*, *kanoi* and *sapporensis* and with anterior margin deeply concave (Fig. 31); sternum 8 (not flattened out) in ventral view is rather pentagonal, although its narrow posterior margin may be straight (Fig. 32). *M. nipponi*
2. Sternum 8 wider and shorter than in *kanoi* and *sapporensis* and with a large and wide bare membranous posterior part (Fig. 14). *M. japonica*
- Sternum 8 narrower and longer than in *japonica* and with a bare membranous posterior part small and narrow (Fig. 40). *M. kanoi* and *M. sapporensis*

Molobratria chujoi Nagatomi, Imaizumi
et H. Nagatomi sp. n.
(Figs. 1, 2, 42)

This species (♀) is similar to *japonica*, *nipponi* and *sapporensis*, but may easily be separated from them by having the external characters shown in the key (a) (couplet 3).

The following description is based on a single female specimen whose antennal segment 3 and hind tarsomeres 3–5 are lacking.



Female. Head: Dark brown to black, and pale yellowish gray tomentose; antenna yellowish brown; palpus, labellum, midventral part of theca, and ocellar triangle shining black; vestiture on head pale yellow, but that on ocellar triangle, area behind ocellar triangle, upper occiput, front, palpus (except base) and antennal segments 1–2 black; hairs behind ocellar triangle short; width of one eye at greatest point 0.5 times length (= height) of eye, 0.9 times width of face at antenna, and 2.4 times distance from antenna to median ocellus; width of front at median ocellus 0.9 times width of face at lowest portion from a direct frontal view, 4.2 times width of ocellar triangle, and 2.6 times distance from antenna to median ocellus; ocellar triangle as wide as long; distance from antenna to median ocellus 0.24 times distance from antenna to lower margin of eye, which is 1.4 times length of face (minus clypeus); when measured along midouter surface, relative lengths of antennal segments 1–2 [segment 3 lacking] 100:62 and their relative widths from the side 62:62.

Thorax: Dark brown to black, and pale yellowish gray (or pale gray) tomentose; mesonotum with 3 broad darker stripes, of which median one is separated by mid vitta and the lateral ones may be obscure in demarcation; hairs and bristles on mesonotum and antepronotum black; hairs on mesonotum very short; hairs on sides of pronotum chiefly black; hairs on pleura pale yellow; *scutellum without hairs and bristles*.

Wing: Membrane yellowish brown to brown; veins yellowish brown to dark brown; halter yellowish (or reddish) brown.

Legs (Figs. 1, 42): Yellowish (or reddish) brown; claw except base black; coxae dark brown to black and pale yellowish gray tomentose; hind femur may have a darkened streak on postero-ventral surface; fore and mid trochanters at ventral apices and hind trochanter at anterior part, each with a small shining black spot; apex of each femur with a pair of lateral shining black spots; coxae pale yellow pilose; femora with very short black

Figs. 1–2. *Molobratria chujoi*, female. 1, Fore basitarsus and apical portion of fore tibia, anterior view; 2, abdomen (including scutellum, postscutellum and halteres), dorsal view.

hairs and short setae; all bristles on tibiae shorter than thicknesses of tibiae; in sigmoid terminal spine of fore tibia, apical black part about 1/2 as long as basal yellowish brown part; relative lengths of segments (excluding coxa and trochanter) of fore leg 205:200:100:35:28:23:30, of mid leg 213:220:65:30:25:23:30, of hind leg 230:233:80:33:?:?:? and in hind leg from the side, relative widths of femur, tibia, and tarsal segments 1-2, 33:30:23:20.

Abdomen (Fig. 2): Yellowish (or reddish) brown; tergum 1, anterior part (before sensory pits) of tergum 2, anterolateral spots on terga 2-6 dark brown to black; sternum 1 and sterna 4-6 (excepting posterior parts) darkened; anterolateral spots on terga 2-3 nearly extending to posterior margin; terga 2-5 with posterolateral yellowish (or pale) gray pollinose spots; dorsum with short recumbent pale yellow pile which becomes longer and bristle-like on sides of tergum 1; venter with recumbent pale yellow pile which is erect on sterna 1-3.

Genitalia: Not examined.

Length: Body 20.1 mm; wing 16.5 mm; fore basitarsus 2.53 mm.

Male. Unknown.

Distribution. Taiwan.

Japanese name: Chûjô-ashinaga-mushihiki.

Holotype: ♀, Sozan, 30. iv. 1933, M. Chûjô.

Holotype is deposited in National Institute of Agro-Environmental Sciences, Tsukuba.

This species is named in honour of Dr. Michio Chûjô, a famous Coleopterist.

Molobratia japonica (Bigot)
(Figs. 3-14)

Dasypogon japonicus Bigot, 1878, Annal. Soc. Entom. France, ser. 5, 8: 411. Type locality: Japan.

Dasypogon takasagense Matsumura, 1916, Thous. Ins. Jap. Addit. 2, p. 322. Type locality: Japan (Takasago, Harima, Honshu). **Syn. n.**

Molobratia japonica Hisamatsu, 1965, Icon. Ins. Jap. Colore Nat. Edita, 3: 202.

One of us (Nagatomi) examined the type (♀) of *takasagense* and no significant difference was found between *takasagense* and *japonica*. Hradský [4] separated *takasagense* from *japonica* by the blackened pattern on abdominal terga 2-7.

However, this character is variable within species and not relied upon.

M. japonica was recorded from Taiwan [21] and Ryukyu Is. [22], but it is highly probable that *chujoi* from Taiwan and *nipponi* from Okinawa I. and Amami Oshima were misidentified as *japonica*.

Among the Japanese species having the yellowish brown legs, *japonica* is characterized as follows: in both sexes, face distinctly wider than in *sapporensis*, and abdominal terga 2-6 without distinct pale yellowish gray pollinose spots at posterolateral corners; posteroventral fin of aedeagal tube bluntly pointed at anterodistal corner, and anterior bar of aedeagus in lateral view wider apically and then narrowed; female sternum 8 with a large bare membranous posterior part.

Male. Head: Dark brown to black, and pale yellowish gray pollinose; antenna (except style) and hypopharynx yellowish brown; palpus, labellum, midventral part of theca, and large part of ocellar triangle shining black; vestiture on head pale yellow but that on ocellar triangle, front opposite ocellar triangle, and antennal segments 2-3 black; in the specimens on hand from Kyushu, vestiture on cerebrale, some strong hairs on upper occiput, hairs on antennal segment 1 and dorso-proximal part of palpus black; width of one eye at greatest point 0.5-0.6 times length (=height) of eye, 1.6-1.9 times width of face at antenna, and 2.0-2.4 times distance from antenna to median ocellus; width of front at median ocellus 0.6-0.8 times width of face at lowest portion from a direct frontal view, 2.0-2.8 times width of ocellar triangle, and 1.1-1.5 times distance from antenna to median ocellus; width of ocellar triangle 0.9-1.0 times its length; distance from antenna to median ocellus 0.3-0.4 times that from antenna to lower margin of eye, which is 1.3-1.5 times length of face (minus clypeus); antenna 0.8-0.9 times length (=height) of eye and 3.0-3.4 times distance from antenna to median ocellus; when measured along midouter surface, relative lengths of antennal segments 1, 2, 3, and style (including spinule) 100: 83(71-91):251(233-273):97(83-108) and their relative widths from the side (except style) 56(50-67):61(57-67):54(43-67); data based on 10 specimens.

Thorax: Dark brown to black, and pale yellowish gray pollinose; humeral and posterior calli and scutellum may be yellowish brown to brown; mesonotum with 3 broad darker stripes, of which median one is separated by mid vitta and the lateral ones may be obscure in demarcation; hairs and bristles on mesonotum and scutellum chiefly or wholly black and those on pleura pale yellow; in the specimens on hand from Kyushu, hairs on anteprenotum black.

Wing: Membrane yellowish brown to brown; veins brown to dark brown; halter yellowish brown to brown.

Legs: Yellowish brown, claw except base black; fore and mid trochanters at ventral apices, and hind trochanter at anterior part, each with a small shining black spot; apex of femur (except ventral part) shining black; coxae pale yellowish gray pollinose and pale yellow pilose; femora with short black hairs which become longer and chiefly pale yellow on ventral surfaces (excepting apical portions); some setae on fore and mid tibiae longer, and all setae on hind tibia not longer than thicknesses of tibiae; in sigmoid terminal spine of fore tibia, apical black part over 1/2 as long as basal yellowish brown part; relative lengths of segments (excluding coxa and trochanter) of fore leg 211(200–221):252(237–288):100:30(28–33):24(21–26):21(19–22):27(26–29), of mid leg 224(216–238):247(235–257):68(65–71):27(26–28):23(21–25):19(18–21):28(26–29), of hind leg 234(223–246):255(238–264):80(77–83):31(27–33):25(22–26):22(21–23):30(28–31), and in hind leg from the side, relative widths of femur, tibia and tarsal segments 1–3, 26(24–28):25(23–28):19(18–21):17(15–19):16(15–18); (N=10).

Abdomen: Yellowish brown, but terga 5–6 shining black, sometimes as well as tergum 7 (except posterior part), anterior border and posterior margin of tergum 4, anterior border of tergum 1 and anterolateral parts of terga 2–3; dorsum with short black hairs which become pale yellow and partly bristle-like on sides of tergum 1 and wholly or partly pale yellow on lateral borders of terga 1–7 and posterior part of tergum 7; venter pale yellow pilose; hairs on genitalia either chiefly pale yellow or chiefly black; hairs on sterna 1–2, sides of terga 1–2 and genitalia longer; anterior

parts of terga 1–6 (which are large on terga 2–3) and posterior parts of sterna 1–6 bare.

Genitalia (Figs. 3–10): In dorsodistal process of gonocoxite, horizontal branch narrower than in *nipponi* at apical portion and without an oblique sclerotized line; in aedeagus, apex of tube curved upward, apical part of posteroventral fin narrower than in *sapporensis*, anterior bar in lateral view wider apically (=anteriorly) and then narrowed and with a darkened inner patch which is longer than wide and rectangular; tube denticulate along lateral margin (except apical portion) and at ventral distal part; in each anterior sclerite of sternum 10, widened part and narrowed process are distinct or abrupt in gradation.

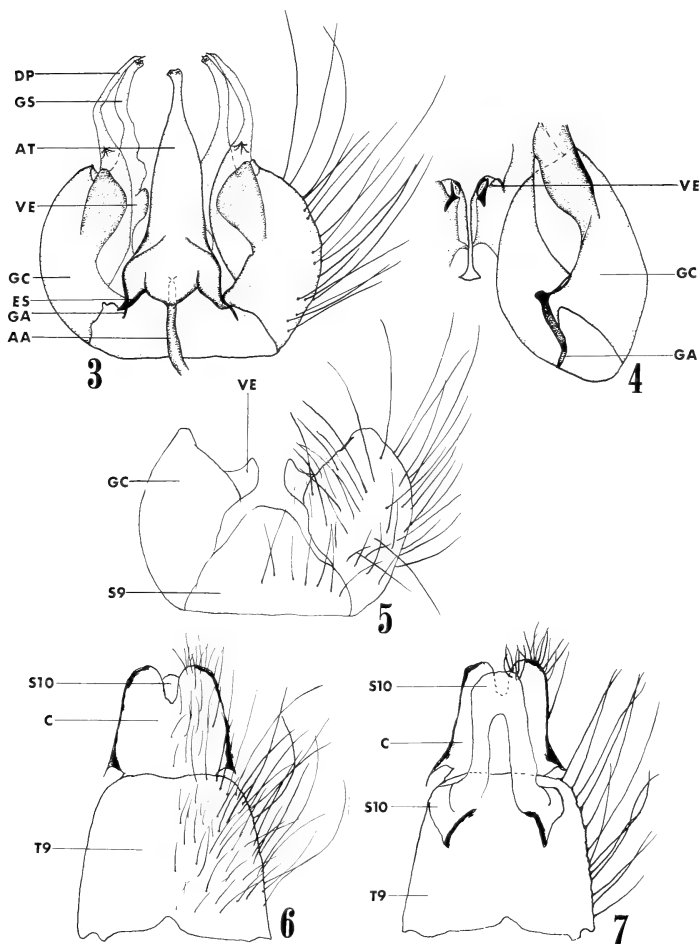
Specimens dissected: 2 ♂♂, Kagoshima City 22 & 27. v. 1961, A. Nagatomi.

Length: Body 19.9–24.4 mm; wing 15.3–19.0 mm; fore basitarsus 2.5–3.2 mm.

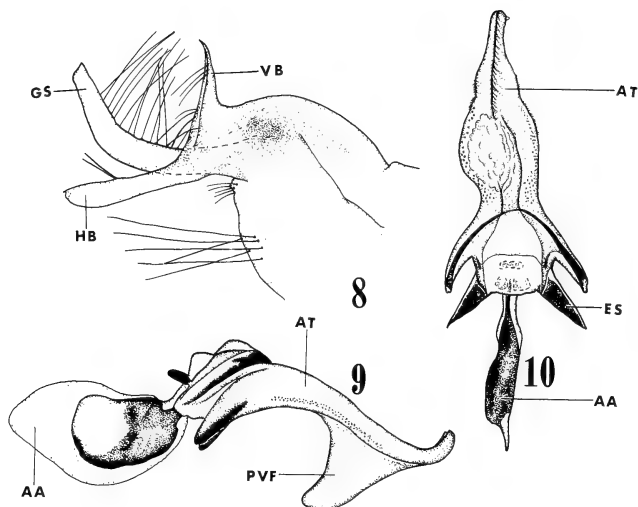
Female. Similar to male except as follows: Head: In some specimens from Kyushu, hairs on antennal segment 1 and on dorsoproximal part of palpus pale yellow as in those from Honshu (this may be so in ♂); no significant structural differences are found between sexes; in 10 specimens measured, width of one eye at greatest point 2.0–2.6 times distance from antenna to median ocellus; width of front at median ocellus 1.2–1.7 times distance from antenna to median ocellus; ocellar triangle 1.0–1.1 times as wide as long; antenna 2.9–3.8 times distance from antenna to median ocellus; when measured along midouter surface, relative lengths of antennal segments 1, 2, 3 and style (including spinule) 100:87(71–100):246(200–283):98(79–140) and their relative widths from the side (except style) 57(43–70):62(57–70):53(43–60).

Legs: Relative lengths of segments of fore leg 210(198–219):245(236–263):100:30(27–33):23(21–25):19(16–21):28(25–30), of mid leg 224(219–233):246(240–256):66(63–68):27(26–28):23(21–24):19(17–21):28(25–30), of hind leg 224(216–231):246(239–256):76(71–80):29(23–31):24(21–26):22(19–23):29(27–31) and in hind leg from the side, relative widths of femur, tibia and tarsal segments 1–3, 27(25–29):26(24–28):20(19–23):18(16–19):17(14–19); (N=10).

Abdomen: Pile on tergum 8 (except sides) may



FIGS. 3-7. Male genitalia of *Molobratria japonica*. 3-4, Dorsal view (in Fig. 4, aedeagus is excluded); 5, ventral view; 6, dorsal view; 7, ventral view. AA, anterior bar of aedeagus; AT, aedeagal tube; C, cercus; DP, dorsodistal process; ES, endophallic sclerite; GA, gonocoxal apodeme; GC, gonocoxite; GS, gonostylus; S9, Sternum 9; S10, sternum 10; T9, tergum 9; VE, inner ventral extension of gonocoxite.



FIGS. 8-10. Parts of male genitalia of *Molobratria japonica*. 8, Gonostylus and dorsodistal process of gonocoxite, outer lateral view; 9-10, aedeagus, lateral and ventral views. AA, anterior bar of aedeagus; AT, aedeagal tube; ES, endophallic sclerite; GS, gonostylus; HB, horizontal branch of dorsodistal process in gonocoxite; PVF, posteroventral fin in aedeagal tube; VB, ventral branch of dorsodistal process in gonocoxite.

be wholly black; pile on cercus pale yellow.

Genitalia (Figs. 11-14): Tergum 8 rather trapezoid, much wider than long, and with anterior margin gently concave; sternum 8 rounded apically and narrower apically than in tergum 8 and with a large bare membranous posterior part.

Specimens dissected: 1♀, Sueyoshi, Kagoshima Pref., 4. v. 1954, S. Taniguchi; 1♀, Iso, Kagoshima City, 27. v. 1961, A. Nagatomi.

Length: Body 19.0-24.5 mm; wing 17.5-20.1 mm; fore basitarsus 2.7-3.4 mm.

Distribution. Japan (Honshu, Shikoku, and Kyushu).

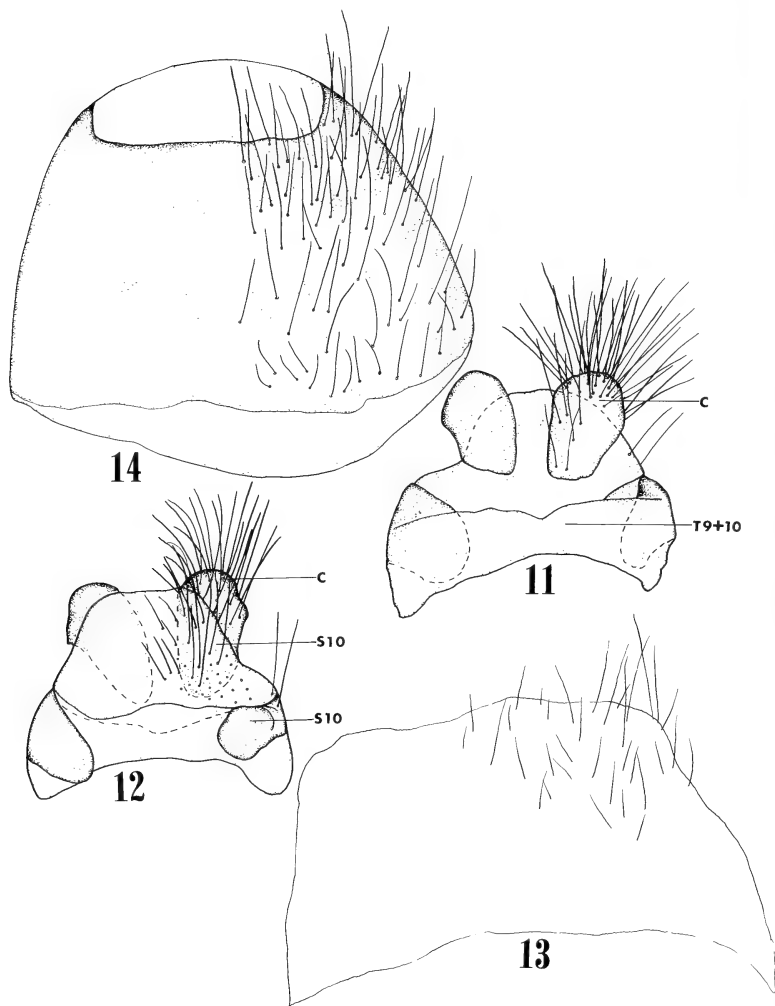
Japanese name: Ashinaga-mushihiki.

Specimens examined (16♂♂, 33♀♀). HONSHU (7♂♂, 12♀♀). Niigata Pref.: 1♂, 1♀, Okutadami, M-Echigo, 25-26. vii. 1955, K. Baba; 1♂, Okutadami, M-Echigo, 26. vii. 1955, Y. Ohmori; 1♀, Nakajo, N-Echigo, 28. vi. 1953, K.

Baba; 1♀, Kurokawa, N-Echigo, 1. vii. 1953, K. Baba; 1♀, Kurokawa, N-Echigo, 11. vi. 1954, K. Baba; 1♀, Kurokawa, N-Echigo, 14. vi. 1956, K. Baba. Tokyo Pref.: 1♀, 23. vi. 1949, Minamitama, N. Fukuhara; 2♂♂, Suginami, 28. v. 1951, N. Fukuhara; 1♀, Minamitama, 17. vi. 1952, I. Hattori; 1♀, 29. v. 1961, J. Minamikawa; 1♀, Kodaira City, 29. v. 1964, J. Minamikawa; 1♀, Takaosan, 5. vii. 1949, I. Hattori. Yamanashi Pref.: 1♀, Kanayama, 30. vi. 1963, A. Nagatomi. Nagano Pref.: 1♂, Kaida-kôgen, 30-31. vii. 1971, A. Nagatomi. Aichi Pref.: Uradani, 14. vi. 1977, K. Ôhara. Hyogo Pref.: 1♀ (type pf *Dasygogon takasagense* Matsumura), Takasago, Harima, S. Matsumura.

SHIKOKU (1♀). Ehime Pref.: 1♀, Matsuyama, 16. v. 1951, T. Shiraki.

KYUSHU (10♂♂, 18♀♀). Kumamoto Pref.: 1♂, 1♀, Gokanoshô, 21. vii. 1968, A. Nagatomi;



FIGS. 11-14. Female terminalia of *Molobratria japonica*. 11-12, Cerci and tergum 9+10, dorsal and ventral views; 13, tergum 8, dorsal view; 14, sternum 8, ventral view. C, cercus; S10, sternum 10; T9+10, tergum 9+10.

1 ♀, Gokanoshō, 20. vii. 1968, R. Ôishi. *Miyazaki Pref.*: 1 ♂, Mt. Wanizuka, 23. v. 1966, A. Tanaka; 1 ♀, Aoidake, 29. v. 1950, S. Kato; 1 ♀, Kuroson-kyo, Ebino City, 18. v. 1976, K. Nicho. *Kagoshima Pref.*: 1 ♀, Mt. Kirishima, 25. v. 1967, A. Tanaka; 1 ♀, Imuta-ike, 16. v. 1965, A. Tanaka; 1 ♀, Akano, Aira-cho, 8. v. 1981, M. Nagayoshi; 1 ♂, Kagoshima City, 22. v. 1961, A. Nagatomi; 1 ♂, 1 ♀, Iso, Kagoshima City, 27. v. 1961, A. Nagatomi; 1 ♀, Iso, Kagoshima City, 4. vi. 1961, A. Nagatomi; 1 ♂, 1 ♀, Iso, Kagoshima City, 19. v. 1963, A. Nagatomi; 2 ♀ ♀, Toso, Kagoshima City, 8. v. 1963, K. Kusigemati; 1 ♂, Toso, Kagoshima City, 16. v. 1963, A. Nagatomi; 1 ♂, Ono-cho, Kagoshima City, 22. iv. 1964, A. Tanaka; 1 ♀, Sueyoshi, Ôsumi, 4. v. 1954, S. Taniguchi; 1 ♂, 1 ♀, Sata, 27–28. iv. 1962, A. Nagatomi; 3 ♀ ♀, Shimadomari, Sata, 1. v. 1966, A. Tanaka; 1 ♂, 1 ♀, Tanegashima, 3–5. v. 1984, S. Yamane; 1 ♂, Tanegashima, 4. v. 1983, K. Tomiyama.

LOCALITY UNKNOWN. 1 ♀, F. Ishitani; 1 ♀, no data.

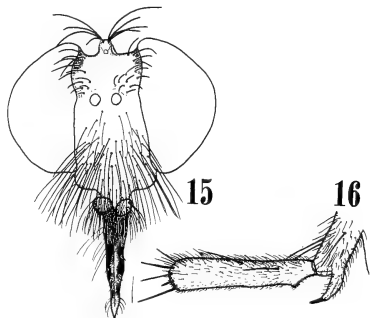
Molobratia kanoi Hradský
(Figs. 15–20, 43)

Molobratia kanoi Hradský, 1980, Trav. Mus. Hist. nat. Gr. Antipa, 22: 453. Type locality: "Meobashi Gummo" (=Maebashi, Gumma Pref., Honshu), Japan.

This species is easily separated from other three Japanese species by having the legs and abdomen entirely dark brown to black and the face wide.

This species is similar to *M. purpuripennis* (Matsumura, 1916) known from Taiwan. Judging from the original description, *purpuripennis* may be distinguished from *kanoi* in the face, cheek, and base of proboscis with pale yellow hairs, legs with white and black hairs, and sides of abdominal dorsum with long white hairs.

Male. Head: Dark brown to black, somewhat velvety; face brownish gray tomentose; labellum shining; vestiture on head wholly black; width of one eye at greatest point 0.5 times length (= height) of eye, equal to width of face at antenna, and 2.5 times distance from antenna to median ocellus; width of front at median ocellus 0.8 times width of face at lowest portion from a direct frontal



FIGS. 15–16. *Molobratia kanoi*. 15, Female head, anterior view; 16, male fore basitarsus and apical portion of fore tibia, anterior view.

view, 3.8 times width of ocellar triangle, and 2.5 times distance from antenna to median ocellus; width of ocellar triangle equal to its length; distance from antenna to median ocellus 0.24 times that from antenna to lower margin of eye, which is 1.3 times length of face (minus clypeus); antenna 0.9 times length (=height) of eye and 4.4 times distance from antenna to median ocellus; when measured along midouter surface, relative lengths of antennal segments 1, 2, 3 and style (including spinule) 100:67:233:42 and their relative widths from the side (except style) 58:50:58.

Thorax: Dark brown to black, somewhat velvety, and more or less brownish gray tomentose; mesonotum with 3 broad stripes where tomentum is denser; median stripe is divided by thin vitta, all hairs or bristles on thorax black; scutellum (on one side) with 3–4 bristles or bristle-like hairs.

Wing: Membrane tinged with dark brown to black; costal cell, subcostal cell, basal portion of marginal cell, etc. may be darker; veins dark brown to black; halter dark brown to black, brownish gray pollinose.

Legs (Fig. 16): Entirely black; pulvilli, empodium, and base of claw yellowish brown; coxae same as pleura and rest of legs with a blue luster; coxae and trochanters with black hairs; each femur

with 3 (or so) dorsal setae near apex and its ventral surface without setae and with black longer bristle-like hairs on basal portion; some bristles on fore and mid tibiae longer than the thicknesses of tibiae as in hind tibia; in sigmoid terminal spine of fore tibia, apical black part roughly 1/2 (0.6 times or so) as long as basal yellowish brown part; relative lengths of segments (excluding coxa and trochanter) of fore leg 207:217:100:40:33:27:30, of mid leg 240:250:77:37:30:27:30, of hind leg 253:267:90:37:33:27:30 and in hind leg from the side, relative widths of femur, tibia, and tarsal segments 1-3, 27:27:23:20:17.

Abdomen: Dark brown to black; dorsum with a blue luster; dorsum with shorter recumbent hairs which become longer on sides of tergum 1; venter with erect hairs which are longer on sternum 1; genitalia with longer erect hairs which become shorter on cerci; all hairs on abdomen black but

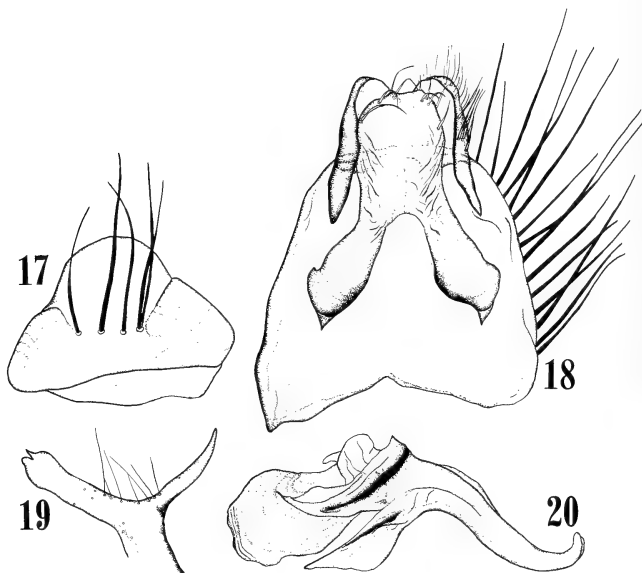
pile on cerci pale.

Genitalia (Figs. 17-20): In dorsodistal process of gonocoxite, apex of horizontal branch with two thicker teeth, of which dorsal one is pointed; sternum 9 with a row of 4 (or 5) bristles in specimen on hand; in aedeagus, apex of tube curved upward, and posteroventral fin entirely absent; apical portion of tube is denticulate on ventral and lateral surfaces, although denticles are minute; anterior bar of aedeagus in lateral view is rather rectangular (except for basal portion) in shape; each cercus apparently separate; in each anterior sclerite of sternum 10, widened part not much inflate outward.

Specimen dissected: 1♂, Mt. Tateshina, Nagano Pref., 23-25. vii. 1947, A. Aoki.

Length: Body 15.1 mm; wing 12.5 mm; fore basitarsus 1.90 mm.

Female. Similar to male except as follows.



FIGS. 17-20. Parts of male genitalia of *Molobrattia kanoi*. 17, Sternum 9, ventral view; 18, cerci, sternum 10 and tergum 9, ventral view; 19, dorsodistal process of gonocoxite, outer lateral view; 20, aedeagus, lateral view.

Head (Fig. 15): Tomentum on face (excepting lower part) pale gray (this may often be so in ♂); no significant structural differences are found between sexes; in 1 specimen measured, front at median ocellus 3.0 times width of ocellar triangle and 2.3 times distance from antenna to median ocellus; antenna 4.15 times distance from antenna to median ocellus; relative lengths of antennal segments 1, 2, 3 and style (including spinule) 100:67:233:50 and their relative widths from the side (except style) 67:50:58.

Legs (Fig. 43): Relative lengths of segments of fore leg 213:213:100:40:33:27:30, of mid leg 233:230:77:37:33:27:30, of hind leg 250:250:87:40:33:27:33 and in hind leg from the side, relative widths of femur, tibia, and tarsal segments 1-3, 30:27:23:20:20.

Genitalia: No significant difference is found between *kanoi* and *sapporensis*.

Specimen dissected: 1♀, Mt. Tateishina, Nagano Pref., 23-25. vii. 1947, A. AOKI.

Length: Body 15.1 mm; wing 13.3 mm; fore basitarsus 1.9 mm.

Distribution. Japan (Honshu).

Japanese name: Kano-ashinaga-mushihiki.

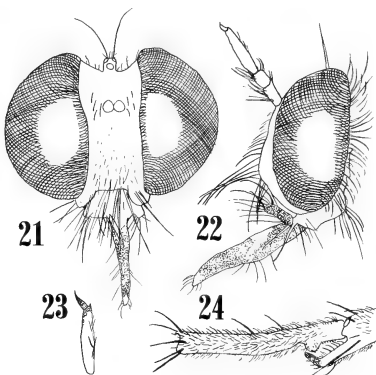
Specimens examined: 1♂, 1♀, Mt. Tateishina (2,000 m), Nagano Pref., 23-25. vii. 1947, A. Aoki.

Molobratria nipponi Hradský

(Figs. 21-32)

Molobratria nipponi Hradský, 1980, Trav. Mus. Hist. nat. Gr. Antipa, 22: 454. Type locality: Mt. Yuwan, Amami Oshima, Japan.

Among the Japanese species having the yellowish brown legs, *nipponi* is characterized as follows: in sigmoid terminal spine of fore tibia, apical black part less than 1/2 as long as basal yellowish brown part; face wider than in *sapporensis*; abdominal terga 2-6 with distinct pale yellowish gray pollinose spots at posterolateral corners (as in *sapporensis*); apex of aedeagal tube not curved upward but directed forward; posteroventral fin of aedeagal tube shorter than in *japonica* and *sapporensis*; anterior bar of aedeagus much wider than in *japonica* and *sapporensis* and somewhat circular; female tergum 8 much longer than in



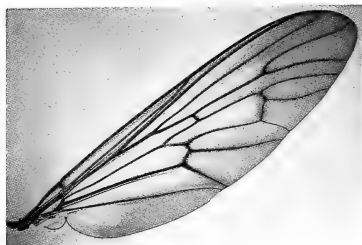
FIGS. 21-24. *Molobratria nipponi*, male. 21-22, Head, anterior and lateral views; 23, antennal segment 3 and style, outer view; 24, fore basitarsus and apical portion of fore tibia, anterior view.

japonica and *sapporensis* and with anterior margin deeply concave.

Male (here described for the first time). Similar to *japonica* except as follows. Head (Figs. 21-23): Often apex of segment 3 darkened (this may be the same in *japonica*); hairs on cerebrale, antennal segment 1, and dorsoproximal part of palpus, and often some strong hairs on upper occiput black (as in the specimens from Kyushu in *japonica*); hairs on face and strong hairs on cerebrale fewer than in *japonica*; width of one eye at greatest point 1.5-1.7 times width of face at antenna (in *japonica*, 1.6-1.9 times); width of front at median ocellus 2.8-3.3 times width of ocellar triangle (in *japonica*, 2.3-2.8 times); when measured along midouter surface, relative lengths of antennal segments 1, 2, 3 and style (including spinule) 100:82(73-89):272(260-300):79(67-89) and their relative widths from the side (except style) 62(55-67):61(55-67):61(50-70); data based on 10 specimens.

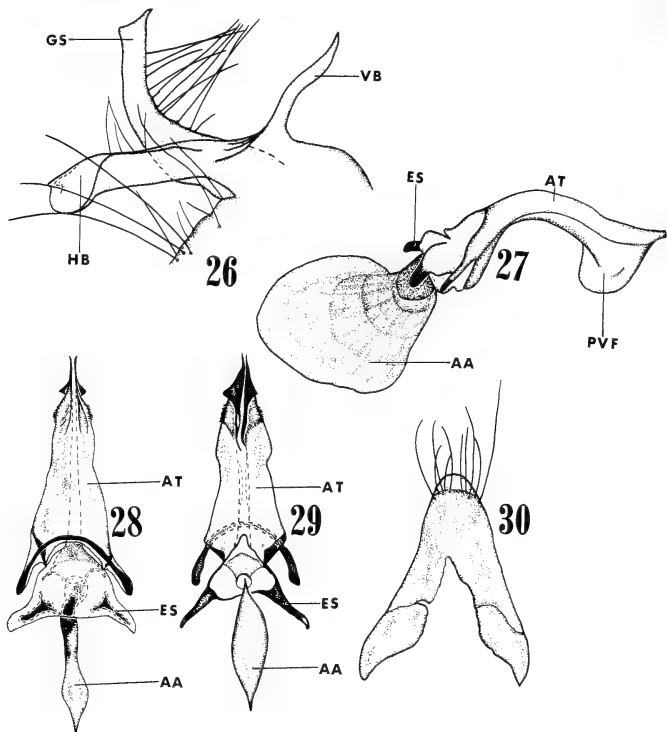
Thorax: Hairs on antepronotum chiefly black.

Wing (Fig. 25): Apical and posterior portions of wing may be more or less darker than rest of

FIG. 25. Male wing of *Molobratria nipponi*.

membrane.

Legs (Fig. 24): Femora have no pale yellow longer hairs; some setae on hind tibia longer than thickness of tibia (as in fore and mid tibiae); in sigmoid terminal spine of fore tibia, apical black part less than 1/2 as long as basal yellowish brown part; relative lengths of segments (excluding coxa and trochanter) of fore leg 193(186-200):205(200-211):100:35(33-37):28(27-29):21(19-23):27(25-29), of mid leg 204(196-211):214(203-222):71(69-74):32(30-33):25(24-27):20(18-22):26(25-27), of hind leg 214(207-221):



FIGS. 26-30. Parts of male genitalia of *Molobratria nipponi*. 26, Gonostylus and dorsodistal process of gonocoxite, outer lateral view; 27-29, aedeagus, lateral, dorsal and ventral views; 30, sternum 10, ventral view. AA, anterior bar of aedeagus; AT, aedeagal tube; ES, endophallic sclerite; GS, gonostylus; HB, horizontal branch of dorsodistal process in gonocoxite; PVF, posteroventral fin in aedeagal tube; VB, ventral branch of dorsodistal process in gonocoxite.

224(213-232) : 79(75-83) : 33(31-34) : 27(25-30) : 22(21-24) : 26(24-29) and in hind leg from the side, relative widths of femur, tibia, and tarsal segments 1-3, 24(22-26) : 22(21-23) : 16(15-17) : 14(13-17) : 13(13-14); (N=9).

Abdomen: Yellowish (or reddish) brown, but anterior borders of terga 4-6 blackened; terga 2-6 with distinct pale yellowish gray pollinose spots at posterolateral corners; hairs on sides of tergum 2 shorter than in *japonica*.

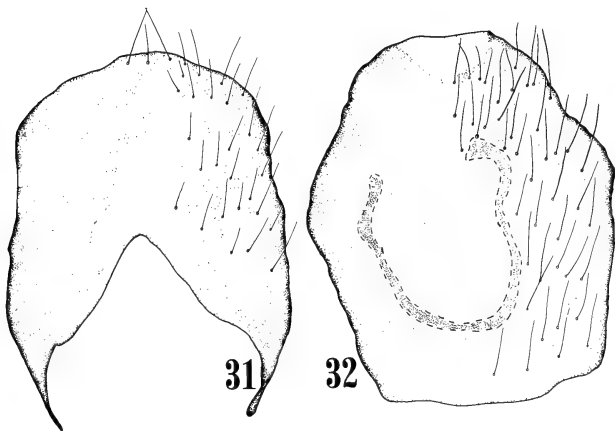
Genitalia (Figs. 26-30): In dorsodistal process of gonocoxite, horizontal branch wider than in *japonica* and *sapporensis* at apical portion and with an oblique sclerotized line; in aedeagus, apex of tube not curved upward but directed forward, posteroventral fin shorter than in *japonica* and *sapporensis* and its apical margin rounded, anterior bar in lateral view much wider than in *japonica* and *sapporensis* and somewhat circular and with darkened patch which is indistinct in demarcation; tube denticulate at ventral surface (except for basal portion) and at antero-[toward base of abdomen] lateral part of ventral fin; in each anterior sclerite of sternum 10, widened part and narrowed part are not abrupt in gradation.

Specimen dissected: 1 ♂, Shinokawa, Amami Oshima, 15. v. 1953, T. Shiraki.

Length: Body 14.0-18.2 mm; wing 12.3-15.2 mm; fore basitarsus 2.3-2.8 mm.

Female. Similar to male except as follows. Head: Hairs on palpus sometimes wholly pale yellow (this may be the same in ♂); no significant structural differences are found between sexes but this species differs from *japonica* as follows: width of one eye at greatest point 1.4-1.6 times width of face at antenna (in *japonica*, 1.6-1.9 times), width of front at median ocellus 2.7-3.3 times width of ocellar triangle (in *japonica*, 2.3-2.8 times) and 1.6-1.8 times distance from antenna to median ocellus (in *japonica*, 1.2-1.7 times); relative lengths of antennal segments 1, 2, 3 and style (including spinule) 100:80(73-83):273(250-300):74(67-80) and their relative thicknesses (except style) 57(50-60):58(50-60):58(50-64); data based on 10 specimens.

Legs: Relative lengths of segments of fore leg 196(190-203) : 208(198-216) : 100 : 35(33-37) : 27(25-30) : 21(19-23) : 27(25-29), of mid leg 207(200-214) : 221(212-228) : 71(68-73) : 31(30-32) : 26(24-28) : 20(18-22) : 27(25-29), of hind leg



FIGS. 31-32. Parts of female terminalia of *Molobratria nipponi*. 31, Tergum 8, dorsal view; 32, sternum 8, ventral view.

214(206–222): 227(217–239): 80(76–83): 33(31–36): 27(25–28): 21(20–22): 28(25–30) and in hind leg from the side, relative widths of femur, tibia, and tarsal segments 1–3, 26(24–28): 23(22–24): 18(16–19): 16(14–17): 15(14–16); (N=10).

Abdomen: Sometimes anterior border of tergum 3 and a band along sensory pits on tergum 2 darkened and sometimes abdomen almost wholly yellowish brown (these may be the same in ♂); pile on tergum 8 and cercus pale yellow.

Genitalia (Figs. 31, 32): Tergum 8 much longer than in *japonica* and *sapporensis* and with anterior margin having a wide and deep concavity; sternum 8 (not flattened out) in ventral view is rather pentagonal, although its narrow posterior margin may be straight; posterior bare membranous part of sternum 8 is much smaller than in *japonica*.

Specimens dissected: 2 ♀♀, Shinokawa, Amami Oshima, 9 & 11. v. 1953, T. Shiraki.

Length: Body 13.6–18.0 mm; wing 12.0–14.7 mm; fore basitarsus 2.1–2.7 mm.

Distribution. Japan (Amami Oshima and Okinawa I.).

Japanese name: Uruma-ashinaga-mushihiiki.

Specimens examined (9 ♂♂, 17 ♀♀): *Amami Oshima* (9 ♂♂, 15 ♀♀): 7 ♂♂, 8 ♀♀, Shinokawa, 9–15. v. 1953, T. Shiraki; 1 ♂, Yuwan, 30. iv. 1953, T. Shiraki; 1 ♀, Yuwan, 8. v. 1953, T. Shiraki; 1 ♂, 2 ♀♀, Naze, 4. v. 1966, K. Kusigemati; 3 ♀♀, 5 & 10. v. 1966, K. Kusigemati; 1 ♀, Asato, 12. vii. 1918, T. Shiraki. *Okinawa I.* (2 ♀♀): 1 ♀, Mt. Yonaha, 8. iv. 1953, T. Shiraki; 1 ♀, Izumi, 29. iv. 1969, S. Yamauchi.

There is 1 ♀ from Okinawa I. (5. v. 1957, T. Takara) whose length is large and 23.4 mm in body, 19.2 mm in wing and 3.5 mm in fore basitarsus. This specimen apparently belongs to *nipponi*.

Molobratia purpuripennis (Matsumura) comb. n.

Dasypogon purpuripennis Matsumura, 1916, Thous. Ins. Jap. Addit. 2, p. 321 & pl. 20, fig. 14. Type locality: Formosa (Horisha).

This species will be redescribed, when new material from Taiwan comes to hand. It is apparently similar to *kanoi* from Japan but may be separated from the latter by having the characters

shown in the key (a) (couplet 2).

The original description by Matsumura is as follows. Male: "Fuscous. Head black pubescent, face with pale yellowish hairs. Proboscis at the extreme apex fulvous, at the base and on the cheeks pale yellowish pubescent, tempora and occiput with black hairs. Antennae black, the first 2 joints with black hairs. Thorax short black pubescent, in the middle with 2 longitudinal grayish stripes, humeri and pleurae grayish yellow pruinose. Wing subhyaline, somewhat infuscated, the second basal cell and the middle part being hyaline, in a certain light reflecting a beautiful purple, veins fuscous. Halteres fuscous, the stems fulvous. Abdomen black, with a purple luster, short black pubescent, on the sides with long white hairs, hypopygium with long black hairs. The upper genital plate of the male on each side inflated in an oval form and each sending backwards a long fuscous hook-like projection, the lower plate broad, nearly quadrate, with fulvous hairs. Legs black, with white and black hairs, tibiae mingling some short fulvous hairs.

Length—22.5 mm, exp. 36 mm.

Hab.—Formosa (Horisha); collected by the author."

Female. Unknown.

Japanese name: Murasaki-ashinaga-mushihiiki.

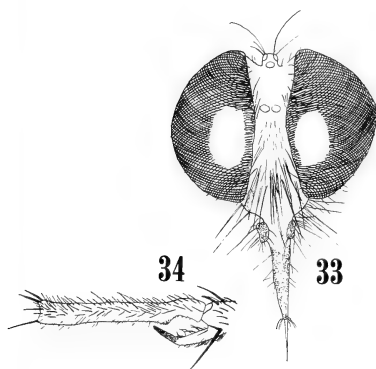
Molobratia sapporensis (Matsumura)

(Figs. 33–41, 44)

Dasypogon sapporensis Matsumura, 1916, Thous. Ins. Jap. Addit. 2, p. 324. Type locality: Japan (Sapporo, Hokkaido).

Molobratia sapporensis Hisamatsu, 1965, Icon. Jap. Col. Nat. Edita. 3: 202.

Among the Japanese species having the yellowish brown legs, *sapporensis* is characterized as follows: in both sexes, face distinctly narrower than in *nipponi* and *japonica*, abdominal tergum 1 shining blue black, abdominal terga 2–6 with distinct pale yellowish gray pollinose spots at postero-lateral corners (as in *nipponi*), and scutellum with no or few hairs; apical part of posteroventral fin in aedeagal tube wider than in *japonica*, and anterior bar of aedeagus without narrowed anterior (= apical) portion (except dorsal corner); bare mem-



Figs. 33-34. *Molobratia sapporensis*, male. 33, Head, anterior view; 34, fore basitarsus and apical portion of fore tibia, anterior view.

braneous posterior part in female sternum 8 small and indistinct.

Male: Similar to *japonica* except as follows: Head (Fig. 33): Apical portion of antennal segment 3 darkened; hairs on antennal segment 1 and cerebrale and some hairs on upper occiput and palpus black in the specimens from Hokkaido and Honshu as well as those from Kyushu; width of one eye at greatest point 2.3-2.8 times width of face at antenna (in *japonica*, 1.6-1.9 times); no significant differences are found in other structural characters between *sapporensis* and *japonica*; in 10 specimens measured, width of one eye at greatest point 1.8-2.6 times distance from antenna to median ocellus; distance from antenna to lower margin of eye 1.5-1.7 times length of face (minus clypeus); antenna 2.7-3.4 times distance from antenna to median ocellus; relative lengths of antennal segments 1, 2, 3 and style (including spinule) 100:79(67-90):248(220-280):96(75-111) and their relative widths from the side (except style) 57(40-67):59(50-67):54(40-67).

Thorax: Humeral and posterior calli and scutellum are the same as rest of thorax in ground colour; *scutellum with no or few hairs*; hairs on antepronotum often black in the specimens from Honshu (this may be so in *japonica*).

Wing: Apical portion and posterior border of wing and apical portions of costal and subcostal cells more or less darker than rest of membrane.

Legs (Fig. 34): Coxae often largely dark brown to black; in the specimens from Kyushu, tarsi and fore tibia (except inner basal portion) darkened; some bristles on hind tibia longer than thickness of tibia (as in fore and mid tibiae); relative lengths of segments (excluding coxa and trochanter) of fore leg 194(188-200):214(209-222):100:31(29-34):24(22-26):19(17-22):25(24-26), of mid leg 211(203-217):220(213-226):68(65-71):27(25-29):23(22-24):19(17-20):25(23-26), of hind leg 217(213-223):225(220-228):76(73-80):29(26-31):24(23-25):20(19-21):26(24-28) and in hind leg from the side, relative widths of femur, tibia, and tarsal segments 1-3, 23(21-26):21(18-23):16(14-20):14(13-17):13(11-15); (N=10).

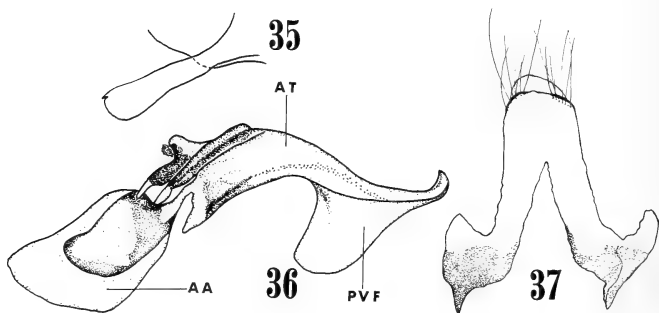
Abdomen: Terga 2-6 with distinct pale yellowish gray pollinose spots at posterolateral corners; tergum 1 shining blue black; in each of terga 2-4, posterior part (except sides) which is variable in extent, and a band along sensory pits shining blue black, as well as anterior border of tergum 2; terga 5-6 (or 5-7) shining blue black as in *japonica*.

Genitalia (Figs. 35-37): In dorsodistal process of gonocoxite, horizontal branch as in *japonica*; in aedeagus, apex of tube curved upward as in *japonica*, apical part of posteroventral fin wider than in *japonica*, anterior bar wider apically (= anteriorly), then not narrowed and with a darker inner patch as in *japonica*; tube denticulate as in *japonica*; in each anterior sclerite of sternum 10, widened part and narrowed process distinct or abrupt in gradation.

Specimens dissected: 1♂, Sasayama, Hyogo Pref., 28. vi. 1963, T. Ishino; 1♂, Kurinodake, Kagoshima Pref., 7. vi. 1963, A. Nagatomi.

Length: Body 14.0-19.8 mm; wing 11.5-15.1 mm; fore basitarsus 2.2-2.9 mm.

Female. Similar to male except as follows. Head: structural differences are not found between sexes; this species differs from *japonica* as follows: width of one eye at greatest point 2.2-2.7 times width of face at antenna (in *japonica*, 1.6-1.9 times); in 10 specimens measured, width of front at median ocellus 1.1-1.4 times distance



FIGS. 35–37. Parts of male genitalia of *Molobratria sapporensis*. 35, Horizontal branch of dorsosidial process in gonocoxite, outer lateral view; 36, aedeagus, lateral view; 37, sternum 10, ventral view. AA, anterior bar of aedeagus; AT, aedeagal tube; PVF, posteroventral fin in aedeagal tube.

from antenna to median ocellus; width of ocellar triangle 0.8–1.0 times its length; distance from antenna to median ocellus 0.3–0.4 times distance from antenna to lower margin of eye; antenna 2.7–3.4 times distance from antenna to median ocellus; relative lengths of antennal segments 1, 2, 3 and style (including spinule) 100:79(67–100):249(217–300):95(73–113) and their relative widths from the side (except style) 59(55–67):61(55–75):55(45–75).

Legs: (Fig. 44): In some specimens from Kyushu, tarsi and hind tibia wholly yellowish brown as in those from Hokkaido and Honshu, in extreme cases; relative lengths of segments of fore leg 196(175–203):216(206–226):100:31(28–33):24(22–26):19(19–20):25(24–27), of mid leg 213(198–225):224(213–235):67(63–70):27(24–29):23(22–24):19(17–20):25(24–28), of hind leg 219(208–229):225(217–238):76(72–80):30(28–31):24(22–26):20(19–22):27(25–28) and in hind leg from the side, relative widths of femur, tibia, and tarsal segments 1–3, 24(22–25):22(19–25):17(14–20):15(14–18):14(11–15); (N=10).

Abdomen: In the specimens from Honshu (probably as well as those from Hokkaido), shining blue black parts of terga 2–4 markedly reduced in extent (bands along sensory pits usually disappear on terga 2–3 or 2–4) and often terga 5–6 largely or partly yellowish brown; pile on tergum

8, cercus and often tergum 7 pale yellow.

Genitalia (Figs. 38–41): Sternum 8 narrower and longer than in *japonica* and its bare membranous posterior part small and indistinct.

Specimens dissected: 1♀, Hataganaru, Ôginosen, Hyogo Pref., 19–23. vii. 1959, A. Nagatomi; 1♀, Suzuka Mountains, Mie Pref., 22. vii. 1962, Z. Yamashita.

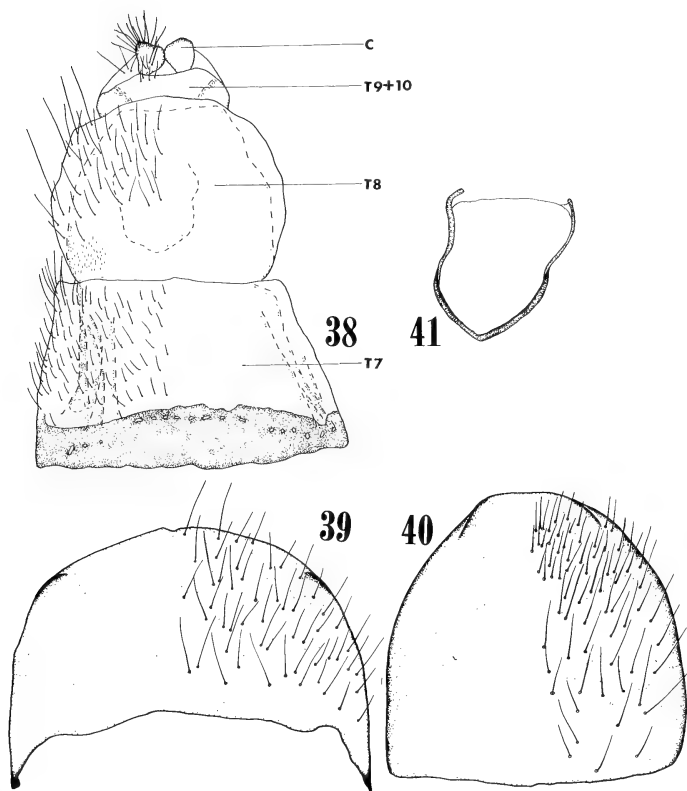
Length: Body 14.9–19.4 mm; wing 12.2–15.7 mm; fore basitarsus 2.2–2.8 mm.

Distribution. Japan (Hokkaido, Honshu, Shikoku and Kyushu).

Japanese name: Sapporo-ashinaga-mushihiki.

Specimens examined (21♂♂, 23♀♀). HOKKAIDO (3♂♂, 1♀). 1♀, Akan, 2. viii. 1939, S. Kinoshita; 2♂♂, Apoi, 27. vi. 1967, K. Kusigemati; 1♀, Touya, 7. vii. 1967, M. Miyazaki.

HONSHU (6♂♂, 17♀♀). Aomori Pref.: 2♀♀, Tsuta-onsen, 6–7. viii. 1953, I. Hattori. Niigata Pref.: 1♂, Yoshigahira, M-Echigo, 3. vii. 1954, Y. Ohmori; 1♀, Kurokawa, N-Echigo, 9. vi. 1955, K. Baba; 1♀, Kurosawadake (1,900 m), S-Echigo, 16. viii. 1967, K. Baba. Tokyo Pref.: 1♀, Hirayama Hill, Minamitama, 6. vii. 1958, I. Hattori. Nagano Pref.: 1♀, Narai, 28. vii. 1969, A. Nagatomi. Ishikawa Pref.: 1♂, Sannomiya, Tsurugi-machi, 4. vi. 1978, I. Togashi; 1♀, Ohsugidani, 29. vi. 1975, I. Togashi. Fukui Pref.: 1♂, Habadaira, Echizen, 16. vii. 1956, K. Iwata. Mie

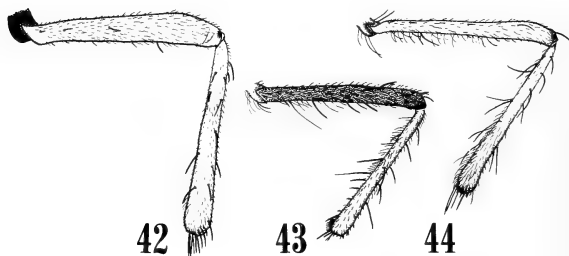


Figs. 38-41. Female terminalia of *Molobratia sapporensis*. 38, Dorsal view; 39, tergum 8, dorsal view; 40, sternum 8, ventral view; 41, genital fork, ventral view. C, cercus; T7, tergum 7; T8, tergum 8; T9+10, tergum 9+10.

Pref.: 1 ♀, Suzuka Mountains, 22. vii. 1962, Z. Yamashita. *Kyoto Pref.*: 1 ♀, Takao, 27. vi. 1955, K. Iwata. *Hyogo Pref.*: 2 ♂♂, Ōginosen, Tazima, 24-26. vii. 1954, F. Gami; 1 ♀, Hataganaru, Ōginosen, Tazima, 19-23. vii. 1959, A. Nagatomi; 1 ♂, Sasayama, Tamba, 28. vi. 1954, T. Ishino; 1 ♀, Sasayama, Tamba, 12. v. 1951, K. Iwata; 1 ♀, Sasayama, Tamba, 8. vii. 1951, K. Iwata; 2 ♀♀,

Sasayama, Tamba, 30. vi. 1953, K. Iwata; 1 ♀, Sasayama, Tamba, 25. vi. 1957, S. Taniguchi. *Shimane Pref.*: 1 ♀, Saigo, Okinoshima, 26. vii. 1966, H. Kadowaki; 1 ♀, Araki, Okinoshima, 12. vii. 1968, H. Kadowaki.

KYUSHU (12 ♂♂, 5 ♀♀). *Fukuoka Pref.*: 1 ♂, Mt. Hiko, 26. vii. 1954, S. Kimoto. *Nagasaki Pref.*: 1 ♂, 1 ♀, Unzen, 27. vi. 1968, T. Shirozu.



FIGS. 42-44. Female hind femur and tibia of *Molobratia* species, anterior view. 42, *M. chujoi*; 43, *M. kanoi*; 44, *M. sapporensis*.

Ōita Pref.: 2 ♀, Tsukumi, 30. v. 1950, A. Nagatomi. *Kumamoto Pref.*: 2 ♂, Gokanoshō, 20. vii. 1966, A. Nagatomi; 2 ♂, Gokanoshō, 20-23. vii. 1966, A. Tanaka. *Kagoshima Pref.*: 1 ♂, 1 ♀, Kurinodake, 7. vi. 1963, A. Nagatomi; 1 ♂, Kurinodake, 16. vii. 1967, A. Tanaka; 1 ♀, Iso, Kagoshima City, 4. vi. 1961, A. Nagatomi; 1 ♂, Kagoshima City, 23. vi. 1961, A. Nagatomi; 1 ♂, Takakuma, Ōsumi, 12. vii. 1960, A. Nagatomi; 2 ♂, Sata, Ōsumi, 24 & 27. v. 1952, H. Hasegawa.

ACKNOWLEDGMENTS

We wish to express our heart-felt thanks to the collectors of the material used in this paper, especially to the late Dr. Tokuchi Shiraki. Our sincere gratitude is also extended to Miss I. Hattori and Mr. N. Fukuhara (National Institute of Agro-Environmental Sciences, Tsukuba) and Dr. K. Kusigemati (Kagoshima University) for their generous aid in various ways.

REFERENCES

- Hull, F. M. (1958) Some species and genera of the family Asilidae (Diptera). *Proc. Ent. Soc. Washington*, **60**: 251-257.
- Bigot, J. M. F. (1878) *Diptères nouveaux ou peu connus*. XV. *Ann. Soc. Ent. de France*, sér. 5, **8**, p. 411.
- Matsumura, S. (1916) *Thousand Insects of Japan*. Additamenta 2. Keiseisha, Tokyo. 474 pp.
- Hradský, M. (1980) Zwei neue Arten der Gattung *Molobratia* Hull, 1962 aus Japan (Diptera, Asilidae). *Trav. Mus. Hist. nat. Gr. Antipa*, **22**: 453-457.
- Iwata, K. and Nagatomi, A. (1962) Prey of some Japanese Asilids (Diptera). *Kontyû*, Tokyo, **30**: 87-100.
- Ionescu, M. A. and Weinberg, M. (1971) *Diptera-Asilidae*. Fauna Republicii Socialiste România. Insecta. Vol. 11, Fascicula 11. Academia Republicii Socialiste România. pp. 1-288. (in Rumanian)
- Weinberg, M. (1977) New data concerning the genus *Molobratia* Hull (Diptera, Asilidae). *Trav. Mus. Hist. nat. Gr. Antipa*, **18**: 261-266.
- Oldroyd, H. (1975) Family Asilidae. In "A catalog of the Diptera of the Oriental Region." Ed. by M. D. Delfinado and D. E. Hardy, vol. II. The University of Hawaii Press, Honolulu, pp. 99-156.
- Hull, F. M. (1962) Robber flies of the world: the genera of the family Asilidae. *Bull. Smithsonian Institution*, **224**: 1-907.
- Theodor, O. (1980) *Diptera: Asilidae*. Fauna Palaestina. Insecta II. The Israel Academy of Sciences and Humanities. Jerusalem. pp. 1-448.
- Papavero, N. (1973) Studies of Asilidae (Diptera) systematics and evolution. I. A preliminary classification in subfamilies. *Arquivos de Zoologia*, **23**: 217-274.
- Papavero, N. (1973) Studies of Asilidae (Diptera) systematics and evolution. II. The tribes of Dasypogoninae. *Arquivos de Zoologia*, **23**: 275-294.
- Theodor, O. (1976) On the structure of the spermathecae and aedeagus in the Asilidae and their importance in the systematics of the family. The Israel Academy of Sciences and Humanities. Jerusalem. pp. 1-175.
- Lehr, P. A. (1988) Family Asilidae. In "Catalogue of Palaearctic Diptera, Vol. 5, Athericidae-Asilidae." Ed. by A. Soós and L. Papp. Akadémiai

- Kiadó, Budapest, pp. 197-326.
- 15 Wood, G. C. (1981) Asilidae. In "Manual of Nearctic Diptera." Vol. 1, Ed. by J. E. McAlpine, B. V. Peterson, G. E. Shewell, H. J. Teskey, J. R. Vockeroth and D. M. Wood, Res. Br., Agric. Can. Monogr., pp. 549-573.
- 16 Engel, E. O. (1930) Asilidae. 24. In "Die Fliegen der palaearktischen Region." Ed. by E. Lindner. E. Schweizerbart'sche Verlagsbuchhandlung, Stuttgart, pp. 1-491.
- 17 Weinberg, M. (1985) *Dasypogon kugleri*, a new species of Asilidae (Diptera) from Yugoslavia. Israel J. Entomol., **19**: 193-196.
- 18 Weinberg, M. (1986) Remarks on genus *Dasypogon* Meigen, 1803 (Diptera, Asilidae), with the description of two new species. Trav. Mus. Hist. nat. Gr. Antipa, **28**: 89-99.
- 19 Weinberg, M. (1987) *Dasypogon gerardi* n. sp. and the designation of the neotype of *Dasypogon diadema* (Fabricius 1781) (Diptera, Asilidae). Trav. Mus. Hist. nat. Gr. Antipa, **29**: 155-164.
- 20 Oldroyd, H. (1969) Diptera Brachycera. Section (a). Tabanoidea and Asiloidea. Handbooks for the identification of British Insects, Vol. 9, Part 4. Royal Entomol. Soc. of London, London, 132 pp.
- 21 Shiraki, T. (1932) Iconographia Insectorum Japonicorum. Hokuryukan, Tokyo. p. 129. (in Japanese)
- 22 Hisamatsu, S. (1965) Iconographia Insectorum Japonicorum Colore Naturali Edit. Vol. 3. Hokuryukan, Tokyo. p. 202. (in Japanese)



Biochemical Systematics of Three Species of the Japanese Long-Tailed Field Mice; *Apodemus speciosus*, *A. giliacus* and *A. argenteus*

MASAKO SAITO¹, NORIMASA MATSUOKA² and YOSHITAKA OBARA

Department of Biology, Faculty of Science, Hirosaki University,
Hirosaki 036, Japan

ABSTRACT—The genetic relationships among two chromosomal races ($2n=48$ and $2n=46$) of *Apodemus speciosus speciosus*, two insular subspecies *A. s. ainu* ($2n=48$) and *A. s. navigator* ($2n=46$), and two related species *A. giliacus* ($2n=48+B's$) and *A. argenteus* ($2n=46$) were examined by electrophoretic analyses of 17 different enzymes. The biochemical dendrogram constructed from the Nei's genetic distances showed the following: (1) Allozymic differentiation between the two chromosomal races was exceedingly low, being equivalent to that observed between local populations of the same species, although they distribute parapatrically with a narrow zone of hybridization. (2) The insular subspecies *A. s. ainu* and *A. s. navigator* have slightly differentiated from *A. s. speciosus* at an allozymic level, and their differentiation has occurred in almost the same divergence time. (3) In a phylogenetic aspect, *A. speciosus* was more closely related to *A. giliacus* than to *A. argenteus*. These findings are well consistent with the karyological relationships among these three *Apodemus* species so far reported. The average value of genetic distances between the two chromosomal races was 0.033, so far as 26 genetic loci were concerned. Such a low genetic distance suggests that the raiation of *Apodemus s. speciosus* has taken place lately in an evolutionary time scale: only some a hundred thousand years ago. The present electrophoretic results strongly support our previous notion that the raiation event of *A. s. speciosus* might have advanced in a stasipatric mode somewhere in a southern part of Japan.

INTRODUCTION

The large Japanese field mouse, *Apodemus speciosus speciosus*, consists of two chromosomal races which have been produced by a Robertsonian chromosome rearrangement [1-5]. They distribute parapatrically, forming a narrow zone of hybridization known as "Toyama-Hamamatsu line" which partitions the field mouse into the northern and southern populations at the middle region of the mainland of Japan, Honshu. This hybrid zone has been reported to be at most 20 km in width [6]. According to Corbet [7], *A. speciosus* is endemic to Japan and classified into eight sub-

species containing the nominate subspecies *A. s. speciosus* and seven insular subspecies. Karyologically, they can be divided into two subgroups: Group I is the $2n=48$ -type which is distributed only in the northward of the hybrid zone including Sado Island, and Group II is the $2n=46$ -type distributing in the southward of the hybrid zone including the neighbouring small islands such as Oki Islands and Tsushima Islands [5]. Karyosystematically, the Honshu population of the northward of the hybrid zone is regarded as a northern race of *A. s. speciosus* or race A, and that of the southward a southern race or race B.

Three possible differentiation processes of the chromosomal races of *A. speciosus* could be proposed as follows: (1) During the glacial period the $2n=48$ -type mice first came into Japan from China through the Korean Peninsula, and thereafter the $2n=46$ -type mice came through the same route [4]. (2) The $2n=48$ -type mice came into Japan

Accepted January 25, 1989

Received October 31, 1988

¹ Present address: Chromosome Research Unit, Faculty of Science, Hokkaido University, Sapporo, Hokkaido 060, Japan.

² To whom reprint requests should be addressed.

through Sakhalin and the $2n=46$ -type ones through the Korean Peninsula, and they contacted at the middle region of Honshu. (3) The $2n=48$ -type mice came into Japan from China through the Korean Peninsula and the $2n=46$ -type mice were newly derived from the former type somewhere in the southern part of Japan, and the latter mice gradually extended their habitat, finally forming the existing pattern of distribution divided by the Toyama-Hamamatsu line [8]. It is self-evident, in the first and second views, that the two types of karyotype had already been differentiated somewhere in the east area of the Eurasian Continent before their migration into Japan. In either case, therefore, the genetic differentiation between the two karyological forms could be expected to be respectable. On the other hand, the third view can be regarded as one of the representative cases of the stasipatric mode of differentiation. If this is the case, the degree of genetic differentiation between the two karyological forms including the insular subspecies should be rather small. For clarifying which of these views is authentic, the biochemical estimation of their genetic distances would be one of the most informative and trustworthy, as described in similar cases of various taxonomic groups of animals [9, 10]. In addition, it would also provide valuable quantitative information on the genetic or evolutionary relationships among three *Apodemus* species distributing in Japan; *A. speciosus*, *A. giliacus* and *A. argenteus*.

With the background mentioned above, we have attempted an electrophoretic study to estimate the degree of the genetic differentiation among two chromosomal races of *A. s. speciosus*, two insular subspecies *A. s. ainu* and *A. s. navigator*, and two related species *A. giliacus* and *A. argenteus*.

MATERIALS AND METHODS

Animals

One hundred seventeen specimens of *Apodemus speciosus*, 3 specimens of *A. giliacus* and 5 specimens of *A. argenteus* were collected at various localities of Honshu, Hokkaido and the neighbouring islands from May, 1984 to March, 1986. Figure 1 shows the collecting localities and population

numbers, of which the populations #1 to #7 correspond to the local populations of *A. s. speciosus* (#1, race A; #2, hybrid zone and #3-7, race B), the populations #8 and #9 to the insular subspecies *A. s. ainu* and *A. s. navigator*, and the populations #10 and #11 to the related species *A. giliacus* and *A. argenteus*, respectively. The collecting localities (the number of specimens examined) of each population were as follows: #1, Zatoh-ishi, Hirosaki (8), Hyakuzawa, Mt. Iwaki (4), Takinosawa, Lake Towada (7) and Mt. Ohdake, Hakkoda (4), Aomori Pref.; #2, Ina (52), Nagano Pref.; #3, Agematsu (11), Nagano Pref.; #4, Nachikatsu-ura (9), Wakayama Pref.; #5, Miyoshi (1), Hiroshima Pref.; #6, Mt. Daisen (3) Tottori Pref.; #7, Shiramine, Ishikawagun (2), Ishikawa Pref.; #8, Rishiri Island (1), Akkeshi (9) and Naganuma, Yuhbarigun (14), Hokkaido; #9, Tohgo, Oki Islands (2), Shimane Pref.; #10, Naganuma, Yuhbarigun (3), Hokkaido; #11, Zatoh-ishi, Hirosaki (2), Aomori Pref.; Shiramine, Ishikawagun (1), Ishikawa Pref. and Nachikatsu-ura (2), Wakayama Pref.

Specimens of the *A. speciosus* complex were identified in principle according to the collecting localities, but those from the hybrid zone by their karyotypes, since three karyological forms (race A, race B and their hybrid) can be found in this area. Chromosome preparation was made according to the protocol described in the previous paper [8]. Table 1 shows the number of specimens of three karyological forms in the populations #2 and #3. Ina (#2) can be regarded as the northern limit of the hybrid zone, and Agematsu (#3) as just the outside of the southern limit based on the composition of three karyological forms in the specimens captured.

Electrophoresis

Liver, skeletal muscle and kidney were cut out from live specimens, and stored at -80°C until being analysed. The procedures for tissue preparation and polyacrylamide gel electrophoresis were almost the same as those described by Matsuoka [11, 12]. Each tissue was individually homogenized in 4 vols of cold 20 mM phosphate buffer (pH 7.0) containing 1 mM EDTA and 0.1 M KCl, using a Potter-Elvehjem glass homogenizer in an

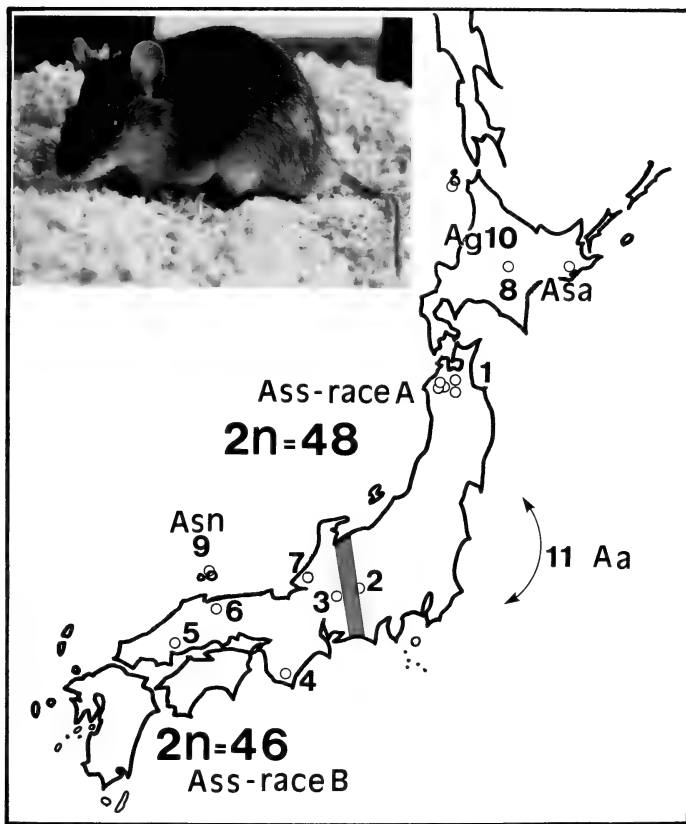


FIG. 1. Collecting localities (#1~#11) of eleven populations of three species of *Apodemus* examined. A thick line of middle Honshu represents a hybrid zone of the races A and B of *A. s. speciosus*. The inset of the upper left is a male race B ($2n=46$) mouse of *Apodemus s. speciosus* Ass: *A. speciosus speciosus*, A5a: *A. speciosus ainu*, Assn: *A. speciosus navigator*, Ag: *A. giliacus*, Aa: *A. argenteus*.

ice-water bath. After centrifugation at $6,100\times g$ for 10 min at 4°C , the clear supernatant was used for electrophoresis. Electrophoresis was carried out on 7.5% polyacrylamide gel [13] using two different types of disc gel apparatuses: $3\times 11\times 75$ mm plastic column and $\phi 7\times 80$ mm glass tube.

After electrophoresis, seventeen enzymes could be detected on the gels in our electrophoretic system. The enzymes assayed in this study, their abbreviations, tissues used, number of loci scored in each enzyme and references for staining methods are listed in Table 2.

TABLE 1. Occurrence frequency of three karyological forms of *A. s. speciosus* in two populations from Nagano Prefecture

Locality	No. of specimens karyotyped			Total
	2n=48	2n=47	2n=46	
#2 (Ina)	29(23)	35(22)	7(7)	71(52)
#3 (Agematsu)			11(11)	11(11)

Numbers in parentheses show the number of specimens used for electrophoretic analysis.

TABLE 2. Enzymes and tissues assayed in the present electrophoretic study

Enzyme	Abbreviation	Tissue	No. of loci scored	Stain reference
α -Glycerophosphate dehydrogenase	α -GPDH	Liver	1	34
Glucose-6-phosphate dehydrogenase	G6PD		1	35
Hexose-6-phosphate dehydrogenase	H6PD		1	36
Nothing dehydrogenase	NDH		1	37
Octanol dehydrogenase	ODH		2	34
6-Phosphogluconate dehydrogenase	6-PGD		1	38
Sorbitol dehydrogenase	SDH		1	38
Superoxide dismutase	SOD		3	34
Xanthine dehydrogenase	XDH		1	38
Malate dehydrogenase	MDH	Kidney	1	38
Malic enzyme	ME		1	34
Fumarase	FUM		1	38
Alkaline phosphate	ALK		1	34
Peroxidase	PO		2	38
Esterase	EST		5	38
Aspartate aminotransferase	AAT	Muscle	1	39
Lactate dehydrogenase	LDH		2	38

RESULTS

The electrophoretic patterns of 17 different enzymes observed in eleven populations from seven taxa of *Apodemus* are diagrammatically shown in Figure 2. From these band patterns, 24–26 genetic loci were obtained in each population. Of them, 15 loci shown in the first and second row of the zymograms: α -GPDH, G6PD, H6PD, SDH, XDH, ALK, ODH-2, EST-1, ME, AAT, LDH-1, LDH-2 and SOD-1~3 were monomorphic in each population. In the course of this study, G6PD and SOD-1 could not be scored in *A. giliacus* and *A. argenteus*. The lack of SOD-1 locus in these species could be assumed as the homozygosity of

null alleles, while in G6PD locus null alleles can not be assumed, judging from the essential physiological function as the key enzyme of the pentose phosphate shunt. Therefore, 25 loci except G6PD were used to compare the *A. speciosus* complex with *A. giliacus* and *A. argenteus*, and 24 loci except G6PD and SOD-1 were used for comparing *A. giliacus* with *A. argenteus*.

The major features of variation in the remaining 11 polymorphic loci (ODH-1, 6-PGD, NDH, MDH, FUM, PO-1, PO-2 and EST-2~5) are summarized as follows: ODH-1 showed single- and triple-banded phenotypes only in *A. s. speciosus*. This variation was interpreted as a diallelic system at a single locus for a dimeric protein, with single-

banded patterns corresponding to the homozygous state and triple-banded patterns to the heterozygous state. In 6-PGD of *A. s. speciosus* and NADP-specific NDH of *A. s. speciosus* and *A. s. ainu*, single- and double-banded phenotypes were observed. This variation was interpreted as a diallelic system at a single locus coding for a monomeric protein. MDH showed double- and triple-banded phenotypes in *A. argenteus*, which were interpreted as representing homozygosity and heterozygosity at a single locus, respectively. On the other hand, the other populations exhibited only a single band of activity having the same mobility. FUM showed single-, double- and triple-banded phenotypes in all the taxa examined, of which all single-banded and one more frequently observed double-banded phenotypes were interpreted as corresponding to the homozygous state, and the other double-banded and triple-banded patterns to the heterozygous state. PO was detected as several bands which were grouped into two zones according to their different staining properties, i.e. the light yellowish brown zone (PO-1) and the dark brown zone (PO-2). PO-1

showed three different band patterns for *A. s. speciosus*, two for *A. s. ainu*, while the other taxa had a single band of activity. Each of these four single band patterns was interpreted as one of the homozygotes of four different alleles. PO-2 showed triple- and fourfold-banded phenotypes in 10 populations except *A. argenteus*, which were interpreted as representing homozygosity and heterozygosity, respectively, while PO-2 of *A. argenteus* showed two sorts of double-banded phenotypes which were interpreted as the homozygosity of different alleles. EST was detected as many bands which were grouped into five zones on the basis of the substrate specificity for α - and β -naphthyl acetate used as the substrate (EST-1~5). EST-1 exhibited a single band of activity showing the same mobility in all the taxa. EST-2 consisted of several bands, which could be interpreted as the products of five different alleles. EST-3 of all taxa and EST-4 of *A. speciosus* complex showed the similar variations to 6-PGD of *A. s. speciosus* and FUM, respectively. EST-4 of *A. giliacus* and *A. argenteus* showed four-fold banded phenotypes having weak activity, and they are assumed to be

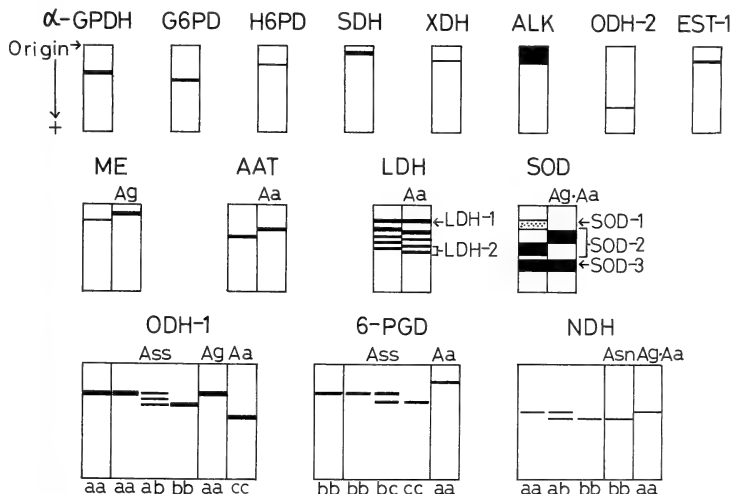


Fig. 2a.

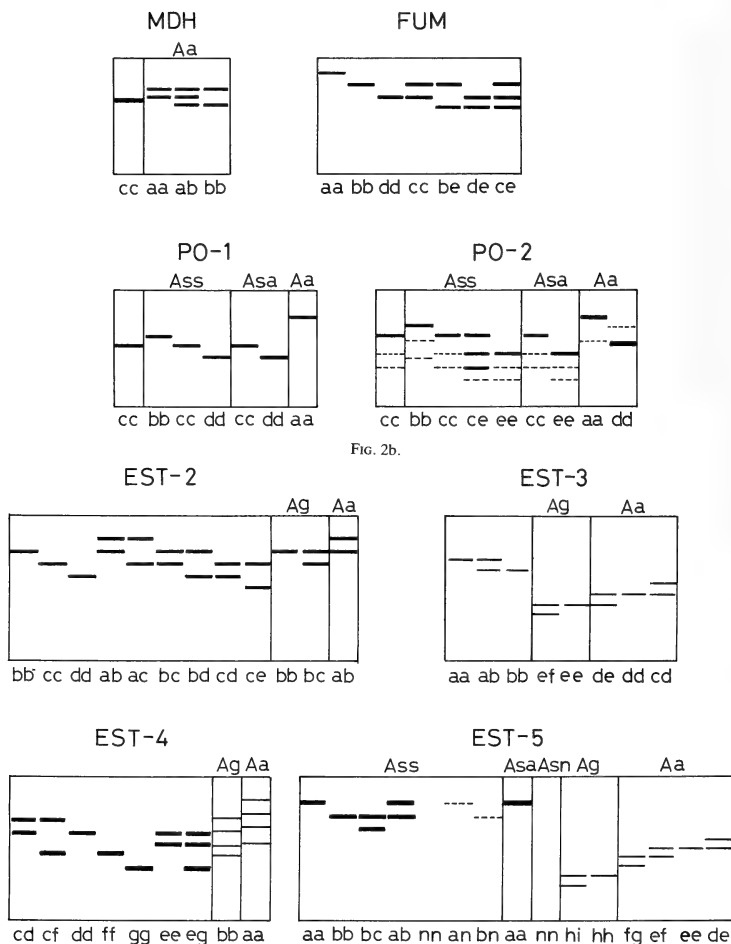


FIG. 2b.

FIG. 2c.

FIG. 2. Electrophoretic patterns of 17 different enzymes in eleven populations of the three species of *Apodemus* examined. The transverse and vertical arrows indicate the origin and direction of mobility, respectively. The genetic loci are numbered downwards from 1, starting with that nearest the origin, i. e., of the lowest mobility. The same abbreviations of the *Apodemus* species as described in Fig. 1 are marked on the top of each banding pattern. No abbreviation represents the taxa other than those marked.

homozygotes of two different alleles. EST-5 was the most active zone of EST. However, the band of EST-5 was not detected in a few specimens. Therefore, several alleles including a null allele were assumed, so that the lack of band was interpreted as homozygosity of null allele and single weak band as heterozygosity with null allele.

The allele frequencies for all loci in 11 populations from three *Apodemus* species are given in

Table 3. As evident from this table, the seven populations of *A. s. speciosus* (#1~#7) shared the same alleles in each locus and the diagnostic locus distinguishing the two chromosomal races could not be obtained. There was no diagnostic locus also in *A. s. speciosus*, *A. s. ainu* and *A. s. navigator*. Only one remarkable property common to the two insular subspecies was observed in EST-5. Although the locus was highly polymor-

TABLE 3. Allele frequencies at 26 genetic loci in eleven populations of the three species of *Apodemus*

Locus	Allele [†]	race A	Hybrid zone	race B					Asa	Asn	Ag	Aa
		#1	#2	#3	#4	#5	#6	#7	#8	#9	#10	#11
<i>α</i> -GPDH	a	1.00	1.00	1.00	1.00	1.00	1.00	1.00	1.00	1.00	1.00	1.00
G6PD	a	1.00	1.00	1.00	1.00	1.00	1.00	1.00	1.00	1.00	NS	NS
H6PD	a	1.00	1.00	1.00	1.00	1.00	1.00	1.00	1.00	1.00	1.00	1.00
LDH-1	a	1.00	1.00	1.00	1.00	1.00	1.00	1.00	1.00	1.00	1.00	1.00
LDH-2	a	1.00	1.00	1.00	1.00	1.00	1.00	1.00	1.00	1.00	1.00	—
	b	—	—	—	—	—	—	—	—	—	—	1.00
MDH	a	—	—	—	—	—	—	—	—	—	—	0.70
	b	—	—	—	—	—	—	—	—	—	—	0.30
	c	1.00	1.00	1.00	1.00	1.00	1.00	1.00	1.00	1.00	1.00	—
NDH	a	0.63	0.62	0.55	0.61	0.50	0.50	1.00	0.25	—	1.00	1.00
	b	0.37	0.38	0.45	0.39	0.50	0.50	—	0.75	1.00	—	—
ODH-1	a	1.00	0.97	1.00	1.00	1.00	1.00	1.00	1.00	1.00	1.00	—
	b	—	0.03	—	—	—	—	—	—	—	—	—
	c	—	—	—	—	—	—	—	—	—	—	1.00
ODH-2	a	1.00	1.00	1.00	1.00	1.00	1.00	1.00	1.00	1.00	1.00	1.00
6-PGD	a	—	—	—	—	—	—	—	—	—	—	1.00
	b	0.91	0.87	1.00	1.00	1.00	1.00	1.00	1.00	1.00	1.00	—
	c	0.09	0.13	—	—	—	—	—	—	—	—	—
SDH	a	1.00	1.00	1.00	1.00	1.00	1.00	1.00	1.00	1.00	1.00	1.00
XDH	a	1.00	1.00	1.00	1.00	1.00	1.00	1.00	1.00	1.00	1.00	1.00
ALK	a	1.00	1.00	1.00	1.00	1.00	1.00	1.00	1.00	1.00	1.00	1.00
AAT	a	—	—	—	—	—	—	—	—	—	—	1.00
	b	1.00	1.00	1.00	1.00	1.00	1.00	1.00	1.00	1.00	1.00	—
FUM	a	—	—	—	—	—	0.67	—	—	—	—	—
	b	0.63	0.49	1.00	1.00	1.00	0.33	0.75	0.93	—	0.67	—
	c	0.35	0.14	—	—	—	—	—	0.07	0.75	0.33	—
	d	—	0.36	—	—	—	—	—	—	—	—	1.00
	e	0.02	0.01	—	—	—	—	0.25	—	0.25	—	—
ME	a	—	—	—	—	—	—	—	—	—	1.00	—
	b	1.00	1.00	1.00	1.00	1.00	1.00	1.00	1.00	1.00	—	1.00
PO-1	a	—	—	—	—	—	—	—	—	—	—	1.00
	b	—	—	0.09	—	—	—	—	—	—	—	—
	c	0.96	1.00	0.91	1.00	1.00	1.00	1.00	0.93	1.00	1.00	—
	d	0.04	—	—	—	—	—	—	0.07	—	—	—
PO-2	a	—	—	—	—	—	—	—	—	—	—	0.80
	b	—	—	0.09	—	—	—	—	—	—	—	—
	c	0.96	0.96	0.91	1.00	1.00	1.00	1.00	0.93	1.00	1.00	—
	d	—	—	—	—	—	—	—	—	—	—	0.20
	e	0.04	0.04	—	—	—	—	—	0.07	—	—	—

TABLE 3. Continued

Locus	Allele [†]	race A		Hybrid zone		race B					Asa	Asn	Ag	Aa
		#1	#2	#3	#4	#5	#6	#7	#8	#9	#10	#11		
SOD-1	n	—	—	—	—	—	—	—	—	—	1.00	—	—	—
	a	1.00	1.00	1.00	1.00	1.00	1.00	1.00	1.00	1.00	—	—	—	—
SOD-2	a	—	—	—	—	—	—	—	—	—	1.00	—	—	—
	b	1.00	1.00	1.00	1.00	1.00	1.00	1.00	1.00	1.00	—	—	—	—
SOD-3	a	1.00	1.00	1.00	1.00	1.00	1.00	1.00	1.00	1.00	1.00	1.00	1.00	1.00
EST-1	a	1.00	1.00	1.00	1.00	1.00	1.00	1.00	1.00	1.00	1.00	1.00	1.00	1.00
EST-2	a	0.02	0.03	—	—	—	—	—	0.04	—	—	—	—	0.50
	b	0.24	0.19	0.18	0.28	—	0.50	—	0.39	0.50	0.67	—	—	0.50
	c	0.67	0.61	0.73	0.72	1.00	0.50	1.00	0.21	0.25	0.33	—	—	—
	d	0.07	0.16	0.09	—	—	—	—	0.26	0.25	—	—	—	—
	e	—	0.01	—	—	—	—	—	—	—	—	—	—	—
EST-3	a	0.07	0.07	0.09	0.11	0.50	—	—	0.04	—	—	—	—	—
	b	0.93	0.93	0.91	0.89	0.50	1.00	1.00	0.96	1.00	—	—	—	—
	c	—	—	—	—	—	—	—	—	—	—	—	—	0.10
	d	—	—	—	—	—	—	—	—	—	—	—	—	0.80
	e	—	—	—	—	—	—	—	—	—	0.83	0.10	—	—
	f	—	—	—	—	—	—	—	—	—	0.17	—	—	—
EST-4	a	—	—	—	—	—	—	—	—	—	—	—	—	1.00
	b	—	—	—	—	—	—	—	—	—	1.00	—	—	—
	c	—	0.06	0.09	—	—	0.17	—	—	—	—	—	—	—
	d	—	0.09	0.18	0.11	—	—	—	0.07	—	—	—	—	—
	e	0.61	0.29	—	—	—	—	—	0.86	—	—	—	—	—
	f	0.35	0.50	0.73	0.89	1.00	0.83	0.50	0.07	0.75	—	—	—	—
	g	0.04	0.06	—	—	—	—	0.50	—	0.25	—	—	—	—
EST-5	n	0.48	0.37	0.18	0.11	1.00	0.67	—	—	1.00	—	—	—	—
	a	0.43	0.45	0.23	0.78	—	0.33	0.50	1.00	—	—	—	—	—
	b	0.09	0.16	0.59	0.11	—	—	0.50	—	—	—	—	—	—
	c	—	0.02	—	—	—	—	—	—	—	—	—	—	—
	d	—	—	—	—	—	—	—	—	—	—	—	—	0.10
	e	—	—	—	—	—	—	—	—	—	—	—	—	0.50
	f	—	—	—	—	—	—	—	—	—	—	—	—	0.30
	g	—	—	—	—	—	—	—	—	—	—	—	—	0.10
	h	—	—	—	—	—	—	—	—	—	0.67	—	—	—
	i	—	—	—	—	—	—	—	—	—	0.33	—	—	—

[†] Alleles are correspondingly lettered from "a", this being the allele of the lowest mobility.

NS: Not scored.

"n" represents null allele.

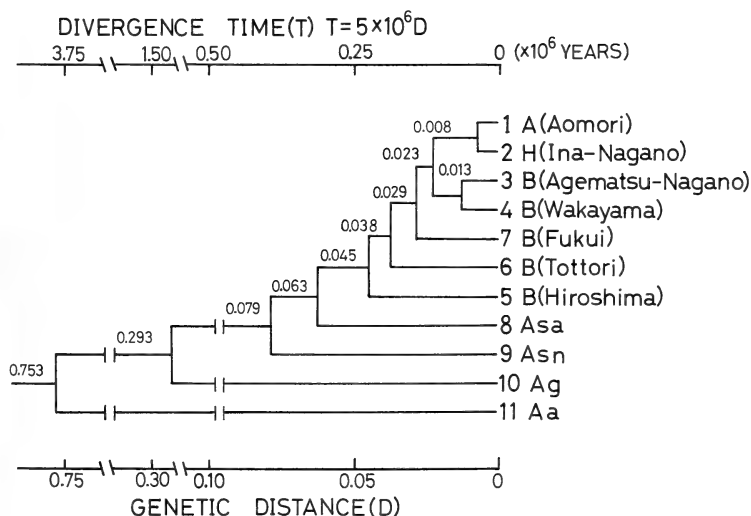
phic in *A. s. speciosus*, it was monomorphic in *A. s. ainu* and *A. s. navigator*, which showed only a single electromorph in all specimens. Interspecific comparison revealed that *A. speciosus* differed from *A. giliacus* in 5 loci (ME, SOD-2 and EST-3~5), while *A. speciosus* differed from *A. argenteus* in 11 loci (LDH-2, MDH, ODH-1, 6-PGD, AAT, PO-1, PO-2, SOD-2 and EST-3~5). Therefore, the four loci (SOD-2 and EST-3~5) were diagnostic, making distinction between *A. speciosus* and the other two *Apodemus* species possible.

We could not find the different pattern of allozymes in either of the two chromosomal races of *A. s. speciosus* and also in the insular subspecies.

Therefore, their genetic differences can be shown only by the slight differences of allele frequencies. Based on the allele frequencies data shown in Table 3, the genetic identity (I) and the genetic distance (D) between each population were calculated by the method of Nei [14]. Table 4 represents the matrices of I and D values between all pairs of 11 populations from the seven taxa of *Apodemus* examined. Figure 3 shows the biochemical dendrogram constructed from the genetic distance (D-value) matrix of Table 4, using the unweighted pair-group arithmetic average (UP-GMA) clustering method of Sneath and Sokal [15].

TABLE 4. Genetic identities (above diagonal) and genetic distances (below diagonal) among eleven populations of the three species of *Apodemus*

	race A		Hybrid zone					race B				Asa	Asn	Ag	Aa
	#1	#2	#3	#4	#5	#6	#7	#8	#9	#10	#11				
#1 <i>Ass</i> (Aomori)	—	.992	.973	.974	.957	.968	.965	.968	.943	.764	.479				
#2 <i>Ass</i> (Ina, Nagano)	.008	—	.980	.981	.959	.975	.972	.961	.944	.760	.499				
#3 <i>Ass</i> (Agematsu, Nagano)	.027	.020	—	.987	.966	.963	.976	.942	.921	.755	.468				
#4 <i>Ass</i> (Wakayama)	.026	.019	.013	—	.961	.967	.974	.955	.914	.756	.465				
#5 <i>Ass</i> (Hiroshima)	.044	.042	.035	.040	—	.956	.937	.897	.927	.738	.449				
#6 <i>Ass</i> (Tottori)	.033	.025	.038	.034	.045	—	.942	.928	.956	.744	.471				
#7 <i>Ass</i> (Fukui)	.036	.028	.024	.026	.065	.060	—	.922	.886	.758	.474				
#8 <i>Asa</i>	.033	.040	.060	.046	.109	.075	.081	—	.901	.732	.454				
#9 <i>Asn</i>	.059	.058	.082	.090	.076	.045	.121	.104	—	.708	.441				
#10 <i>Ag</i>	.269	.274	.281	.280	.304	.296	.277	.312	.345	—	.517				
#11 <i>Aa</i>	.736	.695	.759	.766	.801	.753	.747	.790	.819	.660	—				

FIG. 3. A biochemical dendrogram showing the genetic relationships among eleven populations from seven taxa of three species of *Apodemus*, based on the Nei's genetic distances. A: pure race A population, B: pure race B population, H: mixed population of the race A, race B and their hybrids, others: the same as in Fig. 1.

As evident from Table 4, little differentiation is observed among seven local populations of *A. s. speciosus* (#1~#7) at a protein level. The genetic identity values (I) observed between them are a mean of 0.968 in a range of 0.937~0.992. Further, the difference of I-values between the three subspecies analyzed is also considerably small. The average I-value between *A. s. speciosus* and *A. s. ainu* is 0.939 in a range of 0.897~0.968, while that between *A. s. speciosus* and *A. s. navigator* 0.927 in a range of 0.886~0.956. The range of the intersubspecific I-values obtained overlapped with that of the interpopulational I-values of *A. s. speciosus* in the half of them. Moreover, *A. s. ainu* and *A. s. navigator* are more closely related to the local population of *A. s. speciosus* from Aomori Prefecture (#1) and that from Tottori Prefecture (#6) than to the other local populations, respectively. This finding is in good agreement with their geographic localities shown in Figure 1. Therefore, from a biochemical viewpoint the two insular subspecies analyzed may be considered to be the conspecific local populations of *A. s. speciosus*. On the other hand, the genetic identities between *A. argenteus* and two other species are low (the mean I-values are 0.467 and 0.517, respectively), as compared with the relatively high I-values between *A. giliacus* and the *A. speciosus* complex (the mean I-value is 0.746).

The proportion of polymorphic loci (P) was in a range of 8~35%, the expected average heterozygosity per locus (H_{exp}) was in a range of 4~13% and the observed average heterozygosity per locus (H_{obs}) was in a range of 2~12%. The average heterozygosity of rodents has been reported to be a mean of 5.6% in a range of 1~9% [16]. So, our estimation was not so far from the value mentioned above. The proportion of the polymorphic loci obtained here was also comparable to the values of many other taxonomic groups of animals [17, 18].

DISCUSSION

Interracial and interpopulational relationships of A. s. speciosus

As clearly shown in Figure 3, the D-value be-

tween the race A (Aomori population: #1) and the mixed population of the race A, race B and hybrid form (Ina population: #2) is the smallest ($D=0.008$), although their interval is more than 1,000 km, and the Ina population is more closely related to the Aomori population than to the Agematsu population (#3) which is only 20 km away from Ina locating just on the northern limit of the hybrid zone. This fact may reflect that the mixed population of three karyological forms from the northern limit of the hybrid zone is under the genic influence of the race A to a certain degree. As a whole, *A. s. speciosus* showed a clinal pattern of genetic differentiation varying from north to south.

The interracial D-values were unexpectedly low, being 0.033 on the average in a range of 0.026~0.044. According to Selander *et al.* [19], the interracial D-values for rodents are in a range of 0.010~0.025. Accordingly, it may be reasonable to consider the two karyological forms of *A. s. speciosus* to be in the race level. Applying the Nei's equation of divergence time [20] to the biochemical dendrogram (Figure 3), the raiation of *A. s. speciosus* took place only some a hundred thousand years ago. Thus, the two races of *A. s. speciosus* can be distinguished from each other only by their chromosome constitution, but not by their allozymes and/or their phenetic morphology. In spite of such a high genetic similarity the two races are strictly keeping their own habitat, suggesting some action of a certain kind of isolation mechanism for maintaining their parapatric distribution. The most plausible explanation for this view would be a post-mating isolation mechanism, to which we have referred in the previous paper [21]: the rate of nondisjunction caused by the misdivision during meiotic anaphase I amounts to approximately 28% in the interracial male hybrids, and this unusually high rate of meiotic drive necessarily causes the interracial hybrids to reduce their litter size up to almost three-fourths of that in the homozygotes. Taking these findings into account, the chromosomal races of *A. s. speciosus* may be just on the way to speciation into distinct species or subspecies in spite of a low level of genetic differentiation. Similar mode of speciation has also been proposed to account for the differentiation of

the chromosomal races characterized by different chromosome numbers in two rodent groups: the mole rats of the *Spalax ehrenbergi* complex in Israel and the pocket gophers of the *Thomomys talpoides* complex in the southern Rockies of the United States [22, 23].

Intersubspecific relationships of A. speciosus

According to Britton and Thaler [24], the inter-populational and intersubspecific D-values of *Mus musculus* are 0.013 and 0.220, respectively. The average D-values between *A. s. speciosus* and *A. s. ainu* and that between *A. s. speciosus* and *A. s. navigator* were 0.063 and 0.076 respectively (Table 4). These values are rather equivalent to those between conspecific local populations of *Mus musculus* described above and of many other animal species previously reported [9, 10]. So these three subspecies have undergone little change at a structural gene level. Accordingly, both *A. s. ainu* and *A. s. navigator* can be considered to be still in the level of just local populations of *A. s. speciosus* from genetic and/or biochemical viewpoints. Since the subspecies *A. s. ainu* well corresponds in the karyotype to the race A, and the insular subspecies *A. s. navigator* to the race B, it seems most likely that *A. s. ainu* and *A. s. navigator* might have been derived, without significant genetic differentiation, from the northern and southern local populations of *A. speciosus*, respectively. This suggestion may be supported by the present electrophoretic data indicating that *A. s. ainu* and *A. s. navigator* are more closely related to the local population of *A. s. speciosus* from Aomori Prefecture (#1) and that from Tottori Prefecture (#6) than to the other local populations in their genetic distances, respectively (Table 3). These results may indicate that the Robertsonian rearrangement had already spread far and wide into the southern Honshu population of *A. s. speciosus* prior to its migration into Oki Islands. It is self-evident from the biochemical dendrogram (Figure 3) that the insular subspecies *A. s. ainu* and *A. s. navigator* have differentiated to a certain degree from their nominate subspecies *A. s. speciosus* distributing in the main land of Japan, Honshu, at an allozymic level, although their genetic distances are small.

Interspecific relationships of three Apodemus species

The field mouse *A. giliacus* was newly set up by Kobayashi and Hayata [25] as a distinct species distributing in Hokkaido. This species is characterized by varying number of B-chromosomes [26, 27]. However, the chromosomes of *A. giliacus* ($2n=48+B's$, $NF=48$) are highly homologous in their G-banding pattern to the race A of *A. s. speciosus* ($2n=48$, $NF=56$), excluding the B chromosomes and the sex chromosomes. Taking four pericentric inversions into consideration, their chromosomes mostly correspond to each other, whereas *A. argenteus* ($2n=46$, $FN=52$) chromosomes do not show such a high degree of G-band homology to those of *A. giliacus* as well as to those of *A. speciosus* (unpublished data). Therefore, their genetic relationships (Figure 2) revealed by the present electrophoretic study are well consistent with their karyological relationships. The average D-value 0.293 between *A. speciosus* and *A. giliacus* can be regarded as that of the subspecies or closely related species level of differentiation, when compared with the D-values of the various animal groups already reported [28]. Tsuchiya [29] treated *A. giliacus* as a subspecies of the Korean field mouse *A. peninsulae*, i.e., *A. peninsulae*, *giliacus*, and recently he and his colleagues [30] reported, based on the mtDNA, rDNA and isozyme analyses, that *A. giliacus* may be a synonym of *A. peninsulae*, as Corbet [7] regarded *A. giliacus* as a synonym (or a subspecies) of *A. peninsulae* which is also characterized by the polymorphic B-chromosomes [31, 32]. But, Kuznetsov [33] considered both of them to be races of *A. speciosus*. According to Bekasova *et al.* [31] *A. peninsulae* is closely related to the large Japanese field mouse *A. speciosus*, being included into the subgenus *Alsomys* together with *A. speciosus*. Thus, the taxonomic allocation of *A. giliacus* is still a subject of controversy. The low D-value between *A. speciosus* and *A. giliacus* may also indicate a relatively close relationship between *A. speciosus* and *A. peninsulae*. The small Japanese field mouse *A. argenteus*, on the other hand, differs considerably in morphology from *A. speciosus* and also from *A. giliacus*, although these

three species belong to the same subgenus *Alsomys* [31]. These biochemical and phenetic relationships are also well consistent with the karyological results already mentioned. The average D-value 0.753 between *A. argenteus* and the lineage of *speciosus-giliacus* is comparable to the values observed between different species or closely related genera of many other animals [28], and therefore the present results may suggest that *A.*

argenteus may be remote to some extent in its affinity from the lineage of *speciosus-giliacus*.

The outline of these consideration is simply depicted as a schematic diagram in Figure 4. The diagram shows the stasipatric mode of differentiation of *A. s. speciosus* which can be considered to have been derived from the ancestral form common to *A. agrarius*, since the latter is the only species in Eurasian Continent which shows the

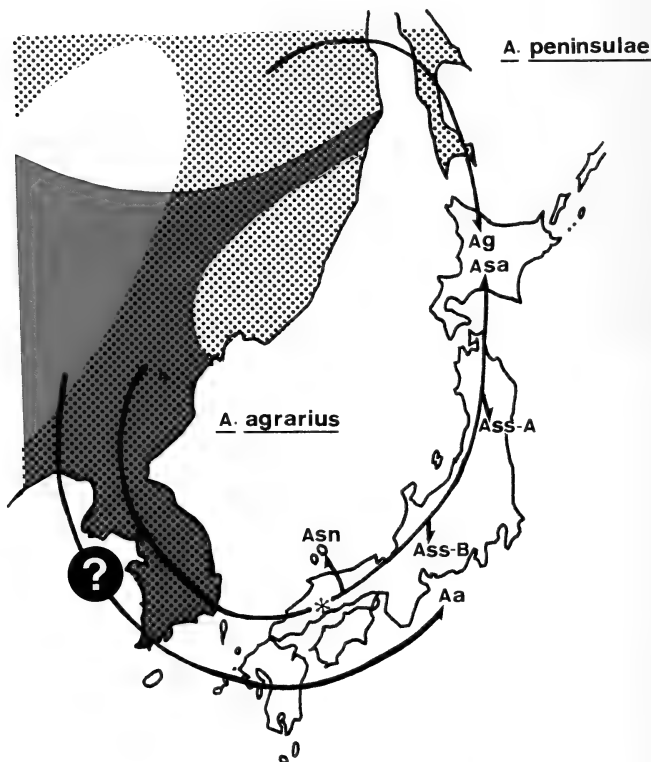


FIG. 4. Probable migration routes of three *Apodemus* species into Japan. Asterisk indicates the generation of a Robertsonian fusion rearrangement somewhere in the southern part of Japan. The shaded part in the continental side represents the distribution area of *A. agrarius* and dotted one that of *A. peninsulae*.

karyotype almost identical to that of the former (race A), and what is more it is distributed in Far East including Korean Peninsula [8]: the chromosomal variants ($2n=46$) of the ancestral form caused by the Robertsonian fusion rearrangement arised somewhere in the south part of Japan, and these variants have been established as a southern race after the acquirement of some advantages overwhelming the parental $2n=48$ -type mice. The insular subspecies *A. s. navigator* might have diverged from a local population of *A. speciosus* in which the Robertsonian rearrangement had already spread far and wide, and the other insular subspecies *A. s. ainu* might have maintained the $2n=48$ karyotype of *A. speciosus* without any chromosome alteration. It is quite confirmative, based on their distribution area and B-chromosome characteristics, that *A. giliacus* has a very close affinity with the Korean field mouse *A. peninsulae*, and its ancestral population has migrated through Sakhalin into Hokkaido and diverged there as a new form, *A. giliacus* according to Kobayashi and Hayata [25] or *A. peninsulae giliacus* according to Corbet [7] and Tsuchiya [29].

The ancestral form of *A. argenteus* can not be inferred from the karyological characteristics, as the karyotype of *A. argenteus* is largely different from any of the *Apodemus* species distributing in the Eurasian Continent. The detailed chromosome banding analysis and the comparative biochemical surveys would be needed for elucidation of this subject.

The comparative electrophoretic study of the Japanese *Apodemus* and the continental *Apodemus* such as *A. agrarius*, *A. peninsulae*, *A. sylvaticus* and *A. chevrieri*, which are distributed in Far East including East Siberia, Korean Peninsula and North East China, would be required to elucidate the speciation process of the *Apodemus* group of Japan.

ACKNOWLEDGMENTS

The authors wish to express their gratitude to Professor Kazuo Saitoh, Department of Biology, Faculty of Science, Hirosaki University, for his valuable suggestions and encouragement throughout this work, and for critical reading of the manuscript. Our thanks are also due to Professor Masaki Takahashi, Marine Biomedical Insti-

tute, Sapporo Medical College, Rishiri Island, Hokkaido, Dr. Nobuhiro Takada, Fukui Medical College, Fukui, Dr. Ikuro Miura, Laboratory for Amphibian Biology, Hiroshima University, Hiroshima, Mr. Azuma Abe, Hirosaki High School, Hirosaki, Mr. Mitsuru Mukohyama, San-nohe High School, San-nohe, Aomori Prefecture and Mr. Yasushi Nagao, Hokkaido Government Office, Sapporo, for their help in collecting the research materials.

REFERENCES

- 1 Yoshida, M. C. and Kobayashi, T. (1966) Notes on the chromosomes of three species of field mice, *Apodemus*. Chrom. Inf. Serv., 7: 18-20.
- 2 Shimba, H. and Kobayashi, T. (1969) A Robertsonian type polymorphism of the chromosomes in the field mouse, *Apodemus speciosus*. Jpn. J. Genet., 44: 117-122.
- 3 Tsuchiya, K. and Yosida, T. H. (1971) Distribution of two chromosomal types of Japanese wood mouse, *Apodemus speciosus*. Ann. Rep. Natl. Inst. Genet., Jpn., 21: 49-50.
- 4 Tsuchiya, K., Moriwaki, K. and Yosida, T. H. (1973) Cytogenetical survey in wild population of Japanese wood mouse, *Apodemus speciosus* and its breeding. Exptl. Anim., 22: 221-229.
- 5 Tsuchiya, K. (1974) Cytological and biochemical studies of *Apodemus speciosus* group in Japan. J. Mammal. Soc. Jpn., 6: 67-87. (In Japanese, with English summary)
- 6 Harada, M., Hamada, S., Koyasu, K. and Miyao, T. (1984) Studies on a contact zone between two chromosomal races of *Apodemus speciosus*. J. Mammal. Soc. Jpn., 10: 101-102. (Abstract)
- 7 Corbet, G. B. (1978) The Mammals of the Palaearctic Region: A Taxonomic Review. Cornell Univ. Press, London/Ithaca, pp. 132-138.
- 8 Saitoh, M. and Obara, Y. (1986) Chromosome banding patterns in five intraspecific taxa of the large Japanese field mouse, *Apodemus speciosus*. Zool. Sci., 3: 785-792.
- 9 Ayala, F. J. (1975) Genetic differentiation during the speciation process. In "Evolutionary Biology". Ed. by T. Dobzhansky, M. K. Hecht and W. C. Steere, Plenum Press, New York, Vol. 8, pp. 1-78.
- 10 Ferguson, A. (1980) Biochemical Systematics and Evolution. Blackie, Glasgow.
- 11 Matsuoka, N. (1981) Phylogenetic relationships among five species of starfish of the genus, *Asterina*: An electrophoretic study. Comp. Biochem. Physiol., 70B: 739-743.
- 12 Matsuoka, N. (1985) Biochemical phylogeny of the sea-urchins of the family Taxopneustidae. Comp. Biochem. Physiol., 80B: 767-771.

- 13 Davis, B. J. (1964) Disc electrophoresis-II. Method and application to human serum proteins. *Ann. N. Y. Acad. Sci.*, **121**: 404-427.
- 14 Nei, M. (1972) Genetic distance between populations. *Am. Natur.*, **106**: 283-292.
- 15 Sneath, P. H. A. and Sokal, P. R. (1973) *Numerical Taxonomy*. Freeman, San Francisco.
- 16 Selander, R. K. and Kaufman, D. W. (1973) Genic variability and strategies of adaptation in animals. *Proc. Natl. Acad. Sci. USA*, **70**: 1875-1877.
- 17 Selander, R. K. and Johnson, W. E. (1973) Genetic variation among vertebrate species. *Ann. Rev. Ecol. System.*, **4**: 75-91.
- 18 Lewontin, R. C. (1974) *The Genetic Basis of Evolutionary Change*. Columbia Univ. Press, New York/London.
- 19 Selander, R. K., Hunt, W. G. and Yang, S. Y. (1969) Protein polymorphism and genic heterozygosity in two European subspecies of the house mouse. *Evolution*, **23**: 379-390.
- 20 Nei, M. (1975) *Molecular Population Genetics and Evolution*. North Holland, Amsterdam.
- 21 Saitoh, M. and Obara, Y. (1988) Meiotic studies of interracial hybrids from the wild population of the large Japanese field mouse, *Apodemus speciosus speciosus*. *Zool. Sci.*, **5**: 813-820.
- 22 Nevo, E. and Shaw, C. R. (1972) Genetic variation in a subterranean mammals, *Spalax ehrenbergi*. *Biochem. Genet.*, **7**: 235-241.
- 23 Nevo, E., Kim, Y. J., Shaw, C. R. and Thaler, C. S. (1974) Genetic variation, selection, and speciation in *Thomomys talpoides* pocket gophers. *Evolution*, **28**: 1-23.
- 24 Britton, J. and Thaler, L. (1978) Evidence for the presence of two sympatric species of mice (genus *Mus* L.) in Southern France based on biochemical genetics. *Biochem. Genet.*, **16**: 213-225.
- 25 Kobayashi, T. and Hayata, I. (1971) Revision of the genus *Apodemus* in Hokkaido. *Annot. Zool. Japon.*, **44**: 236-240.
- 26 Hayata, I., Shimba, H., Kobayashi, T. and Makino, S. (1970) Preliminary accounts on the chromosomal polymorphism in the field mouse, *Apodemus gilvaceus*, a new form from Hokkaido. *Proc. Japan Acad.*, **46**: 567-571.
- 27 Hayata, I. (1973) Chromosomal polymorphism caused by supernumerary chromosomes in the field mouse, *Apodemus gilvaceus*. *Chromosoma*, **42**: 403-414.
- 28 Ayala, F. J. (1982) *Population and Evolutionary Genetics: A Primer*. The Benjamin/Cummings Publishing Company, Menlo Park.
- 29 Tsuchiya, K. (1981) On the chromosome variations in Japanese cricetid and murid rodents. *Mammal. Sci.*, **42**: 51-58. (In Japanese)
- 30 Tsuchiya, K., Sakaizumi, M., Wakana, S., Suzuki, H. and Moriawaki, K. (1988) Genetic relationship between Japanese and continental species of *Apodemus*. *Zool. Sci.*, **5**: 1223. (Abstract)
- 31 Bekasova, T. S., Vorontsov, N. N., Korobitsyna, K. V. and Korabiev, V. P. (1980) B-chromosomes and comparative karyology of the mice of the genus *Apodemus*. *Genetica*, **52/53**: 33-43.
- 32 Bekasova, T. S. and Vorontsov, N. N. (1975) Populational chromosome polymorphism in Asiatic forest mice *Apodemus peninsulae*. *Genetika (Moscow)*, **11**: 89-94. (in Russian with English summary)
- 33 Kuznetsov, B. A. (1965) Order Rodentia. In "Key to the Mammals of the USSR". Ed. by N. A. Bobrinskii, B. A. Kuznetsov and A. P. Kuz'yakin, Izdatel'stvo "Prosveshchenie", Moscow.
- 34 Ayala, F. J., Powell, J. R., Tracey, M. L., Mourão, C. A. and Pérez-Salas, S. (1972) Enzyme variability in the *Drosophila willistoni* group. IV. Genic variation in natural populations of *Drosophila willistoni*. *Genetics*, **70**: 113-139.
- 35 Ayala, F. J., Tracey, M. L., Barr, L. G., McDonald, J. F. and Pérez-Salas, S. (1974) Genetic variation in natural populations of five *Drosophila* species and the hypothesis of the selective neutrality of protein polymorphisms. *Genetics*, **77**: 343-384.
- 36 Matsuoka, N. and Suzuki, H. (1987) Electrophoretic study on the taxonomic relationship of the two morphologically very similar sea-urchins, *Echinostrephus aciculatus* and *E. molaris*. *Comp. Biochem. Physiol.*, **88B**: 637-641.
- 37 Matsuoka, N., Chiba, Y. and Saitoh, K. (1984) Biochemical evidence for the genetic differentiation between two morphologically very similar species of *Neope* (Lepidoptera, Satyridae) from Japan. *Proc. Japan Acad.*, **60B**: 245-248.
- 38 Shaw, C. R. and Prasad, R. (1970) Starch gel electrophoresis of enzymes: A compilation of recipes. *Biochem. Genet.*, **4**: 297-320.
- 39 Marcus, N. H. (1977) Genetic variation within and between geographically separated populations of the sea urchin, *Arbacia punctulata*. *Biol. Bull.*, **153**: 560-576.

[COMMUNICATION]

Superoxide Production by the Haemocytes of the Freshwater Snail, *Biomphalaria glabrata*, Stimulated by Miracidia of *Schistosoma mansoni*

AKIKO SHOZAWA, CHIHARU SUTO and NOBUO KUMADA

Department of Medical Zoology, Nagoya University School of Medicine,
Showa-ku, Nagoya 466, Japan

ABSTRACT—The production of superoxide (O_2^-) by the haemocytes of *Biomphalaria glabrata*, an intermediate host of *Schistosoma mansoni*, was demonstrated by nitroblue tetrazolium (NBT) test. Intact, 4,000 R irradiated and formalin-fixed miracidia (snail-infective larvae) of *S. mansoni* were used as the stimuli. NBT-reduction was observed in the haemocytes incubated with 4,000 R irradiated or formalin-fixed miracidia, whereas only little effect was shown by intact ones. The reduction was inhibited by superoxide dismutase. The results suggest that self/non-self recognition by the haemocytes is involved in the O_2^- production.

INTRODUCTION

It is generally accepted that cellular responses, such as phagocytosis or encapsulation, play a major part in molluscan internal defence. However, little is known about the biochemical processes which occur during the responses [1, 2].

Vertebrate phagocytes stimulated with various agents show a respiratory burst that results in the production of active oxygen metabolites, which contribute to microbicidal activities [3-5]. On the other hand, insect [6] and bivalve [7] haemocytes were reported to be devoid of such antimicrobial system known in vertebrate phagocytes.

Recently, however, Nakamura *et al.* [8] found that haemocytes of the scallop, *Patinopecten yes-soensis*, produce and release hydrogen peroxide (H_2O_2) under phagocytic stimulation *in vitro*. Dikkeboom *et al.* [9] also detected the production

of superoxide (O_2^-) and H_2O_2 by the stimulated haemocytes of the pond snail, *Lymnaea stagnalis*. These results imply that molluscan haemocytes may have some bactericidal or cytotoxic systems comparable to vertebrate phagocytes.

The first aim of this study was to detect the possible production of O_2^- by stimulated haemocytes of *Biomphalaria glabrata*, an intermediate host snail of the human blood fluke, *Schistosoma mansoni*. If it is really produced by the cells, what is the role of O_2^- production in the defence mechanisms of the snail? To answer the question, we tried to stimulate the haemocytes of *B. glabrata* with miracidia (snail-infective larvae) of *S. mansoni*.

MATERIALS AND METHODS

Snails: The pulmonate snails, *B. glabrata* (Puerto Rican strain), which were provided from Department of Parasitology, Hamamatsu University School of Medicine, and Department of Medical Biology, Institute of Basic Medical Sciences, University of Tsukuba, have been maintained in our laboratory since 1985. They were kept in aquaria at 25°C and fed on an artificial diet for the silkworm [10] *ad libitum*. Their susceptibility to *S. mansoni* infection tested in our laboratory was 86% (95% confidence interval: 80% < p < 92%). Adult specimens (shell diameters: 10-15 mm) were placed in distilled water for more than 12 hr before experiments.

Accepted January 26, 1989

Received October 4, 1988

Haemolymph collection

The shell surface of the snail was swabbed with 70% ethanol and dried before use. The snail retracts deeply into its shell and extrudes haemolymph, when it is touched with the point of a glass capillary [11]. In this way, about 15–25 μ l of haemolymph can be obtained from an adult specimen. Haemolymph collected from 20 or more snails was pooled in an ice-cooled, sterile polyethylene sample tube and used within 1 hr. The total haemocyte counts of the haemolymph was ca. 1×10^6 per ml.

Stimuli

S. mansoni (Puerto Rican strain) was provided from Department of Parasitology, Institute of Medical Science, University of Tokyo and has been maintained in our laboratory since 1985. Miracidia were obtained from minced livers of ICR mice (8 weeks post infection with cercariae of *S. mansoni*) by immersing in aged tap water. They were washed twice in sterile, distilled water and used as the intact miracidia. For the preparation of irradiated miracidia, the suspension was adjusted to contain approximately 50 miracidia per ml and exposed to 4,000 R X-ray irradiation generated by Hitachi MBR-1505 R (Hitachi Medico Ltd., Japan). The miracidia were fixed by 3% formalin solution. After 60 min of fixation, they were washed three times and resuspended in sterile, distilled water.

Nitroblue tetrazolium test

O_2^- generation was detected by the histochemical assay using nitroblue tetrazolium (NBT). On a glass slide, 20 μ l of haemolymph was placed, then 10 μ l of sterilized Sminia's snail saline, pH 7.4 (SS; NaCl 249.5 mg, KCl 15.5 mg, $MgCl_2$ 40.7 mg, $CaCl_2$ 64.7 mg in 100 ml of distilled water; pH was adjusted with 0.2 M Tris-HCl, pH 8.0) [12] with or without 2.0 μ g of superoxide dismutase (SOD; 3,000 U/mg protein, from bovine erythrocytes; Sigma) and 5 miracidia were added. As a control, miracidia were omitted and SS alone was added to the haemolymph. After 15 min of preincubation, 10 μ l of 0.2% NBT (Sigma) dissolved in SS was overlaid and incubated for 60 min. All the incubation was done at 25°C in a moist chamber. The slides were fixed in 100% methanol, mounted in glycerol and examined under a phase-contrast microscope. If O_2^- was produced by the cells, yellow, soluble NBT is reduced to blue-black, insoluble formazan. The cells having intracellular formazan granule(s) were considered to be positive for O_2^- production (Fig. 1). At least 500 cells were observed and the percentage of positive cells was determined. Experiments were done in triplicate. Each value is shown by the mean \pm SD.

RESULTS

Both intact and irradiated miracidia transformed into sporocysts and were alive during the incuba-

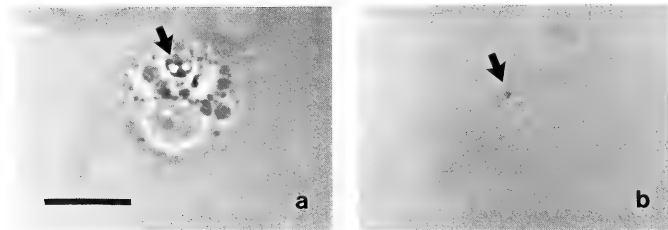


FIG. 1. Phase contrast(a) and light(b) micrographs of a haemocyte of *Biomphalaria glabrata*, which has intracellular formazan granule (arrows) indicating superoxide production. (Bar=10 μ m).

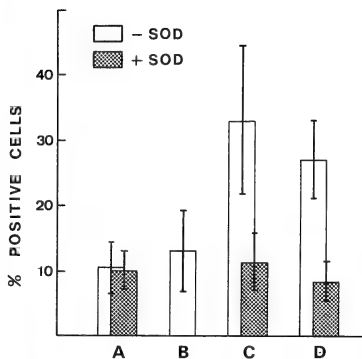


FIG. 2. Percentages of the haemocytes of *Biomphalaria glabrata* having intracellular formazan granule(s). The cells were incubated with (open columns) or without (shaded columns) superoxide dismutase (SOD; final concentration: 50 µg/ml) and stimulated as follows: A, controls without stimuli; B-D, stimulated by intact, 4,000 R irradiated or formalin-fixed miracidia of *Schistosoma mansoni*, respectively. After 15 min of preincubation, nitroblue tetrazolium solution (final concentration: 0.05%) was added and incubated for 60 min at 25°C. Each value represents the mean of triplicate experiments, SD is indicated as a vertical bar.

tion with the haemocytes. Haemocytic encapsulation and adherence against the parasites were never observed in this period.

Percentages of formazan-positive cells are shown in Figure 2. A number of positive cells were observed among the haemocytes incubated with irradiated or formalin-fixed miracidia and the percentages were 33.0 ± 11.4 and 27.0 ± 6.0 , respectively. Only a little effect was shown by intact miracidia (13.0 ± 6.3 %).

SOD inhibited the NBT-reduction by the haemocytes incubated with irradiated or formalin-fixed miracidia; the percentages of the positive cells decreased to 11.4 ± 4.5 and 8.4 ± 3.2 , respectively. The positive rate in the controls (10.5 ± 4.1 %) was unchanged by SOD.

DISCUSSION

In the host-parasite relation between *B. glabrata* and *S. mansoni*, several strains of the host snail are known to be genetically different in their susceptibility to the parasite [13, 14]. When miracidia penetrate to resistant snails, the sporocysts are encapsulated and killed by the haemocytes. The haemocytes of resistant snails were also reported to be cytotoxic to the sporocysts *in vitro* [15]. However, the haemocytes of susceptible ones show little resistance to the parasites *in vivo* [1, 16, 17]. On the other hand, irradiated miracidia of *S. mansoni* are encapsulated by the haemocytes of susceptible snail and fail to develop, though they can penetrate into the host [18]. These cellular responses have been considered to be based on self/non-self recognition by the host, but the killing mechanism(s) remains to be elucidated [2, 15].

The present results clearly indicate that the haemocytes are stimulated by treated (alive and dead) miracidia to produce O₂⁻. The NBT-reduction by the haemocytes stimulated with the miracidia is considered to be similar to the reaction observed in the haemocytes of *L. stagnalis* stimulated with various phagocytic particles or phorbol myristate acetate [9].

Miracidia are generally encapsulated by a number of haemocytes, when the host defence reaction is provoked. NBT-reduction is usually seen in the adherent cells and at the haemocyte/parasite interface in vertebrate haemocytic encapsulation against parasite [19, 20]. In our experiments, probably because of the brief incubation period, neither encapsulation nor adhesion of the haemocytes against any miracidia or sporocysts was observed. However, larger number of formazan positive cells were found around the irradiated or formalin-fixed miracidia than in the other part. This suggests that the positive cells, though they did not adhere to the surface of the parasites, might have some chance to encounter the treated parasites and stimulated during the incubation.

In contrast, the haemocytes seem to be rarely stimulated by the intact miracidia, because the cells incubated with intact ones showed only a slight reduction of NBT. The difference in the haemocytic reactions against intact or treated

miracidia might be to non-self recognition by the haemocytes. Since intact miracidia are recognized as 'self' by the haemocytes of susceptible hosts, they do not induce any cellular reactions [16, 17]. In the similar manner, the haemocytes stimulated by the intact miracidia would have failed to produce O_2^- . Whereas both sporocysts transformed from irradiated miracidia and formalin-fixed ones are recognized as 'non-self' by the host [1, 18]. Therefore, these treated parasites are considered to have provoked the O_2^- production by the haemocytes.

In conclusion, we detected the O_2^- production by the stimulated haemocytes of *B. glabrata*. The results, moreover, indicate that the induction of the cellular response involves self/non-self recognition by the haemocytes. Although the cytotoxicity or microbicidal activities of the oxygen radicals produced by the snail haemocytes have to be further investigated, one can expect that these metabolites would have some roles in the defence system of gastropods.

REFERENCES

- 1 Sminia, T. (1981) In "Invertebrate Blood Cells". Ed. by N. A. Ratcliffe and A. F. Rowley, Academic Press, New York, pp. 191-232.
- 2 Bayne, C. J. (1983) In "The Mollusca vol. 5". Ed. by A. S. M. Saleuddin and K. M. Wilber, Academic Press, New York, pp. 407-486.
- 3 Iyer, G. Y. N., Islam, M. F. and Quastel, J. H. (1961) *Nature*, **192**: 535-541.
- 4 Babior, B. M., Kipness, R. S. and Curnutte, J. T. (1973) *J. Clin. Invest.*, **52**: 741-744.
- 5 Babior, B. M. (1980) In "The Reticuloendothelial System. II. Biochemistry and Metabolism". Ed. by A. J. Sbarra and R. Strauss, Plenum Press, New York, pp. 339-354.
- 6 Anderson, R. S., Holmes, B. and Good, R. A. (1973) *Comp. Biochem. Physiol.*, **43B**: 595-602.
- 7 Cheng, T. C. (1976) *J. Invertebr. Pathol.*, **27**: 263-268.
- 8 Nakamura, M., Mori, K., Inooka, S. and Nomura, T. (1985) *Dev. Comp. Immunol.*, **9**: 407-417.
- 9 Dikkeboom, R., Tijnagel, J. M. G. H., Mulder, E. C. and Van der Knaap, W. P. W. (1987) *J. Invertebr. Pathol.*, **49**: 321-331.
- 10 Horie, Y., Inokuchi, T., Watanabe, K., Nakasone, A. and Yanagawa, K. (1973) *Tech. Bull. Seric. Exp. Station*, **96**: 7-20. (In Japanese)
- 11 Sminia, T. (1972) *Z. Zellforsch.*, **130**: 497-526.
- 12 Sminia, T., Van der Knaap, W. P. W. and Edelenbosch, P. (1979) *Dev. Comp. Immunol.*, **3**: 37-44.
- 13 Richards, C. S. (1975) *Parasitology*, **70**: 231-241.
- 14 Basch, P. F. (1976) *Exp. Parasitol.*, **39**: 150-169.
- 15 Bayne, C. J., Buckley, P. M. and DeWan, P. C. (1980) *J. Parasitol.*, **66**: 413-419.
- 16 Newton, W. L. (1953) *Exp. Parasitol.*, **2**: 242-257.
- 17 Cheng, T. C. and Garrabrant, T. A. (1977) *Int. J. Parasitol.*, **7**: 467-472.
- 18 Lie, K. J., Jeong, K. H. and Heyneman, D. (1983) *Int. J. Parasitol.*, **13**: 301-304.
- 19 Incani, R. N. and McLaren, D. J. (1983) *Parasitology*, **86**: 345-357.
- 20 Leventhal, R. and Soulsby, E. J. L. (1972) *J. Parasitol.*, **58**: 1016-1017.

[COMMUNICATION]

Effect of ATP γ S on Fertilization Envelope
Elevation of Sand Dollar Eggs

YUKIHISA HAMAGUCHI

Biological Laboratory, Tokyo Institute of Technology,
Meguro-ku, Tokyo 152, Japan

ABSTRACT—ATP γ S (adenosine 5'-0-(3-thiotriphosphate)) inhibited cortical granule exocytosis of the sand dollar (*Clypeaster japonicus*) egg at insemination when injected before insemination at concentrations of 33–600 μ M in the cytoplasm. Accordingly the fertilization envelope did not elevate, whereas many sperm were incorporated into the egg and then sperm asters formed. After treatment with Ca ionophore A23187 the fertilization envelope did not elevate from eggs injected with ATP γ S, although the threshold concentration of ATP γ S to inhibit fertilization envelope elevation was higher than that at insemination. These results suggest that ATP γ S would reduce Ca²⁺-sensitivity of cortical granules by means of thiophosphorylation and, therefore, would prevent a transient increase in intracellular free Ca²⁺ concentration at insemination or parthenogenetic activation from inducing cortical granule exocytosis. Another analog, AMPPNP (5'-adenylylimido diphosphate) (< 600 μ M in the egg cytoplasm) did not inhibit fertilization envelope elevation at insemination. However, ATP γ S and AMPPNP at 900 μ M or more in the egg cytoplasm induced the envelope elevation by the injection. AMPPCP (5'-adenylylmethylene diphosphate) showed no effect.

INTRODUCTION

ATP is the fundamental molecule as an energy source for cellular activities, especially for such as the generation of force and movement, the synthesis of biological molecules, and the active transport of molecules. ATP is used as a substrate for more than 100 enzymes not only to utilize high-energy bonds of phosphates by hydrolysis, but also to modify enzymes by phosphorylation in order to

control their activity. Many analogs of ATP have been synthesized and used in order to investigate properties of enzymes [1]. ATP γ S (adenosine 5'-0-(3-thiotriphosphate)), one of phosphate analogs of ATP may be used in place of ATP by kinases, whereas enzymes modified covalently in thiophosphorylated forms by kinases are not favored substrates for phosphatases and, therefore, ATP γ S can possibly control the activities of key enzymes and change cellular activity irreversibly [2]. On the other hand, AMPPCP (5'-adenylylmethylene diphosphate) or AMPPNP (5'-adenylylimido diphosphate), which has non-hydrolyzable linkage between β and γ phosphorus, is not a suitable substrate for any of kinases or any of enzymes which cleave the β - γ linkage of ATP [1] and may affect cellular activities in a manner different from ATP γ S.

In the present study, I investigated the effect of these ATP analogs on fertilization of sand dollar eggs in order to understand the role of phosphorylation in fertilization by means of microinjection because they might not be uptaken easily by the eggs from the surrounding medium. Only ATP γ S inhibited cortical granule exocytosis at insemination, but it did not inhibit sperm incorporation or aster formation, suggesting that ATP γ S might make cortical granules insensitive to Ca²⁺ through thiophosphorylation.

MATERIALS AND METHODS

I obtained gametes of the sand dollar, *Clypeaster japonicus*, by the injection of 0.5 M KCl or sea

water containing 1 mM acetylcholine into the coelomic cavity. The Ca ionophore, A23187 was dissolved at 10 mM in dimethylsulfoxide, diluted to 10 or 20 μ M in artificial sea water (Jamarin, Jamarin Lab. Osaka), and used for parthenogenetic activation. Two to 50 mM of ATP γ S, 25–100 mM AMPPNP, and 25 mM AMPPCP dissolved in 50 mM MOPS (3-(N-morpholino) propanesulfonic acid) (pH. 7.0) were used for injection. 100–400 mM LiCl and 25–100 mM ATP dissolved in 50 mM MOPS (pH. 7.0) were used as controls.

I carried out microinjection at $25 \pm 1^\circ\text{C}$ as

described by Hiramoto [3]. The final concentrations of ATP analogs in the egg cytoplasm were calculated as follows. The injected amount of ATP analogs (the injected volume of the solution multiplied by the concentration of them) was divided by the egg volume of 0.8 nl [4].

RESULTS

The effect of ATP γ S on fertilization or activation of the sand dollar (*Clypeaster japonicus*) egg is summarized in Figure. 1 when ATP γ S was injected

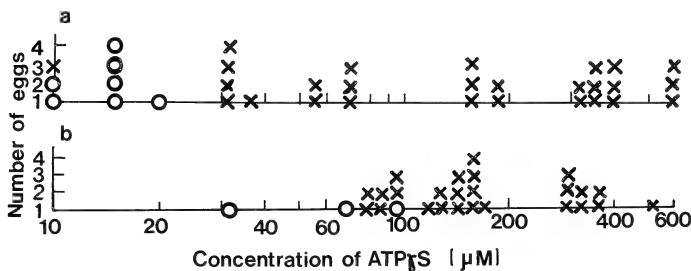


Fig. 1. Effect of ATP γ S injection into unfertilized eggs on fertilization envelope elevation at insemination (a) and activation with A23187 (b). Abscissa; final concentrations of ATP γ S injected into the eggs. o; eggs with the fertilization envelope at insemination or by treatment with A23187. x; eggs without the envelope after insemination or by the treatment. The eggs were counted in case of a when one or more sperm asters were observed in these eggs after insemination.

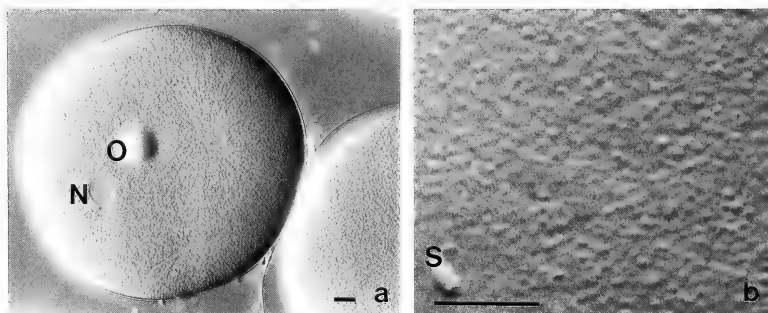


Fig. 2. An egg which was injected with ATP γ S and inseminated after injection. a; three asters are found in this field. O indicates an oil drop introduced at the time of injection, and N synkaryon. b; the cortex of the same egg in a. S indicates a sperm head on the egg surface. It is noted that none of cortical granules disappeared. Bar shows 10 μ m.

at 600 μ M or less in final concentration into the unfertilized one. No significant effect of ATP γ S on egg morphology was observed. However, when the eggs were inseminated after injection of ATP γ S at 33–600 μ M in the cytoplasm, the fertilization envelope did not elevate from any of 26 injected eggs (Fig. 1a). In these eggs, sperm were incorporated and sperm asters were observed (Fig. 2a) although cortical granules appeared intact (Fig. 2b), and the cleavage furrow was developed in some eggs. Seven out of 8 eggs injected with ATP γ S at 20 μ M or less showed fertilization envelope elevation at insemination and developed normally. Occurrence of sperm aster formation suggests that intracellular Ca^{2+} increased in the cytoplasm of the eggs injected with ATP γ S at sperm incorporation.

In order to confirm this possibility, the eggs injected with ATP γ S were treated with Ca ionophore which may increase the intracellular Ca^{2+} and result in fertilization envelope elevation [8]. When 30 eggs injected with ATP γ S at 600 μ M or less in final concentration were incubated in sea water containing 10 or 20 μ M A23187, the fertilization (activation) envelope did not elevate from 27 out of 28 eggs injected with ATP γ S at 80 μ M or more (Figs. 1b and 3), but the fertilization envelope elevated from both of 2 eggs injected with ATP γ S at 70 μ M or less. These results mean that ATP γ S inhibited fertilization envelope elevation, although intracellular Ca^{2+} concentration increased after treatment with Ca ionophore and

that the threshold concentration of ATP γ S to inhibit the elevation after the treatment was higher than that at insemination.

The fertilization envelope elevated from all of 6 eggs injected with ATP γ S at 900 μ M or more in final concentration in the egg cytoplasm shortly after injection without insemination.

Fertilization including the fertilization envelope elevation normally occurred by insemination in 6 eggs injected with AMPPNP at 600 μ M or less in final concentration in the egg cytoplasm. On the other hand, the fertilization envelope elevated from all of 8 eggs injected with AMPPNP at 900 μ M or more in final concentration shortly after injection. No effect was observed when AMPPCP was injected into 5 eggs up to 2000 μ M in the egg cytoplasm and all of them were fertilized normally after insemination.

ATP analogs may deplete some inorganic ions, especially such as Mg^{2+} and Ca^{2+} in the egg cytoplasm because ATP and these analogs chelate them [14] and Li^4 was introduced into the eggs at ATP γ S, AMPPNP, and AMPPCP injection because these analogs were purchased as such Li^+ salt as Li^+ ATP γ S, which might possibly cause some side effects on fertilization of sand dollar eggs. ATP and LiCl were injected into 4 unfertilized eggs at the concentration of up to 1.6 mM in the egg cytoplasm and 10 eggs at the concentration of up to 19 mM as control, respectively. No significant effect was observed after injection and all of the injected eggs were fertilized normally after insemination.

DISCUSSION

ATP γ S inhibited the exocytosis of cortical granules of sand dollar eggs at insemination when it was injected before insemination at low concentration in the cytoplasm, and, accordingly the fertilization envelope did not elevate, although sperm could enter the eggs and sperm asters formed. Occurrence of sperm aster formation indicates Ca^{2+} increase in the egg cytoplasm by two reasons as follows. First, it is well-known that Ca^{2+} concentration increases transiently in the cytoplasm of fertilized eggs were sperm aster forms [5, 6]. Secondly, EGTA which can maintain in-

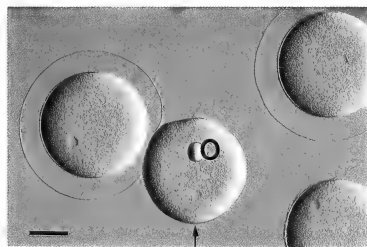


FIG. 3. An egg indicated by arrow which was injected with ATP γ S and treated with 10 μ M A23187 did not induce fertilization envelope elevation, but the other eggs did. Bar shows 50 μ m.

tracellular free Ca^{2+} concentration at such a low level as that in unfertilized eggs by means of injection did not inhibit sperm entrance, but inhibited both cortical granule exocytosis and sperm aster formation [4, 7]. $\text{ATP}\gamma\text{S}$ also inhibited cortical granule exocytosis of the injected eggs after treatment with the Ca ionophore, which is known to increase intracellular Ca^{2+} concentration [8]. It is inferred from these facts that $\text{ATP}\gamma\text{S}$ prevents Ca^{2+} increase from inducing cortical granule exocytosis, though the increase in the cytoplasm of the eggs injected with $\text{ATP}\gamma\text{S}$ occurs both after insemination and by treatment with the Ca ionophore.

Effective concentration of $\text{ATP}\gamma\text{S}$ was much lower in the egg cytoplasm than the cytoplasmic concentration of ATP , which is a few mM [9]. AMPPNP and AMPPCP , which are possible competitive inhibitors of ATP , showed no effect on fertilization envelope elevation at low concentration during fertilization or activation. These facts suggest that $\text{ATP}\gamma\text{S}$ was used not as a substrate for hydrolases but as a substrate for kinases in the egg cytoplasm and that the thiophosphorylated products might reduce Ca^{2+} -sensitivity of cortical granules and inhibit cortical granule exocytosis.

The inhibitory effect of $\text{ATP}\gamma\text{S}$ on fertilization envelope elevation resembles that of local anesthetics such as procaine and urethane [10, 11]. Procaine raised the effective concentration of Ca^{2+} in the egg cytoplasm to elevate the fertilization envelope at the injection of Ca buffers up to such an extremely high level as $40\ \mu\text{M}$ [4]. Reduction of ATP by treatment with metabolic inhibitors also inhibited cortical granule exocytosis after insemination [12, 13], suggesting that the reduction might lower Ca^{2+} -sensitivity of cortical granules [12]. It has not yet been known whether or not these reagents inhibited the exocytosis through phosphorylation.

At millimolar concentration, $\text{ATP}\gamma\text{S}$ and AMPPNP induced cortical granule exocytosis

when injected into sand dollar eggs. It is unknown what kinds of reaction in the egg cytoplasm they would lead induce the exocytosis because they may affect enzymes in the cell as reviewed by Yount [1]. However, one of possibilities is that these two analogs would mimic $\text{GTP}\gamma\text{S}$ (guanosine 5'-0-(3-thiotriphosphate)) by activating a GTP-binding protein because $\text{GTP}\gamma\text{S}$ cause fertilization envelope elevation of sea urchin eggs after injection [14].

ACKNOWLEDGMENTS

I wish to thank Dr. R. Kuriyama of University of Minnesota in USA for her advice on ATP analogs and the Misaki Marine Biological Station for supplying sand dollars.

This work was supported by a Grant-in-Aid from the Ministry of Education, Science and Culture of Japan (62540538).

REFERENCES

- 1 Yount, R. G. (1975) *Ad. Enzymol.*, **43**: 1-56.
- 2 Goody, R. S., Eckstein, F. and Schirmer, R. H. (1972) *Biochim. Biophys. Acta*, **276**: 155-161.
- 3 Hiramoto, Y. (1974) *Exp. Cell Res.*, **87**: 403-406.
- 4 Hamaguchi, Y. and Hiramoto, Y. (1981) *Exp. Cell Res.*, **134**: 171-179.
- 5 Epel, D. (1978) *Curr. Top. Dev. Biol.*, **12**: 185-246.
- 6 Trimmer, V. S. and Vacquier, V. D. (1986) *Ann. Rev. Cell Biol.*, **2**: 1-26.
- 7 Hamaguchi, Y. and Mabuchi, I. (1988) *Cell Motil. Cytoskeleton*, **9**: 153-163.
- 8 Steinhart, R. A. and Epel, D. (1974) *Proc. Natl. Acad. Sci. USA*, **71**: 1915-1919.
- 9 Yanagisawa, T. (1969) *Protein, Nucleic Acid and Enzyme*, **14**: 677-687. (In Japanese)
- 10 Sugiyama, M. (1956) *Exp. Cell Res.*, **10**: 364-376.
- 11 Vacquier, V. D. (1975) *Dev. Biol.*, **43**: 62-74.
- 12 Baker, P. F. and Whitaker, M. J. (1978) *Nature*, **276**: 513-515.
- 13 Okazaki, R. (1956) *Exp. Cell Res.*, **10**: 476-504.
- 14 Turner, P. R., Jaffe, L. A. and Fein, A. (1986) *J. Cell Biol.*, **102**: 70-76.

[COMMUNICATION]

**Development of an *In Vitro* Spermiation System
in the Frog, *Rana nigromaculata***

TOHRU KOBAYASHI, AKIKO OSHIMI and HISAAKI IWASAWA

*Biological Institute, Faculty of Science, Niigata University,
Niigata 950-21, Japan*

ABSTRACT—To clarify the mechanism of spermiation, particularly the release of spermatozoa from Sertoli cells, an *in vitro* spermiation system was developed. Testis pieces were incubated in various conditions, and then the degree of induction of release of spermatozoa from Sertoli cells was evaluated histologically. The induction of spermiation was seen in incubation for 1.5 hr or longer at 18°C following the addition of hCG (10 IU/ml) or bullfrog pituitary glycoprotein (GP: 5 µg/ml). In this system, spermiation was not induced by the addition of insulin, arginine vasotodin (0.01–10 µg/ml) or epinephrine (0.01–1 µg/ml). These results suggest that the release of spermatozoa from Sertoli cells was induced specifically by the addition of gonadotropic substances in this system.

to clarify the mechanism of spermiation. As an *in vitro* spermiation system, it is known that pituitary extracts stimulate spermiation [6], but this *in vitro* system seems to be rather elementary because in this system, the induction of spermiation was evaluated by the presence of spermatozoa in incubation medium. Therefore, as the first step in clarifying the mechanism of spermiation, we developed a new *in vitro* assay system. In this paper, we described in particular an *in vitro* system involved in the release of spermatozoa from Sertoli cells.

INTRODUCTION

In lower vertebrates, spermiation occurs under hormonal control, and the injection of pituitary extracts or gonadotropin (GTH) stimulates spermiation [1–3]. Recently, it was confirmed that a GTH surge was evident around the spermiation period in bullfrogs [4, 5]. Although this evidence indicates the involvement of GTH in anuran spermiation, details of the mechanism have not yet been clarified.

Spermiation consists of the following reactions: 1) release of spermatozoa from Sertoli cells, 2) fluid accumulation in seminiferous tubules, and 3) transport of spermatozoa from seminiferous tubules to efferent ductules [2]. The development of an *in vitro* assay system for spermiation will help

MATERIALS AND METHODS*Animals*

Adult male frogs of *Rana nigromaculata* in October (just before hibernation) were collected at Kanazuka, Niigata Prefecture and maintained in the laboratory at 4°C before use.

Chemicals

Insulin, arginine vasotodin (AVT) and epinephrine (Sigma, St. Louis, Mo.) and hCG (Purigen: Sankyo Co., Tokyo) were purchased from a commercial source. Bullfrog glycoprotein (GP) was supplied by Prof. S. Ishii of Waseda University.

In vitro experiments

Quickly excised testes were placed into ice-cold saline, and fat bodies and mesorchia, including the vasa efferentia were removed. These testes were

cut with scissors into $1 \times 1 \times 2$ mm pieces. Slicing was done in a medium over ice, and the medium was changed once or twice during the procedure. In each series of experiments, testis pieces from only one testis were used. Testis pieces were transferred into plastic dishes, and washed three times in cold medium. Diluted hormones were then added. Testis pieces were incubated usually for 18 hr at 18°C . The response at different times and the temperature were also noted, as described in the following Results' section. After the incubation, testis pieces were transferred into Bouin's solution. They were then embedded in Paraplast (Sherwood Medical, U.S.A.), and serial sections were cut at $5\text{ }\mu\text{m}$ and stained with Carazzi's hematoxylin and eosin.

As incubation media, 70% diluted Medium 199 (Flow Lab., U.S.A.) or Hanks-Hepes saline was used.

Evaluation of the induced spermiation

The degree of spermiation was judged quantitatively as follows. Serial sections were divided into quarters, and three planes were chosen. The total number of seminiferous tubule sections in these three planes was counted (a). These average number was 40 in one testis piece. The total number of spermatozoa and the number of spermatozoa released from the Sertoli cells were counted in each tubule section. The total number of spermatozoa was 100–500 in each tubule section. Then, the percentage of spermatozoa released from the Sertoli cells was calculated in each tubule section. These percentages were divided into five ranges, i.e., 0–20%, 20–40%, 40–60%, 60–80% and 80–100% (Fig. 1). The number of tubules showing each range was counted (b). From these results, the rate for each range in each

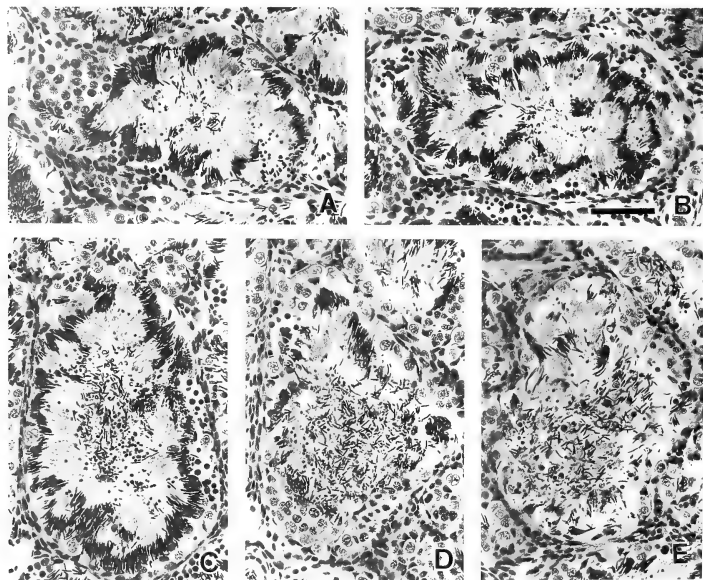


FIG. 1. Degree of spermiation. Rate of released spermatozoa from the Sertoli cells in a seminiferous tubule section was divided into five ranges. A: 0–20%, B: 20–40%, C: 40–60%, D: 60–80%, E: 80–100%. Bottom bar, $50\text{ }\mu\text{m}$.

testis piece, i.e., the rate of spermatozoa release ($b/a \times 100$), was determined.

The results obtained were calculated by one-way analysis of variance followed by Duncan's multiple range test, Student's t-test or Cochran-Cox test.

RESULTS

Effects of incubation medium on testicular condition

Figure 2 shows the rate of spermatozoa released from Sertoli cells during an each incubation time. The effects of plain medium were examined by incubating for 0 to 18 hr at 18°C in Hanks-Hepes or Medium 199. In intact frogs in the present study, a few spermatozoa released from Sertoli cells were seen. This degree indicated the basal level in the present experiment. In the incubation with Medium 199 or Hanks-Hepes, the degree of release of spermatozoa from Sertoli cells was not significant statistically among each incubation time.

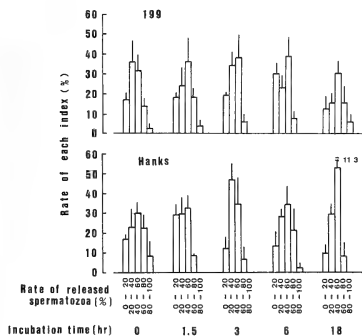


FIG. 2. Effects of incubation time in plain medium on testicular condition at 18°C. The vertical bars represent the mean \pm SEM of the three replicates.

In vitro stimulation of spermiation

In vitro stimulation of spermiation was examined for 18 hr at 18°C following the addition of hCG to the incubation medium (Fig. 3). When hCG was added, the number of seminiferous

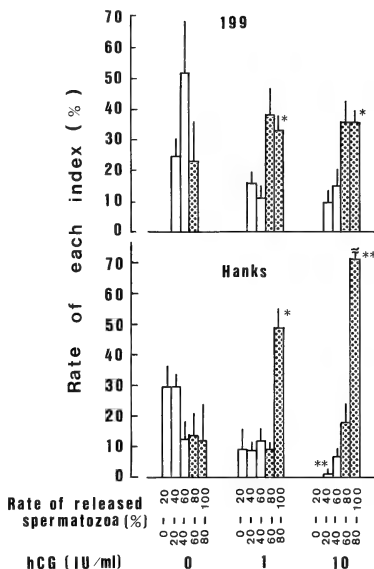


FIG. 3. Effect of hCG on the degree of spermatozoa released from Sertoli cells. Testis pieces were incubated for 18 hr at 18°C. The vertical bars represent the mean \pm SEM of the three replicates. * $p < 0.01$, ** $p < 0.05$ as compared with control.

tubule sections releasing spermatozoa, which had been 0–60%, decreased significantly (Hanks: control, 77, 1 IU/ml, 42, 10 IU/ml, 9.3%; Medium 199: control, 76, 1 IU/ml, 28, 10 IU/ml, 30%), and the rate of tubule sections which had been 60–100%, increased significantly (Hanks: control, 23, 1 IU/ml, 58, 10 IU/ml, 70.7%; Medium 199: control, 24, 1 IU/ml, 72, 10 IU/ml, 76%). Following the addition of hCG, tubule sections in the 0–20% range were no longer seen. With regard to the release of spermatozoa from Sertoli cells, no essential difference was recognized between Hanks-Hepes and Medium 199. From these results, as an index of *in vitro* spermiation induced by agents, the rate of tubule sections showing released spermatozoa, which ranged from 60–100%, was used in the following experiments.

Effect of temperature

The effects of hCG added to Medium 199 on *in vitro* spermiation were examined in incubation for 18 hr at 18 or 25°C (Fig. 4). In the incubation of testis pieces in plain medium, no significant difference between the results obtained at 18 and at 25°C was seen. By adding 1 IU/ml hCG, spermiation was markedly induced. The degree of spermiation induced by adding hCG tended to increase more at 25°C than at 18°C, though this difference was not significant statistically.

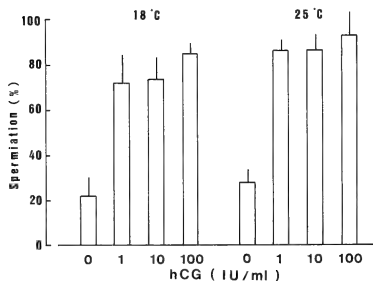


Fig. 4. Effect of incubation temperature on hCG-induced spermiation. Testis pieces were incubated for 18 hr. The vertical bars represent the mean \pm SEM of the three replicates.

Effect of incubation time

From the results of the preliminary experiments, the effect of incubation time following the addition of 10 IU/ml hCG was examined. Incubation was performed at 18°C in Medium 199 or Hanks-Hepes (Fig. 5). The induction of spermiation was significant 1.5 hr after incubation irrespective of the medium employed. The degree of spermiation induced by hCG increased with time in both media, and reached a plateau 6 hr after the start of incubation.

Gonadotropic specificity in the induction of spermiation

Effects of hCG, bullfrog pituitary glycoprotein (GP), insulin, AVT, and epinephrine were tested

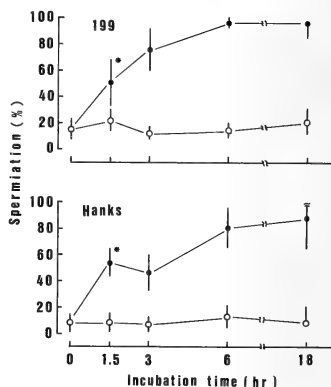


Fig. 5. Time course of spermiation induced by hCG. Testis pieces were incubated at 18°C. The vertical bars represent the mean \pm SEM of the three replicates. Open circle: control, Solid circle: hCG treatment (10 IU/ml). * $p < 0.05$ as compared with control.

for 3 hr at 18°C (Fig. 6). In five tests, the incubation of testis pieces with insulin (0.01–10 μ g/ml), AVT (0.01–10 μ g/ml) or epinephrine (0.01–1 μ g/ml) showed no effects on the induction of spermiation. The addition of a high dose of epinephrine (10 μ g/ml) tended to induce spermiation, but this reaction was not significant statistically. Spermiation was induced significantly by the

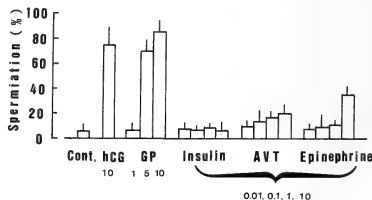


Fig. 6. Effect of human chorionic gonadotropin (hCG; 10 IU/ml), bullfrog pituitary glycoprotein (GP; 1, 5, 10 μ g/ml), and insulin, arginine vasotonsin (AVT) and epinephrine (0.01, 0.1, 1, 10 μ g/ml) on *in vitro* spermiation. Testis pieces were incubated for 3 hr at 18°C. The vertical bars represent the mean \pm SEM of the three replicates.

treatment with 5 or 10 $\mu\text{g/ml}$ GP ($p < 0.05$ or $p < 0.01$) to the same degree as with 10 IU/ml hCG ($p < 0.01$).

DISCUSSION

To our knowledge, there are few reports on a quantitative *in vitro* assay system for GTH-induced spermiation in non-mammalian vertebrates. In the present study, incubation for 1.5 hr or longer in 10 IU/ml hCG solution caused the induction of spermiation. Furthermore, the addition of GP used in the present study also induced spermiation significantly. It is known that *in vivo* spermatozoa appear in urine as early as 20–30 min after the administration of GTH, and numerous spermatozoa are seen in urine ca. 1 hr after the treatment [1, 7–10]. Therefore, with regard to the time for the induction of spermiation, the results obtained in the present study are in good agreement with those of previous *in vivo* experiments.

Temperature is an important factor in regulating the reproductive cycles of temperate zone ectotherms. Numerous reports have been published on the seasonal changes in reproductive activity in anurans with particular regard to temperature [2]. These reports have been postulated that the sensitivity of the testicular function to GTH varies with environmental temperature; Spermatogenesis is stimulated at high temperature, and steroid production at low temperature. Recently, on the properties of *in vitro* binding of bullfrog GTH to the bullfrog testes, Takada *et al.* [11] reported that the binding level at 15°C was higher than at 25°C. In the present study, however, no significant difference was seen in the induction of spermiation between at 18 and 25°C. This may be due to the incubation time (only 18hr). With regard to the effect of temperature on the induction of spermiation, further studies will be necessary.

In the present study, the specificity of gonadotropic substance in spermiation *in vitro* was examined. These results indicated that gonadotropic substances induced spermiation specifically, particularly the release of spermatozoa from Sertoli cells. McCreedy *et al.* [4] and Licht *et al.* [5] reported in bullfrogs that a pronounced GTH

surge was evident during spermiation. This suggests that GTH induced spermiation under physiological conditions. On the other hand, in the present study, it is indicated a high dose of epinephrine (10 $\mu\text{g/ml}$) tended to induce spermiation, though this was less effective than GTH substances. Previous investigators reported that epinephrine induced spermiation [6]. In anurans, however, no innervation was observed in the peripheral region of seminiferous tubules [12–14]; so that the involvement of epinephrine in spermiation under physiological condition is not yet clear.

In conclusion, the *in vitro* assay system used in the present study induced spermiation specifically in incubation for 1.5 hr or longer. In anurans, homologous FSH- and LH-hormones have been purified [15, 16]. However, the involvement of FSH and/or LH in spermiation is not yet clear. Therefore, we think that the *in vitro* spermiation system developed in this study contributes to this area of investigation.

ACKNOWLEDGMENT

We are grateful to Professor S. Ishii of Waseda University for the supply of bullfrog glycoprotein.

REFERENCES

- 1 Galli-Mainini, C. (1947) La Semana Médica, **54**: 337–340.
- 2 Lofts, B. (1974) In "Physiology of the Amphibia." Vol. II. Ed. by B. Lofts. Academic Press, New York. pp. 107–218.
- 3 Nagahama, Y. (1986) In "Vertebrates Endocrinology: Fundamentals and Biochemical Implantations." Ed. by Pang, P. K. T., M. P. Schreibman and A. Gorbman. Academic Press, New York, Vol. I, pp. 399–437.
- 4 McCreedy, B. R., Licht, P., Barnes, R., Rivier, J. and Vale, W. (1982) Gen. Comp. Endocrinol., **46**: 511–520.
- 5 Licht, P., McCreedy, B. R., Barnes, R., and Pang, R. (1983) Gen. Comp. Endocrinol., **50**: 124–145.
- 6 Van Dongen, W. J. and de Kort, E. J. M. (1959) Koninkl. Nederl. Akademie van Wetenschappen-Amsterdam, Ser. C, **62**: 318–326.
- 7 Licht, P. (1973) Gen. Comp. Endocrinol., **20**: 522–529.
- 8 Kobayashi, T. and Iwasawa, H. (1985) Proc. 10th Ann. Meet. Jap. Soc. Comp. Endocrinol., p. 19.

- 9 Van Dongen, W. J., Draisma, R. and de Kort, E. J. M. (1959) Koninkl. Nederl. Akademie van Wetenschappen-Amsterdam, Ser. C, **62**: 327-332.
- 10 Russo, J. and Burgos, M. H. (1969) Gen. Comp. Endocrinol., **13**: 185-188.
- 11 Takada, K., Kubokawa, K. and Ishii, S. (1986) Gen. Comp. Endocrinol., **61**: 302-312.
- 12 Unsicker, K. (1975) Cell Tissue Res., **158**: 215-240.
- 13 Unsicker, K., Axelsson, S., Owman, Ch. and Svensson, K. G. (1975) Cell Tissue Res., **160**: 453-484.
- 14 Kobayashi, T. and Iwasawa, H. (1988) Zool. Sci., **6**: 935-942.
- 15 Takada, K. and Ishii, S. (1984) Zool. Sci., **1**: 617-629.
- 16 Takahashi, H. and Hanaoka, Y. (1981) J. Biochem., **90**: 1333-1340.

[COMMUNICATION]

Reduced Size of Preputial Glands and Absence of Aggressive Behavior in the Genetically Obese (ob/ob) MouseJUNKO YAMASHITA¹, SHIN-ICHI HAYASHI and YUKIO HIRATA²

Department of Nutrition, The Jikei University School of Medicine, Minato-ku, Tokyo 105, and ²Department of Anatomy and Embryology, Tokyo Metropolitan Institute for Neurosciences, Musashidai, Tokyo 183, Japan

ABSTRACT—The preputial gland of freely fed genetically obese (ob/ob) male mice weighed less than that of the lean controls (21 mg vs. 40 mg for unilateral gland). The gland of the ob/ob mice pair-fed with their controls for 45 days was also small (22 mg). The gland of the ob/ob mice, either fed *ad libitum* or pair-fed, contained fewer lipid-secreting cells than that of the lean controls. Upon cohabitation with an unfamiliar male mouse of either ob/ob or lean type, the ob/ob mouse did not exhibit any aggressive behavior which is commonly observed in an adult male mouse housed together with an unfamiliar one. These results indicate that the abnormal feature of the preputial glands in the ob/ob mice is not caused by hyperphagia and is probably related with the absence of aggressive behavior in the ob/ob mice.

INTRODUCTION

We have reported that the genetically obese (ob/ob) mouse has smaller submandibular glands with lower content of nerve growth factor than the lean control [1]. The physiological role of nerve growth factor in the submandibular glands of the mouse has not yet been clarified. Recent reports have shown that a massive amount of nerve growth factor is discharged from the submandibular glands into the bloodstream when adult male mice display aggressive behavior upon cohabitation with un-

familiar male ones [2, 3]. Aggressive behavior is known to be related to the activity of the preputial glands [4-6]. We therefore expected that the ob/ob mice might have abnormal preputial glands and that their aggressive behavior might be different from the lean control's.

In the present study, we investigated the preputial glands of the ob/ob mice histologically, and also examined the effect of food restriction on the glands of these mice since hyperphagia is one of the causes for their obesity [7]. In addition, we observed whether aggressive behavior was provoked in the ob/ob mouse upon cohabitation with an unfamiliar ob/ob or lean mouse.

MATERIALS AND METHODS

The genetically obese (C57BL/6J-ob) and their lean control mice were bred in our laboratory from stock supplied kindly by Dr. M. Miyajima of the Animal Laboratory of Wakayama Medical College. Only male mice were used in this study.

At the age of 50 days, when the ob/ob mice were clearly distinguishable from lean mice, male mice were divided into the ob/ob and lean groups. The mice of each group were group-housed in a polypropylene box (30×20×13 cm) with sawdust, and fed laboratory chow (MF; Oriental Yeast Co. Ltd., Tokyo, Japan). In experiment 1, both the ob/ob and lean control mice were fed *ad libitum*. The experiments were done twice, firstly with four mice for each group and secondly with three mice

Accepted December 27, 1988

Received July 16, 1988

¹ To whom reprint requests should be addressed.

² Present address: Department of Anatomy, School of Medicine, University of the Ryukyus, Okinawa 903-01, Japan.

for each group. In experiment 2, three lean mice were fed *ad libitum*, and three ob/ob mice were subjected to a pair-feeding experiment for 45 days. Thus, food intake of the lean group was measured daily, and the same quantity of food was given to the ob/ob group on the next day. All mice were kept in an air-conditioned room at a temperature of $25 \pm 1^\circ\text{C}$ and a relative humidity of $65 \pm 3\%$ with a 9:00 a.m. to 9:00 p.m. lighting schedule.

At the age of 95 days, each of the ob/ob mice was housed in a polypropylene box with a randomly selected unfamiliar lean or ob/ob mouse and their behaviors were observed for one hr. The mice were then deeply anesthetized with sodium pentobarbital, perfused through the heart with 4% paraformaldehyde in 0.05 M sodium phosphate buffer (pH 7.3) containing 5% sucrose, and then the preputial glands were dissected out. The left preputial gland was freed from adhering adipose and connective tissues, and weighed after the fluid contained in the gland was gently squeezed out according to Hayashi [6]. The right gland was subjected to histological study.

F-test and unpaired Student's t-test were used to compare the results.

RESULTS AND DISCUSSION

In the experiment 1, the preputial glands of the ob/ob mice were smaller and weighed less than those of the lean controls (t-test; $p < 0.01$), while there was no significant difference between their variances (F-test; $p > 0.1$). Since the results of two series of studies were similar for both the ob/ob and lean groups, they were combined in Table 1. The glands of the ob/ob mice had fewer folds with smaller number of lipid-secretory cells than those of lean controls, whereas the size of the lipid-secretory cells in the glands was similar between the two groups.

The abnormalities of the preputial glands in the ob/ob mice were not corrected by food restriction carried out in the experiment 2 (Table 2, Fig. 1). The histological features of the glands of the ob/ob and lean control mice in the experiment 2 were very similar to those of the corresponding groups in the experiment 1. Accordingly, it was concluded that hyperphagia was not the cause of the abnormalities. It is possible, however, that obesity was responsible for that, since the ob/ob mice pair-fed with lean controls still weighed more than

TABLE 1. Body weight and weight of the left preputial gland of male ob/ob and lean mice fed *ad libitum*

Mice	(n)	Body weight(g)	Weight of left preputial gland(mg)
ob/ob	(7)	49.8 ± 1.9^a	21.1 ± 3.1^a
lean	(7)	26.8 ± 0.9	40.0 ± 1.5

The ob/ob and lean mice were each group-housed, and fed *ad libitum*.

Results are mean \pm SEM at the age of 95 days.

^a Significantly different from lean mice ($p < 0.01$).

TABLE 2. Body weight and weight of the left preputial gland of male lean and pair-fed ob/ob mice

Mice	(n)	Body weight(g)		Weight of left preputial gland(mg)
		(50-day-old)	(95-day-old)	
ob/ob	(3)	26.9 ± 0.4^a	38.0 ± 0.7^b	22 ± 3^b
lean	(3)	21.8 ± 1.2	27.2 ± 1.1	40 ± 2

The ob/ob mice were group-housed, and pair-fed with group-housed lean mice. Results are mean \pm SEM for 3 mice of each group. Significantly different from lean mice (a: $p < 0.05$, b: $p < 0.01$).

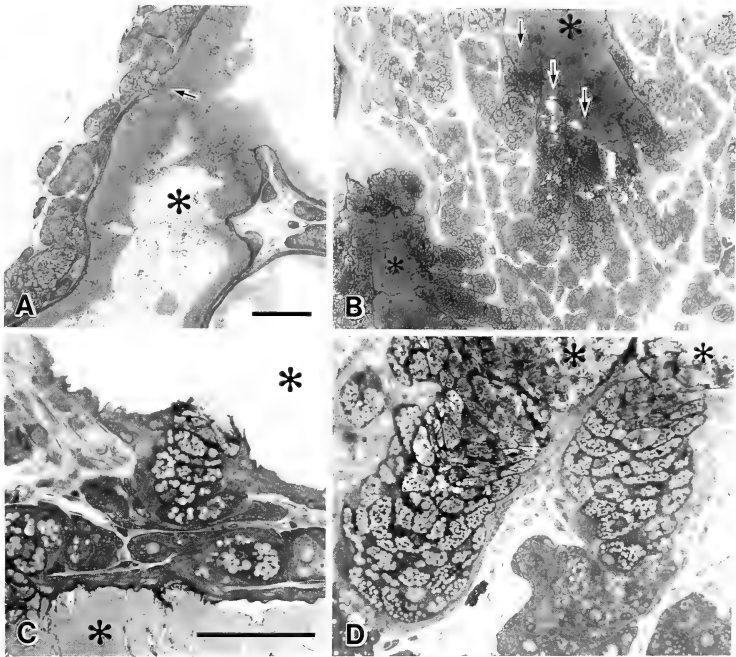


FIG. 1. Photomicrographs of the preputial glands from the ob/ob (A, C) and the lean control (B, D) mice. In the ob/ob mouse of the experiment 2 (body weight 37.4 g, preputial gland 15 mg), the glandular lumen (asterisks) is much wider than that of the lean control (body weight 29.5 g, preputial gland 37 mg), and the secretory acini are less numerous and less complicated than those of the lean mouse. Arrow heads: Opening of the secretory acini into the lumen. 1.5 μ m resin sections stained with toluidine blue/safranin-O. Scale bars: 100 μ m in A and 50 μ m in C and D.

the lean controls. This overweight was probably due to low metabolic rate of the ob/ob mouse compared with the lean control [8].

Meanwhile, intermale spontaneous aggression is a common phenomenon in this species [9]. It is known that the preputial gland of a male mouse plays an important role maintaining the aggressivity not only of a cohabitant male but also of its owner [10]. Hence we supposed that the ob/ob mouse might not elicit aggressive behavior of a cohabitant, and/or not display aggressive behavior

against a cohabitant when it was housed together with an unfamiliar male mouse. We therefore examined their behavior during one hr cohabitation.

Upon cohabitation with a lean mouse, four of ten lean mice in the experiments 1 and 2 attacked a cohabitant 1~5 times with a latency of 2~21 min and sometimes mounted on the cohabitant after fighting. Upon cohabitation with the ob/ob mouse three of them also chased a cohabitant ob/ob mouse and tried to mount 1~3 times with the

latency of 33–36 min. The mounting behavior against the ob/ob mouse was always displayed without mutual aggressive behavior. On the other hand, none of the ob/ob mice displayed any aggressive behavior against a cohabitant, irrespective as to whether it was an ob/ob or lean mouse. In addition, we have often observed that lean mice of the present strain sometimes display intermale aggressive behavior even against familiar lean mice, whereas we have never observed mutual aggressive behavior between ob/ob mice.

The ob/ob mouse shows depressed serum concentration of testosterone [11], and it is also suggested that it has an impaired thyroid function [12]. These hormones are known to be related to the preputial gland weight as well as the aggressiveness in the mouse [13, 14]. Abnormal status of these hormones may directly affect the preputial gland as well as the aggressive behavior. Alternatively, nerve growth factor released from the submandibular glands may play an essential role in the development of preputial glands in the normal mouse and this process may be impaired in the ob/ob mouse, since it is reported that these hormones increase the tissue weight and nerve growth factor content in the submandibular glands of the ob/ob mouse [15]. Further studies are needed to examine these possibilities.

ACKNOWLEDGMENTS

We thank Dr. S. Hayashi of Kagoshima University for valuable advice on measurement of the preputial gland

and Dr. T. Kimura of Tokyo University for helpful information.

REFERENCES

- 1 Yamashita, J., Hirata, Y. and Hayashi, S. (1986) *Int. J. Obesity*, **10**: 461–465.
- 2 Aloe, L., Alleva, E., Böhm, A. and Levi-Montalcini, R. (1986) *Proc. Natl. Acad. Sci.*, **83**: 6184–6187.
- 3 Lakshmanan, J. (1986) *Am. J. Physiol.*, **250**: E386–E392.
- 4 Branson, F. H. and Marsden, H. M. (1973) *Behav. Biol.*, **9**: 625–628.
- 5 Brain, P. F. (1983) *Boll. Zool.*, **50**: 173–187.
- 6 Hayashi, S. (1986) *Physiol. Behav.*, **38**: 299–300.
- 7 Mayer, J., Dickie, M. M., Bates, M. W. and Vitale, J. J. (1951) *Science*, **113**: 745–746.
- 8 Davis, T. R. A. and Mayer, J. (1954) *Am. J. Physiol.*, **177**: 222–226.
- 9 Wimer, R. E. and Fuller, J. L. (1966) In "Biology of the Laboratory Mouse, 2nd edition". Ed. by Green, E. L. *et al.*, McGraw-Hill, New York/Toronto/Sydney/London, pp. 629–653.
- 10 Hayashi, S. (1987) *Zool. Sci.*, **4**: 551–555.
- 11 Swerdloff, R. S., Batt, R. A. and Bray, G. A. (1976) *Endocrinology*, **98**: 1359–1364.
- 12 Wykes, A. A., Christian, J. E. and Andrews, F. N. (1958) *Endocrinology*, **62**: 535–538.
- 13 Mugford, R. A. and Nowell, N. W. (1971) *Physiol. Behav.*, **6**: 247–249.
- 14 Mainardi, D., Mainardi, M., Valenti, G. and Vescovi, P. P. (1981) *Boll. Zool.*, **48**: 319–322.
- 15 Bray, G. A., Shimomura, Y., Ohtake, M. and Walker, P. (1982) *Endocrinology*, **110**: 47–50.

[COMMUNICATION]

Induction of Male Sexual Behaviors by Administration of Testosterone Using Silastic Tubes in Castrated Male and Female Rats

SHINJI KUSAKA, HIROSHI NAGASAWA¹, KOREHITO YAMANOUCHI²
and YASUMASA ARAI³

Application and Training Division, Ciba Corning Diagnostics KK, Shibuya-ku, Tokyo 150, ¹Experimental Animal Research Laboratory, Meiji University, Kawasaki 214, ²Neuroendocrinology, Department of Basic Human Sciences, School of Human Sciences, Waseda University, Mikajima, Saitama 359, and ³Department of Anatomy, Juntendo University School of Medicine, Bynkyo-ku, Tokyo 113, Japan

ABSTRACT—In order to determine a suitable length of Silastic tubes (3.18 o.d. \times 1.57 i.d. mm Dow-Corning) containing testosterone (T) for induction of normal level of male sexual activity, two 5 cm (T10 group) or two 3 cm tubes (T6 group) were implanted subcutaneously in sexually inexperienced castrated males. T10 males showed stronger sexual activity than T6 males and intact control males. Sexual activity of T6 males was almost the same level as that intact males. Ovariectomized females with two 5 cm T-tubes (F10) showed only low level of mounting activity. These results indicate that implantation of two 3 cm Silastic tubes containing T is useful to induce normal level of male sexual activity in castrated male rats.

INTRODUCTION

Adult male rats show a series of male sexual behaviors—mount, intromission and ejaculation, when they find an estrous female [1, 2]. Castration depresses the display of these sexual behaviors and androgen replacement therapy restores these behaviors in males [3–5]. Antiandrogen also suppresses sexual behaviors of males [6]. These results indicate that male sexual behaviors depend

on the blood level of androgen. However, in order to induce the complete male copulatory behavior in castrated male rats, successive subcutaneous injections of androgen for a long period are necessary [7, 8]. Wada [9] reported that administration of androgen using Silastic tubes instead of injections was effective to induce male sexual calling in castrated male Japanese quails. In the present report, since Silastic tubes has been reported to be useful in maintaining a constant blood level of steroids [10, 11], two kinds of length of Silastic tubes containing testosterone (T) were implanted subcutaneously in castrated male rats, in order to restore normal level of behavioral activity.

MATERIALS AND METHODS

Sexually inexperienced Wistar males (210–250 g) and female rats (255–290 g) were maintained under controlled photoperiod (14:10 hr, light:dark) and temperature (24–25°C). Twenty-two males and 7 females were castrated under anesthesia. Seven males without castration served as intact controls. Three weeks after castration, all castrated animals received subcutaneous implantation of T(Sigma) using Silastic medical grade

Accepted January 6, 1989

Received October 27, 1987

³ To whom reprint requests should be addressed.

tubing (3.18 mm o.d. \times 1.57 mm i.d., Dow-Corning, Michigan) according to the technique of Legan *et al.* [10] and Nash *et al.* [11]. Silastic tubing was cut into 3 or 5 cm segments and one end was sealed with Silastic adhesive (Dow-Corning). After allowing to dry, each tube was loosely packed with T and sealed completely. The mean contents of T in 3 and 5 cm tubes were 20.6 ± 0.5 mg and 43.9 ± 1.0 mg, respectively. Before implantation, all tubes containing T were incubated overnight in saline solution. Eight castrated males were subcutaneously implanted with two 3 cm tubes containing T in the right and left back (T6). In other 8 castrated males, a pair of 5 cm tubes with T was implanted (T10). Six castrated males received vacant tubes (controls, T0). In addition, 7 ovariectomized rats were implanted with two 5 cm tubes containing T (FT10).

Behavioral tests were carried out on days 5, 10, 15 and 20 following T implantation. Each experimental rat was adapted in an observation cage (60 \times 50 \times 40 cm) for 3–4 min. Then, a receptive female pretreated with estrogen and progesterone prior to the test was placed with the experimental animal. The observation was continued for 30 min. The receptive female was replaced by another receptive female every 10 min in order to diminish the influence of affinity between the experimental animal and the female. The following standard measures were recorded; mount frequency (MF, number of mounts with thrust and with or without intromission from the start to the first ejaculation or during 30 min if no ejaculation); intromission frequency (IF, number of mounts with intromission); ejaculation frequency (EF, number of ejaculation during 30 min); mount, intromission and ejaculation latencies (ML, IL, EL, time from the introduction of the receptive female to the first occurrence of each behavioral pattern). MF and IF were indicated after converting to the frequency per 5 min. After the end of the test series, all tubes implanted in order to check the reduced amounts of T during implantation in each tube.

RESULTS AND DISCUSSION

All of 6 castrated males which received the

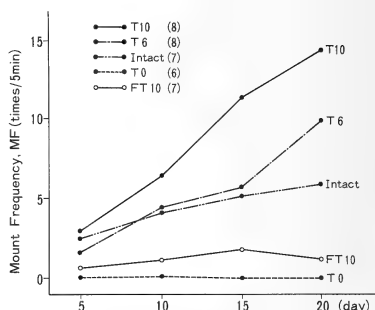


Fig. 1. Effect of subcutaneous implantation of Silastic tubes containing testosterone (T) on mean mount frequency (MF). Castrated male rats were implanted with two 3 cm (T6), two 5 cm (T10) or vacant (T0) tubes. Ovariectomized female rats were implanted with two 5 cm tubes (FT10).

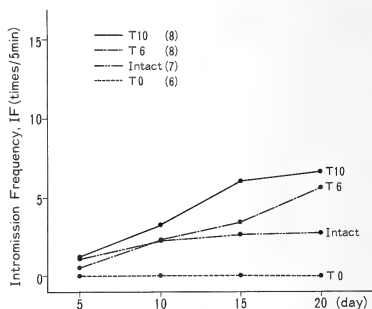


Fig. 2. Effect of implantation of T on mean intromission frequency (IF) in intact males, castrated males and females. T6, castrated males implanted with two 3 cm Silastic tubes containing T; T10, castrated males with two 5 cm tubes; T0, castrated males with vacant tubes.

vacant tubes (T0) showed no sexual behavior throughout. As shown in Figures 1 and 2 and Table 1, the incidence of mounts and intromissions in T0 and intact control males were low in the first test, being not significantly different from that of T0 group. No significant difference in the mean MF and IF was detected among T6, intact and T0

TABLE 1. Incidence (I) and latency (L) of mount and intromission behaviors in each group

Group	DAY 5		DAY 10		DAY 15		DAY 20	
	I	L	I	L	I	L	I	L
MOUNTING								
T6	3/8	125	7/8	18	7/8	14	7/8	8
T10	6/8	311	8/8	14	8/8	5.5	8/8	6
Intact	4/7	70	5/7	11	6/7	9	6/7	46.5
Female	2/7	460.5	4/7	464	4/7	23	4/7	64
INTROMISSION								
T6	2/8	811	5/8	158	6/8	15	7/8	17
T10	5/8	502	7/8	79	8/8	12.5	8/8	18
Intact	4/7	109.5	5/7	60	6/7	22.5	6/7	491
Female	0/7	—	1/7	935	1/7	222	1/7	65

The data in the T0 group are not included in this table, because they did not show male sexual behaviors in 4 tests. L (see): median value.

TABLE 2. Incidence (IE), frequency (EF) and latency (EL) of ejaculation in each group

Group	DAY 10			DAY 15			DAY 20		
	IE	EF+SEM	EL	IE	EF+SEM	EL	IE	EF+SEM	EL
T6	1/8	0.1±0.1	1037	3/8	0.6±0.3	631	3/8	0.6±0.4	1389
T10	3/8	0.5±0.3	1487	6/8	1.0±0.3	1201.5	7/8	1.6±0.3	860
Intact	1/7	0.3±0.3	651	2/7	0.4±0.3	931	3/7	0.6±0.3	1297

The data in the T0 and female groups are not included in this table, because none of them show ejaculatory pattern throughout tests. EL (sec): median value.

groups. Only one intact males achieved to ejaculation in the first test (Table 1). In T10 group, the incidence ($p<0.05$, X^2 -test) and frequency ($p<0.05$, t -test) of mounts (but not intromission) were significantly greater than those in the T0 group. In the second test (day 10), the mean MF and IF of T10, T6 and intact males were significantly larger than those of T0 males. The mean MF and IF of T10 males were still comparable to those of T6 and intact males. In the third test (day 15), however, T10 males became sexually more active, compared to T6 and intact males. The mean MF and IF of T10 males were 11.4 ± 1.2 and 6.1 ± 1.2 , respectively, being significantly greater than those of T6 males ($MF=5.7\pm1.9$, $IF=3.4\pm1.9$) and intact males ($MF=5.2\pm1.7$, $IF=2.6\pm1.1$) ($p<0.025$). Ejaculation was observed in 6 of 8 T10, 3 of 8 T6 and 2 of intact males in the last test (day 20, see

Table 2). The mean MF (14.5 ± 1.4) and IF (6.7 ± 0.9) in T10 males was significantly higher than those in the intact males ($MF=5.9\pm1.8$, $IF=2.7\pm1.3$) ($p<0.01$ and $p<0.05$, respectively). The ML and IL in T10 males were significantly shorter than those of intact controls ($p<0.05$, U -test). In T6 males, the mean MF (9.9 ± 2.4) and IF (5.8 ± 1.9) were not significantly different from those in intact males. T10 males showed ejaculation more frequently than the males of other groups and the mean EF (1.6 ± 0.4) during 30 min was significantly higher than those in T6 and intact males (0.6 ± 0.4 and 0.6 ± 0.3 respectively) ($p<0.05$, t -test). The mean amount of T decreased during 20 days implantation was 3.5 ± 0.7 mg in cm Silastic tubes and 6.6 ± 0.7 mg in 10 cm tubes, respectively.

Thus, the sexual activity in all groups except T0 increased gradually in 4 tests. Cumulative hor-

monal effects may be the most important factor for restoration of sexual behavioral activity in castrated male rats. However, the experience and habituation to testing as an influencing factor cannot be excluded, because an increase in behavioral activity was observed in intact males during the course of the experiment.

The result that castrated males with two 5 cm tubes containing T (T10) showed significantly higher sexual activity than males with two 3 cm tubes (T6) in the present study indicates that male sexual activity is dependent on the length of Silastic tube containing T when implanted subcutaneously to castrated males. To induce sexual activity comparable to that of intact males, implantation of two 3 cm tubes filled with T appears to be enough. Since approximately 3.5 mg of T would be released from 3×2 cm tube for 20 days, T6 males may receive 175 µg of T daily for 20 days. In our previous study, daily injections of 500 µg testosterone propionate (TP) for 21 days were necessary to induce intact male levels of male sexual behaviors in castrated male rats [8]. In general, TP is thought to be more active than T [12] and the effect of the propionate derivative lasts longer. Thus, the use of Silastic tubes for androgen administration seems to be quite favorable to induce male sexual behaviors in castrated males, because a smaller dose of T given by Silastic tubes is enough to induce normal levels of male sexual activity in castrated males. This may be because Silastic tubes can allow the continuous release of steroid contained [10].

In the females with two 5 cm tubes containing (F10), none showed ejaculatory pattern and only one female displayed intromission pattern throughout the test series. Mounting behavior was observed in 4 of 7 females and the mean MF was 0.7 ± 0.5 , 1.2 ± 0.5 , 1.8 ± 0.9 and 1.2 ± 0.6 in 4

tests, respectively. This result confirmed the previous reports that masculine sexual behaviors are very rare in ovariectomized female rats even when treated with high doses of androgen [8, 13].

ACKNOWLEDGMENTS

The authors gratefully thank Dr. M. Wada, Tokyo Medical and Dental University, for his advice about the technique of steroid administration using Silastic tubings. This study was supported by Grants-in Aid to YA from the Ministry of Education, Science and Culture of Japan.

REFERENCES

- 1 Young, W. C. (1961) In "Sex and Internal Secretion". Ed. by W. C. Young, Krieger, Huntington, pp. 1173-1239.
- 2 Dewsbury, D. A. (1979) In "Endocrine Control of Sexual Behavior". Ed. by C. Beyer, Raven, New York, pp. 3-32.
- 3 Davidson, J. M. (1966) *Anim. Behav.*, **14**: 2-3.
- 4 Beyer, C., Larsson, K., Perez-Palacios, G. and Morali, G. (1973) *Horm. Behav.*, **4**: 99-108.
- 5 Hamburger-Bar, R. and Rigter, H. (1977) *Acta Endocrinol.* **84**: 813-828.
- 6 Södersten P., Gray, G., Damassa, D. A., Smith, E. R. and Davidson, J. M. (1975) *Endocrinology*, **97**: 1468-1475.
- 7 Södersten P. and Larsson, K. (1975) *Physiol. Behav.* **14**: 159-164.
- 8 Yamanouchi, K. (1977) *Endocrinol. Japon.* **27**: 499-504.
- 9 Wada, M. (1982) *Horm. Behav.*, **16**: 147-157.
- 10 Legans, S. J., Coon, G. A. and Karsch, F. J. (1975) *Endocrinology*, **96**: 50-56.
- 11 Nash, H. J., Robertson, D. N., Young A. J. M. and Atkinson, L. E. (1978) *Contraception*, **18**: 367-394.
- 12 Larsson, K. (1979) In "Endocrine Control of Sexual Behaviors". Ed. by C. Beyer, Raven, New York, pp. 77-163.
- 13 Pfaff, D. W. (1970) *J. Comp. Physiol. Psychol.*, **73**: 349-358.

Development Growth & Differentiation

Published Bimonthly by the Japanese Society of
Developmental Biologists
Distributed by Business Center for Academic
Societies Japan, Academic Press, Inc.

Papers in Vol. 31, No. 5. (October 1989)

45. **REVIEW:** R. P. Elinson and K. R. Kao: The location of dorsal information in frog early development.
46. R. D. Burke and C. Bouland: Pigmented follicle cells and the maturation of oocytes in the sand dollar, *Dendraster excentricus*.
47. H. Katow: Characterization of vegetal plate cells separated from cytochalasin B-treated blastulae of the sea urchin, *Clypeaster japonicus*.
48. K. Chiba and M. Hoshi: Three phases of cortical maturation during meiosis reinitiation in starfish oocytes.
49. K. Chiba and M. Hoshi: Activation of starfish oocytes modifies their hormone dependent period for 1-methyladenine in meiosis reinitiation.
50. Y. Sendai, T. Ohta and K. Aketa: Involvement of wheat germ agglutinin (WGA)-binding protein in the induction of the acrosome reaction of the sea urchin, *Strongylocentrotus intermedius*. I. WGA affects the ion fluxes associated with the acrosome reaction.
51. Y. Sendai and K. Aketa: Involvement of wheat germ agglutinin (WGA)-binding protein in the induction of the acrosome reaction of the sea urchin, *Strongylocentrotus intermedius*. II. Antibody against WGA-binding protein induces the acrosome reaction.
52. R. McPherson, M. S. Greeley Jr. and R. A. Wallace: The Influence of yolk protein proteolysis on hydration in the oocytes of *Fundulus heteroclitus*.
53. R. Gualtieri, G. Cafiero and P. Andreuccetti: Plasma membrane domains and the site of sperm entrance in *Discoglossus pictus* (Anura) eggs.
54. K. Kawamura, H. Fujita and M. Nakauchi: Concanavalin A modifies allo-specific sperm-egg interactions in the ascidian, *Ciona intestinalis*.
55. M. Dan-Sohkawa and H. Kaneko: Sorting out of presumptive stomach cells of the starfish embryo.

Development, Growth and Differentiation (ISSN 0012-1592) is published bimonthly by The Japanese Society of Developmental Biologists, Department of Developmental Biology, Mitsubishi Kasei Institute of Life Science, Minami-ootani 11, Machida, Tokyo 194, Japan. 1989: Volume 31. Annual subscription for Vol. 31, 1989: U. S. \$ 136.00, U. S. and Canada: U. S. \$ 150.00, all other countries except Japan. All prices include postage, handling and air speed delivery except Japan. Second class postage paid at Jamaica, N.Y. 11431, U. S. A.

Outside Japan: Send subscription orders and notices of change of address to Academic Press, Inc., Journal Subscription Fulfillment Department, 1 East First Street, Duluth, MN 55802, U. S. A. Send notices of change of address at least 6-8 weeks in advance. Please include both old and new addresses. U. S. A. POSTMASTER: Send changes of address to *Development, Growth and Differentiation*, Academic Press, Inc., Journal Subscription Fulfillment Department, 1 East First Street, Duluth, MN 55802, U. S. A.

In Japan: Send nonmember subscription orders and notices of change of address to Business Center for Academic Societies Japan, 16-3, Hongo 6-chome, Bunkyo-ku, Tokyo 113, Japan. Send inquiries about membership to Business Center for Academic Societies Japan, 4-16, Yayoi 2-chome, Bunkyo-ku, Tokyo 113, Japan.

Air freight and mailing in the U. S. A. by Publications Expediting, Inc., 200 Meacham Avenue, Elmont, NY 11003, U. S. A.

NARISHIGE

THE ULTIMATE NAME IN MICROMANIPULATION

OUR NEW MODELS **WR-88** and **MO-102M**
MAKE PRECISION MICROMANIPULATION SO EASY!



SOME FEATURES of THE WR-88 WATER ROBOT MICROMANIPULATOR (3-DIMENSIONAL)

- * Drift-free, the new WR-88 has a DRIFT movement of less than 2 microns.
- * The new WR-88 has a SMOOTH MICRODRIVE MECHANISM.
- * An Aqua Purificate remote control ensures totally vibration-free operation.



NARISHIGE SCIENTIFIC INSTRUMENT LAB.

9-28 KASUYA 4-CHOME SETAGAYA-KU, TOKYO 157, JAPAN
PHONE (INT-L) 81-308-8233, FAX (INT-L) 81-3-308-2005
CABLE : NARISHIGE LABO, TELEX, NARISHIGE J27781

(Contents continued from back cover)

ovarian response to photoperiods in orange-red type medaka	943
------------------------------------------------------------------	-----

Endocrinology

Fujii, K., N. Ohta, T. Sasaki, Y. Sekizawa, C. Yamada and H. Kobayashi: Immunoreactive FMRamide in the nervous system of the earthworm, <i>Eisenia foetida</i>	951
Takada, K., M. Itoh, H. Nishio and S. Ishii: Purification of toad (<i>Bufo japonicus</i>) gonadotropins and the development of their homologous radioimmunoassays	963

Behavior Biology

Yamashita, J., S. Hayashi and Y. Hirata: Reduced size of preputial glands and absence of aggressive behavior in the genetically obese (ob/ob) mouse (COMMUNICATION)	1033
---------------------------------------------------------------------------------------------------------------------------------------------------------------------------	------

Kusaka, S., H. Nagasawa, K. Yamanouch and Y. Arai: Induction of male behaviors by administration of testosterone using silastic tubes in castrated male and female rats (COMMUNICATION)	1037
Terami, H. and M. Watanabe: Excessive transitory migration of guppy populations. III. Analysis of perception of swimming space and a mirror effect	975

Taxonomy and Systematics

Nagatomi, A., H. Imaizumi and H. Nagatomi: Revision of <i>Molobratia</i> from Japan and Taiwan (Insecta, Diptera, Asilidae)	983
Saitoh, M., N. Matsuoka and Y. Obara: Biochemical systematics of three species of the Japanese long-tailed field mice; <i>Apodemus speciosus</i> , <i>A. giliacus</i> and <i>A. argenteus</i>	1005

ZOOLOGICAL SCIENCE

VOLUME 6 NUMBER 5

OCTOBER 1989

CONTENTS

REVIEWS

- Ueck, M., K. Wake and H. Kobayashi: Nervous organization of the pineal complex in lower vertebrates817

- Oami, K. and Y. Naito: Bioelectric control of effector responses in the marine dinoflagellate, *Noctiluca miliaris*833

ORIGINAL PAPERS

Physiology

- Okajima, A. and K. Kumagai: The inhibitory control of prothoracic gland activity by the neurosecretory neurones in a moth, *Mamestra brassicae*851

- Okajima, A., K. Kumagai and M. Watanabe: The involvement of afferent chemoreceptive activity in the nervous regulation of the prothoracic gland in a moth, *Mamestra brassicae*859

- Tamamaki, N.: Visible light reception of accessory eye in the giant snail, *Achatina fulica*, as revealed by an electrophysiological study867

- Tamamaki, N.: The accessory photosensory organ of the terrestrial slug, *Limax flavus* L. (Gastropoda, Pulmonata): morphological and electrophysiological study877

- Shiga, T., Y. Oka, M. Satou, N. Okumoto and K. Ueda: Retinal projections in the himé salmon (landlocked red salmon, *Oncorhynchus nerka*)885

Cell Biology

- Asashima, M., T. Oinuma and S. Komazaki: Electron microscopical and histochemical studies of the spontaneous tumors of *Xenopus laevis*899

- Yashika, K. and P. H. Hashimoto: Annulate lamellae in prothoracic gland cells of brainless pupae of the swallowtail, *Papilio xuthus* (Lepidoptera)907

Immunology

- Shozawa, A., C. Suto and N. Kumada: Superoxide production by the haemocytes of the freshwater snail, *Biomphalaria glabrata*, stimulated by miracidia of *Schistosoma mansoni* (COMMUNICATION)1019

Biochemistry

- Suzuki, T., T. Takagi, K. Okuda, T. Furukohri and S. Ohta: The deep-sea tube worm hemoglobin: subunit structure and phylogenetic relationship with annelid hemoglobin915

Developmental Biology

- Tanaka, A. and M. H. Ross: Tibia to femur ratios of unaltered and regenerated legs of the stumpy mutant of the German cockroach927

- Hamaguchi, Y.: Effect of ATP_γs on fertilization envelope elevation of sand dollar eggs (COMMUNICATION)1023

Reproductive Biology

- Kobayashi, T. and H. Iwasawa: The role of Sertoli cells adjacent to efferent ductules in sperm transport in *Rana porosa porosa* ..935

- Kobayashi, T., A. Oshimi and H. Iwasawa: Development of an *in vitro* spermiation system in the frog, *Rana nigromaculata* (COMMUNICATION)1028

- Awaji, M. and I. Hanyu: Seasonal changes in

(Contents continued on inside back cover)

INDEXED IN:

Current Contents/LS and AB & ES,
Science Citation Index,
ISI Online Database,
CABS Database, INFOBIB

Issued on October 15
Printed by Daigaku Letterpress Co., Ltd.,
Hiroshima, Japan

Vol. 6 No. 6

December 1989

RL
2864
NH

ZOOLOGICAL SCIENCE

An International Journal

**Proceedings of the
Sixtieth Annual Meeting of the
Zoological Society of Japan
October 4-6, 1989
Kyoto**

Vol. 6 No. 6 December 1989

published by Zoological Society of Japan

**distributed by Business Center for Academic Societies Japan
VSP, Zeist, The Netherlands**

ISSN 0289-0003

ZOOLOGICAL SCIENCE

The Official Journal of the Zoological Society of Japan

Editor-in-Chief:

Hideshi Kobayashi (Tokyo)

Managing Editor:

Chitaru Oguro (Toyama)

Assistant Editors:

Yuichi Sasayama (Toyama)

Hitoshi Michibata (Toyama)

Miéko Komatsu (Toyama)

The Zoological Society of Japan:

Toshin-building, Hongo 2-27-2, Bunkyo-ku,
Tokyo 113, Japan. Tel. (03) 814-5675

Officers:

President: Hiromichi Morita (Fukuoka)

Secretary: Hideo Namiki (Tokyo)

Treasurer: Tadakazu Ohoka (Tokyo)

Librarian: Masatsune Takeda (Tokyo)

Editorial Board:

Howard A. Bern (Berkeley)

Horst Grunz (Essen)

Susumu Ishii (Tokyo)

John M. Lawrence (Tampa)

Kazuo Moriwaki (Mishima)

Hidemi Sato (Nagoya)

Ryuzo Yanagimachi (Honolulu)

Walter Bock (New York)

Robert B. Hill (Kingston)

Seiichi Kawashima (Tokyo)

Kosak Maruyama (Chiba)

Tokindo S. Okada (Okazaki)

Hiroshi Watanabe (Tokyo)

Aubrey Gorbman (Seattle)

Yukio Hiramoto (Chiba)

Yukiaki Kuroda (Mishima)

Roger Milkman (Okazaki)

Andreas Oksche (Giessen)

Mayumi Yamada (Sapporo)

ZOOLOGICAL SCIENCE is devoted to publication of original articles, reviews and communications in the broad field of Zoology. The journal was founded in 1984 as a result of unification of Zoological Magazine (1888-1983) and *Annotationes Zoologicae Japonenses* (1897-1983), the former official journals of the Zoological Society of Japan. ZOOLOGICAL SCIENCE appears bimonthly. An annual volume consists of six numbers of more than 1100 pages including an issue containing abstracts of papers presented at the annual meeting of the Zoological Society of Japan.

MANUSCRIPTS OFFERED FOR CONSIDERATION AND CORRESPONDENCE CONCERNING EDITORIAL MATTERS should be sent to:

Dr. Chitaru Oguro, Managing Editor, Zoological Science, Department of Biology, Faculty of Science, Toyama University, Toyama 930, Japan, in accordance with the instructions to authors which appear in the first issue of each volume. Copies of instructions to authors will be sent upon request.

SUBSCRIPTIONS. ZOOLOGICAL SCIENCE is distributed free of charge to the members, both domestic and foreign, of the Zoological Society of Japan. To non-member subscribers within Japan, it is distributed by Business Center for Academic Societies Japan, 6-16-3 Hongo, Bunkyo-ku, Tokyo 113. Subscriptions outside Japan should be ordered from the sole agent, VSP, Utrechtseweg 62, 3704 HE Zeist (postal address: P. O. Box 346, 3700 AH Zeist), The Netherlands. Subscription rates will be provided on request to these agents. New subscriptions and renewals begin with the first issue of the current volume.

All rights reserved. No part of this publication may be reproduced or stored in a retrieval system in any form or by any means, without permission in writing from the copyright holder.

© Copyright 1989, The Zoological Society of Japan

[Publication of Zoological Science has been supported in part by a Grant-in-Aid for
Publication of Scientific Research Results from the Ministry of Education, Science
and Culture, Japan.]

OBITUARY



Nobuo Egami (1925-1989)



Emeritus Professor Nobuo Egami of the University of Tokyo and President of the Zoological Society of Japan died of colon cancer at the age of 64 on the 17th of October 1989. His untimely death has deeply grieved those who knew him and those who worked with him. His death is a great loss to the field of zoological science both in Japan and abroad.

Nobuo Egami was born on the 5th of January 1925 in Kanazawa City in the middle of Honshu on the Japan Sea. In 1941 he entered the Eighth High School (Hachi-kou), Science Course, at Nagoya. Inspired by his teacher of biology, Professor Masao Kumazawa, at the High School, Egami became interested in Zoology. After graduation in 1944, he entered the Zoological Institute of the Faculty of Science, the Imperial University of Tokyo (now the University of Tokyo). On the day of his enrolment in the University, he first encountered the Medaka *Oryzias latipes* actively swimming in a glass aquarium in the corridor of the Institute. This encounter was decisive for his life-long choice of the Medaka as his main experimental animal. At Todai, he became a student of the late Professor Yô K. Okada and pursued studies on sex and reproduction in various invertebrates including bivalves, crustaceans, insects and nematodes for his graduation thesis, while continuing to observe the reproductive function and behavior of the Medaka. Thus, his early papers were concerned with studies on sexuality in the Japanese oyster and in marine copepods (1951-1953) and on geographical variations in the male characters of the Medaka (1954). His full-fledged research on the Medaka, however, began when he graduated from the University in September 1947 and was enrolled in Graduate School at the University of Tokyo, where he initiated his successful scientific career.

In 1949 Egami finished the post-graduate course and was appointed to the position of Assistant (Instructor) in Okada's laboratory and was promoted to Lecturer in 1950. After the retirement of Okada in 1952, Egami collaborated with the late Professor Kiyoshi Takewaki, the pioneer of general and comparative endocrinology of Japan, in his development of the Third Laboratory (Endocrinology and Experimental Morphology Laboratory) of the Zoological Institute. It was at this time that Egami

began his fascinating studies on the reproductive physiology of the Medaka that were to lead to future discoveries on the cell biology and genetic mechanism of aging and carcinogenesis in the Medaka. He examined the effects of hormonal steroids, artificial photoperiodicity and salinity on ovarian growth, appearance of male characters and production of ova by the testis in the Medaka (1954-1959). The male characters generally develop in response to androgenic stimulation. If adult females of the Medaka were kept in water containing methyltestosterone, male characters, such as papillary processes on the joints of the anal fin-rays, developed, owing to enhanced cell proliferation. However, responsiveness to androgen differs among teleost species. He suggested that the difference was not due to the blood level of androgen but to the sensitivity to androgen. Radioimmunoassay was not established at that time, and he studied the metabolism of radiolabeled acetate and progesterone as substrates by the testis. From progesterone, 17 α -hydroxyprogesterone and androstenedione, in addition to a testosterone-like substance, were produced. For these contributions, he was awarded the Zoological Society of Japan Prize in 1963.

In 1961 he was invited to serve as Head of the First Laboratory, Division of Biology, National Institute for Radiological Sciences (NIRS) in Chiba, and later became Director of the Division of Biology. He worked at the NIRS for 9 years before he returned to the University of Tokyo. During this period he initiated and performed his important radiobiological experiments using the Medaka, in collaboration with his colleagues in the NIRS, mentioned below.

He returned to the Zoological Institute, the Faculty of Science, the University of Tokyo, as Professor of the Third Laboratory in 1970. From April 1973 he was in charge of the Laboratory of Radiation Biology, succeeding Dr. Koichi Akita in the post of professor of radiation biology. During this period he continued his work, initiated in the NIRS, on the elucidation of mechanisms of biological action of radiation using teleosts, in particular the Medaka (1961-1985). As a result of his efforts, the value of the Medaka with its relatively simple body architecture was fully recognized in the accurate analysis of radiation effects. He found survival of the Medaka after irradiation decreased in a dose-dependent manner, but that the killing effect was retarded if the irradiated fish were kept at lower temperatures. The low-temperature effect was found to be due to the alteration in the rates of loss and renewal of intestinal epithelial cells. A major series of experiments clearly demonstrated that radiation-induced death was the consequence of the failure of cell renewal systems. These findings have important implications for understanding the mechanisms of aging and carcinogenesis.

As a supervisor of students and younger colleagues, Egami was always warm, helpful, and encouraging. Every morning, he arrived in his office in the Institute around 7 a.m. He enjoyed talking with his young colleagues not only about science but also about any matter of common concern. His conversation with his colleagues, always early in the morning, used to start with "How is it going? Anything interesting, anything new, anything exciting?". This was followed by a brief report, 10 minutes at the most, of any recent advances. From this input, Egami would easily grasp the research progress of all of his colleagues. On one point he was firm; the need to write and publish papers at proper times during the course of an investigation.

During his professorship at the University of Tokyo, Egami served the University as a member of the University Senate, as Dean of the Faculty of Science, as a member of the Graduate School Council, among many other functions. From 1976 to 1978, he was also Director of the University Museum which consists of seventeen departments. Egami exhibited his extraordinary administrative ability to the entire University. This ability cannot be commended too much, if one considers that Dr. Egami never allowed his research activity to slacken even during his busiest administrative days.

Egami was President of the Zoological Society of Japan from 1979 to 1982 and from 1987 until his death. All members of the Society feel great regret at the loss of their distinguished leader. The membership increased markedly after 1970, and along with the diversification of zoology, the Society faced up to some fundamental changes in its structure and function. In particular, a committee was

convened to examine the nature of the official Society publications. During his presidency, it was decided to combine the two existent journals and to create an international journal, "Zoological Science". He stated in the first issue (Vol. 1, No. 1, page 1, 1984) that "as the success of this re-organization hinges on the contents of the journal, we are inexorably dependent upon the criticism and support not only of the Zoological Society of Japan, but of scientists everywhere concerned with zoology and biology". His enthusiasm for the Society and for the broadening of its scope to include new fields of animal biology can be seen in his President's Message in Zoological Science (Vol. 4, p. 957, 1987). As a testament to his memory, a part of this message is cited here: "Our Society is characterized by its dedication to the very wide field of zoology, and by a membership comprising both elder and younger members. It is my desire that our members do not restrict themselves to one narrow field, but instead have an interest in all of biology.—We must not let ourselves become satisfied only with the existence of our Society; instead, it is necessary for us to assert to the world in this day of strong expectation for Life Sciences, our important role and compelling reason for existence. We must preserve free atmosphere and flavor of our Society in which every member can devote himself to his basic and independent research. At the same time, we would like our Society to be a humane, professional group which can contribute to the many problems human beings confront, from bioethical issues which arise in the genetic engineering pursued in biotechnology, to the problems of population, food, and existence."

Egami's contributions to the academic world go far indeed. He served as the member of a number of committees and councils of the Ministry of Education, Science and Culture, the Science and Technology Agency, the Science Council of Japan, and the Japan Society for the Promotion of Science. He was also on the Boards of the National Institute of Genetics in Mishima City and of the National Institute of Basic Biology in Okazaki City. With time Professor Egami assumed increasing responsibility for his fellow scientists, for his University, for the whole of science in Japan.

Egami retired from the University of Tokyo in 1985, but his activity never ceased. He continued his studies on environmental influences on physiological function of the cells of the Medaka, as Professor at Yamaguchi University. Six months later he was appointed Director of the National Institute for Environmental Studies in Tsukuba City, where he encouraged the development of environmental science aimed at harmonizing human beings and their environment. In 1988 Dr. Egami was honored by award of the Medal with Purple Ribbon from the Prime Minister's Office.

Professor Nobuo Egami continued his efforts as a scientist and as a fair and caring human being until the very end of his active life. Shortly before his death, his last book entitled 'Biology Learned from the Medaka' (in Japanese) was published as a result of the devoted effort of his wife Kazuko. More research reports which he wrote while in bed, will be published posthumously. The following verse was found in his will when it was opened by his wife just after his death.

**Haya umare, haya ne, haya oki, haya gatten,
jyoudo he mairu mo, chotto haya meni.
Gasshou**

**"Born in the early part of the year, I was early to rest, early to work, early to judge—
and a little too early to journey to the other side. I give thanks for my life."**

Professor Nobuo Egami is survived by his beloved wife Kazuko, his son Shigeo, and his daughter Michiko.

November 17, 1989

SEIICHIRO KAWASHIMA,

AKIHIRO SHIMA,

AND

HOWARD A. BERN*

Zoological Institute

Faculty of Science

University of Tokyo, and

*Department of Integrative Biology and

Cancer Research Laboratory

University of California at Berkeley

OBITUARY

**Sajiro Makino (1906-1989)**

It is our sad task to announce the death of Dr. Sajiro Makino, one of the world's leading cytogeneticists, whose contributions have exerted a great deal of influence on the development of basic and clinical cytogenetics over several decades.

Dr. Makino was born on June 21, 1906 in Narita, a little town of Shintoism near Tokyo. His interest in the life sciences was fostered during his primary school days. For his effort to improve the breed of white leghorns he was awarded the third prize in a National Fowl Contest. He was then merely 12 years old. Encouraged by his grandfather and high school teachers, the young Makino determined to study genetics, and was enrolled in the Faculty of Agriculture, Hokkaido University, Sapporo where such world-renowned geneticists and biologists as Drs. K. Miyabe, Y. Kuwada, T. Sakamura, S. Matsumura, S. Hatta and H. Kihara were arrayed like glittering stars. His interest in human cytogenetics began in 1928, and he was carefully guided by his mentor, Dr. K. Oguma, who later became the first Director of the National Institute of Genetics in Mishima. It was about that time Dr. Makino encountered E. B. Wilson's book, *The Cell* (1896), which became his life long companion.

Dr. Makino was on the staff of the Zoological Institute, Faculty of Science, Hokkaido University from 1930 through 1969, serving as a full professor for the last 21 years, and was elected to the first Director of Chromosome Research Unit founded in 1969. He taught animal cytogenetics, animal histology, genetics and vertebrate zoology to undergraduate and graduate students. Dr. Makino served for many years as counselor of the Zoological Society of Japan, Genetics Society of Japan, Japanese Society of Human Genetics, and others. He also acted as an editor of several periodicals, such as *Cytologia*, *Cytogenetics*, *Evolution*, *Caryologia*, *Chromosome Information Service* (Editor-in-Chief) and *International Review of Cytology* (advisory Editor). Since his retirement, he became Professor Emeritus of Hokkaido University, and was inducted into the ranks of the National Academy of Science in Japan. In 1976, he was decorated with a medal by the Emperor.

Dr. Makino founded a laboratory for inbred strains of rats and mice in 1943, which later developed

into the Center for Experimental Plants and Animals of Hokkaido University; in 1981, 14 strains of inbred rats and 20 strains of inbred or mutant mice were maintained.

Dr. Makino's publications consist of some 400 scientific articles, 16 books and text books and numerous enlightening articles of interest to cytogeneticists, zoologists and clinicians. His book, "Human Chromosomes", published by North Holland Publishing Company, Amsterdam (1975) is a classic testament for everyone pursuing cytogenetics. "An Atlas of Chromosome Numbers in Animals" was published in 1951 with the help of Dr. W. E. Leonard and revised in 1956. This atlas incorporates chromosome data on a total of 4,850 species of animals, including man. He received many awards from various domestic and international societies for his contribution to both basic and clinical genetics.

One of the contributions for which Dr. Makino has to be remembered is his continuous devotion to and passion for the training of many cytogeneticists during the 40 years of his tenure. His students number as many as 150, of whom more than 80 received their D. Sc. from him. His warm personality attracted many aspiring young people and his ingenious talent as a scientist and teacher influenced everyone studying with him.

It is also worthy of mentioning that he was a staunch believer of science independent of politics. Despite the very difficult times the Japanese experienced during and after the second World War, he was one of the few scientists who refused to carry out the military-backed program.

Dr. Makino loved to nurse and "train" the national flower of Japan, chrysanthemums, for which he won numerous awards. He loved nature. He loved to travel. He loved Sapporo beer. He loved Sapporo ramen noodles. Beyond all, he loved working hard, teaching hard and writing hard. His life was literally the persistent devotion to the development of cytogenetics.

Dr. Makino died of heart failure at his home at the age of 83 on August 6, 1989, shortly after attending his prize-winning chrysanthemums in his garden. Direct disciples, we mourn over the loss of this great cytogeneticist and mentor, whose voice will never be heard again.

HIROSHI HORI, D. Sc.

Professor of Zoology
Hokkaido University

REVIEW

Scanning Electron Microscopy of Vascular Casts: A Methodological Review with Some Comments on the Angioarchitecture of Rat Hypophysis

TAKURO MURAKAMI

*Department of Anatomy, School of Medicine, Okayama University,
Okayama 700, Japan*

ABSTRACT—Scanning electron microscopy of corrosion casts allows three-dimensional visualization of fine vascular beds. The routine methods involved in this microscopy were described with some comments on the blood vascular architecture of rat hypophysis.

INTRODUCTION

Scanning electron microscopy of corrosion casts allows three dimensional visualization of vascular beds. This microscopy developed in 1971 [1] has become a standard tool to demonstrate microcirculatory patterns of various tissues and organs in man and various animals [2-11]. This paper briefly describes the routine methods involved [1-15], and also introduces our recent findings on the blood vascular organizations of rat hypophysis, as obtained by these methods [16].

CASTING MEDIA

Semi-polymerized low viscosity methacrylate mixtures produce satisfactory casts of fine capillaries for scanning electron microscopy. These methacrylate mixtures are prepared in laboratories by warming methyl methacrylate monomer with 2,4-dichlorobenzoyl peroxide (or benzoyl peroxide) [1, 11] or exposing it to ultraviolet light [6]. Commercially available methacrylate or polyester casting media such as Mercor 2B or 2R (Oken Shoji Co, 6-12-17 Ginza, Chuo-ku Tokyo) are usually diluted with 20-40% monomeric methacrylate, to lower their viscosity or to facili-

tate their injection into the fine capillaries [9]. A mixture of methyl and hydroxyethyl methacrylate monomer is very fluid and useful for casting finer vessels such as the bile canaliculi [12].

Prior to injection, each of the casting media is supplemented with catalyst for its prompt and complete polymerization within the vessels. The methacrylate media, including the monomeric methyl and hydroxyethyl methacrylate mixture, are supplemented with 1-2% benzoyl peroxide and N,N-dimethyl aniline [1, 9, 11]; the Mercor media, including the diluted ones (see above), with 1-2% MA (Oken Shoji, see above) [9].

INJECTION OF CASTING MEDIUM

Fresh organs or tissues, including the human autopsy samples, are thoroughly flushed through their arterial vessels with either Ringer or other physiological solutions, to remove blood which interferes with resin injection into the fine capillaries [1-16]. The methacrylate or diluted Mercor casting medium containing the catalyst (see above) is then gently and thoroughly injected through the arteries into the blood vascular beds until the efferent veins of the organs or tissues are filled with the injected medium.

A small amount of the casting medium colored with Sudan III is supplementarily injected, in

order to discriminate the arteries from the veins [9]. The Mercor media are originally colored red (2R) or blue (2B).

REMOVAL OF TISSUE ELEMENTS

The resin-injected specimens are placed for 3 hours or longer in a hot water bath (60°C), to keep their original forms and to accelerate polymerization of the injected resin [1-13]. They are then corroded or macerated in a hot 10% NaOH or KOH solution (60°C) overnight or longer, and washed gently in running tap water overnight or longer [1-13]. The specimens are further immersed in a hot neutral detergent (60°C) overnight or longer, placed in a hot water bath (60°C) overnight or longer, and washed in running tap water overnight or longer [9].

The detergent treatment removes saponified tissue elements and is essentially important to prepare the beautiful casts in the nervous tissues, including the brain. Bony tissues are decalcified in Plank-Rychlo solution containing 7% aluminium chloride, 3% hydrochloric acid and 5% formic acid, prior to the maceration [9].

MOUNTING

Large corrosion casts such as those of the liver and brain are frozen in water and trimmed with razor blades, knives or saws into appropriate blocks for mounting [9]. This trimming eliminates undesired breakages of minute vessels. The trimmed specimens are dried in air or in a critical point drier. Laser beam trimming of the dried specimens is also useful to eliminate such breakages [6].

The trimmed and dried casts are mounted on specimen-holders using conductive paints such as commercially available Dotite paint (Fujikura Kasei Co., Sano, Tochigi), and coated with metals such as gold and platinum in a vacuum evaporator [1-13] or exposed to vaporized osmium tetroxide and hydrazine hydrate [11, 13].

SCANNING ELECTRON MICROSCOPY

Preliminary microdissection of the casts is of importance for demonstration of the vessel or

vessels of interest in the scanning electron microscope [1-13]. The casts coated with metals or impregnated with osmium lose their transparency and facilitate microdissection under a light microscope. The casts thus dissected are again coated with metals and observed with a scanning electron microscope using an acceleration voltage of 5-10 kV. After this scanning, the casts are further dissected, coated with gold and observed in the scanning electron microscope. This series of dissection, metal coating and scanning electron microscopy is repeated for a thorough investigation of the inner structures of the casts. Microdissection includes cutting, fracturing or sectioning of wet, frozen and dried casts with razor blades, forceps and needles in a light microscope.

The osmium vapour treatment imparts electron conductivity to the whole casts and eliminates repeated metal coating during microdissection and scanning electron microscopy [11, 13]. This osmium impregnation is of special value in direct microdissection within the scanning electron microscope [13]. The casts prepared with methyl methacrylate can be softened in a warm ethanol bath with no breakage of vascular connections. This microdissection in ethanol is of value for analysis of such conglomerated capillary beds as those of the kidney glomerulus [2].

Stereo-micrographs are obtained by tilting the cast specimens at tilting angles of 7-10 degrees [9].

COMMENT

The most valuable and reliable findings obtained by scanning electron microscopy of corrosion casts are the details of vascular connections, arrangements and distributions. As an additional finding, it allows a measurement of vascular densities both in organ and tissue. Endothelial nuclear protrusions and cell boundaries are sometimes imprinted in the casts. Valvular structures, including the endothelial cushions, are constantly imprinted. Such imprinting of endothelial structures is enhanced by preliminary perfusion fixation with a low-concentrated (1%) glutaraldehyde. Marks of the resistance of mural elements such as sphincters against the vascular dilation caused by resin injection

tion are also sometimes imprinted in the casts. Furthermore, vascular contractions can be reproduced when injection pressure is adjusted appropriately.

Estimations of specific gravity and weight allow calculation of the volume of the casts. Methacrylate or polyester casting media, including the diluted Mercor medium, reduce their volume by 10–20% when they are hardened. Thus, the calculated values show a 10–20% reduction in the volume of vascular lumina.

Different types of resin are suitable for different types of casting [3–10]. The low viscosity methacrylate or polyester casting media can reproduce even the delicate capillaries found in chick embryo. These media are also available for replication of lymphatic vessels, lung air ways and other tubular systems, including the bile ductules [12, 14, 15]. Reproduction of the bile and other canaliculi is only possible by injection of the monomeric methyl and hydroxyethyl (or hydroxypropyl) methacrylate monomer [12]. Latex or rubber compounds can be injected into lung air ways, but have limited application in casting bile ductules and other fine vessels [9].

Resins vary also in their physical properties. Methacrylate or polyester casts are rigid and show no marked deformations even when they are dried in air way, though such delicate methacrylate casts as those of the bile canaliculi must be freeze-dried [12]. Methacrylate or polyester casts are rather brittle and suited for microdissections of minute vessels, while latex or rubber casts are soft and rather suited for macroscopic isolation of closely packed networks or vascular clusters [9]. Weak or pliable casts can be prepared, even with methacrylate or polyester media, by adding 40–50% hydroxyethyl or propyl methacrylate monomer to the casting media [7].

Positional relations of each vessel or tubule to the tissue elements cannot be examined in the cast samples, since the cast itself is examined in isolation from the surrounding tissue. This deficiency may be supplied by traditional methods such as light microscopy of India ink-injected specimens or other techniques, including the light or transmission electron microscopic examination of serial sections. Despite of these problems of relating the

details of microvascular structures to the surrounding tissues, the herein introduced technique of displaying vascular patterns as independent structures has already shown itself to be valuable in a study of tissue microcirculation, and can be regarded as a useful and basic tool in biological research [1–16].

BLOOD VASCULAR ARCHITECTURE OF RAT HYPOPHYSIS

Ligation of the thoracic aorta and successive thorough-infusion of Ringer's solution and a low viscosity casting medium (semi-polymerized methyl methacrylate mixture or diluted Mercor medium, see above) into the ascending aorta reproduce the whole blood vascular beds, including the hypophyseal ones, of the upper body of the rat (Figs. 1, 2).



Fig. 1. A photograph of the blood vascular replica of an adult rat prepared by thorough injection of a laboratory-prepared low viscosity methyl methacrylate casting medium. Note that the replica alone, without any tissues, reproduces the detailed configurations of the head. $\times 1.5$.

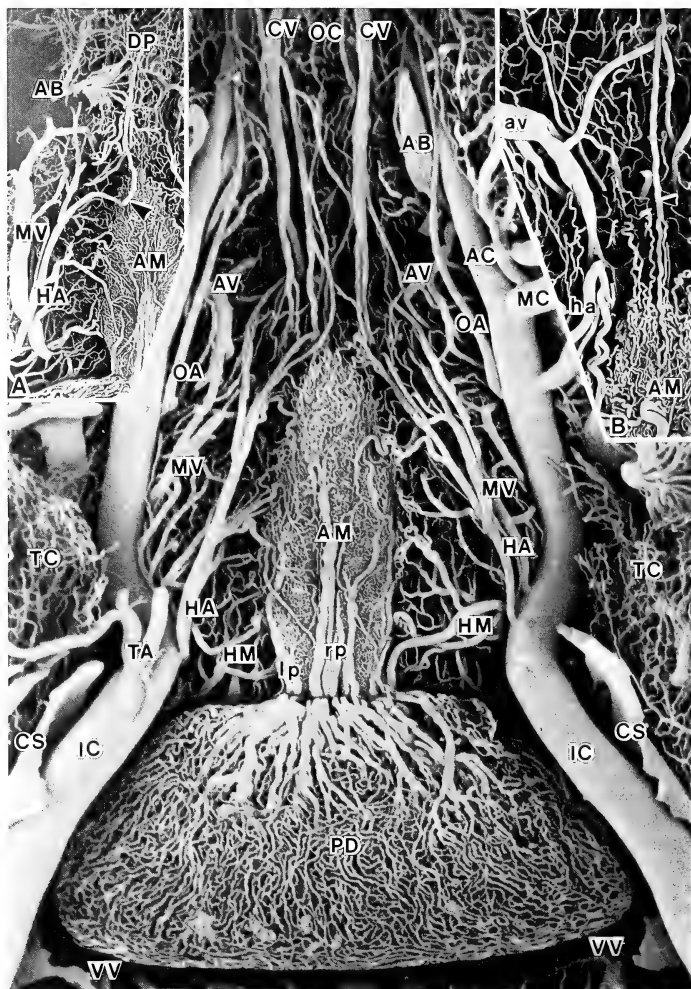


FIG. 2.

The hypophyseal blood vascular beds thus reproduced are isolated together with its connecting hypothalamic vascular bed, coated with gold or exposed to osmium vapor, and observed with a scanning electron microscope (Fig. 2). After this scanning, microdissection each time followed by scanning electron microscopy is repeated, to visualize the inner structures of the hypophyseal beds (Figs. 3-7).

The primary capillary plexus of the hypophyseal portal system originates in the hypophyseal arteries, and surrounds the median eminence and infundibular stalk (Figs. 2, 3). This plexus projects numerous capillary loops into the eminence and stalk (Fig. 3).

The loops are composed of freely anastomosing capillaries, being mainly distributed in the central area of the anterior lip of the median eminence (Figs. 4, 7). The well developed long loops receive their proper afferent arterioles from the arterial terminals in the primary plexus, and emit their proper efferent venules continuous with the long hypophyseal portal vessels (Fig. 4, Insets A and B). The loops in newborn rats are poorly developed, appearing as simple ball-like capillary protrusions of the primary plexus (Fig. 4, Inset C).

Many branches of the hypophyseal arteries penetrate, as the infundibular ascending arterioles, the primary plexus, and continue into the capillary bed of the hypothalamus, especially its basilar and periventricular areas (Fig. 7).

The subependymal capillary network is fairly independent, and located dorsal to the loops (Figs. 3, 6). This network receives some of the infundibular ascending arterioles, and emits the infundibular descending venules (subependymal portal vessels) continuous with the long hypophyseal

portal vessels (Fig. 6). The subependymal network also receives the infundibular descending arterioles from the hypothalamic arteries, and emits the infundibular ascending venules directly continuous with the hypothalamic veins (Fig. 6). Thus, neither a feedback channel nor a retrograde portal route from the hypophyseal capillaries to the hypothalamic capillaries is noted. The subependymal network is denser in the male rats than in the female rats. This network is more developed as the animals are more aged.

The long portal vessels descend into the anterior lobe of the hypophysis to continue into its capillaries (secondary plexus of the hypophyseal portal system), which emit the adenohypophyseal veins (Fig. 2). The long portal vessels can be classified into anterior, lateral and posterior types; they originate in the anterior, lateral and posterior areas of the primary plexus, and run into the anterior lobe from the antero-ventral, antero-lateral and antero-dorsal aspects, respectively (Fig. 2, 5).

The capillary network of the posterior lobe originates in the hypophyseal arteries and emits the neurohypophyseal veins; it also issues the short hypophyseal portal vessels continuous with the capillaries in the anterior lobe (Fig. 5). The short portal vessels are observed most distinguishably in the newborn and young rats (Fig. 5), whereas those in the aged rats are rather slender. The capillary bed of the posterior lobe is continuous with the primary plexus and issues the portal vessels continuous with that of the anterior lobe (see above), so that it should be included in the primary plexus.

The capillary network of the intermediate lobe is only observed in the adult and aged rats; more

Fig. 2. A scanning electron micrograph of the methacrylate-reproduced blood vascular beds of the hypophysis and hypothalamus (newborn rat, ventral view) (From Murakami *et al.* [16]). Note that the capillary bed of the median eminence (AM) issue the long portal vessels (lp and rp, lateral and anterior long portal vessels) continuous with the capillary bed of the anterior lobe (pars distalis of the hypophysis, PD). Inset A shows an aberrant dural branch (arrowhead) of the hypophyseal artery (HA) (newborn rat, ventral view). Inset B shows an aberrant venous branch (arrowhead) which arises from the capillary bed of the median eminence anterior lip (AM) and continues into a branch (av) of the anterior hypothalamic vein (adult female rat, ventral view). AB anterior basal vein, AC anterior cerebral artery, AV anterior hypothalamic vein, CS cavernous sinus, CV apical hypothalamic vein, DP dorsal capillary plexus, HA anterior hypophyseal artery, HM middle hypophyseal artery, IC internal carotid artery, MC middle cerebral artery, OC capillary bed of the optic chiasma, TA trigeminal artery, TC capillary bed of the trigeminal nerve, VV adenohypophyseal vein. $\times 30$, Inset A: 30 , Inset B: 40 .

strictly, it appears at the age of puberty and becomes denser in its meshes as the animals are more aged. This network receives its afferent vessels from the hypophyseal arteries, and emits its efferent vessels (intra-adenohypophyseal portal

vessels) continuous with the capillaries of the anterior lobe (Fig. 6). The capillaries of the intermediate lobe are usually slender, though they become sinusoidal at the estrus.

Fig. 3. Thoroughly replicated and sagittally freeze-cut blood vascular beds of the hypophysis, hypothalamus and adjacent tissues (adult male rat) (From Murakami *et al.* [16]). Note that the capillary bed of the pars intermedia (PI) is inserted between the capillary beds of the pars distalis (PD) and infundibular process (IP), and that the vascular beds of the mamillary body (CM) and paraventricular nucleus (PN) are somewhat denser than that of the hypothalamus (HP). Inset A shows the thoroughly replicated and sagittally freeze-cut blood vascular beds of the hypophysis and hypothalamus of a newborn rat. Note in this inset that no vessel is observed between the pars distalis (PD) and infundibular process (IP). AM capillary bed of the median eminence anterior lip, HC postero-basilar and peri-ventricular part of the hypothalamic capillary bed, HL latero-basilar and peri-ventricular part of the hypothalamic capillary bed, HR antero-basilar and peri-ventricular area of the hypothalamic capillary bed, IS capillary bed of the infundibular stalk, SB subependymal capillary network. $\times 30$, Inset A: $\times 50$.

Fig. 4. Sagittally freeze-cut capillary bed of the median eminence anterior lip (central area) (AM) (aged male rat) (From Murakami *et al.* [16]). Note that the capillary bed of the median eminence (AM) projects numerous loops (CL) consisting of anastomosing capillaries, and that some of the loops are sufficiently long (cl) to reach the subependymal capillary network (SB). Inset A and B show dissected forms of the long loops (adult male rat), where the proper afferent arteriole (thin arrowhead) and efferent venule (thick arrowhead) of the long loop (cl) are clearly observed. Inset C shows the capillary bed of the central area of the median eminence anterior lip (AM) of a newborn rat (dorsal view). Note in this inset that the capillary loops of the newborn rat are small and simple (arrows). rp anterior long portal vessel. $\times 360$, Inset A: $\times 320$, Inset B: 360, Inset C: $\times 300$.

Fig. 5. Blood vascular bed of the infundibular process (newborn rat, dorsal view) (From Murakami *et al.* [16]). Note that the capillary bed of the infundibular process (IP) has additionally given off lateral (dorsal) and posterior short portal vessels (ls and cs) which continue into the capillary bed of the pars distalis (PD) from the medio-dorsal and postero-lateral aspects, respectively. Inset A shows an anterior short portal vessel (rs) connecting the capillary beds of the infundibular process (IP) and pars distalis (PD) from the ventro-anterior aspect. Inset B shows a part of the capsular capillary network of the hypophysis (CH) (adult male rat, dorsal view). AM capillary bed of the median eminence anterior lip, CA anterior cerebellar artery, Co posterior cerebellar artery, HP and hp hypophyseal artery and its branch, NV and nv neurohypophyseal vein and its branch, PM capillary bed of the median eminence posterior lip, cp posterior long portal vessel, hm branch of the hypophyseal artery. $\times 90$, Inset A: $\times 80$, Inset B: $\times 20$.

Fig. 6. A typical posterior intra-adenohypophyseal portal vessel (ci) connecting the capillary beds of the pars intermedia (PI) and pars distalis (PD) (adult male rat) (from Murakami *et al.* [16]). Inset A shows an arteriole (arrowhead) which arises from a branch (hm) of the hypophyseal artery and continues into the capillary bed of the pars intermedia (PI) (adult male rat). Inset B shows a rostral portion of the capillary bed of the pars intermedia (PI) (adult male rat). Note in this inset that the capillary bed of the pars intermedia receives the arterioles or arteriolar capillaries (thick arrowheads) from the branch (hm) of the middle hypophyseal artery and also the capillaries (arrows and thin arrowheads) from the capillary bed of the infundibular process (IP). Inset C shows a typical anterior intra-adenohypophyseal portal vessel (ri) connecting the capillary beds of the pars intermedia (PI) and pars distalis (PD) from the ventro-anterior aspect. LR reaked resin, rs anterior short portal vessel. $\times 150$, Inset A: $\times 50$, Inset B: $\times 90$, Inset C: $\times 80$.

Fig. 7. Subependymal capillary network (SB) and its connecting vessels (aged male rat) (From Murakami *et al.* [16]). Note that the subependymal capillary network (SB) is derived from the peri-infundibular ascending arterioles (pa) and infundibular ascending arterioles (a, b) (see Insets A and B) and connected via the infundibular ascending venules (vh) into the branches (av, mv) of the hypothalamic veins (thick arrowheads) and also via the infundibular descending venule (arrow vp) (see Inset C) into the long portal vein. Also note that this network receives an arteriolar capillary (thin arrowheads, infundibular descending arteriole or arterial capillary) from a branch of the hypophyseal artery (hm). Insets A, B and C show the dissected forms of the a, b and vp vessels. These dissections clearly confirm that the a and b vessels are, closely associated with the loops (c11, c12), the infundibular ascending arterioles (ia) arising from the branches of the anterior hypophyseal arteries (ha), and that the vp vessel is an infundibular descending venule continuous with a long portal vessel (rp). HA hypophyseal artery. $\times 120$, Inset A: $\times 200$, Inset B: $\times 180$, Inset C: $\times 180$.



FIG. 3.

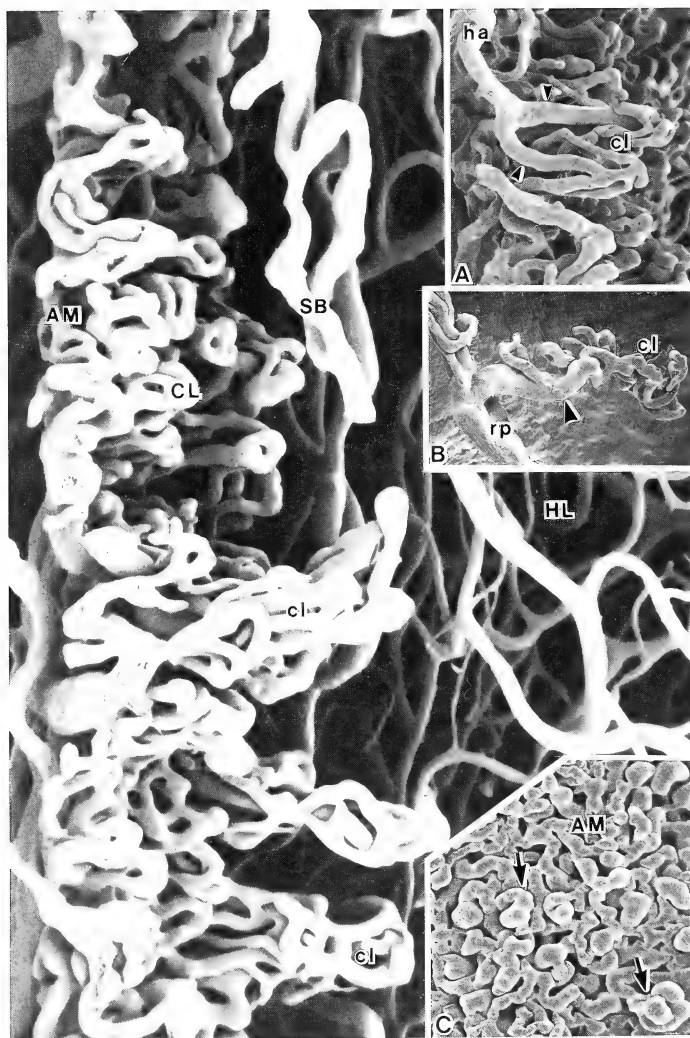


FIG. 4.

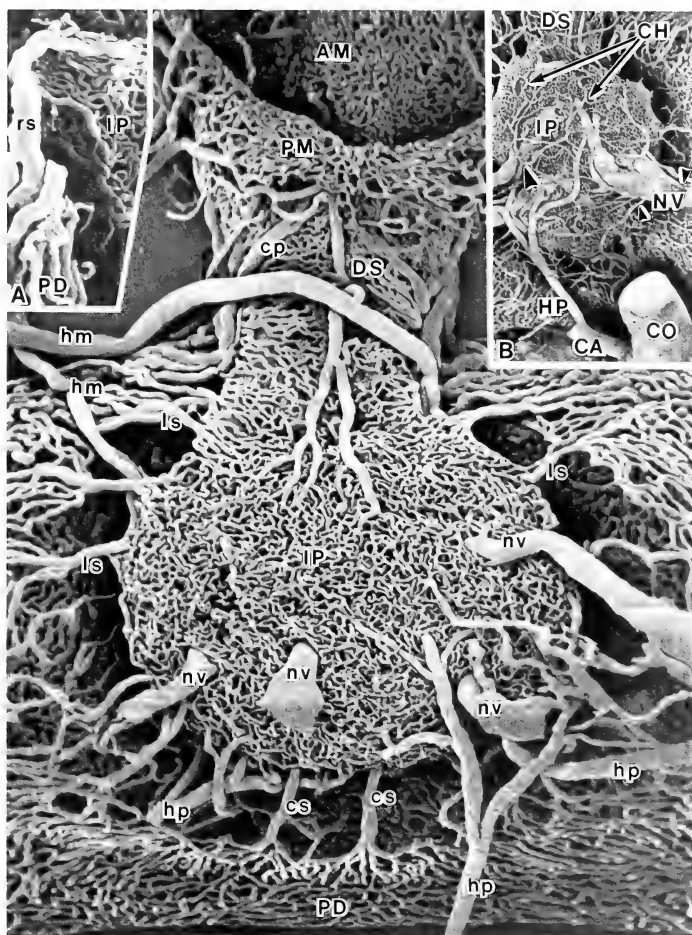


FIG. 5.

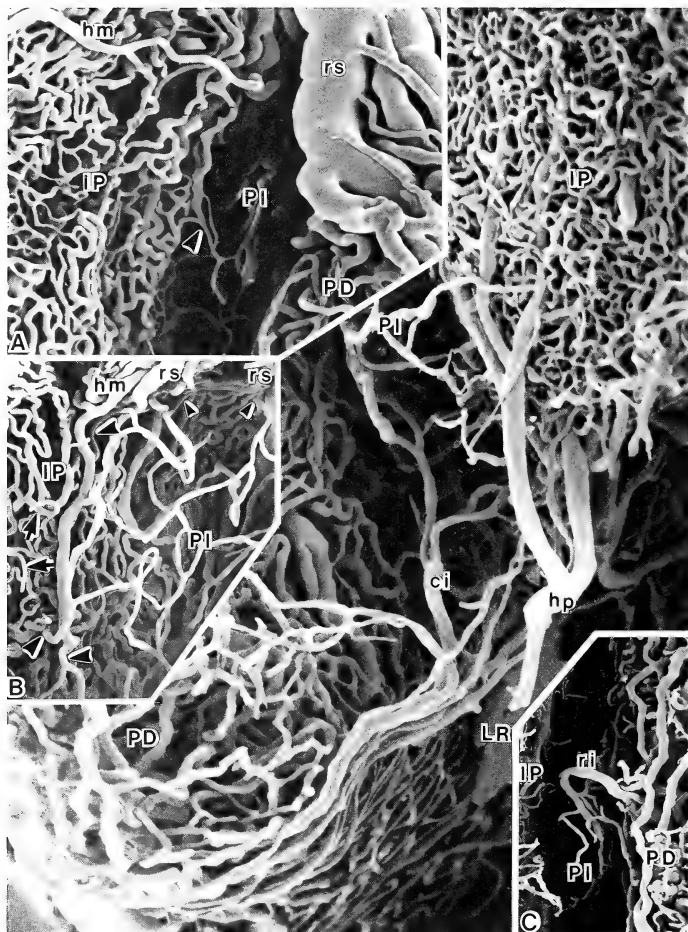


FIG. 6.

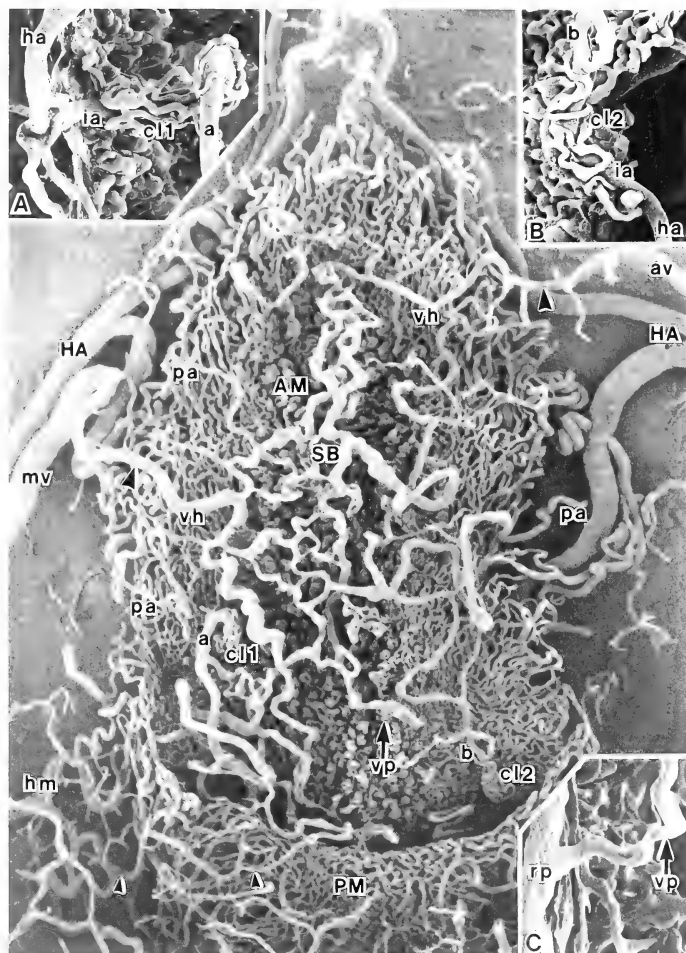


FIG. 7.

ACKNOWLEDGMENTS

This work was supported in part by a research grant, 63570008, from the Ministry of Education of Japan. The author is also indebted to Prof. Tsuneo Fujita (Editor of Arch. Histol. Jpn.) for his kind permission in reproduction of our micrographs [16].

REFERENCES

- 1 Murakami, T. (1971) Arch. Histol. Jpn., **32**: 445–454.
- 2 Murakami, T. (1972) Arch. Histol. Jpn., **34**: 87–107.
- 3 Nowell, J. A. and Lohse, C. L. (1974) SEM Symposium/IITRI/1974: 267–274.
- 4 Murakami, T. (1978) In "Principles and Techniques of Scanning Electron Microscopy". Ed. by M. A. Hayat, Van Nostrand Reinhold, pp. 159–169.
- 5 Gannon, B. J. (1978) In "Principles and Techniques of Scanning Electron Microscopy". Ed. by M. A. Hayat, Van Nostrand Reinhold, pp. 170–103.
- 6 Hodde, K. C. and Nowell, J. A. (1980) SEM Symposium/SEM Inc., **1980/2**: 88–106.
- 7 Murakami, T., Ohtani, O. Ohtsuka, A. and Kikuta, A. (1983) In "Biomedical Research applications of Scanning Electron Microscopy Vol. 3". Ed. by G. M. Hodges and K. E. Carr, Academic Press, pp. 1–30.
- 8 Lametschwandtnr, A., Lametschwandther, U. and Weiger T. (1984) SEM Symposium/SEM Inc., **1984/2**: 663–695.
- 9 Ohtsuka, A., Taguchi, T. and Murakami, T. (1986) The Cell (Tokyo), **18**: 381–384. (in Japanese)
- 10 Christofferson, B. and Nilsson, B. O. (1987) Scanning, **10**: 43–63.
- 11 Murakami, T., Unehira, M., Kawakami, H. and Kubotsu, A. (1973) Arch. Histol. Jpn., **36**: 119–124.
- 12 Murakami, T., Itoshima, T., Hitomi, K., Ohtsuka, A. and Jones, A. L. (1984) Arch. Histol. Jpn., **47**: 223–237.
- 13 Murakami, T., Iida, N., Taguchi, T., Ohtani, O., Kikuta, A., Ohtsuka, A. and Itoshima, T. (1983) SEM Symposium/SEM Inc. **1983**: 235–246.
- 14 Ohtani, O. (1987) Cell Tissue Res., **248**: 365–374.
- 15 Yamamoto, K. and Phillips, M. J. (1986) Anat. Rec., **214**: 67–70.
- 16 Murakami, T., Kikuta, A., Taguchi, T., Ohtsuka, A. and Ohtani, O. (1987) Arch. Histol. Jpn., **50**: 133–176.

REVIEW

Neonatal Estrogenization of the Female Rat: A Useful Model for Analysis of Hypothalamic Involvement of Gonadotropin Release

SHINJI HAYASHI¹ AND MASAHIRO AIHARA²

*Department of Anatomy and Embryology, Tokyo Metropolitan Institute
for Neurosciences, Fuchu, Tokyo 183 and ²Department of Biomolecular
Science, Faculty of Science, Toho University,
Funabashi, Chiba 274, Japan*

ABSTRACT—Sterility induced by neonatal treatment with estrogen in the female rat was briefly reviewed in relation to plasma LH release and hypothalamic levels of LHRH. Intracranial implantation of a minute amount of androgen or estrogen into the hypothalamus of newborn female rats revealed that structures which are relatively wide spread in the hypothalamus are affected by these steroids. The correlation between levels of LH in plasma and levels of LHRH in the hypothalamus was examined. Ovariectomy induced a drastic decrease in the amount of LHRH in the mediobasal hypothalamus (MBH) in neonatally non-treated female rats, while it had little effect in neonatally estrogenized, sterile females. On the other hand, a positive feedback influence of estradiol benzoate (EB) and progesterone (P4) was detectable not only in the neonatally non-treated control but also in sterile rats given 10 µg EB at 1–5 neonatal days. The amount of LHRH in the MBH was significantly decreased by EB+P4 in female rats given EB at 1–10 days neonatally. Intracerebroventricular (ICV) administration of noradrenaline (NA) evoked an increase in plasma LH and a small decrease in LHRH levels in the MBH, both in neonatally non-treated and neonatally EB-treated rats. But the response of the latter was smaller than the former. Thus, neonatal estrogenization might induce a less potent release of LHRH in response to ovariectomy and ICV injected NA. Moreover, since the amount of LHRH in the MBH was significantly larger in the estrogenized rats than in neonatally non-treated females, it suggests that neonatal EB damaged not the system of production of LHRH but its releasing mechanism. The importance of studies on estrogen receptors and chemical factors which influence neuronal development was discussed in relation to sexual determination and differentiation.

I. A HISTORICAL VIEW

Sterility induced by subcutaneous injection of sex steroids

Sexual differentiation of the brain of mammals is generally dependent on the presence or absence of sex steroid hormones during the period when the central nervous system (CNS) is still in an active developmental stage. It was back in the 1930's when Pfeiffer transplanted a testis of a male new-

born rat into a female litter mate and obtained a loss of sexual cyclicity and ovulatory failure. He concluded that a "male type pituitary" developed in the female rat due to a certain "testicular factor" [1].

It was in the 1950's when involvement of the brain in pituitary function became well accepted (see reviews by Harris [2] and Szentágothai *et al.* [3]). The isolation and determination of the amino acid sequence of "gonadotropin releasing factor (s)", which is known as LHRH, was reported in 1971 [4]. Thus, it was made clear that androgenic steroid hormone secreted from the testicular tissue of newborn (late fetus as well) animals determines

Received October 10, 1989

¹ To whom all correspondence should be addressed.

their brain development to be a "male" pattern. If the brain exposure to androgen does not occur during an appropriate period, the brain can not be determined as "male". Thus, this period was defined as the "critical period" [5]. For a recent view of "critical period", see [6].

On the other hand, the pattern of gonadotropin secretion in female rats which received estrogen injection(s) during the neonatal period is very similar to that of the females given androgen. Thus, the question was raised as to whether neonatal "androgenization" is different from neonatal "estrogenization". Naftolin and his group postulated that estrogen, which was converted from androgen by "aromatizing enzyme" in the newborn brain tissue was the main substance in the determination of the sex of the brain [7, 8]. Many experimental data which support this "aromatization hypothesis" are now available, although some reservation is still necessary [9]. Thus, the principle of neonatal "androgenization" is presently deemed the same as that of neonatal "estrogenization".

On the sexual differentiation of the brain, several excellent reviews are available [10, 11].

Intracranial implantation of sex steroids in the newborn rat

Hayashi and Gorski [12] implanted a minute amount of testosterone crystals into the hypothalamus of newborn female rats. After an exposure period of 6 to 72 hrs, the crystals were removed and sterility was examined at 50 and 100 days of age. The microcrystals which had remained in the hypothalamus for more than 48 hrs induced sterility. The effective sites for induction of sterility by the microcrystals seemed to be located throughout the hypothalamus [12].

Hayashi also implanted paraffin micropellets containing a varying amount of estradiol into the hypothalamus, cerebral cortex and under the skin at the nape of female rats 1-2 days old and examined the induction of sterility. From his results, Hayashi concluded that an appropriate amount of estradiol in the hypothalamus induces sterility but not in the thalamus or in the cerebral cortex [13].

These results contradicted reports by Nadler

that paraffin micropellets containing testosterone and implanted in the arcuate/ventromedial hypothalamic nucleus region were more effective for induction of sterility than those in the preoptic/anterior hypothalamic nucleus region [14]. If the aromatization of androgen is truly the prerequisite for neonatal androgen-sterilization, the sites of androgen action and that of estrogen action should be the same in the neonatal brain. The discord between Nadler's finding and ours has remained unresolved.

Autoradiography by Stumpf's group have shown that tritium-labelled estradiol or testosterone accumulates in cell bodies in the medial preoptic area, the ventro-lateral part of the ventromedial hypothalamic nucleus, the arcuate nucleus and the medial amygdala in adult as well as neonatal female rats [15-17]. Similar but slightly different results in the anatomical details were also reported by Pfaff's group in the estrogen concentrating cells [18, 19]. Thus, it is reasonable to assume the "target" site of these steroids in the neonatal brain is also limited in the hypothalamus and/or amygdala. It is noteworthy that the "target" site of estrogen in the brain is not only in the mediobasal and rostral hypothalamus but also in the amygdala. Although sexual dimorphism in the amygdala has been reported by electronmicroscopical studies [20, 21], it is not yet known whether the structures of the limbic area are playing as important a role as those in the hypothalamus.

II. NEONATAL ESTROGENIZATION AND ANDROGENIZATION

Persistent estrus and persistent diestrus: A model of experimental aging

As has been explained, neonatal treatment with androgen has essentially the same (or at least very similar) influence as estrogen does on the gonadotropic activity in the female rat. The main difference in the influence of neonatal estrogen and androgen is found in the development of target organs: e.g., androgen may induce enlargement of the clitoris and failure of vaginal opening, while estrogen may induce hypospadias.

As was previously explained, the effects of

neonatal treatment with androgen and estrogen on the gonadotropic functions at adulthood are very similar. But, we may produce various types of sterile female rats by appropriate selection of treatment conditions such as choice of steroids, route and amount of the material to be given, and duration of injections, etc. For example, neonatal injection of a relatively small amount of androgen (i.e., 10 μ g testosterone propionate (TP) subcutaneously injected at 5 days of age) does not evoke sterility immediately after vaginal opening but accelerates the onset of anovulatory syndrome (delayed anovulatory syndrome, DAS), while a larger amount of androgen (e.g., 1.25 mg TP at 5 days of age) induces persistent estrous and anovulatory syndrome which become apparent immediately after vaginal opening. In contrast, estrogen injection(s) of a relatively low amount and short duration (e.g., a single injection of 10 μ g estradiol benzoate (EB) on the day of birth) evokes persistent vaginal estrus immediately after vaginal opening, while the repetitive injections of larger amount of estrogen (e.g., 100 μ g EB for 10 or more consecutive days from the day of birth) induces persistent diestrous syndrome [22].

Sexual cyclicity of the female rat, which runs regularly in 4–5 day periods at a younger age, become irregular when the rat attain to middle to old age, i.e., from around 200 days of age or more when incidence of vaginal estrus tends to increase. Thus, female rats given sex steroids neonatally seemed to be a good model for the aged animals. In a normally cycling female rat, the brain structure, which is involved in gonadotropin secretion, is exposed regularly to estrogen in general circulation after onset of puberty. This might result in a loss of sexual cycles and ovulatory failure when the rat attains middle to old age. If this hypothesis is true, a large amount of estrogen given shortly after birth might accelerate and accomplish this process in a short duration.

Hypothalamic LHRH and gonadotropin secretion in neonatally estrogenized female rats

Neonatal treatment with estrogen in a female rat evokes loss of cyclicity and ovulatory failure. The gonadotropic potency of these rats is lower than that of neonatally non-treated, control animals.

Plasma LH levels of the sterile rats were significantly lower than that of neonatally non-treated, control rats. An increase in plasma LH in response to the administration of estradiol plus progesterone (E+P4), which is known as positive feedback response, was also examined. The neonatally estrogenized rats had a lower potency in response to the positive feedback effect of these steroid hormones (Fig. 1).

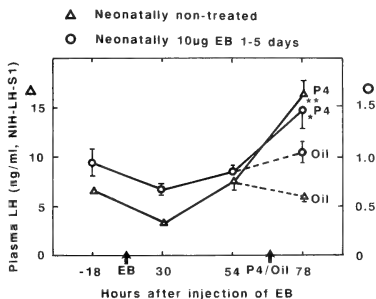


Fig. 1. Plasma LH changes in rats by subcutaneous injection of estradiol (EB) and progesterone (P4). The rats received either subcutaneous injections of 10 μ g EB at 1–5 days of age (circles) or no neonatal injections (triangles). They were ovariectomized at 3 weeks of age. At around 100 days of age, blood was collected through the jugular vein under light ether anesthesia. Eighteen hrs later, EB (10 μ g/0.1 ml sesame oil/100 g BW) was injected subcutaneously. Blood samples were collected further at 30 and 54 hrs after the EB injection. At 71 hrs after EB, progesterone (P4, 2 mg/0.1 ml oil) or only the oil vehicle was given subcutaneously. Seven hrs later, i.e., 78 hrs after EB, the last blood sample was collected. The plasma LH levels of neonatally non-treated controls (triangles; scale is shown at left) were about 10 times higher than those of neonatally estrogenized rats (circles; scale is shown at right). Numbers of samples for each point were 16–20 and those after P4 (solid lines) or oil injection (broken lines) were 9–10. Vertical lines represent standard errors of the means (SEM). Asterisks indicate significant difference between P4 and Oil (*, $p < 0.05$, **, $p < 0.01$).

The amount of LHRH in the hypothalamus was measured by radioimmunoassay. Brain tissue was frozen quickly after decapitation on a dry ice block and kept at -80°C until preparation. During

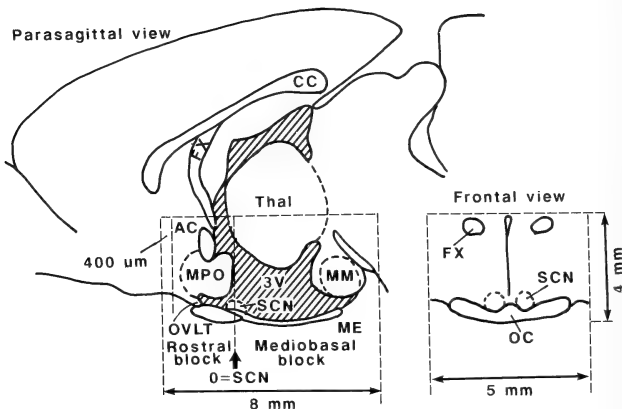


FIG. 2. A diagram showing a hypothalamic block and slice samples. Four serial frontal sections 100 μ m-thick were pooled and deemed as one slice sample of 400 μ m thickness. Abbreviations: AC, anterior commissure; CC, corpus callosum; FX, fornix; ME, median eminence; MM, mammillary body; MPO, medial preoptic nucleus; OC, optic chiasma; OVLT, organum vasculosum lamina terminalis; SCN, suprachiasmatic nucleus; Thal, thalamus; 3V, third ventricle. See text for further explanations.

preparation a hypothalamic block of ca. 5 mm laterally, 8 mm rostral-caudally and 4 mm in depth was mounted on a cryostat chuck and sectioned frontally into 100 μ m thicknesses. Four serial sections were collected and homogenized with 200 μ l of 0.1 N HCl by ultrasonication. The amount of LHRH in portions equivalent to every 400 μ m thickness were therefore measured in a rostral-caudal direction. At the slicing of a hypothalamic block, the section number in which the central part of the suprachiasmatic nuclei (SCN) were located was recorded, so that the rostral-caudal distribution of LHRH in the hypothalamus was compared among different treatments (Fig. 2).

Two clear peaks of LHRH distribution in the hypothalamus were evident. The rostral accumulation of LHRH is due to storage in the organum vasculosum lamina terminalis (OVLT), while the caudal one is ascribable to storage in the median eminence (ME). Our finding confirmed previous studies by immunocytochemistry and radioimmunoassay. The prominent presence of LHRH in the hypothalamus in these structures has been reported in immunocytochemical studies [23,

24] and in studies using radioimmunoassay [25] (Fig. 3).

Ovariectomy reduced the levels of LHRH in the hypothalamus in normally cycling female rats (Fig. 3A). This corresponds well to the increase in plasma LH levels after ovariectomy. It is noteworthy that in neonatally estrogenized females, ovariectomy did not induce a decrease in the level of hypothalamic LHRH (Fig. 3B). Thus, neonatally estrogenized female rats have lost their ability to respond to the loss of plasma estrogen, which is caused by ovariectomy.

As described above, neonatally estrogenized sterile female rats have less ability for LH secretion regardless of the presence or absence of ovaries. However, it is interesting that these females have the ability to increase their plasma level of LH in response to the administration of a combination of estrogen plus progesterone (E + P4), which is known as the positive feedback effect of these steroids (Fig. 1).

Changes in the amount of hypothalamic LHRH content by EB plus P4 injection were examined in the rats which had received 10 μ g EB neonatally

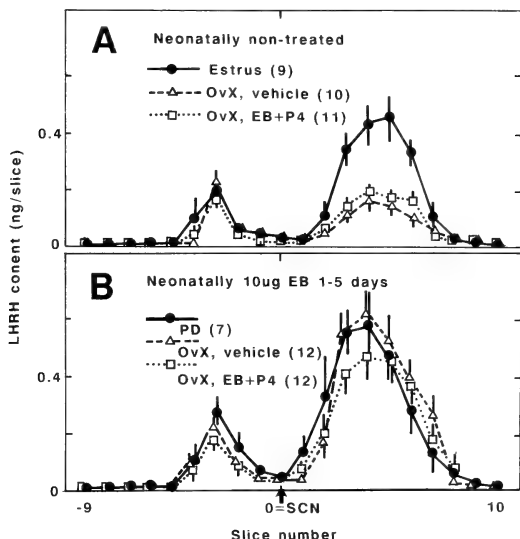


Fig. 3. Rostro-caudal distribution of hypothalamic LHRH levels in neonatally non-treated, control (A) and neonatally estrogenized rats which received 10 μ g EB at 1–5 postnatal days (B). Animals were killed at around 50 days of age. Female rats at vaginal estrus and those showing persistent vaginal diestrus represent animals with ovaries in panels A and B (solid circles with solid lines). Other rats were ovariectomized (OvX) at 22 days and killed 7 hrs after injection of P4 preceded by an injection of EB 71 hrs previous as described in Fig. 1. (OvX, EB + P4) or injections of vehicle only instead of the steroids on the same time schedule (OvX, vehicle). Vertical lines represent SEM. Numbers of animals are shown in parentheses. Ovariectomy induced a drastic decrease in the amount of LHRH in the mediobasal part of the hypothalamus (MBH) in control rats (panel A), but not in neonatally estrogenized rats (panel B). Injection of EB + P4 had a tendency to decrease LHRH levels in the MBH in the estrogenized rats (panel B), while it is not clear in the control rats (panel A).

under different injection schedules, i.e., 10 μ g EB on day of birth, at 1–5 days or 1–10 days. The animals were ovariectomized at 22 days of age and given injections of either EB plus P4 or a vehicle only at around 50 days of age. In the ovariectomized, vehicle injected rats, the amount of LHRH in the mediobasal hypothalamus (MBH) increased gradually according to the duration of the period of neonatal EB injections. EB + P4 induced a significant decrease in LHRH content in the MBH only in the rats treated with EB neonatally for 10 days. In the rats given EB neonatally for 5 days also showed a similar tendency in response to EB + P4, although no statistical difference was de-

tected (Fig. 4). These sterile females, therefore, maintain an ability to respond to the positive feedback influence of E + P4 and release LHRH from the MBH, even though an ovariectomy was not able to release it.

It is known that in ovariectomized female rats, intracerebroventricular (ICV) administration of noradrenaline (NA) evokes an increase in plasma levels of LH [26, 27]. We examined the sensitivity of the hypothalamus to ICV injected NA both in neonatally non-treated, control and neonatally estrogenized female rats. These rats were ovariectomized prepuberally and pretreated with 30 μ g EB/0.1 ml sesame oil 2 days before ICV injection

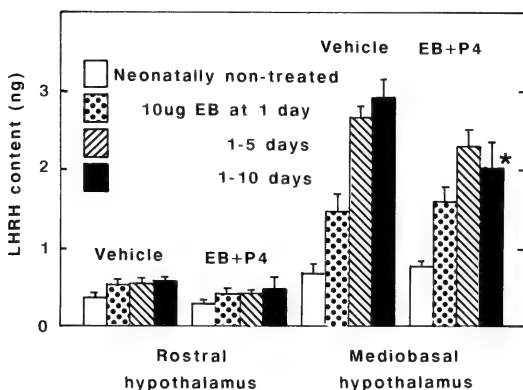


Fig. 4. Hypothalamic content of LHRH in female rats which were neonatally non-treated or recipients of 10 μ g EB injection(s) on the day of birth, at 1-5 or 1-10 days of age. The animals were ovariectomized at 22 days of age and killed at around 50 days as described in Fig. 3. Rostral and mediobasal hypothalami were divided by the slice which contained SCN. Number of rats for each group was 7-9. Vertical lines represent SEM. * indicates a value significantly smaller than the vehicle-injected control ($p < 0.05$). For further details see text.

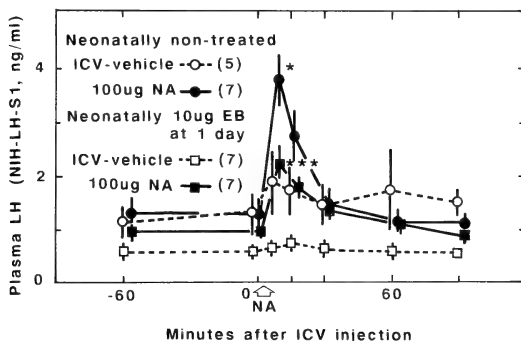


Fig. 5. Plasma LH change induced by intracerebroventricularly (ICV) injected noradrenaline (NA, 100 μ g/2 μ l acid saline) or vehicle. Blood samples were collected from an intra-auricular, indwelling cannula at 60 and 2 min before ICV injection and 7, 15, 30, 60 and 90 min after ICV injection. The rats were ovariectomized previously and primed with 30 μ g EB 2 days before blood sampling. 100 μ g NA, injected through ICV, effectively induced an increase in plasma LH levels within 7 min in both neonatally non-treated and neonatally estrogenized females. However, the response of the former rats was significantly larger than that of the latter rats. Numbers of animals are indicated in parentheses. Asterisks represent significant difference from the values at 2 min before ICV injection of NA: *, $p < 0.05$; ***, $p < 0.001$. Vertical lines represent SEM.

of NA. A 100 μg NA injection induced an increase in plasma level of LH both in neonatally non-treated, control and neonatally estrogenized females, but the peak value of increased plasma LH in the control rats, which was recorded 7 min after ICV injection of NA, was significantly higher than that in neonatally estrogenized females (3.8 ± 0.5 vs. 2.2 ± 0.3 ng NIH-S-1/ml, $N=7$, respectively, $p<0.05$, Fig. 5). We have also examined the rostrocaudal distribution of the hypothalamic LHRH levels in these two types of animals. The brain samples were collected 7 min after ICV administration of either vehicle only or 100 μg NA and processed as described above. A small portion

of LHRH seemed to be released from the MBH by 100 μg NA in both neonatally non-treated and neonatally estrogenized females. But the release of LHRH in the former group of rats seemed more obvious than that in the latter (Fig. 6). Thus, neonatally estrogenized, sterile female rats might be less reactive to ICV injection of NA to release LHRH than neonatally non-treated, control females. This might be one cause for induction of sterility by EB injection(s) during the newborn period.

It is noteworthy that the amount of LHRH in the MBH in neonatally estrogenized, sterile females was significantly larger than that in the normally cycling females. Conversely, plasma levels of LH in neonatally estrogenized females were significantly lower than those in neonatally non-treated, control rats. A similar result was reported by Elkind-Hirsch *et al.* [28]. This fact may indicate that neonatal estrogenization evoked a dysfunction in a mechanism involved in the release of LHRH not in production of LHRH.

III. HYPOTHALAMIC DEAFFERENTATION AND DESTRUCTION IN NEWBORN FEMALES

Rostral structures to the MBH are involved in onset of sexual cycles

Back in 1965, Halász and Pupp transected afferent fibers which input to the MBH and found a loss of sexual cyclicity and ovulatory failure in adult female rats [29, 30]. On the other hand, electrolytic cauterization of the structures anterior to the hypothalamus evoked a loss of sexual cyclicity and ovulatory failure as well. Selective ablation of the medial preoptic nucleus (MPN), a small nucleus located immediately caudal to the OVLT, resulted in ovulatory failure [31]. Since it is known that the neurons which produce LHRH are mainly located in the preoptic/septal area in the anterior hypothalamus, and the suprachiasmatic nucleus (SCN) is the structure which operates biological rhythms, anterior inputs to the MBH seemed important to the onset of sexual cyclicity and ovulation in the female rat.

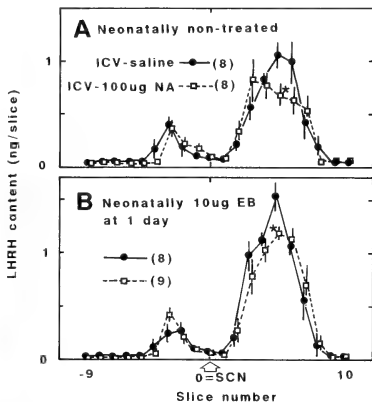


Fig. 6. Rostrocaudal distribution of the hypothalamic LHRH levels in the rats which received an ICV-injection of NA or vehicle only. The animals were non-treated neonatally (panel A) or estrogenized with 10 μg EB on the day of birth (panel B). At around 120 days, they were primed with 30 μg EB and received an ICV-injection of 100 μg NA or vehicle only 2 days later. Brain samples were collected 7 min after the ICV-injection by decapitation. Open squares with broken lines and closed circles with solid lines represent LHRH levels for the animals given NA and vehicle only, respectively. Only a small portion of LHRH in the MBH seemed to be released by NA, which is indicated by an asterisk showing a significant difference from the corresponding slice ($p<0.05$). Numbers of animals are indicated in parentheses.

Hypothalamic deafferentation in newborn females ineffective in inducing sterility

Hayashi and Mizukami transected fiber connections of newborn female rats at 2 days of age to the MBH using a razor blade with a 3 mm width. The anterior deafferentation of the MBH in newborn female rats was ineffective in inducing loss of sexual cyclicity and ovulatory failure in adulthood. On the contrary, similar deafferentation performed in 10-day-old females evoked anovulatory syndrome as is expected by a similar operation in adult females. Thus, neuronal fiber connections which are involved in the onset of sexual cyclicity in the female rat establish themselves between the second and tenth postnatal days [32-34]. These findings are well in accord with the concept of "critical period for induction of anovulatory syndrome by sex steroid hormones" which is the period from the last stage of intrauterine life through around 7 days after birth in the female rat.

Electrolytic destruction in the retrochiasmatic area of the newborn female rat, on the contrary, evokes sterility characterized by ovulatory failure and persistent vaginal estrus [35]. Thus, hypothalamic fiber connections involved in gonadotropic secretion from the pituitary can be considered to establish themselves within the "critical period" under the influence of steroid hormones.

IV. PERSPECTIVES IN THE FUTURE

Involvement of steroid receptors in the sexual differentiation of the brain

When steroid hormones play their role in the target tissue, receptor molecules mediate their action in general. There is no reason why the action of the steroid in the brain is exceptional. Steroid receptors, both for estrogen and androgen, are commonly detected in the hypothalamus [36-38]. By autoradiography of tritiated steroids, several nuclei in the brain are known as sites which accumulate steroids [15, 17-19]. However, scarcely known is the topographical distribution of the estrogen receptors (ER) in the brain of newborn rats. It is important to examine the localization of ER in the newborn rat's brain. Recently, the

genomic sequence of ER has been determined in the human [39], mouse [40], and rat [41]. It is noteworthy that the amount of messenger RNA encoding ER (ER-mRNA) increased upon ovariectomy and decreased upon administration of estrogen in the uterine tissue [42]. The amount of ER, on the contrary, decreases upon ovariectomy and increases upon estrogen administration [43]. Thus, under estrogenic influence, the degradation of ER-mRNA might be suppressed and a relatively small amount of the mRNA is sufficient to produce ER efficiently. The situation is reversed in the pituitary tissue in that by administration of estrogen, ER-mRNA increased [42]. Thus, it is imperative to detect which of these two types of machinery is present in the brain tissue of newborn females.

Mechanism involved in production and release of LHRH in the hypothalamus of the female rat

In neonatally estrogenized rats which release less LH from the pituitary than cycling control females, levels of LHRH in the hypothalamus were significantly higher than that in the cycling rats. This finding supports the idea that sterility induced by neonatal administration of estrogen altered the mechanism involved in the release of LHRH from the median eminence rather than the mechanism to produce LHRH in the hypothalamus.

On the other hand, by an injection of noradrenaline into the cerebroventricle (ICV injected NA), the release of LH from the pituitary was detected in both the neonatally non-treated, ovariectomized and neonatally estrogenized, ovariectomized females. Since a decrease in hypothalamic levels of LHRH was detected by ICV injected NA, the increase in plasma LH was ascribable to a release of LHRH from the median eminence. However, in neonatally estrogenized females, the hypothalamus was less responsive to ICV injected NA than in normally cycling females. Thus, the NA-receptor system might be damaged by neonatal administration of estrogen.

Chemical factors other than sex steroid hormones which are involved in changes of developing brain

Administration of adrenocorticosteroid into

newborn rats delays the onset of biological rhythmicity, which can be examined by diurnal variation of plasma corticosterone levels [44, 45].

Neonatal exposure to thyroxine decreased pituitary and serum TSH levels in adult life [46]. Repetitive injections of TRH to neonatal rats resulted in a blunted response of serum TSH to administration of TRH at adulthood [47]. On the other hand, a classic report by Kikuyama [48] that neonatal administration of reserpine, which depletes stores of catecholamines and serotonin in the brain, suppressed induction of sterility by sex steroids, and more recently, a report by Raum and Swerdloff [49] that phenoxibenzamine, an alpha-adrenergic blocker, prevented neonatal androgenization strongly suggest involvement of neurotransmitters in brain development.

The morphological basis of sexual differentiation induced by neonatal administration of androgen or estrogen was examined by studies of electronmicroscopy. Neonatal administration of sex steroids induces changes in the "wiring pattern" of the dorsomedial preoptic area [50], arcuate nucleus [51, 52] and ventromedial nucleus [53] in the hypothalamus.

It has been revealed that various chemical factors have an influence of the extension of axons and the formation of synapses during development not only in the peripheral but also in the central nervous system (e.g., See review articles by Sanes, 1989 [54], for extracellular matrix molecules; and by Walicke, 1989, for neurotrophic factors [55]). However, at present any direct influence of these chemicals on development and differentiation of brain structures involved in gonadotropic functions is not known. Recently, Yanase *et al.* [56] reported a blockade of neonatal androgenization by an antibody to nerve growth factor. It is still premature to illustrate a complete picture of the correlation between neuronal growth, which includes axonal elongation and synaptic formation, and sexual differentiation. However, these types of studies seem very promising to reveal causes and time sequences of sexual differentiation and the development of brain function in the near future.

ACKNOWLEDGMENTS

This study was supported in part by Grants-in-Aid for Scientific Research from The Ministry of Education, Science and Culture, Japan to S. H. (No. 62840023) and to M. A. (No. 63740438). The radioimmunoassays for hormones were performed in the laboratory of Dr. K. Wakabayashi of the Hormone Assay Center, Endocrinology Institute, Gunma University, Maebashi. The authors would like to express their gratitude for his kindness in allowing us to use his facilities and for his useful discussions.

REFERENCES

- 1 Pfeiffer, C. A. (1936) *Amer. J. Anat.* **58**: 195-225.
- 2 Harris, G. W. (1955) "Neural Control of the Pituitary Gland" Arnold, London.
- 3 Szenthágothai, J., Flerkő, B., Mess, B. and Halász, B. (1968) "Hypothalamic Control of the Anterior Pituitary" Akadémiai Kiadó, Budapest.
- 4 Matsuo, H., Baba, Y., Nair, R. M. G., Arimura, A. and Schally, A. V. (1971) *Biochem. Biophys. Res. Commun.* **43**: 1334-1339.
- 5 Barraclough, C. A. (1961) *Endocrinology*, **68**: 62-67.
- 6 Gorski, R. A. (1988) *Bull. Tokyo Metropol. Inst. Neurosc. (TMIN)*, **16** (Suppl. 3): 67-90.
- 7 Naftolin, F., Ryan, K. J. and Petro, Z. (1972) *Endocrinology*, **90**: 295-298.
- 8 Naftolin, F., Ryan, K. J., Davies, I. J., Reddy, V. V., Flores, F., Petro, Z., Kuhn, M., White, R. J., Takaoka, Y. and Wolin L. (1975) *Recent Prog. Horm. Res.*, **31**: 295-316.
- 9 Hayashi, S. (1976) *Proc. Soc. Exp. Biol. Med.*, **152**: 389-392.
- 10 Dörner, G. (1976) "Hormones and Brain Differentiation" Elsevier, Amsterdam.
- 11 Goy, R. W. and WcEwen, B. S. (1980) "Sexual Differentiation of the Brain" MIT Press, Cambridge.
- 12 Hayashi, S. and Gorski, R. A. (1974) *Endocrinology*, **94**: 1161-1167.
- 13 Hayashi, S. (1976) *Endocr. Japon.*, **23**: 55-60.
- 14 Nadler, R. D. (1972) *Neuroendocrinology*, **9**: 349-357.
- 15 Sar, M. and Stumpf, W. E. (1975) In "Anatomical Neuroendocrinology" Ed. by Stumpf, W. E. and Grant, L. D., S. Karger, Basel. pp. 120-133.
- 16 Sheridan, P. J., Sar, M. and Stumpf, W. E. (1975) In "Anatomical Neuroendocrinology" Ed. by Stumpf, W. E. and Grant, L. D., S. Karger, Basel. pp. 134-141.
- 17 Stumpf, W. E., Sar, M. and Keefer, D. A. (1975) In "Anatomical Neuroendocrinology" Ed. by Stumpf, W. E. and Grant, L. D., S. Karger, Basel. pp. 104-119.

- 18 Pfaff, D. W. (1968) *Science*, **161**:1355-1356.
- 19 Pfaff, D. W. and Keiner, M. (1973) *J. Comp. Neurol.*, **151**:121-158.
- 20 Nishizuka, M. and Arai, Y. (1981) *Brain Res.*, **212**: 31-38.
- 21 Nishizuka, M. and Arai, Y. (1981) *Brain Res.*, **213**:422-426.
- 22 Aihara, M. and Hayashi, S. (1989) *Biol. Reprod.*, **40**: 96-101.
- 23 Merchenthaler, I., Kovács, G., Lovász, G. and Sétáló, G. (1980) *Brain Res.*, **198**: 63-74.
- 24 Kawano, H. and Daikoku, S. (1981) *Neuroendocrinology*, **32**: 179-186.
- 25 Weaton, J. E., Krulich, L. and McCann, S. M. (1975) *Endocrinology*, **97**:30-38.
- 26 Krieg, R. J. and Sawyer, C. H. (1976) *Endocrinology*, **99**: 411-419.
- 27 Handa, R. J., Condon, T. P., Whitmoyer, D. T. and Gorski, R. A. (1986) *Neuroendocrinology*, **43**: 269-272.
- 28 Elkind-Hirsch, K., King, J. C., Gerall, A. A. and Leeman, S. E. (1984) *Neuroendocrinology*, **38**: 68-74.
- 29 Halász, B. and Pupp, L. (1965) *Endocrinology*, **77**: 553-562.
- 30 Halász, B. and Gorski, R. A. (1967) *Endocrinology*, **80**: 608-622.
- 31 Wiegand, S., Terasawa, E. Bridson, W. E. and Goy, R. W. (1980) *Neuroendocrinology*, **31**: 145-157.
- 32 Hayashi, S. and Mizukami, S. (1979) *Neuroendocrinology*, **28**: 145-150.
- 33 Hayashi, S. and Mizukami, S. (1979) *Exper. Neurol.*, **63**: 211-219.
- 34 Hayashi, S., Ooya, E. and Miyabo, S. (1986) *Monogr. neural Sci.*, **12**: 58-63.
- 35 Hayashi, S. and Kawano, H. (1977) *Endocr. Japon.*, **24**: 179-184.
- 36 Kato, J. (1977) In "Receptors and Mechanism of Action of Steroid Hormones, Part II" Ed. by Pasqualini, J. R., Marcer Dekker, N. Y. pp. 603-671.
- 37 Döhler, K. D. (1987) In "Development of Hormone Receptors" Ed. by Csaba, G., Birkhäuser Verlag, Basel. pp. 103-123.
- 38 MacLusky, N. J., Lieberburg, I. and McEwen, B. S. (1979) In "Ontogeny of the Receptors and Reproductive Hormone Action" Ed. by Hamilton, T. H., Clark, J. H., and Sadler, W. A., pp. 393-402.
- 39 Walter, P., Green, S., Green, G., Krust, A., Bornert, J. M., Jeltsch, J. M., Staub, A., Jensen, E., Scrase, G., Waterfield, M. and Chambon, P. (1985) *Proc. Natl. Acad. Sci. USA.*, **82**: 7889-7893.
- 40 White, R., Lees, J. A., Needham, M., Ham, J. and Parker, M. (1987) *Mol. Endocrinol.*, **1**: 735-744.
- 41 Koike, S., Sakai, M. and Muramatsu, M. (1987) *Nucleic Acids Res.*, **15**: 2499-2513.
- 42 Shupnik, M. A., Gordon, M. S. and Chin, W. W. (1989) *Mol. Endocrinol.*, **3**:660-665.
- 43 Aihara, M., Kobayashi, H., Kimura, T., Hayashi, S. and Kato, J. (1988) *Endocr. Japon.*, **35**: 57-70.
- 44 Miyabo, S. and Hisada, T. (1975) *Nature (London)*, **256**: 590-592.
- 45 Miyabo, S., Ooya, E. and Hayashi, S. (1981) *Neuroendocrinology*, **33**: 47-51.
- 46 Bakke, J. L., Lawrence, N. L. and Wilbur, J. F. (1974) *Endocrinology*, **96**: 406-411.
- 47 Kawai, Y., Azukizawa, M., Ashida, N., Kumahara, Y. and Miyai, K. (1983) *Acta Endocr. (Copenh.)*, **104**: 201-205.
- 48 Kikuyama, S. (1967) *Annot. Zool. Japon.*, **34**: 111-116.
- 49 Raum, W. F. and Swerdloff, R. S. (1981) *Endocrinology*, **109**: 273-278.
- 50 Raisman, G. and Field, P. M. (1973) *Brain Res.*, **54**: 1-29.
- 51 Matsumoto, A. and Arai, Y. (1980) *Brain Res.*, **190**: 238-242.
- 52 Matsumoto, A. and Arai, Y. (1981) *Neuroendocrinology*, **33**: 166-169.
- 53 Matsumoto, A. and Arai, Y. (1986) *Neuroendocrinology*, **42**: 232-236.
- 54 Sanes, J. R. (1989) *Ann. Rev. Neurosci.*, **12**: 491-516.
- 55 Walicke, P. A. (1989) *Ann. Rev. Neurosci.*, **12**: 103-126.
- 56 Yanase, M., Honmura, A., Akaishi, T. and Sakuma, Y. (1988) *Neurosci. Res.*, **6**: 181-185.

Proceedings of the
Sixtieth Annual Meeting of the
Zoological Society of Japan

October 4-6, 1989

Kyoto

Suffixal letters of abstract number refer to the abbreviated
subfields of zoology

PH : physiology

GE : genetics

BI : biochemistry

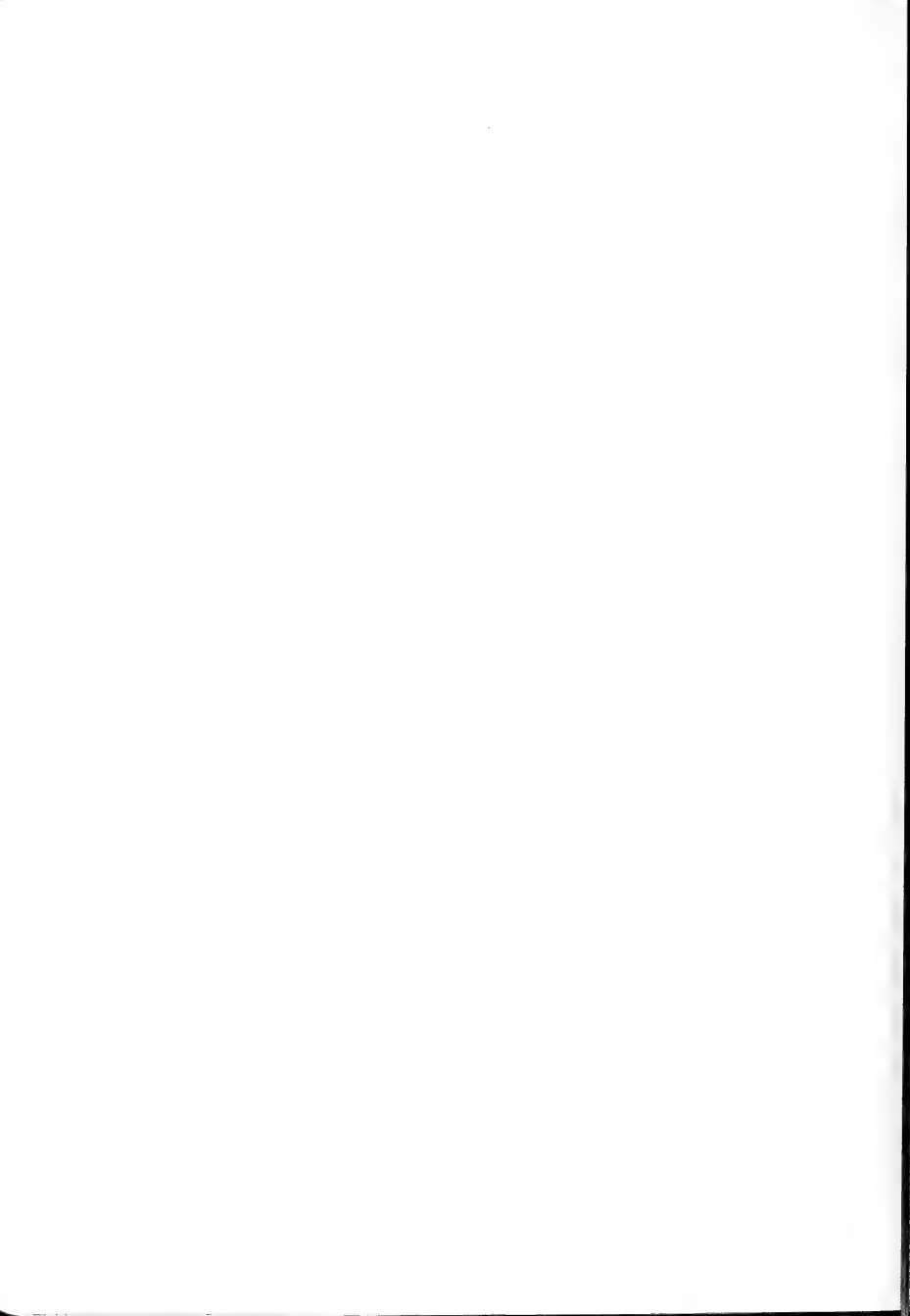
DB : developmental biology

EN : endocrinology

MO : morphology

BE : behavior biology and ecology

TS : taxonomy and systematics



[THE ZOOLOGICAL SOCIETY PRIZE]

Regulation of Gametogenesis in Teleosts

YOSHITAKA NAGAHAMA

Laboratory of Reproductive Biology, National Institute for
Basic Biology, Okazaki 444

It was in 1985 that we identified, for the first time in any vertebrate, $17\alpha, 20\beta$ -dihydroxy-4-pregnen-3-one ($17\alpha, 20\beta$ -DP) as the maturation-inducing substance of amago salmon. Along with estradiol- 17β (E_2), which we identified as the major mediator of oocyte growth, we now have two known biologically important mediators of oocyte growth and maturation in female salmonids, E_2 and $17\alpha, 20\beta$ -DP. It is established that the granulosa cells are the site of production of these two mediators, but their production depends on the provision of precursor steroids (testosterone for E_2 and 17α -hydroxyprogesterone for $17\alpha, 20\beta$ -DP) by the thecal cells (two-cell type model). Thus, normal growth and maturation of the oocyte depend on a high degree of coordination of the interactions of these cell layers.

Microinjection experiments have revealed that $17\alpha, 20\beta$ -DP acts at the oocyte surface; specific $17\alpha, 20\beta$ -DP binding was found in cortices prepared from full-grown rainbow trout oocytes. The early steps following $17\alpha, 20\beta$ -DP action involve the formation of the major cytoplasmic mediator of this steroid, maturation-promoting factor (MPF). MPF activity, assessed by H1-histone kinase activity, cycles during $17\alpha, 20\beta$ -DP-induced maturation of goldfish oocytes; the highest activity occurs at the first and second metaphase. H1 kinase has been purified from mature oocytes of carp. Fractions with the highest kinase activity contained proteins which were recognized by a monoclonal antibody against fission yeast (*S. pombe*) p34^{cdc2} (PSTAIRE).

A steroidogenic shift also occurs in salmonid

testes around the onset of final maturation: from 11-ketotestosterone (11-KT) to $17\alpha, 20\beta$ -DP. *In vitro* studies using different testicular preparations have revealed that the site of $17\alpha, 20\beta$ -DP production is in the sperm, but its production depends on the provision of 17α -hydroxyprogesterone by somatic cells. The site of 11-KT production is in the testicular somatic cell elements.

Recent studies have revealed a role of 11-KT in spermatogenesis and $17\alpha, 20\beta$ -DP in sperm motility. A newly developed organ culture system for Japanese eel testes has proved that 11-KT can induce the entire process of spermatogenesis, *in vitro*, from type A spermatogonia to spermatozoa. $17\alpha, 20\beta$ -DP injection into salmonids caused an increase in the percentage of motile sperm, and raised pH values of the sperm duct. *In vitro* incubation experiments have shown that immotile testicular spermatozoa acquire motility in artificial sperm plasma at a pH greater than 8.5, which also elevates cAMP in spermatozoa. These results suggest the following sequence for the acquisition of motility by sperm: gonadotropin induces the production of $17\alpha, 20\beta$ -DP which acts to increase in sperm duct pH which in turn increases cAMP in sperm allowing the acquisition of motility by sperm.

In conclusion, we have identified three biological mediators of gametogenesis in salmonids. Further studies on the molecular mechanisms of the synthesis and action of these steroidal mediators will certainly provide the basis for a study of the regulation of gametogenesis in vertebrates.

[THE ZOOLOGICAL SOCIETY PRIZE]

Aging of Endocrine Systems in Mammals

SEIICHIRO KAWASHIMA

*Zoological Institute, Faculty of Science, University
of Tokyo, Tokyo 113*

In higher organisms like mammals, regulatory systems, such as, nervous system, endocrine system and immunological surveillance, which surround the cells are extremely important for the function of cells and their alteration may influence the progress of genetic aging program of the cells. Besides these internal environmental factors, some of the external environmental factors act on the organism through the hypothalamo-pituitary system. Therefore, the deterioration of the hypothalamo-pituitary system results in the retardation of adaptability to the environment and causes homeostatic failure.

Our study on age-related changes in various components of endocrine systems in rats and mice shed light on the importance of neuroendocrine regulatory failure for the aging, in particular, of the hypothalamo-pituitary-ovarian system. Results of heterochronic transplantation of the ovary and ovariectomy during early adult life showed that the changes in the hypothalamus was primarily responsible for the induction of senile acyclicity and anovulatory condition. The enhanced prolactin secretion in the rat after the cessation of reproductive period of life was ascribable to the dysfunction of hypothalamic dopaminergic system in both sexes and to longterm stimulatory effects of estrogen in females [1]. In an attempt to retard the occurrence of senile deviation of the estrous cycle and astrocytic gliosis, chlorpromazine was effectively used. Chlorpromazine and centrophenoxine also effectively reduced the accumulation of lipofuscin pigments in neurons in primary culture [2].

Changes of hypothalamic neurosecretory activity with age were apparent in our inbred Wistar/Tw male rats. The increased neurosecretory activity at over 16 months of age was the consequence of polyuria due to renal failure. In these rats the

plasma level of vasopressin and the capacity of acetylcholine agonist binding to the supraoptic nucleus were greater than in young rats, indicating that the neurosecretory activity was properly maintained [3]. Nevertheless, the plasticity of vasopressin neurons for the rearrangement and regrowth of axons after hypophysectomy was retarded at advanced ages [4]. Thus, this component of the neuroendocrine system undergoes its own age-related changes.

Other evidence of the tissue specific 'own' age-related changes was afforded by our study in gonadotropin receptors in the ovary and testis. The number of gonadotropin receptors generally decreased at advanced ages, but the dissociation constants stayed almost the same. For the future analysis on the mechanism of receptor regulation during aging, we have established a new kinetic model during internalization of ligand-receptor complexes and downregulation of gonadotropin receptors in the mouse testis [5, 6]. Application of such approach to other systems may eventually leads to the full understanding of the aging of a given endocrine system and its significance to the body physiology.

- 1 Kawashima, S. and S. Takahashi (1986) In "Pars Distalis of the Pituitary Gland", Ed. by F. Yoshimura and A. Gorbman, Elsevier Sci. Pub., Amsterdam, pp. 51-56.
- 2 Ohtani, R. and S. Kawashima (1983) *Exp. Geront.*, **18**: 105-112.
- 3 Kawashima, S., K. Kawamoto and Y. Kobayashi (1986) *Zool. Sci.*, **3**: 227-244.
- 4 Kawashima, S. (1988) In "New Trends in Aging Research", Ed. by G. Pepeu *et al.*, Fidia Res. Ser., Vol. 15, Liviana Press, Padova, pp. 67-74.
- 5 Tsutsui, K., A. Shimizu, K. Kawamoto and S. Kawashima (1985) *Endocrinology*, **117**: 2534-2543.
- 6 Shimizu, A. and S. Kawashima (1989) *J. Biol. Chem.*, **264**: 13632-13641.

PH 1

DETECTION OF THE GENES INVOLVED IN THE POSTEMBRYONIC NEUROGENESIS OF *DROSOPHILA*. E. Hirose¹, and T. Tanimura². ¹ Dept. Biol., Fac. Sci., Kyushu Univ., Fukuoka, ² Dept. Biol., Fac. Sci., Fukuoka Univ., Fukuoka.

In holometabolous insects, the nervous system is reorganized during metamorphosis to make an adult-specific neural network. To explicate genetic mechanisms involved in the postembryonic neurogenesis, we attempted to identify the genes expressed in subsets of neurons in the CNS of *D. melanogaster* during the larval period. We utilized *E. coli* β -galactosidase gene (*lacZ*) as a reporter. *lacZ* fused to the promoter of *hsp70*, *ftz*, or *P* element were used. The recombinant *P* element was integrated into the genome at a random location by means of a genomic transposase source. In about 56% of 245 [*lacZ*, *ry*⁺] transformants, *lacZ* expression was detected in CNS. Some lines showed similar patterns of *lacZ* expression that can be classified into several groups. Other lines showed unique patterns of expression characteristic to one or a few lines. These lines can be utilized as a specific cell marker. We have also isolated lines in which *lacZ* is expressed in neuroblasts from which adult-specific neurons are produced. These transformants should provide an excellent material to study the molecular mechanisms involved in the postembryonic neurogenesis.

PH 2

EFFECTS OF CYTOSINE ARABINOSIDE ON 2',3'-CYCLIC NUCLEOTIDE 3'-PHOSPHODIESTERASE AND MYELIN FORMATION IN THE ORGANOTYPIC CULTURE OF NEWBORN MOUSE CEREBELLUM. D. SATOMI, Dept. of Biol., Coll. of Arts and Sci., Univ. of Tokyo, Tokyo.

Myelin in the central nervous system is derived from the oligodendrocyte. Newborn mouse cerebellar explants are useful system for the study of myelin formation and oligodendrocyte differentiation. Explants were incubated in the feeding solution containing cytosine arabinoside (10 µg/ml), an inhibitor of DNA synthesis, from first day *in vitro* (1DIV) and from 15DIV. After appropriate periods, cytosine arabinoside treated and control explants were observed microscopically in the living state and then the activity of 2',3'-cyclic nucleotide 3'-phosphodiesterase (CNase), a marker enzyme of myelin, was measured by HPLC. In case of cytosine arabinoside treatment from 1 DIV, 8 DIV explant contained large cells which were grouped or diffusely dispersed. In 22 DIV explant, myelination did not occur and the level of CNase activity was low (3.8 µmol/mg protein/h). On the other hand, in 22 DIV explant treated with cytosine arabinoside from 15 DIV, myelin was formed and the level of CNase activity was nearly the same extent as control (23.6 µmol/mg protein/h). From these results, it was supposed that oligodendrocytes in cerebellar explants differentiate enough for myelin formation during first 2 week incubation.

PH 3

OUTPUT CONNECTIONS OF ASCENDING INTERNEURONS ONTO UROPOD MOTONEURONS IN THE CRAYFISH. M. Sato¹, T. Nagayama² and M. Hisada². ¹Biology, Rakuno Gakuen Univ., Ebetsu, Hokkaido. ²Zool. Inst., Fac. of Sci., Hokkaido Univ. Sapporo.

Intersegmental ascending interneurons originating from the terminal abdominal ganglion of the crayfish receive sensory inputs from the uropods. In addition to the function of these interneurons as the mechanosensory interneurons, we found that many of them also function as pre-motor interneurons to the uropod motor neurons through the local circuits.

Using simultaneous intracellular recording, we characterized the synaptic interactions of these ascending interneurons. Some interneurons seem to make direct monosynaptic connections with certain uropod motor neurons through chemical synapses. Spikes of ascending interneurons elicit consistent and short-latency excitatory or inhibitory postsynaptic potentials (EPSPs or IPSPs) in the motor neurone. There also exist polysynaptic pathways mediated by local non-spiking interneurons from the ascending interneurons to the motor neurones. The ascending interneurons are also frequently mutually interconnected.

PH 4

THE NEURAL ACTIVITY IN THE CRAYFISH BRAIN DURING LATERAL BODY TILT. H. Nakagawa and M. Hisada, Zool. Inst., Fac. Sci., Hokkaido Univ., Sapporo.

The responses of brain neurons to artificial bending of the statocyst hairs were analyzed intracellularly in the immobilized animals. The postsynaptic effect on the oculomotor neurons and the identified descending statocyst interneurons on the simulated lower side were also examined. After the physiological examination, Lucifer Yellow was injected iontophoretically. We characterized fourteen local spiking interneurons with the common morphological properties. They project their neurites to proto- and deutocerebrum. They are classified into four groups of vp1c-B, vp1c-U, vp1c-B and vp1c-U according to the soma position and the laterality of neurite arborization in the protocerebrum. These show either excitatory or inhibitory response to the statocyst stimulation. However, the interneurons found to have output effect to the oculomotor and/or the descending neurons are exclusively of those showing excitatory responses. Two of them are presynaptic to the oculomotor neurons and not to the descending interneurons and remaining three are presynaptic to both the descending interneurons and the oculomotor neurons. We also found that an another type of local spiking interneuron was presynaptic only to the descending interneuron. Of all the neural connections hitherto reported about the equilibrium response in the decapod crustaceans, the central integrative mechanism was thought to be mainly consisted of excitatory ones. However, in this study, we found that the inhibitory connections were also involved. We discussed about the functional meaning of the parallel channels including the local spiking interneurons and the inhibitory responses observed in the statocyst-related interneurons.

PH 5

INPUT AND OUTPUT PATHWAYS IN THE CRICKET GIANT INTERNEURON SYSTEM.

K. Hirota and T. Yamaguchi, Dept. Biol., Fac. Sci., Okayama Univ., Okayama

In the cricket (*Gryllus bimaculatus*) the seven abdominal giant interneurons (GIs: 7-1, 8-1 [MGI], 9-1 [LGI], 9-2, 9-3, 10-2, 10-3) are sensitive to sound and airflow applied to the cercal receptors. The response latencies and the nature of their response to high frequency (50 Hz) electrical stimulation of the cercal nerve indicated that one GI (9-3) and three GIs (MGI, LGI, 9-2) have direct connections with ipsilateral and contralateral cercal receptors, respectively, and the remaining three GIs (7-1, 10-2, 10-3) have direct connections with the bilateral ones. It was also shown that the MGI and 9-3 have indirect connections with the ipsilateral and contralateral cercal receptors, respectively. The LGI and 9-2 never responded to the electrical stimulation of the ipsilateral cercal nerve. Experiments of depolarizing current injection into individual GIs showed that except for the MGI and LGI, the remaining GIs have excitatory connections with all of the motoneurons running through the fifth nerve roots of mesothoracic ganglion, the third nerve roots metathoracic ganglion, the first nerve roots of third abdominal ganglion and the seventh nerve roots of terminal abdominal ganglion, or with some of these motoneurons.

PH 6

IDENTIFICATION OF WIND SENSITIVE INTERNEURONS IN THE TERMINAL ABDOMINAL GANGLION.

Y. Baba and T. Yamaguchi, Dept. Biol., Fac. Sci., Okayama Univ., Okayama

In addition to the seven giant interneurons and fourteen local nonspiking interneurons (Baba and Yamaguchi, 1988), eighteen wind sensitive ascending interneurons (AIs: AI-1 - AI-18), nine wind sensitive local interneurons (SIs: SI-1 - SI-9), and one wind sensitive unpaired neuron have been identified in the terminal abdominal ganglion of the cricket (*Gryllus bimaculatus*). All of these newly identified interneurons were spiking neurons. The AIs could be divided into two groups (unilateral and bilateral AIs) depending on whether their major arborizations occupy both the halves of the terminal abdominal ganglion, or only either half. All of AIs and SIs had directional preferences dependent of the position of the stimulated cercus: especially, each of AI-1, AI-8, AI-12, SI-1 and SI-2 evoked strong excitatory response to wind stimulation to a certain direction. So far as we have examined, electrical stimulation of cercal afferents indicated that all the unilateral AIs receive the sensory input from the cercal receptors contralateral to their somata, and the bilateral AIs and SIs receive the sensory input from the ipsilateral and contralateral cercal receptors or either.

PH 7

PROPRIOCEPTIVE INPUTS AND MOTOR PATTERN GENERATION IN THE STINGING RESPONSE OF HONEYBEE.

H. Ogawa and T. Yamaguchi, Dept. Biol., Fac. Sci., Okayama Univ., Okayama

During the stinging response of the honeybee (rhythmic movements of a pair of lancets around a stylet) two sets of muscles, M198 (protractor) and M199 (retractor) contracted alternatively in succession. There was a linear relation among three parameters of muscle activities: the cycle length of successive electrical discharges of a muscle, the duration of each electrical discharge, and the time lag between electrical discharges of homologous muscles in both sides. The stinging response occurred even in animals which had sensory input from the proprioceptors on the sting (campaniform sensilla and hair plates) removed. In those animals, however, three parameters of muscle activities were weakly relative to each other. When the strength of mechanical stimulation to the proprioceptors on one side was different from that on the opposite side, the muscle activities of both sides did not synchronize with each other, though there was a correlation among three parameters of muscle activities. It is probable that a central pattern generator presents in each half of the terminal abdominal ganglion, and the proprioceptor input is involved in the generation of the normal motor pattern.

PH 8

RESPONSE PROPERTIES OF NONSPIKING GIANT INTERNEURONS IN THE CRAYFISH BRAIN

Y. Okada and T. Yamaguchi, Dept. of Biol., Fac. of Sci., Okayama Univ., Okayama.

In the crayfish brain, three pairs of nonspiking giant interneurons (GI, G2, G3) responded with depolarizing and hyperpolarizing potentials to illumination of the contralateral and ipsilateral eyes, respectively (Okada and Yamaguchi, 1988). In the present experiment, it was found that these interneurons react well also to geotactile stimulation: they evoke depolarizing and hyperpolarizing potentials in response to the body tilts in roll to the ipsilateral and contralateral sides, respectively. The larger the angles of body tilt was, the larger the amplitude of response occurred. The presence of a single light shining the dorsal part of the body had a small influence on the response elicited by the body tilts in roll, except for the onset of illumination. When either statocyst was removed, all the nonspiking giant interneurons respond to the body tilt in roll to either direction even in the dark. However, when both statocysts were removed, the nonspiking giant interneurons responds to the body not in the dark, about in the presence of single light. In this case, the larger the velocity of body tilt was, the larger the amplitude of response occurred.

PH 9

DOPAMINERGIC SENSORY CELLS IN THE GILL EPITHELIUM OF *APLYSIA*.
M. Kurokawa, K. Kuwasawa and M. Otokawa*.
Dept. of Biol., Tokyo Metropolitan Univ.,
*Biol. Lab., Hosei Univ., Tokyo.

An aminergic reticular structure, which we refer to as the neural plexus, has been revealed by glyoxylic acid-induced fluorescence in the gill of *Aplysia kurodai* and *A. juliana*. The plexus contains three types of aminergic cells. One of the three types of the cells is localized in the pinnule epithelium. The cells have a cone cell body with a short dendritic extension and a long process joining reticular nerve fascicles. HPLC analysis of amines in epithelial tissue showed the exclusive presence of dopamine. The cells showed immunoreactivity to antityrosinehydroxylase antiserum. Aminergic varicose processes were seen in areas surrounding neurons in the branchial ganglion (BGNs). BGNs showed excitatory responses to bath-application of dopamine and serotonin. BGNs were also activated by supernatant of the homogenate of the pinnule epithelium. In response to tactile stimuli applied to the gill, BGNs produced compound EPSPs. The EPSPs were depressed by bath-applied haloperidol, but not by methysergide. These results show that the cone cells may be the tactile sensory neurons, and that transmission of sensory impulses from the tactile receptors to BGNs may be mediated by dopamine.

PH 10

THE EFFECT OF OCTOPAMINE TO THE RETRACTOR MUSCLE ACTIVITIES ON THE OVIPOSITOR IN FEMALE CRICKET AND THE ROLE OF DUM NEURON ACTIVITY FROM THE TERMINAL ABDOMINAL GANGLION, *TELEORILLUS COMMODUS*.
H. Ai and N. Ai. Dept. of Biol., Tokyo Gakugei Univ., Koganei, Tokyo.

One of C-5 neurons on the DUM cluster located in the terminal abdominal ganglion has already been reported to have innervation bilaterally for the posterior tergo-sternal muscle (M-4) as retractor on the ovipositor (Ai and Ai, 1989), and also to have closely contact and physiological relationship with the descending neuron. The anterior connective of the above terminal abdominal ganglion being extracellularly stimulated with repetitive pulses, EPSPs were risen frequently with spike potential.

By using intracellular recording electrode penetrated to DUM, the concerned DUM neuron was clearly evoked EPSP and sometimes spike-like potential with high frequency stimulation not low one.

On treatment of octopamine (OA) 10^{-6} M to retractor muscle M-4 of ovipositor, spontaneous and repetitive slow potentials were gradually disappeared intracellularly. But, OA 7 M solution being applied to M-4, these activities were more gradual prolongation in their appearance and decrease in potentiation and then, finally, disappeared.

After treated OA solution was rinsed out of retractor M-4, spontaneous and repetitive action potential were confirmed to have appearance again.

PH 11

DIRECTIONAL SENSITIVITY OF THE LINEAR RESPONSE IN CERCAL NONSPIKING INTERNEURONS OF THE COCKROACH

Y. Kondoh, H. Morishita, T. Arima, and J. Okuma. Wako Research Center, Honda R&D Co. Ltd., Wako, Saitama

In white noise analysis, a cellular response is defined by a series of Wiener kernels produced by a cross correlation of a generalized input, Gaussian white noise, and the evoked response. The first- and second-order Wiener kernels represent the linear and static nonlinear responses, respectively. The stimulus of air displacement modulated in a white noise fashion was applied to the cockroach to analyze the dynamics of the graded response in identifiable, nonspiking local interneurons.

In interneurons H, E and 203, the first-order kernel was biphasic, and closely matched the time differential of a pulse. The waveform of the kernel depends on the direction of the stimulus. For example, in the H-cell, stimulus wind from the side ipsilateral to the cell body produced the on-off type kernel, the initial depolarization followed by a hyperpolarization. This differential waveform was reversed when stimulated on the contralateral side.

The linear models predicted by convolving the first-order kernels with the arbitrary input well simulated the actual response at preferred directions. The stimulus was, however, null for the linear part of the response at a particular direction, as suggested by the large mean square errors (MSEs) of the linear models. The null direction differs between the cell types. The static non-linear components predicted by the second order kernel comprise only a minor part of the response, as indicated by the large MSEs of the second-order models. In conclusion, the graded responses in interneurons H, E, and 203 are nearly linear, and code the time differential of the signal and the direction of its source.

PH 12

IDENTIFICATION OF THE DEUTOCEREBRAL NEURONS RESPONDING TO THE THERMAL STIMULATION IN THE COCKROACH BRAIN

M. Nishikawa, F. Yokohari, and T. Ishibashi
Dept. Biol., Fac. Sci., Fukuoka Univ.,
Fukuoka

Thermal responses of the deutocerebral neurons of the cockroach, *Periplaneta americana*, were recorded extra- and intracellularly. The neurons were morphologically identified by cobalt-lysine intracellular staining.

Most of the deutocerebral neurons responded to cold air stimuli and showed the response pattern of on-phasic-tonic-inhibition type. In the range of temperature examined ($20-30^{\circ}\text{C}$), the impulse frequency increased with increase in temperature drop. Their morphological structures showed the local interneurons which had arborizations in many glomeruli restricted to the antennal lobe. Moreover, other response patterns to cold stimuli were on-phasic type and on-tonic type.

In addition to these neurons, the excitatory responses to warm air stimuli were also recorded. The impulse frequency increased with increase in temperature rise. This type had a short inhibition at the beginning of the stimulus before impulse frequency increased. The morphological structure of this type was also a local interneuron which had arborizations in many glomeruli.

PH 13

RECONSTRUCTION OF MUSHROOM BODY AND NEURO-
NAL RESPONSES TO SEXUAL PHEROMONE IN COCK-
ROACH BRAIN.

T. Shibuya, A. Watanabe, T. Omura and T. Hana-
da. Inst. of Biol. Sci., Univ. of Tsukuba,
Tsukuba.

Responses of the deutocerebral and pro-
tocerebral neurons to periplanone A and B
in the male american cockroach, *Periplaneta
americana*, were recorded intracellularly.
Then neurons were stained by iontophoretic
injection of Lucifer yellow CF. Each
neuron was observed the shape and pathways
of axons in the brain. In the deutocerebrum
, the neurons responded to p-A only arborized
dendrites in the dorsal part of the mac-
roglomerulus. These neurons did almost not
responded to p-B. The neurons which arborized
in both whole and ventral parts responded
well to both p-A and B. These responses
were usually with phasic-tonic-inhibition
(PTI) type as observed in the deutocerebral
neurons of some insects. The extrinsic neu-
rons of protocerebrum also responded to p-
A, -B and mixture of both. However, the
neurons were not divided into a clear few
types. The mushroom body was reconstructed
by the three dimensional method used a com-
puter. Three-D shapes of the calyces, stalk
, α - and β -lobes were analyzed morphologi-
cally. The body have two calyces larger
than that of other insect species relative-
ly in each side of the protocerebrum. The
stalk was long and branched off to the α -
and β -lobes. The α -lobe extended obliquely
to the dorsal side.

PH 14

MORPHOLOGY AND RECEPTIVE FIELDS OF A NEW
POPULATION OF SPIKING LOCAL INTERNEURONES
IN THE METATHORACIC GANGLION OF THE LOCUST
T. NAGAYAMA (Zool. Inst., Fac. of Sci.,
Hokkaido Univ., Sapporo 060 Japan), M.
BURROWS (Dept. of Zool., Univ. of
Cambridge, Cambridge England)

A third population of spiking local
interneurons is found in the metathoracic
ganglion of the locust. All have cell
bodies in a cluster at the ventral,
anteromedial portion of the ganglion.
Their branches are restricted to the same
half of the ganglion as their cell bodies.

Each unilateral interneurons has a
characteristic shape and physiological
action, but they form 3 distinct subgroups
according to their gross morphology and
their mode of operation. Interneurons of
the 1st subgroup have ventral branches
that extend over most of one-half of the
metathoracic neuropil and receive
excitatory inputs from exteroceptors on
the hindleg. Interneurons of the 2nd
subgroup have two main ventral branches
which extend either medially or laterally
and receive inputs from proprioceptors.
Interneurons of the 3rd subgroup have few
ventral branches and are inhibited by
inputs anywhere on the hindleg.

Simultaneous intracellular recordings
revealed that these antero-medial inter-
neurons receive direct excitatory inputs
from the afferents and receive inhibitory
inputs from the midline interneurons.

PH 15

RANDOM OCCURRENCE OF mEJP's AT THE
NEUROMUSCULAR JUNCTION OF *DROSOPHILA* LAR-
VAL BODY WALL MUSCLE.

K. Yamaoka. Natur. Sci. Lab., Toyo Univ.
Asaka Campus, Saitama.

Miniature excitatory junction poten-
tials (mEJP's) at the neuromuscular junc-
tion of the *Drosophila* larval body wall
muscles were examined for randomness by
comparing the raw data to simulated data
obtained by theoretical random model. The
intervals between two adjacent mEJP's dis-
tributed exponentially as expected by ran-
dom theory. Adjacent intervals had no
correlation, and the amplitude of the
event did not correlate with the duration
of the preceding or subsequent intervals.
These results show that mEJP's occur inde-
pendently of each other. However, the
power spectrum of the frequency of the ac-
tually recorded events in time series
showed weak peaks at 1, 0.5, 0.2 and 0.1
Hz, while that of the simulation data
showed no remarkable peaks as a matter of
course because of its randomness.
Consequently, it is suggested that the oc-
currence of mEJP's is basically random,
but the frequency over time can vary.

PH 16

RESPONSE OF THE TARSAL CONTACT CHEMO-
RECEPTOR OF THE CITRUS-FEEDING SWALLOWTAIL
BUTTERFLY RELEASING THE OVIPOSITION BE-
HAVIOR

K. Kusumi and T. Shibuya. Inst. of Biol.
Sci., Univ. of Tsukuba, Ibaraki.

Papilio protenor is one of the Citrus-
feeding swallowtail butterflies. They
recognize their host plant, *Citrus unshu*,
by receiving the chemical components. The
components have been reported to be
Hesperidin, Naringin, Quinic acid,
Chlorogenic acid, L-Synephrine, L-Proline
and L-Stachydrine. We used all components
except L-Stachydrine, and investigated the
activity to release the oviposition be-
havior of each single component.

In the behavioral experiment, the com-
ponents dissolved in the agar substrates
were applied to the female butterflies for
two days, and the laid eggs were counted.
The result is that flavanones, Hesperidin
and Naringin, could release the oviposi-
tion behavior, but any other components
could not.

The electrophysiological experiment
revealed that tarsal sensilla, contact
chemoreceptors, responded well to Narin-
gin, but slightly to Hesperidin. They also
responded well to Quinic acid and
Chlorogenic acid which could not release
the oviposition behavior. This contradic-
tion may be attributed to the ambiguous
amplitude of spikes recorded. L-Synephrine
had an inhibitory effect and L-Proline had
no effect.

PH 17

IMPULSE RESPONSES TO SEXUAL PHEROMONE AND MORPHOLOGY OF ANTENNAL SENSILLUM IN *Spodoptera exigua*.

F. Mochizuki¹ and T. Shibuya² ¹Shin-Etsu Chemical Co. LTD., Tokyo and ²Inst. of Biol. Sci., Univ. of Tsukuba, Ibaraki.

Two kinds of sensillum trichodea, short and long hairs, were observed on the antennae of *Spodoptera exigua*. They can be clearly distinguished under light microscope. The long sensilla trichodea as "type 1" were about 60µm in length. The short sensilla trichodea as "type 2" were about 15µm. In both "type 1" and "type 2" a lot of olfactory pores were observed on them with SEM. Impulse responses from these sensilla to odorants were electrophysiologically recorded. In "type 1", a single sensillum responded with two different amplitude of impulses. The responses were with large impulses to Z9,E12-14:Ac and small ones to Z9-14:OH respectively. Sexual pheromone mimic (Z9-14:Ac) which were changed functional group in minor compound generated not only small impulses, but also large impulses. Moreover, Z9,E12-14:OH generated small impulses. The functional group of sexual pheromone plays an important role as to that olfactory receptor neurons detect the pheromone. "Type 2" trichodea did not respond to both pheromone compounds. However, phenylethyl alcohol as rose odor excited "type 2" neurons well. It seems that the trichodea may play a role of 'generalist' for food-searching behavior.

PH 18

HUMIDITY RESPONSES IN THE ANTENNAL LOBE OF HONEY BEE (*Apis mellifera*).

T. Itoh, F. Yokohari and Y. Tominaga. Dept. of Biol., Fac. of Sci., Univ. of Fukuoka, Fukuoka

Responses to antennal hygro-stimulation were recorded extracellularly from the antennal lobe neurons. The responses were divided into a moist type which was excited in humidity increase, a dry type in humidity decrease. Moist responses were phasic-tonic or tonic in the response time course. Dry responses were phasic-tonic, tonic or phasic. In almost cases, the impulse frequency of both responses was increased with stimulus intensity increase. In some cases, the impulse frequency attained to a maximum at intermediate humidity.

Intracellular cobalt staining revealed several morphological types of hygro-sensitive antennal lobe neurons. One type is a moist responsive local interneuron which arborizes restrictedly in the dorsal and inner lateral region of the antennal lobe. One type is a local interneuron which arborizes widely in the antennal lobe and partly in the dorsal lobe. This type neuron responds to moist and olfactory stimulation (amyl acetate) in different time courses. Other type is an output neuron which innervates a single glomerulus in the dorso-postero region of the antennal lobe and sends an axon toward the protocerebrum.

PH 19

CONDUCTIVE PROPERTIES OF OLFACTORY CILIA. T. Nakamura¹, G. H. Gold, Monell Chemical Senses Center, U.S.A., (¹Present Address: Dept. Appl. Phys. & Chem., Univ. Electro-Communications, Chofu, Tokyo, 182 Japan.)

A cyclic nucleotide-gated ion channel in olfactory cilia observed by patch clamping technique (Nakamura & Gold, 1987, 1988), exhibited similar properties to those of odorant-induced currents in intact receptor cells described by Frings and Lindemann (1988) and Firestein and Werblin (1989). We checked if the voltage change generated by this channel at the cilia can be transmitted to the dorsal portion of the cell. In the cilium, where other kind of channel has not been detected, if the concentration of cAMP was very low ($< 0.1 \mu M$), the membrane resistance might be as high as $10^6 \Omega cm^2$ as reported in rod outer segments (Baylor & Lamb, 1982). Under these conditions, electronic length constant, λ of the cilium was calculated to be a few mm, which suggests that the voltage change could be transmitted to the dorsal portion of the cell. In contrast, at saturated level of cAMP, the ciliary membrane resistance and λ were $5 \Omega cm^2$ and $6 \mu m$ respectively. Then the currents from the distal portion of the cilium would be greatly attenuated. This attenuation may be a part of the olfactory adaptation of the cells. These results are consistent with the hypothesis that cAMP mediates the olfactory transduction.

PH 20

NEURONAL NETWORK IN THE RAT PIRIFORM CORTEX N. Doi¹ and N. Hori² ¹Dept. of Biol., Fac. of Sci., Kyushu Univ., Fukuoka and ²Dept. of Pharmacol., Fac. of Dentistry, Kyushu Univ. Fukuoka.

We investigated the neuronal networks in the rat piriform cortex electrophysiologically by using slice preparation. Pyramidal cells in the piriform cortex receives afferent input from LOT (lateral olfactory tract) fibers and extends its axon (association fiber, AF) toward both rostral and caudal sides. In the present study, we used partially trimmed slice preparations to reveal the existence of the non-LOT inputs.

Experiments using LOT-cut preparation which do not receive the LOT input suggested that the pyramidal cell received excitatory disynaptic inputs, which would be feedforward excitatory inputs mediated by the rostral pyramidal cell. Experiments using LOT-AF fiber separated preparation suggested that the pyramidal cell received the excitatory input from AF fiber, which would be feedback excitatory inputs. The feedforward input was distributed on the apical dendrite of the pyramidal cell. The feedback input was distributed on the apical and basal dendrites of the pyramidal cell. The pyramidal cell received GABAergic inhibitory inputs from the inhibitory interneuron which was sending the axons to the apical and basal dendrites of the pyramidal cell.

PH 21

SINGLE CYCLIC NUCLEOTIDE-ACTIVATED CHANNEL ACTIVITY IN EXCISED PATCHES OF OLFACTORY RECEPTOR CELL SOMA MEMBRANE.
N. Suzuki. Zool. Inst., Fac. of Sci., Hokkaido Univ., Sapporo.

Inside-out membrane patches were excised from the somata of enzymatically isolated bullfrog olfactory receptor cells with a patch pipette filled with divalent cation free solution and were superfused in a microflow chamber. With 0.2 μ M cAMP in the divalent cation free solution, there were current fluctuations which corresponded to the openings and closings of single ion channels. The frequency of channel openings increased with cAMP concentration. There was no obvious desensitization during cAMP stimulation and its effect on the channels was rapidly reversible. The unitary currents which occurred both singly and in short bursts at 1 μ M cAMP had a mean amplitude of 1.4 pA at +60 mV, corresponding to a conductance of 23 pS, and a mean open time of 10 msec. In addition, there were smaller events which were probably other kind of the conductance. The properties of single channels in the soma membrane were the same whether activated by cAMP or cGMP. The mean current increased with the second power of both cAMP and cGMP concentrations, suggesting that there are at least two cyclic nucleotide-binding sites on the channel molecule. With 0.5 mM Mg^{2+} or Ca^{2+} in the cAMP-containing solution, flickering block of the open channel was observed. The reversible flickering block was observed also with 50 μ M Amiloride.

PH 22

PUMPING ACTION OF MOUSE VOMERONASAL ORGAN
T. Hatanaka, Dept. of Biol., Fac. of Educ., Univ. of Chiba, Chiba.

The vasomotor movement of the cavernous vascular tissue of mouse vomeronasal organ was observed by a video camera recording and monitored by a mechanotransducer in order to analyze a pumping action which draw odorants into the receptor mucosa.

This vascular tissue contracted periodically, and the contraction propagated along the vomeronasal organ posteriorly or anteriorly, but in general, a direction of its propagation turned alternatively. These movements had more or less irregular rhythm according to the condition of preparation, but its rhythm was intrinsic and differ from heart beat. This peristalsis like movement contribute to the pumping action and caused periodical activity of the vomeronasal nervous system, bursting responses of receptor cells and accessory olfactory bulb neurons. Some odor stimuli decreased the frequency and increased the amplitude of vasomotor movement to take stimulants fully, showing that this vasomotor movement was influenced by an olfactory input.

PH 23

RESPONSES TO FOOD STIMULI AND MORPHOLOGY OF NEURONS IN THE CEREBRAL GANGLION OF THE TERRESTRIAL SLUGS, *Limax flavus*.
A. Iwama and A. Mizukami, Tsukuba Research Center, SANYO Electric Co., Ltd., Ibaraki.

The terrestrial slugs exhibit food aversion learning after treatment with noxious stimuli during feeding. The nervous systems associated with this type of learning involve the gustatory and the olfactory neural pathways.

To investigate these neural pathways, we used the isolated preparations of CNS with lip(L) or tentacle(T) or both(L-T). The responses to food stimuli of neurons were recorded intracellularly in the cerebral ganglion. After the recordings, these cells were stained with dye injection.

Thirty neurons were examined. Some cells showed excitatory responses to lip stimuli in the CNS-L preparations and to tentacle stimuli in the CNS-T preparations. Two cells responded to only tentacle stimuli in the CNS-L-T preparations.

The somata of most cells stained were located in the dorso-medial region of cerebral ganglion. But the morphological features of them were varied individually. Some cells send their axon into lip nerve or tentacle nerve. Many of them were interganglionic neurons which send their axons into pedal or pleural or buccal ganglia.

PH 24

ADAPTATION AND SENSITIVITY OF THE SUGAR TASTE RECEPTOR CELL OF THE FLY.
M. Ozaki and T. Amakawa, Dept. of Biol., Fac. of Sci., Osaka Univ., Osaka. Dept. of Biol., Col. of Gen. Educ., Kobe Univ., Kobe.

We compared the concentration-response curves of the sugar receptor cell of the fly before and after adaptation with each other. Following adaptation, the shift of the concentration-response curve was seen, depending on the concentration of sugar used for the adaptation and the length of the adapting period. However, the maximum response did not significantly change. Thus, the shift of the concentration-response curve mainly reflects on the reduction of the sensitivity accompanied by the adaptation.

A sensillum contains a sugar, a water, a salt and another taste receptor cells. As for the cross adaptation between these cells, when the sugar receptor cell was exposed to distilled water or salt solution, either of which induces adaptation of the water or the salt receptor cell, respectively, the concentration-response curve for sugar stimulation did not shift.

In a sugar receptor cell, there are two functionally separate receptor sites for sugars, i.e. the P site for glucose, sucrose, etc. and the F site for fructose, D-fructose, etc. As for the cross adaptation between these sites, when the sugar receptor cell was adapted with fructose, the concentration-response curve for sucrose stimulation shifted and vice versa.

PH 25

SUBSPECIES DIFFERENCES IN NEURAL GUSTATORY RESPONSES OF *XENOPUS*

S. Yamashita, H. Kohriyama and S. Kiyohara.
Biol. Inst. Coll. of Lib. Arts, Kagoshima Univ., Kagoshima.

Taste sensitivities of two subspecies of *Xenopus* (*X. laevis laevis* and *X. laevis borealis*) to various chemical stimuli were compared recording integrated responses from the glossopharyngeal nerve.

Thresholds for L-Tyr, L-Trp and L-Phe occurred between 10^{-6} and 3×10^{-5} M in the *X.l.b.*, being 10 to 100 times lower than those for the respective stimuli in the *X.l.l.* The magnitude of the response to each of these stimuli at a given concentration was large in the *X.l.b.* throughout the concentration range tested, compared with the *X.l.l.* Each of other effective 6 amino acids exhibited similar threshold and dose-response curve between the two subspecies.

Of 5 nucleosides tested only adenosine was stimulatory to gustatory receptors of the *X.l.b.*, having the threshold at about 10^{-4} M. Gustatory receptors of the *X.l.l.*, however, caused no responses to adenosine even at 10^{-2} M.

Thresholds of gustatory receptors for bitter substances, quinine and strychnine were about 3×10^{-4} M and 10^{-3} M in the *X.l.b.*, and about 3×10^{-3} M and 10^{-2} M in the *X.l.l.*, respectively. The gustatory responses of the *X.l.l.* to both bitter substances saturated between 10^{-3} and 10^{-2} M, whereas those of the *X.l.b.* resulted in no saturation of responses even at 10^{-2} M.

PH 26

ELECTROPHYSIOLOGICAL STUDIES ON THE DARK ADAPTATION OF COMPOUND EYES OF DARK LEPIDOPTERAN SPECIES.

K. Bandai and E. Eguchi. Department of Biology, Yokohama City University, Yokohama 236, Japan.

In general, the sensitivity recovery during dark adaptation of compound eyes of diurnal insects (apposition eyes) shows a smooth monophasic curve. In superposition eyes of nocturnal insects, their dark adaptation curves are biphasic. The first phase is due to the recovery of sensitivity of a photoreceptor cell itself, whereas the second phase is attributed to the migration of the pigment granules in the iris pigment cells (Bernhard et al. *J. Insect Physiol.* 9:573, 1963).

In this research, dark adaptation curves were electrophysiologically (ERG) determined for the compound eyes of 42 lepidopteran species in 5 different groups; 1) Papilionoidea, 2) Hesperioidae, 3) diurnal sphingids, 4) diurnal moths, 5) nocturnal moths. The dark adaptation curves were recorded by measuring the ERG responses to test flashes (0.3 sec) in every 1 minute during dark adaptation after 3 minutes of light adaptation. Biphasic dark adaptation curves were recorded not only from the superposition eyes but also from the apposition eyes of 12 butterfly species. The comparison of the sensitivity recoveries in dark adaptation among 5 groups represented significant differences between butterflies and nocturnal moths as well as between hesperids and nocturnal moths.

The comparison of the recoveries by the second phase also represented significant differences between butterflies and nocturnal moths as well as between butterflies and diurnal moths.

PH 27

STRUCTURE OF THE LAMINA NEUROPIIL IN THE VISUAL SYSTEM OF THE LARVA OF THE TIGER BEETLE, *CICINDELLA CHINENSIS*.

A. Mizutani and Y. Toh. Dept. of Biol., Fac. of Sci., Kyushu Univ., Fukuoka.

The predatory behavior of the tiger beetle larva depends upon visual information. The visual system of the larva consists of six ocelli and an optic neuropil complex on either side of the head. Each ocellus possesses its own first and second optic neuropil within the complex, which are referred to as the lamina and the lobula, respectively. In the present study, the structure of the lamina of the two large ocelli has been examined. Regularly-spaced reticular axons descend to the bottom of the lamina. Lamina neurons were monopolar. Their cell bodies occur above the lamina layer, and their proximal axons descend through the lamina and end within the lobula. Based upon Golgi staining, lamina neurons were classed into eight types. Some axons horizontally extend a long collateral. Lamina neurons were also divided into groups by their vesicular contents: those which contain clear vesicles, dark vesicles, and clear and cored vesicles and those which contain few vesicles. Synapses occurred between reticular axons and lamina neuron, as well as among lamina neurons. These data suggest that the lamina neuropil is not only an important region for the relay of signals, but also for lateral interaction that is essential for movement detection.

PH 28

GABA AS A NEUROTRANSMITTER OF AN Efferent NEURON IN THE COCKROACH OCELLUS

J. T. LIN, M. MIZUNAMI, Y. TOH and H. TATEDA.
Dept. of Biol., Fac. of Sci., Kyushu Univ., Fukuoka.

Neurotransmitters at synapses from small multimodal, efferent neurons (SM-neurons) to large second-order neurons (L-neurons) of the cockroach ocellus have been examined. Activation of the SM-neuron by cercal stimulation induced a depolarization, a response opposite in sign to that evoked by ocellar illumination. The depolarization induced by ionophoretic application of GABA was about 5 mV in amplitude, and that induced by ACh was about 2 mV. Curare, an antagonist of ACh receptors, failed to inhibit the depolarization of L-neurons caused by cercal stimulation. GABA was effective even after synaptic transmission was blocked by 1 mM cobalt chloride, suggesting a direct effect of GABA on the L-neuron. Picrotoxin and strychnine, antagonists of GABA receptors in the vertebrate nervous system, reversibly depressed the depolarization caused by cercal stimulation and GABA application. Other antagonists such as bicuculline and bicuculline methiodide did not show significant effects on the depolarization of L-neuron. These results suggest that GABA is a transmitter of SM-neurons in the cockroach ocellus, and pharmacological properties of GABA receptors in cockroaches are not identical to those in vertebrates.

PH 29

SYNAPTIC RECTIFICATION MODEL FOR
DIRECTIONAL SELECTIVITY TO MOTION.
M. Mizunami. Dept. of Biol., Fac. of
Sci., Kyushu Univ., Fukuoka.

A cellular model has been proposed for elementary processes of movement detection systems of the fly. The model consists of linear local interactions followed by ON-OFF rectifications. Exponential transfer characteristics are assumed for input-synapses of elementary movement detectors. It has been shown that such nonlinear synapse is the cellular base of rectification in insect visual system. I found that (a) rectifying synapses convert linear (first-order) lateral interaction into quadratic (second-order nonlinear) one, (b) time-averaged outputs of the model well represent time-averaged responses of actual movement detection systems of the fly, (c) dynamics of ON-motion detector of the model well represent dynamics of large-field movement detection system of the fly and (d) dynamics of ON-OFF movement detector of the model explain dynamics of small-field movement detection system of the fly. I propose that (a) synaptic rectification is the cellular base of nonlinear operation underlying movement detection of the fly and (b) elementary movement detectors (EMDs) of the fly consist of two classes, ON-EMDs and OFF-EMDs.

PH 30

A NEUROANATOMICAL STUDY OF THE OPTOKINETIC
NYSTAGMUS IN THE MIDBRAIN OF JAPANESE
DACE.

M. Takizawa and K. Aoki
Life Sci. Inst., Sophia Univ., Tokyo

The optokinetic nystagmus (OKN) in fish is induced by a rotating vertically striped environment in head restrained condition. Optokinetically evoked eye movements are good materials to characterize the relationships between sensory input and motor output and to study the intervening neural circuits with microelectrodes. The responses of units were recorded in and around the thalamic-pretectal region with the stimulation by a rotating vertically striped drum or room light condition. The main responses were tonic type and phasic type, which responded to both rotating drum and room light. The response patterns of the phasic type units were similar to that recorded in the optic tectum. The latency of the phasic type units to the light stimulus was much longer than that of the tonic type units. Therefore it is likely that the phasic type units were recorded from tectal efferents. The tonic type units were probably recorded from the neurons projected directly from the retina. It is suggested that the extracted velocity information for the OKN was recorded in the thalamic-pretectal region.

PH 31

PHYSIOLOGICAL STUDIES ON THE REGENERATED
NEWT RETINA

T. Saito, Y. Yabe and Y. Kaneko. Inst. of
Biol. Sci. Univ. of Tsukuba, Tsukuba, Ibaraki,

The process of retinal regeneration of Japanese newt, *Cynops pyrrhogaster*, was analyzed morphologically and physiologically. (1) ERG recordings during different stages of retinal regeneration were performed on the intact eye using a silver-chloride electrode on the cornea. The first light-evoked responses were seen by day 20 after the operation. The response polarity was either cornea-positive or cornea-negative. The first negative-positive biphasic ERG appeared in eyes from about 30 days post operation. The histological sections of regenerating eyes showed that by 40 days after the operation outer- and inner-plexiform layers were established. (2) The electrical properties of solitary ganglion cells dissociated from the regenerated retina were examined by whole-cell patch-recording method and compared with those of solitary ganglion cells from the normal retina. The spike activities of ganglion cells were seen by day 30 after the operation. The threshold values (about -20mV) and amount of inward current (600pA in maximum) were similar to those of the normal retinal ganglion cells. At this stage of regeneration, ganglion cells had axons, but they did not reach optic tectum.

PH 32

THE EFFECT OF K^+ CONDUCTANCE BLOCKING
REAGENTS ON THE OCCURRENCE OF RETINAL
SPREADING DEPRESSION (SD).

M. Fujimoto, H. Yanase and J. Katayama. Zool.
Inst., Fac. of Sci., Hiroshima Univ.,
Hiroshima.

The retinal spreading depression (SD) has been thought to be generated by the abnormal increase in $[K^+]_o$ in the inner plexiform layer. Retina isolated from bullfrog was immersed in SD-conditioning medium (low Cl^- or high K^+ Ringer's) so that the spontaneous SDs were periodically induced in the dark, and concomitant extracellular potentials (SD potential; SDP) were recorded. The effect of K^+ conductance blocking reagents (TEA, 4-AP, Cs⁺ and Ba²⁺) on the frequency of SD generation was studied using the SDP as an index. These reagents increased the frequency in all cases and decreased their amplitude in general. According to the Müller cell theory, $[K^+]_o$ depolarizes the Müller cells and the resulting extracellular current generates the SDP. Therefore, the small amplitude of the SDP reflects the decreased K^+ current, suggesting that the K^+ -buffering capacity of the Müller cells was partly reduced. Consequently, the frequency of the occurrence of SD increases to compensate for the decreased buffering capacity. The present result is in good agreement with the current Müller cell theory for the origin of SD.

PH 33

INTEGRATION OF COLOR SIGNALS IN THE MEDULLA OF SWALLOWTAIL BUTTERFLY LARVA.
Toshio Ichikawa,
Department of Biology, Faculty of Science, Kyushu University, Fukuoka 812.

Spatial and chromatic properties of medulla neurons which receive input from different optical units (stemmata) of the larval eye in the swallowtail butterfly were examined by illuminating individual stemmata with monochromatic light.

There were many neurons dominated by two or three stemmata located in the frontal (central) region of the eye. The stemmata provided different types of color (opponent) input, thereby the receptive fields of the neurons were spectrally heterogeneous.

Neurons dominated by three stemmata located in the dorsal and lateral (peripheral) regions of the eye showed relatively homogeneous spectral profiles over the receptive fields. A few units were characterized by their tonic or phasic nature of responses.

Neurons dominated by five or all six stemmata had spectrally homogeneous receptive fields. Some neurons showed a spatial summation of responses or a spatial antagonism between central and peripheral or dorsal and ventral parts of the eye.

PH 34

MORPHOLOGICAL BASIS OF THE CAT RETINAL GANGLION CELL RECEPTIVE FIELD AND IMPROVEMENT OF THE SIGNAL TO NOISE RATIO BY COLLECTIVE CODING

Y. Tsukamoto¹, R.G. Smith² and P. Sterling²
¹Dept Anat., Hyogo Col. Med., Nishinomiya
²Dept Anat., Sch. Med., Univ. Penn., Philadelphia, PA, USA

Morphological basis of the receptive field center of the cat retinal ganglion cell has been recently revealed by three dimensional reconstruction of microcircuitry from electron micrographs of serial sections. A ganglion cell collects signals from many cones through several bipolar cells in the area centralis. For the functional significance of the receptive field center, we propose "collective coding" which optimally improves the signal to noise (S/N) ratio of the ganglion cell response. This coding scheme has been developed by expanding the square root law for identical signals to correlated signals. Computer simulation suggests the following. One, the dome-like weighting function produces the maximal S/N improvement for visual scenes with strong spatial autocorrelation. The other, by matching cone density to the ganglion cell collecting area, the retina provides to all beta cells, from center to periphery, the same S/N improvement by a factor of about 4.

PH 35

COLOUR DISCRIMINATION IN THE TRAINED BLOWFLY *LUCILIA CUPRINA*.
T. Fukushi. Department of Biology, Miyagi College of Education, Aramaki-aza-Aoba, Sendai.

The flies trained to one of colours (blue, green, yellow and red) prefer this colour significantly when confronted with a test array of many colour marks consisting of four colours (Fukushi, 1989).

To study what cue of the coloured stimuli (hue or brightness) the fly uses to discriminate between the coloured papers, flies trained to a specific colour or a grey shade were tested on the test array consisting of a colour and three shades of grey, one of the grey shades being similar to blue and green in the fly's subjective brightness and yellow being intermediate between two of grey shades. The flies clearly discriminate blue, green and yellow from the shades of grey, while they confuse red with the darkest grey. After training to two lighter grey shades, the flies can not clearly discriminate between them, although the difference between these two grey shades in the fly's subjective brightness is larger than that between blue and yellow.

These results suggest that the flies discriminate between the colours mainly by the hue of colours.

PH 36

HISTOCHEMICAL DEMONSTRATION WITH HRP STAINING ON THE MEMBRANE BREAKDOWN PROCESS IN BUTTERFLY PHOTORECEPTORS.

Y. Tominaga and M. Shimohigashi. Dept. Biol., Fac. Sci., Fukuoka Univ., Fukuoka.

In order to examine the breakdown pathway of photoreceptor membranes in the compound eye, we observed the endocytotic process in retinula cells of a cabbage butterfly (*Pieris rapae crucivora*) by electron microscopy with horseradish peroxidase staining. In the retinula cells extracellularly stained with HRP, the reaction product was seen at the cell outer surface, the extracellular space or coated pits at the bases of rhabdomeric microvilli, endocytotic vesicles (EV) and multivesicular bodies (MVB). The peroxidase-containing EV mostly gathered adjacent to the rhabdomeres and often kept contact with one another. In MVB, the reaction product was visible at the inner surface of limiting membrane and in the majority of inner small vesicles. This suggests that the outer limiting membrane of MVB may be formed by the fusion of EV membranes. The results show high endocytotic activity confined at the base of rhabdomeric microvilli, as well as the continuity between the endocytosis and the formation of MVB, and clarify the pathway of the membrane breakdown in butterfly's rhabdomere.

PH 37

SYNAPTIC ARCHITECTURE OF 5HT LIKE IMMUNOREACTIVE AND SUSTAINED AMACRINE CELLS; A COMPARATIVE STUDY WITH LIGHT AND ELECTRON MICROSCOPY

Soh Hidaka, Natl. Inst. for Basic Biol., Okazaki, Aichi.

There is so much diversity among amacrine cell population in the vertebrate retina. Amacrine cells play important roles onto the ganglion cells which code the final information of the retinal processing as the spike trains to the visual centers of the brain. It is significant to identify and characterize each group of amacrine cells functionally and morphologically. I identified 5-HT-LI cells with the immunocytochemical method and the sustained amacrine cells with the intracellular staining method. Their morphological properties were determined under LM and EM. The two groups of cells resembled the dendritic branching pattern in the IPL whose primary dendrites mainly ramified eccentrically to their somata, expanding smoothly only into the dorsal direction. I have studied their detailed synaptic connections and reconstructed the synaptic architecture by means of corresponding the EM image on the thin sections with the LM image. The density and the ratio of the converged bipolar/conventional synapses were homologous among the two groups of cells. The synaptic clusters of the ribbon inputs from bipolar cell axons were distributed in each 20-30 μ m. The diverged output synapses of 5-HT-LI cells were found only on other pale dendritic processes, away from the reciprocal sites onto the bipolar. On the other hand, those of sustained cells were restricted to the bipolar axons. That's the dramatic difference among the two populations.

PH 38

SELECTIVE VISUAL LEARNING IN A FOOD-REINFORCED DISCRIMINATION BETWEEN COMPOUND STIMULI IN THE GOLD-FISH, WITH SPECIAL REFERENCE TO STIMULUS CONDITIONS

K. Ohnishi. Dept. of Physiol., Nara Med. Uni., Kashihara

To examine what stimulus conditions induce the selective visual learning (Ohnishi, 1987), the fish were trained to discriminate between stimuli under various stimulus conditions by use of Y maze food-reinforced training technique. A group (n=7) was trained with vertical patterns (2 mm black bar width; 14 mm interval space between bars, ISBs) on red paper vs horizontal patterns on blue paper. After the fish had obtained learned performances, the test trials in which the color and the pattern composing the compound stimuli were separately presented were performed. The percentages of the correct choices were 75.0 \pm 12.5% (35.7 \pm 17.2% in pretraining) in the color tests and 32.9 \pm 16.0% (31.4 \pm 14.6%) in the pattern tests. This indicates the fish selectively learned only color aspect. The color stimuli were discriminated more rapidly than the pattern ones when another groups (n=13) were trained with the separated color or pattern stimuli. When a group (n=7) was trained with vertical patterns (7 mm ISBs) on green paper vs horizontal patterns on blue paper, the percentages of the correct choices were 30.4 \pm 15.9% (33.9 \pm 9.4%) in the color tests and 77.1 \pm 11.1% (41.4 \pm 10.7%) in the pattern tests. This indicates the fish selectively learned only pattern aspect. The pattern stimuli were discriminated more rapidly than the color ones, when another groups (n=14) were trained with the separated color or pattern stimuli. These results show that the fish selectively process and learn only more easily learned aspect between the aspects, which compose visual compound stimuli.

PH 39

BIOGENIC AMINES IN THE FLY OPTIC LOBE SUBSERVING TO THE EXPERIENCE-DEPENDENT DEVELOPMENT OF VISUAL FUNCTION, K. Mimura, Fac. of Liberal Arts, Nagasaki Univ., Nagasaki.

It has been demonstrated in the fleshfly that the development of visual pattern discrimination depends on visual experience for early period of post-emergence and the development is due to the plasticity of neuronal circuits, especially of synaptic transmission, in the optic lobe (Mimura, 1986, 1987, 1988). The present experiment was performed to demonstrate the molecular mechanisms underlying the experience-dependent development. The distribution of biogenic amines, their precursors and metabolites in the optic lobe and the central part of the brain of the fly was analyzed using HPLC with electrochemical detection. Eighteen substances were analyzed at present. Among them, seven biogenic amines and the related substances were optic lobe-specific. These seven substances were compared between LD (light-dark)-reared flies and DD (continuous dark)-reared ones. Quantity of two substances among them increased significantly for early period of post-emergence in LD-reared flies. It is considered, therefore, that these biogenic amines and/or the related substances subserve to the experience-dependent development of visual function, although the two substances were not identified yet.

PH 40

RETINOL LIGANDS OF RETINAL-BINDING PROTEIN IN THE SQUID RETINA

A. Terakita, R. Hara, K. Ozaki and T. Hara. Dept. of Biol., Fac. of Sci., Osaka Univ., Toyonaka, Osaka 560, Japan.

The squid visual cell contains a retinal-binding protein (RALBP) which binds various isomers of retinal and retinol. As reported previously, RALBP is capable of serving as a shuttle for retinal in the rhodopsin-retinochrome system to assist in the regeneration of both photopigments. The present study was aimed at elucidating the fate of retinol ligands of squid RALBP.

When incubated with a membrane preparation of the retina, 11-*cis*-retinol bound to RALBP was changed to 11-*cis*-retinal, though all-*trans*-retinol remained unaffected. This hinted that the retina contains a retinol-dehydrogenase (RDH) specific to the 11-*cis*-retinol ligand of RALBP. In order to make clear the location of RDH, measurements of its enzymatic activity were carried out in serial frozen sections prepared parallel to the retinal surface. A high activity was found in the sections including the areas between the black pigment and the nuclear layers. Since these areas apparently coincide with the location of myeloid bodies in the visual cells, the 11-*cis*-retinol-bearing RALBP would also participate in forming rhodopsin in the rhodopsin-retinochrome system after dehydrogenation of the ligand into retinal. What occurs with the all-*trans*-retinol ligand remains unsolved.

PH 41

MOLECULAR STRUCTURE OF SQUID RETINAL-BINDING PROTEIN (II).

K.Ozaki, A.Terakita, M.Ozaki, R.Hara and T.Hara. Dept. of Biol., Fac. of Sci., Osaka Univ., Toyonaka.

The primary structure of squid retinal-binding protein (RALBP) was deduced from the nucleotide sequence of cDNA, and was confirmed with the amino-acid analysis and sequencing of lysyl polypeptides derived from purified RALBP. The amino-acid compositions of all the peptides recovered (including C-terminal peptide) were consistent with those deduced from cDNA sequence. The N-terminal of RALBP was blocked, and the analysis of the N-terminal peptide by mass spectrometry strongly suggested that the blocking group is an acetyl moiety. RALBP contains 342 amino-acid residues in a single polypeptide chain corresponding to a M.W. of 39,111 (including the blocking group), about 20% smaller than 51,000 estimated by SDS-PAGE and size-exclusion chromatography.

We tried the expression of RALBP in *E.coli* cells. The originally cloned cDNA showed little expression in the pTTQ18 expression vector. To improve the productivity, the polynucleotide at 5' end of cDNA covering the whole 5' nontranslated region and the following 50 nucleotides of translated sequence was eliminated. Although such modification greatly increased the amount of translate, the product showed no retinoid-binding activity, probably due to the abnormal folding or thermal denaturation of the protein.

PH 42

LIGHT- AND VITAMIN A-DEPENDENT SYNTHESIS OF RHODOPSIN IN THE EYE OF *DROSOPHILA*.

T.Ishizaki, M.Ozaki and K.Ozaki. Dept of Biol., Fac. of Sci., Osaka Univ., Toyonaka

Besides the opsin-bound 11-*cis* 3-hydroxyretinal(11-RAL), a considerable amount of all-*trans* 3-hydroxyretinal(AT-RAL) is stored in the dark-adapted eye of *Drosophila*. In order to study the metabolic pathway to form 11-*cis* chromophore of rhodopsin from AT-RAL, we prepared the fly having AT-RAL store but no rhodopsin by feeding them with all-*trans*-retinal in the dark. By a brief irradiation of the fly with intense blue light, AT-RAL was isomerized specifically into 11-*cis* form which was still unbound to opsin. During the subsequent incubation in the dark, 11-RAL was reduced to 3-hydroxyretinol(11-ROL) within 15 min. 11-ROL was then slowly reoxidized to 11-RAL which is to attach to opsin. Since the stored AT-RAL was suggested to be located away from rhodopsin, such a roundabout route (AT-RAL \rightarrow 11-RAL \rightarrow 11-ROL \rightarrow 11-RAL) of chromophore formation might be necessary for retinoid-transport in the eye of *Drosophila*.

In the absence of vitamin A (VA), opsin is not synthesized in the fly retina. Using a DNA fragment of *ninaE* gene as a probe, we examined the presence of opsin mRNA in the head of VA-deficient fly by northern hybridization. The result showed that VA(-) flies possessed as much mRNA of opsin as VA(+) flies, suggesting that VA post-transcriptionally regulates the opsin synthesis in the fly retina.

PH 43

PHOTBLEACHING PROCESS OF CONE VISUAL PIGMENT, IODOPSIN.

Y. Shichida, T. Okada, Y. Imamoto, Y. Kandori, Y. Fukada and T. Yoshizawa. Dept. of Biophys., Fac. of Sci., Kyoto Univ., Kyoto.

In order to get a clue to elucidate the origin of difference in electrophysiological response between rod and cone, photobleaching process of iodopsin was investigated by means of nanosecond laser photolysis at room temperature and compared with that of rhodopsin, rod visual pigment.

Like rhodopsin, iodopsin was bleached to all-*trans* retinal and R-photopsin through batho, lumi, meta I and meta II intermediates. Formation of each intermediates of iodopsin was, however, faster than that of corresponding intermediate of rhodopsin, suggesting that signal transduction process induced by photon absorption of iodopsin is more rapid than that induced by rhodopsin. Furthermore, the decay time constant of meta II intermediate of iodopsin was much shorter than that of rhodopsin. If meta II intermediate of iodopsin as well as that of rhodopsin is a key intermediate which can activate transducin, the GTP binding protein involved in the enzymatic cascade system of photo-transduction, the rapid bleaching of meta II intermediate of iodopsin may explain the photosensitivity of cone lower than that of rod.

PH 44

PHOTOSENSITIVITY AND QUANTUM YIELD OF CHICKEN CONE VISUAL PIGMENT, IODOPSIN.

T.Okano, Y.Fukada, Y.Shichida and T.Yoshizawa. Dept. of Biophys., Fac. of Sci., Kyoto Univ., Kyoto.

In order to elucidate the difference in sensitivity between cone and rod cells we measured the photosensitivities of chicken iodopsin (a red sensitive cone pigment) and rhodopsin (rod pigment) relative to cattle rhodopsin.

Rhodopsin and iodopsin were purified from chicken retinas in the presence of CHAPS and phosphatidylcholine. A photosensitivity of a visual pigment is proportional to a product of its molar extinction coefficient (ϵ) and the quantum yield (ϕ) of the isomerization. The molar extinction coefficients of chicken rhodopsin and iodopsin were estimated to be 41,200 and 47,200, respectively, in comparison with that of cattle rhodopsin (40,600). While, kinetic analyses of photo bleaching of these pigments showed that the relative photosensitivities of chicken iodopsin and rhodopsin to cattle rhodopsin were 0.92 and 1.02. Thus, the quantum yields of chicken iodopsin and rhodopsin were calculated to be 0.53 and 0.68, respectively. These results indicate that only a part of the difference in photosensitivity between rod and cone cells can be ascribed to a difference in sensitivity between two pigments.

PH 45

RETINAL BINDING SITES OF ROD AND RED-SENSITIVE CONE VISUAL PIGMENTS. Y. Fukada¹, T. Okano¹, Y. Shichiida¹, T. Yoshizawa¹ and R.S.H. Liu². Dept. of Biophys., Fac. of Sci., Kyoto Univ., Kyoto and ²Dept. of Chem., Univ. of Hawaii, Honolulu, U.S.A.

A comparative study on the retinal binding sites of the opsin (R-photopsin) from chicken red-sensitive cone visual pigment (iodopsin) and that (scotopsin) from bovine rod pigment (rhodopsin) was performed by use of retinal analogs including geometric isomers of retinal (all-trans, 13-cis, 11-cis, 9-cis and 7-cis) and fluorinated (14-F, 12-F, 10-F and 8-F) and methylated (12-methyl) 11-cis-retinals. Stereo-selectivity of R-photopsin for retinal analogs was almost identical to that of scotopsin, indicating the similar shape of the retinal binding sites of both opsins although the former appears to be located near the protein surface. On the basis of spectral properties of fluorinated analogs, a polar group in the binding site of iodopsin as well as rhodopsin was estimated to locate near the hydrogen atom at the C₁₀ position of the chromophore. Spectral properties of pigment isomers which would have Schiff-base nitrogen at altered position from that of 11-cis pigments suggested that iodopsin would have a Schiff-base weakly hydrogen bonded to the counterion as compared to that of rhodopsin.

PH 46

IMMUNOHISTOCHEMISTRY ON THE LOCALIZATION OF IODOPSIN IN THE VERTEBRATE RETINAS.

A. Kawata, H. Masuda, T. Oishi, Y. Fukada, T. Yoshizawa. Dept. of Biol., Fac. of Sci., Nara Women's Univ., Nara, Dept. of Biophys., Fac. of Sci., Kyoto Univ., Kyoto.

Localization of iodopsin was studied immunohistochemically by using monoclonal antibodies against chicken iodopsin in the retinas of several species of vertebrates from Osteichthyes to Mammalia. In class Aves, the outer segments of cone cells with red and green (double cone) oil droplets were labeled in the Japanese quail (*Coturnix coturnix japonica*) as well as in the chicken (*Gallus gallus domesticus*). In class Reptilia, the outer segments of cones in *Trionyx sinensis japonicus*, *Geoclemys reevesii* (with yellowish-green and red oil droplets) and *Caretta caretta* (with green and orange oil droplets) were stained, but those in *Gekko japonicus* and *Eumeces latiscutatus* were not stained. Four species in class Amphibia (*Rana catesbeiana*, *Hyla arborea japonica*, *Xenopus laevis* and *Cynopoda pyrrhogaster*) and one species in class Mammalia (*Tamias sibiricus*) showed negative staining. In class Osteichthyes, the results in *Pagrus major*, *Limanda yokohamae* and *Zacco temminckii* were negative, while that in *Misgurnus anguillicaudatus* was positive.

PH 47

LOCALIZATION OF VISUAL PIGMENTS IN THE BRAIN OF JAPANESE QUAIL AND FROGS.

H. Masuda, A. Kawata, H. Fujisawa, T. Oishi, S. Kobayashi, Y. Fukada, T. Yoshizawa, and M. Michinome. Dept. of Biol., Fac. of Sci., Nara Women's Univ., Nara, Lab. of Applied Physiol., Coll. of Lib. Arts and Sci., Dept. of Biophys., Fac. of Sci., Kyoto Univ., Kyoto, Dept. of Biol., Fac. of Sci., Konan Univ., Kobe.

Photoreceptors for photoperiodic-gonadal response and entrainment of circadian rhythms have been suggested to exist in the diencephalon of vertebrates except for mammals. Immunohistochemistry with polyclonal antibodies against bovine rhodopsin and monoclonal antibodies against chicken iodopsin were performed on the brains of Japanese quail and frogs (*Rana catesbeiana*, *Xenopus laevis*) as well as HPLC analysis of retinal. In frogs, the outer segments of photoreceptor cells in the pineal organ and the cells close to the third ventricle were labeled with antibodies against rhodopsin, but not with antibodies against iodopsin. HPLC analysis revealed retinal-like substances in both dorsal (including pineal) and ventral diencephalon. In the Japanese quail, immunohistochemistry and HPLC could prove the existence of visual pigments in the pineal, but the results in the diencephalon were not conclusive.

PH 48

VISUAL PIGMENT OF LAMPREY (II)

O. Hisatomi¹, T. Iwasa¹, F. Tokunaga¹ and A. Yasui². ¹Dept. of Phys., Fac. of Sci., Tohoku Univ., Sendai and ²Res. Inst. for Tuberculosis and Cancer, Tohoku Univ., Sendai.

To understand the molecular evolution of visual pigments, we tried to determine the primary structures of proteins in visual pigments from lamprey. We synthesized eight oligonucleotides - mixtures corresponding to eight amino acid sequences conserved well in known visual pigments. Using these oligonucleotides, a DNA fragment was amplified from genomic DNA of lamprey by polymerase chain reaction (PCR). The deduced amino acid sequence of this fragment showed a 80% identity with those of exon 4 of rhodopsins from higher vertebrates, but only ca. 40% identity with human color pigments sequences. We also isolated mRNA from lamprey retina, and obtained a DNA fragment amplified from the cDNA. This fragment contained the previously identified amino acid sequence and the sequence similar to those of exon 5 of rhodopsins from higher vertebrates with a flanking 3'-noncoding sequence. Judging from the amino acid sequence similarities, the cloned DNA fragment is a part of the rhodopsin gene of lamprey.

PH 49

HPLC STUDY OF VISUAL PIGMENT IN PRIMITIVE EYES AND SEASONAL VARIATION OF VISUAL PIGMENT CHROMOPHORE OF COASTAL FISHES.

M. Sugahara¹, K. Ohtsu² and Y. Kito.³
¹Shizyonawate High School., Shizyonawate,
²Ushimado Mar. Lab., Oku³, Dept. of Biol.,
 Fac. of Sci., Osaka Univ., Toyonaka.

We found 11-cis retinal in the primitive eyes of a hydrozoan, Charybdea rastonii and an asteroidean, Asterias amurensis. Retinal was extracted as the oxime-derivatives and analyzed by HPLC. The hydrozoan has small and large ocelli, which contained about 0.2 pmol retinal. The asteroidean ocelli had about 30 fmol retinal. About half of the retinal was in the 11-cis form in both animals. The results suggest that the V.P. in these eyes belongs to rhodopsin family.

The V.P. chromophore of fresh water fish, Zacco platypus showed the seasonal variation of A1/A2 ratio according to environmental temperature. In the coastal fishes of Thalassoma family, the same variation was seen in Pseudolabrus japonicus, but not in Thalassoma cupido and Pteragogus flagellifera. In winter, the former fish is apt to hibernate, and this temperature sensitiveness may concern with the above seasonal variation.

PH 50

COLOR VISION OF FIREFLY SQUID: SPECTRAL DISCRIMINATION OF RHABDOMERIC EYE WITH MULTIPLE LAYERED PHOTORECEPTOR CELLS.

Y. Kito¹, M. Seidou¹, H. Uchiyama¹ and M. Michinome²
¹Dept. of Biol., Fac. of Sci., Osaka Univ., Toyonaka and ²Dept. of Biol., Fac. of Sci., Konan Univ., Kobe.

We found three visual pigments in the eye of the firefly squid, Watasenia scintillans. The outer segment layer of the small area of the ventral retina is thick (600 μ m), and composed of four types of O.S. of photoreceptor cells. One of them projects rhabdomeres in the proximal 200 μ m layer and contains 3-dehydroretinal-based VP of abs. max. at 500 nm, and the second one projects rhabdomeres in the distal layer of 400 μ m and contains 4-hydroxyretinal-based VP of abs. max. at 470 nm. The rest two cells project rhabdomeres in the intermediary zone. In this multiple layered retina, the distal O.S. layer can act as a specific filter on the proximal layers and modify their spectral sensitivities to shift to longer wavelengths. This may improve the color vision of the squid. Denton and Lockett (1989) proposed the similar mechanism in the multiple banked retinas of the deep-sea fishes.

PH 51

LIGHT AND ELECTRON MICROSCOPIC INVESTIGATION OF CELLULAR ARCHITECTURE IN THE RETINA OF THE FIREFLY SQUID, WATASENIA SCINTILLANS II

¹M. Michinome, ²H. Masuda, ³M. Seidou,
⁴H. Uchiyama and ⁵Y. Kito
¹Dept. of Biol., Fac. of Sci., Konan Univ., Kobe Hyogo.
²Dep. of Biol., Fac. of Sci., Osaka Univ., Toyonaka Osaka

The ventral retina just behind a row of large photophores are much thicker than the other parts of retina. In this region, the photoreceptor cells have long outer segments (OS) of 500-600 μ m while the other region have OS of 200-300 μ m. The long OS region in the ventral retina are composed of 3 types of OS. Type 1 are long (600 μ m), while type 2 are short (200 μ m) and type 3 are middle (400 μ m) OS. In the present study, we have investigated the cellular architecture of the short OS region in the dorsal retina. In this region, there is only one type of OS. The microvilli of a single OS form two parallel rows oriented perpendicular to the main axis and opposite each other. The retina cell are organized in more or less straight rows and so arranged that four rhabdomeres come together to form the square structure. In addition to that, the center region of the square rhabdoms are occupied other OS and its rhabdomeres. This regular arrangement does not obtain everywhere. A given retina cell may participate in up to complex of rhabdomeres.

PH 52

CYCLIC NUCLEOTIDES IN THE RETINAE OF CEPHALOPOD AND CRUSTACEA

M. Seidou¹, Y. Kito,¹ K. Ohtsu,² Y. Nakaoka³ and Z. Yamashita,⁴
¹Dept. of Biol., ²Dept. of Bioeng., ³RI center, Osaka Univ., Osaka and ⁴Ushimado Marine Lab., Okayama Univ., Ushimado-cho, Oku, Okayama.

In the eye of the rhabdomeric retina, cyclic GMP and cyclic AMP contents were radioimmunoassayed and compared with visual pigment contents which were determined by HPLC analysis of chromophore. In the dark adapted eye of Octopus ocellatus, one mole cGMP and 15 moles cAMP per 1800 moles of VP were present. A flash exposure which could convert 28 per cent of VP to the meta-form, did not affect the contents of both nucleotides. In the dark adapted eye of the shrimp, Trachypenaeus curvirostris, 6 moles cGMP and one mole cAMP per 200 moles of VP were present. After a flash exposure, cGMP and cAMP contents decreased to one tenth and one fifth. Above results suggest that any ion channels which are opened by the increase in the cGMP and cAMP concentration may not be concerned in the primary phototransduction process of these rhabdomeric photoreceptors.

PH 53

IMMUNOREACTIVITY OF TURTLE PHOTORECEPTORS TO A MONOCLONAL ANTIBODY.

K. Kawamata, T. Ohtsuka. Dept. of Inform. Physiol., Natl. Inst. for Physiol. Sci., Okazaki.

Immunoreactivity of turtle photoreceptors to a monoclonal antibody (Mab 15-18) was studied. Mab 15-18 recognizes the external loop connecting bovine rhodopsin helices IV-V, corresponding to amino acid sequence 190-197. This antibody labels rod outer segment in the mammalian retina, while the same antibody labels cone as well as rod outer segments in the lower vertebrate retinas. We, therefore, investigated cross-immunoreactivity of chromatic subtypes of cones which are labeled by Mab 15-18. Since cone photoreceptors in the turtle retina are morphologically distinguishable by the presence and color of oil droplets located in the inner segments, we were able to correlate directly the subtypes of cones that are immunoreactive to Mab 15-18. After fixation, the whole-mounted retina was incubated in Mab 15-18 (ascites fluid diluted 1:10-3,000), and then labeled outer segments were visualized by the avidin/biotin peroxidase method. Mab 15-18 labeled intensely the outer segments of both rods and green cones. In addition, a weak cross-reactivity was also found in the outer segment of red cones having a pale-green oil droplet and of blue cones. Other morphological subtypes of red cones, cones with a red oil droplet and both members of double cones, showed no labeling. Our results indicate that rhodopsin and green cone opsin have a similar antigenic determinant, and that two different structural forms of red cone opsin may be present in the turtle retina.

PH 54

IMMUNOCYTOCHEMICAL CHARACTERISTICS OF PINEAL ORGAN AND RETINA OF RIVER LAMPREY, *S. Tamotsu* and *Y. Morita*. 1. Dept. Physiol., Hamamatsu Univ. Sch. Med., Hamamatsu.

The pineal complex and the retina of river lamprey, *Lampetra japonica*, were examined immunocytochemically with antisera against opsin and visinin as specific peptide of rod and cone, respectively, and against serotonin as precursor of melatonin. In the retina, short and long photoreceptor exhibited opsin- and visinin-immunoreactivity, respectively. No serotonin-immunoreactivity was observed in the retina with exception of some amacrine-like cells. The opsin-immunoreactivity was located generally in the ventral portion of the pineal organ and was aggregated at the small area of the parapineal organ. The visinin-immunoreactive cells were found peripherally in the former and at the same area as the opsin in the latter. The cells exhibiting serotonin-immunoreactivity were observed in both organs. In the pineal stalk, numerous serotonin-immunoreactive cells showing spherical somata were concentrated. The serotonin-immunoreactive photoreceptor cells in the ventral portion of the end-vesicle of the pineal organ possessed long basal processes. This result reveals at the molecular level that the pineal complex of the lamprey contains rod- and cone-type photoreceptor cells and functions as a photoneuroendocrine organ.

PH 55

IDENTIFICATION OF ACTIN FILAMENTS IN THE PHOTORECEPTOR MICROVILLI OF *DROSOPHILA*

K. Arikawa*† J. L. Hicks* and D. S. Williams*
*School of Optometry, Indiana University, Bloomington IN, USA and †Department of Biology, Yokohama City University, Yokohama, Japan.

It has been previously shown that each rhabdomeric microvillus of invertebrate photoreceptors has a core filament (Blest et al. *Cell Tissue Res*, 233:553, 1982; Saibil, *J Mol Biol*, 158:435, 1982). Saibil (1982) and DeCoutet et al. (*J Cell Biol*, 98:834, 1984) have suggested from biochemical evidence that this core is made of actin, but there is no direct evidence.

In the present study, firstly we labeled L.R. White-embedded ultrathin sections of *Drosophila* retina with monospecific antiactin, followed by a biotinylated secondary antibody and streptavidin-gold. The rhabdomeres and subrhabdomeral cytoplasm were labelled. Secondly, we found that in semi-thin (500nm) frozen retinal sections the rhabdomeres labelled with rhodamine-phalloidin. Finally, we incubated eyes with buffer containing myosin subfragment 1 (S1), and processed them for electron microscopy. S1-decorated filaments were observed with their barbed ends in a dense cap-like structure at the distal end of each microvillus. The filaments extended down the length of the microvilli into the subrhabdomeral cytoplasm. Some microvilli were observed with two or three decorated filaments.

These results indicate that two or more actin filaments form the basis of the cytoskeletal core in each microvillus of *Drosophila* photoreceptors. Similar results have obtained in the photoreceptors of crayfish *Procambarus clarkii*.

Supported by NIH Fogarty International Research Fellowship TW03929 to KA and NIH grant EY07042 to DW.

PH 56

FINE STRUCTURE OF THE RETINA IN A RIVER SNAIL, *SINOTAIA QUADRATUS*.

K. Kawai and H. Sawaki, Dept. of Biology, Naruto Univ. of Education, Naruto, Tokushima

The cellular organization of *Sinotaia* retina was studied by the light and electron (TEM & SEM) microscopes. A large tubular pit-like structure was found at the fundus of the retina, and that its basal end was connected to the main optic nerve with nerve fibers. The existence of such pit-like structure in the retina is particularly interesting, however, its function is still unknown. The distal ends of *Sinotaia* photoreceptor cells are concave and bear numerous long microvilli distally. At these points, *Sinotaia* photoreceptor cells are different from those of *Helix* and *Aplysia*. The soma of *Sinotaia* photoreceptor cells are filled with so-called photic vesicles (about 80 nm diam.), furthermore, cytosome-like electron dense vesicles (about 700 nm diam.) are frequently observed among photic vesicles. In addition to numerous photoreceptor cells and pigmented supportive cells, the ciliary cells, bearing the bundle of about twenty cilia on the distal ends, were frequently observed. The physiological function of the ciliary cell is also of interest.

PH 57

A STUDY ON AXONS OF DERMAL PHOTORECEPTOR CELLS IN *ONCHIDIUM VERRUCULATUM*.N. Katagiri¹, Y. Katagiri², Y. Shimatani², Y. Hashimoto² and E. Aikawa¹¹Dept. of Anat., ²Dept. of Physiol., Tokyo Women's Med. Coll., Tokyo 162

Axons of the dermal photoreceptor (DP) cells were examined through 700 semi-thin serial sections (0.4µm in thickness) of an osmicated specimen at 200 kV with H-700H or at 1000 kV with H-1250M electron microscope. A single axon extending directly from the cell body was recognized in 15 DP cells among a group containing 19 DP cells. It arose laterally from the confined area near the boundary between the distal and proximal parts of the DP cell, traveled a meandering course in the intercellular connective tissue, and finally joined a small papillar nerve bundle which included several axons derived from other DP cells in the group. The axon was variable in size and structure at various parts of its course. The variety will be caused by the retraction and recovery of the papillae according to the movement of the animal. The axon was enclosed with a sheath structure. Along the axon, two types of cells were found; supporting (S) and sheath (Sh) cells. S cells were located adjacent to the surface of the DP cell and their perikaryon was always found near the initial part of the axon. Sh cells were distributed in the connective tissue and enveloped the small papillar nerve. Both S and Sh cells may take part in the formation of the sheath structure.

PH 58

PHOTOPERIODIC-GONADAL RESPONSE IN VITAMIN A DEFICIENT QUAIL WITH RETINOIC ACID REPLACEMENT THERAPY.

T. Oishi¹, A. Kawata¹, K. Oodera², A. Hattori², and I. Shimizu³. ¹Dept. of Biol., Fac. Sci., Nara Women's Univ., Nara, ²Dept. of Anat., St. Marianna Univ. Sch. of Med., Kawasaki, ³Res. Sect. of Environ. Biol., Lab. for Plant Ecol. Studies, Fac. of Sci., Kyoto Univ., Kyoto.

We investigated photoperiodic-gonadal response of retinoic acid replaced vitamin A (VA) deficient quail to clarify the involvement of retinal in this response. Control (VA acetate treated) and VA deficient (retinoic acid treated) quail were placed in LD16:8 or LD8:16 under various light intensity. The response of the cloacal gland, a secondary sex character, was less distinct in VA deficient quail than in controls. The threshold of light intensity for the entrainment of the locomotor activity was almost similar between VA deficient and control quail. The amount of melatonin in the retina was high in dark and low in light in controls, but the difference was not significant in VA deficient quail. HPLC analysis revealed that retinal existed in the retina in VA deficient quail, although they were behaviorally blind. Decreased photoperiodic response suggests that retinal seems to be involved for the photoperiodic photoreception.

PH 59

THE LATENT TIME OF THE STEP-UP PHOTOPHOBIC RESPONSE IN *STENTOR COERULEUS* DEPENDS UPON THE RATIO OF EXTRACELLULAR Ca TO K IONS.

K. Iwatsuki and Y. Kobayashi. Nippon Petrochemicals CO LTD., Tsukuba Life Science Laboratory, Tsukuba

To a sudden increase in light intensity *Stentor coeruleus* responds with a delayed stop and temporary reversal of movement (step-up photophobic response). The latent time of the photoreponse was short when the intensity of the stimulation light was high, whereas the latent time was long when the Ja-value (the ratio of the K concentration to the square root of the Ca concentration in the medium) was low. Both the low and high Ja-value suppressed the photophobic response (The optimum Ja-value = 0.05). It is concluded that the duration of the latent time is determined by the Ja-value and the intensity of the stimulation light respectively. Since the transmembrane potential increases (membrane is hyperpolarized) in lower Ja-value, the threshold for the response rises up in level and the latent time becomes longer. Since the higher Ja-value makes the transmembrane potential decreases (membrane is depolarized), the threshold level goes down. However, in the consequence of the membrane depolarization Ca-channel is inactivated, and the photoreponse is suppressed. Since the photoreponse is affected by the threshold level and the Ca-channel inactivation, the optimum Ja-value exists.

PH 60

AUTONOMIC CHANGE OF RHABDOM VOLUMES IN ISOLATED COMPOUND EYE OF THE GRAPSID CRAB, A STUDY IN CORRELATION WITH A CIRCADIAN CLOCK.

Y. Shimazaki, E. Eguchi, and T. Suzuki¹. Department of Biology, Yokohama City University and ²Department of Pharmacology, Hyogo College of Medicine.

In the compound eye of the grapsid crab *Hemigrapsus sanguineus*, periodic turnover of the photoreceptive membrane causes an 8-fold increase in the rhabdom volume during the night. The rhabdom volume shows circadian changes under continuous darkness, indicating that an intrinsic circadian clock is involved in the process of the membrane turnover (Arikawa et al. *Experientia* 44:219, 1988).

To locate the clocks that control the membrane turnover processes, we investigated the change in the rhabdom volume in *in vitro* preparations. We incubated isolated compound eyes (distal to the basement membrane) and eye-stalks (compound eye plus optic ganglia) for 6 to 8 h in physiological saline at 20°C under various light/dark regimes. Then we compared the rhabdom volume (a percentage of cross sectional area of an ommatidium occupied by a rhabdom, ROR) at different time.

In compound eyes isolated 2.5h before light off (ROR=3.3%) and kept under a LD 12:12 light regime, ROR increased up to 7.9% by 3.5h after light off. ROR of the eyes isolated 2.5h before light onset (12.5%) and kept under LD 12:12 became smaller (3.0%) by 3.5h after the light onset. When the eyes were kept under continuous darkness, the ROR showed the similar results as *in vivo* especially at rhabdom shedding. There are no significant differences between the results of isolated compound eyes and isolated eye-stalks.

The results indicate that 1) autonomic membrane turnover (synthesis and shedding) occurs in the isolated compound eyes, and 2) membrane shedding is controlled by an intrinsic clock within the compound eye.

PH 61

INTERNAL SYNCHRONIZATION OF BILATERAL CIRCADIAN OSCILLATORS IN THE VISUAL SYSTEM OF A CARABID BEETLE.

S. Yamazaki¹, M. Sasak¹ and M. Mizuno².
¹Lab. Entomol., Fac. Agric., and ²Lab. Biol. Cybern., Fac. Eng., Tamagawa Univ., Tokyo.

The interactions between bilateral oscillators of *Apotomopterus insulicola* were investigated by recording ERGs. ERG responses evoked every 10 min by 50 ms flashes (0.05 μ W) of green LEDs placed adjacent to both sides of compound eyes were A/D-converted and stored in a personal computer. ERG amplitudes were analyzed day by day with the least-squares cosine fitting method.

1. ERG amplitudes of both right and left eyes exhibited clear circadian rhythms with the synchronized phase in DD condition.
2. Both sides of ERG rhythms could be entrained by the illumination of one side eye only. Lower threshold light intensity allowing the entrainment was 0.02 μ W.s.
3. The two ERG rhythms from the contralateral eyes could be independently entrained by applying local illumination of different phase-angle. The splitted rhythms with reversed phase-angle were fused in DD after transient of about 7 days.
4. The ERG rhythms of a brain-bisected beetle began to free-run with their own circadian periods after 5 days of arrhythmic period.

PH 62

ENVIRONMENT AND INSECT VISION.

I Gleadall¹, T Hariyama² and Y Tsukahara².
¹NIBB, Okazaki; ²Res. Center for Applied Inform. Sci., Tohoku University, Sendai.
 Insects generally can be divided into two types on the basis of the visual pigment chromophore: 'primitive' types have retinal (A₁), while 'more advanced' insects possess 3-hydroxy-retinal (A₂). However, recent reports indicate that dragonflies (Odonata) and certain beetles (Coleoptera) use both, raising important questions as to the advantages of using A₁ or A₂. We can confirm that 'kamikirimushi' (Coleoptera, Cerambycidae) of the subfamily Lamiinae (e.g. *Anoplophora malasiaca*) contain both, and also that both are present in the Families Gyrinidae (*Gyrinus*), Hydrophilidae (*Hydrophilus*) and Lampyridae (*Hotaruna parvula*, *Luciola cruciata* and *L. lateralis*). These four families of beetles are widely separated phylogenetically, but there are two factors common to three of them: all except the Lamiinae are carnivorous and associated with an aquatic environment. Comparisons are made with other animals containing two chromophores. We note also the possible relevance of three features more common to the Lamiinae than to other members of the Cerambycidae: (i) the elaborate 'girdling' behaviour of the female prior to egg-laying; (ii) the lack of symbiotic fungi to aid in the digestion of lignin; and (iii) a preference for feeding on herbaceous, rather than on woody stems.

PH 63

ISOLATED CENTRAL-PAIR MICROTUBULES FROM *Chlamydomonas*

Reynard¹, Y. Yamada and T. Miki-Yomura. Dept. of Biol., Fac. of Sci., Uchanomizu Univ., Tokyo.

Central-pair microtubules extrude from the tip of elastase-digested axonemes of demembrated *Chlamydomonas* flagella after the addition of ATP (Hosokawa and Y. Yomura, 1987, J.C.B.). Little is known about shape, structure and protein composition of central-pairs.

We isolated central-pairs from axonemes by improved method.

SDS-PAGE showed that central-pair was composed of ~25 protein polypeptides and that major band was tubulin which accounted for ~30% of total proteins of axonemes. Neither bands similar to that of dynein nor ATPase activity were not detected.

Central-pairs in solution had helical structure and their left-handed helix was determined by dark-field microscopy. The pitch was ~2.5 μ m and the diameter was ~3.0 μ m.

Observation under electron microscope revealed that central-sheath projections attached the outside of two singlet microtubules, which were connected each other by a ladder structure. The effects of divalent cations on substructure of central-pair microtubules was examined. In the solution containing 10mM EDTA or 5mM Mg-10mM EGTA (pH 7.5), the central-sheath projections were detached from microtubules partially, whereas the connecting structure of two singlet microtubules remained. In the solution of 10mM EGTA-EDTA, the central-sheath projections were detached completely, although the connecting structure still existed. Most remarkable change was observed in the solution of 1mM Ca, in which connecting structure of singlet microtubules was solubilized, and then singlet microtubules depolymerized.

Gel electrophoresis of central-pair microtubules in the presence or absence of Ca ions revealed change of mobility of two protein polypeptides (67kD, 53kD).

PH 64

FLAZELLA EXTRACTION OF INNER DYNEIN ARMS FROM AN OUTER ARMLESS MUTANT OF *CHLAMYDOMONAS*.

Kenjiro Yoshimura and Keiichi Takahashi. Zool. Inst., Fac. of Sci., Univ. of Tokyo, Tokyo.

Inner dynein arms were extracted from an outer arm deficient mutant of *Chlamydomonas* (*oda 1*) to study the function of these arms. When demembrated axonemes of *oda 1* were treated with a solution containing 0.3 M KCl and 10 μ M ATP for 10 min on ice and then reactivated with 1 mM ATP, they beat with a frequency (14.9 \pm 3.7 Hz, 26 °C) which was much lower than the beat frequency of the untreated axonemes (26.9 \pm 2.6 Hz). When the axonemes were extracted with a solution containing 0.4 M KCl and 10 μ M ATP for 30 sec or longer, they lost their ability to beat. The decrease in beat frequency was dependent on the presence of ATP in the extraction solution; treatment with 0.3 or 0.4 M KCl in the absence of ATP did not affect the beat frequency. The axonemes extracted with 0.3 M KCl in the presence of 10 μ M ATP had the following characteristics: (1) The bend angle and curvature of waveform of the reactivated flagella were the same as before the extraction. (2) In the cross section, 28.5% of the inner arms were lost or appeared feeble. (3) One of the high molecular weight polypeptides of the inner arm was reduced when the extracted axonemes were examined by SDS-urea-PAGE. These results suggest that a part of the inner dynein arm has a function of increasing the flagellar beat frequency but is not essential for flagellar motility.

PH 65

THE OUTER ARM DYNEIN α -HEAVY CHAINS OF SEA URCHIN SPERM FLAGELLA AND EMBRYONIC CILIA ARE DIFFERENT.

K.Ogawa¹, E.Yokota², Y.Hamada³, S.Wada², M.Okuno², and Y.Nakajima¹. Dept. of Cell Biol. and ²Tissue and Cell Culture Lab., NIBB, Okazaki, ³Dept. of Biol., Univ. of Tokyo, Komaba, and ⁴Dept. of Biol., Keio Univ., Yokohama.

Sea urchin sperm outer dynein is a multi-subunits protein composed of α - and β -heavy chains, and three intermediate chains. We prepared monoclonal and affinity-purified polyclonal antibodies to each subunit, and examined whether the embryonic ciliary axonemes of same species contain the polypeptides shared epitopes with them. Ciliary axonemes contained a high molecular weight polypeptides with the exactly same mobility as flagellar β -heavy chain. This polypeptide shared also epitopes with it. In contrast, there was no polypeptide which had the exactly same molecular weight as flagellar α -heavy chain and shared epitopes with it. The western blots showed that ciliary axonemes also contain three polypeptides shared epitopes with the respective flagellar intermediate chain. The present results revealed that the α -heavy chain of flagellar and ciliary outer arm dyneins are different.

PH 66

RESPONSIVENESS OF CILIA DEPENDS ON THEIR GENERATING PART OF CELL SURFACE IN TRITON-GLYCEROL-EXTRACTED *PARAMECIUM*.

M. Noguchi, Y. Nakamura and K. Okamoto. Dept. of Biol., Fac. of Sci., Toyama Univ., Toyama.

We examined the direction that the cilia pointed when observed from above for understanding the control mechanism of the beating direction of cilia by Ca^{2+} and cyclic nucleotides. The ciliated sheets of cell model which stuck to the glass surface were perfused successively with reactivation solutions.

When the ciliated sheets were perfused with the solutions containing cGMP, the cilia tended to change their orientation to 3 o'clock irrespective of the Ca^{2+} concentration. Moreover we found that the cilia on the left-hand field of the cell were more sensitive to cGMP than those on the right-hand field in the presence of micromolar Ca^{2+} . The cilia on the left-hand field of the cell were also more sensitive to cAMP than those on the right-hand field. On the contrary, the cilia on the right-hand field of the cell were more sensitive to Ca^{2+} than those on the left-hand field. These indicate the possibility that uniform change of second messenger concentrations in the all part of the cell is enough to induce such a complicated locomotor behavior as gyration.

PH 67

EFFECTS OF CULTURE TEMPERATURE ON THE K^{+} -INDUCED CILIARY REVERSAL IN *PARAMECIUM*

Y. Shingu and Y. Naitoh. Inst. Biol. Sci., Univ. Tsukuba, Ibaraki 305.

Specimens of *Paramecium caudatum*, cultured at 10, 20 and 30°C respectively, were equilibrated in a standard saline solution (4mM KCl+1mM $CaCl_2$) at 10, 20 and 30°C respectively. Forward swimming velocity was higher when equilibration temperature was higher. Interestingly, the swimming velocity was essentially identical among the specimens cultured at different temperatures when they were equilibrated at their respective culture temperature. Maximum backward swimming velocity of the specimens upon their transfer into a stimulation solution (20mM KCl+1mM $CaCl_2$) at a temperature identical with each equilibration temperature was higher, while duration of the backward swimming was shorter at higher equilibration temperature. Interestingly, the time-integral of the backward swimming velocity, which corresponds to the distance of the backward swimming, was almost identical among the specimens cultured at different temperatures when they were stimulated at their culture temperature. Mechanisms for the adaptations of the motile activity to the culture temperature are discussed in terms of ciliary motile activity and the voltage-sensitive Ca^{2+} channels.

PH 68

THREE DIMENSIONAL SWIMMING BEHAVIOUR OF *PARAMECIUM* UNDER VARIOUS GRAVITATIONAL ENVIRONMENTS

A. Izumi-Kurotani, M. Yamashita¹, Y. Mogami, and S.A. Baba²

1. Institute of Space and Astronautical Science, Sagami-hara
2. Dept. of Biol., Fac. of Sci., Ochanomizu Univ. Tokyo

Negative gravitaxis of ciliates is a biological response to gravitational force at cellular level. Swimming behavior of *Paramecium* is a good marker to elucidate the mechanism of gravity perception and physiological responses of cells. *Paramecium* cell swims spirally and three dimensionally in its media. In order to describe its natural free swimming behavior, Three Dimensional Video Image systems are developed. Cells in a cubic chamber are illuminated by a lamp or light emitting diodes. Front and side view of swimming image are synthesized by a half mirror and projected on single video camera in one way. With a color video camera, two images are colored differently. There is an effect of thermal convection at a strong light injection to the chamber. In such case, a monochromatic video camera with higher sensitivity is adopted as a sensing device. In the second system, front and side views are monitored by two high sensitive video cameras. Two video signals are multiplexed and recorded on a single tape. Those systems developed so far made possible to analyze three dimensional trajectories of cells. Studied are distribution of swimming vector, frequency of change of swimming direction and so forth, under different gravity environments. Experimental apparatus is installed on a free falling capsule for micro gravity experiment. It is possible to observe behaviors under micro gravity and during transient phase from 1 G. For gravity environments higher than 1 G, centrifugal force is applied to the system. From experimental results obtained, regulation of swimming velocity was shown by *Paramecium* in correspond to its swimming angle relative to gravity vector and magnitude of gravity.

PH 69

CAFFEINE-INDUCED CONTRACTION IN VORTICELLA.

K. Kato and Y. Naitoh, Inst. Biol. Sci. Univ. Tsukuba, Ibaraki 305.

Vorticella exhibits an all-or-none type contraction in response to a stimulus. Its contractile mechanism is activated by Ca^{2+} . However, the contraction is seen even in an EGTA-containing solution. This suggests involvement of Ca^{2+} -release from its intracellular storage in the contraction. We, therefore, examined effects of caffeine or ryanodine, which releases Ca^{2+} from sarcoplasmic reticulum (SR) in the skeletal muscle, on the contraction. *Vorticella* contracted repeatedly in a solution containing caffeine. The repetition frequency and the duration of each contraction were greater when the caffeine concentration was higher. The frequency was not affected by changing the external Ca^{2+} or K^+ concentration. The caffeine contraction was seen in a solution containing EGTA. Tetracaine or procaine inhibited the effect of caffeine. Ryanodine binds to Ca^{2+} channels in the SR and kept them open. $1.5 \mu\text{M}$ ryanodine produced a marked increase in the contraction frequency. The present results indicate that the hypothetical Ca^{2+} storage in *Vorticella* is similar in its characteristics to the SR. Endoplasmic reticulum of *Vorticella* seems to correspond to its Ca^{2+} storage.

PH 70

REGULATION OF THE SWIMMING VELOCITY IN SEA-URCHIN LARVAE IN THE GRAVITY FIELD.

S. A. Baba¹, S. Hiruma¹, M. Ooya¹, Y. Mogami¹ and A. Kurotani-Izumiz². ¹Dept. of Biology, Ochanomizu Univ., Tokyo and ²Inst. of Space and Astronaut. Sci., Sagamihara.

We analyzed the swimming velocity V of sea-urchin larvae as a function of the swimming direction θ relative to gravity. Hydrodynamic considerations suggest that the swimming velocity should be matched with, if larvae could not regulate their propulsion, by the equation,

$$V = \sqrt{(P^2 - S^2 \sin^2 \theta) + S \cos \theta},$$

where P is the propulsion and S the sinking speed. It has been demonstrated that gastrulae behave as predicted, whereas the observed velocity of plutei seems to keep a preferred value, significantly different from those predicted (Mogami et al., 1989, J. Exp. Biol. 137: 141-156). We analyzed $V(\theta)$ of larvae in ASW containing percoll at various concentrations. The swimming velocity V_0 of larvae in 13% percoll ASW, in which S was nearly 0, was compared with V_0 in the normal ASW as a control. The observed V_0/V_c from gastrulae varied with θ as predicted by the physical model of the equation above, but V_0/V_c of plutei remained rather constant and suggested regulation of propulsion, which may enable them to get a preferred value of swimming speed in all directions in the gravity field. Analyses of the difference of the downward and upward velocities also suggested regulation of propulsion in pluteus.

PH 71

FLAGELLAR WAVEFORM DURING ROTATION OF THE BEAT PLANE INDUCED BY VIBRATING THE SEA-URCHIN SPERM HEAD.

Chikako Shingyoji, Jun Katada, Kenjiro Yoshimura, and Keiichi Takahashi. Zool. Inst., Fac. of Sci., Univ. of Tokyo, Tokyo.

When the head of a sea urchin sperm is held by a suction pipette and vibrated laterally, the flagellum becomes to beat in phase with, and in the same plane as that of, the imposed vibration; rotating the plane of vibration around the head axis induces rotation ("winding") of the beat plane (Gibbons et al., *Nature*, 325:351-352, 1987). To investigate the mechanism of rotation, we analysed the flagellar waveform of live *Hemicentrotus pulcherrimus* sperm during winding. Throughout the rotation of the beat plane, the planar waveform was not twisted. The asymmetry of bending waves observed in the normally beating sperm was also retained through several cycles of winding. Polystyrene beads attached to a reactivated flagellar axoneme did not rotate with respect to the head axis during winding even though the asymmetric waveform rotated. Preliminary analysis of the flagellar bend angles during winding showed that the asymmetry tended to become smaller when the waveform was in 180° rotated positions than in 0° positions. These results support the view that the flagellum can change the beat plane by changing the pattern of active sliding within the axoneme, and that the wave asymmetry depends on this pattern. What controls the sliding pattern, however, is still to be investigated.

PH 72

EFFECTS OF ATP CONCENTRATION AND Ca^{2+} ON THE PATTERN OF MICROTUBULE SLIDING IN ELASTASE-TREATED AXONEMES OF SEA-URCHIN SPERM FLAGELLA.

Takeshi Kobayashi, Chikako Shingyoji, and Keiichi Takahashi. Zool. Inst., Fac. of Sci., Univ. of Tokyo, Tokyo.

To produce planar flagellar movement, sliding between axonemal microtubules must be controlled in a coordinated manner. The mechanism for such control is lost by treating the axoneme with trypsin, resulting in an overall sliding disintegration upon subsequent reactivation with ATP. Digestion with elastase, however, can produce axonemes which seem to retain part of the control mechanism. When demembrated sea-urchin (*Clypeaster japonicus* and *Hemicentrotus pulcherrimus*) sperm flagella were digested by elastase in the presence of relatively high concentrations ($< 50 \mu\text{M}$) of ATP, the axonemes did not disintegrate into individual microtubules. Instead, sliding episodes were observed only once or twice indicating that active sliding could occur only along an interdoublet site or two. Electron microscopy showed that the sliding took place between a thicker bundle of microtubules consisting of the central pair as well as five or six doublets and a thinner bundle consisting of the rest of the doublets. Judged from the positions of the 5-6 bridge and the orientation of the central pair, the thicker bundles always included doublets 3 and 8. In the presence of Ca^{2+} ($\text{pCa } 3$), the thinner bundle usually contained the 5-6 bridge and slid towards the flagellar base, which is consistent with the result of Sale (*J. Cell Biol.*, 102, 2042-52, 1986) and indicates that in the presence of Ca^{2+} active sliding occurs predominantly between doublets 6 and 7 (or 7 and 8) to form a principal bend. In the Ca-free medium, where both principal and reverse bends would be formed, however, some thinner bundles did not contain the 5-6 bridge, indicating that sliding of a group consisting of doublets 9, 1, and 2 relative to the group consisting of doublets 3 through 8 took place reflecting the event that occurs during the formation of a reverse bend.

PH 73

HIGH-FREQUENCY-VIBRATION OF MICROTUBULES IN FRAGMENTED AXONEMES OF SEA-URCHIN SPERM. S. Kamimura¹ and R. Kamiya². ¹Dept. of Biol., Coll. of Arts and Sci., Univ. of Tokyo, Tokyo and ²Dept. of Mol. Biol., Fac. of Sci., Univ. of Nagoya, Nagoya.

ATP hydrolyzing activity of fragmented axonemes of sea-urchin (*Hemicentrotus pulcherrimus*) sperm flagella has been thought as a motility-independent consumption of ATP because flagellar beat disappears completely by fragmentation. We report the detection of sub-nanometric movement of the microtubules in these 'quiescent' axonemes (Nature, 340:476, 1989). Microbeads (diameter 0.9 μ m) were attached to axonemes and their motion was measured in an angstrom precision and with a time-resolution better than 1 msec using a photoensing system (Appl. Opt., 26:3425, 1987). Microbeads were revealed to vibrate at a high frequency (300Hz at 1 mM of ATP) with an amplitude of about 1-3 nm. The motion was blocked completely by 0.5 μ M of orthovanadate and the frequency depended on MgATP concentration. The apparent Km and Vm were 94 μ M and 340 Hz, respectively. The high-frequency vibration of the axoneme-doubled microbeads would represent motion of doublet microtubules by active dynein arms, i.e. sliding in a molecular scale is occurring being coupled with ATP hydrolysis. New insight into the molecular mechanism of microtubule-sliding by dynein arms is expected by analyzing the new phenomenon.

PH 74

INITIATION OF SALMONID FISH SPERM MOTILITY WITH CALCIUM. M. Okuno. Dept. of Biol., Coll. of Arts & Sci., Univ. of Tokyo, Tokyo, Japan.

The initiation of salmonid fish sperm motility was studied by means of the iontophoresis of Ca^{2+} . Semen of chum salmon was suspended in the solution containing 15 mM KCl in which all of spermatozoa were immotile. When Ca^{2+} was applied to the basal region of the flagellum the initiation of motility was induced approximately 0.1 sec after the onset of the iontophoretic current. When the distance between the tip of the micropipette and the base of flagella was longer the time lag increased even when the tip of the micropipette was very close to the flagellar axis. Therefore, it was likely that calcium influx occurred at the basal region of the flagellum. The initiation of beat also appeared in the basal region of the flagellum when the application of Ca^{2+} was carried out at any place of flagella.

When spermatozoa once obtained motility by the application of Ca^{2+} they continued to beat for more than 20 sec. It was identical to the life time of salmonid fish spermatozoa. When the amount of Ca^{2+} applied was small flagellar motility continued only for a short period, however, the motility was induced again by another application of Ca^{2+} . The total motile time was usually equivalent to the life time generally observed.

PH 75

MICROFLUSHING ANALYSIS OF SPERM MOTILITY. K. Ishida¹ and M. Okuno. ¹Dept. of Urol., Teikyo Univ. Sch. of Med., Tokyo and ²Dept. of Biol., Coll. of Arts and Sci., Univ. of Tokyo, Tokyo.

A new microflushing analysis method for sperm motility is proposed. This method proves continuous observation of reaction process from the beginning till and when the spermatozoa faced to test reagent without adherence to the surface of slide glass during observation. Using this method, always over 90% of sperm motility percentage must reflect native sperm motility, the microflushing method is seemed to be the best method to assay sperm motility. As this method requires only a few amount of specimen, it is also suitable for analysis of spermatozoa of small animals from which we can get it only a trace level.

It was also revealed that the beat frequency of hamster sperm flagellar jumped up to 8 Hz from less than 1 Hz depending on the extracellular Ca^{2+} concentration (more than 7.5×10^{-5} M). Application of 8-bromo-cyclic AMP at 1×10^{-5} M caused similar jump up of the beat frequency of the flagellar. Adenylate cyclase activity of the spermatozoa was increased in the manner similar to that of flagellar depending on the Ca^{2+} concentration. These observations suggest that the increase in the beat frequency of the flagellar is caused basically by the increase in the intracellular concentration of cyclic AMP, and the increase in cyclic AMP is introduced by the increase in the extracellular Ca^{2+} upon ejaculation.

PH 76

ROLES OF OSMOLALITY AND Ca^{2+} IN INITIATION OF SPERM MOTILITY IN MARINE TELEOST S. Oda and M. Morisawa, Misaki Marine Biological Station, Univ. of Tokyo, Miura.

The sperm motility of the marine teleost, puffer (*Fugu niphobles*) was measured using an auto semen analysing system (Cell Soft). Motility was completely inhibited in either an electrolyte or a nonelectrolyte solution isotonic to the seminal plasma (300 mOsm/kg). Motility occurred only when semen was diluted in hypertonic solution (400-1400 mOsm/kg). A maximum swimming velocity (120 μ m/sec) or a maximum beat frequency (90 Hz) was obtained in the 550 mM NaCl solution, the osmolality of which is identical to artificial sea water, suggesting that initiation of sperm motility in marine teleosts is triggered by exposure to hypertonic sea water. Puffer sperm swim in hypertonic solution (550 mM NaCl) containing 10 mM EGTA. They remained quiescent in isotonic solution (120 mM NaCl) even if Ca^{2+} was subsequently added. Thus, Ca^{2+} is not an external factor inducing sperm motility. Sperm motility was induced in isotonic solution when calcium ionophore, A23187 and Ca^{2+} were present. The ionophore-dependent initiation of motility was concentration-dependent. These suggest that Ca^{2+} is an internal factor inducing sperm motility. The change of osmolality at spawning in sea water may cause the release of Ca^{2+} from Ca^{2+} storage in the sperm cell. Ca^{2+} may advance the cascade process of the initiation of sperm motility in marine teleosts.

PH 77

MOTILITY-RELATED STRUCTURAL CHANGES IN THE FLAGELLAR MEMBRANE OF APYRENE SPERMATOZOEA OF BOMBYX MORI CAUSED BY ENDOPEPTIDASES.
H. KASUGA, M. OSAI AND T. AIGAKI
Dept. Biol., Tokyo Metrop. Inst. Geront., Itabashiku, Tokyo.

Motility of apyrene spermatozoa of the silkworm, induced by initiatorin, a multifunctional endopeptidase localized in the glandula prostatica, is accompanied with morphological changes in the flagellar membrane, thinner membrane as well as formation of many slit-like ultrastructures. These structural changes correspond well with motility acquisition of apyrenes *in vivo*. Apyrenes in the male vesicula seminalis were activated by endopeptidases showing a hydrolyzing activity on BAE, trypsin and papain, but not by others, pepsin and collagenase. Apyrenes activated by such BAEases always showed the similar ultrastructural changes in the flagellar membrane to those caused by initiatorin. They are due to partial digestion of acidic proteoglycan localized in the extracellular matrix of the flagellar membrane. Ultrastructural undersurface of the intact flagellar membrane was uniform, but, at that of the trypsin-treated one, many microstrips perpendicular to the flagellum were observed. The existence of these microstrips were also confirmed by observing the surface of the intact flagellar membrane with SEM. They were not distinct probably because of a cover of polysaccharide to the surface.

PH 78

A QUANTITATIVE ANALYSIS OF FLAGELLAR MOVEMENT OF HYPERACTIVATED GOLDEN HAMSTER SPERMATOZOEA.

S. Ishijima and Y. Hamaguchi. Biological laboratory, Tokyo Institute of Technology, O-okayama, Meguro-ku, Tokyo.

Hyperactivation is a dramatic change in beating pattern occurring in the capacitation. This phenomenon is suitable for studying the control mechanisms of flagellar movement. Hyperactivation of hamster sperm can be induced in a medium containing BSA *in vitro*. To examine the feature of hyperactivation, flagellar bends of a hyperactivated spermatozoon were expressed in curvature and compared with those of a intact spermatozoon. The flagellar movement of sperm models in response to Ca^{2+} and cAMP was also expressed in curvature and compared with that of a hyperactivated spermatozoon.

Maximum curvature of the hyperactivated sperm flagella was double at midpiece, while at the other parts, there was not so large difference. Curvature of flagellar bends of reactivated sperm models in 10^{-8} M Ca^{2+} or 150 μ M cAMP was similar to that of the hyperactivated spermatozoa. These experiments show that cAMP in the absence of Ca^{2+} can form the waveform observed in hyperactivated spermatozoa. Recent reports said Ca^{2+} contents did not change so much in hyperactivation, and therefore, cAMP seems to be a most important factor inducing the hyperactivation.

PH 79

MOVEMENT OF F-ACTIN ALONG SINGLE THICK FILAMENTS ISOLATED FROM A MOLLUSCAN SMOOTH MUSCLE.

Akira Yamada, Naokata Ishii, and Keiichi Takahashi.
Zool. Inst., Fac. of Sci., Univ. of Tokyo, Tokyo.

It is known that the direction of movement in the actin-myosin motile system depends on the polarity of the actin filament, but whether it is also influenced by the polarity of the myosin filament is unknown. To answer this question, we studied the movement of actin filaments along thick filaments in a reconstitution motility assay system. Native thick filaments isolated from the anterior byssus retractor muscle of *Mytilus edulis* were placed on a Formvar-coated grid and active movement of fluorescence-labeled F-actin along them was observed. The grid was then fixed and examined electron microscopically to ensure that the movements occurred along single, and not bundles of, filaments. On a single thick filament, we could identify, by watching the movement, the central bare zone: F-actin moved along the thick filament toward this zone and took off on reaching it. F-actin also moved, though very slowly, away from the bare zone along the same filament. The velocity of movement toward the bare zone was about $1 \mu\text{m s}^{-1}$ and that away from the bare zone was about $0.1 \mu\text{m s}^{-1}$. From these results we conclude that the direction of movement of F-actin is not determined by the polarity of the thick filament although the thick filaments show functional bipolarity in terms of the sliding velocity.

PH 80

INITIATION OF FORCE DEVELOPMENT BY CAGED-ATP PHOTOLYSIS IN A MOLLUSCAN SMOOTH MUSCLE.

O. Abe¹, T. Yamada², K. Takahashi¹ and H. Sugi²
¹Zool. Inst., Fac. of Sci., Univ. of Tokyo, Tokyo and ²Dept. of Physiol., Sch. of Med., Teikyo Univ., Tokyo.

Force generating process in *Mytilus* anterior byssal retractor muscle (ABRM) was studied by means of laser photolysis of caged-ATP, an inert photolabile precursor of ATP. Caged-ATP was initially diffused into a saponin-treated rigor muscle bundle (0.2-0.3 mm diameter) in the presence of Ca^{2+} . On sudden production of ATP by photolysis with a single laser pulse, force was produced rapidly after a short delay. Stiffness of the muscle first dropped and then rose, indicating rapid detachment of rigor cross-bridges followed by reattachment with force generation. The rate of force development increased with liberated ATP concentration. The time course of force development could be resolved into three exponential components. The rate constants of the slower components were in the range of $1-2$ and $0.1-0.5 \text{ sec}^{-1}$, and both tended to increase with increasing ATP concentration. The rate constant of the fastest component was about 8 sec^{-1} and independent of the liberated ATP concentration. The fastest component may correspond to the first step of the cyclic reaction leading to force generation, that is reattachment of cross-bridges to thin filaments.

PH 81

STIFFNESS CHANGE OF STARFISH BODY WALL.

T. Motokawa.
Dept. of Biol., Col. of Sci.,
Univ. of the Ryukyus, Okinawa.

The body wall of starfish shows remarkable changes in the stiffness: it becomes stiff when the animal opens prey clams; it is soft when the animal rights itself. Bending tests were performed on the arm of starfish to know how stiff the body wall becomes and to investigate the mechanism of the change. The stiffness of the arm of *Linckia laevigata* without stimulation was 23.4MPa. When the arm was isolated from the body, the stiffness increased by up to 8 times (average stiffness: 60.2MPa; maximum value: 188.9MPa). The studies on *Asterias forbesii* showed that the stiffness increased when the arm was autotomized or was anesthetized with 0.1% MS-222 or with menthol-saturated sea water. The viscosity increase was also observed with the same treatment but the extent of increase was far greater than that of the stiffness increase. Similar changes in the mechanical properties were observed even in the dead arms which were frozen and then thawed in sea water: the stiffness increased by 40 times when they were transferred into distilled water. The large effect of the ionic environment, together with the result that the viscosity change is far greater than the stiffness change, suggests that the catch connective tissue is involved in the stiffness change of the body wall of starfish.

PH 82

MEASUREMENT OF PROPAGATION VELOCITY OF ULTRASONIC WAVE IN SKELETAL MUSCLE USING SCANNING LASER ACOUSTIC MICROSCOPE.

T. Tsuchiya¹, H. Iwamoto¹, Y. Tamura² and H. Sugil¹.
¹Dept. Physiol., Sch. Med., Teikyo Univ., Tokyo
²Dept. Physics, Suzuka Col. Tech., Mie.

It is generally accepted that the contraction of skeletal muscle results from cyclic formation of cross-links between the cross-bridges on the thick filaments and the sites on the thin filaments and the longitudinal stiffness of muscle increases during contraction. On the other hand, we showed that the transverse stiffness of skeletal muscle decreased during contraction using new technique of ultrasonic wave. Present experiment was performed to confirm the above result using scanning laser acoustic microscope (SLAM). Muscle, ileofibularis m. of *Rana japonica*, was set between quartz stage and cover slip, underside of which was coated with gold, and stimulated electrically at room temp.. The SLAM was operated at 100 MHz and interferograms, which were characterized by vertical fringe related to ultrasonic wave velocity, were produced on a CRT in real time (30 frames per sec) and recorded in video-tape. The images were processed by image analyzer and the propagation velocities were calculated from the shift of the interference line of the image during rest and contraction. In all the measurements, the velocities during contraction were clearly slower than in rest, suggesting that the transverse stiffness decreased during contraction.

PH 83

EFFECT OF OCTOPAMINE AND PROCTOLIN ON CONTRACTIONS OF INSECT LEG MUSCLES.

H. Washio, Lab. Neurophysiol. Mitsubishi Kasei Inst. Life Sci. Machida, Tokyo.

The modulatory action of the exogenous octopamine(OA) and proctolin(PR) upon neurally-generated contraction and their direct action were studied on the coxal depressor muscle (135 d) of the cockroach, *Periplaneta americana*. OA increased the contraction and relaxation rates of neurally-generated contraction, while PR increased the basal tension markedly and decreased the relaxation rate.

The PR induced sustained contractures at as low as 10^{-10} M. This contracture was clearly dependent on the external Ca^{2+} . The contracture was completely blocked in a Ca -free saline, and no contracture was seen in the presence of Ca -channel blockers, like Mn^{2+} . Therefore, it is suggested that PR induced contractures are elicited by a calcium entry into the muscle from the external fluid. On the other hand, OA reduced the potassium and caffeine-induced contractures. The effect of OA on the contraction was blocked by the presence of α -adrenergic blocker, phentolamine.

These results indicate that both PR and OA act directly on muscle fibers and might affect some stage of the excitation-contraction coupling mechanism to modify the tension generated by a given level of depolarization.

PH 84

Mechanism for inducing contraction of smooth muscles of sea urchin gonads by a substance present within heamal vessels.

N. Takahashi^{1,2}, N. Sato², M. Takahashi¹ and K. Kikuchi²

¹Marine Biomedical Institute, Sapporo Medical College, Higashirishiri, Hokkaido 097-01 and ²Pathology, Sapporo Medical College, Sapporo 060, JAPAN

In the heamal vessels of the sea urchin, there is present a factor that induces contraction of smooth muscles. It has the features of glycoprotein and a molecular weight of 3,800. The present study was carried out to elucidate the mechanism for this contraction. The following results were obtained: the absence of external Ca^{2+} and the action of Ca^{2+} channel blockers such as Mn^{2+} and verapamil did not cause contraction by this factor to decrease, while the absence of external Na^{+} did cause it to decrease. The effects of Na^{+} channel blockers such as curare and atropin on contraction were examined and confirmed not to inhibit contraction by this factor. However, the Na^{+}/H^{+} antiporter blocker, amiloride, was found to decrease the contraction. It thus follows that the carrier protein of Na^{+}/H^{+} antiporter is essential for contraction by this factor to occur.

PH 85

Myogenic beats induced in the neurogenic heart of the isopod crustacean Ligia exotica
H. Yamagishi, Inst. of Biol. Sci., Univ. of Tsukuba, Tsukuba

The heart beat of the isopod Ligia is neurogenic and each beat follows a burst of nerve impulses generated in the cardiac ganglion. However, when the ganglionic burst lowers in frequency or stops completely, spontaneous electrical activity of the myocardium often appears and the heart beats associated with the activity (myogenic heart beat). To know the physiological properties of the Ligia heart, induction of myogenic heart beats was examined.

With perfusion of tetrodotoxin (TTX) (3×10^{-6} M) containing saline, spontaneous activity of the cardiac ganglion gradually decreased and then stopped completely. Electrical responses of the myocardium to the ganglionic activity also decreased gradually but its spontaneous electrical activity developed progressively. Thus, by application of TTX, the heart was not arrested but continued to beat rhythmically after no ganglionic activity was recorded. By perfusing normal physiological saline, spontaneous activity of the cardiac ganglion gradually recovered and neurogenic heart beats were restored.

These results suggest that the Ligia heart possesses myogenic properties, which are usually masked by neural activity of the cardiac ganglion.

PH 86

Effects of filling pressure and pericardial hormones on the contraction and relaxation rates of the heart of Panulirus japonicus. T. Kuramoto. Inst. of Biol. Sci., Univ. of Tsukuba, Ibaraki 305.

In the isolated heart of the lobster, the maximum rates of rise and fall of heart tension were measured. The systole consists of the first and second contractions (FSC and SSC) under low filling pressure (1.5 kPa). As pressure was raised, FSC increased in both the rise rate and amplitude while SSC decreased. Disappearance of SSC under high pressure (>2.5 kPa) related to a small increase of FSC in both the rise rate and amplitude. Thus the maximum rise rate of the systole was represented by that of FSC. The maximum fall rate of the systole changed in accordance with the change in total amplitude of the systole.

Linear increases in systolic amplitude by pressure were observed only within a narrow range (0-1.5 kPa in filling pressure). Whereas, the linear increase in the maximum rise rate of FSC was found over wider range of pressure (0-3.5 kPa).

Octopamine (1 μ M) increased the maximum rise rate and amplitude of FSC. But during an early period of the response (1 min), the extent of increase in rise rate was very small while the heart rate decreased. SSC was reduced slightly by octopamine. Whereas, serotonin (0.1 μ M) markedly enhanced both the rise rate and amplitude of SSC and mildly those of FSC.

PH 87

DISTRIBUTION OF SEROTONERGIC NEURONS IN THE WHOLE CENTRAL NERVOUS SYSTEM OF A GASTROPODA MOLLUSC, PLEUROBRANCHAEA NOVAEZEALANDIAE. E. Takeda and K. Kuwasawa. Dept. of Biol., Tokyo Metropolitan Univ., Tokyo.

Serotonergic nervous systems of the following central ganglia were immunocytochemically examined; the cerebro-pleural ganglion, the buccal ganglion, the left and right pedal ganglia, the visceral ganglion, the penis ganglion and the glandular sac ganglion. Although immunoreactive neural processes to anti-serotonin antibody were observed almost everywhere in the central nervous system, only in the cerebro-pleural ganglion and the left and the right pedal ganglia, immunoreactive neuron somata were found. There were 15-36 neurons in the cerebro-pleural ganglion, 18-30 neurons in the left pedal ganglion and 28-53 neurons in the right pedal ganglion. Those somata ranged 25-400 μ m in diameter. Almost all nerves, ganglionic nerves running to the periphery, connectives and commissures contained immunoreactive nerve fibers. The visceral ganglion contained no serotonin-immunoreactive neuron somata although a pair of connectives between the visceral and cerebro-pleural ganglia and two nerves arising from the ganglion involved immunoreactive fibers.

There were more immunoreactive neurons in the right pedal ganglion than the left pedal ganglion. This may be due to the presence of a variety of organs in the right side of the body, such as reproductive and cardio-arterial systems.

PH 88

FURTHER EVIDENCE FOR POSTULATED NEUROTRANSMITTERS IN THE HEART OF THE HERMIT CRAB.

T. Yazawa and K. Kuwasawa. Dept. of Biol., Tokyo Metropolitan Univ., Tokyo.

Our previous pharmacological experiments have suggested that neurotransmitters of small cardio-ganglionic neurons (SGNs) and large cardio-ganglionic neurons (LGNs) are, respectively, acetylcholine and dopamine, and that those of acceleratory and inhibitory regulatory neurons are, respectively, dopamine and gamma-aminobutyric acid (GABA). One of three axons contained in the cardio-regulator nerve showed immunoreactivity to anti-GABA antiserum. No neuronal process in the heart showed immunoreactivity to anti-serotonin antiserum although immunoreactive neurons to the serum were found in the thoracic ganglion. Effects of the putative transmitter on membrane conductance were examined. Excitatory effects of acetylcholine and dopamine on LGNs were accompanied by increase of membrane conductance. The inhibitory effect of GABA was also accompanied by increase of membrane conductance of LGNs. Myocardial membrane conductance was increased by dopamine. Both acetylcholine and dopamine enhanced activity of SGNs, and GABA suppressed it. The effects of the drugs on SGNs may indicate that SGNs receive mutual innervation among them, and acceleratory and inhibitory regulatory innervation. All these present results confirmed our previous pharmacological results.

PH 89

CARDIO-ACCELERATORY AND -INHIBITORY NEURONS IN THORACIC GANGLIA OF AN ISOPOD, BATHYNOMUS DOERLEINI.
K. Tanaka and K. Kuwasawa. Dept. of Biol., Tokyo Metropolitan University, Tokyo.

We previously reported that two kinds of cardio-acceleratory neurons, CA1 and CA2 are located in the 2nd and 3rd thoracic ganglia (TG2 and TG3), respectively.

In preparations of an isolated single ganglion (TG2 or TG3) or preparations of connected thoracic ganglia lacking TG1, electrical stimuli applied to connectives anterior and posterior to the ganglion evoked both EPSPs and IPSPs in CA neurons, and stimuli applied to the 2nd roots evoked only EPSPs but no IPSPs. However, in preparations of the thoracic ganglia involving TG1, stimuli to the 2nd roots of TG2 to TG4 evoked IPSPs in CA neurons. Impulses of CA1 and CA2 axons were inhibited by stimuli to the 1st and 3rd roots of TG2 and TG3 in preparations containing TG1. Impulses of CA neurons were never inhibited by these stimuli after TG1 was removed from the preparations.

These results show that the IPSPs in CA neurons induced by stimuli to the peripheral nerves may be due to some interneuron located in TG1. As inactivation of CA1 and CA2 neurons is responsible for cardiac inhibition, as well as activation of cardio-inhibitory (CI) neurons, it is suggested that there is the reflexive center of cardio-inhibitory neural mechanisms in TG1. We found a candidate neuron for CI itself in the TG1 hemisphere.

PH 90

IDENTIFICATION OF NEURONS CONTROLLING BUCCAL MUSCLE MOVEMENT OF THE AFRICAN GIANT SNAIL.

M. Yoshida and M. Kobayashi. Physiol. Lab., Fac. of Integrated Arts and Sciences, Hiroshima Univ., Hiroshima.

Five pairs of neurons controlling the buccal muscle movement were identified in the buccal ganglia of a pulmonate, African giant snail (Achatina fulica Férussac). They were termed R(L)-B1, B2, B3, B4, and B5, respectively. Intracellular staining with fluorescent dye and electrophysiological technique were used for the identification.

Buccal muscles showed cyclical contractions according to the feeding rhythm generated by the central nervous system. All of the neurons identified in the present experiment made excitatory connections onto the muscles which contracted in the radula retraction phase (radula retractor and outer muscle), and some of neurons had electrical coupling each other. B1 and B2 were identical with d-BPN and d-BMN identified by Matsuo et al. (1987). Some neurons innervating the muscle which contracted in the radula protraction phase were also observed, although they have not been identified yet.

PH 91

NEURAL CONTROL OF THE PYLORIC REGION OF STOMACH IN SQUILLA.

K. Tazaki. Biol. Lab., Nara Univ. Educ., Nara.

Muscles of the pyloric region of stomach in Squilla are innervated by motoneurons located in the stomatogastric ganglion. The pyloric constrictor and dilator muscles are sequentially activated by a spontaneous triphasic pyloric output pattern organized by an endogenous oscillatory property of pyloric motoneurons. These muscles can generate all or nothing spikes which are tetrodotoxin-resistant and blocked by a divalent cation of Mn. Spikes of the constrictor muscles are followed by depolarizing afterpotentials which lead to repetitive spike firing. The motoneurons entrain rhythmic spike discharges of these muscles. After isolation from the ganglion, they display an endogenous property of membrane oscillation to generate a train of spikes. Brief depolarizing or hyperpolarizing stimuli can trigger or terminate an oscillatory potential with superimposed spikes to reset its rhythm. Myogenicity under the control of discharges of motoneurons in the constrictor neuromuscular system plays an important role in amplification of rhythmic contractions of muscles in the pyloric region. This system consists of two endogenous oscillators, a motoneuron oscillator and a muscle oscillator.

PH 92

DISTRIBUTION OF CARP AND FMRFAMIDE IN THE CENTRAL NERVOUS SYSTEM AND CIRCUATORY SYSTEM OF AMPHINEURAN MOLLUSCS.

S. Matsumura and K. Kuwasawa. Dept. of Biol., Tokyo Metropolitan Univ., Tokyo.

In the central nervous system and the circulatory systems of Liolophura japonica and Cryptochiton stelleri distribution of two cardio-active peptides was examined using an immunocytochemical method. Anti-FMRFamide antibody and anti-CARP antibody were applied to both sections and whole-mount preparations of the systems. Immunoreactive cells (4-10 μ m in diameter) were found everywhere in the central nervous system. FMRFamide immunoreactive processes were more densely observed than CARP ones in the central nervous system. Immunoreactive plexuses were revealed on the surface of myocardial trabeculae and on the outer surface of the pericardium and the inner surface of the anterior artery. In the heart, FMRFamide-immunoreactive plexuses were more densely distributed than CARP-immunoreactive plexuses, but, in the anterior artery, more CARP immunoreactive plexuses, than FMRFamide ones.

Bath-applied FMRFamide ($>10^{-7}$ M) produced inhibitory effects on both beating rate and force of the pericardium and those of the heart. CARP ($>10^{-8}$ M) also produced inhibitory effects on the pericardium and heart. Excitatory effects of serotonin at a certain concentration on both the heart and pericardium were obstructed by FMRFamide or CARP at the same concentration.

The pericardium and heart may receive inhibitory innervation of the two peptidergic neural plexuses.

PH 93

MODULATORY EFFECTS OF SOME NEUROPEPTIDES ON NEUROMUSCULAR TRANSMISSION OF RADULAR MUSCLES IN A PROSOBRANCH, *RAPANA THOMASIANA*. M. Sakata, M. Yanagawa, Y. Muneoka and M. Kobayashi. Physiol. Lab., Fac. of Integrated Arts and Sci., Hiroshima Univ., Hiroshima.

In pharmacological experiments, it was suggested that FMRFamide and FLRFamide act on the presynaptic sites in the radular protractor and retractor, respectively, to enhance the contraction possibly by increasing the release of transmitters. On the contrary, CARP (Catch-relaxing peptide isolated from the pedal ganglia of a bivalve, *Mytilus edulis*) may act on the post-synaptic sites both in the protractor and retractor to inhibit the contraction. To examine these possibilities, localizations of these peptides within the CNS and peripheral sites were investigated immunohistochemically. Buccal ganglia and radular muscles were fixed on polyester wax and cut in sections of 8-10 μ m, then incubated with polyclonal antisera of FMRFamide and CARP. FMRFamide-like immunoreactive neurons were found on the left-rostral and middle-caudal surfaces of buccal ganglia. There were also many immunoreactive fibers in the radular protractor and retractor. CARP-like immunoreactive neurons were located near the middle-rostral surface of buccal ganglia. These results may support the idea that FMRFamide and CARP have important physiological actions in the regulation of buccal muscle movements.

PH 94

BIOACTIVE PEPTIDES ISOLATED FROM THE PROSOBRANCH MOLLUSC *Fusinus ferrugineus*-1. EXCITATORY PEPTIDES.

Y. Kuroki¹, T. Kanda¹, I. Kubota², Y. Fujisawa¹, Y. Muneoka¹ and M. Kobayashi¹. ¹Faculty of Integrated Arts and Sci., Hiroshima Univ., Hiroshima and ²Suntory Bio Pharma Tech Center, Chiyoda-cho, Osaka-gun, Gunma.

Four excitatory peptides were isolated from the ganglia of *F. ferrugineus*. They are as follows:

PEP₁: A L T N D H F L R F amide

PEP₂: F M R F amide

PEP₃: F L R F amide

PEP₄: G F R M N S S N R V A H G F amide

PEP₁ is a new FMRFamide-related decapeptide. This peptide shows twitch-potentiating action on the radula retractor of the animal at lower concentrations, and at higher than 10⁻⁶M, it elicits a contraction by itself. PEP₂ and PEP₃ are FMRFamide and FLRFamide, respectively. Both of them show contractile action at higher than 10⁻⁶M. PEP₄ is a novel tetradecapeptide. It has contractile effect on the muscle. The peptide does not appear to be a member of any other previously identified peptide family. However, it has potent inhibitory effect on the cardiac activity of *Meretrix lusoria* (Bivalvia) and phasic contraction of the ABRM of *Mytilus edulis* (Bivalvia). Further, two novel tetradecapeptides of which structures are highly homologous with that of PEP₄ have been found in a pulmonate mollusc by Ohta et al. There may exist a family of PEP₄-related peptides in molluscs.

PH 95

BIOACTIVE PEPTIDES ISOLATED FROM THE PROSOBRANCH MOLLUSC *Fusinus ferrugineus*-II. INHIBITORY PEPTIDES.

T. Kanda¹, Y. Kuroki¹, I. Kubota², T. Ikeda¹, Y. Muneoka¹ and M. Kobayashi¹. ¹Faculty of Integrated Arts and Sci., Hiroshima Univ., Hiroshima and ²Suntory Bio Pharma Tech Center, Chiyoda-cho, Osaka-gun, Gunma.

Four inhibitory peptides were isolated from the ganglia of *F. ferrugineus*. Their structures were determined to be as follows:

FIP₁: P M S M L R L amide

FIP₂: P M N M L R L amide

FIP₃: G S L F R F amide

FIP₄: S S L F R F amide

FIP₁ is myomodulin first found in *Aplysia*.

FIP₂ is a new myomodulin-CARP-related peptide (MCRP). MCRPs seem to be widely distributed in molluscs. FIP₁ and FIP₂

show potent inhibitory action on twitch contraction of the radula retractor muscle of *Fusinus* and relaxing action on catch tension of the ABRM of *Mytilus*. FIP₃ and FIP₄ are novel congeneric hexapeptides.

Although the structures of the peptides resemble to those of FMRFamide-related peptides (FaRPs), they do not show FaRP-like excitatory action on the radula muscle but show MCRP-like inhibitory action. In the ABRM, however, the peptides inhibit relaxation of catch in response to repetitive electrical pulses of stimulation. It is supposed that they inhibit the relaxation by acting on the relaxing nerve elements in the ABRM, because they do not inhibit relaxations by serotonin and CARP.

PH 96

BIOACTIVE PEPTIDES REGULATING THE ANTERIOR BYSSUS RETRACTOR MUSCLE OF MYTILUS

Y. Fujisawa¹, I. Kubota², T. Ikeda¹, Y. Muneoka¹. ¹Fac. of Integrated Arts and Sci., Hiroshima Univ., Hiroshima and ²Suntory Bio Pharma Tech Center, Gunma

The neuropeptides in the anterior byssus retractor muscle (ABRM) of *Mytilus* were isolated and purified by HPLC followed by bioassays. The structures of nine peptides were determined as follows:

MIP₁: GSPMFVa MIP₄: LAYPRL(a)

MIP₂: GAPMFVa MIP₅: ASHPRF(a)

MIP₃: DSPFLVa MIP₇: YAPRF(a)

MRP₁: AMPMLRLa MCP₁: ALAGDHFFRa

MCP₂: FMRFa

(One letter abbreviations, a:amide)

MIP₁, MIP₂ and MRP were shown to be the same as the ganglionic peptides, S²-MIP, A²-MIP and CARP, respectively. MIP₃ was considered to be an analogue of S²-MIP and A²-MIP. The sequence analysis of MIP₄ showed that the peptide is highly homologous with the C-terminal sequence of SCP₃, although the actions of these peptides on the ABRM were quite different. MIP₅ and MIP₇ may be also related to MIP₄ and SCP₃. These results suggest that there may exist the -PRX family. MCP₁ was a novel FMRFamide-related decapeptide homologous with *Fusinus* peptide FEP₁. MCP₁ is also unusual because it has -FFRFamide sequence instead of -FMRFamide or -FLRFamide. MCP₂ was shown to be FMRFamide itself.

PH197

TWO NOVEL PEPTIDES ISOLATED FROM THE VENTRAL NERVE CORDS OF URECHIS UNICINCTUS

T. Ikeda¹, Y. Muneoka¹ and I. Kubota². ¹Fac., Integrated Arts and Sci., Hiroshima Univ., Hiroshima. ²Suntory Bio Pharma Tech Center, Chiyoda-cho, Oura-gun, Gunma.

By using the isolated inner circular body-wall muscle of Urechis unicinctus as a bioassay system, ten bioactive peptides were purified from the acid-water extracts of the ventral nerve cords of the worm. Furthermore, fifteen other species of bioactive peptides were suggested to exist in the nerve cord. Some of the purified peptides also showed bioactivities on molluscan muscles.

We determined the structures of two of the purified peptides. These peptides were UEP_A and UEP_C (Urechis excitatory peptide A and C). Their structures are as follows:

UEP_A: AKCSGKWNYSYLKAGAN-OH

UEP_C: TFCITDLNC-OH

The peptides do not appear to be members of any other previously identified peptide family, though UEP_C seems to resemble a little to the crustacean cardioactive peptide (CCAP), PFCNAFTGC-NH₂.

The structure determination experiments of other purified peptides are now in progress.

PH198

BIOACTIVE PEPTIDES ISOLATED FROM THE GANGLIA OF A PULMONATE MOLLUSC, ACHATINA FULICA FÉRUSAC.

N. Ohta¹, H. Matsuo¹, I. Kubota², Y. Muneoka¹ and M. Kobayashi¹. ¹Fac. Integrated Arts and Sci., Hiroshima Univ., Hiroshima and ²Suntory Bio Pharma Tech Center, Gunma.

Several bioactive peptides were isolated from the ganglia of a pulmonate mollusc, Achatina fulica. The penis retractor muscle of this animal was used for bioassay. One of the peptides was shown to be FMRFamide itself. The second peptide termed AES1 (Achatina excitatory substance) induced a contraction of the penis retractor. The structure analysis of this peptide is now in progress. The other two peptides termed AEP283 (Achatina excitatory peptides) enhanced tetanic contraction of the muscle. The structures of the peptides were as follows, and they were structurally related to another novel peptide (FEP4) isolated from a prosobranch mollusc, Fusinus ferrugineus.

GFRQDAASRVAHGY (amide) AEP2

GFRGDAASRVAHGF (amide) AEP3

GFRMNSNRVAHGF amide FEP4

These tetradecapeptides appear not to be members of any other previously identified peptide family both in invertebrates and vertebrates. FEP4 showed bioactivities not only on several muscles of Fusinus and Achatina, but also on the cardiac muscle of Meretrix and the ABRM of Mytilus, both of the bivalvia, Mollusca. These results suggest that there may exist a family of these tetradecapeptides in the Mollusca.

PH199

BIOACTIVE PEPTIDES ISOLATED FROM THE ATRIA OF THE AFRICAN GIANT SNAIL ACHATINA FULICA. K. Fujimoto, N. Ohta, Y. Muneoka and M. Kobayashi. Physiol. Lab., Fac. of Integrated Arts and Sci., Hiroshima Univ., Hiroshima.

Structure and function of peptides isolated from the atria of the African giant snail Achatina fulica were studied. The atria excised from 1,600 snails were processed through acetone extraction, treatment with C-18 cartridges, gel filtration of the retained material, and HPLC separation to isolate bioactive peptides. The atria and the ventricles of the snail were used for bioassay. As the results, three Achatina cardio excitatory substances (ACES-1, 2 & 3) were purified. The structure of ACES-1 was Gly-Phe-Ala-Asp. This appears to be the same peptide with Achatin-1 isolated from Achatina ganglia, which induces an inward current due to Na⁺ in the heart excitatory neuron, PON. The structure of ACES-2 was Arg-Leu-Arg-Phe-Ala. This is an analogue of bag cell peptides (BCPs) isolated from Aplysia bag cells. BCPs (α and γ) as well as ACES-2 enhanced the heart beat of Achatina, although ACES-2 appeared to show stronger enhancing effects than BCPs. ACES-3 was found to be present in larger quantities than ACES-1 or 2 in the atria. ACES-3 showed strong enhancing effects on the contraction of the penis retractor and the buccal muscle of Achatina. It is postulated that this is an atrial hormone-like substance.

PH100

BIOACTIVITIES OF NEURAL COMPLEX EXTRACTS FROM TUNICATE

M. Iwakiri¹, Y. Shudo¹, T. Ikeda² and Y. Muneoka². ¹Dept. of Biol., Fukuoka Univ. of Educ., Munakata and ²Physiol. Lab., Fac. Integrated Arts and Sci., Hiroshima Univ., Hiroshima.

The strips of muscle which were isolated from body wall of Styela plicata, a tunicate, showed contraction or relaxation by electrical stimuli (ES) and some agents (Iwakiri et al., 1984). In the present study, we revealed that the homogenized materials of neural complex of the animal dissolved in physiological saline brought about a marked rhythmic movement on the muscle preparations. The serial gel/sephadex 151-filtrated active fractions were prepared after separating the extracts of homogenized neural complex of Styela into the retained materials (RW) and flow through (FT) with a SEP-PAK¹⁸ reversed-phase column and the activities of each fraction on the muscle preparation of the animal were examined. In the activity-curves based on the muscle contraction and relaxation to RW and FT fractions, more than 10 peaks of the activities were observed. Among these peaks, the activities of fraction No23 (relaxation activity) and No29 (contraction activity) of RW on intestinal, cardiac and abdominal muscle of the frog, Rana limnocharis, were investigated. Both fractions inhibited the rhythmic movement of intestine and the heart beat, and No23 increased the contraction of abdominal muscle by ES and Achr-action. In addition, the former activity was affected by atropine and the latter by curare.

PH 101

IMPROVED METHOD OF CELL-ISOLATION AND CELL CULTURE FOR THE STUDY OF MECHANISM ON PHYSIOLOGICAL MODULATION IN THE MUSCLE.

S. Nagaki and N. A. I. Dept. of Biol., Tokyo Gakugei Univ., Koganei, Tokyo.

Muscle contraction produced by intrinsic chemical modulator, as PGs, makes an intentional move as the typical and essential behavior for animal. But the action mechanism of modulator is not clear. PGs seem to have ability for changing excitability in the muscle. So, it is attacked to prepare excitable cell membrane for the study.

In this study, it is used the cardiac muscle with spontaneous and repetitive action from adult crab, *Sesarma haematochier*, and attempted to make "cultured cardiac muscle by improved method."

At first, adult crab was carefully washed and disinfected by chlorination, and then cardiac muscle was taken out from the isolated heart with fine scissors. The muscle was rinsed with Ca-Mg free salts solution repeatedly. Then, the muscle was cut to fine pieces. In the next, they were centrifuged at 4°C with 3000 rpm for 5 min. Precipitate after these procedure was added to 0.005% trypsin and managed with fine pipette for cutting more pieces. In the last, materials were slowly filtrated. On determination of culture medium, cell-size and its frequency were calculated, and also osmotic pressure were adjusted. Cell-culture was performed under condition for 24hr at 15±1°C. Single cell or cluster were used for experiments of modulator and measurement of membrane potentials.

PH 102

FEEDING AND RESPIRATION IN ADULT LAMPREYS.

R. Kawasaki¹ and C. Rovainen². ¹Col. Biomed. Technol. Niigata Univ., Niigata and ²Dept. Cell Biol. and Physiol., Sch. Med. Washington Univ. St. Louis, MO, USA.

In lampreys, intake of food and oxygen are performed (together in the larva, or separately in the adult) by rhythmic activities of "branchial (or oropharyngeal) muscles". American lampreys (*Ichthyomyzon unicuspis*, juveniles and adults), were tested in lake water of 10°C. After pithing behind the last gill pores, the head was held in an apparatus and the sucker vacuum was monitored with a pressure transducer. EMGs were recorded from the sucker, buccal region (muscles for sucking) and branchial muscles. Minced goldfish meat and skin were extracted. This extract plus food dye was used as test solution.

Feeding behavior was initiated by infusion of the test solution into the sucker cavity; sucker vacuum and EMG recordings showed characteristic profiles of this behavior. Feeding and swallowing was evidenced by the food dye observed in the gut in the dissected lamprey. Infusion of dyed lake-water failed to initiate this behavior, and no colour was observed in the gut.

From our results, "some criteria" for feeding behavior in the lamprey could be originally proposed. Feeding and branchial respiratory movement respectively lasted with their own rhythms, suggesting division of central pattern generator function of "branchial nervous system" for feeding and respiration in adult lampreys.

PH 103

COMPARATIVE STUDIES OF AIRBREATHING FUNCTIONS IN GOBID FISHES-II. CHARACTER IN EPIDERMAL STRUCTURE OF AIRBREATHERS K. IWATA* and I. KAKUTA*. Biol. Labo. Fac. of Edu. Wakayama Univ., Wakayama and *Fac. of Appl. Biol. Hiroshima Univ., Hiroshima

Amphibious fish such as *Periophthalmus cantonensis* (Tobihaeze) is known to have an unique skin: blood capillaries penetrating into epidermis and very large cells locating in the middle layer of epidermis. In the present study, we found another three types of epidermal structures from the dorso-lateral part of skin of other gobid airbreathers as follows: (1) In *Tridentiger obscurus* (Chichibu) with developed scales, the epidermis covering the upperside of intruding scales composes of only 2-3 layers, and its lowest layer has large sized cells, while a very thin epidermal layer covers over the under-surface of intruding scales. (2) In *Chasmichthys doli-cognathus* (Agohaze) with small scales, the cavities of scale pockets lined with the vascularised dermal layer enlarge. (3) In *Luciogobius guttatus* (Mimizuhaze) without scales, the epidermis lined with vascularised dermis composes of the mixed cells: small cells and large cells with vacuoles.

The large cells in the epidermis and the large scale pockets seem to serve as a retention of water in the skin during out of water.

PH 104

VARIATION IN AND OXYGEN-BINDING PROPERTIES OF *DAPHNIA MAGNA* HEMOGLOBIN

M. Kobayashi¹, M. Fujiki¹ and T. Suzuki²

¹Department of Biology, Faculty of Science, Niigata University, Niigata, ²Department of Biology, Faculty of Science, Kochi University, Kochi.

The oxygen-binding and molecular properties of the purified hemoglobin from *Daphnia magna* were investigated. There were inverse correlation between P 50 value (oxygen affinity) and hemoglobin concentration in hemolymph. The P 50 values ranged from 1.1 to 5.3 Torr and the n values (Hill's coefficient) from 1.6 to 1.2 in 0.1 M phosphate buffer of pH 7.2 at 20°C. The purified hemoglobin was separated into at least six components in isoelectric focusing. Although hemoglobin-rich and hemoglobin-poor animals possess the same hemoglobin components, the hemoglobin of the former with high pI values possesses these components in greater amounts. These results indicate that *Daphnia magna* may become acclimated to various oxygen environments through adjustment of the proportions of hemoglobin components differing in affinity and subunit cooperation.

PH 105

EFFECT OF THERMAL ACCLIMATION ON METABOLIC PATHWAYS OF HEART MUSCLE IN GOLDFISH
T.Yonehana and H.Tsukuda. Dept. of Biol.,
Fac. of Sci., Osaka City Univ., Osaka.

The activity of some enzymes and the concentration of some metabolites and others involved in glycolysis and TCA cycle were determined for heart, muscle and liver of goldfish acclimated to 10° or 25°C for more than two months. Enzyme activity was assayed at 25°C for the tissue extract dialyzed for about 20 hours.

The energy charge of heart of 10°-acclimated fish was similar to that of 25°-acclimated fish, but $[NAD^+]/[NADH]$ ratio was higher in 10°-acclimated fish heart. The content of 2-phosphoglycerate, phosphoenolpyruvate, pyruvate and lactate was greater in the heart of 25°-acclimated fish than that of 10°-acclimated fish. There was no difference between two acclimated groups in content of citrate, isocitrate and 2-oxoglutarate. Difference in enzyme activities between two acclimation groups also was not detectable except for pyruvate kinase.

These results suggest that metabolism of heart muscle shifted to more aerobic during cold acclimation. In addition, results for the other tissues suggest that muscle was similar to heart, but liver was relatively anaerobic in cold-acclimated group.

PH 106

BICARBONATE TRANSPORT ACROSS THE SEAWATER EEL INTESTINE

M.Ando¹ and M.V.V.Subramanyam². ¹Lab. of Physiol., Fac. of Integrated Arts & Sci., Hiroshima Univ., Hiroshima, ²Dept. of Sericulture, Bangalore Univ., Bangalore, India

Utilizing a pH stat method, the rates of mucosal and serosal alkalization were measured separately in the seawater eel intestine. These two rates were dependent on contralateral application of DIDS, an inhibitor of HCO_3^- transport, indicating that both the mucosal and serosal alkalization are due to HCO_3^- transport. The mucosal alkalization was enhanced after inhibiting the $Na^+-K^+-Cl^-$ cotransport by treatment with bumetanide, furosemide and Ba^{2+} , suggesting that the HCO_3^- absorption depends on the $Na^+-K^+-Cl^-$ cotransport. After pretreatment with bumetanide, mucosal omission of Cl^- reduced the mucosal alkalization, indicating that the HCO_3^- exit into the lumen depends on luminal Cl^- , i.e. Cl^-/HCO_3^- exchange on the brushborder membrane. This exchanger was not dependent on Na^+ . On the other hand, when serosal Na^+ was removed under the same condition, the mucosal alkalization was reduced, indicating that the HCO_3^- entry from the serosal fluid depends on Na^+ , i.e. $Na^+-HCO_3^-$ cotransport on the basolateral membrane. This symporter did not require Cl^- . Summarizing these results, a possible model for HCO_3^- transport systems is proposed, in relation to Na^+ , Cl^- and water transport.

PH 107

ACCUMULATION OF ^{51}V -LABELED VANADIUM IONS BY ASCIDIAN BLOOD CELLS.

H. Michibata¹, Y. Seki¹, J. Hirata², M. Kawamura³, K. Iwai³, R. Iwata⁴ and T. Ido⁴. ¹Biol. Inst., Fac. of Sci., Toyama Univ., Toyama, ²Fac. of Pharmaceut., Univ. of Tokushima, Tokushima, ³Fac. of Agr., Tohoku Univ., ⁴Cyclotron and Radioisotope Center, Tohoku Univ., Sendai.

Although vanadium ions in seawater are reported to exist as vanadate(V) anion, $H_2VO_4^-$, at a concentration of 35 nM, ascidians belonging to the family Ascidiidae have the highest levels of vanadium ions, 10 mM to 150 mM, in their blood cells. We have examined how ascidians accumulate the metal ions from seawater, using ^{51}V -labeled vanadium ions, which were prepared by irradiation of titanium foils with 18 MeV proton beam at cyclotron of the Cyclotron and RI Center, Tohoku Univ. Blood cells of *Ascidia sydneiensis samea* and *A. gemmata* were incubated with ^{51}V -labeled Na_2VO_4 or $VOSO_4$ at a concentration of 30 nM at 16°C. The influx of vanadium ions was determined by counting the frequency of gamma-rays derived from ^{51}V in the cells. Consequently, it was found that the blood cells of *A. sydneiensis samea* accumulated vanadate(V) ions at influx rate of 5.3×10^{-5} nM/ 10^5 cells/hr and the cells of *A. gemmata* did at influx rate of 2.1×10^{-4} nM/ 10^5 cells/hr. The influx rate of vanadyl(IV) ions was less than one fourth. The half-time for influx of vanadium ions ($t_{1/2}$) was approximately 80 min to 130 min.

PH 108

EXTRACTION OF VANADIUM-BINDING SUBSTANCE (VANADOBIN) FROM A SUBPOPULATION OF SIGNET RING CELLS NEWLY IDENTIFIED AS VANADOCYTES IN ASCIDIANS.

T. Uyama and H. Michibata, Biol. Inst., Fac. of Sci., Toyama Univ., Toyama.

We have previously extracted vanadobin, a substance binding vanadium ions in ascidian blood cells (Michibata et al., 1986). In that experiment, however, it was unclear which blood cell type actually produced and/or contained vanadobin and there was some possibility that the substance might be an artificial complex produced during the experimental process. Therefore, in the present study, we examined which among several types of blood cell contains this substance, using a combination technique involving density gradient centrifugation for cell fractionation, chromatographies for extraction of vanadobin and neutron-activation analysis for determination of vanadium.

Consequently, vanadobin could be extracted only from the subpopulation of signet ring cells and not from that of morula cells in *Ascidia sydneiensis samea*. It was also confirmed that the signet ring cell contained a high amount of vanadium but the morula cell and the other cells do not do so in this species. The data obtained in this study indicate that vanadobin is not an artifact produced during the experimental process but is a native substance contained in the signet ring cells.

PH 109

HIGHLY ACIDIC BLOOD CELLS IN ASCIDIANS CONTAIN HIGH AMOUNTS OF VANADIUM IONS.

Y. Iwata and H. Michibata, Biol. Inst., Fac. of Sci., Toyama Univ., Toyama.

Following Henze's first discovery of 1 N acidity (Henze, 1911), it was widely accepted that a homogenate of ascidian blood cells indicated a low pH value and the mechanism of accumulation of vanadium ions by the cells was associated with the low pH value. However, recent measurements based on new technology including NMR, ESR, and trans-membrane equilibrium gave spurious results of pH values, varied between 1.8 and 7.19.

Since ascidians have six to nine different types of blood cell, one of the reasons for the variation in pH values is probably caused by the measurement of pH without cell fractionation. Therefore, the present study was planned to isolate acidic blood cells and examine whether the cells are identical with the so-called vanadocytes, using a combined technique involving cell fractionation by density gradient centrifugation, a microelectrode for pH measurement and neutron-activation analysis for vanadium determination.

As a result, it becomes clear that in all species examined in the present experiment, signet ring cells contain a high amount of vanadium ions and the layer containing the signet ring cells among four differentiated layers show a low pH value: *Ascidia rhodori*, 2.67; *A. gemmata*, 2.42; *A. sydneiensis* *samea*, 4.20.

PH 110

STRUCTURE OF WATER PERMEATING CELLS IN THE EPIDERMIS OF THE TREEFROG, *Hyla arborea*

Y. Kamishima. Dept. of Biol., Facult. of Sci., Okayama Univ. Okayama 700

Ventral pelvic skin of Japanese treefrogs was extremely permeable to water, while dorsal skin was water-resistant. Larval skin was also water-proof. In this study, larval and adult skins of the treefrog were investigated morphologically in relation to the water permeability. Epidermis of adult frogs consisted of two to three layers of cells, of which outer cells, the granular cells, showed remarkable difference between dorsal and ventral skins. The granular cells in the ventral skin showed very dense cytoplasm and contained small amount of shorter tonofibrils, while those in the dorsal skin were rich in bundles of long tonofibrils and showed moderate cytoplasmic density. Cytoplasmic granules which characterized these cells were scarce in the dorsal cells. The granular cells of the ventral skin showed extensions of cytoplasmic processes by which they interdigitated with neighbouring cells. Granular cells appeared at the late prometamorphic phase and proliferated to cover whole outer surface of the ventral pelvic skin before beginning of the metamorphic climax. During these periods, neural elements appeared among granular cells. A bundle of axons were also observed passing through the basal lamina suggesting innervation in the epidermis.

PH 111

FEEDING AND GROWTH IN HYDRA

Kazumitsu HANAI and Hiroyuki TERADA, Department of Biology, Faculty of Science, Kyushu University 33, Fukuoka

The response of *Hydra* to reduced glutathione is composed of at least 5 components (R1-R5), each of which is specifically depressed by various growth factors. In the body fluids of mammals, that is, cerebrospinal fluid from the rat brain and human serum, R4 depressing activity was observed greatly elevated after food intake. This elevated activity is proposed to be closely related to acidic fibroblast growth factor (aFGF), which may be participated in feeding regulation in the brain.

In *Hydra*, we observed the elevated labelling index of cell proliferation for epithelial cells and interstitial cells, and also observed the R4 depressing activity in culture medium after feeding. It is interesting to see the relationship between the activity which leads to cell proliferation and another which is released into the medium after feeding. To examine closely the latter activity, we extracted the activity from the culture medium after feeding. The activity could be purified after concentration with Butyl-TOYO PEARL by a heparin-Sepharose column and reverse phase HPLC with a C4 column, which are the same chromatographic procedures as aFGF is purified from bovine brains. However, the obtained material was too small for analyses.

PH 112

REGULATION OF IRIDOPHORE MOVEMENTS IN Gobiidae FISHES.

T. Iga, M. Honma and N. Maeno. Dept. of Biol., Fac. Sci., Shimane Univ., Matsue

Regulation of movements of motile iridophores of the paradise goby, *Rhinogobius giurinus* was examined. High K⁺ solution and electric stimulation induced dispersion of the platelets within the cells. These stimuli became ineffective in denervated scale preparations, showing that the movements of the iridophores are under the nervous regulation. Noradrenaline (NA) also induced dispersion of the platelets. The responses of the iridophores to electric stimulation and to NA were inhibited by alpha adrenergic blockers, but not beta adrenergic ones. These results show that the nerve regulating the iridophores is of adrenergic and the transmitter, being assumed as NA, acts on alpha adrenoceptors to induce platelet dispersion. Forskolin was effective in inducing aggregation of the platelets, suggesting that an increase in intracellular cAMP induces platelet aggregation. Melatonin accelerated the aggregation response of the iridophores. The hormone caused platelet dispersion in *Odontobutis* iridophores. This suggests that melatonin receptors include two separate types. Differences in the regulatory mechanisms on movements of iridophores and of leucophores were discussed.

PH 113

CONTROL OF IRIDOPHORE MOVEMENTS OF THE BRACKISH WATER GOBY, GLOSSOGOBius OLIVACEUS.
M. Honma and T. Iga. Dept. of Biol., Fac. Sci., Shimane Univ., Matsue

Iridophores of the brackish water goby, Glossogobius olivaceus are motile. The movements involve intracellular translocation of reflecting platelets, aggregation and dispersion within the cells. Isolated scale preparations were used. The iridophores were light sensitive: the platelets aggregated in darkness and dispersed in lightness. K^+ and electric stimulation caused platelet dispersion of the iridophores. These stimuli became ineffective in denervated preparations. These show that the iridophores are controlled by the nerves. Noradrenaline (NA) also induced the platelet dispersion. The dispersion responses to electric stimulation and to NA were inhibited by alpha antagonists, but not by beta ones, suggesting that the nerve controlling the cells is of adrenergic and the transmitter, NA acts on alpha adrenoceptors to induce platelet dispersion. The existence of beta adrenoceptors was not determined. Melatonin induced aggregation of the platelets. Forskolin and cAMP were effective in inducing platelet aggregation, suggesting that an increase in intracellular cAMP causes aggregation of the platelets.

PH 114

MOTILITY OF THE IRIDOPHORES IN THE NEON TETRA.
H. Nagaishi, K. Miyaji, N. Oshima. Dept. of Biol., Fac. of Sci., Toho Univ., Funabashi.

By the use of the skin pieces isolated from the lateral stripe area of the neon tetra, the responses of the motile iridophores to the neurotransmitters and hormones were examined *in vitro*. The motility of the iridophores present in the lateral stripes was found to be controlled by the sympathetic nervous system in addition to the direct action of light. Adenosine, a co-transmitter accelerated the recovery from the effect of norepinephrine. MCH and melatonin caused the shift of the spectral peak toward longer wavelengths, and alpha-MSH shifted the peak in the opposite direction. Since these peptides and amine were effective only at high concentrations, the substances may not affect the cells *in vivo*. From the optical analysis, it was suggested that the essence of the cell motility might be the change in the inclination of light-reflecting platelets within the iridophores.

Electron microscopic studies revealed that a slender nucleus is present in the lower part of the cell and a pair of stacks of guanine platelets overlie the nucleus. The mechanism controlling the inclination of the platelets within the cells has not been demonstrated on the fine structural level.

PH 115

CALCIUM IONS ON MELANOPHORE MOVEMENTS IN TELEOST FISH.

Y. Miyashita and T. Moriya. Dept. of Biol., Sapporo Med. Coll., Sapporo

The effects of Ca-ionophore A23187 and TMB-8, an intracellular Ca-antagonist, on chromatic nerve transmission and melanophore movements in Lebistes reticulatus and in Betta splendens were studied.

A23187 (above 50 μ M) induced melanosome aggregation in innervated melanophores of both fishes by causing the release of transmitters from chromatic nerve endings. Melanophore cells themselves did not respond to A23187 even with calcium (1.8 mM).

TMB-8 (8-100 μ M) prevented the release of transmitters, resulting in inhibition of melanosome aggregations induced by nervous stimulations in both fishes. With the same concentration of TMB-8, norepinephrine (NE, 0.2-5 μ M) normally caused melanosomes to aggregate but its re-dispersion process was clearly accelerated. The response to NE was independent of extracellular calcium ions; however, the accelerating action of TMB-8 on the re-dispersion was strengthened in a Ca-deficient medium.

In chromatic nerve transmission, both the influx of extracellular calcium and the following mobilization of intracellular calcium seem to be indispensable, while, in response to NE, mobilized intracellular calcium ions seem to be principally utilized. There appear to be several pools of intracellular calcium with differing sensitivities to TMB-8 in chromatic nerves and melanophores of these fishes.

PH 116

FUNCTIONAL CELL MODEL OF TILAPIA MELANOPHORES IN CULTURE.

H. Inagaki, T. Manabe and N. Oshima. Dept. of Biomed. Sci., Fac. of Sci., Toho Univ., Funabashi.

In order to study the mechanism of pigment migration within fish chromatophores, cell model which is permeable to large molecules and retains the ability to move pigment is required. For this purpose, the melanophores treated with Brij 58 in combination with polyethylene glycol can be used (Clark and Rosenbaum, 1982). In former studies, the melanophores were permeabilized using lysis buffer containing 90 mM PIPES, 2.5 mM $MgSO_4$, 10 mM EGTA, 0.15-0.3% Brij 58 and 2.5% polyethylene glycol (pH 6.95). Since PIPES is rather expensive, we examined whether the Tris-HCl buffered lysis solution was usable for the preparation of cell models.

Brij was found to have the strong pigment-aggregating action. A small, temporary aggregation of melanosomes was induced even in the presence of 1 mM theophylline. At concentrations of the detergent higher than 0.1 mM, pigment aggregation advanced further in a dose-dependent manner. The responsiveness of the detergent-treated cells to norepinephrine (NE) and the degree of the recovery from the effects of NE decreased in dependence on concentration of Brij 58 at which cultured melanophores were treated for 45 sec. So, we adopted the lysis solution of the following composition: 130.7 mM NaCl, 2.7 mM KCl, 5.6 mM D-glucose, 5.0 mM Tris-HCl buffer, 0.1-0.15% Brij 58, 2.5% polyethylene glycol and 1 mM theophylline (pH 7.2).

Using the functional cell models of tilapia melanophores, it was shown that vanadate, a inhibitor of dynein ATPase, blocks the aggregation of pigment granules.

PH 117

INOSITOL 1,4,5-TRISPHOSPHATE (IP₃) AGGREGATES PIGMENT IN TILAPIA MELANOPHORES IN CULTURE.

H. Wakatabi, N. Oshima and R. Fujii. Dept. of Biomolecul. Sci., Fac. of Sci., Toho Univ., Funabashi.

It was shown that the motile responses of chromatophores are dependent on the intracellular cAMP level; its increase or a decrease results in the dispersion or the aggregation of chromatosomes. Recent studies have also indicated that the pigment aggregation depends on the intracellular Ca²⁺ level, too. In order to confirm the Ca²⁺ involvement, therefore, the effect of IP₃, which is known to release Ca²⁺ from the intracellular Ca²⁺-storing compartment, was studied on melanophores in primary culture of the tilapia, *Sarotherodon niloticus*. The plasma membrane of the cell had previously been permeabilized by a surfactant, Brij 58. The trisphosphate did aggregate melanosomes within the cell. On the other hand, neither inositol 1,4-bisphosphate (IP₂) nor inositol 1-monophosphate (IP) had such an effect. The IP₃-induced response was not antagonized by alpha-adrenolytics, phentolamine and prazosin. These results led us to conclude that IP₃ must be an intracellular mediator in the signal transduction for aggregating pigment. The present circumstances indicate that the motile response of the pigment cell proceeds by integrating the activities of both Ca²⁺ and cAMP systems.

PH 118

THE INVOLVEMENT OF MICROTUBULE ARRAYS IN MELANOSOME TRANSPORT OF MUTANT-TYPE (BdmR) MEDAKA MELANOPHORES.

S. Negishi. Dept. of Biol., Keio Univ., Yokohama.

The mutant-type (BdmR) medaka possesses characteristic melanophores in which melanosomes scarcely migrate under natural conditions. When melanophores were cultured for 5 to 7 days, however, some of them responded to the dark with incomplete pigment aggregation. Subsequent addition of 10⁻⁶ M α-MSH derived melanosome dispersion of the cells kept in the dark, though the movement required 30 minutes that is 10 times of wild type melanophores. 10⁻⁸ M MCH and 10⁻⁵ M epinephrine were both effective to induce pigment aggregation in BdmR melanophores, though it took 40 to 50 minutes to get only 30% aggregation.

Distribution of microtubules in BdmR melanophores was examined by using the indirect immunofluorescence microscopy. Microtubules were radially arrayed in dark-aggregated melanophores of BdmR, while different microtubule arrays were present in the cells remaining dispersed in the dark, namely, fluorescent bundles were localized abundantly in the periphery, but less detectable in the cell body. This feature was also seen in the cells aggregating incompletely by MCH or epinephrine. These results suggest that the difference in the distribution of microtubules may be closely related to the incomplete pigment transport of BdmR melanophores.

PH 119

PIGMENT-DISPERSING EFFECT OF CHOLERA TOXIN ON MEDAKA LEUCOPHORES

F. Morishita, S. Ishii and K. Yamada, Zool. Inst., Fac. Sci., Hiroshima Univ., Hiroshima.

Effect of cholera toxin (CT), an A-B toxin, on scale leucophores of the medaka, *Oryzias latipes* (miky, bbbrr), was investigated to examine the involvement of stimulatory GTP-binding protein (Gs) in pigment-dispersion response of the cells. CT (5 µg/ml) induced a gradual dispersion of pigment and the cells attained a half dispersed state at 3 hr and finally reached to a fully dispersed state at 5 hr. The B-oligomer of CT had no practical effect, while pretreatment with the oligomer markedly inhibited the cell response to CT. The effect of CT was irreversible, since the dispersion of pigment proceeded even when the medium was substituted for CT-free Ringer at 3 hr. Epinephrine caused a reversible aggregation of pigment in CT-treated dispersed cells through stimulation of alpha₂-adrenoceptors. Forskolin, an activator of adenylate cyclase, induced a reversible and rapid additive dispersion of pigment within CT-treated half dispersed cells. Isoproterenol also caused a further pigment dispersion in CT-treated cells, but the effect was irreversible. These results suggest that Gs is involved in the pigment-dispersion response of medaka leucophores and that CT induced the pigment dispersion through elevation of adenylate cyclase activity via activation of Gs.

PH 120

PIGMENTARY RESPONSE AND ULTRASTRUCTURE OF CHROMATOPHORES OF THE ANTARCTIC TELEOST TREMATOMUS BERNACCHII.

M. Obika¹ and V. B. Meyer-Rochow^{2,1}. Dept. of Biol., Keio Univ., Yokohama and ²Dept. of Biol., Univ. of Waikato, Hamilton, N.Z.

Three types of dermal chromatophores and two types of epidermal chromatophores are found in the integument of this fish that lives under the sea ice of Ross Ice Shelf. Dendritic dermal melanophores and xanthophores have well-developed arrays of cytoplasmic microtubules while smaller, round-shaped iridophores have microtubules only sporadically. Dermal melanophores and xanthophores respond to epinephrine and melanin concentrating hormone (MCH) with rapid pigment aggregation. Theophylline produces pigment dispersion in both cell types. Dermal iridophores that contain stacks of reflecting platelets appear to be immobile. Complete darkness elicits pigment aggregation in most of the dermal xanthophores while melanophores remain dispersed. In densely pigmented dorsal skin, epidermal melanophores and epidermal xanthophores are also observed. Epidermal melanophores with a few slender dendrites do not readily change their morphology but epidermal xanthophores rapidly respond to theophylline with pigment dispersion. The occurrence of epidermal xanthophores is reported for the first time in teleost.

PH 121

MECHANISM OF DARK BAND GENERATION BY SKIN NERVE INCISION: A NEW INTERPRETATION OF PARKER EFFECT

R. Fujii and H. Nishi, Dept. of Biomolecular Sci., Fac. of Sci., Toho Univ., Funabashi.

By using tilapia and some other teleostean species, the mechanism of formation of the dark band, which appears posterior to the site of nerve cutting, was studied. Many observations reported by G.H. Parker, who postulated the presence and the involvement of parasympathetic melanin-dispersing fibers, were not reproducible. The band generation is primarily due to the loss of tonic influences of the melanosome-aggregating sympathetic post-ganglionic fiber by its severance from the center. The circulating melanophore-stimulating hormone (MSH) and the adenine-derived co-transmitter, which lasts longer than the true transmitter, may also be involved in the active dispersion of melanosomes. During the night, the melanophore pigment in the band aggregated, leading to the generation of the reversed, pale band. In the daytime, too, the same phenomenon was inducible by an intraperitoneal injection of melatonin. The band reversal in the night may thus be due to the higher titer of circulating melatonin. When a fish well adapted to a white background was transferred to a dark background, the similar reversal of the denervated band was observable. Thus, melanin-concentrating hormone (MCH) may have a definite role in blanching the band.

PH 122

COLORATION AND LIGHT REFLECTING PROPERTIES OF LONGITUDINAL BAND OF ROSE BITTERLING.

H. Nishi and R. Fujii, Dept. of Biomolecular Sci., Fac. of Sci., Toho Univ., Funabashi.

The rose bitterling, *Rhodeus ocellatus ocellatus*, has a blue-green longitudinal band running about middle part of the posterior trunk. It is about 2.5 mm wide. We found that the band is clearly visible from certain directions, whereas it becomes obscure from others and even practically invisible from below. It was found that iridophores which constitute this band are responsible for the light reflecting properties. Histological examinations indicated that the complex consisting of a melanophore and several iridophores existed in the dermis of the band. It seems that the iridophores may have only a slight ability to change their optical properties through the shift of the distance between adjacent platelets. Pigment movements in underlying melanophores had also only little effect on the iridophores. Hormones, neurotransmitters and electrical nervous stimulation applied to an isolated skin preparation had practically no influence. In schools, individuals of this species seem to make regular ranks, by seeing others' bands. That is, they keep their positions with each other, by recognizing the bright stripe from behind. We suggest that, in this species, this band is of a great importance for their schooling behavior rather than for the communication among individuals.

PH 123

EFFECTS OF LIGHT ON MELATONIN SYNTHESIS IN AN ISOLATED PINEAL ORGAN OF FRESHWATER FISH, ZACCO TEMMINCKII.

I. Takabatake and T. Iga, Dept. of Biol., Fac. of Sci., Shimane Univ., Shimane.

It has been shown that the pineal organ was the site of an active melatonin biosynthesis pathway, and in fish that the synthesis of melatonin in a pineal organ was regulated by direct photoreception. Although many physiological functions of melatonin have been reported, participations of this hormone on behavioral color change in fish are poorly understood. In order to investigate the relation between melatonin synthesis and pineal photoreception, a series of *in vitro* studies using isolated teleost pineal organ were undertaken. The isolated pineal organ was maintained in L-15 medium containing fetal bovine serum and radioactive melatonin precursor (^{14}C -Tryptophan and ^{14}C -5-HT) at 25°C. The chloroform extract was chromatographed using silica gel TLC, and the plate was analyzed by TLC-radioscanner (Berthold, TLC-Multi-Tracemasters LB284). The following results were obtained. (1) An adequate correlation was estimated between the weight of pineal organ and body weight. (2) Melatonin synthesis per unit weight varied with the season. (3) In isolated pineal organ, it appears that melatonin synthesis depends on the change of extrinsic illumination.

PH 124

ANALYSIS OF CRICKET CIRCADIAN RHYTHM BY PHASE RESPONSE CURVE TO LIGHT PULSES

Y. Okada, K. Tomioka and Y. Chiba, Biol. Inst., Yamaguchi Univ., Yamaguchi 753

Male adult crickets, *Gryllus bimaculatus*, show a circadian locomotor rhythm in constant conditions. This rhythm is entrained to light-dark cycle and regulated by a pacemaker in each "optic lamina-medulla-complex" (Tomioka, 1985; Tomioka and Chiba, 1986). We investigated effects of light pulses on free-running locomotor rhythm under constant darkness. Three-hour light pulses gave rise to type-I phase response curve (PRC); phase was delayed during the early subjective night and was advanced during the late subjective night, but did not respond during the middle subjective day. PRC in animals with unilateral lamina-medulla-complex ablated also showed the type-I with quite similar pattern to that in intact animals, indicating that a single pacemaker could regulate a normal phase-response to light. Another noticeable observation pertains to significant difference in free-running period between operated ($23.73 \pm 0.25(\text{SD})$ h, $N=58$) and intact ($23.86 \pm 0.24(\text{SD})$ h, $N=99$; t -test, $p < 0.01$) animals, suggesting the existence of mutual interaction between bilaterally distributed circadian pacemakers.

PH 125

EFFECTS OF COMPOUND EYE PARTIAL REDUCTION ON CIRCADIAN LOCOMOTOR RHYTHM IN THE CRICKET *GRYLLUS BIMACULATUS*
K.Tomioka, Y.Okada and Y.Chiba, Biol.Inst., Yamaguchi Univ., Yamaguchi 753

Adult male crickets (*Gryllus bimaculatus*) show a nocturnal circadian locomotor rhythm, which is driven by the pacemaker in the optic lamina-medulla complex and synchronizes to the light cycle received by the compound eye. To see whether there is any specially differentiated circadian photoreceptor area in the eye, we examined the effect, on entrainability of the locomotor rhythm, of a unilateral reduction of the compound eye in addition to the contralateral removal of optic lobe compound eye system. The operated animals showed a clear nocturnal activity, which, however, revealed some marked differences from that shown by the control animals receiving unilateral optic lamina-medulla compound eye removal. 1. It took more days for some eye-reduced animals than for control animals to establish complete nocturnality after the imaginal molt. 2. Transient cycles needed for reentrainment, following a 6 hour phase advance of light cycle, were in inverse proportion to the number of ommatidia in the reduced eye: the fewer the ommatidia were, the more the transient cycles were. These results suggest that the every area of the compound eye could work as a circadian photoreceptor and that the photic informations from each ommatidium additionally affect the circadian clock to entrain.

PH 126

OUTBREAKS OF LOCUST SWARMING MAY BE CAUSED BY TWO CHRONO-BIOLOGICAL DEFICIENCIES.
Y. Tsukahara¹, I. Gleadall² and T. Hariyama¹.
¹Res. Ctr. for Appl. Inf. Sci., Tohoku Univ., Sendai and ²Natl. Inst. for Basic Biol., Okazaki.

The circadian rhythm of locomotor activity was studied in locusts (1) from the wild (*Locusta migratoria solitaria*, caught in Miyagi Prefecture) and (2) raised in our laboratory (sibling *L. m. solitaria* and *L. m. gregaria*, obtained by changing raising conditions). The eggs of the former required at least a week at cold temperatures to break diapause, and life cycle duration was long (3 months or more). The *L. m. gregaria* siblings acquired the ability to hatch spontaneously, without the need for a cold stimulus. The life cycle of *L. m. gregaria* from this population was less than one month. In continuous darkness, both types of *L. m. solitaria* showed a damped oscillatory circadian rhythm, continuing for more than 3 days. *L. m. gregaria*, however, showed no endogenous rhythm.

These data suggest that outbreaks of locust swarming may be caused by two chrono-biological deficiencies. One is uncoupling of the circadian clock during development and the other is loss of the necessity for diapause. Both deficiencies result in a life cycle duration governed only by temperature and food availability.

Development accelerates rapidly with increasing temperatures.

PH 127

ISOLATION OF AUTOSOMAL CLOCK MUTANTS IN *DROSOPHILA MELANOGASTER*.

A. Matsumoto¹, T. Tanimura², K. Tomioka¹ and Y. Chiba¹, ¹Dept. Biol., Fac. Sci., Yamaguchi Univ., Yamaguchi, ²Dept. Biol., Fac. Sci., Fukuoka Univ., Fukuoka.

Mutants affecting a circadian clock have been isolated in *Drosophila melanogaster*. Among them, period gene on the X chromosome has been extensively studied at a molecular level. Our study aims at the search to the almost unexplored second chromosome. Through mutagenesis with ethylmethane sulfonate, we have established about 1,000 homozygous strains carrying point mutations on the second chromosome. From them, we roughly selected about 100 strains that showed apparently abnormal eclosion rhythms in constant darkness (DD). Then, by recording locomotor activities of these strains in LD12:12 and the ensuing DD, we obtained several candidates of clock mutants. One of these candidates, M-780, shows longer free-running period (25.1±0.4h) than that of the wild type Canton-S (C-S, 24.2±0.3h). The other circadian parameters of M-780, such as phasing, waveform or amplitude, are also different from those of C-S. Additional isolations of a new clock mutant would provide a way to further dissect the complex system of circadian rhythm.

PH 128

PHOTOPERIODIC RESPONSE IN QUALITATIVE AND QUANTITATIVE CHARACTERS

H. Numata and S. Kobayashi, Dept. of Biol., Fac. of Sci., Osaka City Univ., Osaka.

Photoperiodic responses of insects are classified into two types by external manifestations. One is expressed in qualitative characters (QLC) and the other is in quantitative characters (QTC), which is subdivided into threshold and gradual responses (Zaslavski, 1988). We examined the photoperiodic responses in two heteropterans which manifest both QLC and QTC responses.

First, we compared the photoperiodic response for the induction of adult diapause (QLC) and that for the determination of adult body coloration (QTC) in *Riptortus clavatus* Thunberg. The latter had distinct critical photophases and was regarded as a threshold response. Because the response curves in these two responses were similar, we suggest that a common time measurement system is involved in them.

Next, we compared the photoperiodic response for the induction of adult diapause (QLC) and that for the determination of nymphal body coloration (QTC) in *Plautia stali* Scott. The latter was a gradual response without distinct thresholds. Furthermore, there was a noticeable difference in the response curves between these responses. The time measurement system for photoperiodism in this insect must be multiple or flexible.

PH 129

Relationship between reproduction and temperature, photoperiod, density and wing form in a water strider, *Gerris paludum insularis*

T. Harada. Dept. of Biol., Fac. of Sci., Osaka City Univ., Osaka.

First instar nymphs (just after hatching) were reared under long-day (LD=14.5:9.5) or short-day (LD=9.5:14.5) photoperiods at 20°C until the last ecdysis. Then the adults in each group were reared under the long-day or short-day photoperiod at 20°C for 70 days. Eggs were laid by the animals reared under the long-day photoperiod in the nymph and/or adult stage. The adults collected in Dec. were reared at 30°C or 18°C under a short-day (LD=12:12) photoperiod for 30 days. Only the adults at 30°C oviposited. First instar nymphs were reared at 30°C or 18°C under LD=12:12 until the last ecdysis. Then the adults were reared at 24°C under LD=12:12 for 30 days. The adults in the 30°C group laid much more eggs than in the 18°C one. First instar nymphs were reared at high or low population densities, under LD=15.5:8.5 at 25°C until the last ecdysis. The adults in each group were reared in pairs (at 25°C, under LD=15.5:8.5). The adults in the high density group laid less eggs than in the low one. First instar nymphs were reared until the last ecdysis and pairs were made with the adults having the same wing form (at 25°C, under LD=15.5:8.5). Brachypterous females laid more eggs than macropterous females only in the early adult stage (approx. first 18 days).

PH 130

EFFECTS OF THE CROSS-CUT OF THE MEDULLA OBLONGATA AND SPINAL CORD ON THE SWIMMING BEHAVIOR OF THE HAGFISH.

S. Ooka* and H. Kabasawa*. *Atomi Jr. Coll., Tokyo, *Aburatsubo Marine Park Aq., Miura.

The swimming activity of the hagfish was examined by observation and measurement with an infra-red light photocell system. After the cross-cut of the spinal cord, the frontal and hind part of the animal showed the different types of the posture and behavior. We made six experiments of a cut given to each animal at every one-sixth length of the spinal cord (the first cut was made at the top of spinal cord). Swimming behaviors are summarized as follows; (1) swimming in random direction at the bottom in both light and dark period (the 1st and 2nd cut) (2) swimming up to the surface in dark period as the intact animal (5th and 6th cut) (3) a mixture of both types of swimming (3rd and 4th cut). In the experiments of a cross-cut at various parts of medulla oblongata, the animals gradually lost their ability to swim up to the surface with the shift of the cut toward the tail. These results and previous studies indicate that (1) only propulsive movement remains when effects of the brain on the spinal cord are removed, (2) medulla oblongata coordinates the movements and induces the swimming up to the surface, and (3) the brain is responsible for the nocturnal rhythm through the inhibition of the movement during the light period.

PH 131

DISTANCE CALLS IN BENGALIAN FINCHES (*LOCHURA DOMESTICA*): ACOUSTIC CHARACTERISTICS AND PERCEPTUAL SELECTIVITY. K. Okanoya, T. Kimura and K. Aoki. Life Sci. Inst., Sophia Univ., Tokyo

Bengalese finches emit distance calls when they are separated from their mates. Like zebra finches (*Poephila guttata*), these calls are sexually dimorphic in Bengalese finches. Sonographic analysis revealed that two parameters, fundamental frequency and amplitude modulation, were effective in differentiating the calls of males and females.

These two parameters may be used in perceiving sexual identities of distance calls in Bengalese finches. In a pilot study, a male distance call appended with vibrate (amplitude modulations) were less effective than the original call in evoking distance calls from a female. The distance call lowered in pitch (fundamental frequency) were also less effective.

Distance calls from zebra finches and Bengalese finches were used to assess perceptual selectivity in call-back behaviour of Bengalese finches. Both males and females answered more to the conspecific distance calls than to the hetero-specific distance calls. However, the degree of selectivity was higher in males than in females. These experiment may prove to be useful in studying motivational aspects of communicative behaviour. (Work Supported by JSPS fellowship for Japanese Junior Scientists.)

PH 132

GEOTACTIC ORIENTATION IN THE ORB-WEB SPIDER, *ARGIOPE BRUENNICHII*.

K. Taneda, T. Hiramatsu and T. Matsuoka, Dept. of Biol., Fac. of Sci., Kochi Univ., Kochi.

Most snares, or the so-called orb-web spiders, usually orient downwards on their webs. A web containing the spider, *Argiope bruennichii*, was transferred to the laboratory on a square-shaped frame. The frame was kept in a vertical position for 30 min under given experimental conditions. Then the frame was turned up-side down. The spider reoriented itself after mechanical stimulation on the posterior end of its abdomen. The behavior was recorded on video tape. The inclination of the long axis of the abdomen to the vertical axis was measured. The angle was correlated with both directions of gravity and light exposure. The specimen with a small weight adhered to the back of its abdomen tended to reorient within a shorter period of time than one without did. When the abdomen of a specimen was pulled upon using a thread adhered to its dorsal side, the specimen rapidly turned to the rear. The specimen with an amputated leg showed conspicuous orientation behavior. The specimen which prevented the flexion of the whole femoro-patellar or tibio-metatarsal articulations through the use of thin polyethylene tubes, also exhibited the same behavior. The present findings suggest that the orientation of the spider is due to negative phototaxis as well as to the stretch reception of the pedicellus muscle.

PH 133

EFFECTS OF BASAL FOREBRAIN LESIONS ON THE SLEEP MODULATION BY URIDINE AND MURAMYL DIPEPTIDE IN RATS.

M. Kimura-Takeuchi and S. Inoue.
Inst. for Med. Dent. Eng., Tokyo Med. Dent. Univ., Tokyo.

We previously reported that uridine and muramyl dipeptide (MDP) interactively promoted slow wave sleep (SWS) and paradoxical sleep (PS) in unrestrained rats. However, brain sites responsible for the uridine-MDP-mediated sleep modulation have not yet been determined. In order to investigate the sites, we examined whether localized lesions in the basal forebrain could provoke any effect on the nocturnal sleep modulated by uridine and/or MDP administration. Nocturnal 10-h intra-cerebroventricular (i.c.v.) infusion of MDP (2 nmol) resulted in excess SWS (30.7 % above control) in rats with bilateral lateral preoptic area (LPO) lesions. LPO lesions abolished the SWS-promoting action of uridine (10 pmol) but not PS enhancement (15.0 %). Simultaneously infused uridine and MDP promoted both SWS (39.4 %) and PS (24.1 %) in LPO-lesioned rats, but the profile of SWS promotion was similar to that induced by MDP infusion alone in non-lesioned rats. In conclusion, the LPO might be an essential site for the SWS modulation by uridine, while MDP might act on the sites other than the LPO. Thus, uridine and MDP seem to participate in sleep regulation through different sites of action.

PH 134

PLASMA PROTEINS ASSOCIATED WITH HIBERNATION IN CHIPMUNKS

N.Kondo¹ and J.Kondo². ¹Dept. of Muscle Physiol. Mitsubishi Kasei Inst. of Life Sci., Machida, Tokyo and ²Mitsubishi Kasei Corp. Res. Center, Yokohama, Kanagawa.

In a previous HPLC analysis of plasma obtained from chipmunks in hibernating and nonhibernating states, we demonstrated that plasma fraction corresponding to MW 140 kD is markedly reduced in hibernating state. In the present study, the correlation between the changes in this plasma fraction and the beginning of hibernation was investigated in animals exposed to cold (4°C). The reduction of 140 kD plasma fraction observed in hibernating state was indicated to be due to a marked reduction of four proteins (MW 20, 25, 27, 55 kD) included in this fraction. Such 140 kD plasma fraction was reduced in many animals after exposure to cold, then these entered hibernation. However, some animals whose 140 kD plasma fraction was not reduced by cold exposure did not begin hibernating. Furthermore, in animals whose 140 kD plasma fraction was already reduced before exposure to cold, hibernation was rapidly induced by cold exposure. These results suggest that the reduction of four plasma proteins resulting in the reduction of 140 kD fraction is necessary for the beginning of hibernation and relates to the preparation for hibernation.

PH 135

EFFECTS OF ENVIRONMENTAL AGENTS ON HISTAMINE RELEASE FROM RAT PMC STIMULATED WITH SUBSTANCE P. H. Fujimaki, Basic Medical Sciences Division, National Institute for Environmental Studies, Tsukuba, Ibaraki.

The actions of nitrogen dioxide (NO₂), nitrous ions (nitrate and nitrite) and hydrogen peroxide (H₂O₂) on histamine release from rat peritoneal mast cells (PMC) were investigated.

In vitro exposure to 5ppm and 20ppm NO₂ markedly inhibited histamine and β -hexosaminidase release from rat PMC stimulated with substance P, whereas calcium ionophore A23187-stimulated histamine release was not inhibited. When purified PMC were incubated for 30 min with 1mM-50mM nitrous ions, substance P-stimulated histamine release was significantly inhibited by the pretreatment of nitrite. However, nitrate failed to inhibit the histamine release. The pretreatment of PMC with 1 μ M-100 μ M H₂O₂ inhibited the histamine release stimulated with both substance P and A23187. It is concluded that inhaled NO₂ and its chemical intermediates inhibited the histamine release from rat PMC stimulated with substance P.

(Supported in part by grant under the Monbusho International Scientific Research Program).

PH 136

ROLES OF GRANULAR AMOEBOCYTES ON ADHESION/AGGREGATION OF HEMOLYMPH OF HALOCYNTHEA RORETZI.

S.Ohtake, T.Abe, F.Shishikura, and K.Tanaka
Department of Biology, Nihon University School of Medicine, Tokyo.

The fine structure and adhesion/aggregation process *in vitro* of hemocytes of an ascidian, H. roretzi, were examined by TEM and SEM.

Types of hemocytes, based on fine structure, were as follows: Six types of vacuolated or vesicular cells which were classified by the size of vacuole and the kind of inclusion (involving signet ring cells and morula cells), basophilic cells, large granular amoebocytes (LG), fine granular amoebocytes (FG) and lymphocytes.

When the hemolymph contacted with own tunic *in vitro*, cell aggregation was induced within five minutes. The aggregates were formed by only LGs. Twenty minutes after contact with tunic, granules of LG in the center of an aggregate were swollen and fused. FGs elongated filopodia and tightly adhered on the tunic surface. Then, FGs had spread in single layer on the tunic surface 30 min after. The adhesion of FGs around LG aggregates was also observed. These results suggested that two kinds of granular amoebocytes may have important roles on hemostasis and wound healing in the ascidian, by LGs aggregating each other and FGs adhering to LG aggregates and tunic.

PH 137

PHYSIOLOGICAL TEMPERATURE ADAPTATION OF POIKILOtherms: COLD-STABLE MICROTUBULES IN CELLS CULTURED AT LOW TEMPERATURE. II K. Tsugawa, Dept. Nat. Sci., Osaka Women's Univ., Sakai

Microtubules (MT) of the cytoskeleton of cold-acclimated (or adapted) poikilotherms are expected to be stable in cold where they live. In fact, MT of rainbow trout cells, RTG-2, cultured chronically at 5°C are stable at 0°C for at least 16 hr, although those of warm-cultured cells disassembled almost all rapidly (Tsugawa & Takahashi, Comp Biochem Physiol 1987, 87A: 745). The present study showed that the increase in cold stability of MT in the cold-cultured cells is accompanied with an enhanced colcemid-stability of MT.

Cells had been cultured at 23-25°C or 4-5°C for more than 3 years, and log phase cells were exposed to a culture medium containing 0.1 to 5 µM colcemid at 14°C for 3 hr. MT were stained immunofluorescently with a monoclonal anti-β tubulin and FITC-labeled anti-mouse IgG. The network structure of MT in the cold-cultured cells was more stable to colcemid than that in the warm-cultured ones. At 0.33 µM the number of MT reduced to less than half in the latter but almost unchanged in the former. Culture of 24°C-cells at 10°C for 3 months led to some improvement in cold- and colcemid-stability of MT.

PH 138

IMMUNOLocalization AND IN VITRO SECRETION OF THE HEMOLYMPH LECTIN OF THE PEARL OYSTER, Pinctada fucata MARTENSII T. Suzuki, and K. Mori. Natl.Res.Inst. of Aquaculture, Nansai, Mie.

Molluscan hemolymph agglutinates many kinds of vertebrate erythrocytes. However, the producing organ of the lectin responsible for this activity is not known.

We searched for the producing organ of the hemolymph lectin of the pearl oyster by means of immunocytochemistry and in vitro culture. When indirect immunofluorescence was applied to each of the organs examined, only granular cells under the mantle epithelium exhibited apparent granular immunoreaction to the anti-lectin antiserum. In immunoelectron microscopy of the granular cells, small granules of 0.5-1.5 µm in diameter were immunoreactive.

Mantle tissues excised from the dorsal region of the pearl oysters were incubated in the marine molluscan balanced salt solution for 24h. As a control, digestive diverticula were incubated. The medium after incubation with the mantle tissues agglutinated equine erythrocytes, whereas the control medium did not. The hemagglutination activity of the medium was inhibited by both anti-lectin antiserum and galactose which is haptan sugar of the lectin. From these results, we suggest that the mantle produces hemolymph lectin in this animal.

PH 139

AUTOANTIBODIES TO DENATURED SELF ERYTHROCYTES IN HUMAN SERUM AND THE IMMUNE RESPONSE IN MOUSE. T.A. Nomaguchi, Y. Sakurai, Y. Yonezawa and H. Kondo. Dept. of Biol., Tokyo Metropol. Inst. of Gerontol., Tokyo.

Determination of antibodies in human and mouse sera to self erythrocytes denatured with 1% glutaraldehyde (DRBC) was performed. The antibody was determined as agglutination titer of 1% DRBC suspension in PBS to serially diluted serum in a microplate, using anti-IgM and anti-IgG rabbit IgGs.

The positive sera to DRBC in about 1,000 human samples were 94.6% for IgM antibody, 92.0% for IgG antibody in male, and 98.8%, 85.1% in female, respectively. In IgM antibody, female samples showed higher titer than the male, and the incidence at peak titer was 40.6% at 1:80 dilution of serum for female and 33.3% at 1:20 for male, but IgG antibody titer was lower in both sexes.

In the immune experiments used C57BL/6 female mice, IgG antibody was induced by 0.2 ml injection of 1% DRBC. The antigen is T-dependent, since the increasing antibody titers were same levels either DRBC injections with single or Freund's complete adjuvant. An anaphylactic response was also induced by 0.2 ml of 1% DRBC injection during caudal vein in the immunized mice.

This is important as a model for autoimmune system to the 'senescent-related cell antigen' *in vitro* and *in vivo*.

PH 140

RELATIONSHIPS BETWEEN INVASION OF ONCOSPHERES OF TAPEWORM INTO THE DEFINITIVE MOUSE INTESTINAL TISSUE AND PRODUCTION OF ANTI-ONCOSPHERES ANTIBODIES. J. Sasaki, K. Onitake and A. Ito. Dept. of Biol., Fac. of Sci., Yamagata Univ., Yamagata and Dept. of Parasitol., Gifu Univ. Sch. of Med., Gifu.

Antigenicity of oncospheres, cysticercoids and adults of the bile duct tapeworm, *Hymenolepis microstoma*, was analysed by immunoblotting with immune sera of BALB/c mice (i) during patent or prepatent infection with the lumen phase of the parasite and (ii) sensitized orally with live or dead eggs. Mice which had patent infection showed strong antibody responses to all three stage antigens, while mice given prepatent infections showed some antibody responses to cysticercoids and adult antigens only. Although the normal intermediate hosts of this parasite are arthropods, antibodies to some major oncosphere antigens were produced in mice by either oral inoculation of live eggs or ingestion of faeces contaminated with eggs. Antibody were not produced by oral administration of dead eggs. Microscopic observation indicated that oncospheres can invade into the intestinal tissue of mice within 15 min. after egg inoculation. Thus, it seems possible that antibody responses against oncosphere antigens are due to the invasion of oncospheres into the intestinal tissue of definitive host mice.

PH 141

SUPPRESSION OF GENETIC RESISTANCE TO BONE MARROW ALLOGRAFT BY RETICULOENDOTHELIAL SYSTEM (RES)-BLOCKADE CARBON PARTICLES.

S.KADOWAKI, K.J.MORI. Dept. of Biol., Fac. of Sci., Niigata Univ., Niigata.

Bone marrow allografts are rejected in most cases due to genetic resistance of host. There has been evidence that natural killer cells play a major role in genetic resistance to bone marrow transplantatoin. Macrophages are also involved resistance as shown by the findings that agents, which modulate macrophage function, such as silica and carrageenan, suppress genetic resistance to marrow grafts. But these agents might have affected the cells other than macrophage as well. In this study, we used carbon particles which are chemically inert and are phagocytized solely by phagocytic cells in RES, and showed that administration of carbon particles to recipient mice could suppress genetic resistance to allogeneic bone marrow transplantation.

PH 142

PRODUCTION OF NEGATIVE REGULATOR OF IL-3 BY BONE MARROW CELLS IN RESPONSE TO IL-3 STIMULI.

K.Sugimoto and K.J.Mori. Dept. of Biol., Fac. of Sci., Niigata Univ., Niigata.

Co-culture of IL-3 producing leukemic T-cell line, STIL-3, with normal bone marrow cells for 3 days resulted in a significant inhibition of IL-3 activity in the culture supernatant. The supernatant did not inhibit granulocyte-macrophage colony formation. Addition of normal bone marrow cell-conditioned medium had no inhibitory effect on IL-3 activity in the assay system with IL-3 dependent DA-1 cell proliferation. Fractionation of bone marrow cell populations revealed that the 'inhibitor' activity was produced by stem cell-enriched fraction. No inhibitory activity was found in the fraction of T-cells, granulocytes or adherent cells (fibroblasts and macrophages).

Stimulation of stem cell-enriched fraction with IL-3 also resulted in a production of IL-3 inhibitor. Heat-treatment of the supernatant of the culture resulted in a recovery of IL-3 activity.

Ultrafiltration of the supernatant with diallo membrane revealed that relatively large molecular weight (about Mr 100K) fraction strongly inhibited the growth of IL-3 dependent cell lines.

PH 143

LONG LASTING CLONAL DELETION OF T CELLS IN NEONATAL TOLERANCE.

M.Hosono¹, J.Gyotoku¹, S.Ideyama¹, Y.Katsural¹ and M.Kurozumi². ¹Dept. Immunol., and ²Clin. Lab., Chest Dis. Res. Inst., Kyoto Univ.

It is a well known phenomenon that fetal or neonatal administration of allogeneic or semiallogeneic hemopoietic stem cells easily induces immunological tolerance as adult to the corresponding antigenic determinants. Thus induced tolerance, as a model for self tolerance, has long been thought to be due to clonal deletion of immune competent cells, though suppressor cell generation may also be considerable (in the latter case, involved clones should be present but their function must be suppressed by regulatory cells). In this study, we induced neonatal tolerance in newborn BALB/c mice (<24hr after birth) to Mls-1^a (Murine lymphocyte stimulating)-antigenic determinants to which V β -T cell receptor (TCR)-bearing cells are preferentially reactive, and at various ages, frequency of the V β -TCR⁺ cells was investigated. Neonatal administration of Mls-1^a antigens resulted in that ~10% of V β -TCR⁺ cells in untolerized control mice was reduced to less than 1% in the tolerized mice. Suppressor cell generation in tolerance was not evident in the mixture cell experiments. Thus, strongly and directly indicated is that antigen specific deletion of the corresponding T cell clones is a mechanism of neonatal tolerance induction. Lack of the T cell clones in neonatally tolerized animals lasted longer than one year.

PH 144

MORPHOLOGICAL IDENTIFICATION OF 4 STRAINS FROM ACANTHAMOEBA KERATITIS IN JAPAN

H. Horikami and K. Ishii
Laboratory of Biology, Hosei University, Chiyoda-ku, Tokyo 102.

Since first *Acanthamoeba keratitis* was found in Japan (Ishihashi et al., 1988), 5 cases have, so far, recognized accumulatively. Four strains (Fuks, Jike, Tsuk, and Toks strain) isolated from the patients were tried to identify mainly on the basis of morphological features of 100 trophozoites in log phase and 100 cysts of a month old after encystment in each strain. These results were compared with those of *A. castellanii* (Balamuth strain, ATCC 30234) or *A. polyphaga* (Page 3a strain, ATCC 30871). Furthermore, their temperature sensitivities were tested by new convenient method due to size of yeast-free area (plaque) on non-nutrient agar plate coated with a lawn of yeast.

(1) Trophozoites in Fuks, Jike, Tsuk, and Toks strain had a mean length of 25.0, 27.5, 28.5, and 33.0 μ m respectively. And a length-to-breadth ratio (L/B) during active advancing movement in each strain were 2.2, 2.8, 2.7, and 2.7. The mean length of Balamuth and Page 3a strain were 25.8 and 28.2 μ m in each, their L/B 2.2 and 2.4 respectively.

(2) Oostoles covered with opercle were present at the junction of ectocysts and endocysts in all 4 strains. Cysts had a mean diameter of 15.0, 14.7, and 15.3 μ m in each of 4 strains. The mean ray number were 3.6, 5.6, 5.4, and 5.6 respectively. The mean diameter in Balamuth and Page 3a strain were 14.9 and 17.4 μ m, and their mean ray number 2.9 and 1.9 in each.

(3) Judging from the size of the plaque on the agar plate at every certain time during 6 days in 3 different temperatures (23°, 30°, and 37°C), the cells of Fuks showed the fastest proliferation at condition of 30°C, the second is at 23°C and very slow at 37°C. In Toks, the fastest is at 30°C, the second at 37°C, and the slowest at 23°C. Only Jike showed the fastest proliferation at 37°C, and the cell growth declined in proportion to fall of temperature. Tsuk could not grow in this experimental condition. Both Balamuth and Page 3a strain grew fast at 30°C, the second was at 23°C, but could not grow at 37°C.

(4) According to Page's criteria (1967, 1976), Fuks strain is probably *A. castellanii*, and Toks and Jike strain probably *A. polyphaga*. However, Tsuk strain may be a new species at point of large L/B and no proliferation on a lawn of yeast.

PH 145

ESTABLISHMENT AND CHARACTERIZATION OF A SARCOMA-FORMING CELL LINE FROM MURINE BONE MARROW.

K. Shirata¹, T. Suzuki², J. Fujita³ and K. J. Mori¹. ¹Dept. of Biol., Fac. of Sci., Univ. of Niigata, Niigata, ²Dept. of Pathol., Fukushima Med. College, Fukushima and ³Div. of Cancer Pathol., Biomed. Res. Center, Osaka Univ. Med. School, Osaka.

A sarcoma cell line, MS-K, was established from a long-term culture of mouse bone marrow stromal cells. When inoculated into syngeneic C3H/HeN1c mice, the cells formed large necrosis-free tumors, but there was no apparent changes in hematological features nor in general conditions of the tumor-bearing mice. The tumor had a morphology of fibrosarcoma, had adipose tissue and was rich in blood capillaries. Immunohistochemical studies revealed that the cells were negative for Factor VIII, Keratin, Desmin, IGF-I or III, and positive for Vimentin and S-100, indicating that the cells are of lipoblast origin. A significant amount of fat deposition was induced in the cytoplasm of the cells when MS-K cells were cultured in the presence of hydrocortisone and insulin. Antibody staining for oncogene showed that the cells were strongly positive for Ki-ras.

GE 1

KARYOTYPES AND NUCLEOLUS ORGANIZER REGIONS (NORS) IN STARFISH CHROMOSOMES. K. Saitome. Yokohama City Institute of Health, Yokohama.

Comparison of karyotypes in starfish chromosomes has scarcely been carried out in spite of several reports about chromosome numbers. When the air-drying method developed in sea urchin embryos was adapted to starfish with slight modification, good preparation showing definite centromere was obtained. Chromosomes were examined in *Asterina pectinifera* belonging to the order Forcipulatida and *Asterias amurensis* belonging to the order Spinulosida. The following results were obtained; 1) Chromosome numbers were 2n=44 in both species and their size ranged from about 1 to 4 μ m. 2) *A. pectinifera* was characterized by the existence of a pair of metacentrics which was extremely large compared with other metacentrics, while *A. amurensis* did not have one. 3) *A. amurensis* had more metacentrics and acrocentrics than *A. pectinifera*, whereas number of submetacentrics of *A. amurensis* was less than that of *A. pectinifera*. 4) In silver staining, *A. pectinifera* had 2-4 silver-stained NORs and *A. amurensis* possessed 5-6 ones. The definite NORs were observed on the short arm regions of the acrocentrics in both species.

GE 2

CHARACTERIZATION OF MEDAKA HIGHLY REPETITIVE SEQUENCE (OLR1).

K. Naruse, H. Mitani and A. Shima. Zool. Inst., Fac. of Sci., Univ. of Tokyo, Tokyo.

We isolated a DNA fragment (OL9Xba) containing repetitive sequence from Medaka genomic DNA library using OLR1 as a probe and sequenced OLR1 and OL9Xba to determine repetitive unit. The OLR1 contained 883 base-pairs and GC content was 32 percent, while the OL9Xba contained 417 base-pairs and GC content was 40 percent. The 130 bp fragment whose 90 percent of nucleotides was identical was found. Two tandem direct repeats of sequences were observed in this consensus sequence.

From the results of Southern blot analysis, DNA fragment containing the consensus sequence was found to be conserved in *O. latipes*, *O. curvirostris* and *O. luzonensis*. But intensity of hybridization signal using OL9Xba-190 (DNA fragment with 130 bp consensus sequence) as a probe was lower than that of the OLR1-700 (700 bp fragment with the consensus sequence from OLR-1). The OLR1-300 (300 bp fragment without the consensus sequence) showed very low hybridization signal. These results suggest that the DNA fragment containing the consensus sequence was kept in the repeated unit. A possibility that other parts of OLR1 were repeated in the Medaka genome can not be excluded.

GE 3

CHROMOSOME EVOLUTION OF POMACENTRID FISHES (PERCIFORMES) II

A. Takai¹ and Y. Ojima², ¹Osaka Shin-Ai Jogakuin Jr. College, Joto-ku, Osaka and ²The Japan Fish Bioscience Inst., Ashiya.

Karyotypes and distribution of nucleolus organizer regions (NORs) and C-banded heterochromatin of 26 pomacentrid fishes were studied. Chromosome numbers were 2n=48 in all species excepting *Chrysiptera cyanea* with 2n=42; arm numbers ranged from 48 to 92, suggesting the occurrences of karyotype differentiation by pericentric inversions. The karyotype of *Chrysiptera cyanea* has a feature formed by Robertsonian fusions. It was considered that more differentiated karyotypes consisted of more bi-armed chromosomes in general. NORs were located at terminal or interstitial regions of a pair of larger chromosomes, whose morphology was various among the species. The diversity of NOR distribution would have been brought about mainly by pericentric inversions. C-banded heterochromatin showed various distributional patterns. Distribution of a large amount of centromeric and interstitial C-banded heterochromatin was seen in some species. Changes of NOR and C-band distribution in addition to karyotypic changes would have played an important role in speciation. Pomacentridae is a very interesting fish group in relation to diversity of C-band and NOR distribution as well as of karyotypes.

GE4

CHROMOSOME BANDING ANALYSES IN TWO FORMOSAN AND ONE LAOTIAN SPECIES OF GIANT FLYING SQUIRRELS.

T. Oshida¹, H. Sato¹ and Y. Obara². ¹Dept. of Vet. Med., School of Vet. Med. and Anim. Sci., Kitasato Univ., Towada, and ²Dept. of Biol., Fac. of Sci., Hiroshima Univ., Hiroaki.

The giant flying squirrel (GFS) or the genus *Petaurista* is distributed only in India, its neighbouring countries, South East Asia, China and Japan. Few reports have been published concerning the chromosomes of GFS, and thus little has been known to date about the karyo-systematic relationship of this taxonomic group. In this study, we examined, by G-, C-, and NOR-banding techniques, bone marrow and lymphocyte chromosomes of two species of Formosan GFS (*P. petaurista*, red GFS; *P. alborufus*, red and white GFS) and one Laotian species (*Petaurista* sp.) with special attention to their karyological relationship. Their diploid numbers of chromosomes were 38 in all the three species. But, the Laotian GFS resembled *P. alborufus* more closely than *P. petaurista* in the chromosome banding patterns as well as in the chromosome constitution. The relative length of the X chromosomes of these GFS's examined occupied at least 7.22% of the total length of the haploid chromosome complement. So, their large-sized X chromosomes may be worthy of notice as a marked karyological character common to this genus.

GE5

VARIANTS OF RIBOSOMAL DNA REPEATING UNIT TYPES IN *APODEMUS SPECIOSUS*

H. Suzuki¹, K. Tsuchiya², M. Sakaizumi³, S. Wakana⁴, S. Sakurai¹, K. Moriaki⁵. ¹Inst. Med. Sci., The Jikei Univ. School of Med., Tokyo, ²Miyazaki Med. College, The Tokyo Metropol. Inst. Med. Sci., ³Central Inst. Exp. Animals, ⁴Natl. Inst. Genet., Nishima.

The main construction of ribosomal DNA (rDNA) is similar among the different populations of Japanese field mice (*Apodemus speciosus*) (Suzuki et al., 1988). However, we found two variants of rDNA repeating unit types (repetypes) in the individuals collected from Naganuma (Hokkaido pref.) and Nachi (Wakayama pref.). It seemed that each variant was generated from the standard repetype by mutation at the spacer region near the 3' end of the 28S rRNA gene with deletion of about 0.6 kb and 1.6 kb in length, respectively. The variant repetype of Naganuma was also observed in individuals from Bibai, suggesting wide distribution throughout Hokkaido. On the other hand, the variant of Nachi was not observed in other regions near Nachi, such as Taiji, Hongu, and Kumanogawa, suggesting restricted accumulation within small area.

GE6

THE POSITION OF SEX-DETERMINING GENE IN DIFFERENT POPULATIONS OF *RANA NIGROMACULATA* AND *RANA BREVIPODA*.

M. Nishioka and M. Sumida. Lab. for Amphibian Biol., Fac. of Sci., Hiroshima Univ., Hiroshima.

It has been elucidated that the male is heterogametic and the sex-determining gene is linked with the LDH-B and MPI loci on chromosome No. 4 in the Kure and Kumano populations of *R. nigromaculata* and the Konko population of *R. brevipoda*. In the present study, the position of sex-determining gene was examined in nine males belonging to the Hiroshima population of *R. nigromaculata* and eight males belonging to the Maibara population of *R. brevipoda*. The results showed that in 760(92.1%) of the 825 offspring obtained from five of the nine males of *R. nigromaculata*, the sex-determining gene was linked with the MPI and SORDH loci on chromosome No. 4, while in 337(54.7%) and 279(45.3%) of the 616 offspring obtained from the other four males, it was linked and not linked, respectively, with these loci. On the other hand, in 361(53.8%) and 310(46.2%) of the 671 offspring of the eight males belonging to the Maibara population of *R. brevipoda*, the sex-determining gene was linked and not linked, respectively, with the MPI and LDH-B loci on chromosome No. 4, in contrast to the Konko population of the same species. However, it was found that the sex-determining gene was linked with the ME-B locus on chromosome No. 3 in 274(97.9%) of the 280 offspring.

GE7

THE DIFFERENCES IN RECOMBINATION RATE BETWEEN MALES AND FEMALES IN CHROMOSOME NO. 4 OF THE *RANA NIGROMACULATA* GROUP.

M. Nishioka and M. Sumida. Lab. for Amphibian Biol., Fac. of Sci., Hiroshima Univ., Hiroshima.

In the *Rana nigromaculata* group, six enzyme loci, the LDH-B, Pep-B, HK, ENO, MPI and SORDH, are arranged on chromosome No. 4 (Nishioka, Ohtani and Sumida, 1980, 1987). The present study was to confirm the existence of differences between males and females in recombination rate at these loci. The enzymes were analyzed by starch-gel electrophoresis in the 5231 offspring derived from 16 males and seven females of *R. nigromaculata* and *R. brevipoda* which were heterozygous at more than two loci, and the recombination rates between these loci were calculated. The results showed that in *R. brevipoda*, 226(48.6%) of the 465 offspring of the six female parents which were heterozygous at the LDH-B and MPI loci were recombinants. On the other hand, only two (0.1%) were recombinants in the 1591 offspring of the eight male parents which were heterozygous at the two loci. In *R. nigromaculata*, 265(27.3%) of the 972 offspring of a female parent which was heterozygous at four loci, the HK, MPI, Pep-B and SORDH, were recombinants. In the 2203 offspring of the eight male parents which were heterozygous at five loci, the ENO, HK, MPI, Pep-B and SORDH, only two(0.1%) were recombinants. Thus, it was found that the males in both species were extremely small in recombination rate in contrast to females.

GE 8

INVESTIGATION OF DOSAGE COMPENSATION IN THE JAPANESE QUAIL BY COMPARING TWO SEX PHENOTYPES OF SEX CHROMOSOMAL AND AUTOSOMAL GENES

A. Nakamura¹, K. Nishimura² and T. Kaneko¹,
¹Univ. of Shizuoka, Hamamatsu Coll. Hamamatsu.
²Dept. of Biol., Hamamatsu Univ. School of Med., Hamamatsu.

Dosage compensation was investigated by comparing between male and female phenotype in sex chromosomal and autosomal gene of the Japanese quail (*Coturnix coturnix japonica*). The materials used were two strains of imperfect albino, brown quails (sex chromosomal gene), two strains of dilution, white quails (autosomal gene) and wild strain. Color intensity of plumage was compared in the two sexes by quantity measurements. Measurements were taken using a Shimadzu Dual-wavelength flying spot scanner CS-9000 at 370nm-600nm.

The results showed no significant difference between the sexes with respect to male and female phenotype of either autosomal genes or sex chromosomal genes. There was no significant difference between male and female in the manifestation of the albino gene pleiotropism cataract. These results suggest the existence of dosage compensation in Aves.

GE 9

OBSERVATION ON LAMPBRUSH CHROMOSOMES UNDER A SCANNING ELECTRON MICROSCOPE IN *RANA NIGROMACULATA* AND *RANA LESSONAE*.

H. Ohtani. Lab. for Amphibian Biology, Fac. of Sci., Hiroshima Univ., Hiroshima.

The lampbrush chromosomes of *Rana nigromaculata* from Japan and *R. lessonae* from Italy were observed under a scanning electron microscope. In these species, the main axis of each lampbrush chromosome consisted of two fibers, each of which was 100-250 nm in diameter and had numerous lateral loops projecting directly from the fiber. There was no structure called chromomere at the insertion part of each lateral loop. The two fibers of the axis joined with each other at many places, especially in the short segment which was covered with longer lateral loops. The centromere was not observable in the short segment of each lampbrush chromosome of *R. nigromaculata*, while it was evidently observed in each of the lampbrush chromosomes of *R. lessonae*, even though there was no short segment. The centromere of this species was about 4 μ in length and has a perforated node in the middle. The matrices of the lateral loops and the four kinds of landmarks in the two species were constructed of particles which were 70-200 nm in diameter. The characteristic figure of each kind of landmark seemed to be determined by difference in the amount of particles. There was no difference in the figures of landmarks between the two species.

GE 10

COMPARISON OF THE RADIATION-INDUCED MUTATION SPECTRA AMONG THREE LOCI OF THE MEDAKA *ORYZIAS LATIPES*.

A. Shimada and A. Shima. Zool. Inst., Fac. of Sci., Univ. of Tokyo, Tokyo.

During the course of the study on radiation-induced germ cell mutations using the multiple recessive tester Medaka homozygous at the *b*, *lf*, and *gu* loci, we found the difference in mutation spectra among 3 loci. Adult males of the wild type were exposed to 137Cs gamma-rays and mated with females of the tester (*b/b lf/lf gu/gu*). F₁ embryos thus obtained during 1-9 days after irradiation, which correspond to the post-spermatogonial stages of the male gametes at the time of exposure, were scored for total mutation frequency (TMF) during embryonic development as well as viable mutation frequency (VMF) after hatching. The interim results up to August 10, 1989 are presented: (1) TMF at the *b*, *lf*, and *gu* loci were 464E(-5) (=173/37,283), 198E(-5) (=74/37,283), and 154E(-5) (=154/35,848), respectively. (2) VMF at the *b*, *lf*, and *gu* loci were 17.2E(-5) (= 5/29,135), 37.8E(-5) (=11/29,135), and 78.9 E(-5) (=23/29,135). (3) Ratio of the number of TM to that of VM was extremely lower at the *b* locus (0.029) than those at the *lf* (0.15) and *gu* (0.15) loci, indicating that mutants at the *b* locus were prone to die during development. (4) Survival rate after hatching of the viable mutants at the *lf* locus was lower than those at the other two.

GE 11

ON THE POSSIBLE MECHANISM OF THE ADRIAMYCIN-INDUCED ROBERTSONIAN FUSION REARRANGEMENT.

Y. Obara and Y. Kidachi. Dept. of Biol., Fac. of Sci., Hiroshima Univ., Hiroshima.

It is known that the antitumor antibiotic, adriamycin (ADM) can induce with high frequency the Robertsonian fusion rearrangement (Rb-fu) for mouse bone marrow chromosomes (Dulout 1984). In this study, we examined, paying attention to the Rb-fu, the ADR-sensitivity of the bone marrow chromosomes in the large and small Japanese field mice (*Apodemus speciosus* and *A. argenteus*) and the BALB/c mouse. *A. argenteus* was as highly sensitive to the ADR treatment (24 hrs. at a final concentration of 20 mg/kg) as the BALB/c mouse, and its Rb-fu frequency amounted to 20-25/100 metaphases. Whereas, the Rb-fu frequency in *A. speciosus* was approximately one-tenth of that in *A. argenteus*. It was suggested from the fluorescence analysis by the DNA-specific fluorochromes (chromomycin A3 and quinacrine mustard) that the marked difference in the ADR-sensitivity between these two *Apodemus* species may be attributed, at least in part, to the qualitative and quantitative discrepancy of their centromeric C-heterochromatin.

GE 12

RADIOSENSITIVITY OF HUMAN SPERM CHROMOSOMES: COMPARISON BETWEEN X-, γ - AND β -RAYS.

Y. Kamiguchi, H. Tateno and K. Mikamo, Dept. of Biolo. Sci., Asahikawa Med. Col., Asahikawa.

We studied the effects of *in vitro* exposure of ^{137}Cs γ -rays (0.13-1.11 Gy) and tritium β -rays (0.25-1.93 Gy) on human sperm chromosomes, using interspecific *in vitro* fertilization system between human spermatozoa and zona-free hamster oocytes. Total number of 4428 spermatozoa were karyotyped in the former experiment and 2955 in the latter.

The incidence of spermatozoa with radiation-induced structural chromosome aberrations increased linearly with increase of dosage, reaching 50.6% at 1.11 Gy of γ -rays and 72.8% at 1.93 Gy of β -rays, respectively. The incidence of breakage-type aberrations was about 9 times higher than that of exchange-type aberrations. Chromosome-type aberrations occurred far more frequently than chromatid-type aberrations. All of these types of aberrations showed linear dose-dependent increases.

Comparison of these results with our previous data on X-irradiation revealed that human sperm chromosomes were highly vulnerable to X-, γ - and β -rays and that their relative biological effectiveness (RBE) values were similar each other, 0.90 : 1.00 : 0.94.

GE 13

DEVELOPMENT OF THE HYBRIDS BETWEEN DIADEMA SETOSUM AND DIADEMA SAVIGNYI IN SEA URCHINS.

H. Asakura and T. Uehara. Dept. of Biol., Univ. of the Ryukyus, Nishihara, Okinawa.

Two urchins that often co-occur on Okinawa are Diadema setosum and D. savignyi. These species have different seasonal spawning time on Okinawa, with the former spawning in summer and the latter in winter, but there is at least some overlap. Two urchins readily form hybrids in laboratory. Cross-fertilized eggs between D. savignyi (female) and D. setosum (male) developed into young urchins. We could rear only two adults with gametes. Two individuals had no an orange ring around its anus (characteristic of D. savignyi) and had five isolated spots in the apical system (characteristic of D. setosum) and two parallel blue dotted lines and a spot in interambulacral area (partly characteristics of both species). Based on external features of the sperm and color patterns of young or adult urchins, these "experimental" hybrids look like intermediate individuals (natural hybrids?) in the fields. Finally, "experimental" hybrids will be a great help in attacking the problem of natural hybrids between closely related species in the fields.

GE 14

THE MELANOTIC TUMOUR IN ADULT FLIES OF DROSOPHILA MELANOGASTER: AGING EFFECT.

K. Kosuda. Biol. Lab., Faculty of Science, Josai University, Sakado.

In the course of study for aging effect on the mating activity, a new type of the melanotic tumour formation was found in one strain of Drosophila melanogaster. The tumour forming character is heritable. This mutant strain, C-104, is highly inbred and is derived from a natural population in Budapest, Hungary in 1986. The tumours can be detected in the adult stage exclusively in the vicinity of female spermathecae. They could not be found in male flies. They can externally be seen as dense black bodies with unaided eyes, when they grow up well. It was clearly shown that the incidence of tumour development increases as female flies get old and newly emerged flies have no tumours at all. The incidence of tumour development was also shown to be much higher in a high rearing temperature at 29°C. These results suggest that environmental factors accompanied by aging seem to be involved in the formation of melanotic tumours, as well as genetic factors.

GE 15

A MORPHOLOGICAL STUDY ON THE FERTILITY OF INTERSPECIFIC HYBRIDS BETWEEN ORYZIAS LATIPES AND O. CURVINOTUS.

S. Hamaguchi¹ and M. Sakaizumi², ¹Dept. Biol., Coll. Gen. Educ., Niigata Univ., Niigata, ²The Tokyo Metropol. Inst. Med. Sci. Tokyo.

Fertility of interspecific hybrids between O. latipes and O. curvinotus was examined. F1 males could induce normal females to spawn eggs, but could not fertilize eggs. While, when F1 females were mated with normal males, they could lay eggs which accepted sperm to develop normally. Histological observations revealed that most male germ cells could pass through almost entire processes of spermatogenesis, but they deviated from normal course during spermiogenesis. Chromatin condensation in spermatids occurred, but the sperm head of F1 hybrids were of an irregular shape. Their flagellum was also abnormal. More than two flagella were often observed to project from a single cell. Abnormal spermatozoa were phagocytized by Sertoli cells. Most female germ cells in F1 hybrids were degenerated during early stages of meiotic prophase. Only a few of them could enter into diplotene stage, and passed through stages of folliculogenesis and vitellogenesis, developing into fertile ova. These results indicate that the mechanism of impaired gametogenesis in interspecific hybrid was different between males and females.

GE 16

PRODUCTION OF TRIPLOID MEDAKA BY INTERSPECIFIC HYBRIDIZATION BETWEEN CLOSELY RELATED SPECIES OF GENUS *ORYZIAS*
M. Sakaizumi 1 and S. Hamaguchi 2, 1 Dept. of Exp. Anim. Sci., The Tokyo Metropol. Inst. of Med. Sci., Tokyo and 2 Dept. of Biol., Coll. of Gen. Educ., Niigata Univ., Niigata.

We produced interspecific hybrids between *O. curvinotus* and each of four subspecies of *O. latipes* by natural spawning. Males were sterile in every cross, but females layed a few eggs every morning when they were paired with normal *O. latipes* males. About two thirds of the eggs developed normally and adult males and females were obtained.

Allozymic analyses revealed that all backcross progeny were heterozygous at every locus examined. Allozyme patterns and the presence of male progeny suggested that these fish were digenic triploid with one *O. curvinotus* genome and two *O. latipes* genomes. Flowcytometry analysis of DNA content verified this inference.

These results indicated that the eggs produced by hybrid females matured without meiosis and were fertilized with normal *O. latipes* sperm. Allozyme patterns of trigonemic triploids revealed that each allele was expressed approximately evenly in triploid individuals.

GE 17

COMPARISON OF THERMOSENSITIVITY OF TWO INBRED STRAINS OF THE MEDAKA *ORYZIAS* LATIPES.

Y. Kubota and A. Shima. Zool. Inst., Fac. of Sci., Univ. of Tokyo, Tokyo.

By the use of inbred strains (H04C and HB32C) of the Medaka, we are examining whether there is any genetic factor(s) responsible for thermosensitivity. The sensitivity of embryos (st. 20-21) is expressed by the surviving rate of embryos at the next day after heat treatment. At every temperature examined (42, 43 and 44 °C), the HB32C strain was more sensitive than the H04C strain. Interstrain hybrids (H04C ♀ × HB32C ♂) had almost the same sensitivity as that of the H04C strain, while the sensitivity of the reciprocal interstrain hybrids (HB32C ♀ × H04C ♂) was intermediate between the H04C strain and the HB32C strain. Furthermore, the sensitivity of backcross offspring was examined. Interstrain hybrids (HB32C ♀ × H04C ♂) were used as F₁ in the following backcrosses. The backcross offspring (HB32C ♀ × F₁ ♂) showed the same sensitivity as the HB32C strain, and that of backcross progeny (H04C ♀ × F₁ ♂) was intermediate between the H04C strain and the HB32C strain. Other backcross offspring, (F₁ ♀ × HB32C ♂) and (F₁ ♀ × H04C ♂), had almost the same sensitivity as that of the H04C strain. These results suggest that thermosensitivity of the Medaka embryos is under the control of some kinds of maternal effect(s) and also that the sensitivity can be lowered by some factor(s) inherited in the H04C strain and/or increased by those in the HB32C strain.

GE 18

Geographic survey of mitochondrial DNA polymorphism in Korean wild population of the Medaka *Orizias latipes*.

1) T. Yamagishi, T. Nakazawa, 2) M. Sakaizumi, H. Yonekawa, and 3) Sang-Rin Jeon. 1) Dep. Biol., Fac. Sci., Toho Univ., Funabashi, 2) The Tokyo Metropol. Inst. Med. Sci., Tokyo, 3) Dep. Biol., Coll. of Nat. Sci., Sang Myung Women's Univ., Seoul, Korea.

Our previous report showed that the Korean wild population of the freshwater fish *Orizias latipes* is divided into two distinct groups by allozymic variation. In the present study we compared mitochondrial DNA (mtDNA) cleavage patterns after digestion with endonucleases. The results showed that the Korean Medaka have two major haplotypes (A, B). The haplotype A, which was found only in the western coast, consisted of three minor haplotypes (A1, A2, A3). The haplotype B distributed in the eastern and the southern coast. The geographic distribution of the two major haplotypes was similar to that of the two groups distinguished by allozymic variation. The nucleotide sequence divergence between the haplotypes A and B was 5.5% and the divergence time was estimated to be two million years. The two groups of Korean wild population have a complicated geographic distribution in the western coast. But we could not find any hybrid zone in this region. These results suggested that the two groups had been isolated for a long period, and they met again recently in the western coast.

GE 19

BODY COLOR MUTANTS IN MOSQUITO FISH, *GAMBUSIA AFFINIS AFFINIS* AND CRUCIAN CARP, *CARASSIUS AURATUS LANGDORFI*.

H. Tomita. Lab. of Freshwater Fish Stocks, Fac. of Sci., Nagoya Univ., Nagoya.

Two body color mutants were found in mosquito fish, *Gambusia affinis affinis*. The cm mutant has small concentrated melanophores and its body color is blond. The va mutant shows black variegation with dilute and black melanophores, and has dilute iridocytes. These mutants are recessive, autosomal and independent each other. The double recessive (cm va) fish shows light blond in a body color.

In gold fish, *Carassius auratus*, the n mutant is transparent scales which lacks iridocytes in net pattern (Matsui). This was lost. The g mutant which is alike to the n mutant was found (Kajishima). In crucian carp, *Carassius auratus langdorfi*, the ne mutant was detected (Yamamoto). The g and the ne genes are the same ones. The new transparent scale mutant (ne³) was found in *Carassius auratus langdorfi*. This type has transparent scales which is not net pattern. The ne³ is dominant to the ne. The ne alleles are multiple (+> ne>ne). Some of this fish reproduce themselves gynogenetically. The ne like and ne-like types were detected in gynogenetic strains.

GE 20

Geographic difference of molecular heterogeneity due to restriction sites of mitochondrial DNA in *Apodemus speciosus*

S. Nakano¹, H. Suzuki², M. Sakaizumi³, K. Tsuchiya⁴, K. Moriwaki⁵

¹Central Inst. Exp. Animals, ²The Jikei Univ. School of Med.,

³The Tokyo Metropol. Inst. Med. Sci., ⁴Miyazaki Med. College,

⁵Natl. Inst. Genet.

Conventional survey of restriction-fragment polymorphism in mitochondrial DNA of Japanese field mice *Apodemus speciosus* showed that the levels of heterogeneity ($h = n(1 - \sum f_i^2)/(n-1)$, Nei & Tajima 1981) was different among any populations. The observed probabilities that all individuals in Haruna, Nachi and Tanegashima population differed detectably in mtDNA genotype were 0.71, 0.93 and 0.83, respectively. On the other hand the value in Naganuma was 0.14.

Theses showed Haruna, Nachi and Tanegashima population had high level of mtDNA variability, Naganuma population has low level and we found the mtDNA type of Naganuma population was one of the type of Honshu island (example for Haruna population). It was concluded that Hokkaido population of Japanese field mice had gone through bottlenecks during migrating.

GE 21

ISOLATION AND CHARACTERIZATION OF VIRUS-LIKE PARTICLES FROM *Amoeba proteus* STRAIN F.

K. Yazaki¹, K. Ishii² and Y. Tsukii². ¹Tokyo Metropolitan Institute of Medical Science, Bunkyo-ku, Tokyo 113, ²Laboratory of Biology, Hosei University, Chiyoda-ku, Tokyo 102.

An agarose gel electrophoresis of nucleic acid extracted from cells of *Amoeba proteus* strain F presented a distinctive and unique band which was found only in cells of the strain of the Amoeba. Nucleic acid extracted from the band was double-stranded (ds) RNA. (Tsukii & Ishii, Jpn. J. Protozool. 20, 20, 1987). Virus-like particle (VLP) was detected and isolated from the cells. This is the first isolation of virus or VLP from Amoeba cells, and termed ApF-VLP. ApF-VLP is a spherical and about 60nm in diameter, and has no peplomer. The genome is linear dsRNA of about 8.5-9 kbp. From the facts that both dsRNA extracted from the cell and VLP has the same molecular size and linear feature, those dsRNAs are likely to be the same species.

GE 22

ISOLATION OF CLONED NUCLEOLAR VARIANTS FROM XENOPUS CELL LINE

K. Sekiya. Dep. of Biol., Fac. of Sci. Niigata Univ., Niigata

A6 cells, derived from kidneys of an adult male of *Xenopus laevis*, were cultured by K. Hafferty in 1965. The major mode of chromosome number at the 17th subculture was 45, compared with the diploid number of 36. The chromosome number in this cell line changed in the early passage, but still now after 24 years one of differential phenotype, which is characteristic of the organ, has been maintained. When these cells become confluent, they form lots of "domes". Many of cells had 39, 40, or 41 of chromosome number, but unusual chromosomes in number and shape could be seen among normal ones. As we could observe cells with three nucleoli per nucleus in interphase, we used them as an indicator, carried out cloning and could obtain comparatively stable clone. The number of nucleolus corresponds with the maximum number of nucleolar organizer region (NOR) in chromosome, but practically nucleoli fuse mutually and decrease in number. When cloned cells are obtained, the problem of nucleolar number can be excepted as long as the number of NOR does not change. Cloned nucleolar variants are useful in relation to gene expression of rRNA gene.

GE 23

EXPRESSION OF TYROSINASE GENE IN ALBINO MELANOCYTES IN MICE.

S. Tanaka, H. Yamamoto, S. Takeuchi and T. Takeuchi. Biological Institute, Tohoku University, Sendai.

We cloned mouse tyrosinase cDNAs by using anti-tyrosinase antibody and oligonucleotide probe which corresponded to amino acid sequence of the mouse tyrosinase. In order to elucidate regulatory mechanism of the tyrosinase gene, the tyrosinase cDNAs were fused with the authentic genomic 5' putative promoter region and was transfected to cultured albino melanocytes. One of the fused minigenes, the 5' genomic regulatory sequence and Tyrs-J cDNA (mg-Tyrs-J), was shown to produce melanin pigments in the cultured albino melanocytes.

We also introduced the tyrosinase minigene into fertilized eggs of albino mice. Of the 25 animals which developed from the injected eggs, four mice exhibited pigmented coat and eyes. These results indicate that this minigene encodes active tyrosinase protein and that the 5' region contains the sequences controlling the tissue-specific expression.

GE 24

CARRIER MICE OF MUTANT GENES FOR EXENCEPHALY IN THE OFFSPRING OF MALE TREATED WITH EMS.
T. Shimada. Laboratory of biology and Environmental Science, Nagoya College, Toyokake.

Ten, 3 - 4 month-old male mice were received a single i.p. injection of ethyl methanesulfonate (EMS) at 150 mg/kg. Males were mated from day 6 to day 9 after injection with 3 - 4 month-old untreated females to produce F1 progeny for detecting mutations. F1 males were placed at 2 months or older of age, with untreated females. Mating was detected by the presence of a vaginal plug, the females were dissected when 14 or 18 days pregnant, and the fetuses were weighed and scored for exencephalic fetuses. In addition, the data were also collected simultaneously with the study on transmission to F2 generations, and were used to compare effects in the first and second generations.

One among 62 F1 males conceived by 14 mothers proved to be clearly carrier of genes for exencephaly. Three among 20 F2 males from F1-carrier also proved to be carriers of genes for exencephaly. The incidence of exencephalic fetuses was 5.5% (7/127) and 3.7% (8/216) in the F1-carrier and F2-carriers mated with untreated females, respectively. These findings suggest that carrier mice seen in the first and second generations were of genetic origin and could be transmitted to later generations.

BI 1

THE USE OF ACRYLAMIDE GEL BAND AS IMMUNO-ABSORBENT.

M. Kuroda and T. Aizawa. Dept. of Biol., Fac. of Sci. Univ. of Shimane, Matsue

We used gel-bands from SDS-PAGE as an immunoabsorbent for preparing monospecific antibody from anti-sera. Bifunctional reagents are used to crosslink amino group of polyacrylamide to the protein trapped in the gel. Of the 5 crosslinkers tested, EDC, suberimide and glutaraldehyde were found to immobilize protein to the gel-matrix. Side chain modification experiments and kinetics of the crosslinking suggested that the crosslinking reaction took place not between ligands themselves but between acrylamide and the protein. In the present meeting, we showed two examples of the new affinity method by which we had successfully purified specific IgG. Using tropomyosin-immobilized gel-affinity column, specific anti-TM antibody was separated from anti-TM-serum which had been contaminated with unidentified anti-180K protein. We tried another quite heterogeneous anti-serum which was produced by immunizing a rabbit with Z-line containing structure of myofibrils. Immunoblotting experiment showed the antiserum (anti-Z antiserum) contained more than 10 antibodies to muscle structural proteins. Even from this antiserum, only anti-TM was eluted from the gel-affinity column with magnesium chloride. Specific antibody against alpha-actinin was also purified from by the similar procedure.

BI 2

LOCALIZATION OF COFILIN IN CULTURED CHICKEN SKELETAL MUSCLE CELLS.

H. Abe and T. Obinata. Dept. of Biol., Fac. of Sci., Chiba Univ., Chiba 260.

We previously isolated and characterized an actin binding protein of 20 kDa from embryonic chicken skeletal muscle. Since this protein is similar to cofilin, with regards to function, size and antigenicity, we call it muscle-cofilin. In this study, we prepared a monoclonal antibody specific for this protein (MAB-22), and examined its localization in cultured skeletal muscle cells by immunocytochemical methods.

Muscle-cofilin was present diffusely in the cytoplasm, but concentrated in the ruffling membranes and microspikes of growing myotubes. In the myoblasts which attached with each other to fuse, the fluorescence was remarkable at the regions of cell-cell adhesion. The staining by MAB-22 appeared sometimes along the stress fibers and myofibrils. We detected actin-rods which contain cofilin in myotubes by using MAB-22 and anti-actin antibody. It is known that actin-rods which contain cofilin are generated by dimethylsulfoxide (DMSO)-treatment or heat shock in nuclei of non-muscle cells. In the case of myoblasts or myotubes, actin-rods were formed not only in nuclei but also in microspikes by treating with 10% DMSO. However, heat-treatment produced vesicles, but not rods, which were positively stained with both MAB-22 and anti-actin antibody in myotubes.

BI 3

IMMUNOCYTOCHEMICAL AND 2D-PAGE ANALYSES OF C-PROTEIN ISOFORMS IN DEVELOPING AND DEGENERATING MAMMALIAN SKELETAL MUSCLES.
T. Kojima, K. Yabusaki and T. Obinata. Dept. of Biol., Chiba Univ., Chiba 260.

C-Protein is seen as a reliable marker for development and degeneration of avian skeletal muscle, since this protein changes markedly in each occasion. However, little is known as to whether this protein also changes in mammalian skeletal muscle. In this study, we prepared a monoclonal antibody (McAb) (RX-75) to rabbit slow C-protein. Using this McAb together with the other (FC-18) which recognizes both cardiac and fast C-proteins, we examined the type of C-protein in developing, denervated and dystrophic mammalian skeletal muscles.

During the development of fast rectus femoris muscle of mouse, isoform switches of C-protein was observed: at neonatal ages, slow and fast C-proteins co-existed, but the slow isoform decreased as muscle develops. By immunocytochemical methods, we observed that myofibers of small size which lack fast C-protein appeared in denervated fast EDL muscle of rabbit, while the all myofibers contained slow C-protein. In contrast, C-protein in slow soleus muscle was unaffected by denervation. 2D-PAGE analyses confirmed these results. Decrease in fast C-protein was also observed in the dystrophic EDL muscle of mice of dy strain.

BI 4

ANALYSIS OF EMBRYONIC GIZZARD MYOSIN PHOSPHORYLATED WITH PROTEIN KINASE C BY NATIVE PYROPHOSPHATE GEL ELECTROPHORESIS. H. Takano-Ohmuro¹, K. Kohama², K. Oishi¹ and T. Kaminuma¹. ¹The Tokyo Metro. Inst. Med. Sci., Tokyo, ²Dept. Pharmacol. Gunma Univ. Sch. Med., Gunma, ³Dept. Mol. Pharmacol. Meiji College of Pharmacy, Tokyo

Native pyrophosphate gel electrophoresis (PPi PAGE) can separate adult gizzard myosin (Ad.GM) phosphorylated at its regulatory light chain (RLC) with myosin light chain kinase (MLCK) which is an active myosin, from that with protein kinase C (PKC) which is an inactive myosin; the former migrates faster than the latter (Takano-Ohmuro, H. & Kohama, K., 1988 & 1987). Phosphorylation of RLC by PKC activates actomyosin ATPase activity of 12-day-old (12d.) embryonic gizzard myosin (E.GM) but it does not activate that of Ad.GM (de Laneroll, P., et al., 1988).

Embryonic GM contains a unique alkali light chain (L₂₃) but not Ad.GM (Takano-Ohmuro, et al., 1983 & 1985). To investigate whether L₂₃ is involved in the activation of the E.GM by PKC, we analyzed E.GMs of 12d. and 18d. embryo phosphorylated with PKC by PPi PAGE. The mobility of the 12d E.GM increased but that of the 18d E.GM did not. This result strongly suggests that L₂₃ does not play a key role in the activation by PKC in 12d. E.GM. The activation may be possibly caused by presence of new RLC which is expressed in 13d E.GM not in 18d. EGM or Ad.GM (Inoue et al., 1989).

BI 5

ISOLATION OF DYSTROPHIN IN DENATURED FORM FROM RABBIT SKELETAL MUSCLE MYOFIBRILS. T. Murayama¹, S. Kimura¹, K. Maruyama¹ and T. Shimizu². ¹Dept. of Biol., Fac. of Sci., Chiba Univ., Chiba and ²Dept. of Neurol., Fac. of Med., Univ. of Tokyo, Tokyo.

Dystrophin is a product of the muscular dystrophy gene (0.002% of total proteins of normal muscle). The molecular mass was estimated to be 427 kDa from cDNA (Koenig et al., 1988). It is located in sarcolemma and partially purified from rabbit muscle membranes (Campbell and Kahn, 1989).

We have isolated denatured dystrophin from rabbit skeletal myofibrils using a monoclonal antibody against a peptide predicted from position 1526 to 1675 on the human cDNA (AIC).

Myosin-removed myofibrils were extracted with 0.1% Triton X-100 and the extract was fractionated by a hydroxylapatite chromatography. The dystrophin fractions were adsorbed onto a DEAE Toyopearl 650 M column, and dystrophin was selectively eluted with 6 M urea. Pure dystrophin was finally isolated by a gel filtration in the presence of SDS (Asahipak GS-710). The amino acid composition was very close to that deduced from cDNA. The isolated dystrophin showed a value of 440 kDa for molecular mass in the SDS gel electrophoresis.

BI 6

I-PROTEIN BINDS TO LMM.

K. Ohashi and K. Kitano. Dept. of Biol., Fac. of Sci., Chiba Univ., Chiba.

I-protein, which is localized at the A-I junctions of sarcomere, binds to myosin filaments and forms bundles or cage-like aggregates in low ionic strength solutions.

Myosin or LMM was blotted on a nitrocellulose paper sheet and reacted with I-protein in a physiological salt solution. Bound I-protein to myosin was detected with anti-I-protein antibody. I-protein was shown to bind to myosin molecules in the physiological condition, although the affinity was not so strong as in low ionic strength solutions. The mixture of LMM and I-protein dissolved in 0.6 M KCl and 20 mM potassium phosphate buffer (pH 6.5) was diluted with 20 mM potassium phosphate buffer (pH 6.5) to the final KCl concentration of 50 mM. The protein mixture was centrifuged and electrophoresed. I-protein was coprecipitated with LMM and the binding molar ratio was 1:10. LMM at a concentration of 0.15 mg/ml with or without I-protein at a concentration of 0.08 mg/ml was dialyzed against 50 mM KCl buffered with 10 mM potassium phosphate buffer (pH 6.5). Without I-protein, spindle shaped paracrystals of LMM was formed but the axial periodicity was not observed. On the other hand, with I-protein, distinctive axial periodicities of 42 nm and 85 nm was observed on the LMM paracrystals. I-protein seems to bind to the one end of the LMM molecules, because LMM molecule is about 90 nm in length.

BI 7

TO WHICH END OF AN ACTIN FILAMENT DOES β -ACTININ BIND ?

H. Yamamoto, M. Ito and K. Maruyama. Dept. of Biol., Fac. of Sci., Chiba Univ., Chiba.

β -Actinin is one of the first discovered actin regulatory proteins together with α -actinin. In 1977 we reported that it caps the pointed end of an actin filament. This was recently confirmed by Funatsu and Ishiwata (1988). However, Casella and co-workers described that Cap Z caps the barbed end of an actin filament (1986). We have shown that β -actinin and Cap Z are indistinguishable by 2 D electrophoresis and peptide mapping (1987).

We have reinvestigated this problem using highly purified and stable β -actinin preparations. Increase in critical concentration in Mg-K medium, inhibition of elongation of seeds comparable with the action of cytochalasin D, and electron microscopic observations on the growth of arrowheads clearly demonstrated that β -actinin is a barbed-end capping protein. Furthermore, immunofluorescence revealed that β -actinin is located in the Z lines of chicken breast muscle myofibrils.

Hence it is concluded that β -actinin is identical with Cap Z. As for the reason why the pointed end capping was observed in the previous studies is now under investigation.

BI 8

CHARACTERIZATION OF α -CONNECTIN, THE MOTHER MOLECULE OF ELASTIC FILAMENTOUS PROTEIN OF RABBIT SKELETAL MUSCLE.
T. Matsuura, S. Kimura, T. Murayama, S. Ohtsuka, M. Arai and K. Maruyama. Dept. of Biol., Fac. of Sci., Chiba Univ., Chiba.

Connectin is a long filamentous protein linking myosin filament to Z line as an elastic spring in a sarcomere. Quite recently, we have isolated α -connectin from rabbit back muscle (Kimura and Maruyama, '89).

In this study, properties of α -connectin were investigated. The molecular mass was the same as that in whole muscle. The amino acid composition was similar to β -connectin. The rotary shadowed image showed a long filament. The mother molecule (~3000 kDa) was easily split into β -connectin (~2000 kDa) by V8 protease action.

Circular dichroism spectra showed that α -connectin consists of 60% β -sheet and 30% β -turn structures similarly to β -connectin. These secondary structures were not changed by 4 M urea that is used for separation of α - and β -connectins during preparation procedures. Addition of 6 M urea resulted in small changes in CD spectra but the structures were completely restored to the initial state after dialysis to remove urea. On the other hand, a marked change in the secondary structure by 0.1% SDS was partly recovered after extensive dialysis to remove SDS.

BI 9

FRAGMENTATION OF β -CONNECTIN BY SONICATION.
Y. Nakauchi, T. Murayama and K. Maruyama. Dept. of Biol., Fac. of Sci., Chiba Univ., Chiba.

Connectin is a very long, elastic filamentous protein linking myosin filament to Z line in a sarcomere of vertebrate skeletal muscle myofibrils. β -Connectin is a proteolytic product of the mother molecule (α -connectin) but its chain weight is as large as 2 million.

It is well known that an actin filament is fragmented by external force and a big molecule of DNA is also cut into smaller fragments by shearing force and by sonic vibration. In view of very long filamentous structure, we examined fragmentation of β -connectin by shearing force by an SDS gel electrophoresis. Application of a velocity gradient of 1000^{-5} for 5 min in a flow birefringence apparatus did not result in any changes in the size of β -connectin. However, sonication (Tomy Model UR 200P; setting 1, 5 to 30 sec) resulted in breakdown of 2000 kDa β -connectin into various sizes of peptides larger than 400 kDa. The splitting of β -connectin in the presence of 4 M urea, 6 M guanidine-HCl or 0.1% SDS was to a much greater extent than in salt solution. Peptides of smaller than 400 kDa were produced.

BI 10

ARTHROPOD CONNECTIN (1200 kDa).
D. H. Hu, T. Murayama, and K. Maruyama. Dept. of Biol., Fac. of Sci., Chiba Univ., Chiba

It has been established that connectin, an elastic filamentous protein of striated muscle of all the vertebrates is a huge protein of MW of three million.

In the present study, a 1200 kDa protein was isolated from crayfish claw muscle. This protein crossreacted with monoclonal antibodies against chicken muscle connectin and antiserum against the crayfish protein reacted with vertebrate connectin. The amino acid composition was very similar to chicken connectin. Circular dichroism spectra showed that it is rich in the beta sheet structure (60%). Rotary shadowed image was a long flexible filament. Immuno electron microscopy revealed that the 1200 kDa protein was localized in the I band and Z line. These observations demonstrate that the 1200 kDa protein is very similar to vertebrate connectin.

Because of its wide distribution in crustaceans and insects, the 1200 kDa protein is termed arthropod connectin. Projectin of honeybee thoracic muscle is identical with arthropod connectin.

BI 11

ATPASE ACTIVITY OF SEA-ANEMONE MYOSIN.
O. Sato¹, H. Ohmuro² and K. Maruyama¹. Dept. of Biol., Fac. of Sci., Chiba Univ., Chiba and ²Tokyo Metropol. Inst. of Med. Sci., Tokyo.

Sea-anemone, *Actinia equina*, was homogenized with Guba-Straub solution containing ATP and the extract was diluted with water. The precipitate was washed with 0.3 M KCl to remove contaminants and dissolved in 0.6 M KCl. This was subjected to DEAE-Sephadex column chromatography and a trace of actin was removed by HPLC gel chromatography in the presence of 0.6 M KCl.

The purified sea-anemone myosin was electrophoresed in the presence of SDS: it consisted of heavy chain (200 kDa) and four kinds of light chains of low molecular weights. It is not certain whether the different light chains are due to the presence of several myosin isoforms or not.

The KCl-activated (EDTA) ATPase activity of sea-anemone myosin was as high as 0.4 μ moles/mg/min and the Ca-activated one was 0.2 μ moles/mg/min. The Mg-activated ATPase action in the presence of rabbit skeletal actin was as low as 0.1 μ moles/mg/min. Better conditions for the Mg-ATPase are now under a survey.

BI 12

NUCLEOTIDE SPECIFICITY OF *in vitro* TRANSLOCATION SYSTEMS. T. Shimizu, K. Furusawa, S. Ohashi, Y.Y. Toyoshima, and R.D. Vale. 1Res. Inst. Polym. Text., Tsukuba, Ibaraki 305, 2Dept. Biol., Ochanomizu Univ. Ohtsuka, Bunkyo, Tokyo 112, and 3Dept. Pharmacol., Univ. California San Francisco, San Francisco, CA 94143, U.S.A.

The nucleotide specificity of *in vitro* translocation systems, microtubule (MT)-dynein, MT-kinesin and actin-HMM, was investigated with 15 ATP analogues; three deoxy derivatives of ATP, seven adenine modified analogues, and five phosphorothioate analogues. The dynein-based system, with 14S or 22S dynein from *Tetrahymena* cilia, exhibited highly preferred substrate specificity: deoxy derivatives of ATP, 6-N-methyl ATP and ATP α S(Sp) supported the MT gliding of relatively high speed, while formycin triphosphate and ATP γ S induced slow MT gliding. 8-azido ATP supported the MT gliding only with 14S dynein-based system. Since formycin triphosphate, ATP γ S or 8-azido ATP does not support the ciliary reactivation, something other than just MT gliding might be necessary for the reactivation. The kinesin-mediated MT gliding and HMM-supported actin gliding exhibited broad substrate specificity. Although competent for inducing the filament gliding, each ATP analogue gave varied speed of gliding; the variation was more profound with kinesin system than HMM system. These results about the difference in nucleotide specificity of the *in vitro* translocation systems may be useful in knowing which molecular motor is working in a motility-related cellular event.

BI 13

ISOLATION AND CHARACTERIZATION OF A NOVEL DYNEIN IN SEA URCHIN SPERM FLAGELLA. E. Yokota and I. Mabuchi. Department of Biology, College of Arts and Sciences, The University of Tokyo, Meguro-ku, Tokyo 153.

We isolated a novel dynein (C/A dynein), which was composed of C and A band heavy chains, from sea urchin sperm flagella. Sedimentation coefficient of this dynein was estimated by sucrose-gradient centrifugation to be 22-23S. When examined with negatively staining electron microscopy, the molecule appeared to be composed of three domains; two globular domains and one rod like domain. The pattern of UV cleavage of C and A band heavy chain of C/A dynein was different from that of A band heavy chains of 21S outer arm dynein. Furthermore, polyclonal antibody raised against A band heavy chain of C/A dynein did not crossreact with A band heavy chains of 21S dynein. C/A dynein rebound to the axonemes which had been extracted with Triton X-100-0.6 M NaCl solution (TS-axoneme). Electron microscopy of thin sectioned TS-axoneme showed that density at the position of the inner arms increased upon the rebinding. From this result, it was suggested that C/A dynein is a component of inner arms.

BI 14

CONFORMATIONAL CHANGE OF THE ISOLATED β CHAIN OF THE OUTER ARM DYNEIN FROM SEA URCHIN SPERM FLAGELLA COUPLED WITH ATP HYDROLYSIS. K. Inaba and H. Mohri. Department of Biology, College of Arts and Sciences, University of Tokyo, Tokyo.

Conformational changes of the separated α and β chains were examined by tryptic digestion. Tryptic digestion of the β chain yielded faint polypeptides and no significant difference in the digestion pattern was observed in the presence and absence of ATP (ADP) and Vi. On the other hand, tryptic digestion of the β chain in the presence of 2 mM ATP (ADP) and 100 μ M Vi or in the presence of 4 mM ATP γ S produced the polypeptides different from those in the case of no addition. The similar result was obtained with the heavy chains of intact 21S outer arm dynein (Inaba and Mohri '89, J. Biol. Chem. 264, 8384-8388). However, unlike the tryptic digestion pattern of the 21S dynein heavy chains, a 135-kDa polypeptide was consistently produced from the isolated β chain even in the presence of ATP (ADP) and Vi. Tryptic digestion pattern of the 21S dynein reconstituted from the α and β chains (Tang et al. '82, J. Biol. Chem. 257, 508-515) was similar to that of intact 21S dynein; the 135-kDa polypeptide was only slightly produced in the presence of ATP and Vi. The digestion rate constant of the 135-kDa polypeptide from the isolated β chain in the presence of ATP and Vi was significantly decreased as compared with the cases of intact 21S dynein and the reconstituted 21S dynein. These results suggest that association of the α chain with the β chain in the presence of ATP and Vi brings about a certain conformational change of the 135-kDa region.

BI 15

ROTATION OF MICROTUBULES *IN VITRO* BY SEA URCHIN SPERM FLAGELLAR DYNEIN:

Y. Y. Toyoshima, Dept. Biology, Ochanomizu Univ. Tokyo

Rotation and translation of microtubules produced by sperm flagellar dynein from *Hemicentrotus depressus* was examined by *in vitro* motility assay system. Properties of the movement were different from those we observed previously with *Tetrahymena* dynein (Vale & Toyoshima, 1988).

13S dynein was fractionated on the mono Q column. Of 3 major peaks, those contain A and D bands (peak-I and -II) showed rotation as well as translation. The A-band dynein in peak-I and -II showed mapping patterns different from each other and also different from α and β of 21S dynein. These two peak fractions exhibited different motile properties: on peak-I dynein surface, microtubules moved well at ATP concentration lower than 1 mM but became stuck at higher than that; on peak-II dynein surface, microtubules moved well at high ATP concentration but dissociated at lower than 50 μ M. These results are unexpected from ordinary cross-bridge models.

The rotation depended on the translational motion (~ 2.9 rot/ μ m for peak-I; ~ 1.7 rot/ μ m for peak-II). When the rotation speed was plotted against the translation speed, regression lines did not pass through the origin and their slope was different. These results suggest that different kind of dynein motors exist, one mainly for rotation and the other for translation.

BI 16

PREPARATION OF THE GLIDING ACTIVE ATPASE FROM OUTER ARM DEPLETED AXONEMES

S. Wada, M. Okuno, H. Mohri and K. Ogawa*
Coll. of Arts. & Sci., Univ. of Tokyo, Tokyo.
and *Nat. Inst. for Basic Biol., Okazaki.

We prepared the ATPase from the outer arm depleted axonemes of sea urchin sperm flagella by the low salt extraction followed hydroxylapatite column chromatography.

SDS-PAGE revealed that this ATPase had major two high molecular weight peptides (HMWPs). One was the same mobility as α β -chain (component of 21S outer arm dynein; dynein 1), and the other was the same mobility as D-chain (dynein 2). We named the former HMWP α β -like chain and the latter HMWP D-like chain. The anti-21S rabbit antibodies and anti- α β mouse monoclonal antibody didn't cross-react with this ATPase. Therefore, the α β -like chain was different from the α β -chain of the outer arm dynein.

The gliding velocity of microtubules by this ATPase was approximately $3 \mu\text{m}/\text{sec}$ in the presence of 1 mM ATP. This value was less than that of 21S or α β -dyneins. The velocity was dependent on the concentration of ATP. On the other hand, we couldn't observe the gliding of microtubules by GTP, CTP, TTP and UTP. From these result, we assumed this ATPase which contained α β -like chain and D-like chain was a part of the inner arms in sea urchin sperm flagella.

BI 17

TWO GROUPS OF TROPOMYOSIN ISOFORMS WITH DIFFERENT ANTIGENICITY EXIST IN THE SEA URCHIN EGGS.

T. Ishimoda-Takagi, T. Ando and H. Minami.
Dept. of Biol., Tokyo Gakugei Univ., Tokyo.

Tropomyosin (TM) isoforms prepared from eggs of four species of the sea urchin, *Strongylocentrotus intermedius*, *Anthodidaris crassispina*, *Hemicentrotus pulcherrimus* and *Pseudocentrotus depressus*, were analyzed by two-dimensional urea-shift gel electrophoresis and two-dimensional gel electrophoresis with isoelectric focusing. The number, mobility and pI value of the TM isoforms of four species were not identical. Two to four TM isoforms were detected in each species. One or two TM isoforms of each species had the antigenicity common to muscle TM, and had relatively higher pI values than the rest of egg TM isoforms. To investigate the antigenicity of TM isoforms with relatively low pI values, we prepared an antiserum specific to 30K component of *S. intermedius* egg TM isoforms which had relatively low pI value and the antigenicity different from muscle TM. The antiserum cross-reacted with all of the TM isoforms which did not show the cross-reactivity with the antiserum against muscle TM. This result indicated that TM isoforms present in the sea urchin eggs could be divided into two groups with different antigenicity in all of the species examined, and suggested that these groups of TM isoforms had evolved independently during echinoderm evolution.

BI 18

PEPTIDE MAPPING OF 45KDa ACTIN-MODULATING PROTEIN FROM SEA URCHIN EGG AND ITS BINDING SITE ON THE ACTIN MOLECULE

M. Ohnuma and I. Mabuchi. Department of Biology, College of Arts and Sciences, University of Tokyo, Komaba, Tokyo.

45KDa protein which has been purified from a soluble fraction of sea urchin eggs, severs actin filament in the presence of Ca^{2+} and forms a complex with actin. The F-actin severing activity of 45KDa protein was inhibited by phosphatidyl inositol 4,5-bisphosphate (PIP_2). Thus, it is considered that this protein possesses actin-binding, Ca^{2+} -binding, and PIP_2 -binding domains. To localize these domains on the molecule, we first carried out peptide mapping of 45KDa protein using 2-nitro-5-thiocyanato benzoic acid (NTCB) which cleaves proteins at Cys residues. There were 4 Cys residues in the 45KDa protein which were susceptible to NTCB cleavage.

Next, 45KDa protein-binding site on the actin molecule was determined according to the method of Sutoh [K. Sutoh and I. Mabuchi, Biochemistry 25, 6186-6192, (1986)]. The polypeptides which had been obtained by carboxypeptidase Y digestion of actin was cross-linked by water-soluble carbodiimide (EDC) with 45KDa protein. It was shown that the 45KDa protein-binding site on the actin molecule was located in a segment close to the C-terminus of actin.

BI 19

ASSEMBLY OF ACTIN FILAMENTS DURING CLEAVAGE FURROW FORMATION IN THE SEA URCHIN EGG.

I. Mabuchi, Dept. of Biol., Coll. of Arts and Sci., University of Tokyo, Tokyo.

The first cleavage furrow of the sea urchin egg is formed about 1 min after the onset of elongation of egg at anaphase B. Fluorescent staining of actin filaments in fixed eggs with rhodamine-phalloidin revealed that these filaments began to accumulate in the equatorial cortical layer just before the furrowing. The rate of cleavage (rate of reduction of the diameter of the egg at the equator) was accelerated until it reached a constant one about one min after the onset of the furrowing. On the other hand, process of the formation of the contractile ring was investigated by examining the furrow region of the cortical layer isolated on the glass surface. It was revealed that the actin filaments are organized into bundles to form the ring. The involvement of myosin filaments in the contractile ring formation was investigated using an inhibitor for myosin light chain kinase, ML-9. 0.1 mM ML-9 blocked cleavage while nuclear division was not affected. The contractile ring was not formed in these eggs. These results suggest that the contractile ring actin filaments are assembled by the aid of phosphorylated myosin filaments and form bundles during the initial phase of contraction.

BI 20

PRIMARY STRUCTURE OF PROFILINS FROM TWO SPECIES OF ECHINOIDEA AND PHYSARUM. T. Takagi¹, I. Mabuchi², H. Hosoya³, K. Furuhashi⁴ and S. Hatano⁴. ¹Biol. Inst., Fac. of Sci., Tohoku Univ., Sendai, ²Dept. of Biol., Coll. Arts and Sci., Univ. of Tokyo, Tokyo, ³Dept. of Ultrastruct. Res., The Tokyo Metropolitan Inst., of Med. Sci., Tokyo and ⁴Dept. of Mol. Biol., Fac. of Sci., Nagoya Univ., Nagoya.

Profilin is a G-actin-binding protein, the amino acid sequence of which was previously reported for calf, human and *Acanthamoeba*. Here we determined the amino acid sequences of three profilins obtained from eggs of two species of Echinoidea, *Clypeaster japonicus* and *Anthocidaris crassispina* and plasmodium of *Physarum polycephalum*. Two echinoid profilins were composed of 139 amino acid residues and the sequences were 84% identical. However, the homology of these profilins with those from other organisms was not high. On the other hand, *Physarum* profilin was composed of 124 residues and the sequence was homologous with *Acanthamoeba* profilin isoforms, but not with other profilins. The highly conservative sequence of profilins from *Physarum*, *Acanthamoeba*, echinoid and mammalian was found in N-terminal region, which was suggested to be a common actin-binding region. C-terminal region was the next conserved region, which could be the second actin-binding site or the region necessary for preserving the functional structure of this protein.

BI 21

PURIFICATION AND CYTOCHEMICAL LOCALIZATION OF CALPACTIN LIKE PROTEINS FROM SEA URCHIN EGGS.

S. Maekawa¹, M. Toriyama² and H. Sakai¹. ¹Dept. of Biophys. and Biochem., Fac. of Sci., Univ. of Tokyo, Tokyo and ²Fac. of Liberal Arts, Univ. of Shizuoka, Shizuoka.

Calpactin like proteins were screened in sea urchin eggs using a Phenyl Sepharose column and Ca^{2+} -dependent adsorption and elution procedure and two of them (34K and 23K protein) were purified. Both proteins bound actin filament at high Ca^{2+} concentration. The 34K protein showed Ca^{2+} -dependent binding to phosphatidylserine and phosphatidic acid but the 23K protein showed little binding to these phospholipids. Immunoblotting analysis of these proteins using affinity purified antibodies clearly distinguished these proteins. Immunostaining of fixed and sectioned metaphase eggs showed prominent localization of the 23K protein in the mitotic apparatus region and specific exclusion of the 34K protein from this region. These proteins may have quite different roles within the cell.

BI 22

THE ASSEMBLY OF SEA SHELL PARAMYOSIN IN VITRO AND IMMUNOLOGICAL CROSS REACTION OF PARAMYOSIN WITH INTERMEDIATE FILAMENT ANTIBODIES. N. Koike and K. Ohashi. Dept. of Biol., Fac. of Sci., Chiba Univ., Chiba.

Abalone paramyosin dissolved in 0.6 M KCl buffered with 10 mM potassium phosphate buffer (pH 7.5) was diluted with 10 mM potassium phosphate buffer (pH 7.5) into lower KCl concentrations. Final protein concentration was adjusted to 0.15 mg/ml. In case of 10 mM and 25 mM KCl, 10 nm filaments and very fine filaments were observed under an electron microscope. Loose pellet of 10 nm filaments was obtained by centrifugation at 10,000 rpm for 10 min but fine filaments were not precipitated. Bundles of 10 nm filaments were formed at the KCl concentration of 0.05 M and 0.1 M. When the KCl concentration was 0.125 M, paramyosin paracrystals with axial periodicities of 14 nm were observed. These bundles and paracrystals of paramyosin could be collected as white pellets by centrifugation at 10,000 rpm for 10 min. In a 0.225 M KCl solution, paramyosin paracrystals and fine filaments were coexisting. When KCl concentration was decreased by dialysis, the same results as mentioned above were obtained. Antibodies against chicken desmin, vimentin, and keratin reacted with abalone paramyosin. And anti-paramyosin antibody reacted with chicken gizzard desmin and skin keratins but not reacted with erythrocyte vimentin.

BI 23

CLONING AND SEQUENCING OF THE *TETRAHYMENA* 14-NM FILAMENT PROTEIN GENE.

O. Numata, T. Takemasa, Y. Watanabe and J. Chiba. Inst. of Biol. Sci., Univ. of Tsukuba, Tsukuba, Ibaraki 305; Dept. of Biol. Sci. and Tech., Science Univ. of Tokyo, Yamazaki, Noda 278.

Tetrahymena 14-nm filament protein (p49K) has been shown to resemble intermediate filament proteins from mammalian cells in several respects, and to play a role in the oral morphogenesis preceding binary fission. Based on immunofluorescence localization of the p49K during the early stages of conjugation, we suggested that it is involved in some nuclear events during fertilization.

To further investigate the properties of p49K, we isolated the p49K gene from *T. thermophila* cDNA library by using a synthetic oligonucleotide as a probe. The macronucleus of *T. thermophila* was found to contain a single copy of p49K gene. The primary structure of p49K shows 51.5% sequence identity with mitochondria citrate synthase of pig heart, while it shows low sequence identity (29.5%) with human type I keratin. Using the monoclonal antibody, we observed that in log phase cells, immunofluorescence appeared in mitochondria and in oral apparatus. Thus, we speculate that p49K plays crucial roles in fertilization and oral morphogenesis as cytoskeletal protein and in addition may function as an enzyme in mitochondria.

BI 24

STUDIES ON TUBULINS FROM CILIA AND FLAGELLA OF VARIOUS SPECIES. ISUBUNITS AND ISOTYPES K. Nakamura¹, E. Masuyama¹, S. Wada², M. Okuno², and H. Mohri². Dept. of Living Sciences, Hiroshima Women's Univ. Hiroshima and ²Dept. of Biology, College of General Education, Univ. of Tokyo, Tokyo.

In order to understand the biological meanings of micro-heterogeneity of tubulin molecules, we have compared tubulin isotypes from various species; sperm flagella of sea urchin (*Hemicentrotus pulcherrimus*, *Pseudocentrotus depressus*) and oyster (*Crassostrea gigas*), microtubules of oyster egg, and cilia (*Tetrahymena pyriformis*). The analysis using iso-electric focusing has shown that axonemes of these species contain 7-9 tubulin isotypes (alpha 3-5 and beta 4-5) but the egg tubulin from cytoplasmic microtubule has three isotypes (2 alpha and one beta). The dominant isotype originated from an alpha tubulin subunit has the same isoelectric point among the above materials, while each isoelectric point of the main isotype of alkaline region from a beta tubulin differs in species.

Together with these analysis, we have analyzed the homology between alpha and beta tubulin subunits using a personal computer and sequence data of various species. The result has shown that the two subunits evolved in an early stage of the tubulin evolution.

BI 25

SPASMIN LIKE PROTEIN IN THE CILIATE SPIROSTOMUM.

H. Ishida, M. Kuroda, A. Matsuno and Y. Shigenaka¹. Department of Biology, Faculty of Science, Shimane University, Matsue, ¹Laboratory of cell biology, Faculty of Integrated arts and Science, Hiroshima University, Hiroshima.

The large heterotrichous ciliate *spirostomum* is well known for their characteristic twisting contraction. The contraction is easily evoked by external stimuli. The myoneme that is lie just under the cell surface serves the contraction of cell body. It is supposed that the myoneme is calcium-sensitive contractile organella and contracts without hydrolysis of ATP.

The myonemal protein is partially purified from *Spirostomum* by DEAE-column chromatography of the 8M urea extract of the whole cell body. The spasmin-like protein in *Spirostomum* is eluted from DEAE-column at 0.5 M NaCl. This 20Kd protein change mobility with or without Ca²⁺ in SDS polyacrylamide gels. This change of mobility is characteristic of calcium binding proteins.

Rabbit-Antiserum against the spasmin from stalk of *Carchesium* binds to the 20Kd protein of *Spirostomum*.

BI 26

INTERPHASE AND MITOTIC CHROMOSOME STRUCTURE OF DINOFLAGELLATES.

H. Sato¹, J. Cachon², M. Cachon² and Y. Sato³. ¹Sugashima Marine Biol. Lab., Nagoya Univ., Toba, Mie, ²Station Zool., Villefranche-sur-Mer, France and ³Shoin Women's Univ. Nada-ku, Kobe.

Chromosomes of most dinoflagellates persist in condensed state during the cell cycle, and replicated chromosomes segregate without metaphase equatorial plate formation. Striking fact is; chromosomes are consisted with naked DNA molecules and almost no basic protein is exist. Sign of birefringence (BR) is positive in most case and the nature of BR is intrinsic. These facts support that the packed DNA gel is laterally wound in a single coil towards the long axis of individual chromosome.

Some times, ($n_e - n_o$) is measured as high as $+2 \times 10^{-2}$ indicating the molecular alignment of DNA within the chromosome is almost perfect. However, discrepancy still exist between analyses of BR and the electron microscopy and it should be solved in near future.

Based on the chromosomal BR and pattern of chromosomal arrangement, we grouped dinoflagellates into three different types. Type A: All Gymnodinidae, Walnoididae, Pyrocystidae and Proterocentrum. Type B: Armoured dinoflagellates except Adinidae. Type C: Noctulicidae and many parasitic species. Phylogenetic view will be discussed.

BI 27

PURIFICATION AND PROPERTIES OF EARTHWORM ARGININE KINASE.

Y. Yazawa. Dept. of Nutritional physiol., Hokkaido Univ. of Education at Asahikawa, Asahikawa, Hokkaido.

Arginine kinase (AK) was purified and isolated from earthworm with ammonium sulfate fractionation, DEAE-Toyopearl column, gel filtration and hydroxylapatite column chromatography. The molecular weight was estimated as 120K from SDS-PAGE and 240K from gel filtration under the physiological conditions. The amino acid composition was determined and the star diagram was very different from them of other AK. The pH-activity curve for the forward and the reverse reactions showed the increase of the activity with the elevation of pH and optimum at pH9.0. Enzymatic activity was activated by many divalent metal ions.

BI 28

ACTIVITY OF CHOLINE(PHOSPHO)KINASE IN THE MOUSE CEREBRAL CORTEX.

M.Oide. Dept. of Pharmacol., Gunma Univ. Sch. of Med., Maebashi.

Cholinephosphokinase (ChK; EC 2.7.1.32) in the mouse cerebral cortex was partially purified and its properties were investigated. The enzyme activity was assayed according to Weinhold & Rethy (Biochemistry, 13, 5131-5141, 1974) using [14 C]choline as substrate. The labeled phosphorylcholine (a reaction product) was estimated by liquid scintillation spectrometry. Presence of Mg ions was indispensable; the optimum concentration was around 10 mM (when ATP; 10 mM). Ca ions inhibited the ChK activity by 15 % and 45 %, when the concentrations were 0.5 mM and 2 mM, respectively. NaCl, KCl or LiCl showed dual effects; lower concentrations (less than 50 mM) caused some acceleration and higher concentrations than 100 mM exerted considerable inhibition. Hemicholinium-3 inhibited the ChK; 1.25 mM caused 50 % reduction when the choline concentration was 0.25 mM. Intraperitoneal administration of Pyridine-2-aldoxime methiodide (an activator of cholinesterase; 250 mM/kg/day x3) caused a significant ($p < 0.05$) decrease in the cerebral ChK activity. Since acetylcholine (a neurotransmitter) is synthesized also by using choline as substrate, any influence of acetylcholine upon ChK in the living organisms may be suggested.

BI 29

ROLE OF THE (NA,K)ATPASE β -SUBUNIT IN THE BIOGENESIS OF THE ENZYME.

S.Noguchi and M.Kawamura. Dept. Biol., Univ. Occup. & Env. Health, Yahatanishi, Kitakyushu.

(Na,K)ATPase is a membrane-bound enzyme catalyzing ATP-driven transport of Na⁺ and K⁺. It is composed of two heterologous subunits: a catalytic α -subunit of about 110kDa, and an N-linked glycoprotein β -subunit (molecular mass of its protein moiety is about 35kDa). When and in which organellar compartment(s) does the assembly of the α - and β -subunits occur or whether does the β -subunit assist the α -subunit to become correctly and stably expressed in the cell? To answer the question, we have induced the expression of the α - and β -subunit of *Torpedo californica* (Na,K)ATPase in *Xenopus* oocytes. The oocyte system allows the specific programmed synthesis of different subunits in a cell by alternately injecting individual mRNAs.

Here we report that the active $\alpha\beta$ complex was formed in oocytes when the injection of the mRNA for the β -subunit was followed by the injection of the mRNA for the α -subunit, suggesting that the β -subunit acts as a receptor for the newly synthesized α -subunit and facilitates the accumulation of the enzyme in the membrane.

BI 30

GANGLIOSIDES IN CULTURED NEURONS.

M.Ogiso, M.Ohta and S.Hirano. Dept. of Physiology, Toho Univ. Sch. of Med., Tokyo.

Neuronal cells dissociated from 17-day-old fetal rat hemispheres showed developmental changes in ganglioside levels and patterns up to 7 days in culture. The increase of ganglioside contents in cell cultures and the onset of GM1 and GD1a synthesis, which is associated with synaptic membranes, were observed as the neuronal-glia interaction was established. Immunological studies showed characteristic profiles of ganglioside localization. The anti-GM1 antibody cross-reacted only on the cell body at 1 and 3 days and on the neuronal processes as well at 7 days in culture. GD3 ganglioside, the predominant species at 1 day and a precursor of GM1 and GD1a, was detected on the cell body surface at 1 day and on the whole neuron at 3 days. These results suggest that GD3 is retained on endoplasmic reticulum membranes in neurons at 1 day, expressed on the cell surface at 3 days, and transformed to GM1 and GD1a. The incorporation of [3 H]acetylmannosamine into gangliosides was enhanced in coculture of neuronal cells with astroglial cells. Regulation of ganglioside levels by neuronal-glia interaction is also suggested.

BI 31

DEACETYLATION OF ACETYLPUTRESCINE IN RAT TISSUES.

T. Kumazawa, H. Seno and O. Suzuki. Department of Legal Medicine, Hamamatsu University School of Medicine, Hamamatsu.

Acetylputrescine was found to be metabolized directly into putrescine and acetic acid *in vitro* with tissues of the rat. The linearity was observed as a function of incubation time and enzyme concentration, showing that this is an enzymatic reaction. Apparent K_m and optimal pH values for acetylputrescine were 74.5 μ M and 8.3-8.6 for the liver enzyme, respectively. In an attempt to demonstrate differences in properties between the present acetylputrescine-deacetylating enzyme and acetylsermidine deacetylase, we used both radioactive acetylputrescine and N³-acetylsermidine as substrates in experiments for various inhibitors, competitive inhibition by various amine derivatives, subcellular localization, purification study and gel filtration. However, all trials to show differences between them were not successful, but supported that acetylputrescine and N³-acetylsermidine were deacetylated by an identical enzyme, acetylsermidine deacetylase. Nevertheless, it is noteworthy that the present putrescine formation via deacetylation of acetylputrescine gives a new pathway for polyamine re-utilization.

BI 32

CATHEPSIN E IS A PLASMA MEMBRANE-BOUND ASPARTIC PROTEINASE IN MAMMALS.
S. Yonezawa. Dept. of Zoology, Fac. of Sci., Hokkaido Univ., Sapporo.

Cathepsin E is a non-secretory acid protease in mammals. In an attempt to define its destination site in the cell, we examined the subcellular localization pattern of the enzyme in rat livers: Perfused rat livers were homogenized in 0.25M sucrose and differentially centrifuged to obtain nuclear, mitochondrial, lysosomal, microsomal and cytosol fractions. Electrophoretic analysis clearly showed a predominant association of cathepsin E with microsomal fraction, in contrast with an well-known lysosomal association of cathepsin D. When microsomal fraction was resuspended in 57% sucrose, placed under 1M and 0.25M sucrose layers and centrifuged at 75,500xg for 16h to segregate ER-rich (P4) and plasma membrane-rich (P2) fractions, cathepsin E was found to be concentrated in P2 fraction. Although this fraction is known to be heterogeneous and contain Golgi bodies, further sucrose density centrifugation experiments of P2 revealed a distinct difference in distribution pattern between cathepsin E and UDP-GlcNAc:lysosomal enzyme N-acetylglucosaminylphosphotransferase (a marker of cis Golgi). The results thus strongly suggested that cathepsin E is transported to the plasma membrane in rat liver.

BI 33

α , α -TREHALASE FROM ARTEMIA NAUPLIUS
Z.Nambu and F.Nambu-Akiyama.
Dep. of Biol. Sch. of Nursing and Med. Technol. Univ. of Occupational and Environmental Health, Japan. Kitakyushu.

A modified procedure of purifying trehalase from *Artemia* nauplius and the newly investigated nature of the enzyme were presented in this report.

The soluble enzyme was purified more than 1000 fold in the presence of soybean trypsin inhibitor, leupeptin and EDTA by the following 4-step procedures: acetone treatment, DEAE-Sephadex CL-6B, Sephadex G-75 and Con A-Sepharose. The yield of the activity was 30 % and the specific activity was 45 units/mg protein. The enzyme was further purified by chromatofocusing and Sephadex G-75. Although pI of the enzyme was pH 4.8-4.5, most of the enzyme was eluted at pH 4.15-4.00 in the presence of 0.1 % Triton X-100 in the chromatofocusing. Residual activity still retained in the Polybuffer exchanger-94 was eluted by 1.0 M NaCl. Trehalase activity and its molecular weight were not affected by 2-mercaptoethanol. Temperature dependency of the trehalase was investigated; its activity was strongly inactivated over 60° C, and the activation energy was calculated to be 11.0 kcal. The trehalase activity was completely inhibited by 0.1 mM HgCl₂, and monovalent inorganic anions such as I⁻, Br⁻ and Cl⁻ were effective to counteract the inhibition by HgCl₂.

BI 34

CELLOBIASE FROM ARTEMIA NAUPLIUS
-PURIFICATION AND CHARACTERIZATION-
F.Nambu-Akiyama and Z.Nambu
Dep. of Biol. Sch. of Nursing and Med. Technol. Univ. of Occupational and Environmental Health, Japan. Kitakyushu.

In the course of purifying trehalase from *Artemia* nauplius, cellobiase activity was found to be coexistent in the beginning steps, so that we tried to isolate the enzyme.

Soluble cellobiase was isolated from *Artemia* nauplius in the following 5-step procedures: acetone treatment, DEAE-Sephadex CL-6B, Con A-Sepharose, Chromatofocusing and Sephadex G-75. The purified enzyme was shown to be a single band of protein with its activity on SDS-PAGE, its molecular weight being determined to be 86k. The enzyme retained its activity even after the treatment with 2-mercaptoethanol, showing its molecular weight to be 57k. The cellobiase was highly specific for cellobiose and pNP- β -D-glucoside. The K_m value for cellobiose was estimated to be 0.28 mM at the optimum pH of 6.0. Isoelectric point of the enzyme was shown to be pH 6.3-6.6. Effect of temperature on the activity was investigated; the activity was strongly inactivated over 70° C, and the activation energy was calculated to be 11.0 kcal. The activity of the cellobiase was strongly inhibited by 0.1 mM D-glucono δ -lactone and 0.1 mM HgCl₂.

BI 35

MITOCHONDRIAL CYLINDRIN IS A SPECIFIC SUBSTRATE OF ATP-DEPENDENT PROTEASE
S.Nakazawa¹, T.Nakazawa¹, H.Kouyama², S.Watabe², T.Fujii², S.Tatunami², T.Yago², 'Dept. of Biol., Fac. of Sci., Toho Univ., Funabashi, 'Radioisotope Res. Inst., St. Marianna Univ. Sch. Med., Kawasaki.

Mitochondrial cylindrin forming hollow cylinder tube structure was isolated from mitochondrial matrix of pig liver in our laboratory. The molecular weight of this protein was estimated as 25,000 by SDS gel electrophoresis. On the other hand, it was found that a 25k protein (SP-25) in mitochondrial matrix of adrenal cortex is specifically digested by ATP-dependent protease in the mitochondrial matrix. Then comparison of molecular features between both proteins was conducted in this study. Molecular structure of SP-25 observed with electron microscope indicated that SP-25 shows a hollow cylinder tube structure which is completely identical as mitochondrial cylindrin. Both tubes show 13nm and 7nm in outer and inner diameter respectively and consist of six subunits. The tube structure was dissociated in the addition of 1M KI or sonication and reconstructed in the presence of magnesium ions. Furthermore mitochondrial cylindrin from pig liver was crossreacted by polyclonal antibody of SP-25. These common features between both proteins indicate that mitochondrial cylindrin is a specific substrate of ATP-dependent protease.

BI 36

CHANGE IN THE MIDGUT ENZYMES DURING EMBRYONIC DEVELOPMENT OF THE SILKWORM.¹
 T. Suzuki¹, M. Azuma², T. Yoshimura³, M. Eguchi¹
¹Dept. Appl. Biol., Kyoto Inst. Techn., Kyoto.
²Fac. of Agri., Tottori Univ., Tottori.
³Inst. Chem. Res., Kyoto Univ., Kyoto.

We studied the enzymes of two alkaline proteases (APRs) and alkaline phosphatases (ALPs) during embryonic development of the silkworm, and compared the embryonic midgut enzymes with those in the 5th instar.

Activities of ALP isozymes, membrane-bound (m-ALP) and soluble (s-ALP) forms, increased steeply at one day before hatching. As for trypsin-like and chymotrypsin-like APRs, the activities rose markedly after hatching. These enzymes were found to be immunologically identical with those in the midgut of 5th instar larva, although the molecular weight of s-ALP was higher than that of the larval midgut. We also utilized mutants of ALP isozymes; in the s-ALP defective mutant (larval stage), s-ALP was detectable in a similar level to the normal strain in the embryonic stage. Immunohistochemical study showed that m-ALP was discernible at one day before hatching and APRs were observed after hatching at the brush border of columnar cells, whereas s-ALP was detected at the apical surface of goblet cells at one day before hatching. The correspondence of appearance of both ALPs to the development of columnar microvilli and goblet apical surface seems to be important in view of the development of the midgut function.

BI 37

GOBLET CELL ALKALINE PHOSPHATASE IN SILKWORM MIDGUT EPITHELIUM: ITS ENTITY AND FUNCTION AS A SPECIFIC ATPase.

M. Azuma¹, S. Takeda², H. Yamamoto², Y. Endo², M. Eguchi¹, Lab. of Insect Biochem., Fac. of Agri., Tottori Univ., Dept. of Appl. Biol., Kyoto Inst. of Techn., Kyoto.

The insect midgut, in particular that of lepidopteran larvae, contains a high pH fluid (pH 10-11) in its contents. Many enzymes in this tissue have their optimum pH at an alkaline region. To elucidate the insect midgut functions in such a high alkaline environment, we have studied the biochemistry of alkaline phosphatase (ALP) in the silkworm larva, *Bombyx mori*. The purified goblet-ALP is activated by 2 or 3-fold with 5-10mM of MgCl₂ but inhibited with the same concentration of CaCl₂. The purified columnar-ALP was not affected by such metal ions. This Mg²⁺-sensitive ALP also showed ATPase action at pH 8 with Mg²⁺-dependent manner. Since KCl had no effect on ATPase activity of the goblet-ALP, our ATPase differ from K⁺-ATPase, which is responsible for the K⁺ movement between haemocoel and gut lumen. Our ATPase was activated with 50-100mM of KClO₄. This activation is independent of Mg²⁺ and greater than the effect of MgCl₂. Therefore, the goblet-ALP functions as a certain ATPase *in vivo* and this suggests that this ATPase involves in generating and managing the alkalinization of midgut contents.

BI 38

PURIFICATION AND CHARACTERIZATION OF ACID PHOSPHATASE ISOZYMES FROM HAEMOLYMPH OF THE SILKWORM, *Bombyx mori*

M. Matsumoto¹, M. Azuma², M. Eguchi¹
¹Dept. Appl. Biol., Kyoto Inst. Techn.
²Fac. Agric., Tottori Univ.

Five electrophoretic variants, A-E in the haemolymph acid phosphatase (ACP) were found using various inbred strains of the silkworm. These isozymes were considered to be controlled by codominant alleles. The isozyme E was heat labile and showed specificity in some properties.

In this experiment, we purified the isozyme A by ammonium sulfate fractionation, DEAE-Toyopearl, CM-Toyopearl and Hydroxylapatite column chromatographies, and characterized. Ouchterlony's double diffusion test using antiserum against the purified A showed that five isozymes are immunologically identical although an additional precipitate was observed for the isozyme E.

High and lower ACP activities were detected in fat body and midgut, respectively. Immunoblotting using antiserum against purified isozyme A and extracts from the fat body and midgut indicated a protein band corresponding to the purified A in fat body but not in midgut. These results suggest that ACP in the haemolymph would be synthesized in the fat body.

BI 39

PURIFICATION OF THE ZYMOGEN OF A SERINE PROTEASE IN THE PROPHENOLOXIDASE ACTIVATING SYSTEM OF SILKWORM, *BOMBYX MORI*.

H. Kihara and M. Ashida. Biochem. Lab., The Low Temp. Sci., Hokkaido Univ., Sapporo

The prophenoloxidase activating system (a cascade) is present in insect hemolymph. We previously demonstrated that the system is triggered by microbial cell wall components such as β -1,3-glucan and peptidoglycan and that at least two kinds of zymogens of serine protease are the constituents of the system.

The prophenoloxidase activating system in insect has been proposed to play important roles in recognition of foreignness and defense mechanisms against bacteria, fungi, protozoa and parasitic insects invading into insect hemocoel. The proposition was also supported by our recent investigation showing that proteins specifically recognizing the components of fungal cell wall and bacterial cell wall are present in silkworm hemolymph and that the binding of the proteins to the respective microbial cell wall component initiates the activation of the cascade. It is desirable to isolate every component of the cascade to progress our understanding on its roles in insect defense mechanisms.

We developed a method to assay one of the zymogens (precursor of BAEase, which was found as an enzyme hydrolyzing N α -benzoyl-arginine ethyl ester) and purified the zymogen to homogeneity. Some properties of the purified protein were reported.

BI 40

ACTIVATION OF LACCASE-TYPE PROPHENOLOXIDASE IN THE CUTICLE OF INSECT. VI. PROPERTIES OF THE PRO-LACCASE CONSTITUTING PEPTIDES
H.I. Yamazaki. Biol., Lab., Atomi Gakuen Women's Univ., Saitama.

Newly formed cuticles harden and darken immediately after larval-pupal ecdysis. The laccase, a type of phenoloxidase, is found in the cuticular matrix and estimated to play an important role during the hardening and darkening process.

The laccase is ready present in newly ecdysed cuticle as an inactive proform bound in cuticular matrix and it is able to solubilize and activate by proteinases. So, the proteinases seem to be involved in the laccase activation mechanism.

It is a question how the pro-laccase is constituted in cuticular matrix. In order to study the pro-laccase constituting mechanism during ecdysis, immunoreactive peptides in cuticles of *B. mori* were investigated using antiserum raised from purified laccase. The main immunoreactive peptides (68 and 150 kDa) were early detected in the time course of cuticular formation of pharate pupae by SDS-PAGE and immunoblotting analysis. The 150 kDa peptide was estimated to be reduced to 92 and 58 kDa peptides in the course of sclerotization. The pro-laccase constituting process might be present prior to its activation.

BI 41

Site of synthesis of hemagglutinin in the haemolymph of fifth instar larvae of *Bombyx mori*
K. Amanai, S. Sakurai and T. Ohtaki
Department of Biology, Faculty of Science, Kanazawa University, Kanazawa 920

We have reported previously that hemagglutinin in the haemolymph of *Bombyx mori* is a 350kDa protein composed of two different subunits with the molecular weight of 88 and 90kDa, respectively. To identify the site of synthesis of hemagglutinin, fat body, haemocytes, ovary and testis of fifth instar larvae just before gut purge were cultured *in vitro*. A 2-fold dilution assay of the culture medium demonstrated that significant hemagglutinating activity was found in the culture media of haemocytes and ovary. These findings and others suggested that haemocytes were the main site of hemagglutinin synthesis. Immunocytochemical localization in the fixed haemocytes monolayers with monoclonal antibody prepared against *Bombyx* hemagglutinin indicated that hemagglutinin is produced by the granular cells, prohemocytes and undifferentiated plasmatocytes.

BI 42

PROPHENOLOXIDASE ACTIVATION SYSTEM IN THE MOSQUITO, *Aedes Aegypti*
P.T. Brey¹, K. Kinoshita² and M. Ashida²
¹Institut Pasteur, Paris, France, ²Biochem. Lab. The Institute of Low Temp. Sci., Hokkaido Univ., Sapporo.

Malaria and certain other parasitic diseases are transmitted by mosquitoes. Recently, it has been shown that parasite development in the mosquito vector can be arrested by encapsulation of the parasite in a melanin sheath; therefore, blocking transmission of the parasite to its vertebrate host. The implications of parasite transmission blocking in the area of public health are self evident.

This study, the first of its kind in a mosquito vector species, demonstrates the feasibility of studying prophenoeloxidase activation in an insect containing only a few microliters of hemolymph. Mosquito phenoloxidase was found to be in an inactive proenzyme form, prophenoeloxidase. Mosquito prophenoeloxidase system required bivalent cation for its activation; Ca^{++} was found to be the most efficient for activation. Through immunoblotting, using a cross-reactive silkworm anti-prophenoeloxidase IgG antibody, our results strongly suggest that mosquito phenoloxidase resulted from a limited proteolysis. Protease inhibitor experiments reinforce this contention showing the involvement of serine protease(s) with trypsin-like activity in the activation of mosquito prophenoeloxidase.

BI 43

JUVENILE HORMONE ESTERASE REPRESSIVE FACTOR IN THE PLASMA OF PARASITIZED INSECT LARVAE.
Y. Hayakawa. Biochem. Lab. Inst. of Low Temp. Sci., Hokkaido Univ., Sapporo.

Last-instar larvae of the armyworm, *Pseudaletia separata*, parasitized with eggs of the parasitoid wasp, *Apanteles kariyai*, do not initiate metamorphosis. The specific mechanisms whereby parasitism causes suppressed metamorphosis of host insects remain enigmatic. Studies on the endocrinological nature of the effect indicate that plasma JH esterase activity remained low throughout the last-instar while the two major peaks of the enzyme activity were observed in unparasitized last-instar larvae (at Day 3 & 6). Furthermore, a proteinaceous factor, which has a molecular weight of about 15,000 daltons, was found to repress the plasma JH esterase activity. The repressive factor has been purified and the sequence of 25 amino acid residues at the amino terminus was determined as follows: H-Glu-Asn-Phe-Ser-Gly-Gly-Ser-Val-Ala-Gly-Tyr-Met-Arg-Thr-Pro-Asp-Gly-Arg-Ser-Lys-Pro-Thr-Phe-Tyr-Gln-. Injection of about 6.5 pmole of the purified factor into unparasitized last-instar larvae at Days 1 and 2 respectively reduced plasma JH esterase activity by 50% compared to the control* and also resulted in more than a 2-day delay in pupation in 80% of the larvae.

* Control was injected with Ringer solution only.

BI 44

OXIDASES FROM *DROSOPHILA* TESTIS.

Y. Taka, and T. Aotsuka. Dept. of Biol. Fac. of Sci., Tokyo Metropolitan Univ., Tokyo.

We partially purified the testis specific α -hydroxyacid oxidase (HAOX-T) from *Drosophila virilis*. From the results of SDS-PAGE, gel filtration HPLC, and the electrochromatograms of the interspecific hybrids, we inferred HAOX-T is a tetramer of a 40 kDa subunit. The physiological role HAOX-T is not known yet.

As HAOX-T was specific almost only in the *virilis* species group, we have attempted to find the enzyme which replaced the role of HAOX in the testis of the species outside the *virilis* species group. We took notice of aldehyde oxidase (ALDOX) as a candidate. ALDOX was detected in the testis in some *Drosophila* species, and the activity was very high in *D. hydei*. We compared the substrate specificity and the developmental profiles of HAOX-T and ALDOX. ALDOX was active to various aldehydes and some alcohols such as isocamyl alcohol, but we could not find any common substrates for HAOX-T and ALDOX. HAOX-T activity was very low in the very young flies, but the activity increases quickly during the first three days in *D. virilis*. On the other hand, aldehyde oxidase activity in the testis increases rather slowly during the first three days after the eclosion.

BI 45

RECONFIRMATION OF THE INTERNAL STRUCTURE OF LIPOPHORIN USING CONTRAST VARIATION METHOD

C. Katagiri¹, M. Sato² and Y. Katsube².
¹Inst. of Low Temp. Sci., Hokkaido Univ., Sapporo, and ²Inst. for Protein Res., Osaka Univ., Suita.

We have already proposed a three-layer model of lipophorin in insect blood using the small angle X-ray scattering method; a quasispherical particle of diameter 168 Å with an outer shell (thickness 24 Å) of phospholipid and apolipophorin I, a middle layer (thickness 23 Å) of diacylglycerol and apolipophorin II, and a core (radius 37 Å) of hydrocarbons [JBC 262 (1987) 15857-15861]. This model was derived from a simulation analysis in consideration of temperature-dependent structural changes inside the particle. To further reconfirm the internal structure, contrast variation studies were performed by raising the electron density of the solvent by addition of sucrose and the small angle X-ray scattering measured. In the course of adding sucrose, the electron density of the solvent reaches to that of the outer shell at 50% sucrose and the scattering from the outer shell disappears. This method is useful to investigate the internal structure of a particle with a heterogeneous internal electron density. Analysis of the data obtained in this study supports the previously proposed model.

BI 46

THE SITE OF ACTION OF ADIPOKINETIC HORMONE IN LOCUST.

P.Y. Lum and H. Chino, Biochem. Lab., Inst. of Low Temperature Sci., Hokkaido Univ., Sapporo, Japan.

The hypothesis that adipokinetic hormone (AKH) primarily stimulates the fat body lipase in the locust was tested *in vitro*. When the fat body was preincubated with AKH, the level of diacylglycerol (DG) was found to increase by 2 to 3 folds. Calcium ions also found to be needed in the stimulation. Supporting this observation strongly is the data that ionophore *in vivo* mimics the action of AKH. The fat body preincubated with or without AKH was then incubated with hemolymph and the increase of DG in hemolymph was analysed. Both AKH treated and untreated fat body cause the loading of DG onto lipophorin. During the first 90 min the loading rate was almost the same for both, regardless of the difference in DG amount in the fat body, although the absolute amount of DG loaded by lipophorin depends on the DG level in the fat body. Low density lipophorin particles were partially formed in both the incubations after 3 hr. We conclude that AKH plays a direct part in stimulating the fat body lipase to convert TG into DG but not in the loading of DG by lipophorin.

BI 47

BINDING ACTIVE FRAGMENT OF VITELLIN BINDING PROTEIN FROM LOCUSTA MIGRATORIA

K. Yamasaki. Dept., Biol., Tokyo Metropol. Univ. Tokyo.

Vitelin binding activity in ovary of *L.m.* is specific for vitellogenic stage, ovary and species. Two types of VB activity are found in the ovary the first is membrane bound VBP and the second is found in soluble fraction (s-VBP). The two binding activities are stable in organic solvents, ionic and non-ionic detergents and the treatment with nonspecific peptidase, Actinase E. These findings lead us to the point of view that the binding active site in VBP is not present in peptide region. And VB activity was found to be faint in the course of prolonged treatment with Actinase E by the assay methods for binding activity. A possible explanation for the experimental result was the changes of characteristics of VBP by proteolysis. So, it was needed a new binding method to confirm the possibility. A newly developed method was successful for the detection of VB activity on the replica from electrophoretogram.

The actinase treated VBP was analysed by electrophoresis on CA film or PAGE. It was clearly shown that VB activity was released from matrix by proteolysis. The fragmented VBP in Actinase treated fraction was faintly detectable for protein staining by CBB and the activity was found to be poly-dispersed material on SDS and native PAGE.

BI 48

RELATIONSHIP BETWEEN SEASONAL COLOUR DIMORPHISM AND PTERIDINES IN THE SCORPION FLY, *Panorpa japonica*.
M. Nakagoshi, S. Takikawa and M. Tsusue.
Biol. Lab. Kitasato Univ. Sagami-hara.

The scorpion fly, *Panorpa japonica*, displays a colour dimorphism by changing from black to yellow, as we previously reported. The yellow pigment is sepiapterin and the black one is melanin. The quantities of the pigments vary depending upon the colour dimorphism of the insect. The combination of the morphological and biochemical approaches shows that sepiapterin is characteristically located at the pigment granules in the integument of the insect. The granules are spherical or oval in form and contain an internal series of concentric lamellae. From this viewpoint, the fine structure of the granules is similar to pterinosomes in the lower vertebrates.

On the other hand, the contents of various pteridines and the activities of various enzymes (GTP-cyclohydrolase I, 6-pyruvoyl-tetrahydropterin synthase and sepiapterin reductase) were measured at several stages after emergence of both yellow type fly and black one.

The results suggested that GTP-cyclohydrolase I is a key enzyme in the relationship between pteridine metabolism and seasonal colour dimorphism.

BI 49

FURTHER INFORMATION ON THE SYNTHESIS AND STRUCTURE OF PAPILLOCHROME II.
Y. Umebachi, Dept. of Biol., Fac. of Sci., Kanazawa Univ., Kanazawa.

Papillochrome II, a pale yellow pigment of Papilio butterflies, consists of L-kynurenine(K) and N- β -alanyldopamine(NBAD), and the structure has been reported to be N^4 -[α -(3-aminopropionylaminomethyl)-3,4-dihydroxybenzyl]-L-kynurenine, in which the aromatic amino group of K is bonded to the β -carbon of NBAD (Rembold and Umebachi, 1984). There are two kinds of isomers (IIa and IIb) which show opposite optical activity. Yago et al. (1987) reported that Papillochrome IIa and IIb could be synthesized from K and NBAD by phenoloxidase. In the present report, the enzymatic synthesis has been confirmed with mushroom tyrosinase. The enzymatically synthesized IIa and IIb are similar to the natural ones in decomposition-products and chromatographic behaviour. But the *in vitro* synthesized and natural IIa and IIb are different a little from each other in fluorescence and absorption peak. In addition, yellow fluorescent components (IIIa, IIIb, IVa, b, and Va, b) other than IIa and IIb are absent in the *in vitro* incubation mixture, while they are present in the extract of pale yellow scales. There is a possibility that, although the bonding of the aromatic amino group of K to the β -carbon of NBAD occurs in the reaction mixture with phenoloxidase, another factor may be necessary for turning pale yellow.

BI 50

OCCURRENCE OF A PIGMENT GRANULE CONTAINING XANTHOMMATIN-BINDING PROTEIN IN THE EPIDERMAL CELLS OF THE SILKWORM
H. Sawada¹, M. Tsusue¹, T. Yamamoto²
¹ Biol. Lab. Kitasato Univ. Sagami-hara, ² Matsumoto Branch, Sericultural Experiment Station, Matsumoto, Nagano.

The larval color of many strains of *bombyx mori* is determined by the combination of uric acid and various pigments such as xanthommatin, sepiapterin and sepialunazine. Xanthommatin is much more contained in the integuments of quail mutant than in those of other strains. A large amount of uric acid makes the larval color of many strains opaque. In the present study, pigment granules were purified from epidermal tissues of quail mutant by density gradient centrifugation. From the purified granules the pigment was extracted with acidic methanol and identified as xanthommatin by the different two HPLC systems. Pigment protein was obtained after homogenization of the purified granules with buffer. Based on SDS-PAGE analyses, the molecular weight of the pigment protein was estimated to be 13,000, and the glycoprotein detection using ConA-peroxidase was positive. The pigment protein was precipitated by the addition of salt. These data indicate that the binding between the pigment and the protein is steady one. The present study shows that xanthommatin is localized in the pigment granules of the epidermal cells, and it exists in a combined form with the protein.

BI 51

THE ASSEMBLY OF CHICKEN FEATHER KERATIN IN VITRO.
S. Aihara and K. Ohashi. Dept. of Biol., Fac. of Sci., Chiba Univ. Chiba.

Feather keratin was extracted from the fluff barbs of chicken breast feather with a solution containing 6 M urea, 10 mM Tris, 1 mM EGTA, and 0.1% 2-ME (pH 8.5) at 40°C for 4 h. The extract was dialyzed against a low ionic strength solution at a pH of 8.0, 7.5, 7.0, or 6.5. Feather keratin was dispersed in the solution of pH 8.0. As the pH of the solution decreased, keratin became to form white aggregates. At pH 6.5, approximately 70% of the protein was precipitated. Electron microscopic observation revealed that three types of filaments, whose diameters were 3.5, 10, and 20 nm, respectively, were contained in the aggregates. Ten and twenty nanometer filaments were tangled into clusters. Fine filaments of 3.5 nm in diameter usually associated side-by-side and formed large bundles. The bundles of 3.5 nm filaments occupied the minor part of the aggregates. In the presence of 0.1 M KCl, the keratin aggregates increased in the solution of all pHs tested. Forty percent of the protein was precipitated in a solution of 0.1 M KCl and 10 mM Tris-HCl (pH 8.0). Sheet-like structure, which was made of tightly packed 3.5 nm filaments, was observed in the aggregates besides the 3 types of filaments mentioned above. This structure resembled to the electron microscopic image of the thin section of feather rachis.

BI 52

RETINALS ARE BOUND TO LIPOVITELLIN 1 IN *XENOPUS LAEVIS* EGGS.

T. Irie¹, M. Azuma² and T. Seki².
¹Meijo Gakuin High School, Osaka and ²Dept. Health Sci., Osaka Kyoiku Univ., Osaka.

Eggs of *Xenopus laevis* were homogenized in 20mM Tris-HCl buffer (pH 7.4) and centrifuged at 12000rpm for 20min. All the retinals were detected in the precipitate. The precipitate was solubilized in the buffer containing 0.4M NaCl (NaCl-buffer). Retinals were detected in the supernatant after centrifugation. This behavior of retinals is consistent with that of yolk platelets. The proteins of the yolk platelets in the NaCl-buffer were then fractionated with (NH₄)₂SO₄ at 65% saturation. Most retinals were found in the precipitate. This result shows that retinals are bound to lipovitellin, and not to phosphovitin. The lipovitellin fraction obtained was treated with NaBH₄ and SDS, and passed through a Sephacryl S-200 column. Two major peaks of protein were observed in this gel chromatography. The first peak possessed 330nm absorption derived from the retinyl product in contrast to the second peak without this absorption. The first peak was identified, by SDS-PAGE, with lipovitellin 1 and the second with lipovitellin 2. After treatment with NaBH₄, retinals were not extracted with organic solvents from lipovitellin. These results make it clear that retinals are bound to the protein moiety of lipovitellin 1 in *X. laevis* eggs.

One molecule of Retinal against 20-34 molecules of lipovitellin was contained in the eggs of this animal.

BI 53

A CHANGE IN THE STEROL COMPOSITION OF HAMSTER SPERMATOZOA DURING EPIDIDYMAL MATURATION

M. Awano¹, A. Kawaguchi¹, H. Mohri¹ and M. Morisaki². ¹Dept. Biol., Coll. Arts and Sci., Univ. Tokyo, Tokyo, ²Kyoritsu Coll. Pharmacy, Tokyo.

Sterol are the second major class of lipids in the plasma membrane of mammalian spermatozoa and are considered to regulate the membrane fluidity during maturation. In hamster caput epididymal spermatozoa, cholesterol was found to be the main sterol, whereas only a amount of desmosterol was detected. The sterol composition of hamster cauda epididymal spermatozoa was remarkably different from that of caput epididymal spermatozoa. Desmosterol and another main sterol compound accounted for as much as 90% of the total sterol. The latter was identified as cholesta-7,24-dien-3 β -ol by GC-MS analysis. Furthermore, cholesterol and desmosterol were the major components of mouse cauda epididymal spermatozoa, and rabbit, boar and bull ejaculated spermatozoa. The total amount of sterols in hamster spermatozoa remained constant during epididymal maturation. During maturation, however, the desmosterol and cholesta-7,24-dien-3 β -ol levels increased and the cholesterol level decreased. Cholesta-7,24-dien-3 β -ol appears as a sterol in mature spermatozoa and seems to be a characteristic sterol of hamster cauda epididymal spermatozoa.

BI 54

"COLD-ADAPTED" CHARACTERISTICS OF CALCIUM TRANSPORT IN SCALLOP SARCOPLASMIC RETICULUM

M. Abe¹, J. Nakamura¹, T. Watanabe² and K. Konishi¹. ¹Biol. Inst. Fac. of Sci., ²Dept. of Biol., Tohoku Univ., Sendai

Very active preparation of sarcoplasmic reticulum (SR) from scallop adductor striated muscle was obtained by adjusting pH of the solution, which was used in isolating the SR, to 7.0, i.e., the obtained SR had a calcium transport activity of 0.3-1.5 μ mol/mg protein/min at 12 $^{\circ}$ C. The transport activity was studied by comparing with that of SR from rabbit skeletal muscle at 0-50 $^{\circ}$ C. The maximum activities of scallop and rabbit SR were observed at about 25 and 40 $^{\circ}$ C, respectively. At 12 $^{\circ}$ C (average temperature at habitat of scallop), the activity of rabbit SR decreased by about 1/10 of the maximum level. In the case of scallop SR, however, it decreased only by about 1/2. These decreases coincided with decrease in their ATP hydrolysis activities. On the other hand, the content of phosphorylatable calcium-activated ATPase protein in scallop SR was about a half of that in rabbit SR. The present results suggest that, in scallop SR, turn-over rate of the ATP hydrolysis reaction, which is driving force of the calcium transport, is maintained in a high level even at low temperature.

BI 55

STRUCTURE OF VITELLOGENIN GENE OF THE SILKWORM, *Bombyx mori*

K. Yano, M. Toriyama, S. Izumi and S. Tomino
 Dept. Biol. Tokyo Metropol. Univ., Tokyo

Vitellogenin of *Bombyx mori* is composed of two molecules of heavy chain and light chain encoded by separate mRNAs. We cloned a portion of mRNA sequence for each subunit. In RNA blot analysis, each cDNA hybridized with both heavy- and light-chain mRNAs. Furthermore, RNA blot analysis using a series of DNA fragments prepared from the genomic clone suggested that genes for two vitellogenin subunits overlap, and each mRNA is generated by alternative splicing of a common pre-mRNA.

An additional cDNA clone for the vitellogenin heavy chain was isolated and its nucleotide sequence was determined. The combined amino acid sequences deduced from two cDNA clones revealed an open reading frame corresponding to 1436 amino acid residues, which amounts to about 80% of the predicted heavy mRNA sequence. Computer-aided search failed to detect any significant homology in primary structure between the vitellogenin heavy chain and published peptides.

By comparison of nucleotide sequence between genomic and cDNA clones, we found five introns in the heavy chain gene. A sequence homologous to the consensus sequence of splice junction was present in the last exon. This region might be the site of the alternative splicing which gives rise to the light chain mRNA.

BI 56

MOLECULAR STRUCTURE OF SYMBIONIN, A MAJOR PRODUCT OF AN APHID ENDOSYMBIONT *IN VIVO*. K. Kakeda¹, E. Hara², M. Kengaku¹, H. Ishikawa¹. ¹Zool. Inst., Fac. of Sci., Univ. of Tokyo, Tokyo, and ²Shiseido Res. Inst., Tokyo.

We have demonstrated that an endosymbiont of the pea aphid is under a stringent control and synthesizes almost single protein species, symbionin which is supposed to play a key role in the intracellular symbiosis in aphid.

We purified symbionin, which is an acidic protein (pI=5.8) with a molecular mass of 800kDa. Electron micrograph of the negatively stained molecules showed that symbionin is composed of two stacked rings of 7 subunits (63kDa) each. Symbionin and *E. coli* heat shock protein, groEL protein, are very similar in molecular mass and native structure. The groEL protein cross-reacted strongly with polyclonal rabbit antibodies raised against symbionin. Their amino acid compositions were similar and N-terminal 40 amino acid sequences had more than 90% similarity.

These results indicated that symbionin and the groEL protein are homologous to each other. The groEL protein is a member of "chaperonin" family of molecular chaperones which include the Rubisco subunit-binding protein of chloroplasts and mitochondrial heat-shock protein hsp60. Further researches of symbionin must bring important evidence for the endosymbiosis theory for the origin of eukaryotic cell organelles.

BI 57

LOCALIZATION AND SYNTHESIS OF SYMBIONIN IN *ACRTHOSIPHON PISUM* T. Fukatsu¹, E. Hara² and H. Ishikawa³. ¹Zoological Inst., Fac. of Sci., Univ. of Tokyo, and ²Shiseido Res. Inst., Tokyo.

We have successfully purified symbionin and prepared anti-symbionin rabbit antiserum. Using the antiserum we studied immunohistochemically the localization of symbionin on the 5µm thick paraffin sections and the 0.5µm thick Spurr sections of the pea aphid. The major results obtained are as follows: (1) in the aphid tissues, symbionin was detected only in the bacteriocytes, (2) in the bacteriocyte, symbionin was localized in the endosymbionts and was not detected in either nucleus or cytoplasm, (3) in the endosymbiont, symbionin was localized in a characteristic pattern. In an effort to know where symbionin is synthesized, we injected cycloheximide and ³H-leucine into the aphid in order to label newly-synthesized symbionin specifically. Microautoradiogram on the 5µm thick paraffin sections of the labeled aphid indicated that symbionin is synthesized exclusively in the cytoplasm of the bacteriocyte, suggesting that symbionin is synthesized in the endosymbiont.

BI 58

ANALYSIS OF THE GENE ENCODING SYMBIONIN, AN APHID ENDOSYMBIONT-SPECIFIC PROTEIN. C. Ohtaka and H. Ishikawa. Zool. Inst. Fac. of Sci., Univ. of Tokyo, Tokyo.

We have found and previously reported that the heat treatment causes disruption of the symbiotic system of the aphid mycetocyte, and that heat-treated insects cease to synthesize symbionin. To elucidate the molecular mechanism of this response and the function of symbionin, it is necessary to isolate and analyze the gene encoding symbionin.

In this paper we reported analysis of symbionin gene by the method of genomic southern hybridization. We used the groEL gene of *E. coli* as a DNA probe.

We constructed a recombinant plasmid (pOTKGI) carrying the groE genes from a groE transducing phage using pUC19 as a vector. The groEL protein over-produced in JM109/pOTKGI showed an increased cross-reactivity with anti-symbionin antiserum on western blotting, confirming that symbionin is a homolog of the groEL protein immunologically. We analyzed genomic DNA of symbiont by southern hybridization with groE gene fragments from pOTKGI as probes. As a result, unique 5.4kb and 6.5kb fragments were detected from HincII and HindIII digests, respectively. We also analyzed by other restriction endonucleases and determined the target sites of symbionin gene and its flanking regions.

BI 59

THE ROLE OF INTRACELLULAR SYMBIONTS IN NITROGEN METABOLISM IN APHID T. Sasaki and H. Ishikawa. Zoological Inst. Fac. of Sci., Univ. of Tokyo, Tokyo

The levels of uric acid, ammonia and amino acids in the honeydew of symbiotic and sterile, aposymbiotic pea aphids *Acyrthosiphon pisum* were determined. The honeydew of neither symbiotic nor aposymbiotic aphids contained a detectable amount of uric acid. A small amount of ammonia was present in the honeydew of both symbiotic and aposymbiotic aphids. Amino acid composition in the honeydew was compared with that of phloem sap on which aphids feed. Asparagine and glutamine were the two most abundant amino acids in the phloem sap. It was revealed that amino acid composition in the honeydew changed due to age of the aphids. Asparagine and glutamine were smaller in amount in the honeydew of symbiotic adults (21-23 day) than in that of aposymbiotic adults at the same age. In the honeydew of old symbiotic aphids (42-48 day), asparagine was the only amino acid rich in amount. In the honeydew of old aposymbiotic aphids, not only asparagine but glutamine was abundant. When ¹⁴C-labelled glutamine was injected into 19-22 day aphids, its incorporation into symbiotic aphids was significantly higher than that of aposymbiotic aphids. Among several amino acids synthesized from injected glutamine, isoleucine was synthesized exclusively by symbiotic aphids.

BI 60

INITIATION REGION OF TRANSCRIPTION OF THE RIBOSOMAL RNA GENE OF THE PEA APHID.
O.Y.Kwon, K.Ogino, H.Fujiwara and H.Ishikawa. Zool. Inst., Fac. of Sci., Univ. of Tokyo, Tokyo.

A lambda recombinant phage which contains an entire unit of the pea aphid rDNA has been isolated. The rDNA clone was digested with BamHI and XbaI, and resulted fragments were subcloned into the BamHI-XbaI site of plasmid pUC119. Digestion with restriction enzyme KpnI detected 212bp repetitive elements present in the non-transcribed spacer (NTS), whose entire sequence of 3097bp was determined. Each sub-repeat was shown to a characteristic oligo-T tract. The initiation and termination site of the aphid rDNA were determined by the S1-mapping and primer extension method. The initiation site was located at 124bp downstream of the XhoI site of a fragment, which is several hundred nucleotides downstream of the edge of the tandemly-repeating elements in the NTS. Judging from the length heterogeneity of DNA fragment that was protected against S1-nuclease, it was suggested that the termination site may be multiple and the terminal region has a special structure consist of stem-loops. The 5'-end of the 18S rRNA-coding sequence was located at a position 180bp upstream of the XbaI site in a fragment encoding 18S rRNA. The length of external transcribed spacer (ETS) was estimated to be about 800bp.

BI 61

STRUCTURAL ANALYSIS OF CHROMOSOMAL FRAGMENT IN GENETIC MOSAIC FOR LARVAL BODY MARKING OF *BOMBYX MORI*.

H. Fujiwara. Zoological Inst., Fac. of Sci., Univ. of Tokyo, Tokyo.

Several genetic mosaics for larval body marking of the silkworm *Bombyx mori*, have been induced by X-ray irradiation and stably maintained in laboratory stock. Previous studies using genetical and cytological methods indicated that loss of the chromosomal fragments carrying the genes for body marking, during some developmental stages, may give rise to this type of mosaicism. At the molecular level, however, such a chromosomal fragment has not been evidenced for a long time.

Here I report that a DNA molecule of about 2.3-2.5 megabases (Mb) are found specifically in two mosaic strains of mottled P₅, and not in any other phenotype and strain, using pulsed field gradient gel electrophoresis (PFGE). Southern blot hybridization demonstrated that the DNA fragment contains some of chorion gene families which map 6.9% apart from the p₅ locus on the edge of chromosome 2. Some probes containing middle and late chorion genes, showed restriction fragment length polymorphism (RFLP) among individuals in the same generation of mottled P₅ strains. This RFLP was co-inherited with their phenotypes of body marking (p or P₅). The result suggests that the RFLP marker is linked to the chromosomal fragment or directly to the p₅ phenotype.

BI 62

BIOSYNTHESIS OF CUTICLE PROTEINS OF THE SILKWORM *Bombyx mori*: EXPRESSION OF LARVAL AND PUPAL CUTICLE PROTEINS.

H.Nakato, S.Izumi and S.Tomino
Dept. Biol. Tokyo Metropolitan Univ., Tokyo

Biosynthesis of cuticle proteins of the silkworm *Bombyx mori* was studied.

A protein component of the larval cuticle (LCP2) was purified from the urea extract of integument. By use of antibody probes expression of the LCP gene during development was compared with that of the pupal cuticle protein (PCP) gene. LCP2 was not detected in the embryonic extract but was detectable in larvae 10 hours after hatching. Thereafter, LCP2 epitope was present in the integument throughout the larval stage and disappeared at larval-pupal transformation. Two proteins immunologically related to LCP2 were also present in the adult abdominal integument. These proteins are supposed to contain portions of primary structure in common with LCP2.

RNA blot analysis using LCP and PCP cDNA as probes demonstrated that the expression of cuticle proteins is regulated at the mRNA level in a tissue- and stage-specific manner. The LCP2 mRNA in epidermis was maintained at high level until few days after the forth molt and then gradually declined, which strongly suggests the possibility that the expression of the LCP2 gene during the larval development is regulated by juvenile hormone.

BI 63

RABBIT PEPSINOGENS- SEQUENCE OF cDNA, MOLECULAR EVOLUTION, AND EXPRESSION DURING DEVELOPMENT.

T.Kageyama¹, K.Tanabe² and O.Koiwai³
¹Primate Res.Inst., Kyoto Univ., Inuyama,
²Aichi Cancer Ctr.Inst., Nagoya and ³Aichi Colony, Kasugai

Pepsinogens of rabbit stomach were determined during developmental stages. Several zymogens were found and most of them were purified including two infant-specific zymogens and two adult-specific ones. They had different amino acid compositions and N-terminal sequences, a result that showed they were products of different genes. cDNA recombinant clones of 6 zymogens were isolated from cDNA libraries of infant and adult gastric mucosa. Their nucleotide sequences were different from one another. Zymogens were composed of 15-residue signal peptide, 46-residue activation peptide and 326-residue pepsin moiety. Northern analysis using synthetic oligonucleotides as probes showed that expression of each zymogen changed markedly during development.

BI 64

IMMUNOHISTOCHEMICAL DETECTION OF SEA URCHIN NUCLEAR ANTIGEN AGAINST ANTI-MOUSE TOPOISOMERASE II ANTIBODY.
M.Morioka¹, H.Ishikawa¹ & H.Shimada².
¹Zool.Inst., Fac.of Sci., Univ.of Tokyo, Tokyo, ²Zool.Inst., Fac.of Sci., Univ.of Hiroshima, Hiroshima.

Previously, we have reported that the binding of AP4A to nuclear matrix is important in the process of S phase initiation in the cleavage-stage embryos of sea urchin. In this report, we describe the immunohistochemical detection of DNA topoisomerase II (Topo II)-like antigen in sea urchin nuclear matrix which may be one of the AP4A-binding proteins.

The molecular weight of the sea urchin antigen cross-reacted with anti-mouse FM3A Topo II antibody was estimated by immunoprecipitation to be 175kd which is similar to that of mouse Topo II. Immunohistochemical study of the intracellular distribution of this antigen revealed that the antigen is predominantly localized in the interphase nuclei but disappears from the mitotic nuclei. The nuclei retained the antigenicity even after treating the nuclei with DNase, RNase and 2M NaCl, indicating that the antigen is tightly associated with the nuclear matrix, and diffuses out from the nuclei upon nuclear disassembly during mitosis. It was also demonstrated that mouse FM3A Topo II preparation shows the highly specific AP4A-binding activity.

BI 65

ISOLATION OF cDNA FOR SEA URCHIN COLLAGENS. K. Shimizu and K. Yoshizato.
Develop. Biol. Lab., Dept. of Biol., Fac. of Sci., Tokyo Metropolitan Univ., Tokyo.

Biochemical characterization had been performed for collagens derived from test of sea urchin *Asthenosoma iijimai* (Zool. Sci., 4, 1020, Zool. Sci., 5, 1233). The collagens showed characteristics similar to mammalian type I collagen, but were more complex in respect to subunit structures. To get more precise information on sea urchin collagens, we tried to isolate their cDNA. The cDNA library for mRNA in test of *A. iijimai* was constructed using λ gt11 expression vector. Screening of cDNA for collagens was performed by enzyme immuno assay for the β -galactosidase fusion proteins using rabbit anti sea urchin collagens antiserum. As the result, 5 clones were obtained. One of these clones, λ cSUCol-1, was characterized in detail, because inserts of five clones had the same length. The insert of λ cSUCol-1, consist of 1.3 kb, had Sac I and Sma I sites at 0.5 kb. The epitope selection by the fusion protein revealed that cSUCol-1 encoded amino acid sequence common to two of five -chains of sea urchin collagens. The fusion protein had not sensitivity to bacterial collagenase nor affinity to fibronectin. Considering that antiserum used for screening was raised against sea urchin collagens extracted by digesting with pepsin, it is concluded that cSUCol-1 encodes the sequence from non-coding region of C-terminal to a few amino acids of C-terminal region in triple helical domain.

BI 66

TRIPLEX DNA IN 5'FLANKING REGION OF SEA URCHIN ARS GENE.
T.Yamamoto, K.Yamada, K.Akasaka, *S.Irie, H.Shimada. Zool. Inst., Fac. Sci., Hiroshima Univ., *Mitsubishi-kasei Inst. of Life Sci. Machida.

Sea urchin arylsulfatase(Ars) gene that is expressed in stage-specific and cell-lineage-specific manners during embryogenesis contains a polypyrimidic tract of about 200bp in its 5'flanking region. These (dT-dC)n (dA-dG)n runs are found at unexpectedly high levels in eukaryotic genomes. Such sequences show a hypersensitivity to single-strand specific nuclease and the sensitivity is dependent on pH and supercoil density, which indicates that they are adopting a triplex structure. Plasmid containing a polypyrimidic tract were constructed, and assayed for the S1 nuclease sensitivity.

The result showed that only plasmid containing a polypyrimidic tract were sensitive to S1 nuclease digestion at pH 5.0.

This result was interpreted as that the polypyrimidine region of the Ars gene contains a triplex structure at pH 5.0.

Presence of the nuclear proteins that bind to this polypyrimidine region was revealed by a gel shift assay.

BI 67

SEQUENCE ANALYSIS OF THE cDNA FOR A GLOBIN-LIKE GENE OF *PARAMECIUM CAUDATUM*. I.Hirai¹, K.Yamauchi¹, T.Ochiai² and I.Usuki³, ¹Dept. of Biol., Fac. of Sci., Shizuoka Univ., Shizuoka, ²Dept. of Biol., Fac. of Sci., and ³Dept. of Biol., Coll. of Gen. Educ., Niigata Univ., Niigata

We tried to clone the cDNA of *Paramecium caudatum* globins, in order to investigate gene structures of protozoan hemoglobin genes, which are assumed to have primitive type of vertebrate genes. For the purpose, two rabbits was immunized against purified *Paramecium* major hemoglobin with 1.1 kilo dalton. Polyclonal antibody from the rabbits and rat major α -globin cDNA (supplied from Dr. T. Okazaki, Nippon Med. School, Tokyo) were used to screen a *Paramecium* cDNA library in 7×10^5 λ gt11. As the results, one clone with 0.6 kilo base cDNA was obtained with the rat α -globin cDNA probe. The cDNA cloned was composed of more than 471 bases with poly(A) tail, and it was in a homology of 48% to the rat globin cDNA. However, no clone was detected with antibody as far as examined. This may attribute to the fact that the cDNA coding the globin-like protein contains sporadically several TAA and TAG in its sequence. These codons are known to act as terminal signals in *E. coli*, although *Paramecium* can use them as the codons for Gln or Glu.

BI 68

EXPRESSION OF SOME PROTOONCOGENES AND DNA SYNTHESIS IN THE REGENERATING RAT LIVER.
K. Asami, C. Muraiso and H. Matsudaira.
Div. Biol. Natl. Inst. Radiol. Sciences,
Chiba-shi 260.

Expression of several protooncogenes has been reported to occur during pre-replicative phase of liver regeneration. To know the causal relationship between these protooncogene expression and DNA synthesis, the changes in the expression of protooncogenes were examined in relation to the inhibition of DNA synthesis by X rays. Our previous experiments showed that 4.8 Gy of X rays inhibited both the DNA synthesis and the increase in the activity of the nuclear protein kinase specific for histone H1. The level of H-ras, K-ras and c-myc mRNA was elevated during the prereplicative phase of regeneration. The time course of the expression of these protooncogenes was different each other: the K-ras mRNA level reached maximal at 9 h after partial hepatectomy and then decreased continuously, while that of the H-ras mRNA kept high from 9 to 27 h, the peak of DNA synthesis. C-myc was expressed biphasically with peaks at 3 h and 9 h. Their expression was not inhibited with X rays. Thus, the expression of these protooncogenes may not be directly related to the onset of DNA synthesis or a process or processes linking the expression of some protooncogene with the onset of DNA synthesis may be sensitive to X rays.

BI 69

GLUCOSE-STIMULATED PHOSPHORYLATION OF 64 kDa PROTEIN OF HUMAN POLYMORPHONUCLEAR LEUKOCYTES IN A CELL-FREE SYSTEM
M. Shibata^{1,2}, O. Koshio¹, T. Ohoka², S. Mizuno¹ and K. Suzuki¹. ¹Dept. of Antibiotics, National Institute of Health, Tokyo and ²Dept. of Biology, Fac. of Sci., Tokyo Metropol. Univ., Tokyo.

Chemoattractants such as fMet-Leu-Phe (fMLP) and LUCT which is a member of IL-8 family stimulate the phosphorylation of 64 kDa protein (p64) in the ³²P-labeled intact human polymorphonuclear leukocytes. To elucidate the mechanism of the phosphorylation with fMLP- and LUCT-stimulation, we have examined in a cell-free system. Glucose stimulated the phosphorylation of p64, but fMLP did not. The phosphorylation activity existed in the cytosol fraction containing over 30 kDa protein. ³²P-incorporation into p64 was increased in a dose-dependent fashion of glucose with 33 μ M in the maximum stimulation and 1.4 μ M for ED₅₀. ³²P-Phosphoserine was detected by phosphorimino acid analysis of phosphorylated p64. None of glucose derivatives and metabolites of glycolysis stimulated the phosphorylation, but glucose-1-phosphate, glucose-6-phosphate, fructose-6-phosphate and fructose-1,6-diphosphate (1 μ M, respectively) inhibited the phosphorylation stimulated by 1 μ M glucose. Cyclic nucleotides (1 μ M) and protein kinase inhibitors, H-7 (10 μ M), H-8 (10 μ M), W-7 (100 μ M) and staurosporine (50 nM), did not affect the phosphorylation.

These results strongly suggest that the phosphorylation was catalyzed by a glucose-regulated protein kinase.

BI 70

PURIFICATION OF THE PLASMA AMIDOLYTIC ENZYME-INHIBITING SUBSTANCE IN THE HEMOLYMPH OF AN ASCIDIAN, HALOCYNTHIA RORETZI. T. Abe, F. Shishikura, S. Ohtake and K. Tanaka, Department of Biology, Nihon University School of Medicine, Tokyo.

In the previous report (Zool. Sci., 5: 1242, 1988) we have shown that the hemolymph plasma of an ascidian, Halocynthia roretzi, includes amidolytic enzyme(s) and the enzyme-inhibiting substance. We improved the purification methods for the inhibitory substance.

The methods was as follows; hydrophobic interaction chromatography on Toyopearl HW 65 and Butyl Toyopearl 650 (HIC), affinity chromatography (AC) on Heparin-Sepharose 4B, and ion exchange chromatography (IC) on CM Toyopearl 650. The activity was assayed using ascidian plasma or partially purified enzyme as enzyme sources, and Boc-Leu-Gly-Arg-MCA as substrate (Tris-HCl 20mM CaCl₂/pH8.0 30min, 25°C).

This substance was very unstable after HIC and decreased its activity during dialysis. The highly active fraction was finally obtained from IC, however, two bands were recognized in SDS-PAGE with or without 2-mercaptoethanol.

This substance (fraction of AC) inhibits strongly the purified ascidian enzyme and trypsin, moderately thrombin and weakly plasmin. An analysis by Lineweaver-Burk plot showed that the type of inhibition to trypsin was non-competitive.

BI 71

PURIFICATION OF PLASMA ENZYME FROM THE ASCIDIAN, HALOCYNTHIA RORETZI, HEMOLYMPH. AN IMPROVED METHOD.
F. Shishikura, T. Abe, S. Ohtake and K. Tanaka. Dept. of Biol., Nihon Univ. Sch. of Med., Tokyo.

Purification procedures of amidase in hemolymph plasma of H. roretzi have been improved by three steps of chromatography involving hydrophobic interaction chromatography on Toyopearl HW 65, ion exchange chromatography on DEAE-Toyopearl 650 and affinity chromatography on dextran sulfate-Sepharose 4B, where the enzyme fractions and inhibiting-substance were separated by the first step on Toyopearl HW 65. The DEAE fractions which was isolated as almost in pure state was fractionated into four to six enzyme peaks by dextran sulfate-Sepharose 4B. The enzyme was extensively stabilized during the procedures by the addition of 0.1% Brij 35 to the buffer (50 mM Tris-HCl, pH 8.0) and the specific activity of final enzyme fraction is about 5000. Fractions of the enzyme activity were monitored by 10 fluorogenic substrates, which have been demonstrated to be hydrolyzed (Z.S., 4:1021, 1987), resulting slightly differences among the peaks. Our ascidian plasma enzyme found to convert horseshoe crab coagulogen into coagulin (gel-form) which strongly indicates the plasma enzyme has a biological role in the ascidian hemolymph.

BI 72

A CALCIUM-DEPENDENT GALACTOSE-BINDING LECTIN FROM THE TUNICATE POLYANDROCARPA MISAKIENSIS. ISOLATION CHARACTERIZATION AND AMINO ACID SEQUENCE.

T.Suzuki, T.Takagi*, T.Furukohri, K.Kawamura and M.Nakauchi
 Dept. of Biol., Fac. of Sci., Kochi Univ., Kochi;
 *Biol. Inst., Fac. of Sci., Tohoku Univ., Sendai.

A lectin was isolated from the homogenate of the tunicate *Polyandrocarpa misakiensis* by heat treatment, ammonium sulfate fractionation, gel filtration and high-performance ion exchange chromatography. The lectin bound to an immobilized D-galactose column in the presence of calcium ion with a threshold of 500 μ M, and eluted completely with 5 mM EDTA buffer. It did not bind to immobilized D-mannose or N-acetyl-D-galactosamine columns. Thus *Polyandrocarpa* lectin was found to be a calcium-dependent galactose-binding lectin.

The complete amino acid sequence of *Polyandrocarpa* lectin was determined. It is composed of 125 amino acid residues, contains no carbohydrate group, and has a calculated molecular mass of 14,034. The lectin contains four half-cystines, and Cys-21 and Cys-119, and also Cys-96 and Cys-111 form intrachain disulfide bridges, respectively. The amino acid sequence of *Polyandrocarpa* lectin shows about 20-30% homology with those of fly, barnacle, sea urchin, and several vertebrate lectins that belong to C-type lectin. Although the physiological role of *Polyandrocarpa* lectin is not clear, preliminary experiments suggest that the lectin might be related to defense mechanisms because it has a strong antibacterial activity.

BI 73

TISSUE SPECIFICITY OF TROPOMYOSIN ISOFORMS OBTAINED FROM SPINY LOBSTER AND LOBSTER MUSCLES.

M.Itoh, H.Koyama and T.Ishimoda-Takagi.
 Dept. of Biol., Tokyo Gakugei Univ., Tokyo.

We have previously shown that several isoforms of tropomyosin (TM) were contained in the spiny lobsters, *Panulirus japonicus* and *P. cygnus*, and distribution of these isoforms was tissue-specific. To investigate similarity of the distribution of TM isoforms in other species of the lobster, we examined tissue specificity of TM isoforms in the American lobster, *Homarus americanus*, because the muscles of this species have been well characterized morphologically and biochemically. Heterogeneity and tissue specificity of the TM isoforms were similar to those observed in the spiny lobster, although electrophoretic mobilities of the TM isoforms were not identical with those of the spiny lobster and cardiac muscle contained several TM isoforms unique to the cardiac muscle. Since distribution of fast and slow fibers in the claw and abdominal muscles of *H. americanus* had been studied, we examined TM isoforms involved in the fast and slow muscles. The composition of TM isoforms involved in these muscles was distinct from each other. Similar tendency was also observed in the abdominal muscles of *P. japonicus*. These results suggested that tissue specificity of TM isoforms correlated with proportions of fiber types involved in the respective muscle tissue.

BI 74

THE EAR-SHELL MYOGLOBIN IS COMPOSED OF AN UNUSUAL 39 KDA POLYPEPTIDE CHAIN

T.Suzuki, T.Furukohri
 Dep. of Biol., Fac. of Sci., Kochi Univ. Kochi

An unusual myoglobin was isolated from the buccal mass of the ear-shell *Sulculus diversicolor aquatilis*. The myoglobin consists of a 39 kDa polypeptide chain which is about double the size of the unusual myoglobin subunit, contains one heme per molecule, and has an unusual spectral property in the oxy-form. On the basis of these properties and partial amino acid sequencing, we propose that *Sulculus* myoglobin has a didomain structure, and that one of the two domains does not function as an oxygen-binding domain. So far, a myoglobin of this type has not been described in molluscs. The similar type of myoglobin is reported only in the nematode *Ascaris*. (Suzuki & Furukohri (1989) *Experientia* in press)

BI 75

PARAMECIUM OXYMYOGLOBIN: ISOLATION AND STABILITY PROPERTY

Y. TSUBAMOTO and K. SHIKAMA. Biol. Inst., Tohoku Univ., Sendai.

Oxymyoglobin (MbO₂) was isolated directly from *Paramecium caudatum* (syngen 3, stock StG1), cultivated for seven days at 25 °C in a bacteria-free Dryl's solution containing 0.4 % (w/v) reddish bean broth, and was examined for its stability property over the pH range of 4.3-11.3 in 0.1 M buffer at 25 °C. The rate of autooxidation of *Paramecium* MbO₂ to metmyoglobin (metMb) increases rapidly with increasing hydrogen ion concentration, a rate minimum appears at pH 9 and a small increase occurs again at higher values of pH.

Compared with sperm whale MbO₂, as a reference, *Paramecium* MbO₂ was unstable over the whole range of pH studied, but its pH dependence of stability is quite similar to that of sperm whale MbO₂, which has been shown to involve the distal histidine as the catalytic residue in the proton-assisted autooxidation process.

We have also demonstrated that *Paramecium* myoglobin appears in the latter phase of growth curve, whereas cytochrome c occurs constantly.

BI 76

APLYSIA OXYMYOGLOBIN WITH AN UNUSUAL STABILITY PROPERTY: INVOLVEMENT OF TWO KINDS OF CARBOXYL GROUPS
A. Matsuoaka and K. Shikama. Biol. Inst., Tohoku Univ. Sendai.

Unlike mammalian myoglobins, *Aplysia* myoglobin contains only a single histidine residue that combines with the heme iron at the proximal position, and hence lacks the usual distal one. We have recently succeeded in isolating native oxymyoglobin (MbO_2) directly from the radular muscle of *Aplysia kurodai*, a common species around the Japanese coast, and have examined its stability property.

Aplysia MbO_2 is extremely susceptible to autoxidation, and its pH dependence is also unusual, involving two kinds of dissociable group with $\text{pK}_1=4.3$ and $\text{pK}_2=6.1$, respectively. In order to characterize these groups thermodynamically, we have studied the effect of temperature on the dissociation constants, K_1 and K_2 , by analyzing the pH dependence for the autoxidation rate of *Aplysia* MbO_2 at 15, 25 and 35 °C. The resulting thermodynamic parameters for each group were both those to be expected for the ionization of a carboxyl group, and we have therefore concluded that the protonation of these groups is responsible for an increase in its autoxidation rate in the acidic pH range.

BI 77

MOLECULAR ARCHITECTURE OF MICROTUBULE-ASSEMBLY INHIBITOR PROTEIN.

S. Kotani¹, G. Kawai², S. Yokoyama³, and H. Sakai³. ¹Dept. Biochem. Eng. & Sci., Kyushu Inst. Tech., ²Fac. Eng., Yokoyama National Univ., and ³Dept. Biophys. & Biochem., Fac. Sci., Univ. of Tokyo.

The structure of microtubule-assembly inhibitor protein (MIP) was studied by proton nuclear magnetic resonance (NMR) and limited proteolysis. The NMR experiment revealed that about half the amino acid residues in MIP are highly mobile and that the other half fold tightly. By limited proteolysis using subtilisin, we obtained a 17-kDa fragment which retains the activity to inhibit microtubule assembly. NMR analysis indicated that this fragment contains folded region. Most of the acidic residues are clustered in the mobile region. Consequently, MIP consists of two distinct domains; one forms a rigid globule essential for its activity to inhibit microtubule assembly, and the other is highly mobile. The acidic mobile domain tails from the globule. Function and tertiary structure of these two domains appeared to be independent from each other. The mobile domain may be responsible for the function of MIP other than the inhibition of microtubule assembly.

BI 78

BIOPTERIN AND 7-ISO BIOPTERIN SECRETED INTO SALIVA

Terumi Sueoka and Setsuko Katoh. Department of Biochemistry, Meikai University School of Dentistry, Sakado, Saitama 350-02

In the salivary glands, as well as in the brain, the level of tetrahydrobiopterin (BH₄) also seems to control the formation of catecholamines. We examined the secretion of biopterin in human saliva as a reliable standard for the degree of pteridine metabolism in the gland. Whole saliva was collected after the identical stimulation from young adults of similar age during the same time of the day. Saliva was treated with iodine in trifluoroacetic acid and oxidized biopterin was analyzed by a reverse phase HPLC column with the fluorometer. Biopterin (6-dihydroxypropyl pterin) was found in all samples tested (n=9): 1.270 ± 0.255 (male); 1.461 ± 0.624 (female) ng/ml saliva. These were about 60 % of biopterin level in serum. Another fluorescent compound which was identical with 7-iso biopterin (7-dihydroxypropyl pterin, an isomer of biopterin) in retention time on HPLC was found in all samples examined. Although naturally occurring pterins are 6-substituted derivatives, some 7-substituted pterin(s) might exist in saliva at any rate, since 7-carboxypterin could be detected in saliva by HPLC after KMnO_4 -oxidation. The amount of 7-iso biopterin in saliva was less than few % of 6-substituted biopterin. This new pterin was first found most recently in urine from a patient with hyperphenylalanemia. Some loading tests of BH₄ by other workers showed a possible course in the formation of 7-iso biopterin from 6-biopterin.

BI 79

EFFECTS OF METHYLMERCURY CHLORIDE (MM) ON THE SYNTHESIS OF PROTEIN SPECIES IN THE CENTRAL AND PERIPHERAL NERVOUS TISSUES OF THE RAT.

Y. Terui, H. Kasama, S. Onata, and H. Sugano. Dept. of Biochem., Fac. of Sci., Niigata Univ., Niigata.

The accumulated data suggest that inhibition by MM of protein synthesis in nervous tissues is closely related with the neurotoxicity of this agent. The present study was undertaken to clarify whether the synthetic rates of various protein species in nervous tissues of the rat is differentially affected by MM. Poly(A)⁺mRNA fractions or polysomes purified from rat brains were translated in reticulocyte lysate system. The proteins labelled with ³H-Leu(control) or ³⁵S-Met(MM-treat.) were mixed and analyzed by 2D-PAGE. The radioactivity measurement in the protein spots on the gels revealed that the in vivo action of MM on the synthetic rates were not uniform for individual protein species: there were groups of proteins the synthetic rates of which were stimulated, inhibited, and unchanged, respectively, at the symptomatic period of MM intoxication. The qualitatively similar but quantitatively more marked changes were found when the dorsal root ganglion slices from control and MM-treated rats of the latent period of MM intoxication were labelled in vitro and processed as described above.

BI 80

MEMBRANE POTENTIAL OF *PLASMODIUM YOELII*,
A RODENT MALARIA PARASITE.
K. Tanabe and A. Izumo. Lab. of Biol.
Osaka Institute of Technology

Membrane potential of mouse erythrocytes infected with *P. yoelii* was monitored by two methods. Infected erythrocytes were incubated with a cationic permeant dye rhodamine 123 (R123) and localization of R123 was examined by fluorescence microscopy. R123 at 10 $\mu\text{g/ml}$ accumulated in the parasite cytosol but not in the host cell cytosol. At 0.1 $\mu\text{g/ml}$, R123 stained a body resembling a mitochondrion with rod or spherical shape. Cytoplasmic fluorescence disappeared by CCCP, a protonophore, and DCCD, an inhibitor of H^+ -ATPase, but not by KCN, NaN₃, and antimycin A. In contrast, R123 associated with mitochondrion-like body was disappeared by all those inhibitors. Measurements of membrane potential with transmembrane distribution of tetraphenylphosphonium revealed the membrane potential of infected cells to be -49 mV and that of normal cells to be -6 mV. The parasite membrane potential was markedly abolished by CCCP and DCCD but was affected marginally by inhibitors of respiration. These results indicate that *P. yoelii* possesses the plasma membrane and mitochondrial membrane potentials with different biochemical properties.

BI 81

THE PRIMARY STRUCTURE OF EXOGASTRULA-INDUCING PEPTIDE B PURIFIED FROM EMBRYO OF THE SEA URCHIN, *ANTHOCIDARIS CRASSISPINA*.
T. Suyemitsu, Y. Tonogawa and K. Ishihara.
Dept. of Regulation Biology, Fac. of Sci.,
Saitama Univ., Urawa.

The complete amino acid sequence of exogastrula-inducing peptide B purified from embryos of the sea urchin, *Anthocardis crassispina* was determined. S-pyridylethylated peptide B was cleaved with lysyl endopeptidase. The resulting peptides were purified by RP-HPLC. The N-terminal amino acid sequencing of S-pyridylethylated peptide B and the lysyl endopeptidase peptides was achieved with automated Edman degradation. The C-terminal amino acid sequences of S-pyridylethylated peptide B and the lysyl endopeptidase peptides were determined by digestion with carboxypeptidase Y.

The exogastrula-inducing peptide B was a mixture of four peptides, that is, peptide A, A(-), An and An(-) which are the variations of peptide A. The C-terminal amino acid sequences of peptides A(-) and An(-) were -Pro-Arg-Thr, while those of peptides A and An were -Pro-Arg-Thr-Glu. The amino acid residues at position 36 in peptides An and An(-) were replaced from Asp in peptides A and A(-) to Asn. The peptides A, A(-), An and An(-) were composed of 52, 51, 52 and 51 amino acid residues and their molecular weights were calculated to be 5754, 5625, 5753 and 5624, respectively.

DB 1

NERVE NET FORMATION IN BUDDING OF HYDRA
H. Mizumoto^{1,2} and O. Koizumi¹
¹Physiol. Lab., Fukuoka Women's Univ.,
Fukuoka, ²Dept. Biol., Fac. Sci., Kyushu
Univ., Fukuoka

We are studying the nerve net formation using mutants and chimeras of *Hydra magnipapillata*. We reported that the nerve net formation during head-regeneration was controlled by environments provided by epithelial cells in the last annual meeting (Zool. Sci., 5(6), 1255, 1988). All abnormalities were due to epithelial cells, except the defect of 2nd step of multi-headed mutant which are due to nerve cells.

In the present study, we examined the nerve net formation in the budding head using mutants. The abnormalities of nerve net formation due to epithelial cells during head-regeneration were not observed during budding. Only an abnormality due to nerve cells was observed similarly during both regeneration and budding.

DB 2

BASAL DISK FORMATION IN HYDRA, *P. robusta*.
DIFFERENTIATION OF THE BASAL DISK GLAND
CELLS AND THE DNA SYNTHESIS.
Y. Kobayakawa and M. Yuge. Biological
Laboratory, College of General Education,
Kyushu University 01, Fukuoka.

The basal disk gland cells containing amounts of DNA corresponding to 4n differentiate from the peduncle ectodermal epithelial cells containing less than 4n. Then it is suggested that the S-phase is needed for the basal disk gland cell differentiation (Dübel et al., 1987).

We examined this suggestion by studying the BrdU-incorporation. In the foot region of steady state hydra, many ectodermal epithelial cells in the lower region of the peduncle just neighboring to the basal disk incorporated BrdU, while differentiated basal disk gland cells never did. This indicates that the ectodermal epithelial cells go through the S-phase before differentiation into the basal disk gland cells. However, in the foot amputated hydra, some did not incorporate BrdU in the regenerated basal disk gland cells. Treatment with DNA synthesis inhibitor, aphidicholin, through the regeneration period did not suppress the reappearance of monoclonal antibody AE03-positive granules, which are specifically distributed in the basal disk gland cells. Then, we suggest that in the regenerating hydra the S-phase is dispensable for the basal disk gland cell differentiation.

DB 3

CELL LINEAGE RESPONSIBLE FOR THE ADULT SKELETON IN A SAND DOLLAR, PERONELLA JAPONICA.

S.Amemiya, Misaki Marine Biol. Station, Univ. of Tokyo, Kanagawa.

The cell lineage responsible for larval spicules in sea urchins has generally been believed to originate from micromeres of embryos at the 16-cell stage. However, no evidence has ever been provided to indicate the cell lineage giving rise to the adult skeleton. Peronella japonica, a sand dollar distributed only around the coast of Japan, has comparatively large eggs (ca. 0.3 mm in diameter) which develop rapidly to form an adult skeleton within a few days, and is therefore an appropriate material for studying this aspect. I examined the cell lineage responsible for the adult skeleton of P. japonica by three different approaches. First, mesomeres or macromeres were isolated at the 16-cell stage, and mesomere pairs, single macromeres, or aggregates of 8 mesomeres or 4 macromeres were cultured. Second, 4 micromeres or 4 macromeres were cultured in combination with 8 mesomeres in order to form micromere-mesomere or macromere-mesomere aggregates. Third, four macromeres, eight mesomeres or four micromeres were marked by staining them with fluorescent dye at the 16-cell stage, and the embryos were cultured. All of these examinations showed that macromeres were responsible for formation of the adult skeleton.

DB 4

THE ACTIVITY OF PROTEIN THYROSINE KINASE IN CULTURED CELLS DERIVED FROM MICROMERES OF SEA URCHIN EGGS.

S.Kuno, K.Mitsunaga, A.Fujiwara and I.Yasumasu.
Dept. of Biol., Sch. of Educ., Waseda Univ., Tokyo.

In cultured cells derived from micromeres isolated from the 16 cell stage eggs of sea urchin, horse serum is known to be indispensable for them to undergo outgrowth of pseudopodial cables and spicule rods formation in the cable. It was found that these cells produced pseudopodial cables in the presence of insulin. During culture of these cells, the protein tyrosine kinase activity increased at 10hr of culture it became maximum plateau even in the absence of horse serum or insulin. Insulin did not cause any increase in the enzyme activity but caused a marked increase in the radioactivity of tyrosine residue in by hydrolysis of proteins obtained by ^{32}P exposed cultured cells. The increase in protein tyrosine kinase was then followed by the increase in the H7-sensitive protein kinase activity and the casein kinase II activity in the cells kept in the presence of insulin or horse serum. The increase of these enzymes activity was blocked by actinomycin D. The inhibition of H7 sensitive protein kinase by H7 blocked the growth of pseudopodial cables. The cable growth is probably induced with protein phosphorylation by protein tyrosine kinase which result in activation of synthesis of these other protein kinases.

DB 5

SOME DIFFERENCES IN PROTEINS SYNTHESIZED IN VEGETALIZED SEA URCHIN EMBRYOS FROM NORMAL ONES DURING EARLY DEVELOPEMENT.

Y.Iizuka¹, M.Komukai² and I.Yasumasu¹.
¹Dept. of Biol., Sch. of Educ., Waseda Univ., Tokyo, ²Dept. of Pharmacol., Nippon Med. Sch., Tokyo.

Embryos, treated with 55 mM Li^+ in a period between 2.5 hr (the 8-16 cell stage) and 6 hr (the morula stage) developed to early gastrulae with very slight delay of development, if any, and finally became vegetalized ones. Normal and Li^+ -treated embryos were exposed to [^{35}S]-methionine for 2 hr at the pre-hatching blastula, the mesenchyme blastula, the late gastrula and the prism stage. Proteins thus labeled in embryos were analyzed by two dimensional poly acrylamide gel electrophoresis (2D-PAGE) in the range from neutral to alkaline pH. During exposure to Li^+ , one spot on fluorograph of 2D-PAGE in normal embryos were stronger than in vegetalized ones, but at the pre-hatching blastula stage after the exposure of Li^+ , difference in the newly synthesized proteins were hardly found between Li^+ -treated and normal embryos. At the mesenchyme blastula, the late gastrula and the prism corresponding stage, three species of newly synthesized proteins (42, 53 and 60 K protein) were enriched and five species (26, 36, 37, 38 and 55 K protein) were poor in Li^+ -treated embryos. Changes in the rates of synthesis of these proteins are probably responsible for the formation of vegetalized embryos.

DB 6

CDNA CLONING OF Na^+, K^+ -ATPASE IN EMBRYOS OF THE SEA URCHIN, HEMICENTROTUS PULCHERRIMUS.

M.Hatoh¹, M.Mitsunaga², K.Yamada², K.Akasaka³, H.Shimada², and I.Yasumasu¹.
¹Dept. of Biol., Sch. of Educ., Waseda Univ., Tokyo, ²Zool. Inst., Fac. of Sci., Hiroshima Univ., Hiroshima

During early development of sea urchin embryos, Na^+, K^+ -ATPase activity increases after gastrulation. We have tried to isolate a cDNA of Na^+, K^+ -ATPase to study the regulatory mechanism of its gene's transcription and to determine the primary structure.

The cDNA was identified using an oligonucleotide probe derived from a conserved amino acid sequence of cation transport ATPases. About 100,000 clones of the cDNA library constructed from the poly(A⁺) RNA of prism stage embryos were screened with this probe. The longest clone was selected and its nucleotide sequence was determined by dideoxy method.

From the deduced primary structure, this clone includes two ATP analogue-binding sites and one of putative ouabain-binding site. Half region of this clone is very homologous to those of Na^+, K^+ -ATPase in several species of vertebrate, though the other region has little homology. There are at least four hydrophobic regions in the clone.

Amino acid similarity and hydropathy profile comparisons suggest that the isolated cDNA is coding for one of cation transport ATPases, probably Na^+, K^+ -ATPase.

DB 7

EXPRESSION OF Na^+/K^+ -ATPASE DURING EARLY DEVELOPMENT IN EMBRYOS OF THE SEA URCHIN, *HEMICENTROTUS PULCHERRIMUS*.

K. Mitsunaga¹, M. Hatoh², T. Banba¹, K. Yamada¹, K. Akasaka¹, H. Shimada² and I. Yasumasa¹. ¹Dept. of Biol., Sch. of Educ., Waseda Univ., Tokyo, ²Zool. Inst., Fac. of Sci., Hiroshima Univ., Hiroshima.

Activity of Na^+/K^+ -ATPase in sea urchin embryos is found to increase mainly in ectodermal cells following gastrulation. To find out the regulatory mechanism of the increase in Na^+/K^+ -ATPase activity, we examined effects of actinomycin D on the activity and studied its expression by Northern blotting.

Inhibition of transcription by actinomycin D before the mesenchyme blastula stage prevented the increase of the ATPase activity, while the inhibition after the gastrula stage failed to block the increase of the activity.

Northern blot analysis revealed that a cDNA clone, coding the sequence of ATP-binding sites of Na^+/K^+ -ATPase α -subunit, hybridized to about 4.5 Kb mRNA. This mRNA exists in small amounts before hatching and is maximally expressed at the mesenchyme blastula stage. The amount of this mRNA in ectodermal cells isolated from gastrulae was higher than in the other cells.

These results suggest that the increase of Na^+/K^+ -ATPase activity results from the transcription of the gene between the hatched blastula and the mesenchyme blastula stage in presumptive ectodermal cells.

DB 8

THE FACTOR DETERMINING THE DIRECTION OF SPINDLE-AXIS IN DIVIDING NEUROBLASTS OF THE GRASSHOPPER.

K. Kawamura. Lab. of Biol., Rakuno Gakuen Univ., Ebetsu, Hokkaido.

Grasshopper neuroblasts (NB) repeat unequal cytokinesis along the dorso-ventral axis of the embryo to produce a small ganglion cell (GC) to the dorsal side. Since the cleavage furrow is always formed across the spindle equator, the unequal cytokinesis is caused by eccentric location of the spindle which maintains a definite polarity in dividing NB. An electron dense layer (DL) appeared in the cap cell (CC)-side cortex of the NBs at very late prophase. The most conspicuous DL was observed at metaphase. It became fairly rude by the beginning of middle anaphase, and disappeared completely at middle anaphase. The spindle always directed the axis toward the center of the DL. When the spindle body was rotated 90° by a microneedle, the spindle body tended to rotate either backward or forward autonomously to retain the original axis. All rotated spindles in metaphase could return to the original axis, while the recovery rate decreased in later stages. The spindle could not return at all after middle anaphase. The ability of recovering the original spindle-axis occurred only while the DL in CC-side cortex existed. These facts suggest that the DL on the CC-side cortex plays a role in maintaining a definite division axis.

DB 9

FORMATION OF THE CONTRACTILE RING IN THE GRASSHOPPER NEUROBLASTS. N. Yamashiki, Biology, Rakuno Gakuen Univ., Ebetsu, Hokkaido.

In the dividing neuroblasts, the cleavage furrow forms across the middle part of the mitotic apparatus (MA) at late anaphase. When the MA at middle anaphase was rotated or shifted with a microneedle, a cleavage furrow appeared temporarily in the presumptive furrow region and regressed in a few minutes. A new cleavage furrow formed in the cortex close to the equator of MA which was altered the position by the operation. Electron micrographs of intact cells revealed that the microfilaments which aligned perpendicularly to the spindle axis began to appear in the cortex of the presumptive furrow region shortly before the initiation of furrowing. At late anaphase the contractile ring which consisted of the circumferential bundle of the microfilaments was fully formed in the furrowing cortex. In the operated cells aligned microfilaments in the cortex remained for a few minutes after the middle part of MA was removed from the position, and then they were disintegrated. A new contractile ring appeared in the cortex close to the middle part of the MA which was moved to the new position. The MA seems to release the informations toward the cortex to organize the contractile ring across the spindle equator and to maintain the contractility.

DB 10

APPEARANCE OF THE HATCHING ENZYME IN THE DIFFERENTIATING HATCHING GLAND CELLS OF MEDAKA.

S. Yasumasu, T.S. Hamazaki, S. Katow¹, Y. Umino¹, I. Tuchi and K. Yamagami. Life Sci. Inst., Sophia Univ., Tokyo and ¹Natl. Inst. Health, Japan, Tokyo.

The hatching enzyme of medaka is composed of two types of proteases, HCE and LCE. The appearance and the localization of HCE and LCE in the embryos at some developmental stages were examined immunologically by using anti-HCE monoclonal antibody (MAB) and anti-LCE MAB. HCE and LCE were found to be localized in the same hatching gland cells as examined by immunohistochemistry. In the embryos at st. 26, both HCE and LCE were localized evenly in zymogen granules, but the localization of LCE seemed to become uneven in more matured zymogen granules at st. 32. Presence of both HCE and LCE in the extract of the isolated zymogen granules was revealed by western blotting method. Immunocytochemical analyses using the MAB's with immunogold particles showed that HCE was present evenly in a secretory granule after st. 26 through st. 32. It seems, however, that LCE was present only in the periphery of each secretory granule at st. 32, while it was present evenly in a granule at st. 26. These results suggest that HCE and LCE appeared at the same time in the zymogen granules.

DB 11

THE ASSAY OF CHORIOLYTIC ACTIVITY OF THE HATCHING ENZYME IN THE RAINBOW TROUT. Yokoya S. Division of Cell Science, Fukushima Medical College, Fukushima.

To assay the activity of the hatching enzyme of *Salmo gairdneri*, we adopted fluorescence analysis by using fluorescamine and the chorions as the natural substratum of the enzyme. The chorions were isolated from fertilized eggs by forceps. The collected chorions were repeatedly washed 1M NaCl and distilled water and desiccated. The desiccated chorions were grained with a mortar. To solubilize the chorions, they were digested by the Pronase in 0.2M borate buffer at pH 7.5. The proteins from the major peak of Sephacryl-S200 chromatography were used as substrata after succinylation (Schwabe '73) or after labeling with fluorescamine (Sogawa and Takahashi '78). The hatching enzyme used was the hatching medium in which large amounts of contaminating amino acids and proteins contain. Chorio-lytic activity was assayed by three methods, 1) assaying liberated amines from the grained chorion, 2) assaying liberated amines from solubilized succinylated chorion and 3) assaying liberated fluorescent from fluorescamine-labeled chorion. The emission at 475nm was measured by Hitachi F-2000 (excitation 390 nm). During 60-90min incubation, liberated primary amines increased as a function of time in the three methods.

DB 12

INDUCTION OF BRAIN AND SENSORY ORGAN IN ASCIDIAN EMBRYO

H. Nishida.

Dept. of Biology, College of Liberal Arts, Kobe Univ., Kobe.

There is a brain in the tadpole larva of ascidian *Halocynthia roretzi*, and two kinds of pigmented sensory organ exist in the brain. The brain and sensory organ are derived from the blastomeres of animal hemisphere, while vegetal blastomeres are required for induction of these tissue. The inductive interaction for the pigment cell differentiation is accomplished by the middle gastrula (180-cell) stage. Embryos shows compensation regulation when pigment cell progenitors are destroyed by the 32-cell stage. In this study it was reported that the precursor cells of the brain and sensory organs, which were isolated from embryos before the accomplishment of the induction (110-cell stage), did not differentiate epidermis features (morphology of permanent blastula, larval tunic, epidermis specific antigen). Besides, it is suggested that the primordial spinal cord and brain stem cells are enough as inducer of the pigmented sensory organs.

DB 13

ONTOGENETIC STUDY OF PEPSINOGEN EXPRESSION IN LOWER VERTEBRATE STOMACH T. Matsunaga¹, S. Yasugi¹ and M. Asashima². ¹Zool. Inst., Fac. of Sci., Univ. of Tokyo, Tokyo, ²Dept. of Biol., Yokohama City Univ., Yokohama.

The vertebrate pepsinogens	stomachs (Pgs) reactive to anti-chicken embryonic Pg (ECPg) antiserum or anti-chicken adult Pg (ACPg) antiserum.	have
----------------------------	------------------------------------------------------------------------------------------------------------------	------

In the stomachs of adult higher vertebrates, only ACPg-type Pg is expressed. In the present study, the expression of ECPg- and ACPg-type Pgs was examined during the development of fish and amphibians. In the flounder, ECPg- and ACPg-type substances appeared almost at the same time at postclimax stage of metamorphosis. Both types of Pgs are expressed in the adult fish stomach. In the newt, ECPg-type and ACPg-type Pgs first appeared concomitantly at late larval stage, but only ACPg-type Pg was detected after metamorphosis. Those data suggest that ECPg-type Pg works as a digestive enzyme in the adult fish stomach, but its expression was confined to embryonic or larval stage in the course of vertebrate evolution.

DB 14

PEPSIN-LIKE ENZYMES OF FORE-GUT IN METAMORPHOSING TADPOLE OF RANA CATESBEIANA T. Inokuchi, K. Kobayashi and S. Horiuchi Life Sci. Inst., Sophia Univ., Tokyo.

Homogenate of larval fore-gut and metamorphosing stomach and duodenum has acid proteases activity. At first it decreases in stomach, then increases again during metamorphosis. But activity of duodenum doesn't change. Zymogram after polyacrylamide gel electrophoresis (PAGE) shows that pattern of larval fore-gut is same as in the whole region and in metamorphosing duodenum but new bands appear in metamorphosing stomach and esophagus. And pattern of each region of adult is not different from that of froglet. Then these enzymes were purified from adult stomach mucosa. Four peaks (I, II, III and IV) were separated by Q-Sepharose column chromatography. Next step is Sephadex G-75 gel filtration. II and III were further purified by Q-Sepharose rechromatography. According to electrophoretic pattern I, II and III exist only in adult esophagus and stomach, IV exists in larval fore-gut and adult stomach and duodenum. All enzymes were inhibited by pepstatin A, but scarcely inhibited by leupeptin. M.W. of I, II, III and IV are 32000, 34000, 32000, 28000, respectively (Sephadex G-75) and 41000, 42000, 40000 (SDS-PAGE, band of IV was not detected). Optimal pH of I, II, III were between 1.5-2.5 but IV was between 2.0-3.0. By localization and M.W. it suggests that peak I, II and III are pepsin-like enzymes. But we can't identify peak IV now.

DB 15

OBSERVATION ON RELEASE OF PTERINS DURING METAMORPHOSIS OF BULLFROG, RANA CATESBEIANA
T. Manabe, K. Kobayashi and S. Horiuchi.
Life Sci. Inst., Sophia Univ., Tokyo.

When organ culture of tadpole tail fin was attempted by Derby's method, it was found that fluorescent substances were released from tail fin in culture medium in proportion to regression induced by thyroid hormone (T_4). Release of fluorescent substances depended on concentration of T_4 and it was highly increased as tissue involution proceeds. Fluorescent substances released in culture medium mainly consist of biopterin, 6-carboxypterin and isoxanthopterin. It is known that they were highly contained in skin of Rana catesbeiana tadpole. The same response was observed on cultured dorsal skin of tadpole but it was not observed on that of froglet. Moreover, release of pterins was observed during spontaneous metamorphosis particularly in climax, so it is suggested that release of pterins is one of phenomena during metamorphosis.

DB 16

3,3',5-TRIODOTHYRONINE INDUCES COLLAGENASE OF BULLFROG TADPOLE.

K. Oofusa and K. Yoshizato
Lab. of Dev. Biol., Dept. of Biol., Fac. of Sci., Tokyo Metropolitan Univ. Tokyo

The effects of thyroid hormone (TH) on the expression of collagenase were investigated in metamorphosing anuran tadpole tissues by the immunoblot analysis. Collagenase was purified from culture media of back skin explants of tadpoles. The final purity of the enzyme was 98%. Anti-collagenase antisera were made in rabbits. Anti-collagenase IgG was prepared by a protein A column. It was confirmed that the antibody inhibits the activity of the enzyme. Tadpoles of Bullfrogs (Rana catesbeiana) at the TK stage of X were injected with 3×10^{-10} moles $3,3',5$ -triiodo-L-thyronine (T_3) per gram body weight. Four days later, back skin, tail lateral skin, tail muscle and tailfin were obtained from animals. These tissues were homogenized and were subjected to Western-blotting. No proteins reactive with the antibody were observed in the control animals, while the intensely-reactive protein bands were seen in the T_3 -treated ones for back skin. No collagenase was detected for both control and T_3 -treated tadpoles for tail muscle. Tail skins and tailfins showed a weak signal of collagenase in control animals and an intense signal in T_3 treated ones. Increase in collagenase activity known in the metamorphosis is ascribed to the T_3 -induced increase in the amount of enzyme.

DB 17

ONTOGENY OF LEUKOCYTES DERIVED FROM THE BLOOD ISLANDS DURING XENOPUS DEVELOPMENT.
H. Ohinata, S. Tochinali, and Ch. Katagiri,
Zool. Inst., Fac. of Sci., Hokkaido Univ., Sapporo.

Previous immunohistochemical observations employing anti-Xenopus leukocyte monoclonal antibody (XL-1) in combination with a cell tracing technique revealed the occurrence in st.33/34 larvae of non-lymphoid leukocytes which are not derived from VBI. To investigate the relationship of these leukocytes with well-documented, VBI-derived XL-1⁺ cell population, the heart rudiments were removed from st.32 embryos to allow development without blood circulations. In the cardiectomized larvae, XL-1⁺ cells remarkably increased in number in the ventral region during st.40 and st.46-47. When st.22 X. laevis embryos received VBI tissue from the stage matched X. laevis x X. borealis hybrid embryos followed by cardiectomy at st.32, almost all the XL-1⁺ cells at st.45 were derived from the grafted VBI. These results indicate that the XL-1⁺ cells occurring during st.33/34-39 are independent of VBI and constitute a transient population that is replaced by VBI-derived XL-1⁺ cells constituting a major population of leukocytes at st.45 and later.

DB 18

STEM CELLS TO DIFFERENTIATE INTO ADULT EPIDERMAL CELLS IN THE TAIL SKIN OF ANURAN TADPOLES.

T. Kinoshita, H. Takahama and F. Sasaki.
Dept. of Biol., School of Dent. Med., Tsurumi Univ., Yokohama.

In order to examine the existence of stem cells that differentiate into adult epidermal cells within the anuran larval tail, isolated tail skins of Xenopus borealis were transplanted to X. laevis tadpoles at premetamorphosis. Grafts surviving after metamorphosis were detected by Quinacrine staining. When tail skins were transplanted to the back region of host animals, epidermal cells of the grafts survived beyond the climax of metamorphosis. Furthermore, these epidermal cells contained 63kD keratin which is a marker protein specific for adult epidermis. A temporal increase in BrdU incorporation was observed in the normal back epidermis at stage 59, but not in the tail. When the tail skin was cultivated on the back region, cell division of the epidermis at stage 59 increased up to the same level as that of the back skin. In analysis using double immunostaining of BrdU and 63kD keratin, epidermal cells that had divided at stage 59 synthesized 63kD keratin afterwards. These results suggest that anuran tail epidermis contains the stem cells that divide and synthesize the adult-type keratin.

DB 19

CHANGES IN EPIDERMAL CELLS OF RANA
CATESBEIANA FROM LARVAE TO ADULTS.Y. Izutsu¹, K. Yoshizato² and M. Kaiho²

1. Lab. of Dev. Biol., Dept. of Biol., Fac. of Sci., Tokyo Metropolitan Univ.

2. Safety Res. Lab. Yamanouchi Pharma. Co.

It has been known that five types of epidermal cells exist in the bullfrog; apical, skein, basal, granular and cornified cells. We studied on the changes in epidermal cell types during metamorphosis for the skins of tail and body. At the Taylor-kollros stage X, about 20% of the back epidermal cells were basal cells, whereas no basal cells were found in the tail. The lack of basal cells in the tail seems to be responsible for the eventual loss of this tissue at metamorphosis. Furthermore we found out that in body skin the cells stained with anti-A type substance of human blood antibody appeared and increased in numbers in metamorphosis; Anti-A antibody-positive cells are known to be adult-specific differentiated epidermal cells (granular cells). On the other hand, the antigen-containing cells were very few and appeared at the later stage of metamorphosis in the tail. In conclusion, we demonstrate that there is significant difference quantitatively in the nature of epidermal cells between tail and body skins with respect to basal cells and anti-A antibody-positive cells. This difference might be related to the difference in the metamorphic fate of these two tissues.

DB 20

PRESENCE OF THE THYMUS IS REQUISITE FOR THE INDUCTION OF TRANSPLANTATION TOLERANCE BY GRAFTING METAMORPHOSING XENOPUS TADPOLES WITH SEMIXENOGENIC ADULT SKIN.

S. Tochihai, Zoological Institute, Faculty of Science, Hokkaido University, Sapporo

The South African clawed frog, *Xenopus laevis*, can easily be rendered tolerant against semixenogenic (*X. laevis* x *X. borealis*) adult skins grafted before or during metamorphosis. The tolerant state is maintained beyond metamorphosis as evidenced by the specific acceptance of skins of the same haplotype. In order to investigate a possible role of the thymus in tolerance induction, MHC homozygous J-strain *X. laevis* tadpoles were thymectomized at different stages of development along with the semixenogenic adult skin graft at stage 56-57. When tadpoles were thymectomized at stage 52-53 (before) or stage 56-57 (at the same time with skin grafting), tolerance was not inducible. On the other hand, if thymectomy was performed on tadpoles 1 week after the skin grafting, tolerance could be induced in some tadpoles. While thymectomy made at very early stages abrogates the animals' ability to reject non-self grafts because of the lack of effector T cells, thymectomy made at later stages caused the opposite effects resulted in the failure of tolerance induction, or the failure of suppression of graft rejection, as observed above. This indicates, in turn, that in the thymus of metamorphosing tadpoles a population of cells differentiates which has suppressive activities in skin graft rejection. It is also suggested that the precursors of these cells should recognize antigens on grafts prior to their entry into the thymus for further maturation.

DB 21

CHANGES IN LECTIN-BINDING PATTERN OF THE SMALL INTESTINE DURING METAMORPHOSIS IN XENOPUS LAEVIS.

A. Ishizuya-Oka and A. Shimozawa. Dept. of Anat., Dokkyo Univ., Sch. of Med., Tochigi.

The binding of 7 lectins (ConA, DBA, PNA, RCA-I, SBA, UEA-I and WGA) to the small intestine in the metamorphosing *Xenopus* was studied by the ABC method with light microscope. In the epithelium, the pattern of binding to all the lectins except for UEA-I and ConA changed gradually during the metamorphic climax; absorptive cells gradually became positive for DBA, PNA and SBA, and goblet cells for RCA-I and WGA. On the other hand, the change of binding pattern in the connective tissue occurred for ConA, RCA-I and WGA, and rapidly at the beginning of the climax. A stronger binding for ConA and WGA was observed only in fibroblast-like cells close to the epithelium and the basement membrane. At the ultrastructural level, a high density of binding sites labeled with colloidal gold were localized in the vacuoles of the cells. With the progress of development, this localization of binding in the connective tissue became less clear.

These results indicate that lectin histochemistry gives good criteria for distinguishing between adult and larval epithelial cells, and can also be used to identify a particular group of fibroblast-like cells, which may be associated with the epithelial transition from the larval to the adult form during the climax.

DB 22

TEMPORAL AND SPATIAL EXPRESSION OF VITELLOGENIN GENE DURING METAMORPHOSIS OF *Xenopus laevis*

Yoshinori Kawamura, Akira Kawahara and Minoru Amano, Faculty of Integrated Arts and Sciences, Hiroshima University, Hiroshima

The ability of hepatocytes for estrogen-dependent vitellogenin synthesis appears during the metamorphosis of *Xenopus laevis*. In primary cultures of liver parenchymal hepatocytes, we found that a certain fraction of cells obtained from animals before a stage of metamorphic climax acquired this ability in response to thyroid hormone. Thus, metamorphosing animal liver was expected to consist of two types of parenchymal cells, competent and incompetent for vitellogenin synthesis. We investigated the temporal and spatial pattern of vitellogenin gene expression by *in situ* hybridization method.

35S-antisense and sense RNA probes were prepared by *in vitro* run-off transcription of vitellogenin B1 cDNA clone, pvlx10. In addition, we used albumin cDNA clone, pXlalb7420 for control experiments.

The results obtained clearly showed that vitellogenin gene-expressing cells appeared around st. 57 and increased, in scattered fashion, markedly at the metamorphic climax stage. The distribution pattern from animals at st. 65 was finally quite similar to those of albumin gene-expressing cells which did not considerably change during metamorphosis.

The results suggested that almost all parenchymal hepatocytes became competent for vitellogenin synthesis at the late metamorphic climax stage by thyroid hormone-mediated mechanism.

DB 23

CHARACTERIZATION OF A6 CELL LINE DERIVED FROM *XENOPUS LAEVIS*.

A. Fukui and M. Asashima

Department of Biology, Yokohama City University, Yokohama 236.

We have recharacterized the properties of A6 cell line, established by K.A. Rafferty twenty years ago. This cell line had originally derived from the kidney of adult male *Xenopus laevis*. As the results, doubling time was about forty-two hours, plating efficiency was about thirty-four percent, suitable temperature for cell proliferation was twenty-five centigrade. Chromosome number showed heteroploid and mode of chromosome number was thirty-nine. They had a conspicuous secondary constriction in one chromosome which was not observed in normal *Xenopus* chromosomes. There were the same four spots compared normal kidney with A6 cells by two-dimensional gel electrophoresis with silver staining. A6 cells made dome formations, aggregations, tube-like constructions and hollow spheres like a ball after post confluence. We confirmed mono- or two-cell layers by light microscopic observation of cross section of dome structure. We have tried to cell cloning of A6 cells, and we obtained some different types of cell from the morphological observation. They observed like as fibroblast, epitheloid. Some of them made the dome structure in high frequency, and the other formed little. Then we compared with the two kinds of cells which formed dome structure well or few by two-dimensional gel electrophoresis. Though we were not able to find clear different spots, but we could detect some spots showing the decrease of quantity.

DB 24

DEVELOPMENTAL CHANGE OF LOCALIZATION OF ELASTIN mRNA IN MOUSE ORAL CAVITY.

T. Yamaai¹, S. Noji², E. Koyama³ and S. Taniguchi², ¹Dept. of Oral Anat. II, ²Biochem. and ³Maxillofacial Surg. I, Okayama Univ. Dent. Sch., Okayama

The localization of the elastin mRNA during development was investigated in the mouse oral region by a simplified *in situ* hybridization method with riboprobes. C3H mice were fixed by perfusion through the left ventricle with 4% paraformaldehyde in 0.07M Na-cacodylate buffer. Serial sections mounted on slides coated with poly-L-lysine were hybridized with ³⁵S-labeled riboprobes and then made into autoradiograms. A part of the serial sections were stained with resorcin-fuchsin to detect the elastic fibers.

Signal grains were observed first on the proper layer of the vomeronasal organ and the wall of the arterioles at 18-day fetus. They also observed on the proper layer of the alveolar side of the mucogingival junction, transverse palatal ridge, perimysium and periosteum from the neonate. The signal intensity in all tissues became maximum at 1 week old and decreased thereafter. The resorcin-fuchsin positive fibers were found on the same region mentioned above from the neonate. Whereas the staining intensity of them increased gradually and then reached to the adult level after 1 week. These results suggested that the formation of the elastic fibers in the oral proper layer is essentially completed before the weaning.

DB 25

INHIBITION BY HEPARITINASE I OF BRANCHING MORPHOGENESIS OF MOUSE EMBRYONIC SUBMANDIBULAR EPITHELIUM

J. Uematsu, H. Takamatsu and Y. Nakanishi
Department of Chemistry, Faculty of Science, Nagoya University, Chikusa, Nagoya 464.

Extracellular matrix components including collagen have been suggested to be involved in branching morphogenesis of mouse embryonic submandibular epithelium. To further elucidate the matrix organization for epithelial branching, we examined the role of heparan sulfate proteoglycan. A highly purified heparitinase I free of other proteins (*Flavobacterium heparinum*) was therefore introduced into the culture medium (0.2 U/ml). The enzyme completely inhibited the formation of new clefts in the 12- and 13-day glands within 6-10 hours. It also deformed the shape of epithelial lobules from round to rod. Similar effects were observed when heparan sulfate (1 mg/ml) or heparin (75 µg/ml) was added into the medium. In contrast, chondroitin sulfate (1 mg/ml) had no effect. A biochemical analysis of glycosaminoglycans indicated that heparan sulfate in glands prelabeled for 17 hours with radioactive inorganic sulfate completely disappeared during further cultivation for 8 hours with heparitinase I. Whereas, the amount of chondroitin sulfate in the experimental glands decreased slightly. The findings strongly suggest that heparan sulfate proteoglycans in submandibular glands play an important role(s) in forming clefts and maintaining the epithelial morphology.

DB 26

3-DIMENSIONAL IMAGE RECONSTRUCTIONS OF THE DISTRIBUTION OF COLLAGEN III ON THE SURFACE OF MOUSE SALIVARY GLAND EPITHELIUM. K. Ichikawa and Y. Nakanishi.

Dept. of Chem., Fac. of Sci., Nagoya Univ., Chikusa, Nagoya 464.

Our previous studies showed that collagen is one of the regulatory factors of the branching morphogenesis of mouse embryonic submandibular gland. Immunoperoxidase staining experiments indicate that collagen III, which is interstitial and relatively rich in the embryonic period, accumulates at the epithelial-mesenchymal interfaces of the cleft points of the branching epithelium, especially at the bottom and the lateral side of the clefts. Based upon the immunostaining patterns of the serial sections, we reconstructed 3-dimensional (3-D) images of the distribution of collagen III on embryonic salivary epithelium with the personal computer by the use of COSMOZONE 2S software. These 3-D images showed that collagen III is randomly distributed at the interfaces of the mid 12-day gland with no signs of cleft. When cleft formation takes place at the late 12-day stage, the type of collagen begins to localize at the notches and early clefts and accumulates heavily at the bottom of wide clefts of the mid 13-day gland. The findings strongly suggest that collagen III at the bottom of clefts forms a continuous bundle of fibrils encircling the epithelial lobule.

DB 27

DIFFERENTIATION OF THE DIGESTIVE-TRACT ENDODERM OF THE CHICK EMBRYO UNDER THE INFLUENCE OF GIZZARD OR DUODENAL MESENCHYME. S. Matsushita and S. Yasugi², ¹Dept. of Biol., Tokyo Women's Medical College and ²Zool. Inst., Fac. of Sci., Univ. of Tokyo, Tokyo.

The endoderm of various regions of the digestive tract of 6-day chick embryo was cultured in recombination with the gizzard or duodenal mesenchyme of 6-day embryo, in the coelomic cavity of 3-day chick embryo. Gizzard-type differentiation as revealed by appearance of columnar epithelium with apical alcian blue-staining, or intestine-type differentiation expressing sucrase antigen was examined in the recombinates.

In the grafts of various regions of the intact digestive tract, gizzard- or intestine-type differentiation was almost confined to the endoderm of stomach or intestinal region, respectively. In combination with the gizzard mesenchyme, gizzard-type differentiation predominantly appeared in the proventricular or duodenal endoderm, appeared in lower frequency in the oesophageal or jejunal endoderm, and was never found in the ileal endoderm. In combination with the duodenal mesenchyme, intestine-type differentiation could be elicited easily in the gizzard endoderm, but hardly in the oesophageal or proventricular endoderm. Thus, it is likely that the competence for the mesenchyme-induced differentiation is highest in the endoderm of the neighboring regions of the mesenchyme and gets lower in the endoderm of farther regions.

DB 28

ACCUMULATION OF CRYSTALLINS IN CHICKEN DEVELOPMENT

T. Inoue and T. Hirabayashi. Inst. of Biol. Sci., Univ. of Tsukuba, Tsukuba.

The separation and quantification of crystallin subunits in the embryonic and posthatched chicken lens were carried out by two-dimensional gel electrophoresis and an image analysis system in order to know whether accumulation of crystallins was correlated with one another. More than 25 crystallin subunits could be detected on the two-dimensional patterns. Especially, about 20 β -crystallin subunits could be separated by the addition of 7M urea in the second dimension. Crystallin subunits accumulated in different manners. δ -crystallin accumulated rapidly during the early embryonic development and its content was more than 80%, while β -crystallin began to accumulate rapidly after hatching and continued to accumulate. The accumulation patterns of β -subunits were classified into two types. In contrast with β - and δ -, the ratio of α -crystallin to total crystallins was kept approximately 20% during lens development. These experiments suggested differential regulation mechanisms on the accumulation of crystallins.

DB 29

ACCUMULATION OF PROTEIN CONSTITUENTS DURING DEVELOPMENT OF CHICKEN ALD MUSCLE. M. Nomura and T. Hirabayashi. Inst. of Biol. Sci., Univ. of Tsukuba, Tsukuba.

Developmental change of protein constituents in chicken slow muscle, anterior latissimus dorsi (ALD), was examined by two-dimensional gel electrophoresis. Electrophoretic patterns were quantitatively analyzed by image analyzing and photometry. During postnatal development tropoin subunits (tropoin-T and tropoin-C) were coordinately accumulated. Contractile proteins (actin, tropomyosin, myosin light chains) and creatin kinase also showed a moderate coordination in accumulation. The relative ratios of glyceraldehyde-3-phosphate dehydrogenase and aldolase to actin were kept constant during development. These results suggested that the accumulation of contractile proteins in ALD was almost the same as that of, pectoralis major, during postnatal development. On the other hand, glyceraldehyde-3-phosphate dehydrogenase and aldolase in ALD and muscle, pectoralis major differ in the accumulation patterns during postnatal development.

DB 30

FACTORS CONTROLLING EPITHELIAL PROLIFERATION OF MOUSE UTERINE EPITHELIAL CELLS IN PRIMARY SERUM-FREE CULTURE.

H. Fukumachi. Zool. Inst., Fac. of Sci., Univ. of Tokyo, Tokyo.

We have found that mouse uterine epithelial cells proliferate and differentiate in a serum-free primary culture system. When seeded on Matrigel (a reconstituted basement membrane like substratum), they increased slowly in number, but differentiated to form polarized columnar epithelium with junctional complexes, microvilli, and lipid granules, comparable to normal uterine epithelium in vivo. In the previous report, we could not find any effect of estrogens on the epithelial proliferation.

In the present study, we reanalyzed the epithelial proliferation by labeling DNA replicating cells with bromodeoxyuridine, and detecting them immunohistochemically. We found unexpectedly that 17β -estradiol (10^{-7} to 10^{-14} M) significantly inhibited epithelial proliferation in this system. $12-O$ -tetradecanoylphorbol 13-acetate, an activator of protein kinase C, partially stimulated epithelial proliferation. Thus, it is not probable that estrogens directly induce proliferation of uterine epithelial cells, it is more probable that estrogens act on connective tissues to induce secretion of unknown substance(s), which in turn induce epithelial proliferation by activating protein kinase C of epithelial cells in vivo.

DB 31

INDUCTION OF THE DIFFERENTIATION OF OVIDUCTAL EPITHELIAL CELLS IN THE NEWBORN GOLDEN HAMSTER BY ESTROGEN.
H. Abe and T. Oikawa. Developmental and Reproductive Biology Center, Yamagata.

In the golden hamster, the differentiation of oviductal epithelial cells, ciliated and secretory cells, occurs during postnatal period. In this study, the effect of estrogen on the differentiation of oviductal epithelial cells in the newborn golden hamster was studied by electron microscopy. The consecutive injection of estradiol 17- β (E_2) at a dose of 1 μ g/day from 1.5 days after birth induced various ultrastructural changes in the epithelial cells. Ciliogenesis, formation of some ciliary buds and ciliation were found in some epithelial cells on days 1 through 9 of E_2 treatment. On days 2 to 3, the remaining cells contained well-developed Golgi apparatus and extensive RER. Most of them possessed a few secretory granules in the cytoplasm on days 3 to 6 and showed the differentiation into secretory cells. On day 9, many fully mature ciliated and secretory cells were observed. In addition, quantitative data clearly demonstrated that exogenous E_2 induced the differentiation of ciliated and secretory cells. These results suggest that estrogen is a possible differentiation inducing factor of the epithelial cells in newborn golden hamster oviduct.

DB 32

ANALYSIS OF PIG OVIDUCTAL GLYCOPROTEINS.
Y. Maruyama*, H. Abe, K. Takagishi, Y. Hoshi and T. Oikawa. Bio Sci. Laboratory and Develop. & Reprod. Biol. Center, Yamagata.

In some mammals, the oviductal epithelial cells secrete some glycoproteins, which may play an important role for reproductive process. In this study, glycoproteins of the pig oviduct were studied by some immunolabeling techniques using a monoclonal antibody (C8B11) against the golden hamster oviductal glycoprotein (ZP-0). Western blotting analysis revealed that C8B11 reacted with at least three glycoproteins having different molecular weight in flushing fluid of the pig oviduct. Immunofluorescence tests showed that these glycoproteins associated with the zona pellucida of pig eggs matured in vitro. Moreover, C8B11 reacted with the epithelial cells of the pig oviduct. These results suggest that the pig oviductal epithelial cells secrete the zona pellucida binding glycoproteins. In addition, to establish the culture system of mammalian oviductal epithelial cell, we attempted to isolate pig oviductal epithelial cells. The oviductal cells isolated by collagenase were grown fast in the type I collagen coated dish with DMF:Ham's F12 (1:1) supplemented with 10% FCS. These primary and secondary cultured cells contained the materials reacting with C8B11 in the cytoplasm and they were released into the culture supernatant.

DB 33

IMMUNOCYTOCHEMICAL CHARACTERIZATION OF NEURAL CREST-ASSOCIATED MARKERS APPEARING IN GOLDFISH ERYTHROPHOROMA CELLS UNDER DIFFERENTIATION in vitro.
J. Matsumoto¹, T. Akiyama¹ and K. Kitamura²
¹Dept. of Biol., Keio Univ., Yokohama and
²Dept. of Devel. Biol., Mitsubishi-Kasei Inst. of Life Sci., Machida.

Possible distribution of neural crest and melanoblast markers in goldfish erythrophoroma GEM 81 cells in vitro was examined by immunofluorescence using the antibodies, HNK-1 and 2A6. Examinations on cultured goldfish trunk neural crest disclosed that cells in the outgrowth were unequivocally reactive to these antibodies before pigmentation but became non- or less reactive after pigmentation. Assays on GEM cells with HNK-1 indicated that (1) their mother population contains a small number of positively reactive cells, (2) the numbers of such cells are markedly increased upon exposure to DMSO, and (3) their reactivity is gradually weakened with progress of melanogenesis and finally disappeared. Assays on the same cells with 2A6 indicated that their reactivity to this antibody appears transiently after induction of differentiation and soon disappears with the onset of melanogenesis. All these findings indicate that GEM cells are distributed with neural crest and melanoblast markers recognized by HNK-1 and 2A6, the expression of which is closely associated with an earlier stage of their cytodifferentiation.

DB 34

Study on migration and melanophore differentiation of neural crest cells by interspecific transplantation of Xenopus embryo.

M. Nagayoshi and A. Suzuki, Dept. of Biology, Fac. of General Education, Univ. of Kumamoto.

In amphibian embryogenesis, neural crest cells are separated from neural fold during the formation of neural tube. They migrate and differentiate into melanophores, ganglion cells, and so on. We studied on migration of neural crest cells and their differentiation by using interspecific transplantation of albino Xenopus laevis and wild Xenopus borealis embryos. When a part of animal cap of wild X. borealis gastrula was transplanted onto the lateral presumptive neural fold region of albino X. laevis gastrula, many migrated cells with X. borealis nucleus were observed, but a few melanophores were observed at the dorsal region. The neural fold of early X. borealis neurula was transplanted on the same region of X. laevis neurula, most of the cells migrated and well-differentiated melanophores were observed. The neural folds transplanted on the lateral and ventral regions of same developmental stage also produced many migrating cells and well-differentiated melanophores. Mechanisms of migration and melanophore differentiation will be discussed.

DB 35

DIFFERENTIATION IN VITRO OF MOUSE NEURAL CREST CELLS INTO MELANOCYTES.

K. Ito and T. Morita. Dept. of Biol., Coll. of Gen. Educ., Osaka Univ., Osaka.

Mouse neural crest cells differentiate in vitro into melanocytes, only when these cells are in association with the epithelial sheet derived from the explanted neural tube (Ito and Takeuchi, 1984). This fact suggests that the epithelial sheet plays an important role in the development of mouse crest cells into melanocytes. Therefore, the purpose of this study was to analyze the action of the epithelial sheet.

When the explanted neural tube was removed after 48hrs in culture, the epithelial sheet was never formed. By the addition of TPA and cholera toxin (CT) to culture medium, however, melanocytes appeared. Melanocytes differentiated also in the medium containing H-7 (a C-kinase inhibitor) and CT. These results indicate that the functions of the epithelial sheet in the differentiation into melanocytes are substituted for TPA (or H-7) and CT. Thus, the epithelial sheet possesses dual actions; the inhibition of C-kinase activity and the increase of c-AMP concentration. In conclusion, we expect that C-kinase activity and c-AMP content in the neural crest cells influence the commitment to melanocytes, and the commitment occurs when the crest cells still exist in the neural fold.

DB 36

THE EXPRESSION OF PROTO-ONCOGENE *c-kit* IN CULTURED MOUSE NEURAL CREST CELLS AND MELANOCYTES

H. Ono, S. Takeuchi and T. Takeuchi
Biol. Inst., Tohoku Univ., Sendai

It is known that the Dominant-White Spotting (W) locus which affects the differentiation of the neural crest cells into melanocytes encodes the proto-oncogene *c-kit*.

We examined the expression of *c-kit* mRNA in cultured neural crest cells and melanocytes from dorsal skin of new born mice by *in situ* hybridization with three oligonucleotide probes. To culture the neural crest cells, we used two different media, (MEM + 15%FBS, MEM + 15%FBS + TPA + cholera toxin), because it is known that TPA and cholera toxin induce the differentiation of the cultured neural crest cells into melanocytes.

The *c-kit* mRNA was detected in primary cultured melanocytes from dorsal skin of new born mice. On the other hand, the *c-kit* mRNA was not detected in the neural crest cells cultured for 8-13 days in either media. This result seems to indicate that the *c-kit* proto-oncogene expresses only in the terminal phase of the differentiation of neural crest cells into melanocytes.

DB 37

CELLULAR LOCALIZATION AND IDENTIFICATION OF THE ANTIGEN RECOGNIZED BY NEW ANTI-MELANOBLAST ANTIBODY

K. Kitamura¹, M. Sezaki¹, H. Yamamoto² & T. Takeuchi². ¹Dept. of Devl. Biol. Mitsubishi Kasei Inst. of Life Sci., Machida, ²Biol. Inst., Tohoku Univ., Sendai.

The characterization of precursor cells of neural crest-derived cells, such as melanocytes and peripheral nerve cells, is important for the elucidation of the molecular mechanisms underlying differentiation of pluripotent neural crest cells.

Monoclonal antibody "2A6" raised against dorsal skin of chick embryos recognized specifically the migratory neural crest cells (HNK-1 positive) located above the neural tube of stage 20 embryos. Along with development, the intensity of 2A6-staining became strong. Then 2A6-positive cells moved along lateral route and finally homed into epidermis. Immunoelectron microscopic analysis revealed the cellular localization of 2A6-antigen on endoplasmic reticulum, Golgi-apparatus, nuclear membrane and further cell surface. The observed premelanosomes were not immunoreactive. Western blotting showed that the a likely 2A6-antigen is a molecule of 120kd.

These results suggest that differentiation of melanocytes begins with the synthesis of 2A6-antigen and the modification of cell surface with the antigen just after emigration of neural crest cells.

DB 38

SELECTIVE GROWTH AND SERIAL PASSAGE OF MOUSE MELANOCYTES FROM NEONATAL EPIDERMIS IN A HORMONALLY-DEFINED MEDIUM

T. Hirobe. Div. of Biol., Natl. Inst. of Radiol. Sci., Chiba.

Disaggregated epidermal cell suspensions from newborn mouse skin were plated in a medium containing bovine pituitary extract, insulin and transferrin. Fetal bovine serum was added to a concentration of 4 % to the culture medium at the time of plating. After 2 days cells were transferred to serum-free medium to eliminate keratinocyte and fibroblast growth. Preferentially the melanocytes began to grow and after 12 days pure melanocyte populations could be harvested. Melanocytes failed to grow in the absence of the extract. Without keratinocyte and fibroblast growth melanocyte could be subcultured in the serum-free medium supplemented with a conditioned medium of keratinocyte-rich primary cultures. Fetal bovine serum was added at a concentration of 1 % for the first 1 day to support melanocyte attachment. Melanocytes in subculture failed to grow when the cells were cultured with medium free of bovine pituitary extract, medium free of insulin and transferrin or medium free of conditioned medium. These results indicate that the bovine pituitary extract contains a melanocyte growth factor involved in regulating the growth of melanocyte *in vitro* in the presence of keratinocyte-derived factor, insulin and transferrin.

DB 39

OFFSPRING FROM FETAL OVARIES GRAFTED IN MICE STERILIZED BY X-IRRADIATION.
M. Noguchil, M. Murakami¹, and T. Nomura²
¹Biol. Inst., Fac. of Sci., Shizuoka Univ.
Shizuoka, ²Dep. Rad. Biol., Fac. of Med.,
Osaka Univ., Osaka.

In order to manipulate fetal ovaries which contain oocytes in the meiotic prophase and obtain offspring from these ovaries, we examined fertility of the mice sterilized by X-irradiation and then grafted 13.5-19.5 dpc fetal ovaries orthotopically. In 129/Sv-Ev and -Slc strain mice, fetuses from (AY/+ AY/+) and (Sl/+ Sl/+) matings were used as donors and adult females (+/+) as hosts. Hosts were exposed to 100 rad whole body X-irradiation and grafted fetal ovaries in various intervals. Histological examination of host ovaries 56 days after irradiation showed almost elimination of oocytes. Eighty percent of hosts given grafts 28 days after irradiation and mated with males 4 weeks later produced offspring derived from grafts, whereas 4 % of not X-irradiated hosts did so. It is concluded that sterilization by X-irradiation is more useful for obtaining offspring from small fetal ovarian grafts than ovariectomy. Supported by the Special Coordinating Funds for Promoting Science and Technology and a Grant-in-Aid from the Ministry of Education, Science and Culture.

DB 40

OFFSPRING OBTAINED FROM TRANSPLANTATION OF FOETAL MOUSE OVARIES.
H. Hashimoto¹, M. Noguchi² and N. Nakatsujil¹
¹Div. of Dev. Biol., Meiji Inst. of Hlth. Sci., Odawara, ²Biol. Inst., Fac. of Sci., Shizuoka Univ., Shizuoka.

We are trying to develop a new method of introducing foreign genes into mice through manipulation of the primordial germ cells (PGCs). Noguchi and Noguchi (1982) reported that adult female mice transplanted with 13.5-19.5 dpc foetal ovaries bore offspring derived from the transplants. Now, we examined whether similar transplantation can be successfully carried out with 12.5 dpc foetal ovaries which contain proliferating PGCs before entering into meiosis.

C57BL/6-bg/bg (beige mice) foetuses were used as donors and adult C57BL/6 females as hosts. Two weeks after the transplantation, hosts were mated with beige mice. Of 18 host females carrying ovaries not cultured, one was delivered of beige mice. Two of 7 hosts which were transplanted with ovaries cultured for 2 days bore beige mice, and one of 8 hosts carrying 3 day-cultured ovaries did so. These results suggest a novel possibility of using PGCs for genetic manipulation of the germ line.

This study was entrusted by the Science and Technology Agency, using the Special Coordinating Funds for Promoting Science and Technology.

DB 41

REGENERATION OF THE TUNIC CUTICLE IN A COMPOUND ASCIDIAN, BOTRYLLOIDES SIMODENSIS.
Eu. Hirose, Y. Saito & H. Watanabe.
Shimoda Mar. Res. Ctr., Univ. of Tsukuba,
Shimoda, Shizuoka.

The regeneration processes of tunic cuticle were studied by using transmission electron microscopy. After cutting off a part of tunic from a colony, the colony was kept in sea water (SW). Within a few hours, electron dense filaments appeared at the cut surface of the tunic. The filaments aggregated to form a continuous cuticle layer, and fully covered the tunic matrix at the cut surface. After 3-5 days, minute protrusions were formed on the outer surface of the regenerated cuticle. At this time, there were no differences between regenerated and normal cuticles. The processes of cuticle regeneration were very similar to those of the new tunic wall formation in the allogeneic rejection reaction of colony specificity.

The filament formation was observed at the cut surfaces of tunic fragments without zoid, after incubation in SW. The formation also occurred in tunic fragments incubated in NaCl-HEPES (pH 8) which was isotonic to sea water, but was inhibited partially or completely in specimens exposed to some experimental conditions, such as incubation in low pH SW or SW containing EDTA, treatment with DW, detergent, glutaraldehyde or KCN, and freezing and thawing.

DB 42

REGENERATION OF THE NEURAL COMPLEX IN THE COMPOUND ASCIDIAN, POLYANDROCARPA MISAKIENSIS.
Y. Taneda and J. Inoue. Dept. of Biol.,
Fac. of Educ., Yokohama Natl. Univ.,
Yokohama.

Fully developed neural complex of ascidians consists of two different parts, the cerebral ganglion and the neural gland with two ducts which run forward and afterward from the gland. In the compound ascidian, Polyandrocarpa misakiensis, both the zoid from which the neural complex has been removed and the fragment without neural complex have a capacity to regenerate it. Histological study revealed that the ciliated funnel, the opening of neural gland duct, and neural gland duct appeared at first during the regeneration of neural complex. The cerebral ganglion appeared thereafter in the mesenchymal space. It seems likely that the neural gland duct is derived from the atrial epithelium. On the other hand, the cerebral ganglion seems to be formed by the blood cells. Regeneration of the cerebral ganglion from the fragment without neural complex was late compared to that from the neural complex removed zoid.

DB 43

THE ROLE OF ARACHIDONIC ACID CASCADE IN
ASEXUAL DEVELOPMENT OF ASCIDIANS.
K. Kawamura and M. Nakauchi. Dept. of Biol.,
Fac. of Sci., Kochi Univ., Kochi.

Mitosis, aggregation and epithelial transformation of haematopoietic stem cells, haemoblasts, have an important role in morphogenesis of paleal buds in the ascidian, *Polyandrocarpa misakiensis*. We report here that prostaglandins (PGs) are involved in the key step of those phenomena. Indomethacin is a specific inhibitor of cyclooxygenase that mediates the production of endoperoxides from arachidonic acid. In our *in vivo* assay, it blocked both cell division and aggregation of haemoblasts at the concentration as low as 0.4 μ M. In the presence of 1 μ M indomethacin, PGE₂ (15 nM) restored significantly the mitotic activity, but had no apparent effect on cell aggregation. On the other hand, PGE₂ (15 nM) was effective only in the recovery of epithelial transformation of haemoblasts. The results have suggested that mitosis and cell aggregation are governed by mutually distinct metabolic cascades of PGs. Unlike PGE₂, PGE₁ also allowed a heat-shocked, dormant bud to resume asexual development. PGE₂ showed a similar activity as PGE₁, but PGE₂, D₂ and I₂ had no apparent effect on bud development. We suggest that in *P. misakiensis* the early phase of bud development involves an inflammatory aspect.

DB 44

THE INFLUENCE OF SEVOFLURANE ON THE HATCHED CHICKEN.

H. Hasegawa, H. Tanaka and K. Nonoyama.
Dept. of Biol., Aichi Univ. of Educ. Kariya.

The authors examined on the influence of a new anesthetic agent, sevoflurane, to the hatched chicken, especially on the chicken liver damages according to the previous reports. The body weight of 1.5 and 2.0 % treated chicken were suppressed from 16 and 12 days after, respectively, as compared with the control. The ratio of the body weight decrease of treated chickens after 24 days were 13.6 and 16.4 % respectively. The values of serum GOT, GPT and α -GTP of the control were 23.6, 6, 28; on the contrary the values of the treated chicken were 378, 7, 24 (1.5 % treated after 24 days) and 441, 8, 21 (2.0 % after the same days). The variation serum LDH patterns of the control was as follows: LDH 1 = 76.6-78.1, LDH 2 = 11.6-12.3, LDH 3 = 4.7-5.9, LDH 4 = 2.5-3.0 and LDH 5 = 2.1-3.5. And that of the 1.5 % for 20 days treated hatched chicken (total 96 hours) was 48.6, 15.4, 11.6, 5.8, 18.6 and of 2.0 % was 41.1, 17.2, 15.9, 8.2, 17.2 respectively. Many stretched microvilli and lymphatic cells on the surface of disse cavity of the treated chicken liver. Also, the uneven rough surface was observed in the interior of the branch of hepatic arteria. However, not so significant difference was recognized between the treated chicken liver and the control, from the scanning electron microscopic observation.

DB 45

MIGRATION AND DIFFERENTIATION OF VAGAL NEURAL CREST CELLS OF AVIAN EMBRYOS
K. Takiguchi-Hayashi and K. Kitamura
Dept. of Develop. Biol., Mitsubishi Kasei Inst. of Life Sci., Machida, Tokyo 194, Japan

Almost all the vagal neural crest cells of avian embryos migrate through the dorsolateral pathway between ectoderm and somites. The crest-derived cells which enter gut mesenchyme differentiate into the enteric neurons, whereas those which enter ectoderm differentiate into the pigment cells. The purpose of this study is to clarify the regulatory mechanism of migration and differentiation of vagal crest cells.

Using monoclonal antibody 2A6 specific for melanoblasts, we observed temporal difference between the emigration of enteric neuroblasts and that of melanoblasts from the neural tube. Transplantation of quail trunk neural tube and crest into the vagal level of chick embryos revealed that the environment of migration pathway to gut mesenchyme changes after the migration of enteric neuroblasts.

These results suggest that both the intrinsic and extrinsic factors regulate the migration and differentiation of vagal neural crest cells.

DB 46

EFFECTS OF TESTOSTERONE PROPIONATE ON THE POPULATION OF GERM CELLS IN THE GONAD OF DEVELOPING FEMALE QUAIL.

Y. Araki and N. Yamamoto. Dept. of Physiol., Gifu Univ., Sch. of Med., Gifu.

Testosterone propionate (T.P.) (0.25 mg) was injected into the yolk sac of fertilized egg of genetic female quail on day zero stage. The number of germ cells in the cortex and medulla of embryo ovaries from the eleventh to fifteenth days of incubation was estimated. Moreover, the proportion of germ cell numbers to area of gonad (10^{-2} mm²) was estimated and compared with that of treated and control female. That of the left cortex or medulla in the treated female was about 45 or 2 cells on the eleventh day, about 40 or 2 cells on the thirteenth day and about 35 or 2 cells on the fifteenth day. Similar values were obtained for the control (about 40 or 2 cells on the eleventh day, about 45 or 2 cells on the thirteenth day and about 40 or 2 cells on the fifteenth day). On the other hand, that of the right cortex or medulla in the treated female was about 32 or 3 cells on the eleventh day, about 25 or 4 cells on the thirteenth day and about 53 or 9 cells on the fifteenth day. These values were higher than that of the control (about 4 or 2 cells on the eleventh day, about 7 or 2 cells on the thirteenth day and about 33 or 4 cells on the fifteenth day). These results indicate that T.P. induces proliferation of the right cortex while preserving germ cells in the right medulla.

DB 47

DISTALIZATION CAPACITY OF DEVELOPING CHICK PROXIMAL LIMB BUDS
A. Watanabe, K. Ohsugi and H. Ide, Biol. Inst., Tohoku Univ., Sendai.

To examine the distalization capacity of proximal limb buds, distal tip of quail limb bud at stage 21 was grafted onto stage 24-25 chick limb bud stump which contained only presumptive humerus area. The distal tip containing AER was previously X-irradiated (20 Gy) to inhibit the proliferation of mesodermal cells without blocking AER function.

Some cartilage elements appeared at the distal end of humerus 6 days after the grafting. These elements seemed to correspond morphologically to ulna or more distal limb cartilage, and to originate mainly from host stump since they were stained with A223, a chick-specific antibody. Without the grafting of distal tip, no distalization of the stump was observed.

Further, 2-3 days after the grafting, in the distal region of chick stump, AV-1 antigen appeared, which was specifically expressed in some distal region of chick limb bud.

These results suggest that the presumptive humerus area of stage 24-25 chick limb bud is not yet specified irreversibly and retains distalization capacity. By the grafting of distal tip containing AER, some cells of the stump at presumptive humerus level seem to change to AV-1 positive distal cells and form cartilage elements at more distal levels as in the case of limb regeneration.

DB 48

DIFFERENCE IN THE POSITIONAL VALUE-RELATED PROPERTY OF TISSUES FROM THE PROGRESS ZONE OF AVIAN WING BUDS
Koji Uchiyama and Hiroyuki Ide, Biol. Inst., Tohoku Univ., Sendai.

To elucidate the difference in positional value-related property of the progress zone, quail wing bud fragments at different developmental stages were grafted into the progress zone of chick wing buds. Developed chimera wing was examined immunohistochemically with A223 antibody which reacted with chick tissues specifically. Activity of DNA synthesis was histochemically measured with an anti-BrdU monoclonal antibody.

When tissue fragments from the progress zone of stage 25 wing bud were grafted into the progress zone of stage 19-20 wing bud, grafts formed only hand, although the host progress zone developed forearm and hand. The activity of DNA synthesis in the graft was lower than those of stage 20 and 25 wing buds.

When the fragments of the progress zone at stage 20 were grafted into the progress zone of stage 25 wing bud, the grafts formed only distal part of hand.

These results suggest the positional value-related property of the progress zone tissues changes irreversibly during the limb bud development and that the difference in the developmental potency of the grafts in this experiment may be explained by the difference in growth activity of the grafts.

DB 49

THE EFFECT OF RETINOIDS ON DEVELOPING CHICK LIMB BUD.
K. TAMURA, K. OHSUGI, and H. IDE. Biol. Inst., Tohoku Univ., Sendai.

Am80, Am580 and Ch55, synthetic stable analogs of retinoic acid (RA), possess very strong activity in inducing differentiation of the human myelogenous leukemia cell line HL-60 and hardly bind to CRABP (cytoplasmic retinoic acid-binding protein). When these retinoids were locally applied to anterior margin of chick wing bud at stage 20, duplicate formation along the antero-posterior axis was induced as RA. The effective doses of three retinoids in duplicate formation were similar to that of RA.

Since these retinoids were confirmed to mimic the ZPA function, we examined whether they could form normal pattern in ZPA-free limb bud, which usually resulted in truncation of distal parts. When these retinoids were applied to anterior margin and about 1/3 posterior region of limb bud which contained all of ZPA was excised at stage 20, limb pattern developed completely and the digit pattern was reversed.

These results support the idea that RA may affect limb morphogenesis without interaction with CRABP and that RA itself can elongate the limb bud along the proximo-distal axis and form the digit pattern in place of ZPA.

DB 50

TEMPORAL AND SPATIAL CHANGES OF COMPETENCE TO RETINOIC ACID IN CULTURED CHICK LIMB BUD MESODERMAL CELLS.
Hiroyuki Ide, Biol. Inst., Tohoku Univ., Sendai.

Retinoic acid (RA) promoted chondrogenesis in cultured whole distal mesodermal cells of stage 20-24 chick embryos and the competence of the mesodermal cells to RA changed temporally and spatially. As limb bud development proceeded, the cells came to respond to RA at higher concentrations. This suggests that at later stages of limb bud development, the cartilage formation will occur near the ZPA, where RA concentration may be high.

The competence to RA in the distal mesoderm gradually disappeared in a postero-anterior direction and at stage 26, only narrow anterior region of the distal mesoderm was responsive, suggesting that the specification of limb bud cells occurs both in postero-anterior and proximo-distal directions.

Cultured pigment retina of chick embryo inhibited chondrogenesis in the limb bud mesodermal cells and a spaced cartilage nodule pattern formation occurred when the mesodermal cells were surrounded by the pigment retina cells. This spaced nodule formation was promoted by increasing RA concentration.

From these results, cellular mechanisms of limb cartilage pattern formation was discussed.

DB 51

THE CHANGE OF THE EXPRESSION PATTERN OF POSITION SPECIFIC MOLECULE, AV-1, BY RETINOIC ACID IN CHICK LIMB BUDS.
K. Ohsugi, Biological Inst. Tohoku Univ., Sendai.

The AV-1 molecule is a glycoprotein which shows position specific expression during cartilage determination stage in chick limb buds. Indirect immunofluorescence staining and immunoblot analysis showed that the AV-1 molecule was localized on the plasma membrane and was expressed at stage 19-28 in some mesodermal cells of restricted space. At stage 28, it was expressed between the specific precartilaginous regions.

When beads containing retinoic acid of several concentrations were implanted below the AER at the anterior margin of stage 20 limb buds and these buds were allowed to develop, new AV-1 expression pattern became to be observed at 42 hour after the operation. When ZPAs were transplanted instead of retinoic acid containing beads, the same change of the AV-1 expression pattern was observed, however the beginning of the change was observed at 24 hour after the operation.

DB 52

REGENERATION OF BIPOLAR-HEADS AND BIPOLAR-TAILS IN FRESHWATER PLANARIAN.
S. Kurabuchi¹ and Y. Kishida². ¹Dept. of Histol., Sch. of Dentist., The Nippon Dental Univ., Tokyo. and ²Dept. of Biol., Sch. of Educ., Okayama Univ., Okayama.

Regeneration of the pieces 0.5 mm in length made by transverse two amputations in which the second was delayed in some periods after the first, was examined in an asexual form of planarian *Dugesia japonica*. The first amputation was done at the pre- or postpharyngeal region of the body to divide in two parts. After the anterior and posterior parts were reared for various periods until six days, the pieces 0.5 mm in length were prepared by performing the second amputation at the level 0.5 mm anterior to the posterior cut ends of the anterior parts, and 0.5 mm posterior to the anterior cut ends of the posterior parts.

When two amputations were done in the same time, most of pieces regenerated to be normal proportion. However, when the second amputation was delayed for three days from the first, the reversal of the axial polarity was caused in some cases; bipolar-heads in the pieces from the posterior sections whose anterior cut end was made by the first amputation, and bipolar-tails in the pieces from the anterior sections whose posterior cut end was made by the first amputation. Any cases of reversal of polarity was not obtained in the further delay of the second amputation.

DB 53

THE FORMATIONS OF MALFORMED PHARYNX AND NEOPLASIA BY TREATMENT OF CARCINOGEN IN A FRESHWATER PLANARIAN, *Bdellocephala brunnea*.
W. Teshihirogi and T. Hoshina. Dept. of Biol., Fac. of Sci., Hiroshima Univ., Hiroshima.

The effects of carcinogen, benzo (a) pyrene on the formations of pharynx and neoplasia were studied in a planarian, *Bdellocephala brunnea*. Two days after removing the pharynx from pharyngeal cavity, benzo (a) pyrene microcrystal of about 5µg was directly inserted into the pharyngeal cavity. This carcinogen affected morphogenesis of the structure of regenerating pharynx, that is, various duplicative or multiple pharynges were formed in the pharyngeal cavity. Furthermore, neoplasia was induced in a few worms. These malformed pharynges were characterized as overlaps in the anterior part of the main pharynx. This fact is considered to have been caused by the physiological disturbance of the dorso-ventral axis by carcinogen. The induction of neoplasia by carcinogen seems to be closely related with this physiological disturbance. That is, perhaps, as a result of the failure of morphological differentiation, gathered neoblasts have become neoplasia. The low occurrence rate of carcinogen treated neoplasia seems to be related to the high pharynx-formation capacity of the pharyngeal region.

DB 54

ELECTRON MICROSCOPIC STUDIES OF EMBRYONIC DEVELOPMENT OF THE FRESHWATER PLANARIAN, *Bdellocephala brunnea*.
III. THE SYNCYTIUM FORMATION.
T. Sakurai. Div. Cell Sci., Cent. Res. Lab., Fukushima Med. Col., Fukushima.

For the purpose of studying the participation of blastomeres in syncytium formation of yolk cells, planarian embryos were ultrastructurally examined from 2- to 8-cell stages. At the early time of 2-cell stage, special ER-areas are observed in the blastomere cytoplasm. At the late time, a large number of vacuoles are formed within the ER-areas. At the early time of 4-cell stage, those vacuoles once disappear from the cytoplasm, but later on they reappear in the same cytoplasm. At 8-cell stage, neither ER-areas nor vacuoles are found in the cytoplasm where contains a large number of polyplasm.

On the other hand, yolk cells having been aggregating around the blastomeres begin to fuse with one another and embed the latter in the syncytial cytoplasm. The mode of appearance and disappearance of vacuoles is identical to that observed in the 1-cell stage, suggesting that the vacuoles are released three times out of the egg cell and blastomere by 8-cell stage.

Since the syncytium formation is initiated when the vacuole formation and release come to an end, it seems very likely that these vacuoles contain an inductive factor to stimulate yolk cell fusion.

DB 55

FIBROBLASTS TO COLLAGEN INTERACTIONS IN THE PROCESS OF COLLAGEN GEL CONTRACTION
H. Asaga and K. Yoshizato. Dept., Biol., Tokyo Metropolitan University, Tokyo.

We studied the mechanism of the contraction of collagen gel and found that fibroblasts contract differently type I and III collagen gels (contraction speed: I>III, contracted gel size: I<III). The monoclonal antibody A3A5, which recognizes collagen binding domain of fibronectin and inhibits the contraction of type I collagen gel, also suppressed the contraction of type III collagen gel. No contraction of the gels was found when the lectins, ConA, PHA and WGA, were supplied to the culture medium at the concentration 100 μ g/ml, while SBA and PNA had no effect. From these results, we concluded that there is no difference in the molecular mechanism of the recognition of type I and III collagen by fibroblasts. The observed difference of contraction to be due to difference of physical properties of the gels of type I and III collagens. The amounts of the protein synthesized by fibroblasts cultured in collagen gel were markedly suppressed, supporting the idea presented previously that collagen stabilizes the biochemical activities of fibroblasts.

DB 56

STIMULATION OF MOUSE BALB3T3 CELL MIGRATION BY FISH EGG HYOSOPHORINS

K. KITAJIMA¹, Y. INOUE¹, S. INOUE², K. KONNO³, and H. SAKAGAMI³

¹Dept. of Biophys. and Biochem., Fac. of Sci., Univ. of Tokyo, Tokyo, ²School of Pharm. Sci., and ³School of Med., Showa Univ., Tokyo.

Hyosophrin (H-hyosophrin, MW = 100K-200K) is a carbohydrate-rich glycoprotein localized in cortical alveoli of unfertilized fish eggs. H-hyosophrin comprises tandem-repetitions of the identical glycopeptide unit (MW = ~9K). Upon fertilization H-hyosophrin is translocated into the perivitelline space and is completely proteolyzed into repeating units (L-hyosophrin). We initiated a study to elucidate the biological activities of hyosophrins in various cell systems. We report here that L-hyosophrins, but not H-hyosophrins, significantly stimulate the migration of mouse BALB3T3 fibroblasts in the *in vitro* assay system of Stenn. The stimulation effect of *Salmo gairdneri* L-hyosophrin reached a maximal level (twice of control) at above 50 ng/ml. The L-hyosophrins isolated from fertilized eggs of *Plecoglossus altivelis* and *Oryzias latipes* showed similar, but slightly less stimulation activity.

DB 57

ARE THE FILOPODIA OF CHICK GASTRULA MESOBLASTS THE FORCE-GENERATOR IN THEIR LOCOMOTION *IN SITU*?

R. Toyozumi¹ and S. Takeuchi²,
¹Zool. Inst., Fac. Sci., Tokyo Univ.
²Dept. Biol. Sci., Fac. Sci., Kanagawa Univ.

We observed directly the locomotion of mesoblasts in chick embryo at the later primitive-streak stage with the aid of Nomarski's differential interference microscope and of time-lapse cinematography. The blastoderm, the outer adhesive zone of which was discarded, was cultured ventral up at the bottom of whole-slide glass in substitution for the optical opaque vitelline membrane, which gave a good support for the mergin to expand. Mesoblasts were observed to locomote rather straightly (velocity, 130 μ m/hr at the area anterior to Hensen's node). During locomotion, the mesoblasts elongated constantly to the direction to move. Their filopodia were confirmed statistically to distribute significantly along the major axis defined in them when their shapes in SEM photos were approximated to ellapse. With the immuno-fluorescence method, vinculin was recognized to be deposited at the distal end of filopodia.

The mesoblasts *in situ* were considered to make use of the contacts between filopodia and undersurface of epiblasts as supporting points to generate force for locomotion.

DB 58

DEDIFFERENTIATION OF TERMINALLY DIFFERENTIATED MYOTUBES IS INDUCED BY SV40 LARGE T ANTIGEN

T. Endo¹, B. Nadal-Ginard², and T. Obinata¹

¹Dept. of Biol., Fac. of Sci., Chiba Univ., Chiba; ²Harvard Med. Sch., Boston, USA

Terminally differentiated myotubes have been thought to be irreversibly arrested at G₀ phase of the cell cycle. To address whether mature myotubes are able to reenter the cell cycle, we transfected the mouse skeletal muscle cell line C2 with a recombinant plasmid containing the SV40 T antigen gene linked to the Zn²⁺-inducible metallothionein gene promoter. SV40 large T induced by the addition of Zn²⁺ inhibited myogenic differentiation of the cloned transfectants C2SVTts. Remarkably, when large T was induced in the preformed myotubes, host cell DNA synthesis took place. Furthermore, mitosis and cytokinesis represented by the appearance of condensed chromosomes, mitotic spindles, midbodies, and contractile rings were observed. These results indicate that terminally differentiated myotubes are still able to reenter at least one round of the cell cycle by the aid of large T. The levels of expression of the tumor suppressor gene Rb and the myogenic determination gene MyoD were up- and downregulated during differentiation and the above dedifferentiation of C2SVTts cells, respectively. Thus, these gene products might be involved in the regulation of terminally differentiated state.

DB 59

ON THE DIFFERENTIATION OF GERM DISKS IN C3H/HeN-BALB/cA MOUSE AGGREGATION CHIMERAS. C. Tachi¹, M. Yokoyama², H. Kojima². ¹Zoological Inst., Univ. of Tokyo, Tokyo, ²Central Laboratory for Experimental Animals, Kawasaki.

We carried out quantitative analysis of the coat-color patterns of 20 C3H/HeN \leftrightarrow BALB/cA mouse chimeras by means of a video-image analysis system based on personal computer hardware (PC-9801, NEC, Tokyo; IFM-PC, Mitani-shoji, Tokyo); the system was developed by one of the authors and described previously (C. Tachi, 1988; Dev. Genet., 9,121-154). From the results, following tentative conclusions were drawn: 1) in the group of chimeras presently analyzed, the initial steps of the determination of the cranio-caudal axis preferentially took place in the regions of the primary ectoderm where BALB/cA components were predominant; 2) aggregability of the C3H/HeN-derived melanoblasts was inversely related to the ratio between the mean free path of the melanoblasts in the chimeras and that in the normal C3H/HeN mouse; 3) contact inhibition did not develop between C3H/HeN-derived melanoblasts and BALB/cA-derived amelanotic melanoblasts; 4) number of melanoblast clones calculated from the number of the minimal recognizable stripes in the chimeras presently analyzed, was 25-28 arranged unilaterally in the trunk region and closely approximated the number of the somites in the region as suggested previously (C. Tachi, 1988; *ibid.*).

DB 60

DIFFERENTIATION OF BILE DUCT CELLS FROM HEPATOCYTES IN THE RAT EMBRYO.

W. Shiojiri¹, J. Lemire² and N. Fausto². ¹Dept. Biol., ²Fac. Sci., Shizuoka Univ., Shizuoka and ²Dept. Pathol., Div. Biol. Med., Brown Univ., Providence, U.S.A.

Endodermal cells in the rat liver are hepatocytes and bile duct cells. The origin of bile duct cells is still controversial. The present study was undertaken to analyze the differentiation of bile duct cells from hepatocytes with *in situ* hybridization of alpha-foetoprotein (AFP) message and immunostaining of cytokeratin and hepatocyte surface component₆ (HES₂).

F344 strain rats were used. *In situ* hybridization was done according to Evarts et al. (1987). S-labelled probe was prepared from rat AFP cDNA template with *in vitro* transcription method. Sections were also stained doubly with monoclonal antibody against HES₂ and polyclonal antibodies against calf keratin.

AFP message was expressed not only in foetal hepatocytes but also in extrahepatic bile duct cells of young embryos and progenitor cells of intrahepatic bile duct cells. HES₂ was also expressed transiently in the progenitor cells of intrahepatic bile duct cells. These results suggest that all endodermal cells including bile duct cells in the rat liver are derived from AFP-message-positive hepatocytes, and that HES₂-positive differentiated hepatocytes also generate bile duct cells.

DB 61

FUSION OF THE CEPHALIC NEURAL FOLDS OF THE RAT EMBRYO.

M. Matsuda. Dept. Embryol., Inst. Dev. Res., Aichi Prefec. Colony, Kasugai, Japan.

The progression of the fusion of the cephalic neural folds of SD rat embryo was examined by use of an actin-specific antibody. In the rhombencephalic region, actin was detected at the luminal surface of the dorsolateral portions of the neural plate which opened outward. The reduction of the sizes of the area over which actin was distributed proceeded concomitantly with the decrease in area of the luminal surface of the dorsolateral portions of the neural plate. The areas in which actin was distributed at the apices of the neural plate formed the bridge between the two opposing neural folds. These results suggest that the contraction, which may be caused by the contraction of microfilaments, of the luminal surface of the neural plate results in the approach and the fusion of the neural folds. At the forebrain-midbrain boundary, the fusion of the neural folds occurred together with the fusion of the dorsolateral portions of the neural plate. Actin was not found at the luminal surface of the dorsolateral portions of the neural plate which was going to fuse each other.

DB 62

APPEARANCE OF NTA-REACTIVE ANTIGEN IN EMBRYONIC NERVOUS SYSTEM.

M. Miyakawa, Y. Arai¹ and T. Shirai². Depts Anat¹ and Pathol², Juntendo Univ. Sch. Med., Hongo, Tokyo.

Besides thymocytes and a part of T cells natural thymocytotoxic autoantibody (NTA) has been found to bind some neurons in adult mice. The appearance of NTA-reactive antigen was studied immunohistochemically in embryos of BALB/c mouse using monoclonal NTA. The reactivity on thymocytes appeared at embryonic day(E) 16. On the other hand, brain, spinal cord, spinal ganglia, spinal and autonomic nerves and retina were markedly stained at E 11 already. The cell bodies of the ganglia were almost negative but their fibers were positive. In addition to nervous tissues mentioned above, adrenal medulla and fusiform cells located among muscle were reactive. Reactivity of nerves and fusiform cells were especially marked from E 14 to E 16. Optic nerves and sciatic nerves did not show any immunoreactivity in adult mice. Conclusions: 1. The reactivity to NTA appeared earlier in the nervous tissue than the thymocytes. 2. Brain and spinal cord, peripheral nerve fibers and adrenal medullary cells were reactive to NTA in mouse embryo. 3. The change in reactivity during embryonic stage, or between embryos and adults seem to suggest an important role of this antigen in the development.

DB 63

SIALIC ACID-CONTAINING GLYCOPROTEIN IN DEVELOPING RAT NERVOUS SYSTEM AND MUSCLE. T. SEK1, Y. ARAI, Dept. of Anatomy, Juntendo University, Sch. of Medicine, Tokyo.

A monoclonal antibody (Mab) 12E3 was produced against a cell suspension from embryonic rat forebrain. The epitope recognized by Mab 12E3 was spatially and temporally expressed in the embryonic and neonatal rat nervous system and skeletal muscles. Vital immunostaining of cultured cells from the embryonic brain indicates that the antigen is localized on the cell surface. SDS-PAGE and immunoblot analysis of the membrane fraction from neonatal rat brain revealed a broad band around apparent molecular weight 200-280 Kd. The immunoreactivity was abolished following pretreatment of the membrane fraction with neuraminidase (Vibrio cholera), suggesting that the epitope of the antigen contains sialic acid. In the trunk of 12 day embryo, the immunoreactivities were found in the differentiated neurons outgrowing their axon of neural tube and myotomes. At embryonic day 14, the ventral and lateral parts of the spinal cord and skeletal muscles were stained. The immunoreactivities of spinal cord and muscle disappeared by postnatal days 22 and 6, respectively. These results suggest that the sialic acid-containing portion of the glycoprotein plays a possible role in developing nervous system.

DB 64

NEOCORTICAL ANOMALIES IN THE NEW ZEALAND BLACK MOUSE

M.Kamiya, A.Matsumoto, T.Shirai* and Y.Arai. Dept of Anat., *Dept of Pathol., Juntendo Univ. Sch. of Med., Tokyo.

Cerebral anomalies have been reported in the mice from autoimmune strains. The anomalies consist of ectopic cell clusters in the neocortical molecular layer.

We examined the cortical ectopias of the NZB mice morphologically by light and electron microscopes. Axo-somatic synapses as well as axo-dendritic ones were noted in the ectopias, implying that these dislocated cells still possess a synapse-forming capacity. In the cortex just beneath the ectopias, cell packing density was lower than in the adjacent region. Large-sized pyramidal cells, which normally predominate in layer V, were occasionally found in the more superficial layers. The incidences of anomalies in neonatal (1-5 days), prepubertal (2-4 weeks) and adult (3-18 months) mice were 30, 36 and 37 percent, respectively. The results indicate that some pathogenic factor(s) may act on the developing brain of the NZB mice and affect the cortical neurons in acquiring the appropriate laminar positions, rather than in their initial migration from the ventricular proliferative matrix layer to the cortical surface.

DB 65

THE ROLE OF THE NUCLEUS AND THE ASTER IN CLEAVAGE OF *ASTERINA PECTINIFERA* BY MEANS OF MICROMANIPULATION

T. Saiki and Y. Hamaguchi.

Biol. Lab., Tokyo Inst. of Technol., Tokyo

When one aster, two asters, the nucleus, or both the nucleus and an aster were removed from the zygote of the starfish, *A. pectinifera*, the zygote containing two asters cleaved and the zygote containing one aster with or without the nucleus cleaved after duplicating the aster, but the zygote containing only the nucleus did not cleave at all. These were transplanted into the intact zygote or the zygote deprived of the nucleus. When the nucleus was transplanted near two asters into the zygote with or without its own nucleus, a complete mitotic apparatus was formed and, thereafter, mitosis and cleavage completed. When the nucleus was transplanted near one of the asters, it interacted with the aster and made a half spindle, but its karyokinesis never occurred, although the zygote cleaved. When it was transplanted distantly from all of two asters, it stood still and did not interact with any asters. When one or two asters were transplanted, the zygote cleaved into three or four blastomeres at the same time, respectively. These results indicate that two or more asters always induce cytokinesis and that only the nucleus interacting with two asters makes a complete mitotic apparatus, which undergoes karyokinesis.

DB 66

INHIBITORY EFFECT OF MITHRAMYCIN A ON THE CLEAVAGE OF SAND DOLLAR EGGS BY MEANS OF MICROINJECTION

Y. Hamaguchi and M. S. Hamaguchi.

Biol. Lab., Tokyo Inst. of Technol., Tokyo.

Mithramycin A, which has been used for cytochemical staining of DNA and as an anti-tumor drug, was injected into eggs of the sand dollar, *Clypeaster japonicus*.

Mithramycin A has an advantage for observing chromosomes in living cells by its own fluorescence after injection. When the unfertilized egg was injected with mithramycin A and fertilized, or when the fertilized egg was injected with it not later than metaphase, chromosome movement was inhibited after the injection of ca. 4 pg per egg or more, although the spindle formation was not inhibited. However, chromosome movement was not always inhibited when the egg was injected at 4 pg per egg or more after the onset of anaphase. These results indicate that its inhibitory effect on chromosome movement may not be attributable to the inhibition of DNA or RNA synthesis, but that mithramycin A inhibits chromosome segregation directly during anaphase. Furthermore, when mithramycin A was injected into unfertilized eggs at 80 pg per egg or more, synergism of the pronuclei was inhibited after fertilization although the female pronucleus moved to the sperm aster, and, thereafter, the sperm aster moved to the center of the egg with only the female pronucleus.

DB 67

HETEROGENEITY OF MICROTUBULES IN DIVIDING SEA URCHIN EGGS.

M.Oka¹, Y.Hamaguchi¹ and T.Arai². ¹Biol. Lab., Tokyo Institute of Technology, Tokyo, ²Inst. of Basic Med. Sci., Univ. of Tsukuba, Tsukuba.

We investigated the heterogeneities of mitotic microtubules (mts) in sea urchin eggs immunofluorescently. Seven monoclonal antibodies against tubulin were examined and divided into four types in respect to staining pattern: 1. Four antibodies (YL1/2 etc.) stained both the spindle and the aster. 2. An antibody (D2D6) stained the spindle strongly. 3. An antibody (DM1B) stained only the aster. 4. An antibody against acetylated α -tubulin (6-11B-1) did not stain the mitotic apparatus at all. These results suggest that tubulin isoforms of the spindle are somewhat different from tubulin isoforms of the aster.

When the eggs were treated with a mt depolymerizing drug (nocodazole), astral mts depolymerized rapidly, whereas spindle mts remained for a while, and then, became mt bundles gradually, which were stained with DM1B as well as with YL1/2 and D2D6. When the eggs were treated with a mt stabilizing drug (hexylene glycol), many astral and spindle mts polymerized, and many cytasters appeared, although the mitotic apparatus became small with time. YL1/2 and D2D6 stained all of the spindle, asters, and cytasters. DM1B stained cytasters though it stained the mitotic apparatus weakly.

DB 68

ASTER FORMATION IN THE ACTIVATED SEA URCHIN EGGS

A.Nagata, T.Miki-Noumura. Dept. of Biology, Ochanomizu Univ. Tokyo.

Aster formation was studied in sea urchin eggs, after artificially activated by Loeb's double method. Following butyric acid and hypertonic SW treatment, multiple asters are observed in eggs suspended in normal SW with phase contrast and electron microscopy. (Miki-Noumura, 1977. Kuriyama and Borisy, 1983.)

In this study, we used indirect immunofluorescence microscopy to examine tubulin-containing structures in the activated eggs. Small asters appeared during hypertonic treatment. The number of asters increased in accordance with duration of the treatment. After eggs were transferred to normal SW, these small asters disappeared within 15min. But fewer asters reappeared again within 40min. During culture in normal SW these asters grew in size whereas their number was unchanged. Eggs with 1-4 asters actively cleaved and developed to blastula.

It is likely that during hypertonic treatment, organizing centers for asters might be formed or activated, increasing their number as a function of time in hypertonic SW. Disappearance of all asters just after transfer to normal SW was followed by reappearance of fewer asters. The observation suggests that a few organizing centers might remain active or be activated again to organize asters in normal SW.

DB 69

70KDA MICROTUBULE-MODULATING PROTEIN (70KDA PROTEIN) FROM STARFISH OOCYTES II

N. Hosoya¹, H. Hosoya² and H. Mohri¹. ¹Dept. Biol., Univ. Tokyo, Tokyo and ²Dept. Ultrastruct. Res., Tokyo Metro. Inst. Med. Sci., Tokyo.

We previously purified a 70kD microtubule-modulating protein (70kDa protein) from matured oocytes of the starfish, *Asterias amurensis* (Hosoya et al., Zool. Sci. 5, 1287, 1988). The 70kDa protein has three major isoforms identified by isoelectric focusing. The 70kDa protein binds to mammalian brain and echinoderm egg microtubules. It does not promote assembly of brain tubulin, but promotes that of egg tubulin *in vitro* in a concentration-dependent manner. The protein seems to bind to microtubules at a different site from those for brain MAPs, because its binding to microtubules is not inhibited with the saturated amounts of brain MAPs. Immunofluorescence studies indicate that the 70kDa protein specifically localizes on microtubule structures spread widely throughout the cytoplasm, the sperm aster and the microtubules constituting the mitotic apparatus in both meiosis and mitosis. The 70kDa protein is found to exist not only in oocyte but also in nerve cells by immunoblotting technique. It is not detected, however, in sperm flagella. The 70kDa protein may regulate the dynamics of cytoplasmic microtubules.

DB 70

MODE OF THE 51-kDa PROTEIN IN THE CENTRO-SOME AND THE MITOTIC APPARATUS MATRIX

S. Hosoda, K. Ohta, S. Endo and H. Sakai. Dept. of Biophys. and Biochem., Fac. of Sci., Univ. of Tokyo, Tokyo.

The 51-kDa protein is localized in the centrosome and spindle possibly playing an essential role in the formation of mitotic apparatus (MA) in sea urchin eggs. In the centrosome, the 51-kDa protein has been suggested to participate in microtubule (Mt) nucleation, but the role of the 51-kDa protein in the spindle remained to be solved. We have previously shown that the 51-kDa protein in the spindle is associated with a matrix structure (MA matrix, MAM). We isolated MAs under conditions that astral and spindle Mts would depolymerize and found that the 51-kDa protein is still localized in a "meshwork" structure of the MAM as well as in the centrosome. When MAs isolated in a Mt stabilizing buffer and further stabilized by taxol were treated with 0.6M KCl, the 51-kDa protein in the MAM could be solubilized, while the 51-kDa protein in the centrosome could not. Immunoelectron microscopy revealed that the 51-kDa protein was localized in the granular materials in the centrosome of the taxol/salt-treated MA. It was suggested that the 51-kDa protein is incorporated into different structural organizations in the centrosome and the MAM, thereby serving different function. In addition, the 51-kDa protein in the MAM was suggested to be associated with Mts via spindle MAPs.

DB 71

GUANINE NUCLEOTIDE BINDING PROPERTY OF THE MITOTIC APPARATUS ASSOCIATED 51-kDa PROTEIN. K.Ohta, S.Hosoda, S.Endo and H.Sakai. Dept. of Biophys. and Biochem., Fac. of Sci., Univ. of Tokyo, Tokyo.

The 51-kDa protein has been shown to be closely relevant to the aster forming activity of microtubule organizing granules (MTOGs) in the centrosome of sea urchin egg with an essential role in the formation of the mitotic apparatus. We have previously demonstrated that the 51-kDa protein is a GTP binding protein which bears resemblance to the polypeptide elongation factor-1 α . In the analysis of the guanine nucleotide binding property of the 51-kDa protein, it was newly revealed that binding of GTP to the 51-kDa protein was fast (50% in 2 min), and the bound GTP was exchangeable for GDP. The 51-kDa protein bound GTP, GDP, GMPNP and ITP, but little binding was detected for ATP, CTP and UTP. Dissociation constant for GTP (1.1 μ M) was 7 fold higher than that for GDP (0.15 μ M). Furthermore, the 51-kDa protein was shown to possess GTPase activity depending on ribosomes and aminoacyl-tRNA. It was further shown that aster forming activity of MTOGs, in which the 51-kDa protein was a major component, was more sensitive to GDP than spontaneous microtubule formation. We propose a hypothesis that equivalent to other GTP binding proteins the 51-kDa protein represents a molecular signaling mechanism for microtubule initiation in the formation of the mitotic apparatus.

DB 72

ACCUMULATION OF WGA RECEPTORS IN THE CLEAVAGE FURROW DURING CYTOKINESIS IN SEA URCHIN EGGS.

T.Yoshigaki, S.Maekawa and H.Sakai. Dept. of Biophys. and Biochem., Fac. of Sci., Univ. of Tokyo, Tokyo.

Staining of fertilized sea urchin eggs with fluorescein labeled wheat germ agglutinin (WGA) before the first cleavage showed that WGA receptors were concentrated in the cleavage furrow just before and during cytokinesis. In an egg pressed a little and cultured in a thin spacer chamber, WGA receptors first accumulated at the egg surface right above the mid point of the mitotic spindle. Then, a belt-like accumulation of WGA receptors developed on both sides at the surface along the equatorial plane of the spindle, which eventually formed a ring. This observation revealed that the disposition of asters and the distance between asters and cell surface determined the place of the first accumulation of WGA receptors. Colcemid was capable of dispersing the accumulation of WGA receptors only when eggs were treated with the drug early in cytokinesis. This result indicated that microtubules are involved in the accumulation of WGA receptors in a ring-like fashion. Cytochalasin B did not inhibit the first accumulation of WGA receptors of eggs in the thin spacer chamber. We proposed the possibility that the accumulation of WGA receptors is involved in the mechanism of determining the place where the contractile ring is formed.

DB 73

SURFACE CHANGE IN SEA URCHIN EGGS BY THE EFFECT OF CALYCULIN A.

H. Tosuji, K. Miyaji, T. Nakazawa and Y. Kato*. Dept. of Biol., Fac. of Sci., Toho Univ., Funabashi and *Lab. of Mar. Biochem., Fac. of Agric., Univ. of Tokyo, Tokyo.

Calyculin A is a cytotoxic and antitumor substance extracted from marine sponge, *Discodermia calyx*. This substance caused an outgrowth on either fertilized and unfertilized eggs in the several species of sea urchins (*Hemicentrotus pulcherrimus*, *Anthocidaris crassispina* and *Clypeaster japonicus*) within 1 hour after the addition. In the scanning electron microscopic observation, microvilli on the egg surface began to move soon after the addition of calyculin A, and gathered gradually in one point of the egg surface accompanying with microvilli elongation. This "cap formation" was inhibited by the addition of cytochalasin B but not by the addition of colchicine. The area of gathering microvilli was stained with rhodamine-conjugated phalloidin. Therefore, these microvilli shifts induced by calyculin A might be caused by the activation of actin filament.

DB 74

FORMATION OF THE HYALINE LAYER IN SEA-URCHIN EGGS — AS REVEALED BY DEFORMATION DUE TO FIXATION WITH GLUTARALDEHYDE.

N. Usui. Dept. of Anat., Teikyo Univ. Sch. of Med., Tokyo.

The trouble is that fertilized sea-urchin eggs are deformed by fixation with glutaraldehyde (GA). But no deformation occurs in the eggs for a few min after insemination and the eggs possessing neither the fertilization envelope or the hyaline layer (HL). Either or both of these investments must be concerned with this fixation trouble.

To elucidate which structure causes the trouble, the eggs freed from the vitelline coat were fixed with GA every min after insemination. Only the eggs invested by the HL were found deformed. This result allowed examination of the HL formation in a large number of the eggs by light microscopy: The number of deformed eggs and the degree of deformation increased gradually for 5 min after 3 min post-insemination. Thin section study showed that the time exactly corresponded to that for aggregation of material released from the cortical granules to form a cell surface coat, the HL. The HL seems to be formed until 8 min after insemination.

In addition, the present study revealed that when the 8-min eggs with the HL were cultured in Ca²⁺, Mg-free seawater, they kept their spherical shape in GA whereas the 11-min eggs were deformed. It was suggested that some further change occurs in the HL after completion of its formation. This change remains to be studied.

DB 75

CYCLIC APPEARANCE OF CYTOPLASMIC NOR-SILVER STAINED PARTICLES DURING EARLY EMBRYOGENESIS.

R. M. Amikura¹, E. Aikawa¹, H. Yamada² and H. Nagano³. ¹Dep. of Anatomy, Tokyo Women's Medical College, Tokyo, ²Dept. of Mol. Biophys. and Biochem., Yale Univ. U.S.A., ³Central Res. Lab. Yamouchi Pharmaceutical Co. Ltd., Tokyo

The cytoplasmic NOR (nucleolar organizer region)-silver stained particles (CNSPs) were detected in sea urchin embryos. The CNSPs were present during interphase, but not during metaphase and anaphase. They were detected again at telophase. In addition, the CNSPs were specific in the embryos before early blastula stage.

The cyclic appearance of CNSPs was not interfered by the cytochalasin B and aphidicolin. In colchicine treatment, no CNSPs were observed when cell cycles were stopped at metaphase. However, the multi-nuclear cells (eggs) which lacked in CNSPs were formed under cytochalasin B treatment (for 8 hours).

These results suggest that the cyclic appearance of CNSP was controlled by a kind of master (cyclic) signal of cell cycle and highly related to the developmental process.

DB 76

CYTOLOGICAL STUDIES ON THE PARTHENOGENESIS IN STARFISH EGGS: BEHAVIOR OF CHROMOSOMES AND NUCLEI.

S. Washitani-Nemoto¹, K.H. Kato², A. Hino³ and S. Nemoto⁴. ¹Biol. Lab., Hitotsubashi Univ., Kunitachi 186; ²Nagoya City Univ.; ³Kanagawa Univ., and ⁴Ochanomizu Univ..

We have reported that starfish eggs develop parthenogenetically when their polar body (pb) formation is suppressed. Both of activated eggs with either no or one pb develop as tetraploids (2n=44 in *Asterina pectinifera*). We investigated the behavior of chromosomes and nuclei during the period between activation and the 1st cleavage. Fixed eggs were stained with aceto-orcein. (1) Eggs with no pb: As a result of inhibition of pb extrusion, 22 tetrads separated into 88 single chromosomes. After the chromosomes disappeared, a nucleus was formed. After a while, the nucleus broke down, and a diaster was formed, in which 88 bivalents were present. Then the first cleavage occurred. (2) Eggs with one pb: 22 bivalents, retained within egg cytoplasm by inhibition of 2nd pb extrusion, divided into 44 single chromosomes. Then, the 1st appearance of a nucleus was observed. After the nucleus disappeared, a half spindle was formed and chromosomes doubled to 88. Then a nucleus appeared again and the eggs entered into the 1st cleavage cycle. Thus, parthenogenetic embryos become tetraploids.

DB 77

CYTOLOGICAL STUDIES ON THE PARTHENOGENESIS IN STARFISH EGGS: BEHAVIOR OF CENTRIOLES. K.H. Kato¹, S. Washitani-Nemoto², A. Hino³, and S. Nemoto⁴. ¹Nagoya City Univ., Nagoya, 467; ²Hitotsubashi Univ.; ³Kanagawa Univ., and ⁴Tateyama Marine Lab., Ochanomizu Univ..

We reported in starfish that in meiosis II each aster contains only one centriole, whereas in meiosis I each aster has a pair of centrioles (D.G.D. '90). This indicates that no duplication of centrioles occurs during the successive meiotic divisions. When eggs are treated with caffeine just after 1st pb extrusion to suppress 2nd pb formation, they might retain two centrioles. We, using TEM, examined how the meiotic centrioles are converted into the mitotic ones in these eggs of *Asterina pectinifera*. In caffeine seawater the eggs had a pair of centrioles near a cluster of chromosomal vesicles. After returning the eggs to sea water, a nucleus appeared. After a while the nucleus disappeared and then a half spindle was formed. In its aster paired centrioles were observed. In addition, the 3rd centriole was present near the cell surface. After the spindle was disappeared, a nucleus was formed again. Disappearance of the nucleus was followed by the formation of a diaster and a cleavage furrow. Each aster at this stage had a pair of centrioles. These suggest that one of two centrioles within caffeine-treated eggs is duplicated twice coincidentally with the nucleus formation.

DB 78

CELL CYCLE STUDIES OF MICROMERES IN THE EMBRYOS OF SEA URCHIN, *Hemicentrotus pulcherrimus*.

S. Tanaka¹, Kuniko Nakajima¹ and Katsuma Dan². ¹Dept. of Dev. Biol., Mitsubishi-Kasei Inst. of Life Sci., Machida-shi, Tokyo, ²Misaki Marine Biological Station, Koajiro, Miura-shi, Kanagawa.

Microfluorometry of nuclear DNA and other related parameters affords detailed analysis on roles of the cell cycle during embryonic development. In early embryos of sea urchin, accurate microfluorometry have not yet been achieved chiefly due to high background fluorescence emitted from large amount of cytoplasm. To solve such problem, a system of scanning stage controlled multiparametric microfluorometry was developed. At 32 cells stage, parameters of DNA content and amount of BrdU uptake were measured in large and small micromeres. DNA replication initiated about 5 min after the cleavage and completed within 20 min in large micromeres. While in small micromeres, there was further delay of 5 min before entering S phase. In small micromeres, DNA replication continued as long as 9 hr by the stage of ca 350 cells. Rate of DNA replication judged by BrdU incorporation amount was much higher in large micromeres than in small ones. Such great difference in regulation on DNA replication between the large and small micromeres may reflect establishment of different cell lineages upon uneven cell division at 32 cell stage.

DB 79

CELL PROLIFERATION AT VEGETAL HEMISPHERE OF SEA URCHIN EMBRYO AT BLASTULA STAGE. H. Mizoguchi¹ and T. Tanaka². ¹Lab. of Biol., Jun. Col. of Rissio Univ., Saitama, ²Dept. of Develop. Biol., Mitsubishikasei-Inst. of Life Sciences, Tokyo.

In the vegetal hemisphere of sea urchin embryos at blastula stage, cell proliferation was presumed to clarify the cellular mechanism of archenteron formation. Quantitative measurements of cell proliferation was done following 5-bromodeoxyuridine (BrdU) label, assayed by immunocytochemistry using monoclonal antibody against BrdU and streptavidin-biotin peroxidase system.

Treatment of the embryo with BrdU (0.4mM), when started just after hatching, resulted in the production of many mesenchyme-like cells but archenteron was not produced in the embryos. BrdU-caused inhibition of archenteron formation was canceled by excess thymidine. The number of BrdU sensitive cells were increased at the region of vegetal hemisphere during the treatment. Addition of BrdU to the embryo culture, at the mesenchyme blastula and gastrula stage, normal archenteron was formed.

It seems that BrdU sensitive cells in vegetal hemisphere of swimming blastula are participated in archenteron formation.

DB 80

Migration and spicule formation of isolated micromere's and its derived large and small blastomere's descendants of sea urchin embryo. Y. Takahashi and J. Tsukahara. Dept. of Biol., Fac. of Sci., Kagoshima Univ. Kagoshima

In vivo or isolated micromeres (IM) of sea urchin, *A. crassispina*, cleaved unequally to large blastomere (LB) and small one (SB) on the next cleavage cycle. Descendants of them began to migrate at approximately 22 hr after fertilization. Cultivation medium contained horse serum (HS) or blastocoelic fluid (BCF) of *T. gratilla* was used. In the former medium the aggregates derived from IM, SB or LB scattered respectively at approximately uniform velocity within 20 hr. In the latter, LB descendants scattered on the same speed as in the HS, while IM and SB descendants decreased their scattering speed. Later, only in the BCF medium, the descendants not only from IM but also from LB or SB could form spicule(s) at fairly high rate. We also studied that if the medium was exchanged from BCF to HS at appropriate intervals after beginning of scattering or vice versa, descendants from IM on the former condition showed the same scattering figure and could not form spicules, while on the latter it was shown that scattering cells were gathered to make aggregate again and occurred to form spicules.

DB 81

INVOLUTION OF EXTERNAL CELLS DURING STARFISH GASTRULATION. R. Kuraishi and K. Osanai. Mar. Biol. Stn., Tohoku Univ., Aomori.

Intracellular injection of a tracer enzyme, horse radish peroxidase, into one of veg 1 and veg 2 blastomeres of *Asterina pectinifera* at the 32-cell stage revealed that boundary between progenies of veg 1 and veg 2 blastomeres was in the outer layer at the beginning of gastrulation, around the blastopore at the late gastrula stage, and in the archenteron afterwards. This result shows that involution of external cells occurs during starfish gastrulation and that a part of progenies of veg 1 blastomeres differentiate into endodermal cells. When gastrulae were exposed briefly to sea water containing Nile blue, only external cells were deeply stained. As gastrulation proceeded, the archenteron was divided into two regions; anterior, unstained region, which had involuted before the staining, and posterior, stained region, which had newly involuted after the staining. Observation of bipinnariae which had been stained at various stages during the course of gastrulation led to a conclusion that cells in the oesophagus, the stomach, and the intestine had involuted at the early gastrula stage, from the mesenchyme-differentiation stage to the mouth-formation stage, and after the mouth-formation stage, respectively.

DB 82

EFFECT OF ENVIRONMENTAL DIVALENT CATIONS ON THE PERMEABILITY OF SEPTATE JUNCTIONS IN STARFISH LARVAE. Y. Okushima¹, K. Noda², H. Kaneko¹ and M. Dan-Sohkawa¹. ¹Dept. of Biol., Osaka City University, Osaka, ²Tokyo Metropolitan Inst. of Gerontology, Tokyo.

Starfish embryos acquire an epithelial structure, consisting of septate junction and basal lamina, at the blastula stage. The septate junction is known to function as a barrier against molecules from diffusing through an epithelium by way of paracellular routes. In some vertebrate epithelia, it is suggested that the structure and permeability of tight junction, which is the homologous counterpart of invertebrate septate junction, is physiologically regulated. Environmental Ca^{2+} concentration is one of the factors which affect the structure and function of this junction.

To explore the role of divalent cations in the structure and permeability of septate junctions, starfish larvae (early bipinnaria stage) were exposed to sea water containing various concentrations of divalent cations. Permeation of fluorescence labeled macromolecules (FITC-IgG and dextran) into the blastocoel as well as the ultrastructure of the septate junctions under these conditions was observed.

The barrier function against tracer macromolecules was relatively stable at Ca^{2+} concentrations between 1 mM and 9 mM. Macromolecules, however, permeated into the blastocoel under Ca^{2+} depletion, which condition also obscured the septa of septate junctions. Mg^{2+} -free sea water influenced the permeability more weakly than Ca^{2+} -free sea water. Both physiological and morphological changes were reversible. The results suggest that both environmental Ca^{2+} and Mg^{2+} are essential to maintain the structure and function of the septate junction.

DB 83

RELATION BETWEEN BLASTOPORE AND STOMODEUM FORMATION IN DEVELOPMENT OF POND SNAIL, SINOTAIA QUADRATUS.

M. Fukuoaka, M. Tanaka and K. Ishihara, Dept. of Reg. Biol., Fac. of Sci., Saitama Univ., Urawa, Saitama.

Gastropods are generally protostome, except Viviparus (Paludina) whose blastopore is destined to be anus. One of Japanese pond snails, Sinotaia quadratus, was investigated on the development of blastopore and archenteron.

In early gastrula, autonomous fluorescent cells appeared on the tip of archenteron, but not around blastopore. Stomodeum began to invaginate in middle trochophore stage and finally connected to the tip of archenteron where the fluorescent cells were divided into two groups, one was distributed in liver anlage and the other in esophagus. Blastopore lacking fluorescent cells remained unchanged during the stomodeum formation. These facts were confirmed by the microscopic observation of serial paraffin and frozen sections.

These results indicate that blastopore is destined to be anus and mouth opens later on development of embryo, being different from protostomes. The nature of fluorescent substance is unknown but is suggested by the facts that fluorescent cells are in good correspondence in size, position and localization with melanocytes in surface layer of adult liver of the snail.

DB 84

SPECIES SPECIFICITY OF A MONOCLONAL ANTIBODY TO 56- AND 58-KILODALTON-POLYPEPTIDES PRESENT IN THE EGG OF THE STARFISH, ASTERINA PECTINIFERA.

S. Ikegami, T. Mitsuono, M. Kataoka and M. Komatsu*, Dept. of Applied Biol. Sci., Hiroshima Univ., Higashihiroshima-shi and *Dept. of Biol., Fac. of Sci., Toyama Univ., Toyama-shi.

A monoclonal antibody (immunoglobulin G) that reacts specifically with the polypeptides with the molecular weights of 56,000 and 58,000 present in the extract of oocytes of the starfish, *Asterina pectinifera* was prepared. We have shown that the immunoglobulin G reacted with extracts of eggs, morulae, gastrulae, bipinnariae, ovaries, but not with those of brachiolariae, testes, pyrolic ceca, body walls and tube-feet. The immunoglobulin G did not react with extracts of eggs of the starfish *Asterias amurensis* or of several sea urchin species. Among the members of the genus *Asterina*, eggs and embryos of *Asterina batesi* and *Asterina minor* were not reactive whereas blastulae and brachiolariae of *Asterina pseudodelgada pacifica* contain an immunoreactive component. The molecular weight of the component was estimated to be 40,000 by immunoblot analysis. These results represent an example of remarkable phylogenetic alterations of antigen molecules.

Supported in part by a grant from the Nissan Science Foundation.

DB 85

PRESENCE OF CHROMOGRANIN A-RELATED PEPTIDES IN SEA URCHIN EGGS AND SPERM. Y. Fujino¹, A. Fujiwara², I. Yasumasu², T. Fujii¹, ¹Dept. of Pharmacol., Teikyo Univ. Sch. of Med., Tokyo and ²Dept. of Biol., Sch. of Educ., Waseda Univ., Tokyo.

Chromogranin A is known as a Ca^{2+} -binding protein in secretory granules of various secretory glands in mammals.

In the present study, we prepared a polyclonal antibody against chromogranin A, which was extracted and highly purified from the chromaffin granule fraction of bovine adrenal medulla homogenate. The heat stable fractions, obtained from homogenates of unfertilized eggs and sperm of *Hemicentrotus pulcherrimus*, contained several immunoreactive peptides against anti-chromogranin A, revealed by SDS-PAGE followed by immunoblotting using the antiserum. Molecular weights of the almost all peptides in eggs are not similar to those in sperm. Role and the cellular distribution of the chromogranin A-related peptides are unknown at present.

DB 86

AUGMENTATION OF VEGETALIZING EFFECT OF Li^+ BY ML-9 IN SEA URCHIN EGGS. K. Kataoka, A. Fujiwara², I. Yasumasu, Dept. of Biol., Sch. of Educ. Waseda Univ., Tokyo

Pulse treatment with ML-9 for 3 hr starting at 1, 3, 4 and 9 hr after fertilization blocked development of sea urchin but the treatment 2, 5 and 6 hr after fertilization did not exert any inhibitory effects on the development to allow the embryos to develop normal plutei. On the basis of percent inhibition of protein phosphorylation in embryos, estimated by ^{32}P radioactivity in protein fraction following ^{32}P exposure, by ML-9, W-7, W-5, H-7 and HA1004, protein phosphorylation mediated by Ca^{2+} , calmodulin dependent protein kinase seems to be higher in the degree of contribution to overall phosphorylation in embryos than the phosphorylation blocked by H-7 and HA1004 at a period of development between 1 and 4 hr after fertilization and thereafter, it is lower in degree of contribution then mediated by protein kinases sensitive to H-7 and HA1004. Pulse treatment with Li^+ for 3 hr, which was effective for induction of vegetalization when it was initiated 3-4 hr after fertilization, resulted in production of vegetalized embryos in the presence of ML-9 at concentrations of Li^+ lower than those to induce vegetalization in its absence. Inhibition of Ca^{2+} , calmodulin dependent protein kinase seems to support vegetalization of sea urchin embryos.

DB 87

INHIBITION OF PIGMENT CELL FORMATION BY
PROCAINE AND TETRACAINE
IN SEA URCHIN EGGS.A. Fujiwara, K. Kataoka and I. Yasumasu.
Dept. of Biol., Sch. of Educ., Waseda
Univ., Tokyo.

Pigment cells containing echinochromes appeared in embryos at the late gastrula-prim stage. A pulse treatment of eggs for 3 hr with procaine or tetracaine starting at the 8-16 cell stage blocked the formation of pigment cells (judged by the production of echinochromes) at stages later than the prim stage. The same pulse treatment by these compounds, starting at the other stages than the 8-16 cell stage, hardly exerted any strong inhibitory effects on pigment cell formation. Embryos thus treated with these compounds at the 8-16 cell stage became vegetalized ones. However, inhibition of pigment cell formation does not always occur in vegetalized embryos by Li^+ treatment performed in the same manner as the treatment with these compounds. Procaine and Li^+ are known to be able to modulate $[\text{Ca}^{2+}]_i$. Among inhibitors of protein kinases examined in the present study, pulse treatment with ML9 at the 8-16 cell stage blocked pigment cell formation but did not produce vegetalized embryos. Determination of pigment cells, probably occurring at the 8-16 cell stage, seems to be supported by Ca^{2+} -calmodulin dependent protein phosphorylation.

DB 88

HISTOCHEMICAL DETECTION OF ARYLSULFATASE
ACTIVITY IN SEA URCHIN EMBRYOS.K. Akasaka¹, Y. Akimoto², M. Sato³, H. Hirano² and H. Shimada¹.1. Zool. Inst. Fac. of Sci., Hiroshima Univ.
2. Dept. of Anatomy, Kyorin Univ.
School of Med.
3. Zool. Inst. Fac. of Sci., Univ. of Tokyo.

Localization of arylsulfatase activity in the sea urchin embryo was determined histochemically through light and electron microscopy. Histochemical observations by light microscopy revealed that the arylsulfatase activity appears after gastrula stage and that it is restricted to the cells of aboral ectoderm. The enzyme activity is mainly distributed in the apical cellular cytoplasm and is associated with lysosome-like structures which are frequently fused with yolk granules. The intense activity is also detected in the region of endoplasmic reticulum and Golgi apparatus. No enzyme activity is found in the extracellular spaces of embryos.

DB 89

DNA METHYLATION IN SEA URCHIN EMBRYOS.

K. Murofushi and I. Yasumasu. Dept. of Biol., sch. of Educ., Waseda Univ., Shinjuku-ku, Tokyo 169

The rate of DNA methylation, estimated by an exposure of embryos to [methyl-³H] methionine, was high at the morula (8hr after fertilization) and at the gastrula stage (22-24hr). The same was true in the rate of DNA methylation, estimated after the exposure of isolated nuclei to [methyl-³H] S-adenosylmethionine. Exposure of embryos for several hr at the morula stage to SIBA (5'-deoxy-5'-S-isobutyladenosine), which inhibited DNA methylation, caused death of many embryos but embryos, which were still alive even after the exposure, developed normally. The exposure for several hr starting at the early gastrula stage blocked formation of archenteron and pluteus arm. At the former stage, embryos exhibited high rates of DNA methylation and DNA demethylation and the latter stage, high rates of DNA methylation was not accompanied by its high demethylation rate. Demethylation rate was high just before the gastrulation. Electrophoresis of DNA fragments obtained by digestion with several restriction enzymes, showed different distributions of [³H-methyl] labeled regions of DNA at the morula stage from those observed at the gastrula stage.

DB 90

RELATIONSHIPS BETWEEN [ADP-RIBOSYL]ATION OF
NUCLEAR PROTEINS AND DEMETHYLATION OF DNA.
Y. Kamata, I. Yasumasu. Dept. of Biol., Sch. of Educ., Waseda Univ., Tokyo.

The rate of [ADP-ribosylation] of proteins in isolated nuclei, estimated by their exposure to [ade-¹⁴C]NAD⁺, was higher at the morula and the gastrula stage. [ADP-ribosylation] of proteins was blocked by 3-aminobenzamide (3-ABA) and activated by N-methyl-N'-nitro-N-nitrosoguanidine (MNNG) and dimethylsulfate (DMS). These compounds blocked development to cause embryo death at the morula stage and blocked gastrulation at the gastrula stage. In embryos, 3-ABA blocked demethylation of DNA, which was estimated by the decrease in the radioactivity in DNA labeled by exposure of embryos to [methyl-³H] methionine, during culture following the exposure. In isolated nuclei, exposure to [methyl-³H]DMS resulted in labeling DNA. In many cases, considerable decrease in the radioactivity of DNA thus labeled was observed in nuclei during incubation with NAD⁺. The decrease in the radioactivity induced by NAD⁺, accompanied by the release of DNA fragments, was blocked by 3-ABA. In some cases, acceleration of decrease in the radioactivity by NAD⁺ and its blockage by 3-ABA were not so evident as mentioned above, but specific radioactivity of thus released DNA fragments became high in the presence of NAD⁺ and was lowered by 3-ABA. The same was true in nuclei labeled in embryos exposed to [methyl-³H]methionine.

DB 91

INDUCTION OF VITELLOGENIN SYNTHESIS IN *ORYZIAS LATIPES* LARVAE.
Y. Ebina. Div. Cell Sci., Ceny. Res. Lab.,
Fukushima Med. Coll., Fukushima.

Estrogen-dependent synthesis of vitellogenin, the precursor of the major yolk proteins, in the liver of egg-laying vertebrates is an attractive model for gene expression. Our first approach is to find out when vitellogenin synthesis first becomes inducible during embryonic development in *Oryzias latipes*. Dechorionized embryos or larvae of *Oryzias latipes* were transferred to an aqueous solution of 1.0 μ M 17- β -estradiol which was changed daily. After 3 days in estradiol their livers were cultured in 199 medium for 20 hrs. The culture media were analysed immunoblot and Western blot procedures using a monoclonal antibody against yolk egg extract. The result showed that estradiol induced vitellogenin synthesis in liver taken from *Oryzias latipes* larvae. Inducibility first appeared at the 12th day after fertilization (hatching stage).

DB 92

THE CYTOSKELETON SYSTEM IN THE EARLY EMBRYO OF THE MEDAKA, *Oryzias latipes*.
I. THE CORTICAL MICROTUBULE ARRAY IN THE YOLK CYTOPLASMIC LAYER.
T. Kageyama. Department of Biology, Kyoto Prefectural University of Medicine, Kyoto.

In the course of an examination of the microtubule (MT) organization in blastomeres and the syncytial layer around the blastoderm of a teleost, the medaka, I have discovered an extensive meshwork of long MTs throughout the cortical cytoplasmic layer which encloses the yolk sphere. The MTs were visualized immunohistochemically using monoclonal anti-tubulin. The MTs forming meshwork arrange in random direction after the fertilization. The MTs become arranged longitudinally between the 4- and 8-cell stages, and the arrangement persists through the end of epiboly of the blastoderm. The MT array in the yolk cytoplasmic layer (YCL) of the embryo is unique in the independence of MT organizing center and the persistence for a long time. The MT array serves probably for structural support of the YCL and the maintenance of antero-posterior polarity of the embryo during the development. Longitudinally arranged MTs may be responsible for the yolk-like granule migration toward the blastoderm.

DB 93

ISOLATION OF YOLK PHOSPHOPROTEINS OF MEDAKA AND *IN VITRO* AND *IN VIVO* EXAMINATIONS OF THEIR DEGRADATION.
M. Murakami, I. Tuchi, K. Yamagami.
Life Sci. Inst., Sophia Univ., Tokyo.

Four phosphoproteins (PP 1-PP 4) were detected in the yolk of unfertilized eggs as well as blastulae of medaka. By polyacrylamide gel electrophoretic examinations, they were found to be degraded during development. Among them, two kinds of low molecular weight phosphoproteins (PP 3 and PP 4) were isolated by DEAE-cellulose and Toyopearl HW-55S column chromatography and characterized. Both of them contained a large amount of phosphorus and serine (PP 3; 48 mole%, PP 4; 34 mole%) and few aromatic amino acid residues. Molecular weights of PP 3 and PP 4 were 84kD and 47kD, respectively, by Toyopearl HW-55S column chromatography. These characteristics strongly suggest that these are phosphovitins of medaka. To investigate the degradation of yolk phosphoproteins during development, *in vitro* examination was performed by incubating the precipitate of the blastular homogenate either with MCA substrates or with the supernatant of the blastular homogenate. The results suggested participation of some protease in the precipitation of the blastular homogenate. *In vivo* examination showed that the degradation of the yolk phosphoproteins occurred 10 hours after incubation at 30°C of blastulae.

DB 94

MITOCHONDRIAL lrRNA RESTORES POLE CELL-FORMING ABILITY TO UV-STERILIZED DROSOPHILA EMBRYOS
S. Kobayashi and M. Okada, Inst. Biol. Sci., Univ. of Tsukuba, Ibaraki.

Pole cells, determined for germ line, are prevented from forming by uv irradiation at the posterior pole of cleavage embryos. Injection of poly(A)⁺RNA extracted from cleavage embryos restores pole cell-forming ability to the uv-sterilized embryos. To identify the RNA sequence responsible for the restoration, we have isolated single cDNA clone which hybrid-selected poly(A)⁺RNA with the restoration ability. Nucleotide sequence analysis revealed that the cDNA is highly homologous to mitochondrial large ribosomal RNA (lrRNA) gene. This suggests the possibility that the mitochondrial lrRNA is active in the restoration of pole cell-forming ability. To test this possibility directly, sense RNA was transcribed *in vitro* from a full length cDNA of the lrRNA and injected into uv-irradiated embryos. As expected the RNA restored pole cell-forming ability. In contrast, antisense RNA showed no restoration.

DB 95

PHOSPHORYLATION OF A SOMATIC CELL SPECIFIC ANTIGEN IN *DROSOPHILA* EMBRYOGENESIS.

F. Maruo and M. Okada. Inst. Biol. Sci., Univ. of Tsukuba, Tsukuba.

A monoclonal antibody against *Drosophila* ovaries detected an antigen that is produced in nurse cells, transported to the oocyte, and distributed specifically in somatic cells during embryogenesis. The antigen was not found in germ-line cells in the embryo, larvae and male adult. In this study, we characterized this antigen using immunoblot analyses. Immunoblotting after two-dimensional gel separation of the sample from blastoderm embryos resolved the antigen into two series of isoforms that differ in charge and electrophoretic mobility. Low molecular weight group (LMG) and high molecular weight group (HMG) were found between 40 and 50kd in the basic region of the gel. At least 5 and 7 distinct spots differing in charge could be detected in LMG and HMG respectively. Different subsets of isoforms occurred in different stages of oogenesis and embryogenesis. In order to determine the identity of the negatively charged modifications, the samples were treated with some phosphatases before 2-D immunoblotting. The characteristic reductions of acidic isoforms were observed following the enzymatic treatment. This shows that the negatively charged isoforms of the protein are the result of phosphorylation at multiple sites. Stage-specific phosphorylation may regulate the functions of the proteins during embryogenesis.

DB 96

PURIFICATION AND CHARACTERIZATION OF A PROTEASE FROM *XENOPUS* EMBRYOS.

S. Miyata¹, H. K. Kihara¹, N. Furusawa², Y. Nishibe³ and I. Katayama³. ¹Lab. of Res. for Biosynthesis and Metabo. Keio Univ. ²Dep. of Chem. College of Humanities and Science, Nihon Univ. ³First Dep. of Patho. Saitama Medical School.

A protein inhibitor, antipain, interfere with synthesis of RNA and DNA and normal gastrulation in *Xenopus* embryo. Some protease activity is accordingly required for the gene activation and early development. In We are interested in understanding the sequence of events, have now purified the antipain sensitive protease and have raised antiserum against the protease in an attempt to set the stage for further studies of its role in the development. It was demonstrated by immunocytochemical localization with the antiserum that the protease was more abundant in the animal hemisphere and in the ectoderm and mesoderm cells derived from the animal hemisphere. Urea-Papain and hematoxylin-eosin stain ing showed that RNA and nuclei were abundant in the same regions as the elevated concentration of the protease. Therefore, it was suggested that the protease was related to activation of genes that control development into the ectoderm and mesoderm of the animal hemisphere and / or to maintenance of high rates of synthesis of RNA and DNA in the animal hemisphere and in the cells derived from the animal hemisphere.

DB 97

NUCLEAR PROTEIN CONSTITUENTS OF EARLY NEWT EMBRYO.

T. Asao, Biol. Lab., Sch. Med., St. Marianna Univ., Kawasaki.

The electron microscope observation showed that the electron dense moiety surrounding the chromatin occupied a larger space of the nucleus of the neurula than of the blastula.

By washing stepwise in 0, 0.05, 0.1, 0.2, 0.3, 0.4, 0.5, 0.6, and 1.0 M NaCl solution the extract was obtained from the blastula, the middle gastrula and the neurula chromatin (nucleus). The eluate was analyzed in SDS-polyacrylamide gel electrophoresis, followed by detection with silver stain.

The appreciable bands amounted to 34 (16 kd to 340 kd) in the blastula, 40 (15 kd to 340 kd) in the middle gastrula and 58 (11.5 kd to 370 kd) in the neurula. Several bands were commonly present in the three. However, the proteins in 17, 18 and 34 kd which were the main constituents of the neurula extract were not detected in the blastula extract. Results like these showed the sudden appearance of new proteins in the nucleus within a few days.

Gelation of the neurula nucleus by washing in 0.5 M NaCl solution seemed to have some relation to the release of a protein group from 23.5 kd to 27.5 kd. The blastula and gastrula nucleus did not gelate in 0.5 M NaCl washing and were seen to lack proteins in the electrophoresis.

DB 98

MECHANISM OF DORSOVENTRAL AXIS FORMATION IN NUCLEAR TRANSPLANTED *XENOPUS* EGGS.

H. Satoh and A. Shinagawa. Dept. Biol., Fac. Sci., Yamagata Univ., Yamagata 990.

In fertilized amphibian eggs, the dorsoventral axis is established with the dorsal side on the grey crescent, which is formed in the anti-SEP (sperm entry point) side, mediated by the sperm aster. On the other hand, nuclear transplanted anuran eggs, which lack a sperm aster, can develop into embryos with a normal dorsoventral axis. We studied here, using *Xenopus* eggs, how the dorsoventral axis is established normally in nuclear transplanted eggs despite lack of a sperm aster.

We found (1) that no distinct differentiation along the future dorsoventral axis of pigment pattern of the animal surface and cell size at 4- or 8-cell stage occurs in nuclear transplanted eggs, (2) that the subcortical rotation, which is reportedly involved in establishing the dorsoventral axis, however occurs normally in both nuclear transplanted and enucleated eggs as in fertilized eggs and (3) that the degree and direction of the dorsoventral axis in nuclear transplanted eggs appear to be determined in correlation with those of the subcortical rotation as in fertilized eggs.

We conclude that the dorsoventral axis in nuclear transplanted eggs is established by the subcortical rotation, independent of a nucleus, not by differentiation of either pigment pattern of the animal surface or cell size at 4- or 8-cell stage.

DB 99

MESODERMAL INDUCING ACTIVITY BY ACTIVIN A (=EDF) IN *XENOPUS laevis* EMBRYO. M. Asashima¹, H. Nakano¹, K. Kinoshita², and N. Ueno³. ¹Department of Biology, Yokohama City University, Yokohama 236, ²Biological Laboratory, Nippon Medical School, Kawasaki 211, ³Gene Experimental Center, Tsukuba University, Tsukuba 305, Japan

We have examined the mesoderm inducing activities contained in conditioned media of some mammalian cultured cell lines. The mesoderm inducing activities of cultured cell lines were tested by reacting the media with undifferentiated presumptive ectoderms of both *Xenopus* and newt blastulae. Out of 22 cell lines tested, 9 strains such as K-562 and THP-1 had mesoderm inducing activity. The erythroid differentiation activity (EDF activity) was measured for the 22 cell lines comparing with the mesoderm inducing activity. Unexpectedly, evident relation between the two activities were observed. When the explants were treated with activin A (EDF) and inhibin A, high mesoderm inducing activity was observed only by activin A treatment. Activin A is known as a group of TGF- β family proteins and these findings also confirmed the mesoderm inducing activity of TGF- β family proteins. We have obtained three *Xenopus* genomic DNA probes which have high sequence homologies to TGF- β family proteins. They are named M3, B9 and C4. We tested also the mesoderm inducing activity of activin A by immunoblot analysis using anti-myosin antibody and Northern blot analysis using α -actin c-DNA probe.

DB 100

CON A-DORSALIZED VENTRAL MESODERM IS CAPABLE OF NEURAL INDUCTION. M. R. M. Diaz¹, S. Osawal, T. C. Takahashi², K. Takashima² and K. Takata³. ¹Department of Biology, Fac. of Sci., ²Radioisotope Research Ctr., Nagoya Univ. ³Dohu Univ., General Education, Nagoya.

Con A's dorsalizing effect on the ventral mesoderm was found to be concentration dependent, i.e., with increasing concentration, there is a corresponding shift from ventral towards dorsal (muscle and notochord) differentiation. Dorsalization was effectively inhibited by oligomannose-type oligosaccharide, although α -methylmannoside had low inhibitory effect. The decrease in ¹²⁵I-Con A uptake upon addition of the oligosaccharide and no significant dorsalizing effect of Con A-Sepharose suggested that internalization of Con A is a necessary prerequisite of dorsalization.

We designed an experiment to know

1) whether Con A-dorsalized ventral mesoderm has the potential to induce the ectoderm to form neural tissues, 2) at which time this neural inducing potential is acquired. Observations led so far to the following conclusions: There was little possibility that the remaining Con A in/on the ventral mesoderm induced ectoderm explants to form neural tissues. Con A-dorsalized ventral mesoderm certainly acquired neural inducing ability in the early period of dorsalization and its neural inducing potential continued for at least a few days.

DB 101

PUPAL COMMITMENT IN THE WING DISCS OF BOMBYX FIFTH INSTAR LARVAE

M. Miyatani, S. Sakurai, T. Ohtaki. Fac. Science, Kanazawa University.

The timing of commitment change in the wing discs of *Bombyx* fifth instar larvae were examined by manipulating the hormonal conditions of in vitro culture. When cultured with 20-hydroxyecdysone (20-OHE), 28% of day 0 discs (n=80) evaginated while 55% did on day 1 (n=99). Addition of JH to the medium inhibited the evagination of day 1 discs (8%) but the effects gradually decreased to day 4 on which evagination was observed in 42% of the discs. When corpora allata were removed in late 4th instar, evagination of day 0 discs were still inhibited by JH while day 1 discs were not. Contrary, topical application of JH to day 0 of 5th instar larvae inhibited the discs to evaginate on day 1. These results indicate that the change in commitment may occur in responding to the declining titer of hemolymph JH but the low JH titer is not sufficient: the change must occur after the last larval ecdysis since allatectomy did not accelerate the timing of commitment.

DB 102

CYTOSKELETON IN THE PUPAL WING EPIDERMIS OF *PIERIS RAPAE*. A. Yoshida and K. Aoki. Life Sci. Inst., Sophia Univ., Tokyo.

During row development of scale precursor cells, we examined arrangement change of F-actin in the wing epidermis of the early pupa of a butterfly, *Pieris rapae*. We stained F-actin bundles of epidermal cells with rhodamine-phalloidin and also stained their nuclei with DAPI.

1) 20h after pupation. Undifferentiated epidermal cells are closely packed and each of them presents penta-, hexa- or hepta-gonal shape. F-actin bundles are visible along all the cell boundaries. 2) 25h. A few scale precursor cells differentiate. F-actin bundles along their margins are not clearly visible, while the ones along the margins of undifferentiated cells are still visible. 3) 35h. Scale precursors are evenly distributed; they are separated by one or two undifferentiated cell(s). F-actin bundles disappear along all the cell boundaries; they are visible only on the surface of undifferentiated cells (except for the cell boundaries). 4) 40h. Scale precursors are proximodistally elongated. F-actin bundles are invisible along the cell boundaries as at 35h. 5) 45h. Elongated scale precursors form antero-posterior rows; these rows are separated by single or double rows of undifferentiated cells. F-actin bundles appear along all the cell boundaries again at this stage.

DB 103

MORPHOLOGICAL STUDIES ON CORNEAL LENS FORMATION IN THE COMPOUND EYE OF THE ERI-SILK WORM.
S. TAKAHASHI and R. FURUTA. Dept. of Biol., S. Takahashi's Univ., Nara.

We examined the formation of corneal lens in the compound eye of *Samia cynthia ricini* during pupal-adult development. The naked eye discs could be obtained from pupae pre-fixed by injecting glutaraldehyde into the hemocoel. Before apolysis, the surface of the disc consists of small protrusions more or less hexagonally arranged and epidermal cells irregularly arranged. The protrusion is a bundle of processes of four Semper cells. When apolysis initiates, the ecdysial membrane occurs on the disc surface. At this time, a pair of corneagen cells develop on both sides of each protrusion and attach together on the antero-posterior line passing through the protrusion. The corneagen cells deposit outer epicuticle at the surface of the plasma membrane plaques and secrete lens cuticle. We conclude that (1) Semper cells will determine the initial position of an ommatidium, (2) the facet pattern seems to be modulated in relation to the cuticle deposition of corneagen cells, and (3) the ecdysial membrane will be important as a templet when the lens cuticle hardens.

DB 104

INSTABILITY OF THE NUMBER OF SEGMENTS OF UNOPERATED AND REGENERATED MAXILLARY PALPI IN THE MAXILLARY-PALP-ELONGATE (MPE) GERMAN COCKROACH MUTANT.

A. Tanaka and M. H. Ross*. Dept. of Biol., Fac. of Sci., Nara Women's Univ., Nara, *Dept. of Entomol., VPI&SU, Virginia, USA.

Maxillary-palp-elongate (mpe) is a mutant modifying the terminal (5th) segment of the wild-type palpus to a variable number of divisions, increasing the total number of segments up to 9. The supernumerary segments sometimes fuse during postembryonic development. The mutant palpi of both sides of the mouth are often asymmetric in length and in the number of segments. The mutant palpus occasionally carries a prominent bristle, never found in wild type, on the 4th segment, a homologous segment to the tibia of legs. Amputation experiments were carried out at various levels on mpe maxillary palpi. The right palpus was operated in the 2nd instar, and the regenerate was examined in the 4th- and 6th instars. Irrespective of amputated levels from the 1st-2nd to the 6th-7th segment, the total number of segments of a regenerated palpus was irrelevant to that before operation. This suggests that the stump does not regenerate new segments according to a "memory" of the original number of segments. The number of segments of a regenerate was also irrelevant to that of the contralateral palpus, which suggests that the stump does not use the contralateral palpus as a "reference" for the number of segments to be regenerated.

DB 105

IN VITRO INDUCTION OF MEIOSIS IN MALE EEL (*ANGUILLA JAPONICA*)
T. Miura^{1,2}, K. Yamauchi¹, H. Takahashi¹ and Y. Nagahama²

¹ Fac. of Fisheries, Hokkaido Univ., Hakodate, ² Lab. of Reprod. Biol., Natl. Inst. for Basic Biol., Okazaki

In cultivated male eel, germ cells are all type A spermatogonia, and meiotic cells are not observed in testis. However, their maturation can be induced by one HCG injection. In this study, eel testis were cultured with human chorionic gonadotropin (HCG) or 11-ketotestosterone (11-KT) by tissue culture techniques and histological changes in the tissue were observed. In the HCG and 11-KT group, 6 days after the start of culture, Sertoli cells were activated. After 9 days, type A spermatogonia proliferated mitotically. After 18 days, some germ cells started meiosis, and after 21 days, spermatids and spermatozoa were observed in the cultured tissues. In the control group without hormones, the cultured tissues had only type A spermatogonia during the experimental period. These results indicate that 11-KT which is produced by HCG stimulation in the testis can induce the proliferation of spermatogonia, meiosis and spermiogenesis. This phenomenon in the testis may be associated with Sertoli cell activity. This report is the first example in which mitosis, meiosis and spermiogenesis of germ cells are induced by hormonal control in vitro.

DB 106

SEMINIFEROUS TUBULES IN THE TESTIS OF THE LIZARD, *TAKYDROMUS TACHYDROMOIDES* AND THE ABSENCE OF THE WAVE IN THE EPITHELIUM OF THE TUBULE.

M. Chiba. Dept. of Biol., Fukushima Med. Coll., Fukushima.

The morphology of the reptilian seminiferous tubule and the arrangement of the spermatogenic cells in the seminiferous epithelium were studied along the length of the tubule. The general morphology of the tubules was studied by immersing the testis in a 20 percent acetic acid solution. This procedure macerated the testis and enabled to obtain separate tubules. To examine the arrangement of the cell associations, the testis was fixed in Bouin's, embedded in paraffin and cut serially at 10 μ m. Mallory's stained the basement membrane distinctively. Two-dimensional reconstruction maps were made through serial photomicrographs. The tubules started from the rete testis and extended toward the opposite side of the rete. They had blind ends. They did not appear as C-shaped arches as observed in the rat and mouse. The spermatogonia were found in the peripheral area of the tubule and the spermatids were found near the center as observed in the mammalian and avian tubules. No ordinary series of the spermatogenic cell associations were observed in the lizard tubules. This is another feature peculiar to the reptilian seminiferous tubule.

DB 107

ANALYTICAL STUDIES ON THE ULTRASTRUCTURES OF FRESHWATER PLANARIAN SPERMATOZOA.
S. Ishida, Y. Yamashita and W. Teshirogi.
Dept. of Biol., Fac. of Sci., Hiroasaki Univ., Hiroasaki.

A spermatozoon consists of a long thin head, an anterior process and two flagella. The head was separated partially into nucleus, mitochondrion and microtubules by means of water treatment. When the separated head was stained with acridine orange, only nucleus was stained brightly, and distinguished from mitochondrion and microtubules.

Flagellum had so-called "9+1 structure" and separated into nine branches near the end. Each branch consists of one microtubule. The order for branching was as follows. First, the flagellum separated into three branches which include four, three and two microtubules respectively. The three branches were separated more and divided into nine branches. The central microtubule of "9+1" disappeared before branching off.

The acrosome has not been observed in planarian spermatozoa. But dense granules were found in the anterior process. They were taken notice on the relation to acrosomal substance. So, the acrosomal proteolytic activity was examined as a direct demonstration (after Penn and Gledhill, 1972). The result obtained was negative. However, this will be needed further investigation.

DB 108

ADHESION OF MITOCHONDRIA TO NUCLEAR ENVELOPE OF *XENOPUS* SPERMATIDS.
M. Noyori and S. Abe. Dept. of Biol., Fac. of Sci., Kumamoto Univ., Kumamoto.

We have previously reported that mitochondria assemble around nuclear envelope of round spermatids 4-5 hr following second meiotic division. This phenomenon seems to be the first step toward mitochondrial assembly in the middle region of *Xenopus* mature sperm. In the present study, we tried to isolate nuclei of spermatids to find conditions to dissociate mitochondria from the nuclear envelope.

Spermatids were fractionated by BSA gradient in a CelSep chamber, put in a hypotonic solution and homogenized in a teflon homogenizer. The nuclei were purified by centrifugation in 2.1M sucrose solution.

Observation by electron microscopy showed that mitochondria were kept to attach to the nuclear envelope. 10mM CaCl_2 , 10mM MgCl_2 , 10mM EDTA, 1mM EGTA or 0.1-1.0M NaCl could not dissociate the mitochondria from the nuclei. However, treatment with trypsin in the concentration more than 0.0001% dissociated mitochondria from the nuclei of spermatids. These results indicate that integral membrane protein(s) in nuclear envelope of round spermatids and/or mitochondria are involved in adhesion of mitochondria to nuclear envelope.

DB 109

STABILITY OF MANCHETTE (MICROTUBULE BUNDLES) IN NEWT ELONGATE SPERMATIDS.
K. Hashimoto and S. Abe. Dept. of Biol., Fac. of Science, Kumamoto Univ., Kumamoto.

In order to obtain some insights into the role of manchette in nuclear elongation of newt spermatids, we examined the stability of the manchette by treatment with various microtubule (MT)-depolymerizing conditions.

Newt spermatids were fractionated by BSA gradient in a CelSep chamber. The cells were adhered to coverslips coated with PLL and the cell membrane was permeabilized with 0.1% Triton in PEM buffer. The cells were treated with low temp., Ca^{2+} , or both of them and the presence of MT was checked by immunofluorescent microscopy with anti- β tubulin monoclonal antibody. Cytoplasmic tubulin was fractionated by resistance against depolymerizing treatment; 1) soluble tubulin, 2) Ca^{2+} -cold-labile tubulin (round spermatids), 3) Ca^{2+} -cold-stable and colchicine-labile tubulin (manchette).

The MT in round spermatids and Sertoli cells disappeared rapidly by treatment with low temp. or Ca^{2+} . However, manchette structure resisted the treatment for more than 1 hr. 2D-PAGE showed that all fractions contained the same 2 α -tubulin isotypes but fraction 3 contained an unique β -tubulin isotype besides a common one.

DB 110

STAGE-SPECIFIC PROTEIN SYNTHESIS IN AMPHIBIAN SPERMATOGENESIS IN VITRO.
K. Imakado, S. Uno and S. Abe. Dept. of Biol., Fac. of Sci., Kumamoto Univ., Kumamoto.

Stage-specific protein synthesis in *in vitro* spermatogenesis of newt and *Xenopus* was investigated.

Primary spermatocytes and round spermatids were fractionated by BSA gradient in a CelSep chamber. ^{35}S -methionine was incorporated into the cells, washed off, and protein synthesis was analyzed by 2D-PAGE and fluorography. Total proteins were also analyzed by 2D-PAGE and silver stain. Newt sperm were dissected by sonication and fractionated by Percoll.

In *Xenopus*, at least 4 stage-specific polypeptides were observed to be synthesized in primary spermatocytes and round spermatids. In the newt, 5 and 2 polypeptides were observed to be synthesized in primary spermatocytes and round spermatids, respectively. One of the stage-specifically synthesized polypeptides in round spermatids of newt seems to accord with one of the polypeptides present in axial rod of mature sperm.

DB 111

HOW IS THE FLAGELLAR LENGTH OF MATURE SPERM DETERMINED? III. TUBULIN SYNTHESIS IN CULTURED AMPHIBIAN SPERMATIDS.

S. UNO and S. ABÉ. Dept. of Biol., Fac. of Science, Kumamoto Univ., Kumamoto.

In order to elucidate mechanisms that control flagellar length of mature sperm, we studied in synchronous cell suspension cultures flagellar growth, tubulin pool and tubulin synthesis in round spermatids of *Xenopus laevis* and the newt (*Cynops pyrrhogaster*).

Kinetics of flagellar growth showed that the rate and period of flagellar growth in the newt spermatids were 2-3-fold that in *Xenopus* spermatids. The tubulin pool size in newt spermatids was estimated to be about 10-fold greater than that in *Xenopus* spermatids. But even if all of the pool was used for flagellar growth, it could support only about a seventh to a tenth of the flagellar length in mature sperm in either species. Thus, the possibility that the tubulin pool primarily determines flagellar length was excluded. Tubulin synthesis declined over the culture period, but continued in newt spermatids longer than in *Xenopus* spermatids. The period of flagellar elongation almost coincided with the period of tubulin synthesis. Tubulin synthesis and the amount of rRNA in newt spermatids was more than 3-fold greater than that in *Xenopus* spermatids, which may explain the difference in their growth rate of flagella.

DB 112

TRANSITION OF NUCLEAR BASIC PROTEINS DURING SPERMATOGENESIS IN *XENOPUS LAEVIS*.

Yokota, T., K. Takamune, & Ch. Katagiri. Zool. Inst., Fac. Sci., Hokkaido Univ., Sapporo.

Nuclear basic proteins of the sperm of *Xenopus laevis* collected from jelly layer of inseminated eggs were analyzed by acetic acid/urea/Triton X-100 (AUT)-PAGE. The proteins comprised 4 types of sperm basic proteins in addition to somatic type histones H3 and H4 and extremely small amount of H2A and H2B. Amino acid analyses of each purified basic proteins by reversed-phase chromatography revealed that two of these contained more than 30% Arg, while other two contained lesser amount of Arg with a Lys/Arg ratio similar to H1. AUT-PAGE profiles of various stages of spermatogenic cells after fractionation by "Celsp" showed that those before acrosomal vesicle stage contain nuclear basic proteins of typical somatic pattern. Injection of [14 C] Arg into males and fractionation at 15th day of various spermatogenic stage cells for fluorographic analyses revealed that (1) somatic histone synthesis ceases before the primary spermatocyte stage, and (2) all 4 sperm-specific basic protein synthesis commences after the beginning of elongation in spermatids.

DB 113

IMMUNO-ELECTRON MICROSCOPIC LOCALIZATION OF PROTAMINES DURING SPERMATOGENESIS IN ANURANS.

Moriya, M., T. Yokota & Ch. Katagiri. Zool. Inst., Fac. Sci., Hokkaido Univ., Sapporo.

The rabbit antisera were raised against sperm-specific, nuclear basic proteins, protamines, of *Bufo japonicus* and *Xenopus laevis*, respectively. Localization of protamine in spermatogenic cells was studied on testis sections with electron microscopy, employing IgG-conjugated colloidal gold (15 nm in size). In both species, gold particles were localized in high density in mature sperm nuclei but less densely in immature ones. The numbers of gold particles counted on cells at various spermatogenic stages were corrected for unit area of nucleus, cytoplasm and surrounding tissues, on the basis of area determination with a digitizer (MITABLET-II, Graphtec Corp.). The grains appeared first on the nuclei showing first indication of chromatin granulation. Grain density increased gradually concomitant with an increased granulation of nuclear chromatin, and showed a sharp increase at the last stage of maturation with mean values at 63 (*Bufo*) and 35 (*Xenopus*) grains/sq. micron in mature sperm. No significant localization of grains was observed at all in the cytoplasm throughout all spermatogenic stages.

DB 114

PARTIAL CHARACTERIZATION OF PROTAMINE-REMOVING ACTIVITY IN CYTOSOL OF *BUFO JAPONICUS* EGGS.

K. Ohsumi and Ch. Katagiri, Zool. Inst., Fac. of Sci., Hokkaido Univ., Sapporo.

The negatively-charged components of cytosol from mature eggs of *Bufo japonicus* removed protamine from *Bufo* sperm and sperm specific basic proteins (SBPs) but not somatic type histones from sperm of *Xenopus laevis* in 10 min incubation period. The protamine-removing activity (PRA) was quantified by comparing the ratio of SBP/histone H3 in SDS-PAGE profiles of *Xenopus* sperm basic proteins before and after incubation in the cytosol.

The PRA was collected from the cytosol by anion-exchange chromatography on Q-Sepharose and Mono Q as 700 mM KCl eluate (pH 7.4), followed by gel-filtration on Superose 12 as a broad peak at molecular mass of 200-400 kDa. The PRA of the fractionated sample was heat-stable (100°C, 10 min) and sensitive to proteinase K but not to RNase A and DNase I. SDS-PAGE analysis revealed that after incubation of *Bufo* sperm in the fractionated sample, protamine of the sperm was associated with components of the 200-400 kDa fraction, suggesting a relatively strong affinity between them.

DB 115

ISOLATION OF A cDNA CLONE FOR XENOPUS PROTAMINE (SBP2-A).

H. Hiyoshi¹, S. Uno¹, T. Yokota², Ch. Katagiri², H. Nishida², M. Takai³, K. Agata³, G. Eguchi¹, and S. Abe¹. ¹Dept. of Biol., Fac. of Sci., Kumamoto Univ., ²Zool. Inst., Fac. of Sci., Hokkaido Univ., ³Dept. of Dev. Biol., Saga Med. Sch., and ⁴Dept. of Dev. Biol., NIBB.

In order to elucidate when and how protamine genes are expressed in *in vitro* spermatogenesis, we tried to isolate a cDNA clone for *Xenopus* protamine.

A haploid cDNA library (4 x 10⁶ clones) was constructed with λ gt11 from poly(A)⁺ RNA (10 μ g) extracted from 4 x 10⁵ spermatids. Clones were screened by antiserum against *Xenopus* protamine.

Nucleotide sequencing showed that a clone (XHP531) contained a complete coding sequence (234bp), as well as 5'-(70bp) and 3'-(166bp) non-coding regions the latter of which contained poly(A)⁺ tail (20bp). The sequences of N-terminal 11 and C-terminal 15 amino acids completely accorded with those which were obtained from the amino acid analysis of the HPLC-purified peptide fragments obtained by digesting SBP2-A (the main peak in SP3-5 (after Kasinsky)) with V8. Thus, the protamine species which this cDNA encodes was identified to be SBP2-A. Northern blot analysis suggests that the SBP2-A gene is expressed during or before meiosis, and translated at the spermatid-stage.

DB 116

PHYSIOLOGICAL CHARACTERISTICS OF SEMEN AND SPERMATOZOA IN DOMESTIC PIGEONS (COLUMBA LIVIA DOMESTICA)

N. Fujihara, H. Nishiyama¹ and O. Koga. Dept. of Anim. Sci., Kyushu Univ., Fukuoka, ¹Dept. of Anim. Sci., Kyushu Tokai Univ., Kumamoto.

Ejaculated and ductus deferens semen obtained from domestic pigeons were examined. The spermatozoal concentration of the ejaculate was nearly equal to that of semen taken directly from the ducts. Ejaculated semen did not contain aldose, which has been detected in the accessory reproductive fluid produced in other male birds (roosters, drakes, male turkeys). These results suggest that, with the domestic pigeon, no accessory fluid was added to the semen at the time of ejaculation. For observation of *in vitro* viability of pigeon spermatozoa, ejaculated undiluted semen and semen diluted with a phosphate buffer were stored in ice (0-3°C) for a given period of time. A unique phenomenon was that pigeon spermatozoa formed cluster during preservation. Spermatozoa in undiluted semen survived for less than 2 days, while the survival time of those in semen diluted with a buffer solution was more than 2 days. Compared with spermatozoa of roosters, drakes and tom turkeys, the *in vitro* viability of pigeon spermatozoa was extremely short. The storage of undiluted pigeon semen at 0-3°C resulted in a marked increase in the number of deformed spermatozoa as compared with semen diluted with the phosphate buffer.

DB 117

CHANGES IN THE LEVELS OF ADENINE COMPOUNDS IN THE TESTIS OF THE SILKWORM, DURING POST-EMBRYONAL DEVELOPMENT.

M. OSANAI¹, S. NAGAOKA² AND H. KASUGA¹. ¹Dept. Biol., Tokyo Metro. Inst. Geront., Itabashiku, Tokyo and ²Dept. Seric. Sci., Fac. Agr., Tokyo Univ. Agr. Tech., Fuchu.

Quantitative changes in ATP, ADP, AMP, cAMP, adenosine and adenine were measured with growth of testis of *Bombyx mori* from the third larval ecdysis to the adult moth. Wet weight of the testis increases with time from the 4th instar larva and reaches the maximum just after pupation, but thereafter decreases. Contents of ATP per mg protein in the testis are high at the larval stage, but decrease during the pharate pupal stage and maintain the low niveau thereafter. On the contrary, level of AMP per mg protein remains much lower than that of ATP until pharate pupa, and then rises. ADP per mg protein keeps almost a constant level through the entire development. The energy charge showed similar changes to those of the ATP level. The changes in the levels of these three nucleotides are dependent on the activity of cystocyst production: Much cystocysts are produced at a high level of ATP. Relatively high levels of ATP correspond with the formation of many apyrene bundles and the vigorous migration of the two types of spermatozoa, apyrenes and eupyrenes. The quantitative changes of cAMP corresponds well with the important conversion periods in the spermatogenesis.

DB 118

PURIFICATION OF MEMBRANE-BOUND LACTATE BINDING PROTEIN FROM ISOLATED SPERMATOGENIC CELLS OF RATS.

M. Nakamura¹, M. Komukai², S. Okinaga¹ and K. Arai¹. ¹Dept. of OB/Gyn., Sch. of Med., Teikyo Univ., Tokyo, ²Dept. of Pharmacol., Nihon Medical College, Tokyo.

A membrane-bound lactate binding protein was purified from isolated spermatogenic cells of rats. The protein was solubilized with high-salt solution and purified 3,130-fold. Purification steps included ammonium sulfate precipitation and chromatography using Sephadex G-200 and PLC system (Pharmacia). The purified protein had an estimated molecular weight of 56000 by sodium dodecyl sulfate-polyacrylamide gel electrophoresis. This protein may play an important role in the change of the energy metabolism in spermatogenesis of rat testis.

DB 119

CULTURE PATTERNS OF RAT SERTOLI CELL SECRETORY PROTEINS IN A COCULTIVATION CHAMBER

H. Ueda, T. Nishino and S. Fujimoto
Dept. of Anat. II, Sch. of Med., Univ. of
Occup. and Environ. Health, Kitakyushu

Sertoli cells contribute to the formation of a selective permeability barrier responsible for the maintenance of a dual compartment; the basally located blood supply space and the apically located seminiferous tubular lumen. We studied the culture patterns of rat Sertoli cells cocultured with spermatogenic cells or peritubular cells, and the polarized secretion of Sertoli cell-specific proteins in a cocultivation chamber. The number of spermatogenic cells decreased when Sertoli-spermatogenic cell cocultures were prepared on extracellular matrix-coated nylon substrate. Sertoli cells in coculture with spermatogenic or peritubular cells on uncoated microporous substrate, organized continuous sheets displaying polarized protein secretion. While transferrin and S70 were released bidirectionally, S45-S35 heterodimeric protein was released apically. We also found the antigenic homology between Sertoli cell secretory proteins and outer dense fiber polypeptides of the sperm tail. These results indicate that apically released Sertoli cell secretory proteins involve in the sperm tail formation.

DB 120

EARLY STAGE OF GONAD FORMATION IN AN ASCIDIAN, *CIONA SAVIGNYI*, ELUCIDATED BY MONOCLONAL ANTIBODY

T. Okada and M. Yamamoto
Ushimado Marine Lab., Okayama Univ.,
Ushimado, Okayama.

In order to investigate the origin of the germ cell in solitary ascidians, we attempted to make monoclonal antibodies that specifically recognize the germ cell. The antibodies produced against the homogenate of the ovaries of *Ciona intestinalis* were screened by 5 μ m sections of the ovaries of *C. intestinalis* which were fixed for 15 min in methanol (-20°C), dehydrated by ethanol (-20°C) and embedded in polyester wax. We obtained a monoclonal antibody (4Y2F10) that specifically recognized the small oocytes in *C. savignyi*, though in *C. intestinalis* it reacted with the chorion and the cytoplasm of the large oocytes other than the small oocytes.

In *C. savignyi*, the earliest cells were detectable by 4Y2F10 in the tadpole larvae that just began metamorphosis. Stained and unstained cells formed several round clumps. After metamorphosis, more cells became stainable with 4Y2F10 in each cell clump. One clump in each animal seemed to become follicular in shape, others remaining as solid masses. The former may be the rudiment of the ovary.

DB 121

A MONOCLONAL ANTIBODY WHICH REACTS WITH BLOOD CELL AND GERM CELL OF ASCIDIAN *CIONA SAVIGNYI*.

T. Sawada¹, Y. Fujikura¹, S. Tomonaga² and T. Fukumoto¹.
¹Dept. Anatomy Yamaguchi Univ. Sch. Med. and ²Sch. Allied Health Sci., Ube

We immunized mouse with blood cells from *C. savignyi* and got a monoclonal antibody (MAB) 10/46 (subclass IgG3) which reacts with blood cells and germ cells.

In indirect-immunofluorescence study, MAB 10/46 stained minority of blood cells (a part of so-called hemoblasts and signet-ring cells), part of germ cells (sperm, spermatocytes and young oocytes) peribranchial epithelium and pharyngeal wall. MAB 10/46 may recognized a surface antigen because it stained also living blood cells. MAB 10/46 reacted with blood cells of *C. intestinalis* but not with *Halocynthia roretzi* and *Styela clava*.

Thus, germ cells and some blood cells likely have a common antigen on their surface. This might suggest a homology in those cells. MAB 10/46 is not strictly specific for the blood cells and germ cells. However, it would be still expected as an useful tool in the investigation of germ cell-line and in the survey for ascidian cell-surface molecule which is functional and/or characteristic on blood cells and germ cells.

DB 122

SPONTANEOUS MATURATION IN OOCYTES OF THE ASCIDIAN, *HALOCYNTHIA RORETZI*.

K. Sakairi and H. Shirai
Ushimado Marine Laboratory, Fac. of Sci.,
Okayama Univ., Okayama.

In *H. roretzi*, fully grown (immature) oocytes within gonads are arrested in the first meiotic prophase with a large germinal vesicle but spawned oocytes are in the first meiotic metaphase.

Follicle cell-enclosed oocytes (oocyte complex) underwent germinal vesicle breakdown (GVBD) within 1 hr when transferred to natural sea water (NSW, pH8.2). Extrusion of test cells (TC) to perivitelline space and elevation of chorions (Ch) also occurred. We designated these phenomena as the spontaneous oocyte maturation. Oocyte complex incubated in NSW (pH8.2) for about 10 min had already begun to extrude the TC and to raise the Ch.

Low pH sea water (pH5) and a protease inhibitor, leupeptin, inhibited GVBD with concurrent inhibition of the extrusion of TC and the elevation of the Ch. These conditions blocked GVBD only of the oocyte complex within the first 10 min after being transferred to NSW. Addition of actinase caused GVBD even under above-mentioned interference.

Some protease(s) may participate in an early phase in a possible mechanism that triggers GVBD and/or the TC-extrusion and the Ch-elevation.

DB 123

OPTIMUM INCUBATION MEDIUM ON GERMINAL VESICLE BREAKDOWN IN *XENOPUS* OOCYTES.

Y. Hanaka, K. Inai & Y. Shimoda
Inst. Endocrinology, Gunma Univ., Maebashi.

In preliminary experiment, we have confirmed that the germinal vesicle breakdown (GVBD) in *xenopus* oocytes by progesterone is not induced in medium O-R2. This incubation medium was widely used by many investigators when GVBD was induced in vitro. In order to study in further detailed information concerning the influence of various environmental factors on GVBD, we defined optimum incubation medium.

Ovarian fragment containing oocytes were exposed for more than 14 hours to Steinberg's of different concentrations of NaCl. There was a marked inhibition of GVBD induced by progesterone in hypotonic solution from 58 to 101 mM. Maximum response to GVBD was observed at an NaCl concentration of 131 mM. Furthermore, NaCl can be replaced by choline chloride or sucrose, but not by Li chloride. Na ion is not required for GVBD of oocytes by progesterone. The response of GVBD by progesterone is dependent upon the osmolarity of incubation medium. Li may have a toxic effect on oocytes maturation. Ca is essential for inducing GVBD, while Mg appears not to be involved. Optimum K ion to GVBD was observed from 0.17 to 0.67 mM. Two kind of buffer solution (Tris-HCl and HEPES-NaOH) with the pH adjusted from 6.2 to 9.0 was used, and rather a broad maximum response occurred around pH 7.0-8.6. When the oocytes were incubated for a relatively long period in standard solution, the medium become more acid.

DB 124

IN VITRO AMPLIFICATION OF STARFISH MPF

N. Menrai, K. Ookata, A. Shimada and T. Kishimoto. Biol. Lab., Fac. Sci., Tokyo Inst. Technol., Tokyo.

Multiple successive transfer of MPF (maturation-promoting factor)-containing cytoplasm into immature oocytes indicates that MPF has autocatalytic amplification property. We have developed an *in vitro* MPF amplification system to identify the necessary components.

Since in starfish germinal vesicle (GV) contents are known to participate in MPF amplification, GVs were isolated from immature oocytes of *Asterina pectinifera* by centrifugation. Levels of MPF activity was assayed in cell-free system containing interphase extract of *Xenopus* eggs and sperm pronuclei. While isolated GVs alone had no MPF activity, we found that MPF levels increased about four fold during incubation of isolated GVs with crude MPF extract obtained from maturing starfish oocytes, indicating the occurrence of *in vitro* MPF amplification. When isolated GVs were broken by pipetting followed by centrifugation, MPF amplification activity came into the supernatant. Monoclonal antibody that was directed against "PSTAIR" region of the fission yeast cdc2 protein recognized the whole isolated GVs and the precipitate of broken GVs, but not the supernatant of broken GVs. These results indicate that cdc2 product is not included in GV components responsible for *in vitro* MPF amplification.

DB 125

SPONTANEOUS ACTIVATION OF HISTONE H1 KINASE IN CELL-FREE SYSTEM OF IMMATURE STARFISH OOCYTES BY ADDING α -NAPHTHYL PHOSPHATE.

D. Miura and K. Sano. Marine Biol. Station, Fac. of Sci., Hokkaido Univ., Akkeshi.

Histone H1 kinase in immature starfish oocytes is activated during maturation. The latent form of this kinase in immature oocytes is activated when dithiothreitol (DTT) is added to the 10-fold-diluted extracts of immature oocyte (K. Sano, 1987, Dev. Growth Differ., 29, 399). We examined the mechanism of the activation of the histone H1 kinase in this cell-free system of *A. pectinifera*.

When DTT was added to non-diluted original extracts of immature oocytes, the activation of H1 kinase was very low. This suppression of the kinase activation was found to be mainly due to Mg ions and KCl, which were inclusions of the extraction buffer used. NaCl was also inhibitory at 200 mM. The inhibitory action by Mg, KCl and NaCl was found to be cancelled by adding several phosphatase inhibitors, among which α -naphthyl phosphate (α -NP) was most potent. In the presence of 7 mM α -NP and 200 mM NaCl, the activation of H1 kinase in 10-fold-diluted immature oocyte extracts reached the level of maturing oocyte extracts. These results suggest that a certain phosphatase, which can be inhibited by α -NP, exists in immature oocyte extracts and suppresses the activation of H1 kinase by dephosphorylating a certain unknown phosphorylated factor, which seems to be necessary for the activation of histone H1 kinase during oocyte maturation.

DB 126

PERTUSSIS TOXIN BLOCKS 1-METHYLADENYNE-INDUCED DECREASE OF cAMP IN STARFISH OOCYTES

K. Chiba and M. Hoshi. Dept. of Life Sci., Fac. of Sci., Tokyo Institute of Technology, Tokyo.

Maturation of starfish oocytes is reinitiated by 1-methyladenine (1-MA) that binds to the oocyte surface. Pertussis toxin (PTX) ADP-ribosylates a 39 kDa G-protein in the cortex of oocytes and it inhibits 1-MA-induced maturation if microinjected into the cells.

Forskolin, a potent activator of adenylate cyclase, increased the cAMP level 3-fold in the oocyte of *Asterina pectinifera*. When 1-MA and forskolin were concomitantly applied to the cells, the cAMP level increased to 70% of the level fully activated by forskolin only. This difference in the activated level of cAMP was not detectable in PTX-injected oocytes. PTX itself did not change the cAMP level directly. These results suggest that the pertussis toxin-sensitive G-protein is involved in 1-MA dependent regulation of cAMP level.

DB 127

MECHANISMS FOR MAINTAINING GYNOGENESIS: INHIBITION OF REDUCTION OF EGG CHROMOSOMES AND INHIBITION OF MALE PRONUCLEUS FORMATION.

M. Yamashita and Y. Nagahama.

Lab. of Reprod. Biol., Natl. Inst. for Basic Biol., Okazaki.

Triploid gibel carp (crucian carp), *Carassius auratus langsdorffii*, reproduces by gynogenesis. Gynogenesis is maintained by two mechanisms: inhibition of reduction of egg chromosomes during oogenesis and inhibition of male pronucleus formation during fertilization. We have already shown that the inhibition of male pronucleus formation is due to the inhibition of sperm nuclear envelope breakdown. To investigate the mechanism for inhibiting the reduction of the egg chromosomes, we examined gibel carp oocyte maturation induced by 17 α , 20 β -dihydroxy-4-pregnen-3-one. DNA content of the chromosomes was not reduced between the first (MI) and second (MII) meiotic metaphase, as revealed by microfluorometry with DAPI. The first meiotic spindle was tripolar, and the first polar body (PBI) was not extruded. Activity of maturation-promoting factor, detected as histone H1 kinase activity, decreased between MI and MII, indicating that the cell cycle proceeded normally. These results suggest that the formation of a tripolar spindle inhibits PBI formation, therefore preventing reduction of the number of egg chromosomes at this stage of oogenesis.

DB 128

REGULATION OF ADENYLATE CYCLASE ACTIVITY IN AMAGO SALMON GRANULOSA CELLS BY GUANINE NUCLEOTIDE-BINDING PROTEIN

M. Mita¹ and Y. Nagahama²
¹Dept. of Biochem., Teikyo Univ. Sch. of Med., Tokyo, ²Lab. of Reprod. Biol., Natl. Inst. for Basic Biol., Okazaki.

The process of oogenesis in teleosts is largely dependent on steroid hormones which are secreted from ovarian follicle cells under the influence of gonadotropin (GTH). The GTH-induced steroidogenesis is mediated by the adenylate cyclase (AC)-cAMP system.

The present study was designed to investigate the possible function of guanine nucleotide-binding protein (G-protein) and adenylate cyclase in GTH-induced steroidogenesis in granulosa cells of amago salmon (*Oncorhynchus rhodurus*). Chum salmon GTHs stimulated AC activity, but not phosphodiesterase activity. The stimulatory action of GTH required pertussis toxin (PT). PT by itself also stimulated AC activity. GTP analogs (GTP- γ S and Gpp(NH)p) induced the activation of AC in the presence of PT. PT caused incorporation of label of [³²P]NAD into a component of 41 kDa. In contrast, cholera toxin hardly induced ADP-ribosylation. These results strongly suggest that G-protein, most likely Gi or Go, mediates GTH-stimulation of AC activity in amago salmon granulosa cells.

DB 129

SPECIFIC BINDING OF [³H]17 α , 20 β -DIHYDROXY-4-PREGNEN-3-ONE TO CORTEX AND YOLK FRACTIONS FROM FOLLICLE-FREE OOCYTES OF RAINBOW TROUT. M. Yoshikuni and Y. Nagahama

Lab. of Reprod. Biol., Natl. Inst. for Basic Biol., Okazaki.

We have developed a method for preparing follicle-free oocytes from the ovary of rainbow trout. Ovarian fragments are digested with collagenase in trout Ringer, in the presence of protease inhibitors, allowing easy manual removal of the thecal layer. Granulosa cells were removed by rolling theca-free oocytes over Nylon netting in Ca⁺⁺, Mg⁺⁺-free Ringer containing EDTA. Follicle-free oocytes prepared by this method matured *in vitro* on adding 17 α , 20 β -dihydroxy-4-pregnen-3-one (17 α , 20 β -P).

Fractionation was achieved by subjecting the intact oocytes to ultracentrifugation. Membranous fractions of fluffy and cortical layers were obtained by additional homogenizations and ultracentrifugations. These fractions were used for binding assays with 0.1 μ M of [³H]17 α , 20 β -P. High specific bindings existed in cortex and yolk fractions but not in cytosol. The binding to cortex was rapid and saturated within 10 min. Scatchard analysis of competitive binding indicated an apparent dissociation constant of 0.1 μ M and a binding capacity of 0.03 fmol/mg protein. 17 α -Hydroxyprogesterone did not compete with [³H]17 α , 20 β -P, suggesting that the binding observed was not due to metabolizing enzymes.

DB 130

MEASUREMENT OF ζ -POTENTIAL OF HUMAN X- AND Y-CHROMOSOME BEARING SPERM.S. A. ISHIIJIMA, M. OKUNO, AND H. MOHRI.
Dept. of Biol., Coll. of Arts and Sci., Univ. of Tokyo, Tokyo.

Separation of X- and Y-chromosome bearing sperm has significant implications both in animal reproduction and in human reproductive medicine. Our previous analysis of purified human sperm fraction by means of the free-flow electrophoresis revealed that X-bearing sperm had a higher negative charge on the cell surface than did Y-bearing sperm.

In this paper, we examined ζ -potential of human spermatozoa using three different ζ -potential meters (Photal ELS 800, PEN KEM LASER ZEE 501, and 3000) in order to estimate the absolute values under the mild conditions. These measurements provided similar results to those reported previously, i.e. human sperm population was separated into two peaks. The values of two peaks were -13.8mV and -18.4mV.

Then we measured the ζ -potential of spermatozoa fractionated with free-flow electrophoresis. By quinacrine mustard staining, one fraction was 80% F-body positive and regarded as Y-bearing sperm-rich fraction, while the other with less than 5% F-body positive was regarded as X-bearing sperm-rich fraction. The ζ -potentials of the former and the latter were about -12mV and -16mV, respectively, corresponding to those of two peaks obtained with the unseparated sperm samples.

DB 131

IMMUNOLOGICAL ANALYSIS ON SURFACE PROPERTIES OF HUMAN SPERMATOZOA

Y. Nakata¹, T. Nakazawa¹, M. Okuno². ¹Dept. of Biol., Fac. of Sci., Univ. of Toho, Chiba, ²Dept. of Biol., Coll. of Art. and Sci., Univ. of Tokyo, Tokyo.

Mammalian spermatozoa are formed in testis and matures through the epididymis. It has been known that there is a difference in the cell surface between mature X- and Y-bearing spermatozoa. When ζ -potential of spermatozoa was measured X- and Y-bearing spermatozoa represented two peaks as shown by Ishijima et. al. (1989). In this paper, we examined the characteristics of antibodies prepared against human sperm surface components by means of ζ -potential measurement.

BALB/c mouse was immunized with human spermatozoa. The spleen cells were fused with myeloma (PA1) according to the methods of Koller and Milstein. Hybridomas obtained were cultured and the supernatant was collected. Then, we obtained antibodies by 50% saturated ammonium sulfate cut. The antibodies were examined for immunofluorescence of human sperm surface. One of the immunofluorescent positive antibodies (4-27-5), which stained equatorial region, mid-piece and tail were used for further experiment. When human spermatozoa were incubated with the antibody (4-27-5) for 1 hr at room temperature, two peaks of ζ -potential which correspond to the preincubated X- (-8.4 mV) and Y-bearing spermatozoa (-12.4 mV) came to be a single peak (-12.7 mV). It was assumed that the ζ -potential of Y-spermatozoa was shifted and superimposed to that of X-spermatozoa by the reaction with the antibody. Therefore, it was likely that the antibody (4-27-5) recognized the X- or Y-bearing spermatozoa.

DB 132

ELECTRONMICROSCOPIC OBSERVATIONS ON THE PRIMORDIAL GONADAL DEVELOPMENT IN *Cynops pyrrhogaster*, WITH SPECIAL REFERENCE TO THE ORIGIN OF THE GONADAL MEDULLA

Masahiko Kumakura and Hisaaki Iwasawa.
Biol. Inst., Niigata Univ., Niigata

The gonadal medulla was formed by the proliferation of the cells derived from the coelomic epithelium within the primordial gonad. There were some direct contacts between cortical cells and medullary cells of the primordial gonad, and they were covered with a common basal lamina. No intrusion of mesenchymal or blastemal cells from extragonadal regions into the primordial gonad was observed when the medulla was formed. Gonadal sex differentiation occurred directly from the sexually indifferent primordial gonad. In this process, no antagonistic development of the cortex and medulla was recognized. In previous light microscopic studies, it was reported that gonadal sex differentiation is induced by antagonistic substances produced by cortical and medullary regions which have different embryological origins. In the present study, however, the origin of the gonadal medulla was coelomic epithelial cells. In the cortex and medulla, furthermore, the active development of one region did not immediately inhibit the development of the other region. It is conceivable that these phenomena are general in amphibians.

DB 133

LECTIN BINDING IN OVARIES AND TESTIS-OVA PRODUCING TESTIS OF FISH *ORYZIAS LATIPES*.

N. Shibata¹, S. Hamabuchi², and H. Mitsui³
¹Labo. Reprod. Biol., Natl. Inst. Basic Biol., Okazaki, ²Dept. Biol., Coll. Gen. Educ., Niigata Univ., Niigata, ³Inst. Mol. Cell. Biol. Pharm. Sci., Kyoto Pharm. Univ., Kyoto.

Eleven HRP-conjugated lectins were used to study the changes of sugar terminals on cells in ovaries of *Oryzias latipes*. In germ-line cells, no lectins bound to oogonia nor to zygotene to pachytene oocytes. At diplotene stage, after the follicles around oocytes were established, HRP-reaction products of BPA and LCA were found as small granules on their cytoplasm. LCA, LPA, MPA, and PNA bound to pre-granulosa cells around oogonia, and more strongly to follicular granulosa cells around oocytes.

Previously, we reported the binding of lectins in the testis of *O. latipes* and found that the BPA, MPA, and PNA bound to Sertoli cells around oogonia but not to the cells forming testicular cysts. We also found that the Sertoli cells constitute complete follicles around testis-ova. Using these lectins as cell-markers of Sertoli and granulosa cells, we concluded that the follicles formed by Sertoli cells around testis-ova were homologous to granulosa follicles in the normal ovaries.

DB 134

Cortical responses of medaka eggs to sperm, and calcium- or inositol trisphosphate-microinjection.

T. Iwamatsu, K. Onitake* and S. Nakashima
Dept. Biol., Aichi Univ. Educ., Kariya and
*Dept. Biol., Yamagata Univ., Yamagata.

Responses of medaka egg cortex to sperm and calcium- or inositol trisphosphate (IP₃)-injection have been investigated using partially or completely decolorized eggs. In intact eggs, the exocytotic response induced by sperm, IP₃- or calcium-injection is initiated faster at the animal pole region than the vegetal pole region. In denuded eggs, the number of penetrated spermatozoa and swollen sperm heads in the egg cytoplasm was largest at the animal pole region, intermediate at the equatorial region and lowest at the vegetal pole region. This pattern is also observed in lectin(WGA)-treated eggs. In other experiment, centrifugation of immature eggs was used to redistribute the germinal vesicle (GV). These eggs were subsequently denuded after maturation and insemination. This treatment did not alter the pattern of distribution of penetrated spermatozoa. However, the distribution of swollen sperm heads and pronuclei was corresponded to the new site of the GV. We suggest that membrane-specific factor(s) control spermatozoa adherent to the egg plasma membrane, and that GV-specific (possibly diffusible cytosolic) factor(s) regulate the formation of pronuclei.

DB 135

ON THE MODE OF SPERM ENTRY INTO THE MICROPYLAR CANAL IN THE MEDAKA, *ORYZIAS LATIPES*. M. Takano and K. Onitake. Dept. of Biol., Fac. of Sci., Yamagata Univ., Yamagata.

To examine whether the micropyle has active role against the sperm entry or not, the mode of sperm entry into the micropylar canal affected with chemical or physical treatment was observed by Nomarski's microscope and recorded by videotape recorder through it in the medaka, *Oryzias latipes*. The trace of sperm movement on the egg surface recorded by videotape was analyzed with special attention to the sperm on or near the opening of micropyle.

When normal egg was inseminated, most of spermatozoa struck against the wall of micropyle near the opening and entered into the micropylar canal. The striking of spermatozoa against the micropylar wall prior to entry in to micropylar canal was observed when eggs fixed with glutaraldehyde or treated with boiling and periodic acid were inseminated. On the contrast, however, when eggs treated with trypsin were inseminated, spermatozoa struck against the wall of micropyle but a large number of them could not enter into the micropylar canal. It seems probable that there may be some mechanism to introduce the sperm struck against micropylar into micropylar canal which cancelled with trypsin treatment.

DB 136

SCANNING ELECTROMICROSCOPIC OBSERVATION OF THE PROTRUDED STRUCTURES THROUGH MICROPYLAR CANAL JUST AFTER FERTILIZATION IN THE MEDAKA, *ORYZIAS LATIPES*.

K. Onitake¹ and T. Iwamatsu². ¹Dept. of Biol., Fac. of Sci., Yamagata Univ., Yamagata and ²Dept. of Biol., Aichi Univ. of Edu., Kariya.

To examine the polyspermy block in the medaka, *Oryzias latipes*, the eggs were provided at various intervals for the first minute following insemination and fixed for SEM observations. Within the first several seconds after insemination, the spermatozoon attached and fused to the sperm entry site beneath the inner opening of micropylar canal. At this time, small protruded structures were observed near the bottom of micropylar canal. Within 10-15 seconds after insemination, large ball- or long stalk-like structures were protruded outside through the outer opening of micropylar canal, while the first fertilization cone was observed at the sperm fusion site. Supernumerary spermatozoa were contained or trapped in some of those structures. In order to clarify whether the protruded structures were formed by egg activation or not, unfertilized eggs were activated by pricking. Small or large protruded structures were observed in the opening of micropylar canal of eggs fixed at 15 seconds after pricking as same as fertilized eggs. It seems probable that the protruded structures play an important role of the relative

fast polyspermy-block in fertilization.

DB 137

IMMUNOCHEMICAL ANALYSES OF SOME COMPONENTS OF THE EGG ENVELOPE IN MEDAKA. K. Murata, T.S. Hamazaki, I. Iuchi, and K. Yamagami. Life Sci. Inst., Sophia Univ., Tokyo.

Polyclonal anti-chorion glycoprotein (F1) antibody employed so far as a probe for detection of the SF substance [Hamazaki et al., 1985] was found to react not only with the SF substance but with some new substances in the adult fish of medaka. Immunoblotting and immunohistochemical analyses revealed that these new substances were present in blood and the liver of the spawning females and the estrogen-treated males as well as in the ovary of the former. The original anti-F1 antibody was separable into two fractions with different immunoreactivity on immunoblotting analyses; one reacting with only the SF substance and the other reacting specifically with the new substances. The latter antibody fraction was found to be reactive with ZI-1 and ZI-2 but not with ZI-3 [Hamazaki et al., 1987]. It was found that these new substances showed identical electrophoretic mobilities with those of ZI-1 and ZI-2. Thus, the new substances are considered to be closely related to ZI-1 and ZI-2. In medaka, three major components of the ovarian egg envelope, ZI-1, ZI-2 and ZI-3, are possibly formed in the liver under the influence of estrogen and all of them may be named the spawning female-specific (SF) substances.

DB 138

ANALYSES OF CHORION HARDENING IN FISH II. K. Masuda, I. Iuchi and K. Yamagami. Life Sci. Inst., Sophia Univ., Tokyo.

The decrease in solubility of chorion proteins in 1 N NaOH can be regarded as an indication of hardening. Change in the hardness of medaka chorion was quantified under various experimental conditions by determining the amount of the NaOH-soluble protein of the chorion after it was isolated in 10 mM EDTA. When unfertilized eggs were activated by Ca^{2+} -ionophore, A23187 (20 μM), the solubility of their chorion became one fourth of the unhardened chorion by 40 min after activation and the 'hardening' continued to proceed thereafter. Upon incubation in 10 mM Tris-HCl buffered medaka saline containing Ca^{2+} (pH 7.3), the isolated unhardened chorion became hardened gradually, but the hardening proceeded more slowly than did after activation of the intact egg. Two mM Ca^{2+} seemed to be sufficient to cause the 'hardening'. The isolated unfertilized egg chorion was not hardened on exposure to the homogenate of the freshly isolated cortical alveoli. Upon hardening, 75 K and 49 K protein components in the SDS-soluble portion of the inner layer of chorion disappeared as time went on. When unfertilized eggs were treated with either 20 mM cadaverine or 10 mM aminotriazole before A23187-activation, the hardening of the chorion was inhibited in spite of an occurrence of cortical reaction.

DB 139

THE EGG EXUDATE-INDUCED TRANSFORMATION OF VITELLINE COAT ACCOMPANYING FERTILIZATION IN *BUFO JAPONICUS*
HISASHI YAMASAKI AND CHIHIKI KATAGIRI
Zool. Inst., Fac. of Sci., Hokkaido Univ., Sapporo.

When the eggs of *Bufo japonicus* are activated in De Boer (DB) or 1/20DB, their vitelline coats (VCs) lose sensitivity to the sperm lysin within 5 min. This reduced sensitivity to lysin of the VC was more pronounced in the eggs activated in 1/20DB than in DB, and was contrasted with both the hydrolysis of the glycoprotein components and the increase in melting temperatures of VCs that occur only in the eggs activated in 1/20DB (Lindsay et al., 1988). When the egg exudates (AEX) collected from jelly-less activated eggs were added to de-jellied eggs, their VCs became refractory to the sperm lysin. This activity of AEX to reduce the lysin sensitivity of VCs was heat sensitive and dependent on Ca^{2+} , but was not affected at all by several types of protease inhibitors. The activity was absorbed by a preincubation of AEX with fragmented VCs, suggesting the binding of egg-derived molecules to the VCs at fertilization. Immunocytochemical observations employing the anti-AEX rabbit serum showed that the pertinent antigen(s) are localized preferentially on the cortical granules in unfertilized eggs, and after fertilization are deposited on the inner wall of VC and the perivitelline space.

DB 140

YOLK LECTINS IN *XENOPUS* OOCYTES.

N. Yoshizaki, Dept. of Biol., Fac. of Gen. Educ., Gifu Univ., Gifu.

The localization and biochemical nature of yolk platelet lectins (YLS) were examined in *Xenopus laevis* oocytes by immunofluorescent microscopy, PAGE and immunoblotting analyses. An antiserum against cortical granule lectins (CGLs) was used as a probe. Specific, immunofluorescent stain for the lectins was limited to the cortical cytoplasm within 1 μ m from the egg surface of stage I oocytes. The width of stained cortical cytoplasm increased to 4 and 20 μ m in stages II and III oocytes, respectively. In stage IV oocytes, a superficial layer of yolk platelets was stained in addition to the 20 μ m of cortical cytoplasm. Ultrastructural observations showed that the cortical cytoplasm includes multivesicular bodies and dense bodies which are the machinery for yolk formation. The YLS extracted from the isolated yolk platelets and purified by affinity chromatography comprised two distinct proteins, those which apparently correspond to the CGLs, and proteins which appeared as one diffuse band in the native PAGE. The YLS shared the hemagglutination activity specific to D-galactoside residues with the CGLs. The present study indicates that the YLS which aggregate to form CGL-like molecules in the cortical cytoplasm, accumulate in the superficial layer of the yolk platelets in collaboration with yolk formation.

DB 141

ISOLATION AND CHARACTERIZATION OF OVIDUCTIN FROM *XENOPUS LAEVIS* PARS RECTA OVIDUCT.
D.M. Hardy and J.L. Hedrick. Dept. Biochem. & Biophys., Univ. of California, Davis, CA U.S.A.

It was previously shown that conversion of the coelomic (CE) to the vitelline envelope (VE) in *Xenopus laevis* eggs involves a protease from the pars recta oviduct. The protease (oviductin) was purified from pars recta extracts using p-aminobenzamide Sepharose and hydroxylapatite chromatography. The purified enzyme had a $K_m = 58$ μ M and a $k_{cat} = 3.8$ sec⁻¹ for the synthetic substrate PheSerArg-MCA, a pH optimum of 8.0, and a MW = 66K (SDS-PAGE). Its activity was 2X higher in the presence of 200 mM NaCl, and 1.4X higher in the presence of 10 mM $CaCl_2$. Oviductin is a serine active site protease as it was inhibited by several site specific protease inhibitors. The enzyme was reversibly inhibited by Gn-HCl and p-aminobenzamide ($K_i = 7.5$ mM and 4.1 μ M) and irreversibly inhibited by EDTA. The amino acid sequence of the N-terminal end of the polypeptide (28 residues) was homologous to other serine active site proteases with positional identities ranging from 46-64%. Oviductin converted the 43K CE glycoprotein to a 41K glycoprotein analogous to that observed in vivo (VE). The melting temperature of the oviductin treated CE was equivalent to that of the VE. The ultrastructure of the oviductin treated CE was also modified. We conclude that the oviductin isolated here participates in the in vivo conversion of the CE to the VE which occurs in the pars recta oviduct. Supported in part by USPHS research grant HD04906.

DB 142

A SIALOGLYCOPROTEIN RESPONSIBLE FOR SPERM AGGLUTINATION IN THE FISH *TRIBOLodon* EGGS: PURIFICATION, COMPOSITIONS AND IMMUNOHISTOCHEMICAL LOCALIZATION.
S.Kudo¹, S.Inoue², and Y.Inoue³, ¹Dept. of Anat., Gunma Univ. Sch. of Med., Maebashi, ²Sch. of Pharm. Sci., Showa Univ., Tokyo, and ³Dept. of Biophys. Biochem., Univ. of Tokyo, Tokyo

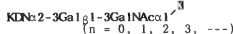
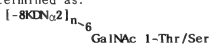
Mature *Tribolodon* eggs crushed were extracted with a solution of 0.8% NaCl. The mixture was filtered through gauze and the filtrate was centrifuged at 5,000 rpm for 30 min. The supernatant was mixed with 1 vol. of 90% phenol, and this mixture was stirred at room temperature for several hours. The aqueous phase was separated by centrifugation for 15 min and dialyzed against distilled water, followed by lyophilization. The partially purified material containing sialoglycoprotein (SGP) and phosphatidyl was applied to a DEAE-Sephadex A-25 column pre-equilibrated with 0.01 M Tris-HCl buffer (pH 8.0) and eluted with a linear gradient of NaCl (0.1-0.5 M). The SGP peak was then subjected to Sephacryl S-200 chromatography following pre-equilibration with the same buffer, in order to separate SGP from phosphatidyl, and eluted with 0.1 M NaCl in the same buffer, to obtain the SGP. The SGP agglutinated fish sperm. Application of antibody against SGP revealed that it was immunohistochemically localized in the cortical alveoli of fish eggs. The SGP is considerably similar in amino acid composition to a SGP responsible for sperm agglutination from carp eggs, but different in carbohydrate composition from the latter. A typical preparation of the present SGP contained 86.3% carbohydrate (by weight %: hexosamines, 34.8; neutral sugars, 45.5; sialic acid, 6.0) and 13.7% protein.

DB 143

DEAMINATED NEURAMINIC ACID (KDN)-RICH GLYCOPROTEIN OF RAINBOW TROUT VITELLINE ENVELOPES: A UNIQUE EGG SURFACE GLYCOPROTEIN WITH SPERM-AGGLUTINATING ACTIVITY

A. Kanamori¹, K. Kitajima¹, Y. Inoue¹, S. Inoue², K. Kudo³
¹Dept. of Biophys. & Biochem., Univ. of Tokyo, Tokyo; ²School of Pharmaceutical Sci., Showa Univ., Tokyo; ³Dept. of Anatomy, Gunma Univ. School of Med., Gunma

Deaminated neuraminic acid-rich glycoprotein (KDN-gp) was isolated from the vitelline envelope of rainbow trout eggs, and was found to have strong sperm-agglutinating activity at 25-50 µg/ml. KDN-gp contains multiple O-linked acidic glycan chains and their structures were determined as:



Oligosaccharides released from KDN-gp were shown to inhibit sperm-agglutination, suggesting sperm to have a unique lectin-like material on their surface. Immunocytochemical study established localization of KDN-gp in the second layer of vitelline envelope.

KDN-gp also agglutinated sperm of *Plecoglossus altivelis* ("ayu"), which is phylogenetically close to *Salmonidae* fishes, but not "medaka" (*Oryzias latipes*) sperm.

DB 144

SPECIES-SPECIFICITY OF DEGENERATION OF URODELE ACCESSORY SPERM.

Y. Iwao¹ and R.P. Elinson². ¹Biol. Inst., Fac. Sci., Yamaguchi Univ., Yamaguchi, Japan. ²Dept. Zool., Univ. Toronto, Toronto, Canada.

To determine species-specificity of sperm nuclear degeneration in physiologically polyspermic urodele eggs, we examined cross-fertilization between various species. *Ambystoma mexicanum*, *A. texanum* or *A. maculatum* sperm did not degenerate in *Cynops pyrrhogaster* eggs. In these cases, sperm migration was poor. This could account for the lack of degeneration, since inhibition by thiabendazole or D₂O of sperm nuclear migration in self-species fertilization can prevent degeneration. *Notophthalmus viridescens* or *Pleurodeles waltl* sperm degenerated in *Cynops* eggs, but *Pleurodeles* sperm sometimes caused heavy polyspermy. *Cynops* sperm did not degenerate in *Notophthalmus* or *Pleurodeles* eggs. Most sperm remaining in the animal hemisphere formed accessory mitotic bipolar spindles. These results indicate that even among the physiologically polyspermic species, sperm respond differently to the egg-cytoplasm with respect to migration and sensitivity to nuclear degeneration.

DB 145

PHORBOL ESTER INDUCES THE DEPOLARIZATION IN ACTIVATED EGGS OF SEA URCHINS.
 S. Tanaka¹, H. Kuroda¹, S. Kanai¹, and S. Obata². ¹MBL, Sch. of Sci., ²Dept. of Anat., Sch. of Med., Nagoya Univ., Toba and Nagoya.

Fertilization enhances the breakdown of phosphatidylinositol (4,5)bisphosphate to inositol (1,4,5)triphosphate (IP₃) and diacylglycerol (DG). DG is known to activate Na/H exchange via C-kinase and to raise intracellular pH (pH_i). We had supposed that the pH_i rise might cause the slow depolarizing component in fertilization potential. However, the pH_i rise by NH₄Cl or high extracellular pH did not elicit depolarization but caused little hyperpolarization. An analogue of DG, phorbol dibutyrate (PDBu), activated Na/H exchange both in unfertilized and fertilized eggs. On the membrane potential, 10 µM PDBu had no effect in unfertilized eggs, but elicited depolarization both in fertilized eggs, and in eggs activated by Ca ionophore. These results indicate that DG does not evoke the depolarization via the pH_i rise. DG might regulate an ion channel and evoke the depolarization.

DB 146

EFFECT OF CTC ON OXYGEN CONSUMPTION ENHANCED BY TREATMENTS WITH ACTIVATING REAGENTS IN SEA URCHIN EGGS.

M. K. Kojima, T. Nakano and S. Nakamura. Dept. of Biol., Fac. of Sci., Toyama Univ., Toyama.

We reported that O₂ consumption of unfertilized sea urchin eggs is enhanced not only by treatments with procaine and NH₄Cl, but also by subthreshold stimulation with Ca ionophore A 23187, insufficient to induce visible cortical changes. In the present study, it was determined whether or not chlortetracycline (CTC), a chelator of membrane-associated calcium, has inhibitory effects on increase of O₂ consumption induced by treatments with activating reagents, such as procaine, NH₄Cl, and A 23187. It was revealed that an increase of O₂ consumption is cancelled by treatments combining 300 µM CTC with 1 µM A 23187, but not treatments combining 300 µM CTC with 10 mM procaine or 10 mM NH₄Cl. These results are quite similar to those obtained by treatments combining above-mentioned activating reagents and TMB-8, an antagonist of intracellular Ca release (Kojima et al., 1988). Therefore, it may be said that Ca ionophore A 23187 induces a release of intracellular membrane-associated Ca, and as a result, a rise of respiration occurs, while weak bases, such as procaine and NH₄Cl can enhance O₂ consumption by stimulation of some metabolic changes which do not directly connect to processes of intracellular Ca release.

DB 147

CHANGES IN THE LEVEL OF ARGININE PHOSPHATE FOLLOWING TREATMENTS WITH ACTIVATING REAGENTS IN SEA URCHIN EGGS.

H.Tsuchida¹, M.K.Kojima¹, S.Nakamura¹, and S.Nemoto¹, Dept. of Biol., Fac. of Sci., Toyama Univ., Toyama and ²Tateyama Marine Lab., Ochanomizu Univ., Tateyama.

We found that O₂ consumption of unf. sea urchin eggs is enhanced by treatments with activating reagents, such as procaine, NH₄Cl, and A23187. Therefore, it was determined whether or not an increase of the ArP content is induced by treatments with above-mentioned three reagents. When unf. eggs are immersed in 10 mM procaine or 10 mM NH₄Cl, the content of ArP increases, while the level of the ArP content does not rise as far as they are exposed to A23187 in lower concentrations, such as 1 μ M, which are enough to provoke enhancement of O₂ consumption but insufficient to induce formation of fertilization membrane. The rise of ArP content following treatments with procaine or NH₄Cl is not affected by TMB-8, an antagonist of intracellular Ca²⁺ release. When eggs are put into Na⁺-free sea water containing 10 mM procaine or NH₄Cl, the ArP content still increases and, this is the true even when eggs just after fertilization are transferred to Na⁺-free sea water. If eggs are treated with nigericine, a K⁺/H⁺ exchanger, the content of ArP decreases. These facts suggest that an increase of the ArP level is not caused by a rise of intracellular pH.

DB 148

STRUCTURAL ANALYSIS OF STARFISH ACROSOME REACTION-INDUCING SUBSTANCE (ARIS)

T.Okinaga and M.Hoshi. Dept. of Life Sci., Fac. of Sci., Tokyo Inst. of Technol., Tokyo

Three egg jelly components, ARIS, Co-ARIS and Oligopeptide(s) are responsible for inducing acrosome reaction in starfish *Asterias amurensis*. ARIS is a highly sulfated glycoprotein. Though saccharide chains of ARIS are thought to play a key role in the induction of the acrosome reaction, information about the chemical structure of ARIS is much limited.

Pronase digested ARIS (P-ARIS), which retained the biological activity of ARIS, was used for the chemical structure analysis. The major sugar components were Fuc, Xyl, Gal, GalNAc. P-ARIS was quantitatively hydrolyzed by mild acid, giving several oligosaccharides. The sulfate groups were eliminated by solvolysis.

DB 149

LOW Na⁺ SEAWATER INDUCES ACROSOME REACTION OF STARFISH IN THE ABSENCE OF EGG JELLY.

T. Amano^{1,2} and M. Hoshi¹. ¹Tokyo Inst. of Technol., Tokyo, ²Tokyo Metropolitan Inst. of Gerontology, Tokyo.

The acrosome reaction (AR) is a key reaction in echinoderm fertilization. Induction of the AR by egg jelly is regulated at the level of the alterations of specific ion permeabilities. However, the induction mechanism of the AR is still unclear.

We find that spermatozoa of the starfish, *Asterina pectinifera*, placed into low Na⁺ (20-25 mM), Ca²⁺-free seawater undergo the AR when Ca²⁺ (final 10 mM) is added to the sperm suspension. This reaction is accompanied by a transient increase in intracellular pH (pHi) followed by acidification, similar to the jelly-induced AR. The changes in pHi depend on extracellular Na⁺, H⁺, K⁺ concentrations. A Ca²⁺-channel antagonist, diltiazem, blocks pHi decrease but does not affect the transient increase in pHi, suggesting that two types of Ca²⁺ entrance systems exist on the sperm plasma membrane. These results suggest that Ca²⁺-channels, Na⁺/H⁺ exchanger, and the change in membrane potential are involved in the low Na⁺-induced AR, like the jelly-induced AR. The low Na⁺-induced AR will provide a novel system for studying the induction mechanism of the AR.

DB 150

VERAPAMIL AND WGA INHIBIT HIGH PH-INDUCED ACROSOME REACTION OF *HEMICENTROTUS PULCHERRIMUS* SPERM

V. Sendai and K. Aketa. Akkeshi Mar. Biol. Stat., Hokkaido Univ., Akkeshi Hokkaido.

It is known that spontaneous acrosome reaction (AR) occurs under high pH (9.0) without the aid of egg jelly. It remains unclear why AR occurs. Since the increases in intracellular Ca²⁺ ([Ca²⁺]_i) and pH (pHi) are necessary for AR induction by egg jelly, we examined the relations of external pH (pHe) to [Ca²⁺]_i and pHi.

High pHe (9.0) caused large increases in both [Ca²⁺]_i and pHi and induced AR of *Hemicentrotus pulcherrimus* (H. p.) sperm. Additionally, not only the former but the latter were suppressed by Ca²⁺ channel blockers such as verapamil and nisoldipine and by WGA, which interacted with a 220 kD membrane glycoprotein, resulting in the inhibition of AR. These inhibitory conditions are identical with those for egg jelly-induced AR.

We suggest that (1) high pH activates Ca²⁺ transport system as dose egg jelly, (2) increase in [Ca²⁺]_i is prerequisite for that in pHi and (3) the 220 kD WGA-binding protein (WGAbp) is involved in regulation of this system.

High pHe did not cause [Ca²⁺]_i and pHi increases and AR of *Strongylocentrotus intermedius* (S. i.) sperm. Some functional differences may exist in WGAbp between H. p. (220 kD) and S. i. (230 kD).

DB 151

MOLECULAR CHARACTERIZATION AND BIOLOGICAL FUNCTION OF THE BASIC PROTEIN FROM *CIONA* INTESTINALIS SPERM.

Y.Satoh, K.Kawamura, and M.Nakauchi.
Dept. Biol., Fac. Sci., Kochi Univ., Kochi.

We have studied adhesive factors of sperm that are involved in sperm-vitelline coat (VC) binding in the ascidian *Ciona intestinalis*. Spermatozoa can attach to a glass or plastic plate other than the VC, however, they are detached easily from the substratum by treating them with acid sea water (1N HCl : sea water = 1:4). Therefore, we have supposed that adhesion molecules of sperm dissolved in acid sea water. The acid extracts showed a major band on Acid Urea-PAGE. It exhibited several biological functions as follows; binding to the VC, the agglutination of unfertilized eggs and the inhibition of sperm-VC binding. The results of molecular characterization showed that it is enriched with Lys and Arg about 44% of amino acids and contains carbohydrates, of which D-glucose is dominant about 80% of total carbohydrates. Thus, this molecule is a basic glycoprotein (isoelectric point ≈ 9.6).

DB 152

ACTIVATION OF GTP-BINDING PROTEINS IN SEA URCHIN SPERM PLASMA MEMBRANE VESICLES.
K.Mikami-Takei and I.Yasumasu. Dept. Biol., Sch. Educ., Waseda Univ., Tokyo.

We have previously reported that two types of GTP-binding protein (G-protein) exist in the sperm plasma membrane of four species of sea urchin (DGD, 31, 397, 1988). In sperm of *H. pulcherrimus*, 45 kDa protein which is ADP-ribosylated by cholera toxin (CT) required 500 mM Mg^{2+} to bind [^{35}S]GTP γ S while 39 kDa protein which is ADP-ribosylated by pertussis toxin (PT) required 0.5 mM Mg^{2+} . [α - ^{32}P]GTP binding to sperm membrane fraction was stimulated by the addition of egg jelly water. The increase of ^{45}Ca uptake into membrane vesicles in response to jelly water diminished after treatment with CT and rather decreased after PT treatment. Both GTP γ S-treated and GTP γ S-treated membrane fraction showed high level of ^{45}Ca uptake regardless of the addition of jelly water. These results suggest that two types of G-protein participate in Ca^{2+} influx triggered by the addition of jelly water but the mechanism of regulation of Ca^{2+} channel should be farther investigated.

DB 153

CO-INSENSITIVE RESPIRATION IN ECHIOROID EGGS.

E.Tazawa¹, A.Fujiwara² and I.Yasumasu².
¹Biol. Inst., Yokohama City Univ., Yokohama and ²Dept. of Biol., Waseda Univ., Tokyo.

It has been found that the respiration of echinoid eggs is hardly blocked by CO and CO-insensitive respiration increase in its rate under white light irradiation. We found that mitochondria isolated from echinoid eggs undergo photo-activated CO-insensitive respiration. Responses of respiration in echinoid eggs to rotenone, antimycin A and TMPD in the presence and absence of CO, observed in the present study, suggest that electron equivalent is transported to molecular oxygen through a bypass of respiratory chain branching from a spin of mitochondrial respiratory chain between flavoproteins and cytochrome b. Difference spectra of eggs obtained in the presence of CO showed the peaks of absorbance corresponding to those of reduced cytochrome b, whereas those obtained in its absence exhibited the reduced peaks of cytochrome aa₃, cytochrome b and cytochrome c. Any absorbance peak corresponding P₄₅₀ was not found in difference spectra of eggs and isolated microsome fraction. Photoactivation of respiration was reversibly induced by light irradiation at wavelength corresponding to those of cytochrome b. Probably, photoactivated cytochrome b-type redox protein mediates electron transport in this CO-insensitive branch of respiratory chain.

DB 154

BIOCHEMICAL AND MORPHOLOGICAL CHANGES IN SPERM AT FERTILIZATION.

A. Hino, Department of Biological Sciences, Kanagawa University, Hiratsuka.

It was reported that the sea urchin sperm which had reacted with glutaraldehyde-fixed eggs were immotile with a quite low respiratory rate (DGD, Vol.22,p813-820). Such quiescent sperm were acrosome-reacted and changed in the shape of their mitochondria which became round-up and spherical figure. The concentrations of adenine nucleotides were measured before and after such morphological changes in the sperm. In the swimming sperm, the ATP level was low but ADP was in high level. On the contrary, in reacted sperm, the ADP level was markedly low and the ATP was as high as in dry sperm. The respiratory rate of quiescent sperm was enhanced by DNP. The electron micrographs showed that the matrix of mitochondria was the condensed conformation in active sperm and the orthodox conformation in reacted one. These results suggest that the energy state of sperm was changed from 3 to 4 after the morphological changes in sperm.

The change in the shape of mitochondria was also observed in the sperm which adhered on intact egg surface. This phenomenon was also observed in the starfish sperm which were interacted with eggs and were induced the acrosome reaction by ARIS and CoARIS. Such change in the shape of sperm mitochondria at fertilization might be comparable to the sperm reaction which is known in the ascidian sperm.

DB 155

PROGRESS OF FORMATION OF CTENII ON THE SCALES IN THE JAPANESE FLOUNDER, *PARALICHTHYS OLIVACEUS*. S. Kikuchi¹ and N. Makino², Kominato Lab., Marine Ecosystems Res. Ctr., Fac. of Sci., ¹Chiba Univ., Amatsu-Kominato 299-54, and Chiba Pref. Fish Farm. Ctr., Katsuura 299-52.

The flounder is covered with the different scales on the each side, the ctenoid scales on the ocular side and the cycloid scales on the blind side respectively. Seikai ('80) reported that the formation of ctenii began from a part of the caudal peduncle on the ocular side and spread to the dorsal and ventral peripheries in an early larval stage. In the present work, we found, in the larval fish with complete ambicoloration, the formation of ctenii spreads from the caudal peduncle to the whole area of the ocular side as does the normal fish. However, the ctenii formation progressed over the edges of the trunk and from the peripheries towards the central part of the blind side. The mode of the ctenii formation in the fish of partial ambicoloration and/or hypomelanosis suggested that this progress of ctenii formation spreads independently of melanization of the skin. Bard ('77) and Murray ('81) advanced an hypothesis in which mammalian coat pattern is determined by diffusion of an unknown factor(s) in a fetal stage through the skin tissue. It is thought that the progress of the ctenii formation of the Japanese flounder is the same mechanism.

DB 156

ELECTRON MICROSCOPIC OBSERVATION OF MATURATION AND FERTILIZATION IN THE BIVALVE, *Laternula limicola*. IV K. Hosokawa¹ and Y. D. Noda², ¹Biol. Lab. Tokyo Dent. Coll. ²Biol. Inst. Fac. Sci. Ehime Univ.

The investments of the bivalve, *Laternula limicola*, were distinguished by three layers; in order, the jelly coat, granular layer and vitelline coat. The vitelline coat was the innermost layer of the investments and composed of a fine fibrillar structure with the microvilli of the oocyte. When the primary oocyte was spawned in sea water, the investments underwent a rapid change. The vitelline coat moved upward from the oocyte surface and that disjoined the microvilli.

However, the vitelline coat again settled on the oocyte surface. As a result of that, interspaces were formed in the investments: (1) the space (SGV) between the granular layer and the vitelline coat, and (2) the perivitelline space between the vitelline coat and the oolemma. At fertilization, the sperm reaction occurred after the sperm entered into the SGV of the investments. A cytoplasmic granule (CG) situated at the posterior end of the sperm mid-piece was similar to a temple bell in shape. A cap of CG (CCG) ruptured and its contents released. The inner membrane of the CCG came into contact with the oolemma. A fertilization cone was formed to fuse an incoming sperm. Sperm penetration into the bivalve egg, *Laternula limicola*, was characterized by a sperm nucleus following close the sperm mitochondria located within the fertilization cone.

DB 157

COILED FILAMENTS OF THE "TRUNCATED CONE" IN JAPANESE ABALONE SPERM Y. Shiroya, and Y. T. Sakai. Biol. Lab., Wayo Women's Univ., Chiba.

A coiled filamentous structure termed 'truncated cone' located in the acrosomal apex of abalone (*Haliotis discus*) sperm transforms into a cylindrical structure of more than 3 times the original height during the acrosome reaction. Studies on the organization of the filaments composing the truncated cone by negative staining, quick-freeze deep-etching and thin sectioning indicated that the truncated cone is composed of about 12 filaments tightly packed with each other. The filament was estimated to be about 3.6 μ m in length and 10 nm in diameter, coiling 2 and half turns from the circular base of the truncated cone.

The acrosome reaction causes the truncated cone to transform into a form of thin cylinder. It was demonstrated that the length of the filament does not change during elongation of the truncated cone and that transformation is due to further coiling up of the filaments up to 5 turns with regular spacing.

Quick-freeze deep-etch images of the truncated cone revealed that each filament appears to have beaded configuration, closely resembling the appearance of intermediate filaments.

DB 158

DETERMINATION OF THE STRUCTURE OF LYSIN BINDING SITES ON VITELLINE COAT: THE PROPERTIES OF LYSIN BINDING SITE. M. Shitara and K. Haino-Fukushima. Dept. of Biol., Fac. of Sci., Tokyo Metropolitan Univ., Tokyo.

Vitelline coat (VC) of lysin of marine Mollusca, *Tegula pfeifferi*, irreversibly binds to VC, bringing about the lysis of VC in stoichiometric and non-enzymatic manner. We tried to purify the lysin-binding sites (LBS) on isolated VC and determine the structure responsible for irreversible binding of lysin.

In this study, three VC fragments denoted as A, B and C were isolated from the alkali-solubilized VC through the steps of V8 proteinase digestion, deglycosylation by trifluoromethane sulfonate, acid degradation by 5.7N HCl of 37° and gel filtration on Sephadex G-50 and Sepharose 4B columns. The molecular weights were estimated as 200K(A), 20K(B) and 5K(C). These fragments construct one molecule of LBS when they are combined in a molar ratio of 1/18:1:1. The LBS reconstructed by A, B and C contains about 4.7% of isolated VC as starting material. The indispensable structures for LBS previously reported, 1) the amino acid and sugar sequence including N-glycosidic bond, 2) the sequence composed with hydrophobic and basic amino acids separate from N-glycosidic bond were ascertained. The chemical composition of A, B and C suggested that those indispensable structures existed in different fragments.

DB 159

CYTOCHALASIN B DOES NOT PREVENT SPERM INCORPORATION IN DENUDED OOCYTES OF STARFISH.

K. Kyoizuka and K. Osanai. Mar. Biol. Stn. Tohoku Univ., Aomori

During fertilization in starfish, actin filaments are involved in sperm entry. Fertilizing sperm of *Asterias amurensis* fuses with the oocyte by the top of the acrosomal process. The fertilization cone begins to form around the acrosomal process, in which actin filaments are detected. Cytochalasin B (1 μ M) prevents fertilization cone formation and sperm incorporation in intact oocytes. Sperm can not pass through egg envelopes in the presence of cytochalasin B. (Kyoizuka and Osanai, 1988).

When denuded (jelly coat and vitelline coat-free) oocytes were inseminated with acrosome-reacted sperm in sea water containing 2 μ M cytochalasin B, the oocytes incorporated the sperm and underwent mitotic nuclear divisions. Electron microscopic examination revealed that the sperm pushed the acrosomal process into the oocyte and then the acrosomal membrane fused with the plasma membrane of the oocyte. A small mass of clear cytoplasm appeared around the fused acrosomal process and incorporated the sperm head.

These results indicate that actin filaments in the acrosomal process and the fertilization cone are required for sperm penetration through egg envelopes, but not for sperm head incorporation.

DB 160

DELAYED SPERM INJECTION AND FERTILIZATION IN PARTHENOGENETICALLY ACTIVATED SAWFLY EGG (*ATHALIA ROSAE*, TENTHREDINIDAE HYMENOPTERA).

M. Sawa¹ and K. Oishi². ¹Div. of Env. Sci., Grad. School of Sci. and Technol., and ²Dept. of Biol., Fac. of Sci., Kobe Univ., Kobe.

Mature unfertilized eggs dissected from ovaries of the turnip sawfly (*Athalia rosae ruficornis* Jakovlev) can be activated in vitro to develop to haploid parthenogenetic males and that these eggs, if injected with sperm and activated, develop as fertilized diploid females in about 10% of the cases (Sawa and Oishi, 1989).

In the present study, we have examined the fate of sperm injected into eggs at various times after activation. About 25% of the eggs activated for 20 min (at the first meiotic telophase) and injected with sperm developed as fertilized diploid females, while about 5% of those activated for 60 min did so. In the hymenopteran system an egg can take two developmental pathways, parthenogenesis or fertilization. The fate of an egg as to which pathway to follow might thus be fixed soon after egg activation.

DB 161

SPERM MORPHOLOGY AND INITIAL STAGES OF SPERM ENTRY INTO EGGS OF THE ROSE BITTERLING, *RHODEUS OCELLATUS OCELLATUS*. T. Ohta. Dept. Biol. Aichi Univ. Educ. Kariya.

A spermatozoon of the rose bitterling has a large mitochondrion but no acrosome. Most of spermatozoa stopped their movement in a physiological saline and began to move in hypotonic solutions. Distribution of intramembranous particles (IMPs) was investigated on PF and EF surfaces of freeze-fractured spermatozoa. Specialized arrays of IMPs on the PF surface, e.g. parallelogram shapes, were seen in portions of sperm heads in front of the centrioles. In other sperm head areas, many IMPs were evenly distributed over the PF surface. The EF surface showed a complementary structure of specialized arrays in similar sperm head regions. Less IMPs were observed on the EF surface than the PF.

Electron microscopic observation of eggs inseminated in fresh water showed the following: (1) Membrane fusion began in most eggs within 10 sec of the beginning of the insemination. (2) It occurred between the sperm head and microvilli just beneath a micropyle. (3) The fertilizing spermatozoon, in most cases, attached to the microvilli at the side of the membrane in which the specialized arrays of IMPs were present.

DB 162

FERTILIZATION OF THE LAMPREY (*LAMPETRA JAPONICA*) EGGS.

W. Kobayashi and T. S. Yamamoto. Zool. Inst., Fac. Sci., Hokkaido Univ., Sapporo.

Upon insemination of the lamprey egg, sperm passed through a jelly mass covering the animal pole of the egg and underwent acrosome reaction when they reached the outer surface of the two-layered vitelline coat; their acrosomal filaments penetrated the thickness of the coat. When the eggs loaded with the Hoechst 33342 were inseminated, a single sperm became fluorescent, even its nucleus remained outside the coat. This indicates that sperm-egg fusion has been established at the tip of acrosomal filament. No other sperm fluoresced. With the separation of egg coat from the ooplasm, the nucleus of fertilizing sperm passed through the outer and inner layers of the coat. The nuclei of excess sperm however remained outside the inner layer. During the perivitelline space formation, thin threads connected the egg coat with the ooplasm. The nucleus of fertilizing sperm moved along the thread and was embedded in the ooplasm. Although cytochalasin B did not disturb the passage through the outer layer of the coat, it inhibited the movement of sperm nucleus through the inner layer of the coat. It was suggested that the fusion of acrosomal filament with the ooplasm is prerequisite to the passage of sperm through the vitelline coat.

DB 163

SPAWNING INDUCTION AND DEVELOPMENT OF THE SEA ANEMONE HALIPLANELLA LINEATA (=H. LUCIAE)
K. Saotome, Tokyo Metropolitan Shinjuku Senior High School, Tokyo

The sea anemones H. lineata were collected in the coast of Miura district, Kanagawa Prefecture. In the laboratory, this species showed a tendency to spawn in the evening during July-August in 1988, 1989. Artificial spawning was induced by desiccation and warming of the anemones about 2-4 hours followed by adding of sea water. Addition of sperm solution to ripe females also induced shedding of eggs.

The process of the development was observed with light microscope at 18°C. The eggs were expelled from female mouth with mucous string and about 130 µm in diameter and pink in color. Cleavage was complete and equal, but the first two cleavage furrows were often not formed. Nuclear divisions without accompanying cytoplasmic divisions took place. Blastula is coeloblastula. Cilia appeared on the surface of the late blastula and it began to swim.

Endoderm formation seems to be by emboly. Apical tuft was formed in the aboral end of the planulae and also nematocysts were made. The planulae secreted mucous thread from their mouth (blastopore) which trailed behind them. The particle like algae or so adhered to the mucous strand and then passed into the gastrocoel.

DB 165

ULTRASTRUCTURAL CHANGES IN NUCLEAR DIFFERENTIATION IN Paramecium caudatum
Y. Yashima Dept. of Biol., Sci. of Lib. Arts and Sci., Iwate Med. Univ., Morioka.

The determination of the nuclear differentiation occurs immediately after the third division of the synkaryon and nuclei near the opposite ends of the cell. The four nuclei situated in the posterior region become macronuclear anlagen and the four in the anterior region become micronuclei.

The purpose of this study was to compare the morphological changes using TEM among the anterior micronuclei, the posterior micronuclei, and other stage micronuclei i.e., the synkaryon and the first division nuclei of the synkaryon including the cytoplasm around the micronuclei.

The remarkable features in both anterior and posterior micronuclei during the nuclear differentiation were membranous structures as lamella which appeared to be derived from the mitochondrial membrane were present in the cytoplasm around the micronuclei in contact with the micronuclear membrane and incorporated into the micronuclei. An particular the membranous structure containing ribosomes was recognized in the posterior micronuclei but was not found in cytoplasm around the synkaryon and the first division nuclei of the synkaryon.

The membranous structures appeared to be formed as follows. One filament appeared to emanate from a mitochondrion. The tip of this filament then enfolded itself forming a spiral membranous structure which in the posterior region sometimes enclosed ribosomes.

DB 164

Micronuclear division inducing factor at meiosis of Paramecium caudatum; an analysis by micromanipulation, II.
K. Mikami, Res. Inst. for Sci. Educ., Miyagi Univ. of Educ., Sendai.

Results of macronuclear elimination at meiosis suggested the existence of two kinds of cytoplasmic factors derived from the macronucleus (mac); one (micDIF) for induction of micronuclear division and the other for its depression. Following results were obtained on the affect of micDIF.

1) When mac was eliminated at a quite early stage of conjugation from either cell of a pair, the micronucleus (mic) in the non-mac cell lacked a typical meiotic prophase but divided twice. The micDIF seemed to migrate easily between mating cells and/or induce division (div.) in lower concentration than other factors. After div. which was induced by micDIF of its mating partner, amount of DNA of each 4 nuclei was measured by microspectrophotometry. Mics in the non-mac cell have the same or half as much DNA as the mics in the mac cell. This means that the 2nd div. occurred without doubling in DNA content after 1st div. as well as in case of meiosis of a mac cell.

2) An assay system was designed for micDIF. The cytoplasm at dividing stage of 1st meiotic division was injected into non-mac pairs prepared by eliminating mics by 6-7 hrs of conj. 23 cells were injected with the cytoplasm so that the mic division was observed in 4 of them. In 17 cells without injection, mic division was not observed.

DB 166

ANALYSIS OF A CONJUGATION-SPECIFIC NUCLEAR ANTIGEN IN PARAMECIUM BY A MONOCLONAL ANTIBODY.

A. Yanagi, Biol. Inst., Fac. of Sci., Tohoku Univ., Sendai.

To know molecular mechanisms controlling conjugation, I obtained a monoclonal antibody against a conjugation-specific antigen in Paramecium caudatum. The antigen appeared in micro- and macronucleus at specific stages during conjugation. The stage-specific manner of its appearance indicates that the antigen is not involved in dividing nuclei during conjugation. So the antigen might have an inhibitory activity to nuclear divisions during conjugation. Using SDS-polyacrylamide gel electrophoresis of a homogenate of conjugating cells followed by electroblotting, it was shown that single positive band existed for the antibody and molecular weight of the antigen was about 60 kDa. This indicates that the antibody reacts specifically with a single antigen in the conjugating cells. Furthermore, the antibody reacted with some nuclear antigen during conjugation in P. multi-micronucleatum and during autogamy in four species of P. aurelia complex. But P. bursaria, Tetrahymena thermophila and spermatozoa of BALB/c mouse were negative for the antibody. This suggests some difference in specificity between the nuclear antigens of "aurelia" group and of the "bursaria" group of Paramecium.

EN1

GONADOTROPIN- AND PROLACTIN-TREATED NEWTS PREFER THE WATER IN WHICH ANIMALS OF THE OPPOSITE SEX HAVE BEEN KEPT.

F.Toyoda and S.Kikuyama. Dept. of Physiol., Nara Med. Coll., Kashihara and Dept. of Biol. Sch. of Educ., Waseda Univ., Tokyo.

In the newt, *Cynops pyrrhogaster*, combination of gonadotropin and prolactin (GTH+PRL) is known to develop various organs involved in reproduction and also to elicit the reproductive behavior. The most significant factor in mate interaction has been considered to be chemical communication. The experiments were conducted to see whether GTH+PRL enhances the responsiveness to the attractant(s) emitted from the specimens of the opposite sex. The container (ϕ 37cm) filled with water (3cm in depth) was divided into 3 sectors where 3 blocks of sponges (5.6 x 7.3 x 3.4cm) containing the water in which the hormone-treated males had been kept, the water in which the hormone-treated females had been kept and the tap water, respectively, were placed. Test animals were individually introduced to the container for 10min every other day during the period of 15 days, the time spent in each sector being recorded. Analyses of the data revealed that the GTH+PRL-treated animals were significantly attracted to the sponge block containing the water in which the newts of the opposite sex had been kept, whereas the saline-treated animals did not exhibit such a tendency. The results indicate that GTH+PRL enhances the responsiveness of the newt to the attractant(s) from the opposite sex.

EN2

EFFECTS OF AMYGDALOID LESIONS ON COPULATORY BEHAVIOR IN MALE RATS.

Y.Kondo, and Y.Arai. Dept. of Anat., Jun-endo Univ. Sch. of Med., Tokyo.

Several studies have reported that lesions in the corticomedial (CMA) but not in the basolateral amygdala (BLA) caused mild decline of copulatory behavior in male rats. In this study, we tried the re-examination of the effects of amygdala lesions. Castrated male rats received radiofrequency lesions of BLA, the rostral part of CMA, or the caudal part of CMA, bilaterally. Three weeks later, all animals were implanted Silastic tubes containing testosterone (T). After the implantation of T, 4 observations of copulatory behavior were carried out every 5 days. Animals were put into observation cage with an estrous female primed with estrogen and progesterone in each observation.

Lesions placed in the rostral part of CMA resulted in severe deficit of copulatory behavior, whereas lesions in the BLA yielded no decrease of mounts, intromissions, and ejaculations compared to sham-operated controls. Although animals with the caudal CMA lesions also showed normal levels of mounts and intromissions, none of these animals achieved ejaculations. These data suggest that though the rostral CMA and the caudal CMA both concern display of copulatory behavior in male rats, the rostral CMA may play a more important role in regulating copulatory behavior than the caudal CMA.

EN3

ROLE OF THE MEDULLARY RAPHE NUCLEUS IN REGULATING MALE SEXUAL BEHAVIORS IN MALE RATS

K. Yamanouchi
Neuroendocrinology, Dept. of Basic Human Sciences, Sch. of Human Sciences, Waseda University, Tokorozawa.

The role of the medullary raphe nucleus, especially raphe obscurus nucleus, in regulating male sexual behaviors was examined in male rats. Male rats were castrated and subjected to brain surgery in the medulla oblongata. The raphe obscurus nucleus, raphe magnus nucleus or gigantocellular nucleus of the reticular formation was destroyed by means of a radiofrequency lesion generator. In addition, castrated control without brain surgery was made. All male rats were implanted subcutaneously with 2 Silastic tubings (5 cm in length, 1.57 x 3.18, i.d. x o.d.) containing testosterone. Sexual behavior tests were carried out on day 7, 14, and 21 after implantation of testosterone. Male rats with raphe obscurus lesions showed low levels of mounting and intromission frequencies, when compared to those of other groups. None of them indicated ejaculation pattern. These results suggest that the raphe obscurus nucleus may be one of the indispensable neural substrates for regulation of male sexual behaviors in male rats.

EN4

EFFECTS OF SEVERAL HORMONES ON THYROID HORMONE METABOLISM IN IMMATURE MASU SALMON, *Oncorhynchus masou*.

H.Yamada, K.Gen and K.Yamauchi. Dept. of Biol., Faculty of Fisheries, Hokkaido Univ., Hakodate.

Effects of estradiol-17 β (E₂), testosterone (T), cortisol (F) and ovine growth hormone (oGH) on serum T₄ and L-T₃ levels and *in vitro* conversion of T₄ to L-T₃ and r-T₃ in the gill and liver were investigated in masu salmon. The generated L-T₃ and r-T₃ were fractionated by reverse phase HPLC system, and the quantities were calculated from their radioactivities.

E₂ depressed circulating T₄ and L-T₃ levels, while T and oGH enhanced the concentrations of T₄ and L-T₃, respectively. F had no effect. E₂ treatment significantly depressed L-T₃ generation, and increased r-T₃ generation in gill and liver. The oGH treatment significantly enhanced L-T₃ generation, but not r-T₃ generation in both tissues. L-T₃ generation was found in the gill following F treatment. T was not effective on both L-T₃ and r-T₃ generation in each tissue.

From these results, it may be mentioned that in masu salmon there are two T₄ deiodination pathways: GH stimulates 5'-monodeiodinase, and E₂ inhibits 5'-monodeiodinase activity and stimulates 5-monodeiodinase activity.

EN5

EFFECTS OF GROWTH HORMONE AND CORTISOL ON THYROXINE METABOLISM IN THE FRESHWATER AND SEAWATER EUROPEAN EEL (*Anguilla anguilla*). K. Gen, H. Yamada and K. Yamauchi. Dept. of Biol., Faculty of Fisheries, Hokkaido Univ., Hakodate.

We investigated the effects of ovine growth hormone (oGH) and cortisol on serum thyroid hormones (T4 and L-T3) and *in vitro* T4 metabolism in the gill and liver of freshwater (FW) or seawater (SW) acclimated European eel. The metabolites were analyzed using reverse phase HPLC. oGH elevated the circulating L-T3 levels in both FW and SW fish. Cortisol increased serum L-T4 levels in FW fish. No effects of the hormones on the gill Na^+ , K^+ -ATPase activity were observed. Cortisol reduced serum sodium concentrations in FW fish. With respect to T4 metabolism in the gill of FW fish, oGH and cortisol caused an increase in L-T3 generation, and cortisol also enhanced r-T3 generation. However, both hormones had no effects on T4 deiodination in the gill of SW fish. In the liver of FW fish, oGH increased L-T3 generation, whereas cortisol enhanced the generation of r-T3. In contrast, oGH stimulated L-T3 generation in the liver of SW fish. These results suggest that oGH and cortisol enhance the conversion of T4 to L-T3 and cortisol also stimulates r-T3 generation, and further indicate that L-T3 may be involved in the improvement of seawater adaptability of the European eel.

EN6

PROLACTIN mRNA LEVELS IN THE CULTURED PITUITARY GLANDS OF BULLFROGS. D. Uchida¹, N. Takahashi¹, S. Kikuyama¹, K. Wakabayashi² and Y. Kato². ¹Dept. of Biol., Sch. of Educ., Waseda Univ., Tokyo. ²Inst. of Endocrinol., Gunma Univ., Gunma.

We have previously reported that both TRH and a substance separated from bullfrog hypothalamus stimulate the release of prolactin (PRL) from the pituitary gland of bullfrogs. Success in molecular cloning of the bullfrog PRL cDNA made it possible to measure the PRL mRNA levels in the pituitary gland using dot hybridization technique. Pituitary glands cultured in the presence of TRH (10^{-9} - 10^{-7} M) and hypothalamic substance (40 ng/ml) for 16 hours markedly elevated the PRL mRNA levels (3-6 times of the control levels). Dopamine (10^{-8} - 10^{-6} M) and CB154 (10^{-8} - 10^{-6} M), which are known to suppress the release of PRL from the bullfrog pituitary gland, lowered the PRL mRNA levels significantly (2/5-1/2 of the control levels). The results indicate that TRH and the hypothalamic substance stimulate not only the release but also the synthesis of PRL and that dopamine and dopamine agonist suppress the release and synthesis of PRL.

EN7

AGE-RELATED CHANGES IN GH mRNA AND PRL mRNA LEVELS IN THE RAT. S. Takahashi¹, S. Kawashima² and H. Seo³. ¹Zool. Inst., Fac. of Sci., Hiroshima Univ. Hiroshima, ²Zool. Inst., Fac. of Sci., Univ. of Tokyo, Tokyo, ³Res. Inst. of Environ. Med., Nagoya Univ., Nagoya.

Pituitary growth hormone (GH) content decreased with aging in male and female rats, and prolactin (PRL) content decreased in male rats and increased in female rats. To study whether the altered pituitary GH and PRL levels in old rats may be related with the changes in mRNA levels, we studied GH mRNA and PRL mRNA levels. Cytoplasmic RNA was extracted by guanidium/hot phenol method. Northern blot analysis was carried out using rat GH cDNA and rat PRL cDNA. Northern analysis exhibited single bands of each mRNA with similar mobility in young (3 months), middle-aged (12 months) and old (18 months) rats. In young females, each mRNA level changed in the estrous cycle. The highest levels of GH mRNA and PRL mRNA were seen at 2nd day of diestrus and estrous day, respectively. GH mRNA levels decreased with aging in both sexes, and PRL mRNA levels decreased in males, but increased in females. Total GH mRNA level in old males was lower than in young males. In females, total GH mRNA levels did not change with aging. Total PRL mRNA levels decreased in old males, but increased in old females. These changes resulted in the changes in pituitary GH and PRL contents.

EN8

EFFECTS OF AGING ON URINARY AND SERUM PARAMETERS FOR RENAL FUNCTION IN THE WISTAR/TW FEMALE RATS. Y. Kobayashi, K. Shimoura and K. Hattori. Dept. of Pharmacol. Shimane Med. Univ., Izumo.

The Wistar/Tw strain female rats show polydipsia after 19 months of age (Mo), while males show it after 16 Mo. Morphological changes in renal glomeruli in young period have been reported. We reported changes of urinary and serum parameters for renal function of male rats with aging. In the present study, the parameters were measured in female rats at 4, 7, 10, 13, 15, 18 and 21 Mo. Urinary protein concentrations increased at 15 Mo and showed a plateau after 18 Mo. Daily excretion of urinary protein increased with aging and showed the maximum at 21 Mo. Urinary creatinine concentrations decreased slowly after 18 Mo. Serum creatinine concentrations, blood urea nitrogen values and glomerular filtration rate did not change with aging, suggesting that the dysfunction of glomeruli was not severe compared with males. On the other hand, urine concentrating rate, calculated from urine and serum creatinine concentrations, reduced slowly with aging. Serum cholesterol and phospholipid concentrations increased with aging. In conclusion, dysfunction of renal glomeruli occurred in younger period and it developed during aging, although the development was slower compared with males. Dysfunction of reabsorption was also occurred at aged rats, which resulted polydipsia.

EN9

CHANGES IN PLASMA ADRENOCORTICAL HORMONE LEVELS DURING THE BREEDING SEASON IN THE TOAD, *BUFO JAPONICUS*

Y. Tasaki¹, M. Itoh¹, S. Ishii¹ and J. C. Wingfield². ¹Dept. of Biology, School of Education, Waseda Univ., Tokyo, ²Dept. of Zoology, Univ. of Washington, Seattle

Aldosterone and corticosterone levels in plasma were determined by radioimmunoassays in toads found under the ground on March 10th (Group A), moving toward a pond between 19 and 21th (B), arriving at the shore of the pond between 22nd and 24th (C), swimming in the pond between 22nd and 24th (D), and having come out from the pond between 24 and 27th (E).

In males, the aldosterone level was highest in Group C (2.90 ± 0.40 ng/ml) and lowest in Group E (0.77 ± 0.13 ng/ml). Females showed similar but less conspicuous changes with no statistically significant difference. Amplexing males showed significantly higher aldosterone levels than solitary ones. The corticosterone level was high in Group B, C, and D with a peak in Group C in both sexes (80.48 ± 2.72 ng/ml in males and 73.51 ± 8.12 ng/ml in females) and lowest in Group A in males (37.65 ± 7.91 ng/ml) and in Group E in females (23.00 ± 7.42 ng/ml). These results suggest that corticosteroids (especially aldosterone) already play some important role before toads come into the breeding pond. Some relation between reproductive behavior and corticosteroid may be expected.

EN10

SEASONAL CHANGES IN THE SENSITIVITY OF THE MALE TOAD (*BUFO JAPONICUS*) PITUITARY GLAND TO THE INJECTION OF MAMMALIAN GONADOTROPIN-RELEASING HORMONE (m GnRH)

Masanori Itoh and Susumu Ishii
Dept. of Biol., Sch. of Edu., Waseda Univ., Tokyo 169

A single intracardiac injection of 2 or 10 μ g/100 g body weight of m GnRH was made to adult male toads in various months. Blood samples were collected by cardiac puncture at intervals of 20 min after the injection, and plasma levels of LH and FSH were determined by homologous radioimmunoassays. Their maximum levels within 100 min after the injection were employed as the responses. The mean LH response was low in May, July and August, showing the minimum (2.53 ng/ml) in July. It clearly increased in November and reached the maximum (26.70 ng/ml) in February and March. The FSH response was also minimal (1.66 ng/ml) in July, and increased in November. The maximum (9.70 ng/ml) was in February. However, the FSH response decreased in March to a level close to that in November, and a similar level was retained in May. Thus, we could show that the *in vivo* sensitivity of the toad pituitary gland changes drastically through the year: almost insensitive in the summer for both LH and FSH and highly sensitive in the breeding season for LH or prior to the breeding season for FSH.

EN11

A SHIFT IN THE STEROID BIOSYNTHETIC PATHWAY IN AMAGO SALMON (*ONCORHYNCHUS RHODURUS*) TESTES ON THE SPERMATIATION

N. Sakai, N. Suzuki* and Y. Nagahama, Lab. of Reprod. Biol., Natl. Inst. for Basic Biol., Okazaki, *Noto Mar. Biol. Lab., Kanazawa Univ., Uchiura, Ishikawa.

Two characteristics of salmonid fishes make them an excellent model to investigate the control of male germ cell development. 1) Germ cells develop synchronously, 2) two important processes of germ cell development appear to be associated with two steroids: spermatogenesis with 11-ketotestosterone (11-KT) and spermiation with 17 α ,20 β -dihydroxy-4-pregnen-3-one (17 α ,20 β -P). A distinct shift, from the production of 11-KT to the production of 17 α ,20 β -P in response to gonadotropin, occurs in the testes of amago salmon around the onset of spermiation. Analysis of steroid biosynthetic pathways showed a shift in activities of testicular enzymes involved in the metabolism of steroids. During spermatogenesis, the testis synthesizes 11-KT by the pregnenolone, 17 α -hydroxypregnenolone, dehydroepiandrosterone pathway. Production of 17 α ,20 β -P results from a change in the pathway, immediately prior to spermiation, to: pregnenolone, 17 α -hydroxypregnenolone, 17 α -hydroxyprogesterone. This is the first demonstration of a shift in the steroid biosynthetic pathway from C19-steroids (androgens) to C21-steroids (progestins) in the testis of a vertebrate.

EN12

DIFFERENT ACTIVITY OF THE RING GLANDS BETWEEN DIAPAUSE DESTINED- AND NON-DIAPAUSE DESTINED LARVAE OF THE FLESH FLY

A. Moribayashi¹, H. Kurahashi², and T. Ohtaki³
¹Dept. of Technology, ²Dept. of Entomology, NIH, Tokyo and ³Biol. Dept., Kanazawa Univ.

Larvae of *Beettherisca peregrina* destined for pupal diapause pupariate one day later than non-diapause destined larvae. By the ligation of mature larvae at the 10th segment, pupariation of the anterior parts was only observed in diapause destined larvae. When ligations were applied behind the 11th segment, the anterior halves of larvae in both cultures could pupariate equally. These facts suggest that an abdominal factor(s) may stimulate the brain to release PTH, that induces ecdysone secretion from the ring gland in non-diapause destined larvae, but in diapause destined larvae the ring gland can secrete ecdysone without the abdominal factor(s).

The isolated ring glands of larvae programmed to diapause could release a certain amount of ecdysone without a brain extract *in vitro*, whereas the ring glands of non-diapause destined larvae did not produce ecdysone. Therefore, the ring glands of mature larvae differentiate by a short day or long day condition, in terms of ecdysone secreting activity and responsiveness to a brain extract (PTH).

EN 13

IS JUVENILE HORMONE INVOLVED IN THE PUPAL METAMORPHOSIS IN DIPTERAN LARVAE?

Shogo Tsuyuki, Sho Sakurai, Tetsuya Ohtaki
Department of Biology, Kanazawa University

Although larval-pupal metamorphosis in insects is considered to be under a hormonal control of juvenile hormone (JH) and ecdysone, it has not been established whether the same mechanism governs the dipteran metamorphosis. We therefore examined whether JH is involved in the dipteran metamorphosis using either whole body of larvae or wing discs of *Sarcophaga peregrina* larvae. Wing discs of early 3rd instar larvae responded to 20-hydroxyecdysone (20-OHE) and evaginated *in vitro*. Addition of JH I to the culture did not affect on the evagination induced by 20-OHE. When larvae were fed on a diet containing JHA (methoprene) from the 1st instar, they underwent normal metamorphosis. JH I injections to the newly ecdysed 3rd instar larvae exerted no effects on their development. These results indicate that the hormonal mechanism underlying in the pupal metamorphosis in *Cyclorhapha* is different from that as established in *Lepidoptera* and *Hemiptera*.

EN 14

BIOASSAY METHOD FOR PROTHORACICOTROPIC HORMONE IN THE SILKWORM, *BOMBYX MORI*, BY USING THE KK-42-TREATED BRAINLESS PUPAE.
H. Fugo. Fac. Agric. Tokyo Univ. Agric. & Technol. Fuchu-shi, Tokyo 183.

Improvement of bioassay method for prothoracicotropic hormone (PTTH) in the silkworm, *Bombyx mori*, was achieved. When the imidazole compound (KK-42: 1-benzyl-5-[(E)-2,6-dimethyl-1,5-heptadienyl]imidazole) was applied on the pupae whose brains had been extirpated just after pupation, the pupal-adult development was completely inhibited in almost all of the animals investigated so far. Though dauer pupae could be prepared only by the extirpation of their brains just after pupation in a specific race of *Bombyx*, these pupae initiated their development spontaneously during 30 to 50 days after operation. In a case of the improved method, pupal-adult development was arrested more than 90 days after the treatment.

The advantages of the improved method for PTTH assay are as follows: 1) arrested states of the animals are steady, 2) many races of *Bombyx* can be used for PTTH assay and 3) sensitivity of the animals for the exogenous PTTH is higher than that of the debrained animals used so far.

It is conclusively demonstrated that brainless pupae treated with imidazole compound (KK-42) are useful materials for the bioassay of PTTH.

EN 15

INTERSPECIES SPECIFICITY OF THE PROTHORACICOTROPIC HORMONES (PTTHs) OF TWO BUTTERFLY AND TWO MOTH SPECIES.

K. Endo, Y. Fujimoto and K. Kumagai¹: Biol. Inst., Fac. of Sci., Yamaguchi Univ. and Biol. Inst., Fac. of Lib. Art, Yamaguchi Univ.² Yamaguchi 1.

Each 1,200 brains obtained from pupae of *Polygonia c-aureum*, pharate pupae of *Papilio xuthus*, moths of *Bombyx mori* and pupae of *Mamestra brassicae* were homogenized in ice-cold acetone, washed in 80% ethanol and extracted with 2% NaCl. Following heating (95°C, 5min) and ammonium sulfate precipitation (80% saturation), the extracts were gel-filtrated using a column of Sephadex G-50 to separate the small and big PTTHs, respectively. Activity of the PTTHs were detected by an *in vitro* assay using the prothoracic glands of *P. c-aureum*, *P. xuthus*, *B. mori* and *M. brassicae* larvae.

Small and big PTTHs of the brain extracts of these 4 insects increased the secretion of ecdysteroids *in vitro* when the larval glands of the same species insects were incubated. In addition, the small PTTHs of *P. c-aureum*, *B. mori* and *M. brassicae* showed interspecies PTTH activity on the glands of *P. xuthus* larvae. But, the big PTTHs of these 4 insects were judged as showing no interspecies tropic action on the larval glands with two exceptions that the big PTTH of *M. brassicae* increased the secretion of ecdysteroids by the incubations of the glands from *P. xuthus* and *B. mori* larvae.

EN 16

PRIMARY STRUCTURE OF PROTHORACICOTROPIC HORMONE (PTTH) OF THE SILKMOTH *BOMBYX MORI*, AS DEDUCED FROM ITS cDNA NUCLEOTIDE SEQUENCE.

A. Kawakami¹, T. Oka¹, H. Adachi¹, A. Mizoguchi¹, M. Iwami¹, H. Kataoka², H. Nagasawa², A. Suzuki², and H. Ishizaki¹. 1: Biol. Inst., Fac. of Sci., Nagoya Univ., Nagoya, 2: Dept. of Agr. Biol. Chem., Fac. of Agr., The Univ. of Tokyo, Tokyo.

By screening a cDNA expression library with an antiserum to PTTH, we characterized 2 types of cDNAs that encode pro-PTTH of the silkmoth *Bombyx mori*. Both cDNAs encode the same protein consisting of the signal peptide, a 2kD peptide, a 6kD peptide, and a 109-amino-acid PTTH subunit. These domains are bounded by proteolytic cleavage signals, indicating that they are post-translationally cleaved. Carbohydrate is presumed to attach to the 41st residue. Together with the amino acid sequencing data, we conclude that the polypeptide moiety of *Bombyx* PTTH is a homodimer composed of 109-amino-acid subunits which are held together by disulfide bonds. *In situ* hybridization experiments demonstrated the localization of PTTH gene transcript in 2 pairs of dorso-lateral neurosecretory cells of the *Bombyx* brain.

EN 17

CLONING OF PROTHORACICOTROPIC HORMONE GENES OF THE SILKMOTH, *BOMBYX MORI*

T.Adachi¹, A.Kawakami¹, H.Kondo¹, M.Iwami¹, H.Kataoka², H.Nagasawa², A.Suzuki² and H.Ishizaki¹, ¹Biol. Inst., Fac. of Sci., Nagoya Univ., Nagoya, ²Dept. of Agr. Chem., Fac. of Agr., Univ. of Tokyo, Tokyo.

A genomic library prepared from the silk glands of the male *Bombyx* was screened with a prothoracicotropic hormone (PTTH) cDNA as probe under a reduced stringent condition for 1.6×10^5 plaques. By this screening, we expected to pick up all PTTH clones with more than 99% probability. Restriction maps were made for six clones among twelve positives and these clones were assigned to two chromosomal loci. Southern analyses of genomic DNA suggested that two or three copies of the PTTH gene existed in the *Bombyx* genome. Nucleotide sequence analyses of one clone proved that this clone contained a PTTH gene and four introns were inserted in the preproPTTH coding region. The amino acid sequence (109 amino acids) of a presumed PTTH subunit deduced from the coding region completely matched that deduced from cDNA. Northern analyses showed a single-size mRNA during larval-pupal development.

EN 18

PRODUCTION OF A MONOCLONAL ANTIBODY TO PROTHORACICOTROPIC HORMONE OF *BOMBYX MORI*. T.Oka¹, A.Mizoguchi¹, H.Kataoka², H.Nagasawa², A.Suzuki², H.Ishizaki¹, ¹Biol.Inst., Fac. of Sci., Nagoya Univ., Nagoya, ²Dept. of Agr. Chem., Fac. of Agr., Univ. of Tokyo, Tokyo.

We obtained a monoclonal antibody which recognized native *Bombyx* prothoracicotropic hormone (PTTH) by immunizing BALB/c mice with a synthetic pentadecapeptide corresponding to the N-terminal amino acid sequence of *Bombyx* PTTH. The specificity of this antibody was confirmed by immunoblotting, bioassay for neutralization, ELISA and immunohistochemistry. The results of bioassay and ELISA indicated that this antibody recognized native PTTH. Binding of this antibody did not abolish PTTH activity, suggesting that the PTTH-receptor-binding site differs from the antibody-binding site. Immunoblotting of brain homogenates suggested that the *Bombyx* PTTH was a dimer protein consisting of 17 KD subunits, which were connected by disulfid-bonds to each other. This antibody immunostained two pairs of neurosecretory cells localizing at the dorso-lateral part of brain and the axons reach the corpora allata, indicating that PTTH is produced by these neurosecretory cells and the corpora allata are the neurohemal organ for PTTH.

EN 19

STRUCTURE AND ORGANIZATION IN *BOMBYX* GENOME OF THE *BOMBYXIN* FAMILY GENES. H.Kondo¹, M.Iwami¹, H.Nagasawa², A.Suzuki² and H.Ishizaki¹, ¹Biol.Inst., Fac. of Sci., Nagoya Univ., Nagoya, ²Dept. of Agr. Chem., Fac. of Agr., Univ. of Tokyo, Tokyo

Bombyxin, a brain peptide of the silk moth *Bombyx mori*, has been shown to consist of highly heterogeneous molecular species. Existence of many gene copies underlies this heterogeneity. We have already isolated 38 distinct clones for bombyxin from the genomic libraries of a *Bombyx* racial hybrid (Kinshu x Showa). These bombyxin genes can be classified into four groups, A, B, C and D according to the nucleotide sequence homology between them. A, B and C comprise respective gene families which consist of at least 10, 12 and 6 copies, respectively. Only a single copy exists for D. We constructed restriction maps of the bombyxin gene families. All the bombyxin genes form a cluster(s) in the *Bombyx* genome. They form generally 2-gene pairs with opposite transcriptional orientation. There are 10 A/B pairs and one B/C pair in the *Bombyx* genome. These paired genes may be coordinately expressed.

EN 20

TEMPORAL AND SPACIAL EXPRESSION OF GENE FAMILIES THAT ENCODE *BOMBYXIN*, AN INSULIN-LIKE PEPTIDE OF *BOMBYX MORI*.

A. Kawakami¹, M.Iwami¹, H.Nagasawa², A.Suzuki², H.Ishizaki¹, ¹Biol.Inst., Fac. of Sci., Nagoya Univ., Nagoya, ²Dep. of Agric.Chem., Fac. of Agric., Univ. of Tokyo, Tokyo.

Bombyxin, an insulin-like peptide of the silkworm *Bombyx mori*, has been identified as a peptide hormone which has the prothoracicotropic activity to another moth, *Samia cynthia ricini*. Multiple genes encoding bombyxins comprise three major families, A, B, and C. In this study, we reported the expression of the three major bombyxin gene families. By applying the *in situ* hybridization technique, bombyxin transcripts of all the three gene families were found to localize in 4 pairs of dorso-medial neurosecretory cells in the brain. Northern blot analyses showed that their expression was at a very low level during embryonic development, but increased dramatically in the period from the 2nd- to 3rd-larval instar. We also found that the three bombyxin gene families were expressed differentially during larval-pupal development, and between male and female. Respective families, especially family B, were expressed dominantly in female larvae on the day before pupation, and probably onward.

EN 21

CHANGES IN HEMOLYMPH TITER OF BOMBYXIN DURING POSTEMBRYONIC DEVELOPMENT OF BOMBYX MORI

H. Saegusa¹, A. Mizoguchi¹, H. Nagasawa², A. Suzuki⁴, and H. Ishizaki¹. ¹Biol. Inst., Fac. of Sci., Nagoya Univ., Nagoya, ²Dept. of Agr. Chem., Fac. of Agr., Univ. of Tokyo, Tokyo.

Bombyxin which is produced by Bombyx brain stimulates the prothoracic glands of Samia cynthia ricini to secrete ecdysone, but its physiological role in Bombyx is not known. To investigate its function in Bombyx, it is necessary to assess the developmental stages at which bombyxin is secreted into hemolymph. First, we obtained a monoclonal antibody which recognized native bombyxin, by immunizing mice with pure bombyxin-II. Then, we developed an RIA system for bombyxin to measure the bombyxin titer in Bombyx hemolymph. Bombyxin titer was low and at an almost constant level during the 4th and early 5th instar. When larvae wandered, the titer began to rise steeply and peaked at the middle of the developing-adult stage. In late developing adults the titer fell, and rose again at the adult emergence. During the developing-adult stage, the titer was higher in female than in male. These results suggest that bombyxin plays some roles at all the developmental stages, especially in pupa-adult development when bombyxin may be involved in the sex-related phenomena.

EN 22

ACTIVATION OF THE PROTHORACIC GLAND OF BOMBYX MORI BY BOMBYXIN IN VITRO

S. Kiriishi¹, S. Sakurai¹, H. Nagasawa², A. Suzuki², H. Ishizaki³.

¹Fac. of Sci., Kanazawa Univ., Kanazawa,

²Fac. of Agr., Tokyo Univ., Tokyo,

³Fac. of Sci., Nagoya Univ., Nagoya.

The brain of Bombyx mori contains 22k-PTTH and bombyxin. Bombyxin is highly active in stimulating the adult development of brainless pupae of Samia cynthia ricini while exhibits no such activity in Bombyx brainless pupae. In spite of the fact that bombyxin possesses no PTTH-like activity in Bombyx, we found that Bombyx prothoracic gland (PG) was activated in the presence of bombyxin at a very high concentration in culture medium in vitro. Effects of bombyxin on Bombyx PG was further studied by comparing the ratio of ecdysone and 3-dehydroecdysone produced by PG in vitro in the presence or absence of either bombyxin or 22k-PTTH. HPLC analysis with a differential radioimmunoassay using S-3 and H-22 antiserum indicated that the ratio was not affected by bombyxin whereas 22k-PTTH increased the amount of dehydroecdysone. These results suggest that bombyxin increases a general physiological activity of the PG cells.

EN 23

WEIGHT CHANGE OF DIAPAUSING OR DEVELOPING PUPA IN SAMIA CYNTHIA PRYERII

A. Koenuma. Dept. of Biology, Fac. of Sci., Univ. of Shinshu, Matsumoto.

Weight of pupa of S. c. pryeri decreases a definite rate during the diapausing period, 0.05-0.08%/day, or the chilling period, 0.1-0.5%/day. The rate of weight decrease of the pupa during adult development is larger than those of both diapausing period and chilling period. The relative weight decrease of the pupa changes with a definite tendency corresponding to the development of the pupa. The tendency of the weight decrease of the ecdysone-injected pupa was almost equal with that of the naturally developing pupa. The relative weight decrease of the pupa changed in a same tendency with the respiration rate during adult development. This fact seems to suggest that the increase of the respiration rate of the pupa is responsible to the increase of the relative weight decrease of the pupa during the adult development. The pupa showing abnormally large weight decrease during diapause resulted in death. Since the normally diapaused pupa showed no such a large weight decrease, a possibility of existence of some kinds of protection mechanism from a desiccation is suggested.

EN 24

A RE-INVESTIGATION OF THE O₂ PERMEABILITY OF THE CHORION IN RELATION TO THE ONSET OF THE EMBRYONIC DIAPAUSE IN THE SILKWORM, Bombyx mori.

H. Sonobe and M. Nakamura, Dept. of Biol., Konan Univ., Kobe

In silkworm eggs, it has been proposed that the decrease in O₂ uptake which accompanies the initiation of diapause may result from a decrease in the air-permeability of the chorion of the eggs (O₂ barrier hypothesis). Thus we measured the amount of O₂ that permeated across the chorion of the pnd mutant by use of an apparatus designed for this purpose. The pnd mutant has a defect that prevents their offspring from entering diapause. However, the embryonic defect is repairable if pnd mutant eggs are fertilized by sperm bearing pnd⁺ gene: the heterozygote can enter diapause. Therefore, if the "O₂ barrier hypothesis" is correct, the O₂ permeability of the chorion of the heterozygote should differ sharply from that of the homozygote at the period when the diapause is triggered by the pnd⁺ gene.

The O₂ permeability of the chorion did not decline appreciably even at the period when O₂ uptake decreased abruptly in the heterozygote. Furthermore, no significant difference in the O₂ permeability of the chorion was detected between the two types of embryos. Therefore, our present results cast doubt on the "O₂ barrier hypothesis". These results are not contradictory to our previous result in the wild type silkworm.

EN 25

ECLSION HORMONE AND MUSCLE CELL DEATH AFTER ECLSION IN *DROSOPHILA MELANOGASTER* K-I. Kimura¹ and J.W. Truman². ¹Lab. of Biol. Hokkaido Univ. of Education, Iwamizawa Campus, Iwamizawa. ²Dept. of Zool. Univ. of Washington, Seattle, USA.

Programmed cell death occurs in the muscular system of newly eclosed adult, *Drosophila melanogaster*. Many of abdominal muscles which were used for eclosion and wing spreading behavior degenerate by 12 hour after eclosion. Ligation experiments showed that the muscle breakdown is triggered by a signal from the anterior region, presumably the head. The signal appears about one hour before eclosion. This timing suggests that eclosion hormone (EH) may be involved. A number of evidence indicate that *Drosophila* has EH. Immunocytochemistry using an antibody against *Manduca* EH stains a pair of cells in the brain of *Drosophila*. Also, injection of extracts of pharate adult heads or of the CNS from wandering larvae of *Drosophila* scores positive for EH activity in a *Manduca* larval ecdisis assay. EH is the first candidate for the signal to induce the muscle breakdown after eclosion in *Drosophila*.

EN 26

CHANGES IN TESTICULAR LH RECEPTORS IN PHOTOSTIMULATED WHITE-CROWNED SPARROWS. K. Kubokawa and J.C. Wingfield. Biol. Dept., Waseda Univ., Tokyo and Zool. Dept., Univ. Washington, Seattle.

We compared binding of chicken LH to testicular receptors of photosensitive (30 and 60 short days, 8L16D), photostimulated (15, and 30 long days, 20L4D) and photorefractory (60 long days, 20L4D) white-crowned sparrows, *Zonotrichia leucophrys gambelii*, in parallel with the sensitivity of the testis to LH by measuring the testosterone release and cAMP content in vitro. The plasma LH level was minimum in the short day birds. It was increased in the photostimulated birds, and then it was decreased in the photorefractory birds to a level close to the short day level. Sensitivities of the testis represented by the cAMP accumulation and testosterone release showed similar changes with the plasma LH. The amount of LH binding was increased in the photostimulated 15 long days birds significantly. However, it was decreased to 2/3 in the 30 long days birds. The LH binding in the photorefractory birds was as low as that in the photosensitive birds. We conclude that the decrease in LH receptors in the photostimulated birds occurs when the testis is still growing. The photorefractoriness may appear early in the LH receptor preceding to the other mechanisms presumably by the down regulation.

EN 27

SEX DIFFERENCE IN PATTERN OF ESTROGEN ACCUMULATION IN BRAIN REGIONS INVOLVED WITH AGGRESSIVE BEHAVIOR OF ZEBRA FINCHES K. Tsutsui, J. C. Wingfield¹, and S. W. Bottjer². Zool. Inst., Fac. of Sci., Hiroshima Univ., Hiroshima, Japan, ¹Dept. of Zool., Univ. of Washington, Seattle, and ²Dept. of Biol., Univ. of Southern California, Los Angeles, USA.

Sexually mature male birds frequently display aggressive actions which are mainly induced by estradiol in the brain. Unlike males, sexually mature female birds show lower levels of aggressive behavior. Some data suggest that elevated levels of estradiol suppress female aggressive action, such as pecking. In order to investigate sex differences in neuroendocrine mechanisms modulating aggressive behaviors, we compared the distribution of estrogen target cells in male and female brain regions involved with aggressive behavior using steroid autoradiographic methods in hypophysectomized zebra finches. Estrogen-accumulating cells were found in the septum, several preoptic and hypothalamic areas, the ventral portion of paleostriatum augmentatum, and the nucleus taeniae (Tn) in the archistriatum. More hormone-accumulating cells were present in females than in males in the Tn which projects to the hypothalamus. In some other regions, no sex difference was detected. It is therefore possible that Tn neurons are activated by estradiol to suppress female aggressive behavior in birds. In contrast, the preoptic area and the hypothalamus may be involved with the control of aggressive behavior in both sexes.

EN 28

CRUSTACEAN HYPERGLYCEMIC HORMONE RECEPTOR AND GUANYLATE CYCLASE IN CRAYFISH HEPATOPANCREAS T. Ezure, M. Ishida, M. Shibata and T. Ohoka. Dept. of Biol., Fac. of Sci., Tokyo Metropolitan Univ., Tokyo.

A hormone-sensitive guanylate cyclase activity was detected in a plasma membrane fraction of crayfish (*Procambarus*) hepatopancreas, as well as in those of heart or intestine. To elucidate the activation mechanism of guanylate cyclase by hormone, enzyme activity and binding of crustacean hyperglycemic hormone (CHH) to the membrane was investigated separately.

CHH was extracted from sinus gland and purified by HPLC on μ Bondasphere phenyl column, iodination was carried out by lactoperoxidase method. Binding assay was effectively detected in presence of 0.1 mM PMSF and 1 μ g BSA. The specific binding activity of ¹²⁵I-CHH and hormone-sensitive guanylate cyclase activity was found in 1,500 x g pellet fraction and could not be detected in 100,000 x g supernatant. Half-maximum saturation of the hormone concentration was estimated to be about 2.0 x 10⁻⁸M.

After tentative solubilization of the membrane, stimulation degree of guanylate cyclase by CHH was considerably increased, but binding activity was hardly detected in the supernatant. Application of Triton X-100 or Lubrol PX resulted also considerable loss of guanylate cyclase stimulation.

EN 29

CHARACTERIZATION AND IMMUNOHISTOCHEMICAL LOCALIZATION OF HAGFISH THYROID IODOPROTEIN. S. Suzuki, K. Fujikura, *Y. Ohmiya and *Y. Kondo. Dept. of Comp. Endocrinol. and *Dept. of Phys. Biochem., Inst. of Endocrinol., Gunma Univ., Maebashi

The thyroid iodoprotein of a hagfish, *Eptatretus burgeri* was characterized. The iodoprotein was not very homogeneous in its apparent molecular mass which decreased with the increase in thyroid hormone/iodotyrosine ratio. Four subfractions with an apparent molecular mass of about 400K Da were purified from one major fraction by size-exclusion and Mono Q ion-exchange HPLC. The subfractions appeared to have the same peptide backbone, since they showed a single band with the same mobility as a 160 K Da protein in SDS/PAGE and the same amino acid composition. Antiserum for iodoprotein was prepared by immunizing rabbits. By western blotting it was shown that the antiserum cross-reacts with the purified iodoprotein and some fractions of thyroid homogenates. The identity and location of the iodoprotein in the thyroid follicle was examined using the peroxidase-antiperoxidase immunocytochemical technique and fluorescein isothiocyanate method. Most of the immunostaining iodoprotein was found within thyroid epithelial cells. The iodoprotein appeared to be localized in cytoplasmic inclusions of various sizes. However, staining was scarcely observed in the follicular lumina.

EN 30

Immunocytochemical studies of proteolytic processing site of proopiomelanocortin (POMC) in rat POMC cells. S. Tanaka, K. Ishikawa¹, M. Nomizu² and K. Kurosuni. Depts. of Morphol. and ¹Physiol., Inst. of Endocrinol., Gunma Univ., and ²KIRIN Brewery Co. Ltd., Maebashi.

ACTH-related peptides in POMC neurons of arcuate nucleus are known to be produced from POMC by intracellular proteolytic cleavage, as well as in corticotrophs and melanotrophs in the pituitary. We constructed a synthetic peptide (ST-1) corresponding to the cleavage site between ACTH and beta-LPH moieties of murine POMC. By using this ST-1 as antigen, specific antibody to POMC was made. When ultrathin frozen sections of rat melanotrophs were immunogold-labeled with anti-ST-1, gold particles were found on immature secretory granules (SG) near the Golgi apparatus, but not on mature SG. Alpha-MSH immunolabeling was observed only on mature SG. Using anti-porcine ACTH which recognizes POMC and ACTH 1-39 but not alpha-MSH, immunolabeling was found both on immature and mature SG. In corticotrophs, many gold particles indicating the presence of POMC (ST-1) were observed on mature and maturing SG, similarly to the result with anti-ACTH.

Immunohistochemical study on POMC neurons of arcuate nucleus demonstrated that POMC (ST-1) located only in perikarya, but not in fibers. With anti-ACTH, alpha-MSH and beta-endorphin, intense immunoreactivity was seen in fibers of POMC neurons.

EN 31

MORPHOLOGY AND FUNCTION OF THE FLASK CELLS IN THE EPIDERMIS OF THE FROG SKINS K. Fujikura, S. Tanaka and S.C. Fujita* Inst. of Endocrinol., Gunma Univ., Maebashi and *Mitsubishi Kasei Inst. of Life Sci., Machida

Adult *Xenopus* could be adapted to 50% seawater, whose osmolality was higher than that of the body fluid, by gradually increasing the salinity and reaching to the final concentration after four weeks. This study was done to elucidate how changes in frog skins are induced by saline treatment. When animals were maintained at 50% seawater for three weeks, we found active molting and marked morphological changes in the flask cells. They increased significantly in number and size. Ultrastructural observations demonstrated that the flask cells contain numerous mitochondria and dense deposits of glycogen, as has been observed the chloride cells of gill epithelium in the teleost. Therefore, its physiological role may be concerned with osmoregulation in combination with the various organs. Adult bullfrog showed also the similar phenomena. Moreover, the monoclonal antibody 188Cl, which was obtained by using bullfrog skins as immunogen, immunostained the perimeter of the flask cells in bullfrog, in addition to some populations of the neurons in dorsal root ganglion and the sciatic nerve and the retina, and the gastrointestinal tract of the chicken. This antibody might be useful probe in clarifying the physiological role and cellular lineage of the flask cells.

EN 32

ULTRASTRUCTURE OF THE GANGLION CELLS OF THE TERMINAL NERVE IN A TROPICAL FISH, DWARF GOURAMI. Y. Oka¹ and M. Ichikawa². ¹Zool. Inst., Fac. of Sci., Univ. of Tokyo, Tokyo and ²Dept. of Anat. & Embryol., Tokyo Metro. Inst. for Neurosci., Tokyo.

It has been recently suggested that the terminal nerve (TN) system may be involved in the control of sexual behavior in teleosts and mammals. We have already shown that, in the brain of the dwarf gourami, the ganglion cells of the TN (TN-ggl cells) are the main sources of the GnRH-ir system. In the present paper we examined by electron microscopy cytology and synaptic inputs of the TN-ggl cells, to give a morphological basis for studying functions of the TN system. The TN-ggl cell bodies had morphological characteristics similar to those of peptide-secreting endocrine cells. Frequent occurrence of coated vesicles in the periphery of the cell bodies were suggestive of membrane retrieval of secretory granules after exocytosis. The adjacent TN-ggl cells were either in direct juxtapositions or made specialized "glomeruloid" cell-to-cell contacts, which may be relevant for the intercellular communications among TN-ggl cells. In the glomeruloid, the somatic processes of the TN-ggl cells received inputs from synaptic terminals having spherical synaptic vesicles and some dense-cored vesicles.

EN 33

CALCITONIN-IMMUNOREACTIVE CELLS PRESENT IN THE NERVOUS SYSTEMS OF SOME INVERTEBRATES
Y. Sasayama¹, A. Katoh¹, C. Oguro¹ and A. Kambe². ¹Dept. of Biol., Fac. of Sci., Toyama Univ., Toyama, ²Dept. of Obst. Gynecol., Fac. of Med., Teikyo Univ., Tokyo.

Calcitonin (CT) is a hypocalcemic hormone secreted from the ultimobranchial gland or C-cells of thyroid in vertebrates. Recently, however, it was reported that in a sea-squirt, calcitonin immunoreactive cells (iCT cells) are present in the neural ganglion. In the present study, nervous systems of some invertebrates were studied by PAP method with anti-salmon calcitonin antiserum to know whether CT is commonly found in invertebrates. As a result, it became clear that in the ribbon worm, *Lineus fuscoviridis* (Nemertinea), the land slug, *Limax flavus* (Mollusca), the polychaete, *Perinereis vancaurica* (Annelida), the earthworm, *Pheretima communissima* and the leech, *Erpobdella lineata* (Annelida), the woodlouse, *Armadillidium vulgare* (Arthropoda), and the beard worm, *Oligobranchia mashihoi* (Pogonophora), iCT cells are present mainly in their brains. There was no fixed pattern in their location. In the ribbon worm and the annelids, however, somewhat regular arrangements were recognized. The number of iCT cells varied in each species, although annelids was the largest in the number. The present results suggest that calcitonin exists commonly among invertebrates.

EN 34

CALCITONIN-IMMUNOREACTIVE CELLS PRESENT IN THE BRAIN OF THE BROOK LAMPREY, LAMPETRA REISSNERI
Y. Sasayama¹, T. Koizumi¹, C. Oguro¹ and A. Kambe². ¹Dept. of Biol., Fac. of Sci., Toyama Univ., Toyama, ²Dept. of Obst. Gynecol., Fac. of Med., Teikyo Univ., Tokyo.

Cyclostomes lack the ultimobranchial gland which is the origin of calcitonin in lower vertebrates. In the brain of the brook lamprey, however, calcitonin-immunoreactive cells (iCT cells) were found by PAP method with anti-salmon calcitonin antiserum. It was known that those are located independently in 2 distinct areas: nucleus hypothalami (NH) and torus semicircularis (TS). Furthermore, it was noted that there are some differences between those 2 groups. The iCT cells in NH are small in size and extend processes to the 3rd ventricle. However, those in TS are large and out of contact with the ventricle. Therefore, it was supposed that these 2 groups of the iCT cells have different functions. Furthermore, serum mineral concentrations were measured in these lampreys. The results showed that the serum Ca and Pi levels are increased with the growth of the fish. Furthermore, it was known that the number of iCT cells in the brain tends to increase with the rise in serum Ca levels as well as with the growth of the lamprey. Therefore, these iCT cells may involve in Ca metabolism and growth of the lampreys.

EN 35

RELEASE OF CALCITONIN FROM ULTIMOBRANCHIAL GLANDS OF THE BULLFROG, *RANA CATESBEIANA*, IN VITRO
C. Oguro, J. Okuyama, T. Ishijima and Y. Sasayama. Dept. of Biol., Fac. of Sci., Toyama Univ., Toyama.

In anuran amphibians, calcitonin (CT) is secreted from the ultimobranchial gland (UB). However, the promoting or suppressing factors of CT secretion have not been known. In the present study, the release of CT from UB of the bullfrog was examined *in vitro*. The UB were incubated in frog salines with 7 different compositions: A) normal saline (Ca 1.1 mM), B) 2 x Ca saline, C) 3 x Ca saline, D) 6 x Ca saline, E) Mg saline (containing 1 mM Mg), F) Pi saline (containing 1.5 mM Pi) and G) 2 x Ca saline + SS (containing 100 ng/ml somatostatin). After the incubation for 72 hr, each medium was administered to rats to know CT amounts released into the medium (rat bioassay). As a result, it was known that medium B is most potent to evoke the depletion of serum Ca levels in rats. However, Ca contents more than medium B did not enhance the release of CT from UB. As well, Mg and Pi did not promote the release. On the other hand, it was noted that medium G suppresses CT release completely. The present results suggest that in UB of the bullfrog *in vitro*, moderate Ca content in medium promotes the release of CT and that somatostatin may be one of the suppressing factors under the present condition.

EN 36

THE ONTOGENY OF IMMUNOREACTIVE ATRIAL Natriuretic Peptide (ir-ANP) IN THE CARDIOCYTES OF *XENOPUS LAEVIS* AND *TRIONYX SINENSIS JAPONICUS*
T. Hirohama, Y. Kasuya, H. Uemura and T. Aoto. Biol. Lab., Kanagawa Dental Coll., Yokosuka.

The ontogeny of ir-ANP in the cardiocytes of developing and adult specimens of *Xenopus laevis* and *Trionyx sinensis japonicus* (Chelonia) was studied using antiserum against α -human ANP. In *Xenopus*, ir-ANP granules were first noted in both the atrial and ventricular cardiocytes at limb-bud stage and increased as development proceeded. The largest number of these granules in atrial and ventricular cardiocytes was observed when the skin of forelimbs began to cornify and, thereafter, the granules tended to decrease prior to metamorphosis. In adult, ir-ANP granules were present moderately in the atrium but scarcely in the ventricle. In *Trionyx*, ir-ANP granules were first noted in cardiocytes of 7-day embryos and the number increased very slowly during the rest of embryonic stage in atrial and ventricular cardiocytes. In the hatching, ir-ANP granules decreased in both atria and ventricles, but abundant Golgi bodies were observed in the former. In adult turtles, the granules aggregated near Golgi bodies in atrial cardiocytes but were scarcely noted in the ventricle. In both species, immunohistochemical reactivity was found to be essentially correlated to the granule population in each stage of ontogeny.

EN 37

DISTRIBUTION OF IMMUNOREACTIVE NEUROPEPTIDES IN THE CENTRAL NERVOUS SYSTEM OF THE AMPHIOXUS, BRANCHIOSTOMA BELCHERIH. Uemura¹, Y. Kasuya¹, and C. Yamada²¹Biol. Lab., Kanagawa Dent. Coll., Yokosuka, ²1st Dept. of Physiol., National Defense Medical Coll. Tokorozawa

Immunohistochemical localizations of several neuropeptides were studied by PAP and ABC methods in the central nervous system of the amphioxus, Branchiostoma belcheri. The perikarya, immunoreactive to antisera against carp urotensin I (UI) or FMRFamide, were found in the anterior portion of the dorsal nerve cord. These immunoreactive perikarya were situated near the ventricle, contacting the cerebrospinal fluid with the apical end. Some axons immunoreactive to UI or FMRFamide antisera ran antero-ventrally to the floor of the cord, while others were found to run longitudinally throughout the entire length of the cord. Axons showing angiotensin II-, β -endorphin-, arginine vasopressin- and oxytocin-like immunoreactivity were also revealed in the cord. No immunoreactivity could be detected to antisera against endothelin I, atrial natriuretic peptide, brain natriuretic peptide, corticotropin-releasing hormone and leucine-enkephalin. No immunoreactivity to any of the antisera used was observed in Hatschek's groove in this study.

EN 38

ULTRASTRUCTURAL AND IMMUNOHISTO- AND IMMUNOCYTOCHEMICAL STUDY OF CULTURED BOVINE ENDOTHELIAL CELLS.

S. Nakamura¹, K. Naruse², M. Naruse² and H. Uemura¹. ¹Biol. Lab., Kanagawa Dental Coll., Yokosuka, ²2nd Dept. of Med., Tokyo Women's Med. Coll., Tokyo.

Cultured endothelial cells (EC) of the bovine pulmonary artery were investigated ultrastructurally and immunohisto- and immunocytochemically using an antiserum against endothelin-1 (ET). Numerous Golgi vesicles and lysosome-related organelles (LRO: primary lysosome, heterophagosome, heterophagolysosome, autophagosome and autophagolysosome) were electronmicroscopically observed, but no secretory granules were found. Immunohistochemical results showed that the cytoplasm of the EC was evenly stained with the antiserum. Immunocytochemical results paralleled these findings: there was an almost even overlay of immunogold particles in the LRO, Golgi vesicles and cytoplasmic matrix. These results suggest that ET may be secreted through the constitutive pathway rather than the granule-mediated pathway and that ET could be taken up into the lysosome.

EN 39

EXOCYTOTIC RELEASE OF NEUROTRANSMITTERS FROM NERVE ENDINGS INNERVATING THE TASTE BUDS AND PANCREATIC ISLETS.

Y. Endo, Dept. of Applied Biology, Kyoto Institute of Technology, Kyoto

It is believed that the taste buds are innervated by sensory, afferent neurons, but some of the nerve fibers have large-cored and small-clear vesicles, which are apparently thought to contain chemical messengers. Using a special fixative containing tannic acid and combining with stimulation of nerves by higher K^+ and Ca^{2+} , I demonstrated the exocytotic release of transmitters from the nerve fibers in the taste buds of rat circumvallate papillae. The exocytosis was found in the non-synaptic sites. These facts indicate that some of the nerve fibers might be efferent and/or reciprocal in nature.

Using the same methods, I also examined on the nerve endings in the pancreatic islets of mice, rats and teleosts. Generally, nerve endings of the autonomic nervous system have no clear synaptic contact with the target tissues. In the pancreatic islets, the exocytotic release of neurotransmitters was found not only at the sites facing the endocrine cells, but also in the sites facing the connective tissues including the pericapillary space.

EN 40

PRIMARY STRUCTURE OF EEL ATRIAL NATRIURETIC PEPTIDE AND ITS RELATIVE POTENCY.

Y. Takei¹, A. Takahashi² and T. Watanabe³. ¹Dept. Physiol. and ²Mol. Biol., Kitasato Univ. Sch. Med., Sagami-hara, and ³Peptide Inst. Inc., Minoh.

From 1690 eel atria (32 g), 5 μ g of pure peptide exhibiting relaxant activity in the chick rectum was isolated, and its primary structure was determined. This peptide, termed eel atrial natriuretic peptide (ANP)-(1-27), has an intramolecular ring structure formed by a disulfide bond, and identical sequences observed in all ANPs so far identified are also conserved except for the replacement of the 11th Arginine with Lysine. Two minor peptides with truncated COOH-termini, corresponding to eel ANP-(3-27) and (5-27), were also identified. The sequence homology of eel ANP is 59% to human and rat ANP, 52% to fowl ANP, and 46% to bullfrog ANP. Thus, the sequence homology of ANP among vertebrates is conversely proportional to the phylogenetic proximity. The biological activity of eel ANP as compared with that of human ANP was 110 times greater for the vasodepressor action in the eel, almost equal for the vasodepressor action in the quail, and 20 times smaller for the vasodepressor and natriuretic action in the rat. Thus, the ANP molecule and its receptor have evolved in parallel during the vertebrate phylogenesis.

EN 41

PRIMARY STRUCTURE OF BULLFROG THYROTROPIN
 M. Sakai¹, S. Kikuyama¹, S. Tanaka²,
 Y. Hanaoka², and H. Hayashi²
¹Dept. of Biol., Sch. of Educ., Waseda
 Univ., Tokyo, ²Inst. of Endocrinol., Gunma
 Univ., Maebashi

Thyroid-stimulating hormone (TSH) was isolated from the pituitary glands of bullfrogs, *Rana catesbeiana*. Both monoclonal antibody against bullfrog FSH α and polyclonal antibody against human TSH β recognized the bullfrog TSH. This TSH was separated into two subunits, α and β , by reverse-phase HPLC after dissociation in 0.1% trifluoroacetic acid/4 M Gu.HCl, followed by reduction and carboxymethylation. The amino acid composition of this α -subunit is almost identical with those of bullfrog LH α and FSH α . Amino acid sequence of N-terminus (25%) and C-terminal half (40%) of TSH α have been determined. In these regions, TSH α was completely identical with bullfrog LH α and FSH α . Thus, we confirmed that this preparation is bullfrog TSH. The N-terminal 45 residues and some peptides obtained from lysyl endopeptidase digest of TSH β were determined. Strikingly, the amino acid sequence of bullfrog TSH β has no homology with those of mammalian TSH β , hitherto known, while β -subunit of bullfrog LH and FSH have resemblance to those of mammalian LH and FSH, respectively.

EN 42

AMINO ACID SEQUENCES OF BULLFROG LH AND FSH.

H. Hayashi¹, T. Hayashi¹ and Y. Hanaoka².
 Dept. of ¹Protein Chemistry and ²Compar.
 Endocrinol., Inst. of Endocrinol., Gunma
 Univ., Maebashi.

Complete amino acid sequences of bullfrog (*Rana catesbeiana*) gonadotropins, LH and FSH, were determined. Both hormones were separated into their subunits by reverse phase HPLC after dissociation in 0.1% trifluoroacetic acid/4 M Gu.HCl. The amino acid sequence was determined by ordinary methods using reduced and carboxymethylated or pyridyl ethylated protein. Asparagine at sugar binding site was confirmed by sequence determination of sugar containing peptides, obtained by lysyl endopeptidase or Arg C digestion, and then deglycosylated with N-oligosaccharide glycopeptidase from almond. The α -subunit of both hormone is composed of 97 amino acid residues, and glycosylated at Asn-57 and 83. Sequence homology of α -subunit between bullfrog and mammalian is about 60%. The β -subunit of LH and FSH is composed of 112 and 107 amino acid residues, respectively. LH- and FSH- β are also glycosylated at Asn-8, and Asn-5 and 22, respectively, as in other's. Sequence homology of β -subunit between bullfrog and mammalian is about 40% for LH and 60% for FSH. However, the profiles of hydrophathy of corresponding subunit are almost the same between species.

EN 43

ISOLATION AND CHARACTERIZATION OF ALDOSTERONE-RELEASING SUBSTANCES IN THE BULLFROG NEUROINTERMEDIATE LOBES.

S. Iwamuro, H. Hayashi*, M. Yamashita,
 N. Mamiya, D. Uchida, and S. Kikuyama.
 Dept. of Biol., Sch. of Educ., Waseda
 Univ., Tokyo. *Inst. of Endocrinol.,
 Gunma Univ., Maebashi.

Two active substances which stimulate aldosterone release from *Xenopus laevis* interrenals both *in vivo* and *in vitro* were isolated from the acid acetone extract of the neurointermediate lobes using C₁₈ SEP-PAK cartridges, Sephadex G-50, and reverse-phase HPLC columns. At the final step of purification, two active principles I and II, both having molecular weight of 1,000, were obtained. The amino acid sequence of I and II are as follows:

I: H-Cys-Tyr-Ile-Gln-Asn-Cys-Pro-Arg
 -Gly-NH₂

II: H-Cys-Tyr-Ile-Gln-Asn-Cys-Pro-Arg
 -Gly-Gly-OH

The sequence of substance I is same as that of AVT. II has an extra glycine residue at the C-terminus of I.

EN 44

DEVELOPMENT OF RADIOIMMUNOASSAY FOR EEL PROLACTIN.

R. Suzuki, S. Hasegawa and T. Hirano.
 Ocean Res. Inst., Univ. of Tokyo, Tokyo.

A highly specific and homologous radioimmunoassay (RIA) for the measurement of prolactin (PRL) in the plasma and the pituitary of the eel was developed using a rabbit antiserum to eel PRL. PRL was purified from the pituitary by gel filtration and HPLC, and exhibited Na⁺ as well as Ca²⁺-retaining activity in hypophysectomized *Fundulus heteroclitus*. Pituitary extract and plasma from the eel exhibited displacement curves parallel to the eel PRL standard. Plasma from chum salmon, rainbow trout, tilapia, goldfish, carp as well as hypophysectomized eel showed negligible cross-reactivity. PRL preparations from chum salmon, tilapia, carp and sheep or growth hormone from eel, chum salmon and sheep did not cross-react with the antibody. The RIA sensitivity was 0.1 ng eel PRL/ml. Intra- and interassay coefficients of variation were 2.4 and 11.8 %, respectively.

The PRL level increased after transfer from seawater (SW) to fresh water (FW). Plasma PRL level decreased after transfer from FW to SW or to Ca²⁺-deficient SW, although the transfer to FW containing 10 mM CaCl₂ did not affect the PRL level.

EN 45

CLONING OF BULLFROG PRL cDNA AND ITS APPLICATION FOR THE MEASUREMENT OF PRL mRNA IN THE PITUITARY OF BULLFROG LARVAE
N. Takahashi¹, K. Yoshihama¹, K. Yamamoto¹, S. Kikuyama¹, K. Wakabayashi², and Y. Kato². ¹Dept. of Biol., Sch. of Educ., Waseda Univ., Tokyo and ²Inst. of Endocrinol., Gunma Univ., Gunma.

Total RNA from bullfrog anterior pituitaries was prepared and cDNA library was constructed in the expression phage vector lambda ZAP. A cDNA clone that reacted with a specific antiserum to bullfrog PRL was obtained and its nucleotide sequence was determined. This clone contained 597bp cDNA insert and coded the full length of the bullfrog PRL molecule. The deduced amino acid sequence was in good accord with the one determined by analyzing the bullfrog PRL fragments obtained by cleavage with enzymes and chemicals (Yasuda et al., 1989). Using the PRL cDNA as a probe, the levels of PRL mRNA in the pituitary of the metamorphosing tadpoles were measured employing dot blot hybridization technique. In the stage 18-21 tadpoles, the pituitary concentration of PRL mRNA were relatively low. At advanced climax stages, the PRL mRNA levels were significantly elevated. At stage 23, 24 and 25 the concentrations were about 2, 3 and 2 times higher than those at preceding stages, respectively.

EN 46

IMMUNOHISTOCHEMICAL STUDY ON PROLACTIN CELLS IN LARVAE OF XENOPUS LAEVIS DURING METAMORPHOSIS.

F. Mizutani¹, Y. G. Watanabe¹, S. Tanaka². ¹Biol. Inst., Fac. of Sci., Niigata Univ., Niigata, ²Dept. of Morph., Inst. of Endocrinol., Gunma Univ., Maebashi

Prolactin(Prl) cells of metamorphosing Xenopus were immunohistochemically studied by the use of anti-bullfrog Prl.

At the light microscopic level sections were stained by the PAP method. Total immunoreactive area gradually increased reaching a peak at St. 62 followed by a slight decrease toward the end of metamorphosis. Relative immunoreactive area, on the other hand, showed a sharp increase from St. 58.

At the electron microscopic level protein A-colloidal gold method was employed. At St. 51, both round and elongated granules were observed in the cytoplasm. At St. 58 Prl cells became generally larger in size and their rich cytoplasm contained many round secretory granules. The size of granules at this stage was larger than that at St. 51. At the end of metamorphosis, or St. 66, most Prl cells had a markedly reduced number of secretory granules.

These data are discussed in relation to the previous data indicating a heightened release of Prl toward the end of metamorphosis.

EN 47

DIFFERENTIATION OF PROLACTIN CELLS IN THE PETAL RAT PITUITARY.
Y. G. Watanabe. Biol. Inst., Fac. of Sci., Niigata Univ., Niigata.

Unlike the adult pituitary, the effect of estrogens on the fetal gland has not been adequately studied. In this study, 1) the pituitary rudiments of fetal rats were treated with estradiol in vitro, and 2) an estrogen analogue that is known to have little binding activity to estrogen-binding-protein was directly injected to fetuses in utero. In both experiments, the number of prolactin(Prl) cells were immunohistochemically investigated.

In vitro, the effect of estradiol on the differentiation of Prl cells increased only when the pituitary rudiments (day 12 of gestation) were cultured in α -MEM that was supplemented with 1% serum. In DMEM/F12 without serum and phenol red, only a few Prl cells were seen in both control and estradiol-treated cultures.

Administration of a synthetic estrogen (RU2858) in utero on day 20 resulted in a marked increase in the number of Prl cells when examined 30 hours later.

Thus, in vivo, estrogens caused the differentiation and/or proliferation of Prl cells in the fetal pituitary near term. Further studies, both in vivo and in vitro, are needed as to whether estrogens are actually involved in early development of Prl cells.

EN 48

EFFECTS OF PRL AND/OR FSH ON GONADOTROPIN RECEPTORS IN ADULT HYPOPHYSECTOMIZED MICE.
M. Takase¹, K. Tsutsui¹ and S. Kawashima².

¹Zool. Inst., Fac. of Sci., Hiroshima Univ., Hiroshima and ²Zool. Inst., Fac. of Sci., Univ. of Tokyo, Tokyo.

Male mice of the C57BL/6NCrJ strain at 90 days of age were given injections of 0.1 mg bromocryptine (brc). Brc injections twice daily for 10 days significantly decreased plasma PRL level, accompanying significant reduction in the testicular LH binding. There was no significant difference in dissociation constant between vehicle-injected and brc-injected groups. Moreover, simultaneous treatment of ovine (o) PRL (100 μ g/day) with brc twice daily for 10 days to other mice having received brc for the preceding 10 days restored the testicular LH receptors to 78.3% of that in control mice, and induced a significant increase in plasma FSH level. Either oPRL or oFSH (2 μ g/day) administration to hypophysectomized (hypox) mice for 10 days from 11th day after the operation augmented the LH binding to the testis, and only oFSH treatment led to increase in Leydig cell numbers. These results suggest that PRL increases LH receptor numbers by the direct effect of PRL and the indirect effect through FSH, and that the mechanism of LH receptor augmentation was different between the two hormones. On the other hand, treatment of rat (r) PRL (20 μ g/day, twice daily for 5 days) to hypox mice beginning at 5-day postoperation had no significant effect in elevating the FSH binding per 4 mg testis. However, simultaneous 5-day injections of rPRL with oFSH (2 μ g/day) nullified the negative down-regulatory effect of oFSH on FSH binding per 4 mg testis. Changes in FSH binding per testis also showed a tendency similar to those in the binding per 4 mg testis. These findings indicate that PRL may have an inhibitory effect on down-regulation of FSH receptors by FSH.

EN 49

INVOLVEMENT OF PROLACTIN IN THE REGULATION OF BLOOD CALCIUM LEVELS IN THE PARATHYROIDECTOMIZED NEWT

K. Matsuda¹, S. Kikuyama¹, Y. Sasayama², and C. Oguro², ¹Dept. of Biol., Sch. of Educ., Waseda Univ., Tokyo, ²Dept. of Biol., Fac. of Sci., Toyama Univ., Toyama.

In the newt, *Cynops pyrrhogaster*, parathyroidectomy brings about a marked decrease in plasma calcium concentrations. The hypocalcemia recovers to a certain extent by 14 days after operation. Experiments were conducted to obtain a direct evidence that endogenous prolactin is involved in this recovery process. The recovery of calcium levels after parathyroidectomy was blocked by the administration of an antiserum against newt PRL. The specimens deprived of both parathyroid and pituitary glands remained in a permanent hypocalcemic state. Administration of newt PRL to the parathyroidectomized and hypophysectomized newts significantly elevated blood calcium levels. After parathyroidectomy, radioimmunoassayable PRL in the blood rose up to 10 times of the value in the sham-operated animal. The results indicate the involvement of PRL in calcium homeostasis in the newt confronted with a shortage of parathormone.

EN 50

IDENTIFICATION AND CHARACTERIZATION OF AN ALDOSTERONE RECEPTOR IN THE TAIL EPIDERMIS OF BULLFROG LARVAE

K. Yamamoto and S. Kikuyama,
Dept. of Biol., Sch. of Educ., Waseda Univ., Nishiwaseda, Shinjuku-ku, Tokyo 169

Aldosterone is known to potentiate the metamorphosis-inducing action of thyroid hormone. The binding of aldosterone to the bullfrog tadpole tail was investigated. Specific binding of [³H]aldosterone at 0°C reached a maximum after 3 hr of incubation. Separation of bound and free hormone was performed by using a hydroxylapatite method. Specific binding of aldosterone was observed in the tail epidermis but not in the tail mesenchyme. Scatchard plot analysis revealed a single class of binding sites with a dissociation constant (Kd) of 8.1 ± 0.3 nM and the maximum number of binding sites of 54.2 ± 2.5 fmol/mg protein. Steroid-binding specificity revealed a significant displacement of the [³H]aldosterone by radioinert aldosterone and, to a lesser extent, glucocorticoids such as corticosterone and cortisol, whereas 17 β -estradiol and testosterone competed very poorly. Sedimentation of epidermal cytosol on sucrose gradient in low salt resulted in only a single peak of radioactivity in 8.0 S area. The number of binding sites was significantly reduced as metamorphosis progressed with no appreciable changes in the Kd value.

EN 51

EFFECT OF ULTIMOBRANCHIALECTOMY ON PLASMA CALCIUM LEVEL IN SNAKES.

M.Yoshihara¹, M.Uchiyama¹, T.Murakami¹, H.Yoshizawa², N.Suzuki³, Y.Sasayama³ and C.Oguro³, ¹Dept. of Oral Physiol., The Nippon Dental Univ., Niigata, ²Dept. of Oral Histol., Matsumoto Dental Coll., Shiojiri, ³Dept. of Biol., Toyama Univ., Toyama.

It is well known that reptilian ultimobranchial gland contains calcitonins which induce hypocalcemia in rats. However, function of calcitonin or ultimobranchial gland has not been clarified in reptile itself.

In the present study, effects of ultimobranchialectomy on plasma calcium level were examined using snakes in various conditions shown below:

- 1) *Elaphe quadrivirgata*: adult, male
- 2) *E. quadrivirgata*: adult, male, high calcium drinking water (0.2 and 0.5% CaCl₂)
- 3) *E. quadrivirgata*: adult, female, 2-3 weeks before ovulation
- 4) *Elaphe climacophora*: just after hatching out
- 5) *Rhabdophis tigrinus tigrinus*: adult, male, calcium infusion (10 mg/kg/hr)
- 6) *E. quadrivirgata*: adult, male, parathyroid hormone (100 U/kg)

No significant differences were found in plasma calcium level between ultimobranchialectomized and sham-operated individuals. The present results apparently indicate that the ultimobranchial gland is not exerting marked influences on systemic plasma calcium concentration in these snakes, at least in the conditions noted above.

EN 52

EFFECTS OF SEX STEROIDS ON GH AND PRL CELLS IN IMMATURE MOUSE ADENOHYPOPHYSIS

M.Motegi and Y.G.Watanabe.

Biol.Inst., Fac.Sci., Niigata Univ., Niigata

The population and proliferation of GH and PRL cells were studied immunohistochemically in the anterior pituitary of immature mice which were treated with sex steroids. Estradiol benzoate (EB;1 μ g) or testosterone propionate (TP;100 μ g) was administered to 7-day-old mice daily for 1 or 2 weeks. On the day of sacrifice, animals received injection of bromodeoxyuridine (BrdU;250mg/kg b.w.) to detect the rate of cell proliferation. The number and density of GH cells were lowered in EB-treated group. EB increased the number and density of PRL cells after 1 and 2 weeks of treatment. TP decreased both the number of GH cells and PRL cells per area, however, it had little effect on the density of GH and PRL cells. The density of BrdU-labeled cells in the anterior pituitary was decreased with age. TP did not alter the rate of cell proliferation in the pituitary during growth. BrdU-labeled cells in EB-treated mice for 1 week were fewer than in controls. BrdU-labeled GH cells decreased with age, and there was no significant difference among 3 groups. Proliferation of PRL cells was greatly stimulated by EB but it was inhibited by TP. Thus, sex steroids treatment in neonatal mice caused a sex difference in the pituitary similar to that observed after puberty.

EN 53

EXPERIMENTAL HEMORRHAGE AND FOLLOWING RESTORATION OF THE MOUSE ANTERIOR PITUITARY. I. Koshimizu and Y. Kobayashi, Dept. of Biol., Fac. of Sci., Okayama Univ., Okayama.

Intense and acute hemorrhage in the anterior pituitary through a mechanism of diapedesis was induced by intraperitoneal injection of 35% glucose at a dose of 0.03ml/g body weight. Extensive necrotic changes and following restoration of the anterior pituitary were investigated with the light and electron microscopes. Degenerative changes due to extravasation of erythrocytes began on day 1 after the injection. The most extensive necrosis occurred on day 3 after hemorrhage. Quantitative light microscopy revealed that the percent volume of necrosis of the anterior pituitary was 74% on day 3, 24% on day 5 and 13% on day 7. Individual differences in aging was recognized in hemorrhage and necrosis. On day 5-7, necrotic area of the gland was gradually replaced by loose connective tissue-like structure consisting of macrophages, fibroblasts, non-glandular cells and free basal lamina. These results indicated that necrosis of the anterior pituitary restores by 7 days after hemorrhage.

EN 54

FINE STRUCTURAL ALTERATIONS IN MOUSE PITUITARY INTERMEDIATE LOBE CELLS FOLLOWING ORAL UREA ADMINISTRATION. M. Okada and Y. Kobayashi, Dept. of Biol., Fac. of Sci., Okayama Univ., Okayama.

In our previous morphometric study, male mice (Jcl/ICR) given a liquid diet (3% powdered milk in 5% glucose) supplemented with 1% urea for 10 days have resulted hypersecretion in pituitary intermediate (PI) cells more significantly than that of the liquid diet alone. In the present study, to eliminate the drinking effect, urea was administered orally mixed in the mouse food at the concentration of 6%, 12% and 24%, respectively, for 14 days, and quantitative changes in PI cells were investigated. The result showed significant alterations in PI cells in a dose dependent manner. In mice fed 24% urea food, the % R-ER (reflecting protein synthesis) increased to 287.5% of the control value, and the numerical density of secretory granules (reflecting secretory granule storage) decreased to 44% of the control value. These results may suggest an involvement of the PI peptides in detoxication or excretion of oral urea ingestion in mice.

EN 55

DEVELOPMENT OF THE HYPOTHALAMO-HYPOPHYSIAL RELATIONSHIP IN SALMON, *Oncorhynchus keta* Naito, N. I., Nakai, Y. I., de Jesus, E. G. Z., Hirano T. 2. ¹Showa Univ. Sch. Med. Tokyo, ²Ocean Res. Inst. Univ. of Tokyo

In the teleost pituitary, direct innervation of hypothalamic nerve fibers is concerned with control of endocrine cell function. Here, we examined chum salmon larvae to reveal the development of pituitary cell-types and hypothalamic nerve fibers projecting into the pituitary during early development (5-10 weeks after fertilization) using immunocytochemical technique. Five cell-types in the adeno-hypophysis (PRL, GH, ACTH, TSH, MSH-cells) were already apparent in the pituitary of embryos at 2 weeks before hatching (5 w. after fertilization). The level of cell-type-differentiation was higher in the rostral than in the caudal area of the embryonic pituitary. One week later, in the neuro-hypophysis (NHP) MCH-positive fibers derived from the nucleus lateralis tuberis (NLT) could be detected. In newly hatched alevins (7 w. after fertilization), nerve fibers from the preoptic nucleus, such as VAT and SRIF-fibers, had also arrived at the NHP and, in addition, adeno-hypophyseal endocrine cells had increased in number and in staining intensity for their specific antisera. These results suggest that some of hypothalamo-hypophyseal relationships may be functional in chum salmon embryos during the last week before hatching.

EN 56

THE APPEARANCE OF GTH-I AND GTH-II IMMUNO-REACTIVE CELLS AND DEVELOPMENT OF THE GONADS IN RAINBOW TROUT, *Salmo gairdneri* T. Sagai, Y. Oota, I. Koshimizu, M. Nozaki³ and H. Kawauchi⁴. ¹Biol. Inst., Fac. of Sci., Shizuoka Univ., Shizuoka, ²Biol. Inst., Fac. of Sci., Okayama Univ., Okayama, ³Primate Res. Inst., Kyoto Univ., Inuyama, ⁴Kitasato Univ., Iwate.

The appearance of each hormone producing cells in the pituitary gland and early development of the gonads were studied immunohistochemically in juvenile rainbow trout. Furthermore, correlation between the appearance of GTH-I and GTH-II immunoreactive cells and the gonadal differentiation was examined. At stage 21, PRL and MSH cells were first detected in the pars distalis (PD) and pars intermedia, respectively. Subsequently, GH, ACTH and TSH cells were appeared in the PD. The fry was hatched just before at stage 30. Then a few GTH-II cells were observed in the PD at stage 32. By this stage, germ cells were observed in the gonads, but they have not sexually differentiated completely. Following stage 35, with the increase in number of GTH-I cells, the gonads more developed and began to differentiate. No GTH-II cell was observed during the early stage of the fry. These results suggest the close correlation between the development of GTH-I cells and gonadal differentiation.

EN 57

ESTROGEN STIMULATES PEPTIDYLARGININE DEIMINASE SYNTHESIS IN RAT PITUITARY TUMOR CELLS IN CULTURE

S. Nagata, M. Yamaguchi, K. Watanabe, K. Inoue* and T. Sensu (Dept. Biochem. Tokyo Metropol. Inst. Gerontol., Tokyo, *Inst. Endoc., Gunma Univ., Gunma)

Effects of 17-beta-estradiol (E_2) on peptidylarginine deiminase (EC 3.5.3.15; PAD) levels in rat pituitary tumor cells were examined using *in vitro* culture system. When growth hormone-producing pituitary tumor cells, MTT/S, were cultured for 2 days with various concentrations of E_2 , PAD activities and its amounts increased in a dose-dependent manner, showing maximum levels at 1 nM E_2 . This increase in PAD activities was evident by 14 hours of culture and become relatively stable after 24 hours. Testosterone, progesterone, and corticosterone were without effects in this respect. Exposure of cells to E_2 increased radiolabeled methionine incorporation into the immunoprecipitable PAD, indicating that E_2 stimulates PAD biosynthesis. When total or poly(A)+-RNA were analyzed by slot blotting and northern blotting, PAD mRNA levels in E_2 -treated MTT/S cells were found more than 4-fold higher than those in non-treated cells. These results indicate that E_2 directly stimulates PAD synthesis in pituitary cells at the transcription level.

EN 58

POSSIBLE ACTION OF ANDROGEN IN FORMATION OF THE ANTEROVENTRAL PERIVENTRICULAR NUCLEUS (AVPV) IN FETAL RATS

H. Sumida, M. Nishizuka*, Y. Kanō, and Y. Arai*. Lab. Anim. Physiol., Fac. Agri., Meiji Univ., Kawasaki and *Dept. Anat., Juntendo Univ. Sch. Med., Tokyo.

To elucidate action of androgen in the AVPV of the preoptic area in fetal rats, some pregnant rats received testosterone propionate (TP) from day 14-18 of gestation, and the rest were given oil. All of the rats were given bromodeoxyuridine (BrdU), a thymidine analogue, on day 15. On day 21 of gestation, fetal brains were processed for histological and immunocytochemical studies using anti-BrdU. The number of AVPV cells and the number of BrdU-immunopositive AVPV cells in TP-treated females were statistically smaller than those of control females. These indicate that androgen induced a reduction of AVPV cells in perinatal rats. Furthermore, based on the fact that the number of pycnotic AVPV cells in TP-treated rats was significantly greater than that of controls, it is concluded that facilitation of cell death following androgen administration underlies the decrease of AVPV cells in prenatal period. On day 21 of gestation, the number of pycnosis in AVPV of male fetuses was remarkably greater than that of females, and the value was comparable to that of TP-treated females. Thus, AVPV of prenatal rats exhibits an apparent sexual dimorphism. The present study clearly documents masculinizing action of androgen in AVPV of prenatal rats.

EN 59

AN IMMUNOHISTOCHEMICAL STUDY OF POLYPEPTIDES AND TYROSINE HYDROXYLASE IN THE SEXUALLY DIMORPHIC ANTEROVENTRAL PERIVENTRICULAR NUCLEUS (AVPV-POA) OF THE RAT

S. Murakami and Y. Arai. Dept. of Anat., Juntendo Univ. Sch. of Med., Tokyo.

The anteroventral periventricular nucleus of the preoptic area (AVPV-POA) has a greater volume in females than in males. This nucleus is thought to be involved in the regulation of the cyclic release of gonadotropin. The counting of the number of neurons in the AVPV-POA indicated that females had a significantly greater number of neurons than males. The possible existence of specific neuronal population correlated with sexual dimorphism of this nucleus examined immunohistochemically. A dense cluster of the α -atrial natriuretic peptide (ANP)-stained cells was found in the region corresponding closely with cytoarchitectonically defined AVPV-POA. However, no sex difference was found in the distribution of ANP-stained cells. Moderate numbers of neurotensin (NT)-, leu-enkephalin (L-ENK)- and tyrosine hydroxylase (TH)-stained cells were found in the AVPV-POA. Sex differences in the distribution of NT- and L-ENK-stained cells were not detected. In contrast, the number of TH-stained cells was a significantly greater in females than males. This sex difference in number of TH-stained cells may be related to the sexually dimorphic function of the nucleus.

EN 60

ANDROGEN REGULATES GAP JUNCTIONS BETWEEN MOTONEURONS IN LUMBAR SPINAL CORDS IN MALE RATS

A. Matsumoto*, A.P. Arnold* and P.E. Micevych†. Dept. of Anat., Juntendo Univ. Sch. Med., Tokyo, *Brain Res. Inst., Univ. California at Los Angeles, Los Angeles.

Gap junctions play an important role in metabolic and electrical coupling between cells. We studied androgenic influence on the occurrence of gap junctions between androgen-sensitive motoneurons in the spinal nucleus of the bulbocavernosus (SNB) in lumbar spinal cords. Adult male rats (Sprague-Dawley) were castrated, and implanted with Silastic capsules containing testosterone (T) or nothing. Four weeks after castration, horseradish peroxidase (HRP) was injected into the bulbocavernosus muscles, and animals were killed 2 days later. The soma and proximal dendritic membranes of 150 HRP-labeled motoneurons were examined ultrastructurally. Of gap junctions observed, 45% were somatodendritic, 35% dendrodendritic and 20% somatosomatic. Castration decreased the number and length of gap junctions by 29% and 39%, respectively. The values in castrates given T were not significantly different from those in controls. These results suggest that androgen regulates the degree of coupling between SNB motoneurons, which may allow synchronization of metabolic and/or electrical activity in the SNB.

EN 61

OVARIAN CONTROL OF OOSTEGITE FORMATION IN *ARMADILLIDIUM VULGARE* (CRUSTACEA, ISOPOD).
S. Suzuki*, K. Yamasaki**.

*Biol. Lab. Kanagawa Pre. Col., Yokohama.
**Dept. Biol. Tokyo Metropol. Univ., Tokyo.

In *A. vulgare*, the oostegites (female secondary characteristic) are formed at molting time followed by egg-laying. The ovarian control for oostegite formation is not confirmed in spite of some experiments using surgical removal of ovaries. Present studies were carried out to find the presence of ovarian factors for oostegite formation.

Young animals (2.9mm in body length) were ovariectomized or andrectomized by removing all rudimentary internal reproductive organs. They grew up to 7.5mm after several months later. These adult sized animals did not develop the oostegites following molts. The individuals over 10mm were used for the experiments. Ovaries from 50 maturing females were homogenized with 200µl of crustacean saline and centrifuged. The supernatant was used as ovarian extract. The extract equivalent with 1/4 ovary was injected. After the first or second post-injection molts, oostegites were formed in ovariectomized females (53%) and andrectomized males (33%). In addition,

if the young males were removed only androgenic glands and testes, the posterior region of reproductive organs differentiated into normal ovaries, and then they developed the oostegites and laid eggs. These results suggest that the maturing ovary contains the factors for the oostegite formation.

EN 62

PRODUCTION OF ANTIBODY TO ANDROGENIC GLAND HORMONE (AGH) AND ITS APPLICATION TO MEASUREMENT OF AGH ACTIVITY.

Y. Hasegawa¹, K. Haino-Fukushima² and Y. Katakura¹. ¹Dept. of Biol., Keio Univ., Yokohama, ²Dept. of Biol., Fac. of Sci., Tokyo Metropolitan Univ., Tokyo.

The androgenic gland hormone (AGH) is the sex determining substance in Crustacea. Antiserum was raised in a rabbit against purified AGH I of *Armadillidium vulgare*. Specificity of the antiserum was confirmed by the immunoblotting experiments. Biological activity of AGH was inhibited by the anti-AGH I IgG. The titer of immune serum was determined using its various dilutions against to the same concentration of AGH I (250 ng / 100 µl). Half-antibody binding was obtained with a dilution of about 1/100. The dose-response curve was obtained by enzyme-linked immunosorbent assay (ELISA) using antiserum at 1/500 dilution. With purified AGH I, a linear response was obtained from about 1.5 to 100 ng / 100 µl. AGH I antiserum bound to AGH I as well as AGH II and the two dose-response curves were quite similar. On DEAE-SPW HPLC, the eighth purification step of AGH, immunoreactivity of each peak correlated with their biological activity. The AGH activity was able to be measured by ELISA, sensitively, rapidly and easily. It can make up the weak points of the bioassay of AGH.

EN 63

SEASONAL CHANGES AND EFFECT OF EYESTALK HORMONE ON THE ULTRASTRUCTURE OF THE ANDROGENIC GLAND OF THE CRAYFISH, *PROCAMBARUS CLARKII*.

Y. Takeuchi, S. Nishikawa and M. Miyawaki. Dept. of Biol., Fac. of Sci., Kumamoto Univ., Kumamoto, 860.

Electron microscopic observations revealed the androgenic gland cell structure changes according to the season of the year. In spring and summer the rER and Golgi bodies are well developed (A type cell). But in autumn and winter the cells have few such organelles; instead there are vacuoles including granules (B type cell). These seasonal differences could be a reflection of seasonal changes in the proportion of two cell types. But these changes in cell structure may simply be seasonal changes in the activity of the single cell type that is correlated with the breeding season of the animals.

Following eyestalk ablation many rER and Golgi complexes with many small dense granules were observed in the gland cells. In contrast, glands from summer animals that were injected with eyestalk homogenates showed an increase in the proportion of B type cells, with the appearance of numerous granules in vacuoles that are apparently formed by blebbing of the outer nuclear membrane. These changes produced by the eyestalk extract makes the hypothesis that eyestalk secretes a hormone that inhibits the activity of the androgenic gland.

EN 64

EFFECTS OF SEX HORMONES ON THE FORMATION OF LIVER HYPERPLASTIC NODULES IN MICE.

S. Suzuki-Morimoto and K. Utsugi. Dept. of Biol., Tokyo Women's Medical College, Tokyo.

Liver hyperplastic nodules (HNs) induced by urethane are formed in male mice earlier and in greater number than in females, so the relation between urethane and sex hormones was investigated. ICR mice were given i.p. injection of urethane from 1 to 3 weeks of age, treated variously from 5 to 20 weeks of age and given phenobarbital from 20 weeks of age. Males were sacrificed at 25 weeks and females at 45 weeks of age. Orchidectomy at 5, 10 and 15 weeks of age decreased the numbers of HNs, but at 20 weeks of age were the same as controls. Orchidectomy at 5 weeks of age and s.c. injection of testosterone from 5 to 20 weeks of age formed almost the same numbers of HNs as controls. S.c. injection of estradiol from 5 to 20 weeks of age decreased the numbers of HNs in both orchidectomized and intact specimens. Ovariectomy at 5 weeks of age increased the numbers of HNs. Ovariectomy and s.c. injection of testosterone from 5 to 20 weeks of age increased the numbers of HNs, but only the injected ones were almost the same as controls and only s.c. injection of estradiol decreased the numbers of HNs. From these results, it is believed that male sex hormone is necessary for a long time as a co-factor for the initiation of urethane and that estrogenic hormone acts as a suppressant.

EN 65

EFFECTS OF THYROID HORMONE DEFICIENCY IN EGGS ON EARLY DEVELOPMENT OF MEDAKA
M. Tagawa and T. Hirano. Ocean Res. Inst., Univ. of Tokyo, Tokyo.

To examine the biological significance of thyroid hormones contained in egg, the hormones were depleted from egg by treating the mother fish with thiourea. Constantly spawning medaka (*Oryzias latipes*) were reared in fresh water with or without thiourea (0.03%). Plasma thyroxine (T4) and triiodothyronine (T3) concentrations before the treatment were 8 and 5 ng/ml, respectively, and decreased to 1/10 of the initial levels after 4 days. Initial concentrations of T4 and T3 in egg were 4 and 1 ng/g, respectively, and decreased to 1/10 after 7 days. During the course of normal development, egg thyroid hormones maintained the initial levels during the first 4 days, and constantly decreased toward hatching (10 days after fertilization). There was no difference between hormone deficient eggs and control eggs in hatchability, the time of hatching and survival under starvation. No difference was seen between the two groups in body weight, body length, condition factor and survival rate 16 days after hatching. These findings indicate that more than 90% of the hormones contained in egg are not essential at least for early development in medaka.

EN 66

EFFECTS OF GROWTH HORMONE INJECTIONS ON BONE METABOLISM IN RAINBOW TROUT

Y. Takagi¹, J. Yamada¹, S. Moriyama² and T. Hirano³, ¹Fac. of Fish., Hokkaido Univ. Hakodate, ²School of Fish. Sci., Kitasato Univ., Sanriku and ³Ocean Res. Inst., Univ. of Tokyo, Tokyo.

Effects of salmon and eel growth hormones (GHs) on bone metabolism were studied in rainbow trout (*Salmo gairdneri*) using the histomorphometric technique. When 0.01 or 0.1 µg/g/week salmon GH (sGH) was injected intraperitoneally 10 times into fed trout, growths in both length and weight were accelerated. Osteoblasts and bone resorptive cells were activated only by injections of higher dose of sGH. When recombinant eel GH (reGH) in a cholesterol pellet was implanted subcutaneously into starved trout (40 µg reGH/18g fish) for 1 week, bone resorptive cells were activated. Osteoblasts were inactive caused by starvation.

The results suggest that GH stimulates both bone formation and resorption via activation of osteoblasts and bone resorptive cells. Bone formation depends on nutritional condition of the fish.

EN 67

EFFECTS OF GONAECTOMY AND SEX STEROIDS ON SEXUALLY DIMORPHIC DEVELOPMENT OF THE MOUSE SUBMANDIBULAR GLAND.
K. Sawada and T. Nomura.
Dept. of Regulation Biol., Fac. of Sci., Univ. of Saitama, Urawa.

The mouse submandibular gland consists of four main parts: the acinus (A), intercalated duct (ID), granular convoluted tubule (GCT) and excretory striated duct (SD), of which GCT are undetectable until about 15 days of age. The GCT began to develop at 20 days, and male GCT were more developed in both the relative occupied area (RA) and the mitotic activities (MA) than female GCT. The MA in male GCT reached a peak at 30 days and then decreased to the female level at 45 days.

Effect of neonatal gonadectomy and sex steroids on sexually dimorphic development of the gland was examined. At 30 days, both RA and MA of GCT in castrated males were similar to those of normal females, but treatment with daily 10 x 10 ug testosterone from 20 days of age increased the MA to the normal male level, but increased the RA slightly. In castrated females, testosterone failed to increase the MA of GCT. Estradiol-17β had no effect in both sexes.

EN 68

PERMANENT CHONDRIFICATION IN THE PELVIS OF NEONATALLY TAMOXIFEN-TREATED MICE
Y. Uesugi, T. Iguchi, N. Takasugi.
Graduate School of Integrated Science, Yokohama City Univ., Yokohama

Permanent chondrification in the pelvic bone of C57BL/Tw mice induced by neonatal exposure to tamoxifen (Tx) was studied. Percent ratios of length and width of the pubis to the longitudinal length of innominate bone (INL) were significantly reduced in the pelvic bone of male and female Tx-treated mice (Tx mice).

The ilium also showed a significant decrease in the ratio of width to INL in both sexes of Tx-treated mice. In adult Tx females, permanent chondrification area in the pubic bone was characterized by a distribution of type II collagen. In 15-day-old Tx females, percent ratio of ossified area in the pubic bone was increased; however, the number of osteoclasts and their nuclei, and ratio of total cell circumference of all osteoclasts to the distance round of the ossified region were reduced significantly. In summary, 1) Tx mainly impairs the ossification of pubis, resulting in permanent chondrification of this part of the pelvic bone. 2) Tx-induced permanent cartilaginous part is characterized by type II collagen. 3) The decreased osteoclast's activity in Tx mice suggests a lowered resorption of the ossified matrix.

EN 69

DECIDUAL CELL REACTION IN PSEUDOPREGNANT RATS BEARING PITUITARY GRAFTS.
Y. Ohta. Biol. Dept., Tottori Univ.
Tottori 680

Decidual cell reaction was investigated in the uterus of pseudopregnant adult rats receiving a single pituitary gland each under the left kidney capsule at 3 months of age. Females with the grafts invariably showed prolonged 14- to 19-day estrous cycles with mucified vaginal smears until ovariectomy performed 1 or 2 months later. The decidual response to uterine trauma was definitely reduced in the pituitary-grafted rats given injections of progesterone alone or in combination with a small amount of estrogen after ovariectomy. By contrast, the control rats bearing isografts of submaxillary glands exhibited 4-day cycles regularly, and always responded positively to the trauma stimulating the formation of massive deciduomata. Ovariectomy at the time of grafting greatly elevated incidence of deciduomata in the pituitary-grafted rats.

The decline in deciduogenic ability of the pseudopregnant rats with ectopic pituitary grafts appears to be largely ascribable to the effect of the continued exposure of the uterus to ovarian steroids, progesterin in particular, rather than to prolactin secreted from pituitary grafts.

EN 70

INCREASE IN BLOOD GLUCOSE LEVEL AND LIVER GROWTH IN SHN MICE BEARING MAMMARY TUMOR CELLS FROM THE CELL LINE 19.
Y. Takamatsu, Y. Uesugi, T. Iguchi, N. Takasugi, K. Kano* Grad. Sch. of Integrated Sci., Yokohama City Univ. and *Fac. Med. Dept. Nutr., Univ. Tokyo.

Spontaneous mammary tumors in female SHN mice cause a hyperglycemic and hyperinsulinemic state accompanied by liver growth. In the present study, growth of liver and mammary tumor was examined in streptozotocin (STZ)-induced hyperglycemic SHN mice with or without insulin (INS) administration. Mammary tumor cells from the cell line 19 established from spontaneous mammary tumor of SHN mice were inoculated into young male SHN mice. Livers in STZ-treated and STZ plus INS-treated mice bearing cell-line 19 tumor cells were larger than those in the intact controls, while the organs in untreated mice bearing the tumor cells were heavier than those in the intact controls. However, there was no statistical difference in liver weight in STZ- and STZ plus INS-treated mice bearing no inoculated tumor cells compared to that in the intact controls. Growth of the inoculated tumor cells was not statistically different between the control hosts and STZ- or STZ plus INS-treated hosts. These findings suggest that factor(s) other than higher blood levels of glucose or insulin plays a role in the growth of liver and mammary tumor.

EN 71

METAMORPHIC CHANGE IN THE SKIN INDUCED BY THYROXINE AT LOW TEMPERATURE IN Hynobius nigrescens LARVAE
Kaeori Yamashita, Hisaaki Iwasawa.
Biol. Inst., Niigata Univ., Niigata

The effects of thyroid hormone at low temperature were studied in Hynobius nigrescens larvae. Stage 63 larvae (Usui-Hamazaki, 1939) were immersed in $6 \times 10^{-6}M$ L-thyroxine Na (T_4) solution at 4, 6, 8, 10 and 12 °C, and metamorphic changes in the external gill, dorsal fin and skin were examined. The control larvae were kept in tap water at 18 °C, and the gill length and dorsal fin height were measured every third day. The larvae of each stage in the control and the larvae treated with T_4 for 50 days were examined histologically. In T_4 -treated larvae at 4 and 6 °C, hardly any metamorphic changes were seen in the gill and fin, and they correspond to those of st.64. In 8 °C, the gill condition corresponds to that of st.66, whereas the height of the fin corresponds to that of st.67. Metamorphic changes in the skin (development of the dermal gland, and degeneration of the Leydig cell and neuromast) in T_4 -treated animals kept at 4 and 6 °C corresponded to those of st.65-66. It is therefore concluded that the effects of T_4 were different in each target organ at low temperature.

EN 72

DEVELOPMENT OF GROWTH HORMONE AND PROLACTIN CELLS IN THE BULLFROG LARVAE.
T. Kobayashi and S. Kikuyama. Dept. of Basic Human Sci., Sch. of Human Sci., and Dept. of Biol., Sch. of Educ., Waseda Univ., Tokyo.

Development and distribution of growth hormone (GH) and prolactin (PRL) cells in the bullfrog, Rana catesbeiana, was studied employing PAP method by using antisera against homologous bullfrog GH and PRL. A few GH cells were first observed in the central region of the anterior pituitary gland of stage 22 (Shurway's classification) embryos. At the same stage, with a short delay of time, immunoreactive PRL cells also appeared in the vicinity of GH cells. Of these PRL-positive cells, a few were also GH-positive. At stage 25, PRL cells began to distribute widely among other pituitary cells, whereas GH cells were found mostly in a dorso-caudal region. In the subsequent larval stages, the characteristics in localization of GH and PRL cells became more prominent. Both GH and PRL cells were increased in number as development progressed. In the pituitary gland of metamorphosing tadpoles and juvenile frogs, the cells stained with both GH and PRL antisera could no longer be found, indicating that GH and PRL are synthesized by two distinct cell groups from later stages of development onwards.

EN 73

LUNG MATURATION IN BULLFROG TADPOLES DURING METAMORPHOSIS

M. Ohkawa, K. Kawamura and S. Kikuyama.
Dept. of Biol., Sch. of Educ., Waseda Univ., Tokyo.

The anuran lung begins to function at advanced stages of metamorphosis. We have already demonstrated by thin layer chromatography that the amount of phosphatidylcholine (PC) (the main surfactant lipid) in the lung of bullfrog tadpoles (*Rana catesbeiana*) markedly increases during climax. Morphological observation was carried out to see the ultrastructural changes in the lung epithelium during metamorphosis. In the prometamorphic (stage X) tadpoles, the lung epithelium is relatively thin and its apical surface is devoid of cytoplasmic processes. Around stage XVIII (prometamorphic stage), the fine cytoplasmic processes appear on the surface of the epithelium and increase in number as metamorphosis progresses. On the basal side, the epithelial cells and the endothelial cells of the capillary form a number of digit-like processes, which intercalate each other. In the epithelium of the climactic animals (stages XXII-XXIV), development of the lamellar bodies is evident. The lamellar bodies are also found in the air space, suggesting that they are released from the epithelial cells. These observations coincide with the biochemical data mentioned above.

EN 74

ROLL OF LOW TEMPERATURE IN THE TERMINATION OF BREEDING ACTIVITY IN JAPANESE QUAIL.

H. Tsuyoshi and M. Wada
Dept. Biol., Sch. Educ., Waseda Univ., Tokyo and Dept. Gen. Educat., Tokyo Med. Dent. Univ., Ichikawa, Chiba

An annual breeding cycle of male Japanese quail is very clear under natural conditions, but gonadal regression is hardly seen by short day treatment in laboratory conditions. We have found, however, that quails transferred from long days to short days always terminate breeding activity if they are kept under constant low temperature (8C). This indicates that environmental factors other than daylength are involved in induction of LH decrease and gonadal regression at the end of a breeding season. Thus we hypothesized changes of temperature is such a factor and conducted a series of experiments.

Matured quails were transferred from 16L8D (19C) to several combinations of daylength and temperature cycles, such as 8L16D (12hr 9C), 12L12D (12hr 9C), and 12L12D (8hr 9C). In all groups, short daylength with certain durations of low temperature lowered plasma LH levels to a reproductively quiescent level. Testes of all these groups regressed completely. The results indicate that an alternation of high and low temperatures is a sufficient factor to terminate LH release and to induce gonadal regression in this species.

EN 75

CHANGES IN SERUM VARIABLES IN JAPANESE QUAIL WHOSE BREEDING ACTIVITY TERMINATED BY SHORT DAYS AND LOW AMBIENT TEMPERATURE

Masaru Wada
Dept. Gen. Educat., Tokyo Med. Dent. Univ., Ichikawa, Chiba

We have observed that a photoperiodic change from long days to short days do not show a steady testicular regression in laboratory conditions and that low ambient temperature together with short days is necessary to reduce circulating LH to a non-breeding level and to regress the testes in Japanese quail. To clarify a mechanism in photoperiodic and temperature regulation of circulating LH decrease, several serum variables were measured in 3 groups of mature male birds; (1) birds kept on long days of 16L8D with 19 C, (2) birds transferred to short days of 8L16D with 19 C, and (3) birds transferred to short days of 8L16D with 12-hour 19 C:12-hour 9 C. Circulating LH and testicular mass significantly reduced to non-breeding levels in Group 3 but body weight, hematocrit, serum osmolality and ion concentrations of Na, K, Cl, Ca, and Mg were not changed in the 3 groups. Serum concentrations of free fatty acids was increased in Group 3 but their composition was not changed. T_4 but not T_3 increased in Group 2 and T_3 but not T_4 increased in Group 3. The results suggest that T_3 and 5'-monodeiodination of T_4 is involved in termination of a breeding season by short days and low temperature.

EN 76

MELATONIN IS NOT INVOLVED IN RHYTHMS OF LOCOMOTOR ACTIVITY AND CROWING BEHAVIOR IN JAPANESE QUAIL

J. Igarashi and M. Wada.
College of Agr. & Vet. Medicine, Nihon Univ., Fujisawa, Kanagawa. and Dept. Gen. Educat., Tokyo Med. Dent. Univ., Ichikawa, Chiba

Crowing behavior and locomotor activity in male Japanese quail is dependent on testosterone, and these behavior have clear circadian rhythms due to a circadian clock mechanism. To clarify an involvement of melatonin in these rhythms, several experiments were conducted. Either pinealectomy or enucleation did not affect crowing rhythms in LD cycle and free-running rhythms under constant dim light at least 10 days. In birds which received both pinealectomy and enucleation, crowing and locomotor activity rhythms were entrained to LD cycles, and showed free-running rhythms in constant dim light. No suppression of locomotor activity and crowing was observed with melatonin implantation. The results indicate that melatonin rhythms are not required for appearance of behavior rhythms in quail, even though a clear rhythm of circulating melatonin exists.

EN 77

SEX-PEPTIDE THAT IS INVOLVED IN THE REGULATION OF SEXUAL BEHAVIOR OF FEMALE *D. MELANOGASTER*.

T.Aigaki¹, M.Bienz², P.S.Chen² and E. Kubli². 1. Dept. of Biol., Tokyo Metropol. Inst. Gerontol., Tokyo, Japan. 2. Zool. Inst. Univ. Zürich, Switzerland.

Mating induces marked changes in the reproductive behavior and physiology of female *D. melanogaster*: 1) mated females switch off their sexual receptivity with a characteristic rejection behavior, 2) ovulation and oviposition are markedly stimulated. We have isolated a peptide (sex-peptide) from the male accessory glands that induces the post-mating responses in virgin females when injected into their abdominal cavities. Amino acid sequencing and oligonucleotide-directed cDNA cloning established that the peptide consists of 36 amino acid residues. We have constructed a hybrid gene in which the sex-peptide cDNA was fused to a heatshock promoter, and introduced into the genome by P element-mediated transformation. A heatshock for 30 min at 37°C induced the behavioral and physiological changes in the transformed virgin females but not in wild type virgins. The results conclusively demonstrated that the sex-peptide is indeed involved in the post-mating reactions in female *D. melanogaster*.

EN 78

MODIFICATION OF FEMALE MOSQUITO CIRCADIAN ACTIVITY BY INTERSUBSPECIFIC COPULATION BETWEEN *CULEX PIPIENS PALLENS* AND *C. P. MOLESTUS*

Y.Shingawa¹, K.Tomioka¹, Y.Chiba¹, and M. Yoshii². ¹Biol. Inst., Fac. of Sci., Yamaguchi Univ., Yamaguchi and ²Dep. of Biol., Fac. of Sci., Okayama Univ., Okayama.

Virgin female circadian activity in the mosquito *Culex pipiens pallens* is diphasic with evening and morning peaks but with almost no activity at night. Insemination brings about a rhythm modifying factor (RMF) released from the male accessory gland, which acts to alter the virgin temporal pattern, strengthening the nocturnality (Yoshii et. al. 1988). A main purpose of the present study was to see if the insemination dependency is observed in the case of interspecific copulation.

Iranian virgin female mosquito, *C. p. molestus* showed a distinct entrained circadian pattern from that of the subspecies, *pallens*; activity continues for a few hours before light-off and after light-on, and occurred to some extent at night. But, after insemination, the day activity disappeared, while the night one was augmented. Thus, insemination affects the temporal pattern in a common way between the two subspecies so that the nocturnality is strengthened. This was reproduced when RMF was conveyed, on interspecific copulation, from *molestus* to *pallens* or vice versa.

EN 79

AN ATTEMPT AT ISOLATING MALE ACCESSORY GLAND SUBSTANCE MODIFYING FEMALE MOSQUITO CIRCADIAN ACTIVITY PATTERN

M.Yoshii¹, T.Yamaguchi¹, Y.Ogura², K.Tomioka², Y.Chiba², and S.Y.Takahashi². ¹Dep. of Biol., Fac. of Sci., Okayama Univ., Okayama, ²Biol. Inst., Fac. of Sci. and ³Biol. Inst., Fac. of Lib.-Arts, Yamaguchi Univ., Yamaguchi.

The diphasic circadian activity pattern of virgin female mosquito (*Culex pipiens pallens*) is modified by an RMF (rhythm modifying factor) conveyed in seminal fluid on copulation. RMF, which is known to be produced in the male accessory gland, may be a protein (Yoshii et al. 1988). We further investigated the properties of RMF, including the molecular weight.

In HPLC analysis (Gel filtration on superose 12 HR column), a high activity was detected in a fraction of less than 1 kD which, however, was not determined for the molecular weight. By Gel filtration with Sephadex G-25, active component was eluted in a void volume fraction of over 5 kD. Being applied to ultrafiltration (Amicon CF25), the activity of RMF was found in both the retentate and the filtrate, though the latter was less active. From these results and previous data, the molecular weight of RMF might be more than 5 kD (probably around 25 kD).

EN 80

EFFECTS OF JUVENILE HORMONE (JH), PROTEIN KINASE C ACTIVATOR AND CALCIUM LEVEL IN HAEMOLYMPH ON DIVISION OF LABOR AND THE PLASTICITY OF TASK SHIFTS AMONG WORKER HONEYBEES (*Apis mellifera* L.)

H.Sasagawa¹, Y.Kuwahara¹, M.Sasaki² and T.Kusano³. ¹Inst. of Appl. Biochem., ²Inst. of Agr. & Foresg., Univ. of Tsukuba, Tsukuba, and ³Fac. of Agr., Tamagawa Univ., Tokyo.

Division of labor (age polyethism) is a characteristic phenomena of the honeybee society and regulated by JH increase in haemolymph with age. Behavioral and physiological effects of methoprene (JHA) and 1-oleoyl-2-acetyl glycerol (OAG, the kinase C activator) on division of labor were examined by topical application of 0.1, 1.0 and 10ug, and 0.4, 4.0 and 40 ug, respectively. Induction of age polyethism by both treatments was demonstrated using a colony of a queen and workers of "isochronological age". OAG treatment accelerated the division of labor just like JHA's. Haemolymph JH of both treatments, determined by a micro-HPLC, became unexpectedly high. Because calcium is essential for activating the kinase C, haemolymph calcium was determined by atomic absorption spectroscopy, to give that calcium levels increased with age until 14 days after emergence and then decreased to low level. These results explain the plasticity of labor-shift, mediated by JH and calcium which activated the kinase C.

MO 1

INNERVATION OF RAT HEPATIC PORTAL SYSTEM
T.Amano, T.Tagawa, Dept. of Anat., Sch.
of Med., Fukuoka Univ., Fukuoka

The aminergic (Amn), cholinergic (Chn) and peptidergic innervations in the proximal and distal portions of rat hepatic portal system were studied using the histochemical and immunohistochemical methods.

Hepatic portal system was well supplied with Amn. Amn were more dense in the distal ones than that of proximal portion. Chn was less dense than that of Amn. No significant difference was present in the Chn distribution between the proximal and distal portions.

Substance P (SP)-like immunoreactive (LI), neurokinin A (NKA)-LI and calcitonin gene-related peptide (CGRP)-LI fibers were observed in the hepatic portal system. They were more dense in the distal ones than in the proximal portion. Vasoactive intestinal polypeptide (VIP)-LI fibers was sparse as compared with other peptidergic fibers and no significant difference was observed in the distribution between the proximal and distal portions. Neuropeptide Y (NPY)-LI fibers were most dense as compared with other four peptidergic fibers. Especially the proximal portion was richly innervated. Several thick nerve bundles were observed to run along the axis of hepatic portal vein.

MO 2

INNERVATION OF CEREBRAL ARTERIES AND INTRACEREBRAL PARENCHYMAL SMALL ARTERIES IN *LEIOTHRIX LUTEA*

T.Tagawa, Y.Enomoto, C.C.Hsu and C.Hirota, Dept. of Anat., Sch. of Med., Fukuoka Univ., Fukuoka

In submammalian vertebrates, autonomic and peptidergic innervations on the cerebral arteries and intracerebral parenchymal small arteries have not been intensively studied. Furthermore, the comparative studies with that of the mammalian species have not been found. Here we report the distributions of aminergic, cholinergic and peptidergic [substance P (SP)-like immunoreactive (LI), neurokinin A (NKA)-LI, calcitonin gene-related peptide (CGRP)-LI, vasoactive intestinal polypeptide (VIP)-LI and neuropeptide Y (NPY)-LI] fibers in *Leiothrix lutea*.

In the cerebral arteries, the internal carotid system is innervated densely by all the nerve fibers except for NPY-LI but the vertebral system is innervated sparsely by all the nerve fibers. In the intracerebral parenchymal small arteries, SP-LI, NKA-LI, CGRP-LI and VIP-LI fibers are observed densely as compared with aminergic, cholinergic and NPY-LI fibers.

MO 3

INNERVATION PATTERN AND ORIGIN OF CEREBULOVASCULAR NERVES IN THE HOUSE SHREW.

K.Ando¹, A.Ishikawa¹ and T.Inokuchi², ¹Biol. Lab., Liberal Arts, Kyushu Sangyo Univ., Fukuoka, ²Dept. Anat II, Kurume Univ., Fukuoka

The overall distribution and origin of nerves emitting catecholamine fluorescence (Can), positive for AChE (AChEn), or with NPY, VIP, SP or CGRP immunoreactivity (NPYn, VIPn, VIPn, SPn and CGRPn) in the cerebral arteries were investigated in the house shrew using histochemical and immunohistochemical techniques. The major arteries of both the internal carotid and vertebral-basilar systems were richly innervated by delicate varicose Can and NPYn fibers from the superior cervical ganglia. Cerebral perivascular AChEn and VIPn appeared to arise mainly from AChE-positive and VIP immunoreactive cell bodies within microganglia found in the nerve bundle that runs close to the sympathetic internal carotid nerve bundle (SICNB) within the tympanic cavity. The presence of ganglion cells has also been demonstrated ultrastructurally in the nerve bundle accompanying the SICNB at the same cranial portion. The ganglion cells had neither catecholamine fluorescence, nor immunoreactivity for NPY, SP and CGRP, although many of them received a supply of SPn and CGRPn. The innervation pattern of AChEn and VIPn was similar in density to that of Can and NPYn, but differed in respect to the presence of longitudinally-oriented fiber bundles. The supply of SPn and CGRPn was very poor. The absence of SPn and CGRPn ascending the caudal part of the VBS may involve that there is no contribution of these two types of sensory nerves to the house shrew cerebrovascular innervation from the cervical dorsal root ganglia.

MO 4

A HISTOLOGICAL STUDY ON THE NERVE INNERVATION IN THE TONGUE OF *CLEMMYS JAPONICA*.
H. Ishihara, Biolog. Lab., Fac. of Sci. & Engineer., Aoyama Gakuin Univ., Tokyo.

The morphology of nerve innervation and nerve endings in the tongue of *Clemmys japonica* was investigated according to the silver impregnation method devised by the present author.

Mucosa: It was found that the nerve plexus in propria mucosa consisted of both autonomic and central nerve fibers showing wavy course. Thick nerve fibers carrying nodes here and there together with fine nerve fibers were observed to enter the epithelium and to end there. Some other nerve fibers were often seen to branch from plexuses in the papilla, penetrate the epithelium and after running for a short distance, end with an argentophile nucleus. The glomerular or termination resembling Meissner's was often observed in papilla.

Lingualis: A small nerve bundles separated from the main nerve bundles were found running in serpentine course in the lingualis. Sometimes the nerve bundles running parallel or obliquely were detected in the lingualis. The nerve endings were seen to appear as spindle termination in the striated muscle.

Capillaries: The autonomic nerve fibers together with sensory nerve fibers were observed to run parallel to capillaries or surround them.

MO 5

DEVELOPMENT OF SEROTONIN AND RFamide-LIKE IMMUNOREACTIVITIES IN THE NERVOUS SYSTEM OF *Paraspadella gotoi* (Chaetognatha).
T. Goto. Dept. Biol., Fac. Educ., Mie University, Mie

The distribution and development of serotonin- and RFamide-like immunoreactivities in the nervous system of the arrowworm were examined by using immunocytochemistry on wholemount preparations. In adults, a single serotonin-like immunoreactive (5HTLI) neuron and numerous RFamide-like immunoreactive (RFaLI) neurons were found in the central nervous system. Based on the structure of the fins, hooks, and eyes, 7 larval stages were recognized. The most obvious features of the stages are as follows: stage 1, newly hatched larva; stage 2, elongation of a continuous lateral-tail fin; stage 3, separation of the lateral and tail fins; stage 4, appearance of hooks; stage 5, pigmentation of eyes; stage 6, attachment by tail adhesive fins; stage 7, prey capture. Stage 1 did not show any immunoreactivity. The 5HTLI neuron first appeared at stage 4 and its axonal pathway became similar to the adult at stage 6. On the other hand, the RFaLI neurons appeared at stage 3 in the ventral ganglion. Some of their somata disappeared at stage 5 and the neuronal architecture was close to the adult at stage 7 although the RFaLI neurons in the cerebral ganglion were complete at the juvenile stage.

MO 6

RESORPTION OF THE DECIDUOUS TEETH IN THE JAPANESE GREATER HORSESHOE BAT, *RHINOLOPHUS FERRUMEQUINUS NIPPON*.
K. Funakoshi¹, Y. Fukue² and S. Tabata³.
¹Biol. Lab., Kagoshima Keizai Univ., Kagoshima, ²Dept. Biol., Fac. Sci., Kyushu Univ., Fukuoka and ³Dept. Oral Anat., Kagoshima Univ. Dental School, Kagoshima.

In the Family Rhinolophidae and Megadermatidae, the deciduous teeth are resorbed prior to birth. In this report, the deciduous dentition of *R. f. nippon* was studied in morphological preparations stained with Alizarin red S and Alcian blue 8GS, and in histological ones stained with Mayer's haematoxylin and eosin. The deciduous dental formula was $di \ 1/2$, $dc \ 1/1$, $dpm \ 2/3 = 32$. In the upper jaw, the primordia of all the deciduous teeth were present at about four weeks before birth. In the lower jaw, the primordia of all the teeth, exclusive of p_3 , were observed at the same stage. At about three weeks before birth, odontoclasts appeared in the dental pulps. The deciduous lower incisors and canines were resorbed, and the two premolars (p_2 , p_4) were located in the alveolar crest at the labial side. The primordia of p_3 occurred slightly upper to the alveoli of the developing permanent premolars (P_4). On the other hand, all the upper deciduous teeth were still retained. At about a week before birth, all deciduous teeth with the exception of the premolars were resorbed. And then, remnants of the deciduous premolars were lost, and the permanent teeth began to erupt at birth.

MO 7

COMPARISON OF IMMUNOREACTIVITY IN ROD OUTER SEGMENTS AMONG VERTEBRATES USING ANTI-CATTLE RHODOPSIN MONOCLONAL ANTIBODIES.
S. Horuchi¹, H. Kobayashi², T. Morita³, Y. Koshida¹ and F. Tokunaga².
¹Dept. of Biol., Coll. of Gen. Educ., and ²Dept. of Biol., Fac. of Sci., Osaka Univ., Toyonaka.

Using monoclonal antibodies (Tokunaga *et al.*, Zool. Sci., 6, 167-171, 1989) against bovine rhodopsin, we reported that these antibodies react to all of the rod outer segments (ROSs) but do not react to the cone outer segments of retinas from cattle, cat, chicken, sparrow, bullfrog and Japanese newt by the fluorescent-isothiocyanate (FITC) indirect immunofluorescence method (Horuchi *et al.*, *ibid.*, 31-34). We applied this time these monoclonal antibodies to the retina of a teleost, medaka (*Oryzias latipes*) and found that ROSs of this species were also FITC positive and the arrangement of ROSs in the retina was clearly shown by this staining. It would be convinced that the epitopes recognized by the antibodies against bovine rhodopsin have been well-preserved in rod cells in vertebrates, and also that these monoclonal antibodies, very specific for ROSs, are useful for our further investigation of the retinal development and morphology.

MO 8

KIDNEY STRUCTURE OF THE CONGOLLI, *PSUEDAPHRITIS URVILLII* (NOTOTHEMIOIDEI, TELEOSTEI).
M. Ogawa, Dept. of Biology, Fac. of Liberal Arts and Science, Saitama Univ., Urawa, Saitama, 338, Japan.

The kidney morphology was examined in the Congolli, *Pseudaphritis urvillii*, a estuarine teleost which inhabits in estuaries and lower reaches of a river of the southern coast of the Australia but is never found in the Antarctic Sea.

The fish were collected in New Town Rivulet, near Sydney, Australia in September. The animals were fixed into 10 % formalin solution. The sections of the kidney were stained with hematoxylin and eosin.

The kidney possesses well-vascularized, numerous glomeruli and Bowman's capsules. There is no distal segment in the nephron. The nephron is specialized into ciliated neck and two proximal segments before entering the collecting tubule. This is the nephron structure of typical marine teleost.

In contrast with most of the Antarctic teleosts with aglomerular kidney which related to the conservation of anti-freeze glycoprotein in the serum, the glomerular kidney of this fish as stated may suggest that it is one of the reasons why they never enter the Antarctic Sea.

MO 9

ANATOMICAL STUDIES ON THE LUNG OF THE AIR-BREATHING FISH (DIPNOI & POLYPTERIDA).

A. Kimura, T. Gomi, Y. Kikuchi, T. Hashimoto and K. Kishi. Dept. of Anat., Sch. of Med., Toho Univ., Tokyo.

In the present study, we observed and compared the lungs of *Protopterus aethiopicus* (Dipnoi) and *Polypterus senegalensis* (Polypterida) in gross anatomical and histological detail by light and electron microscope (SEM & TEM).

The lung structure of *Polypterus* was more simple than that of *Protopterus*, in terms of basic structure. As far as differentiation of the respiratory epithelium, we could find in *Protopterus* a single type having the properties of both Type I, being cells of the squamous lining type and Type II, being cells of the cuboidal secretory type; that is, the thin cytoplasmic projection forms a blood-air barrier and osmophilic lamellated bodies were observed in the cytoplasm. In contrast to *Protopterus*, in *Polypterus*, two types of cells were observed: Type I and Type II, which are found in Anura, Reptilia, Aves and Mammalia. More characteristically, the two types of cells in *Polypterus* were observed in separate areas, that is, Type I cells covered the capillary network, while Type II cells existed in the groove-shaped ciliated tracts, which were mainly arranged in a longitudinal orientation with respect to the lung axis, and included ciliated cells and mucous cells.

MO 10

LIGHT MICROSCOPIC OBSERVATIONS BY VARIOUS STAININGS OF THE LUNGS OF *HYNOBIUS NEBULOSUS* TOKYOENSIS.

Y. Kikuchi, T. Gomi, A. Kimura, T. Hashimoto and K. Kishi. Dept. of Anat., Sch. of Med., Toho Univ., Tokyo.

The lungs of *Hynobius nebulosus* *tokyoensis* were observed mainly by light microscopy as well as gross anatomically and by electron microscopy (SEM & TEM). The lungs were seen to have an airway portion, in that ciliated cells and goblet cells were seen to exist, and a respiratory portion in that respiratory epithelial cells ranging from cuboidal to columnar in shape, were seen to exist. By van Gieson's staining and aldehyde fuchsin staining, smooth muscle was well developed in the airway portion, while the collagen fibers and the longitudinal and circular elastic fibers were well developed in the outer surface of the lungs. Capillary networks were surrounded by circular elastic fibers in the respiratory portion. By PAS reaction, colloidal iron reaction, alcian blue staining and combinations of these stainings, granules of mucopolysaccharides containing acid sulfate groups were seen to exist in the apical cytoplasm of the goblet cells and the respiratory epithelial cells. However, granules stained by Sudan black B staining and by Nile blue staining were observed in the cytoplasm of respiratory epithelial cells; therefore these granules contained lipids.

MO 11

ELECTRON MICROSCOPIC OBSERVATIONS OF THE ALVEOLAR EPITHELIAL CELLS OF THE RAT.

T. Gomi, A. Kimura, Y. Kikuchi, H. Tsuchiya, T. Hashimoto and K. Kishi. Dept. of Anat., Sch. of Med., Toho Univ., Tokyo.

The alveolar epithelial cells of the rat were observed to be of three types. (1) Type I cell (squamous lining type) has a narrow cytoplasm and scant cell organelles. Thin cytoplasmic projections covered the blood capillaries. The blood-air barrier was composed of the epithelium, basement membrane and endothelial cell. (2) Type II cell (cuboidal secretory type) has mitochondria, rER, multivesicular bodies, Golgi apparatus as well as osmophilic lamellated bodies specific to these cells in the cytoplasm. (3) Type III cell (alveolar brush cell) was characterized by long, thick and peculiar microvilli protruding from the apical surface of the cell. It was ellipsoid in shape with a constricted neck and many fine filaments extending from the top of the microvilli to the supranuclear region. Marked junctional complexes were found in the constricted part of the cells. In addition to filaments, there were vesicles, vacuoles, mitochondria, Golgi apparatus, ER, granules, free ribosomes and microtubules in the cytoplasm.

Furthermore, from observations of the alveolar lining layer, we could see a surface film and tubular myelin figures in the hypophase.

MO 12

ON DEGENERATION OF SOFT TISSUES OF THE STALK IN A MUSHROOM CORAL *FUNGIA FUNGITES*

H. Yamashiro¹ and K. Yamazato²
¹Radioisotope Lab., ²Dep. of Biol. Univ. of the Ryukyus, Okinawa.

A mushroom-shaped solitary coral *Fungia fungites* can reproduce asexually by detaching the disc from the stalk as a result of skeletal dissolution at the detachment plane. After detachment, the remained stalk regenerates another disc.

However, the number of discs successively produced by one stalk was very few (1.22 discs per one stalk) than expected. To elucidate why the stalk fails to regenerate, the number of mesenterial filaments and the protein content of the stalk were compared for both pulverizing and non-pulverizing specimens. The results showed that the number of mesenterial filaments and the protein content of the stalk decreased in the pulverizing specimen. Furthermore, before detachment, interseptal spaces of the disc had been already narrowed, by the secondary growth of the septa and columellae near the detachment plane.

The results suggest that marked degeneration of the soft tissues of the stalk during pulverization make their regeneration new discs insufficient or impossible.

MO 13

OBSERVATIONS ON THE REGENERATION OF THE LAND PLANARIAN, BIPALMIUM KEWENSE WHICH PROPAGATES ASEXUALLY, "FISSION".
Y. Shirasawa and N. Makino. Dept. of Biol., Tokyo Med. Coll., Tokyo.

Morphological and histological studies on the head and the pharyngeal regeneration of the B. kewense have been examined in the transected pieces and the spontaneous fissioned ones. This material propagates only asexual fission of the most posterior region. The fissioned tail piece regenerates the head and the pharynx in 2 weeks. And the transected pieces regenerate well also at an interval of 2 weeks after the transection. The histological preparations stained by Gomori's aldehyde fuchsin and H-E stain demonstrate that in three days, a great number of undifferentiated cells approaching to the anterior surface in the area between the ventral nerve cord and the intestinal wall which contains a plenty of AF positive granules. In five to seven days these cells accumulate to form the blastema and construct the head-shape. But in the pharyngeal regeneration, the remarkable accumulation rather delays than in the head, and undifferentiated basophilic cells originated from the intestinal wall were observed in near the expected place of the pharyngeal formation. After the accumulation, the slit was observed in the region at an interval of seven to eight days after the operation.

MO 14

ELECTRON MICROSCOPIC STUDIES ON THE DEDIFFERENTIATION OF THE NERVOUS AND BODY WALL TISSUES IN THE ANTERIOR REGENERATION OF THE FRESH-WATER EARTHWORM, BRANCHIURA SOWERBYI.

M. Shirasawa and N. Makino. Dept. of Biol., Tokyo Med. Coll., Tokyo.

Cytological changes of the ventral ganglion cells and the relation of the body wall cells to the formation of the head-blastema were studied electron microscopically in the anterior regeneration of the fresh-water earthworm, Branchiura sowerbyi. Dedifferentiation of the nerve cells occurs in the most anterior ventral ganglion at an interval of 2-3 days after the decapitation. The cytological changes are as follows. In the nucleus, chromatin gathers thickly and the nucleolus increase in size and density. The long cytoplasmic process is absorbed by autophagosomes, mitochondria decrease in size and number, and RER loses most of ribosomes from the membrane. Cell division is often observed at this stage. As a result, smaller cells with large dense nucleoli and many free-ribosomes appear under the nerve cord. Almost same time, similar cytological changes are observed also in the ventral body wall, especially in the muscle cells, and are suggested to be caused by the contact with the cut end of the nerve cord. Such dedifferentiation spread over the anterior body wall, and with the free nerve cells, these muscle cells form the head-blastema.

MO 15

CELL RENEWAL OF THE LINING EPITHELIUM OF THE PLANARIAN PHARYNGEAL CAVITY.
S. Ishii. Div. Cell Sci., Cent. Res. Lab., Fukushima Med. Col., Fukushima.

Cell renewal of the lining epithelium of the planarian pharyngeal cavity was examined by scanning electron microscopy using 5 species of freshwater triclad. The epithelium consisted of 3 types of cells with characteristic morphology which denoted different stages of cell development: on the luminal surface of cells from Dugesia japonica, young cells had many concentric arrays of labiate folds (rose cells), middle-aged or mature cells smooth-surfaced apical plasma membranes (flat cells), and old cells innumerable thin microvilli (microvillus cells). Nearly parallel results were obtained in other 4 species of planarians (Phagocata kawakatsui, Phagocata vivida, Polycelis auriculata, and Bdellocephala brunnea), although their young cells had more slender surface projections showing some species-specific variations. Discussion was devoted to the cytological implication of cell morphology in connection with the turn-over rate of the epithelia and also the mode of tissue cell recruitment in planarians.

MO 16

STAVATION OF BOTRYOIDAL TISSUE IN THE LEECHES, HIRUDO MEDICINALIS (2)
H. INAMURA. Dept. of Biol., Tokyo Med. Coll., Tokyo.

On searching for sucked blood of leeches, botryoidal tissue have been examined light and electron microscopically. Botryoidal tissue consisted of glandular cells and endothelia. In a fed individual, the cells contained granules of three different types: (1) L1-granules which were oil droplet-like, (2) L2-granules had many particles upon which ACPhase activity had a positive reaction, (3) P-granules which were pigment-like. L2 and P-granules had a limiting membrane. On apical parts of the cells, microvillies shown blood lumen directly, kept taking exocytosis and blood vessel consisted of endothelia. For 2 years hungry leeches have been live, and botryoidal tissue have got black. Cells of the tissue contained quite a few P-granules, some few L2-granules and few L1-granules. On blood luminal parts of the cells, microvillies shown more simple forms than 1 year hungry ones. On basal parts of the cells, entocytosis shown a few invagination to cytoplasm and cell membrane became rugged face. In comparison with 1 year hungry leeches, mitochondria paralleled to cell membrane of basal, lateral and luminal parts shown few, and shown a few in cytoplasm. Golgi apparatus shown a few vesicles on blood luminal parts of cells. It is suggested that blood luminal parts of cells show secretory aspect, and L2-granules show secretory granules, relating to metabolism.

MO 17

IN VITRO HAIR FOLLICLE FORMATION FROM RAT EMBRYONIC CELL AGGREGATES.

M. Watanabe, E. Nagao and S. Ihara. Dept. of Plastic Surg., Kitasato Univ. Sch. of Med., Sagami-hara. Dept. of Biochem. Lab., Inst. of Low Temp. Sci., Hokkaido Univ., Sapporo.

No experimental system has been available yet in which hair follicle is reconstituted *in vitro* from dissociated cells. Moscona, using from mouse embryo cells, reported that hair-follicle-like structure was formed by rotation culture followed by implantation on the chorioallantoic membrane. Its histological appearance was suggestive but not convincing. We tried to establish an *in vitro* system for hair follicle formation, using the lip skin of rat (Sprague-Dawley) fetuses. Cell aggregates were formed by 24h-rotation culture from the single cell suspension obtained by trypsin treatment. Hair follicles carrying hair shaft (up to Hardy stage 6) developed in the aggregate by the subsequent frosting culture for 6-7 days. The optimal conditions for the rotation culture in terms of morphology and follicle formation frequency were as follows: cell density, 1.5×10^6 day-15 embryonic cells/well; and rotation rate, 60 rpm. Electron microscopy demonstrated that the hair follicles thus formed were almost comparable to those developed *in vivo*. That is, the 6 layers characteristic to hair follicle were all detectable. The present experimental system is considered a useful *in vitro* model for hair follicle formation.

MO 18

ANALYSIS OF IN VITRO BEHAVIORS OF DAY-16 AND DAY-18 FETAL RAT MESENCHYMAL CELLS.

Y. Motobayashi and S. Ihara. Dept. Biochem., Kitasato Univ. Sch. Med., Sagami-hara, Kanagawa 228.

We have previously found that day-16 fetal rat (Sprague-Dawley) skin has an ability to close an open wound owing to the function of mesenchymal counterpart in an organ culture system but day-18 skin loses this ability. Here the mesenchymal cell behaviors such as adhesion, spreading, growth, migration, and collagen gel contraction in a cell culture system (in DMEM supplemented with 10% FCS) were examined, using the mesenchymal cells from day-16 and day-18 fetal skin. No significant difference existed between day-16 and day-18 cells in cell adhesion, spreading, proliferation, and migration rate on plastic surface. The extent of collagen gel contraction by the cells did not depend on the fetal age. The addition of hyaluronate or chondroitin sulfate into the gel had no effect on contraction, while heparin inhibited the contraction by both aged cells. In contrast, only day-16 cells was inhibited by heparin when added to the culture medium. Heparin also blocked spreading of day-16 cells on collagen-coated dishes. In conclusion, the constancy of the behavioral properties of mesenchymal cells *per se* do not account for the age-dependent difference in wound closing ability, though the possible difference in binding affinity of mesenchymal cells to collagen should be further investigated.

MO 19

FATE OF PLACENTAL SCARS AND REPAIR OF DESQUAMATION SITE IN UTERINE HORN OF THE MOUSE (DDD STRAIN).

S. Shiraishi, J. Hisano and T. Mōri. Zool. Lab., Fac. of Agr., Kyushu Univ., Fukuoka.

The sequences of repair of desquamation site in the wall of uterine horn, and formation and disappearance of placental scars in the mouse (DDD strain) were macroscopically and light-microscopically followed using primiparous uterine horns from just after parturition (day 0.5) up to day 365. The scars in the mouse persisted for a year after delivery. The area of the scar rapidly decreased until day 21, thereafter showing only a minute decrease. The reduction in the area and changes in colour of the scars coincided with dispersion throughout the desquamation site, congregation into unrepaired portion in the uterine horn and decrease in number of macrophages involving hemosiderin. In the wall of the horn at day 0.5, there were observed conspicuously the cutting part of the circular muscle, lack of the endometrial epithelial cells, dilated blood vessels and many hemorrhage portions. The invasion of numerous neutrophils into the loose connective tissue was also seen. At day 5, the regularly arranged columnar epithelial endometrial cells covered the connective tissue. By day 7, the metrial gland disappeared in the parametrium and the circular muscle was regenerated, thus the desquamation site was presumed to be almost completely repaired by the same day.

MO 20

SEPARATION OF EU- AND HETEROCHROMATIN FROM RAT LIVER NUCLEI, AND THEIR SENSITIVITIES TO NUCLEASE.

M. Hara, K. Yamashita and T. Suzuki. Dept. of Anatomy, St. Marianna Univ. Sch. of Medicine, Kawasaki.

Active chromatin is known to be high sensitive to nuclease compared with inactive one. On the other hand, chromatin is divided into two groups, eu- and heterochromatin, according to the stainability. In order to clarify the correspondence of active or inactive chromatin to eu- or heterochromatin, we investigated the relationships between the stainability and the sensitivity to nuclease.

Chromatin fractions were sedimented by differential centrifugation from sonicated nuclei. No changes in the stainability by hematoxylin were observed with the isolated fraction, eu- and heterochromatin. When the fractions were digested by DNase I, DNA in euchromatin was digested more faster than that in heterochromatin. In the SDS-PAGE analysis, differences between the fractions were noted on protein compositions. Then heterochromatin was digested by DNase after treatment of trypsin, it was changed to be high sensitive to DNase. Results obtained from these experiments reveal that DNA in euchromatin is more sensitive to DNase compared to that in heterochromatin, and some proteins located in each chromatins seem to play important roles to characterize the differences of the structure or of the sensitivity to DNase.

MO 21

CHARACTERIZATION OF HEMIDESMOSOMAL COMPONENTS BY MONOCLONAL ANTIBODIES.
Y. Nishizawa, K. Owari, Molecular Biology, Nagoya University, Nagoya.

The hemidesmosome is a specialized cell-to-substratum junction present in basement membrane zone of stratified and pseudostratified epithelia. Comparing with the desmosome which is a specialized intercellular junction, little is known about the distinctive proteins of the hemidesmosome except a 230kd polypeptide recognized by autoimmune sera of a skin blistering disease, bullous pemphigoid.

We have succeeded in preparing hemidesmosome-rich fraction from bovine cornea. Using this hemidesmosome fraction, we have prepared monoclonal antibodies to hemidesmosomal components. Screening of the antibodies has been done by immunofluorescence microscopy using frozen sections of bovine skin and immunoblotting. In immunofluorescence, special attention was paid to detect hemidesmosomal spots on myoepithelial cells of apocrine sweat glands.

We will here discuss two putative hemidesmosomal components, 200 and 180kd polypeptides. Monoclonal antibodies to these components may be useful as new markers of the hemidesmosome for studying its molecular organization and function and also differentiation of epidermal and other epithelial basal cells.

MO 22

CORRELATIVE ALIGNMENT OF THE BUNDLES OF F-ACTIN AND OF MICROTUBULES IN THE LEADING LAMELLA OF EPITHELIAL MARGINAL CELLS.
Shigeo Takeuchi, Dept. of Biol. Sci., Fac. Sci., Kanagawa Univ., Hiratsuka.

F-actin bundles (FB) in the leading lamella (LL) of epithelial marginal cells were observed to be depleted thoroughly in the presence of colcemid (Col), an inhibitor of elongation of microtubules (MT), suggesting the roles of MT in the alignment of FB. The role of MT in the alignment of FB in LL of epithelial marginal cells were studied.

With the aid of immunofluorescence method or of a fluorescence dye, changes in the distribution of MT, FB, vinculin, α -actinin or microtubules associated proteins (MAPs) of LL in the epithelial marginal cells were followed, when the corneal epithelia of chick embryos were isolated and cultured with Col (0.05 μ g/ml) or CyTB (4 μ g/ml).

Either with Col or with CyTB, the radial alignment of FB in LL disappeared and LL retracted, but left behind the fine cytoplasmic threads bridging cell body and the focal contacts furnished with α -actinin and vinculin. MAPs that were aligned along FB in a normal state, were, in the presence of Col, scattered in the whole cell body, but not, of CyTB.

These results supported our hypothesis that, in the extending LL of marginal cells under locomotion, FB were polymerized at the focal contacts, fasciculated and/or aligned along MT with the aid of MAPs that interlinked FB with MT.

MO 23

MIGRATION OF HUMAN SKIN FIBROBLASTS: EFFECTS OF *IN VITRO* AGING AND DONOR'S AGE.
H. Kondo, Y. Yonezawa and T.A. Nomauchi, Dept. Biol., Tokyo Metropol. Inst. Gerontol., Tokyo 173.

It is widely known that wound healing delays with aging. Since cell migration has an important role in wound healing, we carried out a study to determine whether migratory ability of human skin fibroblasts declined during *in vitro* cellular aging and whether human skin fibroblasts from older donors migrated more slowly than those from younger donors. Cell migration was determined by Stenn's method (1980), which was developed as an *in vitro* model system of wound healing. The migration of human fetal skin fibroblasts (TIG-3S) gradually decreased with successive passages. The same results were obtained when human skin fibroblast lines from adult (age 36) and old (age 77) donors were examined. But their migratory ability decreased in order of fetal, adult and old donors at all stages of passage. Next, the migration between five different skin fibroblast lines from adult (ages 33-40) and old (ages 69-81) donors was compared at relatively early passage levels. The results showed that the old donor skin fibroblast lines migrated at significantly ($p < 0.05$) slower rate than the adult donor skin fibroblast lines. These results implied that migration of human skin fibroblasts declined with *in vitro* aging and *in vivo* aging.

MO 24

CHANGES IN THE FUNCTIONS OF HUMAN VASCULAR ENDOTHELIAL CELLS DURING *IN VITRO* AGING.
K. Yamamoto¹, M. Yamamoto¹ and N. Hasegawa².
¹Dept. Biol., Tokyo Metropol. Inst. Gerontol., Tokyo, ²Div. Cell Biol., Yakult Inst. Microbiol. Res., Kunitachi.

We investigated some properties of human umbilical vein endothelial cells during *in vitro* aging in order to determine whether long-term culture system is proper as a model system of vascular aging. Cell growth potential and cell density decreased during *in vitro* aging. The number of multinucleated cells increased during *in vitro* aging. Prostacyclin production by this long-term culture decreased progressively during *in vitro* aging. The negative charge of the cell surface also decreased during *in vitro* aging. The endothelial cells possessed antibodies to Factor VIII-related antigen during the *in vitro* life span. The angiotensin converting enzyme activity of the cells decreased linearly up to the final passage. The changes in cell growth, cell density, occurrence of multinucleated cells, prostacyclin production and cell surface negative charge during *in vitro* aging were consistent with the previously described changes in vascular endothelial cells during *in vivo* aging. Therefore, we conclude that cumulative cell division is closely involved in the *in vivo* aging of endothelial cells and that this *in vitro* system is suitable for investigating the *in vivo* aging of vascular endothelial cells.

MO 25

SPECIES-SPECIFIC DIFFERENCES IN GROWTH-STIMULATIVE ACTIVITIES OF HEPARIN-BINDING GROWTH FACTORS FROM SERA OF VARIOUS MAMMALS¹ S. Yonezawa¹, H. Kondo¹, R. Hirai², K. Kaji¹ and K. Nishikawa³. (1) Depts. Biol. and Integrated Res., Tokyo Metropol. Inst. Gerontol., Tokyo 173. (2) Sect. Tumor Cell Biol., Tokyo Metropol. Inst. Med. Sci., Tokyo, and (3) Dept. Biochem., Kanazawa Med. Univ., Kanazawa.

Heparin-binding growth factors were separated from various mammals' sera (bovine, human, mouse and rat) using heparin-Sepharose CL-6B column and estimated their growth-stimulative activities by measuring their capabilities to induce DNA synthesis of Balb/c 3T3 cells. Six peaks were obtained: P1; 0.1M NaCl eluted, P2; 0.3M, P3; 0.6M, P4; 1.1M, P5; 1.3M, P6; 1.0M. P5 and P6 were fetus-specific factors. P1 contained EGF and P3 was mostly PDGF. P4 was detected only in rat and mouse sera, showing extremely high activity in rat. We found out that it was a platelet-derived protein of 120,000 molecular weight with some S-S bonds, heat lability and moderate acid stability, which suggested that P4 was a new type of growth factor. The ratio of the total activity (P1+P2+P3+P4+P5+P6) from each serum to that from FBS was 1.65 for calf, 4.18 for human, 11.17 for mouse and 15.40 for rat. These results indicate that growth-stimulative activities from sera of mammals differ in quantity and quality depending on species.

MO 26

GROWTH FACTOR(S) PRODUCED BY HUMAN GLIOMA CELL LINES

K. Kaji (Tokyo Metro. Inst. Gerontol.), S. Kobayashi (Tokyo Metro. Geriatr. Hosp.) & R. Hirai (Tokyo Metro. Inst. Med. Res.)

Human brain tumors of glial origin sometimes induced neovascularization - a massive proliferation of endothelial cells into the tumor tissue - in progression to increased malignancy. Here we tested the possibility whether such glioma derived cells produce an angiogenic growth factor(s). Three human glioma cell lines, Becker, Marcus and U251MG, all produced the human endothelial cell growth factor activity in the conditioned media. Cell homogenates from Becker and U251MG also contained the growth factor activity. Western blot analysis showed that the endothelial cell growth factor activity produced by Becker and U251MG was basic FGF and not acidic FGF. On the other hand, these all three glioma cell lines did not produce PDGF (AA, AB) and TGF β . Becker line could grow in the serum-free medium supplemented with basic FGF, but the other two lines were not stimulated their growth by basic FGF.

These data showed existing evidence for paracrine growth control by all three human glioma cell lines to endothelial cells, and for autocrine growth control by one human glioma line, Becker.

MO 27

THE EFFECTS OF LECTINS ON THE CULTURED GUINEA PIG HARDERIAN GLAND CELLS. Y. Matsuda*, H. Namiki*, Y. Yokoyama, T. Kasama, E. Yasugi, K. Kano and Y. Seyama. Dept. of Physiological Chemistry and Nutrition, Fac. of Medicine, Univ. of Tokyo, Tokyo, *Dept. of Biology, School of Education, Waseda Univ. Tokyo.

The Harderian gland is well developed in rodents. The main function ascribed to the gland is the secretion of oily substances which facilitates the movement of the eyes. The secretory lipid of the Harderian gland of guinea pig is 1-alkyl-2,3-diacylglycerol (ADG) which contains a large amount of branched chain fatty acids. However, the mechanism by which ADG is synthesized has not been clarified. To analyze mechanism of lipid metabolism, we established the methods of culture of the guinea pig Harderian gland cells.

Growth factors including HDGF, aFGF, bFGF, PDGF and EGF except TGF stimulated the growth of the cells but none of growth factors activated the synthesis of ADG. Lectins like PWM and PHA also stimulated, but WGA, Con A and Momordica agglutinin inhibited the growth. Administration of $\mu\text{g/ml}$ WGA to the cultured Harderian gland cells resulted increase of granules which are seen in the organ. The analysis of lipid content of the cells showed the presence of branched chain fatty acids. The increased FCS concentration diminished the number of granules.

MO 28

PURIFICATION AND CHARACTERIZATION OF HARDERIAN GLAND DERIVED GROWTH FACTOR. Y. Yokoyama, Y. Matsuda*, K. Kano, K. Kaji*, and Y. Seyama. Dept. of Physiological Chemistry and Nutrition, Fac. of Medicine, Univ. of Tokyo, Tokyo, *Dept. of Biology, School of Education, Waseda Univ. Tokyo, *Tokyo Metropolitan Institute of Gerontology, Tokyo.

The Harderian gland is located around the posterior half of the eyeball in rodents and other animals. The role of the gland is not clearly defined.

A polypeptide growth factor has been purified from the gland of guinea pig. The activity of this growth factor was determined by the stimulation of ³H-thymidine incorporation into human embryonic fibroblast cells (TIG-3) and cultured guinea pig Harderian gland cells. The growth factor was purified by a TSKgel DEAE-5PW, Blue Sepharose CL-6B, Superose 12 and Aquapore BU500 chromatography. The purified growth factor has a molecular weight of 13K, as determined by SDS-PAGE. These procedures afforded a 43,000-fold purification. This factor had no influence on the K2T1, K2T2 and A2T2 cells which have the strict requirement of FGF for growth. The activity of the factor was inhibited by a protein kinase C inhibitor H7. These results indicated that the Harderian gland derived growth factor is a new growth factor and stimulates cell growth via activation of protein kinase C.

MO 29

VOLATILE GROWTH FACTORS

M.Kariya and H.Namiki
Dept. of Biol., Sch. of Educ., Waseda
Univ., Tokyo.

Volatile substances were collected from the freeze-dried vapor of fetal bovine serum. Frozen serum was freeze-dried under a vacuum, and the vapor was trapped first in a -48°C flask in order to remove water and secondly in a liquid nitrogen-cooled cylinder (-196°C) to collect volatile substances. The whole sample thus prepared showed no growth promoting activities on any types of cells so far checked under various conditions, however, it rather inhibited cell growth. The sample was subsequently processed through a DEAE HPLC column eluted with water and then 20mM HCl. Ten peaks were obtained, among which the 1st, 3rd, 5th, 6th, 9th and 10th fractions showed significant growth promoting activities and, 4th and 8th ones showed significant growth inhibiting activities on TIG-3 cells. Similar effects were observed in case of NBIRGB cells. On the contrary, 3rd fraction exhibited a significant inhibitory effect on Hela cells. Polyamines were thought to be parts of candidates of the growth promoting factors according to their properties and the smell of the sample, however no such evidence were yet demonstrated.

MO 30

ATTEMPT OF IN VITRO CULTURE OF BLOOD CELLS IN THE ASCIDIAN Polyandrocarpa misakiensis
H. Terato, K. Kawamura and M. Nakauchi
Dept. of Biol., Fac. of Sci., Kochi Univ.
Kochi

In order to investigate the mechanism by which hemoblasts undergo the growth, aggregation and epithelial transformation during budding of Polyandrocarpa misakiensis, we attempted in vitro blood cell culture. We also examined the in vitro function of several substances, which have been shown to exhibit a striking effect on in vivo bud development. Blood cells were harvested from developing buds, and inoculated in a plastic dish (2.7×10^5 - 5.3×10^5 cells/cm²) containing TCM 199, fetal calf serum and artificial sea water (3:1:6) adjusted to pH 7.2. The culture medium was exchanged every three days or one week. Under this culture condition, the blood cells proliferated and aggregated to form a cell mass for about two months, although they could not be transferred to the second culture. C-type lectin extracted from P. misakiensis accelerated cell growth and had an apparent anti-bacterial activity. On the other hand, insulin and prostaglandins did not accelerate cell growth in vitro. Next, we attempted blood cell separation by means of Percoll density gradient centrifugation in order to purify hemoblasts. The results showed that hemoblast population were only concentrated upto 25.6% from 18.8% in the natural blood cell population.

MO 31

HEMOLYMPH COAGULATION IN THE LAND SLUG, INCILARIA FRUHSTORFERI COLLINGE.

E.Furuta¹, K.Yamaguchi² and A.Shimozawa¹

¹Dept. of Anat. and ²Lab. of Med. Sci., Dokkyo Univ. Sch. of Med., Tochigi.

The hemolymph coagulation system of the land slug has been investigated. The fresh hemolymph (FH) clotted in the presence of Ca⁺⁺ when exposed to the air. When FH was immediately centrifuged at 160Xg for 10 min at room temperature, the supernatants (CH) were coagulable. FH and CH which were directly treated with FITC Conjugated Rabbit Anti-human Fibrinogen (FITC-anti-HF) showed very strong fluorescence. However, CH which was centrifuged at 4,000Xg for 10 min at 4°C (IH) was incoagulable and when it was treated with FITC-anti-HF, it did not show fluorescence. Readdition of the precipitates of IH caused clotting of IH, and the precipitates contained the platelet-like structures (PLS).

As a positive control, human plasma was used. Moreover, as a negative control, the inhibition test was carried out to make a comparison with those direct immunofluorescent antibody methods. From the results, it is suggested that PLS play a role in the initial stages of coagulation and it possesses a fibrinogen-like protein.

The total protein concentration of the hemolymph was 11.0 mg/ml (Lowry, et al.).

MO 32

ULTRASTRUCTURAL STUDIES ON INITIAL REACTION OF WOUND-HEALING IN THE LAND SLUG, INCILARIA FRUHSTORFERI COLLINGE.

K.Yamaguchi¹, E.Furuta² and A.Shimozawa²

¹Lab. of Med. Sci. and ²Dept. of Anat., Dokkyo Univ. Sch. of Med., Tochigi.

The normal body wall of the land slug consists of the epidermis containing numerous mucus cells, the connective tissues and the muscle layers. The epidermis which covers the dorsal surface possesses fine microvilli, and that which covers the ventral surface has dense cilia. In the mucus layers, there are two kinds of cells. One is the acidophilic and the other is the basophilic. The melanin granule containing cells are often observed among these cells in the dorsal surface.

In this study, the initial reaction of wound-healing was examined. 30 min after wounding, the surface was sealed off by the aggregated platelet-like structures (PLS). As PLS appear to play a role in the hemolymph clotting, this initial stage may prevent further loss of the hemolymph. One hr later, Type I-like (macrophage-like) cells appeared on the surface, became flattened, and then spread over the surface to become a provisional wound covering. Four days after wounding, the epidermis began to cover with undifferentiated epidermal cells over the wound.

MO 33

THE ENDOCRINE CONTROL SYSTEM ABOUT MATURATION OF REPRODUCTIVE ORGANS OF THE SLUG (*LIMAX MARGINATUS*).

N. Seo and N. Makino, Dept. of Biol., Tokyo Med. Coll., Tokyo.

Reproductive organs of immature stage slug were cultured for 21 days. The media contained extract of organs (cerebral ganglia (cg) or subesophageal ganglia (sog) or optic tentacles (ot) or ovotestes (ovt) or hearts (h)) of oviposition stage. The ovt of immature stage had undifferentiated germ cells (ugc) and previtellogenic oocytes. The in vitro ovt showed the enlarge of acini, the continuity oogenesis and the beginning vitellogenesis in all media, and the differentiation of ugc into male germ cells (mgc) till spermatocytes. The mgc and the ugc of the in vitro ovt showed ratio 53:47 (in cg medium), 80:20 (in sog medium), 13:87 (in ot medium), 7:93 (in ovt medium) and 2:98 (in h medium). The in vitro genital tracts with ovt showed fine structures in all media but h medium, especially in ovt medium showed the development of female parts theirs. More neurosecretory cells (nsc) of cg and sog appeared oviposition stage than immature stage. The sog of immature stage had few nsc. The cg of oviposition stage were surrounded with developed dorsal bodies. We might conclude newly from these facts the follow. Neurosecretory of cg and sog have stimulating effects on the differentiation of mgc and the continuity spermatogenesis. Sog surpasses cg in the effects. The dorsal body has not a effect on vitellogenesis. Hormones from ovt control the genital tracts.

MO 34

STRUCTURE AND FINE STRUCTURE OF THE THYMUS AND PERICARDIAL HEMOPOIETIC TISSUE IN THE WHITE STURGEON

A. Chiba,¹ S. Oka¹ and Y. Honma² ¹Dept. of Biol., Nippon Dental Univ., Niigata and

²Sado Mar. Biol. Stat., Fac. of Sci., Niigata Univ., Niigata.

Light and electron microscopic studies were conducted to elucidate the histological architecture of the thymus and pericardial hemopoietic tissue in the white sturgeon, *Acipenser transmontanus*. The thymus as a multilobated organ showed a demarcation between a cortex lymphoid in nature and a medulla rich in epithelial components. Mitosis of thymocytes was more often in the outer cortex. In some of the medullary epithelial cells, secretory activity was strongly intimated. Macrophages, melanomacrophages, and myoid cells were also found. The pericardial hemopoietic tissue appeared as nodular structures, being highly vascularized, innervated by myelinated and unmyelinated fibers, associated with venous sinuses and adipose tissue, and separated into compartments by collagen fibers and fibroblasts. These compartments were occupied mainly with masses of lymphatic cells, macrophages, melanomacrophages, plasma cells, blast cells, and granulocytes were also observed. Thus, differentiation of the microenvironment between these two lymphohemopoietic organs was evident.

MO 35

DISTRIBUTION AND FINE STRUCTURE OF THE SMALL GRANULE-CONTAINING CELLS AND THEIR NERVE TERMINALS IN THE CARDIOVASCULAR CHEMORECEPTOR SYSTEM IN CERVICO-THORACIC REGION OF THE BAT, *Pipistrellus abramus*

S. Kikuchi

Dept. of Biol., Sch. of Liberal Art & Sci., Iwate Medical University, Morioka.

With the glyoxylic acid-induced fluorescence histochemistry, a large cluster of small monoamine-containing cells (coronary body) is found in the right ventricular wall near the origin of the pulmonary artery along the right coronary artery and vein.

Ultrastructurally these small cells are characterized by an abundance of granules (dense-cored vesicles) in the cytoplasm and large nerve terminals. These small granule containing (SGC) cells are in glomus like structures in close proximity to capillaries, of which endothelial cells are fenestrated in the area of contact with the SGC cells. The SGC cells are innervated by large and small nerve terminals. A large terminal frequently makes synaptic connections with two or more SGC cells surrounding it. There are three types of synaptic connections, afferent, efferent and reciprocal, on the SGC cells.

The abundance of the SGC cells and their close resemblance to those of the carotid body suggests a relative importance of the coronary body in the cardiovascular chemoreceptor system of this species.

MO 36

Inner structures of the cerebral vesicle

of the ascidian larva, *Amaroucium* sp. H. Ohtsuki. Inst. Biol., Fac. Educ., Oita Univ., Oita.

The inner structures of the cerebral vesicle of the larvae of *Amaroucium* sp. were investigated by SEM. Swimming larva of this species has three types of sensory organ in the cerebral vesicle: ocellus, statocyte and hydrostatic pressure organ. The ocellus consists of three lens cells, a pigment cell and several retinal cells. The retinal cells project their processes through the pigment cell toward the lens cells. In the cup of the pigment cell, the apical tip of the retinal processes come to show membranous lamellae, embedded in fibrous cytoplasm of the pigment cell. Most of the larvae contain only one statocyte attached to the wall of the cerebral vesicle by a necked junction at anterior, right position to the ocellus. In 2-3% of the larvae, more than two statocytes were found. Three holes are always perforated on the foot piece of the statocyte at the root of the junction. On the floor under the cell body of the statocyte, many fine processes were found encircling the junction of the statocyte. Near the ocellus, some globular structures like those found in other species of *Enterogona* as a hydrostatic pressure organ were also found in this species on the posterior wall of the cerebral vesicle.

MO 37

FINE STRUCTURE OF THE MUSHROOM BODY OF THE LOBSTER COCKROACH, *Nauphoeta cinerea*.

T. Ohmura, T. Shibuya. Inst. of Biol. Sci. Univ. of Tsukuba, Tsukuba.

It is well known that the mushroom body is one of the morphological parts of the protocerebrum in insect brains. The mushroom body on each side of the cockroach protocerebrum was composed of four lobes; two calyces, α - and β -lobe. And the concave of the calyx had many Kenyon cells. Fine structure observed with TEM was as the following:

- (1) The Kenyon cells were about 5 to 7 μ m in diameter. Their nucleus were very large. (about 3 to 6 μ m in diameter.)
- (2) Many intrinsic fibers made synapses with extrinsic fibers in the calyces. Diameter of the fine intrinsic fibers were about 0.2 to 0.4 μ m.
- (3) Many fibers in the stalk run parallel to each other, and branched off to α - and β -lobes.
- (4) Both lobes have many synapses connecting between intrinsic and extrinsic fibers.

3-D-reconstruction of the mushroom body was made to clarify the stereo-shape through a computer by silver stained preparations of the protocerebrum.

MO 38

ULTRASTRUCTURAL INVESTIGATIONS OF THE ADDUCTOR AND DIDUCTOR IN BRACHIOPODA. A. Matsuno. Dept. of Biol., Fac. of Sci., Shimane Univ., Matsue.

Brachiozoa (*Terebratalia*) has two valves located dorsal and ventral to the body. Two pairs of adductors and diductors control the shell movement. The adductors divide into two portions; a cross striated muscular and smooth muscular portions. Ultrastructural characteristics of muscle cells in these three portions are described in the following. (1) A cross striated muscular portion. Muscle cells showed about 7 μ m in diameter, and included thick myofibrils (30 nm in diameter) and thin ones. Well developed T-systems and SR-systems associating to the T-systems were remarkably observed, but Z-disks showed undeveloped form. (2) A smooth muscular portion. Muscle cells measured about 9 μ m in diameter and showed smooth type at the arrangement of myofibrils. Thick myofibrils measured about 60 nm. These muscle cells were supposed to function the "catch muscle", but their features were different from the "catch muscle" in bivalves. (3) A diductor. Muscle cells showed about 6-7 μ m in diameter and included thick myofibrils of about 60-70 nm. They apparently seemed to be smooth muscle cells in a longitudinal section, but after close observations, they seemed to be a peculiar type of smooth muscle cell.

MO 39

ULTRASTRUCTURAL INVESTIGATION ON THE VENTRAL LONGITUDINAL MUSCLE OF A POLYCHAETA, *NEANTHES* SP.

Y. Kawamura and A. Matuno. Dept. of Biol., Fac. of Sci., Simane Univ., Matsue.

The polychaeta (*Neanthes* sp.) has a pair of longitudinal muscles in ventral side of the body. The muscles include obliquely striated muscle cells. Thick filaments, thin filaments, J-rods and SRs are regularly packed in the cells. A longitudinal section shows the sarcomere-like structure between neighboring J-rods. Another longitudinal section that crosses the former section shows the oblique arrangement of units of thick filaments. When muscle contracts, sarcomere-like structures come to short by sliding of thick and thin filaments. At the same time the oblique pattern of thick filaments changes into the cross pattern. According to our closer ultrastructural observations, the muscle cells can be classified into two types by the diameter of their thick filaments; one type cell has 25-30 nm the other has 40-45 nm.

MO 40

PATTERN OF FILAMENT ARRANGEMENT THAT PRODUCES EASILY THEIR BALL-LIKE AGGREGATES IN SMOOTH MUSCLE FIBERS.

K. Terakado. Dept. of Regul. Biol., Fac. of Sci., Saitama Univ., Urawa.

In large scale shortening of body-wall muscle of an ascidian *Halocynthia roretzi*, zigzag folding, twisting and thickening of smooth muscle fibers were generally noticed. A conspicuous structural change, when examined under a transmission electron microscope, was a dense, ball-like aggregation of myofibrils in the contracted fibers. The size of aggregates was various, but it reflected the degree of contraction. The aggregates often caused local thickenings of the fiber. They were consisted of a dense central core(s) and surrounding less-dense region. The former contained concentrated myosin filaments and some actin filaments. The latter consisted of numerous actin filaments interconnecting the core and cell surface. Intermediate filaments were sometimes found in large groups in the latter, but some of them entered into the core region. Accompanying with the aggregation of filaments, many invaginations of the cell membrane toward the core region usually occurred. With regard to the cellular positions that the aggregates occurred, we noticed that they were always formed in the inner cytoplasmic areas surrounded by the cell membrane richly attached by actin filaments.

MO 41

ULTRASTRUCTURAL STUDIES OF THE CAROTID LABYRINTH IN THE NEWT *CYNOPS PYRRHOGASTER*. T. Kusakabe. Department of Anatomy, Yokohama City University School of Medicine, Yokohama.

Fluorescence, light, and electron microscopic observations of the carotid labyrinth of the newt *Cynops pyrrhogaster* showed the presence of glomus cells in the intervascular stroma of the labyrinth. These cells contained many catecholamine-filled dense-cored vesicles (600-1,000 Å in diameter) and their ultrastructure was similar to that of glomus cells reported in many other animal species. In some glomus cells, there was a group of intranuclear inclusion bodies (0.1-0.3 µm in diameter), and long processes were in close contact with endothelial cells (g-e connection) or with pericytes (g-p connection), which have not been reported in the carotid labyrinth so far. Coated pits were often found on the surface of the cell body and its processes. Enclosed by supporting cells, nerve endings lay close to the glomus cells to make synapses. Two types of synapses (efferent and afferent) were found on the glomus cell surfaces. So-called reciprocal synapses were also found. On the basis of these findings, I conclude that the newt glomus cells may have a secretory function in addition to their chemoreceptor function.

MO 42

CELL DEGENERATION IN THE INTERNAL GILLS OF TADPOLES OF THE CRAB-EATING FROG DURING ACCLIMATION TO VARIOUS DILUTIONS OF SEAWATER. M. Uchiyama and H. Yoshizawa. Dept. of Oral Physiol., School of Dentistry at Niigata, The Nippon Dental Univ., Niigata and Dept. of Oral Histol., Matsumoto Dental Coll., Shiojiri.

Ultrastructure of the internal gills was studied in tadpoles of the crab-eating frog, *Rana cancrivora*. The tadpoles (T-K stages XIII-XVII) were acclimated stepwise to variously diluted seawater (tap water-100% SW). The structure of the internal gills is basically identical in both tap water- and SW-adapted tadpoles. The gill epithelia consist of mitochondria-rich cell (MR cell), pavement cell, basal squamous cell and mucous cell. In tap water-adapted tadpoles, numerous MR cells are present and they show signs of apoptotic degeneration. Most of these cells are distinguishable from the mature cells by a high electron density of the cytoplasm and various shrinkages of the cell volume. On the contrary, necrotic cell death besides the apoptosis was observed on gill epithelia in 60% and 100% SW adapted tadpoles. In a wide range of these epithelia, swelling of cells and cellular compartments being followed by disruption were observed. In these tadpoles, cell divisions were frequently observed. It is concluded that the gill epithelium is a tissue that has high ability of cell renewal. This may be favorable in the environment where salinity changes markedly.

MO 43

NUCLEOGENESIS IN PREIMPLANTATION MOUSE EMBRYOS, AS STUDIED WITH ETHANOL PHOSPHOTUNGSTIC ACID (E-PTA) STAINING METHOD. I. Takeuchi and Y. Takeuchi. Inst. Dev. Res., Aichi Prefect. Colony, Kasugai and Gifu Coll. Med. Technol., Seki.

The decondensing sperm nuclei in fertilized mouse eggs were only faintly stained with E-PTA staining method. The nucleoli appearing in the male and female pronuclei were spherical bodies composed of compactly-aggregating fibrillar materials (condensed nucleoli). These nucleoli were intensely stained with E-PTA method. Fibrillar centers locating at the periphery of condensed nucleoli were also intensely stained with E-PTA. In late 1-cell embryos, only cortical zones of the condensed nucleoli were stained with E-PTA, while the inner areas remained to be only faintly stained. Fibrillar centers lost their stainability with E-PTA. In early 2-cell embryos, the condensed nucleoli were homogeneously stained with E-PTA method except for their cortical zone, while in late 2-cell embryos, only the cortical zones of the condensed nucleoli were stained. The pre-incubation of fixed embryos with DTT or SDS resulted in homogeneously intense staining of the condensed nucleoli, suggesting that disulfide crosslinks may be formed in the nucleolar proteins and interfere the penetration of the stain into the condensed nucleoli.

MO 44

ETHANOL-PHOSPHOTUNGSTIC ACID (E-PTA) AND BISMUTH STAINING OF SPERMATID NUCLEOLI IN MOUSE SPERMIOGENESIS. Y. Takeuchi and I. Takeuchi. Gifu Coll. Med. Technol., Seki and Inst. Dev. Res., Aichi Prefect. Colony, Kasugai

The dense fibrillar component (DFC) of the nucleoli in Golgi-phase and cap-phase spermatids was stained with E-PTA method only its cortical zone. Incubation of the fixed testes with DTT before E-PTA staining resulted in homogeneously intense staining of the DFC. Pre-incubation with SDS also resulted in homogeneously intense staining of the DFC in early spermatids, but in late cap-phase spermatids, the electron-density of the inner area of the DFC was only slightly increased. These results suggest the presence of numerous basic proteins in the DFC, and also the formation of disulfide crosslinks in the protein components of the DFC. After bismuth staining en bloc of formaldehyde-fixed (FA-Bi staining) or glutaraldehyde-fixed (GA-Bi staining) testes, the DFC was homogeneously stained with bismuth until the disappearance of nucleoli occurring in acrosome-phase spermatids. The nucleolar fibrillar center (FC) was homogeneously stained with E-PTA, FA-Bi and GA-Bi staining methods. Basic proteins in the DFC and FC may function in the suppression of ribosomal RNA synthesis in round spermatids.

MO 45

TESTICULAR ARCHITECTURE IN THE SALAMANDER, *HYNOBIUS NIGRESCENS*. I. INTERSTITIAL TISSUE AND INTRATESTICULAR EFFERENT DUCTULES.

Tohru Kobayashi and Hisaaki Iwasawa.
Biol. Inst., Niigata Univ., Niigata.

The seminiferous lobules were arranged around the efferent ductules like the spokes of a fan. The spermatogonia were located in the tubules proximal to the efferent ductules. Germ cells in advanced stages were seen in the tubular regions distal to the efferent ductules. Steroid producing cells and myoid cells were always present within the interstitial tissue. When the steroid producing cells were hypertrophied, numerous unmyelinated axons appeared within this tissue. These axons were in close proximity to the steroid producing cells. The presence of the axons in close proximity to the steroid producing cells was not recognized in other amphibians, i.e., *Cynops pyrrhogaster*, *Rana nigromaculata*, *R. porosa* or *Xenopus laevis*. In the efferent ductules, epithelial cells were filamentous and surrounded by myoid cells. Furthermore, unmyelinated nerve fibers were in close proximity to these myoid cells. With regard to the efferent ductules, the structure mentioned above was also seen in *C. pyrrhogaster*.

MO 46

FINE STRUCTURES OF THE SPERMATOPHORES IN THE SQUID, *Todarodes pacificus*.

H. Takahama, T. Kinoshita and F. Sasaki.
Department of Biology, School of Dental Medicine, Tsurumi University, Yokohama.

The structures of the spermatophores in the squid, *Todarodes pacificus*, were observed by light microscopy and electron microscopy, and were analysed by X-ray microanalysis (XMA). Each spermatophore includes a sperm mass, a cement body, an ejaculatory apparatus and some fluid materials, and is covered by an elastic outer tunic. The outer tunic consists of about 20 thin layers with straight microgrooves parallel to one another. This parallel pattern roughly crisscrosses layer by layer. Thickness of the outer tunic is $46 \pm 2 \mu\text{m}$ at the posterior part and $18 \pm 2 \mu\text{m}$ at the anterior end of the spermatophore. The sperm mass, the only cellular component, consists of a sperm rope which coils more than 400 times. Each sperm in the rope is enveloped by fuzzy substances. The cement body, located between the sperm mass and the ejaculatory apparatus, has a hard crust with an arrowhead-like structure. Calcium is detected by XMA in the crust, which is also well-stained with alizarin red. The ejaculatory apparatus consists of tubules, the inner tunic and the inner membrane. After ejaculation, the sperm reservoir which is made from the cement body and the inner tunic is formed at the anterior end of the extruded and reverted ejaculatory apparatus, and encases the sperm mass. The arrowhead-like structure is located at the tip of the reservoir and is suitable for the thrust into the female's tissue.

MO 47

HISTOLOGY OF THE GNATHIID JUVENILE (ISOPODA, CRUSTACEA) PARASITIC ON THE BRANCHIAL WALL OF THE STINGRAY, AND ITS EFFECT ON THE HOST FISH.

Y. Honma¹, A. Chiba² and Ju-shay Ho³.
¹Sado, Mar. Biol. Stat., Niigata Univ., Niigata,
²Dept. of Biol., Nippon Dental Univ., Niigata and
³Dept. of Biol., Calif. State Univ., Long Beach.

While working on the endocrinological studies of the chondrichthyan hypothalamo-hypophyseal system, we noticed the presence of unfamiliar dark parasite stuck on the branchial wall of the stingray (*Dasyatis akajei*). The parasite was diagnosed as a kind of gnathiid isopods in juvenile stage, so-called pranzia. A high incidence of infection of pranzia was found in 2 species of stingrays, *D. akajei* and *Urolophoides matsubaraei*, whereas the infection rate was low in other species of chondrichthyans. Light- and both scanning and transmission electron microscopy was made to learn the fine structure of pranzia and the effect of infection caused by the pranzia. A heavy inflammation was detected in the host tissues consisting of hyperplastic fibrous tissue, congestion of red blood cells, gathering of heterophils, and many macrophages. Compound eyes, brain, ventral nerve cord, blind midgut glands, and an extremely swollen midgut containing a great quantity of blood cells were discriminated. Mouth organs driven deeply into the host branchial wall were paid our attention to the function of blood sucking.

MO 48

DICYEMID PARASITES IN THE KIDNEY OF *OCTOPUS VULGARIS* AND *OCTOPUS MEMBRANEUS*.

H. Furuya, K. Tsuneki, T. Morita, and Y. Koshida. Dept. of Biol., Coll. of Gen. Educ., Osaka Univ., Toyonaka.

Smear preparations of the renal fluid obtained from *Octopus vulgaris* and *Octopus membranaceus* were examined for dicyemid parasites after Carnoy or formalin fixation, followed by Feulgen-hematoxylin or DAPI staining. In the both *Octopus* species, *Dicyema acuticephalum* was found. In *Octopus vulgaris*, *Dicyema misakiense* and the third dicyemid were also found, although the third species has not been identified yet. In all these dicyemid species, various stages of oogenesis, spermatogenesis, and development of infusoriform and vermiform embryos were observed. In a few individuals of *Dicyema misakiense*, both vermiform and infusoriform embryos were found within an axial cell. Electron microscopic observation revealed that peripheral cells of dicyemids were provided with complicated folds, besides cilia, on the cell surface. Extracellular materials were hardly observed between peripheral cells and the axial cell in dicyemids. The DNA content of dicyemid cell nuclei was estimated by cytofluorometry as a preliminary for further studies.

MO 49

THE FINE STRUCTURE OF DICYEMA MISAKIENSIS
K. Hoshide. Biol. Lab., Fac. of Educ.,
Yamaguchi Univ., Yamaguchi

The fine structure of a primary nematode of Dicyema misakiensis was examined by an electron microscope. D. misakiensis was collected in the renal sac of Octopus vulgaris. It has a longitudinal body which consists of three kinds of cells, polar cells, an axial cell and peripheral cells. Each kind of cells has its own characteristic feature. The polar cells are comparatively small and contained high electron dense endoplasm. Lots of mitochondria, vacuoles and endoplasmic reticulum were observed. On the surface of the polar and the peripheral cells two kinds of projections were observed. One kind of projections is normal cilia, containing 9+2 microtubules. The cilia of the anterior tip of polar cells are shorter than those of the other parts. D. misakiensis thrusts those short cilia among the host tissues and holds itself in the renal sac. The other projections are small and short. No microtubule was observed in them. The endoplasm of periphery cells and an axial cell are low electron density and few organelles are contained in them. Vermiform larvae of various developmental stages were observed in the axial cell. They contained high electron dense endoplasm. In the early developmental stage, they had a lot of vacuoles and the surface of the vermiform larvae was smooth. In the later stage they lost the vacuoles but had lots of cilia on their surface.

MO 50

BIREFRINGENT PARTICLES OBSERVED IN
TRICHOPLAX ADHAERENS (PLACOZOA), THE SIMPLE-
EST METAZOAN.

T. Uehara, V.B. Pearse*, and K. Yamazato.
Dept. of Biology and Sesoko Marine Science
Center, Univ. of the Ryukyus, Nishihara-cho
Okinawa and *Dept. of Biology and Institute
of Marine Sciences, Univ. of California,
Santa Cruz, California.

Individuals of Trichoplax adhaerens are small, flat organisms that look somewhat like amebas, but consist of two flagellated epithelium cells. This is the sole species in the phylum Placozoa, established in 1971 by K.G. Grell. The placozoans used in this study were collected from waters off the northwest coast of Okinawa and seawater taken off the central west coast.

All specimens observed microscopically under polarized light displayed a ring of birefringent particles around the edge of the animal. Over 120 such particles were counted in one large individual. Examined by interference microscopy, the particles appeared similar to the rudiments of the spicular calcite skeleton in the gastrula stage of echinoids.

The composition of these particles in placozoans, and their function in the body plan of these simple animals, await further study and comparison with structures in other metazoan phyla.

MO 51

CULTIVATION IN VITRO OF THE INTESTINAL
FLAGELLATES OF THE TERMITE.

I. Yamaoka, Y. Kawamura, K. Doi and R. Murakami. Biol. Inst., Fac. Sci., Yamaguchi Univ., Yamaguchi.

The factors for the symbiotic relation between termites and their intestinal protozoa was examined. The relationship between them in the cellulose digestion is well known, which cellulose eaten by the termite are digested by the intestinal protozoa. Recently it was shown that the termites supply not only cellulose with the intestinal protozoa, but also a kind of cellulase (CMCase). Moreover, it was shown that the environmental factor in the intestine must be added into the factors for the symbiosis. The cultivation in vitro of T. agilis was examined under the several conditions. The flagellates were transplanted into a salt solution (solution-U), but all of them died within 12 hrs. Many species of bacteria were isolated from the intestine of the termite. When conditioned media which incubated with 2 kinds of species of the isolated bacteria were used instead of the solution-U, T. agilis survived for a long period of time. By the addition of CMCase into the conditioned medium second proliferating division of T. agilis was also induced.

MO 52

SOME FACTORS INFLUENCING EXCYSTMENT OF A
HYPOTRICH CILIATE, HISTRICULUS CAVICOLA.
T. Nakamura. Dept. of Biol., Fac. of Sci.,
Kumamoto Univ., Kumamoto.

Excystment of a hypotrich ciliate, Histriculus cavicola, was divided into 4 stages by morphological characteristics detectable under a dissecting microscope. Since the process of a strain, HS-3S, was quite synchronous, it could be useful for the study of ciliate excystment.

In the HS-3S strain, nearly 100% excystment was resulted within 4 h after excystment induction, when excystment was induced in 10x Osterhout's solution at stationary phase. Under this excystment condition, even very young cysts of this strain, 1.5 h after attaining spherical form, could excyst. On the other hand, in the young cysts of KM-1 and KM-2 strains, their excystment was low even in the same excystment condition, but it became high with increasing age of the cysts. In the spontaneously excysted cysts, excystment rate was low in the young cysts, even in HS-3S strain, but it became high with aging of the cysts. Excystment was reversibly inhibited by short-interval observations. The results may suggest that the excystment is influenced by the excystment medium, the age of the cysts, and light and/or vibration caused by observations.

MO 53

CORTICAL MORPHOGENESIS DURING EXCYSTMENT IN A HYPOTRICH CILIATE, *HISTRICULUS CAVICOLA*. T. Yamashita and T. Matsusaka. Dept. of Biol., Fac. of Sci., Kumamoto University, Kumamoto.

Cortical morphogenesis during excystment of a hypotrich ciliate, *Histiculus cavicola*, was observed light and electron microscopically.

At very early phase of excystment, a few kinetosomes appeared *de novo* on the future ventral surface of the cyst and they proliferated to form a cluster. It then splitted into 2 parts; one differentiated into adoral zone of membranelles and the other into cirri on the ventral surface via cirral streaks, and into paroral and endoral membranes. Left and right marginal cirral rows originated from 2 kinetosomal rows appeared at the posterior-left and right sides of the above 2 clusters.

The appearance of kinetosomes on the dorsal surface started later than that on the ventral surface. The kinetosomes first appeared as 3 rows when the cirral streaks developed on the ventral surface. The numbers of rows increased to 6 and then differentiated into 6 dorsal bristle rows. Three caudal cirri were differentiated from the posterior ends of 1st, 2nd and 4th dorsal bristle rows.

The present results clearly showed that cortical morphogenesis during excystment was analogous to that during binary fission.

MO 54

GROWTH PROMOTING SUBSTANCE SECRETED BY THE *JUNYO* MUTANT OF *PARAMECIUM TETRAURELIA*.

Y. Takagi¹, H. Tanabe² and K. Kaji³. ¹Dept. of Biol., Nara Women's Univ., Nara, ²Govt. Indust. Res. Inst., Shikoku, Takamatsu and ³Isotope Lab., Tokyo Metro. Inst. Gerontol., Tokyo.

The *jumyo* mutant of *Paramecium tetraurelia* has a short clonal lifespan and divides slowly in daily reisoletion cultures. When mass cultured, however, it divides as rapidly as the wild type cells. Cell-free fluid of the mutant's mass culture concentrated 100-fold by ultrafiltration, here called crude sample, results in restoration of the normal fission rate in daily reisoletion cultures. The growth promoting substance included in the crude sample was identified as a protein with relative molecular mass (Mr) of 16,000, named *Paramecium* growth factor (ParGF). Crude samples from 10 stocks other than the *jumyo* mutant were tested for their ability to restore the fission rate of the *jumyo* mutant; those from 7 stocks were effective but those from 3 other stocks were ineffective. The ability of restoration that probably indicates the secretion of ParGF was related neither to the genotypes of the *jumyo* and/or *nd169* loci nor to the mating types. Crude sample from the *jumyo* mutant was not substituted for basic FGF to promote growth of human endothelial cells.

MO 55

MICROSURGICAL ANALYSIS OF MUTANT AFFECTING SURFACE ANTIGEN IN *PARAMECIUM TETRAURELIA*. S. Kobayashi and S. Koizumi. Dept. of Biol., Miyagi Coll. of Educ., Sendai.

Mutant strains d48 and d12 cannot express serotype A. Strain d48 contains the A gene in the micronucleus but the gene is lost during macronuclear reorganization because of cytoplasmic defect. The presence of A gene in the d12 of micronucleus has been suggested, but its macronucleus lacks the gene A. Micronuclear transplantations into enucleated cells were performed to analyze those mutants. Wild 51 enucleated cells transplanted d48 micronuclei expressed serotype A. On the contrary, amicronucleate d48 cells transferred 51 micronuclei did not express A. These results indicate that the A gene is present in d48 micronuclei but the cytoplasm is defective. Wild 51 cells transplanted d12 micronuclei could not express A. Amicronucleate d12 cells transplanted normal micronuclei from 51 or d48 showed no expression of A. From these results, it seems that even if d12 of micronucleus contains the gene A, that must be abnormal, and its cytoplasm is also defective as same as d48. Genetic analysis showed that F₁ clones of d12 obtained from crosses to 51 and both F₁ clones of crosses of d12 and d48 frequently express A. These results, therefore, demonstrate that heterozygote of d12 and wild 51 or d48 caused to cure the cytoplasmic defect of d48 or d12 during the development of macronuclei.

MO 56

MONOCLONAL ANTIBODY AGAINST MACRONUCLEUS-SPECIFIC PROTEIN OF *PARAMECIUM CAUDATUM*. M. Fujishima¹, Y. Inoue¹, T. Sawada² and T. Fukumoto². ¹Biol. Inst., Fac. of Sci., Yamaguchi Univ., Yamaguchi and ²Dept. of Anat., Sch. of Med., Yamaguchi Univ., Ube.

Hybridoma clone (MA-1), which produces macronucleus specific monoclonal antibody of *P. caudatum*, was obtained by injecting isolated macronuclei of *P. caudatum* into mice and by following cell fusion between the immunized mouse spleen cells and mouse tumor cells (NS-1). Ouchterlony showed that the antibody is IgG. Immuno-blotting of SDS-PAGE gel showed that a major band of 50 KD and a minor band of 40KD have an antigenicity. Immuno-fluorescence microscopy showed that the antigen was present in the macronucleus of eight syngens of *P. caudatum* and *P. dubosqui*, but not in other *Paramecium* species (*P. aurelia* species, *P. multimicronucleatum*, *P. jenningsi*, *P. bursaria*), other protozoa (*Euplates encysticus*, *Pseudostella levis*, *Tetrahymena thermophila*, *T. pyriformis*, *Amoeba proteus*, *Stentor coeruleus* and *Dictyostelium discoideum*) and blood cells of *Xenopus laevis*, *Bufo bufo japonicum*. Cytoplasmic particles of human granulocyte also showed reactivity. It was found that the antigen of *P. caudatum* appeared in the macronuclear anlagen immediately after the 4 out of 8 postzygotic nuclei differentiate morphologically into the macronuclear anlagen.

MO 57

Immaturity in haploid and diploid clones of *Euplotes woodruffi* syngen I (Ciliophora)
T. Kosaka. Zool. Inst. Fac. of Sci., Hiroshima Univ., Hiroshima.

Conjugation of a unimicronuclear doublet with two singlets produced three kinds of exconjugants: an exconjugant singlet cell, with a micronucleus and a macronucleus, originated from a synkaryont(diploid); an exconjugant singlet with a micro- and a macronucleus from a hemikaryon(haploid); and an exconjugant doublet consisting of two components, one side bearing a micro- and a macronucleus derived from a hemikaryon and another side with those from a synkaryon. Of the two exconjugant singlets, one died in 64% of all cases and both singlets survived and formed clones in 20% of the cases. Using the latter, viability of the exconjugant clones and the length of the immaturity period were compared in diploid and haploid clones. Exconjugants which were considered to have a diploid nuclear apparatus showed an immaturity period of over 40 fissions, while those with a haploid nuclear apparatus produced many clones with short immaturity periods of less than ten fissions and short-life clones. No singlet exconjugant clones, with diploid nuclear apparatus, showed a short immaturity period. The singlets with short immaturity produced F2 clones at a low viability through conjugation, while those with normal immaturity produced F2 clones with a high viability.

MO 58

AN EFFECT OF MICRONUCLEAR TRANSPLANTATION ON EXPRESSION OF MATING TYPE IN *EUPLOTES OCTOCARINATUS*.

K.Sato¹, H.-W.Kuhlmann² and K.Heckmann².
¹Dep. of Biol. Naruto Univ. Naruto and
²Zool. Inst. Münster Univ. Münster, FRG.

The 10 mating types can be distinguished in the ciliate *E. octocarinatus*. The mating types are determined by four codominant alleles (mt¹, mt², mt³, mt⁴) which control the production of four mating-inducing gamones (G₁, G₂, G₃, G₄). The micronucleus (mt², mt³) of the cell (mating type VIII) was transplanted into a amicro-nuclear cell (mating type VII, genotype mt¹, mt⁴) whose micronucleus had been removed. Of the 61 operated cells, 40 cells grew into clones. In 20 of the 40 clones, homotypic pairs were induced by gamones. The 3-5 exconjugants were isolated from each crossbreeding. According to the cross breeding examinations, about 51% of the all exconjugant clones were shown to be clones of the new mating type which conjugated with the 10 mating types cells. The conjugating pairs were homotypic pairs of the progenies. The 11% clones showed mating type VII, the others were in adolescence phase. Also, the micronuclei of mating type VII (mt¹, mt⁴) were transplanted into amicro-nuclear cells of mating type VIII. The new mating type clones appeared in 19% of the progenies. From these results, the micronuclear transplantation appears to have effects on expression of mating type in *E. octocarinatus*.

MO 59

CELL FUSION IN A CILIATE *TETRAHYMENA* III. NUCLEAR CHANGE IN INCOMPLETELY FUSED CELLS. S.Watanabe and T.Sugai. Div. of Biol., Fac. of Sci., Ibaraki Univ., Mito.

Conjugation of ciliate is a sexual process in which meiosis, nuclear exchange, fertilization and nuclear differentiation occur. Conjugating pairs of *Tetrahymena thermophila* were fused by rapid osmotic change (hypotonic shock). Changing degree of the shock, we could obtain two kinds of fused cells; completely fused round cells (CF) and incompletely fused with normal pair like morphology. Synchronized pairs were fused at (A) three prezygotic stages and (B) one post zygotic stage. Nuclear abnormality was studied up to 12 hours after fusion. In both CF and ICF cells fused at (A), (a) micronuclei kept dividing and its number increased beyond normal number(10), (b) many macronuclear anlage were formed, (c) the number of macronuclear anlage decreased to only two which is normal number per cell. In (B) case, no abnormal pattern was observed except nuclear positioning.

This reproducible, controllable fusion system would give more insight into nuclear process during conjugation.

MO 60

THE RELATIONSHIP BETWEEN MORPHOLOGY AND BIOCHEMICAL FUNCTIONS OF ANIMAL CELLS. N.Koseki and K.Yoshizato
Lab. of Dev. Biol., Dept. of Biol., Fac. of Sci., Tokyo Metropolitan Univ.

We found that the changes in cell morphology of anchorage-dependent cells, fibroblasts of human dermis origin in this study, markedly affect the protein synthesis properties quantitatively and qualitatively. The rate of protein synthesis of round and unattached cells on BSA coated dishes, was much lower than that of attached and spread cells. However, amino acid pools of round cells increased 2-fold that of spread cells, suggesting that the observed difference is due to changes in the translational machineries of the cell. Since cell morphology is closely related to cytoskeletons, it is thought that cytoskeletons plays important roles in such a regulation. Then, we attempted to develop a reconstituted cell model (in situ fractionation and reconstruction) to elucidate the role of cytoskeletons. We found that the in situ fractionation procedure gave the morphological intact nuclei and cytoskeletons (actins, vimentins and tubulins) which were still attached to culture plastic. We think these cell-free remnants on plastic are useful as an experimental model system for investigating the relationship between morphology and biochemical functions of cells at molecular levels.

MO 61

REGULATION OF MELANOGENESIS DURING THE HAIR CYCLE OF MICE. II.

Y. Nishitani¹, K. Ito², T. Morita² and Y. Koshida². ¹Nippon Zoki, Pharm. Co., ²Dept. of Biol., Coll. of Gen. Educ., Osaka Univ., Osaka.

We reported in the 59th conference of this society (1988) that the nude mice (C3H/He-nu) were very useful for the study of melanogenesis in skin during the hair cycle.

In the present study, we studied in more detail the transition of melanogenesis during the hair cycle by means of light, electron microscope and primary culture of the nude mouse skin. In anagen during the hair cycle, numerous DOPA-positive melanocytes were observed in the hair bulbs, and DOPA-positive signs were detected in Golgi areas (GERL) of melanocytes. In catagen and telogen, on the other hand, stunted hair bulbs were only found, and the bulbs showed acid phosphatase activity. Moreover, autophagic vacuoles including melanosomes were observed in melanocytes. These results indicate that melanin production is very active in anagen, but melanin degradation by melanosome digestion in autophagic vacuoles occurs in catagen and telogen. In addition, from the results of the primary culture, we expect that the differentiated state of melanocytes in respective stages of the hair cycle is autonomously maintained, even when the surrounding tissues are removed.

MO 62

CHANGES IN THE STRUCTURE OF ENDOMETRIAL EPITHELIAL GLYCOCALYX DURING THE PERIOD FROM SPERM STORAGE TO EARLY PREGNANCY IN THE JAPANESE HOUSE BAT, PIPISTRELLUS ABRAMUS.

T. Mōri and T. A. Uchida. Zool. Lab., Fac. of Agr., Kyushu Univ., Fukuoka.

Spermatozoa inseminated in autumn are stored in both the uterus and the uterovaginal junction for about six months until fertilization in spring. In the uterus, the heads of intact spermatozoa are in close contact with epithelial microvilli which are covered by well-developed glycocalyx with a strong affinity for ruthenium red, phosphotungstic acid, cationized ferritin and ferritin-conjugated Limax flavus (LFA).

Just before ovulation, microvillous glycocalyx commences to change their structure. Spermatozoa begin to be released from microvilli as glycocalyx becomes gross. When glycocalyx exhibits a foamy and tortuous structure, sperm is completely released. At the preimplantation stage, the epithelial cells turn columnar and are characterized by an appearance of developed secondary lysosomes, and all microvilli of the epithelial cells lengthen and are again covered by a great amount of glycocalyx.

MO 63

NEURONAL DIFFERENTIATION FROM THE CELL CULTURE OF THE ANTENNAL IMAGINAL DISC OF SILKWORM, BOMBYX MORI L.

Y. Waku, M. Koike and N. Yoshida. Dep't of Appl. Biol., Kyoto Inst. Technol., Kyoto.

Antennal imaginal discs of the male 5th instar silkworms were excised and disrupted either mechanically or enzymatically. The disrupted discs were cultured *in vitro* using various insect culture media, and the migrated disc cells survived for a long period over 1 year during which various cell proliferation forms were observed. Establishment of the cell lines from the culture is in progress presently.

From the proliferating cell dispersions in culture, many neuroblast-like cells with round contour and small or medium sizes differentiated, then extended their cytoplasmic processes which were mono-, bi- or multipolar in morphology. Finally they transformed to apparent neurons with synapse, varicosities and filopodia etc.. These morphological evidences characteristic to neurons and also the origin of culture (i. e. antennal imaginal discs which are destined to produce numerous neurons during metamorphosis *in vivo*) strongly suggested the success of *in vitro* neurogenesis in this culture system. The most appropriate culture conditions for neurogenesis have been surveyed presently.

MO 64

DYNAMIC ASPECT OF STARFISH PHAGOCYTES: ARE THEY TRYING TO EAT THE SUBSTRATUM BY FORMING SYNCYTIA? S. Towa, M. Oan-Sohkawa and H. Kaneko.

Dept. of Biol., Osaka City University, Osaka.

Phagocytes of the starfish, Asterias amurensis, extend petaloid pseudopodia and float singly in the coelomic fluid. They aggregate in response to contact with foreign bodies, as well as to removal from coelomic cavity. When aggregates are inoculated on cultural substratum such as glass or plastic surface, they adhere, expand and form large syncytia within 12 h. We consider that both of these phenomena, aggregation and syncytium formation on substratum, are reactions of phagocytes against foreign bodies. If this is so, fusion should be an important part of the reaction.

In order to verify the stimuli leading to syncytium formation, the phagocytes were rotary-shake cultured for 18 h either under the presence or absence of the stimulatory influence of latex beads, and were observed by TEM. Fusion was not found in either of these conditions. Instead, extensive folding of cell surfaces was observed between tightly packed cells. Electron dense cell contacts, on the other hand, were found among parallel membranes of adjacent cells in a spreading aggregate at a time period as short as 1.5 h after inoculation. Cytoplasmic connections were sometimes observed in these contacts.

These results suggest that the stimulus to cause phagocyte fusion is cell movement within spreading aggregates and not aggregation itself, duration in an aggregated state or phagocytic stimulus (or adhesion to foreign bodies).

MO 65

TRAPPING OF FOREIGN MATERIALS BY LYMPHOID ORGANS IN THE TELEOST, *ORYZIAS LATIPES*. H. Nakamura¹, A. Shimozawa² and S. Kikuchi². ¹Dept. of Anat., Dokkyo Univ. Sch. of Med., Tochigi and ²Kominato Lab., Chiba Univ., Amatsu-Kominato.

The major phagocytic tissues of the teleost, *Oryzias latipes* comprise the spleen, the kidney and the heart. Although melano-macrophage center (MMC), which is the aggregation of professional phagocytes against antigenic and inert materials, is distributed in these organs, ellipsoids (E) of the spleen, sinusoidal macrophages of the kidney and endothelium of the heart function as the primary barrier against foreign materials.

E showed rapid phagocytosis against colloidal carbon even at low temperatures while slow phagocytosis against some soluble materials such as FITC-dextran. In E, numerous pinocytotic vesicles, loose connection of the endothelial cells, and occasional narrowing of the lumen suggested intra and interendothelial transport pathways. The endothelium, which often lacked basal lamina, was surrounded by a thick wall of argyrophilic fibers and reticular cells (R). R was phagocytic and the ingested carbon was gradually transported to MMC but some was retained within R for a long time (over 50 days). α -Naphthyl acetate esterase yielded brown products in R while DAB peroxidase revealed very little activity in E.

MO 66

PROFOUND SURFACE CHANGES OF IN SITU MACROPHAGES INDUCED BY SUPERIMPOSED ANTIGENS. I. Hori¹ and K. Ryojima². ¹Dept. of Biol., Kanazawa Med. Univ., Uchinada, ²Dept. of Exp. Therap., Cancer Res. Inst., Kanazawa Univ., Kanazawa.

Mice were injected in the footpad with preparations of PSK or sheep erythrocytes (SRBC) or both, and the ultrastructure of subcutaneous macrophages was studied at various intervals after injection.

A single PSK injection induced an extensive accumulation of host cells which consisted of neutrophils, fibroblasts and macrophages. The macrophages phagocytized PSK and kept the PSK for a long time, but they gave rise to only a few cytoplasmic projections. A single SRBC injection induced linear cell arrangements of macrophages in which the phagocytized SRBC were digested rapidly. When PSK-stimulated macrophages were challenged by SRBC, the cells showed very profound surface changes: They sent out numerous long cytoplasmic projections radiating in all directions. Such projections of neighboring macrophages were characterized by the intimate interlocking. This provided massive aggregations of activated macrophages with homogeneous cell profiles.

These results suggest the possibility that intercellular communication among the "activated" macrophages was profoundly elicited and maintained through an intensive interaction of their cytoplasmic projections.

MO 67

MALIGNANT TRANSFORMATION OF MOUSE C3H 10T1/2 CELLS INDUCED BY IONIZING RADIATIONS AND ULTRAVIOLET LIGHT. T. Yamaguchi¹, M. Takahashi² and M. Umeda², ¹Fac.Gen.Educ. and ²Fac.Sci., Ehime Univ. Matsuyama.

Cultured 10T1/2 cells in confluency were irradiated with either ultraviolet (UV: 254 nm), beta (tritiated water), X (250 kVp) or gamma (cobalt-60) rays. The dose-survival and dose-transformation (Tf) curves after protracted beta or gamma irradiation (0.05 to 1 Gy/h) at 4°C were independent on the dose-rate, and the effects per Gy were much higher than those after the same protracted irradiation at 37°C. Therefore, the effect of beta or gamma irradiation at 4°C could be compared with that of a single acute UV (0.67 J/m² per sec) or X (0.5 Gy/min) irradiation. If the cells were exposed to the doses which produced the same mortality among different radiations, the Tf frequencies were in the following order:

UV > beta > X or gamma rays.
The doses required to reduce the survival fraction, for example, to 0.2 were 3.4 J/m², 3.0, 4.0 and 3.8 Gy for UV, beta, X and gamma rays, respectively. The Tf frequencies at these doses were 5.7, 3.0, 1.5 and 1.4 per 1000 surviving colonies, respectively.

BE 1

SIZE STRUCTURE OF DENSE POPULATIONS OF *Ophiura sarsi* (OPHIUROIDEA: ECHINODERMATA) IN THE BATHYAL ZONE AROUND JAPAN. T. Fujita, and S. Ohta. Ocean Res. Inst., Univ. of Tokyo, Nakano, Tokyo.

The epibenthic ophiuroid *Ophiura sarsi* forms dense beds, i.e., high-density populations uniformly covering large area of the sea floor, in the upper bathyal zone around northern Japan. The population density ranged from about 30 to several hundreds individuals per square meter. Size-frequency distributions of *O. sarsi* were polymodal, and were usually dominated by a peak of large-sized individuals. Comparisons of size structure at various localities showed that the size of *O. sarsi* was greatest at lower population densities through probably a density-dependent effect on growth. Consequently the biomass of *O. sarsi* was relatively constant at the different localities.

The maximum size of *O. sarsi* was found to increase with increasing depth in the area off Otsuchi, Pacific coast of northeastern Japan. Relatively strong recruitment was recognized in the shallower part of the dense bed, where *O. sarsi* occurred in the absence of other species of ophiuroids. At greater depths, modes of small individuals were inconspicuous, probably due to interspecific competition with coexisting congeneric species, amongst which *O. sarsi* attained a larger maximum size.

BE 2

ACTIVITY RHYTHM OF *DROSOPHILA* KEPT IN DARKNESS FOR 800 GENERATIONS.
M. Imafuku. Dept. of Zool., Fac. of Sci., Kyoto Univ., Kyoto.

Activity rhythm of the stock of *Drosophila melanogaster* maintained under complete darkness since 1954 (Mori's stock), was investigated. An adult fly was confined in a small cell, and its movements were monitored with an infrared beam penetrating the cell. Three types of experiments were carried out: (1) flies kept in LD (12L-12D) condition from the egg to the whole adult stages, (2) flies kept in LD in the egg and larval stages and shifted to DD condition a few days after into the adult stage, and (3) flies kept in complete darkness over all developmental stages to adult on which a single light pulse was applied. In group (1) their activity was synchronized with the ambient LD cycle, and in groups (2) & (3) circadian rhythms of a 23-24 hour period were detected.

BE 3

FREERUNNING ACTIVITY RHYTHM OF THE NOCTURNAL CRUSTACEAN, *DIMORPHOSTYLIS ASIATICA*.
T. Akiyama. Ushimado Marine Laboratory, Univ. of Okayama, Okayama.

The swimming activity of the nocturnal crustacean, *Dimorphostylis asiatica* was recorded under constant darkness in the laboratory. All the recording showed distinct freerunning rhythmicity with circadian period persisting for 20-40 days of recording period. In accordance with the modality of the pattern, inter and intra-individual variations were observed. Out of 150 recordings, about 70 individuals showed unimodal pattern, about 30 animals bimodal patterns, and the other 50 animals showed modality change during the recording period. Freerunning periods of unimodal patterns were about 2h longer than those of bimodal ones. And the modality change caused the shift of the freerunning periods with the tendency of the periods of unimodal phase to be longer than those of bimodal one. This endogenous rhythmicity possibly show two relatively stable characteristics which express different modality and freerunning periods.

BE 4

LOCOMOTOR ACTIVITY RHYTHM IN THE CRAB *SESARMA PICTUM*.

M. Saigusa. Dept. of Natural Sci., College of Liberal Arts & Sci., Okayama University, Okayama.

The locomotor activity of the crab *Sesarma pictum* was monitored in continuous light (LL), continuous darkness (DD) or 24-h light-dark cycles, and periodical component involved was examined by periodogram, correlogram and naked eyes.

In constant conditions more than half of the experimental animals (62 out of 113 examples) showed arrhythmic activity. The slight periodicity with a circadian component was detected in other 25 specimens, and remaining 26 individuals indicated a remarkable circadian rhythmicity. The endogenous periodicity of these crabs (52 individuals) covered 22.5-40 h (24.8 h in the mean), but obvious difference was seen between male and female crabs as to the degree of its strength.

When crabs were exposed to 24-h light-dark cycles (LD 15:9 or LD 14:10), a 24-h component was more or less detectable for more 80 % of specimens. Correlogram analyses, however, suggested that most of these activity patterns are caused by the direct reaction to the 24-h LD cycles.

BE 5

SEASONAL CHANGE OF THE LOCOMOTOR ACTIVITY RHYTHM OF LOACHES: EFFECTS OF ENVIRONMENTAL FACTORS.

M. Naruse and T. Oishi, Dept. of Biol., Fac. of Sci., Nara Women's Univ., Nara.

We examined the locomotor activity rhythm of loaches kept together in an outdoor water tank. The results are as follows. In winter, the locomotor activity rhythm of loaches showed diurnal activity pattern, and the onset of the activity was in phase with the rising period of water temperature. However, when water temperature became almost constant due to cloudiness or raining, diurnal activity pattern disappeared and the amount of their activity decreased. In summer, the activity became arrhythmic or diurnal, and the relation between activity and water temperature became less clear compared with the activity in winter. Thus, the locomotor activity of loaches changes seasonally and seems to be affected by environmental factors such as light (day length) and temperature. Individual loaches were placed under four conditions (LD16:8, 25°C; LD8:16, 25°C; LD16:8, 10°C; LD8:16, 10°C) in a bioclimatic chamber. The activity mainly showed nocturnal pattern. Thus, the seasonal change in the activity pattern was not reproduced by constant temperature experiments. Daily temperature cycle might be an important factor to control the activity pattern.

BE 6

ENTRAINMENT OF THE CIRCADIAN RHYTHMS IN JAPANESE COMMON NEWT BY MELATONIN INJECTIONS
M. Kikuchi¹, A. Chiba² and K. Aoki¹. ¹Life Sci. Inst., Sophia Univ., Tokyo and ²Dept. of Physiol., St. Marianna Univ. Sch. of Med., Kawasaki.

Daily melatonin injections can entrain the circadian activity rhythms of many species of vertebrates. These data suggest that the circadian rhythm of melatonin concentration provides an internal synchronizing agent in the circadian system. The pineal organ has been shown to possess melatonin synthesizing capabilities and play a role in circadian system of lower vertebrates.

In the present study, the newts were kept in continuous darkness and subcutaneously injected with 10µg of melatonin at the same time each other day to examine its effects on the circadian rhythms of the number of synaptic ribbons in the pineal photoreceptor cells as well as on the circadian activity rhythms. Free-running activity rhythms of the newts were entrained by daily melatonin injections and a similar phase relationship between the rhythms of locomotor activity and synaptic ribbons as has been shown in intact newts were observed. These results suggest the possibility that circadian rhythms of melatonin can synchronize the circadian system of the newts including functions of the pineal organ.

BE 7

ANALYSIS OF DISPLAY PATTERNS IN THE SOCIAL BEHAVIOR OF THE LIZARD, *Japalura polygonata*.

T. Machida¹ and T. Arima². ¹Dept. of Regulation Biol., Fac. of Sci., Saitama Univ., Urawa and ²Dept. of Biol., Fac. of Sci., Kagoshima Univ., Kagoshima.

Patterns of aggressive behavior and courtship behavior in the lizard, *Japalura polygonata*, obtained from the Ryukyu Islands were described and analysed in the laboratory. During aggressive encounters male lizards exhibited the following responses: a) head bobbing, b) dewlap display, c) jaw opening with tongue thrusting, d) lateral body compression, e) crest erection, f) tail whipping, g) biting the root of the tail, h) submissive head nodding, and i) assertion display. It was further observed that the resident male is not always dominant over the intruder, while the larger male generally dominates over the smaller one at the sudden encounter. Distinct regional difference was found in the mode of head bobbings during the challenge display: male lizards from the Okinawa Island exhibited significantly greater number and duration of head bobbings than those from the Miyako Island. No difference was detected in the number and duration of head bobbings in male lizards between aggressive encounters and courtship displays.

BE 8

EFFECTS OF SEX, AGE AND FAMILIARITY ON HUDDLING BEHAVIOR OF MICE
K. Ninomiya and T. Kimura. Dept. of Biol., Coll. of Arts and Sci., Univ. of Tokyo, Tokyo.

Five unrelated mice of the same sex were caged together when they were 3 weeks of age, and their huddling behavior was examined at 4, 8 and 12 weeks of age. At each age, the behavior of mice were videotaped for 48 hr and then analyzed. In males, the tendency to huddle in the light period increased as they grew older, while in the dark period it declined with age. On the other hand, the change in the behavior of females showed no clear correlation with age.

In order to ascertain whether the age-related change in the behavior of males is due to the increase of familiarity, 5 males that were unfamiliar with one another were put into the same cage only during test sessions. In the light period, huddling tendency of these males also increased until 8 weeks of age but declined thereafter, while in the dark period, it decreased with age, as observed in familiar male groups. Interestingly, in the dark period, unfamiliar males tended to huddle more than familiar ones.

It is likely that huddling behavior has some social functions not necessarily related to thermoregulation, and the meaning of the behavior in the light period seems to be different from that in the dark period.

BE 9

WHAT DOES MALE MICE PATERNAL?

F. Matsumoto and T. Kimura. Dept. of Biol., Coll. of Arts and Sci., Univ. of Tokyo, Tokyo.

When isolated in a test cage and exposed to scattered 4 pups, males which had copulated and cohabited with the mate until her delivery showed retrieving behavior and nursing posture in much higher frequency than naive males. These males behaved paternally toward strange pups as well as toward their own pups. This indicates that kin recognition is not important for the onset of paternal behavior.

The male which was kept in a cage with a female but separated from her with a wire mesh barrier for 18 days failed to show any paternal responses to pups. This suggests that sexual interaction is necessary for induction of paternal responses. Males that were allowed to copulate and kept with their mates started to show retrieving behavior in marked frequency as soon as 4 days after copulation.

Finally, males that were isolated from females just after copulation was tested 18 days after isolation. These males retrieved pups as well as those that cohabited with mates for 18 days after copulation.

These results indicate that in male mice, so far as the retrieving behavior is concerned, experience of copulation is the crucial factor for the onset of paternal behavior. Investigation of physiological changes after copulation is needed.

BE 10

COMPARATIVE ANALYSIS OF URINATION PATTERN IN TWO JAPANESE *APODEMUS* SPECIES.
M. Daumae¹ and S. Koyama² ¹Dept. of Biol., Coll. of Arts and Sci., Univ. of Tokyo, Tokyo, ²Dept. of Psychol., Tokyo Woman's Christian Univ., Tokyo.

The urination patterns of the small Japanese field mice (*Apodemus argenteus*) and the Japanese field mice (*A. speciosus*) were compared. In *A. argenteus*, male mice deposited significantly larger number of urine spots in novel environment than female. The presence of other male mice increased the number of their urine spots. Contrastedly, *A. speciosus* showed no sexual difference in urination pattern, and the male mice did not change their urination pattern in the presence of other male. In both species, the number of feces pellets did not show such sexual difference and did not change in the presence of other individual. These results suggest that *A. argenteus* male mice utilize their urine for their communication like urine marking in house mice, but *A. speciosus* do not. In *A. argenteus*, male mice increase their number of urine spots in the presence of conspecific female mice and male mice of *A. speciosus* as well as conspecific male, and there were no significant difference in the increase of the urine spot number among the cases above. The urine marking in *A. argenteus* may not be directed specifically to conspecific individual.

BE 11

CAGE-MATES BEFORE MATURATION AFFECT AGGRESSIVENESS OF MALE MICE.
S. Hayashi. Dept. Biol., Fac. Educ., Kagoshima Univ., Kagoshima.

Each male mouse was reared with either a castrated male (CE & CX) or an intact male (NE & NX) from 35 to 104 days of age. Thereafter, they were isolated for 14 days. CE and NE males were transferred to a cage stained by strange male odors every day. On the other hand, NX and CX males stayed in their original cages. After the isolation, each male was paired with a male of the other group for 20 min, in the meantime social behavior was recorded.

CE males dominated not only CX but NE males. Such dominance was found in neither CX-NX nor NE-NX pairs. Males which had been reared with a castrated male until 69 days of age and thereafter with an intact male dominated males which had been in a reverse cage-mate condition. CE males which could smell an intact male odor until 104 days of age were less aggressive than CE males which could not smell such an odor. These facts suggest that an odor of a cage-mate under 69 days of age is important to determine aggressiveness of male mice.

A strange male odor after maturation enhanced aggressiveness of only CE males although it increased preputial glands of both CE and NE males. A strange male odor affects a hormonal state and behavior in different way.

BE 12

FEEDING BEHAVIOR AND LATERAL LINE SYSTEM IN AXOLOTL, *AMBYSTOMA MEXICANUM*.
H.-A. Takeuchi and H. Namba. Dept. of Biol., Fac. of Sci., Shizuoka Univ., Shizuoka.

Axolotl exhibits a series of feeding behavior to the prey objects moving in the water. Recent investigations have suggested that mechanosensory and electrosensory lateral line systems helped to localize the prey. In the present study, we transected several branches of anterior lateral line nerve (ramus ophthalmicus superficialis: r.o.s.; ramus buccalis: r.buc.), and quantitatively analyzed the effects on the feeding behavior evoked by vibrational stimuli (frequency: 5 Hz). We also examined the central projection of r.o.s. and r.buc. by using the transganglionic transport of cobaltic lysine. Animals with bilateral transection of both r.o.s. and r.buc. exhibited significantly less feeding behavior than sham-operated controls. After transection of only r.o.s., the feeding behavior also decreased, but the significant difference from that of controls was not detected. Neuroanatomical examination showed that both r.o.s. and r.buc. consisted of 3 types of afferent fibers: 1. afferents projecting to the dorsal island of Kingsbury (electrosensory afferents); 2. afferents projecting ventrally to the dorsal island (mechanosensory afferents); 3. trigeminal afferents entering the brain via trigeminal root and projecting most ventrally (cutaneous afferents). The trigeminal afferents were contained more in r.buc. than in r.o.s. The present results suggest that electrosensory, mechanosensory and cutaneous signals mediated by r.buc. and r.o.s. are involved in the release of feeding behavior in axolotl.

BE 13

THE FUNCTION OF TENTACULOZOIDS IN TWO SPECIES OF HYDROZOANS, *STYLACTIS CONCHICOLA* AND *STYLACTIS UCHIDAI* FROM HOKKAIDO.
H. Namikawa. Zool. Inst., Fac. of Sci., Hokkaido Univ., Sapporo.

The colonial hydroids *Stylactis conchicola* and *S. uchidai* have tentaculozooids in addition to gastrozooids and gonozooids. Highly extensible and nematocyst-bearing, tentaculozooids resemble very large tentacles, but their function has been not clear. A close examination of much material revealed that the tentaculozooids most frequently occurred along the boundary between their own colonies and colonies of other sessile animals (sponges, hydrozoans, serpulids, bryozoans and barnacles). Further, the tentaculozooids have only a kind of nematocysts, microbasic euryteles whose function are injection of venomes into targets. While the tentacles of gastrozooids have two kinds of nematocysts, desmonemes whose function is capture of prey by adhesion, and microbasic euryteles which are smaller than those in tentaculozooids. Moreover, bryozoan zooids touched by the tentaculozooids retreated their tentacles into zoocium for 30 minutes. Whereas when touched by the tentacles of gastrozooids of these hydroid species, the bryozoan zooids retreated only for about a minute. All these observations indicate that the tentaculozooids of *S. conchicola* and *S. uchidai* function as an offensive tool for interspecies competition of sessile animals.

BE 14

ORIENTATION OF THE TOAD, *Bufo japonicus*,
TO THE BREEDING POND
Susumu Ishii, Biology Department, School
of Education, Waseda University, Tokyo 169

Our previous studies clarified that toads orient to the breeding pond not by the cue from the pond or by means of the celestial method but presumably by using some geographic knowledge of the migrating route. Our previous experiments in the field revealed that visual disturbances did not reduce the rate of the arrival of toads at the breeding site. In the present study, we disturbed the olfactory sense of experimental toads by injecting a silver nitrate solution (0.5%) into the nasal cavity. In some other toads, the mucosa of a part of the oral cavity was treated with the same solution as the sham-operation. Intact toads were also used as the control. They were kept in a cold room (5°C) for 5 to 10 days for recovery, and then, released at the original location in the field in a warm and humid evening. The experimental toads ($n=25$) could not orient to the pond, while the intact ($n=23$) and sham-operated ($n=19$) toads beautifully oriented to the breeding pond. The average lengths of vectors representing the toad movement in these groups were 0.6, 26.2 and 26.7m, respectively. We concluded that toads memorize the smell of some substances existing locally on the route between the breeding and hibernating sites, and trace back and forth it by olfaction.

BE 15

CHOICE OF LIGHT AND DARKNESS IN THE CRICKET, *GRYLLUS BIMACULATUS*.
I. Nakatani, Dept. of Biol., Fac. of Sci., Yamagata Univ., Yamagata.

A male cricket of the last instar nymph was confined, individually, to an activity chamber with an infra-red sensor. The temperature was kept at a constant of $24 \pm 1^\circ\text{C}$. The signal was activated when the infra-red light beam was interrupted by the cricket. Conditions of light and darkness were interchanged when triggered by a signal. The cricket chose the light and darkness at random and at a rate of about fifty-fifty from the last instar nymph to the beginning of stridulation. The cricket began stridulation at a mean of 4.1 ± 0.2 days following the imaginal molt. Stridulation occurred during the light state and its free running rhythm had a mean period of 24.6 ± 0.1 hours. The rate of darkness chosen per day decreased with stridulation. The mode of the interruption of the infra-red light beam was not changed, though the electricity for the light source was cut off from 18:00 to 06:00. This fact may show that the photoperiod dose not act as a "Zeitgeber" for the locomotory activity of the cricket in the field.

BE 16

CHANGES OF BIOGENIC AMINE LEVELS IN SUBO-ESOPHAGEAL GANGLION OF MAMESTRPA BRASSICAE, LARVAE FOLLOWING TREATMENT WITH CHLORDIME-FORM

T. Shimizu¹, F. Miyagawa² and Y. Tsuchida²
¹National Institute of Health, Shinagawa,
Tokyo 141, ²SRL, Hachioji, Tokyo 192.

We have reported the aberrant wandering and flight behaviours and continuous burst of mandibular movements (CBMM) induced by an octopamine agonist, chlordimeform (CDM) pesticide, and we also suggested CDM exerts its pestistatic action either by disrupting the motor-center neurones in the subo-esophageal ganglion (SG) or by an abnormal electrogenesis of the SG or both (Shimizu et al., 1986).

Changes of biogenic amine levels in the SG of wandering stage larvae following treatment with CDM were investigated by HPLC. The SG contained dopa, octopamine, tyrosine and tyramine. Fifteen min following CDM (2 µg) is injected, the ratio of octopamine/tyrosine was decreased as compared with that of control. Biogenic amine levels detected in SG of the untreated and CDM-injected larvae are discussed in light of the observation that the larvae which was exposed to sublethal concentrations of CDM display pronounced and prolonged CBMM.

BE 17

A FRACTAL MODEL OF ANIMAL BEHAVIOR.
I. Shimada¹ and H. Hara². ¹Dep. Biol. Sci. and ²Fac. Engin., Tohoku Univ.

We constructed a general model of animal behavior based on the results of the distribution of the staying time on the foods in *Drosophila*. The distribution was characterized by linear curves in the log-log plot, that is, fractal properties.

Animal behavior is generally determined by the internal state, that is, CNS of the individual. The internal state, on the other hand, is conditioned by various stimuli in the environment. The level N of the internal state is dynamic, changing along with time. The state is described by the exponential function of N and environmental parameter θ_0 . The state transits to a different state at the critical level N_c . The transition probability, then, is also described by the exponential function of $(N - N_c)$. The lasting time of a behavior (the staying time in our experiment) is naturally defined by a reciprocal of transition probability of the internal state. The parameter θ of transition probability, however, is generally different from θ_0 . The distribution of the lasting time of behavior can be easily calculated and results in the power distribution. Fractal dimension is shown by parameters θ and θ_0 . The upper and lower limits of the lasting time of behavior were discussed based on our model and experiments.

BE 18

SEMILUNAR SPAWNING RHYTHM AND SEX CONVERSION DURING ONE BREEDING SEASON IN A SEA CUCUMBER, *Polycheira rufescens*
M. Tomari and T. Kubota. Dept. of Biol., Kagoshima Univ., Kagoshima 890, Japan.

The sea-cucumber, *Polycheira rufescens* (Apodida, Chridotidae) can be found crowded under pebbles in the tidal zone. In Kagoshima, spawning occurred in July to September. The following points were noticed. (1) Almost all the mature animals released their gametes during 2 days, 1-2 days before every full and new moon. (2) The animal is a hermaphroditic species: when examined 1 day before the every first spawning day, mature individuals were comprised of females with mature eggs (F) and males with motile sperm, which further divided into three groups; with growing eggs of the earlier stage (Me1), the later (Me2) and with no egg (M).

Observations of animals marked with fine thread and put back to shore revealed that individuals, except part of M and sterile ones, changed their sexual types between one spawning and the next regularly in such directions; M to Me1, Me1 to Me2, Me2 to F, and F to M. Thus, the time when M became Me1 differed among M individuals. No definite relationship between these conversion times and body sizes was found.

BE 19

SIZE-DEPENDENT SEX CHANGE OF A PROTANDROUS ANEMONEFISH. *AMPHIPRION FRENATUS*
A. Hattori
Dep. of Biol., Fac. of Sci., Osaka City University, Osaka.

Amphiprion frenatus forms groups consisting of a male-female pair and several nonbreeders. The growth and behavior of marked fish in 34 groups were investigated for 5 months on a fringing reef at Sesoko Island, Okinawa, Japan. The state of gonad development of 64 individuals was studied histologically after field observations. Reproduction occurred in 24 groups (breeding groups). In these groups, the body sizes of females were about twice those of males. The body sizes of the largest and second largest fish in nonbreeding groups were smaller than those in breeding groups. Fish growth was socially controlled. The growth increments of the largest and second largest fish in nonbreeding groups over five months were greater than in breeding groups. Six gonad phases were discriminated. The size distributions of fish with each phase suggest that with growth, the gonads develop from an immature phase through a male phase to a female phase. In this species, the timing of sex change is size-dependent and growth is suppressed by larger fish.

BE 20

EMBRYONIC DEVELOPMENT AND LARVAL DISPERSAL IN THE NERITIDAE (GASTROPODA: PROSOBRANCHIA)
K. Koike, Dept. of Biol., Fac. of Educ., Gunma Univ., Maebashi.

Neritid snails living in the intertidal zone of the sea and in brackish- and freshwater portion of rivers lay egg capsules on various substrata. Egg capsules of 32 species of Neritidae were collected in the Ryukyu Islands and the main island of Japan, and embryonic development in the egg capsules and the larval stages at the time of hatching were observed.

The results revealed that the developmental processes of the Neritidae observed in this study were divided into four types as follows: (1a) 60-200 eggs/egg capsule, trochophore and early veliger with a transparent sac at posterior end of foot, hatch as veliger larvae, long-distance dispersal type. (1b) 80-500 eggs/egg capsule, embryo without transparent sac, hatch as veliger larvae, long-distance dispersal type. (2a) 20-70 eggs/egg capsule, embryo with a transparent sac and a vesicular mass at posterior end of foot, hatch as 2-20 pediveligers, short-distance dispersal type. (2a) 150-200 eggs/egg capsule, embryo with similar characters to 2a, hatch as 2-10 juveniles, adaptation to temperate region. These observations also suggest that the different types of embryonic development have a relation to their phylogeny within the Neritidae.

BE 21

CHOICE OF SPAWNING SITES OF THE SALAMANDER, *HYNOBIUS RETARDATUS*.
T. Sato. Obihiro Centennial City Museum, Obihiro

The spawning sites of the salamander *Hynobius retardatus* were studied in the Tokachi District, Hokkaido during the breeding seasons from 1985 to 1989. Breeding sites were confined at eighty-two points and were divided into three types according to the rate of water flow, high velocity (more than 5 cm/sec), low velocity (less than 5 cm/sec) and standing water, and these occurred at the ratio of 13.4%, 52.4%, and 34.1%, respectively. The mean water depth where the egg sacs were found 3.1 cm. In high velocity areas, the mean water temperature (± 1 SE) was $6.6 \pm 0.54^\circ\text{C}$ at the bottom and $6.6 \pm 0.55^\circ\text{C}$ just beneath the water surface, and these means did not differ significantly ($t=0.12$, $df=16$, $P > 0.90$). In low velocity and standing water, the mean water temperature at the bottom and beneath the water surface differed significantly ($t=4.21$, $df=64$, $P < 0.001$; $t=2.46$, $df=40$, $P < 0.05$). The spawning places in the breeding sites were as follows: on leaves, stems, twigs and roots of plants, stones and rocks, and at the edge of the breeding sites. 82% of the total number of egg sacs were attached to live or dead plants. In standing water, 60.7% of the number of natural enemies (i.e., crayfish and larval caddisflies) were observed; 14.0% and 0% were in low velocity and high velocity, respectively.

BE 22

BREEDING SEASON OF THE BRACKISH WATER BI-
VALVE, *CORBICULA JAPONICA* IN LAKE SHINJI,
JAPAN.
I. SAKAMOTO. Depa. of Biol. Shimane. Med.
Univ., Izumo.

Histological observations of the gonads were made to determine the breeding season of *Corbicula japonica* in Lake Shinji.

The materials were collected from Lake Shinji, at five days interval from April 1987 to March 1988, and have been studied by paraffin section using hematoxylin eosin staining methods. The size of samples used for histological study was the shell length range of 25 to 30 mm.

In both ovary and testis, the beginning of maturing stage was observed in late May. The end of spawning stage was in early October. Spent specimens appeared in mid October.

These results of histological observations suggested that the breeding season of *Corbicula japonica* in Lake Shinji is from late May to early October.

BE 23

ROTIFERA FROM KOYAMA-IKE, IN TOTTORI.
THE LARGEST COASTAL POND OF JAPAN.
M. Sudzuki¹ and K. Fukuta²
¹Biol. Lab., Nihon Daigaku Univ., Omiya
²Biol. Dept., Tottori Univ., Tottori

In the late 1930's when Hada ('37, '39) surveyed this pond the most common rotifers were *B. plicatilis*, *hepatotomus*, *B. angularis*, *K. cruciformis*, *eichwaldi* (salinity: 4.0-4.7‰). The channel connecting Koyama-ike with the Sea of Japan was recently moved and linked with the downstream of Sendai-gawa. While, the pond itself has been contaminated by human activities. The purpose of this approach is to make clear a shift of rotifer composition based on the samples collected from the site near the University on 4/IV, 6/IX, 6/X, 8/XI (1987), 8/IV, 16/V, 17/VIII ('89). The Rotifera found this time: *B. angularis*, *bidens* (D⁺ in XI), *B. e. calyciflorus* (D⁺ in IV), *B. c. dorcus* (VII), *B. u. urceolaris* (IV), *K. c. cochlearis* (IV, V, XI), *K. q. quadrata* (D⁺ in IV), *K. v. tropica* (D⁺ in IX, XI), *N. acuminata* (IV), *N. labis* ssp (IV), *L. acuminata* (IV), *L. flexibilis* (IV), *M. stenroosi* (IV), *P. t. dolichoptera* (IV), *P. t. vulgaris* (D⁺ in XI), *Synchaeta* sp. 1 (XI), *S. sp. 2* (IV), *C. ovalis* (IX), *Cephalodella* sp (VIII), *D. dixon-nuttalli* (VIII), *T. pusilla* (VIII), *Dicranophorus* sp (III), *A. priodontia* (IX), *A. intermedia* (IX), *A. sieboldi* (IX), *E. l. longiseta* (VII, X, IX), *E. l. passa* (D⁺ in IV), *H. mira* (IX, X), *P. sulcata* (VIII), *C. coenobasis* (IV, V, VIII, IX), *Conochilus* sp (IV), Cl⁺ = 174-177 mg/l (30/VII, 1987). As a result, we may consider that water quality has been changed from oligohaline into limnetic (Venice system) at the site investigated.

BE 24

STUDY ON THE ENDOPARASITE OF ANURA

2. PREVALENCE OF HELMINTH IN THE LUNG OF *RANA BREVIPODA POROSA* AND *RANA JAPONICA*.

Y. Sasaki and N. Makino. Dept. of Biology,
Tokyo Med. Coll., Tokyo.

The endoparasites of the frog were studied from July 1987 to July 1989. The frog hosts (*Rana brevipoda porosa* and *Rana japonica*) were captured at Inzai, Chiba Prefecture. Five hundred and twenty four *R. b. p.* were collected and three hundred and twenty seven *R. j.* were collected. The sex ratios of the frogs were approximately equal. Parasites in the lung from each frog was observed at this time. It was observed that, the nematode, *Rhabdias nipponica* and the trematode, *Haematoloechus ranae* were detected in *R. b. p.*, and only *R. nipponica* was detected in *R. j.*. Prevalence of *R. nipponica* and *H. ranae* in the lung of *R. b. p.* was generally low throughout the year for both endoparasites. The intensity of infection, it was noted, was small. In contrast there was a high prevalence all the year round of *R. nipponica* in *R. j.*. The observed occurrence was not such different between males and females. Only *R. nipponica* females, and also parasite spawn were observed in the lung. This worm is known to show the heterogony. It is interesting to note that *R. nipponica* males and females are observed in the free-living exterior environment.

BE 25

THE LIFE AND THE REPRODUCTIVE PHENOMENON IN BIPALMIUM (PLATYHELMINTHES, TURBELLARIAN, TRICLADIDA) OF THE FISSTON TYPE WORM.
N. Makino and Y. Shirasawa, Dept. of Biol.,
Tokyo Med. Coll., Tokyo.

Materials are 2 species of Genus *Bipalium* of the asexual type, these are *Bipalium nobile* and *B. kewense*, and were reared in 18°C laboratory in 3 ~ 5 years.

When *B. nobile* was collected (June, 1984), the worm was about body weight, 7g, and body length, 100cm. under copulation. The worm oviposited a cocoon after 2 weeks. The worm fissioned 6 small pieces from September to December. The larvae took 1.5 years to grow up to 2 ~ 3g. So, perhaps, the collected worm was 3 ~ 4 years old. The worm do not fission since January in 1985. The worm declined little by little in 1988 and separated in to 2 pieces (anterior-posterior or parts). The posterior part never regenerated and then denaturated in September. Thus, it seems 8 ~ 9 years about the longevity. *B. kewense* of another species is the cosmopolitan one. In June, 1986, the worm was collected at Campus of Tokyo Medical College. The worm fissioned 16 times in 9 months from July to next March, usually 1 piece of most posterior part, and then, after half a year, the worm denaturated the posterior part of the body. After recovery, the worm fissioned 19 times in 19 months from November to August, 1989. That is, the worm in younger period showed vigorously fissionable stage. Why does the worm fission? How does the worm fission? The question is the next theme.

TS1

SCANNING ELECTRON MICROSCOPIC OBSERVATIONS ON SPICULES, GEMMULE COATS AND MICROPYLES OF THE FRESHWATER SPONGES, *SPONGILLA ALBA* CARTER, *EUMAPIUS CONFERTUS* (ANNANDALE) AND *TROCHOSPONGILLA LATOUCHIANA* ANNANDALE. Y. Masuda and K. Satoh, Dept. of Biol., Kawasaki Med. Sch., Kurashiki.

All materials were collected from their habitats in Japan. This is the first reported occurrence of *T. latouchiana* in Japan.

Detailed observations using SEM clearly revealed the taxonomic characteristics of the structures of the above three species. The fine characteristic of the structures which seemed to be useful taxonomic characters of intraspecific population were as follows. *S. alba*: 1. Megascleres had microspines on their surface. 2. The foraminal tubule consisted of minute subspherical alveoli which resembled those of the pneumatic layer. *E. confertus*: 1. Gemmoscleres were completely smooth. 2. The base of the gemmule coat consisted of outer and inner gemmular membranes without a pneumatic layer. 3. The layers of the alveolus increased in number toward the micropyle. *T. latouchiana*: 1. Megascleres had spines on their surface. 2. The upper rotule of the gemmosclere had many minute inverted spines and the lower one had a few minute spines at each marginal portion. 3. The micropyle was slightly elevated and surrounded by a narrow collar, which was situated at the center of the saucer-like structure of the outer gemmular membrane.

TS2

MORPHOLOGICAL OBSERVATIONS ON CERATA OF AEOLID NUDIBRANCH, *PHYLLOEUSMIUS SERRATUS*. K. Okawa, Dept. of Gen. Educ., Univ. of Hiroshima, Aomori.

As regards the question of whether the nematocysts derived from coelenterate have an adaptive significance to aeolid nudibranchs, many considerations have been made. Aeolid nudibranchs have evolved their digestive system in the process of acquiring nematocysts of the prey. Grosvenor (1903) described first that nematocysts are used by aeolid nudibranchs as defensive weapons and suggested that the original function of cnidosac might be removal of nematocysts from the digestive system. Morphological observations of *P. serratus* suggest the origin and the role of aeolidacean cnidosacs. The sac organs of *P. serratus* which secrete mucus, are not connected with the digestive system at the tip of cerata. According to the observations I have done so far, the digestive system of this species has not yet evolved to utilize nematocysts to such an extent as suggested by Grosvenor. Therefore, the sac organ found in *P. serratus* might well be said as a prototype of cnidosac.

TS3

NEMATODES OF THE FAMILY MONHYSTERIDAE IN THE GILL CHAMBERS OF "LAND CRABS" FROM THE RYUKYU ISLANDS.

K. Yoshimura, Ube Junior College, Ube.

The gill chambers of 19 species of "land crabs" from the Ryukyu Islands were examined, and two species of *Monhystridium* and a species of *Gammarinema* (Monhystridae; Nematoda) were found. All of these three monhystrids were identical with those previously known from sesarmin crabs of Honshu Island. The longer form of *Monhystridium* were taken from *Parasasarma plicatum* and *P. bidens*, while the shorter one from *Cardisoma hirtipes*, *Grapsus crinipes*, *Chiromantes dehaani*, *Sesarmops intermedium*, *Chasmagnathus convexus*, *Nanhaipotamon yaeyamense*, *Geothelphusa levicervix*, *G. sakamotoana*, *G. aramotoi* and *Candidiopotamon okinawense*. *Nanhaipotamon yaeyamense* and *Candidiopotamon okinawense* were infected with *Gammarinema* sp. too. *Ocypode ceratophthalma* and *Q. cordimana* were not associated with such monhystrids but with a species of *Rhabditis* (Rhabditida).

TS4

THE FIRST OCCURRENCE OF CORONARCTID TARDIGRADE FROM THE SHALLOW WATER.

H. Noda, Seto Mar. Biol. Lab., Kyoto Univ., Shirahama, Wakayama.

A species of the genus *Coronarctus* was found from the shallow water of Japan, although all the members of this genus have so far been known from the abyssal bottom up to the continental shelf. Five specimens of this species were extracted from the sediment sample (amphioxus sand) collected from 40 m depth at the mouth of Tanabe Bay, Wakayama Prefecture.

The present species most resembles *Coronarctus stylisetus* in such characteristics as long cephalic cirri, moderately separated external cirri and absence of the dorsal notch of secondary clava at the level of the insertion of the median cirrus. But it differs from the latter in the shape of the primary and the secondary clavae and the characteristics of the claw. Primary clava is semispherical, not stalked and embedded in the cuticle. Two deep notches are present on the frontal and the ventral border of the secondary clava. The frontal one surrounds the base of the internal cirrus and has the very narrow opening. The ventral one also surrounds the base of the external cirrus and has a moderately narrow opening. The internal claw of the leg IV has two accessory spines. Each the other claws has a single accessory spine.

TS5

CHEILOSTOMATOUS BRYOZOANS FROM SESOKO, OKINAWA
S. F. MAWATARI. Zoological Institute, Faculty of Science, Hokkaido University, Sapporo

The bryozoan material recently collected from Okinawa has led to the description of some new species and extension of ranges in distribution for some ten known species of Cheilostomata.

Adding to 22 known species in the preliminary list (Mawatari, 1987), 20 cheilostomes including 5 new species are reported from Sesoko Island, Okinawa-ken Prefecture, Japan. Among them *Parasmittina* sp. nov. is the most interesting in having characteristic large pores at the borders of zoecia. This species provides another example for the extreme prosperity of *Parasmittina* in tropical seas. The beautiful pinkish colonies of *Hippomenella* sp. nov. have zooids with a pair of lateral suboral avicularia facing distally and ovicells with a pair of large frontal pores. *Cleidochasma* sp. nov. is unique in having a smooth frontal wall without avicularia. The thin and delicate colony of *Bugula* sp. nov. has no avicularia. *Robertsonidra* sp. nov. is characterized by zooids with a central suboral avicularium and evenly perforated large ovicells.

The predominance of *Parasmittina* and *Rhynchosoon* in tropical seas is amply demonstrated by the present bryozoan survey in Okinawa.

TS6

KARYOLOGICAL AND TAXONOMIC STUDIES OF THE DUGESIA SPECIES IN SOUTHEAST ASIA. XV. CHROMOSOMES OF DUGESIA JAPONICA FROM THE SOUTHWEST ISLANDS OF JAPAN.
S. TAMURA¹, I. OKI² and M. Kawakatsu³. ¹Osaka Pref. Inst. Publ. Health, Osaka, ²Osaka Environ. Project Authority, Osaka, ³Biol. Lab., Fuji Women's Coll., Sapporo.

Dugesia japonica consists of 2 subspecies: *D. j. japonica* Ichikawa et Kawakatsu, 1964 (n=8, 2x=16) and *D. j. ryukyensis* Kawakatsu, 1976 (n=7, 2x=14). The results of our previous karyological studies of *D. japonica* indicate that the geographical ranges of the 2 subspecies intermingle in the northern area of the Southwest Islands of Japan (Tamura et al., 1988).

The following results are based upon karyological studies of recently collected animals from the southern area of the Southwest Islands of Japan.

D. j. japonica: Ishigaki Island (3 stations; triploidy) and Iriomote Island (1 station; triploidy) and Yonaguni Island (2 stations; diploidy and triploidy).

D. j. ryukyensis: Okinawa Island (2 stations; diploidy and triploidy) and Miyako Island (1 station; diploidy and triploidy) and Ishigaki Island (1 station; triploidy).

Taxonomic studies of planarians from various of the Southwest Islands of Japan that have accumulated in Kawakatsu's laboratory will be published in a future paper.

TS7

KARYOLOGICAL AND TAXONOMIC STUDIES OF THE DUGESIA SPECIES IN SOUTHEAST ASIA. XVI. TWO TROGLOBITIC SPECIES FROM THAILAND AND SULAWESI (INDONESIA).
M. Kawakatsu¹ and R. W. Mitchell². ¹Biol. Lab., Fuji Women's Coll., Sapporo, ²Texas Tech Univ., Lubbock, Texas, U.S.A.

A troglobitic species of *Dugesia* was collected from pools in Tham Kubi Cave, Kohn Khaen Province, Thailand. This species is small in size (10mm x 2mm preserved) and is completely lacking in body pigmentation and eyes. According to the genital anatomy classification of *Dugesia* spp. from Asia (Kawakatsu et al., 1976), this *Dugesia* sp. belongs to group 2 because of its asymmetrical penis papilla, diaphragm in the penis lumen, lack of a valve at the basal part of the penis papilla and lack of adenodactyl(s). This species was determined to be new based on its external morphology and on the details of its genital anatomy and histology. According to the collector's information, numerous specimens of this species were observed in its cave habitat.

Another troglobitic freshwater planarian was collected from Gua Tanette Cave, located in the Maros Karst of southwestern Sulawesi (Celebes), Indonesia. This species is very small (5mm x 1mm preserved), lacks eyes but has barely perceptible pigmentation on the dorsal surface of the body. All specimens collected were non-sexual, but they appear to be referable to *Dugesia*.

TS8

COMPARATIVE EXTERNAL MORPHOLOGY ON THE SPERMATIZOEA OF FOUR SPECIES, THE FAMILY ECHINOMETRIDA, FOUND ON OKINAWAN REEF FLAT.
Y. Arakaki* and T. Uehara. *Kounan-gakuen, Naha, Okinawa. Dept. of Biology, Univ. of the Ryukyus, Nishihara-cho, Okinawa.

Sperm morphology compared among four types (Type A, B, C, and D) of *Echinometra mathaei*, *Echinostrephus molaris*, *Heterocentrotus mamillatus* and *Colobocentrotus mertensii*. Since the investigation was begun on the four types of *E. mathaei*, it has been suggested that they were possibly four different species. Among the four types, however, the difference between Type C and Type D were ambiguous. In this course of study, however, it was revealed that very interesting fact, which delimits Type C and Type D. The sperm of Type D was very slender and about two times as long as Type A and Type B and 1.6 times as long as Type C. On the other hand, *C. mertensii* has a slender and very long sperm as that of Type D. The other two species, *E. molaris* and *H. mamillatus*, were relatively similar to the sperm of Type A and Type B. Finally, it is obvious that type D is different from the other three types. Why is the sperm of Type D so different from the other types and so resemble to the sperm of *C. mertensii*? So far we can not explain thus results. However, the sperm morphology may give us good information about phylogeny in the Echinometrida.

TS 9

BIOCHEMICAL SYSTEMATICS OF FOUR TYPES OF THE SEA-URCHIN, *ECHINOMETRA MATHAEI*, FROM OKINAWA, JAPAN.

N. Matsuo¹, T. Hatanaka¹, T. Uehara², M. Tsuchiya² and M. Nishihira².
¹ Dept. of Biol., Fac. of Sci., Hirosaki Univ., Hirosaki and ² Dept. of Biol., Fac. of Sci., Univ. of Ryukyus, Okinawa.

Four types of the sea-urchin *Echinometra mathaei* which are distinguishable by several characters such as color pattern of spines are observed on Okinawan reef flats, southern Japan. The taxonomic situation and genetic relationships of four types of the sea-urchin were examined by means of gel electrophoresis of 15 different enzyme systems. The biochemical results showed that they (Type A, B, C and D) were fixed for different alleles at 7 genetic loci of 28 genetic loci scored and did not share gene pools. It clearly shows no gene flow between four types, and is strong evidence for that they are genetically distinct species. Further, the Nei's genetic distances between four types were comparable to those between closely related species in many other animals. The biochemical dendrogram for four types established by the UPGMA clustering method showed that four types are divided into two large clusters (one consists of Type A and C, and other Type B and D): Type A is more closely related to Type C than to other types, and Type B is more closely related to Type D than to other types. It is concluded from the present electrophoretic study that four types of *Echinometra mathaei* are separate, distinct species, on account of their genetic distinction verified. The biochemical dendrogram also showed that these four types diverged from one another in relatively recent geological age of the middle Pleistocene.

TS 10

A STUDY OF THE SHALLOW-WATER ASTEROID FAUNA OF THE AMAMI-RYUKYU ISLANDS.

M. Shigei¹ and M. Saba².
 Misaki Mar. Biol. Stat., Univ. of Tokyo, Kanagawa, ²Ise Senior High School, Mie.

For the purpose of making clearer the asteroid fauna of the Amami-Ryukyu Islands, we made repeated field surveys during 1974-1989 in the shallow waters around such islands as Amami-Oshima, Kakeroma, Tokunoshima, Okinoerabu, Okinawa, Sesoko, Tokashiki, Miyako, Ishigaki, Kuroshima and Iriomote.

We collected a total of 39 species, which much increased our knowledge about the fauna of these islands because the previous studies had revealed only 29 species as a total (Goto, 1914; Djakonov, 1930; Ohshima, 1935; Döderlein, 1935, '36; Hayashi, 1938, '40, '43).

As a whole, the fauna was composed of the tropical, Indo-West Pacific elements as had been considered from the marine environmental conditions around these islands.

The following 7 species were new to Japanese waters:

Archaster laevis H.L. Clark, *Tosia queenslandensis* Livingston, *Dactylosaster cylindricus* (Lamarck), *Gomophia egyptiaca egeriae* A.M. Clark, *Neoferdina cumingi* (Gray), *Nepanthia belcheri* (Perrier), *Valvaster striatus* (Lamarck).

The other two species, *Gymnanthenea* sp. and *Coronaster* sp. are considered to be new to science. We are going to make a systematic description of them.

TS 11

COMPARATIVE STUDIES OF THE FAUNAS OF ECHINOIDS AND ASTEROIDS OF THE SAGAMI SEA.

(1) A REVIEW OF THE SYSTEMATIC STUDIES AND AN ESTIMATION OF THE TOTAL NUMBERS OF SPECIES HITHERTO KNOWN.

M. Shigei. Misaki Marine Biological Station, Univ. of Tokyo, Kanagawa.

It was revealed that the systematic studies of the echinoids and asteroids of the Sagami Sea had been carried out based on the following collections:

R/V Challenger's in 1875, Döderlein's in 1881, Yoshiwara's and Goto's during 1881-early 20th cen., R/V Albatross's in 1906, Mortensen's in 1914, Emperor Showa's during 1926-1941 & 1949-1987, R/V Soyo-Maru's during 1957-1974, Shigei's during 1970-1989.

The systematic studies were as follows: ECHINOIDS; A. Agassiz (1879, '81), Döderlein (1885, '87), Yoshiwara (1897, '98, 1900), Mortensen (1904, '14, '28, '34, '35, '40, '43, '48, '50, '51), A. Agassiz and H.L. Clark (1907), Shigei (1973, '75, '81, '82, '86, '88).

ASTEROIDS; Sladen (1883, '89), Döderlein (1902, '17, '20, '21), Goto (1914), Hayashi (1940, '43, '73), Shigei and Saba (1989).

An attempt to estimate the total number of species hitherto known from the Sagami Sea was made mainly based on my own examination of the Emperor Showa's, Soyo-Maru's and Shigei's collections, and partly on referring to the literatures in the past. The result of estimation was as follows: ECHINOIDS, 84; ASTEROIDS, 70 (-73).

TS 12

TAXONOMIC NOTES ON THE GENUS *OSTRACOTHERES* (CRUSTACEA: PINNOTHERIDAE).

M. Takeda¹ and K. Konishi². ¹Dept. of Zool., Natn. Sci. Mus., Tokyo and ²Natn. Res. Inst. Aquacult., Mie.

The morphology of the genus *Ostracotheres* is characteristic among 28 pinnotherid genera, together with *Xanthasia*, in absence of the dactylus of the maxilliped 3. This genus includes 7 species and they are distributed on the Indo-West Pacific Region: *O. tridacnae* (Ruppell) from the western Indian Ocean and the Red Sea, *O. savignyi* H. Milne-Edwards from the Red Sea, *O. affinis* H. Milne-Edwards from the western Indian Ocean, *O. spondyli* Nobili from the Persian Gulf, *O. cynthiae* Nobili from the western Indian Ocean and the Kei Islands, *O. holothuriensis* (Baker) and *O. subglobosus* (Baker) from South Australia. Recently Pregoner (1988) reviewed Australian species of *Ostracotheres* and he synonymized the Japanese endemic species *O. subquadratus* Sakai with *O. subglobosus*.

A single female specimen of *Ostracotheres* which closely resembles *O. affinis* was collected from Sesoko, Okinawa, Japan; this specimen is distinguished from *O. affinis* by the features that the dorsal surface of the carapace lacks velvet tomentum, and the propodus of the maxilliped 3 is not rounded distally, but obliquely cut along its distal inner margin.

TS 13

DEVELOPMENTAL STAGES OF "NAUPLIUS Y" (CRUSTACEA: FACETOTECTA).

T. Itô, Seto Mar. Biol. Lab., Kyoto Univ., Shirahama, Wakayama.

The general characteristics of the naupliar stages of the "Type-IV group" of facetotectans collected from Tanabe Bay, Japan, and reared in the laboratory are discussed in order to find key characters that can be used to determine the developmental stages of other such nauplii of unknown larval history. The first naupliar stage can be identified by characteristics of the plates on the cephalic shield, such as the possession of four F-plates with no meridional ridges subdividing them. In later stages, plate I-1 comes to be widely separated from I-2 by intervening plate(s) that originate from E-1. Most plates become subdivided either meridionally or latitudinally after the first stage, but many meridional ridges subsequently disappear and long, concentric plates are formed. Hence, the number of plates does not simply increase. In some species, most of the plates disappear in the later stages and the plate pattern becomes useless for stage determination. The setal armature of the antennule is available for this purpose, but it must be used with caution because, in lecitotrophic nauplii, degeneration of setae may take place together with the addition of new setae. Despite the absence of a single key character, stage determination can be done with some confidence on the basis of several characters, but ideally it should be done by individual culture.

TS 14

GEOGRAPHICAL VARIATIONS IN BODY SIZE AND RELATIVE GROWTH OF TWO FORMS OF MACROPHTHALMUS JAPONICUS (BRACHYURA: OCYPODIDAE).

K. Wada, Dept. of Biol. Fac. of Sci., Nara Women's Univ., Nara.

The ocypodid crab *Macrophthalmus japonicus* (De Haan) has been known to consist of two forms (Form V & L) that differ conspicuously in male waving displays. Form V has so far been recorded from Honshu, Shikoku, Kyushu and Tane Is. of Japan, and continental coasts of Yellow Sea and northern East China Sea, whereas Form L from southwestern Honshu, Shikoku, Kyushu and Nansei Shoto Group of Japan, Taiwan, and continental coasts of East China Sea and southern Yellow Sea.

For these two forms, carapace width at puberty, carapace length relative to carapace width, and propodus length of male cheliped relative to carapace width were compared among 16 localities of Japan, Korea and Taiwan. These characters revealed serial variation among localities in the following succession: 1) Form L in Amami-Oshima Is., Okinawa Is. and Miyako Is., 2) Form L in other localities of Japan and Taiwan, 3) Form L in Korea and Form V in Korea and some localities of Japan, and 4) Form V in other localities of Japan. The successive variation seemed to be related with the degree of oceanic to thalassic situations of localities.

TS 15

WATER MITES (HYDRACHNELLAE) FROM HONG KONG.

T. Imamura, Higashi-akatsuka 255-12, Mito City, Ibaraki 311-41.

Up to the present, the following two water mite species (Hydrachnellae) have hitherto reported from Hong Kong by T. Imamura (1976): *Atractides nodipalpis* *nodipalpis* and *Encentridophorus honkongensis* Imamura, 1976. This time, the present author will here give the preliminary report from Hong Kong the following seven families and thirteen genera as follows: Hydrphantidae, *Wandesia* sp.; Torrenticolidae, *Torrenticola* spp.; Hygrobatidae, *Atractides* sp.; Beltridae, *Beltria* sp.; Atridae, *Frontipodopsis* sp., *Axonopsis* sp., *Axonopsis*-like sp., *Lethaxona* sp., *Aturus* sp., *Kongsbergia* sp., *Rharataibia* sp.; Mideopsidae, *Mideopsis* sp. and *Athenemanniidae*, *Mundamella* sp. Among these, all the families and the genera, except the family Hydrphantidae and the genus *Axonopsis*, are all new to the Chinese Continent, and these will include also several new species to science. The present author will soon report them on the descriptive paper in the near future.

TS 16

PHYLOGENY AND A REVISION OF THE SALPINGIDAE (COLEOPTERA) OF JAPAN.

H. Sasaji, Biol. Lab., Fukui Univ., Fukui.

The Othnidae and the Inopeplidae are usually treated as independent families, but are more desirable to be included in the family Salpingidae. The Salpingidae include six subfamilies: Inopeplinae, Othninae, Prostominae, Aegialitinae, Lissodeminae and Salpinginae, as far as the Japanese species are concerned. The Japanese Salpingidae are classified into 10 genera and 27 species. *Trogocryptoides* Champion, 1924 was proposed as a genus of the Cryptophagidae and transferred to *Trogocryptinae* of Othnidae by Crowson (1955). *Prostomia* was described as a member of the Cucujidae, and also included in *Trogocryptinae* by Crowson (1955). But *Prostomia* Grouvelle, 1914 precedes as a valid subfamily name.

Prostomia and *Trogocryptoides* are quite dissimilar to each other in the general appearances, but both show closely related states in the phylogenetically important characters such as mouth parts, tarsi, metendosternites, coxal cavities, etc.

Inopeplus was originally described as a genus of the Cucujidae in Clavicornia, and Crowson (1955) created a new family Inopeplidae in Heteromera. This staphylinid-like beetles are easily distinguishable from the other families of the Cucujoidea by the shortened elytra, but the larval characters show the close relationship to the other groups of the Salpingidae.

Elucutis (=Othnius) is a very compact group in the external appearances, but its fundamental morphological characters show also the close relationship to the other Salpingidae.

TS 17

THE EVOLUTION AND REGRESSION OF THE CORPUS CEREBELLI OF TELEOSTS.

N.Niwa¹, K.Uchihashi². ¹Fukui Senior High School, Kobe, ²Sekihan Laboratory, Akashi.

We have studied the morphological evolution and regression of the corpus cerebelli in about 68 species of Japanese teleosts. The external shape of the corpus cerebelli is classified into 5 types: forward-bending, backward-bending, stick-shaped projection, drop-type projection, and T-shaped projection. The corpus cerebelli becomes most advanced in shape in Scombrina of the Perciformes and the systematic order continues and regresses gradually until the Gadiformes and finally ends up with the tiny drop-type projection. This corresponds very well to ecological behavior in which fish radiate on a large scale from the surface layer to the bottom layer, and the deep sea, regarding the age of the appearance of Perciformes as one peak.

TS 18

THE PRIMITIVITY OF THE TELENCEPHALON OF CLUPEIDAE.

K.Uchihashi. Sekihan Laboratory, Akashi.

Thirteen orders and 92 species of teleosts were examined as to the existence and the whereabouts of the sulcus ypsiliformis and fissura endorhinalis and the existence of an expanded area in the hippocampal region of a forebrain. According to the results, the Clupeidae which have some primitive forebrains, do not have a sulcus ypsiliformis or fissura endorhinalis, and do not exhibit an expanded area of the hippocampal region. This is not found in any of other orders.

TS 19

SPECIES DIFFERENTIATION OF THE RICEFISH IN THAILAND: THE SYMPATRIC SPECIES, *ORYZIAS MELASTIGMA* AND *O. JAVANICUS*.

H. Uwa¹, K. Takata¹, N. Nadee² and W. Magtoon³. ¹Dept. of Biol., Fac. of Sci., Shinshu Univ., Matsumoto, Japan, ²Thai. Inst. of Sci. and Tech. Res., Bangkok and ³Dept. of Biol., Fac. of Sci., Srinakharinwirot Univ. at Bangkok, Bangkok, Thailand.

Two allied species of the ricefish, *Oryzias melastigma* (McClelland) and *O. javanicus* (Bleeker), are distributed from India to Indonesia along the coastal areas of the Indian Ocean. We collected these species from 14 localities in Ranong, Phang Nga, Phuket and Krabi, south Thailand, faced to the Andaman Sea.

They commonly inhabit in the mangrove forest areas, and school together in brackish water. No hybrid fish was detected morphologically in specimens collected from localities. Isozyme studies also revealed no heterozygote among specimens collected from Ranong.

Oryzias melastigma from Ranong had a karyotype 2n=48, NF=48, 24A, while *O. javanicus* from Phuket showed 2n=48, NF=48, 1ST+23A. These karyotypic characteristics in each species are the same as those in *O. melastigma* from India and *O. javanicus* from Singapore, respectively.

These species inhabit sympatrically in south Thailand, and seem to be isolated reproductively at the parental level.

TS 20

THE SYSTEMATIC STUDY OF CYPRINIFORM FISH BY TWO-DIMENSIONAL ELECTROPHORESIS OF LIVER PROTEINS.

J. Miyazaki and T. Hirabayashi. Inst. of Biol. Sci., Univ. of Tsukuba, Tsukuba.

The systematic study by using two-dimensional electrophoresis of protein constituents has been carried out to throw light on confused subfamilial groupings of Cyprinidae by investigating phylogenetic relationships at the molecular level. First, 6 pairs of cypriniform fish, which are different from each other at individual, subspecific, specific, generic, subfamilial, and familial levels, were compared to elucidate applicability of this technique to phylogenetic analyses in this group. Similarity values, based on Aquadro and Avise (1981), decreased as taxonomic levels became higher, indicating reliable applicability of this technique. Secondly, 4 species belonging to different subfamilies were compared in order to investigate phylogenetic relationships of cyprinid subfamilies. Cyprininae and Gobioninae showed the largest similarity value, and Acheilognathinae had large differences from the two subfamilies, suggesting that the former two subfamilies are closely related, and Acheilognathinae is differentiated from them. Leuciscinae was slightly more similar to Cyprininae and Gobioninae than to Acheilognathinae, although the similarity values were not substantially different between Leuciscinae and the other three subfamilies.

TS 21

GENETIC VARIATION IN THE JAPANESE NEWT *CYNOPSIS PYRRHOGASTER* FROM SOUTHERN KYUSHU. T. Hayashi¹ and M. Matsui². ¹Dept. of Zoology, Fac. of Sci., Kyoto Univ., Kyoto and ²Biol. Lab., Yoshida College, Kyoto Univ., Kyoto.

Using horizontal starch gel electrophoresis, we examined allozyme variation of 15 presumptive loci in 290 newts from 16 populations in southern Kyushu. Allozyme data showed that these populations were split into two genetically differentiated groups and their hybrid populations on the basis of substantial differences in electromorph frequencies at three loci (S-Sod-A, Gpi-A and Pgm-A). One group contained six populations from southern part of Miyazaki Prefecture and easternmost part of Kagoshima Pref., whereas another contained eight populations from Kumamoto Pref., most part of Kagoshima Pref. and northern and central parts of Miyazaki Pref. Mean value of Nei's genetic distances between these two groups was 0.155. Hybrid populations were detected from Kunitomi, Miyazaki Pref. and Kanoya, Kagoshima Pref. Between the two groups, introgression occurs along western coast of Kyushu. On the other hand, fixed or almost fixed differences were observed at two loci between populations of different groups in the Miyazaki plains. This indicates that the gene flow between the two groups is restricted in this region.

TS 22

ALLOZYME VARIATION AND SYSTEMATIC RELATIONSHIPS OF SMALL SALAMANDERS FROM HOKKAIDO. M. Matsui¹, T. Hayashi² and T. Sato³. ¹Biol. Lab., Yoshida Coll., Kyoto Univ., Kyoto, ²Dept. Zool., Fac. Sci., Kyoto Univ., Kyoto and ³Obihiro Centennial City Museum, Obihiro.

In order to clarify the systematic relationships among two morphologically different populations of *Hynobius retardatus*, *Salamandrella keyserlingii*, and several small salamander species from Honshu, horizontal starch gel electrophoresis was conducted. The allozyme data from 28 presumptive loci were transformed employing distance procedures. The mean heterozygosity in large-sized *H. retardatus* was extremely larger than that of medium-sized *H. retardatus* or *S. keyserlingii*. Nei's (1978) genetic distance between two types of *H. retardatus* was extremely small, and these were judged to be little differentiated genetically, notwithstanding great differences in adult and egg sac sizes. Both types differed greatly from *S. keyserlingii*, and all of these were genetically fairly well differentiated from *Hynobius* species from Honshu, including lotic and lentic breeding types. Phylogenetic tree derived from distance Wagner network procedure among these species indicated possible common ancestry of *H. retardatus* with *H. kimurae*, but the relationships of the former species with lotic-breeding *Hynobius* requires further examination.

TS 23

SKULL FEATURES OF *H. SADOENSIS* FROM SADO ISLAND.

H. Nambu. Toyama Science Museum. TOYAMA.

Skull of *H. sadoensis* from Sado Island was compared with that of *H. nigrescens* from lowland of Toyama Pref. Skull length measured by soft x ray film is as follows (shown by means \pm SE and ranges, in mm): *H. sadoensis*, 18 males, 14.0 ± 0.09 (13.4-14.5), 7 females, 14.3 ± 0.18 (13.8-15.2); *H. nigrescens*, 19 males, 14.2 ± 0.15 (13.1-15.5), 6 females, 13.8 ± 0.24 (13.2-15). Distance between right and left sphenoids of *H. sadoensis* is wider than that of *H. nigrescens*. In *H. sadoensis*, lateral side of nasals are separated from dorsal projections of maxilla. However, those of *H. nigrescens* touch dorsal projection of maxilla. Prefrontals and frontals of *H. sadoensis* are wider than those of *H. nigrescens*. Vomer teeth series of *H. sadoensis* and *H. nigrescens* are V-shaped and narrow U-shaped, respectively. Posterior tips of vomers are sharper than those of *H. nigrescens*. Numbers of jaw teeth, mandible teeth and vomer teeth of *H. sadoensis* are smaller than those of *H. nigrescens*.

Results of the present observation indicated the following two points. 1) Features of the skull of *H. sadoensis* described by Sato (1940) are partly different from those examined in this study. 2) Features of the skull of *H. sadoensis* are different from those of *H. nigrescens*. Needs of further studies are apparent to establish the taxonomic status of *H. sadoensis*.

TS 24

EFFECTS OF EGG SIZE, TEMPERATURE, FOOD LEVEL AND LARVAL DENSITY ON LARVAL DEVELOPMENT IN THE SALAMANDER *HYNOBIUS NIGRESCENS*

Hisashi Takahashi. Dept. of Biol., Fac. of Sci., Kanazawa Univ., Ishikawa

The inter- and intrapopulation variations in development of larvae derived from eggs having various sizes from two populations (1060 m and 100 m altitude) were examined. Mean egg size was 9.42 mm^3 (ranged from 8.11 to 10.84 mm^3 among clutches) in highland population and 15.06 mm^3 (from 10.35 to 18.61 mm^3) in lowland one. The length of larval period and size at metamorphosis among clutches were compared under different conditions: temperatures (15°C and 20°C), food levels (fed ad libitum and without food half the time) and larval densities (3 and 9 larvae per group). Larval period and size at metamorphosis were significantly differed among clutches and among populations in each condition. Larvae derived from large eggs generally had shorter larval period and smaller size at metamorphosis. In the high temperature, larvae had shorter larval periods and smaller size at metamorphosis. In the high food level, larvae metamorphosed sooner and larger. No significant differences in larval period and size at metamorphosis were seen between larval densities. The relationship between egg size and larval developmental pattern did not change among conditions.

TS 25

COMPARISON OF MATING CALLS AMONG *RANA LESSONAE*, *R. RIDIBUNDA* AND THEIR HYBRIDS.
H. Ueda, Lab. for Amphibian Biol., Fac. of Sci., Hiroshima Univ., Hiroshima

The mating calls of males in *R. lessonae* from Luxembourg and Italy, *R. ridibunda* from Turkey and their reciprocal hybrids were recorded in the laboratory. Their acoustic structures were analyzed by a sound spectrograph.

R. lessonae from Luxembourg had multi-note calls which lasted for 1.02 sec on the average. These calls were consisted of about 24 notes that had the mean time duration of 0.03 sec and showed the dominant frequency at 1.4 kHz. On the other hand, *R. lessonae* from Italy had single-note calls which lasted for 1.8 sec on the average and were composed of about 385 pulses. The calls of this race showed the mean dominant frequency at 2.7 kHz. *R. ridibunda* had multi-note calls which lasted for about 0.41 sec on the average and consisted of about eight notes. The mean time duration was 0.04 sec, showing 5-6 harmonic bands with narrow frequency range. The mean dominant frequency of the calls was at 2.2 kHz.

The mating calls of the males of reciprocal hybrids generally showed intermediate values in most acoustic parameters between those of the two parental species or local races. However, the characteristics of the maternal species or local races were apt to be emphasized especially in call duration and dominant frequency.

TS 26

PHYLOGENETIC ANALYSIS OF THE SCINCID GENUS *EUMECES* IN EAST ASIA.

T. HIKIDA, Dept. Zool., Fac. Sci., Kyoto Univ., Kyoto.

The cosmopolitan skinks of the genus *Eumeces* are distributed in three disjunct regions, North and Middle America, East Asia, and North Africa and West Asia. According to the classification of Taylor (1935), three intrageneric groups occur in East Asia. Recently, two new species were discovered (Hikida, 1989; Hikida and Zhao, 1989) and 16 species have been reported in this region. The *quadrilineatus* group is monotypic and endemic to Asia, but the *obsoletus* and *fasciatus* groups have both East Asian and American members. I examined the external morphology of the species and analyzed the cladistic relationships of the species in the latter two groups, including American relatives. Data matrices were analyzed using PENNY program of PHYLIP ver. 3.2 (Felsenstein, 1989), and MacClade ver. 2.1 (Maddison and Maddison, 1987). Nine alternative tree topologies were discovered for the *fasciatus* group (C.I. = 0.65), while a single tree were obtained for the *obsoletus* group. However, a single American member, *E. obsoletus* shares no apomorphic characters with the East Asian members except for large body size. Thus, at least these East Asian members should be grouped tentatively as another distinct intra-generic group.

TS 27

GEOGRAPHICAL VARIATIONS OF CHROMOSOMES IN JAPANESE SHREW MOLE, *UROTRICHUS TALPOIDES* (MAMMALIA: INSECTIVORA).

M. Harada, Lab. of Experimental Animals, Osaka City Univ. Medical School, Osaka.

Geographical variations in the karyotypes of the Japanese shrew mole (*Urotrichus talpoides*) collected from 23 locations in Japan were examined. Two karyotypes were found, one on each side of a boundary line running through the central part of the mainland of Japan. The only difference was that animals in the west had a large ST pair and that those in the east had an M-MS pair arising from pericentric inversion. The two karyotypes were not found in the same habitat, and chromosomal hybrids were not found in the contact zone. It was interesting that the boundary line was close to that of *Apodemus speciosus* (2n=46 and 48).

TS 28

GENETIC DIFFERENTIATION AND GEOGRAPHICAL DISTRIBUTION OF THE HOUSE MOUSE IN CHINA.

K. Moriwakai, N. Miyashita, H. Yonekawa, Y. Kurihara, H. Suzuki, H. Xingqiao, and Jin Meilei. 1Dept. Cell Genet., Natl. Inst. Genet., Mishima, 2Lab. Animal Sect., Tokyo Metropol. Inst. Med. Sci., Tokyo, 3Dept. Biol., Natl. Inst. Rad. Sci., Chiba, 4Lab. Genet. Eng., Jikei Univ. Med. Coll., Tokyo, 5Shanghai Lab. Anim. Cent., Acad. Sin., Shanghai.

We have already demonstrated that *Mus musculus* species can be divided into four subspecies groups, *domesticus*, *bactrianus*, *castaneus* and *musculus*, based on genetic characters such as electrophoretic patterns of isozymes and serum proteins, RFLPs in Mt-DNAs and rDNAs, chromosome C-banding patterns and others. We also indicated the intersubspecies hybrid nature of the Japanese *M. musculus* which was actually produced by the hybridization of *musculus* and *castaneus* subspecies in the natural habitat. So far, nobody has investigated the genetic status of *Mus musculus* subspecies differentiation in mainland China, though several subspecies have been described in that area. Since 1981, we have surveyed wild populations of *Mus musculus* in China, based on their genetic characters as mentioned above. Mt-DNA RFLPs suggested the possible presence of two subspecies, *musculus* in northern China and *castaneus* in southern China. Analyses of electrophoretic bands of Hbb and RFLPs in rDNA supported the above possibility.

TS 29

AN ORNITHOLOGIST, MINORI OGAWA.
Naohide Isono and Satoko Nagaoki. Dept.
of Biology, Keio University, Yokohama.

Minori Ogawa (1876-1908) was one of the earliest ornithologists in Japan. His works, however, have not been fully determined, except about 30 articles published before his early death.

Recently we found that his notebooks and sketches have been kept in the Inst. of Zool., Fac. of Sci., Univ. of Tokyo. Among them are his daily observation records from 1901 through 1905, and a detailed list on the bird-egg specimens owned by the Institute. Both of them are much useful for studying not only Ogawa's works, but also the contributions of amateur collectors to the bird studies in the Meiji period. The former also gives some interesting information on the distribution of birds in Tokyo and its neighborhood in those days.

The above case is only one example of valuable historical material. Similar documents, records and others may be found in many institutions. They are, however, often forgotten, and even lost with the passage of years. Then they should be listed as soon as possible, and kept in a good condition. We hope the Zool. Soc. of Japan would take an active part in these urgent measures.

TS 30

NOTABLE CHANGE OF SOCIAL FUNCTION OF GRADUATES FROM DEPARTMENT OF BIOLOGY IN JAPAN.

N.Sawada. Matsuyama University, Matsuyama.

Before 1950, number of graduates from department of biology is estimated to be around 70 per year, and most of them engaged in the study of basic biology. Many departments have been established after 1950. Now 34 universities have the biological department (except teacher training course), over 700 students are presumed to graduate now every year. Social function of the graduates must be changed. To prove the change actually, the present occupation of graduates from 10 departments of biology, which was established after 1950, was checked by the alumni lists. The occupation was classified into five groups: research worker, teacher, clinic-related worker, member of enterprise related to biology, occupation unrelated to biology and female without occupation. Number of graduates belong to each group was summed up and the percentage was calculated every year from 1953 to 1982.

The ratio of teacher varied year by year (20%-50%). Member of enterprise increased from 2% to 20%. Research workers decreased in ratio (19%-11%), but doubled in real number. About 5% of graduates engaged in clinical or paramedical work. Half of married females have no constant occupation.

ANNOUNCEMENTS

THE 61ST ANNUAL MEETING OF THE ZOOLOGICAL SOCIETY OF JAPAN

The 61st Annual Meeting of the Zoological Society of Japan will be held at Niigata University from October 3 to 5, 1990. Further information and application forms will be sent to the domestic members in the April issue of 'Biological Science News' (No. 2). The deadline for application is July 14, 1990.

For application from abroad, please contact:

Professor H. IWASAWA
Organizing Committee of the 61st Annual Meeting
of the Zoological Society of Japan
Zoological Institute, Faculty of Science,
Niigata University,
Niigata 950-21, Japan.
Phone: 025(262)6183.

ZOOLOGICAL SCIENCE AWARD

Annual awards for the best original papers have been established through the donation of Narishige Scientific Instrument Laboratory, Tokyo. The sum of about 500,000 yen will be awarded annually at the Annual Meeting of the Zoological Society of Japan to a few papers published in ZOOLOGICAL SCIENCE during the preceding calendar year. Every original papers published in this journal will automatically be candidates for the award. The aim of the award is to encourage contributions to this journal. Selection Committee for the award will be organized every year.

ZOOLOGICAL SCIENCE AWARD 1989 was given to the following four papers.

Saburo Nagata: T cell-specific antigen in *Xenopus* identified with a mouse monoclonal antibody: Biochemical characterization and specific distribution. Vol. 5, No. 1, pp. 77-83, 1988.

Mamiko Ozaki: A possible sugar receptor protein found in the labellum of the blowfly, *Phormia regina*. Vol. 5, No. 2, pp. 281-290, 1988.

Tatsunori Seki, Sakae Kikuyama and Mitsuo Suzuki: Effect of hypothalamic extract on the prolactin release from the bullfrog pituitary gland with special reference to thyrotropin-releasing hormone (TRH). Vol. 5, No. 2, pp. 407-413, 1988.

Naoto Hanzawa, Nobuhiko Taniguchi and Ken-ichi Numachi: Geographical differentiation in populations of Japanese dace *Tribolodon hakonensis* deduced from allozymic variation. Vol. 5, No. 2, pp. 449-461, 1988.

ACKNOWLEDGEMENTS

The Zoological Society of Japan and the Editorial Committee of Zoological Science are grateful to Narishige Scientific Instrument Laboratory Co., Ltd. (President Mr. Eiichi Narishige) for the financial aids for publication of Zoological Science, Volume 6 and constant support for Zoological Science Awards for volumes 1-6.

AUTHOR INDEX

A

Aihara, Masahiro	1059
Akai, Hiromu	615
Arai, Yasumasa	141, 1037
Arikawa, Kentaro	241
Asao, Tezro	715
Asashima, Makoto	899
Awaji, Masahiko	943

B

Badia, Pilar	667
Bhattacharya, Samir	771
Brusle, Solange	789

C

Chiba, Yoshihiko	565
Chieffi, Giovanni	623
Chung, Hae-Moon	1
Clougherty, John J.	813

D

Dixit, Anand S.	129
----------------------	-----

E

Eguchi, Eisuke	241
Endo, Katsuhiko	113
Engström, Wilhelm	15

F

Fujihara, Noboru	731
Fujii, Ken	951
Fujii, Ryoza	477
Fujimoto, Yoshinori	121
Fujiwara, Akiko	63
Fukunaga, Akihiro	541
Furukohri, Takahiro	269, 915

G

Gómez, Tomas	667
Gomi, Toshiaki	675
Gupta, Ayodhya P.	303

H

Hamaguchi, Yukihiisa	1023
Han, Sung S.	303
Hanyu, Isao	943
Harada, Masashi	377
Hasegawa, Hiroshi	1037
Hasegawa, Kou	809
Hasegawa, Masato	289
Hashimoto, Paulo H.	907
Hata, Fumiko	121
Hayashi, Shin-ichi	1033
Hayashi, Shinji	1059
Higashi, Kazuyoshi	675
Higuchi, Keiko	709
Hirano, Tetsuya	83
Hirata, Yukio	1033
Horiuchi, Ryuya	749
Horiuchi, Shinri	31, 321
Hosono, Ryuji	697
Hu, Di Hua	797
Hyodo, Susumu	335

I

Iga, Chie	359
Ikekawa, Nobuo	121
Imada, Masako	45
Imaizumi, Hiroki	983
Inoue, Koji	445
Ishibashi, Satomi	241
Ishii, Susumu	963
Ishikawa, Atsushi	233
Ishikawa, Masaru	599
Ishizaka, Shigeaki	523
Itoh, Masanori	963
Iwamura, Shawichi	345
Iwasa, Tatsuo	167

Iwasaki, Shin-ichi	259, 681
Iwasawa, Hisaaki	935, 1027

K

Kabasawa, Hiroshi	135
Kambegawa, Akira	423, 607, 611
Kamezaki, Naoki	421
Kangstrom, Lars E.	15
Kasukawa, Hiroaki	477
Kasuya, Takahiro	499
Kawashima, Seiichiro	763, 777, 797
Kawashima, Tsuyoshi	801
Kenmochi, Naoya	55, 295
Kikuchi, Yasuhiro	675
Kikuyama, Sakae	345, 757
Kimura, Akihiko	675
Kimura, Ken-ichi	659
Kimura, Mayumi	121
Kimura, Sumiko	797
Kitani, Hiroshi	31
Kobayashi, Hideshi	817, 951
Kobayashi, Kan	259, 681
Kobayashi, Michiyori	269
Kobayashi, Tetsuya	757
Kobayashi, Tohru	935, 1027
Kobayashi, Yasuo	359
Koga, Osamu	731
Koike, Satoshi	351
Kojima, Manabu K.	329
Komazaki, Shinji	899
Koshida, Yutaka	31, 321
Koya, Sakuji	749
Kubota, Shin	147
Kumada, Nobuo	1019
Kumagai, Kanji	113, 659, 851
Kume, Akihide	757
Kuno, Sigeru	697
Kurahashi, Takashi	19
Kuroda, Yukiaki	499
Kusaka, Shinji	1037

L

Larsson, Olle	15
Lattaud, Claude	741
Laubier, Lucien	387
Lorenzo, Antonio	667

M

Maitra, Gaurangi	771
Malacinsky, Gerge M.	1
Mamiya, Naoko	345
Marcel, Roger	741
Maruyama, Koscak	797
Masaki, Tadakatsu	113
Matsuda, Kouhei	423, 607, 611
Matsui, Tomohiko	809
Matsunaga, Takashi	283
Matsuoka, Norimasa	409, 589, 1005
Meyer-Rochow, V. B.	241
Michibata, Hitoshi	289, 639
Minato, Kiyoshi	35, 295
Minh-Nyo, Maung	367, 427
Miura, Tomoyuki	387
Miyaji, Kazuyuki	477
Miyata, Ken	681
Mizuno, Takeo	71, 283
Mollermark, Gunnar	15
Mori, Takao	103
Mukai, Hideo	401
Mukai, Makio	805
Munro, Angus D.	191
Murakami, Takuro	1047
Myohara, Maroko	533

N

Nagasawa, Hiroshi	103
Nagatomi, Akira	983
Nagatomi, Hisako	983
Naito, Tikhiko	541
Naitoh, Yutaka	833
Nakamachi, Tamotsu	121
Nakamura, Shogo	329
Nakazawa, Tohru	801
Nariki, Mayumi	121
Neff, Anton W.	1
Niimi, Shinya	121
Nishio, Hiroshi	963
Nishiyama, Hisayoshi	731
Niwa, Hiroshi	367
Noumura, Tetsuo	351
Numakunai, Takaharu	289

O

Oami, Kazunori	833	Santana, Pino	667
Obara, Yoshitaka	409, 1005	Sasa, Shozo	675
Oda, Shuzitu	401	Sasaki, Tetsuo	951
Ogata, Kikuo	55, 295	Sasayama, Yuichi	423, 607, 611
Ogawa, Mizuho	805	Sassa, Toshihiro	697
Oguri, Mikio	367	Sato, Eiji	649
Oguro, Chitaru	199, 423, 607, 611	Sato, Moriyuki	335
Ohkawa, Muneyoshi	757	Sato, Seiji	167
Ohmi, Chika	329	Satou, Masahiko	885
Ohnishi, Eiji	177	Sawa, Masami	541, 549, 557
Ohta, Suguru	915	Sawada, Isamu	377
Ohtaki, Tetsuya	121	Sawai, Tsuyoshi	709
Ohtsu, Kohzoh	469, 721	Sekizawa, Yoshiyuki	951
Oinuma, Tsutomu	899	Selman, Kelly	211
Oishi, Kugao	541, 549, 557	Shiba, Makoto	269
Oka, Yoshitaka	885	Shibuya, Tatsuaki	19
Okada, Toyohi	391	Shiga, Takashi	885
Okai, Yasuji	523, 603	Shigenaka, Yoshinobu	45
Okajima, Akira	459, 851, 859	Shimazu, Takashi	579
Okamoto, Kiyoshi	233	Shimizu, Akitoshi	91
Okuda, Kazuo	915	Shimizu, Isamu	809
Okuma, Jiro	757	Shimizu, Toshiaki	177
Okumoto, Naoto	885	Shimozawa, Tateo	659
Ooka-Souda, Sadako	135	Shozawa, Akiko	1019
Oommen, Oommen V.	185	Skadhaug, Erik	437
Oshima, Noriko	477	Soeda, Miyabi	675
Oshimi, Akiko	1027	Sonobe, Haruyuki	515
Ozato, Kenhiro	445	Spieler, Richard E.	813
		Su, Wanan C.	233
		Sugino, Yasuo M.	599
		Suiko, Masahito	173
		Suto, Chiharu	1019
		Suzuki, Hirobumi	589
		Suzuki, Tatsuo	241
		Suzuki, Tomohiko	269, 915
		Suzuki, Yuko	487

P

Peng, Tong Xu	155
Peter, M. C. S.	185

R

Radice, Gary	1
Rembold, Heinz	615
Ross, Mary H.	927

S

Saitoh, Masako	1005
Sakai, Tadashi	173
Sakurai, Kazuhiro	721
Sakurai, Sho	121

T

Tabata, Mitsuo	367, 427
Tabata, Nobuyuki	173
Tachi, Chikashi	251
Tagawa, Shin-Ichi	649
Tagawa, Takasuke	233
Takada, Yuko	499
Takagi, Takashi	915
Takagi, Yasuaki	83
Takahashi, Sumio	777

Takao, Masashi	167
Takeda, Masako	487
Takeuchi, Takuji	31, 167
Takikawa, Hiroo	749
Tamamaki, Nobuaki	867, 877
Tanaka, Akira	927
Tanaka, Toshiharu	691
Tanimura, Teiichi	659
Tazawa, Eigoro	63
Tazawa, Hisashi	805
Terada, Koji	963
Terada, Tatsuro	289
Terami, Harue	573, 975
Tewary, Prabha D.	129
Toda, Masanori J.	155
Tokunaga, Fimio	31, 167
Tomioka, Kenji	565

U

Uchibori, Masayuki	763
Uchiyama, Hideho	71
Ueck, Manfred	817
Ueda, Kazuo	885
Urano, Akihisa	335

W

Wada, Keiji	181
-------------------	-----

Wago, Haruhisa	691
Wakamatsu, Yuko	445
Wake, Kenjiro	817
Wallace, Robin A.	211
Watanabe, Masao	459, 859
Watanabe, Munetaka	573, 975
Willis, Judith H.	533

Y

Yamada, Chifumi	951
Yamada, Juro	83
Yamamoto, Masamichi	721
Yamanouchi, Korehito	141, 1037
Yamashita, Junko	1033
Yamauchi, Kiyoshi	749
Yano, Kazuhide	45
Yashika, Kanji	907
Yasugi, Sadao	283
Yasumasu, Ikuo	63
Yoshida, Ikuya	409
Yoshida, Masao	721
Yoshizaki, Norio	507
Yee, Win Win	777

Z

Zenko, Yutaka	289
Zor, Uril	251

AUTHOR INDEX (Abstracts)

A

Abe, Hiroshi	1115
Abe, Hiroyuki	1143
Abe, Michikazu	1128
Abe, Osamu	1092
Abe, Shin-ichi	1162, 1163, 1164
Abe, Takeyuki	1106, 1132
Adachi, Hajime	1180
Adachi, Takashi	1181
Agata, Kiyokazu	1164
Ai, Hiroyuki	1075
Ai, Naohiro	1075, 1098
Aigaki, Toshiro	1092, 1096
Aihara, Shin	1127
Aikawa, Eizo	1087, 1154
Aizawa, Takeshi	1115
Akasaka, Koji	1131, 1136, 1137, 1157
Aketa, Kenji	1172
Akimoto, Yoshihiro	1157
Akiyama, Tadashi	1214
Akiyama, Toyoko	1143
Amakawa, Taisaku	1078
Amanai, Kazuhito	1125
Amano, Minoru	1140
Amano, Toshikazu	1172
Amano, Tsukasa	1197
Amemiya, Shonan	1136
Amikura, Reiko M.	1154
Ando, Koichi	1197
Ando, Masaki	1099
Ando, Tsuyoshi	1119
Aoki, Kiyoshi	1080, 1105, 1160, 1215
Aoto, Tomoji	1185
Aotsuka, Tadashi	1126
Arai, Kiyoshi	1164
Arai, Takao	1152
Arai, Yasumasa	1150, 1151, 1177, 1191
Arakaki, Yuuji	1221
Araki, Yoko	1146
Arikawa, Kentaro	1086
Arima, Takuo	1075, 1215

Arnold, A. P.	1191
Asaga, Hiroaki	1149
Asakura, Hidenori	1112
Asami, Kouichi	1132
Asao, Tezro	1159
Asashima, Makoto	1138, 1141, 1160
Ashida, Masaaki	1124, 1125
Awano, Minoru	1128
Azuma, Masaaki	1124
Azuma, Masami	1128

B

Baba, Shoji A.	1089, 1090
Baba, Yoshichika	1074
Banba, Tomoko	1137
Bandai, Kouichi	1079
Bienz, Mariann	1196
Bottjer, Sarah W.	1183
Brey, Pail T.	1125
Burrows, Malcolm	1076

C

Cachon, Jean	1121
Cachon, Monique	1121
Chen, Pei-Schen	1196
Chiba, Akira	1205, 1208
Chiba, Atsuhiko	1215
Chiba, Joe	1120
Chiba, Kazuyoshi	1166
Chiba, Motoyoshi	1161
Chiba, Yoshihiko	1103, 1104, 1196
Chino, Haruo	1126

D

Dan, Katsuma	1154
Dan-Sohkawa, Marina	1155, 1212
Daumae, Masashi	1216

de Jesus, Evelyn G.	1190
Daiz, Maria Rosario M.	1160
Doi, Kazuyo	1209
Doi, Naomi	1077

E

Ebina, Yukiko	1158
Eguchi, Eisuke	1079, 1087
Eguchi, Goro	1164
Eguchi, Masaharu	1124
Elinson, Richard P.	1171
Endo, Katsuhiko	1180
Endo, Sachiko	1152, 1153
Endo, Takeshi	1149
Endo, Yasuhisa	1124, 1186
Enomoto, Yumiko	1197
Ezure, Tomonobu	1183

F

Fausto, Nelson	1150
Fugo, Hajime	1180
Fujihara, Noboru	1164
Fujii, Tomoko	1123, 1156
Fujii, Ryozo	1102, 1103
Fujiki, Masahiko	1098
Fujikura, Keiko	1184
Fujikura, Yoshihisa	1165
Fujimaki, Hidekazu	1106
Fujimoto, Katsuyuki	1097
Fujimoto, Masaaki	1080
Fujimoto, Sunao	1165
Fujimoto, Yasuhiro	1180
Fujino, Yukio	1156
Fujisawa, Hiromi	1084
Fujisawa, Yuko	1096
Fujishima, Masahiro	1210
Fujita, Jun	1109
Fujita, Shinobu C.	1184
Fujita, Toshihiko	1213
Fujiwara, Akiko	1136, 1156, 1157, 1173
Fujiwara, Haruhiko	1130
Fukada, Yoshitaka	1083, 1084
Fukamachi, Hiroshi	1142
Fukatsu, Takema	1129
Fukue, Yūko	1198
Fukui, Akimasa	1141

Fukumoto, Tetsuo	1165, 1210
Fukuoka, Masao	1156
Fukushi, Tsukasa	1081
Fukuta, Keiko	1219
Funakoshi, Kimitake	1198
Furuhashi, Kiyoshi	1120
Furukohri, Takahiro	1133
Furusawa, Kiyotaka	1118
Furusawa, Noriyuki	1159
Furuta, Emiko	1204
Furuta, Rika	1161
Furuya, Hidetaka	1208

G

Gen, Koichiro	1177, 1178
Gleadall, Ian G.	1104, 1188
Gold, Geoffrey H.	1077
Gomi, Toshiaki	1199
Goto, Taichiro	1198
Gyotoku, Junichiro	1108

H

Haino-Fukushima, Kazu	1192, 1174
Hamada, Yoshi	1089
Hamaguchi, Miyako S.	1151
Hamaguchi, Satoshi	1112, 1113, 1168
Hamaguchi, Yukihisa	1092, 1151, 1152
Hamazaki, Tetsuo S.	1137, 1169
Hanada, Takahisa	1076
Hanai, Kazumitsu	1100
Hanaoka, Youichi	1166, 1187
Hara, Eijirō	1129
Hara, Hiroaki	1217
Hara, Masayuki	1201
Hara, Reiko	1082, 1083
Hara, Tomiyuki	1082, 1083
Harada, Masayoshi	1226
Harada, Tetsuo	1105
Hardy, D. M.	1170
Hariyama, Takahito	1088, 1104
Hasegawa, Hitoshi	1146
Hasegawa, Nobuhiko	1202
Hasegawa, Sanae	1187
Hasegawa, Yuriko	1192
Hashimoto, Koichiro	1145
Hashimoto, Koji	1162

Ishida, Katsumi	1091
Ishida, Makoto	1183
Ishida, Sachiko	1162
Ishihara, Hiroko	1197
Ishihara, Katsutoshi	1135, 1156
Ishii, Kei-ichi	1108, 1114
Ishii, Naokata	1092
Ishii, Saburo	1200
Ishii, Sou	1102
Ishii, Susumu	1179, 1217
Ishijima, Sumio	1092
Ishijima, Sanae A.	1167
Ishijima, Takashi	1185
Ishikawa, Atsushi	1197
Ishikawa, Hajime	1129, 1130, 1131
Ishikawa, Koiichi	1184
Ishimoda-Takagi, Tadashi	1119, 1133
Ishizaki, Hironori	1180, 1181, 1182
Ishizaki, Toshiyuki	1183
Ishizuka-Oka, Atsuko	1140
Isono, Naohide	1227
Ito, Akira	1107
Ito, Kazuo	1144, 1212
Ito, Masaya	1116
Itô, Tatsunori	1223
Itoh, Masaharu	1133
Itoh, Masanori	1179
Itoh, Tsunao	1077
Iuchi, Ichiro	1137, 1158, 1169
Iwai, Kunihiisa	1099
Iwakiri, Minoru	1097
Iwama, Akifumi	1078
Iwamatsu, Takashi	1168, 1169
Iwami, Masafumi	1180, 1181
Iwamoto, Hiroyuki	1093
Iwamuro, Shawichi	1187
Iwao, Yasuhiro	1171
Iwasa, Tatsuo	1084
Iwasawa, Hisaaki	1168, 1194, 1208
Iwata, Katsuya	1098
Iwata, Ren	1099
Iwata, Yukinari	1100
Iwatsuki, Kenji	1087
Izumi, Susumu	1128, 1130
Izumi-Kurotani, Akemi	1089, 1090
Izumo, Akihisa	1135
Izutsu, Yumi	1140

J

Jin, Meilei	1226
-------------------	------

K

Kabasawa, Hiroshi	1105
Kadowaki, Shin-etsu	1108
Kageyama, Takashi	1130
Kageyama, Tetsuo	1158
Kaiho, Masayoshi	1140
Kaji, Kazuhiko	1203, 1210
Kakeda, Keiko	1129
Kakuta, Izuru	1098
Kamata, Yasuyuki	1157
Kambegawa, Akira	1185
Kamiguchi, Yujiroh	1112
Kamimura, Shinji	1091
Kaminuma, Tsuguchika	1116
Kamishima, Yoshihisa	1100
Kamiya, Mie	1151
Kamiya, Ritsu	1091
Kanai, Shigeaki	1171
Kanamori, Akiko	1171
Kanda, Tomoko	1096
Kandori, Hideki	1083
Kaneko, Hiroyuki	1155, 1212
Kaneko, Tomoko	1111
Kaneko, Yûko	1080
Kano, Kazutaka	1194, 1203
Kanô, Yasuhiko	1191
Kariya, Mieko	1204
Kasama, Hidetaka	1134
Kasama, Takeshi	1203
Kasuga, Hiroko	1092, 1164
Kasuya, Yoko	1185, 1186
Katada, Jun	1090
Katagiri, Chiaki	1139, 1163, 1164, 1170
Katagiri, Chihiro	1126
Katagiri, Nobuko	1087
Katagiri, Yasuo	1087
Katakura, Yasutoshi	1192
Kataoka, Hiroshi	1180, 1181
Kataoka, Kenji	1156, 1157
Kataoka, Masanori	1156
Katayama, Isao	1159
Katayama, Jiro	1080
Kato, Koichi H.	1154

Kato, Yukio	1178, 1188	Kishida, Yoshikazu	1148
Kato, Yuko	1153	Kishimoto, Takeo	1166
Katoh, Ayumi	1185	Kitajima, Ken	1149, 1171
Katoh, Kaoru	1090	Kitamura, Kunio	1143, 1144, 1146
Katoh, Setsuko	1134	Kitano, Koichi	1116
Katow, Shigetaka	1137	Kito, Yuji	1085
Katsube, Yukiteru	1126	Kiyohara, Sadao	1079
Katsura, Yoshimoto	1108	Kobayakawa, Yoshitaka	1135
Kawaguchi, Akihiko	1128	Kobayashi, Hiroaki	1198
Kawahara, Akira	1140	Kobayashi, Ken-ichiro	1138, 1139
Kawai, Gota	1134	Kobayashi, Makoto	1095, 1096, 1097
Kawai, Kiyozo	1086	Kobayashi, Michiyori	1098
Kawakami, Atsushi	1180, 1181	Kobayashi, Satoru	1158
Kawakatsu, Masaharu	1221	Kobayashi, Shumpei	1104
Kawamata, Kunihiko	1086	Kobayashi, Shyu	1203
Kawamura, Kazuo	1204, 1133, 1146, 1173	Kobayashi, Shigeo	1084
Kawamura Ken-ya	1137	Kobayashi, Sumiko	1210
Kawamura, Kosuke	1195	Kobayashi, Takeshi	1090
Kawamura Masaru	1122	Kobayashi, Tetsuya	1194
Kawamura, Mieko	1099	Kobayashi, Tohru	1208
Kawamura, Yoshinori	1140	Kobayashi, Yasuo	1190
Kawamura, Yuuki	1206, 1209	Kobayashi, Yumi	1087
Kawasaki, Ryoji	1098	Kobayashi, Yuta	1178
Kawashima, Seiichiro	1178, 1188	Kobayashi, Wataru	1175
Kawata, Atsuko	1084, 1087	Koenuma, Akira	1182
Kawauchi, Hiroshi	1190	Koga, Osamu	1164
Kengaku, Mineko	1129	Kohama, Kazuhiro	1116
Kidachi, Yumi	1111	Kohriyama, Hirohi	1079
Kihara, Hideaki	1124	Koike, Keiichi	1218
Kihara, Hirozi K.	1159	Koike, Mitsuhiro	1212
Kikuchi, Kokichi	1093	Koike, Noboru	1120
Kikuchi, Misao	1215	Koizumi, Osamu	1135
Kikuchi, Shin-ichi	1174, 1213	Koizumi, Sadaaki	1210
Kikuchi, Susumu	1205	Koizumi, Takashi	1185
Kikuchi, Yasuhiro	1119	Koiwai, Osamu	1130
Kikuyama, Sakaé	1177, 1178, 1187 1188, 1189, 1194, 1195	Kojima, Hiroko	1150
Kimura, Akihiko	1199	Kojima, Manabu K.	1171, 1172
Kimura, Ken-ichi	1183	Kojima, Takashi	1115
Kimura, Sumiko	1116, 1117	Komatsu, Miéko	1156
Kimura, Tadashi	1105	Komukai, Masayuki	1136, 1164
Kimura, Takeji	1215	Kondo, Hiroshi	1107, 1202, 1203
Kimura-Tekeuchi, Mayumi	1106	Kondo, Hidehiko	1181
Kinoshita, Kei	1160	Kondo, Jun	1106
Kinoshita, Kuninori	1125	Kondo, Noriaki	1106
Kinoshita, Tsutomu	1139, 1208	Kondo, Yasuhiko	1177
Kiriishi, Shonosuke	1182	Kondo, Yoichi	1184
Kishi, Kiyoshi	1199	Kondoh, Yasuhiro	1075
		Konishi, Kazuhiko	1128

Konishi, Kooichi	1222
Konno, Kunio	1149
Kosaka, Toshokazu	1211
Koseki, Nobumasa	1211
Koshida, Yutaka	1198, 1208, 1212
Koshimizu, Ichiro	1190
Koshio, Osamu	1132
Kosuda, Kazuhiko	1112
Kotani, Susumu	1134
Kouyama, Hiroshi	1123
Koyama, Eiki	1141
Koyama, Hideki	1133
Koyama, Sachiko	1216
Kubli, Eric	1196
Kubokawa, Kaoru	1183
Kubota, Ichiro	1096, 1097
Kubota, Tomoyuki	1218
Kubota, Yoshiko	1113
Kudo, Shigeharu	1170, 1171
Kuhlmann, Hans-Werner	1211
Kumagai, Kanji	1180
Kumakura, Masahiko	1168
Kumazawa, Takeshi	1122
Kuno, Shin-ichi	1136
Kurabuchi, Shingo	1148
Kurahashi, Hiromu	1179
Kuraishi, Ritsu	1155
Kuramoto, Taketeru	1094
Kurihara, Yasuyuki	1226
Kuroda, Hideyo	1171
Kuroda, Masaaki	1115, 1121
Kurokawa, Makoto	1075
Kuroki, Yoshihiro	1096
Kurosumi, Kazumasa	1184
Kurozumi, Mafumi	1108
Kusakabe, Tatsumi	1207
Kusano, Tyuzi	1196
Kusumi, Kiyoshi	1076
Kuwahara, Yasumasa	1196
Kuwasawa, Kiyoaki	1075, 1094, 1095
Kyozuka, Keiichiro	1175
Kwon, O-Yu	1130

L

Lemire, Joan	1150
Lin, Jin Tun	1079
Liu, Robert S. H.	1084

Lum, Pek Yee	1126
--------------------	------

M

Mabuchi, Issei	1118, 1119, 1120
Machida, Takeo	1215
Maekawa, Shohei	1120, 1153
Maeno, Naomi	1100
Magtoon, Wichan	1224
Makino, Naoshi	1174
Makino, Naoya	1200, 1205, 1219
Mamiya, Naoko	1187
Manabe, Tomoko	1101, 1139
Maruo, Fumiaki	1159
Maruyama, Koscak	1116, 1117
Maruyama, Yuko	1143
Masuda, Hiroko	1084, 1085
Masuda, Kaori	1169
Masuda, Yoshiki	1220
Masuyama, Etsuko	1121
Matsuda, Kouhei	1189
Matsuda, Motoko	1150
Matsuda, Yasushi	1203
Matsudaira, Hiromichi	1132
Matsui, Masafumi	1225
Matsumoto, Akira	1151, 1191
Matsumoto, Akira	1104
Matsumoto, Fumio	1215
Matsumoto, Jiro	1143
Matsumoto, Michiya	1124
Matsumoto, Shinji	1095
Matsunaga, Takashi	1138
Matsuno, Akira	1121, 1206
Matsuo, Hironori	1097
Matsuoka, Arika	1134
Matsuoka, Norimasa	1222
Matusoka, Tatsuomi	1105
Matsusaka, Tadao	1210
Matsushita, Susumu	1142
Matsuura, Tetsu	1117
Mawatari, Shunsuke F.	1121
Menrai, Naoto	1166
Meyer-Rochow, Victor B.	1102
Micevych, P. E.	1191
Michibata, Hitoshi	1099, 1100
Michinomae, Masanao	1084, 1085
Michinomae, Masatsugu	1085
Mikami, Kazuyuki	1176

Ohtake, Shin-ichi	1106, 1132
Ohtaki, Tetsuya	1125, 1160, 1179, 1180
Ohtani, Hiromi	1111
Ohtsu, Kohzo	1085
Ohtsuka, Satoshi	1117
Ohtsuka, Teruya	1086
Ohtsuki, Hisashi	1205
Oide, Momoko	1122
Oikawa, Taneaki	1143
Oishi, Kazuhiko	1116
Oishi, Kugao	1175
Oishi, Tadashi	1084, 1087, 1214
Ojima, Yoshiro	1109
Oka, Mikako T.	1152
Oka, Shunya	1205
Oka, Tadanori	1180, 1181
Oka, Yoshitaka	1184
Okada, Manabu	1158, 1159, 1190
Okada, Tetsuji	1083
Okada, Toshiaki	1165
Okada, Yoshinori	1074
Okada, Yasuo	1103, 1104
Okamoto, Kenichi	1089
Okano, Toshiyuki	1083, 1084
Okanoya, Kazuo	1105
Okawa, Keiko	1220
Oki, Iwashiro	1221
Okinaga, Shoichi	1164
Okinaga, Tatsuyuki	1172
Okuma, Jiro	1075
Okuno, Makoto	1089, 1091, 1119, 1121 1167, 1168
Okushima, Yasuo	1155
Okuyama, Junko	1185
Omata, Saburo	1134
Onitake, Kazuo	1107, 1168, 1169
Ono, Hirotake	1144
Oodera, Kizuku	1087
Oofusa, Ken	1139
Ooka, Sadako	1105
Ookata, Kayoko	1166
Oomura, Tomohiro	1076
Oota, Yoshihiko	1190
Ooya, Mayumi	1090
Osanai, Kenji	1155, 1175
Osanai, Minoru	1092, 1164
Osawa, Syozo	1160
Oshida, Tatsuo	1110

Oshima, Noriko	1101, 1102
Otokawa, Minoru	1075
Owaribe, Katsushi	1202
Ozaki, Koichi	1082, 1083
Ozaki, Mamiko	1078, 1083

P

Pearse, Vicki B.	1209
------------------	------

R

Ross, Mary H.	1161
Rovainen, Carl	1098
Ryoyama, Kazuo	1213

S

Saba, Masaki	1222
Saegusa, Hironao	1182
Saga, Tsuyoshi	1190
Saigusa, Masayuki	1214
Saiki, Tomoaki	1151
Saito, Takehiko	1080
Saito, Yasunori	1145
Sakagami, Hiroshi	1149
Sakai, Hikoichi	1122, 1134, 1152, 1153
Sakai, Makoto	1187
Sakai, Noriyoshi	1179
Sakai, Yoshi T.	1174
Sakairi, Kazuhiro	1165
Sakaizumi, Mitsuru	1110, 1112, 1113, 1114
Sakamoto, Iwao	1219
Sakata, Mariko	1096
Sakurai, Sho	1125, 1160, 1180, 1182
Sakurai, Susumu	1110
Sakurai, Takashige	1148
Sakurai, Yoko	1107
Sang-Rin Jeon	1113
Sano, Kiyoshi	1166
Saotome, Kaoru	1176
Saotome, Kyoko	1109
Sasagawa, Hiromi	1196
Sasaji, Hiroyuki	1223
Sakai, Fumie	1139, 1208
Sasaki, Junko	1107
Sasaki, Masami	1088, 1196
Sasaki, Tetsuhiko	1129

Sasaki, Yuri	1219	Shimizu, Isamu	1087
Sasayama, Yuichi	1185, 1189	Shimizu, Katsuhiko	1131
Sato, Hidemi	1121	Shimizu, Takashi	1118
Sato, Hiroshi	1110	Shimizu, Teruo	1116
Sato, Katsuyuki	1211	Shimizu, Toshiaki	1217
Sato Mamoru	1126	Shimoda, Yoichi	1166
Sato Mizunori	1157	Shimohigashi, Miki	1081
Sato, Motoaki	1073	Shimomura, Keiko	1178
Sato, Noriyuki	1093	Shimozawa, Atsumi	1140, 1204, 1213
Sato, Osamu	1117	Shiojiri, Atunori	1159
Sato, Takanori	1218, 1225	Shingu, Yoko	1089
Sato, Yukiko	1121	Shingyoji, Chikako	1090
Satoh, Kuniyasu	1220	Shinkawa, Yasuhiro	1196
Satoh, Hiroyuki	1159	Shiojiri, Nobuyoshi	1150
Satoh, Yoshiaki	1173	Shirai, Toshikazu	1150, 1151
Satomi, Daisaku	1073	Shirai, Hiroko	1165
Sawa, Masami	1175	Shiraishi, Satoshi	1201
Sawada, Hiroshi	1127	Shirasawa, Mikio	1200
Sawada, Kazuhiko	1193	Shirasawa, Yasuko	1200, 1219
Sawada, Nobuaki	1227	Shirata, Katsutoshi	1109
Sawada, Tomoo	1165	Shiroya, Yoko	1174
Sawaki, Hidemitsu	1086	Shishikura, Fumio	1106, 1132
Seidou, Masatsugu	1085	Shitara, Mariko	1174
Seki, Takaharu	1128	Shudo, Yoshinobu	1097
Seki, Yuko	1099	Smith, Robert G.	1081
Sekiya, Kunio	1114	Sonobe, Haruyuki	1182
Sendai, Yutaka	1172	Sterling, Peter	1081
Seno, Hiroshi	1122	Suburamanyam, M. V. V.	1099
Senshu, Tatsuo	1191	Sudzuki, Minoru	1219
Seo, Hisao	1178	Sueoka, Terumi	1134
Seo, Naomi	1205	Sugahara, Michio	1085
Seyama, Yoosuke	1203	Sugai, Toshiro	1211
Sezaki, Mariko	1144	Sugano, Hiroshi	1134
Shibata, Michio	1132, 1183	Sugi, Haruo	1092, 1093
Shibata, Naoki	1168	Sugimoto, Kenkichi	1108
Shibuya, Tatsuaki	1076, 1077, 1206	Sumida, Hiroyuki	1191
Shichida, Yoshinori	1083, 1084	Sumida, Masayuki	1110
Shigei, Michio	1222	Suemitsu, Takashi	1135
Shigenaka, Yoshinobu	1121	Suzuki, Akinori	1180, 1181, 1182
Shikama, Keiji	1133, 1134	Suzuki, Akio	1143
Shima, Akihiro	1109, 1111, 1113	Suzuki, Hitoshi	1110, 1114, 1226
Shimada, Atuko	1111	Suzuki, Kazuo	1132
Shimada, Arata	1166	Suzuki, Norio	1179
Shimada, Hiraku	1131, 1136, 1137, 1157	Suzuki, Noriyo	1078
Shimada, Ichiro	1217	Suzuki, Nobuo	1189
Shimada, Takamichi	1115	Suzuki, Osamu	1122
Shimatani, Yuichi	1087	Suzuki, Reiko	1187
Shimazaki, Youji	1087	Suzuki, Sachiko	1192

Suzuki, Shintaro	1184
Suzuki, Takuro	1201
Suzuki, Takeo	1124
Suzuki, Tatsuo	1087
Suzuki, Tohru	1107
Suzuki, Tomohiko	1098, 1133
Suzuki, Toshimitsu	1109
Suzuki-Morimoto, Shigeko	1192

T

Tabata, Shoji	1198	Takamatsu, Yoshiki	1194
Tachi, Chikashi	1150	Takamune, Kazufumi	1163
Tagawa, Masatomo	1193	Takano, Masayoshi	1169
Tagawa, Takasuke	1197	Takano-Ohmuro, Hiromi	1116
Taka, Yuji	1126	Takase, Minoru	1188
Takabatake, Ikuo	1103	Takasugi, Noboru	1193, 1194
Takagi, Takashi	1120, 1133	Takata, Keisuke	1224
Tanaka, Akira	1161	Takata, Kenzo	1160
Tanaka, Haruo	1146	Takeda, Eiko	1094
Tanaka, Kosuke	1095	Takeda, Masatsune	1222
Tanaka, Kunio	1106, 1132	Takeda, Susumu	1124
Tanaka, Masako	1156	Takei, Yoshio	1186
Tanaka, Satoshi	1114	Takamasa, Tohru	1120
Tanaka, Seiji	1171	Takeshima, Kazuhito	1160
Tanaka, Shigeyasu	1184, 1187, 1188	Taketomi, Yoko	1192
Tanaka, Shoji	1154, 1155	Takeuchi, Hiro-aki	1216
Taneda, Koji	1105	Takeuchi, Ikuo	1207
Takagi, Yasuaki	1193	Takeuchi, Sakae	1114, 1144
Takagi, Yoshiomi	1210	Takeuchi, Shigeo	1149, 1202
Takagishi, Kiyohiko	1143	Takeuchi, Takuji	1114, 1144
Takahama, Hideki	1139, 1208	Takeuchi, Yoshiko	1207
Takahashi, Akiyoshi	1186	Takiguchi-Hayashi, Keiko	1146
Takahashi, Hiroya	1161	Takikawa, Shinichiro	1127
Takahashi, Hisashi	1225	Takizawa, Makoto	1080
Takahashi, Keiichi	1088, 1090, 1092	Tamura, Koji	1147
Takahashi, Masaki	1093	Tamura, Sachiko	1221
Takahashi, Megumi	1213	Tamura, Yoji	1093
Takahashi, Nobuaki	1093	Tamotsu, Satoshi	1086
Takahashi, Noriyuki	1178, 1188	Tanabe, Hiroyuki	1210
Takahashi, Shoji	1161	Tanabe, Kazuyuki	1135
Takahashi, Sumio	1178	Tanabe, Kazushi	1130
Takahashi, Susumu Y.	1196	Taneda, Yasuho	1145
Takahashi, Tadashi C.	1160	Taniguchi, Shigehiko	1141
Takahashi, Yasushi	1155	Tanimura, Teiichi	1073, 1104
Takai, Akinori	1109	Tasaki, Yoko	1179
Takai, Masayuki	1164	Tateda, Hideki	1079
Takamatsu, Hiroshi	1141	Tateno, Hiroyuki	1112
		Tatsunami, Shinobu	1123
		Tazaki, Kenro	1095
		Tazawa, Eigoro	1173
		Terada, Hiroyuki	1100
		Terakado, Kiyoshi	1206
		Terakita, Akihisa	1082, 1083
		Terato, Hiroaki	1204
		Terui, Yasuo	1134
		Teshirogi, Wataru	1148, 1162
		Tochirai, Shin	1139, 1140
		Toh, Yoshihiro	1079

- Tokunaga, Fumio 1084, 1198
 Tomari, Masakazu 1218
 Tominaga, Yoshiya 1077, 1081
 Tomino, Shiro 1128, 1130
 Tomioka, Kenji 1103, 1104, 1196
 Tomita, Hideo 1113
 Tomonaga, Susumu 1165
 Tonegawa, Yasuto 1135
 Toriyama, Masaru 1120
 Toriyama, Mayumi 1128
 Tosuji, Hiroaki 1153
 Toyoda, Fumiyo 1177
 Toyoizumi, Ryuji 1149
 Toyoshima, Yuko Y. 1118
 Towa, Shuichi 1212
 Truman, James W. 1183
 Tsubamoto, Yoshiharu 1133
 Tsuchida, Hirohisa 1172
 Tsuchiya, Hiromasa 1199
 Tsuchiya, Kimiyuki 1110, 1114
 Tsuchiya, Makoto 1222
 Tsuchiya, Teizo 1093
 Tsugawa, Katsuji 1107
 Tsukada, Yutaka 1217
 Tsukahara, Junko 1155
 Tsukahara, Yasuo 1088, 1104
 Tsukamoto, Yoshihiko 1081
 Tsukii, Yuji 1114
 Tsukuda, Hiroko 1099
 Tsuneki, Kazuhiko 1208
 Tsusue, Masao 1127
 Tsutsui, Kazuyoshi 1183, 1188
 Tsuyoshi, Hirohisa 1195
 Tsuyuki, Shogo 1180
- U**
- Uchida, Daisuke 1178, 1187
 Uchida, Teru Aki 1212
 Uchiyama, Hisatoshi 1085
 Uchiyama, Koji 1147
 Uchiyama, Minoru 1189, 1207
 Uchihashi, Kiyoshi 1124
 Ueda, Hiroaki 1226
 Ueda, Hiroshi 1165
 Uehara, Tsuyoshi 1112, 1209, 1221, 1222
 Uematsu, Jun 1141
 Uemura, Haruko 1185, 1186
- Ueno, Naoto 1160
 Uesugi, Yasuo 1193, 1194
 Umebachi, Yoshishige 1127
 Umeda, Masaaki 1213
 Umino, Yukiko 1137
 Uno, Shuhsei 1162, 1163, 1164
 Usui, Noriko 1153
 Usuki, Itaru 1131
 Utsugi, Kazuo 1192
 Uwa, Hiroshi 1224
 Uyama, Taro 1099
- V**
- Vale, Ronald D. 1118
- W**
- Wada, Keiji 1223
 Wada, Masaru 1195
 Wada, Shigeo 1089, 1119, 1121
 Wakabayashi, Katsumi 1178, 1188
 Wakana, Shigeharu 1110, 1114
 Wakatabi, Hoshitsugu 1102
 Waku, Yoshio 1212
 Washio, Hiroshi 1093
 Washitani-Nemoto, Setsuko 1154
 Watabe, Shoji 1123
 Watanabe, Akihiko 1076
 Watanabe, Akihiko 1147
 Watanabe, Hiroshi 1145
 Watanabe, Kazutada 1191
 Watanabe, Mariko 1201
 Watanabe, Satoshi 1211
 Watanabe, Tasuku 1186
 Watanabe, Tsuyoshi 1128
 Watanabe, Yoshio 1120
 Watanabe, Yuichi G. 1118, 1189
 Williams, David S. 1086
 Wingfield, John C. 1179, 1183
- Y**
- Yabe, Yutaka 1080
 Yabusaki, Katsumi 1115
 Yago, Nagasumi 1123
 Yamaai, Tomochiro 1141
 Yamada, Akira 1092

Yamada, Chifumi	1186	Yamazato, Kiyoshi	1199, 1209
Yamada, Hideaki	1177, 1178	Yamazaki, Shin	1088
Yamada, Hisafumi	1154	Yanagawa, Misako	1096
Yamada, Juro	1193	Yanagi, Akira	1176
Yamada, Kazumi	1131, 1136, 1137	Yanase, Hiroshi	1080
Yamada, Koji	1102	Yano, Ken-ichi	1128
Yamada, Naoe	1088	Yashima, Yoichi	1176
Yamada, Takenori	1092	Yasui, Akira	1084
Yamada, Kenjiro	1137, 1158, 1169	Yasugi, Etsuko	1203
Yamagishi, Hiroshi	1094	Yasugi, Sadao	1138, 1142
Yamagishi, Toshiyuki	1113	Yasumasu, Ikuo	1136, 1137, 1156
Yamagiwa, Miho	1191		1157, 1173
Yamaguchi, Keiichiro	1204	Yasumasu, Shigeki	1137
Yamaguchi, Takeo	1213	Yazaki, Kazumori	1114
Yamaguchi, Tsuneo	1074, 1196	Yazawa, Tohru	1094
Yamamoto, Hiroaki	1114, 1144	Yazawa, Yoichi	1121
Yamamoto, Hisashi	1116, 1124	Yokohari, Fumio	1075, 1077
Yamamoto, Kazutoshi	1188, 1189	Yokota, Etsuo	1089, 1118
Yamamoto, Kiyotaka	1202	Yokota, Toshio	1163, 1164
Yamamoto, Mari	1202	Yokoya, Sachihiko	1138
Yamamoto, Masamichi	1165	Yokoyama, Minesuke	1150
Yamamoto, Noriko	1146	Yokoyama, Shigeyuki	1134
Yamamoto, Tadashi S.	1175	Yokoyama, Yoshiko	1203
Yamamoto, Takashi	1131	Yonehana, Tsutomu	1099
Yamamoto, Toshio	1127	Yonekawa, Hiromichi	1113, 1226
Yamanouchi, Korehito	1177	Yonezawa, Satoshi	1123
Yamaoka, Ikuo	1209	Yonezawa, Yumiko	1107, 1202, 1203
Yamaoka, Kageyuki	1076	Yoshida, Akihiro	1160
Yamasaki, Hishashi	1170	Yoshida, Masayuki	1095
Yamasaki, Kenji	1126, 1192	Yoshida, Naoyuki	1212
Yamashiki, Naoko	1137	Yoshigaki, Tomoyoshi	1153
Yamashiro, Hideyuki	1199	Yoshihama, Keiichiro	1188
Yamashita, Kaoru	1194	Yoshihara, Masayoshi	1189
Yamashita, Kayoko	1201	Yoshii, Makoto	1196
Yamashita, Masakane	1167	Yoshikuni, Michiyasu	1167
Yamashita, Masamichi	1089	Yoshimura, Katsuo	1220
Yamashita, Masamiti	1187	Yoshimura, Kenjiro	1088, 1090
Yamashita, Satoru	1079	Yoshimura, Tooru	1124
Yamashita, Tomohiro	1210	Yoshizaki, Norio	1170
Yamashita, Yoshihisa	1162	Yoshizato, Katsutoshi	1131, 1139, 1140
Yamashita, Zinpei	1085		1149, 1211
Yamauchi, Kohei	1161, 1177, 1178	Yoshizawa, Hideki	1207, 1189
Yamauchi, Kiyoshi	1131	Yoshizawa, Tôru	1083, 1084
Yamazaki, Hiroko I.	1125	Yuge, Masahiro	1135

ERRATUM

In the article of Volume 6, number 2, pp. 329-333 entitled "Effect of zinc ion on formation of the fertilization membrane in sea urchin eggs" by Shogo Nakamura, Chika Ohmi and Manabu K. Kojima, upper two lines of right column in page 330 should be deleted.

Development Growth & Differentiation

Published Bimonthly by the Japanese Society of
Developmental Biologists
Distributed by Business Center for Academic
Societies Japan, Academic Press, Inc.

Papers in Vol. 31, No. 6. (December 1989)

56. **REVIEW:** M. Saito: Bioactive sialoglycosphingolipids (gangliosides): Potent differentiation-inducers for human myelogenous leukemia cells
57. **REVIEW:** Y. Iwakura: Mechanism of blastocyst formation of the mouse embryo
58. Y. Yamaguchi and A. Shinagawa: Marked alteration at midblastula transition in the effect of lithium on formation of the larval body pattern of *Xenopus laevis*
59. H. Yokosawa, S. Toratani, Y. Inadome and S. Ishii: Phorbol ester induces elevation of the vitelline coat of eggs of the ascidian *Halocynthia roretzi*
60. Y. Yamazaki and M. Okada: Differences in fine structures between normal and RNA-induced *Drosophila* pole cells
61. Y. Menezes, J. Hamidi, Ch. Khatchadourian and C. Nardon: The murine prepubertal oviduct supports early embryo development *in vitro*
62. K. Itoh and H. Y. Kubota: Expression of neural antigens in normal *Xenopus* embryos and induced explants
63. W. Jiang, G. Peaucellier and W. H. Kinsey: Affinity purification of embryo proteins phosphorylated on tyrosine *in vitro*
64. K. Mikami-Takei and I. Yasumasu: Binding of [³H]nitrendipine to proteins in the plasma membrane of sea urchin sperm
65. R. A. Cameron, T. R. Tosteson and V. Hensley: The control of sea urchin metamorphosis: Ionic effects
66. K. Nishide, T. Nishikata and N. Satoh: A monoclonal antibody specific to embryonic trunk-lateral cells of the ascidian *Halocynthia roretzi* stains coelomic cells of juvenile and adult basophilic blood cells
67. A. Yoshida and K. Aoki: Scale arrangement pattern in a Lepidopteran wing. 1. Periodic cellular pattern in the pupal wing of *Pieris rapae*.

Author Index to Volume 31

Development, Growth and Differentiation (ISSN 0012-1592) is published bimonthly by The Japanese Society of Developmental Biologists, Department of Developmental Biology, Mitsubishi Kasei Institute of Life Science, Minami-ootani 11, Machida, Tokyo 194, Japan. 1989: Volume 31. Annual subscription for Vol. 31, 1989: U.S.\$ 136.00, U.S. and Canada: U.S.\$ 150.00, all other countries except Japan. All prices include postage, handling and air speed delivery except Japan. Second class postage paid at Jamaica, N.Y. 11431, U.S.A.

Outside Japan: Send subscription orders and notices of change of address to Academic Press, Inc., Journal Subscription Fulfillment Department, 1 East First Street, Duluth, MN 55802, U.S.A. Send notices of change of address at least 6-8 weeks in advance. Please include both old and new addresses. U.S.A. POSTMASTER: Send changes of address to *Development, Growth and Differentiation*, Academic Press, Inc., Journal Subscription Fulfillment Department, 1 East First Street, Duluth, MN 55802, U.S.A.

In Japan: Send nonmember subscription orders and notices of change of address to Business Center for Academic Societies Japan, 16-3, Hongo 6-chome, Bunkyo-ku, Tokyo 113, Japan. Send inquiries about membership to Business Center for Academic Societies Japan, 4-16, Yayoi 2-chome, Bunkyo-ku, Tokyo 113, Japan.

Air freight and mailing in the U.S.A. by Publications Expediting, Inc., 200 Meacham Avenue, Elmont, NY 11003, U.S.A.

NARISHIGE

THE ULTIMATE NAME IN MICROMANIPULATION

OUR NEW MODELS **WR-88** and **MO-102M**
MAKE PRECISION MICROMANIPULATION SO EASY!



SOME FEATURES of THE WR-88 WATER ROBOT MICROMANIPULATOR (3-DIMENSIONAL)

- * Drift-free, the new WR-88 has a DRIFT movement of less than 2 microns.
- * The new WR-88 has a SMOOTH MICRODRIVE MECHANISM.
- * An Aqua Purificate remote control ensures totally vibration-free operation.



NARISHIGE SCIENTIFIC INSTRUMENT LAB.

9-28 KASUYA 4-CHOME SETAGAYA-KU, TOKYO 157, JAPAN
PHONE (INT-L) 81-308-8233, FAX (INT-L) 81-3-308-2005
CABLE : NARISHIGE LABO, TELEX, NARISHIGE J27781

Sophisticated Balance between Safety and Centrifugation Capability without Compromise.

Centrifuge in
Integrated with A
Refrigerator

Extra-Quiet
Operation

Ease of Loading/
Unloading
The Rotors

Quick Start/
Quick Stop

High Quality

Triple Safety
Design

Corrosion
Resistance



HIGH SPEED
REFRIGERATED
MICRO CENTRIFUGE

MODEL MR-150

TOMY CORPORATION

1002 SOLEIL NARIMASU BLDG. 31-8, NARIMASU 1-CHOME,
ITABASHI-KU, TOKYO 175 JAPAN
TEL:(03)976-3411 TLX:02723111 TOMYCO J
CABLE:TOMYSHO TOKYO FAX:(GIII G11)(03)930-7010

TOMY SEIKO CO., LTD.

2-2-12, ASAHICHO NERIMA-KU, TOKYO 176 JAPAN
TEL:(03)976-3111

SOLE AGENT

MANUFACTURER

SPECIFICATIONS

Max. Speed
15000 rpm
Max. Centrifugal Force
2000g

ZOOLOGICAL SCIENCE

VOLUME 6 NUMBER 6

DECEMBER 1989

CONTENTS

Obituary	1041
----------------	------

REVIEWS

Murakami, T.: Scanning electron microscopy of vascular casts: A methodological review with some comments on the angioarchitecture of rat hypophysis	1047
Hayashi, S. and M. Aihara: Neonatal estrogenization of the female rat: A useful model for analysis of hypothalamic involvement of gonadotropin release	1059

PROCEEDINGS OF THE 60TH ANNUAL MEETING OF THE ZOOLOGICAL SOCIETY OF JAPAN

Abstracts of papers read by the Zoological Society Prize winners

Nagahama, Y.: Regulation of gametogenesis in teleosts	1071
Kawashima, S.: Aging of endocrine systems in mammals	1072

Abstracts of papers presented at the 60th Annual Meeting of the Zoological Society of Japan

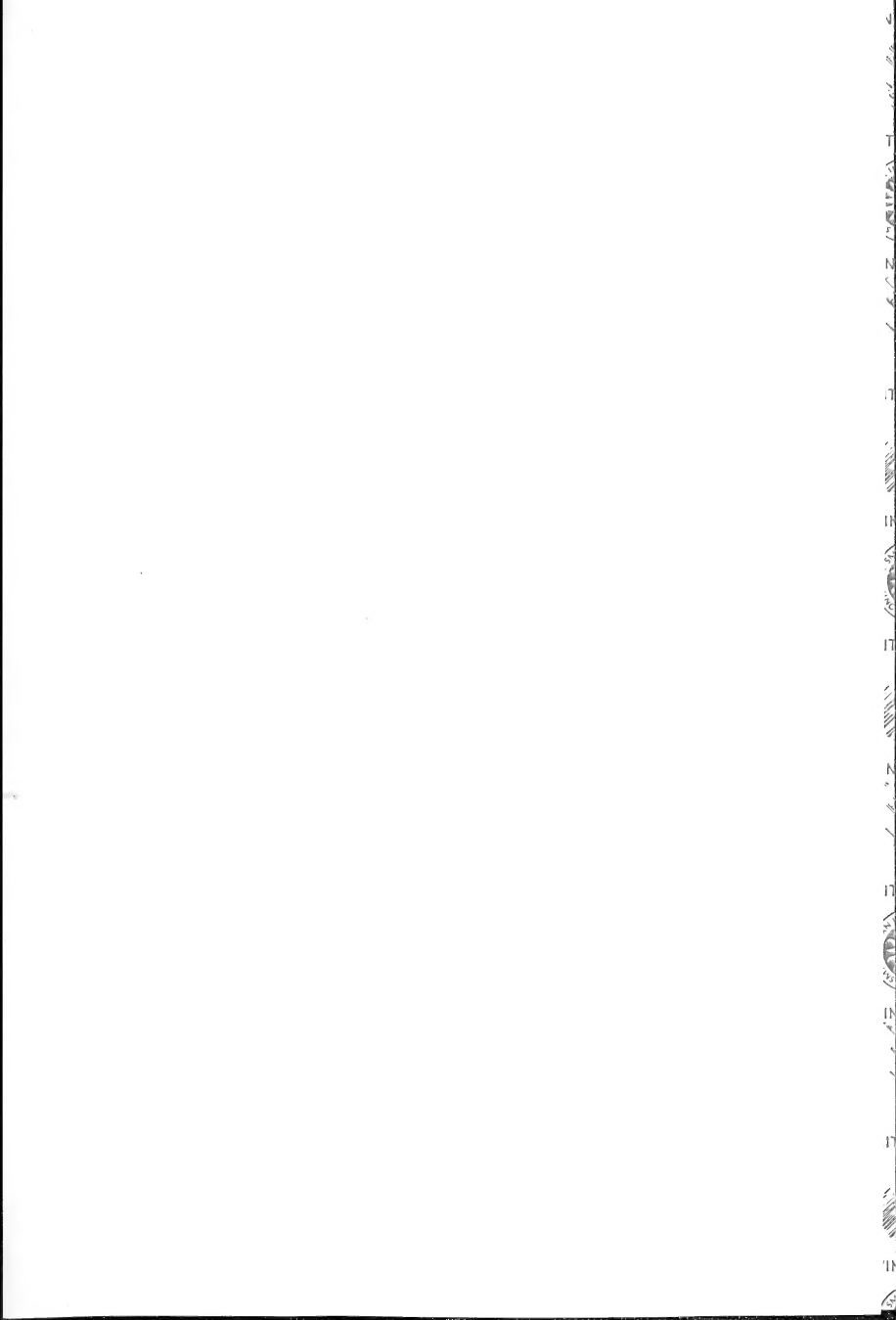
Physiology	1073
Genetics	1109
Biochemistry	1115
Developmental Biology	1135
Endocrinology	1177
Morphology	1197
Behavior Biology and Ecology	1213
Taxonomy and Systematics	1220
Announcements	1230
Author index	1231
Erratum	1246
Contents of ZOOLOGICAL SCIENCE, Vol. 6, Nos. 1-6	i

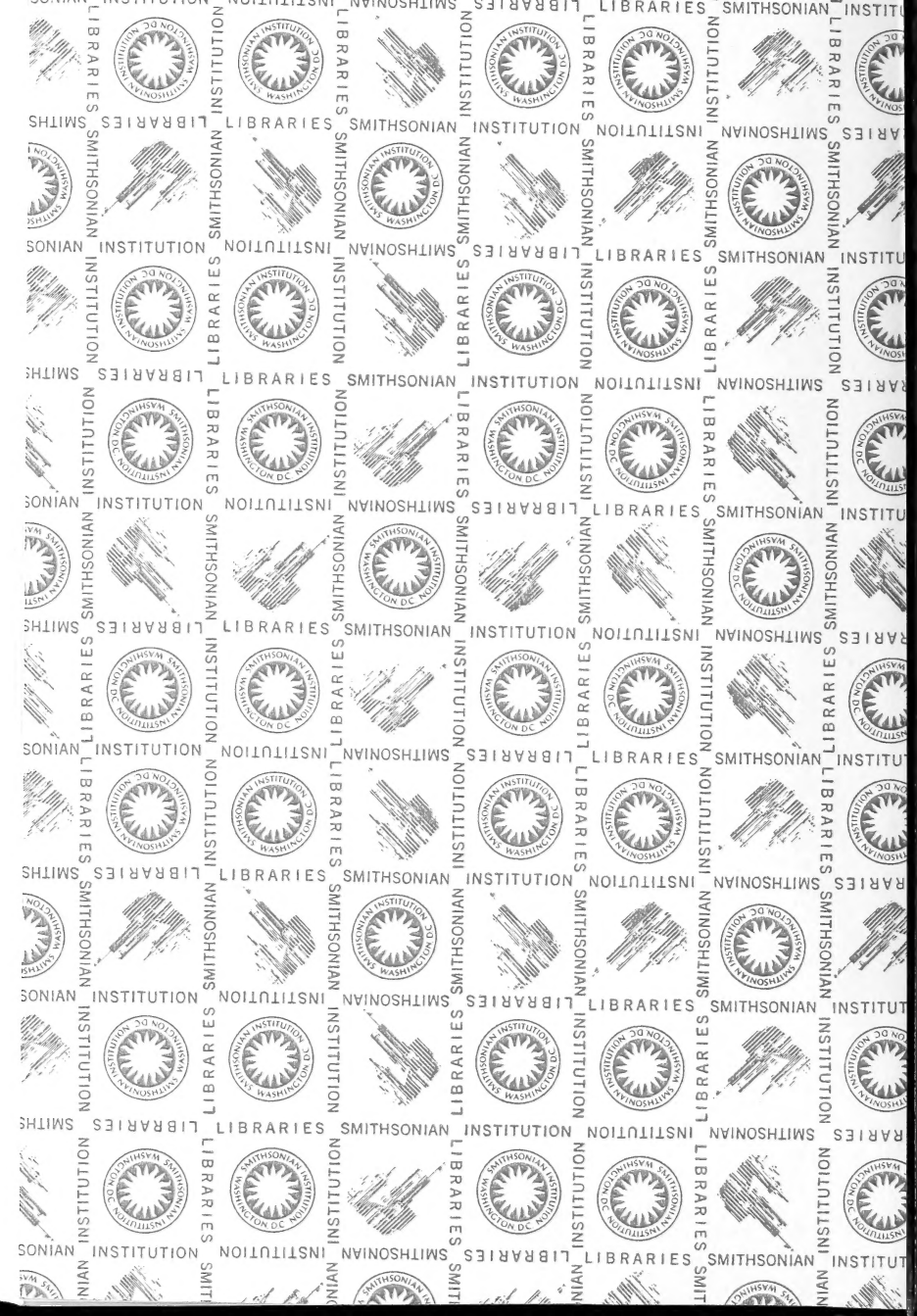
INDEXED IN:

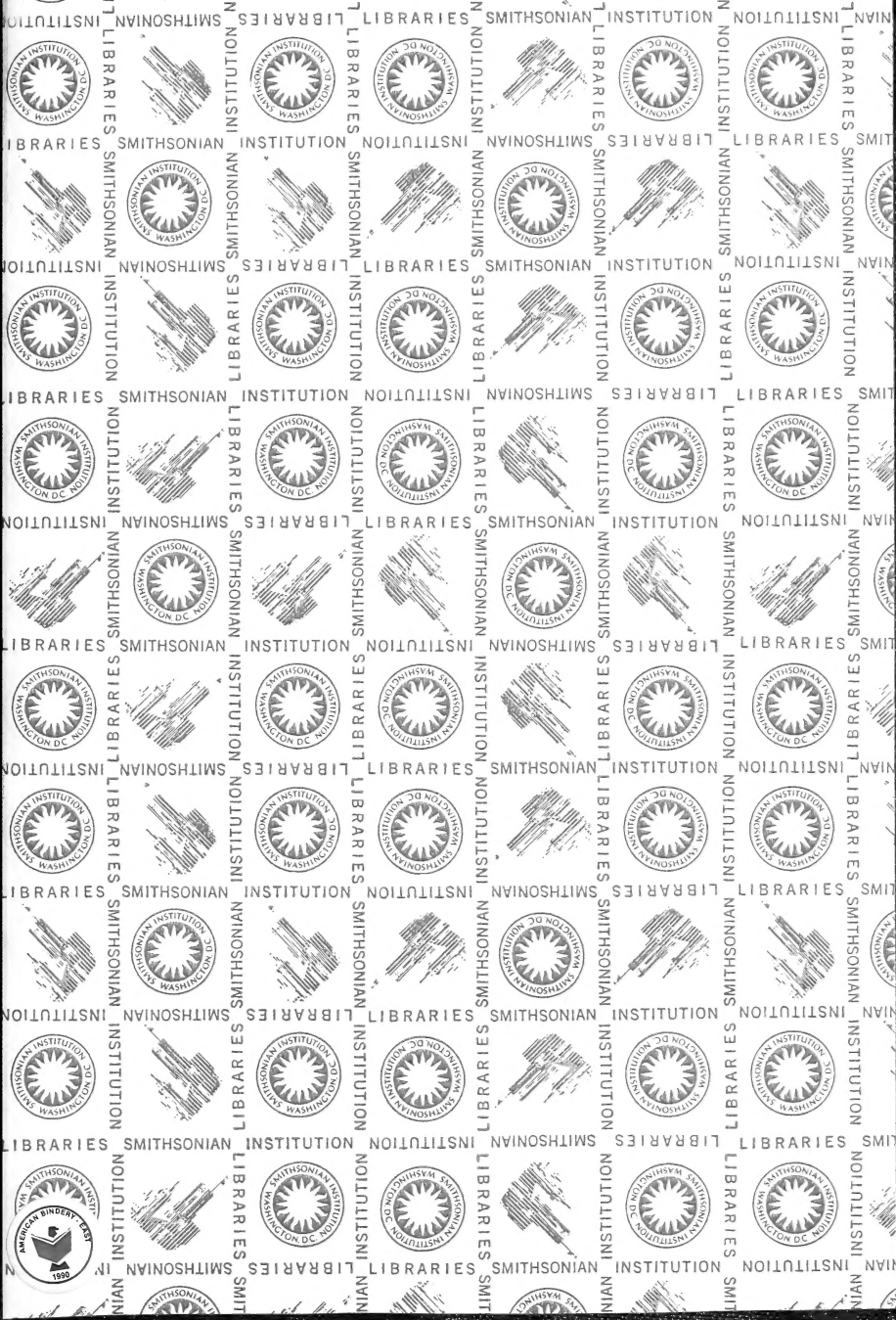
Current Contents/LS and AB & ES,
Science Citation Index,
ISI Online Database,
CABS Database, INFOBIB

Issued on December 15

Printed by Daigaku Letterpress Co., Ltd.,
Hiroshima, Japan







SMITHSONIAN INSTITUTION LIBRARIES



3 9088 01261 2719